



सत्यमेव जयते

INDIAN AGRICULTURAL  
RESEARCH INSTITUTE, NEW DELHI

48050

2/12

I.A.R.I.6.

GIP NLK—H-3 I.A.R.I.—10-5-55—45,000







# Transactions of the Faraday Society

FOUNDED 1903

TO PROMOTE THE STUDY OF ELECTROCHEMISTRY, ELECTROMETALLURGY,  
PHYSICAL CHEMISTRY, METALLOGRAPHY, AND KINDRED SUBJECTS

---

VOL. XLV, 1949

---

48060  
■■■■■■■■■■  
IARI

GURNEY AND JACKSON  
LONDON: 98 GREAT RUSSELL STREET  
EDINBURGH: TWEEDDALE COURT

PRINTED IN GREAT BRITAIN AT  
THE UNIVERSITY PRESS  
ABERDEEN

# SOME OBSERVATIONS ON THE ELECTRO-CHEMISTRY OF URANIUM

By H. G. HEAL

Received 10th February, 1948; as amended, 16th June, 1948

Data on the polarography of uranium salt solutions, in the valencies of three, four, and six are given. These measurements are compared with the older published work on the oxidation-reduction potentials of the uranium ions, and the two sets of figures related by means of the hypothesis of an unstable  $\text{UO}_2^+$  ion, which is also held responsible for the shift of potential of a  $\text{U}^{\text{VI}}\text{-U}^{\text{IV}}$  electrode under illumination. New figures are given for several oxidation-reduction potentials.

The literature references to the electrochemistry of aqueous solutions of uranium salts are numerous and confusing: no connected account of the subject from the electrochemical, as distinct from the analytical or preparative point of view, has appeared. This paper and the one which follows it are an attempt to remedy this deficiency. As a result of the newer investigations, it is now possible to give a plausible general description of the electrode processes in uranium salt solutions, although many details remain to be cleared up. The present paper is a survey of the processes at inert electrodes, while the following one deals with the kinetics of the decomposition of an unstable ion of pentavalent uranium, which plays an important part in the electrode reactions. A note on these subjects has been published.<sup>1</sup>

Recently Kolthoff and Harris, who had been working, unknown to us and simultaneously with us, on the polarography of uranium, published a comprehensive account of their researches.<sup>2, 3, 4</sup> We shall therefore touch only briefly on those results common to both investigations and already published by Kolthoff and Harris.\*

Uranium, in non-complex aqueous solutions of its salts, has three valencies stable enough for solid salts to be isolated, viz. three, four and six. The trivalent salts reduce water, and are therefore difficult to work with. In weakly acid and neutral solutions, complicated hydrolysis reactions, which are not yet fully understood, take place. The predominant ionic form of hexavalent uranium in strongly acid solutions is the uranyl ion,  $\text{UO}_2^{2+}$ , which also forms the solid salts of this valency state. Kolthoff and Harris's polarographic studies and pH measurements of nearly neutral solutions<sup>4</sup> show that this ion is largely hydrolysed to  $\text{UO}_2\text{OH}^+$ , and perhaps partly to  $\text{UO}_2(\text{OH})_2$  in such media, but that hydrolysis is no longer detectable in  $10^{-3}$  M uranyl solutions containing more than about  $5 \times 10^{-4}$  M free HCl. There is little evidence concerning the extent of hydrolysis of  $\text{U}^{\text{IV}}$  and  $\text{U}^{\text{III}}$  ions. We find that  $\text{U}^{\text{IV}}$  solutions precipitate  $\text{UO}_3$ , sometimes only after prolonged standing, in pH's of the order of 3 and over, suggesting the presence of hydrolysed forms of the ion: moreover, salts of  $\text{U}^{\text{IV}}$  cannot be dehydrated without decomposition. These facts, as well as theory, make it unlikely that  $\text{U}^{++++}$  exists in the solutions, and point to  $\text{UO}^{2+}$ ,  $\text{UOOH}^+$  or  $\text{UOH}^{+++}$  as the probable main ionic form of  $\text{U}^{\text{IV}}$  in acid solutions. Polarographic evidence will be quoted to show that

<sup>1</sup> Heal, *Nature*, 1946, **157**, 225.

<sup>2</sup> Kolthoff and Harris, *J. Amer. Chem. Soc.*, 1945, **67**, 1484.

<sup>3</sup> Kolthoff and Harris, *ibid.*, 1946, **68**, 1175.

<sup>4</sup> Kolthoff and Harris, *ibid.*, 1947, **69**, 446.

\* The writer gratefully acknowledges useful private correspondence with W. E. Harris.

the predominant form of  $U^{III}$  in 1 M HCl, or in 0.5 M  $H_2SO_4$ , differs only by one electron from the predominant form of  $U^{IV}$  in the same acid.

One might expect that the potentials of  $U^{IV} - U^{VI}$  and  $U^{III} - U^{IV}$  couples, measured statically, would correspond to the potentials at which the respective ions are oxidised or reduced at an electrode, but the published figures do not by any means correspond. The discrepancies are accounted for in this paper.

### Experimental

Because of the complicated nature of the reactions, the polarograph, which gives information about the concentration of ions and the reversibility of electrode processes as well as mere potentials, was chosen in preference to static electrode potential measurements for our general study. (For the investigation of the kinetics of  $U^{IV}$  decomposition however, a special static-potential apparatus, described in the next paper, was set up.) The polarograph was an ordinary hand-operated apparatus, with a continuously variable applied potential. A separate reference electrode was used throughout. The uranyl sulphate employed contained less than 0.1 % of foreign metals and anions. Uranyl chloride solutions were made up by dissolving equally pure  $UO_3$  in hydrochloric acid. Solutions of  $U^{IV}$  and  $U^{III}$  were prepared by reducing the sufficiently acidified appropriate uranyl solution electrolytically in a cell with mercury cathode and sintered-glass diaphragm.<sup>5</sup> For  $U^{IV}$ , reduction was continued until the solution began to turn brown, then the trace of  $U^{III}$  present oxidised by blowing air through for 1-2 min. For  $U^{III}$ , reduction was continued to the limit, in an atmosphere of hydrogen, which was maintained during transfers. The solutions of  $U^{III}$  were used immediately after preparation.

### Results

The polarograms of acid uranyl solutions contain three reduction-waves at potentials more positive than the hydrogen wave. Those of acid  $U^{IV}$  solutions

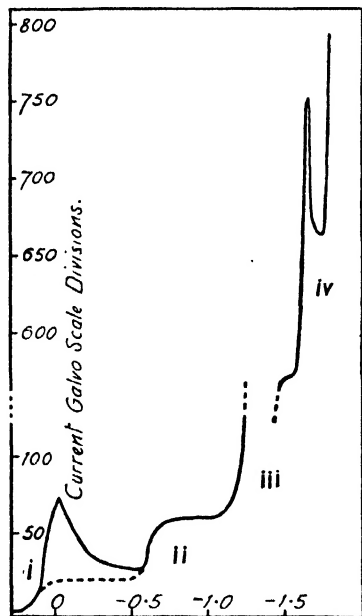


FIG. 1.—Polarogram of 0.001 M  $UO_2Cl_2$ , 0.01 M HCl, 0.1 M KCl, in the absence of a maximum-suppressor. The broken line under the first wave shows the approximate curve in presence of a suppressor.

- (i) First uranyl wave. (ii) Second (composite) uranyl wave. (iii) Hydrogen wave. (iv) Wave probably resulting from reduction  $U^{III}$  to uranium metal.

A part of the hydrogen wave corresponding to 400 scale divisions has been cut out for compactness, as indicated.

contain one reduction-wave, and those of acid  $U^{III}$  solutions one oxidation-wave, in this region of potential. These latter waves correspond in position and height to the third wave in uranyl polarograms for solutions of the same molar con-

<sup>5</sup> Lawrence, *J. Amer. Chem. Soc.*, 1934, **56**, 782.

centration. Potentials on the other side of the hydrogen wave were difficult to investigate, because this wave is very high in solutions acid enough to suppress hydrolysis, and the amplitude of the current fluctuations as the mercury dropped was correspondingly large. However, a high wave was detected in this region in the polarograms of acid uranyl solutions. Fig. 1 shows a typical uranyl polarogram. The first wave, which is the one generally employed in analytical

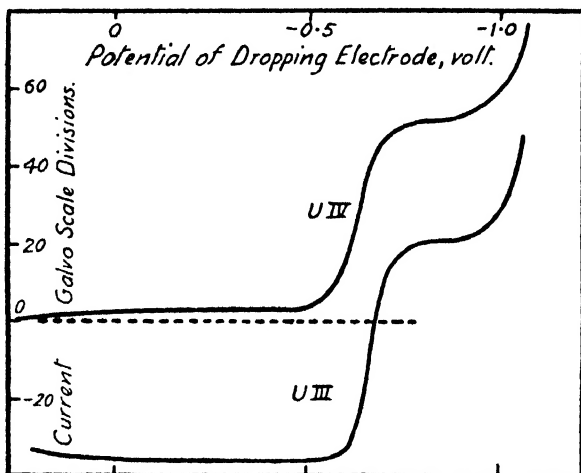


FIG. 2.—Polarograms for 0.07 M  $U^{IV}$  in M HCl (above) and for the same solution after the  $U^{IV}$  had been electrolytically reduced as far as possible (below).

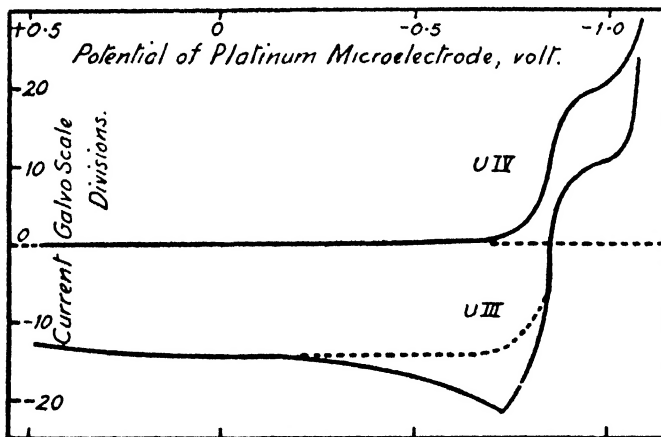


FIG. 3.—Polarograms for 0.01 M  $U^{IV}$  in 0.5 M  $H_2SO_4$  (above) and for the same solution after the  $U^{IV}$  had been electrolytically reduced as far as possible (below). The broken line shows the approximate position of the curve in presence of a maximum-suppressor: the wave-height is estimated from here.

polarography, exhibits on this figure the maximum usually present unless a suppressor is added. The second and third waves are so nearly superimposed that they appear as one, which will be referred to as the "composite wave": this is always the case with chloride solutions, although a slight kink can sometimes be seen halfway up the "wave."

**The  $U^{III}$ - $U^{IV}$  Oxidation-Reduction.**—The interpretation of the waves for this reaction presents no difficulty. Fig. 2 illustrates the reduction-wave for 0.01 M  $U^{IV}$  in M HCl, and the oxidation-wave for the same solution after reduction of the uranium to  $U^{III}$ . The two waves have almost the same half-

wave potential and total height. The part of the "U<sup>III</sup>" wave on the side of the potential axis corresponding to a reduction undoubtedly represents some U<sup>IV</sup> still present in the U<sup>III</sup> solution, which could not be completely eliminated because of the reaction between U<sup>III</sup> and water. Fig. 3 shows the corresponding waves for U<sup>IV</sup> and U<sup>III</sup> in 0.5 M H<sub>2</sub>SO<sub>4</sub> solution. The oxidation-wave has a maximum in this case.

Fig. 4 and 5 show accurate plots of the U<sup>IV</sup> reduction-wave in M HCl and 0.5 M H<sub>2</sub>SO<sub>4</sub> respectively, at 0° C. The graphs of  $\log \frac{i}{i_d - i}$  against potential

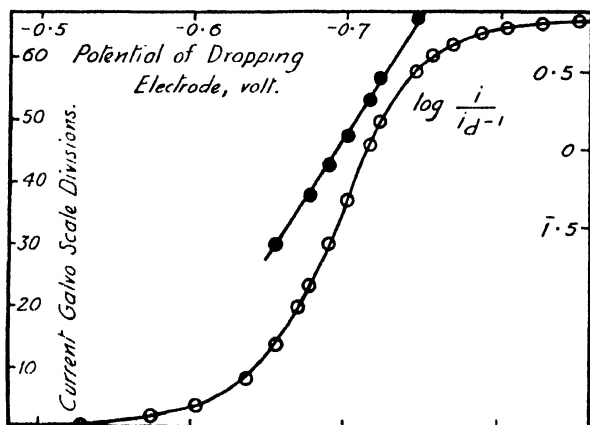


FIG. 4.—Accurate plot of polarographic wave for 0.01 M UCl<sub>4</sub> in M HCl, with  $\log \frac{i}{i_d - i}$  line (shaded circles). Temperature 0° C.

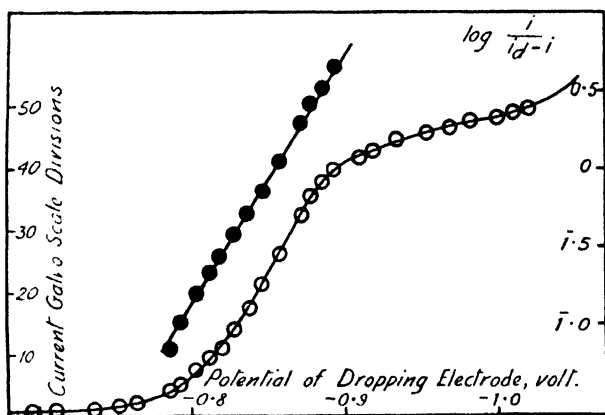


FIG. 5.—Accurate plot of polarographic wave for 0.01 M U(SO<sub>4</sub>)<sub>2</sub> in 0.5 M H<sub>2</sub>SO<sub>4</sub>, with  $\log \frac{i}{i_d - i}$  line (shaded circles). Temperature 0° C.

are also given. These have gradients 0.064 V and 0.061 V, slightly higher than the theoretical 0.058 V for unit valency-change in the reduction. Kolthoff and Harris<sup>2</sup> found 0.08 V and concluded that the reaction was not polarographically reversible. The discrepancy is probably due to the fact that their measurements were made at 25° C and ours at 0° C, and to the large error in the slope measurements.

Comparison of the half-wave potentials and wave heights for the U<sup>IV</sup> and U<sup>III</sup> waves shows that the reduction of U<sup>IV</sup> at the electrode gives rise directly to the predominant form of U<sup>III</sup> present in the U<sup>III</sup> solution. Hydrogen ions

do not participate in the electrode reaction (see later): hence the  $\text{U}^{\text{IV}}$  ions can only differ from the  $\text{U}^{\text{III}}$  ions by one electron. They could thus be  $\text{UO}^{++}$  and  $\text{UO}^+$  respectively, or  $\text{UOH}^{+++}$  and  $\text{UOH}^{++}$ , but not  $\text{UOOH}^+$  and  $\text{UOOH}$ , for this would mean unionised  $\text{U}^{\text{III}}$ . The chief ionic form of  $\text{U}^{\text{IV}}$  must therefore be either  $\text{UO}^{++}$  or  $\text{UOH}^{+++}$ , and the chief form of  $\text{U}^{\text{III}}$  must be  $\text{UO}^+$  or  $\text{UOH}^{++}$ , in acid solutions.

The  $E_{\frac{1}{2}}$  of the  $\text{U}^{\text{IV}}$  reduction-wave\* is  $-0.69$  V in M HCl. This agrees well with the figure  $-0.68$  V obtained by Kolthoff and Harris<sup>3</sup> for M  $\text{HClO}_4$  and  $-0.71$  V for  $0.1$  M HCl. These acids probably, therefore, do not form strong complexes with the ions of  $\text{U}^{\text{III}}$  and  $\text{U}^{\text{IV}}$ , otherwise divergences might be expected. In  $0.5$  M  $\text{H}_2\text{SO}_4$ , on the other hand,  $E_{\frac{1}{2}}$  is  $-0.85$  V, showing that a strong complex with  $\text{U}^{\text{IV}}$  is probably formed. A complex with a dissociation complex of about  $10^{-3}$  would account for the  $E_{\frac{1}{2}}$  value.

The question next arose: would it be possible to oxidise  $\text{U}^{\text{IV}}$  to a higher valency state at an electrode? The polarograms already given showed that no oxidation-wave was found up to  $+0.6$  V, the most positive potential attainable with a dropping mercury electrode in  $0.5$  M  $\text{H}_2\text{SO}_4$ . Accordingly, a still

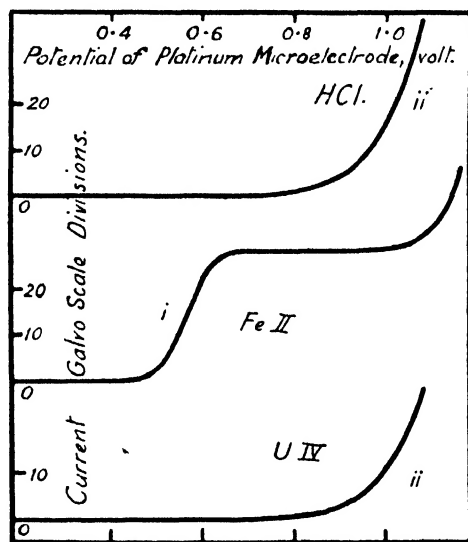


FIG. 6.—Polarograms with platinum microelectrode: for 6 M HCl (above  $0.01$  M  $\text{FeCl}_2$  in 6 M HCl (centre) and  $0.01$  M  $\text{UCl}_4$  in 6 M HCl (below).

- (i)  $\text{Fe}^{++} \longrightarrow \text{Fe}^{+++}$ .
- (ii)  $\text{Cl}^- \longrightarrow \frac{1}{2}\text{Cl}_2$ .

more positive range of potentials was investigated by means of a stationary platinum micro-electrode. The procedure was tested on solutions of  $\text{Fe}^{++}$ , which gives an oxidation-wave in this region. With the same molar concentration of  $\text{U}^{\text{IV}}$ ,  $0.01$  M, in the same acids ( $3$  M  $\text{H}_2\text{SO}_4$  and  $6$  M HCl), and the same current sensitivity, no distinct waves were found before the discharge of oxygen or chlorine (Fig. 6 and 7). However, in  $3$  M  $\text{H}_2\text{SO}_4$  there was a long irregular rise of current, culminating in the evolution of oxygen bubbles: this may have been caused by partial depolarisation of the electrode through reaction of the polarising oxygen with  $\text{U}^{\text{IV}}$ , and consequent reduction of the oxygen overvoltage: it cannot be regarded as a true polarographic wave. These results lead to the, at first sight, surprising conclusion that  $\text{U}^{\text{IV}}$  cannot be oxidised by a primary electrode process although, of course, a secondary chemical oxidation may occur. The polarograms were checked under various conditions. Moreover,

\* All half-wave potentials, referred to as  $E_{\frac{1}{2}}$ , are given on the hydrogen scale for comparison with ordinary electrode potentials. Values quoted from Kolthoff and Harris are also given on this scale; in the original papers, however, they are stated with respect to the saturated calomel electrode.



an attempt to oxidise  $U^{IV}$  electrolytically on the large scale, in  $M$   $HCl$ , by means of a platinum electrode kept at about  $+0.7$  V failed.

**The Uranyl Polarogram.**—Notwithstanding the failure to oxidise  $U^{IV}$  at an electrode,  $U^{VI}$  is reduced at the dropping mercury cathode. A typical uranyl polarogram, similar to those already described in the literature,<sup>3,6,7</sup> is shown in Fig. 8. In moderately acid solution the second "wave" (which in the figure exhibits its composite character) is always nearly twice as high as the first. The conclusion is that three stages of reduction take place in all, each by one unit of valency. If this is so, the slope of the first wave should be that

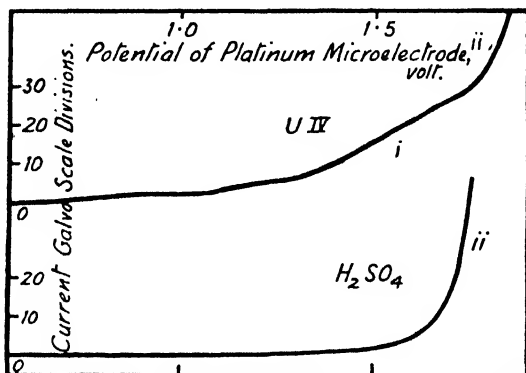


FIG. 7.—Polarograms with platinum microelectrode for  $0.01$  M  $U^{IV}$  in  $3$  M  $H_2SO_4$  (above), and  $3$  M  $H_2SO_4$  alone (below).

(i) Irregular current rise, perhaps due to depolarisation.

(ii)  $HSO_4^- \xrightarrow[e]{+0.0H^-} HSO_4 \xrightarrow{+0.0H^-} HSO_4^- + 1/4 O_2 + 1/2 H_2O$ .

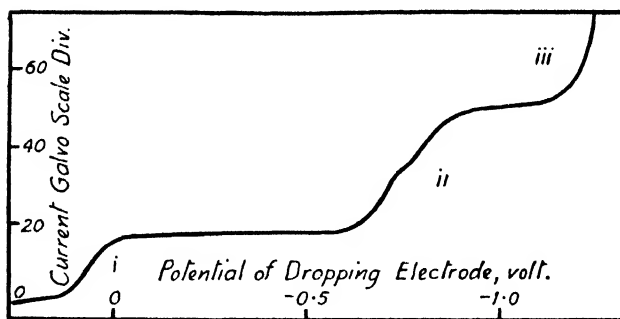


FIG. 8.—Polarogram for  $0.01$  M  $UO_2Cl_2$  in  $0.1$  M  $HCl$  and  $0.9$  M  $KCl$ , with  $0.02$  % gelatin as maximum-suppressor.

(i) First uranyl wave. (ii) Composite uranyl wave. (iii) Hydrogen wave.

for a unit reduction. This wave, together with the corresponding  $\log \frac{i}{i_d - i}$  line, is shown in Fig. 9. The gradient of the latter is  $0.055$  V (theoretical  $0.058$  V for unit valency change at the temperature of the experiment,  $0^\circ C$ );  $E_1$  is  $+0.05$  V. For the corresponding  $E_1$  in  $0.5$  M  $H_2SO_4$  solution, the value  $+0.04$  V was found. Thus it is probable that neither  $UO_2^{2+}$  nor its reduction-product forms a strong complex with  $HCl$  or  $H_2SO_4$ . Trials made by us confirm Kolthoff and Harris's observation that the height of this wave increases markedly as the acidity is increased above about  $0.5$  N.<sup>3</sup>

<sup>6</sup> Herasymenko, *Trans. Faraday Soc.*, 1928, **24**, 267.

<sup>7</sup> Strubl, *Coll. Czech. Chem. Comm.*, 1938, **10**, 466.

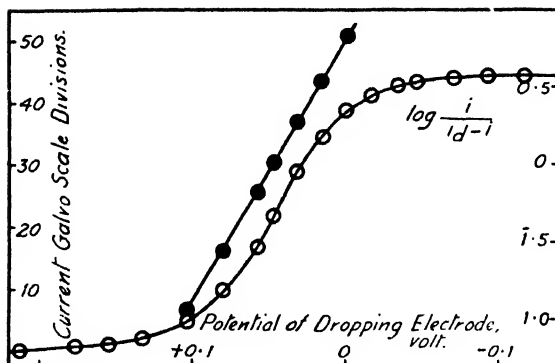


FIG. 9.—Accurate plot of first uranyl wave for 0.01 M  $\text{UO}_2\text{Cl}_2$ , 0.1 M HCl, 0.9 M KCl, with  $\log \frac{i}{i_d - i}$  line (shaded circles). Temperature 0° C.

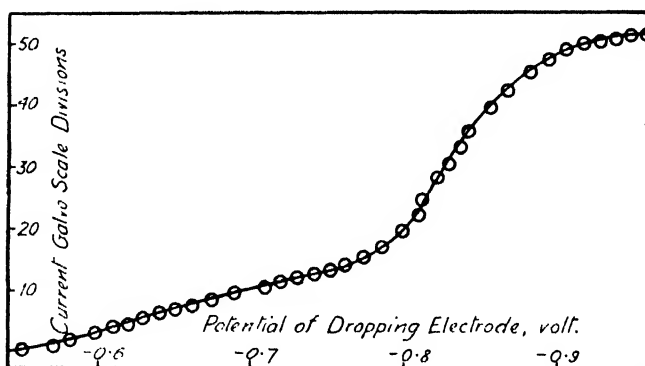


FIG. 10.—Accurate plot of composite wave for 0.01 M  $\text{UO}_2\text{SO}_4$ , 0.05 M  $\text{H}_2\text{SO}_4$ , 0.9 M KCl, with 0.02 % gelatin. Temperature 0° C.

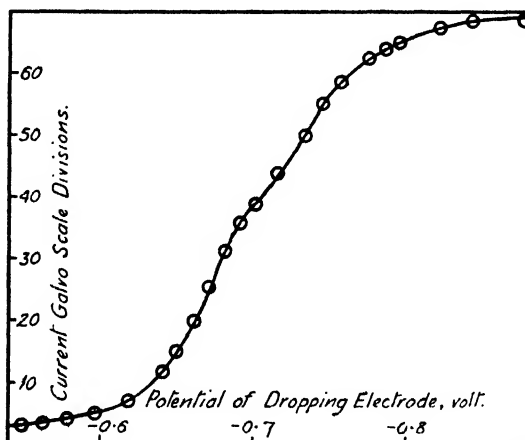


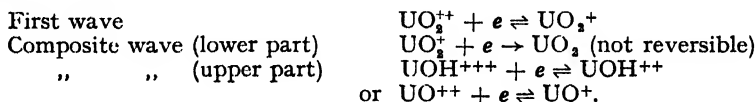
FIG. 11.—Accurate plot of composite wave for 0.01 M  $\text{UO}_2\text{Cl}_2$ , 0.1 M HCl, 0.9 M KCl, with 0.02 % gelatin. Temperature 0° C.

The upper part of the composite wave in the uranyl polarogram corresponds in  $E_1$  to the  $\text{U}^{\text{IV}}\text{-U}^{\text{III}}$  wave, found in the polarograms of  $\text{U}^{\text{III}}$  and  $\text{U}^{\text{IV}}$  solutions. Like the latter, it is displaced by complex-formation to a potential about 0.16 V more negative, in presence of  $\text{H}_2\text{SO}_4$ . This makes the double nature of the wave more evident, and shows that the lower part is irregular in shape, while the upper part is more or less logarithmic (Fig. 10). In chloride solution without  $\text{H}_2\text{SO}_4$  (Fig. 11), the composite wave has a perceptible break.

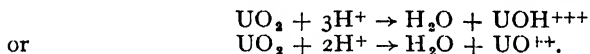
In agreement with Kolthoff and Harris,<sup>8</sup> we found that none of the  $E_1$ 's in the uranyl polarogram is systematically affected by varying the acidity over the range 0.03 N to N. At lower acidities evidence of hydrolysis<sup>4</sup> begins to appear. We conclude that hydrogen ions do not participate in any of the primary electrode reactions.

## Discussion

**The Structure of the Uranyl Polarogram.**—Considering for the moment only that part of the polarogram on the positive side of the hydrogen wave, the starting material for reduction is  $\text{UO}_2^{++}$ , and the last stage of reduction yields  $\text{UO}^+$  or  $\text{UOH}^{++}$ . Since it has been shown that none of the electrode reactions involves hydrogen ions, there must be a purely chemical reaction of inverse hydrolysis at some point. The most probable mechanisms are :



The second reaction, giving rise to the lower part of the composite wave, would produce a solid, perhaps ephemeral, layer on the mercury surface, which would account for the irregular "irreversible" shape of the wave. In order for the upper part of the composite wave to appear, there must be enough acid to convert  $\text{UO}_2$  to  $\text{UOH}^{+++}$  or to  $\text{UO}^{++}$ , i.e.



Kolthoff and Harris noted<sup>4</sup> that in nearly neutral solutions this wave is missing. Pierlé<sup>9</sup> found that a  $\text{UO}_2$  electrode in a uranyl solution took up a potential near that of the second wave, as one would expect if the wave in fact represents a deposition of oxide or hydroxide on the dropping electrode surface.

**The Potential of Uranium Metal against  $\text{U}^{\text{III}}$ .**—This has never been satisfactorily measured. The high wave in the uranyl polarogram coming after the hydrogen wave can only correspond to the reduction  $\text{U}^{\text{III}} \rightarrow \text{U}$  metal. Its  $E_1$  is about  $-1.6$  V. A potential for the  $\text{U}^{\text{III}}\text{-U}$  metal couple in this region is in accordance with the chemical properties of the element, unlike the values given in the older literature.

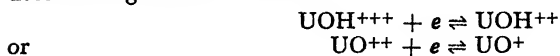
**The Oxidation-reduction Potential of the  $\text{U}^{\text{III}}\text{-U}^{\text{IV}}$  Couple.**—The best values so far obtained for this potential are the  $E_1$  values for the  $\text{U}^{\text{III}}\text{-U}^{\text{IV}}$  wave, which are  $-0.69$  V and  $-0.85$  V in M HCl and 0.5 M  $\text{H}_2\text{SO}_4$  respectively. Luyckx<sup>9</sup> and more recently Khlopin and Gurevitch,<sup>10</sup> measuring with platinum electrodes, obtained very different values, near zero on the hydrogen scale: these workers overlooked the fact that a platinum electrode immersed in such a strongly reducing solution immediately becomes covered with a film of hydrogen, and functions as a hydrogen electrode. (Mercury is the only practicable electrode material in such solutions: it was used in a recent measurement of the vanadium

<sup>8</sup> Pierlé, *J. Physic. Chem.*, 1919, **23**, 517.

<sup>9</sup> Luyckx, *Bull. Soc. chim. Belg.*, 1931, **40**, 269.

<sup>10</sup> Khlopin and Gurevitch, *Bull. Acad. Sci. U.R.S.S.*, 1943, **271**, 381.

redox potentials, where the same difficulty arises.)<sup>11</sup> The potential-determining reaction must be

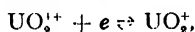


because (i) chemical evidence shows that the  $\text{U}^{\text{IV}}$  can only be present as  $\text{UOH}^{+++}$  or  $\text{UO}^{++}$ , and (ii) polarographic evidence shows that the electrode reaction is simply a one-electron transfer.

**Electrode Reactions of the  $\text{UO}_2^+$  Ion.**—Here it is necessary to account for the following facts.

(i) The standard potential of the  $\text{U}^{\text{VI}}\text{-U}^{\text{IV}}$  couple in acid solutions has been measured by several investigators,<sup>12, 11, 17</sup> with reasonably concordant results. The best measurements available to us, those of Titlestad, give the value  $+0.404$  V on the hydrogen scale. This does not correspond to any of the  $E_1$ 's in the uranyl polarogram. The question therefore arises, whether it is necessary to postulate a different reaction at the platinum electrode, which was employed in these measurements, or whether this potential can be fitted into the polarograph reaction scheme outlined above.

(ii) The general interpretation of the uranyl polarogram, and the slope of the  $\log \frac{i}{i_d - i}$  line for the first wave, show that an ion of quinquavalent uranium is formed in the first reduction,



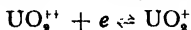
yet the large scale electrolytic reduction of uranyl solutions does not yield a salt of quinquavalent uranium, nor are such salts known at all.

(iii) The Becquerel effect: the potential of a platinum electrode in a mixed  $\text{U}^{\text{IV}}\text{-U}^{\text{VI}}$  solution, with respect to any suitable reference electrode, drifts to a more negative value under illumination. The initial drift, and the return to the normal potential after the light is shut off, are both exponential in character, and occupy periods of the order of seconds or minutes.

An ordinary redox equilibrium does not explain this.<sup>12, 14, 15, 16</sup> The following hypothesis will account for these observations. The ion  $\text{UO}_2^+$  is unstable but is not reduced to  $\text{U}^{\text{IV}}$  at the potential of the first uranyl wave, and persists in the neighbourhood of the dropping electrode until it undergoes disproportionation with another ion of the same kind into  $\text{U}^{\text{IV}}$  and  $\text{U}^{\text{VI}}$ . At moderate acidities, this reaction is still too slow to affect the shape of the wave, but above about 0.5 N acidity this is no longer the case. Kolthoff and Harris showed<sup>3</sup> that the increase in height could be explained qualitatively by supposing that the rate of decomposition increased with acidity and temperature. In our next paper we give numerical values for the rate constant of the disproportionation, obtained by a different method. We assume that the  $\text{UO}_2^+$  ion is not only formed by reduction of  $\text{UO}_2^{++}$ , but is always present in mixed  $\text{U}^{\text{VI}}\text{-U}^{\text{IV}}$  solutions at a concentration determined by a formation-disproportionation equilibrium



We now postulate that the potential-determining reaction at a platinum electrode is the same as that at the dropping mercury electrode, viz.



<sup>11</sup> Jones and Colvin, *J. Amer. Chem. Soc.*, 1944, **66**, 1547.

<sup>12</sup> Baur, *Z. physik. Chem.*, 1908, **63**, 689.

<sup>13</sup> Luther and Michie, *Z. Elektrochem.*, 1908, **14**, 829.

<sup>14</sup> Titlestad, *Z. physik. Chem.*, 1910, **72**, 264.

<sup>15</sup> Schiller, *ibid.*, 1912, **80**, 656.

<sup>16</sup> Trümpler, *ibid.*, 1915, **90**, 385.

<sup>17</sup> McCoy and Bunzel, *J. Amer. Chem. Soc.*, 1909, **31**, 367.

but that in the former case the concentrations of the two ions are grossly unequal, whereas in the latter case they are of the same order: i.e. the  $U^v$  concentration is very small when the  $U^v$  is in equilibrium with  $U^{vi}$  and  $U^{vi}$ , but is much larger in the neighbourhood of the dropping electrode, where reduction is continuously taking place.  $E_{\frac{1}{2}}$  is approximately equal to the standard potential for this electrode reaction, which corresponds to equal concentrations of  $U^{vi}$  and  $U^v$ :\* it is +0.05 V.

The potential of a platinum electrode in a mixed  $U^{vi}$ - $U^{iv}$  solution should therefore be given approximately by the Nernst equation:

$$E \simeq 0.05 + \frac{RT}{F} \ln \frac{[UO_2^{++}]}{[UO_2^+]}$$

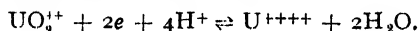
Titlestad gives the value +0.404 V for  $E$  at M concentration in each of  $U^{vi}$ ,  $U^{iv}$  and  $H^+$ . If this figure is substituted in the Nernst equation, the concentration of  $U^v$  in such a solution turns out to be about  $10^{-8}$  M. This is consistent with the value  $10^{-8}$ , set as the lower limit for the equilibrium constant

$$K = \frac{a_{UO_2^{++}} \cdot a_{UO_2^{+}}}{a_{UO_2^+}^2 \cdot a_{H^+}}$$

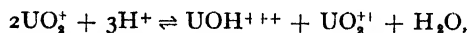
by Kolthoff and Harris, from their polarographic measurements.<sup>3</sup> It is too low a concentration to be detected chemically or spectroscopically. Titlestad found that the equation

$$E = E_0 + \frac{RT}{2F} \ln \frac{[UO_2^{++}][H^+]^4}{[U^{++++}]}$$

fitted the observed variations of the platinum electrode potential with the concentrations (assuming that all the  $U^{iv}$  was present as  $U^{++++}$ ), and concluded that the electrode reaction was



An exact quantitative comparison of the results given by the hypothesis of quinquavalent uranium with Titlestad's potential equation is out of the question, because the charge on the  $U^{iv}$  ion is not known, and the required activity coefficients cannot be estimated even approximately: however, the following considerations show that there is no obvious inconsistency. Assuming first that the ionic form of  $U^{iv}$  is mainly  $UOH^{+++}$ , the total disproportionation reaction (not necessarily occurring in one stage) will be



the activity of  $U^v$  at equilibrium is therefore

$$a_{U^v} = \text{const.} \sqrt{\frac{a_{U^{iv}} \cdot a_{U^{vi}}}{a_{H^+}^3}}.$$

The Nernst equation for the  $U^{vi}$ - $U^v$  electrode is

$$E = 0.05 + \frac{RT}{F} \ln \frac{a_{UO_2^{++}}}{a_{UO_2^+}},$$

and substituting this value of the  $U^v$  activity gives

$$E = 0.05 + \frac{RT}{2F} \ln \frac{[UO_2^{++}][H^+]^3}{[UOH^{+++}]} + \frac{RT}{F} \ln (\text{const.})$$

plus a logarithm containing the activity coefficients. This equation agrees with Titlestad's, except that the  $H^+$  concentration occurs to the third instead of the fourth power. However, the activity coefficient

\* This is the case so long as decomposition of the  $U^v$  is not so rapid as to affect the wave-height: this requirement is fulfilled in acidities below 0.5 N.<sup>3</sup>

factor also varies with the ionic strength of the solution, and therefore with the acidity, in such a way that this power is in effect increased. If one assumes alternatively that the  $U^{IV}$  is present as  $UO^{++}$ , the  $H^+$  concentration enters as the square into the Nernst equation; moreover, the activity-coefficient factor would not vary much with acidity, for the  $U^{VI}$  and  $U^{IV}$  ions have the same charge. This assumption is, therefore, not in good agreement with Titlestad's observations, and these results tend to support the belief that  $UOH^{+++}$  is the predominant form of ionic  $U^{IV}$  in acid solutions.

As regards the Becquerel effect, we postulate that the  $U^V$  concentration in a  $U^{IV}$ - $U^{VI}$  solution is increased by illumination. This demands an increased rate of reaction between  $U^{VI}$  and  $U^{IV}$ , which is plausible, because of the well-known activation of the uranyl ion by light.\* At constant intensity of illumination, the  $U^V$  concentration attains a steady value higher than in darkness. The consequences of this hypothesis are examined qualitatively in our next paper. The existence of a purely chemical stage in the reduction of ionic  $U^{VI}$  or  $U^V$  to ionic  $U^{IV}$  is the reason why the reverse oxidation cannot be made to take place electrolytically at the same potential. The removal of an additional electron from  $UOH^{+++}$ , or from  $UO^{++}$  as the case may be, would not lead to the known form  $U^V$ , and requires too great an energy to be possible in the accessible range of potential.

This work was performed at the Montreal Laboratories of the National Research Council of Canada.

*National Research Council of Canada,  
Chalk River,  
Ontario.*

\* Dr. Weiss of Newcastle has kindly drawn our attention to his own publications on the photochemistry of uranium, in which an unstable  $UO_2^+$  was postulated as an intermediate stage in the photochemical reduction of  $UO_2^{++}$ .

---

## UNSTABLE IONS OF QUINQUAVALENT URANIUM

BY H. G. HEAL AND J. G. N. THOMAS

*Received 10th February, 1948; as amended 16th June, 1948*

The formation and disproportionation of an unstable  $UO_2^+$  ion in  $H_2SO_4$  solutions of  $U^{IV}$  and  $U^{VI}$  have been studied. The technique was to measure the potential of a platinum reference electrode in the solution, which is determined by the  $U^{VI}/U^V$  activity ratio.  $U^V$  is formed by reaction of  $U^{VI}$  with  $U^{IV}$ , which is accelerated by light, and by electrolytic reduction of  $U^{VI}$ , attaining a maximum concentration of approximately  $10^{-8}$  M under the conditions of our experiments. Its disproportionation is of the second order in  $U^V$ , and approximately of the first order in  $H^+$ . The activation energy of the disproportionation is about 9,500 cal. A number of values for the rate constants are given.

---

In the preceding paper it was shown that the electrochemical behaviour of uranium solutions was consistent with the hypothesis of an unstable ion of quinquavalent uranium. It was postulated that this ion is present at a minute equilibrium concentration in mixed  $U^{VI}/U^{IV}$  solutions, and that this concentration may be temporarily increased, either by reduction of the  $U^{VI}$  at an electrode, or by illuminating the solution. This paper describes experiments which show that the unstable substances formed in

these two ways are actually identical, and yield approximate values for the rate constant of the disproportionation of the  $U^V$ . Several writers have described the drift of the platinum electrode potential under illumination, giving various qualitative explanations.<sup>1, 2</sup> The drift during electrolytic reduction was observed by Luyckx,<sup>3</sup> who, however, did not realise that it was connected with the light-effect and gave a rather improbable explanation for it.

### Principles of the Method

According to our hypothesis,  $U^V$  disproportionates spontaneously into  $U^{IV}$  and  $U^{VI}$ . The disproportionation must be of the second order in  $U^V$ , but is of uncertain order as regards hydrogen-ion concentration. At equilibrium, in darkness, this disappearance of  $U^V$  is balanced by formation of  $U^V$  at an equal rate by reaction between  $U^{IV}$  and  $U^{VI}$ . When an electrode at a more negative potential than that determined by the  $U^{VI}/U^V$  equilibrium is introduced, or when light falls on the solution,  $U^V$  is produced more quickly, and its concentration rises over a period of time to a new equilibrium value, falling gradually to the "darkness value" again when the light is shut off, or reduction stops, as the case may be. These changes in  $U^V$  concentration are reflected in changes of the potential of a platinum reference electrode in the solution, which potential, according to the hypothesis, is determined solely by the  $U^{VI}/U^V$  activity ratio. Our procedure was as follows: the  $U^V$  concentration was temporarily increased by reduction and illumination successively in the same uranium solution, and the potential of a free platinum electrode was plotted as a function of time, as it returned to equilibrium during the disproportionation of the excess  $U^V$ . From the curve it was possible to determine the rate constant for the disproportionation. The objects were to test the theory generally by ascertaining whether the potential-shift followed the equation predicted for it, and whether the curve was the same after illumination as after reduction; and, if all was satisfactory in this respect, to measure the rate constants for various compositions of solution, studying especially the variations of decomposition velocity with acidity and temperature.

In the following discussion, concentrations will be used everywhere in place of activities. This is strictly justified in dealing with the time-variation of the potential, for the concentrations of the major constituents of the solution did not vary appreciably, during an individual experiment, and the activity coefficients were therefore practically constant. When the results for different solutions are compared, however, correction should be made for the variation of activity coefficients. Since such corrections could not reasonably be estimated for the complex ionic mixtures involved, we attempted to keep the ionic strength constant by adding a neutral salt in the series in which the acidity was varied (see Experimental). In the temperature variation series the only variation of activity coefficients was that due to temperature changes, which is probably rather small. The effect of varying the activity coefficients would be twofold, viz., upon the potential measurements, and upon the reaction velocity.

We assume that the first stage of the disproportionation mechanism is a reaction between  $2UO_2^+$  and  $nH^+$  ions.\*

It is, of course, very unlikely that  $n$  would be greater than one, although probably two or four  $H^+$  ions participate before the end-products

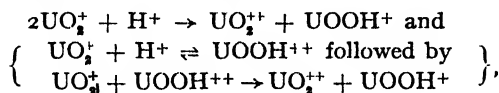
<sup>1</sup> Tillestad, *Z. physik. Chem.*, 1910, **72**, 264.

<sup>2</sup> Baur, *ibid.*, 1908, **63**, 689. Schiller, *ibid.*, 1912, **80**, 656. Trümpler, *ibid.*, 1915, **90**, 385.

<sup>3</sup> Luyckx, *Bull. Soc. chim. Belg.*, 1931, **40**, 269.

\* Writing  $H^+$  instead of  $H_2O^+$  for convenience.

(stable  $U^{IV}$  and  $U^{VI}$  ions) are reached. The velocity of disproportionation is determined by the first stage. There is no physical distinction between the reactions (taking  $n = 1$ , for example)



and the same reasoning applies to both. Hence the rate of disproportionation is given by  $k[H^+]^n C^2$ , where  $C$  is the instantaneous  $U^V$  concentration. At the same time, however,  $U^V$  is being formed out of  $U^{IV}$  and  $U^{VI}$ . The rate of formation does not depend on  $C$ , and it is equal, in darkness, to the rate of disproportionation of  $U^V$  at equilibrium. Let the equilibrium concentration of  $U^V$  for a given solution be  $C_E$ ; then the rate of formation of  $U^V$  in darkness, from  $U^{VI}$  and  $U^{IV}$ , is  $k[H^+]^n C_E^2$ . The net rate of disappearance of  $U^V$  is therefore

$$k[H^+]^n (C^2 - C_E^2) = -\frac{dC}{dt}.$$

This is a form of the ordinary second-order equation, and yields when integrated

$$t = \frac{1}{2K[H^+]^n C_E} \ln \frac{C + C_E}{C - C_E} + \text{constant}.$$

If now the concentration at zero time is defined as  $C_0$ , then

$$t = \frac{1}{2K[H^+]^n C_E} \ln \frac{C + C_E}{C - C_E} \times \frac{C_0 - C_E}{C_0 + C_E}.$$

The concentrations can all be expressed in terms of potentials, which are the quantities actually measured. Let the instantaneous potential of the platinum reference electrode be  $E$ , the potential at zero time  $E_0$ , and the equilibrium potential  $E_E$ , all measured with respect to the half-wave potential of the first uranyl wave.

This is close to the standard potential for the  $UO_2^+ - UO_2^{++}$  couple.\* Thus

$$E = -\frac{RT}{F} \ln \frac{C}{[UO_2^{++}]},$$

etc. When these values are substituted in the velocity equation, the following result emerges:

$$t = \frac{\exp \frac{E_E F}{RT}}{2K[H^+]^n [UO_2^{++}]} \left\{ \ln \tanh \frac{E_0 F}{2RT} - \ln \tanh \frac{E F}{2RT} \right\},$$

where  $E' = E_E - E$ ,  $E'_0 = E_E - E_0$ .

$E'_0$  is the divergence of the (arbitrary) starting potential from the equilibrium potential and  $E'$  the corresponding divergence of the instantaneous potential. ( $E'_0$  is, of course, constant for a given run.)

The graph of  $t$  against  $\log \tanh \frac{E F}{2RT}$  should be a straight line, from the slope of which  $K$  can be determined. This equation actually fits the results very satisfactorily.

\* There is a small divergence due to the departure from equality of the two activity coefficients and the two diffusion coefficients. However, if the half-wave potential is measured in a solution of similar composition to that used for the experiment, similar activity coefficient factors enter at both ends of the potential difference measured, and tend to cancel each other. The diffusion coefficient ratio is close to 1 and introduces only a trifling error.



A similar argument gives the corresponding expression for the shift of potential away from the equilibrium value when the solution is lit by light of constant intensity :

$$t = \frac{\exp \frac{E_0 F}{RT}}{2K[H^+]^n[UO_2^{+}]^m} \left\{ \ln \tanh \frac{E'' F}{2RT} - \ln \tanh \frac{E_0'' F}{2RT} \right\},$$

where

$$E'' = E_F - E_0$$

and

$$E_0'' = E - E_0.$$

Here  $E$  and  $E_F$  are as before, and  $E_0$  is the steady potential reached under illumination.

All the uranium solutions for which results are given here contained sulphate and bisulphate as the only anions. Hydrochloric acid solutions would have been more convenient for estimating the hydrogen-ion concentration, but for some unexplained cause the Becquerel effect is not observed in  $U^{VI} - U^{IV}$  solutions in  $HCl$  (although a solution containing no  $U^{IV}$  may display it<sup>2</sup>). We made a few trials with chloride solutions and found a potential shift on reduction, but no light effect. This deserves further examination, and it would also be interesting to study  $HClO_4$  solutions.

A mercurous sulphate electrode containing 0.5 M  $H_2SO_4$  was used as "fixed" reference electrode against which to measure the potential of the platinum electrode, because it did not introduce chloride ion and was also convenient for measuring the required half-wave potential.

Since the absolute values of  $K$  depend upon an exponential function of the measured potentials, they are inevitably subject to large errors (a factor of 2 is not improbable). The error is mostly due to the exponential term in the gradient expression. The relative accuracy of the  $K$  values for varying acidity and temperature should be considerably better than this, probably within 10 % error, and the error in the gradient from a single line is not above 5 %. To minimise the errors in the  $E_F$  values for the different solutions of the acidity series, the junction-potentials between mercurous sulphate electrode and uranium solution were corrected for (see Experimental).

## Experimental

The uranium solutions were prepared from 99.9 %  $UO_2SO_4$  and crystalline  $U(SO_4)_2 \cdot 4H_2O$  prepared therefrom by electrolytic reduction. The two salts and the  $H_2SO_4$  were analysed for  $U^{IV}$ ,  $U^{VI}$ , free acid, and  $SO_4^{2-}$  as required.

Two sets of measurements were made, using different pieces of apparatus. In the first, (Fig. 1), the excess  $U^{VI}$  could be produced either by electrolytic reduction or by illumination: this was used to compare the two effects, and for some  $K$  measurements with varying total uranium concentration and varying  $U^{VI}/U^{IV}$  ratio. The second apparatus (Fig. 2) allowed only of illumination, but was easier to set up and more reliable, and was employed in studying the variation of velocity with acidity and temperature.

The mode of setting-up need not be described, except to state that the mercurous sulphate electrode was filled to such a level that when it was placed in the uranium solution a little of the latter entered its side-tube (which had a fine tip). The tightly-packed glass wool in the side-tube then maintained a durable boundary between the solutions, and prevented traces of mercurous sulphate from passing into the main solution. For some time before the runs, and during them, a slow stream of oxygen-free argon, saturated with water vapour at the temperature of the thermostat, was passed through the cell.

The platinum electrode was cleaned with chromic-nitric acid mixture, rinsed and heated to redness just before immersion. It always required at least an hour to reach the equilibrium potential, and in some cases (especially when the acidity or the total uranium concentration was low) as much as 16 hr.

This observation is in itself evidence that one of the potential-determining ions is present at very low concentration. Once the steady potential was reached, however, the response to light or electrolysis was instantaneous. The initial potential of the electrode, upon immersion, was often several hundred millivolts from the equilibrium value.

Mechanical stirring mixed the  $U^V$ , formed irregularly in different parts of the solution by reduction or light, uniformly throughout. It was continued during the potential measurements in order to minimise any local variations in the rate of decomposition due to the presence of platinum surfaces. Actually no such effects were observed, and the stirring made little difference to the results.

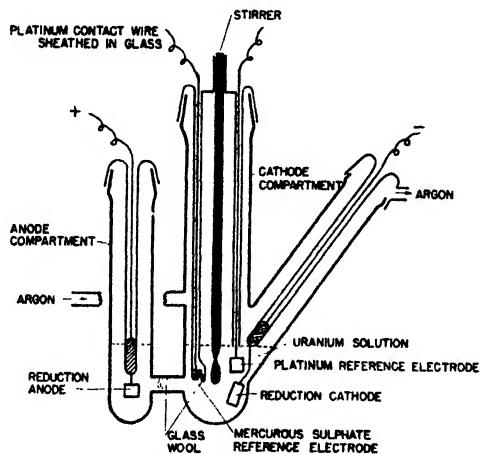


FIG. 1.—Apparatus for determining rate constant of  $U^V$  disproportionation, first form.

The procedure in making a run was as follows. The cell was kept in darkness for  $\frac{1}{2}$  hr. or more, and the equilibrium potential measured with a Leeds and Northrup potentiometer calibrated to 0.05 mV on a spiral slide-wire. The galvanometer was a highly-sensitive mirror instrument with a large series resistance. When an electrolytic reduction was to be carried out, the electrolysis electrodes, which had previously been unconnected, were attached to a source

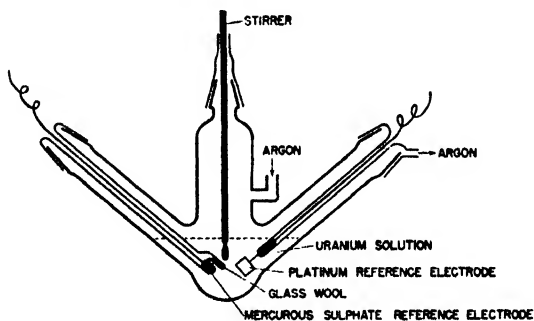


FIG. 2.—Rate-constant apparatus, second form.

of potential giving about 2.5-3 V. A few seconds of electrolysis sufficed to produce enough  $U^V$ , accompanied by a shift of 30-100 mV in the platinum electrode potential, for good measurement. The electrolysis current was disconnected, and the return of the potential to its equilibrium value followed with a stopwatch. The potentiometer was always set a little in advance of the actual potential, noting the time when the galvanometer spot crossed the zero. The whole proceeding was carried out with the cell in darkness. For an illumination

run, the uranium solution was lit for 30 sec. or so by a 200-W lamp held against the side of the thermostat. The potential-shift was of the same order of magnitude as with reduction.

In measuring the half-wave potential, the uranium concentration proved to be too high for satisfactory plotting of the wave: it was accordingly reduced from 0.05 M in  $U^{IV}$  and  $U^{VI}$ , the value employed in most of the  $K$  determinations, to 0.02 M in  $U^{IV}$  and  $U^{VI}$ . This changes the activity coefficients somewhat and introduces an error into the absolute  $K$  values, but does not affect their relative accuracy. No significant variation of  $E_1$  with temperature was found between 20° and 40°. The value was  $-0.618$  V against the  $Hg_2SO_4$  electrode containing 0.5 M  $H_2SO_4$ .

For the series in which the acidity was varied, the variable junction-potential between mercurous sulphate electrode and uranium solution (0.5 mV) was corrected for as follows. Two mercurous sulphate half-cells, one containing 0.5 M  $H_2SO_4$  and the other the uranium solution under study, were connected first by a bridge of 0.5 M  $H_2SO_4$  and then by one of saturated  $KNO_3$ ; the difference between the potentials of these two chains was taken as the junction-potential. This correction is not claimed to be better than an order of magnitude, but it is in any case a small correction.

The variation of ionic strength in the series with varying acidity might have had an effect on the reaction rate comparable with that expected from the  $[H^+]$  variation. The ionic strength was, therefore, kept approximately constant by adding potassium bisulphate so as to maintain a constant total molar concentration of  $H_2SO_4$  and  $KHSO_4$ .<sup>\*</sup> The hydrogen-ion activities of the various solutions were determined by careful measurement of the pH's with a glass electrode, the measurements being checked several times.

## Results

In every case in which the time-potential curves were plotted both after illumination and after reduction, they were found to be practically identical. Fig. 3 shows a typical pair of curves. The  $\log \tanh \frac{E'F}{2RT} - t$  lines corresponding to these curves are given in Fig. 4. They are good straight lines, as was always the case, with almost equal gradients. (The final points of the potential-time curve, for which the accuracy of measurement is very low, were omitted in plotting these lines.) It is clear that the time-potential equation proposed above fits the results well, and that the unstable substances produced by light and by reduction of  $U^{VI}$  are the same.

The rate-constant values and other information are tabulated below.  $K'$  denotes the product  $K[H^+]$ , which is given by the gradient of the line. From Table I it can be seen that  $K'$  is proportional to the first power of the hydrogen-ion activity, and that if  $K'$  is divided by this activity a reasonably constant figure for  $K$  is obtained.

TABLE I.—INFLUENCE OF  $H^+$  ACTIVITY. TEMPERATURE 30.4° C

$H_2SO_4$ Conc. (molar)	$H^+$ Activity (molar)	$E$ (volt)	Junction- pot. (volt)	$U^{VI}$ Conc. at Equilibrium (molar)	$K'$ (l. mole. <sup>-1</sup> sec. <sup>-1</sup> )	$K = \frac{K'}{[H^+]}$ (l. mole. <sup>-1</sup> sec. <sup>-1</sup> )
0.5	0.48	0.3048	$-0.0012$	$4.32 \times 10^{-7}$	$5.79 \times 10^3$	$1.21 \times 10^4$
0.425	0.37	0.3006	$+0.0008$	$5.00 \times 10^{-7}$	$4.51 \times 10^3$	$1.22 \times 10^4$
0.4	0.335	0.2971	$+0.0019$	$5.80 \times 10^{-7}$	$4.32 \times 10^3$	$1.29 \times 10^4$
0.375	0.30	0.2894	$+0.0031$	$7.80 \times 10^{-7}$	$3.79 \times 10^3$	$1.25 \times 10^4$
0.35	0.26	0.2847	$+0.0040$	$9.31 \times 10^{-7}$	$2.84 \times 10^3$	$1.08 \times 10^4$
0.325	0.23	0.2806	$-0.0051$	$10.92 \times 10^{-7}$	$2.76 \times 10^3$	$1.18 \times 10^4$

The junction-potentials signify the potential of the uranium solution against the  $H_2SO_4$  in the mercurous sulphate electrode.

All solutions contained 0.05 M of  $U^{VI}$  and 0.05 M  $U^{IV}$ , and enough  $KHSO_4$  to make the total molar concentration of  $H_2SO_4$  and  $KHSO_4$  up to 0.5.

<sup>\*</sup> At the suggestion of Prof. E. A. Guggenheim.

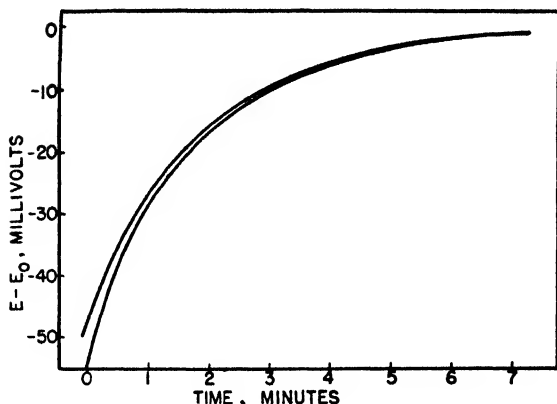


FIG. 3.—Typical potential-time curves. The two are for the same solution: the upper curve represents the return to equilibrium after illumination, the lower curve the same after reduction.

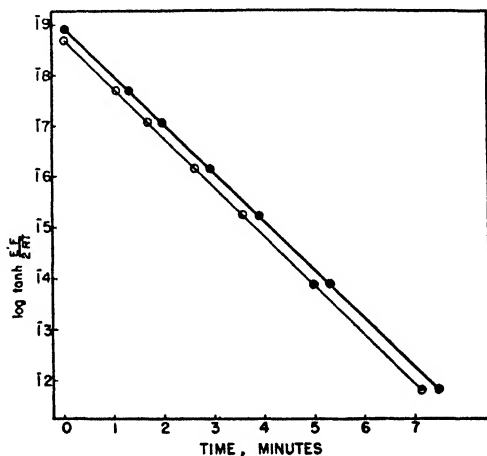


FIG. 4.—The  $\log \tanh E'F/2RT$  — time lines corresponding to the curves of Fig. 3.

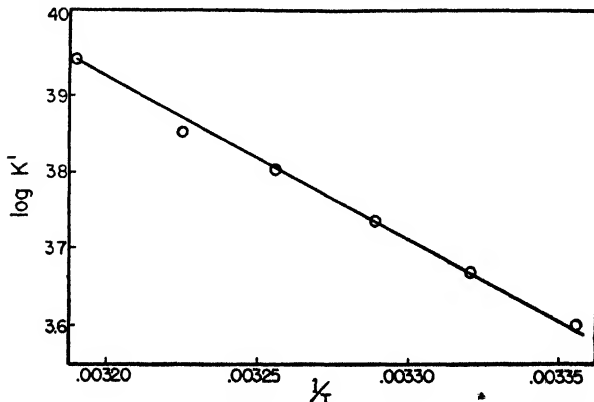


FIG. 5.—Variation of disproportionation velocity with temperature. Graph of  $\log K'$  against  $1/T$  for the data of Table II.

Table II gives the variation of  $K'$  with temperature for a given solution. The graph of  $\log K'$  against  $1/T$  is a satisfactorily straight line (Fig. 5), from the slope of which the activation energy 9,500 cal. is obtained. This result is not corrected for the variations of the half-wave potential, the activity coefficients or, most serious, the hydrogen-ion activity with temperature. The error may therefore amount to 20-30 %.

TABLE II.—INFLUENCE OF TEMPERATURE

Temperature (°C)	$E_E$ (volt)	$U^{IV}$ Concentration at Equilibrium (molar)	$K'$ (l. mole. <sup>-1</sup> sec. <sup>-1</sup> )
25.0	0.3023	$3.88 \times 10^{-7}$	$4.01 \times 10^3$
28.0	0.3031	$4.22 \times 10^{-7}$	$4.67 \times 10^3$
31.0	0.3039	$4.59 \times 10^{-7}$	$5.45 \times 10^3$
34.0	0.3069	$4.57 \times 10^{-7}$	$6.33 \times 10^3$
37.0	0.3103	$4.52 \times 10^{-7}$	$7.08 \times 10^3$
40.3	0.3123	$4.65 \times 10^{-7}$	$8.82 \times 10^3$

The solution was 0.05 M  $U^{IV}$ , 0.05 M  $U^{VI}$  and 0.5 M  $H_2SO_4$  throughout.

Table III and IV contain the data for variation of  $K'$  with  $U^{IV}/U^{VI}$  ratio and with varying total uranium concentration.  $K'$  should be a constant for all these measurements if the ionic strength and  $H^+$  activity were fixed. These requirements are not fulfilled in practice, but the variations of  $K'$  are not very large, and are at any rate qualitatively consistent with expectations. (Since the mode of ionisation of  $U^{IV}$  is not known, it was impossible to control these factors effectively.) The letter  $e$  and  $i$  denote figures for reduction and illumination respectively; the two sets of  $K'$  values agree well.

TABLE III.—INFLUENCE OF  $U^{VI}/U^{IV}$  RATIO. TEMPERATURE 30.4° C

$U^{IV}$ Concentration (molar)	$E_E$ (volt)	$U^{VI}$ Concentration at Equilibrium (molar)	$K'$ (l. mole. <sup>-1</sup> sec. <sup>-1</sup> )
0.015 $e$	0.325	$3.3 \times 10^{-7}$	$5.6 \times 10^3$
0.015 $i$	0.324	3.5 "	5.2 "
0.025 $e$	0.323	3.2 "	4.9 "
0.025 $i$	0.323	3.2 "	5.0 "
0.050 $e$	0.308	3.8 "	5.4 "
0.050 $i$	0.308	3.8 "	5.2 "
0.075 $e$	0.303	2.3 "	7.9 "
0.075 $i$	0.302	2.4 "	7.6 "
0.085 $e$	0.285	2.8 "	7.8 "
0.085 $i$	0.285	2.8 "	7.4 "
0.092 $e$	0.278	1.9 "	6.0 "
0.092 $i$	0.278	1.9 "	6.0 "
0.097 $e$	0.263	1.3 "	11.6 "
0.097 $i$	0.264	1.2 "	9.8 "

All solutions contained 0.5 M  $H_2SO_4$  and 0.1 M U in all.  $e$  denotes an electrolysis run,  $i$  an illumination run.

Titlestad (loc. cit.) gives a number of tables of figures for the Becquerel effect. These fit the two time-potential equations given in this paper, though not as well as our own data. The divergences, however, are not systematic and are undoubtedly due to lower accuracy in the measurements. The  $K$  values deduced from Titlestad's figures are of the same order of magnitude as ours.

TABLE IV.—INFLUENCE OF TOTAL U CONCENTRATION. TEMPERATURE 30.4° C

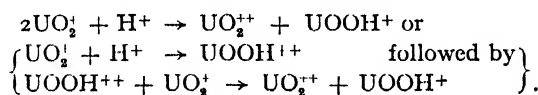
Total U Concentration (molar)	$E_E$ (volt)	$U^V$ Concentration at Equilibrium (molar)	$K'$ (l. mole. <sup>-1</sup> sec. <sup>-1</sup> )
0.03 <i>e</i>	0.301	$1.5 \times 10^{-7}$	$7.3 \times 10^3$
0.03 <i>i</i>	0.302	1.4 "	7.6 "
0.05 <i>e</i>	0.305	2.2 "	6.0 "
0.05 <i>i</i>	0.305	2.2 "	6.4 "
0.07 <i>e</i>	0.310	2.5 "	6.6 "
0.07 <i>i</i>	0.310	2.5 "	6.9 "
0.10 <i>e</i>	0.308	3.8 "	5.4 "
0.10 <i>i</i>	0.308	3.8 "	5.2 "

The solutions all contained 0.5 M.  $H_2SO_4$  and equal gram-molecular concentrations of  $U^{IV}$  and  $U^{VI}$ . The slow increase of  $K'$  as the U concentration is reduced is probably due to increasing  $H^+$  activity.

*e* denotes an electrolysis run, *i* an illumination run.

### Discussion

In general, the results afford plausible confirmation of the existence of unstable  $UO_2^+$  ions, and the behaviour postulated for them in the preceding paper and by Weiss and by Kolthoff and Harris. The decomposition of  $UO_2^+$  seems to be second-order in  $UO_2^+$  and first-order in  $H^+$ . The mechanism can therefore be represented by



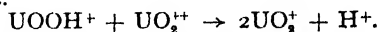
The observed rate of reaction is very much below that calculated simply from the approximate collision frequency of  $UO_2^+$  ions, and the known activation energy. This is attributable in part to the participation of hydrogen ions and in part to the effect of orientation of the colliding particles, which is normally very important in such complex reaction-systems. There may be several modes of disproportionation, of which this is the most important.

The greatest equilibrium concentration of  $U^V$  observed was about  $10^{-6}$  M. This might be increased towards a value detectable, for example, spectroscopically, by increasing the concentrations of  $U^{VI}$  and  $U^{IV}$  and reducing the acidity. However, hydrolysis sets a limit to this, and it is doubtful whether an increase greater than 10 times could be achieved. Under strong light or with vigorous reduction the concentration may increase temporarily 20 times.

The activated complex formed between  $U^{IV}$  and  $U^{VI}$  ions might break up either into two  $U^V$  ions or into  $U^{IV}$  and  $U^{VI}$  again. In the latter case the uranium atoms may exchange. If a solution of  $U^{VI}$  were mixed with one of  $U^{IV}$ , one or other containing a tracer quantity of one of the short-lived uranium isotopes, an exchange of the active constituent between the valency states should be observed. The rate of exchange would be the total due to both modes of decomposition of the activated complex, while the rate of exchange via  $U^V$  is known from the results just given. Hence one could deduce the rate of exchange by the second mechanism.

There is not enough experimental material to give a definite notion of the mechanism of formation of  $U^V$  from  $U^{VI}$  and  $U^{IV}$ , but on electrostatic grounds it is likely that reaction takes place mainly between  $UO_2^{1+}$  on the one hand and  $UOOH^+$  or  $UO_2$  on the other hand, rather than with  $UOH^{2+}$ . These hydrolysed forms of  $U^{IV}$  are, according to evidence

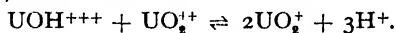
given in the foregoing paper, present only at small concentrations in moderately acid solutions, where  $\text{UOH}^{+++}$  is probably the predominant form of  $\text{U}^{\text{IV}}$ . If we assume that  $\text{UOOH}^+$  is the chief species of  $\text{U}^{\text{IV}}$  reacting to give  $\text{U}^{\text{V}}$ , the reaction of formation is simply the reverse of the disproportionation, viz.



Low acidity would favour the hydrolysis of  $\text{UOH}^{+++}$  to  $\text{UOOH}^+$ , and hence lead to higher equilibrium concentrations of  $\text{U}^{\text{V}}$ . A similar argument applies if  $\text{UO}_2$  is the reacting species. Quantitatively the equilibrium  $[\text{U}^{\text{V}}]$  should be given by

$$[\text{UO}_2^+] \simeq \text{constant} \sqrt{\frac{[\text{UOH}^{+++}][\text{UO}_2^{++}]}{[\text{H}^+]^3}},$$

in terms of the experimental concentrations of  $\text{U}^{\text{VI}}$  and  $\text{U}^{\text{IV}}$  at moderate acidities. This expression follows from the equation for the total equilibrium between  $\text{U}^{\text{IV}}$ , and  $\text{U}^{\text{V}}$  and  $\text{U}^{\text{VI}}$ :



Therefore  $\text{UO}_2^+$  should be roughly proportional to  $[\text{H}^+]^{-1/2}$ , for fixed concentrations of  $\text{U}^{\text{IV}}$  and  $\text{U}^{\text{VI}}$  and at moderate acidities. Now it was postulated that the potential of a platinum electrode in such solutions is determined by the equation

$$E \simeq 0.05 + \frac{RT}{F} \ln \frac{[\text{UO}_2^{++}]}{[\text{UO}_2^+]},$$

from which all the  $\text{U}^{\text{V}}$  concentrations in the tables have been calculated. Those given in Table I do vary roughly as the  $-3/2$  power of the  $\text{H}^+$  activity, as expected from the above argument. The function of  $\text{U}^{\text{IV}}$  in the reaction can be regarded simply as the reduction of  $\text{U}^{\text{VI}}$ , and, in principle, any other reducing agent of suitable strength should form  $\text{U}^{\text{V}}$  from  $\text{U}^{\text{VI}}$ .

These experiments were carried out at the Montreal Laboratories of the National Research Council of Canada.

National Research Council of Canada,  
Chalk River,  
Ontario.

Royal College of Science,  
Imperial College,  
S.W.7.

## BOND DISSOCIATION ENERGIES IN POLYATOMIC MOLECULES OF THE TYPE $\text{MX}_n$

BY H. A. SKINNER

*Received 23rd March, 1948*

The inter-relation of bond dissociation energies and bond energy terms in polyatomic molecules of the type  $\text{MX}_n$  is discussed for molecules  $\text{MX}_n$  in which the value of  $n$  exceeds the valence of the atom  $\text{M}$  in its ground state. Bond dissociation energies in the Group II halides are listed, and an attempt made to explain the marked weakness in  $D(\text{M}-\text{X})$  relative to  $D(\text{X}-\text{MX})$  in these compounds. The special case of the tetravalent compounds of  $\text{C}$  (in particular  $\text{CH}_4$ ) is considered, and some reasons given for questioning whether the latent heat of sublimation of carbon can be deduced from a knowledge of  $D(\text{CH}_3-\text{H})$  *per se*.

In a recent paper, Long and Norrish<sup>1</sup> have re-emphasised a point that seems first to have been made by Mecke<sup>2</sup> in 1930—namely, that since tetravalent compounds of carbon must derive from a tetravalent state

<sup>1</sup> Long and Norrish, *Proc. Roy. Soc. A*, 1946, **187**, 337.

<sup>2</sup> Mecke, *Nature*, 1930, **125**, 526.

of the C atom, the energy of excitation from the ground to the tetravalent state enters directly into computations of the bond energies in the case of compounds of carbon. Long and Norrish identify the appropriate tetravalent state of the C atom as the excited state  $^4S$ , which has recently been shown by Shenstone <sup>3</sup> to lie some 96.4 kcal. above the ground state,  $^3P$ .

A detailed discussion of the state of the carbon atom in tetravalent compounds was given by Van Vleck <sup>4</sup> in 1934, who concluded that the valence state of C is not identical with any one of the six atomic states belonging to the configuration  $sp^3$ , but "is instead to be regarded as a linear combination of these." Van Vleck computed that the valence state of C lies about 164 kcal. above the ground-state level, in case where the C atom forms tetrahedral  $sp^3$ -hybridised bonds.

Irrespective of argument concerning the "correct" value to be ascribed to the energy of the excitation process within the C atom, the necessity for an internal excitation remains: and in so far as this point is granted in respect of C compounds, it is equally necessary to consider the effect of internal excitation processes in all compounds of the type  $MX_n$ , where the value of  $n$  is greater than the valency of the atom M in its ground state, e.g. in all compounds of the Group II elements.

Pauling <sup>5</sup> in deriving his table of mean bond energy terms,\* obtained the  $\bar{E}(M-X)$  value for a compound  $MX_n$  from

$$\bar{E}(M-X) = Q_a/n, \quad . \quad . \quad . \quad . \quad . \quad . \quad (1)$$

where  $Q_a$  = heat of formation of  $MX_n$  (gas) from ground state atoms. Long and Norrish differ from Pauling, obtaining their mean bond-energy terms from

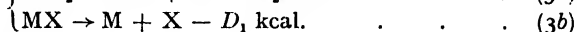
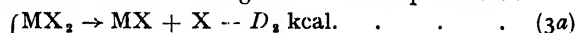
$$\bar{E}^*(M-X) = Q_a^*/n, \quad . \quad . \quad . \quad . \quad . \quad . \quad (2)$$

where  $Q_a^*$  measures the heat of formation of  $MX_n$  (gas) from suitably excited atoms. Both  $\bar{E}$  and  $\bar{E}^*$  are defined quantities and neither has any particular advantage over the other for general thermochemical purposes: for the specific purpose of correlating mean bond-energy terms with bond-dissociation energies it may, in certain cases, be more reasonable to choose  $\bar{E}^*$  rather than  $\bar{E}$  terms.

In this paper we are primarily concerned with the general way in which internal excitation energy terms may reflect themselves in observed bond-dissociation energies in  $MX_n$  compounds. The experimental data we can quote are regrettably small, and in this respect the subject as a whole appears blurred. A more thorough examination of the problem requires much further study on the stepwise dissociation energies in  $MX_n$  compounds.

### Compounds of Type $MX_2$

Representing the bond-dissociation energies of the two processes:



by  $D_1$  and  $D_2$  it follows that

$$(D_1 + D_2) = Q_a \quad . \quad . \quad . \quad . \quad . \quad . \quad (4)$$

where  $Q_a$  is the heat of formation from normal atoms. Reliable values of  $D_1$  have been obtained for the series  $HgX$  ( $X = Cl, Br, I$ ) by Wieland <sup>7</sup> from spectroscopic studies. Values of  $Q_a$  are known with fair accuracy

<sup>3</sup> Shenstone, *Physic. Rev.*, 1947, **72**, 411.

<sup>4</sup> Van Vleck, *J. Chem. Physics*, 1934, **2**, 20 and 297.

<sup>5</sup> Pauling, *Nature of the Chemical Bond* (Cornell, 1939).

\* We are here employing the suggested nomenclature of Butler and Polanyi,<sup>6</sup> in order to distinguish between the two commonly used meanings of "bond-energy."

<sup>6</sup> Butler and Polanyi, *Trans. Faraday Soc.*, 1943, **39**, 19<sup>a</sup>.

<sup>7</sup> Wieland, *Helv. physic. Acta*, 1939, **12**, 295; 1941, **14**, 549; *Helv. chim. Acta*, 1941, **24**, 1285.



for the  $\text{HgX}_2$  (gas) molecules from thermochemical heats of formation.<sup>8</sup> Accordingly, both  $D_1$  and  $D_2$  values are reasonably well established in case of the mercuric halides: these are given in Table I.

TABLE I.—BOND-DISSOCIATION ENERGIES IN  $\text{HgX}_2$  \*

Molecule	$Q_0$ (kcal.)	$D_1$ (kcal.)	$D_2$ (kcal.)	$(D_2 - D_1)$
$\text{HgCl}_2$ . . .	104.5	24	80.5	56.5
$\text{HgBr}_2$ . . .	87.9	16.4	71.5	55.1
$\text{HgI}_2$ . . .	69	12	57	45

TABLE II.—BOND-DISSOCIATION ENERGIES IN  $\text{MX}_2$  COMPOUNDS(a)  $D_1$  values

Molecule	$D_1$ (kcal.)	Experimental Method	Reference
$\text{CdCl}_2$	$\geq 46$	Activation-energy of reaction of Cd with $\text{Cl}_2$	11
	$> 31 < 47$	Na-flame reaction with $\text{CdCl}_2$	12
	$51 \pm 20$	Linear Birge-Sponer extrapolation	13
$\text{CdBr}_2$	$> 21 < 35$	Na-flame with $\text{CdBr}_2$	12
	$(65 \pm 25)$	Linear Birge-Sponer	13
$\text{CdI}_2$	$> 8 < 20$	Na-flame with $\text{CdI}_2$	12
	$32 \pm 5$	Linear Birge-Sponer	13
$\text{ZnCl}_2$	$\geq 50$	Activation energy of reaction of Zn with $\text{Cl}_2$	11
	46.5	Na-flame with $\text{ZnCl}_2$	12
	$58 \pm 20$	Linear Birge-Sponer	13
$\text{ZnI}_2$	$41 \pm 15$	Linear Birge-Sponer	13
$\text{BeCl}_2$	$69 \pm 15$	Linear Birge-Sponer	13
$\text{MgCl}_2$	$62 \pm 20$	Linear Birge-Sponer, graphical Birge-Sponer	13
$\text{CaCl}_2$	63.6	Predissociation	13

(b)  $D_1$  and  $D_2$  values

Molecule	$Q_0$	$D_1$	$D_2$	$(D_2 - D_1)$
$\text{CaCl}_2$ . . .	(240)	63.6	(176)	(112)
$\text{MgCl}_2$ . . .	(198)	$62 \pm 20$	$(136 \pm 20)$	$(74 \pm 40)$
$\text{BeCl}_2$ . . .	216	$69 \pm 15$	$147 \pm 15$	$78 \pm 30$
$\text{CdCl}_2$ . . .	(130)	$46 \pm 5$	$(84 \pm 5)$	$(38 \pm 10)$
$\text{CdBr}_2$ . . .	(111)	$35 \pm 10$	$(76 \pm 10)$	$(41 \pm 20)$
$\text{CdI}_2$ . . .	82	$25 \pm 10$	$57 \pm 10$	$32 \pm 20$
$\text{ZnCl}_2$ . . .	(146)	$50 \pm 5$	$(96 \pm 5)$	$(46 \pm 10)$
$\text{ZnI}_2$ . . .	(94)	$41 \pm 15$	$(53 \pm 15)$	$(12 \pm 30)$

<sup>8</sup> Bichowsky and Rossini, *Thermochemistry of Chemical Substances* (Reinhold, 1936).

<sup>9</sup> Wehrli and Milazzo, *Helv. chim. Acta*, 1943, **26**, 1025.

<sup>10</sup> Polanyi and Schay, *Z. physik. Chem. B*, 1928, **1**, 30. Ootuka and Schay, *ibid.*, 1928, **1**, 62. Ootuka, *ibid.*, 1930, **7**, 407.

<sup>11</sup> Hartel and Polanyi, *Trans. Faraday Soc.*, 1928, **24**, 606.

<sup>12</sup> Horn, Polanyi and Sattler, *Z. physik. Chem. B*, 1932, **17**, 220.

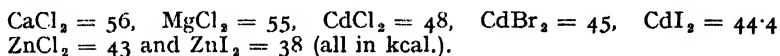
<sup>13</sup> Gaydon, *Dissociation Energies* (Chapman and Hall, 1947).

\* These data are taken from the paper by Wehrli and Milazzo,<sup>9</sup> which draws attention to some of the points raised here.

The significant feature of Table I, is the magnitude of the difference,  $(D_2 - D_1)$ : or, alternatively, the *weakness* of the binding in  $\text{HgX}$  relative to that in  $\text{HgX}_2$ . That there is a marked difference in the bond-dissociation energies of the two  $\text{Hg}-\text{X}$  bonds in the mercuric halides was inferred several years ago by Polanyi and co-workers<sup>10</sup> from studies of the reactions of Na vapour with  $\text{HgX}_2$ . The recent spectroscopic data provide confirmation of the earlier conclusions.

It would be of interest to know whether the feature  $D_2 > D_1$ , so clearly revealed in the  $\text{HgX}_2$  molecules, is general for the compounds of Group II, or whether it is specific to the compounds of Hg. Relatively little is known of the  $D_1$  and  $D_2$  values for the other halides of Group II, and the data we have collected together in Table II are a good deal less reliable than those given in Table I.

The  $Q_0$  values for the halides listed are derived from  $Q$ , (cryst.) values quoted by Bichowsky and Rossini,<sup>8</sup> and heats of sublimation estimated from data given by Kelley<sup>14</sup> (except for  $\text{CaCl}_2$  and  $\text{MgCl}_2$ , for which we have assumed a reasonable value). The following heats of sublimation were used:



The  $D_1$  values are chosen as the most probable in the light of the variable experimental data given in Table II (a).

We may conclude that the  $(D_2 - D_1)$  values for the halides listed in Table II, although subject to fairly wide limits of error, are positive in sign. The feature noted in Table I ( $D_2 > D_1$ ), would thus appear to be general for the halides of Group II.

In terms of the Heitler-London theory of valence, the elements of Group II are zero-valent in their atomic ground states,  $^1\text{S}$ . The formation of a stable covalent type of bond by an atom M of Group II, requires an initial excitation of the M atom to the divalent valence state. Although it may be incorrect to identify the valence state of M with one of the divalent atomic states,  $^3\text{P}$ , we may expect that the excitation energy involved is not *less* than the energy of the transition  $\text{M}(^1\text{S}) \rightarrow \text{M}(^3\text{P})$ . On the close approach of a univalent atom or group X to the atom M, there are (in first-order approximation) three "ideal" states that can be formulated—

(a) The state  $\text{M}^\circ\text{X}$ , i.e., the totally repulsive state deriving from the ground-state of  $\text{M}(^1\text{S})$ .

(b) The state  $\text{M}^*-\text{X}$ , i.e. the covalent state deriving from the excited valence state of M.

(c) The state  $\text{M}\bar{\text{X}}$ , i.e. the ion-pair resulting from an electron transfer from  $\text{M} \rightarrow \text{X}$ .

Each of the "ideal" states, (a), (b), (c), is of the same multiplicity (one unpaired electron), and perturbations between the three states are allowed in terms of the Kronig selection rules. The ground state of  $\text{MX}(^2\Sigma)$  would then be identified as the deepest of the perturbed states. An alternative mode of description starts by writing the eigenfunction  $\Psi(\text{MX}, ^2\Sigma)$ , as a linear combination of the eigenfunctions describing the three "ideal" states—

$$\Psi(\text{MX}) = a\Psi(\text{M}^\circ\text{X}) + b\Psi(\text{M}^*-\text{X}) + c\Psi(\text{M}\bar{\text{X}}) \quad (5)$$

where  $a$ ,  $b$ ,  $c$  are mixing coefficients.

A schematic representation of the origin of the ground-state of  $\text{MX}$  is given in the potential-energy (P.E.) diagram shown in Fig. 1 (the example

<sup>14</sup> Kelley, U.S. Dept. Bur. Mines Bull., 1935, 383.

chosen is for  $MX = \text{HgCl}$ ). Curve A represents the P.E. curve for the ion-pair,  $\text{Hg}^+\bar{\text{Cl}}$ , and curve B the P.E. curve for the covalent molecule,  $\text{Hg}^*\text{—Cl}$ . Interaction between curves A and B (ionic-covalent resonance) is presumed to yield the dotted curve H. This latter intersects curve C (representing the repulsive state  $\text{Hg}^0\text{Cl}$ ), and by interaction with it is presumed to give the ground-state curve G. As pictured in Fig. 1, the

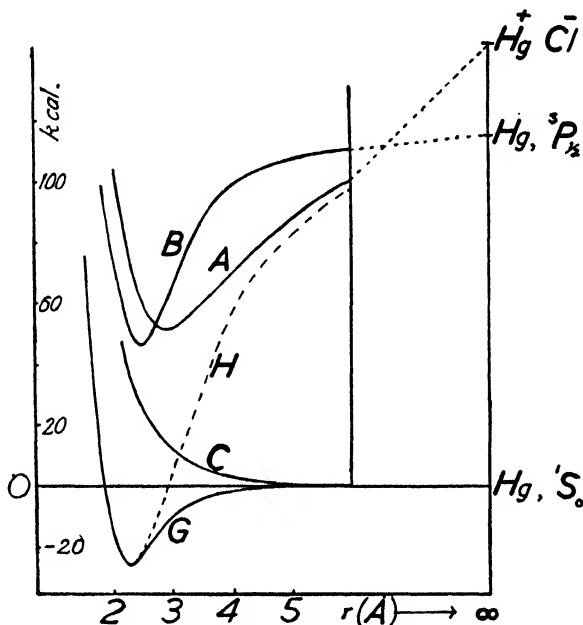


FIG. 1.—Potential-energy curves for  $\text{HgCl}$ .

The ionic curve A is drawn from a Born-Mayer potential function :

$$V(r) = -e^2/r + b e^{-r/\rho} + I_{\text{Hg}} - E_{\text{Cl}}$$

where  $\rho = 0.345 \text{ \AA}$ ,  $I_{\text{Hg}}$  = ionisation potential of Hg, and  $E_{\text{Cl}}$  = electron affinity, of Cl. The constant  $b$  was evaluated from the equilibrium condition,  $[dV/dr]_{r_i} = 0$ ,

where  $r_i$  = equilibrium bond length in the ion-pair,  $\text{Hg}^+\bar{\text{Cl}}$ . We have estimated  $r_i$  ( $\text{Hg}^+\bar{\text{Cl}}$ ) at  $2.86 \text{ \AA}$ : this value is  $0.07 \text{ \AA}$  larger than  $r_i$  in gaseous  $\text{KCl}$  ( $2.79 \text{ \AA}$ ), to comply with the larger crystal radius of  $\text{Hg}^+$  relative to  $\text{K}^+$ .

The covalent curve B is drawn from a Morse function assuming probable values for the equilibrium bond length, force constant and dissociation energy. Our estimation  $\bar{E}^*(\text{Hg—Cl}) \sim 65 \text{ kcal}$ . is perhaps the least certain of these. Curve C is purely schematic. It will be noted that these values require  $R_1(\text{HgCl})$  to have a relatively high figure,  $71 \text{ kcal}$ . This may at first sight seem far too large, since Hg is not normally regarded as a highly electropositive element. But, it should be recollected that it is the covalent state  $\text{Hg}^*\text{—Cl}$  with which the ionic state is in resonance, and the excited state of Hg from which  $\text{Hg}^*\text{—Cl}$  derives is very much more electropositive than is the normal Hg atom.

The value of  $\alpha$  is assumed to be  $112 \text{ kcal}$ .

effect of the term  $a\Psi(M^0X)$  in (5) is primarily to cause a dissociation of the ionic-covalent hybrid H into *normal atoms*. Virtually, we assume the coefficient  $a \rightarrow$  zero in the region  $r(\text{Hg—Cl}) \rightarrow r_e$ , and becomes unity as  $r \rightarrow \infty$ .

This description of the nature of the binding in the specific case of  $\text{HgCl} (^3\Sigma)$ , enables us to write the dissociation energy  $D_1$  in the form

$$D_1 = \bar{E}^*(\text{Hg—Cl}) + R_1(\text{HgCl}) - \alpha, \quad (6)$$

where

$\bar{E}^*$  (Hg—Cl) = covalent bond energy in  $\text{Hg}^*\text{—Cl}$ ,

$R_1(\text{HgCl})$  = resonance energy (ionic-covalent) in  $\text{HgCl}$ .

$\alpha$  = excitation energy required to raise  $\text{Hg}(^1S)$  to the divalent valence state.

In the general case,  $\text{MX}$ , eqn. (6) may be written :

$$D_1(\text{MX}) = \bar{E}^*(\text{M—X}) + R_1(\text{MX}) - \alpha. \quad (7)$$

The formation of the second Hg—Cl bond in  $\text{HgCl}_2$  can occur on close approach of a Cl atom to  $\text{HgCl}$  without additional internal excitation of the Hg atom, which in  $\text{HgCl}$  already carries an unpaired electron. The gain in energy accompanying the formation of the second bond may be expressed (as shown in the energy diagram, Fig. 2) through the equation

$$(D_1 + D_2) = 2\bar{E}^*(\text{Hg—Cl}) + R_2(\text{HgCl}_2) - \alpha. \quad (8)$$

The term  $R_2$  in (8) measures the *total* resonance energy in the  $\text{HgCl}_2$  molecule, relative to the covalent structure  $\text{Cl—Hg}^*\text{—Cl}$ , and includes the contribution from structures  $\bar{\text{Cl}} \text{Hg}^{\ddagger} \bar{\text{Cl}}$ , and  $\text{Cl—Hg}^{\ddagger} \bar{\text{Cl}}$  (twice). Combining eqn. (6) and (8) one obtains

$$D_2 = \bar{E}^*(\text{Hg—Cl}) + (R_2 - R_1) \quad (9)$$

and

$$(D_2 - D_1) = \alpha + R_2 - 2R_1. \quad (10)$$

The eqn. (10) may be generally applied to the compounds  $\text{MX}_2$  of Group II.

It is not simple to estimate the terms  $R_2$  and  $R_1$  even approximately by theoretical calculation. Nevertheless, eqn. (10) enables us to make some predictions concerning the probable trend in the energy difference  $(D_2 - D_1)$  as the atom M is varied. Thus,

(a)  $(D_2 - D_1)$  is most likely to be a large positive quantity in case where the excitation energy  $\alpha$  is large, and the terms in  $R$  are small—i.e. when  $\alpha$  is large, and the bonds  $\text{M—X}$  are essentially covalent in character.

(b) In case where  $\alpha$  is a relatively small quantity, it is still possible for  $(D_2 - D_1)$  to be a large positive quantity if  $R_2 > 2R_1$ . One might suggest that this latter condition is favoured in  $\text{MX}_2$  compounds in which the  $\text{M—X}$  bonds are predominantly ionic in character, by virtue of an appreciable contribution to  $R_2$  from the resonance involving the

totally ionic structure  $\bar{\text{X}} \text{M}^{\ddagger} \bar{\text{X}}$ .

We may now refer back to Tables I and II. Whilst we may not know the correct values for the excitation energies  $\alpha$  in the Group II elements, we might expect the  $\alpha$  values to run parallel to the excitation energies required for the transitions  $^1S \rightarrow ^3P$  in the isolated atoms. The free atom excitation energies are : \*

Hg = 112, Zn = 92.5, Cd = 87, Be = 62.5, Mg = 62, and Ca = 43 kcal.

\* The excitation energies quoted are for the atomic transitions  $\text{M}(^1S_0) \rightarrow \text{M}(^3P_1)$ .

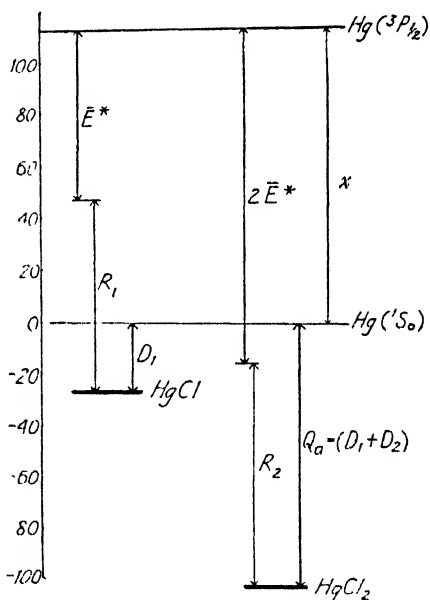


FIG. 2.—Energy diagram for  $\text{HgCl}$ ,  $\text{HgCl}_2$ .

The effect of the term in  $\alpha$  on  $(D_2 - D_1)$  may therefore be expected to be largest in the case of  $\text{HgX}_2$  compounds, and least in case of  $\text{CaX}_2$  compounds. On the other hand, it is customary to describe the compounds of Mg and Ca as essentially ionic in character, and it is not improbable that the ionicity of the  $\text{M}-\text{X}$  bonds is greatest in the Ca and Mg halides, and least in the Hg halides. The combined effect of a falling  $\alpha$  value and increasing ionicity in the series of halides Hg, Zn, Cd, Be, Mg, Ca would be to render  $(D_2 - D_1)$  large and positive in all these compounds.

An interesting class of compounds is provided by the dialkyls of Group II,  $\text{MR}_2$  (where R is an alkyl radical). In these one would expect the ionic-covalent resonance-energy terms ( $R_1$  and  $R_2$ ) to be smaller than in the corresponding halides,  $\text{MX}_2$ , in view of the electropositive position of C relative to the halogens. In this event, the conditions are perhaps most suitable to a large difference between  $D_1$  and  $D_2$  values. But thermal and dissociation energy data are almost completely lacking in this field. Some recent thermal data on the dialkyls of cadmium and zinc,<sup>15</sup> and some old combustion heats on the alkyls of mercury<sup>16</sup> provide  $(D_1 + D_2)$  values for these metal-carbon bonds, but give no information on the individual bond dissociation energies. In the case of  $\text{Hg}(\text{CH}_3)_2$  Berthelot's combustion heat \* corresponds to a value of *ca.* 35 kcal. for the sum  $(D_1 + D_2)$  of the  $\text{Hg}-\text{CH}_3$  bond energies. If the difference  $(D_2 - D_1)$  is large in this case (as we would anticipate), it follows from the small value of the sum  $(D_1 + D_2)$  that the  $\text{Hg}-\text{CH}_3$  radical must be very weakly bonded and unstable. At the moment, however, there is insufficient experimental evidence available to show whether or not this expectation is met.

A set of experimental data which can be fitted into the scheme relates to the dissociation energies in the series of diatomic molecules, MH and  $\text{MH}^+$ , the values for which are listed in Table III (data taken from Gaydon<sup>13</sup>).

TABLE III.—DISSOCIATION ENERGIES IN MH AND  $\text{MH}^+$ 

Molecule	$D_1$ (kcal.)	$\alpha = ({}^1S_0 \rightarrow {}^3P_1)$	$\Delta = D(\text{MH}^+) - D(\text{MH})$
$\text{BeH}^+$ . . .	$74 \pm 5$	62.5	$21 \pm 11$
$\text{BeH}$ . . .	$53 \pm 6$		
$\text{MgH}^+$ . . .	$48 \pm 5$	62	$2 \pm 17$
$\text{MgH}$ . . .	$46 \pm 12$		
$\text{ZnH}^+$ . . .	$65 \pm 10$	92.5	$45 \pm 10$
$\text{ZnH}$ . . .	19.5		
$\text{CdH}^+$ . . .	$48 \pm 10$	87	$32 \pm 10$
$\text{CdH}$ . . .	15.7		
$\text{HgH}^+$ . . .	$69 \pm 20$	112	$60 \pm 20$
$\text{HgH}$ . . .	8.6		

It is noticeable that the  $D_1$  values are larger in the  $\text{MH}^+$  molecule-ions than in the molecules (with a possible exception in the case  $\text{M} = \text{Mg}$ ). A trend in the observed direction might be anticipated in view of the fact that the  $\text{MH}^+$  molecule-ions can be formed from the  $\text{M}^+$  univalent ions

<sup>15</sup> Carson, Hartley and Skinner, *Nature*, 1948, **161**, 725; and unpublished results.

<sup>16</sup> Berthelot, *Compt. rend.*, 1899, **129**, 918.

\* We suspect that the heat of formation of mercury dimethyl, derived from the heat of combustion by Berthelot is not very reliable. Even if  $(D_1 + D_2)$  as quoted is in error by as much as 10 kcal., we would still expect  $D_1$  to be very small.

without the necessity of a prior excitation within the ion. Thus,

$$D_1(\text{MH}) = \bar{E}^*(\text{M}-\text{H}) + R_1(\text{MH}) - \kappa, \quad (11)$$

whereas

$$D_1(\text{MH}^+) = \bar{E}(\text{M}-\text{H}) + R(\text{MH}^+) \quad (12)$$

The covalent energy  $\bar{E}^*(\text{M}-\text{H})$  is almost certainly a *larger* quantity than the term  $\bar{E}(\text{M}-\text{H})$  since the former relates to a bond of type ( $sp - s$ ) whereas the latter describes a bond type ( $s - s$ ). Moreover, whereas the term  $R(\text{MH}^+)$  must be a small or zero quantity (one cannot postulate ionic-covalent resonance in the  $\text{MH}^+$  molecule-ions) the terms  $R_1(\text{MH})$  may be an appreciable positive quantity. We may therefore conclude that  $D_1(\text{MH}^+)$  will, in general, exceed  $D_1(\text{MH})$  by an amount appreciably *less* than the excitation energy  $\kappa$ . This is borne out by comparison of the  $\Delta$  values in Table III with the  $\kappa(^1S \rightarrow ^3P)$  values, which we assume to be *minimum* values of the valence-state excitation energies in the Group II elements.

From eqn. (7),

$$D_1(\text{MX}) = \bar{E}^*(\text{M}-\text{X}) + R_1(\text{MX}) - \kappa, \quad (7)$$

we may obtain

$$\Delta D_1 \left[ \begin{smallmatrix} \text{MX} \\ \text{MX}_1 \end{smallmatrix} \right] = \Delta \bar{E}^* \left[ \begin{smallmatrix} \text{MX} \\ \text{MX}_1 \end{smallmatrix} \right] + \Delta R_1 \left[ \begin{smallmatrix} \text{MX} \\ \text{MX}_1 \end{smallmatrix} \right] \quad (13)$$

where the terms in  $\Delta$  measure *differences* in  $D_1$ ,  $\bar{E}^*$ , and  $R_1$  values. The terms  $\bar{E}^*(\text{M}-\text{X})$ , measuring *covalent* bond energies, decrease down the series  $\text{X} = \text{H}, \text{F}, \text{Cl}, \text{Br}, \text{I}$  (for a given  $\text{M}$ ). The terms  $R_1(\text{MX})$ , which we have regarded as ionic-covalent resonance energies, increase with increasing electronegativity of  $\text{X}$ , i.e. increase along the series  $\text{X} = \text{H}, \text{I}, \text{Br}, \text{Cl}$  and  $\text{F}$ . Hence, in eqn. (13), when  $\text{X}_1 = \text{H}$ , and  $\text{X}_2 = \text{I}$ , we expect  $\Delta D_1$  to be the sum of a positive term,  $\Delta \bar{E}^*$  (probably of the order 30 kcal.), and a negative term,  $\Delta R_1$ , which would seem to be of the same order of magnitude. Applying (13) to the case  $\text{X}_1 = \text{H}$ ,  $\text{X}_2 = \text{F}$ , the positive term  $\Delta \bar{E}^*$  is now reduced (probably to 20 kcal.), whereas the negative term  $\Delta R_1$  will be very much increased. Our general expectation, from (13), is to find that for a given  $\text{M}$ , the  $D_1(\text{MX})$  values should increase along the series  $\text{X} = \text{H}$  (smallest) to  $\text{X} = \text{F}$  (largest). The listed values of  $D_1(\text{MX})$  in Table IV reveal this trend quite clearly. For comparison, we have added (at the end of Table IV) the  $D_1(\text{MX})$  values for the case of a typical ionic molecule ( $\text{M} = \text{Na}$ ) and a typical covalent molecule ( $\text{M} = \text{CH}_3$ ). The strong resemblance to the ionic, rather than the covalent example may be noted.

TABLE IV.— $D_1(\text{MX})$  VALUES FOR  $\text{M} = \text{GROUP II ELEMENT}$  IN KCAL.

Bond	M—H	M—I	M—Br	M—Cl	M—F
M = Be	53	—	—	69	92
Mg	46	—	58	62	74
Ca	39	58	—	64	73
Sr	38	46	—	58	62
Zn	19	30	40	50	—
Cd	16	25	35	46	—
Hg	8	12	17	25	32
Na	47	72	88	98	115
CH <sub>3</sub>	102	55	68	* 81	—

The application of (13) to the interesting case where  $X_1 = H$  and  $X_2 = CH_3$ , leads to the conclusion that the  $D_1(MCH_3)$  dissociation energies should lie very close to the  $D_1(MH)$  values, for we would expect  $\Delta \bar{E}^*$  to be a small positive term and  $\Delta R_1$  to be a small negative term (the electronegativities of C and H lying close together). Our suggestion earlier that  $D_1(HgCH_3)$  is probably small would then fit in with the small value (8 kcal.) for the  $D_1(Hg-H)$  value.

One further point of interest in respect of the  $MX_2$  and  $MX$  compounds of Group II concerns the bond lengths in these molecules. Bond lengths are known from spectroscopic<sup>17</sup> measurements in the MH diatomic molecules, and from electron-diffraction studies of a few dihalides.<sup>18</sup> In Table V we give the values of the "effective" radius of the M atom in various MX bonds, obtained by subtraction of the covalent radius of the X atom from the observed bond-length.

TABLE V.—EFFECTIVE RADII OF M ATOMS IN MX AND  $MX_2$ 

Be	Mg	Ca	Zn	Cd	Hg	Compounds
0.97	1.36	1.63	1.22	1.39	1.37	Hydrides
0.64	1.03	1.30	—	—	—	Fluorides
—	—	—	—	1.24	1.24	Chlorides
—	—	—	—	1.25	1.30	Bromides
—	—	—	1.10	1.27	1.28	Iodides

The effective radii are noticeably less in the halides than in the hydrides, especially so in the case of M—F bonds. We are inclined to the view that the main factor responsible for the contractions in these bonds rests in their large ionic character, as has been suggested by Stevenson and Schomaker.<sup>19</sup> The large contraction in M—F bonds, and the smaller contraction in M—Cl and M—Br bonds, would agree with the general picture of a decreasing, although still appreciable, ionic nature from the fluorides through to the hydrides.

### Compounds of Group III

The elements of Group III are monovalent in their atomic ground-states, and an internal excitation is required to allow the formation of compounds of the type  $MX_2$  or  $MX_3$ . The energy diagram for the series  $MX$ ,  $MX_2$  and  $MX_3$  ( $M = \text{Group III element}$ ) is shown in Fig. 3, and leads to the set of equations:

$$D_1 = \bar{E}(M-X) + R_1(MX) \quad . \quad . \quad (14a)$$

$$(D_1 + D_2) = 2\bar{E}^*(M-X) + R_2(MX_2) - \alpha \quad . \quad (14b)$$

$$(D_1 + D_2 + D_3) = 3\bar{E}^*(M-X) + R_3(MX_3) - \alpha \quad . \quad (14c)$$

As before, the terms in  $R$  measure resonance energies relative to the covalent structures  $MX$ ,  $M^*X_2$  and  $M^*X_3$ . The term  $\bar{E}(M-X)$  measures the energy of the covalent  $p$  bond: whether or not the terms  $\bar{E}^*(M-X)$  are identical in (14b) and (14c) is doubtful, for whilst we can reasonably describe the bonds in  $MX_3$  as  $sp^2$  hybrids, the bonds in  $MX_2$  may be either  $sp^2$  or  $sp$  hybrids. Pauling<sup>5</sup> has estimated that the strength of binding

<sup>17</sup> Quoted by Herzberg, *Molecular Spectra and Molecular Structure* (1939), p. 484.

<sup>18</sup> Hassel and Strömme, *Z. physik. Chem. B*, 1938, **38**, 466. Lister and Sutton, *Trans. Faraday Soc.*, 1941, **37**, 406. Maxwell and Mosley, *Physic. Rev.*, 1940, **57**, 21.

<sup>19</sup> Stevenson and Schomaker, *J. Amer. Chem. Soc.*, 1941, **63**, 37.

in  $sp$  and  $sp^2$  bonds is almost identical, so that it might be a good enough approximation for our present purpose to presume that the terms  $\bar{E}^*(M-X)$  in (14b) and (14c) are the same. We cannot further assume that  $\bar{E}(M-X)$  and  $\bar{E}^*(M-X)$  are equal, since Pauling's calculated strengths of hybrid bonds show  $sp^2$  binding to be much stronger than  $p$  binding.

From eqn. (14) we may rearrange to obtain

$$D_1 = \bar{E}(M-X) + R_1 \quad . \quad . \quad . \quad . \quad . \quad (15a)$$

$$D_2 = 2\bar{E}^*(M-X) - E(M-X) + (R_2 - R_1) - \alpha \quad (15b)$$

$$D_3 = \bar{E}^*(M-X) + (R_3 - R_2) \quad . \quad . \quad . \quad . \quad . \quad (15c)$$

Since  $\bar{E}^*(M-X) > \bar{E}(M-X)$ , we may write the difference between them as  $\Delta E$ , where  $\Delta E$  is a positive quantity. Eqn. (15b) then becomes

$$D_2 = E^*(M-X) + \Delta E + (R_2 - R_1) - \alpha \quad . \quad . \quad . \quad (15d)$$

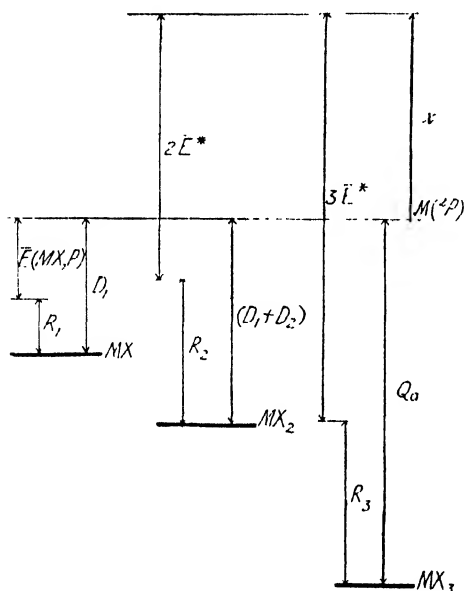


FIG. 3.—Energy diagram for MX, MX<sub>2</sub>, MX<sub>3</sub>.

Comparing eqn. (15d) and (15c), we see that if  $\alpha$  is a large enough quantity,  $D_3$  is likely to exceed  $D_2$ . On the other hand, if  $\alpha$  is not a large term in itself, the weakening effect of the excitation energy on  $D_2$  may be more or less completely offset by the term in  $\Delta E$ .

It may be objected that the eqn. (15) are inadequate, in so far as our description has not taken note of the effect of multiple-bonded structures

of the type  $X_2\bar{M} = \bar{X}$ , and their contribution to the total resonance in MX<sub>3</sub> compounds (Pauling has suggested that such structures are of major importance in, e.g., BF<sub>3</sub>). Account of such resonance can be included in our treatment, *without* alteration to the equations as written, if we recognise that the resonance energy terms in  $R$  may arise, not exclusively from ionic-covalent interaction, but also from interaction with multiple-bonded structures.\* It becomes, of course, far more difficult to

\* A similar criticism can be levelled against the treatment we have given in the Group II compounds. If double-bonding is a serious factor in the halides of Group II, our equations remain unaltered, but our interpretation of the terms in  $R$  as ionic-covalent resonance energies would be inadequate.



assess, even roughly, the relative magnitudes of the resonance energy terms  $R_1$ ,  $R_2$  and  $R_3$ . For this reason it is difficult at present to progress beyond the equations we have given, and conclusions that can be drawn from the equations are at best tentative. The most certain of these is that in case where  $x$  is a large term, the dissociation energy  $D_2$  will be the smallest of the three  $D$  values.

Only in one sample (that of the indium halides) is there sufficient experimental data to derive the individual values of the three dissociation energies,  $D_1$ ,  $D_2$  and  $D_3$ . Significantly, it is apparently the case that here  $D_2$  is considerably smaller than either  $D_1$  or  $D_3$ . The data on the  $\text{InX}_3$  compounds (mainly due to Wenk<sup>20</sup>) are listed in Table VI. Apart from this single example (which is not a very favourable one, since the  $\text{In}-\text{X}$  bonds are predominantly ionic in character and the terms in  $R$  are therefore large), there are no experimental determinations of  $D_2$  for other Group III compounds.

TABLE VI.—BOND-DISSOCIATION ENERGIES IN  $\text{InX}_3$ 

Compound	$Q_a$ (kcal.)	$D_1$	$D_2$	$D_3$
$\text{InCl}_3$	(253)	104	46	(103)
$\text{InBr}_3$	(215)	85	42	(88)
$\text{InI}_3$	(170)	69	42	(59)

Values of  $Q_a$  are estimated, using data given by Bichowsky and Rossini, and assuming the heat of sublimation of  $\text{InX}_3$  (cryst.) to be 15 kcal. for all  $\text{InX}_3$  compounds. Probably, actual heats of sublimation are less than we have assumed.  $D_1$  and  $D_3$  values are from Wenk.<sup>20</sup>

### Compounds of Group IV

The Group IV elements are divalent in their atomic ground-states and, by analogy with the earlier discussion, it is necessary to assume an internal excitation at the step,  $\text{MX}_2 + \text{X} \rightarrow \text{MX}_3$ . A possible \* energy diagram for  $\text{MX}$ ,  $\text{MX}_2$ ,  $\text{MX}_3$  and  $\text{MX}_4$  (where  $M$  now refers to a Group IV element) is shown in Fig. 4, and corresponds to the equations:

$$D_1 = \bar{E}(\text{MX}, p) + R_1 \quad (16a)$$

$$(D_1 + D_2) = 2\bar{E}(\text{MX}, p) + R_2 \quad (16b)$$

$$(D_1 + D_2 + D_3) = 3\bar{E}^*(\text{MX}, sp^2) + R_3 - x \quad (16c)$$

$$(D_1 + D_2 + D_3 + D_4) = 4\bar{E}^*(\text{MX}, sp^3) + R_4 - x, \quad (16d)$$

from which may be obtained:

$$D_1 = \bar{E}(\text{MX}, p) + R_1 \quad (17a)$$

$$D_2 = \bar{E}(\text{MX}, p) + (R_2 - R_1) \quad (17b)$$

$$D_3 = 3\bar{E}^*(\text{MX}, sp^2) - 2\bar{E}(\text{MX}, p) + (R_3 - R_2) - x \quad (17c)$$

$$D_4 = 4\bar{E}^*(\text{MX}, sp^3) - 3\bar{E}^*(\text{MX}, sp^2) + (R_4 - R_3). \quad (17d)$$

The terms in  $R$  measure resonance energies with respect to the covalent structures  $\text{MX}$ ,  $\text{MX}_2$ ,  $\text{M}^*\text{X}_3$  and  $\text{M}^*\text{X}_4$ , and the terms in  $\bar{E}$  the covalent bond energies of  $p$ ,  $sp^2$ , and  $sp^3$   $\text{M}-\text{X}$  bonds. If we denote the difference

<sup>20</sup> Wenk, *Helv. phys. Acta*, 1941, 14, 355.

\* The energy diagram is referred to as a "possible" one, since there is an alternative possibility, namely that the excitation to a higher valence state occurs at the step  $\text{MH} + \text{H} \rightarrow \text{MH}_2$ . Furthermore, the valence state of the  $M$  atom may not lie at the same  $x$  as the state of hybridisation of the  $\text{M}-\text{X}$  bonds changes.

$\bar{E}^*(MX, sp^3) - \bar{E}(MX, p)$  by  $\Delta E$  (where  $\Delta E$  is a positive term) eqn. (17c) may be rewritten as

$$D_3 = \bar{E}^*(MX, sp^3) + 2\Delta E + (R_3 - R_2) - \alpha. \quad (17e)$$

Whereas in our discussion on the  $MX_2$  (Group II) and  $MX_3$  (Group III) compounds, we have been led to expect low dissociation energies (relatively) for those bonds ( $D_1$  and  $D_2$  respectively) affected by the term in  $\alpha$ , the case is less certain in the  $MX_4$  compounds of Group IV. As (17e) shows, the weakening effect of the term in  $\alpha$  on  $D_3$  is offset by the term  $2\Delta E$ , which may be large enough more or less completely to compensate for  $\alpha$ .

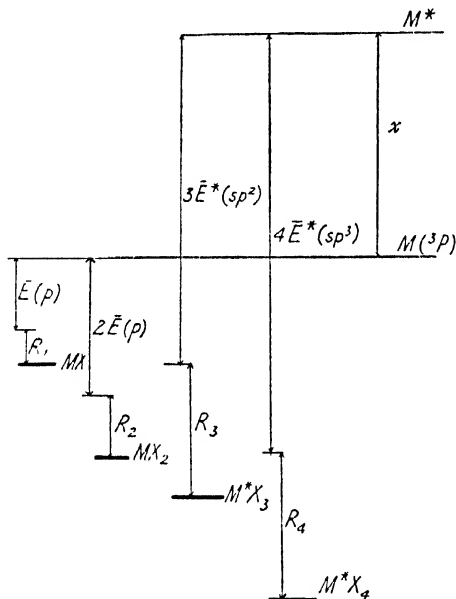


FIG. 4.—Energy diagram for  $MX$ ,  $MX_2$ ,  $MX_3$ ,  $MX_4$ .

There are practically no experimental data available for  $MX_4$  compounds which provide values for  $D_3$ . Only in the case of  $SnX_4$  are the data sufficient to allow an estimation of the individual values  $D_3$  and  $D_4$ . The relevant thermal data are summarised in Table VII.

TABLE VII— $Q_a$  VALUES IN  $SnX_3$  AND  $SnX_4$

Molecule	$Q_f$ (gas)	$Q_a$	$(D_1 + D_2)$	$(D_3 + D_4)$
$SnCl_3$ . . .	(58)	(194)	194	—
$SnCl_4$ . . .	118	312	194	118
$SnBr_3$ . . .	(32)	(164)	164	—
$SnBr_4$ . . .	83	269	164	105
$SnI_3$ . . .	(9)	(138)	138	—
$SnI_4$ . . .	?	(225)	138	(87)

$Q_f$  values estimated from data given by Bichowsky and Rossini,<sup>8</sup> with heats of vaporisation from Fisher and Gewehr.<sup>21</sup> Heats of fusion assumed at 5 kcal. (for  $SnX_3$  compounds). Heat of vaporisation of  $SnBr_4$  estimated at 9 kcal.

$Q_a$  ( $SnI_4$ ) is an estimated value.

<sup>21</sup> Fischer and Gewehr, *Z. anorg. Chem.*, 1939, **242**, 161.

The  $Q_s(\text{SnX}_3)$  provide the sum  $(D_1 + D_3)$ , and  $Q_s(\text{SnX}_4)$  the sum  $(D_1 + D_3 + D_3 + D_4)$ : from the difference we may obtain  $(D_3 + D_4)$ . Experimental determinations of the  $D_4$  values in  $\text{SnCl}_4$  and  $\text{SnI}_4$  have been made by studies on the photodissociation of these compounds by Terenin and Tschubarov,<sup>22</sup> who quote  $D_4 \sim 76$  kcal. in  $\text{SnCl}_4$ , and  $D_4 \sim 60$  kcal. in  $\text{SnI}_4$ . Substitution of these into our equation for  $(D_3 + D_4)$  yields

$$\begin{aligned} D_3(\text{SnCl}_4) &\sim 42.6 \text{ kcal.} \\ D_3(\text{SnI}_4) &\sim 27 \text{ kcal.} \end{aligned}$$

If we assume a value for  $D_4$  ( $\text{SnBr}_4$ ) midway between the  $D_4$  values in  $\text{SnCl}_4$  and  $\text{SnI}_4$ , the estimated values of  $D_3(\text{SnBr}_4)$  is 37 kcal. In all these cases,  $D_3$  is much less than  $D_4$ . Independent experimental evidence of relatively small  $D_3$  values in  $\text{SnX}_4$  compounds is provided by the Na-flame reactions with  $\text{SnX}_4$ , which have been discussed by Ogg and Polanyi.<sup>23</sup>

The special case of the tetravalent compounds of C has already been mentioned by Long and Norrish,<sup>1</sup> who were mainly concerned to show that the experimental value<sup>24</sup> of 102 kcal. for  $D_4$  in  $\text{CH}_4$  provides evidence for the "low" value ( $L = 126$  kcal.) for the heat of sublimation of graphite, and necessitates a value of *ca.* 60-70 kcal. for the excitation energy ( $\chi$ ) in C. The argument of Long and Norrish is, however, based essentially on the tacit assumption that the bond-energy term values  $E^*(\text{C}-\text{H})$  in  $\text{CH}_4$  and in the methyl radical are of similar magnitude. The experimental data place  $E^*(\text{C}-\text{H})$  in  $\text{CH}_4$  at  $(L + \chi)/4 + 56.5$  kcal., and  $E^*(\text{C}-\text{H})$  in the methyl radical at  $(L + \chi)/3 + 41.3$  kcal. If the  $E^*(\text{C}-\text{H})$  values are assumed equal, then it follows that  $(L + \chi) = 182.4$  kcal. But, since the CH bonds in free methyl are probably of a different type (trigonal, or  $sp^2$  bonds) from the tetrahedral  $sp^3$  bonds in  $\text{CH}_4$  (see Penney<sup>25</sup> and Voge<sup>26</sup>) it is a considerable assumption to presume that the two  $E^*(\text{C}-\text{H})$  are equal or even approximately so. Moreover, it does not require a large difference between the two  $E^*(\text{C}-\text{H})$  values to make a serious change in the corresponding value  $(L + \chi)$ : e.g., if we assume  $E^*(\text{C}-\text{H})$  in methyl is only 5 kcal. greater than  $E^*(\text{C}-\text{H})$  in  $\text{CH}_4$ , the value  $(L + \chi)$  then becomes 242.4 kcal. In view of the very sharp dependence of  $(L + \chi)$  on the assumed difference in the  $E^*(\text{C}-\text{H})$  values in  $\text{CH}_3$  and  $\text{CH}_4$ , we are forced to conclude that it would be risky to adopt the "low" value for  $L$  on the basis of the Long and Norrish argument alone—although it may still be that the "low" value is the correct one.

It is instructive to apply the type of argument used by Long and Norrish in the case of  $\text{CH}_4$  to other examples. In the case of  $\text{H}_2\text{O}$ , for which experiment has given the values  $D(\text{O}-\text{H}) \sim 102$  kcal., and  $D(\text{H}-\text{OH}) \sim 119$  kcal., the mean bond-energy term  $E(\text{O}-\text{H})$  lies midway at 110.5 kcal. If, however, we choose to measure the total energy of  $\text{H}_2\text{O}$  with respect to the divalent valence state of the oxygen atom, which Mulliken<sup>27</sup> has estimated to lie *ca.* 16 kcal. above the ground state,  $^3P$ , we obtain 118.5 kcal. for the mean bond-energy term  $E^*(\text{O}-\text{H})$ . In this particular example, there is a very close correlation between  $E^*(\text{OH})$  and  $D(\text{H}-\text{OH})$  which is interesting, and may be significant. But, in the example of  $\text{HgCl}_2$ , an identity between  $D(\text{Cl}-\text{HgCl})$  and  $E^*(\text{HgCl})$  would require a value of 56.5 kcal. for the excitation energy to the valence state of Hg. This is only *half* the energy of the atomic transition  $\text{Hg}(^1S) \rightarrow \text{Hg}(^3P)$ , and we have already pointed out that it seems

<sup>22</sup> Terenin and Tschubarov, *Acta Physicochim.*, 1937, **7**, 1.

<sup>23</sup> Ogg and Polanyi, *Trans. Faraday Soc.*, 1935, **31**, 1375.

<sup>24</sup> Kistiakowsky and van Artsdalen, *J. Chem. Physics*, 1944, **12**, 469.

<sup>25</sup> Penney, *Trans. Faraday Soc.*, 1935, **31**, 734.

<sup>26</sup> Voge, *J. Chem. Physics*, 1936, **4**, 581.

<sup>27</sup> Mulliken, *J. Chem. Physics*, 1934, **2**, 782.

improbable that the "valence state" of divalent Hg can lie at a lower level than the lowest of the Hg  $^3P$  levels.

According to the description we have given, the inter-relation between  $D$  and  $E^*$  values is not simple, and we should not expect an identity between these terms except in special circumstances. Nevertheless, it is desirable to examine whether there is a description by means of which it may be possible to expect values of  $\alpha$  as low as 60-70 kcal. in C, and 50-60 kcal. in Hg. In this connection, the paper by Voge<sup>26</sup> is of interest, in that he shows that the value of the excitation energy to the valence state in C is very much reduced below van Vleck's estimation if the valence state is considered to be built up from configurations  $s^2p^2$  and  $p^1$  in addition to the configurations  $sp^3$ . It may be that in the case of Hg, inclusion of configurations  $s^2$  in the valence state could lead to a lower value of  $\alpha$  than we have considered possible. But, by so doing, the conception of the valence state is rendered rather vague and indefinite: it seems more profitable to regard the valence state as something quite specific, and to conclude, if necessary, that a simple 1:1 correlation between  $D$  and  $E^*$  values will not in general be found.

The author wishes to express his thanks to Prof. M. Polanyi for advice during the preparation of this paper, and also to Dr. H. D. Springall for many useful discussions.

*Chemistry Department,  
University of Manchester,  
Manchester, 13.*

---

## MOLECULAR FORCE FIELDS

### PART VI.—DISTORTIONS OF BOND-FORMING ORBITALS AND THE EFFECT ON MOLECULAR VIBRATIONS

By J. W. LINNETT AND P. J. WHEATLEY

*Received 15th April, 1948*

The possibility of the bonding orbitals of a central atom changing their hybridisation in such a manner as to follow the outer atoms during bending vibrations has been discussed. The effect of this on the bending vibration of a non-linear triatomic symmetrical molecule has been examined, and it has been shown that the bending vibration would occur more easily if there were such orbital following. However, since there is only one bending vibration in such a molecule, the concept cannot be tested. In tetrahedral molecules with several bending vibrations there are four relevant directions in which the orbitals might follow the surrounding atoms. It has been shown that in one of these directions there can be no orbital following, and the relative increase in potential energy for the other three types of distortion has been obtained. It is proposed to include the increase in potential energy due to orbital following in the full potential energy function of tetrahedral molecules, and the results obtained from this modified form of the O.V.F.F. will be given in a subsequent paper.

Heath and Linnett<sup>1</sup> have shown that a field based on Pauling's theory of directed valency<sup>2</sup> accounts better for the vibration frequencies of certain molecules than does the simple valency force field (S.V.F.F.). They called this field, which differs from the S.V.F.F. only in its treatment of angular displacements, the orbital valency force field (O.V.F.F.). According

<sup>1</sup> Heath and Linnett, *Trans. Faraday Soc.* (in press).

<sup>2</sup> Pauling, *J. Amer. Chem. Soc.*, 1931, **53**, 1367.



to such an extent as to minimise the energy. Therefore  $\Delta\beta$  can be related to  $\Delta\alpha$  by

$$2 \frac{dV}{d\Delta\beta} = -4k_\alpha(\Delta\alpha - \Delta\beta) + 2k_\beta\Delta\beta = 0. \quad (4)$$

Hence

$$\Delta\beta = \frac{2k_\alpha}{2k_\alpha + k_\beta} \Delta\alpha. \quad (5)$$

When (5) is substituted in (3), we obtain

$$2V = \frac{2k_\alpha k_\beta}{2k_\alpha + k_\beta} (\Delta\alpha)^2. \quad (6)$$

If  $k_\beta$  is infinite and there is no orbital following then it will be seen that (6) reduces to (1), i.e. the formula for the simple O.V.F.F. However, if  $k_\beta$  is finite and there is orbital following

$$\frac{2k_\alpha k_\beta}{2k_\alpha + k_\beta} < k_\alpha$$

and the bending distortion is easier than if there were no orbital following.

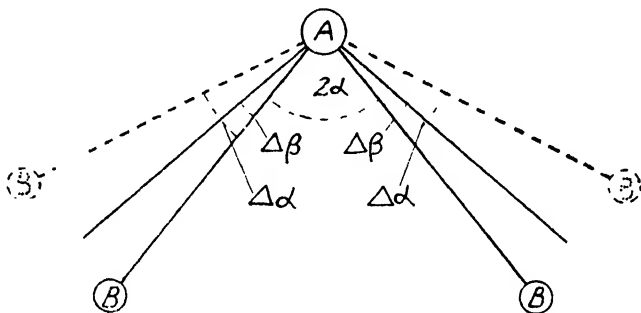


FIG. 1.

It is not possible to test this hypothesis with triatomic molecules since there is only one bending vibration and the relative magnitudes of  $k_\alpha$  and  $k_\beta$  cannot be determined. It was decided, therefore, to apply the above considerations to methane and the four deuterated methanes.

### Wave Mechanical Treatment of the Distortions in $\text{CH}_4$

The  $s$  and  $p$  eigenfunctions with the same total quantum number do not differ very much in their mean values of  $r$ .<sup>2</sup> Their dependence on  $\theta$  and  $\phi$  is given by

$$\begin{aligned} s &= 1, & p_x &= \sqrt{3} \sin \theta \cos \phi, \\ p_y &= \sqrt{3} \sin \theta \sin \phi, & p_z &= \sqrt{3} \cos \theta, \end{aligned}$$

where the normalisation factors are equivalent for all. The best bond-forming orbitals are obtained when these four ( $s$ ,  $p_x$ ,  $p_y$  and  $p_z$ ) are combined to form four equivalent orbitals directed towards the corners of a tetrahedron. One set of these, which are directed towards four of the corners of a cube in the manner shown in Fig. 2 are<sup>3</sup>

$$\begin{aligned} \psi_1 &= \frac{1}{2}s + \frac{1}{2}p_x + \frac{1}{2}p_y + \frac{1}{2}p_z, \\ \psi_2 &= \frac{1}{2}s - \frac{1}{2}p_x - \frac{1}{2}p_y + \frac{1}{2}p_z, \\ \psi_3 &= \frac{1}{2}s - \frac{1}{2}p_x + \frac{1}{2}p_y - \frac{1}{2}p_z, \\ \psi_4 &= \frac{1}{2}s + \frac{1}{2}p_x - \frac{1}{2}p_y - \frac{1}{2}p_z. \end{aligned}$$

The lines in Fig. 2 represent the directions in which the bonding orbitals have their maximum values.

<sup>2</sup> Pauling, *The Nature of the Chemical Bond* (Cornell University Press) § 14.

Let us suppose that the orbitals are distorted by change of hybridisation in the manner indicated by the arrows in Fig. 3. This distortion might be expected to occur during a vibration of  $\text{CH}_4$  of analogous form, so that the orbitals would follow the movements of the atoms. Now if the bonding orbitals 1 and 2 are to be distorted as in Fig. 3 the  $p_x$  contribution to each must increase equally, and the  $p_x$  and  $p_y$  contributions must remain the same, since the two orbitals remain equivalent. Thus we may write

$$\begin{aligned}\psi_1 &= \frac{1}{2}s(1 + C) + \frac{1}{2}p_x(1 + B) + \frac{1}{2}p_y(1 + B) + \frac{1}{2}p_z(1 + A), \\ \psi_2 &= \frac{1}{2}s(1 + C) - \frac{1}{2}p_x(1 + B) - \frac{1}{2}p_y(1 + B) + \frac{1}{2}p_z(1 + A).\end{aligned}$$

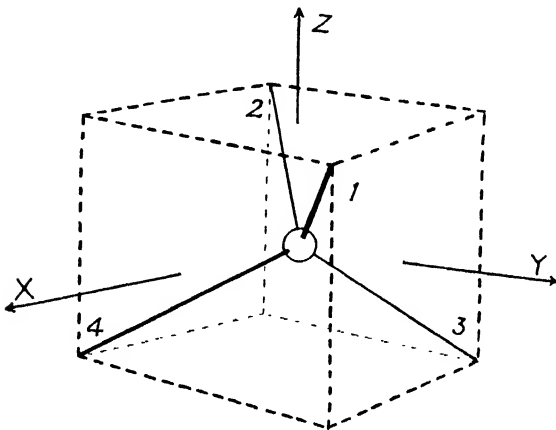


FIG. 2.

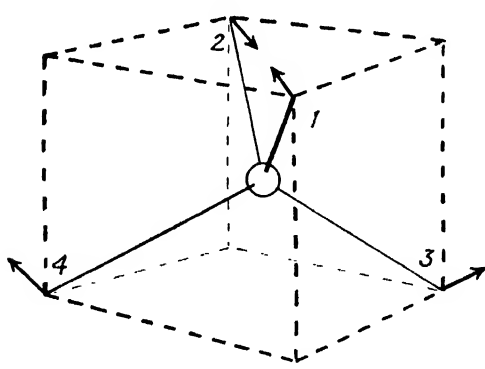


FIG. 3.

By a similar set of arguments the distorted orbitals 3 and 4 must be given by

$$\begin{aligned}\psi_3 &= \frac{1}{2}s(1 + F) - \frac{1}{2}p_x(1 + E) + \frac{1}{2}p_y(1 + E) - \frac{1}{2}p_z(1 + D), \\ \psi_4 &= \frac{1}{2}s(1 + F) + \frac{1}{2}p_x(1 + E) - \frac{1}{2}p_y(1 + E) - \frac{1}{2}p_z(1 + D).\end{aligned}\quad (7)$$

When distorted the four orbitals must remain orthogonal to one another and they must remain normalised. Application of these conditions to the above eqn. (7) enables  $B$ ,  $C$ ,  $D$ ,  $E$  and  $F$  to be eliminated and gives

$$\begin{aligned}\psi_1 &= \frac{1}{2}s(1 - A - A^2) + \frac{1}{2}p_x + \frac{1}{2}p_y + \frac{1}{2}p_z(1 + A), \\ \psi_2 &= \frac{1}{2}s(1 - A - A^2) - \frac{1}{2}p_x - \frac{1}{2}p_y + \frac{1}{2}p_z(1 + A), \\ \psi_3 &= \frac{1}{2}s(1 + A) - \frac{1}{2}p_x + \frac{1}{2}p_y - \frac{1}{2}p_z(1 - A - A^2), \\ \psi_4 &= \frac{1}{2}s(1 + A) + \frac{1}{2}p_x - \frac{1}{2}p_y - \frac{1}{2}p_z(1 - A - A^2).\end{aligned}\quad (8)$$

The first orbital  $\psi_1$  has its maximum value when

$$\left\{ \frac{1}{2}(1 - A - A^2) + \frac{\sqrt{3}}{2} \sin \theta_1 \cos \phi_1 + \frac{\sqrt{3}}{2} \sin \theta_1 \sin \phi_1 + \frac{\sqrt{3}}{2}(1 + A) \cos \theta \right\} \quad (9)$$

has its maximum value. It is easily shown that this occurs when  $\phi_1 = \frac{\pi}{4}$

and when 
$$\tan \theta_1 = \frac{\sqrt{2}}{1 + A} \quad (10)$$

which means that 
$$\sin \theta_1 = \frac{\sqrt{2}}{\sqrt{3}}(1 - \frac{1}{3}A)$$

and 
$$\cos \theta_1 = \frac{1}{\sqrt{3}}(1 + \frac{2}{3}A - \frac{1}{3}A^2). \quad (11)$$

Thus the maximum value  $M_1$  of  $\psi_1$  is

$$M_1 = \frac{1}{2}(1 - A - A^2) + \frac{1}{2}(1 - \frac{1}{3}A) + \frac{1}{2}(1 - \frac{1}{3}A) + \frac{1}{2}(1 + A)(1 + \frac{2}{3}A - \frac{1}{3}A^2) = 2 - \frac{1}{3}A^2. \quad (12)$$

In the undistorted form the orbital 1 makes an angle  $\theta_1^\circ$  with the  $z$ -axis for which  $\tan \theta_1^\circ = \sqrt{2}$ . The angular distortion of the orbital,  $\theta_1 - \theta_1^\circ = \Delta\theta_1$ , may therefore be calculated using (10). It is found to be

$$\Delta\theta_1 = -\frac{\sqrt{2}}{3}A. \quad (13)$$

Substitution of (13) in (12) gives

$$M_1 = 2 - \frac{2}{3}(\Delta\theta_1)^2. \quad (14)$$

The orbital 2 is distorted through  $\Delta\theta_2 = -\frac{\sqrt{2}}{3}A$  also. A similar

calculation shows that  $\Delta\theta_3 = \Delta\theta_4 = -\frac{\sqrt{2}}{3}A$ . Hence the maximum values of all four distorted orbitals are given by eqn. (14), which may be written in general as

$$M = 2 - \frac{2}{3}(\Delta\theta)^2, \quad (15)$$

where

$$\Delta\theta = \Delta\theta_1 = \Delta\theta_2 = \Delta\theta_3 = \Delta\theta_4,$$

and

$$M = M_1 = M_2 = M_3 = M_4.$$

If the strength or bonding energy of the bond is proportional to  $M^n$  (Pauling has taken  $n = 2$ )<sup>4</sup>,

$$S = M^n = 2^n - (n \times 2^{n-1}) \times \frac{2}{3}(\Delta\theta)^2,$$

terms containing higher powers of  $\Delta\theta$  being negligible for small displacements. Thus

$$-V' \propto \Sigma S = 4 \times 2^n - (n \times 2^{n-1}) \times 6(\Delta\theta)^2,$$

and

$$\Delta V' \propto (n \times 2^{n-1}) \times 6(\Delta\theta)^2. \quad (16)$$

This, ideally, is equivalent to the part of the energy change given in (2) for the case of the molecule  $AB_3$ .

Let us now consider the possibility of distorting the orbitals, by changing hybridisation, in the manner shown in Fig. 4. In this case all the orbitals will remain equivalent. This means that the contribution of  $p_z$  to all of them would have to increase and in a set of equations like (8),  $A$  would have to equal  $D$ . Likewise  $B$  would have to equal  $E$ , and  $C$  would have to equal  $F$ . But from the normalisation condition this is impossible, i.e.  $A, B, C, D, E$  and  $F$  would have to be zero. Therefore it is impossible to distort the orbitals in the manner shown in Fig. 4 and it would be impossible for the bonding orbitals to follow a vibration of analogous form.

<sup>4</sup> Pauling and Sherman, *J. Amer. Chem. Soc.*, 1937, **59**, 1450.



The orbital distortions shown in Fig. 5 and 6 can be treated in a manner similar to that of the distortion shown in Fig. 3. The result for the distortion shown in Fig. 6 is that, if each of the three orbitals is distorted through  $\Delta\theta'$

$$-V' \propto \Sigma S = 4 \times 2^n - (n \times 2^{n-1}) \times 9/2(\Delta\theta'')^2,$$

$$\text{or} \quad \Delta V' \propto (n \times 2^{n-1}) \times 9/2(\Delta\theta'')^2. \quad (17)$$

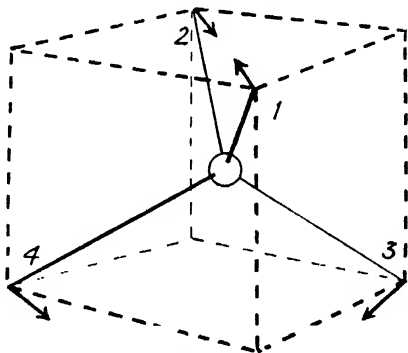


FIG. 4.

The result for the distortion shown in Fig. 5 is that, if the angle between orbital 1 (or 2) and the plane of orbitals 3 and 4 changes by  $\Delta\theta'$ ,

$$-V' \propto \Sigma S = 4 \times 2^n - (n \times 2^{n-1}) \times 3/4(\Delta\theta')^2,$$

$$\text{or} \quad \Delta V' \propto (n \times 2^{n-1}) \times 3/4(\Delta\theta')^2. \quad (18)$$

The above considerations allow us to choose a following constant  $k$ , such that, for the distortion shown in Fig. 3, we may write

$$\Delta V' = 6k_r(\Delta\theta)^2. \quad (19)$$

Then, for the distortion shown in Fig. 5,

$$\Delta V' = 3/4k_r(\Delta\theta')^2 \quad (20)$$

and for that shown in Fig. 6,

$$\Delta V' = 9/2k_r(\Delta\theta'')^2. \quad (21)$$

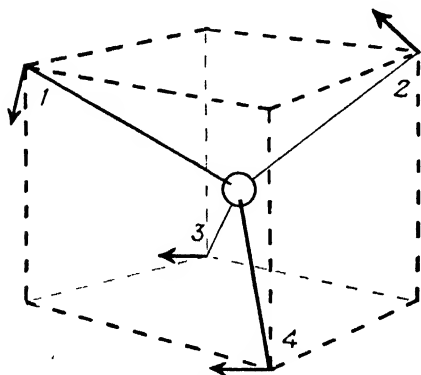


FIG. 5.

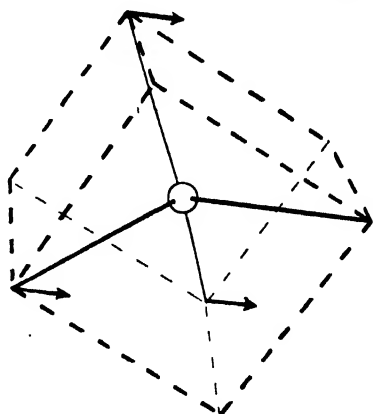


FIG. 6.

These expressions for the increase in P.E. due to orbital following may then be included in the full P.E. function for each type of vibration analogous to each type of distortion. The full P.E. functions for the bending vibrations will then include two constants: (a) an orbital bending

constant and (b) an orbital following constant. Since there are several bending vibrations in tetrahedral molecules, it will be possible to determine the relative magnitudes of these two constants.

### Conclusion

The most important conclusions to be drawn from this study are: (1) that bending vibrations will occur more easily in certain molecules than would be expected from the simple O.V.F.F., if the bonding orbitals are able to follow the movement of the atoms by change of hybridisation; and (2) that in methane it is possible for the bonding orbitals to follow the atoms during certain vibrations by change of hybridisation (Fig. 3), but impossible for them to follow the atoms during other vibrations (Fig. 4) because change of hybridisation in the sense required is not possible. Conclusion (2) should enable us to test the hypothesis because it predicts that certain bending vibrations of methane and its derivatives should occur more easily than others. This will be done in a subsequent paper.

We wish to thank Prof. C. A. Coulson and Mr. H. C. Longuet-Higgins for helpful discussions.

*Inorganic Chemistry Laboratory,  
Oxford.*

## MOLECULAR FORCE FIELDS

### PART VII. THE APPLICATION OF THE CONCEPT OF ORBITAL FOLLOWING TO METHANE AND THE DEUTEROMETHANES

By J. W. LINNETT AND P. J. WHEATLEY

*Received 15th April, 1948*

In the present paper we have examined the application of the orbital valency force field, combined with the conception of orbital following by change of hybridisation which has been put forward in Part VI, to the vibrations of methane and its deuterated derivatives. It was found that the field accounted well for the vibration frequencies, the average error between calculated and observed values being 1 %.

In the previous paper<sup>1</sup> it was pointed out that, if the bonding orbitals of an atom were able, by change of hybridisation, to follow the attached atoms during a bending vibration, the effective force constant for that particular deformation would be reduced. The object of the present paper is to examine the application of this idea to methane and its four deuterated derivatives. In the previous paper, we studied the way in which the bonding energy of the tetrahedral orbitals of carbon changed for small deviations from the tetrahedral configuration. The decrease in bonding energy (i.e. increase in potential energy) depends on the form of the distortion. The results that were obtained are summarised below. For a distortion of the type shown in Fig. 1a no following of the orbitals is possible. For distortions of the types shown in Fig. 1b, 1c and 1d, the increases in potential energy due to orbital following are given, respectively, by

$$\Delta V' = 6k_r(\Delta\theta)^2,$$

$$\Delta V' = 3/4k_r(\Delta\theta')^2,$$

$$\Delta V' = 9/2k_r(\Delta\theta'')^2.$$

and

<sup>1</sup> Linnett and Wheatley, *Trans. Faraday Soc.* (preceding paper).

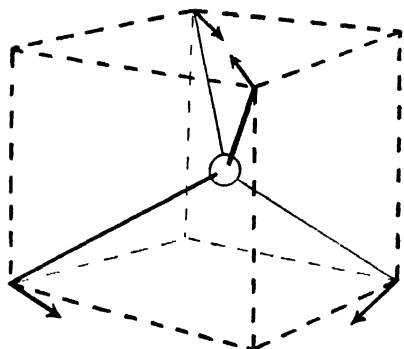


FIG. 1a.

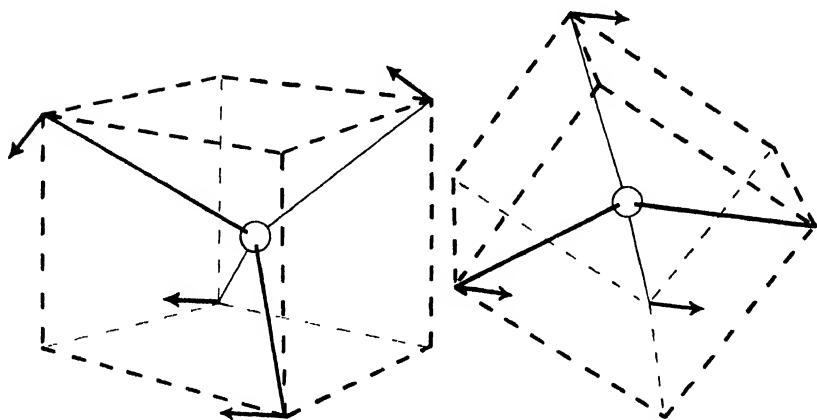
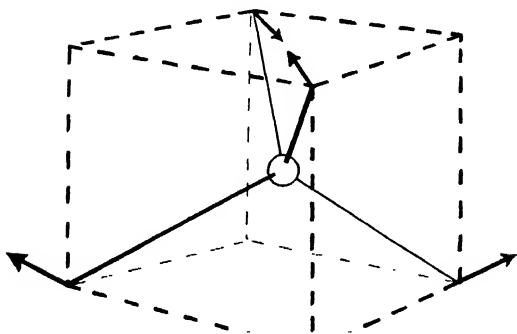


FIG. 1c.

FIG. 1d.

### Experimental Frequencies

The spectra of methane and the deuteromethanes have been investigated by both infra-red and Raman spectrography,<sup>2</sup> and the results have been considered and tabulated by Herzberg.<sup>3</sup> Not all of the frequencies are assigned to the different symmetry classes and this had

<sup>2</sup> MacWood and Urey, *J. Chem. Physics*, 1936, **4**, 402. Ginsburg and Barker, *ibid.*, 1935, **3**, 668. Benedict, Morikawa, Barnes and Taylor, *ibid.*, 1937, **5**, 1.

<sup>3</sup> Herzberg, *Infra-red and Raman Spectra* (D. Van Nostrand and Co. Inc.), p. 309.

first to be done by means of the product rule.<sup>4</sup> The secular equations from which the frequencies may be calculated, using the simple valency force field,<sup>5</sup> are given in Appendix I. Table I gives a list of the experi-

TABLE I.—THE OBSERVED VALUES FOR THE FUNDAMENTAL VIBRATION FREQUENCIES OF METHANE AND THE DEUTEROMETHANES AND CALCULATED VALUES USING THE S.V.F.F.

$T$  = triply-degenerate vibrations.  
 $E$  = doubly-degenerate vibrations.  
 $A$  = non-degenerate vibrations.  
 $SS$  = vibrations symmetric to both the HCH and DCD planes.  
 $AA$  = vibrations antisymmetric to both the HCH and DCD planes.  
 $SA$  = vibrations symmetric to the HCH and antisymmetric to the DCD plane.  
 $AS$  = vibrations antisymmetric to the HCH and symmetric to the DCD plane.

	$\times 10^5$ dyne $\times$ cm. <sup>-1</sup>		Stretching Vibrations			Bending Vibrations		
	$k_1$	$k_{\theta/r^2}$	Calc. cm. <sup>-1</sup>	Exp. cm. <sup>-1</sup>	% Diff.	Calc. cm. <sup>-1</sup>	Exp. cm. <sup>-1</sup>	% Diff.
CH <sub>4</sub>	5.0	0.88	3067 $T$ 2902 $A$	3020 $T$ 2914 $A$	+ 1.53 - 0.43	1491 $E$ 1331 $T$	1526 $E$ 1306 $T$	- 2.29 + 1.93
CH <sub>3</sub> D	5.0	0.88	3067 $E$ 2966 $A$ 2200 $A$	3030 $E$ 2982 $A$ 2205 $A$	+ 1.32 - 0.54 - 0.23	1441 $E$ 1324 $A$ 1168 $E$	1477 $E$ 1306 $A$ 1156 $E$	- 2.44 + 1.38 + 1.04
CH <sub>2</sub> D <sub>2</sub>	5.0	0.88	3066 $SA$ 2995 $SS$ 2291 $AS$ 2161 $SS$	3020 $SA$ 2974 $SS$ 2255 $AS$ 2139 $SS$	+ 1.52 + 0.71 + 1.60 + 1.03	1413 $SS$ 1291 $AA$ 1239 $AS$ 1105 $SA$ 1026 $SS$	1450 $SS$ 1285 $AA$ 1235 $AS$ 1090 $SA$ 1034 $SS$	- 2.55 + 0.47 + 0.32 + 1.38 - 0.77
CHD <sub>3</sub>	5.0	0.88	3032 $A$ 2280 $A$ 2105 $E$	2992 $A$ 2269 $A$ 2141 $E$	+ 1.34 + 0.88 - 1.68	1269 $E$ 1024 $E$ 1010 $A$	1299 $E$ 1046 $E$ 982 $A$	- 2.31 - 2.15 + 2.85
CD <sub>4</sub>	5.0	0.88	2287 $T$ 2053 $A$	2258 $T$ 2085 $A$	+ 1.20 + 1.54	1055 $E$ 999 $T$	1054 $E$ 996 $T$	+ 0.09 + 0.35
			Average . .			Average . .		
			1.11			1.49		

mental frequencies in their symmetry classes, and also calculated values using the S.V.F.F. Only two constants are required :

$k_1$ , a valency stretching constant =  $4.95 \times 10^5$  dyne cm.<sup>-1</sup>,  
 and  $k_{\theta/r^2}$ , an angle-bending constant =  $0.88 \times 10^5$  dyne cm.<sup>-1</sup>.

These two constants explain all the frequencies with an average error of less than 1.5 %, and a maximum error of less than 3 %.

Although the agreement is quite satisfactory, the S.V.F.F. is not altogether an adequate field. It breaks down as soon as molecules containing heavier atoms are considered, and, further, its treatment of the bending vibrations is essentially artificial. The orbital valency force field (O.V.F.F.), introduced by Heath and Linnett,<sup>6</sup> considers bending vibrations strictly in accordance with modern theories of directed valency, and on this consideration alone is worthy of attention.

<sup>4</sup> Redlich, *Z. physik. Chem., B*, 1935, **28**, 371.

<sup>5</sup> Ref. 3, p. 168.

<sup>6</sup> Heath and Linnett, *Nature*, 1948, **161**, 314; *Trans. Faraday Soc.* (in press).

### The O.V.F.F. Applied to Methane and the Deuteromethanes

The O.V.F.F. also requires two constants:  $k_1$ , a valency stretching constant, and  $k_{H/r^2}$ , a constant allowing for the departure from maximum overlap of the hydrogen or deuterium atoms. The secular equations from which the frequencies may be calculated, using the O.V.F.F., are given in Appendix II.

When the experimental values for the frequencies of  $\text{CH}_4$  and  $\text{CD}_4$  are substituted in the secular equations, it is found that the doubly-degenerate bending vibrations (Fig. 2) require

$$k_{H/r^2} = 1.35 \times 10^5 \text{ dyne cm.}^{-1},$$

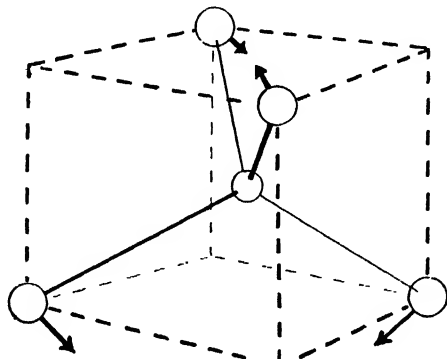


FIG. 2.

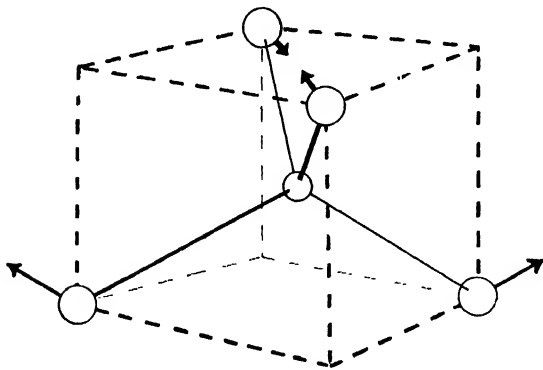


FIG. 3.

whereas the triply-degenerate vibrations (Fig. 3) require for the bending constant

$$k_{H/r^2} = 0.86 \times 10^5 \text{ dyne cm.}^{-1}.$$

It will be seen that the bending motion represented in Fig. 2 has a larger force constant than that shown in Fig. 3. Reference to Fig. 1 shows that the orbitals can follow the vibration in Fig. 3 but cannot follow that in Fig. 2. The idea put forward in the previous paper immediately offers an explanation as to why the effective force constant is greater for the doubly- than for the triply-degenerate vibration, for orbital following by change of hybridisation reduces the effective force constant in the case of the triply-degenerate bending vibration.

Analogous results were obtained for the molecules  $\text{CH}_3\text{D}$  and  $\text{CHD}_3$ . In these molecules, the symmetric vibrations needed a value for  $k_{H/r^2}$  :

of  $0.84 \times 10^6$  dyne cm.<sup>-1</sup>, and the degenerate vibrations a value of  $1.1 \times 10^6$  dyne cm.<sup>-1</sup>. The fact that the constant for the symmetric vibrations is less than that for the degenerate vibrations is consistent with the view that the orbitals of the carbon atom can follow more easily the motion of the surrounding atoms during a symmetric than during a degenerate vibration.

### The Application of the Idea of Orbital Following to the above Molecules

Since the relative increase in potential energy (P.E.) resulting from following of the orbitals in different angular distortions is known, it is possible to incorporate this in the P.E. function, and to obtain the secular equations in terms of three constants:

$k_1$ , a valency stretching constant,

$k_{H/r^2}$ , a constant allowing for the departure from maximum overlap of the hydrogen or deuterium atoms,

and  $k_{f/r^2}$ , the orbital following constant.

An example is given to show the application of both rotation of the orbitals of the carbon atom as a whole and of following of the carbon atom orbitals in obtaining the full P.E. function. Fig. 4 shows the co-ordinates

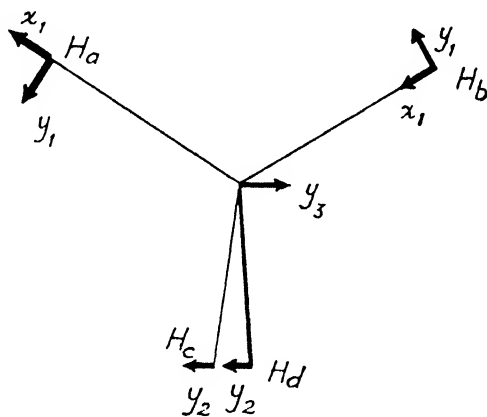


FIG. 4.

that can be used for one of the triply-degenerate vibrations of  $\text{CH}_4$ . It will be seen that this bending vibration corresponds to the distortion shown in Fig. 1c. This vibration is antisymmetric to the plane through the atoms C,  $\text{H}_c$  and  $\text{H}_d$ , but symmetrical to the plane through C,  $\text{H}_a$  and  $\text{H}_b$ . Hence rotation of the orbitals of the carbon atom as a whole about the axis which is perpendicular to the plane of C,  $\text{H}_a$  and  $\text{H}_b$ , lies in the plane of C,  $\text{H}_c$  and  $\text{H}_d$ , and passes through the carbon atom can lead to a better overlap of the carbon and hydrogen bond-forming orbitals. This will lower the P.E. Let the orbitals be rotated  $\gamma$  about this axis in an anticlockwise direction. The angle between the new atomic direction  $\text{CH}_a$  (i.e. the line from the centre of the carbon atom to the centre of the atom  $\text{H}_a$ ) and the direction in which the carbon bond-forming orbital has its maximum value after rotation will be

$$\left( \frac{y_1}{r} + \frac{1}{\sqrt{3}} \times \frac{y_3}{r} - \gamma \right).$$

The angle will be the same for the  $\text{CH}_b$  atomic direction and its bond-forming orbital. For the atomic directions  $\text{CH}_c$  and  $\text{CH}_d$  the corresponding angles will be

$$\left(\frac{y_2}{r} + \frac{y_3}{r} + \frac{\gamma}{\sqrt{3}}\right).$$

At the same time as this overall rotation of the orbitals occurs, the carbon bond-forming orbitals may follow the movement of the surrounding atoms through an angle  $\Delta\theta'$  by changing their hybridisation. Let us suppose for simplicity of treatment that this type of orbital following operates entirely by altering the direction of the orbitals to atoms  $\text{H}_a$  and  $\text{H}_b$ , leaving those to atoms  $\text{H}_c$  and  $\text{H}_d$  in their original directions. Then the angles between the distorted  $\text{CH}_a$  and  $\text{CH}_b$  atomic directions and the directions in which the orbitals have their maximum values will be

$$\left(\frac{y_1}{r} + \frac{1}{\sqrt{3}} \times \frac{y_2}{r} - \gamma - \Delta\theta'\right).$$

We could equally well have supposed that  $\Delta\theta'$  operated on the orbitals to  $\text{CH}_c$  and  $\text{CH}_d$  or to have been divided between  $\text{CH}_a$  and  $\text{CH}_b$  on the one hand and  $\text{CH}_c$  and  $\text{CH}_d$  on the other. However, any of these is related to the one we have chosen to consider by the application of the orbital distortion we have selected followed by a rotation of the orbitals as a whole, and we could imagine this rotation as a whole to be included in the  $\gamma$  we have already used.

Then the P.E. arising from angular distortion only is

$$V = k_H \left( \frac{y_1}{r} + \frac{1}{\sqrt{3}} \cdot \frac{y_2}{r} - \gamma - \Delta\theta' \right)^2 + k_H \left( \frac{y_2}{r} + \frac{y_3}{r} + \frac{\gamma}{\sqrt{3}} \right)^2 + \frac{3}{4} k_f (\Delta\theta')^2. \quad (1)$$

where the last term is the increase in P.E. resulting from the distortion of the orbitals by change of hybridisation (see Introduction and Fig. 1).

The rotation of the orbitals  $\gamma$  and the orbital following by change of hybridisation  $\Delta\theta'$  will occur to such an extent as to minimise the P.E. To determine the values of  $\gamma$  and  $\Delta\theta'$  which will minimise the P.E. we

equate  $\frac{dV}{d\gamma}$  and  $\frac{dV}{d\Delta\theta'}$  to zero and obtain

$$\gamma = \frac{\frac{9}{4} k_f y_1 - \sqrt{3} k_H y_2 - \frac{3\sqrt{3}}{4} k_f y_2 - \sqrt{3} k_H y_3}{r(k_H + 3k_f)}, \quad (2)$$

$$\Delta\theta' = \frac{k_H y_1 - \frac{4}{\sqrt{3}} k_H y_3 + \sqrt{3} k_H y_2}{r(k_H + 3k_f)}. \quad (3)$$

When (2) and (3) are substituted in (1) we obtain for the minimum value of the angular contribution to the P.E.

$$V = \frac{3k_H k_f}{r^2(k_H + 3k_f)} \left\{ \frac{1}{2} y_1 + \frac{\sqrt{3}}{2} y_2 + \frac{2}{\sqrt{3}} y_3 \right\}^2. \quad (4)$$

The full P.E. function, including bond stretching, is then given by

$$V = k_1 \left( x_1 + \frac{\sqrt{2}}{\sqrt{3}} y_3 \right)^2 + \frac{3k_H k_f}{r^2(k_H + 3k_f)} \left\{ \frac{1}{2} y_1 + \frac{\sqrt{3}}{2} y_2 + \frac{2}{\sqrt{3}} y_3 \right\}^2. \quad (5)$$

From this expression the secular equation may be obtained in the normal manner.<sup>7</sup>

The secular equations from which the frequencies may be calculated using the O.V.F.F., modified by the introduction of the concept of orbital following, are given in Appendix III. With

$$k_1 = 4.95 \times 10^5 \text{ dyne} \times \text{cm.}^{-1},$$

$$k_H/r^2 = 1.362 \times 10^6 \text{ dyne} \times \text{cm.}^{-1},$$

and

$$k_f/r^2 = 0.798 \times 10^6 \text{ dyne} \times \text{cm.}^{-1},$$

<sup>7</sup> Ref. 3, p. 72.

the calculated values of the frequencies are given in Table II. The average deviation for the bending vibrations is 1.19 % with a maximum of 2.44 % for the 982 cm.<sup>-1</sup> vibration of CHD<sub>3</sub>, and for the stretching vibrations is 0.81 % with a maximum of 2.15 % for the 2141 cm.<sup>-1</sup> vibration of CHD<sub>3</sub>. The numerical agreement between the calculated and observed frequencies is better than the S.V.F.F. gives.

TABLE II.—CALCULATED VALUES OF THE VIBRATION FREQUENCIES OF METHANE AND THE DEUTEROMETHANES USING THE O.V.F.F., COMBINED WITH THE IDEA OF ORBITAL FOLLOWING

*T* = triply-degenerate vibrations.

*E* = doubly-degenerate vibrations.

*A* = non-degenerate vibrations.

*SS* = vibrations symmetric to both the HCH and DCD planes.

*AA* = vibrations antisymmetric to the HCH and DCD planes.

*SA* = vibrations symmetric to the HCH and antisymmetric to the DCD plane.

*AS* = vibrations antisymmetric to the HCH and symmetric to the DCD plane.

	dyne × cm. <sup>-1</sup> × 10 <sup>6</sup>			Stretching Vibrations			Bending Vibrations		
	<i>k<sub>i</sub></i>	<i>k<sub>H/r</sub></i> <sup>2</sup>	<i>k<sub>f/r</sub></i> <sup>2</sup>	Calc. cm. <sup>-1</sup>	Exp. cm. <sup>-1</sup>	% Diff.	Calc. cm. <sup>-1</sup>	Exp. cm. <sup>-1</sup>	% Diff.
CH <sub>4</sub>	4.95	1.362	0.798	3050 <sup>T</sup> 2887 <sup>A</sup>	3020 <sup>T</sup> 2914 <sup>A</sup>	+1.02 -0.93	1514 <sup>E</sup> 1322 <sup>T</sup>	1526 <sup>E</sup> 1306 <sup>T</sup>	-0.79 +1.21
CH <sub>3</sub> D	4.95	1.362	0.798	3051 <sup>E</sup> 2951 <sup>A</sup> 2189 <sup>A</sup>	3030 <sup>E</sup> 2982 <sup>A</sup> 2205 <sup>A</sup>	+0.69 -1.04 -0.73	1459 <sup>E</sup> 1315 <sup>A</sup> 1164 <sup>E</sup>	1477 <sup>E</sup> 1306 <sup>A</sup> 1156 <sup>E</sup>	-1.22 +0.69 +0.69
CH <sub>2</sub> D <sub>2</sub>	4.95	1.362	0.798	3020 <sup>SA</sup> 2980 <sup>SS</sup> 2256 <sup>AS</sup> 2150 <sup>SS</sup>	3020 <sup>SA</sup> 2974 <sup>SS</sup> 2255 <sup>AS</sup> 2139 <sup>SS</sup>	— +0.20 +0.04 +0.51	1424 <sup>SS</sup> 1312 <sup>AA</sup> 1233 <sup>AS</sup> 1097 <sup>SA</sup> 1044 <sup>SS</sup>	1450 <sup>SS</sup> 1285 <sup>AA</sup> 1235 <sup>AS</sup> 1090 <sup>SA</sup> 1034 <sup>SS</sup>	-1.79 +2.10 -0.16 +0.64 -0.97
CHD <sub>3</sub>	4.95	1.362	0.798	3017 <sup>A</sup> 2277 <sup>A</sup> 2094 <sup>E</sup>	2992 <sup>A</sup> 2269 <sup>A</sup> 2141 <sup>E</sup>	+0.84 +0.35 -2.15	1279 <sup>E</sup> 1026 <sup>E</sup> 982 <sup>A</sup>	1299 <sup>E</sup> 1046 <sup>E</sup> 982 <sup>A</sup>	-1.54 -1.91 +2.44
CD <sub>4</sub>	4.95	1.362	0.798	2276 <sup>T</sup> 2042 <sup>A</sup>	2258 <sup>T</sup> 2085 <sup>A</sup>	+0.79 -2.05	1071 <sup>E</sup> 992 <sup>T</sup>	1054 <sup>E</sup> 996 <sup>T</sup>	+1.61 -0.36
				Average		0.81	Average		1.19

It is possible to estimate theoretically the ratio between *k<sub>H</sub>* and *k<sub>r</sub>*. Suppose we consider the distortion of the form shown in Fig. 1*d*. Consider the three orbitals which are equivalent with respect to the fourth as a symmetry axis. The magnitude of any one of these undistorted tetrahedral orbitals at an angle  $\Delta\theta$  from the true tetrahedral direction can be shown to be

$$M = 2 - \frac{3}{2}(\Delta\theta)^2.$$

And if the strength is proportional to  $M^n$  (see Part VI) :

$$-V' \propto 2^n - (n \times 2^{n-1}) \times \frac{3}{2}(\Delta\theta)^2.$$

This is the same for all three equivalent bonds. For the motion symmetric to the axis of the fourth bond, the fourth bond maintains its strength at  $2^n$ , and for the four bonds

$$-V' \propto 4 \times 2^n - 3\{n \times 2^{n-1} \times \frac{3}{2}(\Delta\theta)^2\}.$$



But this is, theoretically, the change of energy when there is distortion of the molecule with no orbital following; i.e. when

$$\begin{aligned}\Delta V' &= \frac{3}{2}k_H(\Delta\theta)^2, \\ \therefore \frac{3}{2}k_H &= \frac{9}{4}k_f, \\ \therefore \frac{k_H}{k_f} &= 1.5.\end{aligned}$$

The present calculations give

$$\frac{k_H}{k_f} = \frac{1.362}{0.798} = 1.71.$$

The agreement between the theoretical and experimental ratios is therefore quite pleasing.

By putting the constants  $k_H$  and  $k_f$  into eqn. (3) it is possible to calculate the extent to which the orbitals follow the movement of the surrounding atoms. It is found that they follow to the extent of about 25 % of the angle through which the atoms move for a vibration corresponding to the distortion shown in Fig. 1c.

### Conclusion

Our general conclusion is, therefore, that the O.V.F.F. combined with the conception of orbital following gives a very satisfactory interpretation of the vibrations of methane and its deuterated derivatives. Moreover, the force field does more than merely explain the experimental frequencies. It gives a definite picture of the electron distribution within a molecule as the molecule vibrates, and thus throws light on the more fundamental forces acting within a molecule, which the somewhat artificially conceived S.V.F.F. cannot do.

We wish to thank Imperial Chemical Industries for providing us with a calculating machine.

### APPENDIX I

#### Secular Equations using the S.V.F.F.



NON-DEGENERATE

$$\lambda - k_1 \left\{ \frac{1}{m_H} \right\} = 0, \quad \text{where } \lambda = 4\pi^2\nu^2, \nu \text{ being a vibrational frequency.}$$

DOUBLY-DEGENERATE

$$\lambda - \frac{k_\theta}{r^2} \left\{ \frac{3}{2m_H} \right\} = 0.$$

TRIPLY-DEGENERATE

$$\lambda^2 - \lambda \left\{ k_1 \left( \frac{1}{m_H} + \frac{4}{3m_C} \right) + \frac{k_\theta}{r^2} \left( \frac{1}{m_H} + \frac{8}{3m_C} \right) \right\} + \left\{ k_1 \frac{k_\theta}{r^2} \left( \frac{1}{m_H^2} + \frac{4}{m_H m_C} \right) \right\} = 0.$$



SYMMETRIC

$$\begin{aligned}\lambda^3 - \lambda^2 \left\{ k_1 \left( \frac{1}{m_H} + \frac{1}{m_D} + \frac{4}{3m_C} \right) + \frac{k_\theta}{r^2} \left( \frac{1}{m_H} + \frac{8}{3m_C} \right) \right\} \\ + \lambda \left\{ k_1^2 \left( \frac{1}{m_H m_D} + \frac{1}{m_H m_C} + \frac{1}{3m_D m_C} \right) \right. \\ \left. + k_1 \frac{k_\theta}{r^2} \left( \frac{1}{m_H^2} + \frac{4}{m_H m_C} + \frac{1}{m_H m_D} + \frac{8}{3m_D m_C} \right) \right\} \\ - \left\{ k_1^2 \frac{k_\theta}{r^2} \left( \frac{1}{m_H^2 m_D} + \frac{1}{m_H^2 m_C} + \frac{3}{m_H m_D m_C} \right) \right\} = 0.\end{aligned}$$

## DEGENERATE

$$\begin{aligned} \lambda^3 - \lambda^2 \left\{ k_1 \left( \frac{1}{m_H} + \frac{4}{3m_C} \right) + \frac{k_0}{r^2} \left( \frac{7}{4m_H} + \frac{3}{4m_D} + \frac{8}{3m_C} \right) \right\} \\ + \lambda \left\{ k_1 \frac{k_0}{r^2} \left( \frac{7}{4m_H^2} + \frac{3}{4m_H m_D} + \frac{5}{m_H m_C} + \frac{1}{m_D m_C} \right) \right. \\ \left. + \frac{k_0^2}{r^4} \left( \frac{9}{16m_H^2} + \frac{15}{16m_H m_D} + \frac{3}{m_H m_C} + \frac{1}{m_D m_C} \right) \right\} \\ - k_1 \frac{k_0}{r^2} \left\{ \frac{9}{16m_H^2} + \frac{15}{16m_H^2 m_D} + \frac{15}{4m_H^2 m_C} + \frac{9}{4m_H m_D m_C} \right\} = 0. \end{aligned}$$

CH<sub>2</sub>D<sub>2</sub>

## ANTISYMMETRIC-ANTISYMMETRIC

$$\lambda - \frac{k_0}{r^2} \left\{ \frac{3}{4m_H} + \frac{3}{4m_D} \right\} = 0.$$

## ANTISYMMETRIC-SYMMETRIC

$$\begin{aligned} \lambda^2 - \lambda \left\{ k_1 \left( \frac{1}{m_D} + \frac{4}{3m_C} \right) + \frac{k_0}{r^2} \left( \frac{3}{4m_H} + \frac{1}{4m_D} + \frac{8}{3m_C} \right) \right\} \\ + \left\{ k_1 \frac{k_0}{r^2} \left( \frac{1}{4m_D^2} + \frac{3}{4m_H m_D} + \frac{1}{m_H m_C} + \frac{3}{m_D m_C} \right) \right\} = 0. \end{aligned}$$

## SYMMETRIC-SYMMETRIC

$$\begin{aligned} \lambda^4 - \lambda^3 \left\{ k_1 \left( \frac{1}{m_H} + \frac{1}{m_D} + \frac{4}{3m_C} \right) + \frac{k_0}{r^2} \left( \frac{5}{4m_H} + \frac{5}{4m_D} + \frac{8}{3m_C} \right) \right\} \\ + \lambda^2 \left\{ k_1^2 \left( \frac{1}{m_H^2 m_D} + \frac{2}{3m_H m_C} + \frac{2}{3m_D m_C} \right) \right. \\ \left. + k_1 \frac{k_0}{r^2} \left( \frac{1}{4m_H^2} + \frac{1}{4m_D^2} + \frac{1}{2m_H m_D} + \frac{13}{3m_H m_C} + \frac{13}{3m_D m_C} \right) \right. \\ \left. + \frac{k_0^2}{r^4} \left( \frac{3}{2m_H m_D} + \frac{2}{m_H m_C} + \frac{2}{m_D m_C} \right) \right\} \\ - \lambda \left\{ k_1^2 \frac{k_0}{r^2} \left( \frac{1}{4m_H^2 m_D} + \frac{1}{4m_D^2 m_H} + \frac{1}{6m_H^2 m_C} + \frac{1}{6m_D^2 m_C} + \frac{13}{3m_H m_D m_C} \right) \right. \\ \left. + k_1 \frac{k_0^2}{r^4} \left( \frac{6}{m_H m_D m_C} + \frac{3}{2m_H^2 m_D} + \frac{3}{2m_H m_D^2} + \frac{2}{m_H^2 m_C} + \frac{2}{m_D^2 m_C} \right) \right\} \\ + \left\{ k_1^2 \frac{k_0^2}{r^4} \left( \frac{3}{2m_H^2 m_D} + \frac{3}{m_H^2 m_D m_C} + \frac{3}{m_H m_D^2 m_C} \right) \right\} = 0. \end{aligned}$$

To obtain the secular equations for the molecules CHD<sub>3</sub> and CD<sub>4</sub>, replace  $m_H$  by  $m_D$  and  $m_D$  by  $m_H$  in the equations for CH<sub>2</sub>D<sub>2</sub> and CH<sub>4</sub>, respectively. The secular equation headed Antisymmetric-symmetric for the molecule CH<sub>2</sub>D<sub>2</sub> refers to those vibrations which are symmetric to the plane containing the carbon and the two deuterium atoms and antisymmetric to the plane containing the carbon and the two hydrogen atoms. To obtain the equation for the vibrations symmetric to the HCH and antisymmetric to the DCD plane, interchange  $m_H$  and  $m_D$  in this equation.

## APPENDIX II

## Secular Equations using the O.V.F.F.

CH<sub>4</sub>

## NON-DEGENERATE

$$\lambda - k_1 \left\{ \frac{1}{m_H} \right\} = 0.$$

## DOUBLY-DEGENERATE

$$\lambda - \frac{k_H}{r^2} \left\{ \frac{1}{m_H} \right\} = 0.$$

## TRIPLY-DEGENERATE

$$\lambda^3 - \lambda \left\{ k_1 \left( \frac{1}{m_H} + \frac{4}{3m_C} \right) + \frac{k_H}{r^2} \left( \frac{1}{m_H} + \frac{8}{3m_C} \right) \right\} \\ + \left\{ k_1 \frac{k_H}{r^2} \left( \frac{1}{m_H^2} + \frac{4}{m_H m_C} \right) \right\} = 0.$$


---

CH<sub>3</sub>D

## SYMMETRIC

$$\lambda^3 - \lambda^2 \left\{ k_1 \left( \frac{1}{m_H} + \frac{1}{m_D} + \frac{4}{3m_C} \right) + \frac{k_H}{r^2} \left( \frac{1}{m_H} + \frac{8}{3m_C} \right) \right\} \\ + \lambda \left\{ k_1^2 \left( \frac{1}{m_H m_D} + \frac{1}{m_H m_C} + \frac{1}{3m_D m_C} \right) \right. \\ \left. + k_1 \frac{k_H}{r^2} \left( \frac{1}{m_H^2} + \frac{1}{m_H m_D} + \frac{4}{m_H m_C} + \frac{8}{3m_D m_C} \right) \right\} \\ - \left\{ k_1^2 \frac{k_H}{r^2} \left( \frac{1}{m_H^2 m_D} + \frac{1}{m_H^2 m_C} + \frac{3}{m_H m_D m_C} \right) \right\} = 0.$$

## DEGENERATE

$$\lambda^3 - \lambda^2 \left\{ k_1 \left( \frac{1}{m_H} + \frac{4}{3m_C} \right) + \frac{k_H}{r^2} \left( \frac{1}{8m_H} + \frac{5}{8m_D} + \frac{8}{3m_C} \right) \right\} \\ + \lambda \left\{ k_1 \frac{k_H}{r^2} \left( \frac{1}{8m_H^2} + \frac{5}{8m_H m_D} + \frac{9}{2m_H m_C} + \frac{5}{6m_D m_C} \right) \right. \\ \left. + \frac{k_H^2}{r^2} \left( \frac{3}{8m_H^2} + \frac{5}{8m_H m_D} + \frac{2}{m_H m_C} + \frac{2}{3m_D m_C} \right) \right\} \\ - \left\{ k_1 \frac{k_H^2}{r^4} \left( \frac{3}{8m_H^2} + \frac{5}{8m_H m_D} + \frac{5}{2m_H^2 m_C} + \frac{3}{2m_H m_C m_D} \right) \right\} = 0.$$

To obtain the secular equations for CHD<sub>3</sub> and CD<sub>4</sub> replace  $m_H$  by  $m_D$  and  $m_D$  by  $m_H$  in the secular equations for CH<sub>3</sub>D and CH<sub>4</sub> respectively.

## APPENDIX III

## Secular Equations using the O.V.F.F. combined with the idea of Orbital Following

CH<sub>4</sub>

## NON-DEGENERATE

$$\lambda - k_1 \left\{ \frac{1}{m_H} \right\} = 0.$$

## DOUBLY-DEGENERATE

$$\lambda - \frac{k_H}{r^2} \left\{ \frac{1}{m_H} \right\} = 0.$$

## TRIPLY-DEGENERATE

$$\lambda^3 - \lambda \left\{ k_1 \left( \frac{1}{m_H} + \frac{4}{3m_C} \right) + \left[ \frac{3k_H k_f}{r^2(k_H + 3k_f)} \right] \left( \frac{1}{m_H} + \frac{4}{3m_C} \right) \right\} \\ + \left\{ k_1 \left[ \frac{3k_H k_f}{r^2(k_H + 3k_f)} \right] \left( \frac{1}{m_H^2} + \frac{4}{m_H m_C} \right) \right\} = 0.$$


---

CH<sub>3</sub>D

## SYMMETRIC

$$\lambda^3 - \lambda \left\{ k_1 \left( \frac{1}{m_H} + \frac{1}{m_D} + \frac{4}{3m_C} \right) + \left[ \frac{3k_H k_f}{r^2(k_H + 3k_f)} \right] \left( \frac{1}{m_H} + \frac{8}{3m_C} \right) \right\} \\ + \lambda \left\{ k_1^2 \left( \frac{1}{m_H m_D} + \frac{1}{m_H m_C} + \frac{1}{3m_D m_C} \right) \right. \\ \left. + k_1 \left[ \frac{3k_H k_f}{r^2(k_H + 3k_f)} \right] \left( \frac{1}{m_H^2} + \frac{1}{m_H m_D} + \frac{4}{m_H m_C} + \frac{8}{3m_D m_C} \right) \right\} \\ - \left\{ k_1^2 \left[ \frac{3k_H k_f}{r^2(k_H + 3k_f)} \right] \left( \frac{1}{m_H^2 m_D} + \frac{1}{m_H^2 m_C} + \frac{3}{m_H m_D m_C} \right) \right\} = 0.$$

## DEGENERATE

$$\begin{aligned}
& \lambda^3 - \lambda^2 \left\{ k_1 \left( \frac{1}{m_H} + \frac{4}{3m_C} \right) + \frac{k_H}{r^2} \left( \frac{3}{4m_H} + \frac{1}{4m_D} \right) \right. \\
& \quad + \left[ \frac{3k_H k_f}{r^2(k_H + 3k_f)} \right] \left( \frac{5}{8m_H} + \frac{3}{8m_D} + \frac{8}{3m_C} \right) \Big\} \\
& \quad + \lambda \left\{ k_1 \frac{k_H}{r^2} \left( \frac{3}{4m_H} + \frac{1}{4m_H m_D} + \frac{1}{3m_C m_D} + \frac{1}{m_H m_C} \right) \right. \\
& \quad + k_1 \left[ \frac{3k_H k_f}{r^2(k_H + 3k_f)} \right] \left( \frac{5}{8m_H} + \frac{3}{8m_H m_D} + \frac{1}{2m_D m_C} + \frac{7}{2m_H m_C} \right) \\
& \quad + \frac{k_H}{r^2} \left[ \frac{3k_H k_f}{r^2(k_H + 3k_f)} \right] \left( \frac{3}{8m_H} + \frac{5}{8m_H m_D} + \frac{2}{3m_D m_C} + \frac{2}{m_H m_C} \right) \Big\} \\
& \quad - \left\{ k_1 \frac{k_H}{r^2} \left[ \frac{3k_H k_f}{r^2(k_H + 3k_f)} \right] \left( \frac{3}{8m_H} + \frac{3}{2m_H m_D m_C} + \frac{5}{8m_H^2 m_D} + \frac{5}{2m_H^2 m_C} \right) \right\} = 0.
\end{aligned}$$

CH<sub>2</sub>D<sub>2</sub>

## ANTISYMMETRIC-ANTISYMMETRIC

$$\lambda - \frac{k_H}{r^2} \left( \frac{1}{2m_H} + \frac{1}{2m_D} \right) = 0.$$

## ANTISYMMETRIC-SYMMETRIC

$$\begin{aligned}
& \lambda^2 - \lambda \left\{ k_1 \left( \frac{1}{m_D} + \frac{4}{3m_C} \right) + \left[ \frac{3k_H k_C}{r^2(k_H + 3k_f)} \right] \left( \frac{3}{4m_H} + \frac{1}{4m_D} + \frac{8}{3m_C} \right) \right\} \\
& \quad + \left\{ k_1 \left[ \frac{3k_H k_f}{r^2(k_H + 3k_f)} \right] \left( \frac{1}{4m_D} + \frac{3}{4m_H m_D} + \frac{1}{m_H m_C} + \frac{3}{m_D m_C} \right) \right\} = 0.
\end{aligned}$$

## SYMMETRIC-SYMMETRIC

$$\begin{aligned}
& \lambda^4 - \lambda^3 \left\{ k_1 \left( \frac{1}{m_H} + \frac{1}{m_D} + \frac{4}{3m_C} \right) + K_C \left( \frac{1}{2m_H} + \frac{1}{2m_D} + \frac{4}{3m_C} \right) - K_E \left( \frac{4}{3m_C} \right) \right\} \\
& \quad + \lambda^2 \left\{ k_1^2 \left( \frac{1}{m_H m_D} + \frac{2}{3m_H m_C} + \frac{2}{3m_D m_C} \right) \right. \\
& \quad + k_1 K_C \left( \frac{1}{2m_H} + \frac{1}{2m_D} + \frac{1}{m_H m_D} + \frac{2}{m_H m_C} + \frac{2}{m_D m_C} \right) \\
& \quad + (K_C^2 - K_E^2) \left( \frac{1}{4m_H m_D} + \frac{1}{3m_H m_C} + \frac{1}{3m_D m_C} \right) - k_1 K_E \left( \frac{4}{3m_H m_C} + \frac{4}{3m_D m_C} \right) \Big\} \\
& \quad - \lambda \left\{ k_1^2 K_C \left( \frac{2}{m_H m_D m_C} + \frac{1}{2m_H^2 m_D} + \frac{1}{2m_H m_D^2} + \frac{1}{3m_H^2 m_C} + \frac{1}{3m_D^2 m_C} \right) \right. \\
& \quad + k_1 (K_C^2 - K_E^2) \left( \frac{1}{m_H m_D m_C} + \frac{1}{4m_H^2 m_D} + \frac{1}{4m_H m_D^2} + \frac{1}{3m_H^2 m_C} + \frac{1}{3m_D^2 m_C} \right) \\
& \quad - k_1^2 K_E \left( \frac{4}{3m_H m_D m_C} \right) \Big\} \\
& \quad + \left\{ k_1^2 (K_C^2 - K_E^2) \left( \frac{1}{4m_H^2 m_D^2} + \frac{1}{2m_H^2 m_D m_C} + \frac{1}{2m_H m_D^2 m_C} \right) \right\} = 0,
\end{aligned}$$

where

$$K_C = \frac{k_H(k_H + 6k_f)}{r^2(k_H + 3k_f)}.$$

and

$$K_E = \frac{k_H^2}{r^2(k_H + 3k_f)}.$$

To obtain the secular equations for the molecules CHD<sub>3</sub> and CD<sub>4</sub>, replace  $m_H$  by  $m_D$  and  $m_D$  by  $m_H$  in the equations for CH<sub>2</sub>D<sub>2</sub> and CH<sub>4</sub>, respectively. The secular equation headed Antisymmetric-symmetric for the molecule CH<sub>2</sub>D<sub>2</sub> refers to those vibrations which are symmetric to the plane containing the carbon and the two deuterium atoms and antisymmetric to the plane containing the carbon and the two hydrogen atoms. To obtain the equation for the vibrations symmetric to the HCH and antisymmetric to the DCD plane, interchange  $m_H$  and  $m_D$  in this equation.

*Inorganic Chemistry Laboratory,  
Oxford.*

# A SEMI-MICRO LOW-TEMPERATURE CALORIMETER, AND A COMPARISON OF SOME THERMODYNAMIC PROPERTIES OF METHYL ALCOHOL AND METHYL DEUTEROXIDE

BY L. A. K. STAVELEY AND A. K. GUPTA

*Received 16th April, 1948; as revised 6th August, 1948*

An adiabatic low-temperature calorimeter is described with which measurements of heats of phase changes and heat capacities from room temperature down to temperatures accessible with liquid nitrogen can be made on substances liquid or gaseous under ordinary conditions. Only 4.5 cm.<sup>3</sup> of the condensed substance are required, and it is considered that the results obtained are accurate to within 0.5 %. The calorimeter has been used to compare the heat capacities from -180° C to 0° C, the heats of evaporation at 0° C, and the heats and temperatures of transition and fusion of CH<sub>3</sub>OH and CH<sub>3</sub>OD. Of the two, CH<sub>3</sub>OD has the lower melting point, a smaller heat and entropy of fusion, and the higher heat and entropy of vaporisation, and although its transition temperature is higher than that of CH<sub>3</sub>OH, the heat and entropy change of the transition are smaller for the deuterated compound. With both alcohols, the form stable above the transition temperature can be supercooled, and the low-temperature form slightly superheated. The nature of the transition (which is of the lambda-point type) is briefly discussed, and reasons given for thinking that it probably involves a change in intermolecular bonding, perhaps similar to that which occurs between the two forms of resorcinol, rather than that it is due to, or is accompanied by, the onset of the rotation of the molecules in the lattice. As a test of the accuracy of the results obtained with the calorimeter, measurements have been made of the heats of transition and fusion of carbon tetrachloride, which are recorded in the Appendix.

One of the many important results of experimental studies of the thermal properties of solids at low temperatures has been the discovery of numerous transitions, which, unlike a normal change from one condensed phase of a pure substance to another, do not take place abruptly at a well-defined temperature, but over a temperature range. These unsharp transitions (sometimes known as lambda-points) are manifestations of changes which involve an increase in disorder and which are co-operative in the sense that the transformation from the low-temperature form with the greater internal order to the high-temperature disordered form begins gradually but becomes more facile as the degree of disorder increases. It is still not known with certainty precisely what alterations in the disposition or behaviour of the particles composing the lattice occur. It is unlikely that they are always the same, since such transitions have been found in substances of widely different chemical types. It has often been supposed that lambda-points mark the change from a librational motion of molecules or ions in the crystal lattice to their comparatively free rotation, but though this interpretation may sometimes be true there are various reasons for thinking that it cannot hold universally.

Both the occurrence and character of transitions are very sensitive to the chemical nature of the solid. One of two chemically similar substances may have one or more transitions, the other none: or both may exhibit transitions, but with different characteristics. When, however, the molecules or ions in a compound contain hydrogen atoms—and this is true of many substances exhibiting lambda-points—it is possible by

substituting deuterium for hydrogen to change those properties of the particles which depend on their mass without altering the field of force surrounding them. Thus, this substitution will increase the moment of inertia of the particles but lower the frequency of their lattice vibrations and hence their zero-point energy, and the vibrations will become less anharmonic. Even these relatively small changes are sometimes sufficient to alter qualitatively the properties of the solid. For example,  $\text{CD}_4$  shows two lambda-points while  $\text{CH}_4$  has only one,<sup>1</sup> while  $\text{HBr}$  and  $\text{DBr}$  have three and two unsharp transitions respectively.<sup>2</sup>

Since slight and predictable changes in the behaviour of the particles in the lattice may be made by isotopic replacement, comparison of the thermal properties of suitably chosen hydrogen and deuterium compounds is a promising method of investigating the dependence of such properties on the nature of the component particles. In particular, the comparison might be expected to increase our knowledge of the causes of lambda-points and the factors determining their characteristics. Kelley<sup>3</sup> found from heat-capacity measurements that methyl alcohol shows a lambda-point about  $18^\circ\text{C}$  below the melting-point, and Smyth<sup>4</sup> later suggested that this may mark the onset of the rotation of the molecules in the lattice about the  $\text{C}-\text{O}$  axis. Since the molecule of this substance contains functionally different hydrogen atoms, it was thought that a comparison of the properties of  $\text{CH}_3\text{OH}$ ,  $\text{CH}_3\text{OD}$ , and  $\text{CD}_3\text{OH}$  might be interesting. The investigation of the last of these compounds has been held up by the present shortage of heavy water. Measurements have, however, been made of the heat capacities from  $-180^\circ\text{C}$  to  $0^\circ\text{C}$ , heats and temperatures of transition and fusion, and heats of evaporation of  $\text{CH}_3\text{OH}$  and  $\text{CH}_3\text{OD}$ .

## Experimental

**The Calorimeter.**—This was much smaller than those usually employed in low-temperature work, the calorimeter itself having a capacity of  $4.5\text{ cm}^3$ . The apparatus was, in fact, designed to give results sufficiently accurate to detect unambiguously differences in the properties of hydrogen and deuterium compounds which would only be available in small quantities.

The apparatus was of the adiabatic vacuum type, in which heat exchange between the calorimeter and its surroundings is nullified by keeping the surroundings at the same temperature as the calorimeter. In its general construction it was similar to the numerous instruments of the same kind which other workers have used, and of these it perhaps resembled most closely that described by Eucken and Schröder.<sup>5</sup> Energy was supplied electrically via a constantan heating-coil, and temperatures were measured with a platinum resistance thermometer.

Fig. 1 shows the calorimetric apparatus. The mass of the calorimeter (1) was such that its thermal capacity was roughly equal to that of its contents, but preliminary experiments had shown that when solid methyl alcohol is heated considerable strain can be imposed on the walls enclosing it, and it therefore seemed to be unwise to reduce the thermal capacity of the calorimeter at the risk of making its walls dangerously thin. The thermometer (3) was insulated from the calorimeter by silk and bakelite varnish. The heating-coil (4) was wound on a copper tube and insulated from it by rice paper and bakelite varnish. Thicker leads were soldered to the heating-coil so that the junctions were inside the copper tube, and these leads were brought into thermal contact with the tube on leaving it to ensure that all the heat generated in the coil was transferred to the calorimeter, and none of it lost by conduction down the leads outside the calorimeter.

In order to achieve adiabatic working, both the copper mantle (6) and the inlet tube (5) were provided with heating-coils. That on the mantle had a

<sup>1</sup> Bartholomé, Driks and Eucken, *Z. physik. Chem.*, A, 1938, **139**, 371.

<sup>2</sup> Clusius and Popp, *ibid.* B, 1940, **46**, 81.

<sup>3</sup> Kelley, *J. Amer. Chem. Soc.*, 1929, **51**, 180.

<sup>4</sup> Smyth and Hitchcock, *ibid.*, 1934, **56**, 1084; Smyth and McNeight, *ibid.*, 1936, **58**, 1597.

<sup>5</sup> Eucken and Schröder, *Z. physik. Chem.*, B, 1938, **41**, 308.

resistance of *ca.* 1000 ohms, and that on the inlet tube (which was wound over a length of 2 cm., at a distance of 6 cm. from the calorimeter) a resistance of *ca.* 300 ohms. Copper-constantan thermocouples fixed to the calorimeter, the inlet tube (just below the heating coil), and to the copper rods (12) enabled temperature differences between these parts of the apparatus to be detected.

The purpose of the copper vessel (7) was to increase the thermal capacity of the mantle and to extend the range of the apparatus to lower temperatures in the usual way (i.e. by filling the space in (7) with a liquefied gas through the valve (8), and then pumping out through the outlet (9)). It also enabled the leads to be cooled to the temperature of the calorimeter, which was essential in view of its very small thermal capacity. The German silver tube (11) was soldered at the roof of the copper vessel (7) to a copper tube which passed through this vessel. This copper tube, after insertion of the cable of leads, was filled with Wood's metal. On leaving the lower end of the copper tube the cable was

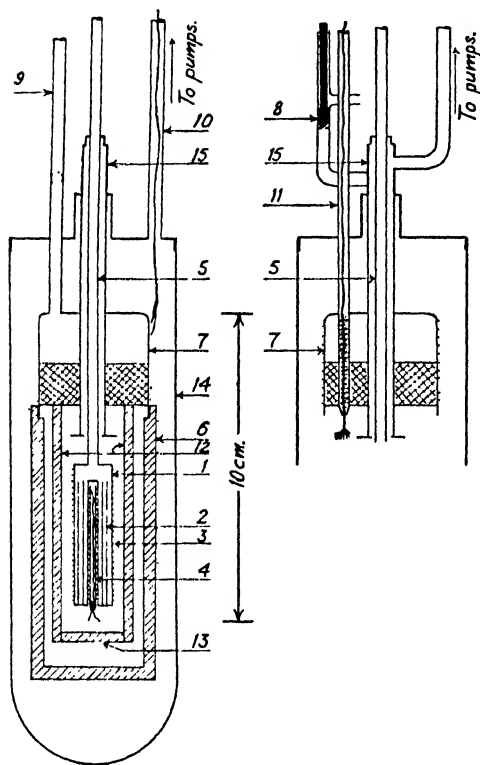


FIG. 1.—The calorimeter. The diagram on the right shows the upper part of the apparatus as seen from the right-hand side of the complete diagram. (1) Cylindrical copper calorimeter, wall thickness 0.5 mm.; (2) concentric, perforated copper cylinders, 0.1 mm. thick, to hasten the attainment of thermal equilibrium; (3) platinum resistance thermometer, s.w.g. 48,  $\Omega = 327$  ohms at  $0^{\circ}\text{C}$ ; (4) constantan heating-coil, s.w.g. 48,  $\Omega = 420$  ohms at  $0^{\circ}\text{C}$ ; (5) German silver inlet tube to calorimeter, 3 mm. diam., wall thickness 0.1 mm.; (6) cylindrical copper mantle; (7) copper vessel half filled with lead; (8) valve; (9), (10), (11) German silver tubes; (12) copper rods; (13) copper cross-piece joining copper rods; (14) chromium-plated brass can, wall thickness 1 mm.; (15) German silver tube.

split into its component wires, and each was wound ten times round one of the copper rods (12) soldered to the underside of the copper vessel (7) or round the cross-piece (13) joining the lower ends of these rods. These rods served a dual purpose in supporting the leads and in completing the transference to the mantle of the heat conducted down them.

The Dewar vessel containing the refrigerant (liquid oxygen or a mixture of solid carbon dioxide and alcohol) was supported on a stand with an arrangement for the fine control of its height. This made it possible to adjust the depth of immersion of the apparatus in the refrigerant so that the temperature of the junction of the tubes (5) and (15) was only very slightly less than that of the calorimeter, or alternatively very slightly higher when the vapour pressure of the contents of the calorimeter was such as to make it imperative to eliminate any possibility of condensation at a cold spot in the inlet tube (5).

**The electrical measurements and the calibration of the platinum resistance thermometer.**—The resistance at the ice-point was easily determined by immersing the whole calorimeter in pure, melting ice. To obtain

further calibration points, which had to be fairly numerous as the thermometer was not strain-free, use was made of the accurate measurements recorded in the literature of the triple-points and vapour pressures of methane, phosphine, and ammonia. Each of these substances was condensed into the calorimeter and the resistance of the thermometer at the triple-point determined. The condensed gas was then warmed up in steps of about  $6^{\circ}\text{C}$ , the calorimeter was brought to constant temperature at the end of each heating period, and simultaneous measurements of the vapour pressure of the liquefied gas and thermometer resistance made. From the numerous pairs of resistance-temperature values so obtained a calibration curve was constructed and utilised as described in Ostwald-Luther's *Physikochemische Messungen*.\*

This method of calibrating the thermometer had the advantage that it could be quickly repeated at any time. Frequent repetitions did in fact prove necessary, as stresses were sometimes set up in the calorimeter when it contained solid  $\text{CH}_3\text{OH}$  or  $\text{CH}_3\text{OD}$  which apparently caused a slight stretching of the wire. The success of this method of calibration depends on the purity of the substances used and on the accuracy of the vapour pressure readings. The preparation and purification of the three gases is described below. Vapour pressures were determined with an accuracy of  $0.02\text{ mm}$ , or better with a manometer with which readings were made on a Société Gènevoise glass scale by means of a built-in travelling microscope.

The necessary triple-point and vapour pressure data for ammonia and phosphine were taken from the papers of Overstreet and Giauque<sup>6</sup> and Stephenson and Giauque<sup>7</sup> respectively. For methane, insertion of our own value of the triple-point pressure in the vapour pressure formula of Henning and Stock<sup>8</sup> gave  $90.68^{\circ}\text{K}$  as the triple-point, which agrees with the figure reported by Clusius and Weigand.<sup>9</sup>

As regards the measurement of energy input, the resistance of the constantan heating-coil in the calorimeter was determined as a function of temperature, and the rate at which heat was supplied during any measurement was found by a potentiometric determination of the current flowing through the coil, which was between 5 and 30 mA. Current was supplied by a battery of accumulators which discharged during the "off" periods through a stabilizing resistance. The heating time was determined by means of an electrically operated stop-watch which had been calibrated against a standard clock. It was actuated by a double-throw switch which simultaneously started and stopped the current through the calorimetric heating-coil.

**The method of measuring heat capacities.**—A suitable quantity of the liquid to be studied was condensed into the calorimeter from a detachable trap connected to the vacuum line. The amount of liquid transferred to the calorimeter was found from the change in weight of the trap. The calorimeter was then brought to a steady temperature by suitable adjustment of the depth of immersion of the apparatus in the cooling-bath and of the currents flowing through the heating-coil on the copper mantle (6) and the coil on the inlet tube (5). With practice, it was possible to hold the temperature of the calorimeter constant to  $0.001^{\circ}\text{C}$  for the period of time required for an average heat capacity determination. Such determinations were, however, made with a temperature drift before and after the actual heating period so long as the drift did not exceed  $0.001^{\circ}\text{C/min.}$ , although in measurements in the transition regions of  $\text{CH}_3\text{OH}$  and  $\text{CH}_3\text{OD}$  (where very small temperature changes consequent on the application of small quantities of heat had to be measured), the working was made as truly adiabatic as possible. The heating period was usually between 10 and 20 min., and the temperature rise  $2^{\circ}$  to  $5^{\circ}$ , the final temperature of one measurement serving as the initial temperature of the next. The heat capacity of the empty calorimeter was carefully determined from  $-180^{\circ}\text{C}$  to  $0^{\circ}\text{C}$ .

**Preparation and purification of the substances used.**—**METHANE** was prepared from purified methyl iodide via the Grignard compound, and fractionated at the temperature of boiling oxygen in a column of the type described by Clusius and Riccoboni.<sup>10</sup> The purity of the main fraction was tested

\* In later work with this calorimeter, five gases have been used for calibrating the resistance thermometer (methyl chloride, methyl bromide, phosphine, methane, and ethylene). The range  $0^{\circ}\text{C}$  to  $-180^{\circ}\text{C}$  can then be covered almost without a break.

<sup>6</sup> Overstreet and Giauque, *J. Amer. Chem. Soc.*, 1937, **59**, 254.

<sup>7</sup> Stephenson and Giauque, *J. Chem. Physics*, 1937, **5**, 149.\*

<sup>8</sup> Henning and Stock, *Z. Physik*, 1921, **4**, 226.

<sup>9</sup> Clusius and Weigand, *Z. physik. Chem.*, B, 1940, **46**, 1.

<sup>10</sup> Clusius and Riccoboni, *ibid.*, 1939, **38**, 81.



by measurement of the triple-point pressure at different stages of melting. There was no detectable drift in the pressure values, the mean of which was  $87.75 \pm 0.04$  mm., somewhat higher than the value of 87.4 mm. recorded by Frank and Clusius.<sup>11</sup>

PHOSPHINE was prepared from phosphonium iodide by the method of Stephenson and Giauque.<sup>7</sup> It was fractionated in the same column in a bath of alcohol maintained at  $-98^\circ\text{C}$ . The triple-point pressure of the main fraction again showed no drift as melting proceeded. The mean value was  $27.45 \pm 0.07$  mm., slightly higher than the figure of  $27.32 \pm 0.02$  mm. given by Stephenson and Giauque.

AMMONIA from a cylinder was passed through a cotton-wool filter and solid KOH and condensed. After being repeatedly cooled in liquid oxygen and pumped out, it was twice fractionally sublimed. The middle fraction of the second sublimation gave a constant value for the triple-point pressure of  $45.60 \pm 0.02$  mm. (cf. Overstreet and Giauque,<sup>6</sup> 45.58 mm.; Thode,<sup>12</sup> 45.61 mm.).

METHYL ALCOHOL. An A.R. sample was first dried over lime, then fractionated, and further drying of the middle fraction carried out by treating it with magnesium according to the method of Bjerrum and Zechmeister.<sup>13</sup> It was again fractionated, and the middle fraction used in the calorimetric experiments:  $d_4^{20}$  was 0.79216 (cf. 0.79134, *Int. Crit. Tables*).

METHYL DEUTEROXIDE,  $\text{CH}_3\text{OD}$ .—This was prepared by treating magnesium methylate with  $\text{D}_2\text{O}$ . 6.4 g. purified methyl alcohol were refluxed with 2.4 g. magnesium for several days in an all-glass apparatus, and the surplus methyl alcohol removed by condensation into a cooled trap while the magnesium methylate was kept at  $50^\circ\text{C}$ . The methylate was then treated with 2.5 g. of 99.6%  $\text{D}_2\text{O}$  at  $50^\circ\text{C}$  for three days. The crude  $\text{CH}_3\text{OD}$  was then dried over lime which had been heated *in vacuo* for two days, then refluxed over a small quantity of magnesium methylate. Further treatment with magnesium (with which the liquid now reacted very readily) produced no change in its density, and the product was freed from traces of dissolved hydrogen and condensed into the calorimeter.  $d_4^{20}$  was 0.81269.

**The accuracy of the results obtained with the calorimeter.**—The values recorded by different observers for the thermal properties of a given substance frequently disagree by much more than would be expected from the estimated experimental errors. Comparison of the results furnished by a given calorimeter with those of independent workers would therefore seem to be desirable in any case, and essential here in view of the unusually small capacity of the calorimeter.

From smoothed curves drawn through the plot of our experimental values of the molar heat capacity of  $\text{CH}_3\text{OH}$  against temperature, we have derived values at  $10^\circ$  intervals which are compared in Table I with the figures obtained in the same way from Kelley's<sup>9</sup> results. There is no systematic deviation between the two sets of figures, and the mean (arithmetical) difference is about 0.5%. Our figure for the heat of fusion of the same substance is about 0.3% lower than that of Kelley. The heats of transition do not agree so well, our value being 170 cal./mole, as against 154.3 cal. but, as explained later, the evaluation of this quantity is rather arbitrary. Our value for the molar heat of evaporation of  $\text{CH}_3\text{OH}$  at  $0^\circ\text{C}$ ,  $9,207 \pm 20$  cal., is about 0.2% higher than that of Flock, Ginnings, and Holton,<sup>14</sup> which appears to be the most accurate figure available for comparison.

In order to extend these comparisons to another substance, measurements were made of the heats of fusion and transition of carbon tetrachloride. This substance was selected since it can easily be obtained in a very pure state, and because what seemed to be a very accurate determination of the quantities concerned had been carried out by Johnston and Long.<sup>15</sup> Our results are recorded in Table VII in the Appendix, and compared there with those of Johnston and Long. It will be seen that their values, particularly that for the heat of fusion, are not in good agreement with our own, but some time after the latter had been obtained, values were published by Hicks, Hooley, and Stephenson,<sup>16</sup>

<sup>11</sup> Frank and Clusius, *ibid.*, 1939, 42, 410.

<sup>12</sup> Thode, *J. Amer. Chem. Soc.*, 1940, 62, 581.

<sup>13</sup> Bjerrum and Zechmeister, *Ber.*, 1923, 56, 897.

<sup>14</sup> Flock, Ginnings and Holton, *Bur. Stand. J. Res.*, 1931, 6, 881.

<sup>15</sup> Johnston and Long, *J. Amer. Chem. Soc.*, 1934, 56, 31.

<sup>16</sup> Hicks, Hooley and Stephenson, *ibid.*, 1944, 66, 1064.

which agree very closely with ours. It is perhaps significant that the results of Johnston and Long are low, and that in some of their determinations of the heat of fusion the heating of the solid was started at temperatures unusually close to the melting-point in measurements of this kind. In the light of these comparisons, it would appear that errors in the heat capacities and heats of phase changes obtained with our calorimeter are not, on the average, greater than 0.5 %.

## Results

The heat capacity of both alcohols was measured from 90° to 273° K. Two independent runs were carried out on each substance. The results are plotted in Fig. 2 and 3. Values of  $C_p$  per mole at 10° intervals, interpolated from smooth

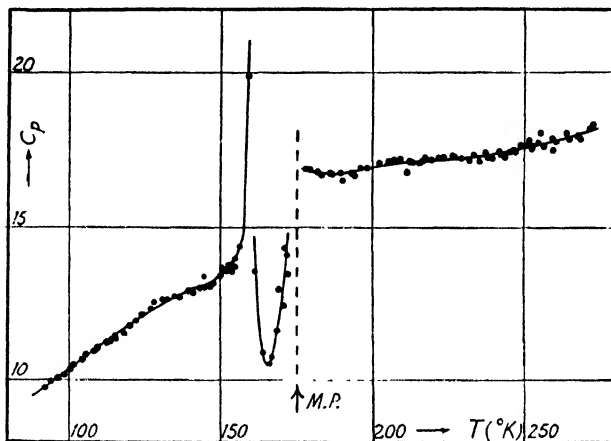


FIG. 2.—Molar heat capacity of  $\text{CH}_3\text{OH}$ .

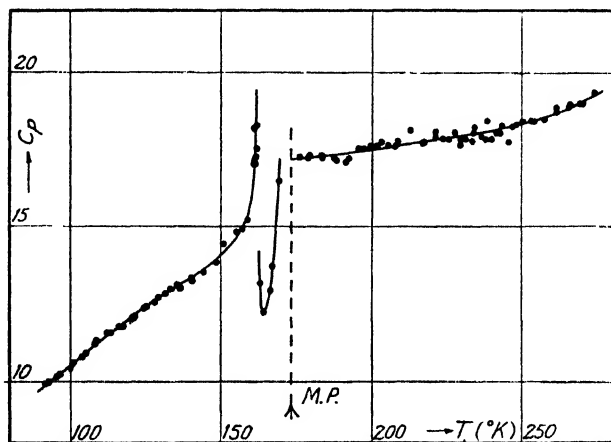


FIG. 3.—Molar heat capacity of  $\text{CH}_3\text{OD}$ .

curves drawn through the experimental points, are recorded in Table I, except for the regions between the beginning of the transition and the melting-point, for which interpolated  $C_p$  values at smaller temperature intervals are given in Table II. By rapidly cooling the high-temperature solid modifications of the two alcohols they could be preserved for a long while well below the transition temperatures. On warming up these supercooled forms to a few degrees below

the transition temperatures, the change to the low-temperature forms took place with liberation of the heat of transition. All measurements on the low-temperature forms of the alcohols were therefore made after each had been kept a little below its transition temperature for a time sufficiently long to ensure that conversion to the low-temperature modification was complete.

TABLE I.—MOLAR HEAT CAPACITY OF  $\text{CH}_3\text{OH}$  AND  $\text{CH}_3\text{OD}$  AT  $10^\circ$  INTERVALS

$C_p$  values

Temp. $^\circ\text{K}$	$\text{CH}_3\text{OH}$ (This research)	$\text{CH}_3\text{OH}$ (Kelley)	$\Delta C_p^*$	$\text{CH}_3\text{OD}$
90	9.58	9.71	-1.4	9.66
100	10.36	10.47	-1.1	10.48
110	11.10	11.16	-0.5	11.26
120	11.83	11.78	+0.4	12.01
130	12.50	12.37	+1.0	12.72
140	12.89	12.96	-0.5	12.32
150	13.45	13.51	-0.4	14.18

Transition region. See Table II.

180	16.79	16.78	0	17.25
190	16.72	16.78	-0.4	17.31
200	16.98	16.88	+0.6	17.52
210	17.11	16.97	+0.8	17.70
220	17.16	17.04	+0.7	17.83
230	17.24	17.20	+0.2	17.91
240	17.36	17.40	-0.2	18.04
250	17.56	17.62	-0.3	18.29
260	17.82	17.89	-0.4	18.63
270	18.11	18.19	-0.4	19.04

\*  $\Delta C_p$  represents  $C_p$  (this research) minus  $C_p$  (Kelley) as a percentage.

The unit for  $C_p$  and all energy quantities throughout this paper is the  $15^\circ\text{C cal.} \equiv 4.1833 \text{ int. joules.}$

TABLE II

MOLAR HEAT CAPACITY OF  $\text{CH}_3\text{OH}$  AND  $\text{CH}_3\text{OD}$  IN THE TRANSITION REGION

$\text{CH}_3\text{OH}$		$\text{CH}_3\text{OD}$	
Temp., $^\circ\text{K}$	$C_p$	Temp., $^\circ\text{K}$	$C_p$
153	13.6	152	14.6
155	13.8	154	14.75
157	14.4	156	14.85
157.73	45	158	15
157.75	60		15.5
157.85	121	160.65	40
157.96	62	161.1	120
158.4	25.2	162	16
159.5	19.9	163	13
162	13.0	164	12.3
164	11.0	166	12.7
166	10.55	168	14.3
168	10.9	—	—
170	11.7	—	—
172	12.9	—	—

It was also found possible with both alcohols to superheat the low-temperature form to  $0.5^\circ$  to  $1^\circ$  above the temperature at which the heat capacity for the substance when in an equilibrium condition reaches its maximum value. Moreover, in the heat capacity measurements in this region, equilibrium was reached only after a long time (sometimes several hours), and this militated against accurate determinations of the true  $C_p$  values and of the transition temperatures (i.e. the temperature at which  $C_p$  reaches its maximum). By carrying out a large number of  $C_p$  determinations with small energy inputs in the neighbourhood of these temperatures, they were assigned the values of  $157.8^\circ \pm 0.1^\circ$  K for  $\text{CH}_3\text{OH}$  (cf.  $157.4^\circ$  K, Kelley;<sup>3</sup>  $161.1^\circ$  K, Parks<sup>11</sup>), and  $161.1^\circ \pm 0.1^\circ$  K for  $\text{CH}_3\text{OD}$ .

Heats of transition were found by measuring the heat absorbed on warming up each alcohol from a temperature below the transition region to that point between the transition temperature and the melting point at which  $C_p$  is a minimum, and subtracting from this the "normal" heat intake for the given temperature rise. This was evaluated by extrapolating to the transition temperature the "normal"  $C_p$  against  $T$  curves above and below the transition. These extrapolations are somewhat arbitrary, particularly in view of the narrow intervals between the transition and melting points. The "normal"  $C_p$ - $T$  relationship in this interval, both for the determination of heats of fusion and transition, was taken to be that given by the experimental values between  $166^\circ$  and  $171^\circ$  K for  $\text{CH}_3\text{OH}$  and between  $164^\circ$  and  $167^\circ$  K for  $\text{CH}_3\text{OD}$ . The results of the experiments on the heats of transition are recorded in Table III.

TABLE III.—HEATS OF TRANSITION OF  $\text{CH}_3\text{OH}$  AND  $\text{CH}_3\text{OD}$ 

Temp. interval	Cal. supplied	$\int C_p \times dT$ (calorimeter + contents)	Molar heat of transition
<b><math>\text{CH}_3\text{OH}</math>. Transition temp. <math>157.8^\circ</math> K. Mass of sample <math>3.0043</math> g.</b>			
$151.05$ - $166.31$	$56.652$	$40.816$	$168.9$
$150.77$ - $166.01$	$56.638$	$40.830$	$168.6$
$151.00$ - $166.17$	$56.639$	$40.415$	$173.0$
		Mean	$170 \pm 2$ cal.
<b><math>\text{CH}_3\text{OD}</math>. Transition temp. <math>161.1^\circ</math> K. Mass of sample <math>2.9118</math> g.</b>			
$155.13$ - $165.06$	$42.177$	$28.458$	$155.7$
$155.00$ - $164.94$	$42.177$	$28.507$	$155.1$
$154.76$ - $164.58$	$42.030$	$28.221$	$156.7$
		Mean	$155.8 \pm 1$ cal.

TABLE IV.—MELTING POINTS OF  $\text{CH}_3\text{OH}$  AND  $\text{CH}_3\text{OD}$ 

$\text{CH}_3\text{OH}$		$\text{CH}_3\text{OD}$	
% Melted	Temp., $^\circ$ K	% Melted	Temp., $^\circ$ K
4	$175.19$	25	$173.25$
21	$175.31$	46	$173.40$
39	$175.35$	67	$173.48$
57	$175.38$	87	$173.50$
75	$175.38_7$	—	—
93	$175.39_3$	—	—
99	$175.40$	—	—

The mean value for  $\text{CH}_3\text{OH}$  ( $170 \pm 2$  cal.) is higher than that for  $\text{CH}_3\text{OD}$  ( $155.8 \pm 1$  cal.).

The melting point of each alcohol was determined by the usual method of melting the solid in stages and recording the equilibrium temperature at each

stage. One such set of observations for each alcohol is recorded in Table IV. Owing to the strain to which the calorimeter appeared to be subjected when the alcohols were solidified and later melted in it, with a consequent alteration of the characteristics of the platinum thermometer, it was considered advisable to carry out several determinations of each melting point, each determination being preceded and followed by recalibration of the thermometer. For  $\text{CH}_3\text{OH}$ , four determinations of the melting-point did not differ by more than  $0.08^\circ$  and gave a mean of  $175.37^\circ \pm 0.04^\circ \text{K}$  (cf.  $175.22^\circ \text{K}$ , Kelley;  $175.3^\circ \text{K}$ , Parks<sup>17</sup>). Four values were also obtained for the melting point of  $\text{CH}_3\text{OD}$ . These covered a range of  $0.15^\circ \text{K}$ , the mean being  $173.52^\circ \pm 0.08^\circ \text{K}$ .

The results from which the heats of fusion were estimated are given in Table V. The molar heat of fusion of  $\text{CH}_3\text{OH}$ ,  $755.1 \pm 3 \text{ cal.}$ , (cf.  $757.2$ , Kelley;  $759.4$ , Parks), is considerably higher than that of  $\text{CH}_3\text{OD}$  ( $726.0 \pm 3 \text{ cal.}$ ).

TABLE V.—HEATS OF FUSION OF  $\text{CH}_3\text{OH}$  AND  $\text{CH}_3\text{OD}$ 

Temp. interval	Cal. supplied	$\int C_p \times dT$ (calorimeter + contents)	Molar heat of fusion
$\text{CH}_3\text{OH}$ . Melting point $175.37^\circ \text{K}$ . Mass of sample $3.0043 \text{ g}$ .			
173.54-176.56	79.596	9.119	751.7
173.20-177.10	83.203	12.239	756.9
166.13-177.00	103.702	32.752	756.7
		Mean	$755.1 \pm 3 \text{ cal.}$
$\text{CH}_3\text{OD}$ . Melting point $173.52^\circ \text{K}$ . Mass of sample $2.9118 \text{ g}$ .			
171.30-175.66	76.384	12.567	724.3
171.06-175.44	76.384	12.495	725.1
164.58-175.26	96.161	31.976	728.5
		Mean	$726.0 \pm 3 \text{ cal.}$

In measuring the heats of evaporation, the whole calorimeter was immersed in melting ice, and the alcohols evaporated isothermally at a temperature of about  $-0.5^\circ \text{C}$ , so that there was no risk of the evaporated alcohol vapour condensing in the outlet tube. This vapour was condensed in a detachable trap cooled in liquid air and its amount determined by weighing. Isothermal evaporation was achieved by controlling the rate of flow of the vapour into the condensation trap by means of a metal valve of the type described by Sagers,<sup>18</sup> so that the vapour pressure of the alcohol in the calorimeter (as observed on the accurate manometer) was constant throughout. For  $\text{CH}_3\text{OH}$  this pressure was  $29.42 \text{ mm.}$ , and for  $\text{CH}_3\text{OD}$   $27.30 \text{ mm.}$  The vapour pressures at the ice-point were found to be  $30.42$  and  $28.30 \text{ mm.}$  respectively. Determinations were made on both alcohols at two different rates of energy input, the results of which are recorded in Table VI, together with the apparent molar heats of evaporation derived from them. These apparent values vary with the rate of energy input since the calorimeter gains some heat from its surroundings during the evaporation. The mean values of these apparent heats of vaporisation were plotted against the time taken for the evaporation and linearly extrapolated to zero heating time (corresponding to infinitely rapid evaporation). The validity of this procedure has been discussed by Frank and Clusius.<sup>11</sup> Small corrections were applied to the extrapolated values (which referred to  $-0.5^\circ \text{C}$ ) to obtain the molar heats of evaporation at  $0^\circ \text{C}$ , giving  $9,207 \pm 20 \text{ cal.}$  for  $\text{CH}_3\text{OH}$  and  $9384 \pm 20 \text{ cal.}$  for  $\text{CH}_3\text{OD}$ . Values of the heat of vaporisation of  $\text{CH}_3\text{OH}$  at this temperature given in the literature are  $9192.1$ ,<sup>14</sup>  $9263$ ,<sup>19</sup> and  $9360.5$ <sup>20</sup> cal.

In each determination of the heat of evaporation the calorimeter was initially full, and about  $1 \text{ cm.}^3$  only was evaporated in any one experiment, which brought the level of the liquid down to the top of the heating coil. If more alcohol than

<sup>17</sup> Parks, *J. Amer. Chem. Soc.*, 1925, **47**, 338.

<sup>18</sup> Sagers, *J. Sci. Instr.*, 1935, **12**, 93.

<sup>19</sup> Young, *Proc. Roy. Dublin Soc.*, 1910, **12**, 374.

<sup>20</sup> Jahn, *Z. physik. Chem.*, 1893, **11**, 787.

this was distilled off, high values for the heat of evaporation were obtained, since some of the heat supplied was communicated to the ascending vapour.

TABLE VI.—HEATS OF EVAPORATION OF  $\text{CH}_3\text{OH}$  AND  $\text{CH}_3\text{OD}$   
Temp. of measurements  $\sim -0.5^\circ\text{C}$

Heating time (sec.)	Cal. supplied	g. alcohol evaporated	App. molar heat of evaporation
$\text{CH}_3\text{OH}$			
5718	230.21	0.8082	9127
5716	230.13	0.8045	9166
5738	231.02	0.8098	9141
2636	229.73	0.8009	9191
2536	229.73	0.8027	9170
2535	229.64	0.7944	9263

Value of true heat of evaporation obtained by extrapolation to zero heating time and corrected to  $0^\circ\text{C} = 9207\text{ cal.}$

$\text{CH}_3\text{OD}$			
5715	230.09	0.8202	9271
5715	230.09	0.8252	9215
5715	230.09	0.8203	9210
1799	162.97	0.5797	9291
2535	229.64	0.8124	9342
2535	229.64	0.8128	9337

Value of true heat of evaporation obtained by extrapolation to zero heating time and corrected to  $0^\circ\text{C} = 9384\text{ cal.}$

## Discussion

At present there is scarcely sufficient information on the thermal properties of hydrogen and deuterium compounds to enable us to decide with certainty what generalisations, if any, can be made on the effect of isotopic replacement on these properties. This lack of data for comparison must, therefore, limit the discussion of the results for  $\text{CH}_3\text{OH}$  and  $\text{CH}_3\text{OD}$ , though these may prove more illuminating when considered together with the same information for  $\text{CD}_3\text{OH}$  and  $\text{CD}_3\text{OD}$ , which it is hoped to obtain in due course. In so far as the few fairly complete investigations do suggest any regularities in the effects on melting and transition characteristics of replacing hydrogen by deuterium, these are covered by the following statements.

(1) The temperature of a transition is usually raised, the increase in this temperature being greater than the change in the melting-point. The heat and entropy change of the transition are also increased.

(2) The melting-point may be either raised or lowered, but for un-associated substances it is more often lowered. Lowering of the melting-point seems to be accompanied by a drop in the heat of fusion, and a very slight decrease in the entropy of fusion.

The results for  $\text{CH}_3\text{OH}$  and  $\text{CH}_3\text{OD}$  conform with these statements except that the entropy change of the transition is less for  $\text{CH}_3\text{OD}$  than for  $\text{CH}_3\text{OH}$ . We agree with Kelley that this transition is not of the first order. In forming this conclusion, its apparently gradual onset (which might be due to an effect produced by impurities similar to pre-melting) is perhaps less significant than the failure to end at a well-defined temperature, which is what would be expected in a first-order transition in a slightly impure substance. As has already been observed, the transition in both alcohols is accompanied by marked inertia; both superheating of the low-temperature form and super-cooling of the high-temperature form are possible. This is noteworthy, since transitions

which occur as near to the melting point as those in these alcohols are usually free from hysteresis effects, which are more commonly observed when the transition temperature lies well below the melting point.<sup>21</sup>

It was found that when methyl alcohol was cooled rapidly in a strong hard-glass tube to liquid-air temperature, and then allowed to warm up slowly, the glass tube frequently cracked before the alcohol melted. As the alcohol was probably largely preserved on cooling in its supercooled high-temperature modification, which would change to the low-temperature form on slowly warming up to the transition temperature, it seems not unlikely that the low-temperature form is the less dense of the two modifications. It would be worth while to submit this conclusion to direct experiment since, if it be true, it suggests that there may be some resemblance between the transition in methyl alcohol and that in resorcinol investigated by Robertson and Ubbelohde.<sup>22</sup> The high-temperature  $\beta$ -form of resorcinol is more dense than the low-temperature  $\alpha$ -modification, the change  $\alpha \rightarrow \beta$  involving a distortion of the intermolecular hydroxyl bonds such that the molecules are brought closer together. Moreover, the transition in resorcinol, like that in methyl alcohol, is accompanied by considerable hysteresis and by an entropy change of much the same magnitude. Quite possibly, therefore, the transition in methyl alcohol involves a rearrangement of intermolecular hydroxyl bonds leading to a more closely packed structure. In view of the strong, directional intermolecular forces, it seems much less likely, for this particular substance, that the onset of molecular rotation (whether about three axes or one) can be held responsible for, or accompanies, the change to the high-temperature form.

The values recorded for the heats of vaporisation of  $\text{CH}_3\text{OH}$  and  $\text{CH}_3\text{OD}$  show that the latter substance is the more highly associated in the liquid state. This is particularly evident if, following Hildebrand, the entropies of vaporisation are compared at such temperatures that the molar volumes of the vapours are equal. Using the results recorded above for the vapour pressures and heats of vaporisation at  $0^\circ\text{C}$ , the entropy of vaporisation of  $\text{CH}_3\text{OH}$  is  $33.70 \text{ cal. mole}^{-1} \text{ deg.}^{-1}$  at  $0^\circ\text{C}$ , and that of  $\text{CH}_3\text{OD}$  at the temperature ( $1.22^\circ\text{C}$ ) at which the vapour has the same molar volume as  $\text{CH}_3\text{OH}$  at  $0^\circ\text{C}$  is  $34.17 \text{ cal. mole}^{-1} \text{ deg.}^{-1}$ . The entropies of vaporisation of  $\text{H}_2\text{O}$  and  $\text{D}_2\text{O}$  when compared on the same basis stand in the same relation. In the neighbourhood of their triple points the entropy of vaporisation of  $\text{D}_2\text{O}$  exceeds that of  $\text{H}_2\text{O}$  by about one unit. It is also interesting to observe that with methyl alcohol, as with water, the molar volume of the deuterium compound is the greater. (The figures at  $20^\circ\text{C}$  are  $40.66 \text{ cm.}^3$  for  $\text{CH}_3\text{OD}$  and  $40.49 \text{ cm.}^3$  for  $\text{CH}_3\text{OH}$ .)

We are indebted to the Government Grant Committee of the Royal Society and to Imperial Chemical Industries, Ltd., for financial help, and we also wish to thank Dr. B. Lambert for providing the manometer, and Mr. J. H. E. Jeffes for assisting us with the measurements on carbon tetrachloride.

**Appendix.**—As a check on the results obtained with the calorimeter, determinations were made of the heats of fusion and transition of carbon tetrachloride. The melting point of the sample used changed by  $< 0.005^\circ$  over the range 20 to  $90\%$  melted. The experimental observations are recorded in Table VII, and our values for the heats of transition and fusion are compared there with those of other workers. Of these, those determined most recently (by Hicks, Hooley and Stephenson) are in excellent agreement with our own.

<sup>21</sup> Eucken and Schröder, *Nach. Ges. Wiss. Göttingen*, 1938, 3 (5), 65.

<sup>22</sup> Robertson and Ubbelohde, *Proc. Roy. Soc., A*, 1938, 167, 122, 136.

TABLE VII.—HEATS OF FUSION AND TRANSITION OF CARBON TETRACHLORIDE

Heat of transition. (Transition temp. = 225.75° K)

Mass sample (g.)	Temp. interval	Cal. supplied	$\int C_p \times dT$ (calorimeter + contents)	Molar heat of transition
6.4131	222.65-228.33	62.794	17.015	1098.2
6.4131	222.99-228.65	62.991	17.090	1096.3
6.4717	223.50-227.93	59.256	13.270	1093.1
			Mean value	1096 cal.

(Other values : Latimer,<sup>23</sup> 1100 ; Johnston and Long,<sup>15</sup> 1080.8 ; Stull,<sup>24</sup> 1100 ; Hicks, Hooley and Stephenson,<sup>16</sup> 1095 cal.)

Heat of fusion. (Melting point = 250.2° K)

6.3115	248.20-252.65	38.564	13.910	600.9
6.3115	248.20-253.38	40.972	16.229	603.1
6.5147	248.48-252.19	37.156	11.600	603.5
6.5147	248.59-251.25	33.849	8.465	599.4
			Mean value	602 cal.

(Other values : Latimer,<sup>23</sup> 644 ; Johnston and Long,<sup>15</sup> 577.2 ; Stull,<sup>24</sup> 581 ; Hicks, Hooley, and Stephenson,<sup>16</sup> 601 cal.)

*The Inorganic Chemistry Laboratory,  
Oxford.*

<sup>23</sup> Latimer, *J. Amer. Chem. Soc.*, 1922, **44**, 90.

<sup>24</sup> Stull, *ibid.*, 1937, **59**, 2726.

## THE POLARISABILITIES OF BONDS

### PART II.—BOND REFRACTIONS IN THE ALKANES

BY B. C. VICKERY AND K. G. DENBIGH

*Received 5th May, 1948*

The molar refractions of the paraffins are examined to determine how accurately the observed data can be represented by a simple system of bond refractions and to what extent deviations can be related to structural factors. The molar refractions of the 196 alkanes considered, normal and branched, can be calculated from the bond parameters  $[CH] = 1.674$  and  $[CC] = 1.296$  with an average discrepancy from the observed value of less than 0.5 %. A methyl branch in the 2-position leads to a slight but real increase in molar refraction relative to the normal isomer, 2 : 2-dimethyl branching leads to a considerably larger increase. All other forms of branching lead to a decrease in molar refraction, the decrease being the greater according to (i) the degree of branching, (ii) the length of the branching chain.

In an earlier paper by one of the authors<sup>1</sup> a general survey was made of the possibility of regarding the polarisability of a molecule as being primarily located in the *bonds*. The data on the molecular refraction of substances was therefore analysed directly in terms of bond refractions, in place of the older analysis of Brühl, Landolt and Eisenlohr in terms of atomic refractions. In our earlier paper, data on the Kerr constant and depolarisation factor were also used, in order to determine the anisotropy of the bond ellipsoid, i.e. the relative ease of electron displacement in directions along and at right-angles to the bond axis.

<sup>1</sup> Denbigh, *Trans. Faraday Soc.*, 1940, **36**, 936.





Values for the constants  $a$  and  $b$  are obtained by suitable mathematical methods from the observed values of  $R$  for a series of alkanes.

Second,  $a$  and  $b$  are represented as combinations of bond refractions. In this case,  $b$  is the  $-\text{CH}_3$  increment, and is given by the equation

$$b = [\text{CC}] + 2[\text{CH}] \quad (2)$$

where  $[\text{CC}]$  and  $[\text{CH}]$  are the  $\text{C}-\text{C}$  and  $\text{C}-\text{H}$  bond refractions. The constant  $a$  can be represented as

$$a = [\text{CC}] + 6[\text{CH}]. \quad (3)$$

Inserting the calculated values for  $a$  and  $b$  in these equations and solving gives values for  $[\text{CC}]$  and  $[\text{CH}]$ .

The calculation of  $a$  and  $b$  in eqn. (1) is essentially the problem of determining the "best" straight line through a number of experimental points. A fallacy in the method originally used by Berthelot,<sup>5</sup> Landolt<sup>6</sup> and Brühl<sup>7</sup> has been pointed out by Angus,<sup>8</sup> and Van der Hulst<sup>9</sup> has similarly criticised the method of Eisenlohr.<sup>10</sup> We prefer to determine the "best" straight line by a procedure which is the equivalent to the method of least squares.<sup>10</sup>

Suppose we have  $N$  members of a homologous series (not necessarily consecutive members), whose molar refraction  $R$  is represented by eqn. (1). Putting  $x = n - 2$ , we have

$$b = \frac{N\sum(x[R]) - \sum x \sum [R]}{N\sum x^2 - (\sum x)^2}, \quad (4)$$

$$a = \sum [R]/N - b\sum x/N. \quad (5)$$

From the values of  $a$  and  $b$  so calculated, we can obtain calculated molar refractions, and a difference ( $\Delta$ ) between observed and calculated values for each member of the series. The standard error for our value of  $b$  is then given by the square root of the sampling variance  $V_b$ , which is calculated thus:

$$V_b = \frac{N\sum \Delta^2}{(N-2)(N\sum x^2 - (\sum x)^2)}. \quad (6)$$

Two values of  $b$  may be compared by means of a  $t$ -test of significance. The sampling variances of the two values are summed, and the square root ( $S$ ) of this sum is taken. The value of  $t$  is obtained by dividing the difference between the two values of  $b$  by  $S$ . The probability that a value of  $t$  as large as that obtained is compatible with the hypothesis that the values of  $b$  do not differ significantly, can now be estimated. This is done by examination of a table of  $t$ , such as that given by Fisher and Yates,<sup>11</sup> using the requisite number of "degrees of freedom" (in this case equal to four less than the total number of observed values from which the two values of  $b$  have been calculated).

## The Data

Several extensive compilations of refractive index (for the  $D$  line) and density data for alkanes have been made during the last few years.<sup>12-14</sup> Data for the first 43 normal alkanes and 153 branched alkanes used in this paper are shown in Tables I and II. The values of Ward and Kurtz have been used when these were available, otherwise those of Egloff, Francis or Landolt-Bornstein.

<sup>5</sup> Berthelot, *Ann. Chim. Phys.* (3), 1856, 48, 342.

<sup>6</sup> Landolt, *Pogg. Ann.*, 1864, 123, 611.

<sup>7</sup> Brühl, *Z. physik. Chem.*, 1891, 7, 140.

<sup>8</sup> Angus, *Ann. Reports*, 1941, 38, 32.

<sup>9</sup> Van der Hulst, *Rec. trav. chim.*, 1940, 59, 1219.

<sup>10</sup> Eisenlohr, *Z. physik. Chem.*, 1891, 7, 140.

<sup>11</sup> Fisher and Yates, *Statistical Tables for Biological, Agricultural and Medical Research*, 1943.

<sup>12</sup> Egloff, *Physical Properties of Hydrocarbons*, Vol. 1, 1935.

<sup>13</sup> Ward and Kurtz, *Ind. Eng. Chem. (Anal.)*, 1938, 10, 559.

<sup>14</sup> Francis, *Ind. Eng. Chem.*, 1943, 35, 442; 1944, 36, 256.

The tables also show  $[R]$ , the molar refraction calculated from the observed density and refractive index according to the Lorenz-Lorentz formula, using the atomic weights  $C = 12.01$ ,  $H = 1.0078$ .

The remaining columns show  $[R']$ ,  $[R'']$ , values of the molar refraction using parameters derived as explained below, and also  $\Delta' = [R - R']$ ,  $\Delta'' = [R - R'']$ .

**The Normal Alkanes.**—As the basis of our preliminary examination of the normal alkanes, we have taken only the lower members whose physical properties are known with considerable accuracy, and have restricted ourselves, in the first instance, to eight alkanes about whose properties there is close agreement among the three main compilers, viz. the normal alkanes  $C_8$  to  $C_{11}$  and  $C_{16}$ .

From the observed molar refractions for these alkanes, the following values were calculated :

$$a = 6[CH] + [CC] = 11.339, \quad . \quad . \quad . \quad (7)$$

$$b = 2[CH] + [CC] = 4.644, \quad . \quad . \quad . \quad (8)$$

$$V_b = 1.57 \times 10^{-1}, \quad \sqrt{V_b} = 0.00125 \text{ (standard error of } b \text{)}.$$

Solving between (7) and (8), we obtain

$$[CH] = 1.674, \quad [CC] = 1.296.$$

These values were used to calculate molar refractions for all the alkanes, including those with branched chains. The results of this procedure are seen in Tables I and II, in which  $[R']$  is the molar refraction so calculated and  $\Delta'$  is the discrepancy between observed and calculated values,  $\Delta'$  being positive when the observed value is greater than the calculated.

Over the whole range of alkanes considered the average discrepancy is 0.43 %. Further examination shows that the positive discrepancies, which average 0.37 %, occur predominantly among the higher normal alkanes, while the negative discrepancies, averaging 0.46 %, lie almost wholly among the branched alkanes.

The reality of the exaltation of the higher members of the normal alkanes relative to the lower can be tested statistically. For this purpose the best straight line is fitted to the observed molar refractions for normal alkanes  $C_{17}$  to  $C_{43}$ , with the results :

$$a' = 10.346, \quad b' = 4.697, \quad V_b' = 4.4 \times 10^{-5}.$$

The  $CH_2$ -increment, 4.697, is thus appreciably larger than the value, 4.644, for the lower members. This difference is certainly not due to random causes, as shown by a  $t$ -test of significance :

$$t = \frac{b' - b}{\sqrt{V_b + V_b'}} = 7.8.$$

$$\text{Degrees of freedom} = 35. \quad P \ll 0.001.$$

The probability that it is a random difference is thus quite negligible. It may be, however, that the apparent exaltation is not a genuine structural effect. Two possible explanations are (a) systematic contamination of the experimental samples by paraffins of higher molecular weight ; (b) a temperature effect—many of the higher members were studied at temperatures considerably above 20° C.

On the other hand, an exaltation does not occur among the higher *branched* alkanes and it appears, therefore, that it may be a genuine structural peculiarity of the straight-chain compounds. A similar effect has been observed by Gibling<sup>18</sup> with regard to the parachor.

**The Branched Alkanes.**—As shown in the last section the branched alkanes in general show an appreciable depression of the molar refraction. To test whether this was due to particular types of branching, the

<sup>18</sup> Gibling, *J. Chem. Soc.*, 1941, 299.

branched alkanes were separated into groups according to their structures, and the observed refractions of each group were compared statistically, by the *t*-test described earlier, with those of the normal isomers. In these tests only alkanes with 16 carbon atoms or less were studied, to avoid any possible interference from long-chain exaltation. This analysis revealed the following statistically significant results.

TABLE I.—NORMAL ALKANES

Carbon Atoms	$d_4^t$	$n_D^t - 1$	Ref.	$R$	$R'$	$\Delta'$	Notes
1	—	—	15	6.588	6.695	-0.107	
2	—	—	16	11.35	11.339	+0.011	
3	—	—	12	15.857	15.988	-0.126	
4	—	—	12	20.800	20.627	+0.173	
5	0.6264	0.3577	12	25.271	25.271	0	
6	0.6594	0.3751	12	29.918	29.915	+0.003	
7	0.6837	0.3877	12	34.557	34.559	-0.002	
8	0.7028	0.3976	12	39.191	39.203	-0.012	
9	0.7179	0.4056	12	43.843	43.847	-0.004	
10	0.7298	0.4120	12	48.510	48.491	+0.019	
11	0.7404	0.4173	13	53.119	53.135	-0.016	
12	0.7495	0.4217	13	57.740	57.779	-0.039	
13	0.7568	0.4266	14	62.491	62.423	+0.068	
14	0.7636	0.4296	14	67.053	67.007	-0.046	
15	0.7689	0.4330	13	71.793	71.711	+0.082	
16	0.7741	0.4352	13	76.354	76.355	-0.001	
17	0.7778	0.4374	13	81.055	80.999	+0.056	at 25° C
18	0.7767	0.4307	12	85.787	85.643	+0.144	at 28° C
19	0.7854	0.4404	13	90.170	90.287	-0.117	
20	0.7888	0.4434	13	95.030	94.931	+0.099	
21	0.7766	0.4356	13	99.761	99.576	+0.185	
22	0.7778	0.4361	14	104.42	104.22	+0.20	
23	0.7797	0.4367	14	109.00	108.87	+0.13	at 47.4° C
24	0.7694	0.4303	14	113.76	113.51	+0.25	at 65° C
25	0.7713	0.4320	14	118.59	118.15	+0.44	at 65° C
26	0.7780	0.4357	14	123.16	122.79	+0.37	at 60° C
27	0.7753	0.4345	14	128.00	127.44	+0.56	at 65° C
28	0.7792	0.4368	14	132.66	132.08	+0.58	at 61.6° C
29	0.7789	0.4364	14	137.33	136.72	+0.61	at 65° C
30	0.7769	0.4352	14	142.06	141.37	+0.69	at 70° C
31	0.7789	0.4356	14	146.51	146.01	+0.50	at 70° C
32	0.7798	0.4364	14	151.29	150.66	+0.63	at 70° C
33	0.7725	0.4323	14	156.17	155.31	+0.86	at 84° C
34	0.7738	0.4329	14	160.81	159.95	+0.86	at 84° C
35	0.7751	0.4334	14	165.41	164.59	+0.82	at 84° C
36	0.7819	0.4362	14	169.58	169.23	+0.35	at 76° C
37	0.7780	0.4345	14	174.55	173.88	+0.67	at 84° C
38	0.7749	0.4326	14	179.28	178.52	+0.76	at 90° C
39	0.7771	0.4358	14	184.65	183.16	+1.49	at 84° C
40	0.7785	0.4363	14	189.21	187.81	+1.40	at 84° C
41	0.7784	0.4366	14	194.07	192.46	+1.61	at 84° C
42	0.7803	0.4375	14	198.66	197.10	+1.56	at 84° C
43	0.7810	0.4378	14	203.28	201.75	+1.53	at 84° C

Notes.—(1)  $t = 20^\circ \text{C}$  unless otherwise stated.

(2) In some cases  $d$  or  $n$  have been corrected using a correction formula (ref. 17) to bring them to the same temperature.

<sup>15</sup> Tausz and Hornung, *Z. tech. Physik*, 1927, **8**, 338.

<sup>16</sup> Stuckert, *Z. Elektrochem.*, 1910, **16**, 37; Friberg, *Z. Physik*, 1931, **73**, 216; Lowery, *Proc. Roy. Soc. A*, 1931, **133**, 188.

<sup>17</sup> Lipkin and Kurtz, *Ind. Eng. Chem. (Anal.)*, 1941, **13**, 291, also ref.<sup>18</sup>

TABLE II.—BRANCHED ALKANES

Carbon Atoms	Cpd. No.	Carbon Skeleton	$d'_4$	$n_D^{20} - 1$	Ref.	R	R'	$\Delta'$	R''	$\Delta''$
5	44		0.6197	0.3539	13	25.302	25.271	-0.03	25.297	0
	45		0.613	0.3513	13	25.409	—	-0.14	25.323	+0.09
6	46		0.6532	0.3715	13	29.946	29.915	-0.03	29.941	0
	47		0.6640	0.3764	13	29.806	—	-0.11	29.772	+0.03
7	48		0.6493	0.3690	13	29.931	—	+0.02	29.967	-0.04
	49		0.6615	0.3750	13	29.819	—	-0.10	29.967	-0.15
7	50		0.6787	0.3850	13	34.596	34.559	+0.04	34.585	+0.01
	51		0.6870	0.3887	13	34.469	—	-0.09	34.416	+0.05
7	52		0.6737	0.3823	13	34.635	—	+0.08	34.611	+0.02
	53		0.6745	0.3832	13	34.666	—	-0.11	34.611	+0.05

54		0.6951	0.3920	13	34.324	—	— 0.23	34.442	— 0.12
55		0.6900	0.3804	13	34.375	—	— 0.18	34.637	— 0.26
56		0.6932	0.3911	13	34.349	—	— 0.21	34.273	+ 0.08
57		0.6984	0.3937	13	34.294	—	— 0.26	34.315	— 0.02
58		0.6980	0.3936	13	39.107	39.203	— 0.10	39.229	— 0.12
59		0.7051	0.3980	13	39.097	—	— 0.11	39.060	+ 0.04
60		0.7090	0.3992	13	38.984	—	— 0.22	39.060	— 0.08
61		0.6953	0.3930	13	39.207	—	+ 0.00	39.255	— 0.05
62		0.6943	0.3928	13	39.245	—	+ 0.04	39.255	— 0.01
63		0.6918	0.3916	13	39.281	—	+ 0.08	39.281	0
64		0.7195	0.4043	13	38.850	—	— 0.35	38.917	— 0.07
65		0.7123	0.4013	13	38.985	—	— 0.22	39.086	— 0.10

TABLE II.—BRANCHED ALKANES (*continued*)

Carbon Atoms	Cpd. No.	Carbon Skeleton	$d_4^i$	$n_D^{20} - 1$	Ref.	$R$	$R'$	$\Delta'$	$R''$	$\Delta''$
8	66		0.7173	0.4030	13	38.859	39.203	-0.34	39.112	-0.25
	67		0.7258	0.4074	13	38.772	—	-0.43	38.943	-0.17
	68		0.7197	0.4045	13	38.856	—	-0.35	39.112	-0.26
	69		0.7211	0.4002	14	38.372	—	-0.83	39.307	-0.93
	70		0.7096	0.4006	13	39.073	—	-0.13	38.917	+0.16
	71		0.6993	0.3952	13	39.175	—	-0.03	39.086	+0.09
	72		0.7130	0.4017	13	38.981	—	-0.22	38.959	+0.02
	73		0.7182	0.4029	13	38.801	—	-0.40	38.985	-0.18
9	74		0.7274	0.4078	13	38.719	—	-0.48	38.816	-0.10
	75		0.7134	0.4032	13	43.888	43.847	+0.04	43.873	+0.01



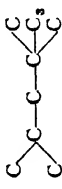
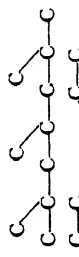


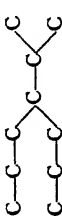



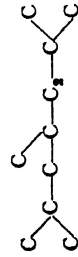



TABLE II.—BRANCHED ALKANES (*continued*)

Carbon Atoms	Cpd. No.	Carbon Skeleton	$d_4^t$	$n_D^{20} - 1$	Ref.	$R$	$R'$	$\Delta'$	$R''$	$\Delta''$
9	88		0.7048	0.4031	14	44.414	43.847	+ 0.57	43.756	+ 0.66
	89		0.7233	0.4090	14	43.835	—	- 0.01	43.587	+ 0.25
	90		0.7266	0.4090	14	43.636	—	- 0.21	43.603	+ 0.03
	91		0.7407	0.4156	13	43.412	—	- 0.43	43.603	- 0.19
	92		0.7266	0.4106	14	43.785	—	- 0.06	43.629	+ 0.16
10	93		0.7522	0.4197	13	43.119	—	- 0.73	43.359	- 0.24
	94		0.7365	0.4125	14	43.373	—	- 0.47	43.655	- 0.28
	95		0.7429	0.4178	14	43.485	—	- 0.36	43.418	+ 0.07
	96		0.7242	0.4089	13	48.559	48.491	+ 0.07	48.517	+ 0.04
	97		0.7335	0.4125	13	48.314	—	- 0.18	48.348	- 0.03



TABLE II.—BRANCHED ALKANES (*continued*)

Carbon Atoms	Cpd. No.	Carbon Skeleton	$d_4^i$	$n_D^{20} - 1$	Ref.	$R$	$R'$	$\Delta'$	$R''$	$\Delta''$
10	110		0.7346	0.4143	14	48.427	48.491	- 0.06	48.374	+ 0.05
	111		0.7198	0.4057	13	48.519	—	+ 0.03	48.400	+ 0.12
	112		0.7514	0.4200	14	47.916	—	- 0.57	48.003	- 0.09
	113		0.7360	0.4141	13	48.314	—	- 0.18	48.184	+ 0.13
	114		0.7412	0.4171	14	48.280	—	- 0.21	48.210	+ 0.07
11	115		0.7380	0.4154	14	48.316	—	- 0.17	48.247	+ 0.07
	116		0.7566	0.4230	13	52.603	53.135	- 0.53	53.043	- 0.44
	117		0.7439	0.4176	13	52.904	—	- 0.23	53.017	- 0.11
	118		0.7331	0.4123	13	53.084	—	- 0.05	53.043	+ 0.04
	119		0.7507	0.4205	13	52.742	—	- 0.39	52.891	- 0.15

120		0.7465	0.4200	14	52.741	—	— 0.39	52.828	— 0.09
121		0.7484	0.4205	14	52.905	—	— 0.23	52.891	+ 0.01
122		0.7470	0.4203	14	52.982	—	— 0.15	52.891	+ 0.09
123		0.7527	0.4238	13	57.717	57.779	— 0.06	57.636	+ 0.08
124		0.7514	0.4231	14	57.732	—	— 0.05	57.636	+ 0.10
125		0.7630	0.4275	13	57.373	—	— 0.41	57.545	— 0.17
126		0.7925	0.4402	14	56.663	—	— 1.12	57.597	+ 0.07
127		0.7542	0.4225	14	57.446	—	— 0.33	57.493	— 0.05
128		0.7572	0.4240	13	57.397	—	— 0.38	57.662	— 0.26
129		0.7477	0.4187	14	57.490	—	— 0.29	57.740	— 0.25
130		0.7559	0.4228	13	57.354	—	— 0.42	57.472	— 0.12
131		0.7496	0.4220	13	57.739	—	— 0.04	57.498	+ 0.24

12

TABLE II.—BRANCHED ALKANES (*continued*)

Carbon Atoms	Cpd. No.	Carbon Skeleton	$d_1^t$	$n_D^{20} - 1$	Ref.	R	R'	$\Delta'$	R''	$\Delta''$
12	132		0.7675	0.4316	14	57.515	57.779	-0.26	57.291	+0.22
	133		0.7655	0.4320	13	57.709	—	-0.07	57.524	+0.18
	134		0.7519	0.4228	14	57.658	—	-0.12	57.535	+0.12
	135		0.7560	0.4251	14	57.620	—	-0.16	57.535	+0.09
13	136		0.7632	0.4279	14	57.404	—	-0.37	57.291	+0.11
	137		0.7443	0.4182	14	57.691	—	-0.09	57.524	+0.17
	138		0.7576	0.4244	13	62.143	62.423	-0.28	62.280	-0.14
	139		0.7633	0.4271	14	62.021	—	-0.40	62.475	-0.45
14	140		0.7692	0.4287	13	61.873	—	-0.55	62.332	-0.46
	141		0.7580	0.4242	14	62.084	—	-0.34	62.306	-0.22





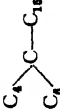
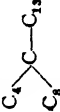


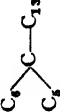
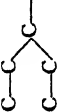


TABLE II.—BRANCHED ALKANES (*continued*)

Carbon Atoms	Cpd. No.	Carbon Skeleton	$d_4^i$	$n_D^{25} - 1$	Ref.	$R$	$R'$	$\Delta'$	$R''$	$\Delta''$
15	154		0.7746	0.4333	14	71.307	71.711	-0.40	71.404	-0.10
	155		0.7787	0.4348	13	75.844	76.355	-0.51	76.069	-0.22
16	156		0.7841	0.4368	13	75.624	—	-0.73	75.741	-0.12
	157		0.7789	0.4366	13	76.097	—	-0.26	76.111	-0.02
17	158		0.7858	0.4369	14	75.474	—	-0.88	75.867	-0.39
	159		0.7700	0.4360	14	81.649	80.999	+0.65	80.385	+1.28
18	160		0.7806	0.4385	13	85.662	85.643	+0.02	85.669	0
	161		0.7924	0.4428	13	85.108	—	-0.53	85.357	-0.25
163	162		0.7871	0.4397	14	85.157	—	-0.49	85.155	0
	163		0.7911	0.4421	14	85.129	—	-0.51	85.029	+0.10

164		0.7924	0.4430	14	85.141	—	— 0.50	85.155	— 0.01
165		0.7911	0.4444	14	85.515	—	— 0.13	85.336	+ 0.18
166		0.7864	0.4413	13	94.929	94.931	0	94.957	— 0.03
167		0.7885	0.4412	14	94.656	—	— 0.27	94.697	— 0.04
168		0.7928	0.4411	13	94.680	—	— 0.25	94.687	— 0.01
169		0.7950	0.4430	14	103.57	104.22	— 0.65	104.27	— 0.70
170		0.7968	0.4463	13	104.00	—	— 0.22	103.91	+ 0.09
171		0.7984	0.4442	14	103.37	—	— 0.85	103.66	— 0.29
172		0.7978	0.4462	14	113.23	113.51	— 0.28	113.54	— 0.31
173		0.8054	0.4502	14	113.04	—	— 0.47	112.94	+ 0.10
174		0.8012	0.4472	14	112.97	—	— 0.54	113.20	— 0.23
175		0.8017	0.4487	14	117.92	118.15	— 0.23	117.84	+ 0.08



TABLE II.—BRANCHED ALKANES (*continued*)

Carbon Atoms	Cpd. No.	Carbon Skeleton	$d_i^1$	$n_D^{20} - 1$	Ref.	R	R'	$\Delta'$	R''	$\Delta''$
26	176		0.8031	0.4488	14	122.42	122.79	-0.37	122.65	-0.23
	177		0.8057	0.4503	14	122.38	—	-0.41	122.48	-0.10
	178		0.8040	0.4499	14	122.54	—	-0.25	122.48	+0.06
	179		0.8041	0.4498	14	122.50	—	-0.29	122.48	+0.02
	180		0.8046	0.4500	14	122.47	—	-0.32	122.48	-0.01
	181		0.8038	0.4497	14	122.52	—	-0.27	122.48	+0.04
	182		0.8040	0.4497	14	122.49	—	-0.30	122.48	+0.01
	183		0.8069	0.4507	14	122.29	—	-0.50	122.55	-0.26
	184		0.8092	0.4517	14	122.17	—	-0.62	122.48	-0.31
	185		0.8029	0.4491	14	122.52	—	-0.27	122.53	-0.01



- (a) Methyl substitution, except at the end of a chain, causes a depression in the refraction of  $0.143 \pm 0.016 \text{ cm}^3 \text{ mole}^{-1}$  per methyl group.
- (b) Ethyl substitution causes a depression of  $0.244 \pm 0.026 \text{ cm}^3 \text{ mole}^{-1}$  per ethyl group.
- (c) Longer side chains give rise to an average depression of  $0.307 \pm 0.030 \text{ cm}^3 \text{ mole}^{-1}$ .
- (d) In sharp distinction to (a), a methyl group in the 2-position causes an exaltation of  $0.026 \pm 0.011 \text{ cm}^3 \text{ mole}^{-1}$ .

The probability that these results are due to random error is less than 0.001 in the first three cases and less than 0.05 in (d).

It is of interest that Wibaut and Langedijk<sup>19</sup> on the basis of an examination of some 24 alkanes carefully prepared by themselves and their collaborators, came to similar conclusions.

Molar refractions for the alkanes can be calculated, using the branching effects derived above to correct the values  $[R']$  calculated from the parameters  $[\text{CH}] = 1.674$  and  $[\text{CC}] = 1.296$ . The results are shown in column  $[R'']$  of Table II.

The average discrepancy  $\Delta''$  is now only 0.20 %, approximately equally distributed among positive and negative values. The corrections for branching have therefore, both reduced the average discrepancy from 0.43 % to 0.20 %, and have also removed the predominance of negative discrepancies among the branched alkanes.

### Bond Types

The analysis so far has been based on fixed values for the refraction of the C—C and C—H bonds, together with the small correcting factors, (a)-(d), for the branching effects. An alternative procedure, of a type previously used by Huggins,<sup>2</sup> in connection with the Gladstone-Dale formula, is to make a distinction between the various types of C—C and C—H bonds which occur in the alkanes and to attribute specific values of the refraction to each type of bond. Thus the C—C bonds may be classified according to the number of C—C neighbours each type has around it. There are then four types of C—H bond and ten types of C—C bond, allowing for the symmetry of arrangement of the neighbouring atoms.

A scheme of this kind is theoretically more attractive than that which was adopted in the previous section. Armed with fourteen parameters, one might also expect to reduce the discrepancies to a very small amount. We have carried out a great many calculations and have come to the conclusion, however, that the procedure is too ambiguous for reliable bond values to be obtained. The most that can be said with any degree of confidence is that as the number of C—C neighbours around a particular C—C bond increases, so its contribution to the molar refraction diminishes, if it is assumed that the refraction of the C—H bonds remain unchanged.

Moreover, such calculations take into account only the change in refraction due to branching. The following effects still lie outside the scope of the scheme :

- (1) the exaltation in the long chain normal hydrocarbons,
- (2) the different effect of methyl substitution according to the position in the chain (see (a) and (d) above),
- (3) the effect on refraction of the *length* of the side chains, analysed at (a), (b) and (c) above.

All these effects have real statistical significance. They are due, perhaps, to specific geometrical factors which affect the density of the liquid

<sup>19</sup> Wibaut and Langedijk, *Rec. trav. chim.*, 1940, **59**, 1219.

<sup>20</sup> The methods indicated below can be studied in such books as Mather, *Statistical Analysis in Biology* (1946).

and thereby its molar refraction, and thus supplement, or limit the application of, an analysis based purely on bond types. Any complete account of molar refractions in the alkanes would have to provide parameters for such further structural effects as well as for fourteen bond types.

The complexity of such a system makes computation difficult, the numerical values obtained are of doubtful validity, and the array of parameters is not of real use. In the future development of a system of bond refractions, it seems that the most satisfactory procedure will be to attribute the best average values to each bond of a distinctive type, e.g. C—H, C—C, C=C, C—Cl, etc. These values will then be regarded as constant to the *first approximation* in all compounds. At the *second approximation*, instead of seeking to account for the inevitable small deviations by means of a sub-classification of the bond types, it will be preferable to make a statistical computation of the magnitude of the disturbing effects, as in the previous section. These remarks do not in any way impair our view that the bond system is superior to the atomic system of refractions. The latter is subject to the same limitations, together with the larger ones which are avoided in the bond system.

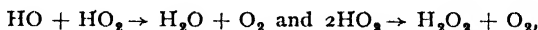
*Imperial Chemical Industries Ltd.,  
Butterwick Research Laboratories,  
Welwyn, Herts.*

## THE TERMINATION REACTION IN THE PHOTOLYSIS OF HYDROGEN PEROXIDE IN DILUTE AQUEOUS SOLUTIONS

BY (THE LATE) D. E. LEA \*

*Received 19th May, 1948*

The quantum yields for the decomposition of 0.01 M aqueous  $\text{H}_2\text{O}_2$  have been determined over a wide range of intensities of light absorbed. At low intensities the quantum yield ( $\gamma$  = molecules  $\text{H}_2\text{O}_2$  decomposed per quantum) is found to be proportional to  $I_{\text{abs}}^{-1/2}[\text{H}_2\text{O}_2]$  in confirmation of the results of other workers at higher concentrations; but at high intensities  $\gamma$  reaches a limiting value =  $1.39 \pm 0.11$  independent of  $I_{\text{abs}}$  and the acidity. It is concluded that either or both the reactions,

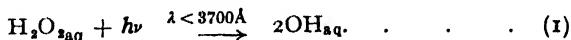


and hence also the reaction,  $\text{HO} + \text{H}_2\text{O}_2 \rightarrow \text{H}_2\text{O} + \text{HO}_2$ , must be occurring. The reactions,  $2\text{HO} \rightarrow \text{H}_2\text{O}_2$  or  $\text{H}_2\text{O} + \text{O}$  are not excluded, but are considered unlikely.

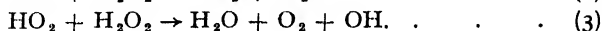
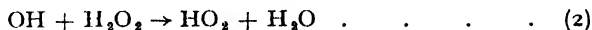
There is ample evidence, both direct and from sector experiments, that the rate of photolysis of hydrogen peroxide in dilute aqueous solution,

\* Dr. D. E. Lea died on 16th June, 1947, and this note has been written by F. S. Dainton, of the Laboratory of Physical Chemistry, Cambridge, after consulting Dr. Lea's practical note-books and inspecting parts of Dr. Lea's dismantled apparatus. Whilst F. S. D. accepts all responsibility for this publication he wishes to state that the purpose of, and many of the conclusions drawn from these experiments, although not written in Dr. Lea's notes, were explicitly stated by Dr. Lea at a colloquium held towards the end of 1946 and also separately to F. S. D. at a later date. The work described was only a part of Dr. Lea's programme, but it was nevertheless deemed advisable to publish his results thus far obtained.

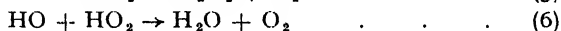
is proportional to the square root of the intensity of the absorbed light<sup>1</sup> and the first power of the hydrogen peroxide concentration.<sup>2</sup> Quantum yields much larger than unity are observed and the reaction is considered to be an unbranched chain reaction in which the initial photochemical act may be written



Confirmation for this view is afforded by the fact that hydrogen peroxide is a photosensitiser<sup>3</sup> for the polymerisation of water-soluble vinyl compounds just as the electron-transfer reaction,  $\text{Fe}^{++} + \text{H}_2\text{O}_2 \rightarrow \text{Fe}^{+++} + \text{OH}$ , which is also a source of hydroxyl radicals, is a thermal sensitiser.<sup>4</sup> The propagation reactions are likely to be those of the Haber-Weiss scheme,<sup>5</sup> viz.:



The termination reaction must involve mutual destruction of the chain centres in pairs, and there are three possible paired combinations of HO and HO<sub>2</sub> in which this may be achieved:



In principle it is possible to devise experiments to distinguish whether (4a), or (4b), or (5) and (6) are the termination reactions. The method is to conduct experiments at such high light intensities and low hydrogen peroxide concentrations that the reaction ceases to be a chain reaction and merely consists of the groups of consecutive reactions (1) + (4a), or (1) + (4b), or (1) + (2) + (5), or (1) + (2) + (6). This condition will be readily recognised since the reaction rate will then be directly proportional to the absorbed light intensity and correspondingly the quantum yield will have fallen to a steady value independent of the light intensity. If  $k_1$  is the quantum yield of the primary act (i.e. reaction (1)) the steady values of the observed quantum yield (molecules of H<sub>2</sub>O<sub>2</sub> destroyed), for the consecutive reaction corresponding to the above groups would be  $0$ ,  $k_1$ ,  $2k_1$ ,  $2k_1$  respectively.

An earlier investigation made by Heidt<sup>6</sup> indicated that such a limiting value to the quantum yield might be attained by using a powerful light source, but very high H<sub>2</sub>O<sub>2</sub> concentrations were employed. In the present work the quantum yield has been measured over a 50,000-fold intensity variation for solutions of concentration  $10^{-3}$  M.

## Experimental

(1) **Optical Arrangement.**—The light source used was a high-voltage gas-filled mercury-vapour lamp, consisting of 30 cm. quartz tubing of diameter 0.8 cm. wound in a close spiral of about 3.3 cm. diameter. The pitch of the spiral was about 1.2 cm. and there were three complete windings. At 10 cm. distance

<sup>1</sup> Allmand and Style, *J. Chem. Soc.*, 1930, 596; Kornfeld, *Z. physik. Chem. B*, 1935, **29**, 205; Dain and Pusekin, *J. Physic. Chem. Russ.*, 1938, **4**, 478; Qureshi and Rahman, *J. Physic. Chem.*, 1932, **36**, 664.

<sup>2</sup> Kornfeld, *loc. cit.*, Henri and Wurmser, *Compt. rend.*, 1913, **157**, 126; Taylor and Anderson, *J. Amer. Chem. Soc.*, 1923, **45**, 654.

<sup>3</sup> Dainton, *J. Physic. Chem.*, 1948, **52**, 490, and unpublished data.

<sup>4</sup> Baxendale, Evans, *et al.*, *Trans. Faraday Soc.*, 1946, **42**, 155, 668, 675.

<sup>5</sup> Haber and Weiss, *Proc. Roy. Soc. A*, 1934, **147**, 333.

<sup>6</sup> Heidt, *J. Amer. Chem. Soc.*, 1932, **54**, 2840.

\* This reaction was not considered by Dr. Lea.

along a radius, the intensity of the full light emitted by the lamp when operating at a current of 3 mA, was found from thermopile measurements to be about  $10^4$  ergs  $\text{cm}^{-2}$   $\text{sec}^{-1}$ . In the centre of the lamp the intensity was eighty times this value. The reaction vessels consisted of small, clear, quartz test-tubes of internal diameter 1.22 to 1.29 cm., external diameter 1.48 to 1.58 cm., and overall length 1.6 cm.

(II) **Procedure.**—Samples of B.D.H. A.R. hydrogen peroxide, freed from stabiliser, were redistilled in a Pyrex apparatus under reduced pressure and collected in a quartz receiver in which they were diluted with carefully distilled water as required. The molar extinction coefficient over the whole wavelength range emitted by the mercury lamp was determined by measurements on such samples placed in a standard quartz cell of length 1.0 cm. From the known intensity distribution inside and outside the lamp helix, the geometry of the reaction cells and the average molar extinction coefficient, the number of ergs of light energy absorbed per  $\text{cm}^3$  per sec. could be calculated.

In each run 1.2 ml. standardised  $10^{-2}$  M hydrogen peroxide solution were placed in a quartz test-tube provided with a glass dust cover. This cell was then clamped at the desired position relative to the lamp. After suitable time intervals samples of about 0.02 ml. volume were withdrawn by a micro-pipette and transferred to a small glass absorptiometer cell containing a weighed amount of about 0.5 ml. titanous sulphate in N  $\text{H}_2\text{SO}_4$ . After reweighing, the solution was thoroughly mixed by sucking up and down several times through a dry pipette. The percentage transmission of blue light (Ilford Violet filter No. 601) permitted by the resulting yellow-coloured solution was then measured in a simple photo-electric absorptiometer. By comparison with a calibration curve the amount of hydrogen peroxide added could then readily be determined. For each run  $\log_{10} (\text{H}_2\text{O}_2)$  was plotted against time and found to give a satisfactory straight line over periods of up to 5 hr. at the higher intensities; thus confirming the apparent first order of the reaction.

Some further experiments were carried out using a 1-in-4 rotating sector driven through a gear system by an A.C. synchronous motor.

## Results

The quantum yields obtained under the two conditions of constant illumination are given in Table I. In Fig. 1 these values of the quantum yield were plotted against  $\log_{10} I_{\text{abs}} - \log_{10} (6.03 \times 10^{14})$ . The data for intermittent illumination are given in Table II.

TABLE I

Lamp Operating Conditions	Position of Reaction Cell	Molar Concentration of $\text{H}_2\text{O}_2$	Acidity	$I_{\text{abs}}$ (quanta $1. \rightarrow 1 \text{ sec.}^{-1} \times (6.03 \times 10^{14})^{-1}$ )	Quantum Yields (mol. $\text{H}_2\text{O}_2$ decomposed/quantum)
	cm. from helix				
D.C. 3 mA	80	0.034	none added	4.4	48.4
" "	40	"	"	$2.4 \times 10^1$	20.7
" "	80	0.01	"	1.27	33.6
" "	40	"	"	7.06	8.94
" "	20	"	"	$2.47 \times 10^1$	5.11
" "	11	"	pH 3.5	$6.05 \times 10^1$	3.53
" "	10	"	none added	$7.9 \times 10^1$	3.38
" "	5	"	"	$2.12 \times 10^2$	1.57
" "	5	"	pH 3.1	"	1.78
A.C. 25 mA	20	"	" 3.5	$2.63 \times 10^2$	1.26
" "	11	"	" 1.0	$5.65 \times 10^2$	1.46
" "	10	"	" "	$7.8 \times 10^2$	1.20
" "	5	"	" "	$2.12 \times 10^3$	1.15
" "	5	"	" 3.5	"	1.40
D.C. 3 mA	inside helix	"	" 3.1	$5.63 \times 10^3$	1.56
" "	"	"	none added	"	1.48
A.C. 25 mA	"	"	pH 3.5	$5.8 \times 10^4$	1.49
" "	"	"	" 1.0	"	1.37

TABLE II

$[H_2O_2] = 0.01$  M; pH = 5; cell at 20 cm. from lamp running at 3 mA on D.C.  $I_{abs}$  for continuous illumination at this distance =  $24.7$  (quanta  $l.^{-1} sec.^{-1} \times (6.03 \times 10^{14})$ ) and quantum yield under these conditions =  $5.11$ . Interpolated values of  $\gamma$  at 0.25 this value of  $I_{abs} = 9.7$ : 1 in 4 sector used throughout.

Sector speed rev. sec. $^{-1}$	0.043	0.475	0.52	21	38	$\sim 100$
$\log_{10}$ (time of 1 rev.)	1.3665	0.3233	0.284	$\bar{2}.677$	$\bar{2}.42$	$\sim \bar{2}.0$
Quantum yield ( $\gamma$ )	7.89	7.51	7.89	9.0	9.4	9.0

### Discussion

Table I and Fig. 1 show clearly that for 0.01 M  $H_2O_2$  solutions irradiated with the unfiltered light of a gas-filled mercury-vapour lamp, the quantum yield decreases to a limiting value as the intensity is increased. This relation appears to be unaffected by the presence of added sulphuric acid within the pH range 1-6. The averaged limiting value of the quantum yield is  $1.39 \pm 0.11$ , and obtains at intensity values greater than  $2.4 \times 10^{17}$  quanta  $l.^{-1} sec.^{-1}$ . At lower intensities the quantum yield is proportional to  $I_{abs}$  as is shown by the fact that the equation of the full curve drawn in Fig. 1 is  $\gamma\sqrt{I_{abs}} = 6.12 \times 10^6$  molecules quanta $^{-1} l.^{-1} sec.^{-1}$ , and also by the sector experiments. In the latter the value of the quantum yield at high sector speeds is almost 8, i.e. 1.8 times the value of the quantum yield for continuous illumination with this incident intensity,

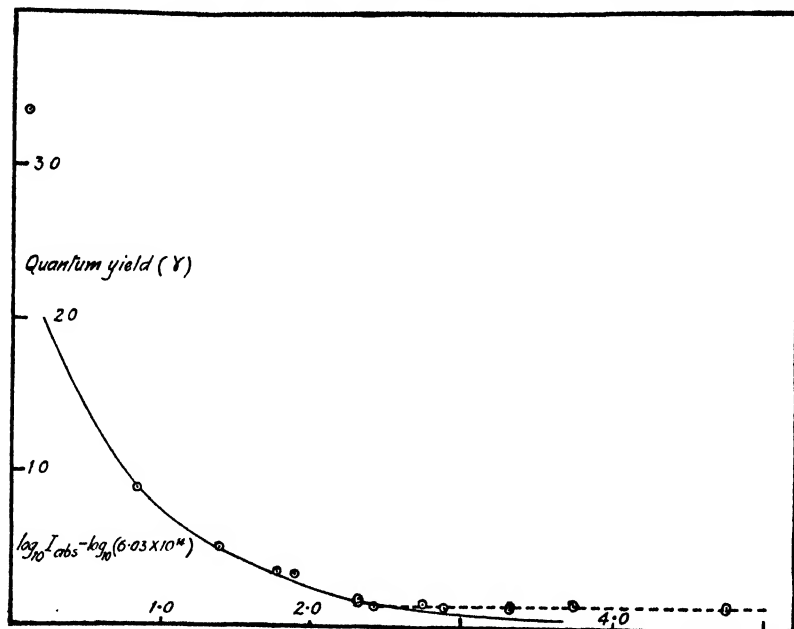


FIG. 1.

whereas a two-fold increase in quantum yield would have been expected for  $n = \frac{1}{2}$  in the expression, rate =  $k I_{abs}^n$ , using a 1-in-4 sector. That the rate depends on a power of the light intensity less than unity is substantiated by the decrease of quantum yield with falling sector speed

shown in Table II. This decrease begins at a sector revolution time of about 0.5 sec.; but it will be observed that even at the longest times employed (23 sec.) the quantum yield has not fallen to the limiting value of 5 anticipated theoretically on the basis of a  $\sqrt{I_{abs}}$  relation. This is in agreement with Allmand and Style's results at higher concentrations.

In all the experiments carried out at high intensities appreciable amounts of  $H_2O_2$  were decomposed and the concentration decreased according to a first-order law, as would be expected if rate =  $K I_{abs}$  and  $I_{abs} = k^1 I_0 [H_2O_2]$ , where  $I_0$  is the incident light intensity. At low intensities the data for the decay of  $[H_2O_2]$  fit an order 1.5 better than unity. This suggests that the expression for the rate in this region is  $K(I_{abs})^{1/2} [H_2O_2]$ . In agreement with this, the quantum yields appropriate to 0.034 M  $H_2O_2$  are respectively 4.0 and 3.85 times the values at the lower concentrations for the same value of  $I_{abs}$ .

The conclusions to be drawn from these experiments are as follows.

(a) Aqueous solutions of hydrogen peroxide of 0.01 M concentration undergo photolysis by a chain mechanism provided the intensity of light absorbed is less than  $\sim 10^{17}$  quanta  $l^{-1}$  sec.<sup>-1</sup>. Under these conditions the rate is found to be proportional to  $I_{abs}^{1/2} [H_2O_2]$  in accordance with the results of previous workers and the Haber-Weiss mechanism.

(b) At intensities greater than  $\sim 3 \times 10^{17}$  quanta  $l^{-1}$  sec.<sup>-1</sup> the rate is proportional to  $I_{abs}$  only and the reaction is no longer a chain reaction. The limiting value of the quantum yield under these conditions is  $1.39 \pm 0.11$ , i.e. greater than unity, and therefore excludes the possibility that either reaction (4a) or (4b), followed by  $O \rightarrow \frac{1}{2}O_2$ , is occurring. It follows that some  $HO_2$  radicals are formed, presumably by reaction (2), and that some if not all the radicals are removed by reaction (5) or (6).

The results do not exclude the possibility that the quantum yield of the primary act (=  $k_1$ ) is less than unity and hence that (4b) is not occurring at all.

(c) The fact that the values of the quantum yield appear to be independent of pH suggests that the various reactions take place as written in (1), (2), and (3), and do not involve  $HO_2^-$  or  $O_2^-$  ions, the concentration of which must have been very different in those experiments carried out in the presence of sulphuric acid from those with no added acid present.

*Physical Chemistry Laboratory,  
The University,  
Cambridge.*

## THE THERMAL DECOMPOSITION OF EXPLOSIVES

### PART II. CYCLOTRIMETHYLENETRINITRAMINE AND CYCLOTETRAMETHYLENETETRANITRAMINE

BY A. J. B. ROBERTSON

*Received 20th May, 1948*

The decomposition of both liquid cyclotrimethylenetrinitramine (cyclonite) and cyclotetramethylenetetranitramine follows the unimolecular equation, the Arrhenius frequency factors being very large. The unimolecular uncatalysed decomposition of cyclonite in dilute solution in dicyclohexyl phthalate and trinitrotoluene has a frequency factor approaching the normal value. A more concentrated solution of cyclonite decomposes faster than the dilute solutions; this fact and the anomalous frequency factor for the pure liquid are explained in terms of a chain reaction of short length with a temperature dependent chain length. Analyses of the gaseous products are given, which with the kinetic data show trinitrotoluene to behave effectively as an inert solvent with respect to cyclonite.



In an enquiry into the sensitiveness of explosives to external stimuli it was considered desirable to examine the thermal decomposition of the important explosives cyclotrimethylenetrinitramine (cyclonite or hexogen) and cyclotetramethylenetetranitramine in the liquid phase.

### Experimental

The methods used for determining the decomposition rate from the pressure increase due to the gaseous products and for analysis of the gases were those described previously.<sup>1</sup>

**Decomposition of Cyclotrimethylenetrinitramine.**—This was examined above the m.p. (203° C). With quantities of material sufficiently small to avoid explosion, the thermal decomposition of cyclonite followed the unimolecular equation over the whole temperature range 213–299° C, the half-life being 410 sec. at 213° C and 0.25 sec. at 299° C. The reaction rate was the same with the sample in Pyrex glass bulbs or between copper and mica surfaces, and in the presence of air, nitrogen or hydrogen at various pressures up to atmospheric (provided the conditions used did not lead to an explosive decomposition). *In vacuo*, the substance vaporised and distilled from the hot zone before decomposing appreciably. Further recrystallisation of the material from acetone was without effect on the rate. This was also independent of mass at the lower temperatures when quantities from 4–45 mg. were used. At the higher temperatures only a few mg. were used to avoid explosions. From the pressure-time curves unimolecular constants ( $k$ ) were derived as described before<sup>1</sup> and on plotting  $\log_{10} (k \times 10^3)$  against  $1/T$  the points shown in Fig. 1 were obtained.

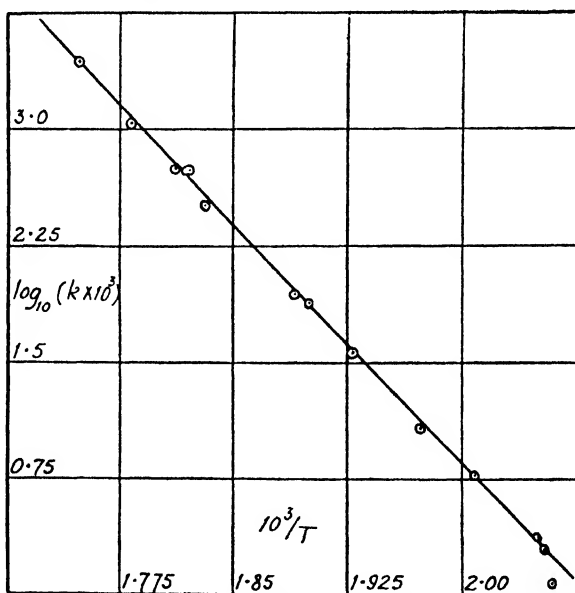


FIG. 1.—Decomposition of cyclonite.

A straight line fitted to the points by the method of least squares gave for the unimolecular constant the expression

$$k \text{ (sec.}^{-1}\text{)} = 10^{18.5} e^{-47.5 \text{ kcal./RT.}}$$

It is necessary to consider whether the high value of the frequency factor could be due to self-heating. The independence of rate and mass at the lower temperatures, with the identity of rate at different inert gas pressures, shows self-heating not to be significant. At the higher temperatures these tests fail as explosion then occurs with larger quantities and at higher gas pressures, but the absence of explosion with a few mg. of material at 10 cm. gas pressure gives

<sup>1</sup> Robertson, *Trans. Faraday Soc.* 1948, **44**, 677.

some indication. It follows from the thermal explosion theories of Semenov<sup>2</sup> and Frank-Kamenetsky<sup>3</sup> that when self-heating becomes of the order  $RT^2/E$ , where  $E$  is the activation energy of the reaction and  $T^\circ$  K the temperature of the vessel, a stable decomposition is no longer possible and explosion ensues. In the glass bulbs the very thin layers of cyclonite could be decomposed at  $312^\circ\text{C}$  without explosion, the reaction rate being somewhat too great to determine with accuracy. The degree of self-heating at this temperature should therefore be less than  $RT^2/E$  or  $14^\circ\text{C}$ . Self-heating should not therefore raise the temperature at  $299^\circ\text{C}$  by more than a few degrees. With these considerations the error in  $E$  in the above equation was estimated as 2000 cal./mole.

**Reaction Products.**—Analyses were made of the gases evolved from cyclonite at  $225$  and  $267^\circ\text{C}$ , nitrogen being initially present at 6 cm. pressure to reduce vaporisation. The results expressed as moles of product from one mole of cyclonite are shown in Table I. A considerable solid residue was also obtained. Considerable quantities of formaldehyde and water were also noted. The composition of the products is slightly dependent on temperature. The production of formaldehyde and nitrous oxide suggests the primary step in the decomposition to be the transfer of an oxygen atom from an  $-\text{NO}_2$  group to a neighbouring  $-\text{CH}_2-$  group, possibly through a transient oxiazol structure,  $\cdot\text{CH}_2\cdot\text{O}\cdot\text{NO}\cdot\text{N}\cdot\text{CH}_2\cdot$ . The radical remaining after elimination of  $\text{HCHO}$  could give both nitrous and nitric oxide by direct elimination, or further oxidation of the other neighbouring methylene group to formaldehyde by the  $-\text{NNO}$  residue at the end of the chain could lead to the elimination of nitrogen. Further

TABLE I.—DECOMPOSITION PRODUCTS OF CYCLONITE

Temp.	NO	N <sub>2</sub> O	N <sub>2</sub>	H <sub>2</sub>	CO	CO <sub>2</sub>
225° C	0.54	0.98	1.16	0.09	0.40	0.48
267° C	0.75	0.76	1.03	0.06	0.29	0.44

steps of this kind could occur in the remaining residue accompanied by the formation of complex condensation products.

**Decomposition of Cyclotrimethylenetrinitramine in Dicyclohexyl Phthalate Solution.**—To investigate further the origin of the very large frequency factor for cyclonite the decomposition in dilute solution was examined. Solutions containing 2 and 5 % of cyclonite in dicyclohexyl phthalate were prepared at  $150^\circ\text{C}$  and a 20 % solution at  $190^\circ\text{C}$ , the mixtures being subsequently handled as a solid. Visual observation showed the complete solution of the cyclonite. About 1 min. was required for preparing the solutions, the extent of decomposition during this time being negligible. To prevent distillation of the solvent during the decomposition experiments nitrogen was present, usually at 10 cm. pressure.

The pressure-time curves for the 2 and 5 % solutions followed the unimolecular equation closely above  $250^\circ\text{C}$  apart from an initial complication due to the 10 sec. or so required for thermal equilibrium to be attained with the large quantity (about 30 mg.) of solvent present, and by a pressure rise due to vaporisation of part of the solvent. In view of these effects any slight autocatalysis at the start of the decomposition would not have been detected in the higher temperature experiments. Below about  $250^\circ\text{C}$  some autocatalysis became observable from an initial linear portion of the pressure-time curve, the effect becoming more noticeable at lower temperatures until at  $200^\circ\text{C}$  the linear relation persisted while the pressure of products rose to half its final value, the curve then following a first-order equation. In order to justify the derivation of rate constants from the pressure-time curves it was necessary to verify that their shape was not appreciably influenced by supersaturation of gaseous products in the solvent. The pressure-time curves were the same for 2 % and 5 % solutions at gas pressures from 10 to 40 cm. except at the highest temperatures ( $280$ – $290^\circ\text{C}$ ) when the unimolecular constant was about 25 % greater at 40 cm. pressure than at 10 cm. pressure. An opposite effect would be expected if much supersaturation occurs; the increased rate was considered to be due to increased

<sup>2</sup> Semenov, *Chemical Kinetics and Chain Reactions* (Oxford, 1935), chap. 17.

<sup>3</sup> Frank-Kamenetsky, *J. Physic. Chem. U.S.S.R.*, 1939, **13**, 738; *Acta Physico-chim.*, 1939, **10**, 365.

self-heating arising from a less vigorous stirring and dispersive action of the bubbles of gaseous decomposition products at the higher inert gas pressures.<sup>1</sup> These observations together with the vigorous bubbling observed and the absence of the deviations in the pressure-time curve to be expected to arise in case of supersaturation according to Pedersen<sup>4</sup> were taken as indicating this not to be occurring to a significant extent. Unimolecular constants were derived from those pressure-time curves which followed the unimolecular equation throughout with Guggenheim's equation.<sup>5</sup> Where an initial linear portion of the curve was observed the slope of this with the final pressure rise gave the unimolecular constant for the initial decomposition before the accumulation of autocatalyst.

The temperature variation of the decomposition rate in the ester is shown in Fig. 2. At the highest temperatures the unimolecular constants are rather less than is to be expected from the other results. The reaction may be sufficiently rapid (the half-lives being only a few seconds) to make the rate of disengagement of gas from the solvent an appreciable factor. These high temperature points were therefore disregarded in drawing the straight line shown, which gave for the decomposition rate of cyclonite in 5 % ester solution over the temperature range 201-280° C the expression

$$k \text{ (sec.}^{-1}\text{)} = 10^{15.46} e^{-41 \text{ kcal./RT}}.$$

This expression also represented the decomposition rate in 2 % solution. The decomposition rate in solution is therefore less than that of the pure liquid, the difference increasing with temperature.

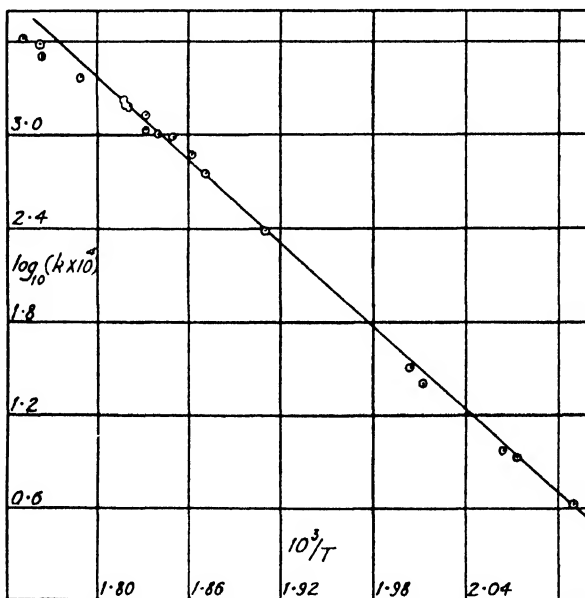


FIG. 2.—Decomposition of cyclonite in dicyclohexyl phthalate.

**Decomposition in 20 % Solution.**—The diminution of the decomposition rate of cyclonite in dilute solution suggests that a chain reaction of very short length may be involved in the pure liquid-phase reaction, the development of which is impeded by the presence of solvent. In this case more concentrated solutions of the explosive should decompose more rapidly than weaker solutions. The decomposition of a 20 % solution was therefore investigated at 273° C, this temperature being below that at which disengagement of gas may be an interfering factor, but sufficiently high for the difference between the decomposition rate of the pure explosive and the dilute solutions to be readily measur-

<sup>4</sup> Pedersen, *J. Amer. Chem. Soc.*, 1927, **49**, 2681.

<sup>5</sup> Guggenheim, *Phil. Mag.*, 1926, **2**, 538.

able (the rates differ by a factor of 3). The decomposition of the 20 % solution followed the unimolecular equation with  $k = 0.164 \text{ sec}^{-1}$ , which is some 30 % above the value for 2 and 5 % solutions at this temperature. An increase of this order is in agreement with theoretical expectations as mentioned later.

**Autocatalysis.**—The formation of a relatively stable catalytic substance by the decomposition of cyclonite in the ester at the lower temperatures was demonstrated by using the liquid remaining from a 5 % solution decomposed at  $224^\circ \text{C}$  for 40 min. as the solvent for a new 5 % solution. The new initial rate for the decomposition at  $224^\circ \text{C}$ . was then nearly equal to the final catalysed rate for the first experiment, but autocatalysis was less marked in the second experiment. The thermal stability of the catalyst is clearly considerably greater than that of cyclonite. Further recrystallisation of the solvent had no effect on the extent of autocatalysis.

**Gaseous Products.**—The products from the 5 % solution at  $225^\circ \text{C}$  are shown in Table II as moles of product from 1 mole of cyclonite. Nitrogen at 6 cm. pressure was used to prevent distillation of the mixture from the hot bulb. The residual ester was brown and showed a m.p. depression of  $4.7^\circ \text{C}$ .

TABLE II.—DECOMPOSITION PRODUCTS OF CYCLONITE IN ESTER SOLUTION

NO	N <sub>2</sub> O	N <sub>2</sub>	H <sub>2</sub>	CO	CO <sub>2</sub>
0.15	1.13	0.89	0.05	0.16	0.35

The reaction in solution leads to more N<sub>2</sub>O and less NO and N<sub>2</sub> as compared with the pure liquid. This is consistent with the intermediate oxidiazol hypothesis already mentioned rather than a scheme involving the breaking of the C—NNO<sub>2</sub> bond as the first step, when the NNO<sub>2</sub> radicals in solution might be expected to rearrange to give two NO molecules.

**Decomposition of Cyclotrimethylenetrinitramine in Trinitrotoluene Solution.**—1 % and 5 % solutions of cyclonite in T.N.T. were prepared at about  $150^\circ \text{C}$ . The T.N.T. was found to behave effectively as an inert

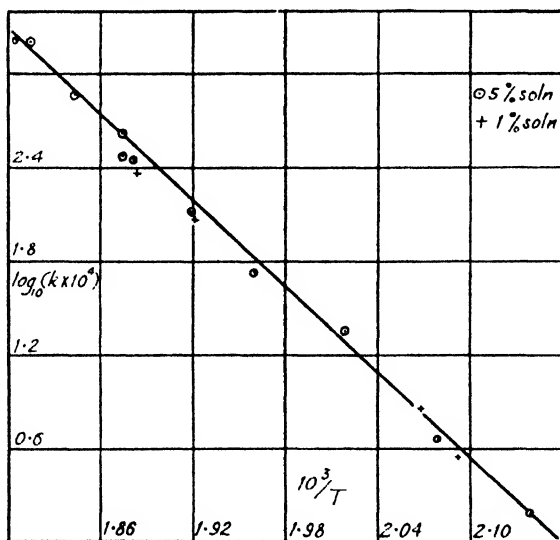


FIG. 3.—Decomposition of cyclonite in T.N.T.

solvent for the cyclonite up to the highest temperatures used ( $281^\circ \text{C}$ ). This observation is in conformity with earlier work of Farmer<sup>6</sup> and Hinshelwood,<sup>7</sup> who studied the decomposition of tetryl in T.N.T. as a solvent at much lower

<sup>6</sup> Farmer, *J. Chem. Soc.*, 1920, 117, 1603.

<sup>7</sup> Hinshelwood, *ibid.*, 1921, 119, 721.

temperatures. The cyclonite decomposition was examined in the presence of nitrogen, usually at 10 cm. pressure up to 250° C, and at 20-40 cm. pressure up to 281° C, to prevent boiling of the T.N.T. (at 10 cm. T.N.T. boils at 267°C).<sup>8</sup> Similar pressure-time curves were obtained with the 1 % and 5 % solutions and with inert gas pressures from 10 to 40 cm. The shape of the curves closely resembled those obtained in the ester solution; the initial linear portion persisted for about half the decomposition at 200° C, and became less marked with increasing temperature, until above about 250° C no deviation from the unimolecular equation was detectable. After the cyclonite decomposition the pressure continued to increase slowly as the T.N.T. underwent its usual autocatalytic decomposition.<sup>8</sup> The change in the pressure-time curves from the cyclonite to the T.N.T. decomposition was sufficiently well defined to enable the pressure change due to the cyclonite decomposition to be determined to within 5-10 %. The initial reaction rate constant was determined as before. The temperature variation of  $k$  over the range 194.5-281° C is shown in Fig. 3 and is given by the expression

$$k \text{ (sec.}^{-1}\text{)} = 10^{15.55} e^{-41.5 \text{ kcal./RT}}$$

The decomposition rate of cyclonite in T.N.T. solution is again less than that of the pure liquid to an extent dependent on temperature, and in the temperature range examined it is slightly less than that in the ester solution.

**Gaseous Products.**—Analyses were carried out with 5 % solutions at 220° C with 16 cm. nitrogen initially present and at 264° C with 20 cm. nitrogen. The results are given in Table III as moles of product from 1 mole of cyclonite.

TABLE III.—DECOMPOSITION PRODUCTS OF CYCLONITE IN T.N.T. SOLUTION

Temp.	NO	N <sub>2</sub> O	N <sub>2</sub>	H <sub>2</sub>	CO	CO <sub>2</sub>
220° C.	0.70	0.63	1.65	0.20	0.57	0.83
264° C.	1.02	0.47	1.33	0.30	0.32	0.85

The variation with temperature of the relative quantities of the various products is very similar to that observed with cyclonite alone (Table I). At both temperatures rather more nitrogen and carbon appears in the gas phase as the products mentioned from the decomposition in T.N.T. There is probably some slight decomposition of the T.N.T. induced by the cyclonite. At 225° C the residual T.N.T. had a light brown colour and its m.p. had been depressed ½-1° C. At 264° C more interaction occurred as the residual T.N.T. had a dark red colour and drops of a red liquid could also be seen.

**Decomposition of Cyclotetramethylenetetranitramine.**—The decomposition was examined in glass bulbs with 5 cm. air or hydrogen present to prevent vaporisation and distillation of the explosive, and in the copper ovens

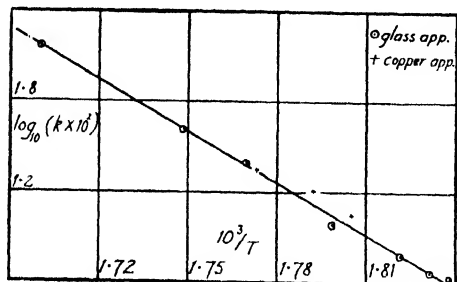


FIG. 4.—Decomposition of cyclotetramethylenetetranitramine.

apparatus<sup>1</sup> with air present at atmospheric pressure. *In vacuo*, the substance readily vaporised and condensed on the cooler parts of the apparatus without undergoing appreciable decomposition. Above 280° C the explosive melted rapidly, the liquid decomposition following the unimolecular equation. In experiments at 271, 273 and 276° C a time of 20-50 sec. elapsed before complete liquefaction during which an accelerative reaction much slower than the ensuing first-order reaction was observed. It seems possible that some preliminary decomposition occurs lowering the melting-point. The half-life for the liquid phase decomposition was 16 sec. at 271° C and 0.45 sec. at 314° C. The temperature variation of the unimolecular constant  $k$  is shown in Fig. 4 and was represented by the expression

$$k \text{ (sec.}^{-1}\text{)} = 10^{19.7} e^{-52.7 \text{ kcal./RT}}$$

<sup>8</sup> Robertson, *Trans. Faraday Soc.* (in press).

The frequency factor is even greater than that for cyclonite. No effect of mass was observed on varying the quantity used from 1-7 mg. A non-explosive decomposition was obtained with 2.3 mg. at 337° C, the rate being too rapid to determine accurately. The error in  $E$  in the equation above was estimated as 2,000 cal./mole.

Addition of 24 % of cyclotetramethylenetetranitramine to cyclonite made no difference to the decomposition rate of the latter in the temperature range 241-251° C, the mixture decomposing as one substance at the normal rate for cyclonite.

**Reaction Products.**—From the liquid explosive decomposed at 280° C. for 2 min. the products shown in Table IV were obtained (moles per mole explosive).

TABLE IV.—DECOMPOSITION PRODUCTS OF  
CYCLOTETRAMETHYLENETETRANITRAMINE

NO	N <sub>2</sub> O	N <sub>2</sub>	CO	CO <sub>2</sub>
0.95	1.51	1.16	0.57	0.64

Formaldehyde and water were also formed. The products are similar to those from cyclonite, and a similar decomposition mechanism may be postulated.

### Discussion

Both the cyclic nitroamines examined undergo a liquid-phase decomposition which proceeds in accordance with the unimolecular equation, and in the case of cyclonite the independence of decomposition rate with concentration in the 1-5 % range shows the true unimolecular character of the reaction. For both explosives the decomposition rate can be expressed by an Arrhenius equation  $Ae^{-E/RT}$  with an extremely large value for the frequency factor. In the case of cyclonite, however, a significant diminution in the frequency factor towards the normal value is observed for the decomposition in dilute solution in two solvents of different chemical type. At the melting point of cyclonite the decomposition rate of the pure liquid is only slightly greater than that of the dilute solutions, but as the temperature is raised the difference between the two becomes steadily greater. At a temperature where the difference is considerable there is also a significantly faster rate of decomposition of cyclonite in 20 % solution in dicyclohexyl phthalate as compared with 5 % solution.

The kinetic expressions for the decomposition of cyclonite in T.N.T. and the ester could be subject to experimental errors arising from autocatalysis and self-heating. Autocatalysis in solution is less marked at the higher temperatures used and is not detectable above 250° C for experimental reasons. Since in deriving the Arrhenius equations initial rates not influenced by autocatalysis were determined at the lower temperatures, and unimolecular constants possibly slightly increased by autocatalysis at the higher temperatures, any errors in the temperature coefficient from this cause would increase both  $A$  and  $E$  above the true values for the intrinsic decomposition: making the most unfavourable assumptions a possible error from autocatalysis of 2,000 cal./mole in  $E$  was estimated, corresponding to a variation in  $A$  of about 10 times. Any errors due to self-heating also tend to increase both  $A$  and  $E$  since the effect is more marked at higher temperatures. It may be noted from theoretical considerations that self-heating is not necessarily diminished by dilution of the explosive with inert material. For infinite slabs, spheres and cylinders of liquid in which an exothermic reaction is taking place with a heat of reaction  $q$  per unit volume, the amount by which the

temperature in the centre of the material exceeds that of the boundaries ( $T^\circ$  K) increases with increase of a non-dimensional parameter<sup>3</sup>  $d^2(q/K) Ae^{-E/RT} / E/RT^2$  where  $d$  measures the size of the material (it is half the thickness of the slab or the radius of the cylinder or sphere) and  $K$  is a quantity defined in the same way as thermal conductivity, but which may be numerically increased to allow for forced convection. For a sphere, dilution of the explosive to  $n$  times its original volume diminishes  $q$  by  $n$  times (for the same reaction rate) and increases  $d^2$  by  $n^{2/3}$  times, so that if  $K$  remains the same self-heating is diminished. For a cylinder,  $q$  is diminished  $n$  times and  $d^2$  increased  $n$  times, so for constant  $K$  self-heating is unchanged. For an infinite slab self-heating is increased by dilution. Actually it is probable that  $K$  is decreased by dilution on account of the less vigorous stirring by the bubbles of gaseous products, and self-heating of a thin-layer of explosive at the bottom of the bulb may well be increased by dilution. The independence of rate with concentration variations of 1.5 % does not necessarily indicate absence of self-heating, and it is therefore important to make observations at different gas pressures.

Taking these points into consideration it was concluded that the values of  $E$  for the reaction in solution were probably not in error by more than 2,000 cal./mole and the most likely errors would increase both  $A$  and  $E$ . The different kinetic expressions for the decomposition of cyclonite in dilute solution and in the condensed liquid phase were considered to have a sufficiently sound experimental basis to justify theoretical discussion.

The increased decomposition rate of pure liquid cyclonite as compared with the solutions suggests that short chain reactions are involved in the pure liquid. If the probability of one decomposing molecule directly inducing the decomposition of a neighbouring molecule is  $p$ , each act of primary activation leads to the decomposition of  $(1 - p)^{-1}$  molecules. As the explosive molecules are separated by inert solvent the chain development is increasingly inhibited. If the assumption is made that the true decomposition rate of cyclonite uncomplicated by chain reactions is given by the experiments in dilute dicyclohexyl phthalate solution,  $p$  can be evaluated. Thus at  $205^\circ\text{C}$ ,  $k$  for pure cyclonite is  $0.00076 \text{ sec.}^{-1}$  compared with  $0.00058$  for the solution, whence  $0.00076/0.00058 = (1 - p)^{-1}$  and  $p = 0.236$ . At  $273^\circ\text{C}$  the values of  $k$  are  $0.37$  and  $0.125$ , whence  $p$  is  $0.662$ . Thus in a range of temperature so great that the decomposition rate of cyclonite varies by 640 times, a variation of  $p$  by less than 3 times suffices to increase the Arrhenius frequency factor by some 1000 times.

The simplest way of estimating the chain length in solution is to multiply  $p$  by the molar fraction  $M$  of cyclonite present in solution, each act of activation leading to the decomposition of  $(1 - Mp)^{-1}$  molecules. For 20 % solutions of cyclonite in the ester at  $273^\circ\text{C}$ ,  $M = 0.27$  and  $p = 0.662$ , whence the chain length becomes 1.22. The decomposition rate should exceed the limiting rate in very dilute solution by 22 %. By experiment, the rate was 30 % greater. The agreement seems reasonable considering the very simple nature of the calculation. These arguments would also predict the rate in 5 % solution to exceed that in 2 % solution by 3 %. This difference, however, would lie within the experimental error.

It follows from these views that the entropy of activation used in the activated complex theory is not extremely large for the cyclonite decomposition. This is in conformity with the views already expressed concerning the primary decomposition step, which does not involve any great disorganisation of the molecule. The transfer of an oxygen atom from a nitro group to a neighbouring methylene group can occur in six distinct ways, which might suffice to increase the frequency factor to six times the normal value: the experimental value for the dilute solutions can therefore be regarded as showing little anomaly.

The author has much pleasure in thanking Prof. E. K. Rideal for many discussions. This work forms part of a programme carried out at the Department of Colloid Science, Cambridge, jointly with the Department of Chemistry, Bristol, and the author thanks Dr. C. E. H. Bawn, Mr. L. A. Wiseman and Mr. G. K. Adams, for information on their work. This paper is published by permission of the Chief Scientist, Ministry of Supply.

*Davy-Faraday Lab.,  
Royal Institution,  
Albemarle St., W.1.*

## KINETIC STUDIES IN THE CHEMISTRY OF RUBBER AND RELATED MATERIALS

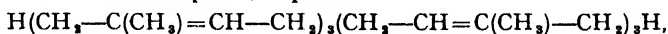
### VII. THE MECHANISM OF CHAIN PROPAGATION IN THE OXIDATION OF POLYISOPRENES

By J. L. BOLLAND AND P. TEN HAVE

*Received 24th May, 1948*

A kinetic investigation has been made of the interaction of the hexa-isoprene, squalene, with oxygen in presence of benzoyl peroxide, both in absence and presence of hydroquinone. The mechanism by which oxidation chains are propagated and terminated in these systems is identified and shown to be formally analogous to that already determined for the oxidation of mono-olefins and 1:4-dienes. The identity of the chain propagation reactions in the oxidation of polyisoprenes is discussed: the diperoxide type of primary oxidation product obtained with this class of olefin required the occurrence of a four-stage chain propagation cycle.

Recent work has established that the major primary autoxidation product of the hexa-isoprene,<sup>1</sup> squalene



and of the di-isoprene,<sup>2</sup> 2:6-dimethyl-octadiene-2:6, is in both cases a diperoxide in contrast to the mono-hydroperoxidic products formed by the autoxidation of mono-olefins and 1:4-dienes (e.g.<sup>3, 4, 5</sup>). It should be emphasised that this diperoxide is formed even in the initial stages of autoxidation and is, therefore, to be regarded as formed in the propagation steps of the oxidation chains and not as a result of secondary reactions of a mono-hydroperoxidic primary product. In this paper we choose for kinetic study two oxidation systems involving squalene which give the most direct means of comparing the chain-propagation mechanism for the polyisoprene with those of the other (mono- and 1:4-di-) olefins already examined.<sup>6, 7, 8, 9</sup> The first selected system is the benzoyl peroxide initiated oxidation of squalene, the second the same system in presence of certain phenolic antioxidants.

\* Seconded by The Netherlands Indies Government to the B.R.P.R.A.

<sup>1</sup> Bolland and Hughes, *J. Chem. Soc.* (in press).

<sup>2</sup> Bolland and Hughes, unpublished work.

<sup>3</sup> Farmer and Sundralingam, *J. Chem. Soc.*, 1942, 121.

<sup>4</sup> Farmer and Sutton, *ibid.*, 1943, 119.

<sup>5</sup> Bolland and Koch, *ibid.*, 1945, 445.

<sup>6</sup> Bolland, *Proc. Roy. Soc. A*, 1946, 186, 218.

<sup>7</sup> Bolland and Gee, *Trans. Faraday Soc.*, 1946, 42, 236.

<sup>8</sup> Bolland, *Trans. Faraday Soc.*, 1948, 43, 669.

<sup>9</sup> Bolland and ten Have, *ibid.*, 1947, 43, 201.



## Experimental

The experimental technique of oxidation rate measurement was that already described.<sup>6, 9</sup> Squalene was obtained from basking shark liver oil. After removal of saponifiable components, the oil was subjected to successive fractional molecular distillations in a still of the falling-film type.<sup>10</sup> The squalene (2 % solution in 40-60° petrol ether) was finally purified by passage through a 20 cm. alumina chromatographic column. The saturated hydrocarbon, used when required as diluent, was a normal paraffin mixture of setting point 38.9° C supplied by the Burma Oil Company.

2 : 6-dimethyl-octadiene-2 : 6, prepared by the reduction of purified geraniol with sodium in liquid ammonia, was kindly supplied by Dr. R. F. Naylor.

## I. Benzoyl Peroxide Initiated Oxidations

(a) SQUALENE.—The manner in which the rate of oxidation of squalene depends on the concentration of benzoyl peroxide [ $\text{Bz}_2\text{O}_2$ ], oxygen pressure  $p$  and squalene concentration  $[\text{RH}]$  is illustrated by Fig. 1 and 2 and Table I

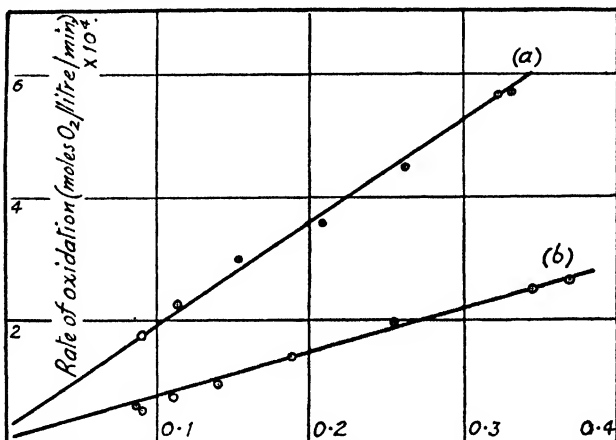


FIG. 1.—Influence of benzoyl peroxide concentration on rate of oxidation at 45° C and 100 mm Hg. oxygen pressure. (a) Squalene ; (b) 2 : 6-Dimethyl-octadiene-2 : 6.

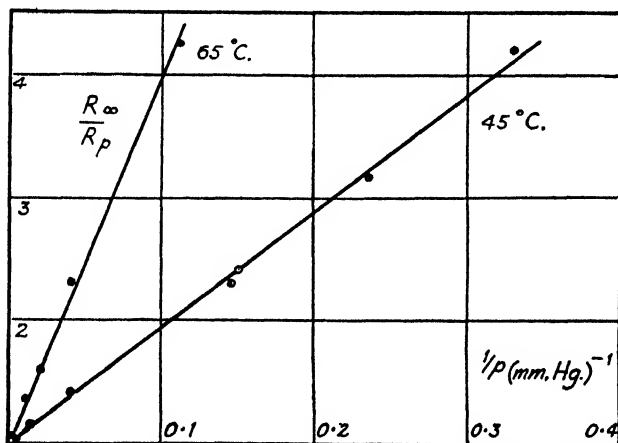


FIG. 2.—Influence of oxygen pressure on rate of oxidation ( $R_p$ ) of squalene at 45° C ( $[\text{Bz}_2\text{O}_2] = 0.0510$  moles/l.) and 65° C ( $[\text{Bz}_2\text{O}_2] = 0.0372$  moles/l.).  $R_{\infty}$  represents the rate of oxidation at infinite oxygen pressure.

<sup>10</sup> Farmer and Sutton, *J. Soc. Chem. Ind.*, 1946, **65**, 164.

respectively. From the effect of these various parameters when varied individually the oxidation rate equation in the temperature range 45-65° C approximates closely to the form :

$$\text{Rate} = c [\text{Bz}_2\text{O}_2]^{\frac{1}{2}} [\text{RH}] \frac{p}{\lambda + p} + f([\text{RH}], p) \quad (1)$$

where  $c$  and  $\lambda$  are constants and  $p$  is the oxygen pressure. The function  $f([\text{RH}], p)$ , (i.e.  $C [\text{Bz}_2\text{O}_2]$  etc.) attributable to the occurrence of oxidation chains not initiated

TABLE I.—INFLUENCE OF  $[\text{RH}]$  ON RATE OF OXIDATION AT 45° C

$p$ (mm. Hg)	$[\text{Bz}_2\text{O}_2]$ Moles/l.	$[\text{RH}]$	Rate (moles/l./min.) $\times 10^4$	Rate/ $[\text{RH}]$ * (min. <sup>-1</sup> ). $\times 10^6$
(a) Squalene 100	0.0682	12.6	4.45	3.60
		4.92	1.68	3.42
		2.05	0.70	3.41
		1.00	0.33	3.30
(b) 2 : 6-Dimethyl-octadiene-2 : 6 100	0.0642	11.2	1.94	1.73
		5.60	0.93	1.67
		3.10	0.52	1.68
		1.68	0.27	1.62
		0.98	0.170	1.73

by benzoyl peroxide, is of importance only at low  $[\text{Bz}_2\text{O}_2]$ . The values of  $c$  and  $\lambda$  required to define eqn. (1) at several temperatures are collected in Table II. The present data are incomplete in one minor respect : the dependence of  $\lambda$  on  $[\text{RH}]$  has not been determined.

(b) 2 : 6-DIMETHYL-OCTADIENE-2 : 6.—A parallel investigation of the oxidation kinetics of this di-isoprene led to precisely the same form of rate equation as (1). For example, the dependence of rate on  $[\text{Bz}_2\text{O}_2]$  and  $[\text{RH}]$  is included in Fig. 1 and Table I respectively. Experimental determinations of  $c$  and  $\lambda$  are included in Table II.

The overall energies of activation ( $E_a$ ) for the oxidation of these two hydrocarbons, based on the temperature coefficient of  $c$ , are 23.5 and 24.0 kcal./mole respectively. The temperature coefficient of  $\lambda$  corresponds to an energy term ( $E_\lambda$ ) of 12 kcal./mole in the case of squalene.

Owing to the volatility of 2 : 6-dimethyl-octadiene-2 : 6, the limiting oxygen pressure below which reliable rate measurements could be made was too high for precise values of  $\lambda$  to be obtained. No attempt has therefore been made to measure the temperature coefficient in this case, and indeed the one figure quoted (at 45° C) may be subject to ca. 30 % error.

**Comparison with Kinetics for other Olefins.**—(a) FORM OF RATE EQUATION.—Comparison of the rate equation (1) with those obtained for the benzoyl peroxide initiated oxidation of three such dissimilar olefins as ethyl linoleate,<sup>8</sup> methyl oleate<sup>11</sup> and tetralin<sup>12</sup> reveals at once that the kinetic

TABLE II

Temp. (°C)	(moles/l.) <sup>c</sup> $\frac{1}{t}$ min. <sup>-1</sup> ( $\times 10^4$ )	$\lambda$ mm. Hg
(a) Undiluted squalene		
35	0.44	3.8
45	1.47	9.6
55	4.35	—
65	13.0	30
(b) Undiluted 2 : 6-dimethyl-octadiene-2 : 6		
35	0.21	—
45	0.78	6
55	2.35	—
65	6.9	—

\*  $[\text{RH}]$  is expressed in moles isoprene residues/l.

<sup>11</sup> Bolland, Part VIII of present series.

<sup>11a</sup> Bolland, Part XI of present series.

<sup>12</sup> Bateman and Gee, *Proc. Roy. Soc. A* (in press).



and  $k_2$  are each in close accord for the polyisoprenes and the most similar type of mono-olefin. The argument that the chain carriers concerned in the oxidation of squalene and 2:6-dimethyl-octadiene-2:6 are (as for the mono-olefin) of the R— and RO<sub>2</sub>— types is therefore undoubtedly strong.

## II. Benzoyl Peroxide Initiated Oxidation of Squalene in Presence of Phenolic Inhibitors

(a) **Hydroquinone.**—A somewhat detailed examination of the kinetic characteristics of the oxidation of squalene, initiated by benzoyl peroxide, in presence of hydroquinone has been carried out in a similar manner to an earlier study of the corresponding ethyl linoleate system.<sup>9</sup> Measurements of the initial rate of oxidation  $(R_a)_0$  under a series of systematically varied conditions of benzoyl peroxide  $[Bz_2O_2]_0$ , hydroquinone  $[Hq]_0$  and squalene  $[RH]_0$  concentrations, oxygen pressure and temperature are recorded in Table III. These data may

TABLE III

$[\text{Hq}]_0$ mole per litre			$\rho$ (num)	Temp. (°C)	$(R_a)_0$ $R_u$ $K$ mole/l./min.			$t_{\frac{1}{2}}$ (min.)	$n/\alpha$
$\times 10^4$	$\times 10^3$				$\times 10^4$	$\times 10^4$			
(a) Variation of $[\text{Hq}]_0$									
0.458	7.68	12.6	100	45	0.487	5.62	0.089	25	2.5
0.783	7.29	12.6	100	45	0.309	5.50	0.100	44	2.4
0.783	7.71	12.6	100	45	0.305	5.64	0.095	40	2.3
1.85	7.06	12.6	100	45	0.121	5.40	0.097	85	2.0
1.88	8.09	12.6	100	45	0.150	5.77	0.106	80	2.1
3.77	8.55	12.6	100	45	0.074	5.90	0.100	—	—
(b) Variation of $[\text{Bz}_2\text{O}_2]_0$									
0.937	0.86	12.6	100	45	0.042	2.22	0.101	—	—
1.45	2.38	12.6	100	45	0.066	3.35	0.108	160	1.7
1.57	10.7	12.6	100	45	0.237	6.56	0.107	53	2.2
(c) Variation of $[\text{RH}]_0$									
0.95	7.20	4.80	100	45	0.090	2.07	0.095	—	—
0.80	8.05	2.65	100	45	0.061	1.20	0.090	—	—
(d) Variation of oxygen pressure									
1.65	7.52	12.6	11	45	0.108	538	0.080	90	2.4
0.80	7.52	12.6	15	45	0.218	538	0.077	40	2.3
(e) Variation of temperature									
3.57	7.14	12.6	100	52	0.240	11.7	0.078	65	2.2
3.53	8.29	12.6	100	52	0.292	12.5	0.082	60	2.3
0.353	6.22	12.6	100	38	0.151	2.38	0.119	70	2.7
0.525	6.22	12.6	100	38	0.105	2.38	0.123	—	—

be used to make four points of comparison between the effects of hydroquinone on the oxidation of squalene and ethyl linoleate respectively.

(i) **FORM OF RATE EQUATION.**—In presence of benzoyl peroxide and hydroquinone the rate of oxidation of ethyl linoleate conforms to the rate equation

$$(R_a)_0 = \text{const. } R_i \frac{[RH]_0}{[Hq]_0} \quad (4)$$

$$= K \times \frac{R_u^a}{[RH]_0[Hq]_0} \quad (5)$$

where  $R_i$  represents the rate of chain initiation (in presence of appreciable amounts of benzoyl peroxide,  $k_1$ ,  $[Bz_2O_2]_0$ ) and  $R_u$  the corresponding rate of oxidation in absence of hydroquinone:  $K$  is a constant. Application of this relation

to the data in Table III gives the values of  $K$  recorded therein. Apart from a slight dependence of  $K$  on oxygen pressure (which will, for the moment, be neglected) eqn. (5) accords well with the experimental facts. The mechanism of inhibition is thus formally analogous to that found for ethyl linoleate. The main chain-termination step may, therefore, be identified as interaction between a hydroquinone molecule and a chain carrier of the peroxide-radical type ( $Y$  in the formal scheme R1-R6), the propagation reactions remaining unchanged



(ii) EFFICIENCY OF TERMINATION REACTION,  $k_9$ .—By application of stationary state methods to the reaction scheme (R1-R3, R9) the constant  $K$  may be evaluated in terms of the individual velocity coefficients:

$$K = k_6/k_3k_9 \quad (6)$$

In comparing the values of  $K$  obtained for ethyl linoleate and squalene, the olefin concentrations are best expressed in terms of moles reactive groups/l. (assuming the number in the ethyl linoleate and squalene molecules to be one and six respectively). The values of  $K$  at 45° C are then 0.100 for squalene and (using the rates of uninhibited oxidation given ref. <sup>8</sup>) 0.032 (mole/l. min.) for ethyl linoleate. Utilising the known figures for  $k_3k_6^{-1}$ —0.0268 for squalene (cf. above) and 0.162 (mole/l. min.)<sup>-1</sup> for ethyl linoleate—it is possible to estimate from (6) the quantity  $k_9k_6^{-1}$ . For squalene at 45° C then,  $k_9k_6^{-1}$  is 373 compared with 194 (moles/l. min.)<sup>-1</sup> for ethyl linoleate. Recalling Bateman and Gee's demonstration<sup>12</sup> that  $k_6$  is very similar for ethyl linoleate and the di-isoprene 2:6-dimethyl-octadiene-2:6, the reactivity towards hydroquinone—and presumably therefore the essential chemical nature—of the peroxide radical chain carriers in the oxidation of ethyl linoleate and squalene are similar.

(iii) ACTIVATION ENERGIES.—A further—though much less sensitive—test of the quantitative correspondence between the oxidation of ethyl linoleate and squalene in presence of hydroquinone lies in the overall energy of activation ( $E_a$ ). Since

$$(R_3)_0 = R_i \frac{k_3[RH]}{k_9[Hq]},$$

$$E_a = E_i + E_3 - E_9 \quad (7)$$

where  $E_i$ ,  $E_3$  and  $E_9$  are the activation energies of the initiation process and the reactions (R3) and (R9) respectively. The experimental values of  $E_a$  are 38 and 42 kcal./mole respectively for ethyl linoleate and squalene. From the overall energies of activation of the uninhibited benzoyl peroxide initiated oxidation of these two olefins (cf. ref. <sup>8</sup> and above)

$$(E_3)_{\text{squalene}} - (E_3)_{\text{linoleate}} = 3.0 \text{ kcal./mole. Applying eqn. (7),}$$

$$(E_9)_{\text{squalene}} - (E_9)_{\text{linoleate}} = -1.0 \text{ kcal./mole.}$$

This energy difference must be regarded as not significant in view of the large activation energies on which its derivation is based.

(iv) REMOVAL OF INHIBITOR.—In the case of the oxidation of ethyl linoleate in presence of hydroquinone,<sup>9</sup> the latter was apparently removed from the system as a result of participation in reaction (R9). A method was described for estimating the ratio  $n/\alpha$  (where  $n$  is the number of oxidation chains terminated by one hydroquinone molecule and  $\alpha$  is the number of chains initiated by the decomposition of one benzoyl peroxide molecule). Application of this method to the present set of data gave the values of  $n/\alpha$  included in Table III. From their constancy over a wide range of experimental conditions, it follows that here also the major proportion of the hydroquinone is destroyed in the course of the termination reaction. The mean value of  $n/\alpha$  is ca. 2.3, in excellent agreement with the figure (2.1) obtained from the earlier data on ethyl linoleate.

(b) Other Phenolic Inhibitors.—The chain-terminating efficiencies of seven other phenolic compounds have been determined by measurements of the type reported above for hydroquinone. A systematic study of the influence of the various concentration variables was not attempted. There was, however, every indication that in each case the initial rate of oxidation was inversely proportional to the concentration of antioxidant  $[AH]_0$ . The several values of  $K$  so obtained are collected in Table IV.

The increase in antioxidant efficiency with decreasing oxidation-reduction potential observed for the members of both types of phenolic compound parallels their inhibitory effect on the oxidation of ethyl linoleate.<sup>13</sup> It is, however, noteworthy that the phenols are, on the average, some eight times more effective

<sup>13</sup> Bolland and ten Have, *Faraday Soc. Discussions*, 1947, 2, 252.

in terminating oxidation chains in squalene than in ethyl linoleate, while the corresponding ratio in the case of the hydroquinone is no more than two. The explanation of this disparity is not apparent from these preliminary measurements.

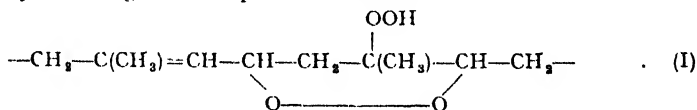
The influence of oxidation-reduction potential on inhibitor efficiency taken together with the measurements on the rate of removal of hydroquinone from the oxidising system (Table III) serves to emphasise that the terminating reactions operative in the two olefins are chemically very similar.

### Discussion

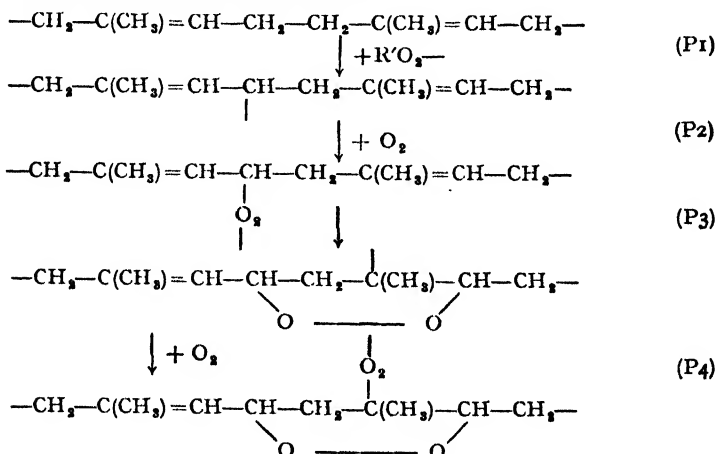
The complete identification of the main oxidation products of squalene and dihydromyrcene by standard organic chemical methods presents very real difficulties.<sup>14</sup> The application of certain analytical methods to determine the number and type of the oxygen-containing chemical groupings in the oxidised hydrocarbons and their fully hydrogenated derivatives can, however, establish all but the finer structural details of the primary oxidation product. Thus it is found<sup>1,2</sup> that in each oxidised polyisoprene molecule (a) four atoms of oxygen are present, (b) two of which form a hydroperoxide and (c) two a cyclic peroxide grouping, while (d) two oxygen atoms, one from each grouping, are attached to adjacent carbon atoms in the polyisoprene chain.

The kinetic investigations outlined in the previous two sections prove that the oxidation mechanism for polyisoprenes conform to the same formal pattern (R1-R6) as that for the various olefins and unsaturated esters which form  $\alpha$ -mono-hydroperoxides as primary oxidation products. Moreover, the very similar rates found for the respective elementary reactions involved in the oxidation of squalene and comparable mono-olefins implies that the chain carriers concerned in the oxidation of these two types of olefins are chemically very similar.

These conclusions as to the chemical nature of the primary product and the chain carriers on the one hand, and the form of the elementary reactions by which it is formed on the other are most satisfactorily reconciled by ascribing to the diperoxide the structure:

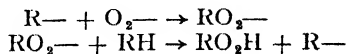


This formulation obviously embodies each of the four conclusions drawn from analytical investigation. The reasons for preferring this particular structure to others which also fulfil these same analytical requirements are detailed elsewhere.<sup>1</sup> The diperoxide is visualised as being formed by the following four-stage chain propagation cycle—



This last peroxide radical then abstracts an  $\alpha$ -methylenic hydrogen from another isoprene residue to complete the diperoxide structure (I) and reproduce the first step (P<sub>1</sub>) in the cycle.

The four-stage propagation cycle (P<sub>1</sub>-P<sub>4</sub>) will lead to kinetics indistinguishable from the two-stage propagation cycle :



appropriate to the oxidation of olefins giving mono-hydroperoxidic products only if the *intramolecular* process (P<sub>3</sub>) is much more efficient than the alternative *intermolecular* reaction involving the transfer of an  $\alpha$ -methylenic hydrogen from another olefin molecule (analogous to step (P<sub>1</sub>))—or indeed from the neighbouring  $\alpha$ -methylene groups in the same molecule. One factor which may determine which reaction will preponderate is the exothermicity of the competing processes.<sup>15</sup> In olefins containing more than one double bond, however, the relative positioning between unsaturated centres may be critical in so far as the possible formation of intramolecular cyclic products is concerned. The 1 : 5-diene structure found in polyisoprenes\* would appear to be the most favourable in this respect since reaction (P<sub>3</sub>) leads to formation of a six-membered ring. The formation of six- and five-membered cyclic products appears to be common in polyisoprenic systems; thus they appear as major products in the thermal depolymerisation of rubber<sup>17</sup> (i.e. dipentene) and its interaction with H<sub>2</sub>S<sup>18</sup> and sulphur.<sup>19</sup> In each case the most plausible mechanisms conform to the pattern suggested in the present instance: attack by the reagent at one unsaturated centre is followed by intramolecular reaction of the product so formed with the neighbouring unsaturated centre. It is not safe to conclude that the occurrence of the second intramolecular step is dictated entirely by the favourable steric conditions, until the role of the hyperconjugation effects suggested by Bateman and Jeffrey<sup>20</sup> has been more completely determined.

This work forms part of the programme of fundamental research on rubber undertaken by the Board of the British Rubber Producers' Research Association.

*The British Rubber Producers' Research Association,*  
48, 50, 52 Tewin Road,  
Welwyn Garden City,  
Herts.

\* It is unlikely that methyl substitution at the double bond will have much influence in determining the predominant mode of reaction since it is known to increase somewhat the reactivity of the unsaturated centre towards radicals attacking at both the  $\alpha$ -methylene position<sup>11</sup> and the double bond.<sup>16</sup>

<sup>16</sup> Bolland and Gee, *Trans. Faraday Soc.*, 1946, **42**, 244.

<sup>17</sup> Nozaki, *J. Polymer Sci.*, 1946, **1**, 455.

<sup>18</sup> Bolland and Orr, *Trans. Inst. Rubber Ind.*, 1946, **21**, 133.

<sup>19</sup> Naylor, *J. Polymer Sci.*, 1946, **1**, 305.

<sup>20</sup> Farmer and Shipley, *ibid.*, 1946, **1**, 293.

<sup>20</sup> Bateman, *Trans. Faraday Soc.*, 1942, **38**, 367; Bateman and Jeffrey, *Nature*, 1943, **152**, 446; Bateman and Jeffrey, *J. Chem. Soc.*, 1945, 211; Jeffrey, *Proc. Roy. Soc. A*, 1945, **183**, 388.

# STATISTICAL THERMODYNAMICS OF MIXTURES OF NORMAL PARAFFINS

By H. TOMPA

Received 28th May, 1948

Guggenheim's treatment of the statistical thermodynamics of mixtures is extended to the case of mixtures of molecules of different lengths, where all molecules are built up of identical end segments and identical middle segments. The resulting formulæ are applied to Brønsted and Koefoed's measurements on mixtures of normal paraffins.

## 1. Introduction

Brønsted and Koefoed<sup>1</sup> have published the results of an investigation in which they measured the vapour pressure of the volatile component in three binary systems of normal paraffin hydrocarbons; they found that in each case their experimental results were given with very great accuracy by expressions of the form  $\log \gamma_1 = -AN_2^2$ , where  $\gamma_1$  is the activity coefficient of the volatile component,  $A$  is a constant at a given temperature, and  $N_2$  is the mol. fraction of the non-volatile component. They also introduce the "concept of congruence," calling solutions congruent which contain the same ratio of  $\text{CH}_3$  to  $\text{CH}_2$  units, independent of how they are made up into molecules within the range considered; by using this concept they are able to derive the three constants  $A$  of the three systems considered from one general constant. All experiments were carried out at one temperature and no conclusions can be drawn therefore about the heat of mixing.

The expression given by Brønsted and Koefoed may be formally derived for a type of solution called "strictly regular" by Fowler and Guggenheim.<sup>2</sup> A solution is defined as strictly regular if the molecular volumes and free volumes of the components are roughly equal and are additive in solution; if a co-ordination number can be defined in such a way that each molecule is surrounded by the same number of molecules; if the molecules pack similarly in the pure components and can be assumed to pack in the same way in a mixture; and if interactions between molecules other than nearest neighbours can be neglected. With these assumptions an expression of the form found by Brønsted and Koefoed can be derived for the activity coefficient, provided the heat of mixing is small (or if the co-ordination number is assumed to be infinite, though co-ordination numbers larger than 12 have no physical meaning). The constant  $A$  is then proportional to the energy of interaction of unlike molecules, in excess of the mean of the energies of interaction of like molecules, and it can be shown that the entropy of mixing is equal to the ideal entropy of mixing.

It is noteworthy that this interpretation of Brønsted and Koefoed's results would predict that heat is evolved on mixing—indeed, as the activity coefficients are all less than unity, any assumption which is equivalent to taking the entropy of mixing as nearly ideal, will lead to heat evolved on mixing. This in itself is most unusual for non-polar components. A much more serious objection would be, however, the neglect

<sup>1</sup> Brønsted and Koefoed, *Kgl. Danske Vid. Selsk., Mat.-fys. Medd.*, 1946, 22, No. 17, 1.

<sup>2</sup> Fowler and Guggenheim, *Statistical Thermodynamics* (Camb. Univ. Press, 1939), p. 351.



of the influence of the different molecular sizes. Now Guggenheim<sup>3, 4</sup> has developed the statistical thermodynamics of mixtures of molecules of different sizes, whether or not the energy of interaction is zero; the assumption is made that each molecule occupies a certain number of sites on a quasi-lattice. It is easily verified that the formulæ for zero energy of interaction give values for the activity coefficients which are far below those observed by Brønsted and Koefoed (see later); the formulæ for non-zero energy of interaction are, however, not directly applicable, for the following reason: Guggenheim's formulæ are derived from a model in which the molecules of one type are built up of identical segments, and the energies of interaction are those between the different types of segments. But all normal paraffins are built up of the same segments (the units may be taken as the  $\text{CH}_2$  and  $\text{CH}_3$  groups) and the energies of interaction between different molecules should be the same as between molecules of the same kind. The most plausible way to account for a heat of mixing is to assume that there are different energies of interaction between end groups and middle groups. As the ratio of end groups to middle groups changes on mixing molecules of different lengths, there will be a finite heat of mixing. It is the purpose of this paper to derive the statistical thermodynamics of this case, and to apply the formula derived to Brønsted and Koefoed's results.

## 2. Statistical Treatment

The treatment given below follows very closely Guggenheim's method.<sup>4</sup>

Let us consider a mixture of a number of molecules of different lengths, each molecule of kind  $i$  occupying sites of a quasi-lattice; we assume that all molecules are built up of identical end segments  $e$  and identical middle segments  $m$ , so that each molecule contains two end segments  $e$  and  $(r_i - 2)$  middle segments  $m$ ; we assume the chains to be open and unbranched.

We shall use the following symbols:

$z$	co-ordination number of the lattice,
$r_i$	number of sites occupied by a molecule of kind $i$ ,
$zq_i$	number of pairs of sites in which each molecule of kind $i$ participates (other than pairs of its own consecutive segments),
$e_i$	fraction of these in which an end segment participates,
$m_i = 1 - e_i$	fraction of these in which a middle segment participates,
$n_i$	number of molecules of kind $i$ ,
$zX_{ee}, zX_{em}, zX_{mm}$	numbers of pairs of sites occupied as indicated by the subscripts,
$W_{ee}, W_{em}, W_{mm}$	energies of interaction of pairs of sites occupied as indicated by the subscripts.

We also define  $x_i, y_i, \xi_e, \xi_m, \alpha$ , by the following equations:

$$\begin{aligned}
 x_i &:= (q_i n_i) / \sum_i q_i n_i, \\
 y_i &:= (r_i n_i) / \sum_i r_i n_i, \\
 \xi_e &:= \sum_i e_i x_i, \\
 \xi_m &:= 1 - \xi_e = \sum_i m_i x_i, \\
 \alpha &= z[W_{em} - \frac{1}{2}(W_{ee} + W_{mm})]/kT.
 \end{aligned}$$

<sup>3</sup> Guggenheim, *Proc. Roy. Soc. A*, 1944, **183**, 203.

<sup>4</sup> Guggenheim, *ibid.*, 1944, **183**, 213.



where  $\rho_i$  is the number of possible configurations of a molecule, when one of its segments occupies a given site.

It can be verified fairly easily that these conditions are satisfied by an expression very similar to Guggenheim's eqn. (5.1) :<sup>4</sup>

$$\log g(n_i, \bar{X}_{em}) = \log g(n_i) + \log \frac{(z\bar{X}_{ee}^*)!}{(z\bar{X}_{ee})!} + \log \frac{(z\bar{X}_{mm}^*)!}{(z\bar{X}_{mm})!} + \log \frac{(z\bar{X}_{em}^*)!}{(z\bar{X}_{em})!} \frac{2^z \bar{X}_{em}}{2^z \bar{X}_{em}^*}. \quad (15)$$

The  $\bar{X}^*$  can be obtained from eqn. (10), (11), (12) by putting  $\kappa = 1$ . By substituting these values eqn. (15) becomes

$$\begin{aligned} \log g(n_i, \bar{X}_{em}) &= \sum_i n_i \log \rho_i - \sum_i \log n_i! - (\frac{1}{2}z - 1) \log \left( \sum_i r_i n_i \right)! \\ &+ z \log \left( \xi_e \sum_i q_i n_i \right)! + z \log \left( \xi_m \sum_i q_i n_i \right)! - \frac{1}{2}z \log \left( \xi_e \sum_i q_i n_i - \bar{X}_{em} \right) \\ &- \frac{1}{2}z \log \left( \xi_m \sum_i q_i n_i - \bar{X}_{em} \right)! - z \log \bar{X}_{em}! \quad . \quad . \quad (16) \end{aligned}$$

The free energy of the assembly is

$$F/kT = - \sum_i n_i \log f_i - \log g(n_i, \bar{X}_{em}) + \alpha \bar{X}_{em}, \quad . \quad (17)$$

where the  $f_i$ 's are the partition functions for the internal degrees of freedom of the molecules fixed to a definite set of sites, assumed separable from the configurational part and assumed to contain suitable factors to make  $W_{ee} = W_{mm} = 0$ .

The partial potentials  $\mu_i$  and the absolute activities  $\lambda_i$  are related to the free energy by the usual equations

$$\mu_i = kT \log \lambda_i = (\partial F / \partial n_i)_{T, n_j}. \quad . \quad . \quad (18)$$

Using Stirling's theorem and eqn. (10) we get from eqn. (16), (17) and (18)

$$\lambda_i = \frac{n_i}{f_i \rho_i \sum_j r_j n_j} \left( \frac{\sum_j r_j n_j}{\sum_j q_j n_j} \right)^{\frac{1}{2} z q_i} \left( \frac{1 - \kappa \xi_m}{\xi_e} \right)^{\frac{1}{2} z q_i e_i} \left( \frac{1 - \kappa \xi_e}{\xi_m} \right)^{\frac{1}{2} z q_i m_i}. \quad (19)$$

By putting  $n_i = 1$  and all other  $n_j = 0$  we obtain the absolute activity  $\lambda_i^0$  of the pure component  $i$ ;  $\xi_e$ ,  $\xi_m$  and  $\kappa$  are to be replaced by  $e_i$ ,  $m_i$  and  $\kappa_i$  respectively, where  $\kappa_i$  is the root lying between 0 and 2 of the equation

$$\kappa_i = 1 - \kappa_i^2 e_i m_i (e_i^{2/\alpha} - 1) \quad . \quad . \quad (20)$$

The ratio of the absolute activity of a component in the mixture to that of the pure component is then

$$\frac{\lambda_i}{\lambda_i^0} = y_i \left\{ \frac{x_i}{y_i} \left[ \frac{(1 - \kappa \xi_m) e_i}{(1 - \kappa_i m_i) \xi_e} \right]^{e_i} \left[ \frac{(1 - \kappa \xi_e) m_i}{(1 - \kappa_i e_i) \xi_m} \right]^{m_i} \right\}^{\frac{1}{2} z q_i}. \quad (21)$$

Putting  $\alpha = 0$ , i.e.  $\kappa = \kappa_i = 1$ , we recover Guggenheim's eqn (8.7)<sup>3</sup>

$$\frac{\lambda_i^*}{\lambda_i^0} = y_i \left\{ \frac{x_i}{y_i} \right\}^{\frac{1}{2} z q_i}, \quad . \quad . \quad (22)$$

so that eqn. (21) can be written

$$\frac{\lambda_i}{\lambda_i^0} = \frac{\lambda_i^*}{\lambda_i^0} \left\{ \left[ \frac{(1 - \kappa \xi_m) e_i}{(1 - \kappa_i m_i) \xi_e} \right]^{e_i} \left[ \frac{(1 - \kappa \xi_e) m_i}{(1 - \kappa_i e_i) \xi_m} \right]^{m_i} \right\}^{\frac{1}{2} z q_i}. \quad (23)$$

It is easier to obtain the expression for the free energy of mixing  $\Delta F$  from eqn. (23) than from eqn. (17); the result is

$$\Delta F/kT = \sum_i n_i \log (\lambda_i/\lambda_i^0) = \sum_i [\frac{1}{2}zq_i n_i \log x_i - (\frac{1}{2}zq_i - 1)n_i \log y_i] \\ + \frac{z}{2} \sum_i q_i n_i \left[ \xi_s \log \frac{1 - \kappa \xi_m}{\xi_s} + \xi_m \log \frac{1 - \kappa \xi_s}{\xi_m} - e_i \log \frac{1 - \kappa_i m_i}{e_i} \right. \\ \left. - m_i \log \frac{1 - \kappa_i e_i}{m_i} \right], \quad . \quad . \quad . \quad . \quad (24)$$

where the first sum on the right-hand side equals  $\Delta F^*/kT$ .

The energy of mixing  $\Delta E$  can be calculated from eqn. (13), substituting for  $X_{sm}$  its equilibrium value (10), and from expressions analogous to eqn. (13) for the pure components. The result is

$$\Delta E = kT\alpha \sum_i q_i m_i [\kappa \xi_s \xi_m - \kappa_i e_i m_i] \quad . \quad . \quad . \quad (25)$$

It can be verified easily that (24) and (25) satisfy the Gibbs-Helmholtz equation.

Numerical calculation of  $\lambda_i/\lambda_i^0$  from eqn. (23) for application to experimental data is tedious; it is, however, possible to obtain an expansion in powers of  $\alpha$ , valid for small values of  $\alpha$ , which are, after all, the most likely to occur in practice. We shall carry the calculation up to the quadratic term in  $\alpha$ .

We need first an expansion of  $\kappa$ . From the equation defining  $\kappa$  we obtain

$$\kappa = 1 - 2(\alpha/z)\xi_s \xi_m - 2(\alpha/z)^2 \xi_s \xi_m (\xi_s - \xi_m)^2 \quad . \quad . \quad (26)$$

and an analogous expression for  $\kappa_i$ , obtained by replacing  $\xi_s$  and  $\xi_m$  in eqn. (26) by  $e_i$  and  $m_i$  respectively. Substituting these values in eqn. (20) and expanding by the multinomial theorem, we obtain by a calculation which is rather lengthy, but not otherwise difficult,

$$\lambda_i/\lambda_i^0 = (\lambda_i^*/\lambda_i^0) \{1 + \alpha q_i (e_i - \xi_s)^2 + (\alpha^2/z) q_i (e_i - \xi_s)^2 [(\xi_s - \xi_m)^2 - 2e_i m_i \\ + (\frac{1}{2}zq_i - 1)(e_i - \xi_s)^2]\}. \quad (27)$$

If, on the other hand, a given set of experimental data is to be fitted by an equation of the form of eqn. (23), treating  $\alpha$  as an adjustable parameter, it is most convenient to calculate  $\lambda_i/\lambda_i^0$  from eqn. (27) for several trial values of  $\alpha$ , and then, if necessary, to calculate the exact values of  $\lambda_i/\lambda_i^0$  from eqn. (23) with a suitable value of  $\alpha$ ; a small final adjustment in  $\alpha$  may be made and the final value of  $\lambda_i/\lambda_i^0$  calculated, assuming its increase to be proportional to the increase in  $\alpha$  and using eqn. (28), which is derived from eqn. (23)

$$\frac{d(\lambda_i/\lambda_i^0)}{d\alpha} = \frac{\lambda_i}{\lambda_i^0} q_i \left\{ \frac{\kappa}{2 - \kappa} (e_i \xi_m + m_i \xi_s - \kappa \xi_s \xi_m) - \kappa_i e_i m_i \right\} \quad . \quad (28)$$

### 3. Application to Brønsted and Koefoed's experiments

Brønsted and Koefoed measured the vapour pressure of the volatile component—which we shall for convenience call the solvent—throughout the whole range of concentrations at 20.00° C in the three systems hexane-cetane, heptane-cetane and hexane-dodecane, all being normal paraffins, and hence calculated the activity coefficient  $\gamma_1$  of the solvent, referred to the pure solvent as standard state:  $\gamma_1 = \lambda_1/(N_1 \lambda_1^0)$ . Correction for gas imperfection was, of course, applied. Denoting the three systems by 6-16, 7-16 and 6-12, the solvent by the suffix 1 and the solute by 2, Brønsted and Koefoed found that the experimental results could be represented very accurately by the expressions

$$\begin{array}{ll} 6-16: & \log_{10} \gamma_1 = -0.0480 N_2^2 \\ 7-16: & \log_{10} \gamma_1 = -0.0400 N_2^2 \\ 6-12: & \log_{10} \gamma_1 = -0.0175 N_2^2 \end{array} \quad ,$$

Several runs were carried out on each system, the total number of points recorded in the three systems being 56, 51 and 23. To show the accuracy with which the expressions fit the experimental data, the standard deviations of the experimental values of  $\gamma_1$  from the values given by the formula were calculated; they are 0.0012, 0.0016 and 0.0027.

To see whether formulæ of the type of eqn. (20) can be found which would represent the experimental data, values of  $\gamma_1^* = \lambda_1^*/(N_1\lambda_1^0)$  were first calculated for  $z = 4$  and  $z = 8$  by eqn. (22) with the values  $r_1 = 6$ ,  $r_2 = 16$ ;  $r_1 = 7$ ,  $r_2 = 16$ ; and  $r_1 = 6$ ,  $r_2 = 12$ , at intervals of 0.2 of  $N_1$ . As these figures have some interest in themselves, they are given in Table I.

TABLE I.—CALCULATED VALUES OF  $\gamma_1^*$ 

$N_1$	0	0.2	0.4	0.6	0.8
System Z					
6-16 { 4 . .	0.7217	0.7779	0.8400	0.9058	0.9674
{ 8 . .	0.7080	0.7656	0.8299	0.8989	0.9646
7-16 { 4 . .	0.7839	0.8324	0.8834	0.9344	0.9786
{ 8 . .	0.7735	0.8234	0.8764	0.9299	0.9769
6-21 { 8 . .	0.8400	0.8793	0.9189	0.9562	0.9865
{ 8 . .	0.8299	0.8710	0.9128	0.9526	0.9852

Values of  $\gamma_1$  were then calculated with suitably chosen  $\alpha$  as described in the last paragraph of the preceding section; the final adjustment in  $\alpha$  was made by the method of least squares, so as to make the sum of the squares of the differences of  $\gamma_1$  as calculated and as given by Brønsted and Koefoed's formula at  $N_1 = 0.2, 0.4, 0.6$  and  $0.8$ , a minimum.  $N_1 = 0$  was not included as it is outside the experimental range. Table II gives the resulting values of  $\gamma_1$ , together with Brønsted and Koefoed's figures, and also the values of  $\alpha$  used.

TABLE II.—EXPERIMENTAL AND CALCULATED VALUES OF  $\gamma_1$  AND VALUES OF  $\alpha$  USED

$N_1$	0	0.2	0.4	0.6	0.8	$\alpha$
System						
6-16 { B and K .	0.8954	0.9317	0.9610	0.9825	0.9956	—
{ Z = 4 . .	0.9016	0.9321	0.9601	0.9830	0.9969	1.046
{ Z = 8 . .	0.8953	0.9296	0.9608	0.9855	0.9989	0.975
7-16 { B and K .	0.9120	0.9428	0.9674	0.9854	0.9963	—
{ Z = 4 . .	0.9186	0.9437	0.9664	0.9847	0.9964	1.041
{ Z = 8 . .	0.9149	0.9424	0.9670	0.9862	0.9975	0.991
6-12 { B and K .	0.9605	0.9745	0.9856	0.9936	0.9984	—
{ Z = 4 . .	0.9594	0.9783	0.9859	0.9945	0.9992	1.038
{ Z = 8 . .	0.9560	0.9729	0.9865	0.9958	0.9999	0.941

To bring out the agreement of the calculated values with the experimental formula even more strikingly, their differences have been plotted in Fig. 1 for  $z = 8$  and Fig. 2 for  $z = 4$ , with the experimental formulæ as datum lines; the standard deviations of the experiments from Brønsted and Koefoed's formulæ are also shown. The agreement is seen to be very satisfactory, the main discrepancy being that for  $z = 8$  the calculated values of  $\gamma_1$  approach unity too quickly with increasing  $N_1$ . As  $\alpha$  represents the same physical quantity in each of the systems, the three values for  $z = 4$  should be identical, as well as the three values at  $z = 8$ ; though

$\alpha$  for  $z = 4$  need not be the same as for  $z = 8$ . Again, the agreement is very satisfactory, especially for  $z = 4$ .

The model chosen in which all C atoms occupy points of a regular lattice

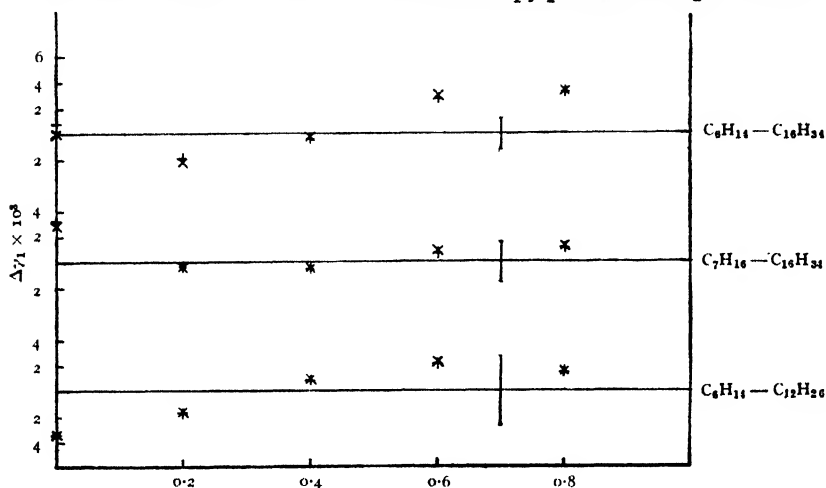


FIG. 1

× Full values of  $r$ .  
 +− Half values of  $r$ .  
 I Standard deviation of exponential.

is not quite satisfactory, since the C—C distance in a normal paraffin is 1.54 Å, but the C atoms of different molecules can hardly approach closer

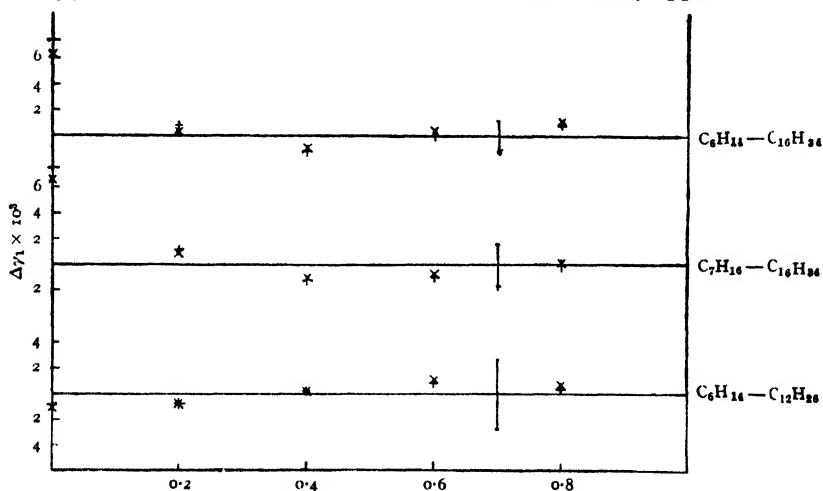


FIG. 2

× Full values of  $r$ .  
 + Half values of  $r$ .  
 I Standard deviation of exponential.

than twice that distance. It was thought therefore worth while to see whether halving all values of  $r$ , i.e. considering the systems as 3-8,  $3\frac{1}{2}$ -8 and 3-6, would give an even better fit; this is equivalent to regarding

$C_2H_6$  and  $C_2H_4$  as the fundamental units of the molecules (the value  $3\frac{1}{2}$  for  $r_1$  cannot correspond, of course, exactly to a physical picture). The calculation was carried out exactly as before; the values of  $\gamma_1^*$  are given in Table III, values of  $\gamma_1$ , together with the experimental data and the values of  $\alpha$  used, in Table IV. The differences of the calculated and

TABLE III.—CALCULATED VALUES OF  $\gamma_1^*$ 

$N_1$	0	0.2	0.4	0.6	0.8
System Z					
3-8 $\begin{cases} 4 \\ 8 \end{cases}$	$\begin{cases} 0.7399 \\ 0.7150 \end{cases}$	$\begin{cases} 0.7940 \\ 0.7720 \end{cases}$	$\begin{cases} 0.8530 \\ 0.8351 \end{cases}$	$\begin{cases} 0.9145 \\ 0.9025 \end{cases}$	$\begin{cases} 0.9709 \\ 0.9661 \end{cases}$
$3\frac{1}{2}$ -8 $\begin{cases} 4 \\ 8 \end{cases}$	$\begin{cases} 0.7979 \\ 0.7788 \end{cases}$	$\begin{cases} 0.8441 \\ 0.8279 \end{cases}$	$\begin{cases} 0.8924 \\ 0.8800 \end{cases}$	$\begin{cases} 0.9388 \\ 0.9322 \end{cases}$	$\begin{cases} 0.9807 \\ 0.9779 \end{cases}$
3-6 $\begin{cases} 4 \\ 8 \end{cases}$	$\begin{cases} 0.8530 \\ 0.8351 \end{cases}$	$\begin{cases} 0.8898 \\ 0.8752 \end{cases}$	$\begin{cases} 0.9266 \\ 0.9160 \end{cases}$	$\begin{cases} 0.9608 \\ 0.9545 \end{cases}$	$\begin{cases} 0.9880 \\ 0.9858 \end{cases}$

experimental figures are also included in Fig. 1 and Fig. 2. There is no significant difference between the results for the systems 6-16, 7-16 and 6-12 and the results for 3-8,  $3\frac{1}{2}$ -8 and 3-6.

TABLE IV.—EXPERIMENTAL AND CALCULATED VALUES OF  $\gamma_1$  AND VALUES OF  $\alpha$  USED

$N_1$	0	0.2	0.4	0.6	0.8	$\alpha$
System						
3-8 $\begin{cases} \text{B and K} \\ Z = 4 \\ Z = 8 \end{cases}$	$\begin{cases} 0.8954 \\ 0.9028 \\ 0.8962 \end{cases}$	$\begin{cases} 0.9317 \\ 0.9326 \\ 0.9298 \end{cases}$	$\begin{cases} 0.9610 \\ 0.9599 \\ 0.9607 \end{cases}$	$\begin{cases} 0.9825 \\ 0.9824 \\ 0.9853 \end{cases}$	$\begin{cases} 0.9956 \\ 0.9965 \\ 0.9989 \end{cases}$	$\begin{cases} — \\ 0.613 \\ 0.526 \end{cases}$
$3\frac{1}{2}$ -8 $\begin{cases} \text{B and K} \\ Z = 4 \\ Z = 8 \end{cases}$	$\begin{cases} 0.9120 \\ 0.9195 \\ 0.9153 \end{cases}$	$\begin{cases} 0.9428 \\ 0.9439 \\ 0.9424 \end{cases}$	$\begin{cases} 0.9674 \\ 0.9662 \\ 0.9669 \end{cases}$	$\begin{cases} 0.9854 \\ 0.9844 \\ 0.9861 \end{cases}$	$\begin{cases} 0.9963 \\ 0.9963 \\ 0.9975 \end{cases}$	$\begin{cases} — \\ 0.607 \\ 0.534 \end{cases}$
3-6 $\begin{cases} \text{B and K} \\ Z = 4 \\ Z = 8 \end{cases}$	$\begin{cases} 0.9605 \\ 0.9596 \\ 0.9561 \end{cases}$	$\begin{cases} 0.9745 \\ 0.9738 \\ 0.9728 \end{cases}$	$\begin{cases} 0.9856 \\ 0.9859 \\ 0.9864 \end{cases}$	$\begin{cases} 0.9936 \\ 0.9945 \\ 0.9957 \end{cases}$	$\begin{cases} 0.9984 \\ 0.9990 \\ 0.9998 \end{cases}$	$\begin{cases} — \\ 0.611 \\ 0.507 \end{cases}$

No matter how good the agreement between the observed and calculated values of  $\gamma_1$  is, the real test of the theory is, of course, whether the heats of mixing predicted with these values of  $\alpha$  will be experimentally

TABLE V.—CALCULATED VALUES OF HEAT OF MIXING

$Z$	6-16	3-8	7-16	$3\frac{1}{2}$ -8	6-12	3-6
System						
4	42.0	37.3	29.1	25.3	22.6	20.5
8	48.2	45.5	33.2	31.2	26.4	25.1

confirmed; this test will have to stand over until experimental data on heats of mixing are available. The calculated heats of mixing in calories, when  $\frac{1}{2}$  mol of solvent and  $\frac{1}{2}$  mol of (liquid) solute are mixed at 20.00° C to give 1 mol of solution of mol fraction  $\frac{1}{2}$ , are shown in Table V; there is a marked dependence on  $z$  and also on the absolute values of  $r$ .

It is worth while to point out that all heats are heats taken up, leading to positive deviations of  $\gamma_1$  from the athermal case and to decreasing  $\gamma_1$  with increasing temperature.

The author acknowledges his indebtedness to a remark of Prof. E. A. Guggenheim at the General Discussion of the Faraday Society in September, 1946; <sup>5</sup> his thanks are due to Dr. C. H. Bamford for clarifying discussions.

*Courtaulds, Limited,  
Research Laboratory,  
Maidenhead, Berks.*

<sup>5</sup> Guggenheim, *Trans. Faraday Soc.*, 1946, **42B**, 45.

## A NEW METHOD FOR EXTRAPOLATING DIELECTRIC POLARISATION DATA TO INFINITE DILUTION AND RECALCULATION OF THE APPARENT MOLECULAR POLARISATION AND DIPOLE MOMENT OF NITRO- BENZENE IN VARIOUS SOLVENTS

BY J. W. SMITH AND D. CLEVERDON

*Received 21st November, 1947; as revised 9th August, 1948*

It has been observed that in many cases the dielectric constants of dilute solutions of polar compounds in non-polar solvents can be represented accurately by equations of the form,  $\epsilon_{12} = \epsilon_1 + \alpha w_2 + \alpha' w_2^2$ , where  $\alpha$  and  $\alpha'$  are constants. Utilising this and the linear variation of the specific volume of the solution with  $w_2$ , a method of deducing the apparent molecular polarisation at infinite dilution, and hence for computing its apparent dipole moment, has been developed. The application of the method to existing data for dilute solutions of nitrobenzene in various solvents shows these to be more consistent with one another than is indicated by the values of  $P_2$  and  $\mu$  derived from them by the investigators, and probable values for these functions at 25° C have been deduced. For most solvents the values of  $P_{2\infty}$  lie on, or near, a straight line when plotted against  $(\epsilon_1 - 1)/(\epsilon_1 + 2)$ , but benzenoid solvents appear to be exceptional.

The values recorded in the literature for dipole moments determined through measurements on dilute solutions show in some cases wide discrepancies, even when the same solvent has been used by each of the observers concerned. This is due in part to the various methods by which the moments have been derived from polarisation data, and particularly to the extent to which allowance has been made for atomic polarisation, but apart from these factors the actual values of the total molecular polarisation at infinite dilution reported by different workers have varied considerably. This is an unsatisfactory state of affairs, especially in view of the important questions of molecular structure elucidated by the application of such data and the interest centred around the "solvent effects." Owing to this circumstance it has become usual, when studying any particular group of compounds, for an investigator to make his own measurements on all the compounds with which he is concerned, even though many of these have been studied before, so as to obtain results of a more truly comparable order.



Few attempts have been made, however, to analyse the causes of these discrepancies, or to correlate the available data so as to obtain reliable mean figures. In some cases the lack of accord is due to inaccuracy of measurement either of the dielectric constants concerned or of the densities. This seems to have arisen, particularly in earlier investigations, not only from the use of unsuitable equipment but also from a lack of appreciation of the necessity for accurate temperature control. Allowing that the measurements are reasonably exact, however, the usual method of applying them leads to considerable uncertainties. It involves calculation of the mean molecular polarisation  $P_{12}$  of the solution, which is given by

$$\frac{\epsilon_{12} - 1}{\epsilon_{12} + 2} = \frac{M_1 f_1 + M_2 f_2}{d},$$

where  $\epsilon$ ,  $d$ ,  $M$  and  $f$  denote the dielectric constant, density, molecular weight and mole fraction, respectively, whilst the subscripts 1, 2 and 12 refer to the solvent, solute and solution, respectively. By writing  $P_{12} = P_1 f_1 + P_2 f_2$  and assuming that  $P_1$  remains constant at its value for the pure solvent, values of  $P_2$  at various concentrations can be deduced.

To derive the apparent dipole moment  $\mu$ , however, it is necessary to determine the limiting value of  $P_2$ , i.e.  $P_{2\infty}$  at infinite dilution, where no dipole interaction can occur and the system more closely resembles that of gas molecules at low pressures. The difficulty in evaluating this arises from two causes. Firstly there is no knowledge of the manner in which  $P_2$  varies with  $f_2$ , and hence no theoretical basis for the extrapolation. Secondly, as it involves the difference between two terms which are nearly equal the percentage uncertainty in the value of  $P_2 f_2$  is fairly high, and increases as  $f_2$  is diminished, so the values derived for  $P_2$  at low concentrations may be subject to appreciable error. This has caused some investigators to omit measurements at very low concentrations, where they should be most valuable, owing to the inexactitude of the  $P_2$  value deduced, whilst others have, in their extrapolation, assigned too great a weight to measurements in this region, leading to incorrect drawing of the  $P_2$ - $f_2$  curve.

An alternative method has involved plotting either  $P_2 f_2$ , or  $P_{12}$ , against  $f_2$ , in which case every point has equal weight, the value of  $P_{2\infty}$  being deduced from the slope of the tangent to the curve at  $f_2 = 0$ , but this is an equally hazardous procedure.

There has always been a tendency to picture  $P_2$  as a linear function of  $f_2$ , although the examination of most data tends to suggest that  $P_2$  increases more rapidly at low concentration than would be anticipated from the linear law. On the other hand, it has been evident to most workers in this field that at low concentrations  $\epsilon_{12}$  and  $d$ , or better the specific volume ( $v_{12}$ ), are approximately linear functions of  $f_2$  or of the weight fraction ( $w_2$ ) of solute.

Hedestrand<sup>1</sup> pointed out that if  $\epsilon_{12}$  and  $d$  vary linearly with  $f_2$ , the value of  $P_{2\infty}$  can be calculated directly. Le Fèvre and Vine,<sup>2</sup> on the other hand, preferred to assume that  $\epsilon_{12}$  and  $d$  are linear functions of  $w_2$ . Perhaps the most constructive proposal, however, has been that of Halverstadt and Kumler,<sup>3</sup> who suggested that for the solutions of many compounds at low concentrations both  $\epsilon_{12}$  and  $v_{12}$  are linear functions of  $w_2$ , and that if this relationship is written in the form

$$\epsilon_{12} - \epsilon_1 = \Delta\epsilon = \alpha w_2 \text{ and } v_{12} - v_1 = \Delta v = \beta w_2,$$

then the specific polarisation of the solute at infinite dilution is given by

$$p_{2\infty} = \frac{3\alpha v_1}{(\epsilon_1 + 2)^2} + (v_1 + \beta) \cdot \frac{\epsilon_1 - 1}{\epsilon_1 + 2} \quad (1)$$

<sup>1</sup> Hedestrand, *Z. physik. Chem. B*, 1929, **2**, 428.

<sup>2</sup> Le Fèvre and Vine, *J. Chem. Soc.*, 1937, 1805.

<sup>3</sup> Halverstadt and Kumler, *J. Amer. Chem. Soc.*, 1942, **64**, 2988.

By using this relationship Halverstadt and Kumler demonstrated that several series of data, from which appreciably different values of  $P_{\infty}$  and  $\mu$  had been derived, were actually in accord with one another. The results calculated by their method were generally higher than those which had been derived by the more usual methods, and in some cases approximated to the values which had been found from measurements on the vapour. The higher values of  $P_{\infty}$  derived by this method, however, are anomalous. In many cases, as was first pointed out by Sugden,<sup>4</sup>  $P_2$  decreases with increasing solute concentration in such a manner as to be a linear function of the volume polarisation  $(\epsilon_{12} - 1)/(\epsilon_{12} + 2)$  of the solution. If these extrapolations of Halverstadt and Kumler are correct, it must be inferred that this linearity holds down to very low concentration, but that an abrupt change in  $P_2$  then occurs as  $w_2$  approaches zero. This is not very probable.

Halverstadt and Kumler's approach, however, has the advantage over the other forms of linear relationship in that when no volume change is associated with the dissolution of a liquid solute in the solvent the linear relationship between  $v_{12}$  and  $w_2$  holds strictly. In general,  $(v_1 + \beta)$  represents the partial specific volume of the solute at low concentrations, and hence linearity of  $v_{12}$  with  $w_2$  is to be expected in most cases over the concentration ranges usually employed.

The present authors consider that the anomalous  $P_{\infty}$  values found by Halverstadt and Kumler are due to the manner in which they evaluate  $\alpha$ . They assume that "with the usual methods of handling, the solutions are exposed longer to air than is the pure solvent, and consequently the solutions may absorb more water vapour than the solvent," and also that "even if rigid methods are used to exclude moisture, each  $\epsilon$  value for the different solutions depends on a single solvent measurement of  $\epsilon_1$ , and consequently the latter is much more heavily weighted than any single solution measurement of  $\epsilon$ ." Therefore they derive the dielectric constant of the pure solvent by extrapolating the  $\epsilon_{12} - w_2$  data linearly to  $w_2 = 0$ , the intercept giving the value of  $\epsilon_1$  used in deriving  $p_2$ , whilst the slope of the line gives the value of  $\alpha$ .

No exception could be taken to this method if the extrapolated values of  $\epsilon_1$  approximated to, or were within, experimental error of the observed values, but in many cases the figure obtained was far outside the limits of such error. Also, in reliable series of data the published  $\epsilon_{12}$  values are not isolated measurements but the result of several measurements on each solution. If handling of the solution is found to result in variation of the experimental figure, the handling technique is modified to eliminate such errors. Again it is customary to submit the "blank" solvent specimen to the same handling as a solution, so it is difficult to see why  $\epsilon_{12}$  values should change so considerably without variation of  $\epsilon_1$ . If the solute is hygroscopic, for instance, and causes the anomaly, the effect will vary with concentration, and the slope of the  $\epsilon_{12} - w_2$  curve will be erroneous in any case. Also, whilst it is recognised that the weakness of most methods is that undue weight is placed on the measurements on the pure solvent, it is nevertheless usual to determine  $\epsilon_{12}$  values with respect to an assumed value for  $\epsilon_1$ , and this reference point is returned to repeatedly, especially when fresh batches of solvent are used, so that it is established very accurately. Hence it seems illogical to discard completely this assumed value of  $\epsilon_1$  as a point on the  $\epsilon_{12} - w_2$  curve.

In most cases the extrapolated value of  $\epsilon_1$  obtained by Halverstadt and Kumler's method is lower than the observed value. Closer inspection of a large amount of data shows that, even at very low concentrations, the  $\epsilon_{12} - w_2$  plot is definitely curved and generally concave upwards, so the best straight line leads to a value of  $\epsilon_1$  lower than the true value.

<sup>4</sup> Sugden, *Nature*, 1934, 133, 415.

On the other hand the authors have observed that the variation of  $\epsilon_{12}$  with concentration can be represented for dilute solutions as

$$\epsilon_{12} = \epsilon_1 + \alpha w_2 + \alpha' w_2^2 \quad (2)$$

Hence  $\Delta\epsilon/w_2$  should vary linearly with  $w_2$ . With a very few exceptions which are being further studied, this relation has been found to hold to values of  $w_2$  in excess of 0.1 in the case of solutes of relatively low dielectric constant, which have low values of  $\alpha$ , whilst when  $\alpha$  is high it holds fairly well up to values of  $\Delta\epsilon$  ranging from about 0.8 to 1.0. Above these concentrations departures from linearity occur requiring extra terms, which are to be anticipated if the variation of  $\epsilon_{12}$  with  $w_2$  is of one of the forms

$$\Delta\epsilon/w_2 = 1/(A - Bw_2) \text{ or } 1/(A - Bw_2) + 1/(C + Dw_2),$$

such as are predicted by most solvent effect equations. The method of computing  $p_{2\infty}$ ,  $P_{2\infty}$  and  $\mu$  now proposed is based on the application of eqn. (2).

### The Method of Computing

Differentiation of the relation

$$p_{12} = p_1 + (p_2 - p_1)w_2 = (\epsilon_{12} - 1)v_{12}/(\epsilon_{12} + 2)$$

with respect to  $w_2$  shows that eqn. (1) will hold if  $\alpha$  and  $\beta$  are taken as the limiting values of  $\Delta\epsilon/w_2$  and  $\Delta v/w_2$  respectively at infinite dilution, i.e. at  $w_2 = 0$ , and if  $p_1$  does not change with  $w_2$ . This last limitation is also imposed on the more usual extrapolation methods of deriving  $p_{2\infty}$  and  $P_{2\infty}$ . The problem is, therefore, reduced to one of determining  $\alpha$  and  $\beta$ .

To determine the value of  $\alpha$  the method adopted is to plot  $\Delta\epsilon/w_2$  against  $w_2$  and extrapolate the values linearly to  $w_2 = 0$ , proportionately greater weight being given to the points corresponding to higher values of  $w_2$ , where the experimental accuracy in the determination of  $\Delta\epsilon/w_2$  is the greatest. In the case of precise measurements this plot shows very exactly the concentration, if any, above which departures from linearity occur, and the values for such concentrations are disregarded in making the extrapolation.

Since, in general,

$$\beta = (v_{12} - v_1)/w_2 = \Delta v/w_2,$$

one specific volume determination should suffice to evaluate  $\beta$ , but, owing to the small magnitude of  $\Delta v$  the inaccuracy in some cases may be appreciable. If a definite trend occurs in the values of  $\Delta v/w_2$  as deduced from the determinations at various concentrations, the simple relationship evidently does not hold and the same procedure has to be adopted as for deriving  $\alpha$ . Usually the values vary only slightly and in a random manner, within the limits of possible experimental error, so that a mean value can be taken such as was utilised by Halverstadt and Kumler. This may be derived by the method of least squares as  $\bar{\beta} = \Sigma w_2 \Delta v / \Sigma w_2^2$ , in which the weight put on each  $\Delta v$  value is proportional to  $w_2$ , i.e. to its probable accuracy, or more simply as  $\Sigma \Delta v / \Sigma w_2$ , which in most cases leads to values indistinguishable from those deduced by the least squares method.

Once the values of  $\alpha$  and  $\beta$  have been ascertained  $p_{2\infty}$  can be calculated directly by eqn. (1), the values of  $\epsilon_1$  and  $v_1$  used being the actual values measured or assumed for the pure solvent.

This method still involves an extrapolation to infinite dilution of values derived from measurements at various low concentrations, but it has the advantage of being a linear extrapolation, based on reasonable assumptions, of experimental data prior to combining these into polarisation terms, where the individual experimental errors become disguised. Further, it is a simple matter to determine the probable limits of error in the values of  $\Delta\epsilon/w_2$  for each measurement and therefore to determine the limits of error in  $\alpha$ .

The application of this procedure to data from various sources shows it to be a very searching method for comparing the results obtained by various investigators. In some cases it has been shown that measurements were in serious error, although this was not brought to light by the values of  $P_{12}$  or of  $P_2$  because the changes in  $\epsilon_{12}$  and  $v_{12}$ , erring in opposite senses, have compensated one another. It also permits some comparison between data for different temperatures because, although the value of  $\alpha$  changes with temperature, the  $\Delta\epsilon/w_2 - w_2$  lines for two

TABLE I

SUMMARY OF RECORDED DATA FOR THE MOLECULAR POLARISATION AND DIPOLE MOMENT OF NITROBENZENE IN SOLUTION

Solvent	Temp. °C	Observers	$P_{\infty}$ cm. <sup>3</sup>	$P_E$ cm. <sup>3</sup>	$P_{E+A}$ cm. <sup>3</sup>	$P_{\mu}$ cm. <sup>3</sup>	$\mu$ (D)
Benzene	10	Rau and Narayanaswamy <sup>5</sup>	*378.1	—	—	—	3.96
	18.5	Hassel and Uhl <sup>6</sup>	335	—	—	—	3.98
	20	Tiganik <sup>7</sup>	366	32.7	32.7	333.3	3.97
		Müller <sup>8</sup>	361	32	32	329	3.95
		Rau and Narayanaswamy <sup>5</sup>	*360.8	—	—	—	3.98
	20.7	Bergmann and others <sup>9</sup>	382	33.0	33.0	349	4.08
	22	Poltz <sup>10</sup>	358.3	30.7	35.3	323.0	3.93
	24	Lange <sup>11</sup>	—	33	—	—	3.84
	25	Williams and Schwingel <sup>12</sup>	348	33	33	315	3.90
		Le Fèvre and Russell <sup>13</sup>	*371.7	32.7	32.7	339.0	4.05
			347	32.7	32.7	314	3.90
		Le Fèvre and Le Fèvre <sup>14</sup>	*367.0	32	32	335	4.03
			360	32	32	328	4.0
		Jenkins <sup>15</sup>	353.8	32.6	32.6	321.2	3.94
		Chang <sup>16</sup>	337	33	33	304	3.83
		Nukada <sup>17</sup>	—	—	—	—	3.96
		Pal <sup>18</sup>	351	33	33	318	3.916
	27	Davis and others <sup>19</sup>	353	32.7	34.3	318.7	3.96
	30		†352	32.7	34.3	317.7	3.95
		Rau and Narayanaswamy <sup>5</sup>	*360.1	—	—	—	3.99
Toluene	40	Rau and Narayanaswamy <sup>5</sup>	*349.7	—	—	—	3.99
	18.5	Hassel and Uhl <sup>6</sup>	—	—	—	305	3.83
Naphthalene	85	Briegleb <sup>20</sup>	240	32	32	208	3.73
Cyclohexane	10	Rau and Narayanaswamy <sup>5</sup>	*395.1	—	—	—	4.06
	20	Rau and Narayanaswamy <sup>5</sup>	*385.8	—	—	—	4.07
	25	Jenkins <sup>15</sup>	369.0	32.6	32.6	327.4	3.97
	30	Rau and Narayanaswamy <sup>5</sup>	*376.3	—	—	—	4.09
	40	Rau and Narayanaswamy <sup>5</sup>	*366.1	—	—	—	4.09
Decalin	20	Müller <sup>8</sup>	381	31	31	350	—
	25	Jenkins <sup>15</sup>	352.9	32.6	32.6	320.3	3.93
n-Hexane	25	Jenkins <sup>15</sup>	372.5	32.6	32.6	339.9	4.05
"Hexane"	10	Rau and Narayanaswamy <sup>5</sup>	*399.5	—	—	—	4.08
	20	Müller <sup>8</sup>	377	32	32	345	4.05
		Rau and Narayanaswamy <sup>5</sup>	*389.8	—	—	—	4.10
	25	Williams and Ogg <sup>21</sup>	346	32	32	314	3.89
	30	Rau and Narayanaswamy <sup>5</sup>	*379.6	—	—	—	4.10
	40	Rau and Narayanaswamy <sup>5</sup>	*367.3	—	—	—	4.10

\* Derived by Hedestrand method <sup>1</sup> or modified Hedestrand method. <sup>13</sup>† Extrapolated by Hoecker's method. <sup>23</sup><sup>5</sup> Rau and Narayanaswamy, *Proc. Indian Acad. Sci. A*, 1935, **1**, 489.<sup>6</sup> Hassel and Uhl, *Z. physik. Chem. B*, 1930, **8**, 199.<sup>7</sup> Tiganik, *ibid.*, 1931, **13**, 440.<sup>8</sup> Müller, *Physik. Z.*, 1933, **34**, 700.<sup>9</sup> Bergmann, Engel and Sandor, *Z. physik. Chem. B*, 1930, **10**, 412.<sup>10</sup> Poltz, *ibid.*, 1933, **20**, 353.<sup>11</sup> Lange, *Z. Physik*, 1925, **33**, 173.<sup>12</sup> Williams and Schwingel, *J. Amer. Chem. Soc.*, 1928, **50**, 362.<sup>13</sup> Le Fèvre and Russell, *J. Chem. Soc.*, 1936, 495.<sup>14</sup> Le Fèvre and Le Fèvre, *ibid.*, 1936, 1136.<sup>15</sup> Jenkins, *ibid.*, 1934, 482.<sup>16</sup> Chang, *J. Chinese Chem. Soc.*, 1933, **1**, 107.<sup>17</sup> Nukada, *Nic. Chem.*, 1932, **5**, 41.<sup>18</sup> Pal, *Phil. Mag.*, 1930, **10**, 265.<sup>19</sup> Davis, Bridge and Svirbely, *J. Amer. Chem. Soc.*, 1943, **65**, 858.<sup>20</sup> Briegleb, *Naturwiss.*, 1934, **22**, 105.<sup>21</sup> Williams and Ogg, *J. Amer. Chem. Soc.*, 1928, **50**, 95.

TABLE I—*cont.*

Solvent	Temp. °C	Observers	$P_{\infty}$ cm. <sup>3</sup>	$P_E$ cm. <sup>3</sup>	$P_{E+A}$ cm. <sup>3</sup>	$P_{\mu}$ cm.	$\mu$ (D)
Dioxane	10	Rau and Narayanaswamy <sup>5</sup>	*366.8	—	—	—	3.90
	20	Rau and Narayanaswamy <sup>5</sup>	*358.6	—	—	—	3.91
	30	Rau and Narayanaswamy <sup>5</sup>	*350.0	—	—	—	3.93
	30.1	Davis and others <sup>19</sup>	361	32.7	34.3	326.7	3.99
Heptane	40	Rau and Narayanaswamy <sup>5</sup>	*341.9	—	—	—	3.94
	40	Rau and Narayanaswamy <sup>5</sup>	*400.7	—	—	—	4.09
	20	Rau and Narayanaswamy <sup>4</sup>	*390.0	—	—	—	4.10
	30	Rau and Narayanaswamy <sup>5</sup>	*378.4	—	—	—	4.10
Carbon tetra- chloride	40	Rau and Narayanaswamy <sup>5</sup>	*366.6	—	—	—	4.10
	10	Pal <sup>18</sup>	373	33	33	340	3.92
		Rau and Narayanaswamy <sup>5</sup>	*386.1	—	—	—	4.00
	20	Müller <sup>8</sup>	362	32	32	330	—
		Pal <sup>18</sup>	359.3	33	33	329.3	3.92
		Rau and Narayanaswamy <sup>5</sup>	*375.8	—	—	—	4.02
	25	Jenkins <sup>15</sup>	353.1	32.6	32.6	320.5	3.93
	30	Pal <sup>18</sup>	350.3	33	33	317.3	3.94
		Rau and Narayanaswamy <sup>5</sup>	*305.1	—	—	—	4.02
	40	Pal	343	33	33	310	3.95
		Rau and Narayanaswamy <sup>5</sup>	*353.8	—	—	—	4.02
	50	Pal	335.3	33	33	302.3	3.96
Carbon disulphide	20	Müller <sup>8</sup>	326	31	31	295	3.74
	25	Williams and Ogg <sup>21</sup>	346	—	—	—	3.89
Ether		Jenkins <sup>15</sup>	310.0	32.6	32.6	277.4	3.66
	25	Higasi <sup>22</sup>	243	32	32	211	3.2
Chloroform	18	Hassel and Uhl <sup>6</sup>	—	—	—	230.5	3.30
	25	Jenkins <sup>15</sup>	241.2	32.6	32.6	208.6	3.17
Chlorobenzene		Le Fèvre and Russell <sup>13</sup>	*225.3	33	33	192	3.05
			218	33	33	185	2.99
	18.5	Hassel and Uhl <sup>6</sup>	—	—	—	169.6	2.83
	25	Le Fèvre and Russell	*161.3	33	33	128	2.49
			158	33	33	125	2.46

temperatures only a few degrees apart will be expected to lie almost parallel with each other, since the value of  $\alpha'$  will not change very rapidly with change of temperature.

In general, however, the most striking result of the application of the method has been the degree of accord which has been observed between the results of different investigators when these are reduced to a comparable basis, even though their published values of  $\mu$  derived from them may differ quite appreciably. This gives grounds for the belief that the method will afford more truly comparable dipole moment values than have been deduced hitherto. In the present communication the method will be illustrated by published measurements on solutions of nitrobenzene in various solvents.

### Applications of Method

**Nitrobenzene.**—As nitrobenzene is a common compound with a high dipole moment, and, moreover, one in which the dipole axis of the molecule lies along the axis of maximum polarisability, it has been considered most extensively in relation to solvent effects, and measurements on its solutions in a number of solvents have been made by several investigators. Recorded data are summarised in Table I, where  $P_{\infty}$  indicates the values derived by the observers by extrapolation of the  $P_2 - f_2$  plot except where otherwise stated.  $P_E$  and  $P_{E+A}$  are the electronic and total distortion polarisations deduced or assumed by them, and  $P_{\mu}$  and  $\mu$  are the orientation polarisation and apparent dipole moment, respectively, derived from these figures. Where two methods have been used

\* Derived by Hedestrand method<sup>1</sup> or modified Hedestrand method.<sup>13</sup>

<sup>22</sup> Higasi, *Sci. Pap. Inst. Physic. Chem. Res., Japan*, 1934, **24**, 63.

<sup>23</sup> Hoecker, *J. Chem. Physics*, 1936, **4**, 431.

for interpreting the measurements the results of both are given. Some early results, such as those of Lange,<sup>11</sup> in which the value of  $P_{\infty}$  in various other solvents was virtually assumed to be the same as had been observed for solutions in benzene, have been omitted from this list. Nevertheless, there is a great variation in the results obtained by different workers using the same solvent at the same temperature; for instance, for solutions in benzene at 25° the values of  $P_{\infty}$  vary from 304 to about 340 cm.<sup>3</sup>, whilst the values of  $\mu$  reported vary from 3.82 to 4.08 D. These variations are as great as those observed on passing from one solvent to another, so it is a matter of some importance to investigate the causes of the divergences, as only when the results are reduced to a comparable basis can any true correlation of  $P_{\infty}$  or of  $\mu$  with the characteristics of the solvent be expected.

The application of the method developed in this paper to the data for benzene solutions will be considered in detail, whilst the results of similar treatment for solutions in other solvents are summarised.

**SOLUTIONS IN BENZENE.**—A plot of the recorded values of  $P_2$  against  $f_2$  shows that the early results of Williams and Schwingel are rather low, whilst those of Chang and of Wehrle are very erratic, but the figures reported by other investigators all lie on, or reasonably near to, a smooth curve. The fact that the extrapolation of this curve has led to such diverse values of  $P_2$  has arisen principally through the extrapolation being based on insufficient data to give a true indication of the trend of the  $P_2 - f_2$  curve. The collected data suggest that a better mean extrapolation would lead to a value of  $P_{\infty}$  somewhat higher than that of Jenkins but lower than the values deduced by Le Fèvre and his collaborators by the Hedestrand method.

The results of applying the method described in this paper to the more consistent series of measurements are shown in Table II, which shows the values of  $\epsilon_1$  and  $v_1$  found by the observers and the values of  $\alpha$ ,  $\alpha'$ , and  $\beta$  deduced from the experimental data for the solutions, together with the values of  $P_{\infty}$  and of  $\mu$  derived from the latter. In the calculation of  $\mu$ , the value of  $P_{E.A.}$  has

TABLE II  
SUMMARISING DATA FOR SOLUTIONS OF NITROBENZENE IN BENZENE

Temp. °C.	Observers	$\epsilon_1$	$v_1$	$\alpha$	$\alpha'$	$\beta$	$P_{\infty}$ cm. <sup>3</sup>	$\mu$ (D)
10	Rau and Narayanaswamy	2.303	1.1254	13.41	7.3	-0.304	376.6	3.951
20	Tiganik	2.2825	1.1388	14.61	6.3	-0.314	365.5	3.954
	Rau and Narayanaswamy	2.283	1.1392	14.73	6.5	-0.314	368.3	3.971
22	Poltz	2.280	1.1409	14.22	10.0	-0.307	357.8	3.920
25	Le Fèvre and Le Fèvre	2.2725	1.1445	14.22	13.7	-0.328	359.0	3.948
	Le Fèvre and Russell	2.2725	1.1445	14.05	13.8	-0.316	355.7	3.928
	Le Fèvre (combined)	2.2725	1.1445	14.30	11.3	-0.316	361.5	3.964
	Jenkins	2.2727	1.1447	14.34	8.0	-0.331	361.9	3.966
	Jenkins (combined)	2.2727	1.1447	14.32	9.0	-0.317	362.0	3.967
30	Rau and Narayanaswamy	2.263	1.1533	14.04	5.8	-0.323	359.3	3.983
	Davis and others	2.2574	1.1538	13.78	9.0	-0.327	353.8	3.949
40	Rau and Narayanaswamy	2.243	1.1678	13.37	4.7	-0.336	350.3	3.991

been assumed to be 36.2 cm.<sup>3</sup>, the value found by Groves and Sugden<sup>25</sup> for the vapour phase. Table III shows the data for the individual solutions, together with the values of  $\epsilon_{12}$  and  $v_{12}$  calculated by means of the values of  $\alpha$ ,  $\alpha'$  and  $\beta$  deduced.

Generally speaking, the apparent moments derived in this way are more consistent than the values as originally deduced, and, further, the reasons for the differences found are more readily apparent. Thus the high values obtained by Rau and Narayanaswamy, not only for benzene solutions but also for solutions in some of the other solvents, arise in part from the fact that they used the original Hedestrand method of calculation. In addition to this, however, the increase in dielectric constant found on passing from the pure solvent to the solution was, particularly at low concentrations, greater than observed elsewhere, leading to slightly high values of  $\alpha$  and low values of  $\alpha'$ .

<sup>25</sup> Jenkins and Sutton, *J. Chem. Soc.*, 1935, 609.

TABLE III

DIELECTRIC CONSTANT AND DENSITY DATA FOR SOLUTIONS OF NITROBENZENE  
IN BENZENE AT VARIOUS TEMPERATURES

$w_2 \times 10^3$	$\epsilon_{12}$ (obs.)	$v_{12}$ (obs.)	$\Delta\epsilon/w_2$	$\Delta v/w_2$	$\epsilon_{12}$ (calc.)	$v_{12}$ (calc.)
10° C (Rau and Narayanaswamy)						
4.418	2.999	1.1119	15.75	-0.305	2.998	1.1120
5.301	3.140	1.1094	15.79	-0.302	3.140	1.1093
7.235	3.456	1.1034	15.94	-0.304	3.456	1.1034
20° C (Tiganik)						
0.8366	2.4051	1.1362	14.66	-0.31	2.4051	1.1362
1.634	2.5227	1.1337	14.70	-0.31	2.5229	1.1337
3.229	2.7612	1.1286	14.82	-0.315	2.7609	1.1286
6.372	3.2385	1.1188	15.01	-0.314	3.2385	1.1188
20° C (Rau and Narayanaswamy)						
4.418	2.948	1.1254	15.01	-0.312	2.948	1.1253
5.301	3.083	1.1226	15.09	-0.313	3.083	1.1226
7.235	3.383	1.1164	15.20	-0.314	3.383	1.1165
20.7° C (Bergmann, Engel and Sandor)						
0.5748	2.3713	1.1373	15.43	-0.33	—	1.1373
0.9745	2.4325	1.1360	15.38	-0.33	—	1.1360
1.5013	2.5085	1.1343	15.07	-0.326	—	1.1343
4.3116	2.9353	1.1251	15.14	-0.327	—	1.1251
22° C (Poltz)						
1.421	2.481	1.1365	14.14	-0.31	2.484	1.1365
1.669	2.521	1.1358	14.44	-0.304	2.520	1.1358
2.042	2.574	1.1346	14.39	-0.308	2.574	1.1346
2.440	2.632	1.1334	14.44	-0.309	2.632	1.1334
2.691	2.672	1.1326	14.57	-0.310	2.670	1.1326
3.179	2.741	1.1310	14.50	-0.310	2.742	1.1311
3.269	2.756	1.1309	14.56	-0.306	2.756	1.1308
25° C (Le Fèvre and Russell)						
5.2872	3.0537	1.1278	14.78	-0.316	3.0599	1.1278
10.525	3.9011	1.1112	15.47	-0.316	3.8978	1.1112
10.635	3.9239	1.1108	15.53	-0.316	3.9234	1.1108
25° C (Le Fèvre and Le Fèvre)						
2.516	2.6390	1.1357	14.56	-0.34	2.6395	1.1363
3.198	2.7411	1.1344	14.65	-0.316	2.7411	1.1344
3.628	2.8067	1.1325	14.72	-0.331	2.8062	1.1330
25° C (Jenkins)						
2.396	2.6224	1.1366	14.60	-0.336	2.6208	1.1367
2.634	2.6559	1.1357	14.54	-0.341	2.6559	1.1360
3.535	2.7894	1.1330	14.62	-0.334	2.7895	1.1330
4.510	2.9356	1.1299	14.70	-0.328	2.9357	1.1298
5.409	3.0717	1.1271	14.77	-0.325	3.0716	1.1268
25° C (Jenkins and Sutton)						
8.772	3.597	1.1168	15.10	-0.318	3.598	1.1169
10.81	3.928	1.1101	15.30	-0.320	3.926	1.1104
13.20	4.326	1.1028	15.55	-0.317	4.320	1.1027
14.19	4.490	1.0999	15.63	-0.316	4.487	1.0997
18.29	5.224	1.0868	16.14	-0.316	—	1.0868
24.33	6.372	1.0678	16.85	-0.316	—	1.0676
29.25	7.373	1.0524	17.44	-0.315	—	1.0520
30.79	7.704	1.0477	17.64	-0.311	—	1.0462

TABLE III—*cont.*

$w_2 \times 10^3$	$\epsilon_{12}$ (obs.)	$v_{12}$ (obs.)	$\Delta\epsilon/w_2$	$\Delta v/w_2$	$\epsilon_{12}$ (calc.)	$v_{12}$ (calc.)
30° C (Rau and Narayanaswamy)						
4.418	2.895	1.1391	14.30	-0.321	2.895	1.1390
5.301	3.024	1.1361	14.35	-0.324	3.024	1.1362
7.235	3.309	1.1299	14.46	-0.323	3.309	1.1299
30° C (Davis, Bridge and Svirbely)						
0.5953	2.3397	1.15188	13.82	-0.318	2.3397	1.15182
0.6950	2.3534	1.15148	13.81	-0.329	2.3536	1.15150
0.7436	2.3609	1.15141	13.91	-0.317	2.3604	1.15134
0.9740	2.3921	1.15068	13.83	-0.317	2.3926	1.15059
1.330	2.4430	1.14920	13.96	-0.344	2.4423	1.14942
1.720	2.4958	1.14817	13.86	-0.326	2.4970	1.14815
1.846	2.5156	1.14777	13.99	-0.325	2.5159	1.14774
1.922	2.5254	1.14755	13.95	-0.324	2.5255	1.14749
1.971	2.5315	1.14732	13.91	-0.327	2.5314	1.14733
2.338	2.5828	1.14613	13.92	-0.327	2.5846	1.14613
3.120	2.6957	1.14350	14.02	-0.329	2.6952	1.14355
4.151	2.8440	1.14012	14.16	-0.329	2.8433	1.14020
40° C (Rau and Narayanaswamy)						
4.418	2.843	1.1531	13.58	-0.333	2.843	1.1530
5.301	2.965	1.1499	13.62	-0.337	2.965	1.1500
7.235	3.235	1.1435	13.71	-0.336	3.235	1.1435

On the other hand, the measurements of Jenkins are very regular and the  $\epsilon_{12}$  measurements accord well with the later results of Jenkins and Sutton,<sup>24</sup> which, however, lie beyond the concentration range over which eqn. (2) holds. There is, however, a rather abrupt change in the value of the  $\Delta\epsilon/w_2$  ratio between the two series of measurements, a result partly confirmed by the two series of measurements of Le Fèvre but not borne out by the data of Tiganik for 20° C or of Davis for 30° C, in both of which series the measurements were extended to very low concentrations. The figures shown under Jenkins (combined) in Table II are deduced from a mean value of  $\beta$  for the two series and a value of  $\alpha$  derived from the figures of Jenkins and the data for the lowest concentration solutions of Jenkins and Sutton, and are introduced to show that the value of  $\alpha$  deduced is only slightly in error even when results slightly outside the linearity range are included.

The figures of Le Fèvre are much more consistent with the other data than would be anticipated from the values of  $P_{2\infty}$  and  $\mu$  derived by them. Le Fèvre and Russell obtained a very low value by extrapolating the  $P_2 - f_2$  curve because they made three measurements only and these at rather high and not widely differing concentrations, so the slope of extrapolated curve was insufficiently steep. The high values derived by their modified Hedestrand method, on the other hand, is due to the circumstance that at the three concentrations studied the value of  $\Delta\epsilon/w_2$  is much higher than at low concentrations, and the assumption that this value is the same as at infinite dilution can lead to very considerable errors. The values of  $\alpha$ ,  $\alpha'$  and  $\beta$  derived by considering the two series of measurements together are very close to the corresponding figures deduced from the measurements of Jenkins and have been used in deriving the values of  $\epsilon_{12}$  (calc.) and  $v_{12}$  (calc.) shown in Table III.

The results of Davis and his co-workers at 30° C appear at first sight to be somewhat erratic, but comparison of the observed and calculated values of  $\epsilon_{12}$  and  $v_{12}$  shows this to be due to the very low concentration range covered.

Of the data not analysed here the dielectric constants were recorded to two places of decimal only in the results of Williams and Schwingel, Wehrle, and Chang, whilst Hassel and Uhl studied too few solutions of low concentration to permit analysis. The  $\epsilon_{12}$  values obtained by Bergmann and his co-workers are erratic and the values of  $\Delta\epsilon/w_2$  decrease initially with increasing  $w_2$  but pass

<sup>24</sup> Groves and Sugden, *J. Chem. Soc.*, 1934, 1094.



TABLE IV—SUMMARISING DATA FOR SOLUTIONS OF NITROBENZENE IN OTHER SOLVENTS

Temp. °C	Observers	$\epsilon_1$	$v_1$	$\alpha$	$\beta$	$P_{\infty}$ cm. <sup>3</sup>	$\mu$ (D)
TOLUENE							
18.5	Hassel and Uhl	[2.383]	[1.1526]	13.92	[-0.332]	340.1	3.789
24	Lange	2.380	1.159	13.65	-0.335	336.5	3.802
100	Lange	2.204	1.274	9.12	-0.372	274.5	3.704
<i>p</i> -XYLENE							
20	Fairbrother <sup>25</sup>	2.268	1.1614	14.00	-0.340	359.8	3.920
40	Fairbrother <sup>25</sup>	2.234	1.1852	12.60	-0.351	337.6	3.910
60	Fairbrother <sup>25</sup>	2.200	1.2106	11.45	-0.367	319.9	3.913
80	Fairbrother <sup>25</sup>	2.165	1.2294	10.52	-0.382	306.6	3.933
100	Fairbrother <sup>25</sup>	2.131	1.2655	9.67	-0.392	294.2	3.949
120	Fairbrother <sup>25</sup>	2.097	1.2947	8.87	-0.397	282.3	3.964
CYCLOHEXANE							
10	Rau and Narayanaswamy	2.039	1.2692	12.88	-0.425	396.8	4.066
20	Rau and Narayanaswamy	2.023	1.2845	12.30	-0.430	387.3	4.083
25	Jenkins	2.016	1.2922	11.36	-0.434	362.8	3.972
	Jenkins and Sutton	2.016	1.2022	11.38	-0.445	363.1	3.973
30	Rau and Narayanaswamy	2.007	1.3004	11.71	-0.441	376.8	4.090
40	Rau and Narayanaswamy	1.992	1.3165	11.15	-0.450	366.7	4.094
DECALIN							
25	Jenkins	2.1624	1.1353	13.43	-0.284	354.4	3.922
HEXANE							
0	Müller	1.922	1.4593	10.45	-0.635	390.0	3.956
10	Rau and Narayanaswamy	1.923	1.4518	10.54	-0.646	390.6	4.031
20	Müller	1.912	1.4573	10.06	-0.643	377.2	4.023
	Rau and Narayanaswamy	1.907	1.4715	10.11	-0.670	382.8	4.057
25	Williams and Ogg	1.904	1.4706	9.12	-0.649	348.4	3.887
	Jenkins	1.887	1.5117	9.50	-0.703	373.9	4.038
	Jenkins and Sutton	1.887	1.5117	9.20	-0.7013	362.7	3.969
	Jenkins (combined)	1.887	1.5117	9.50	-0.701	373.8	4.038
30	Rau and Narayanaswamy	1.892	1.4919	9.62	-0.697	373.1	4.091
40	Rau and Narayanaswamy	1.877	1.5124	9.10	-0.713	360.4	4.055
HEPTANE							
10	Rau and Narayanaswamy	1.928	1.3957	11.08	-0.587	393.7	4.049
20	Rau and Narayanaswamy	1.915	1.4122	10.55	-0.590	382.7	4.056
30	Rau and Narayanaswamy	1.902	1.4292	10.03	-0.599	371.4	4.057
40	Rau and Narayanaswamy	1.889	1.4476	9.51	-0.625	359.3	4.048
DECANE (Di-isoamyl)							
20	Fairbrother <sup>25</sup>	1.983	1.3822	10.71	-0.545	369.8	3.980
40	Fairbrother <sup>25</sup>	1.956	1.4120	9.83	-0.550	353.2	4.012
60	Fairbrother <sup>25</sup>	1.928	1.4440	8.88	-0.584	332.0	3.995
80	Fairbrother <sup>25</sup>	1.901	1.4782	8.19	-0.611	318.5	4.018
100	Fairbrother <sup>25</sup>	1.873	1.5149	7.51	-0.632	304.6	4.028
120	Fairbrother <sup>25</sup>	1.846	1.5540	6.88	-0.646	291.5	4.032
DIOXAN							
10	Rau and Narayanaswamy	2.353	0.9612	17.84	-0.144	365.5	3.880
20	Rau and Narayanaswamy	2.328	0.9716	17.00	-0.138	357.2	3.904
30	Rau and Narayanaswamy	2.3035	0.9825	16.18	-0.141	348.4	3.915
30.1	Davis and others	2.1965	0.9784	15.48	-0.138	347.1	3.907
40	Rau and Narayanaswamy	2.278	0.9936	15.36	-0.143	339.3	3.921

TABLE IV.—*cont.*

Temp. °C	Observers	$\epsilon_1$	$v_1$	$\alpha$	$\beta$	$P_{\infty}$ cm. <sup>3</sup>	$\mu$ (D)
CARBON TETRACHLORIDE							
10	Pal	2.245	0.6198	27.10	0.194	373.6	3.934
10	Rau and Narayanaswamy	2.256	0.6203	27.51	0.189	377.3	3.946
20	Müller	2.236	0.6274	25.50	0.202	359.1	3.915
	Pal	2.224	0.6273	25.80	0.191	364.2	3.947
	Rau and Narayanaswamy	2.237	0.6277	26.18	0.196	367.7	3.967
25	Jenkins (combined)	2.2277	0.6310	24.99	0.194	355.2	3.925
30	Pal	2.203	0.6350	24.45	0.192	355.7	3.961
	Rau and Narayanaswamy	2.218	0.6355	24.83	0.196	357.2	3.970
40	Rau and Narayanaswamy	2.199	0.6434	23.59	0.191	347.0	3.970
	Pal	2.185	0.6429	23.25	0.190	344.5	3.954
50	Pal	2.163	0.6510	22.28	0.189	338.1	3.975
CARBON DISULPHIDE							
0	Müller	2.694	0.7741	24.0	0.081	349.4	3.722
20	Müller	2.640	0.7916	21.0	0.060	322.2	3.685
24	Lange	2.618	0.8026	20.42	0.014	319.0	3.689
25	Jenkins (combined)	2.6328	0.7963	20.20	0.055	313.7	3.661
CHLOROFORM							
25	Le Fèvre and Russell	4.7240	0.6811	30.50	0.134	225.3	3.021
	Jenkins	4.7210	0.6758	33.75	0.136	241.8	3.150
ETHER							
25	Wehrle	4.55	1.4049	13.7	-0.026	217.7	2.960
	Higasi	4.25	1.4149	15.12	-0.040	247.6	3.196
CHLOROBENZENE							
25	Wehrle	5.22	0.9093	9.96	-0.058	125.4	2.075
	Le Fèvre and Russell	5.6120	0.90839	17.10	-0.077	161.0	2.455

through a minimum and then increase, suggesting that the value taken for  $\epsilon_1$  is too low compared with the  $\epsilon_1$ ,  $\epsilon_2$  values.

**SOLUTIONS IN OTHER SOLVENTS.**—A summary of the results obtained by treating the experimental data for solutions of nitrobenzene in other solvents by the new method is shown in Table IV. As in the case of benzene, the results generally confirm the tendency for the apparent moment to increase with rise of temperature, i.e. with decreasing  $\epsilon_1$ , although there are a few anomalies. There are only scanty data for toluene solutions, including very few measurements at low concentrations, but these are as consistent as can be expected under the circumstances. The measurements of Fairbrother on solutions in *p*-xylene lead to the conclusion that in this solvent  $\mu$  is lower than in benzene. Of the series of measurements on hexane solutions only Jenkins and Jenkins and Sutton specify that the *n*-isomer was used, the other measurements having been made, presumably, in an isomeric mixture. This may account for the great differences of density of the pure solvent quoted by the various investigators. The results of Müller and of Jenkins show close accord, but the rate of increase of  $\epsilon_1$  with concentration found by Rau is, in this case and also in cyclohexane and carbon tetrachloride solutions, appreciably higher than found by other observers. His figures for heptane solutions indicate that the apparent moment is practically the same as in hexane, whilst Fairbrother's data for decane solutions, which are sufficiently consistent for  $\mu$  to be calculated approximately from them, although two solutions only were studied, suggest that in that solvent

<sup>20</sup> Wehrle, *Physic. Rev.*, 1931, **37**, 1135.

<sup>21</sup> Fairbrother, *J. Chem. Soc.*, 1934, 1848.

$\mu$  is only slightly higher than in benzene. The revised method of calculation brings the results of Rau and of Davis for dioxan solutions into line, although the  $\epsilon_1$  values given by Rau are much too high and suggest that he may have used a wet sample. Of the other results the most surprising discrepancy appears in the figures for solutions in chloroform at 25° C as determined by Jenkins and by Le Fèvre and Russell, respectively. Although their  $\epsilon_1$  values differ by only about 0.002, their  $\nu_1$  values differ by 1 % and the values of  $\alpha$  derived from their  $\epsilon_{12}$  data by 10 %. This system evidently requires re-investigation, as do solutions of nitrobenzene in ether and in chlorobenzene where extremely contradictory results have been reported.

### Discussion

An analysis of the probable values of  $P_2$  and of  $\mu$  at 25° C in the various solvents considered is given in Table V. The most striking feature is that, with the exceptions of benzene, xylene and chlorobenzene, the values of  $P_{2\infty}$  not only decrease regularly with increasing  $\epsilon_1$  but, as has been pointed out by Sugden and others, the decrease is almost linear with  $(\epsilon_1 - 1)/(\epsilon_1 + 2)$ . Also, as was indicated by Goss<sup>28</sup> the values of  $P_1$  for solutions of various concentrations in hexane, decalin, cyclohexane and carbon tetrachloride, when calculated on the assumption that  $P_1$  remains unchanged with concentration, all fall near the same curve when plotted against  $\epsilon_{12}$  or  $(\epsilon_{12} - 1)/(\epsilon_{12} + 2)$ , although the curve in the case of the latter function is more linear than is indicated by the relationship

$$P_2 = A - B \cdot \frac{\epsilon_{12} - 1}{\epsilon_{12} + 2} - B \frac{(\epsilon_{12} - 1)^2}{(\epsilon_{12} + 2)^2}$$

then suggested by Goss.

TABLE V.—PROBABLE VALUES OF THE APPARENT MOLECULAR POLARISATION AT INFINITE DILUTION AND APPARENT DIPOLE MOMENT OF NITROBENZENE IN VARIOUS SOLVENTS AT 25° C

	$\epsilon$	$P_{2\infty}$ (cm. <sup>2</sup> )	$\mu$ (D)
n-Hexane . . . . .	1.887	373.8	4.038
Decane (di-isoamyl) . . . . .	1.976	366.2	3.984
Cyclohexane . . . . .	2.016	362.8	3.972
Decalin . . . . .	2.162	354.4	3.922
Dioxan . . . . .	2.204	352.8	3.910
Carbon tetrachloride . . . . .	2.228	355.2	3.925
p-Xylene . . . . .	2.260	354.3	3.917
Benzene . . . . .	2.273	362.0	3.967
Carbon disulphide . . . . .	2.633	313.7	3.661
Ether . . . . .	4.25	247.6	3.196
Chloroform . . . . .	4.722	241.8	3.150
Chlorobenzene . . . . .	5.612	161.0	2.455

As against this, the values of  $P_{2\infty}$  for solutions in benzene and xylene calculated on the same assumption are higher than would be expected in comparison with other solvents and the scanty data for toluene suggest that the value for this solvent is also anomalously high. If the value of  $P_1$  for these solvents decreases with increasing  $\epsilon_{12}$  the true values of  $P_{2\infty}$  are even higher still. On the other hand, the value for chlorobenzene is lower than would be expected in relation to other polar solvents of high  $\epsilon_1$ , or even in relation to liquid nitrobenzene itself. One is led to infer, therefore, that  $\epsilon_{12}$  is the dominating but not the exclusive factor in determining the molecular polarisation of a solute. Further than this, however, the precision with which the value of  $P_1$  in several solvents

<sup>28</sup> Goss, *J. Chem. Soc.*, 1935, 502.

depends on the  $\epsilon_{12}$  of the solution and is almost independent of the chemical nature or physical shape of the solvent molecule, appears to be too exact to be coincidental. Hence it seems that these should be regarded as "normal" solvents and the other solvents as more or less abnormal.

In his later study, Goss,<sup>29</sup> using the method of intercepts, recalculated the values of  $P_1$  for nitrobenzene in carbon tetrachloride solutions on the assumption that  $P_1$  also varies with  $\epsilon_{12}$ . Such treatment has been applied to the solutions in other solvents by a modification of the extrapolation method described in this paper, in which the solutions are regarded as comprising solute in a solvent consisting of a solution of lower concentration. When the figures of Jenkins and Sutton are treated by this method they lead to a series of more or less parallel curves, but in no instance do the curves for two solvents coincide with one another, so it is to be inferred that if such treatment is correct, there is a strong specific factor in each case dependent on the solvent itself which determines the rate of change of  $P_1$  with concentration. The curve for carbon tetrachloride solutions lies in the midst of the others and there is nothing to suggest that it represents any more fundamental behaviour than in the other cases, such as might be anticipated from the symmetry of its molecule. As this state of affairs is much more complex than would be anticipated from the variation with  $\epsilon_{12}$  of the values of  $P_{2\infty}$  for the various solvents, which remain unchanged on the basis of the intercept method, and the values of  $P_1$  at finite concentrations as deduced by the more usual method, one is led to doubt the applicability of the intercept method to this problem. The limitations imposed by the method have been discussed by one of us elsewhere.<sup>30</sup>

*Department of Chemistry,  
Battersea Polytechnic,  
London, S.W.11.*

<sup>29</sup> Goss, *J. Chem. Soc.*, 1937, 1915.

<sup>30</sup> Smith, *Sci. Prog.*, 1948, 36, 492.

---

## ELECTROMETRIC MEASUREMENT OF THE FREE ENERGY OF FORMATION OF NAPHTHALENE PICRATE

BY R. P. BELL AND J. A. FENDLEY

*Received 21st September, 1948*

The free energy of formation of naphthalene picrate from its solid components has been determined by a direct electrometric method and found to be 2070 cal./mole at 25° C, in good agreement with other measurements.

---

If an excess of solid naphthalene picrate is shaken with water it partly decomposes to give solid naphthalene and a solution of picric acid of fixed equilibrium concentration. It was pointed out by Brönsted<sup>1</sup> that the affinity of formation of naphthalene picrate from its solid constituents could be obtained from the E.M.F. of two cells of the type,

Hydrogen electrode | Picric acid solution | Picrate electrode,  
one containing a solution saturated with picric acid and the other a solution

<sup>1</sup> Brönsted, *Z. physik. Chem.*, 1911, 77, 284.

in equilibrium with solid naphthalene picrate. Brönsted suggested using a mercury-mercurous picrate electrode, but was not able to carry out measurements because the hydrogen electrode was depolarised by reduction of the picric acid: he was therefore compelled to use an indirect and laborious electrometric method. The present paper describes a direct determination using a mercurous picrate electrode and a glass electrode in place of the hydrogen electrode.

Naphthalene picrate was prepared by mixing alcoholic solutions of the two components, and the saturated aqueous solutions were obtained by rotating excess of picric acid or naphthalene picrate with water for 16 hr. at approximately 25° C. No description of mercurous picrate could be found in the literature. It was precipitated as yellow needles by mixing solutions of sodium picrate and mercurous nitrate, washed with water, alcohol and ether, and dried in air. It deflagrates on heating, but could not be made to detonate. The mercurous picrate electrode was made by spreading a thin layer of solid over a pool of mercury, and the solutions investigated were shaken with mercurous picrate before use. Inter-comparison of several of these electrodes using the same solution of picric acid and a Tinsley potentiometer showed differences of less than 0.2 mV. The measurements with glass electrode were made with a Cambridge bench pH-meter. The E.M.F. was recorded to 0.5 mV, and the same glass electrode was used alternately in rapid succession in the two cells, thus minimising errors due to asymmetry potentials and instability of the measuring circuit. The following values were obtained for the difference in the E.M.F. of the two cells: 89, 90, 90, 88.5, 90.5, 90, 89.5, 90.5 mV; mean 90 mV. This corresponds to a free energy of formation of  $90 \times 23.0 = 2070$  cal./mole at 25° C. This value agrees exactly with the data of Brönsted, who gives 2050 cal./mole at 20° with a temperature coefficient of 4 cal./mole degree, and is in reasonable agreement with the less accurate value of 2080 cal./mole at 3° C obtained by Brown<sup>2</sup> from cryoscopic measurements in nitrobenzene.

*Physical Chemistry Laboratory,  
Oxford.*

<sup>2</sup> Brown, *J. Chem. Soc.*, 1925, 345.

---

## REVIEWS OF BOOKS

**Natural Philosophy through the Eighteenth Century and Allied Topics.** (Commemoration Number to mark the 150th Anniversary of the foundation of the Magazine.) Edited by ALLAN FERGUSON, M.A., D.Sc. (Taylor and Francis Ltd., 18 Red Lion Court, E.C.4, 1938. Pp. viii + 164. Price 15s.)

This commemoration number of an "institution" like the *Philosophical Magazine* is an event of much more than passing interest, the kind of congratulation that observes with a nod that Number One-hundred-and-fifty has been reached. It is nothing less than proof positive of the robust condition of an enterprise that has known cloudy skies, dark and even crucial days. For what it has done, for what it is, and for what it yet may be, we proffer our felicitations and greetings.

The contents of this *Festschrift* are distinguished, both in themselves, and on account of those who have written them. They deal with the development of Natural Philosophy during the Eighteenth Century, and thus bring the reader squarely up to the year 1798, when that resolute

graduate of Glasgow Alexander Tillock (*né* Tullock) founded the *Philosophical Magazine*. It is needless to recite the list of names—proprietors and editors—who have guided it since then : in their several generations they provide evidence enough of the undiluted distinction upon which it has been possible to draw. And for the most part, this is true of the contributors no less. It is interesting to note that Sir J. J. Thomson published his first paper in the "*Phil. Mag.*," and also his last. "J. J." was ever a friend of the goings-on at the top of the stair in Red Lion Court. Never, probably, in the history of science has a privately-owned and sponsored periodical commanded such a galaxy of talent.

We approach now what is before us in this special issue : papers on the magazine itself, on astronomy, physics, chemistry, mathematics, engineering and invention, and scientific instruments in the seventeenth-hundreds. In addition are contributions dealing with scientific periodicals and societies, and the teaching of the physical sciences. One and all, they tell of unrelenting thought, experiment and movement, fitful at times, but never retrograde.

Into such a world, Tillock brought his new venture. Its outstanding characteristic was its atmosphere of scholarship ; specialisation had not yet started to erode beauty of expression and versatility of interest. Kelvin's inaugural lecture at Glasgow University was composed and delivered in Latin. It is significant that an obituary notice of him, by the late Sir Joseph Larmor was considered by its author as his finest literary composition. All of which goes to show the store set upon style by these giants of the past.

Natural philosophers in those days assuredly did not lack physical courage : the study of electrostatics (ahead of electrodynamics) needed evidence of static charge, and shocks—often quite heavy ones—were the commonly accepted method of interpreting "feeling is believing." All of which puts one in mind of William Stukeley, who matriculated at Corpus (Cambridge) in 1704. "I often prepared the *pulvis fulminans*," he wrote, "and sometime surprized the whole college with a sudden explosion. I cur'd a lad once of an ague with it by a fright." As the Laurence Professor observed a full two centuries later—"Young Stukeley was a thorough scientist."

Those were great days ; experimentalists were a little amateurish perhaps, and not always prudent, but they were accumulating potential and paving the way for the advent of the *Philosophical Magazine*.

The concluding contribution, that on scientific education at the end of the century is most illuminating, and not a little appropriate. Dr. Sherwood Taylor tabulates the kind of higher instruction, starting from none whatever, that men of science received. If formal courses came their way, they were in mathematics or in medicine. The upshot, as might be expected, appears to be that innate ability is impervious to method, and emerges triumphant, come what may. One interesting point is that technology made a brave show during the period under review ; lack of academic training seemingly counted for little.

Much of this is relevant to our present distress. It is not the task of a reviewer however to draw the moral, obvious as it is, but to return whence we set out, in wishing these great pages "many happy returns of the day."

F. I. G. R.

**Handbook of Textile Technology No. 3. The IDENTIFICATION OF TEXTILE MATERIALS.** (The Textile Institute, Manchester). Pp. 10. Price 5s.)

This handbook is the work of a committee under the chairmanship of Mr. J. M. Preston, the members of which are concerned with fibre identification. It is published as a Tentative Textile Specification and comments and suggestions for its improvement are invited.

In addition to the few pages of text which are written concisely, the book contains four tables (A-D) of which A and B remind one of those used in qualitative chemical analysis. Tables A and B are for a preliminary analysis of fibres, Table A being devised for use without a microscope, Table B with a microscope. Table C is an extensive one giving the reactions of different fibres in twenty different tests, most of these being based on staining and solubility, and illustrates the complications which may now beset one in the identification of textile fibres. It would have been helpful if the specific or more important tests for individual fibres had been set out in heavy type. Table D introduces a somewhat novel feature in that the variation in the density of the fibres is used as a sorting test. The fibres cut into short lengths are immersed in liquids of varying density and sorted into groups according to whether they float or sink.

The handbook contains twenty-five plates showing photomicrographs of longitudinal and cross-section of various fibres, the originals being supplied by Messrs. Courtaulds Ltd., the British Cotton Industries Research Association, and the Wool Industries Research Association. The text contains interesting material on chemical and physical properties of fibres, a major part being devoted to the description of the various rayons. Among interesting features are methods for detection of urea and formaldehyde in crease-resist treated fabrics, detection of titanium in delustrated materials, the cutting of cross-sections, notes on mounting of sections and a table giving the dimensions of vegetable fibres.

The handbook should prove of value to all concerned with the technology of fibres and represents the combined experience of many experts giving a large amount of useful information in an amazingly small compass.

J. B.

## CORRIGENDA

Vol. 44, 1948:

Page 627. *The legend of Fig. 1 should read—*

FIG. 1 —Surface tension of the system  
ether-acetone.      O—calculated  
points ( $l = \frac{2}{3}$ ,  $m = \frac{1}{3}$ ), X—observed  
points.

*The legend of Fig. 2 should read—*

FIG. 2. —Composition of surface layer  
( $v'_B$ ) as function of composition of  
bulk phase ( $x_B$ ) for the system ether-  
acetone.

{ O—calculated points with  $l = \frac{1}{2}$ ,  $m = \frac{1}{2}$ .  
X—calculated points with  $l = \frac{2}{3}$ ,  $m = \frac{1}{3}$ .

„ 948. 5 lines from bottom of page—

*For co-volume read co-area.*

„ 954. 4 lines up from Summary—

*For co-volume read co-area.*





# THE ENERGIES OF VAPORISATION, VISCOSITY AND COHESION AND THE STRUCTURE OF LIQUIDS

BY L. GRUNBERG AND A. H. NISSAN

*Received 19th September, 1947; as revised 3rd August, 1948*

According to the type of forces which exist between molecules, liquids may be classified as non-polar and polar. In the former only dispersion forces are active, whilst in the latter dipole interaction plays an important part. In polar liquids dipole interaction is counteracted by thermal motion. Thus at low temperatures dipole interaction may lead to the formation of stable molecular aggregates, whilst at higher temperatures it may manifest itself only by hindrance to rotation. Steric factors such as the accessibility of the dipoles are also of primary importance.

For non-polar, and for polar, unassociated liquids it is found that the free energy of viscosity equals the work of cohesion, whilst for polar associated liquids, the energy of viscosity is greater than the work of cohesion. The difference between these energies can be attributed to the energy of association per bond. In vaporisation, all the bonds are broken and the ratio between the energy of vaporisation and the energy of viscosity or the work of cohesion gives the statistical value of the number of bonds per molecule. This value is generally found to lie between 3 and 4.

Polar, associated liquids can be grouped into two distinct classes. If unassociated in the vapour the energy of vaporisation contains the energy of dissociation and the ratio  $E_v/E_{visc}$  describes the arrangement of the molecules. If the vapour is associated, the ratio  $E_v/W_c$  gives an indication of the symmetry of the arrangement.

From the difference between  $F_{visc}$  and  $W_c$  and the dipole moment, the degree of association can be determined. This calculation was carried out for water and alcohols. Esters are found to be unassociated, in spite of the high value of the dipole moment. This is due to steric inaccessibility of the dipoles. Amongst the ketones, only acetone is partly associated at ordinary temperature, whilst higher ketones are found to be unassociated.

---

## 1. Introduction

At present the most convenient way of studying the structure of liquids is by means of X-rays or by means of model experiments in determining the distribution function. Both these methods give the probability of finding the centres of other molecules at a certain distance from a central molecule. The interpretation of the results is very difficult and still rather controversial. It may, therefore, prove fruitful to try an alternative approach to the problem. In a liquid the molecules are restricted from developing the full kinetic motion by the interaction with neighbouring molecules. In investigating to what extent the full development of kinetic motion is restricted, it may be possible to gain insight into the structure of liquids. We have three methods by means of which this can be measured:

- (1) by measuring the energy required to vaporise a molecule, i.e. to impart to a molecule the full kinetic motion by transferring it into the vapour phase;
- (2) by measuring the energy content of the surface of a liquid, since this energy derives from the energy necessary to form a surface;

- (3) by measuring the energy required to transfer a molecule in the liquid from one equilibrium position to another. This energy can be deduced from the variation of the coefficient of viscosity with the temperature.

In the absence of a rigorous mathematical treatment of the liquid state a number of postulates and assumptions will have to be made. These can only be justified by the fact that they help to explain certain phenomena in a reasonable way; but they cannot claim absolute or general validity. Thus, for example, only molecular liquids will be considered in which the interaction between particles in the liquid is due to secondary valence forces. Liquids in which ionic forces are prevalent and metallic liquids will not be considered in the present work.

## 2. Assumptions

It is thought useful to state explicitly the assumptions and definitions we accept as the basis of the present work.

The attractive forces between molecules are assumed to arise from—

(1) The dispersion effect, which is a temperature-independent function of the distance between molecules, their polarisabilities and ionisation potentials.

(2) The orientation effect<sup>1</sup> of molecules possessing permanent dipole moments. The potential for the parallel position is given by the approximate equation.

$$V(r) = -\frac{2\mu_1\mu_2}{r^3} \quad . \quad . \quad . \quad . \quad (1)$$

For the antiparallel position it is taken to be

$$V(r) = -\frac{\mu_1\mu_2}{r^3}, \quad . \quad . \quad . \quad . \quad (2)$$

where  $\mu_1$  and  $\mu_2$  are the dipole moments of the molecules and  $r$  is the distance between the centres of the dipoles.

(3) The induction effect<sup>2</sup> which is given by

$$\mu_i = \alpha F \quad . \quad . \quad . \quad . \quad (3)$$

and

$$V(r) = -\frac{2\mu^2\alpha}{r^6}, \quad . \quad . \quad . \quad . \quad (4)$$

where  $\mu_i$  is the induced moment acquired by a molecule of polarisability  $\alpha$  when placed in an electric field of strength  $F$  and  $\mu$  is the moment of the inducing dipole.

Depending on the magnitude and nature of the attractive forces, molecules of liquids will show variable degrees of being "associated" in clusters.

On the basis of the above assumptions and the fact that melting of solids results in only small (10 to 20 %) increase in specific volume (excepting water and a few other materials which contract), we arrive at a model of a liquid, in which the arrangement of the molecules does not differ materially from that of the corresponding solid, except in the following respects.

(i) The arrangement of molecules in repeating unit cells is localised and the symmetry is lost over large distances. Whilst, therefore, it would be incorrect to speak of a molecular lattice in liquids, it is quite justified to assign to every central molecule an average number of "nearest neighbours." From the abundance of unoccupied sites and from the short range of the order it is clear that the number of nearest neighbours has a statistical value if averaged over the whole liquid and need not necessarily be a whole number. The symmetry of the "unit cell" does not perpetuate

<sup>1</sup> Keesom, *Physik Z.*, 1921, **22**, 120, 643; 1922, **23**, 225.

<sup>2</sup> Debye, *ibid.*, 1920, **21**, 178; 1921, **22**, 302.

itself throughout the liquid, but is lost a few molecular diameters from the central molecule.

(ii) The arrangement is limited in time as well as in space. Molecules continuously leave and join the clusters.

(iii) Whilst in the solid the existence of unoccupied sites is the exception, the number of "holes"<sup>3</sup> has a definite statistical value in the liquid.

(iv) Whilst in the solid the rotation of the molecules is to the greatest extent restricted, in the liquid (except for those liquids in which strong orientating forces are operative) the rotational degrees of freedom are not impaired. This fact may be responsible for the higher specific heat of the liquid as compared with the solid and also leads to the following important simplification in the treatment of the liquid. If free rotation of the molecules of a liquid can be assumed, then the volume swept by the rotating molecule will, in the simpler types of liquid, approach spherical symmetry. The description of the arrangement of the molecules as that of spherical particles, approaches the actual conditions to a greater extent in the liquid, than it would in the corresponding solid.

These form the basic assumptions for the present work. Before proceeding to the exposition of the use of the three energies of vaporisation, cohesion and viscosity in elucidating the structure of the liquids, these energies will be briefly defined and explained.

### 3. Definitions

**The Energy of Vaporisation.**—The internal energy only will be considered, i.e. the energy required to vaporise one mole of the liquid at constant volume. It is therefore defined by the equation,

$$E_v = M(l - p(v_v - v_l)) \quad (5)$$

where  $E_v$  = the internal molar latent heat of vaporisation,  $M$  = the molecular weight,  $l$  = the latent heat of vaporisation per gram of liquid,  $p$  = the vapour pressure,  $v_v$  = the specific volume of the vapour,  $v_l$  = the specific volume of the liquid.  $E_v$  thus equals the molar latent heat minus the work of expansion from the liquid to the vapour volume.

Certain limitations exist for polar liquids. If, in the process of vaporisation, the molecular aggregates, due to the directed polar forces are dissolved, then  $E_v$  contains the increments due to all three types of attraction, the dispersion, the orientation and the induction effects. If, however, the molecular aggregates are so stable that the vapour contains also associations of, say, two molecules,  $E_v$  contains a fraction of the polar increments, this fraction being determined by the degree of association in the liquid and in the vapour. If the degree of association is the same in the liquid and in the vapour, then  $E_v$  measures only the increment of the potential energy due to the dispersion forces.

**$E_b$  and Bonds between Molecules.**—The potential energy may be considered localised in definite bonds between molecules and a certain bond strength can be assigned to the field existing between a pair of molecules in interaction. Let the central molecule be surrounded by  $n$  nearest neighbours and the potential energy between the central molecule and the neighbours be equal to  $E_b$ . Since every bond belongs to two molecules the average bond strength is given by the equation:

$$\text{Bond strength} = 2E_b/n \quad (6)$$

This relation will be used later when different symmetrical arrangements of the molecules will be considered.

**The Work of Cohesion.**—This quantity has been defined by Harkins<sup>4</sup> as:

$$\text{Work of cohesion} = 2 \times \text{surface energy} \quad (7)$$

<sup>3</sup> Eyring, *J. Chem. Physics*, 1936, 4, 283.

<sup>4</sup> Harkins, *J. Amer. Chem. Soc.*, 1921, 43, 35.

In order to transform the work of cohesion into a molar quantity an *a priori* knowledge of the arrangement of the molecules in the surface layer is required. This knowledge is, however, not available and a simple *a priori* assumption must be made for this purpose.

Let  $\gamma$  = the surface energy in cal./unit area,  $N$  = Avogadro's number and  $V$  = the molar volume. If the volume per molecule is given by  $V/N$ , then the number of molecules per unit surface area of liquid is given by  $(N/V)^{1/2}$ . The surface energy per molecule will be  $\gamma V^{1/2}/N^{1/2}$  and the molar surface energy  $\gamma N^{1/2} V^{1/2}$ . From (7) we can now derive the work of cohesion,  $W_c$ , i.e.

$$W_c = 2\gamma N^{1/2} V^{1/2}. \quad (8)$$

Polar, associated liquids again require special consideration. In such a liquid an imaginary plane (passing between, but not through individual molecules) will pass through and between associated complexes. If the plane of surface formation follows the imaginary plane, then the formation of the surface will cause the dissociation of the associated complexes through which the plane passes. The surface tension (and therefore  $W_c$ ) of such a fresh surface would be greater than if surface formation would occur without dissociation. The lifetime of the "dissociated" molecule can only be of the order of  $10^{-12}$  sec. before it enters again into an associated complex. This means that the surface tension of a freshly formed surface of an associated liquid may be higher than that of the "aged" surface after  $10^{-12}$  sec. The work of cohesion calculated from the ordinarily measured surface tension will not contain increments of energy due to the dissociation of associated complexes (i.e. the increments of the orientation and induction effects). The alternative consideration that surface formation occurs without dissociation leads to the same result.

It can, therefore, be concluded that whilst for non-polar and polar, unassociated liquids the molar work of cohesion measures the strength of the bonds broken when the surface is formed, for polar associated liquids it does not contain the dissociation energy increments of these bonds.

**The Number of Bonds Equivalent to  $W_c$ .**—The number of bonds which are broken in the process of surface formation will depend on the geometrical arrangement of the molecules. Considering different arrangements in a unit cell round a central molecule we can stipulate that the energy of surface formation will be equal to the energy of the smallest number of bonds which have to be broken in order to "uncover" the central molecule. For the simpler types of molecular arrangements such as tetrahedral (co-ordination number 4) and octahedral (co-ordination number 6), the breaking of a single bond is sufficient to create the surface. For more complicated arrangements such as cubic body-centred (co-ordination number 8), cubic close-packing (co-ordination number 12), hexagonal close-packing (co-ordination number 12) we must consider the smallest number of molecules which have to be removed from the unit cell in order to uncover the central molecule and also to what extent the other molecules forming part of the unit cell are affected by this process. With models one finds that the smallest number of molecules which have to be removed from the unit cell in the formation of a surface are 2 for cubic body-centred, 3 for cubic close-packing and 3 for hexagonal close-packing. In counting the number of bonds broken per molecule uncovered, 1 bond is broken in cubic body-centred, 1.5 bonds in cubic close-packing and 1.5 bonds in hexagonal close-packing. The value of  $W_c$  thus corresponds to the energy of 1, 1.5 and 1.5 bonds respectively. It must, however, be remembered that calculation of  $W_c$  according to eqn. (8) gives an approximate value of that quantity, which may differ by a factor of the order of unity from the value characteristic of the different geometrical arrangements. Since the knowledge of the arrangement of the molecules is not available, eqn. (8) was used for *a priori* calculations of  $W_c$ . The general conclusions are not affected to any great extent by the approximate nature of eqn. (8).

**The Energy of Viscosity.**—The viscosity of liquids can be represented by an equation of the type :

$$\eta = K\phi_1(T, v)e^{\phi_2(T, v)},$$

where  $\eta$  = the coefficient of viscosity,  $K$  = a constant characteristic of the liquid and  $\phi_1(T, v)$  and  $\phi_2(T, v)$  are functions of the temperature and volume. If the empirical data are examined it is found that for normal liquids both functions vary only slightly with the temperature and the volume, so that a simplified equation,

$$\eta = Ae^{E_{\text{visc}}/RT} \quad (9)$$

can be used. The fact that  $A$  and  $E_{\text{visc}}$  are nearly constant for normal liquids can be ascertained by plotting  $\log \eta$  against  $1/T$ . This yields, in most cases, very nearly a straight line. Polar, associated liquids yield lines of appreciable curvature.

Eqn. (9) was first proposed by de Guzman.<sup>5</sup> Most theories on the viscosity of liquids agree on the fact that an exponential term of the form  $e^{E_{\text{visc}}/RT}$  should be used. The mechanism of viscosity in the light of the structure of liquids considered in the present work will be made the subject of a future publication. At present it is sufficient to discuss the significance of the term  $E_{\text{visc}}$  as considered by previous workers. According to Andrade,<sup>6</sup>  $E_{\text{visc}}$  is the energy of interaction between a pair of molecules of the liquid. Frenkel<sup>7</sup> considers  $E_{\text{visc}}$  to be the energy required to liberate a molecule from the sphere of co-ordination and to effect a jump into a new equilibrium position. Numerous attempts<sup>8</sup> have been made to relate  $E_{\text{visc}}$  to van der Waals' constant  $a$ , to the latent heat of vaporisation<sup>9</sup>, to the internal pressure<sup>9</sup> and to the latent heat of fusion.<sup>10</sup> These theories seem to indicate that  $E_{\text{visc}}$  represents the energy required to break certain bonds between molecules. This process is thus analogous to that of surface formation and one may expect some definite relationship between  $E_{\text{visc}}$  and  $W_c$ . If the values of  $W_c$  calculated according to eqn. (8) are compared with the values of  $E_{\text{visc}}$  obtained from the tangent of the curve  $\log \eta$  against  $1/T$ , they are found to be nearly identical.<sup>11</sup> For polar, associated liquids,  $E_{\text{visc}}$  is greater than  $W_c$ . As has been pointed out,  $W_c$  does not contain the increments of bond energy originating from the orientation and induction effects. Unless one assumes that a different mechanism of flow exists for polar and non-polar liquids (which is unlikely), important conclusions can be drawn from the inequality of  $E_{\text{visc}}$  and  $W_c$  for polar associated liquids.

(i) Since for these liquids  $E_{\text{visc}}$  is greater than  $W_c$  the difference between these energies can be attributed to the energy of dissociation.

(ii) The transfer of molecules in the viscous flow of liquids may, at least in part, be a unimolecular process, since the energy of dissociation forms part of the energy of activation of that process.

(iii) The fact that the energy of dissociation is contained in  $E_{\text{visc}}$  explains the curvature of the graphs  $\log \eta$  against  $1/T$  for associated liquids. The energy of dissociation will decrease with the degree of association which will vary considerably with the temperature.

#### 4. The Structure of Liquids

**The Geometrical Arrangement of Molecules and the Relationship between the Three Energies.**—It has been shown that the relationship between  $E_c$  and bond strength is given by

$$\text{Bond strength} = zE_c/n,$$

$n$  being the co-ordination number.

<sup>5</sup> de Guzman, *Ann. Soc. Esp. fís. y quim.*, 1913, 11, 353.

<sup>6</sup> Andrade, *Phil. Mag.*, 1934, 17, 497, 698.

<sup>7</sup> Frenkel, *Z. physik*, 1926, 35, 662; *Trans. Faraday Soc.*, 1937, 33, 58.

<sup>8</sup> Friend, *ibid.*, 1935, 31, 542.

<sup>9</sup> MacLeod, *ibid.*, 1923, 19, 6.

<sup>10</sup> Ward, *ibid.*, 1937, 33, 92.

<sup>11</sup> Grunberg and Nissan, *Nature*, 1944, 154, 146.

The bond strength for different geometrical arrangements of the molecules was calculated. The values are given in Table I.

TABLE I

Type of Arrangement	Co-ordination number, $n$	Bond Strength
Tetrahedral . . . . .	4	$E_v/2$
Octahedral . . . . .	6	$E_v/3$
Cubic body-centred . . . . .	8	$E_v/4$
Cubic close-packing . . . . .	12	$E_v/6$
Hexagonal close-packing . . . . .	12	$E_v/6$

From the number of bonds which are broken per molecule in the process of surface formation for different geometrical arrangements and the relationship between bond strength and  $E_v$  given in Table I, the relationship between  $E_v$  and  $W_c$  (or  $E_{visc}$ ) can be calculated for different arrangements of the molecules of a liquid. The results of these calculations are given in Table II.

TABLE II

Type of Arrangement	Number of Bonds Equal to $W_c$ (or $E_{visc}$ ).	Characteristic Ratio, $E_v/W_c$ (or $E_v/E_{visc}$ )
Tetrahedral . . . . .	1	2
Octahedral . . . . .	1	3
Cubic body-centred . . . . .	1	4
Cubic close-packing . . . . .	1.5	4
Hexagonal close-packing . . . . .	1.5	4

If, therefore, the ratios  $E_v/W_c$  (or  $E_v/E_{visc}$ ) are found to approximate to any of the values given in column 3 of Table II, then the arrangement of the molecules can be said to correspond to the type given in column 1 of the Table. The characteristic ratio need not necessarily be an integer, since the co-ordination number,  $n$ , of liquids can only have a statistical value, which may approximate the figures given in Table II. Further the approximations involved in equating  $E_v$  to the potential energy in calculating  $W_c$  and  $E_{visc}$  may introduce errors which are difficult to assess. Table III gives the values of  $E_v$ ,  $W_c$ ,  $E_{visc}$  and the ratios  $E_{visc}/W_c$ ,  $E_v/W_c$ ,  $E_v/E_{visc}$  for a number of non-polar and polar, unassociated liquids.

As can be seen from Table III, the ratio  $E_{visc}/W_c$  is very close to unity. The values of  $E_v/W_c$  and  $E_v/E_{visc}$  vary mostly between 3 and 4, indicating that the arrangements of the molecules in these liquids corresponds to systems of high symmetry.

When considering polar, associated liquids, i.e. liquids in which  $E_{visc} > W_c$ , one important distinction must be made. This distinction is based on the type of energy measured by  $E_v$ .

GROUP A. If, on vaporisation, the associated complexes are dissociated, so that the resulting vapour contains only unassociated molecules then  $E_v$  contains apart from the increment due to the dispersion forces, also the increments due to dipole interaction, i.e. the energy of dissociation of the complexes. Since  $E_{visc}$  contains the dissociation increment (while  $W_c$  does not), it is clear that the geometrical arrangement will be defined by the ratio  $E_v/E_{visc}$ . The ratio  $E_v/W_c$  for this class of liquids may be expected to be far greater than 4. Typical liquids of this group

TABLE III

$$E_{\text{visc}} \approx W_e$$

No.	Substance	°C	$E_e$ kcal./mole	$W_e$ kcal./mole	$E_{\text{visc}}$ kcal./mole	$E_{\text{visc}}/W_e$	$E_e/W_e$	$E_e/E_{\text{visc}}$
1	n-Hexane	0	7.14	2.09	1.94	0.928	3.42	3.68
	"	20	6.86	1.92	1.84	0.958	3.57	3.73
	"	40	6.58	1.73	1.69	0.976	3.80	3.89
2	n-Octane	0	7.66	2.24	2.24	1.000	3.42	3.42
	"	20	7.62	1.93	2.04	1.057	3.95	3.74
	"	40	7.58	1.74	2.02	1.160	4.36	3.75
3	Benzene	20	7.59	2.33	2.53	1.086	3.26	3.00
	"	30	7.43	2.24	2.42	1.080	3.32	3.07
	"	50	7.26	2.09	2.31	1.105	3.48	3.14
4	m-Xylene	20	8.52	2.88	3.02	1.048	2.96	2.82
5	o-Xylene	20	8.52	2.97	3.26	1.097	2.87	2.62
6	CCl <sub>4</sub>	10	7.30	2.38	2.61	1.096	3.07	2.80
	"	20	7.21	2.29	2.51	1.096	3.15	2.87
	"	30	7.08	2.20	2.44	1.109	3.22	2.90
7	CHCl <sub>3</sub>	10	7.46	2.14	2.05	0.958	3.49	3.64
	"	20	7.19	2.04	1.93	0.946	3.52	3.73
	"	60	6.64	1.70	1.71	1.006	3.91	3.88
8	CH <sub>3</sub> Cl <sub>3</sub>	20	6.30	1.70	1.61	0.946	3.70	3.91
9	ClH <sub>2</sub> C · CH <sub>2</sub> Cl	10	7.78	2.47	2.41	0.975	3.15	3.23
	"	20	7.67	2.39	2.32	0.970	3.21	3.31
	"	40	7.43	2.22	2.25	1.013	3.35	3.31
10	C <sub>2</sub> H <sub>5</sub> Br	10	6.15	1.81	1.85	1.020	3.41	3.32
	"	20	6.07	1.73	1.75	1.010	3.51	3.47
	"	40	5.95	1.57	1.60	1.020	3.79	3.72
11	n-C <sub>3</sub> H <sub>7</sub> Br	20	7.16	1.89	1.82	0.960	3.79	3.93
12	BrH <sub>2</sub> C · CH <sub>2</sub> Br	50	8.45	2.80	2.60	0.930	3.02	3.25
13	Argon	-186	1.70	0.50	0.52	1.040	3.40	3.27
14	Oxygen	-183	1.45	0.42	0.41	0.976	3.45	3.54
15	C <sub>2</sub> H <sub>5</sub> OC <sub>2</sub> H <sub>5</sub>	20	5.91	1.52	1.54	1.014	3.89	3.84
16	CH <sub>3</sub> CHO	0	5.61	1.38	1.42	1.029	4.07	3.95
17	CH <sub>3</sub> COC <sub>2</sub> H <sub>5</sub>	0	7.66	2.14	2.24	1.050	3.58	3.42
	"	20	7.46	1.99	2.10	1.050	3.75	3.55
	"	20	6.40	1.55	1.64	1.058	4.13	3.90
18	HCOOCH <sub>3</sub>	20	6.40	1.55	1.64	1.058	4.13	3.90
19	CH <sub>3</sub> COOCH <sub>3</sub>	10	7.57	1.90	1.84	1.033	3.98	4.12
20	C <sub>2</sub> H <sub>5</sub> COOCH <sub>3</sub>	10	8.22	2.13	2.12	0.996	3.86	3.88
21	C <sub>2</sub> H <sub>5</sub> COOCH <sub>2</sub>	10	8.58	2.32	2.31	0.995	3.70	3.72
22	HCOOC <sub>2</sub> H <sub>5</sub>	10	7.50	1.80	1.81	1.006	4.17	4.14
23	C <sub>2</sub> H <sub>5</sub> COOC <sub>2</sub> H <sub>5</sub>	0	8.38	2.19	2.24	1.023	3.84	3.74
24	HCOOC <sub>2</sub> H <sub>5</sub>	10	8.52	2.11	2.20	1.043	4.04	3.87
25	C <sub>2</sub> H <sub>5</sub> COOC <sub>2</sub> H <sub>5</sub>	10	9.07	2.35	2.25	0.957	3.86	4.04

are water and the lower aliphatic alcohols, which are associated in liquid form and unassociated (except at low temperatures) in the vapour form.

GROUP B. If the vapour contains association complexes, say double molecules, then the dissociation increment is not measured by  $E_e$  and the geometrical arrangement will be defined by the ratio  $E_e/W_e$ . The ratio  $E_e/E_{\text{visc}}$  can be expected to be lower than the values found for normal liquids shown in Table III. A typical liquid in this group is acetic acid, which contains double molecules in the vapour.

Table IV shows the results of the calculations for some associated liquids.

On examining the data contained in Table IV, it is found that in all examples the ratio  $E_{\text{visc}}/W_e$  exceeds unity. An interesting example is acetone, which at 10° C gives a value of 1.26, while at 20° C the ratio is only 1.09, indicating the decrease in association with increase in temperature.

For most substances cited in Table IV, the ratio  $E_e/W_e$  far exceeds the values characteristic for different geometrical arrangements. These



liquids are associated while there is less association in the corresponding vapour. The ratio  $E_e/E_{\text{visc}}$  for these liquids lies between 2 and 4, which constitute the limits characteristic for different geometrical arrangements.

**Dipole Interaction and Association.**—Whilst the ratios of the different energies give an indication as to the symmetry of the arrangement of the molecules, the difference between  $E_{\text{visc}}$  and  $W_e$ , being equal to the energy of dissociation per bond (for the simpler molecular arrangements), may be used for investigating dipole interaction and association.

Let us consider a liquid in which all the molecules take part in associated complexes. For such a liquid one may write:

$$\frac{E_{\text{visc}} - W_e}{N} = E(r)_{\text{dipole interaction}}, \quad . \quad . \quad . \quad (10)$$

TABLE IV

$$E_{\text{visc}} > W_e$$

No.	Substance	°C	$E_e$ kcal./mole	$W_e$ kcal./mole	$E_{\text{visc}}$ kcal./mole	$E_{\text{visc}}/W_e$	$E_e/W_e$	$E_e/E_{\text{visc}}$
1	Water	0	10.17	2.10	4.80	2.29	4.84	2.12
		10	10.06	2.06	4.56	2.22	4.89	2.21
		20	9.95	2.02	4.15	2.06	4.93	2.40
		30	9.82	1.99	3.85	1.94	4.94	2.55
		40	9.71	1.94	3.63	1.87	5.00	2.68
		50	9.59	1.91	3.44	1.80	5.02	2.79
		60	9.46	1.86	3.32	1.78	5.09	2.85
		70	9.30	1.81	3.20	1.77	5.14	2.91
		80	9.23	1.77	3.04	1.72	5.22	3.04
2	CH <sub>3</sub> OH	100	8.96	1.67	2.85	1.70	5.36	3.14
		0	8.77	1.15	2.56	2.23	7.62	3.43
		20	8.50	1.08	2.48	2.30	7.88	3.43
		30	8.37	1.05	2.46	2.34	7.96	3.40
		50	8.10	0.98	2.44	2.49	8.26	3.32
3	C <sub>2</sub> H <sub>5</sub> OH	10	9.94	1.42	3.32	2.34	7.00	3.00
		20	9.78	1.38	3.29	2.38	7.08	2.97
		40	9.45	1.30	3.26	2.51	7.27	2.90
		50	9.31	1.25	3.22	2.58	7.45	2.89
4	CH <sub>3</sub> CH <sub>2</sub> CH <sub>2</sub> OH	20	11.02	1.71	4.41	2.58	6.44	2.50
		40	10.63	1.61	4.39	2.73	6.60	2.42
		60	10.19	1.51	4.37	2.89	6.75	2.33
		80	9.80	1.41	4.34	3.08	6.95	2.26
5	CH <sub>3</sub> CH <sub>2</sub> CH <sub>2</sub> CH <sub>2</sub> OH	0	12.46	2.04	4.67	2.29	6.10	2.67
		20	12.07	2.01	4.64	2.31	6.01	2.60
		50	11.26	1.85	4.59	2.48	6.08	2.45
6	Acetone	0	7.60	1.83	2.30	1.26	4.15	3.30
		20	7.24	1.70	1.86	1.09	4.26	3.89
7	CH <sub>3</sub> Cl	0	4.35	1.11	1.66	1.50	3.92	2.62
		10	4.24	1.03	1.63	1.58	4.12	2.60
		20	4.12	0.95	1.59	1.67	4.34	2.59
8	HCOOH	10	5.98	1.75	3.87	2.21	3.42	1.55
		20	5.90	1.71	3.63	2.12	3.45	1.62
		50	5.50	1.59	3.22	2.02	3.46	1.71
9	CH <sub>3</sub> COOH	20	6.31	1.67	2.90	1.74	3.78	2.18
		50	5.95	1.52	2.70	1.77	3.91	2.20
		75	5.62	1.39	2.50	1.80	4.04	2.25
10	CH <sub>3</sub> CH <sub>2</sub> COOH	20	7.52	1.91	2.45	1.28	3.94	3.07
11	CH <sub>3</sub> CH <sub>2</sub> CH <sub>2</sub> COOH	20	10.87	2.23	2.99	1.34	4.87	3.53
		50	10.56	2.03	2.93	1.44	5.20	3.61
		100	9.96	1.73	2.88	1.66	5.76	3.46
12	CH <sub>3</sub> CHCOOH	20	10.57	2.08	2.75	1.32	5.08	3.85
		50	10.26	1.90	2.67	1.41	5.40	3.85
		100	9.66	1.56	2.57	1.65	6.19	3.76

and since  $E(r)_{\text{dipole interaction}}$  may be considered as the summation of the orientation and induction effects, by using eqn. (1), (2) and (4), then

$$\frac{E_{\text{visc}} - W_c}{N} = \frac{2\mu^2}{r^3} + \frac{2\mu^2\alpha}{r^6} \quad . \quad . \quad . \quad (11)$$

for parallel, and

$$\frac{E_{\text{visc}} - W_c}{N} = \frac{\mu^2}{r^3} + \frac{2\mu^2\alpha}{r^6} \quad . \quad . \quad . \quad (12)$$

for anti-parallel arrangement of the dipoles. By rearranging these equations, the dipole moment  $\mu$  is given by

$$\mu_{\text{par}} = \sqrt{\frac{E_{\text{visc}} - W_c}{N} \cdot \frac{r^3}{2 + 2\alpha/r^3}} \quad . \quad . \quad . \quad (13)$$

and

$$\mu_{\text{antipar}} = \sqrt{\frac{E_{\text{visc}} - W_c}{N} \cdot \frac{r^3}{1 + 2\alpha/r^3}} \quad . \quad . \quad . \quad (14)$$

Whilst eqn. (11) to (14) are valid for liquids in which degree of association is unity, i.e. all the possible dipole interaction bonds are formed, a correction is necessary for liquids in which the degree of association is less than unity, i.e. only the fraction  $\beta$  of the possible dipole interaction bonds are formed. If eqn. (13) and (14) were used for this condition, a dipole moment would be obtained, which would have a smaller value than the dipole moment obtained by usual methods. If the dipole moment from other measurements is available, the degree of association  $\beta$  can be calculated. For a partially associated liquid

$$\frac{E_{\text{visc}} - W_c}{N} = \beta E(r)_{\text{dipole interaction}} \quad . \quad . \quad . \quad (15)$$

Hence

$$\beta = \left( \frac{\mu_{\text{calc.}}}{\mu_{\text{obs.}}} \right)^2 \quad . \quad . \quad . \quad . \quad (16)$$

where  $\mu_{\text{calc.}}$  is the value of  $\mu$  obtained from eqn. (13) and (14) and  $\mu_{\text{obs.}}$  the value of  $\mu$  obtained from other measurements, e.g. dielectric constant and density.

Mostly the conditions are more complicated than those outlined above. The relative orientation of the dipoles may conform neither to a parallel or an antiparallel position and the geometrical arrangement of the molecules may be such that  $E_{\text{visc}}$  and  $W_c$  may be equivalent to more than one bond. These factors must in all cases be taken into account.

## 5. Applications of Results

**Normal Liquids.**—In Table II it has been shown that values of  $E_v/W_c$  (or  $E_v/E_{\text{visc}}$ ) between 2 and 4 are characteristic for certain arrangements of the molecules. These results in Table III suggest that the co-ordination number in normal liquids may vary between 6 and 12. The actual proportions of the various arrangements present cannot, however, be elucidated by the method employed.

There are many indications in the literature that co-ordination numbers in liquids may be about 12 (e.g. liquid mercury and xenon<sup>12</sup>). The values of  $E_v/W_c$  (or  $E_v/E_{\text{visc}}$ ) given in Table III vary between 3 and 4. From Tables I and II we find that the ratios 3, 4, 4 and 4 correspond to co-ordination numbers of 6, 8, 12 and 12 respectively. If the co-ordination numbers in normal liquids would be 12, then only ratios of 4 would have been found in Table III. Lower co-ordination numbers may thus be considered to play an important part in liquids.

**Water.**—The structure of the ice lattice has been investigated by means of X-ray data by many workers. It appears that in ice the oxygen atoms are situated in the centre of a tetrahedron, and are surrounded by four hydrogen atoms. Since every hydrogen atom is common to two tetrahedra, the ratio

<sup>12</sup> Campbell and Hildebrand, *J. Chem. Physics*, 1943, 11, 330, 334.

H/O = 2/1 is maintained throughout the crystal. This structure is similar to that existing in certain modifications of silica, such as tridymite. Bernal and Fowler<sup>13</sup> investigated the structure of liquid water using X-ray data. These workers concluded that, in order to account for the low density of water, it is necessary to assume that the open tetrahedral structure characteristic for ice should exist also in water. Three types of arrangement are said to exist in water—

- (i) tridymitic ice-like structure existing below 4° C;
- (ii) quartz-like structure existing at ordinary temperatures;
- (iii) close-packing as an ideal liquid. This arrangement is favoured by increasing temperature.

There is no question of a mixture of volumes with different structures. At all temperatures the time-average structure of liquid water is macroscopically homogeneous, but the average arrangement of the molecules resembles to a certain extent one of the three types. The maximum of the density of water at 4° C can be explained by a change of type (i) to type (ii), since the latter corresponds to a closer approach of the oxygen atoms.

Additional evidence that at ordinary temperatures the structure of water differs considerably from that of an ordinary close-packed liquid, can be derived from the fact that between 0 and 30° C the viscosity of water decreases with the increase in pressure, whilst the viscosity of other liquids increases with the pressure. These facts have been observed by Bridgman.<sup>14</sup> This can be interpreted as due to the breakdown of the open tetrahedral structure under the action of pressure.

If the ratios  $E_{\text{visc}}/W_e$ ,  $E_e/W_e$  and  $E_e/E_{\text{visc}}$  for water (Table IV) are examined it is found that

(i)  $E_{\text{visc}}/W_e$  is appreciably greater than unity. Water is therefore, according to the arguments brought forward in the present work, an associated liquid.

(ii)  $E_e/W_e$  is greater than 4, water is therefore mainly dissociated in the vapour form.

(iii)  $E_e/E_{\text{visc}}$  increases from a value of 2.12 to a value of 3.14 as the temperature increases from the melting to the boiling point. From Table II, a ratio equal to 2 is characteristic for the tetrahedral arrangement of the molecules, whilst close-packing is characterised by a ratio of 4. The values of the ratio  $E_e/E_{\text{visc}}$  thus confirm that the arrangement of the molecules in water is in part tetrahedral. The extent of close-packing increases with the increase in temperature. The valence angle on the oxygen atom in water is of the order of 104°, very close to the value of the regular tetrahedral angle of 109°. The arrangement of the dipoles in water is thus neither parallel nor antiparallel and to a first approximation an angle of about 52° may be assumed between associated dipoles. The bond strength due to the orientation effect will then be equal to  $1.231\mu^2/r^3$ . The correction for the induction effect will still be of the order of  $2\mu^2\alpha/r^6$ , so that—

$$\text{Bond strength (orientation + induction)} = \mu^2/r^3 (1.231 + -2\alpha/r^3) \quad (17)$$

With  $\mu = 1.84 \times 10^{-18}$  D and  $r = 2.76$  Å (for tridymitic arrangement at 0° C) we calculated a value of 3.23 kcal. for  $N$  bonds. This figure can now be compared with the value for the hydrogen-bond from latent heat data. The heat of sublimation of ice is 11.62 kcal./mole (the latent heat of fusion is 1.44 kcal./mole and the internal latent heat of vaporisation 10.18 kcal./mole). If we assume that the contribution of the dispersion forces to  $2N$  bonds equals  $2W_e$  i.e. 4.20 kcal./mole the value of the hydrogen bond becomes 7.42 kcal./mole or 3.71 kcal./ $N$  bonds. The values of 3.23 and 3.71 kcal. are lower than the value of 4.5 kcal. given by Pauling.<sup>15</sup> The discrepancy arises from difference in the estimation of the dispersion contribution to the bond.

Using the data for  $(E_{\text{visc}} - W_e)$  and the values of  $r = 2.76$  Å for the tridymitic structure (below 4° C) and of  $r = 2.71$  Å for the quartz-like structure (above 4° C) we calculated the degree of association of water between 0 and 100° C. The results are given as curve I in Fig. 1. Alternative values of the degree of association were calculated from  $(E_{\text{visc}} - W_e)$  and the value of 3.71 kcal./ $N$  bonds obtained from latent heat data. These values are shown as curve II in Fig. 1. A check on these calculations can be obtained by considering

<sup>13</sup> Bernal and Fowler, *J. Chem. Physics*, 1933, 1, 513.

<sup>14</sup> Bridgman, *The Physics of High Pressure* (Bell & Sons, 1931).

<sup>15</sup> Pauling, *The Nature of the Chemical Bond* (Cornell, 1940).

the amount of dissociation occurring during melting. The latent heat of fusion is 1.44 kcal./mole. Expressing this as a fraction of  $2N$  hydrogen bonds, according

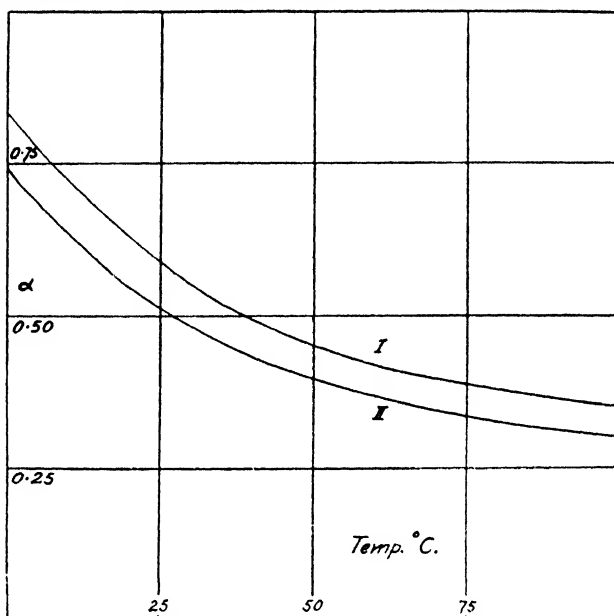


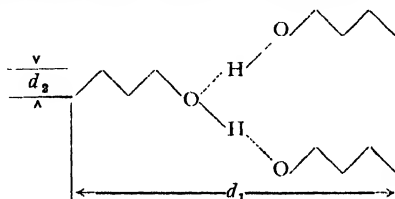
FIG. 1.

to the electrostatic model or to latent heat data, we obtain 0.22 and 0.19 respectively. The corresponding values for the degree of association of water at 0° C from  $(E_{\text{visc}} - W_e)$  are 0.84 and 0.73 showing tolerable agreement with the fusion data.

**Alcohols and Fatty Acids.**—These two groups of substances show important differences in their behaviour. If the values of  $E_{\text{visc}}/W_e$ ,  $E_v/W_e$  and  $E_v/E_{\text{visc}}$  (Table IV) are examined it is found that both alcohols and acids show the criterion of association, namely  $E_{\text{visc}}/W_e > 1$ . The alcohols show ratios  $E_v/W_e > 4$  and  $E_v/E_{\text{visc}}$  between 2.4. They can therefore be regarded as associated in the liquid, although mainly dissociated in the vapour. Formic and acetic acids show values of 3.4 for  $E_v/W_e$  whilst  $E_v/E_{\text{visc}}$  is much smaller. This seems to indicate that these substances are associated both in the liquid and in the vapour.

It is interesting to note that the values for  $E_v/W_e$  and  $E_v/E_{\text{visc}}$  of the higher acids are similar to those obtained with the alcohols. This indicates that these acids are less associated in the vapour than formic and acetic acids.

A great number of X-ray measurements have been taken on alcohols<sup>16</sup> and acids.<sup>17, 18, 19, 20, 21</sup> Two principal distances can be observed with these compounds. One of these distances increases only slightly as one ascends the homologous series and can be attributed to the distance between the hydrocarbon chains ( $d_2$ ). The other distance ( $d_1$ ) increases with chain length and can be attributed to the distance between the ends of two associated molecules—  
e.g. alcohol molecules :



<sup>16</sup> Stewart and Morrow, *Physic. Rev.*, 1927, **30**, 232.

<sup>17</sup> Morrow, *ibid.*, 1928, **31**, 10.

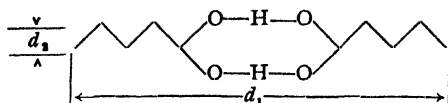
<sup>18</sup> Katz, *Z. Physik*, 1927, **45**, 97; 1928, **46**, 392.

<sup>19</sup> Krishnamurti, *Indian J. Physics*, 1928, **2**, 355; 1930, **4**, 449.

<sup>20</sup> de Smedt, *Bull. Roy. Soc. Belg.*, 1924, **10**, 366.

<sup>21</sup> Sogani, *Indian J. Physics*, 1928, **2**, 491.

and acid molecules :



The values of  $d_1$  and  $d_2$  are given in Table V.

TABLE V

Substance.	$d_1(\text{\AA})$ .	$d_2(\text{\AA})$ .
Methyl alcohol . . . . .	5.35	3.81
Ethyl alcohol . . . . .	7.82	4.07
<i>n</i> -Propyl alcohol . . . . .	9.92	4.43
<i>n</i> -Butyl alcohol . . . . .	11.30	4.48
Formic acid . . . . .	5.20	3.65
Acetic acid . . . . .	5.90	4.17
Propionic acid . . . . .	6.00	4.39
Butyric acid . . . . .	8.5	4.64

From these data and the probable configuration of the associated complexes one can deduce that the orientation of the dipoles in alcohols and acids is anti-parallel. For methyl alcohol using  $\mu = 1.68 \times 10^{-18}$  D and  $r = 2.7$  Å we obtained a value of 2.67 kcal./N hydrogen bonds. In order to calculate the degree of association it is necessary to make an *a priori* assumption as to the number of bonds corresponding to  $E_{\text{visc}}$  and  $W_e$ . Assuming this figure to be about 1.5 (since  $E_e/W_e$  is about 3.4), we find  $(E_{\text{visc}} - W_e)/1.5$  at 20° C to be about 0.93 kcal./N bonds and the degree of association to equal 0.34.

We calculated a value of about 2.7 kcal. for the hydrogen bond in methyl alcohol whilst Pauling<sup>18</sup> reports a value of 6.2 kcal. Ordinarily the strength of the hydrogen bond is obtained by subtracting the contribution of the dispersion forces from the total bond strength. The accuracy thus depends on the estimation of the contribution of the dispersion forces. It was shown above that by using  $W_e$  as an expression of the dispersion increment tolerable agreement can be obtained for the value of the hydrogen bond in water from the electrostatic attraction and latent heat data. We shall proceed in the opposite direction for methyl alcohol and try to evaluate the number of nearest neighbours from latent heat data and  $W_e$ , using the value of the hydrogen bond obtained from the electrostatic model.

A molecule of methyl alcohol can form 2 hydrogen bonds, so that there are N such bonds in a mole. The latent heat of sublimation of methyl alcohol is about 9.3 kcal./mole and if the hydrogen bond equals 2.7 kcal./mole, then at the melting point the contribution of the dispersion is about 6.6 kcal./mole. At the melting point the value of  $W_e$  can be estimated to be about 1.6 kcal. If  $W_e$  is equivalent to 1.5 bonds we find that the dispersion forces are equivalent to about 6 bonds per molecule. This shows that a molecule of methyl alcohol at the melting point is probably surrounded by 12 nearest neighbours. This result cannot be obtained from Pauling's value of the hydrogen bond in methyl alcohol.

We calculated the value of the hydrogen bond in other alcohols and found for ethyl alcohol 2.74, for *n*-propyl alcohol 2.61 and for *n*-butyl alcohol 2.80 kcal./N bonds. Making the same assumptions as for methyl alcohol, the degree of association from  $(E_{\text{visc}} - W_e)$  at 20° C is for ethyl alcohol 0.46, for *n*-propyl alcohol 0.69 and for *n*-butyl alcohol 0.67.

The strength of the hydrogen bond in formic<sup>22</sup> and acetic<sup>23</sup> acids, reported in the literature is 7.06 and 8.2 kcal. respectively. From the electrostatic model we calculated values of 2.56 and 2.93 kcal. Pauling<sup>18</sup> comments on the highly ionic character of the bond in these substances. Thus it seems that the pure dipole attraction accounts only for about 36 % of the total bond strength.

It is of interest to calculate to what extent viscous flow is a monomolecular process in formic and acetic acids. Assuming that  $E_{\text{visc}}$  and  $W_e$  represent

<sup>22</sup> Coolidge, *J. Amer. Chem. Soc.*, 1926, **50**, 2166.

<sup>23</sup> Macdougall, *ibid.*, 1936, **58**, 2585.

the energy of 1.5 bonds, the dissociation energy per  $N$  bonds is 1.28 and 0.82 kcal. at 20°C. Viscous flow in formic and acetic acid is about 18 and 10 % a monomolecular process.

**Esters.**—Steric effects may render the dipole "inaccessible" and thus prevent dipole interaction. This is best illustrated by the results obtained with organic esters. Although highly polar substances ( $\mu$  varies from 1.7 to 2.0), the esters are unassociated liquids, due to the shielding effect of the hydrocarbon chains. As shown in Table III,  $E_{visc} \simeq W_e$ , whilst the values of  $E_e/W_e$  and  $E_e/E_{visc}$  approximate a value of 4 very closely. Thus esters, in contrast to alcohols and acids, and in spite of the high value of the dipole moment, are "normal" liquids, characterised mainly by close packing.

**Ketones.** The influence of steric effects may vary also within the same groups of compounds. Thus whilst acetone shows the criteria of a partly associated liquid, higher ketones such as methyl ethyl ketone or diethyl ketone, although highly polar, are unassociated. The accessibility of the dipoles is reduced by an increase in the chain length of the substituent groups. Methyl groups afford a certain amount of shielding, as can be seen from the fact that acetone is only partially associated.

Dr. Rosin Industrial Research  
Co., Ltd.,  
Wembley,  
Middlesex.

The Bowater Paper Corporation, Ltd.,  
Central Research Laboratories,  
Northfleet,  
Kent.

---

## ON PHASE-CHANGE PROCESSES IN IRON-SILICON ALLOYS

BY K. M. GUGGENHEIMER AND H. HEITLER

Received 23rd January, 1948; as revised 17th August, 1948

Various phase-change processes in the solid state of the iron-silicon system which have been observed previously by measuring the magnetic saturation intensities as functions of temperature have been studied with respect to their reaction kinetics. Quasi-monomolecular and bimolecular reactions have been found and some activation energies have been determined.

---

Measurements of the magnetic saturation intensity of ferro-magnetic materials can be used to establish the presence of certain magnetic phases.<sup>1, 2, 3, 4</sup> In a recent paper,<sup>4</sup> a study of the magnetic properties of the iron-silicon system, carried out in the years 1942-46, was described in some detail. It was shown that it is possible to determine the phase composition of these alloys and important details of the phase diagram. Further, the magnetic method can be used to investigate reactions occurring in the solid state. The use of this method appears to be possible even in a case where alloys undergo complicated phase changes. In this paper, an attempt has been made to consider the reaction kinetics of these phase-change processes.

### Experimental and Results

The experimental procedure previously described<sup>4</sup> was briefly as follows. All specimens were kept at a controlled temperature until they had reached a well-defined equilibrium state and then quenched; they were then submitted to a heat treatment at a chosen temperature for various lengths of time. After

<sup>1</sup> Sucksmith, *Proc. Roy. Soc. A*, 1939, **170**, 551; **171**, 525.

<sup>2</sup> Pickles and Sucksmith, *ibid.*, 1940, **175**, 331.

<sup>3</sup> Hoselitz and Sucksmith, *ibid.*, 1943, **181**, 303.

<sup>4</sup> Guggenheimer, Heitler and Hoselitz, *J. Iron Steel Inst.*, 1948, 192.

each heat treatment a magnetic saturation intensity-temperature curve ( $\sigma-T$  curve) was obtained by use of a magnetic balance. The  $\sigma$ -values were measured from room temperature to temperatures well beyond the Curie point at intervals of 10-15°. It was found that three different magnetic phases, the  $\alpha$ -solid solution, the  $\alpha'$ -phase and the  $\eta$ -phase can occur.

The first task was, therefore, to determine the exact composition and the magnetic characteristics of the pure phases. The main data are contained in Table I. It can be seen that they are widely different and therefore easily distinguishable from each other in the  $\sigma-T$  curves.

TABLE I

	% Si	Curie Temp. (° C)	$\sigma$ at		
			Room Temp.	150° C	300° C
Pure iron . . . . .	0	768	217.8	—	—
$\alpha$ -phase (saturated solid solution) . . . . .	17.1	555	119	113	100
$\alpha'$ -phase . . . . .	20.8	270	68	45.3	9.4
$\eta$ -phase . . . . .	23.2	120	75	15.4	2.0
$\epsilon$ -phase . . . . .	33.4	non-magnetic	—	—	—

The composition of the pure phases given by other authors whose investigations were carried out prior to or simultaneous with this work may be of interest for comparison.

TABLE II

Author	% Si			
	$\alpha$	$\alpha'$	$\eta$	$\epsilon$
Stoughton and Greiner <sup>5</sup> . . . . .	15	—	25	33.4
Osawa and Murata <sup>6</sup> . . . . .	15	18.6	23.2	33.4
Lipson and Weill <sup>7</sup> . . . . .	16	—	23.2	33.4
Farquhar, Lipson and Weill <sup>8</sup> . . . . .	15.1	20.2-20.6	23.2	33.4

The part of the resulting phase diagram, as far as it has been established by the magnetic measurements, is shown in Fig. 1. In the solidus there are four main equilibrium regions in which the three magnetic phases are in stable states.

(i) Between 0 and 17.1 % Si right up to the liquidus there is an extensive region of an  $\alpha$ -solid solution of silicon in iron.

(ii) Between 17.1 and 33.4 % Si up to about 830° C the saturated  $\alpha$ -solid solution is in equilibrium with the non-magnetic  $\epsilon$ -phase.

(iii) Between about 19 and 33.4 % Si in the temperature region 830° C-1030° C the  $\eta$ -phase is stable and in equilibrium with the  $\alpha$ -phase below 23.2 % Si and with the  $\epsilon$ -phase above it.

(iv) Between about 19 and 33.4 % Si at temperatures above 1030° C the  $\alpha'$ -phase is stable and in equilibrium with the  $\alpha$ -phase below 20.8 % Si and with the  $\epsilon$ -phase above it.

The horizontal boundaries were of no particular interest for the present work and therefore not specifically determined.

With the aid of the magnetic values of the pure phases it was then possible to analyse all experimental curves with respect to the amounts of each phase

<sup>5</sup> Stoughton and Greiner, *Metals Handbook* (Amer. Soc. Metals, Cleveland, 1939), B96.

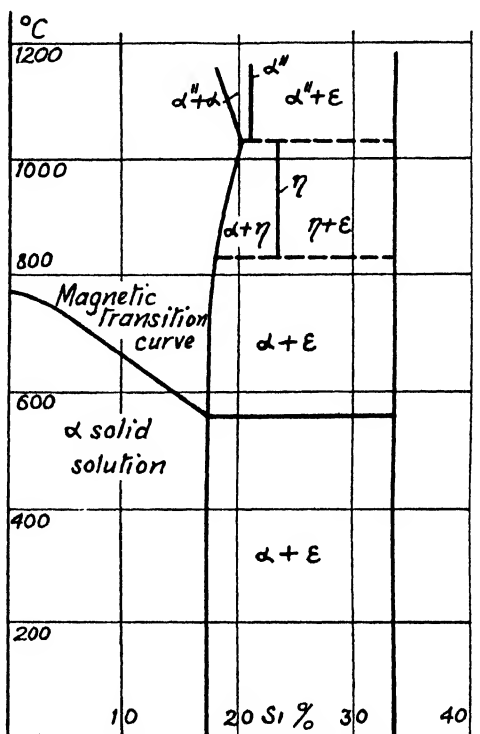
<sup>6</sup> Osawa and Murata, *Nippon Kinzoku Cakkai-Si*, 1940, 4, 228.

<sup>7</sup> Lipson and Weill, *Trans. Faraday Soc.*, 1943, 39, 13.

<sup>8</sup> Farquhar, Lipson and Weill, *J. Iron Steel Inst.*, 1945, 457.

present and to study the transition from one equilibrium region into another as function of temperature and duration of heat treatment. In particular, the transition of the  $\alpha''$ -equilibrium into that of the  $\alpha$ - was investigated in great

FIG. 1.—Phase boundaries determined magnetically.  
 — Phase boundaries determined by magnetic analysis.  
 - - - Not accurately determined.



detail. Some resulting curves are shown in Fig. 2-4 in which the fractional weight  $\omega$  of the magnetic phases present are given as a function of time of anneal. Fig. 2 shows a specimen with 27.5 % Si annealed at 650° C and Fig. 3 another

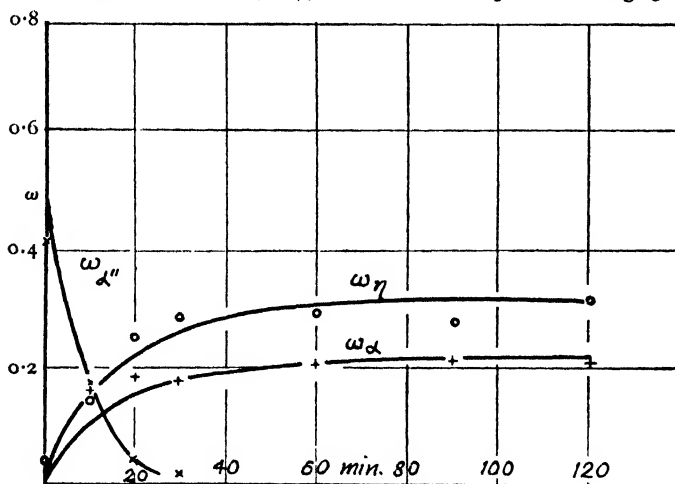


FIG. 2.—Change of  $\omega_{\alpha}$ ,  $\omega_{\alpha''}$  and  $\omega_{\eta}$  with time of anneal at 650° C in a specimen with 27.5 % silicon. Drawn out curves calculated acc. to eqn. (8)-(10) and Table V.



one with 25 % Si annealed at 550 and 608° C. It can be seen that the magnetic  $\alpha''$ -phase decomposes and the two other magnetic phases  $\alpha$  and  $\eta$  are produced. The rate of decay of  $\alpha''$  and the formation of  $\alpha$  and  $\eta$  are slow enough to allow the determination of the reaction velocities.

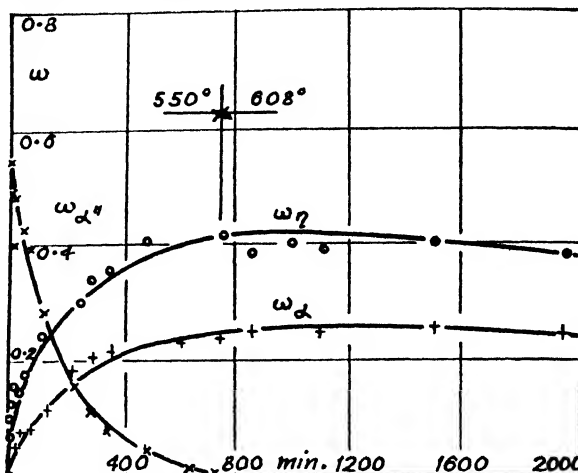


FIG. 3.—Change of  $\omega_\alpha$ ,  $\omega_{\alpha''}$  and  $\omega_\eta$  with time of anneal at 550° and 608° C in a specimen with 25 % silicon. Drawn out curves calculated acc. to eqn. (8)-(10) and Table VI.

However, the  $\eta$ -phase is not stable, but passes through a maximum and disappears again after much longer heat treatment. At the same time the amount of the  $\alpha$ -phase increases until equilibrium with the  $\epsilon$ -phase is reached. The results of a 23 % Si specimen heat treated at 735° C are shown in Fig. 4. The decay rate of the  $\alpha''$ -phase has been too rapid to be measured, but the subsequent decay of  $\eta$ - and increase of  $\alpha$ -are easily observable.

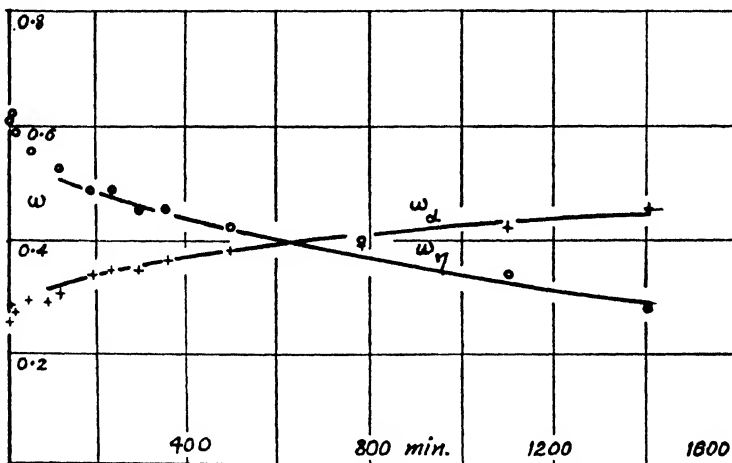


FIG. 4.—Change of  $\omega_\alpha$  and  $\omega_\eta$  with time of anneal at 735° C in a specimen with 23 % silicon. Drawn out curves calculated acc. to eqn. (8)-(10) and Table V.

### Discussion

**Quasi-monomolecular Reactions.**—The results of the magnetic analysis are quantitative. They can serve as a basis for treating the phase-change processes as chemical reactions and for investigating the reaction

kinetics. From Fig. 2 and 3 it can be seen that the amount  $\omega_{\alpha'}$  which disappears is equal to the sum of  $\omega_{\alpha} + \omega_{\eta}$  which are produced. The reaction is therefore



The  $\epsilon$ -phase does not enter this reaction.

A further confirmation of this reaction is provided by calculating the amount of silicon involved in it. If the observed  $\omega$ -values are multiplied by the corresponding silicon contents of the pure phases (see Table I), the sum  $Si_{\alpha} + Si_{\alpha'} + Si_{\eta}$  must be constant. This condition is approximately fulfilled (cp. Table III).

TABLE III

Heat Treatment			$\omega$				Si %				
Spec.	Temp. °C	Duration	$\alpha$	$\alpha''$	$\eta$	$\epsilon$	$\alpha$	$\alpha''$	$\eta$	$\epsilon$	$\Sigma Si$
25 %	1100	2 hr.	0.001	0.668	0.000	0.331	0.0	14.0	0.0	11.1	25.1
"	550	10 min.	0.038	0.498	0.125	0.339	0.6	10.4	2.9	11.3	25.2
"	550	6 hr.	0.224	0.026	0.410	0.340	3.8	0.5	9.5	11.4	25.2
"	550	7 days	0.296	0.000	0.360	0.344	5.1	0.0	8.3	11.5	24.9

The second reaction, that is the slow decay of  $\eta$ -, results in an increase of the  $\alpha$ -phase as shown in Fig. 4. Since the silicon content of  $\alpha$ -is smaller than that of  $\eta$ -, the non-magnetic  $\epsilon$ -phase must also increase. The reaction is, therefore,



The chemical formulae which correspond best to the silicon content of the pure phases (Table IV) are :

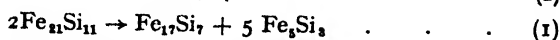
TABLE IV

	Formula	% Si	Temp. °C
$\alpha''$	$Fe_{21}Si_{11}$	20.84	750
$\alpha$	$Fe_{17}Si_7$	17.14	"
$\eta$	$Fe_8Si_3$	23.17	"
$\epsilon$	$FeSi$	33.44	"

Thus the first reaction must have the form :



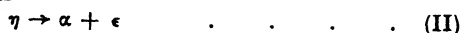
or



The factors, however, which are involved in this stoichiometric formulation, have only a formal significance. The crystallites of the different phases are large homogeneous complexes. For this reason, the reactions in the solid state are of the first-order with respect to each phase, and the following formulation for indicating the chemical units which react together is to be preferred,



For the second reaction one has



i.e.



or



These chemical units ( $n_x$ ) which react together possess masses which can be expressed in units of atomic weight. If the empirical weights per cent.  $\omega_x$  of each phase are divided by the molecular weight  $M_x$  of these chemical units, one obtains the number of these units present in 1 g. of the specimen, e.g.,  $n_\alpha = \omega/M_\alpha$ , where  $M_\alpha$  is according to (1),  $17 \times 55.84 + 7 \times 28.06 = 1146$ . In a similar way one obtains

$$n_{\alpha''} = \frac{\omega_{\alpha''}}{2963}; \quad n_\eta = \frac{\omega_\eta}{1817}; \quad n_\epsilon = \frac{\omega_\epsilon}{671}$$

With the aid of these units it is possible to formulate the differential equations for the reactions as follows. The decay of  $\alpha''$  in reaction (I) is quasi-monomolecular,

$$\frac{dn_{\alpha''}}{dt} = -k_1 n_{\alpha''}, \quad . \quad . \quad . \quad (3)$$

where  $k_1$  is the velocity constant of the  $\alpha''$  decay. The  $\eta$ -phase is created in reaction (I) with the same constant  $k_1$  and decays in reaction (II) with the velocity constant  $k_2$ , therefore,

$$\frac{dn_\eta}{dt} = k_1 n_{\alpha''} - k_2 n_\eta \quad . \quad . \quad . \quad (4)$$

The  $\alpha$ -phase is formed in reaction (I) with constant  $k_1$  and in (II) with velocity constant  $k_2$ , thus

$$\frac{dn_\alpha}{dt} = k_1 n_{\alpha''} + k_2 n_\eta \quad . \quad . \quad . \quad (5)$$

The  $\epsilon$ -phase increases in reaction (II) with the velocity constant  $k_2$ , according to

$$\frac{dn_\epsilon}{dt} = k_2 n_\eta \quad . \quad . \quad . \quad (6)$$

The initial conditions are, for  $t = 0$ ,

$$n_{\alpha''}(0) = n_{0\alpha''}; \quad n_\epsilon(0) = 0; \quad n_\alpha(0) = 0; \quad n_\eta(0) = 0 \quad . \quad (7)$$

The integration of equations (3)-(6) gives

$$n_{\alpha''} = n_{0\alpha''} e^{-k_1 t}; \quad . \quad . \quad . \quad (8)$$

$$n_\eta = \frac{k_1 n_{0\alpha''}}{k_1 - k_2} (e^{-k_2 t} - e^{-k_1 t}); \quad . \quad . \quad . \quad (9)$$

$$n_\alpha = n_{0\alpha''} (2 - e^{-k_1 t}) - \frac{n_{0\alpha''}}{k_1 - k_2} (k_1 e^{-k_2 t} - k_2 e^{-k_1 t}); \quad . \quad (10)$$

$$n_\epsilon = n_{0\alpha''} - \frac{n_{0\alpha''}}{k_1 - k_2} (k_1 e^{-k_2 t} - k_2 e^{-k_1 t}) + n_{0\alpha''} \quad . \quad (11)$$

According to eqn. (8),  $\alpha''$  decays exponentially. The plot of  $\log n_{\alpha''}$  against time gives a straight line, the slope of which gives a measure of the velocity constant  $k_1$ . The same velocity constant  $k_1$  can be obtained from the observed initial formation of  $\alpha$  and  $\eta$  (eqn. (4) and (5)). The velocity varies appreciably with the temperature of anneal (cf. Table VI).

The  $\eta$ -phase passes through a maximum, and decays also exponentially for times  $t \gg k_1^{-1}$ . Straight lines are also obtained if  $\log n_\epsilon$  is plotted against time. The constants are given in Table VI. It is found that  $k_2$  is much smaller than  $k_1$ .

After the two constants  $k_1$  and  $k_2$  are determined, theoretical curves can be constructed. They are the curves drawn in Fig. 2-4, and describe the experimental results for the whole time of observation, within the experimental error.

The change of the velocity constants with temperature can best be described by

$$k_1 = 6.7 \times 10^6 e^{-20,000/T} \quad . \quad . \quad (12)$$

$$\text{and} \quad k_2 = 1.1 \times 10^3 e^{-16,000/T} \quad . \quad . \quad (13)$$

A third quasi-monomolecular reaction has been observed, namely,

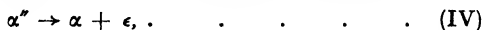


at temperatures above 1030° C. The chemical reaction corresponds to



The reaction takes place within a few hours. The lowest velocity constant observed was  $k_v = 7.5 \times 10^{-8} \text{ sec.}^{-1}$  but this is probably already influenced by the back reaction during cooling.

Formally a fourth monomolecular reaction is possible, namely,



or

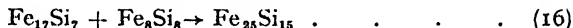


However, this reaction has not been observed. According to the phase diagram, it could only occur below 850° C but there the  $\alpha''$  decay proceeds always according to reaction (I), that is,  $\alpha'' \rightarrow \alpha + \eta$  and these two phases are always formed in the ratios expected by this latter formula.

**Quasi-bimolecular Reactions.**—Formally, all four reactions so far described could also occur in the reverse direction at suitable temperatures. The reverse reaction to (II), namely,



or



has been observed at between 900 and 1000° C. A series of specimens with varying silicon content has been investigated at 950° C and the formation of  $\eta$  observed over increasing times of anneal. Since two different phases have to react together to form a new one, the reaction cannot in general proceed according to the law of monomolecular reaction. An attempt has been made, therefore, to apply the equation for bimolecular reactions, viz.,

$$\frac{dn_\eta}{dt} = k_v(n_{0\alpha} - n_\eta)(n_{0\epsilon} - n_\eta) \quad \text{(17)}$$

where  $n_{0\alpha}$  and  $n_{0\epsilon}$  are the initial concentrations of the  $\alpha$ - and  $\epsilon$ -phase respectively, and  $n_\eta$  is the concentration of the  $\eta$ -phase as a function of time. The integration of this equation leads to

$$k_v t = \frac{1}{n_{0\alpha} - n_{0\epsilon}} \ln \frac{n_{0\epsilon} (n_{0\alpha} - n_\eta)}{n_{0\alpha} (n_{0\epsilon} - n_\eta)} \quad \text{(18)}$$

Table V gives the result for four specimens between 23 % and 30 % silicon for heat treatments between about 6 and 10 hr. at 950° C.

TABLE V

% Si	Time (hr.)	$k_v$ (sec. <sup>-1</sup> mol. <sup>-1</sup> cm. <sup>3</sup> )
23	8½	$1.5 \times 10^{-3}$
25	9½	$1.4 \times 10^{-3}$
27.5	6½	$1.3 \times 10^{-3}$
30	6½	$1.4 \times 10^{-3}$

It can be seen that for the above times of anneal, eqn. (18) fits the experimental results surprisingly well for this wide range of silicon contents, and leads to the same velocity constant in all four cases, thus confirming the mechanism of bimolecular reaction. However, the formation of the  $\eta$ -phase slows down considerably after longer periods of anneal, presumably owing to the influence of diffusion which must take place before the reaction can be completed. Even after several weeks of anneal traces of  $\alpha$  are found.

Another reaction  $\alpha + \epsilon \rightarrow \alpha''$ , . . . . . (VI)

or  $\text{Fe}_{17}\text{Si}_7 + \text{Fe}_4\text{Si}_4 \rightarrow \text{Fe}_{21}\text{Si}_{11}$  . . . . . (19)

has also been observed and measured. Formally, it is the reverse of reaction (IV) which, however, has not been observed. Reaction (VI) takes place at temperatures above  $1030^\circ\text{C}$ . The velocity has been measured at  $1140^\circ\text{C}$ . The evaluation of the experimental data of several specimens with different silicon contents shows again that eqn. (18) can be applied and leads to a constant of velocity of the order of magnitude  $k_{v1} = 8 \times 10^{-3} \text{ sec.}^{-1} \text{ mol.}^{-1} \text{ cm.}^3$  though the fluctuations are bigger than those in reaction (V).

The reverse of reaction (III) takes the form

$\alpha'' + \epsilon \rightarrow \eta$ , . . . . . (VII)

or  $\text{Fe}_{21}\text{Si}_{11} + \text{Fe}_4\text{Si}_4 \rightarrow \text{Fe}_{25}\text{Si}_{15}$ , . . . . . (20)

and occurs between  $900$  and  $1030^\circ\text{C}$ . It has been found in the present investigation and is effectively completed within a few hours. This reaction is the most suitable one to bring the  $\eta$ -phase into equilibrium with the  $\epsilon$ -phase and with a specimen of 23 % Si it was possible to obtain the  $\eta$ -phase in its pure form. The magnetic intensity  $\sigma$  reaches its maximum value in the series of specimens which show the  $\eta$ -phase as the only magnetic phase. It seems that this phase is distinguished by exceptional hardness and resistance to chemical attack. More detailed measurements have still to be performed to determine the velocity constant.

The reverse of reaction (I) is

$\alpha + \eta \rightarrow \alpha''$ , . . . . . (VIII)

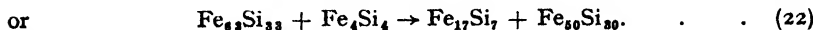
or  $\text{Fe}_{17}\text{Si}_7 + \text{Fe}_{25}\text{Si}_{15} \rightarrow \text{Fe}_{42}\text{Si}_{22}$ , . . . . . (21)

It can occur above  $1030^\circ\text{C}$  in specimens containing 19-23 % Si, but being a bimolecular reaction it may be slower than the monomolecular reaction (III),  $\eta \rightarrow \alpha'' + \epsilon$ , with the reaction (VI),  $\alpha + \epsilon \rightarrow \alpha''$ , following the production of the  $\epsilon$ -phase. All reactions with  $\alpha''$  as end-product are known to be complete within a few hours.

TABLE VI

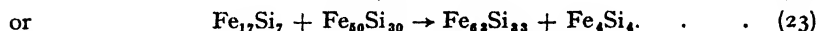
	Reaction Temp. ( $^\circ\text{C}$ )	Reaction Velocity (sec. $^{-1}$ )	Activation Energy (cal.)
(I) $\alpha'' \rightarrow \alpha + \eta$	500 550	$1.8 \times 10^{-5}$ $9.2 \times 10^{-5}$	40,000
(II) $\eta \rightarrow \alpha + \epsilon$	650	$1.2 \times 10^{-4}$	
	608	$1.6 \times 10^{-3}$	
	735	$1.2 \times 10^{-6}$	
	750	$7.0 \times 10^{-6}$	
(III) $\eta \rightarrow \alpha'' + \epsilon$	811	$1.3 \times 10^{-5}$	32,000
	811	$3.0 \times 10^{-5}$	
	1140	$7.5 \times 10^{-5}$	
(IV) $\alpha'' \rightarrow \alpha + \epsilon$	850	Not observed	
(V) $\alpha + \epsilon \rightarrow \eta$	950	$1.4 \times 10^{-3} \text{ sec.}^{-1} \text{ mol.}^{-1} \text{ cm.}^3$	
(VI) $\alpha + \epsilon \rightarrow \alpha''$	1100	$8.0 \times 10^{-3}$ " "	
(VII) $\alpha'' + \epsilon \rightarrow \eta$	950	Completed within a few hours	
(VIII) $\alpha + \eta \rightarrow \alpha''$	1030	" " "	
(IX) $\alpha'' + \epsilon \rightarrow \alpha + \eta$	950	Probably (I) + (V)	
(X) $\alpha + \eta \rightarrow \alpha'' + \epsilon$	1030	Probably (III) + (VI)	

Specimens with Si content between 20.8 % and 23.2 % and with the initial composition of  $\alpha''$  and  $\epsilon$  (stable at above 1030° C) go over into  $\alpha$  and  $\eta$  at lower temperatures. This reaction has been investigated at 950° C. It may occur according to



This would mean a double transformation of two phases into two other phases. There is, however, the possibility, and also some empirical indication, that initially  $\alpha''$  goes over into  $\alpha + \eta$  according to (I) and that  $\epsilon$  reacts together with the newly-created  $\alpha$  in forming the stable  $\eta$  according to (V),  $\alpha + \epsilon \rightarrow \eta$ . The total reaction is completed within a few hours.

The reverse of reaction (IX) is



It can take place at above 1030° C for specimens between 20.8 and 23.2 % Si. The total reaction is completed more quickly than (IX) but the mono-molecular reaction (III),  $\eta \rightarrow \alpha'' + \epsilon$ , is probably faster than (X) and must be followed by (VI),  $\alpha + \epsilon \rightarrow \alpha''$ .

In the following, all the reactions investigated are listed together with the determined velocity constants and activation energies.

*Department of Natural Philosophy, H. H. Wills Physical Laboratory,*  
*University of Glasgow. University of Bristol.*

## THE SEPARATION OF THE OXYGEN ISOTOPES BY THERMAL DIFFUSION

BY R. H. DAVIES

*Received 12th February 1948; as revised 26th October, 1948*

The results given by Lauder for the separation of oxygen isotopes in a thermal diffusion column are extended to take account of the  $^{17}\text{O}$  atoms. It is shown that the efficiency of the columns is approximately that predicted by the theory of Furry, Jones and Onsager.

In a recent experimental paper by Lauder<sup>1</sup> the amount of enrichment of the heavy oxygen isotopes obtained in a thermal diffusion column was estimated by measuring the density excess of water prepared from the oxygen. The normal concentrations of the oxygen isotopes  $^{16}\text{O}$ ,  $^{17}\text{O}$ ,  $^{18}\text{O}$ , are in the proportions 2494 : 1 : 5 and, since the enrichment obtained was small, it was assumed that all the density excess in any sample of heavy oxygen water could be attributed with little error, to an increased quantity of  $^{18}\text{O}$ . The method of calculation used by Lauder was not given in his paper but it is interesting that, from the data which he gave, the final concentrations of both  $^{17}\text{O}$  and  $^{18}\text{O}$  can be calculated. This calculation is carried out below.

It is also interesting to compare the experimental results with the theoretical analysis of Furry, Jones and Onsager<sup>2</sup> and this is done in the following section. Their theory predicts a separation factor which agrees roughly with that actually obtained by Lauder.

<sup>1</sup> Lauder, *Trans. Faraday Soc.*, 1947, **43**, 626.

<sup>2</sup> Furry, Jones and Onsager, *Physic. Rev.*, 1939, **55**, 1083.

### Calculation of the Final $^{17}\text{O}$ and $^{18}\text{O}$ Concentrations

In the single-stage column described in Part I of Lauder's paper, let  $c$  be the concentration of  $^{18}\text{O}$ ,  $c_i$  referring to the concentration at the top of the column,  $c_z$  to that at a distance  $z$  down the column,  $c_f$  to that at the bottom and  $c_0$  to the original concentration. Let  $c'$ ,  $c'_i$ , etc., refer to the corresponding concentrations of  $^{17}\text{O}$ .

Using Furry, Jones and Onsager's notation,<sup>3</sup> at equilibrium we have a separation factor,

$$\frac{c_f}{c_i} = \left(\frac{c'_f}{c'_i}\right)^2 = \exp(2AL), \quad (1)$$

where  $L$  is the length of the column and  $A$  is a quantity determined by the characteristics of the column and the gas (see below). (The value of  $A$  for  $^{17}\text{O}$ - $^{18}\text{O}$  mixtures should be very nearly one-half that for  $^{18}\text{O}$ - $^{16}\text{O}$  mixtures.) Two further relations follow from the conservation of the two isotopes in the column, flask and piping. Let  $\mu_1$  be the mass of oxygen per unit length of column when the cold wall temperature is  $T_1^\circ \text{K}$ ,  $\rho_T$  the density of oxygen at  $T^\circ \text{K}$ , and  $r_1$ ,  $r_2$ , the radii of the cold wall and the hot wire respectively. Taking the volume of the flask and piping as 10,800 ml., and 700 ml., for that of the column, the temperature of the cold wall as  $20^\circ \text{C}$  (unstated in the paper), and  $27^\circ \text{C}$  for that of the gas in the flask and piping, and 400 cm. for the length of the column, we have for the conservation of  $^{18}\text{O}$ ,

$$c_0\{10800 \rho_{300} + 400 \mu_1\} = \mu_1 \int_0^L c_z dz + 10800 c_i \rho_{300} \quad (2)$$

and for the conservation of  $^{17}\text{O}$ ,

$$c'_0\{10800 \rho_{300} + 400 \mu_1\} = \mu_1 \int_0^L c'_z dz + 10800 c'_i \rho_{300} \quad (3)$$

For Maxwellian molecules,  $\mu_1$  is given by<sup>3</sup>

$$\mu_1 = \pi r_1^2 \rho_{T_1} 2t_1 \cdot \exp(t_1^2) \cdot \int_{t_1}^{t_2} \exp(-t^2) dt,$$

where<sup>4</sup>  $\frac{t_2}{t_1} = \frac{T_2}{T_1} = 3.70$ , ( $T_2^\circ \text{K}$  = temp. of hot wire),

and  $\log_e \left(\frac{r_2}{r_1}\right) = \frac{1}{2}(t_2^2 - t_1^2) = \log_e(21.07)$ .

These values give  $\mu_1 = 1.1465 \rho_{T_1} \text{ g./cm.}$  At equilibrium, we have

$$c_s = c_i \exp(2Az). \quad (4)$$

From these equations we may estimate the concentrations and separation factors for  $^{17}\text{O}$  and  $^{18}\text{O}$  for the density excess (700 p.p.m.) obtained at the optimum pressure. Taking a volume containing 2500 molecules of normal water, its weight is proportional to

$$W_0 = (2494)18 + (1)19 + (5)20 = 45011.$$

The weight of a corresponding volume of heavy-oxygen water is proportional to

$$W_1 = 2500\{(1 - c_f - c'_f)18 + (c'_f)19 + (c_f)20\}.$$

The excess density is, therefore

$$\frac{W_1 - W_0}{W_0} = \frac{(2c_f + c'_f)2500 - 11}{45011} = 700 \text{ p.p.m.} \quad (5)$$

<sup>3</sup> Jones and Furry, *Rev. Mod. Physics*, 1946, 18, 211.

<sup>4</sup> Jones and Furry, *ibid.*, 171.

Eliminating  $c_f$  and  $c'_f$  from (5) by means of (2), (3), (4) and substituting for  $\mu_1$ ,  $c_0$ , and  $c'_0$ , the equation,

$$\frac{10 \exp 2x}{\frac{\exp 2x - 1}{2x} + 23.00} + \frac{\exp x}{\frac{\exp x - 1}{x} + 23.00} = 1.771,$$

is obtained, where  $x = AL$ . The solution of this is  $x = 0.725$ , giving from (1), a separation factor

$$\exp 2AL = \frac{c_f}{c_i} = 4.26, \quad . \quad . \quad . \quad (6)$$

and percentages

$$c_f = 0.81 \%, \quad c'_f = 0.081 \%, \quad c_i = 0.191 \%, \quad \text{and} \quad c'_i = 0.039 \%.$$

The value  $c_f + c'_f = 0.89 \%$  compares with  $0.9 \%$  given in the paper, but  $c_i + c'_i = 0.23 \%$  is somewhat larger than the  $0.18 \%$  quoted by Lauder.

Another estimate of the separation factor may be obtained from Part II of Lauder's paper, in which a four-stage column is described. Let  $c_f$ ,  $c'_f$  now refer to the concentrations at the bottom of the fourth column, and  $c_i$ ,  $c'_i$  to those at the bottom of the first column. Assuming an approximately exponential approach to equilibrium, it seems likely, from Fig. 6 of the paper, that the excess density of a sample from the bottom of the fourth column, had equilibrium been reached at the optimum pressure, would not have exceeded 40,000 p.p.m. Taking this value, we have

$$\frac{(2c_f + c'_f)2500 - 11}{45011} = 40,000 \text{ p.p.m.}$$

and

$$\frac{c_f}{c_i} = \left( \frac{c'_f}{c'_i} \right)^2 = \exp 6AL.$$

With  $c_i = 0.2 \%$ ,  $c'_i = 0.04 \%$ , these equations give  $c_f = 36 \%$ ,  $c'_f = 0.54 \%$  and

$$\exp 2AL = 5.64. \quad . \quad . \quad . \quad (7)$$

### Theoretical Efficiency of the Column

A third estimate of the separation obtainable at the optimum pressure may be made from the theory of Furry, Jones and Onsager<sup>2</sup> as developed for the hot wire column by Furry and Jones<sup>6</sup> and by Jones and Furry.<sup>6</sup> Using the following values: for the gas  $\alpha = 0.00903^7$ ,  $D = 0.215 \text{ cm.}^2/\text{sec.}$ ,<sup>8</sup>  $\rho_{T_1} = 1.331 \times 10^{-3} \text{ g./sec.}$ ,<sup>9</sup>  $\eta = 2.039 \times 10^{-4} \text{ poise}$ <sup>10</sup> evaluated for a force index  $\nu = 7.6$ <sup>11</sup> and  $T_1 = 20^\circ \text{ C}$ ; and for any one of the columns:  $L = 400 \text{ cm.}$ ,  $r_1 = 0.75 \text{ cm.}$ ,  $r_2 = 0.0375 \text{ cm.}$ ,  $T_2 = 810^\circ \text{ C}$ ,  $P = 31.25 \text{ cm. Hg}$ ,  $P_0 = 76 \text{ cm. Hg}$ , the transport factors<sup>12</sup> are

$$H = \frac{2\pi(\alpha\rho^2g)}{6! \left(\frac{\eta}{T_1}\right)} \cdot r_1^4 \cdot \left(\frac{P}{P_0}\right)^2 \cdot h\left(\frac{r_1}{r_2}; \frac{T_2}{T_1}\right) = 3.583 \times 10^{-1} \text{ g./sec.}$$

$$K_c = \frac{2\pi\left(\frac{\rho^3g^2}{D\eta^3}\right)}{9!} \cdot r_1^8 \cdot \left(\frac{P}{P_0}\right)^4 \cdot k_c\left(\frac{r_1}{r_2}; \frac{T_2}{T_1}\right) = 9.448 \times 10^{-5} \text{ g. cm./sec.}$$

$$K_d = 2\pi(D\rho)_{T_1} \cdot r_1^2 \cdot k_d\left(\frac{r_1}{r_2}; \frac{T_2}{T_1}\right) = 8.436 \times 10^{-4} \text{ g. cm./sec.}$$

Therefore, assuming  $K_p = 0$  (see below)

$$\begin{aligned} K_c/K_d &= 0.11, \quad 2AL = HL/(K_c + K_d) = 1.528 \\ \exp(2AL) &= 4.61 \quad . \quad . \quad . \quad (8) \end{aligned}$$

<sup>5</sup> Furry and Jones, *Physic. Rev.*, 1946, **69**, 459.

<sup>6</sup> Jones and Furry, *ibid.*, 151.

<sup>7</sup> Jones and Furry, *ibid.*, 157.

<sup>8</sup> Chapman and Cowling, *Mathematical Theory of Non-Uniform Gases*, 1939, 248, 251.

<sup>9</sup> Kaye and Laby, *Tables*.

<sup>10</sup> Chapman and Cowling, *ref.*<sup>8</sup>, 221, 229.

<sup>11</sup> Chapman and Cowling, *ibid.*, 223.

<sup>12</sup> Jones and Furry, *ref.*<sup>5</sup>, 172.



## Discussion

The values taken for  $h$ ,  $K_o$ ,  $K_d$  above apply strictly only to a gas consisting of Maxwellian molecules (force index  $\nu = 5$ ), and for  $\alpha$  independent of temperature. Certainly  $H$  would be strongly influenced by any marked temperature dependence in  $\alpha$  and  $K_e$  should be larger for oxygen than for Maxwellian molecules, although  $K_d$  should be fairly accurate.<sup>13</sup> In the first estimate, from the behaviour of a single column, apart from uncertainties in the volumes taken, the separation factor may be too small as  $\mu$  will be larger for oxygen molecules than for Maxwellian molecules.<sup>14</sup> In the second, the calculated factor is probably greater than that which would be obtained at equilibrium at the optimum pressure.

In all the above, it is assumed that the  $^{18}\text{O}$  and  $^{17}\text{O}$  atoms occur in molecules of  $^{18}\text{O}$   $^{18}\text{O}$  and  $^{17}\text{O}$   $^{18}\text{O}$  only. In the second estimate, therefore, in which the concentration of  $^{18}\text{O}$  is of the same order as that of  $^{18}\text{O}$  in the fourth column, a considerable proportion of  $^{18}\text{O}$   $^{18}\text{O}$  molecules must be formed, and the value of  $A$  for this column will be somewhat different from that for the other three.

There is no question of turbulence being caused solely by a too rapid convective flow, as the Reynolds number for the flow, approximately  $^{15} 2(K_e/K_d)^{1/2} \simeq 2/3$ , is much smaller than the usual limiting value for a hot wire column of about 25.

The values given in eqn. (6), (7), (8) for the separation factor agree quite well among themselves and also with the value 5 quoted by Lauder, and indicate that there was little parasitic flow ( $K_p$ ) within the columns.

The author wishes to express his thanks to Mr. J. T. Kendall for his interest, to Sir Arthur P. M. Fleming, C.B.E., D.Eng., Director of Research and Education, and to Mr. B. G. Churcher, M.Sc., M.I.E.E., Manager of the Research Department, Metropolitan-Vickers Electrical Co. Ltd., for permission to publish this paper.

Research Department,  
Metropolitan-Vickers Electrical Co. Ltd.,  
Trafford Park,  
Manchester, 17.

<sup>13</sup> Jones and Furry, ref.<sup>5</sup>, 213.

<sup>15</sup> Jones and Furry, *ibid.*, 173.

<sup>14</sup> Simon, *Physic. Rev.*, 1946, **69**, 601.

<sup>16</sup> Jones and Furry, *ibid.*, 207.

## STUDIES IN MEMBRANE PERMEABILITY

## PART V. ACTIVATION ENERGY OF DIFFUSION AND MEMBRANE POTENTIALS OF POTASSIUM CHLORIDE THROUGH CUPRIC FERROCYANIDE

BY J. D. TOLLIDAY, E. F. WOODS AND E. J. HARTUNG

Received 3rd March, 1948

Additions to the apparatus previously described have been made in order to measure the permeability of a membrane to electrolytes over a temperature range of 0° to 35° C. A constant flow apparatus for the measurement of membrane potentials has been constructed.

The dependence of the properties of cupric ferrocyanide membranes on the electrochemical nature of the membrane has been established by both potential difference and permeability studies. The activation energy for the diffusion of KCl through nine membranes has been determined. A relation between the potential to KCl and the rate of penetration of KCl through thirteen membranes has been established.

Earlier work in this laboratory on cupric ferrocyanide membranes has dealt with the determination of permeabilities and potentials towards different electrolytes,<sup>1, 2, 3</sup> as well as adsorption phenomena by the membranes.<sup>4</sup> This paper attempts to correlate these membrane properties and also to study the temperature coefficient of the diffusion process.

### Experimental

**The Membranes.**—For our work, the most suitable support so far tried is hardened filter paper,<sup>1</sup> and specially selected discs of Whatman No. 50 papers were used throughout this work.

The membranes were prepared by the method of Austin, Hartung and Willis,<sup>2</sup> but their finding that no increase in thickness occurred after the first two days was not confirmed. After removal from the dialysing jar, the membranes were soaked on alternate days in copper sulphate and potassium ferrocyanide solutions. This treatment was continued until rigid, evenly dispersed structures were obtained, the last treatment being always with potassium ferrocyanide unless otherwise stated. Gurchot<sup>5</sup> found that the membranes are attacked by bacteria, and to minimise this effect thymol was placed in all solutions in which membranes were stored, and also in the electrolyte solutions used in the permeability determinations.

Microtome sections of several membranes showed that a very dense layer of precipitate existed near the surfaces of the paper, with sparse distribution in the centre. Under the microscope, the layers of precipitate appeared continuous and gave no indication of the possibility of mechanical leakage.

**Permeability Measurements.**—The apparatus used for permeability determinations was essentially the same as the constant flow apparatus used by Austin, Hartung and Willis.<sup>2</sup> Previously the apparatus had been used to measure the permeability of the membranes at 25° C only. Measurements now being required at temperatures ranging from 0° to 35°, a second thermostat kept at 25° ( $\pm 0.02^\circ$ ) was installed to bring the effluent from the permeability cell to

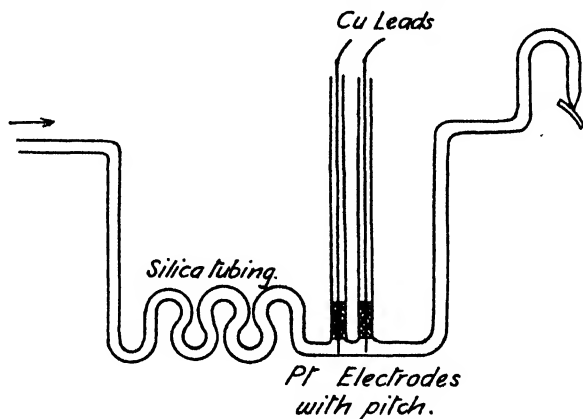


FIG. 1.

this temperature, at which the conductivity was measured. This device avoided much work in determining conductivity-concentration curves at different temperatures. The cell effluent was led into the second thermostat as in Fig. 1, the diameter of the silica tubing being such that at the maximum rate of flow there was a lag of 7 min. between the cell and measuring electrodes. These electrodes, of stout platinised-platinum wire, were placed as closely together as practicable to make the cell-constant small. They were held in position by distilled commercial pitch and led out through the top of the thermostat by stout copper leads. The effluent outlet was firmly clamped to the thermostat by an adjustable screw.

<sup>1</sup> Hartung, Kelly and Wertheim, *Trans. Faraday Soc.*, 1937, **33**, 398.

<sup>2</sup> Austin, Hartung and Willis, *ibid.*, 1944, **40**, 520.

<sup>3</sup> Willis, *ibid.*, 1942, **38**, 169.

<sup>4</sup> McMahon, Hartung and Walbran, *ibid.*, 1940, **36**, 515.

<sup>5</sup> Gurchot, *J. Physic. Chem.*, 1926, **30**, 83.

For working at lower temperatures, tap water was led through a large coil of copper tubing in an ice bath and then through copper tubing interwoven between the apparatus in the thermostat. The water then passed through the condenser jacket to ensure that the temperature difference between the distilled water entering the thermostat and the water in the thermostat was small, thus minimising bubble formation due to dissolved air. By regulating the flow of tap water so that it would maintain the thermostat just below the desired temperature, the ordinary heating and cut-out system maintained the thermostat accurately at the lower temperature.

The oscillator and null-point bridge detector showed a symmetrical wave form and were found to be reliable to one part in 500 at 50,000 ohm.

**Potential Measurements.**—At first, the potential measurements were carried out using the Michaelis apparatus.<sup>6</sup> However, on filling the cell, the potential immediately commenced to drop, and steady readings could not be obtained. Unmack<sup>7</sup> has discussed the conditions under which stirring is a necessity in membrane potential measurements to overcome effects of diffusion, and it was therefore decided to allow the two electrolyte solutions of different concentrations (N/10, N/100) to flow slowly past the sides of the membrane, which was firmly clamped in a vertical position between rubber washers. The size of the cell (47 mm. diam.) was the same as that used in the permeability apparatus, so that an identical membrane could be used in both. Care was taken to ensure that no air bubbles were present in the cell, filling being carried out by applying suction at the top of the storage flasks. The rate of flow was adjusted by means of taps at the bottom of the storage flasks, and the solutions were run by short leads into beakers connected by agar bridges to the electrodes. No temperature control was attempted, but the temperature of the solutions was recorded for each series of measurements. It was assumed that the streaming potential could be neglected with such relatively high concentrations of strong electrolyte as were used. The rate of flow was varied from 60 ml./hr. to 150 ml./hr. without appreciable variation in potential.

## Results and Discussion

One of the main difficulties of studies on the behaviour of a cupric ferrocyanide membrane towards different electrolytes<sup>1, 2, 3, 4</sup> was the dependence of the properties of the membrane upon the order in which the various electrolyte solutions were placed in contact with it. The potential measurements obtained using various anions (potassium salts) illustrate this phenomenon.

TABLE I.—MEMBRANE POTENTIALS (Potassium salts, Concentration Ratio N/10, N/100, Dilute side positive)

Membrane 1			Membrane 2		
Day	Anion	Potential (mV)	Day	Anion	Potential (mV)
1	Cl <sup>-</sup>	21.8	1	Cl <sup>-</sup>	5.6
2	SO <sub>4</sub> <sup>-</sup>	42.2	2	Cl <sup>-</sup>	5.4
3	SO <sub>4</sub> <sup>-</sup>	41.8	3	NO <sub>3</sub> <sup>-</sup>	11.2
4	NO <sub>3</sub> <sup>-</sup>	26.9	6	SO <sub>4</sub> <sup>-</sup>	43.6
5	NO <sub>3</sub> <sup>-</sup>	26.8	7	Cl <sup>-</sup>	16.1
8	Cl <sup>-</sup>	24.9	8	Cl <sup>-</sup>	12.8
9	Cl <sup>-</sup>	24.8	9	Cl <sup>-</sup>	11.9
10	C <sub>2</sub> O <sub>4</sub> <sup>-</sup>	47.2	10	Cl <sup>-</sup>	11.4
11	IO <sub>3</sub> <sup>-</sup>	46.0	13	Cl <sup>-</sup>	12.2
12	BrO <sub>3</sub> <sup>-</sup>	44.0	14	Br <sup>-</sup>	17.0
13	ClO <sub>3</sub> <sup>-</sup>	43.3	15	I <sup>-</sup>	28.1
15	Cl <sup>-</sup>	38.3			
16	Cl <sup>-</sup>	38.1			
17	CrO <sub>4</sub> <sup>-</sup>	46.1			
18	Fe(CN) <sub>6</sub> <sup>=</sup>	49.4			

<sup>6</sup> Michaelis, *Kolloid-Z.*, 1933, 62, 1.

<sup>7</sup> Unmack, from Manegold and Kalauch, *ibid.*, 1939, 86, 186.

It is seen that, after contact with other anions, particularly bivalent ions, the potential of the membranes towards the chloride ion is increased. In the case of membrane 2, contact with  $\text{SO}_4^{2-}$  ions increased the potentials towards  $\text{Cl}^-$  from 5.5 mV to 16.1 mV, showing that adsorption of  $\text{SO}_4^{2-}$  ions had occurred. The direct measurements of Hartung,<sup>8</sup> as well as the indirect work by Sen<sup>9</sup> and Hayashi,<sup>10</sup> support ionic adsorption by cupric ferrocyanide. The sign of the potential in the above case shows the membranes to be electrically negative in character, and this is increased by the adsorption of the bivalent anions as shown by the variation in the value of the reference chloride ion in the above series. A considerable portion of the  $\text{SO}_4^{2-}$  adsorption is irreversible, as shown by the fact that, after contact with other anions, the potential towards  $\text{Cl}^-$  ion did not drop to the original value (5.6 mV) even after 6 days.

Even allowing for this variation, the order of the potential values, in decreasing magnitude, given by various anions (constant cation) is—

$\text{Fe(CN)}_6^{4-}$ ,  $\text{C}_2\text{O}_4^{2-}$ ,  $\text{CrO}_4^{2-}$ ,  $\text{SO}_4^{2-}$ ,  $\text{IO}_3^-$ ,  $\text{BrO}_3^-$ ,  $\text{ClO}_3^-$ ,  $\text{I}^-$ ,  $\text{Br}^-$ ,  $\text{NO}_3^-$ ,  $\text{Cl}^-$ . The higher the potential, the lower is the expected permeability, and in this regard the above series corresponds almost exactly with the permeability series obtained by Austin, Hartung and Willis,<sup>2</sup> who found the order of permeability in decreasing magnitude to be—

$\text{Cl}^-$ ,  $\text{Br}^-$ ,  $\text{NO}_3^-$ ,  $\text{I}^-$ ,  $\text{IO}_3^-$ ,  $\text{SO}_4^{2-}$ ,  $\text{C}_2\text{O}_4^{2-}$ ,  $\text{Fe(CN)}_6^{4-}$ .

The order of potentials obtained by us differs slightly from that of Willis<sup>2</sup> but is substantiated by Austin.<sup>11</sup> Because of the variation of the charge on the membrane (probably primarily due to adsorption) throughout such a series of measurements involving different anions, little significance can be attached to the actual magnitude of results obtained, unless the membrane can be stabilised to each electrolyte in turn and reproducible values obtained.

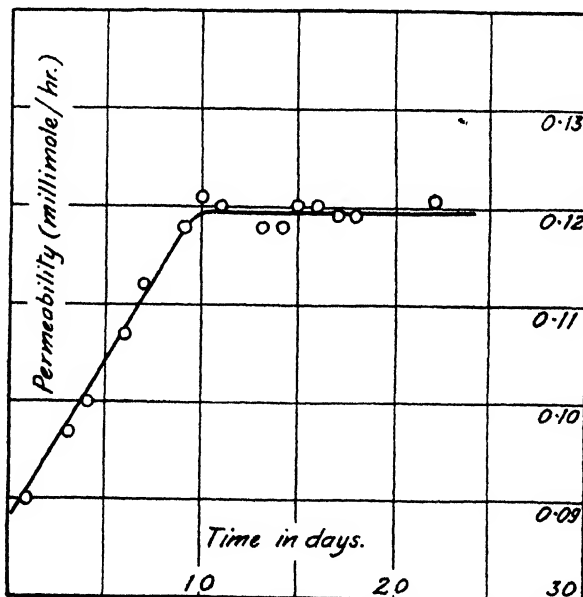


FIG. 2.

<sup>8</sup> Hartung, *Trans. Faraday Soc.*, 1920, **15**, 170.

<sup>9</sup> Sen, *J. Physic. Chem.*, 1925, **29**, 517.

<sup>10</sup> Hayashi, *Kolloid-Z.*, 1926, **39**, 209.

<sup>11</sup> Austin, private communication, 1945.

To see if this could be done, the Michaelis apparatus\* was used to determine the potential of a cupric ferrocyanide membrane towards KCl from day to day, the membrane being stored in distilled water between the measurements. No steady state was reached after 30 days, nor was there systematic variation of potential with time. The same membrane was then stored in N/10 electrolyte between determinations and the potential observed for a further 16 days. It was now found that after 7 days the membrane reached a steady state and the potential measurements were reproducible to within 1 mV for at least a further 9 days. However, on diluting the storage electrolyte to N/100, unsystematic variation without the attainment of a steady state was observed up to 45 days.

To see if contact with electrolyte of sufficient concentration would enable a steady and reproducible permeability value to be obtained, the permeability of a membrane to M/5 KCl at 25° was observed for 22 days. During these measurements, the electrolyte solution was allowed to remain in contact with the membrane, no washing with water being carried out at any stage. Fig. 2 shows that after 9 days a steady state is obtained, the actual overall variation in the concentration of the lower effluent then being 0.00012 g. KCl per litre.

Similar results with other membranes showed that cupric ferrocyanide can be established to KCl, and in all subsequent determinations the membranes were stored in N/10 KCl containing a crystal of thymol for at least 10 days before use.

**Correlation between Permeability and Potential.**—Some membranes were prepared under as nearly identical conditions as possible and were stabilised before use. The potential was always measured immediately after the permeability determinations and, where convenient, beforehand as well. After stabilising, the permeability of a membrane to M/5 KCl was determined on consecutive days, and if these agreed, measurements at various temperatures were carried out. The initial aim was to carry out the following determinations on each membrane: (a) temperature coefficient expressed in terms of activation energy for diffusion of KCl (M/5); (b) potential to KCl (N/10, N/100); (c) permeability to  $K_2SO_4$  (M/5) at 18°; and (d) potential to  $K_2SO_4$ , but after three such series, it was apparent that the sulphate determinations could not be done successfully in conjunction with the chloride determinations, as the  $K_2SO_4$  equilibrium was established very slowly, and consequently the time taken to complete the series was excessive. Steady conductivity measurements of the lower effluent using  $K_2SO_4$  could not be obtained on any one day, and these measurements showed an increase in permeability with time. Since adsorption of sulphate ions would tend to decrease the permeability, this does not explain the phenomenon. With a membrane which allows the passage of only 0.03 millimole of  $K_2SO_4$  per hour, peptisation may occur because of the low concentration of electrolyte in the lower effluent. This would tend to desorb ions, thus giving an increased permeability value.

The results on membrane No. 12 shown in Table II are typical of the KCl determinations, the order in which measurements were made being given by the vertical column.

These results give a very roughly linear plot. This has also been claimed by Falinski<sup>12</sup> for free diffusion and is usually the case when the temperature range is small. We have, however, followed the generally accepted practice of plotting  $\log P$  against  $1/T$  (Fig. 3) as this gives some physical significance to the temperature coefficient of diffusion by enabling an "activation energy" for the process to be calculated. The approximately linear curve gives an activation energy of 5100 cal./mole.

The potentials at room temperature for 13 similar membranes and the activation energies for the diffusion of KCl for 9 of these are plotted

<sup>12</sup> Falinski, *Compt. rend.*, 1944, 218, 754; 1944, 218, 938.

TABLE II.—MEMBRANE NO. 12. KCl M/5

$T$ Temperature (°C)	$P$ Permeability (millimole/hour)	
18.0	0.0474	
18.0	0.0467	} Permeability at 18° C = 0.0474 millimole/hr.  Potential after permeability determinations— 1st day 37.6 mV 2nd day 37.3 mV (Temperature 19° C)
21.4	0.0533	
18.0	0.0474	
21.4	0.0535	
25.4	0.0609	
13.0	0.0412	
30.0	0.0677	

against the permeabilities at 18° in Fig. 4. These activation energies all lie between 4950 and 5250 cal./mole. Free diffusion coefficients for KCl quoted in the literature vary considerably even for the same concentration, but the values correspond generally to an activation energy between 3700 and 4400 cal./mole. In spite of the limitations of the experimental material, there is evidence that the energy barrier which the ions must surmount in passing the membrane is greater than that for free diffusion. This is as expected, the membrane barrier in the case of ions being mainly electrostatic. An indication was obtained during preliminary work that the activation energy for membrane diffusion of  $K_2SO_4$  (M/5) was of the order of 5900 cal./mol.

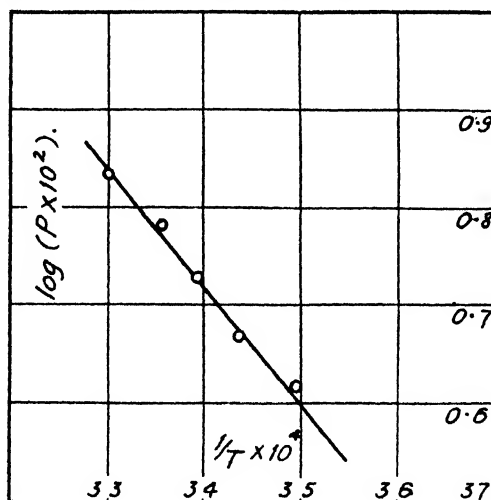


FIG. 3.

The poor correlation shown in Fig. 4 between membrane potential and permeability for KCl for the more permeable membranes compares unfavourably with that obtained by Wilbrandt<sup>13</sup> for HCl through collodion. We believe this to lie in the less reproducible geometrical structure of copper ferrocyanide membranes as compared with collodion. As high membrane potential is associated with low permeability, the presence in an otherwise fine-pored structure of a relatively small number of wide irregular pores, in which the electrical charge density is not sufficient

<sup>13</sup> Wilbrandt, *J. Gen. Physiol.*, 1934-5, **38**, 933.

to oppose effectively the entrance of one of the ions, may have a considerable effect on the permeability, but relatively little effect on the potential. Wilbrandt found indeed that collodion from different sources gave little correlation between permeability and potential.

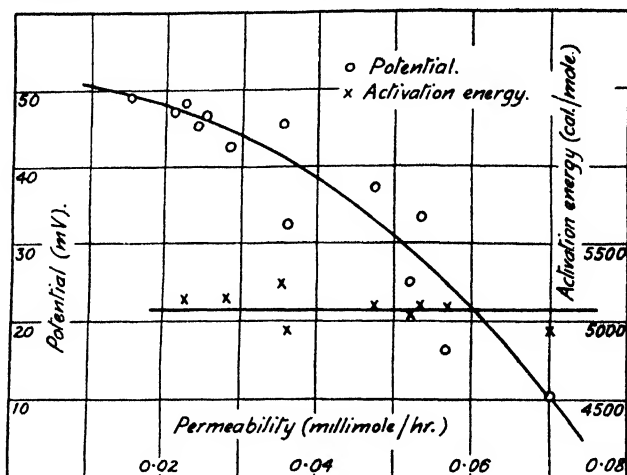


FIG. 4.

**Adsorption of  $\text{CuSO}_4$  and  $\text{K}_4\text{Fe}(\text{CN})_6$  on the Membranes.**—Austin, Hartung and Willis<sup>2</sup> found that treatment with  $\text{K}_4\text{Fe}(\text{CN})_6$  enhanced the selectivity of the membrane and decreased the permeability to ions, whereas treatment with  $\text{CuSO}_4$  increased the permeability to ions. Corresponding to these changes in permeability, Austin<sup>11</sup> found corresponding changes in potential; adsorption of  $\text{K}_4\text{Fe}(\text{CN})_6$  increased the potential with N/10 and N/100 KCl, and adsorption of  $\text{CuSO}_4$  decreased it and in the latter case may even reverse the surface charge on the membrane. As Austin had only tested one membrane in such potential measurements, they were repeated. A membrane was treated with  $\text{CuSO}_4$  for 3 days and was found to have an initial potential towards KCl of  $-39.8$  mV. The variation of potential with time was observed. For the first 23 days, the membrane was stored in distilled water between determinations, and it was found that between the twelfth and twenty-third days the values only varied over 2 mV, the value after 23 days' observations being  $-26.6$  mV. The potential towards  $\text{KNO}_3$  was then studied, the membrane being stored in distilled water between measurements, and it was found that, although the results varied more than with KCl, no great change in potential occurred. After the thirty-first day, the value was  $-19.0$  mV. The storage medium was then changed to N/10  $\text{KNO}_3$ , and a rapid rise in potential was obtained; the potential reversed in sign and after a further 10 days rose to a steady value of  $+35.5$  mV. As before, storage in dilute electrolyte did not give a steady value.

The rapid rise of potential on storing membranes treated by  $\text{Cu}^{++}$  solutions in potassium salt solution suggests an exchange between  $\text{K}^+$  and  $\text{Cu}^{++}$  ions. McMahon, Hartung and Walbran<sup>4</sup> found in their adsorption experiments on  $\text{Cu}_2\text{Fe}(\text{CN})_6$  a slight cationic displacement of  $\text{Cu}^{++}$  by  $\text{Na}^+$ . We confirmed this by treating a membrane with  $\text{CuSO}_4$  for 3 days and washing with distilled water until no more copper was desorbed, as indicated by sodium diethyl dithiocarbamate. The membrane had a negative potential. On the addition of M KCl, a rapid liberation of  $\text{Cu}^{++}$  occurred, giving a very strong positive test for  $\text{Cu}^{++}$ , and the potential became positive. Quantitative estimations on two membranes showed that  $0.094$  and  $0.165$  mg. respectively of  $\text{Cu}^{++}$  were liberated per  $\text{cm}^2$  of membrane.

Two membranes prepared in the usual way were kept, one in M/5  $\text{CuSO}_4$  for 3 months, the other in M/5  $\text{K}_4\text{Fe}(\text{CN})_6$  for the same period. They were then tested for potential and permeability; the latter showed a constant potential of 49 mV after one week, and the permeability was 0.0153 millimole/hr. The former had an initial potential of -21.5 mV, which rose to a maximum value of +26 mV in 2 months, the membrane being kept in contact with N/10 solution on one side, N/100 on the other. This rise in potential is attributed to slow liberation of  $\text{Cu}^{++}$  ions.

The permeability and activation energy of diffusion of KCl of this membrane were then determined and the activation energy found to be 4500 cal./mole, which is markedly lower than the values previously obtained for the ferrocyanide-treated membranes.

Three membranes whose activation energies and potentials had been determined were treated with  $\text{Cu}^{++}$  ions for 48 hr., then kept in fresh changes of M KCl until no more  $\text{Cu}^{++}$  could be detected in the solution, and the activation energies and potentials redetermined. The results are shown in Table III. It is seen that treatment with  $\text{Cu}^{++}$  yields

TABLE III

Membrane No.	Ferrocyanide Treated.			Copper Treated and Restabilised to KCl.		
	Potential (mV)	Permeability (millimole/hr.)	Activation Energy (cal./mol.)	Potential (mV)	Permeability (millimole/hr.)	Activation Energy (cal./mol.)
21	45.3	0.0356	5250	26.0	0.0874	4400
22	48.6	0.0223	5150	29.5	0.0631	4250
27	42.3	0.0284	5150	28.3	0.0449	4850

membranes of higher permeability and correspondingly lower potentials and activation energies. This must be due to a decrease in the net negative charge on the membrane. Further work is being done on the adsorption of  $\text{Cu}^{++}$  on  $\text{Cu}_4\text{Fe}(\text{CN})_6$  membranes.

*Chemistry Laboratories,  
University of Melbourne,  
Australia.*

## POLARISABILITY AND DIELECTRIC CONSTANT OF IONIC CRYSTALS \*

BY B. SZIGETI

*Received 25th March, 1948*

The polarisability of a crystal is connected with its natural frequencies. It follows from papers by Lyddane and Herzfeld, and Fröhlich and Mott, that in static fields or for very long external waves the polarisability varies with the shape of the material. In the case of short waves, on the other hand, the polarisability is independent of the shape of the material but depends on whether the wave is longitudinal or transverse. It is shown that the Clausius-Mosotti formula connecting the polarisability  $\alpha$  with the dielectric constant  $\epsilon$  i.e.  $(\epsilon - 1)/(\epsilon + 2) = (4\pi/3)\alpha$ , holds if  $\alpha$  is the polarisability of a sphere in very long external waves; the Drude formula,  $\epsilon - 1 = 4\pi\alpha$ , is valid if  $\alpha$  is the polarisability for short transverse waves, while for short longitudinal waves  $4\pi\alpha = (\epsilon - 1)/\epsilon$ .

\* Parts of this paper are based on E.R.A. Report Ref. L/T 203.



In terms of the normal vibrations of the crystal, the polarisation is divided into high-frequency or ultra-violet and low-frequency or infra-red parts. The first contains purely electronic displacements and the second both displacements of ions as a whole (atomic polarisation) and shifts of the electrons relative to the nuclei. The interaction of the atomic and electronic displacements in the course of the infra-red polarisation is separated into short-range and long-range effects. Although the short-range interaction should vanish in an ideal hetero-polar crystal with cubic lattice, experimental data show that it has quite considerable values even in alkali halides.

An often recurring difficulty in dielectric theory is the connection between polarisability and dielectric constant. This is connected with the question, what is the effective field which polarises the material. The polarisability  $\alpha_m$  of a single molecule is defined by

$$\mu = \alpha_m E,$$

where  $\mu$  is the dipole moment induced on the molecule if the field  $E$  acts upon it. Similarly, for a macroscopic material we can define  $\alpha$  the polarisability per unit volume by

$$P = \alpha E_{\text{eff.}}, \quad (1)$$

where  $P$  is the polarisation per unit volume if an effective field of value  $E_{\text{eff.}}$  acts upon the material. The inherent difficulty is the value of the effective field. The Drude formula puts it equal to the average macroscopic field  $E$ , i.e.  $E_{\text{eff.}} = E$  which leads to the simple connection between the dielectric constant  $\epsilon$  and the polarisability,

$$\epsilon - 1 = 4\pi\alpha. \quad (2)$$

The Clausius-Mosotti Lorentz-Lorenz formula, on the other hand, is based on the argument that the macroscopic field  $E$  is the sum of the field due to external sources and of the internal field which is due to all the dipoles induced in the material. In order to obtain the effective field acting on a particle, the contribution of this particle, the "self-field", has to be deducted from  $E$ , since the particle is not polarised by its own field. This argument results in

$$E_{\text{eff.}} = E + 4\pi P$$

for isotropic materials, from which the well-known formula

$$\frac{\epsilon - 1}{\epsilon + 2} = \frac{4\pi}{3}\alpha \quad (3)$$

is derived.

Since we are here interested mainly in ionic crystals, we can restrict ourselves to materials which contain no permanent dipoles. It is then customary to divide the polarisability into two parts

$$\alpha = \alpha_a + \alpha_e,$$

where the atomic polarisability  $\alpha_a$  arises from the displacements of ions as a whole and the electronic polarisability  $\alpha_e$  from the displacement of the electron cloud relative to the nuclei.  $\alpha_e$  can be expressed with the aid of the optical refractive index  $n$ , and the Drude formula (2) then leads to

$$\epsilon - 1 = 4\pi\alpha_a \quad (4)$$

while the Clausius-Mosotti equation (3) gives

$$\frac{\epsilon - 1}{\epsilon + 2} - \frac{n^2 - 1}{n^2 + 2} = \frac{4\pi}{3}\alpha_e \quad (5)$$

where  $\epsilon$  denotes the static dielectric constant.

The Clausius-Mosotti formula is based on the idea that we draw a sphere around each particle, molecule or ion; the particle is assigned a polarisability consisting of atomic and electronic parts, and the field

acting upon it, the "local field," is taken as the value of the field at the centre of the sphere minus the self-field of the particle. This is a good approximation for organic materials, where the intermolecular forces are so weak that the subdivision of the material into molecules each having its own polarisability independently from the others is a good approximation. But the formula breaks down for ionic crystals. The theorem yields for ionic crystals,

$$\frac{n^2 - 1}{n^2 + 2} = \frac{4\pi}{3}(\alpha_{e,1} + \alpha_{e,2}),$$

where  $\alpha_{e,1}$  and  $\alpha_{e,2}$  are the electronic polarisabilities of the two constituent ions, and should have the same value for the same kind of ions in all compounds, irrespectively of the other ion. Measurements on alkali halides show, however, that this is not quite true.<sup>1</sup>

As pointed out by Heckmann,<sup>2</sup> the reason why the Clausius-Mosotti theorem breaks down for ionic crystals is that the ions partially overlap. In this case the concept of drawing a sphere with one ion inside and all others outside does not work. The interaction of the ions is not the same as it would be for point dipoles, and putting the effective field acting on an ion equal to the value of the field at its centre is a bad approximation. Also, the oscillations of the ions are strongly coupled so that they cannot be considered as individual oscillators each having its own polarisability independently of the others.

### I. Infra-red and Ultra-violet Polarisation Waves

In order to relate the polarisability with the fundamental properties of the material, we introduce the natural frequencies of the crystal. It turns out that in this case neither the division of the polarisability into atomic and electronic contributions nor the concept of the local field are useful.

The reason against division into atomic and electronic polarisations is that they are not independent quantities. The distribution of the electron cloud depends on the interatomic distance and the displacements of ions therefore induce a shift of the electron cloud. This effect, which was first pointed out by Eucken and Büchner,<sup>3</sup> is a short-range effect, since it only depends on displacements of near neighbours. There is also another type of interaction between atomic and electronic polarisations, for the field set up by the displacements of the ions polarises the electrons and vice versa. This interaction through the internal field is a long-range effect, for the contribution of distant as well as of near dipoles to the field acting on a particle is important. This is because while the field of a dipole decreases as  $1/r^3$ , the number of dipoles at distance  $r$  from a particular lattice point increases as  $r^3$ .

In the case of ionic crystals we are dealing with small displacements so that we can assume a harmonic potential. In classical physics it is then possible to separate the polarisation in terms of the normal vibrations of the crystal which are independent of each other and each of which has its own frequency. A similar treatment is possible in quantum-mechanical dispersion theory, where the polarisation is ascribed to a number of virtual oscillators so that we may again separate it into independent contributions, each corresponding to a characteristic frequency of the crystal. In other words, we may write the polarisation as  $P = p_1 + p_2 + \dots$  where each term is the contribution of one of these oscillators. The independence of these contributions implies that they do not interact with each other and any one of them is independent of the values of all the other  $p$ 's.

<sup>1</sup> Mott and Gurney, *Electronic Processes in Ionic Crystals* (Oxford University Press, 1940), p. 18.

<sup>2</sup> Heckmann, *Z. Krist.*, 1925, 61, 250.

<sup>3</sup> Eucken and Büchner, *Z. physik. Chem. B*, 1934, 27, 321.

The polarisation connected with these infra-red vibrations is sometimes called atomic polarisation, but we shall refer to it as infra-red polarisation in this paper, since the electronic contribution to it is quite considerable and can hardly be considered as a mere satellite to the atomic polarisation. The displacements of electrons are not determined by the neighbouring nuclei alone, but also by the long-range internal field, which depends on the nature of the wave. While electronic and atomic contributions reinforce each other for transverse infra-red waves, they have opposite signs for longitudinal waves (cp. eqn. (32), (28) and Table I).

where  $m_k$  is the mass of the  $k$ th atom.

In a perfectly polar crystal each ion carries a charge  $ze$ , valency times electronic charge. If the lattice vibrations consisted of displacements of ions as a whole, then the dipole moment would be given by

$$\mu_j = e \sum_k z_k x_{kj} = eq_j \sum_k z_k c_{kj}, \quad (8)$$

$z_k$  being the valency of the  $k$ th ion. In general the electronic shells are also deformed by the atomic displacements and then eqn. (8) does not hold. But in any case  $\mu_j$  certainly vibrates in phase with the atoms and is proportional to the atomic displacements and to  $q_j$ . This fact is expressed by eqn. (7), which also holds for crystals in which the charge is less than  $ze$ .

Let us now consider the crystal in the course of its  $j$ th normal vibration. In absence of an external field the potential energy of each basic unit is  $\frac{1}{2}\omega_j^2 q_j^2$ , where  $\omega_j$  is  $2\pi$  times the frequency. The displacement  $q_j$  is connected with a uniform polarisation throughout the crystal, giving rise to an internal field. The potential energy is due partly to the action of short-range forces and partly to the long-range interaction through the internal field.

If the crystal is in the same state of polarisation but there is an additional external field present, then the total electric field in the crystal is

$$E = E_{\text{ext.}} + E_{\text{int.}}, \quad (9)$$

$E_{\text{ext.}}$  being the field due to external and  $E_{\text{int.}}$  to internal sources. We assume, for the time being, that the external field has the same value everywhere in the crystal. The potential energy of a basic unit now is

$$\frac{1}{2}\omega_j^2 q_j^2 - E_{\text{ext.}} \frac{\partial \mu}{\partial q_j} q_j, \quad (10)$$

where  $(\partial \mu / \partial q_j) q_j$  is the dipole moment connected with displacement  $q_j$  and only  $E_{\text{ext.}}$  has to be considered in the second term.  $E_{\text{int.}}$  is determined by  $q_j$  and for a given configuration its value is the same whether or not there is an external field acting; its effect is therefore contained in the term  $\frac{1}{2}\omega_j^2 q_j^2$ . The internal field due to the other normal vibrations or to the ultra-violet polarisation  $P_u$  need not be considered either, since, according to what has been said in the previous section, these do not interact with  $q_j$ .

The expression (10) is the potential energy of a harmonic oscillator whose equilibrium position is

$$\bar{q}_j = E_{\text{ext.}} \frac{\partial \mu / \partial q_j}{\omega_j^2}.$$

Inserting this result into eqn. (7) we have, in presence of an external field

$$\bar{M}_i = E_{\text{ext.}} N v \sum_j \frac{(\partial \mu / \partial q_j)^2}{\omega_j^2}.$$

The infra-red polarisation is  $P_i = \bar{M}_i / v$ , where the mean value of  $M_i$  is used since we have to average over fluctuations in time. Putting

$$\alpha_i = N \sum_j \frac{(\partial \mu / \partial q_j)^2}{\omega_j^2} \quad (11)$$

we have

$$P_i = \alpha_i E_{\text{ext.}}, \quad (12)$$

where  $\alpha_i$  may be identified as the infra-red contribution to the polarisability which is now defined in terms of the natural frequencies of the material. Comparing (12) with (1) shows that the effective field is due to external sources only, because the effect of the internal field is contained in the frequencies and therefore in  $\alpha_i$ . All the difficulty in calculating the interaction with the internal field is contained in the  $\partial \mu / \partial q_j$ 's.

Similarly to (12) we may define a high-frequency or ultra-violet polarisability  $\alpha_u$  by

$$P_u = \alpha_u E_{\text{ext.}} \quad (13)$$

and a total polarisability  $\alpha$  by

$$\begin{aligned} P &= \alpha E_{\text{ext.}}, \\ \alpha &= \alpha_i + \alpha_u. \end{aligned} \quad (14)$$

where

$\alpha_u$  is determined by the frequencies of the ultra-violet virtual oscillators in a similar way as  $\alpha_i$  is given by (11), but we shall not need this connection.

Using the definition of the dielectric constant

$$\epsilon - 1 = 4\pi P/E, \quad (15)$$

eqn. (14) can be written

$$\epsilon - 1 = 4\pi\alpha E_{\text{ext.}}/E. \quad (16)$$

While  $\epsilon$  is, of course, independent of the shape of the material,  $\alpha$  is not, because it contains the interaction through the internal field. Lyddane and Herzfeld<sup>4</sup> have shown for the infra-red polarisation that if the external field has the same value everywhere in the crystal, i.e. in case of static fields or waves very long compared with the size of the material, then the interaction through the internal field depends on the shape of the material. Following their argument it is easy to show that for such external fields  $\alpha_u$  as well as  $\alpha_i$  depends on shape.

If the material is a slab polarised across, which is the usual case for the dielectric in a condenser, then it is known from electrostatics that

$$E_{\text{int.}} = -4\pi P = -(\epsilon - 1)E \quad (17)$$

the second equation following from (15). The negative sign is used since polarisation and internal field have opposite directions. On the other hand, if the slab is polarised along one of its long axes,

$$E_{\text{int.}} = 0. \quad (18)$$

While if the material is a sphere

$$E_{\text{int.}} = -(4\pi/3)P = -3(\epsilon - 1)E. \quad (19)$$

Inserting, in turn, (17), (18) and (19) into (9), we have

for the slab polarised across,  $E_{\text{ext.}}/E = \epsilon$ ;

for the slab polarised along,  $E_{\text{ext.}}/E = 1$ ;

and for the sphere,  $E_{\text{ext.}}/E = (\epsilon + 2)/3$ .

$E_{\text{ext.}}$  is the field due to external sources and is, of course, not identical with the dielectric displacement of macroscopic theory. Inserting these values of  $E_{\text{ext.}}/E$ , in turn, into (16) gives

$$\left. \begin{aligned} (\epsilon - 1)/\epsilon &= 4\pi\alpha_{\perp} \\ \epsilon - 1 &= 4\pi\alpha_{\parallel} \\ \frac{\epsilon - 1}{\epsilon + 2} &= \frac{4\pi}{3}\alpha_s \end{aligned} \right\} \quad (20)$$

where  $\alpha_{\perp}$ ,  $\alpha_{\parallel}$  and  $\alpha_s$  denote the polarisabilities across and along a slab, and of a sphere, respectively. These equations show how strongly the polarisability depends on shape. For alkali halides, for instance,  $\epsilon \approx 5$ , so that  $\alpha_s/\alpha_{\perp} \approx 2.1$  and  $\alpha_{\parallel}/\alpha_{\perp} \approx 5$ .

### III. Short Longitudinal and Transverse Waves

So far we have considered the case that the wave-length of the external field is very long compared with the size of the material. The case when

<sup>4</sup> Lyddane and Herzfeld, *Physic. Rev.*, 1938, **54**, 846.

the wave-length of  $E_{\text{ext.}}$  is short compared with the material but still very long compared with the unit cell is also of interest since this is the case for infra-red, visible and near ultra-violet rays. As infinitely long external waves can interact only with the normal vibrations of the crystal with infinite wave-length, so for shorter waves the summation in eqn. (6) and (11) extends over those vibrations of the crystal which have the same wave-length and direction of polarisation as the external field, since for all other vibrations the interaction energy  $-\mu E_{\text{ext.}}$  vanishes when summed over the whole crystal. While the natural frequencies are different for longitudinal and transverse vibrations,<sup>4, 5</sup> they do not vary with wave-length down to much shorter waves than considered here.<sup>6</sup> It will be shown presently that the  $\partial\mu/\partial q_i$ 's are also independent of the wavelength. Eqn. (11) can therefore be written,

$$\left. \begin{array}{l} \text{for longitudinal waves,} \\ \text{and for transverse waves,} \end{array} \right\} \begin{array}{l} \alpha_{li} = \sum \frac{(\partial\mu/\partial q_i)^2}{\omega_{li}^2} \\ \alpha_{ti} = \sum \frac{(\partial\mu/\partial q_i)^2}{\omega_{ti}^2} \end{array} \quad . \quad . \quad . \quad . \quad (21)$$

where the indices  $li$  and  $ti$  refer to longitudinal and transverse infra-red waves, respectively. We have neglected the dependence of the polarisability on the frequency of the external field, for we shall restrict ourselves to the case that this frequency is much lower than all the  $\omega$ 's appearing in eqn. (21).

In connection with the external field, it has been shown by Lyddane and Herzfeld<sup>7</sup> and by Fröhlich and Mott<sup>8</sup> that when the wave-length of  $E_{\text{ext.}}$  is smaller than the material, then the internal field is independent of the shape of the material and depends on whether the wave is longitudinal or transverse. These authors only considered infra-red polarisation waves but their results are obviously also valid for the ultra-violet part of the polarisation. Since the wave-length is large compared with the lattice dimensions, within any microscopic region comprising a large number of atoms we may regard both the polarisation and  $E_{\text{int.}}$  as uniform. The authors quoted have shown that for longitudinal waves,

$$E_{\text{int.}} = -4\pi P, \quad . \quad . \quad . \quad . \quad (17a)$$

$$\text{while for transverse,} \quad E_{\text{int.}} = 0, \quad . \quad . \quad . \quad . \quad (18a)$$

where  $E_{\text{int.}}$  and  $P$  refer, of course, to the same microscopic region. These last two equations are identical with (17) and (18), respectively. Therefore, with the same procedure as equations (20) were derived, we obtain

$$\epsilon - 1/\epsilon = 4\pi\alpha_l; \quad \epsilon - 1 = 4\pi\alpha_t \quad . \quad . \quad . \quad (22)$$

and comparison with (20) shows that

$$\alpha_l = \alpha_1; \quad \alpha_t = \alpha_{11} \quad . \quad . \quad . \quad . \quad (23)$$

Eqn. (23) must hold separately for the infra-red and ultra-violet polarisations, as these are independent of each other. Thus

$$\left. \begin{array}{l} \alpha_{lu} = \alpha_{1u}; \quad \alpha_{lt} = \alpha_{1t} \\ \alpha_{tu} = \alpha_{11u}; \quad \alpha_{tt} = \alpha_{11t} \end{array} \right\} \quad . \quad . \quad . \quad . \quad (24)$$

or

$$\left. \begin{array}{l} \sum \frac{(\partial\mu/\partial q_i)^2}{\omega_i^2} = \sum \frac{(\partial\mu/\partial q_1)^2}{\omega_1^2} \\ \sum \frac{(\partial\mu/\partial q_i)^2}{\omega_i^2} = \sum \frac{(\partial\mu/\partial q_{11})^2}{\omega_{11}^2} \end{array} \right\} \quad . \quad . \quad . \quad (21a)$$

<sup>5</sup> Fröhlich and Mott, *Proc. Roy. Soc. A*, 1939, **171**, 496.

<sup>6</sup> Born and Göppert-Meyer, *Handb. Physik*, 1933, **24** (2), 638.

<sup>7</sup> An error contained in Lyddane and Herzfeld's paper has been corrected subsequently.<sup>7</sup>

<sup>8</sup> Lyddane, Herzfeld and Sachs, *Physic. Rev.*, 1940, **58**, 1008.

Since it also follows from the paper by Lyddane and Herzfeld that every  $\omega_i$  is equal, in the present approximation, to an  $\omega_{\perp}$ , we may also conclude that every  $\partial\mu/\partial q_i$  is equal to the corresponding  $\partial\mu/\partial q_{\perp}$ . This can also be seen as follows. The near neighbourhood of any basic unit may be regarded as uniformly polarised in the course of all vibrations considered here, so that the short-range interaction is the same in each case. The long-range interaction is also the same for the longitudinal and  $\perp$  case, because the internal field is the same. In the present approximation, therefore, the potential energy of a basic unit is the same function of its displacement co-ordinates in these two cases, which means that both the normal displacements and the corresponding restoring forces are the same. This demonstrates the equality of corresponding  $\omega$ 's and  $\partial\mu/\partial q$ 's for longitudinal and  $\perp$  vibrations. The only difference is that for  $\perp$  all unit cells vibrate with the same amplitude while for longitudinal waves they have different amplitudes in different microscopic regions. By a similar argument the same equality holds between the  $\omega_i$ 's and  $\omega_{\parallel}$ 's, and the  $\partial\mu/\partial q_i$ 's and  $\partial\mu/\partial q_{\parallel}$ 's, respectively.

#### IV. The Various Formulae for Infra-red Polarisability.

Eqn. (20) and (22) must hold separately for the ultra-violet and the infra-red polarisations. The ultra-violet parts of these equations can be written :

$$\left. \begin{aligned} \frac{n^2 - 1}{n^2} &= 4\pi\alpha_{\perp u} = 4\pi\alpha_{\perp u} \\ n^2 - 1 &= 4\pi\alpha_{\parallel u} = 4\pi\alpha_{\parallel u} \\ \frac{n^2 - 1}{n^2 + 2} &= \frac{4\pi}{3}\alpha_{su} \end{aligned} \right\} \quad . \quad . \quad . \quad (25)$$

where  $n^2$ , the square of the optical refractive index, is the high-frequency dielectric constant. This is the only polarisation that takes place if the frequency of the external field is higher than the characteristic frequencies of the lattice vibrations. Subtracting eqn. (25) from the corresponding eqn. (20) and (22) we obtain for the low-frequency or infra-red contribution

$$\left. \begin{aligned} \frac{\epsilon - 1}{\epsilon} - \frac{n^2 - 1}{n^2} &= 4\pi\alpha_{\perp, i} = 4\pi\alpha_{\perp, i} \\ \epsilon - n^2 &= 4\pi\alpha_{\parallel, i} = 4\pi\alpha_{\parallel, i} \\ \frac{\epsilon - 1}{\epsilon + 2} - \frac{n^2 - 1}{n^2 + 2} &= \frac{4\pi}{3}\alpha_{s, i} \end{aligned} \right\} \quad . \quad . \quad (26)$$

Eqn. (26) give the dependence of infra-red polarisability on the shape of the material and the nature of the external wave. The second of these equations has the same form as (4) and the third is similar to (5). It is seen, therefore, that if we replace in those equations  $\alpha_a$  by  $\alpha_i$ , both these seemingly contradictory formulae are correct. The Clausius-Mosotti formula (5) is correct if  $\alpha$  means the static polarisability of a sphere; while (4) is correct if  $\alpha$  is the polarisability for transverse waves. The correction, however, that  $\alpha_a$  should be replaced by  $\alpha_i$ , i.e. that the electronic contribution to the infra-red polarisation should be taken into account, is important.

It is also worth remembering that the Clausius-Mosotti formula is used in two different ways, viz. in a macroscopic and a microscopic sense (cp. Fröhlich<sup>6</sup>). In the first case it connects the dielectric constant with the macroscopic polarisability of the whole material, like eqn. (26). The microscopic Clausius-Mosotti formula, on the other hand, uses the polarisabilities of the individual molecules or ions. In case of ionic crystals this is not correct, for the ions are not independent oscillators and have therefore no well-defined individual polarisabilities.

If the crystal contains only two kinds of atoms, then each of the  $\alpha_i$ 's in (26) contains only one term, i.e. there is only one  $\omega_{i,i}$ , one  $\omega_{i,i'}$  and one  $\omega_{g,i}$ , connected with the polarisation in any principal direction. For non-cubic crystals, the  $\alpha$ 's, the  $\omega$ 's and the  $\partial\mu/\partial q$ 's are, of course, different for the different principal directions. The connection between the various infra-red frequencies and  $\partial\mu/\partial q$ 's has been calculated for diatomic crystals by Lyddane, Sachs and Teller.<sup>8</sup> Introducing the frequency  $\nu$ , where  $2\pi\nu = \omega$ , and dropping the index  $i$  from  $\nu_i$  and  $\partial\mu/\partial q_i$ , their results are, in our notation

$$\left. \begin{aligned} \nu_l^2 &= \frac{\epsilon}{n^2} \nu_i^2 \\ \nu_s^2 &= \frac{\epsilon + 2}{n^2 + 2} \nu_i^2 \end{aligned} \right\} \quad . \quad . \quad . \quad . \quad (27)$$

$$\frac{\partial \mu}{\partial q_1} = n^2 \frac{\partial \mu}{\partial q_1} = \frac{n^2 + 2}{3} \frac{\partial \mu}{\partial q_3}, \quad (28)$$

where, for non-cubic crystals, all quantities refer to the same principal direction. The only approximation contained in these results is the one used throughout in the present paper, namely that the displacements are small so that both the dipole moment  $\mu$  and the restoring force is of first order in  $q$ . In a following publication these calculations will be extended to other crystals, but now we shall restrict ourselves to crystals for which eqn. (27) and (28) are valid, i.e. for which each  $\alpha_i$  contains only one term.

TABLE I

Substance	$z$	Lattice type	$\epsilon$	$n^2$	$\epsilon - n^2 = 4\pi\alpha_f$	$\lambda_f$ (cm. <sup>-1</sup> )	$\left(\frac{n^2+2}{3}\right)^2$	$s$
LiF	1	NaCl	9.27	1.92	7.35	32.6	1.71	0.87
NaF	1	NaCl	6.0	1.74	4.26	40.6	1.56	0.93
NaCl	1	NaCl	5.62	2.25	3.37	61.1	2.01	0.74
NaBr	1	NaCl	5.99	2.62	3.37	74.7	2.37	0.69
NaI	1	NaCl	6.60	2.91	3.69	85.5	2.68	0.71
KCl	1	NaCl	4.68	2.13	2.55	70.7	1.90	0.80
KrBr	1	NaCl	4.78	2.33	2.45	88.3	2.08	0.76
KI	1	NaCl	4.94	2.69	2.25	102.0	2.45	0.69
RbCl	1	NaCl	5	2.19	2.81	84.8	1.95	0.84
RbBr	1	NaCl	5	2.33	2.67	114.0	2.08	0.82
RbI	1	NaCl	5	2.63	2.37	129.5	2.38	0.89
CsCl	1	CsCl	7.20	2.60	4.60	102	2.34	0.84
CsBr	1	CsCl	6.51	2.78	3.73	134	2.53	0.79
TiCl	1	CsCl	31.9	5.10	26.8	117	5.6	1.08
CuCl	1	ZnS	10	3.57	6.43	53	3.45	1.10
CuBr	1	ZnS	8	4.08	3.92	57	4.10	0.995
MgO	2	NaCl	9.8	2.95	6.85	17.3	2.73	0.88
CaO	2	NaCl	11.8	3.28	8.52	27.4	3.10	0.76
SrO	2	NaCl	13.3	3.31	9.99	47	3.14	0.58
ZnS	2	ZnS	8.3	5.07	3.23	33	5.57	0.48
CaF <sub>2</sub>	2	CaF <sub>2</sub>	8.43	1.99	6.44	51.5	1.77	0.74
SrF <sub>2</sub>	2	CaF <sub>2</sub>	7.69	2.08	5.61	69	1.85	0.65
BaF <sub>2</sub>	2	CaF <sub>2</sub>	7.33	2.09	5.24	73	1.86	0.70
Rutile ⊥	2	TiO <sub>2</sub>	89	6.82	82.18	{ 30.5 41	8.7 8.7	0.88 0.65
Rutile	2	TiO <sub>2</sub>	173	8.42	164.58	{ 41 50	12.1 12.1	0.79 0.65

<sup>8</sup> Lyddane, Sachs and Teller, *Physic. Rev.*, 1941, **59**, 673.

<sup>9</sup> Fröhlich, *Theory of Dielectrics* (Clarendon Press) (in press).



Eqn. (28) shows that the ratios of the various  $\partial\mu/\partial q$ 's depend only on  $n^2$  and not on  $\epsilon$ . This is because the displacements of the nuclei are the same in all cases, being determined by the ratio of masses, and only the displacement of the electron cloud relative to the nuclei is different for the various cases, and this involves  $n^2$ .

### V. Long-range and Short-range Interaction between Atomic and Electronic Displacements

Among eqn. (26) the second is of chief interest, since only the transverse frequency can be obtained from the absorption spectrum. Substituting for  $\alpha$ , this equation gives

$$\epsilon - n^2 = N \frac{(\partial\mu/\partial q_t)^2}{\pi v_t^2} \quad . \quad . \quad . \quad (29)$$

This equation has been derived by Lyddane, Sachs and Teller. We shall now separate the effect of long-range and short-range interaction in  $\partial\mu/\partial q_t$ . Although  $E_{\text{int.}} = 0$  for transverse waves, this does not mean that the long-range interaction vanishes, since  $E_{\text{int.}}$  is the field due to all dipoles, not only to the distant ones, and contains the self-field of any particle considered. As Lorentz has shown, it is in the case of a uniformly polarised sphere that the long-range interaction vanishes. It is therefore  $\omega_s$  and  $\partial\mu/\partial q_s$  which are independent of long-range forces.

In case of a perfectly polar crystal, if the electron shells were rigid so that the lattice vibrations contained no electronic polarisation, the dipole moment induced by the infra-red vibration would be given by eqn. (8). Born showed that for this case

$$\partial\mu/\partial q_s = ze\sqrt{1/m_1 + 1/m_2} \quad . \quad . \quad . \quad (30)$$

$m_1$  and  $m_2$  being the masses of the positive and negative ions, respectively. If the electron shells are deformable then eqn. (30) gives the contribution of the atomic polarisation alone, i.e. the polarisation due to the displacement of ions as a whole without distorting their electron shells. This is indicated by the index  $a$  after  $\partial\mu/\partial q$ .

Eqn. (30) was derived by Born under the assumption of central forces, but it actually holds whether the forces are central or not, for cubic and anisotropic crystals, as long as the electron shells are rigid. The condition that the centre of gravity of each unit cell is at rest,

$$m_1 x_+ + m_2 x_- = 0$$

and the normalisation condition of normal co-ordinates,

$$m_1 x_+^2 + m_2 x_-^2 = q^2,$$

imply that

$$x_+ - x_- = q\sqrt{1/m_1 + 1/m_2}.$$

Substituting this last equation into (8) and differentiating results in eqn. (30).

For deformable ions which do not overlap the Lorentz theorem holds and the field exerted on an ion by all others vanishes in a uniformly polarised sphere if the lattice is cubic. In this case the field set up by the displacements of ions does not act on electrons and the infra-red  $\alpha_s$  does not contain electronic polarisation. Therefore, for this ideal case eqn. (8) holds and  $\partial\mu/\partial q_s$  is given by (30). For longitudinal or transverse waves, on the other hand, the long-range interaction does not vanish and such infra-red waves do contain electronic polarisation. Eqn. (28) shows that  $\partial\mu/\partial q_t$  is larger and  $\partial\mu/\partial q_l$  smaller than  $\partial\mu/\partial q_s$ ; this shows that for longitudinal waves electronic and atomic polarisations have opposite sign, while for transverse waves they have the same sign.

In real crystals, however, the ions always overlap to some extent. The Lorentz theorem is then not valid and there is a field acting on each ion

due to its neighbours. even in a uniformly polarised sphere. We may put

$$\left. \begin{aligned} \mu_B &= sze(x_+ - x_-) \\ \partial\mu/\partial q_B &= sze\sqrt{1/m_1 + 1/m_2} \end{aligned} \right\} \quad . \quad . \quad . \quad (31)$$

where  $s$  is a correction factor for deviation from ideal heteropolar behaviour and depends on the short-range dipolar interaction. The long-range interaction still vanishes, since this is of course not affected by the overlap of neighbouring ions.  $\partial\mu/\partial q_B$  and  $s$  therefore depend on short-range forces only.

With the aid of (27) and (31), eqn. (29) can be transformed into

$$\epsilon = n^2 + \left(\frac{n^2 + 2}{3}\right)^2 s^2 \frac{(ze)^2 N}{\pi \nu_i^2} \left(\frac{1}{m_1} + \frac{1}{m_2}\right). \quad . \quad . \quad . \quad (32)$$

While Born's well-known equation for rigid ions is

$$\epsilon = n^2 + \frac{(ze)^2 N}{\pi \nu_i^2} \left(\frac{1}{m_1} + \frac{1}{m_2}\right).$$

The first term in (32) is the contribution of the ultra-violet and the second of the infra-red polarisation. This second term contains two factors not present in Born's equations; both take account of the electronic contribution to infra-red polarisation.  $s$  represents the short-range interaction of electronic and atomic displacements, while the factor  $\left(\frac{n^2 + 2}{3}\right)^2$  appears because the long-range interaction does not vanish for transverse waves. The necessity for correcting for the short-range interaction has been pointed out by Heckmann,<sup>2</sup> Eucken and Büchner,<sup>3</sup> Mott and Littleton<sup>10</sup> and others. Lyddane, Sachs and Teller<sup>8</sup> took both long-range and short-range interaction together into account. The present formula (32) separates long-range and short-range effects and makes it possible to calculate the short-range factor  $s$ .

Since eqn. (30) is also valid for anisotropic crystals if the electron shells are rigid, eqn. (31) and (32) are valid for all crystal structures,  $s$  still being the correction factor for the short-range interaction of atomic and electronic polarisations. In anisotropic crystals, however,  $s$  is not equal to unity even in an ideal heteropolar material, since the short-range dipolar interaction does not vanish in such crystal structures even if there is no overlap. In non-cubic crystals the quantities connected by eqn. (30), (31) and (32), of course, all refer to the same principal direction.

For triatomic crystals with two equal atoms, such as  $\text{CaF}_2$  or  $\text{TiO}_2$ , Born's result is, for rigid electron shells

$$\partial\mu/\partial q_a = ze\sqrt{1/m_1 + 1/2m_2} \quad . \quad . \quad . \quad (30a)$$

where  $m_1$  is the mass and  $z$  the charge of the ion with the higher valency. Instead of (32) we then have

$$\epsilon = n^2 + \left(\frac{n^2 + 2}{3}\right)^2 s^2 \frac{(ze)^2 N}{\pi \nu_i^2} \left(\frac{1}{m_1} + \frac{1}{2m_2}\right) \quad . \quad . \quad . \quad (32a)$$

where  $\left(\frac{n^2 + 2}{3}\right)^2$  and  $s^2$  again stand for the electronic contributions to the infra-red polarisation.

## VI. Short-range Interaction and Polarity

All quantities in eqn. (32) and (32a) can be determined experimentally except  $s$ . Table I contains data for those materials for which the experimental data are available. All these materials are cubic, with the exception of rutile. Values for  $\epsilon$  and  $n^2$  are taken from Mott and Gurney<sup>1</sup>

<sup>10</sup> Mott and Littleton, *Trans. Faraday Soc.* 1938, **34**, 485.

and from Landolt-Börnstein.  $\lambda_i$ , the vacuum wave-length for transverse vibrations, is taken from absorption measurements by Barnes<sup>11</sup> for alkali halides and TiCl and from Parodi<sup>12</sup> for the other substances. There is some doubt about rutile. This material, being tetragonal, should have two absorption maxima corresponding to polarisation along the two kinds of axes. The absorption spectrum has been measured by Parodi who finds three maxima, at 30.5, 41 and 50 $\mu$ , one of which must be secondary. From the data given by that author it is not possible to decide which two of these three are the main maxima;  $\lambda_i$  for polarisation perpendicular to the long axis is therefore either 30.5 or 41 $\mu$ , and parallel to the main axis either 41 or 50 $\mu$ . The calculations have been carried out for these various possibilities.

The last column in Table I contains values for the short-range factor  $s$ , calculated from eqn. (32) and (32a). The experimental data for alkali halides seem well established and one may expect, therefore, that the  $s$  values calculated for these substances are accurate within a few per cent., although the figures for some of the other materials may be less reliable.

For an ideal heteropolar material  $s$  ought to be unity and it is therefore rather surprising to find that alkali halides have  $s$  values round about 0.8. On the other hand, for materials like CuCl, CuBr and TiCl, whose chemical and physical properties indicate that their polarity is weaker than that of alkali halides,  $s$  is about unity or even larger. This shows that  $\partial\mu/\partial q_s$  and  $s$  do not necessarily decrease with decreasing polarity. The reason is probably as follows.

The conclusion that  $s$  should be unity rests on the following two assumptions usually made in connection with an ideal heteropolar lattice—

(1) That the charge on each ion is  $ze$  and that in each ion the centre of the electronic charges coincides with the nucleus;

(2) that the change in electrostatic interaction due to the displacement of the ions can be described by the effect of point dipoles located at the lattice points. From this it follows that the Lorentz theorem holds, i.e. if in a crystal of spherical shape and of cubic lattice structure all negative ions are displaced with respect to the positive ions, then there is no force tending to polarise the electrons and consequently the centres of positive and negative charges in each ion still coincide after the displacement.

According to current views the first assumption is correct in the case of alkali halides, and a departure of  $s$  from unity therefore seems to indicate that in these materials the second assumption is at fault. The reason for this may be either that the charge distribution around the ions is not spherical, or that the ions overlap to some extent, or that the non-electrostatic short-range forces tend to distort the ions when they are displaced relative to each other. For most other ionic crystals, probably neither of the two assumptions is exactly true.

One might expect to find a particularly large difference between  $s$  and unity if the ions penetrate considerably into each other<sup>1</sup> or if the bond has partial homopolar character and its polarity changes rapidly with the distance between the atoms.<sup>3</sup> The effects on  $s$  of these various departures from ideal heteropolar behaviour may however have different signs and this is probably the reason why  $s$  is not a measure of the polarity of the crystal. For instance, the fact that  $s$  in CuBr is much nearer to unity than in alkali halides is presumably due to the circumstance that in CuBr various effects of opposite sign counterbalance each other.

In conclusion, I wish to thank Prof. H. Fröhlich for many very helpful discussions on this subject, and the British Electrical and Allied Industries Research Association for permission to publish this paper.

*Dept. of Theoretical Physics,  
University of Liverpool.*

<sup>11</sup> Barnes, *Z. Physik*, 1932, **75**, 723.

<sup>12</sup> Parodi, *Compt. rend.*, 1937, **204**, 1636; **205**, 906 and 1224; 1939, **206**, 1717.

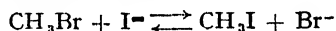
# THE INFLUENCE OF THE SOLVENT ON THE KINETICS OF REACTIONS BETWEEN IONS AND POLAR MOLECULES

BY E. A. MOELWYN-HUGHES

*Received 12th July, 1948*

The kinetics of the reactions of certain methyl halides with halogen ions have been investigated in acetone solution. A comparison of the results with those previously found for the same reactions in hydroxylic media indicates that the influence of the solvent on the rates of reactions between ions and polar molecules is principally, and almost entirely, to effect a change in the energy of activation.

The solvent influences the velocity of chemical change in a variety of ways, which, though not fully understood, seem to depend on the nature (polar, ionic, non-polar, etc.) of the reactants. In an attempt to find how the solvent affects the velocity of reactions between ions and polar molecules, the following substitutions



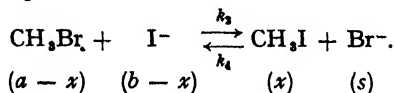
were kinetically investigated in aqueous<sup>1</sup> and in methyl alcoholic<sup>2</sup> solutions. Changing the solvent from water to methyl alcohol merely resulted in an increase of about 50 % in the velocity coefficients. The change in energy of activation was not detectable for the forward reaction, and amounted to only a few hundred calories per gram-molecule for the reverse process. These are surprisingly small effects. The present work extends the investigation of the same two reactions to acetone as a solvent. It is now found that the velocity constants are increased by factors of the order of magnitude of one thousand. Moreover, the collision term  $A$  in the equation,

$$k = A e^{-E_A/RT}, \quad (1)$$

remains sensibly unchanged, so that the alteration in rate as we pass from one solvent to another is to be ascribed almost entirely to a change in the apparent energy of activation  $E_A$ .

## Formulation of the Chemical Kinetics

The kinetics of these reactions in acetone solution are not quite the same as in the hydroxylic media because interaction with the solvent does not now occur, and because KBr is precipitated from solution in the early stages of the interaction of  $\text{CH}_3\text{Br}$  and KI. Employing the same notation as in previous papers, and denoting the solubility of KBr by  $s$ , we have the following scheme—



Integration of the differential equation

$$\frac{dx}{dt} = k_3(a-x)(b-x) - k_4sx \quad (2)$$

<sup>1</sup> *Trans. Chem. Soc.*, 1938, 779.

<sup>2</sup> *Trans. Faraday Soc.*, 1939, 35, 368.

gives the following expressions for the velocity coefficient

$$k_2 = \frac{1}{2\beta bt} \ln \left[ \frac{a - (\alpha - \beta)x}{a - (\alpha + \beta)x} \right], \quad . \quad . \quad . \quad (3)$$

and for the fractional change

$$(x/a) = [\alpha + \beta \coth (k_2 \beta bt)]^{-1}, \quad . \quad . \quad . \quad (4)$$

where

$$\alpha = \frac{1}{2} \left( 1 + \frac{a}{b} + \frac{sk_4}{bk_2} \right) \quad . \quad . \quad . \quad (5)$$

and

$$\beta^2 = \alpha^2 - (a/b). \quad . \quad . \quad . \quad (6)$$

It is clear from eqn. (4) that, as  $t$  becomes infinite, the value of  $x$  is given by the equation

$$x = \frac{a}{\alpha + \beta} = b(\alpha - \beta). \quad . \quad . \quad . \quad (7)$$

Expressing the four concentrations corresponding to infinite time in terms of  $x_\infty$ , it follows that

$$\frac{sx_\infty}{(a - x_\infty)(b - x_\infty)} = \frac{k_2}{k_4}, \quad . \quad . \quad . \quad (8)$$

in accordance with a zero rate of reaction (eqn. (2)).

In problems of this kind, the work is simplified by a determination of the static values,  $s$  and  $(k_2/k_4)$ , prior to the kinetic values  $k_2$  and  $k_4$ , in which we are chiefly interested.

### Experimental and Results

The methyl bromide used was drawn from the same cylinder as that used in earlier work.<sup>3</sup> Kahlbaum's *acetone pro analysi* was distilled in small batches over anhydrous sodium sulphate in an all-glass apparatus, collecting samples boiling in the range 56.4 to 56.6° C. A large volume was prepared and stored in a 12-litre Pyrex vessel fitted with a delivery tube and a phosphorus pentoxide vent. Solutions of  $\text{CH}_3\text{Br}$  in this solvent were prepared as required in the bubbling apparatus previously described, and at a total pressure of 525 mm. Hg. Solutions of KI in acetone were made by weight in 1-litre ground-stoppered Erlenmeyer flasks, fitted with delivery tubes. The concentrations of the reactant solutions could be determined, by repetition, to within  $\pm 0.1$  millimole per litre. Not so high an accuracy is claimed for estimations relating to single samples of solutions expressed during the course of the runs. The concentration of inorganic halide ( $\text{Br}^-$  and  $\text{I}^-$ ) was measured by Volhard's method, and that of the total halide ( $\text{Br}^-$ ,  $\text{I}^-$ ,  $\text{CH}_3\text{Br}$  and  $\text{CH}_3\text{I}$ ) by the same method after overnight digestion with excess potash at 100° C. The concentration of inorganic iodide was determined by titration with standard potassium iodate solution,



in the presence of cold chloroform and strong HCl. Blank experiments showed this method of analysis to be reliable in the presence of acetone,  $\text{CH}_3\text{Br}$  and KBr. The solubility limit of KBr is reached in the early stages of the experiments, and thereafter the salt is quantitatively precipitated. This fact makes it possible to follow the course of the reaction by titrating filtered samples with either  $\text{KIO}_3$  or  $\text{AgNO}_3$ . The latter method of analysis is the quicker, and was therefore chiefly employed. The results obtained, using a filter plug of mixed glass and cotton wools, were consistent.

**Equilibrium Analyses.**—Equilibrium analyses of the final solutions can be carried out at temperatures too high to allow of accurate kinetic measurements. Some representative results are shown in Table I. The calculated values are those given by eqn. (8).

**Solubilities and Equilibrium Constants.**—Excess of dry, finely powdered KBr and KI were sealed off in contact with dry acetone in vessels which were fixed to a platform rotating in the thermostat at 200 rev./min. After not less than a day, the solubilities were determined volumetrically for filtered samples

TABLE I.—EQUILIBRIUM CONCENTRATIONS (MILLIMOLES/LITRE)

[CH <sub>3</sub> Br] <sub>0</sub> = <i>a</i>	[I <sup>-</sup> ] <sub>0</sub> = <i>b</i>	[CH <sub>3</sub> Br] <sub>∞</sub> = ( <i>a</i> - <i>x</i> <sub>∞</sub> )		[I <sup>-</sup> ] <sub>∞</sub> = ( <i>b</i> - <i>x</i> <sub>∞</sub> )	
		Obs.	Calc.	Obs.	Calc.

(T = 273·13° K, sk <sub>4</sub> /k <sub>2</sub> = 1·36)					
14·4	14·4	3·5	3·8	2·9	3·8
28·7	28·7	5·5	5·6	5·5	5·6
33·6	33·6	6·3	6·2	6·3	6·2
42·7	14·4	29·4	29·0	1·2	0·7
44·7	14·4	30·9	30·9	0·6	0·6
57·4	57·5	8·8	8·2	7·3	8·3

(T = 307·78° K, sk <sub>4</sub> /k <sub>2</sub> = 1·56)					
6·6	6·2	2·4	2·7	2·0	2·3
13·2	12·3	4·3	4·2	3·4	3·3
19·8	18·5	5·6	5·4	4·3	4·1
26·4	24·6	6·7	6·6	4·9	4·8
33·0	30·8	8·2	7·5	6·0	5·3

(T = 328·10° K, sk <sub>4</sub> /k <sub>2</sub> = 1·69)					
6·6	6·3	2·5	2·7	2·2	2·4
13·1	12·7	4·1	4·1	3·6	3·6
19·8	19·0	5·4	5·4	4·6	4·6
26·4	25·4	6·7	6·3	5·7	5·3
33·0	31·7	7·5	7·3	6·2	6·0

or gravimetrically after removal of solvent. The solubilities of both salts increase with the wetness of the solvent. The results for the purest and driest

TABLE II.—THE SOLUBILITIES (IN MILLIMOLES/LITRE) OF KI AND KBr IN ACETONE

<i>T</i> ° K	KI Obs.	KBr	
		Obs.	Calc.
273·07	—	1·53	1·53
287·89	185	1·39	1·38
291·01	180	—	—
298·08	164	—	—
302·97	—	1·20	1·26
307·75	142	—	—
317·41	—	1·16	1·17
328·10	105	1·10	1·10

solvent used are summarised in Table II. The calculated values for KBr are those given by the equation—

$$s \text{ (millimoles/litre)} = 0·219 e^{+1055/RT} \quad (9)$$

The heat evolved on the dissolution of KI at 298·1° K is 2500 cal., but the heat effect at higher temperatures is greater, and an equation of the form of eqn. (9) is consequently not applicable. There appear to be no previously determined reliable values for the solubility of KBr in acetone. The present data for KI are in reasonable agreement with some of the published values<sup>4</sup> but are lower than those given by Walden.<sup>5</sup> The present results may therefore indicate an incomplete dryness of the solvent. An inspection of Walden's data, however, shows that he obtained higher 'solubilities' for samples shaken for a long time.

<sup>4</sup> Coney and Hahn, *A Dictionary of Chemical Solubilities* (Macmillan, 1921).

<sup>5</sup> Walden, *Z. physik. Chem.*, 1906, **55**, 715.

It is thus possible that his values were too low. Fortunately, the solubility of this salt is not needed for the present investigation. By combining the data of Tables I and II, we obtain the following expression (see Table III) for the dependence on temperature of the ratio of the two velocity coefficients:

$$k_3/k_4 = 4.06 \times 10^{-2} e^{1810/RT} \quad (10)$$

TABLE III.—RATIOS OF THE BIMOLECULAR CONSTANTS

T° K	$sk_4/k_2$	$s$	$k_3/k_4$	
			Obs.	Calc.
273.18	1.36	1.53	1.136	1.145
288.15	1.44	1.38	0.956	0.963
307.78	1.56	1.23	0.783	0.783
328.10	1.69	1.10	0.652	0.652

**Velocity Constants.**—Water has a retarding effect on the rate of reaction, and not until precautions had been taken to ensure its absence, or at least its presence in a constant proportion, could reproducible results be obtained. The data of the preceding sections allow an evaluation of the functions  $\alpha$  and  $\beta$  for solutions of any composition at any temperature. The most direct way of determining the velocity coefficient is by plotting the logarithmic term in eqn. (3) as a function of time. This method has the advantage of affording a check—very

TABLE IV.—VELOCITY CONSTANTS AT 273.13° K ( $K = 1.136$ )

$(\alpha + \beta)$	$(\alpha - \beta)$	$t$ (min.)	$a - x$ (millimoles/litre)	$k_2 \times 10^2$ (litres (mole sec.) <sup>-1</sup> )
1.241	0.807	0	28.7	—
		4	23.9	2.93
		7	21.9	2.60 (?)
		12	18.0	2.93
		18	15.6	2.79
		24	13.4	2.90
		34	11.2	2.89
		50	9.2	2.82
		$\infty$	5.6	—
Average $2.88 \pm 0.09$				
1.322	0.757	0	14.37	—
		5.5	12.11	3.98
		11	10.62	3.79
		21	8.49	3.99
		32	7.30	3.76
		43.5	6.21	3.91
		$\infty$	3.84	—
Average $3.88 \pm 0.12$				

necessary in rapid reactions—on any error in the starting time. Alternately,  $k_2$  may be calculated, as shown in Table IV, for each analytical datum. With equimolar reactants, to which the figures refer, the velocity constant is reproducible to within  $\pm 3\%$  of the mean value. The ability of eqn. (4) to reproduce the fractional change as a function of time is shown in Table V, the data in which also refer to equimolar reactants. Values of the hyperbolic co-tangent were taken from Milne-Thomson and Crombie's *Standard Four-Figure Mathematical Tables* (Macmillan, 1931).

TABLE V.—THE APPLICABILITY OF EQN. (4)

( $T = 273.13^\circ \text{K}$ .  $\alpha = 1.0118$ .  $\beta = 0.1517$   
 $k_2 = 2.15 \times 10^{-2}$  litres (mole sec.) $^{-1}$ )

$t$ (min.)	100( $x/a$ )	
	Obs.	Calc.
0	0	0
7	33.6	33.9
13	48.9	48.6
20	59.1	58.9
28	66.4	66.3
35	71.8	70.6
44	74.6	74.5
$\infty$	85.7	85.9

**The Effects of Concentration and Temperature.**—Varying the concentration of  $\text{CH}_3\text{Br}$  has no detectable effect on the velocity of reaction. Increasing the concentration of  $\text{KI}$ , however, causes a considerable decrease in rate, which can be understood in two ways.

(1) According to an elementary theory of reactions between ions and polar molecules<sup>6</sup> the logarithm of the velocity coefficient may be expected to vary linearly with respect to the ionic concentration,  $j$  (g.-ions/litre):

$$\left(\frac{d \ln k_2}{dj}\right)_P = \frac{\pi N e^2 z_n \mu_A \cos \theta}{125 (DkT)^2} \quad (11)$$

Here  $N$  is the Avogadro number,  $e$  the electronic charge,  $k$  the Boltzmann constant,  $z_A$  the valency of the ion, and  $\theta$  the angle which it subtends with respect to the positive end of the dipole of moment  $\mu_A$ . The maximum value of the theoretical gradient at  $298.1^\circ \text{K}$  ( $\theta = 0$ ;  $\mu_A = 1.86 \times 10^{-18} \text{D}$ ) becomes  $-1.90$  if we accept the value of the dielectric constant ( $D = 34.0$ ) for the continuous medium. The experimental gradient is greater by a factor of about 5. Any reasonable adjustment in  $D$  brings experiment and theory closer together.

(2) The magnitude of the gradient and its change with respect to concentration suggest, as a more likely explanation, that the salt is not completely ionised at the dilutions used. As no definite increase in  $k_2$  could be detected during a given run, despite the continuous decrease in ionic strength, it may be doubted whether the true salt effect is as high as it would appear to be according to the present experiments. The influence on the rate of dilution in comparable reactions which have been examined with greater precision in ethyl alcoholic solution<sup>7</sup> can be fully explained as due to the increasing ionisation of the salt.

The value of  $k_2$  extrapolated to infinite dilution at  $273.21^\circ \text{K}$  is  $6 \times 10^{-2}$  litres (mole sec.) $^{-1}$ .

The technique adopted here does not allow of an extensive study of the temperature effect. To cope with these relatively fast reactions, methods other than the analytical one were tried. They included a dilatometric method, and the use of a differential tensimeter, with pure acetone as manometer liquid. Both methods involved too long a delay at the start of the reactions, and had to be abandoned. The results are summarised in Table VI, the last column of which gives velocity coefficients for the forward reaction according to the equation

$$k_2 = 1.15 \times 10^{10} e^{-14,840/RT} \quad (12)$$

Combining with eqn. (10), we obtain for the reverse reaction:

$$k_4 = 2.83 \times 10^{11} e^{-16,150/RT} \quad (13)$$

The errors in the energies of activation have been estimated as  $\pm 1200$  and  $\pm 1500$  cal. respectively.

<sup>6</sup> *The Kinetics of Reaction in Solution*, 2nd Ed. (Oxford, 1947), p. 132.

<sup>7</sup> Hardwick, *Trans. Chem. Soc.*, 1935, 141; Mitchell, *ibid.*, 1937, 1792; Woolf, *ibid.*, 1937, 1172.



TABLE VI

THE INFLUENCE OF SALT CONCENTRATION AND TEMPERATURE ON  $k_2$ 

T° K	j(g.-moles/litre)	$k_2 \times 10^3$ (litres/(mole sec.) <sup>-1</sup> )	
		Obs.	Calc.
273·13	0·0560	2·15	—
273·13	0·0272	2·88	—
273·13	0·0128	3·88	3·90
283·94	0·0128	10·6	10·5
290·65	0·0127	19·5	19·5

## Discussion

The data summarised in Table VII indicate clearly that, as far as these two reactions in three solvents are concerned, the effect of the medium is almost exclusively an effect on the activation energy. Thus, for example, the velocity of reaction between KBr and  $\text{CH}_3\text{I}$  is increased about 5000 times on passing from methyl alcohol to acetone. If the collision frequency were the same in the two media, we would expect a difference of 5000 cal. in the energies of activation. The observed difference is  $5250 \pm 2500$  cal. Comparable information on other reactions of the type

TABLE VII.—THE INFLUENCE OF SOLVENTS ON THE KINETICS OF REACTIONS BETWEEN IONS AND POLAR MOLECULES

Reaction	Solvent	$k$ at 298·1 K (litres/(mole sec.) <sup>-1</sup> )	$A$ (litres/(mole sec.) <sup>-1</sup> )	$E$ (cal./mole)
$\text{CH}_3\text{Br} + \text{I}^- \rightarrow \text{CH}_3\text{I} + \text{Br}^-$	$\text{CH}_3\text{OH}$	$9·42 \times 10^{-4}$	$2·26 \times 10^{10}$	$18,250 \pm 250$
	$\text{H}_2\text{O}$	$6·84 \times 10^{-4}$	$1·68 \times 10^{10}$	$18,260 \pm 130$
	$(\text{CH}_3)_2\text{CO}$	$3·55 \times 10^{-1}$	$1·15 \times 10^{10}$	$14,340 \pm 1200$
$\text{CH}_3\text{I} + \text{Br}^- \rightarrow \text{CH}_3\text{Br} + \text{I}^-$	$\text{CH}_3\text{OH}$	$7·98 \times 10^{-5}$	$3·91 \times 10^{11}$	$21,400 \pm 400$
	$\text{H}_2\text{O}$	$4·61 \times 10^{-5}$	$1·08 \times 10^{10}$	$19,620 \pm 440$
	$(\text{CH}_3)_2\text{CO}$	$4·09 \times 10^{-1}$	$2·83 \times 10^{11}$	$16,150 \pm 1500$
$3:5(\text{NO}_2)_2\text{C}_6\text{H}_3\text{Cl} + \text{I}^- \rightarrow$	$\text{C}_2\text{H}_4(\text{OH})_2$	$1·06 \times 10^{-10}$	$3·50 \times 10^{10}$	$28,000 (?)$
$3:5(\text{NO}_2)_2\text{C}_6\text{H}_3\text{Cl} + \text{CH}_3\text{O}^- \rightarrow$	$\text{CH}_3\text{OH}$	$2·50 \times 10^{-8}$	$4·27 \times 10^{10}$	$16,680 \pm 1050$

under consideration seems to be lacking, but an interesting comparison, illustrating the same point, is provided by the kinetic constants found for the reactions of 3:5-dinitrochlorobenzene with the iodide ion in ethylene glycol solution<sup>8</sup> and with the methoxyl ion in methyl alcoholic solution.<sup>9</sup> Reactions of the methyl halides in ethylene glycol solution are now consequently being investigated.

Department of Physical Chemistry,  
The University,  
Cambridge.

<sup>8</sup> Bennett and (Miss) Vernon, *Trans. Chem. Soc.*, 1938, 1783.

<sup>9</sup> Talen, *Thesis* (Leiden, 1927); see *Tables Annuelles*.

# THE ELECTRONIC STRUCTURE OF THIOPHENE AND RELATED MOLECULES

BY H. C. LONGUET-HIGGINS

Received 9th August, 1948

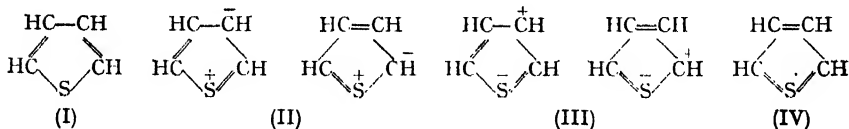
The idea of *pd* hybridisation in thiophene explains the general similarity between thiophenes and their benzene analogues, and when followed up leads to correct conclusions as to the small chemical differences between the two classes of compound.

It is well known that there is a very close similarity in physical and chemical properties between aromatic hydrocarbons containing the group  $\text{—CH=CH—}$  and the corresponding sulphur compounds in which this group is replaced by formally bivalent sulphur  $\text{—S—}$ . This similarity extends to those properties which are usually believed to depend on the mobile electrons, such as the near ultra-violet absorption spectrum,<sup>1</sup> the first ionisation potential,<sup>2</sup> the resonance energy<sup>3</sup> and the behaviour in substitution reactions, all of which properties may be considered under the convenient heading of "aromatic character". On the other hand, furan and pyrrole, although somewhat aromatic in character, are much less so than thiophene; and similar relations hold between the higher analogues of these molecules.

It is the purpose of this note to suggest why there should be this close resemblance between thiophene derivatives and benzene derivatives, and why this resemblance should not extend so markedly to derivatives of furan and pyrrole.

## Nature of Atomic Orbitals

One fundamental difference between sulphur on the one hand and nitrogen or oxygen on the other is that, whereas oxygen and nitrogen have only *s* and *p* atomic orbitals available for bonding, sulphur has also five *d* orbitals in its valence shell. The possibility that some of these *3d* orbitals may be used for bonding in thiophene has been discussed before, notably by Schomaker and Pauling,<sup>4</sup> who adopted a valence-bond approach to the problem. From a consideration of bond lengths, resonance energies and dipole moments these authors concluded that all the following types of structure were important in thiophene—



The relative weights assigned to the different types of structure were: type I, 70 %; type II, 20 %; types III and IV, 10 %. Of these structures those of types III and IV must involve the sulphur *d* orbitals, because in such structures the sulphur atom has a deficit of electrons in its

<sup>1</sup> Milazzo, quoted by Walsh, *Quart. Rev.*, 1948, **2**, 85.

<sup>2</sup> Price, *Chem. Rev.*, 1947, **41**, 257.

<sup>3</sup> Wheland, *The Theory of Resonance* (Wiley, New York, 1944).

<sup>4</sup> Schomaker and Pauling, *J. Amer. Chem. Soc.*, 1939, **61**, 1779.

valence shell. Schomaker and Pauling introduced the decet structures to reconcile the relatively low resonance moment of thiophene with its high aromatic character, as indicated by the resonance energy and C—S bond length. Their arguments are qualitatively convincing, but give no means of assessing the weights of different structures in more complicated analogues of thiophene when bond lengths and dipole moments are not available; this is a general weakness of the valence-bond method, that it is not easily extended to the quantitative investigation of large molecules.

The method of molecular orbitals, on the other hand, is particularly suitable for the investigation of large molecules, because it provides a definite and manageable technique for determining electronic structures, once the values of certain parameters have been fixed. We shall therefore use this method in the present paper. It turns out that, if the participation of the sulphur  $3d$  orbitals is taken into account, then the atomic and molecular orbitals of the  $\pi$ -electrons in a thiophene derivative correspond closely with those of the analogous benzene derivative. (Such a correspondence is not possible in pyrrole and furan derivatives, because the available atomic orbitals are always one fewer than in the benzene analogue.)

To establish this correspondence, let us consider a molecule containing the group  $\text{>CH—S—CH<}$ . It is convenient to define co-ordinates in the molecule, with the S atom as origin. The  $x$  and  $y$  axes then bisect the C—S—C angle externally and internally respectively, and the  $z$  axis is perpendicular to the molecular plane. Denote the  $2p_z$  atomic orbitals of the C atoms by  $\phi_a$  and  $\phi_b$ . Then on the S atom there are three atomic

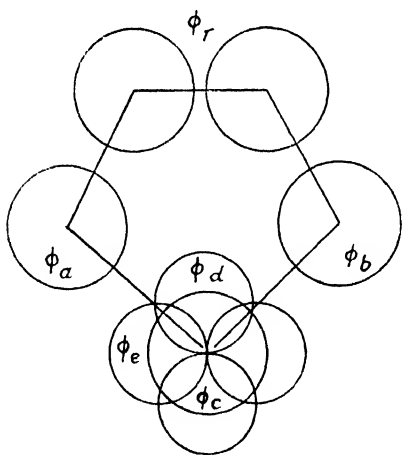


FIG. 1.

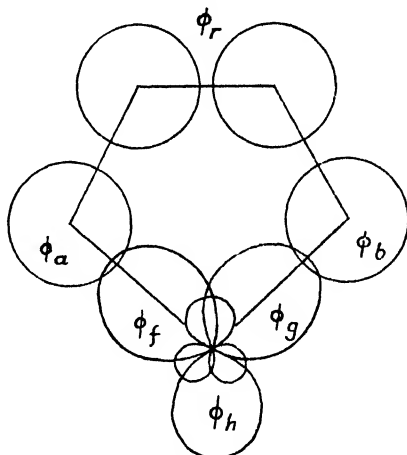


FIG. 2.

orbitals which can conjugate with  $\phi_a$  and  $\phi_b$ , namely  $3p_z$ ,  $3d_{yz}$  and  $3d_{xz}$ , which have nodal planes corresponding to their suffixes, and which we shall denote by  $\phi_c$ ,  $\phi_d$ , and  $\phi_e$  respectively.<sup>5</sup> For completeness let us denote the other atomic orbitals of the system collectively by  $\phi_r$ . The geometrical disposition of the various atomic orbitals under discussion is illustrated in Fig. 1, where the molecular plane is understood to be a plane of anti-symmetry.

Then by symmetry

$$S_{ac} = S_{bc}, \quad S_{ad} = S_{bd}, \quad \text{and} \quad S_{ae} = -S_{be},$$

where  $S_{ac} (= \int \phi_a \phi_c d\tau)$  is the overlap integral [between  $\phi_a$  and  $\phi_c$ , and so on.

<sup>5</sup> Pauling, *Nature of the Chemical Bond* (Cornell Univ. Press, Ithaca, New York, 1939).

### Hybridisation of $p$ and $d$ Orbitals

We now proceed to define hybrid atomic orbitals  $\phi_f$ ,  $\phi_g$ ,  $\phi_h$ , as follows—

$$\left. \begin{aligned} \phi_f \} &= \frac{S_{ac}S_{ae}\phi_c + S_{ad}S_{ae}\phi_d \pm (S_{ac}^2 + S_{ad}^2)\phi_e}{\{(S_{ac}^2 + S_{ad}^2)(S_{ac}^2 + S_{ad}^2 + S_{ae}^2)\}^{\frac{1}{2}}} \\ \phi_g \} &= \frac{S_{ad}\phi_c - S_{ac}\phi_d}{(S_{ac}^2 + S_{ad}^2)^{\frac{1}{2}}} \end{aligned} \right\}$$

Their approximate form is shown in Fig. 2. The significance of  $\phi_f$ ,  $\phi_g$  and  $\phi_h$  is that they are the only linear combinations of  $\phi_c$ ,  $\phi_d$  and  $\phi_e$  satisfying the following conditions—

$$\begin{aligned} S_{ff} &= S_{gg} = S_{hh} = 1, \\ S_{fh} &= 0 = S_{gh}, \\ S_{ah} &= 0 = S_{bh}, \\ S_{ag} &= 0 = S_{bg}, \\ S_{af} &= S_{bg}. \end{aligned}$$

These last relations follow quite simply from the fact that  $\phi_c$ ,  $\phi_d$ , and  $\phi_e$  are orthogonal and normalised. It should be noted, however, that  $\phi_f$  and  $\phi_g$ , although both orthogonal to  $\phi_h$ , are not orthogonal to one another.

### The Secular Equations

Since  $\phi_f$ ,  $\phi_g$  and  $\phi_h$  are linearly independent, we may use them in setting up the secular equations for the molecular  $\pi$ -orbitals. As is well known,<sup>6</sup> these equations give the coefficients  $c_i$  and the energy  $E$  for a molecular orbital expressed in the form  $\sum_j c_j \phi_j$ . There is one equation for each atomic orbital, that for  $\phi_i$  being

$$c_i(H_{ii} - E) + \sum_j c_j(H_{ij} - S_{ij}E) = 0,$$

where  $H_{ij}$  stands for  $\int \phi_i H \phi_j d\tau$ , the resonance integral between  $\phi_i$  and  $\phi_j$ .

Mulliken<sup>7</sup> has made computations of the resonance and overlap integrals for pairs of atomic orbitals in a few simple molecules, and has shown that over quite a range of interatomic distances the relationship

$$H_{ij} \approx F S_{ij}$$

holds approximately, where  $F$  is a constant with the dimensions of energy. On the rather bold assumption that this relationship holds quite generally, the secular equations corresponding to  $\phi_a$ ,  $\phi_f$  and  $\phi_h$  may be written thus—

$$c_a \frac{H_{aa} - E}{F - E} + \sum_r c_r S_{ar} + c_f S_{af} = 0,$$

$$c_f \frac{H_{ff} - E}{F - E} + c_a S_{fa} + c_g S_{fg} = 0,$$

and

$$c_h \frac{H_{hh} - E}{F - E} = 0,$$

with similar equations for  $\phi_g$  and  $\phi_e$ . The last equation shows that  $\phi_h$  is itself a molecular orbital; this must be so, as it does not interact with any of the other  $\phi$ 's.

Now let us write down the secular equations for the benzene analogue of the thiophene derivative. Denote by  $\phi'_a$ ,  $\phi'_b$ ,  $\phi'_c$  the atomic orbitals corresponding to  $\phi_a$ ,  $\phi_b$ ,  $\phi_c$ , and by  $\phi'_f$ ,  $\phi'_g$  the  $2p_z$  orbitals of the two carbon atoms which replace the sulphur atom (see Fig. 3). Then the secular equations corresponding to  $\phi'_a$  and  $\phi'_f$  are—

$$c'_a \frac{H'_{aa} - E'}{F - E'} + \sum_r c'_r S'_{ar} + c'_f S'_{af} = 0$$

$$c'_f \frac{H'_{ff} - E'}{F - E'} + c'_a S'_{fa} + c'_g S'_{fg} = 0,$$

<sup>6</sup> Coulson and Longuet-Higgins, *Proc. Roy. Soc. A*, 1947, **191**, 39.

<sup>7</sup> Mulliken, *Report of Conference on the Chemical Bond* (Paris, 1947), (in press).

with similar equations for  $\phi'_b$  and  $\phi'_g$ . (The primes are intended as a reminder that we are now discussing the benzene analogue.) These equations are formally identical with those for the thiophene derivative, except that there is no equation analogous to that involving  $c_h$ . Further,

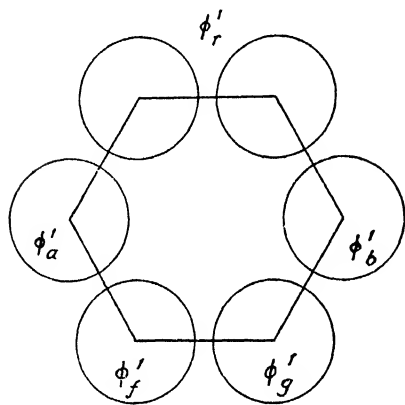


FIG. 3.

all the other secular equations are identical in the two molecules, since they are associated with atomic orbitals  $\phi_r$  or  $\phi'_r$  which are remote from the seat of difference. Now the molecular orbital  $\phi_h$  is almost certainly of too great energy to be occupied in the ground state, and is therefore mainly  $3d$  in character; for were it occupied there would be only four aromatic electrons left in the thiophene ring, which seems very unlikely on chemical grounds. So if we can find independent evidence that  $S_{af}$ ,  $S_{fg}$  and  $H_{ff}$  are nearly the same as  $S'_{af}$ ,  $S'_{fg}$  and  $H'_{ff}$ , this will imply a close correspondence in energy and form between the molecular

orbitals of the thiophene derivative and its benzene analogue, and hence between their electronic structures, at least in the ground state.

**Ionisation Potentials.**—Fortunately, such evidence is available from various sources. The first piece of evidence comes from a comparison of the first ionisation potentials of hydrogen sulphide and ethylene.<sup>2</sup> It is almost certain that in both these molecules the first ionisation is removal of a  $\pi$ -electron having as nodal plane the plane of the molecule. This means that in ethylene, whose  $p$  atomic orbitals are closely similar to  $\phi'_f$  and  $\phi'_g$ , the first ionisation potential will be given by the expression

$$(H'_{ff} + H'_{fg})/(S'_{ff} + S'_{fg}) = (H'_{ff} + FS'_{fg})/(1 + S'_{fg}),$$

which is the energy of the orbital  $(\phi'_f + \phi'_g)$ .

Now in hydrogen sulphide the most easily ionised  $\pi$ -electron moves in an orbital similar to  $\phi_e$ , so the first ionisation potential of  $\text{H}_2\text{S}$  will be equal to  $H_{ee}$ . But we can express  $H_{ee}$  in terms of  $H_{ff}$ , etc., in the following manner. As suggested above,  $\phi_h$  is mainly  $3d$  in character, which implies that  $S_{ad}/S_{ae}$  is small. Therefore  $\phi_a$  makes only a small contribution to  $\phi_f$  and  $\phi_g$ , and so  $\phi_f + \phi_g$  will be nearly equal to  $\phi_e$ , apart from a normalisation factor. It follows that  $H_{ee}$  is given by the expression—

$$(H_{ff} + H_{fg})/(S_{ff} + S_{fg}) = (H_{ff} + FS_{fg})/(1 + S_{fg}).$$

It will be apparent that if  $H_{ff} = H'_{ff}$  and  $S_{fg} = S'_{fg}$ , the ionisation potentials of ethylene and  $\text{H}_2\text{S}$  will be nearly equal; in fact they are 10.50 and 10.47 volts respectively. This close coincidence does not, of course, prove that  $H_{ff}$  and  $S_{fg}$  are equal to  $H'_{ff}$  and  $S'_{fg}$ —more extensive investigation may reveal a cancellation of errors—but it is at least consistent with that hypothesis.

**Resonance Energies.**—The second line of evidence is from resonance energies. Values of 29 and 31 kcal./mole have been given for the resonance energy of thiophene,<sup>3,4</sup> and that of benzene is close to 40 kcal., this figure being if anything too large.<sup>5</sup> The difference between these figures can be used to give an idea of the difference between  $H_{af}$  and  $S_{af}$  on the one hand and  $H'_{af}$  and  $S'_{af}$  on the other, assuming, as above, that  $H_{ff} = H'_{ff}$ ,  $S_{fg} = S'_{fg}$ .

If the overlap between adjacent atomic orbitals is formally neglected, the binding energies of the molecular orbitals in a hydrocarbon take the

form  $k_j\beta$ , where  $k_j$  are numbers and  $\beta$  is the carbon-carbon resonance integral. If overlap is not neglected, the total binding energy of the mobile electrons takes the form  $\sum_j k_j G / (1 + k_j S)$ , where  $S$  is the overlap integral

for a CC bond,  $G$  is a constant, and the summation is taken over the occupied molecular orbitals.<sup>8</sup> Now for benzene the values of  $k_j$  are 2, 1, 1, and for ethylene just 1. So in these molecules the binding energies of the mobile electrons are respectively

$$G \left\{ \frac{2}{1+2S} + \frac{1}{1+S} + \frac{1}{1+S} \right\} \text{ and } G \left\{ \frac{1}{1+S} \right\}.$$

Similarly, in thiophene if it is assumed that  $H_{ff}$ ,  $H_{fs}$  and  $S_{fs}$  have the same values as the corresponding integrals in benzene, and that  $S_{af}/S_{af'} = H_{af}/H_{af'} = \alpha$ , then the unsaturation energy of thiophene is given by the expression

$$G \left\{ \frac{k_1}{1+k_1S} + \frac{k_2}{1+k_2S} + \frac{k_3}{1+k_3S} \right\},$$

where  $k_1\beta$ ,  $k_2\beta$ ,  $k_3\beta$  are the three lowest roots of the secular equations when overlap is formally neglected and the resonance integral between  $\phi_a$  and  $\phi_f$  (and that between  $\phi_b$  and  $\phi_s$ ) is assigned the value  $\alpha\beta$ . Actually, the values of  $k_1$ ,  $k_2$ ,  $k_3$  are—

$$\begin{aligned} k_1 &= \frac{1}{2}(1 + \sqrt{5 + 4\alpha^2}), \\ k_2 &= 1, \\ k_3 &= \frac{1}{2}(-1 + \sqrt{5 + 4\alpha^2}). \end{aligned}$$

The quantity  $\alpha$  is what we are interested in at the moment. Its value can be determined from resonance energies once  $G$  and  $S$  are known. Now  $S$  is known<sup>8</sup> to be close to  $\frac{1}{4}$ . So in terms of  $G$  the resonance energy of benzene is

$$G \left\{ \frac{2}{1+2S} - \frac{1}{1+S} \right\} = \frac{8G}{15} = 40 \text{ kcal./mole, whence } G = 75 \text{ kcal.};$$

and since  $k_2 = 1$ , the resonance energy of thiophene is given by the expression

$$G \left\{ \frac{k_1}{1+k_1S} + \frac{k_3}{1+k_3S} - \frac{2}{1+S} \right\} = 30 \text{ kcal.}$$

But  $G$  and  $S$  are known, and  $k_1$  and  $k_3$  are functions of  $\alpha$  alone. The last equation can therefore be solved for  $\alpha$  yielding the value  $\alpha = 0.8$ . (A lower value for the resonance energy of benzene would imply a value of  $\alpha$  closer to unity.)

The above discussion may be summarised as follows. By taking into account the participation of the sulphur  $3d$  orbitals in the  $\pi$ -conjugation of a thiophene derivative we obtain a set of secular equations identical with those for the corresponding benzene derivative, except that (i) in the case of the thiophene derivative the secular equations have an extra solution corresponding to a localised non-bonding molecular orbital on the sulphur atom, this orbital probably having too high an energy to be occupied in the ground state, and (ii) the integrals  $H_{af}$  and  $S_{af}$  (and also  $H_{bs}$  and  $S_{bs}$ ), which determine the conjugation with the sulphur atom, are about 20% lower than the corresponding integrals in benzene. This means that it is possible to elucidate the electronic structure of any thiophene derivative from that of the benzene analogue by applying first-order perturbation theory to the latter.

**Bond Orders in Thiophene.**—As an example of the procedure just mentioned, we shall calculate the bond orders and bond lengths in thiophene. It is known<sup>9</sup> that if the resonance integral of a bond in benzene is multiplied by  $(1+y)$ , where  $y$  is small, the order of the bond itself is

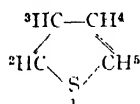
<sup>8</sup> Wheland, *J. Amer. Chem. Soc.*, 1941, **63**, 2025.

<sup>9</sup> Coulson and Longuet-Higgins, *Proc. Roy. Soc. A*, 1948, **193**, 450.

increased by  $13\gamma/54$ , and the orders of the  $\sigma$ -,  $m$ - and  $p$ -bonds are increased by  $-11\gamma/54$ ,  $+7\gamma/54$  and  $-5\gamma/54$  respectively. Now in view of the analogy just established, the orders of the bonds in thiophene are the same as those we should find in benzene if we could somehow distort the molecule so as to reduce the resonance integrals of bonds 1—2 and 5—6 by one-fifth. Since the mobile orders of the CC bonds in benzene are  $2/3$ , it follows that in the distorted molecule they would be as follows—

$$p_{12} = 0.59 = p_{56}, \quad p_{23} = 0.73 = p_{45}, \quad p_{34} = 0.61$$

( $p_{16}$  has no analogy in thiophene). From curves of bond order against bond length it follows that in thiophene the bond orders and lengths should be

	$C_2-S$	$C_2-C_3$	$C_3-C_4$	—
	0.59	0.73	0.61	Mobile order
	$1.68 \pm 0.02$	1.38	1.40	Length in Å

The uncertainty in the C—S bond length arises from the uncertainty as to what values should be taken for the normal lengths of single and double bonds between carbon and sulphur. The calculated bond lengths may be compared with those given by Schomaker and Pauling on the basis of an electron-diffraction investigation, namely

$C_2-S$	$C_2-C_3$	$C_3-C_4$	Å.
$1.74 \pm 0.03$	(1.35)	(1.44)	

The parentheses indicate that the C—C bond lengths were assumed to have the values given in the determination of the C—S bond length; so not too much weight is to be attached to the difference between the calculated and observed values.

**Dipole Moments.**—It is of interest to enquire why thiophene has a dipole moment of only 0.6D, whereas that of tetrahydrothiophene is 1.5D. Schomaker and Pauling explained this difference by supposing that thiophene has a resonance moment of about 1D arising from the unequal contribution of type II and type III structures (see earlier); but this implies that the carbon atoms in thiophene should bear negative charges of the same order of magnitude as in furan, which has an estimated resonance moment of 0.95D, and that therefore thiophene should be about as reactive chemically as furan.<sup>11</sup> On the other hand, according to the present hypothesis that  $H_{ij} = H'_{ij}$ , it follows that the net charges at the carbon atoms in thiophene will be zero, as in benzene; and this agrees with the fact that thiophene is much more similar chemically to benzene than to furan, but at first sight leaves unexplained the apparent resonance moment of thiophene. However, on closer inspection the difficulty disappears. Since the available atomic orbitals in thiophene are arranged in a hexagon, and all their coulomb integrals are equal, it follows from a general theorem that the mean number of  $\pi$ -electrons in each is unity.<sup>10</sup> But this does not imply that the moment due to the  $\pi$ -electrons is zero, because the hybrid orbitals  $\phi_i$  and  $\phi_j$  are asymmetric. In fact, there will be in thiophene a "hybridisation moment" due to the  $\pi$ -electrons which is not present in tetrahydrothiophene. Such a hybridisation moment cannot be present in furan, because the only atomic orbital on the oxygen atom which can take part in the conjugation is the  $2p_z$  orbital, which is centred on the oxygen nucleus. It is difficult to assess the magnitude of the hybridisation moment in thiophene *a priori*, because the overlap integrals governing the form of  $\phi_i$  and  $\phi_j$  are not known; but a value of 1D is quite reasonable on the assumption that these orbitals are directed more or less along the S—C bonds.

It therefore seems probable that the differences in dipole moment between furan and thiophene and their tetrahydroderivatives arise from

<sup>10</sup> Coulson and Rushbrooke, *Proc. Camb. Phil. Soc.*, 1940, **36**, 193.

essentially different causes: that in furan it is a resonance moment which is responsible for the observed lowering of dipole moment, but that in thiophene the lowering is produced by hybridisation of the  $\pi$ -orbitals on the sulphur atom.

**Reactions.**—As regards the chemical reactions of thiophene, two points may be made here. First, since two of the resonance integrals in thiophene are slightly less than the corresponding ones in benzene, the electronic structure of thiophene will be intermediate between that of benzene and that of butadiene, being closer to that of benzene. Therefore one can understand why thiophene is rather more susceptible to attack than benzene, and why such attack normally takes place at the 2- rather than at the 3-position. The second point concerns the effect of substitution on the thiophene nucleus, which will be determined by the "mutual polarisabilities" of the various pairs of atoms.<sup>11</sup> Now in butadiene the mutual polarisability of positions 1 and 2 is much greater ( $-0.402$ ) than that of positions 2 and 3 ( $-0.045$ ), so the same will be true to a lesser extent in the carbon skeleton of thiophene. This idea is borne out by the properties of 2:4-dimethyl-thiazole, in which the 2-methyl group is readily oxidised and condenses with ketonic reagents, whereas the 4-methyl group is unreactive.<sup>12</sup>

The author is much indebted to Prof. C. A. Coulson for helpful criticism.

Balliol College,  
Oxford.

<sup>11</sup> Coulson and Longuet-Higgins, *Proc. Roy. Soc. A*, 1947, **192**, 16.

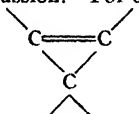
<sup>12</sup> Dr. W. A. Waters drew the author's attention to this point.

## THE STRUCTURES OF ETHYLENE OXIDE, CYCLOPROPANE, AND RELATED MOLECULES

BY A. D. WALSH

Received 9th August, 1948

Evidence bearing upon the structures of the ethylene oxide and cyclopropane molecules is discussed. It is shown that many of the salient properties of these molecules are not isolated facts but related and all connected with a particular valency condition of the C atoms involved. This valency or hybridisation condition is closer to that employed in olefines than in paraffins. The C valencies towards H, for example, are close to  $sp^3$  in nature. The orbitals within the 3-membered ring formed by bringing together  $CH_2$  groups as they exist in olefines are discussed: they appear to lead to a probability pattern that can partly be regarded as a generalisation of the pattern in the  $C=C$  bond of ethylene to an extra dimension. Certain advantages follow by very simple arguments from the discussion. For example the structures of the *spiro*-pentane molecule and the group



find a natural explanation; and a partial explanation is afforded of why the ozone molecule does not adopt the form of an equilateral triangle.

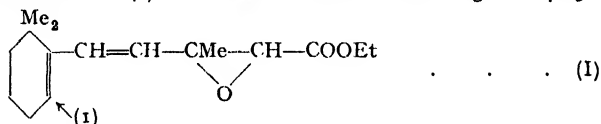
The purpose of this paper is to consider the evidence bearing upon the problem of the structures of the molecules of ethylene oxide, cyclopropane and related substances.



**Ethylene Oxide and its Derivatives.**—Some of the general properties of ethylene oxide (polymerisation and addition reactions) may be called "unsaturation properties" and have been held by Zimakov<sup>1</sup> to argue some resemblance of electronic structure to olefines.

We have photographed the far ultra-violet absorption spectrum of propylene oxide<sup>2</sup> and have found it to show strong continuous absorption from about 1750 Å. This compares with the onset of strong ultra-violet absorption by olefines at wavelengths slightly shorter than 1800 Å (ethylene, 1745 Å), by paraffins at much shorter wavelengths (ethane, ~1350 Å) and by simple ethers at rather longer wavelengths (~1950 Å). One might argue, therefore, that ethylene oxide contains electrons bound with a degree of "tightness" more similar to that of the  $\pi$  electrons of olefines than to the electrons of normal C—C and C—O bonds.

When the C=C group is joined by single bonds to other unsaturated groups, the longest wavelength absorption moves far to long wavelengths and increases considerably in intensity. In order to test further the analogy between ethylene oxide derivatives and olefines, it is therefore important to study spectroscopically a molecule where the epoxy group is joined by a single bond to unsaturated groups. This has been done by Heilbron, Johnson, Jones and Spinks.<sup>3</sup> They find that the long wavelength absorption of the glycidic ester (I) has  $\lambda_{\max.} = 2860$  Å and  $\log \epsilon = 4.25$ ;



that is, the absorption occurs at much longer wavelengths and has much higher intensity than that of, say, butadiene or ethyl acetate. The absorption approaches indeed the character of that of octatrienic acid ( $\lambda_{\max.} = 3030$  Å,  $\log \epsilon = 4.57$ , for hexane solution;  $\lambda_{\max.} = 2960$  Å for alcohol solution). Evidently the epoxy group acts like a C=C link with slightly reduced conjugating power, continuing the conjugated chain from carbon atom (1) all the way to the COOEt group. Similarly, there is spectroscopic evidence<sup>4</sup> of conjugation occurring between a benzene nucleus and an olefine oxide ring, e.g. in  $\alpha$ -phenyl propylene oxide. The spectroscopic data thus agree with the conclusion from general properties that there is some essential similarity between the electronic structures of ethylene oxide derivatives and of unsaturated molecules.

Phibbs, Darwent and Steacie,<sup>5</sup> studying mercury-photosensitised reactions, find that ethylene oxide reacts principally like unsaturated, and only to a minor extent like saturated, hydrocarbons.

As regards the nuclear symmetry of the ethylene oxide molecule, the Raman and infra-red spectra can be interpreted on the basis of a model in which the C, C, O atoms form an isosceles triangle and the two CH<sub>2</sub> planes lie at right-angles to the C<sub>2</sub>O plane.<sup>6</sup> Although this is not unambiguous proof of the correctness of the model, there is little doubt that the above symmetry is highly probable (cf. the evidence given below for the symmetry of the related molecule cyclopropane) and we shall take it as correct. Linnett<sup>7</sup> has calculated the stretching-force constant of the CH link in ethylene oxide ( $5.0 \times 10^5$  dyne/cm.) and found

<sup>1</sup> Zimakov, *Acta Physicochim.*, 1946, **31**, 401.

<sup>2</sup> Walsh (unpublished work). At very low pressures, sharp bands were also visible from about 1520 Å. If the association of these with propylene oxide is confirmed, there is little doubt that they are due to Rydberg transitions of the non-bonding oxygen electrons.

<sup>3</sup> Heilbron, Johnson, Jones and Spinks, *J. Chem. Soc.*, 1942, 727.

<sup>4</sup> Campbell, Linden, Godshalk and Young, *J. Amer. Chem. Soc.*, 1947, **69**, 881.

<sup>5</sup> Phibbs, Darwent and Steacie, *J. Chem. Physics*, 1948, **16**, 39.

<sup>6</sup> Herzberg, *Infra-red and Raman Spectra* (Van Nostrand, 1945).

<sup>7</sup> Linnett, *Nature*, 1947, **159**, 400.

it to lie closer to that of the CH bond in ethylene (5.1) than to that of a methylene group in a paraffin (4.6). On the basis of electron diffraction photographs,<sup>8</sup> a length  $1.56 \pm 0.05$  Å has been suggested for the separation of the carbon atoms. The length suggested for the CH bonds (1.05 Å) is considerably less than the length found in methane<sup>9</sup> (1.094 Å) and nearer to the lengths reported for ethylene<sup>8</sup> (1.071 Å) and acetylene<sup>9</sup> (1.059 Å). Not much stress can be put upon this point since the figure 1.05 Å for ethylene oxide is subject to rather wide uncertainty ( $\pm 0.07$  Å), but it is at least permissive evidence of similarity between the CH bonds of ethylene oxide and those of unsaturated hydrocarbon molecules. It fits the force constant data.

**Cyclopropane and its Derivatives.**—Cyclopropane, with certain reagents, gives additive products. It is slowly attacked by bromine yielding 1:3-dibromopropane, whereas cyclobutane and the higher homologues, in contrast, yield substitution products if any reaction occurs. Similarly, HBr immediately converts cyclopropane into propyl bromide, but does not attack the higher homologues. There is thus some evidence, even if slight, from the general properties of cyclopropane for a similarity between its electronic structure and that of unsaturated molecules.<sup>9</sup>

Particular interest therefore attaches to its spectroscopic properties. The far ultra-violet absorption spectrum is continuous below  $1950$  Å;<sup>10</sup> that is, it starts at wavelengths very much longer than those at which  $\sigma$  C—C electrons absorb. In itself this does not tell us more than that there are electrons in the molecule much more weakly bound than those found in normal C—C single bonds. A more interesting study will be that of molecules containing cyclopropyl groups joined to C=C or C=O groups, so that we may know whether, as with epoxy groups, the characteristic phenomena of conjugation appear. Conjugation results in the so-called  $N \rightarrow V$  transition\* moving to long wavelengths and increasing in intensity; and, in the special case of carbonyl compounds, in the  $N \rightarrow A$  transition\* behaving likewise. Several authors (see Rogers and Roberts<sup>11</sup> and Rogers<sup>12</sup>) have shown that molecules containing cyclopropyl groups show these effects characteristic of conjugation. Thus Klotz<sup>13</sup> has shown that *i*-cholestadiene, containing the group  $\text{CC}=\text{C}$

shows an absorption peak around  $2100$  Å, that is, at a wavelength much longer than those of the peaks shown by simple olefines and close to the region of  $N \rightarrow V$  absorption by butadiene derivatives. Similarly, the  $N \rightarrow A$  transition of cyclopropyl methyl ketone<sup>14</sup> occurs at  $3670$  Å ( $\epsilon_{\text{max.}} = 23,500$ ) as compared with formaldehyde and crotonaldehyde

$$(\lambda_{\text{max.}} = 3490 \text{ Å}; \epsilon_{\text{max.}} = 18,200)$$

$$(\lambda_{\text{max.}} = 3770 \text{ Å}; \epsilon_{\text{max.}} = 26,600).$$

There is thus close similarity between epoxy and cyclopropyl rings in their spectroscopic properties. Each is able to conjugate with unsaturated groups.

The conclusion that cyclopropyl rings can conjugate with unsaturated groups is also reached from quite different lines of attack. Thus Robinson<sup>15</sup> as early as 1916 on organic chemical evidence was led to postulate the conjugating power of a cyclopropyl group; and Kohler and Conant<sup>16</sup>

<sup>8</sup> Ackermann and Meyer, *J. Chem. Physics*, 1936, 4, 377.

<sup>9</sup> For the general properties of cyclopropane and their resemblance to those of olefines, see Fuson, Gilman's *Organic Chemistry* (Wiley, 1938), vol. 1, p. 36.

<sup>10</sup> Ashdown, Harris and Armstrong, *J. Amer. Chem. Soc.*, 1936, 58, 850.

<sup>11</sup> Rogers and Roberts, *ibid.*, 1946, 68, 843.

<sup>12</sup> Rogers, *ibid.*, 1947, 69, 2544.

<sup>13</sup> Roberts and Green, *ibid.*, 1946, 68, 214.

<sup>14</sup> Robinson, *J. Chem. Soc.*, 1916, 109, 1042.

<sup>15</sup> Kohler and Conant, *J. Amer. Chem. Soc.*, 1917, 39, 1404.

\* For the explanation of these symbols, see papers by Mulliken in *J. Chem. Physics*, 1939.

<sup>16</sup> Klotz, *ibid.*, 1944, 66, 88.

showed, with reference to several reactions, that the properties of a cyclopropyl ring attached to a carbonyl group are not fundamentally different to those of the corresponding  $\alpha$ ,  $\beta$  unsaturated carbonyl compounds.

The infra-red and Raman spectra of cyclopropane make it very probable that the planes of the  $\text{CH}_2$  groups are at right-angles to the plane of the ring. Probably the C atoms lie at the corners of a  $60^\circ$  triangle with

the  $\text{CH}_2$  planes bisecting the  $\hat{\text{C}}\text{C}\hat{\text{C}}$  angles. The  $60^\circ$  triangle is supported by electron diffraction photographs which yield  $1.53 \pm 0.03 \text{ \AA}$ <sup>17</sup> and  $1.535 \text{ \AA}$ <sup>18</sup> for the CC distance. Saksena,<sup>19</sup> assuming an equilateral CCC triangle and the H atoms to lie at tetrahedral corners out of the ring plane, has calculated the stretching-force constant of the C—C bond to be  $4.04 \times 10^5$  dyne/cm. (suggesting a slight weakening relative to ethane) and that of the C—H bonds to be  $4.91 \times 10^5$  dyne/cm. (suggesting a strength not far from those of methane and ethylene). Bonner,<sup>20</sup> by cruder methods, suggests a similar C—C stretching-force constant. Linnett<sup>7</sup> calculates the CH stretching force constant as  $5.0 \times 10^5$  dyne/cm. as compared with the values  $5.1 \times 10^5$  dyne/cm. for ethylene and  $4.6 \times 10^5$  dyne/cm. for a methylene group in a paraffin chain. It had earlier been remarked<sup>21</sup> that considerable strength of the cyclopropane C—H bonds, relative to cyclobutane and ordinary paraffins, was indicated by the fact that, whereas with the latter compounds several intense Raman lines occur between 2850 and 3000  $\text{cm}^{-1}$ , compounds containing cyclopropane rings give no intense Raman lines in the region much below 3000  $\text{cm}^{-1}$ . The force constant data thus indicate a similarity between the C—H bonds of cyclopropane and those of ethylene. The CH bond length ( $1.08 \text{ \AA}$ ) found by Bastiansen and Hassel<sup>18</sup> does the same.

One might, therefore, expect the  $\text{H}\hat{\text{C}}\text{H}$  angle to be close to  $120^\circ$ . Spinrad<sup>22</sup> found an external valency angle  $\text{H}\hat{\text{C}}\text{H}$  of  $98^\circ$  from dipole moment data, but his calculations involved the assumption that the bond moment of C—Cl is the same in di- as in mono-chloro cyclopropane and the purity of his materials has been questioned both by himself and by others.<sup>23</sup> Smith,<sup>24</sup> from the moment of inertia determined from the infra-red spectrum, arrived at an exterior  $\text{H}\hat{\text{C}}\text{H}$  angle of  $136^\circ$ . Skinner,<sup>25</sup> however, has shown that the moment of inertia determined by Smith is compatible with the model of Bastiansen and Hassel,<sup>18</sup> involving an angle close to  $120^\circ$ . Bastiansen and Hassel recently investigated the electron diffraction of cyclopropane by the rotating sector method. They concluded from their photographs that the angle  $\text{H}\hat{\text{C}}\text{H}$  was certainly greater than tetrahedral and gave it as  $118.2^\circ$  with a probable error not greater than  $\pm 2^\circ$ . An electron diffraction investigation of the related molecule 1 : 1-dichloro-cyclopropane<sup>26</sup> gives the  $\text{Cl}\hat{\text{C}}\text{Cl}$  angle as  $112 \pm 4^\circ$ . The slightly smaller value of this angle than of the corresponding angle in the Bastiansen and Hassel model for cyclopropane itself is to be expected since the  $\text{Cl}\hat{\text{C}}\text{Cl}$  angle in 1 : 1-dichloro-ethylene<sup>28</sup> ( $116 \pm 2^\circ$ ) is known to be slightly less than the  $\text{H}\hat{\text{C}}\text{H}$  angle in ethylene ( $118^\circ$ ,<sup>27</sup>  $119^\circ$   $55'$ ).<sup>28</sup>

<sup>17</sup> Pauling and Brockway, *J. Amer. Chem. Soc.*, 1937, **59**, 1223.

<sup>18</sup> Bastiansen and Hassel, *Saertrykk av Tids. Kjem. Bergvesen Met.*, 1946, **6**, 71.

<sup>19</sup> Saksena, *Proc. Indian Acad. Sci. A*, 1939, **10**, 449.

<sup>20</sup> Bonner, *J. Chem. Physics*, 1937, **5**, 293.

<sup>21</sup> Kohlrausch and Skrabal, *Monatsh.*, 1937, **70**, 44, 377.

<sup>22</sup> Spinrad, *J. Amer. Chem. Soc.*, 1946, **68**, 617.

<sup>23</sup> O'Gorman and Schomaker, *ibid.*, 1946, **68**, 1138.

<sup>24</sup> Smith, *Physic. Rev.*, 1941, **59**, 924.

<sup>25</sup> Skinner, *Nature*, 1947, **160**, 902.

<sup>26</sup> Brockway, Beach and Pauling, *J. Amer. Chem. Soc.*, 1935, **57**, 2693.

<sup>27</sup> Thompson, *Trans. Faraday Soc.*, 1939, **35**, 697.

<sup>28</sup> Gallaway and Barker, *J. Chem. Physics*, 1942, **10**, 88.

Theoretically it can be understood in terms of the replacement of H by Cl evoking more  $p$  character in the C valency to which it is attached,<sup>29</sup> though the matter is complicated by the direct interaction of the two Cl atoms and of the weakly bound ring electrons (or  $\pi$  electrons in the case of 1:1-dichloro-ethylene) with the Cl lone pair electrons.\* Finally, electron diffraction studies of the related molecule *spiro*-pentane<sup>31</sup> yield an exterior  $\widehat{\text{HCH}}$  angle of  $120 \pm 8^\circ$ . One may conclude that the evidence is rather strongly in favour of an angle not far removed from  $120^\circ$ . Provisionally at least, it is best to take as correct the Bastiansen and Hassel value of  $\widehat{\text{HCH}} = 118^\circ$ .

The conclusion from the spectrum of cyclopropane, that the molecule contains electrons weakly bound in comparison with those occupying normal  $\sigma$  C—C orbitals, is also reached by consideration of the high value of the quenching cross-section of cyclopropane for cadmium resonance radiation.<sup>32</sup> This cross-section increases greatly if weakly bound (e.g.  $\pi$ ) electrons are present, the value for cyclopropane being such as to place it midway between olefines and paraffins.

Day and Pease<sup>33</sup> studied the vapour-phase oxidation of cyclopropane and found that it did not give the cool flames that are so characteristic of the oxidation of compounds containing paraffinic  $\text{CH}_2$  groups. The rate of slow oxidation with cyclopropane was slower and the ignition temperatures higher than with either propylene or propane. Ethylene also oxidises slowly relative to propylene and gives rise to no cool flames. The *reduced* reactivity to oxidation of these molecules relative to paraffins, in spite of their containing more weakly bound electrons, is especially noteworthy. The oxidation characteristics of cyclopropane are, therefore, permissive of there being a similarity between the structure of the molecule and that of ethylene.

Rather strong evidence that the C valencies towards H in cyclopropane are close to the  $sp^2$  hybrid type characteristic of ethylenic C atoms is provided by a study of the dipole moment of cyclopropyl chloride. This moment (1.75D) is 0.3D less than the values for *isopropyl* chloride and cyclopentyl chloride.<sup>14, 22</sup> Consideration of inductive effects on the basis of the usual strained ring structure for cyclopropane would lead to the expectation of a moment as large or larger than that of *isopropyl* chloride, since the electrons in the ring must be considered weakly bound and therefore particularly polarisable. Also, Rogers and Roberts<sup>11</sup> point out that one would expect the moment of cyclopropyl chloride, on a strained ring basis, to be as large or larger than that of cyclopentyl chloride since the polarisable matter is concentrated more nearly in the line of the original dipole due to the small CCC angle. The difference in moments induced in the hydrocarbon parts of these molecules should be no more than that between the moments of *isopropyl* chloride and 3-chloro-heptane, for which identical moments have been reported. The low dipole moment of cyclopropyl chloride is at once understandable if we suppose that the C atom to which the Cl atom is attached is a trigonal one. A trigonal C atom has a higher electronegativity in its  $sp^2$  valencies than has a tetrahedral C atom in its  $sp^3$  valencies,<sup>29</sup> so that largely because of this (combined with some delocalisation of the Cl lone-pair electrons)

<sup>29</sup> Walsh, *Discussions Faraday Soc.*, 1947, **2**, 18.

<sup>30</sup> Pauling and Brockway, *J. Amer. Chem. Soc.*, 1935, **57**, 2684.

<sup>31</sup> Donohue, Humphrey and Schomaker, *ibid.*, 1945, **67**, 332.

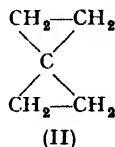
<sup>32</sup> Steacie and LeRoy, *J. Chem. Physics*, 1943, **11**, 164.

<sup>33</sup> Day and Pease, *J. Amer. Chem. Soc.*, 1941, **63**, 912.

\* In  $\text{CH}_2\text{Cl}_2$  the repulsion of the two Cl atoms evidently overcomes the electronegativity-hybridisation effect, since  $\widehat{\text{ClCCl}}$  is greater than  $\widehat{\text{HCH}}$  in  $\text{CH}_4$ .<sup>30</sup> In 1:1-dichloro-ethylene the Cl—Cl repulsion can be considered as largely cancelled by the interaction of the Cl lone pair and CC  $\pi$  electrons, so that the electronegativity-hybridisation effect has a clearer field.

vinyl and phenyl chlorides have lower dipole moments than the corresponding paraffinic chlorides. Rogers<sup>13</sup> provides other dipole moment evidence for near-trigonal C atoms in cyclopropyl groups.

**Spiro-pentane.**—The compound *spiro*-pentane,  $C_5H_8$ , was first prepared by Murray and Stevenson.<sup>34</sup> The substance is remarkably stable. The formula (II) was assigned to it on the grounds of its mode of preparation, its chemical properties and its Raman spectrum. Electron diffraction investigations<sup>31</sup> have confirmed this arrangement of the C nuclei and shown the planes of the two rings to be at right-angles and the angle HCH to be  $120 \pm 8^\circ$ . Infra-red studies<sup>35</sup> provide confirmatory evidence for the  $D_{3d}$  structure.



### Discussion

The similarity of the ethylene oxide and cyclopropane structures in several important points—for example, their spectra, their conjugating power and the strength of their C—H bonds—is evident from the review of their properties. This is very satisfactory for it is a well-known principle of valency theory that a group XH commonly has properties rather similar to those of the “fused nucleus.” It should be possible to exchange O for  $\text{CH}_2$  without making a fundamental difference to the nature of the molecule: this, indeed, is what is observed.

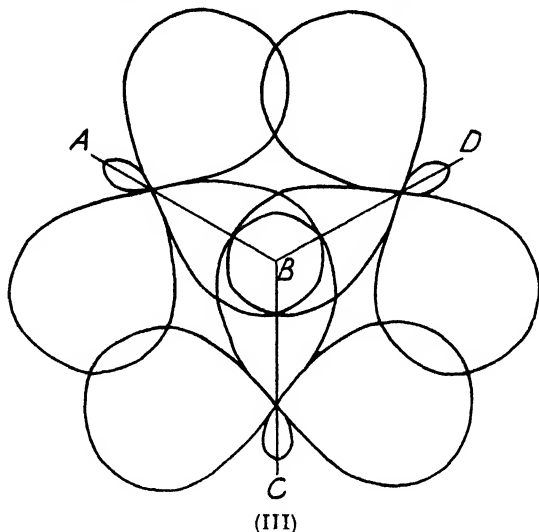
More important, however, is that evidence from many independent sources indicates that the hybridisation state of the C valencies in these molecules is close to that of the C atoms in ethylene. The low dipole moment of cyclopropyl chloride indicates a C valency towards hydrogen in cyclopropane close to  $sp^2$ . Evidence as to the external valency angle in cyclopropane does likewise. The magnitude of the C—H stretching-force constant in both ethylene oxide and cyclopropane leads to the same end. Other evidence is at least permissive. Most important of all the property of conjugating power leads to a similar conclusion. From a molecular-orbital point of view, the phenomena of conjugation are essentially due to the increase of “available space,” into which we can fit the wavelengths that characterise the possible  $\pi$  orbitals. The available space is conceived as formed by the sideways overlap of  $2p$  atomic orbitals (abbreviated to AOs) on neighbouring C atoms. The magnitude of the conjugating power of cyclopropyl and olefine oxide groups must mean that there are present in these groups molecular orbitals (MOs) which are largely built from  $2p$  AOs and thus inevitably give proper sideways overlap with  $2p$  AOs of parallel axis on neighbouring C atoms. Cyclopropane and ethylene oxide are therefore built from C atoms that are using an approximately pure  $2p$  AO. This fits the idea that these C atoms are close to ethylenic in nature, i.e. are forming three hybrid  $sp^2$  valencies at  $120^\circ$  in a plane and one pure  $p$  valency of axis at  $90^\circ$  to this plane.

It is important to stress this conclusion that the C atoms in cyclopropane and ethylene oxide have much similarity in their hybridisation condition to those in ethylene. Cyclopropane and ethylene oxide can be regarded as formed from  $\text{CH}_2$  groups whose C atoms are in a state of hybridisation close to that of ethylenic C atoms. It is this significant conclusion that any successful theory of these molecules has to explain and whose implications have to be drawn out.

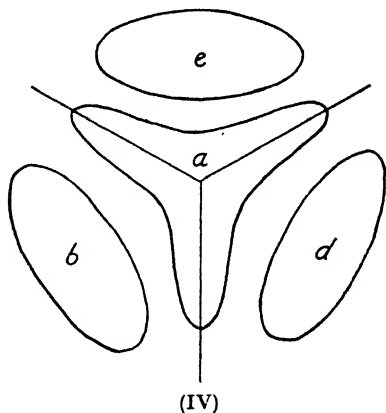
<sup>34</sup> Murray and Stevenson, *J. Amer. Chem. Soc.*, 1944, **66**, 812.

<sup>35</sup> Cleveland, Murray and Galloway, *J. Chem. Physics*, 1947, **15**, 742.

**The Orbitals in the CCC and CCO Rings.**—A survey of the facts relating to the ethylene oxide and cyclopropane molecules clearly makes the natural starting point for an electronic description of the binding in



these molecules that of bringing together  $\text{CH}_2$  groups in an ethylenic rather than a paraffinic state. One enquires what happens when  $\text{CH}_2$  groups are brought together whose C valencies towards H are  $sp^3$  in type and whose planes are at  $90^\circ$  to the CCC ring plane. MOs in the resulting hypothetical cyclopropane molecule are formed by the overlap of  $2p$  AOs whose axes lie in the plane of the ring. Other MOs are formed by the overlap of hybrid  $sp^3$  AOs whose axes also lie in the plane of the ring. The overlap is shown in (III). AB, CB, DB are  $\text{CH}_2$  planes at  $90^\circ$  to the paper. One then asks how the electrons are distributed in such a system. From the general symmetry of the overlap picture one would suppose the probability pattern of the electrons in the resultant MOs to have something of the character of (IV). This can be justified as follows (cf. Sugden<sup>36</sup>).



If we assume that the CH orbitals are localised, but that the MOs formed by the overlap of the similar AOs ( $\psi_1, \psi_2, \psi_3$ ), one from each C atom in the ring, are non-localised, then these latter MOs are given by<sup>37</sup>

$$\frac{1}{\sqrt{3}}(\psi_1 + \psi_2 + \psi_3) \quad . \quad . \quad . \quad . \quad (1)$$

$$\frac{1}{\sqrt{2}}(\psi_1 - \psi_2) \quad . \quad . \quad . \quad . \quad (2)$$

$$\frac{1}{\sqrt{6}}(\psi_1 + \psi_2 - 2\psi_3) \quad . \quad . \quad . \quad . \quad (3)$$

<sup>36</sup> Sugden, *Nature*, 1947, 160, 367.

<sup>37</sup> Mulliken, *J. Chem. Physics*, 1935, 1, 492.

The first of these represents a wave having no nodes in the available space ; the second a wave with a nodal line passing through atom (3) and bisecting the (1)-(2) line ; and the third a wave with a nodal line passing through the centre of gravity and at  $90^\circ$  to the nodal line of the second MO. (2) and (3) are degenerate, the degeneracy arising from the twofold symmetry of the available space. The problem and the forms of the resulting MOs are very similar to those involved in determining the  $\pi$  orbitals of benzene. In the constituent AOs used to form the non-localised MOs, however, benzene and our hypothetical cyclopropane molecule are very different. In the former, the overlap is of the "sideways" type between  $2p$  AOs of axes perpendicular to the plane of the ring. In the latter it is as (III). (III) involves two types of overlapping AOs. In so far as these do not mix, there will be therefore a set of three possible MOs as (1), (2), (3) where  $\psi_1, \psi_2, \psi_3$  represent the hybrid  $sp^2$  AOs and another set where  $\psi_1, \psi_2, \psi_3$  represent the  $2p$  AOs of (III).

Considering the set derived from the  $sp^2$  AOs, (1) will clearly give rise to strong bonding between all the carbon nuclei. (2) and (3) will give rise to rather strong anti-bonding since they involve more nodes than anti-nodes in the CC lines. Considering the set derived from the  $2p$  AOs lying in the plane of the ring, clear diagrams of these have been given by Sugden.<sup>36</sup> Their peculiarity is that, whereas in the former set, orbital (1) was bonding and the two degenerate orbitals (2) and (3) were anti-bonding, here orbital (1) is anti-bonding and the two degenerate orbitals (2) and (3) have a net bonding effect.

Thus two electrons occupy an orbital of type (1) where  $\psi_1, \psi_2, \psi_3$  represent hybrid  $sp^2$  AOs. Their probability pattern is the three-pronged area  $a$  in (IV). Four electrons occupy the two degenerate orbitals of type (2) and (3) where  $\psi_1, \psi_2, \psi_3$  represent  $2p$  AOs in the plane of the ring. Their probability pattern is the connected three-lobed area  $bdc$ . Their effect is partly anti-bonding and (to a greater extent) partly bonding.

We have assumed, however, non-localised orbitals in the ring. (III) probably implies not only some character as (IV), but also some localised bond character. The overlap between any pair of  $2p$  AOs is neither "sideways" nor "endwise." In so far as it is the latter, the resulting MO is compact and overlaps little with the third  $2p$  AO, i.e. localised bonds at  $b, d, e$  result,  $a$  is vacated and its component AOs, mixed with the original C AOs, cause some change towards tetrahedral  $sp^3$  valencies.

In this way one can see that the  $\widehat{\text{HCH}}$  angle will not be quite as large as  $120^\circ$  and that the conjugating power will be somewhat reduced relative to an ethenoid group. The angle between the  $2p$  axes, however, is such that sideways overlap, with resulting non-localisation, will be greater than endwise, so that the C valencies towards H will be nearer  $sp^2$  than  $sp^3$ .

Qualitatively, therefore, one can understand the nature of the cyclopropane molecule by regarding it as formed from three initially ethylenic  $\text{CH}_2$  groups, i.e. by orbitals overlapping as (III). The result appears to be to give ring orbitals partly as (IV), but with some tendency towards bonds localised in particular CC distances. Further, light is shed on the stability of cyclopropane for there is a total of three bonding orbitals in which we can accommodate without trouble the six electrons that have to be fed into the CCC orbitals.

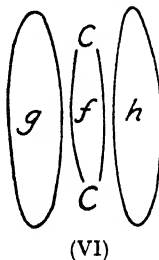
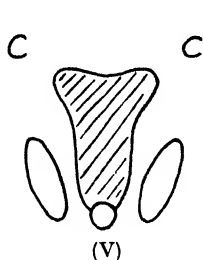
Independent of the precise forms of the resulting MOs, however, the experimental evidence leading to (III) as representing to a considerable extent the overlap involved in cyclopropane and related molecules is strong.

In ethylene oxide the probability pattern would be similar to (IV), except that the presence of the dipole (1.88D) means  $e$  is now tenuous,  $b$  and  $d$  are drawn downwards and the upper prongs of  $a$  are contracted ; (V) results.

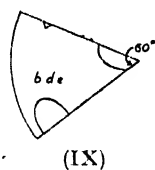
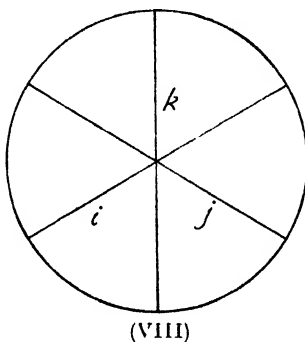
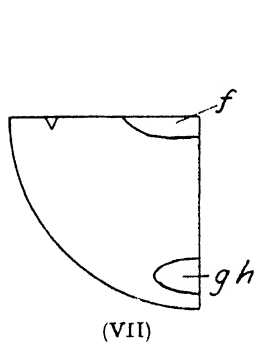
**Implications.**—The implications and advantages of the discussion so far are —

(1) It shows how many of the salient properties of cyclopropane and ethylene oxide are not isolated but connected and, therefore, to some extent deducible one from another.

(2) It explains the peculiar relation of cyclopropane to ethylene. The probability pattern (IV) is in a sense a generalisation to 3 centres of the orbital picture (VI) which has been evolved to explain 2-centre



unsaturation.\* *f* represents the  $\sigma$ , and *gh* the  $\pi$  orbital. (That (IV) and (VI) are the same geometrical pattern applied to two and three centres respectively can be shown by folding filter papers. Fold a paper along two diameters at  $90^\circ$ : cut it as in (VII). Fold a second paper along



three diameters at  $60^\circ$  (VIII), bringing *i* to *j* and then *k* to *ij*: cut as in (IX) which is similar to (VII). On opening out, *f* becomes *a*, *gh* become *bdc*.) In an older theory of the  $C\equiv C$  link in ethylene the two CC bonds were regarded as both of the same nature and the "anomalies" in the properties of ethylene (relative to the paraffins) were attributed to strain due to distortion of the bonds from the tetrahedral directions. While that theory is held it is expected that cyclopropane should show some unsaturation character, for any two C atoms in it can be regarded as joined by two curved lines (one proceeding via a third C atom). The quantum mechanical description of  $\diagdown C\equiv C \diagup$ , in discarding the older theory, has led to much progress in understanding the properties of  $\diagdown C\equiv C \diagup$  groups (particularly (a) the spectroscopic properties of conjugation and (b) the properties of the valencies external to the  $C\equiv C$  (e.g.  $H\hat{C}H$  in ethylene)), but has destroyed the "naturalness" of the unsaturation of cyclopropane. In evolving the new theory for ethylene, an obligation was incurred—but apparently not recognised—to reconsider the structure of cyclopropane in the light of the new ideas on ethylene. That the old theory for ethylene is by no means completely unsatisfactory is found in more than one recent

\* We may conveniently term the unsaturation in cyclopropane 3-centre unsaturation to distinguish it from the 2-centre unsaturation of ethylene and the 4-centre unsaturation of cyclobutane.



example.<sup>38</sup> In the same way the theory of bent bonds in cyclopropane is a useful one but not adequate for explaining the conjugating properties and the nature of the valencies external to the ring (e.g.  $\widehat{\text{HCH}}$  in cyclopropane).

Much of the old idea of strain can be translated into terms of hybridisation. Translation from one description to another is always well worth making for it frequently deepens insight. Thus to translate the older idea of the  $\text{P}_4$  molecule as a strained tetrahedron into the terms of hybridisation<sup>39</sup> is to realise why  $\text{N}_4$  does not exist. In the same way a translation of the strained ring theory of cyclopropane into hybridisation terms is likely to deepen our understanding of this and related molecules, just as a similar translation has done with ethylene. The two cases go together and it is not surprising that the probability picture indicated for cyclopropane should be a generalisation of that thought to hold for ethylene.

(3) It ascribes to cyclopropane or ethylene oxide an orbital picture which, whatever its precise details, explains such properties as the conjugating power of epoxy or cyclopropyl groups, in the same way as the conjugating power of  $\text{C}=\text{C}$  groups is explained. In the neighbourhood of any C atom the orbital  $b d e$  must look like the AO from which it is partly composed. For conjugation the groups must set themselves such that their plane of the ring is parallel to the axis of neighbouring  $2p$  AOs, i.e. perpendicular to the plane of a conjugated side-chain. Molecules containing  $\text{CC}=\text{C}=\text{C}$  groups therefore afford examples of conjugated

carbon chains that are not co-planar.

(4) Granted the stability of cyclopropane, it explains the stability of *spiro*-pentane and certain other molecules. The essential feature of the overlap picture (III) is that any C atom should have a  $2p$  AO of axis in the plane of the ring and a hybrid AO pointing towards the centre of gravity of the ring. This feature could be retained if one of the  $\text{CH}_2$  groups were replaced by an acetylenic C atom. The hybrid AO pointing towards the centre of the ring would now be  $sp$  in nature, the two H atoms would be replaced by a second  $2p$  AO of axis perpendicular to the plane of the ring and a second  $sp$  AO would project at  $180^\circ$  to the first. In other words one could build a second ring having a plane at  $90^\circ$  to the first. The existence of *spiro*-pentane with its two rings at  $90^\circ$  therefore becomes a simple consequence of the overlap picture (III). In contrast, from the "strained ring" viewpoint, *spiro*-pentane looks a most improbable molecule. Incidentally, further homologues should be possible by changing other  $\text{CH}_2$  groups for acetylenic C atoms. In these homologues, adjacent rings will always be at  $90^\circ$  and the chain of rings will look like the stems of certain cacti.

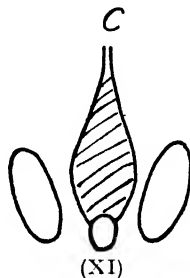
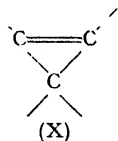
The essential feature of the overlap picture (III) could also be retained if two of the C atoms were changed from the trigonal to digonal hybridisation condition. The  $2p$  AOs of axis in the plane of the ring and the hybrid AOs pointing towards the centre of gravity of the ring remain much as in (III); but one now has on each of two C atoms another  $2p$  AO of axis at  $90^\circ$  to the plane of the ring. In other words a true  $\pi$  bond can now be formed and the prediction is that, if cyclopropane is stable, the group (X) should have considerable stability. It is important that such groups have been reported.<sup>40</sup> Some of the properties of molecules

<sup>38</sup> Bernstein, *J. Chem. Physics*, 1947, **15**, 284; cf. Lewis and Calvin, *Chem. Rev.*, 1939, **25**, 281.

<sup>39</sup> Arnold, *J. Chem. Physics*, 1946, **14**, 351. For an older viewpoint, see Skinner *Trans. Faraday Soc.*, 1945, **41**, 645.

<sup>40</sup> See Schlatter, *J. Amer. Chem. Soc.*, 1941, **63**, 1733; Feist, *Ber.*, 1893, **26**, 750; Haerdi and Thorpe, *J. Chem. Soc.*, 1925, **127**, 1237. I am indebted to Prof. F. O. Rice and Prof. C. K. Ingold for calling my attention to the work of Schlatter and Feist respectively.

containing (X) can be predicted from knowledge of the correlations between properties and valency hybridisation,<sup>39</sup> and should be capable of experimental test in the future. From the viewpoint of bent bonds, (X) looks most improbable.



To recapitulate, the facts show that (III) is very largely the overlap picture involved in the cyclopropane ring. (III) somehow possesses stability. Some indication of why this is so has been given. But, independent of the interpretation, the idea that six electrons fed into orbitals resulting from overlap as in (III) confers stability explains the stability of *spiro*-pentane and the group (X).

(5) We have argued that (III) implies not only some character as (IV), but also some localised bond character. The  $60^\circ$  angle between the  $2p$  axes in cyclopropane implies that the former is more important than the latter, in accord with the C valencies towards H being nearer  $sp^2$  than  $sp^3$ . In cyclobutane the angles are such that localisation is greater and 4-centre unsaturation less. Even in cyclohexane, however, a greater tendency (than in paraffins) towards  $2p$  character in the C valencies to C and of  $2s$  in the C valencies to H appears to be shown by CC weakness<sup>41</sup> and (in spite of the CH bonds being  $2^\circ$  ones) CH strength (shown by combining thermochemical data with the fact of CC weakness).

(6) (V) has the merit that it gives a possible explanation of a fact that has been stressed by Robinson,<sup>42</sup> namely, the resemblance of ethylene oxide to acetaldehyde: for a  $\text{>C=O}$  group has the MO picture (XI) which clearly has some resemblance to (V). The resemblance is, no doubt, increased because the length of the perpendicular from the O to the CC line (calculated from the electron diffraction data) is  $1.20 \text{ \AA}$ , which is close to the  $\text{C=O}$  length in acetaldehyde ( $1.22 \text{ \AA}$ ). The possibility of isomerisation of ethylene oxide to acetaldehyde doubtless increases the apparent resemblance still further. The resemblance presumably only concerns the  $\text{>C=O}$  group of  $\text{CH}_3\text{CHO}$ . The CH bonds of ethylene oxide are certainly stronger than those of  $\text{CH}_3\text{CHO}$  (a fact reflected in differences found between the reactions of H atoms with ethylene oxide and aldehydes<sup>43</sup>).

(7) The discussion affords a partial explanation of why the ozone molecule does not adopt the shape of an equilateral triangle. If it *did* adopt such a shape, then it would be expected that possible MOs would be built from (a) hybrid or  $2p$  AOs pointing to the centre of the ring, (b)  $2p$  AOs of axis in the plane of the ring, (c)  $2p$  AOs of axis at  $90^\circ$  to the plane of the ring. Those resulting from (a) and (b) would be as in cyclopropane, and, as already explained, could accommodate just six electrons in bonding MOs. Those resulting from (c) would be  $\pi$  orbitals extending over the whole triangle. Only one of them (of form given by

<sup>41</sup> Sutherland and Ramsay, *Proc. Roy. Soc. A*, 1947, **190**, 243; Walsh, *Trans. Faraday Soc.*, 1946, **42**, 779. <sup>43</sup> Robinson, *Nature*, 1947, **160**, 162.

<sup>42</sup> Trost, Darwent and Steacie, *J. Chem. Physics*, 1948, **16**, 353.

(i)) would be bonding. Two electrons could be accommodated in this and the remaining four would have to go into anti-bonding orbitals. Relative to cyclopropane, one therefore has an additional net anti-bonding effect.

In other words, as three O atoms are brought together to form an equilateral triangle,  $2p$   $\pi$  lone pairs of electrons repel each other. It is not therefore surprising that the ozone molecule prefers a different nuclear arrangement. Something of this anti-bonding effect must be present in the carbonate ion, but here it is much weaker owing to the greater O—O distances. It is very weak in cyclopropane relative to ozone because the electrons causing the repulsion in  $O_3$  are localised in  $C_sH_3$  in CH orbitals that (i) are so tightly bound and (ii) have such a position, that they overlap very little.

In a similar way, light is thrown upon the problem why, although  $(CH_2)_3$  and  $(CH_2)_2O$  exist,  $(CH_2)O_2$  is not known. For  $(CH_2)O_2$  to have a similar structure to  $(CH_2)_3$  and  $(CH_2)_2O$ , it would have to accommodate four electrons in  $\pi$  orbitals and two of these would have to go into a strongly anti-bonding  $\pi$  orbital between the O atoms.

**Other Related Molecules.**—The structure of ethylene sulphide may be interpreted similarly to that of ethylene oxide. Linnett<sup>7</sup> finds the stretching force constant of its CH bonds to be the same as those of ethylene oxide and cyclopropane. Ethylene imine<sup>44</sup> shows the same polymerisation tendencies as ethylene oxide and may also be interpreted structurally like ethylene oxide: NH is expected in valency theory to resemble  $CH_2$  and O.

**Note on Other Work.**—In the present paper the electronic structure of cyclopropane has been considered from the starting point of bringing together ethylenic  $CH_2$  groups. This is a natural approach because a survey of the facts suggests the path from it to the ultimate goal to be short. The work is largely empirical in its nature, being concerned with the recognition and fitting together of the various facts and then, accepting these facts, with the drawing-out of their implications. Obviously, however, other starting points are possible. A preliminary description of a more fundamental treatment has been given by Coulson and Moffitt.<sup>45</sup> This starts with a model containing three filled localised orbitals, one associated with each CC distance, and, like the old strain theory, stresses that the lines of maximum charge density do not necessarily coincide with the CC directions. The energy of cyclopropane is expressed in terms of a function expressing the degree of hybridisation (regarded as a variational parameter) in the ring valencies employed. Minimisation of the energy then yields predictions of properties of the molecule. Two of these in particular are in accord qualitatively with the present discussion, namely, that the  $\widehat{HCH}$  angle should be greater than tetrahedral, i.e. some way towards  $120^\circ$ , and that some delocalisation of the ring electrons is present so that to some extent they occupy orbitals with a connected density pattern rather like *bde* of (IV). However, in its preliminary form, the treatment yields an  $\widehat{HCH}$  angle of only  $113^\circ$  instead of the Bastiansen-Hassel value of  $118^\circ$  and it deals as yet with only a limited selection of the facts including for example, no explicit account of the conjugating power of cyclopropyl groups and the structures of related molecules like *spiro*-pentane.

Laboratory of Physical Chemistry,  
Cambridge.

<sup>44</sup> Jones, Langsjoen, Neumann and Zomlefer, *J. Org. Chem.*, 1944, **9**, 125.

<sup>45</sup> Coulson and Moffitt, *J. Chem. Physics*, 1947, **15**, 151.

# BOND ORDERS AND OTHER CRITERIA OF DOUBLE-BOND CHARACTER

By V. GOLD

Received 12th September, 1948

A comparison is made between the bond order, the  $\pi$ -bond dissociation energy ( $W$ ) and the  $\pi$ -electron energy loss ( $Y$ ) on saturating a bond in a conjugated system, all calculated on the basis of Hückel's approximate molecular-orbital method. It is shown that a rough correlation exists between these calculated parameters. The results are applied to a discussion of the kinetics of *cis-trans* isomerisation and of the thermodynamics of double-bond addition reactions. It follows from this that, in so far as the basic theory is valid, bond orders may be used in certain cases as an approximate index of chemical as well as physical double-bond character.

## 1. Physical Significance of Bond Order

According to classical valency theory the links between two carbon atoms can be rigidly classified as single, double or triple bonds. The application of quantum mechanics to valency problems has shown that such a sharp classification is incorrect, and that most bonds are to be assigned non-integral bond orders.<sup>1, 2, 3</sup> In the cases considered here, i.e. conjugated systems in which "single" and "double" bonds alternate, this order lies between 1 and 2 for all bonds and, according to Coulson's definition<sup>3</sup>—employing the calculus of the method of molecular orbitals<sup>4</sup>—tends to the same value (1.637) for both "single" and "double" bonds in the middle of an infinitely long conjugated polyene chain.

To illustrate the physical significance of Coulson's bond order (B.O.), its definition (for a bond linking atoms  $r$  and  $s$ ) may be stated in the form<sup>3</sup>

$$(\text{B.O.})_{rs} = 1 + p_{rs} = 1 + \frac{1}{2} \frac{\partial E}{\partial \beta_{rs}},$$

where  $E$  is the total electronic energy of the  $\pi$ -electrons in the molecule and  $\beta_{rs} = \int \phi_r H \phi_s d\tau$  (resonance integral). The mobile bond order  $p_{rs}$  which is the contribution from the  $\pi$ -electrons to the total bond order can thus be interpreted<sup>3</sup> as "a measure of the force tending to change the length of that bond, in the configuration in which all bonds are supposed equal in length, only forces due to mobile electrons being considered." Bond orders on this scale run closely parallel to those on the scale defined by Penney<sup>2</sup> on the basis of the valence-bond method. The physical reality of bond orders is firmly established through their good correlation with experimentally determined bond lengths.<sup>5</sup>

The bond order is essentially a "static" property and does not claim to provide an index for "dynamic" double-bond character, as exemplified by stiffness to rotation or reactivity for addition reactions, as chemists sometimes expect it to do. It is the object of the present survey to examine whether bond orders do, nevertheless, bear some relation to the energy

<sup>1</sup> Pauling, Brockway and Beach, *J. Amer. Chem. Soc.*, 1935, **57**, 2705.

<sup>2</sup> Penney, *Proc. Roy. Soc., A*, 1937, **158**, 318.

<sup>3</sup> Coulson, *ibid.*, 1939, **169**, 413.

<sup>4</sup> Hückel, *Z. Physik.*, 1931, **70**, 204; **72**, 310; 1932, **76**, 628.

<sup>5</sup> Lennard-Jones and Coulson, *Trans. Faraday Soc.*, 1939, **35**, 811.

parameters which should govern these "dynamic" criteria of double-bond character.

## II. The Quantity $W$

In the first place we shall consider the behaviour of the energy quantity  $W$ , defined as the amount of  $\pi$ -electron energy lost by the molecule on reducing the interaction of the  $\pi$ -electrons across the bond concerned to zero, without any accompanying change in the energy of interaction of the  $\sigma$ -electrons ( $W$  is therefore equivalent to the bond dissociation energy of the  $\pi$ -bond). This process is purely hypothetical but may, in certain cases, bear some relation to the ease of rotation about the bond. It is assumed that the  $\pi$ -electrons will then assume the more localised arrangement appropriate to the force-field of the new frame, e.g. on stopping the  $\pi$ -electron interaction across the middle bond in butadiene each half of the molecule will assume the  $\pi$ -electron distribution obtained by solution of the secular equation for ethylene. In order to make the comparison of the quantity  $W$  with Coulson's bond orders internally consistent Hückel's approximation of the molecular-orbital method<sup>4</sup> is used for deriving the  $\pi$ -electron energy of both the original molecule ( $E$ ) and of the disturbed frame ( $E'$ ). The principle of the calculation is then illustrated by the case of the central bond in 1:3-butadiene where we may say that we solve the secular equations

$$\begin{vmatrix} \alpha - \epsilon & \beta & 0 & 0 \\ \beta & \alpha - \epsilon & \beta & 0 \\ 0 & \beta & \alpha - \epsilon & \beta \\ 0 & 0 & \beta & \alpha - \epsilon \end{vmatrix} = 0 \quad (1)$$

and

$$\begin{vmatrix} \alpha - \epsilon' & \beta & 0 & 0 \\ \beta & \alpha - \epsilon' & 0 & 0 \\ 0 & 0 & \alpha - \epsilon' & \beta \\ 0 & 0 & \beta & \alpha - \epsilon' \end{vmatrix} = 0 \quad (2)$$

differing only in the elements  $H_{23}$ ,  $H_{32}$  corresponding to the bond 2-3 across which the  $\pi$ -interaction is broken. The second equation will, of course, factorise to give two identical two-row determinants corresponding to the two isolated ethylene halves. The value of  $E$  (or  $E'$ ) is then obtained by allotting the  $\pi$ -electrons pairwise to the lowest energy levels  $\epsilon$  (or  $\epsilon'$ ) obtained as roots of these equations and then summing the energies for all  $\pi$ -electrons ( $\alpha$  = Coulomb integral =  $\int \phi_r H \phi_r d\tau$ ).

As the term involving  $\alpha$  remains unchanged,  $(E - E')$  is given by the difference in the  $\pi$ -electron coupling energies (i.e. the terms involving  $\beta$  in the expression for the  $\pi$ -electron energy).

Table I illustrates the evaluation of  $W$  for three bonds in diphenylbutadiene.

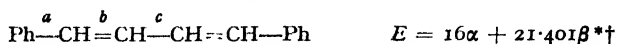
Table II gives a summary of the results of these calculations for typical compounds, using in the main values given in the literature.<sup>6, 7, 8</sup> Published values of Coulson's bond orders are listed for comparison wherever

<sup>6</sup> Hückel, *Z. Elektrochem.*, 1937, **43**, 775.

<sup>7</sup> Wheland, *J. Amer. Chem. Soc.*, 1941, **63**, 2025.

<sup>8</sup> Syrkin and Diatkina, *Acta Physicochim.*, 1946, **21**, 641, 921.

TABLE I

EVALUATION OF  $W$  FOR VARIOUS BONDS IN DIPHENYLBUTADIENE

Bond $r-s$	Conjugated System left after Breaking $\pi$ -Interaction across $r-s$	$(E' - 16\alpha) \times \beta^{-1}$	$\frac{W \times \beta^{-1}}{=(E - E') \times \beta^{-1}}$	(B.O.) $_{rs}$
<i>a</i>	Benzene + phenylbutadiene	$(8.00 + 12.932^*) - 20.932$	0.469	1.444 *
<i>b</i>	$\text{Ph}\dot{\text{C}}\text{H}_2 + \text{PhCH}=\text{CH}-\dot{\text{C}}\text{H}_2$	$(8.721 + 11.385^*) = 20.106$	1.295	1.758 *
<i>c</i>	$2 \times \text{styrene}$	$(2 \times 10.424) = 20.848$	0.553	1.501 *

\* New calculations.

† The value 24.401 given by Hückel <sup>6</sup> is evidently a misprint.

possible. In Fig. 1 the values of B.O. are plotted against  $W$ , where in addition to the results of Table I a few unpublished results <sup>9</sup> of B.O.

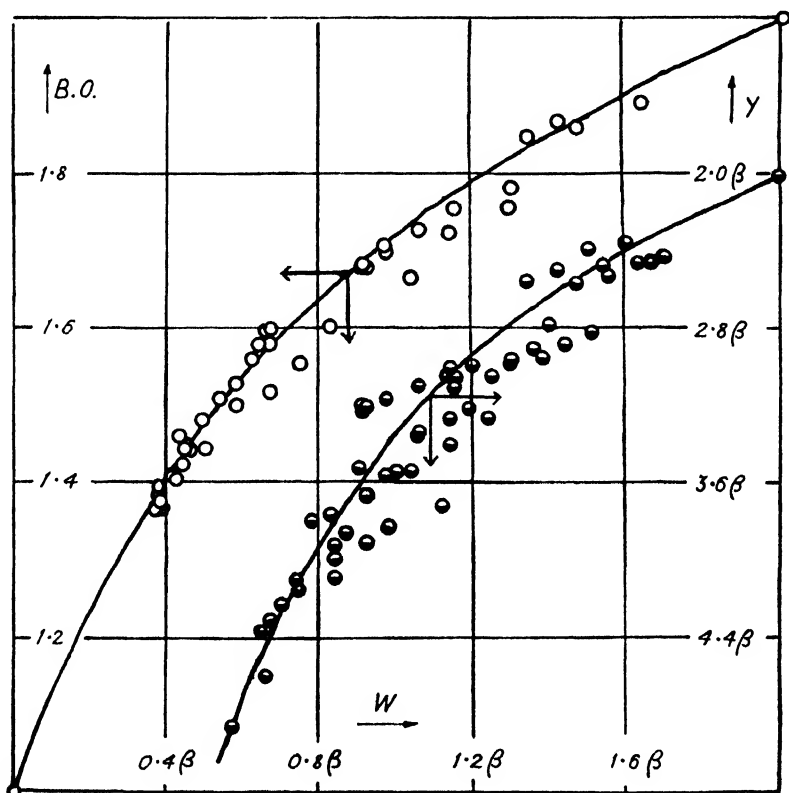


FIG. 1.

have been included. It is seen that a fair correlation exists and that  $W$  increases as B.O. increases, although  $dW/d(\text{B.O.})$  is by no means constant

<sup>9</sup> Coulson (unpublished calculations).

TABLE II

Molecule	Bond	B.O. †	$W$ $\times \beta^{-1}$	$W$ (kcal.)	$Y$ $\times \beta^{-1}$
$\text{CH}_2^a=\text{CH}^b-\text{CH}=\text{CH}_2$	<i>a</i>	1·894	1·64	29·5	2·47
	<i>b</i>	1·447	0·47	8·5	4·47
$\text{CH}_2^a=\text{CH}^b-\text{CH}^c=\text{CH}-\text{CH}=\text{CH}_2$	<i>a</i>	1·871	1·42	25·6	2·49
	<i>b</i>	1·483	0·49	8·8	—
	<i>c</i>	1·785	1·30	23·4	2·96
$\text{CH}_2^a=\text{CH}^b-\text{CH}^c=\text{CH}^d-\text{CH}=\text{CH}-\text{CH}=\text{CH}_2$	<i>a</i>	1·862	1·47	26·5	2·56
	<i>b</i>	1·495	0·56	10·1	—
	<i>c</i>	1·758	1·15	20·7	3·05
	<i>d</i>	1·529	0·58	10·4	—
$\text{CH}_2=(\text{CH}-\text{CH}=\text{CH})_{11}\text{CH}_2$	<i>a</i>	1·850	1·34	24·1	2·54
	<i>b</i>	1·507	0·54	9·7	—
	<i>c</i>	1·731	1·06	19·1	3·09
	<i>d</i>	1·562	0·62	11·2	—
	<i>e</i>	1·700	0·98	17·6	3·16
	<i>f</i>	1·582	0·67	12·1	—
	<i>g</i>	1·686	0·91	16·4	3·21
	<i>h</i>	1·591	0·66	11·9	—
	<i>i</i>	1·686	0·92	16·6	3·20
	<i>j</i>	1·596	0·67	12·1	—
	<i>k</i>	1·677	0·91	16·4	3·21
	<i>l</i>	1·597	0·67	12·1	—
$\text{Ph}-\text{CH}^a=\text{CH}^b-\text{CH}_2$	<i>a</i>	1·408*	0·42	7·6	—
	<i>b</i>	1·912*	1·70	30·6	2·42
$\text{Ph}-\text{CH}^a=\text{CH}^b-\text{CH}^c=\text{CH}^d-\text{CH}_2$	<i>a</i>	—	0·46	8·3	—
	<i>b</i>	—	1·38	24·8	2·93
	<i>c</i>	—	0·51	9·2	—
	<i>d</i>	—	1·55	28·0	2·51
$\text{Ph}-\text{CH}^a=\text{CH}^b-\text{CH}^c=\text{CH}^d-\text{CH}^e=\text{CH}_2$	<i>a</i>	—	0·50	9·0	—
	<i>b</i>	—	1·20	21·6	2·99
	<i>c</i>	—	0·57	10·3	—
	<i>d</i>	—	1·25	22·5	3·04
	<i>e</i>	—	0·53	9·5	—
$\text{Ph}-\text{C}^a(\text{CH}_2^b)_2$	<i>a</i>	1·371	0·38	6·8	—
	<i>b</i>	—	0·92	16·6	3·91
$\text{Ph}-\text{CH}^a=\text{CH}^b-\text{Ph}$	<i>a</i>	1·421*	0·45	8·1	—
	<i>b</i>	1·820*	1·44	25·9	2·88
$\text{Ph}-\text{CH}^a=\text{CH}^b-\text{CH}^c=\text{CH}-\text{Ph}$	<i>a</i>	1·444*	0·47	8·5	—
	<i>b</i>	1·758*	1·30	23·4	2·98
	<i>c</i>	1·501*	0·55	9·9	—
$\text{Ph}-\text{C}^a(\text{CH}^b=\text{CH}_2^d)_2$	<i>a</i>	—	0·31	5·6	—
	<i>b</i>	—	1·40	25·2	2·78
	<i>c</i>	—	0·36	6·5	—
	<i>d</i>	—	1·60	28·8	2·35
$\text{Ph}-\text{C}^a(\text{Ph})=\text{CH}_2^b$	<i>a</i>	—	0·39	7·0	—
	<i>b</i>	—	1·51	27·2	2·81
$\text{Ph}-\text{C}^a(\text{Ph})=\text{C}^b(\text{Ph})-\text{H}$	<i>a</i>	—	0·38	6·8	—
	<i>b</i>	—	1·24	22·3	3·26
	<i>c</i>	—	0·45	8·1	—
$\text{Ph}-\text{C}^a(\text{Ph})=\text{C}^b(\text{Ph})-\text{Ph}$	<i>a</i>	—	0·46	8·3	—
	<i>b</i>	—	1·12	20·2	3·72

TABLE II—continued

Molecule	Bond	B.O.†	$W$ $\times \beta^{-1}$	$W$ (kcal.)	$Y$ $\times \beta^{-1}$
	a	—	1.63	29.4	2.44
	b	—	0.44	7.9	—
	c	—	0.66	11.9	4.60
	a	—	1.36	24.5	2.90
	b	—	0.43	7.7	—
	c	—	1.66	29.9	2.43
	a	—	0.50	9.0	—
	b	—	1.14	20.5	3.40
	c	—	0.47	8.5	—
	a	—	0.42	7.6	—
	b	—	0.98	17.6	3.82
	a	—	0.84	15.1	3.92
	a	—	0.50	9.0	—
	b	—	1.00	18.0	3.54
	c	—	1.14	20.5	3.04
	a	—	0.74	13.3	4.10
	a	—	0.38	6.8	—
9 : 9'-Dianthryl	9 : 9'	—	0.43	7.7	—
Benzene	—	1.667	1.04	18.7	3.53
	a	1.555	0.75	13.5	4.16
	b	1.725	1.14	20.5	3.26
	c	1.603	0.83	14.9	3.76
	d	—	—	—	3.68
	e	—	—	—	4.16
	f	—	—	—	4.74
	a	—	0.78†	14.0	3.79
	b	—	1.19†	21.4	3.21
	c	—	0.70†	12.6	4.23
	d	—	0.87	15.7	3.85
	e	—	—	—	4.92
	f	—	—	—	3.63
	g	—	—	—	3.31
	h	—	—	—	3.85
	i	—	—	—	4.23
	a	—	1.34†	24.1	3.07
	b	—	0.65†	11.7	4.37
	c	—	0.84†	15.1	4.09†
	d	—	1.06†	19.1	3.33
	e	—	0.92†	16.6	3.66
	f	—	1.06†	19.1	3.35
	g	—	0.84†	15.1	3.99
	h	—	—	—	4.56
	i	—	0.57	10.3	4.86

† Approximate value only.

† Taken chiefly from ref. 5.

\* New calculations.



and is much greater at high bond orders than at low ones. The scatter of the points is not excessive, as such a variety of compounds, both cyclic and open-chain, is represented by them, so that a rough estimate of  $W$  can be made if the value of the bond order is known, or vice versa.

A different approach to the problem of the connection between B.O. and  $W$  would be the mathematical examination of the relation

$$W_{rr} = - \int_0^\beta \frac{\partial E}{\partial \beta_{rr}} \cdot d\beta_{rr} = 2 \int_0^\beta p_{rr} \cdot d\beta_{rr} \quad (3)$$

### III. Rotation about "Unsaturation" Bonds

When a part of a molecule which is linked to the rest of the molecule through a bond with partial double-bond character is rotated out of coplanarity with the other part, the interaction of the  $\pi$ -orbitals between the two parts becomes weakened and falls practically to zero when the planes of the carbon atoms are oriented at right-angles to one another. This orientation represents the configuration of maximum  $\pi$ -electron energy in the course of rotation about that link. Subject to other factors present, some of which will be noted below, the perpendicular orientation may then be regarded as the transition state and  $W$  may be thought of as the contribution from the  $\pi$ -electrons to the heat of activation for *cis-trans* isomerisation. This idea has been mentioned before<sup>10</sup> but its consequences do not seem to have been systematically examined before. In the case of ethylene a more detailed treatment has been attempted by Penney,<sup>11</sup> and more recently by Mulliken and Roothaan.<sup>12</sup> The first objection to be raised against the simple procedure is the fact that the molecule with the non-coplanar orientation of its parts is not correctly represented by a secular equation of the type of eqn. (2); for example, as  $\beta$  is a composite quantity<sup>7, 12</sup> it is incorrect to put  $H_{12} = H_{21} = 0$  in this instance but, for the present argument, it seems hardly justifiable to seek such refinement of the theory which would render the treatment too laborious. As we are mainly interested in the comparison of different bonds the absolute error thus introduced will probably cancel out to a large extent.

It is assumed that no steric hindrance is present in the molecule, so that it is normally in the coplanar form possessing the full amount of resonance energy. This assumption is probably justified in the case of the *trans*-polyene chains but is not quite correct for *cis* structures. Complications due to hyperconjugation have been neglected.<sup>13</sup>

Apart from the  $\pi$ -electrons the  $\sigma$ -electrons may contribute to the activation energy of isomerisation. In a multiple bond the length of the  $\sigma$ -bond is compressed to below its ordinary value and, when the interaction of the  $\pi$ -electrons is stopped, the link will expand to the single-bond distance and thus contribute to the stability of the transition state. The lengths of the other bonds in the molecule will also adjust themselves to different lengths in the transition state owing to the general redistribution of the  $\pi$ -electrons.

A possible method of taking account of these energies has been outlined by Lennard-Jones<sup>13</sup> and could be extended to the present calculations. However, it has been shown that Hückel's method yields consistent results even when such energy terms are neglected, provided that an appropriate value of  $\beta$  is chosen which apparently absorbs the error thus introduced. (The value chosen is  $\beta = -18$  kcal.)

For rotation about bonds, designated conventionally as "single" bonds, the heats of activation calculated in this manner are reasonable.

<sup>10</sup> Coulson, *Proc. Roy. Soc. Edin. A*, 1941, **61**, 115.

<sup>11</sup> Penney, *Proc. Physic. Soc.*, 1934, **46**, 333. Mulliken and Roothaan, *Chem. Rev.*, 1947, **41**, 219.

<sup>12</sup> Mulliken, Rieke and Brown, *J. Amer. Chem. Soc.*, 1941, **63**, 41.

<sup>13</sup> Lennard-Jones, *Proc. Roy. Soc. A*, 1937, **158**, 280.

The general trend of the data is consistent with the known fact that it is—if at all possible—extremely difficult to isolate separate geometrical isomers about “single” bonds (except through the completely different cause of steric hindrance, as in the diphenyls) because when the two isomers are separated by only a low energy barrier the less stable form will be rapidly converted to the more stable isomer. (Because of some steric hindrance the *cis*-form is generally the less stable isomer. For stilbene the energy difference between *cis*- and *trans*-forms has been experimentally estimated<sup>14</sup> as 2.7 kcal. Carotenoid isomers, differing only in the geometrical isomerism of one “double” bond, appear to have an energy difference of about 1-2 kcal.) For these reasons it is probable that the mechanism of *cis-trans* isomerisation about “single” bonds is, in fact, of the simple type considered here. However, it must again be emphasised that many factors have been neglected in this calculation (e.g. steric hindrance, hyperconjugation) so that no reliance is to be placed on the absolute magnitude of any individual activation energy calculated.

The difference in electronic energy between the perpendicular and coplanar forms must also be included in the steric hindrance calculations for the rate of isomerisation of sterically-hindered diphenyl derivatives.<sup>15</sup> As the transition state is in this case the coplanar form (or very close to it) the effect operates in the direction of reducing the activation energy.

For formal “double” bonds, on the other hand, the calculated values of the heat of activation do not agree with experience. For instance, the thermal isomerisation of (*cis*-) isostilbene  $\rightarrow$  (*trans*-) stilbene has been thoroughly investigated<sup>16</sup> and found to have an activation energy of  $\sim 43$  kcal., so that an experimental value of  $\sim 46$  kcal. (corrected for the difference in energy content of the *cis*- and *trans*-forms mentioned above), should be compared with the calculated estimate of 25.9 kcal. A different value of  $\beta$  could modify these results somewhat, but the explanation of the failure of the calculation in this case is probably a more fundamental one.

There is a difference in kind (and not only of degree) between rotation about “single” and “double” bonds by the mechanism considered in that each isolated portion of the molecule contains an even number of electrons in the former case but contains an odd number when the double bond is rotated. The energy level calculated by the simple molecular-orbital method lies between the singlet and triplet levels of the rotated molecule. If the reaction goes only through singlet states, about half the singlet-triplet separation must then be added on to the value of  $W$ . If some switching over to the triplet state can occur, the heat of activation can have a much lower value, but this would probably be accompanied by a decrease of the frequency factor. Arguments of this kind were advanced by Magee, Shand and Eyring<sup>17</sup> to explain the different activation energies of *cis-trans* isomerisation reactions of ethylene derivatives. (Assuming, say, a singlet-triplet separation of  $\sim 40$  kcal., and the calculated level to lie half-way, a more reasonable value for the heat of activation of stilbene isomerisation would be obtained.) The failure of the calculation for the “double”-bond case may also be connected with the possibility that the shortcomings of our procedure, pointed out in the first paragraph of this section, have graver consequences here than in the “single”-bond case.

An examination of bond orders and values of  $W$  will, therefore, lead to too low an estimate for the energy barrier of “double”-bond rotation. More quantitative experimental work on *cis-trans* isomerisations of long-

<sup>14</sup> Branch and Calvin, *The Theory of Organic Chemistry* (New York, 1941), p. 340.

<sup>15</sup> Westheimer and Mayer, *J. Chem. Physics*, 1946, **14**, 733. Westheimer, *ibid.*, 1947, **15**, 252.

<sup>16</sup> Kistiakowsky and Smith, *J. Amer. Chem. Soc.*, 1934, **56**, 638.

<sup>17</sup> Magee, Shand and Eyring, *ibid.*, 1941, **63**, 677.

chain polyenes would greatly help our understanding of the problem. The existing data in this field<sup>18</sup> may also be tentatively interpreted as indicating a larger difference in stiffness to rotation between "single" and "double" bonds than is predicted by the over-simplified theory.

As a purely theoretical problem it is of interest to consider whether the bonds in the middle of an infinitely long polyene chain could still be reasonably distinguished as "single" and "double." From the point of view of bond order (and therefore bond length and stretching-force constant) the bonds will be identical. From the point of view of stiffness to rotation they will differ owing to the singlet-triplet splitting. If, however, in the infinitely long chain these levels become indistinguishable this difference will again disappear.

#### IV. Addition to "Unsaturation" Bonds

Ease of addition reactions is often taken as a measure of double-bond character so that the question arises, whether this reactivity is in any way to be related to bond orders or  $W$ .

The present approach to this problem is again an empirical one. Addition to an unsaturation bond involves a change in the  $\pi$ -electron energy (and this change will be termed  $Y$ ), a change of hybridisation at the carbon atoms on the seat of addition and formation of the links between these C atoms and the added groups. If we can now make the assumption that these two latter processes are energetically identical for a series of unsaturated bonds, it should be possible to predict from a knowledge of  $Y$  (which will be calculated by the molecular-orbital method), the relative stabilities of addition products to different bonds, i.e., the nature of the addition products when these are in thermodynamic equilibrium with one another. The smaller  $Y$  is numerically, the greater will be the stability of that addition product.\* The last column of Table II gives values of  $Y$  calculated in this manner. If we now plot  $Y$  against  $W$  (Fig. 1) it becomes apparent that some measure of correlation does exist.<sup>21</sup> As  $W$  has been shown to be roughly related to B.O., this result may be stated in the form that—very approximately—the higher the bond order of a linkage in a conjugated hydrocarbon the greater will be its (exothermic) heat of hydrogenation or its tendency to break and suffer addition across it, as measured by the equilibrium constant of the reaction. At first sight this statement may appear paradoxical, as it implies that a "tighter" link (as measured by the stretching force constant) will be less stable thermodynamically. The general scatter of the points clearly indicates, however, that this is only a broad statistical generalisation and that, even without considering factors other than resonance energies, this rule has many individual exceptions. It is noteworthy that only points for molecules for which "starring" is impossible and for which the Hückel method is no longer self-consistent<sup>22</sup> fall completely off the curve.

The calculation of  $Y$  predicts correctly the nature of the dihydro-derivatives of naphthalene and phenanthrene. For anthracene the prediction is slightly in error, as it leads one to expect the 1:2 dihydro-derivative to be slightly more stable than the *meso*-compound actually

<sup>18</sup> Zechmeister, *Chem. Rev.*, 1944, **34**, 267.

<sup>19</sup> Pauling and Sherman, *J. Chem. Physics*, 1933, **1**, 679.

<sup>20</sup> Syrkin and Diatkina, *Acta. Physicochim.*, 1941, **14**, 105.

<sup>21</sup> Cf. Waters, *J. Chem. Soc.*, 1948, 730.

<sup>22</sup> Coulson and Rushbrooke, *Proc. Camb. Phil. Soc.*, 1940, **36**, 193.

\* A treatment of hydrogenation of some benzenoid hydrocarbons on these lines has also been given by Pauling and Sherman,<sup>19</sup> using the valence-bond method, and recently by Syrkin and Diatkina,<sup>20</sup> using Hückel's molecular-orbital method. 1:4 addition to conjugated systems can in principle also be considered in this manner.

obtained. There are many possible causes of this, e.g. (a) the possibility that the 1 : 2 compound is not isolated because the 9 : 10 addition proceeds more rapidly by a different mechanism and thermodynamic equilibrium between the forms is not attained, or (b) the existence of ring-strain in the 1 : 2 dihydronaphthalene which can only be relieved if the 3 : 4 double-bond is bent out of the plane of the naphthalene ring, thus decreasing the resonance energy. Argument (b) is probably of importance in some of the other examples, but there the difference in resonance energy between different products is large enough for this smaller term not to make such a decisive difference to the result. However, such refinements are beyond our scope at present.

A prediction of the reactivity of unsaturation bonds as measured by the velocity of addition reactions cannot be made without adequate consideration of the mechanism of the reaction. Consideration of the stability and velocity of formation of addition products are of importance to the theory of carcinogenic activity of compounds containing a phenanthrene skeleton. It has been pointed out that there may be a relation between activity and bond order,<sup>23</sup> but this is probably only an indirect consequence of the fact, pointed out above, that bond orders are empirically connected to energy parameters, such as *W* and *Y*, and perhaps also to the activation energy for an addition reaction between the carcinogenic *K* region of the hydrocarbon and tissue (or an oxidation <sup>24</sup>), so that the bond order-activity relation may in future be given a more logical interpretation in terms of the stability or velocity of formation of some addition compound inducing cancerous growth.

The author wishes to thank Prof. C. A. Coulson and Dr. D. W. G. Style for valuable comments, and Prof. Coulson also for permission to use some of his unpublished calculations of bond orders.

*Department of Chemistry,  
King's College,  
London, W.C.2.*

<sup>23</sup> Pullmann, *Ann. Chim.*, [12], 1947, 2, 5.

<sup>24</sup> Anderson, *Nature*, 1947, 160, 893.

---

## THE REDUCTION OF NITROCOMPOUNDS AT THE DROPPING-MERCURY CATHODE

### PART III—THE NITRORESORCINOLS \*

BY J. PEARSON

*Received 20th September, 1948*

The reduction at the dropping-mercury cathode of the nitroresorcinols is simpler than that of the nitrobenzenes and nitrophenols; reduction is complete in one stage to the amines at all hydrogen ion concentrations. Reduction proceeds through the intermediary of cathodically-deposited hydrogen atoms, and the presence of two hydroxyl groups appears to prevent the formation of phenyl-ammonium ions. In the compounds studied, hydrogen bonding counteracts any stabilising effect of the extra hydroxyl group on the nitrogroups, as compared with the nitrophenols.

\* This communication forms part of a thesis submitted in January, 1946, to the University of London in partial fulfilment of the requirements for the Degree of Ph.D.

The reduction at the dropping-mercury cathode of nitrophenols is more complex than that of the nitrobenzenes and nitrotoluenes.<sup>1,2</sup> The nitroresorcinols contain two hydroxyl groups and the investigation has been extended to these compounds to ascertain whether the complexity would increase.

### Experimental

The technique and apparatus employed was that previously described,<sup>1,2</sup> except that measurements were made in media of pH 2.0, 4.0, 6.0, 8.0, 9.2 and 10.0. The concentration range studied was 0.1-1.0 millimolar. Typical polarographic records, taken at pH 2.0, are depicted in Fig. 1; the concentrations, in millimoles per litre, are indicated.

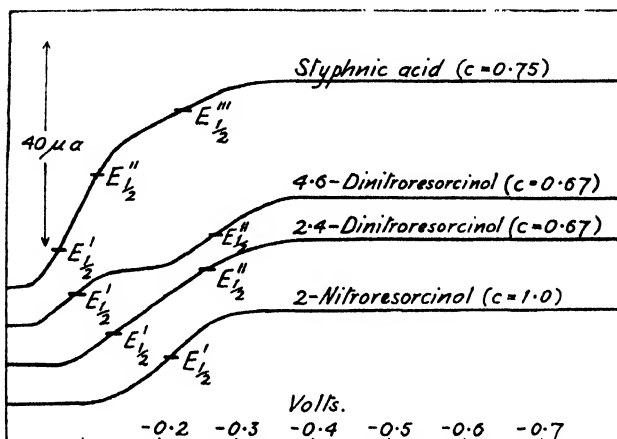


FIG. 1.

### Results

At all hydrogen ion concentrations, 2-nitroresorcinol gave rise to a single polarographic wave. The value of the diffusion-current constant ( $K = i_d / C.m.^{2/3}t^{1/6}$ ) varied between 9.9 and 10.2. The number of electrons involved in the reduction must therefore have been six ( $n = K/1.7$ ).<sup>1</sup>

In media of pH higher than 4.0, 2:4-dinitroresorcinol produced doublet waves, their separation increasing with pH. The components were of equal height and the  $K$ -values for the final limiting currents were approximately 20.0. The reduction therefore proceeded in two 6-electron stages. At pH 2.0 and 4.0, the two components merged to a single wave, similar to that of *m*-dinitrobenzene.<sup>1</sup> The waves were not well defined in alkaline media, so that half-wave potentials are not given with any certainty.

4:6-Dinitroresorcinol behaves in a manner similar to that of the 2:4-isomer, except that, even at pH 2.0, it exhibited separate component waves. The diffusion-current constants of these were approximately 10.2 and 20.4.

Styphnic acid (2:4:6-trinitroresorcinol) exhibited waves almost identical in shape to those of picric acid.<sup>3</sup> At pH 2.0 and 4.0 the single waves had  $K$ -values of 29.3. Doublet waves were recorded at pH 6.0 and 8.0 ( $K$ -values approx. 20.0 and 29.3). At lower hydrogen ion concentration, three components were visible, the third wave having a large "spread" and, therefore, not very definite. The respective diffusion-current constants were 10.1, 20.3 and 29.1. The reduction proceeded in three stages, involving apparently 6, 12 and 17 electrons. The first two stages were probably reductions of nitro- to amino-groups whilst, by analogy with Lingane's result for picric acid,<sup>3</sup> the final product was possibly di-(dihydroxydiaminophenyl)-hydrazine.

<sup>1</sup> Pearson, *Trans. Faraday Soc.*, Part I, 1948, **44**, 683.

<sup>2</sup> Pearson, *ibid.*, Part II, 1948, **44**, 692.

<sup>3</sup> Lingane, *J. Amer. Chem. Soc.*, 1945, **67**, 1916.

The half-wave potentials and  $n$ -values are given in Table I. Where a single wave represented a 12- or a 17-electron reduction, half-wave potentials have been estimated for the two or three components. In all instances, half-wave potentials were independent of, and diffusion-currents were proportional to, concentrations.

TABLE I

pH	2.0		4.0		6.0		8.0		9.2		10.0	
Constant	$E_{\frac{1}{2}}$	$n$	$E_{\frac{1}{2}}$	$n$	$E_{\frac{1}{2}}$	$n$	$E_{\frac{1}{2}}$	$n$	$E_{\frac{1}{2}}$	$n$	$E_{\frac{1}{2}}$	$n$
2-Nitroresorcinol	-0.21	6	-0.32	6	-0.41	6	-0.50	6	-0.61	6	-0.72	6
2 : 4-Dinitroresorcinol	-0.14	6	-0.21	6	-0.30	6	-0.55	6	-0.86	6	(-0.97)	6
	-0.26	12	-0.35	12	-0.50	12	-0.80	12	-1.14	12	(-1.20)	12
4 : 6-Dinitroresorcinol	-0.09	6	-0.19	6	-0.28	6	-0.40	6	-0.63	6	(-0.73)	6
	-0.27	12	-0.40	12	-0.52	12	-0.74	12	-0.95	12	(-1.04)	12
Styphnic acid	-0.07	6	-0.15	6	-0.25	6	-0.38	6	(-0.57)	6	(-0.70)	6
	-0.12	12	-0.24	12	-0.38	12	-0.60	12	(-0.89)	12	(-1.05)	12
	-0.23	17	-0.48	17	-0.55	17	-0.82	17	(-1.17)	17	(-1.30)	17

The values of  $E_{\frac{1}{2}}$  (corrected for  $iR$  drop) are in volts against a saturated calomel electrode, and those of  $n$  are the total number of electrons involved in the reduction causing the diffusion current. The values in parenthesis are somewhat uncertain because of lack of definition of the waves.

### Discussion

Contrary to expectation, the introduction of two hydroxyl groups into a polynitrobenzene molecule resulted in simplification of the reduction processes as compared with those of the nitro-benzenes, -toluenes and -phenols. The nitrogroups were reduced without exception, at all pH's, in single stages. Astle and Stephenson<sup>4</sup> have made the same observation with 2- and 4-nitroresorcinols. This uniformity of behaviour seems to imply that there was no change in the nature of the initial materials or their reduction products as pH was increased.

TABLE II

	V/pH unit
2-Nitroresorcinol . . . . .	0.051
2 : 4-Dinitroresorcinol (first wave) . .	0.037
(second wave) . . . . .	0.049
4 : 6-Dinitroresorcinol (first wave) . .	0.047
(second wave) . . . . .	0.067
Styphnic acid (first wave) . . . . .	0.038
(second wave) . . . . .	0.055
(third wave) . . . . .	0.069

The relationship between half-wave potential and pH was linear up to about pH 9 for 2-nitroresorcinol, up to about pH 6 for the dinitroresorcinols, and up to just less than pH 6 for styphnic acid. Beyond these values, the reduction potential increased more rapidly with rise of pH, as has also been found for the mononitroresorcinols by Astle and

<sup>4</sup> Astle and Stephenson, *J. Amer. Chem. Soc.*, 1943, **65**, 2399.

Stephenson.<sup>4</sup> This increased effect is attributed to salt formation, the difference in the point at which the increase starts being presumably connected with the acid strength of the compounds. Since there was no break in the  $E_1$ -pH relationships nor a change in reduction process at about pH 3.5, as with the nitrobenzenes,<sup>1</sup> it must be assumed that the presence of the two hydroxyl groups prevented formation of phenyl-ammonium ions. The slope of the  $E_1$ -pH lines, up to the pH's mentioned above, are given in Table II. Here also, as with the nitro-benzenes and -toluenes, the value of  $E_1'' - E_1'$  increased with pH.

The individual waves produced by the reduction of the various nitro-groups of the nitroresorcinols were almost identical in shape with those produced by the nitro-benzenes, -toluenes, and -phenols. It follows that the slope of the plots of cathode potential against  $\log [i/(i_a - i)]$  will be similarly identical. Some typical values, for reduction in a medium of pH 2.0, are given in Table III, with the slopes to be expected if the reductions were reversible, i.e. 0.0591/n.

TABLE III

Compound	n	Slope	Expected Slope
2-Nitroresorcinol . . . . .	6	0.080	0.010
4 : 6-Dinitroresorcinol (first wave) . . .	6	0.055	0.010
(second wave) . . . . .	6	0.058	0.010
Styphnic acid (first part of composite wave)	12	0.055	0.005

It is seen that the values of the slopes are similar to those reported for the nitrocompounds in Parts I and II of this series. In fact, three of them are remarkably close to the 0.059 predicted from the theoretical considerations in Part I,<sup>1</sup> and give added confirmation to the conclusion that the reduction proceeded via the intermediary of cathodically-deposited hydrogen atoms.

The introduction of a hydroxyl group into nitrobenzene molecules leads to more negative reduction potentials, i.e. the +T electron-donating influence of this group stabilises the nitrogroups and makes them less susceptible of reduction, unless hydrogen bonding intervenes.<sup>2</sup> Since the nitrogroups in the nitroresorcinols were reduced completely in one stage at all pH's it is perhaps not legitimate to compare their half-wave potentials with those of the nitro-benzenes and -toluenes. Nevertheless, certain half-wave potentials, at pH 2.0 in V against a saturated calomel electrode, have been set out in Table IV.

TABLE IV

Compound	Volt	Compound	Volt	Compound	Volt
Nitrobenzene .	-0.27	<i>o</i> -Nitrophenol	-0.23	2-Nitroresorcinol	-0.21
		<i>m</i> -Nitrophenol	-0.25		
		<i>p</i> -Nitrophenol	-0.35		
<i>o</i> -Dinitrobenzene	-0.11 -0.30	2 : 4-Dinitrophenol	-0.14 -0.32	2 : 4-Dinitroresorcinol	-0.14 -0.26
		2 : 6-Dinitrophenol	-0.09 -0.24	4 : 6-Dinitroresorcinol	-0.09 -0.27
1 : 3 : 5-Trinitrobenzene	-0.06 -0.13 -0.21	Picric acid	(-0.11) (-0.19) (-0.37)	Styphnic acid	-0.07 -0.12 -0.23

From Table IV it will be seen that any stabilising influence of the extra hydroxyl group was strongly countered, probably by hydrogen bonding between the nitro- and hydroxyl groups. Thus the reduction potentials of 2-nitro-, 2 : 4- and 4 : 6-dinitroresorcinols were almost identical with those of the nitro- and dinitro-phenols, respectively. Styphnic acid was even more readily reduced than picric acid, the  $E_1$  values being essentially the same as those of trinitrobenzene. It is unfortunate that a sample of 5-nitroresorcinol was not available for examination, for in that compound hydrogen bonding is not possible and the true effect of the additional hydroxyl group might have been found.

Acknowledgement is made to the Chief Scientist, Ministry of Supply, for permission to publish this work, which was carried out in a branch, formerly of the Armament Research Department, but now of the Explosives Research and Development Establishment.

*British Iron and Steel Research Association,  
Skelty Hall,  
Swansea.*

---

## THE EFFECT OF PRESSURE ON THE VOLUME, THERMODYNAMIC PROPERTIES AND CRYSTALLINITY OF POLYTHENE

BY W. PARKS AND R. B. RICHARDS

*Received 27th September, 1948*

The compressibility of polythene has been measured at 25-160° C and at pressures up to 2000 atm. by an adaptation of the method described by T. W. Richards. The compressibility decreases as pressure increases except in the case of the compression of initially liquid polythene to a point at which crystallisation begins; in this case the solidification is accompanied by an increase in compressibility.

The compressibility at 1-100 atm., which rises to a maximum as the melting point is approached, is comparable with that of a liquid or of rubber, rather than that of a crystalline solid. The melting point is raised by pressure at a rate of about 0.02° C atm.<sup>-1</sup>. From the  $P$ - $V$ - $T$  data and specific heat data previously determined the effect of pressure and temperature on the entropy, heat content and internal energy of polythene has been calculated. From the internal energy changes the effect of pressure on the proportion of crystalline material is estimated. The rise in temperature on adiabatic compression of polythene or on free expansion as in extrusion can be read from the entropy or heat content charts.

---

Measurements of the effect of temperature on the volume and the heat content of polythene have been published;<sup>1, 2</sup> the results indicated that as temperature is increased there is a continuous rise in the proportion of amorphous matter in the solid state, the last traces of crystalline matter disappearing at the temperature commonly referred to as the melting point (110-115° C for normal samples). Examination by X-ray methods give qualitative support to this view.<sup>3</sup> On cooling, the reverse

<sup>1</sup> Hunter and Oakes, *Trans. Faraday Soc.*, 1945, 41, 49.

<sup>2</sup> Raine, Richards and Ryder, *ibid.*, 1945, 41, 56.

<sup>3</sup> Bunn and Alcock, *ibid.*, 1945, 41, 317.



processes occur with relatively little hysteresis. Statistical thermodynamical theories have been put forward in which the crystalline-amorphous complex is regarded as being in an equilibrium state at each temperature and equations are set up to represent the amorphous content as a function of temperature.<sup>4, 5</sup>

Measurement of the compressibility and of the effect of pressure on the thermodynamic properties of polythene has been undertaken because it was expected that abnormal results would be obtained as a result of the composite crystalline-amorphous structure of the polymer. Hydrocarbons, both in the solid and liquid state, have high compressibilities. In the case of polythene as pressure is increased it is to be expected that the equilibrium between crystalline and amorphous matter will be displaced with an increase in the proportion of the more dense crystalline phase, leading to an extra volume decrease and an abnormally high compressibility. Wood, Bekkedahl and Gibson<sup>6</sup> have shown that the melting point of partially crystalline rubber is increased by pressure, and the polythene compressibility measurements have been extended to temperatures above the normal melting point to cover the phenomenon of solidification under pressure. The range covered is 25-160° C at pressures up to 2000 atm.

### Experimental

The sample of polymer used in this work was similar to that used by Raine, Richards and Ryder<sup>7</sup> for specific heat measurements. The apparatus used for the compressibility measurements was a stainless steel adaptation of the glass piezometer used by T. W. Richards and his co-workers.<sup>7</sup>

The polythene surrounded by mercury is contained in the vessel A (Fig. 1) which is sealed at the bottom by a flat plate B secured by the nut C. Screwed to the top of the vessel is a steel tube D inside which is a glass insulating tube E, shaped at the bottom to join on to the constriction at the entrance to the vessel. The metal contact F, which is in the form of four stainless steel vanes terminating in a thin platinum wire, rests in the bottom of the glass tube with the wire projecting into the constriction in the vessel. The contact is located by the spring G which is compressed by the screw on the cap H through an insulating glass bush J. A glass funnel L enters the tube through a Neoprene stopper K in the cap and reaches to within 1 cm. of the top of the contact. The outside of the funnel is coated with platinum and is joined by a thin copper wire to the spring which, therefore, completes the electrical connection between the platinumised funnel and the platinum wire contact below.

The polythene used is in the form of a cylinder (of volume about 12 cm.<sup>3</sup> at the lower temperatures), and is put into the vessel through the base. The remaining space in the vessel is filled with mercury and the bottom joint is made. The metal tube D is then fixed and the air is extracted from the vessel by a high-vacuum pump. The vessel and contents are now brought to the required temperature, and the mercury level is adjusted so that it is just at the top of the constriction. The rest of the apparatus is then assembled, the glass tube being filled with water at 25° C and 75° C and with glycerine at higher temperatures. The piezometer, when filled, is put into a pressure vessel of capacity 300 ml. which has about 20 ml. of mercury in the bottom, the remaining space being filled with oil. The water or glycerine in the glass tube in the piezometer prevents the mercury surface from being contaminated by the oil. The electrical connection from the contact is brought out of the pressure vessel through a glass insulated cone<sup>8</sup> which is connected by thin copper wire to the platinum on the outside of the glass funnel. The electrical circuit is completed through the mercury and the wall of the pressure vessel by a milliammeter, a 2-volt cell and a resistance, so that when the mercury in the piezometer is touching the platinum contact a small current is recorded. The pressure vessel is immersed in an oil thermostat. Pressure is applied by a Cailletet press and is gradually raised until the mercury is forced away from the contact, breaking

<sup>4</sup> Frith and Tuckett, *Trans. Faraday Soc.*, 1944, **40**, 251.

<sup>5</sup> Richards, *ibid.*, 1945, **41**, 127.

<sup>6</sup> Wood, Bekkedahl and Gibson, *J. Chem. Physics*, 1945, **13**, 475.

<sup>7</sup> Richards, *J. Amer. Chem. Soc.*, 1912, **34**, 975.

<sup>8</sup> Welbergen, *J. Sci. Instr.*, 1933, **10**, 247.

the electrical circuit. The pressure is then slowly released until contact is just remade. This is repeated until a steady pressure reading is obtained indicating that the heat of compression has been dissipated. Three Bourdon tube pressure gauges, of ranges 0-250 atm., 0-1000 atm. and 0-3000 atm. which had been checked against a pressure balance,<sup>9</sup> were used to measure the pressures. The pressure difference between the make and break of the contact was very small. At the lower pressures it was less than 1 atm. and was never greater than 5 atm. which is the limit of sensitivity of the gauges used at the higher pressures.

When the first point has been established the pressure is released, a further weighed quantity of mercury is introduced into the piezometer, and the pressure at which the contact is broken is again determined as above. This is repeated as often as necessary until a pressure of 2000 atm. is reached. In order to put the mercury into the piezometer without it coming into contact with oil and without breaking the main pressure joint, a glass tube, filled with water or glycerine, is passed through a plug hole in the top of the vessel, through the oil, and under the water or glycerine in the piezometer. The mercury can then be poured down this tube without danger of contamination. The volume change between atmospheric pressure and the lowest pressure at which the contact is broken is obtained by extrapolation and consequently it is most desirable to have this first point near to atmospheric pressure. This in practice is not difficult.

Experiments were carried out at two different temperatures with mercury only in the piezometer, and from these, knowing the compressibility of mercury the change in volume of the vessel can be found. Bridgman's figures for the compressibility of mercury<sup>10</sup> were extrapolated as a linear function to these higher temperatures. The total volume change of the mercury is small compared with that of the polythene, and there can be no appreciable error as a result of this extrapolation.

Owing to the limited diameter of the pressure vessel it was not possible to design the piezometer with the mercury exit in the shape of a U-tube leaving the bottom of the vessel. As a result, at those temperatures where the polythene was very plastic or fluid, precautions had to be taken to prevent the upthrust of the mercury forcing the polythene through the constriction and out of the vessel. At 95° C and 105° C this was achieved by enclosing the polythene, surrounded by mercury, in a thin rubber bag. At higher temperatures the polythene was held under a single-ended inverted cylinder of thin stainless steel. In this case it was necessary to reduce the amount of polythene in order that the cylinder could be of such a size that there was a clearance between it and the walls of the vessel of at least 2 mm. This was to allow a free passage of mercury and prevent the trapping of air during the evacuation.

## Results

**Pressure-Volume-Temperature Relation for Polythene.**—The effect of pressure on the volume of 1 g. of polythene at 25, 75, 95, 105, 110, 120, 140 and 160° C is shown in Fig. 2. The points for 1 atm. are based on thermal expansion measurements carried out on this sample of polythene by Miss J. Phillipson using the method described by Hunter and Oakes.<sup>1</sup>

The main features of the *P-V-T* chart are the pronounced curvature in the pressure-volume lines, the increase in compressibility as the temperature approaches the melting point and the breaks in the volume pressure curves for temperatures above the melting point at 1 atm. (111° C) at the pressures at which the sample solidifies. During the experimental work it was noted that close to these break points equilibration was rather slow, a consequence possibly both of time factors in crystallisation and of the relatively large temperature changes which, as will be shown later, occur in the neighbourhood of the melting point during adiabatic compression or expansion.

The compressibility  $\kappa = \frac{1}{V} \times \frac{dV}{dP}$  for 1-100 atm. is plotted in Fig. 3 as a function of temperature. Figures for molten paraffin wax<sup>11</sup> are shown for comparison; the compressibility of this material is greater than that of molten polythene but varies with temperature in a similar manner. A point is also given for the hypothetical value of the compressibility at 23° C of a paraffin containing about 1000 carbon atoms obtained by an extrapolation of the linear plot of the compressibilities of liquid paraffins from hexane to hexadecane<sup>12</sup>

<sup>9</sup> Michels, *Ann. Physik*, 1923, **72**, 285.

<sup>10</sup> *Int. Crit. Tables*, **3**, 47.

<sup>11</sup> *Ibid.*, **2**, 146.

<sup>12</sup> *Ibid.*, **3**, 37.

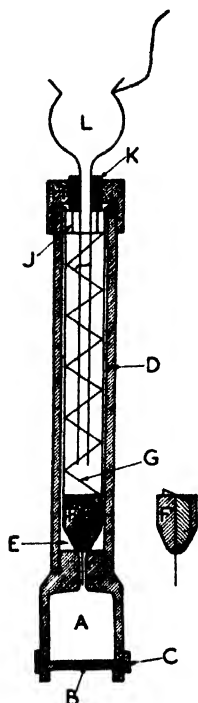


FIG. 1.—Apparatus for compressibility measurements.

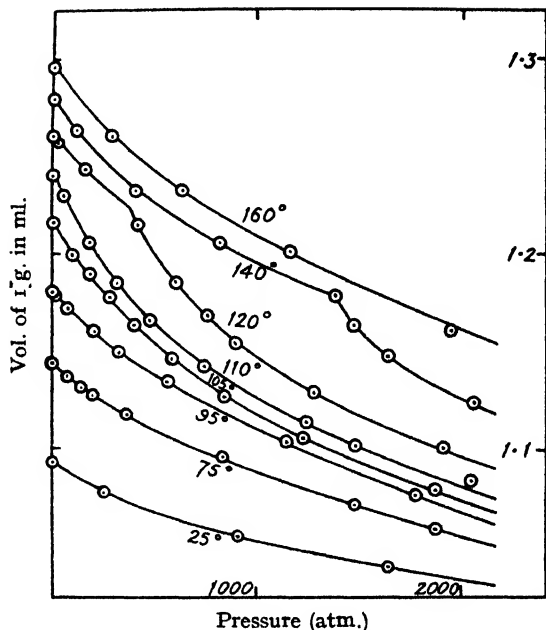


FIG. 2.—Volume (ml.) of 1 g. polythene at 25–160° C. as a function of pressure, in atm.

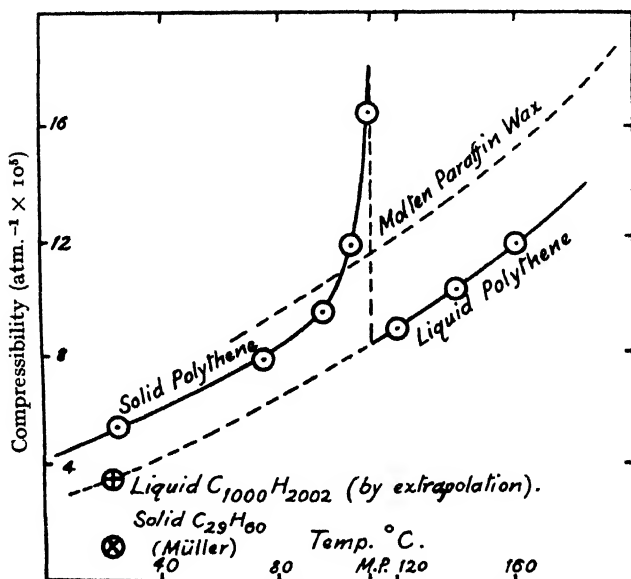


FIG. 3.—Compressibility of polythene as function of temperature.

against the reciprocals of the number of carbon atoms in the chain. This point is in reasonable accord with an extrapolation to 23° C of the compressibilities of liquid polythene, and lies appreciably below the line for solid polythene.

No direct measurements of the compressibility of crystalline paraffins appear to have been carried out, but Müller<sup>13</sup> has measured the effect of pressure on the X-ray spacings of solid paraffins and his results for  $C_{29}H_{60}$  indicate a volume compressibility about one-tenth of the value for polythene at ordinary temperatures.

Some compressibility figures for other materials are shown in Table I for comparison with the data for polythene. Polythene is one of the most compressible solids for which data are available and is more compressible than water.

TABLE I.—COMPRESSIBILITIES OF POLYTHENE AND OF LIQUIDS AND SOLIDS (1-100 ATM., ORDINARY TEMPERATURES)

Substance (and reference).	Compressibility atm. <sup>-1</sup> × 10 <sup>4</sup>
Polythene . . . . .	5.5
Pentane <sup>12</sup> . . . . .	19
Hexadecane <sup>12</sup> . . . . .	7.6
Benzene <sup>12</sup> . . . . .	9.7
Rubber (unvulcanised) <sup>14</sup> . . . . .	5.5
Water <sup>12</sup> . . . . .	4.3
Mercury <sup>10</sup> . . . . .	0.4
Iron <sup>10</sup> . . . . .	0.06
Sodium chloride <sup>10</sup> . . . . .	0.4

The data for polythene are also shown in the form of volume-temperature curves at a series of pressures in Fig. 4 based on the data given in Fig. 2 but

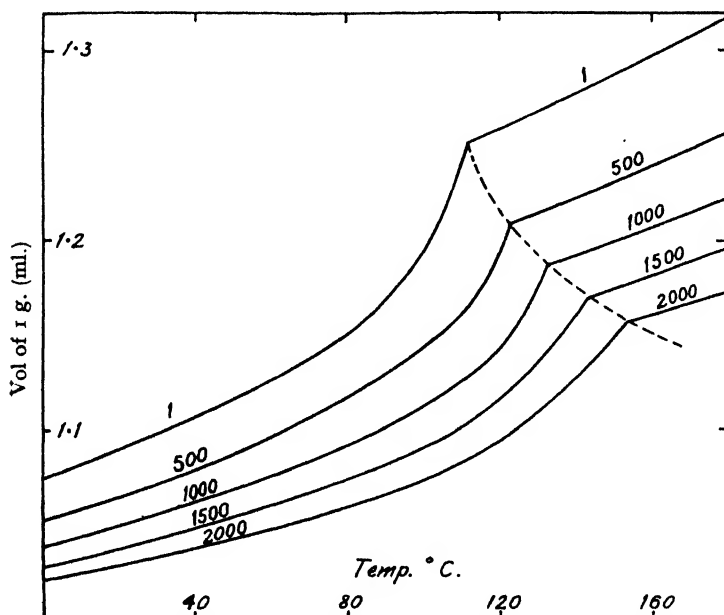


FIG. 4.—Volume of 1 g. polythene at 500, 1000, 1500 and 2000 atm. smoothed to give a self-consistent family of curves. This demonstrates clearly the shift to higher temperatures of the melting point and of the temperature zone during which the proportion of amorphous material is increasing rapidly.

<sup>13</sup> Müller, *Proc. Roy. Soc. A*, 1941, 178, 227.

<sup>14</sup> Wood, *Proc. Rubber Tech. Conf.* (London, 1938), p. 933.

**The Effect of Pressure on Thermodynamic Properties.**—From the  $P$ - $V$ - $T$  data and previously-determined heat capacity measurements at ordinary pressures for a similar sample of polythene the changes with pressure and temperature of the entropy ( $S$ ) total heat content ( $H$ ) and internal energy ( $E$ ) of 1 g. of polythene have been calculated. The stages in the calculations are as follows—

1. Calculation of the entropy-temperature curve for 10–160° C at 1 atm. from the available heat content-temperature data,<sup>2</sup> with an extrapolation down to 0° C. A graphical method is used in the summation of

$$S_{T_2} = S_{T_1} + \int_{T_1}^{T_2} \frac{C_p}{T} \cdot dT$$

and values of the entropy  $S$  are obtained, taking the value at 0° C as zero.

2. Calculation of the changes in entropy with pressures at various constant temperatures.

Since

$$\left[ \frac{\partial S}{\partial P} \right]_T = - \left[ \frac{\partial V}{\partial T} \right]_P,$$

then

$$\Delta S = \int_{P_1}^{P_2} dS = \int_{P_1}^{P_2} - \left[ \frac{\partial V}{\partial T} \right]_P dP.$$

For each temperature the values of the slopes of the  $V$ - $T$  curves at 1, 250, 500, 750, 1000, 1500, 2000 atm. obtained from Fig. 2 were plotted against the pressure and the values of  $\Delta S$  were calculated graphically. From these values and the values of  $S$  for 1 atm. at various temperatures obtained in (1) above, a chart of  $S$  as a function of  $T$  for various pressures was constructed. The curves for 1, 500, 1000, and 2000 atm. are given in Fig. 5.

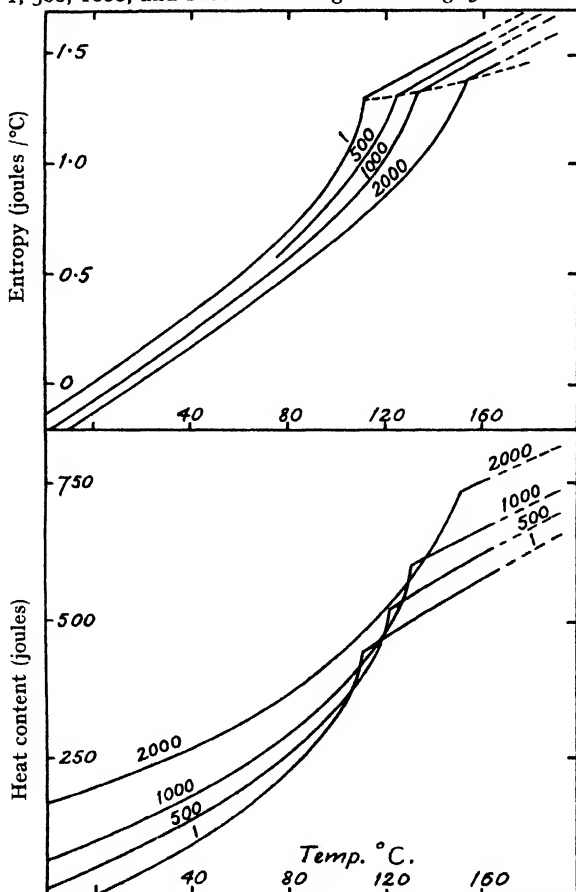


FIG. 5 and 6.—Entropy-temperature and heat content-temperature curves for 1 g. polythene at 1, 500, 1000, 2000 atm.

The heat-content temperature curve for 1 atm. is taken from the work of Raine, Richards and Ryder<sup>2</sup> with extrapolation to 0° C, putting  $H = 0$  at 0° C. The effect of pressure on heat content at constant temperature is given by

$$\Delta H = \int_{P_1}^{P_2} \left\{ V - T \left[ \frac{\partial V}{\partial T} \right]_P \right\} dP.$$

This is evaluated partly from a plot of  $V$  against  $P$  and partly from the change in entropy with pressure as in (2) above. From these values of  $\Delta H$  and the data, at 1 atm. heat content-temperature curves for various pressures are calculated. Curves for 1, 500, 1000, and 2000 atm. are given in Fig. 6.

Internal energy values are calculated from the above heat content values using the relation

$$E = H - PV.$$

They are plotted in Fig. 7 as  $E$ - $P$  curves at a series of temperatures, as it will be convenient to use the data in this form in a discussion of the effect of pressure on the crystalline-amorphous equilibrium.

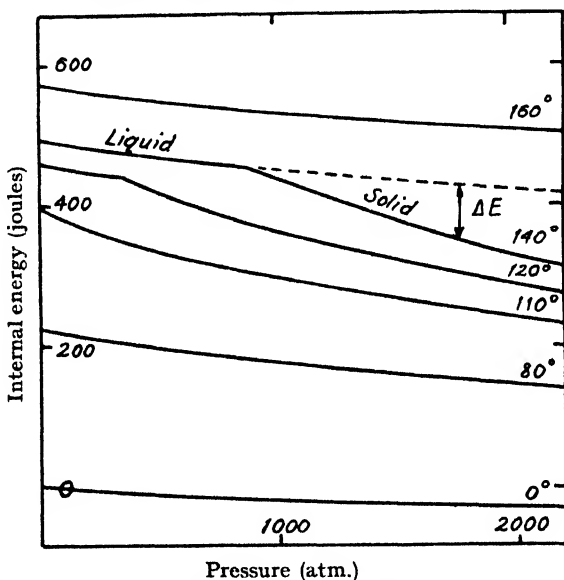


FIG. 7.—Effect of pressure on the internal energy of 1 g. polythene at 0-160° C.

## Discussion

(a) **The Effect of Pressure on the Melting Point.**—The temperature of the break in the  $V$ - $T$  curve corresponding to the temperature above which the polymer is completely amorphous (the melting point) rises as pressure increases at the rate of about 0.02° C atm.<sup>-1</sup>. A direct measurement of the effect of pressure on the melting point was made by observing the pressure at which a polythene film, supported in a pressure vessel with glass windows, became opaque at a temperature above the melting point. A figure of about 750 atm. at 130° C was obtained, compared with 800 atm. by interpolation from the break-points of the  $P$ - $T$  curves.

Wood, Bekkedahl and Gibson<sup>6</sup> have measured the effect of pressure on the melting point of frozen ("stark") rubber; the figure at low pressures is about 0.037° C atm.<sup>-1</sup>.

For a single-component system, the effect of pressure  $P$  on the melting point  $T_F$  is given by

$$\frac{dT_F}{dP} = \frac{T_F \times \Delta V}{L},$$

where  $\Delta V$  and  $L$  are the volume change on melting and latent heat of fusion. In the case of polythene it is difficult to apply this formula because melting occurs over a temperature range; using the  $V$ - $T$  and  $H$ - $T$  curves for polythene, we can, however, make crude estimates of the volume and heat content which solid polythene would have at its melting point if no increase<sup>1</sup> in amorphous content occurred over the range 20-111° C. We have<sup>2</sup> then  $T_F = 384$ ,  $\Delta V = ca. 0.08$  ml. and  $L = ca. 170$  joules/g. =  $ca. 1600$  ml.-atm.  $dT_F/dP$  is hence  $0.019^\circ \text{C atm.}^{-1}$ , in good agreement with the experimental value. Gee<sup>15</sup> has shown similar agreement between observed and calculated values for rubber and points out that despite the complexities of the melting process in a polymer the overall process can be treated thermodynamically as a simple phase change, i.e. as if it were a transition in a one-component two-phase system.

(b) **The Effect of Pressure on the Degree of Crystallinity.**—It has been pointed out above that the high compressibility of solid polythene can be attributed to an increase in the proportion of the more dense crystalline material under pressure. It is of interest to attempt to calculate quantitatively the extent of this crystallisation under pressure. This could be done if the separate compressibilities of the crystalline and the amorphous regions were known and if it could be assumed that these compressibilities were unaffected by changes in the proportions of crystalline material. Changes with pressure of the X-ray spacings have been measured for solid paraffins by Müller;<sup>18</sup> using his data on  $\text{C}_{22}\text{H}_{46}$  and an extrapolation from the data for liquid polythene (guided by the liquid paraffin data as in Fig. 3) for the separate compressibilities of the crystalline and amorphous regions in the polythene, it can be shown that an increase in pressure from 1 to 100 atm. would increase the proportion of crystalline material by about 1%; the increase of crystallinity falls off as the pressure increases further.

An alternative method of estimating the change in crystallinity with pressure is based on calculations of the change in internal energy  $E$ . This method is most useful at temperatures near the melting point where the proportion of crystalline material is relatively small. It is seen from Fig. 7 that the effect of pressure on  $E$  in the liquid state is relatively small, but that when solidification occurs there is a more rapid decrease in internal energy. A value can be calculated for  $\Delta E$ , the difference between the internal energy of the partly crystalline solid and the extrapolated value for the internal energy if the sample were amorphous at the same temperature. The difference in internal energy between an entirely crystalline and an entirely amorphous long chain paraffin ( $\Delta E'$ ) at 1 atm. and 25° C is<sup>2</sup> about 236 joules/g. and to a first approximation this may be regarded as constant when pressure or temperature is increased. If we assume that the internal energy of a crystalline-amorphous complex varies linearly with the proportion of crystalline material, then  $\Delta E'$  is equal to the proportion of crystalline material. The effect of pressure on crystallinity at temperatures in the range 100-160° C, calculated as above, is shown in Fig. 8. To use this method with any confidence at lower temperatures, account would have to be taken of the effect of pressure and temperature on the internal energy difference between entirely crystalline and entirely amorphous paraffins. It can be shown that the values for  $\Delta E'$  of 236 joules/g. would be too great at the higher pressures, but the values cannot be assessed reliably. At ordinary temperatures  $\Delta E$  is of the order of 190 joules/g. and varies little with temperature, and the value for the degree of crystallinity then becomes sensitive to the value of  $\Delta E'$ .

The large increases in the degree of crystallinity at temperatures around 110° C when pressure is applied are very striking.

<sup>15</sup> Gee, *Quart. Rev.*, 1947, 1, 265.

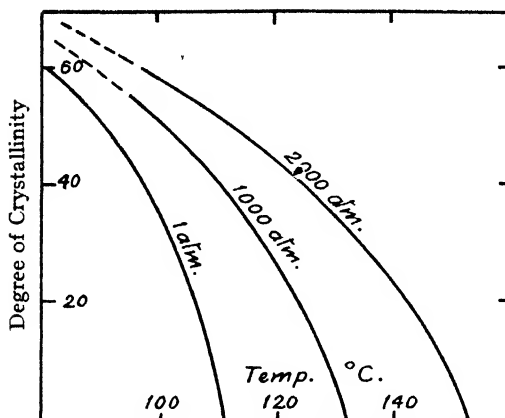


FIG. 8.—Effect of pressure on degree of crystallinity near the melting point (approximate).

(c) **Temperature Changes on Adiabatic Compression and on Free Expansion.**—From the entropy and heat-content charts it is possible to read off the temperature changes when polythene is compressed or allowed to expand. Compression of polythene, if no heat is lost during the compression and if the polythene is at all stages in equilibrium with the pressure (i.e. if crystallisation occurs rapidly enough), is a process of constant entropy. From Fig. 5 we see that isentropic compression from 1 to 2000 atm. would cause a rise in temperature from 20° C to 35° C, i.e. from 100 to 128° C or from the melting point (111° C) to 148° C and of the liquid from 140 to 163° C. On the other hand it is seen that despite these temperature rises it is never possible to melt polythene by adiabatic compression, because the entropy at the melting point rises as pressure rises. If the above approximate calculations of the proportion of crystalline material at various pressures and temperatures are combined with the entropy data, it can be shown that the effect of adiabatic compression on polythene, over most of the range of pressures and temperatures covered by this work, is to increase the proportion of crystalline material in spite of the temperature rise.

Continuous expansion of molten polythene at an extrusion nozzle or spinneret approximates to a constant heat-content process, and the changes in temperature can be read from Fig. 6.

The very large temperature rise on expansion of the solid at constant heat content is of interest. Expansion from 2000 atm. would cause a temperature rise from 20 to 80° C and expansion from about 5000-6000 atm. at ordinary temperatures would melt the polythene. It is, however, difficult to see how such an expansion could be carried out in practice.

The authors wish to acknowledge the advice given during the course of this work by Mr. G. Feachem and Mr. E. Hunter. The piezometer was made by Mr. P. van Ulden, Mr. H. J. Welbergen and Mr. J. Williamson.

*Imperial Chemical Industries Research Department,  
Alkali Division, Northwich.*



# THE IGNITION OF CORDITE BY HOT GASES

BY R. C. BRIAN AND C. A. McDOWELL

*Received 29th September, 1948*

Hot air at known temperatures, from 16° C to 400° C, and at various known velocities was blown on specimens of cordite and the induction period for the ignition recorded. It was found that a plot of  $\log t$  (induction period in seconds) against  $10^3/T$  was approximately linear over the region investigated. The average values of  $A$  and  $E$  for H.S.C. cordite found were  $1.59 \times 10^{-6} \text{ sec.}^{-1}$ , and 17,000 cal./mole<sup>-1</sup> respectively; the corresponding values for S.C. cordite being  $3.98 \times 10^{-6} \text{ sec.}^{-1}$  and 14,000 cal./mole<sup>-1</sup>.

There have been many experimental studies of the rate of burning of cordites<sup>1, 2</sup> but little investigation of the kinetics of the ignition of this type of propellant. It is well known that the ignition of cordite at high temperatures is a very rapid process, and the experimental investigation of this phenomenon is beset with difficulties. Cordite can, however, be ignited at temperatures above 200° C by hot non-incandescent gases, and the ignition process under these conditions is characterised by an induction period of the order of seconds.

## Experimental

Laboratory air was pumped through an electrically-heated furnace; the rate of flow being measured by means of a calibrated glass flow-meter. The temperature of the hot air emerging from the furnace was measured with a calibrated Alumel-Chromel thermocouple.

The cordite specimen was attached by thermally insulated clips to a brass disc, the surface of which was covered by  $\frac{1}{4}$ -in. thick asbestos sheeting to insulate it thermally from the cordite. The disc was so arranged that it could be rotated in a plane at right-angles to the direction of the air stream and at a fixed distance from the exit orifice of the furnace. The thermocouple was attached to the disc so as to enable the temperature of the air stream to be measured in the same plane as the surface of the cordite specimen.

Experiments were performed with different rates of flow of the hot air, and at temperatures from 160° to 400° C. When the temperature of the air was constant, the disc was rotated rapidly until the cordite specimen was positioned centrally in the hot air beam, and observations were made of the time from the air impinging on the cordite surface to the point at which explosive ignition occurred.

## Results

It was found difficult to bring about the ignition of cordite at temperatures less than 220° C. At all temperatures above approximately 220° C, after an induction period depending on the temperature of the hot air, ignition was observed. Initially, a few small blisters appeared on the cordite surface, after a short time the number rapidly increased until the surface became sintered, at which point decomposition set in. After a further interval, the surface softened, and ultimately began to "flow" from regions of high pressure in the impinging air-stream. Decomposition was very rapid at this juncture and was quickly followed by a slight explosion, when ignition occurred immediately.

In Fig. 1 the logarithm of the induction period in seconds is plotted against the reciprocal of the absolute temperature of the hot air beam for a typical run.

<sup>1</sup> Crow and Grimshaw, *Phil. Trans. A*, 1931, **230**, 387.

<sup>2</sup> Cranz, *Lehrbuch der Ballistik* (Berlin, 1926), Vol. 1.

From this graph it is clear that the experimental results are governed by the usual linear relation,  $\log_{10} t = C + B/T$ , found to hold for the explosive ignition of mixtures of oxygen and hydrocarbons, etc.,<sup>3</sup> nitroglycerine and trotyl,<sup>4</sup> lead styphnate,<sup>5</sup> and mercury fulminate,<sup>6</sup> and other explosives.<sup>7</sup>

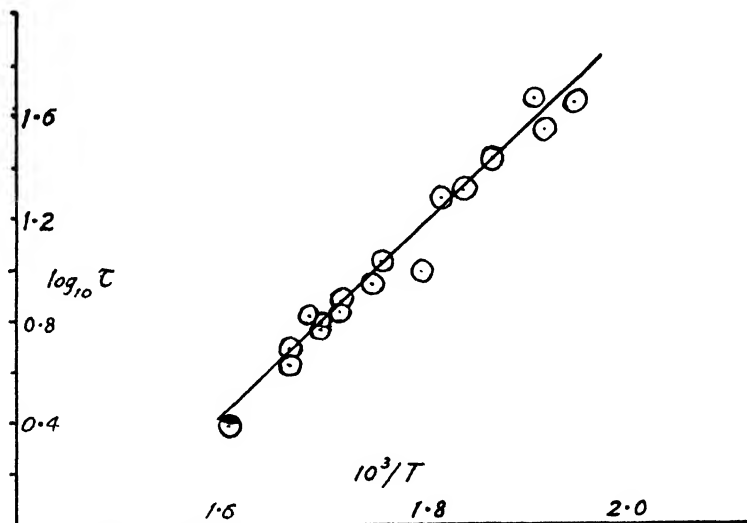


FIG. 1.

Table I contains the values of  $A$  and  $E$  calculated from the graphs of  $\log t$  against  $10^3/T$  for different rates of flow of the impinging stream of hot air and for two different cordites, assuming that the temperature variation of the induction period is given by  $t = Ae^{E/RT}$

TABLE I

THE ACTIVATION ENERGY FOR THE IGNITION OF CORDITE BY HOT AIR.

Type of Cordite	Linear Velocity of Air Stream (cm./sec.)	$A$ (sec. <sup>-1</sup> )	$E$ (cal./mole)
H.S.C.	3140	$7.9 \times 10^{-7}$	16,720
	2700	$2.5 \times 10^{-6}$	17,600
	2460	$4.0 \times 10^{-6}$	16,450
	3700	$7.9 \times 10^{-7}$	17,900
	3570	$2.5 \times 10^{-6}$	16,230
S.C.	2860	$4.0 \times 10^{-6}$	14,200

We should like to thank Prof. C. E. H. Bawn for many interesting discussions during the course of this work. This paper is based on work carried out in the Armament Research Department, Ministry of Supply, and is published by permission of the Chief Scientist.

Department of Inorganic and Physical Chemistry,  
Liverpool University.

<sup>3</sup> Semenov, *Chemical Kinetics and Chain Reactions* (Oxford, 1935).

<sup>4</sup> Roginsky, *Physik. Z. Sowjet.*, 1932, **1**, 640.

<sup>5</sup> Hailes, *Trans. Faraday Soc.*, 1933, **29**, 544.

<sup>6</sup> Garner and Hailes, *Proc. Roy. Soc. A*, 1933, **139**, 576. Garner, Gomm and Hailes, *J. Chem. Soc.*, 1933, 1393.

<sup>7</sup> Copp, Napier, Nash, Powell, Skelly, Ubbelohde and Woodward, *Phil. Trans. A*, 1948, **241**, 197.

## REVIEWS OF BOOKS

**The Chemistry of High Polymers.** By C. E. H. BAWN. (Butterworths Scientific Publications, London, 1948.) Pp. ix + 249. Price 17s. 6d. net.

In this book Prof. Bawn has attempted to present the basic ideas of polymer chemistry and physics in a reasonably condensed form. The first part deals with the principal types of polymerisation reactions, and discusses the information which may be obtained from a quantitative study of the kinetics of the processes involved. The emphasis here is on the general methods of attack rather than on the detailed chemical reactions of particular systems, though some discussion is attempted of the more complicated and controversial topics of organic chemistry (e.g. the effect of oxygen on polymerisation and chain scission).

The remainder of the book deals with the thermodynamics of solutions and gels, methods of studying molecular weights and molecular-weight distributions, the structure of high polymers as revealed by X-rays and other means, and the relation of mechanical properties to structure. This section includes the statistical treatment of long-chain molecules and its application to the problem of rubber elasticity.

Though in matters of detail specialists will no doubt find points which may be criticised in the light of the most recent knowledge, this book can be unreservedly recommended as an introduction to this wide and rapidly extending subject. The author has succeeded in producing a very readable text from rather widely scattered sources, and has restricted the mathematical detail to the minimum necessary for an intelligent exposition of the quantitative aspects of the subject. The reader who requires to follow any particular line in more detail will find adequate references to the original papers.

L. R. G. T.

**Annual Reports on the Progress of Chemistry for 1947.** (The Chemical Society, London, 1948.) Pp. 327. Price 20s.

The forty-fourth volume of this well-known and valued survey of the progress of Chemistry includes reports on General and Physical Chemistry, Inorganic Chemistry, Organic Chemistry, Biochemistry, and Analytical Chemistry. The first part, which will probably be most interesting to members of the Faraday Society, has a report on the kinetics of electrode processes and one on far ultra-violet spectra. The section on Inorganic Chemistry has a short but informative account of the transuranic elements and a long and rather speculative article on intermediate compounds in inorganic reactions. In the Organic Chemistry section there is a survey of fluoro-hydrocarbons and related compounds, terpenes and steroids. The Analytical Chemistry section contains a brief summary of the applications of statistics in chemical analysis. The volume, although containing a large amount of material and full references to the literature

is on the whole very readable, and amply fulfils the purpose of the reports in providing surveys of topics of special interest which are likely to be of value to students, research workers and all who wish to keep abreast of modern developments in the science. The printing is very good, but the paper is rather thin, and attention should be given to improvement of this in future issues. At a time when plenty of excellent paper is available for quite worthless publications, those who might be expected to do something in helping important scientific publications to get their share of what is good should fulfil their obligations.

J. R. P.

**An Introduction to the Chemistry of Carbohydrates.** By JOHN HONEYMAN. (Oxford University Press, 1948.) Pp. 143. Price 15s. net.

This book will, without doubt, prove of great value to students of carbohydrate chemistry.

The monosaccharides are dealt with skilfully and the author has not hesitated to include modern work. Presumably, owing to limitations of space, an occasional lack of balance may be detected, for example, in the section on disaccharides where the synthetic work of B. Helferich is not mentioned. Space could have been saved in the chapter on polysaccharides by modifying the formulæ for starch (p. 129) and dextrin (p. 131) which are likely to be confusing to students and could be simplified. One sympathises with Dr. Honeyman in his attempts to introduce important references, but in some cases he runs into difficulties by selecting one author as the key, for example, in connection with the constitution of chondrosamine (p. 80) and the synthesis of cellobiose (p. 96). Furthermore, it is unfortunate that the dates for references to chain length determinations by end-group assay (pp. 124, 126, 132) are given as 1928 and not 1932. The high quality of the book can be judged by the fact that this last is one of the few actual errors, apart from a few misprints, and, although everyone will not agree with the formula ascribed to inulin (p. 133), the author is to be congratulated on the production of a readable text-book on carbohydrates which is sure of a warm welcome.

E. G. V. P.

**Multiple-Beam Interferometry of Surfaces and Films.** By S. TOLANSKY. (Geoffrey Cumberlege, at the Oxford University Press, 1948.) Pp. viii + 187. Price 18s.

Prof. Tolansky's earlier books, *Fine Structure in Line Spectra and Nuclear Spin* (Methuen, 1934), *High Resolution Spectroscopy* (Methuen, 1946), and *Introduction to Atomic Physics* (Longmans, Green and Co., 1942) will be familiar to many. In this latest work he describes in the same clear crisp style his techniques for studying fine-scale topography and optical properties of surfaces and thin films. These techniques were developed since 1942 at Manchester University and are now being continued at Royal Holloway College, London University, and the many illustrations here show well that peculiar beauty and sharpness of detail which are now widely known and appreciated.

As the preface points out, the methods described in this book will be valuable to chemists, crystallographers, metallurgists and others, as well as to the optics specialist. The first four chapters will be especially helpful to these general users, since they introduce briefly but clearly the important cases of two-beam and multiple-beam interference, the silvering technique, and silver-modified Newton's rings applied to direct estimation of phase-change in the reflection of light by metals. The results obtained by multiple-beam methods (Fizeau fringes) applied to the topography of quartz, mica, selenite and calcite are discussed in Chapter V. Chapter VI on crossed Fizeau fringes from diamonds, and Chapter VII on doubly silvered films (of mica) describe extensions of the technique. Next, in Chapter VIII, come the important "fringes of equal chromatic order", and in Chapters IX, X, and XI applications to mica, calcite and diamonds. Chapter XII shows how the methods can be applied to opaque substances and metals, XIII discusses replica techniques, XIV the principles of interferometric colour filters and monochromators, and XV non-localised multiple-beam fringes.

Apart from the techniques and the general topographical results, the high-lights are the data obtained about phase-change in reflection at metal surfaces (p. 43), birefringence measurements throughout a large spectral range (p. 114), measurement of thickness of thin films (p. 147), and details of interferometric colour filters (p. 161 ff.). The topographical results on crystal cleavage are important, especially for mica (pp. 61-2), though the frequent comparison with electron microscopy is hardly appropriate. The often-made reference to cleavage steps as being a number of *molecules* high, or flat to one *molecule*, is also an unfortunate misconception in relation to ionic crystals, where there are no distinct molecules present, and it is an anachronism from the 18th century period of Haüy and Romé de L'Isle.

It is also desirable to note that these interferometric methods give an *average* film thickness where the surface has roughnesses of the order of a few atomic diameters in extent, as electron-diffraction reflection photographs show is in general the case with silver or similar deposits. The references to film thicknesses and silver-film densities (not actual silver density, which is effectively a constant) should therefore be understood in this way.

Finally, the reader will be perhaps only temporarily disconcerted by several errors in the references (correct the second [23] on p. 45 to [24]; [24] on p. 57 to [25]; [29] on p. 43 to [20]; and add [16] after figure 16 on p. 30); and by the lack of references in the later chapters even where a date follows an author's name (p. 181). In general, however, the book is well produced and will be much used and appreciated.

H. W.

# DIAMAGNETIC SUSCEPTIBILITY OF AMMONIUM COMPOUNDS

BY M. E. BEDWELL, J. F. SPENCER AND V. C. G. TREW

Received 24th July, 1946, as amended 21st July, 1948

The diamagnetic mass susceptibility of the ammonium halides in solution and in the solid state has been determined, and values for the gram ionic susceptibility of the ammonium ion in various co-ordination states have been deduced, using the appropriate anionic correcting constants. The molar susceptibility and co-ordination number show a linear relationship for each halide, and extrapolation gives values of molar susceptibility for the free ions. Measurements have also been made on nine further compounds of ammonium, and an estimate of the susceptibility of the ammonium ion has been made in those cases where data are available.

Comparison of the experimental figures with those calculated theoretically indicates that the extrapolated experimental figures for free ions are in closest agreement with theoretical values calculated by Slater's method.

The systematic investigation of the diamagnetic susceptibility of polar compounds has been undertaken by a number of workers in recent years. In 1932 Kido<sup>1</sup> measured the magnetic susceptibility of certain alkali and ammonium salts. He noted a linear relationship between molar magnetic mass susceptibility and the number of electrons in the cation for the series of alkali salts with the same anion, and a similar relationship for the halide series with the same cation. From these results he deduced values for the ionic mass susceptibility of alkali and halide ions but made no attempt to allow for variation of co-ordination numbers in the salts concerned. Later Brindley and Hoare<sup>2,3,4</sup> carried out a systematic investigation of the diamagnetic susceptibility of the alkali halides showing that slightly greater values for the susceptibility of the salts were obtained in the dissolved state than in the solid state. This conclusion was supported by the subsequent work of Flordal and Frivold<sup>5</sup> and of Fahlenbrach.<sup>6</sup> Brindley and Hoare also derived values for the ionic susceptibility of anions and cations in different co-ordination states, investigating the influence of adjacent ions upon the ion concerned. More recently Klemm<sup>7</sup> has suggested values for a large number of ionic susceptibility constants, in which he has made corrections for the co-ordination effects, while Frivold and Olsen<sup>8</sup> have made similar corrections in the case of the alkali halides. On theoretical grounds Klemm<sup>7</sup> and Trew<sup>9</sup> independently have pointed out that the ionic susceptibilities of a related series e.g. alkali metal or halogen ions should not be a linear function of the number of electrons in the ion, but should be related to the numerical periodicity of the electron shells of the ions concerned.

<sup>1</sup> Kido, *Sci. Rep. Tohoku Imp. Univ.*, 1932, **21**, 149, 288, 869; 1933, **22**, 835.

<sup>2</sup> Brindley and Hoare, *Proc. Roy. Soc. A*, 1935, **152**, 342.

<sup>3</sup> Brindley and Hoare, *ibid.*, 1937, **159**, 395.

<sup>4</sup> Brindley and Hoare, *Trans. Faraday Soc.*, 1937, **33**, 268.

<sup>5</sup> Flordal and Frivold, *Ann. Physik*, 1935, **23**, 425.

<sup>6</sup> Fahlenbrach, *ibid.*, 1935, **24**, 485.

<sup>7</sup> Klemm, *Z. anorg. Chem.*, 1941, **246**, 347.

<sup>8</sup> Frivold and Olsen, *Auhandl. Norsk. Vidensk. Akad.*, 1940, **2**, 16.

<sup>9</sup> Trew, *Trans. Faraday Soc.*, 1941, **37**, 476.

Kido's apparently linear results would seem to arise mainly from a neglect of co-ordination effects.

Less attention has been paid to salts of ammonium than to those of the alkali metals and there is considerable variation in the results of different investigators. The present work was undertaken to investigate the general additivity relationships for the ammonium salts, and to study the influence of co-ordination upon the susceptibility of the ammonium ion.

## Experimental

**Preparation of Compounds.**—Wherever possible A.R. materials were used and these were further purified by careful recrystallisation. The compounds were especially examined for ferromagnetic impurities, iron, nickel and cobalt, and only materials giving negative reactions were used for the magnetic measurements. In all cases, as a further test of purity, the anion content of the compounds was determined and material rejected for which duplicate analyses varied by more than 0.2 % from the theoretical amount. All specimens were carefully dried before use.

**Measurement of Susceptibility.**—Magnetic susceptibility measurements were carried out at room temperature, using a modified Gouy method, precautions being taken to eliminate various sources of error and obtain concordant results as described in previous papers.<sup>10, 11</sup>

## Results

Tables I(a) and (b) summarise the results obtained for the diamagnetic susceptibility of the ammonium halides in the solid state and in aqueous solution, and of the other salts investigated. The values in solution were calculated, assuming additivity, from the relationship

$$\chi_{\text{measured}} = w_1\chi_{\text{solvent}} + w_2\chi_{\text{solute}}$$

where  $w_1$  and  $w_2$  are weights per cent. of solvent and solute respectively. The last column shows the susceptibility values obtained by other investigators, where these are available.

TABLE I.—DIAMAGNETIC MASS SUSCEPTIBILITY OF AMMONIUM COMPOUNDS<sup>1</sup>

(a)

Compound	State	Co-ordination Number	$-10^6 \cdot \chi_M$	$-10^6 \cdot \chi_M$ (literature)
NH <sub>4</sub> F *	Solid	4	$23.0 \pm 0.04$	$24.5^1$
	Solution 16.9 %	4	$23.5 \pm 0.11$	
NH <sub>4</sub> Cl *	Solid	8	$36.7 \pm 0.21$	$34.2,^1 35.7,^{12} 36.2^{13}$
	Solution 16.8 %	4	$38.5 \pm 0.16$	—
NH <sub>4</sub> Br	Solid	8	$47.0 \pm 0.30$	$47.4,^1 46.7,^{12} 46.2^{13}$
	Solution 16.7 %	4	$49.8 \pm 0.30$	—
NH <sub>4</sub> I *	Solid	6	$64.4 \pm 0.15$	$66.0,^1 69.5,^{12} 64.1^{13}$
	Solution 16.8 %	4	$66.4 \pm 0.16$	—

The % composition of solutions refers to grams solute per 100 g. solution.

\* The experimental data for the ammonium halides (with the exception of the bromide), in the solid state have been previously published<sup>9</sup> but are included here for the purposes of detailed discussion in relation to co-ordination number.

<sup>10</sup> Trew and Watkins, *Trans. Faraday Soc.*, 1933, **29**, 1310.

<sup>11</sup> French and Trew, *ibid.*, 1945, **41**, 439.

<sup>12</sup> Duchemin, *Compt. rend.*, 1931, **199**, 571.

<sup>13</sup> Dinsdale and Long, *Proc. Leeds Phil. Soc.*, 1937, **3**, 270.

(b)

Compound	State	$-10^6 \cdot \chi_M$	$-10^6 \cdot \chi_M$ (literature)
$\text{NH}_4\text{NO}_3^*$	Solid	$32.6 \pm 0.16$	$33.6^1$
	Solution 14.1 %	$38.9 \pm 0.27$	
$\text{NH}_4\text{VO}_3$	Solid	$-8.1 \pm 0.23$	$-14.04,^{14} -14.04^{15}$
$\text{NH}_4\text{OH}$	Solution 35 %	$31.5 \pm 0.15$	—
$(\text{NH}_4)_2\text{SO}_4$	Solid	$67.0 \pm 0.70$	$75.4,^{16} 63.2^{12}$
$(\text{NH}_4)_2\text{SO}_4 \cdot \text{H}_2\text{O}$	Solid	$70.3 \pm 0.67$	—
$(\text{NH}_4)_2\text{S}_2\text{O}_8$	Solid	$75.1 \pm 0.59$	—
$(\text{NH}_4)_2\text{CrO}_4$	Solid	$-1.0 \pm 0.38$	—
$(\text{NH}_4)_2\text{Cr}_2\text{O}_7$	Solid	$-37.8 \pm 0.75$	—
$(\text{NH}_4)_6\text{Mo}_7\text{O}_{24} \cdot 4\text{H}_2\text{O}$	Solid	$163.1 \pm 0.84$	—

### Discussion

The experimental figures for the susceptibility of the ammonium halides in Table I(a) are in good agreement with previously published values,<sup>1, 12-16</sup> the closest agreement being with the most recent results, those of Dinsdale and Long.<sup>13</sup> It will be noted that the values for the susceptibilities of salts in solution are slightly higher than the corresponding values for the solid state. This result is in agreement with the observations of Brindley and Hoare<sup>2-4</sup> for the alkali halides and was explained by them as due to the reduction in the co-ordination number of the ions when in the dissolved state. In order to investigate this effect more fully, values for the susceptibility of salts containing the ammonium ion in various states of co-ordination have been calculated from the experimental figures of Table I.

For strongly polar salts, such as the alkali halides, it can be assumed that the molar diamagnetic susceptibility is solely made up of the sum of the ionic susceptibility values for the anion and the cation, provided that the ions are in the same co-ordination state. This assumption has been shown to hold for the salts of the alkali halides and thus should be applicable to the ammonium salts. In the crystalline state the co-ordination number of the ammonium ion is known for the various halides, and for large ions in solution can be taken as four.<sup>17</sup> The experimental molar susceptibility thus represents the sum of the susceptibility values for the cation and anion in the particular co-ordination state of the crystal in question, and values for other states require to be calculated. This can be done by a method similar to that used by Brindley and Hoare<sup>3</sup> for the alkali ions, using the values given by them for the susceptibility of halide ions in various co-ordination states. From the experimental molar susceptibilities, complete sets of values can thus be obtained for the four ammonium halides in four-, six-, and eight-fold co-ordination. Table II (columns 2-5) shows the values obtained in this way. The detailed calculation by which the figures were obtained for co-ordination number eight provides an illustration of the method involved. Subtracting the values<sup>3</sup> for the susceptibility of the chloride and bromide ions in eight-fold co-ordination from the respective experimental molar susceptibilities (Table I) gives a value for the susceptibility of the ammonium ion in eight-fold co-ordination, thus : \*

<sup>14</sup> Ray Chaudhuri, *Indian J. Physics*, 1936, **10**, 245.

<sup>15</sup> Meyer, *Ann. Physik*, 1899, **68**, 325.

<sup>16</sup> Gray and Farquharson, *Phil. Mag.*, 1930, **10**, 191.

<sup>17</sup> Bernal and Fowler, *J. Chem. Physics*, 1933, **1**, 515.

\* All molar and ionic diamagnetic susceptibility values quoted in the text are given in c.g.s. units  $\times (-10^6)$ , and paramagnetic values in c.g.s. units  $\times 10^6$ .



$$\chi_{\text{NH}_4\text{Cl}(\text{s})} - \chi_{\text{Cl}^-(\text{s})} = \chi_{\text{NH}_4^+(\text{s})} \quad \text{and} \quad \chi_{\text{NH}_4\text{Br}(\text{s})} - \chi_{\text{Br}^-(\text{s})} = \chi_{\text{NH}_4^+(\text{s})}$$

$$36.7 - 22.9 = 13.8 \quad 47.0 - 33.4 = 13.6$$

whence a mean value of  $\chi_{\text{NH}_4^+(\text{s})} = 13.7$  is obtained.

TABLE II.—THEORETICAL, EXPERIMENTAL AND DERIVED DIAMAGNETIC SUSCEPTIBILITIES ( $-10^6\chi$ ) FOR THE AMMONIUM ION AND SALTS WITH VARIOUS CO-ORDINATION NUMBERS

C.N. = Co-ordination number. Values in brackets are the derived values. Addition of the corresponding values for the singly charged halide ion, in each case, gives the figures in columns 7-9.

	Experimental and Derived Values $\times (-10^6)$ c.g.s.					Theoretical Values $\times (-10^6)$ c.g.s.		
	Crystal C.N.8	Crystal C.N.6	Crystal C.N.4	Aqueous Solution C.N.4	Extrapol. Value C.N.zero	Method of Pauling	Method of Slater	Method of Angus
$\text{NH}_4^+$	13.7	13.8	—	14.2	14.5	15.1	15.0	13.9
$\text{NH}_4\text{F}$	(22.4)	(23.2)	23.0	23.5	(24.6)	23.2	23.1	21.0
$\text{NH}_4\text{Cl}$	36.7	(38.0)	—	38.5	(40.7)	44.1	40.3	36.3
$\text{NH}_4\text{Br}$	47.0	(48.3)	—	49.8	(52.3)	69.1	54.3	49.0
$\text{NH}_4\text{I}$	(62.5)	64.4	—	66.4	(70.2)	95.1	73.6	68.1

The theoretical figures were calculated as follows. In the ammonium ion the unit positive charge is considered as divided approximately equally among the five atoms,<sup>30</sup> each having a resultant charge of about  $+0.2$ . Using the theoretical susceptibility values for atoms with whole number charges which have been calculated by the Pauling,<sup>26</sup> Slater,<sup>27</sup> and modified Slater (Angus)<sup>28</sup> methods, we have, in terms of  $-10^6\chi$  the following values:

	Pauling		Slater		Angus	
$\text{N}^{+1}$	$0.2 \times 5.91$	1.2	$0.2 \times 5.36$	1.1	$0.2 \times 4.67$	0.9
$\text{N}^0$	$0.8 \times 8.28$	6.6	$0.8 \times 7.93$	6.3	$0.8 \times 6.73$	5.4
$\text{H}^{+1}$	$4 \times 0.2 \times 0$	0.0	$4 \times 0.2 \times 0$	0.0	$4 \times 0.2 \times 0$	0.0
$\text{H}^0$	$4 \times 0.8 \times 2.273$	7.3	$4 \times 0.8 \times 2.370$	7.6	$4 \times 0.8 \times 2.370$	7.6
	$\therefore \chi_{\text{NH}_4^+} = 15.1$		$\therefore \chi_{\text{NH}_4^+} = 15.0$		$\therefore \chi_{\text{NH}_4^+} = 13.9$	

From this figure, calculated values for the molar susceptibilities of the two remaining halides, ammonium fluoride and iodide with co-ordination number eight can be obtained by addition of the values for these anions with that co-ordination number:

$$\chi_{\text{NH}_4^+(\text{s})} + \chi_{\text{F}^-(\text{s})} = \chi_{\text{NH}_4\text{F}(\text{s})} \quad \text{and} \quad \chi_{\text{NH}_4^+(\text{s})} + \chi_{\text{I}^-(\text{s})} = \chi_{\text{NH}_4\text{I}(\text{s})}$$

$$13.7 + 8.7 = 22.4 \quad 13.7 + 48.8 = 62.5$$

Similar calculations give the remaining figures in Table II (columns 2-5). The value for the fluoride ion with co-ordination number eight is not given by Brindley and Hoare. For the sake of completing the data on the ammonium ion, a value for the fluoride ion in eight-fold co-ordination, could this be realised, was estimated by assuming a percentage change on passing from co-ordination number six to eight of the same order as for the chloride ion. It will be seen that the average change in molar susceptibility for a change in co-ordination number of two units is 3%. This may be compared with a similar figure of about 4% for the caesium halides obtained by Brindley and Hoare.<sup>1</sup>

Values for the ionic susceptibility of the ammonium ion with various co-ordination numbers follow from the experimental results. Thus,

subtracting the value for the susceptibility of the halide ion in the appropriate state,  $\chi_{\text{NH}_4^+(s)} = 13.7$  from the chloride and bromide measurements, and  $\chi_{\text{NH}_4^+(s)} = 13.8$  from the iodide measurement. Values for the susceptibility of the ammonium ion in the dissolved state calculated by means of Brindley and Hoare's suggested values for halide ions in solution<sup>4</sup> are not, however, satisfactory. Thus, if the values  $\chi_{\text{F}^-}(\text{dissolved}) = 10.3$ ,  $\chi_{\text{Cl}^-}(\text{dissolved}) = 25.1$ ,  $\chi_{\text{Br}^-}(\text{dissolved}) = 36.4$  and  $\chi_{\text{I}^-}(\text{dissolved}) = 54.2$  are subtracted from the measured susceptibility values, the susceptibility of the ammonium ion in solution follows, namely  $\chi_{\text{NH}_4^+}(\text{dissolved}) = 13.2$  from the fluoride measurement, 13.4 from the chloride, 13.4 from the bromide and 12.2 from the iodide, all values lower than those in the solid state with higher co-ordination number. An alternative method for assessing the contribution of the ammonium ion to the total susceptibility in the dissolved state, that is not dependent on the absolute magnitude of the halide ion contribution, is to assume that the same proportional contribution of the total susceptibility is made by anion and cation whether in the solid state or in solution.

The ratio

$$\frac{\chi_{\text{NH}_4^+}(\text{dissolved})}{\chi_{\text{NH}_4\text{X}}(\text{dissolved})} = \frac{\chi_{\text{NH}_4^+}(\text{cryst.})}{\chi_{\text{NH}_4\text{X}}(\text{cryst.})}$$

(where  $\text{NH}_4\text{X}$  signifies the halide salts) will give the required value for  $\chi_{\text{NH}_4^+}(\text{dissolved})$  since  $\chi_{\text{NH}_4^+}(\text{cryst.})$  is as given above for the six- and eight-fold co-ordination states; the values for the susceptibility of the salt in solution and in the solid state are as in Table I and hence  $\chi_{\text{NH}_4^+}(\text{dissolved})$  follows. This method gives  $\chi_{\text{NH}_4^+}(\text{dissolved}) = 14.5$  from the chloride, 14.4 from the bromide and 13.8 from the iodide, representing a mean value of 14.2 for the susceptibility of the ammonium ion with co-ordination number four in the dissolved state. This value is higher than that obtained for the six- and eight-fold co-ordination states and hence is in line with the general trend of increase in susceptibility with fall in co-ordination number. This method for obtaining a value for  $\chi_{\text{NH}_4^+}(\text{dissolved})$  is supported by the application of an equation relating the diamagnetic susceptibility of an ion in solution to that in the solid state proposed recently by Lee.<sup>18</sup> Pointing out that the transfer of an ion from the crystalline state to solution involves the two factors of an increase in susceptibility due to a release of the ion from a strong field in which mutual deformation occurs, and a counter effect of a deformation of some of the water molecules due to the introduction of an ion into their vicinity, which will of course lower the susceptibility of the solution, he suggests a relationship  $-\chi_s = a_1(-\chi_c) - b_1$ , where  $-\chi_s$  and  $-\chi_c$  are the ionic susceptibilities in solution and the solid state respectively expressed in  $10^6$  c.g.s. units and  $a_1$  and  $b_1$  are constants. For univalent anions and cations,  $a_1 = 1.09$  and  $b_1 = 1.0$ . Lee shows that this relationship holds to within  $\pm 0.3$  unit of susceptibility for the alkali and halide ions. Applying this to the present data and taking  $\chi_{\text{NH}_4^+}(\text{cryst.}) = 13.7$ , the calculated value for  $\chi_{\text{NH}_4^+}(\text{dissolved}) = 13.9$  in good agreement with the experimental value of 14.2 obtained above, on the assumption that the proportional change in susceptibility is the same for each univalent ion on transferring from the solid state to the dissolved state. Thus the susceptibility of the ammonium ion in solution is 14.0 rather than 16 units of susceptibility tentatively suggested by Brindley and Hoare.<sup>4</sup>

If the susceptibility values of Table II (columns 2-5) are plotted against the appropriate co-ordination number of the salt in question the points lie on five straight lines, one for the ammonium ion and one for each

<sup>18</sup> Lee, *J. Chinese Chem. Soc.*, 1945, **12**, 81.

halide, a result similar to that for the alkali halides. Extrapolation of the straight lines to zero co-ordination number gives the values shown in column 6 of Table II. These may be taken to represent the susceptibility values for the free ion in the case of ammonium, and for the state of zero co-ordination number for the salts, i.e. a state in which the co-ordination effects have been eliminated. These susceptibility values may be compared with theoretical values.

It has already been pointed out<sup>9</sup> that on plotting the experimental results for the solid halides of Table I against the effective charge of the anion, a graph results which shows the periodicity expected from the change in number of electrons in the electron shells of the anion on passing from fluoride to iodide, and that this graph is reasonably parallel with those for the alkali salts. A slight deviation from the parallel relationship occurs with ammonium iodide and fluoride due to the difference in co-ordination number of the ammonium ion in these salts from that in the chloride and bromide.

In Table I(b) where the co-ordination number data are inadequate, the values for the susceptibility of the ammonium ion were calculated in those cases where data for the anionic contribution to the susceptibility were available, although no allowance could be made for change in co-ordination number. A value of  $\chi_{\text{NR}_4^+} = 13.7$  was obtained for the susceptibility of the ammonium ion in the nitrate and  $\chi_{\text{NH}_4^+} = 13.5$  in the sulphate, using the anionic values suggested previously.<sup>9</sup> These values are in good agreement with that obtained from the halide series showing that any change in co-ordination number has only a small effect. Since no experimental anionic values were available for the thiosulphate, chromate, and dichromate ions, these were estimated from recent experimental measurements on the sodium and potassium salts of these anions by subtracting the cationic contributions.\* The considerable variation in the experimental susceptibility values of different investigators for the same salt make the conclusions rather uncertain, but the results are

\* The method of calculation is as follows :

$\chi_{\text{Na}_2\text{S}_2\text{O}_3} = 61.8$ ,<sup>19</sup> whence subtracting twice  $\chi_{\text{Na}^+} = 6.8$ <sup>9</sup> gives  $\chi_{\text{S}_2\text{O}_3^{2-}} = 48.2$ .

Correspondingly from  $\chi_{\text{K}_2\text{S}_2\text{O}_3} = 75.9$ ,<sup>20</sup> subtracting twice  $\chi_{\text{K}^+} = 14.9$ <sup>9</sup> gives  $\chi_{\text{S}_2\text{O}_3^{2-}} = 46.1$ , giving a mean  $\chi_{\text{S}_2\text{O}_3^{2-}} = 47.2$ . This, subtracted from the experimental figure for ammonium thiosulphate in Table I(b), gives the value  $\chi_{\text{NH}_4^+} = 14.0$ . Kido's<sup>1</sup> figure for the susceptibility of sodium thiosulphate trihydrate was not used in this calculation since if the full value for the susceptibility of the three molecules of water of crystallisation is subtracted it gives a very much lower value for the susceptibility of the anion than either of the other two values used.

(2) The paramagnetic susceptibility of sodium chromate is  $\chi_{\text{Na}_2\text{CrO}_4} = 19.4$ ,<sup>21</sup> and  $\chi_{\text{Na}_2\text{CrO}_4} = 11.0$ ,<sup>22</sup> whence the paramagnetic susceptibility  $\chi_{\text{CrO}_4^{2-}} = 33.0$  and  $24.0$ , subtracting twice  $\chi_{(\text{dia.})\text{Na}^+}$ . Similarly from the paramagnetic values for the susceptibility of  $\text{K}_2\text{CrO}_4 = 4.0$ ,<sup>22, 23</sup> and  $0.0$ ,<sup>21</sup> the paramagnetic susceptibility  $\chi_{\text{CrO}_4^{2-}} = 25.8$ ,  $25.8$ ,  $29.8$ , giving a mean of the five values of  $\chi_{\text{CrO}_4^{2-}} = 27.8$  for the paramagnetic susceptibility of the chromate ion, and hence  $\chi_{(\text{dia.})\text{NH}_4^+} = 13.4$  from the data for ammonium chromate in Table I.

(3) Similarly the values available for the paramagnetic susceptibility of potassium dichromate are  $\chi_{\text{K}_2\text{Cr}_2\text{O}_7} = 37.9$ ,<sup>24</sup>  $54.0$ ,<sup>21</sup>  $31.8$ ,<sup>14</sup>  $15.0$ ,<sup>22</sup> whence the paramagnetic value  $\chi_{\text{Cr}_2\text{O}_7^{2-}} = 64.5$  follows as a mean value, giving  $\chi_{(\text{dia.})\text{NH}_4^+} = 13.4$ .

<sup>19</sup> Pascal, *Compt. rend.*, 1921, 173, 712.

<sup>20</sup> Farquharson, *Phil. Mag.*, 1932, 14, 1003.

<sup>21</sup> Gray and Dakers, *ibid.*, 1931, 11, 297.

<sup>22</sup> Tilk and Klemm, *Z. anorg. Chem.*, 1939, 240, 355.

<sup>23</sup> Trew, *Trans. Faraday Soc.*, 1936, 32, 1655.

<sup>24</sup> Endo, *Sci. Rep. Tohoku Imp. Univ.*, 1925, 14, 479.

included as they give a value for the susceptibility of the ammonium ion of the same order of magnitude as that derived from the halide salts. Thus  $\chi_{\text{NH}_4^+} \approx 14.0$  from the thiosulphate measurement and 13.4 from both chromate and dichromate.

**Comparison of Theoretical and Experimental Diamagnetic Susceptibilities.**—A number of methods for calculating theoretical diamagnetic susceptibilities have been proposed,<sup>25-28</sup> and have been frequently discussed so that details need not be given here. The theoretical susceptibilities for the ammonium ion, calculated by the methods of Pauling,<sup>25</sup> Slater,<sup>27</sup> and Angus,<sup>28</sup> are summarised in Table II (columns 7-9). Following the method originally applied by Gray and Cruickshank,<sup>29</sup> allowance has been made for the partial shift in charge, due to unequal sharing of electrons as determined from dipole measurements. The theoretical values for the susceptibilities of the halides have been calculated assuming that the linkings between the ammonium and halide ions are completely polar. It will be seen that for the ammonium ion itself, the theoretical molar susceptibility calculated by Angus' method,  $\chi_{\text{NH}_4^+} = 13.9$ , agrees most closely with the experimental value,  $\chi_{\text{NH}_4^+} = 13.6-13.8$ , for the ion in combination with univalent anions in solid crystals. The values obtained when the experimental susceptibilities of the salts are extrapolated to co-ordination number zero are in closest agreement with susceptibilities calculated by Slater's method in which semi-empirical rules for obtaining the screening constants in the ions are used.

An increasing divergence between theoretical and experimental susceptibilities occurs as the effective atomic number of the salt increases, a result similar to that found for the alkali and other salts.<sup>9, 23, 31</sup> For all the halides except the fluoride, calculations by Pauling's method give, as in these other cases, theoretical susceptibilities which are higher than the experimental for salts of heavier ions. When, however, as in Slater's method of calculating atomic and ionic susceptibilities, modified screening constants are used for the *N*-shell of electrons and beyond, the resultant theoretical susceptibility is brought very much closer to that for the salt corrected for the co-ordination effects, as a comparison of column 6 with column 8 of Table II will show. Angus' further suggestion that the contribution of *s* and *p* shells of electrons to the susceptibility should be computed separately, brings the final calculated molar susceptibility below the experimental values corrected for co-ordination effects, and so would appear unjustified by the experimental results.

Bedford College,  
Regents Park,  
London, N.W.1.

<sup>25</sup> Pauling, *Proc. Roy. Soc. A*, 1927, **114**, 181.

<sup>26</sup> Hartree, *Proc. Camb. Phil. Soc.*, 1928, **89**, 111; *Proc. Roy. Soc. A*, 1933, **141**, 282.

<sup>27</sup> Slater, *Physic. Rev.*, 1930, **36**, 57.

<sup>28</sup> Angus, *Proc. Roy. Soc. A*, 1932, **136**, 569.

<sup>29</sup> Gray and Cruickshank, *Trans. Faraday Soc.*, 1935, **31**, 1491.

<sup>30</sup> Pauling, *Nature of the Chemical Bond* (1940).

<sup>31</sup> Brindley, *Phil. Mag.*, 1931, **13**, 786.

# THE DISSOCIATION CONSTANT OF HYDROGEN PEROXIDE AND THE ELECTRON AFFINITY OF THE HO<sub>2</sub> RADICAL

BY M. G. EVANS AND N. URI

Received 6th September, 1948

Measurements are described on the dissociation constant of hydrogen peroxide in aqueous solution and from these measurements at different temperatures the heat of dissociation is evaluated. This value has enabled us to estimate the electron affinity plus the solvation energy of the O<sub>2</sub>H radical. Values of  $\Delta G$ ,  $\Delta H$  and  $\Delta S$  for the dissociation of water and hydrogen peroxide are compared. Measurements are also reported on the proton affinity of H<sub>2</sub>O<sub>2</sub>. Calculations based on existing data are given for the electron affinities and solvation energies of OH, O<sub>2</sub>H, O<sub>2</sub> and O<sub>2</sub><sup>-</sup>.

**Introduction.**—The strengths of the various bonds in molecules and radicals of oxygen and hydrogen atoms are of importance in discussions of the energetics of many oxidation reactions both in the gas phase and in solution. The electron affinities of radicals and the solvation energies of the ions are quantities which are required in considering many electron-transfer reactions in solution. In this paper we present new measurements concerning the dissociation constant and the proton affinity of hydrogen peroxide in aqueous solution and use these values together with existing data to obtain some of the fundamental quantities referred to above. Many of these quantities have been evaluated by Weiss<sup>1</sup> but the data which are now available enable one to make more certain estimates.

**The Dissociation Constant of Hydrogen Peroxide.**—In 1912 Joyner<sup>2</sup> evaluated the hydrolysis of NaHO<sub>2</sub> by measuring (a) the ratio of saponification of ethyl acetate in the presence of NaHO<sub>2</sub>, (b) the distribution of undissociated hydrogen peroxide between water and amyl alcohol, and (c) the conductivity of a solution of NaHO<sub>2</sub>.

He obtained the following values for the acid dissociation of hydrogen peroxide in dilute aqueous solution at 0° C :

METHOD (a)	METHOD (b)	METHOD (c)
0.77 × 10 <sup>-12</sup>	0.59 × 10 <sup>-12</sup>	0.64 × 10 <sup>-12</sup>

He also measured the heat of the reaction,



at 0° C, by direct thermochemical measurement of the heat of neutralisation and obtained a value of  $\Delta H^\circ = + 8.6$  kcal. The lack of any consideration of the influence of ionic strength in Joyner's experiments has necessitated a re-determination of the dissociation constant of H<sub>2</sub>O<sub>2</sub>, taking into account the influence of the ionic strength of the solution.

It has been shown by Reichert and Hull<sup>3</sup> that the glass electrode is

<sup>1</sup> Weiss, *Trans. Faraday Soc.*, 1935, **31**, 966 and 668.

<sup>2</sup> Joyner, *Z. anorg. Chem.*, 1912, **77**, 103.

<sup>3</sup> Reichert and Hull, *Ind. Eng. Chem. (Anal.)*, 1939, **11**, 311.

suitable for the measurement of pH in peroxide solutions. We have used aqueous solution of  $\text{H}_2\text{O}_2$  up to 2 M concentration and in this range we consider that the ions present are hydrated  $\text{H}_3\text{O}^+$ ,  $\text{OH}^-$  and  $\text{HO}_2^-$ , and that the concentration of  $\text{H}_2\text{O}_2$  is negligible. We can, therefore, treat the system as a dissociating weak acid and have used the Alkali glass electrode which is now applicable over a pH range of 9-14. We have measured the pH of an  $\text{H}_2\text{O}_2$ -NaOH mixture at various concentrations of sodium perchlorate and at different temperatures. For the evaluation of the pK of dilute  $\text{H}_2\text{O}_2$  up to 2 M the modified Henderson buffer equation has been used :

$$\text{pH} = \text{pK} + \log \frac{[\text{Na}^+]}{[\text{H}_2\text{O}_2]_0 [\text{Na}^+]} - 0.5\sqrt{\mu} + C'\mu \quad (1)$$

It should be added that under the working concentrations the reaction  $\text{OH}^- + \text{H}_2\text{O}_2 \rightarrow \text{HO}_2^- + \text{H}_2\text{O}$  can be regarded as practically complete and thus eqn. (1) is applicable. Fig. 1 shows the dependence of the pH

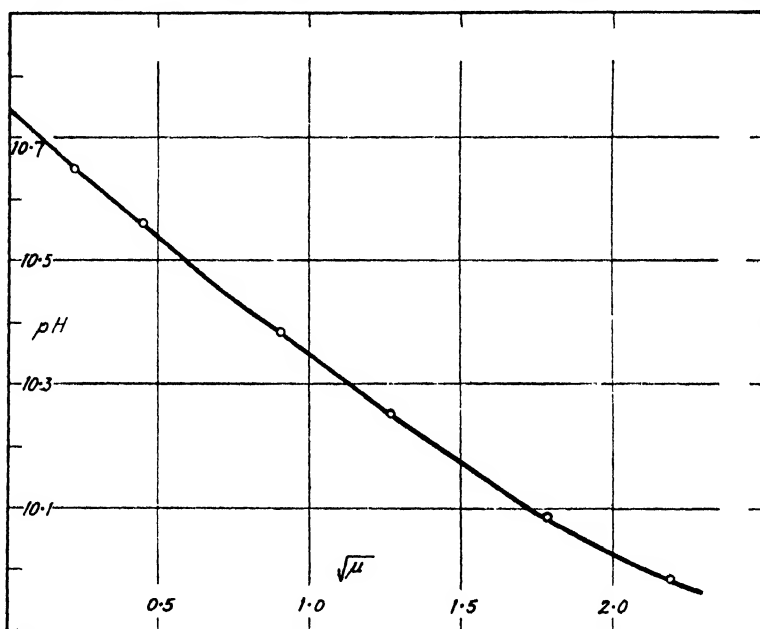


FIG. 1.— $[\text{H}_2\text{O}_2] = 0.55 \text{ M}$ ,  $[\text{NaOH}] = 0.05 \text{ M}$ ,  $\text{pH} = (\text{pK} - 1) - 0.5\sqrt{\mu} \pm 0.08\mu$ .  
Curve corresponding to  $\text{pH} = (\text{pK} - 1) - 0.5\sqrt{\mu} + 0.08\mu$ .

at constant concentrations of 0.05 M NaOH and 0.55 M  $\text{H}_2\text{O}_2$  at a constant temperature of 20° C on the square root of the ionic strength. The variation of the ionic strength of the solution was effected by the addition of sodium perchlorate as neutral electrolyte. From these data the values of  $C'$  and pK have been calculated; the pK value was found to be  $11.75 \pm 0.02$ , which corresponds to a dissociation constant of

$$1.78 \pm 0.1 \times 10^{-12}$$

at 20° C ( $C' = 0.08$ ).

The variations in the value of  $K$  at 20° C determined under the same experimental conditions are shown in Table I. The error in the estimation of the dissociation constant is about  $\pm 5\%$ . The average value of  $K$  at 20° C at zero ionic strength is  $1.78 \times 10^{-12}$ .

<sup>4</sup> Jenkins, *Trans. Faraday Soc.*, 1945, 41, 138.

TABLE I

Expt.	Solution	$K$ (20° C, $\mu = 0$ )	pK
1	0.55M $\text{H}_2\text{O}_2$ + 0.05M NaOH	$1.75 \times 10^{-12}$	11.76
2	"	$1.79 \times 10^{-12}$	11.75
3	"	$1.70 \times 10^{-12}$	11.77
4	"	$1.88 \times 10^{-12}$	11.73

The complete function for the temperature dependence of  $K$  for a weak acid has the form,<sup>3</sup>

$$\log K = A/T + \frac{B \log T}{T} + \frac{C \log^2 T}{T} + D.$$

In this case with the large value of  $A$  we can neglect  $B$  and  $C$  in the small temperature interval between 15° and 35° C. The Alkali glass electrode proved suitable for measurement between 15° and 40° C only. Above 35° C, however, the hydrogen peroxide decomposition is too rapid, so that the effective range for our measurement was within the above-mentioned limit. A straight line is obtained when pK is plotted against  $1/T$  (Fig. 2). The value  $\Delta H$  for the reaction



calculated from the slope of the graph corresponds to + 8.2 kcal. The values obtained are generally in good agreement with those of Joyner.<sup>3</sup>

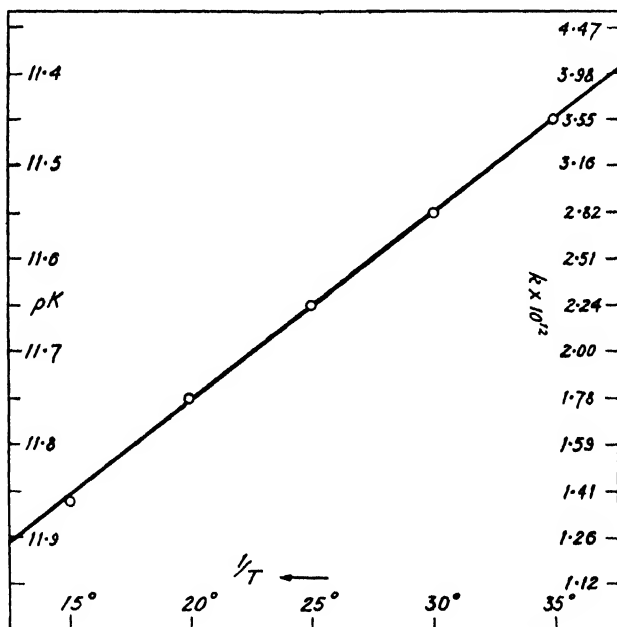
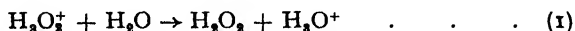


FIG. 2.

At high concentrations of  $\text{H}_2\text{O}_2$ , a striking increase in the hydrogen ion activity has been found. This corresponds to the effect of superacidity observed also in concentrated acetic acid.<sup>5</sup> This suggests that  $\text{H}_3\text{O}_2^+$  is formed and that  $\text{H}_2\text{O}_2$  is a weaker base than  $\text{H}_2\text{O}$ .

<sup>5</sup> Glasstone, *Electrochemistry of Solutions* (3rd Ed., 1945), p. 181.

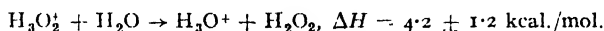
**The Proton Affinity of  $\text{H}_2\text{O}_2$ .**—The above observation suggests that in the reaction



the equilibrium lies over on the right. We have measured the heat of the above change in this following way. Firstly, the heat of dilution of 88 % and 96 %  $\text{H}_2\text{O}_2$  in a large excess of water was measured and by extrapolation a value for the heat of dilution of pure  $\text{H}_2\text{O}_2$  obtained. Secondly, the heat of mixing was measured of a normal perchloric acid solution in 40 M  $\text{H}_2\text{O}_2$  with a large excess of N  $\text{HClO}_4$  solution in water. The temperature increases were measured on a Beckmann thermometer, and the thermal capacities of the systems measured electrically. The results obtained for the heats of dilution are shown in Table II.

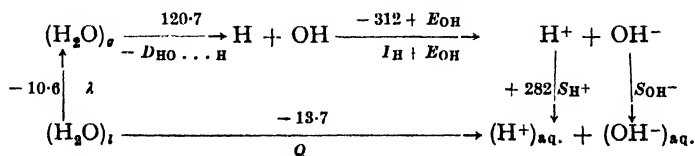
TABLE II

Conc. $\text{H}_2\text{O}_2$	Reaction	$\Delta H$ (kcal./mol.)
88 %	$\text{H}_2\text{O}_2 \rightarrow \text{H}_2\text{O}_2$ (aq.)	- 0.65
96 %	$\text{H}_2\text{O}_2 \rightarrow \text{H}_2\text{O}_2$ (aq.)	- 0.71
100 %	$\text{H}_2\text{O}_2 \rightarrow \text{H}_2\text{O}_2$ (aq.)	- 0.74



In the determination of the heat of dilution of pure hydrogen peroxide ( $\sim 43$  M) the increase in temperature on diluting the hydrogen peroxide with the twelve-fold excess of water was of the order of  $2^\circ$ . The difference in the temperature increase, however, caused by the heat of dilution of  $\sim 40$  M  $\text{H}_2\text{O}_2$  and that of N  $\text{HClO}_4$  in 40 M  $\text{H}_2\text{O}_2$ , with a twelve-fold excess of water in the first case and with a solution of N  $\text{HClO}_4$  in water in the second was of the order of  $0.25^\circ$ - $0.30^\circ$  only. Hence the latter result involves a considerable experimental error. From the difference between these two heats of dilution and extrapolation to pure  $\text{H}_2\text{O}_2$  the heat of the above reaction can be calculated. The experimental results are given in Table II.  $\Delta H$  for the above reaction was evaluated as  $-4.2 \pm 1.2$  kcal./mol. The value of  $\Delta H$ , which is a measure of difference between the proton affinity of  $\text{H}_2\text{O}_2$  and  $\text{H}_2\text{O}$ , is in keeping with the observation that  $\text{H}_2\text{O}_2$  is a weaker base than  $\text{H}_2\text{O}$ . If the entropy change in reaction (1) is negligibly small, then  $\Delta G^\circ \sim \Delta H^\circ$  and  $-4.2$  kcal. and the equilibrium constant  $K \approx 10^3$ .

**The Electron Affinity and Solvation Energy of the OH and  $\text{HO}_2$  Radicals.** (a) Baughan, Evans and Polanyi<sup>6</sup> gave a cycle from which the electron affinity could be obtained from the solvation energy of OH. In the light of new data we now revise this cycle.



The revised value of  $D_{\text{HO} \dots \text{H}}$  is obtained from the heat of formation of water<sup>7</sup> and the value of  $D_{\text{H} \dots \text{O}}$  of Dwyer and Oldenburg.<sup>8</sup> This leads to a value  $(E_{\text{OH}} + S_{\text{OH}^-}) = 147.6$  kcal.

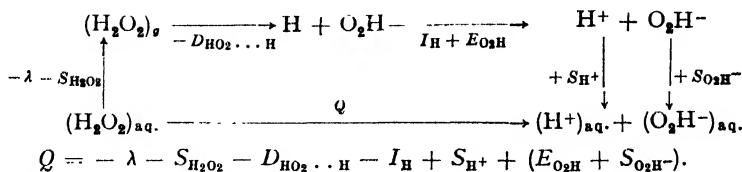
<sup>6</sup> Baughan, Evans and Polanyi, *Trans. Faraday Soc.*, 1941, **37**, 377.

<sup>7</sup> Bichowsky and Rossini, *Thermochemistry of Chemical Substances* (New York, 1936).

<sup>8</sup> Dwyer and Oldenburg, *J. Chem. Physics*, 1944, **12**, 357.

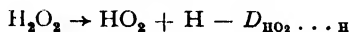


(b) The value of  $(E_{\text{O}_2\text{H}} + S_{\text{O}_2\text{H}^-})$  can be obtained from the following cycle.



The value  $Q = -8.2$  kcal./mol. is given in § 1 of this paper. The latent heat of vaporisation of pure  $\text{H}_2\text{O}_2$  is given by Bichowsky and Rossini<sup>7</sup> as  $+11.6$  kcal./mol.;  $S$  the heat of dilution of pure  $\text{H}_2\text{O}_2$  from our own experiments, is  $+0.74$  kcal./mol.

The value of  $D_{\text{H}_2\text{O}_2 \dots \text{H}}$  corresponding to the heat of the reaction



is uncertain. On the assumption that the energy of the  $-\text{O}-\text{O}-$  bond is the same in  $\text{HO}_2$  as in  $\text{H}_2\text{O}_2$  a value of  $D_{\text{H}_2\text{O}_2 \dots \text{H}}$  of 100 kcal. is obtained. Sokolov,<sup>8</sup> however, suggests that the energy of the  $\text{O}-\text{O}$  bond in  $\text{HO}_2$  is increased by about 2 kcal. over that in  $\text{H}_2\text{O}_2$ .<sup>10</sup> This would give a value of  $D_{\text{H}_2\text{O}_2 \dots \text{H}}$  of 102 kcal. Walsh<sup>11</sup> on the other hand suggests a value of the energy of the  $-\text{O}-\text{O}-$  bond in  $\text{HO}_2$  of 80-90 kcal. which would lead to a value for  $D_{\text{H}_2\text{O}_2 \dots \text{H}}$  of 70-80 kcal. Using the above values for the bond energy, the values of  $(E_{\text{O}_2\text{H}} + S_{\text{O}_2\text{H}^-})$  obtained range over 136 to 106 kcal. It is not possible at present to give a more certain value of  $(E_{\text{O}_2\text{H}} + S_{\text{O}_2\text{H}^-})$ .

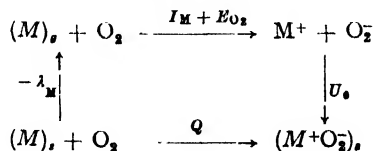
It is interesting to compare the entropy change of dissociation of  $\text{H}_2\text{O}$  and  $\text{H}_2\text{O}_2$ . The thermodynamical constants at  $20^\circ\text{C}$  for the two reactions are given in Table III.

TABLE III

Reactions	pK	$\Delta H$ (kcal.)	$\Delta S$ (cal./deg.)	$\Delta G$ (kcal.)
$\text{H}_2\text{O} \rightarrow \text{H}_3\text{O}^+ + \text{OH}^-$	15.81	13.7	-25.5	21.2
$\text{H}_2\text{O}_2 \rightarrow \text{H}_3\text{O}^+ + \text{HO}_2^-$	11.75	8.2	-25.7	15.8

We note that the difference in  $\Delta G^\circ$  is determined almost entirely by the difference in  $\Delta H^\circ$  and that the value of  $\Delta S^\circ$  for the two reactions is practically identical. This would seem to indicate that the solvation of the two ions  $\text{OH}^-$  and  $\text{O}_2\text{H}^-$  in water is very similar and that the difference between  $(E + S)$  for  $\text{OH}$  and  $\text{O}_2\text{H}$  is mainly a difference in the electron affinity.

**The Electron Affinity of Oxygen.**—(a) A value of this can be obtained from the cycle,



if the latent heat of vaporisation  $\lambda$  of the metal  $\text{M}$ , the ionisation potential  $I_{\text{M}}$  of  $\text{M}$  and the heat of formation  $Q$  of the ionic  $(\text{M}^+\text{O}_2^-)$  can be calculated.

<sup>8</sup> Sokolov, *Acta Physicochim.*, 1944, **19**, 208.

<sup>10</sup> Skinner, *Trans. Faraday Soc.*, 1945, **41**, 645.

<sup>11</sup> Walsh, *J. Chem. Soc.*, 1948, 331.

The heats of formation of  $\text{KO}_2$ ,  $\text{RbO}_2$  and  $\text{CsO}_2$  have been determined as 67.5, 68.8 and 70.5 kcal. respectively.<sup>7, 12</sup>

The crystal structure of these solids have been investigated by Helms and Klemm.<sup>13</sup> The solids have been found to be of the sodium chloride type, the  $\text{O}_2^-$  ion is, however, an asymmetric ion having a major axis of 4.04 Å and a minor of 3.02 Å. The asymmetry of the ion necessitates an evaluation of the Madelung constant for such a lattice. This was determined by summing the terms  $z^2e^2/d$  for the interaction between the ion at the origin and the other ions within a cube, the faces of which cut through the planes of atoms, and summing the rapidly converging energy series which is obtained by this method, when the cube is extended. The recent investigation by Helms and Klemm referred to above provided us with the necessary interionic distance. The lattice energy  $U_0$  is given by

$$U_0 = \frac{Ne^2 A}{(r_{M^+} + r_{m_i})} \left(1 - \frac{1}{n}\right)$$

in which  $N$  is Avogadro's number,  $A = 1.644$  the Madelung constant for this distorted sodium chloride type lattice,  $r_{M^+}$  the radius of the positive ion,  $r_{m_i}$  the minor radius of the oxygen ion and  $n$ , the Born exponent, = 10. Table IV gives the data used in the Born-Haber cycle, the calculated lattice energies and the resulting electron affinity of the oxygen molecule in the gas phase.

TABLE IV

Solid	$\lambda_M$	$I_M$	$Q$	$r_{M^+}$	$U_0$	$E_{O_2}$	Mean $E_{O_2}$
$\text{KO}_2$	21.7	99.6	67.5	1.33	172.2	16.6	} 15.8
$\text{RbO}_2$	19.0	95.0	68.8	1.48	168.2	16.4	
$\text{CsO}_2$	19.1	89.4	70.5	1.69	164.5	14.5	

The solvation energy of the  $\text{O}_2^-$  ion has been calculated assuming free rotation of the ion in solution, and treating the ion as a sphere of average radius 1.70 Å. The value obtained in this way is 70.0 kcal. Thus the value of  $(E + S)_{O_2} = 85.8$  kcal.

(b) The second electron affinity of the oxygen molecule can be obtained from a similar cycle to the one above involving the heats of formation of solids of the type  $M^{++}\text{O}_2^-$ . The crystal structures of the Ba, Sr and Ca peroxides have been determined by Bernal and all have the calcium carbide type lattice. The  $\text{O}_2^-$  ion is an ellipsoid with major and minor axial diameters of 5.12 Å and 3.34 Å respectively. The Madelung constant of such a lattice has been evaluated as 1.636 and in the same way as used above the lattice energies have been calculated. Table V gives the data used in the Born-Haber cycle and the resulting values of the energy change in the reaction,

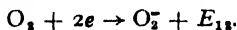


TABLE V

Solid	$\lambda_M$	$(I_1 + I_2)_M$	$Q$	$r_{M^{++}}$	$U_0$	$E_{12}$	Mean $E_{12}$
$\text{BaO}_2$	49.1	349.0	144.2	1.36	647	-104.7	} -112.5
$\text{SrO}_2$	47.0	383.8	154.9	1.13	998	-115.5	
$\text{CaO}_2$	475	412.9	155.5	0.99	735	-117.3	

<sup>12</sup> Machu, *Das Wasserstoffperoxyd und die Perverbindungen* (Wien, 1937).

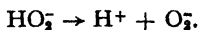
<sup>13</sup> Helms and Klemm, *Z. anorg. Chem.*, 1939, **241**, 97.

It is interesting to note that whereas the first electron affinity of the oxygen molecule in the gas phase is positive the sum of the first and second electron affinities is negative.

We have evaluated the heat of solution of the O<sub>2</sub><sup>-</sup> ion in water using a mean ionic radius of 1.97 Å as  $S_{O_2} = 210$  kcal. Thus we have

$$(E_{11} + S_{O_2}) = +97.5 \text{ kcal.}$$

From these figures we would expect the second dissociation of H<sub>2</sub>O<sub>2</sub> to be extremely small due to the high endothermicity  $\sim 100$  kcal. of the step,



*Chemistry Department,  
The University,  
Leeds.*

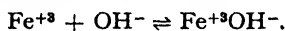
## THE [Fe(OH)]<sup>+</sup> AND [Fe(O<sub>2</sub>H)]<sup>+</sup> COMPLEXES

By M. G. EVANS, PHILIP GEORGE AND N. URI

*Received 6th September, 1948*

The properties of an ion pair complex between Fe<sup>3+</sup> and O<sub>2</sub>H<sup>-</sup> ions in aqueous solution are described for the first time. The equilibrium constant and the thermodynamical quantities  $\Delta G^\circ$ ,  $\Delta H^\circ$  and  $\Delta S^\circ$  are evaluated and compared with those for the complex Fe<sup>3+</sup>OH<sup>-</sup>. The absorption spectrum has been measured and the differences between this spectrum and that for Fe<sup>3+</sup>OH<sup>-</sup> are discussed, on the assumption that both are electron-transfer spectra, in terms of the electron affinities of OH and O<sub>2</sub>H.

Rabinowitch and Stockmayer<sup>1,2</sup> have measured the absorption spectrum of the complex Fe<sup>3+</sup>OH<sup>-</sup> in aqueous solution and combining this result with the data of Bray and Hershey<sup>3</sup> have determined the thermodynamical quantities  $\Delta G^\circ$ ,  $\Delta H^\circ$  and  $\Delta S^\circ$  for the reaction,



In this communication we report a similar investigation for the complex Fe<sup>3+</sup>O<sub>2</sub>H<sup>-</sup>.

### Experimental and Results

Aqueous solutions of ferric ions and concentrated hydrogen peroxide have a deep brown colour under conditions where the colour due to the [Fe<sup>3+</sup>OH<sup>-</sup>] complex is negligible. We have investigated the dependence of the intensity of this colour on the concentration of ferric ions, hydrogen peroxide and on pH. At the very low concentration of ferric ion at which we have worked the rate of decomposition of H<sub>2</sub>O<sub>2</sub> is slow and does not interfere with the measurements.

The optical density has been measured by means of a photocell colorimeter using a 4 cm. cell and the Ilford filter 601 corresponding to the spectral region of 430 mμ. The hydrogen ion activity was measured in the equilibrium system by means of a glass electrode.

At constant H<sub>2</sub>O<sub>2</sub> concentration and constant H<sup>+</sup> activity the optical density of the solution is a linear function of the initial ferric ion concentration (Fig. 1). At constant ferric ion concentration and H<sup>+</sup> activity the change of the optical density with H<sub>2</sub>O<sub>2</sub> concentration is shown in Fig. 2 up to a concentration of H<sub>2</sub>O<sub>2</sub> = 33 M.

Fig. 3 shows the change of optical density with change of pH and we note that increasing pH increases the optical density. These general observations

<sup>1</sup> Rabinowitch and Stockmayer, *J. Amer. Chem. Soc.*, 1942, **64**, 335.

<sup>2</sup> Rabinowitch, *Rev. Mod. Physics*, 1942, **14**, 112.

<sup>3</sup> Bray and Hershey, *J. Amer. Chem. Soc.*, 1934, **56**, 1889.

are consistent with the assumption that the colour is due to the formation of a complex  $\text{Fe}^{+3}(\text{O}_2\text{H}^-)$ . In these solutions therefore, we are dealing with the equilibria :

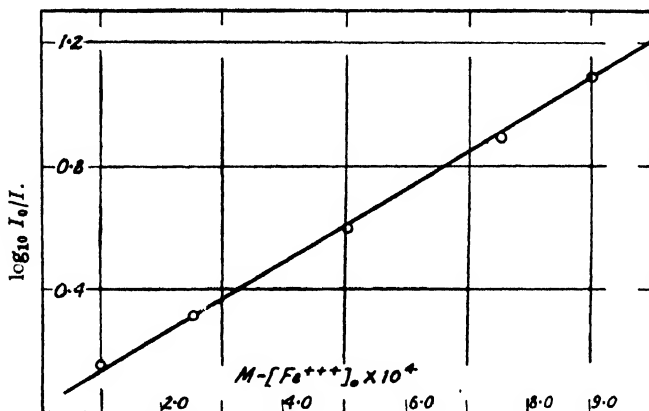
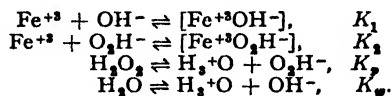


FIG. 1.— $[\text{H}_2\text{O}_2] = 9\text{M}$ ,  $\mu = 0.1$ ,  $t = 20^\circ\text{C}$ ,  $\text{pH} = 1.77$ .  
4 cm. cell, Ilford Filter 601 (430 m $\mu$ ).

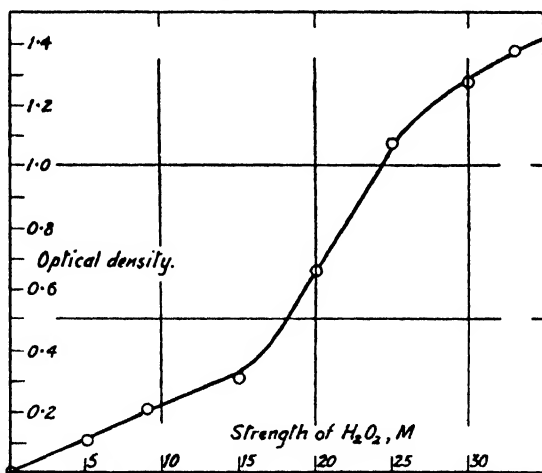


FIG. 2.— $[\text{Fe}^{+3}]_0 = 5 \times 10^{-3}\text{M}$ ,  $[\text{HClO}_4] = 0.5\text{M}$ ,  $t = 20^\circ\text{C}$ ,  
4 cm. cell, Ilford Filter 601 (430 m $\mu$ ).

The concentration of  $[\text{Fe}^{+3}\text{O}_2\text{H}^-]$  is given in terms of the initial  $\text{Fe}^{+3}$  ion concentration  $[\text{Fe}^{+3}]_0$  by

$$\frac{[\text{Fe}^{+3}\text{O}_2\text{H}^-]}{[\text{Fe}^{+3}]_0 - [\text{Fe}^{+3}\text{O}_2\text{H}^-] \left( 1 + \frac{K_1}{K_2} \frac{[\text{OH}^-]}{[\text{O}_2\text{H}^-]} \right)} = K_2 [\text{O}_2\text{H}^-] \quad (1)$$

whence

$$[\text{Fe}^{+3}\text{O}_2\text{H}^-] = \frac{K_2 [\text{O}_2\text{H}^-] [\text{Fe}^{+3}]_0}{1 + K_2 [\text{O}_2\text{H}^-] \left( 1 + \frac{K_1}{K_2} \frac{[\text{OH}^-]}{[\text{O}_2\text{H}^-]} \right)} \quad (2)$$

The work reported in the previous paper<sup>4</sup> on the evaluation of the dissociation constant for H<sub>2</sub>O<sub>2</sub> enables us to test eqn. (2) on the assumption that the optical density of the solutions is a linear function of Fe<sup>+</sup>O<sub>2</sub>H<sup>-</sup>.

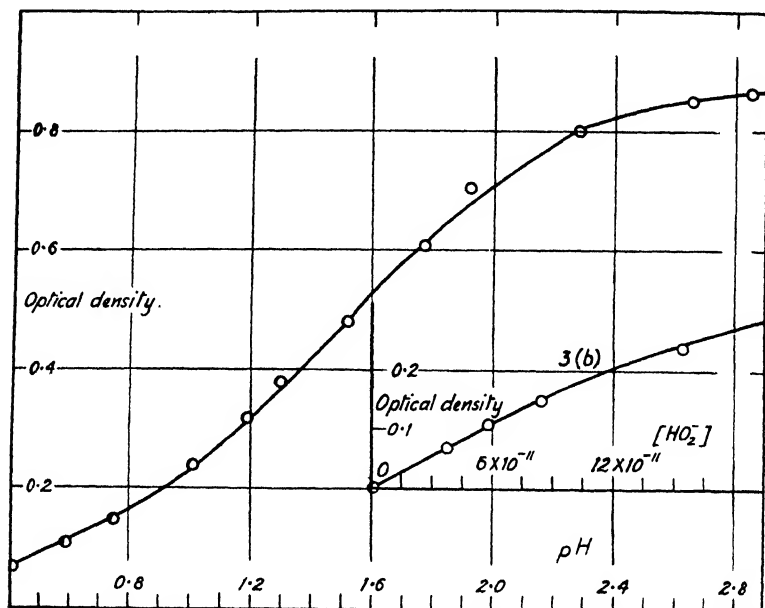


FIG. 3.—[H<sub>2</sub>O<sub>2</sub>] = 9 M, [Fe<sup>+</sup>]<sub>0</sub> = 5 × 10<sup>-4</sup> M, *t* = 20° C, HClO<sub>4</sub> used as acid, 4 cm. cell, Ilford filter 601 (430 mμ).

We see from eqn. (2) that (a) the optical density should be linear with respect to the initial ferric ion concentration [Fe<sup>+</sup>]<sub>0</sub> as found (see Fig. 1); (b) at low pH, where

$$(K_2[\text{O}_2\text{H}^-] + K_1[\text{OH}^-]) \ll 1,$$

the optical density should be linear with respect to O<sub>2</sub>H<sup>-</sup> (see Fig. 3(b)). The concentration of O<sub>2</sub>H<sup>-</sup> may be varied either by a change of H<sup>+</sup> at constant H<sub>2</sub>O<sub>2</sub> or by a change of H<sub>2</sub>O<sub>2</sub> at constant pH. The first variation is shown in Fig. 3 and the second in Fig. 2. Eqn. (2) is only applicable up to H<sub>2</sub>O<sub>2</sub> of about 10 M, where the superacidity effect already referred to becomes marked. We wish, however, to draw attention to the very marked increase in the optical density above 15 M. The reasons for this change, which might arise from the formation of a ferric perhydrate, we do not fully understand at present and we have limited our discussion to these concentrations for which eqn. (2) is applicable. (c) At high pH and high H<sub>2</sub>O<sub>2</sub>, where

$$K_2[\text{O}_2\text{H}^-] \gg 1 + K_1[\text{OH}^-]$$

the optical density should become independent of the pH (see Fig. 3).

Since the molar extinction coefficient of [Fe<sup>+</sup>O<sub>2</sub>H<sup>-</sup>] is unknown eqn. (2) cannot be used to obtain an absolute value of the concentration of Fe<sup>+</sup>O<sub>2</sub>H<sup>-</sup> and hence a value of K<sub>2</sub>. We can, however, obtain a value of K<sub>2</sub> from the optical density δ of two solutions differing only in H<sup>+</sup> ion activity. Eqn. (2) could be expressed

$$\delta \propto [\text{Fe}^+\text{O}_2\text{H}^-] = \frac{K_2 K_3 \frac{[\text{H}_2\text{O}_2]}{[\text{H}^+]} [\text{Fe}^+]_0}{(1 + K_2 K_3 \frac{[\text{H}_2\text{O}_2]}{[\text{H}^+]} (1 + \frac{K_1 K_3 [\text{H}_2\text{O}_2]}{K_2 K_3 [\text{H}_2\text{O}_2]}))},$$

<sup>4</sup> Evans and Uri, *Trans. Faraday Soc.*, 1948, 44, 224.

and since the concentration of  $\text{Fe}^{+3}$  ion is  $5 \times 10^{-4}$  M compared with  $\text{H}_2\text{O}_2 \sim 9$  M and  $\text{H}_2\text{O} \sim 45$  M, the equilibrium concentrations of  $\text{H}_2\text{O}_2$  and  $\text{H}_2\text{O}$  are the same as their initial concentrations. Hence by comparing optical densities of solutions differing only in  $\text{H}^+$  activity we have

$$\frac{\delta_1}{\delta_2} = \frac{[\text{H}^+]_2}{[\text{H}^+]_1} \frac{1 + K_2 K_p \frac{[\text{H}_2\text{O}_2]}{[\text{H}^+]_2} \left(1 + \frac{1}{K_2} K\right)}{1 + K_2 K_p \frac{[\text{H}_2\text{O}_2]}{[\text{H}^+]_1} \left(1 + \frac{1}{K_2} K\right)},$$

and

$$K_2 = \frac{(\delta_2/[\text{H}^+]_1 - \delta_1/[\text{H}^+]_2)}{\frac{K_p}{[\text{H}^+]_1[\text{H}^+]_2} (\delta_1 - \delta_2) [\text{H}_2\text{O}_2]} - K,$$

where

$$K = \frac{K_1 K_w}{K_p} \times \frac{[\text{H}_2\text{O}]}{[\text{H}_2\text{O}_2]}.$$

The measurements were made in the presence of  $\text{NaClO}_4$  as neutral electrolyte and the ionic strength of the solutions was 0.1.

From 15 combinations of pairs from a series of 6 experiments in the pH range 1 to 2 where eqn. (3) holds, the average value of  $K_2$  obtained was

$$K_2 = 2.05 (\pm 0.4) \times 10^9$$

at  $20^\circ\text{C}$ . The fluctuations of about 20 % due to the inaccuracy involved in the constants  $K_1$  and  $K_2$  as well as to the experimental method itself are indicated in brackets. The value of  $K_p$  used was that given in the previous publication ( $K_p = 1.78 \times 10^{-12}$  at  $20^\circ\text{C}$ ) and the value of  $K_1$  that determined by Bray and Hershey<sup>3</sup> ( $K_1 = 5 \times 10^{11}$  at  $20^\circ\text{C}$ ).

Colorimetric measurements have been made at various temperatures in the range  $7.5^\circ\text{C}$  to  $40^\circ\text{C}$ . These measurements together with the known temperature dependence of  $K_p$  have enabled us to calculate the temperature dependence of  $K_2$  (Fig. 4). Table I gives the value of  $\Delta G^\circ$ ,  $\Delta H^\circ$  and  $\Delta S^\circ$  for the formation

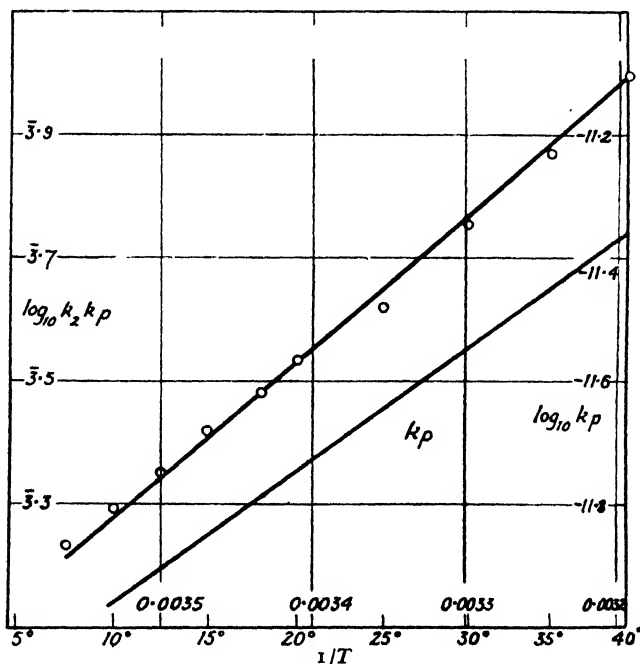


FIG. 4.

of the  $\text{Fe}^{+3}\text{O}_2\text{H}^-$  complex and these are compared with those corresponding to the formation of  $\text{Fe}^{+3}\text{OH}^-$ .

TABLE I

Reaction	$\Delta G^\circ$ at 20° (kcal./mol.)	$\Delta H^\circ$ (kcal./mol.)	$\Delta S^\circ$ (kcal./mol.° C)
$\text{Fe}^{+3} + \text{O}_2\text{H}^- \rightarrow \text{Fe}^{+3}\text{O}_2\text{H}^-$	-12.5	$1.8 \pm 0.6$	+49
$\text{Fe}^{+3} + \text{OH}^- \rightarrow \text{Fe}^{+3}\text{OH}^-$	-15.9	$-1.2 \pm 1$	+50

The S-shaped form of the relation between the optical density  $\delta$  and pH leads to a maximum slope at a hydrogen ion concentration given by

$$[\text{H}^+]_{\text{max.}} = K_1 K_2 [\text{H}_2\text{O}_2] + K_1 K_w [\text{H}_2\text{O}].$$

Under these experimental conditions where

$$K_1 K_2 \gg K_1 K_w \frac{[\text{H}_2\text{O}]}{[\text{H}_2\text{O}_2]}$$

the above condition is approximately

$$[\text{H}^+]_{\text{max.}} = K_1 K_2 [\text{H}_2\text{O}_2].$$

This maximum occurs at pH  $\sim 1.5$  for  $[\text{H}_2\text{O}_2] = 9\text{M}$ . In the absence of hydrogen peroxide, i.e. for the  $\text{Fe}^{+3}\text{OH}^-$  complex, the maximum slope occurs at pH  $\sim 3.0$ .

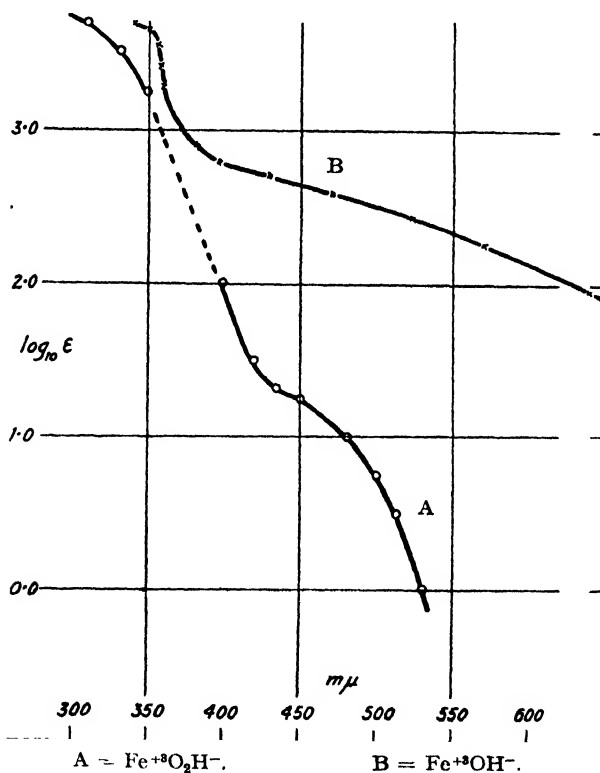


FIG 5.

The maximum corresponds to the point at which

$$\frac{[\text{Fe}^{+3}(\text{O}_2\text{H}^-)]}{[\text{Fe}^{+3}]} = 1, \text{ or } \frac{[\text{Fe}^{+3}\text{OH}^-]}{[\text{Fe}^{+3}]} = 1,$$

i.e. to the point at which 50% of the ferric ions present are converted into the complex.

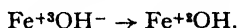
With the association constant of  $[\text{Fe}(\text{HO}_2)]^{++}$  established, the absorption spectrum of the complex was determined by means of a spectrograph combined with a Hilger sector photometer. Below  $370 \text{ m}\mu$  a correction for the  $\text{H}_2\text{O}_2$  absorption had to be made. The absorption curve, which is presented in Fig. 5 is in its shape characteristic of an electron-transfer spectrum (cf. Rabinowitch<sup>3</sup>), but it differs from the  $[\text{Fe}(\text{OH})]^{++}$  curve obtained by Rabinowitch (loc. cit.) in the following features. Its maximum shows a red-shift of about  $40 \text{ m}\mu$  ( $310\text{--}350$ ), and furthermore the absorption in the visible region is considerably larger. For the purpose of comparison both curves were put on to one figure. At  $430 \text{ m}\mu$  the wave length at which the optical density was measured the approximate molar extinction coefficients for  $[\text{Fe}(\text{HO}_2)]^{++}$ ,  $[\text{Fe}(\text{OH})]^{++}$  and  $[\text{Fe}(\text{H}_2\text{O}_6)]^{+++}$  are 500, 20 and 0.1 respectively.

Bohnson and Robertson<sup>5</sup> stated that a violet colour was formed when ferric ions were introduced into concentrated hydrogen peroxide which they erroneously (as it seems) attributed to the formation of ferrate. As a matter of fact we have also obtained this colour when we worked with A.R.  $\text{H}_2\text{O}_2$  supplied by B.D.H. It was observed, however, that this violet colour disappears within a short time, the rate of disappearance being dependent on pH of the solution. Since neither is  $\text{H}_2\text{O}_2$  considerably decomposed nor does ferric ion disappear in this interval of time, any real reaction product of ferric ion and hydrogen peroxide in equilibrium with the reactants would be maintained at an equilibrium concentration. Our assumption was that this colour might be due to impurities caused by traces of aromatic hydroxy-compounds contained in the  $\text{H}_2\text{O}_2$ , which gave a similar colour reaction with ferric ions. Moreover, these hydroxy-compounds are not oxidised by  $\text{H}_2\text{O}_2$  itself whereas they are rapidly destroyed by a  $\text{Fe}^{+++} - \text{H}_2\text{O}_2$  mixture. Further evidence to support this assumption is brought forward: (1) by the fact that no similar colour was formed when a sample of  $\text{H}_2\text{O}_2$  obtained by distillation of the A.R. sample was used; (2) that by the addition of sodium salicylate not only was a similar violet colour obtained, but even the rate of disappearance of the colour showed a similar dependence on the pH of the reaction mixture.

## Discussion

1. In our discussion of the dissociation constant of  $\text{H}_2\text{O}_2$ , we remarked on the fact that the entropy change of the reaction was practically identical with that for the dissociation of water. This observation implied that the entropy of the  $\text{O}_2\text{H}^-$  ion in aqueous solution is very similar to that of  $\text{OH}^-$ . It is interesting therefore to note that in the comparison given in Table I the entropy change of the formation in aqueous solution of the ion pair  $\text{Fe}^{+3}\text{O}_2\text{H}^-$  is very close to that for the formation of  $\text{Fe}^{+3}\text{OH}^-$ —again emphasising the similarity of these ions  $\text{OH}^-$  and  $\text{O}_2\text{H}^-$  in an aqueous solution.

2. We note that the maximum of the absorption spectrum curve of the complex  $\text{Fe}^{+3}\text{O}_2\text{H}^-$  as compared with that for  $\text{Fe}^{+3}\text{OH}^-$  is displaced towards the red by a wave-length difference corresponding to approximately 10 kcal. Rabinowitch<sup>3</sup> has attributed the absorption spectrum in the case of the  $\text{Fe}^{+3}\text{OH}^-$  complex to the electron-transfer process,



The energy change  $\Delta\epsilon_1$  involved in this process will be given by

$$\Delta\epsilon_1 = -\Delta H_{\text{Fe}^{+3}\text{OH}^-} + I_{\text{Fe}^{+2}} - E_{\text{OH}} - S_{\text{OH}^-} + S_{\text{OH}} + Q_1$$

in which  $\Delta H_{\text{Fe}^{+3}\text{OH}^-}$  is the heat of formation of the ion pair  $\text{Fe}^{+3}\text{OH}^-$  from the separated ions  $(\text{Fe}^{+3})_{\text{aq.}}$  and  $(\text{OH}^-)_{\text{aq.}}$ ,  $E_{\text{OH}}$  the electron affinity of the OH radical in the gas phase,  $S_{\text{OH}^-}$  and  $S_{\text{OH}}$  the heats of solution from the gas phase of the  $\text{OH}^-$  ion, and radical respectively,  $I_{\text{Fe}^{+2}}$  the ionisation potential of  $\text{Fe}^{+2}$  in aqueous solution and  $Q_1$  the energy change required to bring the separated particles  $(\text{Fe}^{+2})_{\text{aq.}}$  and  $(\text{OH})_{\text{aq.}}$  into a configuration identical with that of the  $(\text{Fe}^{+3}\text{OH}^-)$  ion pair.

If we assume that in the case of the  $\text{Fe}^{+3}\text{O}_2\text{H}^-$  complex the adsorption

<sup>5</sup> Bohnson and Robertson, *J. Amer. Chem. Soc.*, 1923, **45**, 2493.



spectrum, in the region of the maximum at least, arises from a process similar to that described above, the energy change  $\Delta\epsilon_2$  is given by

$$\Delta\epsilon_2 = -\Delta H_{\text{Fe}^{+2}\text{O}_2\text{H}^-} + I_{\text{Fe}^{+2}} - E_{\text{O}_2\text{H}} - S_{\text{O}_2\text{H}^-} + S_{\text{O}_2\text{H}} + Q_2,$$

and

$$(\Delta\epsilon_1 - \Delta\epsilon_2) = -(\Delta H_{\text{Fe}^{+2}\text{OH}^-} - \Delta H_{\text{Fe}^{+2}\text{O}_2\text{H}^-}) - (E_{\text{OH}} - E_{\text{O}_2\text{H}}) - (S_{\text{OH}^-} - S_{\text{O}_2\text{H}^-}) + (S_{\text{OH}} - S_{\text{O}_2\text{H}}) + (Q_1 - Q_2).$$

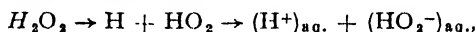
In this equation we know the following terms:

$$(\Delta H_{\text{Fe}^{+2}\text{OH}^-} - \Delta H_{\text{Fe}^{+2}\text{O}_2\text{H}^-}) = (-1.2 - 1.8) = -3.0 \text{ kcal.}$$

On the assumption that the heats of solution of OH and  $\text{O}_2\text{H}$  radicals are identical with those of  $\text{H}_2\text{O}$  and  $\text{H}_2\text{O}_2$  respectively:

$$(S_{\text{OH}} - S_{\text{O}_2\text{H}}) = (10.6 - 12.3) = -1.7 \text{ kcal.}$$

The term  $(E_{\text{OH}} + S_{\text{OH}^-}) - (E_{\text{O}_2\text{H}} + S_{\text{O}_2\text{H}^-})$  is much less certain. We are here dealing with an absorption process in which the position of the centres is unchanged whereas in estimating the value of the term  $(E_{\text{O}_2\text{H}} - S_{\text{O}_2\text{H}^-})$  from the cycle based on



changes in the internuclear separation of the centres are taken into account. On the basis of the previous paper, however, it is clear that the term  $(E_{\text{OH}} + S_{\text{OH}^-}) - (E_{\text{O}_2\text{H}} + S_{\text{O}_2\text{H}^-})$  is positive to at least a value of 11 kcal., which would correspond to the observed shift in the absorption maximum from 310  $\text{m}\mu$  to 350  $\text{m}\mu$ .

It is interesting to note that the change in the maximum of the absorption spectrum does follow at least qualitatively the change in the electron affinity plus solvation energy between OH and  $\text{O}_2\text{H}$  in the same way as found by Rabinowitch in the change from  $\text{Fe}^{+3}\text{Cl}^-$  to  $\text{Fe}^{+3}\text{Br}^-$ .

3. There is, however, in the case of  $\text{Fe}^{+3}\text{O}_2\text{H}^-$  a very marked absorption in the whole visible spectrum which is not observed in the case of  $\text{Fe}^{+3}\text{OH}^-$ .

We hope to discuss this point in a subsequent publication.

*Chemistry Department,  
The University,  
Leeds.*

## THE HEAT OF THE REACTION BETWEEN FERROUS IONS AND HYDROGEN PEROXIDE IN AQUEOUS SOLUTION

By M. G. EVANS, J. H. BAXENDALE AND N. URI

*Received 6th September, 1948*

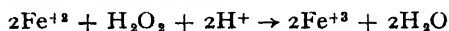
Experimental determinations are reported on the heat of reaction between ferrous ions and hydrogen peroxide in aqueous solution. These results lead to a value of +38 kcal. for the heat of the reaction of



This value, together with the quantities used in the previous publications, enables one to obtain a value for the ionisation potential of ferrous ions in aqueous solution which is in good agreement with the value obtained by other methods.

In the preceding publications we have discussed values for the heat of dissociation of  $\text{H}_2\text{O}_2$  into OH radicals, the electron affinity of OH

radicals and the heat of solution of  $\text{OH}^-$  ions. By direct thermochemical measurement of the heat of the reaction



we can obtain some confirmation of the correctness of the values adopted.

### Experimental

The experiments were carried out in a calorimeter consisting of the thermally insulated reaction vessel (of 500 ml. volume) which was covered by a rubber stopper containing a number of holes for a Beckmann thermometer, a stirrer, an inlet tube and a heating coil for electrical calibration. Both the reaction vessel and the inlet tube were filled with the reacting liquids, after the latter were slightly warmed and kept constant at  $25^\circ$ . The inlet tube was enlarged at its bottom end to a sphere which was entirely immersed in the reaction liquid so that the solution (normally 20 ml.) to be poured from the sphere of the inlet tube into the reaction vessel would for all practical purposes keep the same temperature as the bulk of the liquid in the reaction vessel during the cooling period of fifteen minutes preceding zero time. At zero time the sphere of the inlet tube was broken by means of a glass rod. The composition of the reaction mixtures as well as the observed values for  $\Delta T$  are shown in Table I.

TABLE I

<i>Experiment</i>	$\Delta T$
(1) 230 ml. $[\text{N HClO}_4 + 0.05 \text{ M H}_2\text{O}_2]$ diluted with 20 ml. $1.40 \text{ M FeSO}_4$ (containing $0.01 \text{ N HClO}_4$ )	$+ 2.27^\circ$
(2) Expt. (1) repeated	$+ 2.23^\circ$
Mean $\Delta T = 2.25^\circ$	
(3) 230 ml. $\text{N HClO}_4$ diluted with 20 ml. $\text{H}_2\text{O}$	$+ 0.02^\circ$
(4) Expt. (3) repeated	$+ 0.04^\circ$
(5) 230 ml. $\text{N HClO}_4$ diluted with 20 ml. $\text{FeSO}_4$ ( $1.40 \text{ M}$ ) (containing $0.01 \text{ N HClO}_4$ )	$- 0.47^\circ$
(6) Expt. (5) repeated	$- 0.44^\circ$

Two calibration experiments gave in exact agreement  $1 \text{ kcal.} \sim \Delta T = 3.55^\circ$ . The differences in the specific heat in the final reaction mixtures (which all contain  $\text{N HClO}_4$ ) are negligible.

As Haber and Weiss<sup>1</sup> pointed out, no hydrogen peroxide is decomposed when ferrous sulphate is poured into dilute hydrogen peroxide (no local excess of  $\text{H}_2\text{O}_2$  is effected by this procedure, which might cause  $\text{OH}$  radicals produced in the first step to react with  $\text{H}_2\text{O}_2$  rather than with  $\text{Fe}^{+2}$ ), and the stoichiometric ratio  $\Delta\text{H}_2\text{O}_2/\Delta\text{Fe}^{+2} = 0.5$ . It has also been found that  $\text{H}^+$  ions inhibit the cycle reaction leading to  $\text{O}_2$  formation. With the mixing procedure adopted and the acid concentration of  $\text{N HClO}_4$ , any decomposition of  $\text{H}_2\text{O}_2$  seems to be practically excluded. By this high initial acid concentration only a comparatively small change is effected by  $\text{H}^+$  consumed in the reaction. We therefore obtain for reaction (1) from the results of Table I:

Direct measurement	$\Delta T = + 2.25$
Correction for acid dilution	$\Delta T = + 0.04$
Correction for $\text{FeSO}_4$ dilution	$\Delta T = - 0.47$
Corrected value	$\Delta T = + 2.68$

The *negative* heat of dilution of  $\text{FeSO}_4$  is remarkable. Since the small positive heat of acid dilution is included in Expt. (5) and (6) the value obtained in (5) was used for the correction instead of the mean of both experiments. From  $\Delta T = 2.68^\circ$  we obtain for the heat of reaction (1)

$$\frac{2.68}{3.55 \times 1.15} \times 10^3 = 65.5 \text{ kcal.}$$

Taking into account the experimental precision, the value of 65.5 kcal. may be regarded as accurate within  $\pm 3\%$  (corresponding to  $\pm 2 \text{ kcal.}$ ). With the known value for the heat of neutralisation one obtains for the heat of the reaction,

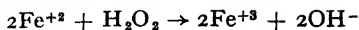


a value of  $\sim 38 \text{ kcal.}$

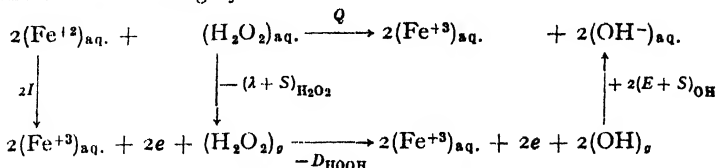
<sup>1</sup> *Proc. Roy. Soc. A*, 1934, **147**, 334.

## Discussion

We can express the heat of the reaction



in terms of the following cycle :



in which the symbols have the following significance—

$I$  = ionisation potential of  $\text{Fe}^{+2}$  ions in aqueous solution ;

$\lambda$  = latent heat of evaporation of  $\text{H}_2\text{O}_2$  ;

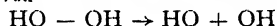
$S$  = heat of solution of  $\text{H}_2\text{O}_2$  in aqueous solution ;

$D$  = heat of dissociation of  $\text{H}_2\text{O}_2 \rightarrow 2\text{HO}$  in the gas phase ;

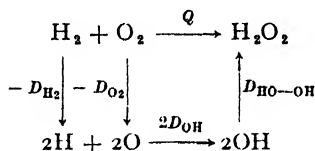
$-S$  = electron affinity of the  $\text{OH}$  radical plus the heat of solvation of the  $\text{OH}^-$  ion.

$$Q = 2I - (\lambda + S)_{\text{H}_2\text{O}_2} - D_{\text{HOOH}} + 2(E + S)_{\text{OH}}$$

In previous publications we have referred to the evaluation of  $S_{\text{H}_2\text{O}_2}$  and  $(E + S)_{\text{OH}}$ . The heat of the reaction



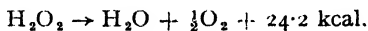
is obtained from the cycle :



$$\text{i.e.} \quad Q = -D_{\text{H}_2} - D_{\text{O}_2} + 2D_{\text{O}-\text{H}} + D_{\text{HO}-\text{OH}}$$

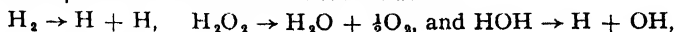
The value of  $Q$  which has been experimentally determined is given by Bichowsky and Rossini<sup>2</sup> as 33.6 kcal. The work of Dwyer and Oldenburg<sup>3</sup> gives a value for the term  $D_{\text{O}-\text{H}} = 100.1$  kcal. Using these values together with the value  $D_{\text{H}_2} = 104.1$ <sup>4</sup> and  $D_{\text{O}_2} = 118.2$ <sup>6</sup> we find  $D_{\text{HO}-\text{OH}} = 55.7$  kcal.

A similar calculation has been made by Skinner<sup>5</sup> for an evaluation of the various bond strengths involved and these values lead to 56 kcal. for the heat of the above reaction. Another cycle can be built on the reaction



Using the above values and the value  $D_{\text{H}-\text{OH}} = 120.7$  kcal. from the heat of formation of water,<sup>2</sup> this leads to a value of 55.5 kcal. The average of the observations is 55.6 kcal.

Recently<sup>6</sup> a value of 50.9 kcal. has been suggested by Hold, McLane and Oldenburg. The difference of approximately 5 kcal. arises out of small discrepancies between their heat values for



and those adopted by us.

<sup>2</sup> Bichowsky and Rossini, *Thermochemistry of Chemical Substances* (New York, 1936).

<sup>3</sup> Dwyer and Oldenburg, *J. Chem. Physics*, 1944, **12**, 357.

<sup>4</sup> Herzberg, *Molecular Spectra and Molecular Structure* (1939).

<sup>5</sup> Skinner, *Trans. Faraday Soc.*, 1945, **41**, 645.

<sup>6</sup> Hold, McLane and Oldenburg, *J. Chem. Physics*, 1948, **16**, 229.

The values we adopt are :

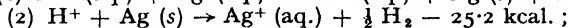
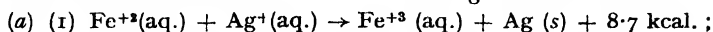
$$\lambda_{\text{H}_2\text{O}_2} = 11.6 \text{ kcal.}, S_{\text{H}_2\text{O}_2} = 0.7 \text{ kcal.}, D_{\text{HOOH}} = 55.6 \text{ kcal.}$$

and  $(E + S)_{\text{OH}} = 147.6 \text{ kcal.}$

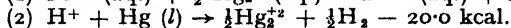
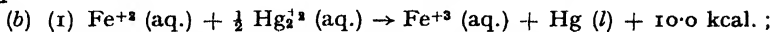
These measurements therefore lead to a value of  $I$  :

$$I = \frac{1}{2}(-Q - \lambda_{\text{H}_2\text{O}_2} - S_{\text{H}_2\text{O}_2} - D_{\text{HOOH}} + 2(E + S)_{\text{OH}}) \\ = 94.7 \text{ kcal.}$$

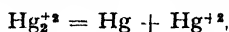
Values of  $I$  can be obtained from the following measurements : <sup>2</sup>



and

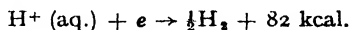


In view of the possible complications involved in reactions (b) arising from the association of the  $\text{Hg}_2^{+2}$  ion, the disproportionation equilibrium,

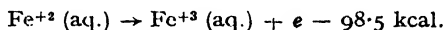


as well as the anomalies in the dissociation of mercury salts, we consider the value obtained from (a) to be the more reliable.

Using the value of



we obtain



Another approximate evaluation of  $I$  can be obtained from the E.M.F. of the cell



which corresponds at a temperature of  $25^\circ \text{C}$  to a free energy change of  $\Delta G = 17 \text{ kcal.}$  Neglecting, in this approximation, the entropy change which may correspond at most to about 5.6 kcal. and identifying the free energy change with the change in heat content we obtain a value of 99 kcal. The entropy change in the above reaction is negative and thus reduces the value of  $I$  to approximately 95 kcal.

We conclude therefore that the values of the individual terms we have chosen in the above thermochemical calculations are well-based and reasonable estimates.

*Chemistry Department,  
The University,  
Leeds.*

# AN EVALUATION OF THE DIFFUSION COEFFICIENT FOR CHLOROFORM IN POLYSTYRENE FROM SIMPLE ABSORPTION EXPERIMENTS

By J. CRANK AND G. S. PARK

*Received 7th October, 1948*

Experimental data for the rates of sorption and desorption of chloroform by polystyrene sheet are presented. Diffusion is considered to be the rate-controlling process and the diffusion coefficient is found to vary considerably with concentration of chloroform. The diffusion coefficient-concentration relation is derived from the sorption-time curves by a new method.

It has been known for some time that in many systems diffusion processes do not obey Fick's law of diffusion, and that for systems in which one component is a high polymer the deviations are often considerable. The deviation which arises frequently is one in which the diffusion coefficient varies with concentration of the diffusing substance but is not otherwise a function of the space or time variables. The present paper describes a method of studying such a variation quantitatively. The method is applied to the diffusion of chloroform in polystyrene.

The measurement of a variable diffusion coefficient is not an easy matter, firstly, because there are considerable experimental difficulties and secondly, because the formal mathematical solutions of the diffusion equation, which exist for the non-steady state, only apply to the case of a constant diffusion coefficient. The two main kinds of experimental methods which have been used are both designed to avoid the necessity of solving the diffusion equation in the subsequent evaluation of the diffusion coefficient. The first involves the analysis of data giving the concentration of diffusing substance as a function of time and distance. Thus Neale and Garvie<sup>1</sup> have obtained the diffusion coefficient for the dye Sky Blue 1F in Cellophane sheet by analysing a number of concentration-distance curves for various values of the time variable. Matano<sup>2</sup> showed, for the inter-diffusion of two metals that, provided each metal is effectively semi-infinite in extent, the diffusion coefficient-concentration relation can be obtained by analysis of a single concentration-distance curve at a fixed time. This mathematical analysis has recently been applied to concentration-distance curves obtained by an interferometric technique in a study of the diffusion of solvents and swellers into cellulose acetate.<sup>3</sup> It appears that a comparable method, using a single concentration-time curve at a fixed spatial co-ordinate, could be used for determining the diffusion-concentration relationship, though no instance of the use of such a method is known to the authors. The mathematical analysis involved in these methods is simple but the measurement of concentration-distance-time data usually demands a refined micro-analytical technique and for low diffusion coefficients the time needed to carry out a number of successive experiments of this kind becomes prohibitively long.

The second kind of experiment is based on measurements of the flux of material through a membrane under steady-state conditions, i.e. when no material is accumulating at any point in the membrane. King<sup>4</sup> has

<sup>1</sup> Neale and Garvie, *Trans. Faraday Soc.*, 1938, **34**, 335.

<sup>2</sup> Matano, *J. Physics, Japan*, 1932-33, **8**, 109.

<sup>3</sup> Crank and Robinson (not yet published).

<sup>4</sup> King, *Trans. Faraday Soc.*, 1945, **41**, 479.

applied this method to the diffusion of water through horn keratin and has shown that if  $F(C_0, C_1)$  is the flux of material through the membrane when the concentrations at the two sides of the membrane are  $C_0$  and  $C_1$  respectively, then

$$F(C_0, C_1) = \frac{1}{l} \int_{C_0}^{C_1} D(C) dC, \quad . \quad . \quad . \quad (1)$$

where  $l$  is the thickness of the membrane and  $D(C)$  the diffusion coefficient is a function of concentration  $C$ . On differentiating (1) with respect to  $C_0$ , keeping  $C_1$  constant, we have

$$D(C_0) = -l \frac{\partial}{\partial C_0} F(C_0, C_1). \quad . \quad . \quad . \quad (2)$$

so that if  $F$  is measured for a number of different values of  $C_0$  keeping  $C_1$  fixed (usually for convenience  $C_1 = 0$ ), the diffusion coefficient may be obtained by use of (2). Unfortunately, the apparatus needed for such experiments tends to be complicated and this is especially so for low values of the diffusion coefficient. Furthermore, for these low values the time that must elapse before a steady state is achieved is very great (for a membrane 0.03 cm. thick and  $D$  having the constant value  $10^{-9}$  cm.<sup>2</sup> sec.<sup>-1</sup> the time is of the order of 10 days). Thus in order to carry out a number of experiments of either of the above general kinds in a reasonable time, several sets of apparatus would be required to run concurrently and often this is not possible when the apparatus is complicated.

For these reasons it was decided to explore the possibilities of obtaining the diffusion coefficient-concentration relation from the comparatively simple measurements of overall rate of absorption curves. No exact relation similar to eqn. (1) has been deduced for the non-steady state, but it has been shown elsewhere<sup>5</sup> that an approximation to  $\int_0^{C_0} D dC$  can be obtained from absorption-time curves, so that analysis of a number of such curves for different regains  $C_0$  at the surface of the sheet or membrane allows the  $D$ - $C$  relation to be deduced by a differentiation analogous to that of eqn. (2).

The rate of uptake of chloroform by polystyrene has been measured at various partial pressures of the former and the method suggested has been applied to the absorption-time curves. The order of the error involved in applying the approximate relation to this system is examined and used as a basis of a method of successive approximations by which the diffusion coefficient-concentration relation can be obtained to any degree of accuracy warranted by the experimental data.

## Experimental

**Materials.**—The polystyrene used was obtained from B.X. Plastics in sheet form under the trade name Styrafoil. It was of the order of 0.1 mm. thick and its density was found to be 1.051 g./cm.<sup>3</sup>. Its intrinsic viscosity  $[\eta]$  in litres/base mole at 25° C in toluene was 11.97 and hence, using the relationship,

$$[\eta] = 3.04 \times 10^{-3} M^{0.65}, \quad . \quad . \quad . \quad (3)$$

obtained by Bamford and Dewar,<sup>6</sup> where  $M$  is the "viscosity average" molecular weight, a value of 340,000 is obtained for the molecular weight.

The chloroform was of A.R. quality. The methyl alcohol, present as an oxidation inhibitor, was removed by refluxing with phosphorus pentoxide followed by distillation. The purified material was kept in a dry state. Dibutyl phthalate used as a diluent for the chloroform was technical material. It was dried over calcium chloride and was then purified by distillation under reduced pressure. Only the middle fractions were used in these experiments.

<sup>5</sup> Crank and Henry, (submitted for publication).

<sup>6</sup> Bamford and Dewar, *Proc. Roy. Soc. A*, 1948, **192**, 329.

**Procedure.**—Rectangular pieces of polystyrene sheet were suspended in vessels each containing an atmosphere maintained at a fixed partial pressure of chloroform by means of dibutyl phthalate-chloroform mixtures, and kept in a thermostat at 25° C. The partial pressure of chloroform was different in each vessel. The mass of each polystyrene specimen was estimated from time to time by rapid weighing on an aperiodic balance. This weighing did not appreciably disturb the system as its duration was of the order of seconds in experiments lasting from two to sixty days. The thickness of each specimen was estimated from its area, dry weight and known density.

**The Effect of Still Air.**—It may be argued that since the presence of air produces a gradient of concentration of chloroform vapour in the diffusion vessel, this could be the cause of the variation in the rates of uptake of chloroform which are shown in Fig. 1 and discussed later in the paper. It is easy

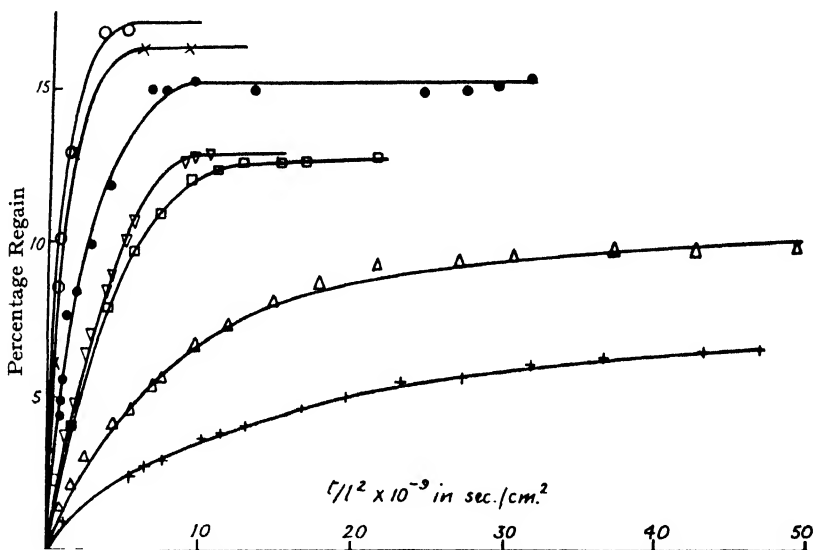


FIG. 1.—Rate of uptake of chloroform by polystyrene sheet at 25° C.

to see, however, even in the worst case, i.e. when the rate of sorption is highest, that the gradient of chloroform concentration in the air is negligibly small. Thus a rate of transfer of chloroform of 2 mg./hr. corresponds to a gradient of about  $2 \times 10^{-4}$  mg. cm.<sup>-2</sup>, taking the diffusion coefficient of chloroform in air to be approximately 0.1 cm.<sup>2</sup> sec.<sup>-1</sup>. This gradient is negligible since the equilibrium concentration of chloroform in the air is of the order of 0.5 mg. cm.<sup>-3</sup>. An attempt to estimate the effect of air was made by carrying out one experiment in a vessel from which all air had been removed. The results of this experiment are shown in Table I. Other conditions were the same as for the experiment carried out in the presence of air and it is seen that even in this case of a high chloroform concentration, no effect of air can be detected.

TABLE I.—EFFECT OF AIR ON THE RATE OF UPTAKE OF CHLOROFORM BY POLYSTYRENE SHEET AT 25° C

Experiment	% Regain of Chloroform	$t/l^2 \times 10^{-9} \text{ sec./cm.}^2$
In presence of air . . . . .	1.9	0.0893
	3.3	0.193
	6.1	0.483
In absence of air . . . . .	3.3	0.194

## Results and Discussion

**The Effect of Heat of Sorption.**—King and Cassie<sup>7</sup> have shown for the rapid uptake of water vapour by wool, when the effect of air is removed, that the rate-determining step of the sorption process is the rate of loss of heat of sorption from the wool material. That this is not likely to be the case in our experiments is evident from a consideration of the most rapid sorption. The heat of mixing of polystyrene and chloroform is not likely to be very high and so the heat of sorption can be taken as being roughly equal to the latent heat of vaporisation of chloroform, which is about 60 cal./g. The specimen absorbs less than 2 mg. in the first hour so the heat absorbed is of the order of  $0.002 \times 60 = 0.12$  cal. The mass of the specimen is about 100 mg. and its specific heat about  $0.3$  cal. deg.<sup>-1</sup> at 25°C so that the increase of temperature would be roughly 4°C if there were no loss of heat. In actual fact the heat loss will reduce this figure considerably and so temperature change will be an unimportant factor in the sorption process.

### Absorption-Time Curves and Derivation of Diffusion Coefficients.

For the special case in which the diffusion coefficient is constant and equal to  $D_0$  say, the appropriate formal mathematical solution of the diffusion equation may be written in the convenient form,

$$\frac{M_t}{M_\infty} = 1 - \frac{8}{\pi^2} \sum_{m=0}^{\infty} \frac{1}{(2m+1)^2} \exp \{-D_0(2m+1)^2 \pi^2 t/l^2\}, \quad (4)$$

where  $M_t$  is the total amount of chloroform absorbed by the polystyrene sheet of thickness  $l$  at time  $t$  and  $M_\infty$  the equilibrium sorption attained theoretically after infinite time. The application of this solution to the present problem is based on the assumption that immediately the polystyrene sheet is placed in the chloroform atmosphere, the concentration of chloroform at each surface of the sheet attains a value corresponding to the equilibrium regain for the vapour pressure of chloroform in that atmosphere, i.e. the concentration acquired instantaneously on the surface is that attained throughout the polystyrene after infinite time. The surface concentration is assumed constant throughout the sorption process, and the polystyrene is considered to be initially free of chloroform. In deriving eqn. (4) the thickness  $l$  of the sheet is assumed to remain constant as diffusion proceeds, but in practice as the chloroform enters the polystyrene swelling occurs and the thickness increases. Eqn. (4) can still be applied, however, provided the concentration and thickness are measured in suitable units. Thus if a new unit of length is chosen such that unit increment in length includes unit mass of polystyrene per unit area of sheet, then the thickness of the sheet remains constant on the new scale, being equal to the mass of polystyrene sheet per unit area initially, i.e. equal to the product of the initial thickness and the density. In terms of the new unit of length, concentration is defined as the mass of chloroform per unit mass of polystyrene in any element of overall volume, which is the usual way of measuring regain. The diffusion coefficient measured in this way is defined as the flux of chloroform across unit area of a section, which moves so that the mass of polystyrene on each side of it remains constant, divided by the space gradient of concentration at the section measured on the new scales. For present purposes in order to apply (4) to a swelling sheet it is convenient to let  $l$  denote the initial thickness measured in cm. and to include the (density)<sup>3</sup> factor in the diffusion coefficient  $D_0$ . The relation between the diffusion coefficient measured in this way and diffusion coefficients obtained by other methods, is discussed fully in another paper.<sup>8</sup>

<sup>7</sup> King and Cassie, *Trans. Faraday Soc.*, 1940, **36**, 445.

<sup>8</sup> Crank and Hartley (submitted for publication).



It is readily seen from (4) that the value of  $t/l^2$  for which  $M_t/M_\infty$  has any given value is independent of  $M_\infty$  when the diffusion coefficient is constant. In particular it is easy to show that the value of  $t/l^2$  for which  $M_t/M_\infty = \frac{1}{2}$ , conveniently written  $(t/l^2)_{\frac{1}{2}}$ , is given by

$$\left(\frac{t}{l^2}\right)_{\frac{1}{2}} = -\frac{1}{\pi^2 D_0} \ln \left\{ \frac{\pi^2}{16} - \frac{1}{9} \left( \frac{\pi^2}{16} \right)^2 \right\}, \quad (5)$$

approximately, the error being about 0.001 %. Thus we have

$$D_0 = 0.04939 / (t/l^2)_{\frac{1}{2}}, \quad (6)$$

and hence, if an experimental absorption-time curve is obtained for a system in which the diffusion coefficient is constant, the value of this constant can be determined by use of (6).

Inspection of the curves of Fig. 1 shows at once that  $(t/l^2)_{\frac{1}{2}}$  is not independent of  $M_\infty$ , and therefore that the diffusion coefficient is not constant. Application of eqn. (6) to each of the curves of Fig. 1 yields some mean value  $\bar{D}$ , say, of the variable diffusion coefficient averaged over the range of concentration appropriate to each curve. Values of  $(t/l^2)_{\frac{1}{2}}$  and  $\bar{D}$  are presented in Table II. A separate paper<sup>5</sup> describes

TABLE II.—DIFFUSION COEFFICIENTS FOR CHLOROFORM IN POLYSTYRENE AT 25° C. ALL DIFFUSION COEFFICIENTS ARE IN CM.<sup>2</sup>/SEC.  $\times 10^{-10}$

% Regain at Equilibrium = $C_0$	$(t/l^2)_{\frac{1}{2}}$ sec./cm. <sup>2</sup> $\times 10^{10}$	$\bar{D}$ expt.	1st Approximation			2nd Approximation		
			$\frac{1}{C_0} \int_0^{C_0} D dC$ cm. <sup>2</sup> /sec. $10^{-10}$	$D$	$\bar{D}$ calc.	$\frac{1}{C_0} \int_0^{C_0} D dC$ cm. <sup>2</sup> /sec. $10^{-10}$	$D$	$\bar{D}$ calc.
5.0	—	0.024 (extrap.)	0.024	0.024 (extrap.)	0.024	0.024	0.024	0.024
7.5	1.130	0.0437	0.0437	0.110	0.0504	0.039	0.12	0.044
9.9	0.620	0.0797	0.0797	0.288	0.103	0.062	0.29	0.080
12.9	0.288	0.171	0.171	0.780	0.238	0.125	0.40	0.17
13.2	0.248	0.199	0.199	0.970	0.276	0.144	0.54	0.20
15.1	0.151	0.326	0.326	3.36	0.585	0.216	1.6	0.33
16.3	0.0583	0.846	0.846	10.5	1.20	0.583	6.6	0.85
16.8	0.0481	0.972	0.972	16.0 approx.	—	—	—	—

an attempt to discover the significance of the  $\bar{D}$  values measured in this way. Numerical solutions of the diffusion equation were evaluated for a number of variable diffusion coefficients of the general form

$$D = 1 + f(C/C_0),$$

and by applying (6) to the absorption-time curves so calculated,  $\bar{D}$  values were obtained. In Table III the  $\bar{D}$  values for several diffusion coefficients are compared with the corresponding values of

$$(1/C_0) \int_0^{C_0} D dC,$$

which are readily calculated from the known relation between  $D$  and  $C$ . The data for sorption presented in Table III show that  $\bar{D}$  provides a reasonable approximation to

$$(1/C_0) \int_0^{C_0} D dC.$$

The data for desorption and the mean data are discussed later.

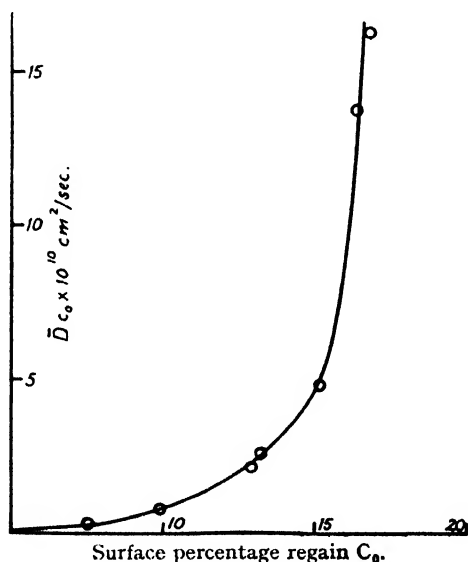
TABLE III.—SIGNIFICANCE OF  $\bar{D}$  FOR SOME EMPIRICAL DIFFUSION COEFFICIENTS OF THE FORM,  $D = 1 + f(c)$ , WHERE  $c = C/C_0$ 

$f(c)$	$\int_0^1 D dC = \frac{1}{C_0} \int_0^{C_0} D dC$	Absorption		Desorption		Mean of Absorption and Desorption	
		$\bar{D}$	% Error*	$\bar{D}$	% Error*	$\bar{D}$	% Error*
10c	6.00	7.14	+19	4.44	-26	5.79	-3
7.5c	4.75	5.66	+19	3.64	-23	4.65	-2
4.8c	3.40	4.15	+22	2.58	-24	3.36	-1
2.5c	2.25	2.77	+23	1.66	-26	2.22	-1
4.8c <sup>3</sup>	2.20	2.55	+16	1.80	-18	2.17	-1
4.8c <sup>1/3</sup>	4.60	4.88	+6	4.20	-9	4.54	-1
100c <sup>2</sup> e <sup>-10c</sup>	2.38	1.98	-17	2.62	+10	2.31	-3
14.8c(1-c)	3.47	3.42	-1	3.42	-1	3.42	-1

Thus by deducing a value of  $\bar{D}$  from each of the experimental curves of Fig. 1 and assuming the approximate relation

$$\bar{D} = \frac{1}{C_0} \int_0^{C_0} D dC, \quad (7)$$

a graph showing  $\bar{D}C_0$ , that is,  $\int_0^{C_0} D dC$ , as a function of  $C_0$  can be drawn as in Fig. 2. Numerical or graphical differentiation of the curve with

FIG. 2.— $\bar{D}C_0$  as a function of  $C_0$ .

respect to the upper limit  $C_0$  gives a first approximation to the relation between  $D$  and  $C$ , which is shown in Fig. 3, together with the  $\bar{D}$ - $C$  curve for comparison. The numerical data are given in Table II.

\* This is the error involved in assuming  $\bar{D} = \frac{1}{C_0} \int_0^{C_0} D dC$  expressed as a percentage of  $\frac{1}{C_0} \int_0^{C_0} D dC$ .

The approximate diffusion coefficient shown in Fig. 3 varies much more rapidly with concentration than did any of the relations examined in Table III, and so the error involved in assuming eqn. (7) may be

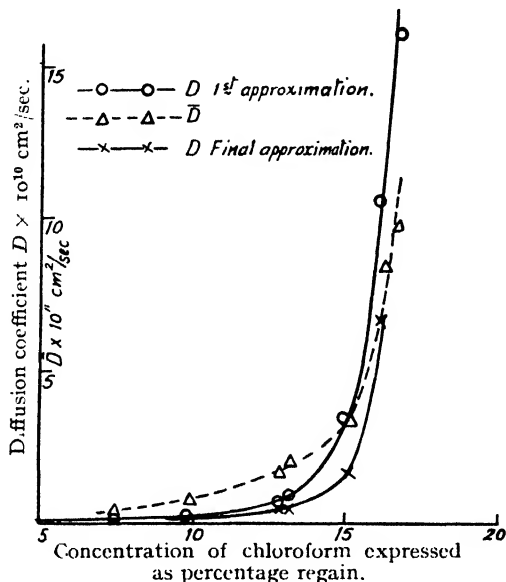


FIG. 3.

expected to be correspondingly greater. In order to estimate the errors in the present work, calculations of the absorption-time curves were carried out, using the mathematical methods described elsewhere,<sup>5</sup> and the  $D$ - $C$  relation shown as the first approximation in Fig. 3. The  $\bar{D}$  values derived from these calculations are shown in Table II, column 6. Comparison of these calculated  $\bar{D}$  values with the experimental  $\bar{D}$  values, and therefore with the first estimate of

$$(1/C_0) \int_0^{C_0} D \, dC,$$

shows the errors involved in use of (7). Hence the correct relationship between  $\bar{D}$  and

$$(1/C_0) \int_0^{C_0} D \, dC$$

for the calculated  $D$ - $C$  relation can be plotted and from this a second approximation to

$$(1/C_0) \int_0^{C_0} D \, dC$$

can be read off for each of the experimentally determined values of  $\bar{D}$ . By repeating the differentiation, a second approximation to the diffusion coefficient  $D$  is obtained from which new  $\bar{D}$  values are calculated, which when compared with the second approximation to

$$(1/C_0) \int_0^{C_0} D \, dC$$

provide improved corrections to eqn. (7). The process can be repeated if necessary till the calculated values of  $\bar{D}$  agree with the experimental values on which the successive approximations are based.

The successive steps in the process of calculation may be summarised as follows—

- (i) Plot  $M_t/M_\infty$  against  $t/l^2$  for various values of  $C_0$ .
- (ii) Deduce  $\bar{D}$  for each of the curves plotted in (i), using eqn. (6), and plot  $\bar{D} C_0$  against  $C_0$ .
- (iii) Differentiate this curve to obtain a first approximation to the  $D$ - $C$  relation.
- (vi) Compute curves of  $M_t/M_\infty$  against  $t/l^2$  for various  $C_0$ 's, using this first approximation to  $D$ , and hence derive a set of calculated  $\bar{D}$  values.
- (v) Plot the  $\bar{D}$  values calculated in (iv) against the values of

$$(1/C_0) \int_0^{C_0} D dC$$

from which the first approximation to the  $D$ - $C$  relation was derived.

- (vi) Read off from this curve

$$(1/C_0) \int_0^{C_0} D dC$$

for each experimental value of  $\bar{D}$  and replot against  $C_0$ .

- (vii) Differentiate to obtain a second approximation to the  $D$ - $C$  relation.
- (viii) Repeat the process till the calculated values of  $\bar{D}$  agree with the experimental values to within the required degree of accuracy.

Table II shows that after only two stages in the approximation the diffusion coefficient  $D$  is determined as accurately as the experimental data permit. No attempt has been made to improve the value of the diffusion coefficient for the concentration 16.8 % regain because the experimental data and the process of graphical differentiation are very uncertain for the high regains. The lowest regain at which measurements were made was 7.5 %. A value of  $D$  at 5.0 % regain was obtained by extrapolating the  $D$ - $C$  curve and  $D$  was assumed constant at this extrapolated value of  $0.024 \times 10^{-10}$  cm.<sup>2</sup>/sec. for lower regains for purposes of calculation. The final form of the diffusion coefficient-concentration relation is compared with the first approximation in Fig. 3. The essential features of this relation are not substantially changed by the mathematical refinement, although the accuracy of the results is improved considerably.

**Comparison of Sorption and Desorption-Time Curves.**—If instead of taking the value of  $(t/l^2)_{\frac{1}{2}}$  for sorption, the value for desorption is taken a second set of  $\bar{D}$  values can be obtained. The data of Table III show that the  $\bar{D}$  values calculated from the empirical diffusion coefficients for desorption represent the integrated mean diffusion coefficients to much the same order of accuracy as do those derived from sorption data. The means of the  $\bar{D}$  values derived from sorption and desorption in Table III are seen to provide a much better approximation to

$$(1/C_0) \int_0^{C_0} D dC$$

than either of the values taken separately.

For this reason, measurements of rates of desorption of chloroform from polystyrene were carried out on samples with initial equilibrium regains of 15.1 % and 9.9 %. A current of dry air at 25° C was passed over the samples which were weighed from time to time. The desorption data are shown graphically in Fig. 4. For the case of 15.1 % regain,  $(t/l^2)_{\frac{1}{2}}$  for desorption is roughly four times as great as for sorption; whereas when the equilibrium sorption is 9.9 % the two values of  $(t/l^2)_{\frac{1}{2}}$  are about the same. In both cases the last stages of desorption are extremely slow.

This kind of effect is to be expected qualitatively since in the later

stages of desorption the concentration in the sample is everywhere much less than 15.1 % so that the operative diffusion coefficient is a mean over a range of low concentrations only, whereas in the case of sorption the

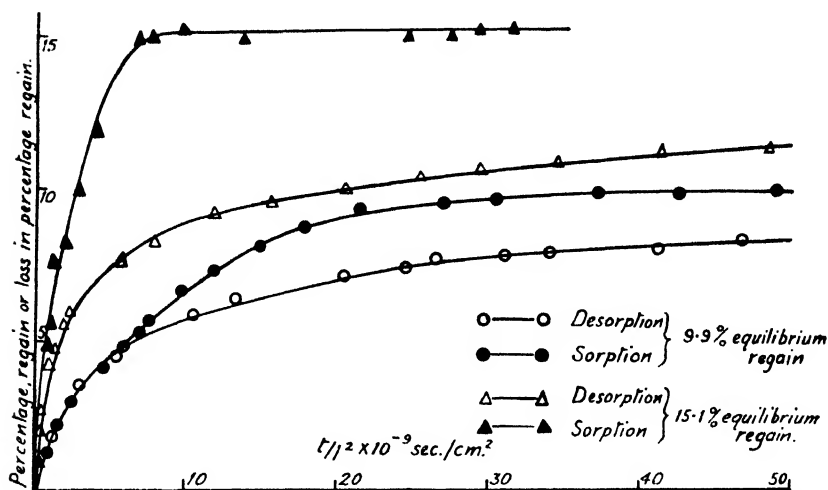


FIG. 4.—Rate of loss of chloroform by polystyrene sheet at 25° C compared with the rate of uptake of chloroform by the same material at 25° C.

average is taken over a range of high concentrations only. The former will thus include only low values of the diffusion coefficient and the latter only high values for the kind of diffusion coefficient shown in Fig. 3 and hence the last stages of desorption will be relatively slow. Where  $\bar{D}$  increases several-fold throughout the concentration range a considerable effect is to be anticipated.

The differences between the sorption and desorption curves of Fig. 4 are much greater than for any of the diffusion coefficients considered in Table III. For this reason the value of  $\bar{D}$  was calculated at various stages of both sorption and desorption for 15.1 % equilibrium regain by comparing the experimental curves with the mathematical solution of eqn. (4). The results obtained are shown in Table IV and it is seen that  $\bar{D}$  for the desorption process decreases rapidly as desorption proceeds but  $\bar{D}$  for sorption is roughly constant for a considerable part of the process. This suggests that in sorption  $\bar{D}$  represents an average taken over all concentrations of chloroform from zero to 15.1 % until more than 50 % equilibrium regain has been absorbed, whereas in desorption the range of concentration over which the average is taken decreases almost from the start.

TABLE IV.—CALCULATION OF  $\bar{D}$  FROM SORPTION AND DESORPTION CURVES

$M_t/M_\infty$	$\bar{D}t/l^2$ (Calc.)	$t/l^2 \times 10^{-10}$ Sorption sec./cm. <sup>2</sup>	$\bar{D} \times 10^{10}$ cm. <sup>2</sup> /sec.	$t/l^2 \times 10^{-10}$ Desorption sec./cm. <sup>2</sup>	$\bar{D} \times 10^{10}$ Desorption cm. <sup>2</sup> /sec.
0.357	0.025	0.090	0.276	0.180	0.138
0.504	0.050	0.152	0.326	0.579	0.086
0.698	0.100	0.306	0.326	3.17	0.032
0.887	0.200	0.576	0.354	> 7	0.028

This is confirmed by the calculated curves of Fig. 5, which shows

how the concentration of chloroform varies with distance through the sample at the time for which  $M_t/M_\infty = \frac{1}{2}$ , in the case where the equilibrium regain is 15.1 %. The shape of the curve for sorption is of the

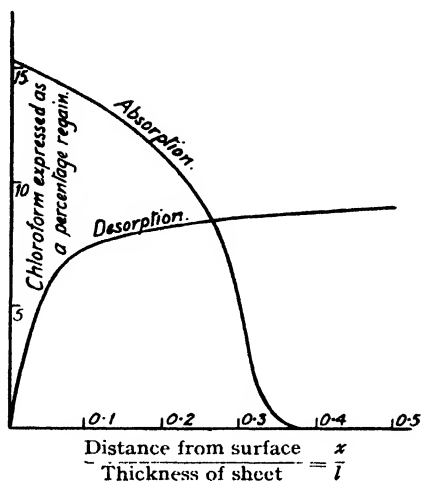


FIG. 5.—Calculated concentration-distance curves  $M_t/M_\infty = \frac{1}{2}$ .

familiar form associated with a diffusion coefficient which increases with concentration increasing, and it is clear that the concentration at the centre of the sheet is still effectively zero and the sheet is still behaving as a semi-infinite one when  $M_t/M_\infty = \frac{1}{2}$ . The corresponding curve for desorption shows that here the concentration at the centre of the sheet has already fallen considerably below the value of 15.1 % from which it started. Because of these considerations only the sorption measurements have been used as described above in determining the diffusion coefficient-concentration relation.

The authors' thanks are due to Mr. E. P. Cummins for technical assistance, and to Miss M. E. Henry, who carried out the computational work.

Research Laboratory,  
Courtaulds Limited,  
Maidenhead, Berks.

# THE SURFACE TENSION OF AQUEOUS SOLUTIONS OF $\alpha : \beta$ -DIHYDROXY- $\gamma$ -ARYLOXYPROPANES

BY A. C. R. DEAN AND W. BRADLEY

Received 25th October, 1948

The surface tensions of various  $\alpha : \beta$ -dihydroxy-aryloxypropanes in aqueous solution have been determined. Substitution of alkyl, alkoxyl and carbo-alkoxyl groups in the benzene nucleus of the  $\alpha$ -phenyl ether of glycerol increases the capillary activity of the parent compound, the effect increasing with increase in the chain-length of the substituent. The increase in capillary activity is greatest with alkyl substituents and least with alkoxyl substituents. The effect of a substituent diminishes in the order:  $p > m > o$ .

Halogen substitution in the benzene nucleus increases the capillary activity of the parent compound, the effect increasing with increase in the atomic weight of the substituent. Amino substitution in the benzene nucleus reduces the capillary activity of the parent compound. Acylating the amino group increases the capillary activity of an amino derivative, the effect increasing with increase in the chain-length of the acyl group.

The areas occupied by the glycerol ether molecules at the surface of an aqueous solution, have been calculated and the orientation of the molecules is discussed.

There does not appear to be any simple relation between the surface activity of an aryl ether of glycerol and its ability to relax skeletal muscle.

---

The mon-aryl ethers of glycerol form a group of simple compounds many of which show interesting biological properties. The  $\alpha$ - $p$ -chloro-phenyl ether of glycerol inhibits the growth of *B. coli*, *Staph. aureus*, *Ps. pyocyanea*, *Proteus vulgaris*, *B. paratyphosus* and *B. dysenteriae* at concentrations in the range 0.15-0.2 %<sup>1</sup> and several members of the group cause relaxation of skeletal musculature when administered to humans or laboratory animals.<sup>2</sup> The muscle-relaxing property is the more interesting because of its importance for medicine and surgery and it has become desirable to determine its physical and chemical basis. In the present communication the surface activity of a range of  $\alpha : \beta$ -dihydroxy- $\gamma$ -aryloxypropanes is described and the results considered in relation to the muscle-relaxing properties of the compounds.

The compounds investigated were supplied by members of the B.D.H. research staff. The muscle-relaxing potencies were determined in the B.D.H. Biological Department. The compounds comprised  $\alpha : \beta$ -dihydroxy- $\gamma$ -phenoxypropane and a number of its derivatives including alkyl, alkoxyl, hydroxyalkyl, halogen, amino, acylamino and carbo-alkoxy derivatives.

## Experimental

The surface tensions were determined at 25°C by the maximum bubble pressure method of Sugden.<sup>3</sup> Benzene, purified by the method of Richards<sup>4</sup> was used to standardise the apparatus, which was similar to that described by Sugden. Quayle and Smart<sup>5</sup> have stressed the necessity of keeping the tubes vertical, and their method for confirming this by taking a second reading after

<sup>1</sup> Hartley, *Quart. J. Pharm.*, 1947, **20**, 388.

<sup>2</sup> Berger and Bradley, *Brit. J. Pharm.*, 1946, **1**, 265.

<sup>3</sup> Sugden, *J. Chem. Soc.*, 1924, 27.

<sup>4</sup> Richards and Shipley, *J. Amer. Chem. Soc.*, 1914, **36**, 1825.

<sup>5</sup> Quayle and Smart, *ibid.*, 1944, **66**, 937.

rotating the tubes through  $180^\circ$  has been adopted. The purity of the compounds was established by analysis, followed by recrystallisation until solutions prepared from successive fractions had similar surface tensions at a given concentration.

## Results and Discussion

**The Effect of Substitution in the Benzene Nucleus on the Capillary Activity of  $\alpha : \beta$ -Dihydroxy- $\gamma$ -phenoxypropane.**—The surface tension-concentration curve (Fig. 1) of the phenyl ether of glycerol in aqueous solution is that of a typical capillary-active substance.<sup>6</sup> Substitution in

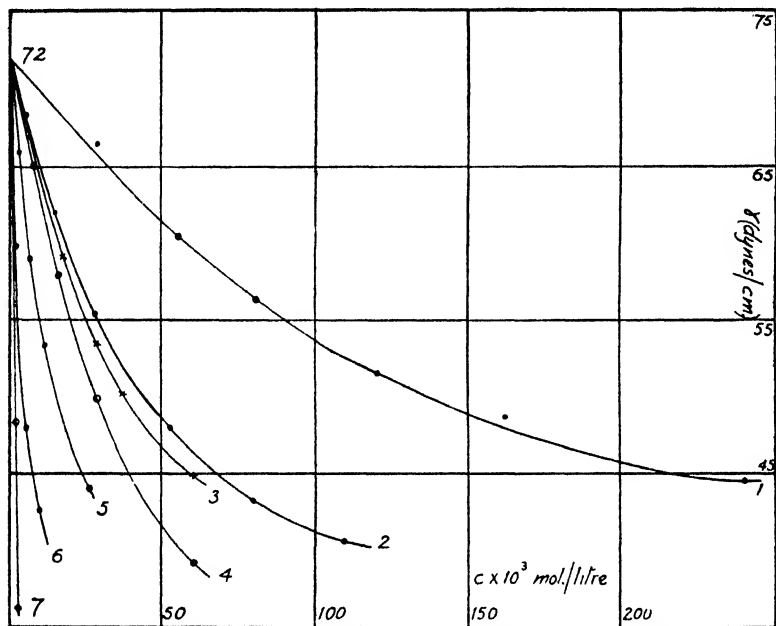


FIG. 1.—Alkyl substituents in the phenyl nucleus of  $\alpha : \beta$ -dihydroxy- $\gamma$ -phenoxypropane.

- |                      |                      |                      |
|----------------------|----------------------|----------------------|
| 1. Parent compound.  | 2. <i>o</i> -Methyl. | 3. <i>m</i> -Methyl. |
| 4. <i>p</i> -Methyl. | 5. <i>o</i> -Ethyl.  | 6. <i>o</i> -Propyl. |
|                      | 7. <i>p</i> -Butyl.  |                      |

the benzene nucleus of alkyl, alkoxy, carbo-alkoxy or halogen radicals increases the capillary activity of the parent compound, whilst amino substitution in the *p*-position to the glycerol side-chain reduces the capillary activity.

**Alkyl Substitution.**—The capillary activities of the homologues of  $\alpha : \beta$ -dihydroxy- $\gamma$ -phenoxypropane increase as the chain length of the substituent increases. Results are recorded in Fig. 1. An alkyl group has the greatest effect when it occupies the *p*-position. It is less effective in the *m*-position and least in the *o*-position. The comparison is expressed more clearly in Fig. 5, where the capillary equivalent concentrations (i.e. the concentrations which reduce the surface tension of water to 50 dynes/cm.) are graphed. The ratio of the capillary equivalent concentrations of *o*- and *p*-substituted methyl compounds is 1.64, whilst with the corresponding butyl compounds it is 1.22. It will be shown later that the area of the surface occupied by the molecule is least with the substituent in the *p*-position and greatest with the substituent in the *o*-position. The increased surface activity with *p*-substitution is then



explained by a greater number of molecules being able to enter the surface layer of the solution.

The solubility of the *o*-tolyl ether of glycerol is  $70.9 \times 10^{-3}$  g. mol./litre but supersaturated solutions may be prepared by cooling a solution which is saturated at a higher temperature. The surface tensions of supersaturated solutions were determined up to a concentration of  $110.6 \times 10^{-3}$  g. mol./litre, the  $\gamma$ - $c$  curve continuing regularly into this supersaturated region (Fig. 1) showing that above the normal solubility limit molecules are still able to enter the surface layer.

**Alkoxy Substitution.**—Alkoxy substitution increases the capillary activity of the parent compound in a similar manner to alkyl substitution (Fig. 2) but the effect is smaller than that of an alkyl group having the

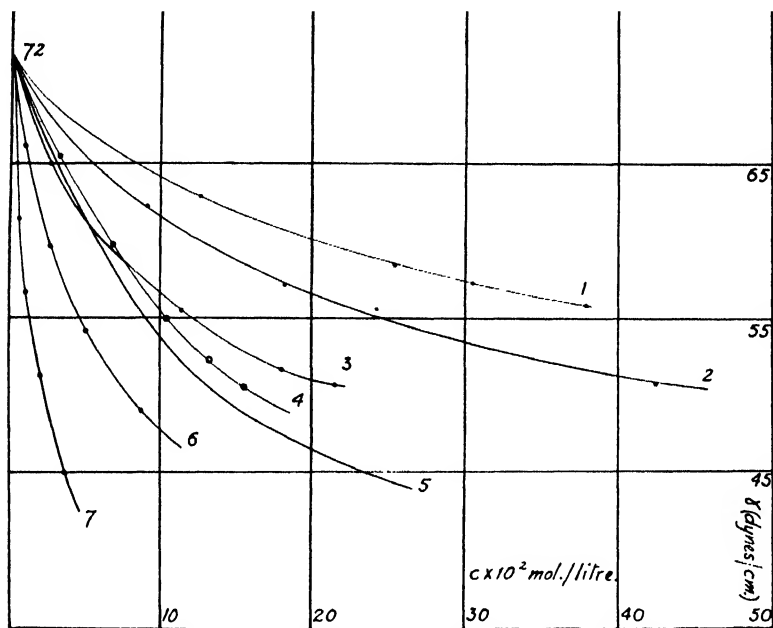


FIG. 2.—Alkoxy substituents in the phenyl nucleus of  $\alpha$ : $\beta$ -dihydroxy- $\gamma$ -phenoxypropane.

- |                             |                       |                      |
|-----------------------------|-----------------------|----------------------|
| 1. <i>o</i> -Hydroxymethyl. | 2. <i>o</i> -Hydroxy. | <i>o</i> -Methoxy.   |
| 4. <i>p</i> -Methoxy.       | 5. Parent compound.   | 6. <i>o</i> -Ethoxy. |
|                             | 7. <i>o</i> -Propoxy. |                      |

same number of carbon atoms, and the concentrations required for capillary equivalent solutions are approximately five times greater than those for the corresponding alkyl compounds. The capillary activity increases as the homologous series is ascended and *p*-substitution has a greater effect than *o*; the ratio of the capillary equivalent concentrations for *o*- and *p*-substituted methoxy compounds is 1.61 (*o/p* methyl = 1.64).

**Carbo-alkoxy Substitution.**—The capillary equivalent concentrations of the carbo-alkoxy derivatives lie between those of the alkyl and the alkoxy derivatives (Fig. 5). The surface tension-concentration curves are given in Fig. 3.

**Halogen Substitution.**—In general, halogen substitution increases the capillary activity of the parent compound, the effect increasing with the increase in atomic weight of the substituent (Fig. 3). *p*-Substitution has a greater effect on the capillary activity than *o*-substitution, the ratio of the capillary equivalent concentrations for *o*- and *p*-chloro compounds being 1.22.

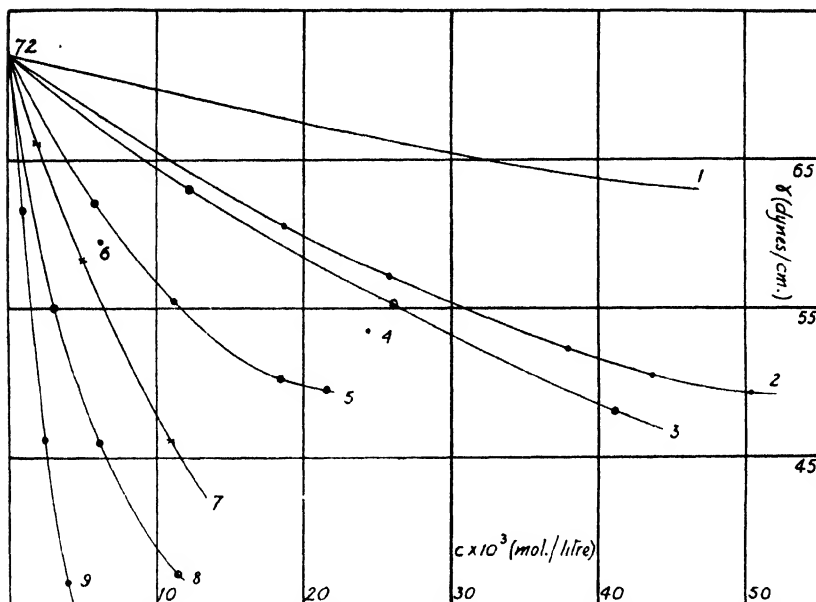


FIG. 3.—Halogen and carboalkoxy substituents in the phenyl nucleus of  $\alpha : \beta$ -dihydroxy- $\gamma$ -phenoxy propane.

- |  |                           |                                       |
|--|---------------------------|---------------------------------------|
| 1. Parent compound                     | 2. <i>o</i> -Chloro.      | 3. <i>p</i> -Chloro.                  |
| 4. <i>o</i> -Bromo (solubility limit). | 5. <i>p</i> -Carboethoxy. | 6. <i>o</i> -Iodo (solubility limit). |
| 7. <i>m</i> -Methyl <i>p</i> -chloro.  | 8. <i>p</i> -Carbobutoxy. | 9. <i>p</i> -Carbobutoxy.             |

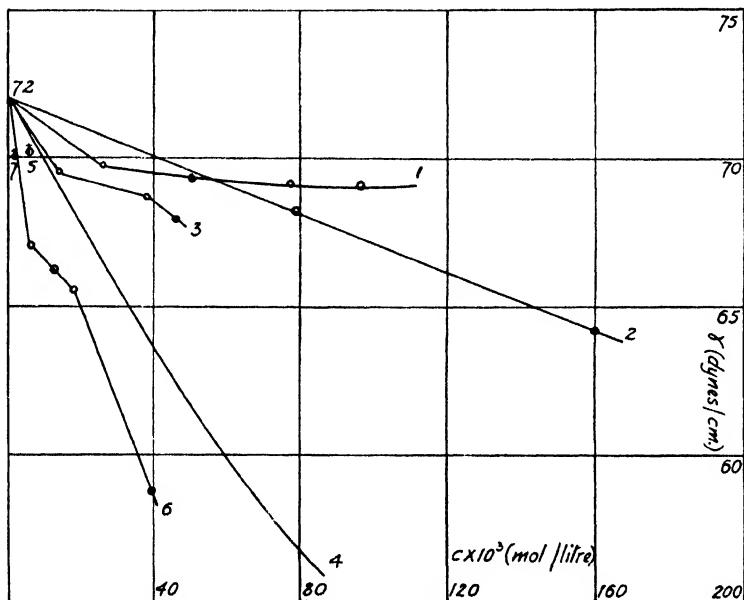


FIG. 4.—Amino and acylamino substituents in the phenyl nucleus of  $\alpha : \beta$ -dihydroxy- $\gamma$ -phenoxy propane.

- |                            |   |                              |
|----------------------------|---|------------------------------|
| 1. <i>p</i> -Acetylamino.  | 2. <i>p</i> -Amino.                           | 3. <i>p</i> -Propionylamino. |
| 4. Parent compound.        | 5. <i>p</i> -Furoylamino (solubility limit).  |                              |
| 6. <i>p</i> -Butyrylamino. | 7. <i>p</i> -Benzoylamino (solubility limit). |                              |

**Amino and Acylamino Substitution.**—The introduction of an amino group into the *p*-position of the benzene nucleus of  $\alpha$ : $\beta$ -dihydroxy- $\gamma$ -phenoxypropane reduces the capillary activity of the parent compound. Replacement of the hydrogen in the amino group by an acyl group reverses this effect, the capillary activities increasing in the order: aminophenyl, acetylaminophenyl, propionylaminophenyl, phenyl and butyrylaminophenyl. With higher concentrations ( $c \times 10^3 > 58$  moles/litre) the aminophenyl derivative has a greater capillary activity than the acetylaminophenyl derivative. The *p*-furoylaminophenyl and *p*-benzoylaminophenyl derivatives have slightly higher capillary activities than the parent compound, but are very sparingly soluble (Fig. 4).

**The Relationship between the Capillary Equivalent Concentrations and the Number of Carbon Atoms.**—The concentrations of the glycerol ethers necessary to reduce the surface tension of water to 50 dynes/cm. (capillary equivalent concentrations) are given in Fig. 5. Ferguson<sup>7</sup>

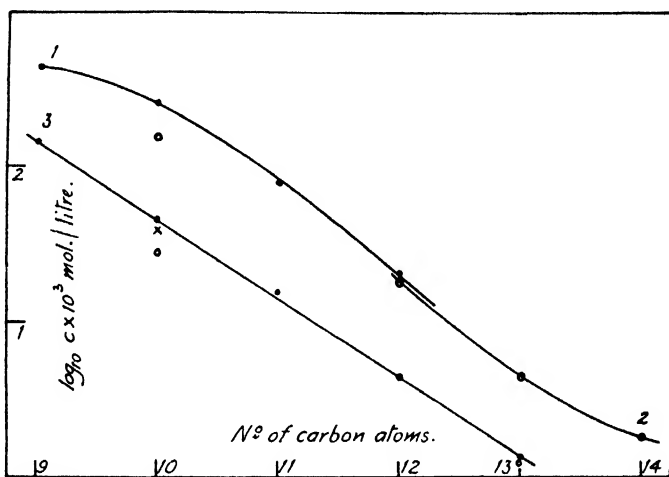


FIG. 5.—The relationship between the capillary equivalent concentrations and the number of carbon atoms in the molecule.

1. Alkoxy substituents. 2. Carboalkoxy substituents. 3. Alkyl substituents  
— *o*-Compounds. × *m*-Compounds. O *p*-Compounds.

has shown that in the homologous series of the normal primary alcohols there is a linear relationship between the logarithm of this concentration and the number of carbon atoms. The *o*-alkyl-substituted glycerol ethers show a similar relationship, as also does the alkoxy series. *o*-Hydroxyphenyl  $\alpha$ -glycerol ether is unique. The relationship does not hold with carbo-alkoxy substituents.

With the less soluble compounds, e.g. the *o*-bromo, *o*-iodo, *p*-amino, *p*-acetyl amino, *p*-propionyl amino, *p*-butyryl amino, *p*-benzoyl amino and *p*-furoyl amino derivatives of  $\alpha$ : $\beta$ -dihydroxy- $\gamma$ -phenoxypropane it was not possible to obtain sufficiently high concentrations to reduce the surface tension of water to 50 dynes/cm.

**The Adsorption of Glycerol Ethers in Aqueous Solution.**—From the Gibbs equation Schofield and Rideal<sup>8</sup> have derived the relationship

$$FA/RT = 2.303 F/S,$$

where  $F = \gamma_0 - \gamma$ ,  $A$  is the area occupied by a molecule in the surface

<sup>7</sup> Ferguson, *Proc. Roy. Soc. B*, 1939, **127**, 391.

<sup>8</sup> Schofield and Rideal, *ibid. A*, 1925, **109**, 69.

and  $S$  is the slope of the curve relating  $F$  and  $\log_{10} c$  ( $c$  = molar concentration). Using this equation the areas occupied by the glycerol ether molecules in the surface have been calculated; they are given in Table I. The molecular volumes were calculated from the densities of the solutions, and it is assumed that these values apply to the surface layer.

TABLE I.—THE ADSORPTION OF SUBSTITUTED PHENYL  $\alpha$ -GLYCEROL ETHERS

Substituent in Phenyl Nucleus	Molal Volume (cm. <sup>3</sup> )	Volume of One Molecule Å <sup>3</sup>	Concentration of Solution (mol./l. $\times 10^3$ )	Area (Å <sup>2</sup> )	Thickness of film (Å)
Nil . . .	168.4	278	{ 229.1 241.0 30-60 110.6*	38.7 31.6 37.9 37.9	— 8.8 7.9 7.9
<i>o</i> -Methyl . .	182.3	301	10-50	39.6	8.1
<i>o</i> -Ethyl . . .	196.3	324	5-20	44.6	7.8
<i>o</i> -Propyl . .	210.7	348	14-60	36.6	8.2
<i>m</i> -Methyl . .	182.5	301	15-60	30.3	10.0
<i>p</i> -Methyl . .	182.4	301	19-50	34.3	9.8
<i>o</i> -Chloro . .	202.8	335	23.41	27.3	12.2
<i>p</i> -Chloro . .	203.0	335	53.215	52.8	—
<i>o</i> -Methoxy . .	198.4	327	85	51.7	—
<i>o</i> -Ethoxy . .	212.4	351	18-35	45.6	—
<i>o</i> -Propoxy . .	227.0	374	6-21.5	43.5	—
<i>p</i> -Carboethoxy . .	240.5	397	5.8-11.7	32.1	—
<i>p</i> -Carbopropoxy . .	254.0	419	2.4-4.4	25.5	—
<i>p</i> -Carbobutoxy . .	268.1	442			—

= Supersaturated solution.

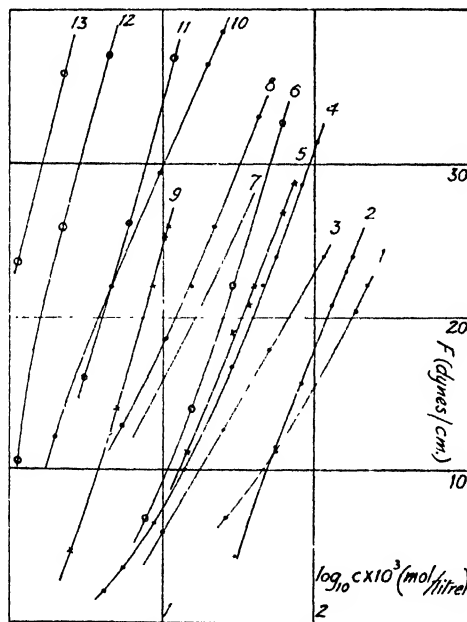


FIG. 6.—The relationship between surface pressure and concentration.

- |                       |                             |                                       |
|-----------------------|-----------------------------|---------------------------------------|
| 1. <i>o</i> -Methoxy. | 2. Parent compound.         | 3. <i>o</i> -Ethoxy.                  |
| 4. <i>o</i> -Methyl.  | 5. <i>m</i> -Methyl.        | 6. <i>p</i> -Methyl.                  |
| 7. <i>o</i> -Propoxy. | 8. <i>o</i> -Ethyl.         | 9. <i>m</i> -Methyl <i>p</i> -chloro. |
| 10. <i>o</i> -propyl. | 11. <i>p</i> -Carbopropoxy. | 12. <i>p</i> -Carbobutoxy.            |
|                       |                             | 13. <i>p</i> -Butyl.                  |

In all the cases examined the relationship between  $F$  and  $\log_{10} c$  was practically linear (Fig. 6) and hence the Milner equation,<sup>9</sup>

$$(\gamma_0 - \gamma)/\gamma_0 = \alpha + \beta \log c$$

(where  $\gamma_0$  is the surface tension of water and  $\alpha$  and  $\beta$  are constants), can be used to predict the surface tension of aqueous solutions of glycerol ethers within the concentration limits of the experiments.

From an examination of films of phenols, Adam<sup>10</sup> has shown that the cross-sectional area of the benzene nucleus is  $24 \text{ \AA}^2$ . In the case of phenol Goard and Rideal<sup>11</sup> came to a similar conclusion and suggested that the phenol molecule lay on the surface of the water with the hydroxyl group drawn inwards, leaving the plane of the molecule at right-angles to the surface. A similar orientation would be expected of the molecules of the glycerol ethers. Examination of Table I shows that the areas occupied by the *p*-chlorophenyl ether and the *p*-carbobutoxyphenyl ether are  $27 \text{ \AA}^2$  and  $25.5 \text{ \AA}^2$  respectively, whilst those of the *p*-methyl phenyl ether and the phenyl ether are  $30 \text{ \AA}^2$  and  $31.6 \text{ \AA}^2$ . These areas are in fairly good agreement with those found by Adam and Rideal when it is considered that concentrations are used instead of activities. If this orientation is correct it would be expected that molecules with substituents in the *o*- and *m*-positions would occupy a larger surface area than those with a *p*-substituent. This is the case, since the *o*- and *m*-methyl phenyl ethers have a larger surface area than the *p*-homologue, and a similar relationship holds for the *o*- and *p*-chlorophenyl ethers. It is interesting to note that as the *o*-alkyl series is ascended the areas increase progressively, the thickness of the film remaining practically constant at  $8 \text{ \AA}$ .

In the *o*-alkoxy series and in the case of the *p*-carboethoxy ether the surface areas are much larger, probably because at the highest concentrations which could be obtained the surface layer is not packed with molecules and hence the molecules are not oriented with their long axes at right-angles to the surface. In methyl derivatives the area is greatest with substitution in the *o*-position and least in the *p*-position.

**Pharmacological Activity and Surface Activity.**—A number of simple derivatives of  $\alpha : \beta$ -dihydroxy- $\gamma$ -phenoxy-propane are able to bring about relaxation of skeletal muscles in small laboratory animals.<sup>2</sup> They also decrease the surface tension of water in various degrees.  $\alpha : \beta$ -Dihydroxy- $\gamma$ -(*p*-aminophenoxy)-propane, which is unable to relax skeletal muscle, has little effect on surface tension. Whilst surface activity appears to contribute to the muscle-relaxing power of glycerol ethers, however, other factors, too, must come into play. Thus  $\alpha : \beta$ -dihydroxy- $\gamma$ -(2-methylphenoxy)-propane is more effective as a muscle relaxant than any related simple ether, whilst its surface activity is in no sense abnormal.

The authors thank the directors of The British Drug Houses, Ltd., for permission to publish this paper.

Research Dept.,  
The British Drug Houses, Ltd.,  
London, W.1.

<sup>9</sup> Milner, *Phil. Mag.*, 1907, **13**, 96.

<sup>10</sup> Adam, *Physics and Chemistry of Surfaces* (1946), p. 54.

<sup>11</sup> Goard and Rideal, *J. Chem. Soc.*, 1925, 1673.

# THE EFFECTS OF SUBSTITUENTS IN THE NAPHTHALENE RING

## PART I. THE BASIC STRENGTHS OF THE MONONITRO-NAPHTHYLAMINES

BY ALEXANDER BRYSON

Received 1st November, 1948

The basic strengths of the 14 mononitro-naphthylamines have been measured in aqueous solution. The effect of a nitro group in the same nucleus as an amino group is similar to that in the nitroanilines but the reduction in basic strength is greater when quinonoid contributions are possible and smaller if the groups are in *meta* positions. The difference between  $\alpha$  and  $\beta$  positions is increased. When the nitro group is in the other nucleus the effect is much smaller and is mainly inductive. Quinonoid contributions cause a further decrease in basicity of about 0.3 units. The difference between the basic nature of the amino group in the  $\alpha$  and  $\beta$  positions is largely eliminated.

3-nitro-2-naphthylamine is 10,000 times stronger than 1-nitro-2-naphthylamine. This provides further evidence for the substantial contribution of the Erlenmeyer formula in the structure of naphthalene.

---

A great deal of work has been done on derivatives of the benzene series to determine the influence of substituents on acid-base equilibria and on reaction rates. As a result much light has been thrown on the interplay of inductive and resonance effects while the "ortho effect" still defies complete explanation. Comparatively little systematic work of a like nature has been published on naphthalene compounds, although much thought has been given to the nature of the bonds in the naphthalene nucleus. The quantum-mechanical treatment by Pauling and Wheland and others<sup>1</sup> indicates that the degree of double bonding between the carbon atoms in naphthalene varies considerably, and that it is appreciably greater between  $C_1-C_2$ , than between  $C_2-C_3$ , while for the central link  $C_9-C_{10}$ , the amount should be intermediate in value. These conclusions are not unsupported by experimental evidence. McLeish and Campbell<sup>2</sup> have shown that the bromine atom in 1-bromo-2-naphthylamine is readily removed by boiling with piperidine while 3-bromo-2-naphthylamine is unaffected. 5-Bromo- and 6-bromo-2-naphthylamine and also 8-chloro-1-naphthylamine show the same lack of reactivity. This phenomenon is taken to be an expression of the resistance of the 2:3- and the binuclear-substituted compounds to the inductive and mesomeric polarizations which are necessary for the reaction with an anionoid reagent to succeed. Arnold and Sprung<sup>3</sup> and Bergmann and Hirshberg<sup>4</sup> have reported acid-base equilibria in various hydroxy-naphthaldehydes and halogen-substituted naphthoic acids. In both cases there is an observable difference between the  $C_1-C_2$  and the  $C_2-C_3$  compounds. Fieser and Lothrop<sup>5</sup>

<sup>1</sup> Pauling and Wheland, *J. Chem. Physics*, 1933, **1**, 362.

<sup>2</sup> McLeish and Campbell, *J. Chem. Soc.*, 1937, 1103.

<sup>3</sup> Arnold and Sprung, *J. Amer. Chem. Soc.*, 1938, **60**, 1153.

<sup>4</sup> Bergmann and Hirshberg, *J. Chem. Soc.*, 1936, 331.

<sup>5</sup> Fieser and Lothrop, *J. Amer. Chem. Soc.*, 1935, **57**, 1459; 1936, **58**, 2050.

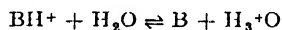
have investigated the diazo coupling of dihydroxy-naphthalenes, and have concluded that the arrangement of the bonds in the naphthols corresponds to the Erlenmeyer structure (I) and that this structure represents a condition of considerable rigidity. The available chemical evidence on the naphthalene system has been adequately covered by Fieser.<sup>6</sup>



(I) It seems, however, that little systematic experimental work has been done on the effects of substituents in various positions of an already substituted naphthalene compound, especially in relation to the transmission of resonance effects from one ring to the other. The earliest attempt was by Eberbach<sup>7</sup> who determined by conductivity methods in 1893 the dissociation constants of the ten available amino-naphthalene sulphonic acids. Hampson and Weissberger<sup>8</sup> and Vassiliev and Syrkin<sup>9</sup> have measured and discussed the dipole moments of the chloro-naphthalenes and ten of the nitro-naphthylamines respectively. Hodgson and Hathway<sup>10</sup> have attempted to correlate the colour of the nitro-naphthylamines with their electronic structure and have also discussed substitution in the naphthalene ring in a number of papers.<sup>11</sup>

### Experimental and Results

The present author therefore decided to investigate the influence of the nitro group in various positions on the basic strength of the amino group in the nitro-naphthylamines. The last of the fourteen isomers, viz., 2:3 and 2:7 nitro-naphthylamine have recently been prepared by Hodgson and his collaborators and the series is relatively easy to prepare. (For a summary of available methods, see Hodgson and Hathway.<sup>12</sup>) These substances are yellow, orange or red; they are but slightly soluble in water producing yellow or orange solutions even in concentrations less than 0.001 M, and they are all weak bases. Their basic strengths as measured by the  $pK_a$  values for the reaction



vary from 3.16 to -1.6. Extensive hydrolysis of the salts occur and it is thus impossible to determine the  $pK$  values by the usual potentiometric titration. In this research the values were determined by the titration of a dilute solution of the nitro-amine, ca. 0.0005 M with a suitable acid, the pH being measured with a glass electrode and the progress of salt formation being followed by the use of the Spekker absorptiometer. The salts are practically colourless and correction may be made for any absorption due to these. The whole operation of titration, pH measurement and drum reading was carried out in a 4 cm. cell, and since it is difficult to control the temperature, the results are given for room temperature. Hall and Sprinkle<sup>13</sup> have given temperature corrections of -0.013 to -0.020 pH per °C for aromatic amines, but such corrections do not alter the significance of the results, since the alteration is not more than 0.1 unit at most.

The  $pK_a$  values between 2.2 and 3.2 were determined in very dilute solutions and should approximate to thermodynamical constants. The accuracy of these values can be taken as  $\pm 0.05$  pH unit. For the remaining three bases whose values are +0.54, -1.0 and -1.6 the figures are much more speculative since they were measured in strongly acid solution. They can be considered as having little more than comparative value.

The results are given in Table I. Melting points from the literature are taken from Hodgson and Hathway;<sup>12</sup> dipole moments are from Vassiliev and Syrkin.<sup>9</sup>

<sup>6</sup> Gilman, *Organic Chemistry*, Chap. 3.

<sup>7</sup> Eberbach, *Z. physik. Chem.*, 1893, **11**, 608.

<sup>8</sup> Hampson and Weissberger, *J. Chem. Soc.*, 1936, 353.

<sup>9</sup> Vassiliev and Syrkin, *Acta Physicochim.*, 1941, **14**, 414.

<sup>10</sup> Hodgson and Hathway, *Trans. Faraday Soc.*, 1945, **41**, 115; 1947, **43**, 643.

<sup>11</sup> Hodgson and Hathway, *J. Soc. Dyers Col.*, 1945, **61**, 283; 1946, **62**, 241; 1947, **63**, 109; 1947, **63**, 46.

<sup>12</sup> Hodgson and Hathway, *ibid.*, 1947, **63**, 231.

<sup>13</sup> Hall and Sprinkle, *J. Amer. Chem. Soc.*, 1932, **54**, 3469.

TABLE I  
 BASIC STRENGTHS OF THE MONONITRONAPHTHYLAMINES

	Position of Substituents		Colour	M.p.		pK <sub>a</sub>	t °C	Dipole Moment
	NH <sub>2</sub>	NO <sub>2</sub>		Expt.	Literature			
Mononuclear substituted compounds	1	2	yellow	144	144	-1.6	20	4.89
	1	3	"	135.5	136	2.27	20	5.14
	1	4	"	191	191	0.54	20	6.97 <sup>(a)</sup>
	2	1	orange	127	127	-1.0	20	4.47
	2	3	red	135		2.93	25	—
	2	4	"	98	140 <sup>(b)</sup> 98.5	2.98 2.61	25	4.62
Binuclear substituted compounds (Quinonoid contributions likely)	1	5	red	118.5 <sup>(c)</sup>	119	2.80	25	5.22
	1	7	"	134	134	2.83	20	—
	2	6	gold	203	203	2.90	21	7.10 <sup>(a)</sup>
	2	8	red	105 <sup>(c)</sup>	104.5	2.86	25	4.47
Binuclear substituted compounds (Quinonoid contributions unlikely)	1	6	red	166	167	3.15	20	—
	1	8	orange-red	97.5 <sup>(c)</sup>	97	2.79	23	3.12
	2	5	red	144 <sup>(c)</sup>	146	3.16	25	5.03
	2	7	yellow	181	184	3.13	21	—

(a) Dipole moments measured in benzene; all others are in dioxan.

(b) The author is indebted to Dr. H. H. Hodgson for a sample of this compound.

(c) In the preparation of these compounds the nitration was carried out at -25° C using solid CO<sub>2</sub> in the nitrating bath.

For comparison, Table II gives relevant figures for naphthylamines, nitronaphthalenes, aniline and its derivatives.

TABLE II

Compound	pK <sub>a</sub> (25°)	Dipole Moment
α-Naphthylamine . . . .	3.92 <sup>1</sup> , 4.0 <sup>2</sup>	1.49 <sup>4</sup>
β-Naphthylamine . . . .	4.11, <sup>1</sup> 4.3 <sup>2</sup>	1.77 <sup>4</sup>
Aniline . . . . .	4.6 <sup>1</sup>	1.54 <sup>4</sup>
m-Nitroaniline . . . . .	2.65, * 2.6 <sup>2</sup>	—
p-Nitroaniline . . . . .	1.1 <sup>2</sup>	6.17 <sup>4</sup>
o-Nitroaniline . . . . .	-0.05, * -0.17, <sup>3</sup> -0.25 <sup>2</sup>	4.26 <sup>4</sup>
Nitrobenzene . . . . .	—	4.01 <sup>4</sup>
α-Nitronaphthalene . . . .	—	3.98 <sup>4</sup>
β-Nitronaphthalene . . . .	—	4.36 <sup>4</sup>

\* This research; values are for 21° C.

<sup>1</sup> Hall and Sprinkle, *J. Amer. Chem. Soc.*, 1932, **54**, 3468.

<sup>2</sup> Farmer and Wurth, *J. Chem. Soc.*, 1904, **85**, 1713.

<sup>3</sup> Hammett and Paul, *J. Amer. Chem. Soc.*, 1934, **56**, 837.

<sup>4</sup> Vassiliev and Syркин, *loc. cit.*

**Measurement of Dissociation Constants.**—The compounds were all recrystallized from water before saturated solutions were prepared. For those compounds with pK values between 2.2 and 3.2 the procedure



was as follows. The solution of the nitroamine was diluted with water to obtain a series of concentrations from saturated to 0.1 saturated. These solutions were placed in 4 cm. Spekker cells and the drum readings noted. The 601 violet filter was used throughout. If the graph of drum reading against concentration did not approach a straight line, more dilute solutions were used until this was obtained. This dilution curve was used subsequently to determine the amount of nitroamine during the titration of 25 ml. solution with N/10 HCl from a microburette, the pH being measured concurrently by a glass electrode (Cambridge model potentiometer) calibrated at 3.57 with potassium hydrogen tartrate. About 10 successive additions of 0.1 ml. of acid were made, this being sufficient to produce up to 70 % salt formation. To determine the absorption due to the salt, 1 ml. 10 N HCl was added and the blank so obtained was used to correct the individual drum readings. The following figures illustrate the measurements with 8-nitro-2-naphthylamine.

TABLE III  
WATER SETTING 1.30; FILTER, 601 VIOLET; TUNGSTEN LAMP

ml. 0.1 N HCl	0.1	0.2	0.3	0.35	0.4	0.5	0.55	0.6	0.7	0.9
pH	3.56	3.22	3.11	3.04	2.98	2.86	2.80	2.77	2.69	2.61
Drum reading	1.20	1.065	1.005	0.955	0.90	0.80	0.78	0.77	0.68	0.61
Corrected drum reading	1.20	1.055	0.995	0.945	0.885	0.78	0.76	0.75	0.66	0.59
Fraction neutralization	0.16	0.295	0.345	0.385	0.435	0.52	0.53	0.54	0.60	0.65
pK <sub>a</sub> (calc.)	2.84	2.86	2.83	2.85	2.87	2.89	2.85	2.84	2.88	2.88

Av. = 2.86

Drum reading with 1 ml. 10 N HCl in cell = 0.025

For the very weakly basic amines the method was altered since much stronger acids were necessary and were used in greater amounts, dilution effects then becoming important. In these cases the required amount of acid was added to 25 ml. nitroamine solution, the solution was cooled and made up to 30 ml. The concentration-drum reading curve was prepared from nitroamine solutions diluted in the ratio of 30/25. The pH was measured to zero on the pH meter using 0.1 N HCl (pH, 1.08<sub>5</sub>) as calibrating solution. The blank was impossible to measure in these cases and was taken as 0.04. Figures for 4-nitro-1-naphthylamine are given in Table IV:

TABLE IV

5 N HCl	0.5	1.0	1.5	2.0	2.5	3
pH	1.20	0.87	0.71	0.60	0.48	0.40
pK <sub>a</sub> (calc.)	0.53	0.51	0.50	0.55	0.54	0.58

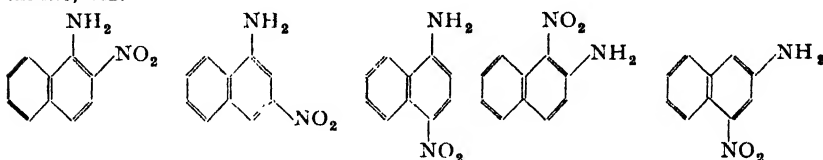
Av. 0.54

The same procedure was used for *o*-nitroaniline, the constant with 70 % HClO<sub>4</sub> being -0.05. With 36 N H<sub>2</sub>SO<sub>4</sub> the readings on the pH meter for the first three additions of acid were 0.35, 0.17, and 0.02, giving constants of -0.02, -0.10, and -0.05 in agreement with the above. By continuing the titration with conc. H<sub>2</sub>SO<sub>4</sub> and using the value of the constant as -0.05, it was possible to calculate apparent pH values for solutions up to a normality of 4.6. Using such values, the titration of the very weak bases 2-nitro-1-naphthylamine and 1-nitro-2-naphthylamine gave values of -1.6 and -1.0 respectively. These values can be regarded as approximate, but the nature of the enquiry does not demand greater accuracy.

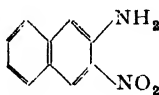
### Discussion

It is possible to predict by analogy with the benzene series that the mononuclear-substituted nitronaphthylamines should be similar in properties to the nitroanilines and that wherever ionic contributions of a quinonoid type are present the strength of the base should be considerably decreased. For the binuclear-substituted compounds the influence of the nitro group should be less and quinonoid contributions should have a small but appreciable effect on the basic strength. In general these predictions are borne out by the figures in Table I. There are, however, some deviations. We are, in addition, concerned with the matter of the difference in degree between the  $\alpha$  and  $\beta$  positions and with the influence of the nitro group on the basic strength of the amino group in these two positions. In order to discuss this it is convenient to classify the nitronaphthylamines in four groups.

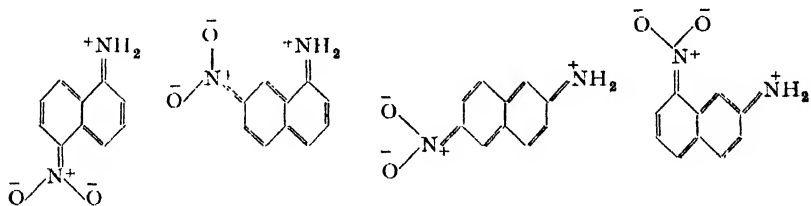
1. The mononuclear-substituted compounds except 3-nitro-2-naphthylamine, viz.



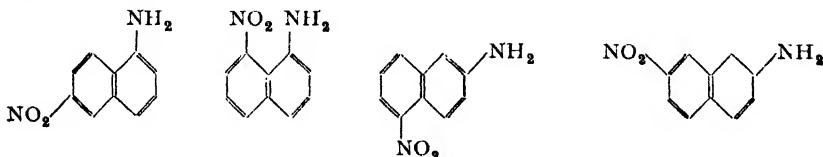
2. 3-Nitro-2-naphthylamine



3. Binuclear-substituted compounds in which there is the possibility of quinonoid contributions of the following types,

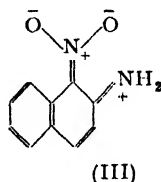
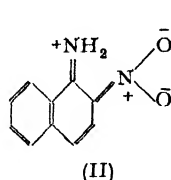


4. Binuclear-substituted compounds in which no possibility exists of such contributions,



Members of the first group show the same relative characteristics as the nitroanilines. Both the *ortho* substituted compounds are exceedingly weak bases with  $pK_a$  values of  $-1.6$  for 2-nitro-1-naphthylamine and  $-1.0$  for 1-nitro-2-naphthylamine, and both are much weaker than *o*-nitro-aniline ( $-0.05$ ). This is clearly due to the greater double-bond character of the C<sub>1</sub>—C<sub>2</sub> linkage with the result that the states (II) and (III) make a substantial contribution to the resonance hybrid of the base. 4-Nitro-1-naphthylamine is completely analogous to *p*-nitro-aniline. In the

two *meta* compounds, the difference between the  $\alpha$ -amino and  $\beta$ -amino groups is preserved, although both bases are stronger than would be expected, e.g., 4-nitro-2-naphthylamine has the same value as *m*-nitro-aniline. It will be observed that in all the members of this group the



difference between the strengths of the  $\alpha$  and  $\beta$  compounds has been maintained and even widened.

The other member of the mononuclear-substituted series, 3-nitro-2-naphthylamine is quite exceptional. Its  $pK_a$  value of 2.98 makes it 10,000 times stronger as a base than 1-nitro-2-naphthylamine. It thus provides further evidence of the notable difference between the  $C_1-C_2$  and the  $C_2-C_3$  bonds and indicates the smaller double-bond character of the latter. It is indeed surprising that 3-nitro-2-naphthylamine is a stronger base than 4-nitro-2-naphthylamine in spite of the fact that the former is an *ortho* compound. One explanation of this remarkable result is that the relative fixation of the bonds due to the substantial contribution of the Erlenmeyer structure should lead to a Mills-Nixon effect in which the nitro and amino groups are brought closer together. Jenkins<sup>14</sup> has concluded that the strength of aromatic bases can be explained mainly on inductive grounds, the potential at the amino nitrogen atom being influenced by the inductive effect of the  $-\text{NO}_2$  dipole. If the direction of the dipole moment becomes more nearly parallel with that of the amino group its effect will be reduced and the basic strength of the amino group increased. The difference between 1-nitro-2-naphthylamine and 3-nitro-2-naphthylamine is much greater than in other equivalent cases quoted in the literature (Table V).

TABLE V

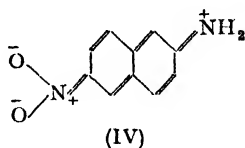
Compound	$pK_a$
1-Hydroxy-2-naphthaldehyde <sup>3</sup> . . . .	7.86
2-Hydroxy-1-naphthaldehyde <sup>3</sup> . . . .	8.27
3-Hydroxy-2-naphthaldehyde <sup>3</sup> . . . .	9.93
1-Chloro-2-naphthoic acid <sup>4</sup> . . . .	3.80
3-Chloro-2-naphthoic acid <sup>4</sup> . . . .	4.37

The effect of hydrogen bonding on the basic strengths of nitro amines is not known, but it is likely to be more noticeable in the 1 : 2 than in the 2 : 3 compounds owing to the higher double-bond character of the  $C_1-C_2$  bond.\*

The remaining two groups comprise firstly, the binuclear-substituted nitro-naphthylamines in which the contributions of the ionic or quinonoid

\* An examination of the infra-red spectra of the mononitro-naphthylamines has shown that whereas there is considerable hydrogen bonding in the cases of 2-nitro-1-naphthylamine and 1-nitro-2-naphthylamine, hydrogen bonding does not occur in 3-nitro-2-naphthylamine: both the amino and the nitro bonds were examined. This difference is most simply attributed to the high proportion of double-bond character in the  $C_1-C_2$  bond. (Private communication, Dr. D. E. Hathway.)

states should be noticeable. Such contributions as the following (IV) are, however, of less significance than in the mononuclear-substituted compounds because of the greater charge separation, but the effect is quite definite and results in a lowering of the  $pK_a$  values of the group



by approximately 0.3 unit under those for the remaining binuclear-substituted group. This last group contains the compounds in which no important contributions of a quinonoid type involving the two nitrogen atoms can be expected, and they are therefore the most basic of all the nitro-naphthylamines, the average value for three members being 3.15. (It will be observed that if corrections are applied for temperature variations, the figures are somewhat further apart but not more than 0.1 pH unit.) The only exception is 8-nitro-1-naphthylamine (2.79) but *peri*-derivatives generally show anomalous behaviour. In this case we must postulate that the angle between the  $-\text{NO}_2$  dipole and the C—N link of the amino group is about the same as that for the 2-nitro-3-naphthylamine since the inductive effect of the  $-\text{NO}_2$  group is about the same in both cases. Bergmann and Hirshberg<sup>4</sup> report  $pK_a$  values for 3-chloro-2-naphthoic acid and 8-chloro-1-naphthoic acids of 4.37 and 4.05 respectively which show similar trends ( $\alpha$ - and  $\beta$ -naphthoic acids, 3.69 and 4.17).

The values for the  $\alpha$  and  $\beta$  compounds in each of the binuclear-substituted groups are surprisingly close and indicate that the difference between the basic nature of the amino group in the  $\alpha$  and  $\beta$  positions has been largely but not completely eliminated when the nitro group is in the second ring. The effect of the nitro group in these compounds is mainly inductive and deactivating, and the reduction in basic strength compared to the parent naphthylamine is not more than 1 unit. This is in marked contrast to the effect of the nitro group in the mononuclear-substituted compounds where the distinction between the  $\alpha$ - and  $\beta$ - $\text{NH}_2$  groups is even more marked than in the parent substances. Further evidence is required to test whether this behaviour is general, and in a subsequent paper the amino-sulphonic acids will be discussed in this connection. It may be observed that while the  $pK_a$  values of anthracene 1- and 2-carboxylic acids are 3.69 and 4.2 respectively, those for anthraquinone 1- and 2-carboxylic acids<sup>14</sup> are 3.37 and 3.42. This evidence seems to confirm the above observation although the possible effect of hydrogen bonding should not be overlooked.

**Dipole Moments and Basic Strengths.**—The available figures for the dipole moments of the nitro-naphthylamines given in Table I do not permit a satisfactory correlation with the basic strengths. The values for the 1:4 and 2:6 compounds show the expected exaltation of dipole moment but the 1:5 compound has a value close to that calculated from the moments of the individual groups. Nevertheless, the basic strengths of the 1:5 and 2:6 compounds are almost equal. Both 1-nitro-2-naphthylamine and 8-nitro-2-naphthylamine have the same dipole moment (4.47) while their basic strengths ( $pK_a$  values,  $-1.0$  and  $+2.86$ ) are widely different. It is clear that no simple relation exists between these physical properties.

It was hoped that the results obtained for the  $pK_a$  values would serve as a suitable test for the contention of Jenkins<sup>14</sup> that  $pK$  values are proportional to the potential established by the  $-\text{NO}_2$  dipole at the functional

<sup>14</sup> Jenkins, *J. Chem. Soc.*, 1937, 1137.

<sup>15</sup> Lauer, *Ber., B.*, 1937, 70, 1288.

atom. Until more information is available about the dipole moment of the  $-\text{NO}_2$  group in different positions in the molecule and how it is influenced by other groups, it is impossible to do this. Assuming the values of the dipole moments of the  $-\text{NO}_2$  group to be 3.98 and 4.36 in the  $\alpha$  and  $\beta$  positions, only rough agreement with the principle is found.

Thanks are due to Prof. R. J. W. Le Fevre, Dr. F. H. Reuter, and Messrs R. M. Gascoigne, R. A. Eade and G. K. Hughes for helpful discussion.

*Chemistry Department,  
Technical College,  
Sydney, Australia.*

## MOLECULAR FORCE FIELDS

### PART VIII. THE VIBRATION FREQUENCIES OF SOME OCTAHEDRAL $\text{XY}_6$ MOLECULES

BY D. F. HEATH AND J. W. LINNETT

*Received 8th November, 1948*

We have examined the application of the orbital valency force field and simple valency force field, both including reasonable repulsion between non-bonded atoms, to the molecules  $\text{SF}_6$ ,  $\text{SeF}_6$  and  $\text{TeF}_6$ . It is found that the O.V.F.F. reproduces the observed frequencies much more satisfactorily than does the S.V.F.F. However, the simple O.V.F.F. does not account satisfactorily for the frequency of the vibration of symmetry  $F_{2u}$  which is lower than might have been expected. It is suggested that it is possible that during the vibration the bonding orbitals of the central atom accommodate themselves to the distortion by a change of hybridization rendering the distortion easier.

We have also studied the frequency values suggested by Begeleisen, Mayer, Stevenson and Turkevich for  $\text{UF}_6$  in relation to the frequencies of  $\text{SF}_6$ ,  $\text{SeF}_6$  and  $\text{TeF}_6$  and the application of the O.V.F.F. to those hexafluorides. It is found that the suggested values are not exactly what would have been anticipated. This is discussed and possible explanations are considered.

In Part III<sup>1</sup> of this series we described a new molecular force field which was based on the modern view that directed valency bonds are to be related to the form of the atomic orbitals. This field was therefore called the orbital valency force field. It was further applied to tetrahedral molecules in Parts IV<sup>2</sup> and V<sup>3</sup> where it was shown to be superior to the simple valency force field. The necessity of including terms in the potential energy (P.E.) function to allow for the repulsion between non-bonded atoms had been demonstrated in Part II<sup>4</sup> and further confirmed in Parts III, IV and V. The present paper describes the application of the orbital valency force field (O.V.F.F.) combined with the necessary repulsion terms to the octahedral molecules  $\text{SF}_6$ ,  $\text{SeF}_6$  and  $\text{TeF}_6$ . We also include a consideration of the vibration frequencies of the molecule  $\text{UF}_6$ .

The octahedral molecules,  $\text{XY}_6$ , of symmetry  $O_h$  each show six fundamental vibration frequencies. One vibration is non-degenerate (Class  $A_{1g}$ ), one is doubly degenerate (Class  $E_g$ ) and four are triply degenerate

<sup>1</sup> Heath and Linnett, *Trans. Faraday Soc.*, 1948, **44**, 873.

<sup>2</sup> Heath and Linnett, *ibid.*, 1948, **44**, 878.

<sup>3</sup> Heath and Linnett, *ibid.*, 1948, **44**, 884.

<sup>4</sup> Heath and Linnett, *ibid.*, 1947, **44**, 561.

(two in Class  $F_{1u}$  and one each in classes  $F_{2g}$  and  $F_{3u}$ ).<sup>5</sup> The forms of these (one member of each degenerate set) are shown in Fig. 1, in which

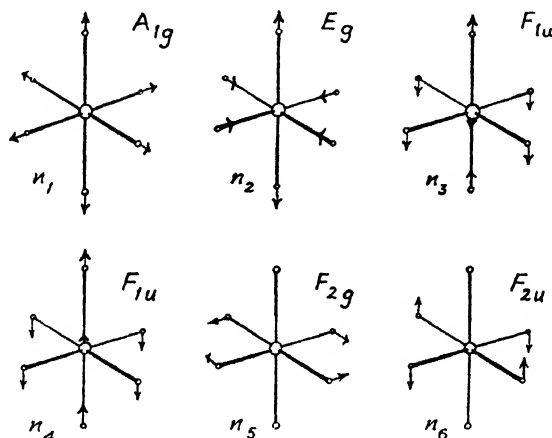


FIG. 1.—The fundamental vibrations of  $XY_6$  molecules of symmetry  $O_h$ .

the vibration frequencies are labelled  $n_1 \dots n_6$ ;  $n_1$ ,  $n_2$ , and  $n_3$  are associated with essentially valency vibrations, and  $n_4$ ,  $n_5$ , and  $n_6$  with essentially deformation vibrations.  $n_1$ ,  $n_2$ , and  $n_3$  are allowed to appear in the Raman spectrum,  $n_3$  and  $n_4$  are allowed to appear in the infra-red spectrum,  $n_6$  is not allowed to appear in either because the vibration of Class  $F_{2u}$  is forbidden for both the Raman and infra-red spectrum. This means that only the first five fundamental vibration frequencies can be directly determined spectroscopically.  $n_6$  has to be obtained either from combination tones or from specific heat data and it is therefore less accurate.

The frequencies of  $SF_6$ ,  $SeF_6$  and  $TeF_6$  are given in Table I. These

TABLE I.—VIBRATION FREQUENCIES OF  $XY_6$  MOLECULES IN  $CM.^{-1}$

Molecule	$n_1$	$n_2$	$n_3$	$n_4$	$n_5$	$n_6$
$SF_6$ . .	775	644	665	617	524	363
$SeF_6$ . .	708	662	787	461	405	245
$TeF_6$ . .	701	674	752	370	313	165

are obtained from a paper of Bartholomé and Sachse.<sup>6</sup> These workers suggested that certain anharmonicity corrections should be made to the observed frequencies but as their arguments for the magnitudes of the corrections to be applied do not seem altogether sound we have used the observed values uncorrected for anharmonicity.  $n_4$  for  $TeF_6$  was not directly observed but was derived from overtones. It seems to us that any value between 340 and 370  $cm.^{-1}$  would account satisfactorily for the overtones observed and one cannot therefore fix the value more closely than this. The frequency  $n_6$  is determined for all these molecules

<sup>5</sup> Herzberg, *Infra-red and Raman Spectra of Polyatomic Molecules* (Van Nostrand Co. Inc., 1945), p. 123.

<sup>6</sup> Bartholomé and Sachse, *Z. physik. Chem. B*, 1935, **28**, 257. Eucken and Ahrens, *ibid.*, 1934, **26**, 297. Eucken and Bartels, *ibid.*, 1921, **98**, 461. Eucken and Bertram, *ibid.*, 1936, **31**, 361. Yost, Steffens and Gross, *J. Chem. Physics*, 1934, **2**, 311.

by combining spectroscopic and specific heat data. Consequently this frequency may easily be in error by 20 cm.<sup>-1</sup>.

**Calculations.**—In obtaining an expression for the vibration frequencies we have used a P.E. function based on the simple O.V.F.F. with repulsion between the non-bonded atoms. That is, it has the form :

$$2V = 2B' \sum_j \Delta r_{ij} + k_1 \sum_j (\Delta r_{ij})^2 + k'\beta \sum_j (\Delta \beta_{ij})^2 - 2B \sum_{jk} \Delta R_{jk} + 2A \sum_{jk} (\Delta R_{jk})^2,$$

where  $i$  represents the central atom and  $j, k$ , etc., the outer atoms;  $\Delta r_{ij}$  is the increase in the bond length  $r_{ij}$  from the value in the equilibrium configuration and  $\Delta R_{jk}$  is the increase in the distance between the non-bonded atoms  $j$  and  $k$  from the value which  $R_{jk}$  has in the equilibrium configuration;  $\Delta \beta_{ij}$  is the angle the line from the central atom to atom  $j$  makes with the line in which the particular orbital has its maximum value, and it measures the movement of the atom away from the direction in which the orbitals of the two atoms show maximum overlap (see Part III).<sup>1</sup>  $B', k_1, k', B$  and  $A$  are constants. The second and third are the O.V.F.F. stretching and bending force constants. The fourth and fifth are those which represent the repulsion between the non-bonded atoms expressed in the form (see Part II),<sup>4</sup>

$$V = -B\Delta R + A(\Delta R)^2,$$

where  $B = -(dV/dR)_0$  and  $A = \frac{1}{2}(d^2V/dR^2)_0$ ,

these differentials being taken where  $R$  has the value for the equilibrium configuration. The first term involving  $B'$  is necessary so that  $V$  shall be a minimum when  $\Delta r, \Delta \beta$  and  $\Delta R$  are all zero.

The expressions for the six vibration frequencies of the octahedral molecules in terms of  $k_1, k_\beta, A$  and  $B/R$  are given below ( $k_\beta = k_\beta'/r^3$ );  $m_1$  is the mass of the central atom X and  $m_2$  is the mass of the outer atom Y. In addition we have given the expressions that would be obtained for the vibration frequencies using a P.E. function based on the S.V.F.F. with repulsion terms. The S.V.F.F. bending constant is designated by  $k_\alpha'$ ;  $k_\alpha (= k_\alpha'/r^2)$  appears in the formulae. Throughout the formulae we use  $\lambda_i = 4\pi^2 n_i^2$ .

#### CLASS $A_{1g}$

Both O.V.F.F. and S.V.F.F.

$$\lambda_1 = (k_1 + 8A)/m_2.$$

#### CLASS $E_g$

Both O.V.F.F. and S.V.F.F.

$$\lambda_2 = (k_1 - \frac{8B}{3R} + \frac{8}{3}A)/m_2.$$

#### CLASS $F_{1u}$

Both O.V.F.F. and S.V.F.F.

$$\begin{aligned} \lambda_3 + \lambda_4 &= f_{11}(1/m_2 + 2/m_1) + f_{22}(4/m_1 + 1/m_2) - 4\sqrt{2} \times f_{12}/m_1, \\ \lambda_3 \times \lambda_4 &= (f_{11}f_{22} - f_{12}^2)(1/m_2^2 + 6/m_1m_2), \end{aligned}$$

where

$$\begin{aligned} f_{11} &= (k_1 - 2B/R + 4A), \\ f_{12} &= (2\sqrt{2}A - \sqrt{2}B/R), \\ f_{22} &= (k_\beta + 3B/R + 2A) \text{ for the O.V.F.F.,} \\ f_{22} &= (2k_\alpha + 3B/R + 2A) \text{ for the S.V.F.F.} \end{aligned}$$

CLASS  $F_{2g}$ 

$$\lambda_5 = (k_\beta + 2B/R + 4A)/m_2 \text{ for the O.V.F.F.,}$$

$$\lambda_5 = (4k_\alpha + 2B/R + 4A)/m_2 \text{ for the S.V.F.F.}$$

CLASS  $F_{2u}$ 

$$\lambda_6 = (k_\beta + 2A)/m_2 \text{ for the O.V.F.F.,}$$

$$\lambda_6 = (2k_\alpha + 2A)/m_2 \text{ for the S.V.F.F.}$$

In introducing the repulsion constants into our calculations we have followed the procedure of Parts III and IV in which we supposed that the function  $a/R^{12}$  provided a sufficiently close approximation to the P.E. function for the interaction of the non-bonded atoms at the distances existing in the molecules with which we were concerned (i.e. at separations less than that at the minimum of the van der Waals' curve).<sup>7</sup> By doing this we are able to fix  $B/R$  once we have chosen  $A$  for  $B/R = \frac{1}{2}A$ , if  $V = a/R^{12}$ . (This will be discussed in more detail in a subsequent paper.) So in treating these molecules we have three adjustable constants per molecule— $k_1$ ,  $k_\beta$  and  $A$  if the O.V.F.F. is used and  $k_1$ ,  $k_\alpha$  and  $A$  if the S.V.F.F. is used. The results of our calculations of  $n_1 \dots n_6$  (those frequencies that can be directly observed spectroscopically) are shown in Table II. This Table lists the constants used and compares the

TABLE II. COMPARISON OF CALCULATED AND OBSERVED FREQUENCIES (IN CM.<sup>-1</sup>). THE CONSTANTS  $k_1$ ,  $k_\alpha$ ,  $k_\beta$ ,  $A$  AND  $B/R$  ARE GIVEN IN UNITS OF  $10^6$  DYNE/CM.

Molecule	$k_1$	$k_\alpha$ and $k_\beta$	$A$	$B/R$	$n_1$	$n_2$	$n_3$	$n_4$	$n_5$	% Error	
										$n_1, n_2, n_3,$	$n_4, n_5$
SF <sub>6</sub>	Observed				775	644	965	617	525	--	--
OVFF	3.55	1.15	0.425	0.0655	787	635	971	622	516	1.19	0.98
SVFF	3.7	0.4	0.4	0.0615	785	639	954	571	545	1.00	5.72
SeF <sub>6</sub>	Observed				708	662	787	461	405	--	--
OVFF	4.3	1.00	0.1875	0.0290	720	650	802	463	402	1.8	0.58
SVFF	4.3	0.25	0.20	0.307	726	657	794	382	408	1.3	8.94
TeF <sub>6</sub>	Observed				701	674	751	370 346	313	—	—
OVFF	4.85	0.78	0.075	0.0115	698	660	775	351	313	1.31	0
SVFF	4.9	0.20	0.080	0.0123	704	674	780	277	320	1.28	9
Average errors					.	.	OVFF			1.33	0.52
							SVFF			1.19	8.0
Average overall errors					.	.	OVFF			0.92	
							SVFF			4.6	

frequencies calculated with those observed. It also lists the average percentage error for the frequencies of the valency vibrations ( $n_1$ ,  $n_2$  and  $n_3$ ) and the average percentage error for the frequencies of the bending vibrations ( $n_4$  and  $n_5$ ). It will be seen that the O.V.F.F. with repulsion accounts for the observed frequencies very well, the average difference between calculated and observed being under 1 %. The S.V.F.F. with repulsion is much less successful. Moreover, the S.V.F.F. succeeds with the frequencies of the valency vibrations but fails with the frequencies of the deformation vibrations. It appears therefore that the O.V.F.F.

<sup>7</sup> See ref. 2 and Fowler and Guggenheim, *Statistical Thermodynamics* (C.U.P.), p. 285.



treatment of angular distortion is much more satisfactory than the S.V.F.F. treatment. The conclusion reached for the  $\text{BF}_3$ -type molecules in Part III, and for the  $\text{CCl}_4$ -type molecules in Part IV and for the  $\text{SO}_4^{2-}$ -type ions in Part V is therefore confirmed in this study of the octahedral molecules.

It remains to consider the calculation of  $n_6$  for these three molecules. The results of calculations using O.V.F.F. and S.V.F.F. are compared with the observed frequencies in Table III—the force constants listed in Table II were used to calculate  $n_6$ . It will be seen that the observed fre-

TABLE III.—COMPARISON OF CALCULATED AND OBSERVED FREQUENCIES (IN  $\text{cm}^{-1}$ ) FOR  $n_6$ . THE FORCE CONSTANTS LISTED IN TABLE II WERE USED

Molecule	Values of $n_6$ ( $\text{cm}^{-1}$ )		
	Observed	O.V.F.F.	S.V.F.F.
$\text{SF}_6$ . . .	363	423	378
$\text{SeF}_6$ . . .	245	350	284
$\text{TeF}_6$ . . .	165	288	224

quencies are less than those calculated using either force field. The frequencies calculated using S.V.F.F. are nearer than those calculated using O.V.F.F. but with both  $\text{SeF}_6$  and  $\text{TeF}_6$  the values calculated using S.V.F.F. are not at all in agreement with the observed figures. We can therefore only conclude that both the ordinary S.V.F.F. and the ordinary O.V.F.F. as described in Part III do not account for the low value of  $n_6$ .

The low value of  $n_6$  means that this vibration occurs very easily. That is, when this type of distortion occurs the restoring force coming into play is relatively small. This would be the case if the directed atomic orbitals of the central atom were able to change their orientation by change of hybridization in such a way as to follow the vibration of symmetry class  $F_{2u}$  ( $n_6$ ).<sup>8</sup> If that is the true explanation of the low value of  $n_6$  we have an example here that is similar to that examined by Linnett and Wheatley for methane.<sup>9</sup> We have shown that the possibility that the bonding orbitals of the central atom change their hybridization in such a way as to follow the  $F_{2u}$  vibration is not forbidden by the symmetry of the distortion, so that such a following is allowed. We have shown that orbital following during the vibration by change of hybridization is forbidden for the bending vibration of symmetry  $F_{2g}$ , but is allowed for that of symmetry  $F_{1u}$ . The results obtained for  $n_4$  and  $n_5$  indicate that there is no more orbital following for the  $F_{1u}$  vibration than for the  $F_{2g}$  vibration. Since no orbital following is possible for the  $F_{2g}$  vibration this must mean that there is no change of hybridization of the bonding orbitals of the central atom during the  $F_{1u}$  vibration. This suggests that a change of hybridization of the orbitals in such a way as to distort them according to the symmetry of class  $F_{1u}$  is so difficult that, though it is allowed, it does not occur appreciably. We are not, at present, able to offer any explanation for this. However, distortion according to the symmetry of class  $F_{2u}$  does seem to be possible because of the low values of  $n_6$  in all these molecules. It is interesting that the distortion in class  $F_{2u}$  is such as to bring the four distorted bonds towards a tetrahedral configuration (see Fig. 1) and it may be that this should be considered when seeking an explanation of why the bonds seem to accommodate themselves to the distortion of symmetry class,  $F_{2u}$ .

<sup>8</sup> Linnett and Wheatley, *Trans. Faraday Soc.*, 1949, **45**, 33.

<sup>9</sup> Linnett and Wheatley, *ibid.*, 1949, **45**, 39.

**Uranium Hexafluoride.**—Begeleisen, Mayer, Stevenson and Turkevich<sup>10</sup> have recently suggested values for the vibration frequencies of  $\text{UF}_6$ . Their suggestions are summarized in Table IV. We will con-

TABLE IV.—VIBRATION FREQUENCIES OF  $\text{UF}_6$  AS ASSIGNED BY BEGELEISEN, MAYER, STEVENSON AND TURKEVICH

Vibr.	Freq. ( $\text{cm.}^{-1}$ )	How Observed
$\nu_1$	656	Observed in Raman spectrum
$\nu_2$	511	Observed in Raman spectrum, more faintly than $\nu_1$
$\nu_3$	640	Observed as strong absorption band in infra-red spectrum
$\nu_4$	200	From combination bands in infra-red spectrum
$\nu_5$	200	Observed in Raman spectrum of $\text{UF}_6$ solution
$\nu_6$	130	From combination bands in infra-red spectrum

sider these frequencies in relation to the frequencies of  $\text{SF}_6$ ,  $\text{SeF}_6$  and  $\text{TeF}_6$ . We have not made detailed calculations for  $\text{UF}_6$  because, as will be seen from the considerations presented below, there seems to be a major difference between its vibrational behaviour and that of  $\text{SF}_6$ ,  $\text{SeF}_6$  and  $\text{TeF}_6$  if the frequencies suggested in Table IV are correct. Of course,  $\text{UF}_6$  must be electronically very different from the other hexafluorides because uranium has an atomic number six greater than the previous inert gas whereas Se and Te are at the end of a long period having an atomic number sixteen greater than the previous inert gas and two less than the next inert gas. Electronically we have the state of affairs that, for S, Se and Te, the least tightly-bound electrons are those in a  $p$ -shell whereas this is not the case for uranium. The bonding electrons used by uranium in  $\text{UF}_6$  are therefore probably quantized quite differently as regards their subsidiary quantum numbers from those used by S, Se and Te in  $\text{SF}_6$ ,  $\text{SeF}_6$  and  $\text{TeF}_6$ . In the latter the bonding orbitals of the central atom are almost certainly six  $sp^3d^2$  hybrids, but uranium probably uses quite different bonding orbitals in  $\text{UF}_6$ . It has been suggested that  $\text{UF}_6$  is not octahedral<sup>11</sup> but the recent spectroscopic evidence of Begeleisen, Mayer, Stevenson and Turkevich seems to indicate that it is, and, in what follows, we have presumed that the molecule has the symmetry of the Group  $O_h$ .

In the series  $\text{SF}_6$ ,  $\text{SeF}_6$ ,  $\text{TeF}_6$ ,  $\text{UF}_6$  the fluorine atoms get farther apart as the atomic number of the central atom increases. This will mean that the repulsion terms become smaller on passing up the series. Reference to the formulae for  $\nu_1$  and  $\nu_2$  shows that the difference between these two frequencies should get smaller as repulsion between the non-bonded atoms (and  $A$ ) decreases. When  $A$  and  $B$  are zero  $\nu_1$  and  $\nu_2$  should be equal. Reference to Table I shows that the observed values of  $(\nu_1 - \nu_2)$  do in fact decrease on passing from  $\text{SF}_6$  (131) through  $\text{SeF}_6$  (46) to  $\text{TeF}_6$  (27) in the manner that would be expected. But the suggested figures for  $\text{UF}_6$ , where the FF separation is still greater ( $\nu_1 = 656$  and  $\nu_2 = 511$  and  $(\nu_1 - \nu_2) = 145$ ) do not continue this expected trend and in fact  $(\nu_1 - \nu_2)$  is greater for  $\text{UF}_6$  than for  $\text{SF}_6$ . There seem to be two possibilities. In the first place the suggested frequencies for  $\text{UF}_6$  may be in error. If this is so, it would seem most likely that  $\nu_1$  is correct but  $\nu_2$  incorrect, for  $\nu_1$  appears more intensely in the Raman effect than  $\nu_2$ . If the suggested values for  $\nu_1$  and  $\nu_2$  are correct, the large difference between them, and the fact that  $\text{UF}_6$  does not follow the series of  $\text{SF}_6$ ,  $\text{SeF}_6$  and  $\text{TeF}_6$  could be ascribed to the difference that exists electronically

<sup>10</sup> Begeleisen, Mayer, Stevenson and Turkevich, *J. Chem. Physics*, 1948, 16, 442.

<sup>11</sup> Braune and Pinnow, *Z. physik. Chem. B*, 1937, 35, 239.

between  $\text{UF}_6$  and the other hexafluorides. The low value of  $n_3$ , relative to  $n_1$ , would result in the  $k_1$  derived from  $n_3$  being less than that derived from  $n_1$ . This would indicate that the distortion corresponding to  $n_3$  occurs more readily than that corresponding to  $n_1$  presumably because the bonding electrons could change their orbitals in such a way as to make this distortion less difficult.

In the series  $\text{SF}_6$ ,  $\text{SeF}_6$ ,  $\text{TeF}_6$ ,  $(n_3 - n_1)$  decreases, being 180, 79 and 51 for these three molecules respectively. Examination of the algebraic formulae shows that this decrease in  $(n_3 - n_1)$  is likewise due to the decrease in  $A$  as the fluorine atoms become farther apart. For  $\text{UF}_6$ ,  $(n_3 - n_1)$  equals -16, whereas a continuation of the above series would have suggested that  $(n_3 - n_1)$  for  $\text{UF}_6$  should at any rate be in the range +10 to +40. Now  $n_1$  is the most reliably determined Raman frequency and  $n_3$ , except for the difficulty of a possible Fermi degeneracy, is the most reliably determined infra-red frequency. If the possibility of Fermi degeneracy were neglected  $n_3$  would be even smaller which would make  $(n_3 - n_1)$  more abnormal in relation to  $\text{SF}_6$ ,  $\text{SeF}_6$  and  $\text{TeF}_6$ . It is unlikely that  $n_3$  is greater than 640. So the abnormality of  $\text{UF}_6$  here seems to be real. It appears that the deformation corresponding to  $n_3$  is less difficult than that corresponding to  $n_1$ .

In the series  $\text{SF}_6$ ,  $\text{SeF}_6$ ,  $\text{TeF}_6$ ,  $(n_4 - n_5)$  decreases in passing along the series (as  $A$  decreases and  $n_1$  increases) being 92, 56 and *ca.* 40 in these three molecules. In  $\text{UF}_6$ ,  $n_4$  and  $n_5$  are given the same value by Begeleisen, Mayer, Stevenson and Turkevich. That this should be approximately true would be anticipated though we might have expected  $n_4$  to be rather greater than  $n_5$ .

As regards  $n_6$  it again appears that the frequency is lower than one might expect because the simple O.V.F.F. predicts that when  $A$  and  $B$  are small, as they should be in  $\text{UF}_6$ ,  $n_6$  and  $n_5$  should be approximately equal. The low value of  $n_6$  therefore indicates that the distortion corresponding to this fundamental frequency ( $F_{3u}$ ) occurs more readily than would be anticipated from the O.V.F.F. and that its behaviour is therefore similar to that of  $n_6$  in  $\text{SF}_6$ ,  $\text{SeF}_6$  and  $\text{TeF}_6$ .

To summarize the above there seem to be two alternatives—(i) The values of  $n_1$ ,  $n_3$ ,  $n_4$ ,  $n_5$  and  $n_6$  suggested by Begeleisen, Mayer, Stevenson and Turkevich have relative magnitudes which are quite similar to what would be expected from consideration of  $\text{SF}_6$ ,  $\text{SeF}_6$  and  $\text{TeF}_6$ , though  $n_3$  would have been expected to be a little greater than  $n_1$  instead of a little less. But the suggested value of  $n_4$  is quite different from what would be expected by considering  $\text{SF}_6$ , etc., and the application of the simple O.V.F.F. or S.V.F.F. to these molecules. Both of these considerations would have suggested that  $n_3$  should be in the range 600 to 650  $\text{cm}^{-1}$ . It is interesting that five of the six fundamental frequencies given by Begeleisen, Mayer, Stevenson and Turkevich do have relative values to be expected from examining  $\text{SF}_6$ , etc., and perhaps this suggests that the sixth ( $n_3$ ) should also have a magnitude consistent with an examination of the other hexafluorides. If  $n_3$  were changed to a value between 600 and 650  $\text{cm}^{-1}$  it would be necessary to alter one of the other frequencies slightly to account for the thermodynamic data. However, the exact magnitudes of  $n_4$  and  $n_6$  are uncertain and a very small decrease in these small triply-degenerate frequencies would compensate for the increase of the doubly-degenerate  $n_3$  from 511 to about 625. Also, if  $n_3$  were changed from 511 to about 625 it would not be possible to explain the faint infra-red bands as neatly as is done by Begeleisen, Meyer, Stevenson and Turkevich. But until we know more about the intensity of overtones and combination levels it is difficult to be sure that we should only consider binary combination levels as is done by Begeleisen, Mayer, Stevenson and Turkevich. Also, because there are vibration frequencies of the order of 100 to 200  $\text{cm}^{-1}$ , transitions from excited vibrational levels might appear faintly. (ii) If the values suggested by Begeleisen, Mayer,

Stevenson and Turkevich are correct the fact that the magnitude of  $n_s$  for  $UF_6$  does not bear the same relation to the other frequencies that it does in  $SF_6$ ,  $SeF_6$  and  $TeF_6$ , might be a result of the different quantization of the bonding electrons of uranium from those of S, Se and Te. One way in which this might be tested is by an examination of the Raman and infra-red spectra of  $WF_6$  and  $MoF_6$ .

In conclusion we wish to thank Imperial Chemical Industries for the loan of a calculating machine, and Prof. C. A. Coulson for most valuable discussions.

*Inorganic Chemistry Laboratory,  
Oxford.*

---

## MERCURY CUT-OFFS FOR THE CONTROLLED INTRODUCTION OF GAS

BY J. C. P. MIGNOLET

*Received 29th July, 1948; as revised, 10th November, 1948*

A simple introducer and two micro-introducers of the mercury cut-off type are described, by means of which volumes of gas down to 0.2 mm.<sup>3</sup> are easily introduced.

---

When trying to use a simple U-shaped mercury cut-off for the introduction of gas from a generator at atmospheric pressure into an evacuated reservoir, the gas flow will generally get out of control after the first few bubbles have entered. This trouble cannot be stopped by raising the mercury reservoir and mercury is blown into the system. The explanation is simple: when the first few bubbles escape the length of the mercury column is temporarily reduced. Since the resistance to flow is low, the rate of gas flow greatly increases and more mercury is forced upward; the process is thus self-accelerating. This difficulty can be avoided in a number of ways <sup>1, 2, 3</sup> the simplest being to insert a capillary in the path of the gas.

### Experimental

**Type A Introducer.**—This method is used in Type A introducer (Fig. 1) which may be considered as a modification of Benton and White's cut-off.<sup>3</sup> By suitable choice of capillary, the gas flow can be adjusted by the height of the mercury reservoir since the flow is proportional to the distance by which the latter is lowered below the cut-off level H. Thus, the gas flow can be made approximately the same as that from a generator and purifying system without risk of producing a depression in them. Single bubbles are easily introduced. Type A introducers are believed to be superior to the well-known porcelain or sintered glass type as regards simplicity and flexibility and for use in introducing small measured volumes (see Types A and B microintroducers derived from Type A). They are, however, inferior when large gas flows are to be handled.

The dimensions of the introducers used are as follows. The capillary has

<sup>1</sup> Stock, *Z. Elektrochem.*, 1917, **33**, 23. Klemenck, *Die Behandlung und Reindarstellung von Gasen* (1938), p. 14.

<sup>2</sup> Stock, *Z. Elektrochem.*, 1933, **39**, 256. Wansbrough-Jones, *Proc. Roy. Soc. A.*, 1936, **127**, 530.

<sup>3</sup> Benton and White, *J. Amer. Chem. Soc.*, 1930, **52**, 2328.

a bore of 0.2 to 0.3 mm. and a length of 15 cm. The long limb has an internal diameter of 1 cm.; its length is 120 cm. from the top to the junction with the short limb and 15 cm. from the junction to the bottom. The maximum permissible flow is about 0.5 l./hr. when the pressure in the system is of the order of 0.01 mm. Hg. At higher pressures it can be increased to several litres per hour since the bubble "explosions" become less violent.

**Type A Micro-introducer.**—For the introduction of small volumes (under 1 ml.) it is advisable to connect a burette-tube and a "bubble-cutter" between

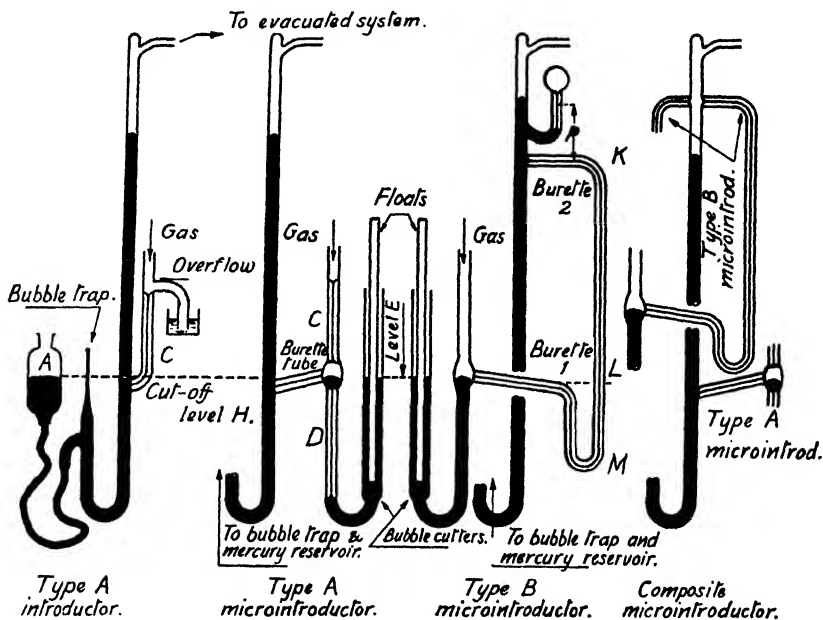


FIG. 1.

the long limb and the safety capillary C (Fig. 1). The mode of operation is quite simple. The float of the "bubble-cutter" is raised above level E, and the mercury reservoir is raised until the burette-tube and the "bubble-cutter" are filled with mercury to E. The mercury reservoir is slowly lowered until the burette contains the required volume of gas and then the float is pushed down, thereby isolating the gas contained in the burette. As the float is pushed farther down, the gas bubble travels first down the burette tube and then up the main limb. The smallest volume of gas that can be introduced is about 10 to 20 mm.<sup>3</sup> Smaller bubbles stick on their way, usually at the junction; attempts to reduce this volume were unsuccessful.

**Type B Micro-introducer.**—Another micro-introducer (Fig. 1) was found to be quite satisfactory. Here the bubble is led through a capillary at a higher level where its volume is much greater. The operation is the same as with Type A. Finally, the mercury reservoir is lowered to bring the mercury under the junction so as to avoid trapping any gas. Long bubbles are measured in burette 1. Short bubbles are measured with a considerable magnification in burette 2, the pressure being read on the capillary manometer. The gas bubbles are easily brought to rest by acting only on the float. For volumes over 0.2 mm.<sup>3</sup>, with capillaries of 0.5 mm. diam. or larger, Type B micro-introducers are quite satisfactory. For smaller volumes, difficulties arise as narrower capillaries have to be used. A burette having a 0.2 mm. diam. capillary was rejected because the mercury meniscus moved jerkily, thereby making it difficult to make short bubbles and to measure them in burette 2.

One Type A and several Type B micro-introducers can be combined together (as shown schematically in Fig. 1) with a common mercury reservoir and long limb without risk of interference. Two such composite micro-introducers have been in use for one year and found to be quite satisfactory. Their accuracy

was checked in special tests in which bubbles of measured lengths were introduced into a known volume and the pressures measured. For the last one, the following cross-sections were found :

Type	Cross-sections	
	Calibration with Mercury (mm. <sup>2</sup> )	Introduction Experiment (mm. <sup>2</sup> )
A . . .	1.98	1.99 ; 1.97 ; 1.97
B-burette 1 .	0.379 ; 0.381	0.384 ; 0.374 ; 0.383 ; 0.382
B-burette 2 .	0.327 ; 0.329	0.294 ; 0.298 ; 0.320 ; 0.304

The errors in the cross-sections using burette 2 were mainly due to errors in bubble length caused by sticking.

**Miscellaneous Details.**—The safety capillary is somewhat troublesome when Type A micro-introducer is used as a simple introducer. It causes the mercury to oscillate in the "bubble-cutter" and the gas flow to be broken up into groups of bubbles succeeding one another very closely. These undesirable oscillations can be avoided by lowering the mercury level in the "bubble-cutter" by means of the float.

In contradistinction to Type A micro-introducers, those of Type B work only within a limited range of gas pressure in the main limb: i.e. from 0 to  $p_{\text{gen}} - \Delta p_{\text{KL}}$ , where  $p_{\text{gen}}$  is the pressure in the gas generator (about 1 atm.) and  $\Delta p_{\text{KL}}$  is the difference in pressure between points K and L. For larger  $p$ , the burette tube is filled with mercury and cannot be emptied by lowering the mercury reservoir.

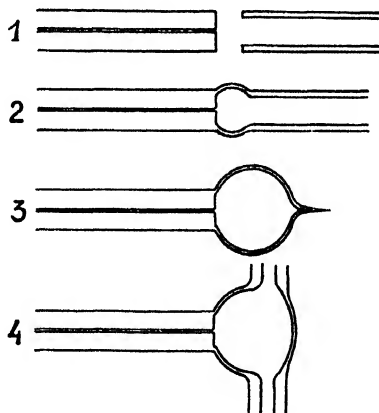


FIG. 2.

The junction between the bubble-cutter and the burette-tube must be carefully made if small bubbles are to be "cut." The usual tapering joint is inadequate. Fig. 2 shows the principal stages in blowing a correct junction. The joint and the bulb should be rather thin, especially with ordinary glass.

My best thanks are due to Prof. L. D'Or for his interest in this work and for facilities to carry it out, and to Prof. H. W. Melville for kindly correcting the manuscript. I am indebted to Dr. A. Orzechowski for drawing my attention to Benton and White's cut-off.

*Institut Walthère Spring,  
Université de Liège, Belgium.*

# A STUDY OF THE FINE STRUCTURE OF CARBONACEOUS SOLIDS BY MEASUREMENTS OF TRUE AND APPARENT DENSITIES

## PART I. COALS

By ROSALIND E. FRANKLIN

*Received 18th November, 1948*

The true density of a series of coals was measured with helium gas and apparent densities were measured with methanol, water, *n*-hexane and benzene liquids. From the results obtained, the following conclusions were drawn.

Helium fills rapidly and completely the pore space of coals ground to pass a 72 B.S. sieve, and measures the true density of the coals. The pore space of coals ground to pass a 72 B.S. sieve is filled by methanol almost completely in a few hours. There is a contraction of  $2.6 \times 10^{-8}$  cm.<sup>3</sup> for each cm.<sup>2</sup> of surface covered by methanol. Water, *n*-hexane and benzene fill the pores space of some low rank coals practically completely. The apparent densities of such coals in these liquids are high owing to the contraction which accompanies adsorption. *n*-Hexane and benzene penetrate only very slowly into the pore space of some coals owing to the relatively large diameters of the molecules of these liquids. There is no appreciable volume of closed pores in coals.

The accessibility of the pore space of a coal to liquids and gases varies with rank in a manner similar to the porosity and adsorptive properties. Coals of high porosity have the most open pore structure. The pores in coals contain numerous fine constrictions, and the variation in the accessibility of the pore space from one coal to another is related to a variation in the width of these constrictions rather than in the mean diameter of the pores. The width of the constrictions is of the same order as the diameters of simple molecules and is smallest in coals containing between 89 % and 93 % carbon.

---

**The Apparent Density of Porous Solids.**—It is well known that the apparent density of finely porous solids and of solids possessing large specific surfaces is highly dependent on the method of measurement. The variation may be attributed in the main to two factors which influence the results in opposite directions. Values greater than the true density of the solid may result from the decrease in volume which accompanies adsorption of the filling fluid; alternatively, slow or incomplete penetration of the pores by the fluid may lead to low apparent density values. In the latter case a density drift (or increase of apparent density with time) is frequently observed. These considerations apply to a wide range of organic and inorganic colloidal materials and are well illustrated by the many measurements which have been made on charcoals. A selection of these is given in Table I; it is clear that very varied results may be obtained with a single charcoal, and also that the values obtained with a given series of liquids may fall into different order when different charcoals are used.

The results quoted in Table I show that both incomplete penetration of the pores and the contraction due to adsorption may be important. Thus the apparent density values are intimately related to the fine structure of the solid investigated; they depend not only on the properties of the liquid and the density of the solid, but also on the nature and extent of the surface of the solid, the size and accessibility of the pores, and the extent to which the accessibility of the pores and inner surfaces may be influenced by deformation of the solid resulting from interaction with the liquid.

The object of the present work was to use measurements of true and apparent densities to investigate the inner structure of coals, the variation of structure with rank (see later), and the nature of the interaction between coal surfaces and certain liquids.

TABLE I.—APPARENT DENSITIES OF CHARCOALS IN LIQUIDS

Liquid	Harkins and Ewing <sup>1</sup>	Firth <sup>2</sup>		Cude and Hulett <sup>3</sup>	Culbertson and Weber <sup>4</sup>	Corriez <sup>5</sup>
	Activated coconut charcoal	Coconut charcoal	Sugar charcoal	Coconut charcoal	Active charcoal	Sugar charcoal
Water . . .	1.84	1.90	1.79	1.85	1.86	1.88
Chloroform . . .	1.99	2.18	2.22	—	—	—
Benzene . . .	2.01	1.96	1.98	1.80	2.01	1.65
Carbon disulphide . . .	2.06	—	—	1.98	2.03	1.97
Acetone . . .	2.11	—	—	—	2.05	—
Ethyl alcohol . . .	—	2.00	1.96	—	2.01	—

#### Significance of Density Measurements made with Helium.—

The choice of helium for the measurement of the "true" density of a number of porous solids has been dictated by its small molecular diameter which should enable it to penetrate into very fine pores, and by its small van der Waals' field resulting in negligible adsorption on solids at room temperature. It is not, however, self-evident that a "true" density can be assigned to a complex and fine-structured material such as coal. If the solid contains closed pores which are inaccessible to all fluids including helium, then it may be necessary to define arbitrarily whether or not such spaces are to be included in the "true" volume of the material. Further, as has been well emphasised by Hermans,<sup>6</sup> density is essentially a macroscopic property, and irregularities of molecular dimensions cannot be measured by attempting to pack molecules into the available space. Thus, if the structure of the solid is such that "pores" of a few Ångströms diameter occupy an appreciable fraction of the total volume, then measurements made with helium (molecular diameter 2Å) will give an apparent density which has no precise or fundamental significance. Hermans considers that in the case of cellulose "there is no longer a conclusive reason to believe that any special preference should be given to the density found in helium, or that it would have any particular physical meaning." All the evidence resulting from the present work, however, tends to show that for coals helium may be used to measure a well-defined property which may reasonably be called the true density. In particular, it may be mentioned here that although the fine structure and micro-pore volume are known to vary widely from one coal to another, the density measured in helium is a function of chemical composition only.<sup>7</sup> Further evidence that helium measures the true density of coals is given in later sections of this paper.

**The Physical Structure of Coal.**—Coals of different rank form a series of related materials representing different (though not necessarily

<sup>1</sup> Harkins and Ewing, *J. Amer. Chem. Soc.*, 1921, **43**, 1787.

<sup>2</sup> Firth, *Trans. Faraday Soc.*, 1923, **19**, 444.

<sup>3</sup> Cude and Hulett, *J. Amer. Chem. Soc.*, 1920, **42**, 391.

<sup>4</sup> Culbertson and Weber, *ibid.*, 1938, **60**, 2695.

<sup>5</sup> Corriez, *Thesis* (Paris, 1937).

<sup>6</sup> Hermans, *Contribution to the Physics of Cellulose Fibres* (Elsevier Publishing Co., 1946), p. 62.

<sup>7</sup> Franklin, *Fuel*, 1948, **27**, 46.



successive) stages in the process of "coalification" which started with the decay of plant material in a peat-bog and led to the formation of lignites, sub-bituminous coals, anthracites and peranthracites. Investigations of the colloidal structure of coals are described in a series of papers presented to a Conference on the "Ultra-fine Structure of Coals and Cokes," and the subject has also been reviewed by Bangham.<sup>8</sup> Griffith and Hirst<sup>9</sup> measured the heat of wetting in methanol of some two hundred coals, and, with the aid of adsorption data due to Maggs,<sup>10</sup> gave evidence that the *surface area* of coals accessible to methanol varies from about 20 to 200 m.<sup>2</sup>/g. The relation between the surface area and rank of coals is shown in Fig. 1, where the heat of wetting in methanol is plotted against the volatile content of the coal.\*

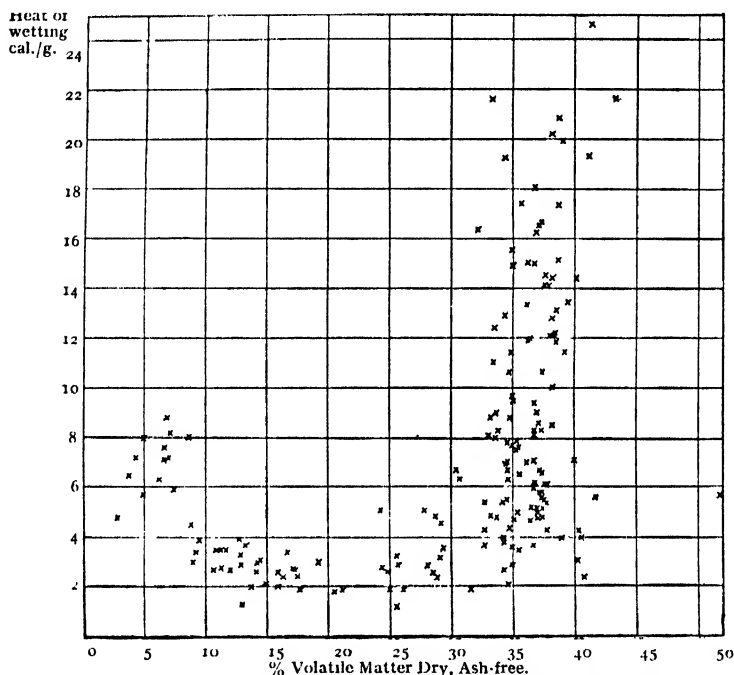


FIG. 1.—The heat of wetting—volatile matter classification.

The *porosity* of a large number of coals was measured by King and Wilkins,<sup>11</sup> who used mercury to measure the lump density and water for the "true" density. Porosity values ranged from about 2 % to 20 %, the variation of porosity with rank being similar to that of the heat of wetting in methanol. The highest porosities were found among the low rank coals, and the lowest in coals of about 89 % carbon content. Measurements by Dunningham<sup>12</sup> again reveal a similar relationship between *inherent moisture content* and rank.

<sup>8</sup> Bangham, *Ann. Reports*, 1943, 40, 29.

<sup>9</sup> Griffith and Hirst, *Conference on the Ultrafine Structure of Coals and Cokes* (B.C.U.R.A., 1944), p. 80.

<sup>10</sup> Maggs, *ibid.*, (B.C.U.R.A., 1943), p. 95.

\* The volatile content of a coal is closely related to its rank, and 1 cal. of heat of wetting in methanol is equivalent to approximately 10 m.<sup>2</sup> of surface (see ref. 8).

<sup>11</sup> King and Wilkins, *Conference on the Ultrafine Structure of Coals and Cokes* (B.C.U.R.A., 1943), p. 46.

<sup>12</sup> Dunningham, *ibid.*, p. 57.

Bangham<sup>8, 13</sup> has postulated that coals have a micellar structure, the micelles being bound to one another principally by van der Waals' forces. Evidence of this is drawn from the behaviour of coal in solvents,<sup>14</sup> from adsorption and surface area measurements,<sup>9, 10</sup> from the rheological behaviour of coal<sup>13</sup> and from the low-angle scattering of X-rays.<sup>15</sup> The decrease in surface area and porosity with increasing rank (up to about 89 % carbon content) is attributed to a process analogous to syn-eresis. In the present work, measurements of true and apparent densities have yielded further information concerning the size and distribution of the pores in coals, and, on the basis of the results, the micellar theory is further developed.

### Experimental

**Materials.**—**COALS.** A list of the twelve coals used, together with their carbon contents and heats of wetting in methanol is given in Table II. All the samples were of "bright" coals (i.e. they contained a preponderating amount of vitrain). Except where otherwise stated, all measurements were made on coals ground to pass a 72 B.S. sieve, precautions being taken to avoid an undue proportion of fines.

TABLE II.—ANALYSES OF COALS

Coal	Locality	Carbon %	Heat of Wetting in Methanol cal./g.
A	Ireland	95.2	6.2
B	S. Wales	94.7	7.7
C	S. Wales	94.2	7.6
D	S. Wales	91.7	2.8
E	Kent	90.9	2.5
F	S. Wales	89.7	2.0
G	Derbyshire	84.6	5.8
H	Yorkshire	83.5	8.8
J	Staffordshire	82.9	10.4
K	Northumberland	82.4	16.6
L	Nottinghamshire	81.3	11.8
M	Northumberland	80.6	17.1

**HELIUM.** "Spectroscopically pure" helium was supplied by British Oxygen Co. Ltd.

**LIQUIDS.** Water was freshly distilled; methanol and benzene of A.R. grade and *n*-hexane boiling at 67°-69° C were used.

**Measurement of Densities with Helium.**—A diagram of the apparatus is given in Fig. 2. In essentials it was the same as that of Smith and Howard.<sup>16</sup> The operation consisted in (1) thorough evacuation of the apparatus, (2) measurement of the temperature and pressure of a quantity of helium in the calibrated bulb F, (3) transfer of the helium through the capillary tube G into the calibrated bulb A which contained the sample, and (4) measurement of the temperature and pressure of the helium in the bulb A. This gave the free volume in the bulb A and hence the volume of the sample. The sample was weighed after the bulb was removed from the apparatus at the end of the experiment.

The bulb F, at room temperature, was surrounded by a water jacket fitted with thermometer and stirrer; the bulb A was in a water-bath supported on the platform P and maintained at  $25 \pm 0.01^\circ$  C. During the preliminary evacuation the water bath was replaced by an electric oven. Pressure measurements were made by adjusting the mercury level to a fixed mark B (viewed through a

<sup>13</sup> Bangham, *Conference on the Ultrafine Structure of Coals and Cokes* (B.C.U.R.A., 1943), p. 18.

<sup>14</sup> Kiebler, *Ind. Eng. Chem.*, 1940, **32**, 1389.

<sup>15</sup> Riley, *Conference on the Ultrafine Structure of Coals and Cokes* (B.C.U.R.A., 1943), p. 232.

<sup>16</sup> Smith and Howard, *Ind. Eng. Chem.*, 1942, **34**, 43.

telescope) and observing the height of the mercury in the capillary tube G. The capillary tube was carefully selected for uniformity of bore (mean diam. 1.16 mm., maximum deviation 0.004 mm.) and mounted against an engraved steel scale which was read to 0.1 mm.

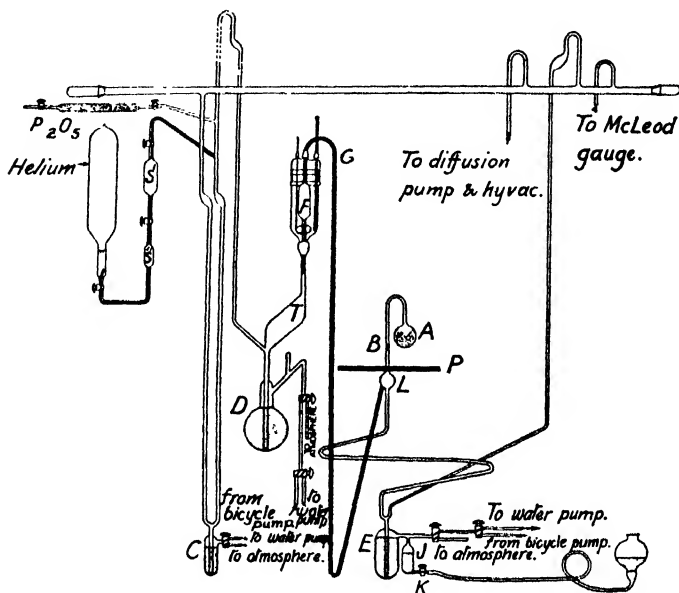


FIG. 2.

When coal is heated *in vacuo*, evolution of gas continues, at a steadily decreasing rate, for long periods of time. Further increase of temperature is always accompanied by further evolution of gas. It was therefore necessary to select arbitrarily an evacuation schedule which, whilst heating the coal sufficiently to ensure that measurable quantities of gas would not be disengaged subsequently at room temperature, yet would not cause significant structural changes. In practice, the sample was heated to 90°-100° C until a pressure of less than  $10^{-4}$  mm. (with the pumps running) was obtained, the minimum period of heating being 16 hr. The sample was previously evacuated elsewhere in order to reduce its tendency to scatter when evacuated in the density apparatus. It was established that minor variations in the above procedure did not influence the results.

The first reading of the pressure of helium in the sample bulb was made as rapidly as possible; it was generally completed 30-40 sec. after the gas first entered the bulb. Further readings were taken at intervals until no further change was observed in 24 hr. In general, coals showed no density drift in helium provided sufficient time was allowed for the sample to come to the temperature of the thermostat before the gas was admitted.

Duplicate determinations of the free-space in the bulb did not differ by more than 0.1 %. The recorded density values are therefore accurate to  $\pm 0.2$  %.

**Measurement of Apparent Densities in Liquids.**—The coal samples, contained in calibrated glass bulbs, were evacuated as described above. The bulbs were then sealed, the sealed tips were broken off while immersed in the liquid, and the bulbs placed in a thermostat at  $25 \pm 0.02^\circ$  C before levelling the liquid and weighing. The density drift was often considerable, and in order to obtain comparative data it was necessary to make measurements after standard periods of immersion. Except where otherwise stated, all densities recorded were measured after 24 hr. immersion and all density drifts are given as the percentage difference between the density values obtained after 2 hr. and after 24 hr. immersion. Duplicate measurements did not differ by more than 0.5 % even when large density drifts occurred.

**Lump Density.**—For the measurement of the lump density of coals, single lumps were dried to constant weight in an air-oven at 105° C, smeared with a

thin film of vaseline, and re-weighed rapidly in air and in water. The possibility of errors due to large ash inclusions or other irregularities was eliminated by making measurements on five or six different lumps of each coal.

**Correction of Densities for Mineral Matter.**—An approximate correction for mineral matter was applied to all the density values recorded. Wandless and Macrae,<sup>17</sup> who made a detailed study of one coal, showed that the error involved in correcting for mineral matter on the basis of *ash* density and *ash* content is not appreciable so long as the ash content is small. The corrected density is given by

$$d = \frac{ad'(100 - A)}{100a - Ad'},$$

where  $d'$  is the observed density,  $a$  the density of the ash and  $A$  the ash content per cent. The correction amounts to less than 2 % for all the coals used in the present investigation.

**Measurement of Heat of Wetting.**—Heats of wetting of coals in liquids were measured by the routine method developed in the B.C.U.R.A. laboratories by Griffith and Hirst.<sup>9</sup>

## Results

**Control Experiments with Helium.**—Preliminary experiments showed that under the conditions of the density measurements helium penetrates rapidly and completely into the pores of all the coals investigated. Equilibrium was always rapidly established, and, below a certain size limit, the density was independent of the particle size of the material (Table IV, column 3). Further, the results were not altered when the period of evacuation at 90°-100° C was extended from 16 hr. to 10 days.

TABLE III.—APPARENT DENSITIES OF THE COALS

Coal	Helium		Methanol		Water		n-Hexane		Benzene	
	Density (g./cm. <sup>3</sup> )	Drift (%)	Density after 24 hr. (g./cm. <sup>3</sup> )	Drift (% 2 hr. to 24 hr.)	Density after 24 hr. (g./cm. <sup>3</sup> )	Drift (% 2 hr. to 24 hr.)	Density after 24 hr. (g./cm. <sup>3</sup> )	Drift (% 2 hr. to 24 hr.)	Density after 24 hr. (g./cm. <sup>3</sup> )	Drift (% 2 hr. to 24 hr.)
A	1.645	0.0	1.700	0.3	1.630	0.0	1.497	0.8	1.518	1.5
B	1.517	0.0	1.556	0.1	1.488	0.0	1.433	1.9	1.450	2.9
C	1.497	0.0	1.549	0.1	1.475	0.0	1.425	2.0	—	—
D	1.361	0.4	1.374	0.4	1.318	0.0	1.300	0.3	1.293	0.3
E	1.337	0.0	1.352	0.2	1.305	0.0	1.297	0.3	1.299	0.6
F	1.311	0.0	1.333	0.6	1.291	0.0	1.286	0.3	1.297	0.3
G	1.293	0.0	1.334	0.6	1.297	0.0	1.276	0.7	1.286	1.3
H	1.301	0.0	1.357	0.6	1.307	0.0	1.262	1.8	1.276	2.5
J	1.302	0.0	1.402	0.7	1.333	0.0	1.297	0.8	1.292	1.3
K	1.305	0.0	1.387	0.4	1.326	0.0	1.329	1.8	1.342	1.4
L	1.317	0.0	1.387	0.5	1.328	0.0	1.272	2.2	1.321	2.6
M	1.341	0.0	1.327	0.3	1.370	0.0	1.374	2.9	—	—

**The True and Apparent Densities of Twelve Coals.**—The apparent densities and density drifts of the twelve coals described in Table II were measured in methanol, water, *n*-hexane and benzene, and true densities were measured with helium. The results are given in Table III, and in Fig. 3 the densities are plotted against the carbon content of the coals. The main feature of the results are—

- (1) The density in methanol is in every case the highest.
- (2) Densities in *n*-hexane and in benzene are in general lower than the true density (measured with helium). Two low rank coals are exceptions.
- (3) Where the apparent densities in *n*-hexane and in benzene differ appreciably, the value given by *n*-hexane is the lower.
- (4) Apparent densities in water are lower than the true density for high rank coals and higher for low rank coals. The change occurs between 82 % and 85 % carbon content.

<sup>17</sup> Wandless and Macrae, *Fuel*, 1934, 13, 4.

TABLE IV.—INFLUENCE OF PARTICLE SIZE ON APPARENT DENSITY

Coal	Size	Helium		Methanol		Water		n-Hexane	
		Density (g./cm. <sup>3</sup> )	Drift (%)	Density after 24 hr. (g./cm. <sup>3</sup> )	Drift (% 2 hr. to 24 hr.)	Density after 24 hr. (g./cm. <sup>3</sup> )	Drift (% 2 hr. to 24 hr.)	Density after 24 hr. (g./cm. <sup>3</sup> )	Drift (% 2 hr. to 24 hr.)
F	(1) Through 14 B.S. on 1/32 in. . . . .	1.298	0.0	1.315	2.2	1.285	0.9	1.273	0.0
	(2) Through 72 B.S. . . . .	1.299	0.0	1.331	1.1	1.283	0.0	1.271	0.4
	(3) Through 72 B.S. . . . .	1.311	0.0	1.333	0.6	1.289	0.0	1.281	0.3
	(4) Through 240 B.S. . .	1.307	0.0	1.335	0.2	1.285	0.0	1.291	0.6
K	(1) Through 14 B.S. on 1/32 in. . . . .	1.292	0.0	1.373	0.4	1.311	0.0	1.316	2.2
	(2) Through 72 B.S. on 100 B.S. . . . .	1.294	0.0	1.371	0.6	1.318	0.0	1.318	2.1
	(3) Through 72 B.S. . . . .	1.305	0.0	1.386	0.4	1.327	0.0	1.330	1.8
	(4) Through 240 B.S. . .	1.305	0.0	1.380	0.5	1.336	0.0	1.339	1.8

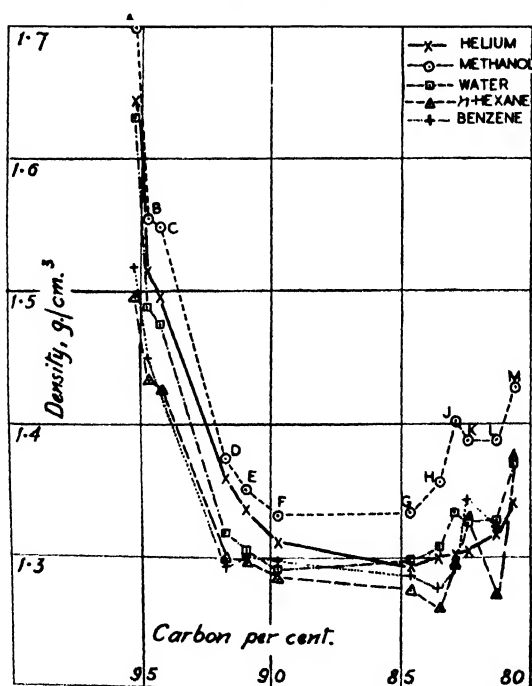


FIG. 3.

- (5) (a) There is, in general, no density drift in helium. One coal showed a small drift.  
 (b) There is no density drift in water.  
 (c) Density drifts in methanol are generally small (0.2-0.6 %).  
 (d) Considerable density drifts in *n*-hexane and benzene are observed with some coals.

(6) TRUE DENSITIES.—The significance of the values obtained for the true densities of coals is discussed elsewhere.<sup>7</sup> It is shown that for all the coals investigated the true specific volume is a linear function of the hydrogen content, and extrapolation gives 1.85 g./cm.<sup>3</sup> for the density of a "coal" of zero hydrogen content. This relationship indicates that there is a characteristic molecular or atomic packing which is common to all coals and very different from that of graphite (density, 2.26 g./cm.<sup>3</sup>).

These measurements provide a general survey of the way in which the apparent densities of coals vary with rank and with the nature of the fluid used to make the measurement. The following series of subsidiary measurements were made to assist in elucidating the results.

- (1) To ascertain the significance of the low apparent densities of some coals in water, *n*-hexane and benzene, the lump densities of the coals c, d, f, h and k were measured as described above, and from the lump densities and the densities in helium the true porosities were calculated. The results are given in Table IV.  
 (2) To investigate further the density drifts and low apparent density values, the dependence of the results on the particle size of the coal was studied. Results obtained with coals f and k prepared in four size grades are given in Table V.

TABLE V.—POROSITY OF COALS

Coal	Density * of Dry Lump (g./cm. <sup>3</sup> )	Porosity Calc. from Density in Helium (%)
C	1.364	10.1
D	1.313	4.7
F	1.301	3.2
H	1.214	7.7
K	1.151	12.3

\* Densities not corrected for mineral matter.

- (3) The strong influence of the chemical character of the coal surface on the values of the apparent densities in liquids was confirmed by measurements made on oxidised coals. Samples of coals f and k, ground to pass 72 B.S.S., were spread in thin layers in a well-ventilated air oven at 105°C for 36 days. The densities and heats of wetting before and after oxidation are given in Table VI.

TABLE VI.—INFLUENCE OF OXIDATION ON APPARENT DENSITIES AND HEATS OF WETTING

Material	Helium		Methanol			Water			<i>n</i> -Hexane		
	Density (g./cm. <sup>3</sup> )	Drift (%)	Density after 24 hr. (g./cm. <sup>3</sup> )	Drift (% 24 hr. to 24 hr.)	Heat of Wet-ting (cal./g.)	Density after 24 hr. (g./cm. <sup>3</sup> )	Drift (% 24 hr. to 24 hr.)	Heat of Wet-ting (cal./g.)	Density after 24 hr.	Drift (% 24 hr. to 24 hr.)	Heat of Wet-ting (cal./g.)
Coal f	1.311	0.0	1.333	0.6	2.0	1.291	0.0	0.6	1.286	0.3	1.8
Coal f, oxidised	1.359	0.0	1.400	0.7	3.4	1.357	0.1	3.5	1.321	0.0	2.3
Coal k	1.305	0.0	1.387	0.4	16.6	1.326	0.0	9.5	1.329	1.8	4.9
Coal k, oxidised	1.427	0.0	1.577	1.1	22.6	1.479	0.4	12.3	1.371	1.4	1.5

## Discussion

**Apparent Densities in Methanol: Compression of the Adsorbed Liquid.**—The apparent density in methanol exceeds the density in helium for all the twelve coals investigated. It has been shown above that helium penetrates rapidly and completely into the pores of coals ground to pass a 72 B.S. sieve. Moreover, measurements on the two widely different coals F and K (Table V) show that the pores of coals ground to pass a 72 B.S. sieve are also completely filled by methanol in 24 hr.; density drifts in methanol are small and decrease with decreasing particle size, and density values after 24 hr. are practically independent of particle size. The difference between the density values obtained with helium and with methanol must therefore be attributed to the contraction which accompanies adsorption.

The contraction per g. of coal is given by  $(V_{\text{He}} - V_{\text{MeOH}})$ , where  $V_{\text{He}}$  is the specific volume in helium and  $V_{\text{MeOH}}$  the apparent specific volume in methanol. This function is found to be directly proportional to the heat of wetting of the coal in methanol, for eleven of the twelve coals investigated (Fig. 4), the contraction being 0.0026 cm.<sup>3</sup> per calorie heat of wetting. Only coal J is represented by a point lying well above the line, but the heat of wetting of this coal was liberated exceptionally slowly and the value recorded is known from other evidence to represent a gross under-estimate.\*

Maggs<sup>10</sup> has shown that the heat of wetting of coals in methanol is 1 cal./10 m.<sup>2</sup> of surface, and this is the same as the figure obtained by

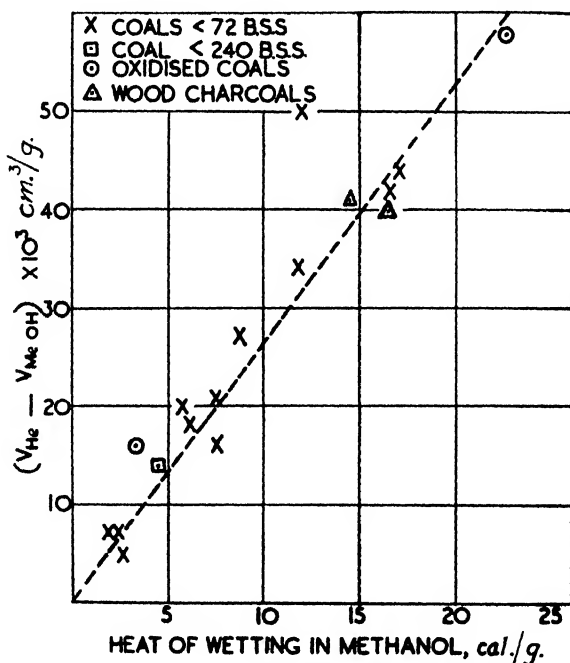


FIG. 4.

Bangham<sup>8</sup> for charcoal. The heat of wetting in methanol may therefore be taken as a measure of the specific surface of the coals, modified coals

\* Owing to the limitations of the calorimeter used, heats of wetting could only be measured during the first 10 to 20 min. after immersion. Specific volumes measured after 2 hr. immersion rather than after 24 hr., were therefore used in obtaining the values of  $(V_{\text{He}} - V_{\text{MeOH}})$  shown in Fig. 4.

and charcoals discussed here. The linear relationship in Fig. 4 then shows that the contraction due to adsorption is proportional to the surface area covered. The fact that the line passes through the origin confirms that methanol and helium penetrate to an approximately equal extent into the pore structure.

It is important to note that the contraction per unit area of adsorbing surface is found to be of equal magnitude for charcoals, anthracites, coals of low rank and highly oxidised coals in spite of the widely differing physical and chemical properties of these materials. The contraction cannot, therefore, be attributed either to incipient solution or to contraction in the solid substance.

Taking a heat of wetting of 1 cal. to represent 10 m.<sup>2</sup> of surface the observed contraction is  $2.6 \times 10^{-9}$  cm.<sup>3</sup> per cm.<sup>2</sup> of surface, or about 60 % of the volume which would be occupied by a monolayer of methanol on the surface of the solid if no contraction occurred. Thus, even if the contraction were spread evenly throughout the absorbed material (coals absorb the equivalent of from 3 to 5 molecular layers of methanol at saturation pressure at 25° C), it is surprisingly large. Measurements involving charcoals and cellulosic materials indicate, however, that the large contraction observed when methanol is adsorbed on coals is not exceptional.

Several authors have calculated the hydrostatic pressure required to produce the observed contraction in the adsorbed film, but it seems that such calculations can have little meaning since the adsorbed film and the forces responsible for its formation are essentially anisotropic, and the structure and properties of the film differ from those of the bulk liquid. Direct measurements of the volume occupied by water vapour on cellulose<sup>18</sup> and by organic vapours on charcoal<sup>19</sup> have shown that the greatest contraction occurs for small quantities of vapour adsorbed, when the lateral film pressure is very small and the volume change must be attributed almost entirely to the close approach of the adsorbate molecules to the surface atoms of the adsorbent. It seems probable, therefore, that the greater part of the large contraction observed when methanol is adsorbed on coal occurs in the direction perpendicular to the adsorbing surface.

**Apparent Densities in *n*-Hexane and Benzene.**—The apparent densities of coals in *n*-hexane and benzene show considerable drifts, and the values obtained after 24 hr. immersion are lower than the corresponding densities in helium for all except two of the coals investigated. Penetration of the pores by these liquids is slow and incomplete, and the extent of penetration varies with the rank of the coal. In the coals D, E and F, the liquids are almost completely excluded from the pores: the drifts are exceptionally slow, and for coal D the apparent density in *n*-hexane after 2 hr. immersion is still very near the lump density. The densities of the anthracites in *n*-hexane are much lower than in helium, but comparison with the lump density shows that the liquids penetrate to a considerable part of the pore space. The coals K and M, for which the apparent densities in *n*-hexane are higher than in helium, are both low rank coals of high porosity. It appears, therefore, that the accessibility of the pores of coals to *n*-hexane and benzene is at a minimum for coals containing between 89 % and 93 % carbon, and increases for coals of higher or of lower rank, being greatest for low rank coals of high porosity. That is, the *accessibility* is closely related to the *porosity*.

*n*-Hexane and benzene readily wet the surfaces of coals, and the viscosity of *n*-hexane is very low. The poor penetrating power of the liquids cannot, therefore, be attributed either to a wetting angle greater than 90°

<sup>18</sup> Stamm and Seborg, *J. Physic. Chem.*, 1935, **39**, 133. Stamm and Hanson, *ibid.*, 1937, **41**, 1007.

<sup>19</sup> Danforth and Devries, *J. Amer. Chem. Soc.*, 1939, **61**, 873.



or to high viscosity, but must be associated rather with the relatively large size of the benzene and *n*-hexane molecules. The molecule of *n*-hexane is considerably larger than that of benzene, and, where the apparent densities of a coal in the two liquids differ appreciably, the *n*-hexane value is the lower.

The above results therefore suggest that the width of the pores or of constrictions in the pore system in coals is of the same order as the diameters of the molecules used for the density measurements. These fine pores or constrictions are smallest in coals containing between 89 % and 93 % carbon. In the coal *n* the pores or constrictions are so narrow that even helium (molecular diameter 2 Å) penetrates somewhat slowly, a small density drift being observed.

It may be noted that the low apparent densities in *n*-hexane or benzene are always associated with long, slow drifts. This was observed also with other organic liquids of relatively large molecular size; even the heavy oil supplied for a Hyvac rotary pump showed a prolonged density drift, indicating slow penetration. This behaviour may probably be attributed to slow distortion of the coal substance by the spreading pressure in the adsorbed films, and is in sharp contrast with that of carbonised coals; the more rigid structure of the latter resists deformation by adsorbed films at 25° C, and, if the molecules of a given liquid are too large to enter the pores, then the liquid is totally excluded and there is no density drift.<sup>30</sup>

**Apparent Densities in Water.**—The apparent density in water is greater than the density in helium for coals of less than about 84 % carbon content. For high rank coals, on the other hand, it is intermediate between the values obtained with helium and *n*-hexane, being close to the low, *n*-hexane value for coals containing between 89 % and 93 % carbon, and nearly equal to the helium value for the highest rank anthracite (Fig. 3). Thus, as in the case of *n*-hexane and benzene, the accessibility of the pores and inner surfaces of coals to water is greatest for low rank coals of high porosity, passes through a minimum for coals containing between 89 % and 93 % carbon, and increases again with increasing rank among the anthracites.

The failure of water to fill completely the pores of high rank coals cannot be due to the size of the water molecule, since the molecule of methanol is larger, and apparent densities in methanol are high. Moreover, the absence of any density drift suggests that the cause of low apparent densities in water is different from that of the low values obtained with *n*-hexane and benzene. This difference is also revealed by the measurements made on samples of coals *r* and *k* ground to various sizes (Table V). Finer grinding increases the apparent density of both coals in *n*-hexane, and the drift for coal *r* is also increased. In water, on the other hand, the apparent density of coal *r* remains constant and that of coal *k* is increased, but in neither case is a density drift introduced.

It seems, therefore, that the low apparent densities of high rank coals in water is an effect associated with their poor wettability. That the external surfaces of coals *n* and *r* (91.7 % and 89.7 % carbon respectively) are not easily wetted by water was shown when attempts were made to measure their densities by immersing the sample (not previously evacuated) in the boiling liquid in a simple density bottle. The particles were not wetted even after prolonged boiling, and apparent densities as low as 0.7 g./cm.<sup>3</sup> were recorded.\* With coals *c* and *k*, on the other hand, the

<sup>30</sup> Franklin, *Coal Res.*, 1946, p. 37.

\* Striking proof of the way in which poor wettability (due to a large angle of contact) may influence apparent densities in water even after evacuation was obtained with a sample of the commercial carbon black P33. The material was evacuated at 90° C for three days, after which time the particles adhered to one another, and the substance could be shaken about in the glass bulb in the

results agreed well with the apparent densities measured in water after evacuation.

There is an apparent contradiction between these results and some later work by Maggs<sup>21</sup> who found that even high rank coals adsorb at saturation pressure, sufficient water vapour to fill all the pores. The discrepancy may perhaps be due to the fact that Maggs used water vapour whereas in the present work the coal was always placed in direct contact with the liquid. High rank coals contain adsorbed methane, the last traces of which are difficult to remove, and it may be that water vapour can replace the gas molecule by molecule, whereas the presence of liquid water impedes its escape.

**Dimensions of the Pores in Coals.**—Comparison of the porosity of coals as measured by King and Wilkins with the heat of wetting in methanol as measured by Griffith and Hirst suggests that the porosity is approximately proportional to the surface area. It follows that, for any given structural model, the mean diameter of the pores is approximately the same in all coals. Measurements of the porosity of the coals C, D, E, H, and K confirm this observation. Assuming that 1 cal. of heat of wetting in methanol corresponds to 10 m.<sup>2</sup> of surface, then, if the pore space in coals consists in uniform, cylindrical, non-intersecting pores, the mean pore diameter in all coals is about 40 Å. Alternatively, if the solid consists of equally spaced cubes of coal substance, the distance of separation between the cubes would be about 12 Å. The dimensions of the regions of continuous coal substance would, of course, vary with the surface area of the coal.

It has been shown, however, that coals do not behave as if they all contain uniform pores whose size is independent of rank. The pores of coal containing between 89 % and 93 % carbon are the least easily penetrated by liquids and among both low rank coals and anthracites permeability increases with increasing porosity. Similar observations have been made by Graham<sup>22</sup> who has pointed out that the permeability to methane and to moisture varies widely from one coal to another, the permeability of many anthracites and some low rank coals being low whereas other low rank coals and also the highest rank anthracite have a high permeability.

Since the mean pore diameter in all coals is approximately equal while the permeability varies widely, it must be presumed that the pores are not uniform along their length but contain fine constrictions, and that the accessibility of the pore space to liquids and gases is determined by the size and frequency of these constrictions rather than by the mean pore diameter. On this hypothesis, the pores are most highly constricted in coals containing between 89 % and 93 % carbon, while low rank coals of high porosity have the most open pore structure.

The configuration of the fine pores must be intimately related to the way in which the coal micelles are bound together, and the variation of the pore structure with the rank of the coal must be associated with the changes in micellar structure which occur during coalification. If the decrease in surface area and porosity which occurs with increasing rank up to about 90 % carbon be attributed to an increase in the size of the micelles, then the decreasing accessibility of the pores is in no way explained. The results suggest, rather, that the changes in pore structure

form of a hemispherical lump with a partly shiny surface. Its density in helium was 1.89 g./cm.<sup>3</sup>. When attempts were made to measure the density in water the solid floated, and approximate measurements gave values of about 0.8 g./cm.<sup>3</sup>, showing that atmospheric pressure was not sufficient to force the water into the evacuated spaces between the loosely aggregated particles.

<sup>21</sup> Bond, Griffith and Maggs, *Faraday Soc. Discussions*, 1948, 3, 29.

<sup>22</sup> Graham, *Conference on the Ultrafine Structure of Coals and Cokes* (B.C.U.R.A., 1943), p. 151.

at this stage are due to a *closer compacting of the coal micelles*. In a later paper a simple model based on this hypothesis is developed and is shown to be consistent with a wide range of experimental results in addition to those described above.

The work was carried out at the British Coal Utilisation Research Association.

The author wishes to thank Dr. D. H. Bangham and Dr. W. Hirst for much helpful discussion and advice.

*Laboratoire Central des Services Chimiques de l'État,  
12 quai Henri IV,  
Paris IV,  
France.*

---

## THE KINETICS OF THE TRANSIENT STATE IN A CONTINUOUS REACTION SYSTEM

By J. D. JOHNSON AND L. J. EDWARDS

*Received 29th November, 1948*

A three-vessel, continuous flow laboratory reactor is described, which may be used for preparative work or for the study of reaction kinetics. Equations for the rate processes in an  $n$ -vessel reactor are derived, including the build-up of product during the earlier stages before equilibrium has been attained. The performance of the apparatus is tested by following the increase in concentration when a solution of KCl entering the vessel is allowed to come to equilibrium. It is shown that the build-up of  $[Cl^-]$  in each compartment closely follows the predicted course and the behaviour of the apparatus deviates only very little from the ideal. The ammonolysis of chloroacetic acid to glycine is studied in the reactor and the conversion is compared with those obtaining in the batch process and in the tubular reactor.

Certain types of reaction, particularly those in which some of the reactants are in large excess, are carried out on an industrial scale by a continuous process in order to obtain the maximum yield of product under economical conditions. The vessels used for this process may be either of the continuous flow tubular reactor type, or may consist of a number of stirred mixers in series with one another. When the number of vessels in series becomes very large and the volume of each vessel correspondingly small, the system approaches the tubular reactor in performance. Both of these systems have been shown to give better results than the ordinary batch type of reaction vessel.<sup>1</sup>

On the laboratory scale, the use of continuous flow reactors is less frequent, partly owing to the greater practical difficulties in setting up the apparatus and partly because the need for economy of materials and best use of available reaction space is usually of minor importance. In some cases, however, the use of a series reactor offers advantages which may outweigh these objections.

This paper describes the application of a three-vessel system to the study of a typical slow reaction between two materials, one of which is in large excess. Although only three vessels were used in the experimental work the rate processes for an  $n$ -vessel reactor are derived in the theoretical section. A tubular type of reactor would be impracticable for slow processes on the laboratory scale owing to the great length which would be necessary to obtain the requisite degree of reaction.

The kinetics of a continuous process differ from those of a batch process

<sup>1</sup> Denbigh, *Trans. Faraday Soc.*, 1944, **40**, 352.

inasmuch as the reaction is extended in space rather than in time. When equilibrium has been reached, a stationary state is set up in each vessel of the series and, in general, it is only required to know the value of these equilibrium concentrations. In cases where reaction is slow, however, it may be some days before equilibrium conditions are attained in all vessels. Here it is advisable to follow the build-up of reaction product in each vessel from the start of the process, otherwise several days may elapse before it can be quite certain that the reaction is proceeding as planned. With a complete knowledge of the theoretical progress of reaction in the early stages before equilibrium is reached it is possible to check, at the earliest possible moment, such faults as inefficient stirring, back diffusion of products or irregularities in feed rates.

### Progress of Continuous Flow Reaction between Two Components

The reaction to be considered is of the type,



where P is the product required in best yield.

#### Notation

$n$	number of vessels or compartments in the reactor,
$V_1, V_2, V_3, \dots V_n$	volume of individual vessels or compartments,
$Q$	total volume of all vessels or compartments,
$v_x, v_y$	rate of flow of solutions of components X and Y into first vessel,
$v$	rate of flow of products from last vessel, equal to sum of $v_x$ and $v_y$ ,
$x_0, y_0$	active concentrations of components X and Y in the inflowing liquids,
$t$	time elapsed from start of reaction,
$x_1, x_2, x_3, \dots x_n$	concentrations of X in vessels after time $t$ ,
$y_1, y_2, y_3, \dots y_n$	concentrations of Y in vessels after time $t$ ,
$y_m$	assumed concentration of Y in all vessels for the pseudo-monomolecular reaction,
$p_1, p_2, p_3, \dots p_n$	concentration of P in vessels after time $t$ ,
$k$	velocity constant of the bimolecular reaction,
$x'_1, x'_2, x'_3, \dots x'_n$	concentration of X in vessels after time $t$ in the special case when $k = 0$ ,
$E$	efficiency with which the total space, $Q$ , is being used compared to a tubular reactor of equal volume.

In deriving the rate equations for the continuous flow series reactor, the following assumptions are made—

1. The volume of connecting pipes between compartments is negligibly small.
2. Instantaneous perfect mixing takes place in each compartment.
3. No back diffusion of active components occurs between compartments.
4. The feed rates of components and effluent rate of product are perfectly uniform.
5. No volume fluctuations occur in the contents of each compartment.
6. The whole process is carried out under uniform conditions of temperature and pressure.

The component Y will be taken to be in large excess throughout the system; this is effected by making  $v_y > v_x$  and  $y_0 > x_0$  and filling all compartments with Y at concentration  $y_0$  before starting the flow of reactants. Under such conditions  $y \gg x$  throughout the reaction and

the bimolecular reaction with velocity constant  $k$  may be taken as monomolecular with respect to X. Then the rate of increase of  $x$  in each vessel is given by—

$$\frac{dx_1}{dt} = \left( \frac{x_0 v_x}{v} - x_1 \right) \frac{v}{V_1} - kx_1 y_1, \quad . \quad . \quad . \quad (1)$$

$$\frac{dx_2}{dt} = (x_1 - x_2) \frac{v}{V_2} - kx_2 y_2, \quad . \quad . \quad . \quad (2)$$

$$\frac{dx_3}{dt} = (x_2 - x_3) \frac{v}{V_3} - kx_3 y_3, \quad . \quad . \quad . \quad (3)$$

$$\frac{dx_n}{dt} = (x_{n-1} - x_n) \frac{v}{V_n} - kx_n y_n. \quad . \quad . \quad . \quad (4)$$

On integration, assuming  $y_1, y_2, \dots, y_n$  to be constant, these equations lead to the following expressions for  $x$ :

$$x_1 = \frac{x_0 v_x}{a_1 V_1} [1 - \exp(-a_1 t)], \quad . \quad . \quad . \quad . \quad . \quad (5)$$

$$x_2 = \frac{x_0 v_x v}{a_1 a_2 V_1 V_2} \left[ 1 - \frac{a_2}{a_2 - a_1} \exp(-a_1 t) - \frac{a_1}{a_1 - a_2} \exp(-a_2 t) \right], \quad (6)$$

$$x_3 = \frac{x_0 v_x v^2}{a_1 a_2 a_3 V_1 V_2 V_3} \left[ 1 - \frac{a_2 a_3}{(a_2 - a_1)(a_3 - a_1)} \exp(-a_1 t) \right. \\ \left. - \frac{a_1 a_3}{(a_1 - a_2)(a_3 - a_2)} \exp(-a_2 t) - \frac{a_1 a_2}{(a_3 - a_2)(a_1 - a_3)} \exp(-a_3 t) \right] \quad (7)$$

$$x_n = \frac{x_0 v_x v^{n-1}}{a_1 a_2 \dots a_n V_1 V_2 \dots V_n} \left[ 1 - F_1 \exp(-a_1 t) \right. \\ \left. - F_2 \exp(-a_2 t) - \dots - F_n \exp(-a_n t) \right], \quad (8)$$

where the factor  $a_n$  represents  $\frac{v + k y_n V_n}{V_n}$  and the coefficients  $F_1, F_2, F_3, \dots, F_n$  become increasingly complex as  $n$  increases.

If no reaction takes place between the components X and Y there will still be a change of concentration when they are fed into the vessels containing Y due to the mixing effect alone. Under these conditions the values of  $x'$  are found by putting  $k = 0$  in eqn. (5) to (8) when

$$x'_1 = \frac{x_0 v_x}{v} \left[ 1 - \exp\left(-\frac{vt}{V_1}\right) \right], \quad . \quad . \quad . \quad . \quad . \quad (9)$$

$$x'_2 = \frac{x_0 v_x}{v} \left[ 1 - \frac{V_1}{V_1 - V_2} \exp\left(-\frac{vt}{V_1}\right) - \frac{V_2}{V_2 - V_1} \exp\left(-\frac{vt}{V_2}\right) \right], \quad (10)$$

$$x'_3 = \frac{x_0 v_x}{v} \left[ 1 - \frac{V_1^2}{(V_1 - V_2)(V_1 - V_3)} \exp\left(-\frac{vt}{V_1}\right) - \frac{V_2^2}{(V_2 - V_1)(V_3 - V_1)} \exp\left(-\frac{vt}{V_2}\right) \right. \\ \left. - \frac{V_3^2}{(V_2 - V_3)(V_3 - V_1)} \exp\left(-\frac{vt}{V_3}\right) \right], \quad (11)$$

$$x'_n = \frac{x_0 v_x}{v} \left[ 1 - F'_1 \exp\left(-\frac{vt}{V_1}\right) - F'_2 \exp\left(-\frac{vt}{V_2}\right) \right. \\ \left. - F'_3 \exp\left(-\frac{vt}{V_3}\right) - \dots - F'_n \exp\left(-\frac{vt}{V_n}\right) \right]. \quad (12)$$

The value of  $p$  in any vessel is given by a simple multiple of the difference between the concentration of X which would have been present if no reaction had occurred and the concentration present when reaction does occur, i.e.,

$$p_n = m(x'_n - x_n), \quad . \quad . \quad . \quad . \quad (13)$$

$m$  being a small integer, usually unity.

**Vessels of Equal Volume.**—When the volumes of all vessels are equal, eqn. (5) to (8) still hold if  $V$  is substituted for the various values of  $V_n$ .

Substitution of equal values of  $V$  in eqn. (9) to (12) for the case when  $k = 0$  leads to indeterminate results. Here the original rate processes have to be rewritten—

$$\frac{dx'_1}{dt} = \left( \frac{x_0 v_r}{v} - x'_1 \right) \frac{v}{V}, \quad . \quad . \quad . \quad . \quad (14)$$

$$\frac{dx'_2}{dt} = (x'_1 - x'_2) \frac{v}{V}, \quad . \quad . \quad . \quad . \quad (15)$$

$$\frac{dx'_3}{dt} = (x'_2 - x'_3) \frac{v}{V}, \quad . \quad . \quad . \quad . \quad (16)$$

$$\frac{dx'_n}{dt} = (x'_{n-1} - x'_n) \frac{v}{V}, \quad . \quad . \quad . \quad . \quad (17)$$

Integration leads to the expression—

$$x'_n = \frac{x_0 v_r}{v} \left[ 1 - \left( 1 - \frac{v}{V} - \frac{v^2}{2V^2} t^2 - \dots - \frac{v^{n-1}}{(n-1)! V^{n-1}} t^{n-1} \right) \exp \left( -\frac{v}{V} t \right) \right], \quad (18)$$

Eqn. (18) is equivalent to the expression for "bye-passing" (26) derived by Denbigh.<sup>1</sup> Denbigh uses the term "bye-passing" to describe what occurs in the vessels when  $k = 0$ . The authors prefer to define "bye-passing" as the difference between the concentrations of product in theory and in fact due to deviations from ideal behaviour in the apparatus.

The values of  $p$  for vessels of equal volumes are again determined by eqn. (13) using the values of  $x$  and  $x'$  given by eqn. (5) to (8) and (18) respectively.

As  $y \gg x$  the value of  $y$  is approximately constant in all vessels at all times. Actually there is a slight decrease in  $y$  from  $y_0$  at zero time to  $y_0 v_v/v$  at infinite time. The maximum error due to the assumption of a constant value for  $y$  will be illustrated in the experimental section below, where curves are constructed for each of the extreme values of  $y$ . As the equilibrium level in each vessel is ultimately of major interest it is better to use  $y_0 v_v/v$  for calculations involving the final state. For following the reaction in its initial stages, however, closer agreement is obtained by using  $y_0$  or even an average value  $\frac{y_0}{2} \left( 1 - \frac{v_v}{v} \right)$ .

When the value of  $y$  is chosen as  $y_m$  in all vessels the eqn. (5) to (8) lead to indeterminate results on substitution. The rate processes must again be rewritten—

$$\frac{dx_1}{dt} = \frac{x_0 v_r}{V} - x_1 \left( k y_m + \frac{v}{V} \right), \quad . \quad . \quad . \quad (19)$$

$$\frac{dx_2}{dt} = \frac{x_1 v}{V} - x_2 \left( k y_m + \frac{v}{V} \right), \quad . \quad . \quad . \quad (20)$$

$$\frac{dx_3}{dt} = \frac{x_2 v}{V} - x_3 \left( k y_m + \frac{v}{V} \right), \quad . \quad . \quad . \quad (21)$$

$$\frac{dx_n}{dt} = \frac{x_{n-1} v}{V} - x_n \left( k y_m + \frac{v}{V} \right), \quad . \quad . \quad . \quad (22)$$

Integration leads to the expression

$$x_n = \frac{x_0 v_r v^{n-1}}{a_m^n V^n} \left[ 1 - \left( 1 + a_m t + \frac{1}{2} a_m^2 t^2 + \dots + \frac{1}{(n-1)!} a_m^{n-1} t^{n-1} \right) \exp (-a_m t) \right], \quad (23)$$

where  $\frac{v + k V y_m}{V}$  is represented by  $a_m$ .

Thus for the pseudo-monomolecular reaction in vessels of equal volume the concentration of product in the  $n$ th vessel will be—

$$p_n = \frac{mx_0 v_x}{v} \left[ 1 - \left( 1 + at + \frac{1}{2} a^2 t^2 + \dots + \frac{1}{(n-1)!} a^{n-1} t^{n-1} \right) \exp(-at) \right. \\ \left. - \left( \frac{v}{a_m V} \right)^n \left\{ 1 - \left( 1 + a_m t + \frac{1}{2} a_m^2 t^2 + \dots + \frac{1}{(n-1)!} a_m^{n-1} t^{n-1} \right) \exp(-a_m t) \right\} \right], \quad (24)$$

where  $v/V$  is represented by  $a$ .

After a long time the equilibrium value for  $p_n$  becomes

$$(p_n)_{t \rightarrow \infty} = \frac{mx_0 v_x}{v} \left[ 1 - \left( \frac{v}{a_m V} \right)^n \right]. \quad (25)$$

With a very large number of vessels  $p_n$  would approach the value corresponding to complete reaction, i.e., disappearance of component X from the effluent liquid. Under these conditions:

$$(p_n)_{\substack{t \rightarrow \infty \\ n \rightarrow \infty}} = \frac{mx_0 v_x}{v}. \quad (26)$$

The number of vessels necessary to achieve a specific degree of completeness of reaction is readily calculable from (25) and (26). Thus, for 99% completion,

$$1 - \left( \frac{v}{a_m V} \right)^n = 0.99,$$

or

$$n = \frac{2}{\log_{10} \frac{a_m V}{v}}. \quad (27)$$

If the total reaction volume is limited by considerations of bench space, etc., it is important to know the efficiency with which the available space is being used in comparison to that of a tubular reactor of the same total volume.

From (25),

$$(p_n)_{\substack{t \rightarrow \infty \\ nV=Q}} = \frac{mx_0 v_x}{v} \left[ 1 - \left( \frac{v}{v + \frac{kQy_m}{n}} \right)^n \right].$$

Inverting  $\left( \frac{v}{v + \frac{kQy_m}{n}} \right)^n$  and expanding the binomial

$$\left( 1 + \frac{kQy_m}{nv} \right)^n = 1 + \dots + \frac{n(n-1)(n-2) \dots (n-r+1)}{r!} \left( \frac{kQy_m}{nv} \right)^r + \dots$$

the general term reduces to  $\frac{1}{r!} \left( \frac{kQy_m}{v} \right)^r$  as  $n \rightarrow \infty$ , hence the series approaches  $\exp \left( \frac{kQy_m}{v} \right)$ . For a large number of vessels of total volume  $Q$  or a tubular reactor of the same volume the limiting concentration of product approaches

$$(p_n)_{\substack{t \rightarrow \infty \\ n \rightarrow \infty \\ nV=Q}} = \frac{mx_0 v_x}{v} \left[ 1 - \exp \left( - \frac{kQy_m}{v} \right) \right], \quad (28)$$

and the efficiency with which the available reaction space is being used is therefore

$$E = \frac{1 - \left( \frac{v}{v + \frac{kQy_m}{n}} \right)^n}{1 - \exp \left( - \frac{kQy_m}{v} \right)}. \quad (29)$$

### Experimental

**Apparatus.**—The final layout of the three-vessel laboratory reactor is illustrated in Fig. 1. The vessels were made from Pyrex glass with Quickfit B24

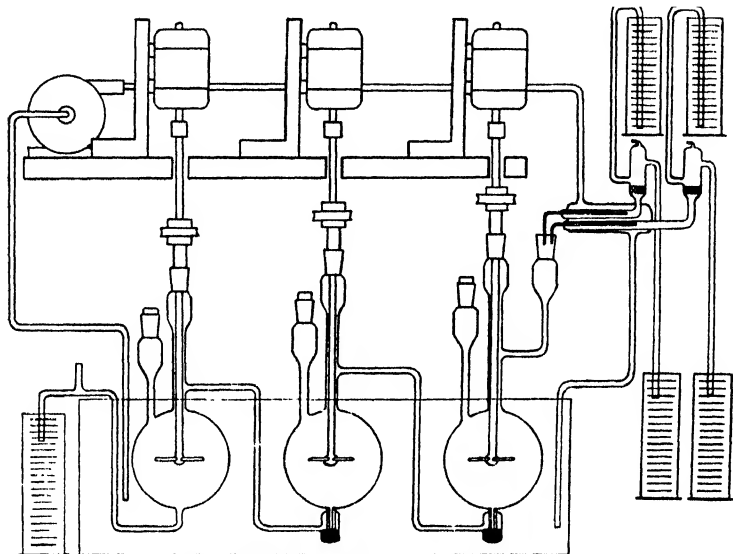


FIG. 1.—Three vessel reactor.

joints and stirrer heads. The total reaction space was 1665 ml., each vessel having a capacity of  $555 \pm 5$  ml. A thermostat bath at  $25^\circ \text{C}$  was used to control the temperature throughout all experiments.

In arriving at this design of apparatus the following points were taken into consideration.

1. Each vessel was fitted with an independent motor whose speed (*ca.* 300 rev./min.) was regulated by a rheostat. Earlier experiments using a single motor to stir the first vessel with belt drives to the other two were unsuccessful; irregular stirring due to the slipping or breaking of the belts at various times made it difficult to follow the course of reaction with any accuracy.

2. It was important that the level of liquid in each vessel should remain constant throughout a run. This was effected partly by uniform stirring and partly by providing the vessels with long, narrow necks through which the stirrer shafts passed with the minimum of clearance. The liquid level in each vessel was arranged to fall approximately halfway up the narrow part of the neck so that the effect of any residual variation in stirrer speed on the volume of liquid present in the vessel was practically eliminated.

3. The diffusion of liquid from one vessel to the previous one was prevented by means of a small mercury seal at the base of each vessel (except the last). The mercury pressure to be overcome was less than 1 mm. so that it was necessary to have a difference of about 1 cm. in the liquid levels of successive compartments. At the start of a run the vessels were filled with the component in excess and this solution was run slowly into the first vessel until the levels in all vessels had settled down to a steady state with all stirrers in operation. Once this state had been achieved the introduction of a small volume of liquid into the first vessel was followed by the discharge of an equal volume of liquid from the last vessel within a few seconds. This arrangement was preferred to having the vessels in cascade as the latter device necessitated three thermostat baths and considerably more headroom.

4. To obtain slow, steady delivery rates into the first vessel, fairly long capillary feeds were necessary. Some trouble was experienced in earlier trials owing to blockage of these capillaries by small particles of foreign matter. This was overcome by incorporating sintered-glass filters into the feed lines. The uniformity of the flow rate was further enhanced by the constant-head device illustrated and by jacketting each capillary with water circulated from the main



thermostat bath. With these precautions, a steady delivery rate could be maintained indefinitely. The total delivery in any given period of time was determined by the change of levels in the upper and lower graduated vessels attached to the constant-head device. The upper vessels were refilled and the lower ones emptied from time to time as occasion demanded.

5. Each compartment of the reactor was fitted with an additional neck for sampling purposes. Samples withdrawn at any one time never exceeded 1 ml. per vessel and the total volume of samples taken during a run was usually of the order of 1 % of the total volume of reaction liquid involved in the run.

**Performance of the Apparatus when  $k = 0$ .**—The behaviour of the apparatus was tested in the absence of chemical reaction by filling all compartments with water and running in water and an aqueous solution of KCl. The concentrations of KCl were determined in each of the three vessels at various times by titration of 1 ml. samples. The theoretical curves were calculated from eqn. (18) using the following data :

$$\begin{array}{ll} X = \text{KCl solution;} & Y = \text{water.} \\ x_0 = 0.5; & v_a = 0.967 \text{ ml./min.} \\ v_v = 11.26 \text{ ml./min.;} & v = 12.227 \text{ ml./min.} \\ & V = 555 \text{ ml.} \end{array}$$

These curves and the experimental points are shown in Fig. 2. The agreement

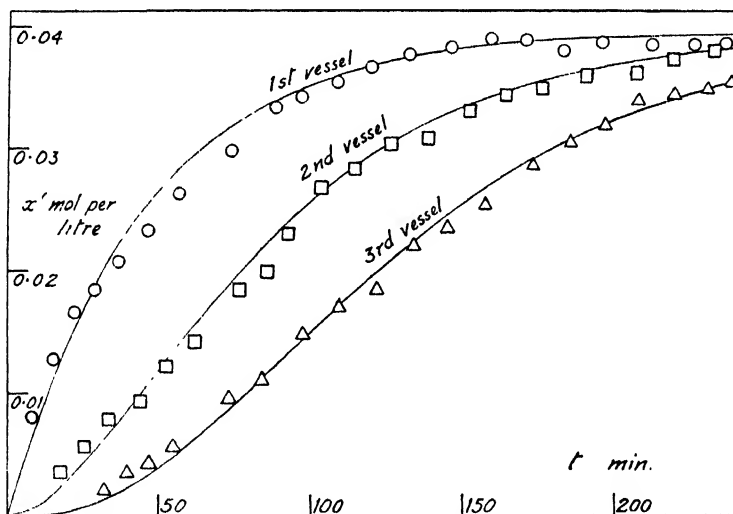
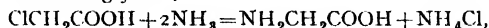


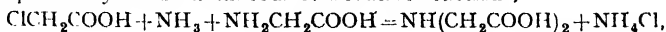
FIG. 2.—Performance of the apparatus when  $k = 0$ .

between experiment and theory shows that the apparatus is operating under conditions which closely approximate to the assumptions made in deriving the rate equations, hence "bye-passing" is negligible.

**Preparation of Glycine.**—The reaction between aqueous ammonia and chloro-acetic acid to form glycine,



is accompanied by the simultaneous consecutive reactions,



and



The presence of a large excess of ammonia increases the chances of fruitful encounters with chloroacetic acid molecules and decreases the likelihood of the formation of the imidoacetic acids. In a quantitative study of the reaction,<sup>2</sup> Robertson showed that using a molar ratio of 1/15 chloroacetic acid to ammonia the yield of glycine was 58 %, whereas a 95 % yield resulted if the ratio was increased to 1/220. In the latter case the quantity of by-products formed was small.

<sup>2</sup> Robertson, *J. Amer. Chem. Soc.*, 1927, **49**, 2889.

This reaction, requiring a very large excess of one reactant to give a good yield of the desired product, is ideally suited to a continuous process. Before carrying out the main run, however, a small batchwise experiment was performed using the same reactants at the same working temperature in order to determine the value of  $k$  for the reaction. The reactants used were:

X = chloroacetic acid solution (104 g./l.).

Y = ammonia solution (245 g./l.).

For the batch ammonolysis, 17.26 ml. X and 200 ml. Y were mixed in a stoppered flask at 25° C and titrated at intervals to determine the Cl<sup>-</sup> liberated (which is equivalent to the glycine formed). These quantities correspond to a molar ratio of 1/152, the same value as used in the subsequent run in the continuous flow reactor. A plot of

$$\log_{10} \frac{[Cl^-]_{\infty}}{\infty[Cl^-] - [Cl^-]_t}$$

against  $t$  is shown in Fig. 3. The slope of the best curve through the experimental points is equal to  $ky_0/2.303$ , or

$$k = \frac{2.303 \times 0.08518 \times 217.26}{14.41 \times 200} = 0.0148 \text{ l.mol.}^{-1} \text{ hr.}^{-1}.$$

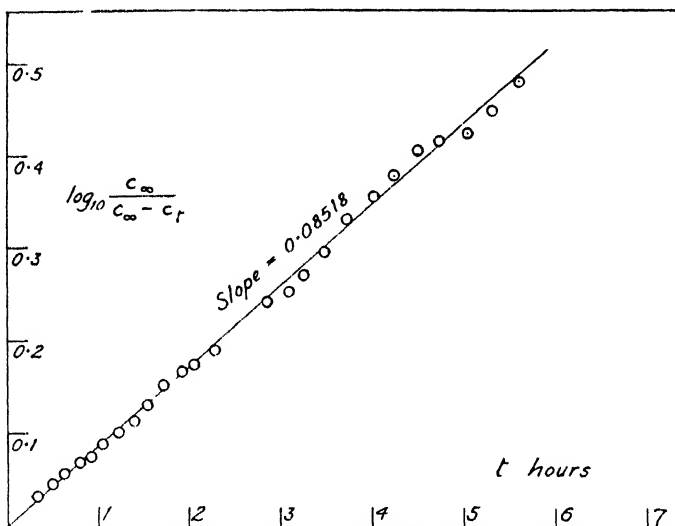


FIG. 3. Determination of  $k$  for the glycine reaction.

Thus, for the continuous process, the data required to calculate the theoretical progress of the reaction were:

$$x_0 = 1.100 \text{ mol./l.}$$

$$v_x = 0.00505 \text{ l./hr.}$$

$$v = 0.06355 \text{ l./hr.}$$

$$Q = 1.665 \text{ l.}$$

$$k = 0.0148 \text{ l.mol.}^{-1} \text{ hr.}^{-1}$$

$$y_0 = 14.41 \text{ mol./l.}$$

$$v_y = 0.0585 \text{ l./hr.}$$

$$V = 0.555 \text{ l.}$$

$$m = 1$$

$$y_0 v_y / v = 13.27 \text{ mol./l.}$$

Using 13.27 and 14.41 as the extreme values of  $y_m$  substitution in eqn. (24) gave the theoretical limits within which the glycine concentration (i.e. the [Cl<sup>-</sup>]) should lie at any time.

From eqn. (25), taking  $y_m = 13.27$

$$(p_1)_{t \rightarrow \infty} = 0.05521 \text{ (63.2 \% conversion),}$$

$$(p_2)_{t \rightarrow \infty} = 0.07556 \text{ (86.4 \% conversion),}$$

$$(p_3)_{t \rightarrow \infty} = 0.08304 \text{ (95.0 \% conversion).}$$

And from (26)

$$(p_n)_{t \rightarrow \infty} = 0.08741 \text{ (100.0 \% conversion).}$$

To attain 99 % completion of reaction, from (27)

$$n = \frac{2}{\log_{10} \left( 1 + \frac{0.0148 \times 0.555 \times 13.27}{0.06355} \right)} = 4.6,$$

i.e. 5 vessels would be required.

The efficiency with which the available reaction space is being used, calculated from (29), is shown in Table I.

TABLE I.—EFFICIENCY OF USE OF REACTION SPACE

$n$	$E$ (%)
1	84.21
2	92.70
3	95.56
4	96.90
5	97.66
6	98.13
7	98.46
8	98.69
9	98.86
10	99.00
$\infty$	100.00
(tubular reactor)	

In Fig. 4 the heavy black lines indicate the limits of error due to the variation of  $\gamma$ . It is clear that the error involved is small and may be neglected in comparison with the other experimental errors. The final equilibrium concentrations after about four days' reaction were:

Vessel 1, 0.0555; Vessel 2, 0.0770;

Vessel 3, 0.0843.

These values were in fairly good agreement with the values predicted from eqn. (25), and the progress of the reaction in its earlier stages is, on the whole, in reasonable agreement with theory. The major source of variation was due to the tendency for the ammonia solution to lose strength over long periods, whilst the disturbance to the system in the neighbourhood of 24 hr. was due to a change of shifts at that time. From Table I it may be seen that little gain in efficiency is effected by the use of more

than three or four vessels on the laboratory scale. On a production scale, however, a large number of vessels or a tubular reactor might be preferable.

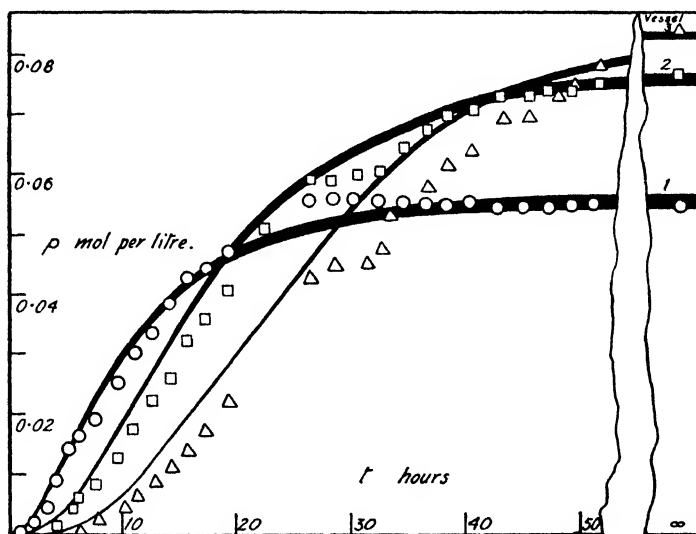


FIG. 4.—Progress of the glycine reaction.

To confirm that glycine had been formed simultaneously to a degree comparable with that of the chloride ion, formal titrations were performed on samples from the second and third vessels after equilibrium had been reached. The concentrations found were

Vessel 2, 0.0739; Vessel 3, 0.0792,

which amount to

$$(0.0739/0.07556)100 = 97.8 \%$$

and

$$(0.0792/0.08304)100 = 95.1 \%$$

theoretical respectively. It may be concluded that if another vessel had been placed in series with the three actually used, the yields of chloride ion and of glycine would have been about 99 % and 96 % respectively of the amounts theoretically possible after the lapse of an infinite time in a batch reaction. Alternatively, these better yields would have resulted in the existing apparatus if more concentrated ammonia had been used, since an increase in  $y_m$  has the effect of raising the asymptotic concentration of resultants. This was not done in the experiment described owing to the difficulty in preventing variations in strength of the ammonia solution at very high concentrations.

The glycine was isolated from the effluent from the last vessel by evaporating to dryness and extracting the ammonium chloride with methanol. The residue gave only a faint chloride reaction and one crystallisation from water served to purify it. No attempt was made to recover the ammonia in the laboratory; on a plant scale this would be done by means of a stripping column and absorber or some such standard method.

### Discussion

In the glycine reaction described above, the time required to attain equilibrium in the last vessel was more than three days. The process was followed from start to finish in order to test the agreement between the experimental results and the derived rate equations. In practice, much time could be saved by allowing the reactants to come to equilibrium by filling the reaction vessel with the two reactants fed simultaneously in appropriate ratio and, after allowing sufficient time to elapse for equilibrium to be sensibly attained, restarting the feeds of the two materials. Using the same solutions of ammonia and chloroacetic acid it can be shown that the steady state would be attained some 15 hr. after the start of a run. With other reactions it may not be feasible to proceed in this manner because of some particular hazard; a violent heat evolution, for example, would make it essential to fill the reactor with one of the reactants only.

The continuous flow reactor can be used, if so desired, for much faster reactions than the ammonolysis of chloroacetic acid. The hydrolysis of ethyl acetate with 2.5N HCl, a process whose velocity constant is about ten times as great as the glycine reaction, was carried out with satisfactory results in the apparatus described.

The applications of a multi-compartment reactor are not limited to preparative work. The apparatus may be used to determine the velocity constant of any reaction taking place therein. This may be done by comparing the equilibrium concentrations of product in any two of the compartments. For example, from (25) it may be shown that if

$$\begin{aligned} \frac{(p_2)_{t \rightarrow \infty}}{(p_1)_{t \rightarrow \infty}} &= r, \\ k &= \frac{v}{V y_m} \left( \frac{2-r}{r-1} \right). \end{aligned} \quad (30)$$

For the glycine reaction,  $r = 0.077/0.0555 = 1.387$ ,  
giving  $k = 0.0137$

in fair agreement with the figure obtained by the direct method. With such a slow reaction there is no point in determining  $k$  in this manner. When the reaction is very rapid, however, the continuous flow method offers a distinct advantage, especially when the number of vessels is fairly large. The extension of the reaction in space rather than in time enables its course to be plotted at leisure.

The authors wish to record their thanks to the directors of Beecham Research Laboratories, Ltd., for permission to publish this work.

*Brockham Park,  
Betchworth,  
Surrey.*

# A THEORETICAL STUDY OF SOME NON-BENZENOID HYDROCARBONS

## PART I

By R. D. BROWN

Received 9th December, 1948

The results of calculations of electron densities, free valences, bond orders and bond lengths are presented for some non-benzenoid aromatic hydrocarbons of symmetry  $V_h$ . The chemistry of these molecules is discussed briefly, and it is concluded that, although all but one are so far unknown, they would all be reasonably stable once formed.

**Introduction.**—In recent years a growing interest, both experimental and theoretical, has been evinced in the so-called non-benzenoid hydrocarbons.<sup>1</sup> Theoretically these are of interest because it is for just these compounds that the valence-bond and molecular-orbital methods disagree. The molecular-orbital treatment is less reliable for these hydrocarbons than for the more common alternant hydrocarbons,<sup>2</sup> but the results of such a treatment are of particular interest to the organic chemist because it is only for these non-alternant hydrocarbons that the electron densities differ from unity. It is true that this is precisely where the inconsistency lies in the molecular-orbital treatment but it seems likely that the results will be qualitatively correct, and in any case the experimental testing of the results to be presented below will provide evidence of the validity or otherwise of this assumption.

In view of the recent discussion of aromatic substitution by Waters<sup>3</sup> it seems useful to compare the chemistry of the molecules as predicted on the one hand by the  $\pi$ -electron density results and on the other by the polarization energy method as developed by Wheland.<sup>4</sup> The interrelation of polarization energy values with the  $\pi$ -electron densities seems very probable although it has so far not been possible to give a rigorous proof of this.<sup>5</sup>

In this paper the  $\pi$ -electron densities, bond orders, bond lengths and free valences of the hydrocarbons, pentalene, heptalene, fulvalene\* and biphenylene, all belonging to the symmetry group  $V_h$ , are reported. In succeeding papers the polarization energies, resonance energies and spectra of these compounds will be discussed and the results of a similar treatment of other non-benzenoid hydrocarbons of lower symmetry will be presented.

**Method of Computation.**—The details of the LCAO approximation are too well known to merit reproduction here.<sup>6</sup> As the inclusion of a finite overlap integrals makes no difference to the resultant  $\pi$ -electron densities or related quantities, the calculations were carried through assuming  $S = 0$ .

<sup>1</sup> Baker, *J. Chem. Soc.*, 1945, 265; Horn, Nunn and Rapson, *Nature*, 1947, 160, 829; Craig and Maccoll, *ibid.*, 1948, 161, 481.

<sup>2</sup> Coulson and Longuet-Higgins, *Proc. Roy. Soc. A*, 1947, 192, 18.

<sup>3</sup> Waters, *J. Chem. Soc.*, 1948, 727.

<sup>4</sup> Wheland, *J. Amer. Chem. Soc.*, 1942, 64, 900.

<sup>5</sup> Coulson, private communication.

\* The name *fulvalene* is suggested for the so-far unknown "aromatic" hydrocarbon, related to fulvene, with the structure indicated in the diagrams.

<sup>6</sup> Longuet-Higgins and Coulson, *Trans. Faraday Soc.*, 1947, 43, 87.

The bond lengths were found using the graph of bond order against bond length already published.<sup>7</sup> As hyperconjugation occurs in two of the molecules used as standards in preparing the graph (viz. ethane, ethylene) a second plot was drawn making allowance for this but the results by the two graphs did not differ significantly. As a rough indication of the magnitude of the change introduced by allowing for hyperconjugation the values derived from both graphs have been included in one case.

The free valences were computed following the method of Coulson<sup>8</sup> assuming that  $N_{\text{max.}} = 4.680$ .

**Results.**—The  $\pi$ -electron densities are shown in Fig. 1, the free

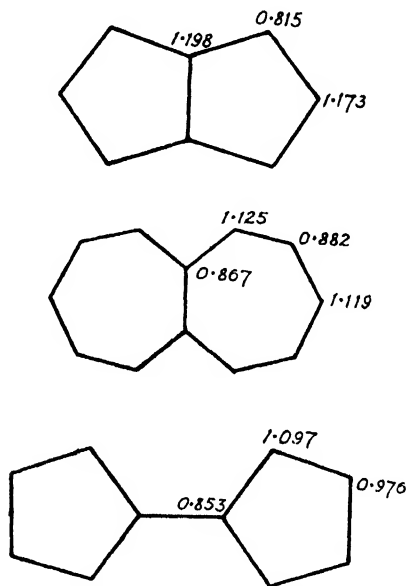


FIG. 1.—Electron densities.

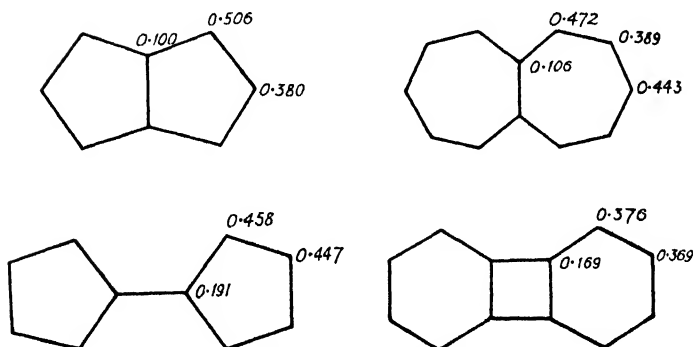


FIG. 2.—Free valences.

valences in Fig. 2, the bond orders in Fig. 3, and the bond lengths in Å in Fig. 4. It is tempting to predict the chemistry of these molecules from

<sup>7</sup> Brown, *ibid.*, 1948, **44**, 984.

<sup>8</sup> Mulliken, Rieke and Brown, *J. Amer. Chem. Soc.*, 1941, **63**, 54.

<sup>9</sup> Coulson and Longuet-Higgins, *Rev. Sci.*, 1947, **85**, 929.

the results given. In the following the usual assumptions have been made: electrophilic attack and nucleophilic attack are assumed to occur

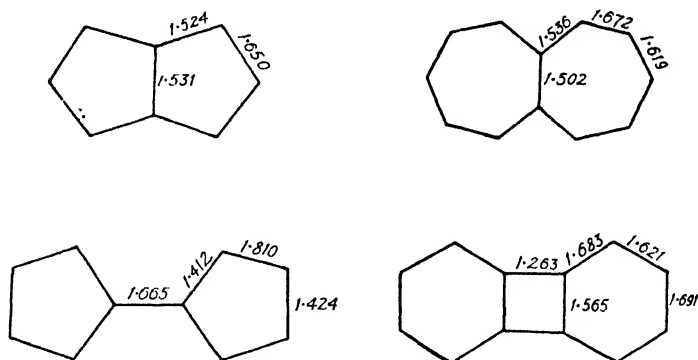


FIG. 3.—Bond orders.

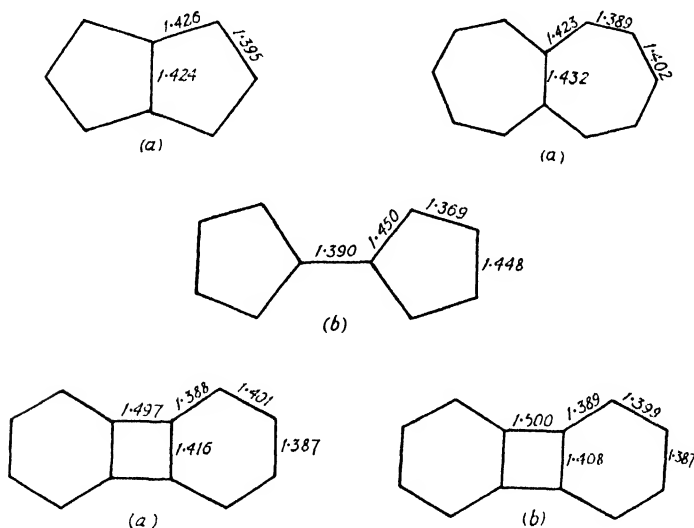


FIG. 4.—Bond lengths.

(a) Ignoring hyperconjugation.

(b) Allowing for hyperconjugation.

at the positions of highest and of lowest  $\pi$ -electron density respectively, and free radical attack at the point of highest free valence. These predictions of course provide a means for experimentally determining the reliability of the MO treatment of non-alternant hydrocarbons.

**Pentalene.**—The  $\pi$ -electron densities\* of pentalene are seen to deviate considerably from unity, rather more, for example, than in azulene.<sup>10</sup> There are only two possible positions of chemical attack and the present data suggest that electrophilic substitution will occur† at position 2, and nucleophilic attack at position 1. The free valences are quite high

\* The electron densities have already been published (Coulson and Rushbrooke, *Proc. Camb. Phil. Soc.*, 1940, **36**, 193) but have not been discussed in terms of the chemistry.

<sup>10</sup> Coulson and Longuet-Higgins, ref. 9; Brown, ref. 7.

† The numbering system employed is given at the end of the paper.

compared with those of azulene or naphthalene,<sup>9</sup> but lower than those of fulvene and ethylene.<sup>9</sup> The results indicate that radical attack will take place at position 1.

The bond orders and consequently also the bond lengths do not vary very much, especially as compared with those of azulene or naphthalene,<sup>10</sup> and are reasonably close to the benzene value (1.667). In particular the bond common to the two rings has a higher bond order than the corresponding bond in azulene or naphthalene.<sup>10</sup> This latter result is in complete contrast to the results of Craig and Maccoll<sup>11</sup> who obtained an order of less than unity for this bond. It is true that they used the valence-bond method in their work but it is generally found that the agreement between the two methods is excellent.

The above results lead one to expect that pentalene, once formed, would be a reasonably stable substance, more stable than, say, fulvene although still quite reactive chemically. This, of course, does not mean that the molecule would necessarily be formed easily because its chemical stability is not directly related to the activation energy of formation. The absence of bonds of order above 1.7 indicates that pentalene would tend to undergo substitution rather than addition in reactions such as bromination.

**Heptalene.**—For heptalene the electron densities do not diverge from unity quite as much as in the case of pentalene. The results indicate that electrophilic substitution will occur at position 1 and nucleophilic attack at position 2. The free valences are smaller than for pentalene and the maximum value of 0.47 at position 1 is much the same as the maxima for phenanthrene and anthracene.<sup>9</sup> Thus it is to be expected that oxidation, reduction, etc., will occur with about the same ease as for anthracene and phenanthrene.

The bond orders show a greater spread of values than those for pentalene but still not as much as azulene or naphthalene. It may be noted that the bond common to the two rings still has an order greater than that of azulene.

In view of these results it may reasonably be expected that heptalene also would be quite stable when formed, perhaps more stable than pentalene. However, the possibility of a non-planar configuration, not allowed for in the above computations, cannot be ruled out. Again the fact that all bond orders lie well below 1.7 suggests that substitution rather than addition will be the rule in reactions such as bromination.

**Fulvalene.**—The  $\pi$ -electron densities for this molecule show less variation than those of either of the above two molecules or of azulene. The figures point to electrophilic substitution at position 1 and nucleophilic attack at position 2. The largest free valence is 0.46 which is quite close to that of heptalene and consequently fulvalene may be expected to behave in much the same way as this molecule in reactions involving free radicals.

The most striking thing about the bond orders is the degree of bond fixation in the five-membered rings. This indicates that fulvalene would be less aromatic in character than the other hydrocarbons and in particular the 1:2 bond would be prone to undergo addition reactions. Thus, for example, the sequence: butadiene (1.894), acenaphthylene (1.796), fulvene (1.778), phenanthrene (1.775), naphthalene (1.725), of the orders of the most reactive bond in each molecule, is also, as far as one can judge from the experimental data, that of increasing tendency to substitution. We see that fulvalene falls between butadiene and acenaphthylene.

The results just discussed for fulvalene imply that it would be quite stable when prepared but would behave more like an unsaturated than an aromatic compound. Further, in contrast to fulvene, it would not be expected to polymerize.

<sup>11</sup> Craig and Maccoll. ref. 1.



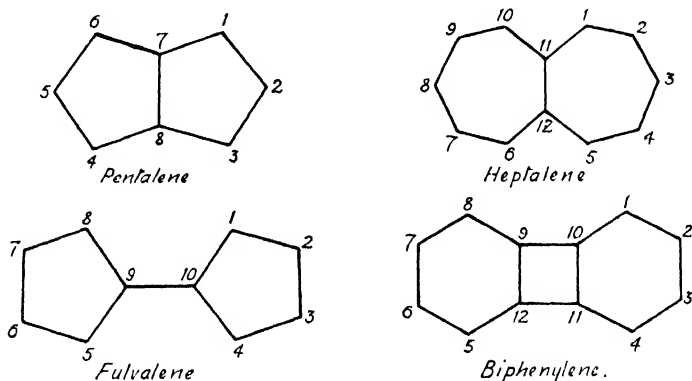
**Biphenylene.**—As biphenylene is an alternant,<sup>2</sup> the electron densities all come out to unity and consequently it is not included in Fig. 1. The maximum free-valence value for this molecule is nearly as low as that of benzene (0.35) suggesting that biphenylene would not be reactive towards free radicals.

The bond orders have already been reported<sup>13</sup> but are reproduced here to complete the data for this molecule. The main point of interest is the low order of the 9:10 bond, even compared with the corresponding bond in biphenyl (1.370).

The chemistry of biphenylene will be considered more fully when the polarization energies are published.

I should like to thank Dr. F. N. Lahey for his helpful criticism of the manuscript, and also Mr. I. H. Belyca for preparing the diagrams.

**Appendix.**—The numbering system employed :



Chemistry Department,  
University of Melbourne,  
Victoria,  
Australia.

<sup>13</sup> Waser and Schomaker, *J. Amer. Chem. Soc.*, 1943, **65**, 1451.

## REVIEWS OF BOOKS.

**/ Crystal Structures (First Section).** By RALPH W. G. WYCKOFF.  
(Interscience Publishers Inc., New York & London, 1948.) Price 48s.

This book is a compilation of crystal structures following the general arrangement of the second edition of the author's "Structure of Crystals." Since this field is rapidly extending with a consequent appearance of new material each year, this publication, which is an experiment using loose-leaf binding and vari-typing, is most welcome. It aims to provide a satisfactory up-to-date survey capable of addition by the issue of supplementary pages and the replacements of existing pages. This method presents difficulties in pagination and the volume has no indexes. Instead, the book is divided into chapters, each of which is sub-divided into Text, Tables, Illustrations and Bibliography. These groups are paged separately. The index problem is overcome by having a table of contents

based on chemical composition and each chapter is provided with one or more master tables listing the crystals considered in it. In practice, one can quickly locate the type of compound about which one requires information. The bibliography starts from 1934; for earlier references, the reader must consult that given in the author's previous two volumes. Illustrations of the packing of atoms in crystals are based on those in "Structure of Crystals" and it is planned to have a figure for each well-established type of structure by the later issue of supplementary pages. The terminology conforms to that used in the International Tables. In order to emphasize relationships between structures and to preserve brevity of description, structures of low symmetry are not uniquely defined and there is a disregard of many conventionally accepted axial assignments. The space group symbols of Schoenflies are included for those accustomed to a designation independent of axial sequence.

This section, the first of three, is concerned with inorganic structures and deals with the elements, and the compounds,  $RX$ ,  $RX_2$ ,  $R_mX_n$ ,  $R_nMX_2$ ,  $R_nMX_3$  and  $RMX_4$  — this will be completed in Section II by the inclusion of  $R_n(MX_4)_p$ ,  $R_n(MX_6)_p$ ,  $R_nMX_p$ , hydrates, silicates and miscellaneous structures.

No critical survey of the results has been made and no indication of the accuracy of the spacing measurements is included. Particular attention is given to interatomic distances and atomic and ionic sizes; there seems to be a real danger here that such discussions may give the appearance of critical authority where none is intended.

This book is costly, but will save many a weary hour searching the literature and it is felt that the complete publication will be well worth the money spent since we must anticipate that the supplementary and replacement pages will maintain the contents up-to-date at comparatively low costs. The experiment of producing books of this character should be encouraged since not only is the average reader disinclined to buy later editions for the sake of a few additions or emendations, but there is a greater probability that the author will adhere to his intention of revising the text at frequent intervals.

**British Chemical Nomenclature.** By A. D. MITCHELL. (Edward Arnold & Co., London, 1948.) Pp. viii + 156. Price 21s.

This book is a most welcome addition to the small number which has been published in the United Kingdom on the subject of chemical nomenclature and indexing; particularly is this so since in the U.S.A. this important aspect of chemical literature is given more detailed study and prominence and one might quote many examples where British usage differs from that adopted by the Americans. This book is really a record of the magnificent work which the Chemical Society has accomplished in formulating rules to cover a large variety of compounds, and as a tribute to the successive editors of the Journal and those many British chemists who have helped in advising them in this difficult and complex task. It is therefore fitting that this volume is dedicated to the late Dr. Clarence Smith who did so much to foster the high standard of the publications of the Chemical Society.

The author, as assistant editor for some twenty years, has contributed to this in no small measure, and one can think of nobody better fitted to expound and clarify this complex subject of nomenclature. It may be suggested that the volume appears rather prematurely because the decisions of one or two international conferences have still to be confirmed or announced. One can imagine, however, that this statement could be made at any time during the next five to ten years with the same force. Nevertheless, it is particularly unfortunate that the author should give on p. 6 the conventions for symbols adopted by the Chemical Society, the Physical Society and the Faraday Society in 1937, since various changes proposed by the Royal and allied Societies have been largely accepted at an international level. It is suggested that this paragraph should be corrected and enlarged in future editions.

This book should be in the possession of all libraries; it will be a particularly useful guide to authors in preparing their contributions to British Journals. Perhaps one can hope that at some future time interested Societies might subsidize its publication so that it could be purchased at a lower price by penurious research workers!

**Preparations and Characteristics of Solid Luminescent Materials.**

By F. SEITZ and G. FONDA. (John Wiley and Sons, Inc., New York, and Chapman & Hall, Ltd., London, 1948.) Pp. xvi + 459. Price 30s.

Members of the Faraday Society will be particularly interested in this book. It comprises the twenty-nine papers read at a three-days' symposium sponsored by The Division of Electron Optics of The American Physical Society, held in October 1936 at Cornell University. As can be anticipated, under the joint editorship of Dr. F. Seitz and Dr. G. Fonda the volume preserves a well-balanced presentation between the viewpoints of the theoretical physicist and the experimentalist.

The first eight papers are introductory in design and provide a broad and rapid survey of the field for the general reader. They have the character of reviews on recent developments and include such topics as the theoretical treatment of the storage of luminescent energy, the conception of trapping states, the general characteristics and methods of preparation of luminescent substances, including infra-sensitive phosphors, and the constitution and structure of such substances.

The remaining papers contain original work, both experimental and theoretical, and are representative of current research. These are grouped in three main divisions, factors affecting fluorescents, the storage of luminescent energy and a miscellaneous group including such aspects as the photochemical effect of short ultra-violet radiation on phosphors, multiple bands in fluorescent spectra and the print-out effect in silver halide crystals. Short discussions follow each paper and the concluding session, under the chairmanship of Prof. H. A. Bethe, took the form of a general and informal discussion of current problems grouped under various headings.

It is interesting to note that, bearing in mind the Discussions of the Faraday Society, all contributors with the exception of one, were American. The only representative of the English group of workers in this field was Garlick of Birmingham; no-one of the large and active Dutch schools

was represented. This would appear to be a pity since those familiar with this wide field will recognize that in their absence the symposium cannot be regarded as complete. Perhaps this is evidenced in the general similarity of thought and treatment, and the possible lack of stimulus in the discussion. On the other hand, one must recognize the loss which the English and Continental workers have suffered in not having had the opportunity of personally attending this conference. If the reason is that the English scientists can afford neither time nor money for such meetings, then some responsible organization should help to alleviate such hardship. If, however, the scientists in the States feel that English and Continental workers have little to contribute, then, as the Faraday Society attempts to do by its Discussions, we must make every effort to encourage our American friends to come to England, and hope that we may disillusion them!

However, we give this book our heartiest recommendation; it is a valuable record which will be appreciated not only by specialists but by the general reader, and it is exceedingly good value at the price.

**Electrons, Atoms, Metals and Alloys.** By W. HUME-ROTHERY. (The Louis Cassier Co. Ltd., 1948). Pp. vii. + 371. Price 30s.

An enthusiastic and patient young scientist who had graduated in Honours Physics or Physical Chemistry some time between 1930 and 1939, chanced upon an older and much depressed metallurgist who had taken his degree in Metallurgy or Chemistry before the advent of the quantum theory. They had both attended a four-day conference on the Theory of Alloy Structures arranged by the new Institute of Physical Metallurgy. The metallurgist, already worried by his production problems, gave up the struggle after two days had been spent on the simpler problem of the ideal crystal in which strange symbols, equations involving  $e^{2\pi i}$ , and Brillouin zones appeared; the young scientist, however, thought that the mathematical physicists had "come clean". The book is presented in the form of a dialogue between these two people. The young scientist recognizes that the older metallurgist is both too busy and too deeply entrenched in the old groove ever to delve deeply into the new work, but insists that it should be possible for him to grasp the general ideas of the newer outlook. In this way the author, by means of tutorial discussion, seeks to provide an introduction to those who found his *Atomic Theory for Students of Metallurgy* somewhat heavy going. Part I begins with an account of the early theory of the hydrogen atom, develops the idea of electron waves and builds up the wave-mechanical picture of the hydrogen atom and the general theory of the heavier elements. In Part II, the free electron theory is introduced and the concept of Brillouin zones is discussed; the crystal structures of elements and the nature of the binding forces are dealt with and the problem of ferromagnetism and plastic deformation introduced. Part III is concerned with the nature of alloys and deals with such topics as electron compounds, superlattice structures and interstitial compounds. Part IV is short (about forty pages) and lightly touches upon the structure of the nucleus; it includes a discussion on disintegrations, fundamental particles and the fission of the nucleus.

The book was written for those engaged in metallurgical industry and not primarily for the University student. However, despite this, the latter is recommended to *study* it. It has little that the senior student will find contrary to the treatment in more advanced text-books and he may get a better insight into the real meaning of the fundamental ideas than he might have obtained from a mass of mathematical symbolism. To the less able it will provide a readable, entertaining and stimulating exposition; to the lecturer it will help to provide new ways of presenting his subject.

The book is printed on excellent paper, but it is a pity that there has been departure from orthodoxy in the use of symbols; that chemical elements are sometimes printed in italics and sometimes (correctly) in roman, and that there are quite a few typographical errors. There is an embarrassing array of diagrams, many of which are instructive and novel. Unfortunately, such a large number, however, has meant that some of them are printed two pages away from the relevant text. The book, being of the more "popular" type, should, it is felt, be priced more moderately.

**Literature Search on Dry Cell Technology.** By MARJORY BOLEN and B. H. WEIL. (State Engineering Experimental Station, Georgia Institute of Technology, Atlanta, Georgia, 1948.) Pp. 700.

This book is the result of a systematic search of all the literature on dry batteries and material of their construction, sponsored by the Battery Branch Signal Corporation, Engineering Laboratories of Fort Monmouth, New Jersey, and carried out by the State Engineering Experimental Station, Georgia Institute of Technology, Atlanta, Georgia. The search covers a period starting about the 1890's to the present day. Both literature and patents have been abstracted, some 278 pages being devoted to abstracts of literature, and 330 pages to patents of all Nations. The book is completed by a very full Index occupying some 60 pages, and in all 3,654 abstracts are given.

This book contains the most exhaustive survey of dry cell literature ever made, and is undoubtedly of considerable value to those working on this subject. It has been reproduced by photographing typescript, but is sufficiently clear to read without difficulty. The abstracting has been well carried out, sufficient information being given for the reader to ascertain the subject matter of the article or patent concerned. The full particulars and dates of all articles and patents are incorporated.

E.A.O.

# CORRIGENDUM

1948 Vol. 44.

P. 690. Eqn. (6) *should read*

$$E = E_0 - 0.0591 \cdot \log \left[ \frac{k_A}{k} \cdot \frac{i}{i_d - i} \cdot \frac{1}{C_H^0} \right]. \quad (6)$$



# INDUCED REACTIONS OF HALOGENS IN AQUEOUS SOLUTION

## PART I. REACTIONS IN THE SYSTEM IODINE-THIOSULPHATE-NITRITE

BY R. O. GRIFFITH AND R. IRVING

*Received 28th May, 1948*

The reactions occurring in aqueous solutions containing  $I_2$ ,  $Na_2S_2O_3$ , and  $NaNO_2$  buffered to pH's in the neighbourhood of 6 have been studied by analytical methods. It is found that the thiosulphate is oxidized to both tetrathionate and sulphate, but that no significant amounts of nitrite are consumed. A mechanism is suggested for the nitrite-catalyzed reaction between  $S_2O_3^{--}$  and  $I_2$  which leads to the formation of sulphate.

Berthoud and Berger<sup>1</sup> noted that it was not possible to obtain the theoretical end-point in the titration of iodine with sodium thiosulphate in the presence of a nitrite and they subjected the matter to further study. They found, carrying out the titrations in acetate buffers by running the thiosulphate into solutions of iodine containing potassium nitrite, that the ratio of thiosulphate consumed to the amount theoretically required for formation of  $Na_2S_4O_6$  was less than unity and tended towards a limiting value of 0.5 at high concentrations of nitrite and low concentrations of thiosulphate. They further stated that none of the thiosulphate was converted into sulphate, but this statement has been contradicted by Kurtenacker and Spielhaczek,<sup>2</sup> who found considerable sulphate in all solutions of iodine together with nitrite which they had decolorized with thiosulphate. In our work we have carried out measurements essentially similar to those of Berthoud and Berger, but with wider variation of experimental conditions, and have obtained results not in agreement with the conclusions of those investigators.

### Experimental

The reactions occurring in systems containing  $I_2$ ,  $NaNO_2$ , and  $Na_2S_2O_3$  are extremely fast and cannot be followed kinetically. The method we have adopted therefore is to determine the stoichiometry of the *net* reaction under a variety of conditions, in the hope that the results would give some indication of the kinetics of the processes occurring. It is to be noted that, apart from the reaction between thiosulphate and iodine and the induced reaction involving the three reactants, there is the possibility in these systems of reaction between nitrite and iodine<sup>3</sup> and of reaction between nitrite and thiosulphate.<sup>4</sup> Neither of these reactions need be taken into account, however, as each is much too slow to exert any significant effect under the conditions of this work. The results we have obtained may conveniently be presented under two heads: (a) determination of the ratio

$$R = \frac{\text{molecules } I_2 \text{ consumed}}{\text{molecules } Na_2S_2O_3 \text{ consumed}}$$

(b) quantitative determination of the end-products of the reaction.

<sup>1</sup> Berthoud and Berger, *J. Chim. physique*, 1928, **25**, 562.

<sup>2</sup> Kurtenacker and Spielhaczek, *Z. anorg. Chem.*, 1934, **217**, 321.

<sup>3</sup> Durrant, Griffith and McKeown, *Trans. Faraday Soc.*, 1936, **32**, 999.



All reaction mixtures were buffered to avoid complications due to free nitrous acid; pH's between about 6 and 7.2 were used, most of the experiments being carried out in phosphate buffers, though a few determinations of  $R$  and most of the quantitative analyses of the end-products were effected using acetate buffers.

(1) **Determinations of  $R$ .** Values of  $R$  were obtained by adding known amounts of thiosulphate solution to buffered solutions containing iodine and nitrite, the amounts of thiosulphate being insufficient to decolorize all the iodine. The remaining iodine was then determined by addition of sodium arsenite and back-titration with iodine. Preliminary experiments showed that the values of  $R$  obtained in this way depend on (i) the rate at which the thiosulphate solution is run in, and (ii) the method of stirring during the addition, but are independent of (iii) the volume of thiosulphate run in under our experimental conditions and (iv) the time the reaction mixture is allowed to stand before addition of sodium arsenite. The last of these results implies that the reactions occurring in the system are fast and further that any reactions consuming  $I_2$  in the systems which result, i.e.  $I_2 + NO_2^- \rightarrow S_4O_6^{2-}$  (or other sulphur compound formed from the  $S_2O_3^{2-}$ ) are negligibly slow. As regards effects (i) and (ii) neither is of large magnitude. For example, the effect on  $R$  of the rate of addition of  $Na_2S_2O_3$  was tested by comparing the  $R$  values obtained (a) by running in the thiosulphate solution from a fast-flowing pipette (time required 3-4 sec.) with those (b) obtained by running in the thiosulphate drop by drop (time of addition about 70 sec.). Using the same method of stirring throughout, examples of the results obtained are:

$$[KH_2PO_4] = 0.0375; [Na_2HPO_4] = 0.01875; [NaNO_2] = 0.075; \\ [I_2]_{init.} = 0.0006; [KI] = 0.01. \text{ Units are g. mol./l.}$$

[Thiosulphate] (g. mol./l.)	$R$			
	$3 \times 10^{-3}$	$10^{-3}$	$2 \times 10^{-4}$	$5 \times 10^{-5}$
Method (a) .	1.17	1.68	3.03	3.88
Method (b) .	1.19	1.66	2.86	3.57

These and other results show that the rate of addition of the thiosulphate has an influence on the value of  $R$ , that the effect is not pronounced, that with very low concentrations of thiosulphate the  $R$  values obtained by running in the thiosulphate "in bulk" are greater than those using drop-by-drop addition, while with higher concentrations ( $3 \times 10^{-3}$  g. mol./l. and over) there is a tendency for the reverse statement to hold true. Similarly, the method of agitation of the solution during the addition of thiosulphate is found to exert a definite though not a very large effect. Thus in corresponding experiments, adding the thiosulphate drop-by-drop, values of  $R$  obtained were:

Method of Agitation	$R$	
Solutions hand-shaken .	3.27	2.07
Solutions motor-stirred .	3.49	2.29

The standard procedure adopted to determine  $R$  was as follows. Into a 300 ml. Erlenmeyer flask were introduced 5 ml. buffer solution, 5 ml.  $NaNO_2$  solution, 20 ml.  $I_2$ -KI solution together with the volume of water necessary to make the average volume 40 ml., the average volume being defined as that of the reaction mixture when one-half of the pre-determined volume of thiosulphate solution had been added. The latter was run in drop by drop at approximately the same rate in each experiment (2 drops/sec.) and during the addition the reaction mixture was kept agitated by uniform hand-shaking. Blank experiments were also carried out in which water (instead of thiosulphate solution) was run into the buffered mixture of iodine and nitrite to find the corrections for any loss of iodine by vaporization or reaction with nitrite. A repeat

of each experiment was carried out; the results show reproducibility of  $R$  values to within 1-2 %. It is further to be noted that the results obtained by any other standard procedure would present the same general picture as those to be given, though the individual  $R$  values in the two sets would in general differ to some extent.

All the experiments were carried out at room temperature ( $16^{\circ}$ - $20^{\circ}$  C), no special precautions being needed to work within narrower limits as it was found that the  $R$  values are relatively insensitive to temperature. In general, lowering the temperature from  $18^{\circ}$  to  $0^{\circ}$  C diminishes  $R$  by about 10 %.

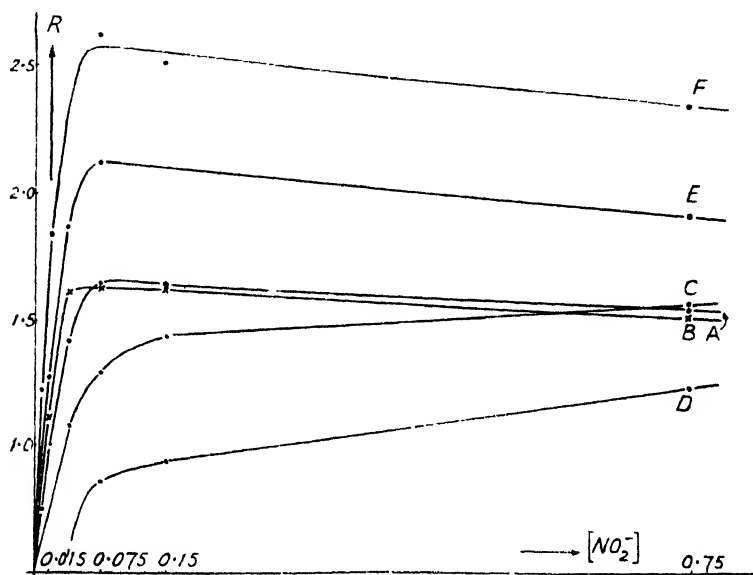


FIG. 1.

Series	[KH <sub>2</sub> PO <sub>4</sub> ]	[Na <sub>2</sub> HPO <sub>4</sub> ]	[ΣI <sub>2</sub> ]	[ΣI <sup>-</sup> ]	[S <sub>2</sub> O <sub>3</sub> <sup>2-</sup> ] added
A	0.0375	0.0187	0.00061	0.01	0.001
B	0.0375	0.0187	0.00061	0.0025	0.001
C	0.0375	0.0187	0.00061	0.05	0.001
D	0.0375	0.0187	0.00061	0.25	0.001
E	0.0375	0.0187	0.0025	0.01	0.001
F	[HAc] 0.125	[NaAc] 0.00625	0.00025	0.01	0.00019

Concentrations in g. mol. or g. ion per litre.

Fig. 1-3 give an indication of the type of results obtained. It is found that: (1)  $R$  values range between 0.5 and 4.0, the limiting value of 4.0 being approached using moderate concentrations of  $\text{NO}_2^-$  and running in a very dilute ( $M/20,000$ ) solution of thiosulphate.

(2) Increase in concentration of  $\text{NO}_2^-$  in general increases  $R$ , but in the presence of low concentrations of  $\text{I}^-$  a maximum value of  $R$  is soon reached, beyond which further increase in  $[\text{NO}_2^-]$  has practically no effect.

(3) Increase in concentration of iodine increases  $R$ .

(4) Increase in  $[\text{I}^-]$  diminishes  $R$ , except at very low concentrations of  $\text{I}^-$  where no effect is found.

(5) Neither change in pH nor change of buffer constituents affects  $R$  within the limits of  $[\text{H}^+]$  of  $10^{-6}$  to  $5 \times 10^{-8}$  g. ion/l.

(II) **End-products of the Reaction.** Qualitatively it was found, in disagreement with Berthoud and Berger,<sup>1</sup> that sulphate is always formed in the reaction between thiosulphate and iodine when nitrite is present, and that the sulphate formation is accompanied by an increase in acidity of the reaction mixture. Quantitative determinations were made of the tetrathionate and sulphate formed and acid liberated, together with iodine and thiosulphate consumed. It was unfortunately not feasible to trace the fate of the nitrite, but the quantitative data obtained prove that no appreciable amounts of nitrite can be consumed during the reaction. The method used to determine the other resultants was to run in thiosulphate into the buffered solution containing  $I_2$

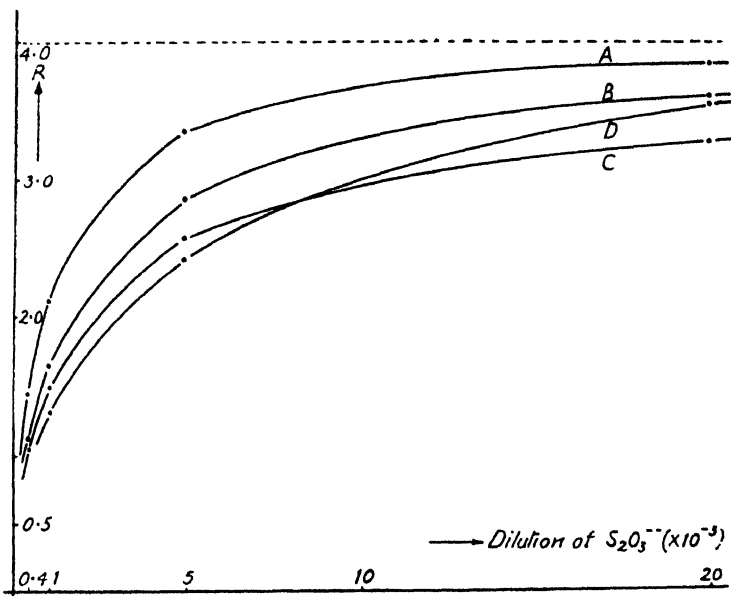


FIG. 2.

Series	$[KH_2PO_4]$	$[Na_2HPO_4]$	$[I_2]$	$[I^-]$	$[NO_2^-]$
A	0.0375	0.0187	0.0025	0.01	0.075
B	0.0375	0.0187	0.00061	0.01	0.075
C	0.0375	0.0187	0.00061	0.01	0.75
D	0.0375	0.0187	0.00025	0.01	0.075

Concentrations in g. mol. or g. ion per litre.

and  $NO_2^-$  until the colour of the iodine just disappeared. Aliquot portions of the resulting solution were then analyzed: (i) for sulphate by precipitation as  $BaSO_4$  and weighing, (ii) for tetrathionate by addition of excess sulphite forming thiosulphate, which was titrated with iodine after addition of formaldehyde to bind the excess sulphite, and (iii) for increase in acidity by titration with standard NaOH, using phenolphthalein.

In order to avoid the possibility of decomposition of tetrathionate (with formation of sulphate) in hot solutions, sulphate was determined by precipitation of  $BaSO_4$  in the cold. 3 %  $BaCl_2$  solution was run very slowly with efficient stirring into the solution to be analyzed. After two hours' standing the precipitate was filtered, ignited and weighed. Blank experiments were carried out with known amounts of  $K_2SO_4$  together with tetrathionate, KI,  $NaNO_2$  and buffer constituents, each in concentration of the same order as those in the actual experiments. With weights of  $BaSO_4$  precipitate of from 0.04 to 0.09 g., the blank experiments agreed with the theoretical to within about 1.5 %. For

the estimation of tetrathionate also, appropriate blank experiments were made to find the conditions under which, by Kurtenacker's method, tetrathionate could be determined when present in low concentration (about 0.002 M) in presence of nitrite. The chief matter requiring attention is, as mentioned by Kurtenacker and Spielhaczek, the pH of the solution when the final titration of  $I_2$  is effected. This pH had not to be less than about 5.4, and the blank experiments gave the amount of acetic acid that could safely be added to the solution before the final titration in order to obtain satisfactory results. It is considered that the estimations of tetrathionate should be accurate to within about 2 %.

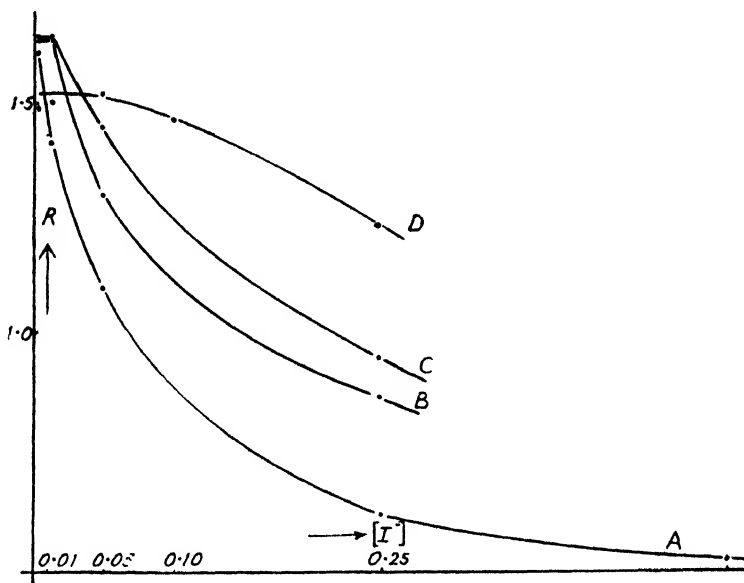


FIG. 3.

Series	$[KH_2PO_4]$	$[Na_2HPO_4]$	$[I_2]$	$[NO_2^-]$	$[S_2O_5^{2-}]$ added
A	0.0375	0.0187	0.00061	0.045	0.001
B	0.0375	0.0187	0.00061	0.075	0.001
C	0.0375	0.0187	0.00061	0.15	0.001
D	0.0375	0.0187	0.00061	0.75	0.001

Concentrations in g. mol. or g. ion per litre.

In these determinations, the concentration of iodine in g. mol./l.  $[I_2]$  in the original solution was varied from 0.003 to 0.03,  $[I^-]$  from 0.01 to 0.12,  $[NO_2^-]$  from 0.03 to 0.72 g. ion/l. The buffer ratio  $[NaAc]/[HAc] = 20/1$  was used, though the concentrations of the buffer constituents were varied. A few experiments were also done with phosphate buffers in the ratio  $[Na_2HPO_4]/[KH_2PO_4] = 1/2$ . The concentration of added thiosulphate was varied between 0.0004 and 0.1 g. mol./l. Some of the results obtained in this way are given in Table I. ( $\Delta S_4O_8^{2-}$ ,  $\Delta H^+$ ,  $\Delta SO_4^{2-}$  = moles tetrathionate, moles acid, moles sulphate formed.)

The results as seen in Table I on page 310 and other results show that under all conditions:

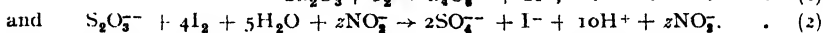
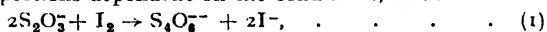
- the ratio of moles  $H^+$  formed to moles sulphate formed = 5.0;
- moles thiosulphate consumed = 2 (moles tetrathionate formed) +  $\frac{1}{2}$  (moles sulphate formed), i.e. no sulphur compounds other than tetrathionate and sulphate are produced;
- moles  $I_2$  consumed = moles tetrathionate formed + 2 (moles sulphate formed).

TABLE 1

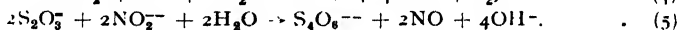
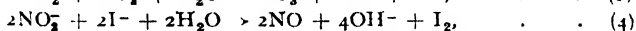
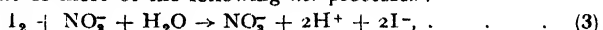
Temp. = 18° C; [NaAc]/[HAc] = 20/1

Concentrations in Initial Solution g. mol. or g. ion per l.			Conc. of Added $\text{Na}_2\text{S}_2\text{O}_3$ g. mol./l. $\times 10^3$	Moles $\text{S}_2\text{O}_3^{--}$ Consumed $\times 10^4$	Moles $\text{I}_2$ Consumed $\times 10^4$	g. ion $\times 10^4$		
$[\text{I}_2]$	$[\text{I}^-]$	$[\text{NO}_2^-]$				$\Delta\text{S}_4\text{O}_6^{--}$	$\Delta\text{H}^+$	$\Delta\text{SO}_4^{--}$
0.02655	0.1067	0.08000	24.22	27.29	19.10	12.97	15.44	3.104
0.03158	0.1263	0.06317	25.58	40.45	30.00	18.74	28.15	3.602
0.002045	0.04054	0.03243	5.070	4.177	3.624	1.881	4.34	0.881
0.002134	0.04348	0.03478	5.175	8.035	7.123	3.527	8.505	1.724
0.01491	0.0375	0.1000	2.656	7.682	11.93	2.899	20.36	4.158
0.01878	0.0250	0.7200	0.4124	3.894	9.390	—	21.32	4.383

It follows from these that the total reaction is compounded of two *net* processes, which occur in varying proportions dependent on the conditions, viz.:



The nitrite is thus not permanently consumed, and so acts solely as a catalyst. For consumption of the nitrite to occur, it would be necessary to add to reactions (1) and (2), one or more of the following *net* processes:



If any or all of these take place to a significant extent, however, the experimental results (a), (b) and (c) could not simultaneously hold true; it must, therefore, be inferred that (1) and (2) are the sole *net* processes which have to be considered. On this basis, it follows that if in any experiment,  $x$  is the fraction of the thiosulphate converted into tetrathionate, and  $R$  is the ratio of

$$(\text{moles } \text{I}_2 \text{ consumed})/(\text{moles } \text{Na}_2\text{S}_2\text{O}_3 \text{ consumed}),$$

then  $x = (8 - 2R)/7$ , so that fraction of thiosulphate forming sulphate

$$= 1 - x = \frac{2R}{7} - \frac{1}{7}.$$

A plot of  $R$  against  $(1 - x)$  should thus be a straight line with a slope of  $2/7 = 0.286$ . The results plotted in Fig. 4 show satisfactory agreement, the slope of the straight line plotted being 0.273.

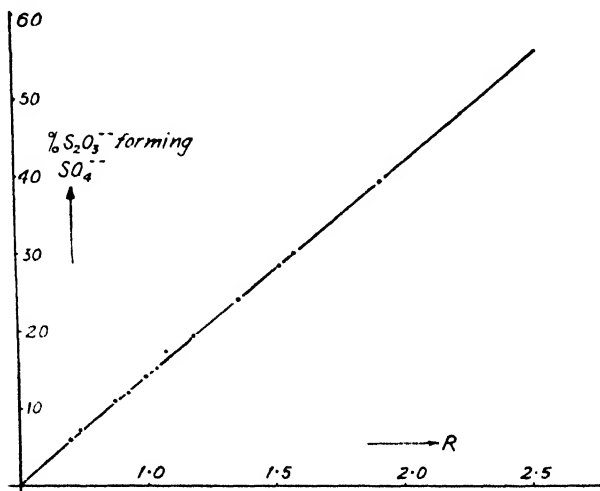
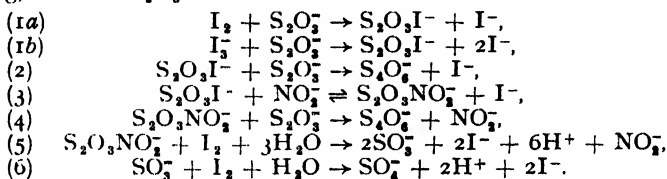


FIG. 4.

## Discussion

The results given above show that in the presence of nitrite the reaction between iodine and thiosulphate leads not only to tetrathionate formation, but also to the production of sulphate, that with sufficiently dilute thiosulphate the fraction oxidized to sulphate approaches unity, and that no significant amount of nitrite is consumed in the change. The mechanism suggested by Berthoud and Berger<sup>1</sup> for the reactions in these systems need not be discussed, as it was based on an erroneous limit for  $R$ , and further it takes no account of sulphate formation. We propose the following mechanism, which will account qualitatively for most of our results and which is based on the hypothesis that the first product of the reaction between thiosulphate and iodine is, as suggested by Raschig,<sup>4</sup> the ion  $S_2O_3I^-$ .



All these reaction steps are regarded as fast reactions, but, to interpret our results, it is necessary to make the following assumptions in respect of relative rates: (i) that in presence of moderate concentrations of nitrite, tetrathionate formation via (3) and (4) is faster than via (2), and (ii) except at fairly high concentrations of iodide the equilibrium (3) lies well over to the right-hand side. Reactions (1a), (1b) and (2) are postulated as those taking place also when  $I_2$  reacts with  $S_2O_3^{2-}$  in absence of  $NO_2^-$ , except that under these conditions it may also be necessary to take into account the reversals of (1a) and (1b); the reasons for the choice of this mechanism for the  $I_2 - S_2O_3^{2-}$  reaction will be given in a subsequent paper.

It is not possible to deal quantitatively with the reaction kinetics on the basis of this or of any other mechanism, since the part-reactions are so rapid that they are practically completed during the time of addition of the thiosulphate, so that the system is not a homogeneous one, but qualitatively this mechanism accounts for the experimental findings. The effect of concentration of added thiosulphate is seen to be in the sense that increasing dilution of thiosulphate will diminish tetrathionate formation (i.e. increase sulphate formation), since reactions (2) and (4) which produce tetrathionate will—due to the lowered concentration of  $S_2O_3^{2-}$ —be more retarded than reaction (5) which leads to sulphate formation. The effect of increasing  $[SI_2]$  is found experimentally to result in an increase of  $R$ , i.e. increased sulphate formation. This is due partly to an increased rate of reaction (5), and partly to the fact that the increase in the rates of (1a) and (1b) will cause a reduced concentration of  $S_2O_3^{2-}$  available for the tetrathionate-forming reactions (2) and (4). The effects of  $[I^-]$  and  $[NO_2^-]$  are to some extent bound together. We may consider them as follows. At low  $[I^-]$ , the reversal of process (3) may be neglected. At low  $[I^-]$  and very low  $[NO_2^-]$  much  $S_4O_6^{2-}$  is formed by reaction (2), but on increasing  $[NO_2^-]$  the rate of reaction (3) increases and the concentration of  $S_2O_3NO_2^-$  increases at the expense of that of  $S_2O_3I^-$ . If now a fair proportion of the resulting  $S_2O_3NO_2^-$  reacts by (5) this will cause a sharp rise in  $R$  with increasing  $[NO_2^-]$  as found experimentally. At higher concentrations of  $NO_2^-$ , however, a state will be reached when all the  $S_2O_3I^-$  formed in (1a) and (1b) reacts by (3) to form  $S_2O_3NO_2^-$  and reaction (2) does not occur. Under these conditions a certain fraction of the  $S_2O_3NO_2^-$  reacts by (5), the remainder by (4) yielding a value of  $R$

<sup>4</sup> Raschig, *Ber.*, 1915, 48, 2088.

which depends on the concentrations of  $I_2$ ,  $I^-$  and thiosulphate. Increase of  $[NO_2^-]$  beyond this limiting value should not affect  $R$ . This is approximately what is found experimentally, though there is a slight tendency for the  $R$  values to fall at higher values of  $[NO_2^-]$  than the limiting. The effect of  $[I^-]$  on  $R$  at moderate and high values of  $[I^-]$  ( $[I^-] > 0.02$  g. ion/l.) is ascribed to the reduction by tri-iodide formation of the concentration of free iodine with consequent reduction in the rate of reaction (5), which leads to sulphate formation. The effect of increase of  $[NO_2^-]$  at these concentrations of iodide will, in general, be similar to that at low  $[I^-]$ , except that we must now consider (3) to be an equilibrium and take account of the reversal. This will have the effect that the attainment of the concentration of  $NO_2^-$  at which the limiting value of  $R$  is reached is delayed, i.e. the mechanism will qualitatively predict the type of  $R - [NO_2^-]$  curve found, namely, an initial more or less steep rise followed by a slow rise at higher concentrations of  $[NO_2^-]$ . There is, however, one experimental result which this mechanism does not account for, viz., the absence of any effect of  $[I^-]$  on  $R$  at low values of  $[I^-]$  ( $[I^-] > 0.02$ ) and not too low values of  $[NO_2^-]$ . The theory predicts that under all conditions  $R$  should decrease with increasing  $[I^-]$  and we can suggest no satisfactory explanation of this anomaly.

In this system we have thus an example of selective direction of the course of reaction by catalysis, somewhat similar to the catalytic effect of molybdic acid on the reaction between thiosulphate and hydrogen peroxide, studied by Abel.<sup>5</sup> In that process, just as in the processes dealt with in this paper, the uncatalysed reaction leads to tetrathionate, the catalyzed process to sulphate. The mechanisms of the catalyses in the two cases would, however, appear to be very different.

*Muspratt Laboratory of Physical and Electro-Chemistry,  
Department of Inorganic and Physical Chemistry,  
University of Liverpool.*

<sup>5</sup> Abel, *Z. Elektrochem.*, 1912, 18, 705.

## A THEORETICAL STUDY OF THE OXIDATION-REDUCTION POTENTIALS OF QUINONES

BY M. G. EVANS, J. GERGELY \* AND J. DE HEER †

*Received 6th September, 1948*

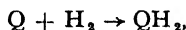
Using the molecular-orbital method we have evaluated the energy of the ten  $\pi$  and eight  $\pi$  electrons in hydroquinones and quinones respectively. This has enabled us to express the resonance or delocalization energy of the electrons as a function of parameters, corresponding to the electronegativity of the oxygen atoms and the bond energy in the  $C=O$  bonds. Although exact values of these parameters are not known, the important theorem emerges, that in a series of related quinones the contribution to the total resonance energy arising from these parameters is a constant. These calculations have enabled us to discuss the oxidation-reduction potential of quinones without making the early untenable assumption of a complete localization of electrons in the  $C=O$  bonds. A small difference which now appears between the calculated and observed oxidation-reduction potentials of *o*- and *p*-quinones we attribute to a hydrogen-bond stabilization of the reduced form of the *o*-compounds.

\* British Council Scholar, Dept. of Biochemistry, University of Budapest ; now at the Dept. of Physical Biology, National Institute of Health, Bethesda, U.S.A.

† Ramsay Memorial Fellow, The Netherlands.

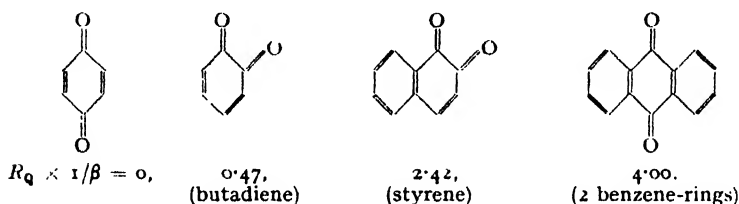
## I. Introduction

It has been shown by Evans<sup>1</sup> and Diatkina and Syrkin<sup>2</sup> that the important term in determining the free-energy changes in a series of reactions of the type,



(in which  $Q$  represents a quinone) is the difference in resonance energy ( $R_{QH_2} - R_Q$ ) between the hydroquinone and the quinone. In both these previous publications the resonance energy of the hydroquinone was set equal to that of the corresponding hydrocarbon. The resonance energy of the quinone was evaluated in two ways.

(a) **The localized-bond approximation.**<sup>1, 2</sup>—Here it was assumed that the  $p_z$  electrons of the oxygen and the adjacent carbon were localized in the  $C=O$  bond and support for this assumption was adduced from the reduced diamagnetic anisotropy of *p*-benzoquinone as compared with that of hydroquinone and benzene. Moreover, the greater binding energy in  $C=O$  seemed to give some theoretical support to this idea. By making use of this assumption,  $R_Q$  was approximated in a way which will be clear from the following examples—



Combining this approximation for  $R_Q$  with that referred to above for  $R_{QH_2}$ , a linear relationship was obtained between the oxidation potential  $E_0$  and  $(R_{QH_2} - R_Q)$ . In fact, two parallel straight lines were obtained in this way; there was a large discrepancy between the values calculated for the *o*- and *p*-quinones. As this discrepancy could, however, be removed by choosing the benzoquinones as standards in the two series,<sup>1</sup> it was concluded that it was due to the extreme assumption of complete localization in the  $C=O$  bonds which lead to a constant difference between the *o*- and *p*-compounds. Comparison with experimental heats of reduction<sup>3</sup> confirmed what was to be expected on theoretical grounds, namely, that this approximation under-estimates  $R_Q$ .

(b) **Quinodimethane approximation.**<sup>2</sup>—Here  $R_Q$  is put equal to the resonance-energy of the corresponding (hypothetical) quinodimethane; e.g. *p*-benzoquinone is put equal to the resonance energy of  $H_2C=\text{benzene ring}=\text{CH}_2$ , calculated directly by the molecular-orbital method.

Spectroscopic evidence for the similarity of  $\pi$  electronic states in conjugated ketones and the corresponding unsaturated hydrocarbons has been given by McMurry;<sup>3</sup> the structure of the region of strong long-wavelength absorption for the corresponding molecules is so similar that the transition process is very probably the same in each case ( $N \rightarrow V_1$  transitions in Mulliken's terminology). McMurry points out that an additional weak absorption, which appears only in the spectra of  $C=O$  compounds (both saturated and unsaturated), involves excitation of an essentially non-bonding electron, localized largely on the oxygen atom.

As Syrkin and Diatkina themselves remark, this method must appreciably over-estimate  $R_Q$ , as in quinodimethanes the delocalization of  $\pi$  electrons will be more complete than in the corresponding quinones. Indeed, comparison with experimental heats of reduction confirms this.<sup>3</sup>

<sup>1</sup> Evans, *Trans. Faraday Soc.*, 1946, **42**, 113.

<sup>2</sup> Diatkina and Syrkin, *Acta Physicochim.*, 1946, **21** (5), 921.

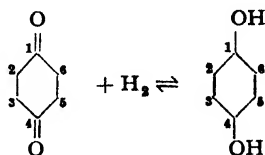
<sup>3</sup> McMurry, *J. Chem. Physics*, 1941, **9**, 241.



The purpose of this present work is to improve on the approximations referred to above by taking into account the greater binding energy of the electrons in the C=O bonds, the greater electronegativity of the O atoms and the tendency to conjugation through the entire system.

## II. Outline of Method

Consider a reaction of the type—



The energy,  $E_1$ , of  $Q$ , apart from the energy of inner-shell electrons, can be analyzed into the following terms—

$$E_1 = 2D_{C_2-C_3} + 4D_{C_1-C_2} + 4D_{C-O-H} + 2D_{C-O} + D_{H-H} + 4E_{p_0} + E_{\pi\pi}, \quad (1)$$

where all  $D$ 's refer to  $\sigma$  bond energies between the atoms indicated in the subscripts. Fig. 1a shows diagrammatically the assignment of  $p$  electrons to the carbon-oxygen skeleton. On each of the oxygens there is a doubly-occupied  $p_z$  orbital, whose symmetry-axis is in the plane of the ring. The energy of an electron in such an orbital is denoted by  $E_{p_0}$ . The energy of the system of 8 mobile electrons originally in  $p_z$  orbitals is denoted by  $E_{\pi\pi}$ .

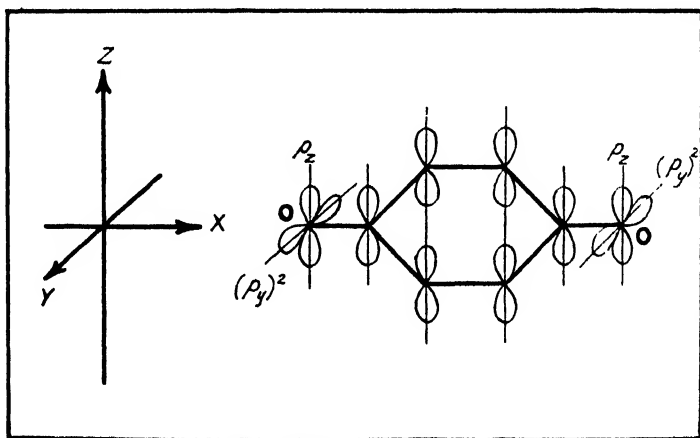


FIG. 1a

Similarly the relevant part of the energy of the hydroquinone,  $E_2$ , can be expressed—

$$E_2 = 2D'_{C_2-C_3} + 4D'_{C_1-C_2} + 4D'_{C-O-H} + 2D'_{C-O} + 2D_{O-H} + E_{10\pi}, \quad (2)$$

where the  $D$ 's have the same significance as the  $D$ 's in eqn. (1) and reference to Fig. 1b shows that we now have to consider the energy of 10 mobile electrons originating from  $8p_z$  orbitals.

Thus for the energy change in the reaction under discussion we have

$$E_2 - E_1 = \Delta E = \Delta D_\sigma - D_{H-H} + 2D_{O-H} - 4E_{p_0} + E_{10\pi} - E_{\pi\pi}, \quad (3)$$

where  $\Delta D_\sigma$  denotes the total change in  $\sigma$  bond energy, resulting from the

changes in the bond lengths concerned. Strictly speaking  $\Delta D_\sigma$  may be different for different quinones (in the reduction of naphthoquinones for example, changes in ten, not six, C—C  $\sigma$  bonds are involved). However, in the reduction of those more complicated *o*- and *p*-quinones to which the discussion is restricted, we may assume the changes in bond length as taking place in the "quinoid aromatic nucleus" only and consequently the change in energy  $\Delta D_\sigma$  may be taken as a constant throughout the series. Furthermore, the value of  $E_{p_0}$  (eqn. (1)) may be taken as a constant throughout a series of quinones. Thus, if we change from one quinone to another the energy change  $\Delta E$  in eqn. (3) will be governed by changes in  $(E_{10\pi} - E_{8\pi})$ , the difference between the total binding energy of 10 and 8 mobile  $\pi$  electrons in  $QH_2$  and  $Q$  respectively.

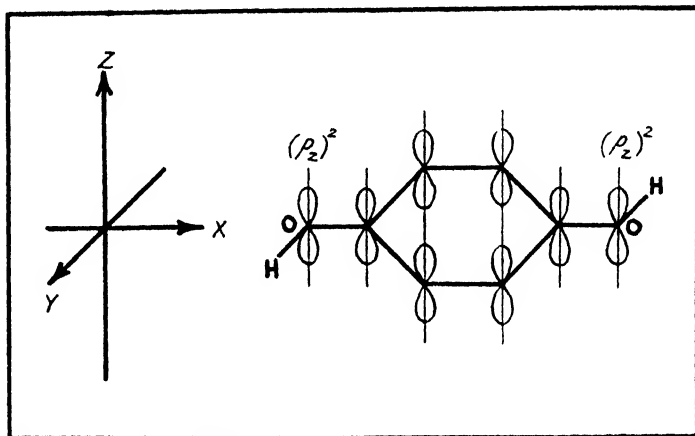


FIG. 1b

We have calculated  $E_{8\pi}$  and  $E_{10\pi}$  by means of the molecular-orbital method as it was first used for substituted aromatic compounds by Pauling and Wheland.<sup>4</sup>

In the secular equations, which are readily set up and factorized by making use of the appropriate symmetry-group, we introduce the following parameters :

- (i)  $\delta$ , expressing (in terms of the resonance integral  $\beta$ ) the difference between the electronegativity of the oxygen and carbon atoms ;
- (ii)  $\rho$ , being the ratio of the resonance-integral of the C=O bonds to those of the C=C bonds (the latter all taken equal to  $\beta$ ) ;
- (iii)  $k$ , expressing the change in the electronegativity of the C atoms adjacent to the O atoms, as the result of an inductive effect, by an amount  $k\delta\beta$ .

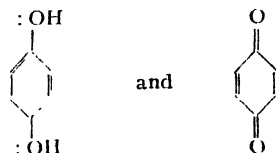
We neglect overlap integrals between adjacent orbitals. Wheland<sup>5</sup> has shown that this does not essentially change the results for the ground state of hydrocarbons molecules. For hetero-molecules the error involved in this approximation is still the subject of investigation by several authors.

After assigning certain values to the parameters  $\delta$ ,  $\rho$  and  $k$ , the factorized secular equations are solved numerically. To obtain  $E_{10\pi}$  and  $E_{8\pi}$  we have to assign to the five and four molecular orbitals with the lowest energy the 10 and 8 $\pi$  electrons respectively.

<sup>4</sup> Pauling and Wheland, *J. Amer. Chem. Soc.*, 1935, **57**, 2091.

<sup>5</sup> Wheland, *J. Amer. Chem. Soc.*, 1941, **63**, 2025.

It is convenient at this stage to express our results not in terms of differences between the total energy of  $\pi$  electrons but as the difference in resonance energy,  $R_{QH_2} - R_Q$  of the compounds concerned. We will take as our datum line for the definition of resonance energy (essentially delocalization energy) the total energy  $E_{loc.}$  of the  $\pi$  electrons in hypothetical localized bond structures of the type—



Then  $R_{QH_2} = E_{10\pi} - E_{loc.}^{QH_2}$  and  $R_Q = E_{8\pi} - E_{loc.}^Q$ .

Thus  $E_{10\pi} - E_{8\pi} = R_{QH_2} - R_Q + (E_{loc.}^Q - E_{loc.}^{QH_2})$ .

The last term is the same throughout a series of *o*- or *p*-quinones, provided that the same parameters  $\delta$ ,  $\rho$  and  $k$  are assigned in all these molecules.

There are at least two serious objections to this type of calculation.

(i) In order to obtain true solutions of the problem of the self-consistent field, we ought to assign parameters to all centres and bonds which would correspond to the true electron distribution in the molecule. Here, since we are only assigning parameters to a limited number of centres and bonds, the solutions we obtain are only a first approximation.

(ii) Secondly, the exact magnitudes of the parameters  $\delta$ ,  $\rho$  and  $k$ , which are used, are unknown. Some idea of the value of  $\delta$  may be deduced from the difference in the ionization potentials of C and O atoms, while a value of  $\rho$  may be obtained from the energy difference between a C=O bond and a C—O— bond at the distance concerned. In most cases the complete set of parameters is chosen so as to give the best possible agreement with certain experimental data.\*

The striking success of the approximation for  $R_{QH_2}$  combined with the "localized-bond approximation" for  $R_Q$  discussed above strongly suggests that only some additive factors, constant throughout the series within the accuracy required, have been neglected. The aim of the present investigation therefore was to find theoretical support for this suggestion and to show that the variation of  $(R_{QH_2} - R_Q)$  throughout the series is independent of a definite choice of the parameters and, moreover, to remove the objections inherent in the assumption of complete localization.

### III. Results

**A. Hydroquinones.**—Calculations were carried out for five compounds, these being chosen because, owing to their symmetry properties, the corresponding secular equations could be reduced appreciably by means of group theory. The results are given in Table I. We notice that with two different sets of parameters which give quite different absolute values of the resonance energies, the difference between the resonance energy of the  $QH_2$  and the corresponding hydrocarbon (this latter value denoted by  $R_{e,h}$ ) is fairly constant throughout the series.

**B. Quinones.**—The results of our calculations for four quinones, together with those of Diatkina and Syrkin\* for eight quinodimethanes are given in Table II. It is to be noted that the total resonance energy  $R_Q$  differs from that of the rings attached to the quinone system,  $R'$ , by a fairly constant amount. Rings attached to the quinone system are shown in heavy type in the diagram on the opposite page.

\* See, for example, Wheland, *J. Amer. Chem. Soc.*, 1942, **64**, 900.

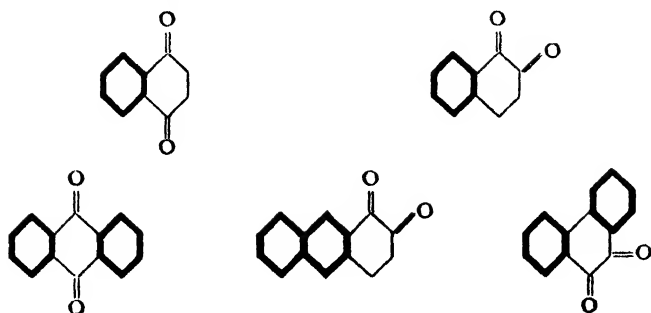

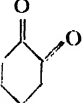
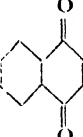
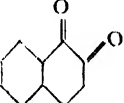
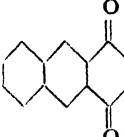
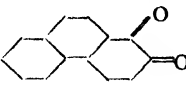
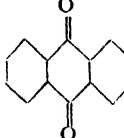
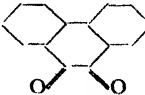


TABLE I  
(All values of  $R$  to be taken  $\times \beta$ )

Parameters Compound	$\delta = 2$ $k = 0$ $\rho = 1$			$\delta = 2$ $k = 0.1$ $\rho = 2$		
	$R_{QH_2}$	$R_{c.h.}$	Difference	$R_{QH_2}$	$R_{c.h.}$	Difference
	2.60	2.00	0.60	4.26	2.00	2.26
	2.60	2.00	0.60	4.28	2.00	2.28
	4.30	3.68	0.62	5.99	3.68	2.31
	4.28	3.68	0.60	6.06	3.68	2.38
	5.96	5.32	0.64	7.76	5.32	2.44

TABLE II

(All values of  $R$  to be taken  $\times \beta$ )

Compound	Parameters	$\delta = 0$ $k = 0$ $\rho = 1$			$\delta = 2$ $k = 0$ $\rho = 1$			$\delta = 2$ $k = 0.1$ $\rho = 2$		
		$R_Q^*$	$R'$	Difference	$R_Q$	$R'$	Difference	$R_Q$	$R'$	Difference
		1.94	0.00	1.94	1.80	0.00	1.80	1.40	0.00	1.40
		1.92	0.00	1.92	1.73	0.00	1.73	1.42	0.00	1.42
		3.82	2.00	1.82	3.91	2.00	1.91	3.39	2.00	1.39
		3.79	2.00	1.79						
		5.50	3.68	1.82						
		5.52	3.68	1.84						
		5.68	4.00	1.68	5.92	4.00	1.92	5.45	4.00	1.45
		5.72	4.00	1.72						

\* Calculated by Diatkina and Syrkin.<sup>2</sup>

## IV. Discussion

We have to evaluate ( $R_{QH_i} - R_Q$ ). It will be seen from Tables I and II that both these depend on the values of the parameters  $\delta$ ,  $\rho$  and  $k$ , the exact magnitudes of which are not known. Furthermore, two *different* sets of parameters have to be assigned to  $QH_i$  and  $Q$  respectively. It appears from the results, however, that both  $R_{QH_i}$  and  $R_Q$  can be expressed as a sum of two terms:

- (i) a term independent of the parameters,  $R_{c.h.}$  and  $R'$ , defined above;
- (ii) a term dependent on the parameters, but fairly constant throughout the series.

Mathematically this can be expressed as follows—

$$R_{QH_i}^i(p) = R_{c.h.}^i + a(p) \quad . \quad . \quad . \quad (4a)$$

$$R_Q^i(p') = R' + b(p'), \quad . \quad . \quad . \quad (4b)$$

where  $p$  and  $p'$  stand for the set of parameters assigned to  $QH_i$  and  $Q$  respectively and  $a$  and  $b$  are functions of these parameters, but constant throughout the series in which  $i$  denotes a particular member. The calculations by Syrkin and Diatkina for a series of quinodimethanes<sup>2</sup> now appear as a special case (when  $\delta = k = 0$  and  $\rho = 1$ ) of eqn. (4b).

It can easily be verified that any other way of splitting  $R_{QH_i}$  and  $R_Q$  into a parameter-independent and a parameter-dependent term does not make the latter a constant throughout the series. For example, if in splitting up  $R_Q(p')$  we put  $R_{c.h.}$  in place of  $R'$  we obtain for  $b(p')$  the values as given in Table III. The theoretical explanation of these facts is the subject of a further investigation.

TABLE III  
( $R_Q - R_{c.h.}$ )  $\times 1/\beta$

Compounds \ Parameters	$\delta = 0$ $k = 0$ $\rho = 1$	$\delta = 2$ $k = 0$ $\rho = 1$	$\delta = 2$ $k = 0.1$ $\rho = 2$
<i>o</i> -Benzoquinone . . . .	-0.06	-0.20	-0.60
<i>p</i> -Benzoquinone . . . .	-0.08	-0.27	-0.58
1:4-Naphthoquinone . . .	+0.14	+0.23	-0.29
9:10-Anthraquinone . . .	+0.36	+0.61	+0.14

From eqn. (4a and b) we get—

$$\Delta R^i = (R_{c.h.}^i - R') + (a - b). \quad . \quad . \quad . \quad (5)$$

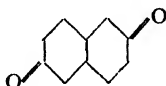
The importance of this result lies in this fact that  $(a-b)$  is constant throughout the series for a given set of parameters. Thus, in relating  $\Delta R$  to  $E_0$ , we can in effect deal with  $(R_{c.h.} - R')$ .

Another important point is seen from Tables I and II, namely, that the values of both  $R_Q$  and  $R_{QH_i}$  are practically the same for corresponding *o*- and *p*-compounds for all values of the parameters taken. The values of  $R_Q$  for five pairs of compounds as calculated by Diatkina and Syrkin never differ more than 0.04 $\beta$ . It is very striking, as our own calculations show for the benzoquinones, that a close agreement between  $R_{p-q}$  and  $R_{p-q}$  still persists if we allow for a certain degree of localization by assigning positive  $\delta$ 's and  $\rho$ 's  $> 1$ .

An assumption of *complete* localization in the C=O bonds gave differences in  $R_{p-q}$  and  $R_{p-q}$  of the order of 0.45 $\beta$ . Thus it appears that although one might expect a certain degree of localization from the bigger electron affinity of O and the greater binding energy in C=O, it is clearly incorrect to treat this part of the system as an independent localized one.

One must carry through a molecular-orbital calculation for the entire molecule and localization must be taken care of by means of introducing suitable parameters in the secular equation.

To summarize, we have discovered that in a series of *o*- and *p*-quinones,  $R_Q$  and  $R_{QH_2}$  can be expressed as a sum of two terms, one of which can be treated as a conjugated hydrocarbon by the molecular-orbital method, whereas the other term, though a function of theoretically-defined but unknown parameters, appears to be relatively constant throughout the series. This regularity does not apply to quinones of the type—



Moreover, the changes in  $\sigma$  bond energies accompanying are not confined to one portion of the structure, but occur throughout the entire molecule.

It is interesting to note, that neither does the regularity discussed above apply to hypothetical compounds of the structure—



This quinone, as is seen from Table IV, has an abnormal low resonance energy.

TABLE IV

$$R_Q \times 1/\beta$$

Compound	Parameters	$\delta = 0$ $k = 0$ $\rho = 1$	$\delta = 2$ $k = 0$ $\rho = 1$	$\delta = 2$ $k = 0.1$ $\rho = 2$
		3.82	3.91	3.39
		3.79	—	—
		3.52	3.54	2.92

Thus, our additivity rule does not apply here. We hope to discuss the reasons for this in a later publication.

In Table V the values of  $R_{QH_2}$ ,  $R_Q$  and  $(R_{QH_2} - R_Q)$  have been collected together with the oxidation-reduction potentials,  $E_0$ , of the corresponding system. In Fig. 2a the differences given in the fourth column of this Table are plotted against  $E_0$ . We get two straight lines of slope 0.82. However the *o*- and *p*-compounds still lie on different lines, although the difference in their intercepts has by this more precise treatment been

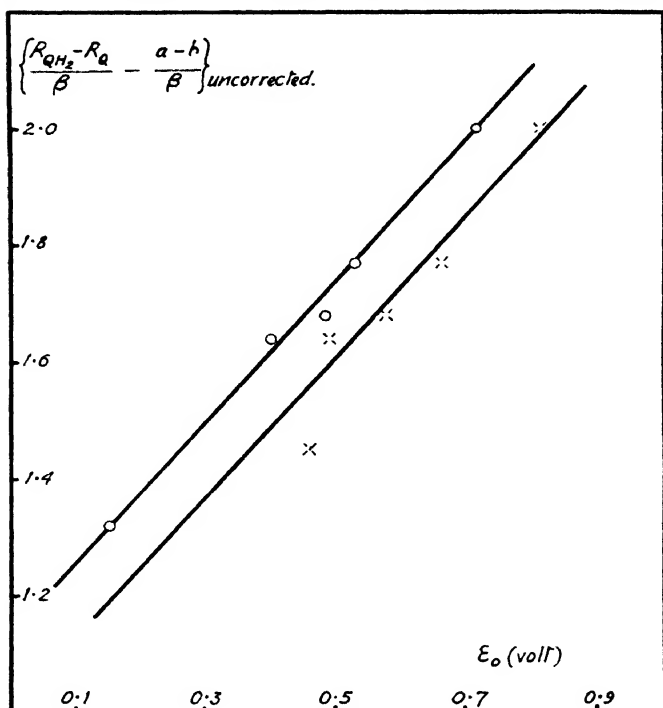


FIG. 2a.

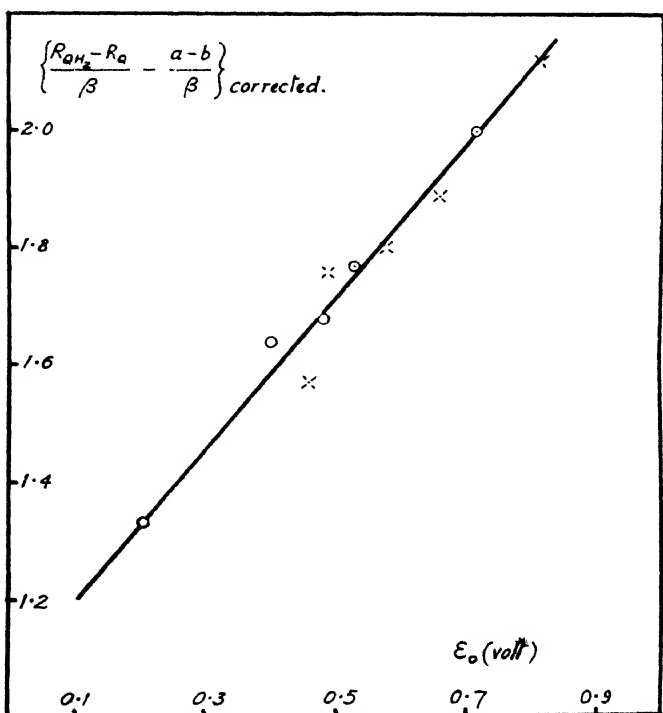




TABLE V

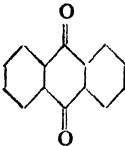
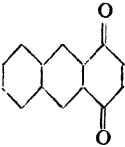
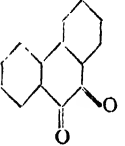
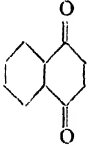
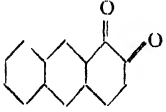
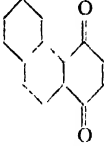
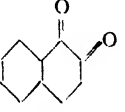
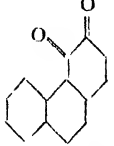

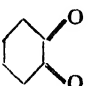
Compound	$E_0$ (volt)	$(R_{QH_2} - a) \times 1/\beta$ $= R_{o.h.}$	$(R_Q - b) \times 1/\beta$ $= R'$	$(R_{QH_2} - R_Q) -$ $-(a - b) \times 1/\beta$	Corrected for Bonding
	0.154	5.32	4.00	1.32	1.32
	0.401	5.32	3.68	1.64	1.64
	0.460	5.45	4.00	1.45	1.57
	0.484	3.68	2.00	1.68	1.68
	0.490	5.32	3.68	1.64	1.76
	0.530	5.45	3.68	1.77	1.77
	0.576	3.68	2.00	1.68	1.80
	0.660	5.45	3.68	1.77	1.89

TABLE V—(continued)

Compound	$E_0$ (volt)	$(R_{QH_2} - a) \times 1/\beta$ = $R_{c.h.}$	$(R_Q - b) \times 1/\beta$ = $R'$	$(R_{QH_2} - R_Q) -$ $-(a - b) \times 1/\beta$	Corrected for Bonding
	0.715	2.00	0.00	2.00	2.00
	0.813	2.00	0.00	2.00	2.12

reduced from 0.56 $\beta$  to 0.12 $\beta$ . By reference to Tables I and II it is clear that this difference between the *o*- and *p*-quinones does not arise from the method of calculation and we must therefore conclude that it is a real difference, arising from some factor we have not heretofore taken into account.

Such a factor, which is mentioned by Branch and Calvin,<sup>7</sup> is the possibility of hydrogen bonding in the *o*-hydroquinones. We would suggest therefore that the discrepancy of 0.12 $\beta$  is to be attributed to the neglect of this effect. This amounts to the assumption of an extra stabilization in the *o*-hydroquinones of 0.12 $\beta$  which is a reasonable value for this type of hydrogen bonding. The results corrected in this way are shown in Fig. 2b.

<sup>7</sup> Branch and Calvin, *Theory of Organic Chemistry* (New York, Prentice Hall, 1941).

Dept. of Physical and Inorganic Chemistry,  
The University,  
Leeds.

## RATE COEFFICIENTS IN THE POLYMERIZATION OF METHYL METHACRYLATE

### PART I

By M. H. MACKAY AND H. W. MELVILLE

Received 13th September, 1948

The photopolymerization of methyl methacrylate in the liquid phase has been studied. The rate coefficients and activation energies for propagation and termination have been determined by a modified sector method giving  $k_p = (4.1 \pm 0.5) \times 10^8$ ;  $k_t = (6.8 \pm 1.2) \times 10^7$  l. g.-mol.<sup>-1</sup> sec.<sup>-1</sup> at 35.9° C and  $E_p = (4.4 \pm 1.0)$  kcal. per g.-mol.;  $E_t =$  zero. The results are compared with the corresponding figures which are available for styrene and for vinyl acetate and are applied to published data on monomer reactivity ratios.

The kinetics of the polymerization of liquid methyl methacrylate have been the subject of a number of papers.<sup>1</sup> The general features of the reaction are now established and it appeared therefore that the reaction might be suitable for the evaluation of the absolute rate coefficients concerned in the process by making use of photochemical technique coupled with the rotating-sector method of measuring the life-time of polymer radicals as has already been done with vinyl acetate.<sup>2</sup> There is now a further objective in obtaining values for these coefficients. A considerable amount of work on the composition of copolymers makes it possible to get relative values of growth coefficients for the interaction of one kind of radical with two kinds of monomer. The value of the absolute coefficient for methyl methacrylate then makes it possible to calculate absolute values in copolymerization processes, and thus makes available a very extensive set of reactivities in regard to radical double-bond interactions.

Apart from the above matters the behaviour of the methyl methacrylate molecule is peculiar in many respects and it was essential to try and elucidate some of these features more extensively. For example, in the gas-phase polymerization three kinds of reaction can take place.<sup>3</sup> Polymerization may be induced by atomic hydrogen but the polymers formed are of low molecular weight. Polymerization is also induced by direct absorption of ultra-violet radiation. In addition, however, polymerization proceeds in the dark for long periods of time after the light is cut off. While it is now certain that the first two reactions are radical processes—the first, monoradical polymerization and the second, probably a diradical process—the nature of the third process is much more obscure and therefore merited further investigation. As has already been pointed out in the case of vinyl acetate polymerization, gas-phase reactions can become rather complicated because of the fact that the polymer molecule forms a new phase in the system and therefore the reaction tends to become heterogeneous in the sense that monomer has to be taken up by the growing polymer radical as a necessary preliminary to reaction. It was therefore important to find whether this kind of effect could be obtained in the liquid phase where the above-mentioned complications are absent and there might be a possibility of getting a better insight into the origin of this special type of reactivity.

The first paper, therefore, gives a description of the kinetics of the reaction with emphasis on the evaluation of the rate coefficients. The second paper deals with a number of other observations on the behaviour of this system.

### Experimental and Results

Methyl methacrylate, supplied containing 0.1 % hydroquinone, was purified by washing repeatedly with NaOH to remove inhibitor, then with distilled water. It was then dried quickly over anhydrous calcium chloride and filtered into the reservoir on the vacuum line. The monomer was distilled twice *in vacuo*, and finally into the reaction vessels which were sealed off. Throughout, the monomer was protected from strong light. Other purification methods had been tried such as the following. The washed monomer was distilled under nitrogen at about 20 mm. pressure, and washed with ferrous sulphate solution, then with distilled water. It was then dried, degassed and allowed to stand *in vacuo* in the light until some polymerization had taken place and the liquid had become viscous. The monomer was then distilled from the polymer *in vacuo* and re-distilled as before.

<sup>1</sup> Norrish and Brookman, *Proc. Roy. Soc. A*, 1939, **171**, 147. Norrish and Smith, *Nature*, 1942, **150**, 336. Schulz and Blaschke, *Z. physik. Chem. B*, 1942, **51**, 75. Schulz and Harborth, *Die makromol. Chem.*, 1947, **1**, 106. Trommsdorff, *B.I.O.S. Report*, No. 363, Item 22. Baxendale, Evans and Kilham, *Trans. Faraday Soc.*, 1946, **42**, 668; *J. Polymer Sci.*, 1946, **1**, 466. Bamford and Dewar, *Faraday Soc. Discussions* 1947, **1**.

<sup>2</sup> Burnett and Melville, *Proc. Roy. Soc. A*, 1947, **189**, 456.

<sup>3</sup> Melville, *ibid.*, 1937, **163**, 511.

The first method, however, was found to be most reliable, giving a product which was thermally stable at the temperatures employed (20-50° C) and gave reproducible photo-polymerization results.

Benzoquinone was purified by repeated steam distillation, thorough drying and sublimation. Benzoyl peroxide was purified by dissolving in chloroform, filtering and precipitating the benzoyl peroxide by pouring into methyl alcohol. It was then filtered off, dried and stored in a vacuum desiccator.

Silica reaction vessels were used as shown in Fig. 1, having a capacity of about 3.5 ml. They were calibrated by addition of water from a microburette. The reaction vessels were cleaned by filling with chromic acid mixture overnight, washing with distilled water and filling with sulphurous acid solution again overnight; then washing repeatedly and filling with distilled water until required. The reservoir and receivers on the vacuum line were cleaned in the same way, then flamed out thoroughly *in vacuo*.

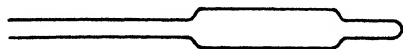


FIG. 1.—Silica reaction vessel.

The source of light was an Osira 125 W high-pressure mercury arc-lamp run off the 230 V A.C. mains. The glass cover was removed and a silica tube used as envelope. A rectangular metal screen, bent to fit inside the silica tube, reflected the light in the direction of the reaction vessel in an approximately parallel beam. In carrying out experiments in the determination of rate coefficients, it is important to be sure that the radiation is not completely absorbed in a layer of monomer much less in thickness than that of the reaction vessel itself. Experiments were made with a variety of glass filters to find the longest wavelengths capable of initiating reaction at a measurable speed and light of wavelength up to about 3600 Å was found to be effective. When a Corning filter No. 014 was used, having the transmission given in Table I, the rate of polymerization was reduced by a factor of two as compared with the full radiation from the Osira lamp. Therefore at least half of the photochemically-active radiation lies above 3000 Å, and, since the powerful 3130 Å line is cut down ten times in intensity by the use of this filter, the fraction will actually be considerably greater. The molar decadic extinction coefficient of methyl methacrylate at 3000 Å is 0.01<sup>4</sup> and only 10 % of the light of this wavelength is absorbed in passing through the reaction vessel used. This means that for all practical purposes the light is uniformly absorbed throughout the reaction vessel.

TABLE I.—TRANSMISSION BY CORNING 014 FILTER

Wavelength (Å)	3050	3130	3180	3230	3260	3300	3350	3390	3470	3650
% Trans- mission	0	10	20	30	40	50	60	70	80	90

Preliminary experiments had shown that the light used caused no decomposition of liquid methyl methacrylate or of the polymer.

A rectangular glass tank was used as thermostat. The Osira lamp was immersed in this and the silica envelope and reaction vessel clamped firmly to the steel-rod framework surrounding the tank. A brass screen with a rectangular window was interposed between lamp and reaction vessel, to cut off all light except that passing through the window. The screen was fitted on one side with grooves and a stop for holding filters or screens as required and on the other side with a shutter sliding smoothly in grooves, so that the window could be kept open or shut or intermittent illumination obtained. The lamp, window and screen were carefully aligned vertically and horizontally and the lamp and screen kept fixed.

The course of polymerization was followed dilatometrically, the meniscus in the reaction vessel capillary being observed by means of a cathetometer. This method was accurate up to about 20 % polymerization in the capillaries used but at higher conversions the meniscus became distorted due to the increasing viscosity of the mixture. To calibrate the dilatometric method, at the end of each of a series of runs at one temperature, the contents of the reaction vessel were washed out completely with acetone and the polymer precipitated by slow

<sup>4</sup> Goodeve, *Trans. Faraday Soc.*, 1938, **34**, 1239.

### 326 POLYMERIZATION OF METHYL METHACRYLATE

addition of excess methyl alcohol with constant stirring. The polymer was allowed to settle for some hours, then filtered off on a weighed sintered-glass crucible and washed with methyl alcohol. The polymer was obtained as a very bulky porous precipitate which dried to constant weight in about 3 days at 80° C. From the weight of polymer obtained and the original volume and density of the monomer, the % polymerization was calculated for each run and the (linear) relationship between % decrease in volume and % polymerization established for the experimental temperature. This was then repeated at another temperature (Fig. 2 and 3).

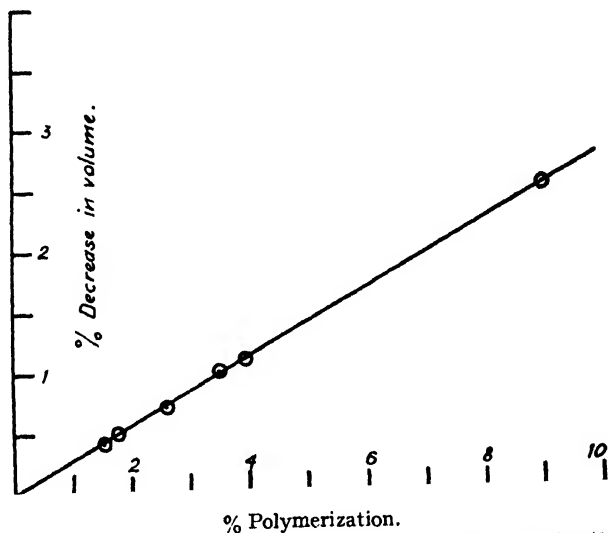


FIG. 2.—Measurement of the conversion factor (%-polymerization/%-decrease in volume); temperature = 20.9° C; conversion factor = 3.60.

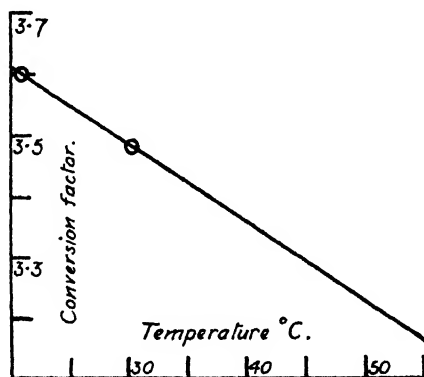


FIG. 3.—Conversion factor as a function of temperature for extrapolation.

**Molecular Weight Measurements.**—Where absolute molecular weights were required, the osmotic molecular weight was measured; but where only relative values were needed, the intrinsic viscosity was found as this was much less laborious and less polymer was required. To determine the number average molecular weight of a sample, this was dissolved in distilled benzene to give

30 ml. solution (1 %, if sufficient polymer were available) and the solution was filtered. The dynamic osmotic pressure of this solution was then found. The osmometer used was a modified, thermostatted form of that described by Fuoss and Mead<sup>5</sup> used with bacterial cellulose membranes.<sup>6</sup> Full details of osmometer construction, membrane preparation and experimental technique have been given by Masson and Melville.<sup>7</sup> The solution was run out of the osmometer and the concentration determined by evaporating a weighed amount of solution at 100° C to constant weight. This method involves an error due to residual solvent which remains in the polymer film and is not driven off by prolonged heating at 100° C. To estimate this error, experiments have been carried out<sup>8</sup> in which similar solutions of polymethyl methacrylate in benzene were evaporated at 100° C to constant weight in the usual way and the weighing bottle then placed in a molecular still and heated to 110° C in high vacuum, again to constant weight. This caused a loss in weight equal to 6.3 % of the apparent weight of polymer, i.e. the true weight of polymer was equal to 93.7 % of the apparent oven-dried weight. This correction was applied to all concentration measurements. The osmotic pressure was measured for a series of concentrations obtained by successive dilutions of the original solution. The cell constant was found (after each two osmotic pressure measurements or, when it was found to vary, after each single measurement) with solvent on both sides of the membrane. The experimental values of  $\pi$  were plotted against concentration  $c$ . Points on this smoothed curve were used to plot  $\pi/c$  against  $c$  and extrapolate to zero concentration as in Fig. 4. Then if  $\bar{M}_n$  is the number average molecular weight of the polymer,

$$\bar{M}_n = RT / \left( \frac{\pi}{c} \right)_{c=0}$$

Viscosity measurements were carried out in Ostwald-type viscometers of similar dimensions and therefore approximately equal rates of shear. About 0.05 g. of the dry polymer was weighed out into a clean 100 ml. bottle with ground stopper and 50 ml. distilled benzene added. The polymer was dissolved by slow end-over-end rotation in a tumbling machine and the resulting solution filtered through a sintered-glass crucible. To obtain the concentration of the filtered solution, two 10 ml. samples were successively evaporated on a weighed watch glass at 100° C to constant weight and the correction for residual solvent was applied as before. Before use, the viscometers were steeped in chromic acid mixture then washed with distilled water, then acetone and dried by compressed air. After one determination they were washed out three times with acetone, dried and used again; after the second they were washed out with acetone, then distilled water and steeped in chromic acid mixture for some hours. This was found necessary in order to obtain consistent results. The experimental accuracy required has been indicated by Gee.<sup>9</sup> Three viscometers were rigidly held in a brass stand which was placed in the thermostat and fixed to the framework, two plumb-lines giving the vertical in two perpendicular directions. Three concentrations of each polymer solution were used, the original solution being diluted in the viscometers. By using three stop-watches, the viscosities of the three concentrations could be measured at the same time.

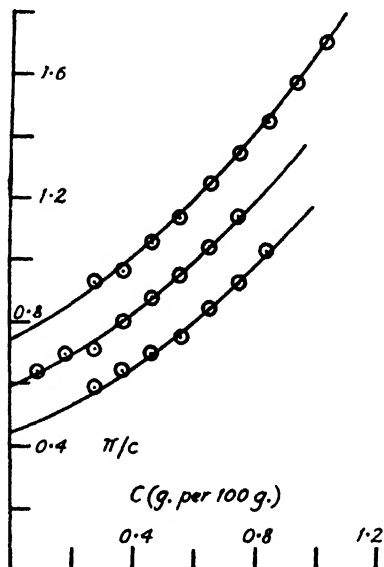


FIG. 4.—Extrapolation of  $\pi/c$  against  $c$ .

<sup>5</sup> Fuoss and Mead, *J. Physic. Chem.*, 1943, **47**, 59.

<sup>6</sup> Cruickshank, Masson, Melville and Menzies, *Nature*, 1946, **157**, 74.

<sup>7</sup> Masson and Melville, *J. Polymer Sci.*, 1948 (in press).

<sup>8</sup> Grassie, *ibid.* (in press).

<sup>9</sup> Gee, *Trans. Faraday Soc.*, 1940, **36**, 1162.

## 328 POLYMERIZATION OF METHYL METHACRYLATE

The intrinsic viscosity  $[\eta]$  was obtained by extrapolating the expressions—

$$[\eta] = \lim_{c \rightarrow 0} \eta_{sp}/c$$

and

$$[\eta] = \lim_{c \rightarrow 0} \{1/c \ln(1 + \eta_{sp})\}.$$

The mean rate of shear in the viscometers was always greater than 1000 sec.<sup>-1</sup>, at which value  $[\eta]$  is not sensibly dependent on rate of shear.<sup>10</sup>

Since the intrinsic viscosity was used as a means of interpolation for the measurement of molecular weights, it was necessary to calibrate the method against osmotic measurements made on the same unfractionated samples. The intrinsic viscosities of photopolymers for which  $\overline{M}_n$  had been determined osmotically were measured in benzene solution at 20° C and a linear relationship was found between  $\overline{M}_n$  and  $[\eta]^{0.77}$ , as shown in Fig. 5, in accordance with the equation,

$$\overline{M}_n = 3.32 \times 10^5 [\eta]^{1.0.77}$$

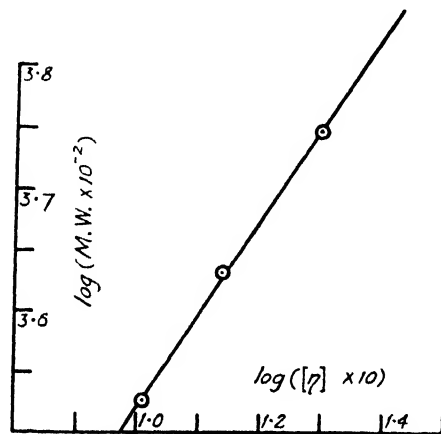


Fig. 5.—Intrinsic viscosity of the photopolymer as a function of osmotic molecular weight.

This is not in agreement with the results of Baxendale, Bywater and Evans<sup>11</sup> for unfractionated polymers produced by the reduction-activation technique, but it must be emphasized that poly-disperse materials were being used.

**The Photopolymerization Reaction.**—No measurable thermal polymerization occurred at the temperatures used (20–50° C). In reaction vessels at room temperature in the dark, the monomer showed no apparent increase in viscosity after several weeks.

The reaction showed no detectable induction period and was apparently independent of polymer concentration in the initial stages and over a considerable % conversion (Fig. 6). In the later stages of the reaction there was a "gel" effect, the rate increasing rapidly with time (Fig. 7). The "gel" acceleration set in at a lower % conversion under conditions leading to higher molecular weights, i.e. at higher temperatures and at lower light intensities. The relative molecular weight, measured by the intrinsic viscosity, remained constant during the "zero-order" phase of the reaction and increased during the "gel" stage, as shown in Table II.

TABLE II.—INTRINSIC VISCOSITY OF THE POLYMER

### 1. Initial phase of reaction at 20.9° C

%-Conversion	1.8	2.7	3.9	5.5	9.0
$[\eta]$	1.2	1.0	1.1	1.0	1.2

### 2. Initial and "gel" phase at 30.15° C (see Fig. 7)

%-Conversion	3.6	5.2	15	25	45
$[\eta]$	1.4	1.4	1.7	1.8	1.8

<sup>10</sup> Davies, *Porton Report*, 1944, No. 2598. Toms and Hall, *ibid.*, No. 2599.

<sup>11</sup> Baxendale, Bywater and Evans, *J. Polymer Sci.*, 1946, 1, 237.

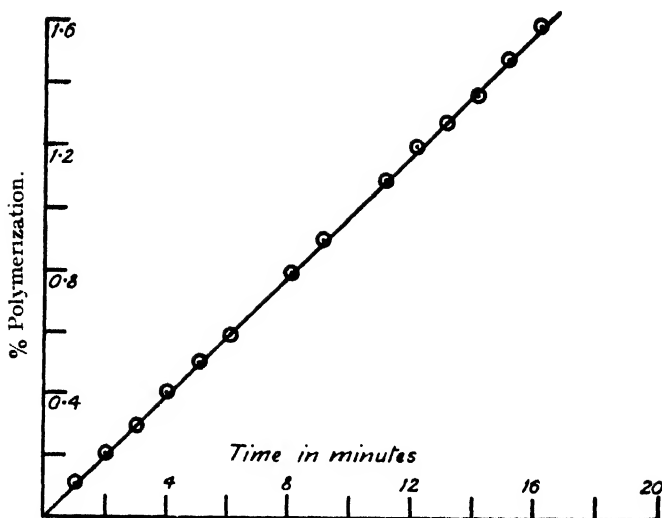


FIG. 6.—Photopolymerization as a function of time at 36.5° C

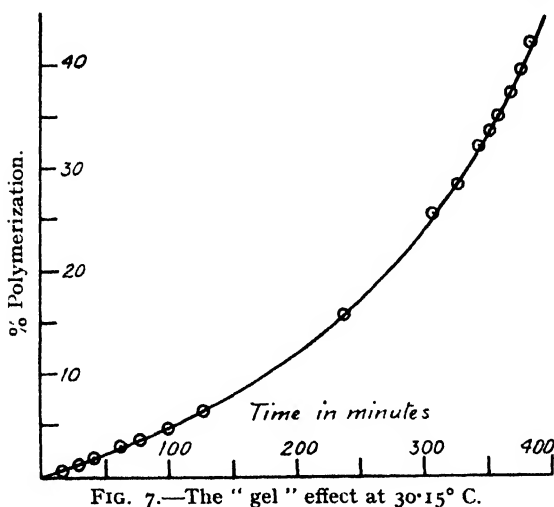


FIG. 7.—The "gel" effect at 30.15° C.

Prolonged exposure to air, after filling the reaction vessel *in vacuo* in the usual way, was found to have little effect on the polymerization.

TABLE III.—THE EFFECT OF AIR (Temperature = 35.9° C)

	Induction Period (sec.)	Steady Rate (% conversion per min.)	$[\eta]$ of Polymer
In air . . . .	24	0.106	0.88
<i>In vacuo</i> . . . .	0	0.102	0.97

**The Effect of Temperature.**—The rate of polymerization was measured in one run at three different temperatures in succession, the reaction vessels being kept in a vacuum flask with solid  $\text{CO}_2$  while the thermostat temperature



### 330 POLYMERIZATION OF METHYL METHACRYLATE

was being altered. At the same time, complete runs to about 11 % polymerization were carried out at two different temperatures under the same intensity and the osmotic molecular weights of the polymers formed were measured to

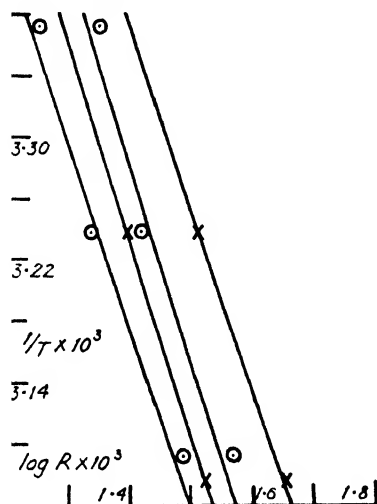


FIG. 8.—The overall activation energy for photopolymerization.

find the effect of temperature on the mean chain-length. Plotting  $\log$  (relative rate) against the reciprocal of the absolute temperature, as in Fig. 8, gives an overall activation energy of  $3.7 \pm 0.2$  kcal. per g. mol.

TABLE IV.—EFFECT OF TEMPERATURE ON MEAN CHAIN LENGTH

Temperature °C	Rate $\times 10^5$ (g. mol. $\times 1.1^{-1} \times \text{sec.}^{-1}$ )	Osmotic Chain Length $\bar{\nu}_n$
35.9	12.76	3360 $\pm$ 100
50.67	17.42	4280 $\pm$ 150

These figures give an activation energy for mean chain length of  $3.3 \pm 0.5$  kcal. per g. mol.

**The Effect of Intensity.**—To measure the intensity exponent of the reaction, the rate of polymerization was measured in one run in the same reaction vessels at 35.9° C, (a) under the full intensity from the lamp and (b) with the intensity reduced by covering the window with successive calibrated screens. The intensity exponent had a mean value of 0.48 at the beginning of the reaction (Fig. 9), but increased with increasing polymer concentration as shown in Fig. 10. Complete runs were also carried out to about 11 % polymerization under different light intensities and the molecular weights of the polymers were measured osmotically.

The value (0.48) of the intensity exponent measured in the initial stages of the reaction shows that mutual termination only takes place. It is not possible to discriminate kinetically between disproportionation and combination. In a monoradical system either mechanism is possible, the mean chain-length being twice as great with combination as with disproportionation. If, however, the growing chains are diradicals, termination by combination would cause the linking-up of chains into successively larger units; in the steady state the number of growing chains would be constant but the mean chain-length would increase apparently without limit other than that imposed by any simultaneous transfer reaction.

In this paper, the assumption is made that the system is a diradical one. There is no direct experimental evidence on this point but the following arguments support the assumption while not affording proof. Firstly, so far as is

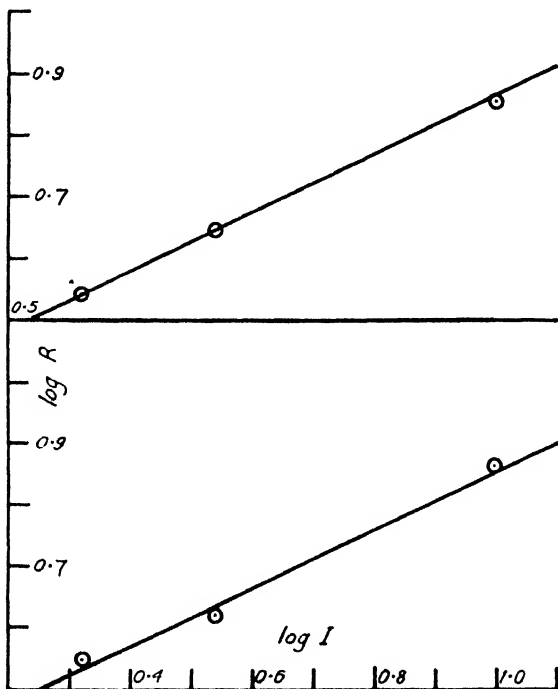


FIG. 9.—Intensity exponent at beginning of photopolymerization at 35.9° C.

known, molecules of this kind are not decomposed by light of the wavelengths used. It would be possible for dissociation into radicals to take place without any decomposition being observed, owing to the rapid recombination of the

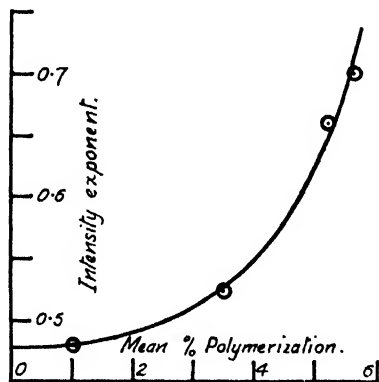


FIG. 10.—Intensity exponent as a function of mean %-conversion at 35.9° C.

radicals in the liquid phase. The maximum opportunity for survival of such radicals occurs in the gas phase but, whereas polymerization is initiated by light of longer wavelengths, photodecomposition of methyl methacrylate is

## 332 POLYMERIZATION OF METHYL METHACRYLATE

caused only by light of wavelengths less than  $2200 \text{ \AA}$ .<sup>3</sup> In the photopolymerization of vinyl acetate,<sup>2</sup> as in the thermal polymerization of styrene,<sup>12</sup> it has been shown that diradicals are produced. By analogy, it seems reasonable to assume that this is the case with methyl methacrylate also. Assuming the system to be a diradical one, there is no experimental evidence for combination; finite molecular weights have been obtained in all experiments, the chain-length remains constant during the course of the normal polymerization and increases with rise in temperature. (If the chain-length were determined solely by a transfer reaction, it would decrease with rise in temperature since such reactions in general have a considerable activation energy.<sup>13</sup>) Also the molecular weights obtained in the photoreaction are comparable with those obtained in the benzoyl peroxide-sensitized polymerization, a known monoradical reaction (see Part II), so that the occurrence of combination to any significant extent is unlikely. Evans<sup>14</sup> has shown by kinetic and osmotic molecular-weight and

TABLE V.—EFFECT OF INTENSITY ON MEAN CHAIN LENGTH

Temperature =  $35.9^\circ \text{C}$ 

Relative Intensity $I_{\text{rel.}}$	Rate $\times 10^5$ (g. mol. $\times 1.1 \times \text{sec.}^{-1}$ )	Osmotic Chain Length $\bar{\nu}_n$	$(\bar{\nu}_n \times I_{\text{rel.}}) \times 10^{-3}$
100	12.76	$3360 \pm 100$	33.6
34.6	7.61	$5600 \pm 200$	32.9

terminal-group estimations that in the polymerization of methyl methacrylate in aqueous solution combination of radicals apparently does occur. It is possible that in this case in presence of hydrogen peroxide there may have been transfer involving peroxide molecules giving terminal hydroxyl groups and still making it possible for there to be disproportionation of methyl methacrylate radicals.

The figures given in Table V show that the product  $(\bar{\nu}_n \times I_{\text{rel.}})$  at  $35.9^\circ \text{C}$  is constant within the accuracy of measurement of  $\bar{\nu}_n$ . This means that the osmotic chain-length at this temperature is determined solely by the termination reaction and transfer does not play a significant part in the reaction, i.e. the mean kinetic chain-length is equal to the osmotic chain-length. Also, since the mean chain-length remains constant during the normal polymerization reaction, the mean chain-length  $\bar{\nu}_n$  is equal to the instantaneous chain-length,  $\nu_n$ , so that the rate of initiation of chains can be obtained directly from the rate of polymerization and osmotic chain-length.

**Measurement of the Life-time of the Active Polymer.**—Since the overall rate of polymerization is proportional to the square-root of the intensity of the absorbed light and is constant during a considerable initial period of the reaction, the life-time of the active polymer can be determined by the use of intermittent illumination, applying the theory as developed by Burnett and Melville.<sup>3</sup> A preliminary experiment was made with a rotating sector to find the approximate life-time. The reaction vessel was immersed in a small copper tank with silica windows, through which water was circulated from a thermostat at  $35.9^\circ \text{C}$ . It was illuminated by an Osira lamp and a black metal disc cut with two  $90^\circ$  sectors was fitted up to rotate in the path of this beam of light. The sector disc was mounted and driven as described by the above authors and the speed of the motor was varied and measured in a similar way. Since the sector-opening was much larger than the area of the reaction vessel, there was no danger of scanning. The rate of polymerization was measured for steady illumination and for intermittent illumination with different sector speeds. The sector was allowed to run at constant speed for 10–15 min. before each measurement but it was found difficult to obtain uniform rotation at very low speeds. No variation in rate with sector speed was found down to the slowest speeds accurately obtainable, i.e. the life-time under these conditions was greater than about  $1/5$  sec.

<sup>12</sup> Kern and Feuerstein, *J. prakt. Chem.*, 1941, **158**, 186. Melville and Watson, *Trans. Faraday Soc.* (in press).

<sup>13</sup> Bamford and Dewar, *Proc. Roy. Soc. A*, 1948, **192**, 309.

<sup>14</sup> Evans, *J. Chem. Soc.*, 1947, 266

The experiments were continued with the set-up described below where better temperature regulation was obtainable. Intermittent illumination was obtained by manual operation of the sliding shutter, timed by a 1/10 sec. stopwatch. This method, although tedious, had the advantage over a sector method of giving an abrupt transition between light and dark conditions and avoided any possibility of scanning. The reaction vessel was given equal alternate periods of light and dark so that this was equivalent to the use of a 1/1 sector (i.e.  $r = 1$  in Burnett and Melville's notation). The life-time was determined at 35.9° C and the mean molecular weight of the polymer formed under steady illumination at that intensity was measured osmotically. For the life-time

TABLE VI.—SECTOR EXPERIMENT

Under steady illumination,

$$R_{st} = 2.75 \times 10^{-3} \text{ (cm. per min. decrease in height)}$$

$$R_{st} \times 2.4 = 1.94 \times 10^{-3} \text{ (cm. per min. decrease in height)}$$

Time of Flash (sec.) $\times 10^3$	Rate (cm. per min.) $\times 10^3$
4.45	2.00
6.8	2.04
17.48	2.01
18.45	1.95

measurements, three reaction vessels were used in succession and, with each, several observations were made of the fall in meniscus level during five minutes of steady illumination, for no illumination, and for two different rates of flashing. The mean values were taken in each case. In making each measurement, to correct for any end-effect, the shutter was worked for one minute and the initial meniscus reading taken. The shutter was then worked for five minutes and the final reading taken. The life-time was determined in the same way under a lower intensity for which the osmotic mean molecular weight was also measured. The measurements were then repeated at two other temperatures.

It was necessary to correct the observed rates for the simultaneous dark reaction which was measured during the period of no illumination. The correction has been discussed by Noyes and Leighton<sup>15</sup> and depends on the mechanisms of the two reactions. If the light and dark reactions follow independent paths, the total rate will be the sum of the two rates taken independently. Also when the light and dark rates involve one or more of the same secondary processes, if the concentration of the rate-determining intermediate varies directly with the light intensity or concentration of reactants, the total rate will again be the sum of the light and dark rates taken independently. If, however, proportionality to the square-root of the light intensity or concentration of a reactant is involved, the total rate will be equal to the square-root of the sum of the squares of the light and dark rates. In the present instance, if it is assumed that the dark reaction is a free-radical reaction, the propagation (and probably also the termination) process will be common to both reactions; also the rate of the photopolymerization is proportional to the square-root of the light intensity. The correction was therefore applied as follows.

If  $R_T$  = observed total rate of polymerization ;  
 $R_L$  = rate of light reaction ;  
 $R_D$  = rate of dark reaction ;  
 then  $R_L = (R_T^2 - R_D^2)^{1/2}$ .

All rate measurements were made within the first few % polymerization so that in every instance the dark rate was relatively small (see Part II) and remained constant within experimental accuracy during the period of the experiments. The correction, applied as above, was in most cases zero and always less than 3 % of the mean observed total rate. Under these conditions, any discrepancy between the dark rate during illumination and the measured dark rate due to its decay during the one-minute interval preceding measurement would not be large enough to affect the results significantly.

<sup>15</sup> Noyes and Leighton, *The Photochemistry of Gases* (Reinhold, 1941).

## 334 POLYMERIZATION OF METHYL METHACRYLATE

The preliminary experiment with the rotating sector had shown that the rate for high-flashing speeds was related to the steady rate by

$$R = R_{st.}/2^{\frac{1}{2}},$$

so that although high speeds were not obtainable by the shutter technique, the rate at high speeds could be taken as  $R_{st.}/2^{\frac{1}{2}}$ . For each set of measurements at a particular rate of flashing, the ratio of the corrected mean rate to that at high speeds was calculated as in Table VIII and the corresponding value of  $\log m$  was found from Burnett and Melville's theoretical curve for  $\nu = 1$  (Fig. 11), and hence the life-time,

$$\tau = t/m,$$

where  $t$  is the duration of the light flash. (Tables IX-XI.)

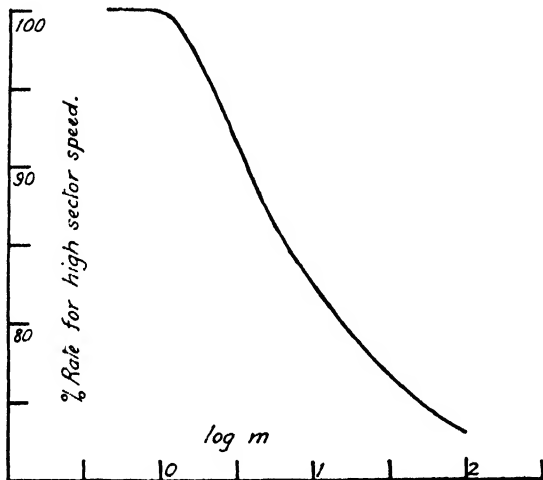
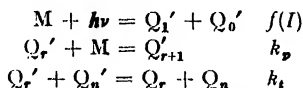


FIG. 11.—Theoretical curve of Burnett and Melville.

From this value of  $\log m$ , the value of  $\log \{[2f(I)]^{\frac{1}{2}} \times t\}$  was subtracted where  $2f(I)$  is the rate of initiation of chains (Table VII) to give directly  $\log k_t^{\frac{1}{2}}$  and hence  $k_t$ ;  $k_p$  was then calculated from the mean value for  $k_t$ . In their calculation of rate coefficients, Burnett and Melville made no distinction between monoradical and diradical systems and although they assumed diradicals, their notation would seem to imply a monoradical system. This has led to some confusion regarding the precise significance of their results. Considering each radical end individually, the kinetic scheme for a diradical system without transfer may be represented as follows.



where  $Q_r'$  represents an active "half-chain" of length  $r$  units, and  $Q_r$  represents an inactive "half-chain" of length  $r$  units. The rate of production of "half-chains" is  $2f(I)$ . Assuming disproportionation, the mean chain-length  $\bar{\nu}_n$  is equal to twice the mean "half-chain" length; also the mean "half-chain" length is equal to the instantaneous "half-chain" length, i.e. to the ratio:

$$\frac{\text{Rate of consumption of monomer}}{\text{Rate of production of "half-chains"}} = \frac{-d(M)/dt}{2f(I)}.$$

Hence

$$\bar{\nu}_n = 2 \frac{-d(M)/dt}{2f(I)}$$

and the rate of production of "half-chains" is

$$2f(I) = 2 \frac{-d(M)/dt}{\bar{\nu}_n}$$

The coefficients  $k_p$ ,  $k_t$  refer respectively to the interaction of one growing chain-end with a monomer molecule and to the mutual interaction of two growing chain-ends without any regard to the other ends of the chains which may also be growing or may have already been terminated.

TABLE VII.—CALCULATION OF RATES OF CHAIN INITIATION

Temperature °C	Overall Rate $\times 10^6$ (g. mol. l. <sup>-1</sup> $\times$ sec. <sup>-1</sup> ) $R$	Number Average Chain Length $\bar{\nu}_n$	Rate of Initiation $\times 10^6$ (einstein l. <sup>-1</sup> $\times$ sec. <sup>-1</sup> ) $2R/\bar{\nu}_n = 2f(I)$
35.9 (a)	12.76	3360 $\pm$ 100	7.60
35.9 (b)	7.01	5600 $\pm$ 200	2.50
23.6	5.56	4700 $\pm$ 150	2.36
50.5	10.51	7590 $\pm$ 300	2.77

TABLE VIII.—MEASUREMENT OF LIFE-TIME AT 50.5° C

(Example of experimental data.)

Conditions	Rate (cm. drop per 5 min. $\times 10^3$ )	Corrected Mean Rate $R_L = (R_T^2 - R_D^2)^{1/2}$	% Rate for High Flashing Speeds
$R_T$ , steady illumination	61, 62, 63, 62	62.0	—
$R_D$ , no illumination	1, 1, 1, 1	—	—
$R_T$ , 2 sec. flash	42, 42, 40, 40	41.0	93.5
$R_T$ , steady illumination	62, 62, 63	62.3	—
$R_D$ , no illumination	2, 2, 0, 1	—	—
$R_T$ , 2 sec. flash	40, 40, 41	40.3	91.5
$R_T$ , steady illumination	52, 52, 51, 52	51.7	—
$R_D$ , no illumination	1, 2, 1, 1	—	—
$R_T$ , 2 sec. flash	34, 34, 35, 33	34.0	92.9
$R_T$ , 5 sec. flash	32, 31, 30, 32	31.2	85.3

TABLE IX. - CALCULATION OF  $\tau$  AND  $k_t$  AT 35.9° C

$t$ (sec.)	% Rate for High Flashing Speeds	$\log [(2f(I))^{1/2}t]$	$\log m$	$\tau$ (sec.)	$\log k_t^{\dagger}$	$k_t \times 10^{-7}$ (l. g.-mol. <sup>-1</sup> sec. <sup>-1</sup> )
(a) 1	95.3	4.440	0.330	0.47	3.890	6.0
2	89.2	4.741	0.603	0.50	3.862	5.3
2	87.8	4.741	0.675	0.42	3.934	7.4
2	87.0	4.741	0.710	0.39	3.969	8.7
Mean				0.44		6.8
(b) 2	92.3	4.500	0.467	0.68	3.967	8.6
5	85.5	4.898	0.800	0.79	3.902	6.4
5	86.0	4.898	0.770	0.85	3.872	5.4
Mean				0.77		6.8

(a) Mean value of  $k_t = (6.8 \pm 1.2) \times 10^7$  l. g.-mol.<sup>-1</sup> sec.<sup>-1</sup>.

In the steady state,  $d(\Sigma Q'_r)/dt = 2f(I) - k_t(\Sigma Q'_r)^2 = 0$ ,

$$\text{therefore } (\Sigma Q'_r)^2 = \frac{2f(I)}{k_t} = 11.11 \times 10^{-10},$$

$$\text{and } (\Sigma Q'_r) = 3.33 \times 10^{-5} \text{ g.-mol. l.}^{-1}.$$

Rate of polymerization,  $R = k_p(\Sigma Q'_r)(M)$ ,

$$\text{therefore } k_p = R/(\Sigma Q'_r)(M) = (4.1 \pm 0.5) \times 10^2 \text{ l. g.-mol.}^{-1} \text{ sec.}^{-1}.$$

## 336 POLYMERIZATION OF METHYL METHACRYLATE

- (b) Mean value of  $k_t = (6.8 \pm 1.2) \times 10^7$  l. g.-mol.<sup>-1</sup> sec.<sup>-1</sup>;  
 as above,  $(\Sigma Q'_r) = 1.91 \times 10^{-8}$  g.-mol. l.<sup>-1</sup>;  
 and  $k_p = (4.0 \pm 0.5) \times 10^3$  l. g.-mol.<sup>-1</sup> sec.<sup>-1</sup>.

TABLE X.—CALCULATION OF  $\tau$  AND  $k_t$  AT 23.6° C

$t$ (sec.)	% Rate for High Flashing Speeds	$\log [(2f(I))^{1/2}t]$	$\log m$	$\tau$ (sec.)	$\log k_t \frac{1}{2}$	$k_t \times 10^{-7}$ (l. g.-mol. <sup>-1</sup> sec. <sup>-1</sup> )
2	93.7	4.488	0.403	0.79	3.915	6.8
2	94.2	4.488	0.380	0.83	3.892	6.1
5	85.4	4.886	0.805	0.78	3.919	6.9
Mean				0.80		6.6

- Mean value of  $k_t = (6.6 \pm 0.4) \times 10^7$  l. g.-mol.<sup>-1</sup> sec.<sup>-1</sup>;  
 as above,  $(\Sigma Q'_r) = 1.89 \times 10^{-8}$  g.-mol. l.<sup>-1</sup>;  
 and  $k_p = (3.1 \pm 0.2) \times 10^3$  l. g.-mol.<sup>-1</sup> sec.<sup>-1</sup>.

TABLE XI.—CALCULATION OF  $\tau$  AND  $k_t$  AT 50.5° C

$t$ (sec.)	% Rate for High Flashing Speeds	$\log [(2f(I))^{1/2}t]$	$\log m$	$\tau$ (sec.)	$\log k_t \frac{1}{2}$	$k_t \times 10^{-7}$ (l. g.-mol. <sup>-1</sup> sec. <sup>-1</sup> )
2	92.9	4.522	0.442	0.72	3.920	6.9
5	85.3	4.920	0.805	0.78	3.885	5.9
2	91.5	4.522	0.500	0.63	3.978	9.0
2	93.5	4.522	0.410	0.78	3.888	6.0
Mean				0.73		6.9

- Mean value of  $k_t = (6.9 \pm 1.0) \times 10^7$  l. g.-mol.<sup>-1</sup> sec.<sup>-1</sup>;  
 as above,  $(\Sigma Q'_r) = 2.00 \times 10^{-8}$  g.-mol. l.<sup>-1</sup>;  
 and  $k_p = (5.8 \pm 0.6) \times 10^3$  l. g.-mol.<sup>-1</sup> sec.<sup>-1</sup>.

These experimental results show that the coefficients  $k_p$ ,  $k_t$  do not vary significantly with chain length. Within the experimental accuracy,  $k_t$  is also independent of temperature, i.e. the most probable value of the activation energy

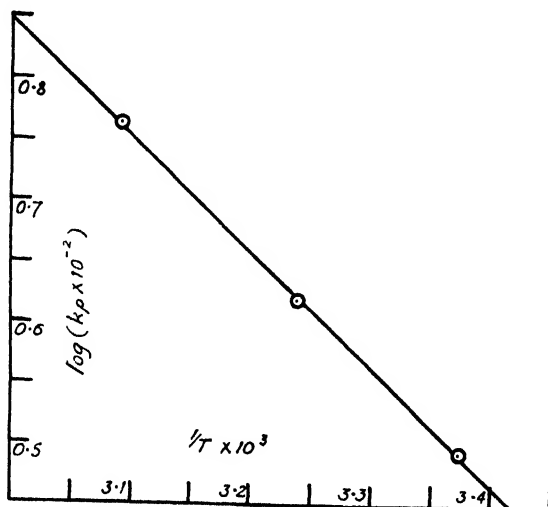


FIG. 12.—The activation energy for the propagation reaction.

for termination,  $E_t$ , is zero. Plotting  $\log(k_p \times 10^{-3})$  against the reciprocal of the absolute temperature as in Fig. 12 gives an activation energy for propagation,  $E_p = (4.4 \pm 1.0)$  kcal. per g.-mol. With the notation given above the rate of polymerization is

$$-d(M)/dt = k_p(M)\Sigma(Q_r).$$

In the steady state,

$$2f(I) = k_t(\Sigma Q_r)^2,$$

and

$$-d(M)/dt = k_p(M)\left[\frac{2f(I)}{k_t}\right]^{\frac{1}{2}};$$

so that the overall activation energy is given by

$$E_T = E_p + \frac{1}{2}E_{2f(I)} - \frac{1}{2}E_t; \quad (i)$$

also

$$\bar{\nu}_n = \frac{-d(M)/dt}{f(I)} = \frac{2k_p(M)}{[2f(I)k_t]^{\frac{1}{2}}},$$

and the activation energy for chain-length is given by

$$E_{\bar{\nu}_n} = E_p - \frac{1}{2}E_{2f(I)} - \frac{1}{2}E_t. \quad (ii)$$

The experimental results obtained were  $E_T = (3.7 \pm 0.2)$ ,  $E_{\bar{\nu}_n} = (3.3 \pm 0.5)$  kcal. per g.-mol.; so that within experimental accuracy  $E_{2f(I)}$  is zero, as would be expected for photochemical initiation. With the values obtained for  $E_p$ ,  $E_t$ ,  $E_{2f(I)}$ , eqn. (i) gives an overall activation energy of  $(4.4 \pm 1.4)$  kcal. per g.-mol. as compared with the experimental value of  $(3.7 \pm 0.2)$  kcal.

$$k_p \text{ is defined by } k_p = A_p e^{-E_p/RT}$$

i.e.

$$A_p = k_p e^{E_p/RT} = 5 \times 10^5 \text{ l. g.-mol.}^{-1} \text{ sec.}^{-1}$$

$$\text{also } k_t \text{ is defined by } k_t = A_t e^{-E_t/RT}$$

i.e.

$$A_t = k_t e^{E_t/RT} = 10^8 \text{ l. g.-mol.}^{-1} \text{ sec.}^{-1}.$$

TABLE XII.—RATE COEFFICIENTS AND ACTIVATION ENERGIES FOR METHYL METHACRYLATE

Temperature °C . . . . .	23.6	35.9	35.9	50.5
$-d(M)/dt \times 10^5$ (g.-mol. l. <sup>-1</sup> sec. <sup>-1</sup> ) . . . . .	5.56	12.76	7.01	10.51
$\bar{\nu}_n$ . . . . .	4700	3360	5600	7590
$2f(I) \times 10^8$ (einstein l. <sup>-1</sup> sec. <sup>-1</sup> ) . . . . .	2.36	7.60	2.50	2.77
$\tau$ (sec.) . . . . .	0.80	0.44	0.77	0.73
$k_p \times 10^{-2}$ (l. g.-mol. <sup>-1</sup> sec. <sup>-1</sup> ) . . . . .	3.1	4.1	4.0	5.8
$k_t \times 10^{-7}$ (l. g.-mol. <sup>-1</sup> sec. <sup>-1</sup> ) . . . . .	6.6	6.8	6.8	6.9
$E_p$ (kcal. g.-mol. <sup>-1</sup> ) . . . . .	4.4	—	—	—
$E_t$ (kcal. g.-mol. <sup>-1</sup> ) . . . . .	0	—	—	—
$A_p$ (l. g.-mol. <sup>-1</sup> sec. <sup>-1</sup> ) . . . . .	$5 \times 10^5$	—	—	—
$A_t$ (l. g.-mol. <sup>-1</sup> sec. <sup>-1</sup> ) . . . . .	$10^8$	—	—	—

The figures given in Table XIII show some consistencies between the coefficients and activation energies for the different monomers. Allowing for temperature differences, the propagation rate coefficients are reasonably consistent and decrease in the order vinyl acetate > methyl methacrylate > styrene. The values of  $k_t$  except for styrene, show less agreement. Propagation in each case requires an activation energy of about 5 kcal.; termination on the other hand is activated only slightly or not at all. The temperature-independent factors are in reasonable agreement, giving an average value for  $A_t/A_p$  of  $6 \times 10^3$ .

From work on the composition of copolymers, monomer reactivity ratios



# 338 POLYMERIZATION OF METHYL METHACRYLATE

have been obtained for a large number of two-component systems.<sup>18</sup> By combining the ratios for systems containing methyl methacrylate with the value for the propagation rate coefficient for methyl methacrylate, absolute values are obtained for the rate coefficients for reaction of a methyl methacrylate radical with different monomer molecules, as in Table XIV.

TABLE XIII.—COMPARISON OF RATE COEFFICIENTS AND ACTIVATION ENERGIES

Reference	Styrene		Vinyl Acetate		Methyl Methacrylate	
	16	13	2	19.	17 (this paper)	
Temperature °C . . . .	30	25	15.9	25	0	35.9
$k_p$ (l. g.-mol. <sup>-1</sup> sec. <sup>-1</sup> ) . . . .	52.0	18.7	770	1100	42.7	400
$k_t \times 10^7$ (l. g.-mol. <sup>-1</sup> sec. <sup>-1</sup> ) . . . .	1.05	0.28	310	8.0	0.47	6.8
$E_p$ (kcal. g.-mol. <sup>-1</sup> ) . . . .		6.5	4.4			4.4
$E_t$ (kcal. g.-mol. <sup>-1</sup> ) . . . .		2.8	0			0
$A_p$ (l. g.-mol. <sup>-1</sup> sec. <sup>-1</sup> ) . . . .		$1 \times 10^8$	$2 \times 10^8$			$5 \times 10^8$
$A_t$ (l. g.-mol. <sup>-1</sup> sec. <sup>-1</sup> ) . . . .		$3 \times 10^8$	$3 \times 10^8$			$10^8$

If the monomer reactivity ratio of the methyl methacrylate radical with a given monomer is  $\sigma$ , the rate coefficient for reaction of that monomer with a methyl methacrylate radical is given by  $k_p/\sigma$ . Extrapolation of the plot in Fig. 12 gave  $k_p = 7.0 \times 10^2$  l. g.-mol.<sup>-1</sup> sec.<sup>-1</sup> at 60° C.

TABLE XIV.—RATE COEFFICIENTS FOR REACTION OF MONOMERS WITH METHYL METHACRYLATE RADICALS AT 60° C

Monomer	Monomer Reactivity Ratio, $\sigma^{18}$	Absolute Rate Coefficient (l. g.-mol. <sup>-1</sup> sec. <sup>-1</sup> ) $\times 10^{-2}$
Butadiene . . . . .	0.25	28.0
Styrene . . . . .	0.46	15.2
Methacrylonitrile . . . . .	0.67	10.4
Methyl methacrylate . . . . .	1.00	7.0
Acrylonitrile . . . . .	1.35	5.2
Vinylidene chloride . . . . .	2.53	2.8
Vinyl acetate . . . . .	20	0.35
Allyl acetate . . . . .	23	0.30

One of us (M. H. M.) is indebted to Bakelite Ltd. for financial assistance during the course of this work (1946-48).

Chemistry Department,  
University of Aberdeen.

<sup>18</sup> Valentine (unpublished).

<sup>17</sup> Bamford and Dewar, ref. 1.

<sup>18</sup> Mayo, Lewis and Walling, *Faraday Soc. Discussions* 1947, 1.

<sup>19</sup> Swain and Bartlett, *J. Amer. Chem. Soc.*, 1946, 68, 2381.

# DISSOCIATION ENERGIES OF CARBON BONDS, AND RESONANCE ENERGIES IN HYDRO- CARBON RADICALS

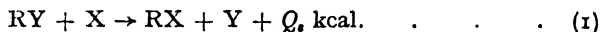
By J. S. ROBERTS AND H. A. SKINNER

Received 18th September, 1948

Values of the heats of formation  $Q_f(R)$  of a number of alkyl radicals are derived from thermal and other data. These are used to compile lists of bond dissociation energies  $D(R-X)$ , where  $R=Me, Et, Pr, sec.-Pr, tert.-Bu, allyl, benzyl, acetyl, formyl, vinyl, phenyl, -C\equiv CH$ , and  $-C\equiv N$ , and  $X=H, OH, NH_2$ , a halogen, or another alkyl radical. Equations are given relating the bond-dissociation energy  $D(R-Y)$  to the resonance energy in  $RY$  and in the radical  $R$ . The dissociation energies  $D(R-H)$  are discussed in terms of the theory of hyperconjugation. Empirical conjugation energies in  $RH$  and  $R$  are listed. Calculations of the conjugation energies and bond lengths in hydrocarbons and hydrocarbon radicals are given, leading to  $D(R-H)$  values in fair agreement with experiment. Substitution heats of a number of reactions are listed and discussed.

## 1. Introduction

Although few *direct* measurements of bond dissociation energies in carbon compounds have as yet been made, it is possible, as Baughan and Polanyi<sup>1</sup> have pointed out, to assess a bond dissociation energy  $D(R-Y)$  if another,  $D(R-X)$ , is known and the "substitution heat,"  $Q_s$ , of the reaction



is obtainable from thermochemical heats of formation. Accordingly, one can estimate *indirectly* bond dissociation energies of a large number of bonds despite the fact that few absolute measurements have been made.

The substitution heat in (1) is given by :

$$Q_s = \Delta Q_f \left[ \begin{smallmatrix} RX \\ RY \end{smallmatrix} \right] + \Delta Q_f \left[ \begin{smallmatrix} Y \\ X \end{smallmatrix} \right] \quad (2)$$

where the terms in  $\Delta Q_f$  measure the *difference* in the heats of formation ( $Q_f$ ) of gaseous  $RX$  and  $RY$ , and of  $Y$  and  $X$ , from *elements* in their standard states. The bond dissociation energies  $D(R-X)$  and  $D(R-Y)$  are given by the equations,

$$\begin{cases} D(R-X) = Q_f(RX) - Q_f(R) - Q_f(X) & (3a) \\ D(R-Y) = Q_f(RY) - Q_f(R) - Q_f(Y) & (3b) \end{cases}$$

which may be combined to give

$$\Delta D \left[ \begin{smallmatrix} R-X \\ R-Y \end{smallmatrix} \right] = \Delta Q_f \left[ \begin{smallmatrix} RX \\ RY \end{smallmatrix} \right] + \Delta Q_f \left[ \begin{smallmatrix} Y \\ X \end{smallmatrix} \right] = Q_s \quad (4)$$

The various  $D(R-Y)$  values given by Baughan and Polanyi were derived by use of eqn. (4), in which the experimental  $D(R-I)$  values of Butler and Polanyi<sup>2</sup> served as the known  $D(R-X)$  values. Alternatively, one could use *any* known bond dissociation energy,  $D(R-X)$ , to give

<sup>1</sup> Baughan and Polanyi, *Nature*, 1940, **146**, 685.

<sup>2</sup> Butler and Polanyi, *Trans. Faraday Soc.*, 1943, **39**, 19.

## 340 DISSOCIATION ENERGIES OF CARBON BONDS

$Q_f(R)$  in eqn. (3a), and thence substitute into eqn. (3b) to derive an unknown  $D(R-Y)$  value.

A list of  $Q_f(R)$  values for a number of organic radicals is presented in Table I. These were calculated from the thermal data given in column 4, and the experimental bond dissociation energies in column 3. The values refer to room-temperature conditions (25° C).

TABLE I  
 $Q_f(R)$  VALUES IN KCAL. MOL.<sup>-1</sup>

Process	R	$D(R-X)$	$Q_f(RX)$	$Q_f(R)$
$CH_4 \rightarrow CH_3 + H$	Me	102 <sup>a</sup>	17.9	-32.1
$C_2H_6 \rightarrow C_2H_5 + H$	Et	97.5 <sup>b</sup>	20.2	-25.3
$C_3H_8 \rightarrow C_3H_7 + H$	Pr	95.5 <sup>c</sup>	24.8	-18.7
	<i>sec.</i> -Pr			-14 <sup>d</sup>
$Me_3CI \rightarrow Me_3C + I$	<i>tert.</i> -Bu	45 <sup>e</sup>	16.3	-3.2
$C_6H_5CH_3 \rightarrow C_6H_5CH_2 + H$	Benzyl	77.5 <sup>f</sup>	-11.9	-37.4
$HCO \rightarrow CO + H$	Formyl	26 <sup>g</sup>	—	0.4
$CH_3CO \rightarrow CO + CH_3$	Acetyl	17 <sup>g</sup>	—	11.3
$CH_3 \cdot CH = CH_2 \rightarrow C_2H_5 + H$	Allyl	78 <sup>h</sup>	-4.9	-30.9
$Me \begin{array}{c} \diagup \\ C=CH_2 \end{array} \rightarrow \begin{array}{c} Me \\ \diagup \\ CH_2 \\ \diagdown \\ C=CH_2 \end{array} + H$	2-Me allyl	76 <sup>h</sup>	3.3	-20.7
$C_2H_4 \rightarrow C_2H_3 + H$	Vinyl	102 <sup>j</sup>	-12.5	(-62.5)
$C_2H_2 \rightarrow C_2H + H$	$\cdot C \equiv CH$	121 <sup>k</sup>	-54.2	(-123.2)
$C_6H_6 \rightarrow C_6H_5 + H$	Phenyl	102 <sup>j</sup>	-19.8	(-69.8)
$C_2N_2 \rightarrow 2CN$	$\cdot C \equiv N$	127 <sup>l</sup>	-73.6	(-100.3)

(a) Kistiakowsky and v. Artsdalen,<sup>3</sup>  $102 \pm 2$ ; Baughan and Polanyi,<sup>1</sup> 102.5; Patat,<sup>4</sup> 102.5; Stevenson,<sup>5</sup> 101 + 4.

(b) Andersen and v. Artsdalen,<sup>6</sup>  $99 \pm 2$ ; Baughan and Polanyi,<sup>1</sup> 97.5; Steacie and Phillips,<sup>7</sup> 95; Stevenson,<sup>5</sup> 96 + 4.

(c) This is an estimate; Baughan and Polanyi give 95.

(d) Obtained by interpolation of the  $Q_f(R)$  in the series Me, Et, *sec.*-Pr, *tert.*-Bu.

(e) Butler and Polanyi;<sup>2</sup> Butler, Mandel and Polanyi.<sup>8</sup>

(f) Szwarc.<sup>9</sup>

(g) Gorin.<sup>10</sup> For a discussion on these values, see Steacie.<sup>11</sup>

(h) Szwarc.<sup>12</sup>

(j) This is an estimate by Laidler<sup>13</sup> based on the experimental work of Taylor and Smith.<sup>14</sup> But see Stevenson<sup>15</sup> for a much lower value (92 kcal.).

(k) Cherton;<sup>16</sup> but see Steacie and Le Roy.<sup>17</sup>

(l) Hogness and Ts'ai;<sup>18</sup> Robertson and Pease;<sup>19</sup> Glockler;<sup>20</sup> but see White,<sup>21</sup> who quotes a higher value (146 kcal.) for  $D(NC-CN)$ .

Values given in brackets are rather uncertain: otherwise the error in the quoted values lies within 2-3 kcal.

<sup>3</sup> Kistiakowsky and v. Artsdalen, *J. Chem. Physics*, 1944, **12**, 469.

<sup>4</sup> Patat, *Z. Physik. Chem.*, B, 1936, **32**, 290.

<sup>5</sup> Stevenson, *J. Chem. Physics*, 1942, **10**, 291.

<sup>6</sup> Andersen and v. Artsdalen, *ibid.*, 1944, **12**, 479.

<sup>7</sup> Steacie and Phillips, *Can. J. Res. B*, 1938, **16**, 303.

<sup>8</sup> Butler, Mandel and Polanyi, *Trans. Faraday Soc.*, 1945, **41**, 298.

<sup>9</sup> Szwarc, *J. Chem. Physics*, 1948, **16**, 128.

<sup>10</sup> Gorin, *ibid.*, 1939, **7**, 256.

<sup>11</sup> Steacie, *Atomic and Free Radical Reactions* (Reinhold, 1946).

<sup>12</sup> Szwarc, *J. Chem. Physics* (in press).

<sup>13</sup> Laidler, *ibid.*, 1947, **15**, 712.

<sup>14</sup> Taylor and Smith, *ibid.*, 1939, **7**, 390; 1940, **8**, 543.

<sup>15</sup> Stevenson, *J. Amer. Chem. Soc.*, 1943, **65**, 209.

<sup>16</sup> Cherton, *Bull. soc. chim. Belg.*, 1943, **52**, 26.

<sup>17</sup> Steacie and Le Roy, *J. Chem. Physics*, 1944, **12**, 117.

<sup>18</sup> Hogness and Ts'ai, *J. Amer. Chem. Soc.*, 1932, **54**, 123.

<sup>19</sup> Robertson and Pease, *ibid.*, 1942, **64**, 1880.

<sup>20</sup> Glockler, *J. Chem. Physics*, 1948, **16**, 600.

<sup>21</sup> White, *ibid.*, 1940, **8**, 463.

From the listed  $Q_f(R)$  values, we have used eqn. (3b) and available thermal data to estimate the  $D(R-Y)$  values collected together in Tables IIA and IIB. The heats of formation  $Q_f(RY)$  used in compiling these have been selected from among the best at present available, and are listed separately below. In cases where there is reason to suspect that the  $Q_f$  value quoted may be in error by more than 1 or 2 kcal. mol.<sup>-1</sup>, an asterisk is placed against the doubtful figure.

### 1. Hydrocarbons

Data for the hydrocarbons were taken from the *Selected Values of Thermodynamic Constants* (National Bureau of Standards, U.S.A.),<sup>22</sup> except the following:

Diphenyl . . . . .	-41.2	Brull ; <sup>23</sup> $\lambda_p$ by Wolf. <sup>24</sup>
Diphenyl methane . . . . .	-33.2	Parks ; <sup>25</sup> $\lambda_p = 12.7$ , by Wolf.
Dibenzyl . . . . .	-28.0	Ref. <sup>25</sup> , and <sup>24</sup> .
Diallyl . . . . .	-20.8	Kistiakowsky. <sup>26</sup>
Phenyl acetylene . . . . .	-75.8*	Quoted by Wheland. <sup>27</sup>

### 2. Alcohols

MeOH . . . . .	48.10	Rossini <sup>28</sup>
EtOH . . . . .	56.27	Rossini <sup>28</sup>
PrOH . . . . .	62.19	Rossini <sup>28</sup>
sec.-l'roH . . . . .	65.9	Parks ; <sup>29</sup> $\lambda_p$ by Parks <sup>30</sup>
tert.-BuOH . . . . .	77.0	Raley <i>et al.</i> <sup>31</sup>
Allyl OH . . . . .	30.7	Kistiakowsky <sup>32</sup>
Benzyl OH . . . . .	25*	Stohmann ; <sup>33</sup> $\lambda_p = 12$ kcal. (assumed)
Phenol . . . . .	24*	Quoted by Wheland <sup>27</sup>
HCO . OH . . . . .	86.7	N.B.S. <sup>22</sup> Table 23-4
CH <sub>3</sub> CO . OH . . . . .	97.4*	N.B.S. Table 23-5 : and $\lambda_p = 19$ kcal (assumed)

### 3. Aldehydes and Ketones

CH <sub>2</sub> O . . . . .	27.7	N.B.S., <sup>22</sup> Table 23-4
CH <sub>3</sub> CHO . . . . .	39.8	N.B.S., Table 23-5
EtCHO . . . . .	46	We have estimated this value
PrCHO . . . . .	52.5	We have estimated this value
Allyl-CHO . . . . .	20.6	We have estimated this value
Benzaldehyde . . . . .	11.2*	Quoted by Wheland <sup>27</sup>
CH <sub>3</sub> COCH <sub>3</sub> . . . . .	51.75	Miles and Hunt <sup>34</sup>
Et . COCH <sub>3</sub> . . . . .	58.17	Crog and Hunt ; <sup>35</sup> $\lambda_p = 8.95$ kcal.
Pr . COCH <sub>3</sub> . . . . .	65.1	Swietoslawski ; <sup>36</sup> $\lambda_p = 11$ kcal.
sec.-Pr . COCH <sub>3</sub> . . . . .	66.8	Swietoslawski ; <sup>36</sup> $\lambda_p = 11$ kcal.
Vinyl-CHO . . . . .	20*	Moureu ; <sup>37</sup> $\lambda_p = 9$ kcal. (assumed)
CH <sub>3</sub> CO . CHO . . . . .	65.8	Moulds and Riley ; <sup>38</sup> $\lambda_p = 8$ kcal. (assumed)

\*  $Q_f(RY)$  values (kcal. mol.<sup>-1</sup>).

<sup>22</sup> Rossini, *Tables of Selected Values of Chemical Thermodynamic Constants* (Bureau of Standards, Washington, 1948).

<sup>23</sup> Brull, *Gazz. chim. ital.*, 1935, **65**, 19.

<sup>24</sup> Wolf and Weghofer, *Z. physik. Chem. B*, 1938, **39**, 194.

<sup>25</sup> Parks, West, Naylor, Fujii and McClaine, *J. Amer. Chem. Soc.*, 1946, **68**, 2524.

<sup>26</sup> Kistiakowsky, Ruhoff, Smith and Vaughan, *ibid.*, 1936, **58**, 146 ; see also Coops, Mulder, Dinske and Smittenberg, *Rec. Trav. Chim.*, 1946, **65**, 128.

<sup>27</sup> Wheland, *The Theory of Resonance* (John Wiley, 1944). (The heats of combustion quoted by Wheland are taken from an unpublished table of combustion heats compiled by Kharasch and Brown.)

<sup>28</sup> Rossini, *Bur. Stand. J. Res.*, 1934, **13**, 189.

<sup>29</sup> Parks and Moore, *J. Chem. Physics*, 1939, **7**, 1066.

<sup>30</sup> Parks and Barton, *J. Amer. Chem. Soc.*, 1928, **50**, 24.

<sup>31</sup> Raley, Rust and Vaughan, *ibid.*, 1948, **70**, 88.

<sup>32</sup> Dolliver, Gresham, Kistiakowsky, Smith and Vaughan, *ibid.*, 1938, **60**, 440.

<sup>33</sup> Stohmann, *Z. physik. Chem.*, 1890, **6**, 334.

<sup>34</sup> Miles and Hunt, *J. Physic. Chem.*, 1941, **45**, 1346.

<sup>35</sup> Crog and Hunt, *ibid.*, 1942, **46**, 1162.

<sup>36</sup> Swietoslawski, *J. Amer. Chem. Soc.*, 1920, **42**, 1092.

<sup>37</sup> Moureu, Boutaric and Dufraisse, *J. chim. Physique*, 1921, **18**, 333.

<sup>38</sup> Moulds and Riley, *J. Chem. Soc.*, 1938, 621.

## 4. Amines

MeNH <sub>2</sub> . . . . .	6.7	N.B.S.; <sup>23</sup> Table 23-14
EtNH <sub>2</sub> . . . . .	11.6	N.B.S.; <sup>23</sup> Table 23-43
PrNH <sub>2</sub> . . . . .	17.2*	Derived from Thomsen's data <sup>30</sup>
Allyl-NH <sub>2</sub> . . . . .	-6.9*	Derived from Thomsen's data <sup>30</sup>
tert.-BuNH <sub>2</sub> . . . . .	32*	Quoted by Wheland <sup>23</sup>
Benzyl-NH <sub>2</sub> . . . . .	-15*	Petit; <sup>40</sup> $\lambda_p = 10$ kcal. (assumed)
Aniline . . . . .	-16.7*	Quoted by Wheland <sup>27</sup>
HCO . NH <sub>2</sub> . . . . .	49.0	Roth; <sup>41</sup> and $\lambda_p = 11.0$ kcal. (assumed)
CH <sub>3</sub> CO . NH <sub>2</sub> . . . . .	60.9	Quoted by Wheland <sup>27</sup>
NC . NH <sub>2</sub> . . . . .	-27.7*	Salley and Gray; <sup>42</sup> and $(\lambda_p + \lambda_f) = 13$ kcal. (assumed)

## 5. Chlorides

MeCl . . . . .	19.6	N.B.S.; <sup>23</sup> Table 23-7
EtCl . . . . .	25.1	N.B.S.; <sup>23</sup> Table 23-35
PrCl . . . . .	29.7*	Derived from Thomsen's data <sup>30</sup>
Allyl-Cl . . . . .	-0.6*	Derived from Thomsen's data <sup>30</sup>
Vinyl-Cl . . . . .	-7.5*	N.B.S.; <sup>23</sup> Table 23-35
Chlorobenzene . . . . .	-12.5	Hubbard, Knowlton, Huffmann <sup>43</sup> and $\lambda_p = 9$ kcal. (assumed)
tert.-BuCl . . . . .	42.5	Kistiakowsky <sup>44</sup>
CH <sub>3</sub> COCl . . . . .	59.0	Carson and Skinner <sup>45</sup>
CNCl . . . . .	-34.5	N.B.S.; <sup>23</sup> Table 23-19

## 6. Bromides

MeBr . . . . .	8.6	From data by Bak <sup>46</sup>
EtBr . . . . .	13.0	N.B.S.; <sup>23</sup> Table 23-40
tert.-BuBr . . . . .	30.9	Kistiakowsky <sup>44</sup>
Allyl-Br . . . . .	-12.1*	Gellner and Skinner <sup>47</sup>
Benzyl-Br . . . . .	-15.6*	Gellner and Skinner <sup>47</sup>
CH <sub>3</sub> COBr . . . . .	46.6	Carson and Skinner <sup>45</sup>

## 7. Iodides

MeI . . . . .	-2.8	Carson, Hartley and Skinner <sup>48</sup>
EtI . . . . .	1.1*	From Thomsen's data <sup>30</sup>
tert.-BuI . . . . .	16.3	Ogg <sup>49</sup>
CH <sub>3</sub> COI . . . . .	31.8	Carson and Skinner <sup>47</sup>
CNI . . . . .	-54.6	N.B.S.; <sup>23</sup> Table 23-20
Allyl-I . . . . .	-22.0*	Gellner and Skinner <sup>47</sup>
Benzyl-I . . . . .	-26.4*	Gellner and Skinner <sup>47</sup>

## 8. Cyanides

HCN . . . . .	-31.2	N.B.S.; <sup>23</sup> Table 23-13
MeCN . . . . .	-21.0	N.B.S.; <sup>23</sup> Table 23-43
Vinyl-CN . . . . .	-43.7	Davis and Wiedemann <sup>50</sup>
Allyl-CN . . . . .	-38*	Bruylants; <sup>51</sup> $\lambda_p = 10$ kcal. (assumed)
Phenyl-CN . . . . .	-48*	Berthelot; <sup>52</sup> $\lambda_p = 11$ kcal. (assumed)
Benzyl-CN . . . . .	-43*	Berthelot; <sup>52</sup> $\lambda_p = 11$ kcal. (assumed)
C <sub>2</sub> N <sub>2</sub> . . . . .	-73.6	N.B.S.; <sup>23</sup> Table 23-43

\*  $Q_f(\text{RY})$  values (kcal. mol.<sup>-1</sup>).

<sup>30</sup> Thomsen, *Thermochemischen Untersuchungen* (Barth, Leipzig, 1882); see also Kharasch, *Bur. Stand. J. Res.*, 1929, **2**, 359.

<sup>40</sup> Petit, *Ann. chim. phys.* 1889, **18**, (6), 145.

<sup>41</sup> Roth, quoted in Landolt-Bornstein (1937).

<sup>42</sup> Salley and Gray, *J. Amer. Chem. Soc.*, 1948, **70**, 2650.

<sup>43</sup> Hubbard, Knowlton and Huffmann, *A.C.S. Abstr.* (March, 1948).

<sup>44</sup> Kistiakowsky and Stauffer, *J. Amer. Chem. Soc.*, 1937, **59**, 165.

<sup>45</sup> Carson and Skinner, *J. Chem. Soc.* (in press).

<sup>46</sup> Bak, *Det. Kgl. Danske Vid. Sels.*, 1948, **24**, 9.

<sup>47</sup> Gellner and Skinner, *J. Chem. Soc.* (in press).

<sup>48</sup> Carson, Hartley and Skinner, *Proc. Roy. Soc. A*, 1948 (in press).

<sup>49</sup> Jones and Ogg, *J. Amer. Chem. Soc.*, 1937, **59**, 1943.

<sup>50</sup> Davis and Wiedemann, *Ind. Eng. Chem.*, 1945, **37**, 482.

<sup>51</sup> Bruylants and Christiaen, *Bull. soc. chim. Belg.*, 1925, **34**, 144.

<sup>52</sup> Berthelot and Petit, *Ann. chim. phys.*, 1889, **18**, (6), 107.

The  $D(R-Y)$  values given in Tables IIA and IIB are naturally dependent upon the accuracy of the  $Q_f(R)$  values given in Table I. Errors in  $Q_f(R)$  enter correspondingly into  $D(R-Y)$ : those  $D(R-Y)$  values based upon an uncertain  $Q_f(RY)$  are marked by an asterisk. The following  $Q_f(Y)$  values in kcal. (taken from N.B.S. ref. <sup>53</sup>) have been used:

$$Q_f(H) = 52.0; Q_f(Cl) = 29.0; Q_f(Br) = 26.7; \\ Q_f(I) = 25.5; Q_f(OH) = 10.0.$$

For  $Q_f(NH_2)$  we have used  $Q_f(NH_2) = -44$  kcal., corresponding to Geib's value for  $D(NH_2-H)$  of 107 kcal.<sup>53</sup> This may be appreciably in error, for the experimental values so far reported<sup>54</sup> for the dissociation energy  $D(NH_2-H)$  vary from 117 kcal. to < 103 kcal. The mean bond-energy term in  $NH_3$  is 93 kcal. mol.<sup>-1</sup>, and, by analogy with the case of the  $H_2O$  molecule, one might reasonably expect  $D(NH_2-H)$  to exceed this mean value by some 10 kcal.; Geib's value seems a fair one to choose from this point of view.

TABLE IIA  
 $D(R-Y)$  VALUES FOR C-C BONDS (KCAL.)

R	Me	Et	Pr	sec-Pr	tert-Bu	C <sub>6</sub> H <sub>5</sub> -	C <sub>6</sub> H <sub>5</sub> CH <sub>2</sub> -	Vinyl	Allyl	-CHO	-COMe	-C≡CH	-C≡N
Me	84.4	82.2	80.6	77.5	74.8	90.0	62.4	89.7	62.7	71.2	72.6	111.0	112.2
Et	82.2	80.4	79.0	76.2	72.7	88.0	60.8	87.5	61.2	70.9	72.2	108.8	—
Pr	80.6	79.2	77.4	74.4	71.0	86.0	59.4	86.2	59.6	70.9	72.5	107.4	—
sec-Pr	77.5	76.2	74.4	70.5	66.0	82.9	—	83.4	56.6	—	69.5	—	—
tert-Bu	74.8	72.7	71.0	66.0	60.1	—	—	79.8	—	—	—	—	—
C <sub>6</sub> H <sub>5</sub> -	90.0	88.0	86.6	82.9	—	102.4	74.0	101.2	—	80.6*	—	117.2*	122.8*
C <sub>6</sub> H <sub>5</sub> CH <sub>2</sub> -	62.4	60.8	59.4	—	—	74.0	46.8	—	—	—	—	—	94.4*
Vinyl	89.7	87.5	86.2	83.4	79.8	101.2	—	102.4	67.8	82.1*	—	—	118.8
Allyl	62.7	61.2	59.6	56.6	—	—	—	67.8	41.0	51.1	—	—	92.9*
-CHO	71.5	70.9	70.9	—	—	80.6*	—	82.1*	51.1	—	54.1	—	—
-COMe	72.6	72.2	72.5	69.5	—	—	—	—	—	54.1	—	—	—
-C≡CH	111.0	108.8	107.4	—	—	117.2*	—	—	—	—	—	—	—
-C≡N	111.4	—	—	—	—	122.1*	94.7*	119.1	93.2*	—	—	—	127.0

TABLE IIB  
 $D(R-Y)$  VALUES IN KCAL. MOL.<sup>-1</sup>

R	H	-OH	-NH <sub>2</sub>	Cl	Br	I
Me	102	91.2	82.8	80.7	67.4	55.0
Et	97.5	92.6	80.9	79.4	64.6	52*
Pr	95.5	92.8	79.9*	77.4*	—	—
sec-Pr	90.8	90.9	—	—	—	—
tert-Bu	86.5	91.0	79.2	74.7	60.8	45.0
Phenyl	102	104.8*	97.1*	86.3	—	—
Benzyl	77.5	73.4*	66.4*	—	48.5*	36.5*
Vinyl	102	—	—	84.0	—	—
Allyl	78	72.6	68.0*	59.3*	45.5*	34.4*
CHO	79.3	96.3	92.6	—	—	—
-COCH <sub>3</sub>	80.5	97.2	93.6	76.7	62.0	46.0
-CN	121.1	—	116.6*	94.8	—	71.2

<sup>53</sup> Geib, *Z. Elektrochem.*, 1938, **44**, 81; see also, Wicke, *Naturwiss.*, 1942, Band 20.

<sup>54</sup> Bonhoeffer and Harteck, *Grundlagen der Photochemie* (Steinkopff, Dresden, 1933); Terenin and Neumin, *Bull. Acad. Sci. U.R.S.S.*, 1936, **4**, 1.

## 2. Gradations in Bond Dissociation Energies

In a theoretical discussion given by Baughan, Evans and Polanyi<sup>55</sup> in 1941, the *gradations* in bond dissociation energies  $D(R-Y)$ , down a series in which R changes, were attributed to two main causes—

(a) the effect of changes in the “radical resonance energy” of the radical R ;

(b) the effect of changing ionic character in the bonds  $R-Y$ .

The expression “radical resonance energy” was used as a measure of the energy stabilisation in the free radical R arising from  $\pi$ -electron conjugation (e.g., as in the allyl radical), and/or from  $\pi$ -hyperconjugation (e.g., as described by Wheland<sup>56</sup> in the alkyl radicals). Baughan, Evans, and Polanyi's theory is not quite complete, in that it does not take full account of other factors (of which, for example,  $\pi$ -hyperconjugation is perhaps the most important) which might lead to an energy stabilisation in the molecule  $RY$  itself.

In cases where the bond  $R-Y$  is virtually non-polar, it would be sufficient to assess the total delocalisation-energy\* in both the molecule  $RY$ , and the radical R. Representing the total delocalisation energy in  $RY$  by  $\pi(RY)$ , and correspondingly in the radical by  $\pi(R)$ , the bond dissociation energy  $D(R-Y)$  is given as

$$D(R-Y) = D_0(R-Y) + \pi(RY) - \pi(R). \quad (5)$$

In this equation,  $D_0(R-Y)$  is a constant, independent of R, so that the difference between the bond dissociation energies  $D(R_1-Y)$ , and  $D(R_2-Y)$ , is given by

$$\Delta D \begin{bmatrix} R_1-Y \\ R_2-Y \end{bmatrix} = \Delta \pi \begin{bmatrix} R_1Y \\ R_2Y \end{bmatrix} - \Delta \pi \begin{bmatrix} R_1 \\ R_2 \end{bmatrix} \quad (6)$$

where the terms in  $\Delta$  signify differences.

Eqn. (6) might reasonably be applied to the hydrocarbons ( $Y = H$ ), but it is questionable that it should hold where the atom or group Y is highly electronegative (e.g. when  $Y = Cl, Br, -OH$ , etc.). When the bond  $R-Y$  is polar, there is a part of the energy,  $D(R-Y)$ , to which Pauling<sup>58</sup> has referred as the “ionic resonance energy”. In an isolated  $A-B$  bond, this ionic resonance energy is taken as the difference between the actual (observed) dissociation energy  $D(A-B)$ , and a *mean* of the two dissociation energies  $D(A-A)$  and  $D(B-B)$ , and is generally larger, the more the two atoms A, B, differ from each other in the property broadly described by “electronegativity”. In like manner, we might expect a part of the dissociation energy  $D(R-Y)$  to be due to ionic resonance, and possibly to be larger, the greater the electronegativity difference between the radical R, and the group or atom Y. We might try to allow for this extra ionic resonance energy by adding a term to eqn. (5), thus,

$$D(R-Y) = D_0(R-Y) + \pi(RY) + \chi_i(RY) - \pi(R), \quad (7)$$

in which  $\chi_i(RY)$  is the ionic resonance energy term.

With this addition to eqn. (5), eqn. (6) correspondingly becomes

$$\Delta D \begin{bmatrix} R_1-Y \\ R_2-Y \end{bmatrix} = \Delta \pi \begin{bmatrix} R_1Y \\ R_2Y \end{bmatrix} + \Delta \chi_i \begin{bmatrix} R_1Y \\ R_2Y \end{bmatrix} - \Delta \pi \begin{bmatrix} R_1 \\ R_2 \end{bmatrix} \quad (8)$$

which is identical with the equation derived by Baughan, Evans and Polanyi, except for the inclusion of the term in  $\Delta \chi_i \begin{bmatrix} R_1Y \\ R_2Y \end{bmatrix}$ .

<sup>55</sup> Baughan, Evans and Polanyi, *Trans. Faraday Soc.*, 1941, **37**, 377.

<sup>56</sup> Wheland, *J. Chem. Physics*, 1934, **2**, 474.

<sup>57</sup> Coulson, *Quart. Rev.*, 1947, 144.

<sup>58</sup> Pauling, *Nature of the Chemical Bond* (Cornell Univ. Press, 1939), p. 48.

\* For an account of the meaning of the terms “delocalisation energy,  $\pi$ - and  $\sigma$ -hyperconjugation,” see Coulson.<sup>57</sup>

It is recognised from general chemical experience that different organic radicals  $R_1, R_2, \dots$ , differ from one another in their electronegativity and polarisability properties.<sup>59</sup> By analogy with simple diatomic systems  $A-B$ , one might anticipate that the ionic resonance energy terms in  $R_1Y$  and  $R_2Y$  are not necessarily identical, particularly so when the two radicals are widely separated in electronegativity.

Eqn. (8) should not, however, be interpreted too literally. The subdivision of the energy of the  $R-Y$  bond into independent and separate parts is largely artificial, for the terms in  $\chi(RY)$  and  $\chi_i(RY)$  are both functions of the electronegativity of  $Y$ , and in this sense are mutually bound up with each other.

### 3. Resonance Energies in Free Radicals

The term  $\chi(R)$  in eqn. (7) should measure the *total* delocalisation energy in the free radical  $R$ . In the most *general* case,  $\chi(R)$  might be regarded as composed of three parts,

$$\chi(R) \approx \chi_\pi(R) + h_\pi(R) + h_\sigma(R), \quad (9)$$

where  $\chi_\pi(R)$  is the  $\pi$ -electron conjugation energy (or the "1st-order conjugation energy," in the terminology of Mulliken<sup>60</sup>),

$h_\pi(R)$  is the  $\pi$ -hyperconjugation energy,

$h_\sigma(R)$  is the  $\sigma$ -hyperconjugation energy.

In many cases, one or more of the terms in (9) will be relatively unimportant compared with the others.

In the important example of the alkyl radicals, where the term in  $\chi_\pi(R)$  is zero, approximate calculations of the  $\pi$ -hyperconjugation energy terms  $h_\pi(R)$  have been reported by Baughan, Evans and Polanyi, who obtained the values quoted below—

R = Me	Et	Pr	sec.-Pr	tert.-Bu
$h_\pi = 0$	7.0	8.6	14.1	21.2 kcal.

Details of these calculations were not given by the authors, so that one is unaware of the assumptions made in deriving the figures. There is little reason, however, to doubt that the general trend,

$$(h_\pi(\text{tert.-Bu}) > h_\pi(\text{sec.-Pr}) > h_\pi(\text{Pr})),$$

is a sound conclusion, although the absolute values quoted are less certain.

The important paper on hyperconjugation by Mulliken, Rieke and Brown,<sup>60</sup> gives a description of an application of the method of molecular orbitals to the calculation of  $\pi$ -hyperconjugation energies in hydrocarbon molecules. We have considered it of interest to apply Mulliken's method to the calculation of these same quantities in hydrocarbon *radicals*. The complete evaluation of  $\chi(R)$ , as given by eqn. (9), is hardly practicable at the present time, unless certain simplifying assumptions are made.

### 4. Standard Bond-energy Terms.

The empirical estimation of resonance energies in hydrocarbons depends initially upon a choice of a set of standard bond-energy terms,  $E(C-C)$ ,  $E(C=C)$ ,  $E(C-H)$ , etc. One then compares the observed total energy of formation with the calculated energy obtained by summing the  $E$  values over all the bonds in the molecule. This procedure in its simplest form makes no attempt to discriminate between  $C-H$  or  $C-C$

<sup>59</sup> Kharasch and Grafflin, *J. Amer. Chem. Soc.*, 1925, **47**, 1948.

<sup>60</sup> Mulliken, Rieke and Brown, *ibid.*, 1941, **63**, 41.



bonds which differ in respect of their hybridisation characteristics (e.g.  $sp^3$ ,  $sp^2$ , or  $sp$  bonding), or to distinguish between bonds differing in their immediate environment (e.g. primary, secondary and tertiary C—H bonds). Yet it is well known, for example, that the bond lengths and force constants of C—H bonds in  $CH_4$ ,  $C_2H_4$  and  $C_2H_2$  show distinct differences from one another and that the force constants of primary, secondary and tertiary C—H bonds are not identical. The set of C—H and C—C bond energies described below attempts in a general way to make allowance for these factors.

(a) **Tetrahedral,  $sp^3$ -bonds.**—The C—C bond in diamond is usually regarded as a standard C—C bond: but, as both Mulliken and Coulson have pointed out, the diamond bonds are appreciably strengthened by hyperconjugation effects, and the *standard* bond should be taken as a weaker and longer bond than occurs in diamond itself. We shall therefore write

$$E(C-C)sp^3-sp^3 = L/2 - \alpha \quad . \quad . \quad . \quad (10)$$

where  $L$  is the latent heat of sublimation of carbon, and  $\alpha$  is the unknown strengthening per C—C bond in diamond, due to hyperconjugation.

The term  $E(C-H)sp^3$  for the standard primary tetrahedral C—H bond, is obtainable from the heat of formation of gaseous ethane. The heat of formation *from atoms* ( $Q_a$ ) is  $(2L + 332.2)$  kcal. (we are expressing all the bond-energy terms for use at room temperature): if the *net* delocalisation energy,  $\kappa(C_2H_6)$ , in ethane, is taken into account, we may set up the identity,

$$Q_a(C_2H_6) = 2L + 332.2 = E(C-C)sp^3-sp^3 + 6E(C-H)sp^3 + \kappa(C_2H_6). \quad (11)$$

Combining eqn. (10) and (11), one obtains

$$E(C-H)sp^3 = L/4 + 55.37 + \alpha/6 - \kappa(C_2H_6)/6, \quad . \quad . \quad . \quad (12)$$

which may be written in shorter form, by introducing a quantity,

$$\gamma = (\alpha - \kappa(C_2H_6)), \quad . \quad . \quad . \quad (13)$$

as

$$E(C-H)sp^3 = L/4 + 55.37 + \gamma/6. \quad . \quad . \quad . \quad (14)$$

Mulliken, Rieke and Brown adopt the view that the  $E(C-H)$  term values are slightly less for secondary and tertiary C—H bonds than for primary C—H bonds. The reason for this seems far from clear, although it may be that it allows for repulsive forces between non-bonded atoms, and/or for deviations from pure  $sp^3$ -bonding. We shall similarly write  $E(C-H)$  for secondary and tertiary C—H bonds as less than  $E(C-H)sp^3$  by amounts  $\lambda_1$  and  $\lambda_2$  respectively, without specifying the magnitudes of these constants.

(b) **Trigonal,  $sp^2$ -bonds.**—From the experimental value

$$D(CH_3-H) = 102 \text{ kcal.},$$

and the heat of formation of  $CH_4$ , it follows that

$$Q_a(CH_3) = (L + 123.9 \text{ kcal.}).$$

There are grounds for the belief that the bonds in the methyl radical are trigonal in character (Penney,<sup>61</sup> Voge,<sup>62</sup>) so that the C—H bonds in  $CH_3$  might be regarded as standard trigonal bonds, strengthened somewhat by  $\sigma$ -hyperconjugation. Writing the net delocalisation energy in  $CH_3$  as  $\kappa(CH_3)$ , it follows that

$$E(C-H)sp^2 = L/3 + 41.3 - \kappa(CH_3)/3. \quad . \quad . \quad . \quad (15)$$

The term  $E(C=C)$  may be obtained by combining eqn. (15) with  $Q_a(C_2H_4)$ . The equation is

$$Q_a(C_2H_4) = 2L + 195.5 \text{ kcal.} = 4E(C-H)sp^2 + E(C=C) + \kappa(C_2H_4) \quad (16)$$

leading to

$$E(C=C) = 2L/3 + 30.3 + 4/3\kappa(CH_3) - \kappa(C_2H_4). \quad . \quad . \quad . \quad (17)$$

<sup>61</sup> Penney, *Trans. Faraday Soc.*, 1935, **31**, 734.

<sup>62</sup> Voge, *J. Chem. Physics*, 1936, **4**, 581.

If it is permissible to assume that the *difference* (if any) between  $E(\text{C—H})sp^3$  and  $E(\text{C—H})sp^2$  is matched by a like difference between  $E(\text{C—C})sp^2-sp^3$  and  $E(\text{C—C})sp^2-sp^2$ , and also between  $E(\text{C—C})sp^2-sp^3$  and  $E(\text{C—C})sp^2-sp^2$ , expressions for these latter quantities can then be written down. These are given later.

(c) **Digonal, *sp*-bonds.**—If it is assumed (as Mulliken does) that the bonds in acetylene are standard digonal bonds, one then has

$$E(\text{C}\equiv\text{C}) + 2E(\text{C—H})sp = Q_a(\text{C}_2\text{H}_2) = 2L + 49.8 \text{ kcal.} \quad (18)$$

Although eqn. (18) is not sufficient to enable us to write down explicit expressions for  $E(\text{C}\equiv\text{C})$  and  $E(\text{C—H})sp$ , it is only necessary to add the assumption that the difference between  $E(\text{C—H})sp$  and  $E(\text{C—H})sp^3$  is matched by a similar difference between

$$E(\text{C—C})sp-sp^3 \text{ and } E(\text{C—C})sp^3-sp^3,$$

in order to write down the resonance energies in the alkyl-substituted acetylenes.

From the heat of formation of allene, one may obtain

$$E(\text{C}\equiv\text{C}), \text{ allene,} = 5L/6 - 2\alpha(\text{CH}_3)/3 - \frac{1}{2}\alpha(\text{C}_2\text{H}_4) - 1.6 \text{ kcal.} \quad (19)$$

The allene  $\text{C}\equiv\text{C}$  bond is not necessarily the same as the ethylene  $\text{C}=\text{C}$ , in view of the digonal hybridisation of the central C atom in allene.

Summarising these various bond-energy terms, we have the expressions given in Table III.

TABLE III

## STANDARD BOND-ENERGY TERM VALUES

$$\begin{cases} \text{(i)} & E(\text{C—H})sp^3 = L/4 + 55.37 + \gamma/6 \\ \text{(ii)} & E(\text{C—H})sp^2 = L/3 + 41.3 - \alpha(\text{CH}_3)/3 \\ \text{(iii)} & E(\text{C—C})sp^2-sp^3 = L/2 - \alpha \\ \text{(iv)} & E(\text{C—C})sp^3-sp^2 = 7L/12 - 14.07 - 7\alpha/6 - \alpha(\text{CH}_3)/3 + \alpha(\text{C}_2\text{H}_4)/6 \\ \text{(v)} & E(\text{C—C})sp^2-sp^2 = 2L/3 - 28.14 - 4\alpha/3 - 2\alpha(\text{CH}_3)/3 + \alpha(\text{C}_2\text{H}_4)/3 \\ \text{(vi)} & E(\text{C}\equiv\text{C}) = 2L/3 + 30.3 + 4\alpha(\text{CH}_3)/3 - \alpha(\text{C}_2\text{H}_4) \\ \text{(vii)} & E(\text{C}\equiv\text{C}), \text{ allene} = 5L/6 - 2\alpha(\text{CH}_3)/3 - \frac{1}{2}\alpha(\text{C}_2\text{H}_4) - 1.6. \end{cases}$$

## 5. Empirical Resonance Energies

Given the set of bond-energy term values listed in the previous section, it is a simple matter to derive empirical *net* resonance energies in saturated and unsaturated hydrocarbons from their heats of formation, values for which are now quite accurately known in many cases. For instance, the net resonance energy in benzene is derived from

$$\alpha(\text{C}_6\text{H}_6) = Q_a(\text{C}_6\text{H}_6) - \sum E(\text{bonds})$$

or,

$$\alpha(\text{C}_6\text{H}_6) = Q_a(\text{C}_6\text{H}_6) - \{6E(\text{C—H})sp^3 + 3E(\text{C}\equiv\text{C}) + 3E(\text{C—C})sp^2-sp^3\}$$

at

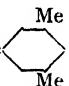



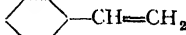
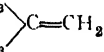
$$\alpha(\text{C}_6\text{H}_6) = 37.9 + 4\gamma + 3\alpha(\text{C}_2\text{H}_4) + 3\alpha(\text{C}_2\text{H}_6). \quad (20)$$

$\alpha(\text{C}_6\text{H}_6)$  includes the hyperconjugation energy in benzene, in addition to the  $\pi$ -electron or 1st-order conjugation energy of the six  $\pi$ -electrons of the ring. It is useful to define a quantity  $\alpha'(\text{C}_6\text{H}_6)$ , obtained from  $\alpha(\text{C}_6\text{H}_6)$  by subtracting  $3\alpha(\text{C}_2\text{H}_4) + 3\alpha(\text{C}_2\text{H}_6)$ . In general, for any hydrocarbon containing  $n$  formal  $\text{C—C}$  bonds, and  $m$  formal  $\text{C}\equiv\text{C}$  bonds, the quantities  $\alpha'$  are related to the quantities  $\alpha$  by the equation

$$\alpha'(\text{RH}) = \alpha(\text{RH}) - n\alpha(\text{C}_2\text{H}_6) - m\alpha(\text{C}_2\text{H}_4) \quad (21)$$

In Table IV, a list of  $\alpha'$  values is given for a number of hydrocarbons and hydrocarbon free radicals. They are all based on *experimental* heats of formation, and might conveniently be referred to as the *empirical* resonance energies ( $\alpha'$  values).

TABLE IV  
 EMPIRICAL RESONANCE-ENERGIES ( $\alpha'$ ) IN HYDROCARBONS

Molecule	$\alpha'$ (kcal.)
$C_2H_6$	$37.9 + 4\gamma$
$C_6H_5 \cdot CH_3$	$39.0 + 4\frac{1}{2}\gamma$
<i>p</i> -Xylene	$40.0 + 5\frac{1}{2}\gamma$
1 : 3 : 5-Me 	$41.3 + 6\gamma$
	$79.0 + 8\gamma$
	$102.7 + 12\gamma$
	$81.0 + 9\frac{1}{2}\gamma$
 $-CH=CH_2$	$41.9 + 5\frac{1}{2}\gamma$
$CH_3-CH=CH_2$	$0.9 + \frac{2}{3}\gamma$
$CH_3-CH=CH-CH_3$ ( <i>trans</i> -)	$1.42 + \frac{2}{3}\gamma$
$CH_3$ 	$2.35 + \frac{2}{3}\gamma$
$C_2H_5-CH=CH_2$	$(2\lambda_1 - 1.3) + \frac{2}{3}\gamma$
$CH_2=CH-CH=CH_2$	$5.0 + \frac{2}{3}\gamma$
$CH_2=CH-CH_2-CH_2=CH_2$	$(4\lambda_1 - 2.5) + \frac{2}{3}\gamma$
$CH_3-C \equiv CH$	$3.13 + \frac{2}{3}\gamma$
$CH_3-C \equiv C-CH_3$	$5.5 + \frac{2}{3}\gamma$
$C_2H_6$	0
<i>n</i> -Propane	$(2\lambda_1 - 2.14) + \frac{2}{3}\gamma$
<i>n</i> -Butane	$(4\lambda_1 - 3.88) + \frac{2}{3}\gamma$
<i>n</i> -Pentane	$(6\lambda_1 - 5.4) + 2\gamma$
$Me_3CH$	$(\lambda_2 - 2.2) + \frac{2}{3}\gamma$
$Me_4C$	$-0.7 + 2\gamma$
Cyclohexane	$(12\lambda_1 - 11.0) + 4\gamma$
1:3-Cyclohexadiene	$(4\lambda_1 - 1.0) + 4\gamma$
<i>n</i> -Octane	$(12\lambda_1 - 10.6) + 4\gamma$
Ethyl	$[CH_3] + \frac{2}{3}\gamma$
Propyl	$[CH_3] + \frac{2}{3}\gamma + (2\lambda_1 - 0.1)$
<i>sec</i> -Pr	$[CH_3] + \frac{2}{3}\gamma + 4.6$
<i>tert</i> -Bu	$[CH_3] + 2\gamma + 8.7$
Benzyl	$[CH_3] + 5\frac{1}{2}\gamma + 59.1$
Allyl	$[CH_3] + \frac{2}{3}\gamma + 20.4$
2-Me allyl	$[CH_3] + 2\gamma + 23.9$

The reference structures with respect to which the  $\alpha'$  values are measured are in most cases unambiguous (e.g. benzene); the less obvious cases include the alkyl radicals, and the allene molecule. For these, the reference structures were taken as follows:

Allene: 4 CH,  $sp^3$  bonds: 2 C=C (allene) bonds.

Ethyl: 3 CH,  $sp^3$  primary bonds: 2 CH,  $sp^3$  bonds: C—C,  $sp^3-sp^3$ .

*sec*-Pr: 6 CH,  $sp^3$  primary bonds: CH,  $sp^3$ : 2 C—C,  $sp^3-sp^3$ .

*tert*-Bu: 9 CH,  $sp^3$  primary bonds: 3 C—C,  $sp^3-sp^3$ .

Where comparison is possible, a close agreement may be noted between the  $\alpha'$  values of Table IV and the "resonance energies" of Pauling—

if we were to assume  $\gamma = 0$ . But there seems no way of deciding from the empirical data alone on the probable value of  $\gamma$ : and, to proceed further, one is forced to make a number of *ad hoc* assumptions. Mulliken, Rieke and Brown have already pointed out that there may be more than one particular set of initial assumptions leading to a self-consistent scheme. In this respect, the scheme as set out here can make no claim to be either more "correct" or less arbitrary than others used previously.

## 6. Calculated Resonance Energies

The method of Mulliken, Rieke and Brown enables calculations to be made of the quantities  $\kappa_{\pi}(\text{RH})$  and  $h_{\pi}(\text{RH})$  in terms of the resonance integrals  $\beta_{\text{CC}}$  (regarded as a variable with distance,  $r(\text{C}-\text{C})$ ), and  $\beta_{\text{CH}}$  (assumed to be a constant). The absolute values of  $\beta_{\text{CC}}$  and  $\beta_{\text{CH}}$  are chosen to give a good fit between calculated and empirical resonance energies in a number of selected reference molecules. e.g. benzene and butadiene.

It is to be noted from Table IV and eqn. (21) that the total net resonance energy,  $\kappa(\text{RH})$  in a hydrocarbon includes terms in  $\kappa(\text{C}_2\text{H}_4)$  and  $\kappa(\text{C}_2\text{H}_2)$ . Neither of these latter can be given a definite experimental value, and it is necessary to allot arbitrarily chosen numerical values to one, or both, of these two quantities.

There are some other difficulties that we may briefly mention. From the expression for  $E(\text{C}-\text{H})sp^3$  and the heat of formation of  $\text{CH}_4$ , one obtains

$$\kappa(\text{CH}_4) = 4.4 - 2/3\gamma \text{ (kcal.)}, \quad . \quad . \quad . \quad (22)$$

so that, unless  $\gamma$  is given the seemingly impossibly large value of 6.6 kcal.,  $\kappa(\text{CH}_4)$  is not zero. In our view,  $\gamma$  is probably a small positive quantity, and  $\kappa(\text{CH}_4)$  is then of the order 3 or 4 kcal. Coulson<sup>57</sup> has elsewhere remarked that  $h_{\pi}(\text{CH}_4)$  is necessarily zero, so that the positive value of  $\kappa(\text{CH}_4)$  is presumably to be attributed to a positive value of  $h_{\sigma}(\text{CH}_4)$ .

TABLE V.— $\beta_{\text{CC}}$  VALUES AT DIFFERENT C—C INTERNUCLEAR DISTANCES

$r(\text{C}-\text{C})$	$C_s$	$C_d$	$\beta_{\text{CC}}$	$-dC_s/dr$	$-d\beta/dr$
1.555	0	14.67	24.8	0	66.1
1.53	0.21	11.49	26.5	17.1	69.5
1.49	1.50	7.01	29.4	48.5	74.8
1.45	4.16	3.44	32.5	85.4	80.6
1.41	8.43	1.03	35.85	128.9	86.4
1.38	12.82	0.12	38.5	166.0	90.8
1.34	20.59	0.35	42.3	222.9	97.0
1.30	30.77	2.55	46.3	288.7	103.0
1.26	43.78	7.10	50.5	365.1	109.1
1.22	60.1	14.45	55.0	453.0	115.0
1.20	69.7	19.3	57.3	502.0	117.8

In the  $-\text{CH}_3$  radical (as in  $\text{CH}_4$ ), the term in  $h_{\pi}$  is again zero, but it does not follow that  $\kappa(\text{CH}_3)$  can be given a zero value. It seems probable to us that the terms  $h_{\sigma}(\text{CH}_3)$  and  $h_{\sigma}(\text{CH}_2)$  are similar in magnitude, and in this paper we have presumed a value of 3 kcal. for  $\kappa(\text{CH}_3)$ . But we readily admit the arbitrary and rather unsatisfactory character of this choice.

In case of ethane (and higher hydrocarbons) where the terms in  $h_{\pi}(\text{RH})$  are not zero, Mulliken *et al.* assume an identity between  $\kappa(\text{RH})$  and  $h_{\pi}(\text{RH})$ . How far it is justifiable to do this is open to question, although it is perhaps the best one can do at present. The same assumption has been made in the calculations given here.

We have used different values for the resonance integrals  $\beta_{\text{CC}}$  and  $\beta_{\text{CH}}$  from those used previously:  $\beta_{\text{CH}}$  was taken as a constant, equal to 125 kcal.;  $\beta_{\text{CC}}$  assumed to be a parameter varying with the C—C distance, had the values listed in Table V.

## 350 DISSOCIATION ENERGIES OF CARBON BONDS

The  $\beta_{00}$  values were obtained by the method of Lennard-Jones<sup>63</sup> from the equation,

$$2\beta_{00}(r) = \Delta + C_c(r) - C_d(r), \quad (23)$$

where  $\Delta$  measures the energy difference between

$$E(\text{C}=\text{C}) \text{ and } E(\text{C}-\text{C})sp^2-sp^2,$$

and  $C_c(r)$ ,  $C_d(r)$  are the energies of compression and/or extension of the standard C—C and C=C bonds from their equilibrium length to length  $r$ . The value of  $\Delta$ , as given by our equations for these standard bond energies, is

$$\Delta = 58.45 + 2\chi(\text{CH}_3) + 4/3\gamma + \chi(\text{C}_2\text{H}_6) - \chi(\text{C}_2\text{H}_4). \quad (24)$$

Perhaps the simplest assumption to make in respect of (24) is that the terms in  $(\text{CH}_3)$ ,  $\gamma$ ,  $\chi(\text{C}_2\text{H}_4)$  and  $\chi(\text{C}_2\text{H}_6)$  mutually cancel, leaving  $\Delta \sim 58$

TABLE VI. — 3RD-ORDER CONJUGATION ENERGIES:  $\delta_r$ -VALUES

$r(\text{C}-\text{C})$ in Å	$\delta_r$ in kcal.
1.55	2.50
1.53	2.76
1.49	3.40
1.45	4.20
1.41	5.10
1.39	5.60
1.38	5.90
1.34	7.08

kcal. This compares with the recommended value of Baughan and Polanyi for the energy of the "second-half" of the C=C double-bond. But it is clear that eqn. (24) allows a wide choice in the value of  $\Delta$ , according to the values one may choose for the unknowns in the equation. The calculations given here are based upon an assumed  $\Delta = 64.5$  kcal., to comply with our preferred values for the terms  $\gamma$ ,  $\chi(\text{C}_2\text{H}_6)$  and  $\chi(\text{C}_2\text{H}_4)$  employed later. There is no special reason, at present, to prefer a value for  $\Delta$  as high as we have taken: except that it does seem to be necessary to use a value of  $\Delta$  of the order 62-65 kcal. if the quantity  $\chi(\text{CH}_3)$  is as much as 3 kcal.

The compression energies,  $C_c(r)$  and  $C_d(r)$  were calculated from Morse functions,  $C = D\{e^{-a(r-r_e)} - 1\}^2$ , in which the exponent  $a$  was obtained from the relationship  $a = \sqrt{k_e/2D}$  where  $k_e$  is the bond force-constant. The assumed values of  $k_e$  were:

$$k_e(\text{C}-\text{C}), sp^2-sp^2 = 4.5 \text{ dynes/cm.}; k_e(\text{C}=\text{C}) = 7.8 \text{ dynes/cm.}$$

obtained from a smooth plot of  $k_e$  against  $r_e(\text{C}-\text{C})$  for various C—C bonds, using data of Crawford and Brinkley<sup>64</sup> Bonner,<sup>65</sup> and Herzberg.<sup>66</sup> Values of  $C_c(r)$  and  $C_d(r)$  in the region  $r(\text{C}-\text{C}) = 1.30 - 1.55$  Å are given in Table V. It should be noted that the equilibrium bond-lengths of C—C and C=C assumed here refer to the lengths of the *standard* bonds, and are not necessarily identical with the observed bond lengths in ethane and ethylene.

The quantities denoted by  $\delta_r$  in Mulliken's paper (3rd-order conjugation energies), measuring the hyperconjugation energy from the interaction of quasi- $\pi$  electrons in adjacent C—H bonds, and given by

$$\delta_r = 2\{\sqrt{\beta_{00}^2(r) + 4\beta_{\text{CH}}^2} - 2\beta_{\text{CH}}\} \quad (25)$$

are recalculated with the  $\beta_{00}$  and  $\beta_{\text{CH}}$  values preferred here in Table VI.

The calculated conjugation energies in some selected hydrocarbons are summarised in Table VII. The inter-relation between the various computed quantities,  $R$ ,  $R_v$ , and  $C$ , which here have the same meaning as these same symbols in reference<sup>60</sup>, is simply:

$$\chi(\text{RH}) = R_v + R - C. \quad (26)$$

<sup>63</sup> Lennard-Jones, *Proc. Roy. Soc. A*, 1937, **158**, 280.

<sup>64</sup> Crawford and Brinkley, *J. Chem. Physics*, 1941, **9**, 69.

<sup>65</sup> Bonner, *J. Amer. Chem. Soc.*, 1936, **58**, 34.

<sup>66</sup> Herzberg, *Infra-red and Raman Spectra* (van Nostrand, New York, 1945).

The terms in  $C$  (measuring the skeleton compression energies), were read off for each C—C bond from the curves of  $C_s(r)$  and  $C_d(r)$  (but see later for some modifications to this procedure).

TABLE VII

## CONJUGATION ENERGIES AND BOND LENGTHS IN HYDROCARBONS

Molecule	C—C Bond Distances (Å)		Conjugation Energies (kcal.)					
	Calc.	Obs.	Computed					Empirical $\pi'(\gamma = 0.6)$
			$R_z$	$R_y$	$C$	$\pi$	$\pi'$	
$C_2H_2$	1.55	1.55 ± 0.03	2.50	2.50	0.4	4.6	0	0
$C_2H_4$	1.33 <sup>†</sup>	1.34 ± 0.01	0	7.20	0.4	6.8	0	0
$C_2H_6$	1.18 <sup>‡</sup>	1.205	—	—	—	—	0	0
$C_6H_6$	1.39 <sup>‡</sup>	1.39 ± 0.02	73.8	32.5	31.8	74.5	40.3	40.3
Butadiene	(1) 1.34 <sup>‡</sup> (2) 1.45 <sup>‡</sup>	(1) 1.35 ± 0.02 (2) 1.46 ± 0.03	11.8	17.7	3.7	25.8	7.6	5.8
Propylene	(1) 1.34 (2) 1.52	(1) 1.34 (2) 1.54	4.44	10.02	1.26	13.2	1.8	1.3
<i>trans</i> -CH <sub>3</sub> —CH=CH—CH <sub>3</sub>	(1) 1.35 (2) 1.52	(1) 1.34 (2) 1.53 ± 0.02	8.86	12.6	1.9	19.6	3.6	2.2
Isobutene	(1) 1.35 (2) 1.52	(1) 1.34 (2) 1.54 ± 0.02	8.08	12.6	1.9	19.7	3.7	3.15
Allene	1.32 <sup>‡</sup>	1.330	11.2	11.2	0.6	21.9	8.3	?
CH <sub>3</sub> —C≡CH	(1) 1.19 (2) 1.46 <sup>‡</sup>	(1) 1.205 (2) 1.47	5.4	5.4	2.6	8.2	3.6	3.53
CH <sub>3</sub> —C≡C—CH <sub>3</sub>	(1) 1.19 (2) 1.46 <sup>‡</sup>	(1) 1.20 (2) 1.47 ± 0.02	10.8	10.8	5.2	16.4	7.2	6.3
Diacetylene	(1) 1.19 <sup>‡</sup> (2) 1.38 <sup>‡</sup>	(1) 1.19 ± 0.02 (2) 1.36 ± 0.03	12.3	12.3	6.9	17.7	13.1	*13 ± 10

\* An estimate by Mulliken, Rieke and Brown.<sup>64</sup>

The computed conjugation energies are rather sensitive to the assumed C—C bond lengths, the experimental values for which are in most cases uncertain to  $\pm 0.02$  Å. Accordingly, to give greater internal consistency, we have used *calculated* bond-lengths in the computations of the conjugation energies. The bond-length calculations were made by the method described by Lennard-Jones:<sup>65</sup> these calculations required values for the differentials  $d\beta_{CO}/dr$  and  $dC_s/dr$ , which were obtained from the Morse curves previously mentioned. Our method of calculation included the by no means insignificant effects of  $\pi$ -hyperconjugation on the C—C bond-lengths.<sup>†</sup> It was assumed that the C—H bonds remain of constant length: this is in accord with the conclusions reached by Mulliken *et al.* on this point.

Coulson<sup>67</sup> has pointed out that the "atomic radius" of carbon is probably variable with the state of hybridisation of the C atom, so that the equilibrium bond lengths of the standard bonds should differ in the direction:

$$r_s(C-C)sp^3-sp^3 > r_s(C-C)sp^2-sp^2 > r_s(C-C)sp-sp.$$

<sup>67</sup> Coulson, *V. Henri Memorial Vol.*, Liege (1948).

<sup>†</sup> Thus, e.g., the C=C bond-length in ethylene is shorter than the length of the standard C=C bond. The ethylene bond-length is calculated from the equations,

$$\frac{\partial F}{\partial r} = 0 = 2 \frac{d\beta_{CO}}{dr} + \frac{d\delta_r}{dr} - \frac{dC_s}{dr},$$

where

$$\frac{d\delta_r}{dr} = 2\beta_{CO} \frac{d\beta}{dr} / \sqrt{\beta_{CO}^2 + 4\beta_{CH}^2}.$$

The point is of importance in our calculations of conjugation energies and bond lengths, insofar as both  $C_s(r)$  and  $dC_s/dr$  at a given internuclear separation will differ for two different bond-types, e.g. C—C,  $sp^3-sp^3$  and C—C,  $sp-sp$ . Strictly, one should construct a family of Morse curves for each type of C—C bond. This we have not done, but have made allowance for the radii changes by an appropriate shift in the zero from which  $C_s(r)$  and  $dC_s/dr$  are measured, corresponding to the following assumed standard bond-lengths:

$$\begin{array}{ll} r_s(\text{C—C})sp^3-sp^3 = 1.585 \text{ \AA} & r_s(\text{C—C})sp^3-sp^2 = 1.570 \text{ \AA} \\ r_s(\text{C—C})sp^2-sp^2 = 1.555 \text{ \AA} & r_s(\text{C—C})sp^2-sp = 1.55 \text{ \AA} \\ r_s(\text{C—C})sp-sp = 1.510 \text{ \AA} & \end{array}$$

On the other hand,  $\beta_{CC}$  and  $d\beta_{CC}/dr$  have been assumed to be independent of the state of hybridisation of the C atoms bonded together, and to be functions of  $r(\text{C—C})$  only.

The agreement between observed and calculated\* bond lengths in Table VII is quite good. In the single case where the calculated bond-length is certainly in error by as much as 0.02 Å (i.e. in the acetylene molecule) there are special reasons why this lack of agreement might occur: this is adequately discussed elsewhere by Robertson and Dunitz.<sup>68</sup> Indeed, there is a close agreement between our calculated value (1.183 Å) and the value (1.185 Å) for the pure triple bond recommended by the above-mentioned authors.

The comparison between calculated and empirical  $\pi'(\text{RH})$  values in Table VII is based upon the following assumed values:

$$\begin{array}{l} \pi(\text{C}_2\text{H}_2) = 4.6 \text{ kcal.} : \pi(\text{C}_2\text{H}_4) = 6.8 \text{ kcal.} : \\ \alpha = 5.2 \text{ kcal.} : \gamma = 0.6 \text{ kcal.} : \pi(\text{CH}_3) = 3.0 \text{ kcal.} \end{array}$$

Here, the agreement is by no means exact, although generally within  $\pm 2$  kcal. Compared with the agreement obtained by Mulliken, Rieke and Brown, our  $\beta_{CC}$  and  $\beta_{CH}$  values are less successful. On the other hand the scheme set out here might claim to have attempted a greater degree of internal consistency. The removal of the constraint imposed on the  $\beta_{CC}$  values by eqn. (23), or the replacement of the  $C_s(r)$  and  $C_d(r)$  Morse functions by other well-chosen functions could, perhaps, yield a "better" set of  $\beta$  values than those we have used. Whether such adjustments are worth seeking seems doubtful, for the assumption of orthogonality implicit in this sort of treatment is perhaps the greatest weakness in the method. Recent work by Mulliken and co-workers<sup>69</sup> is highly significant in this latter respect, although on the other hand, Wheland<sup>70</sup> has concluded that the orthogonality assumption is not a serious weakness where hydrocarbons are being discussed.

Table VIII summarises the results of calculations of the bond length and conjugation energies in a number of hydrocarbon free-radicals. The calculations follow the Mulliken method, and the same  $\beta_{CC}$  and  $\beta_{CH}$  values were assumed as in the calculations on the RH molecules. As examples of the method of calculation we may quote the case of the ethyl and sec.-propyl radicals.

(a) ETHYL RADICAL.— $R_z$  calculated as a 3-electron problem, involving the free electron on the  $-\dot{\text{C}}\text{H}_2$  group, and the  $[\pi]$  electrons of the quasi- $\pi[\chi]\text{C—H}$  bond in the  $-\text{CH}_2$  group:

$$\left\{ \begin{array}{l} R_z = 2(\sqrt{\beta_{CH}^2 + \beta_{CO}^2} - \beta_{CH}) \\ R_y = \delta_r. \end{array} \right\} \quad . \quad . \quad . \quad (27)$$

<sup>68</sup> Robertson and Dunitz, *J. Chem. Soc.*, 1947, 1145.

<sup>69</sup> Mulliken and Rieke, *J. Amer. Chem. Soc.*, 1941, 63, 1770; Roothan and Mulliken, *J. Chem. Physics*, 1948, 16, 118.

<sup>70</sup> Wheland, *J. Amer. Chem. Soc.*, 1941, 63, 2025.

\* Observed bond lengths are in the main electron diffraction values (see Wheland<sup>71</sup>). Calculated bond lengths given to the third place of decimals are more exactly determined than the others.

(b) *sec.-PROPYL RADICAL*.— $R_{\pi}$  calculated as a 5-electron problem, involving the free electron on the  $> \dot{\text{C}}\text{H}$ , and the  $[\pi]$  electrons of the quasi- $\pi[\pi]\text{C}-\text{H}$  bonds in the two  $-\text{CH}_3$  groups:

$$\begin{cases} R_{\pi} = 2\{\sqrt{\beta_{\text{CH}}^2 + 2\beta_{\text{CO}}^2} - \beta_{\text{CH}}\} \\ R_{\nu} = 2\delta_{\pi} \end{cases} \quad (28)$$

TABLE VIII  
CONJUGATION ENERGIES AND BOND-LENGTHS IN RADICALS


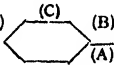
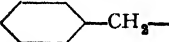
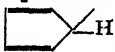
Radical	C—C Bond Lengths (Å)	Conjugation Energies (kcal.)					$Q_f(\text{R})$ Calc.	
		Calc.	Computed					
			$R_{\pi}$	$R_{\nu}$	$C$	$\pi$		$\pi'$
Ethyl . . . . .	1.49 <sup>6</sup>	6.66	3.30	1.95	8.0	3.4	—25.3	
sec.-Pr . . . . .	1.49 <sup>7</sup>	13.03	6.60	3.9	15.8	6.6	—15.8	
tert.-Bu . . . . .	1.49 <sup>8</sup>	19.30	9.9	5.8	23.4	9.6	—6.5	
Allyl . . . . .	1.39 <sup>9</sup>	31.0	11.2	11.4	30.8	19.4	—35.7	
2Me-allyl . . . . .	(1) 1.39 <sup>6</sup> (2) 1.52	35.0	14.0	11.8	37.2	21.2	—23.4	
$\text{CH}_2=\text{CH}-\dot{\text{C}}\text{H}-\text{CH}=\text{CH}_2$	(1) 1.37 <sup>1</sup> (2) 1.42 <sup>2</sup>	47.4	21.9	15.3	54.0	30.6	—44.6	
 . . . . .	1.413	66.0	25.2	26.5	64.8	37.4	—45.4	
Vinyl . . . . .	1.28 <sup>7</sup>	0	17.6	2.2	15.4	8.6	?	
Propargyl . . . . .	(1) 1.20 <sup>6</sup> (2) 1.38 <sup>5</sup>	23.1	7.9	9.3	21.7	17.1	—79.7	
Benzyl (D)  (B) (A)	(A) 1.39 (B) 1.41 (C) 1.38 (D) 1.39	102.8	38.8	44.8	96.8	58.0	—44.7	

TABLE IX.—CALCULATED  $D(\text{R}-\text{H})$  VALUES

R	$Q_f(\text{RH})$	$Q_f(\text{R})$ Calc.	$D(\text{R}-\text{H})$ kcal.	
			Calc.	Obs.
Et	20.2	—25.3	97.5	97.5
<i>sec.-Pr</i>	24.8	—15.8	92.6	90.8
<i>tert.-Bu</i>	31.5	—6.5	90.0	86.5
$-\text{CH}_2-\text{C}\equiv\text{CH}$	—44.3	—79.7	87.4	—
 $-\text{CH}_2-$	—11.9	—44.7	84.8	77.5
Allyl	—4.9	—35.7	82.8	78
2-Me-allyl	3.3	—23.4	78.7	76
$\text{CH}_2=\text{CH}-\dot{\text{C}}\text{H}-$	—25.6	—44.6	71.0	—
 $-\text{H}$	—32.4	—45.4	65.0	—

The calculated  $\pi'$  value for vinyl is insufficient to allow an estimation of  $D(\text{C}-\text{H})$  in ethylene: it would be necessary to know the absolute strengths of diagonal  $\text{C}-\text{H}$  and  $\text{C}-\text{C}$  bonds to do this. In case of the allene molecule, which yields the propargyl radical on removal of a H atom, we can obtain (from the calculated  $Q_f$  of the propargyl radical) the bond dissociation energy  $D(\text{H}_2\text{C}:\text{C}:\text{CH}-\text{H})$  as 85.2 kcal.



The calculated  $Q_r(R)$  values of Table VIII, taken in conjunction with eqn. (3), lead to the calculated bond dissociation energies  $D(R-H)$  listed in Table IX.

The comparison of calculated and observed  $D(R-H)$  values in Table IX shows that the general *trend* is correctly reproduced, although the absolute values do not compare as closely as one might wish. The most serious discrepancies occur with  $D(\text{benzyl}-H)$  and  $D(\text{tert.-Bu}-H)$ , and in the former, at least, the experimental value is now well established, so that here the calculated value is undoubtedly badly at fault. One could perhaps remove these discrepancies by a more suitable choice of  $\beta$  values. But, in case of the benzyl and allyl radicals, where the bond distances are closely similar to those found in the benzene molecule, we do not think it would be easy to fit the observed  $x'$  in *benzene*, and in the benzyl or allyl radicals, by a mere change in the assumed  $\beta_{CC}$  values alone. Although a closer agreement between observed and calculated  $D(C-H)$  values in toluene and propylene could be attained by an *upgrading* of  $\beta_{CC}$  values, this step would then destroy the good agreement between observed and calculated  $x'$  values for benzene.

The comparative failure of the scheme to include the benzyl and allyl radicals could be sought in many of the assumptions it has been necessary to make, among which two in particular ought to be mentioned.

(a) The assumption (also made by Mulliken *et al.*, and admitted to be rather questionable) that the hyperconjugation energy in the benzene molecule may be calculated from  $h_\pi = 6\delta_r$  ( $r = 1.398 \text{ \AA}$ ). This leads to a calculated value not very different from the sum,

$$3x(C_2H_6) + 3x(C_2H_4).$$

Similarly, in allyl and benzyl the calculated  $h_\pi$  terms (i.e. the  $R_\pi$  of Table VIII) almost exactly balance with the subtraction ( $x - x'$ ), so that

$$h_\pi \sim nx(C_2H_6) + mx(C_2H_4),$$

where  $n$ ,  $m$  are the number of C—C and C=C bonds in the reference structures. In such systems as these, where the  $\pi$ -electrons are almost completely delocalised, there is some doubt whether the hyperconjugation energies can be assessed by the methods we have used. In particular, an erroneous assessment of the hyperconjugation energy in the benzene molecule is serious, for it destroys the usefulness of this as a standard against which it is usual to calibrate  $\beta_{CC}$  values in the region  $r(C-C) \sim 1.4 \text{ \AA}$ .

(b) The assumption that it is *not* a source of error to neglect the non-zero values of the orthogonality integrals  $S$ . Wheland<sup>70</sup> has examined this assumption for hydrocarbons, and concluded it is a reasonable one to make. But, one might note that Wheland's calculations were not made from the starting-point of a dependence of  $\beta_{CC}$  on the distance

TABLE X

Molecule	$r(C-C)$	$S$	$R_\pi$ (calc.)
Benzene . . . .	1.398	0.245	1.078 $\beta_{CC}^*$
Allyl . . . . .	1.390	0.249	0.484 $\beta_{CC}^*$
$C_6H_5-$ . . . . .	1.413	0.24	1.091 $\beta_{CC}^*$

$r(C-C)$ . In Table X we give some results of calculations of  $R_\pi$  in the systems benzene, allyl, and cyclo pentadienyl, based on the bond lengths in these molecules given in Tables VII and VIII, and using the  $S$  values recommended by Mulliken and Roothan.<sup>69</sup> The quantities are listed in terms of the new resonance integrals,  $\beta_{CC}^*$ , appropriate to the case where orthogonality is included.

If we now equate  $R_\pi$  (benzene) in Table X, to the same quantity as given in Table VII, we obtain  $\beta_{CC}^*$  (benzene) = 68.5 kcal. Assuming a similar

variation in  $\beta_{\text{CO}}^*$  with  $r(\text{C}-\text{C})$  as is shown by  $\beta_{\text{CO}}$ , the values  $\beta_{\text{CO}}^*$  (allyl)  $\sim 69.5$ , and  $\beta_{\text{CO}}^*$  ( $\text{C}_3\text{H}_5$ )  $\sim 67$  kcal. are obtained. This set of values leads to:

	$R_{\text{C}}$ (Tables VII, VIII)	$R_{\text{C}}$ (Table X)
Benzene . . .	73.8	73.8
Allyl . . .	31.0	33.6
$\text{C}_3\text{H}_5$ — . . .	66.0	73.0

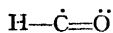
In case of allyl, the inclusion of orthogonality does not make a marked difference to the calculated  $R_{\text{C}}$ , although it is interesting that the difference is in the direction required to bring a closer agreement between the observed and calculated bond dissociation energy in propylene. The  $R_{\text{C}}$  value for  $\text{C}_3\text{H}_5$ — is more seriously altered by the inclusion of orthogonality, (unless the rate of change of  $\beta_{\text{CO}}^*$  with distance is much sharper than the corresponding rate of change in  $\beta_{\text{CO}}$ ), but until the experimental value of the bond-dissociation energy in cyclo pentadiene is known, we cannot say which treatment gives the better agreement. However, calculations of this sort are not strictly fair, for we should also examine the effects of including the orthogonality integrals on the calculated bond lengths.

In concluding this section we might claim that the *main* features shown by existing experimental knowledge of different  $D(\text{C}-\text{H})$  values are explicable in terms of the scheme we have used. But refinements to the scheme are clearly desirable, and it may be that one would see more certainly the direction in which refinements are to be made when more numerous and accurate experimental data on  $D(\text{C}-\text{H})$  values are available.

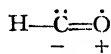
## 7. The Radicals $-\text{CHO}$ and $\text{CH}_3\text{CO}-$

The low values of  $D(\text{H}-\text{CHO})$  and  $D(\text{CH}_3\text{CO}-\text{H})$  relative to  $D(\text{CH}_3-\text{H})$  and  $D(\text{CH}_3\text{CH}_2-\text{H})$  are suggestive of a large radical resonance energy in the formyl and acetyl radicals. Mulliken, Rieke and Brown, commenting on molecules containing the  $\text{C}=\text{O}$  linkage (acetone, acetaldehyde) have previously drawn attention to the fact that there would seem to be a remarkably large and powerful hyperconjugation effect associated with the carbonyl group. The weakness of the  $\text{C}-\text{H}$  bonds in formaldehyde and acetaldehyde points to a carry over of this conjugation on a larger scale to the free radicals.

It is possible to formulate a three-electron bond resonance in the radicals  $-\text{CHO}$  and  $\text{CH}_3\text{CO}$ ,



(I)



(II)

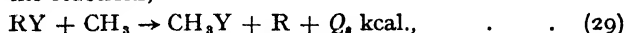
which would provide a considerable resonance stabilisation of these radicals. The chief objection to this suggestion is the theoretical one that the three-electron bond does not normally occur between atoms of widely different electronegativity. It might be that the superimposition of the three-electron bond on to the *double-bond already existing* in the carbonyl group is possible in view of the charge distribution in the carbonyl bond itself, which may, in effect, "remove" the large electronegativity difference that exists between free C and O atoms. In any case, we must recognise the existence of a powerful stabilisation in the formyl and acetyl radicals, which must lie in an increased binding between the C and O atoms.

## 8. Substitution Heats

Comparing the  $D(\text{R}-\text{Y})$  values given in Table IIB with a similar list by Baughan and Polanyi, there are some new features revealed by

our more complete set of data. The trend, noted by Baughan and Polanyi, of a fall in  $D(R-Y)$  as R changes down the series R=Me, Et, Pr, *sec.*-Pr, *tert.*-Bu, remains—this fall being most marked in cases where Y = H, CH<sub>3</sub>, and decreasing in the direction I > Br > Cl. In case where Y=OH, as previously noted, the  $D(R-Y)$  values are almost constant. But we may now note that this constancy disappears when R is extended beyond *tert.*-Bu to include R=allyl and benzyl. In all cases,  $D(R-Y)$  shows a substantial fall from the values in *tert.*-Bu Y as we pass to allyl-Y or benzyl-Y, including the case where Y = OH. We may also note that the —NH<sub>2</sub> group behaves in a manner roughly between that of —OH and —Cl.

The variations in  $D(R-Y)$  may be expressed in terms of the substitution heats of the reactions,



where  $Q$  is the energy difference  $\Delta D \left[ \begin{smallmatrix} CH_3-Y \\ R-Y \end{smallmatrix} \right]$ .

$Q$  values are listed in Table XI for the series R = Et, Pr, *sec.*-Pr, *tert.*-Bu, allyl, and benzyl, for R = vinyl, phenyl, —CHO, and COCH<sub>3</sub>, and for R=—CN. The main feature of Table XI is the general fall in  $Q$ , as we pass from Y=H to Y=OH, following the order in which the Y groups are arranged. An exception is provided by the —CN radical, whose behaviour seems to be quite anomalous.

The three terminal columns in Table XI list the quantities  $\Delta Q \left[ \begin{smallmatrix} H \\ Y \end{smallmatrix} \right]$ , where

$$\Delta Q \left[ \begin{smallmatrix} H \\ Y \end{smallmatrix} \right] = \Delta D \left[ \begin{smallmatrix} CH_3-H \\ R-H \end{smallmatrix} \right] - \Delta D \left[ \begin{smallmatrix} CH_3-Y \\ R-Y \end{smallmatrix} \right] \quad (30)$$

for Y=CH<sub>3</sub>, Cl and OH. Referring back to eqn. (8) of § 2, it may be seen that  $\Delta Q \left[ \begin{smallmatrix} H \\ Y \end{smallmatrix} \right]$  is expressible in the form,

$$\Delta Q \left[ \begin{smallmatrix} H \\ Y \end{smallmatrix} \right] = (\Delta x_i + \Delta x) \left[ \begin{smallmatrix} RY \\ CH_3Y \end{smallmatrix} \right] - (\Delta x_i + \Delta x) \left[ \begin{smallmatrix} RH \\ CH_4 \end{smallmatrix} \right] \quad (31)$$

TABLE XI  
SUBSTITUTION HEATS,  $RY + CH_3 \rightarrow CH_3Y + R$

R \ Y	H	CH <sub>3</sub>	I	Br	Cl	NH <sub>2</sub>	OH	$\Delta Q \left[ \begin{smallmatrix} H \\ CH_3 \end{smallmatrix} \right]$	$\Delta Q \left[ \begin{smallmatrix} H \\ Cl \end{smallmatrix} \right]$	$\Delta Q \left[ \begin{smallmatrix} H \\ OH \end{smallmatrix} \right]$
Et .	4.5	2.2	3.0*	2.8	1.3	1.9	-1.4	2.3	3.2	5.9
Pr .	6.5	3.8	—	1.9	3.3*	2.9*	-1.6	2.7	3.2	7.1
<i>sec.</i> -Pr	11.2	6.9	—	—	—	—	0.3	4.3	—	10.9
<i>tert.</i> -Bu	15.5	9.6	10.0	6.6	6.0	3.6	0.2	5.9	9.5	15.3
Allyl .	24	21.7	20.6	21.9	21.4	14.8*	18.6	2.3	2.6	5.4
Benzyl	24.5	22.0	18.5	18.9	—	16.4*	17.8	2.5	—	6.7
Vinyl .	0	-5.3	—	—	-3.3	—	—	5.3	3.3	—
Phenyl	0	-5.6	—	—	-5.6	-14.3*	-13.6	5.6	5.6	13.6
Formyl	22.7	13.2	—	—	—	-9.8	-5.1	9.5	—	27.8
Acetyl	21.8	11.8	9.0	5.4	4.0	-10.8	-6.0	10.0	17.4	27.8
C≡N	-19.1	-27.0	-16.2	—	-14.1	-33.8	—	9.0	-5.0	—

The theory of Baughan, Evans and Polanyi omits the terms in  $\Delta x$  from eqn. (31), and since  $\Delta Q \left[ \begin{smallmatrix} H \\ Y \end{smallmatrix} \right]$  is usually positive, requires that, in general,

$$\Delta x_i \left[ \begin{smallmatrix} RY \\ CH_3Y \end{smallmatrix} \right] > \Delta x_i \left[ \begin{smallmatrix} RH \\ CH_4 \end{smallmatrix} \right].$$

There is a certain measure of support for this from the empirical fact that  $\Delta Q_s \left[ \begin{smallmatrix} \text{H} \\ \text{Y} \end{smallmatrix} \right]$  have the largest numerical values the more electronegative the atom or group Y. But it seems to us doubtful that one should put *full* weight on to the  $\Delta x_i$  terms, and in certain cases there is little question that the terms in  $\Delta x$  are important. For example, the very large values of  $\Delta Q_s \left[ \begin{smallmatrix} \text{H} \\ \text{Y} \end{smallmatrix} \right]$  in case of the acetyl radical ( $\text{Y}=\text{Cl}, \text{OH}$ ), are certainly due, in part at least, to the fact that  $\Delta x \left[ \begin{smallmatrix} \text{RY} \\ \text{CH}_3\text{Y} \end{smallmatrix} \right] > \Delta x \left[ \begin{smallmatrix} \text{RH} \\ \text{CH}_3 \end{smallmatrix} \right]$ . The importance of hyperconjugation in acetyl chloride, represented in valence bond formulation by the contribution from the structure  $\text{CH}_3-\text{C} \begin{smallmatrix} \text{O}^- \\ \text{Cl}^+ \end{smallmatrix}$ , is generally recognised.

The *negative* value of  $\Delta Q_s \left[ \begin{smallmatrix} \text{H} \\ \text{Cl} \end{smallmatrix} \right]$  in case of the  $-\text{CN}$  radical is particularly interesting. Writing out eqn. (31) in full, we have

$$\Delta Q_s \left[ \begin{smallmatrix} \text{H} \\ \text{Cl} \end{smallmatrix} \right] = \Delta x_i \left[ \begin{smallmatrix} \text{CNCl} \\ \text{CH}_3\text{Cl} \end{smallmatrix} \right] + \Delta x \left[ \begin{smallmatrix} \text{CNCl} \\ \text{CH}_3\text{Cl} \end{smallmatrix} \right] - \Delta x_i \left[ \begin{smallmatrix} \text{HCN} \\ \text{CH}_3 \end{smallmatrix} \right] - \Delta x \left[ \begin{smallmatrix} \text{HCN} \\ \text{CH}_3 \end{smallmatrix} \right]. \quad (32)$$

Of the four terms in (32), the first is probably negative, for both Cl and  $-\text{CN}$  are strongly electronegative in character, and ionic structures  $\overset{+}{\text{CN}}\overset{-}{\text{Cl}}$  or  $\overset{+}{\text{CN}}\overset{+}{\text{Cl}}$  should be of slight importance, whereas in  $\text{CH}_3\text{Cl}$ , the ionic structure  $\overset{+}{\text{CH}_3}\overset{-}{\text{Cl}}$  is believed to be a major contributor to the resonance in this molecule. The second term is certainly positive, due to the importance of the structure  $\overset{-}{\text{N}}=\text{C}=\overset{+}{\text{Cl}}$ , which is reflected in the very short C—Cl bond length in this molecule. The third term may be negative, in view of the acidic character,  $\overset{+}{\text{H}}\overset{-}{\text{CN}}$ , of HCN, whilst the fourth term is probably a small positive one. The argument is purely qualitative, but one may note that the large positive term is offset by two negative terms—which are apparently sufficient to render  $\Delta Q_s$  finally negative.

In the case of  $Q_s \left[ \begin{smallmatrix} \text{H} \\ \text{CH}_3 \end{smallmatrix} \right]$  for the  $-\text{CN}$  radical, which is a *positive* quantity, the term corresponding to the first one in eqn. (32), is now positive, whilst the second also retains a positive value (compare  $x'$  values for  $\text{CH}_3-\text{C}\equiv\text{H}$  and for  $\text{CH}_3-\text{CH}_3$ ). In this example, we have two, possibly three, positive terms offset by only a single, probably small, negative term.

These examples illustrate that a full explanation of the gradations in R—Y bond energies requires an assessment of the stability of RY both in terms of hyperconjugation and ionic character. In the special case of R—H bonds, one can present a reasonable picture in terms of hyperconjugation effects alone: but, in the more general case where the R—Y bond is polar, the problem is more complex—and although, here, it *may* be (as Baughan, Evans and Polanyi assumed), the ionic factor is of prime importance, it remains to be proved whether or not this is the case. At present, we lack a reliable instrument of calculation both of ionic and hyperconjugation resonance energies in polar molecules, so that the questions remain to a large extent, open ones.

The authors express thanks to Prof. C. A. Coulson for comments and suggestions during the preparation of this paper.

Chemistry Department,  
University of Manchester,  
Manchester 13.

# TRANSIENT FLOW OF GASES IN SORBENTS PROVIDING UNIFORM CAPILLARY NETWORKS OF MOLECULAR DIMENSIONS

By R. M. BARRER

Received 29th September, 1948

A kinetic treatment has been developed for interpreting flow transients in a constant volume but variable pressure sorption system in which the equilibrium distribution of sorbate between gas phase and sorbent follows Henry's law. The results have made possible an analysis of flow transients in a variety of zeolitic media providing uniform capillary networks the channels in which have diameters of molecular magnitudes. Both positive and negative temperature coefficients in the relative sorption velocities were observed, the former predominating. Both kinds of temperature coefficient find a natural explanation in terms of the diffusion theory developed, and true energies of activation,  $E$ , for interstitial diffusion have been obtained. These support the view that a periodic potential field is encountered by the diffusing molecule within the crystal. Among various crystals the energy  $E$  ranged from 12,000 cal./atom (Kr) to 2500 cal./mol. ( $H_2$ ). The value of  $E$  depends on the radius of the sorbate molecule and also on the radius and the valence of the cations Li, Na, K,  $NH_4$ , Ca, and Ba in a series of base-exchange mordenites. At the lowest temperatures adsorption upon external crystal surfaces became measurable and exerted a characteristic influence, the theory of which was developed, upon the kinetics of intra-crystalline flow. By base exchange it was possible to modify systematically the character of the interstitial channels of mordenite, and so to produce a number of new molecular sieve sorbents with potential uses in separating the inert gases from one another or from atmospheric gases. For a series of gases in a given zeolite increased relative sorption velocities were in general found to be associated with decreasing molecular dimensions and decreasing affinities of the gases for the zeolite. Levynite behaved as a molecular sieve sorbent rather similar to Ca-mordenite.

**1. Introduction.**—Some insight has been gained into the nature of interstitial solid solutions of gases in zeolitic crystals and of diffusion in such crystals. Important factors include the polarizing power of the interstitial cation; <sup>1, 2</sup> the polarizability and polarity of the occluded molecule; <sup>1, 3</sup> the dimensions and shape of the sorbed molecule relative to those of the interstitial channels; <sup>2, 3, 4</sup> the duration and severity of heating and evacuation, depending on a balance between degree of dehydration and of lattice collapse; <sup>4, 5, 6, 7</sup> and the presence of foreign molecules in the interstitial channels.<sup>6</sup> Diffusion rates, in addition to being modified by the above factors, depend on the amount of sorbate occluded and on the state of subdivision of the crystals.<sup>7, 8, 9</sup>

<sup>1</sup> Barrer, *Trans. Faraday Soc.*, 1944, **40**, 555.

<sup>2</sup> Lowenstein, *Z. anorg. Chem.*, 1909, **63**, 69.

<sup>3</sup> Barrer, *J. Soc. Chem. Ind.*, 1945, **44**, 130; *Brit. Pat.* No. 548, 905; *U.S. Pat.* No. 2, 306, 610.

<sup>4</sup> Barrer and Ibbitson, *Trans. Faraday Soc.*, 1944, **40**, 206.

<sup>5</sup> Lamb and Woodhouse, *J. Amer. Chem. Soc.*, 1936, **58**, 2637.

<sup>6</sup> Emmett and de Witt, *ibid.*, 1943, **65**, 1253.

<sup>7</sup> Barrer and Riley, *J. Chem. Soc.*, 1948, 133.

<sup>8</sup> Barrer, *Trans. Faraday Soc.*, 1941, **37**, 590.

<sup>9</sup> Barrer and Ibbitson, *ibid.*, 1944, **40**, 195.

Robust anionic framework zeolites—among others, chabazite, gmelinite, analcite, mordenite and levynite—provide, when dehydrated, regular networks of capillaries of diameters no bigger than those of small molecules; <sup>8, 10, 11</sup> but apart from silica glass, which is permeable to hydrogen, helium and neon, <sup>12</sup> there are few substances porous on this fine scale. Base exchange reactions described elsewhere <sup>13</sup> made available a series of mordenite crystals enriched in the cations  $\text{Li}^+$ ,  $\text{Na}^+$ ,  $\text{K}^+$ ,  $\text{NH}_4^+$ ,  $\text{Ca}^{++}$  and  $\text{Ba}^{++}$ . The dehydrated crystals provide uniform capillary networks of molecular dimensions and were used in the present investigation of flow transients of simple gases in such networks. The present kinetic investigation parallels a similar study <sup>14</sup> of sorption equilibria between the inert gases and chabazites hydrothermally enriched in  $\text{Na}^+$ ,  $\text{K}^+$ ,  $\text{NH}_4^+$ ,  $\text{Cs}^+$ ,  $\text{Ca}^{++}$ ,  $\text{Sr}^{++}$  and  $\text{Ba}^{++}$ . Another zeolite, levynite, falls naturally among the mordenites studied in this paper, on the basis of its molecular sieve and sorptive characteristics. <sup>11</sup>

**2. Experimental.**—Synthetic and base-exchange mordenites were prepared hydrothermally, and details of preparation are given elsewhere. <sup>13</sup> A sample of levynite was made available by the courtesy of Dr. Philips. Pure gases ( $\text{H}_2$ ,  $\text{O}_2$ ,  $\text{N}_2$ , Ar, Ne, and He) were supplied by the British Oxygen Co., as was a sample of Krypton + 4 % Xenon. Ethane was taken from a cylinder, dried and fractionated; ammonia was prepared by a method already indicated. <sup>9</sup>

Heterogeneous equilibria and flow transients involving gas-sorbent systems were measured using the volumetric method in a double sorption system. <sup>9</sup> The zeolites were outgassed for periods of 4-5 hr. at 300-340° C before use, and between runs.

## Results.

**3. Preliminary Data.**—Typical isotherms are shown in Fig. 1 for synthetic mordenite and for levynite. All the zeolites examined were excellent sorbents of those gases the molecules of which were small enough to be accommodated interstitially within the crystal. The isotherms are qualitatively of Langmuir type, comparable with those in various zeolitic media already investigated. <sup>4, 9</sup> Isotherms were, however, determined only incidentally to the kinetic studies to provide further information concerning flow transients.

Since outgassing conditions may modify the rate of interstitial flow, the rate of sorption of ethane in a synthetic mordenite was measured under progressive outgassing conditions (Fig. 2). Progressive outgassing did within limits alter the rate of sorption, but this trend eventually ceased, leaving active sorbents.

**4. Kinetic Laws Governing Transient Flow.**—In zeolites the diffusion coefficient,  $D$ , depends on the sorbate concentration. <sup>7</sup> For this reason the charges of gas used were small and did not correspond at equilibrium to more than 2 % of saturation, except for levynite where the figure was 10 %. In this range of concentration the usual Fick laws may be taken to be valid, and, moreover, at least in the higher temperature range, many of the sorbates distributed themselves between solid and gaseous phases according to Henry's law.

Many of the kinetic data initially obeyed the expression,

$$Q_t/Q_\infty = k'\sqrt{t}$$

where  $Q_t$  denotes the amount occluded at time  $t$ , and  $Q_\infty$  is the amount sorbed at equilibrium (Fig. 2). A  $\sqrt{t}$ -diffusion law is known to be valid under conditions approaching those in a constant pressure sorption

<sup>10</sup> Barrer, *Ann. Reports*, 1944, **41**, 31.

<sup>11</sup> Barrer, *Nature*, 1947, **159**, 508.

<sup>12</sup> Cf. Barrer, *Diffusion in and through Solids* (C.U.P., 1941), Chap. 3.

<sup>13</sup> Barrer, *J. Chem. Soc.*, 1948, 2158.

<sup>14</sup> Barrer and Riley (in preparation).

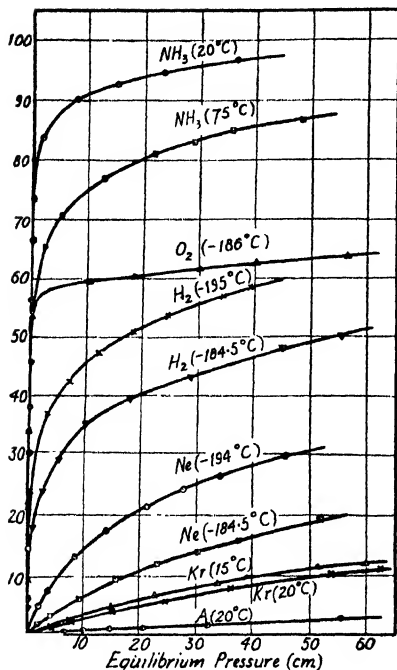


FIG. 1a.—Typical isotherms obtained using synthetic sodium mordenite as sorbent. Isotherms for  $\text{NH}_3$  were obtained on one sample and all other isotherms on a second sample. Ordinates:  $\text{cm}^3$  sorbed at N.T.P. per g.

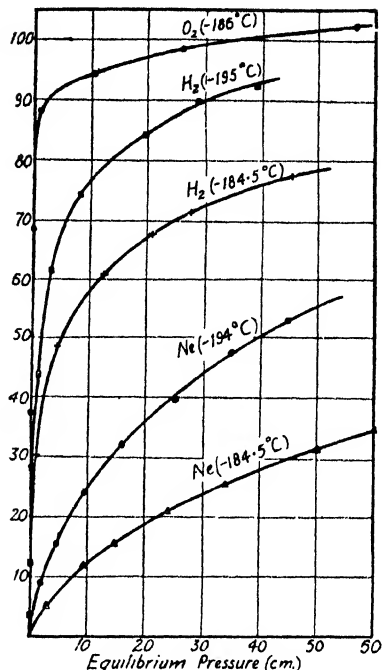


FIG. 1b.—Typical isotherms obtained using levynite as sorbent. Ordinates:  $\text{cm}^3$  sorbed at N.T.P. per g.

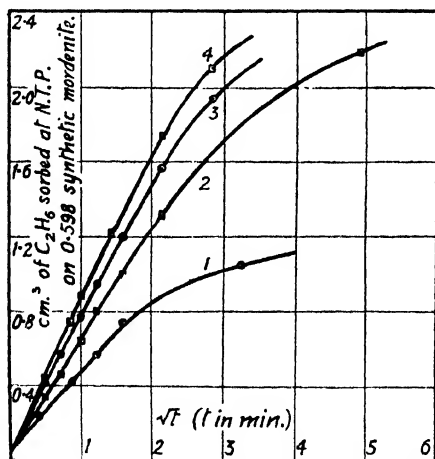


FIG. 2.—Influence of outgassing conditions upon the rate of occlusion of  $\text{C}_2\text{H}_6$  by synthetic sodium mordenite.

Curve 1: 3 hr. outgassing at  $225^\circ\text{C}$ .

Curve 2: As curve 1 + 2 hr. outgassing at  $270^\circ\text{C}$ .

Curve 3: As curve 2 + 7 hr. outgassing at  $287^\circ\text{C}$ .

Curve 4: As curve 3 + 4 hr. outgassing at  $287^\circ\text{C}$ .

The initial dose of  $\text{C}_2\text{H}_6$  corresponded in each run to  $3.36 \text{ cm}^3$  at N.T.P.

process,<sup>4, 7</sup> but its theoretical interpretation and range of applicability in a constant volume but variable pressure sorption system is not known. This problem is therefore considered in Appendix II, where it is shown that a  $\sqrt{t}$ -law again arises in the equivalent forms:

$$\left. \begin{aligned} \frac{Q_t}{Q_\infty} &= 6 \frac{K+1}{K} \sqrt{\frac{\tau}{\pi}} \\ &= \frac{6}{a} \left( \frac{K+1}{K} \right) \sqrt{\frac{Dt}{\pi}} \\ &= \left( \frac{6}{a} + \frac{2Ak}{V_g} \right) \sqrt{\frac{Dt}{\pi}} \\ &= \frac{6}{a} \frac{Q_0}{(Q_0 - Q_\infty)} \sqrt{\frac{Dt}{\pi}} \end{aligned} \right\} \quad (14)$$

where  $D$  denotes the diffusion coefficient,  $t$  is the time,  $a$  the radius of a sphere of the sorbent and  $A$  is the surface area of the sphere;  $k$  is the distribution coefficient of the sorbate between the gas phase and the sorbent,\* and  $K = V_g/V_s k$ , where  $V_g$  is the volume of the gas phase and  $V_s$  the volume of the sorbent.  $Q_0$  is the quantity of gas initially in the gas phase, and the sorbent is regarded as being free of sorbed gas when  $t = 0$ .

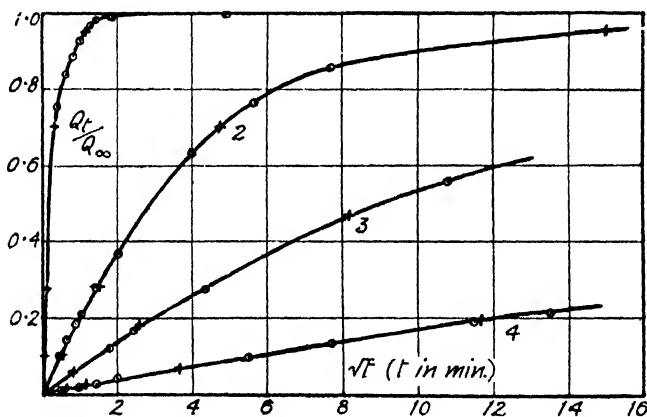


FIG. 3.—Representation of transient flow by eqn. (2).

Curve 1: Neon in Li-mordenite at  $-185^\circ \text{C}$ .

$1/K = 2.50$ ;  $\sqrt{D}/a = 0.285$ .

Curve 2: Neon in Ca-mordenite at  $-185^\circ \text{C}$ .

$1/K = 2.54$ ;  $\sqrt{D}/a = 0.0214$ .

Curve 3: Krypton in Ba-mordenite at  $24^\circ \text{C}$ .

$1/K = 0.86$ ;  $\sqrt{D}/a = 0.0122$ .

Curve 4: Krypton in Levynite at  $0^\circ \text{C}$ .

$1/K = 0.96$ ;  $\sqrt{D}/a = 0.00273$ .

○ = Experimental points.

× = Points calculated from eqn. (2).

The  $\sqrt{t}$ -law illustrated in Fig. 2 may be extended by using eqn. (11), Appendix II:

$$\frac{Q_t}{Q_\infty} = (K+1) \left\{ 1 - \frac{1}{\alpha + \beta} \left[ \alpha e^{-\alpha^2 \tau} (1 + \text{erf } \alpha \sqrt{\tau}) - \beta e^{-\beta^2 \tau} (1 + \text{erf } \beta \sqrt{\tau}) \right] \right\}, \quad (11)$$

where  $\alpha$  and  $\beta$  are the roots of  $x^3 - 3x/K - 3/K = 0$ . Fig. 3 shows the

\*  $k = \frac{\text{conc. in the sorbent}}{\text{conc. in the gas phase}}$ , and the equations apply to the case where Henry's law governs the distribution of gas between sorbent and gas phase (see Appendix II).





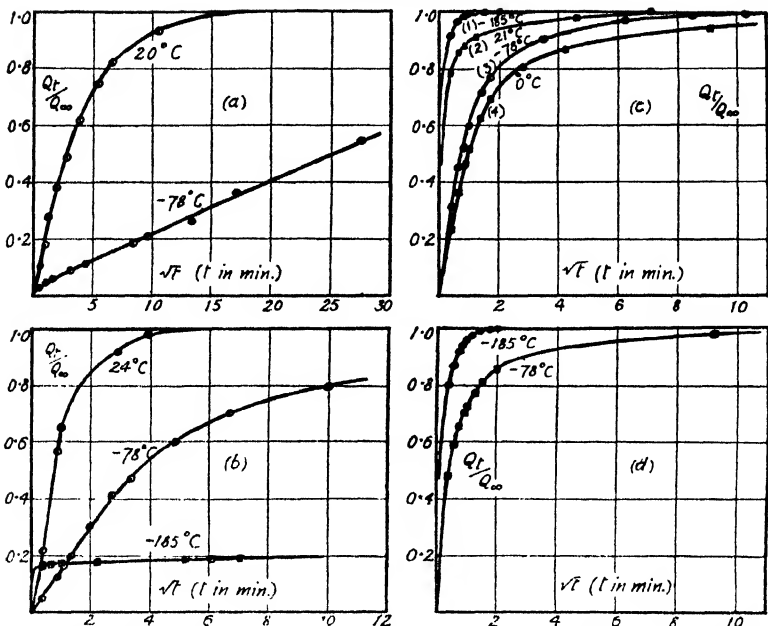


FIG. 5.—Examples of positive and negative temperature coefficients in transient flow of gases in zeolitic sorbents.

(a) Kr in synthetic Na-mordenite.

(b) A in Ba-mordenite.

(c) Curves 1 and 2 refer to  $N_2$  in  $NH_4$ -mordenite, and curves 3 and 4 to Kr in the same sorbent.

(d) A in  $NH_4$ -mordenite.

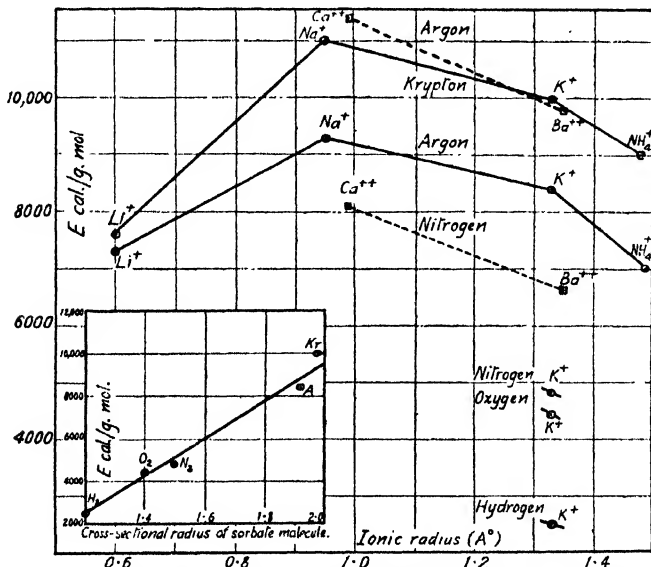


FIG. 6.—Relation between the true energy of activation,  $E$ , for diffusion and the cationic radius in a series of base exchange mordenites, for a given sorbate molecule. Inset is shown the relation between the true energy of activation,  $E$ , and the cross-sectional radius of a series of sorbate molecules for a given base-exchange mordenite, here K-mordenite.

with eqn. (14), and thence obtain

$$\log \frac{\left\{ \frac{d(Q_i/Q_\infty)}{d\sqrt{t}} \times \frac{Q_0 - Q_\infty}{Q_0} \right\}_{T_1}}{\left\{ \frac{d(Q_i/Q_\infty)}{d\sqrt{t}} \times \frac{Q_0 - Q_\infty}{Q_0} \right\}_{T_2}} = \frac{E}{2.303 \times 2} \left\{ \frac{1}{T_2} - \frac{1}{T_1} \right\} \quad (2)$$

This relation serves to give the true energy  $E$  with some accuracy, and was applied to a number of appropriate data. The results are summarized in Table I, which also gives relative values of  $D$ , determined from eqn. (14) for various gases in a given sorbent.

TABLE I.—TRUE ENERGIES OF ACTIVATION AND RELATIVE DIFFUSION CONSTANTS FOR FLOW IN CRYSTALS

Crystal	Gas	Relative Value of $D$	True Energy of Activation $E$ (cal./mol.)
Li-mordenite	Kr	1 ( $-78^\circ \text{C}$ )	7,600
	A	240 ( $-78^\circ \text{C}$ )	7,300
NH <sub>4</sub> -mordenite	Kr	1 ( $16^\circ \text{C}$ )	9,000
	A	90 ( $16^\circ \text{C}$ )	7,000
Na-mordenite	Kr	1 ( $20^\circ \text{C}$ )	11,000
	A	110 ( $20^\circ \text{C}$ )	9,300
K-mordenite	Kr	1 ( $-78^\circ \text{C}$ )	10,000
	A	130 ( $-78^\circ \text{C}$ )	8,400
	N <sub>2</sub>	510 ( $-78^\circ \text{C}$ )	4,800
	O <sub>2</sub>	1,100 ( $-78^\circ \text{C}$ )	4,400
	H <sub>2</sub>	2,600,000 ( $-78^\circ \text{C}$ )	2,500
Ba-mordenite	A	1 ( $-78^\circ \text{C}$ )	9,800
	N <sub>2</sub>	60 ( $-78^\circ \text{C}$ )	6,600
Ca-mordenite	A	1 ( $-78^\circ \text{C}$ )	11,500
	N <sub>2</sub>	9 ( $-78^\circ \text{C}$ )	8,100
	O <sub>2</sub>	650 ( $-78^\circ \text{C}$ )	—
Levynite	Kr	1 ( $-78^\circ \text{C}$ )	12,000
	A	170 ( $-78^\circ \text{C}$ )	9,400
	N <sub>2</sub>	260 ( $-78^\circ \text{C}$ )	—
	Nc	—	2,600

Relative values of  $D$  give a good idea of the magnitude of the molecular sieve effects found. As the temperature is lowered further, the relative values usually diverge still more, often very greatly.

The value of  $E$  depends in a striking way upon the radius of the interstitial cation in a series of base-exchange mordenites. For the monovalent cations lower values of  $E$  are associated with both large and small ions (NH<sub>4</sub><sup>+</sup> and Li<sup>+</sup>), and the largest value of  $E$  occurs with an ion of intermediate size (Fig. 6). The maximum in the curve of  $E$  against ionic radius indicates that two factors must act in opposition. One suggestion is that the larger the ion the more deformable or softer it becomes; but on the other hand when undeformed it blocks the interstitial channel more completely than a small ion. If this view is correct,  $E$  must be associated partly with sorbate-cation interaction. In the transition state for each unit diffusion process the sorbate molecule squeezes between the cation and the anionic oxygens of the "wall" of the channel. This in turn must press the cation against the opposite "wall."\*

\* That equilibrium sorption sites are in close association with the cations has already been indicated. Thus the affinity of gases for some base-exchange mordenites is in the same order as the polarizing power of the cations.<sup>1</sup>

Fig. 6 shows that divalent cations give a different curve of  $E$  against ionic radius from monovalent cations. A possible reason may be offered. Since each divalent cation replaces two monovalent ones, the number of occupied sites will be reduced to half the original number when exchange is complete. In order best to neutralize anionic charge, each divalent cation may be placed intermediate in position between two original monovalent cation sites. It will, in general, then offer a different resistance to sorbate diffusion.

Inset in the same figure the true energy of activation  $E$  for diffusion in  $K$ -mordenite is plotted against the radius of the smallest cross-section of the sorbate molecules (see § 6). There is clearly a relation between these quantities which is qualitatively compatible with the view given above of the transition state in each unit act of diffusion.

**6. Molecular Sieve Properties of the Crystals.**—There are two ways of considering the relative rates of intra-crystalline flow. Firstly, one may compare the relative sorption rates of a given gas in a series of the sorbents, as in Fig. 7, and secondly, one may consider these rates for different sorbates in a given sorbent (Fig. 8). Only a few of the results are shown graphically, but the actual rate sequences are more fully summarized in Tables II and III. Both tables reveal a fairly regular

TABLE II.—RELATIVE RATES OF INTRA-CRYSTALLINE FLOW OF A GIVEN GAS IN A SERIES OF CRYSTALS

Gas	Temperature °C	Relative Rate Sequence for Various Crystals *
Kr . . . .	-78 20	NH <sub>4</sub> > Li > Na > K NH <sub>4</sub> > Li > Na > Ba > K > Lev > Ca
Ar . . . .	-78 20	Li > NH <sub>4</sub> > Na > Ba > Lev > Ca Li > NH <sub>4</sub> , Na > Ba > Lev > Ca
Ne . . . .	-185	Li > Ba > K > Lev > Ca
N <sub>2</sub> . . . .	-185 -78 20	Li > NH <sub>4</sub> > Ba > Ca, K NH <sub>4</sub> , Ba > Lev > Ca NH <sub>4</sub> , Ba > Ca
O <sub>2</sub> . . . .	-185 -78	NH <sub>4</sub> , Li, Ba > Lev > Ca > K Li > Ba > NH <sub>4</sub> > Ca > K
H <sub>2</sub> . . . .	-185 -78	Na, Li > Ba > Lev > Ca > NH <sub>4</sub> > K Li > NH <sub>4</sub> > K

\* Li = lithium-rich mordenite. Na = sodium-rich mordenite. K = potassium-rich mordenite. NH<sub>4</sub> = ammonium-rich mordenite. Ba = barium-rich mordenite. Ca = calcium-rich mordenite. Lev = levynite.

pattern of results, modified by some exceptions. Table II shows that Li, NH<sub>4</sub> and Na mordenites present more accessible capillary networks than do Ca and K mordenite or levynite, while Ba mordenite is in an intermediate position. Among factors determining such sequences are the particle size, modified resistance to interstitial diffusion produced by base exchange and variations in the affinity of the gas for the minerals (Fig. 9, Appendix II).

The effect of the varying affinity of a given gas for a series of sorbents may be eliminated by determining the quantity  $D/a^2$  ( $a$  being the mean particle diameter). For the flow of argon at  $-78^\circ\text{C}$  the results in Table IV were obtained. The great range in values of  $D/a^2$  among the sorbents makes it unlikely that variations in the particle diameter alone can account for it. A large part of the variation may reasonably be ascribed to

modifications in intra-crystalline mobility of the sorbate due to base exchange of the sorbent.

TABLE III.—RELATIVE INTRA-CRYSTALLINE RATES OF FLOW OF VARIOUS GASES IN A GIVEN MOLECULAR SIEVE ZEOLITE

Crystal	Temperature (°C)	Order of Relative Rates (for a given Time Interval)
Li-mordenite . .	-185 -78 20	H <sub>2</sub> , O <sub>2</sub> > N <sub>2</sub> > Ne > A O <sub>2</sub> , N <sub>2</sub> > A > Kr O <sub>2</sub> , N <sub>2</sub> > A > Kr
Na-mordenite (synthetic) . .	-185 -78 20	O <sub>2</sub> , H <sub>2</sub> > Ne > A A > Kr A > Kr
K-mordenite . .	-185 -78 20	H <sub>2</sub> > O <sub>2</sub> > N <sub>2</sub> > A H <sub>2</sub> > O <sub>2</sub> > N <sub>2</sub> > A > Kr O <sub>2</sub> , N <sub>2</sub> > A > Kr
NH <sub>4</sub> -mordenite . .	-185 -78 20	H <sub>2</sub> , O <sub>2</sub> > N <sub>2</sub> > A H <sub>2</sub> > O <sub>2</sub> , N <sub>2</sub> > A > Kr O <sub>2</sub> > N <sub>2</sub> , A > Kr
Ca-mordenite . .	-185 -78 20	He > H <sub>2</sub> > Ne > O <sub>2</sub> > N <sub>2</sub> , A O <sub>2</sub> > N <sub>2</sub> > A N <sub>2</sub> > A > Kr
Ba-mordenite . .	-185 -78 20	He > H <sub>2</sub> , O <sub>2</sub> > Ne > N <sub>2</sub> > A O <sub>2</sub> > N <sub>2</sub> > A N <sub>2</sub> > A > Kr
Levynite . .	-185 -78 20	H <sub>2</sub> , O <sub>2</sub> > Ne > N <sub>2</sub> > A N <sub>2</sub> > A > Kr A > Kr

In Table III the relative sorption rate sequences are independent of the fineness of subdivision of the sorbent. Marked molecular sieve effects arise, and in any one zeolite the velocity sequence which tends to be preserved is

$$\text{Kr} < \text{A} < \text{N}_2 < \text{O}_2, \text{Ne} < \text{H}_2 < \text{He}$$

TABLE IV.— $D/a^2$  (IN MIN.<sup>-1</sup>) FOR ARGON AT -78° C IN A SERIES OF CRYSTALS

Crystal	$D/a^2$
Ca-mordenite . . . .	$1.51 \times 10^{-8}$
Levynite . . . . .	$7.6 \times 10^{-7}$
K-mordenite . . . . .	$2.8 \times 10^{-6}$
Ba-mordenite . . . . .	$5.5 \times 10^{-6}$
Na-mordenite . . . . .	$3.8 \times 10^{-5}$
Li-mordenite . . . . .	$4.0 \times 10^{-4}$
NH <sub>4</sub> -mordenite . . . .	$1.35 \times 10^{-3}$

although some exceptions occur. The relative affinities of the gases for synthetic mordenite and levynite (see Fig. 1) are

$$\text{Kr} > \text{A}, \text{N}_2, \text{O}_2 > \text{H}_2 > \text{Ne} > \text{He} \text{ (in Na-mordenite)}$$

$$\text{O}_2 > \text{H}_2 > \text{Ne} > \text{He} \text{ (in levynite)}$$

and similar series are found in chabazite and other zeolites.<sup>1, 15</sup> Thus

<sup>15</sup> Barrer, *Proc. Roy. Soc. A*, 1938, 167, 392, 406.

the greater the affinity of the gas for the zeolite the less easily does interstitial flow occur. That is, the *increase* in the rate of flow due to the higher affinity of a sorbate for the crystal, as shown in Fig. 9, is more than offset by the decrease in intrinsic mobility. A consideration not previously

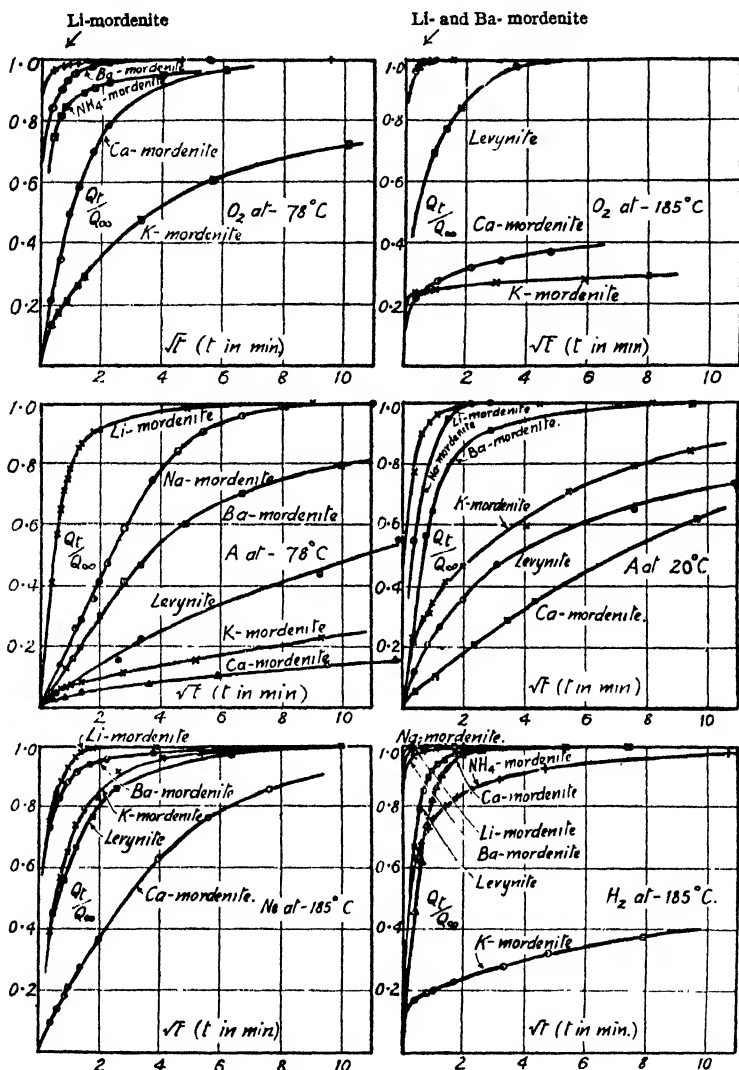


FIG. 7.—Relative sorption rates of each of several sorbates in levynite and in a series of mordenites modified by base-exchange. A great measure of control over the sorption rate can be exercised by a suitable choice of base-exchange mordenite.

referred to here, which must modify mobility in a channel that sheathes the diffusing molecule closely, is the shape and dimension of the molecule. Dividing the sorbates into two groups depending on their shape one has

(i) Spherical atoms :

Kr	A	Ne	He
(3.94)	(3.84)	(~3.20)	(~2.0)

(ii) Dumbell-shaped molecules :

N <sub>2</sub>	O <sub>2</sub>	H <sub>2</sub>
(3.0)	(2.8)	(2.4)

There are now no exceptions to the order of the sorption rates in each series considered separately. The figures in brackets are the diameters of the spherical noble gas atoms, and the cross-sectional diameter normal to their long axis for the dumbbell-shaped molecule.<sup>16</sup> Recombining the series (a) and (b) in descending order of these dimensions then gives a reasonable guide to the actual sorption rate series (neon and oxygen sometimes giving interchanged rates).

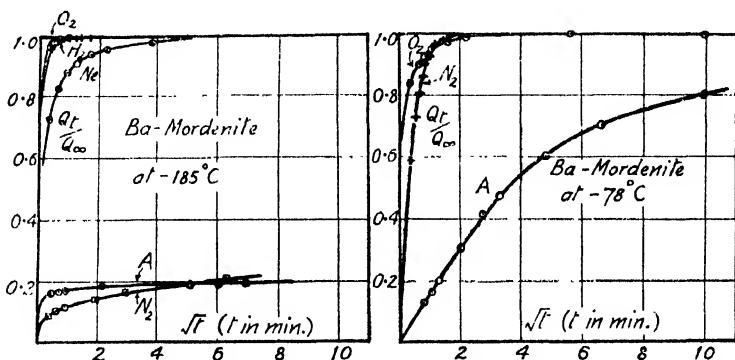


FIG. 8.—Examples of the molecular sieve action of Ba- and Ca-mordenites towards different simple gases, as expressed by selectivity in the rates of sorption at  $-185^{\circ}\text{C}$  and  $-78^{\circ}\text{C}$ . For other examples see Fig. 4.

**7. Discussion.**—The results obtained indicate that one may prepare artificially a much greater diversity of molecular sieves than has previously been realised,<sup>3, 10</sup> a range of such products being possible, within limits set by a given anionic framework. An interesting practical aspect of these sorbents is the possibility of using them to separate the inert gases from one another or from oxygen, nitrogen and hydrogen. At the lowest temperatures ( $-78^{\circ}\text{C}$ ,  $-185^{\circ}\text{C}$ , and  $-195^{\circ}\text{C}$ ) great differences in sorption rates occur among appropriately chosen gas pairs. Many possibilities of resolving gas mixtures occur. At  $-185^{\circ}\text{C}$ , Ba-mordenite sorbs  $\text{O}_2$ ,  $\text{Ne}$  and  $\text{H}_2$  rapidly, and  $\text{N}_2$  and  $\text{A}$  only slowly; Ca-mordenite sorbs  $\text{H}_2$  and  $\text{He}$  rapidly, and  $\text{N}_2$  and  $\text{A}$  slowly; while levyntite sorbs  $\text{O}_2$ ,  $\text{H}_2$  and  $\text{H}_2$  rapidly and  $\text{A}$  slowly. Similar large differences in rates suggest that Na-mordenite could resolve  $\text{A}$ — $\text{Kr}$  mixtures or Ca-mordenite resolve  $\text{O}_2$ — $\text{A}$  mixtures. Many other possibilities arise.

#### Appendix I.—Sorption Kinetics in a Constant Volume Variable Pressure System

Occlusion of a fixed quantity of gas released at time  $t = 0$  into a fixed volume, where it is sorbed by a zeolite in the form of a powder of spherical particles, can be treated by methods recently developed in dealing with heating or cooling of spheres in a stirred fluid.<sup>17, 18</sup>

We will consider first a single sphere of sorbent of radius  $a$ , and then generalize the result for a powder of small spheres. Let  $V_g$  denote the volume of the gas phase, and  $V_s$  the volume of the sorbent. At  $t = 0$ ,  $Q_0 = u_0 V_g$  of gas is released into the volume  $V_g$  in contact with sorbent, where  $u_0$  is the initial gas phase

<sup>16</sup> These dimensions for the inert gases Kr, A, Ne are the closest distance of approach between atoms in their crystals (Slater, *Introduction to Chemical Physics* (McGraw Hill Book Co., 1939), p. 416). For He an approximate figure given by Melville and Farkas, *Experimental Methods in Gas Reactions* (MacMillan and Co., 1939), p. 2) is used, and for  $\text{N}_2$ ,  $\text{O}_2$  and  $\text{H}_2$ , the van der Waals' atomic radii are taken (Pauling, *The Nature of the Chemical Bond* (Cornell Univ. Press, 1940), p. 189).

<sup>17</sup> Paterson, *Proc. Physic. Soc.*, 1947, **59**, 50.

<sup>18</sup> Carslaw and Jaeger, *Conduction of Heat* (O.U.P., 1947), p. 205.

concentration of sorbate. The general isotherm relating the concentration between gas phase concentration of sorbate ( $u$ ) and sorbate concentration ( $v$ ) in the sorbent is

$$\frac{k_1 u}{1 + k_2 u} = v, \quad . \quad . \quad . \quad . \quad . \quad (1)$$

but the diffusion problem can be solved only for the two limiting cases

$$k_1 u = v \text{ (Henry's law)} \quad . \quad . \quad . \quad . \quad . \quad (1a)$$

$$k_1/k_2 = v \text{ (saturation of sorbent)} \quad . \quad . \quad . \quad . \quad . \quad (1b)$$

Solutions corresponding to (1b) are well known (cf. eqn. (16), Appendix II); we are interested in solutions corresponding to (1a).

The boundary conditions are:

$$\frac{\delta(rv)}{\delta t} = \frac{D\delta^2(rv)}{r^2} \text{ for } r < a < 0; t < 0, \quad . \quad . \quad . \quad . \quad . \quad (2)$$

$$\left. \begin{aligned} v &= v_0 \text{ for } a < r < 0, t = 0, \\ v &= k_1 u \text{ at } r = a, t > 0, \\ u &= u_0 \text{ for } r > a, t = 0, \end{aligned} \right\} \quad . \quad . \quad . \quad . \quad . \quad (3)$$

and

$$V_s \frac{\delta u}{\delta t} + 4\pi a^2 D \frac{\delta v}{\delta r} = 0, \text{ at } r = a, t > 0. \quad . \quad . \quad . \quad . \quad . \quad (4)$$

We now define a quantity  $K_1$  by

$$K_1 = V_s/(k_1 V_s). \quad . \quad . \quad . \quad . \quad . \quad (5)$$

It is then possible to proceed by standard methods to show that after a time interval  $t_1$ ,<sup>18</sup>

$$v_1 - v(r) = \frac{1}{K_1 + 1} \left[ \frac{Q_0}{V_s} + v_0 \right] + \frac{6a}{r} \left( \frac{Q_0}{V_s} - K_1 v_0 \right) \sum_{\alpha_1 n} \frac{\sin \alpha_1 n r}{\sin \alpha_1 n a} \times \frac{\exp(-\alpha_1 n^2 \tau_1)}{9(K_1 + 1) + \alpha_1 n^2 a^2 K_1^2}, \quad (6)$$

where

$$\tau_1 = \frac{D_1 t_1}{a^2} \quad . \quad . \quad . \quad . \quad . \quad (7)$$

and where  $\alpha_1 n$  is the  $n$ th positive root of the equation,

$$\tan \alpha_1 a = \frac{3a\alpha_1}{3 + K_1 a^2 \alpha_1^2} \quad . \quad . \quad . \quad . \quad . \quad (8)$$

In the gas phase the concentration  $u$  follows from (6) where  $\tau = a$ , since  $u_1 = v_1/k_1$ ;

$$u_1 = \frac{1}{(K_1 + 1)k_1} \left[ \frac{Q_0}{V_s} + v_0 \right] + \frac{6}{k_1} \left( \frac{Q_0}{V_s} - K_1 v_0 \right) \sum_{\alpha_1 n} \frac{\exp(-\alpha_1 n^2 \tau_1)}{9(K_1 + 1) + \alpha_1 n^2 a^2 K_1^2}. \quad (9)$$

$Q_1$ , the quantity of gas remaining unsorbed after time  $t_1$ , is simply  $V_g \times u_1$ , while  $Q_s$ , the quantity sorbed, is

$$Q_0 + v_0 V_s - Q_1.$$

The important special cases of eqn. (6) and (9) where the sorbent was initially gas-free are applied in § 4 to suitable data (where sorption approximately followed Henry's law).

The solutions obtained can be generalized from the single sphere to a powder of spherical particles all of the same size,  $N$  in number. In this case if  $v_s$  is the volume of a single small sphere,  $V_s = N v_s$ . For each such particle of radius  $a$ , the boundary condition (4) for example, becomes

$$\frac{V_s}{N} \frac{\delta u}{\delta t} + 4\pi a^2 D_1 \frac{\delta v}{\delta r} = 0, \quad . \quad . \quad . \quad . \quad . \quad (4a)$$

since the behaviour of each sphere is as if it alone were enclosed in a volume  $V_s/N$  of the gas phase and left to come to equilibrium with the gas. Eqn. (6) to (9) then refer to each separate particle on replacing  $V_s$  by  $V_s/N$ ;  $V_s$  by  $v_s$ ; and  $a$  by  $a_1$ . The total amount sorbed is then  $N \times$  (the amount sorbed by a single particle).



### Appendix II.—The Validity and Range of Application of a $\sqrt{t}$ -Law in a Constant Volume Sorption System

When  $v_0 = 0$ , eqn. (6) leads to the following expression for  $Q_t/Q_\infty$  in a constant volume system where at equilibrium occlusion follows Henry's law :

$$\frac{Q_t}{Q_\infty} = 1 - 6K(K+1) \sum \frac{\exp(-\alpha_n^2 \tau)}{9(K+1) + \alpha_n^2 a^2 K^2}, \quad (10)$$

where  $\tau = Dt/a^2$ . The series in eqn. (10) is only slowly convergent for small  $\tau$  and cannot readily account for the  $\sqrt{t}$ -law. A solution alternative to eqn (10) can, however, be used :<sup>15</sup>

$$\frac{Q_t}{Q_\infty} = (K+1) \left\{ 1 - \frac{1}{\alpha + \beta} \left[ \alpha e^{-\alpha^2 \tau} (1 + \operatorname{erf} \alpha \sqrt{\tau}) - \beta e^{-\beta^2 \tau} (1 + \operatorname{erf} \beta \sqrt{\tau}) \right] \right\}, \quad (11)$$

where  $\alpha$  and  $\beta$  are the roots of the equation,

$$x^2 - 3x/K - 3/K = 0. \quad (12)$$

Both exponentials and error functions can be expanded as series and for small values of  $\sqrt{\tau}/K$  only first terms need be considered, to give

$$\frac{Q_t}{Q_\infty} = -(K+1) \left\{ 2(\alpha + \beta) \sqrt{\frac{\tau}{\pi}} + (\alpha^2 + \alpha\beta + \beta^2)\tau + 2(\alpha^3 + \beta^2)(\alpha + \beta) \frac{\tau^{3/2}}{\sqrt{\pi}} \right\} \quad (13)$$

$$= \frac{3(K+1)}{K} \left\{ 2\sqrt{\frac{\tau}{\pi}} - \left(1 + \frac{3}{K}\right)\tau + 6\left(\frac{3}{K^2} + \frac{2}{K}\right) \frac{\tau^{3/2}}{\sqrt{\pi}} \right\}. \quad (13a)$$

For small enough values of  $\sqrt{\tau}/K$  the first term in eqn. (13) or (13a) is dominant, and the  $\sqrt{\tau}$  law is valid. This law takes the following equivalent forms :

$$\left. \begin{aligned} \frac{Q_t}{Q_\infty} &= \frac{6(K+1)}{K} \sqrt{\frac{\tau}{\pi}} \\ &= \frac{6}{a} \frac{K+1}{K} \sqrt{\frac{Dt}{\pi}} \\ &= \left( \frac{6}{a} + \frac{2Ak}{V_s} \right) \sqrt{\frac{Dt}{\pi}} \\ &= \frac{6}{a} \frac{Q_0}{(Q_0 - Q_\infty)} \sqrt{\frac{Dt}{\pi}}, \end{aligned} \right\} \quad (14)$$

where  $A$  is the external surface area of the sorbent, and

$$1/K = kV_s/V_s,$$

(cf. Appendix I) and so is proportional to the distribution coefficient  $k$  of gas between gaseous and solid phases.\* Thus the physical significance of the initial slope of curves of  $Q_t/Q_\infty$  against  $\sqrt{t}$  (Fig. 2) differs from that in a constant pressure system where †

$$\frac{Q_t}{Q_\infty} = \frac{Av_0}{Q_\infty} \sqrt{\frac{Dt}{\pi}} \quad (14a)$$

and, as we have shown for sorption at constant volume, permits the evaluation of true energies of activation for diffusion (§ 5).

Eqn. (11) has been used to calculate  $Q_t/Q_\infty$  when the  $\sqrt{t}$ -law is no longer valid, and Fig. 3 shows that it is possible to describe the whole course of the experimental  $Q_t/Q_\infty$  against  $\sqrt{t}$  curves with some accuracy in favourable cases. In Fig. (9) are shown curves of  $Q_t/Q_\infty$  against  $1/K$  for various fixed values of  $\tau$ , again calculated from eqn. (2), the purpose of which is to show that *the rate of sorption increases greatly as the Henry's law distribution coefficient rises*, for fixed values of  $D$ . The importance of this is referred to in § 5 and 6.

\*  $1/K$  is very easily calculated from experimental data, since

$$\frac{1}{K} = \frac{Q_\infty}{(Q_t - Q_\infty)} = \frac{\text{Amount of gas in zeolite}}{\text{Amount of gas not sorbed}}$$

†  $v_0$  is the initial concentration just within the surface of the sorbent as before, but is now constant for the duration of the experiment.

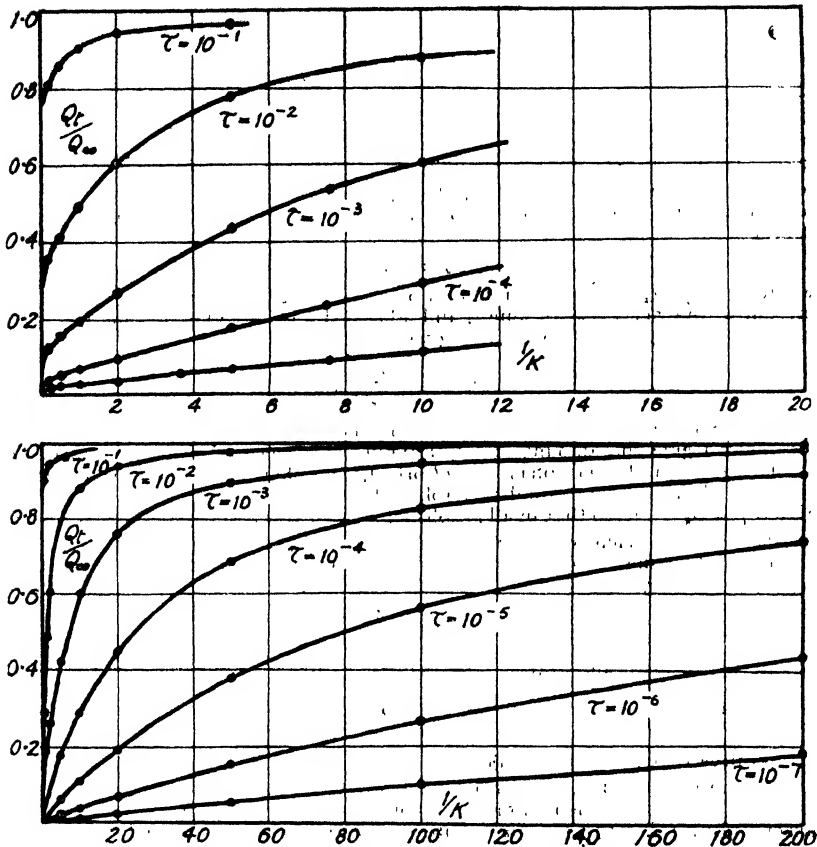


FIG. 9.—The influence of  $1/K = Q_{\infty}/(Q_i - Q_{\infty})$ , and hence of the distribution coefficient, upon the relative sorption rate for various constant values of  $\tau = Dt/a^2$ .

### Appendix III.—Deviations from the "Ideal" Kinetic Laws

Departures from the  $\sqrt{t}$ -law and from eqn. (10) and (11) were found over a range of values of  $Q_i/Q_{\infty}$ , and might be ascribed to several causes—

(a) HETEROGENEITY IN SIZE OF SORBENT PARTICLES. This heterogeneity was unavoidable to some extent. In many cases, however, it was not sufficient to invalidate the  $\sqrt{t}$ -law, or the successful use of eqn. (11) for a number of systems, as the results of § 4 clearly show.

(b) DEVIATIONS FROM A HENRY'S LAW DISTRIBUTION OF GAS BETWEEN GASEOUS AND SOLID PHASES. The occlusion isotherm is of Langmuir type (Fig. 1) so that, in the notation of Appendix I,

$$v = \frac{k_1 u}{1 + k_2 u}, \quad (15)$$

where  $k_1$  and  $k_2$  are constants. At high pressures and lower temperatures  $v_1$ , the interstitial sorbate concentration, then becomes independent of its gas phase concentration,  $u$ , giving saturation of sorption just within the ingoing surface. Then

$$\frac{Q_t}{Q_{\infty}} = 1 - \frac{6}{\pi^2} \sum_{n=1}^{\infty} \frac{1}{n^2} \exp(-n^2 \pi^2 \tau) \quad (16)$$

to which, for small  $\tau$ , eqn. (14a) corresponds. Conditions for eqn. (16) are for the permanent and noble gases only likely to apply at the lowest experimental temperatures, but the possibility remains that then sorption may commence

according to eqn. (16) or (14a) and change as the pressure falls to one obeying eqn. (10) or (11). No exact solution of the diffusion equation has been obtained for the general boundary condition of eqn. (15).

(c) SURFACE ADSORPTION AS DISTINCT FROM OCCLUSION. Adsorption upon external surfaces of the powder has two effects upon the kinetics of occlusion. Adsorption corresponded in extreme cases to about 1 cm.<sup>3</sup> at N.T.P. of gas, compared with an initial total gas charge of about 4 cm.<sup>3</sup> at N.T.P. Adsorption, unlike occlusion, was always virtually instantaneous, and therefore gave rise to a "foot" in the curves of  $Q_t/Q_\infty$  against  $\sqrt{t}$ , illustrated in Fig. 4. The second influence of adsorption is upon the *slope* of these curves. At any moment conservation of mass gives

$$Q_0 = Q_g + Q_a + Q_i, \quad (17)$$

where  $Q_0$ ,  $Q_g$ ,  $Q_a$  and  $Q_i$  are amounts of gas initially present in the gas phase, present in the gas phase at time  $t$ , and adsorbed and occluded at time  $t$ , respectively. The adsorption isotherm is given by

$$Q_a = \frac{\delta Q_g}{1 + \gamma Q_g}, \quad (18)$$

where  $\delta$  and  $\gamma$  are constants. It does not matter, in deriving the eqn. (10) or (16), which give the amount of *interstitially* sorbed gas, whether the remainder of the gas is in the gas phase or adsorbed, provided equilibrium between adsorbed and free gas is rapidly established. However, the observational data give  $Q'_t = Q_i + Q_a$ , so that in all graphs (cf. Fig. 3, 4) it is  $Q'_t/Q_\infty$  which is plotted against  $\sqrt{t}$ . In such a system, however,  $Q_a$  is itself a function of time, and therefore the kinetic laws become more complex. Substituting for  $Q_a$ , using eqn. (18), one has

$$Q'_t = Q_i + \frac{\delta Q_g}{1 + \gamma Q_g}, \quad (19)$$

where  $Q_g$  from (17) and (18) is given by

$$Q_g = \frac{-(1 + \delta - \gamma(Q_0 - Q_i)) + \sqrt{[(1 + \delta - \gamma(Q_0 - Q_i))^2 + 4\gamma(Q_0 - Q_i)]}}{2\gamma}, \quad (20)$$

the positive root alone being taken.

We are interested in the form of the  $Q'_t/Q_\infty$  against  $\sqrt{t}$  curves in order or see how far the modified diffusion theory predicts curves in accordance with observations (cf. Fig. 4). In zeolites, adsorption upon external surfaces is normally a less energetic process than occlusion. Therefore when Henry's law is obeyed for occlusion a similar law should be obeyed for adsorption. On the other hand when occlusion corresponds to saturation of interstitial sites the adsorbed layer may vary between saturation of surface sites and the Henry's law range. The full diffusion equation obtained by substituting eqn. (20) and either (10) or (16) in (19) is clearly complex, so that it is better to consider several limiting cases:

(i) *Henry's law for adsorption coupled with saturation just within the sorbent surface for occlusion.*

The general relation  $Q'_t = Q_i + Q_a$  now reduces to

$$Q'_t = \frac{Q_i}{1 + \delta} + \frac{\delta \cdot Q_0}{1 + \delta}, \quad (21)$$

where  $Q_i$  is given by eqn. (16) or (14a). For small values of  $\tau$ ,

$$\frac{Q'_t}{Q_\infty} = \frac{Av_0}{(1 + \delta)Q_\infty} \sqrt{\frac{Dt}{\pi}} + \frac{\delta Q_0}{1 + \delta Q_\infty}, \quad (22)$$

and the last term gives the magnitude of the "foot". The slope of the curve is reduced in the ratio  $1/(1 + \delta)$  from its value according to eqn. (14a).

(ii) *Saturation both for adsorption and just within the surface for occlusion.*

The relation  $Q'_t = Q_i + Q_a$  now becomes

$$Q'_t = \frac{\delta}{\gamma} + Q_i \quad (23)$$

with  $Q_i$  given by eqn. (16) or (14a). For small values of  $\tau$ ,

$$\frac{Q'_t}{Q_\infty} = \frac{Av_0}{Q_\infty} \sqrt{\frac{Dt}{\pi}} + \frac{\delta}{\gamma Q_\infty} \quad (24)$$

(iii) *Henry's law both for adsorption and for occlusion.*

$Q'_t$  again is given by eqn. (21), and  $Q_t$  by (10), (11), or (14). For small values of  $\sqrt{t}/K$ , one obtains, for example,

$$\frac{Q'_t}{Q_\infty} = \frac{6}{a(1+\delta)} \frac{Q_0}{Q_0 - Q_\infty} \sqrt{\frac{Dt}{\pi}} + \frac{\delta Q_0}{(1+\delta)Q_\infty} \quad (25)$$

With modified slope, the  $\sqrt{t}$ -law of eqn. (14) is again valid. The intercepts  $\frac{\delta Q_0}{(1+\delta)Q_\infty}$  or  $\frac{\delta}{\gamma Q_\infty}$  correspond to the "foot" in the curves of  $Q_t/Q_\infty$  against  $\sqrt{t}$  noted at lower temperatures (Fig. 4). During sorption one may have a transition from one of these limiting cases to another; for example, a natural sequence is from (ii) to (i) and from (i) to (iii). In these ways then, adsorption modifies the kinetics of diffusion, and accordingly the flow transients examined in § 4 refer to data in which adsorption was shown to be negligible by the absence of a "foot" in the rate curve.

Marischal College,  
The University,  
Aberdeen.

Bedford College,  
Regent's Park,  
N.W.1.

## THE RESIDUAL AFFINITY OF CONJUGATED AND RESONATING HYDROCARBONS

BY WILLIAM MOFFITT

Received 30th September, 1948

The reactivity of conjugated and resonating hydrocarbons has been discussed in the light of recent work by Daudel and Pullman. It has been found that a more satisfactory analysis of their calculations may be made. By postulating that the initial ease of attack, by the members of a restricted class of reagents, of the electron associated with a particular carbon atom is inversely correlated with the strength of the binding there, residual affinities have been defined for each of these atoms. Since the strength of this binding is measured by the Penney-Dirac bond orders, and the law of combination for these is linear, the residual affinities are very simply related to these bond orders and may be calculated from them. The feasibility of our postulate has been demonstrated by appeal to the known properties of particular molecular systems. The formal status of the original method of Daudel and Pullman is then examined and its applicability discussed.

**1. Introduction.**—The recent work of Daudel and Pullman<sup>1</sup> has shown that the contribution of multiple-excited structures to the ground states of a series of aromatic compounds is large. The question how these structures are to be interpreted is thus raised in an acute form. With an adaptation of the procedure of Svartholm,<sup>2</sup> they have sought to explain the reactivity of these compounds by means of a not entirely satisfactory analysis of the "distribution of electron density" in the molecule. Their method bears an obvious resemblance to the bond order of Pauling, Brockway and Beach,<sup>3</sup> and suffers from the same lack of a fundamental mathematical basis.

In this paper we show that the true status of this approach is an approximation to a well-defined procedure based on spin-theory and thus directly related to the Penney-Dirac<sup>4</sup> bond order. Short of a complete treatment of activation complexes, which is not possible in the present

<sup>1</sup> Daudel and Pullman, *J. Physique Rad.*, 1946, **7**, 59, 74, 105.

<sup>2</sup> Svartholm, *Arkiv. Kem. Min. Geol. A*, 1941, **15**, (13), 1.

<sup>3</sup> Pauling, Brockway, Beach, *J. Amer. Chem. Soc.*, 1935, **57**, 2705.

<sup>4</sup> Penney, *Proc. Roy. Soc. A*, 1937, **158**, 306.

state of the HLSP\* theory,<sup>5</sup> we have shown that we may predict the relative reactivities at the various positions of aromatic molecules by making a very simple and feasible assumption; this enables us to relate a considerable range of unsaturation reactivities in hydrocarbon chemistry.

## 2. The Procedure of Daudel and Pullman

### (a) THE *s*- AND *l*-ZONES OF DAUDEL AND PULLMAN

It is helpful to consider how Daudel and Pullman<sup>1</sup> have interpreted the procedure initiated by Svartholm.<sup>3</sup> A distinction is drawn between effective and formal, or ineffective, bonds; the Kekulé structures for benzene contain three effective bonds, whereas the Dewar structures each contain one formal and two effective bonds. These are pictured as consisting of electronic charges localized in *l*- and *s*-zones (*zones de liaison* and *zones de sommet*) respectively.

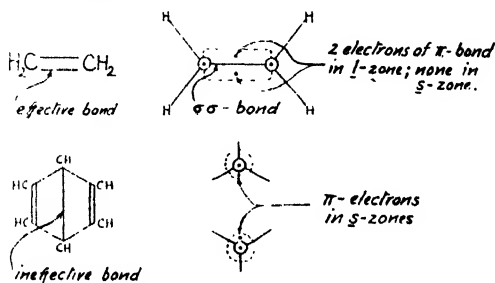


FIG. 1.

Accordingly, the following symbolism (by means of which numbers are finally attached to the various zones) is adopted:

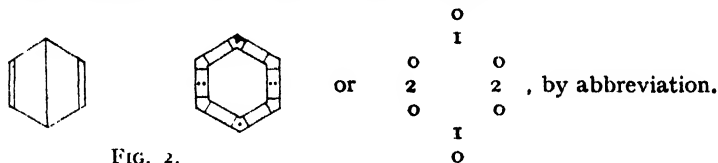


FIG. 2.

Svartholm supposed that a satisfactory description of the molecule as a whole could be obtained by superposing all such diagrams for its singly-excited structures, to each of which he gave equal weight. The reactivity at any particular carbon atom (or the free electron density there) is to be associated with the number in the corresponding *s*-zone. For example, naphthalene has 16 singly-excited structures from which a molecular diagram may be constructed by addition:

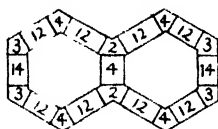
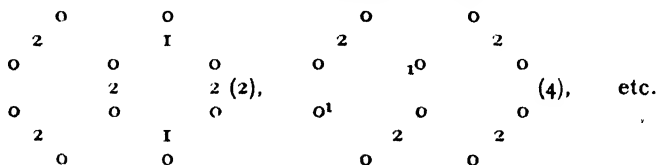


FIG. 3.

\* HLSP = Heitler, London, Slater, Pauling.

<sup>5</sup> Pauling, *J. Chem. Physics*, 1933, 1, 280.

We notice that the  $\alpha$ - and  $\beta$ -positions are associated with numbers 4 and 3 respectively; Daudel and Pullman consider this to offer an elegant demonstration of the greater reactivity of naphthalene at the  $\alpha$ -position compared to the  $\beta$ -position.

### (b) GENERALIZATION

In HLSP theory the complete wave function for any particular molecule is of the form

$$\psi = \sum_{\alpha} a_{\alpha} \psi^{\alpha},$$

where we may write down the  $\psi^{\alpha}$  representing the individual structures of the molecule, but we must determine  $a_{\alpha}$ 's by a variational treatment, setting

$$\frac{\partial E}{\partial a_{\alpha}} = 0, \text{ for all } \alpha.$$

Let us assume, with Daudel and Pullman, that this wave function is approximately of the form

$$\psi = \sum_n a_n \left\{ \sum_v \psi_{nv}^* \right\}, \quad (v = 1, \dots, \beta_n),$$

where  $\{\psi_{nv}^*\}$  denotes the sequence of the  $n$ -ply-excited structures,  $\beta_n$  in number—that is to say, we suppose the weight of each of the structures belonging to a given degree of excitation to be the same. This assumption is not necessary, but it is generally made to facilitate calculations.

Then if  $N_{ni}$  is the number of  $n$ -ply excited structures which contain ineffective bonds terminating at carbon atom  $C_i$ , and  $Z_n$  is the weight associated with all the  $n$ -ply excited structures, the absolute charge, in units of the electronic charge  $e$ , on the  $s$ -zone at this  $C_i$  is

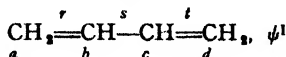
$$Q_{si} = \sum_n Z_n N_{ni}, \quad Z_n = |a_n|^2 / \sum_n \beta_n |a_n|^2.$$

Similarly, if  $M_{nk}$  is the number of  $n$ -ply excited structures which contain a certain effective bond  $k$ , the absolute charge in the corresponding  $l$ -zone is

$$Q_{lk} = 2 \sum_n Z_n M_{nk}.$$

We note that  $Q_{lk}$  is exactly twice the bond order of Pauling, Brockway and Beach<sup>2</sup> associated with the bond  $k$  in this approximation.

It is as well to remark here that these  $Q$ 's cannot be treated as dynamical variables even in the restricted sense (see later). For butadiene, for example, using the independent structures



and



we obtain, as is well known, the secular equation

$$\begin{vmatrix} 2x - 3 & x - 3 \\ x - 3 & 2x \end{vmatrix} = 0, \text{ where } x = (E - E_0)/J.$$

so that for the ground state the exchange energy and wave function are respectively,

$$E - E_0 = \sqrt{3} \times J \text{ and } \psi = (1 + \sqrt{3})\psi^I + \psi^{II}.$$

Accordingly,

$$Q_{sa} = \frac{1}{5 + 2\sqrt{3}} = 0.118 = Q_{sd}, \quad Q_{sb} = 0 = Q_{sr},$$

$$Q_{tr} = \frac{4(2 + \sqrt{3})}{5 + 2\sqrt{3}} = 1.764 = Q_{tt}, \quad Q_{ts} = \frac{2}{5 + 2\sqrt{3}} = 0.236,$$

which numbers, as we shall see, may be used to describe the reactivity of the molecule.

Now  $\psi^I$  and  $\psi^{II}$  are not the only pair of independent structures that we could have used as basis for our wave function  $\psi$ . With equal justification we could use the alternative representation



and



$\psi^{II}$  and  $\psi^{III}$  are equally satisfactory zeroth-order functions, since  $\psi^{III}$  belongs to the same (identical) representation of the molecule's point group as do  $\psi^{II}$  and  $\psi^I$ . In this event we obtain the same energy as before and the wave function

$$\psi' = \frac{1}{2}(1 + \sqrt{3}) \psi^{II} - \psi^{III},$$

giving

$$Q'_{sa} = 1 = Q'_{sd}, \quad Q'_{sb} = \frac{2}{4 + \sqrt{3}} = 0.348 = Q'_{sr},$$

$$Q'_{tr} = 0 = Q'_{tt}, \quad Q'_{ts} = \frac{2(2 + \sqrt{3})}{4 + \sqrt{3}} = 1.303.$$

Now although  $\psi'$  may be shown to be the same as  $\psi$  apart from a normalizing factor, the  $Q$ 's are obviously very different from the  $Q$ 's and in no way reflect the chemical properties of the molecule. This illustrates the dependence of the  $Q$ 's on the particular set of independent structures chosen. In future we shall assume that the  $Q$ 's are calculated in terms of that representation, which we may call rational, involving the least excitation—i.e. maximized with respect to  $\beta_0, \beta_1, \dots$ , in that order. (An alternative characterization for a rational representation will be given in a later section.)

#### (c) CHEMICAL REACTIVITY AND THE $Q$ 'S

In order to correlate the  $Q$ 's with the chemical reactivity of hydrocarbons with  $\pi$ -electrons, Daudel and Pullman postulate that

- (i) the relative ease of substitution reactions is measured by the electronic density  $Q_s$  in the corresponding  $s$ -zone;
- (ii) the relative ease of atomic additions is associated with the same factor  $Q_s$ ;
- (iii) molecular addition reactions proceed the more readily for high electronic charge densities in the appropriate  $l$ -zone  $Q_l$  and, if possible, high charges  $Q_s$  on both the corresponding  $s$ -zones.

Thus, using the rational representations for ethylene and benzene, we obtain the following molecular diagrams:

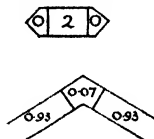


FIG. 4.

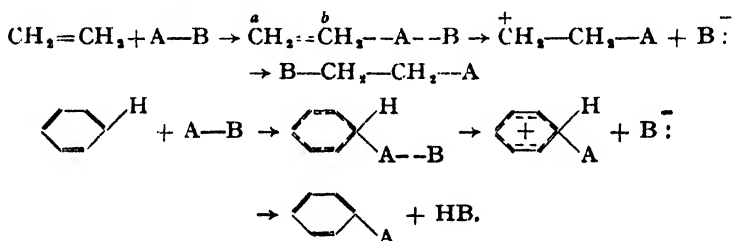
The characteristic addition reactions of the olefines are now ascribed to the fully charged *l*-zone ( $Q_i = 2$ ), whereas the aromatic character of benzene, in particular its vulnerability to substitution reactions, is associated with its charged *s*-zones ( $Q_s = 0.07$ ). The relative ease of substitution in, and addition to, condensed ring systems, such as naphthalene and anthracene may be explained along these lines; so also may certain reactions such as the Diels-Alder synthesis.

### 3. Criticism of this Procedure

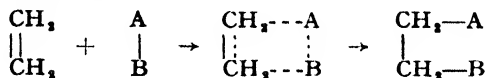
#### (a) CONCERNING REACTION MECHANISMS

In beginning to criticize the procedure outlined in the preceding section, we are perhaps struck by the rather sweeping classification of reactions into three types. We prefer to proceed rather more cautiously in first examining only that rather large class of the reactions of these hydrocarbons with electrophilic reagents which may give rise either to additions or to substitutions.

The study of chemical kinetics has led to the current view in which this class of reactions is envisaged as occurring through a rate-determining and essentially linear transition state involving only three centres—or four centres in a Lowry mechanism (see below)—and leading to the ionization of the reagent, which we call AB:



(It is not suggested that ions  $\overset{+}{\text{CH}_2}-\text{CH}_2-\text{A}$  always exist as such; it is extremely likely that in most cases the transition state is stabilized by the simultaneous approach of a basic catalyst (for example, an  $\text{H}_2\text{O}$  molecule or  $\text{B}^-$ , to  $\text{C}_a$ , so that the identities of these ions may very well be lost by such a Lowry mechanism). It seems to have been fairly conclusively demonstrated that the above mechanisms are apposite and that the four-centre additions



are relatively rare, at least for members of this class.

Let us reconsider Daudel and Pullman's discussion of chemical reactivities; we now find that for reactions with electrophilic reagents the transition state is essentially linear and three-centred for both substitutions and additions. We cannot, therefore, accept the third postulate of § 2 (c), which would appear in every case to imply a four-centred mechanism; we are, in fact, led to associate such additions with charged *s*-zones in the same way as for substitutions. But this would imply that benzene is more reactive than ethylene with respect to the attack of electrophilic reagents—an unhappy conclusion.


#### (b) CONCERNING *l*- AND *s*-ZONES

In the light of our previous comments we must enquire in what sense we may accept the distinction between electrons in *l*- and *s*-zones, that

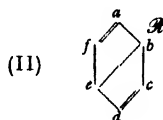
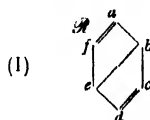


is between those participating in effective and purely formal bonds respectively. Both sets of electrons have their spins coupled (anti-parallel in pairs) but whereas in the one case the coupling is accompanied by an energy of binding measured by the corresponding exchange integral, in the other this integral is negligible, so that the coupling energy is effectively zero.

Let us consider the approach, to a (fictitious) molecule represented

by the Dewar structure , of any reagent  $\mathcal{R}$  belonging to a certain

class. We characterize this class of reagents by the condition that they each potentially contain an electron in a  $\sigma$ -orbital with which an unsaturation  $\pi$ -electron of the hydrocarbon to be attacked may be coupled to form a  $\sigma\sigma$  bond. (This class of reagents  $\mathcal{R}$  contains the class of electrophilic reagents  $AB$  and that of the atomic reagents  $X$ , such as bromine  $Br$  or hydrogen  $H$ , as sub-classes.)



If the direction of approach is as in (I), the permutation group for the molecule remains essentially unchanged at first and, since the coupling between  $a$  and  $f$  cannot easily be broken, the initial interaction is a repulsion which may be assessed in the usual way by means of a term,  $-\frac{1}{2}(J_{Ra} + J_{Rf})$ . If, however, the mode of incidence follows (II), the situation is quite different. Since the energy of uncoupling of the formal bond between  $b$  and  $e$  is zero, the permutation group for the molecule is altered at the outset and, in the ground state of the ensuing complex with  $\mathcal{R}$ , the electron associated with the  $\pi$ -orbital of  $b$  is coupled with another in the appropriate  $\sigma$ -orbital of the reagent  $\mathcal{R}$ , giving rise to an attraction  $J_{Rb}$ , approximately.

Thus, if we regard those electrons which are coupled in effective bonding as localized in  $l$ -zones and the "available" electrons, which only bond ineffectively, as situated in the corresponding  $s$ -zones, we find that we may conventionally represent the state of affairs by means of the "distribution of electron density" envisaged by Svartholm—providing we do not suppose that this localization is genuinely spatial in origin.

### (c) PURE (EIGEN-) STATES AND PURE VALENCE STATES

Since we have managed to give a more precise meaning to the zone diagram for a single structure  $\psi^\alpha$ , it is clearly in the method of combination, i.e. in the definition of the  $Q_i$ 's and  $Q_j$ 's, that the weakness of the Daudel and Pullman procedure is to be found. It seems to us that a confusion has arisen between the expansion  $\psi_m = \sum_{\tau} a_{\tau} \psi^{\tau}$  of the representative of a

mixed state  $\psi_m$  in terms of the representatives  $\psi^{\tau}$  of its constituent pure (eigen-) states, and the expansion  $\psi = \sum_{\alpha} a_{\alpha} \psi^{\alpha}$ , of the wave function  $\psi$  of a (complex) pure state in terms of simpler (variational) functions  $\psi^{\alpha}$ .

In the former case, the  $\psi^{\tau}$  are the mutually orthogonal eigenfunctions of pure states belonging to the eigenvalues  $\xi_{\tau}'$  of a complete set of commuting observables  $\xi$ . Any observation of  $\xi$  necessarily yields some  $\xi_{\tau}'$  for its result so that immediately afterwards the observed system is in the pure state  $\psi^{\tau}$ . The probability of obtaining any particular result is given by the weight  $\omega_{\tau} = |a_{\tau}|^2 / \sum |a_{\tau}|^2$  of the pure state in the initial

mixed state  $\psi_m$ . (A stationary state  $\psi^\tau$ , in general, is one for which  $\xi$  is the Hamiltonian and  $\xi^\tau$  the energy.)

In the latter case, however, the  $a_\alpha$ 's are chosen so as to obtain the best possible approximation to the pure state  $\psi$ . For our purposes the structures  $\psi^\alpha$ , which are not even orthogonal, obviously do not represent constituent pure states in the above sense. Nor is the decomposition

$\psi = \sum_{\alpha} a_{\alpha} \psi^{\alpha}$  unique since, as we have seen for butadiene, the number of

possible structures is always greater than the number of independent structures, except for the simplest case of ethylene. Thus although the term  $|a_{\alpha}|^2 / \sum_{\alpha} |a_{\alpha}|^2$  may indicate the relative importance of the structure

$\psi^{\alpha}$  in the variational calculation using some particular set of independent structures, it may not be given the logical status of a quantum-mechanical weight  $\omega_r$ .

We therefore find that the Daudel and Pullman assessment of the "electronic densities" to be associated with the various zones of a molecule is an entirely arbitrary procedure; we have been misled in our ready acceptance of the "weight" factors  $Z_n$ . It is unfortunate, and possibly in some way accounts for the confusion, that the structures  $\psi^{\alpha}$  are often known as "pure" valence states. A "pure valence state" is an electronic condition that could exist by itself whereas the  $\psi^{\alpha}$  could not.

#### 4. The Residual Affinities

##### (a) THE VECTOR MODEL

Let us, following Penney,<sup>4</sup> begin by formulating the HLSP procedure in terms of the cosine coupling of spin vectors. Dirac<sup>5</sup> has given the general solution of our problem—that of determining the perturbation energy for a system whose representative is an antisymmetrical combination of atomic orbitals (AO's)  $\phi_i$ —in the form

$$E = \text{const.} - \frac{1}{2} \sum_i \sum_{j>i} (1 + 4\mathbf{s}_i \cdot \mathbf{s}_j) J_{ij}.$$

The quantities  $-\frac{1}{2}(1 + 4\mathbf{s}_i \cdot \mathbf{s}_j)$  here play their role as eigenvalues of operators permuting AO's which, being peculiar to an approximation combining AO's in this manner, may be considered as dynamical variables in the restricted sense. For given values of the exchange integrals

$$J_{ij} \equiv \iint \phi_i^*(1) \phi_j^*(2) \mathbf{H} \phi_i(1) \phi_j(2) d\tau_1 d\tau_2,$$

the  $\mathbf{s}_i \cdot \mathbf{s}_j$  are determined by minimizing the energy  $E$ , subject to the conditions imposed by the eigenvalues of the integrals of the motion  $\mathbf{S}^2, \mathbf{S}_z$ . Now to our approximation, in which non-adjacent interactions are neglected and all other exchange integrals are supposed to be equal, we may distinguish between effective and ineffective bonding as follows. Whenever  $J_{ij} = J \neq 0$ , we say that the orbitals  $\phi_i, \phi_j$  are joined by a partial bond of order  $p_{ij}$  determined by the relative spin orientation of the electrons associated with these orbitals; conventionally

$$p_{ij} = -\frac{4}{3}(\mathbf{s}_i \cdot \mathbf{s}_j),$$

so that if these spins are anti-parallel, as for the  $\pi$ -electrons in ethylene,  $p_{ij} = 1$ , whereas for random coupling  $p_{ij} = 0$ . If, however,  $J_{ij} \approx 0$ , then the bonding is ineffective and even the smallest of perturbations of the appropriate symmetry may destroy this purely formal coupling which we call

$$r_{ij} = \frac{4}{3}(\mathbf{s}_i \cdot \mathbf{s}_j).$$

<sup>5</sup> Dirac, *Quantum Mechanics* (2nd ed., 1934), Ch. 10.

## (b) THE RESIDUAL AFFINITIES

Intuitively, therefore, it is clear that the initial ease of attack of a reagent  $\mathcal{R}$  at carbon atom  $C_i$  of a molecule is a function of the total amount of ineffective bonding in which the electron associated with  $\phi_i$  participates, and the question arises how we are to assess this.

Let us first confine ourselves to those molecules for which the eigenvalues of  $\mathbf{S}^2$  and  $\mathbf{S}_z$  are equal to zero. The law of combination of the individual spin vectors being linear, we find that

$$\sum_j' (\mathbf{s}_i \cdot \mathbf{s}_j) = (\mathbf{s}_i \cdot \sum_j' \mathbf{s}_j) = (\mathbf{s}_i \cdot \mathbf{S}) = (\mathbf{s}_i \cdot \mathbf{s}_i),$$

or, since the eigenvalue of  $\mathbf{S}^2$  is equal to 0,

$$-\frac{1}{2} \sum_j' (\overline{\mathbf{s}_i \cdot \mathbf{s}_j}) = -\frac{1}{2} \{(\overline{\mathbf{s}_i \cdot \mathbf{S}}) - (\mathbf{s}_i \cdot \mathbf{s}_i)\} = -\frac{1}{2} \{0 + \frac{1}{2}(\frac{1}{2} + 1)\} = 1,$$

the summation  $\sum_j'$  being taken over all  $j \neq i$ . But  $-\frac{1}{2} \sum_j' (\overline{\mathbf{s}_i \cdot \mathbf{s}_j}) = \sum_j' t_{ij}$

where  $t_{ij} = p_{ij}$  if the coupling  $(\overline{\mathbf{s}_i \cdot \mathbf{s}_j})$  is effective and  $t_{ij} = r_{ij}$  if the coupling is ineffective. Thus if  $\sum_j' r_{ij}$  and  $\sum_j' p_{ij}$  denote the total ineffective and

effective coupling associated with the spin vector  $\mathbf{s}_i$ , we find that, say,

$$\sum_j' r_{ij} = 1 - \sum_j' p_{ij} = r_i.$$

It is clear that the numbers  $r_i$ , thus defined, perform that function which the  $Q_{ii}$ 's of Daudel and Pullman had set out to perform; we may therefore call them the residual affinities, attached respectively to the carbon atoms  $C_i$  of a conjugated or resonating system. They are dynamical variables (in the restricted sense of Dirac<sup>6</sup>) and thus independent of the particular choice of structures which we choose to facilitate our calculations. Let us see if we can find a more direct meaning for the  $r_i$ —one which may help to justify our future usage.

(c) A FURTHER PROPERTY OF THE  $r_i$ 

The exchange energy of a particular molecule may be written in the form,

$$\begin{aligned} E - E_0 &= V = R - 2 \sum_i \sum_{j>i} (\overline{\mathbf{s}_i \cdot \mathbf{s}_j}) J_{ij} \\ &= R + \frac{1}{2} \sum_i \left\{ \sum_j' t_{ij} J_{ij} \right\}, \end{aligned}$$

where  $R = -\frac{1}{2} \sum_i \sum_{j>i} J_{ij}$  is the total exchange repulsion, and the last term,

in which summation over pairs  $\sum_i \sum_{j>i}$  has been replaced by the equivalent

summation  $\frac{1}{2} \sum_i \left\{ \sum_j' \right\}$ , measures the energy of coupling. We may say that

the electron associated with  $C_i$  is bound with an exchange energy of coupling  $\frac{1}{2} \sum_j' t_{ij} J_{ij}$  or  $\frac{1}{2} \sum_j' p_{ij} J_{ij}$  in our approximation. The residual affinity

$r_i = 1 - \sum_j' p_{ij}$  therefore describes the differential lability or the initial

ease of displacement of the electron on  $C_i$ . (For an ethylenic carbon atom  $r_i = 0$ , which is a useful standard.)

Our rather indirect spin criterion may now be replaced by the more immediate condition which may be formulated. If we assume that the

ease of attack at the carbon atoms of an unsaturated molecule is inversely correlated with the strength of the electronic binding there, then the activation energies of reactions with molecules  $\mathcal{R}$  (§ 3(b)) may be correlated with the appropriate residual affinities  $r_i$ . The ultimate justification for this assumption lies in the correspondence between prediction and observation to which it gives rise—we shall show it to be appropriate in a later section—but it is unfortunately a necessary assumption. The HLSP theory in its present form is incapable of dealing in a quantitative manner with ionic structures, without which these activation complexes (or indeed any aromatic compounds with substituents of electromeric propensity) cannot be adequately described.

## 5. Application to Particular Molecules

### (a) THE DOMAIN OF THE RESIDUAL AFFINITIES $r_i$

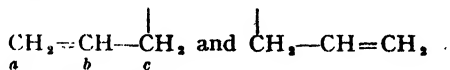
In order to illustrate the chemical significance of the range of residual affinities, we shall first deal with three standard molecules: ethylene, benzene and the free radical  $\text{CH}_2 \cdot \text{CH} \cdot \text{CH}_2$ .

(i) Ethylene may be regarded as being in a pure valence state; the complete set of  $\psi^\alpha$  contains only one member so that  $p$  (ethylene) = 1,  $r$  (ethylene) = 0.

(ii) Benzene with five independent structures yields, independently of their particular choice,  $p$  (benzene) = 0.623, and

$$r \text{ (benzene)} = 1 - 2(0.623) = -0.246.$$

(iii)  $\text{CH}_2 \cdot \text{CH} \cdot \text{CH}_2$ . In treating free radicals (doublet ground states) by the HLSP method, the free electron in each structure is formally coupled with that in an orbital at infinity, which may here be identified with an orbital  $\phi_p$  of the attacking reagent  $\mathcal{R}$ . Accordingly the permutation group for the molecule (which is then treated under Pauling's rules for singlet states) has been "prepared" for this attack and the correct  $r_i$  is simply the factor  $-\frac{1}{3}(\mathbf{1}_i \times \mathbf{1}_p)$ . For this particular free radical there are two structures



from which we obtain the results,

$$r_a = +\frac{1}{3} = r_c, \quad r_b = -\frac{1}{3}; \quad p = +\frac{1}{3}.$$

Thus olefinic reactivities lie near  $r_i = 0$ , whereas those of aromatic molecules are to be found in the range around  $r_i = -0.25$ . The positive range of the  $r_i$  covers the reactivities of the free radicals. (For a "pure" free radical, with no resonance,  $r_i = 1$ .)

### (b) BUTADIENE, NAPHTHALENE AND ANTHRACENE

For butadiene, which we have examined in considering the  $Q_n$ 's, the following results are obtained:

$$p_r = 0.911 = p_i \quad \text{and} \quad p_s = 0.333,$$

so that

$$r_a = 1 - 0.911 = 0.089 = r_d,$$

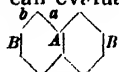
$$r_b = 1 - 0.911 - 0.333 = -0.244 = r_c.$$

Thus we may account for the high reactivity of butadiene at its outer carbon atoms—a reactivity which surpasses that of ethylene.

For naphthalene we should have to explain the preferential attack by  $\mathcal{R}$  of its  $\alpha$ -position, whereas for anthracene we ought to find particularly reactive *meso*-positions. The bond orders for both these molecules have been calculated on the basis of certain simplifying assumptions which the

## 382 CONJUGATED AND RESONATING HYDROCARBONS

work of Sherman,<sup>7</sup> and Daudel and Pullman,<sup>1</sup> has justified. Accordingly we can evaluate the  $r_1$  without any difficulty.



For naphthalene, Penney<sup>4</sup> gives

$$p_A = 0.433, p_B = 0.530, p_a = 0.516, p_b = 0.690$$

from which it is readily verified that

$$r_A = -0.206; r_B = -0.220,$$

in agreement with our expectations, from chemical evidence. (We note that both  $|p_a - p_b| = 0.174$  and  $|p_b - p_B| = 0.160$  are small—this is later shown to characterize aromaticity and consequently vulnerability to substitution, as is found.)



For anthracene Michailov<sup>8</sup> has calculated the following bond orders:

$$p_b = 0.491, p_c = 0.715, p_B = 0.491, p_a = 0.587,$$

whence the residual affinities are

$$r_1 = -0.191, r_2 = -0.206, r_3 = -0.174.$$

These quantities evidently reproduce the chemical behaviour of this compound.

## 6. Review of the Daudel and Pullman Procedure

### (a) MATHEMATICAL STATUS

Writing the wave function for a molecule in the form  $\psi = \sum_{\alpha} a_{\alpha} \psi^{\alpha}$ ,

we find that

$$Z_{\alpha} = |a_{\alpha}|^2 / \sum_{\alpha} |a_{\alpha}|^2 = |a_{\alpha}|^2 / N^2, \text{ say,}$$

$N$  being a normalizing constant. We now define numbers  $\rho_{ij}^{\alpha}$ ,  $\xi_{ij}^{\alpha}$  and  $\eta_{ij}^{\alpha}$  for each structure  $\psi^{\alpha}$ , such that  $\rho_{ij}^{\alpha} = 1$  or 0 according as the electrons on  $C_i$  and  $C_j$  are paired in  $\psi^{\alpha}$  or not, and  $\rho_{ij}^{\alpha} = \eta_{ij}^{\alpha}$  or  $\xi_{ij}^{\alpha}$  according as  $C_i$  and  $C_j$  are adjacent ( $J_{ij} = J \neq 0$ ) or not ( $J_{ij} \approx 0$ ), respectively. It is then found that

$$Q_{ii} = \sum_{\alpha} Z_{\alpha} \left\{ \sum_j^{\dagger} \xi_{ij}^{\alpha} \right\} - N^{-2} \sum_{\alpha} |a_{\alpha}|^2 \left\{ \sum_j^{\dagger} \xi_{ii}^{\alpha} \right\},$$

$$Q_{ik} = 2 \sum_{\alpha} Z_{\alpha} \eta_k^{\alpha} - 2N^{-2} \sum_{\alpha} |a_{\alpha}|^2 \eta_k^{\alpha},$$

where  $k$  refers to a particular effective bond  $i-j$ . We note that, if  $\sum_k^i$  denotes summation over the effective bonds terminating on  $C_i$ , then

$$Q_{ii} = 1 - \sum_k^i \frac{1}{2} Q_{ik}.$$

Let us see how these quantities are related to the energy  $E$  of the molecule. We have

$$E = \int \psi^* \psi d\tau = \int \psi^* \mathbf{H} \psi d\tau,$$

or

$$E = \sum_{\alpha} \sum_{\beta} a_{\alpha}^* a_{\beta} (\alpha | \beta) = \sum_{\alpha} \sum_{\beta} a_{\alpha}^* a_{\beta} (\alpha | \mathbf{H} | \beta),$$

where

$$(\alpha | \beta) = \int \psi^{\alpha*} \psi^{\beta} d\tau \text{ and } (\alpha | \mathbf{H} | \beta) = \int \psi^{\alpha*} \mathbf{H} \psi^{\beta} d\tau$$

may be determined with the aid of the rules laid down by Pauling.<sup>8</sup>

<sup>7</sup> Sherman, *J. Chem. Physics*, 1934, **2**, 488.

<sup>8</sup> Michailov, *Acta Physicochim.*, 1946, **21**, 387.

Clearly

$$\begin{aligned}(\alpha | \mathbf{H} | \alpha) &= E_0 - \frac{1}{2} \sum_i \sum_{j>i} J_{ij} + \frac{3}{2} \sum_i \sum_{j>i} \rho_{ij}^\alpha J_{ij} \\ &= E_0 + R + \frac{3}{2} \sum_k \eta_k^\alpha J,\end{aligned}$$

where  $E_0$  is the Coulomb energy. If we were to neglect non-diagonal terms (e.g.  $(\alpha | \mathbf{H} | \beta)$  with  $\alpha \neq \beta$ ) we then find that, as an approximation to  $E$ , we have the quantity  $E'$ , where

$$E' \times N^2 = (E_0 + R) \cdot N^2 + \frac{3}{2} \sum_\alpha |a_\alpha|^2 \sum_k \eta_k^\alpha \cdot J,$$

or

$$E' = E_0 + R + \frac{3}{2} \sum_k Q_{ik} \cdot J.$$

To this approximation, then, we may relate the  $Q$ 's with our  $p$ 's and  $r$ 's as follows:

$$Q_{ik} = 2p_k \text{ and } Q_{ii} = r_i$$


since  $\sum_k = \frac{1}{2} \sum_i \sum_j$  and because  $Q_{ii} = 1 - \sum_k^i \frac{1}{2} \cdot Q_{ik}$ .

In general the quantity  $E'$  depends upon the particular set of independent structures selected, so that the  $Q$ 's will, at best, be significant only in that representation for which the approximation of neglecting the non-diagonal elements of the energy matrix is most appropriate—i.e. with that set of structures  $\psi^\alpha$  which gives the closest approach of  $E'$  to  $E$ . We might therefore expect to obtain apposite  $Q$ 's (of relative significance) by use of such "rational" representations (see also § 2 (b), above) for a particular family of molecules. But we must also expect trouble if we compare the  $Q$ 's of one family (e.g. the polythenes: ethylene, butadiene, etc. . . .) with those of another (say, the polyacenes: benzene, naphthalene, anthracene, . . .)—since although the errors accompanying this approximation may remain dormant for, or nearly constant throughout, the members of one class, we have no reason to suppose that they should do so for the whole range of these hydrocarbons.

### (b) APPLICABILITY

Whenever we can use  $Q$ 's in this relative sense for a particular class of compounds, we expect bond lengths and force constants to be functions of the  $Q_i$ 's and reactivities to parallel the  $Q_i$ 's. This appears to be so for the class of polyacenes and for the class of polyenes. We cannot, however, follow Daudel and Pullman in their analysis of the relative reactivities of ethylene and benzene which are the lowest members of these quite different families. They have used their charge densities in an absolute sense postulating that highly charged  $l$ -zones lead to additions and that highly-charged  $s$ -zones alone lead to substitutions. But we have shown in § 3 (a) that the transition states for both these classes of reactions are generally quite analogous, and that the ease of attack should therefore in both cases be assessed by  $r_i$  alone (to which  $Q_{ii}$  is supposed to be an approximation). Why, then, is there this correlation of  $Q_i$  with addition reactions?

Before answering this question, let us return to the mechanism of attack by the electrophilic AB of the molecules ethylene and benzene.

We recall that the ion  lost  $H^+$ , with characteristic aromaticity,

to give the substituted benzene. That  $B^-$  is not added instead is explained by the great stability of the highly resonating benzene ring system which would be broken by addition of  $B^-$ . Now if  $C_i$  has two nearest neighbours,  $C_a$  and  $C_b$ , with which it makes bonds  $m$  and  $n$ , we may associate such full resonance with  $C_i$  by requiring that  $|p_{ia} - p_{ib}|$  or  $|Q_{im} - Q_{in}|$  be small.

Accordingly, instead of assuming that additions require high  $l$ -zone charges at the bond they attack, we characterize substitutions by means of low  $|p_{ia} - p_{ib}|$ , or  $|Q_{im} - Q_{in}|$ , associating their readiness to occur, however, with  $r_i$  or  $Q_{ii}$ . That the  $Q_i$ 's would suggest benzene to be more reactive than ethylene is taken as an indication that these two compounds belong to different families which are not mutually  $Q_i$ -comparable. We note in passing that most hydrocarbons appear to be  $Q_i$ -comparable.

For larger molecules the additional labour in calculating  $p$ 's (and hence  $r$ 's), after the secular equation has been solved, may be considerable. In these cases we must use the  $Q_i$ 's in order to determine the properties of the various bonds and the  $Q_i$ 's for the chemical reactivity. Providing we do so relatively, and bear in mind their limited domain of applicability, this should lead to significant predictions.

## 7. Appendix

In § 5 we calibrated our residual affinities  $r_i$  against certain standard molecules. For some purposes and for completeness it may be useful to have a more fundamental criterion, namely a value of  $r_i$  for the most inert carbon atom of a given type. Since interactions between nearest neighbours only are considered, and the exchange integrals are taken as equal for these, we shall find it convenient to distinguish between three different sorts of carbon atom: Those with only one, class (i), say, two, (ii), and three, (iii), nearest neighbours, respectively. As examples of these we have the carbon atoms of ethylene, benzene and those common to two nuclei in polynuclear hydrocarbons. (This classification may also be useful on other, e.g. steric, grounds.) For carbon atoms of the type (i), it is obvious that maximum bonding, and therefore minimum affinity, occurs when  $p = 1$  and  $r = 0$ .

Consider now the more general case of a carbon atom  $i$  surrounded by  $n$  carbon atoms  $j$  ( $= 1, \dots, n$ ) in a plane containing  $i$ . The only non-negligible  $\pi$  exchange integrals are those of the form  $J_{ij}$  and these are supposed equal to  $J$ . (As an example of this, we have already encountered the case  $n = 2$  for the free radical  $\text{CH}_2 \cdot \text{CH} \cdot \text{CH}_2$ .) The perturbing Hamiltonian may be written in the form

$$\mathbf{V}^n = -\frac{1}{2} \sum_{j=1}^n (1 + 4\mathbf{s}_j \cdot \mathbf{s}_i) J = - (n/2 + 2\mathbf{S}_n \cdot \mathbf{s}_i) J,$$

where  $\mathbf{S}_n = \sum_j \mathbf{s}_j$ . Now it is easily shown that with this particular form

for  $\mathbf{V}^n$ ,  $\mathbf{S}_n^2$  and  $\mathbf{s}_i^2$ , as well as  $\mathbf{S}^2$  (where  $\mathbf{S} = \mathbf{S}_n + \mathbf{s}_i$ ), commute with  $\mathbf{V}^n$  and are therefore constants of the motion. Accordingly and because

$$2\mathbf{S}_n \cdot \mathbf{s}_i = \mathbf{S}^2 - \mathbf{S}_n^2 - \mathbf{s}_i^2,$$

the energy eigenvalues are

$$E^n = E_0^n + R^n - \{S(S+1) - S_n(S_n+1) - s_i(s_i+1)\}J.$$

Now the strength of the  $\pi$  bonding at carbon atom  $i$  will be a maximum when the spins of the electrons on neighbouring atoms  $j$  are free to couple with  $\mathbf{s}_i$  in the strongest possible way—i.e. when these spins are not pre-emptively aligned owing to the presence of other conjugating parts of a molecule. The ground state of the hypothetical molecule (of  $(n+1)$  atoms and only  $n$  effective exchange interactions) which we have been considering, therefore exhibits the electron associated with  $i$  in its most strongly bound form. When a group of  $(n+1)$  such atoms is found in a molecule of  $m > (n+1)$  carbon atoms, of course,  $(\mathbf{S}_n + \mathbf{s}_i)^2$  will no longer, in general, be a "good quantum number". Accordingly, although the molecule as a whole may be in a singlet state, any conclusions as to the limit properties of atom  $i$  which we may draw by assigning an eigenvalue other than 0 to the operator  $(\mathbf{S}_n + \mathbf{s}_i)^2$ , will not be invalidated.

Consider first the case  $n = 2$ . Since  $J$  is negative the ground state is the doublet for which  $S = \frac{1}{2}$ ,  $S_n = 1$ ,  $s_i = \frac{1}{2}$ :

$$r_i = 1 - \sum_j p_{ij} = 1 + \sqrt{\frac{1}{2} S_n \cdot s_i} = -\frac{1}{2}.$$

Similarly when  $n = 3$ , the triplet ground state has quantum numbers  $S = 1$ ,  $S_n = \frac{3}{2}$ ,  $s_i = \frac{1}{2}$ , so that

$$r_i = 1 + \sqrt{\frac{1}{3} S_n \cdot s_i} = -\frac{1}{3}.$$

(These results which we have obtained by means of the vector model could also, of course, have been deduced less systematically by means of the more usual HLSP procedure; the method which we have followed is, however, also more simple here and serves to illustrate the direct use of Dirac's formula.)

The lowest residual affinities associated with electrons on carbon atoms of classes (i), (ii) and (iii) are therefore 0,  $-\frac{1}{2}$  and  $-\frac{1}{3}$  respectively. If we wished to avoid negative signs in our definition of residual affinities, we could retain this classification of carbon atoms according to their situations and redefine quantities relative to these three standard values.

Coulson<sup>9</sup> has recently suggested that the molecular orbital method may also be used to predict reactivity. Analogous quantities  $r_i = 1 - \sum_j p_{ij}$  may also be defined for these calculations, and arguments similar to those used above, lead to minimum affinities at  $r = 0$ ,  $(1 - \sqrt{2})$  and  $(1 - \sqrt{3})$  respectively.

NOTE.—More recently, to conform with current usage, Daudel<sup>10</sup> has changed his nomenclature somewhat so that now  $Q_{ik}$  is called the free valence number and  $\frac{1}{2}Q_{ik}$  the bond order.

The writer would like to acknowledge the receipt of a grant from the Board of the British Rubber Producers' Research Association, and the benefit of certain discussion with Prof. C. A. Coulson.

New College,  
Oxford.

<sup>9</sup> Coulson, *Trans. Faraday Soc.*, 1946, 42, 265.

<sup>10</sup> Daudel *et al.*, *Rev. Sci.*, 84, 489.

## SOME NEW ASPECTS OF THE STRENGTH OF ALLOYS \*

BY GEORGE-MARIA SCHWAB

Received 25th October, 1948

It is shown that the temperature coefficient of the Brinell hardness of metals can be represented by a bi-exponential formula, leading to the assumption of two different processes with different activation energies, of which the larger one,  $E_2$ , is connected with the formation of new perturbation centres. The Brinell hardness of the phases  $\alpha$ ,  $\beta$ ,  $\gamma$ ,  $\epsilon$ ,  $\eta$  of the Hume-Rothery systems, Cu—Zn, Cu—Sn, Ag—Zn and Ag—Cd, is measured between 20 and 450° C in a special apparatus and evaluated according to the above theory. A maximum of  $E_2$

\* Contribution from the Dept. of Inorganic, Physical and Catalytic Chemistry, of the Institute "Nicolao Canellopoulos," Piraeus, Greece.



appears to be exhibited by the  $\gamma$ -phases of all the systems, which at the same time accounts for their hardness maxima at room temperature. It is concluded that the dislocation of atoms is the more difficult the more the first Brillouin zone of a lattice is electron-saturated.

Transitions of cubic body-centred to hexagonal phases of the same composition cause an increase of hardness and vice versa. Silver and its alloys show a hardness anomaly around 300°, which may be due to a reversible, and sometimes retarded, mosaic-structure transition.

In a survey of published data of the Brinell hardness of Hume-Rothery alloys, a summary of which has been published previously,<sup>1</sup> it was found (i) that the hardness increases with the proportion of the polyvalent component within the  $\alpha$ -phases (ii) that the hardness has a sharp maximum at the composition of the  $\gamma$ -phases, and (iii) that  $\beta$ -,  $\epsilon$ - and  $\eta$ -phases have about the same hardness values as the saturated  $\alpha$ -phases. In a number of publications from this laboratory<sup>2</sup> the same rules have been shown to hold accurately for the activation energy of the formic acid dehydrogenation using Hume-Rothery alloys as catalysts. In these reactions and also with the specific electric resistance the influence of electron concentration could be explained by Mott and Jones' theory of these alloys,<sup>3</sup> in terms of the degree of electron saturation of the first Brillouin zone. Therefore, an attempt was made<sup>1</sup> to explain the variation of hardness on similar lines. It was supposed that in a Brillouin zone which was nearly filled by conductivity electrons, as is the zone of the  $\gamma$ -phases, a diminution of the zone volume will encounter considerable opposition. Such a diminution, involving an increase of certain atom distances, was considered as a necessary condition for the formation and propagation of lattice dislocations in the mechanism of plastic gliding.

In a discussion on this topic<sup>4</sup> the question was raised as to how far this hypothesis, based on data for ordinary temperatures, would be applicable at other temperatures in view of the effect of temperature on the hardness. It was therefore suggested by the author that the critical activation energy of plastic deformation should show a similar variation. In the present paper an experimental approach to this problem is presented.<sup>5</sup>

First, an approximate mathematical treatment of the temperature coefficient of the Brinell hardness is derived from existing theories and experimental data. Then, measurements on Hume-Rothery alloys are described and evaluated using the above theory, and tentative conclusions are drawn. Some special phenomena encountered in this work is also discussed.

**The Temperature Dependence of Brinell Hardness.**—It is generally admitted that the Brinell or "sphere-indenting" hardness is not a clearly defined nor a strictly reproducible measure of the magnitude of the intrinsic plasticity of a material, because (i) it does not correspond to a state of homogeneous stress distribution, (ii) work-hardening occurs during the indenting process, (iii) plastic after-flow is observed. In spite of this, a relation to the elastic limit or yield stress, sufficiently consistent for practical purposes, can be stated (see e.g. the recent work of Tabor).<sup>6</sup> It is probably due to these shortcomings that no special theory for the temperature dependence of hardness seems to exist in the literature.

<sup>1</sup> Schwab, *Experientia*, 1946, **2**, 103.

<sup>2</sup> Schwab and Karatzas, *Z. Elektrochem.*, 1944, **50**, 204; Schwab, *Trans. Faraday Soc.*, 1946, **42**, 689; Schwab and Pesmatjoglou, *J. Physic. Chem.*, 1948, **52**, 1040, and forthcoming publications.

<sup>3</sup> Mott and Jones, *The Theory of the Properties of Metals and Alloys* (O.U.P. 1936).

<sup>4</sup> *Proc. XI. Int. Cong. Chem.* (London, 1937).

<sup>5</sup> See the preliminary communication at the meeting of the Swiss Chemical Society, 2nd Feb., 1948; *Chimia*, 1948, **2**, 124.

<sup>6</sup> Tabor, *Proc. Roy. Soc. A*, 1948, **192**, 247.

For the same reason, the treatment proposed below is to be considered as a first approximation, which accounts for the broad effects of temperature and composition.

One could tentatively assume that the hardness, i.e. the load at which a sphere ceases to penetrate into the material, is identical or proportional to the critical shearing stress which produces a perceptible deformation velocity. A theoretical equation for the plastic deformation velocity has been formulated by Smekal<sup>7</sup> and improved by Becker<sup>8</sup> and Orowan.<sup>9</sup> According to it, the gliding velocity  $v$  is given by

$$v = \alpha c \frac{E(1 - \sigma/\sigma_0)^2}{RT}, \quad (1)$$

$E$  being the critical increment for the movement of a perturbation centre,  $\sigma$  the stress applied,  $\sigma_0$  the critical stress at  $0^\circ$  K, and  $\alpha$  a proportionality factor, containing the number of perturbation centres present and the deformation produced by their movement. The idea is that the necessary thermal activation energy is diminished by the activation produced by the applied stress. For the critical stress  $\sigma_k$  which produces a certain critical deformation velocity  $v_k$ , we obtain

$$\sigma_k = \sigma_0 - \sigma_0 \sqrt{(RT/E)(\alpha - \log v_k)} = A - B\sqrt{T}. \quad (2)$$

This equation, according to Kochendörfer<sup>10</sup> well represents the temperature dependence of critical shearing stresses as taken from stress-strain curves. An attempt to apply it to some of the few existing temperature-hardness curves is shown in Fig. 1. The values marked

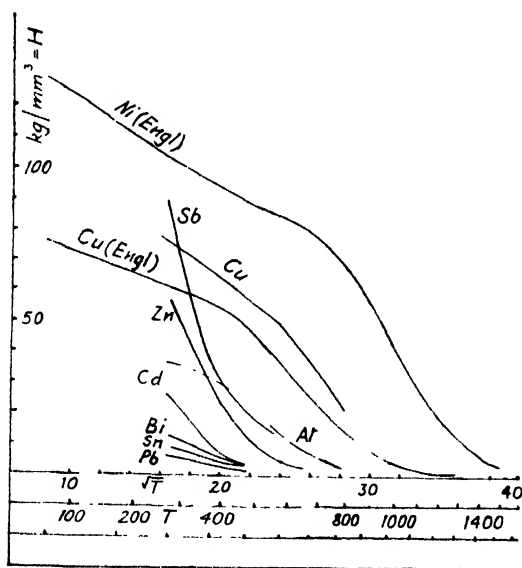


FIG. 1.

Engl are of Engl and Katz,<sup>11</sup> the rest are cone hardnesses of Ludwik,<sup>12</sup> these being known to be about 25 % lower than sphere hardnesses. The result is disappointing. Not only is  $B$  not constant, but even its variation is not uniform.

<sup>7</sup> See Smekal, *Erg. exakt. Naturwiss.*, 1936, **15**, 130, et seq.

<sup>8</sup> Becker, *Z. Physik*, 1925, **26**, 919.

<sup>9</sup> Orowan, *ibid.*, 1934, **89**, 605.

<sup>10</sup> Kochendörfer, *Plastische Eigenschaften von Kristallen und metallischen Werkstoffen* (Berlin, 1941).

<sup>11</sup> Engl and Katz, *Z. Physik*, 1937, **106**, 1.

<sup>12</sup> Ludwik and Schimmer, *Z. physik. Chem.*, 1916, **91**, 232.

The fact that the true temperature function is of an exponential form was first observed by Schischokin<sup>13</sup> who was also the first to make systematic measurements of temperature coefficients on some alloy systems and to state the influence of composition.<sup>14</sup> His empirical equation is

$$H = ae^{-bt}, \quad (3)$$

$H$  being the hardness,  $t$  temperature °C,  $a$  and  $b$  constants. This shows that the hardness cannot appear exclusively in the exponent, as does  $\sigma$  in (1), but that some sort of viscosity equation is more adequate. We therefore write

$$v = \sigma \alpha' e^{-\frac{E(1-\sigma/\sigma_0)}{RT}} \quad (4)$$

This equation denotes that the deformation produced by the mobility of a perturbation centre is not constant but proportional to the stress applied as in viscous flow. In this form, the expression is transcendental, but by assuming  $\sigma_0 \gg \sigma$  it takes the more convenient form:

$$v = \sigma \alpha' e^{-E/RT} \quad (5)$$

This assumption requires that the energy produced by the applied stress is small compared with the total mobility energy. The assumption is justified *a posteriori*, at least at high temperatures, by the  $E_k$  values found, which, even allowing for a notch factor of 500, are much higher than the work done by critical stresses over mean atomic distances.

If, again, we define "hardness" as the critical stress  $\sigma_k$  which produces a certain, just perceptible, deformation velocity  $v_k$  (or a magnitude proportional to  $\sigma_k$ ), we obtain

$$H = \sigma_k = \frac{v_k}{\alpha' e^{-E/RT}} = A e^{E/RT}, \quad (6)$$

which leads to

$$\ln H = \ln A + (E/R) \times (1/T). \quad (7)$$

In Fig. 2,  $\log H$  is plotted as a function of  $1/T$  for those examples shown in Fig. 1. It is seen that in this plot all the curves have the same characteristics. In the low temperature region they are approximately straight

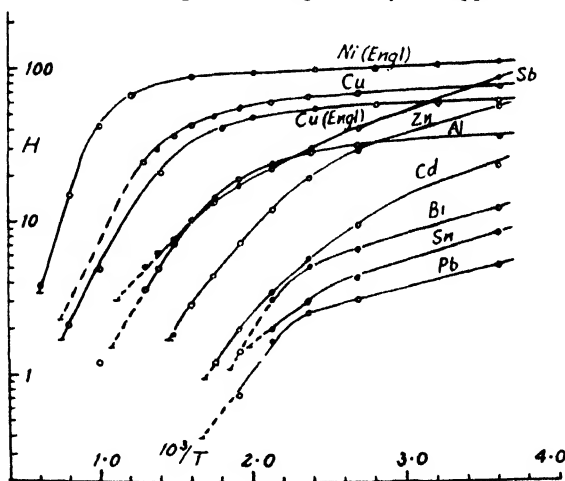


FIG. 2.

lines of small slope, corresponding to eqn. (7), whereas at higher temperatures the hardness falls rather steeply. If the low-temperature branches are extrapolated to higher temperatures, and  $1/H$  (extrapol.) values

<sup>13</sup> Schischokin, *Z. anorg. Chem.*, 1930, **189**, 263.

<sup>14</sup> Schischokin and Agajewa, *ibid.*, 1930, **193**, 237.

thus obtained are subtracted from those of  $1/H$  (observed), it is found in all the examples cited that the reciprocal of this difference obeys a second exponential law of the form of eqn. (7) to a good approximation. Hence, the whole curves can be represented by

$$H = \frac{1}{Ae^{-E_1/RT} + Be^{-E_2/RT}} \quad (8)$$

The circles in Fig. 2 have been calculated according to this equation using the constants given in Table I.

TABLE I.—HARDNESS CONSTANTS OF METALS

Material	$E_1$ (kcal.)	log $A$	$E_2$ (kcal.)	log $B$
Ni ( <i>Engl.</i> )	0.178	-1.89	14.62	1.30
Cu ( <i>Engl.</i> )	0.169	-1.65	8.96	1.22
Cu	0.228	-1.71	7.27	0.46
Sb	1.644	-0.64	7.64	1.25
Zn	1.187	-0.80	8.05	2.31
Al	0.365	-1.30	8.22	1.70
Cd	1.690	-0.04	8.22	2.95
Bi	1.325	-0.05	14.34	5.68
Sn	1.415	+0.18	9.42	3.58
Pb	1.187	+0.20 <sub>6</sub>	17.80	7.40

The agreement is good although no special care was taken to select the best values of the constants. Thus, eqn. (8) is a suitable expression for representing the temperature coefficient of hardness.

It assumes that the high-temperature branch of the curves also approximates to a straight line at higher temperatures so that the whole curves consist of two rectilinear branches of different slope and a transition curve connecting them. This fact, although it appears somewhat obscured by the termination of the curves near the melting point, has been observed previously by Dushman<sup>15</sup> who evaluated the high-temperature branches in a similar way and calculated  $E_2$  values.

Eqn. (8) is not without a theoretical significance. It corresponds to the expression

$$v = \sigma(\alpha e^{-E_1/RT} + \beta e^{-E_2/RT}), \quad (9)$$

for the deformation velocity. Exactly the same equation is known to hold for the electrolytic conductivity of certain semi-conductors, again with  $E_2 > E_1$ . In that case, it is interpreted (see Jost<sup>16</sup>) on the assumption that at high temperatures the crystal is in disorder equilibrium, the energy of disorder being  $E_2 - E_1$  in our notation, whereas at low temperatures the disorder equilibrium is "frozen-in" and the existing disordered ions can move if they acquire an activation energy  $E_1$ . By analogy, one is tempted to suggest that the deformation velocity is also determined by two mechanisms. At low temperatures, pre-existing perturbation centres, probably situated in cracks and internal surfaces (Smekal) are immobile when they acquire the small thermal energy  $E_1$  while at higher temperatures new perturbation centres are formed by establishment of the disorder equilibrium, the sum of their energies of formation and movement being  $E_2$ .

Tammann and his co-workers have determined by different frictional methods the temperature at which exchange of sites will begin and found that for different metals it is about 0.35 of the (absolute) fusion temperature  $T_f$ . Similarly, Botschwar<sup>17</sup> found the temperature at which

<sup>15</sup> Dushman, *Proc. Amer. Soc. Test. Mat.*, 1929, **29**, (2), 7.

<sup>16</sup> Jost, *Diffusion und Chemische Reaktion in festen Stoffen* (Dresden and Leipzig, 1937), p. 77.

<sup>17</sup> Botschwar, *Z. anorg. Chem.*, 1926, **157**, 319; 1928, **176**, 46.

marked recrystallization occurs to be  $0.43 T_s$ . Now, the transition from the low-temperature to the high-temperature mechanism of deformation, i.e. the change of slope in Fig. 2, always occurs at about  $(0.65 \pm 0.1) T_s$ . The applicability of this rule points again to a connection between the high temperature deformation and the occurrence of mobile atoms. As the critical increment of deformation is lower and the reduced temperature of the onset of this is higher than in self-diffusion, recrystallization, etc., one could conclude that the perturbation centres of deformation have lower energies and lower entropies of formation than completely mobile atoms, probably because they are groups of dislocated atoms.

In the following discussion, eqn. (8) will be used as a preliminary basis of discussion of the influence of temperature and composition on the hardness of Hume-Rothery alloys. From this point of view, the question is whether the critical energies  $E_1$  and  $E_2$ , for Hume-Rothery alloys, depend on the electron concentration and the lattice type.

Theoretically,  $E_1$  need not be precisely constant because, in view of its low value (Table I), any effect of the applied stress in the sense of eqn. (4) is not excluded. But no important conclusions should be drawn from these values. As for  $E_2$ , it is clear from Fig. 2 that its determination from the high-temperature slope is uncertain due to the limited temperature range available. This applies still more to the alloy curves discussed below. In this respect it is of practical importance to observe that all the metals in Fig. 2 show a fusion-point hardness of about  $1.5 \text{ kg./mm.}^2$ , the value decreasing somewhat with the melting point. This fact is of help in obtaining a good extrapolation of the high-temperature branch of the experimental curves. In any case, in view of the said uncertainty, stress will be laid on the qualitative sequence of the slopes rather than on their accurate values.

## Experimental

**Method.**—The apparatus used for the measurement of the temperature coefficient is shown in actual size in Fig. 3. Its principle is to measure the hardness at different temperatures with the same sample so as to be independent of casual differences of the samples. The coin-shaped sample A is placed on an iron anvil B. The channel in B contains a copper-constantan thermocouple, sealed in glass, with its soldered ends close to the sample. A ball-bearing steel sphere C rests below on the surface of the sample A, carried above in an eccentric recess of the iron piston D. The apparatus is enclosed by an iron tube E which can be heated from outside by an insulated heating coil. E is packed at the bottom with asbestos wool so that a slow stream of carbon dioxide, entering at F, displaces the air inside during the experiments and prevents oxidation of the sample and the sphere. At G, by means of a Brinell press, a measured load can be applied gradually and removed after measured intervals of time. Between every two indentations D is revolved by means of the handle H through a definite angle (usually  $45^\circ$ ). This moves the sphere over the sample to a new position, so that eight indentations, corresponding to eight different temperatures, can be formed in a circle upon the same sample, without dismounting. (The rotation of A during the displacements of C is prevented by a suitable device.)

The diameter of the indentations was measured using a microscope with a micrometer eyepiece in two perpendicular directions to an accuracy of  $1/400 \text{ mm.}$ , and from the mean value  $d$ , the sphere diameter  $D$  and the load  $P$ , the Brinell hardness was calculated by the usual formula,

$$H = \frac{2P}{\pi D(D - \sqrt{D^2 - d^2})} \quad (10)$$

Most measurements were made with a load of  $35.6 \text{ kg.}$  spheres of  $6.5 \text{ mm.}$  diam. over a period of 1 min. The very low hardnesses were measured with  $15.8 \text{ kg.}$  load, and double measurements with both loads were the same. Most of the runs were carried out at rising temperature between  $20^\circ$  and  $450^\circ \text{ C}$  in steps of about  $50\text{--}60^\circ$ ; sometimes smaller intervals were used. Normally, runs with decreasing temperature gave identical results; exceptions will be noted.

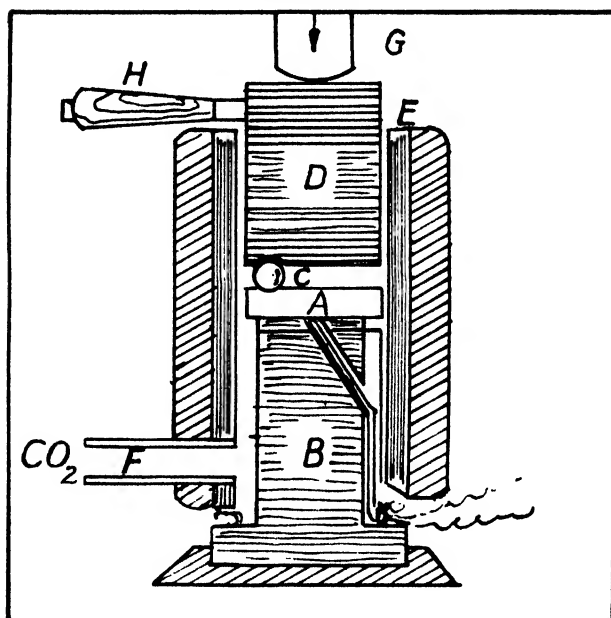


FIG. 3.

**Materials.**—Four alloy systems were chosen which form true Hume-Rothery phases: Cu—Zn, Cu—Sn, Ag—Zn and Ag—Cd. The copper used was pure electrolytic wire. The silver, prepared from halide residues by reduction with

TABLE II.—ALLOYS FOR HARDNESS MEASUREMENTS

1st Metal	2nd Metal	Content of 2nd Metal Atomic %      % by Weight		Electron Concentration	Phase	M.p. (°C)
Cu	Zn	0	0	1.0	Cu	1083
		30	29.5	1.30	$\alpha$	890
		44.4	43.7	1.44	$\beta$	860
		65	64.4	1.64	$\gamma$	760
		83	82.6	1.83	$\epsilon$	480
		100	100	2.0	$\eta = \text{Zn}$	419
Cu	Sn	0	0	1.0	Cu	1083
		30.6	19.1	1.57	$\gamma$	582
		36.3	23.4	1.70	$\gamma + \epsilon$	582
		40.4	26.7	1.81	$\epsilon$	680
		67	52	2.56	$\eta$	420
Ag	Zn	0	0	1.0	Ag	961
		17.5	26	1.26	$\alpha$	760
		36.5	49	1.49	$\beta(\zeta)$	700
		50	62	1.62	$\gamma$	650
		70	78	1.78	$\epsilon$	580
		100	100	2.0	$\eta = \text{Zn}$	419
Ag	Cd	0	0	1.0	Ag	961
		39.4	38.4	1.38	$\alpha$	700
		52.5	51.5	1.52	$\beta$	680
		62.9	62.0	1.62	$\gamma$	640
		74.5	73.8	1.74	$\epsilon$	500
		100	100	2.0	$\eta = \text{Cd}$	321

Zn + HCl, contained a few per cent. of Zn which did not affect the present measurements (it increases the hardness of chemically pure silver by 4 kg./mm.<sup>2</sup>). Zn and Cd were Kahlbaum *pro analysi* preparations. The alloys were prepared by fusing together weighed amounts of the components in ceramic crucibles under a protective melt of NaCl, CaCl<sub>2</sub> and borax. Special care was needed in the preparation of the Ag—Zn and Ag—Cd alloys because of their high heats of formation and low boiling points. Here, Zn or Cd was fused and silver foil gradually dissolved in the melt. The alloys were cast in asbestos moulds and the coin-shaped samples filed and polished. Sometimes they were annealed at 300–400°, but no perceptible hardness difference was observed, except in the case of  $\epsilon$ -Ag—Cd (see later).

The compositions of the alloys tested are tabulated in Table II.

The melting points tabulated (which were used as aids in extrapolation) are the temperatures of the first appearance of a liquid phase, as shown in the respective phase diagrams.

### Results

Some observations were made in order to check the method as to the uncertainties produced by plastic flow and by work-hardening. The results are presented in Fig. 4. The hardness is plotted logarithmically as a function of

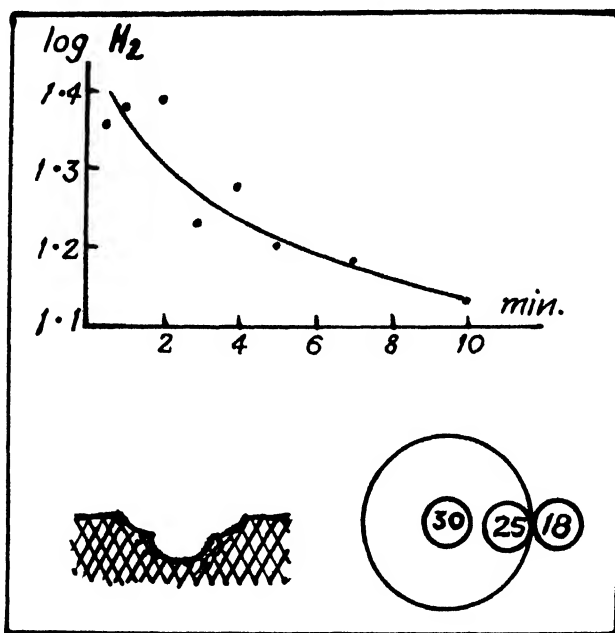


FIG. 4.

the indenting time in the upper part. The experiment was made with  $\alpha$ -Ag—Zn at 364° C ( $10^3/T = 1.575$ ). The scattering is due to temperature fluctuations. It is seen that at this temperature a considerable after-flow occurs, but that the 1 min.-value, used throughout this investigation, is not much affected by it. The work-hardening during the indentation was examined by first making some large indentations on a silver surface with a 11.41 mm. sphere (load 35.6 kg.), and then measuring the hardness at different points within these indentations with a 3.12 mm. sphere (load 15.8 kg.). The cross-section of two combined indentations is shown below on the left and some typical results on the right. In fact, the centre of an indentation is remarkably hardened, but this effect, not very large as compared with the strong temperature influence, is certainly less with the small indentations of a 6.5 mm. sphere and at elevated temperatures.

The final results are given in the form of  $\log H - 1/T$  diagrams in the Fig. 5-8, for the systems Cu—Zn, Cu—Sn, Ag—Zn and Ag—Cd respectively. In

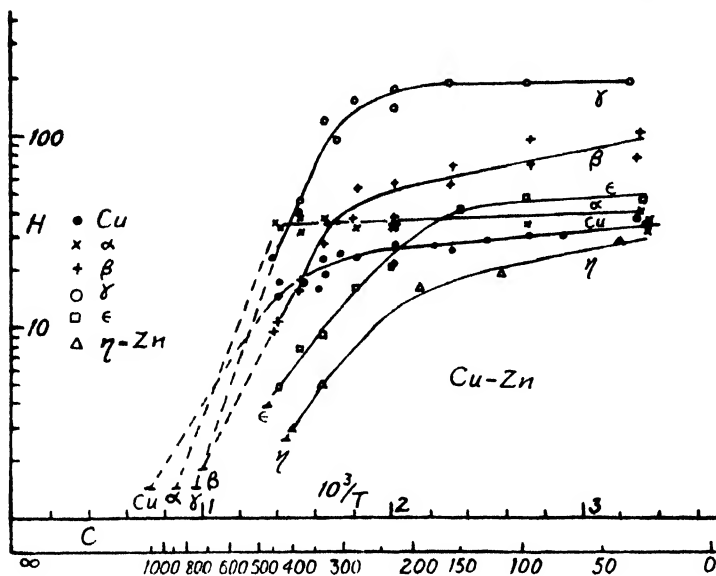


FIG. 5.

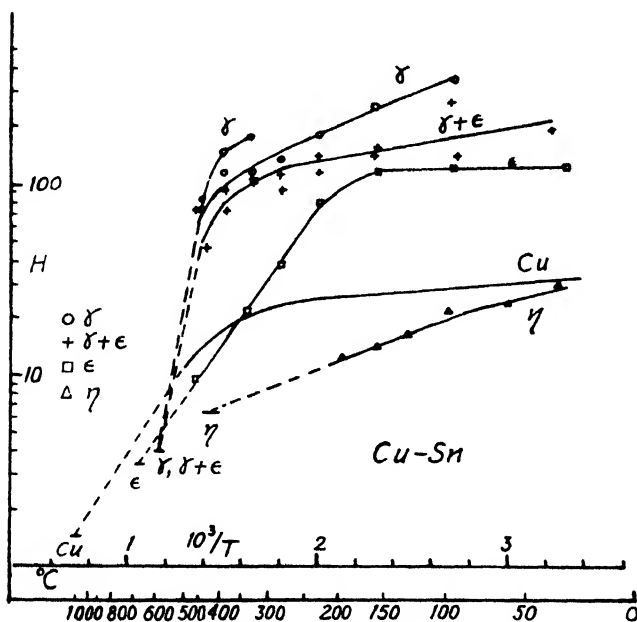


FIG. 6.

Fig. 5 and 6 single measurements are given, to indicate the degree of reproducibility with different samples. In Fig. 7 and 8 some of these points are omitted for the sake of clarity. The interrupted sections of the curves have been extrapolated by using the final slope of the measured high-temperature branches and the fact (see above) that the hardness at the melting-point does not exceed a few units.



## STRENGTH OF ALLOYS

Some particular remarks concerning the silver alloys are necessary. In the Ag-Zn system the normal cubic body-centred phase  $\beta$  is stable only above  $250^\circ$ ,<sup>18</sup> below which temperature it changes into the hexagonal  $\zeta$  structure.

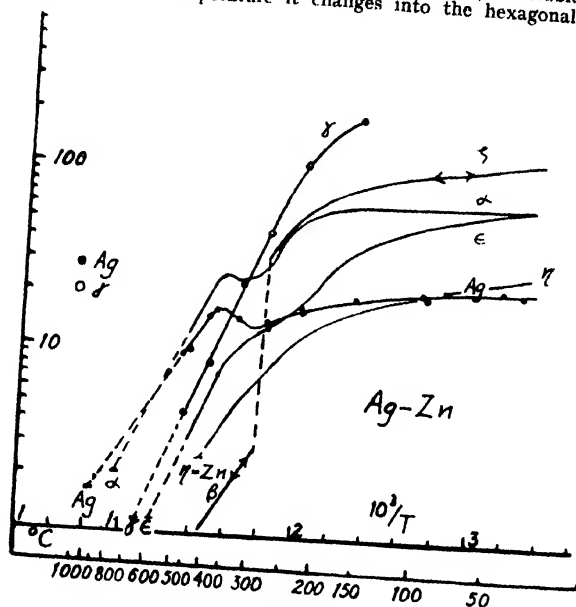


FIG. 7.

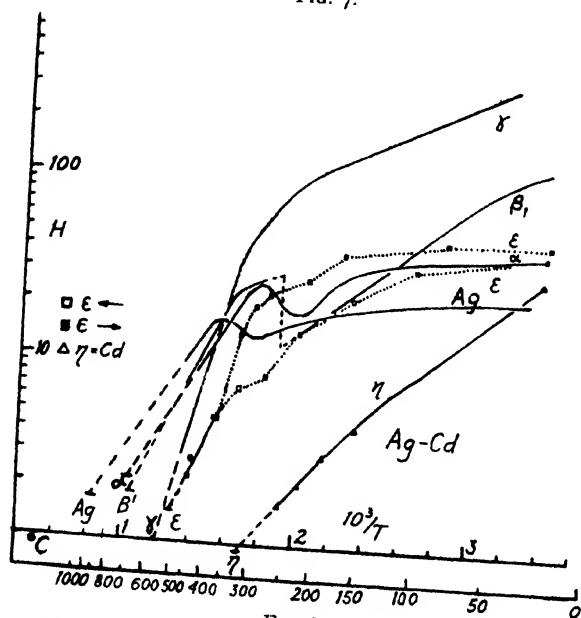


FIG. 8.

Usually, hexagonal structures are harder than cubic ones, because only one glide plane (0001) exists instead of two in the cubic lattices (111 and 100). Correspondingly, a large and reversible jump in hardness is observed near the transi-

<sup>18</sup> Hansen, *Der Aufbau der Zweistofflegierungen* (Berlin, 1936).

tion temperature. In the system Ag—Cd the  $\beta$  phase shows an inverse transition: below  $240^\circ$  the  $\beta'$  phase, being an ordered body-centred cubic lattice, is stable, and above this temperature the hexagonal  $\beta_1$  phase. Correspondingly, an increase of hardness is to be expected on passing through the transition point in an ascending direction, as is in fact observed. The hysteresis loop of  $\epsilon$ -Ag—Cd for which one experiment only has been recorded in the figure, will be discussed below.

### Discussion

For the soft metals Zn and Cd our curves coincide in a satisfactory manner with those of Fig. 2. For copper our values are lower by a factor of about 2. This is probably due to work-hardening affecting the literature values which were obtained with very much greater loads.

In the four systems examined, the hardness at room temperature and generally at low temperatures shows the same variation as stated previously.<sup>1</sup> It rises from the value of pure copper or silver through the  $\alpha$  and  $\beta$  phases to a maximum at the  $\gamma$  phase and descends again over the  $\epsilon$  to the  $\eta$  phase. The question is, how far can this variation be accounted for by the magnitude of the energy values, i.e. of  $E_1$  and  $E_2$ . This can be answered without the tedious and not very accurate full analysis of the constants of all the curves (cf. Table I). The slopes of the low-temperature and high-temperature branches of the curves give directly an approximate picture of the variations of  $E_1$  and  $E_2$ .

$E_1$  is generally small and, consequently, of little influence on the hardness values; intersections of curves belonging to subsequent phases do not occur in the low-temperature region. Moreover, no systematic variability of  $E_1$  can be discovered.

The contrary is true of  $E_2$ . It is clearly seen that in all the four systems the high-temperature branches of the  $\gamma$ -curves show the maximal slope. The high-temperature slopes, partly based on an extrapolation, cannot claim a high accuracy, but it proved impossible, taking into account the initial slopes observed and the melting points, to apply different extrapolations without bias which do not give a maximum slope for the  $\gamma$ -curves. With the reservations due to the uncertainties mentioned above, an approximate evaluation of  $E_2$  from the curves has been attempted in Table III.

TABLE III.—APPROXIMATE  $E_2$  VALUES FOR ALLOYS (KCAL.)

System	Phase	Pure	$\alpha$	$\beta$	$\gamma$	$\gamma + \epsilon$	$\epsilon$	$\eta$
Cu—Zn	.	7.3	12	9	13.5	—	6.5	6.8
Cu—Sn	.	7.3	—	—	23	20	6.5	2
Ag—Zn.	.	7	8.6	7	10	—	10	6.8
Ag—Cd.	.	7	7.5	9	16	—	9.4	5.2

From these numbers it again appears that  $E_2$  is greatest in the  $\gamma$ -phases, and this would mean, as pointed out previously, that in these phases, due to the high degree of saturation of the Brillouin zone, the energy needed for the formation of perturbation centres, is highest. (The secondary maxima encountered in the  $\alpha$ -phases of the two Zn systems, if real, are probably due to secondary effects, e.g. of atom size.)

Such a systematic variation of  $E_2$  would also give an explanation of the parallel variation of the low-temperature hardnesses, which it produces in the following way. At the melting point the hardness of different metals is close to a universal low value of, say,  $1.5 \text{ kg./mm.}^2$ . Starting from this value, at decreasing temperatures, the hardness increases corresponding to the steeper or flatter slope  $E_2/R$ ; at a temperature of

0.65 of the melting point it reaches a value depending on this slope (and the (not very variable) melting temperature), and from then on it changes little in the low-temperature region.

A peculiarity is shown by all alloys containing silver. Around 300° silver itself already shows a transitory minimum of hardness, and the same minimum is observed also in  $\alpha$ -Ag—Zn and  $\alpha$ -Ag—Cd. (With the latter it has been proved to occur at rising and at falling temperatures.) In  $\epsilon$ -Ag—Zn the phenomenon is still observed as an inflexion of the curve. In  $\epsilon$ -Ag—Cd it manifests itself as a hysteresis loop. At rising temperatures the curves are very similar to that of  $\epsilon$ -Ag—Zn whereas at decreasing temperatures a normal two-branch curve is obtained. The whole phenomenon, and especially the hysteresis loop, is similar to a retarded allotropic transition, as if the low-temperature branches of the curves belong to another and softer modification than the high-temperature branches. It is remarkable, perhaps, that the hardness anomaly is found just in the temperature range of the phase transitions  $\zeta \rightarrow \beta$  of Ag—Zn and  $\beta_1 \rightarrow \beta'$  of Ag—Cd.

No definite phase transitions are known in the  $\alpha$ - and  $\epsilon$ -phases. It was thought that an order-disorder transition possibly occurs. Even with unalloyed silver this would be possible in view of its small Zn content (see above). However, chemically pure silver, prepared by repeated HCl precipitation and dissolution in ammonia and reduction with iron (which is insoluble in silver) also gives the anomaly although to a smaller degree. The occurrence of an order-disorder transition or a phase transition, hitherto overlooked, was checked in a calorimetric apparatus which clearly indicated the  $\zeta \rightarrow \beta$  transition of Ag—Zn and the order-disorder transition of  $\beta$ -Cu—Zn. No anomaly could be discovered in  $\alpha$ -Ag—Zn nor in  $\epsilon$ -Ag—Cd.

The anomaly was found neither with copper nor with gold. These two elements differ from silver mainly in one common property, the easier transition of an electron from the  $d$ -shell into the conductivity ( $s$ ) band, manifested by valency change and by the reddish colour of the free metals. It was tentatively supposed that this electron transition might occur in silver and its alloys in an exceptionally narrow temperature range and thus bring about an increase of electron concentration and, consequently, of hardness. This is not very likely because the transition requires a quantum of less than 320 m $\mu$ ., i.e. energies of more than 89 kcal./g. atom., and thus cannot proceed thermally at 300°. Moreover, no resistance anomaly is known for silver in this range. We searched for a thermoelectric anomaly of silver, but without any result.

The only possible explanation appears to be the assumption of Zwicky of a reversible transition of the mosaic block structure, as found by Cohen<sup>19</sup> for Cd, Zn, Sb, Cu and Bi and by Götz<sup>20</sup> for Bi. For silver, Cohen calculated a transition point of 260° C from an anomaly of the temperature coefficient of the specific heat, although Jänecke,<sup>21</sup> using anomalies of the pressure coefficient and of thermoelectric effect, concluded that a transition existed at 120°. (See also Hedvall and Colliander.<sup>22</sup>) It is possible that a transition of this kind may be perceptible as a hardness anomaly, as  $\alpha$  in eqn. (1) and (9) will depend on the mean free path of a perturbation. Probably, in absence of this anomaly, the relation of  $E_s$  and the structure of the phases would be more evident.

*Dept. of Inorganic, Physical and Catalytic Chemistry,  
Institute "Nicolaos Canellopoulos,"  
Piraeus, Greece.*

<sup>19</sup> Cohen, *et al.*, *Z. physik. Chem.*, 1913, **85**, 419; 1914, **87**, 409, 419; 1915, **89**, 489, 638.

<sup>20</sup> Goetz and Jacobs, *Physic. Rev.*, 1937, **51**, 151, 159; *Proc. Acad. Sci. Wash.*, 1930, **16**, 99.

<sup>21</sup> Jänecke, *Z. physik. Chem.*, 1915, **90**, 313.

<sup>22</sup> Hedvall and Colliander, *Z. anorg. Chem.*, 1940, **243**, 234.

# FRIEDEL-CRAFTS POLYMERIZATIONS

## PART I. THE EFFECT OF SOLVENT ON THE POLYMERIZATION OF OLEFINS BY STANNIC CHLORIDE

BY D. C. PEPPER

Received 9th November, 1948

The rate and degree of polymerization of olefins at 25° C by Friedel-Crafts catalysts are markedly increased by increase in the dielectric constant of the medium. Traces of moisture reduce the rate of polymerization in solvents of high dielectric constant, but appear to increase it in hydrocarbons. Solutions of stannic chloride in solvents of high dielectric constant show appreciable conductivities in presence of traces of water. In nitroparaffins, very high conductivities are observed, which are not due to moisture. It is concluded that the polymerization has an ionic mechanism, but that, in solvents of high dielectric constant at least, it does not involve hydrate ions. In solvents of low dielectric constant the hydrate may play a part.

The polymerization of olefins induced thermally or by organic peroxides and similar substances is now generally recognized to be a free-radical chain reaction. The kinetics of such polymerizations have been completely explained on the radical chain theory, and recently successful measurements have been made of the activation energies and frequency factors of all the elementary kinetic steps.<sup>1, 2</sup>

Such polymerizations are relatively slow; the overall activation energies lie in the range 15-30 kcal., and temperatures at 50-150° C are needed to give conveniently measurable rates of reaction. In contrast, when the polymerization is induced by acids or Friedel-Crafts catalysts, striking differences in the character of the reaction are observed. Reaction proceeds rapidly, often explosively, at room temperatures and even below -100° C.<sup>3, 4</sup> The overall activation energy must, therefore, be very low—in the single case reported it was found to be about 3 kcal.<sup>5</sup> At normal temperatures the chain-length of the polymers is short (mol. wt. 10<sup>3</sup>-10<sup>4</sup>), but high molecular weights may be obtained at very low temperatures.<sup>4, 6</sup>

It has been concluded that in such polymerizations the active chain carrier is an ion or polarized molecule.<sup>7, 8a, 9</sup> This is a plausible inference from the nature of the effective catalysts, since Friedel-Crafts catalysts can readily give rise to ions or electron-accepting fragments, and from the low activation energies involved, since ionic reactions occur by electron transfers which require much lower activation energies than do normal reactions involving the breaking of covalent bonds. It must be noted,

<sup>1</sup> Burnett and Melville, *Proc. Roy. Soc. A*, 1947, **189**, 456.

<sup>2</sup> Bamford and Dewar, *ibid.*, 1948, **192**, 309.

<sup>3</sup> Staudinger and Breusch, *Ber.*, 1929, **62**, 442.

<sup>4</sup> Thomas, Sparks and Frohlich, *J. Amer. Chem. Soc.*, 1940, **62**, 276.

<sup>5</sup> Williams, *J. Chem. Soc.*, 1940, 775.

<sup>6</sup> Hershberger, Reid and Heligman, *Ind. Eng. Chem.*, 1945, **37**, 1073.

<sup>7</sup> Hulbert *et al.*, *Ann. N.Y. Acad. Sci.*, 1943, **44**, 371.

<sup>8</sup> Price, (a) *ibid.*, 1943, **44**, 351; (b) *Reactions at C=C Double Bonds* (New York, 1946).

<sup>9</sup> Evans and Polanyi, *J. Chem. Soc.*, 1947, 252.

however, that a low value of the overall activation energy could arise for quite a different reason, viz., if the activation energy of the chain termination reaction is very high (since  $E_{\text{overall}}$  is a composite quantity and in the simplest case is equal to  $E_{\text{initiation}} + E_{\text{propagation}} - E_{\text{termination}}$ ).

The precise nature of the chain initiator and the details of the kinetic steps are still not clear. Polanyi and co-workers<sup>9, 10, 11</sup> have shown that  $\text{SnCl}_4$  or  $\text{TiCl}_4$  alone are insufficient to initiate the polymerization of isobutene at low temperatures and that a "co-catalyst" must also be present. Effective co-catalysts are water, *tert*-butyl alcohol, sulphuric acid and various organic acids. Norrish and Russell<sup>12</sup> have made a similar observation with stannic chloride and regard either the mono- or the dihydrate as the effective initiator. Kinetic evidence which might support an ionic chain mechanism is meagre and uncertain of interpretation<sup>13, 14</sup> and some doubt has been expressed whether a stationary state is in fact established.

**Scope of this Paper.**—The experiments described here, with styrene and  $\alpha$ -methyl styrene catalyzed by stannic chloride, are part of a general exploration of the characteristics of Friedel-Crafts polymerizations. The particular approach here is the investigation of the effect of the dielectric nature of the solvent medium, and the detection of ions by measurements of electrical conductivity. Any reaction involving the formation or destruction of ions will be influenced by the dielectric constant of the medium; data here presented show that at 25° C both the rate and degree of polymerization are markedly increased by increase in the dielectric constant of the solvent used. Due to anomalies caused by variable traces of water, the results are at best only semi-quantitative, but the main effect remains clear. One remarkable feature is that traces of moisture are found to decrease the rate of polymerization in solvents of high dielectric constant, that is, the reverse of the effect found at low temperatures in hydrocarbon or other low dielectric solvents. The results of electrical conductivity measurements are complicated. Considerable concentrations of ions can be detected in solutions of stannic chloride in high dielectric solvents, but these are found to arise largely, if not entirely, from hydrate or other complexes, and the relatively high conductivities produced obscure the contribution (if any) of ions in the polymerization chain. The hydrate appears to play no part in the polymerization in high dielectric solvents.

## Experimental

The polymerizations were carried out in stoppered Pyrex test-tubes in a thermostat at 25° C. When temperature equilibrium had been reached, the appropriate amount of catalyst solution was added and samples for analysis withdrawn from time to time in a pipette. The disadvantages of such an open system are obvious in a reaction sensitive to traces of moisture, but in this preliminary investigation it was decided to accept them in view of its simplicity and convenience. In later, more accurate, kinetic measurements a dilatometric method was used, which will be described in a subsequent paper. The rates quoted in Tables VI and VII were obtained by this method.

The course of polymerization was followed by estimation of the unchanged monomer by bromination of its double-bond. Since the polymer itself has a double-bond, allowance for this must be made. A known volume of monomer-polymer solution was added to excess bromine solution (0.3 N in  $\text{CCl}_4$ ) \* and allowed to stand for  $\frac{1}{2}$  min. In this time addition to the double-bond is sensibly complete and the excess bromine can be estimated by addition of aqueous KI

<sup>10</sup> Evans, Meadows and Polanyi, *Nature*, 1947, **160**, 869.

<sup>11</sup> Plesch, Polanyi and Skinner, *J. Chem. Soc.*, 1947, 257.

<sup>12</sup> Norrish and Russell, *Nature*, 1947, **160**, 543.

<sup>13</sup> Eley and Pepperc, *Trans. Faraday Soc.*, 1947, **44**, 112.

\* A 0.3 N solution is used since at this concentration the partial vapour pressures of bromine and solvent are approximately equal, so that any evaporation does not change the composition of the solution.

and titration with thiosulphate. Potassium iodate is then added and the thiosulphate titration continued to estimate HBr produced by substitution. Little substitution occurred in the bromination of the monomers or poly  $\alpha$ -methyl styrene, but with polystyrene it was quite marked.

The polymers were isolated from samples or at the end of the reaction by shaking the solutions with water, and steam-distilling to remove solvent and any unchanged monomer. This method was quite satisfactory for polystyrenes but with poly  $\alpha$ -methyl styrenes it was difficult to remove the last traces of monomer. The molecular weights quoted for poly  $\alpha$ -methyl styrenes are, therefore, likely to be somewhat lower than their true values. In some cases polymers were isolated by precipitation by methyl alcohol. Except with the lowest polymers, where some of the polymer remained dissolved, this method gave products of the same molecular weight as those isolated by steam distillation.

The molecular weights of  $\alpha$ -methyl styrene polymers were determined by bromination of the terminal double-bond. This method is not suitable for polystyrenes, which were, therefore, measured by the determination of their intrinsic viscosities in benzene at 25° C. The molecular weights were calculated from Bamford and Dewar's relations,<sup>2</sup>\*

$$[\eta] = 4.57 \times 10^{-3} M^{0.65},$$

where  $M$  = mol. wt.,  $[\eta] = \lim (\eta_{sp})/c$ , and  $c$  = concentration in base moles (104 g.) per litre.

Conductivities were measured in a small cell of conventional type, consisting of a stoppered Pyrex test-tube with circular platinum electrodes sealed through the wall at the bottom of the tube. This cell had a constant of 0.156 and required a minimum of 2 ml. solution. Since results of the highest accuracy were not required at this stage the simplest conductivity bridges were used—at first, a Kohlrausch bridge and later, a Mullard bridge accurate to 2 %. The latter had a "magic eye" null-point detector instead of telephones, which made it much more convenient and rapid in use.

**Materials.**—The  $\alpha$ -methyl styrene used was supplied by the Distillers Company. It had been fractionally distilled through a column equivalent to 50 theoretical plates (b.p. 163.9–164.2° C at 745 mm.). Despite this treatment it still contained about 6 % isopropyl benzene (from which it had been made by dehydrogenation). However, this merely acts as a diluent and does not otherwise affect the polymerization. The  $\alpha$ -methyl styrene slowly oxidizes in presence of air to acetophenone and formaldehyde and the liquid becomes opalescent and eventually deposits a white solid (paraformaldehyde?). Before use it was distilled at reduced pressure in an atmosphere of nitrogen (b.p. 78° C at 20 mm.;  $n_D^{20} = 1.5361$ ).

Styrene was obtained from I.C.I. Plastics and contained traces of hydroquinone to inhibit the spontaneous oxidation and polymerization (radical chain). This inhibitor does not prevent the stannic chloride catalysis but it was, nevertheless, removed by shaking with NaOH, drying over Na and vacuum distillation (b.p. 46° C at 15 mm.;  $n_D^{20} = 1.5445$ ).

Stannic chloride was distilled in all-glass apparatus (b.p. 114–115° C). Elaborate precautions to remove HCl and hydrates (a very difficult task<sup>6,14</sup>) were not taken. For use as a catalyst it was diluted to 1 % by volume in the appropriate solvent.

All solvents were dried (over  $P_2O_5$  where practicable) and distilled through a 12-in. spiral glass column. Nitrobenzene chars considerably if heated with  $P_2O_5$  and must, therefore, be shaken with solid NaOH before distillation.  $P_2O_5$  also reacts with nitroparaffins forming a yellow sol. These solvents were, therefore, dried successively over  $CaCl_2$  and anhydrous copper sulphate.

## Results

**(a) Polymerization in Different Solvents.**—A series of polymerizations of  $\alpha$ -methyl styrene, at constant monomer and catalyst concentrations, was carried out in solvents of different dielectric constant, ranging from cyclohexane

\* Bamford and Dewar's relation refers to low molecular weight polystyrenes prepared at low conversions by a radical mechanism, and containing  $CCl_3$  end-groups. It may not, therefore, give exact results with the polymers described here. However, until the  $\eta$ -mol. wt. relation of these polymers has been experimentally determined, it may be taken as giving a better relative comparison of molecular weights than the simple Staudinger equation of Kemp and Peters.

<sup>14</sup> Baxter and Starkweather, *J. Amer. Chem. Soc.*, 1920, **42**, 906.

( $\epsilon = 1.9$ ) to nitrobenzene ( $\epsilon = 36$ ). No induction period was observed, and the polymerizations proceeded at steady rates over about the first 25 % of reaction, subsequently slowing down as monomer was consumed. In the solvents of high dielectric constant an appreciable rise of temperature took place. Table I shows the initial rate (of disappearance of monomer in moles  $\text{l.}^{-1} \text{ min.}^{-1}$ ) and the maximum temperature rise, together with molecular weight (number average) of the polymer produced.

TABLE I.—EFFECT OF DIELECTRIC CONSTANT OF SOLVENT

$$[M]_0 = 1.36. \quad [\text{SnCl}_4] = 4.5 \times 10^{-3} \text{ mole l.}^{-1} \quad T = 25^\circ \text{C}$$

Solvent	$\epsilon$	$\Delta T$ (max.) $^\circ\text{C}$	Rate $\times 100$ mole $\text{l.}^{-1} \text{ min.}^{-1}$	Mol. Wt.
Cyclohexane . . .	1.9	0.5	1.25	500
Bromobenzene . . .	5	0.6	1.45	430
Ethylene dichloride . . .	10	1.5	3.3	1200
Nitroethane . . .	28	6	20.4	(680)
Nitrobenzene . . .	36	16	150	8500

\* In ref. 15 this catalyst concentration was given by mistake as  $0.9 \times 10^{-3}$ .

Because of the non-isothermal nature of these reactions the above rates are not strictly comparable, but the variation due to different temperature is not likely to be great, in view of the low activation energies usual with this type of reaction. The results shown may, therefore, be taken to demonstrate a marked influence of solvent medium on the rate and degree of polymerization.

A similar series of experiments was carried out with styrene. The rates of polymerization were not measured, but the molecular weights were found (Table II) to show a similar increase in dielectric constant of the solvent.

TABLE II.—EFFECT OF SOLVENT ON MOL. WT. OF POLYSTYRENE

$$[M]_0 = 1.74. \quad [\text{SnCl}_4] = 9 \times 10^{-3} \text{ mole l.}^{-1} \quad T = 25^\circ \text{C}$$

Solvent	$\epsilon$	$[\eta]$	Mol. Wt.
Cyclohexane . . . .	1.9	0.66	2040
Benzene . . . . .	2.3	0.68	2190
Ethylene dichloride . . . .	10	1.04	4200
Nitroethane . . . . .	28	1.07	4450
Nitrobenzene . . . . .	36	1.62	8300

To eliminate as far as possible specific chemical effects of the solvent, a series of experiments was performed in which the dielectric constant was varied by varying the composition of benzene-nitrobenzene mixtures. The results are given in Table III, the dielectric constant of the mixed solvents being estimated from the values given at  $16^\circ \text{C}$  in *Int. Crit. Tables*. Steady initial rates were observed in all solvents except pure benzene which showed an induction period of 90 min. followed by a relatively rapid rate. In general, higher rates and molecular weights were found in the mixtures of higher dielectric constant.

TABLE III.—STYRENE IN BENZENE-NITROBENZENE MIXTURES

$$[M]_0 = 1.74. \quad [\text{SnCl}_4] = 9 \times 10^{-3} \text{ mole l.}^{-1} \quad T = 25^\circ \text{C}$$

Vol. % nitrobenzene	$\epsilon$	$-dM/dt \times 100$	$[\eta]$	Mol. Wt.
0	2.3	(0.3)	0.63	1,900
25	7.5	0.12	1.06	4,400
50	14.0	1.1	1.58	8,000
62.5	18.5	4	1.58	8,000
75	23.0	7	1.75	9,400
100	36.0	26	1.82	10,000

Qualitative evidence was also obtained that the same solvent effect is shown in the polymerization of styrene by other catalysts ( $\text{H}_2\text{SO}_4$ ,  $\text{FeCl}_3$ ), and of *n*-butyl vinyl ether by stannic chloride. In each case a greater and more rapidly developed heat evolution was observed in nitrobenzene than in cyclohexane.

(b) **The Detection of Ions.**—Solutions of stannic chloride in high dielectric solvents were found to be conducting, indicating the presence of appreciable concentrations of ions. At a concentration of  $9 \times 10^{-3}$  moles per litre the following conductivities were observed at 25° C.

TABLE IV

Solvent	$\kappa$	$\kappa \times 10^6$ mhos
Benzene . . . . .	2.3	Not measurable
Bromobenzene . . . . .	5	Not measurable
Ethylene dichloride . . . . .	10	0.3-5 sensitive to $\text{H}_2\text{O}$
Nitrobenzene . . . . .	36	4-20 sensitive to $\text{H}_2\text{O}$
Nitropropane . . . . .	21	200
Nitroethane . . . . .	28	300
Nitromethane . . . . .	38	770

Similarly, the conductivity of stannic chloride in benzene-nitrobenzene mixtures increases with the proportion of nitrobenzene. It was found also that, on the addition of styrene, the conductivity fell as the polymerization proceeded, the change in conductivity being in any given experiment approximately proportional to the extent of polymerization. These observations immediately suggest that the effect of dielectric constant on the polymerization is due to a higher concentration of initiating ions (and possibly also of an ionic chain carrier) existing in the solvents of higher dielectric constant. However, there are two objections to this simple theory; that in ethylene dichloride and nitrobenzene the conductivity appears to be variable and in the nitroparaffins it is anomalously high.

**The Effect of Water on Conductivity.**—The higher values of conductivity quoted above for ethylene dichloride and nitrobenzene were obtained with batches of solvent dried in the usual way and stored for several weeks in stoppered bottles opened occasionally to the atmosphere. Solutions made with freshly dried and distilled solvents gave the lower figures. Moreover, the conductivity in freshly dried solvents appears to be only slightly dependent on the amount of  $\text{SnCl}_4$  present, as shown in Table V. The variation is so little greater than experimental error that it may be due to variable traces of water still present in the solvent rather than to a real effect of  $\text{SnCl}_4$  concentration.

TABLE V  
In Nitrobenzene

$[\text{SnCl}_4] \times 10^3$ $\kappa \times 10^6$	0.55 0.97-1.2	1.1 1.3	9 2.5-3.3	11.5 3.4-3.6	90 4.2-5.1
---	------------------	------------	--------------	-----------------	---------------

In Ethylene Dichloride

$[\text{SnCl}_4] \times 10^3$ $\kappa \times 10^6$	5.5 0.19-0.27	11.2 0.22	92 0.30
---	------------------	--------------	------------

If measured traces of water be added to solutions of stannic chloride in nitrobenzene, a linear increase of conductivity with concentration of water is observed. Fig. 1 shows the results in three different concentrations of  $\text{SnCl}_4$ . The traces of water were introduced by adding small volumes of nitrobenzene saturated with water at 15° C (containing  $1.33 \times 10^{-4}$  mole  $\text{H}_2\text{O}$  per ml.). The concentration of  $\text{SnCl}_4$  was kept constant by simultaneously adding equal volumes of a solution of double strength.



In 50/50 mixtures of benzene and nitrobenzene, and in ethylene dichloride a linear dependence is also found.

It will be noted that all the curves in Fig. 1 are more or less superimposed and that the two at higher concentrations of  $\text{SnCl}_4$  have the same slope. In the most dilute solution (Curve 3) the curve falls below linearity as the molar ratio  $\text{H}_2\text{O}/\text{SnCl}_4$  exceeds unity. These results imply that as long as the stannic chloride is in excess, the conductivity depends only on the added water. If it

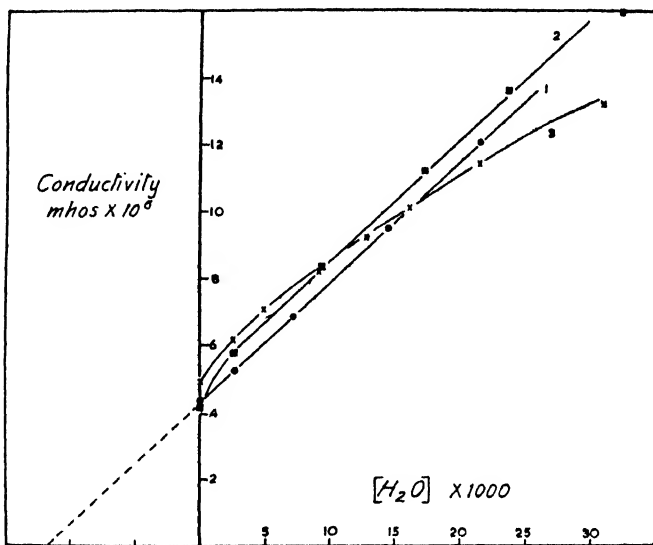


FIG. 1.—The effect of  $\text{H}_2\text{O}$  on conductivity of  $\text{SnCl}_4$  in nitrobenzene.

Curve 1.  $[\text{SnCl}_4] = 9 \times 10^{-2}$  mole/litre; 2.  $[\text{SnCl}_4] = 4.5 \times 10^{-2}$  mole/litre; 3.  $[\text{SnCl}_4] = 9 \times 10^{-3}$  mole/litre.

be assumed that pure  $\text{SnCl}_4$  in completely anhydrous nitrobenzene has negligible conductivity, then the initial conductivities shown in Fig. 1 correspond to the presence in the solvent of about  $1 \times 10^{-2}$  mole  $\text{H}_2\text{O}$  per litre (i.e. 0.02 % w./w.). Such a small amount of water might have been picked up in the brief exposure to air during the making up of the solution or from the multilayer of water adsorbed on the surface of imperfectly dried glass apparatus.

The conclusion must be, therefore, that the conductivities observed in nitrobenzene and ethylene dichloride are largely, if not entirely, due to ions produced by hydration or hydrolysis of the stannic chloride and not to its dissociation or interaction with the solvent. This conclusion does not apply to the solutions in nitroparaffins. The very high conductivities observed in these solvents are, if anything, increased by more careful drying, and are definitely reduced by the addition of water. These solutions are being studied further and there is some spectroscopic evidence that the conductivities are due to the formation of ionizable complexes with the solvent.

**The Effect of Water on Polymerization.**—Contrary to expectations, more careful drying of the solvent is found to *increase* the rate of polymerization of styrene in ethylene dichloride and nitrobenzene, and the addition of traces of moisture to reduce it.

The same effect was found qualitatively at higher concentrations of stannic chloride in nitrobenzene ( $9 \times 10^{-2}$ ). Here the rate of polymerization was more than twice as fast in freshly dried solvent as in solvent stored several weeks. It seems, therefore, that in high dielectric solvents water raises the conductivity but lowers the polymerization rate, i.e. the processes of hydration and polymerization are not directly associated, as postulated in low dielectric solvents at low temperatures.

TABLE VI.—EFFECT OF WATER ON THE POLYMERIZATION OF STYRENE

	[H <sub>2</sub> O] moles per litre × 10 <sup>3</sup>	$\kappa$ mhos × 10 <sup>8</sup>	$-dM/dt$ × 10 <sup>5</sup>
<b>In Ethylene Dichloride</b>			
$[M]_0 = 1.74$ $[SnCl_4] = 4.5 \times 10^{-3}$	0	0.15	12.7
	1.5	0.18	8.5
	7.5	0.20	5.9
	60	0.07 (solution cloudy)	0
<b>In Nitrobenzene</b>			
$[M]_0 = 1.74$ $[SnCl_4] = 9 \times 10^{-4}$	0	1.36	5.73
	.3	2.2	2.05

In hydrocarbons (benzene and cyclohexane) at 25° C the polymerization was found to be irreproducible—giving induction periods of variable length and some unaccountably slow reactions. However, in one series of experiments in benzene the addition of water was found to cause a definite increase in polymerization rate (Table VII).

TABLE VII

Solvent: Benzene  $[M]_0 = 1.74$   $[SnCl_4] = 9 \times 10^{-3}$  moles l.<sup>-1</sup>

[H <sub>2</sub> O] Added	$-d[M]/dt \times 100$
0	4.17
0	5.13
$2 \times 10^{-3}$	8.17
$4 \times 10^{-3}$	9.2

### Discussion

The experiments quoted in Tables I-III must all have been affected to a small (and variable) extent by traces of water. The relative rates of polymerization and molecular weights obtained in different solvents cannot, therefore, be taken as strictly quantitative. However, due to the opposite effect of water on the polymerization in high and low dielectric solvents it follows that in strictly anhydrous systems the effect of solvent would be even more marked. Hence it must be concluded that there is a real effect of dielectric constant on the polymerization. This constitutes strong evidence in favour of an ionic mechanism.

The stationary concentration of ions in an ionic chain reaction need only be very small and may, or may not, be detectable by the methods used here. The appreciable conductivities observed in ethylene dichloride and nitrobenzene are very largely, if not entirely, due to hydration by contaminating moisture and, moreover, in any one solvent are associated with low rather than high rates of polymerization (Table VI). That is, the ions detected here are not those taking part in the polymerization chain. Such ions are presumably present, but their contribution to the conductivity of the solution is very small or, at any rate, is completely masked by that of the much higher concentration of ions derived from hydrate. Since the large majority of the ions present—the hydrate ions—play no part in the polymerization, the fall in conductivity during the reaction must be attributed to the decrease in ionic mobility as the viscosity of the solutions increases.

The above observations imply that in high dielectric solvents the active catalyst is anhydrous  $\text{SnCl}_4$  and not hydrate, a conclusion at variance with previous results in low dielectric solvents at very low temperatures. The conflict may perhaps be resolved if a slight difference in mechanism is postulated in the two cases. The high dielectric solvents, where ionization is favoured, the active initiator may be a true ion formed from a catalyst-monomer or catalyst-solvent complex. In such a case the presence of moisture or any substance competing for the stannic chloride would reduce the effective concentration of the catalyst and hence the rate of polymerization. In solvents of low dielectric constant such complexes may be expected to be less stable and to be present in much smaller concentrations if at all. However, even in these solvents hydrates could still readily be formed which, though their dissociation would be difficult, might still provide the small concentration of ions necessary for initiation.

The effect of dielectric constant on the polymerization, while providing general confirmation of the ionic nature of the reaction, gives little detailed information about the individual kinetic processes. From the fact that the chain length as well as the rate of polymerization is increased by high dielectric constant, it was concluded that the termination rate is strongly reduced.<sup>15</sup> This would suggest that the termination step is the combination of ions of different sign rather than a simple dissociation of the polymer ion. However, this deduction is valid only if no transfer processes are operating and is not borne out by kinetic experiments (cf. Part II) in ethylene dichloride, which indicate spontaneous rather than combination termination. The influence of dielectric constant being greater on rate than on molecular weight suggests that the initiation process is strongly affected, as would be any reaction producing ions.

The high conductivity of stannic chloride in nitro-paraffin solutions is very interesting in itself, but its significance in the polymerization of olefines in these solvents is still uncertain. The rates observed in nitroethane are as expected from its dielectric constant, although the molecular weights appear to be anomalously low. In nitromethane, the polymerization seems to occur at about the same rate as in nitrobenzene, but measurements are inaccurate since the polymer is insoluble and separates during the reaction. These systems are being studied further.

*Trinity College,  
Dublin.*

<sup>15</sup> Pepper, *Nature*, 1946, **158**, 789.

---

## FRIEDEL-CRAFTS POLYMERIZATIONS

### PART II. THE KINETICS OF POLYMERIZATION OF STYRENE BY STANNIC CHLORIDE

BY D. C. PEPPER

*Received 9th November, 1948*

Experiments are reported on the stannic chloride catalyzed polymerization of styrene in solution in ethylene dichloride at 25° C. The initial rate of polymerization is found proportional to the square of the styrene concentration and to the first power of the stannic chloride concentration. The molecular weight is proportional to the styrene concentration and independent of that of stannic chloride. A kinetic scheme is suggested involving monomer-catalyst initiation and a unimolecular termination process. The catalyst is taken to be the anhydrous stannic chloride and not its hydrate.

The kinetics of polymerization of olefines by Friedel-Crafts catalysts have been little explored, in contrast to the immense amount of work on radical-catalyzed polymerizations. There is much qualitative information, but hardly any quantitative data. This is, no doubt, partly due to the intractable nature of the reactions; the catalysts are hygroscopic and difficult to handle; the reactions are very fast and hard to control; polymers of high molecular weight are produced only at very low temperatures where kinetic work is difficult.

Gwynn Williams<sup>1</sup> and Eley and Pepper<sup>2</sup> have investigated the stannic chloride catalyzed polymerization at room temperature of styrene and *n*-butyl vinyl ether respectively, but at the time of their work the importance of traces of water was not realized, and the interpretation of some of their results is uncertain. Plesch, Polanyi and Skinner<sup>3</sup> and Norrish and Russell<sup>4</sup> have shown that for isobutene at low temperatures (*ca.* -100° C) polymerized by the weaker Friedel-Crafts catalysts TiCl<sub>4</sub> and SnCl<sub>4</sub>, the presence of water is essential and have postulated that the polymerization is initiated by ions derived from the hydrates of these halides. The most active Friedel-Crafts catalyst BF<sub>3</sub> appears to induce polymerization without the intermediacy of water in the liquid phase at low temperatures, but not in the gas phase.<sup>5</sup>

In recent work<sup>6, 7</sup> the author has shown that the effect of water depends on the medium employed. At 25° C in solutions of stannic chloride in solvents of high dielectric constant (nitrobenzene, ethylene dichloride) moisture produces ions, presumably by hydration or hydrolysis, but reduces the rate of polymerization. The catalyst under these conditions seems, therefore, to be the anhydrous halide rather than the hydrate. Nevertheless, there is evidence that the polymerization in these solvents involves ionic processes, since both the rate and chain length are strongly increased the higher the dielectric constant.

In the experiments reported here, ethylene dichloride was chosen as the solvent, since in it steady rates of polymerization are obtained without the induction periods usually observed in hydrocarbons and carbon tetrachloride.

## Experimental

**Methods.**—The method of following the polymerization by bromination of unchanged monomer, used previously by Williams and by the author is convenient, but has the disadvantage that the reaction vessel must frequently be opened for the removal of samples. In a reaction sensitive to moisture this is a serious drawback. A very convenient method is to follow the viscosity of the polymerizing solution.<sup>2, 7</sup> This was tried in several preliminary experiments, but it was found that in certain cases, where relatively high molecular weight polymers were formed, the relation between polymer concentration and log viscosity was no longer linear. In such cases it was not possible to deduce accurately the course of the reaction from a single measurement of concentration at the end of the reaction.

A dilatometric method was finally chosen. These polymerizations are strongly exothermic and if the reaction vessel is a simple cylindrical bulb the temperature in the interior of the liquid may rise several degrees above that of the thermostat. Apart from its effect on the kinetics, such a temperature rise seriously impairs the accuracy of dilatometric methods, due to the thermal expansion of the solution. The dilatometers finally used in these experiments had the form of an annulus, as shown in Fig. 1. They were made of Pyrex

<sup>1</sup> Williams, *J. Chem. Soc.*, 1940, 775.

<sup>2</sup> Eley and Pepper, *Trans. Faraday Soc.*, 1947, **44**, 112.

<sup>3</sup> Plesch, Polanyi and Skinner, *J. Chem. Soc.*, 1947, 257.

<sup>4</sup> Norrish and Russell, *Nature*, 1947, **160**, 543.

<sup>5</sup> Evans, Meadows and Polanyi, *ibid.*, 1947, **160**, 869.

<sup>6</sup> Pepper, (a) *Nature*, 1946, **158**, 789; (b) *Trans. Faraday Soc.* (preceding paper).

<sup>7</sup> Foord, *J. Chem. Soc.*, 1940, 48.

and contained about 4 ml. solution. By reason of their annular shape, no part of the solution was more than 1 mm. (and the bulk about  $\frac{1}{2}$  mm.) from a surface cooled by the thermostat liquid. In practice, this design was very successful and no expansion effects due to rise of temperature were observed.

The dilatometer was clamped rigidly in a thermostat at 25° C. Monomer and catalyst solutions were brought to temperature equilibrium in stoppered Pyrex test-tubes in the thermostat, and at zero time the appropriate volumes mixed. About 4 ml. was then withdrawn by a pipette and run quickly into the dilatometer. By this method dilatometer readings could be obtained within  $1\frac{1}{2}$  min. of the start of the experiment.

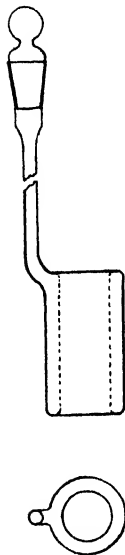


FIG. 1.—The Dilatometer.

The fall of the meniscus in the dilatometer tube was followed very accurately by a cathetometer reading to 0.01 mm. Since the dilatometers had different capacities and slightly different volumes were used in each run, the final contraction ( $\Delta h_{\infty}$ ) was different in each case and the simple rates of fall of the meniscus were not comparable. To derive the rate of polymerization,  $1/\Delta h_{\infty} \times dh/dt$ , the experiment was in many cases followed to completion to obtain  $\Delta h_{\infty}$ . However, when the systems were left for long periods (24-28 hr.) anomalies sometimes occurred, such as the formation of bubbles, or slight distillation of solvents to the upper part of the dilatometer. It was, therefore, found more reliable to calculate  $\Delta h_{\infty}$  from the initial volume and the known concentration of monomer.

The theoretical change of volume can be calculated from the densities of styrene monomer (0.9056 g. cm.<sup>-3</sup>) and polymer (1.070 g. cm.<sup>-3</sup>) to be 0.170 cm.<sup>3</sup> g.<sup>-1</sup>. If the mixing properties of monomer and polymer with the solvent are the same, the same volume change will be shown by solutions. Calibration of the dilatometer tubes, therefore, makes it possible to calculate the expected change of height corresponding to complete polymerization. Table I shows good agreement between calculated and observed values of  $\Delta h_{\infty}$  for solutions of concentration 181 g./l.

At the end of the experiment the solution was carefully washed out of the dilatometer and the solvent and any unchanged monomer removed by steam distillation. By this method the polymer was isolated quantitatively in a light flaky form very suitable for filtration and drying. Traces of stannic hydroxide formed by hydrolysis of the catalyst remained embedded in the polymer and were removed by dissolving in benzene and filtration. Molecular weights were determined from the intrinsic viscosities in benzene at 25° C, using Bamford and Dewar's relation,<sup>8</sup>

$$[\eta] = 4.57 \times 10^{-3} M^{0.65},$$

TABLE I.—CALIBRATION OF DILATOMETERS

Dil. No.	Calibration of Tube (mm./ml)	V (ml.)	$\Delta h_{\infty}$ (mm.)	$\Delta h_{\infty}/V$	$\Delta h_{\infty}/V$ (Calc.)
I . .	174	4.32	23.0	5.32	5.36
		4.33	23.5	5.44	
		4.22	22.2	5.25	
II . .	167	3.75	19.3	5.15	5.13
		3.75	18.6	4.96	
III .	167	4.44	22.6	5.09	5.13

where  $M$  = mol. wt.,  $[\eta] = \lim_{c \rightarrow 0} (\eta_{sp}/c)$ ,  $c$  = base mole (104 g)/l. The polymers obtained in this work were all of relatively low molecular weight (up to 10,000) but nevertheless, it was necessary to extrapolate the viscosities to zero concentration. Values of the intrinsic viscosity so obtained were reproducible to 1 %.

<sup>8</sup> Bamford and Dewar, *Proc. Roy. Soc. A*, 1948, 192, 309.

Monomer and solvent were purified and dried (over Na or  $P_2O_5$ ), as described in the previous paper,<sup>6b</sup> and stored in stoppered bottles in a large desiccator. All-glass apparatus was dried at  $110^\circ\text{C}$  before use and cooled in a stream of air dried by passing through  $P_2O_5$ .

### Results

With the dilatometers described above the course of polymerization could be followed conveniently from a time about  $1\frac{1}{2}$  min. after the start of the reaction. No induction periods greater than this time were ever observed so they were assumed to be absent even over shorter periods. The fall of the meniscus proceeded continuously at a decreasing rate as monomer was consumed, but over about the first 20 % of reaction the rate was sensibly constant, permitting extrapolation to zero height in the tube and accurate determination of the initial rate.

**The Effect of Stannic Chloride Concentration.**—A series of experiments was performed at constant monomer concentration (20 % by volume, 1.74 moles per litre) in ethylene dichloride, with different catalyst concentration over a tenfold range. Reproducible results (Table II, Fig. 2) were obtained, indicating a linear dependence of rate, and molecular weights independent of stannic chloride concentration.

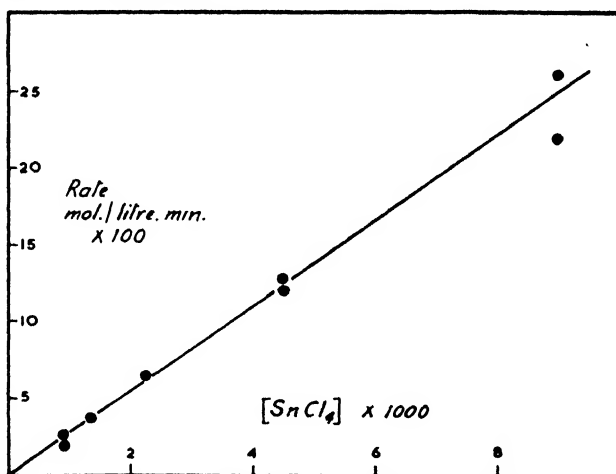


FIG. 2.—The dependence of rate on concentration of stannic chloride.

TABLE II.—THE EFFECT OF STANNIC CHLORIDE CONCENTRATION

$[M]_0 = 1.74$  (in ethylene dichloride)  $T = 25^\circ\text{C}$

Expt.	$[\text{SnCl}_4] \times 10^3$	$\frac{dh}{dt}$ (mm./min.)	$\frac{1}{\Delta h_\infty} \times \frac{dh}{dt} \times 10^3$	$-\frac{d[M]}{dt} \times 10^3$	$[\eta]$	Mol. wt.
96	0.9	0.20	1.04	1.81	1.82	10,000
97	0.9	0.33	1.43	2.49	1.85	10,400
98	1.35	0.40	2.08	3.61	—	—
95	2.25	0.86	3.7	6.45	1.88	10,700
90	4.5	1.60	6.93	12.0	1.85	10,400
91	4.5	1.64	7.26	12.6	1.86	10,500
89	9.0	2.95	12.55	21.8	1.84	10,300
114	9.0	3.34	14.8	25.9	(1.22)	(5,500)

These molecular weights are rather greater than expected in this solvent at this monomer concentration—usually values of 5000-5500 are obtained, as in Expt. 114. The higher values, in Expt. 89-97, were traced to a slight contamination of the batch of monomer with polymer produced photochemically or by oxidation on storage. This (radical-induced) polymer has a much higher molecular weight than that produced by the stannic chloride; hence, very small traces are enough to raise the average molecular weight quite considerably. However, in the above experiments this error affects all the results equally and does not impair the conclusion that the molecular weight of the polymer is independent of the catalyst concentration.

**The Effect of Styrene Concentration.**—Where the dielectric constants of monomer and solvent are different, as in this case, we must expect a composite effect of monomer concentration on rate of polymerization and molecular weight.

TABLE III.—THE EFFECT OF STYRENE CONCENTRATION

Volume %			$[M]_0$	$-\frac{d[M]}{dt} \times 100$	$[\eta]$	Mol. Wt.
Styrene	Benzene	Ethylene Dichloride				
5	15	80	0.435	0.96	0.59	1750
10	10	80	0.870	5.02	0.86	3100
			0.870	4.38	—	—
15	5	80	1.305	11.1	1.01	4100
			1.305	18.1	0.99	3900
20	0	80	1.74	25.9	1.22	5500
			1.74	21.8	—	—

Two influences will operate simultaneously: (a) the normal kinetic effect of increasing rate with increasing monomer concentration, and (b) an opposite effect due to the reduction of dielectric constant as the monomer (hydrocarbon) content increases. Such a composite effect has been observed by Norrish and Russell<sup>4</sup> in mixtures of isobutene and ethyl chloride.

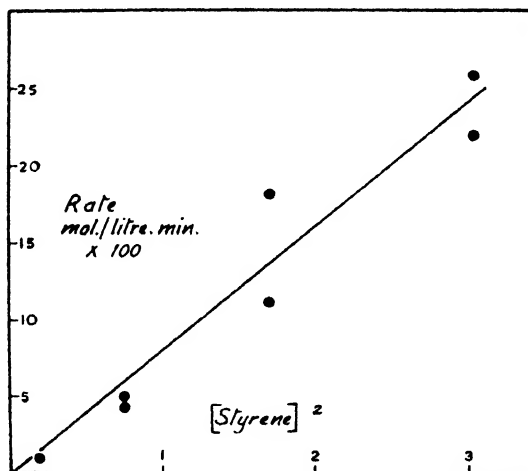


FIG. 3.—The dependence of rate on styrene concentration.

To obtain the true kinetic effect of monomer concentration, the dielectric constant of the solution must be kept constant while the monomer content is varied. This was achieved in these experiments by carrying out the polymerizations in ternary mixtures of ethylene dichloride, styrene and benzene. The dielectric constant of the solutions was kept effectively constant by keeping a fixed proportion of ethylene dichloride to total hydrocarbon and the monomer

concentration varied by altering the proportion of styrene to benzene. Under these conditions no falling off of rate due to decrease of dielectric constant was observed up to the highest monomer concentration used, 20 % by volume or 1.74 mole/litre.

Fig. 3 shows the rate of polymerization plotted against the square of the styrene concentration. The straight line seems justified, though the scatter of points makes it just possible that a cube relation would also fit. However, a log-log plot gives an exponent of 2.3, so the second power relation is more plausible.

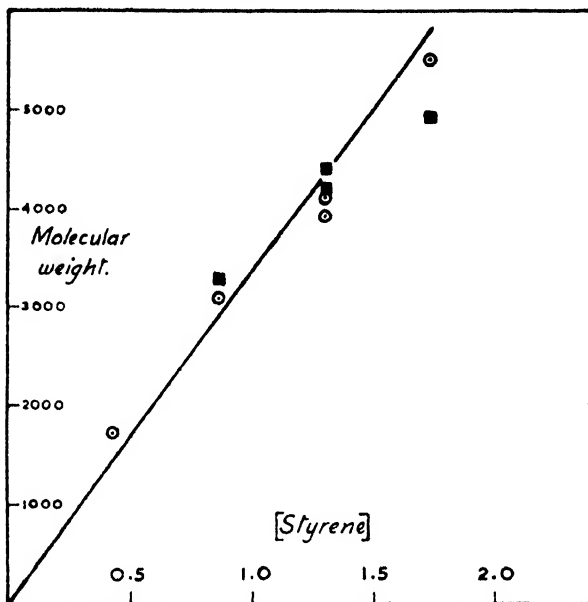


FIG. 4.—The effect of initial styrene concentration on molecular weight.

The molecular weights are best described as directly proportional to the monomer concentration. As can be seen from Fig. 4, the points at the highest monomer concentration lie somewhat below the linear relation, but a plot against the square root of the concentration shows a much greater deviation. In Fig. 4 the circles refer to polymer isolated from the dilatometer at the end of the reaction and the squares to samples taken at about 50-80 % polymerization.

### Discussion

The above results lead to the kinetic relations—

- (i) Rate proportional to  $[M]^3 \times [c]$ , where  $[M]$  = styrene conc.,  $[c]$  =  $\text{SnCl}_4$  conc. ;
- (ii) Mol. wt. proportional to  $[M]$  (independent of  $[c]$ ).

These relations confirm previous results as far as comparisons are possible. Thus a linear dependence of rate on catalyst concentration was found also by Williams<sup>1</sup> with styrene, Eley and Pepper<sup>2</sup> with vinyl *n*-butyl ether, and Norrish and Russell<sup>4</sup> with *isobutene* (though here the catalyst appears to be the hydrate). Similarly, the independence of molecular weight of catalyst concentration was observed by Williams, and by the author in unpublished data on the polymerization of styrene in benzene and in nitrobenzene. There is conflict between the results reported here and those of Williams on the effect of monomer concentration on rate, which he records as proportional to the third or fourth power of the concentration. However, this dependence was derived from an analysis of the rate over the whole course of the reaction, a method now regarded as unreliable in polymer kinetics.



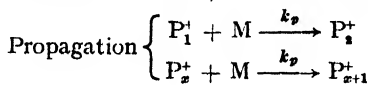
An apparent discrepancy between the results in this paper and that of Williams on the effect of monomer concentration on molecular weight is due to a different method of calculation from the intrinsic viscosity. If the molecular weight be taken as directly proportional to the intrinsic viscosity, then the results of Table III show proportionality between the molecular weight and the square root of the monomer concentration, as recorded by Williams. However, such a linear (Staudinger) relation between intrinsic viscosity and molecular weight is now known to be generally invalid, and Bamford and Dewar<sup>9</sup> have found for low molecular weight polystyrenes that

$$[\eta] = 4.57 \times 10^{-3} \times M^{0.55}.$$

If the molecular weights are calculated from this relation, one finds a linear dependence on the monomer concentration.

One weakness in the molecular weight data reported here is that they refer to polymer isolated at the end of the reaction. Samples taken during the reaction (55-80 % polymerization) have, as a rule, slightly (*ca.* 5 %) greater average molecular weights, indicating that the molecular weight falls as the monomer concentration decreases, as shown also by the series of experiments at different initial monomer concentration. However, if the dependence is in fact linear, as suggested, it is immaterial when the samples are taken.

The above kinetic relations can be explained by the very simple scheme suggested by Eley and Pepper,<sup>2</sup> viz.:



Making the usual assumptions of a stationary state and identity of all the propagation rate constants, we derive:

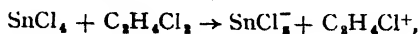
$$\text{Rate} = \frac{k_i \times k_p}{k_t} \times [M]^2[C],$$

$$\text{Mol. wt.} = \frac{k_p}{k_t} \times [M].$$

Such a scheme leads to the observed relations, and by providing for the liberation of the catalyst in the termination process, accounts for the formation of many polymer chains per molecule of catalyst (about 40 at the lowest catalyst concentration and 4 at the highest).

An alternative explanation of this fact, and also of the relatively low molecular weights found in this type of polymerization, is that chain transfer by monomer or solvent is taking place. However, this would necessitate more complicated kinetic dependences than those found above, and there is as yet no other evidence for such transfer processes in this system. Eley has recently found evidence for monomer transfer in related systems.<sup>9</sup>

The nature of the monomer-catalyst complex is not specified, but a plausible suggestion would be the polarized molecule proposed by Price.<sup>10</sup> On the other hand, the marked effect of the dielectric constant of the solvent on these polymerizations strongly suggests that true ions play a part. If so, a possible initiating mechanism might be the reaction of stannic chloride with the solvent, e.g.



<sup>9</sup> Eley (private communication).

<sup>10</sup> Price, *Reactions at C=C Double Bonds* (New York, 1946).

followed by combination of one or other ion with the monomer. Similar reactions<sup>11</sup> are known with  $\text{AlCl}_3$ , and there is evidence for some ionization process such as this in solutions of stannic chloride in nitroparaffins where large conductivities are shown.

The observed catalyst and monomer dependencies do not agree with kinetic schemes involving termination by combination of a polymer ion with another ion of opposite sign, or by mutual combination of oppositely-charged polymer ions. The suggestion of such a termination process advanced earlier by the author,<sup>6a</sup> based on general arguments from the effect of dielectric constant on the molecular weight is, therefore, not borne out by the kinetic evidence.

Such bimolecular termination reactions have been proposed by Polanyi<sup>12</sup> and by Norrish and Russell<sup>4</sup> in polymerizations where the hydrate of the catalyst appears to be the effective initiator. Here it is difficult to assess the role of water with certainty. Small traces of water were no doubt present in the systems here described (due to access from the air, or already present as hydrate in the stannic chloride), but certainly played no dominant part. If the hydrate were responsible for the initiation one would not expect the observed smooth dependence of rate on stannic chloride concentration, since the amount of hydrate would depend on the (arbitrary) concentration of water. Moreover, the addition of small traces of water is found definitely to retard the polymerization in ethylene dichloride (and in nitrobenzene) at 25° C. The conclusion seems to be that under these conditions the catalyst is the anhydrous halide (or ions derived from it) rather than the hydrate.

Further work is needed to settle this and other obscure points. It is not impossible that different mechanisms operate at -100° and at 25° C, since processes energetically unfavourable at the lower temperature might well be quite rapid at the higher. Also, the dielectric nature of the medium may affect the mechanisms as well as the rate of any one process; in solvents of high dielectric constant processes involving true ionic dissociation will be favoured, while at low dielectric constant only polarized molecules may result.

*Trinity College,  
Dublin.*

<sup>11</sup> Wertyporoch and Firla, *Annalen*, 1933, **500**, 287.

<sup>12</sup> Polanyi, *Nature*, 1946, **158**, 223.

---

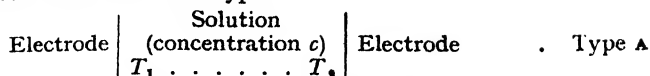
## THERMAL DIFFUSION POTENTIALS IN NON-ISOTHERMAL ELECTROLYTIC SYSTEMS

BY H. J. V. TYRRELL AND G. L. HOLLIS

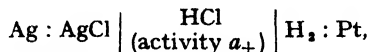
*Received 15th November, 1948*

In general, the presence of a temperature gradient in an electrolyte gives rise to a potential gradient, the thermal diffusion potential. Potentials of this type have been studied in cells consisting of two electrodes immersed in the same electrolyte, one electrode being heated relative to the other. It has been shown that they are approximately independent of the total ionic concentration, and of the absolute temperature of the system, but are greatly influenced by the presence of  $\text{H}^+$  or  $\text{OH}^-$ . The experimental data have been considered in the light of an equation derived from rate process theory, and the possibility of obtaining absolute values for thermal diffusion potentials discussed.

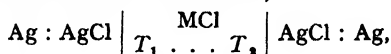
If a non-isothermal cell of the type :



is set up, taking simple precautions to prevent mixing by thermal convection, the measured E.M.F., while constant and characteristic, cannot be calculated from the conventional temperature coefficient of the electrode. This quantity is invariably measured in an isothermal cell of the type,<sup>1</sup>

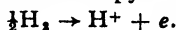


the standard E.M.F.,  $E^\circ$ , being measured over a range of temperature. The potential of the normal hydrogen electrode is arbitrarily assumed to be zero at all temperatures,<sup>2</sup> and  $dE^\circ/dT$  is termed the temperature coefficient of the silver-silver chloride electrode. The difference between the observed value of the E.M.F. for the cell,



and that calculated from  $dE^\circ/dT$  depends on the total ionic composition of the solution. It is due partly to the arbitrary assumption that the normal hydrogen electrode has a temperature coefficient of zero, and partly to the existence of a potential between the hot and cold portions of the electrolyte arising from the tendency of different ions to diffuse at different rates under a thermal gradient, and analogous to the diffusion potential which exists across a concentration gradient in such a solution. These potentials are termed "thermal diffusion potentials" in the present paper.

Non-isothermal systems of the above type have been studied by several workers with the object of calculating the true temperature coefficient of the hydrogen electrode and the entropy change in the electrode reaction,



The majority measured the E.M.F.  $\Delta\phi$  of Type A cells over a range of temperature and employed entropy data<sup>3</sup> or conventional temperature coefficients of electrodes<sup>4</sup> in their calculations. Alternatively, the heat absorbed or evolved at the electrode when 1 g. ion of substance was dissolved from, or deposited at, the electrodes (molar Peltier heat  $\Pi$ ) was measured<sup>5</sup> and related to the value of  $d\phi/dT$  for the corresponding Type A cell by a relation similar to the Thomson equation for metallic thermocouples,

$$\Pi = z_i F T (d\phi/dT),$$

where  $z_i$  is the valency of the ion to which the electrode is reversible. Lange and Hesse found the equation to hold fairly well,  $\Pi$  varying with the ionic composition of the electrolyte in the same way as  $d\phi/dT$ .<sup>6</sup> The dependence of the experimental values upon the total ionic concentration showed the existence of thermal diffusion potentials, and in order to calculate the true temperature coefficient of the hydrogen electrode it is necessary to determine their value, although this fact was not always recognised.<sup>7</sup> All previous attempts to calculate them have been based on their thermodynamic derivation in terms of the empirical "entropies of transfer," due to Eastman,<sup>8</sup> and to Wagner.<sup>9</sup> The entropy of transfer

<sup>1</sup> Harned and Ehlers, *J. Amer. Chem. Soc.*, 1932, **54**, 1350.

<sup>2</sup> Lewis and Randall, *Thermodynamics* (McGraw-Hill, 1923), p. 431.

<sup>3</sup> E.g. Bernhardt and Crockford, *J. Physic. Chem.*, 1942, **46**, 473.

<sup>4</sup> Gilbert, *Faraday Soc., Discussions*, 1947, **1**, 320.

<sup>5</sup> Lange and Hesse, *Z. Elektrochem.*, 1932, **38**, 428.

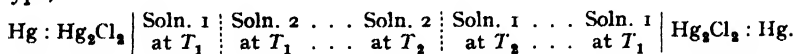
<sup>6</sup> Lange and Hesse, *ibid.*, 1933, **39**, 374.

<sup>7</sup> E.g. Kolthoff and Tekelenburg, *Rec. Trav. Chim.*, 1927, **46**, 18.

<sup>8</sup> Eastman, *J. Amer. Chem. Soc.*, 1928, **50**, 292.

<sup>9</sup> Wagner, *Ann. Physik*, 1929, **3**, 629; 1930, **6**, 370.

of an ion was defined as the entropy decrease of the system at one point and increase at another when 1 g. ion was removed from the first point and transferred to the second point within the system, and values were calculated by Eastman from some early data of Podzus on cells of the type,



For this purpose, Eastman assumed a relation between the magnitude of the Soret effect and the mobilities of the ions which had little experimental basis. Any errors in these entropies of transfer would of course lead to errors in the computed temperature coefficients. In addition, these refer to the concentrations at which the experiments were carried out, not to the "normal" electrode. Thus the results of different workers cannot readily be compared.

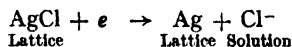
The Eastman-Wagner thermodynamic treatment yields an expression for  $d\phi/dT$  in terms of the true temperature coefficient of the normal electrode  $d\phi^\circ/dT$ , the activity of the ion, and the thermal diffusion potential  $J$ . It is shown in this paper that  $(d\phi^\circ/dT) + J$  can be obtained by an extrapolation method using a modified Eastman-Wagner equation. Values of this quantity have been calculated from new data on Type A cells using silver, silver-silver bromide, and silver-silver chloride electrodes, and from some of the earlier values. The nature of thermal diffusion potentials is discussed in the light of these results, and an equation derived from rate process theory.

### Theoretical

(i) **Extrapolation Formula.**—The thermodynamic treatment of Eastman and Wagner yields the following equation,

$$d\phi/dT = -\Delta S/z_e F - S_e^*/F - \sum n_+ S_+^*/F + \sum n_- S_-^*/F \quad (1)$$

where  $S_e^*$ ,  $S_+^*$ ,  $S_-^*$  are entropies of transfer of electrons in the metallic conductor, of cations and of anions respectively in the solution,  $n_+$ ,  $n_-$  the transport numbers of the ions, and  $\Delta S$  the entropy change per g. mol. in the reaction (considering silver-silver chloride electrodes),



$\Delta S$  may be written in terms of the partial molar entropies,

$$\Delta S = \bar{S}_{\text{Ag}} + \bar{S}_{\text{Cl}^-} - \bar{S}_{\text{AgCl}} - \bar{S}_e.$$

The only variable in this equation is the partial molar entropy of the chloride ion which may be written,

$$-\bar{S}_{\text{Cl}^-} = d\mu_{\text{Cl}^-}/dT = d\mu_{\text{Cl}^-}^\circ/dT + R \ln a_{\text{Cl}^-} + RT d/dT (\ln a_{\text{Cl}^-}),$$

$$\therefore \bar{S}_{\text{Cl}^-} = \bar{S}_{\text{Cl}^-}^\circ - R \ln a_{\text{Cl}^-} - RT d/dT (\ln a_{\text{Cl}^-}),$$

Substituting in (1),

$$\begin{aligned} \frac{d\phi}{dT} = & -\frac{\Delta S^\circ}{F} + \frac{R}{F} \ln a_{\text{Cl}^-} + \frac{RT}{F} \frac{d}{dT} (\ln a_{\text{Cl}^-}) \\ & - S_e^*/F - \sum n_+ S_+^*/F + \sum n_- S_-^*/F, \end{aligned}$$

where  $\Delta S^\circ$  is the entropy change per g. mol. in the above reaction when the solution contains chloride ions at unit activity. The conducting electrons in the electrode lattice at the temperature of the electrode are regarded as being in the standard state. This standard state thus differs for each electrode system but this fact may be neglected in the present

discussion. The  $S^*$  terms may be put equal to some quantity  $J$ , the "non-isothermal" part of the measured value of  $d\phi/dT$ . Of the remaining terms,  $\ln a_{\text{cl-}}$ , and  $d/dT (\ln a_{\text{cl-}})$  are unknown at finite concentrations. However,

$$d/dT (\ln a_i) = -\bar{L}_i/RT^2,$$

where  $\bar{L}_i$  is the relative partial heat capacity of the  $i$ th ion. In dilute solutions, for a univalent ion in a uni-univalent electrolyte, the simple Debye-Hückel theory gives, for an aqueous solution at  $25^\circ\text{C}$ ,

$$\log_{10} f_i = -0.50 \sqrt{\mu},$$

$$\therefore d\phi/dT = 2.303R/F \log_{10} c_{\text{cl-}} + \frac{2.303R}{2F} \sqrt{\mu} = \frac{d\phi^\circ}{dT} - \frac{\bar{L}_{\text{cl-}}}{FT} + J,$$

writing  $d\phi^\circ/dT$  for  $-\Delta S^\circ/F$ . Terms on the left-hand side can be measured or computed; of those on the right,  $d\phi^\circ/dT$  is constant,  $\bar{L}_{\text{cl-}}/(FT)$  tends to zero as  $c \rightarrow 0$ , and  $J$  tends to some limiting value  $J'$ . Thus  $(d\phi^\circ/dT) + J'$  can be found by plotting the left-hand side against some suitable function of  $c$ , say  $\sqrt{c}$ , and extrapolating to zero.

(ii) **Calculation of Thermal Diffusion Potential by Rate Process Theory.**—The method used by Glasstone, Laidler, and Eyring for the calculation of the diffusion of an electrolyte under the influence of a concentration gradient<sup>10</sup> may be adapted for this purpose. Using this it can be shown that the net rate of transfer of the  $i$ th ion in the forward direction is:

$$N\lambda c_i(k' - k'')(1 + \alpha w/kT) + N\lambda c_i(k''/kT) \times w,$$

where  $k'$ ,  $k''$  are the specific rates in the forward and backward directions respectively,  $\lambda$  the distance between two successive equilibrium positions of the ion,  $c_i$  the concentration,  $w$  the work done in moving it from one equilibrium position to the next, and  $\alpha$  the proportion of ions in the activated state. If  $\Delta G_i^\ddagger$  is the free energy of activation of transfer,

$$k' = kT/h \exp [-\Delta G_i^\ddagger/RT],$$

$$k'' = k/h.(T + \lambda dT/dx) \exp [-(\Delta G_i^\ddagger + \lambda d/dx(\Delta G_i^\ddagger))/R(T + \lambda dT/dx)],$$

$$\simeq k/h.(T + \lambda dT/dx) \exp [-\Delta G_i^\ddagger/RT] \exp [-\lambda d/dx(\Delta G_i^\ddagger)/RT].$$

$$\therefore k' - k'' = kT/h \exp [-\Delta G_i^\ddagger/RT] \times (\lambda/RT \times d/dx(\Delta G_i^\ddagger)) - k'' \lambda d/dx(\ln T),$$

$$\simeq k''(\lambda/RT \times d/dx(\Delta G_i^\ddagger) - \lambda \times d/dx(\ln T)).$$

$\therefore$  Net rate of transfer

$$= N\lambda^2 c_i k'' \left( \frac{1}{RT} \times \frac{d}{dx}(\Delta G_i^\ddagger) - \frac{d}{dx}(\ln T) \right) + \frac{N\lambda c_i k''}{kT} \times w.$$

Now,

$$w = \lambda \times dE/dx \times z_i e,$$

$$D_i = \lambda^2 k_i'',$$

where  $dE/dx$  is the potential gradient in the solution,  $z_i$ ,  $D_i$  the valency and diffusion coefficient respectively of the ion, and  $e$  the electronic charge.

$\therefore$  Net rate of transfer

$$= ND_i c_i \left[ \frac{1}{RT} \times \frac{d}{dx}(\Delta G_i^\ddagger) - \frac{d}{dx}(\ln T) \right] + \frac{ND_i c_i z_i}{kT} \times e \times \frac{dE}{dx}$$

$$= \frac{ND_i c_i z_i F}{RT} \left[ \frac{1}{z_i F} \times \frac{d}{dx}(\Delta G_i^\ddagger) - \frac{RT}{z_i F} \times \frac{d}{dx}(\ln T) + \frac{dE}{dx} \right].$$

<sup>10</sup> Glasstone, Laidler and Eyring, *Theory of Rate Processes* (McGraw-Hill, 1941), p. 552.

At equilibrium, the rates of transfer for each ion are equal. Thus, for a uni-univalent electrolyte,

$$\begin{aligned} & \frac{ND_+cF}{RT} \left[ + \frac{1}{F} \times \frac{d}{dx}(\Delta G_+^*) - \frac{RT}{F} \frac{d}{dx}(\ln T) + \frac{dE}{dx} \right] \\ &= - \frac{ND_-cF}{RT} \left[ - \frac{1}{F} \frac{d}{dx}(\Delta G_-^*) + \frac{RT}{F} \frac{d}{dx}(\ln T) + \frac{dE}{dx} \right]. \\ \therefore \frac{dE}{dx} &= \frac{R}{F} \times \frac{D_+ - D_-}{D_+ + D_-} \left( \frac{dT}{dx} \right) - \frac{1}{F} \times \frac{D_+ \frac{d}{dx}(\Delta G_+^*) - D_- \frac{d}{dx}(\Delta G_-^*)}{D_+ + D_-}. \end{aligned}$$

Changing the variables this becomes,

$$\frac{dE}{dT} = - \frac{D_+ (d/dT(\Delta G_+^*) - R) - D_- (d/dT(\Delta G_-^*) - R)}{D_+ + D_-}.$$

But it may be shown that,

$$D_i = \frac{RT}{z_i^2 F^2} \times A_i,$$

where  $A_i$  is the equivalent conductivity of the ion.

$$\frac{dE}{dT} = - \frac{A_+ (d/dT(\Delta G_+^*) - R) - A_- (d/dT(\Delta G_-^*) - R)}{F \times (A_+ + A_-)}.$$

The terms  $(d/dT(\Delta G_i^*) - R)$  are entropy terms and can be put equal to  $+S_i^*$ , Eastman's entropy of transfer, i.e. the rate process theory and the thermodynamic approach give identical equations for the thermal diffusion potential. The remaining "non-isothermal" term in the Eastman-Wagner equation arises from thermo-electric effects in the conductor which have not been considered in the above.

## Experimental

Solutions were prepared from the purest available materials. Because of the high resistance of the cell used, potential measurements were made with a Marconi pH meter, Type TF 511D. This limited the accuracy to about 1 mV, and it was not therefore necessary to use highly purified electrolytes.

Silver electrodes were made by heating a paste of silver oxide and water on a platinum spiral in an alcohol flame until a spongy mass of silver was formed. Silver-silver chloride electrodes were made from these by anodic treatment in dilute HCl.<sup>4</sup> Silver-silver bromide electrodes were prepared in the dry way<sup>11</sup> by heating a paste of 90 % silver oxide and 10 % silver bromate to about 700° C (alcohol flame or electric furnace). These were more satisfactory than those prepared by decomposition of silver oxide and subsequent electrolysis.

Two types of cell were used, the design of both being such that concentration changes round the electrodes were minimized. One consisted of two electrode vessels connected by a long bridge of narrow glass tubing bent so as to reduce thermal diffusion between the electrodes. The other, used in the majority of the experiments, was an H-type cell, the upright limbs, containing the thermometers and the electrodes, having jackets through which water could be circulated. A three-way glass tap was placed in the narrow transverse limb, measurements of the E.M.F. of the cell being made with this tap closed. The temperature gradient in this cell lay mainly in the transverse limb. The third leg of the three-way tap could be used for checking the potential of each test electrode against an external standard. All experiments in this cell were carried out in an atmosphere of purified nitrogen, electrolyte saturated with the gas being forced over from an auxiliary flask, and stirred by passing a slow stream of the gas through each limb of the cell. Both water-jackets were filled, one being heated gently with a microburner, and the other kept cool by passing a slow stream of water through. Temperatures were measured to the nearest fifth of a degree by means of thermometers placed close to the electrodes; these had been previously checked against one another over the whole working range. The upper limit of this was fixed at 50° C. If heated above this temperature

<sup>11</sup> Keston, *J. Amer. Chem. Soc.*, 1935, **57**, 1671.

the electrodes sometimes failed to return to their reversible value on cooling to room temperature. The cell was blackened externally as a precaution against light effects at the electrodes.

When the vessel was filled with solution, one limb was heated gently until the difference in temperature was about  $10^{\circ}\text{C}$ , and the microburner removed. The electrode was left for a few minutes to come to thermal equilibrium with its immediate surroundings, and a reading taken of the E.M.F.  $\Delta\phi$  of the cell, the temperature difference  $\Delta T$  being noted simultaneously. This was repeated at gradually increasing temperature intervals until the electrode reached a temperature of not more than  $50^{\circ}\text{C}$ . The cell was then allowed to cool, simultaneous readings of E.M.F. and the temperatures of the two electrodes being taken. Results were rejected if the cooling curve did not coincide with the heating curve, or if the heated electrode did not return to its original potential. No special precautions were taken to keep the cold electrode at a constant temperature, and its temperature sometimes changed by a degree or two; this was not important since the temperature difference was measured at each potential reading, and the variation of  $\Delta\phi$  with  $\Delta T$  was found to be linear within the limits of experimental error.

### Results

The results obtained in the present work show that over the temperature range  $20^{\circ}\text{--}50^{\circ}$ ,  $\Delta\phi$ , the observed E.M.F. of a Type A cell was approximately a linear function of  $\Delta T$ , the temperature difference between the electrodes. Approximately two hundred curves of this type were obtained, a small selection being shown in Fig. 1. A slight flattening of the curve sometimes occurred at

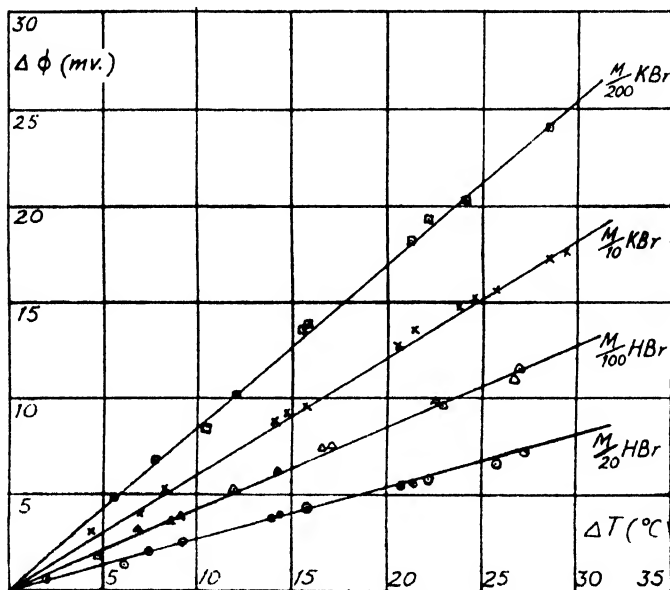


FIG. 1.—Variation of  $\Delta\phi$  with  $\Delta T$ .

the upper end of the temperature range but when a mean slope  $d\phi/dT$  was calculated for each experiment by the method of averages,<sup>12</sup> the experimental points did not deviate from the calculated line by more than the experimental error. The values used in the subsequent calculations were the means of results from two experiments on each of two different electrodes, the spread not being greater than  $\pm 0.01\text{ mV}/^{\circ}\text{C}$  except in one or two cases. In all cases, a positive value of  $d\phi/dT$  signifies that the heated electrode was positive.

<sup>12</sup> Davies, *Empirical Equations and Nomography* (McGraw-Hill, 1943), p. 4.

The validity of the extrapolation formula derived from the Eastman-Wagner equations was tested by plotting

$$(d\phi/dT - 2.303R/F \times \log_{10} c + 2.303R/2F \times \sqrt{\mu})$$

against  $\sqrt{c}$  for bromide solutions (silver-silver bromide electrodes) and chloride solutions (silver-silver chloride electrodes) (Fig. 2) using data obtained during the present investigation together with those of Bernhardt and Crockford.<sup>3</sup>

TABLE I.—EXTRAPOLATED VALUES OF  $(d\phi/dT) + J'$ , AND UNCORRECTED VALUES FOR THE PARTIAL IONIC ENTROPY OF THE HYDROGEN ION

Electrode	Electrolyte	$(d\phi/dT) + J'$ (mV/°C)	$\bar{S}_{H^+}^0$ (cal. mole <sup>-1</sup> deg. <sup>-1</sup> )	Reference
Ag-AgCl	HCl	$-0.145 \pm 0.005$	+3.7	A
		$-0.130 \pm 0.002$	+3.4	B
		$-0.10 \pm 0.02$	+2.7	C
	LiCl	$+0.21 \pm 0.01$	-4.4	B
	KCl	$+0.210 \pm 0.005$	-4.4	B
	NaCl	$+0.205 \pm 0.005$	-4.3	A
		$+0.205 \pm 0.005$	-4.3	B
	NH <sub>4</sub> Cl	$+0.230 \pm 0.010$	-4.7	A
		$+0.200 \pm 0.005$	-4.7	B
Ag-AgBr	NaBr	$+0.320 \pm 0.01$	-3.3	A
	NH <sub>4</sub> Br	$+0.37 \pm 0.01$	-4.4	A
	KBr	$+0.365 \pm 0.005$	-4.2	A
	75% KBr-25% HBr	$+0.180 \pm 0.015$	-0.03	A
	50% KBr-50% HBr	$+0.105 \pm 0.005$	+1.71	A
	25% KBr-75% HBr	$+0.045 \pm 0.005$	+3.05	A
	HBr	$+0.00 \pm 0.01$	+4.1	A
Ag	AgNO <sub>3</sub>	$-0.22 \pm 0.01$	-3.1	A
		-0.26	-2.1	D
		-0.27	-1.9	C
	25% HNO <sub>3</sub> -75% AgNO <sub>3</sub>	-0.35	-0.06	A

A. Direct measurement, 20°-50° C, this paper.

B. Direct measurement, 25°-35° C.<sup>3</sup>

C. Peltier heat, 25° C.<sup>5, 6</sup>

D. Direct measurement, 20°-60° C.<sup>13</sup>

For dilute solutions the ordinates were, in general, almost constant, suggesting that the non-isothermal portion of the E.M.F. was almost independent of concentration. The gradual decrease shown at higher concentrations may have been due to the inadequacy of the extrapolation formula, the increasing importance of the  $d/dT (\ln a_i)$  term, to variations in  $J$ , or to combinations of these factors.

Where possible, the published data together with those obtained in the present work have been extrapolated to zero concentration in this way, the results, together with the estimated errors in extrapolation, being shown in Table I, Richards' data on calomel electrodes,<sup>14</sup> and some Peltier heat measurements of Lange and Hesse<sup>5, 6</sup> were unsuitable, the concentrations studied being limited and the results inconsistent with the extrapolation equation. In order to provide a basis for comparison between different electrodes, values for  $\bar{S}_H^0$  uncorrected for thermal diffusion effects have been calculated.

<sup>13</sup> Burian, *Z. Elektrochem.*, 1931, **37**, 238.

<sup>14</sup> Richards, *Z. physik. Chem.*, 1897, **24**, 39.



A few experiments were carried out on 50/50 mixtures of KOH and KBr using silver-silver bromide electrodes. In the most dilute solutions (N/1000, N/2000 in Br<sup>-</sup>) the E.M.F. was increased by about 0.16 mV/°C by the presence of OH ions. In the more concentrated solutions the increase was greater (0.38 mV/°C in a solution N/100 in Br<sup>-</sup>) but the electrodes appeared to be affected by the presence of the high concentration of alkali.

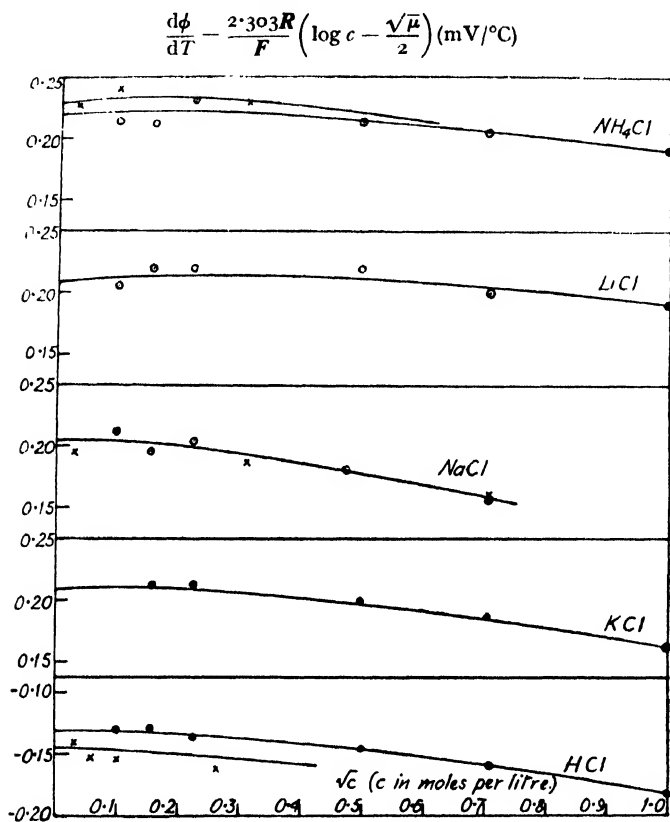


FIG. 2a Extrapolation curves for Ag-AgCl electrodes.

○ Bernhardt and Crookford (3)

× This paper.

### Discussion

Fig. 2 shows that the mean  $d\phi/dT$  values can be represented quite well by a modified equation of the Eastman-Wagner type, using the simple Debye-Hückel expression to represent the activity coefficient of the ion, the terms  $(d\phi^{\circ}/dT) + J + d/dT (\ln a_i)$  remaining approximately constant up to 0.1 M.  $(d\phi^{\circ}/dT) + J'$  could therefore be determined by extrapolation with fair accuracy, and, being independent of concentration, was more useful for comparison purposes than were individual  $d\phi/dT$  values.

It is clear from the data assembled in Table I that the most important factor influencing the values of  $(d\phi^{\circ}/dT) + J'$  was the presence of hydrogen or hydroxyl ions. With the convention adopted in this paper, that the heated electrode is taken as positive, it is evident that the thermal diffusion potential had a larger negative value in solutions containing hydrogen ions than in solutions of neutral salts. The difference was approximately independent of the nature of the electrodes and of the other ions present,

$$\frac{d\phi}{dT} - \frac{2.303R}{F} \left( \log c - \frac{\sqrt{\mu}}{2} \right) (\text{mV}/^\circ\text{C})$$

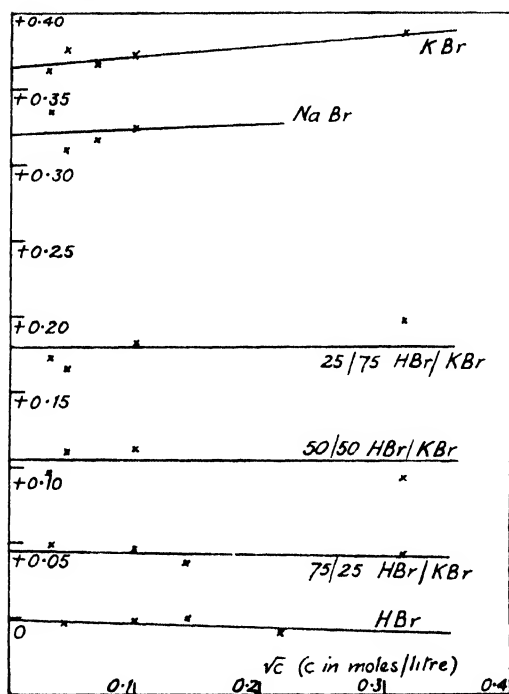


FIG. 2b.—Extrapolation curves for Ag-AgBr electrodes. This paper.

$$\frac{d\phi}{dT} - \frac{2.303R}{F} \left( \log c - \frac{\sqrt{\mu}}{2} \right) (\text{mV}/^\circ\text{C})$$

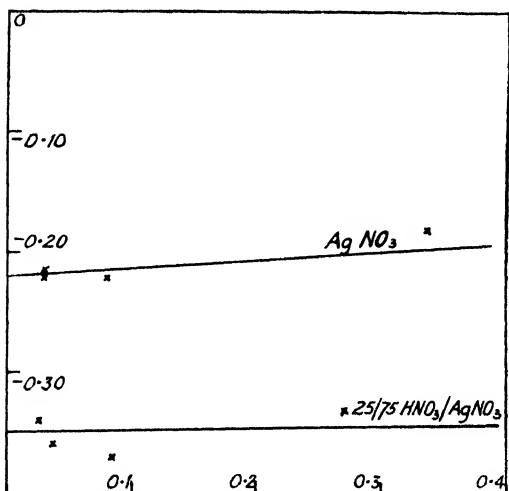


FIG. 2c.—Extrapolation curves for Ag electrodes. This paper.

the difference between HCl and KCl solutions with silver-silver chloride electrodes being almost the same as that between HBr and KBr solutions with silver-silver bromide electrodes. A similar effect was observed for mixtures of silver nitrate and nitric acid with silver electrodes, the diminution being approximately that found for silver-silver bromide electrodes in a mixture of bromides containing the same proportion of acid. The differences observed between individual neutral salts were comparatively small, and in most cases no larger than the experimental error, but addition of potassium hydroxide increased the E.M.F. of a silver-silver bromide cell containing KBr by a considerable amount. These effects can be qualitatively explained in terms of the different rates of diffusion of ions under a temperature gradient. Diffusion occurs from the hot to the cold end of the cell (Soret effect) and ions like  $H^+$  and  $OH^-$  would be expected to diffuse more rapidly than others. At equilibrium, the rate of diffusion of all ions must be equal, and a potential which opposes the migration of the faster ions and accelerates that of the slower ones must therefore exist in the solution, i.e. the thermal diffusion potential will reduce the E.M.F. of the thermal cell when hydrogen ions are present, and increase it when hydroxyl ions are present.

Both the Eastman-Wagner thermodynamic treatment, and the rate process theory approach outlined above, yield equivalent expressions for  $J$  in terms of the transport numbers and the entropies of transfer, or the entropies of activation of transfer of the ions present. The entropy terms cannot, at present, be related to known thermodynamic quantities. Eastman assumed the entropies of transfer to be constant over the range  $15^\circ$ – $35^\circ$ , almost independent of concentration, and positive. The rate process expression requires that

$$\begin{aligned} d/dT(\Delta G_i^\ddagger) - R &= S_i^\ddagger, \\ -\Delta S_i^\ddagger - R &= S_i^\ddagger. \end{aligned}$$

or

There is probably some restriction in the activated state for ionic transfer and  $\Delta S_i^\ddagger$  is therefore negative.  $S_i^\ddagger$  is thus greater than  $-2$  cal./deg.  $-\Delta S_i^\ddagger$ , and positive if  $-\Delta S_i^\ddagger > R$ .  $\Delta H^\ddagger$  can be obtained from the variation in ionic mobility with temperature, and hence  $d/dT(\Delta H_i^\ddagger)$ . On differentiating the Gibbs-Helmholtz equation,

$$\frac{d^\ddagger}{dT}(\Delta G_i^\ddagger) = -\frac{1}{T} \times \frac{d}{dT}(\Delta H_i^\ddagger),$$

i.e. for  $d/dT(\Delta G_i^\ddagger)$  and hence  $S_i^\ddagger$ , to be independent of  $T$ ,  $\Delta H_i^\ddagger$  must also be independent of  $T$ . This is not the case, as can be seen from Table II,  $\Delta H_i^\ddagger$  decreasing as  $T$  increases. This table was constructed from values of ionic mobilities at infinite dilution obtained by Owen and Sweeton<sup>15</sup> and Gunning and Gordon.<sup>16</sup> Therefore,  $d/dT(\Delta G_i^\ddagger)$  must increase with temperature, the change being roughly the same for all ions. The effect on the thermal diffusion potential in acid solutions is, however, comparatively small. For  $H^+$  ions,  $d/dT(\Delta G_i^\ddagger)$  increases by  $3.11$  cal./deg. over the range  $288^\circ$ – $328^\circ$  K, the increase for the chloride ion being much the same.

$$\begin{aligned} \text{Increase in } J \text{ over this range} &\simeq (n_{H^+} - n_{Cl^-}) 3.11 \text{ cal./deg.} \\ &\simeq 0.08 \text{ mV/}^\circ\text{C.} \end{aligned}$$

At the upper end of the range therefore, the experimental point in the  $\Delta\phi/dT$  curve should lie about  $1.6$  mV below the straight line drawn through the points lying at the lower end of the temperature range. This ignores any temperature variation of  $d\phi^\circ/dT$ , and would be much less and possibly of a different sign in neutral salts. Thus the maximum theoretical variation in  $J$  is little more than the experimental error in the present experiments and is, in practice, complicated by the unknown variation in  $d\phi^\circ/dT$ . Data

<sup>15</sup> Owen and Sweeton, *J. Amer. Chem. Soc.*, 1941, **63**, 2811.

<sup>16</sup> Gunning and Gordon, *J. Chem. Physics*, 1942, **10**, 126.

for a more refined analysis do not exist, but it may be said that the observed values for the temperature coefficient of the mobilities of ions are consistent with the available results on thermal cells, and may account for the slight flattening of the  $\Delta\phi/\Delta T$  curves near the upper temperature limit for acid solutions.

TABLE II.—HEATS OF ACTIVATION OF TRANSFER AT INFINITE DILUTION (CAL./MOLE) CALCULATED FROM CONDUCTIVITY DATA<sup>15, 16</sup>

Ion Species Temp. °K	H+	Na+	K+	Cl- (HCl)	Cl- (KCl)
278	3090	—	—	4580	—
288	2710	3980	3680	3930	3880
298	2415	3845	3435	3610	3560
308	2165	3640	3205	3385	3325
318	1942	3380	3020	3215	3135
328	1770	—	—	3070	—
338	1630	—	—	2950	—

The entropies of transfer deduced by Eastman from Podzus' data were used by Bernhardt and Crockford<sup>3</sup> to correct their observed  $d\phi/dT$  values for thermal diffusion potentials. A constant  $d\phi^0/dT$  value for the hydrogen electrode was obtained; the corrections were small except with HCl solutions. This constancy is not unexpected since their experimental data were obtained in essentially the same way as those of Podzus.

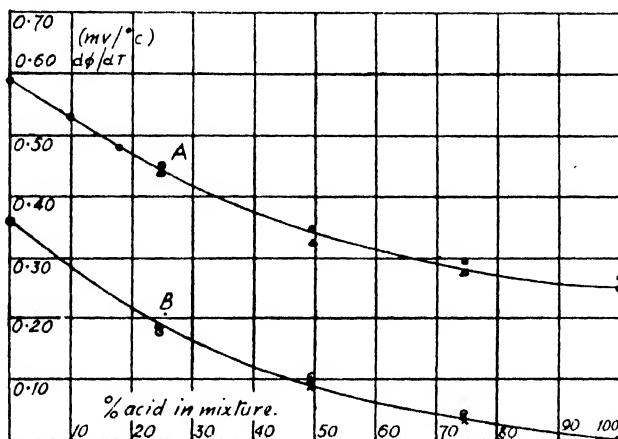


FIG. 3.—A ○ Richards' data on KCl-HCl mixtures (N/2).

× Eastman's equation.

△ ( $n_+ - n_-$ ) 0.504 mV/°C.

B ○ Extrapolated data on KBr-HBr mixtures (this paper).

× Eastman's equation.

△ ( $n_+ - n_-$ ) 0.536 mV/°C.

Eastman's figures may also be applied to the results of Richards on mixtures of HCl and KCl using calomel electrodes,<sup>14</sup> and to the present results on mixtures of HBr and KBr using silver-silver bromide electrodes; a value of  $S_{tr}^*$  being calculated from data on pure HBr and KBr (3.6 cal./deg.). Fig. 3 shows the observed results, those calculated from Eastman's formula, and those calculated assuming the entropies of transfer of all the ions to be identical, i.e. that  $J$  can be represented by an equation

of the form  $K(n_+ - n_-)$ , where  $K$  is an empirical constant calculated from the observed difference between the pure solutions. It can be seen that both formulae fit the results quite well, the form of the curve being due mainly to the very high transport number of the hydrogen ion. The values of  $S_+^*$  used are comparatively unimportant. Accurate data on these mixtures would allow  $S_+^*$  values to be calculated without the assumptions made by Eastman provided the results were extrapolated to zero concentration.

Several authors have used data on non-isothermal cells to calculate the "true" temperature coefficient of the hydrogen electrode. In some cases the existence of thermal diffusion potentials<sup>7, 17</sup> has been ignored, in others they were calculated by Eastman's method.<sup>8</sup> For neutral chlorides, the corrections are not large and Gilbert<sup>4</sup> calculated an uncorrected value for the normal electrode of about  $-1.0$  mV/°C from experiments on KCl with silver-silver chloride electrodes. Bernhardt and Crockford's<sup>3</sup> data extrapolated to obtain  $d\phi^\circ/dT$  after correction for  $J'$ , gave a value of about  $-0.86$  mV/°C. These figures may be compared with a value of  $-0.43$  mV/°C obtained from a direct measurement in N sulphuric acid.<sup>17</sup> Deviations from the value of about  $-0.9$  mV/°C in other published figures are due to neglect of the thermal diffusion potentials. This value of course would be affected somewhat by changes in Eastman's values for entropies of transfer. In addition, all measurements on non-isothermal cells are subject to an unknown error arising from the tendency to reach Soret equilibrium. Not only may concentration changes round the electrodes influence the E.M.F. of the cell, but the thermal diffusion potential will decrease as the equilibrium is reached and the net transference of ions ceases. No detailed study of these changes has yet been made, and it is possible that the existing values for thermal diffusion potentials are too small, having been calculated from data on cells where Soret equilibrium may have been partly attained. This was true for the cells used in the present work since a temperature gradient in the heated limb was unavoidable. The experimental technique used did not permit the detection of any change in  $d\phi/dT$  with time corresponding to changes in the degree to which Soret equilibrium had been attained, and this is being made the subject of a separate study.

True temperature coefficients of electrodes and thermal diffusion potentials become important in certain problems concerned with the effect of temperature on the corrosion of metals when it may be desirable to compare the potentials of corroding electrodes at different temperatures. Comparison of the E.M.F. of cells of the type,

Metal | Solution | Reference electrode

at different temperatures does not give information about the change in potential at the metal-solution interface unless the change in potential of the reference electrode is known, while measurements in non-isothermal cells involve thermal diffusion potentials. These are independent of the total concentration at high dilutions, but will vary considerably with the pH under these conditions. For this reason non-isothermal systems should not be used in any study of corrosion by natural waters unless precautions to avoid changes in thermal diffusion potentials are taken.

### Conclusions

(1) The variation in potential with temperature of a non-isothermal cell may be expressed at concentrations below  $0.1$  M by an equation of the form :

$$\frac{d\phi}{dT} = \frac{d\phi^\circ}{dT} + \frac{2.303R}{z_+F} \log_{10} c_+ - \frac{2.303}{2z_+F} \sqrt{\mu} + J,$$

<sup>17</sup> Bircher and Howells, *J. Amer. Chem. Soc.*, 1926, 48, 34.

where  $J$  is the thermal diffusion potential and  $d\phi^\circ/dT$  is the temperature coefficient of the standard electrode.

(ii)  $J$  is approximately independent of the total concentration, and of the absolute temperature, but is greatly influenced by the presence of hydrogen or hydroxyl ions.

(iii) It arises from the tendency of ions to diffuse at different speeds under a thermal gradient, the sign being such as to equalise these diffusion rates. The great effect of  $H^+$  and  $OH^-$  is due to their high diffusion rates, those of other ions being apparently much smaller and approximately equal.

(iv) Identical expressions for  $J$  may be calculated thermodynamically and by a simple rate process method, of the form (for uni-univalent electrolyte),

$$n_+ S^* - n_- S^*$$

where  $S^*$  is an entropy of transfer which cannot at present be calculated from other data. It is not independent of  $T$  and the rate process theory equation allows its variation to be calculated from the temperature coefficients of ionic mobilities. The effect on  $J$  is too small to be detected in the available data.

(v) Thermal diffusion potentials may be of importance in electrochemical studies of corrosion phenomena.

*Department of Chemistry,  
Sheffield University,  
Sheffield 10.*

---

## REVIEWS OF BOOKS

**Catalytic, Photochemical, Electrolytic Reactions (Technique of Organic Chemistry, Vol. II).** Editor—ARNOLD WEISSBERGER (Interscience Publishers, Inc., New York and London, 1948.) Pp. ix + 219. Price 30s.

It requires judgment and wisdom successfully to produce a series such as the *Technique of Organic Chemistry* of which the present book is the second volume. The field to be covered is broad and, in consequence, difficult to survey; the subject-matter ranges from the construction of high-pressure apparatus used by the chemical engineer to the minute and delicate glassware of the microchemist. The reader may be a plant manager in an industrial organization not primarily concerned with organic chemistry, who requires some details of a pneumatically-operated pressure-control valve; or he may be a young postgraduate in search of the approximate magnitude of the energy output of a 1000-watt filament lamp in a certain range of wave lengths—each can expect to find an answer somewhere in this series.

Most chemists—and those directly concerned—with organic chemistry may well be in the minority—will have some acquaintance with the contents of Vol. I. The present volume deals with catalytic reactions (U. I. Komarewsky and C. H. Ries), photochemical reactions (W. A. Noyes, Jr., and V. Boekelheide) and electrolytic reactions (S. Swann, Jr.), each section covering about 70 pages. As is inevitable, the approach, presentation and standard of each section differ widely; the comments of a reviewer will in the same way depend on his interest and his requirements.

The chapter on catalytic reactions can best be summarized in terms of the references cited. In "the preparation of catalysts," some 50 % of these refer to journals devoted to chemistry and, commendably, <sup>the</sup> details of important preparations are given in full; the remainder of the chapter is devoted to a few pages on laboratory technique normally used in academic research, and about fifty pages to the techniques of the chemical engineer, wherein nearly all references are to engineering journals or journals of industrial chemistry. Thus the material is of interest and primary importance to the technologist and few chemists will find that the chapter caters for their needs. Contrariwise, the second chapter may be regarded by some as a model of what the average organic chemist would like to have as a guide in setting up photochemical experiments, e.g. there are lists of filters from mercury arc lines, detailed instructions on how to use an uranyl oxalate actinometer, etc.—other readers will, however, complain that some material is discussed in a cursory manner and would prefer the elimination of semi-quantitative guides to allow the inclusion of more advanced techniques.

The third chapter has a brief and elementary account of general "theory" together with a description of some simple techniques illustrated by a number of procedures. It includes reactions in which inorganic intermediates are formed and a variety of syntheses by electrolytic reduction, oxidation, cathodic and anodic coupling, and substitution are given. It would be difficult to justify this chapter except for reasons of completeness.

Considering the volume as a whole, the standard is below that of Volume I and many will find it a somewhat disappointing book.

# THE KINETICS OF IONIC POLYMERIZATIONS

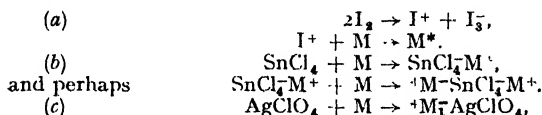
## PART I. THE POLYMERIZATION OF VINYL OCTYL ETHER CATALYZED BY IODINE

BY D. D. ELEY AND A. W. RICHARDS

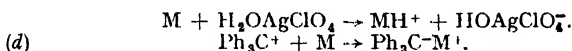
Received 11th November, 1948

The kinetics of polymerization of vinyl 2-ethyl hexyl ether have been measured in the presence of the catalysts, iodine, stannic chloride, silver perchlorate, and cresol solutions of triphenylmethyl chloride. In the last case, the conditions suggest that the polymerization is initiated by the carbonium ion. In the first three cases the accelerating influence of solvents of high dielectric constant supports the view that the polymerizations involve an ionic mechanism.

The scheme of reaction thus involves positive ion or electrophilic initiation. If M indicates monomer, we have



or since water has an accelerating influence,



Termination of the chain is by a spontaneous loss of activity, thus explaining the kinetics in the stannic chloride case. With iodine and silver perchlorate, both the low value for the molecular weight of the polymer and its independence of monomer concentration support the operation of a transfer mechanism for these catalysts. The growing polymer possibly transfers its activity via a catalyst molecule or fragment, since the effect depends on the catalyst employed.

An unsolved problem is the specific effect of water, which accelerates the reaction catalyzed by silver perchlorate, but has no effect on the reaction catalyzed by stannic chloride.

There exist few kinetic measurements on ionic polymerizations, in marked contrast to the wealth of data available for radical polymerizations. Investigations of this kind are urgently needed, to help sort out the speculations on reaction mechanism already available. We have accordingly studied the polymerization of 2-ethyl hexyl vinyl ether (vinyl octyl ether, V.O.E.) in the presence of four separate catalysts, iodine, stannic chloride and two new agents not previously used in polymerizations, silver perchlorate and triphenyl methyl chloride. The vinyl ethers have been the subject of a classical paper by Chalmers,<sup>1</sup> who established their susceptibility to iodine and halide catalysts, and assembled numerous data on their properties. The kinetics of polymerization of *n*-butyl vinyl ether by stannic chloride were subsequently studied by Eley and Pepper.<sup>2</sup> Satisfactory data at higher catalyst concentrations were precluded in their case by the non-isothermal conditions prevailing. Even at lower catalyst concentrations a stationary state was never properly set up. However, the general results and kinetic scheme resulting

<sup>1</sup> Chalmers, *Can. J. Res. B*, 1932, **7**, 464.

<sup>2</sup> Eley and Pepper, *Trans. Faraday Soc.*, 1947, **43**, 112.



from this investigation have been confirmed and extended in our new work. We have found that vinyl octyl ether polymerizes more slowly than the vinyl *n*-butyl ether, and that in all cases a satisfactory stationary state is set up, a necessary prerequisite for the usual analysis of kinetic data. We have replaced our original viscometric technique by the simpler dilatometric method of following the reaction. We have found that all four catalysts fit into the same simple kinetic scheme. By far the larger part of our work has been with the iodine catalyst, so we devote our first paper to this. Originally, the catalytic power of iodine in this reaction set us a quite specific problem, in view of its inhibitory effects on radical polymerizations. This paper will show how it fits into the general scheme of ionic catalysis.

### Experimental

The reaction velocity was followed in a 9 ml. dilatometer, which was filled with catalyst solution and diluent, cooled and pumped and the requisite volume of cooled monomer added under conditions of high vacuum. The dilatometer

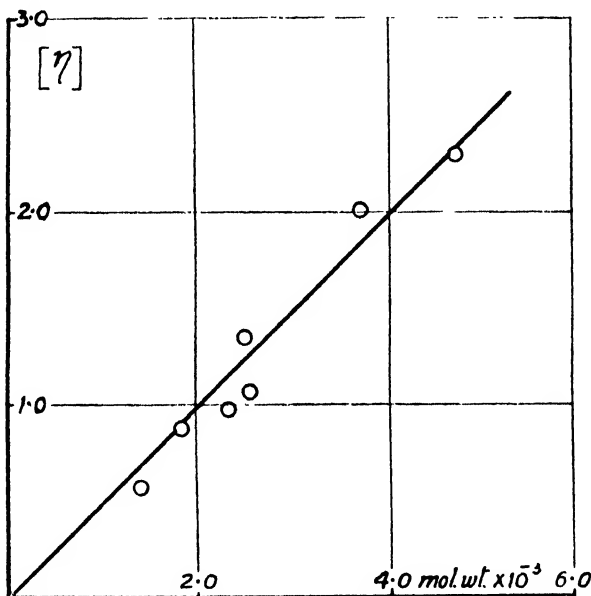


FIG. 1.—Intrinsic viscosity  $[\eta]$  plotted against the cryoscopic molecular weight.

was sealed off and could be stored in liquid air if necessary, until required. It was placed in the thermostat at 25° C at zero time, and volume measurements taken with a cathetometer reading to 0.01 mm. The volume per cm. of dilatometer capillary was about 0.06 ml. in all cases, and was accurately calibrated.

If the dilatometer contains  $\Delta n$  g. of monomer, then since the density ( $D_4^{25}$ ) of polymer and monomer is 0.890 and 0.812 g. cm.<sup>-3</sup> respectively, the molecular weight of the monomer is 156 and the volume of the dilatometer 9 ml., the polymerization velocity  $R$  in mole litre<sup>-1</sup> min.<sup>-1</sup> is

$$R = \frac{6.61}{dt} \frac{d\Delta v}{dt}$$

where  $\Delta v$  is the contraction of the solution in ml. at time  $t$ . A high-vacuum technique was necessary because the vinyl ether formed a peroxide on standing in air, which markedly inhibited the reaction (see later).

In general, the dilatometer was opened at 20% polymerization and the polymer separated for molecular weight determination. This was done by

shaking the reaction mixture with N/100 sodium thiosulphate solution, which effectively destroyed the catalyst. The polymer solution was separated and pumped for 5 hr. at 60° C and 15 mm. Hg pressure. This sufficed to remove all monomer and solvent and yielded the polymer, a sticky viscous material varying from light yellow to dark brown in colour. It was established that no degradation occurred in this process. Thus, no change was found in the specific viscosity of polymer pumped for 12 hr. under the above conditions, or even subsequently on heating for 2 days in air at 90° C.

The molecular weights of the polymer were determined by the Staudinger method. In each case the viscosity of a petrol ether solution was measured at four or five different concentrations, and the intrinsic viscosity  $[\eta]$  determined by extrapolation of the plot of  $\eta_{sp.}/c$  against  $\eta_{sp.}$ , which was linear in all cases. Fig. 1 shows  $[\eta]$  plotted against the cryoscopic value of the molecular weight  $M$  for a series of samples.<sup>3</sup> If we express  $c$  in base mole per litre, then

$$[\eta] = 5.0 \times 10^{-4} M.$$

**Materials.**—The monomer, 2-ethyl hexyl vinyl ether (b.p. 75-76° at 32 mm.) was kindly supplied by The Distillers Company, Ltd., Research Department. It was freshly distilled in high vacuum before use. The solvent petrol ether was shaken with concentrated sulphuric acid, washed, dried and fractionated; the 60-68° fraction was collected. The ether and ethylene dichloride were also dried and distilled before use: A.R. iodine was sublimed and used as a 0.5 % solution in the solvent concerned.

## Results

**The Time Course of the Reaction.**—In this paper values of  $[C]$  are invariably given as millimole per litre (mmole/l.) and  $[M]$  as moles per litre (mole/l.). Fig. 2 gives a set of curves at various values of  $[C]$ , the catalyst concentration,

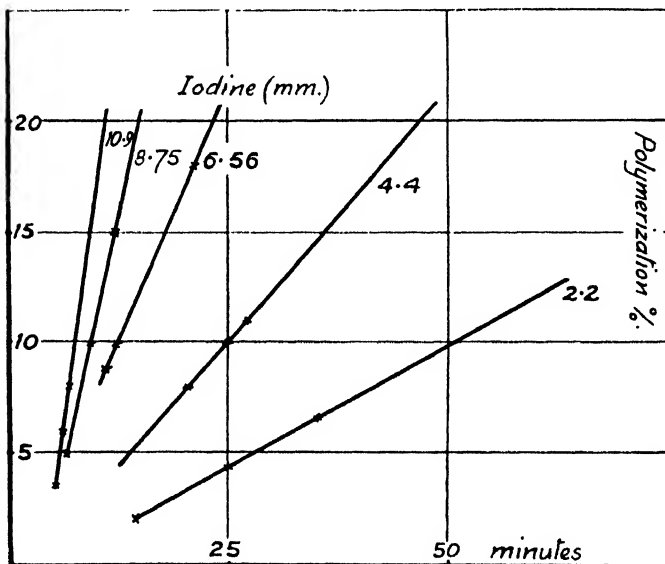


FIG. 2.—The time course of polymerization.

for a monomer concentration  $[M]$  of 0.6 mole/l. There is a small period of induction due to the warming-up of the dilatometer, after which a true stationary velocity of polymerization is set up. The velocities of polymerization are calculated from the initial slopes of these curves; in fact, these approximate closely to straight lines over as much as 5 % of polymerization. All values of the velocity of reaction— $d[M]/dt$  are given in mole l.<sup>-1</sup> min.<sup>-1</sup>.

<sup>3</sup> Huggins, *Ind. Eng. Chem.*, 1943, 35, 980.

**The Kinetics of the Reaction.**—The results in Fig. 3 and 4 show that in all three solvents at 25° C the velocity of polymerization follows the law,

$$-dM/dt = k[M][C]^2,$$

where  $[M]$  is the concentration of monomer and  $[C]$  the concentration of catalyst.

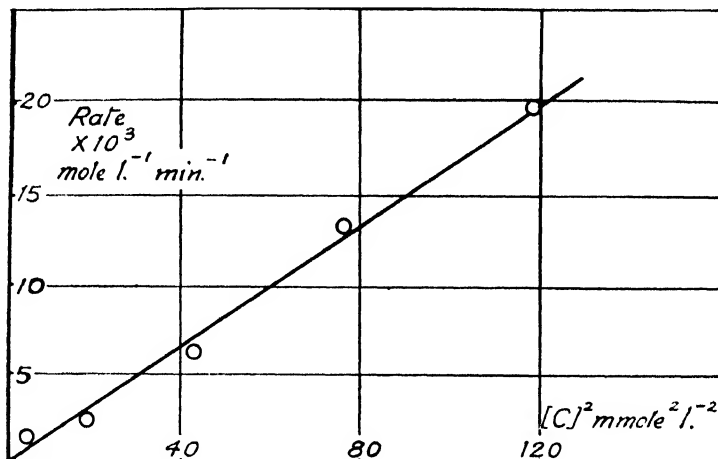


FIG. 3 (a), (b), (c).—Effect of catalyst concentration  $[C]$  on reaction velocity (a) petrol ether, (b) diethyl ether, (c) ethylene dichloride.

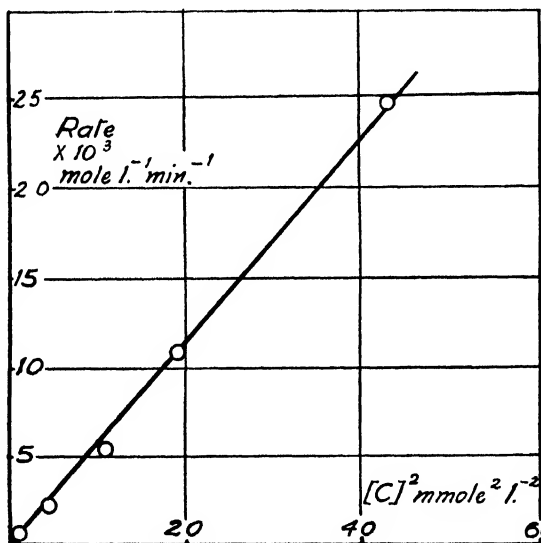


FIG. 3 (b).

In varying the catalyst concentration, the monomer concentration was held constant at 0.6 mole/l. In varying the monomer concentration the catalyst concentration was held constant at 2.2 mmole/l. for petrol ether solvent, 4.4 for diethyl ether and 0.55 for ethylene dichloride. Each series of experiments has given a value for the velocity constant  $k$ .

It is satisfactory that the characteristic kinetics were also observed in diethyl ether as solvent, since in this case the dielectric constant of the mixture does not

change with increasing monomer concentration. The discrepancy between the values of  $k$  as determined from variations of  $[M]$  and variation of  $[C]$  almost certainly resides in this point. There is no discrepancy in the case of diethyl ether as solvent.

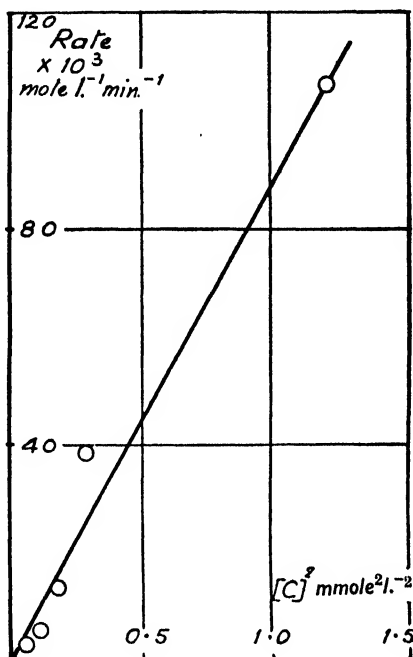


FIG. 3 (c).

**The Molecular Weight of the Polymers.**—Table II shows that variations in monomer or catalyst concentration exert no systematic effect on the molecular weight of the polymer at 20 % polymerization, in all three solvents.

TABLE I.—RATE CONSTANTS

Solvent	$k$ (l. <sup>2</sup> mole <sup>-2</sup> min. <sup>-1</sup> )
Petrol ether . . .	$\begin{cases} 0.8 \times 10^9 \\ 0.3 \times 10^9 * \end{cases}$
Diethyl ether . . .	$\begin{cases} 1.0 \times 10^9 \\ 1.0 \times 10^9 \end{cases}$
Ethylene dichloride . .	$\begin{cases} 213 \times 10^9 \\ 147 \times 10^9 * \end{cases}$

\* Value for  $[M]$  constant.

Further, the molecular weight stayed steady throughout the reaction up to 100 % polymerization, which strongly supports our subsequent assumption of a stationary concentration of active species. It was observed, however, that a large rise in molecular weight could occur *after* 100 % polymerization, if the reaction mixture were left with the catalyst undestroyed. Thus we took a particular case of a polymer of mol. wt. 1400 ( $[M] = 0.6$  mole/l.,  $[C] = 4.4$  mmole/l.) with results shown in Table III.

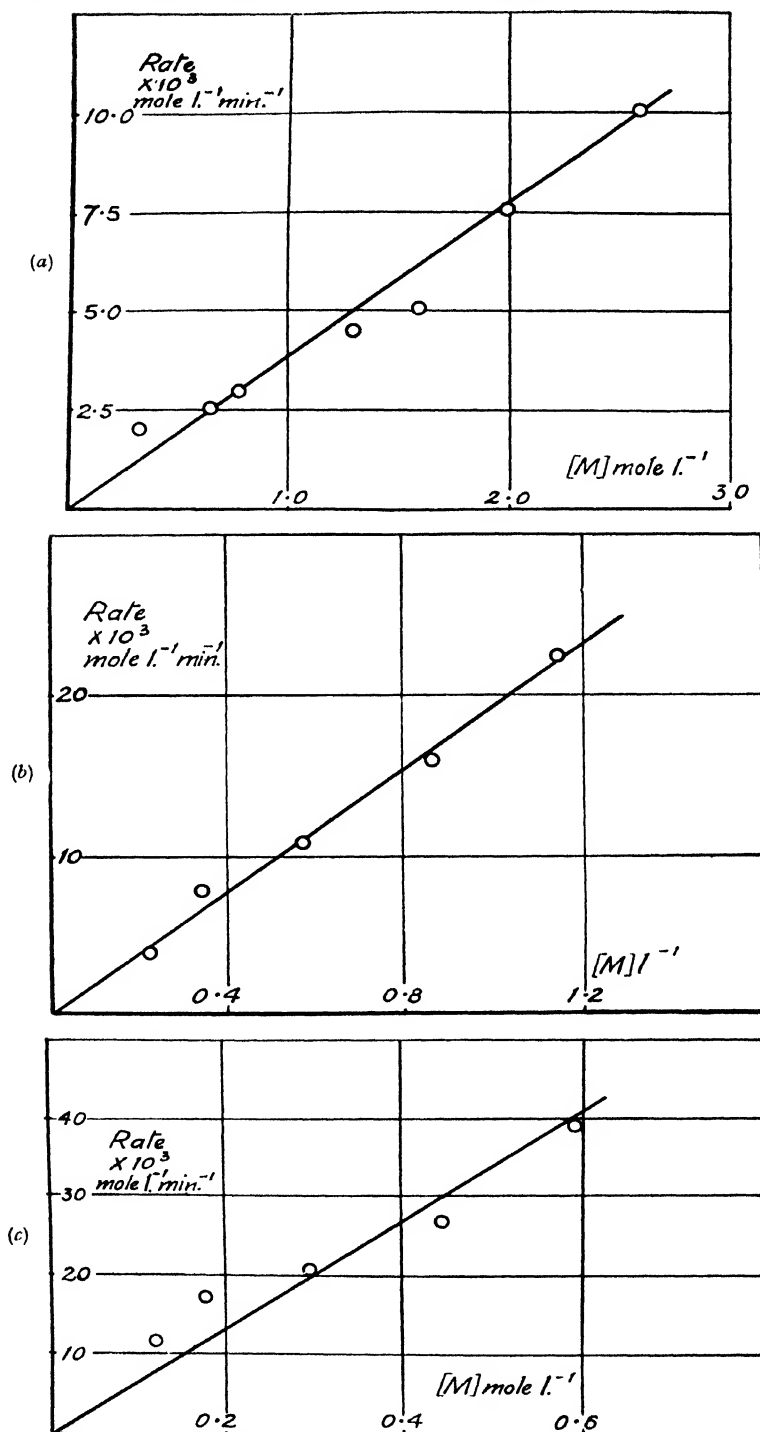


FIG. 4 (a), (b), (c).—Effect of monomer concentration  $[M]$  on reaction velocity (a) petrol ether, (b) diethyl ether, (c) ethylene dichloride.

From the point of view of this investigation it was most important to destroy the catalyst efficiently and isolate the polymer immediately.

TABLE II.—MOLECULAR WEIGHT OF POLYMER  
(20 % polymerization, 25° C)

Petrol Ether		Diethyl Ether		Ethylene Dichloride	
[M] = 0.6 mole/l.		[M] = 0.58 mole/l.		[M] = 0.6 mole/l.	
[C] mmole/l.	Mol. wt.	[C] mmole/l.	Mol. wt.	[C] mmole/l.	Mol. wt.
2.18	1000	1.1	800	1.1	1050
4.37	1600	2.18	800	0.55	780
6.56	980	3.3	1000	0.44	780
8.75	1100	4.37	1000	0.35	1050
10.9	980	6.56	800	0.33	780
[C] = 2.2 mmole/l.		[C] = 4.4 mmole/l.		[C] = 0.55 mmole/l.	
M mole/l.	Mol. wt.	M mole/l.	Mol. wt.	M mole/l.	Mol. wt.
0.78	1400	0.23	800	0.6	750
1.3	1000	0.35	800	0.45	780
1.6	1600	0.58	950	0.3	750
2.6	950	0.87	800	0.18	750
		1.15	800		

TABLE III.—INCREASE IN MOLECULAR WEIGHT AFTER 100 %  
POLYMERIZATION

Time (hr.) .	1.0	1.33	1.66	2	17	25	40	90	240
Mol. wt. $\times 10^{-3}$ .	1.4	1.4	2.0	2.0	2.4	2.6	2.8	3.4	6.4

**Effect of Dielectric Constant of Solvent.**—Pepper's results with stannic chloride- $\alpha$ -methyl styrene make it important to investigate this effect.<sup>4</sup> We find a most marked increase of velocity with dielectric constant, in agreement with Pepper. The velocity constant increases approximately exponentially with  $\epsilon$ , as shown in Fig. 5. On the other hand, the molecular weight at 20 % polymerization is quite unaffected. We have extended these results to acetone ( $\epsilon = 25D$ ), where the velocity was immeasurably fast and the molecular weight still only 1100.

**Effect of Temperature.**—The effect of temperature on the reaction velocity has been determined for standard conditions;  $[C] = 4.4$  mmole/l.,  $[M] = 0.6$  mole/l. for petrol ether, and  $[C] = 0.1$  mmole/l.,  $[M] = 0.6$  mole/l. for ethylene dichloride. The results are shown in Fig. 6, from which "overall" activation energies of 10,000 cal. (petrol ether) and 16,000 cal. (ethylene dichloride) are calculated. The increased polymerization velocity in the solvent of higher dielectric constant is thus not due, as one might at first sight expect, to a lower overall energy of activation.

Increased temperature has only a small effect on the molecular weight of the product, leading to a decrease, as shown in Table IV. The experiments are under comparable conditions, and special care was taken with the molecular weight determinations.

<sup>4</sup> Pepper, *Nature*, 1946, 158, 789.

In each case we have an "activation energy" of about  $-3300$  cal./mol.

**Iodine Analysis.**—There is no reason at present to do otherwise than assume the polymer is an ordinary linear vinyl polymer. It is of interest to analyze for catalyst fragments (iodine) and double bonds.

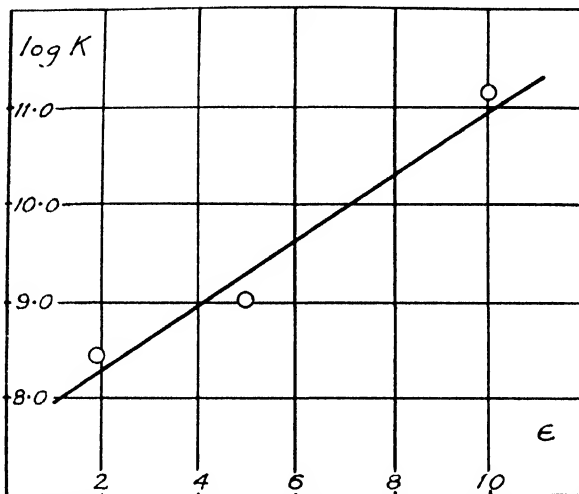


FIG. 5.—Dependence of  $\log_{10} k$  on dielectric constant of solvent  $\epsilon$ .

In the first place, polymerization mixtures at 100 % polymerization were treated with an excess of aqueous N/100 sodium thiosulphate and then back titrated with aqueous N/100 iodine solution until the blue starch-iodine complex was formed. Thus, for example, a reaction mixture which had been polymerized with 2 ml. 0.5 % iodine solution was examined. This amount of iodine equals 8.0 ml. N/100 thiosulphate. However, at completion of reaction

TABLE IV.—EFFECT OF TEMPERATURE ON MOLECULAR WEIGHT

Petrol Ether		Ethylene Dichloride	
[M] = 0.6 mole/l.; [C] = 4.4 mmole/l.		[M] = 0.6 mole/l.; [C] = 0.1 mmole/l.	
t° C	Mol. wt.	t° C	Mol. wt.
25	1800	25	1050
35	1500	40	780
40	1200	46	780
44	1000	52	700
48	1000	56	640

the titration value was only 3.8 ml., showing that over half the added iodine was chemically bound in either the polymer or the solvent, and was not available for titration. This result (up to 80 % of iodine being bound) was found in a series of 10 experiments.

If the polymer were isolated by the ordinary method, analysis showed it to contain no iodine, and we were thus set the problem as to the destination of the iodine. In following up this problem we have found that the iodine-polymer bond is so weak that the iodine is removed by the usual isolation treatment. If, however, we take the solution of polymer, from which free iodine has been removed by titration with thiosulphate, and isolate the polymer by prolonged

pumping at room temperature, we secure a polymer containing iodine, and a satisfactory iodine balance.

EXPT. 142. 5.25 mg. polymer  $\equiv$  0.17 mg. AgI  $\equiv$  0.090 mg.  $I_2$ .

Total polymer = 0.5 g.  $\equiv$  0.0086 g.  $I_2$ .

Quantity in solution  $\equiv$  0.00127 g.  $I_2$ .

0.00987 g.

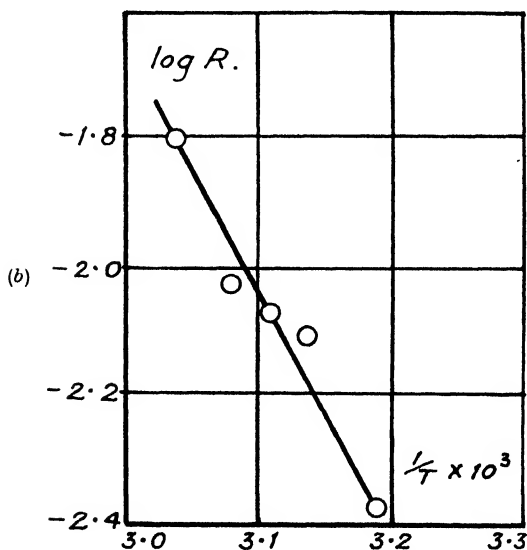
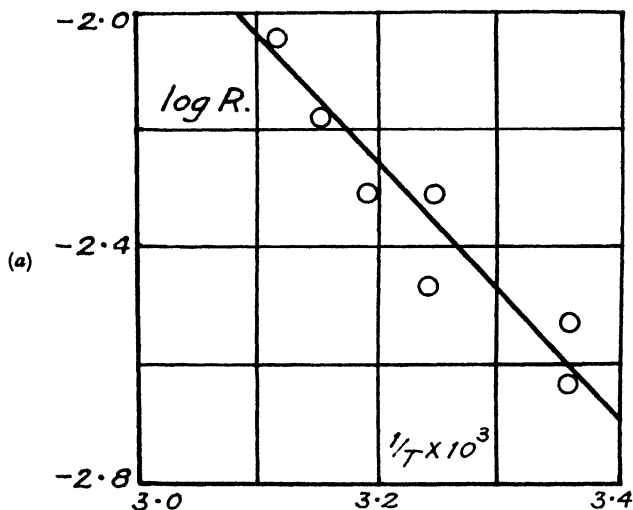


FIG. 6 (a), (b).—The activation energy of polymerization (a) petrol ether (b) ethylene dichloride.

The figure of 0.00987 agrees with the amount originally added of 0.01 g.

EXPT. 144. Total polymer  $\equiv$  0.007 g.  $I_2$ .

Quantity in solution  $\equiv$  0.0038 g.  $I_2$ .

0.0108 g.

The figure of 0.0108 agrees with the amount originally added of 0.01 g.



The molecular weight of the polymer in Expt. 144 was determined cryoscopically as 1250. It is thus easily calculated that 1 g. mole polymer contains 1.37 g. atoms iodine.

It was found possible to remove the iodine from the polymer quantitatively by standing the polymer solution over aqueous potassium iodide plus starch solution. There seemed to be an equilibrium, since as the iodine was removed from solution by titration with sodium thiosulphate, more iodine passed into the free state, turning the starch blue. Thus, in Table V we show the amount of thiosulphate added to remove the blue colour as it reformed.

TABLE V.—REMOVAL OF IODINE FROM POLYMER

Time (days)	0	1	2	3	6	10	16	20	24
Ml. N/10 thiosulphate	2.0	1.0	1.0	1.0	1.0	1.0	0.5	0.2	0.1

Since the quantity of iodine originally added equals 8.0 ml. thiosulphate, we see that we have recovered nearly all of it by this treatment.

**Double-Bond Analysis.**—A known solution of bromine in carbon tetrachloride was added to the polymer dissolved in the same solvent, and left standing for several hours. Excess potassium iodide plus starch was then added and the mixture titrated with sodium thiosulphate. This technique was found to give the right result of one double bond per molecule for the vinyl ether monomer. Several experiments on the polymer gave  $\frac{1}{2}$  g. molecule of bromine, that is, half a double bond, per molecule.

We interpret these results to mean that the dead polymer contains one double bond per molecule, but a certain number of these bonds have been iodinated. Thus we may qualitatively link up the deficiency of double bonds with the excess of iodine found in the polymer over one atom per polymer molecule. However, the low value found may not be significant, as the estimation of unsaturation in this type of system is a difficult matter.

**Effect of Added Inhibitors.**—Early observations on effects of oxygen suggested an investigation of added peroxides. Benzyl peroxide and vinyl ether peroxide were found to lead to a marked induction period, and a lowering of molecular weight of the product as isolated at 100 % polymerization. Butyl alcohol in amounts up to 0.2 mmole/l. had a similar effect but above this concentration the induction period decreased to zero and a very rapid reaction set in. The results are recorded in Table VI, but it should be noted that the molecular weights were obtained on products isolated some roughly constant time after 100 % polymerization, and are therefore not comparable with those given in the rest of this paper.

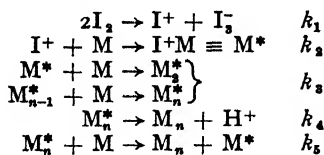
TABLE VI.—EFFECT OF ADDED BUTYL ALCOHOL

Butyl Alcohol (mmole/l.)	$R \times 10^3$	Mol. wt.	Induction Period (min.)
0	1.9	3000	—
0.1	2.4	3100	15
0.2	2.7	2900	25
0.5	3.4	2760	20
1.0	3.7	1460	5
1.5	4.7	1160	5
4.0	15.25	560	0

The effects here are very comparable with those found by Eley and Pepper in stannic chloride—*n*-butyl vinyl ether.<sup>8</sup> As these authors remarked, the combination of increased rate with decreased mol. wt. suggests that butyl alcohol acts by catalyzing transference of activity from a growing chain to a monomer.

## Discussion

The results fit into a simple kinetic scheme, developed from that originally given by Eley and Pepper.<sup>2</sup>



Stationary concentrations of the intermediates  $\text{I}^+$  and  $\text{M}^*$  may safely be assumed. Thus

$$k_1[\text{I}_2]^2 - k_2[\text{I}^+][\text{M}] = 0 \quad \text{and} \quad \text{I}^+ = \frac{k_1}{k_2} \frac{[\text{I}_2]^2}{[\text{M}]} \quad (1)$$

$$k_3[\text{I}^+][\text{M}] - k_4[\text{M}^*] = 0 \quad \text{M}^* = \frac{k_3}{k_4} [\text{I}^+][\text{M}] \quad (2)$$

Thus 
$$[\text{M}^*] = \frac{k_1}{k_4} [\text{I}_2]^2$$

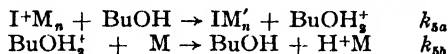
and 
$$-\frac{d[\text{M}]}{dt} = k_3[\text{M}^*][\text{M}]$$

$$= \frac{k_1 k_3}{k_4} [\text{I}_2]^2 [\text{M}] \quad (3)$$

This dependence of velocity on  $[\text{M}]$  and  $[\text{I}_2]$  is that found experimentally. The average molecular weight is given by

$$\text{Mol. wt.} = \frac{k_2[\text{M}^*][\text{M}]}{k_4[\text{M}^*] + k_5[\text{M}^*][\text{M}]} = \frac{k_2[\text{M}]}{k_4 + k_5[\text{M}]}$$

The experimental results require that the molecular weight is independent of monomer concentration, and therefore we may suppose that the transfer process is the most important and  $k_5[\text{M}] \gg k_4$ . There seems little doubt that transfer processes may play an important part in determining the mol. wt. in these ionic polymerizations. This is brought out by comparing these results with those with the stannic chloride catalyst in the next paper, and also by inhibitors like butyl alcohol which lower the molecular weight while increasing the velocity of reaction. Any normal termination reaction would result in a parallel *decrease* in reaction velocity. The chemistry of these transfer reactions, that is, whether electrons, hydrogen ions, or even  $\text{I}^+$  ions are transferred, remains obscure at present. Butyl alcohol may well act by accepting an  $\text{H}^+$ .



If we ignore the starting of chains by transfer, each polymer molecule should contain one iodine atom and one double bond. If we allow for a certain subsequent degree of iodination of the double bond, our results indicate that this is so. The presence of a terminal double bond explains the viscosity increase in polymer mixtures, containing catalyst, *after* 100 % polymerization, shown in Table III. The existence of transfer mechanisms means that some polymer molecules will contain no iodine except that arising from subsequent iodination of the double bond. The discrepancy of a half atom of bromine ( $2 - 1 - \frac{1}{2} = \frac{1}{2}$ ) might arise in this way.

*A priori* we should expect a solvent of increased dielectric constant to act mainly by raising  $k_1$ , where two electric charges are developed.

In all the other cases electric charge is conserved, and the solvent should have no effect. Thus we should expect an increase in rate but little effect on molecular weight, as observed.

The apparent activation energy is

$$RT^2 \frac{\partial \ln k}{\partial T} = RT^2 \frac{\partial \ln \frac{k_1 k_3}{k_4}}{\partial T} = E_1 + E_3 - E_4.$$

The apparent activation energy for the effect of temperature on molecular weight is clearly

$$E_{\text{Mol. wt.}} = E_3 - E_4.$$

These two equations cannot determine the four unknowns, so not much progress can be made. It is, however, interesting that the "more rapid" solvent, ethylene dichloride, has the higher activation energy. The dielectric constant of the solvent, then, in this case must act mainly on the entropy of activation.

In conclusion we would mention briefly some physical evidence in favour of the bimolecular ionization of iodine that we have assumed to explain our kinetic results. Electrolytic transport measurements<sup>5</sup> on ICl in nitrobenzene have established the formation of  $I^+$  and  $ICl_2^-$  and the existence of  $I_3^-$  is well known in aqueous solution. Crowne, working in this laboratory,<sup>6</sup> has made transport measurements on solutions of  $I_2$  in ethylene dichloride, using a potential drop of 6,000 V to secure an adequate current. He finds some evidence for the postulated process of ionization. However, a preliminary examination of the conductance of iodine solutions has given results in apparent disagreement with this transport work, so the question remains open pending further investigation.

<sup>5</sup> Sandonnini and Borgello, *Atti. accad. Lincei, classe sci. fis. mat. nat.*, 1937, 25, 46.

<sup>6</sup> Crowne (unpublished results).

## PART II. THE POLYMERIZATION OF VINYL OCTYL ETHER CATALYZED BY STANNIC CHLORIDE AND OTHER CATALYSTS

In this paper we have established the kinetics of polymerization of 2-ethylhexyl vinyl ether under the influence of stannic chloride and two other catalysts. These other catalysts, silver perchlorate and the triphenylmethyl carbonium ion, may be expected to be catalysts for our reaction, since they fall into that general class of acids described by Lewis.<sup>1</sup> With silver perchlorate it was qualitatively established by a measurement of temperature rise that the polymerization was fastest in the solvent acetone ( $\epsilon = 25D$ ), slower in ether ( $\epsilon = 4.3D$ ), and slowest in petrol ether ( $\epsilon = 1.9D$ ); with stannic chloride the reaction was faster in ethylene dichloride ( $\epsilon = 10D$ ) than in petrol ether ( $\epsilon = 1.9D$ ). That is, the reaction is accelerated in solvents of high dielectric constant  $\epsilon$  and the polymerization is probably ionic in type.<sup>2</sup> Triphenyl methyl chloride was found to be most active in certain solvents known to be specific ionizing solvents for this substance, namely chloroform- $SO_2$  and *m*-cresol.<sup>3</sup> The intense yellow colour of these solutions indicated the presence of the carbonium ion.<sup>4</sup> Once these results had been established, we proceeded directly towards a detailed examination of the reaction kinetics.

<sup>1</sup> Lewis, *J. Franklin Inst.*, 1938, 226, 293.

<sup>2</sup> Pepper, *Nature*, 1946, 158, 789.

<sup>3</sup> Walden, *Ber.* 1902, 35, 2018; Hantsch, *ibid.*, 1921, 54, 2573.

<sup>4</sup> Hammett, *Physical Organic Chemistry* (McGraw-Hill, 1940), p. 53.

## Experimental

**Materials.**—STANNIC CHLORIDE.—A good many experiments were made with fresh B.D.H. material, since excellent reproducibility was achieved, the results agreeing with those obtained on material carefully distilled as below. In later experiments, particularly on the effects of water, the stannic chloride was distilled six times in high vacuum, using a temperature gradient of  $-20^{\circ}$  to  $-60^{\circ}$  C. This gave a colourless liquid, plus usually a very small amount of a white solid, probably a stannic chloride hydrate, which tended to distil with the halide.

SILVER PERCHLORATE.—This was prepared by Gomberg's method.<sup>5</sup> The white crystals are exceedingly hygroscopic. They were kept over phosphorus pentoxide and heated to constant weight at  $120^{\circ}$  C before making up solutions.

TRIPHENYL METHYL CHLORIDE from B.D.H. was used without further purification.

SOLVENTS AND MONOMER were carefully dried and distilled before use.

**Procedure.**—The rate of polymerization and molecular weights of the polymer (at 20 % polymerization) were measured as in Part I. In view of the observations of Polanyi, Evans *et al.*<sup>6,7</sup> and Norrish and Russell,<sup>8</sup> it was decided

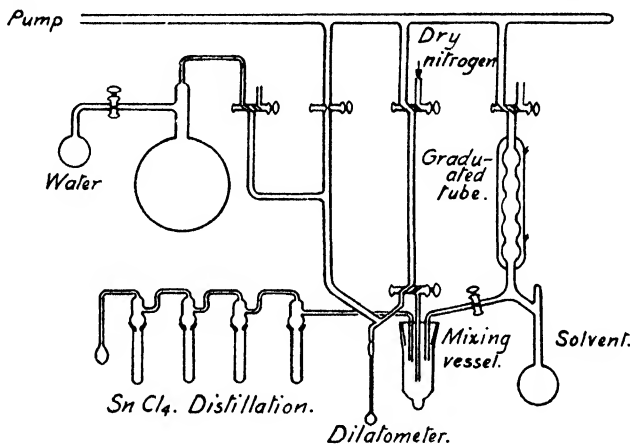


FIG. 1.—Apparatus for filling dilatometer.

to investigate the  $\text{SnCl}_4$  reaction under extreme conditions of dryness, and in the presence of known amounts of water. The apparatus is shown in Fig. 1, silicone grease being used on all taps.  $\text{SnCl}_4$  was distilled six times, finally into the 1 ml. graduated test at the bottom of the mixing vessel. A known amount of solvent could then be distilled into the mixing vessel, and the  $\text{SnCl}_4$  dissolved by the application of a small flame, which served to boil the solvent and mix the two liquids. The stannic chloride solution in the solvent could then be sucked up into the burette through the two-way tap lubricated with silicone grease, and a measured volume of solution discharged into the dilatometer containing monomer and solvent. At this stage a known volume of water vapour could be condensed into the dilatometer from the large bulb shown. The walls of the bulb were made hydrophobic according to the method used by Norrish and Russell,<sup>8</sup> so as to eliminate loss of water by adsorption.

## Results

The systems examined were :

- (a) vinyl octyl ether- $\text{SnCl}_4$ -petrol ether ;
- (b) vinyl octyl ether- $\text{AgClO}_4$ -diethyl ether ;
- (c) vinyl octyl ether- $(\text{C}_6\text{H}_5)_3\text{CCl}$ -*m*-cresol.

It will be convenient to describe the results on the three systems together.

<sup>5</sup> Gomberg, *J. Amer. Chem. Soc.*, 1923, **45**, 398.

<sup>6</sup> Plesch, Polanyi and Skinner, *J. Chem. Soc.*, 1947, 257.

<sup>7</sup> Evans and Polanyi, *ibid.*, 1947, 252.

<sup>8</sup> Norrish and Russell, *Nature*, 1947, **160**, 57.

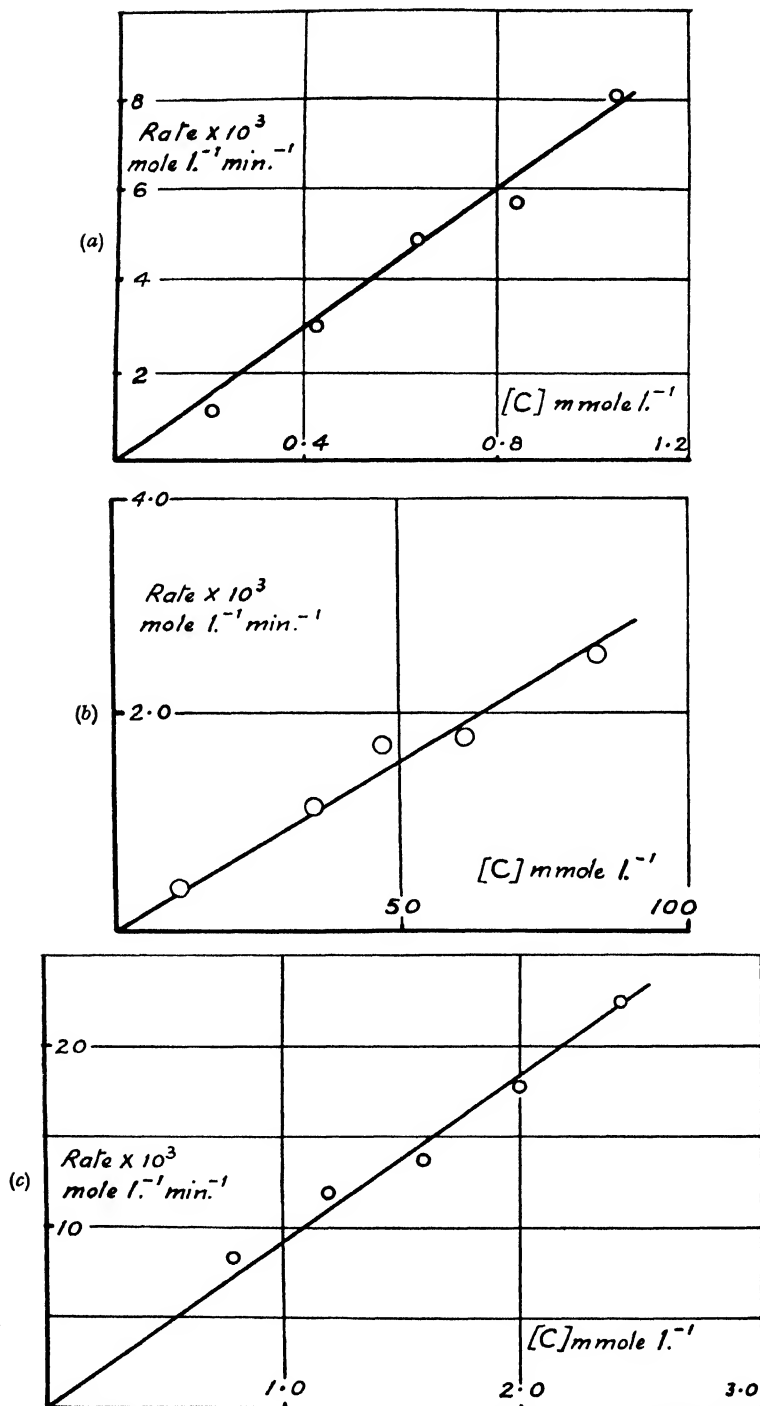


FIG. 2 (a), (b), (c).—Effect of catalyst concentration  $[C]$  on reaction velocity (a) with  $\text{SnCl}_4$  catalyst, (b)  $\text{AgClO}_4$ , (c)  $(\text{C}_6\text{H}_5)_3\text{CCl}$ .

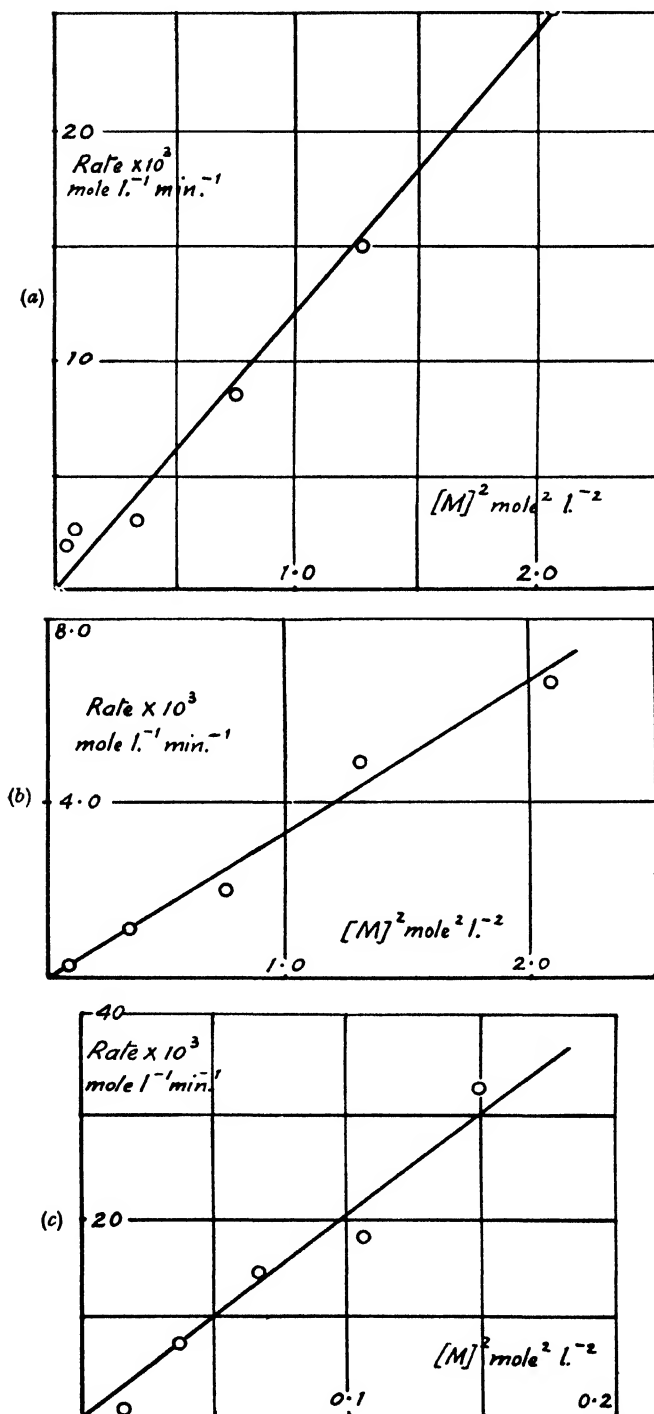
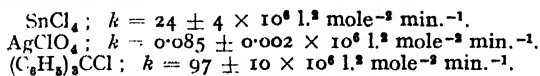


FIG. 3. (a), (b), (c).—Effect of monomer concentration  $[M]$  on reaction velocity (a) with  $\text{SnCl}_4$  catalyst, (b)  $\text{AgClO}_4$ , (c)  $(\text{C}_6\text{H}_5)_3\text{CCl}$ .

**The Reaction Kinetics.**—Fig. 2(a-c) show the effect of varying  $[C]$  at constant  $[M]$  and Fig. 3(a-c) the effect of varying  $[M]$  at constant  $[C]$ . It is clear that in all cases the results fit the formula for the rate of reaction  $R$ ,

$$R = k[C][M]^2.$$

The values of  $k$  are, at 25° C :



**The Molecular Weight of the Polymers.**—It is best to discuss the results for  $\text{SnCl}_4$  and  $\text{AgClO}_4$  separately.

**STANNIC CHLORIDE.**—As found by Eley and Pepper<sup>9</sup> for  $\text{SnCl}_4$ -*n*-butyl vinyl ether, there was some increase in molecular weight during the course of the reaction with this catalyst. The results below refer to polymers isolated at 20 % polymerization.

TABLE I.—EFFECT OF  $[\text{SnCl}_4]$  AND  $[M]$  ON MOLECULAR WEIGHT (25° C)

Variation of $[C]$		Variation of $[M]$	
$[M] = 0.44 \text{ mole/l.}$		$[C] = 0.42 \text{ mmole/l.}$	
$[C] \text{ mmole/l.}$	Mol. wt. $\times 10^{-3}$	$[M] \text{ mole/l.}$	Mol. wt. $\times 10^{-3}$
1.28	7.3	0.15	4.0
0.85	7.5	0.30	5.6
0.64	7.0	0.60	11.0
0.425	6.4	0.87	20.0
0.31	7.0	1.45	20.0
0.10	1.0		
0.05	0.75		

Except at the lowest values of  $[C]$  the molecular weight is independent of  $[C]$ . On the other hand, the molecular weight varies directly with  $[M]$  up to the highest concentrations, where it becomes constant (Fig. 4). Summarizing, over a fairly large range of conditions,

$$\text{Mol. wt.} = \text{const. } [M].$$

#### SILVER PERCHLORATE.

TABLE II.—EFFECT OF  $[\text{AgClO}_4]$  AND  $[M]$  ON MOLECULAR WEIGHT (25° C ; 20 % POLYMER)

Variation of $[C]$		Variation of $[M]$	
$[M] = 0.6 \text{ mole/l.}$		$[C] = 36.3 \text{ mmole/l.}$	
$[C] \text{ mmole/l.}$	Mol. wt.	$[M] \text{ mole/l.}$	Mol. wt.
12	1200	0.3	1200
36.3	1400	0.6	1400
48.5	1500	0.88	1700
60.5	1400	1.15	1800
85	1500	1.45	2500

The molecular weight of the polymer is definitely unaffected by  $[C]$  but shows a tendency to increase with  $[M]$ .

<sup>9</sup> Eley and Pepper, *Trans. Faraday Soc.*, 1947, **43**, 112.

**Effect of Temperature.**—Results are only available for stannic chloride. Fig. 5 shows a plot leading to a value for the activation energy of 10,000 cal. mole<sup>-1</sup>. Increased temperature has a marked effect in lowering the molecular weight of the polymer.

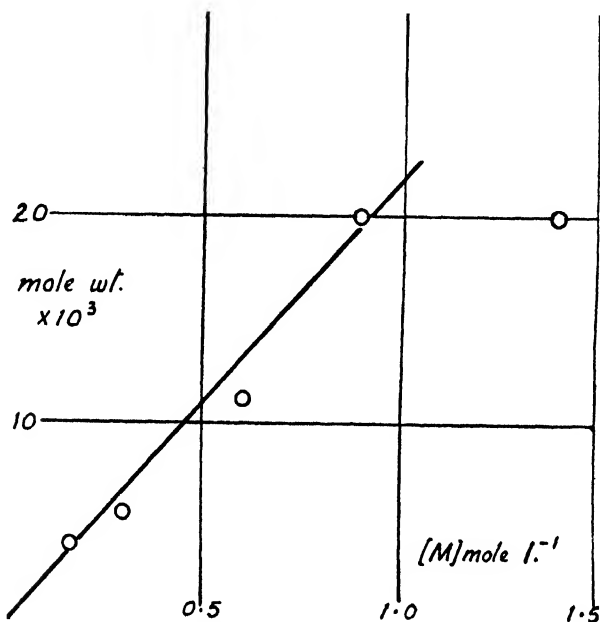


FIG. 4.—Effect of monomer concentration  $[M]$  on molecular weight of polymer at 25° C for  $\text{SnCl}_4$  catalyst.

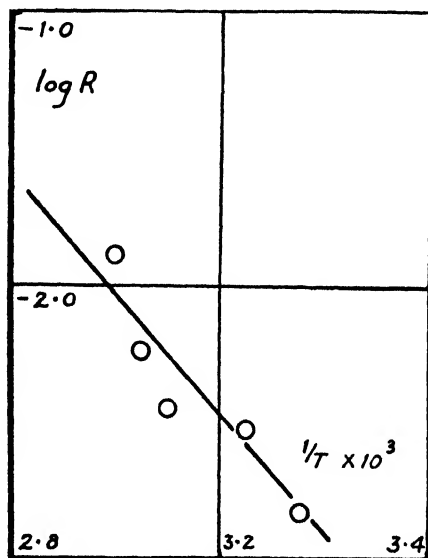


FIG. 5.—The activation energy of the polymerization catalyzed by  $\text{SnCl}_4$ .



Here  $\log [M]$  is only approximately linear against  $1/T$  over the range 25–50° C, and the corresponding heat term is about  $-3,300$  cal. Above 50° C this negative heat term increases most sharply, the molecular weight falling four-fold over ten degrees.

TABLE III.—EFFECT OF TEMPERATURE ON MOLECULAR WEIGHT  
(20 % POLYMER)

[M] = 0.6 mole/l. [C] = 0.2 mmole/l.	
$T^{\circ}\text{C}$	Mol. wt. $\times 10^{-3}$
25	6.0
35	5.5
50	4.0
55	3.0
60	1.0

**Analysis for Double Bonds.**—A solution of bromine in carbon tetrachloride was added to the polymer in the same solvent. The same technique was employed as with the iodine polymer. 0.27 g. of polymer (mol. wt. 6,000), were found to take up 0.0155 g. bromine, yielding a result of two double bonds per polymer molecule (prepared with stannic chloride).

TABLE IV.—ADDITION OF MOISTURE

[M] = 0.6 mole/l. [C] = 3.2 mmole/l. 25° C	
% Water Present	Rate $\times 10^{-3}$ mole l. <sup>-1</sup> min. <sup>-1</sup>
0	34.1
0.045	34.4
0.09	33.6
0.135	34.6

**The Effects of Water.**—(a) **Stannic Chloride.** Small amounts of water were added to the anhydrous system, of magnitude similar to that which had a marked effect on the  $\text{SnCl}_4$ -isobutene system.<sup>8</sup> Table IV shows that the initial rate of polymerization was completely uninfluenced by this addition.

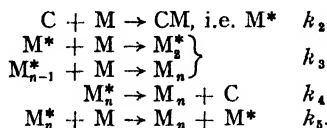
(b) **Silver Perchlorate.**—Water was added to silver perchlorate by allowing the anhydrous salt to stand over water for a certain time. One sample was then dissolved in ether for use as a polymerization catalyst, while another sample was investigated for its water content. The subject was not studied quantitatively, but the accelerating influence of moisture is clearly shown in Table V.

TABLE V.—ADDITION OF MOISTURE

[C] mmole/l.	[M] mole/l.	$[\text{H}_2\text{O}]$ mmole/l.	Rate $\times 10^3$ mole. l. <sup>-1</sup> min. <sup>-1</sup>
36.3	0.6	0	1.11
0.066	0.3	0.26	94
0.088	0.3	0.35	158

### Discussion

These results fall into the kinetic scheme already applied to the case of the iodine catalyst:

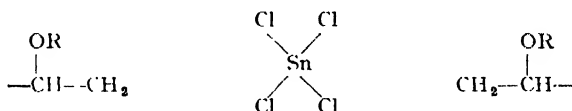


For stationary conditions, which are probably not widely departed from,

$$\begin{aligned}
 -\frac{d[M]}{dt} &= \frac{k_2 k_3}{k_4} [C][M]^2 \\
 \text{M.W.} \propto \text{D.P.} &= \frac{k_3[M]}{k_4 + k_5[M]}
 \end{aligned}$$

where M.W. signifies molecular weight, and D.P. degree of polymerization of product.

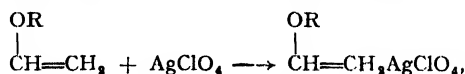
These reaction velocity kinetics are found in all cases. For silver perchlorate, since M.W. is independent of monomer concentration, we may assume that a transfer mechanism ( $k_5$ ) is operative, and indeed the very low molecular weights found would support this view. Markedly higher molecular weights, up to 20,000, were found for stannic chloride as catalyst. In part it is possible that this is due to the fact that the co-ordination number of tin is six and stannic chloride may therefore be assumed to start *two* chains. (We shall seek further evidence on this point.)



Even so, each half molecule is larger than the polymer molecules obtainable with iodine or silver perchlorate, so in the stannic chloride system we may suppose that transfer effects are weak. This view is strongly supported by the kinetic results that the molecular weight is proportional to  $[M]$ , therefore  $k_5[M] \ll k_4$ , and spontaneous termination is the main chain-ending mechanism. Incidentally, the assumption that one stannic chloride molecule may start two chains would agree with the analytical result that each polymer molecule contains two double bonds. At the higher concentrations of monomer we might expect  $k_5[M]$  to become larger than  $k_4$ , which would lead to a flattening out of the mol. wt.- $[M]$  curve as shown in Fig. 4.

With triphenyl methyl chloride the solvent is such that we may assume that the substance is largely ionized, and that the triphenyl methyl carbonium ion,  $\text{Ph}_3\text{C}^+$ , is the activating catalyst. This species will then start one polymer chain, like  $\text{I}^+$ , and silver perchlorate.

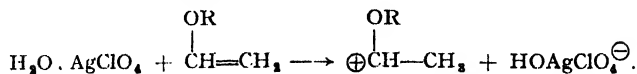
The absence of an effect of water on  $\text{SnCl}_4$ -vinyl ether is to be compared with its demonstrated effect<sup>9</sup> on  $\text{SnCl}_4$ -isobutene at  $-78^\circ\text{C}$ , but the difference may reside in the difference in monomers or temperatures. The isobutene reaction at  $-78^\circ\text{C}$  with  $\text{TiCl}_4$  and  $\text{BF}_3$  has been stated to be heterogeneous.<sup>10, 11</sup> The marked effect of water on silver perchlorate suggests that in this case, besides the initiation step,



<sup>10</sup> Plesch, *Nature*, 1947, 160, 868.

<sup>11</sup> Evans, Meadows and Polanyi, *ibid.*, 869.

We have a hydrogen-ion initiation analogous to that suggested for  $\text{TiCl}_4$ -isobutene by Polanyi *et al.*<sup>8</sup>,



Our results show that effects of water on catalysts are highly specific, and it is scarcely worth while attempting to draw up mechanisms as yet. The further interesting point is that a comparison of the molecular-weight results with stannic chloride and those with iodine and silver perchlorate suggests that in some way transfer mechanisms are effected by the catalyst present. It is therefore unlikely that the transfer merely involves the passage from polymer to monomer of a terminal hydrogen ion. The transfer mechanism may then involve transfer of catalyst or a catalyst fragment.

In the case of stannic chloride, the activation energy from the rate measurements  $E_R$  is given in terms of the contribution for the separate steps by

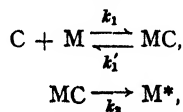
$$E_R = E_s + E_2 - E_4 = 10,000 \text{ cal./mole.}$$

Since we have decided that for this catalyst we may neglect transfer effects to a first approximation at 25° C,

$$E_{\text{M.w.}} = E_s - E_4 = -3,300 \text{ cal./mole.}$$

Thus,  $E_s$  is 13,300 cal./mole.

It may be, of course, that the initiation step is composite, viz.,



in which case the activation energy will be

$$E_R = E_s + q + E_2 - E_4,$$

where  $q$  is the heat of formation of the complex, and  $E_s$  for the initiation step is 13,300 -  $q$ . However, in the absence of further evidence we prefer not to elaborate this hypothesis. The strong increase of  $E_{\text{M.w.}}$  as we raise the temperature we may attribute to the onset of transfer reactions with a high value of  $E_s$ , so that

$$E_{\text{M.w.}} (55-60) = E_s - E_2 \sim -40,000 \text{ cal./mole.}$$

We should then expect that at 60° C with  $\text{SnCl}_4$ , the molecular weight would become independent of monomer concentration, but unfortunately we have no evidence on this point. Taylor and Tobolski<sup>12</sup> and Dainton and Ivin<sup>13</sup> have recently stressed the effects of depolymerization occurring simultaneously with polymerization. Such an effect would also lead to a rapid decrease in molecular weight of the product with increase in temperature but, in the authors' view, is unlikely in the present case, where no indication of a ceiling rate of polymerization was found.

These results may throw some light on the process of low-temperature polymerization, exemplified in the use of  $\text{BF}_3$ ,  $\text{AlCl}_3$  or  $\text{SnCl}_4$ , with vinyl ether,<sup>14</sup>  $\alpha$ -methyl styrene<sup>15</sup> or isobutene at -80° C.<sup>16</sup> By working at these low temperatures one eliminates transfer reactions which lead to

<sup>12</sup> Taylor and Tobolski, *J. Amer. Chem. Soc.*, 1945, **67**, 2063.

<sup>13</sup> Dainton and Ivin, *Nature*, 1948, **162**, 705.

<sup>14</sup> Mueller-Cunradi and Pieroh, *U.S. Pat.* 2,061,934.

<sup>15</sup> Hersberger, Reid and Heiligmann, *Ind. Eng. Chem.*, 1945, **37**, 1073.

<sup>16</sup> Thomas, Sparks, Frohlich, Otto and Mueller-Cunradi, *J. Amer. Chem. Soc.*, 1940, **62**, 276.

low molecular weight products. The choice of a catalyst for low-temperature polymerizations will then involve at least two factors: (1) the activation energy for initiation should be low enough for the catalyst to act at  $-80^{\circ}\text{C}$ ; (2) the catalyst should be unfavourable to the transfer reaction. Since the existence of low-temperature polymerizations of the vinyl ethers means that  $E_3 \sim 2,000$  cal./mole, we may estimate the activation energy of spontaneous termination  $E_4$  as  $\sim 5,000$  cal./mole.\*

The authors' grateful thanks are due to The Distillers Company Ltd., who supported the research financially and with liberal supplies of monomeric vinyl ether.

*Dept. of Chemistry,  
The University,  
Bristol.*

\* *Note added in proof*: This calculation assumes an  $A$  factor for the propagation reaction of  $10^6$ , as found by Burnett and Melville in the photopolymerization of vinyl acetate (*Proc. Roy. Soc. A*, 1947, **189**, 456). A normal  $A$  factor of  $10^4$  would give  $E_3 \sim 7,000$  cal./mole and  $E_4 \sim 10,000$  cal./mole.

---

## THE VIBRATIONAL ASSIGNMENT FOR TETRACHLOROETHYLENE

### AND SOME REMARKS ON THE FORCE CONSTANT OF THE $\text{C}=\text{C}$ BOND IN THAT MOLECULE

By P. TORKINGTON

*Received 18th November, 1948*

It is shown that the force constant for  $\text{C}=\text{C}$  stretching in tetrachloroethylene takes a normal ethylenic value if a constant for interaction between  $\text{C}-\text{C}$  and  $\text{C}-\text{Cl}$  stretching is introduced into the potential function. A complete frequency-assignment for  $\text{C}_2\text{Cl}_4$  is given, which allows of an interpretation of all additional observed frequencies as overtones and combinations.

---

There have been a number of investigations of the infra-red and Raman spectra of tetrachloroethylene, but the vibrational assignment has remained incomplete.<sup>1</sup> Calculations of the potential function of the molecule have been carried out. With the three strong polarized Raman lines assigned to the Class  $A_g$  fundamentals, it was found that the force constant of the  $\text{C}=\text{C}$  bond was abnormally low (between 6 and  $7 \times 10^5$  dynes/cm.) ; a value of about  $8 \times 10^5$  may be obtained by using the frequency  $383$   $\text{cm}^{-1}$  for the  $A_g \hat{\text{C}}\text{Cl}_2$  deformation,<sup>2</sup> but this Raman line has now been shown to be spurious.<sup>3</sup> It is of interest that a normal value for the  $\text{C}=\text{C}$  stretching constant is obtained, using the obvious assignment for the  $A_g$  fundamentals, if a term for interaction between  $\text{C}=\text{C}$  and  $\text{C}-\text{Cl}$

<sup>1</sup> Wu, *Vibrational Spectra and Structure of Polyatomic Molecules* (J. W. Edwards, Michigan, U.S.A., 1946). Herzberg, *Infra-red and Raman Spectra of Polyatomic Molecules* (D. van Nostrand Co., Inc., New York; London: Macmillan & Co., Ltd., 1945).

<sup>2</sup> Duchesne, *Nature*, 1938, **142**, 256.

<sup>3</sup> Wittek, *Z. physik. Chem. B*, 1940, **48**, 1.

stretching is introduced into the potential function. A constant of magnitude  $0.51 \times 10^5$  dynes/cm. (i.e. only  $\sim 1/20$ th  $k_{C=C}$ ), gives

$$k_{C=C} = 9.59 \times 10^5 \text{ dynes/cm. ;}$$

with an additional constant for interaction between  $C=C$  stretching and  $CCl_2$  deformation, (analogous to the necessary constant in ethylene)<sup>4</sup> small variations from this value can be produced.<sup>5</sup> The  $C=C$  bond in tetrachloroethylene can therefore be regarded as normal; relatively large interactions of the type introduced are to be expected on theoretical grounds.<sup>6</sup> It may be observed that only a slight decrease in  $\nu_{C=C}$  is produced by one or two chlorine atoms,<sup>7</sup> and that fluorine, which has greater powers of conjugation than chlorine, raises  $\nu_{C=C}$ .<sup>8</sup> Further, the value of this frequency in ethylene- $D_4$ , where there is no question of abnormality in the  $C=C$  bond, is  $1515 \text{ cm}^{-1}$ ; <sup>9</sup> it seems most unlikely that the more normal value in  $C_2Cl_4$  is associated with a highly abnormal force constant.

In Table I is suggested a complete vibrational assignment\* for tetrachloroethylene—

TABLE I

	$A_g$	$A_u$	$B_{1g}$	$B_{1u}$	$B_{2g}$	$B_{2u}$	$B_{3u}$	
$\nu_{C=C}$	1571	—	—	—	—	—	—	} $\text{cm}^{-1}$
$\nu_{C-Cl}$	447	—	512	—	—	913	782	
$\delta_{CCl_2}$	237	—	—	—	—	—	387	
$\delta_{CCl}$	—	—	347	185	215	332	—	
$\delta_{twist}$	—	135	—	—	—	—	—	

The previous assignment of 332 to  $B_{1u}$  and 512 to  $B_{2u}$  leads to far too high a value for the force constant for non-planar bending; the values given here for these modes are deduced from combination bands which cannot be explained without their introduction.  $215 \text{ cm}^{-1}$  can be taken as identical with the Raman frequency at  $218 \text{ cm}^{-1}$ . The non-planar force constants  $d$  are then as follows. For co-ordinates  $r_{C-Cl}(\Delta\theta_1 \pm \Delta\theta_2)$ , where 1, 2 denote the two ends of the molecule, and  $\Delta\theta$  is the angle for non-planar bending,

$$\left. \begin{aligned} d_{B_{1u}} &= 0.0258 \\ d_{B_{2u}} &= 0.0078 \end{aligned} \right\} \times 10^5 \text{ dynes/cm.,}$$

the subscripts referring to the symmetry-class of the vibration. Taking  $r_{C-Cl} = 1.69 \text{ \AA}$ ,  $r_{C=C} = 1.35 \text{ \AA}$ , and all angles  $120^\circ$ , the constant for the

angle  $C=C-Cl_2$ , derived from both modes, is found to be  $0.096 \times 10^{-11}$  dynes cm. radian<sup>-1</sup>. This shows quite satisfactory agreement with the similar constant in phosgene<sup>10</sup> ( $0.086 \times 10^{-11}$ ). It seems unsatisfactory to assign the very weak Raman line at  $1000 \text{ cm}^{-1}$  to the  $B_{2g}$   $C-Cl$  stretching mode; this would lead to a very high  $C-Cl$  stretching constant, so we take instead the medium Raman line at  $512 \text{ cm}^{-1}$ . The twisting frequency is calculated from the twisting constant in ethylene,<sup>†</sup> accepting a vibration frequency of  $800 \text{ cm}^{-1}$  for that molecule.<sup>11</sup> ‡ In general support of the assignment given above, we may observe that the mean

<sup>4</sup> See e.g. Kilpatrick and Pitzer, *J. Res. Nat. Bur. Stand.*, 1947, **38**, 191.

<sup>5</sup> Torkington, *J. Chem. Physics* (in press).

<sup>6</sup> Coulson and Longuet-Higgins, *Proc. Roy. Soc. A*, 1947, **191**, 39.

<sup>7</sup> Thompson and Torkington, *ibid.*, 1945, **184**, 21.

<sup>8</sup> *Idem.*, *Trans. Faraday Soc.*, 1945, **41**, 236; Torkington, *Nature*, 1949, **163**, 464.

<sup>9</sup> De Hemptinne, Jungers and Delfosse, *J. Chem. Physics*, 1938, **6**, 319.

\* For the symmetry classification, see Herzberg,<sup>1</sup> pp. 107, 108.

<sup>10</sup> Torkington, *Proc. Roy. Soc. A* (in press).

of the two  $\text{CCl}_2$  deformation frequencies is  $312 \text{ cm.}^{-1}$ , close to the accepted value for a single group; the large difference between the two individual frequencies here denotes the occurrence of considerable interaction. The two planar  $\text{CCCl}$  rocking modes are both of the expected order of magnitude; the value in vinylidene chloride,<sup>7</sup> where there is only one  $\text{CCl}_2$  group, is  $375 \text{ cm.}^{-1}$ . The order of the  $B_{3u}$  and  $B_{3g}$  C—Cl stretching frequencies is paralleled by the C—F stretching frequencies in  $\text{C}_2\text{F}_4$ ,<sup>8</sup>  $\nu_{B_{3u}}$  having the exceptionally high value in both molecules. All other observed frequencies can be interpreted as combinations as shown in Table II.

TABLE II

$\nu \text{ cm.}^{-1}$	Intensity	Activity	Assignment	Species
464	(w)	R	$2 \times 237$	$A_g$
574	(w)	R	$(387 + 185)$	$B_{2g}$
631	(vw)	R	$(782 - 135)$	$B_{3g}$
726	(vw)	R	$(512 + 215)$	$B_{3g}$
755	(m)	I.R.	$(2 \times 215 + 332)$	$B_{2u}$
784	(vw)	R	$(913 - 135)$	$B_{2g}$
			$(185 + 215 + 387)$	$A_g$
802	(s)	I.R.	$(2 \times 215 + 387)$	$B_{3u}$
1000	(vw)	R	$(447 + 347 + 215)$	$B_{3g}$
1025	(w) (p)	R	$2 \times 512$	$A_g$
1441	(w)	R	$(185 + 347 + 913)$	$B_{2g}$
1819	(w)	R	$2 \times 913$	$A_g$
1998	(w)	R	$(1571 + 447)$	$A_g$

(R indicates Raman spectrum; I indicates infra-red; *s*, *m*, *w*, *vw* indicate intensity strong, medium, weak, very weak; *p* indicates polarized Raman line.)

The discrepancies found between observed and calculated combinations are in general of the order expected for a molecule containing polar bonds; it should be remembered that the frequencies here are taken from both Raman and infra-red spectra, and refer variously to gas, liquid and solution. It may be objected that a triple combination should not be employed for the infra-red band at  $802 \text{ cm.}^{-1}$ , but the combination is of the same species as the fundamental at  $782 \text{ cm.}^{-1}$ ; it is therefore justifiable to assume that Fermi resonance occurs here, leading to the intensity observed.

*Physical Chemistry Laboratory,  
Oxford.*

† The justification for this is perhaps not very obvious; but if we assume that the twisting function is largely determined by the  $\pi$ -electrons which lead to the stable planar configuration, then since the double bond in  $\text{C}_2\text{Cl}_4$  has been shown to be probably normal, presumably the twisting function is not essentially different in  $\text{C}_2\text{H}_4$  and  $\text{C}_2\text{Cl}_4$ .

<sup>11</sup> Eucken and Parts, *Z. physik. Chem. B*, 1933, **20**, 184. Burcik, Eyster and Yost, *J. Chem. Physics*, 1941, **9**, 118.

‡  $825 \text{ cm.}^{-1}$  is now generally accepted as the value of the twisting frequency in ethylene, it being assumed that  $1656 \text{ cm.}^{-1}$  in the Raman spectrum is its first overtone. But there will be considerable anharmonicity in this mode, which makes the estimate only approximate in any event. A larger twisting constant would improve the fit for the Raman line at  $631 \text{ cm.}^{-1}$  in  $\text{C}_2\text{Cl}_4$ ; there is an alternative for the line at  $784 \text{ cm.}^{-1}$ .

# THE LACTONIZATION OF $\gamma$ -HYDROXYSTEARIC ACID IN A MONOLAYER

BY J. T. DAVIES

Received 25th November, 1948

On account of the variation of film properties with temperature, the apparent energy of activation and probability factor in the acid-catalyzed lactonization of  $\gamma$ -hydroxystearic acid monolayers rise considerably at high pressures, in good agreement with statistical calculations. The decrease in rate of reaction at constant temperature can also be predicted, and is in accord with experiment. Although little new information about the mechanism of this particular reaction has been gained, the temperature variation of  $\phi$ , the "accessibility" factor, which controls the effective concentration of reacting groups in the surface, is possibly a phenomenon of more general occurrence in monolayer reactions. Suggestions for future work to verify predictions from the statistical analysis are made.

In 1892 Henry<sup>1</sup> investigated the kinetics of the acid-catalyzed lactonization of  $\gamma$ -hydroxyvaleric acid, and found that the reaction velocity was closely proportional to the hydrogen ion concentration. Taylor and Close<sup>2</sup> confirmed the observation of Henry that in the presence of HCl the equilibrium state corresponded to 92 % conversion of the acid to lactone, but found that the catalytic influence of HCl was not strictly proportional to the hydrogen ion concentration as determined by conductivity measurements. Some years later, Garrett and Lewis<sup>3</sup> showed the velocity to be dependent on the viscosity of the solution, and postulated that the slow step must be bimolecular, being the collisions of suitably activated hydroxy-acid molecules and hydrogen ions. The energy of activation of the lactonization process was found to decrease from 16,100 cal./mole for reaction in 0.01 N HCl, to 15,050 cal./mole in 0.1 N HCl.

Taylor and Close<sup>4</sup> carried out very careful measurements on the same system, showing that the velocity constant should strictly be corrected for the reverse reaction occurring simultaneously, though this effect was not great. They put forward the idea that there was a "proportionality between reaction velocity and the thermodynamic activity of the hydrogen ions."

Rolfe and Hinshelwood<sup>5</sup> have considered the reaction between methyl alcohol and acetic acid. They demonstrated that the reaction was third order, depending on the collision of an acid molecule, an alcohol molecule and a catalyst, in this case another acetic acid molecule. The energy of activation  $E$  and the probability factor  $p$  were found to be 13,000 cal./mole and  $5 \times 10^{-9}$  respectively if the number of degrees of freedom involved in  $E$  be taken as two: if it is greater,  $p$  becomes even smaller. When a correction for the temperature coefficient of the collision number of the solvent molecules, since these are involved in the activated collisions, was employed,  $p$  increased to  $1.5 \times 10^{-7}$ . The authors advanced three possible reasons for this small probability:

- (i) that a precise orientation of the molecules is necessary for reaction,
- (ii) that the reacting molecules must be in a suitable internal phase,
- (iii) that quantum-mechanical restrictions of some kind make the transition probability in the activated systems very small.

<sup>1</sup> Henry, *Z. physik. Chem.*, 1892, **10**, 96.

<sup>2</sup> Taylor and Close, *J. Amer. Chem. Soc.*, 1917, **39**, 422.

<sup>3</sup> Garrett and Lewis, *ibid.*, 1923, **45**, 1091.

<sup>4</sup> Taylor and Close, *J. Physic. Chem.*, 1925, **29**, 1085.

<sup>5</sup> Rolfe and Hinshelwood, *Trans. Faraday Soc.*, 1934, **30**, 935.

Williamson and Hinshelwood<sup>6</sup> esterified acetic acid in methanol solution, using HCl as catalyst. The rate was found to be accurately expressed by

$$dx/dt = K[\text{HAc}][\text{CH}_3\text{OH}_2^+],$$

in which square brackets denote concentrations, after a correction for the distribution of hydrogen ions between the water formed as a product of reaction and the alcohol solvent was taken into account.  $E$  was found to be 10,200 cal./mole and  $p$  was  $1.17 \times 10^{-5}$ . If, however, a  $\text{CH}_3\text{OH}$  molecule is involved in the activating collision, the viscosity correction raises  $E$  to 12,680 cal./mole and  $p$  to  $0.78 \times 10^{-5}$ . The probability that a methanol molecule is present is taken as unity, since the encounter of the reactant molecules is calculated to be comparatively long. The efficiency of the collisions is thus very much greater with the ionic catalyst and, indeed, the factor  $0.78 \times 10^{-5}$  can be explained on the basis of the simplest kind of steric considerations.

The possibility of controlling the activation energy and the probability factor of a reaction by altering the film pressure of a monolayer of reactant has been pointed out by several workers. Alexander and Rideal<sup>7</sup> showed that, in the alkaline hydrolysis of trilaurin films, the energy of activation increased from 10,000 to 16,100 cal./mole as  $\pi$ , the film pressure, was changed from 5.4 dynes/cm. to 16.2 dynes/cm., the probability factor  $p$  increasing under the same conditions from  $1.1 \times 10^{-6}$  to  $4.1 \times 10^{-5}$ . The same authors found that ethyl palmitate monolayers, partially expanded at room temperature, hydrolysed on alkali with an energy of activation of 12,000 cal./mole, close to the value for the analogous reaction in homogeneous solution of 11,300 cal./mole. The  $p$  factor of this reaction was  $0.9 \times 10^{-5}$ . In contrast, a condensed film of methyl stearate hydrolysed under similar conditions with an activation energy of 17,400 cal./mole, gave a  $p$  factor of 0.12. Similarly,  $\alpha\alpha'$ -dipalmitin, which formed a condensed monolayer, hydrolysed with an energy of activation of about 20,000 cal./mole, of the same order of magnitude as for tripalmitin, the films of which were also condensed. The highly expanded films of  $\alpha$ -monopalmitin, however, gave a value of only 15,000 cal./mole.

Mittelmann and Palmer<sup>8</sup> found that the activation energy in the oxidation of triolein films with permanganate was dependent on the film pressure, though they pointed out that their values were only very rough.

By analogy with such experiments as these, studies of the lactonization of monolayers of  $\gamma$ -hydroxystearic acid might cast light on the nature of the fundamental process, since  $E$  and  $p$  may be functions of the film pressure, and hence of the configuration and orientation of the long-chain molecules in the surface. Fosbinder and Rideal<sup>9</sup> showed that the velocity of hydrolysis of a monolayer of  $\gamma$ -stearolactone was a function of surface pressure, and, more recently, Kögl and Havinga<sup>10</sup> investigated the lactonization process as a surface reaction. These latter authors made no measurements of  $E$  and  $p$ , however, nor of the influence of pressure on reaction velocity.

## Experimental

A sample of  $\gamma$ -hydroxystearic acid (m.p.  $87^\circ\text{C}$ ) was kindly donated by Dr. F. Kögl.  $\gamma$ -Stearolactone, for use in determining the characteristics of mixed films, was prepared from Kahlbaum pure oleic acid, according to the method of Clutterbuck,<sup>11</sup> and purified to constant melting point by four recrystallizations from pure methylated spirit, and a final wash with redistilled ethanol (m.p.

<sup>6</sup> Williamson and Hinshelwood, *Trans. Faraday Soc.*, 1934, **30**, 1145.

<sup>7</sup> Alexander and Rideal, *Proc. Roy. Soc. A*, 1937, **163**, 70.

<sup>8</sup> Mittelmann and Palmer, *Trans. Faraday Soc.*, 1942, **38**, 506.

<sup>9</sup> Fosbinder and Rideal, *Proc. Roy. Soc. A*, 1933, **143**, 61.

<sup>10</sup> Kögl and Havinga, *Rec. trav. chim.*, 1940, **59**, 601.

<sup>11</sup> Clutterbuck, *J. Chem. Soc.*, 1924, **125**, 2330.



## 450 LACTONIZATION OF $\gamma$ -HYDROXYSTEARIC ACID

50.1°-50.3° C.; Kögl and Havinga,<sup>10</sup> 53° C.; Fosbinder and Rideal,<sup>9</sup> 50° C.; Clutterbuck,<sup>11</sup> 52-53° C.). Constant boiling HCl was used in making the solutions, and the normalities were checked by titration. Film pressures and potentials were measured in the usual way.

The second-order velocity constant  $k$  was evaluated from the expression,

$$k = \frac{1}{t[H^+]} \ln \left( \frac{\Delta V_0 - \Delta V_\infty}{\Delta V_t - \Delta V_\infty} \right), \quad . \quad . \quad . \quad (1)$$

where  $\Delta V$  is the film potential and  $t$  the time elapsed since the beginning of the reaction. In practice, the slope of a plot of  $\log_{10} (\Delta V_t - \Delta V_\infty)$  against  $t$  was employed to evaluate  $k$ . The validity of (1) depends on the existence of a linear relation between  $\Delta V$  and composition of the film, a condition which was found to be obeyed satisfactorily at the various pressures by spreading mixed films. At 2 dynes/cm., however, a change of state to a condensed film as reaction proceeded made accurate measurements impossible. After reacting till  $\Delta V$  was constant, the film gave characteristics corresponding closely with those of a film of  $\gamma$ -stearolactone under the same conditions, so that no correction for the reverse reaction was necessary.

### Results

Force-area and potential-area curves of  $\gamma$ -hydroxystearic acid and  $\gamma$ -stearolactone agreed closely with those of Adam<sup>12</sup> (who found that on N/50 and N HCl the  $\pi$ - $A$  curves were similar) and Fosbinder and Rideal.<sup>9</sup> Between

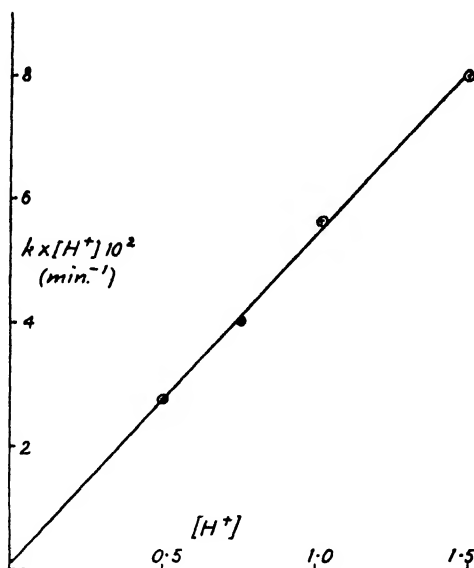


FIG. 1.—Rate of lactonization against  $[H^+]$ .  $\pi = 16$  dynes/cm.  $t = 20^\circ \text{C}$ .

0.5 N HCl and 1.5 N HCl at 20° C and at 16 dynes/cm., the bimolecular lactonization constant was  $5.40 \pm 0.12 \times 10^{-2}$  l. mole<sup>-1</sup> min.<sup>-1</sup>. The rate of reaction is thus proportional to the concentration of HCl, and the straight line passed between the observed points on the graph of rate of reaction against  $[H^+]$  according to the method of least squares, showing that the rate is practically zero at zero concentration of acid (Fig. 1).

Fig. 2 shows the plot of  $\log_{10} k$  against  $10^3/T$ , where  $T$  is the absolute temperature, for the reactions at 16 dynes/cm. and 5 dynes/cm. It is seen that in the former case the slope of the plot is constant over the temperature range 8° C-20° C, when  $E = 17,400$  cal./mole, but that above 20° C the plot deviates

<sup>12</sup> Adam, *Proc. Roy. Soc. A*, 1933, 140, 223.

from linearity, and  $E$  increases. At 5 dynes/cm. in the temperature range  $20^{\circ}\text{C}$ – $30^{\circ}\text{C}$ ,  $E$  is found from the slope to be 11,600 cal./mole. Under these conditions the film is expanded. The experimental difficulties due to change

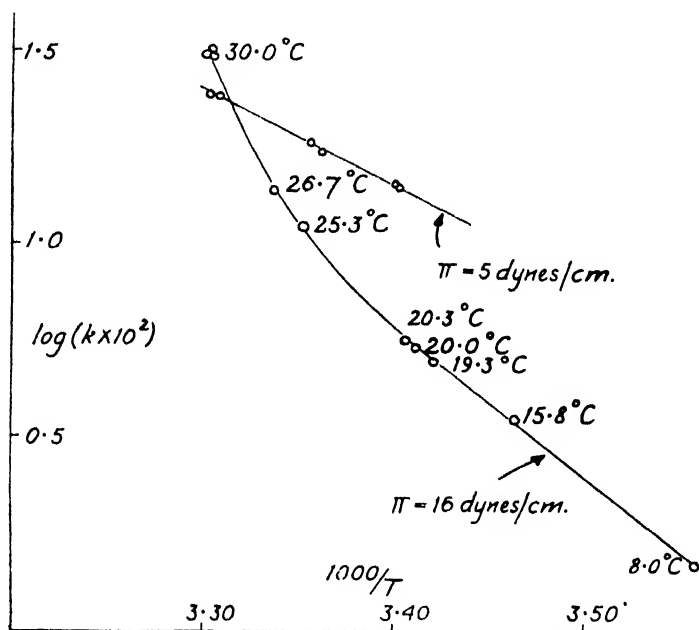


FIG. 2.— $E$  at 16 dynes/cm. = 17,400 cal./mole.  
 $E$  at 5 dynes/cm. = 11,600 cal./mole.

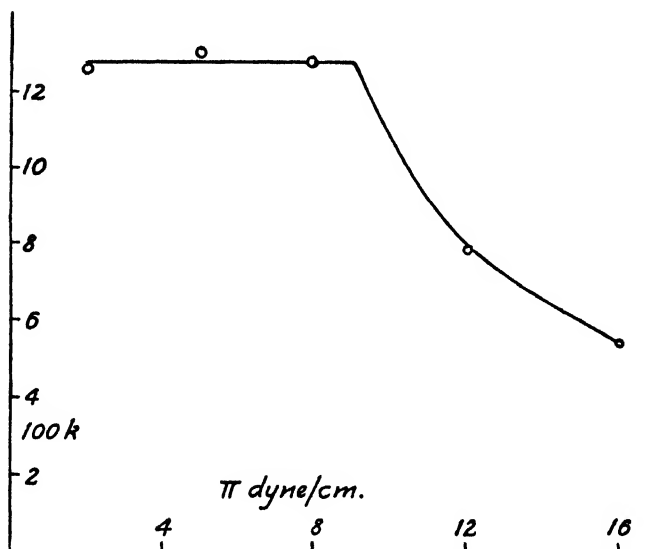


FIG. 3.—Variation of reaction rate with film pressure at  $20^{\circ}\text{C}$  and on  $\text{N HCl}$ .

in the state of the film as reaction proceeded became very great at temperatures below  $20^{\circ}\text{C}$  for the reaction at 5 dynes/cm., and accurate measurements of the velocity constant were impossible under these conditions. The probability

factors for the lactonization at 5 dynes/cm. and 16 dynes/cm were calculated by the method of Fosbinder and Rideal<sup>9</sup> to be  $4.3 \times 10^{-5}$  and 0.38 respectively.

The effect of pressure on the reaction velocity at constant temperature of 20° C is shown in Fig. 3 for substrates of N HCl. The rate is practically unchanged till the film pressure exceeds about 9 dynes/cm., thereafter decreasing as the film condenses, being reduced to less than half the former value at  $\pi = 16$  dynes/cm.

### Discussion

**The Accessibility Factor.**—The proportionality between the rate and the concentration of HCl in the substrate shows that the following factors need not be taken into account :

- (i) ionization in the monolayer, which would cause deviations from direct proportionality (Davies<sup>13</sup>) ; ionization occurs, however, in films of acids and alcohols at higher substrate concentrations of HCl, according to Schulman and Hughes ;<sup>14</sup>
- (ii) kinetic activity factors ;
- (iii) autocatalysis ;
- (iv) solvent-catalysed lactonization.

The slower reaction at higher pressures can be correlated, as explained below, with the inaccessibility of the —OH or —CO<sub>2</sub>H group to the substrate, so that it appears that, in view of the high energy of activation, the hydroxyl and carboxyl groups and the hydroxonium ion must all be present when the slow step occurs. This conclusion is in agreement with the work of Rolfe and Hinshelwood.<sup>5</sup>

Mittelman and Palmer<sup>8</sup> have put forward an interpretation of the retardation of the velocity of oxidation of triolein monolayers spread on aqueous permanganate, in terms of the configuration of the long chains, and the probability that the double bond will lie in the surface. This probability is given by  $\phi$ , the accessibility factor, i.e.

$$\phi = \frac{\sum_{\beta} e^{-G/\mathcal{R}T}}{\sum_{\alpha} e^{-G/\mathcal{R}T}}, \quad \dots \quad (2)$$

in which  $G = \frac{N(\pi + \gamma) al}{4 \cdot 18 \times 10^7} + 800$  cal./mole.

$G$  is the energy in cal./mole of a particular configuration in the surface,  $\mathcal{R}$  is in cal./mole deg.  $T$  is the absolute temperature,  $N$  the Avogadro number and  $\gamma$  a measure of the work required (in erg cm.<sup>-2</sup>) to remove a long chain from a vertical position and to extend it horizontally on the surface against the cohesive energy of the film molecules themselves ;  $a$  and  $l$  are the width and length (which increases discretely) of the hydrocarbon chain lying in the surface, expressed in cm.  $\pi$  is the film pressure in dyne/cm., and  $\sum_{\beta}$  and  $\sum_{\alpha}$  denote summations over all the configurations

with the double bond in the surface, and over all possible configurations respectively. The value of 800 cal./mole is the energy required to bend a hydrocarbon chain through  $2\pi/3$  radians relative to a CH<sub>3</sub> group (Pitzer<sup>15</sup>). When the chain is unbent, either lying vertically or horizontally in the surface, this value is not included. The cohesive energy of the film is evidently low in films of triolein which has *cis* double bonds in the long chain, since Mittelman and Palmer showed they could write  $\gamma = 0$  and obtain satisfactory agreement with the observed  $\phi$  at various pressures.

<sup>13</sup> Davies, *Advances in Surface Chemistry* (Report of Bordeaux Conference), 1948 (in press).

<sup>14</sup> Schulman and Hughes, *Proc. Roy. Soc. A*, 1932, 138, 436.

<sup>15</sup> Pitzer, *J. Chem. Physics*, 1940, 8, 711.

If the polar carboxyl group is spherical, and occupies  $20 \text{ \AA}^2$  in the surface, the area  $A$  in  $\text{\AA}^2$  at any pressure,  $\pi$ , is given by

$$A = 20 + 10^{16} \frac{\sum_a a l e^{-G/RT}}{\sum_a e^{-G/RT}} \quad (3)$$

Mittelmann and Palmer obtained good correspondence with the experimental  $\pi$ - $A$  plot of triolein using eqn. (3), again taking  $\gamma$  as zero.

In the consideration of  $\gamma$ -hydroxystearic acid the analysis is more complicated. Not only is there the high energy of adsorption of the CHOH group to take into account, but the work done against film cohesion will be far from zero. In addition, the possibility of the chains having been bent several times cannot be neglected, nor can that of the  $\text{CO}_2\text{H}$  group being forced above the surface while the CHOH group is adsorbed there. Further, the  $\text{CO}_2\text{H}$  group may be pushed below the surface while the CHOH group is still in the water surface, though this configuration will not be possible in the close-packed structures at higher pressures and lower temperatures. The most probable configurations, however, are those of an L-shaped molecule with the carboxyl group adsorbed at the surface, and the OH group in, or just out of, the surface.

The term  $\gamma a l$  has been replaced in this study by

$$Wh (b/2 + l),$$

where  $W$  is the work of cohesion in  $\text{erg/cm}^2$  between hydrocarbon surfaces. This expression follows from consideration of the hydrocarbon chain lying in the surface (Fig. 4) causing a triangular prism to be formed

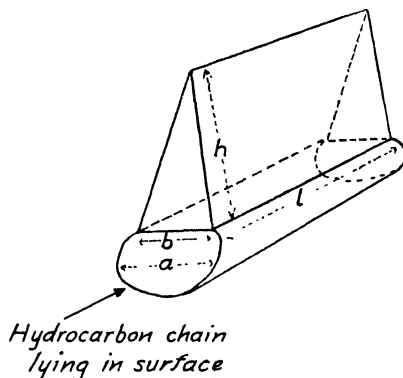


FIG. 4.

in the chains still standing upright. The width and length of the base of this will be  $b$  and  $l$  respectively, so that the area of hydrocarbon surface pulled away from an equal area is

$$h(b/2 + l),$$

where  $h$  is the slant height of the prism, and is practically equal to the perpendicular height.

The exact evaluation of  $h$  and  $b/2$ , however, is not easily made, nor is it certain whether  $W$  the cohesive energy includes the polar head group or the hydrocarbon chains alone. The value of  $Wh$  for various states of the film may be found, however, from the force-area curves, using a value of  $20 \text{ \AA}^2$  for the area per vertical chain, so that

$$A = 20 + 10^{16} \frac{\sum_a a l e^{-G'/RT}}{\sum_a e^{-G'/RT}}, \quad (4)$$

454 LACTONIZATION OF  $\gamma$ -HYDROXYSTEARIC ACID

where the symbols have the same significance as in (3), except that  $G$  is now replaced by

$$G' = \frac{N(Wh(b/2 + l) + \pi al)}{4.18 \times 10^7} + 800n + H, \quad (5)$$

where  $n$  is the number of times any chain is bent, and  $H$  is an energy term, calculated below, expressing the work of adhesion of the  $\text{CHOH}$  group, or work of immersion of a  $\text{CH}_2$  group, or that of raising a  $\text{CO}_2\text{H}$  group from the surface. From models,  $b$  is taken as  $2.6 \times 10^{-8}$  cm.

TABLE I.—EFFECT OF TEMPERATURE ON  $A$  AND  $\phi$   
 $\pi = 16$  dynes/cm.

$t^\circ\text{C}$	$Wh$ (cal. mole $^{-1}$ Å $^{-1}$ )	$A$ (calc.) (Å $^2$ )	$A$ (obs.) <sup>a</sup> (Å $^2$ )	$\phi$ (calc.)
8	318	25.7	25.5	0.368
20	250	28.2	28.0	0.501
26	160	33.0	32.5	0.695
27	94	35.3	35.5	0.786
30	60	38.2	38.3	0.836

TABLE II.—EFFECT OF  $\pi$  ON  $A$  AND  $\phi$  AT CONSTANT TEMPERATURE OF  $30^\circ\text{C}$   
Film expanded,  $Wh = 60$  cal. mole $^{-1}$  Å $^{-1} = 42 \times 10^{-8}$  erg/cm.

$\pi$ (dyne/cm.)	$A$ (calc.) (Å $^2$ )	$A$ (obs.) <sup>a</sup> (Å $^2$ )	$\phi$ (calc.)
6	48.9	50.5	0.885
12	42.4	42.8	0.853
16	38.2	38.3	0.836

TABLE III.—EFFECT OF  $\pi$  ON  $A$  AND  $\phi$  AT CONSTANT TEMPERATURE OF  $8^\circ\text{C}$   
Film condensed,  $Wh = 318$  cal. mole $^{-1}$  Å $^{-1} = 221 \times 10^{-8}$  erg/cm.

$\pi$ (dyne/cm.)	$A$ (calc.) (Å $^2$ )	$A$ (obs.) <sup>a</sup> (Å $^2$ )	$\phi$ (calc.)
6	27.6	28.2 (extrapolated)	0.453
12	26.4	27.6	0.397
16	25.7	25.5	0.368
24	24.6	23.1	0.300

$G'$  is defined as zero when  $l = 0 = n$ , so that the state of zero energy is that in which the chains are vertical with only the carboxyl group in the water surface.

By trial and error with different  $Wh$  values and temperatures, eqn. (4) was fitted to the force-area curves of Fosbinder and Rideal. The values of  $Wh$ ,  $T$  and  $\pi$  at different areas are summarized in Tables I, II and III, from which the agreement with experiment can be judged. Since  $Wh$  is now known,  $\phi$  may be calculated by a method analogous to that given above (eqn. (2)), and has the values given in Tables I, II and III at the different temperatures, pressures, and film cohesions.

The summation of probabilities that the group can react has been made over those configurations in which the  $\text{CO}_2\text{H}$  and  $\text{CHOH}$  groups in the same molecule are immersed in the substrate. Fig. 5 shows that  $\phi$ , derived from Fig. 3 and the calculated accessibility value of 0.90 at low pressures, is close to the theoretical values, obtained using the values of  $Wh$  from the  $\pi$ - $A$  curves. The change to the condensed state at higher

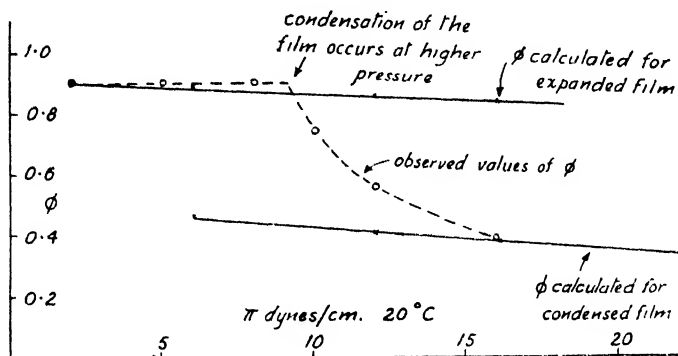


FIG. 5.—Variation of rate of lactonization on  $\text{N HCl}$  with film pressure. The observed values are derived from Fig. 3, and that at 10 dynes/cm. is interpolated.

pressures is reflected in the shift of the observed  $\phi$  from the theoretical curve for expanded films to that for condensed films in the region of condensation of the film.

It is to be noted that  $\partial(-\phi)/\partial\pi$  and  $\partial(-A)/\partial\pi$  (from Fig. 5 and the data of Fosbinder and Rideal<sup>9</sup> respectively) are both greatest at about  $\pi = 10$  dynes/cm. at  $20^\circ\text{C}$ , and decrease continuously at higher pressures when further condensation occurs.

The configurations taken into account in the calculations of  $A$  and  $\phi$  are indicated in Fig. 6, where a line represents the  $-\text{CH}_2-\text{CH}_2-$  chain,

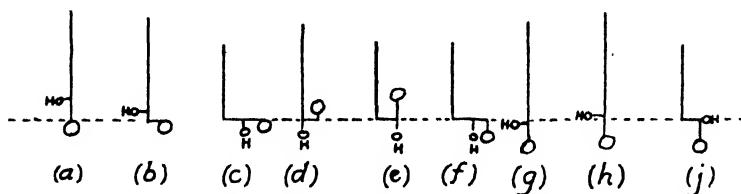


FIG. 6.

and O refers to the polar head group. The broken line represents the water surface configurations, with variable numbers of carbon atoms lying in the surface; types (c), (f), (g) and (j) were considered in the term  $\sum_{\beta} e^{-G'/RT}$ , and all the forms were taken into account in evaluating  $\sum_{\alpha} e^{-G'/RT}$  and  $\sum_{\alpha} a e^{-G'/RT}$ . Positions (g) and (h) were considered only in the expanded films.

The values of  $H$  (eqn. (5)) in each form were known from appropriate selections of the following energies—

- (i) work to lift  $\text{CHOH}$  from surface, 1,700 cal./mole;
- (ii) work to lift  $\text{CO}_2\text{H}$  from surface, 1,600 cal./mole;
- (iii) work to immerse  $\text{CO}_2\text{H}$  in water,<sup>18</sup> 437 cal./mole;
- (iv) work to immerse  $\text{CH}_2$  in water,<sup>18</sup> 625 cal./mole.

<sup>18</sup> Adam, *The Physics and Chemistry of Surfaces*, 3rd ed. (Oxford), p. 122.

The work done in lifting the CHO groups out of the water surface and replacing them by hydrocarbon chains is given by the energy of adhesion to water of a long-chain alcohol less that for a long-chain hydrocarbon. The values of Harkins<sup>17</sup> of 91.8 ergs/cm.<sup>2</sup> and 46.0 ergs/cm.<sup>2</sup> for *n*-octyl alcohol and *n*-octane respectively, are different by 45.8 ergs/cm.<sup>2</sup>, which, at an area of 25 Å<sup>2</sup> per CHO group, is 1,700 cal./mole, as given above. In the case of long-chain acids, the work of adhesion to water less the work of adhesion of a hydrocarbon chain gives the energy required to lift the CO<sub>2</sub>H group out of the surface and replace it by a CH<sub>3</sub> group. The work of adhesion of oleic acid<sup>17</sup> is 89.8 ergs/cm.<sup>2</sup>, and that of a hydrocarbon chain (*n*-octane) is 46.0 ergs/cm.<sup>2</sup>. The difference, 43.8 ergs/cm.<sup>2</sup> at an area of 25 Å<sup>2</sup> per molecule, is 1,600 cal./mole.

That the exact values of  $H$  employed, and the omission of some of the more unlikely configurations, have little effect on the relation of  $\phi$  to  $A$  can be seen by comparing Tables II and III with Table IV, in which the

TABLE IV.—EFFECT OF  $\pi$  AND  $\gamma$  ON  $A$  AND  $\phi$  AT CONSTANT TEMPERATURE  
OF 20° C;  $a = 4.6$  Å

$\pi$ (dyne/cm.)	$\gamma$ (dyne/cm.)	$A$ (calc.) ( $\text{\AA}^2$ )	$A$ (obs.) <sup>a</sup> ( $\text{\AA}^2$ )	$\pi$ (calc.)
0	8	62.8	62.5	0.940
4.7	8	54.5	53.0	0.913
8	8	49.4	47.8	0.894
12	8	44.0	43.3 *	0.848
16	8	42.0	39.5 *	0.801
0	5.1	29.9	29.6 *	0.567
4	5.1	29.0	28.8 *	0.526
9	5.1	27.9	28.0	0.478
12.6	5.1	27.2	26.8	0.444
16	5.1	26.5	25.2	0.406
23	5.1	25.5	23.5	0.354

\* Value extrapolated from curves outside the region of change of state.

figures were calculated using the simpler form of eqn. (5), replacing the term

$$[\pi al + Wh(b/2 + l)] \text{ by } (\pi + \gamma)al,$$

where

$$\gamma a \approx Wh \quad . \quad . \quad . \quad . \quad . \quad (6)$$

since  $b/2$  is small compared with  $l$  in most configurations. Only forms (a), (b) and (c) are taken into account in Table V, and the energy of removing a CHOH group from the surface is taken as 1,500 cal./mole (Fosbinder and Rideal<sup>6</sup>).

In the expanded films  $\phi$  calculated by the simplified method varies slightly more with changes in  $\pi$  than does the more exact  $\phi$ , but in the condensed films  $\phi$  calculated by the approximate method is uniformly less than that in Table III by about 0.05. In the two cases the agreement of the calculated and observed areas is similar.

**The Numerical Values of  $Wh$  and  $\gamma$ .**—For condensed films,  $Wh$  is found to be  $318 \text{ cal. mole}^{-1} \text{ \AA}^{-1}$ . This gives  $W = 221/h \text{ ergs/cm.}^2$ , the units of  $h$  now being  $\text{\AA}$ . The work of cohesion of *n*-octane<sup>17</sup> is  $43.5 \text{ ergs/cm.}^2$ , so that  $h = 5.1 \text{ \AA}$ . This value appears very reasonable from a model, the measured height above the horizontal hydrocarbon chain of a prism such as that postulated here being  $5.7 \text{ \AA}$ . At lower pressures, when the film is expanded,  $Wh = 60 \text{ cal. mole}^{-1} \text{ \AA}^{-1}$ , or  $W = 41.7/h \text{ ergs/cm.}^2$ , when  $h$  is expressed in  $\text{\AA}$ , giving  $h = 0.96 \text{ \AA}$ . This means that

<sup>17</sup> Harkins, Brown and Davies, *J. Amer. Chem. Soc.*, 1917, **39**, 354.

the less rigid nature of the structure allows the wedge-shaped cavity to be nearly filled up again with hydrocarbon chains. Adam<sup>18</sup> summarizes the evidence for the flexibility of long chains. That Mittelmann and Palmer could write for triolein films  $\gamma = 0$  shows that in this case the *cis* double bonds permit a very loose and mobile arrangement of the hydrocarbon chains.

In eqn. (6),  $a$  is the width of a hydrocarbon chain, taken as  $4.6 \text{ \AA}$ , following Mittelmann and Palmer;  $\gamma a$  is thus calculated from the figures of Table IV to be  $234 \times 10^{-8} \text{ erg/cm.}$  and  $37 \times 10^{-8} \text{ erg/cm.}$  for the condensed and expanded films respectively. These values agree quite well with those of the more rigorous form of analysis, of  $221 \times 10^{-8} \text{ erg/cm.}$  and  $42 \times 10^{-8} \text{ erg/cm.}$

Langmuir<sup>19</sup> has given a different method of considering expanded monolayers, regarding them as duplex films, and writing the equation of state,

$$(\pi + \pi_0)(A - A_0) = kT,$$

where  $k$  is the Boltzmann constant.

For liquid expanded films of myristic acid, Langmuir obtained values of  $11.2 \text{ dynes/cm.}$  for  $\pi_0$  and, at  $20^\circ \text{C}$ ,  $15.6 \text{ \AA}^2$  for  $A_0$ . Though this equation of state is different from (4), it may be noted that the value of  $\gamma$  of  $8 \text{ dynes/cm.}$  (Table IV) is not very different from  $\pi_0$  for myristic acid.

Whereas Langmuir suggested that micelles are formed during the condensation of the film, no such definite picture need be considered in the present work. The values of  $Wh$  in Table I may be the average for a number of separate molecules, or they may equally well be the averages for separate molecules and micelles.

**The Change of  $E$  with Pressure.**—The results of previous workers on the energies of activation and rates of reaction of monolayers at constant pressures, together with those of the present work, show an interesting common characteristic, namely that although the energy of activation and the probability factor may vary by as much as  $6,000 \text{ cal./mole}$  and a factor of  $10^4$  respectively, the actual rates of reaction measured at room temperatures do not vary greatly. Further, in the present work as well as in that of Mittelmann and Palmer, the decrease in rate at higher pressures can be explained in terms of concentrations of reacting groups in the surface, without taking into account electrical redistributions in the molecule, changes of mechanism of reaction, potential barriers at the surface, or the changed energy of activation. This suggests that the apparent increase in the energy of activation in the lactonization of  $\gamma$ -hydroxystearic acid may not be independent of  $\phi$ .

If we write

$$k = \phi p Z e^{-E/RT}, \quad (7)$$

where  $Z$  is the collision rate, and  $p$ ,  $Z$  and  $E$  are independent of film pressure and temperature, the decrease in  $k$  at higher pressures by a factor determined solely by  $\phi$  follows immediately.

Taking logarithms of (7) and differentiating at constant pressure,

$$\left( \frac{\partial \ln k}{\partial (1/RT)} \right)_\pi = \left( \frac{\partial \ln \phi}{\partial (1/RT)} \right)_\pi - E = E', \quad (8)$$

where  $E'$  is defined as

$$- \left( \frac{\partial \ln k}{\partial (1/RT)} \right)_\pi$$

Thus

$$E' = E + RT^2 / \phi \left( \frac{\partial \phi}{\partial T} \right)_\pi, \quad (9)$$

or

$$E' = E + \Delta E. \quad (10)$$

<sup>18</sup> Adam, *Proc. Roy. Soc. A*, 1930, **126**, 366.

<sup>19</sup> Langmuir, *J. Chem. Physics*, 1933, **1**, 756.



In completely expanded films  $\phi$  is assumed constant, a procedure which is discussed below. So, for reaction at 5 dynes/cm. above  $20^\circ\text{C}$ ,  $\Delta E = 0$ . In the partially expanded films, however, as the temperature is raised  $Wh$  will decrease, and consequently  $\phi$  will increase (Table I), ultimately tending to unity. Thus

$$\left(\frac{\partial\phi}{\partial T}\right)_\pi > 0$$

and  $E'$  measured for this type of film will exceed  $E$ . For reaction of  $\gamma$ -hydroxystearic acid this temperature range will be  $8^\circ$ - $33^\circ\text{C}$  for films at 16 dynes/cm.

It may well be significant that the films giving high  $E'$  values at higher pressures or in the condensed state show this change of state about the temperature and pressure range in which the kinetics at constant pressure were studied. Furthermore, this temperature range is usually not far from room temperature. If the head group is larger than the hydrocarbon chain in cross-sectional area or if it may be bent (as in the case of the glycerides), squeezing out or buckling of some of the reactant groups may occur, decreasing  $\phi$  at higher film pressures, as was the case for  $\gamma$ -hydroxystearic acid. It is of interest to note<sup>20</sup> that the work of adhesion of the ester group to water less that of a long-chain hydrocarbon is 29 ergs/cm.<sup>2</sup>, or 1.100 cal./mole at  $25\text{ \AA}^2$  per group. In other words, the apparent increase in  $E'$  may perhaps be related to an increasing concentration of reacting groups in the surface at higher temperatures.

**The Magnitude of  $\Delta E$ .**—In Table I, for the case of  $\gamma$ -hydroxystearic acid, the values of  $\phi$  between  $8^\circ\text{C}$  and  $20^\circ\text{C}$  give

$$(\partial\phi/\partial T)_{\pi=16} = 0.133/12.$$

Taking mean values of  $\phi$  and  $T$  of 0.434 and  $287^\circ\text{K}$ ,

$$\Delta E = RT^2/\phi(\partial\phi/\partial T)_{\pi=16} = 4,200 \text{ cal./mole.}$$

The observed value is 5,800 cal./mole.

Between  $20^\circ$  and  $26^\circ\text{C}$ ,

$$(\partial\phi/\partial T)_{\pi=16} = 0.194/6,$$

and the mean values of  $\phi$  and  $T$  are 0.598 and  $296^\circ\text{K}$ , so

$$\Delta E = 9,400 \text{ cal./mole.}$$

This means that the plot of  $\log_{10} k$  against  $1/T$  will not be linear in this region of temperature, the numerical value of the slope increasing, as was found experimentally (Fig. 2). The experimental value of  $\Delta E$  under the same conditions is found from the same graph to be 12,300 cal./mole. Above  $25^\circ\text{C}$ ,  $\Delta E$  increases still further, and at  $30^\circ\text{C}$  the rate is actually slightly greater than in the film at 5 dynes/cm. From the simple statistical theory it can be seen that if  $Wh$  has the same value at 5 dynes/cm. and 16 dynes/cm. at  $30^\circ\text{C}$  (since in both cases the films are expanded),  $\phi$  will be about 0.8 or 0.9 in each case (Table II).

The case of reaction at 16 dynes/cm. can be considered from a slightly different viewpoint. When the  $\text{CHOH}$  group is not in the surface, an approaching  $\text{H}_3\text{O}^+$  ion can react to form the intermediate complex if, and only if, energy sufficient to bring the  $\text{CHOH}$  group on to or below the aqueous interface be available. This extra energy appears in the rate equations as an apparent increase in the energy of activation of the lactonization process at 16 dynes/cm.

**Assumptions made in the Application of the Statistical Theory to the Calculation of  $\Delta E$ .**—(i)  $Wh$  is constant with change of temperature in the expanded state of the film. Table V gives values of  $\phi$  for the expanded state, using the simplified method of calculation, at three different temperatures. It is seen that

$$(\partial\phi/\partial T)_{\pi, Wh} = -1 \times 10^{-4},$$

<sup>20</sup> Adam, *The Physics and Chemistry of Surfaces*, 3rd ed. (Oxford), p. 154.

giving a negligible value of  $\Delta E$ . Further, the  $\pi$ - $A$  curves of Fosbinder and Rideal show that there is no increase in film area at 5 dynes/cm. between 17° and 33° C.

(ii) No other effects than *concentration* of reactant groups in the surface contribute to  $\Delta E$ .

TABLE V.—EFFECT OF TEMPERATURE ON  $\phi$  AND  $A$  AT CONSTANT  $\pi$  AND  $\gamma$

$\pi$ (dyne/cm.)	$\gamma$ (dyne/cm.)	$t^\circ\text{C.}$	$A$ (calc.) ( $\text{\AA}^2$ )	$\phi$ (calc.)
5	8	10	53.54	0.912
5	8	20	54.00	0.911
5	8	30	54.46	0.910
14	51	10	27.75	0.424
14	51	20	26.96	0.432
14	51	30	27.24	0.442

$$(\partial\phi/\partial T)_{\pi=5, \gamma=8} = -1 \times 10^{-4} \quad (\partial A/\partial T)_{\pi=5, \gamma=8} = 4.6 \times 10^{-2}$$

$$(\partial\phi/\partial T)_{\pi=14, \gamma=51} = +9 \times 10^{-4} \quad (\partial A/\partial T)_{\pi=14, \gamma=51} = 2.5 \times 10^{-2}$$

(iii) The  $p$  factor and  $Z$  in eqn. (7) are independent of temperature.

(iv) The configurations and energies taken into account in the complete theory are the only significant ones, and that it is only in expanded films that the unbent vertical chain can have both the CHOH and  $\text{CO}_2\text{H}$  groups hydrated at the same time. At lower areas, the close-packing of the film is assumed to make this condition impossible.

(v) The energy, 1700 cal./mole, required to remove the CHOH group from the water surface is independent of temperature and pressure.

The accuracy of the statistical method generally may be judged from Table I. A change of  $Wh$  from 60 to 94 cal. mole $^{-1}$   $\text{\AA}^{-1}$  (an increase of 57 %), decreases  $\phi$  by 6 %, and the calculated area by 7.6 %. In all cases  $(\partial\phi/\partial T)_{\pi, \gamma}$  is very small (Table V). The comparison of the complete and simplified methods of calculation has already been given.

**The Case of Reaction at Constant Area.**—This can be considered most simply by writing

$$A = f(\pi + \gamma, T).$$

Differentiating,

$$\frac{dA}{dT} = \left( \frac{\partial A}{\partial(\pi + \gamma)} \right)_T \frac{d(\pi + \gamma)}{dT} + \left( \frac{\partial A}{\partial T} \right)_{(\pi + \gamma)}.$$

At constant area  $dA = 0$ , and further, since  $(\partial A/\partial T)_{(\pi + \gamma)}$  is known from Table V to be  $2.5 \times 10^{-2} \text{\AA}^2/\text{deg.}$  when  $(\pi + \gamma) = 65$  dynes/cm., and  $(\partial A/\partial(\pi + \gamma))_T$  is, from Table IV,  $(27.2 - 25.5/12.6 - 23) = -0.16$ ,

$$(\partial(\pi + \gamma)/\partial T)_A = +0.16.$$

But

$$\left( \frac{\partial\phi}{\partial T} \right)_A = \left( \frac{\partial\phi}{\partial(\pi + \gamma)} \right)_A \left( \frac{\partial(\pi + \gamma)}{\partial T} \right)_A$$

and the term

$$\left( \frac{\partial\phi}{\partial(\pi + \gamma)} \right)_A$$

can be found, at a calculated area per molecule of  $27.2 \text{\AA}^2$ , from the data of Tables IV and V, to be  $(0.444 - 0.442)/(63.6 - 65)$ , i.e.  $-1.4 \times 10^{-3}$ . Thus

$$(\partial\phi/\partial T)_{27.2\text{\AA}^2} = -2.3 \times 10^{-4},$$

$$\therefore \Delta E = \frac{RT^2}{\phi} \left( \frac{\partial\phi}{\partial T} \right) = -90 \text{ cal./mole}$$

using a value of  $\phi$  of 0.443 and  $T = 298^\circ \text{K}$ . For reaction at  $54.5^\circ \text{Å}^\circ$ , the data of Tables IV and V give  $\Delta E = -51 \text{ cal./mole}$ . So for reactions carried out at constant areas the theory predicts that  $\Delta E$  will be negligible, or at any rate very small, both at high and low areas. It is perhaps significant that Fosbinder and Rideal,<sup>9</sup> hydrolyzing  $\gamma$ -stearolactone at constant area, found  $E$  and  $p$  values of 12,500 cal./mole and  $8.2 \times 10^{-6}$  respectively. They pointed out that these values are close to those for analogous bulk reactions. The pressures of the film at the upper end of the temperature range in which they worked would be of the order of 16 dynes/cm.

**The  $p$  Factor.**—Using the value of  $E'$  and the method of Fosbinder and Rideal,  $p'$ , the apparent  $p$  factor, is given by

$$k = p'Ze^{-E'/RT}.$$

But

$$k = \phi pZe^{-E/RT}, \quad . \quad . \quad . \quad . \quad (7)$$

$$\therefore p = \frac{p'e^{\Delta E/RT}}{\phi},$$

since

$$E' = E + \Delta E. \quad . \quad . \quad . \quad . \quad (10)$$

Indicating the pressures by subscripts, and using the values of  $\Delta E$  and  $\phi$  of 4,200 cal./mole and 0.434 for the temperature range  $8^\circ\text{--}20^\circ \text{C}$ ,

$$p_{16} = p' \times 14.5 \times 10^{-4},$$

or, using the value of 0.38 for  $p'$ ,  $p_{16} = 5.5 \times 10^{-4}$ . Similarly,

$$p_6 = 4.3 \times 10^{-5} \times 1.13 = 4.8 \times 10^{-5}.$$

The difference between  $p_{16}$  and  $p_6$  is clearly very much less than between  $p'_{16}$  and  $p'_6$ .

Further work on the energies of activation for the lactonization of  $\gamma$ -hydroxystearic acid, carried out at different constant areas should give a valuable check on the applicability of the results derived from a comparatively simple model of the reactant molecule. Study of reactions in which  $\Delta E$  is large, over a much wider temperature range should also yield interesting information, but the experimental difficulties in making accurate measurements under these conditions would become increasingly severe.

The author is indebted to Prof. E. K. Rideal for continual interest in this work. He is also grateful to Mr. K. I. Sutherland for stimulating criticism and discussion, and to the Council of Canterbury University College, New Zealand, for an award of the Lord Rutherford Memorial Research Fellowship.

*Davy-Faraday Research Laboratory,  
Royal Institution,  
London.*

# SOME APPLICATIONS OF THE VALENCE-BOND METHOD TO PROBLEMS OF MOLECULAR STRUCTURE

## PART I. CALCULATIONS OF THE BOND LENGTHS OF THE HYDROGEN HALIDES

BY ERNEST WARHURST

*Received 25th November, 1948*

It has been shown that the experimental data indicate that *single* bonds, which are usually described in terms of resonance between ionic and covalent structures, exhibit contractions which are approximately directly proportional to the resonance energy. The covalent radius of hydrogen has been discussed and reasons for the choice of a value of 0.32 Å have been given. The bond lengths of the hydrogen halides have been calculated by means of the valence-bond method. An expression for the bond length of the actual state of the molecule has been obtained from the first derivative of the secular equation with respect to internuclear separation. An approximate evaluation of the dependence of the resonance integral on internuclear separation has been made which enables the bond-length expression to be used quantitatively. The results are in satisfactory agreement with the experimental data. A number of the approximations used have been discussed critically. It has been shown that the agreement between experimental and calculated bond lengths is independent of quite drastic alterations in some of the uncertain parameters. It has been demonstrated that the simple valence-bond treatment of dipole moments in terms of ionic character leads to the result that a negative sign for  $(r_0 - r_1)$ , i.e. bond contraction, is the only relationship between  $r_0$  and  $r_1$  which is compatible with the conclusions of other authors concerning the change in dipole moment with internuclear separation for the hydrogen halides.

### Introduction

The calculation of the lengths of carbon-carbon bonds in unsaturated molecules by the valence-bond method is now well known due, chiefly, to the work of Pauling<sup>1</sup> and Penney<sup>2</sup> and their collaborators. The position is by no means as satisfactory for the case of molecules which contain covalent bonds between atoms of different electronegativity, i.e. covalent bonds which possess partial ionic character. The valence-bond method treats such molecules in terms of resonance between pure covalent\* and ionic structures. There has already been a certain amount of discussion concerning the effect of this type of resonance on bond length.<sup>3</sup> Some

<sup>1</sup> Pauling, *The Nature of the Chemical Bond* (Cornell University Press), p. 171, *et seq.* Pauling, Brockway and Beach, *J. Amer. Chem. Soc.*, 1935, **57**, 2705.

<sup>2</sup> Penney, *Proc. Roy. Soc. A*, 1937, **158**, 306.

\* A "pure covalent structure" is considered to be one in which all the members of the particular type of bond under consideration in the molecule are "pure covalent bonds." A "pure covalent bond" between the centres A and B is defined as follows. The wave function describing this bond is a conventional Heitler-London function without ionic terms (or, at least, with only small and equal contributions corresponding to  $\overset{+}{A}\overset{-}{B}$  and  $\overset{-}{A}\overset{+}{B}$ ). It is envisaged as an overlapping, without distortion, of the two atomic eigenfunctions concerned, hence, as a first approximation, the bond is assumed to have no dipole moment. It is also assumed that the dissociation energy of such a bond is given approximately by Pauling's geometric mean rule and the normal internuclear separation by the sum of the covalent radii.

<sup>3</sup> Schomaker and Stevenson, *J. Amer. Chem. Soc.*, 1941, **63**, 37.

aspects of this problem have been treated qualitatively by the writer<sup>4</sup> and more recently we have published the results of some calculations of the bond lengths of the hydrogen halides.<sup>5</sup> In the present paper the empirical evidence concerning the effect of ionic character on the lengths of *single* bonds is examined and certain conclusions with regard to covalent radii, particularly for the case of hydrogen, are described. A more extensive and critical discussion of the calculation of the bond lengths in the case of the hydrogen halides, especially with regard to a number of uncertainties in the method, is presented. Some modifications in the earlier method<sup>5</sup> have been made and the results of these improved calculations are given.

Bond length calculations for unsaturated hydrocarbon molecules can, in principle, be carried out in all cases starting from two basic bond lengths, viz. the C—C and the C=C distances. Little uncertainty attaches to the assignment of values to these quantities. This is, unfortunately, not so for instances of resonance between ionic and covalent structures; here, each case considered involves specific values for the normal internuclear separation in the two structures. For pure covalent structures Pauling<sup>6</sup> has suggested the rule of additivity of covalent radii in order to obtain the required internuclear separation for a bond in such a pure state. The usual method for determining the covalent radius of an atom A consists in taking half the A—A distance observed in the diatomic molecule or in a molecule which contains A atoms linked together by a pure covalent bond (or a "normal covalent single bond") unperturbed by resonance with any other type of structure. On this basis, Pauling<sup>6</sup> arrived at the conclusion that partial ionic character had a negligible effect on bond length since the observed lengths of many bonds, e.g. C—F, which possess considerable ionic character, were found to be practically identical with the appropriate covalent radius sums. Cases of bonds deviating from additivity are treated by Pauling in terms of resonance involving multiple-bond structures. However, this view does not seem very plausible if use is made of the revised values for the covalent radii of fluorine, nitrogen and oxygen.<sup>8</sup> Many bonds which conformed to additivity on the basis of Pauling's radii are now accepted to exhibit considerable contractions.

It has been recognized<sup>3, 9</sup> that some of these instances of bond contraction cannot be explained satisfactorily by resonance involving multiple-bond structures and that resonance between ionic and covalent structures also causes a contraction in bond length relative to the sums of covalent radii. This feature is illustrated by Fig. 1 and 2. In Fig. 1 bond contraction, i.e. ( $r_{\text{obs.}}$ —covalent radius sum), is plotted against  $R_{\text{ic}}$ , the extra ionic resonance energy of the bond. This quantity  $R_{\text{ic}}$ , which is a convenient approximate measure of the ionic character of a bond, has been derived in the well-known manner by using Pauling's geometric mean rule,<sup>10</sup> viz. for a bond between atoms A and B,

$$R_{\text{ic}} = D_{\text{AB}} - \sqrt{D_{\text{AA}} \times D_{\text{BB}}}$$

where  $D_{\text{AB}}$  is the observed bond energy and  $D_{\text{AA}}$  and  $D_{\text{BB}}$  the bond energies in the structures A—A and B—B which involve normal covalent bonds. Pauling's bond energy values have been used.

The points shown in Fig. 1 result from a search of the literature for experimental data concerning predominantly covalent *single* bonds which do not involve hydrogen and for which the participation of structures containing multiple bonds between the two atoms is ruled out as far as

<sup>4</sup> Warhurst, *Trans. Faraday Soc.*, 1944, **40**, 26.

<sup>5</sup> Warhurst, *Victor Henri Memorial Symposium* (Liege, 1948), p. 57.

<sup>6</sup> Pauling, *loc. cit.*<sup>1</sup>, Chap. V.

<sup>7</sup> Pauling, *J. Amer. Chem. Soc.*, 1932, **54**, 3570, and 988.

<sup>8</sup> Pauling, *loc. cit.*<sup>1</sup>, pp. 230 and 232.

<sup>9</sup> Burawoy, *Trans. Faraday Soc.*, 1943, **39**, 79.

<sup>10</sup> Pauling *loc. cit.*<sup>1</sup>, p. 50.

possible. Accordingly, data are not included for cases in which empty  $d$  orbitals, likely to be used in multiple bond formation, are available, e.g. in the halides of elements of the second and higher rows of the Periodic Table. In some of the cases shown in Fig. 1 multiple-bond formation

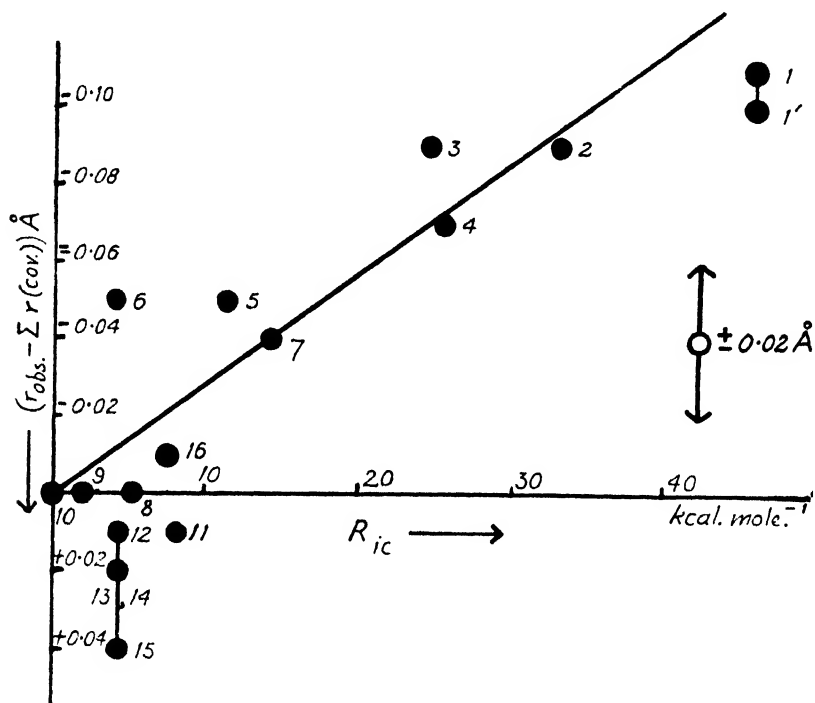


FIG. 1.

The points in Fig. 1 are all obtained from electron-diffraction data, with the exception of 1 which is from a recent spectroscopic value for the C—F bond in  $\text{CH}_3\text{F}$  given by Bernstein and Herzberg, *J. Chem. Physics*, 1948, **16**, 36. The arrows in the figure indicate the uncertainty of the best electron-diffraction measurements ( $\pm 0.02 \text{ \AA}$ ). The experimental observations concern the following molecules:

- |                                       |  |  |
|---------------------------------------|--|--|
| 1'. $\text{CH}_3\text{—F}$ (a)        | 8. $\text{ICl}$ (c)  | 13. $\text{CH}_3\text{N} \begin{smallmatrix} \text{Cl} \\ \text{Cl} \end{smallmatrix}$ (e) |
| 2. $\text{NF}_3$ (b)                  | 9. $\text{CH}_3\text{—Br}$ (a)   | 14. $(\text{CH}_3)_2\text{N—Cl}$ (e)   |
| 3. $\text{CH}_3\text{O—CH}_3$ (a)     | 10. $\text{CH}_3\text{—I}$ (d)   | 15. $(\text{CH}_3)_2\text{N—Cl}$ (a)   |
| 4. $\text{ClF}$ (c)                   | 11. $\text{CH}_3\text{—Cl}$ (a)  | 16. $(\text{CH}_3)_3\text{Si—CH}_3$ (a)  |
| 5. $\text{F}_2\text{O}$ (c)           | 12. $\text{CH}_3\text{N} \begin{smallmatrix} \text{Cl} \\ \text{Cl} \end{smallmatrix}$ |  |
| 6. $\text{Cl}_2\text{O}$ (c)          |  |  |
| 7. $(\text{CH}_3)_2\text{N—CH}_3$ (a) |  |  |

(a) Wheland, *The Theory of Resonance* (John Wiley & Sons, Inc., New York, 1944), Appendix.

(b) Schomaker, unpublished observation quoted by Bauer, *J. Amer. Chem. Soc.*, 1947, **69**, 3104.

(c) Schomaker and Stevenson, *ibid.*, 1941, **63**, 37.

(d) Pauling, *The Nature of the Chemical Bond*, p. 167.

(e) Skinner and Sutton, *Trans. Faraday Soc.*, 1944, **40**, 164.

could be envisaged by introducing structures of the type  $\text{B}^+ = \text{AB}^-$ . It does not seem very plausible, on the grounds of stability, that such structures can make significant contributions in most of the cases given in Fig. 1. For C-halogen bonds participation of this type of structure,

i.e.  $\bar{B}C = \overset{+}{H}al$ , has been rendered extremely unlikely by restricting consideration to the methyl derivatives. Similarly, the structure  $\bar{C}N = \overset{+}{Cl}$  is not considered to participate to an appreciable extent in the molecules  $(CH_3)_3NCl$  and  $(CH_3)_3N \begin{smallmatrix} Cl \\ \diagup \\ Cl \end{smallmatrix}$ , from which the data for the N—Cl bond have been derived.

Fig. 2 shows a similar plot for the X—H bonds of hydride molecules, but, in this case, for reasons which are mentioned later, the quantity  $(r_{obs.} - r_x)$ , i.e. the difference between the observed bond length and the covalent radius of the X atom, has been plotted against  $R_{ic}$ .

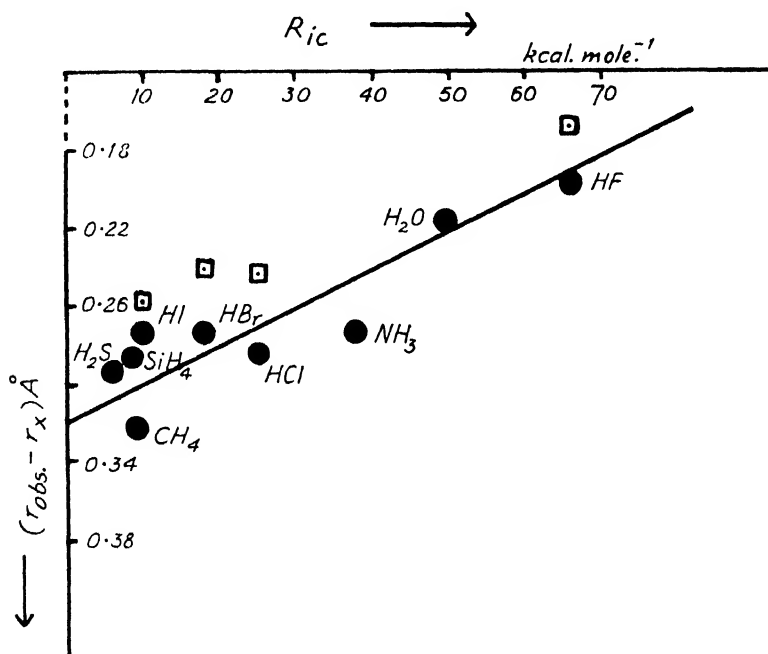


FIG. 2.

All the bond-length data in Fig. 2 are spectroscopic values. Data for HF, HCl, HBr and HI from Herzberg, *Molecular Spectra and Molecular Structure*, Vol. I, *Diatomic Molecules* (Prentice-Hall, Inc., New York, 1939). Data for H<sub>2</sub>O, NH<sub>3</sub>, H<sub>2</sub>S, SiH<sub>4</sub> and CH<sub>4</sub> from Herzberg, *Infra-red and Raman Spectra of Polyatomic Molecules* (Van Nostrand Co. Inc., New York, 1945).

The points indicated □ are the calculated values for the hydrogen halides from Table III.

Fig. 1 and 2 demonstrate a number of points which are of considerable interest.

(1) In the case of the hydride molecules there is no possibility of multiple bonding. In view of this, the very similar trends shown by both Fig. 1 and 2 are considered to add further strong support to the view that multiple bonding plays a negligible part in the molecules which have been used to provide the data of Fig. 1. The data for both sets of molecules are regarded as demonstrating that resonance between ionic and covalent structures causes a contraction in bond length which increases

in magnitude very approximately in a linear manner with increase in ionic character.\*

(2) Fig. 1 and 2 are also considered to provide strong support for the concept of covalent radii, in the sense that a set of radii for atoms can be derived by the method mentioned above (with the exception of hydrogen which is discussed below), the appropriate sums of which do give satisfactory values for the observed bond lengths, provided the ionic character and partial double-bond character of the bonds are negligible. Of course, the number of such cases is small. In other words, the sums of such radii provide a useful basis from which to discuss anomalies in bond length in terms of resonance effects.

(3) The data in Fig. 2 are plotted in such a way that the value of the ordinate for an X—H bond which possesses zero ionic character should correspond to the covalent radius of hydrogen as defined in the last paragraph. The linear trend of the points extrapolates to an intercept of 0.31 to 0.33 Å for  $R_{10} = 0$  and it seems highly unlikely that the extrapolation could tend to an intercept of 0.37 Å. It is concluded, therefore, that the appropriate value for the covalent radius of hydrogen is 0.31 to 0.33 Å and not 0.37 Å as obtained by taking half the internuclear separation in the hydrogen molecule. It is perhaps not so surprising that the method which identifies the covalent radius of an atom with one half the internuclear separation in the diatomic molecule should break down in the case of hydrogen, since in this diatomic molecule there are no electrons present other than the two which constitute the bond. Another factor which may be important in this connection is that the bond in the hydrogen molecule arises from the overlapping of two *s* eigenfunctions. This *s*—*s* type of bond does not occur in any of the molecules dealt with in Fig. 1 and 2, nor does it occur in any of the A—A bonds from which the covalent radii of all the other atoms have been derived.

The choice of a value for the covalent radius of hydrogen affects the details of the calculations of bond lengths in hydride molecules insofar as it influences the values for the normal internuclear separation,  $r_1$ , for the pure covalent structures. Two complete sets of calculations for the hydrogen halides have been made, based on covalent radii of 0.32 Å and 0.37 Å for hydrogen. Most of the details and discussion presented in this paper refer to the former value since, for the reasons given above, it is considered to be by far the more plausible choice. Some results based on the value of 0.37 Å are also given in order to demonstrate that the success of the calculations in reproducing the main features of the experimental data is not dependent on a specific value for this quantity.

Since the observed lengths of covalent bonds which possess partial ionic character are smaller than the corresponding covalent radius sums, and since the latter are invariably smaller than the sums of the appropriate ionic radii, it is clear that resonance between ionic and covalent structures produces the curious consequence that the observed length of such a bond does not lie between the extreme values corresponding to the covalent and ionic structures but has a value which is less than either. An acceptable description of these bonds in terms of resonance of this kind must, therefore, be able to account for this important feature.

The hydrogen halides provide the simplest case for an attack on the problem since other factors such as multiple bonding, changes in hybridization and degeneracy in the ionic state can be excluded from consideration.

\* Schomaker and Stevenson\* arrived at a similar conclusion and expressed this in the form of an empirical relationship. However, the issue does not emerge so clearly from their paper since they applied the relationship to a large number of bonds which probably possess multiple-bond character.



### Derivation of the Bond-Length Equation

Consider the case of a diatomic molecule AB, for which the actual state of the molecule is described in terms of a resonance between a pure covalent state A : B, and an ionic state A<sup>+</sup>B<sup>-</sup>, containing an "extreme ionic bond". Let  $\psi_1$ ,  $V_1$  and  $r_1$ ,  $\psi_2$ ,  $V_2$  and  $r_2$  and  $\psi_a$ ,  $V_a$  and  $r_a$  represent the wave function, potential energy and normal internuclear separation for the covalent state I, the ionic state II and the actual state of the molecule, respectively. The quantities  $r_1$ ,  $r_2$  and  $r_a$  are special values of the general parameter  $r$  and correspond to minimum values of the respective potential energies. The  $\psi$ 's and  $V$ 's are functions of  $r$ , the subscripts merely indicate the state to which these quantities relate. The valence-bond approximation for  $\psi_a$  is then written

$$\psi_a = a_1\psi_1 + a_2\psi_2, \quad . \quad . \quad . \quad . \quad . \quad (0)$$

where  $a_1$  and  $a_2$  are the "participation coefficients" for the two states I and II. If  $\psi_a$  is normalized and  $\psi_1$  and  $\psi_2$  are normalized and assumed to be mutually orthogonal, then the energy of the actual state of the molecule is given by the lower root of the secular equation,

$$V_a = \frac{1}{2}V_1 + \frac{1}{2}V_2 - \left\{ \left( \frac{V_2 - V_1}{2} \right)^2 + W^2 \right\}^{\frac{1}{2}}, \quad . \quad . \quad . \quad (1)$$

where 
$$W = \int \bar{\psi}_1 H \psi_2 d\tau = \int \bar{\psi}_2 H \psi_1 d\tau$$

is the so-called resonance or overlap integral. An alternative form of eqn. (1) is

$$R = -S/2 + \{(S/2)^2 + W^2\}^{\frac{1}{2}}, \quad . \quad . \quad . \quad . \quad (2)$$

where 
$$R = V_1 - V_a \quad . \quad . \quad . \quad . \quad . \quad (2a)$$

is the resonance energy referred to state I and

$$S = V_2 - V_1 \quad . \quad . \quad . \quad . \quad . \quad (2b)$$

is the energy of separation between the two states I and II. Defined in this way  $R$  is always positive. For the hydrogen halides  $S$  is also positive, since  $V_2 > V_1$ .

Corresponding to pure state I we have  $S$  large and positive and  $S \gg W$ . Corresponding to pure state II we have  $S$  large and negative and  $-S \gg W$ .

The resonance integral is given by

$$W = -\{R(R + S)\}^{\frac{1}{2}} \quad . \quad . \quad . \quad . \quad (3)$$

and the participation coefficients are given by

$$1 - a_1^2 = a_2^2 = \frac{R}{2R + S} \quad . \quad . \quad . \quad . \quad (4)$$

From (2) and (4) it is evident that in the transition from a pure state I structure ( $R = 0$ ,  $S = +\infty$ ) to a pure state II structure

$$(R = +\infty, S = -R = -\infty),$$

$a_1^2$  varies without discontinuity from 0 to 1, as expected.

Differentiation of eqn. (1) or (2) with respect to internuclear separation, introduction of the condition  $(dV_a/dr)_{r_a} = 0$ , and the approximation that over the relevant range of  $r$  the potential energies of states I and II can be represented by parabolic functions,

i.e. 
$$\left( \frac{dV_1}{dr} \right)_{r_1} = k_1(r_a - r_1) \quad \text{and} \quad \left( \frac{dV_2}{dr} \right)_{r_2} = k_2(r_a - r_2),$$

leads to the following expression for the bond length  $r_a$ :

$$r_a = r_1 + \frac{1}{\left(\frac{1-a_2^2}{a_2^2}\right)\frac{k_1}{k_2} + 1} \left\{ (r_2 - r_1) + \frac{2W}{k_2 \times R} \times \frac{dW}{dr} \right\}, \quad (5)$$

where  $k_1 = \left(\frac{d^2V_1}{dr^2}\right)_{r_1}$  and  $k_2 = \left(\frac{d^2V_2}{dr^2}\right)_{r_2}$

are the restoring force constants for the pure covalent and ionic bonds, respectively. Using (3) and (4), this equation can be cast into the form,

$$r_a = r_1 + \frac{1}{\left(\frac{R+S}{R}\right)\frac{k_1}{k_2} + 1} \left\{ (r_2 - r_1) + \frac{2}{k_2} \sqrt{\frac{R+S}{R}} \times \frac{d}{dr} \left( -\sqrt{R(R+S)} \right) \right\}. \quad (5a)$$

If it is not assumed that  $\psi_1$  and  $\psi_2$  are orthogonal and the orthogonality integral,  $\int \psi_1 \psi_2 d\tau$ , is denoted by  $\delta$ , then it can be easily shown that differentiation of the more general secular equation gives the following expression for the bond length,

$$r_a = r_1 + \frac{1}{\left(\frac{a_1^2}{a_2^2}\right)\frac{k_1}{k_2} + 1} \left\{ (r_2 - r_1) + \frac{2(W - \delta V_a)}{k_2 R} \times \frac{d}{dr} (W - \delta V_a) \right\}, \quad (5b)$$

and the following relationships hold:

$$\frac{a_1^2}{a_2^2} = \frac{R+S}{R} \quad \text{and} \quad (W - \delta V_a) = -\sqrt{R(R+S)}.$$

It can be seen that substitution of these relationships into (5b) leads to an expression which is identical with (5a). Now the parameters  $R$  and  $S$  are the ones which are most directly available from empirical data and others, such as  $a_1^2$ ,  $W$ , etc., have to be evaluated from these. The values of  $R$  and  $S$ , at  $r = r_a$ , which should be substituted in the bond-length expression are thus independent of the nature of the assumption concerning the orthogonality integral. Hence the fact that, expressed in terms of  $R$  and  $S$ , eqn. (5) and (5b) both reduce to (5a) means that the values of  $r_a$  calculated by the present method are independent of the nature of this assumption. For simplicity the method is discussed in the following sections in terms of the formulation based on the assumption  $\delta = 0$ .

The second derivative of eqn. (1) gives the general expression,

$$\begin{aligned} \frac{d^2V_a}{dr^2} &= (1 - a_2^2) \frac{d^2V_1}{dr^2} + a_2^2 \frac{d^2V_2}{dr^2} \\ &+ \frac{\left(\frac{dV_1}{dr} - \frac{dV_a}{dr}\right) \left(\frac{dV_2}{dr} - \frac{dV_a}{dr}\right)}{R + S/2} - \frac{W \left(\frac{d^2W}{dr^2}\right) + \left(\frac{dW}{dr}\right)^2}{R + S/2}. \end{aligned} \quad (6)$$

Eqn. (6), (1), (2), (3), (4) and (6) hold for all values of  $r$ , eqn. (5) specifically refers to  $r = r_a$ . In using any one of these equations for a particular internuclear separation the values of the parameters should, strictly, refer to that particular value of  $r$ .

Before describing the details of the application of eqn. (5) for the calculation of bond lengths a number of points must be dealt with first.

## The Description of the Ionic State II

The potential energy  $V_2$  and its first and second derivatives with respect to  $r$  have been obtained by the use of the Born and Mayer

expression.<sup>11</sup> Relative to the zero corresponding to dissociation into neutral atoms, to which  $V_a$  and  $V_1$  are also referred, the expression becomes

$$(V_2)_r = e^2 \left\{ -\frac{1}{r} + \frac{\rho \times e^{(r_0 - r)/\rho}}{r_0^2} \right\} + I_H - E_X, \quad (7)$$

where

$e$  = the electronic charge,  
 $I_H$  = the ionization potential of hydrogen,  
 $E_X$  = the electron affinity of the halogen,

and  $\rho$  = a constant, the magnitude of which is discussed below. General expressions for  $(dV_2/dr)_r$  and  $(d^2V_2/dr^2)_r$ , and the specific quantity  $(d^2V_2/dr^2)_r = k_2$  can easily be obtained by differentiation of eqn. (7).

The values obtained previously by the writer<sup>4</sup> for  $r_0$ , the normal inter-nuclear separation in the ionic state, for HCl, HBr and HI have been used in eqn. (7). The same approach applied to HF gives  $r_0 = 1.10 \text{ \AA}$ . Some uncertainty attaches to these values for molecules such as the hydrogen halides, but variations of  $0.10 \text{ \AA}$  in the  $r_0$  values have no marked effect on the calculated bond lengths. Much more drastic changes in the parameters of the ionic state produced by changes in the constant  $\rho$  are discussed below.

From a study of data for alkali metal halides Born and Mayer<sup>11</sup> derived a value of  $0.345$  for the constant  $\rho$ . Some doubt may be felt in the use of this value in eqn. (7) and its derivatives, since the positive ion is a proton. It was considered that the effect of changes in  $\rho$  on the results of the calculations merited careful examination. An indication of the direction in which changes in  $\rho$  ought to be made, compared with the value  $0.345$ , in order to apply more accurately to an ion pair  $H^+X^-$  can be obtained in the following way. Pauling and Wilson consider<sup>12</sup> that one of the excited states of the hydrogen molecule is to be identified with the ionic structure  $H^+H^-$ . This state is characterized by  $r_0 = 1.30 \text{ \AA}$ ,  $\omega_0 = 1338 \text{ cm}^{-1}$  and  $D = 79 \text{ kcal. mole}^{-1}$ , corresponding to dissociation into  $H(2s) + H(1s)$  which gives  $D^1 = 140 \text{ kcal. mole}^{-1}$  for dissociation into  $H^+ + H^-$ . Zener and Kemble<sup>13</sup> and Zener and Guillemin<sup>14</sup> have expressed similar views, although calculations failed to give the degree of ionic character of this state at  $r = r_0$ . Using the Born and Mayer equation, the value of  $\rho$  which gives a reasonable "fit" for both  $D^1$  and  $k_2$  (calculated from  $\omega_0$ ) can readily be found. The result is,  $\rho \sim 0.55$ . It cannot be considered that this value is likely to be the correct one for our calculations, since the exact nature of this excited state of hydrogen is not sufficiently well established. The result, however, does indicate strongly that if the Born and Mayer expression is accepted as a reasonable function to describe the energy of ionic states in which the positive ion is a proton, then a value of  $\rho$  somewhat larger than  $0.345$  should be employed. Accordingly, two completely parallel sets of calculations have been carried out with two different values of  $\rho$ ; one value ( $0.333$ ) being close to the Born and Mayer value, the other ( $0.400$ ) being somewhat greater. The two values of  $\rho$  result in different calculated values for  $V_2$  and its derivatives with respect to  $r$ . The changes in  $V_2$  are relatively small, but for first and particularly second derivatives of  $V_2$  they are quite drastic, in some cases amounting to a factor of two. However, the quantities  $S$ ,  $W$ ,  $k_1$  and  $\gamma$ , and the calculated bond contractions and bond lengths, the evaluations of which depend in various ways on these parameters of the ionic state, turn out to be surprisingly insensitive to the changes in  $\rho$ . This, fortunately, is particularly the case for the bond lengths. The two different values of  $\rho$  produce variations in the calculated bond contractions of less

<sup>11</sup> Born and Mayer, *Z. Physik.*, 1932, **75**, 1.

<sup>12</sup> Pauling and Wilson, *Introduction to Quantum Mechanics* (McGraw-Hill, 1935), p. 354.

<sup>13</sup> Zener and Kemble, *Physic. Rev.*, 1929, **33**, 512.

<sup>14</sup> Zener and Guillemin, *ibid.*, **34**, 999.

than 10 % and variations in the calculated bond lengths of less than 2 % for all the hydrogen halide molecules. Such variations are not regarded as significant in view of the approximate nature of the method. All the results of calculations presented in this paper are based on  $\rho = 0.400$ , which is considered to be the more plausible of the two values.

### The Resonance Energy and the Energy of Separation

The quantities  $R$  and  $S$  as defined by eqn. (2a) and (2b) are dependent on  $r$  and the derivation of values for these two parameters from values of  $V_a$ ,  $V_1$  and  $V_2$  requires some consideration. For substitution in eqn. (5), the appropriate values of  $R$  and  $S$  should strictly refer to  $r = r_a$ . This presents a number of difficulties, one of which arises from the lack of knowledge of certain parameters for the pure covalent state I. For this state Pauling's<sup>8</sup> additivity rule for covalent radii provides an approximate value for  $r_1$ , and his geometric mean rule<sup>10</sup> an approximate value,  $V_{a.m.}$ , for the potential energy which, presumably, should apply to  $r = r_1$ . Nothing further is known concerning this state. The correct \* values of  $R$  and  $S$  for  $r = r_a$  are

$$R = (V_1)_{r_a} - D_0 \quad \text{and} \quad S = (V_2)_{r_a} - (V_1)_{r_a}.$$

But  $(V_1)_{r_a}$ , which is slightly different from  $V_{a.m.}$  since  $r_a \neq r_1$ , is unknown. Further, the evaluation of  $(V_2)_{r_a}$  from eqn. (7) involves a knowledge of  $r_a$ . If considerations are transferred from  $r_a$  to  $r_1$ , for which the value of  $V_1$  is known, i.e.  $V_{a.m.}$ , then the correct values of  $R$  and  $S$  are

$$R = V_{a.m.} - (V_a)_{r_1} \quad \text{and} \quad S = (V_2)_{r_1} - V_{a.m.}$$

It is clear that  $S$  can be evaluated without knowledge of  $r_a$ , but for  $R$  the quantity  $(V_a)_{r_1}$  is slightly different from  $D_0$  and its evaluation by means of, say, a Morse function requires a knowledge of  $r_a$ . These difficulties could be removed by adopting a method of calculation based on successive approximation. Such a method, however, in order to constitute a real improvement on the less rigorous methods described below, would require independent data concerning  $k_1$ ,  $W$  and its dependence on  $r$ . This is not available; indeed these quantities have to be calculated indirectly from  $R$  and  $S$ .

Two alternative approximations for values of  $R$  and  $S$  for use in eqn. (5) have been adopted. The first uses

$$R = V_{a.m.} - D_0 \quad \text{and} \quad S = (V_2)_{r_1} - V_{a.m.}$$

Both  $R$  and  $S$  can thus be evaluated without knowledge of  $r_a$ . The second approximation uses the correct values for  $R$  and  $S$  for  $r = r_1$ , i.e.

$$R = V_{a.m.} - (V_a)_{r_1} \quad \text{and} \quad S = (V_2)_{r_1} - V_{a.m.}$$

In this case the value of  $r_a$  enters into the calculations in a minor way in the evaluation of  $(V_a)_{r_1}$ . The approximate values of  $k_1$ , obtained by a method described in a subsequent section, enable rough estimates to be made of the inaccuracies introduced by use of these approximations. The effect on the calculated bond lengths is relatively small and, furthermore, is offset by another factor arising from the assumption of parabolic potential energy curves for states I and II in the derivation of eqn. (5). This point is discussed in a later section.

### The Form of the Resonance Integral $W^\dagger$

A knowledge of the dependence of  $W$  on internuclear separation in the region  $r \approx r_a$  is required for the evaluation of  $dW/dr$  (and for the

\* The term "correct" is used in the sense that the potential energies for the actual state and states I and II are properly referred to the same value of  $r$ . The values of the potential energy obtained from Morse and Born and Mayer equations are, of course, realized to be approximations.

† If the calculation of bond lengths is approached from the more general standpoint, i.e. it is not assumed that  $\psi_1$  and  $\psi_2$  are orthogonal, then the considerations of the present section concerning the dependence of  $W$  on internuclear separation should be taken to apply to the function  $(W - \delta V_a)$  instead of  $W$ .

less important quantity  $d^2W/dr^2$ ). Any rigorous formulation of such integrals as functions of  $r$  would probably be much too complicated for the present treatment. A more empirical approach has, therefore, been adopted. The problem would be simple if, for a given molecule,  $W$  could be evaluated for a number of values of  $r$ . This is not possible on account of the lack of knowledge concerning the covalent state I. The problem thus presents some difficulty.

A number of qualitative considerations point to the conclusion that in the region  $r \approx r_0$ , as  $r$  increases  $W$  decreases in magnitude, i.e.  $dW/dr$  is positive, since  $W$  is negative. In the first place, the magnitude of  $W$  is related to the spatial overlapping of the wave functions  $\psi_1$  and  $\psi_2$ . This overlapping probably decreases as  $r$  increases, becoming zero at  $r = \infty$ . Secondly, in the treatment of unsaturated hydrocarbon molecules by the valence-bond method, overlap integrals between different valence-bond structures can all be expressed approximately as a numerical coefficient multiplied by  $\alpha$ , the well-known interchange integral for two electrons on adjacent carbon atoms. It does not seem unreasonable to assume that in the region of internuclear separations of the order of covalent bond lengths  $dW/dr$  will have the same sign as the derivatives of the above type of overlap integral, and therefore the same sign as  $d\alpha/dr$ . Likewise the sign of  $d\beta/dr$ , in which  $\beta$  is the molecular-orbital analogue of the integral  $\alpha$ , might reasonably be assumed to indicate the sign of  $dW/dr$ . The integrals  $\alpha$  and  $\beta$  can be related approximately to empirical data, and evaluated over a range of  $r$ , and it is clear from the work of Lloyd and Penney<sup>15</sup> and Lennard-Jones<sup>16</sup> that  $d\alpha/dr$  and  $d\beta/dr$  are both positive. Further evidence for a positive sign for  $dW/dr$  is given below.

As mentioned above, the exact form of  $W$  as a function of  $r$  would doubtless be very complicated. However, the work of Born and Mayer<sup>11</sup> and Pauling<sup>17</sup> has amply demonstrated that over a limited range of internuclear separation the repulsion between two ions, for which a quantum-mechanical treatment with a simple model yields a very complicated and unwieldy expression (see, for example, Pauling's paper<sup>17</sup>) can be adequately represented by a single exponential or a single inverse power term. It is therefore suggested that the dependence of  $W$  on  $r$  in the region  $r \approx r_0$  can be represented sufficiently accurately for present purposes by the expression

$$W_r = W_{r_i} e^{-\gamma(r-r_i)}, \quad (8)$$

in which  $W_r$  and  $W_{r_i}$  are the values of the resonance integral at the internuclear separations  $r$  and  $r_i$ , respectively. There remains the evaluation of the constant  $\gamma$  and the determination of its sign, which the above qualitative considerations indicate to be positive ( $dW/dr$  positive). In the Born and Mayer equation the constant  $\rho$  is found to be the same for a wide variety of ion pairs. As a first approximation the same situation has been assumed to hold for  $\gamma$  in the case of the hydrogen halides. Support for this assumption and further indication that the sign of  $\gamma$  is positive arises from the following considerations. The only value of  $r$  for which  $R$  and  $S$ , and hence  $W$ , can be evaluated correctly is  $r = r_1$ . If, for the four hydrogen halides, the values of  $\log W_{r_1}$ , so obtained are plotted against  $r_1$  the points lie well on a straight line, indicating that these values of  $W$  satisfy an equation of the type (8) with a positive sign for  $\gamma$ .

The assumption has now been made that the value of  $\gamma$  obtained from the slope of this line when used in eqn. (8) represents approximately the dependence of  $W$  on  $r$  in the region  $r \approx r_0$  for each individual hydrogen halide. One crude way of interpreting this assumption is that we consider

<sup>15</sup> Lloyd and Penney, *Trans. Faraday Soc.*, 1939, **35**, 835.

<sup>16</sup> Lennard-Jones, *Proc. Roy. Soc. A*, 1937, **158**, 280.

<sup>17</sup> Pauling, *Z. Krist.*, 1928, **67** (3/4 Heft.), 377.

that the stretching and compressing of, say, the HCl molecule alters  $W$  in a manner given roughly by the variations in  $W$  brought about by changing the HCl molecule into structures resembling the two neighbouring halide molecules. HF corresponding to compression and HBr corresponding to extension. This approach is regarded as no more than a rough approximation, but, failing more rigorous methods, it was considered worthwhile to investigate the consequences of its use in evaluating bond lengths by means of eqn. (5).

### The Force Constant for the Pure Covalent State I

This quantity  $k_1$ , which occurs in eqn. (5), is not obtainable directly from experimental data. In the first method of calculation of bond lengths, described in the next section, the approximation  $k_1 \approx k_a$  has been employed. However,  $k_1$  can be calculated approximately from eqn. (6), the second derivative of the secular equation. For  $r = r_1$ ,

$$(dV_1/dr)_{r_1} = 0, \quad (d^2V_1/dr^2)_{r_1} = k_1$$

and (6) reduces to

$$\begin{aligned} \left( \frac{d^2V_a}{dr^2} \right)_{r_1} &= (1 - a_2^2)k_1 + a_2^2 \left( \frac{d^2V_2}{dr^2} \right)_{r_1} \\ &+ \frac{\left[ \frac{dV_a}{dr} \left( \frac{dV_a}{dr} - \frac{dV_2}{dr} \right) \right]_{r_1}}{R + S/2} - \frac{\left[ W \frac{d^2W}{dr^2} + \left( \frac{dW}{dr} \right)^2 \right]_{r_1}}{R + S/2}, \quad (9) \end{aligned}$$

in which  $R$  and  $S$  can be correctly formulated as

$$V_{G.M.} - (V_a)_{r_1} \quad \text{and} \quad (V_2)_{r_1} - V_{G.M.}$$

respectively. The appropriate values of  $V_a$ ,  $dV_a/dr$  and  $d^2V_a/dr^2$  can be obtained by the use of a potential function, e.g. a Morse function; those for  $V_2$ ,  $dV_2/dr$  and  $d^2V_2/dr^2$  can be obtained from (7);  $W$ ,  $dW/dr$  and  $d^2W/dr^2$  can be obtained from (3) and (8) together with the value of  $\gamma$  determined by the method described in the previous section. The participation coefficient is evaluated from (4). Eqn. (9) thus contains only one unknown,  $k_1$ .

The calculated values of  $k_1$  are shown in Table III. Similar approximate calculations of  $k_1$  have been made using the function suggested by Dunham<sup>18</sup> for the evaluation of the parameters for the actual state of the molecule. The Dunham equation, neglecting powers of  $(r - r_a)$  greater than the fourth, can be written

$$(V_a)_r = \frac{\hbar_a}{2}(r - r_a)^2 \left[ 1 + \frac{\alpha_1}{r_a}(r - r_a) + \frac{\alpha_2}{r_a^2}(r - r_a)^2 \right].$$

The constants of the Dunham equation for the hydrogen halides were taken from the paper of Hulbert and Hirschfelder.<sup>19</sup> This latter method gave values of  $k_1$  which did not differ significantly from those obtained by the use of a Morse function.

Although the method outlined above for the calculation of  $k_1$  is formally correct there are a number of reasons why no great accuracy can be attributed to the results. In the first place,  $d^2W/dr^2$  has to be evaluated by means of the second derivative of eqn. (8), which equation is only regarded, at best, as being able to provide approximate values of  $dW/dr$ . Secondly, the use of Morse or Dunham functions and the Born and Mayer equation for the evaluation of first and particularly second derivatives of energy is not expected to yield other than approximate values. For example, the best available data, by means of which the potential energy of the actual state of the molecule can be formulated, are derived from

<sup>18</sup> Dunham, *Physic. Rev.*, 1932, **41**, 713 and 721.

<sup>19</sup> *J. Chem. Physics*, 1941, **9**, 61.

the vibrational levels of the molecule. For each hydrogen halide molecule the potential energy change  $D_0 - (V_0)_{r_1}$ , corresponding to a change in internuclear separation from  $r_0$  to  $r_1$ , is much smaller than the energy spacing of the lower vibrational levels. This is particularly the case for HCl, HBr and HI. In other words, the formulation of potential energy curves by means of Morse or Dunham functions has to make use of data which is much too "coarse-grained" for present purposes, especially with regard to the evaluation of second derivatives of energy. Accordingly, the calculated values of  $k_1$  are merely regarded as an alternative approximation to the use of  $k_1 \approx k_0$  for the evaluation of bond lengths by means of eqn. (5). Fortunately, there is only a slight difference between the results obtained by the two methods.

### The Calculation of the Bond Lengths

Differentiation of eqn. (8) gives

$$(dW/dr)_r = -\gamma W_r.$$

Substituting this in (5) and using (3) gives the convenient expression :

$$-\Delta = r_0 - r_1 = \frac{1}{\left(\frac{1-a_2^2}{a_2^2}\right)\frac{k_1}{h_2} + 1} \left\{ (r_0 - r_1) - \frac{2\gamma(R+S)}{h_2} \right\}; \quad (10)$$

$\Delta$  may be termed the bond contraction.

The evaluation of the parameters of the right-hand side of this equation has been dealt with in previous sections. The data shown in Table I

TABLE I

Molecule	$-D_0$	$-V_{0.M.}$	$k_0$	$r_0$	$r_0$ (obs.)	$r_H = 0.32$		$r_H = 0.37$	
						$r_1$	$\Delta$ (obs.)	$r_1$	$\Delta$ (obs.)
HF .	147.5	81.0	1385	1.10	0.917	1.04	0.12 <sub>3</sub>	1.09	0.17 <sub>3</sub>
HCl .	102.7	77.3	742	1.50	1.275	1.31	0.03 <sub>5</sub>	1.36	0.08 <sub>5</sub>
HBr .	87.3	69.0	591	1.60	1.414	1.46	0.04 <sub>4</sub>	1.51	0.09 <sub>4</sub>
HI .	71.4	61.2	463	1.75	1.604	1.65	0.04 <sub>8</sub>	1.70	0.09 <sub>8</sub>

Energies are given in kcal. mole<sup>-1</sup>, force constants in kcal. mole<sup>-1</sup> Å<sup>-2</sup> and internuclear separations in Å.

$r_H$  = covalent radius of hydrogen.

have been taken from the following sources.  $D_0$  and  $V_{0.M.}$  from Pauling's book ;<sup>20</sup> values of  $k_0$  have been calculated from fundamental vibration frequencies ;<sup>21</sup> observed internuclear separations have been taken from Herzberg's book ;<sup>22</sup> values of  $r_1$  have been obtained from the covalent radii given by Schomaker and Stevenson,<sup>8</sup> with the exception of the covalent radius of hydrogen, which has been discussed fully in the introduction ; the values of  $r_0$  have been discussed in a previous section of this paper.

### Methods of Calculation of the Bond Lengths

(i) Without introducing the value of  $r_0$  in any way into the calculations, the approximations

$$R = V_{0.M.} - D_0 \quad \text{and} \quad S = (V_0)_{r_1} - V_{0.M.}$$

<sup>20</sup> *Loc. cit.*<sup>1</sup>, p. 52.

<sup>21</sup> Kohlrausch, *Der Smekeal-Raman Effekt* (Springer, 1938), p. 124.

<sup>22</sup> *Molecular Spectra and Molecular Structure*, Vol. I, *Diatomc Molecules* (Prentice-Hall, New York, 1939).

have been used. Using these, approximate values of  $W$  can be obtained by means of eqn. (3). The values of  $\log W$  when plotted against  $r_1$  lie quite well on a straight line giving a value for the constant  $\gamma$  of eqn. (8). The approximation  $k_1 \approx k_a$  has been used. Table II gives the calculated values of  $\Delta$  and  $r_a$  based on  $\rho = 0.400$  and  $0.32 \text{ \AA}$  for the covalent radius of hydrogen. Table IV gives the calculated values of  $\Delta$  and  $r_a$  based on  $\rho = 0.400$  and  $0.37 \text{ \AA}$  for the covalent radius of hydrogen.

TABLE II

Molecule	$R$ (appr.) $V_{0.M.} - D_0$	$S$ (appr.) $(V_0)r_1 - V_{0.M.}$	$-W$	$a_2^{\frac{1}{2}}$	$k_2$	$\Delta$ (calc.)	$\Delta$ (obs.)	$r_a$ (calc.)	$r_a$ (obs.)
HF .	66.5	103.5	106.3	0.281	187	0.137	0.12 <sub>3</sub>	0.90 <sub>3</sub>	0.917
HCl .	25.4	138.4	64.5	0.134	172	0.09 <sub>4</sub>	0.03 <sub>5</sub>	1.21 <sub>6</sub>	1.275
HBr .	18.3	141.1	54.0	0.103	162	0.08 <sub>7</sub>	0.04 <sub>6</sub>	1.37 <sub>3</sub>	1.414
HI .	10.2	148.9	40.3	0.060 <sub>2</sub>	147	0.06 <sub>4</sub>	0.04 <sub>6</sub>	1.58 <sub>6</sub>	1.604

Energies are given in kcal. mole<sup>-1</sup>, force constants in kcal. mole<sup>-1</sup> Å<sup>-2</sup> and internuclear separations in Å.

Born and Mayer constant  $\rho = 0.400$ ;  $\gamma = 1.52$ , from the plot of  $\log W$  against  $r_1$ .

The observed and calculated values of  $r_a$  and  $\Delta$  are based on  $r_H = 0.32 \text{ \AA}$ .

(ii) This method refers the values of all the parameters of eqn. (10) to  $r = r_1$ , for which internuclear separation  $R$  and  $S$  can be "correctly" evaluated. Values of  $W_{r_1}$  are obtained by means of eqn. (3) and a value of  $\gamma$  from the plot of  $\log W_{r_1}$  against  $r_1$ . The calculated values of  $k_1$  are used. The calculated values of  $\Delta$  and  $r_a$  based on  $\rho = 0.400$  and  $0.32 \text{ \AA}$  for the covalent radius of hydrogen are shown in Table III, and the corresponding values of  $(r_a - r_x)$  are plotted in Fig. 2.

TABLE III

Molecule	$R$	$S$	$-W$	$a_2^{\frac{1}{2}}$	$k_1$ (calc.) (Morse)	$\Delta$ (calc.)	$\Delta$ (obs.)	$r_a$ (calc.)	$r_a$ (obs.)
HF .	58.8	103.5	97.7	0.266	1027	0.15 <sub>1</sub>	0.12 <sub>3</sub>	0.88 <sub>9</sub>	0.917
HCl .	25.1	138.4	64.1	0.133	872	0.07 <sub>5</sub>	0.03 <sub>5</sub>	1.23 <sub>5</sub>	1.275
HBr .	17.6	141.1	52.9	0.099 <sub>7</sub>	598	0.07 <sub>8</sub>	0.04 <sub>6</sub>	1.38 <sub>2</sub>	1.414
HI .	9.7	148.9	39.2	0.057 <sub>6</sub>	431	0.06 <sub>1</sub>	0.04 <sub>6</sub>	1.58 <sub>9</sub>	1.604

Energies are given in kcal. mole<sup>-1</sup>, force constants in kcal. mole<sup>-2</sup> Å<sup>-2</sup> and internuclear separations in Å.

Born and Mayer constant  $\rho = 0.400$ ;  $\gamma = 1.44$  from plot of  $\log W$  against  $r_1$ ;  $R$ ,  $S$ ,  $W$  and  $a_2^{\frac{1}{2}}$  refer to  $r = r_1$ .

The observed and calculated values of  $r_a$  and  $\Delta$  are based on  $r_H = 0.32 \text{ \AA}$ .

These calculated values of  $\Delta$  and  $r_a$  given in Tables II, III and IV require correction in two respects. Firstly, as mentioned in a previous section, the correct values of  $R$  and  $S$  for  $r = r_a$  cannot be obtained in a simple manner and both methods of calculation have employed approximations. Secondly, there is the assumption, usually made in calculations of this kind, that the energy curves for states I and II are parabolic over the relevant region of  $r$ . Rough estimates of these two corrections can be made by using the calculated values of  $k_1$ , together with a Morse function, to define an energy curve for state I. The corrections turn out to be opposite in sign and calculations show that allowance for both would not produce modifications in the  $\Delta$  and  $r_a$  values which are likely to exceed



0.03 Å. Since no very great significance is attached to the absolute magnitudes of the calculated values, this is not regarded as serious.\*

TABLE IV

Molecule	R (appr.) $V'_{\text{G.M.}} - D_0$	S (appr.) $(V_2/r_1 - V'_{\text{G.M.}})$	-W	$a_2^2$	$\Delta$ (calc.)	$\Delta$ (obs.)	$r_a$ (calc.)	$r_a$ (obs.)
HF	66.5	103.0	106.1	0.282	0.14 <sub>1</sub>	0.17 <sub>3</sub>	0.94 <sub>9</sub>	0.917
HCl	25.4	136.8	64.2	0.136	0.09 <sub>8</sub>	0.08 <sub>8</sub>	1.26 <sub>2</sub>	1.275
HBr	18.3	140.0	53.9	0.104 <sub>7</sub>	0.09 <sub>0</sub>	0.09 <sub>8</sub>	1.42 <sub>0</sub>	1.414
HI	10.2	148.2	40.2	0.060 <sub>8</sub>	0.06 <sub>8</sub>	0.09 <sub>8</sub>	1.63 <sub>4</sub>	1.604

Energies are given in kcal. mole<sup>-1</sup>, force constants in kcal. mole<sup>-1</sup> Å<sup>-2</sup> and internuclear separations in Å.

Born and Mayer constant  $\rho = 0.400$ ;  $\gamma = 1.55$ , from the plot of  $\log W$  against  $r_1$ .

The observed and calculated values of  $r_a$  and  $\Delta$  are based on  $r_H = 0.37$  Å.

## Discussion

The results given in Tables II, III and IV all show the same general features as the experimental values, i.e. that  $r_a < r_1$  for all four hydrogen halides, and the magnitude of  $\Delta$  is largest for HF, the molecule with the largest ionic character. The agreement between calculated and experimental values is much better for the two extreme cases, HF and HI, than for the two intermediate cases, HCl and HBr.

It has been pointed out previously by the writer<sup>4</sup> that bond contractions could be explained by the resonance integral term of eqn. (5) possessing a negative sign and a greater magnitude than the term  $r_2 - r_1$ . The work described in the present paper adds very strong support to this suggestion. It is interesting to note that, unlike the case of unsaturated hydrocarbon molecules, for resonance between ionic and covalent structures the bond length turns out, in certain circumstances, to be a parameter which behaves like the energy, i.e. for the actual state of the molecule, the value does not lie between those for the two valence-bond structures but is lower than either.

Pauling, Brockway and Beach<sup>1</sup> and Penney<sup>2</sup> have developed by the valence-bond method, general curves connecting the length of carbon-carbon bonds with "percentage double-bond character" and "bond order," respectively. Unfortunately, for the case of ionic-covalent resonance, no general equation connecting bond length with ionic character can be developed, since the quantities  $r_2$ ,  $r_1$ ,  $k_1$  and  $k_2$  are not constant for all molecules which exhibit this type of resonance. However, it is of some interest to examine qualitatively for a given case the behaviour of  $r_a$ , as given by eqn. (5) or (10), for variations in  $a_2^2$  brought about by altering the position of the ionic potential-energy curve relative to that for the covalent state. For the limit,

$$a_2^2 = 0, R = 0 \text{ and } S = +\infty,$$

\* The results for HF shown in Tables II, III and IV are based on the value of 63.5 kcal. mole<sup>-1</sup> for the dissociation energy of F<sub>2</sub>. Recent work (Schmitz and Schumaker, *Z. Naturforsch.*, 1947, 2a, 359, 362) has indicated that 33 kcal. mole<sup>-1</sup> is probably a better value for this quantity. On this basis  $D_0(\text{HF}) = 132.4$  and  $V'_{\text{G.M.}} = 58.4$  kcal. mole<sup>-1</sup>. These changes, however, are found to produce a negligible effect on the calculated values of  $\Delta$  and  $r_a$ . For example, recalculation by method (i) shows that  $\Delta$  is increased by only 0.012 Å. The value of  $W$  is changed by less than 1 %, so the plot for the evaluation of  $\gamma$  is not affected.

corresponding to a pure covalent state, eqn. (5) and (10) reduce to  $r_a = r_1$  and  $dr_a/dS$  is found to be positive. For the limit

$$a_2^2 = 1, \quad R = +\infty, \quad S = -\infty,$$

corresponding to a pure ionic state, the equations reduce to  $r_a = r_2$  and  $dr_a/dS$  is found to be negative. Thus, as the ionic potential-energy curve is lowered from an infinite height above that of the pure covalent state,  $r_a$  first decreases from the initial value of  $r_1$  and as the ionic energy curve recedes to an infinite depth below that of the covalent state, near the limit,  $r_a$  increases towards the value  $r_2$ . Somewhere between these limits  $r_a$  must pass through a minimum. Unfortunately, the expression of  $dr_a/dS$  is rather complicated and a simple generalization concerning the location of this minimum does not appear possible.

The conclusion, arrived at in this paper, that the valence-bond method provides a convincing explanation of the fact that  $r_a$  is less than both  $r_1$  and  $r_2$  finds most striking support in considerations of the dependence of the dipole moment of these molecules on internuclear separation. A more complete treatment of this topic will form the subject of a later publication. In the present paper a brief qualitative discussion is given, insofar as it provides strong evidence for the sign of the quantity  $(r_a - r_1)$ .

The work of Bartholmé<sup>23</sup> and Bell and Coop<sup>24</sup> has indicated that for the molecules HCl, HBr and HI,  $d\mu_a/dr$  at  $r = r_a$  is negative, where  $\mu_a$  is the dipole moment for the actual state of the molecule. The simple valence-bond treatment, i.e. neglecting orthogonality, leads to the following expression for  $\mu_a$ ,

$$\mu_a = a_2^2 \mu_i = a_2^2 e r$$

in which  $\mu_i$  is the moment in the ionic state and  $e$  is the electronic charge. That this simple expression is a fairly satisfactory approximation for the hydrogen halides and a number of other molecules has been demonstrated by Fairbrother,<sup>25</sup> Wall,<sup>26</sup> and Baughan, Evans and Polanyi.<sup>27</sup> By means of eqn. (4), (2a) and (2b) this expression becomes

$$\mu_a = \left( \frac{V_1 - V_a}{\bar{V}_1 + \frac{1}{V_2} - 2\bar{V}_a} \right) e r.$$

Differentiation with respect to  $r$  gives

$$\left( \frac{d\mu_a}{dr} \right)_{r_a} = e a_2^2 \left[ 1 + \frac{r_a}{R} \left\{ (1 - a_2^2) \frac{dV_1}{dr} - a_2^2 \frac{dV_2}{dr} \right\} \right]$$

in which all parameters on the right-hand side assume the values corresponding to  $r = r_a$ . Now  $(dV_2/dr)_{r_a}$  will be negative since  $r_a$  must be less than  $r_2$  for the lower root of the secular equation, which represents the actual state of the molecule. Hence this expression can only give the required negative sign for  $(d\mu_a/dr)_{r_a}$  if  $(dV_1/dr)_{r_a}$  is negative, i.e. if  $r_a$  is less than  $r_1$ , which corresponds to a contraction in bond length relative to the sum of the covalent radii. It is to be noted that this conclusion does not involve any assumptions concerning either the dependence of the resonance integral on internuclear separation or the evaluation of  $r_1$ . Indeed, the above considerations can be regarded as extremely strong evidence for the choice of a positive sign for  $dW/dr$  which has been discussed at an earlier stage in this paper.

If bond contractions are accepted as a general consequence of ionic character (or at least for cases in which this factor is large) then a part, and possibly all, of the contractions observed for the polyhalides of carbon,

<sup>23</sup> Bartholmé, *Z. physik. Chem., B*, 1933, **23**, 131.

<sup>24</sup> Bell and Coop, *Trans. Faraday Soc.*, 1938, **34**, 1209.

<sup>25</sup> Fairbrother, *ibid.*, 1937, **33**, 1507.

<sup>26</sup> Wall, *J. Amer. Chem. Soc.*, 1939, **61**, 1051; 1940, **62**, 800.

<sup>27</sup> Baughan, Evans and Polanyi, *Trans. Faraday Soc.*, 1941, **37**, 377.

silicon, tin, etc., must be attributed to resonance between ionic and covalent structures. Pauling<sup>28</sup> attributes these contractions to the participation of multiple-bond structures. This view requires considerable modification. The treatment of polyhalogenated compounds is complicated by the fact that the ionic state is degenerate. Some calculations on the bond lengths of such compounds will be described in a further publication.

*Chemistry Department,  
The University,  
Manchester.*

<sup>28</sup> *Loc. cit.*<sup>1</sup>, Chap. VII.

---

## SOME APPLICATIONS OF THE VALENCE-BOND METHOD TO PROBLEMS OF MOLECULAR STRUCTURE

### PART II. CALCULATIONS OF THE EFFECT OF SOLVATION ON THE FORCE CONSTANTS OF BONDS WHICH POSSESS PARTIAL IONIC CHARACTER

BY ERNEST WARHURST

*Received 25th November, 1948*

It has been pointed out that the experimental data reveal an approximate linear relationship between the reduction in vibration frequency which occurs when certain gases are liquefied or dissolved in non-ionizing solvents and the logarithm of the dielectric constant of the solvent. The sensitivity of the vibration frequency to changes in dielectric constant has been shown to increase with increase in the ionic character of the bonds concerned. The writer's method<sup>1</sup> for calculating the effect of solvation on force constants has been extended to include changes in bond length resulting from solvation and to include the results of an attempt to formulate the dependence of the resonance integral on internuclear separation. The more complete method has been applied to the cases of HF and HCl. The results of the calculations for HCl are in qualitative agreement with the experimental observations. For HF the agreement is dependent on the nature of certain assumptions in the method.

---

### Introduction

In a previous publication<sup>1</sup> the writer put forward an explanation of the decrease in vibration frequency observed for HCl, HBr and HI when these substances are liquefied or dissolved in non-ionizing media. This entailed considerations of the effect of ionic character on bond-force constants. In the light of the foregoing paper (Part I) on the effect of ionic character on bond lengths it seemed advisable to re-examine some aspects of the force-constant calculations, particularly with regard to certain simplifying assumptions which were made. The following sections consist of a more complete treatment of the force-constant problem together with a critical discussion of some aspects of the method. The treatment has also been extended to include the case of HF, for which the effect of ionic character on bond length is most pronounced.

### The Experimental Data

The reduction in vibration frequency brought about by solvation has been observed for many substances, the molecules of which are usually considered

<sup>1</sup> Warhurst, *Trans. Faraday Soc.*, 1944, 40, 26.

to contain bonds which possess partial ionic character. The solvation of a molecule produces a change in molecular environment. The dielectric constant of the medium surrounding the molecule is increased compared with that for the gaseous state.

In some cases, for example HCl, HF and the OH frequency in  $\text{H}_2\text{O}$ ,  $\text{CH}_3\text{OH}$ ,  $\text{C}_2\text{H}_5\text{OH}$  and  $\text{C}_6\text{H}_5\text{OH}$ , the data in the literature are sufficiently extensive to demonstrate, for each case, an approximately linear relationship between

$$\frac{\Delta\nu}{\nu_{\text{gas}}} = \frac{\nu_{\text{gas}} - \nu_{\text{sol.}}}{\nu_{\text{gas}}}$$

and the logarithm of the dielectric constant  $\epsilon$  of the surrounding medium. The data for some of these molecules show that this holds over a very wide range of

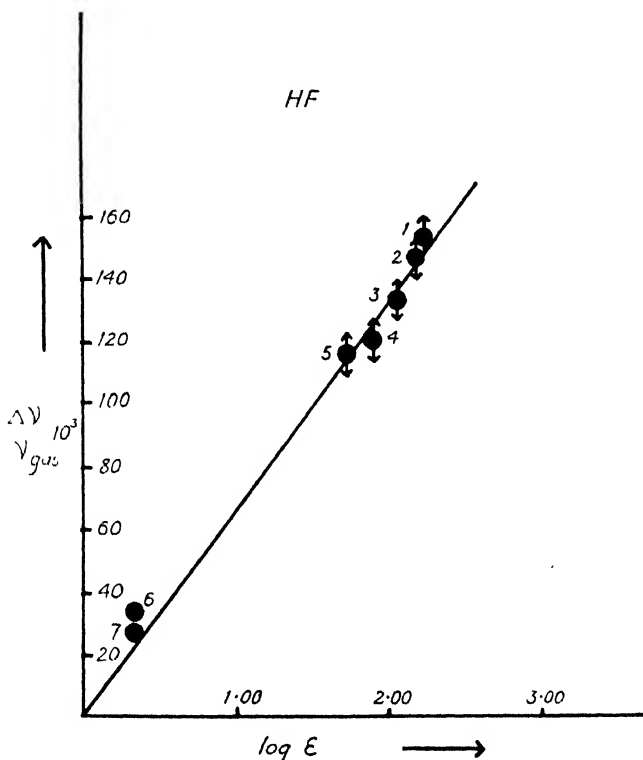


FIG. 1.

Points 1 to 5 are from observations on the  $0 \rightarrow 3$  band of liquid HF in the temperature range  $19^\circ \text{C}$  to  $-75^\circ \text{C}$  by Wahrhaftig (*J. Chem. Physics*, 1940, 8, 350). Values of  $\epsilon$  for this temperature range are taken from Fredenhagen and Dahmlos (*Z. anorg. Chem.*, 1929, 178, 272). Points 6 and 7 are from data given by Bushwell, Maycock and Rodebush (*J. Chem. Physics*, 1940, 8, 362) for dilute solutions of HF in  $\text{CCl}_4$  ( $0 \rightarrow 1$  band).

dielectric constant changes. Graphs illustrating this linear relationship have been constructed from data for the pure liquids at various temperatures and for the sharp monomer band in dilute solutions of the particular substance. For these conditions the nature of the medium surrounding a given solute molecule is known with certainty, i.e. pure solvent and  $\epsilon$  can be given a definite value. This is not necessarily so for solutions which are not dilute; the solvation shell may then consist of both solute and solvent molecules. Fig. 1 and 2, typical

graphs, show the data for HF and HCl.\* This linear relationship which is obtained for all these molecules together with the fact that, for example with HF, the points obtained from observations on the pure liquid, corresponding to a solvation shell of HF molecules and large values of  $\epsilon$ , lie on the same straight line as the points for a dilute solution in  $\text{CCl}_4$ , corresponding to a solvation shell of  $\text{CCl}_4$  molecules and a very small value of  $\epsilon$ , provides in the writer's opinion strong evidence for the essentially electrostatic nature of the intermolecular forces which constitute the hydrogen bond, even in the cases for which this bond is very strong.

The graphs also demonstrate that the sensitivity of the vibration frequency towards dielectric constant changes, as given by the slopes of the lines, i.e.

$$\frac{1}{\nu_{\text{gas}}} \times \frac{d(\Delta\nu)}{d \log \epsilon}$$

increases with increase in the ionic character of the bonds concerned.

### Method of Calculation

The writer has interpreted the effect of the increase in dielectric constant of the surrounding medium resulting from solvation as a lowering

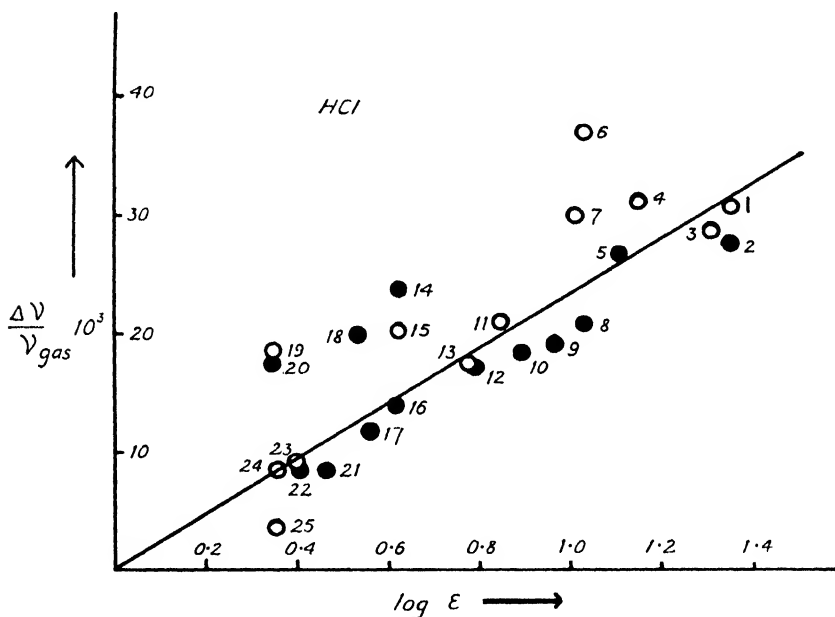


FIG. 2.

The data used in Fig. 2 was taken from the following sources: West and Arthur, *J. Chem. Physics*, 1937, **5**, 10; West and Edwards, *ibid.*, 1937, **5**, 14; West, *ibid.*, 1939, **7**, 795; Plyler and Williams, *Physic. Rev.*, 1936, **49**, 215; Williams, *ibid.*, 1936, **50**, 720. The points denoted by ○ are from measurements of the  $0 \rightarrow 1$  vibration, those denoted by ● from the  $0 \rightarrow 2$  vibration. The solvent and temperature (in °C) of the measurements are indicated below.

1. $\text{SO}_2$ , - 65.	7. HCl, - 90.	13. $\text{C}_6\text{H}_5\text{Cl}$ , + 20.	19. $\text{CCl}_4$ , + 20.
2. $\text{SO}_2$ , - 65.	8. HCl, - 100.	14. $\text{PCl}_3$ , - 65.	20. $\text{CCl}_4$ , + 20.
3. $\text{CH}_3\text{COCl}$ , - 65.	9. HCl, - 72.	15. $\text{PCl}_3$ , - 65.	21. HCl, + 48.
4. $\text{C}_2\text{H}_5\text{Br}$ , - 65.	10. HCl, - 44.	16. HCl, + 25.	22. HCl, + 55.
5. $\text{POCl}_3$ , + 20.	11. $\text{CHCl}_3$ , - 65.	17. HCl, + 35.	23. $\text{SiCl}_4$ , - 65.
6. HCl, - 100.	12. HCl, - 13.	18. $\text{PCl}_3$ , + 20.	24. $\text{C}_6\text{H}_6$ , + 20.
			25. $\text{C}_6\text{H}_6$ , + 20.

\*The points are rather scattered due to, in many cases, experimental inaccuracies arising from the diffuse nature of the bands.

\* A more extensive presentation of the graphs for all these molecules will be given in a later publication. The present paper is concerned with a theoretical treatment of the problem.

of the potential energy of the ionic state, i.e. a reduction in  $S$ , and a consequent increase in resonance energy and ionic character of the bond. In view of the fact that it is known that solvation increases the dipole moments of HCl, HBr and HI this approach seems very plausible.<sup>3</sup> A method was developed for calculating the effect of the increase in ionic character arising from solvation on the force constant of the molecule. The method makes use of the second derivative of the secular equation, eqn. (6), Part I, which for  $r = r_a$  becomes

$$k_a = \left( \frac{d^2 V_a}{dr^2} \right)_{r_a} = (1 - a_1^2) \left( \frac{d^2 V_1}{dr^2} \right)_{r_a} + a_2^2 \left( \frac{d^2 V_2}{dr^2} \right)_{r_a} + \frac{\left( \frac{dV_1}{dr} \times \frac{dV_2}{dr} \right)_{r_a}}{R + S/2} - \frac{\left[ W \left( \frac{d^2 W}{dr^2} \right) + \left( \frac{dW}{dr} \right)^2 \right]_{r_a}}{R + S/2}. \quad (1) \dagger$$

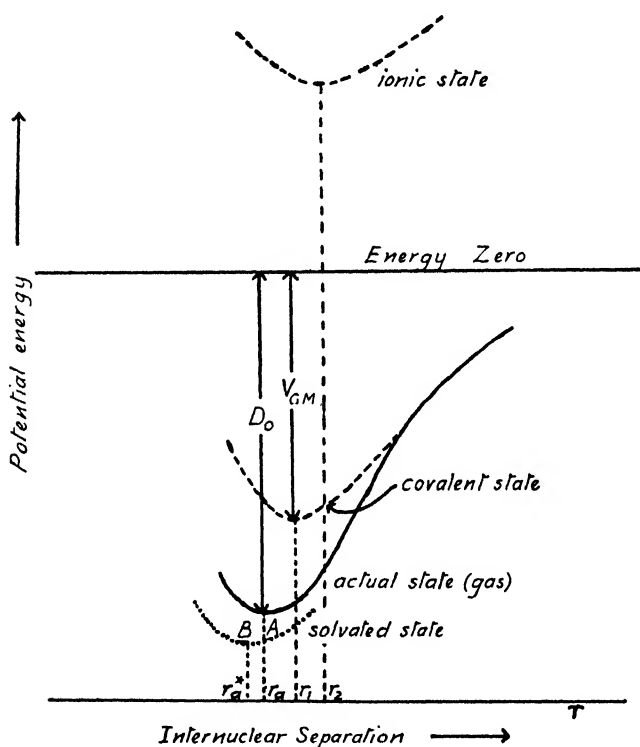


FIG. 3.

The complete calculation of the effect of solvation on the bond force constant can be conveniently dealt with in two stages. Firstly, application of eqn. (1) to the gaseous and solvated states gives the change in second derivative of the potential energy at  $r = r_a$  brought about by solvation

<sup>3</sup> Fairbrother, *Trans. Faraday Soc.*, 1937, **33**, 1507.

† The notation used in this paper is identical with that employed in Part I. In order to avoid confusion it must be pointed out that in the earlier publication<sup>1</sup> the quantities  $\left( \frac{d^2 V_1}{dr^2} \right)_{r_a}$  and  $\left( \frac{d^2 V_2}{dr^2} \right)_{r_a}$  were, unfortunately, abbreviated to  $k_1$  and  $k_2$  respectively.

i.e. the ratio of  $k_a$  to  $\left(\frac{d^2V_a}{dr^2}\right)_{r_a}^*$  can be found, where  $\left(\frac{d^2V_a}{dr^2}\right)_{r_a}^*$  applies to the solvated state and corresponds to point A in Fig. 3. Secondly, if solvation causes any change in bond length, say from  $r_a$  to  $r_a^*$ , and this can be evaluated, then the ratio of  $\left(\frac{d^2V_a}{dr^2}\right)_{r_a}^*$  to the true force constant,  $k_a^* = \left(\frac{d^2V_a}{dr^2}\right)_{r_a^*}^*$ , for the solvated state (corresponding to the point B in Fig. 3) can be calculated by the use of a suitable potential function for the energy of the solvated state.

In the earlier paper dealing with HCl, HBr and HI molecules a number of simplifications were introduced into the method. The calculations were based on Pauling's value of 0.30 Å for the covalent radius of hydrogen. This yields values of  $r_1$  which are very close to the corresponding  $r_a$  values. Hence the conclusion that ionic character, in the case of these compounds, had no effect on bond length was adopted and it was considered reasonable to assume that the further increase in ionic character resulting from solvation would also have no effect on the bond length. Thus

$$k_a^* = \left(\frac{d^2V_a}{dr^2}\right)_{r_a}^*$$

and the third term of eqn. (1) vanishes. Further, with the condition  $r_1 = r_a$ , a plausible argument was advanced which indicated that the magnitude of the fourth term might be negligibly small. Eqn. (1) then reduces to

$$k_a = \left(\frac{d^2V_1}{dr^2}\right)_{r_a} - a_2^2 \left[ \frac{d^3V_1}{dr^3} - \frac{d^3V_1}{dr^3} \right]_{r_a}.$$

It was shown that this simple equation gave results of the correct sign and very roughly the right order of magnitude for the force constant changes.

Returning to the more detailed method, as shown in earlier sections of this paper, there is strong evidence that ionic character shortens a bond relative to the sum of covalent radii. The writer accordingly concludes that if the present interpretation of the solvation of a hydrogen halide molecule, which entails an increase in ionic character, is accepted, then it is reasonable to assume that the solvation probably causes a further contraction in bond length, at least when only small changes in  $a_2^2$  are involved, i.e.  $r_a^* < r_a$ .† An approximate evaluation of  $r_a^*$  can be made by application of eqn. (10) Part I, to the solvated state. Hence, in principle, it is possible to refine the earlier calculations and to calculate the true force constant for the solvated state by evaluating  $\left(\frac{d^2V_a}{dr^2}\right)_{r_a}^*$  from eqn. (1) and from this  $k_a^*$  can be found using the calculated value of  $r_a^*$  and a suitable potential function for the energy of the solvate state.‡ Of the various functions which allow for anharmonicity both the Morse and the Dunham functions have been considered. For these small changes in internuclear separation, i.e.  $r_a - r_a^*$ , the two functions give practically identical results. On the grounds of ease of computation the

† This would not be true if the ionic character of the bond were equal to or greater than the critical value corresponding to a minimum bond length (see the discussion in Part I). This point is referred to again in connection with the results of the force constant calculations for HF.

‡ Since eqn. (10), Part I, only gives approximate results for bond lengths, the calculated values of  $r_a^*$  have been corrected by the factor  $r_a(\text{obs.})/r_a(\text{calc.})$ . Similar considerations apply to eqn. (1) with respect to the quantities  $k_a$  and  $\left(\frac{d^2V_a}{dr^2}\right)_{r_a}^*$ .

Dunham function was chosen with *anharmonicity constants the same as those used for the gaseous molecule*.

This more elaborate method which attempts to allow for changes in bond length consequent upon solvation has been applied to the cases of HF and HCl. The calculations also incorporate the writer's conclusions with regard to the dependence of  $W$ , the resonance integral, on  $r$ , in so far as eqn. (8) of Part I has been used to evaluate approximately the fourth term in eqn. (1). The results are shown in Table I. The calculations are based on values of  $r_1$  derived from the choice of 0.32 Å for the covalent radius of hydrogen and they consist in a determination of the relative magnitudes of  $k_a$ ,  $\left(\frac{d^2V_a}{dr^2}\right)_{r_a}^*$  and  $k_a^*$  for a uniform lowering of the ionic potential energy curve of 20 kcal. The calculations have been carried out using various alternative assumptions concerning the nature of each of the energy curves for the actual state, the solvated state and state I. The alternatives are indicated in columns 2, 3 and 4 of Table I.

TABLE I

Molecule	Covalent State	Gas State	Solvated State	$k_a / \left(\frac{d^2V_a}{dr^2}\right)_{r_a}^*$	$k_a^* / \left(\frac{d^2V_a}{dr^2}\right)_{r_a}^*$	$k_a^* / k_a$	Percentage Change in $k_a^\dagger$
HF	Morse	Morse	Dunham	1.047	1.070	1.022	+ 2.2
HF	Morse	Morse	Parabola	1.047	1.000	0.955	- 4.5
HF	Parabola	Parabola	Parabola	1.040	1.000	0.962	- 3.8
HCl	Morse	Morse	Dunham	1.042	1.019	0.977	- 2.3
HCl	Morse	Morse	Parabola	1.042	1.000	0.960	- 4.0
HCl	Parabola	Parabola	Parabola	1.045	1.000	0.957	- 4.3
HCl †	Morse	Morse	Dunham	1.033	1.019	0.986	- 1.4
HCl †	Morse	Morse	Parabola	1.033	1.000	0.968	- 3.2
HCl †	Parabola	Parabola	Parabola	1.032	1.000	0.969	- 3.1

† These results are based on  $\rho = 0.333$  in Born and Mayer equation. The remainder of the results shown in the Table are based on  $\rho = 0.400$ , which is considered the better of the two alternative values.

‡ Application of Kirkwood's equation (*J. Chem. Physics*, 1934, 2, 351) to the solvation of the dipole of the ionic state II gives the following expression for the lowering of the potential energy of the ionic state :

$$\Delta V_s = - \frac{e^2 r_2^2}{x^3} \left( \frac{\epsilon - 1}{2\epsilon + 1} \right),$$

where  $e$  is the electronic charge,  $\epsilon$  the dielectric constant of the surrounding medium and  $x$  is the radius of the cavity in the medium into which the dipole is placed and within which the dielectric constant is assumed to be unity. This expression with values of  $x$  based on van der Waals' distances of closest approach for the molecules, together with the experimental data of Fig. 1 and 2 enable rough estimates to be made of the percentage decrease in force constant which should result from a lowering of the ionic curve by 20 kcal. The results are—

$$\begin{cases} \text{HF, } x = 1.27 \text{ Å, } \sim 2.8 \% \text{ decrease in } k_a, \\ \text{HCl, } x = 1.65 \text{ Å, } \sim 1.1 \% \text{ decrease in } k_a. \end{cases}$$

With  $x \equiv r_a$  the results are—

$$\begin{cases} \text{HF, } x = 0.92 \text{ Å, } \sim 1.0 \% \text{ decrease in } k_a, \\ \text{HCl, } x = 1.28 \text{ Å, } \sim 0.5 \% \text{ decrease in } k_a. \end{cases}$$

The parameters of the right-hand side of eqn. (1) which are affected by solvation are  $a_s^2$ ,  $R$  and  $S$ . The changes in these brought about by a lowering of the potential energy of the ionic state by 20 kcal. can be obtained from eqn. (2a), (2b) and (4) of Part I. The other parameters, the values of which at  $r = r_a$  are not affected by solvation, have been



evaluated as follows.  $W$  and its derivatives, which are assumed to remain constant, from eqn. (3) and (8) of Part I;  $V_s$  and its derivatives from the Born and Mayer equation (7) of Part I, and  $V_1$  and its derivatives by the use of a potential function for the energy of the covalent state together with values of  $k_1$  calculated by the method described in Part I.

### Discussion

The first point that emerges from the calculations is that, for both HCl and HF,  $\left(\frac{d^2V_a}{dr^2}\right)_{r_a}^*$  is always less than  $k_a$ , independent of the assumptions concerning the nature of the energy curves. The values given in column 5 of Table I are all greater than unity. If the potential-energy curve for the solvated state were parabolic then it would also follow that

$$k_a^* = \left(\frac{d^2V_a}{dr^2}\right)_{r_a}^* < k_a,$$

in agreement with the experimental observations. This result is independent of any changes in bond length consequent upon solvation. However, using an anharmonic function for the solvated state  $k_a^*$  is greater than  $\left(\frac{d^2V_a}{dr^2}\right)_{r_a}^*$  (see column 6 of Table I) and this offsets the above-mentioned decrease in the second derivative of the potential energy. The ratio  $k_a^*/k_a$ , values for which are given in column 7 of Table I, thus depends on the relative magnitudes of these two opposing factors. For HCl the results show that  $k_a^*/k_a$  is always less than unity, in qualitative agreement with experiment. Rough estimates, from the experimental data, of the decrease in force constant resulting from a 20 kcal. decrease in  $V_s$  are given in a footnote to Table I. The quantitative agreement between theory and experiment is not good, but this is not regarded as serious in view of the uncertainties which are involved in the calculations. For HF, when the Dunham function is used for the energy of the solvated state, the ratio  $k_a^*/\left(\frac{d^2V_a}{dr^2}\right)_{r_a}^*$  turns out to be larger than  $k_a/\left(\frac{d^2V_a}{dr^2}\right)_{r_a}^*$  and hence  $k_a^*/k_a$  is somewhat larger than unity, which is contrary to the experimental observations.

It does not seem very plausible that the failure of the method to predict the correct sign for the change in the force constant of the HF molecule indicates that the treatment is not applicable to this case and that the cause of the decrease in the vibration frequency of this molecule must be of a fundamentally different nature from that which operates in the case of HCl, particularly when it is noted that this failure only arises in special circumstances, viz. when the anharmonicity constants applicable to the gaseous molecule are *imposed unchanged on the solvated state*. The great similarity of the experimental data for the two compounds is strong evidence against such a view. The writer is of the opinion that the cause of the discrepancy lies in one or more of the factors which are discussed immediately below.

The most serious of the uncertainties which enter into these force-constant calculations also operate in the evaluation of  $k_1$ , the force constant of the covalent state, and they have thus already been discussed in the section of Part I dealing with the calculation of  $k_1$ . The consequent errors will certainly be much larger for the case of HF than for the case of HCl. For example,  $r_a^* - r_a$  and  $r_a - r_1$  are both much larger in the former case and the assumed potential functions and the first and second derivatives of the secular equation and eqn. (8) Part I have to be relied upon to give estimates of the changes in various parameters over much wider ranges of internuclear separation. Further, the assumption concerning anharmonicity of the potential energy curve of the solvated

state has an important effect on the ratio  $k_a^*/k_a$  since it governs the ratio  $k_a^*/\left(\frac{d^2V_a}{dr^2}\right)_{r_a}^*$ . It is clear that if the increased resonance between the ionic and covalent states in addition to lowering the energy of the actual state of the molecule also reduces the anharmonicity, making the energy curve more parabolic in nature, then the ratio  $k_a^*/\left(\frac{d^2V_a}{dr^2}\right)_{r_a}^*$  would be reduced and this effect might be sufficiently pronounced to result in values of less than unity for the ratio  $k_a^*/k_a$ . It is to be noted in this connection that, in the extreme case, the assumption of a parabolic form for the energy of the solvated state does result in a value of less than unity for this ratio in the case of HF as well as for HCl.

A further reason for the discrepancy may be as follows. It is expected on theoretical grounds, as indicated in Part I, that the perturbation of a given covalent state by an increasing ionic contribution should cause the bond length for the actual state to pass through a minimum. It may well be that the ionic character of HF is very near to the critical value which corresponds to a minimum bond length and that the further increase in ionic character due to solvation has no appreciable effect on the bond length or may even cause a slight increase in bond length. Hence

$$k_a^* < \left(\frac{d^2V_a}{dr^2}\right)_{r_a}^*,$$

in these circumstances. Eqn. (10) Part I, whilst providing a reasonable approximation for the bond length in the gaseous HF molecule, may be too crude an expression to reveal this feature.

It might be argued that any treatment of the solvation of these molecules which entails a decrease in internuclear separation must inevitably result in an increase in force constant on the grounds of such empirical relationships as, for example, Badger's rule.<sup>3</sup> This does not seem to be a valid conclusion in the writer's opinion, since there is no theoretical justification for the general applicability of such rules and, further, none of the series of molecules, to which these rules may be applied successfully, form a sequence which corresponds to a constant pure covalent bond perturbed by varying ionic contributions, which is the situation envisaged in the present treatment of the solvation of a hydrogen halide molecule.

It is concluded that, although the more complete force-constant calculations are rather complicated and uncertain in some respects, the results, particularly for HCl, demonstrate that a decrease in force constant due to solvation and a simultaneous decrease in bond length (which the considerations of Part I indicate to be a probable consequence of solvation) are quite compatible. The nature of the experimental data concerning vibration frequencies discussed at the beginning of Part II and the general features of the observations on bond contractions, illustrated in Fig. 1 and 2 of Part I, are considered to indicate strongly that both these phenomena originate from the same cause, namely, the ionic character of the bonds. The success of the bond-length calculations and the qualitative success of the force-constant calculations (although only of a qualified nature in the case of HF) add further support to this view and provide, in the writer's opinion, adequate justification for the use of Pauling's concept of resonance between ionic and covalent structures in the treatment of certain problems which involve bonds between atoms of different electro-negativity.

*Chemistry Department,  
The University,  
Manchester.*

<sup>3</sup> *J. Chem. Physics*, 1934, **2**, 128; 1935, **3**, 710.

# ELECTRONIC STRUCTURE AND DIPOLE MOMENT OF THE HYPOTHETICAL CROSS-CONJUGATED ISOMER OF CYCLO-OCTATETRAENE

BY G. BERTHIER AND B. PULLMAN

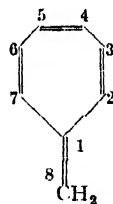
Received 24th November, 1948

The methods of resonance and of molecular orbitals are used to study the molecules of methylenecycloheptatriene and cycloheptatriene itself. It is concluded that electrons tend to move into 5-rings and out of 7-rings. This effect should be revealed experimentally in a study of dipole moments.

The structure of cyclo-octatetraene has been a matter of considerable interest during the last few years.<sup>1</sup> Though the question cannot yet be considered as being definitely settled, either theoretically or experimentally, chemical evidence seems to indicate that this molecule may also react in two other tautomeric forms; namely, as a bicyclo- (2 : 2 : 0)-octa-2 : 4 : 7-triene or a 1 : 2 : 4 : 5-dimethylenecyclohexa-2 : 5-diene. These two isomers differ from the classical form in the number of double bonds present in the molecules. Theoretically there exists also the possibility of two cross-conjugated isomers possessing the same number of double bonds as the classical form. One of those, the *p*-benzoquinodimethane (A) has recently been obtained by Szwarc<sup>2</sup> and its electronic configuration has been studied by Coulson, Craig, Maccoll and Pullman.<sup>3</sup> The other one, the methylenecycloheptatriene (B) does not seem to have been synthesized yet and it is therefore of particular interest to theoretical chemists who seldom find an opportunity of dealing with a simple and yet unknown molecule.



(A)



(B)

The apparent structure of (B) would lead one to suppose that it plays in the case of cyclo-octatetraene a role similar to that played by fulvene in the case of benzene.

The electronic structure of fulvene has been studied recently by the valence-bond (v.b.) and the molecular-orbital (m.o.) methods with much care<sup>4</sup> and the results are as follows. The two methods lead to a similar picture of the distribution of bond orders and free valencies but they disagree completely in the diagram of charge concentration. The v.b. method suggests a uniform charge distribution, similar to that existing

<sup>1</sup> For a review, see Campbell, *Ann. Reports* 1947, **44**, 120, to which may be added a recent paper by Pink and Ubbelohde, *Trans. Faraday Soc.*, 1947, **44**, 708.

<sup>2</sup> Szwarc, *Faraday Soc. Discussions*, 1947, **2**, 45.

<sup>3</sup> *Faraday Soc. Discussions*, 1947, **2**, 36. See also A. Pullman, Berthier and B. Pullman, *Bull. Soc. chim.*, 1948, **15**, 450.

<sup>4</sup> A. Pullman, B. Pullman and Rumpf, *Bull. Soc. chim.*, 1948, **15**, 280, 757; Coulson, Craig and Maccoll, *Proc. Physic. Soc.*, 1948, **61**, 22.

in the more common hydrocarbons, while the m.o. method indicates a non-uniform charge distribution and predicts the existence of a dipole moment. When more precise calculations are carried out, in which account is taken of the variation of the resonance integral with bond length, the theoretical dipole moment is in good agreement with the experimental one measured by Wheland.<sup>5</sup> The charge shift is in the direction going from the external C atom towards the pentagonal ring so that the terminal carbon bears a positive charge while all the others contain an excess of negative electricity.

We have now studied in the same way the structure of (B). In the v.b. calculations use has been made of the set of formulae presented in Fig. 1. When all the monoexcited structures are supposed to have the

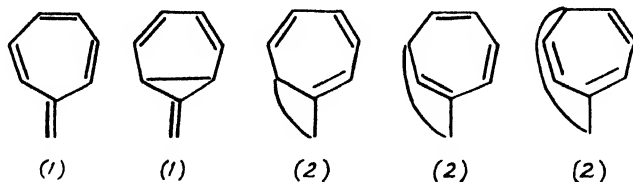


FIG. 1.

same relative weight, the total importance of this group of formulae is 17 %, the Kékulé formula representing thus a contribution of 83 % to the real structure of the molecule. The v.b. molecular diagram<sup>6</sup> indicating the distribution of bond orders and free valencies is given in Fig. 2. The neglect of ionic structures in this v.b. treatment leads to a uniform charge distribution (each C atom having 1 electron around it), which is presumably a very poor result.

In the m.o. calculations an approximate diagram was first constructed with all the resonance integrals uniformly put equal to  $\beta$ . The results obtained together with the presumed relation between carbon-carbon

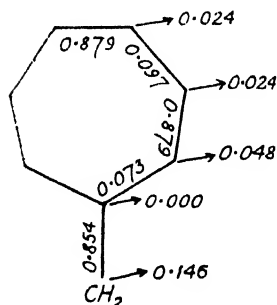


FIG. 2.

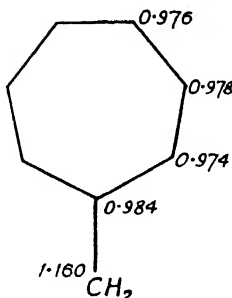


FIG. 3a.

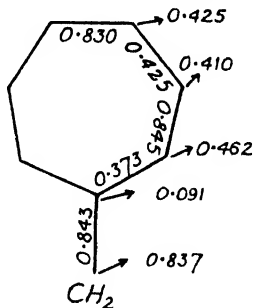


FIG. 3b.

bond length and resonance integral<sup>7</sup> then lead to a second diagram constructed with the assumption that when the resonance integrals of the C=C bonds of (B) are taken equal to  $\beta$ , those of the C—C links should be taken equal to  $0.8\beta$ . Fig. 3a represents then the distribution of electrical charge and Fig. 3b the distribution of bond orders and free valencies.<sup>8</sup>

<sup>5</sup> Reported by Mulliken, *Colloque International sur la Nature de la liaison Chimique* (Paris, April 1948); (*J. Chim. Physique*, in press).

<sup>6</sup> Daudel and A. Pullman, *Compt. rend.*, 1946, **222**, 663; A. Pullman, *Ann. Chim.*, 1947, **2**, 5; Daudel, *Compt. rend.*, 1947, **223**, 946.

<sup>7</sup> Mulliken, Rieke and Brown, *J. Amer. Chem. Soc.*, 1941, **63**, 41.

<sup>8</sup> Coulson, *Proc. Roy. Soc. A*, 1939, **169**, 413; *Faraday Soc. Discussions*, 1947, **2**, 9.

As could have been presumed on account of previous results, the charges are not uniform and the molecule should thus have a dipole moment of the approximate magnitude of 2.35 D. *But the most interesting point is that this dipole moment should lie in a direction opposite to that calculated for fulvene: the external carbon is negative, while all those of the heptagonal ring are positively charged.*

General difficulties which exist in the application of the m.o. method to odd-numbered rings<sup>9</sup> forbid us from considering this result as rigorous. Besides, steric factors may prevent complete planarity and thus reduce the conjugation. But the good agreement found between theory and experiment in the case of fulvene leads to a similar expectation in the case of (B), especially as the field is more "self-consistent" in this last example. The real dipole moment is probably somewhat smaller than the calculated one.

Two further points may be treated in relation to the present results.

(i) THE STRUCTURE OF CYCLOHEPTATRIENE.—It has been shown<sup>10</sup> that the structure of cyclopentadiene is, in a general way, quite similar to that of fulvene. When a proper account is taken of the hyperconjugation of the  $C=H_2$  group, and even when the possible inductive effect

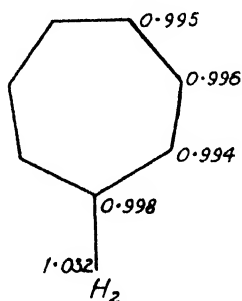


FIG. 4a.

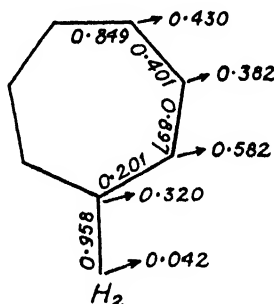


FIG. 4b.

is neglected, there is a charge shift from the methylene grouping towards the pentagonal ring and the resultant dipole moment practically agrees with the experimental one (0.45-0.53 D).<sup>11</sup> The introduction of the inductive effect would raise the theoretical moment.

When similar calculations (hyperconjugation alone) are carried out for cycloheptatriene they indicate a dipole moment *in a direction opposite to that observed in cyclopentadiene*. This is indicated in Fig. 4a (Fig. 4b represents the distribution of bond orders and free valence), constructed (after preliminary calculations) by supposing

$$\begin{aligned}\beta_{C=H_2} &= 2\beta_{C=C} \\ \beta_{C_1-C_2} &= \beta_{C_1-C_7} = 0.6\beta_{C=C} \\ \beta_{C_3-C_4} &= \beta_{C_5-C_6} = 0.8\beta_{C=C}\end{aligned}$$

The corresponding dipole moment would be equal approximately to 0.35 D. It cannot be asserted that this should be the real value and direction of the dipole in this molecule as the inductive effect, which would act in the reverse direction, cannot at present be easily taken into account. But we may say that *the dipole moment of cycloheptatriene should be smaller in absolute value than that of cyclopentadiene and that the probability that*

<sup>9</sup> Coulson and Rushbrooke, *Proc. Camb. Phil. Soc.*, 1940, **36**, 193.

<sup>10</sup> B. Pullman and Berthier, *Bull. Soc. chim.*, 1948, **15**, 551, 788.

<sup>11</sup> Syrkin and Shott-Lvova, *Acta Physicochim.*, 1944, **19**, 379. Hannay and Smyth, *J. Amer. Chem. Soc.*, 1946, **68**, 244.

it is in a reverse direction must be recognized. It should also be mentioned that the results obtained for cyclopentadiene (and for its homologues indene and fluorene) have accounted quite well for the presence and the variation of acid strength in this group of molecules. The total absence of acidic properties in cycloheptatriene may then be explained by the change of polarity, inducing a negative charge on the external  $H_1$ .

(ii) THE STRUCTURE OF AZULENE.—A theoretical study of the electronic structure of this compound <sup>12</sup> led to the conclusion that the molecule should possess a large dipole moment. All the carbons of the pentagonal ring are negative while those of the heptagonal ring are positive. The calculations for fulvene and for (B) throw some light on this problem as they enable us to correlate the charge transfer in azulene with a *fundamental tendency of the mobile electrons to leave heptagonal rings and to concentrate in pentagonal ones*. It may be added that in hexagonal rings even cross-conjugation does not bring about any appreciable charge shift.<sup>3</sup>

Institut du Radium,  
11 Rue Pierre Curie,  
Paris 5.

<sup>12</sup> Coulson and Longuet-Higgins, *Rev. Sci.*, 1947, p. 929. A. Pullman and Berthier, *Compt. rend.*, 1948, **227**, 677.

*Added in Proof:* For further developments see: Berthier and Pullman, Geometrical configuration and dipole moment of conjugated compounds, *Colloque International sur les Polarisabilités Moléculaires* (Paris, April 1949) and *Bull. Soc. Chim.* (in press).

---

## THE ULTRA-VIOLET ABSORPTION OF THE PROTEINS OF THE GROUND NUT (*ARACHIS HYPOGAEA*)

BY A. C. R. DEAN

*Received 20th December, 1948*

The ultra-violet absorption of the globulins of the ground nut has been examined at pH 7.3 and 11.0. "Mixed protein" (total globulins of Johns) and arachin have identical spectra. This agrees with Johnson's ultracentrifugal evidence that they are equilibrium states of the same molecule. Variations in pH within the experimental range cause reversible changes in the absorption. This has been shown to be due to the ionization of the tyrosine groups in the protein molecule.

Extinction coefficients calculated in terms of the tyrosine, tryptophane and cystine present do not agree quantitatively with the observed absorption of arachin. The discrepancies in the tryptophane content of the protein as determined by various workers have been discussed in relation to its absorption. The absorption of conarachin at pH 7.3 can be explained in terms of the tyrosine, tryptophane and cystine present but at pH 11.0 there is no agreement. At pH 7.3 the spectra of conarachin and archin are similar, but not identical, whilst at pH 11.0 the spectra have little resemblance.

---

The globulins of the ground nut were first investigated by Ritthausen <sup>1</sup> and later by Johns and Jones,<sup>2</sup> who have shown that they can be extracted from oil-free ground nut meal with sodium chloride; the latter workers

<sup>1</sup> Ritthausen, *Arch. Ges. Physiol.*, 1880, **21**, 81.

<sup>2</sup> Johns, Jones *et al.*, (a) *J. Biol. Chem.*, 1916, **28**, 77; (b) *ibid.*, 1917, **30**, 33; (c) *ibid.*, 1918, **36**, 491; (d) *ibid.*, 1924, **62**, 183.

claim to have isolated two globulins, arachin and conarachin, from these extracts. In a more detailed investigation Jones and Horn<sup>3</sup> have stated that arachin could be isolated by dilution of the sodium chloride extract and subsequent acidification, or by 40 % saturation with ammonium sulphate, whilst conarachin could be isolated by dialysis of the filtrate from the arachin precipitation. More recently Johnson<sup>4</sup> in the course of a study of these globulins by ultracentrifugal methods has shown that these two procedures do not yield the same product. Dilution followed by acidification produces a protein having two sedimenting species, whilst 40 % saturation with ammonium sulphate results in one sedimenting species only. This paper reports the results of an investigation of the ultra-violet absorption of the globulins isolated by this method, the fraction containing two sedimenting species being referred to as "mixed protein" and that with one sedimenting species as arachin.

### Experimental

**Apparatus.**—The spectra were measured between 2200 and 3200 Å with a Hilger Medium Quartz Spectrograph fitted with a Spekker spectrophotometer and using a tungsten steel arc as light source. The wavelength scale on the instrument was standardized against the spectra of the mercury and copper arcs, these being compared with the data of Plotnikow<sup>5</sup> for mercury and against a photograph of the copper spectrum supplied by Hilger.

**Extraction of Mixed Protein.**—50 g. oil-free ground nut meal was shaken with 250 ml. 10 % aqueous sodium chloride overnight, centrifuged, and the clear liquid filtered and diluted to 1 l. with distilled water and left overnight. The precipitated protein was centrifuged, washed with distilled water, and dried *in vacuo* over calcium chloride.

**Extraction of Arachin.**—The sodium chloride extract of ground nut meal was 40 % saturated with ammonium sulphate, centrifuged, and the precipitate washed with distilled water and then dialyzed in a cellophane tube against running water and finally against distilled water until free from sulphate and chloride. The protein was dried in the same way as mixed protein.

**Extraction of Conarachin.**—The filtrate left after the precipitation of the arachin with ammonium sulphate was allowed to stand overnight, filtered, and the filtrate dialyzed as with arachin. Dialysis was continued until the conarachin separated out (2-3 days). During this period the surface of the liquid was covered with toluene to inhibit bacterial growth. The conarachin was dried in the same manner as the other proteins.

The purity of mixed protein, arachin and conarachin was determined by nitrogen analysis. All contain 18.2-18.3 % N.

**Amino Acids.**—Samples supplied by B. D. H. and Ashe were used and were recrystallized where necessary until the same sample showed no difference in absorption after successive recrystallizations.

**Preparation of Solutions.**—Mixed protein was examined in 10 % aqueous sodium chloride solution at pH 5.5 and in phosphate buffer at pH 7.3 and 11.0. In all cases the pure solvent was used in the compensating cell of the photometer. Solutions were examined 2½ hr. after preparation, and pH's were determined with a glass electrode immediately before and after the spectroscopic examination.

**Calculation of Results.**—The Bunsen-Roscoe extinction coefficient was used throughout, i.e.

$$E = \frac{1}{cd} \log_{10} \frac{I_0}{I_{\infty}}$$

where  $c$  = concentration in g./ml. ;

$d$  = thickness in cm. ;

$I_{\infty}$  = intensity of transmitted radiation (of original intensity  $I_0$ ) after passing through the solution.

<sup>3</sup> Jones and Horn, *J. Agric. Res.*, 1930, **40**, 673.

<sup>4</sup> Johnson, *Trans. Faraday Soc.*, 1946, **42**, 36.

<sup>5</sup> Plotnikow, *Photochemische Versuchstechnik* (Leipzig, 1912), p. 277.

## Results

The absorption curves for mixed protein, arachin and conarachin are given in Fig. 1 and 3. Since the absorption of mixed protein was similar at pH

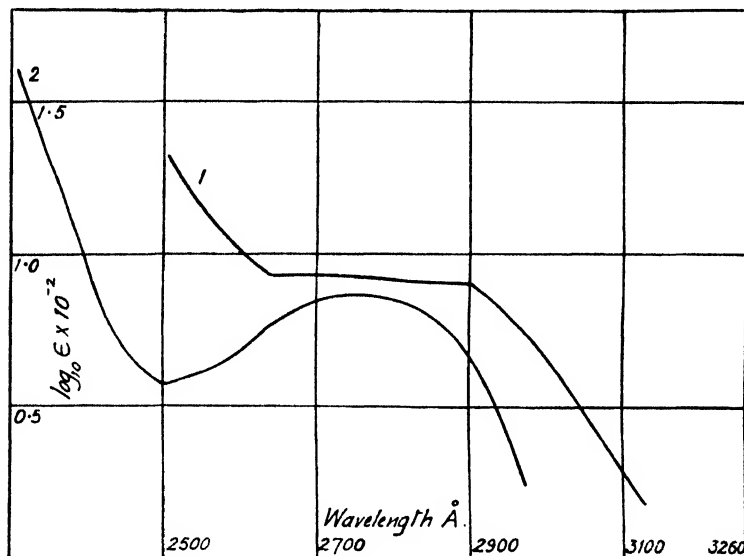


FIG. 1

Mixed Protein or Arachin

1. pH 11.0 2. pH 7.3

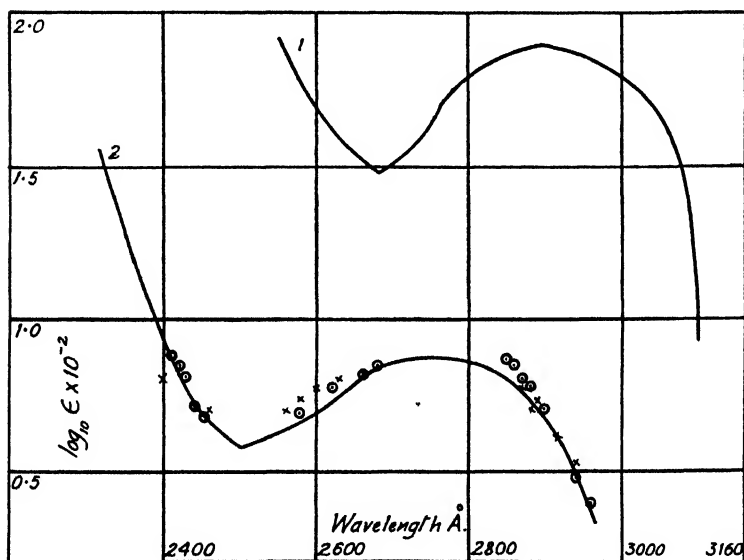


FIG. 2

1. Tyrosine pH 11.0

2. Mixed Protein pH 7.3

x = Protein at pH 12.5 reduced to pH 3.0

o = Protein at pH 7.3 increased to pH 12.0 and then reduced to pH 8.0



5.5 and 7.3 the absorption curves for arachin and conarachin were determined at pH 7.3 and 11.0 only.

Mixed protein has a typical protein absorption curve with a minimum at 2500 Å and a maximum at 2740-2760 Å at pH 7.3. At pH 11.0 the absorption is increased, the minimum tends to disappear, the maximum is flattened out and the whole curve is shifted towards higher wavelengths. This change with increasing alkalinity was shown to be reversible by dissolving mixed protein in sodium hydroxide at pH 12.5 and reducing the pH to 3.0 immediately with hydrochloric acid, and by dissolving the protein in phosphate buffer at pH 7.3,

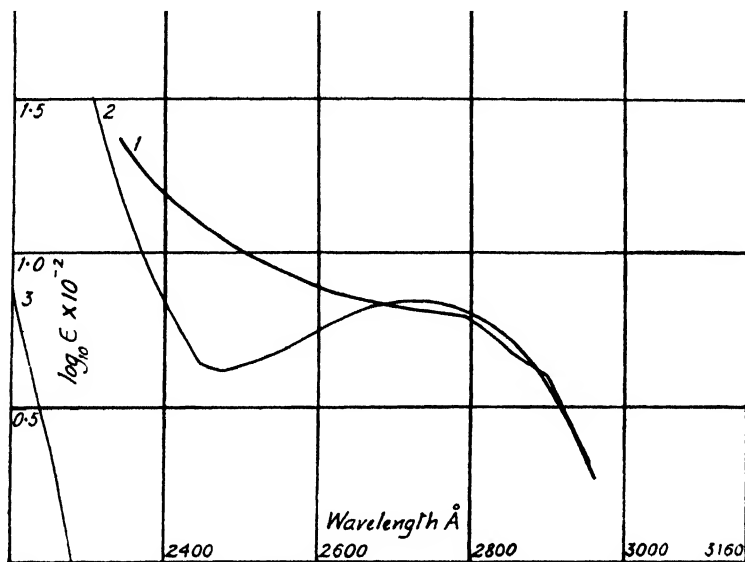


Fig. 3

1. Conarachin pH 11.0
2. " pH 7.3
3. Arginine, Aspartic Acid, Glutamic Acid and Lysine pH 7.3 and 11.0

increasing the pH to 12.0 and immediately reducing it to pH 8.0. In both cases the ultra-violet absorption agreed substantially with the values previously obtained at pH 7.3 (Fig. 2). Exact agreement was not to be expected since the stability limit of the protein molecule is pH 11.0.

Arachin has a similar absorption curve to mixed protein at pH 7.3 and 11.0. The absorption curve for conarachin resembles that for arachin at pH 7.3, whilst at pH 11.0 the curve flattens out but the shift towards higher wavelengths is not as great (Fig. 3).

## Discussion

**The Identical Ultra-Violet Absorption of Mixed Protein and Arachin.**—Mixed protein and arachin have practically identical ultra-violet absorptions at pH 7.3 and 11.0. This is readily understood by a consideration of the methods of extraction and the amino acid content of the fractions. The ground nut globulins are extracted with aqueous sodium chloride and from the extract Johns and Jones<sup>2</sup> obtained by dilution, either with or without acidification, a fraction which they called total globulins. By treatment of the sodium chloride extract with ammonium sulphate another fraction, arachin, was obtained. These fractions are identical with the mixed protein and arachin respectively of this paper. Later Jones and Horn<sup>3</sup> claimed that arachin was obtained both by acidification and by ammonium sulphate precipitation, but

Johnson,<sup>4</sup> using ultracentrifugal technique, has shown that these fractions are not identical. He showed that the fraction obtained by dilution contained two sedimenting species, with sedimentation constants 14.6 and 9.5, and that obtained by ammonium sulphate precipitation contained only one sedimenting species, with sedimentation constant 14.6. Moreover, the slower sedimenting species had its origin in the dissociation of the larger molecule, the degree of dissociation depending on the extent of dilution.

Kotasthane and Narayana<sup>6</sup> and Milone and Everitt,<sup>7</sup> using all these methods to isolate mixed protein and arachin, have examined their nitrogen content and amino acid composition. Their results are given in Table I and it will be seen that the nitrogen content and amino acid

TABLE I.—THE AMINO ACID COMPOSITION OF THE GROUND NUT GLOBULINS

Amino Acid	Mixed Protein	Arachin	Conarachin	Reference
Arginine . .	13.26-13.68	13.55-13.96	13.07-14.10	8
Aspartic acid . .	—	5.25	—	2c
Cystine . .	1.24-1.42	0.85-1.17	1.57-1.64	9
Glutamic acid . .	—	16.69	—	2c
Histidine . .	1.58-1.67	1.88-1.92	1.83-1.99	2b
Leucine . .	—	3.88	—	2c
Lysine . .	4.49-4.69	4.35-4.98	4.82-6.04	8
Phenylalanine . .	—	2.60	—	2c
Proline . .	—	1.37	—	2c
Tryptophane . .	0.58-0.66	0.66-0.69	0.93-1.07	8
	—	1.80	1.78	9
Tyrosine . .	4.80-5.48	5.43-5.69	3.09-3.23	8

Figures refer to percentage of dried protein.

Mixed protein, arachin and conarachin contain 18.1-18.3 % total N.

composition of these fractions are practically identical. Since the ultra-violet absorption of proteins has been explained by various authors in terms of their amino acid composition it is not surprising that the absorption spectra of mixed protein and arachin should be identical. As was suggested by Johnson,<sup>4</sup> the name arachin used by Jones and Horn<sup>3</sup> to designate both fractions is satisfactory, since both are identical chemically and differ only in molecular weight, the difference being due to dissociation of the larger molecule. This dissociation has no effect on the ultra-violet absorption.

#### Amino Acid Composition and Absorption Spectrum of Arachin.—

It is well known that the ultra-violet absorption of aliphatic amino acids is slight and continuous, whilst that of aromatic amino acids is much greater and is selective. Of the amino acids in arachin (Table I), leucine and proline do not absorb beyond 2330 and 2362 Å respectively,<sup>8</sup> histidine beyond 1950 Å,<sup>9</sup> whilst a mixture of arginine, aspartic acid, glutamic acid and lysine does not absorb beyond 2280 Å (Fig. 3). Obviously any absorption above 2500 Å is not due to these acids. Cystine in acid and alkaline solutions absorbs continuously between 2200 and 3000 Å, but this absorption is very slight.<sup>6</sup> The aromatic amino acids, phenylalanine, tyrosine and tryptophane, absorb strongly in the same region as the protein band. Coulter<sup>5</sup> has shown that absorption in proteins above 2500 Å is due to these aromatic amino acids, phenylalanine absorbing between

<sup>6</sup> Kotasthane and Narayana, *Proc. Indian Acad. Sci. B*, 1937, 376.

<sup>7</sup> Milone and Everitt, *Proc. Soc. Expt. Biol. Med.*, 1942, 51, 82.

<sup>8</sup> Ley and Arends, *Z. physik. Chem. B*, 1932, 17, 177.

<sup>9</sup> Coulter, Stone and Kabat, *J. Gen. Physiol.*, 1936, 19, 739.

2530 and 2690 Å and being responsible for only a small part of the absorption in terms of amount rather than spectral extent. Much of the larger part between 2700 and 2900 Å is due to tyrosine and tryptophane. Clearly any absorption above 2600 Å should be due mainly to tyrosine, tryptophane and cystine. The absorption of phenylalanine<sup>10</sup> and tryptophane<sup>11</sup> alters very little with changing pH; the absorption of tyrosine, however, increases greatly, and the maximum is shifted to higher wavelengths, with increasing alkalinity. This change is due to progressive ionization of the hydroxyl group, and is reversible.<sup>10</sup> It will be remembered that by reducing the pH from 11 to 7.3 it was possible to restore the absorption curve to its original position. These changes clearly depend on the amount of phenoxide ion of tyrosine present.

Can the absorption spectrum of arachin be quantitatively explained in terms of these absorbing amino acids? Arnold and Kistiakowsky<sup>12</sup> have shown why amino acids should retain their spectral character in the protein molecule, and Crammer and Neuberger<sup>11</sup> have been able to explain the absorption of insulin between pH 1 and 13 in terms of its absorbing amino acids. They were unable to explain the absorption of egg albumin, however, since the tyrosine groups in this protein are not free to ionize to the same extent as in the free amino acid.

The arachin molecule, assuming Johnson's molecular weight of 396,000, contains 14 to 20 cystine groups. The extremes in the analytical figures for tyrosine permit 119 to 125 tyrosine residues per molecule for arachin and 105 to 119 residues for mixed protein. With tryptophane the results of Kotasthane<sup>6</sup> and Milone<sup>7</sup> differ greatly, and permit 13 and 35 groups per molecule respectively. Extinction coefficients were calculated for the arachin molecule at pH 7.3 and 11.0 in terms of both tryptophane values, the extremes and a mean value for tyrosine and 20 cystine groups. They appear in Table II. The absorption of cystine above 2600 Å is very slight and the difference in the extinction coefficients when 14 or 20 groups are used is insignificant. Since the hydroxyl group of tyrosine is not ionized at pH 7.3 ( $\text{OH pK} = 10.15$ <sup>11</sup>), the values of Crammer and Neuberger at pH 1 were used, and the absorption of tryptophane at pH 7.3 and 11.0 was obtained from their values by extrapolation. The data of Ley and Arends were used for cystine and the absorption of tyrosine at pH 11.0 was obtained from Fig. 2.

At pH 7.3 the calculated and experimental values differ widely at all wavelengths when 13 tryptophane groups are assumed. With 35 groups per molecule the agreement is much better, thus confirming the estimation of Milone and Everitt. At this pH tyrosine absorbs mainly between 2700 and 2900 Å, and over this range the agreement is best with 105 tyrosine groups per molecule, though increasing this to 125 groups per molecule increases the absorption by only about 5%. Assuming 105 tyrosine and 35 tryptophane groups, the calculated values are too low from 2600 to 2650 Å and at 2900 Å, correct at 2700 and 2850 Å, and too high at the maximum, 2750 to 2800 Å. Below 2700 Å phenylalanine would be absorbing, and would account for the low calculated values, but between 2700 and 2850 Å tyrosine and tryptophane are not absorbing in the protein to the expected extent.

At pH 11.0 the calculated results are much too low from 2600 to 2750 Å, fairly good agreement being reached between 2800 and 3000 Å only. This excessive absorption diminishes slowly from 2600 to 2700 Å and then very rapidly from 2700 to 2800 Å. Phenylalanine again may be responsible at the lower wavelengths, but this cannot explain the anomaly in the region 2700 to 2800 Å since no absorption bands due to it have been reported above 2700 Å.<sup>9</sup> The solutions at pH 11.0 were much darker

<sup>10</sup> Stenstrom and Reinhard, *J. Physic. Chem.*, 1925, **29**, 1477.

<sup>11</sup> Crammer and Neuberger, *Biochem. J.*, 1943, **37**, 303.

<sup>12</sup> Arnold and Kistiakowsky, *J. Amer. Chem. Soc.*, 1932, **54**, 1713.

in colour than at pH 7.3 and there is evidence that phosphate buffer accelerates the oxidation of tyrosine.<sup>13</sup> Such pigment production may contribute towards the excessive absorption, the effect being masked above 2800 Å due to the strong absorption of the phenoxide ion of tyrosine. The maximum of tyrosine at pH 11.0 is 2900 Å. It is significant that the experimental values are still higher than the calculated values at 3000 Å, the region where pigment corrections are usually calculated, and tyrosine is still absorbing strongly at this wavelength.

TABLE II.—MOLAR EXTINCTION COEFFICIENTS OF ARACHIN.

		A	2600	2650	2700	2750	2800	2850	2900	2950	3000
pH 7.3	$\epsilon \times 10^{-5}$	Found	1.90	2.42	2.87	2.93	2.81	2.48	1.83	—	—
		Calc.	1. 1.07	1.44	1.90	2.19	2.14	1.50	0.67	—	—
			2. 1.76	2.31	2.88	3.20	3.34	2.52	1.48	—	—
			3. 1.72	2.22	2.78	3.15	3.21	2.44	1.46	—	—
			4. 1.82	2.38	2.99	3.30	3.45	2.59	1.49	—	—
			5. 1.54	1.96	2.39	2.70	2.78	2.08	1.42	—	—
pH 11.0	$\epsilon \times 10^{-5}$	Found	3.96	3.37	3.41	3.33	3.29	3.25	3.19	2.53	1.78
		Calc.	2. 2.18	2.09	2.25	2.64	3.24	3.15	2.90	2.13	1.60
			3. 2.08	2.03	2.19	2.56	3.12	3.01	2.75	1.98	1.63
			4. 2.27	2.15	2.30	2.71	3.35	3.27	3.04	2.25	1.85

1. 13 tryptophane, 116 tyrosine and 20 cystine groups per molecule.

2. 35 " 116 " 20 " " "

3. 35 " 105 " 20 " " "

4. 35 " 125 " 20 " " "

5. 35 " 70 " 20 " " "

TABLE III.—MOLAR EXTINCTION COEFFICIENTS OF CONARACHIN

		A	2600	2650	2700	2750	2800	2850	2900	2950
pH 7.3	$\epsilon \times 10^{-5}$	Found	0.97	1.10	1.18	1.17	1.11	0.92	0.60	0.36
		Calc.	0.66	0.91	1.03	1.10	1.18	0.93	0.61	0.28
pH 11.0	$\epsilon \times 10^{-5}$	Found	1.29	1.17	1.12	1.09	1.02	0.81	0.68	0.37
		Calc.	0.75	0.69	0.84	0.97	1.17	1.09	0.58	0.28

15 tryptophane, 30 tyrosine and 11 cystine groups per molecule.

The stability limit for the arachin molecule appears to be pH 11.0. At higher alkalinity it is degraded into polydisperse fractions of low molecular weight ( $M$  less than 10,000),<sup>4</sup> and for this reason the absorption was not determined above pH 11.0.

**The Ultra-Violet Absorption Spectrum of Conarachin.**—Conarachin, the fraction isolated by Johns, Jones and co-workers by dialysis of the filtrate after precipitation of the arachin with ammonium sulphate, has a similar, but not identical, absorption to arachin at pH 7.3, but at pH 11.0 the absorption and the shift of the band towards higher wavelengths are not so great. In the ultracentrifugal examination of this fraction the sedimentation diagrams were ill-defined but the crude sedimentation constant was in reasonable agreement with that for the slower sedimentating species in mixed protein produced by the dissociation

<sup>13</sup> Bowman, *J. Biol. Chem.*, 1941, **141**, 877.

of the larger arachin molecule.\* On the basis of a molecular weight of 170,000 conarachin should contain 30 tyrosine, 11 cystine and 15 tryptophane groups per molecule, taking the higher tryptophane content of Milone as correct.

Extinction coefficients calculated with this amino acid composition are in agreement with the experimental values at pH 7.3 except in the region of the spectrum below 2700 Å where phenylalanine would again be absorbing. At pH 11.0 the calculated absorption is too low over the entire spectrum except between 2800 and 2850 Å. The high experimental values can be attributed to the same causes as in the case of arachin.

In conclusion it will be seen from Table I that arachin and conarachin are very similar with regard to amino acid composition, differing only in tyrosine and cystine content. Cystine has little effect on the absorption. At pH 7.3 the absorption of conarachin above 2700 Å can be explained in terms of the tyrosine, tryptophane and cystine present, whereas no such agreement is found for arachin using either the reported analytical data for tyrosine (4.8-5.7 %) or the content which has been found to give agreement in the case of conarachin (3.2 % tyrosine) (Table II, No. 5).

If conarachin is identical with the slower sedimenting species produced by the dissociation of the larger arachin molecule, this dissociation must take place in such a manner that conarachin has a lower percentage of tyrosine than arachin.

The author wishes to express his appreciation to Dr. F. D. Miles for helpful discussion and criticism and to Mr. H. Hutchinson for experimental assistance. Acknowledgements are due to the directors of I.C.I. (Nobel Division) for permission to publish the paper.

*Research Department,  
The British Drug Houses Ltd.,  
London W. 1.*

## THE HOMOGENEOUS DECOMPOSITION OF ETHYL NITRATE

BY G. K. ADAMS AND C. E. H. BAWN

*Received 4th December, 1947; as revised 14th January, 1949*

The gaseous decomposition of ethyl nitrate over the temperature range 180-215° C obeys the first-order law,  $k = 10^{15.8} e^{-39.9/RT}$ . It is suggested that the primary step in the decomposition is the breaking of the  $C_2H_5O-NO_2$  bond and that the measured activation energy corresponds to the  $-O \cdots NO_2$  bond strength. The ethoxy fragments react to form acetaldehyde which is subsequently oxidized to CO and  $CO_2$ . The  $O-NO_2$  bond energy of 39.9 kcal. is shown to be consistent with  $-O-H$  bond energy in ethyl alcohol of 95.8 kcal.

The nitrate esters, which constitute an important group of explosives, possess the characteristic grouping,  $-O-NO_2$ , attached to a carbon atom, and all show a very marked thermal instability. Like other explosive systems they possess the characteristic property, depending on external conditions, of passing in a short time interval from the quiescent state to explosion or detonation. In order to discover the nature of the chemical processes which influence and control the burning of nitrate esters and to elucidate the causes of their instability, a kinetic study was made of the thermal decomposition of ethyl nitrate, in the hope that

this would provide a working model for the understanding of the decomposition reactions of the more complex molecules. The gaseous decomposition was shown to obey a first-order relationship and the analysis of the products at various stages indicated that the primary stage of the reaction was the breaking of the  $\text{—O—NO}_2$  bond. This process required an activation energy of 39.9 kcal.\*—a value almost identical with that reported by Appin, Chariton and Todes<sup>1</sup> for the decomposition of methyl nitrate vapour.

### Experimental

The reaction velocity was measured in the usual manner by observing the increase in pressure at constant volume and temperature. Ethyl nitrate, carefully purified by fractional distillation, was stored in a small bulb A. This bulb was joined via a tap to a larger bulb B (volume 100 ml.) which was connected by a tap and narrow bore tubing to a Pyrex decomposition vessel C (volume 130 ml.). The reaction vessel was heated by means of an electric furnace, the temperature of which was maintained constant to better than  $\frac{1}{2}^\circ\text{C}$  over the period of an experiment. The pressure in the reaction vessel was determined in the initial experiments (runs 1-13) by the use of a Pyrex Bourdon gauge sealed directly to the vessel, and in subsequent experiments by a short mercury manometer read by means of a telescope and scale. It was found that the vapour in the narrow tube leading to the manometer acted as a buffer and prevented interaction of the reactive gases produced with the mercury.

In carrying out an experiment, ethyl nitrate in trap A, which had been carefully freed from all dissolved gases by repeated freezing and evacuation, was evaporated into bulb B at a known pressure. The amount of vapour in B was controlled by changing the temperature of the storage bulb A, and could be varied between a pressure of 16.1 mm. at  $0^\circ\text{C}$  and 51.3 mm. at  $20^\circ\text{C}$ . The vapour in B was admitted to the reaction vessel by opening for a short period the tap which connected it with B.

### Results

The experiments showed that ethyl nitrate vapour decomposed with a measurable velocity at pressures of 30-50 mm. in the temperature range  $180\text{--}215^\circ\text{C}$ . Above this temperature, explosive decomposition occurred shortly after admitting the vapour to the decomposition vessel and although only a few observations were made, these indicated the existence of a lower explosion limit. Visual observation during the decomposition process proved the formation of nitrogen peroxide as shown by the production of its characteristic brown colour. It was noted that the intensity of the colour increased in the early stage of the reaction, but as the decomposition progressed the colour slowly disappeared and was hardly perceptible when reaction was complete. As is established later in this paper, the disappearance of the nitrogen peroxide occurred as a result of its participation in secondary oxidation processes.

During any run the pressure increased regularly up to the stage of complete decomposition but the total pressure change accompanying the reaction was very variable and fluctuated between an increase of 85 to 112 % of the initial pressure of the nitrate. Under all conditions, however, the initial reaction rate was found closely to obey the first-order law,

$$k = \frac{1}{t} \ln \frac{p_\infty - p_t}{p_\infty - p_i}$$

The plot of  $\log (p_\infty - p_t)$  against  $t$  for the individual experiments gave good straight lines, from the slope of which  $k$  was determined. Above 60 % decomposition  $k$  decreased rapidly especially at the higher temperatures. This decrease and the variability of the final pressure was shown to be due to secondary oxidative reactions and also to the condensation of aldehydes produced in these

\* Since this paper was completed Phillips (*Nature*, 1947, **160**, 753) has reported activation energies from 34-47 kcal. for the primary process in the dissociation of a large number of mono- and poly-nitrates in the gaseous and liquid phases.

<sup>1</sup> Appin, Chariton and Todes, *Acta Physicochim.*, 1936, **5**, 655.

processes in the short connecting tube of the reaction vessel. The results are summarized in Table I.

TABLE I

No. of Expt.	Temp. (° C)	Initial Pressure (mm.)	% Increase in Pressure	$k \times 10^{-4}$ (sec. <sup>-1</sup> )
6	180.0	—	—	3.47
7	186.5	30.0	112	5.88
8	192.0	34.0	99	9.91
9	193.5	35.0	102	11.8
10	201.0	40.0	109	18.4
11	194.0	36.5	108	11.6
13	187.5	43.0	100	6.98
16	202.0	44.0	89	25.1
17	214.0	45.0	87	66.4
18	203.0	39.0	85	26.0
19	215.0	44.0	99.5	78.3
20	185.0	41.5	104	4.26
21	191.5	44.2	91	8.13
22	180.0	33.0	108	2.77
23	190.5	41.0	—	8.45
24	196.0	35.5	112	10.6
25	200.0	45.0	96.5	23.0
26	199.5	31.7	112	18.6
27	207.0	35.0	102	41.0

**Effect of Surface.**—Rate measurements carried out with the reaction vessel packed with Pyrex tubing \* corresponding to a 7.4 times increase in surface showed that at 183.5° C the surface had no influence on the reaction. The velocity constant in the packed vessel agreed within  $\pm 6\%$  of that in the unpacked vessel. The average analysis of the product gases in several runs carried out in the packed vessel at 183.5° C showed the following results: NO, 65-68 %; CO<sub>2</sub>, 24-25 %; CO, 7-10 %. These agree closely with the data obtained in the unpacked reaction vessel and show that the reaction follows the same course in both systems. The addition of 25-40 % argon to the reactants was also without influence on the reaction rate. It may therefore be concluded that the reaction occurs homogeneously.

**Temperature Coefficient of the Reaction.**—The values given in Table I are shown in Fig. 1 in the form of a  $\log_{10} k - 1/T$  plot. The values of  $B$  and  $E$  in the Arrhenius expression,  $k = B e^{-E/RT}$ , calculated by method of least squares, are given by the expression,

$$k = 10^{15.8} e^{-39.9/RT}.$$

The scattering of the individual points from the straight line was due primarily to the variability in the final pressure mentioned above.

**The Products of the Reaction.**—The gaseous products of the reaction were analyzed by separation into two fractions (1) the gases not condensed when the products were passed through a trap cooled by liquid oxygen; (2) the gases condensed at liquid oxygen temperature but removed when the trap was replaced by a bath at  $-78^\circ\text{C}$ . The first fraction contained nitric oxide, carbon monoxide, nitrogen, and in some instances, hydrogen, whilst the second fraction consisted of carbon dioxide, nitrous oxide, together with aldehyde vapours and a small amount of nitrogen peroxide and nitric oxide. On account of the difficulty of accurately analyzing the aldehyde in the second fraction, the latter, together with the nitrogen peroxide was in many cases (Table II) retained and the  $\text{N}_2\text{O} + \text{CO}_2$  separated by using a bath at  $-120^\circ\text{C}$ . The gas samples were analyzed by standard methods,† viz., (1) carbon monoxide by oxidation to CO<sub>2</sub>,

\* The authors are indebted to Messrs E. H. Pollard and R. M. H. Wyatt for these measurements.

† Complete details of the method of gas analysis employed will be published as a separate communication.

using copper oxide at 500°, followed by absorption in potash, (2) NO by absorption in aqueous chromous chloride, (3) N<sub>2</sub> by difference, (4) H<sub>2</sub> by combustion over CuO at 300°, (5) carbon dioxide by potash absorption, (6) N<sub>2</sub>O by difference and by conversion to nitrogen over Cu—CuO at 500° C. The results of analyses of the final products are summarized in Table II.

TABLE II

Temp. (°C)	% NO	% CO	% H <sub>2</sub>	% N <sub>2</sub>	% CO <sub>2</sub>	% N <sub>2</sub> O	Remarks
185-190	60.0	8.9	—	1.2	23.4	3.2	Average analyses of Expt. 20-23 (Table I)
200	67.1	9.8	—	1.0	18.0	3.4	Average Expt. 24-27
202	65.1	8.0	—	1.6	22.1	3.0	
210	53.7	7.5	—	1.5	25.7	11.6 *	*N <sub>2</sub> O + some NO
230	32.8	46.8	12.2	4.1	3.2	0.9	Flame
240	48.6	36.6	8.6	2.1	2.2	1.0	

The presence of hydrogen in the gases when explosion occurs is probably a consequence of the establishment of the water gas equilibrium at the temperature of the explosion.

The residue in the trap at -120° and -78° C after removal of the gaseous product was shown to contain acetaldehyde by use of the dimedone aldehyde reagent. The precipitate formed had a melting point identical with the derivative prepared from fresh acetaldehyde. This was confirmed by a mixed melting point.

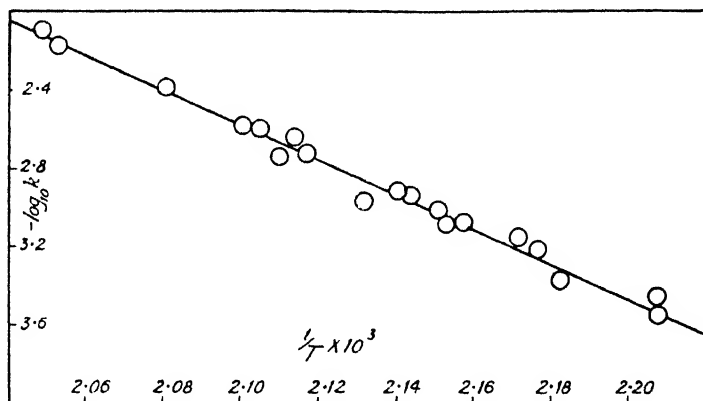


FIG. 1.

**Course of the Reaction.**—During the reaction, nitrogen peroxide was produced but this disappeared as the reaction progressed and at the end of the decomposition, as judged from the colour of the gases, the percentage nitrogen peroxide present was very small. The formation and disappearance of nitrogen peroxide during the reaction was determined in the following way: an investigation of the reaction between nitrogen peroxide and aqueous solutions of urea and amido-sulphonic acid showed that with known amounts of nitrogen peroxide the volume of nitrogen produced by reaction was half that of the volume of nitrogen peroxide used. The results obtained by this method of analysis at two temperatures, together with that of the other nitrogen oxides formed, are shown in Table III.

It is evident from these results that the nitrogen peroxide present at its highest concentration in the earlier stages of the reaction, is consumed in oxidative processes with the formation of an approximately equivalent volume of nitric oxide.



**Reaction Mechanism.**—The above results indicate that the primary decomposition process is the breaking of the  $\text{—O—NO}_2$  linkage, and that this reaction requires an activation energy of 39.5 kcal., viz.

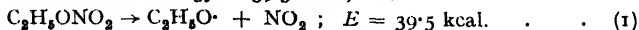
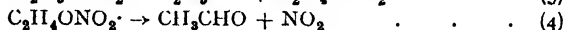
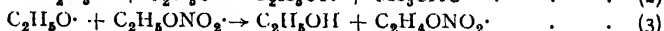
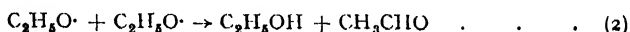


TABLE III

Temp. (° C)	Initial Pressure of $\text{C}_2\text{H}_5\text{ONO}_2$ (mm.)	Time in Reaction Vessel (min.)	Atoms N/molecules $\text{C}_2\text{H}_5\text{ONO}_2 \times 100$		
			$\text{NO}_2$	NO	$\text{N}_2\text{O}$ (approx.)
180	33.0	40	44	15	2
180	33.0	85	55	30	2
190	40.0	21	63	27	3
190	40.0	30	—	56	3
190	40.0	60	32	65	3
190	40.0	91	6.0	86	3

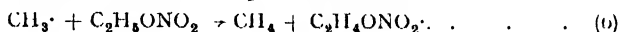
The nitrogen peroxide formed is consumed in subsequent oxidative reactions with the formation of carbon monoxide and dioxide. The actual reactions taking place cannot be stated with certainty, although it has been established experimentally that acetaldehyde is one of the intermediate products and it is assumed that it is formed from the ethoxy radical by one of the following reactions:



The formation of aldehydes by the direct thermal dissociation of the intermediate ethoxy radical according to



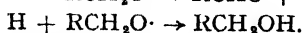
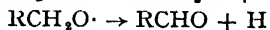
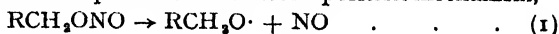
can be ruled out, since the experimental results neither indicated the formation of formaldehyde nor methane which would have been expected by reaction of the methyl radical produced with undecomposed nitrate or other intermediates:



The formation of  $\text{CO}$ ,  $\text{CO}_2$  and  $\text{NO}$  probably results from oxidation of aldehydes or alcohols produced by nitrogen peroxide. This evidence is very strongly supported by independent investigations by Dr. F. H. Pollard in this laboratory of the gaseous reaction between  $\text{NO}_2$  and aldehydes. It has been found that aldehyde vapours and  $\text{NO}_2$  react together very rapidly at temperatures above  $160^\circ\text{C}$  and that the  $\text{NO}_2$  is reduced almost quantitatively to nitric oxide and the aldehydes oxidized to carbon monoxide and dioxide.

### Discussion

It is of interest to compare the pyrolysis of the nitrate with those of the nitrite esters. The latter have been extensively investigated by Steacie and his co-workers,<sup>2</sup> who have postulated the decomposition mechanism,

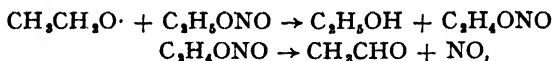


The activation energy for the overall decomposition was 37,700 cal. for the ethyl ester. By studying the decomposition of ethyl nitrite at very low pressures, using a flow method, Rice and Rodowskas<sup>3</sup> proved the formation of free radicals by their attack on metallic mirrors and showed

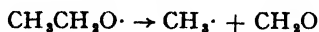
<sup>2</sup> Steacie and Katz, *J. Chem. Physics*, 1937, **5**, 125 (where previous references are given).

<sup>3</sup> Rice and Rodowskas, *J. Amer. Chem. Soc.*, 1935, **57**, 350.

that the activation energy of the radical-forming process was about 35,000 cal., and corresponded to the primary process (1). This was followed by

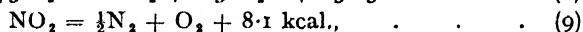
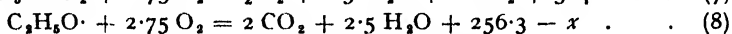
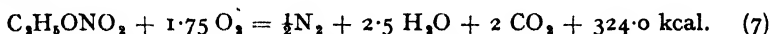


which, like Steacie's scheme, accounts for the experimental products. At low pressures Rice and Rodowskas also assume the occurrence of the reactions,



and the subsequent reaction of the methyl radical to give methane.

The difference between the dissociation energies of the nitrate and nitrite esters can be evaluated from thermochemical data<sup>4</sup> in the following manner :



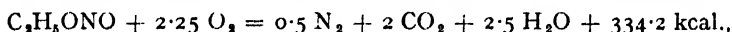
which, on subtracting (8) and (9) from (7), gives



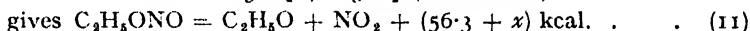
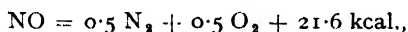
where  $x$  is the heat of dissociation of the —OH bond in ethyl alcohol, viz.



The corresponding data on the heat of formation of ethyl nitrite,



combined with (8) and



The difference of 3.3 kcal. in heat of the primary dissociation process of ethyl nitrite and nitrate respectively corresponds closely to the difference in activation energies for the two reactions, viz. 37.7 kcal. for the nitrites and the value of 39.5 kcal. for the nitrate. The kinetic measurements of Rice and Rodowskas refer directly to the energy of dissociation of the O—NO bond and the agreement with the higher pressure kinetic values is so close that it may be assumed as a good approximation that the measured values of  $E$  for the nitrite and nitrate correspond to the dissociation energies of the O—NO and O—NO<sub>2</sub> bonds respectively. No other measurements of these values have been reported, but they may be determined from (10) and (11), if a reliable value could be assigned to  $x$ . Conversely, from the value of the —O—NO<sub>2</sub> bond and eqn. (11) the dissociation energy of the —O—H bond in ethyl alcohol  $x$  is found to be 95.8 kcal.

The authors wish to express their thanks to Prof. W. E. Garner and E. L. Hirst for their interest in this work.

*Department of Chemistry,  
University of Liverpool.*

<sup>4</sup> Landolt-Bornstein, *Physik. Chem. Tabellen*, II, p. 1619.

## REVIEWS OF BOOKS

### Organic Reagents Used in Gravimetric and Volumetric Analysis.

By JOHN F. FLAGG. (Interscience Publishers, Inc., New York, 1948.) Pp. xiv + 300. Price 36s.

The author states in his preface that the function of his volume is "to describe the various organic reagents (precipitants) used in gravimetric and volumetric analysis; to indicate the type of analysis in which they may be used; and to provide proved directions for their use." It may be said at once that this object has been largely achieved.

The first four chapters, occupying some 79 pages, are devoted to "theory" and include excellent accounts of organic compounds as precipitants for inorganic ions, some properties of organometallic precipitates, separations by means of organic reagents, and theory of the solubility of salts with a common anion. This is followed by a short chapter (12 pages) on "technique"; the reviewer feels that its brevity renders it of limited value to a beginner and the experienced analyst will probably prefer to have such subjects as quantitative bromination included under oxine. The remaining 186 pages are devoted to a detailed account of the various special reagents: in addition to simple determinations, full details are provided of their application to practical problems such as the analysis of steels, alloys, and ores. References to recent literature are given throughout.

The reviewer was rather disappointed to find that the following organic reagents were not discussed:  $\beta$ -naphthoquinoline (for cadmium), *m*-nitrobenzoic acid (for thorium), pyrogallol (for bismuth), *p*-aminoacetophenone (for palladium), and sodium 6-chloro-5-nitrotoluene-3-sulphonate (for potassium). Such omissions tend to reduce the usefulness of the book. A new edition might well include an account of these and at least a bibliography of all other organic reagents which have been used in quantitative inorganic analysis. Literature references to the preparation of the various reagents would be welcomed by many.

The proof reading has been carefully carried out. The following minor errors have been noted: p. 131, for *perchloride* read *perchloric*; p. 243, for *De Varda's* read *Devarda's*; the formula for tetraphenylarsonium chloride contains pentavalent arsenic. The instruction on p. 222 to filter through a "Jena G4 sintered-glass crucible" reads rather strangely in a book written in the U.S.A. during 1948. The production of the book is excellent, but the price of 36s. is rather high by British standards.

A. I. V.

# THE THEORY OF MOLECULAR DISTILLATION AND ITS EXPERIMENTAL VERIFICATION

BY R. S. BRADLEY AND A. D. SHELLARD

*Received 11th October, 1948*

The theory of molecular distillation for binary mixtures is discussed, and is shown to be applicable to measurements on mixtures of normal hexadecane with (a) normal tetradecane and (b) normal pentadecane. Values of the vapour pressure of (a) and (b) have been determined at 40 and 46° C respectively.

In the so-called molecular or ideal distillation a freely flowing jet of vapour, coming off a liquid surface in a hard vacuum, is condensed on a cooled surface. Under ideal conditions the path is short and the vapour pressure is such that the flow is of the "molecular" type studied by Knudsen, i.e. collisions between molecules play an unimportant role. The distillation of mixtures using a molecular still cannot be followed in the usual way by means of the change in boiling point, and Hickman and his co-workers<sup>1</sup> have therefore had recourse to the introduction of "constant yield oil", and have studied the "elimination curve" determined from the quantities carried over at various ranges of temperature. Hickman considers that the separation achieved is poor, and states that a difference of boiling point of 100° C is required for good separation, but points out that this disadvantage may be compensated by the low temperature employed.

We have used a simple molecular still for the purification of the higher paraffin hydrocarbons, for studies on the rates of evaporation.<sup>2</sup> In order to characterize the distillation we have kept the temperature constant at some figure convenient for fairly fast distillation (say 10-20. g./hr.), and have determined the quantities distilling over as a function of the time. When this laboratory technique is applied to specially prepared mixtures of long chain normal paraffins it appears that considerably better separations are possible than those obtained by Hickman under industrial conditions. A theoretical study, which we believe to be new, is given below, together with the experimental results for hydrocarbon mixtures.

**The Theory of the Distillation of Binary Mixtures at Constant Temperature in a Molecular Still.**—Suppose that at any time there are in the distilland  $w_1$  and  $w_2$  g. of molecules 1 and 2, the molecular weights of which are  $M_1$  and  $M_2$ , and saturated vapour pressures of the pure components  $p_{10}$  and  $p_{20}$  respectively. Let the effective area of the condensing surface be  $A$ , and the partial vapour pressures  $p_1$  and  $p_2$ . If we suppose that the condensing surface is cool enough for the vapour pressure at this surface to be negligible in comparison with the vapour pressure at the liquid surface, and that the evaporation coefficient is unity, which holds for the hydrocarbons we have studied,<sup>2</sup> then

$$\frac{dw_1}{dt} = -p_1 \left( \frac{M_1}{2\pi RT} \right)^{\frac{1}{2}} A, \quad \dots \quad (1)$$

<sup>1</sup> Hickman, *Amer. Sci.*, 1945, **33**, 205; *Chem. Rev.*, 1944, **34**, 51.

<sup>2</sup> Bradley and Shellard, *Proc. Roy. Soc. A* (submitted for publication).

$$\frac{dw_2}{dt} = -p_2 \left( \frac{M_2}{2\pi RT} \right)^{\frac{1}{2}} A, \quad . \quad . \quad . \quad . \quad (2)$$

where

$$p_1 = p_{10} \times \frac{w_1/M_1}{w_1/M_1 + w_2/M_2}, \quad . \quad . \quad . \quad . \quad (3)$$

$$p_2 = p_{20} \frac{w_2/M_2}{w_1/M_1 + w_2/M_2}, \quad . \quad . \quad . \quad . \quad (4)$$

if Raoult's law holds;  $T$  is the absolute temperature of the distilland.

Hence 
$$\frac{dw_1}{dw_2} = \frac{p_{10} w_1}{p_{20} w_2} \left( \frac{M_2}{M_1} \right)^{\frac{1}{2}} \quad . \quad . \quad . \quad . \quad (5)$$

If 
$$\beta = \left( \frac{M_1}{M_2} \right)^{\frac{1}{2}} \frac{p_{10}}{p_{20}}, \quad . \quad . \quad . \quad . \quad (6)$$

on integrating we obtain

$$w_1 = \gamma w_2^\beta, \quad . \quad . \quad . \quad . \quad . \quad (7)$$

$$\gamma = \frac{w_{10}}{w_{20}^\beta} \quad . \quad . \quad . \quad . \quad . \quad (8)$$

where  $w_{10}$  and  $w_{20}$  are the initial weights in the distilland.

If  $w_1$  in eqn. (4) is replaced by the value given by (7), we obtain in place of (2)

$$\begin{aligned} \frac{dw_2}{dt} &= -p_{20} \frac{w_2 M_1}{w_1 M_2 + w_2 M_1} \left( \frac{M_2}{2\pi RT} \right)^{\frac{1}{2}} \times A \\ &= -p_{20} \frac{M_1}{M_1 + M_2 \gamma w_2^{\beta-1}} \left( \frac{M_2}{2\pi RT} \right)^{\frac{1}{2}} \times A. \end{aligned}$$

The last equation gives on integration

$$M_1 w_2 + \frac{M_2 w_1}{\beta} = -p_{20} M_1 \left( \frac{M_2}{2\pi RT} \right)^{\frac{1}{2}} A t + \delta_2, \quad . \quad . \quad . \quad (9)$$

where  $\delta_2$  is a constant given by

$$M_1 w_{20} + M_2 w_{10}/\beta = \delta_2.$$

A similar result is obtained from (1), viz.

$$M_2 w_1 + \beta M_1 w_2 = p_{10} M_2 \left( \frac{M_1}{2\pi RT} \right)^{\frac{1}{2}} A t + \delta_1 \quad . \quad . \quad . \quad (10)$$

From (9), (10) and (6) it is clear that

$$\beta \delta_2 = \delta_1.$$

Eqn. (9) at first sight appears difficult to solve for  $w_2$  at a given time. It is, however, very easy to draw up a table of times corresponding to a range of values of  $w_2$ , since

$$t = \left( \frac{2\pi RT}{M_2} \right)^{\frac{1}{2}} \frac{1}{p_{20} M_1 A} \{ \delta_2 - M_1 w_2 - M_2 \gamma w_2^\beta / \beta \} \quad . \quad . \quad . \quad (11)$$

It is, therefore, a simple matter to plot  $t$  as a function of  $w_2$ , and hence  $w_2$  can be read off from the graph for any value of  $t$ . The theory may also be checked by plotting the function

$$\phi(w_2) = M_1 w_2 + M_2 \gamma w_2^\beta / \beta$$

as a function of  $t$ , when a straight line should be obtained. It should be noted that  $w_1$  and  $w_2$  refer to the distilland, i.e. to the liquid in the still; the quantities which have been distilled are  $w_{10} - w_1$ , and  $w_{20} - w_2$ . The simple theory is easily extended to polycomponent mixtures.

## Experimental

A simple Pyrex pot molecular still was used, as the falling film type, although more efficient, introduces complications which are difficult to assess theoretically. Approximately 40 ml. of liquid was heated by the thin platinum spiral A, which was soldered by means of nickel to tungsten leads passing into mercury in the tubes B. Leads from a 20 V mains transformer dipped into B, and a current up to 3 A could be obtained, using a variable resistance. The condensate was collected in six sample tubes C. Each sample tube passed through a hole in a circular aluminium plate which rested on pips fused to the tube D, the bottom of the tube being supported on a second aluminium plate. The tube D terminated in a dry socket, the core of which, E, was fused to a second cone which could be rotated by means of F in a socket lubricated by Apiezon grease. The sample tubes, aluminium plates and tube D could be removed by means of a hook engaging in the wire G. Vacuum wax was used on the large ground-joints. The temperature of the liquid could be read on a thermometer inserted into a pool of mercury in the bottom of the tube I. The apparatus was exhausted to  $10^{-5}$  cm. Hg by means of a mercury-vapour pump backed by an oil pump, with a liquid-air trap just before the apparatus.

For reasons of analysis we have used only binary liquids. A mixture consisting of 20.8 g. of pure *n*-hexadecane and 14.7 g. of pure *n*-tetradecane was distilled at 40° C at a pressure of  $10^{-4}$ - $10^{-5}$  cm. Hg. Six samples, 2.4 g. each, were collected, and the time required to collect each sample was recorded. The residue in the still, 11 g., set to a crystalline mass and gave at 25° C the same refractive index as pure *n*-hexadecane.

TABLE I.—CALIBRATION CURVE FOR COMPOSITION-REFRACTIVE INDEX FOR  $n\text{-C}_{14}\text{H}_{30} + n\text{-C}_{16}\text{H}_{34}$ 

Wt. % $\text{C}_{14}$	$n_D^{25}$	Wt. % $\text{C}_{14}$	$n_D^{25}$
0	1.43308	60	1.42966
10	1.43247	70	1.42916
30	1.43147	100	1.42745
50	1.43006	—	—

The six samples of distillate were then mixed and the distillation was repeated. Results for both runs are recorded in Table II.

TABLE II.—MOLECULAR DISTILLATION OF  $n\text{-C}_{14}\text{H}_{30} + n\text{-C}_{16}\text{H}_{34}$ 

Fraction No.	Wt. of Fraction (g.)	Wt. $\text{C}_{16}$ in Fraction (g.)	Wt. $\text{C}_{14}$ in Fraction (g.)	Time to Collect each Fraction (min.)	Temp. °C
Expt. 1: 20.8 g. $\text{C}_{16}$ + 14.7 g. $\text{C}_{14}$					
I	2.404	0.26	2.14	—	20-40
II	3.972	0.64	3.33	10	40
III	3.798	0.83	2.97	10	40
IV	3.990	1.28	2.72	16	40
V	4.154	2.37	1.78	26	40
VI	4.023	3.70	0.32	34	40
VII	11.0	11.0	0	(left in still)	—
Expt. 2: 19.64 g. $\text{C}_{16}$ + 13.10 g. $\text{C}_{14}$					
I	3.70	0.41	3.29	—	17-40
II	3.809	0.69	3.12	7	40
III	3.350	0.84	2.51	8	40
IV	3.723	1.34	2.38	12	40
V	3.763	2.30	1.46	20	40
VI	4.308	4.09	0.22	30	40
VII	9.82	9.82	0	(left in still)	—

The refractive index of the six samples was determined, using a Pulfrich refractometer, and thence the composition could be calculated from the calibration curve of refractive index against % composition by weight. The latter was

found to be linear, and the spread of values of refractive index is sufficient to give reasonably accurate compositions, as is seen from the data of Table I.

In Expt. 1 the weight of  $C_{14} + C_{16}$  recovered was 33.34 g., i.e. ca. 2 g. was lost, but in Expt. 2 the loss was only 0.2 g.; some of this was lost in the trap. Since fraction I was collected over a rising temperature it was rejected for the purpose of verifying the theory, and distillation was assumed to start at fraction II. Thus for Expt. 1 it was assumed that the initial weights of  $C_{16}$  and  $C_{14}$  in the still were respectively  $20.8 - 0.26 = 20.54$  g., and  $14.7 - 2.14 = 12.56$  g. Similarly for Expt. 2,  $w_{10} = 19.64 - 0.41 = 19.23$  and  $w_{20} = 13.10 - 3.29 = 9.81$ , where  $w_{10}$  and  $w_{20}$  are taken to be the initial values of  $w_1$  and  $w_2$  respectively.

From the data above the weights of  $C_{14}$  and  $C_{16}$  left in the still at the instants at which the sample tubes were filled could be calculated, and a composition-time curve could be drawn for the distilland (Table III). The shape of this curve is indicative of a good separation in the latter part of the runs, when almost pure hexadecane was recovered; the boiling points of  $n-C_{14}H_{30}$  and  $n-C_{16}H_{34}$  are quoted as  $251.0^\circ$  and  $280.0^\circ$  C respectively.<sup>3</sup> Although the temperature has been maintained constant in order to facilitate the theoretical analysis and give a clear picture, it might be expedient when the last fractions are much less volatile than the first, to increase the temperature towards the end of the distillation; the separation curve is, however, more difficult to interpret.

TABLE III

1 =  $n-C_{16}H_{34}$ . 2 =  $n-C_{14}H_{30}$ . VALUES OF  $\phi$  ARE CALCULATED IN A LATER SECTION

$\frac{\%}{n-C_{16}H_{34}}$ in Distil- land	$w_1$ (g.)	$w_2$ (g.)	$t$ (min.)	$\frac{\phi}{1000}$	$\frac{\%}{n-C_{16}H_{34}}$ in Dis- tilland	$w_1$ (g.)	$w_2$ (g.)	$t$ (min.)	$\frac{\phi}{1000}$
Expt. 1					Expt. 2				
62	20.54	12.56	0	36.9	66.2	19.23	9.81	0	34.1
68.3	19.90	9.23	10	35.1	73.5	18.54	6.69	7	32.3
75.3	19.07	6.26	20	33.0	80.9	17.70	4.18	15	30.3
83.4	17.79	3.54	36	30.3	90.3	16.36	1.80	27	27.5
89.8	15.42	1.76	62	26.0	97.6	14.06	0.34	47	23.4
89	11.72	1.44	96	19.8	98.9	9.97	0.12	77	16.6
100	11.0	0	(left in still)		100	9.82	(left in still)		

Evidently Expt. 2 is the more accurate. The whole of the above experimental procedure, except that the refractive index curve was assumed to be linear, was repeated with mixtures of  $n-C_{16}H_{32}$  and  $n-C_{16}H_{34}$ , with the results listed in Table IV.

TABLE IV

EXPT. 3

22.88 g.  $n-C_{16}H_{34}$  + 9.81 g.  $n-C_{16}H_{32}$ . 1 =  $C_{16}$ . 2 =  $C_{15}$ 

Frac- tion No.	Wt. of Fraction (g.)	Wt. $C_{16}$ in Fraction (g.)	Wt. $C_{15}$ in Fraction (g.)	Time to fill each Frac- tion (min.)	Temp. °C	$w_1$ (g.)	$w_2$ (g.)	$t$ (min.)	$\frac{\%}{C_{16}}$ in Distilland	$\frac{\phi}{1000}$
I	3.908	1.407	2.501	—	15.46	—	—	—	—	—
II	4.018	2.090	1.928	9	46	21.47	7.31	0	74.6	14.9
III	3.653	2.192	1.461	9	46	19.38	5.38	9	78.3	13.2
IV	3.942	2.680	1.262	10	46	17.19	3.92	18	81.4	11.5
V	3.750	2.850	0.900	11	46	14.51	2.66	28	84.5	9.5
VI	4.358	3.660	0.698	12	46	11.66	1.76	39	86.9	7.6
VII	8.441	8.441	0	(Left in still)		8.441	0	51	88.3	5.2
									100	—

Loss = 0.6 g.  $w_{10} = 22.88 - 1.407 = 21.47$ .  $w_{20} = 9.81 - 2.50 = 7.31$

<sup>3</sup> Egloff, *Physical Constants of Hydrocarbons*, Vol. I.

It is evident that even for this mixture, the components of which differ in boiling point<sup>3</sup> by only 12° C, the separation is good for the end fraction, since almost a third of the original  $n\text{-C}_{16}\text{H}_{34}$  is recovered almost pure. In addition for reasons which will be evident in the theoretical section following, we have distilled  $n\text{-C}_{16}\text{H}_{34}$  at 47° C, with the following results:

Expt. 4.	Fraction II.	wt. = 3.528 g.,	time to collect = 13 min.
	III.	wt. = 3.579 g.,	" " = 13 "
	IV.	wt. = 3.487 g.,	" " = 13 "

The mean weight collected in 13 min. was 3.53 g. As would be expected the rate of distillation was constant.

**Application of the Theory to the Experiments.**—For the calculation of the values of  $\beta$ , a knowledge of the vapour pressures is necessary. Vapour pressure equations of the Antoine type have been given by Thomson,<sup>4</sup> but these are derived from data at higher temperatures, and are unsuitable for extrapolation to 40–47°. We have determined the vapour pressure of liquid  $n\text{-C}_{16}\text{H}_{34}$  at 20–35° C; and have shown<sup>2</sup> that the results may be represented by the equation  $\log_{10} P \text{ cm.} = -4189/T + 10.260$ . This gives for  $P$  at 40°, 46°, 47° the respective values  $0.77 \times 10^{-3}$ ,  $1.36 \times 10^{-3}$ , and  $1.50 \times 10^{-3}$  cm. Mr. G. C. S. Waghorn, working under the direction of one of us (R.S.B.) has determined the vapour pressures of  $n$ -tetradecane, using the Knudsen technique. Reasonably concordant values were obtained using holes of different sizes for the effusion of the vapour. The mean results are as follows:  $n$ -tetradecane at 40° C ( $6.08 \pm 0.05$ )  $\times 10^{-3}$  cm. Hg;  $n$ -pentadecane at 46° C ( $3.82 \pm 0.03$ )  $\times 10^{-3}$  cm. Hg.

For the mixture  $n$ -tetradecane and  $n$ -hexadecane we calculate  $\beta = 0.1196$ . The values of  $\phi = M_1 w_2 + M_2 w_1 / \beta$ , where liquid 1 is  $n$ -hexadecane and liquid 2

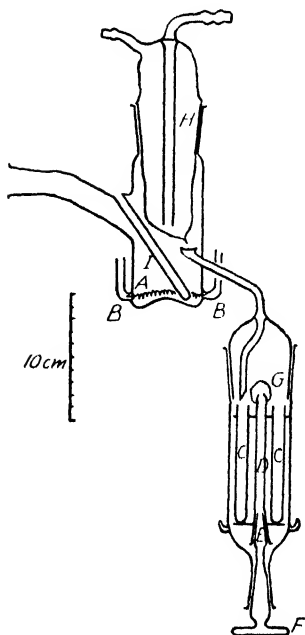


FIG. 1.

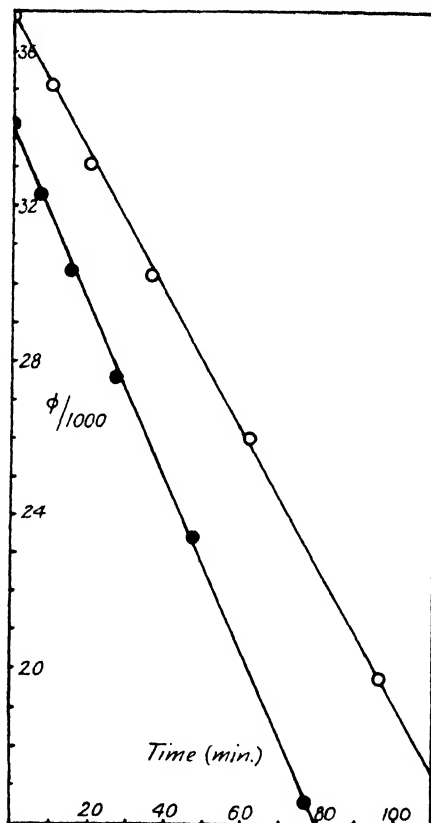


FIG. 2.

<sup>4</sup> Thomson, *Chem. Rev.*, 1946, 38, 1.



*n*-tetradecane, are given in Table III, and are plotted in Fig. 2. It will be seen that  $\phi$  against  $t$  is a good straight line, with slightly different values of the slope for Expt. 1 and 2. Since the value of  $A$ , the area of the condensing surface is somewhat indeterminate, we have calculated  $A$  from the equation:

$$\frac{d\phi}{dt} = -p_{s0}M_1\left(\frac{M_2}{2\pi RT}\right)^{\frac{1}{2}} \times A.$$

The values of  $d\phi/dt$  for Expt. 1 and 2 are respectively 178 and 229 per min., giving a mean value of  $A = 5.3 \text{ cm.}^2$ . This is less than the area estimated by sticking paper on the curved surface, viz.  $17 \text{ cm.}^2$ . However, the effective condensation area is indeterminate by direct measurement, and our calculated result is of the right order.

Similarly, for *n*-pentadecane (2) and *n*-hexadecane (1), we find  $\beta = 0.3447$ . The values of  $\phi$  are given in Table IV, and it will be seen from Fig. 3 that  $\phi$

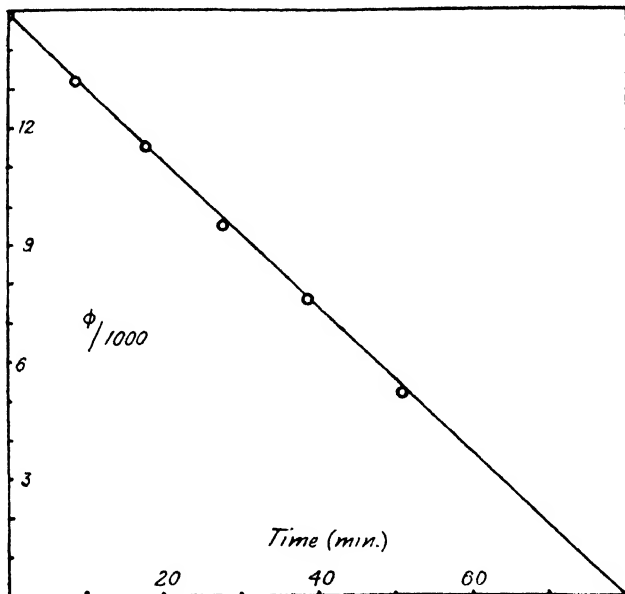


FIG. 3.

is a linear fraction of  $t$ .  $d\phi/dt = 188$  per min., giving  $A = 7.58 \text{ cm.}^2$ .

These values of the condensing area are in rough accord, and are approximately the same as the area deduced from the results for cetane alone at  $47^\circ \text{C}$ . For cetane alone

$$\frac{dw}{dt} = p\left(\frac{M}{2\pi RT}\right)^{\frac{1}{2}} \times A,$$

giving  $A = 6.12 \text{ cm.}^2$ .

### Discussion

In so far as the calculated results for the condensing area are of the same order as the measured value, which is difficult to compute, it would appear that the course of the molecular distillation is adequately covered by classical theory. The low value for the calculated area may be due to impedance in the molecular flow owing to collision of hydrocarbon molecules with one another. This departure from the simple theory will increase with the vapour pressure, and we consider that the term molecular distillation should be confined to examples in which the molecular flow is approximately ideal and relatively free from gas collisions between evaporating molecules and air molecules or between pairs of evaporating molecules.

The mean free path of the hydrocarbon molecules, for collision with one another, is difficult to compute, since the temperature and concentration were changing from the liquid surface to the cold surface. We have determined the collision area of the hydrocarbons for collision with molecules of air,<sup>5</sup> and an estimate may be made from these of the collision area and mean free path  $\lambda_{11}$  for collisions between hydrocarbon molecules. For *n*-hexadecane at 15° C,  $\lambda_{11} = 1.9$  cm., at 40° C,  $\lambda_{11} = 0.12$  cm., if the concentration of molecules at the two temperatures is that appropriate to the corresponding saturated vapour pressure. For *n*-tetradecane at 40° C,  $\lambda_{11} = 0.015$  cm. For ideal conditions it is clear that the evaporation path, which varied from 2 to 4 cm. as the distillation proceeded, should have been shorter. Our aim in this work, however, was not to make the conditions of distillation as ideal as possible, but rather to examine a convenient and simple laboratory still and to see to what extent the ideal behaviour was obeyed, and to determine the separation which could be effected.

For this reason the liquid was not stirred and it is possible that some denudation of the more relative component occurred from the surface layers. The method of heating from the bottom gave rise to convection currents, however, and the low rate of distillation also favoured mixing of the liquid. It is clear that surface denudation could not have been a major factor, otherwise the rate of distillation in the early stages would have dropped to that of the less volatile component.

The low value of the calculated area is unlikely to be due to residual air, since the rate of evaporation in the presence of air is given by

$$Am\alpha \left( \frac{p}{kT} \right) \left( \frac{kT}{2\pi m} \right)^{\frac{1}{2}} \times \frac{1}{1 + \alpha \left( \frac{kT}{2\pi m} \right)^{\frac{1}{2}} \frac{(l - \Delta)}{D}}$$

for a single component of vapour pressure  $p$ , molecular mass  $m$  and evaporation coefficient  $\alpha$ ;  $l$  is the length of the diffusion path,  $D$  the diffusion coefficient and  $\Delta$  the distance from the liquid surface to the region of highest concentration of vapour molecules.<sup>5</sup> As the air pressure is reduced the rate of evaporation passes asymptotically towards the vacuum rate, and beyond a certain low air pressure further reduction in the air pressure makes little difference to the rate of evaporation, a point also stressed by Carman.<sup>6</sup>

Our thanks are due to the Shell Marketing and Refining Company Ltd. for a grant to defray part of the cost of the apparatus, and for generously allowing one of us (A.D.S.) to take up the work in Leeds while in their employ. Our thanks are also due to Prof. M. G. Evans for his interest in the work.

*Department of Inorganic and Physical Chemistry,  
The University of Leeds.*

<sup>5</sup> Bradley and Birks (*Proc. Roy. Soc. A*, submitted for publication).

<sup>6</sup> Carman, *Trans. Faraday Soc.*, 1948, **44**, 529.

# THE TRANSFER OF SODIUM AND POTASSIUM IONS BETWEEN MUSCLE AND THE SURROUNDING MEDIUM

BY E. J. HARRIS AND G. P. BURN

*Received 1st November, 1948*

The kinetics of the transfer of alkali metal ions between an assembly of cells, such as make up a muscle, and the surrounding medium depend on two factors, the rate of diffusion of the ions in the extra-cellular space and the rate of crossing the cell boundaries. Equations describing the time course of the process have been solved for the special cases of sodium and potassium ions being transferred into the cells of a thin sheet of muscle.

The transfer of the sodium ion takes place as if it were the sum of diffusion and permeation processes. From experimental data it was possible to deduce the diffusion constant of the ion in the extra-cellular space ( $2.6 \times 10^{-6}$  cm.<sup>2</sup> sec.<sup>-1</sup>), the cell permeability (0.0005 cm. hr.<sup>-1</sup>), the fraction of extra-cellular space (0.1-0.3), and the ratio of the internal to the external sodium concentration (0.14-0.28).

The potassium ion transfer involves both diffusion and permeability constants implicitly; by assuming a diffusion constant the permeability constant was obtained (0.0034 cm. hr.<sup>-1</sup>). This permeability constant was found to be independent of the concentration of KCl in the Ringer's solution in the range 0.015 % KCl to 0.09 % KCl. The effect of loss of potassium from the cells on the permeability is discussed.

Figures for the permeability of frog erythrocytes to potassium ( $9 \times 10^{-6}$  cm. hr.<sup>-1</sup>) and sodium ( $2 \times 10^{-6}$  cm. hr.<sup>-1</sup>) were obtained.

---

Before radioactive tracer elements became available the study of the rate of loss or accumulation of inorganic ions in muscle cells had to be conducted by using solutions either richer, or poorer, in the chosen ion than the normal physiological surroundings, so that the changing concentration resulting from the cells' activity could be followed analytically. In order to obtain a set of results relating to different times of exposure to the medium it was necessary either to use a large number of separate specimens, or to make some assumption to relate an observable physical change (e.g. swelling) with the amount of ion which had entered. These experiments merely gave information regarding the net change of the amount of the ion, which was the difference between the amount gained and the amount lost during the experiment. Under physiological conditions, a steady state prevails and the internal concentration of the ion does not change, although by use of isotopes to provide labelled ions, distinct physically but similar chemically, it is possible to observe the dynamic state of the equilibrium, and to measure the rates at which ions enter and leave the cells under various conditions. It is important to obtain information on the "equilibrium" state, which prevails *in vivo*: the use of solutions containing too great an excess or deficiency of the alkali metal ions can lead to alterations in the properties of the cell membrane which vitiate conclusions drawn concerning the resistance it offers to the ions under physiological conditions. The application of radioactive isotopes permits the assay of the amount of an ion which is in the tissue sample at any time during the experiment, so a curve relating the amount of the ion transferred from solution to tissue, or vice versa, to the time elapsed, can be drawn for each specimen. When the external concentrations have been properly selected the concentration of the ion being studied

does not change in the chemical sense, it is the change in the proportion of labelled (i.e. associated with a certain radioactivity) material which allows the transfer to be followed. In this case the transfer becomes statistically an exchange process, the number of ions passing in one direction being equal to the number passing in the opposite direction.

A number of observations made by the isotope technique have been recorded concerning the exchange of sodium or potassium ions between muscle and plasma.<sup>1, 2, 3, 4</sup> Krogh<sup>5</sup> has reviewed the subject up to 1946. It appears that frog muscles have failed to show complete exchangeability of their potassium, and this has been discussed in terms of unionized complexes and impermeable barriers. The former explanation is generally discounted, and no final conclusion has been reached. There are few exact measurements of the rate of exchange of potassium ions *in vivo* because the plasma concentration of the labelled ion changes rapidly following injection. In order to make calculations of the ion transfer it would be necessary to have a record of the plasma radioactivity, and preferably to keep the proportion of labelled ions constant by continuous injections. Such procedure is hardly possible with small animals like frogs. Noonan, Fenn, and Haegge<sup>6</sup> found that the exchange of potassium was affected by blood circulation and denervation of the muscle. The exchange reached about 10 % in an hour in live and perfused frog muscles. Dean<sup>7</sup> found a similar figure for the exchange taking place between an isolated frog muscle and Ringer's solution, whether in an atmosphere of oxygen or nitrogen.

Radio-sodium uptake has been used to measure the extra-cellular space of muscles.<sup>8, 9</sup> The latter authors<sup>9</sup> were aware that the sodium also exchanged with intracellular material, and Krogh<sup>3</sup> found that the value for the "extra-cellular space" based on the uptake of radio-sodium was 50 % greater than the space as measured by the uptake of thiocyanate ion. Ussing<sup>4</sup> has reported a half-period of  $\frac{1}{2}$  hr. for the penetration of radio-sodium into an isolated frog sartorius.

It proves difficult to distinguish that part of the sodium which is present in the cells from that present in the extra-cellular space, and tracer methods do not of themselves assist in the matter. It is only if the exchange of the one sort proceeds with a velocity sufficiently different from that of the other that a distinction can be made. There does not appear to be any evidence that the sodium associated with the muscle cells is really inside the membrane, as distinct from being adsorbed in the cell wall material. In the discussion of results it is convenient to use the adjective "internal," applied to that part of the sodium which does not exchange as fast as that present in the extra-cellular volume, but there is no evidence as to the location of this less rapidly exchangeable part, and the formulation remains similar if, in fact, the internal sodium is adsorbed.

The kinetics of transfer processes taking place through membranes were discussed by Collander and Barlund.<sup>10</sup> They distinguished two limiting cases, one when the transfer was controlled by a thin layer contributing all the resistance, and the other when a uniform resistance was encountered. The former leads to an equation involving a permeability constant, which includes an unknown factor related to the membrane thickness and has the dimensions length/time, while the latter

<sup>1</sup> Hahn and Hevesy, *Acta Physiol. Scand.*, 1941, **2**, 51.

<sup>2</sup> Heppel, *Amer. J. Physiol.*, 1939, **128**, 449.

<sup>3</sup> Krogh, *Acta Physiol. Scand.*, 1944, **7**, 221 and 238.

<sup>4</sup> Ussing, *Nature*, 1947, **160**, 262.

<sup>5</sup> Krogh, *Proc. Roy. Soc. B*, 1946, **133**, 140.

<sup>6</sup> Noonan, Fenn and Haegge, *Amer. J. Physiol.*, 1941, **132**, 474 and 612.

<sup>7</sup> Dean, *J. Cell. Comp. Physiol.*, 1940, **15**, 189.

<sup>8</sup> Hevesy and Rebbe, *Acta Physiol. Scand.*, 1940, **1**, 347.

<sup>9</sup> Manery and Bale, *Amer. J. Physiol.*, 1941, **132**, 215.

<sup>10</sup> Collander and Barlund, *Acta Fenn. Bot.*, 1933, **11**, 1.

corresponds to the diffusion process and involves the diffusion constant with dimensions (length)<sup>2</sup>/time. Hill <sup>11</sup> and Eggleton, Eggleton and Hill <sup>12</sup> had already shown that diffusion accounts for the gain and loss of lactic acid, oxygen, and urea by muscles. A concentration gradient is encountered and the basic equation for the one-dimensional case (an infinite sheet) is

$$\frac{d[S]}{dt} = \frac{D}{\lambda^2} \frac{d^2[S]}{dx^2}, \quad . \quad . \quad . \quad (1)$$

in which  $D$  is the diffusion constant and  $\lambda$  is the factor by which the distance the substance has to travel between the outer surface and any point inside is increased by reason of obstacles.

Evidently diffusion must limit the equilibration between the external medium and the extra-cellular fluid of the isolated muscle.<sup>13</sup> When applying this consideration to tracer experiments there is no chemical concentration gradient, but nevertheless, the effect of the Brownian movements is to lead to a movement of labelled ions into those parts of the system occupied by unlabelled ions, and vice versa, provided no energy barrier greater than several times  $kT$  is interposed. For the purpose of diffusion calculations we can therefore treat the labelled and unlabelled ions as distinct species. Returning to the first case of Collander and Barlund,<sup>10</sup> suppose we have to deal with a system which maintains an ion  $S$  inside the confines of a membrane at a concentration different from its concentration outside. The probability of transfer of an ion from outside to inside will be supposed proportional to the outside concentration  $[S_o]$  and the probability of the reverse transfer will be taken as proportional to the inside concentration  $[S_i]$ . In a cell, therefore, with surface area  $A$ , the net amount going in per unit time is

$$\kappa_1 A [S_o] - \kappa_2 A [S_i],$$

where  $\kappa_1$  and  $\kappa_2$  are constants. If then  $V$  be the volume of the cell the rate of increase of concentration inside will be

$$(\kappa_1 [S_o] - \kappa_2 [S_i]) A / V.$$

Calling  $\kappa_1 A / V$ ,  $k_1$  and  $\kappa_2 A / V$ ,  $k_2$  we have

$$\frac{d[S_i]}{dt} = k_1 [S_o] - k_2 [S_i]. \quad . \quad . \quad . \quad (2)$$

Krogh's "permeability constant" is  $\kappa_2$  which is equal to  $V k_2 / A$ , while Conway's <sup>14</sup> is  $\kappa_1$  which is  $V k_1 / A$ .

Provided the cell is in equilibrium with its surroundings the rate of change of  $[S_i]$  is zero and

$$k_1 [S_o] = k_2 [S_i].$$

In order to distinguish labelled ions they will be denoted  $S^*$  and unlabelled ions  $S'$ .  $S$  will be taken to refer to all ions, whether labelled or not. The experiment is usually conducted in a large volume of external solution, or one which is renewed, so the outside concentration of  $S^*$  or  $S'$  as the case may be, remains constant. It is then possible to eliminate either  $k_1$  or  $k_2$  and obtain  $k_{eliminated}$  for the steady state,

$$\frac{d[S_i^*]}{dt} = -k_2 [S_i^*], \quad . \quad . \quad . \quad (2a)$$

for the external solution all unlabelled, and

$$\frac{d[S_i^*]}{dt} = k_1 [S_i'] - k_2 [S_i^*], \quad . \quad . \quad . \quad (2b)$$

for the external solution all labelled. The integrals are, respectively,

$$-k_2 t = \ln \frac{[S_i^*]}{[S_i^*]_{t=0}} \quad . \quad . \quad . \quad (3a)$$

<sup>11</sup> Hill, *Proc. Roy. Soc. B*, 1929, **104**, 39.

<sup>12</sup> Eggleton, Eggleton and Hill, *ibid.*, 1928, **103**, 620.

<sup>13</sup> Harris and Burn, *Nature*, 1948, **162**, 929.

<sup>14</sup> Hill, *Proc. Roy. Soc. B*, 1930, **109**, 267.

and

$$-k_2 t = \ln \left\{ 1 - \frac{[S_i^*]}{[S_i]} \right\}. \quad (3b)$$

When comparing the properties of cell membranes it is the amount of ion being transferred per unit time and area which is of interest, as was realized by Mullins, Fenn, Noonan and Haeghe<sup>15</sup> in their work on erythrocyte permeability. Under steady state conditions this amount is given by either  $k_1[S_0]V/A$  or  $k_2[S_i]V/A$ , which are equal. Conway based his arguments on the quantity  $k_1V/A$ , which does not express the amount of ion being gained or lost by the cell per unit area and time until multiplied by  $[S_0]$ .

Preliminary measurements of the rate of exchange of alkali metals between isolated frog sartorii and gastrocnemii and the surrounding solution showed that the rate depended upon the dimensions of the muscle. This indicates that diffusion plays at least some part in the process, for the basic permeability equation only involves the volume/surface ratio of the cells, and not the size of the bundle when several or many cells are examined together. It is accordingly necessary to consider a system in which the ions only reach the cell boundaries after diffusion through the interspaces. The cells are supposed to have an internal concentration  $[S_i]$  and to be in steady state conditions with external concentration  $[S_0]$ . At time zero, the bundle of cells is transferred to a new solution, having a concentration  $[S_0^*]$  of labelled ions. The problem is then to find the amount of labelled ion present in the assembly (muscle cells plus interstitial fluid) after any time  $t$ . The ions  $S^*$  move into the interspaces by diffusion, and are always subject to the possibility of transfer to the interior of a cell according to eqn. (2). After time  $t$  the concentration of labelled ion in the cells will be changing at a rate,

$$\frac{\partial [S_i^*]}{\partial t} = k_1[S^*] - k_2[S_i^*], \quad (2c)$$

$[S^*]$  and  $[S_i^*]$  being functions of position and time. The rate of build up of the labelled ions in the cells plus interspaces is defined by eqn. (1a),

$$\frac{D}{\lambda^2} \times \frac{\partial^2 [S^*]}{\partial x^2} = a \times \frac{\partial [S^*]}{\partial t} + b \times \frac{\partial [S_i^*]}{\partial t}, \quad (1a)$$

in which  $a$  is the fraction by volume occupied by extra-cellular fluid and  $b$  is the fraction by volume occupied by intra-cellular fluid. The solutions of the simultaneous equations (2c) and (1a) have been given us by Mr. Wigglesworth of the Mathematics Department, University College, London. For both sides of the infinite sheet exposed to the solution having concentration  $[S_0^*]$  at  $t = 0$ , the sheet having uniform concentrations  $[S_0]$  in the interspaces, and  $[S_i]$  in the cells at  $t = 0$ , and sheet thickness  $l$ , they are

$$[S^*] = [S_0^*] + \sum_0^{\infty} \phi_{2n+1} \sin (2n+1) \frac{\pi x}{l}, \quad (4)$$

$$\text{and} \quad [S_i^*] = \frac{k_1}{k_2} [S_0^*] + \sum_0^{\infty} \psi_{2n+1} \sin (2n+1) \frac{\pi x}{l}, \quad (5)$$

in which

$$\phi_{2n+1} = \frac{-4[S_0^*]}{(2n+1)\pi} \times \left[ \frac{\alpha_2(k_2 + \alpha_1) \exp(\alpha_1 t) - \alpha_1(k_2 + \alpha_2) \exp(\alpha_2 t)}{(\alpha_2 - \alpha_1)k_2} \right], \quad (4a)$$

and

$$\psi_{2n+1} = \frac{-4[S_0^*]}{(2n+1)\pi} \times \frac{k_1}{k_2} \times \left[ \frac{\alpha_2 \exp(\alpha_1 t) - \alpha_1 \exp(\alpha_2 t)}{(\alpha_2 - \alpha_1)} \right]. \quad (5a)$$

<sup>15</sup> Mullins, Fenn, Noonan and Haeghe, *Amer. J. Physiol.* 1941, **135**, 93.

The average values of  $[S^r]$  and  $[S_i^r]$  over the thickness  $l$  are

$$[\bar{S}^r] = [S_0^r] + \sum_0^{\infty} \frac{2}{(2n+1)\pi} \times \phi_{2n+1}, \quad (4b)$$

and

$$[\bar{S}_i^r] = \frac{k_1}{k_2} [S_0^r] + \sum_0^{\infty} \frac{2}{(2n+1)\pi} \times \psi_{2n+1}. \quad (5b)$$

The exponents  $\alpha_1$  and  $\alpha_2$  are the roots of a quadratic and are given by

$$\left[ ak_2 + bk_1 + (2n+1)^2 \frac{\pi^2 D}{\lambda^2 l^2} \right] \pm \left[ \left( ak_2 + bk_1 + (2n+1)^2 \frac{\pi^2 D}{\lambda^2 l^2} \right)^2 - 4ak_2(2n+1)^2 \frac{\pi^2 D}{\lambda^2 l^2} \right]^{\frac{1}{2}} \quad (6)$$

2a

This result shows that the time constants involve  $D/\lambda^2$  and the constants  $k_1$  and  $k_2$ , one of which can be eliminated as before. It will be seen that measurements made on an assembly of cells do not directly furnish a value for either diffusion constant or membrane permeability unless it happens that one of the processes takes place at a very different rate to the other. When it is desired to apply the equations to a muscle exposed on one side only,  $l$  is to be replaced by  $2l$ .

**The Transfer of the Potassium Ion.**—In order to make use of the equations above it is necessary to make approximations. In the majority of muscles the values of  $a$  and  $b$  are not far from 0.13 and 0.67 respectively. In the potassium transfer experiments we have used solutions such that the ratio of external to internal concentration was between 0.1 and 0.014. From the steady state equation this sets the ratio  $k_2/k_1$ . Then  $ak_2/bk_1$  has the range 0.02-0.0033. It is, therefore, allowable to neglect  $ak_2$  and its multiples with respect to the same multiples of  $bk_1$ . The roots  $\alpha_1$  and  $\alpha_2$  can then be obtained. They are

$$\alpha_1 \approx -\frac{1}{a} \left[ bk_1 + (2n+1)^2 \frac{\pi^2 D}{\lambda^2 l^2} \right],$$

$$\alpha_2 \approx -\frac{k_2(2n+1)^2 \frac{\pi^2 D}{\lambda^2 l^2}}{bk_1 + (2n+1)^2 \frac{\pi^2 D}{\lambda^2 l^2}}.$$

Putting these into eqn. (4b) and (5b) the values of the mean concentrations of labelled ion in the extra-cellular and intra-cellular fluids at time  $t$  after immersion in a solution of constant concentration are found.

For extra-cellular potassium,

$$\frac{[\bar{K}^r]}{[\bar{K}_0^r]} = 1 - \frac{8}{\pi^2} \sum_0^{\infty} \frac{\frac{\pi^2 D}{\lambda^2 l^2} \exp(\alpha_1 t) + \frac{bk_1}{(2n+1)^2} \exp(\alpha_2 t)}{bk_1 + (2n+1)^2 \frac{\pi^2 D}{\lambda^2 l^2}}, \quad (7)$$

and for intra-cellular potassium,

$$\frac{[\bar{K}_i^r]}{[\bar{K}_0^r]} = \frac{k_1}{k_2} + \frac{8}{\pi^2} \sum_0^{\infty} \left[ \frac{ak_1 \times \frac{\pi^2 D}{\lambda^2 l^2} \times \exp(\alpha_1 t)}{\left( bk_1 + (2n+1)^2 \frac{\pi^2 D}{\lambda^2 l^2} \right)^2} - \frac{k_1 \exp(\alpha_2 t)}{k_2 (2n+1)^2} \right]. \quad (8)$$

In order further to simplify (8) put  $bk_1$  equal to  $r(\pi^2 D/\lambda^2 l^2)$ . The first values of  $\alpha_1$  are

$$\alpha_1 = \begin{array}{cccc} n=0 & 1 & 2 & 3 \\ -\frac{k_2}{1+r} & -\frac{9k_2}{9+r} & -\frac{25k_2}{25+r} & -\frac{49k_2}{49+r} \end{array}$$

If  $r$  is not much more than unity (and practical values justify this) it will be sufficient to take only the first two terms as differing from those of the series,

$$\sum_0^{\infty} \frac{e^{-k_2 t}}{(2n+1)^2} = \frac{\pi^2}{8} e^{-k_2 t}$$

so that

$$\sum \frac{e^{-\alpha_1 t}}{(2n+1)^2} = \frac{\pi^2}{8} \exp(-k_2 t) + \left[ \exp\left(\frac{-k_2 t}{1+r}\right) - \exp(-k_2 t) \right] + 0.111 \left[ \exp\left(\frac{-9k_2 t}{9+r}\right) - \exp(-k_2 t) \right].$$

Also the value of  $\alpha_1$  proves to be some hundred times  $\alpha_2$ , so the first term including  $\exp(\alpha_1 t)$  rapidly becomes negligible. In the experiments to be described this is true after 500 sec., so eqn. (7) and (8) become

$$\frac{[\bar{K}^*]}{[K_0^*]} = 1 - \frac{8}{\pi^2} \sum_0^{\infty} \frac{bk_1 \exp(\alpha_2 t)}{\left(bk_1 + (2n+1)^2 \frac{\pi^2 D}{\lambda^2 l^2}\right)(2n+1)^2} \quad \text{for } t > 500 \text{ sec.}, \quad (7a)$$

and

$$\frac{[\bar{K}_i^*]}{[K_0^*]} = \frac{k_1}{k_2} \left\{ 1 - 0.812 \left[ 0.121 \exp(-k_2 t) + \exp\left(\frac{-k_2 t}{1+r}\right) \right] + 0.111 \exp\left(\frac{-9k_2 t}{9+r}\right) \right\}. \quad (8a)$$

When the assay of the amount of labelled ion is made, both the intra- and the extra-cellular ions are observed together, so that strictly a weighted mean of the concentrations given by the above equations should be compared with experimental results. The relative amount of extra-cellular potassium is generally a few % of the total, as indeed is stated by the original condition that  $ak_2/bk_1 = 0.02-0.0033$ , so in the interpretation of the experiments it is only necessary to use eqn. (8a). It is interesting, however, to calculate the fraction of labelled potassium present in the interspace fluid after various times. From experimental values of the constants it is found that the mean concentration of labelled ion is 56.86 % of the external concentration during many hours.

When the experiment is conducted by immersing a muscle containing labelled potassium (the whole of the muscle potassium at the start can then be regarded as labelled) in an unlabelled solution  $[K^*]$  the equations describing the loss of labelled ion are obtained by the substitution

$$[K^*] = [K] - [K^*],$$

so that (7a) and (8a) become

$$\frac{[\bar{K}^*]}{[K_0^*]} = \frac{8}{\pi^2} \sum_0^{\infty} \frac{bk_1 \exp(\alpha_2 t)}{\left(bk_1 + (2n+1)^2 \frac{\pi^2 D}{\lambda^2 l^2}\right)(2n+1)^2} \quad \text{for } t > 500 \text{ sec.}, \quad (7b)$$

and

$$\frac{[\bar{K}_i^*]}{[K_0^*]} = 0.812 \frac{k_1}{k_2} \left[ 0.121 \exp(-k_2 t) + \exp\left(\frac{-k_2 t}{1+r}\right) + 0.111 \exp\left(\frac{-9k_2 t}{9+r}\right) \right]. \quad (8b)$$

**The Transfer of the Sodium Ion.**—Provided that eqn. (2), with the proper significance attached to the constants, describes the rate of exchange of the "internal" sodium it is unnecessary to know its location in the cell. It is only in the light of experiment that it is possible to suggest a suitable approximation to allow the solution of eqn. (6). An



experimental plot of the time-course of the loss of radio-sodium from a muscle is shown in Fig. 1. The process can be resolved into the sum of an exponential with time constant 40-60 min., and a more rapid exchange which has the shape of a diffusion curve. It will be recalled that more than half the sodium of the muscle is present in the extra-cellular space, and it would be expected that this fraction would undergo exchange with the external solution by diffusion.

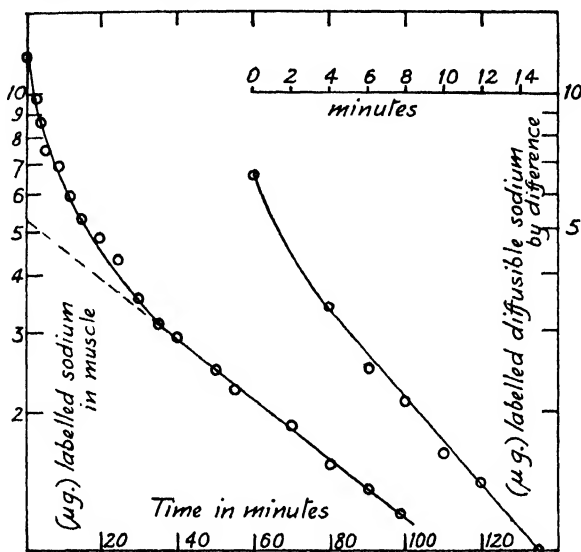


FIG. 1.

It appears, then, that the process of diffusion between the inter-spaces and the external solution is more rapid than the exchange with the "internal" sodium. Assume

$$\frac{\pi^2 D}{\lambda^2 l^2} \gg ak_2 + bk_1$$

in order to find  $\alpha_1$  and  $\alpha_2$ . Then,

$$\alpha_1 \approx -(2n+1)^2 \frac{\pi^2 D}{al^2 \lambda^2},$$

and

$$\alpha_2 \approx -k_2.$$

Using this approximation the equations relating the mean concentrations of labelled sodium to the external concentration of labelled sodium into which the muscle was placed at  $t=0$  are

$$\frac{[\bar{Na}^+]}{[Na_0^+]} = 1 - \frac{8}{\pi^2} \sum_{n=0}^{\infty} \frac{\exp(\alpha_1 t)}{(2n+1)^2}, \quad (9a)$$

and

$$\frac{[\bar{Na}_i^+]}{[Na_0^+]} = \frac{k_1}{k_2} \left\{ 1 + \left[ \frac{8}{\pi^2} \times \frac{k_2}{\pi^2 B} \sum_{n=0}^{\infty} \frac{\exp(\alpha_1 t)}{(2n+1)^2} \right] - \exp(\alpha_2 t) \right\}, \quad (10a)$$

where  $B \equiv D/al^2 \lambda^2$ .

The root  $\alpha_1$  varies with  $n$ , but the other is constant. The series appearing in (9a) has been evaluated by Hill<sup>11</sup> for variable  $Bt$  (his  $kt/b^2$ ). It is plotted in Fig. 2 on semi-logarithmic paper in order to demonstrate that it approximates to an exponential at higher values of  $Bt$ , and that

the intercept of the exponential on the ordinate axis is at  $1/1.235 = 0.81$  of the true initial value. This results if terms other than the first are ignored. The series in (10a) differs but little from  $\exp(-\pi^2 Bt)$ .

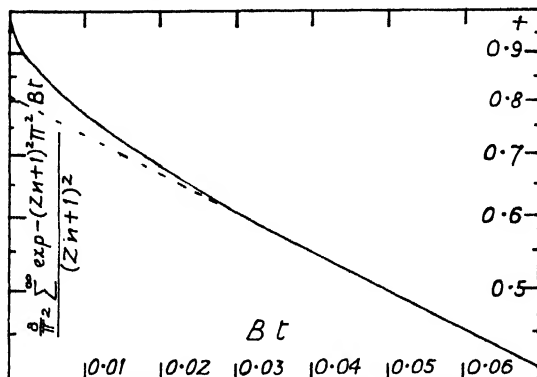


FIG. 2.

The quantity actually observed in the experiments is a mean of the intra- and extra-cellular sodium (when the absorption of the radiation used to estimate the content of labelled sodium is a constant fraction, see Appendix 2). A sample composed of fraction  $a$  by volume of extra-cellular fluid, and  $b$  of internal solution (with which the sodium concentration  $[Na_i]$  is associated) will undergo the exchange process according to a composite equation made up by multiplying (9a) by  $a$ , and (10a) by  $b$ , and adding, thereby giving (11a),

$$\frac{a[\overline{Na'}] + b[\overline{Na''}]}{[Na_0]} = \left(a + b \frac{k_2}{k_1}\right) - \left\{ \frac{8}{\pi^2} \sum \left[ \frac{a}{(2n+1)^2} - \frac{bk_1}{(2n+1)^4 \pi^2 B} \right] \exp(\alpha_1 t) \right\} - \frac{bk_1}{k_2} \exp(-k_2 t). \quad (11a)$$

The condition, implied in the original approximation, that  $bk_1/\pi^2 B$  should be small compared with unity is borne out by experiment (e.g. one value found is 0.002). Therefore (11a) is in effect the sum of a diffusion function  $\sum \frac{\exp(-\pi^2 Bt)}{(2n+1)^2}$  and an exponential term, in accordance with the observations.

When the loss of labelled sodium to an unlabelled solution is followed the relation

$$[Na'] + [Na''] = [Na],$$

which merely states that the total sodium, irrespective of label, is constant, enables appropriate equations to be derived, (11b) being the composite equation corresponding to (11a),

$$\frac{a[\overline{Na'}] + b[\overline{Na''}]}{[Na_0]} = \frac{8}{\pi^2} \sum \frac{a}{(2n+1)^2} \exp(\alpha_1 t) + \frac{bk_1}{k_2} \exp(-k_2 t). \quad (11b)$$

The ratio of the sodium which follows the diffusion law to the total which undergoes exchange is

$$ak_2/(bk_1 + ak_2),$$

provided equilibrium between labelled and unlabelled ions has been reached. For a muscle with 0.13 by volume of interspace and  $k_1/k_2 = 0.15$ , the ratio is 0.565. As the fraction  $a$  increases the proportion of diffusion law material increases.

In order to deduce  $B = D/al^2\lambda^2$  and  $k_1$  from the results, the graphs as exemplified in Fig. 1, were treated as follows. The exponential line was produced back to the ordinate axis, and its time constant ( $1/k_1$ ) found. The exponential was subtracted from the experimental curve and the difference was replotted on an expanded time-scale so that the time course of the diffusion process was obtained. The time required for diffusion to have reduced the quantity of ion to some fraction of its initial value was read off and compared with the value of  $B\pi^2t$  plotted in Fig. 2, whence  $B = D/al^2\lambda^2$  was evaluated. The thickness  $l$  of the specimen was sometimes measured directly, but generally use was made of a calibration established between the muscle weight and the square of the thickness, between which an approximately linear relation exists when the muscle length does not vary greatly. The fraction  $a$  was deduced from the observed ratio of the concentration of labelled sodium following the diffusion law to the concentration of labelled sodium in the medium in which the muscle had been prepared. The ratio of exchangeable internal sodium to external sodium concentration was found by comparing the concentration of labelled sodium in the muscle following the exponential law to the concentration of labelled sodium in the medium.

### Experimental

All measurements of radio-activity were made using glass Geiger-Müller tubes constructed in the laboratory, in conjunction with a commercial scaling unit. The times at which all readings were taken were noted in order to apply correction for the decay of radio-activity. Check assays were made at intervals on solutions of known dilution, and corrections for resolving time and background activity were made when required. The muscle was tied either round the counter tube or on to a glass frame into which the counter could be fitted. In the first arrangement only the outer surface of the specimen was exposed to the solution, but the frame allowed nearly the whole surface to be exposed. The experiments were conducted by observing the radio-activity of the muscle initially, and then immersing it, still tied to the counter, or frame, in the desired solution. It was removed at intervals and the radio-activity again measured. When the specimen was being soaked in radio-active solution the adhering solution was removed before counting by twice dipping into an inactive solution of the same strength. This procedure was only applied in the potassium experiments in which loss by diffusion from the interspaces is insignificant compared to the total potassium in the muscle. Care was necessary to ensure that adsorption of radio-active material on the glass did not lead to error. The comparatively weak solutions used for the potassium experiments did not give trouble. The assay of the radio-activity was usually completed in 2 min. or less, more than 400 counts being observed so that statistical errors have a probable deviation of  $\pm 3\%$ . At the end of the period of soaking the muscle was dissolved in a little acid and after dilution with water the solution was assayed in a counter made specially for dealing with a small volume (2 ml.) of liquid. The radio-activity of the muscle solution was compared with that of a standard made up from the original radio-active material in order that the quantity of radio-active ion in the muscle at the end of the experiment could be calculated. From that figure it was possible to convert to the quantity present at the commencement of the experiment by use of the appropriate counting results obtained when the muscle was intact.

In order to follow the rapid loss of radio-active sodium which takes place in the first 10 min. of soaking the method was modified, the counter being kept in operation continuously while the washing solution was circulated round the muscle.

Muscles containing radio-potassium were prepared by injecting 10 mg. active KCl + 10 mg.  $\text{CaCl}_2$  dissolved in 2 ml. water on the day previous to dissection. The calcium chloride appeared to counteract the toxicity of the potassium. Muscles containing radio-sodium were made either by injection of 10 mg. NaCl in 1 ml. water, or by soaking isolated muscles in Ringer's solution made up from radio-sodium chloride. Some analyses of samples of plasma, erythrocytes and muscles were made. For chemical analysis the material was subjected to wet oxidation in silica flasks and the methods detailed in the Appendix were applied.

## Results

**The Effect of Storage of the Muscles.**—It has frequently been observed that even after the most careful dissection there is a slow loss, or "leakage" of the potassium of the fibres.<sup>16</sup> This can have a considerable influence upon the measured rates of exchange of the potassium ion, for not only is there a movement of potassium ion, but also the concentration of potassium in the interspaces will be increased above the concentration in the external solution. As the rate of exchange varies with the potassium concentration a rather complicated situation is set up. It is easy to calculate the distribution of potassium concentration in the extra-cellular fluid which results from leakage, the necessary equations have been given by Hill (cp.<sup>11</sup> § B, p. 50). If the effective diffusion constant of the ion in the interspaces be taken as  $3 \times 10^{-6}$  cm.<sup>2</sup>/sec. and the rate of leak is 5 % of the internal potassium concentration per hour, say, 175  $\mu$ g. cm.<sup>-3</sup> of tissue (67 % cell fluid) per hour, in absence of loss by diffusion this would lead to an increase of the concentration in the interstitial fluid (13 % by volume) of  $175/0.13 \times 3600 = 0.375$   $\mu$ g. cm.<sup>-3</sup> sec.<sup>-1</sup>. Then with a muscle 0.1 cm. thick, exposed on one side only, the concentration of potassium in the interstitial fluid at the unexposed side, when loss by diffusion at the exposed side is in progress will be

$$[K] = [K_0] + \frac{1}{2} \times \frac{0.01 \times 0.375 \times 0.13}{3 \times 10^{-6}} = [K_0] + 81 \mu\text{g. cm.}^{-3},$$

where  $[K_0]$  is the concentration in the external solution. Over the thickness of the muscle the mean concentration will be

$$[\bar{K}] = [K_0] + \frac{1}{3} \times \frac{0.01 \times 0.375 \times 0.13}{3 \times 10^{-6}} = [K_0] + 54 \mu\text{g. cm.}^{-3}$$

so when in 0.015 % KCl Ringer's the mean potassium in the interspaces is over 1.6 times the external concentration. The loss of potassium from the assembly (cells plus interspace fluid) will be equal to the loss from the cells minus the increase of potassium in the interspaces, i.e.  $175 - (54 \times 0.13) = 168$   $\mu$ g. per cm.<sup>3</sup> tissue per hour, when of thickness 0.1 cm., with one side exposed. For comparison the amount of potassium exchanging per cm.<sup>3</sup> tissue (67 % cells) in 0.015 % KCl Ringer's solution is 90  $\mu$ g./hr. The effect of the potassium leakage is greater than would be expected because it is found that the factor  $k_2$  which determines the exchange rate is proportional to the potassium concentration in the interspaces, which is, in the first example, over 1.6 times the external concentration (when in 0.015 % KCl Ringer's solution). The internal potassium of a "leaking" muscle will, therefore, exchange at a greater rate than that of one which is not leaking. It has been found that fairly consistent results for rate of exchange were obtained by avoiding periods of soaking exceeding 4.5 hr., and by not working with lower concentrations of potassium chloride than 0.03 % in the Ringer's solution. It is likely that several of the experiments carried out in 0.015 % KCl Ringer's solution have indicated too high a rate of exchange because of the presence of leakage. All experiments in which the loss of labelled potassium was followed in 0.015 % KCl Ringer's solution gave high values for  $k_2$ .

TABLE I.—THE UPTAKE OF LABELLED SODIUM DURING STORAGE IN RINGER'S SOLUTION

Muscle wt. (g.)	Sodium Content (calc.) $\mu$ g.	Radio-Sodium Uptake after			> 3 hr.	K Content $\mu$ g.	
		8 min. $\mu$ g.	1 hr. $\mu$ g.	3 hr. $\mu$ g.		Fresh	Stored
<i>Sartorius</i>							
0.085	58.6	32.5	55.5	55	89 (17 hr.)	210	160
0.041	28.3	23	29	33	51 ( 8 hr.)	140	110
<i>Gastrocnemius</i>							
0.22	128	64	110	114			
0.24	132	76	114	130			
0.34	192	98	163	183			
0.18	172	99	186	—			
	(analysis)						

When a muscle is stored in Ringer's solution made with labelled NaCl the content of labelled sodium becomes nearly constant after an hour, and corresponds to what would be expected if all the muscle sodium had exchanged, based on an assumed value of 0.18 for  $a$  for sartorii and 0.13 for gastrocnemii. If the storage is prolonged until an appreciable potassium loss has taken place it is found that an additional amount of sodium is absorbed. By comparison of the chemical analyses of a pair of muscles, the one taken directly, and the other after long storage, the potassium loss could be found, and compared with the increase of sodium measured by the radio-activity. The two quantities proved to be nearly chemically equivalent.

**The Kinetics of the Loss of Labelled Sodium from Sartorii.**—Muscles were prepared with a content of labelled sodium and then treated with a solution free from radio-active ions. The loss of radio-activity was followed. Observations making up such an experiment are illustrated in Fig. 1. The values of the exchange constants, and of the effective diffusion constant of sodium in the interspaces are tabulated in Table II. In order to calculate  $k_1$  from  $k_2$ , assuming a constant internal sodium concentration, the relation,

$$\frac{[Na_i]}{[Na_0]} = \frac{\text{Labelled sodium following exponential law} \times 1.06}{\text{Muscle Wt.} \times \text{Labelled sodium per g. external soln.} \times \bar{W}_m \times (1 - a)}$$

was used. The factor 1.06 is the ratio of the density of muscle cells to that

TABLE II.—SUMMARY OF RESULTS OF SODIUM TRANSFER MEASUREMENTS

Temp. °C	$D/\lambda^2$ cm. <sup>2</sup> /sec.	$a$	$[Na_i]/[Na_0]$	$k_1$ hr. <sup>-1</sup>	$k_2$ hr. <sup>-1</sup>	Solution used
(a) Muscles taken 20 hr. after injection of labelled saline.						
17	$2.1 \times 10^{-6}$	0.13	0.28	0.26	0.9	Ringer's soln.
17	1.9 "	0.21	0.28	0.42	1.54	+0.022 % KCl
17	2.4 "	0.14	0.14	0.19	1.33	" "
19	2.7 "	0.21	0.18	0.20	1.11	" " Mean $D/\lambda^2$
10	2.3 "	0.13	0.14	0.23	1.62	" " $2.64 \pm 0.25$
18	2.8 "	0.19	0.15	0.27	1.82	" " $\times 10^{-6}$ cm. <sup>2</sup> /sec.
8	2.2 "	0.17	0.20	0.28	1.32	" "
18	3.2 "	0.22	0.20	0.33	2.86	" " Mean $k_1$
19	3.2 "	0.29	0.15	0.19	1.22	0.015% KCl 0.26 $\pm$ 0.02 hr. <sup>-1</sup>
16	3.2 "	0.21	0.27	0.25	0.91	" " Mean $a = 0.19$
16	3.5 "	0.17	0.23	0.22	0.95	" " Mean $[Na_i]/[Na_0] = 0.20$
19	3.5 "	0.26	0.19	0.27	1.36	0.045% KCl
16	2.5 "	0.20	0.18	0.14	0.77	0.06% KCl
17	2.5 "	0.19	0.18	0.45	2.50	0.06% KCl
16	1.2 "	0.18	$0.11 \times 2^*$	0.15	0.68	Ringer's soln. +
10	2.3 "	0.11	$0.05 \times 2$	0.10	1.00	50 % NaCl replaced by
10	2.3 "	0.12	$0.065 \times 2$	0.135	1.00	" " dextrose
12	3.2 "	0.21	$0.18 \times 4^*$	1.0	1.38	75 % of NaCl "
12	2.3 "	0.20	$0.085 \times 4$	0.42	1.25	" " "
12	1.6 "	0.10	$0.095 \times 4$	0.77	2.00	" " "
(b) Muscles prepared by soaking in Ringer's solution made up with labelled NaCl.						
17	$4.0 \times 10^{-6}$	0.20	0.174	0.32	1.82	Ringer's soln. +
17	2.8 "	0.13	0.103	0.18	1.76	0.022 % KCl (soaked 1.3 hr.)
17	2.1 "	0.24	0.186	0.11	0.61	0.06 % KCl (soaked 1.8 hr.)
						0.022 % KCl (soaked 2 hr.)

\* The value of the ratio determined by the experiment refers to the conditions under which the muscle was prepared, viz. by being exposed to the labelled lymph of the living frog. In order to deduce  $k_1$  from the  $k_2$  found in the soaking-out experiment the ratio referred to the soaking-out solution must be used, which is 2 or 4 times the experimental figures; provided the internal sodium concentration does not change during the experiment.

of Ringer's solution (cp. Hill,<sup>14</sup>);  $W_m$  is the fraction by weight of non-protein in the cell material (taken as 0.8). For sodium the corrections for water content of the plasma and the effect of dissolved protein approximately cancel out. The fraction by volume of extra-cellular space  $a$  was similarly found from

$$a = \frac{\text{Labelled sodium following diffusion law} \times 1.05}{\text{Muscle Wt.} \times \text{Labelled sodium per g. external soln.}}$$

The factor 1.05 is the ratio of the density of whole muscle (with approximately 15 % interspace) to that of Ringer's solution.

The theoretical equations were developed for a thin sheet of infinite extent. No great error is introduced if they are applied to a thin, flat muscle like the sartorius. They do not apply to the gastrocnemius, for not only is this muscle of circular section, but also its dimensions are such that the rate of diffusion is approximately equal to the rate of permeation. As a consequence the loss of labelled sodium from such a muscle follows a diffusion law, but the additional sodium in the cells prolongs the process and makes the apparent "diffusion constant" considerably lower than the true value.

■ The following remarks can be made about the preceding results.

(1) The effective value of the diffusion constant in the interspaces  $D/\lambda^2$  is about  $\frac{1}{2}$  of the value of  $D$  in free solution.

(2) The constant  $k_1$  is not significantly altered by changes of 10° C in the temperature, nor by changes in the concentration of potassium chloride in the Ringer's solution between 0.015 % and 0.06 %.\*

(3) Substitution of dextrose for up to half the sodium chloride does not lead to a considerable alteration in  $k_1$  or  $k_2$ , but when three-quarters is so substituted  $k_1$  is increased if the internal sodium concentration remains constant during the experiment. This point could not be checked, so it is possible that the muscles lost sodium in this solution.

(4) Taking a mean fibre diameter of 80  $\mu$  the volume/surface ratio is 0.002 cm. and  $\kappa_1 = k_1 V/A$  is 0.00052 cm./hr. for freshly dissected muscles, corresponding to a sodium flux of 1.33  $\mu\text{g. cm.}^{-2} \text{ hr.}^{-1}$ .

**The Transfer of the Potassium Ion.**—Referring to eqn. (7) and (8) developed for the potassium ion, it will be seen that the exponents involve both diffusion and permeation constants implicitly. No convenient separation into

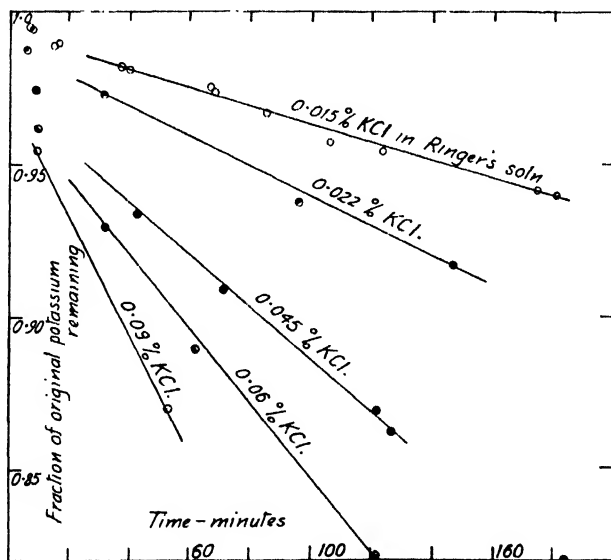


FIG. 3.

"fast" and "slow" fractions takes place. Fig. 3 illustrates some experimental results, the fraction of the potassium left unexchanged being plotted against time of immersion in Ringer's solutions having various concentrations of KCl.

\* See Note added in proof.

In order to deduce  $k_2$  (and from it,  $k_1$ ) it is necessary to assume a figure for  $D/\lambda^2$ , the effective diffusion constant of potassium in the interspaces. The value we have used is  $3 \times 10^{-6}$  cm.<sup>2</sup>/sec. rather higher than the sodium ion value, because in free solution the potassium ion has a diffusion constant of  $16 \times 10^{-6}$  compared with  $11.5 \times 10^{-6}$  cm.<sup>2</sup>/sec. for sodium at 18° C.

In Fig. 4 the function

$$\frac{8}{\pi^2} \left[ 0.121 \exp(-k_2 t) + \exp\left(\frac{-k_2 t}{1+r}\right) + 0.111 \exp\left(\frac{-9k_2 t}{9+r}\right) \right]$$

has been plotted for varying  $k_2 t$  and  $r = bk_1(4)l^2\lambda^2/\pi^2 D$ . If the time required for a given fractional exchange of potassium is known and the value of  $\pi^2 D/(4)al^2$  is calculated it is possible to find  $k_2$  by successive approximation, a likely value for  $r$  being assumed initially.  $k_1$  is obtained from  $k_2$  by use of the relation  $k_1/k_2 = [K_i]/[K_o]$ , which must hold if the internal potassium concentration remains constant during the experiment.

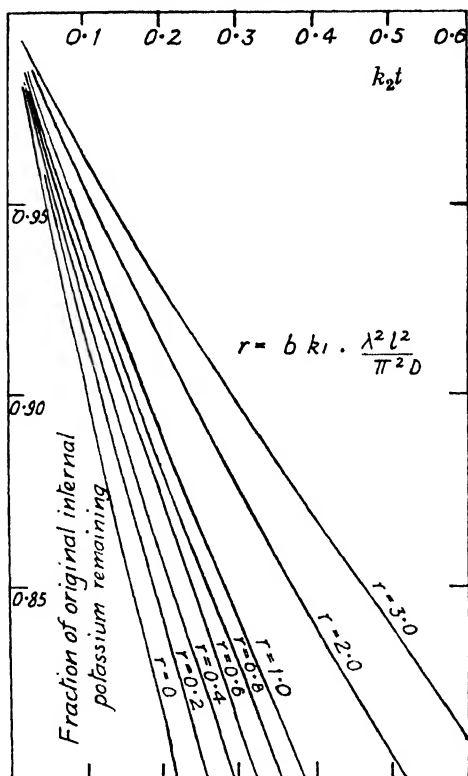


FIG. 4.

The experimental figures were used to calculate  $1 - [K_i^*]/[K_i]$  when the muscle was exposed to a labelled solution, and  $[K_o^*]/[K_o]_{(t=0)}$  when the loss of labelled ion from the muscle to the solution was being followed. The resulting figures were plotted as exemplified in Fig. 3. From the plots the time for a given fractional exchange was found. As there was generally an abrupt change at the commencement, probably related to an adsorption effect, the time equal zero intercept of the ratio was used as the initial value rather than the theoretical value (unity). When plotting results obtained in the higher strengths of potassium it was found convenient to use the root of the time as abscissæ, as the fractional exchange was found to be linearly related to the root of the time after about 10 % exchange. Table III summarizes the results. The majority were obtained by the method of soaking the muscle in labelled solution, as the effect of potassium leakage is less than when using the alternative method. The methods are distinguished by *In* and *Out* respectively. Those runs made with the muscle exposed on both sides by use of the frame are distinguished by the word *Spaced*.

TABLE III.—POTASSIUM ION TRANSFER

Solution	[K <sub>1</sub> ]/[K <sub>0</sub> ]	Temp. °C	r	k <sub>1</sub> hr. <sup>-1</sup>	k <sub>2</sub> hr. <sup>-1</sup>	Method	Notes
Ringer's + 0.015 % KCl	62.5	5	0.6	1.7	0.028	In	(1)
		5	0.3	1.2	0.020	"	
		8	0.6	2.4	0.038	"	
		12	0.6	1.7	0.028	"	
		16	0.35	2.0	0.032	"	
		17	0.6	1.5	0.024	"	
			Mean	1.75	0.028		
Ringer's + 0.022 % KCl	42.8	5	0.6	1.0	0.023	In	Spaced (2)
		7	0.7	1.8	0.042	Out	
		10	0.12	2.0	0.046	In	
		10	0.7	1.8	0.043	"	
		12	0.7	1.7	0.040	"	
		15	0.35	1.4	0.032	"	
		15	0.55	1.7	0.040	"	
			Mean	1.61	0.038		
Ringer's + 0.045 % KCl	20.8	5	0.25	1.5	0.071	In	Spaced "
		5	0.3	2.4	0.116	Out	
		8	0.8	1.9	0.092	"	
		10	0.15	1.7	0.082	In	
		10	0.15	1.6	0.077	"	
		12	0.6	1.6	0.078	"	
		17	0.6	1.9	0.091	"	
		17	0.3	1.4	0.070	"	
			Mean	1.75	0.085		
Ringer's + 0.06 % KCl	15.65	8	0.8	2.1	0.134	In	(3)
		10	0.6	1.2	0.078	Out	
		17	0.6	1.8	0.114	In	
			Mean	1.70	0.109		
Ringer's + 0.09 % KCl	10.4	5	0.45	1.6	0.156	In	
		5	0.4	1.6	0.153	Out	
		17	0.6	1.9	0.210	In	
			Mean	1.67	0.173		
K <sub>2</sub> SO <sub>4</sub> (0.095M)/ Dextrose (0.22M) = 7/2	0.855	17	0.10	0.36	0.41	Out	(4)
		17	0.14	0.26	0.29	"	
		17	0.10	0.31	0.35	"	
			Mean	0.31	0.35		

Notes.—(1) Two similar sets of figures, one obtained with 0.02 % CaCl<sub>2</sub> in the solution, and the other with 0.04 %.

(2) Two similar sets of figures, one obtained in usual unbuffered solution, and the other with 1 % 0.1 M phosphate buffer, pH 7.

(3) Two similar sets of figures, one with 0.02 % CaCl<sub>2</sub> in the solution, and the other with 0.06 %.

(4) The muscles are reversibly inexcitable in this medium. The figures were obtained for comparison with some electrical measurements made by Dr. B. Katz. The derivation of  $\alpha_1$  and  $\alpha_2$  is less applicable than in other cases because  $ak_2/bk$ , has become comparatively large (0.23).



The following points emerge from these figures—

(1) The exponent  $k_2$  is a linear function of the potassium ion concentration up to the equivalent of 0.09 % KCl. On the contrary  $k_1$  is independent of the external solution in the range studied, and is 1.7 hr.<sup>-1</sup>.

(2) On the basis of a volume/surface ratio of 0.002 cm. the permeability constant  $\kappa_1 = k_1 V/S$  comes to 0.0034 cm./hr. In 0.015 % KCl Ringer's solution the amount of potassium ion leaving, and entering, the cell per unit area per hour is 0.27  $\mu\text{g.}$ , and this amount increases linearly with the external potassium concentration up to 0.09 % KCl.

(3) No systematic temperature effect can be observed as a result of changes of temperature \* of 10° C.

(4) Increases of the calcium ion concentration, or presence of phosphate buffer do not exert an appreciable influence on the permeability.

**Ion Transfer between Frog Erythrocytes and Plasma.**—It was thought to be worth comparing muscle cells with some other cells. As the experiments furnished samples of erythrocytes which had been soaked *in vivo* in labelled plasma the necessary analyses were made in order to deduce their permeability constants.

Figures have been published by Mullins, Fenn, Noonan and Haeghe<sup>16</sup> for the permeabilities of various erythrocytes to potassium, together with a few results for sodium. They made use of an equation similar to (2) and defined their permeability constant as

$$k_2 = [K_i] V_i / A,$$

$V_i$  and  $A_i$  being the volume and surface area of the cell, and  $[K_i]$  its internal potassium concentration. We have written  $k_2$  for their  $k$  in order to show its identity with our  $k_2$ . There are some errors in their equations (ref. <sup>16</sup>, pp. 97, 98). Their eqn. (2) should read

$$x_0 = a - x_i \frac{[K_i] V_i}{[K_0] V_0} \quad \dots \quad (11)$$

in which  $a$  is the initial specific activity of the external potassium,  $x_i$  is the specific activity of the internal potassium,  $[K_0]$ ,  $x_0$  and  $V_0$  are respectively the potassium concentration, specific activity, and volume of the external solution. When the external specific activity varies with time, being related to the gain of labelled atoms by the internal medium according to (11) the integral is

$$\ln \left[ 1 - \frac{x_i}{a} \left( 1 + \frac{[K_i] V_i}{[K_0] V_0} \right) \right] = - \frac{p A_i t}{[K_i] V_i} \left( 1 + \frac{[K_i] V_i}{[K_0] V_0} \right) \quad \dots \quad (12)$$

TABLE IV.—EXCHANGE BETWEEN FROG ERYTHROCYTES AND PLASMA IN APPROXIMATELY 20 HR. FOLLOWING INJECTION OF 10 MG. OF LABELLED ALKALI CHLORIDE

Final Specific Activity of Plasma	Final K Content of Plasma ( $\mu\text{g./g.}$ )	Final Specific Activity of Cells	K Content of Cells (mg./g.)	$k_2$ (hr. <sup>-1</sup> )	$k_1$ (hr. <sup>-1</sup> )
POTASSIUM					
0.110	426	0.007	2.59	0.004	0.024
0.037	602	0.015	2.50	0.028	0.116
0.116	232	0.010	3.67	0.005	0.079
0.040	350	0.012	2.90	0.018	0.15
0.048	330	0.012	1.90	0.114	0.081
SODIUM					
	Final Na Content ( $\mu\text{g./g.}$ )		Na Content (mg./g.)		
0.046	2800	0.006	0.90	0.007	0.002
0.087	3340	0.027	0.90	0.019	0.005
0.078	1950	0.028	0.67	0.014	0.009
0.152	2230	0.061	0.40	0.020	0.004

\* See Note added in proof.

Proceeding, as did Mullins *et al.*, to the case when the external specific activity does not vary, which corresponds to  $V_0 \rightarrow \infty$ , the equation is

$$\ln \left( 1 - \frac{x_t}{a} \right) = \frac{-pA_t t}{V_0} \equiv -k_2 t,$$

corresponding to our (3b). The final equation in the quoted work omitted  $a$ , which must determine  $x_t$  at  $t = \infty$ .

The results we obtained for the two alkali metals are tabulated below. They show considerable variations of both permeability and alkali metal content, this may be a consequence of the gross amount of alkali chloride injected.

The values of  $k_1$  and  $k_2$  were obtained from the final activities, no allowance being made for the variation during the experiment. In two additional experiments separated erythrocytes were stored for 20 hr. in Ringer's solution made up with labelled sodium chloride. From the measurements of radio-activity, and sodium content, the value  $0.003 \text{ hr.}^{-1}$  for  $k_1$  was obtained. While there are insufficient data to establish the point it is likely that, as in the muscle cells, the value of  $k_2$  is a function of the external concentration of the ion. Mullins' value of  $k_2$  for potassium was  $0.016 \text{ hr.}^{-1}$  and his  $[K_0]$  was  $2.97 \text{ mg./g.}$  He also gave some figures for the cell dimensions which make the volume/surface ratio  $4.27 \times 10^{-4} \text{ cm.}$ , from which the permeability constant can be calculated.

**The Results of Changes in the Conditions on the Permeability.**—The experiments have usually been confined to the investigation of the results of changes in the concentration of potassium or sodium ion, or of the temperature, upon the permeability of the muscle. Under given conditions there is a wide variation from specimen to specimen, and to establish a correlation a considerable number of experiments are required unless the effect is gross. For example, changes of temperature of up to  $10^\circ \text{C}$  were insufficient to give rise to a significant variation of the permeability.\*

The rate of the potassium exchange was affected in a regular way by the concentration of potassium in the external solution, corresponding to a constant value of the permeability constant ( $\kappa_1$ ). There was no obvious influence on the sodium exchange. Conway<sup>16, 17</sup> contends that an increased potassium concentration should reduce the permeability to sodium. Ussing<sup>4</sup> found no such influence on the rate of penetration of a frog sartorius.

The range of variation of the concentrations of the ions making up the solution is limited, for on the one hand loss of salts from the muscle takes place, and on the other the membrane becomes inexcitable. In order to apply the simpler equations it is necessary to restrict work to solutions in which the muscle maintains a constant concentration of salts and a constant weight. In solutions with low KCl content there is a loss of potassium and this may even take place in  $0.015 \%$  KCl Ringer's solution.<sup>18</sup> In K-free Ringer's solution, Stanton<sup>19</sup> found the loss to be  $3 \%$  of the total potassium in  $\frac{1}{2} \text{ hr.}$  It was unaffected by pH between 6 and 8. We have also observed that the potassium permeability is unaffected by pH in the range 5-7. Many of the muscles become inexcitable in Ringer's solution with  $0.06 \%$  KCl, though excitability is restored by washing in normal Ringer's solution.

In order to vary the concentration of sodium it was necessary to maintain osmotic equilibrium by adding e.g. dextrose. Thus, the chloride concentration was subject to simultaneous variation. When more than half the sodium chloride was replaced, the muscle became reversibly inexcitable, and the membrane permeability ( $\kappa_1$ ) to sodium increased or loss of internal sodium took place.

The influence of narcotics on permeability has been discussed by Danielli and Davson.<sup>20</sup> There are very few figures relating the permeability to the concentration of narcotic. An important qualitative result due to Davson is that some substances reduce the rate of penetration of sodium and increase the rate for potassium. Observations made on the plasma potassium level *in vivo* may probably be related to a shift in the steady state conditions of potassium in certain cells. Keys in 1938 confirmed that adrenaline injection brings about a rise in plasma potassium in the case of cats, dogs, and rabbits, although it had an opposed result in human beings. If the injected substance causes a change in the ratio of  $k_1/k_2$  (or  $\kappa_1/\kappa_2$ ) there will be a change in the ratio of

\* See Note added in proof.

<sup>16</sup> Conway, *Irish J. Med. Science*, 1947 (Oct.-Nov.).

<sup>17</sup> Conway and Hingerty, *Biochem. J.*, 1948, **42**, 372.

<sup>18</sup> Horton, *J. Physiol.*, 1930, **70**, 389.

<sup>19</sup> Stanton, *J. Gen. Physiol.*, 1923, **5**, 461.

<sup>20</sup> Danielli and Davson, *The Permeability of Natural Membranes* (1944).

$[K_i]/[K_o]$ . Following the loss or inactivation of the substance the ratios will return to normal. The technique described here could be used to investigate the effects of such substances on isolated tissues.

Although calcium is supposed to have a specific effect on muscle, it was not found that changes in the concentration of  $CaCl_2$  between 0.02 and 0.06 % gave rise to significant alteration of the potassium permeability.

**The Specific Activities of Muscles and Plasma.**—The specific activity of the plasma measured at the end of the period following injection is not accurate for the calculation of the kinetics of penetration of ions *in vivo* because there is a continuous loss of labelled ion going on all the time. After 20 hr. it was frequently found that the muscle specific activity exceeded that of the plasma. This comes about because the muscle specific activity is a time integral of the product of the instantaneous rate of penetration and the concentration of labelled material in the surrounding medium. The latter is falling continuously so the muscle activity will pass through a maximum value at some time following injection and will not be simply related to the final value of the plasma activity. The figures quoted below do not, therefore, prove that the muscle sodium and potassium are fully exchangeable.

TABLE V.—COMPARISON OF SPECIFIC ACTIVITIES AT 20 HR. AFTER INJECTION OF 10 MG.  $K^+$  OR  $Na^+$  CHLORIDE

Sodium		Potassium	
Muscle	Plasma	Muscle	Plasma
0.18	0.197	0.118	0.110
0.084	0.078	0.078	0.043
0.176	0.17	0.08	0.116
0.247	0.299	0.107	0.04
0.08	0.078	0.126	0.048
0.34	0.30	0.077	0.08
0.136	0.152	0.12	0.08
0.10	0.146	—	—

**Sodium Activity in the Potassium Samples.**—One explanation offered for the failure to reach equilibrium between the specific activities of muscle and plasma potassium in Hevesy's experiments has been that there might be radio-sodium contamination of his potassium. In the experiments described here the presence of radio-sodium would only interfere in the "soaking-in" experiments, as the organism itself effects a purification of the potassium when a labelled muscle is prepared. In order to decide whether any important amount of sodium activity was associated with our potassium samples, some were dissolved, inactive sodium chloride added and the potassium precipitated as perchlorate which was reconverted to chloride. No significant loss of specific activity was found. In the samples prepared by bombardment of chlorides an appreciable radio-phosphate activity is found, amounting to 0.05 % of the total activity on the day following receipt of the sample.

**The Equilibration between Extra-Cellular Potassium and External Potassium.**—It is of interest to calculate the degree of exchange between the extra-cellular potassium and that in the external solution. The rate of exchange is considerably less than would be found if the ions had only to pass round impermeable obstacles because the concentration is controlled in part by the large reserve amount of potassium present in the cells. Taking as one example the case of an ordinary muscle put at time zero into a labelled Ringer's solution containing 0.015 %  $KCl$  eqn. (7) is applied, using the figures from Table III.

$$k_1 \ 2.25 \text{ hr.}^{-1} = 6.25 \times 10^{-4} \text{ sec.}^{-1}, \quad bk_1 = 4.2 \times 10^{-4} \text{ sec.}^{-1}.$$

$$k_2 \ 0.036 \text{ hr.}^{-1} = 10 \times 10^{-6} \text{ sec.}^{-1}.$$

An average sartorius has  $l^2 = 0.01 \text{ cm.}^2$ , so  $\pi^2 D/l^2 = 2 \times 10^{-3} \text{ sec.}^{-1}$  (for the muscle exposed both sides). The roots  $\alpha_1$  and  $\alpha_2$  are multivalued, but for  $t > 100 \text{ sec.}$  we need take only the first value of  $\alpha_1$  and the first two of  $\alpha_2$ , i.e.

$$\alpha_1 \ (n = 0) = 1.1 \times 10^{-2} \text{ sec.}^{-1}, \quad \alpha_2 \ (n = 0) = 0.83 \times 10^{-5} \text{ sec.}^{-1}$$

$$\alpha_2 \ (n = 1) = 0.93 \times 10^{-5} \text{ sec.}^{-1}.$$

The fraction of the extra-cellular potassium which has undergone exchange after various times is—

$t$ (sec.)	100	400	1,000	10,000
$[K]/[K_0]$	0.637	0.861	0.862	0.944

A similar calculation for 0.06 % KCl in the Ringer's solution provides the following figures—

$t$ (sec.)	100	400	1,000	10,000
$[K]/[K_0]$	0.531	0.560	0.568	0.650

Thus the labelled potassium in the extra-cellular fluid is far from reaching the concentration of labelled ion in the external solution even after some considerable time, and that the concentration of labelled potassium after 400 sec. immersion is nearly equal to that present in the interspaces for a further two hours. The term in  $\exp(\alpha_1 t)$  describes the course of the initial rush of labelled ions into the extra-cellular spaces, afterwards a slow increase proceeds, limited by the rate of exchange of the potassium in the fibres. The initial phase is over in less than 400 sec.

### Discussion

The sodium exchange measurements made *in vitro* have provided information about the diffusibility of the ion round the fibres making up the muscle, and also about the rate of penetration of the fibres. The diffusion constant is reduced from the free solution value ( $11.5 \times 10^{-6}$  cm.<sup>2</sup>/sec.) to a mean value of about a  $\frac{1}{4}$  of this. If the ions had to traverse the semi-circumferences of a number of cylinders on their way between the outside and the interior of the muscle bundle they would cover a distance  $\pi/2$  times the measured distance, so the value of  $l^2$  used in the calculation of  $D$  should be increased in the ratio  $\pi^2/4$  to the measured value. This would raise our mean value of  $D$  to  $6.5 \times 10^{-6}$  cm.<sup>2</sup>/sec., about half the free solution value. It is unfortunate that it is not possible to measure the value of  $D$  for the potassium ion owing to its rapid exchange with the intra-cellular potassium.

TABLE VI -- CELL PERMEABILITY FIGURES

Ion	Cell	$k_1$ , cm./hr.	Original Source
Na	Frog muscle	$5.2 \times 10^{-4}$	This paper
Na	Rat muscle	$13.8 \times 10^{-4}$	Heppel (K deprived rats)
Na	Cat erythrocyte	$5 \times 10^{-6}$	Mullins, Fenn, Noonan and Haeg
Na	Dog erythrocyte	$14 \times 10^{-6}$	Cohn and Cohn
Na	Frog erythrocyte	$2 \times 10^{-6}$	This paper
K	Frog muscle	$3.4 \times 10^{-3}$	This paper
K	Rat muscle	$5 \times 10^{-2}$	Noonan, Fenn and Haeg
K	Rat muscle	$1.6 - 5 \times 10^{-2}$	Hahn and Hevesy
K	Rabbit muscle	$3.2 \times 10^{-3}$	Hahn and Hevesy
K	Frog erythrocyte	$4 \times 10^{-5}$	This paper
K	Frog erythrocyte	$9 \times 10^{-6}$	Mullins, Fenn, Noonan and Haeg

The permeability measurements lead to the conclusion that the "permeability constant" obtained by multiplying  $k_2$  of eqn. (2a) or (2b) by the volume/surface ratio is *not* independent of the external concentration. On the other hand  $k_1$  (in eqn. (2)) is found to be constant as is implied in the formulation, as long as the internal concentration of the ion remains constant. Following Conway, the most useful figure to quote is the product  $k_1 \times$  (volume/surface). The use of a mean volume/surface ratio is liable to lead to difficulties, because in muscles the fibre diameters have such a wide range of values. The mean value should take account of the distribution of the volume/surface ratios in relation to the volume of the muscle.

The results we have obtained *in vitro* indicate how necessary it is to allow for the limiting effect of diffusion when trying to study cell permeability, unless single cells can be used. The relative importance of diffusion *in vivo* will depend on the blood supply brought by the capillaries. Fenn, Noonan, and Haeger in their experiments on potassium exchange concluded that blood supply influences the rate of exchange, for stimulation of an isolated muscle did not affect the exchange rate, whilst stimulation *in vivo* did so. Similarly, Hahn and Hevesy found the exchange accelerated when their rats were made to swim. We may compare the figures collected by Krogh from a number of sources for permeability measured *in vivo* (with no allowance made for diffusion), with our results. For this purpose we have recalculated to  $\kappa_1 = k_1$  volume/surface, keeping the units cm. per hour (Conway,<sup>18</sup> (Table IX) does not state the units of  $P_0$ , which is our  $\kappa_1$ ).

The final figure is doubtful as we had to assume that the plasma potassium of the frogs was about equal to the concentration we found in ours.

Measurements made *in vivo*, in which no correction for the delaying effect of diffusion have been made, provide values of  $\kappa_1$  higher than we find *in vitro*. Unfortunately, they refer to different animals, so it is not possible to estimate the influence which diffusion plays *in vivo*. The increased rate of exchange which has been observed to result from increased blood circulation is likely to be related to a reduction of the diffusion path by the opening up of more capillaries. If  $l$  be reduced two-fold, the number  $r$  is reduced. In a small muscle this will lead to a reduction of the time for 50 % potassium exchange by a factor of about 30 %.

The combined diffusion-permeation process must come into play whenever one has to deal with an exchange taking place between an assembly of cells and their surroundings. Measurements of diffusion constant and permeability have to be considered in this light. For example, Stella<sup>21</sup> found the "diffusion constant" for phosphate in muscle to have value  $0.8 \times 10^{-7}$  cm.<sup>2</sup>/sec. He considered the possibility of phosphate entering the cells, but concluded that the important part of the process was occurring in the interspaces. It is now known that phosphate exchanges with intracellular phosphate, and becomes incorporated in organic compounds in the cells, so the uptake of phosphate is a complex process. The diffusion constant of phosphate ions in the interspaces in a preliminary experiment has been found to be  $2 \times 10^{-6}$  cm.<sup>2</sup>/sec. and Stella's low figure is a result of loss of phosphate from the interspaces to the cells, which retards the attainment of equilibrium between solution and interspaces.

We are indebted to Prof. A. V. Hill for having made this work possible, and for his constant advice; and to Dr. B. Katz for help, particularly with the method of dissection. The isotopes were obtained from the Atomic Energy Research Establishment; we must express our appreciation of the arrangements made to provide a continuous supply of these short-lived materials. The expenses of this research have been borne in part by a grant from the Government Grants Committee of the Royal Society to one of us (E. J. H.).

#### Appendix I. Method of Analysis

The residue from the acid digestion was evaporated to dryness in a silica beaker to remove all acid. Following this, alternative procedures were applied. Quantities of up to about 0.2 mg. of potassium were estimated by a method described to us by Dr. Davson, using sodium cobaltinitrite. The residue was taken up in 1 ml. water, 1 ml. 20 % sodium acetate and 2 ml. 20 % sodium cobaltinitrite in N/10 acetic acid added. After standing overnight the precipitate was collected in a small Gooch crucible using well-oxidized asbestos. The solid potassium cobaltinitrite was washed with 10 ml. N/10 acetic acid,

<sup>21</sup> Stella, *J. Physiol.*, 1928, 66, 12.

using four portions of 2.5 ml. The crucible was then transferred to a boiling tube to which was added 2 ml. 25 %  $H_2SO_4$  and 2 ml. N/50 permanganate and the precipitate stirred into the liquid. The contents of the boiling tube were brought, gently, nearly to the boil, then 1 ml. N/50 oxalic acid was added and the excess oxalic acid was titrated with N/50 permanganate. A series of calibrations was carried out on known potassium solutions.

Sodium was estimated by a modification of Salit's<sup>22</sup> method, using zinc uranyl acetate. It was found that treatment with calcium oxide did not remove all the phosphate in the samples and this was confirmed using radio-active phosphate. As a result the figures obtained are liable to be too high when phosphate is present. It was also observed that the ethyl alcohol used to reduce the solubility of the precipitate reacts with the reagent forming acetaldehyde. No difficulty was experienced when dealing with plasma samples, on account of their low phosphate content. Various procedures using either a zinc or magnesium reagent to remove the phosphate have been tried, but a reliable method has not yet been evolved.

## Appendix II. The Error Introduced by the Absorption of Radiation in the Thickness of the Specimen

The assay of the radio-activity of the specimens of muscle relies upon the ionization produced in the Geiger counter by the  $\beta$ - and  $\gamma$ -radiation emitted from the radio-active atoms distributed in the material. In their passage through the specimen the particles are absorbed, and some reduction of the intensity of the radiation takes place. An error will be introduced if the measured radio-activity corresponding to one distribution of radio-active atoms be compared with that given by some other distribution, because the absorption will weight the result in favour of the radio-active atoms nearest to the counter. The less the change in the distribution during the experiment, and the less the absorption loss the lower will be the error. If the muscle be exposed both sides the error due to absorption will be less than when one surface is in contact with the counter; accordingly, calculations of the influence of absorption on the observed mean radio-activity have only been carried out for the latter case.

It was first necessary to measure the fractional transmission of the detected radiation through various thicknesses of a medium similar to tissue. For this purpose sheets of moist filter paper were used, about 75 % of the mass being water. Fig. 5 shows the fractional transmission of the radiation from sodium, and potassium, through various thicknesses of material measured in  $mg. cm^{-2}$ , as it is the mass of matter rather than its nature which is important for  $\beta$ -particle absorption.

Considering the case of a muscle 0.1 cm. thick, exposed to the solution only on the side remote from the counter; it is found that the absorption reduces the detected radiation from a uniform distribution of potassium to 0.878 of the no-absorption value. Now, after the experiment has been in progress for a time, more potassium will have been lost from the external surface than from the interior. Using eqn. (5) to calculate the concentration at the inner surface at  $k_2 t = 0.2$  and for  $r = 1$  (an average muscle) the fraction unexchanged is 0.916; from eqn. (8b) the mean fraction unexchanged is 0.891, and from eqn. (3b) the fraction unexchanged at the outer surface is 0.819. From the three figures an otherwise arbitrary distribution was constructed, and multiplied by the fractional transmission values appropriate to the various thicknesses. The mean value of the resulting curve was 0.7855 of the initial no-absorption value, and the

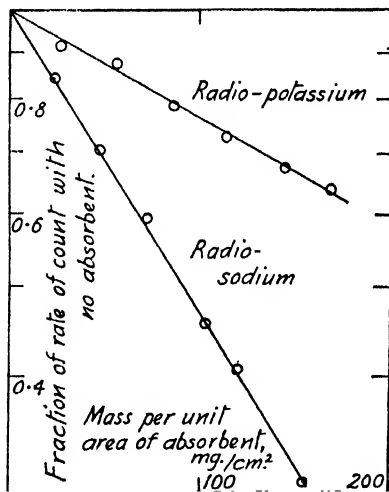


FIG. 5.

<sup>22</sup> Salit, *J. Biol. Chem.*, 1932, **96**, 659.

fractional decrease of labelled ion content which will be observed is  
 $0.7855/0.878 = 0.895$ ,

instead of the true value 0.891.

It would be anticipated that the error will be greater when observing the sodium ion, for not only is the absorption greater, but in addition the distribution passes through a phase when it is less uniform. During the first few minutes of the experiment the sodium in the interspaces is exchanging with that in the solution, and that at the inner surface may not have exchanged at all, while the outer has exchanged all its extra-cellular ions. The situation is improved, however, by the presence of the less exchangeable "internal" sodium, which makes up, say, 50 % of the total. The boundary conditions are then at inner surface, no exchange, at outer surface, 50 % exchange. From (11b) at  $t = 30$  sec. mean fraction unexchanged 0.887. Constructing a distribution to fit these values, having in fact no exchange over 55 % of the total thickness, and multiplying by the sodium absorption values the mean level measured comes to 0.643 of the initial value in absence of absorption. The initial value, which is uniform, is reduced by absorption to 0.701, so the fractional diminution of labelled ion which is observed at the end of 30 sec. is  $0.643/0.701 = 0.918$ , instead of the true value 0.887. Thus the apparent exchange (8.2 %) in the first few minutes is only about 80 % of the true figure (11.3 %). When the loss of extra-cellular sodium is completed the distribution becomes uniform again, and there is no error introduced by absorption.

In view of the variation from specimen to specimen it was not considered worth applying corrections to the observed figures.

*Note added in proof.*—Further experiments, which will be reported later, indicate that the temperature coefficient of the potassium transfer process is about 2.1 per 18° C. and of the sodium transfer process about 2.5 per 18° C.

*Biophysics Research Unit,  
 University College, London.*

## THE ACTION OF COLLOIDAL ELECTROLYTES ON BACTERIA, WITH PARTICULAR REFERENCE TO SOAPS AND SOAP-PHENOL MIXTURES

### PART V.—THE EFFECT OF ADDITIVES KNOWN TO INFLUENCE SURFACE ACTIVITY

BY ANNE AGAR AND A. E. ALEXANDER

*Received 16th November, 1948*

The work described here is an extension of earlier studies of the bacteriological activity of soap-phenol mixtures and its interpretation in terms of physico-chemical factors, of which surface activity and micelle formation were shown to be of great importance.

In the present investigation a variety of soaps (anionic, cationic and non-ionic) have been studied, both alone and in admixture with the following substances; inorganic salts, chloroform, pentachlorethane, phenol, tribromophenol and hexyl resorcinol. The bacteriostatic and bactericidal activities of the mixtures were measured and compared with the changes in physico-chemical properties, particularly the surface activity as measured by the depressant power upon surface or interfacial tension. The results obtained fit in well with the general picture presented earlier.

In earlier papers of this series it was shown how certain bacteriological responses, particularly rates of killing, in mixed soap and soap-phenol systems, appeared to be related to changes in adsorption and could readily

be explained in terms of accepted colloid-chemical concepts (Alexander *et al.*<sup>1</sup>). The present investigation concerns the effect of a number of additives known to influence the surface activity (as measured by the power of lowering the surface, or interfacial, tension) of these systems and of other soap-drug combinations. Changes in surface activity are compared with changes in bactericidal and bacteriostatic activity and the results so found fit in well with the general picture presented earlier. (See also Trim and Alexander.<sup>2</sup>)

### Experimental

**Materials.**—The soaps employed fall into three types, anionic (Aerosol OT and Aerosol MA, referred to as AOT and AMA respectively), cationic (cetyl pyridinium bromide (CPB)), and non-ionic or neutral (cetyl alcohol condensed with ethylene oxide, molar ratio *ca.* 1/30, ref. no. C99408 from I.C.I. Ltd., Dyestuffs Division, Blackley). The chloroform, pentachlorethane, hexyl resorcinol and phenol were pure laboratory samples. The tribromophenol was prepared by brominating phenol.

**Biological Tests.**—For studying bacteriostatic action a 1 % peptone medium was employed, the extent of growth being observed visually after 24 and 48 hr. incubation. All solutions were adjusted to pH 7 before mixing. If necessary, sub-cultures were made into another tube of peptone water to confirm growth. Bactericidal activity was assessed by means of the modified Rideal-Walker technique, or by viable counts, as used in Part III of this series.

**Measurement of Surface Activity.**—As in our earlier work the interfacial tension against medicinal paraffin was measured by means of a micrometer syringe. These measurements also enabled the critical concentration for micelle formation to be determined.

### Results and Discussion

For convenience the experimental results are sub-divided into a number of sections according to the principal systems studied.

(a) **Anionic Soaps and Salts.**—Addition of inorganic salts to soap solutions, provided this does not cause precipitation by chemical reaction or by physical "salting-out", increases the surface activity of the mixture and lowers the critical concentration for micelle formation. In accord with the Schulze-Hardy rule the effect is greatly influenced by the valency of the ion with opposite charge to that on the organic soap ion, e.g. on a molar basis  $\text{CaCl}_2$  has much more influence than  $\text{NaCl}$  upon anionic soaps, and  $\text{Na}_2\text{SO}_4$  much more than  $\text{NaCl}$  upon the cationic type. Fig. 1 shows some typical results.

Bacteriostatic tests were carried out using *B. Coli* and *Staph. aureus* as test organisms, AMA and AOT as anionic soaps, and  $\text{NaCl}$  and  $\text{CaCl}_2$  as added salts. *B. Coli* is rather too insensitive to anionic soaps to be really suitable, but a typical result with AMA after 24 hr. is shown in Table I.

TABLE I.—BACTERIOSTATIC EFFECT OF AMA, ALONE AND IN THE PRESENCE OF SALTS, UPON *B. Coli*

Concentration AMA (%)	1.25	1.0	0.63	0.50	0.32	0.25	0.16	0.12
AMA alone . . . . .	+	+	+	+	+	+	+	+
AMA + 1 % $\text{NaCl}$ . . .	—	—	—	+	+	+	+	+
AMA + 0.1 % $\text{CaCl}_2$ . .	—	—	—	—	+	+	+	+

(+ = growth of *B. Coli* after 24 hr. incubation.)

<sup>1</sup> Alexander *et al.*, 1948 (in press) (Symposium on Recent Advances in Surface Chemistry, held at Bordeaux, October, 1947).

<sup>2</sup> Trim and Alexander, 1948 (in press) (Soc. Expt. Biol., Symposium on Selective Toxicity and Antibiotics, held at Edinburgh, July, 1948).



Table II shows some typical results with *Staph. aureus*, which is much more sensitive to soaps.

TABLE II.—BACTERIOSTATIC EFFECT OF AOT, ALONE AND IN THE PRESENCE OF SALTS, UPON *Staph. aureus*

Concentration AOT (%)	0.125	0.063	0.032	0.016	0.008	0.004	0
AOT alone (24 hr.) . . .	—	—	—	—	±	+	+
(48 hr.) . . .	—	—	±	±	+	+	+
AOT + 1 % NaCl (24 hr.) .	—	—	—	—	—	±	+
(48 hr.) .	—	—	—	±	±	+	+

Addition of salts thus lowers the limiting bacteriostatic concentration, so that these results on bacteriostasis fall into line with those on bactericidal activity obtained by other workers (e.g. Hill and Hunter <sup>3</sup>), and with the increased surface activity as shown by Fig. 1.

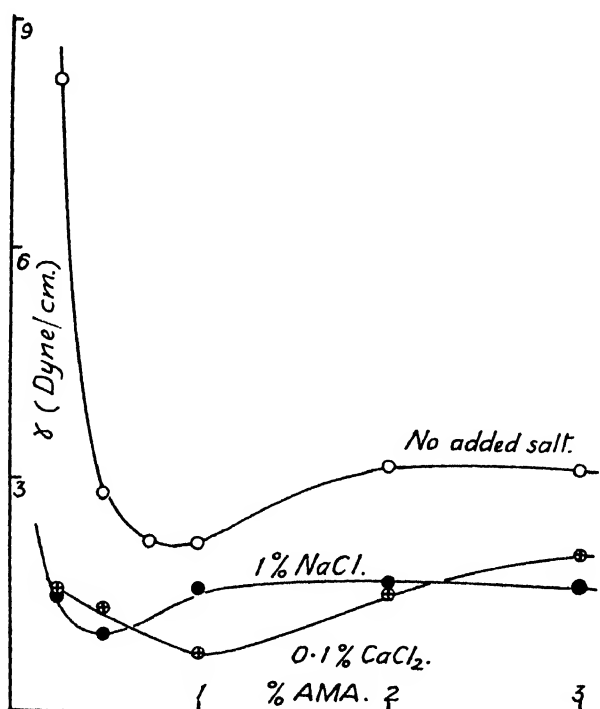


FIG. 1.—The interfacial tension, against medicinal paraffin, of the anionic soap Aerosol MA, alone and in the presence of added salts. All solutions contain 0.54 % phenol.

(b) **Soaps and Phenols.**—In our previous study of soap-phenol systems and *B. Coli* an anionic soap was used so as to avoid complications due to the toxicity of the soap itself. With the cationic soaps, which are themselves very toxic, low concentrations in admixture with phenols lead to a pronounced synergism, as shown below. Only dilute solutions

<sup>3</sup> Hill and Hunter, *Nature*, 1946, 158, 585.

have been studied since the possibility of obtaining detoxication of the phenol when micelles are present is here obscured by the toxicity of the soap.

Table III shows a typical bactericidal test, using *B. Coli* and the modified Rideal-Walker technique, for the cationic soap CPB (0.001 %), alone and in the presence of 0.5 % phenol or 0.015 % hexyl resorcinol (HR). As will be seen, the mixtures are very much more toxic than either component alone.

TABLE III

*B. Coli*, RIDEAL-WALKER TEST

Concentrations of CPB, phenol and hexyl resorcinol (HR), 0.001 %, 0.5 % and 0.015 % respectively

Time (min.)	Phenol alone	HR alone	CPB alone	Phenol + CPB	HR + CPB
5	+	+	+	—	+
10	+	+	+	—	—
20	+	+	+	—	—
30	+	+	+	—	—
40	+	+	+	—	—
60	+	+	+	—	—
120	+	—	+	—	—
180	+	—	—	—	—
240	+	—	—	—	—
360	+	—	—	—	—

In view of their apparent potency it was felt worth while to test these mixtures against the very resistant organism *B. pyocyaneus*. Table IV shows that similar results were obtained. (HR concentration 0.02 % and not 0.015 % as above.) Table IV also includes data using the same

TABLE IV

*B. Pyocyaneus*, RIDEAL-WALKER TEST

Concentrations of CPB, AMA, phenol and hexyl resorcinol, 0.001 %, 1 %, 0.5 % and 0.02 % respectively

Time (min.)	Phenol alone	HR alone	CPB alone	AMA alone	Phenol + CPB	HR + CPB	Phenol + AMA
2½	+	+	+	+	—	—	—
5	+	+	+	+	—	—	—
10	+	+	+	+	—	—	—
20	+	+	—	+	—	—	—
40	+	+	+	+	—	—	—
60	+	+	—	+	—	—	—
90	+	+	+	+	—	—	—
120	—	+	+	+	—	—	—
180	—	+	—	+	—	—	—
240	—	—	—	+	—	—	—

test organism with phenol (0.5 %), in the presence of the anionic soap AMA, used at its critical concentration (*ca.* 1 %) where its synergistic effect is at a maximum. As will be seen, this mixture is as toxic as that with the cationic soap. Since anionic soaps are much less readily detoxicated by proteins, serum, etc., such mixtures may be of practical interest.

The question of the effect of soaps upon insoluble antiseptics is of some importance, particularly in elucidating certain problems associated with permeability and drug action (see section (d) and also Trim and Alexander <sup>2</sup>).

Tribromphenol was chosen as a suitable water-insoluble phenol; *B. Coli* grew quite freely in a nutrient medium saturated with it. Saturated solutions in various concentrations of the anionic soap AMA were prepared and examined for bacteriostatic and bactericidal activities, with the results shown in Table V.

TABLE V

(a) Bacteriostatic effect of AMA saturated with tribromphenol upon *B. Coli*

Concentration AMA (%)	4	3	2.5	2.0	1.5	1.0	0.75	0.5	0.25
AMA alone	—	—	+	+	+	+	+	+	+
AMA + tri- bromphenol	—	—	—	—	—	+	+	+	+

(+ = growth of *B. Coli* after 48 hr. incubation.)

(b) Bactericidal effect of AMA saturated with tribromphenol upon *B. Coli*

Concentration AMA (%)	4	2	1	0.5	0.25	0
Time (min.)						
1	—	—	—	—	+	+
3	—	—	—	—	—	+
5	—	—	—	—	—	+
10	—	—	—	—	+	+
20	—	—	—	—	+	+
40	—	—	—	—	+	+
60	—	—	—	—	+	+
120	—	—	—	—	—	+
180	—	—	—	—	—	+
240	—	—	—	—	—	—

Some variation in the bactericidal results was found, due it is believed, to difficulties in obtaining saturated solutions, but the marked increase in activity when soap micelles are present was always observed. This increase may be due either to an increased rate of transport of the drug to the bacterial surface, or to the soap modifying the surface layer of the bacterium and so allowing the phenol to enter more readily. It seems probable that both factors would be involved although the former would appear to be the more important since *B. Coli* will tolerate such high soap concentrations.

(c) **The Effect of Salts upon Soap-Phenol Mixtures.**—As pointed out in (a) above, salts increase the surface activity of soap solutions. It was therefore thought desirable to see if addition of salts to soap-phenol mixtures increased their bactericidal activity. Tables VI and VII show some typical results obtained on adding respectively 1 % NaCl and 0.1 % CaCl<sub>2</sub> to 0.54 % phenol-AMA mixtures. The surface activity of the mixtures is shown in Fig. 1.

In agreement with expectation both salts increase the bactericidal activity of the soap-phenol mixture, and CaCl<sub>2</sub> is much more effective than NaCl when compared on a molar basis.

TABLE VI.—*B. Coli*, RIDEAL-WALKER TEST

AMA, 0.54 % phenol								AMA, 0.54 % phenol + 1 % NaCl							
% AMA	3	2	1	0.75	0.5	0.25	0	3	2	1	0.75	0.5	0.25	0	
Time (min.)															
2½	+	+	—	+	+	+	+	+	+	—	+	+	+	+	
5	+	+	—	+	+	+	+	+	—	—	—	+	—	+	
10	+	+	—	+	+	+	+	—	—	—	—	—	+	+	
20	+	—	—	+	+	+	+	—	—	—	—	—	+	+	
40	+	—	—	—	+	+	+	—	—	—	—	—	—	+	
60	+	—	—	—	—	+	+	—	—	—	—	—	—	+	
90	+	—	—	—	—	+	+	—	—	—	—	—	—	+	
120	+	—	—	—	—	+	+	—	—	—	—	—	—	+	
240	+	—	—	—	—	—	+	—	—	—	—	—	—	+	

TABLE VII.—*B. Coli*, RIDEAL-WALKER TEST

AMA, 0.54 % phenol								AMA, 0.54 % phenol + 0.1 % CaCl <sub>2</sub>							
% AMA	3	2	1	0.75	0.5	0.25	0	3	2	1	0.75	0.5	0.25	0	
Time (min.)															
2½	+	+	+	+	+	+	+	+	+	+	+	+	+	+	
5	+	+	+	+	+	+	+	+	+	+	+	+	+	+	
10	+	+	+	+	+	+	+	+	+	+	+	+	+	+	
20	+	+	+	+	+	+	+	+	+	—	—	+	+	+	
40	+	—	—	+	+	+	+	+	—	—	—	+	+	+	
60	+	—	—	—	+	+	+	+	—	—	—	—	+	+	
90	—	—	—	—	—	+	+	—	—	—	—	—	+	+	
120	—	—	—	—	—	+	+	—	—	—	—	—	+	+	
240	—	—	—	—	—	+	+	—	—	—	—	—	—	+	

(d) Soaps and Non-surface active Antiseptics (CHCl<sub>3</sub> and C<sub>2</sub>HCl<sub>3</sub>).—

For comparison with the surface-active phenolic type of antiseptic, chloroform and pentachlorethane were chosen as typical lipid-soluble substances practically devoid of surface activity. Such comparisons, particularly as concerns soap effects, are of great importance in elucidating the mechanism of drug penetration. (See Trim and Alexander.<sup>9</sup>)

Some typical Rideal-Walker tests using chloroform in the presence of anionic, cationic and non-ionic soaps are shown in Tables VIII and IX.—(Test organism, *B. Coli*.)

TABLE VIII.—ANIONIC SOAPS, *B. Coli*, RIDEAL-WALKER TEST

(a) AMA, 0.4 % CHCl <sub>3</sub>						(b) AOT, 0.35 % CHCl <sub>3</sub>			
% AMA	5	2.5	1.25	0.62	0	% AOT	1.0	0.1	0
2½ min.	+	+	—	+	+	2½ min.	+	+	+
5 "	+	+	—	+	+	5 "	+	+	+
10 "	+	—	—	+	+	10 "	+	+	+
20 "	—	—	—	+	+	20 "	+	—	+
40 "	—	—	—	—	—	30 "	+	—	+
60 "	—	—	—	—	—	40 "	+	—	+
90 "	—	—	—	—	—	60 "	+	—	+
120 "	—	—	—	—	—	90 "	+	—	+
180 "	—	—	—	—	—	120 "	+	—	—
						300 "	+	—	—

TABLE IX

CATIONIC AND NON-IONIC SOAPS, *B. Coli*, RIDEAL-WALKER TEST0.3 %  $\text{CHCl}_3$ ; 0.001 % CPB; 5 % C99408 (non-ionic soap)

Time (min.)	$\text{CHCl}_3$ alone	CPB alone	C99408 alone	$\text{CHCl}_3$ + CPB	$\text{CHCl}_3$ + C99408
2½	+	+	+	—	+
5	+	+	+	(+)	+
10	+	+	+	—	+
20	+	+	+	—	+
40	—	+	+	—	+
60	—	+	+	—	+
90	—	+	+	—	+
120	—	+	+	—	+
180	—	—	+	—	—
240	—	—	+	—	—

With the anionic soaps we notice an activation up to the micelle point and a detoxication when micelles are present, just as with the phenols. (Critical concentrations *ca.* 1.1 % for AMA, *ca.* 0.1 % for AOT.) On the other hand, at the concentrations used the cationic soap is seen to give an activation, the non-ionic one a marked inhibition. Since micelles are present in the latter case, but not in the former, such behaviour is to be expected on the general theory presented earlier.

Pentachlorethane, unlike chloroform, is so insoluble in water that its saturated solution (provided suspended droplets are removed) is without effect upon *B. Coli*. In the presence of soap micelles its solubility increases and the activity of such saturated systems was examined. Table X presents the results for AMA and for the non-ionic soap C99408, using *B. Coli* and the Rideal-Walker technique. Essentially the same behaviour was observed with *B. pyocyaneus*.

TABLE X

*B. Coli*, RIDEAL-WALKER TEST

(a) AMA saturated with $\text{CHCl}_3$				(b) C99408 saturated with $\text{C}_2\text{HCl}_3$			
% AMA	4.0	1.0	0	% C99408	5.0	0.25	0
Time (min.)				Time (min.)			
1½	—	—	+	1	+	+	+
3	—	—	+	5	—	+	+
6	—	—	+	10	—	+	+
10	—	—	+	20	—	+	+
20	—	—	+	40	—	+	+
40	—	—	+	60	—	+	+
60	—	—	+	120	—	+	+
120	—	—	+	180	—	+	+
180	—	—	+	240	—	—	+
360	—	—	+	360	—	—	+

The biological activity is seen to be greatly increased when soap micelles are present, although the thermodynamic activity of the pentachlorethane is not affected, since the solution exists in equilibrium with the pure liquid in all cases. This indicates that in these systems diffusion to the bacterial surface is the process which determines the overall biological response.

(e) **Ionized Soaps in the Presence of Non-Ionic Soaps.**—Unlike ionized soaps those of the non-ionic type appear to exert no retarding influence upon bacterial growth. (The difference may be due to the lower surface activity of the latter, although adequate data to test this are lacking.) It would thus be anticipated that, when present in the micellar state, the non-ionic type would be able to detoxicate ionized soaps by adsorbing them on to their micellar surfaces. This theory was tested by examining the bacteriostatic activity of AOT and CPB (anionic and cationic respectively), in the presence and absence of the non-ionic soap C99408.

TABLE XI

(a) Bacteriostatic effect of AOT in presence of non-ionic soap C99408

% AOT	0.25	0.125	0.063	0.031	0.015	0.008	0.004	0.002	0
AOT + 5 % C99408 .	—	+	+	+	+	+	+	+	+
AOT + 2.5 % C99408 .	—	—	+	+	+	+	+	+	+
AOT + 1 % C99408 .	—	—	—	+	+	+	+	+	+
AOT + 0.25 % C99408 .	—	—	—	—	—	+	+	+	+
AOT alone .	—	—	—	—	—	—	—	+	+

(b) Bacteriostatic effect of CPB in presence of non-ionic soap C99408

% CPB	0.2	0.1	0.075	0.05	0.025	0.01	0.005	0.001
CPB + 5 % C99408 .	—	+	+	+	+	+	+	+
CPB + 2.5 % C99408 .	—	—	—	+	+	+	+	+
CPB + 1 % C99408 .	—	—	—	+	+	+	+	+
CPB + 0.25 % C99408 .	—	—	—	—	+	+	+	+
CPB alone .	—	—	—	—	+	+	+	+

(+ = growth of *Staph. aureus* in 1 % peptone after 48 hr. incubation.)

Table XI shows that, as the concentration of the non-ionic soap increases, so does the concentration of ionized soap necessary to inhibit growth, the effect being particularly clear with AOT.

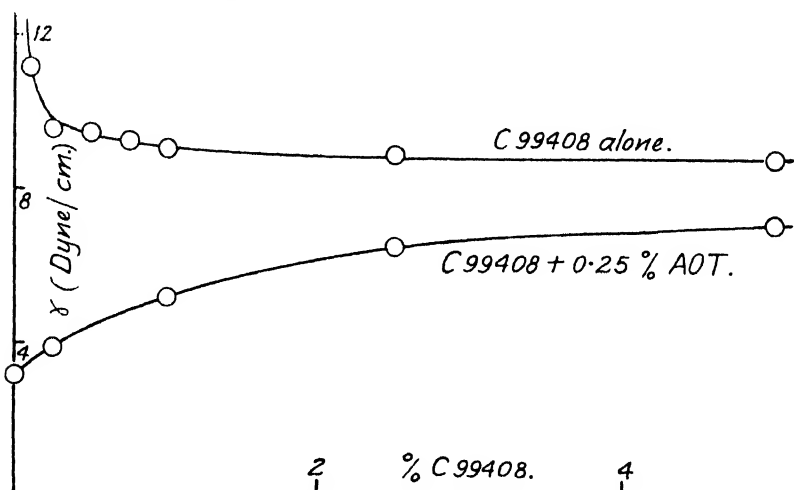


FIG. 2.—The interfacial tension, against medicinal paraffin, of the non-ionic soap C99408, alone and in the presence of 0.25 % Aerosol OT.

Fig. 2 gives the interfacial activity, against medicinal paraffin at 25° C, of the non-ionic soap alone and in the presence of 0.25 % AOT. The former shows that micelles commence to form around 0.2 %, the latter that AOT is being taken up by the micelles. At 5 % C99408, the interfacial tension is seen to be almost back to its value in the absence of AOT, showing that under such conditions the concentration of unbound AOT in the solution is quite small, in agreement with the bacteriological findings.

(f) **The Effect of Serum.**—As is well known, the presence of serum markedly reduces the activity of most bactericidal agents. The effect is particularly noticeable with the cationic soaps, due to their ready precipitation by the oppositely charged protein molecules. A number of the soap-antiseptic mixtures tested above were also examined in the presence of serum (1/1 by volume), using the Rideal-Walker technique. As expected the presence of serum greatly reduced the bactericidal activity, the reduction being least in the case of AMA,  $C_2HCl_5$ , and AMA-tribromphenol mixtures. Some typical results with *B. Coli* are shown in Table XII.

TABLE XII  
*B. Coli*, RIDEAL-WALKER TEST

(a) AMA saturated with $C_2HCl_5$					(b) AMA saturated with tribromphenol		
Serum absent			Serum present		Serum present		
% AMA	2.5	1.0	2.5	1.0	2.5	1.0	0
Time (min.)							
1	—	—	+	+	+	+	+
5	—	—	+	+	—	+	+
10	—	—	+	+	—	+	+
20	—	—	+	+	—	+	+
40	—	—	—	+	—	+	+
60	—	—	—	+	—	+	+
120	—	—	—	+	—	+	+
240	—	—	—	+	—	+	+
360	—	—	—	+	—	+	+

Compare Table XII (b) with Table V (b).

**Conclusions.**—The results obtained here, covering a wide range of soap-drug systems, are in good agreement with the general picture advanced in our earlier papers. The two factors of surface activity and of micelle formation are clearly of particular importance. Further work is in progress to examine in more detail the way in which drugs are adsorbed by, and then penetrate inside, the bacterial cell.

We are indebted to the American Cyanamid Co. for the Aerosols, to Dr. M. A. Phillips for the cetyl pyridinium bromide, to I.C.I. Ltd. for the neutral detergents and to the Director and staff of the Public Health Laboratory Service, Cambridge, for much help with cultures and media. Mr. G. Stainsby kindly prepared the tribromphenol and gave valuable assistance with the interfacial tension measurements.

This work was made possible by a grant from the Medical Research Council, to whom our thanks are due.

Department of Colloid Science,  
University of Cambridge,  
Free School Lane, Cambridge.

# THE OXIDATION OF HYDROCARBONS

## OBSERVATIONS ON THE HIGH-TEMPERATURE REACTION

BY M. F. R. MULCAHY

Received 18th November, 1948

The rates of oxidation of several substances containing 3 carbon atoms per molecule have been measured under comparable conditions over a range of temperature. The differences in reaction rate observed in the low-temperature range ( $< \sim 300^\circ \text{C}$ ) largely disappear in the high-temperature range ( $> \sim 400^\circ \text{C}$ ). Other evidence that the marked structural sensitivity characteristic of the low-temperature oxidation is absent in the high-temperature reaction is reviewed.

As it is improbable that the high-temperature reaction is peroxidic in character, the absence of a large influence of hydrocarbon structure on the rate of the high-temperature reaction supports the view that in the low-temperature region the structural effect is associated with the nature of the peroxide taking part in the reaction.

The slow combustion of a hydrocarbon may proceed by one or other of two mechanisms according to the temperature. At pressures in the region of atmospheric, the "low-temperature" mechanism is operative up to about  $300^\circ \text{C}$ , but above about  $400^\circ \text{C}$ , the "high-temperature" mechanism becomes predominant. The intermediate temperature range is characterized by a slackening in the reaction rate which, with increasing temperature, may pass through a maximum before increasing again.

The kinetics of both high- and low-temperature reactions are complex; in each there is an induction period followed by acceleration to a maximum rate. However, the detailed kinetic properties of the reaction in the two temperature ranges differ in a number of ways.<sup>1-7</sup> For example, the maximum rate is strongly dependent on the oxygen concentration in the high range but practically independent of it in the low range.<sup>1, 7, 8</sup>

A remarkable feature of the low-temperature oxidation is the large effect of the structure of the hydrocarbon molecule on the rate of reaction. The rate increases very strongly with increasing chain length of the hydrocarbon but is depressed by branching of the hydrocarbon chain.<sup>8</sup> It is also sensitive to the presence and position of a substituent in the molecule.<sup>8</sup>

It is generally recognized that in the low-temperature mechanism, peroxides play an essential part and that their formation and subsequent decomposition in large measure govern the course of the reaction. Recently Hinshelwood and Cullis<sup>4</sup> have shown that a number of the kinetic peculiarities of the low-temperature reaction may be accounted for on the assumption that the reaction rate depends on the rate of

<sup>1</sup> Pease, *J. Amer. Chem. Soc.*, 1938, **60**, 2244.

<sup>2</sup> Cullis, Hinshelwood, Mulcahy and Partington, *Faraday Soc. Discussion*, 1947, **2**, 111.

<sup>3</sup> Prettre, *Bull. Soc. chim.*, 1932, (4) **51**, 1132.

<sup>4</sup> *Idem*, *Compt. rend.*, 1936, **203**, 561.

<sup>5</sup> *Idem*, *Acta Physicochim.*, 1938, **9**, 581.

<sup>6</sup> Aivazov and Neumann, *ibid.*, 1936, **4**, 575.

<sup>7</sup> Day and Pease, *J. Amer. Chem. Soc.*, 1941, **63**, 912.

<sup>8</sup> Cullis, Hinshelwood and Mulcahy, *Proc. Roy. Soc. A*, 1949, **196**, 160.



breakdown of peroxide (ROOR or ROOH) by fission at the O—O bond to give two radicals (RO· and OR or OH). And they suggested that the extreme sensitivity of the reaction rate to the structure of the hydrocarbon (RH) may be correlated with the effect of the structure of R on the strength of the neighbouring O—O bond.<sup>2, 8</sup>

In this paper it is proposed to examine to what extent the structure sensitivity is present in the high-temperature mechanism. Attention is devoted to derivatives of propane with which hydrocarbon it appears most convenient to carry out rate measurements over a large temperature range.

The experimental procedure was similar to that followed in previous investigations in this laboratory.<sup>2, 9</sup>

## Results

The effect of substituents on the maximum rate ( $\rho_{\max}$ ) of reaction (as measured by the rate of pressure rise  $dp/dt$ ) at low temperature may be illustrated by comparison of the rates obtained with the 3-carbon molecules in Table I. The figures refer to experiments with 30 mm. of each substance (separately) and 250 mm. oxygen in the same reaction vessel at 298° C.\* The effect of a hydroxy group is particularly noteworthy: substituted in the end position it causes about a 3-fold increase in rate, but in the middle position it depresses the rate to about 1/30 that of propane or less.†

TABLE I

Compound	Structure	$\rho_{\max}$ , mm./min.
<i>n</i> -Propyl chloride. . . .	C—C—C—Cl	~ 28
<i>n</i> -Propyl alcohol . . . .	C—C—C—OH	7.2
Propylene . . . . .	C—C=C	3.2
Propane . . . . .	C—C—C	2.6
<i>iso</i> -Propyl alcohol . . . .	C—C—C   OH	≠ 0.09

In view of the complex rate-temperature relationship which is known to exist with propane, it is of interest to examine the relative rates of oxidation of the substances over a range of temperature. It was possible to do this with all except *n*-propyl chloride which gave rise to a cool flame at about 295° C. Fig. 1 shows the effect of temperature on the maximum rates of 30 mm. "hydrocarbon"—250 mm. oxygen mixtures and includes some results obtained with acetone.

The change in mechanism, most obvious with propane, is also apparent in the propylene and *n*-propyl alcohol curves. The behaviour of *iso*-propyl alcohol is somewhat different, the curve becomes linear below about 425° and continues in this fashion at least down to 325° C.‡

However, the most interesting aspect of Fig. 1 is the fact that the differences in rate observed at low temperatures (Table I) tend to disappear at high tem-

\* Mulcahy, *Trans. Faraday Soc.* (to be published).

† The figures were obtained by interpolation or extrapolation from the curves of Fig. 1. The propane at the lowest temperatures contained 1 % added acet-aldehyde which reduced the induction period but very probably made little difference to the rate.<sup>2</sup>

‡ The effect of a Cl atom is similar; the oxidation rate of the *iso*-chloro compound could not be determined because it undergoes oxygen-catalyzed pyrolysis rather than oxidation.<sup>8</sup> However, there is no doubt that its rate of oxidation under the above conditions is less than that of propane.

§ It is possible that *iso*-propyl alcohol at the lower temperatures undergoes oxygen catalyzed pyrolysis rather than oxidation (cf. *iso*-propyl chloride<sup>9</sup>). For this reason the rate is given as an upper limit in Table I. The lower (linear) part of the *iso*-propyl alcohol curve is not shown in Fig. 1.

peratures. For example, at 298° there is a 30-fold difference between the rates of propane and *iso*-propyl alcohol, but above 440° the rates of both substances are the same. Similarly, at 298° *n*-propyl alcohol reacts 2.2 times faster than propylene, but above 380° the rates are almost the same, the difference being of the order of the experimental error. Unfortunately, because of the high reaction rates it was not possible to make measurements with the latter two substances at temperatures higher than those given, but it appears probable from Fig. 1 that if measurements could be made at a sufficiently high temperature,

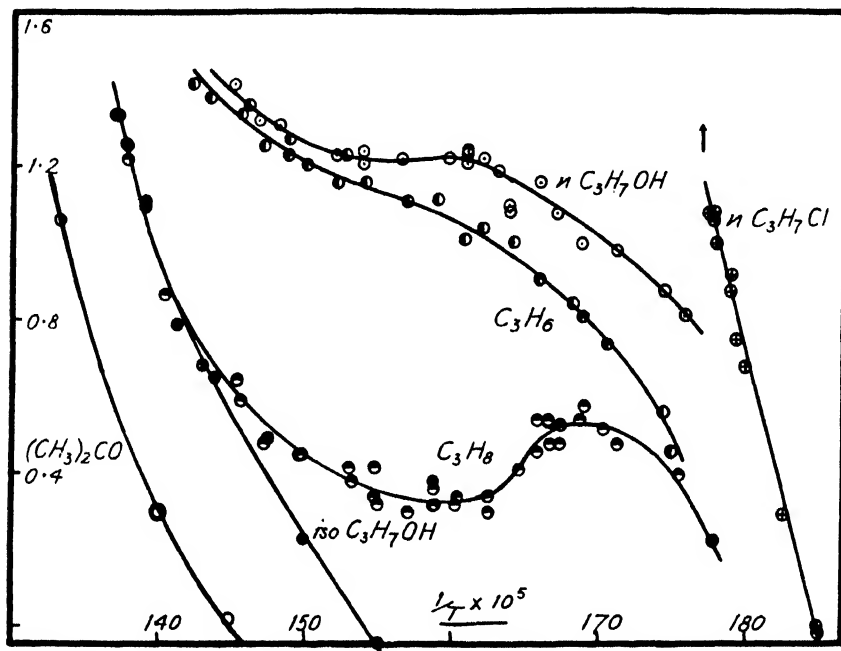


FIG. 1.—The influence of temperature on the maximum oxidation rates of 30 mm. *n*-propyl chloride, *n*-propyl alcohol, propylene, propane, *iso*-propyl alcohol and acetone with 250 mm. oxygen ( $\log_{10} \rho_{\max}$  as ordinate against  $1/T$ ).

little difference would be found in the oxidation rates of propane, propylene, *n*- and *iso*-propyl alcohols.

It appears that acetone oxidizes more slowly than these substances at high temperatures, but again the difference in rate from that of propane, propylene or *n*-propyl alcohol is evidently much greater at low temperatures (cf. McCormac and Townend<sup>10</sup> who have shown that acetone is very unreactive below about 350°).

### Discussion

There is evidence that the contrast between the low-temperature and high-temperature comparative oxidation rates of related compounds is a general phenomenon. The effect is discernible in the experiments of Townend and others on the ignition characteristics of a number of compounds.\* For example, the ignition curves for corresponding mixtures of ethane, ethyl alcohol and acetaldehyde with air obtained by Kane,

<sup>10</sup> McCormac and Townend, *J. Chem. Soc.* 1938, 238.

\* The minimum pressure under which ignition occurs in a mixture of hydrocarbon and oxygen under specified conditions of concentration and temperature is a rough measure of the "oxidizability" of the hydrocarbon and, in fact, the relative ease of ignition of a substance runs approximately parallel to its rate of reaction.

Chamberlain and Townend<sup>11</sup> show that, whereas in the low-temperature range (200–300°) the minimum ignition pressures are widely different, in the high-temperature range, above ~400°, the differences are very much less marked. Moreover, the curves draw continually closer together with increasing temperature. The comparative behaviour of propane, *n*-propyl alcohol and propionaldehyde, of butane and *isobutane*<sup>11</sup> and even of *n*-hexane and cyclohexane<sup>12</sup> and cyclohexene<sup>13</sup> is similar. It is also evident<sup>12</sup> that the effect of the length of the hydrocarbon chain on the rate of oxidation is very much reduced in the high-temperature range.\*

The effect of structural factors on the rate of reaction is clearly much more marked at low than at high temperatures. It is unlikely that the high-temperature reaction is peroxidic in character and there can be little doubt that the slackening in rate of the low-temperature reaction with increasing temperature above 300° is connected with the gradual disappearance of peroxides from the reaction mechanism. This may be due either to decomposition of the peroxide giving products which do not participate further in the main reaction or, more probably, to peroxide not being formed because of a decomposition in an earlier step in the mechanism. In either case, the fact that a large influence of hydrocarbon structure is not found with the high-temperature reaction is evidence for the view that in the low-temperature region the structural effect is associated with the nature of the peroxide taking part in the reaction.

It seems most likely that the high-temperature reaction proceeds via less complex intermediates and involves radicals of simpler type—simple alkyl radicals, oxygen atoms, hydroxyl radicals and the like—which are produced less readily at low temperatures. Indeed, in its more-than-linear dependence on both hydrocarbon and oxygen concentrations, the reaction is reminiscent of the hydrogen–oxygen reaction. However, its auto-catalytic character indicates the presence of a fairly stable intermediate in the mechanism. This may possibly be a lower aldehyde, perhaps formaldehyde (cf. Norrish and Foord,<sup>14</sup> Norrish,<sup>15</sup> Walsh<sup>16</sup>).

Another factor which may be of some importance in determining the kinetic properties of the high-temperature reaction is the increased probability at high temperatures of the initial attack on the hydrocarbon molecule occurring at the end of the chain, i.e. at a CH<sub>3</sub> group. At low temperatures, attack apparently occurs mainly at CH and CH<sub>2</sub> groups,<sup>17, 8</sup> a fact which may be correlated with the superior C—H bond strength within the CH<sub>3</sub> group.<sup>18, 19</sup> The exceptional inertness of methane, ethane and acetone towards oxidation at low temperatures is thus, at least in some measure, accounted for. Presumably with these substances under ordinary conditions, the rate of initiation of the oxidation only becomes appreciable at temperatures at which peroxides are no longer formed or stable and consequently the reaction proceeds by the high-temperature mechanism. Molecules containing (paraffinic) CH or CH<sub>2</sub> groups may still be attacked mainly at these groups at high temperatures, but as the temperature is increased, attack on the methyl groups will make an

\* Cf. also the experiments of Burgoyne, Tang and Newitt<sup>13</sup> from which the effect may be seen to be present with various alkyl-substituted benzene derivatives.

<sup>11</sup> Kane, Chamberlain and Townend, *ibid.*, 1937, 436.

<sup>12</sup> Townend, *Chem. Rev.*, 1937, 21, 259.

<sup>13</sup> Burgoyne, Tang and Newitt, *Proc. Roy. Soc. A*, 1940, 174, 379.

<sup>14</sup> Norrish and Foord, *ibid.*, 1936, 157, 503.

<sup>15</sup> Norrish, *Colloque sur la cinétique des réactions de combustion en phase gazeuse* (Paris, 1948).

<sup>16</sup> Walsh, *Trans. Faraday Soc.*, 1947, 43, 305.

<sup>17</sup> *Idem*, *ibid.*, 1946, 42, 269.

<sup>18</sup> Smith and Taylor, *J. Chem. Physics*, 1939, 7, 390.

<sup>19</sup> Hinshelwood, *J. Chem. Soc.*, 1948, 531.

increasingly important contribution to the rate of initiation. This may be of some consequence for the subsequent reaction steps, since the degradation products which follow end-attack may be expected to be different from those resulting from attack in a more central part of the molecule.

The best thanks of the author are due to Prof. Sir Cyril Hinshelwood, F.R.S., for his advice and interest in this work. The author is a member of the staff of the Division of Tribophysics of the Council for Scientific and Industrial Research, Australia.

*Physical Chemistry Laboratory,  
South Parks Road,  
Oxford.*

---

## ACTIVE METHYL RADICALS IN THE PHOTOLYSIS OF DIMETHYL MERCURY\*

BY M. K. PHIBBS AND B. DE B. DAKWENT

*Received 30th November, 1948*

The effect of temperature on the photolysis of dimethyl mercury in the presence of hydrogen has been re-investigated. Particular attention has been paid to the low-temperature reaction and to the effect of inert gas on the temperature coefficient of the rate of formation of methane. The results indicate that the methyl radicals produced photochemically possess considerable energy carried over from the initial split.

The photochemical decomposition of organic compounds has been used as a method of producing free radicals for the study of the reactions of those radicals with various substances. Thus Taylor and his students<sup>1</sup> have measured the activation energies of the kinetically important reactions of methyl radicals with hydrogen and various hydrocarbons by studying the effect of temperature on the rate of formation of methane when dimethyl mercury was decomposed photochemically in the presence of large excesses of hydrogen or hydrocarbons.

In general, if the energy per quantum of the light used is greater than that necessary to break the bond of the parent molecule, thus producing the free radicals, the excess energy would be expected to be present in the dissociation fragments, thus leading to the production of active radicals with energy greater than the thermal value. Cunningham and Taylor used  $\lambda = 2550 \text{ \AA}$  with energy of about 100 kcal./einstein; the Hg—C bond strength is probably only about 34 kcal./mole.<sup>†</sup> The dynamics of the system  $\text{Hg} + 2\text{CH}_3$  (treated as rigid bodies) show that

\* Contribution No. 1930 from the National Research Council, Ottawa, Canada.

<sup>1</sup> (a) Cunningham and Taylor, *J. Chem. Physics*, 1938, **6**, 359; (b) Smith and Taylor, *ibid.*, 1939, **7**, 390.

<sup>†</sup> The combined energies of the two Hg—C bonds in dimethyl mercury may be shown, by thermochemical considerations (Bichowsky and Rossini, *Thermochemistry of Chemical Substances* (Reinholds, N.Y., 1936), assuming the strength of the C—C bond in ethane to be 86 kcal., to be about 34 kcal. Sidgwick and Springall (*Nature*, 1945, **156**, 599) have calculated the strength of the second Hg—C bond in dimethyl mercury to be 4.0 or 15.5 kcal./mole, depending on the value adopted for the heat of atomization of carbon. Since there is some uncertainty attached to this figure, we have assumed the strength of the second Hg—C bond to be zero and that of the first to be 34 kcal./mole. The actual value adopted will have little effect on our conclusions.

about 90 % of the 66 kcal. excess energy will be located in the methyl radicals. Thus it would be expected that the primary act should lead to the production either of one  $\text{CH}_3$  with about 60 kcal./mole excess energy and one "thermal"  $\text{CH}_3$  or to two  $\text{CH}_3$ 's each with about 30 kcal./mole in excess of the value corresponding to the temperature.

The excess energy present in the radicals produced in the initial photochemical act (photo-radicals) should be a function of the energy (wave length) of the exciting light. Consequently the work of Cunningham and Taylor has been repeated using the narrow cadmium singlet line at  $\lambda = 2288 \text{ \AA}$  to obtain some information about the nature of these photo-methyl radicals, and the effect of adding an inert gas ( $\text{CO}_2$ ) to deactivate excited radicals has been investigated.

### Experimental

Dimethyl mercury was prepared by the method of Gilman and Brown.\* It was dried with fused calcium chloride and stored in a glass bulb connected to the apparatus through a mercury cut-off. The hydrogen was taken from a cylinder of electrolytic gas and purified by passage through a hot palladium tube. Carbon dioxide was taken from a cylinder filled by the Carbonate Company Limited, Montreal; it was stated to be 99.5 % pure and was dried by passage over phosphorus pentoxide, freed from permanent gases by prolonged evacuation at liquid-air temperature and stored in a large bulb.

The apparatus was similar to that used by Cunningham and Taylor.<sup>1</sup> The reaction cell was a quartz cylinder 10 cm. long with plane quartz windows; the volume was about 245 cm.<sup>3</sup>. Mercury cut-offs were used throughout because of the high solubility of dimethyl mercury in stopcock grease. A cylindrical furnace was used for high temperatures ( $25^\circ$  to  $250^\circ \text{C}$ ) and a water thermostat for experiments between  $0^\circ$  and  $50^\circ \text{C}$ . In all cases the temperature was controlled manually to within  $\pm 1^\circ \text{C}$  and the temperature variation along the cell did not exceed  $3^\circ \text{C}$ . The light source was a cadmium-neon discharge lamp which had strong lines at 2288  $\text{\AA}$  and 3261  $\text{\AA}$  with only very weak lines between. The lamp was run at  $280^\circ \text{C}$  on 110 mA from a Jefferson sign transformer.

The procedure adopted was essentially the same as that used by Cunningham and Taylor.<sup>1</sup> Mercury dimethyl was introduced to the appropriate pressure (50 mm. Hg) into the cell and then frozen out in a side tube at  $-78^\circ \text{C}$ ; carbon dioxide, when used, was added next and frozen out in the same side tube at  $-183^\circ \text{C}$ . The desired pressure of hydrogen was then admitted and the cell and side-tube sealed off. The cell and its contents were placed in the furnace or thermostat 15 min. before starting the photolysis to allow thermal equilibrium to be attained. At the end of the experiment the cell was resealed to the apparatus by means of an internal seal which could be broken by a magnetic hammer and most of the hydrogen removed by pumping on a hot palladium tube with the cell in liquid air. The methane was rendered free from any residual hydrogen, by compressing the gases on to hot copper oxide, and its volume measured. Ethane was pumped off with the cell at  $-126^\circ \text{C}$  and the amount measured.

### Results

The results are given in Table I. The thermal experiments (No. 8, 9 and 15) were carried out to obtain correction factors for the effect of the thermal reaction on the photochemical experiments. Expt. 19 affords an additional correction for the methane produced thermally during the preliminary "warm-up" period of 15 min. at  $250^\circ \text{C}$ ; at lower temperatures this correction was negligible. Expt. 17 was carried out with the lamp on but with a 2-mm. Correx D filter which removes completely light of wave length shorter than 2800  $\text{\AA}$ ; the rate of formation of methane in this experiment is almost identical with that of Expt. 15 in which no light was admitted to the cell, showing that the strong line at 2288  $\text{\AA}$  is probably the only significantly effective light in these experiments. In Expt. 22 to 32 inclusive a new lamp of slightly greater intensity was used and the results corrected for comparison with preceding runs by the use of a factor  $0.0140/0.0154 = 0.91$  obtained by comparing Expt. 20 and 23. A further correction for light intensity was necessary in Expt. 30 which was carried out in a water thermostat instead of in the furnace; this factor was 2.67, the average

\* Gilman and Brown, *J. Amer. Chem. Soc.*, 1930, **52**, 3314.

TABLE I.—THE PHOTOLYSIS OF DIMETHYL MERCURY IN THE PRESENCE OF HYDROGEN

Vol. of cell = 245 cm.<sup>3</sup>. Pressure of Hg(CH<sub>3</sub>)<sub>2</sub> = 50 mm. Hg.Pressure of H<sub>2</sub> = 200 mm. Hg

Expt. No.	Temp. °C	Time (hr.)	CH <sub>4</sub> Production (cm. <sup>3</sup> /hr.)		C <sub>2</sub> H <sub>6</sub> (cm. <sup>3</sup> /hr.)
			Found	Corrected	
A. Thermal Experiments					
8	250	1.0	2.03	—	—
9	200	2.08	0.258	—	0.0065
15	150	2.0	0.0088	—	0.0013
19a	250	(0.25)	0.440	—	—
17b	150	2.00	0.0078	—	—
B. Photochemical Experiments					
11	150	2.00	0.339	0.331	0.357
12	200	0.50	1.316	1.058	0.372
13	250	0.33	4.83	2.58	0.435
14	102	6.83	0.074	0.074	—
16	107	2.00	0.085	0.085	0.300
20	52	20.00	0.0140	0.014	0.232
23c	52	11.08	0.0154	0.014	0.277
27c	25	20.75	0.00883	0.00801	0.250
30d	2	8.33	0.00208	0.00554	0.103
31d	24	6.0	0.00269	0.00715	0.139
32d	50	3.50	0.00594	0.0158	—
24e	53	13.00	0.0117	0.0106	—
25e	26	21.00	0.00436	0.00396	—
26e	50	12.08	0.0087	0.0079	—
27e	51	13.25	0.0091	0.0083	—
28e	25	19.00	0.0040	0.00365	—

(a) Effect of preliminary 15 min. "warm-up" period—0.110 cm.<sup>3</sup>/hr. CH<sub>4</sub> produced.

(b) Lamp on—2-mm. Correx D filter.

(c) New lamp of slightly greater intensity.

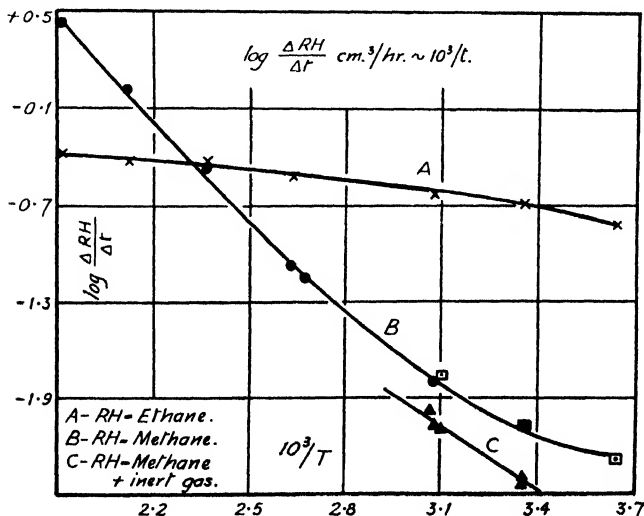
(d) Water thermostat—press. Hg(CH<sub>3</sub>)<sub>2</sub> = 20 mm.(e) CO<sub>2</sub> added—400 mm.

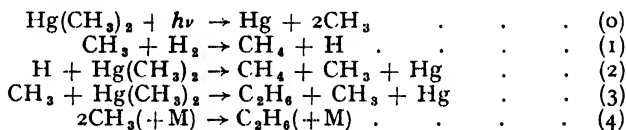
FIG. 1.

of 2.36 ( $= 0.0154/0.00594 \times 0.91$ ) from Expt. 23 and 32, and 2.98 ( $= 0.00883/0.00269 \times 0.91$ ) from Expt. 22 and 31. These corrections were used only for the convenience of obtaining one continuous curve instead of two or three widely separated curves for the determinations of activation energy. Expt. 24 to 28 inclusive were carried out with 400 mm.  $\text{CO}_2$  as well as the 50 mm.  $\text{Hg}(\text{CH}_3)_2$  and 200 mm.  $\text{H}_2$  (except in 30, 31 and 32 in which 20 mm.  $\text{Hg}(\text{CH}_3)_2$  were used) to investigate the effect of an inert gas on the reaction at low temperatures.

The effect of temperature on the rate of production of methane and ethane is shown in Fig. 1. Satisfactorily straight lines are obtained in the  $\ln k - 1/T$  plot for ethane (Curve A) and methane (Curve B) between  $250^\circ$  and  $100^\circ\text{C}$ , the slopes indicate activation energies of 1.0 and 9.1 kcal./mole respectively. Below  $100^\circ\text{C}$  the curve for methane production deviates considerably and apparently continuously from the straight line indicating a decrease in activation energy with decrease in temperature. A small (2.0 kcal./mole) but significant increase in activation energy is obtained at low temperatures by the addition of carbon dioxide (Curve C).

### Discussion

The activation energy (9.1 kcal./mole) for the production of methane above  $100^\circ\text{C}$  agrees well with that found by Cunningham and Taylor<sup>1</sup> using light of less energy and with the value obtained from purely thermal experiments.<sup>3</sup> The obvious inference is that, above  $100^\circ\text{C}$ , the majority of the methyl radicals did not have any energy in excess of the thermal value and the experimentally determined activation energy is therefore independent of the method by which they are produced. This is in agreement with the following mechanism, similar to that originally proposed by Cunningham and Taylor:—



which, by the usual stationary state treatment gives

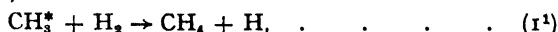
$$\begin{aligned} [\text{CH}_3] &= \left( \frac{2I_a}{k_4} \right)^{\frac{1}{2}}, \\ [\text{H}] &= \left( \frac{k_1[\text{H}_2]}{k_2[\text{A}]} \right) \left( \frac{2I_a}{k_4} \right)^{\frac{1}{2}}, \\ \frac{d}{dt}[\text{CH}_4] &= 2k_1[\text{H}_2] \left( \frac{2I_a}{k_4} \right)^{\frac{1}{2}}, \quad . \quad . \quad . \quad (a) \end{aligned}$$

where  $\text{A} = \text{Hg}(\text{CH}_3)_2$ . At high temperatures, where reactions (1) and (2) are rapid, the majority of the methyl radicals will be formed by the chain series (1) and (2) and will actually be thermal methyl radicals. However, the above mechanism does not explain the decreased value of  $E_1$  at low temperatures as found in these experiments and which seemed to be present in Cunningham and Taylor's results at low temperatures, nor the slight but definite increase in the low temperature value of  $E_1$  by the addition of carbon dioxide.

If the radicals produced in the initial photochemical act possess excess energy the above mechanism may be modified slightly by writing equation (0) as



and adding the reaction,



<sup>3</sup> Steacie, *Atomic and Free Radical Reactions* (Reinhold Publishing Corp., New York, 1946), p. 294.

where  $\text{CH}_3^*$  represents a methyl radical with excess energy from the initial photochemical act. We now have

$$\frac{d}{dt}[\text{CH}_3] = BI_a + 2k_1\left(\frac{2I_a}{k_4}\right)^{\frac{1}{2}}[\text{H}_2]. \quad (b)$$

With the above mechanism  $B$  has the value of 4. This is obviously wrong since at low temperatures the quantum yield of methane production is much less than unity whereas eqn. (b) demands a minimum value of 4. However, if deactivating reactions, such as



be included,  $B$  will involve the ratio of  $k_1/k_5$  which may be very small and thus agree with experiment. Eqn. (b) differs from (a) by the presence of the temperature independent term  $BI_a$  and predicts that, at high temperatures where

$$2k_1\left(\frac{2I_a}{k_4}\right)^{\frac{1}{2}}[\text{H}_2] \gg BI_a,$$

$E_1$  will be the same as found for thermal methyl radicals, but at low temperatures where

$$BI_a > 2k_1\left(\frac{2I_a}{k_4}\right)^{\frac{1}{2}}[\text{H}_2],$$

$E_1$  will approach zero as found experimentally.\* Qualitative support for eqn. (b) is obtained by the fact that Cunningham and Taylor, using a higher intensity, found that the value of  $E_1$  started to decrease at a higher temperature than in the present investigation which is in agreement with eqn. (b).

More direct evidence in favour of eqn. (b) is obtained by the increase of  $E_1$  through the addition of carbon dioxide at low temperatures. Although a reduction in the rate of formation of methane by addition of  $\text{CO}_2$  at any one temperature is partly due to the increase in the frequency of three-body collisions, favouring reaction (4), it is unlikely that such a process could result in an increased temperature dependence of the rate. It is far more likely that the effect of the addition of carbon dioxide is due to an increase in the rate of reaction (5), leading to a decreased concentration of active methyl radicals and, in effect reducing the value of  $BI_a$  in eqn. (b).

Hence the results obtained lead to the belief that the excess energy of the initial act, as shown by the dynamics of the system, resides in the methyl radicals. The alternative of an electronically excited mercury atom is, of course, eliminated by the fact that the lowest (triplet) state lies 112 kcal. above the ground state.

The indications<sup>4</sup> are that reaction (1) has a very low steric factor of the order of  $10^{-4}$ , and one would expect nearly all the active methyl radicals produced in the initial act to lose their excess energy by collision before reaction (1') could occur. However, it has been shown<sup>5</sup> that vibrational energy is not readily lost on collision and it is likely that the photo-methyl radicals, if vibrationally active, could experience as many as  $10^6$  collisions before losing their excess energy. Also the low steric factor probably would apply only to reaction (1) and not to (1'), since it is probable that a large amount of energy in excess of  $E_1$  would increase the steric factor to approximately unity.

Division of Chemistry,  
National Research Council,  
Ottawa, Ontario.

\* We have assumed  $E_4$  to be zero since it is generally accepted that the recombination of free radicals does not require any real energy of activation.

<sup>4</sup> (a) Patat, *Z. physik. Chem. B*, 1936, **22**, 274, 294; (b) Steacie, Darwent and Trost, *Faraday Soc. Discussions*, 1947, **1**.

<sup>5</sup> Zener, *Physic. Rev.*, 1931, **37**, 556; Terenin and Neuman, *Acta Physicochim.*, 1942, **16**, 1.



# INDUCED REACTIONS OF THE HALOGENS IN AQUEOUS SOLUTION

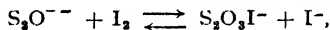
## PART II. REACTIONS IN THE SYSTEMS $I_2-S_2O_3^{2-}-N_3^-$ AND $I_2-S_4O_6^{2-}-N_3^-$

BY G. DODD AND R. O. GRIFFITH

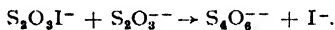
Received 9th December, 1948

The reaction between  $NaN_3$  and  $I_2$  in aqueous solution with liberation of  $N_2$  is induced by both  $Na_2S_2O_3$  and  $Na_2S_4O_6$ , and studies of both processes have been made over fairly wide ranges of conditions. The induction by  $Na_2S_4O_6$  which yields  $H_2SO_4$  and  $N_2$  is slow, and kinetic measurements have been made by determining the rates of consumption of iodine and of production of  $N_2$ . The effect of  $[I^-]$  on both rates is characterized by a pronounced minimum in the region of  $[I^-] \approx 0.01-0.02$ . The results are accounted for in terms of a chain mechanism, involving the intermediates  $S_2O_3I^-$  and  $S_2O_3N_3^-$  (or  $S_2O_3^-$ ), with different primary steps in the regions of low  $[I^-]$  and high  $[I^-]$ . The latter correspond to the first steps in reactions which have been found to take place in absence of  $N_3^-$ , viz. the reaction between  $S_4O_6^{2-}$  and  $I_2$  in presence of very low  $[I^-]$  and the reaction between  $S_4O_6^{2-}$  and  $I^-$ . The former of these has been studied kinetically but as yet no mechanism is proposed for it.

The products of reaction in  $S_2O_3^{2-}-I_2-N_3^-$  systems include  $S_4O_6^{2-}$ ,  $H_2SO_4$  and  $N_2$ . The reactions are too fast to follow by ordinary kinetic methods and experimental work has been limited to investigation of the over-all stoichiometry and of the relation between  $I_2$  consumed to  $Na_2S_2O_3$  consumed under a variety of conditions. A possible chain mechanism for the reaction is suggested. Based on this work an experimental method was evolved by means of which the rate of the direct reaction between  $Na_2S_2O_3$  and  $I_2$  could be measured in mixtures containing excess  $I_2$ , and a reaction mechanism derived from these data is proposed for the  $I_2-S_2O_3^{2-}$  reaction. The mechanism suggested is



followed by

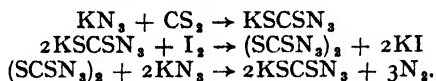


Raschig<sup>1,2</sup> discovered that the addition of small amounts of  $Na_2S_2O_3$  (or  $Na_2S$ ) induces a vigorous reaction between  $I_2$  and  $NaN_3$  in aqueous solution, nitrogen being evolved; in absence of the catalyst no reaction between  $I_2$  and  $NaN_3$  can be detected. Though the induced reaction has been used as a means of estimating azide and as a sensitive test for the detection of various compounds of sulphur, no detailed quantitative study of the process appears to have been made, and insufficient data exist to throw much light on its mechanism. Published work bearing on these induced reactions may be briefly summarized. Raschig carried out a few qualitative measurements on the system  $I_2-S_2O_3^{2-}-N_3^-$  and showed that  $H_2SO_4$  is one of the resultants of the reactions which occur. He also showed that in the system  $S_2O_3^{2-}-I_2$  there is formed a catalyst whose life under certain conditions can be of the order of minutes. Browne

<sup>1</sup> Raschig, *Chem.-Ztg.*, 1908, **32**, 1203.

<sup>2</sup> Raschig, *Ber.*, 1915, **48**, 2088.

and Hoel<sup>3</sup> investigated the reaction between  $\text{KN}_3$  and  $\text{I}_2$  induced by  $\text{CS}_2$  and concluded that the probable mechanism is :



The mechanism was supported by the preparation and isolation of the two intermediates  $\text{KSCSN}_3$  and  $(\text{SCSN}_3)_2$ , together with the observation that the addition of small amounts of either of these two substances to a  $\text{KN}_3$ - $\text{I}_2$  mixture free from  $\text{CS}_2$  results in a vigorous oxidation of the azide. Friedman<sup>4</sup> has studied the reaction between  $\text{NaN}_3$  and  $\text{I}_2$  induced by a number of sulphur-containing compounds, including  $\text{Na}_2\text{S}_2\text{O}_3$ . By measuring the  $\text{N}_2$  evolution from a Barcroft apparatus he determined the ratio ( $U$ ) of moles  $\text{NaN}_3$  decomposed to moles of sulphur compound consumed. In general, a very rapid evolution of  $\text{N}_2$  occurred in the first few minutes, followed by a much slower evolution subsequently. The fast reaction was ascribed to the action of the  $\text{R-SH}$  compound in initiating a chain whose chain-breaking process was the conversion of the  $\text{R-SH}$  molecule into the disulphide  $\text{R-S-S-R}$ ; the much slower reaction to a reaction between  $\text{NaN}_3$  and  $\text{I}_2$  induced by the disulphide. Only one experiment with  $\text{Na}_2\text{S}_2\text{O}_3$  was carried out; the value of  $U$  obtained for the fast initial reaction under the conditions of this experiment was about 11. Though Raschig,<sup>2</sup> Friedman<sup>4</sup> and Weiss<sup>5</sup> have advanced mechanisms for the induced reaction in the system  $\text{I}_2$ - $\text{S}_2\text{O}_3^{2-}$ - $\text{N}_3^-$ , none is supported by adequate experimental evidence. In the present work we have carried out over a fairly wide range of conditions experiments on the reactivity of these systems; we have further studied the analogous system  $\text{I}_2$ - $\text{S}_4\text{O}_6^{2-}$ - $\text{N}_3^-$ , the direct  $\text{I}_2$ - $\text{S}_2\text{O}_3^{2-}$  reaction in absence of azide, and the reaction between  $\text{S}_4\text{O}_6^{2-}$  and  $\text{I}_2$  which is found to take place at very low concentrations of iodide. By correlation of all the data, it has been possible to advance mechanisms, which, though in some respects speculative, account satisfactorily for the reactivity of these systems.

## Experimental

**System  $\text{I}_2$ - $\text{S}_2\text{O}_3^{2-}$ - $\text{N}_3^-$ .**—Owing to the great rapidity of the reactions in these systems, kinetic methods are not available to follow them; our work has thus been confined to determining the stoichiometry of the reaction and the amount of reaction induced by unit amounts of thiosulphate under a variety of conditions. The data thus comprise determinations of the ratio  $R$  of (moles  $\text{I}_2$  consumed)/(moles  $\text{Na}_2\text{S}_2\text{O}_3$  consumed) and quantitative estimation of the end-products of the reaction.

Values of  $R$  were determined by running small amounts of thiosulphate solution into solutions containing azide and iodine, buffered with acetic acid—sodium acetate, and determining the excess iodine by addition of sodium arsenite and back-titration with standard iodine. This method is similar to that employed in the study of the  $\text{I}_2$ - $\text{S}_2\text{O}_3^{2-}$ - $\text{NO}_2^-$  system described in Part I of this series,<sup>6</sup> and, except that the  $\text{I}_2$ - $\text{S}_2\text{O}_3^{2-}$ - $\text{N}_3^-$  system is the more sensitive to variation in experimental method, similar remarks in regard to the effect on  $R$  of the method of adding thiosulphate and of mode of stirring apply to both systems. As described in Part I, here also in order to obtain comparable and reproducible results, a standard procedure was adopted, which consisted in the addition of the thiosulphate solution drop by drop at the rate of approximately one drop per second into the remainder of the reaction mixture, which was briskly swirled by hand during the addition. As the system (either in presence or absence of  $\text{S}_2\text{O}_3^{2-}$ ) is not light-sensitive, and as the  $R$  values are not very temperature-dependent, non-thermostatted reaction flasks of clear glass were used, and the

<sup>3</sup> Browne and Hoel, *J. Amer. Chem. Soc.*, 1922, **44**, 2106.

<sup>4</sup> Friedman, *J. prakt. Chem.*, 1935, **146** (ii), 179.

<sup>5</sup> Weiss, *Trans. Faraday Soc.*, 1947, **43**, 119.

<sup>6</sup> Griffith and Irving, *ibid.*, 1949, **45**, 305.

data obtained relate to room temperature, from 17° to 20° C. Fig. 1-4 are representative of the results obtained. These and other data show that values of  $R$  found range from 0.5 (the limiting value in absence of  $N_3^-$ ) to 50, though higher values could result by extending the range of conditions of experiment. They increase with increasing  $[N_3^-]$  and with increasing  $[I^-]$ , in each case the increase being the more marked at low concentrations.  $R$  increases with decreasing concentration of added  $S_2O_3^{2-}$ , the increase being the greater at low  $[S_2O_3^{2-}]$ . The effect of variation of  $[I_2]$  on  $R$  is inappreciable, while, in general, decrease of temperature from 18° to 1° C increases  $R$  by about 20 %. Increase in  $[H^+]$  tends to diminish  $R$ . As in the presence of sufficient strong mineral acid the

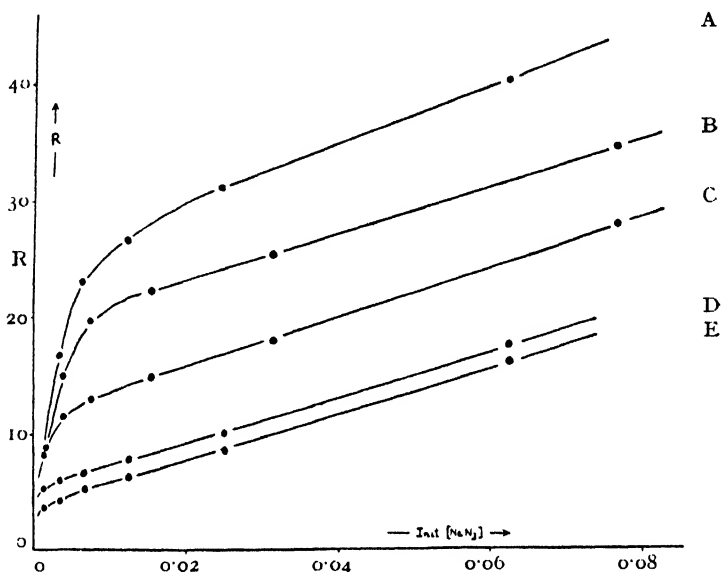


FIG. 1

Series	Init. $[I^-]$
A	0.2500
B	0.06153
C	0.01230
D	0.00200
E	Nil

In all Series :—

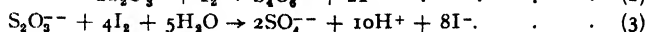
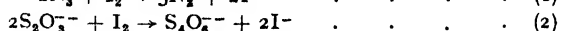
$$\text{Init. } [I_2] = 0.000250 \text{ or } 0.000300$$

$$\text{Init. } \frac{[NaAc]}{[HAc]} = \frac{0.01250}{0.00625} \text{ or } \frac{0.01538}{0.00769}$$

$$[Na_2S_2O_3] \text{ added} = N/10,000$$

oxidation of azide is completely inhibited, it appears that  $HN_3$  does not react with  $I_2$  in the presence of  $Na_2S_2O_3$  and that reaction occurs only with free  $N_3^-$  ion. The observed decrease of  $R$  with increase of  $H^+$  in the range tested in our experiments can be ascribed mainly, if not entirely, to the corresponding decrease in the effective  $[N_3^-]$  due to increase in the ratio  $[HN_3]/[N_3^-]$ . It may finally be noted here that, as dealt with later,  $S_4O_6^{2-}$  also catalyzes the reaction between  $NaN_3$  and  $I_2$ , but, compared with the  $S_2O_3^{2-}$  catalysis, the speed of the reaction involving  $S_4O_6^{2-}$  is very small and catalysis by  $S_4O_6^{2-}$  can be entirely neglected under the conditions of the experiments of this section.

Quantitative estimation of the end-products showed that the *net* reactions taking place are :



The experiments were carried out by addition of  $\text{Na}_2\text{S}_2\text{O}_3$  solutions to mixtures of known composition of  $\text{I}_2$ ,  $\text{KI}$ ,  $\text{NaN}_3$  and buffer constituents until all the  $\text{I}_2$  present had been exactly consumed, followed by analysis of the resulting colourless solution and/or by the measurement of  $\text{N}_2$  evolved.  $\text{S}_4\text{O}_6^{2-}$  was determined by the method of Kurtenacker and Goldberg,<sup>7</sup> consisting in the reduction of  $\text{S}_4\text{O}_6^{2-}$  to  $\text{S}_2\text{O}_3^{2-}$  by  $\text{KCN}$ , addition of mineral acid and titration of the  $\text{S}_2\text{O}_3^{2-}$  with standard  $\text{I}_2$ . Unfortunately, for the range of concentrations of  $\text{S}_4\text{O}_6^{2-}$  M/800-M/4000, in which chief interest lies, it was not found possible to obtain results with an accuracy better than  $\pm 5\%$ ; with stronger solutions data of reasonable accuracy could be obtained and determinations of  $\text{S}_4\text{O}_6^{2-}$  were made in solutions in which  $\text{S}_4\text{O}_6^{2-}$ , as end-product, was present in concentrations exceeding M/800. Sulphate was determined by precipitation as  $\text{BaSO}_4$  and weighing; to avoid any possible decomposition of tetrathionate the precipitation

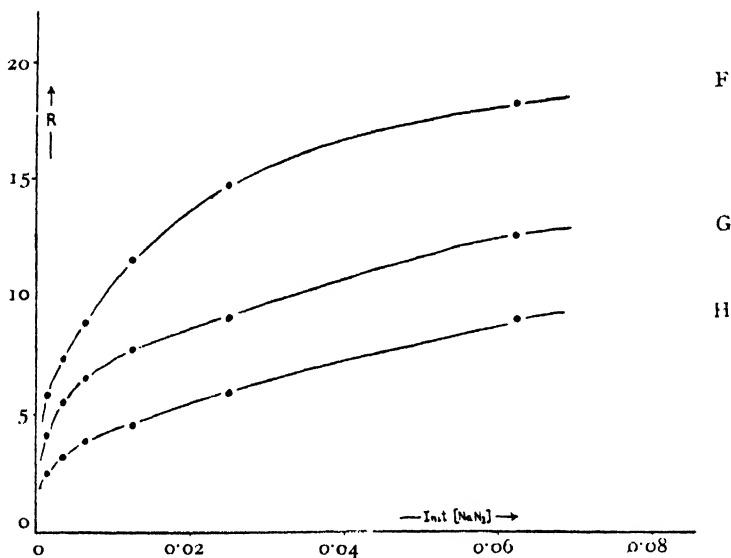


FIG. 2

Series	$[\text{Na}_2\text{S}_2\text{O}_3]$ added	In all Series :—	
F	N/10,000	Init. $[\text{I}_2]$	= 0.002786
G	N/1,000	Init. $[\text{I}^-]$	= 0.007500
H	N/200	Init. $\frac{[\text{NaAc}]}{[\text{HAc}]}$	= $\frac{0.01250}{0.00625}$

was effected in the cold, blank experiments being made to find the best conditions for accurate analyses. Estimations of  $\text{S}_4\text{O}_6^{2-}$  and  $\text{SO}_4^{2-}$  in the solutions resulting from the running-in of N/50 thiosulphate into various mixtures of the other reactants showed that at least 98 % of the S in the  $\text{S}_2\text{O}_3^{2-}$  was accounted for as  $\text{S}_4\text{O}_6^{2-}$  and  $\text{SO}_4^{2-}$ . In view of the estimated experimental errors in the two determinations it is not considered that the remaining 2 % is of significance, and the most probable conclusion is that in the induced reaction the only products containing S are  $\text{S}_4\text{O}_6^{2-}$  and  $\text{SO}_4^{2-}$ . This view is supported by the results of experiments in which the  $\text{N}_2$  evolved was measured in a nitrometer. Table I summarizes the data of some experiments in which thiosulphate was run into the reaction mixture of the composition indicated until the iodine was decolorized, the evolved  $\text{N}_2$  measured and the  $\text{SO}_4^{2-}$  in the colourless solution determined. In the last two columns are given the percentages of  $\text{S}_2\text{O}_3^{2-}$  converted to  $\text{SO}_4^{2-}$  obtained (a) by direct determination of  $\text{BaSO}_4$  and (b) from the amount of  $\text{N}_2$

<sup>7</sup> Kurtenacker and Goldberg, *Z. anal. Chem.*, 1927, 166, 177.

evolved assuming that the only *net* processes occurring are (1), (2) and (3). The agreement between the two is regarded as sufficient to justify the assumption made.

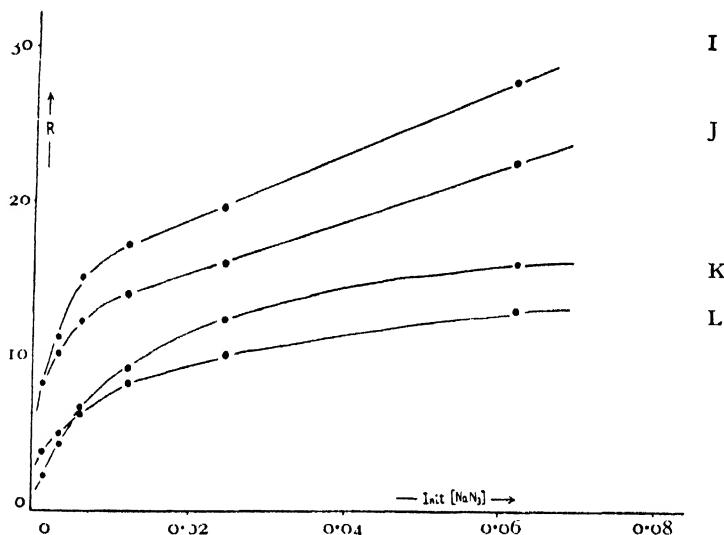


FIG. 3

Series	Temp.	Init. $[H^+]$
I	1° C	$1.8 \times 10^{-6}$
J	Room	$1.8 \times 10^{-6}$
K	1° C	$90.0 \times 10^{-6}$
L	Room	$90.0 \times 10^{-6}$

*In all Series :-*  
 Init.  $[SI_2] = 0.00025$   
 Init.  $[I^-] = 0.0100$   
 $[Na_2S_2O_3 \text{ added}] = N/10,000$

Some experiments were also made to determine the increase of acidity of the reaction mixture, the stoichiometric relation (3) requiring the formation of 10 moles of  $H^+$  for each mole of  $S_2O_3^{2-}$  oxidized to sulphate. The results obtained

TABLE I

Initial Concentrations (g.-mole (or g.-ion)/l.)					Conc. of added $S_2O_3^{2-}$ (approx.)	% $S_2O_3^{2-}$ converted to $SO_4^{2-}$	
$[SI_2]$	$[I^-]$	$[N_3^-]$	$[NaAc]$	$[HAc]$		(a)	(b)
0.02858	0.1143	0.07143	0.01429	0.007143	N/1000	60.6	59.8
0.02500	0.1000	0.1250	0.01250	0.006250	N/1000	50.8	53.7
0.02858	0.5714	0.07143	0.01429	0.007143	N/1000	50.0	48.9
0.02500	0.5000	0.1250	0.01250	0.006250	N/1000	42.5	41.4
0.02858	0.1143	0.07143	0.01429	0.007143	N/500	42.1	42.4
0.02858	0.1143	0.07143	0.01429	0.007143	N/200	23.5	25.2
0.02858	0.1143	0.07143	0.01429	0.007143	N/100	17.0	18.3

were only about one-half to three-quarters of the expected values, but the discrepancies are due to loss of the very volatile  $HN_3$  when the reaction is carried out in open flasks or beakers. In a closed apparatus with a trap containing NaOH solution through which passed the evolved  $N_3$  together with any  $HN_3$  in the gaseous phase, the results found were in reasonable agreement with the theoretical values.

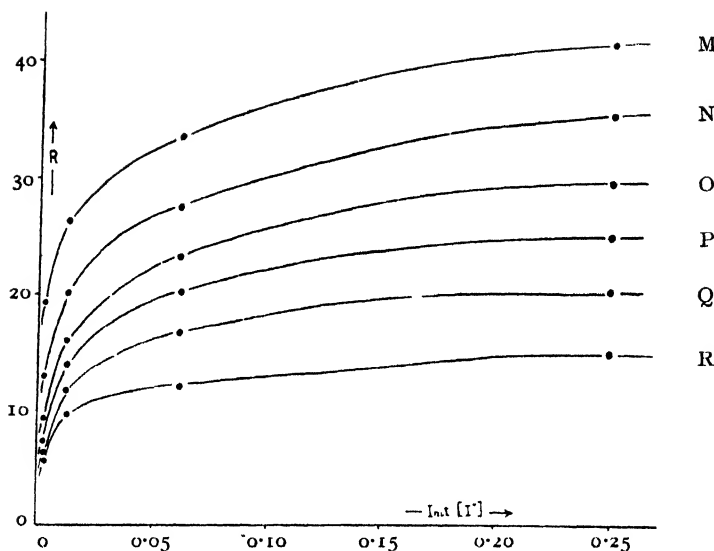


FIG. 4

Series	Init. [NaN <sub>3</sub> ]
M	0.0700
N	0.0400
O	0.0200
P	0.0100
Q	0.0050
R	0.0025

In all Series :—

$$\text{Init. } [\Sigma \text{I}_2] = 0.00025 \text{ or } 0.00030$$

$$\text{Init. } \frac{[\text{NaAc}]}{[\text{HAC}]} = \frac{0.01250}{0.00625} \text{ or } \frac{0.01538}{0.00769}$$

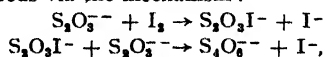
$$[\text{Na}_2\text{S}_2\text{O}_3] \text{ added} = N/10,000$$

The results of experiments of the type of those in Table I are briefly summarized in Table II, in which  $P$  is the percentage of the  $\text{S}_2\text{O}_3^{2-}$  converted into  $\text{SO}_4^{2-}$  and  $Q'$  is the ratio of moles of  $\text{N}_3^-$  decomposed to moles of  $\text{S}_2\text{O}_3^{2-}$  converted into  $\text{SO}_4^{2-}$ . The table gives the effect of increasing the concentrations of  $\text{N}_3^-$ ,  $\text{I}^-$ ,  $\Sigma \text{I}_2$  and  $\text{S}_2\text{O}_3^{2-}$  on these variables.

TABLE II

	[N <sub>3</sub> <sup>-</sup> ]	[I <sup>-</sup> ]	[ΣI <sub>2</sub> ]	[S <sub>2</sub> O <sub>3</sub> <sup>2-</sup> ]
$P$	Nearly independent	Nearly independent	Increases slightly	Marked decrease more marked at low [S <sub>2</sub> O <sub>3</sub> <sup>2-</sup> ]
$Q'$	Increases slightly	Increases slightly	Independent	Independent

**The Reaction between Na<sub>2</sub>S<sub>2</sub>O<sub>3</sub> and I<sub>2</sub>.**—Raschig<sup>3</sup> has shown that a solution prepared by adding thiosulphate solution to an excess of a solution of iodine (e.g. a mixture of equimolar amounts of I<sub>2</sub> and Na<sub>2</sub>S<sub>2</sub>O<sub>3</sub>) retains some catalytic activity, as measured by its action when poured into a solution of NaN<sub>3</sub>, for a time of 1-2 min. He suggested that the direct reaction between I<sub>2</sub> and Na<sub>2</sub>S<sub>2</sub>O<sub>3</sub> proceeds via the mechanism :



and that the catalytic activity of a mixture of  $I_2$  and  $Na_2S_2O_3$  such as the one mentioned above is due to the presence of the catalyst  $S_2O_3I^-$ , which under certain conditions has a detectable life-period, and which, it is presumed, can initiate reactions leading to the oxidations of azide. As the mechanism of the direct  $I_2$ — $Na_2S_2O_3$  reaction is of prime importance in formulating a mechanism, of the reactions in the system  $I_2$ — $S_2O_3^{2-}$ — $N_3^-$ , we have attempted to obtain quantitative data from experiments of the type which Raschig carried out qualitatively, i.e. we have carried out determinations of the rate of reaction in mixtures of  $Na_2S_2O_3$  and excess  $I_2$ . The rate of this direct reaction we have found to be strongly accelerated by increase of  $[I^-]$ , but, by working with mixtures containing  $I_2$  and  $Na_2S_2O_3$  of initial concentrations of the order of  $M/2000$  and  $KI$  of initial concentrations of the order  $M/600$ — $M/150$ , it has been found possible to measure the reaction rate over periods of two hours or more.

The experiments were made by adding  $Na_2S_2O_3$  solution to an excess of an  $I_2$ — $KI$  solution in a thermostatted flask, withdrawing samples from time to time, and determining the concentration of "active"  $S_2O_3^{2-}$  in each sample. The "active"  $S_2O_3^{2-}$ , designated by  $\Sigma S_2O_3^{2-}$ , is defined as the  $S_2O_3^{2-}$  not converted into  $S_4O_6^{2-}$ , i.e. it is the sum of the free unchanged  $S_2O_3^{2-}$  together with the  $S_2O_3^{2-}$  present in the form of some active intermediate, such as, for example, the  $S_2O_3I^-$  intermediate postulated by Raschig. The concentration of  $\Sigma S_2O_3^{2-}$  in each sample was determined from the extent of reaction, measured in terms of consumption of iodine, when the sample was added to a standard "indicator" mixture of  $I_2$ ,  $KI$ ,  $NaN_3$  and buffer. Empirically an "indicator" mixture was sought, whose sensitivity (i.e.  $R$  value = moles  $\Sigma I_2$  consumed in the mixture per mole of  $S_2O_3^{2-}$  added) was fairly constant for the range  $N/4000$ — $N/20,000$  of concentration of added thiosulphate. Such an "indicator" was found in a mixture of the composition:

$[\Sigma I_2] = 0.0250$ ;  $[I^-] = 0.125$ ;  $[N_3^-] = 0.125$ ;  $[NaAc] = 0.025$ ;  $[HAc] = 0.0125$ , as is shown by the following  $R$  values found when 24.75 ml. of solutions of  $Na_2S_2O_3$  of various strengths were run under standardized conditions\* into 50 ml. of the "indicator."

Conc. of added $Na_2S_2O_3 \times 10^4$	2.488	1.986	1.192	0.9930	0.4965
$R$	42.24	42.99	44.51	42.46	44.65
				(Mean $R = 43.65$ )	

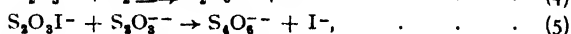
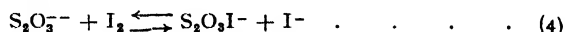
Thus by running a 24.75 ml. sample of the reacting mixture of  $Na_2S_2O_3$  and  $I_2$  into 50 ml. of this "indicator" under the same standard conditions and determining the moles iodine consumed ( $x$ ) in the "indicator," we obtain the concentration in the sample of "active"  $S_2O_3^{2-}$ , viz.:

$$[\Sigma S_2O_3^{2-}] = \frac{x \times 1000}{24.75 \times 43.65}$$

The data obtained in this way for a typical reaction mixture are shown in Table III.

From this and the other experiments it was found that the decrease in  $[\Sigma S_2O_3^{2-}]$  with time follows a bimolecular course, and bimolecular velocity constants  $k_{b1}$  (l. moles<sup>-1</sup> min.<sup>-1</sup>) were calculated from "point to point" in each experiment. The results are summarized in Table IV.

The fifth column of Table IV gives the mean values of  $k_{b1}$ , found in experiments classified into four groups according to ionic strength and temperature. Inspection of these values shows that the rate of reaction as given by the  $k_{b1}$ 's is strongly accelerated by  $[I^-]$  and is retarded by  $[\Sigma I_2]$ . This behaviour can be accounted for in terms of Raschig's mechanism slightly modified. We postulate the mechanism to be



with (4) a rapidly established equilibrium well over to the right-hand side, and (5) the rate-determining reaction. On this basis, if  $k_5$  is the velocity constant

\* 24.75 ml. of the  $Na_2S_2O_3$  solution was delivered from a fast-flowing pipette (time of delivery 4 sec., with no drainage time) into 50 ml. of the "indicator" contained in a 250 ml. Erlenmeyer flask, the flask being briskly swirled by hand during the mixing process. Excess of standard  $As_2O_3$  solution was then added and the excess back-titrated with standard iodine.

of reaction (5),  $K$  the equilibrium constant of (4), i.e.  $K = \frac{[S_2O_3I^-][I^-]}{[S_2O_3^{2-}][I_2]}$  and

$K_3$  the tri-iodide equilibrium constant  $\frac{[I^-][I_2]}{[I_3^-]}$ , it follows that

$$\frac{d[S_4O_6^{2-}]}{dt} = k_3[S_2O_3I^-][S_2O_3^{2-}] = \frac{k_3[S_2O_3I^-]^2[I^-]\{K_3 + [I^-]\}}{KK_3[SI_2]}$$

If it be assumed that equilibrium (4) is nearly completely over to the right, then  $[S_2O_3I^-]$  can be identified with  $[S_2O_3^{2-}]$  measured during each run. Hence

$$\frac{d[S_4O_6^{2-}]}{dt} = k_{b1}[S_2O_3^{2-}]^2 = \frac{k_3[SI_2][I^-]\{K_3 + [I^-]\}}{K^2K_3[SI_2]}$$

and 
$$\frac{k_{b1}[SI_2]}{[I^-]\{K_3 + [I^-]\}} = \frac{k_3}{KK_3} = \text{const.} = k_x \text{ (say).}$$

TABLE III

Temp. = 20° C.      Initial concentrations       $\left\{ \begin{array}{l} [SI_2] = 0.0006600 \\ [I^-] = 0.001667 \\ [S_2O_3^{2-}] = 0.0003164 \\ [NaNO_3] = 0.09733 \end{array} \right.$   
Ionic strength ( $\mu$ ) = 0.100      (g.-mole (or g.-ion)/l.)

Time (min.)	$\Delta t$	$x \times 10^4$	$[S_2O_3^{2-}] \times 10^4$	$\Delta[S_2O_3^{2-}] \times 10^4$	$k_{b1} \times 10^{-2}$
1.00		2.024	1.886		
5.00	4.00	1.737	1.619	0.267	2.19
	8.00			0.362	2.22
13.00	16.00	1.349	1.257	0.3711	2.08
29.00	32.00	0.9504	0.8859	0.3506	2.31
61.00		0.5744	0.5353		

Thus if the experimental values of  $k_{b1}$  are multiplied by the factor

$$[SI_2]/[I^-]\{K_3 + [I^-]\} (= F),$$

the values of the product  $k_x$  should be constant. The seventh and eighth columns of Table II give the mean concentrations during the runs of  $[SI_2]$  and  $[I^-]$  (corrected for tri-iodide formation using  $K_3 = 1.20 \times 10^{-3}$  at 20° and  $1.57 \times 10^{-3}$

\* It is to be noted that to obtain values of  $x$  it is necessary to know the  $[SI_2]$  in the sample of reaction mixture. It is, however, not possible to calculate this quantity until both the mechanism of the  $I_2-S_2O_3^{2-}$  reaction and the amount of  $S_2O_3^{2-}$  in the sample are known. Hence, to obtain an approximate value of the iodine in the sample the assumption was made that the  $I_2-S_2O_3^{2-}$  reaction had gone to completion. Thus, for the reaction mixture of Table III the  $[SI_2]$  at completion is given by  $0.0006600 - 0.0003164/2 = 0.0005018$ ; a 24.75 ml.-sample at completion thus contains  $0.1242 \times 10^{-4}$  moles  $I_2$ , and this value is used throughout in obtaining  $x$ . This procedure, though an approximation, introduces only a small error, since the consumption of iodine in the "indicator" is large compared with the amount of iodine in the sample. In the experiment of Table III, by the time the first sample was removed  $[S_2O_3^{2-}]$  had fallen from 0.0003164 to 0.0001886 moles/l., that is, during the mixing process and the following minute the reaction had proceeded to nearly half completion, and after this initial disturbance the comparatively slow rate was measurable. An effect of this magnitude—up to two-thirds completion of the reaction by the time of taking the first sample—was observed in the majority of the experiments, and is discussed later. In the experiment of Table III the value of the amount of iodine in the first sample thus cannot differ by more than about  $0.07 \times 10^{-4}$  moles from the value  $0.1242 \times 10^{-4}$  moles calculated on the basis that the reaction had gone to completion. This possible error of  $0.07 \times 10^{-4}$  is an error in the value  $x = 2.024 \times 10^{-4}$ , i.e. an error of about 3.5 %; the error in succeeding samples is progressively less.



TABLE IV

Temp. = 20° C (except for Group D)

Initial concentrations (g.-mole (or g.-ion)/l.)				$k_{b1}$ $\times 10^{-2}$	$[S_2O_3^{2-}]_m$ $\times 10^4$	$[I_2]_m$ $\times 10^4$	$[I^-]_m$ $\times 10^3$	$k_\alpha$ $\times 10^{-4}$	$k_\beta$ $\times 10^{-3}$
$[I_2]$ $\times 10^4$	$[I^-]$ $\times 10^3$	$[S_2O_3^{2-}]$ $\times 10^4$	$\mu^*$						
Group A									
6.51	1.67	6.43	0.0036	1.23	1.34	2.63	2.15	0.449	3.39
6.51	1.67	3.22	0.0026	0.743	1.53	4.14	1.74	0.599	4.34
6.51	1.67	1.63	0.0022	0.606	1.16	5.11	1.55	0.730	5.23
3.27	1.67	1.63	0.0022	0.987	0.98	1.96	1.71	0.388	2.92
6.64	6.67	6.60	0.0087	8.55	1.14	2.77	7.09	0.403	4.79
6.64	6.67	3.32	0.0077	5.32	1.33	4.32	6.63	0.442	4.30
6.64	6.67	1.65	0.0072	3.99	1.03	5.30	6.39	0.436	3.90
3.30	6.67	3.27	0.0077	13.28	0.69	1.33	6.88	0.317	5.67
3.30	6.67	1.63	0.0072	8.61	0.77	2.10	6.65	0.347	4.45
Group B									
6.55	1.67	6.54	0.064	3.63	1.00	2.78	2.14	1.41	6.38
6.54	1.67	3.29	0.064	2.07	1.17	4.31	1.74	1.74	7.38
6.54	1.67	1.64	0.064	1.73	0.95	5.25	1.54	2.16	8.99
6.63	6.67	6.60	0.064	17.57	0.86	2.90	7.08	0.870	7.88
6.61	6.67	3.32	0.064	10.58	1.05	4.45	6.62	0.908	6.06
6.63	6.67	1.65	0.064	8.69	0.88	5.37	6.38	0.965	5.79
Group C									
6.50	1.67	6.32	0.100	3.81	1.05	2.90	2.11	1.58	7.10
6.60	1.67	3.16	0.100	2.20	1.21	4.41	1.72	1.93	8.15
6.57	1.67	1.66	0.100	1.80	1.03	5.23	1.54	2.24	9.32
6.61	6.67	6.60	0.100	21.22	0.69	2.96	7.07	1.08	9.59
6.63	6.67	3.32	0.100	14.31	0.89	4.53	6.61	1.25	8.29
6.64	6.67	1.65	0.100	11.78	0.81	5.41	6.38	1.32	7.90
Group D (Temp. = 30°)									
6.57	1.67	6.62	0.0036	1.79	1.31	2.60	2.18	0.568	5.50
6.57	6.67	6.62	0.0086	10.02	1.08	2.72	7.11	0.440	6.23

at 30°), and the ninth column the derived values of  $k_\alpha$ . Inspection of these values shows that in each of the groups, the values of  $k_\alpha$  tend to increase with increase of  $[I_2]_m$  and to fall with increase of  $[I^-]_m$ , and hence to increase with increasing  $F$ . These discrepancies indicate that the equilibrium position of (4) is not so far over to the right-hand side as has been assumed above; from the deviations we may obtain approximate values of  $K$  and  $k_2$  as follows.

By definition of  $K$  we have

$$\frac{[S_2O_3I^-]}{[S_2O_3^{2-}]} = KK_3F = K'F,$$

where  $K' = KK_3$ . Further,

$$k_1[S_2O_3I^-][S_2O_3^{2-}] = k_{b1}[S_2O_3^{2-}]^2$$

and

$$[S_2O_3^{2-}] = [S_2O_3I^-] + [S_2O_3^{2-}],$$

from which

$$k_2 = \frac{k_{b1}(1 + K'F)^2}{F}.$$

By trial and error values of  $K'$  are found which on substituting in the above equation makes  $k_2$  most constant in each group. The values of  $K'$  so derived are 0.7 for the experiments of Group A and 0.4 for the experiments of Groups

\* For reaction mixtures with  $\mu > 0.01$ , the ionic strength was increased to the indicated value by addition of  $NaNO_3$ .

B and C. These correspond to values of  $K$  of about 580 for Group A, and 330 for Groups B and C. We shall assume that  $K$  for Group D is also 580, giving  $K' = KK_2 = 0.9$ . With these values of  $K'$ , the  $k_2$ 's given in the last column of Table IV were calculated from the observed values of  $k_{b1}$ . Though some slight errors are involved in this procedure, since the values of  $[S_2I_2]_m$  and  $[I^-]_m$  (and hence also of  $F$ ), all based on the assumption that the equilibrium (4) lies nearly completely over to the right, are not now quite correct, the experimental data are not sufficiently accurate to warrant more elaborate calculations, but it is considered that, as they stand, they provide substantial evidence for the mechanism proposed and that they yield values of  $K$  and  $k_2$  of the rough order of magnitude of those summarized in Table V.

TABLE V

Ionic Strength	Temp. (°C)	$K$	$k_2 \times 10^{-3}$
0.002-0.008	20	580	4.3
0.06	20	330	7.1
0.10	20	330	8.4
0.002-0.008	30	(580)	5.9

It is to be noted that on the basis of the mechanism  $[S_2I_2]$  should increase over the period of reaction for which measurements can be made. This follows because after the initial rapid formation of  $S_2O_3I^-$ , reaction (5) is maintained by the re-conversion of part of the  $S_2O_3I^-$  back into  $S_2O_3^-$  and  $I_2$  by the reverse reaction in equilibrium (4), and hence  $[S_2I_2]$  increases. The predicted rise in  $[S_2I_2]$  during the course of reaction was found and followed experimentally by measuring the light absorption of an  $I_2$ - $Na_2S_2O_3$  mixture by means of a Hilger Spekker absorptiometer. For example, with a reaction mixture of initial composition

$$[S_2I_2] = 0.000657, [S_2I^-] = 0.00267, [S_2O_3^-] = 0.000649,$$

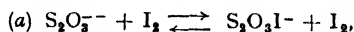
reacting at room temperature (ca. 18°) in a cell of 1 cm. thickness, the following values of  $\alpha d$  were obtained, using a violet filter.

Time (min. from start)	2.0	5.0	10.0	20.0	30.0	40.0
$\alpha d$	0.401	0.406	0.410	0.430	0.438	0.440

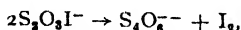
Though a part of this increase in  $\alpha d$  with time may be due to an increase in  $[S_2I^-]$ , leading to an increased ratio of  $[I_2]/[I_2]$  and, since  $\alpha_{I_2} > \alpha_{I_2^-}$  for  $\lambda = 4300\text{\AA}$ , to an increased absorption of light, it is not difficult to show that the effect is much too big to be accounted for in this way, and we can conclude that the main part of the increase must be due to an increase in  $[S_2I_2]$ , as predicted by the mechanism.

To test the validity of the experimental method for determining  $[S_2S_2O_3^-]$  in reacting mixtures of  $I_2$  and  $S_2O_3^-$ , a few of the experiments of Table III were repeated, but instead of running samples into the  $I_2$ -KI- $NaNO_3$  "indicator" mixture, the latter was replaced by a suitable  $I_2$ -KI- $NaNO_2$  mixture. A study of the reactivity of  $S_2O_3^-$ - $I_2$ - $NO_2^-$  systems<sup>6</sup> has shown that  $R$  values between 0.5 and a maximum of 4.0 are obtainable. Hence by employing a procedure analogous to that described above, it is possible to determine the  $[S_2S_2O_3^-]$  in each sample of a reacting  $S_2O_3^-$ - $I_2$  mixture from the extent of reaction induced in an  $I_2$ -KI- $NaNO_2$  "indicator" mixture. The sensitivity of the "indicator," however, is very low, and the data are subject to considerable error, yet the method yields approximate values of  $k_{b1}$  which are found to be in reasonable agreement with those given above.

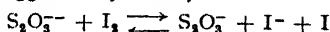
Other mechanisms have been considered, e.g.



followed by



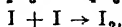
and (b) the mechanism suggested by Weiss,<sup>5</sup>



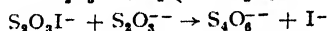
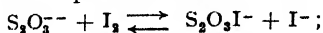
followed by



and

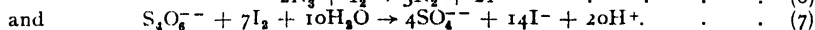


but none is consistent with the experimental data; hence the mechanism



appears to us to be the most likely course of the reaction between thiosulphate and iodine.

**System  $\text{I}_2\text{--S}_4\text{O}_6^{2-}\text{--N}_3^-$ .**—The reactions occurring in these systems are measurably slow and can be followed by ordinary kinetic methods, if the concentrations of reactants are not too high, and determinations of the rate of reaction have been made at 20° and 30° C in the presence of acetate buffers. Analysis of the end-products showed that the only *net* processes taking place are:



This was shown by preparing reaction mixtures of compositions similar to those employed in the kinetic experiments and allowing the reaction to proceed to completion at 20°, that is, until all the initial iodine had been consumed, sufficient  $\text{NaN}_3$  being present to ensure an excess of this salt at the end of the run. The total volume of  $\text{N}_2$  evolved was measured in a nitrometer and the sulphate in the resulting colourless solution was determined by precipitation and weighing as  $\text{BaSO}_4$ . Table VI shows the type of result obtained.

TABLE VI

Temp. = 20°;  $[\text{I}_2]_{\text{init.}} = 0.001974$ ;  $[\text{HAc}] = 0.0333$ ;  $[\text{NaAc}] = 0.0333$   
Conc. in g.-mole (on g.-ion)/l.

$[\text{N}_3^-]_{\text{init.}}$	$[\text{S}_4\text{O}_6^{2-}]_{\text{init.}}$	$[\text{I}^-]_{\text{init.}}$	% $\text{S}_4\text{O}_6^{2-}$ converted into $\text{SO}_4^{2-}$	
			( $\alpha$ )	( $\beta$ )
0.004167	0.01667	0.100	0.423	0.465
0.008333	0.008333	0.100	0.488	0.448
0.008333	0.008333	0.050	0.546	0.534

In the last two columns are given the percentage conversions of the initial tetrathionate into sulphate, ( $\alpha$ ) as given directly by sulphate determination, and ( $\beta$ ) as inferred from the volume of  $\text{N}_2$  evolved and total iodine consumed on the basis of (6) and (7) being the sole *net* reactions.

For kinetic measurements at 20° it was found that reaction mixtures containing  $[\text{I}_2]$ ,  $[\text{NaN}_3]$  and  $[\text{Na}_2\text{S}_4\text{O}_6]$  in the range 0.0004–0.002 M gave conveniently measurable rates. The data of the analyses quoted above show that the percentage conversion of  $\text{Na}_2\text{S}_4\text{O}_6$  into  $\text{Na}_2\text{SO}_4$  in such mixtures is very small. Hence it was not practicable to measure the rate of sulphate formation during a run either by determination of  $\text{SO}_4^{2-}$  formed or of  $\text{S}_4\text{O}_6^{2-}$  remaining. The rate of sulphate formation had therefore to be obtained indirectly as follows. Reaction mixtures were divided into two portions. From one portion samples were removed from time to time,  $[\text{I}_2]$  in the samples determined by titration, and hence the over-all rate of reaction in terms of  $[\text{I}_2]$  determined. The other portion was placed in a Warburg apparatus, the rate of evolution of  $\text{N}_2$  determined, and hence, in terms of eqn. (6), the rate of consumption of  $\text{I}_2$  used in oxidizing  $\text{NaN}_3$ . Subtraction of this latter rate from the over-all rate of iodine consumption gives the rate of iodine consumed in oxidizing tetrathionate, and one-seventh of this is rate of disappearance of tetrathionate.

Preliminary measurements of the over-all rate showed that variation of  $[\text{I}^-]$  has a striking effect on the rate. With zero initial  $[\text{I}^-]$  a comparatively high rate of reaction is found. Increase of  $[\text{I}^-]$  strongly retards the reaction, until a minimum is reached in the region of  $[\text{I}^-]$  between 0.01 and 0.02 M. Increase of  $[\text{I}^-]$  beyond this region progressively accelerates the reaction, the rate becoming about proportional to  $[\text{I}^-]^2$  when  $[\text{I}^-] = 0.4$ . Fig. 5 illustrates this behaviour for reaction mixtures at 20° containing initially

$$\begin{aligned} [\text{I}_2] &= 4 \cdot 10^{-4}, & [\text{N}_3^-] &= [\text{S}_4\text{O}_6^{2-}] = 1.67 \times 10^{-3}, \\ [\text{NaAc}] &= 3.33 \times 10^{-2}, & [\text{HAc}] &= 1.67 \times 10^{-2}, \end{aligned}$$

with varying  $[I^-]$ . In the plot the rate is expressed as  $k_{0(\Sigma I_2)} = -\frac{\Delta[\Sigma I_2]}{\Delta t}$

measured for the first time interval. It thus appears probable that at least two mechanisms are operative, one predominating in the region of very low  $[I^-]$ , with the rate retarded by  $I^-$ , and the other predominating in the region of medium and high  $[I^-]$ , with the reaction catalyzed by  $I^-$ . This conclusion receives support from the discoveries (a) that  $I_2$  reacts with  $Na_2S_4O_6$  in absence

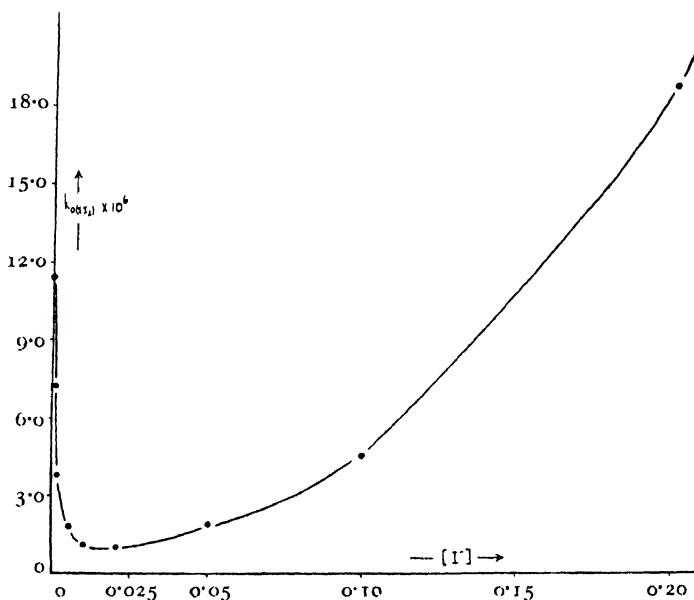


FIG. 5

of  $NaN_3$  in solutions of very low  $I^-$  content and, (b) that at high concentrations of reactants a reaction between  $Na_2S_4O_6$  and  $I^-$  can be detected, also in absence of  $NaN_3$ . These direct reactions are discussed later in this paper; for the present we shall assume that two distinct mechanisms operate in the reactions in  $I_2-S_4O_6^{2-}-N_3^-$  mixtures and deal separately with the data pertaining to the regions of  $[I^-]$  above and below 0.01 M.

TABLE VII

Temp. = 20° C;  $[NaAc] = 0.0333$ ;  $[HAc] = 0.0167$  g. mole/l.

Initial concentrations (g.-mole (or g.-ion/l.))				$k_{0(\Sigma I_2)} \times 10^4$	$k_{uni(N_3^-)} \times 10^3$	$k_{0(S_4O_6^{2-})} \times 10^7$	$Q_0$
$[\Sigma I_2] \times 10^4$	$[I^-]$	$[N_3^-] \times 10^3$	$[S_4O_6^{2-}] \times 10^4$				
8.28	0.40	1.67	3.33	7.73- 3.39	8.63	1.28	73.0
4.09	0.20	1.67	16.7	15.9-11.4	18.1	3.45	53.7
4.09	0.20	1.67	8.33	7.93- 5.92	9.59	1.44	84.6
16.49	0.20	0.833	3.39	1.57- 0.77	3.28	0.44	32.0
16.49	0.20	3.33	8.49	10.5- 5.12	6.11	1.68	70.1
4.09	0.10	1.67	17.0	4.49- 3.89	4.77	1.40	43.5
8.25	0.05	1.67	33.8	4.70- 2.77	4.75	1.33	41.0
16.47	0.05	0.833	33.3	3.20- 1.84	5.21	1.39	21.4
4.09	0.05	3.33	17.0	3.20- 2.93	1.61	0.86	49.2
4.08	0.02	1.67	16.7	1.00- 0.73	0.74	0.37	29.2

Table VII summarizes the results of some of the experiments (about one-third of the total) carried out at medium and high  $[I^-]$ . In this table  $k_{0(\Sigma I_2)}$  and  $k_{0(S_4O_6^{2-})}$  are zero-molecular constants with respect to  $\Sigma I_2$  and  $S_4O_6^{2-}$  respectively. The former of these was found to fall slightly during a run; in the Table are given the first and last values determined. The rate of evolution of  $N_2$  was found to be unimolecular with respect to  $N_3^-$  and the Table gives mean values for each experiment of

$$k_{\text{uni}(N_3^-)} = \frac{1}{t_2 - t_1} \log_e \frac{[N_3^-]_1}{[N_3^-]_2}$$

The last column gives values of the ratio

$$Q_0 = (\text{moles } NaN_3 \text{ decomposed}) / (\text{moles } Na_2S_4O_6 \text{ consumed})$$

over the time the reaction was followed.

From these and other data not listed, it is found that the dependence of the various rates measured on the concentration of reactants and of iodide in this region of  $[I^-]$  is as summarized in Table VIII.

TABLE VIII

	Dependence on			
	$[\Sigma I_2]$	$[I^-]$	$[N_3^-]$	$[S_4O_6^{2-}]$
Overall rate of consumption of $I_2$	Independent	$\propto [I^-]^z$ $z > x > 1$	$\propto [N_3^-]^y$ $y$ slightly less than 1	Proportional
Rate of $NaN_3$ decomposition	Independent	$\propto [I^-]^z$ $z > x > 1$	Proportional	Proportional
Rate of consumption of $Na_2S_4O_6$	Independent	Proportional	$\propto [N_3^-]^z$ $z$ approx. 0.5	Proportional
$Q_0$	Independent	Increases slightly with inc. $[I^-]$	$\propto [N_3^-]^z$ $z$ approx. 0.5	Independent

We have also made a number of similar kinetic experiments in  $N_3^-$ — $S_4O_6^{2-}$ — $I_2$  systems in the presence of low concentrations of iodide ( $[I^-]_{\text{init.}} < 0.006$ ). These yielded values of  $Q_0$  in the range from 10 to 45, with rates of reactions markedly retarded by  $I^-$ . Since here there is a considerable increase of  $[I^-]$  during each run, it has so far been found difficult to make an exact assessment from the data of the effect of concentrations of  $\Sigma I_2$ ,  $S_4O_6^{2-}$ ,  $N_3^-$  and  $I^-$  on the rates of reaction; consequently we shall not deal further at present with the reactivity of such systems in presence of low  $[I^-]$ .

**The Reactions between  $S_4O_6^{2-}$  and  $I^-$  and  $S_4O_6^{2-}$  and  $I_2$ .**—As indicated earlier,  $S_4O_6^{2-}$  is found to react directly under certain conditions both with  $I^-$  and  $I_2$ , and these reactions (or their initial steps) must play important roles in the reactivity of the system  $S_4O_6^{2-}$ — $I^-$ — $N_3^-$  in the regions respectively of high and low  $[I^-]$ . Both reactions are complicated, particularly the  $S_4O_6^{2-}$ — $I^-$  reaction, on which we have made only a few qualitative measurements. The  $S_4O_6^{2-}$ — $I_2$  reaction can only be measured at very low concentrations of iodide; for it we have obtained some quantitative data, but not sufficient to establish a mechanism.

Dealing first with the  $S_4O_6^{2-}$ — $I^-$  reaction, the following experiment indicates the formation during the course of the reaction of appreciable amounts of a substance which reacts rapidly with iodine or induces azide to do so. To 130 ml. of a solution of composition:

$$[\Sigma I_2] = 0.000413, \quad [I^-] = 0.200, \quad [N_3^-] = 0.00667, \\ [NaAc] = 0.0333, \quad [HAc] = 0.0167$$

at 20° C were added 20 ml. M/400  $\text{Na}_2\text{S}_4\text{O}_6$  in 1.5 M KI solution, which had previously been heated to 65° C for 30 min. and then cooled to 20° C. However, even before all the  $\text{Na}_2\text{S}_4\text{O}_6$  solution had been added, all the iodine in the reaction mixture was completely consumed. In an identical reaction mixture, but without pre-heating of the  $\text{Na}_2\text{S}_4\text{O}_6$  with KI, the time required for complete consumption of the iodine was over an hour. Qualitative tests showed that the mixture of  $\text{Na}_2\text{S}_4\text{O}_6$  and KI used above after heating would itself react with iodine and also contained sulphate and  $\text{H}^+$ . A few attempts were made to follow the course of the direct reaction between  $\text{S}_4\text{O}_6^{2-}$  and  $\text{I}^-$  at 20°, using fairly high concentrations of reactants ( $[\text{I}^-] = 1.00$ ;  $[\text{S}_4\text{O}_6^{2-}] = 0.02\text{--}1.00$ ), by titrating samples with  $\text{I}_2$ . Using unbuffered solutions, the reaction followed a marked autocatalytic course; in phosphate or acetate buffers, the rates of reaction were much less and the degree of autocatalysis not so pronounced. Among the ultimate products are  $\text{H}_2\text{S}$ , free S,  $\text{SO}_4^{2-}$  and  $\text{H}^+$ . Of chief interest for our purpose of discussing the mechanism of the reactions in  $\text{I}_2\text{--S}_4\text{O}_6^{2-}\text{--N}_2^-$  systems is the fact that a direct reaction between  $\text{S}_4\text{O}_6^{2-}$  and  $\text{I}^-$  does take place at 20° and that one of the products in the early stages of the reaction is a compound which reacts immediately with  $\text{I}_2$ . This product is not  $\text{SO}_3^{2-}$  and is most probably  $\text{S}_2\text{O}_3^{2-}$ .

On the reaction between  $\text{S}_4\text{O}_6^{2-}$  and  $\text{I}_2$ , which yields  $\text{SO}_4^{2-}$ ,  $\text{H}^+$  and  $\text{I}^-$ , we have carried out kinetic measurements at 20° C in presence of acetate buffers and in the presence of initial  $[\Sigma\text{I}^-]$  ranging from zero to 0.009. The reaction was followed by determination of  $[\Sigma\text{I}_2]$  by titration in samples withdrawn from time to time. Table IX summarizes the results.

TABLE IX

Temp. = 20°;  $[\text{NaAc}] = 0.0250$ ;  $[\text{HAc}] = 0.0125$  g. mole/l.

Initial Concentrations (g.-mole (or g.-ion)/l.)			$k_{\text{uni}} \times 10^2$	$[\text{I}^-] \times 10^4$		$k' \times 10^2$
$[\Sigma\text{I}_2] \times 10^4$	$[\text{S}_4\text{O}_6^{2-}] \times 10^4$	$[\Sigma\text{I}^-] \times 10^4$		First sample	Last sample	
3.36	0.937	Nil	2.80-0.84	0.750	5.56	5.80
3.36	1.87	Nil	4.37-1.33	0.930	5.45	5.00
*3.36	1.87	Nil	4.26-1.50	1.08	5.63	5.24
6.72	1.87	Nil	3.25-0.51	1.62	10.77	4.91
3.36	3.75	Nil	7.16-2.05	1.43	5.61	4.27
6.51	3.75	Nil	5.09-0.81	1.66	10.76	3.96
3.25	7.50	3.06	5.37-1.51	3.18	9.00	3.24
3.25	15.0	3.06	7.73-2.28	3.44	8.87	2.60
3.33	15.0	8.66	3.23-1.39	7.68	14.55	2.99
3.33	30.0	8.66	4.64-2.18	8.03	14.58	2.38
†3.17	0.937	Nil	9.32-3.82	1.69	5.72	29.7
†6.35	1.87	Nil	7.35-2.40	3.13	12.03	23.5

\*  $[\text{NaAc}] = 0.0250$ ,  $[\text{HAc}] = 0.0025$  g.-moles/l.; † Temp. = 20°.

In the fourth column of Table VIII are given first-order constants ( $k_{\text{uni}}$ ) with respect to  $\Sigma\text{I}_2$ . These fall markedly in each run; the values given are those relating to the first and last time intervals in each experiment. The concentration of tetrathionate in all these experiments decreases only slightly, and the fall in  $k_{\text{uni}}$  with time is thus probably to be referred to the large increase in  $[\text{I}^-]$  which occurs in each run; columns 5 and 6 give the concentrations of  $\text{I}^-$ , corrected for tri-iodide formation, in the first and final samples taken from the reaction mixture. Comparison of the results of Expt. (2) and (3) indicates that  $[\text{H}^+]$  has no significant effect on the rate over the range of  $[\text{H}^+]$  tested. Insufficient work has been done to derive the exact dependence of the rate on the concentrations of reactants and of iodide, but application of the equation,

$$k' = k_{\text{uni}} \frac{\{K_3 + [\text{I}^-]_m\}[\text{I}^-]_m}{K_3} [\text{S}_4\text{O}_6^{2-}]_m^{-1},$$

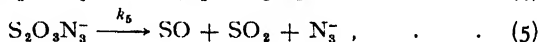
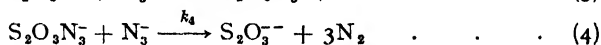
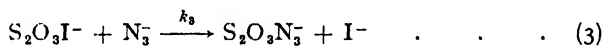
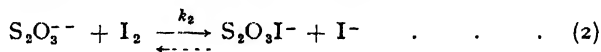
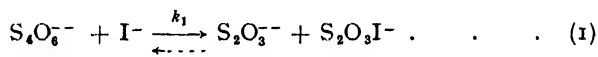
where  $[\text{I}^-]_m$  and  $[\text{S}_4\text{O}_6^{2-}]_m$  are the mean concentrations of free  $\text{I}^-$  and  $\text{S}_4\text{O}_6^{2-}$  respectively in the time interval for which  $k_{\text{uni}}$  was determined and  $K_3$ , the

tri-iodide equilibrium constant, has the values 0.0012 at 20° and 0.00157 at 30°, appears to give reasonable constancy of  $k'$  in each experiment. The mean values of  $k'$  are given in the last column; it is seen that these fall as  $[S_4O_6^{2-}]$  is increased. However, in these experiments the increase in  $[S_4O_6^{2-}]$  was accompanied by an increase in ionic strength, and thus there is a possibility that the fall in  $k'$  may be referred to an effect of ionic strength. Further work will thus be necessary before the mechanism of this reaction can be usefully discussed. These preliminary experiments show, however, that tetrathionate is oxidized by  $I_2$  at low concentrations of  $I^-$ ; the initial step (or steps) of this reaction will form the catalyst which is responsible for the reaction between  $I_2$  and  $N_3^-$  induced by  $Na_2S_4O_6$  at very low concentrations of iodide.

### Reaction Mechanisms

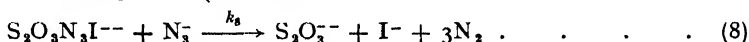
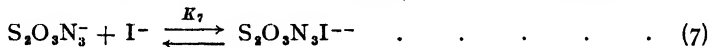
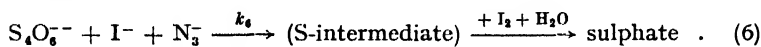
It is convenient first to deal with the mechanism of reaction in  $I_2-S_4O_6^{2-}-N_3^-$  systems, for which quantitative measurements of rates of reaction have been obtained over a fairly wide range of conditions. As there are grounds for the belief that the reactivity of these systems is closely linked with that of  $I_2-S_2O_3^{2-}-N_3^-$  systems, for which direct kinetic measurements are not available, the mechanism of the latter can best be discussed in the light of the mechanism adopted for the former.

Discussing first the kinetics of the reactions in  $I_2-S_4O_6^{2-}-N_3^-$  systems in the presence of medium and high  $[I^-]$ , one of the outstanding features of the experimental data (see Table VII) is the large values of  $Q_0$  obtained. Thus, depending on the conditions, 20-100 moles of  $NaN_3$  are oxidized to  $N_2$  per mole of  $Na_2S_4O_6$  oxidized to sulphate. It is therefore considered that the mechanism of  $N_3^-$  decomposition involves a reaction chain. A plausible and simple chain mechanism is the following:



(followed by rapid oxidation of SO and  $SO_2$  by  $I_2$  to sulphate). The initial step postulated is the slow reaction (1), which is the reverse of the second reaction assumed to take place when  $I_2$  reacts with  $S_2O_3^{2-}$ . It receives some justification from the fact given above that at high concentrations a reaction between  $S_4O_6^{2-}$  and  $I^-$  can be detected, yielding a product (probably  $S_2O_3^{2-}$ ) which reacts rapidly with  $I_2$ . In the absence of  $N_3^-$  and with moderate and low concentrations of  $S_4O_6^{2-}$  and  $I^-$  reaction (1) is not detectable, and the equilibrium lies nearly completely over the left. In the presence of  $I_2$  and  $N_3^-$ , however, the small amounts of  $S_2O_3^{2-}$  and  $S_2O_3I^-$  are immediately converted into the intermediate  $S_2O_3N_3^-$  by the fast reactions (2) and (3). Since in  $S_2O_3^{2-}-I_2-N_3^-$  systems the reactions are practically instantaneous, it follows that after the slow process (1) forming  $S_2O_3^{2-}$ , all the succeeding reactions must be very rapid. Processes (2), (3) and (4) constitute the chain. Consideration of the experimental data leads to the conclusion that the chain-breaking process is probably closely linked with the formation of sulphate, and, after the consideration of other possibilities, process (5) is suggested. This mechanism yields, by the assumption of stationary state concentrations for  $S_2O_3^{2-}$ ,  $S_2O_3I^-$ , and  $S_2O_3N_3^-$  expressions for  $k_0(LI_2)$ ,  $k_{uni}(N_3^-)$ ,  $k_0(S_4O_6^{2-})$  and  $Q_0$  which can be compared in respect of their dependence on concentration variables with the experimental data summarized in Table VIII. It is found in this way that the mechanism satisfies most of the data,

but does not account for the observed increase of rate of  $S_4O_6^{--}$  consumption with increase of  $[N_3^-]$  nor for the observed dependence of rates of consumption of  $SI_3$  and of decomposition of  $N_3^-$  on the concentration of iodide. These defects may be remedied on the basis of the above scheme by the addition of further reactions to the mechanism. It appears that (a) one must postulate the occurrence of an additional sulphate-forming reaction whose velocity is increased by increase of  $[N_3^-]$  but which does not result in decomposition of  $N_3^-$ , and (b) there exists an extra enhancing effect of  $[I^-]$  on the chain which is not taken account of by reactions (1)-(5). These considerations lead us to postulate the following additional reactions to the scheme :



Here process (6) is represented in a purely formal manner, and process (7) is regarded as a maintained equilibrium. With these additions to reactions (1)-(5), the following rate expressions are obtained, if it is assumed for simplicity that reactions (4) and (8) have equal intrinsic speeds,\* i.e.  $k_4 = k_8$  :

$$k_0(SI_2) = [S_4O_6^{--}][I^-] \left\{ \frac{2k_1k_4[N_3^-](K_7 + [I^-])}{k_8K_7} + 7(k_6[N_3^-] + k_1) \right\}$$

$$k_{unl}(N_3^-) = \frac{4k_1k_4[S_4O_6^{--}][I^-](K_7 + [I^-])}{k_8K_7}$$

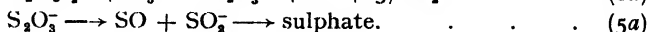
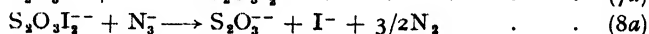
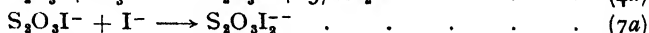
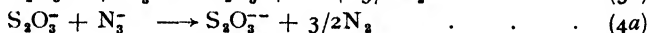
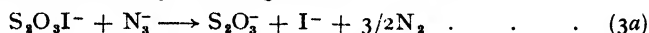
$$k_0(S_4O_6^{--}) = [S_4O_6^{--}][I^-](k_6[N_3^-] + k_1)$$

$$Q_0 = \frac{4k_1k_4[N_3^-](K_7 + [I^-])}{k_8K_7(k_6[N_3^-] + k_1)}$$

Qualitatively these equations are in accord with the experimental findings as given in Table VIII, and quantitatively they reproduce the data (Table VII) fairly well with the following values of the constants :

$$k_1 = 0.00045; \quad k_4/k_6 = 9500; \quad k_8 = 0.349; \quad K_7 = 0.11,$$

all based on concentrations in moles/litre, and time in minutes. It may be noted that an alternative chain to the one given above is equally probable, as the two are kinetically indistinguishable. This is :



Here, instead of  $S_2O_3N_3^-$ , the postulated chain carrier is the radical ion  $S_2O_3^-$ , whose existence has previously been postulated by several investigators, for example by Evans and Baxendale.\*

As regards the reaction in the region of very low  $[I^-]$ , it is possible that the same intermediates  $S_2O_3I^-$  and  $S_2O_3N_3^-$  take part, but until further data are obtained for the reaction and for the reaction between  $S_4O_6^{--}$  and  $I_2$  in absence of  $N_3^-$ , the reaction mechanism cannot be profitably discussed.

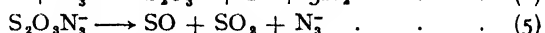
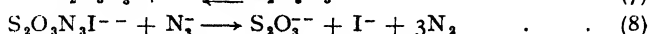
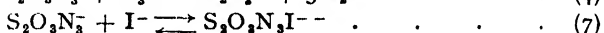
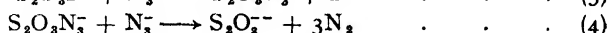
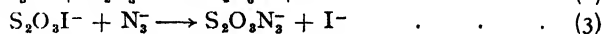
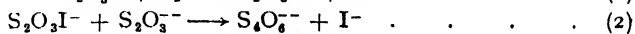
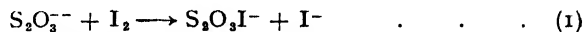
Turning now to the reactivity of  $I_3-S_2O_3^{--}-N_3^-$  systems, for which the experimental data have been given in Fig. 1-4, and Tables I and II,

\* If this assumption is not made, no essential difference in the form of the resulting expression ensues.

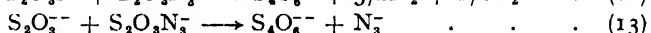
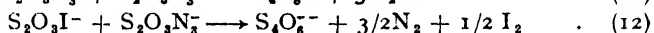
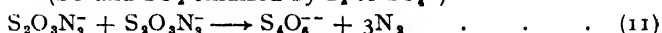
\* Evans and Baxendale, *Trans. Faraday Soc.*, 1946, **42**, 197.



the formulation of a reaction mechanism in absence of quantitative rate measurements presents difficulties, though some help is afforded from the fact that the proposed steps must be reconcilable with the data for the direct  $I_2$ - $Na_2S_2O_3$  reaction and the  $I_2$ - $Na_2S_4O_6$ - $NaN_3$  induced reaction considered above. The following tentative mechanism, all the steps of which, except (11)-(13), have been previously put forward, is suggested :



(SO and  $SO_2$  oxidized by  $I_2$  to  $SO_4^{2-}$ )



It has been mentioned earlier that the values of  $R$  obtained depend to a considerable extent on the method of addition of  $Na_2S_2O_3$  to the rest of the reaction mixture and on the mode of agitation during the addition. The process of mixing is thus of importance, and it is even possible that the total reaction occurs in the immediate vicinity of the regions in which the drops of  $Na_2S_2O_3$  solution meet the remainder of the reaction mixture, so that the reaction is practically completed before the solution is homogeneous. The initial steps in the reaction are the same as those in the direct  $I_2$ - $S_2O_3^{2-}$  reaction. For the latter we have evidence that the rate of formation of  $S_4O_6^{2-}$  is much greater initially than would be anticipated from the subsequent course of reaction; the probable explanation is that during the mixing process owing to high local concentrations of  $S_2O_3^{2-}$  and  $S_2O_3I^-$  the rate of reaction (2) is much enhanced, with the consequence that one-half to two-thirds of the thio-sulphate has disappeared before the first reading can be taken, though the subsequent course of the reaction may be quite slow. In the presence of azide this tendency for the reaction to take place before the solution can become homogeneous must be considerably greater, because in place of the slow reaction (2), the much faster reaction (3) together with its successors occurs. In presence of moderate and high  $[N_3^-]$  reaction (2) will be practically eliminated, and most of the tetrathionate which is then formed, must result from other processes. We must therefore postulate the occurrence of reactions such as (11)-(13) (and possibly also similar reactions with the complex  $S_2O_3N_3I^-$  replacing  $S_2O_3N_3^-$ ) as chain-breaking reactions forming  $S_4O_6^{2-}$ , at least one of these being intrinsically much faster than (2). The chain-continuing processes we postulate are the same as those in  $S_4O_6^{2-}$ - $I_2$ - $N_3^-$  systems in presence of moderate and high  $[I^-]$ , as also is the chain-breaking process forming  $SO_4^{2-}$ . Considering the two systems, in both we have the same active intermediates,  $S_2O_3^{2-}$ ,  $S_2O_3I^-$ ,  $S_2O_3N_3^-$  and  $S_2O_3N_3I^-$ . In the  $Na_2S_4O_6$ - $I_2$ - $NaN_3$  system these active bodies are true intermediates in the sense that their concentrations are extremely low and may be kinetically regarded as stationary. In  $Na_2S_2O_3$ - $I_2$ - $NaN_3$  systems, however, the addition of  $Na_2S_2O_3$  to the reaction mixture is equivalent to the addition of active catalyst in concentration very much higher than that of a true intermediate. The total reaction is complete within a very short time and probably within a limited volume, and the concentration of "active  $S_2O_3^{2-}$ " is thus falling during this short time from its initial value to zero. Hence the concentration of the catalysts cannot be regarded as

kinetically stationary, and it is not possible to deal quantitatively with this or any other mechanism. It is clear, however, that the "average" concentration of the catalysts must be very much higher in these systems than in  $S_4O_6^{2-}-I_2-N_3^-$  systems, and that, though reactions (11)-(13) might be of importance in the former they, and also reaction (2), may not need to be considered in the latter systems.

Reference may be made to one feature of the scheme. The effect of increase of  $[I^-]$  is to increase the chain length (i.e. increase  $R$ ); the mechanism accounts for this by the assumption of equilibrium (7) together with the postulate that the complex  $S_2O_3N_3I^-$  does not decompose as readily as  $S_2O_3N_3^-$  to give products (SO and  $SO_2$ ) easily oxidized by  $I_2$  to sulphate. It is found, however, that the other halide ions  $Br^-$  and  $Cl^-$  also exert a similar, but smaller effect, on the value of  $R$ , while  $NO_3^-$  has no effect. Thus for a certain reaction mixture (containing 0.002 M KI) the value of  $R$  obtained was 11.6; for the same mixture but with addition of KI or KBr or KCl, or  $KNO_3$  to make each concentration of salt 0.248 M, the values of  $R$  were respectively 35.7, 21.8, 13.0 and 11.6. This observation thus lends some support to the assumption of the formation of complex, not specific to iodide, formed between halide and some reacting entity.

So far as the nature of the reaction permits a judgment to be made, the experimental data can be qualitatively interpreted in terms of this mechanism. It is realized, however, that further work employing more refined technique and with closer attention to the mixing process will be necessary before this or any other mechanism can be adequately tested; for the present we may perhaps claim that the above scheme (or the alternative with the radical ion  $S_2O_3^-$  replacing  $S_2O_3N_3^-$ ) does not conflict with any of the available evidence obtained from studies of both  $S_4O_6^{2-}$  and  $S_2O_6^{2-}$  systems, and has at least some claims for consideration.

*Muspratt Laboratory of Physical and Electrochemistry,  
Department of Inorganic and Physical Chemistry,  
University of Liverpool.*

## INDUCED REACTIONS OF THE HALOGENS IN AQUEOUS SOLUTION

### PART III. REACTIONS IN THE SYSTEMS $N_3^- - Br_2$ , $N_3^- - Br_2 - S_2O_3^{2-}$ AND $N_3^- - Br_2 - S_4O_6^{2-}$

BY R. O. GRIFFITH AND R. IRVING

*Received 9th December, 1948*

This paper deals with the kinetics of (a) the uncatalyzed reaction in aqueous solution between  $NaN_3$  and  $Br_2$  and (b) of the same reaction in presence of  $Na_2S_2O_3$  or  $Na_2S_4O_6$ . Measurements of the speed of the direct reaction (a) at temperatures 0°, 10° and 20° under a variety of conditions indicate that the mechanism is (I)  $N_3^- + Br_2 \rightleftharpoons N_3Br_2 \rightleftharpoons N_3Br + Br^-$ ; (II)  $N_3Br + N_3^- \rightarrow 3N_2 + Br^-$ , with the equilibria (I) rapidly established and (II) the rate-determining reaction. Support for the existence of strong complex formation which must be assumed to account for the kinetic data is afforded by determinations of the equilibrium constant for  $N_3^- + Br_2 \rightleftharpoons N_3Br + Br^-$  by partition and spectrophotometric methods, and, in general, the results can be quantitatively interpreted in terms of the mechanism.

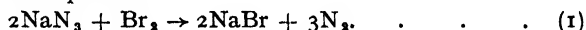
(b) In the presence of  $Na_2S_2O_3$  or  $Na_2S_4O_6$  the reactions in systems containing  $NaN_3$  and  $Br_2$  are extremely rapid. Together with the fast oxidation of  $Na_2S_2O_3$  or  $Na_2S_4O_6$  to sulphate there is a concomitant rapid induced oxidation

of  $N_3^-$  by  $Br_2$ . Determinations of the ratio of moles  $N_3^-$  oxidized to moles  $Na_2S_2O_3$  (or  $Na_2S_4O_6$ ) oxidized show that there is a strong parallelism between the action of  $Na_2S_2O_3$  and that of  $Na_2S_4O_6$ . Values of this ratio increase with increasing dilution of  $Na_2S_2O_3$  ( $Na_2S_4O_6$ ); the high values obtained (up to 110) indicate a chain mechanism for the induced reaction. A mechanism of such a type, applicable to both inducing agents and involving  $S_2O_3Br^-$  and  $S_2O_3N_3^-$  as intermediates, is suggested

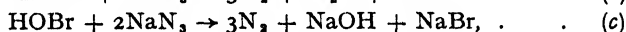
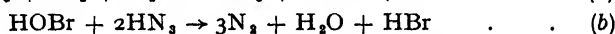
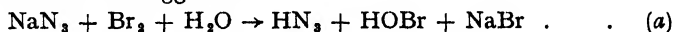
In Part II of this series of papers,<sup>1</sup> the induced reactions in the systems  $I_2-N_3^--S_2O_3^{2-}(S_4O_6^{2-})$  were considered; this paper deals with the reactivity of the analogous systems with bromine replacing iodine. Since, however, bromine also reacts directly with azide, it has been necessary first to study the non-induced reaction in the attempt to elucidate its kinetics.

### A. Kinetics of the Reaction Between Bromine and Azide in Aqueous Solution

When sodium azide is added to an aqueous solution of bromine, the colour of the mixture at once fades to a pale-straw, and nitrogen is evolved according to the over-all equation:



The reaction is kinetically measureable at ordinary temperatures and a few determinations of the rate have been made by Spencer,<sup>2</sup> who followed the course of reaction iodometrically at a temperature of 15° C. No quantitative treatment of his data was attempted, but the following reaction mechanism was suggested:



in which (a) is very fast, (b) and (c) relatively slow and rate-determining, with (c) faster than (b). We have carried out measurements of the rate of reaction over a wider range of conditions than Spencer's, with the result that his mechanism is not considered to be satisfactory, and should be replaced by one in which the compound  $N_3Br$  is an intermediate. We have also carried out a few experiments on the kinetics of the reaction between  $Cl_2$  and  $NaN_3$  in aqueous solution; these indicate that the mechanism of this reaction is analogous to that of the bromine reaction.

### Experimental

The reaction between  $Br_2$  and  $NaN_3$  has been followed at temperatures of 0°, 10° and 20° C in unbuffered solutions, in presence of phosphate buffers, in presence of mineral acid, with and without the addition of  $KBr$ , and in presence and absence of neutral salt ( $KNO_3$ ). Two methods of determining the extent of reaction have been used. In the one mostly employed, the rate of decrease of concentration of bromine was determined by pipetting off samples of the reaction mixture, running these into acidified  $KI$  solution and titrating the liberated iodine with thiosulphate. (Provided enough mineral acid is present, azide does not interfere with the iodine-thiosulphate titration.) In some experiments the course of the reaction has been determined by measuring the rate of evolution of nitrogen, using for this purpose a modified Warburg apparatus. Satisfactory agreement between the rates inferred for a given reaction mixture from the two methods shows that the stoichiometry of the *net* reaction is as given by eqn. (1).

We define the rate of reaction in terms of the equation,

$$-\frac{1}{2} \frac{d[EN_3^-]}{dt} = -\frac{d[2Br_2]}{dt} = k_{01}[EN_3^-][2Br_2] \quad (2)$$

<sup>1</sup> Dodd and Griffith, *Trans. Faraday Soc.* (preceding paper).

<sup>2</sup> Spencer, *J. Chem. Soc.*, 1925, 127, 216.

though the kinetics are more complex than given by this equation, in which  $[\text{N}_3^-]$  and  $[\text{Br}_2]$  are the concentrations (moles/litre) of total azide and total bromine respectively, and  $t$  is in minutes.  $k_{bt}$  is now found experimentally to be dependent on the concentration of bromide in the system, but also, and even to a greater extent, on the ratio of  $[\text{N}_3^-]/[\text{Br}_2]$ . For example it is found that when in a given experiment  $[\text{N}_3^-]/(2[\text{Br}_2]) > 1$ ,  $k_{bt}$  increases during the run; when  $[\text{N}_3^-]/(2[\text{Br}_2]) < 1$ ,  $k_{bt}$  decreases; and in systems in which  $[\text{N}_3^-]/(2[\text{Br}_2]) = 1$ ,  $k_{bt}$  remains constant. These are tantamount to the statement that  $k_{bt}$  increases with increasing ratio of  $[\text{N}_3^-]/(2[\text{Br}_2])$ , and we have therefore determined values of  $k_{bt}$  as a function of this ratio. The experiment, details of which are given in Table I, is typical of the type of result obtained.

TABLE I

Temp. = 20° C;  $[\text{Br}_2]_{\text{init.}} = 0.007087$ ;  $[\text{N}_3^-]_{\text{init.}} = 0.008$ ;  
 $[\text{KBr}]_{\text{init.}} = 0.100$ . Conc. in moles or g. ions/l.

$t$ (min.)	$t_2 - t_1$ (min.)	$10^3 [\text{Br}_2]$	$10^3 [\text{N}_3^-]$	$[\text{N}_3^-]/2[\text{Br}_2]$	$k_{bt}$
2.27	28.41	7.003	7.832	0.5354	0.259
30.68		6.630	7.086	0.5182	0.225
77.20	46.42	6.187	6.200	0.4782	0.206
152.27	75.17	5.669	5.164	0.4328	0.191
244.65	92.38	5.219	4.264	0.3875	0.165
355.73	111.08	4.860	3.546		

Here the values of  $k_{bt}$  are worked out for each time interval, together with the corresponding mean values of the ratio  $[\text{N}_3^-]/(2[\text{Br}_2])$ .

Fig. 1 shows some of the results obtained at a temperature of 20° from experiments with three different initial concentrations of KBr, the values of  $k_{bt}$  being plotted as a function of  $[\text{N}_3^-]/(2[\text{Br}_2])$ . It is doubtless true that  $k_{bt}$  depends not only on this ratio, but also on the absolute values of the concentrations of reactants. In all these experiments, however,  $[\text{Br}_2]_{\text{init.}}$  was approximately constant, varying between 0.006 and 0.008, and thus during the course of the experiments  $[\text{Br}_2]$  lay in the range of concentrations between 0.008 and about 0.002; over this range of concentration of  $\text{Br}_2$  the results show that  $k_{bt}$  is to a sufficiently good approximation a function only of  $[\text{N}_3^-]/(2[\text{Br}_2])$  at constant  $[\text{Br}^-]$ . Curves of shapes similar to those shown in Fig. 1 are also obtained from experiments at 10° and 0° C. It is seen that for small values of  $[\text{N}_3^-]/(2[\text{Br}_2])$  the values of  $k_{bt}$  (and of rates of reaction) are very small, for values of the same ratio in the neighbourhood of 0.5 to 1.0 there is a rapid rise in  $k_{bt}$  as the ratio is increased, and that the curve for each concentration of  $\text{Br}^-$  reaches a limiting value at high values of  $[\text{N}_3^-]/(2[\text{Br}_2])$ , the limiting value decreasing with increasing  $[\text{Br}^-]$ . Fig. 1 also shows that in general the reaction is retarded by bromide, except at low values of the ratio  $[\text{N}_3^-]/(2[\text{Br}_2])$ . A few experiments have been carried out to determine the effect of ionic strength  $\mu$  on the reaction rate. In two series of experiments, both with  $[\text{Br}^-]_{\text{init.}} = \text{zero}$ , the one with  $\mu = 0.02$  and the other (by addition of  $\text{KNO}_3$ ) with  $\mu = 0.12$ , the plots of  $k_{bt}$  against  $[\text{N}_3^-]/(2[\text{Br}_2])$  fall on the same curve, showing that the effect of ionic strength is here inappreciable. However, an effect can be detected by employing a larger increase in  $\mu$ . Thus it is found that in the presence of 0.1 M KBr increasing the ionic strength from 0.22 to 0.82 by addition of  $\text{KNO}_3$  increases the rate of reaction by about 17 %.

The effect of  $[\text{H}^+]$  on the rate is found to be nil in the region of pH 7. Thus, in three experiments in which  $\mu = 0.82$  and  $[\text{Br}^-] = 0.1$ , (a) with the solution unbuffered, (b) in the presence of 0.1 M  $\text{Na}_2\text{HPO}_4 + 0.2$  M  $\text{KH}_2\text{PO}_4$ , and (c) in the presence of 0.1 M  $\text{Na}_2\text{HPO}_4 + 0.4$  M  $\text{KH}_2\text{PO}_4$ , the values of  $k_{bt}$  compared at the same ratios of  $[\text{N}_3^-]/(2[\text{Br}_2])$  were found to be the same. Even at still higher pH's where the hydrolysis of  $\text{Br}_2$  might be expected to be considerable, the rate is still found to be the same as in the unbuffered solution. For

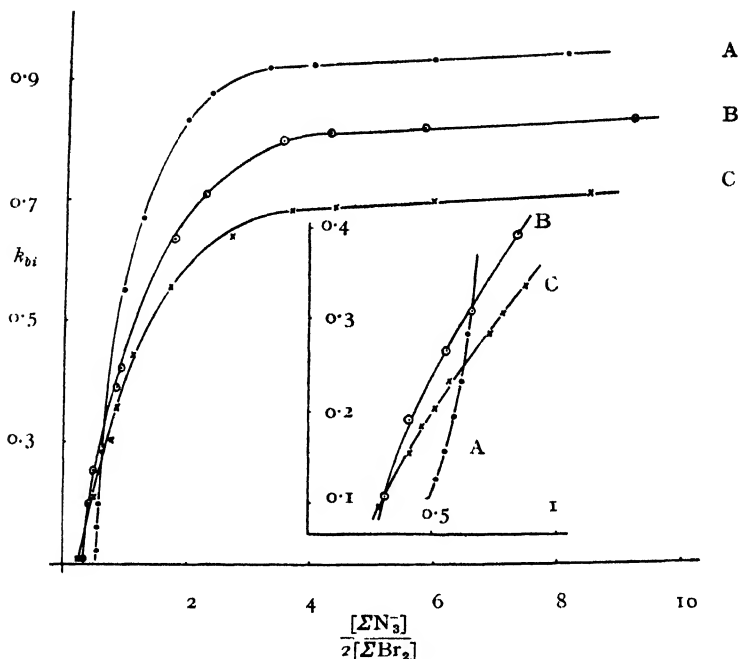


FIG. 1.

A: zero initial KBr

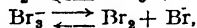
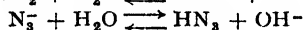
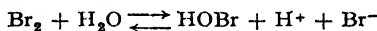
B: 0.1 M KBr

C: 0.2 M KBr

example, the same rates were found at 10° C in two reaction mixtures each containing initially



but mixture (1) containing in addition 0.75 M NaNO<sub>3</sub> and mixture (2) 0.2444 M Na<sub>2</sub>HPO<sub>4</sub> + 0.0056 M KH<sub>2</sub>PO<sub>4</sub>. If we assume that the *only* equilibria we need take into account in these solutions are:

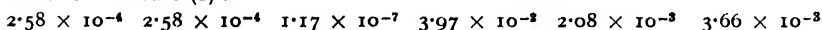


together with, in (2),  $\text{H}_2\text{PO}_4^- \rightleftharpoons \text{H}^+ + \text{HPO}_4^{2-}$ ,

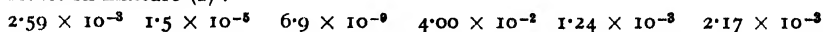
we calculate, using the values: ionization constant of HN<sub>3</sub> = 1.8 × 10<sup>-5</sup>, hydrolytic constant of bromine = 1.45 × 10<sup>-9</sup>, second ionization constant of phosphoric acid (at μ = 0.8) = 3.0 × 10<sup>-7</sup>, and equilibrium constant for tri-bromide decomposition = 0.057, the following initial concentrations in the two reaction mixtures:



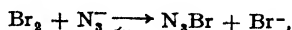
Reaction mixture (1):



Reaction mixture (2):



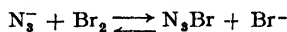
Inspection of these figures shows that if these are the only equilibria concerned, Spencer's view that the reaction rate is determined chiefly by the product [HOBr][N<sub>3</sub><sup>-</sup>] (or [HOBr][N<sub>3</sub><sup>-</sup>]<sup>2</sup>) cannot be maintained. However, the fact that the same rate is observed in these two experiments is to be regarded as an indication that the basis of the calculation is incorrect, and that strong formation of some other compound must be assumed. We shall show that the probable equilibrium is



with the equilibrium well over to the right-hand side; introduction of this into the scheme will make it possible for the concentrations of the rate-determining constituents in reaction mixtures (1) and (2) to be practically the same.

Although, as the above results show, variation of  $[H^+]$  in the region of pH from about 6.3 to 8.4 has no influence on the rate of reaction, increase of  $[H^+]$  does retard the reaction at lower pH's, i.e. when mineral acid is added giving a pH of 5 or less, so that significant amounts of azide are present as  $HN_3$ . Later reference will be made to this. Finally, it may be noted that in strong alkaline solution, when all the bromine is present as  $OBr^-$ , no reaction with  $N_3^-$  can be detected.

**Complex Formation in  $Br_2-N_3^-$  Mixtures.**—Spencer<sup>2</sup> has prepared and isolated the compound  $N_3Br$  by passing bromine vapour over solid sodium azide, and has examined its properties; the methods of determining  $N_3Br$  given below are essentially those of Spencer, and shown by him to give accurate results. Assuming that the equilibrium



is set up in aqueous solution, and that this equilibrium (together with the tri-bromide equilibrium) is the only one that needs to be taken into account, attempts have been made to determine the equilibrium constant

$$K = \frac{[N_3Br][Br^-]}{[Br_2][N_3^-]}$$

by two methods, (a) by partition methods with  $CCl_4$  as the second phase, and (b) by spectrophotometric determination of the concentration of bromine.

(a) If a mixture of  $N_3^-$  and  $Br_2$  in aqueous solution be shaken with  $CCl_4$ , analysis of the  $CCl_4$  layer shows that it contains both bromine and nitrogen. If the free bromine in the  $CCl_4$  layer be determined by spectrophotometric means (i.e. assuming that  $N_3Br$  or any other complex does not absorb), it is then found that the ratio of atoms of nitrogen to atoms of the remainder of the bromine is 3/1, showing that the  $CCl_4$  has extracted from the aqueous layer a mixture of bromine and a compound of empirical formula  $N_3Br$ . There is thus good ground for the view that  $N_3Br$  must also be present in the aqueous layer. In the partition method used for determining  $K$ , a  $CCl_4$  solution containing  $N_3Br$  and  $Br_2$  was prepared as above and this solution was shaken with an aqueous solution of  $KBr$  of known strength until equilibrium was attained. The  $CCl_4$  solution was analyzed both before and after shaking as follows: (i) by running a sample into acidified  $KI$  and titrating with thiosulphate, (ii) by treating a sample with  $NaOH$  containing  $H_2O_2$  and titration of the excess alkali with acid, (iii) a portion of the neutral solution formed in (ii) was titrated with  $AgNO_3$  using  $K_2CrO_4$  indicator, (iv) the remainder of the solution formed in (ii) was treated with excess  $AgNO_3$ , the solution boiled with  $HNO_3$  to decompose the  $AgN_3$  and drive off the  $HN_3$  formed, and the cooled solution titrated with  $KCN$ . The aqueous layer after equilibrium with the  $CCl_4$  layer was attained was analyzed for  $[2Br_2] + [N_3Br]$  by treating a sample with acidified  $KI$  solution and titrating with thiosulphate. The experiments carried out at 20° C by this method yielded a value of  $K$  of about 200, and a value for the partition coefficient of  $N_3Br$  between  $CCl_4$  and  $H_2O$  of about 24. The value of

$$K_s = \frac{[Br_2][Br^-]}{[Br_3^-]}$$

was taken to be 0.057.<sup>3</sup>

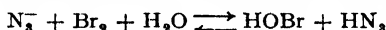
(b) More experiments have been done and probably a more accurate value of  $K$  obtained with the spectrophotometric method. Solutions of known content of bromine, bromide and azide were prepared—in all of them  $[2Br_2]$  had to be greater than  $[N_3^-]$  in order to cut down the rate of reaction—and their light absorptions immediately determined and compared with those of solutions of identical content of bromine and bromide in absence of azide. The absorption measurements were made at room temperature (about 18° C) either with a "Spekker" absorptiometer using blue and violet light or with a Beckmann absorptiometer at three wavelengths 4300, 4400 and 4700 Å, the total concentration of bromine (i.e.  $[Br_2] + [Br_3^-] + [N_3Br]$ ) being between 0.003 and 0.0003. Assuming that absorption by  $N_3Br$  is negligible, the results of Table II were obtained.

<sup>3</sup> Griffith, McKeown and Winn, *Trans. Faraday Soc.*, 1932, 28, 752.

TABLE II.—VALUES OF  $K$ 

[KBr] = 0.05		
$K = 221, 245, 235, 321, 234, 321, 320, 261$		Mean : $270 \pm 10$
[KBr] = 0.10		
$K = 304, 272, 274, 339, 277, 306, 279, 289, 283, 433, 316, 388, 282, 390$		Mean : $317 \pm 9$
[KBr] = 0.20		
$K = 267, 303, 293, 303, 325, 291, 424, 332, 388, 341, 328, 427, 455$		Mean : $344 \pm 11$

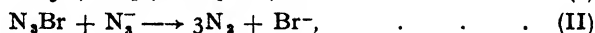
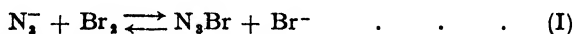
Though the values of  $K$  are not very concordant, the divergences are probably within the experimental errors of the method; it is seen that the experiments indicate strong complex formation, with a value of  $K$  in the neighbourhood of 300, a value in moderate agreement with the estimate of 200 given by the partition experiments. There is also an indication from the figures of the table that  $K$ , as calculated, increases somewhat with increasing concentration of bromide. In these experiments no corrections for the hydrolysis



have been made; these would be small and would, in general, have the effect of reducing  $K$  by 2-3 %.

### Reaction Mechanism

The type of curves shown in Fig. 1 for the variation of  $k_{bi}$  with the ratio  $[\text{N}_3^-]/(2[\text{Br}_2])$  is consistent with the mechanism:



with (I) a maintained equilibrium and (II) the rate-determining reaction. If, as we have found to be the case, the equilibrium constant of (I) is high, so that under our experimental conditions there is a large immediate conversion of the reactants into  $\text{N}_3\text{Br}$ , the general form of the curves is easily accounted for. At high ratios of  $[\text{N}_3^-]$  to  $[\text{Br}_2]$  practically all the bromine is present as  $\text{N}_3\text{Br}$ , and  $[\text{N}_3^-]$  is nearly equal to  $[\text{N}_3\text{Br}]$ ; the rate of reaction will thus become proportional to  $[\text{N}_3\text{Br}][\text{Br}_2]$ , i.e.  $k_{bi}$  will be a constant in this region. At low ratios of  $[\text{N}_3^-]$  to  $[\text{Br}_2]$  practically all the azide is present as  $\text{N}_3\text{Br}$ , and as there is very little  $\text{N}_3^-$  left for reaction (II) to occur, the rate of reaction will be very small. The effect of  $\text{Br}^-$  at these low ratios of  $[\text{N}_3^-]$  to  $[\text{Br}_2]$  is also consistent with the mechanism. But the effect of  $\text{Br}^-$  at high ratios of  $[\text{N}_3^-]$  to  $[\text{Br}_2]$  is not accounted for; the scheme as written above predicts that at all bromide concentrations the same limiting value of  $k_{bi}$  at high ratios of  $[\text{N}_3^-]$  to  $[\text{Br}_2]$  should be attained, whereas experimentally the limiting value decreases with increasing concentration of bromide. The discrepancy may be removed by the assumption of an additional equilibrium forming the complex  $\text{N}_3\text{Br}_2^-$ , i.e. by writing instead of (I),



The magnitude of

$$K' = \frac{[\text{N}_3\text{Br}_2^-]}{[\text{N}_3\text{Br}][\text{Br}^-]}$$

may be estimated from the experimental data from which Fig. 1 was constructed. At 20° C the limiting  $k_{bi}$ 's for  $[\text{Br}^-] = 0.2, 0.1$  and approximately zero are about 0.75, 0.87 and 1.06 respectively. On the basis that the concentration of  $\text{N}_3\text{Br}_2^-$  is negligible in the solution with  $[\text{Br}^-] \approx 0$  and on the assumption that  $\text{N}_3\text{Br}_2^-$  does not react further with  $\text{N}_3^-$ , the ratio of concentrations of  $\text{N}_3\text{Br}_2^-$  to  $\text{N}_3\text{Br}$  in the limit at the other bromide concentrations may be calculated, and it is found that  $K' = 2.18$  for  $[\text{Br}^-] = 0.1$  and 2.07 at  $[\text{Br}^-] = 0.2$ , i.e.  $K'$  has a value of about 2.1. Some support to the presumed existence of the complex  $\text{N}_3\text{Br}_2^-$  and to

a value of  $K'$  of this magnitude is afforded by the spectrophotometric determinations of the equilibrium constant  $K$ . It can be shown that if  $N_3Br_2^-$  formation occurs, the apparent  $K$ 's as calculated from the spectrophotometric determinations should increase with increasing concentration of bromide; the increase which is in fact found is of the order of magnitude corresponding to that which a  $K'$  of 2.1 would produce.

On the basis of this mechanism the velocity constant  $k$  of the rate-determining reaction (II) at 20° has the value 1.06, the limiting value of  $k_{bi}$  at very low concentrations of bromide; further, the value of  $k_{bi}$  in any other reaction mixture at 20° is given by :

$$k_{bi} = \frac{k[N_3Br][N_3^-]}{[NBr_2][N_3^-]}$$

in which  $[N_3Br]$  and  $[N_3^-]$  are the actual concentrations of the reactants in the system. These concentrations have been calculated for the experiments of Fig. 1, using the values  $K = 300$ ,  $K' = 2.1$ ,  $K_s = 0.057$ , and hence calculated values of  $k_{bi}$  derived. The results are shown in Fig. 2, in which the observed and calculated  $k_{bi}$ 's are plotted for three

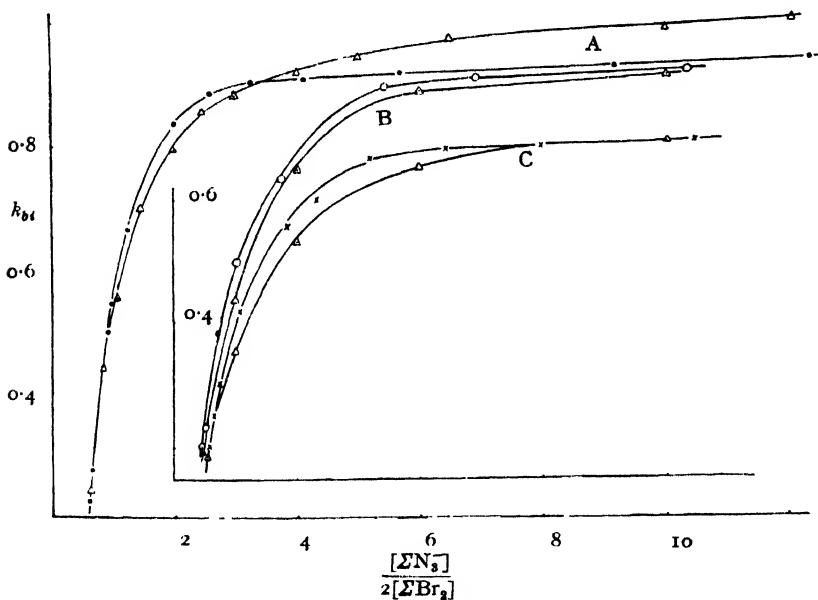


FIG. 2.

A: zero initial KBr  
B: 0.1 M KBr  
C: 0.2 M KBr

Δ Calculated  
● Experimental  
○ Experimental  
× Experimental

series of experiments at 20°. It is seen that the agreement between theory and experiment is fairly good, and substantiates the mechanism. A still better agreement could probably be obtained by appropriate slight alterations in the values of the constants  $k$ ,  $K$  and  $K'$ .

The temperature coefficient of  $k_{bi}$  between 10° and 20° under conditions of low  $[Br^-]$  and of high ratios of  $[ΣN_3^-]/2[ΣBr_2]$  is found to be 3.21; under such conditions the observed temperature coefficient is that of the rate-determining reaction (II), whose velocity coefficient is  $k$ . The reaction



has thus an energy of activation of 19.2 kcal. Though it is not possible



to derive from the data any estimate of the effect of temperature on the equilibrium constant  $K$ , the temperature dependence of  $K'$  can be obtained. Thus at high ratios of  $[\Sigma N_3^-]/[\Sigma Br_2]$  and at a bromide concentration of 0.1 the temperature coefficient between 10° and 20° of  $k_{br}$  is found to be 3.59; combination of this with the previously-mentioned temperature coefficient of 3.21 leads to a value of  $K'$  of 3.5 at 10° compared with 2.1 at 20°.

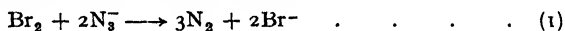
Finally, a few kinetic experiments have been carried out in which, by addition of HCl, a considerable fraction of the azide was converted into  $HN_3$ , so that the azide in the reaction mixture was present partly as  $N_3^-$ , partly as  $HN_3$  and partly as  $N_3Br$ . It is not considered necessary to give details of these; they are entirely consistent with the view that the rate of reaction between  $HN_3$  and  $N_3Br$  is negligible compared with that between  $N_3^-$  and  $N_3Br$ .

## B. Induced Reactions in the Systems $Br_2-N_3^-S_2O_3^{2-}$ and $Br_2-N_3^-S_4O_6^{2-}$

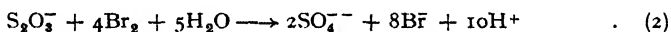
The reaction between  $NaN_3$  and  $Br_2$  can be catalyzed by either  $Na_2S_2O_3$  or  $Na_2S_4O_6$ . The catalyzed reactions take place practically instantaneously, so that they cannot be followed kinetically. They are also as fast, so far as can be judged, under conditions for which the direct reaction between  $NaN_3$  and  $Br_2$  is very slow, such as, for example, when  $[\Sigma Br_2] = [\Sigma N_3^-]$ .

### Experimental

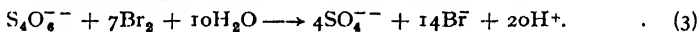
Under conditions approximating to those used in the main series of experiments we have found that the *net* reactions occurring in these systems are:



and either



or



This was shown by running an excess of bromine solution of known concentration drop by drop into a solution of thiosulphate (or tetrathionate) and azide in presence of phosphate buffer ( $[KH_2PO_4]/[Na_2HPO_4] = 4/1$ ), and measuring the nitrogen evolved in a nitrometer. The excess bromine was then estimated by addition of sodium arsenite and back-titration with iodine. The amount of bromine consumed was compared with that estimated on the basis of the above equations; several experiments of this type were done and in all very satisfactory agreement between the observed and calculated bromine consumptions was found.

When bromine and thiosulphate react in absence of azide, there may or may not be, depending on the conditions of reaction, complete conversion of the thiosulphate into sulphate. If thiosulphate is run drop by drop into a bromine solution, buffered as above, between 99 and 100 % of the thiosulphate is oxidized to sulphate; if, however, the thiosulphate is run in quickly the odour of  $H_2S$  is apparent, and the amount of thiosulphate needed to decolorize the bromine is greater than for drop-by-drop addition. Also when bromine is run into a solution of thiosulphate  $H_2S$  formation ensues, especially when the ratio (moles  $Br_2$ )/(moles  $S_2O_3^{2-}$ ) is less than 4/1. Thus in two experiments in which 0.05 M  $Br_2$  was run quickly into 0.01 M thiosulphate in presence of phosphate buffer, the results of analyses of the resulting solutions were:

(Mixture (i) : (Moles  $Br_2$ )/(Moles  $S_2O_3^{2-}$ ) = 2/1 ;

Mixture (ii) : (Moles  $Br_2$ )/(Moles  $S_2O_3^{2-}$ ) = 3/1).

	(i)	(ii)
Percentage of original $S_2O_3^{2-}$ remaining	9.2	1.62
" " " " converted to $S_4O_6^{2-}$	53.0	43.58
" " " " " $SO_3^{2-}$	0.0	0.47

The resulting solutions were clear, no sulphur separating out, but in each the odour of  $H_2S$  was apparent. Analyses for  $H_2S$ ,  $SO_4^{2-}$  and other compounds



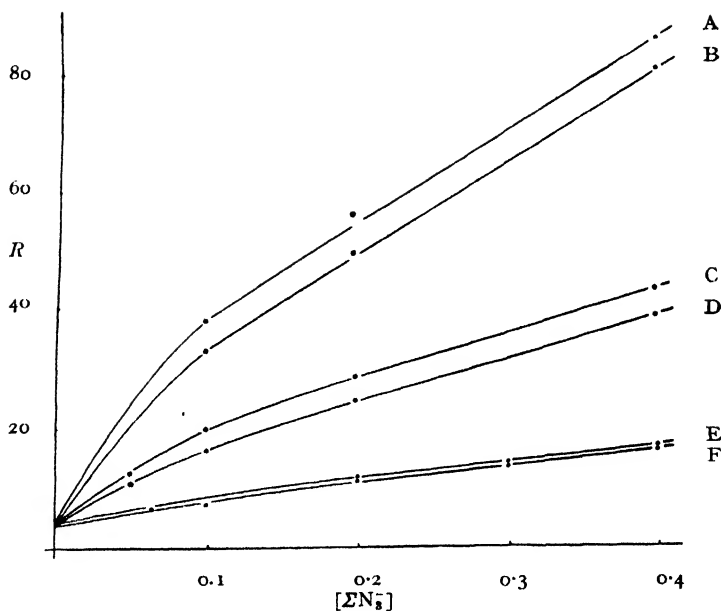


FIG. 3.

In all series :

$[\Sigma Br_2] = 0.025$   
 A :  $[S_2O_3^{2-}] = 0.0002$   
 C :  $[S_2O_3^{2-}] = 0.001$   
 E :  $[S_2O_3^{2-}] = 0.01$

$[Br^-] = 0.50$   
 B :  $[S_4O_6^{2-}] = 0.0001$   
 D :  $[S_4O_6^{2-}] = 0.0005$   
 F :  $[S_4O_6^{2-}] = 0.005$

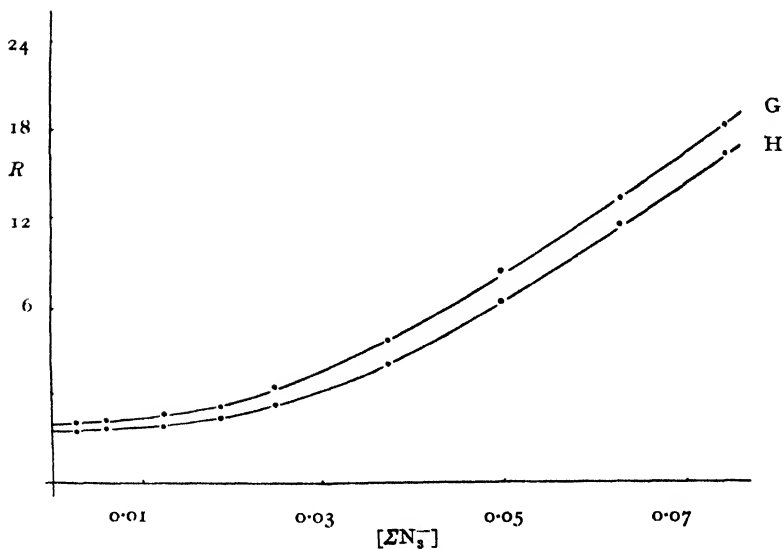


FIG. 4.

In both series :

$[\Sigma Br_2] = 0.025$   
 F :  $[S_2O_3^{2-}] = 0.01$

$[\Sigma Br^-] = 0.50$   
 G :  $[S_4O_6^{2-}] = 0.005$

abscissa. Other experiments, details of which will not be given, have been made to determine the effect on  $R$  of varying  $[\text{Br}^-]$ ,  $[\Sigma\text{Br}_2]$  and temperature. The whole of the results may be summarized as follows. The most striking feature of the determinations of  $R$  is the parallelism between the data for  $\text{S}_2\text{O}_3^{2-}$  and for  $\text{S}_4\text{O}_6^{2-}$ . Under all comparable experimental conditions  $R_{\text{S}_2\text{O}_3^{2-}}$  and  $R_{\text{S}_4\text{O}_6^{2-}}$  at equivalent concentrations of inducing agent are nearly the same,  $R_{\text{S}_2\text{O}_3^{2-}}$  being slightly the greater, the difference between the two varying between 0.5 under conditions when  $R$  is small to about 6 when  $R$  is large. Another feature of the results is the high values which  $R$  can attain; the highest value measured is 113. The effect of increasing  $[\text{N}_3^-]$  is to increase  $R$ . With method (a) the increase is approximately linear from zero  $[\text{N}_3^-]$  onwards; with method (b) the increase in  $R$  is inappreciable at low concentrations of azide, but an approximately linear increase begins at a concentration of azide near that of the bromine in the system. The effect of decreasing  $[\text{S}_2\text{O}_3^{2-}]$  is to increase  $R$ , and from Fig. 5 it would appear that as  $[\text{S}_2\text{O}_3^{2-}]$  approaches zero  $R$  increases without limit. A similar behaviour is found with  $\text{S}_4\text{O}_6^{2-}$ . The effect of  $[\Sigma\text{Br}_2]$

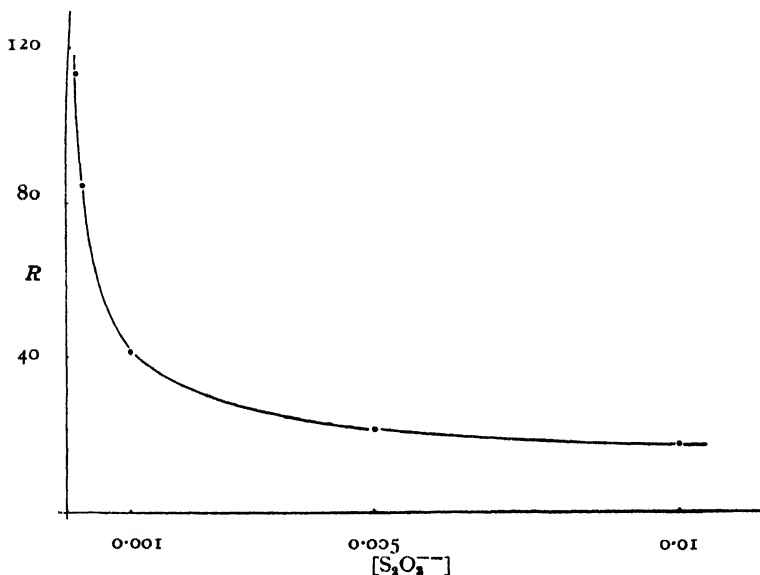


FIG. 5.

$$[\Sigma\text{N}_3^-] = 0.40$$

$$[\Sigma\text{Br}_2] = 0.025$$

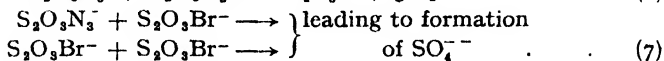
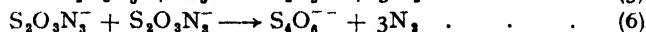
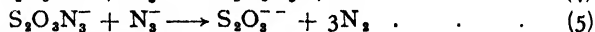
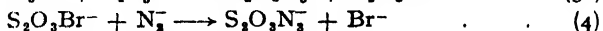
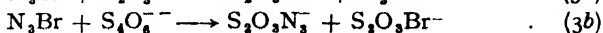
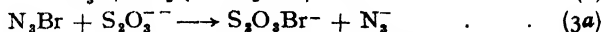
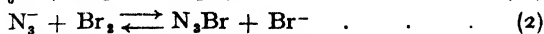
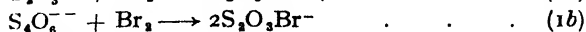
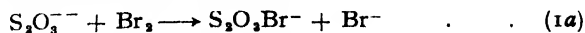
$$[\text{Br}^-] = 0.50$$

on both  $R_{\text{S}_2\text{O}_3^{2-}}$  and  $R_{\text{S}_4\text{O}_6^{2-}}$  depends on the method employed in the determination. With method (a),  $R$  increases slightly with increasing  $[\Sigma\text{Br}_2]$ , the increase being the more pronounced the higher the concentration of azide. Using method (b), however,  $R$  diminishes with increasing  $[\Sigma\text{Br}_2]$ . The effect of bromide on  $R_{\text{S}_2\text{O}_3^{2-}}$  and  $R_{\text{S}_4\text{O}_6^{2-}}$  is nil when method (a) is used; with method (b),  $R$  increases with increasing  $[\text{Br}^-]$ . Finally  $R$  is only slightly temperature-dependent, as reducing the temperature from 18° to 0° only lowers  $R$  by about 10 %.

### Reaction Mechanism

In the experiments described above, 1 mole  $\text{S}_2\text{O}_3^{2-}$  ( $\frac{1}{2}$  mole  $\text{S}_4\text{O}_6^{2-}$ ) consumes 4 moles (3.5 moles) of  $\text{Br}_2$ ; simultaneously  $R_{\text{S}_2\text{O}_3^{2-}} - 4$  ( $R_{\text{S}_4\text{O}_6^{2-}} - 3.5$ ) moles of  $\text{Br}_2$  are consumed by reaction with  $\text{N}_3^-$ . The similarity under all conditions between the  $R_{\text{S}_2\text{O}_3^{2-}}$  and  $R_{\text{S}_4\text{O}_6^{2-}}$  values at equivalent concentrations shows that the mechanisms in the two reacting systems are in some way very closely associated; it is also clear, in view of the high  $R$  values which can be realized that chain mechanisms

must be operative. The following mechanism will account qualitatively for the various effects that have been observed.



All these reactions are postulated as being very fast; in addition it appears necessary to postulate that reactions (1a), (1b), (3a) and (3b) are intrinsically faster than the direct reaction (2), and probably that they are also faster than all the other reactions. The intermediary catalysts suggested are  $\text{S}_2\text{O}_3\text{Br}^-$  and  $\text{S}_2\text{O}_3\text{N}_3^-$ ; reactions (1) or (3), (4) and (5) or (6) constitute the chain; reactions (7) are chain-breaking and lead to sulphate formation and cessation of reaction. The conditions of reaction are such that it is not possible to deal quantitatively with the kinetics of reaction on the basis of this or any mechanism, but qualitatively the above scheme accounts satisfactorily for the experimental results. The differences between the results obtained by methods (a) and (b) are accounted for in terms of formation of  $\text{N}_3\text{Br}$  by reaction (2). Though it is assumed that  $\text{N}_3\text{Br}$  can react with  $\text{S}_2\text{O}_3^{--}$  or  $\text{S}_4\text{O}_6^{--}$  by reaction (3), it is postulated that a reaction between  $\text{N}_3\text{Br}$  and  $\text{S}_2\text{O}_3\text{N}_3^-$  analogous to reaction (5) either does not take place or is too slow to need consideration. In method (b), then, in which  $\text{S}_2\text{O}_3^{--}$  ( $\text{S}_4\text{O}_6^{--}$ ) is run into a mixture of  $\text{Br}_2$  and  $\text{NaN}_3$ ,  $\text{N}_3\text{Br}$  formation has already taken place and if conditions are such that most of the  $\text{EN}_3^-$  is present as  $\text{N}_3\text{Br}$  the value of  $R$  will not greatly exceed 4 (or 3.5). This will account for the behaviour illustrated in Fig. 4, in which with increasing  $[\text{EN}_3^-]$ ,  $R$  first remains nearly constant at 4 (3.5), until a concentration of  $[\text{EN}_3^-]$  is reached which permits of significant concentrations of free  $\text{N}_3^-$  being present. It also accounts—by displacement of the equilibrium (2)—of the effects of concentrations of bromine and bromide on  $R$  using method (b). With method (a) it follows, on the basis that reactions (1) are faster than the formation of  $\text{N}_3\text{Br}$  by reaction (2), that free  $\text{N}_3^-$  will be available for reactions (4) and (5) to occur, and it is clear that  $R$  should increase with increasing  $[\text{EN}_3^-]$  throughout the whole range of concentration of  $[\text{EN}_3^-]$ , as is found experimentally. It should be noted, however, that  $\text{N}_3\text{Br}$  formation does take place using method (a), as there is time between the addition of each drop for equilibrium (2) to establish itself, but since fresh  $\text{N}_3^-$  is continually being added, the chain length of the reaction is little affected. Thus using this method at low  $[\text{EBr}_2]$  and high  $[\text{EN}_3^-]$  it was found that when about 0.5 ml. out of a total of 5.0 ml. of the mixture of  $\text{NaN}_3$  and  $\text{Na}_2\text{S}_2\text{O}_3$  ( $\text{Na}_2\text{S}_4\text{O}_6$ ) had been run into the bromine solution the reaction mixture was practically colourless, indicating that a high percentage of the  $\text{Br}_2$  was present as  $\text{N}_3\text{Br}$ . The value of  $R$  was still high, indicating that, as postulated by reactions (3a) and (3b), the complex  $\text{N}_3\text{Br}$  can maintain the concentration of catalyst. Thus the catalyst  $\text{S}_2\text{O}_3\text{Br}^-$  can be formed by reaction with  $\text{S}_2\text{O}_3^{--}$  or  $\text{S}_4\text{O}_6^{--}$  either from  $\text{Br}_2$  or  $\text{N}_3\text{Br}$ , but for propagation of a chain the presence of free  $\text{N}_3^-$  is necessary and the chain length increases with increasing concentration of free  $\text{N}_3^-$ .

In terms of the mechanism it can be seen if reactions (1a) and (1b) are of equal speed (and also reactions (3a) and (3b)) then under comparable conditions  $R_{\text{S}_2\text{O}_3^{--}}$  should be greater than  $R_{\text{S}_4\text{O}_6^{--}}$  by 0.5.

Actually it is found that the difference is 0.5 when low  $R$  values are realized, e.g. at high  $[S_2O_8^{2-}]$  and low  $[N_2]$ , but the differences become the greater the higher the values which  $R$  attain. A simple way of accounting for this result would appear to be the assumption that reactions (1b) and (3b) are somewhat faster than reactions (1a) and (3a) respectively. This would result in a greater average concentration of catalyst being present when  $S_4O_6^{2-}$  is used than with  $S_2O_8^{2-}$ , and, since the rate of formation of  $SO_4^{\cdot -}$  is according to (7) proportional to the square of the catalyst concentration while the rate of  $N_2$  formation according to (5) and (6) is proportional to the catalyst concentration raised to a power between 1 and 2,  $R_{S_2O_8^{2-}} - 4$  will be somewhat bigger than  $R_{S_4O_6^{2-}} - 3.5$ , and the difference will be the greater as the  $R$ 's increase. Finally, the dependence of  $R$  on  $[S_2O_8^{2-}]$  (or  $[S_4O_6^{2-}]$ ) at constant  $[N_2]$  given by Fig. 5 is accounted for by the theory in a qualitative manner on the same basis, namely that the rates of the chain-breaking reactions increase with catalyst concentration and hence with concentration of added  $S_2O_8^{2-}$  faster than do the rates of the reactions which yield nitrogen and continue the chain; hence  $R$  decreases with increase of concentration of  $S_2O_8^{2-}$  or  $S_4O_6^{2-}$ . The theory can be applied to yield a quantitative relation between  $R$  and  $[S_2O_8^{2-}]$ , but only if certain further assumptions be made. Thus, if it is postulated that (i) reactions (1) are extremely rapid, so that the  $S_2O_8^{2-}$  is almost completely converted into  $S_2O_8Br^-$  before the remaining reactions take place to an appreciable extent, (ii) that the magnitude and the nature of the reaction zone around the drop is not dependent on the concentration of  $S_2O_8^{2-}$  in the drop; and (iii) that the ratio of  $[S_2O_8Br^-]$  to  $[S_2O_8N_2]$  in the reacting system is independent of the concentration of  $S_2O_8^{2-}$ , it may be shown that, with constant  $[N_2]$ ,

$$R_{S_2O_8^{2-}} - 4 \propto \frac{k + [S_2O_8^{2-}]}{[S_2O_8^{2-}]},$$

where  $k$  is a constant and  $[S_2O_8^{2-}]$  is the concentration of  $S_2O_8^{2-}$  in the solution which is being run into the remainder of the reaction mixture. This relation is in general agreement with the data of Fig. 5, both yielding plots of  $1/(R_{S_2O_8^{2-}} - 4)$  against  $[S_2O_8^{2-}]$  passing through the origin and concave to the  $[S_2O_8^{2-}]$  axis, but quantitatively the data cannot be well fitted into a relation of the above type. However, though assumption (iii) is probably justified, the others are open to much doubt, and it is not surprising that a simplified treatment will not reproduce the experimental results.

*Muspratt Laboratory of Physical and Electrochemistry,  
Department of Inorganic and Physical Chemistry,  
University of Liverpool.*

## THE OXIDATION OF HYDROCARBONS

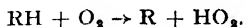
### SOME OBSERVATIONS ON THE INDUCTION PERIOD

BY M. F. R. MULCAHY

*Received 29th December, 1948*

In the low-temperature oxidation of *n*-butane, propylene and (probably) isobutane the reciprocal of the induction period increases linearly with the product of the hydrocarbon and oxygen concentrations. This simple relationship contrasts with the more complicated and different effects of the reactants on the maximum reaction rate subsequently attained under the same conditions.

In explanation it is suggested that whereas the maximum rate is dependent on the rate of (delayed) chain-branching, the inverse induction period is proportional to the rate of chain initiation, which is assumed to occur by the reaction,



Some observations are made on the effects of the nature of the surface and of the temperature on the length of the induction period.

Not the least remarkable feature of the reaction between hydrocarbons and oxygen is the existence of a well-marked induction period. In suitable circumstances, this may extend over many hours and yet be followed by rapid reaction. It is most probably associated with the gradual "auto-catalytic" rise in concentration of an intermediate substance, the subsequent decomposition or reaction of which causes the reaction to proceed. For the low-temperature reaction there is evidence that the intermediate substance is a comparatively stable peroxide<sup>1, 2</sup> which by decomposing in the manner,



confers on the reaction the characteristics of "degenerate" chain branching.<sup>1, 2</sup>

This mechanism will explain, in a general way, the initial slowness of reaction and the gradual acceleration to a maximum rate,<sup>3, 4</sup> but the more precise conditions which determine the duration of the induction period are largely unknown. It may be expected that the elucidation of these factors will give some insight into the early stages of the reaction and consequently into the mechanism of the reaction as a whole. The question has received comparatively little attention probably mainly on account of the inherent experimental difficulties. The length of the induction period is extremely sensitive to changes in the state of the surface of the reaction vessel and, unless proper precautions are taken, varies erratically from one experiment to the next.

It is the purpose of this paper to record some observations on the induction period and to point out significant differences between the kinetic properties of the reaction in its early stages and those which are found when it has reached its maximum velocity.

## Experimental

Known pressures of the hydrocarbon and oxygen were admitted to an evacuated silica vessel at constant temperature and the progress of the reaction followed manometrically. The induction period was defined as the time taken for the reaction to reach the standard rate of pressure increase of 0.5 mm./min. This rate was, in general, small compared with the maximum rate ultimately reached. This definition, rather than the usual one involving the time taken for a standard small pressure increase, was chosen because it does not involve a small difference measured from the initial pressure reading and because it seems to be more amenable to theoretical treatment.<sup>1</sup>

To obtain consistent results for successive reactions it was found necessary to standardize the evacuation procedure, the vessel being pumped out for 10 min. after the vacuum (no discharge) had been reached. When the reaction vessel was allowed to remain for any considerable time above room temperature (e.g. overnight), the first subsequent run invariably gave a longer (sometimes considerably so) induction period than an experiment carried out immediately after the usual evacuation procedure. On the other hand, the admission of air to the hot evacuated vessel resulted in shorter induction periods. This latter effect persisted through many subsequent experiments; consequently it was necessary to maintain the vacuum in the vessel between successive runs.

<sup>1</sup> Cullis, Hinshelwood, Mulcahy and Partington, *Faraday Soc. Discussion*, 1947, **2**, 111.

<sup>2</sup> Walsh, *Trans. Faraday Soc.*, 1946, **42**, 269; 1947, **43**, 297, 305.

<sup>3</sup> Semenov, *Chemical Kinetics and Chain Reactions* (Oxford Univ. Press, 1935).

When these factors had been recognized it became possible to obtain reasonably consistent results. The reproducibility improved as the number of experiments increased, presumably because the walls of the vessel became coated with a uniform layer of oxidation products.

### Results

**The Influence of Reactant Concentrations on the Length of the Induction Period.**—Some results obtained with *n*-butane at 263° C are given in Fig. 1 in which the reciprocal of the induction period ( $\theta$  min.) is plotted against

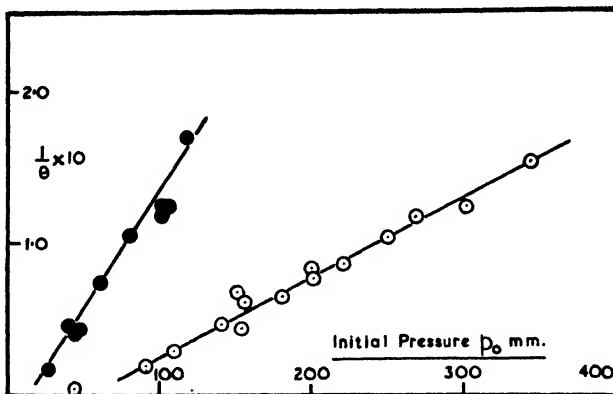


FIG. 1.—*n*-Butane-oxygen mixtures (263° C). The variation of the inverse induction period (min.<sup>-1</sup>) with the pressures of the reacting gases.

Full circles : butane varied, oxygen = 250 mm.

Open circles : oxygen varied, butane = 80 mm.

the partial pressure of the reactant for each of two series of experiments: (a) in which the initial oxygen pressure was kept constant (250 mm.) and the hydrocarbon pressure altered (black circles), and (b) in which the initial hydrocarbon pressure was constant (80 mm.) and the oxygen varied (open circles).

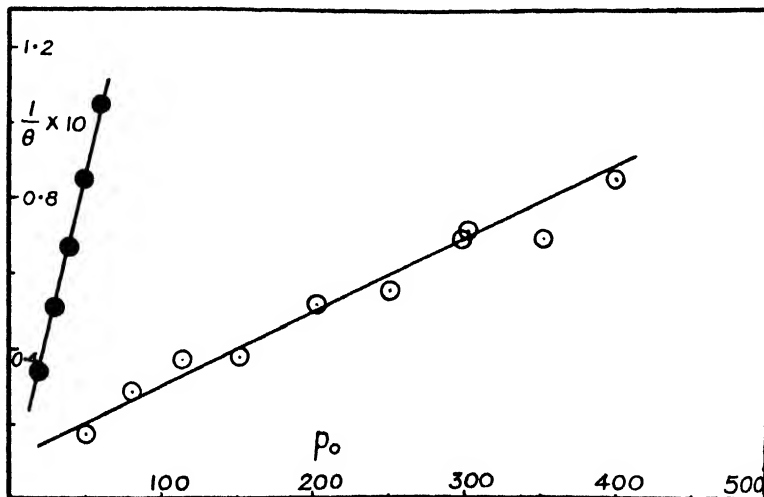


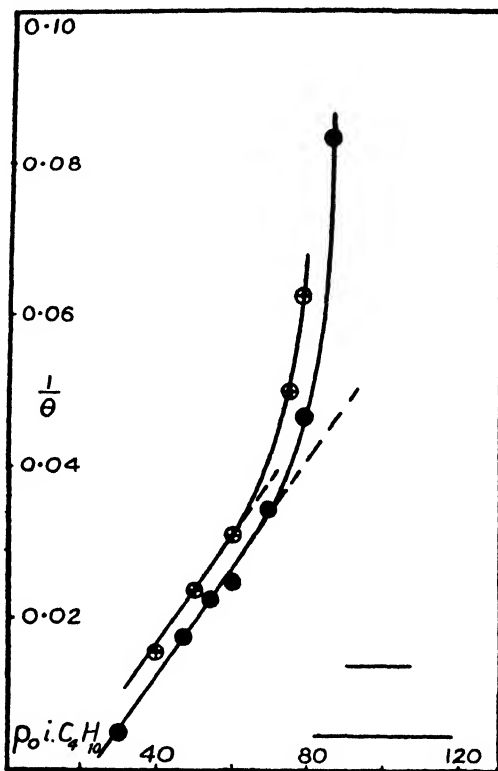
FIG. 2.—Propylene-oxygen mixtures (298° C). The variation of the inverse induction period with the pressures of the reacting gases.

Full circles : propylene varied, oxygen = 400 mm.

Open circles : oxygen varied, propylene = 50 mm.



It will be seen that the reciprocal of the induction period increases linearly with both the oxygen and the butane concentrations. A similar result was found for the dependence of  $1/\theta$  on oxygen concentration with 50 mm. butane at 259° C.



● Before air admitted.

⊕ After air admitted.

FIG. 3.—Isobutane-oxygen mixtures (289.5°). The variation of the inverse induction period with the isobutane pressure ( $O_2 = 250$  mm. in all experiments). Two series of experiments.

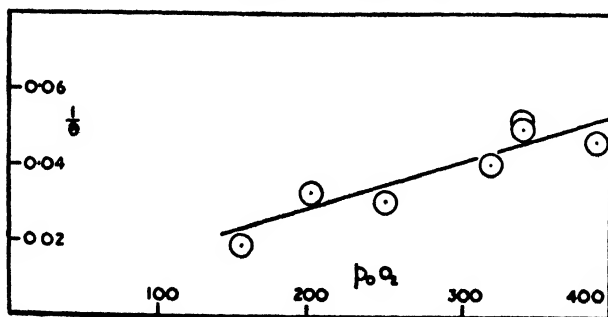


FIG. 4.—Isobutane-oxygen mixtures (289.5°). The variation of  $1/\theta$  with oxygen pressure (isobutane = 60 mm.).

The same result was obtained with propylene. Fig. 2 shows the results of two series of experiments at 298° with 400 mm. constant initial oxygen pressure and 50 mm. constant initial propylene pressure respectively. The results of experiments with isobutane at 289.5° are given in Fig. 3 and 4. Fig. 3 refers to two

series of experiments each with the reaction vessel surface differently treated (see later) but otherwise under similar conditions of 250 mm. constant initial pressure of oxygen and various *isobutane* pressures. It appears that at the lower pressures  $1/\theta$  increases linearly with the *isobutane* pressure but at higher pressures increases more rapidly.\* The variation  $1/\theta$  with oxygen pressure at 289.5° is shown in Fig. 4. These experiments were rather less precise than usual, but the results are compatible (at least) with a linear relationship between  $1/\theta$  and the oxygen concentration.

It will be observed that the results for *n*-butane, *isobutane* and propylene, three hydrocarbons of diverse structure, are the same: the reciprocal of the induction period increases linearly with the concentrations of both oxygen and hydrocarbon.† This raises the question whether in fact it increases linearly with the product of the two concentrations. Neglecting, for the moment, the fact that the straight lines representing the  $1/\theta$  concentration relationships in general do not pass through the origin, this may be tested in the following way.

If the induction period is dependent on the reactant concentrations according to an expression of the form,

$$1/\theta = K[O_2][H.C.], \quad (A)$$

the variation of  $1/\theta$  in the experiments with variable hydrocarbon concentration will be given by

$$1/\theta = kC_0[H.C.],$$

where  $C_0$  = the constant oxygen pressure, e.g. 250 mm. in the *n*-butane experiments. Similarly in the experiments with various oxygen pressures the expression (A) leads to

$$1/\theta = kC_H[O_2],$$

where  $C_H$  = the constant hydrocarbon pressure, e.g. 80 mm. in the *n*-butane experiments. But  $kC_0$  and  $kC_H$  are the slopes of the linear relationships in each case, therefore

$$\frac{S_H}{S_0} = \frac{\text{slope of straight line with variable hydrocarbon}}{\text{slope of straight line with variable oxygen}}$$

$$\text{should be } \frac{kC_0}{kC_H} = \frac{C_0}{C_H}.$$

Comparisons of the ratio of the observed slopes with that of the initial constant concentrations for the three hydrocarbons are given in Table I.

TABLE I

Hydrocarbon	$C_0$ mm. Hg	$C_H$ mm. Hg	$S_H$ min. <sup>-1</sup> mm. Hg <sup>-1</sup>	$S_0$ min. <sup>-1</sup> mm. Hg <sup>-1</sup>	$C_0/C_H$	$S_H/S_0$
<i>n</i> -Butane (259° C)	—	50	—	$3.33 \times 10^{-4}$	—	—
<i>n</i> -Butane (263° C)	250	80	$1.56 \times 10^{-3}$	$5.32 \times 10^{-4}$	3.1	2.9
Propylene . . .	400	50	$1.67 \times 10^{-3}$	$1.96 \times 10^{-4}$	8.0	8.5
<i>Isobutane</i> . . .	250	60	$7.2 \times 10^{-4}$	$(1.2 \times 10^{-4})$	4.2	(6)

Considering the nature of the experiments, Table I shows good agreement between the relative slopes observed and those expected from the ratio of the initial constant partial pressures. Consequently it may be inferred that the dependence of the induction period on the reactant concentration is of the form,

$$1/\theta = k[O_2][H.C.],$$

and not

$$1/\theta = k'[O_2] + k''[H.C.].$$

The linear plots of  $1/\theta$  against initial reactant concentration generally do not pass through the origin. This may be due partly to the nature of the definition chosen for the induction period, but it appears from some experiments

\* It is possible that the departure from linearity may be due to inadequacy of the definition chosen for the induction period under conditions leading to high reaction rates.

† This may not hold for the hydrocarbon dependence under conditions such that a high reaction rate is subsequently attained.

with *n*-butane that the displacement from the origin, at least in the case of the hydrocarbon dependence, varies with the nature of the surface. Fig. 5 shows

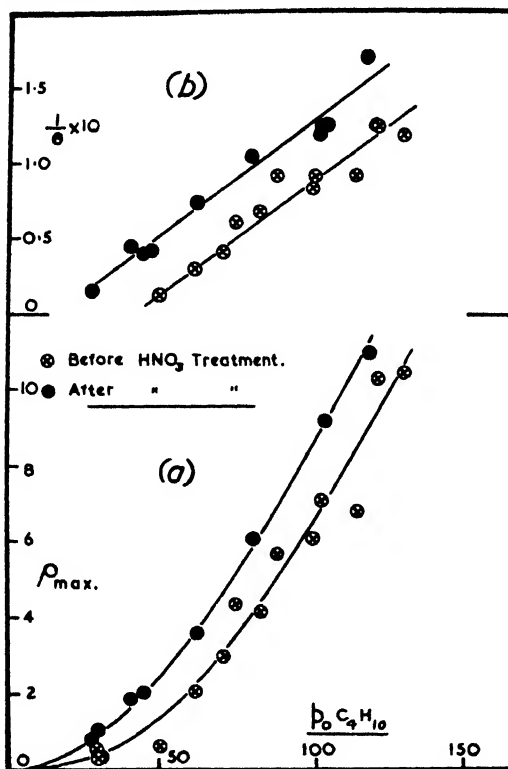


FIG. 5.—*n*-Butane-oxygen mixtures (263° C). Influence of surface treatment on variation of (a) maximum rate and (b) inverse induction period with hydrocarbon pressure ( $O_2 \approx 250$  mm. in all experiments).

the effect of treating the reaction vessel surface with nitric acid vapour (and air) at 263° on subsequent reactions with 250 mm. initial oxygen pressure at 263°. The induction period (Fig. 5b) was reduced, for example with 80 mm. butane, from 23 to 10 min. But though the absolute values at any one concentration are different, the slope of the linear relationship between  $1/\theta$  and the hydrocarbon concentration is within the experimental error the same before and after the surface treatment. (Fig. 5a gives the maximum rates corresponding to the induction periods in Fig. 5b.) A similar effect is discernible in experiments with isobutane (Fig. 3) in which the surface was heated for 24 hr. in contact with air.

It seems therefore that the length of the induction period is best represented by

$$1/\theta = k[O_2][H.C.] \pm F_s, \quad (B)$$

where  $F_s$  is a function of the surface conditions which does not involve  $[H.C.]$  (and, in view of the relationship between  $1/\theta$ ,  $[O_2]$  and  $[H.C.]$ , probably not  $[O_2]$ ).\*

\* According to eqn. (B), for a given hydrocarbon, the intercepts made on the  $1/\theta$  axis by the straight lines representing  $kC_0[H.C.]$  and  $kC_H[O_2]$  should be equal ( $F_s$ ), provided that the surface conditions are identical in both series of experiments. In each of Fig. 1 and 2 (*n*-butane and propylene), the intercepts are nearly equal, though this is not the case with the isobutane experiments (cf. Fig. 3 and 4). However, in the latter case the intercept of the variable oxygen curve is somewhat doubtful, and in the variable oxygen experiments the reaction vessel was in a more active state than in either series of the variable isobutane experiments.

However, it will be necessary to examine this expression in the light of further experiments which are in progress in this laboratory.

### The Contrast between the Inverse Induction Period and the Maximum Rate

(a) **The Effect of Reactant Concentrations.**—It has been pointed out previously<sup>1</sup> in connexion with the oxidation of *n*-butane that the influence of the reactant concentrations on the induction period is quite different from their effect on the maximum rate.\* The maximum rate-concentration relationships are more complex and, moreover, different for each reactant; the rate increases rapidly with hydrocarbon concentration, but above a certain concentration becomes practically independent of the concentration of oxygen.

Fig. 6 shows the maximum rates ( $\rho_{\max}$ ) obtained with propylene at 298° and should be compared with the corresponding results for the induction period given in Fig. 2. The contrast between the linear influence of both reactant concentrations on  $1/\theta$  and their more complicated and different effects on the rate is again evident. Isobutane at 289° was found to behave similarly.

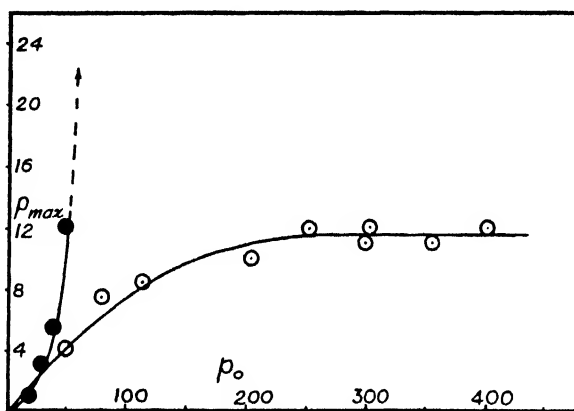


FIG. 6. —Propylene-oxygen (298°). Variation of the maximum rate (mm./min.) with the pressures of the reactants.

Full circles : propylene varied, oxygen = 400 mm.

Open circles : oxygen varied, propylene = 50 mm.

(b) **The Effect of Temperature.**—The induction period is more sensitive to the effect of temperature than the maximum rate. This is shown particularly well in experiments with propylene. The curve shown in Fig. 7 was obtained by plotting  $\log \rho_{\max}$  against  $1/T$  for mixtures of 30 mm. propylene and 250 mm. oxygen from 300 to 430° C.<sup>4</sup> † The points shown, however, refer to  $\log 1/\theta$  plotted against the same scale of  $1/T$ . It will be seen that the reciprocal induction period and maximum rate increase in parallel fashion with increasing temperature. However, the vertical scale referring to  $\log 1/\theta$  is twice that which refers to  $\log \rho_{\max}$ . This means that at any temperature the "activation energy" derived from the reciprocal induction period under these circumstances is double that of the maximum rate.‡

\* i.e. the tangent to the steepest part of the S-shaped pressure-time curve. At this point the concentration of peroxide reaches its maximum value, the rate of destruction becoming equal to the rate of formation.

<sup>4</sup> Mulcahy, *Trans. Faraday Soc.* (in press).

† The curve shows the gradual transition between the "low" and the "high" temperature reaction mechanisms.

‡ The coincidence may be to some extent fortuitous, since the rates and induction periods at the different temperatures were determined with constant pressures of propylene and oxygen. The correction of the values to constant concentrations depends on the form of the dependence on concentration in



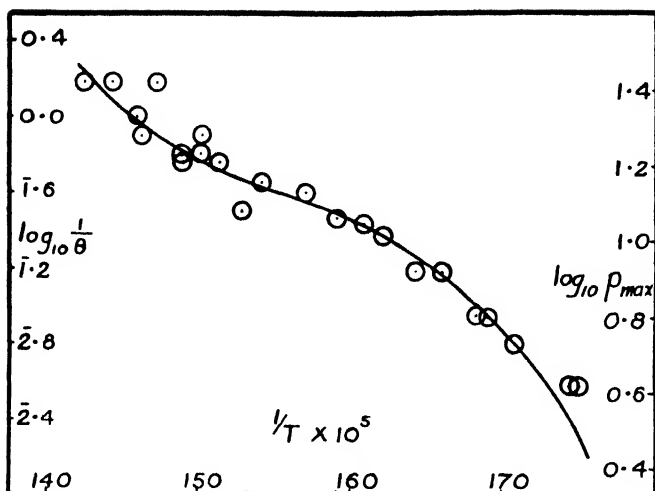


FIG. 7.—Propylene-oxygen. Variation of maximum rate and inverse induction period with temperature (30 mm. propylene-250 mm. oxygen).

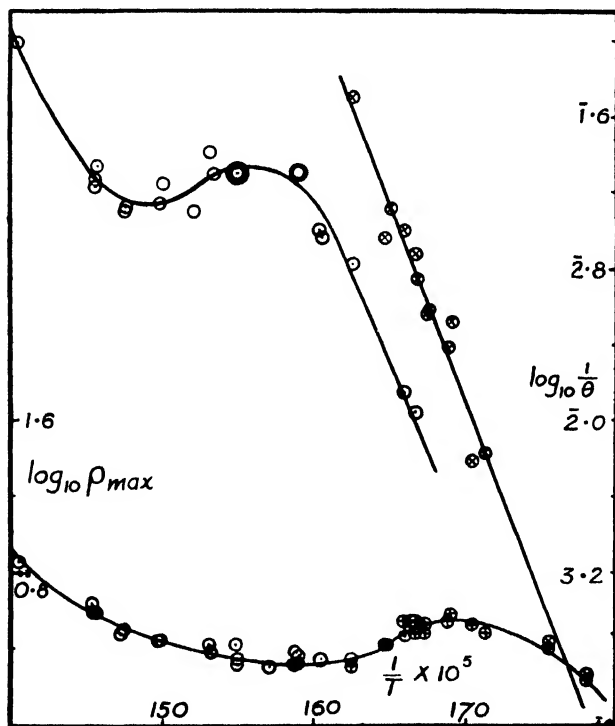


FIG. 8.—Propane-oxygen. Variation of maximum rate (lower curve) and inverse induction period (upper curves) with temperature.

Open circles : propane 30 mm., oxygen 250 mm.

Crossed circles : propane 29.7 mm., oxygen 250 mm., acetaldehyde 0.3 mm.  
(vertical crosses refer to  $\log \rho_{\max}$ , diagonal crosses to  $\log 1/\theta$ ).

Since  $[RH]$  and  $[O_2]$  will not differ appreciably from the initial concentrations,

$$[ROOH] = \frac{k_1 k_4}{k_3} [RH][O_2]t,$$

i.e. the rate of reaction at any time  $t$

$$= \rho = K'[ROOH] = K' \frac{k_1 k_4}{k_3} [RH][O_2]t;$$

consequently 
$$\bar{\rho} = K' \frac{k_1 k_4}{k_3} [RH][O_2]\theta,$$

where  $\bar{\rho}$  is the rate at the end of the induction period. Hence

$$1/\theta = K[RH][O_2].$$

The scheme therefore leads to the correct relationship between the length of the induction period and the concentrations.

The above scheme does not attempt to explain the surface dependent term in the expression,

$$1/\theta = K[RH][O_2] \pm F_s.$$

Though this relationship requires further investigation, it seems likely that, superimposed on a mechanism such as that just described, there is another which involves a surface reaction of zero order with respect to the reactants.

The more complicated dependence of the maximum rate on the concentrations can be attributed to the increased importance of chain-branching breakdown and consequent autocatalytic formation of peroxide. In fact, it has been shown that a reaction mechanism involving formation and decomposition in a manner similar to that indicated above leads to the correct concentration relationships.\*

In connection with the effect of temperature on the induction period it may be remarked that the initiation reaction,



probably requires a high activation energy since it is endothermic at least to the extent of 30-40 kcal./mole.<sup>9</sup>

Speculation on the influence of the surface must await further experimental evidence. More information is required concerning the relative importance of its functions in initiating and terminating chains.

The author is very much indebted to Prof. Sir Cyril Hinshelwood, F.R.S., for his advice throughout the work described in this paper. His best thanks are also due to Dr. C. F. Cullis for many interesting discussions.

The author is a member of the staff of the Division of Tribophysics of the Council for Scientific and Industrial Research, Australia.

*The Physical Chemistry Laboratory,  
South Parks Road,  
Oxford.*

\* In the original scheme <sup>1</sup> reaction (4) was considered to be



However, the mechanism involving the formation of hydroperoxide seems more plausible and leads (though not unequivocally) to the same  $\rho_{\max.}$ -concentration relationship. The derived constants in the rate expression involve the rate constants of the elementary steps in a more complicated way than in the corresponding expression derived from the original scheme.

The approximation made previously <sup>1</sup> in considering the induction period does not give the same result with both reactions (4) and (4a) and for this reason the treatment given above is preferred.

<sup>9</sup> Cf. Walsh, *J. Chem. Soc.*, 1948, 331.

# STUDIES OF SOAP SOLUTIONS

## PART I. THE FATTY ACID SOAPS AND THEIR HYDROLYSIS IN AQUEOUS SOLUTIONS

BY G. STAINSBY AND A. E. ALEXANDER

*Received 18th January, 1949*

A simple molecular treatment of the hydrolysis of soap solutions is derived, based upon the assumption that mixed micelle formation occurs between fatty acid molecules (formed by hydrolysis) and soap ions. The main features of the hydrolysis curves obtained by Powney and Jordan from pH measurements are established quantitatively. From such experimental data interesting conclusions upon the dissociation constants of the higher fatty acids and upon the variation of the ratio  $\frac{\text{soap ions in micelle}}{\text{fatty acid molecules in micelle}}$  with total soap concentration are drawn.

The effect of alcohols upon the hydrolysis curve is estimated in a semi-quantitative manner, on the basis of a simple competition between fatty acid and alcohol molecules for the limited number of sites in the micelles.

While studying the solubilization of polar compounds, such as phenols, by soap solutions it became necessary to examine in detail the behaviour of the fatty acid soaps. These, like all salts of weak acids, are hydrolyzed in aqueous solution. The extent of the hydrolysis is of importance in relation to the colloidal nature of soap solutions, and is of great interest in connection with the mechanism of detergent action, and with the stabilization of foams and emulsions. A number of investigations dealing with the problem are reported in the literature, the most exhaustive being that of Powney and Jordan,<sup>1</sup> who, by means of the glass electrode, measured the degree of hydrolysis of a large number of sodium soaps (laurate, myristate, palmitate, stearate, oleate, linoleate, ricinoleate) as a function of concentration and of temperature.

A typical set of curves is that for sodium palmitate, reproduced as Fig. 1. All the soaps show a remarkably similar general behaviour, the curves for the different soaps merely being displaced along the concentration and hydrolysis axes. Thus it is clear that any explanation must be of quite a general nature and capable of accounting for the following facts :

- (i) increase of temperature and of chain-length results in an increase in hydrolysis ;
- (ii) the degree of hydrolysis goes through a minimum and then through a maximum as the concentration increases ;
- (iii) the curve of degree of hydrolysis against concentration becomes, at high soap concentrations, parallel to the curve for very low soap concentrations.

It will be shown below that a general quantitative explanation, derived from simple molecular considerations,\* accounts for the essential experimental features and offers, in addition, considerable quantitative

<sup>1</sup> Powney and Jordan, *Trans. Faraday Soc.*, 1938, **34**, 363.

\* In a private communication Dr. G. S. Hartley has pointed out that by consideration of surface and bulk pH's essentially similar conclusions may be reached.



information upon the formation and structure of micelles in aqueous solutions of the fatty acid soaps.

The present explanation is to be compared with that suggested in qualitative terms by Powney and Jordan<sup>1</sup> who state "the abnormal

hydrolysis of soap solutions can be reasonably explained on the assumption that the rise in hydrolysis to a maximum is due to the formation of an insoluble acid soap, as suggested by McBain, and that the subsequent decrease of hydrolysis at higher soap concentrations is brought about by the formation of an acid soap of a more soluble type, possibly having a preponderance of neutral soap in its composition."

Similar views to those of Powney and Jordan have also been advanced and formulated quantitatively by Ekwall. He and his co-workers studied, by means of turbidity<sup>2</sup> and pH<sup>3,4</sup> measurements, the hydrolysis of certain soaps and interpreted their results on a theory involving the stepwise formation of a series of acid soaps.<sup>5</sup> We cannot support this idea as the definite compounds postulated do not appear to exist under the experimental conditions for normal hydrolysis studies.

#### Derivation of the General

**Equation.**—Salts of the lower fatty acids (e.g. sodium acetate), unlike the soaps, show no

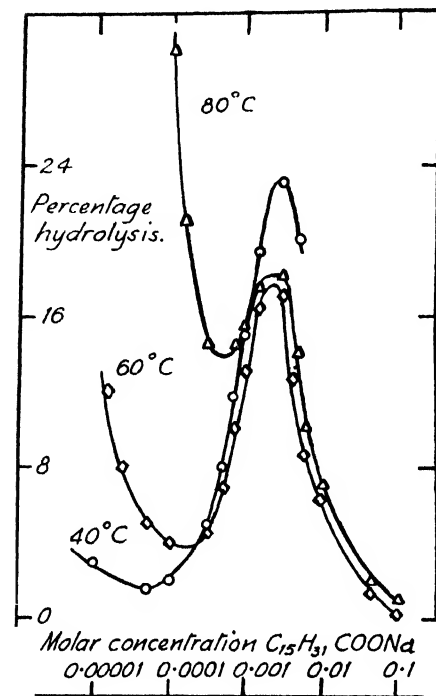
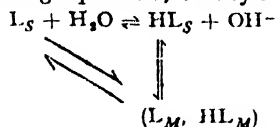


FIG. 1.—Hydrolysis-concentration curves for sodium palmitate.

increase in hydrolysis with increasing concentration. Neither do they form colloidal aggregates in aqueous solutions. Undoubtedly, therefore, the formation of colloidal aggregates (normally termed micelles) in aqueous soap solutions, is closely related to the unusual hydrolysis behaviour of the higher fatty acid salts. It is well known that solutions of, say, potassium laurate form micelles above a certain critical concentration, and it is to be expected that, by virtue of their structure, these micelles will tend to solubilize molecules of undissociated fatty acid, just as with alcohols and other polar organic molecules. Effectively, therefore, the fatty acid molecules produced by hydrolysis are removed from solution, and the equilibrium between salt and acid is displaced in the direction of increased hydrolysis. The micellar surfaces thus resemble a macroscopic oil-water interface.

When micelles are present the state of affairs in solution may be represented by the following equilibria, clearly intimately linked :



<sup>2</sup> Ekwall, *Kolloid-Z.*, 1936, **77**, 320.

<sup>3</sup> Ekwall and Lindblad, *ibid.*, 1941, **94**, 42.

<sup>4</sup> Ekwall, *ibid.*, 1941, **97**, 71.

<sup>5</sup> Ekwall, *ibid.*, 1940, **92**, 141.

For convenience, sodium ions are omitted completely. The micelle ( $L_M$ ,  $HL_M$ ) is represented as a mixed aggregate, as it contains both soap ions ( $L$ ) and unionized fatty acid molecules ( $HL$ ).

The following notation is employed :

$C$  = total soap concentration in g.-moles/litre.

$V$  = total volume of solution, in litres.

$V_M$  = volume (in litres) occupied by the mixed micelle in  $V$  litres of soap solution.

Symbols, such as  $HL_S$ ,  $L_M$ , etc., without brackets denote *total* amounts in g.-moles. (i.e. in  $V$  litres of solution).

Brackets denote concentrations in g.-moles per litre, e.g.  $[HL_S]$  is concentration of fatty acid in g.-moles/litre of solution,  $[HL_M]$  is concentration of fatty acid in g.-moles/litre of the mixed micelle.

Braces denote activities,

i.e.  $\{HL_S\} = [HL_S] \times f_{HL_S}$ , where  $f_{HL_S} \rightarrow 1$  as  $C \rightarrow 0$ .

Subscript  $S$  refers to molecular solution

Subscript  $M$  refers to the micelle.

$$K_F = \frac{[HL_M]}{[HL_S]}, \quad K_D = \frac{[L_M]}{[L_S]}.$$

Now the hydrolysis constant, as normally defined, using concentrations, is

$$K_h = \frac{[OH^-][HL_S]}{[L_S]}, \quad (1)$$

and, whatever the value of  $C$ ,  $[OH^-] = \beta C$ , where  $\beta$  is the degree of hydrolysis. Below the micellar region

$$K_h = \frac{\beta^2 C}{1 - \beta} \quad (1a)$$

Moreover,

$$HL_S + HL_M = \beta CV, \quad (2)$$

and

$$L_S + L_M = (1 - \beta)CV. \quad (3)$$

Eqn. (2) may be written

$$\beta CV = [HL_S] \times V + K_F [HL_S] V_M \quad (4)$$

If now we introduce  $\rho$ , the density of the mixed micelle,

$$V_M = \frac{HL_M + L_M}{\rho} \quad (5)$$

$\rho$  is derived from the usual densities (in g./cm.<sup>3</sup>) and molecular weights of the fatty acid molecules and soap ions. If these densities are taken as unity, and the small difference in molecular weight is ignored, then  $\rho = 10^3/M$ , where  $M$  is the molecular weight of the soap.\* Numerically, these approximations in the calculation of  $\rho$  are not significant for the present purpose. From (5),

$$\begin{aligned} V_M &= \frac{1}{\rho} (\beta CV - HL_S + (1 - \beta)CV - L_S), \\ &= \frac{V}{\rho} (C - [HL_S] - [L_S]). \end{aligned}$$

Substituting for  $V_M$  in (4) we obtain

$$\beta C = [HL_S] \left\{ 1 + \frac{K_F}{\rho} (C - [HL_S] - [L_S]) \right\}. \quad (6)$$

But

$$[HL_S] = \frac{K_h \times [L_S]}{\beta C} \text{ by eqn. (1),}$$

i.e.

$$\beta^2 C^2 = K_h [L_S] \left\{ 1 + \frac{K_F}{\rho} \left( C - [L_S] - \frac{K_h [L_S]}{\beta C} \right) \right\} \quad (7)$$

\* The units of  $\rho$  are g.-mole/litre.

Strictly eqn. (7) is not accurate as thermodynamic values of  $K_h$  and  $K_F$  have not been employed. Using activity coefficients defined as above, eqn. (7) becomes

$$\beta^2 C^2 = -\frac{K_h \times f_{LS} \times [L_S]}{f_{HL_S} \times f_{OH}} \left\{ 1 + \frac{K_F}{\rho} \times \frac{f_{HL_S}}{f_{HL_M}} \left( C - [L_S] - \frac{K_h [L_S]}{\beta C} \times \frac{f_{LS}}{f_{HL_S} \times f_{OH}} \right) \right\} \quad (8)$$

The necessary activity coefficients are not known by other means, but they would not appear to differ markedly from unity since deductions from eqn. (7), which assumes that they are unity at all concentrations, are confirmed experimentally within the fairly large error necessitated by certain approximations.\* Eqn. (7) cannot be used as it stands because both  $K_F$  and  $[L_S]$  depend upon  $C$ . However, if  $C_S$  is the critical concentration for micelle formation (as normally measured) two extreme cases arise which considerably simplify the mathematics.

CASE I.— $C \gg C_S$ .

For all the systems under discussion  $K_h/\beta C \ll 1$ , and is of the order of  $10^{-4}$ .

E.g. sodium myristate :

$$\begin{array}{ll} (a) \ 80^\circ \text{C} : K_h \sim 10^{-7} & (b) \ 25^\circ \text{C} : K_h \sim 10^{-9} \\ \beta \sim 10^{-1} & \beta \sim 10^{-2} \\ C \sim 10^{-3} & C \sim 10^{-3} \end{array}$$

i.e.  $K_h [L_S]/\beta C$  can be neglected in comparison with  $[L_S]$ . Eqn. (7) then reduces to

$$\beta^2 C^2 = K_h [L_S] \left\{ 1 + \frac{K_F}{\rho} (C - [L_S]) \right\},$$

$$\text{i.e.} \quad \beta^2 C^2 \simeq K_h [L_S] \left\{ 1 + \frac{K_F}{\rho} \times C \right\} \quad . \quad . \quad . \quad . \quad (8)$$

Now  $\rho \sim 3 - 4$ ,  $C \sim 10^{-1}$  molar ;  $K_F \sim 10^5 - 10^8$ ,

$$\therefore \quad \frac{K_F \times C}{\rho} + 1 \simeq \frac{K_F C}{\rho},$$

$$\text{i.e.} \quad \rho \beta^2 C = K_h [L_S] \times K_F. \quad . \quad . \quad . \quad (9)$$

$$\text{or} \quad K_h = \frac{\beta^2 C \rho}{[L_S] K_F}.$$

Had no micelles formed, for very small values of  $C$  ( $= C_1$ ) the normal expression for  $K_h$  would have been (eqn. (1a)),

$$K_h = \beta^2 C_1, \quad \text{if } \beta \ll 1.$$

When  $C \gg C_S$ , again  $\beta \ll 1$  if  $C$  is sufficiently large. Thus, for the same small value of  $\beta$ ,

$$\frac{C}{C_1} = \frac{[L_S] K_F}{\rho}.$$

The experimental results for  $\beta$  against  $C$  (see Fig. 1), show that the curve before the minimum runs parallel to that beyond the maximum, and hence it follows that  $C/C_1 = \text{const}$ . Thus, for  $C \gg C_S$ ,  $K_F [L_S]$  is constant, and since there is good evidence that the concentration of simple molecules  $[L_S]$ , does not vary much once micelles are present, then  $K_F$  is also a constant. Values of  $K_F$  cannot, however, be found until  $[L_S]$  is known. This may be extracted from the literature or can be obtained directly from the data of Powney and Jordan, as follows.

\* Note eqn. (8) does not contain  $f_M$  which would certainly vary considerably with concentration.

Re-writing eqn. (7) in the form,

$$\beta^2 = \frac{K_h[L_S]}{C^2} \left\{ 1 + \frac{K_F}{\rho} (C - [L_S]) \right\},$$

and putting  $[L_S] = c_S$ ,

we have

$$\beta^2 C^2 - \frac{K_h K_F}{\rho} \times c_S \times C + c_S K_h \left( \frac{K_F \times c_S}{\rho} - 1 \right) = 0, \quad (10)$$

i.e. if  $C > C_S$ , there are two values of  $C$  for a given value of  $\beta$ . Moreover, there will be a maximum value of  $\beta$  ( $= \beta_{\max.}$ ) given when  $C = C_{\max.}$  and eqn. (10) has only one root. Then

$$C_{\max.} = \frac{K_h K_F c_S}{2 \beta_{\max.}^2 \times \rho}, \quad (11)$$

$$\text{and} \quad \frac{K_h^2 K_F^2 c_S^2}{\rho^2} = 4 \beta_{\max.}^2 \times c_S K_h \left( \frac{K_F c_S}{\rho} - 1 \right) \quad (12)$$

To a first approximation, eqn. (12) reduces to

$$\beta_{\max.}^2 = \frac{K_F K_h}{4 \rho}, \quad (13)$$

and thus  $C_{\max.} = 2c_S$ , i.e.  $c_S$  can be obtained from the maximum in the curve. For a given soap it is well known that the critical concentration for micelle formation increases only slowly with temperature; it is not surprising therefore, that the maxima in the experimental curves should all occur at about the same soap concentration. Probably the best values in the literature for critical concentrations are given in the paper by Klevens.<sup>6</sup> In Table I the values of  $c_S$  calculated as above from the hydrolysis data are compared with the experimental values of Klevens. The agreement is clearly very reasonable.

TABLE I.—THE CRITICAL CONCENTRATION FOR THE FORMATION OF SOAP MICELLES

	$C_{11}H_{23}CO_2Na$	$C_{15}H_{27}CO_2Na$	$C_{16}H_{31}CO_2Na$	$C_{17}H_{33}CO_2Na$
Expt. (Klevens)	$2.4 \times 10^{-2}$	$6.6 \times 10^{-3}$	$2 \times 10^{-3}$	$5 \times 10^{-4}$
Calc. from hydrolysis data	$1-2 \times 10^{-2}$	$3 \times 10^{-3}$	$1.3 \times 10^{-3}$	$5 \times 10^{-4}$

All concentrations in moles/litre. Values at 60° C.

TABLE II.—CALCULATED VALUES OF  $10^{-5} K_F$  FOR VARIOUS SODIUM SOAPS AT VARIOUS TEMPERATURES

	25° C	40° C	60° C	80° C
Laurate	9.0	4.5	0.6	0.15
Myristate	28	10	1.4	0.16
Palmitate	—	162	10.4	0.51
Stearate	—	344	130	8.3
Oleate	104	52.5	2.1	0.16

Knowing  $[L_S]$ ,  $K_F$  then follows; the values so found are set out in Table II. Two generalizations may be made from this Table; firstly

<sup>6</sup> Klevens, *J. Physic. Chem.*, 1948, **52**, 130.

that  $K_F$  decreases with increasing temperature,\* secondly that  $K_F$  increases markedly with chain length. Since  $K_F$  effectively represents a partition coefficient it should increase with the number of carbon atoms in the chain, and by a constant factor of *ca.* 3 per  $\text{CH}_2$  group, just as

with other properties such as surface activity, oil-water partition coefficient, etc. (see for example, Ferguson<sup>7</sup>).

Fig. 2 shows that the increase of  $\log K_F$  with chain length is indeed approximately linear, and that  $K_F$  varies by the usual factor of 3 as found for successive members of a straight chain series (Traube's rule).

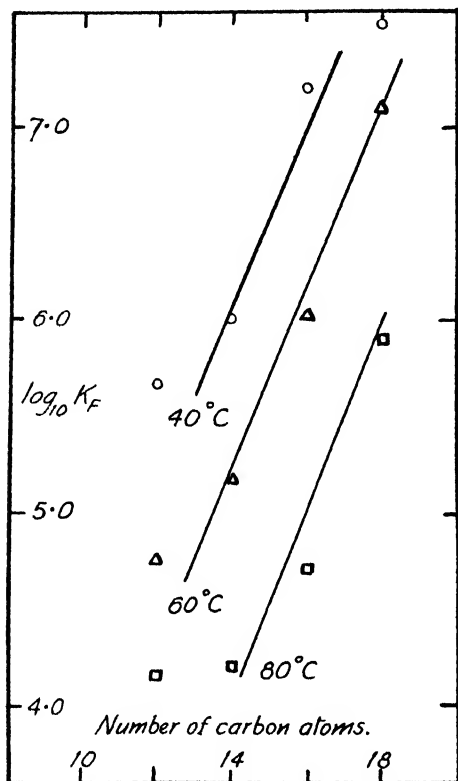


FIG. 2.—The dependence of  $K_F$  upon the number of carbon atoms in the paraffin chain. The slope of the straight lines has been calculated from Traube's rule (see text).

be expected to be the same for all the saturated acids. Such values of  $K_a^*$  can be compared with values for  $K_a$  obtained from eqn. (13) (see Table III). The wide discrepancy which clearly exists cannot be accounted for by micellar activity coefficients since, with the exception of the laurates at low temperatures, the thermodynamic  $K_a$ 's do not give the experimental  $\beta - C$  curves in the pre-micellar region ( $C \sim 10^{-3}$  M). However, using the values of  $K_a$  calculated from  $\beta_{\max}$ , there is quite good agreement between the observed and calculated curves at these low soap concentrations. Unfortunately there are little data available on activity coefficients of soap solutions. The most useful for the present

#### CASE II. $C \ll C_S$ .

Before this region can be considered it is necessary to know the values of  $K_a$ ,  $K_a^*$  (thermodynamic value) could be obtained from the ionic product of water ( $K_w$ ) and the thermodynamic dissociation constant of the acid ( $K_a$ ) if the latter were known with sufficient accuracy. Dippy<sup>8</sup> has collected data on the dissociation constants of the saturated fatty acids up to nonoic; the insolubility of the higher members prevents a direct measurement. From this data it would seem quite likely that  $K_a$  (thermodynamic) might be almost independent of chain-length above, say, six or seven carbon atoms, i.e. at the same temperature,  $K_a^*$  might

\* From graphs of  $\log_{10} K_F$  against  $1/T$ , values of  $\Delta H_F$ , the change in heat content for the transformation,

fatty acid in solution  $\rightleftharpoons$  fatty acid in mixed micelle,

have been obtained. It is hoped to discuss this aspect in some detail in a later paper of this series.

<sup>7</sup> Ferguson, *Proc. Roy. Soc. B*, 1939, **127**, 387.

<sup>8</sup> Dippy, *Chem. Rev.*, 1939, **25**, 151.

purpose comes from the work of McBain and Barker,<sup>9</sup> but the lowest concentration investigated was  $10^{-2}$  M. At this concentration (micelles present) the activity coefficients were of the order of 0.8 to 0.9, certainly not differing from unity by a factor of ten or one hundred. It would seem more plausible, therefore, to take activity coefficients as unity and to ascribe the above discrepancy to a change in  $K_a$  with chain-length. Column 5 in Table III shows values of  $K_a$  so found, uncorrected for activity coefficients. The change is in the expected direction, viz., a decrease in  $K_a$  with increasing chain-length. The marked temperature dependence of  $K_a$  seems not unreasonable if the long paraffin chains are coiled in solution to decrease as far as possible the hydrocarbon-water interface.

TABLE III

	°C	$10^7 K_h$ Calc.	$10^7 K_h$ Obs.	$10^5 K_a$	$10^4 c_F$	$10^7$ Satn. Sol.	$10^7$ Total Acid at min.
Sodium Laurate	25	0.009	0.007	1.7	7	2.9	6.5
	40	0.020	0.006	6.2	6	3.5	6.5
	60	0.094	0.079	1.6	30	4.4	60
	80	0.26	0.31	1.1	100	5.2	130
Sodium Myristate	25	—	0.065	0.18	30	0.9	2.0
	40	—	0.1	0.40	50	1.2	6.0
	60	—	0.75	0.17	75	1.5	72
	80	—	6.7	0.052	380	2.0	350
Sodium Palmitate	40	—	0.47	0.084	30	3.7	7.5
	60	—	4.4	0.029	100	0.47	60
	80	—	93	0.0037	660	0.58	900
Sodium Stearate	40	—	1.2	0.031	16	1.3	4.8
	60	—	2.1	0.06	23	1.7	10
	80	—	40	0.0087	125	2.2	190

Column 3.  $K_h$  calculated from  $K_w^{(6)}$  and  $K_a^{(4)}$ .

4.  $K_h$  calculated from  $\beta_{\max}$ .

5.  $K_a$  calculated from column 4 and  $K_w$ .

6.  $c_F$  obtained from column 4.

7. Saturation solubility ( $\times 10^4$ ) of fatty acid in water.

All concentrations are in moles/litre.

In the above calculations the values of  $K_w$  used by Powney and Jordan to compute  $\beta$  had to be employed. These values were taken from the work of Lorenz and Bohi<sup>10</sup> and are not in agreement with the "best" values given in the International Critical Tables.

Having decided upon the values of  $K_h$  to be used it is of interest to derive another equation for the dependence of  $\beta$  upon  $C$  in the region  $C \ll C_s$ . Using eqn. (3) we obtain

$$(1 - \beta)C = [L_s] \left\{ 1 + \frac{K_D}{\rho} (C - [L_s] - [HL_s]) \right\} \quad (14)$$

But  $[L_s] = \frac{\beta C \times [HL_s]}{K_h}$  by eqn. (1)

$$\therefore \frac{1 - \beta}{\beta} \times K_h = [HL_s] \left\{ 1 + \frac{K_D}{\rho} \left[ C - [HL_s] \left( 1 + \frac{\beta C}{K_h} \right) \right] \right\} \quad (15)$$

Here both  $[HL_s]$  and  $K_D$  will depend upon  $C$ .

<sup>9</sup> McBain and Barker, *Trans. Faraday Soc.*, 1935, **31**, 149.

<sup>10</sup> Lorenz and Bohi, *Z. physik. Chem.*, 1909, **66**, 733.

For soap solutions the critical concentration for micelle formation as measured here ( $C_S$ ) and, for example, by Klevens is much higher than the value at the minimum of the hydrolysis curves. Yet in order to explain why these curves are not normal some type of aggregation, beginning in the region of the minimum value of  $\beta$ , seems essential. From eqn. (1) it is clear that, at a given  $C$ ,  $\beta$  will be raised if fatty acid molecules are effectively removed from solution by being incorporated into some sort of colloidal aggregate, such as a soap micelle. However, it seems well established from other properties (e.g. conductivity, density, interfacial tension, refractive index, etc.) that soap micelles normally form over a narrow range of concentration; certainly not approaching the factor of ten which would be required here. An alternative explanation would be that *fatty acid* aggregates are formed at the requisite low

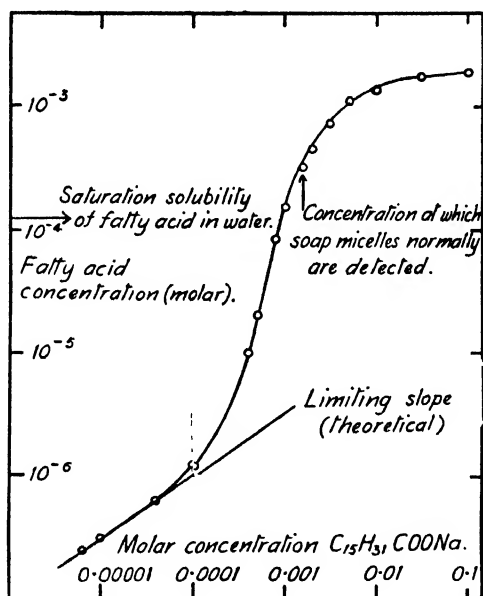


FIG. 3.—The total concentration of palmitic acid in aqueous solutions of sodium palmitate at 40° C.

concentration (say about  $0.1C_S$  or so), beginning at a fatty acid concentration which is some definite fraction of its saturation solubility. Since the latter increases with temperature<sup>11</sup> (see Table III) it follows that the minimum in the curve would move to higher soap concentrations and to higher degrees of hydrolysis as the temperature is raised.

The idea of fatty acid aggregates is not new, probably the first indication being given by the work of Jones and Bury<sup>12</sup> upon butyric acid. Further support comes from the solubilization data for organic substances in soap solutions. With soaps which do not hydrolyze in solution the solubility appears to increase quite sharply at the critical micellar concentration (e.g. Hartley<sup>13</sup>—*trans*-azobenzene in cetyl pyridinium chloride solutions) whereas with the fatty acid soaps appreciable increases in solubility are noted well before this point (e.g. *trans*-azobenzene in sodium laurate solutions; <sup>14</sup> see also Fig. 3 given by Merrell

<sup>11</sup> Ralston and Hoerr, *J. Org. Chem.*, 1942, 7, 546.

<sup>12</sup> Jones and Bury, *Phil. Mag.*, 1927, 4, 841.

<sup>13</sup> Hartley, *J. Chem. Soc.*, 1938, 1968.

<sup>14</sup> Unpublished work of the authors.

and Getty<sup>15</sup>—Orange O.T. in potassium laurate—and Fig. 3 and 5 of Kolthoff and Stricks<sup>16</sup>—dimethyl aminobenzene in sodium laurate and in sodium caprylate). If  $c_F$  is the concentration of fatty acid molecules at which aggregation commences, and if we assume that  $c_F$  is approximately a constant then eqn. (15) becomes

$$K_h \times \frac{1 - \beta}{\beta} = c_F \left\{ 1 + \frac{K_D}{\rho} \left[ C - c_F \left( 1 + \frac{\beta C}{K_h} \right) \right] \right\}.$$

On rearrangement this transforms into

$$\frac{K_h}{\beta} = c_F - c_F^2 \times K_D + C \left( \frac{c_F K_D}{\rho} - \frac{c_F^2 K_D \beta}{\rho K_h} \right).$$

At the minimum  $\delta\beta/\delta C$  is zero. If  $K_D$  is taken as a constant over small ranges of concentration then

$$\frac{\delta\beta}{\delta C} \left( \frac{C \times c_F^2 K_D}{\rho K_h} - \frac{K_h}{\beta^2} \right) = \frac{c_F K_D}{\rho} - \frac{c_F^2 \times K_D \beta}{\rho K_h},$$

or

$$K_h = c_F \times \beta_{\min}. \quad (16)$$

$K_h$  is known,  $\beta_{\min}$  can be obtained from the curve and so  $c_F$  may be found. Table III shows  $c_F$  so calculated, also the saturation solubilities in water and the total fatty acid at the soap concentration for minimum hydrolysis. Clearly aggregation occurs before saturation, the difference between the two decreasing at higher temperatures. Graphs of  $\log c_F - 1/T$  and  $(\log c_{\text{sat.}}) - 1/T$  yield interesting results, but discussion upon them is being postponed for a later paper.

### CASE III. THE REGION BETWEEN THE MAXIMUM AND THE MINIMUM IN THE HYDROLYSIS CURVE.

It is of interest to consider in more detail the change from the fatty acid aggregates which we have postulated as forming initially to the soap micelles which eventually contain only soap ions. This may best be done in the following simple manner, without using the equations already derived.

From the  $\beta - C$  curves it is possible to obtain the *total* fatty acid concentration, since this is merely equal to  $\beta C$  (see Fig. 3). At high soap concentrations this clearly tends to zero, whereas at low soap concentrations, for small values of  $\beta$ , the slope of the graph of  $\log \beta C - \log C$  should be 0.5. This follows from eqn. (1):

$$\begin{aligned} K_h \times (1 - \beta)C &= (\beta C)^2, \\ \text{i.e. } \log K_h + \log C &\doteq 2 \log \beta C, \end{aligned}$$

$$\text{or } \frac{\delta \log (\beta C)}{\delta \log C} = 0.5.$$

The limiting slope of 0.5 is reached at soap concentrations just before the minimum in the hydrolysis curve, and it is in this region that aggregation to fatty acid micelles sets in.

By means of Fig. 3 it is possible to obtain the ratio:

$$\frac{\text{Amount of micellar fatty acid in 1 l. soln.}}{\text{Amount of free fatty acid in 1 l. soln.}}$$

for various total soap concentrations, if  $[HL_S] = c_F = \text{const.}$  Only if  $C > C_S$  can  $K_F$  be found from this ratio since, if  $C < C_S$ , it is necessary to know  $K_D$  in order to determine the volume occupied by the micelles. Consider, for example, sodium palmitate solutions at 40° C. When  $\beta = 0.23$ ,  $C = 3.0 \times 10^{-3}$  M,  $c_F = 2 \times 10^{-7}$  M and the molar ratio is

<sup>15</sup> Merrill and Getty, *J. Physic. Chem.*, 1948, **52**, 774.

<sup>16</sup> Kolthoff and Stricks, *ibid.*, 1948, **52**, 915.



3,500. Now the volume of the micelles is equal to  $1.5 \times 10^{-3}/3.6$  l. (approx.), since  $\rho = 3.6$  and  $C_s = 1.5 \times 10^{-3}$  M. Thus  $K_F$ , which is the ratio expressed in concentrations, is equal to  $3,500 \times \frac{3.6 \times 10^3}{1.5}$ , or  $8.5 \times 10^6$ . This is in fair agreement with the steady value ( $16 \times 10^6$ ) found from the parallel displacement of the hydrolysis curves at very high and very low soap concentrations (Table II).

Further interest centres around the ratio

$$\frac{\text{total micellar soap}}{\text{total micellar fatty acid}},$$

i.e. the number of soap ions to every fatty acid molecule in a micelle. The variation of this ratio with total soap concentration is shown for sodium palmitate at  $40^\circ\text{C}$  in Fig. 4. In order to obtain this diagram

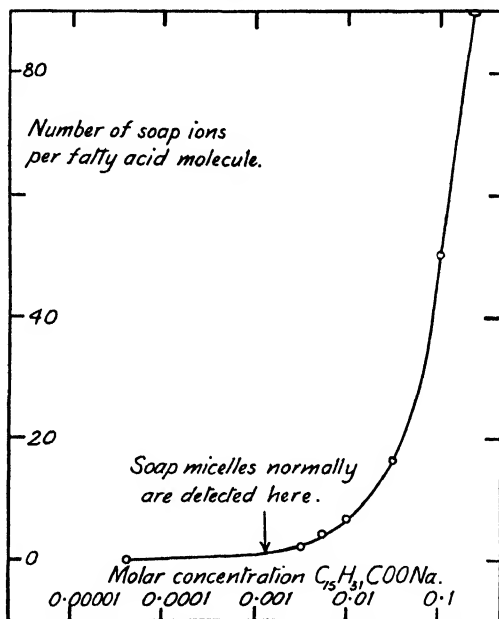


FIG. 4.—The composition of the micelles in sodium palmitate solutions at  $40^\circ\text{C}$ .

it has been assumed that when  $C > C_s$  there remains in solution a concentration of single soap ions equal to  $C_s$ . Clearly when  $C \gg C_s$  the ratio will become very large indeed, and when  $C$  is in the region of  $C_{min}$ , the ratio tends to zero. For the above system, when  $C = C_{max.}$ , the ratio is two soap ions to every fatty acid molecule. If  $K_D$  were known for all values of  $C$  the concentration range from  $C_{min.}$  to  $C_s$  could be analyzed quantitatively, but as this is not so, a smooth curve joining the parts for which  $C > C_s$  and  $C \approx C_{min.}$  has been drawn. From this curve it follows that when  $C = C_s$  (i.e. at the critical concentration for soap micelles as normally measured) the ratio of soap ions to fatty acid molecules is not far from unity. This is a result of very great interest in view of the well-known stability of the acid soaps of composition NaL, HL.

**Hydrolysis in Aqueous Alcohol.**—Powney and Jordan<sup>1</sup> also present data upon the effect of normal alcohols in decreasing the hydrolysis of sodium oleate (0.003 M) at  $25^\circ\text{C}$ . They suggest that this is due to an increase in the solubility of the fatty acid in aqueous alcohol so that at no time is the solubility limit exceeded. Possibly this solubility is a contributory factor but it is not, in our view, the major one.

It is well established that soap micelles solubilize alcohol molecules, the solubilization increasing with increasing chain-length of the alcohol for the lower members at any rate. In a solution containing both alcohol and free fatty acid (formed by hydrolysis) there will exist a competition for the limited number of sites in the soap micelles so that, if the alcohol is in great excess, no increase in the total amount of fatty acid can be obtained by solubilization: the hydrolysis, therefore, remains at a normal value. On this view, with increasing chain-length of the alcohol, a given diminution in hydrolysis should require a progressively lower alcohol concentration (Traube's rule). This is what has been found,<sup>1</sup> e.g. the concentrations necessary to reduce the degree of hydrolysis from 7% to 1% are 26%, 18%, 9% and 5% for MeOH, EtOH, PrOH and BuOH respectively.

Since the addition of alcohols to soap solutions lowers the critical micellar point it is to be expected that as the alcohol concentration increases the 'maximum' in the hydrolysis curves ( $C_{\max.} = 2C_S$ ) should move to lower soap concentrations. The limit is reached when the solution is saturated with alcohol, in which event the maximum and minimum of the hydrolysis curve become identical and a normal curve results.

A semi-quantitative analysis of these phenomena may be made on the general lines advanced in this paper, and may be exemplified by the system *n*-butyl alcohol-sodium oleate at 25°C. Using the equations already derived for the hydrolysis in aqueous solutions the following figures are obtained:

$$\begin{aligned} K_h \text{ (from } \beta_{\max.}) &= 7.4 \times 10^{-9} \text{ g.-moles/l.} \\ K_F &= 1 \times 10^7, \\ C_S &= 1 \times 10^{-5} \text{ M} \end{aligned}$$

(compare, for example, the value  $0.7 - 1.2 \times 10^{-3}$  M given by Harkins *et al.*<sup>17</sup>). It will be assumed that  $K_h$  is not affected by the alcohol present, and in order to determine values of  $K_F$  the density of the mixed micelle  $\rho$  will be taken as 3.3 independent of the alcohol concentration. As the alcohol concentration increases to saturation  $\rho$  will change from 3.3 to about 1.3, but this variation in  $\rho$  is not known quantitatively.

Before  $K_F$  can be found it is necessary to know how  $C_S$  changes as alcohol is added to the solution. This may be estimated in a very approximate manner from the known variation of the critical micellar concentration of Aerosol M.A. solutions when phenol is added.<sup>14</sup> The estimation should not be seriously in error as phenol and *n*-butyl alcohol have similar solubilities in water at 25°C, and require similar volumes in micelles.

With these assumptions  $K_F$  may be computed for various values of  $\beta$  (i.e. for various alcohol concentrations) from the separation of the hydrolysis curves at high and low soap concentrations, i.e. from  $K_F C_S / \rho$ . When 4.7% alcohol is present  $K_F$  has fallen by a factor of 10.

It is interesting to obtain some idea of how  $\beta_{\max.}$  changes with the addition of alcohol. Now

$$\beta_{\max.} = \frac{K_F K_h}{4\rho}, \text{ (eqn. 13)}$$

$$\text{i.e.} \quad \beta_{\max.} = \frac{K_F C_S}{\rho} \times \frac{K_h}{4C_S}.$$

$K_F C_S / \rho$  is known from Powney and Jordan's data.  $K_h$  has been calculated from the value of  $\beta_{\max.}$  when no alcohol is present.  $C_S$  is known, approximately, from the addition of phenol to soap solutions. Thus  $\beta_{\max.}$  can be calculated at various alcohol concentrations. Knowing  $\beta_{\max.}$  and the value of  $\beta$  when  $C = 0.003$  M, the general shape of the hydrolysis

<sup>17</sup> Corrin, Kleven and Harkins, *J. Chem. Physics*, 1946, 14, 480.

curve in the presence of various concentrations of *n*-butyl alcohol may be estimated. This is how Fig. 5 has been obtained. Clearly, when the solution is saturated with alcohol a normal hydrolysis curve should result.

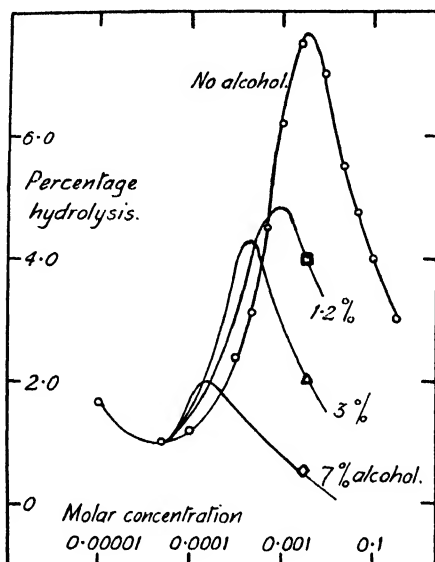


FIG. 5.—The effects of *n*-butyl alcohol upon the hydrolysis-concentration curve for sodium oleate at 25° C.

The correctness of the above ideas may be tested by predicting the alcohol concentration necessary to reduce the degree of hydrolysis to a given value, say one-half of that in pure water. Again the system sodium oleate-*n*-butyl alcohol will be considered. Suppose, in the sodium oleate micelles, there is a fixed number of sites available for solubilized fatty acid and alcohol molecules. Then the concentration in the micelles of the alcohol molecules ( $C_M^A$ ) will be given by

$$C_M^A = C_B^A \times e^{-\Delta G^A/RT},$$

where  $\Delta G^A$  is the free energy of adsorption and  $C_B^A$  the concentration of the alcohol in bulk solution. The corresponding quantity for the fatty acid molecules ( $C_M^F$ ) will then be

$$C_M^F = C_B^F \times e^{-\Delta G^F/RT},$$

where  $\Delta G^F$  is the free energy of adsorption of the fatty acid and  $C_B^F$  its concentration in bulk solution. Let us make the reasonable assumption that to reduce  $\beta$  by 50 % the number of alcohol molecules in the soap micelles must equal the number of fatty acid molecules. Hence

$$C_M^A = C_M^F,$$

i.e.

$$C_B^A \times e^{-\Delta G^A/RT} = C_B^F \times e^{-\Delta G^F/RT}.$$

Now  $\Delta G^F = -RT \log_e K_F$  and  $\Delta G^A = -RT \log_e K_A$ , and for oleic acid, which has a value of  $K_F$  close to that for palmitic acid due to the presence of the double bond (see Table II)  $K_F \approx \text{const.} \times 3^{18}$ . The corresponding value for  $C_4H_9OH$  would be  $K_F \approx \text{const.} \times 3^4$  (Traube's rule).

Thus  $C_B^A = C_B^F \times e^{(-\Delta G^F - \Delta G^A)/RT} = C_B^F \times 3^{12}$ .

From the minimum in the hydrolysis curve in the absence of alcohol,

$$C_B^F = 0.01 \times 5 \times 10^{-5} = 5 \times 10^{-7} \text{ M.}$$

Thus  $C_B^A = 5 \times 10^{-7} \times 3^{12} \text{ M} = 0.26 \text{ M} = 1.9 \%$ .

i.e. a 1.9 % solution of *n*-butyl alcohol should reduce the hydrolysis of sodium oleate at 25° C to 3.5 %. The experimental value found by Powney and Jordan is 1.8 %. The agreement is excellent considering the approximations made in the calculation, and it would seem that the general interpretation presented here is substantially correct.

We are indebted to Dr. G. S. Hartley for helpful discussions and to the D.S.I.R. for financial assistance to one of us (G.S.).

*Department of Colloid Science,  
Cambridge.*

## AN EMPIRICAL EQUATION FOR THE RESONANCE ENERGY OF POLYCYCLIC AROMATIC HYDROCARBONS

BY (THE LATE) P. G. CARTER

*Received 7th July, 1948; as revised 3rd February, 1949*

The Branch-Calvin relation between the corrected normal potential of an aromatic quinone and the number of Kekulé structures in the hydroquinone  $N_H$  and quinone  $N_Q$  is altered to the logarithmic form,

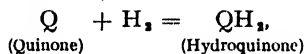
$$E_0(\text{corr.}) = 0.26 + 0.65 \ln N_H/N_Q.$$

From this an equation is derived for the resonance energy  $R$  of an aromatic, fused-ring hydrocarbon:

$$R/\beta = 0.6D + 1.5 \ln N - 1,$$

where  $D$  is the number of double bonds and  $N$  the number of Kekulé structures. A comparison with values of  $R/\beta$  calculated by the method of molecular orbitals shows that the equation is valid for bi- to undeca-cyclic hydrocarbons.

The possibility of a relation between the normal reduction potentials of aromatic quinones and the change of resonance energy in passing from the quinone to the hydroquinone has been discussed by Branch and Calvin,<sup>1</sup> Evans,<sup>2</sup> Berliner<sup>3</sup> and Diatkina and Syrkin;<sup>4</sup> all are agreed that such a relation should exist, but their methods of attack on the problem differ. In the reaction,



the oxidation-reduction potential  $e_0$  is given by

$$-n\mathbf{F}e_0 = \Delta G = \Delta H - T\Delta S, \quad (1)$$

all symbols having their usual thermodynamic meaning. As pointed out by the first authors,  $\Delta H$  can be considered to consist of two parts,  $\Delta H'$

<sup>1</sup> Branch and Calvin, *The Theory of Organic Chemistry* (New York, Prentice-Hall Inc., 1945).

<sup>2</sup> Evans, *Trans. Faraday Soc.*, 1946, **42**, 113.

<sup>3</sup> Berliner, *J. Amer. Chem. Soc.*, 1946, **68**, 49.

<sup>4</sup> Diatkina and Syrkin, *Acta Physicochim.*, 1946, **21**, 921.

which represents the change of the energy as calculated from accepted bond energy values, and  $\Delta R$  the resonance energy change. In the reduction of a series of quinones,  $\Delta S$  (which largely consists of the loss of the entropy of a mole of hydrogen gas) and  $\Delta H'$  are both approximately the same for each member. Accordingly, eqn. (1) may be approximately rewritten :

$$nFE_0 = k + \Delta R, \quad . \quad . \quad . \quad (2)$$

$k$  being a constant equal to  $\Delta H' - T\Delta S$ . Plausible values of  $\Delta H'$  and  $\Delta S$  for this reaction at 298° K indicate that  $k$  will be small. Branch and Calvin relate the change of resonance energy  $\Delta R$  to the function  $\frac{N_H - N_Q}{N_H + N_Q}$ , where  $N_H$  and  $N_Q$  are the number of Kekulé structures in the hydroquinone and quinone respectively. This function seems impossible to justify (it will be discussed below), but Branch and Calvin's plot of  $e_0$  against  $\frac{N_H - N_Q}{N_H + N_Q}$  is reasonably good, and after correcting the measured potential for steric and other effects ( $E_0$  (corr.)), surprisingly so. The whole range of available data for both *o*- and *p*-quinones of the mono- to penta-cyclic fused-ring systems fit into a relation of the form :

$$E_0(\text{corr.}) = a + b \left( \frac{N_H - N_Q}{N_H + N_Q} \right). \quad . \quad . \quad . \quad (3)$$

Evans<sup>2</sup> calculates  $\Delta R$  by the method of molecular orbitals on the assumption of localization of bonds, a procedure also used by Diatkina and Syrkin,<sup>4</sup> and obtains linear relations with  $E_0$ , the lines for *o*- and *p*-quinones being parallel. This method necessitates the calculation of the resonance energy for the hydrocarbon residue corresponding to each quinone and hydroquinone.

Berliner<sup>3</sup> has confirmed eqn. (2) by using for  $\Delta R$  the difference in empirical resonance energies obtained from combustion data, and finds that the plot of  $e_0$  against  $\Delta R$  for the range benzoquinone to anthraquinone is a straight line passing through the origin.

**The Change of Resonance Energy in a Reaction.**—There can be no doubt of the validity of eqn. (2), yet Branch and Calvin's formulation of  $\Delta R$  cannot be reconciled with it; there is no way in which  $\frac{N_H - N_Q}{N_H + N_Q}$  can be separated (as it must be, since  $\Delta R = R_H - R_Q$ ) into two terms involving separately  $N_H$  and  $N_Q$ . The difficulty is resolved by the following considerations.

In an aromatic hydrocarbon consisting of two portions linked by a single-bond or a resonance-blocking group (for example, diphenyl) the resonance energy is approximately the sum of the resonance energies of the component rings, but the number of Kekulé structures is the product; this suggests that if the resonance energy of an aromatic hydrocarbon is a function of the number of Kekulé structures, that function must be a logarithmic one. In addition resonance energy is known to increase approximately linearly with an increase in the number  $D$  of carbon-carbon double-bonds (cf. the polyenes<sup>5</sup>) and the possibility arises that the resonance energy of a fused-ring, aromatic hydrocarbon may be expressed by an empirical equation of the form,

$$R = a + bD + c \ln N \quad . \quad . \quad . \quad (4)$$

For the resonance energy of a hydroquinone we will set

$$R_H = a_H + bD_H + c \ln N_H, \quad . \quad . \quad . \quad (5)$$

that is, the resonance energy of a hydroquinone is equal to the resonance energy of the corresponding hydrocarbon,

$$R = a + bD + c \ln N,$$

<sup>5</sup> Lennard-Jones and Coulson, *Trans. Faraday Soc.*, 1939, **35**, 811.

plus an increment (independent of both  $D$  and  $N$ ) equal to  $a_H - a$ ; such increment including both the extra resonance due to the presence of the hydroxy groups and any steric or inductive effects which arise from the structure of the hydroquinone. Similarly, for each quinone,

$$R_Q = a_Q + bD_Q + c \ln N_Q, \quad (6)$$

where  $D_Q$  refers to the number of carbon-carbon double bonds and  $N_Q$  the number of Kekulé structures in the hydrocarbon resulting from omission of the  $C=O$  groups from the structure of the quinone. Thus both  $a_H$  and  $a_Q$  will be expected to vary from substance to substance, whereas  $b$  and  $c$  should be constant.

From eqn. (2), (5), and (6) :

$$k + \Delta R = nF e_0 = k + (a_H - a_Q) + b(D_H - D_Q) + c \ln N_H/N_Q,$$

or 
$$E_0 - \frac{(a_H - a_Q)}{nF} = \frac{b'}{nF} + \frac{c}{nF} \ln \frac{N_H}{N_Q}, \quad (7)$$

since  $D_H - D_Q = 1$  (and  $b'$ , the new constant,  $= k + b$ ). The second term on the left-hand side of (7) is in the nature of a correction to the normal potential for the effects mentioned above; lack of data prevents its evaluation, but the assumption that it is equal to the correcting factor used by Branch and Calvin is justified by the results below. Eqn. (7) written as

$$E_0 (\text{corr.}) = \frac{b'}{nF} + \frac{c}{nF} \ln \frac{N_H}{N_Q} \quad (8)$$

is confirmed by the good fit to a straight line obtained by plotting  $E_0$  (corr.) against  $\log N_H/N_Q$ : from the data of Table I the values of the coefficients

TABLE I  
From Branch and Calvin<sup>1</sup>

Quinone	$N_H$	$N_Q$	$e_0$	$E_0$ (corr.)
<i>p</i> -Benzo . . . . .	2	1	0.71	0.71
$\alpha$ -Naphtha . . . . .	3	2	0.48	0.53
1 : 4-Anthra . . . . .	4	3	0.40	0.45
9 : 10-Anthra . . . . .	4	4	0.15	0.25
1 : 4-Phenanthra . . . . .	5	3	0.53	0.61
1' : 2'-Benzanthra . . . . .	7	6	0.23	0.36
1' : 2' : 5' : 6'-Dibenzanthra . . . . .	12	9	0.27	0.42
<i>o</i> -Benzo . . . . .	2	1	0.81	0.71
$\beta$ -Naphtha . . . . .	3	2	0.58	0.51
9 : 10-Phenanthra . . . . .	5	4	0.46	0.41
1 : 2-Phenanthra . . . . .	5	3	0.66	0.59
3 : 4-Phenanthra . . . . .	5	3	0.62	0.57
1 : 2-Anthra . . . . .	4	3	0.49	0.42
1' : 2'-Benzanthra-3' : 4' . . . . .	7	6	0.43	0.38
Chrysene . . . . .	8	6	0.47	0.45
Picene . . . . .	13	10	0.47	0.45

$b'/nF$  and  $c/nF$  are found (least squares) to be 0.259 and 0.648 respectively, the standard errors being 0.008 and 0.02. The final form of the equation for the corrected potential is therefore

$$E_0 (\text{corr.}) = 0.26 + 0.65 \ln N_H/N_Q. \quad (9)$$

Eqn. (9) gives results as good as those from Branch and Calvin's relation, and is superior in that the term involving  $N_H$  and  $N_Q$  may be expressed as a difference of a function of the variables.

A possible explanation of the success of the form

$$(N_H - N_Q)/(N_H + N_Q)$$

may lie in the result of expansion of a logarithm as a series :

$$\ln x = 2(x - 1)/(x + 1) + \dots ;$$

for

$$x = N_H/N_Q$$

this first term becomes

$$2(N_H - N_Q)/(N_H + N_Q).$$

**The Resonance Energy of Fused-ring Aromatic Hydrocarbons.**

—The values of  $b/nF$  and  $c/nF$ , found from the reduction potential relation, when multiplied by  $nF$  and inserted in (4) give

$$R = a + 11.987D + 29.968 \ln N \text{ kcal.} \quad (10)$$

The value of the constant  $a$  must be determined from empirical resonance energies, and of the three known sets<sup>6, 10</sup> the value of 36.0 kcal. for benzene ( $D = 3$ ,  $N = 2$ ), derived from Kistiakowsky's work on hydrogenation, has been selected. The resulting value of  $a$  is  $-20.732$  kcal., and the equation for the resonance energy,

$$R = -20.732 + 11.987D + 29.968 \ln N.$$

This may be re-expressed, with negligible extra error, as

$$R = 20.0 (0.6D + 1.5 \ln N - 1) \quad (11)$$

The coefficient outside the parentheses is approximately equal to the value in kcal. of the resonance integral  $\beta$  so that finally :

$$R/\beta = 0.6D + 1.5 \ln N - 1. \quad (12)$$

This equation was derived in 1944, but until recently data were lacking for making a comprehensive check of its accuracy; the required data are

TABLE II

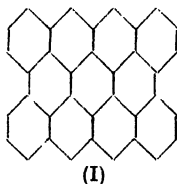
Hydrocarbons	D	N	R/ $\beta$				
			Empirical Eqn. (12)	Syrkin and Diatkina	Bradburn, Coulson and Rushbrooke	Combustion Data	
						(a) Wheland, <sup>6</sup> Chap. 3, Table 6 $\beta = 22.3$ kcal.	(b) Dewar <sup>10</sup> $\beta = 17.2$ kcal.
Naphthalene . . .	5	3	3.65	3.68	3.73	3.45	3.60
Anthracene . . .	7	4	5.28	5.32	5.21	5.20	5.12
Phenanthrene . . .	7	5	5.61	—	—	5.83	—
Naphthacene . . .	9	5	6.81	6.94	6.68	—	—
Chrysene . . .	9	8	7.52	7.20	—	7.31	—
Pyrene . . .	8	6	6.49	6.48	—	6.82	—
Triphenylene . . .	9	9	7.70	7.24	—	—	—
Perylene . . .	10	9	8.30	8.24	8.11	—	—
Dibenzanthracene . . .	11	12	9.33	8.92	—	—	—
Pentacene . . .	11	6	8.29	8.54	8.14	—	—
Hexacene . . .	13	7	9.72	10.12	9.58	—	—
Heptacene . . .	15	8	11.1	—	11.03	—	—
Coronene . . .	12	20	10.7	10.64	10.56 <sup>8</sup>	—	—
Chalkacene . . .	15	27	12.9	—	12.56	—	—
meso-Naphthdi- anthrene . . .	14	16	11.6	—	11.66	—	—
Octacene . . .	17	9	12.5	—	12.48	—	—

<sup>6</sup> Wheland, *Theory of Resonance* (New York, Wiley and Sons, 1944).

contained in a paper by Syrkin and Diatkina,<sup>7</sup> and in one (in press) by Bradburn, Coulson and Rushbrooke; the molecular-orbital method is used in both cases. These two sets of resonance energies, and three calculated by eqn. (12) are compared in Table II. Bradburn, Coulson and Rushbrooke's values (in terms of a resonance integral  $\gamma$ ) have been obtained in terms of  $\beta$  by multiplication by two.

The last two columns of Table II list values of  $R/\beta$  from combustion data, (a) from figures given by Wheland,<sup>8</sup> and (b) from a publication by Dewar;<sup>10</sup> to reconcile the results with one another and with the values of  $R/\beta$  calculated by the molecular-orbital method, it is necessary to have different values of the resonance integral for the two cases; these have been taken as 22.3 and 17.2 kcal. respectively. The latter value is that used by Syrkin and Diatkina.<sup>7</sup>

Good agreement is obtained throughout the range from bicyclic naphthalene to the three octacyclic compounds at the bottom of Table II, and this agreement extends as far as the undecacyclic hydrocarbon (I).



For substances having an increasing number of rings over eleven agreement becomes progressively less satisfactory; this is of no practical disadvantage, because such substances (even if they are known) are rarely or never encountered. A statistical examination of the material has shown that the standard deviation of the empirical and calculated values of  $R/\beta$  (Table II, columns 5-8) about the empirical equation

$$R/\beta = 0.6D + 1.5 \ln N - 1$$

is 0.207. The constants in this empirical equation are derived from the constants of eqn. (9) which are calculated from empirical data, and are therefore subject to error. The effect of these errors on the values of  $R/\beta$  obtained from the equation is not large compared with the standard error of 0.207 about the empirical equation, as shown by the following selected values:

Anthracene	( $N = 4, D = 7$ ): $\sigma(R/\beta) = 0.050$ ;
Dibenzanthracene	( $N = 12, D = 11$ ): $\sigma(R/\beta) = 0.087$ ;
meso-Naphthdianthrene	( $N = 16, D = 14$ ): $\sigma(R/\beta) = 0.131$ .

The combined standard error when using the empirical equation to estimate  $R/\beta$  for the above three selected hydrocarbons is, respectively, 0.213, 0.224, and 0.245.

Eqn. (12) does not apply to ring systems containing other than six-membered rings, nor is it applicable to polyphenyl types without modification to allow for the extra resonance energy due to coupling of the phenyl residues. It is surprising that satisfactory results are obtained by using only Kekulé structures, particularly in view of Pullman's calculations,<sup>9</sup> which show that in the series of linear ring hydrocarbons the Kekulé structures become less and less important compared with excited structures as the number of rings increases.

**Applications of Eqn. (12).**—From eqn. (1) and (12):

$$\Delta G = \Delta H' - T\Delta S - 20.0(0.6\Delta D + 1.5 \ln N_2/N_1).$$

<sup>7</sup> Syrkin and Diatkina, *Acta Physicochim.*, 1946, **21**, 641.

<sup>8</sup> Coulson, *Nature*, 1944, **154**, 797.

<sup>9</sup> (Mde.) Pullman, *Thesis* (University of Paris, Masson et Cie, 1946).

<sup>10</sup> Dewar, *Trans. Faraday Soc.*, 1946, **42**, 767.



This equation has been applied to the elucidation of various observations in the polycyclic aromatic series, for example hydrogenation, oxidation, isomerization, Diels-Alder additions, and nucleophilic reactions of ketones, and it is intended to publish such applications in the near future.

The author's thanks are due to Prof. M. G. Evans, F.R.S., and to Prof. C. A. Coulson for helpful discussions, and to the latter for his kind permission to refer to the results of unpublished molecular-orbital calculations; also to a number of colleagues, including Dr. O. L. Davies, for his statistical calculations.

*Imperial Chemical Industries Ltd.,  
Research Laboratories,  
Hexagon House,  
Manchester, 9.*

---

## REVIEWS OF BOOKS

**Elasticity and Anelasticity of Metals.** BY CLARENCE M. ZENER.  
(University of Chicago Press, in the U.S.A.; Cambridge University Press, in Great Britain and Ireland.) Pp. ix + 170. Price 22s. 6d. net.

"*Anelasticity* has been chosen to denote that property of solids in virtue of which stress and strain are not single-valued functions of one another in that low stress range in which no permanent set occurs and in which the relation of stress to strain is still linear"—that defines what this book is mainly about. Elasticity is disposed of in a valuable summary of thirty pages. This starts immediately with crystal elasticity, but preserves simplicity by concentrating on the case of cubic symmetry. The author then turns to anelasticity. The elastic after-effect was made a scientific topic by Weber in 1825: it became a favourite subject of learned theory about fifty years later and the mathematical methods devised by Boltzmann and others then have been repeatedly rediscovered ever since: spring-and-dashpot analogues, first devised by Poynting and Thomson, have also suffered subsequent elaboration, without much gain in understanding. Zener is too good a scholar to waste time in such distractions: his account of the formal theory is brief and to the point, and his main contribution here is a presentation which is not restricted, for example, to the case that only a small fraction of the stress relaxes. The review of methods of measurement covers only eight pages, constituting a briefly critical index to the literature. Chapter VII, "Physical Interpretation of Anelasticity," covers the remaining three-fifths of the book.

The sort of physical explanations dealt with are most concisely indicated by the frontispiece, "A typical relaxation spectrum," which shows six damping maxima in the frequency range  $10^{-12}$  to  $10^6$  sec.<sup>-1</sup>, attributed to intercrystalline thermal currents (peak frequency  $10^5$ ), transverse thermal currents ( $10^2$ ), interstitial solute atoms ( $10^{-1}$ ), twin boundaries ( $10^{-5}$ ), the grain boundary ( $10^{-8}$ ) and pairs of solute atoms ( $10^{-12}$ ). Such a frequency as  $10^{-12}$  sec.<sup>-1</sup> is naturally an extrapolated one: the temperature dependence of a relaxation frequency is of course one of the most important facts about it, besides providing a means of

simplifying its observation. This is an imaginary case, but there is no doubt of the separate reality of the phenomena, several of which are the discovery of Zener and his school. Those at the higher frequencies are explained beyond dispute. One can query the detail of some of the interpretations for the "mechanical" band of frequencies below  $10^{-1}$ . Here Zener diverges rather widely from current English thought, in attributing small importance to dislocations: his preference is for a picture of "viscous-like behaviour" in slip-bands and in grain boundaries. This divergence would be entirely acceptable, if he would distinguish a little more clearly between "These experiments are explicable by this theory" and "These experiments conclusively prove the truth of this theory." However, the closing sections of Chapter VII are clearly meant to be somewhat speculative and controversial. The reviewer has the hardihood to think that some of these sections may be significantly different by the time the author writes his next edition; if so, that will indicate progress to which Zener, and this little book, have been major contributors.

F. C. F.

**Physical Aspects of Colour** BY P. J. BOUMA. (Philips, Eindhoven, 1947.) Pp. 312.

The late Dr. Bouma was an illuminating engineer who wrote this, book in a foreign language, during the closing phase of an incurable disease, and under the shadow of the German occupation. It is, therefore, not surprising that he has disdained the prevailing fashion of endeavouring to establish a bubble reputation for brilliance by shining his light into the observer's eyes, but has chosen rather to direct it on to his subject. The vague hinterland between objectivity and subjectivity is lit up by his clarity and sincerity of approach, in the reconciliation of the apparently objective Newtonian analysis of colour with the subjective attitude of the Goethe philosophy, in which the observer's eye, with its limited trichromatic sensibility, replaces Newton's sun as the central point of the universe.

The content of the book is well defined by the sub-title, "An Introduction to the study of Colour Stimuli and Colour Sensations."

S. M. N.

**Symposium on Internal Stresses in Metals and Alloys.** Published by the Institute of Metals. Pp. viii + 485.

This book contains a collection of 36 papers presented to the Institute of Metals in October 1947, on various aspects of internal stresses in metals and alloys. The papers are classified into the measurement, origin, control, removal and effects of these stresses, presenting the reader with a comprehensive account of the present state of knowledge on this subject, and should be of great value to engineers, metallurgists and physicists. The theme running throughout the book is admirably expressed by Prof. Hugh O'Neill, who introduces his paper with the comment "Residual stresses, like fire and water, are good servants, but bad masters".

Papers on the measurement of internal stress by mechanical, magnetic, electrical and X-ray methods are included, and it is apparent from the work of Dr. W. A. Wood, Dr. H. Lipson, Mr. D. E. Thomas and Mr. G. B. Greenough that a precise interpretation of the relation between internal stress and X-ray line broadening is still a matter of controversy. The increased strain resistance of metals obtained by shot-peening and autofrettage, which processes pre-stress the material, are important advances which are likely to be increasingly developed. The origin and nomenclature of internal stresses are considered by Dr. E. Orowan and Prof. F. C. Thompson, and Lazlo's theoretical papers critically reviewed by Mr. F. R. N. Nabarro. It is shown that internal stresses exist as a result of differences of thermal expansions of separate phases. Boas' and Honeycomb's work on the plastic deformation obtained by submitting non-cubic metals to thermal cycles is summarized by Dr. F. P. Bowden. It is of interest to point out here that similar effects have been found with iron, a cubic metal, when the thermal cycles are at the  $\gamma$ - $\alpha$  transformation temperature.

An invaluable feature of many of the papers is the attention drawn to problems on which much work still requires to be done. The formula derived by Sir Lawrence Bragg,  $\gamma = 5.5 s/t$ , where  $\gamma$  is the elastic limit of strain,  $s$  the interatomic distance, and  $t$  the mean glide distance during deformation, can only be checked when the order of magnitude of  $t$  is known. Similarly, it is pointed out by Prof. J. H. Andrew and Dr. H. Lee that a complete understanding of hydrogen embrittlement must depend on further knowledge of crystallite sizes and mosaic blocks, to be associated with the  $t$  of Bragg's equation. The important problem of calculating the stresses in large masses of steel cooling from the austenitic region has been carried out by Mr. J. E. Russell. This author indicates that because of the meagre data available, no precise figures are obtainable. Heat emission and volumetric changes during transformation and the rheological behaviour of iron at high temperatures were largely unknown.

The work of Dr. E. Orowan and Mr. J. F. Nye on transparent polycrystalline material observed under strain with a polarizing microscope might well have been included as a complete paper, for this elegant technique for observing and measuring stresses should prove to be of great value in assessing physical theories. The suggestion of Mr. D. O. Sproule for the development of ultrasonic methods of measuring internal stress is worthy of serious consideration. Such a method has the dual advantage of being non-destructive and of exploring the metal in depth. Finally, it would have been worth while to include a subject index, for the papers presented form an invaluable reference work on the subject of internal stress in metals.

J. S.

**Electrons, Atoms, Metals and Alloys.** BY W. HUME-ROTHERY.  
(The Louis Cassier Co. Ltd., 1948.) Pp. vii + 371. Price 25s.

The price of the above book, reviewed in the *Trans. Faraday Society*, 1949, 45, 303, was erroneously given as 30s. The published price is 25s. and, in consequence, the statement that "the book, being of the more 'popular' type, should, it is felt, be priced more moderately," is regretted and withdrawn.

# DIELECTRIC LOSS IN SWOLLEN RUBBER

By A. SCHALLAMACH AND P. THIRION

*Received 19th January, 1949*

It is shown experimentally that the dielectric loss-tangent curves of swollen vulcanized rubbers as function of the temperature have one maximum if the swelling agent is non-polar but two maxima if it is polar. Rubber swollen in polar solvent differs therefore in its dielectric behaviour from polar liquid mixtures which have in general only one loss-tangent maximum<sup>1</sup> and it is suggested that this difference is due to the chain structure of the rubber.

In a recent paper,<sup>1</sup> it was shown that binary polar mixtures containing only non-associated, or only associated, liquids have normal loss-factor against temperature curves with one clear maximum. On the other hand, the dielectric characteristics of mixtures of a non-associated and an associated liquid are not normal, and their loss-factor curves have two well-marked maxima when the dielectric losses in the two components are comparable. It was deduced from these findings: (1) that dielectric relaxation involves a relatively large volume, and (2) that mixtures of a non-associated and an associated liquid are inhomogeneous on the molecular scale.

Vulcanized rubber and other high polymers behave dielectrically like liquids with a long relaxation time, as far as can be judged by the frequency- and temperature-dependence of their dielectric constants. If the analogy is complete, vulcanized rubber swollen in polar solvents should behave dielectrically like a liquid mixture but the experiments reported here show that in fact rubber swollen in polar solvents exhibits invariably two loss-tangent maxima. These results contradict the findings of Alexandrov and Dzhan<sup>2</sup> who obtained only one maximum in the system rubber-bromobenzene.

## Experimental

The measurements were carried out at frequencies from 100 kc./sec. to 40 Mc./sec., using a resonance method. As this band is too small to cover the frequency dispersion range, we measured, as a rule, the temperature dispersion at different constant frequencies. The rubber samples were put into a small, shielded, parallel-plate condenser which fitted into the thermostat described in an earlier communication<sup>3</sup> where also details of the experimental method are given. Measurements could be made at temperatures from  $-180^{\circ}\text{C}$  to  $+70^{\circ}\text{C}$ . As the dimensions of the rubber changed considerably in such a wide temperature range we determined only the loss-tangents in the calculation of which the dimensions of the sample cancel out.

Most of the experiments were made with a vulcanizate of natural rubber compounded as follows: Crepe 100, S 3, ZnO 2, accelerator 0.3, and cured at  $142^{\circ}\text{C}$  for 30 min. Some measurements were made with a cured Neoprene of the following composition: Neoprene GN 100, stearic acid 0.75, MgO 4, ZnO 1, accelerator 0.5, antioxidant 2 and cured for 30 min. at  $142^{\circ}\text{C}$ . The swelling agents were: *n*-heptane, medicinal paraffin, isoamyl bromide, bromobenzene, di-*n*-butyl ether, all of which were commercial products, and di-geranyl ether which was kindly made for us by Dr. Naylor. These liquids, with the

<sup>1</sup> Schallamach, *Trans. Faraday Soc.*, 1946, **42A**, 180.

<sup>2</sup> Alexandrov and Dzhan, *Tech. Phys. U.S.S.R.*, 1938, **5**, 836.

<sup>3</sup> Schallamach, *Trans. Faraday Soc.*, 1946, **42**, 495.

exception of bromobenzene, were chosen because they do not crystallize at low temperatures. Special care was taken to ensure that equilibrium between solvent and rubber had been established before measurements were begun. The swollen samples were left for at least 24 hr. in nitrogen, at room temperature with the mobile solvents and at 60° C with medicinal paraffin and di-geranyl ether.

## Results

Fig. 1 shows the influence of the imbibition of non-polar solvents on the loss-tangent of vulcanized rubber. The curves are in all cases displaced towards lower temperatures as compared with the dry rubber but the effect of

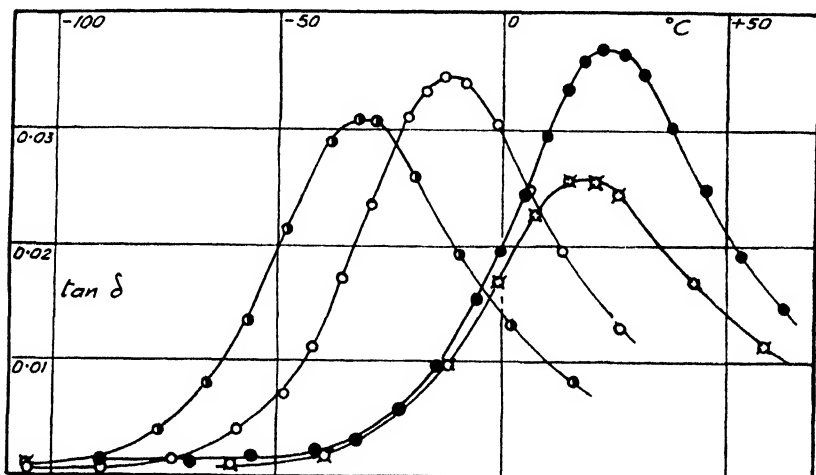


FIG. 1.—Loss-tangent of vulc. nat. rubber dry (●) and swollen with 28.7 % of *n*-heptane (○), with 58 % of *n*-heptane (◐) and with 60 % of med. paraffin (△) at 4.4 Mc./sec. against temperature °C.

medicinal paraffin is small in this respect. As for the height of the peaks, it should be remembered that the dielectric loss in the swollen rubber is, of course, smaller but that for a given concentration of dipoles the maximum will be the larger the lower the temperature at which it occurs.

Fig. 2 shows loss-tangent curves of rubber with different concentrations of isoamyl bromide. This graph indicates two dispersion regions, most clearly so for the sample containing 30.8 % by volume of the bromide. At this frequency,  $\tan \delta$  for the pure liquid has its maximum at about  $-120^{\circ}\text{C}$ . The relative heights and position of the maxima show that the peak at the higher temperatures is associated with the rubber, and the low-temperature peak with the solvent. The heights of the maxima are temperature-dependent as seen in Fig. 3 where dispersion curves at two different frequencies are given for a constant concentration of 30 % bromide. The rubber peak becomes more pronounced at lower temperatures and frequencies. This is the normal trend in dielectric measurements, but the solvent-maximum becomes at the same time lower and broader. We do not think that this abnormal frequency dependence is in any way a peculiarity of the rubber because it can be observed in other viscous mixtures. We found, for example, that a mixture containing 70 % medicinal paraffin and 30 % isoamyl bromide gave the following loss-factor maxima:

Frequency (kc./sec.)	Temp. (°C)	Loss-factor
8540	— 89	0.313
100	— 117	0.239

The effect may be due to a temperature-dependent distribution of relaxation times.

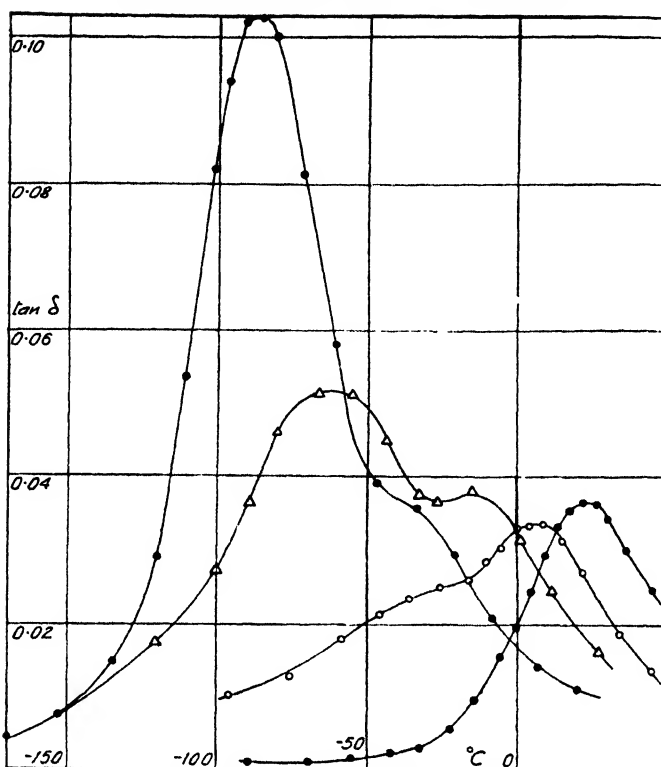


FIG. 2.—Loss-tangent of vulc. nat. rubber dry (●) and swollen with 11.6 % (○), 30.8 % (△) and 61.8 % (◐) of isoamyl bromide at 4.4 Mc./sec. against temperature °C.

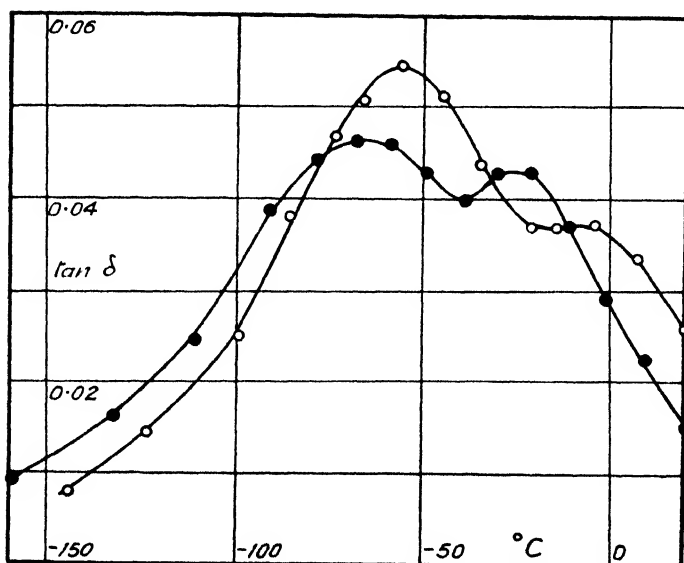


FIG. 3.—Loss-tangent of vulc. nat. rubber swollen with 30 % of isoamyl bromide at 9.2 Mc./sec. (○) and at 1.18 Mc./sec. (●) against temperature °C.

In order to satisfy ourselves that the irregularities of the loss-tangent curves are not simply due to the temperature variation, we determined in this one case the frequency dispersion at constant temperature. The result, as shown in Fig. 4, although not giving the complete dispersion range, confirms the existence of a double maximum.

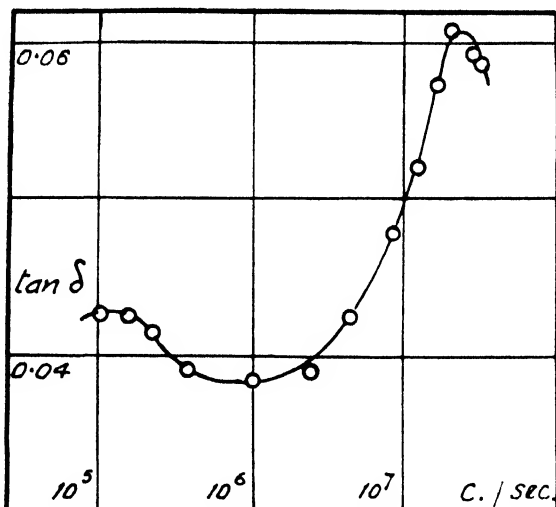


FIG. 4.—Loss-tangent of vulc. nat. rubber with 26 % of isoamyl bromide at a constant temperature of  $-36^{\circ}\text{C}$  against frequency.

Measurements with bromobenzene as solvents were difficult because this liquid crystallized out at even moderately low temperatures but it was possible to show (Fig. 5) that there are again two maxima of the loss-tangent. Hysteresis

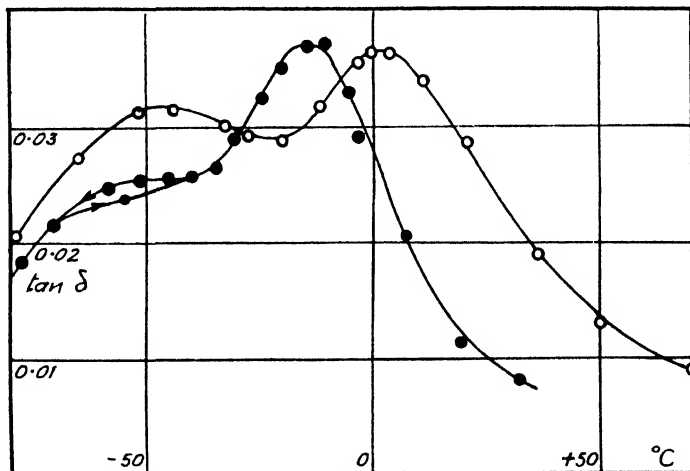


FIG. 5.—Loss-tangent of vulc. nat. rubber swollen with 27.6 % of bromobenzene at 8.90 Mc/sec. (O) and at 1.48 Mc/sec. (●) against temperature  $^{\circ}\text{C}$ .

found between measurements with falling and with rising temperature is indicated by the arrows in the curve for 1.48 Mc/sec. and is obviously due to crystallization. The system rubber-bromobenzene was not studied in detail, but our data do not bear out the findings of Alexandrov and Dzhan<sup>2</sup> as mentioned above.

Results obtained with di-*n*-butyl ether are given in Fig. 6. The ether being less polar than *iso*amyl bromide, its influence is not very marked when present in a low concentration; there is, however, another effect which is best seen at low concentrations and consists in a small maximum at rather low temperatures,

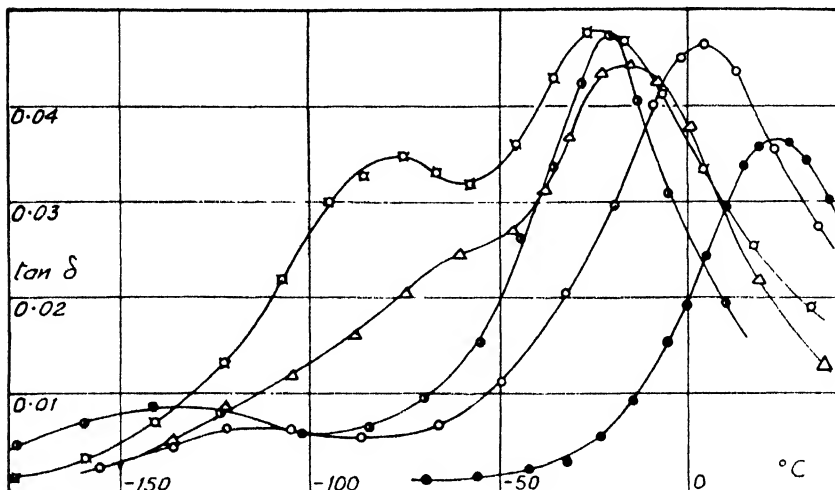


FIG. 6.—Loss-tangent of vulc. nat. rubber dry (●) and swollen 19.4 % (○), 42.5 % (Δ) and 66 % (□) of di-butyl ether at 4.4 Mc./sec., and with 19.4 % at 0.23 Mc./sec. (●) against temperature °C.

i.e.  $-114^{\circ}\text{C}$  at 4.4 Mc./sec. and  $-140^{\circ}\text{C}$  at 0.23 Mc./sec. This new maximum disappears, or is masked, at higher concentrations where the loss-tangent curves become similar to those of the bromides.

Fig. 7 gives the loss-tangent curves of the system rubber-digeranyl ether

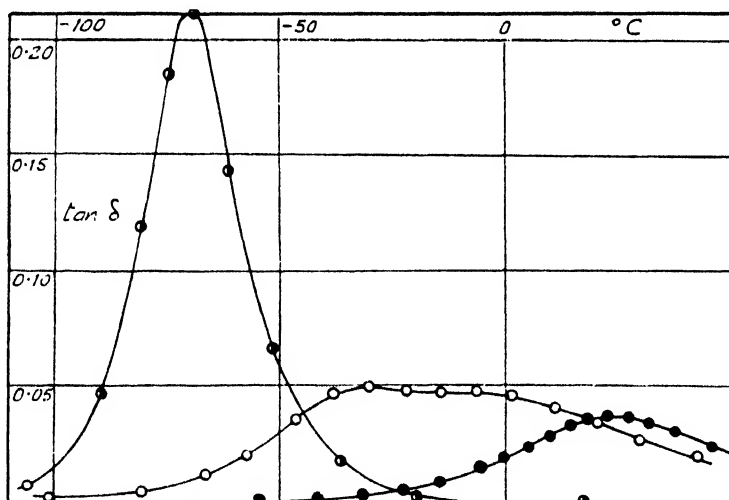


FIG. 7.—Loss-tangent of vulc. nat. rubber (●), of di-geranyl ether (●) and of the rubber swollen with 58 % of the ether (○) at 4.4 Mc./sec. against temperature °C.

and of the pure ether. A rather high volume fraction was used because the dielectric constant of this ether is low and it would not show up very well in lower concentrations. There appear to be two maxima although the resolution is not very good because of the proximity of the original peaks.



Finally, we give in Fig. 8 the dielectric losses in Neoprene, and in Neoprene swollen by 51 % of *isoamyl* bromide. Neoprene is, of course, strongly polar so that a high volume fraction of the bromide was necessary. The figure shows

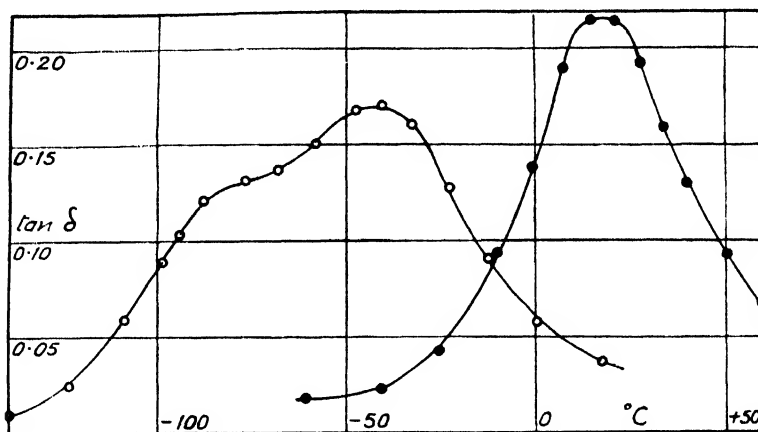


FIG. 8.—Loss-tangent of cured Neoprene (●) and of Neoprene swollen with 51 % of *isoamyl* bromide (○) at 4.4 Mc./sec. against temperature °C.

that the effect of the solvent on this synthetic rubber is essentially the same as on natural rubber, with the only difference that the losses in the Neoprene are larger than in the bromide.

### Discussion

Whatever the solvent, the loss-tangent curves of swollen rubber have at least one maximum which must be attributed to the rubber itself. This maximum is shifted towards lower temperatures by an amount which depends on the molecular weight, and so on the viscosity, of the solvent. This is shown graphically in Fig. 9 where logarithms of the dielectric relaxation time  $\tau$  ( $= 1/2\pi$  frequency) are plotted against the reciprocal of the absolute temperature at which the rubber-maxima occur. It will be seen that heptane and *isoamyl* bromide have approximately the same effect for the same degree of swelling but that the displacement of the peak becomes less as one progresses to liquids of higher molecular weight until one reaches medicinal paraffin which has very little effect. Mobile solvents increase therefore the mobility of the rubber-dipoles, and in their action they are similar to plasticizing agents, such as diphenyl, in polyvinyl chloride and other high polymers.

The appearance of a second maximum when the solvent is polar shows that rubber- and solvent-dipoles move independently. Although these curves look very much like the loss factor curves of non-homogeneous liquid mixtures,<sup>1</sup> there is little reason to assume that the effect is here due to a non-random distribution of the solvent. All the liquids which we used are good swelling agents, the internal energy-changes accompanying swelling are very small and the plasticizing action of the solvents can only be understood as brought about by random distribution. We might also point out that the solvents in swollen rubber are subject to the reverse of plasticization in that their loss-tangent maxima are brought by the rubber to much higher temperatures than those of the pure liquids. The only case where there is a suspicion of inhomogeneity is rubber swollen in di-*n*-butyl ether. The pure liquid relaxes with a frequency of 20 Mc./sec. at  $-114^{\circ}\text{C}$  so that the small maximum occurring below  $-100^{\circ}\text{C}$  when the concentrations are low (Fig. 6) suggest that there

was some free ether in the system but it is possible that this was due to the freezing-out of liquid at low temperatures.

Having ruled out inhomogeneity as an explanation of the two maxima their existence could be explained as a concentration effect. Assuming that each S atom forms one dipole, one has only one dipole to each 16 isoprene units in a rubber containing 3 % of combined S. The average distance between these dipoles is comparatively large even if the rubber is only lightly swollen, and it is possible that rubber- and solvent-dipoles cannot relax simultaneously because the zone involved in dielectric relaxation is too small. This effect must show up at a certain degree of dipole dilution but it cannot wholly account for our results because it does not explain the two maxima of swollen Neoprene (Fig. 8) where the dipole concentrations are of the same order of magnitude as in some liquid mixtures which exhibit only one relaxation mechanism.<sup>1</sup>

We suggest that the two relaxation mechanisms in swollen rubbers are a specific effect of the chain structure of the rubbers. The chain structure imposes an additional restriction on the motion of rubber dipoles and it appears that the relaxation of a rubber dipole is conditioned by another type of activation than that of liquid dipoles.

We wish to thank Dr. R. F. Naylor for having prepared for us the digeranyl ether.

The work reported above forms part of the programme of fundamental research undertaken by the Board of the British Rubber Producers' Research Association.

*The British Rubber Producers' Research Association,  
Tewin Road,  
Welwyn Garden City,  
Herts.*

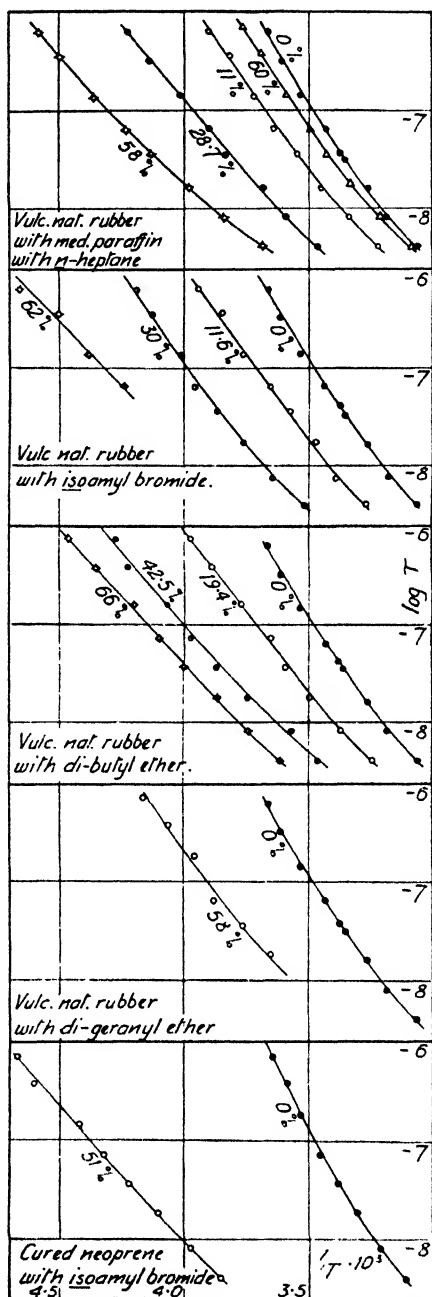


FIG. 9.  $\log \tau = f(1/T)$  for nat. rubber and Neoprene swollen with the indicated percentages of solvent.

In the uppermost section of the figure:  $\Delta$  denotes vulcanized natural rubber swollen with medical paraffin and  $\circ$   $\bullet$   $\times$  with *n*-heptane.

# TABLES OF OSMOTIC AND ACTIVITY COEFFICIENTS OF ELECTROLYTES IN AQUEOUS SOLUTION AT 25° C

By R. A. ROBINSON AND R. H. STOKES.\*

Received, 25th January, 1949

The concluding part<sup>1</sup> of *A Thermodynamic Study of Bivalent Metal Halides in Aqueous Solution* contained tables of the osmotic and activity coefficients of 45 electrolytes of 2-1 and 1-2 valency type. The values were based on isopiestic data and had all been recalculated to conform to the most recent values of the four reference electrolytes on which the interpretation of the isopiestic data depended, viz., sodium and potassium chloride,<sup>2</sup> calcium chloride and sulphuric acid.<sup>1, 3, 4</sup> As considerable effort has been expended on obtaining values for these four electrolytes, it is our hope that they are reliable and not likely to require substantial modification; it should therefore be of use to compile tables of the osmotic and activity coefficients of electrolytes of other valency types, also recalculated to be consistent with the data for the four reference electrolytes and with the data for the 1-2 and 2-1 salts. Tables have been given by Lewis and Randall<sup>5</sup> and by Guggenheim<sup>6</sup> (most of the data relating to the freezing point) and, more recently, by Harned and Owen,<sup>7</sup> but the tables given in this paper are more extensive and consist mainly of data which have been revised in the light of recent knowledge of our reference electrolytes.

**Definitions.**—If an electrolyte in aqueous solution at a stoichiometric concentration  $m$  (in mole/1000 g. water), dissociates into  $\nu$  ions of which  $\nu_+$  are cations and  $\nu_-$  anions, the mean ionic molality is defined by

$$m_{\pm} = (\nu_+^{\nu_+} \nu_-^{\nu_-})^{1/\nu} m, \quad . \quad . \quad . \quad . \quad (1)$$

and the "practical" activity coefficient is defined by

$$\bar{G} = \bar{G}_m^0 + \nu RT \ln \gamma_{\pm} m_{\pm}, \quad . \quad . \quad . \quad . \quad (2)$$

$\bar{G}$  being the partial molal free energy (per mole electrolyte) and  $\bar{G}_m^0$  the free energy in a standard state so chosen that  $\gamma_{\pm} \rightarrow 1$  as  $m_{\pm} \rightarrow 0$ .

There is also a "rational" activity coefficient defined by

$$\bar{G} = \bar{G}_N^0 + \nu RT \ln f_{\pm} N_{\pm} \quad . \quad . \quad . \quad . \quad (3)$$

$N_{\pm}$  being the mean ionic mole fraction,

$$N_{\pm} = m_{\pm} / (55.51 + \nu m). \quad . \quad . \quad . \quad . \quad (4)$$

The two activity coefficients are related by

$$\ln f_{\pm} = \ln \gamma_{\pm} + \ln (1 + 0.018 \nu m). \quad . \quad . \quad . \quad . \quad (5)$$

Similarly there is a "practical" osmotic coefficient  $\phi$  defined in terms of the partial molal free energy of the solvent by

$$\bar{G}_{H_2O} = \bar{G}_{H_2O}^0 - \phi RT \nu m / 55.51, \quad . \quad . \quad . \quad . \quad (6)$$

\* Imperial Chemical Industries Fellow, University of Cambridge.

and a "rational" osmotic coefficient  $g$  given by

$$\bar{G}_{\text{H}_2\text{O}} = \bar{G}_{\text{H}_2\text{O}}^0 + gRT \ln N_{\text{H}_2\text{O}} \quad (7)$$

where  $N_{\text{H}_2\text{O}} = 55.51/(55.51 + \nu m)$ .

The two osmotic coefficients are related by

$$g = \phi(1 + 0.009 \nu m) \quad (8)$$

Unlike eqn. (5), eqn. (8) is only an approximation but the error introduced is not larger than the experimental errors of measurement; thus, even at  $\nu m = 8$ , eqn. (8) gives  $g/\phi = 1.072$  instead of 1.070.

In this paper we shall be concerned with the practical osmotic coefficient  $\phi$  and the practical activity coefficient which, for brevity, we shall write as  $\gamma$ . Moreover, the water activity, given by

$$\bar{G}_{\text{H}_2\text{O}} = \bar{G}_{\text{H}_2\text{O}}^0 + RT \ln a_w \quad (9)$$

and the relative vapour pressure of the solution,

$$p/p^0 = a_w,$$

can be obtained from the osmotic coefficient by the relation,

$$\phi = -55.51/\nu m \ln a_w,$$

or

$$\log_{10} a_w = \log_{10} p/p^0 = -0.007824 \nu m \phi.$$

Calculation of  $\phi$  from  $\gamma$  and the converse is made by some form of the Gibbs-Duhem equation. The procedure outlined by Randall and White<sup>8</sup> is convenient for the calculation of  $\gamma$  if values of  $\phi$  are known, using the equation,

$$-\ln \gamma = \int_{m=0}^m (1 - \phi) d \ln m; \quad (10)$$

it is often convenient to use the equivalent integrals,

$$\int (1 - \phi)/m dm, \quad \text{or} \quad 2 \int (1 - \phi)/\sqrt{m} d\sqrt{m}$$

for graphical or tabular integration. As a matter of computation the calculation of  $\phi$ , if  $\gamma$  is known, presents more difficulty and this has recently been considered by Stokes.<sup>9</sup>

Many of the data given in the following Tables have been obtained by isopiestic vapour pressure measurements. The experimental results of this method are expressed as pairs of molalities of solutions of equal vapour pressure, one solution being that of the electrolyte being studied and the other that of one of the reference electrolytes, such as sodium chloride or sulphuric acid, whose  $\phi$  and  $\gamma$  values are thought to be known with considerable accuracy. It must be emphasized, however, that any errors in the  $\phi$  and  $\gamma$  values of the reference electrolytes is reflected in the  $\phi$  and  $\gamma$  values for other salts and any change in the data for the reference electrolytes entails extensive recalculation for other salts. The isopiestic measurements having been made, if  $m_R$  is the molality of the solution of the reference electrolyte and  $m$  that of the salt being studied, a plot of the isopiestic ratio,  $R = m_R/m$ , against  $m$  is made. Usually there is no difficulty in drawing a smooth curve through the points from which values of  $R$  at round values of  $m$  can be read. (Any undue scattering of the points is to be regarded with suspicion; it will occur with volatile electrolytes such as hydrochloric acid or salts like ferric chloride which exhibit ageing effects.) From these values of  $R$ , the osmotic coefficient is calculated by the equation,

$$\nu \phi = \nu_{\text{ref}} R \phi_{\text{ref}}, \quad (11)$$

it being assumed that  $\phi_{\text{ref}}$  has been tabulated at close intervals over a wide concentration range of the reference electrolyte. Thus  $\phi$  can be obtained upwards from the lowest concentration (about 0.1  $m$ ) at which the isopiestic method works. It should be noted that there is no difficulty in obtaining  $\phi$  at the lowest concentration because the osmotic coefficient is derived directly from the experimental data. To obtain  $\gamma$ , however, an integration must be made as in eqn. (10) which introduces the difficulty that we do not know

$$\int_{m=0}^{m=0.1} (1 - \phi) d \ln m.$$

If we proceed by an alternative, although essentially equivalent, method using an equation given by Robinson and Sinclair:<sup>10</sup>

$$\ln \gamma = \ln \gamma_R + \ln R + \int_0^{m_R} (R - 1) d \ln \gamma_R m_R, \quad (12)$$

we have the same difficulty of not knowing the value of the integral between  $m = 0$  and  $m = 0.1$ . In many cases where both electrolytes are of the same valency type, it is possible to extrapolate the  $R$  against  $m$  curve to unity at  $m = 0$  with considerable confidence, in which case the integral in eqn. (12) can be evaluated. In some cases  $\gamma$  at  $m = 0.1$  is known from other measurements, e.g. data for the zinc halides are available from E.M.F. work. The  $\gamma$  values given by the isopiestic method are, therefore, accurate relative to the value at  $m = 0.1$  but the latter does not necessarily have high accuracy; in some cases such as sodium chloride or calcium chloride,  $\gamma$  at  $0.1 m$  is known with accuracy from other measurements and we should be reluctant to change the values selected. In other cases, e.g. sodium iodide, the values at  $0.1 m$  are known with fair certainty by extrapolation of the  $R$  curve to  $m = 0$  and, whilst the values at  $0.1 m$  given in the following Tables are subject to change, we doubt if they are in error by more than perhaps 0.005 in  $\gamma$ . Of course, if the  $\gamma$  values at  $0.1 m$  are changed, then the  $\gamma$  values at other concentrations must be changed *pro rata*. In some cases, however, particularly with salts of high valency type, e.g. aluminium sulphate, the values selected for  $m = 0.1$  are little more than a guess and almost certainly open to revision. Such values we have indicated in the following Tables by enclosing them in parentheses.

**Osmotic and Activity Coefficients.**—The following Tables give practical osmotic and activity coefficients at 25°. We have included data for one non-electrolyte, sucrose,<sup>10, 11, 12</sup> which should be useful as a reference solute for isopiestic measurements on other non-electrolytes, but we have omitted data derived from isopiestic work on glycerol and urea<sup>12</sup> and an interesting series of measurements on 18 amino-acids.<sup>13</sup> Some recent determinations on sodium and potassium acid sulphate<sup>14</sup> have also been omitted because, whilst the isopiestic data enable the vapour pressures to be calculated, the dissociation of the bisulphate ion makes  $\phi$  and  $\gamma$  values of little use. In addition, reference only is made to measurements<sup>15</sup> on a series of sodium salts of fatty acids up to the caprate.

The following notes will enable some estimate of the reliability of the data given in the Tables to be made.

Some of the data depend on isopiestic measurements only and no confirmation is available from other techniques. This holds for the following salts: lithium iodide, perchlorate, nitrate, acetate and toluenesulphonate; sodium chlorate, perchlorate, bromate, nitrate, acetate, toluenesulphonate, thiocyanate and phosphate; potassium fluoride, chlorate, bromate, nitrate, acetate, toluenesulphonate, thiocyanate and phosphate; the five rubidium salts; caesium bromide, iodide, nitrate and acetate; silver nitrate; the three thallium salts, magnesium, manganese and nickel sulphate; all the trivalent metal salts (for lanthanum chloride independent isopiestic measurements are in good agreement); potassium ferrocyanide and ferricyanide; aluminium and chromium sulphate and thorium nitrate.

With some it is possible to compare the osmotic and activity coefficients with those derived from freezing point measurements but there are seldom sufficient heat content data available to estimate the temperature correction exactly; nevertheless, it is found that the activity coefficients at  $0.1 m$  usually agree within 1 % at the two temperatures; only in the case of lithium nitrate, potassium nitrate, potassium chlorate and sodium acetate do differences of up to 2 % appear but the heat content data available are not sufficient to tell us if this difference is real or due to error in the activity coefficients at either temperature.

**Hydrochloric Acid**—The values of  $\gamma$  between  $0.1$  and  $4 m$  are taken from the very careful work of Harned and Ehlers,<sup>16</sup> interpolated at some concentrations by means of the Debye-Hückel constants given by Harned and Ehlers. Osmotic coefficients have been calculated by the method outlined by Stokes.<sup>9</sup> Randall and Young<sup>17</sup> quote values of  $\gamma$  between  $1.2$  and  $4 m$  which are, on the average, 0.35 % higher (i.e. a difference equivalent to 0.18 mV). The data in the Tables for concentrations above  $4 m$  are taken from the paper of Randall and Young, some intermediate values being obtained by Besselian interpolation. The values above  $4 m$  are supported by the data of Åkerlöf and Teare<sup>18</sup> whose  $\gamma$  values exhibit an average deviation of 1 % from those of Randall and Young.

**Hydrobromic Acid.**—The  $\gamma$  values are from Harned, Keston and Donelson;<sup>19</sup> interpolation has been made at some concentrations by the use of their Debye-Hückel constants and  $\phi$  has been calculated by the procedure of Stokes.<sup>9</sup>

**Hydriodic Acid.**—The values depend on isopiestic data only.<sup>20</sup>

**Perchloric Acid.**—The isopiestic  $\phi$  values agree within 1 % with those derived from the direct vapour pressure measurements of Pearce and Nelson.<sup>21</sup> Their  $\gamma$  values are, however, very different.

**Nitric Acid.**—The  $\gamma$  values are those obtained from freezing point measurements by Hartman and Rosenfeld<sup>42</sup> with some interpolations added. The  $\phi$  values are computed from these.

**Lithium Hydroxide.**— $\gamma$  values are from the E.M.F. measurements of Harned and Swindells<sup>22</sup> with interpolations at some concentrations.

**Lithium Chloride and Bromide.**—The isopiestic data are confirmed up to 2 *m* by the E.M.F. values of Harned<sup>23</sup> which agree within 0.8 % with the isopiestic values; above 2 *m*, however, there are considerable differences and, because the lithium amalgam electrode is known to be erratic, we think that the isopiestic data are to be preferred.

**Sodium Hydroxide.**—Up to 2 *m*,  $\gamma$  values interpolated from the E.M.F. measurements of Harned<sup>24</sup> and of Harned and Hecker<sup>25</sup> have been used; above 2 *m* we have used the isopiestic measurements of Stokes:<sup>26</sup> it should be noted that the values of  $\gamma$  due to Åkerlöf and Kegeles<sup>27</sup> are considerably different—by about 3 %.

**Sodium Fluoride.**—Attention should be drawn to the E.M.F. measurements of Ivett and De Vries<sup>28</sup> which do not agree well with the  $\gamma$  values tabulated from isopiestic data.

**Sodium Chloride.**—Harned's<sup>23</sup> E.M.F. values of  $\gamma$  (extending up to 4 *m*) do not differ from those in the Tables by more than 0.004 in  $\gamma$  at any concentration and only differ on the average by 0.3 %. Similar data by Harned and Nims<sup>30</sup> give an average difference of 0.5 %, there being a difference of 0.009 in  $\gamma$  at 4 *m*. The  $\gamma$  values of Olynyk and Gordon<sup>31</sup> between 1.5 and 6 *m* agree within 0.3 % whilst  $\phi$  values calculated from the direct vapour pressure measurements of Negus<sup>31a</sup> agree within 0.2 % from 1 to 5 *m*.

**Sodium Bromide.**—The isopiestic data quoted in the Tables agree within 0.2 % with the E.M.F. data of Harned and of Harned and Crawford<sup>32</sup> up to 2 *m*; between 2.5 and 4 *m* their data are higher by about 1.5 %.

**Sodium Iodide.**—The isopiestic data are in good agreement with the values quoted by Harned,<sup>23</sup> the average difference being 0.3 % in  $\gamma$  up to 1 *m* (the highest concentration at which E.M.F. measurements were made).

**Potassium Hydroxide.**—Up to 4 *m* we have used values calculated from the E.M.F. measurements of Harned and Cook<sup>33</sup> and above 4 *m* those of Åkerlöf and Bender.<sup>34</sup>

**Potassium Chloride.**—The values quoted in the Tables agree with those of Harned<sup>23</sup> and of Harned and Cook<sup>33</sup> with an average deviation of 0.4 %. Moreover, the direct vapour pressure measurements of Lovelace, Frazer, and Sease<sup>35a</sup> can be corrected from 20° to 25° to give values of  $\phi$  which agree within 0.3 %.

**Potassium Bromide and Iodide.**—The values in the Tables for the bromide, taken from isopiestic data, are within 0.3 % of those given from E.M.F. data by Harned.<sup>23</sup> Similarly, the data for the iodide agree within 0.3 % up to 1 *m* above which the E.M.F. values are 2 % higher.

**Caesium Hydroxide.**—The data quoted are derived from the E.M.F. measurements of Harned and Schupp.<sup>36</sup>

**Caesium Chloride.**—The data in the Tables, from isopiestic measurements, exhibit an average deviation of only 0.5 % from the E.M.F. data of Harned and Schupp.

**Copper Sulphate.**—The E.M.F. data of Nielsen and Brown<sup>37</sup> are within 2 % of the isopiestic  $\gamma$  values whilst the values of Wetmore and Gordon<sup>38</sup> are within 1.5 %.

**Zinc Sulphate.**—Bray<sup>39</sup> has made measurements which yield activity coefficients which differ, on the average, by less than 2 % from the isopiestic values quoted.

**Cadmium Sulphate.**—The E.M.F. data of LaMer and Parkes<sup>40</sup> do not agree with the isopiestic values that we have used, there being differences of the order of 13 %.

TABLE I.—OSMOTIC COEFFICIENTS AT 25° C

<i>m</i>	HCl	HBr	HI	HClO <sub>4</sub>	HNO <sub>3</sub>	LiOH	LiCl	LiBr	LiI	LiClO <sub>4</sub>	LiNO <sub>3</sub>
0.1	0.943	0.948	0.953	0.947	0.940	0.920	0.939	0.943	0.952	0.951	0.938
0.2	0.945	0.954	0.969	0.951	0.935	0.902	0.939	0.944	0.966	0.959	0.935
0.3	0.952	0.964	0.984	0.958	0.936	0.890	0.945	0.952	0.980	0.971	0.940
0.4	0.963	0.978	1.001	0.966	0.940	0.881	0.954	0.960	0.995	0.985	0.946
0.5	0.974	0.993	1.019	0.976	0.944	0.875	0.963	0.970	1.008	0.999	0.954
0.6	0.986	1.007	1.038	0.988	0.950	0.869	0.973	0.981	1.022	1.013	0.962
0.7	0.998	1.023	1.057	1.000	0.957	0.866	0.984	0.993	1.034	1.027	0.970
0.8	1.011	1.038	1.075	1.013	0.964	0.863	0.995	1.007	1.049	1.043	0.978
0.9	1.025	1.054	1.094	1.026	0.971	0.861	1.006	1.021	1.063	1.058	0.987
1.0	1.039	1.072	1.113	1.041	0.979	0.860	1.018	1.035	1.080	1.072	0.997
1.2	1.067	—	1.153	1.072	0.994	0.863	1.041	1.067	1.111	1.104	1.015
1.4	1.096	—	1.193	1.106	1.009	0.866	1.066	1.098	1.143	1.137	1.033
1.6	1.126	—	1.233	1.141	1.025	0.870	1.091	1.130	1.176	1.170	1.052
1.8	1.157	—	1.273	1.175	1.042	0.872	1.116	1.163	1.212	1.204	1.070
2.0	1.188	—	1.315	1.210	1.060	0.875	1.142	1.196	1.250	1.238	1.088
2.5	1.266	—	1.424	1.305	1.106	0.882	1.212	1.278	1.351	1.328	1.134
3.0	1.348	—	1.535	1.406	1.154	0.886	1.286	1.364	1.467	1.419	1.181
3.5	1.431	—	—	1.511	—	0.889	1.366	1.467	—	1.512	1.227
4.0	1.517	—	—	1.622	—	0.892	1.449	1.578	—	1.595	1.270
4.5	1.598	—	—	1.738	—	—	1.533	1.687	—	—	1.312
5.0	1.680	—	—	1.860	—	—	1.619	1.793	—	—	1.352
5.5	1.763	—	—	1.981	—	—	1.705	1.891	—	—	1.387
6.0	1.845	—	—	2.106	—	—	1.791	1.989	—	—	1.420
Ref.	16	19	20	41	42	22	10, 43	44, 45	10	46	47, 48

<i>m</i>	LiAc	LiTol	NaOH	NaF	NaCl	NaBr	NaI	NaClO <sub>3</sub>	NaClO <sub>4</sub>	NaBrO <sub>3</sub>	NaNO <sub>3</sub>
0.1	0.935	0.928	0.925	0.924	0.932	0.934	0.938	0.927	0.930	0.918	0.921
0.2	0.928	0.917	0.925	0.908	0.925	0.928	0.936	0.913	0.920	0.896	0.902
0.3	0.929	0.912	0.929	0.898	0.922	0.928	0.939	0.904	0.915	0.883	0.890
0.4	0.931	0.908	0.933	0.891	0.920	0.929	0.945	0.897	0.912	0.873	0.881
0.5	0.935	0.906	0.937	0.886	0.921	0.933	0.952	0.892	0.910	0.865	0.873
0.6	0.940	0.906	0.941	0.882	0.923	0.937	0.959	0.888	0.909	0.857	0.867
0.7	0.945	0.905	0.945	0.879	0.926	0.942	0.967	0.885	0.910	0.851	0.862
0.8	0.951	0.905	0.949	0.876	0.929	0.947	0.975	0.883	0.911	0.845	0.858
0.9	0.956	0.905	0.953	0.874	0.932	0.953	0.983	0.882	0.912	0.839	0.854
1.0	0.962	0.905	0.958	0.872	0.936	0.958	0.991	0.880	0.913	0.833	0.851
1.2	0.975	0.904	0.969	—	0.943	0.969	1.007	0.878	0.916	0.824	0.845
1.4	0.988	0.902	0.980	—	0.951	0.983	1.025	0.876	0.920	0.815	0.839
1.6	1.001	0.899	0.991	—	0.962	0.997	1.043	0.874	0.925	0.808	0.835
1.8	1.014	0.894	1.002	—	0.972	1.012	1.061	0.875	0.930	0.804	0.830
2.0	1.027	0.893	1.015	—	0.983	1.028	1.079	0.876	0.934	0.800	0.826
2.5	1.061	0.899	1.054	—	1.013	1.067	1.120	0.879	0.947	0.792	0.817
3.0	1.093	0.912	1.094	—	1.045	1.107	1.188	0.881	0.960	—	0.810
3.5	1.123	0.930	1.139	—	1.080	1.150	1.243	0.886	0.975	—	0.804
4.0	1.153	0.951	1.195	—	1.116	1.199	—	—	0.991	—	0.797
4.5	—	0.972	1.255	—	1.153	—	—	—	1.008	—	0.792
5.0	—	—	1.314	—	1.192	—	—	—	1.025	—	0.788
5.5	—	—	1.374	—	1.231	—	—	—	1.042	—	0.787
6.0	—	—	1.434	—	1.271	—	—	—	1.060	—	0.788
Ref.	47	47	24, 25, 26, 27	29	2	44, 49	44	50	46	51	47

Ac = Acetate. Tol = Tolueneulphonate.

TABLE I.—OSMOTIC COEFFICIENTS AT 25° C (*Cont.*)

<i>m</i>	NaAc	NaTol	NaCNS	NaH <sub>2</sub> PO <sub>4</sub>	KOH	KF	KCl	KBr	KI	KClO <sub>3</sub>	KBrO <sub>3</sub>	KNO <sub>3</sub>
0.1	0.940	0.924	0.937	0.911	0.944	0.930	0.927	0.928	0.932	0.913	0.910	0.906
0.2	0.939	0.907	0.934	0.884	0.936	0.919	0.913	0.916	0.922	0.887	0.881	0.873
0.3	0.945	0.897	0.935	0.864	0.938	0.915	0.906	0.910	0.918	0.867	0.858	0.851
0.4	0.951	0.887	0.938	0.847	0.944	0.914	0.902	0.906	0.917	0.849	0.837	0.833
0.5	0.959	0.880	0.943	0.832	0.953	0.915	0.899	0.904	0.917	0.832	0.816	0.817
0.6	0.967	0.874	0.948	0.819	0.962	0.916	0.898	0.904	0.918	0.816	—	0.802
0.7	0.977	0.867	0.953	0.808	0.972	0.919	0.897	0.904	0.919	0.802	—	0.790
0.8	0.986	0.861	0.958	0.798	0.983	0.923	0.897	0.905	0.922	—	—	0.778
0.9	0.994	0.855	0.963	0.789	0.993	0.926	0.897	0.906	0.924	—	—	0.767
1.0	1.002	0.849	0.969	0.780	1.003	0.931	0.897	0.907	0.926	—	—	0.756
1.2	1.018	0.837	0.979	0.765	1.026	0.941	0.899	0.910	0.931	—	—	0.736
1.4	1.038	0.824	0.990	0.751	1.051	0.951	0.901	0.914	0.937	—	—	0.718
1.6	1.057	0.811	1.002	0.739	1.076	0.962	0.904	0.917	0.943	—	—	0.700
1.8	1.074	0.799	1.014	0.729	1.100	0.973	0.908	0.922	0.950	—	—	0.684
2.0	1.092	0.787	1.025	0.721	1.125	0.984	0.912	0.927	0.957	—	—	0.669
2.5	1.137	0.763	1.055	0.705	1.183	1.014	0.924	0.941	0.974	—	—	0.631
3.0	1.181	0.748	1.086	0.696	1.248	1.048	0.937	0.955	0.990	—	—	0.602
3.5	1.223	0.738	1.118	0.691	1.317	1.084	0.950	0.969	1.006	—	—	0.577
4.0	—	0.733	1.150	0.691	1.387	1.124	0.965	0.984	1.021	—	—	—
4.5	—	—	—	0.694	1.459	—	0.980	1.000	1.032	—	—	—
5.0	—	—	—	0.699	1.524	—	—	1.015	—	—	—	—
5.5	—	—	—	0.706	1.594	—	—	—	—	—	—	—
6.0	—	—	—	0.713	1.661	—	—	—	—	—	—	—

Ref. 47 47 52 53 33, 34 29 2 44, 49 44, 54 51 55 47

<i>m</i>	KAc	KTol	KCNS	KH <sub>2</sub> PO <sub>4</sub>	RbCl	RbBr	RI	RNO <sub>3</sub>	RbAc	CsOH	CsCl	CtBr
0.1	0.943	0.921	0.926	0.901	0.923	0.922	0.921	0.903	0.943	0.942	0.917	0.917
0.2	0.944	0.901	0.911	0.868	0.907	0.905	0.901	0.871	0.945	0.939	0.897	0.896
0.3	0.951	0.886	0.904	0.843	0.898	0.897	0.896	0.847	0.952	0.940	0.885	0.882
0.4	0.958	0.873	0.900	0.823	0.893	0.892	0.890	0.826	0.961	0.949	0.875	0.873
0.5	0.968	0.860	0.897	0.805	0.889	0.888	0.886	0.809	0.971	0.960	0.869	0.865
0.6	0.977	0.847	0.896	0.789	0.887	0.886	0.884	0.794	0.981	0.970	0.864	0.861
0.7	0.987	0.834	0.895	0.773	0.886	0.884	0.881	0.781	0.992	0.982	0.861	0.857
0.8	0.997	0.822	0.895	0.760	0.886	0.882	0.880	0.768	1.002	0.992	0.859	0.854
0.9	1.007	0.809	0.894	0.747	0.885	0.881	0.879	0.756	1.013	1.003	0.858	0.852
1.0	1.017	0.798	0.894	0.736	0.885	0.881	0.878	0.745	1.023	1.014	0.857	0.850
1.2	1.038	0.775	0.893	0.716	0.886	0.880	0.878	0.725	1.046	—	0.856	0.849
1.4	1.060	0.751	0.892	0.698	0.888	0.881	0.878	0.706	1.068	—	0.856	0.848
1.6	1.081	0.732	0.892	0.683	0.890	0.882	0.880	0.689	1.091	—	0.857	0.848
1.8	1.103	0.715	0.893	0.669	0.893	0.884	0.882	0.673	1.114	—	0.859	0.850
2.0	1.123	0.700	0.894	—	0.896	0.887	0.886	0.656	1.137	—	0.862	0.852
2.5	1.177	0.664	0.898	—	0.905	0.893	0.893	0.620	1.192	—	0.869	0.859
3.0	1.228	0.637	0.903	—	0.916	0.899	0.901	0.588	1.248	—	0.879	0.866
3.5	1.274	0.615	0.908	—	0.928	0.907	0.911	0.561	1.302	—	0.889	0.874
4.0	—	—	0.912	—	0.941	0.916	0.921	0.538	—	—	0.900	0.884
4.5	—	—	0.917	—	0.952	0.924	0.931	0.516	—	—	0.912	0.892
5.0	—	—	0.921	—	0.966	0.934	0.940	—	—	—	0.924	0.901
5.5	—	—	—	—	—	—	—	—	—	—	—	—
6.0	—	—	—	—	—	—	—	—	—	—	—	—

Ref. 47 47 52 53 10, 56 44, 56 44, 56 47, 56 47, 56 36 10, 36 44, 56

Ac = Acetate. Tol = Toluene-sulphonate.



TABLE I.—OSMOTIC COEFFICIENTS AT 25° C. (*Cont.*)

<i>m</i>	CsI	CsNO <sub>3</sub>	CsAc	AgNO <sub>3</sub>	TiClO <sub>4</sub>	TiNO <sub>3</sub>	TiAc	CuSO <sub>4</sub>	MgSO <sub>4</sub>	ZnSO <sub>4</sub>	CdSO <sub>4</sub>
0.1	0.916	0.902	0.945	0.903	0.900	0.881	0.913	0.561	0.606	0.590	0.565
0.2	0.895	0.869	0.947	0.870	0.867	0.833	0.891	0.515	0.562	0.533	0.513
0.3	0.880	0.842	0.954	0.847	0.842	0.800	0.876	0.494	0.540	0.506	0.490
0.4	0.870	0.820	0.964	0.827	0.821	0.775	0.865	0.478	0.529	0.492	0.476
0.5	0.863	0.802	0.975	0.811	0.804	—	0.855	0.469	0.522	0.483	0.466
0.6	0.858	0.787	0.986	0.795	—	—	0.849	0.462	0.518	0.476	0.458
0.7	0.855	0.774	0.996	0.779	—	—	0.843	0.458	0.517	0.473	0.452
0.8	0.852	0.761	1.006	0.766	—	—	0.838	0.457	0.518	0.473	0.450
0.9	0.849	0.748	1.016	0.754	—	—	0.833	0.456	0.520	0.474	0.449
1.0	0.846	0.736	1.026	0.742	—	—	0.829	0.461	0.525	0.478	0.452
1.2	0.842	0.715	1.049	0.720	—	—	0.823	0.473	0.542	0.489	0.461
1.4	0.839	0.695	1.072	0.699	—	—	0.818	0.491	0.567	0.508	0.476
1.6	0.836	—	1.095	0.680	—	—	0.814	—	0.597	0.533	0.496
1.8	0.834	—	1.119	0.662	—	—	0.810	—	0.630	0.566	0.522
2.0	0.832	—	1.142	0.646	—	—	0.807	—	0.666	0.602	0.551
2.5	0.827	—	1.196	0.609	—	—	0.801	—	0.780	0.717	0.632
3.0	0.822	—	1.251	0.576	—	—	0.796	—	0.922	0.861	0.726
3.5	—	—	1.306	0.550	—	—	0.789	—	—	1.033	0.832
4.0	—	—	—	0.523	—	—	0.783	—	—	—	—
4.5	—	—	—	0.502	—	—	0.777	—	—	—	—
5.0	—	—	—	0.483	—	—	0.772	—	—	—	—
5.5	—	—	—	0.467	—	—	0.766	—	—	—	—
6.0	—	—	—	0.452	—	—	0.760	—	—	—	—
Ref.:	44, 56	47, 56	47, 56	57	56	56	56	58	58	58	58

<i>m</i>	MnSO <sub>4</sub>	NiSO <sub>4</sub>	AlCl <sub>3</sub>	SeCl <sub>4</sub>	CrCl <sub>3</sub>	YCl <sub>3</sub>	LaCl <sub>3</sub>	CeCl <sub>3</sub>	PrCl <sub>3</sub>	NdCl <sub>3</sub>	SmCl <sub>3</sub>
0.1	0.587	0.581	0.819	0.797	0.811	0.789	0.788	0.782	0.784	0.783	0.789
0.2	0.538	0.533	0.841	0.827	0.833	0.810	0.800	0.805	0.801	0.801	0.809
0.3	0.516	0.508	0.889	0.868	0.875	0.847	0.833	0.835	0.830	0.832	0.841
0.4	0.501	0.488	0.947	0.917	0.926	0.892	0.871	0.872	0.866	0.871	0.879
0.5	0.490	0.475	1.008	0.969	0.983	0.939	0.912	0.914	0.905	0.913	0.921
0.6	0.481	0.465	1.074	1.027	1.045	0.989	0.955	0.955	0.945	0.954	0.964
0.7	0.475	0.458	1.145	1.090	1.111	1.042	0.998	1.007	0.996	1.006	1.019
0.8	0.472	0.456	1.220	1.156	1.181	1.100	1.052	1.057	1.046	1.056	1.074
0.9	0.472	0.456	1.299	1.222	1.250	1.161	1.102	1.107	1.100	1.110	1.128
1.0	0.475	0.459	1.382	1.291	1.319	1.223	1.154	1.158	1.154	1.165	1.186
1.2	0.485	0.472	1.560	1.430	1.443	1.354	1.266	1.264	1.271	1.283	1.302
1.4	0.504	0.492	1.749	1.572	—	1.491	1.384	1.387	1.388	1.404	1.427
1.6	0.527	0.517	1.951	1.718	—	1.631	1.502	1.504	1.507	1.527	1.554
1.8	0.556	0.551	2.175	1.869	—	1.780	1.623	1.638	1.631	1.656	1.686
2.0	0.588	0.589	—	—	—	1.940	1.748	1.777	1.759	1.789	1.824
2.5	0.677	0.708	—	—	—	—	—	—	—	—	—
3.0	0.782	—	—	—	—	—	—	—	—	—	—
3.5	0.909	—	—	—	—	—	—	—	—	—	—
4.0	1.048	—	—	—	—	—	—	—	—	—	—
Ref.:	58	58	59	59	60	59	59, 61	59	59	59	62

Ac = Acetate. Tol = Toluene sulphonate.

TABLE I.—OSMOTIC COEFFICIENTS AT 25° C (*Cont.*)

<i>m</i>	EuCl <sub>2</sub>	Cr(NO <sub>3</sub> ) <sub>3</sub>	K <sub>3</sub> Fe(CN) <sub>6</sub>	K <sub>4</sub> Fe(CN) <sub>6</sub>	Al <sub>2</sub> (SO <sub>4</sub> ) <sub>3</sub>	Cr <sub>2</sub> (SO <sub>4</sub> ) <sub>3</sub>	Th(NO <sub>3</sub> ) <sub>4</sub>
0.1	0.794	0.795	0.727	0.595	0.420	0.414	0.675
0.2	0.812	0.818	0.695	0.556	0.390	0.401	0.685
0.3	0.842	0.860	0.682	0.535	0.391	0.412	0.705
0.4	0.882	0.906	0.678	0.518	0.421	0.437	0.734
0.5	0.926	0.953	0.676	0.506	0.477	0.473	0.770
0.6	0.971	1.003	0.676	0.498	0.545	0.524	0.807
0.7	1.027	1.055	0.679	0.494	0.625	0.585	0.846
0.8	1.082	1.111	0.685	0.494	0.718	0.657	0.885
0.9	1.137	1.168	0.694	0.501	0.809	0.740	0.925
1.0	1.193	1.227	0.705	—	0.922	0.832	0.965
1.2	1.310	1.343	0.727	—	—	1.031	1.044
1.4	1.438	1.456	0.750	—	—	—	1.120
1.6	1.570	—	—	—	—	—	1.192
1.8	1.707	—	—	—	—	—	1.259
2.0	1.853	—	—	—	—	—	1.325
2.5	—	—	—	—	—	—	1.455
3.0	—	—	—	—	—	—	1.546
3.5	—	—	—	—	—	—	1.616
4.0	—	—	—	—	—	—	1.659
4.5	—	—	—	—	—	—	1.688
5.0	—	—	—	—	—	—	1.706
Ref. :	62	60	63	56	56	60	63

TABLE II.—ACTIVITY COEFFICIENTS AT 25° C

<i>m</i>	HCl	HBr	HI	HClO <sub>4</sub>	HNO <sub>3</sub>	LiOH	LiCl	LiBr	LiI	LiClO <sub>4</sub>	LiNO <sub>3</sub>	LiAc
0.1	0.796	0.805	0.818	0.803	0.791	0.760	0.790	0.796	0.815	0.812	0.788	0.784
0.2	0.767	0.782	0.807	0.778	0.754	0.702	0.757	0.766	0.802	0.794	0.752	0.742
0.3	0.756	0.777	0.811	0.768	0.735	0.665	0.744	0.756	0.804	0.792	0.736	0.721
0.4	0.755	0.781	0.823	0.766	0.725	0.638	0.740	0.752	0.813	0.798	0.728	0.709
0.5	0.757	0.789	0.839	0.769	0.720	0.617	0.739	0.753	0.824	0.808	0.726	0.700
0.6	0.763	0.801	0.860	0.776	0.717	0.599	0.743	0.758	0.838	0.820	0.727	0.691
0.7	0.772	0.815	0.883	0.785	0.717	0.585	0.748	0.767	0.852	0.834	0.729	0.689
0.8	0.783	0.832	0.908	0.795	0.718	0.573	0.755	0.777	0.870	0.852	0.733	0.688
0.9	0.795	0.850	0.935	0.808	0.721	0.563	0.764	0.789	0.888	0.869	0.737	0.688
1.0	0.800	0.871	0.963	0.823	0.724	0.554	0.774	0.803	0.910	0.887	0.743	0.689
1.2	0.840	—	1.027	0.858	0.734	0.542	0.796	0.837	0.955	0.931	0.757	0.693
1.4	0.876	—	1.098	0.900	0.745	0.532	0.823	0.874	1.007	0.979	0.774	0.700
1.6	0.916	—	1.175	0.947	0.758	0.525	0.853	0.917	1.063	1.034	0.792	0.709
1.8	0.960	—	1.260	0.998	0.775	0.518	0.885	0.964	1.127	1.093	0.812	0.719
2.0	1.009	—	1.356	1.055	0.793	0.513	0.921	1.015	1.198	1.158	0.835	0.729
2.5	1.147	—	1.641	1.227	0.846	0.503	1.026	1.161	1.418	1.350	0.896	0.762
3.0	1.316	—	2.015	1.448	0.900	0.494	1.156	1.341	1.715	1.582	0.966	0.798
3.5	1.518	—	—	1.726	—	0.487	1.317	1.584	—	1.866	1.044	0.837
4.0	1.762	—	—	2.08	—	0.481	1.510	1.897	—	2.18	1.125	0.877
4.5	2.04	—	—	2.53	—	—	1.741	2.28	—	—	1.215	—
5.0	2.38	—	—	3.11	—	—	2.02	2.74	—	—	1.310	—
5.5	2.77	—	—	3.83	—	—	2.34	3.27	—	—	1.407	—
6.0	3.22	—	—	4.76	—	—	2.72	3.92	—	—	1.506	—

Ac = Acetate.

TABLE II.—ACTIVITY COEFFICIENTS AT 25° C (*Cont.*)

<i>m</i>	LiTol	NaOH	NaF	NaCl	NaBr	NaI	NaClO <sub>3</sub>	NaClO <sub>4</sub>	NaBrO <sub>3</sub>	NaNO <sub>3</sub>	NaAc
0.1	0.772	0.766	0.765	0.778	0.782	0.787	0.772	0.775	0.758	0.762	0.791
0.2	0.723	0.727	0.710	0.735	0.741	0.751	0.720	0.729	0.696	0.703	0.757
0.3	0.695	0.708	0.676	0.710	0.719	0.735	0.688	0.701	0.657	0.666	0.744
0.4	0.674	0.697	0.651	0.693	0.704	0.727	0.664	0.683	0.628	0.638	0.737
0.5	0.659	0.690	0.632	0.681	0.697	0.723	0.645	0.668	0.605	0.617	0.735
0.6	0.647	0.685	0.616	0.673	0.692	0.723	0.630	0.656	0.585	0.599	0.736
0.7	0.638	0.681	0.603	0.667	0.689	0.724	0.617	0.648	0.569	0.583	0.740
0.8	0.630	0.679	0.592	0.662	0.687	0.727	0.606	0.641	0.554	0.570	0.745
0.9	0.623	0.678	0.582	0.659	0.687	0.731	0.597	0.635	0.541	0.558	0.752
1.0	0.617	0.678	0.573	0.657	0.687	0.736	0.589	0.629	0.528	0.548	0.757
1.2	0.605	0.681	—	0.654	0.692	0.747	0.575	0.622	0.507	0.530	0.769
1.4	0.595	0.686	—	0.655	0.699	0.763	0.563	0.616	0.489	0.514	0.789
1.6	0.586	0.692	—	0.657	0.706	0.780	0.553	0.613	0.473	0.501	0.809
1.8	0.575	0.700	—	0.662	0.718	0.799	0.545	0.611	0.461	0.489	0.829
2.0	0.568	0.709	—	0.668	0.731	0.820	0.538	0.609	0.450	0.478	0.851
2.5	0.558	0.743	—	0.688	0.768	0.883	0.525	0.609	0.426	0.455	0.914
3.0	0.556	0.784	—	0.714	0.812	0.963	0.515	0.611	—	0.437	0.982
3.5	0.559	0.835	—	0.746	0.865	1.053	0.508	0.617	—	0.422	1.057
4.0	0.566	0.903	—	0.783	0.929	—	—	0.626	—	0.408	—
4.5	0.575	0.985	—	0.826	—	—	—	0.637	—	0.396	—
5.0	—	1.077	—	0.874	—	—	—	0.649	—	0.386	—
5.5	—	1.181	—	0.928	—	—	—	0.662	—	0.378	—
6.0	—	1.299	—	0.986	—	—	—	0.677	—	0.371	—

<i>m</i>	NaTol	NaCNS	NaH <sub>2</sub> PO <sub>4</sub>	KOH	KF	KCl	KBr	KI	KClO <sub>3</sub>	KBrO <sub>3</sub>	KNO <sub>3</sub>
0.1	0.765	0.787	0.744	0.798	0.775	0.770	0.772	0.778	0.749	0.745	0.739
0.2	0.709	0.750	0.675	0.760	0.727	0.718	0.722	0.733	0.681	0.674	0.663
0.3	0.674	0.731	0.629	0.742	0.700	0.688	0.693	0.707	0.635	0.625	0.614
0.4	0.648	0.720	0.593	0.734	0.682	0.666	0.673	0.689	0.599	0.585	0.576
0.5	0.627	0.715	0.563	0.732	0.670	0.649	0.657	0.676	0.568	0.552	0.545
0.6	0.609	0.712	0.539	0.733	0.661	0.637	0.646	0.667	0.541	—	0.519
0.7	0.593	0.710	0.517	0.736	0.654	0.626	0.636	0.660	0.518	—	0.496
0.8	0.579	0.710	0.499	0.742	0.650	0.618	0.629	0.654	—	—	0.476
0.9	0.566	0.711	0.483	0.749	0.646	0.610	0.622	0.649	—	—	0.459
1.0	0.554	0.712	0.468	0.756	0.645	0.604	0.617	0.645	—	—	0.443
1.2	0.532	0.716	0.442	0.776	0.643	0.593	0.608	0.640	—	—	0.414
1.4	0.511	0.723	0.420	0.800	0.644	0.586	0.602	0.637	—	—	0.390
1.6	0.493	0.730	0.401	0.827	0.647	0.580	0.598	0.636	—	—	0.369
1.8	0.476	0.737	0.385	0.856	0.652	0.576	0.595	0.636	—	—	0.350
2.0	0.460	0.744	0.371	0.888	0.658	0.573	0.593	0.637	—	—	0.333
2.5	0.427	0.779	0.343	0.974	0.678	0.569	0.593	0.644	—	—	0.297
3.0	0.402	0.844	0.320	1.081	0.705	0.569	0.595	0.652	—	—	0.269
3.5	0.383	0.854	0.305	1.215	0.738	0.572	0.600	0.662	—	—	0.246
4.0	0.368	0.897	0.293	1.352	0.779	0.577	0.608	0.673	—	—	—
4.5	—	—	0.283	1.53	—	0.583	0.616	0.683	—	—	—
5.0	—	—	0.276	1.72	—	—	0.626	—	—	—	—
5.5	—	—	0.270	1.95	—	—	—	—	—	—	—
6.0	—	—	0.265	2.20	—	—	—	—	—	—	—

Ac = Acetate. Tol = Toluenesulphonate.

TABLE II.—ACTIVITY COEFFICIENTS AT 25° C (Cont.)

<i>m</i>	K $\overline{\text{Ac}}$	K $\overline{\text{Tol}}$	KCNs	KH <sub>2</sub> PO <sub>4</sub>	RbCl	RbBr	RbI	RbNO <sub>3</sub>	Rb $\overline{\text{Ac}}$	CsOH	CsCl	CsBr
0.1	0.796	0.762	0.769	0.731	0.764	0.763	0.762	0.734	0.796	0.795	0.756	0.754
0.2	0.766	0.702	0.716	0.653	0.709	0.706	0.705	0.658	0.767	0.761	0.694	0.694
0.3	0.754	0.662	0.685	0.602	0.675	0.673	0.671	0.606	0.756	0.744	0.656	0.654
0.4	0.750	0.632	0.663	0.561	0.652	0.650	0.647	0.565	0.753	0.739	0.628	0.626
0.5	0.751	0.605	0.646	0.529	0.634	0.632	0.629	0.534	0.755	0.739	0.606	0.603
0.6	0.754	0.582	0.633	0.501	0.620	0.617	0.614	0.508	0.759	0.742	0.589	0.586
0.7	0.759	0.560	0.623	0.477	0.608	0.605	0.602	0.485	0.766	0.748	0.575	0.571
0.8	0.766	0.541	0.614	0.456	0.599	0.595	0.591	0.465	0.773	0.754	0.563	0.558
0.9	0.774	0.523	0.606	0.438	0.590	0.586	0.583	0.446	0.782	0.762	0.553	0.547
1.0	0.783	0.506	0.599	0.421	0.583	0.578	0.575	0.430	0.792	0.771	0.544	0.538
1.2	0.803	0.476	0.587	0.393	0.572	0.565	0.562	0.402	0.815	—	0.529	0.523
1.4	0.827	0.448	0.577	0.369	0.563	0.556	0.551	0.377	0.840	—	0.518	0.510
1.6	0.854	0.424	0.569	0.348	0.556	0.547	0.544	0.356	0.869	—	0.509	0.500
1.8	0.881	0.404	0.562	0.332	0.551	0.541	0.537	0.338	0.900	—	0.501	0.493
2.0	0.910	0.386	0.556	—	0.546	0.536	0.533	0.321	0.933	—	0.495	0.486
2.5	0.995	0.347	0.546	—	0.539	0.526	0.524	0.285	1.023	—	0.484	0.474
3.0	1.086	0.317	0.538	—	0.536	0.520	0.518	0.257	1.126	—	0.478	0.465
3.5	1.181	0.292	0.533	—	0.536	0.516	0.516	0.234	1.240	—	0.474	0.460
4.0	—	—	0.529	—	0.538	0.514	0.515	0.216	—	—	0.473	0.457
4.5	—	—	0.526	—	0.541	0.514	0.516	0.200	—	—	0.473	0.455
5.0	—	—	0.524	—	0.546	0.515	0.517	—	—	—	0.474	0.453
5.5	—	—	—	—	—	—	—	—	—	—	—	—
6.0	—	—	—	—	—	—	—	—	—	—	—	—

<i>m</i>	CsI	CsNO <sub>3</sub>	Cs $\overline{\text{Ac}}$	AgNO <sub>3</sub>	TiClO <sub>4</sub>	TiNO <sub>3</sub>	Ti $\overline{\text{Ac}}$	CuSO <sub>4</sub>	MgSO <sub>4</sub>
0.1	0.754	0.733	0.799	0.734	0.730	0.702	0.750	(0.150)	(0.150)
0.2	0.692	0.655	0.771	0.657	0.652	0.606	0.686	0.104	0.105
0.3	0.651	0.602	0.761	0.606	0.599	0.545	0.644	0.083	0.088
0.4	0.621	0.561	0.759	0.567	0.559	0.500	0.614	0.071	0.076
0.5	0.599	0.528	0.762	0.536	0.527	—	0.589	0.062	0.068
0.6	0.581	0.501	0.768	0.509	—	—	0.570	0.056	0.062
0.7	0.567	0.478	0.776	0.485	—	—	0.553	0.052	0.057
0.8	0.554	0.458	0.783	0.464	—	—	0.539	0.048	0.054
0.9	0.543	0.439	0.792	0.446	—	—	0.526	0.045	0.051
1.0	0.533	0.422	0.802	0.429	—	—	0.515	0.043	0.049
1.2	0.516	0.393	0.826	0.399	—	—	0.496	0.039	0.045
1.4	0.501	0.368	0.853	0.374	—	—	0.480	0.037	0.044
1.6	0.489	—	0.883	0.352	—	—	0.466	—	0.042
1.8	0.479	—	0.916	0.333	—	—	0.454	—	0.042
2.0	0.470	—	0.950	0.316	—	—	0.444	—	0.042
2.5	0.450	—	1.041	0.280	—	—	0.422	—	0.044
3.0	0.434	—	1.145	0.252	—	—	0.405	—	0.049
3.5	—	—	1.263	0.229	—	—	0.389	—	—
4.0	—	—	—	0.210	—	—	0.376	—	—
4.5	—	—	—	0.194	—	—	0.364	—	—
5.0	—	—	—	0.181	—	—	0.354	—	—
5.5	—	—	—	0.169	—	—	0.344	—	—
6.0	—	—	—	0.159	—	—	0.335	—	—

 $\overline{\text{Ac}}$  = Acetate.  $\overline{\text{Tol}}$  = Toluene sulphonate.

<i>m</i>	ZnSO <sub>4</sub>	CdSO <sub>4</sub>	MnSO <sub>4</sub>	NiSO <sub>4</sub>	AlCl <sub>3</sub>	SeCl <sub>2</sub>	CrCl <sub>3</sub>	YCl <sub>3</sub>	LaCl <sub>3</sub>	CeCl <sub>3</sub>	PrCl <sub>3</sub>	NdCl <sub>3</sub>
0·1	(0·150)	(0·150)	(0·150)	(0·150)	(0·337)	(0·320)	(0·331)	(0·314)	(0·314)	(0·309)	(0·311)	(0·310)
0·2	0·104	0·102	0·106	0·105	0·305	0·288	0·298	0·278	0·274	0·273	0·273	0·272
0·3	0·083	0·082	0·085	0·084	0·302	0·282	0·294	0·269	0·263	0·261	0·260	0·261
0·4	0·071	0·069	0·073	0·071	0·313	0·287	0·300	0·271	0·261	0·260	0·258	0·259
0·5	0·063	0·061	0·064	0·063	0·331	0·298	0·314	0·278	0·266	0·264	0·262	0·264
0·6	0·057	0·055	0·058	0·056	0·356	0·316	0·335	0·291	0·274	0·272	0·268	0·272
0·7	0·052	0·050	0·053	0·052	0·388	0·339	0·362	0·307	0·285	0·286	0·281	0·284
0·8	0·048	0·046	0·049	0·047	0·429	0·369	0·397	0·329	0·302	0·302	0·297	0·301
0·9	0·046	0·043	0·046	0·044	0·479	0·403	0·436	0·355	0·321	0·320	0·316	0·321
1·0	0·043	0·041	0·044	0·042	0·539	0·443	0·481	0·385	0·342	0·342	0·338	0·344
1·2	0·040	0·038	0·040	0·039	0·701	0·544	0·584	0·462	0·398	0·395	0·395	0·403
1·4	0·038	0·035	0·038	0·036	0·936	0·677	—	0·566	0·470	0·469	0·467	0·480
1·6	0·036	0·034	0·037	0·035	1·284	0·853	—	0·701	0·561	0·559	0·558	0·577
1·8	0·035	0·032	0·036	0·034	1·819	1·089	—	0·884	0·677	0·684	0·675	0·704
2·0	0·035	0·032	0·035	0·034	—	—	—	1·136	0·825	0·847	0·825	0·867
2·5	0·037	0·032	0·035	0·035	—	—	—	—	—	—	—	—
3·0	0·041	0·033	0·038	—	—	—	—	—	—	—	—	—
3·5	0·048	0·035	0·042	—	—	—	—	—	—	—	—	—
4·0	—	—	0·048	—	—	—	—	—	—	—	—	—

<i>m</i>	SmCl <sub>3</sub>	EuCl <sub>2</sub>	Cr(NO <sub>3</sub> ) <sub>3</sub>	K <sub>2</sub> Fe(CN) <sub>6</sub>	K <sub>4</sub> Fe(CN) <sub>6</sub>	Al <sub>2</sub> (SO <sub>4</sub> ) <sub>3</sub>	Cr <sub>2</sub> (SO <sub>4</sub> ) <sub>3</sub>	Th(NO <sub>3</sub> ) <sub>4</sub>
0·1	(0·314)	(0·318)	(0·319)	(0·268)	(0·139)	(0·0350)	(0·0458)	(0·279)
0·2	0·278	0·282	0·285	0·212	0·100	0·0225	0·0300	0·225
0·3	0·267	0·270	0·279	0·184	0·081	0·0176	0·0238	0·203
0·4	0·266	0·270	0·281	0·167	0·070	0·0153	0·0207	0·192
0·5	0·271	0·276	0·291	0·155	0·062	0·0143	0·0190	0·189
0·6	0·280	0·286	0·304	0·146	0·056	0·0140	0·0182	0·188
0·7	0·296	0·303	0·322	0·140	0·052	0·0142	0·0181	0·191
0·8	0·314	0·322	0·344	0·135	0·048	0·0149	0·0185	0·195
0·9	0·336	0·345	0·371	0·131	0·046	0·0159	0·0194	0·201
1·0	0·362	0·371	0·401	0·128	—	0·0175	0·0208	0·207
1·2	0·424	0·436	0·474	0·124	—	—	0·0250	0·224
1·4	0·509	0·525	0·565	0·122	—	—	—	0·246
1·6	0·616	0·641	—	—	—	—	—	0·269
1·8	0·756	0·792	—	—	—	—	—	0·296
2·0	0·940	0·995	—	—	—	—	—	0·326
2·5	—							

TABLE III.—OSMOTIC AND ACTIVITY COEFFICIENTS AT HIGH CONCENTRATIONS ( $m > 6$ )

HCl			HClO <sub>4</sub>		LiCl		LiBr		LiNO <sub>3</sub>	
<i>m</i>	$\phi$	$\gamma$	$\phi$	$\gamma$	$\phi$	$\gamma$	$\phi$	$\gamma$	$\phi$	$\gamma$
7	2.008	4.37	2.365	7.44	1.965	3.71	2.206	5.76	1.485	1.723
8	2.163	5.90	2.629	11.83	2.143	5.10	2.432	8.61	1.541	1.952
9	2.315	7.94	2.901	19.11	2.310	6.96	2.656	12.92	1.591	2.19
10	2.444	10.44	3.167	30.9	2.464	9.40	2.902	19.92	1.633	2.44
11	2.559	13.51	3.433	50.1	2.607	12.55	3.150	31.0	1.668	2.69
12	2.663	17.25	3.688	80.8	2.730	16.41	3.356	46.3	1.700	2.95
13	2.760	21.8	3.935	129.5	2.830	20.9	3.581	70.6	1.727	3.20
14	2.853	27.3	4.166	205.0	2.915	26.2	3.776	104.7	—	—
15	2.944	31.1	4.393	322.0	2.978	31.9	3.912	146.0	—	—
16	3.033	42.4	4.608	500.0	3.023	37.9	4.025	198.0	—	—
17	—	—	—	—	3.044	43.8	4.110	260.0	—	—
18	—	—	—	—	3.057	49.9	4.173	331.0	—	—
19	—	—	—	—	3.060	56.3	4.216	411.0	—	—
20	—	—	—	—	3.063	62.4	4.217	485.0	—	—

KOH			NaOH		AgNO <sub>3</sub>	
<i>m</i>	$\phi$	$\gamma$	$\phi$	$\gamma$	$\phi$	$\gamma$
7	1.81	2.88	1.567	1.603	0.426	0.142
8	1.96	3.77	1.707	2.01	0.408	0.129
9	2.09	4.86	1.853	2.55	0.393	0.118
10	2.22	6.22	1.993	3.23	0.378	0.109
11	2.36	8.10	2.131	4.10	0.371	0.102
12	2.50	10.5	2.262	5.19	0.363	0.096
13	2.60	13.2	2.382	6.50	0.356	0.090
14	2.66	15.8	2.488	8.04	—	—
15	2.76	19.6	2.574	9.74	—	—
16	2.87	24.6	2.643	11.53	—	—
17	—	—	2.694	13.47	—	—
18	—	—	2.730	15.41	—	—
19	—	—	2.756	17.38	—	—
20	—	—	2.772	19.33	—	—

SODIUM HYDROXIDE									
<i>m</i>	21	22	23	24	25	26	27	28	29
$\phi$	2.780	2.780	2.773	2.764	2.749	2.731	2.712	2.693	2.678
$\gamma$	21.3	23.1	24.8	26.5	28.0	29.5	30.9	32.2	33.7

TABLE IV.—OSMOTIC AND ACTIVITY COEFFICIENTS OF SUCROSE AT 25 C

<i>m</i>	0.1	2	0.3	0.4	0.5	0.6	0.7	0.8	0.9	1.0	1.2	1.4
$\phi$	1.008	0.017	1.024	1.033	1.041	1.050	1.060	1.068	1.079	1.088	1.108	1.129
$\gamma$	1.017	0.34	1.051	1.068	1.085	1.105	1.125	1.144	1.165	1.188	1.233	1.283

<i>m</i>	1.6	8	2.0	2.5	3.0	3.5	4.0	4.5	5.0	5.5	6.0	
$\phi$	1.150	1.169	1.189	1.240	1.288	1.334	1.375	1.414	1.450	1.482	1.511	
$\gamma$	1.335	1.387	1.442	1.590	1.751	1.924	2.101	2.310	2.481	2.680	2.878	

Finally, we wish to express our thanks to the Chemical Society, a grant from whose Research Fund has made much of this work possible.

University of Malaya,  
Singapore.

Laboratory of Physical Chemistry,  
Cambridge.

# REFERENCES.

- <sup>1</sup> Stokes, *Trans. Faraday Soc.*, 1948, **44**, 295.
- <sup>2</sup> Robinson, *Trans. Roy. Soc. N.Z.*, 1945, **75**, 203.
- <sup>3</sup> Shankman and Gordon, *J. Amer. Chem. Soc.*, 1939, **61**, 2370.
- <sup>4</sup> Stokes, *ibid.*, 1947, **69**, 1291.
- <sup>5</sup> Lewis and Randall, *Thermodynamics* (McGraw-Hill Book Co. Inc., New York, 1923).
- <sup>6</sup> Guggenheim, *Phil. Mag.*, 1935, **19**, (7), 588; 1936, **22**, (7), 322.
- <sup>7</sup> Harned and Owen, *Physical Chemistry of Electrolytic Solutions* (Reinhold Publishing Corp., New York, 1943).
- <sup>8</sup> Randall and White, *J. Amer. Chem. Soc.*, 1926, **48**, 2514.
- <sup>9</sup> Stokes, *ibid.*, 1945, **67**, 1686.
- <sup>10</sup> Robinson and Sinclair, *ibid.*, 1934, **56**, 1830.
- <sup>11</sup> Robinson, Smith and Smith, *Trans. Faraday Soc.*, 1942, **38**, 63.
- <sup>12</sup> Scatchard, Hamer and Wood, *J. Amer. Chem. Soc.*, 1938, **60**, 3061.
- <sup>13</sup> Smith and Smith, *J. Biol. Chem.*, 1937, **117**, 209; **121**, 607; 1940, **132**, 47, 57.
- <sup>14</sup> Stokes, *J. Amer. Chem. Soc.*, 1948, **70**, 874.
- <sup>15</sup> Smith and Robinson, *Trans. Faraday Soc.*, 1942, **38**, 70.
- <sup>16</sup> Harned and Ehlers, *J. Amer. Chem. Soc.*, 1933, **55**, 2179.
- <sup>17</sup> Randall and Young, *ibid.*, 1928, **50**, 989.
- <sup>18</sup> Åkerlöf and Teare, *ibid.*, 1937, **59**, 1855.
- <sup>19</sup> Harned, Keston and Donelson, *ibid.*, 1936, **58**, 989.
- <sup>20</sup> Harned and Robinson, *Trans. Faraday Soc.*, 1941, **37**, 302.
- <sup>21</sup> Pearce and Nelson, *J. Amer. Chem. Soc.*, 1933, **55**, 3075.
- <sup>22</sup> Harned and Swindells, *ibid.*, 1926, **48**, 126.
- <sup>23</sup> Harned, *ibid.*, 1929, **51**, 416.
- <sup>24</sup> Harned, *ibid.*, 1925, **47**, 676.
- <sup>25</sup> Harned and Hecker, *ibid.*, 1933, **55**, 4838.
- <sup>26</sup> Stokes, *ibid.*, 1945, **67**, 1689.
- <sup>27</sup> Åkerlöf and Kegeles, *ibid.*, 1940, **62**, 620.
- <sup>28</sup> Ivett and De Vries, *ibid.*, 1941, **63**, 2821.
- <sup>29</sup> Robinson, *ibid.*, 1941, **63**, 628.
- <sup>30</sup> Harned and Nims, *ibid.*, 1932, **54**, 423; Harned and Cook, *ibid.*, 1939, **61**, 495.
- <sup>31</sup> Olynyk and Gordon, *ibid.*, 1943, **65**, 224.
- <sup>32</sup> Negus, *Thesis* (Johns Hopkins University, 1922).
- <sup>33</sup> Harned and Crawford, *J. Amer. Chem. Soc.*, 1937, **59**, 1903.
- <sup>34</sup> Harned and Cook, *ibid.*, 1937, **59**, 496.
- <sup>35</sup> Åkerlöf and Bender, *ibid.*, 1948, **70**, 2366.
- <sup>36</sup> Harned and Cook, *ibid.*, 1937, **59**, 1290.
- <sup>37</sup> Lovelace, Frazer and Sease, *ibid.*, 1921, **43**, 102.
- <sup>38</sup> Harned and Schupp, *ibid.*, 1930, **52**, 3886.
- <sup>39</sup> Nielsen and Brown, *ibid.*, 1927, **49**, 2423.
- <sup>40</sup> Wetmore and Gordon, *J. Chem. Physics*, 1937, **5**, 60.
- <sup>41</sup> Bray, *J. Amer. Chem. Soc.*, 1927, **49**, 2372.
- <sup>42</sup> LaMer and Parkes, *ibid.*, 1931, **53**, 2040.
- <sup>43</sup> Robinson and Baker, *Trans. Roy. Soc. N.Z.*, 1946, **76**, 250.
- <sup>44</sup> Hartman and Rosenfeld, *Z. physik. Chem.*, 1933, **164**, 377.
- <sup>45</sup> Robinson, *Trans. Faraday Soc.*, 1945, **41**, 756.
- <sup>46</sup> Robinson, *J. Amer. Chem. Soc.*, 1935, **57**, 1161.
- <sup>47</sup> Robinson and McCoach, *ibid.*, 1947, **69**, 2244.
- <sup>48</sup> Jones, *J. Physic. Chem.*, 1947, **51**, 516.
- <sup>49</sup> Robinson, *J. Amer. Chem. Soc.*, 1935, **57**, 1165.
- <sup>50</sup> Robinson, *ibid.*, 1946, **68**, 2402.
- <sup>51</sup> Robinson, *Trans. Faraday Soc.*, 1939, **35**, 1217.
- <sup>52</sup> Jones, *J. Amer. Chem. Soc.*, 1943, **65**, 1353.
- <sup>53</sup> Jones and Froning, *ibid.*, 1944, **66**, 1672.
- <sup>54</sup> Robinson, *ibid.*, 1940, **62**, 3131.
- <sup>55</sup> Stokes, *Trans. Faraday Soc.*, 1945, **41**, 685.
- <sup>56</sup> Robinson and Wilson, *ibid.*, 1940, **36**, 738.
- <sup>57</sup> Jones, *J. Amer. Chem. Soc.*, 1947, **69**, 2066.
- <sup>58</sup> Robinson, *ibid.*, 1937, **59**, 84.
- <sup>59</sup> Robinson and Tait, *Trans. Faraday Soc.*, 1941, **37**, 569.
- <sup>60</sup> Robinson and Jones, *J. Amer. Chem. Soc.*, 1936, **58**, 959.
- <sup>61</sup> Mason, *ibid.*, 1938, **60**, 1638.
- <sup>62</sup> Smith, *ibid.*, 1947, **69**, 91.
- <sup>63</sup> Robinson, *Trans. Faraday Soc.*, 1939, **35**, 1229.
- <sup>64</sup> Mason, *J. Amer. Chem. Soc.*, 1941, **63**, 220.
- <sup>65</sup> Robinson and Levien, *Trans. Roy. Soc. N.Z.*, 1946, **76**, 295.

# THE ADSORPTION OF LONG CHAIN POLAR COMPOUNDS FROM SOLUTION ON METAL SURFACES

By E. B. GREENHILL

Received 28th January, 1949

The adsorption isotherms of long chain polar substances on metal powder have been determined. The results show that saturation of the surface, giving a unimolecular layer, occurs at very low concentrations with strongly adsorbed substances such as stearic acid, whereas alcohols and esters require much higher concentrations. Although the initial rate of adsorption from solution is very rapid, final equilibrium may not be reached for many hours.

The adsorption process appears to be the same for thoroughly cleaned and reduced powders as for oxide-coated powders. With the clean powders, however, the amount of adsorption is increased in some cases owing to an increase in the surface area brought about by the reduction and degassing procedure at 200°-250° C.

A comparison is made of the adsorption results and the boundary lubricating properties of acids, alcohols, and esters. There is some discrepancy in the behaviour of the alcohol, since it is more readily adsorbed on metal powders than the ester, whereas it appears to possess poorer lubricating properties. With the fatty acid and ester, however, there is close agreement between the frictional behaviour and the adsorption measurements. The fatty acid, which is more readily adsorbed (and which may react to form the metal soap) is a more effective boundary lubricant than the ester.

It has generally been assumed that long chain polar compounds are adsorbed on metal surfaces, and that these adsorbed layers are responsible for the boundary lubricating properties of solutions of these substances in oils and other solvents. There are many references in the literature which deal with the lubrication of metals by polar substances dissolved in various solvents, but few which refer to a study of the adsorption process in detail.

The adsorption of polar compounds at the liquid-mercury interface has been studied by Barnard and Wilson<sup>1</sup> and more recently by Wolf,<sup>2</sup> but their results cannot be applied directly to the lubrication of solid metal surfaces by adsorbed polar substances. Heymann and Boye<sup>3</sup> have investigated the adsorption of a homologous series of fatty acids on gold powder. No adsorption was observed for the higher acids such as myristic acid.

Very recently, Zisman and co-workers<sup>4</sup> have studied the formation of oleophobic monolayers on metal surfaces immersed in solutions of long chain polar compounds. While not measuring adsorption directly, these workers have thrown considerable light on the formation of monolayers on metals, a problem of fundamental importance in boundary lubrication.

The only direct investigation of adsorption and boundary lubrication has been carried out by Hutchinson<sup>5</sup> using non-metallic solids. The

<sup>1</sup> Barnard and Wilson, *Ind. Eng. Chem.*, 1922, 14, 682.

<sup>2</sup> Wolf, *Z. angew. Chem.*, 1942, 55, 295.

<sup>3</sup> Heymann and Boye, *Kolloid-Z.*, 1932, 59, 153.

<sup>4</sup> Bigelow, Picket and Zisman, *J. Colloid Sci.*, 1946, 1, 513.

<sup>5</sup> Hutchinson, *Trans. Faraday Soc.*, 1947, 63, 439.



adsorption from solution of a large range of polar compounds on finely divided sodium fluoride was studied, and the results were applied to the lubrication of similar solids by the same solutions.

This paper is concerned with a preliminary investigation of the adsorption of polar compounds from solution on finely divided metal powders.

### Experimental

The adsorption was measured by the method of Hutchinson.<sup>8</sup> Appropriate volumes of solution, before and after adsorption, were spread on to a surface balance and the decrease in concentration due to adsorption calculated from the decrease in area of the film at constant pressure. This method has the great advantage that it is applicable to any water-insoluble long chain polar compound and is therefore very suitable for the type of compounds used as boundary lubricants.

Copper, silver, iron, nickel and platinum powders were used, sufficient quantities being obtained to enable all the adsorption experiments to be carried out on the same batch of powder. The copper was prepared by electrolysis, the silver by chemical precipitation, the iron from iron carbonyl and the nickel was probably reduced from the oxide. The platinum powder was a special non-porous sample. The powders were thoroughly dried in a vacuum desiccator before use and were shown to be free from grease contamination by washing with clean benzene and spreading the washings on the surface balance. Usually, the powders were not freed from oxide or from adsorbed vapours, but some experiments showed that cleaned and reduced powders give similar results.

The long chain polar compounds used were stearic acid, m.p.  $69.3^{\circ}\text{C}$ , ethyl stearate, m.p.  $30.6^{\circ}\text{C}$  and octadecyl alcohol, m.p.  $58^{\circ}\text{C}$ . A.R. benzene which had been dried and redistilled over sodium was used as the solvent and no surface-active contaminant was detected in it when a sample was spread on a surface balance.

The initial concentrations of the solutions used were determined by diluting a known volume and spreading a portion of this solution on a surface balance by means of a micro-pipette; this gave a more accurate value than that obtained by direct weighing. In the adsorption experiments 5 ml. of the solution were added to a stoppered tube containing a known weight (2.5 g.) of metal powder and the whole shaken at frequent intervals for 4 hr. At the end of this period a known volume of the solution was diluted, spread on the surface balance and the adsorption calculated. Satisfactory agreement between duplicate experiments was obtained. To standardize conditions, the tubes were placed in a thermostat maintained at  $22^{\circ}\text{C}$  while adsorption was taking place and the surface balance measurements were made at a constant pressure of 26 dynes/cm. This method was used successfully up to concentrations of 50 mg./ml.; at higher concentrations the experimental errors involved in the determination of the concentration become of the same order of magnitude as the change in concentration due to adsorption itself and the method becomes useless.

### Results

**(a) The Adsorption Isotherm.**—Adsorption isotherms for stearic acid, octadecyl alcohol and ethyl stearate at  $22^{\circ}\text{C}$  are shown in Fig. 1, 2 and 3, in which the adsorption in mg./g. powder is plotted against the concentration of solution in contact with the adsorbent after 4 hr. The isotherms show that the maximum adsorption of stearic acid on all metals is attained at much lower concentrations than with the alcohol and the ester. Very strong solutions are necessary before any appreciable adsorption of the ester occurs, so that the results for the ester are subject to considerable error and must be considered as approximate values indicative of general trends. It is also interesting to note that a plot of the concentration  $C$  against  $Cm/x$ , where  $x$  mg. of adsorbate is adsorbed on  $m$  g. of powder does not give a straight line for the alcohol or the ester. This shows that the isotherms are not of the simple Langmuir type. It is not possible to test the validity of the Langmuir equation for the acid with the present data, since results at very low concentrations have not been obtained.

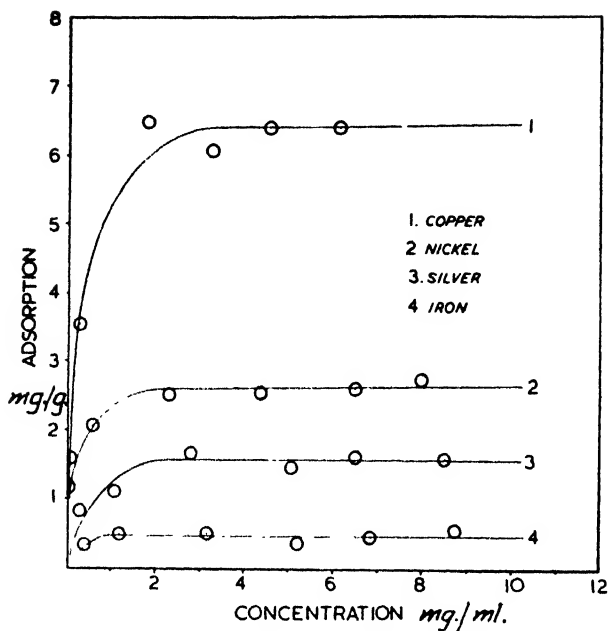


FIG. 1.—Adsorption isotherms for stearic acid on metal powders from benzene solution at 22° C.

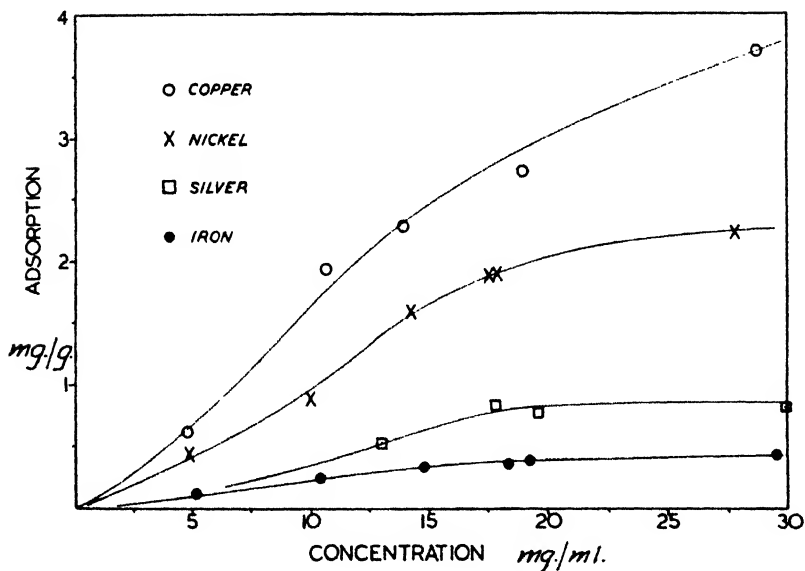


FIG. 2.—Adsorption isotherms for octadecyl alcohol on metal powders from benzene solution at 22° C.

The adsorption of the above compounds is almost certainly unimolecular. Harkins and Gans <sup>7</sup> have assumed this for acids, and have proposed a new method for determining the surface area of a powder based upon the adsorption of a suitable acid from solution. This method was used by Hutchinson <sup>8</sup> in his work on ionic crystals. Two assumptions are involved, (a) that at maximum adsorption the surface is covered by a close-packed oriented monolayer, and (b) that the area occupied by each molecule is the same as on an aqueous surface—that is, approximately 20 sq. Å. Further support for these assumptions was obtained in the present work from area measurements on iron powder. The area calculated from the adsorption of stearic acid was 2100 cm.<sup>2</sup>/g., a value in good agreement with that calculated from the mean diameter of the spherical particles, 1730 cm.<sup>2</sup>/g. Similar comparisons for the other powders were not possible owing to the very irregular nature of the particles. Areas of the other powders calculated from adsorption data are as follows—copper 27,200 cm.<sup>2</sup>/g., silver 6,800 cm.<sup>2</sup>/g., nickel 11,100 cm.<sup>2</sup>/g., platinum 13,600 cm.<sup>2</sup>/g. The area of copper powder is very doubtful since some chemical reaction between the powder and stearic acid was observed.

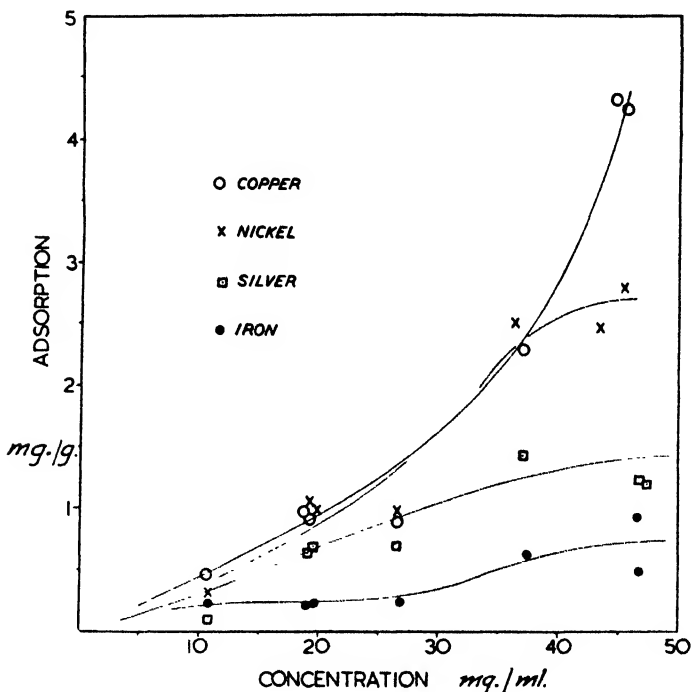


FIG. 3.—Adsorption isotherms for ethyl stearate on metal powders from benzene solution at 22° C.

It is interesting to consider these results in connection with frictional measurements made using solutions of these compounds in paraffin oil as boundary lubricants. Frewing <sup>6</sup> has shown that a solution containing from 0.1 to 1.0 % of stearic acid will readily lubricate most metals, while concentrations of at least 50 % of ethyl stearate are necessary for the lubrication of steel surfaces.<sup>6</sup> Since the concentrations used by Frewing are of the same order as those found necessary to give a close-packed monolayer in the adsorption experiments, this indicates that a close-packed monolayer is required for effective lubrication. However, several workers have shown that alcohols are not effective boundary lubricants on any metal surfaces, either in the pure liquid

<sup>6</sup> Frewing, *Proc. Roy. Soc., A*, 1944, **182**, 270.

<sup>7</sup> Harkins and Gans, *J. Amer. Chem. Soc.*, 1931, **53**, 2805.

<sup>8</sup> Hutchinson, *Trans. Faraday Soc.*, 1947, **63**, 443.

state or in hydrocarbon solution. The adsorption data show that alcohols are more strongly adsorbed than esters, so that they should be superior to esters as lubricants. A possible explanation of this anomaly is that esters may be hydrolyzed to some extent on the surface, forming some free acid, especially at high concentrations.

Nearly all boundary lubrication investigations have been concerned with paraffin oil solutions but it is unlikely that great differences would occur with other hydrocarbon solvents provided that equilibrium conditions have been established. For instance, solubilities of long chain polar compounds do not vary a great deal in the various hydrocarbons, so that the adsorption equilibria might be expected to be similar in each case. Adsorption experiments carried out with hexane as solvent gave similar results to those obtained using benzene.

**(b) The Effect of Oxide and Other Adsorbed Films.**—The powders for which the adsorption isotherms were determined, were free from surface-active impurities and were dry, but there is little doubt that they were covered by a relatively thick oxide film and/or adsorbed gas films. These are the conditions normally encountered in friction experiments so that the above results should be used when discussing the effect of adsorption on lubrication. It is, however, of interest to determine the effect on adsorption of removing the oxide and adsorbed gases. For this purpose samples of metal powder were alternately outgassed and reduced in hydrogen at 200-250° for three days after which the glass bulbs in which the metal was contained were sealed off while still under vacuum. When required the bulbs were broken into the benzene solution.

Table I shows some results for the adsorption of stearic acid on reduced and oxidized powders. In all cases the initial concentration of stearic acid was 10 mg./ml. and the adsorption was measured after the solution had been in contact with the powder for 4 hr.

TABLE I.—ADSORPTION OF STEARIC ACID FROM BENZENE  
10 MG./ML. AFTER 4 HR. AT 22° C

Powder	Oxidized Powder Adsorption mg./g.	Reduced Powder Adsorption mg./g.
Ag . . .	1.27	1.48
Cu . . .	10.30	14.50
Fe . . .	0.51	0.76
Ni . . .	3.48	3.43
Pt . . .	3.20	4.77

It will be seen that the amount of acid adsorbed increases when the powder is degassed and reduced at 200-250° C. This suggests that the surface area may be increased slightly during the treatment. If higher temperatures are used, the powders sinter badly.

**(c) The Rate of Adsorption.**—Except with copper, the initial rate of adsorption of stearic acid is extremely rapid, approximately 90 % of the 4-hr. adsorption occurring in the first 5 min. It was found that a stearic acid solution left in contact with copper powder for many hours developed a pale blue colour, presumably due to the formation of the copper soap. Since the maximum adsorption of alcohol and ester on copper is attained considerably more rapidly than with stearic acid, it would seem that the slow chemical reaction is interfering with the adsorption process in some way. The rates of adsorption from a 1 % solution of stearic acid in benzene on both oxidized and reduced powders are shown in Fig. 4. These results show that the rates of adsorption are similar for oxidized and reduced powders.

If the adsorption is allowed to proceed for periods longer than 4 hr., further increases in the amount of adsorption often occur. This is illustrated by the data given in Table II.

It will be seen that this increase amounts only to a few per cent. for iron and nickel, but for copper and silver it is rather greater. This increase may be associated with slow chemical reaction with copper, and possibly with a slow absorption into the interstices of the powder. (Examination under the microscope showed the powder to consist of extremely irregular particles.) With copper, chemical reaction is probably the more important factor. This is supported by the observation that the effect is more marked for the fatty acid,

especially at high concentrations, than for the ester or alcohol. With silver, however, there is also an appreciable increase in adsorption with time for the alcohol and ester. Since chemical reaction between the silver powder and the alcohol is very unlikely this suggests that the effect is due to a slow absorption into the interstices of the powder. A similar explanation probably also applies to the other metals examined and it is clear that, in general, complete equilibrium is not attained for many hours.

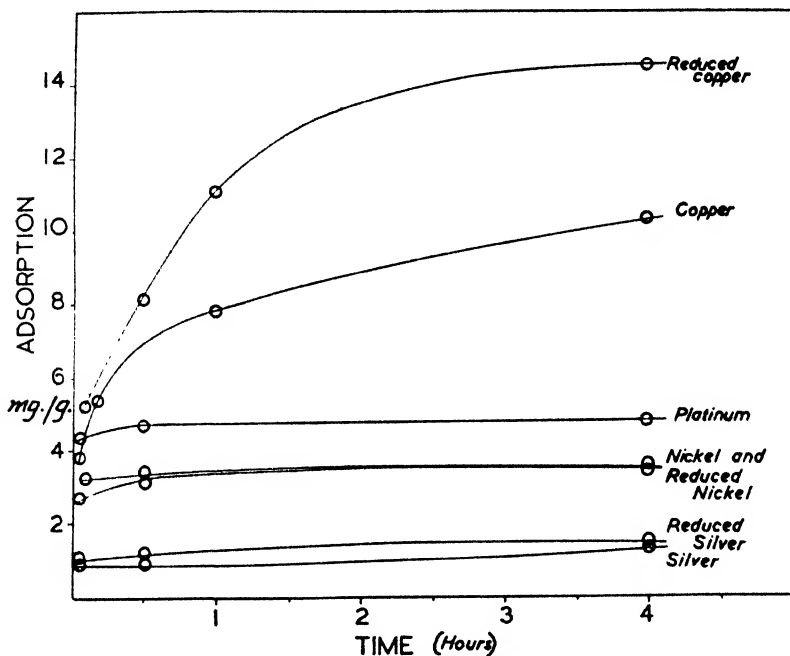


FIG. 4.—Graph showing the rates of adsorption of stearic acid from benzene solution 10 (mg./ml.) on metal powders.

It must be pointed out that the results shown in Table II were obtained using various batches of powder, so that they may not be consistent with each other, nor with the results quoted earlier in the determination of the isotherm.

TABLE II.—ADSORPTION OF STEARIC ACID FROM BENZENE SOLUTION

Initial Concentration mg./ml.	Metal	4-hr. Adsorption mg./g.	24-hr. Adsorption mg./g.
1.66	Cu	3.54	3.89
	Fe	0.44	0.47
	Ni	2.04	2.31
3.76	Ag	1.72	2.24
	Cu	7.04	8.70
	Fe	0.52	0.52
	Ni	2.50	2.70
5.61	Cu	5.90	6.53
	Fe	0.38	0.41
	Ni	2.45	2.55
9.38	Ag	1.59	1.70
	Cu	6.29	8.33
	Fe	0.58	0.58

This work was carried out in the Department of Physical Chemistry, Cambridge, as part of a joint programme between the Research Laboratory on the Physics and Chemistry of Rubbing Solids, Cambridge, and the Division of Tribophysics, Council for Scientific and Industrial Research, Australia. I should like to express my thanks to Mr. S. G. Daniel for his assistance in the experimental work and to Dr. F. P. Bowden for his encouragement and advice during the course of this investigation. I am also indebted to the Ministry of Supply (Air) for grants to the Laboratory and to C.S.I.R. (Australia) for a research award.

*Research Laboratory on the Physics  
and Chemistry of Rubbing Solids,  
Department of Physical Chemistry,  
Cambridge.*

*Division of Tribophysics,  
C.S.I.R., Australia.*

---

## THE LUBRICATION OF METAL SURFACES BY MONO- AND MULTI-MOLECULAR LAYERS

BY E. B. GREENHILL

*Received 28th January, 1949*

A study has been made of the boundary lubricating properties of stearic acid, ethyl stearate, octadecyl alcohol and the stearates of copper and silver. Layers of these compounds were deposited, by the Langmuir-Blodgett method, on a flat metal surface and the friction between this surface and a clean slider of the same metal was measured. The minimum number of layers required to provide effective lubrication depends on the compound and metal used. Where a metal can be lubricated by a solution of one of these compounds in paraffin oil one or three deposited layers suffice but where a paraffin solution does not provide lubrication more than three layers are necessary. This indicates that where paraffin solutions do effect lubrication the sliding surfaces are only separated by the monolayer adsorbed on each surface. The results for platinum and silver show that metal stearates are more effective lubricants than stearic acid itself.

The temperatures at which these deposited layers cease to lubricate have been determined. In agreement with the results of other workers it is shown that breakdown of lubrication occurs at the bulk melting point of the compound except with stearic acid on a reactive metal where lubrication persists up to a temperature which corresponds roughly to the softening point of the appropriate metal soap.

---

The comprehensive investigations of Hardy<sup>1</sup> showed that thin films of polar compounds were effective boundary lubricants when only a few molecules thick. He suggested that an oriented monolayer of polar material was responsible for the boundary lubricating properties observed. Using the Langmuir-Blodgett technique for the deposition of monolayers, this suggestion has been confirmed by Langmuir,<sup>2</sup> Akamatu and Sameshima,<sup>3</sup> Isemura,<sup>4</sup> and Bowden and Leben.<sup>5</sup> These workers have either used glass or steel surfaces and have shown that the same initial lowering of the coefficient of friction is observed for a monolayer as for an excess of the lubricant.

<sup>1</sup> Hardy, *Collected Works* (Camb. Univ. Press, 1936).

<sup>2</sup> Langmuir, *Trans. Faraday Soc.*, 1920, **15**, 62.

<sup>3</sup> Akamatu and Sameshima, *Bull. Chem. Soc. Japan*, 1936, **11**, 791.

<sup>4</sup> Isemura, *ibid.*, 1940, **15**, 467.

<sup>5</sup> Bowden and Leben, *Phil. Trans. A*, 1940, **239**, 1.

Working with relatively thick layers of pure substances, Tabor<sup>6</sup> showed that the majority of long chain boundary lubricants have sharply defined transition temperatures which are reversible. At this temperature, the frictional coefficient rises sharply and the type or nature of the sliding may change. In many cases the transition temperature corresponds to the bulk melting point of the lubricant, but it is definitely above the melting point when certain reactive metals such as cadmium and copper are lubricated by fatty acids. Bowden, Gregory and Tabor<sup>7</sup> have suggested that fatty acids lubricate above their melting points when they react with the metal surface to form metallic soap films which lubricate up to their softening or melting points.

Hughes and Whittingham<sup>8</sup> and Frewing<sup>9</sup> have observed similar changes with mono- and multi-layers deposited by the Langmuir-Blodgett technique on stainless steel surfaces. The actual transition temperatures observed are similar to those found for an excess of the same lubricant.

Much of this work on monolayers has been conducted with layers of doubtful composition, since some workers have used ordinary tap water as substrate for the deposition. Acid layers deposited in this way will contain a large proportion of calcium or other soaps. Also, nearly all workers have employed glass or stainless steel surfaces. This investigation is concerned with the lubricating properties and transition temperatures of mono- and multi-layers of pure acids, esters and metallic soaps deposited from conductivity water on a range of metal surfaces. It was hoped in this way to confirm and extend the results of previous workers and to throw further light on the boundary lubricating process.

### Experimental

The apparatus used for the measurement of friction coefficients and transition temperatures of boundary films was similar to that used by Bowden and Leben.<sup>10</sup> The load applied between the sliding surfaces was 4 kg. and the speed of sliding was approximately 0.007 cm. sec<sup>-1</sup>. The temperature of the lower surface was controlled by means of a heating element placed inside the hollow metal box on which the lower surface was mounted. The temperature was measured by means of a specially designed copper-constantan thermocouple which was pressed on to the surface by means of a spring. This thermocouple consisted of 0.035 mm. diameter wires sealed into a glass tube, the end of which was ground down until the wires were exposed. The end was made slightly convex and was coated with a layer of copper or silver in an evaporation apparatus.

In this way the thermocouple possessed a small heat capacity and made thermal contact over a relatively large area, so that heat losses into the thermocouple were small and almost independent of the load and of the nature of the metal plate. For a plate temperature of 100° C, for example, the error in the thermocouple reading was of the order of a few degrees C. Similar errors are likely to occur due to the conduction of heat from the plate into the slider. This was considerably reduced by constructing the slider in the form of a small metal tip mounted in an insulating glass holder. However, even with un-insulated sliders, theory and experiment show that for most of the metals used, for a plate temperature of 100° C the temperature drop is no greater than about 5° C if the slider and plate are of the same metal. With the insulated sliders the error is even smaller. Since similar metals were used in all the following experiments the surface temperatures may be considered reliable to within a few degrees C.

The lower plate was heated continuously at a slow uniform rate (that used when the thermocouple was calibrated) during each determination of the transition temperature.

<sup>6</sup> Tabor, *Nature*, 1940, **145**, 308 and 1941, **147**, 609.

<sup>7</sup> Bowden, Gregory and Tabor, *ibid.*, 1945, **156**, 97.

<sup>8</sup> Hughes and Whittingham, *Trans. Faraday Soc.*, 1942, **38**, 9.

<sup>9</sup> Frewing, *Proc. Roy. Soc. A*, 1942, **181**, 23.

<sup>10</sup> Bowden and Leben, *ibid.*, 1939, **169**, 371.

In all cases except that of stainless steel, the metals used were spectroscopically pure. The lower plates were approximately 3 in.  $\times$   $\frac{1}{2}$  in.  $\times$   $\frac{1}{8}$  in. in size and were polished on grade 600 emery paper under water prior to an electrolytic degreasing process as recommended by Blodgett.<sup>11</sup> The specimen is made the cathode in a bath containing 20 g. NaOH in 1 l. of 95 % methyl alcohol using a current of 1-1.5 A. The hemispherical sliders were all polished on 600 emery paper in a high-speed chuck and thoroughly rubbed on clean, degreased cloth to remove any traces of emery.

The long chain compounds investigated were stearic acid, m.p. 69.3° C; octadecyl alcohol, m.p. 58° C; ethyl stearate, m.p. 30.6° C. These compounds were spread from a petroleum ether solution on the water surface of a Langmuir trough. Pure oleic acid or castor oil served as suitable piston oils, the latter being preferable for the ester and soap films. The water used in the trough was doubly distilled, a quartz still being used for the second distillation. For the deposition of soap films, the pH was adjusted to approximately 9.5 by the addition of a solution containing 30 g.  $\text{KHCO}_3$ /l., 0.6 g. KOH/l., and 4 g.  $\text{NH}_4\text{OH}$  (0.880)/l. A small concentration, usually  $5 \times 10^{-6}$  mole/l. of the appropriate metal ion was obtained by the addition of A.R. salt. A fatty acid monolayer spread on the trough under these conditions will react to give a substantially pure soap: the actual composition of the films was not investigated (see Langmuir,<sup>12, 13</sup>). In order to avoid irregularities in the films deposited on the metal surfaces, the metals were raised and lowered through the water surface by an electrically driven device. In this way mono- and multi-layers could be deposited, though with the alcohol it was possible to deposit only the single monolayer.

## Results

(a) **The Effect of Film Thickness.**—For efficient boundary lubrication, each metal requires a characteristic number of molecular layers of each lubricant. When a sufficient number is present, sliding is smooth and the coefficient of friction is reduced to a value which is roughly independent of the metal at temperatures below the transition point. The coefficient of friction usually lies between 0.08 and 0.12 although occasional values as low as 0.05 have been observed on the softer metals. Once this value has been reached no further change occurs as the lubricating layer becomes thicker. Table I shows the minimum number of layers required by each metal for acid, ester and soap films. These results refer to films deposited on the lower plate only; no films were deposited on the slider.

TABLE I.—MINIMUM NUMBER OF MOLECULAR LAYERS REQUIRED FOR ADEQUATE BOUNDARY LUBRICATION

Metal	Acid	Ester	Soap (Cu or Ag Stearate)
Stainless steel (18/8)	3	3	1
Copper	3	5 or 7	3
Silver	7	11 or 13	3
Cadmium	3	—	—
Nickel	3	—	3
Platinum	10	—	ca. 9

After some preliminary work with acid films cadmium was not used owing to the difficulty of preparing a clean, polished surface unaffected by immersion in water.

It will be seen that metallic soaps are the most efficient lubricants and that steel is the metal lubricated most easily. These observations are consistent with the results obtained when an excess of lubricant or a solution in paraffin oil is employed. For example, a 1 % solution of stearic acid in paraffin oil will lubricate steel, copper and cadmium, but not silver and platinum. Similarly, pure esters or their solution only lubricate steel effectively. It is seen that those metals which are lubricated under these conditions are those which require one or three molecular layers deposited from a Langmuir trough.

<sup>11</sup> Blodgett, *J. Amer. Chem. Soc.*, 1935, **57**, 1007.

<sup>12</sup> Langmuir and Schaefer, *ibid.*, 1936, **58**, 284.

<sup>13</sup> Langmuir and Schaefer, *ibid.*, 1937, **59**, 2400.



It must be remembered that when the lubricant is applied directly to the surfaces an adsorbed monolayer is formed on each of the sliding surfaces, whilst in the above experiments the layers are deposited only on the lower surfaces. Further, layers deposited by the dipping method are probably less perfect than those adsorbed from solution. For these reasons it can be assumed that the behaviour of three monolayers deposited on one surface is not significantly different from a monolayer adsorbed on to both surfaces. These results therefore show that on reactive surfaces "one or two" monolayers of fatty acid are sufficient to provide effective lubrication. On non-reactive metals many more layers are necessary. If, however, films of metallic soap are deposited on the surfaces, even a non-reactive metal such as silver is lubricated by 3 monolayers. This again emphasizes the effectiveness of soap films in boundary lubrication.

(b) **Transition Temperatures of Mono- and Multi-layers.**—The transition temperatures of these films were measured as soon as possible after their deposition on the metal surfaces. The results are the mean of several determinations on *freshly* prepared surfaces and sliders. Some metals appeared to give less reproducible results than others so that in these cases six or more determinations were made. With all precautions, it was found that the agreement between successive results was occasionally better than 5° C and never worse than 10° C.

Transition temperatures are recorded in Table II for acid, ester, alcohol and soap films. These temperatures are those which correspond to the complete breakdown in lubrication. In all cases, the number of layers given in column 3 is the minimum required to give the effective lubrication at room temperature.

TABLE II.—TRANSITION TEMPERATURES OF MONO- AND MULTI-LAYERS

Metal	Lubricant	Number of Layers	Transition Temperature °C
Stainless steel (18/8)	Stearic acid	3	130
	Ethyl stearate	3	78
	Octadecyl alcohol	1	40-45
	Silver stearate	1	140 } Very
	Copper stearate	1	148 } variable
Copper.	Stearic acid	3	90
	Ethyl stearate	7	31
	Silver stearate	3	127
	Copper stearate	3	94
Silver . . . .	Stearic acid	5	69
	Ethyl stearate	—	No lubrication for 11 layers
	Silver stearate	3	113
	Copper stearate	3	96
Nickel . . . .	Silver stearate	3	112
	Copper stearate	3	110
Cadmium . . . .	Stearic acid	3	90
Platinum . . . .	Stearic acid	27*	69
	Silver stearate	10	122
	Copper stearate	10	120

(\* Not minimum thickness.)

Experiments show that there is a tendency for the transition temperature to increase slightly as the thickness of the layer is increased above the minimum, but the difference is usually small.

According to the theory proposed by Bowden, Gregory and Tabor<sup>7</sup> the transition temperatures of pure fatty acids on metals with which they can react ought to be the same as those for layers of the appropriate metal soap. Copper lubricated by three layers of stearic acid should then behave similarly to copper

lubricated by three layers of copper stearate. Table III shows that this is indeed the case: for stearic acid on copper, lubrication persists up to 90° C while for the copper soap itself lubrication is effective up to approximately the same temperature. On the other hand, as we saw before, unreactive metals such as platinum or silver are not lubricated by fatty acid films above their melting point. If, however, a metal soap of sufficient thickness is directly applied to these surfaces the lubrication is effective up to a much higher temperature. For example, with copper stearate films on silver, lubrication persists up to 96° C whereas for stearic acid the transition temperature is the melting point, 69° C. These results support the view that the lubrication of copper by stearic acid is due to the formation of a surface film of copper stearate. The results further suggest that the lubrication observed is essentially a property of the soap film itself and is not markedly dependent on the nature of the substrate.

TABLE III.—TRANSITION TEMPERATURES FOR FILMS OF MINIMUM THICKNESS REQUIRED FOR LUBRICATION

Metal	Lubricant			
	Stearic acid, m.p. 69° C	Copper stearate, m.p. 111° C	Silver stearate m.p. 180° C	Excess Stearic Acid, m.p. 69° C
Copper . . .	90	94	125	108
Silver . . .	69	96	113	69
Platinum . .	69	120	122	69

Bowden, Gregory and Tabor<sup>7</sup> and Gregory and Spink<sup>14</sup> have associated the final transition temperature with the bulk softening point of the metal soap. The softening or melting points of copper and silver stearates, recorded by Lawrence,<sup>15</sup> are given in Table III. It will be seen that transition temperatures and melting points are of the same order for copper stearate, but large discrepancies occur with silver soaps. Since metallic soaps soften over quite a large temperature range and have ill-defined melting points, discrepancies of this order are only to be anticipated. When the melting point is sharp, as with pure acids, esters, and hydrocarbons, there is usually a close agreement between transition temperatures and bulk melting points. This is shown by stearic acid layers on silver and platinum surfaces where no chemical reaction occurs.

Using monolayers, Frewing<sup>9</sup> and Gregory and Spink<sup>14</sup> have observed temporary rises in the frictional force which occur at temperatures below the final transition temperature. In the present work, similar changes have been observed in "soap" films. Copper and silver stearate films show definite fluctuations of the coefficient of friction at 60-80° C, i.e. near the melting point of stearic acid. These fluctuations may be due to the melting of some free acid present in the film (even when deposited at a pH of 9.5) or the soap films themselves may undergo a phase change near the melting point of the acid from which they are derived.

This work was carried out in the Department of Physical Chemistry, Cambridge, as part of a joint programme between the Research Laboratory on the Physics and Chemistry of Rubbing Solids, Cambridge, and the Division of Tribophysics, Council for Scientific and Industrial Research, Australia. I should like to express my thanks to Dr. F. P. Bowden and Dr. Tabor for their advice and encouragement during the course of this work. I am also indebted to the Ministry of Supply (Air) for grants to the Laboratory, and to C.S.I.R. (Australia) for enabling me to carry out this work at Cambridge.

*Research Laboratory on the Physics  
and Chemistry of Rubbing Solids,  
Department of Physical Chemistry,  
Cambridge.*

*Division of Tribophysics,  
C.S.I.R., Australia.*

<sup>14</sup> Gregory and Spink, *Nature*, 1947, **159**, 403.

<sup>15</sup> Lawrence, *Trans. Faraday Soc.*, 1938, **34**, 660.

# DIFFUSION IN MEDIA WITH VARIABLE PROPERTIES

## PART I. THE EFFECT OF A VARIABLE DIFFUSION COEFFICIENT ON THE RATES OF ABSORPTION AND DESORPTION

BY J. CRANK AND M. E. HENRY

*Received 4th February, 1949*

Numerical solutions of the diffusion equation in one dimension are obtained for a number of diffusion coefficients varying in different ways with the concentration of the diffusing substance, in order to see how the form of the diffusion coefficient influences the relative behaviour of the absorption and desorption-time curves. In all the cases examined it is found that, when the diffusion coefficient increases uniformly with increasing concentration, absorption is quicker than desorption throughout, but that, when the diffusion coefficient decreases with increasing concentration, the reverse is true. When the diffusion coefficient first increases, passes through a maximum value and finally decreases as concentration increases, the absorption and desorption-time curves may cross each other and the conditions for which this occurs are examined.

The accuracy of an approximation to  $\int D \, dC$  is considered and on the basis of this approximation a new method of evaluating the diffusion coefficient-concentration relation from experimentally determined absorption-time curves is suggested.

---

**1. Introduction.**—Earlier experimental work on diffusion was largely concerned with measurements of a diffusion coefficient in systems for which it was reasonable to suppose that this coefficient was constant. Similarly, the formal mathematical solutions of the diffusion equation which have been developed, at least for the non-steady state, are almost entirely confined to the special case of a constant diffusion coefficient. In many systems, however, the diffusion coefficient not only varies but varies so considerably that conclusions based on the assumption of a constant coefficient may be entirely misleading, and some of the most interesting features of the systems may be overlooked. Such systems, which include the diffusion of organic liquids and vapours into polymer films and into fibres are now being extensively studied not only because of their importance in fundamental research work but also because they are of considerable technological interest to the textile and other industries.

It seems desirable, therefore, to consider, in as general a way as possible, some of the properties associated with a variable diffusion coefficient. In the present paper the problem is approached by evaluating approximate numerical solutions of the diffusion equation for a number of diffusion coefficients varying in different ways with the concentration of diffusing substance. The method of obtaining the mathematical solutions is described briefly but the emphasis of the paper is on the behaviour of the calculated absorption and desorption-time curves associated with the different diffusion coefficients.

A method of deducing the relation between the diffusion coefficient and concentration from a number of experimentally determined absorption or desorption-time curves is suggested on the basis of the results presented in this paper.

**2. The Diffusion Equation and some Transformations.**—Suppose a sample of material in the form of an infinite plane sheet of thickness  $2l$  is immersed in a bath of liquid or vapour of infinite extent. If it is assumed that the rate-determining process controlling the absorption of liquid or vapour by the sheet is one of diffusion, the absorption process can be examined by evaluating solutions of the appropriate form of the diffusion equation. It will be convenient to refer throughout to the diffusing liquid or vapour as the penetrant, a term which can include solvents as well as swelling agents.

Since the diffusion is here one-dimensional, the diffusion equation is

$$\frac{\partial C}{\partial t} = \frac{\partial}{\partial x} \left( D_1 \frac{\partial C}{\partial x} \right), \quad (1)$$

where  $C$  is the concentration of the penetrant,  $D_1$  the diffusion coefficient assumed to be a function of  $C$  only,  $t$  is the time variable and  $x$  the space variable. In order to study the rate of absorption, solutions of (1) are required subject to the boundary conditions

$$C = C_0, \quad x = -l, \quad x = +l, \quad t > 0, \quad (2)$$

and the initial condition

$$C = 0, \quad -l < x < l, \quad t = 0. \quad (3)$$

In practice the thickness  $2l$  of the sheet can only be assumed constant as diffusion proceeds if the molal volume of the penetrant molecules is effectively zero within the sheet. In general this is not so, and usually as the sheet absorbs penetrant its volume is increased, that is, the sheet swells. This implies that, in terms of the space variable  $x$ , the condition (2) is to be applied on a moving boundary, the motion of the boundary depending on the solution of (1) which itself depends on the motion. This awkward situation can be avoided by introducing a new variable of length  $z$ , defined such that unit increment in  $z$  always includes unit mass of the material of the sheet, and therefore the range in  $z$  between the two faces of the sheet is constant, being equal to the mass of the sheet per unit area. Provided the concentration of penetrant is also defined in terms of  $z$ , i.e. is defined as the mass of penetrant per unit mass of sheet in any element of overall volume, the diffusion equation and the boundary conditions for the swelling sheet are found to take the same form as (1), (2) and (3). The relevant diffusion coefficient is defined as the ratio of the flux of penetrant across unit area of a section fixed so that the mass of sheet on either side of it remains constant, to the space gradient of concentration of penetrant at the section, both the concentration and its gradient being measured in terms of the new variable  $z$ . These transformations apply whether the molal volumes of the material of the sheet and of the penetrant are independent of composition or not, and so the following treatment of equations (1), (2) and (3) is of general application to both swelling and non-swelling sheets except in so far as there may be complicating features other than the change of volume.

It is convenient to introduce the non-dimensional variables

$$c = C/C_0, \quad \xi = x/l, \quad \tau = D_0 t/l^2, \quad D = D_1/D_0, \quad (4)$$

where  $D$  is a function of  $c$  conveniently written in the form,

$$D = 1 + f(c), \quad (5)$$

so that  $D_0$  is the value of  $D_1$  when  $c = 0$ . Equations (1), (2) and (3) then reduce to

$$\frac{\partial c}{\partial \tau} = \frac{\partial}{\partial \xi} \left( D \frac{\partial c}{\partial \xi} \right), \quad (6)$$

$$c = 1, \xi = -1, \xi = 1, \tau > 0, \quad . \quad . \quad . \quad (7)$$

$$c = 0, -1 < \xi < 1, \tau = 0. \quad . \quad . \quad . \quad (8)$$

**3. Evaluation of Numerical Solutions.**—In the early stages of diffusion, when the concentration of penetrant has not become appreciable at the centre of the sheet, the problem reduces to one of diffusion into a semi-infinite sheet with constant surface concentration, i.e. considering the surface  $\xi = 1$ , solutions of (6) are required for the conditions,

$$c = 1, 1 - \xi = 0, c \rightarrow 0, 1 - \xi \rightarrow \infty, \tau > 0, \quad . \quad . \quad . \quad (9)$$

$$c = 0, 1 - \xi > 0, \tau = 0. \quad . \quad . \quad . \quad (10)$$

For these conditions Boltzmann<sup>1</sup> has shown that the concentration may be expressed as a function of a new variable  $\eta$  where

$$\eta = (1 - \xi)/2\sqrt{\tau}. \quad . \quad . \quad . \quad (11)$$

The partial differential equation (6) then reduces to an ordinary differential equation in  $\eta$ , namely

$$+ 2\eta \frac{dc}{d\eta} = \frac{d}{d\eta} \left( D \frac{dc}{d\eta} \right), \quad . \quad . \quad . \quad (12)$$

and the required solutions must satisfy the conditions

$$c = 1, \eta = 0, c \rightarrow 0, \eta \rightarrow \infty. \quad . \quad . \quad . \quad (13)$$

Numerical solutions of (12) can be obtained for a given relation between  $D$  and  $c$ , using a standard iterative method of integration.<sup>2</sup> Thus on integration, eqn. (12) may be written

$$c = 1 - A \int_0^{\eta} \frac{1}{D} \exp \left\{ - \int_0^{\eta} \frac{2\eta}{D} d\eta \right\} d\eta, \quad . \quad . \quad . \quad (14)$$

where  $A$  is a constant determined by the conditions (13). By taking  $D$  to have the constant value  $D = 1$ , which is its value at  $c = 0$ , a first approximation to  $c$  may be evaluated and it is in fact the well-known solution

$$c = 1 - \operatorname{erf} \eta, \quad . \quad . \quad . \quad (15)$$

where 
$$\operatorname{erf} \eta = \frac{2}{\pi^{1/2}} \int_0^{\eta} e^{-x^2} dx. \quad . \quad . \quad . \quad (16)$$

It is usually found in practice for the diffusion coefficients considered here that when  $\eta > 4.0$ ,  $c$  is effectively zero, which indicates the relevant range in  $\eta$  over which the integration must be carried out, i.e. the condition  $c = 0$ ,  $\eta > 4.0$  replaces  $c \rightarrow 0$ ,  $\eta \rightarrow \infty$  in practice. Using (15) and (5),  $D$  is evaluated at equal intervals in  $\eta$  (every 0.1 in  $\eta$  was found to be satisfactory for most cases considered) and hence (14) is evaluated to give a second approximation to  $c$  at each  $\eta$ , having first determined  $A$  so that (13) is satisfied. The process is repeated till successive approximations to  $c$  agree to within the order of accuracy required. If the error function solution (15) is taken as the first approximation, corresponding values of  $c$  after the fourth and fifth approximations differ by less than 5 in the third decimal place in all cases considered here. With a little experience this order of accuracy can be achieved after only one or two approximations by making a better first estimate of the solution than is afforded by (15). If  $c = 0$  at the chosen upper limit of  $\eta$ , e.g.  $\eta = 4.0$ , but  $dc/d\eta \neq 0$ , then the iteration is repeated for a higher upper limit of  $\eta$ . The suggestion that this method might prove suitable in this case was made to us by Prof. D. R. Hartree.

<sup>1</sup> Boltzmann, *Ann. Physik., Leipzig*, 1894, **53**, 959.

<sup>2</sup> Levy and Baggott, *Numerical Studies in Differential Equations* (Watts, 1934).

The transformation (11) is only useful in the early stages of diffusion when the concentration at the centre of the sheet is effectively zero. For later times the original equation (6) must be used. Approximate numerical solutions can be evaluated by replacing the derivatives with respect to both  $\xi$  and  $\tau$  in a particular way by finite difference ratios, and details of a convenient iterative procedure have already been published.<sup>3</sup> The application of the method to the present problem needs only a brief explanation.

From symmetry, only half the sheet need be considered, and the condition  $c = 1$ ,  $\xi = -1$  can be replaced by

$$\frac{\partial c}{\partial \xi} = 0, \quad \xi = 0. \quad . \quad . \quad . \quad . \quad (17)$$

The range  $0 \leq \xi \leq 1$  is divided into  $p$  equal intervals  $\delta\xi$ , and  $c_{m-1}$ ,  $c_m$  and  $c_{m+1}$  denote concentrations at time  $\tau$  at the points  $(m-1)\delta\xi$ ,  $m\delta\xi$  and  $(m+1)\delta\xi$  respectively. If the corresponding concentrations at time  $\tau + \delta\tau$  are denoted by  $c'_{m-1}$ ,  $c'_m$  and  $c'_{m+1}$  respectively, the appropriate finite difference form of (6) may be written

$$c'_m = c_m + \frac{\delta\tau}{2(\delta\xi)^2} [\bar{D}_{m+\frac{1}{2}}\{(c'_{m+1} + c_{m+1}) - (c'_m + c_m)\} \\ - \bar{D}_{m-\frac{1}{2}}\{(c'_m + c_m) - (c'_{m-1} + c_{m-1})\}], \quad (18)$$

where  $\bar{D}_{m+\frac{1}{2}}$ ,  $\bar{D}_{m-\frac{1}{2}}$ , the mean values of  $D$  in the interval  $\delta\tau$  at the points  $(m + \frac{1}{2})\delta\xi$  and  $(m - \frac{1}{2})\delta\xi$ , are taken to be the values of  $D$  for concentrations  $(c'_{m+1} + c_{m+1} + c'_m + c_m)/4$  and  $(c'_{m-1} + c_{m-1} + c'_m + c_m)/4$  respectively. Equations (18) for different  $m$  in the range  $0 < m < p$  form a set of simultaneous algebraic equations for  $c'_m$  as a function of  $m$ , given  $c_m$  for each value of  $m$ , which are solved iteratively as described in the earlier paper.<sup>3</sup> The boundary condition  $c = 1$ ,  $\xi = 1$  means  $c_p = 1$ , and using (17) the special equation for  $m = 0$  is

$$c'_0 = c_0 + \frac{\delta\tau}{(\delta\xi)^2} [\bar{D}_{\frac{1}{2}}\{(c'_1 + c_1) - (c'_0 + c_0)\}], \quad (19)$$

since  $c_{-1} = c_{+1}$ ,  $\bar{D}_{-\frac{1}{2}} = \bar{D}_{\frac{1}{2}}$ .

An alternative method of treating eqn. (6) is to use a transformation suggested by Eyres, Hartree and others.<sup>4</sup> Thus on introducing a modified concentration  $s$  defined by the relation

$$s = \int_0^c D \, dc, \quad . \quad . \quad . \quad . \quad (20)$$

eqn. (6) reduces to

$$\frac{\partial s}{\partial \tau} = D \frac{\partial^2 s}{\partial \xi^2}, \quad . \quad . \quad . \quad . \quad (21)$$

of which the appropriate finite difference form is

$$s'_m = s_m + \frac{(D'_m + D_m)\delta\tau}{4(\delta\xi)^2} [(s'_{m+1} + s_{m+1}) - 2(s'_m + s_m) + (s'_{m-1} + s_{m-1})], \quad (22)$$

which takes the special form,

$$s'_0 = s_0 + \frac{(D'_0 + D_0)\delta\tau}{2(\delta\xi)^2} \{(s'_1 + s_1) - (s'_0 + s_0)\}, \quad . \quad . \quad (23)$$

where  $m = 0$ . Both the forms (18) and (22) have been used in the present work, and in general (22) is to be preferred since introduction of the means  $\bar{D}_{m+\frac{1}{2}}$ ,  $\bar{D}_{m-\frac{1}{2}}$  is avoided.

<sup>3</sup> Crank and Nicolson, *Proc. Camb. Phil. Soc.*, 1947, **43**, 50.

<sup>4</sup> Eyres, Hartree, Ingham, Jackson, Sarjant and Wagstaff, *Phil. Trans. Roy. Soc. A*, 1946, **240**, 1.

Evaluation of (14) gives values of  $c$  at a number of values of  $\eta$  in the range  $0 < \eta < \eta_{lim}$ , where  $\eta_{lim}$  is the value of  $\eta$  at which  $c$  becomes effectively zero, i.e.  $c < 0.001$  in this work. The condition that this shall occur at some  $\xi$  satisfying  $\xi > 0$ , i.e. that the sheet is still behaving as a semi-infinite one, is that  $2\tau^{\frac{1}{2}}\eta_{lim} < 1$  (see 11) and this condition determines the latest time  $\tau$  at which the semi-infinite sheet solution is valid. When  $\xi$  values are converted into  $\eta$  values by (11), the solution of (14) provides values of  $c$  at a number of values of  $\xi$  at this time, from which to start the iterative solution of eqn. (18) or (22). Eqn. (12) must be used for small  $\tau$  because the presence of a singularity at  $\tau = 0$  makes the use of finite difference ratios inaccurate in that neighbourhood. The singularity is removed by (11).

If  $M_t$  denotes the total amount of penetrant absorbed by the sheet at time  $t$  and  $M_\infty$  the equilibrium absorption attained theoretically after infinite time, then

$$\frac{M_t}{M_\infty} = \frac{\int_0^l C dx}{lC_0} = - \int_0^1 c d\xi = 2\tau^{\frac{1}{2}} \int_0^\infty c d\eta. \quad (24)$$

The corresponding problem in desorption calls for solutions of the same diffusion eqn. (16) with the boundary conditions

$$c = 0, \quad \xi = -1, \quad \xi = 1, \quad \tau = 0, \quad (25)$$

replacing (7), and the initial condition

$$c = 1, \quad -1 < \xi < 1, \quad \tau = 0 \quad (26)$$

replacing (8). If  $M_t$  is the amount of penetrant desorbed now, and  $M_\infty$  is the amount desorbed after infinite time, then

$$\frac{M_t}{M_\infty} = 1 + \int_0^1 c d\xi = 1 - 2\tau^{\frac{1}{2}} \int_0^\infty c d\eta. \quad (27)$$

Thus the rates of absorption and desorption are readily calculated from the results of evaluating (14) and (18) or (22).

In general for all the forms of diffusion coefficient considered, values of  $c$  were evaluated at intervals of 0.10 in  $\eta$ , though occasionally for the desorption process it was necessary to use intervals of 0.05 near the surface of the sheet and also sometimes permissible to use intervals 0.20 towards the upper end of the range in  $\eta$ . In the finite difference equations the range in  $\xi$  was divided into 8 intervals, i.e.  $p = 8$ . The value of  $\delta\tau$  used depended somewhat on the relation between  $D$  and  $C$  but usually  $\delta\tau/(\delta\xi)^2 = 1/10$  approximately.

**4. Absorption and Desorption-Time Curves.**—DIFFUSION COEFFICIENTS INCREASING AND DECREASING UNIFORMLY WITH CONCENTRATION INCREASING. Using the methods described above, the overall rates of absorption and desorption of penetrant by a plane sheet of material have been calculated for a number of diffusion coefficients varying in different ways with the concentration of the penetrant. The relation between the diffusion coefficient and the concentration need not necessarily be known in algebraic form; an empirical relation, given for example in graphical form, can be handled just as easily by the methods of this paper. In the present work, algebraic relations have been chosen for simplicity in reference.

The simplest type of variable diffusion coefficient considered is one which increases linearly with concentration throughout the range, i.e. in terms of the nomenclature used above,

$$D = 1 + ac, \quad (28)$$

where  $a$  is a constant. Numerical solutions have been evaluated for  $a = 10.0, 7.5, 4.8, 2.5, 0.0$ ; the last value implies the constant diffusion

coefficient  $D = 1$  and a well-known formal solution exists for this case.<sup>5</sup> The value 4.8 was used instead of 5.0 because calculations for this value had already been carried out in connection with other work on the diffusion of direct dyes into cellulose. Values of  $D_0 t/l^2$  for absorption are tabulated in Table I for each value of  $a$  at intervals of 0.1 in  $M_t/M_\infty$  and the corresponding values for desorption are tabulated in Table II. Fig. 1 shows the absorption and desorption-time curves for  $D = 1 + 10c$ . Both curves have an infinite gradient at  $t = 0$  and at all subsequent times the absorption curve lies above that for desorption. This behaviour is to be contrasted with that for a constant diffusion coefficient when the

TABLE I.—RATE OF ABSORPTION DATA.  $D = 1 + ac$ 

$M_t/M_\infty$	$D_0 t/l^2$				
	$a = 10.0$	$a = 7.5$	$a = 4.8$	$a = 2.5$	$a = 0.0$
0.0	0	0	0	0	0
0.1	0.001	0.001	0.002	0.003	0.008
0.2	0.004	0.006	0.008	0.012	0.031
0.3	0.010	0.012	0.015	0.025	0.071
0.4	0.018	0.020	0.030	0.045	0.124
0.5	0.028	0.035	0.048	0.073	0.197
0.6	0.041	0.048	0.067	0.110	0.286
0.7	0.054	0.065	0.092	0.153	0.403
0.8	0.072	0.090	0.131	0.208	0.565
0.9	0.100	0.125	0.188	0.290	0.848

TABLE II.—RATE OF DESORPTION DATA.  $D = 1 + ac$ 

$M_t/M_\infty$	$D_0 t/l^2$				
	$a = 10.0$	$a = 7.5$	$a = 4.8$	$a = 2.5$	$a = 0.0$
0.0	0	0	0	0	0
0.1	0.001	0.003	0.003	0.006	0.008
0.2	0.006	0.010	0.012	0.020	0.031
0.3	0.010	0.020	0.026	0.037	0.071
0.4	0.020	0.033	0.046	0.066	0.124
0.5	0.045	0.055	0.077	0.120	0.197
0.6	0.068	0.088	0.131	0.166	0.286
0.7	—	—	0.198	0.241	0.403
0.8	—	—	—	—	0.565
0.9	—	—	—	—	0.848

absorption and desorption curves coincide as indicated by the single curve of Fig. 1 for  $D = 6$ , which is the mean  $D$ . Both the absorption and desorption processes occur more rapidly for  $D = 1 + 10c$  than for  $D = 1$ , a result which is discussed in detail below (§ 5). Curves of similar shape and properties to those of Fig. 1 are obtained by plotting the data of Tables I and II for the intermediate values of  $a$ .

The linear dependence of  $D$  on  $c$  is a special case of a relation of the form

$$D = 1 + ac^n. \quad (29)$$

Values of  $D_0 t/l^2$  for absorption and desorption are tabulated at the values of  $M_t/M_\infty$  shown in Table III for diffusion coefficients of the type (29)

<sup>5</sup> Carslaw and Jaeger, *Conduction of Heat in Solids* (Oxford, the Clarendon Press, 1947).



having  $a = 4.8$  and  $n = 1/3$ , and 3, respectively. The values for  $n = 1$  are, of course, to be found in the columns headed  $a = 4.8$  in Tables I and II. Absorption and desorption-time curves are shown in Fig. 2 for  $n = 3.0$  and  $0.0$ . It is obvious from (29) that  $n = 0$ ,  $a = 4.8$ , correspond to the constant value  $D = 5.8$  and in Fig. 2 the absorption and desorption curves are seen to coincide for this value of  $n$ . For  $n = 3$  the absorption curve lies wholly above the desorption curve as in Fig. 1. These curves and the data of Table III show that for a given value of  $a$  the rates of absorption and desorption are both greater the lower the value of the exponent  $n$ .

TABLE III.—ABSORPTION AND DESORPTION DATA.  $D = 1 + ac^n$ 

$M_t/M_\infty$	$D_0 t/l^2$			
	$a = 4.8; n = 1/3$		$a = 4.8; n = 3$	
	Absorption	Desorption	Absorption	Desorption
0	0	0	0	0
0.1	0.001	0.003	0.003	0.005
0.2	0.006	0.009	0.012	0.019
0.3	0.014	0.017	0.027	0.043
0.4	0.021	0.029	0.046	0.072
0.5	0.041	0.047	0.079	0.110
0.6	0.059	0.066	0.114	0.165
0.7	0.082	0.097	0.154	0.257
0.8	0.114	0.140	0.204	—
0.9	0.168	—	0.270	—

The data presented in Tables I, II and III suggest that whenever the diffusion coefficient increases throughout with increasing concentration the whole process of desorption takes place more slowly than the corresponding absorption process, and in particular the final stages of desorption proceed very slowly compared with the final stages of absorption. This latter is a well-known phenomenon in the drying of polymer sheets and fibres and is to be expected on grounds of general reasoning since as desorption proceeds, the concentration throughout the sheet approaches zero and hence only the small values of the diffusion coefficient associated with low concentrations are operative, whereas, in the last stages of absorption the concentration is everywhere high and tending to the value  $c = 1$  so that the rate is determined by the larger values of  $D$  only.

If  $(1 - c)$  is written for  $c$ , the diffusion eqn. (6) is unchanged in form but the boundary conditions (7) and the initial condition (8), which formerly referred to absorption, now become the conditions for desorption, and similarly the original conditions (25) and (26) for desorption become those for absorption. This means that the solution for absorption when  $D$  is a given function of  $c$ , is also the solution for desorption when  $D$  is the same function of  $(1 - c)$ , and vice versa. For example, the curve labelled absorption in Fig. 1 for  $D = 1 + 10c$  is also the desorption curve for  $D = 1 + 10(1 - c)$ . In this way the following general conclusions about the absorption and desorption processes associated with a diffusion coefficient of this kind may be drawn without further calculation. When the diffusion coefficient decreases uniformly as the concentration increases, the desorption-time curve lies wholly above the absorption curve and in particular the last stages of absorption proceed always more slowly than the last stages of desorption. If  $D$  is of the form

$$D = 1 + a(1 - c)^n,$$

the above data show that when  $n = 0$  both absorption and desorption

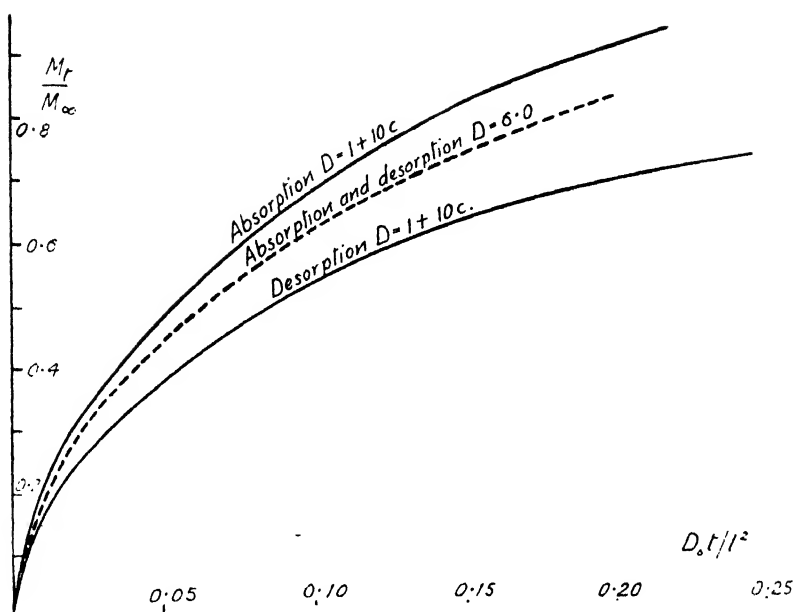


FIG. 1.

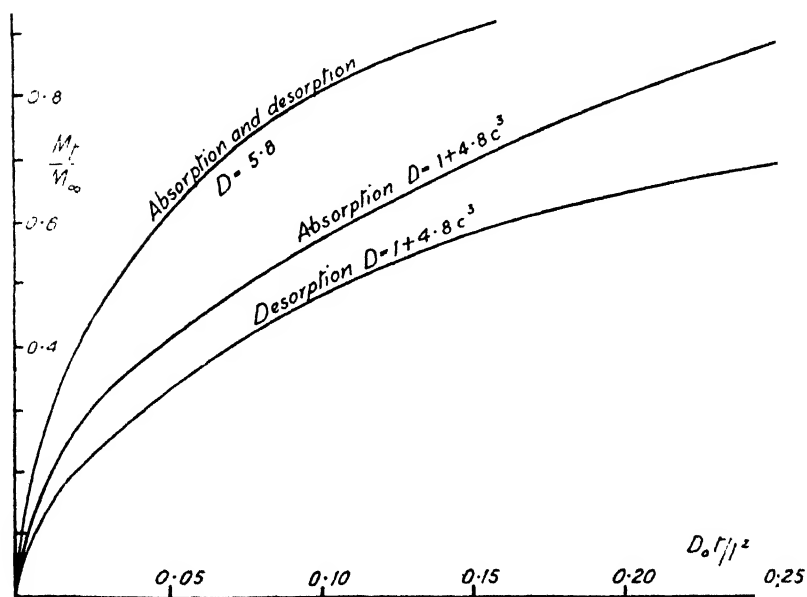


FIG. 2.

are quicker the larger  $a$  is, and for a given  $a$  both processes are slower the larger  $n$  is.

THE DIFFUSION COEFFICIENT PASSES THROUGH A MAXIMUM. In Fig. 3, three different diffusion coefficients are plotted as functions of concentration. They correspond to the algebraic relations:

$$D = 1 + 14.8c(1 - c), \quad (30)$$

$$D = 1 + 100c^2 e^{-10c^2}, \quad (31)$$

$$D = 1 + 100(1 - c)^2 e^{-10(1-c)^2}, \quad (32)$$

All three satisfy the conditions  $D = 1$  when  $c = 0$  and  $c = 1$ , and the maximum value of  $D$  is approximately 4.7 in each case. Eqn. (30) is

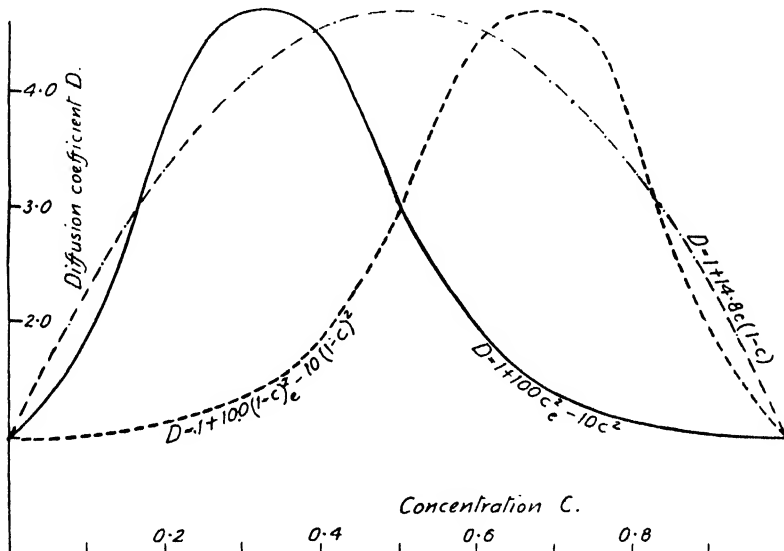


FIG. 3.

a symmetrical form in which this maximum occurs at  $c = 0.5$ , while the maximum values for (31) and (32) are at  $c = 0.3$  and  $0.7$  respectively, since (32) follows immediately from (31) by writing  $(1 - c)$  for  $c$ . The rates of absorption and desorption data for these diffusion coefficients are presented in Table IV. Since (30) is symmetrical in  $c$  and  $(1 - c)$  it follows from what was said above that for the boundary conditions considered throughout this work the absorption and desorption-time curves are coincident, and this is, of course, true for any symmetrical relation between  $D$  and  $c$ . The results show that for  $D$  given by (31) with a maximum at  $c = 0.3$  the desorption curve lies wholly above that for absorption, while the opposite is true for the relation (32) where the maximum value of  $D$  occurs at  $c = 0.7$ .

The relative behaviour of the absorption and desorption-time curves is affected by the relative values of the diffusion coefficient at  $c = 0$  and  $c = 1$ , and also by the position of the maximum in the  $D$ - $c$  curve if one occurs. This suggests that, in some cases, the desorption curve may be above the absorption curve in the early stages of diffusion but later may cross it so that the final stages of desorption are again slower than those of absorption. This is likely to occur when there is a maximum in the diffusion coefficient-concentration relation and when the value of  $D$  at  $c = 1$  is greater than at  $c = 0$ .

In order to study this behaviour a diffusion coefficient-concentration relation of the form,

$$D = 1 + \alpha \operatorname{erf}(\beta c) + \gamma c, \quad (34)$$

was used, where  $\alpha$ ,  $\beta$ ,  $\gamma$  are constants for any one curve. There is no significance in the precise form of (34) except that it leads to diffusion

TABLE IV.—ABSORPTION AND DESORPTION DATA

$$(a) D = 1 + 14.8c(1 - c)$$

$$(b) D = 1 + 100c^2 e^{-10c^2}$$

$$(c) D = 1 + 100(1 - c)^2 e^{-10(1-c)^2}$$

$M_t/M_\infty$	$D_0 t/l^2$		
	Absorption and Desorption for (a)	Absorption for (b) Desorption for (c)	Absorption for (a) Desorption for (b)
0.0	0	0	0
0.1	0.003	0.005	0.004
0.2	0.009	0.016	0.013
0.3	0.021	0.027	0.027
0.4	0.037	0.065	0.049
0.5	0.058	0.102	0.077
0.6	0.086	0.159	0.112
0.7	0.127	0.244	0.159
0.8	0.188	—	0.226
0.9	0.320	—	—

coefficient-concentration curves of the desired form and is convenient to handle numerically. From (34) and (16) we have

$$\frac{dD}{dc} = \frac{2\alpha\beta}{\pi^{\frac{1}{2}}} e^{-\beta^2 c^2} + \gamma = 0 \quad (35)$$

when  $D$  has a maximum value. All curves given by (34) pass through the point  $D = 1$ ,  $c = 0$ . The three further conditions that  $D$  shall have a prescribed value at  $c = 1$  and a given maximum value at a prescribed value of  $c$ , can be satisfied by suitable choice of the parameters  $\alpha$ ,  $\beta$ ,  $\gamma$ , the desired values being readily determined by use of (34) and (35). A typical curve of this family, actually the one given by

$$D = 1 + 4.62 \operatorname{erf}(6.10c) - 3.12c, \quad (36)$$

which satisfies the conditions,

$$D = 1, c = 0, D = 2.5, c = 1, dD/dc = 0, D = 4.7, c = 0.25, \quad (37)$$

is shown in Fig. 4. The absorption and desorption-time curves for this diffusion coefficient are shown in Fig. 5. The curves intersect at

$$D_0 t/l^2 = 0.86.$$

For values of  $D_0 t/l^2$  less than this, desorption proceeds more rapidly than absorption but after the intersection the desorption curve lies below that for absorption. This to be contrasted with the absorption and desorption curves shown in Fig. 6, which do not intersect and which are for a diffusion coefficient of the form,

$$D = 1 + 29.86 \operatorname{erf}(0.98c) - 23.40c. \quad (38)$$

This diffusion coefficient is also shown in Fig. 4 where it is seen to differ from that defined by (36) in that it has a maximum value at  $c = 0.6$  instead of  $c = 0.25$ . The numerical data used to plot the curves of Fig. 5 and 6 and also for a further diffusion coefficient of the same general shape having a maximum value at  $c = 0.125$ , are tabulated in Table V. It is clear from inspection of these data that, keeping the end points of the diffusion coefficient-concentration curves fixed at  $D = 1$  and  $D = 2.5$  and the maximum value of  $D = 4.7$ , as the position of the maximum value moves from  $c = 1$  to  $c = 0$  there is first a range of positions of the maximum for which the whole process of desorption is slower than absorption. Continuing to move the position of the maximum towards

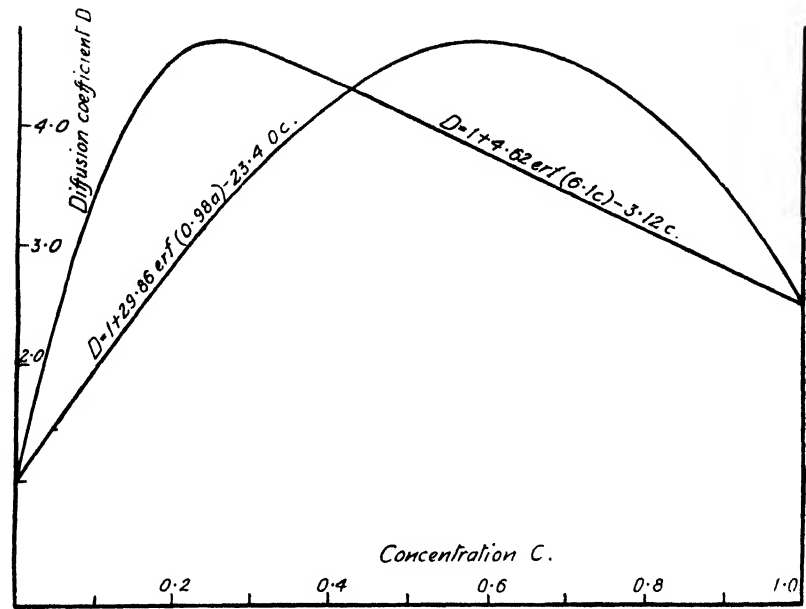


FIG. 4.

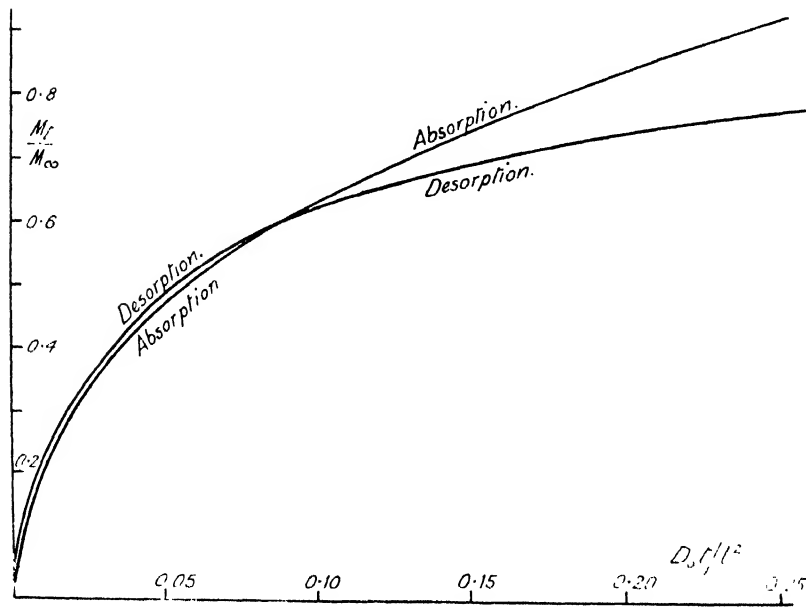


FIG. 5.

$c = 0$  there is evidently a further range of positions for which the desorption and absorption curves intersect, the point of intersection occurring at successively larger values of  $D_0 t/l^2$  as the position of the maximum

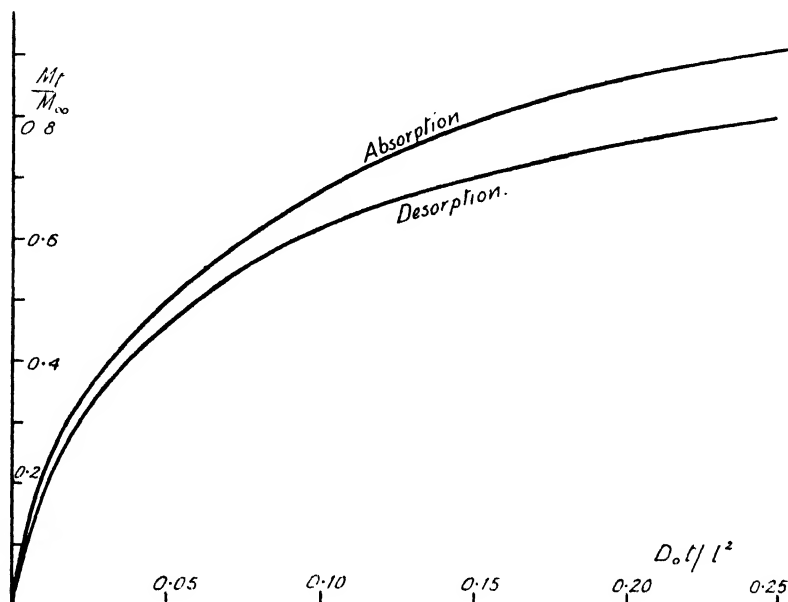


FIG. 6.

moves towards  $c = 0$ . There is some intermediate position of the maximum for which the desorption curve crosses the absorption curve at the origin only and this is the limiting case between absorption and desorption curves which intersect for  $t > 0$  and those which do not. It is difficult to detect the positions of the intersections occurring near the origin, and hence to determine the limiting case, when the absorption and

TABLE V.—ABSORPTION AND DESORPTION DATA

$$D = 1 + 2 \operatorname{erf}(\beta c) + \gamma c$$

$M_t/M_\infty$	$D_0 t/l^2$					
	$\alpha = 4.06, \beta = 14.50, \gamma = -2.56$		$\alpha = 4.62, \beta = 6.10, \gamma = -3.12$		$\alpha = 29.86, \beta = 0.98, \gamma = -23.40$	
	Absorption	Desorption	Absorption	Desorption	Absorption	Desorption
0	0	0	0	0	0	0
0.1	0.003	0.002	0.003	0.002	0.004	0.005
0.2	0.010	0.008	0.013	0.011	0.010	0.011
0.3	0.020	0.017	0.021	0.020	0.018	0.021
0.4	0.036	0.031	0.036	0.033	0.034	0.038
0.5	0.057	0.049	0.058	0.053	0.052	0.061
0.6	0.086	0.072	0.088	0.088	0.076	0.093
0.7	0.123	0.108	0.127	0.158	0.111	0.155
0.8	0.175	0.164	0.178	—	0.158	0.252
0.9	0.245	0.242	0.243	—	0.246	—

desorption curves are plotted against  $(D_0 t/l^2)$  since the gradients of both curves become infinite at  $D_0 t/l^2 = 0$ . By plotting against  $(D_0 t/l^2)^{\frac{1}{2}}$ , however, this difficulty is removed, since the curves are linear for small values of  $D_0 t/l^2$ , a property which follows directly from relations (24) and (27).

It is found that the limiting position of the maximum for which intersection of the absorption and desorption curves occurs at  $D_0 t/l^2 = 0$  (in which case the rates of absorption and desorption are equal at  $t = 0$ ), is about  $c = 0.26$ . When the maximum occurs at higher values of  $c$  than this, desorption is slower than absorption right from  $D_0 t/l^2 = 0$ , but when the maximum lies in the range  $0 < c < 0.26$  the desorption curve is first above the absorption curve but crosses it later so that the final stages of desorption are again slower than those of absorption.

Still confining attention to the general form of variable diffusion coefficient expressed by (34), it is to be expected that the critical position of the maximum for which the absorption and desorption curves have equal gradients in the neighbourhood of  $t = 0$  when plotted against  $(D_0 t/l^2)^{\frac{1}{2}}$  will vary as the value of  $D$  at  $c = 1$  is caused to vary, taking the maximum value to  $D$  to remain constant and the condition  $D = 1$ ,  $c = 0$  to be satisfied in all cases. This expectation is confirmed by the results presented graphically in Fig. 7, where the critical position of the

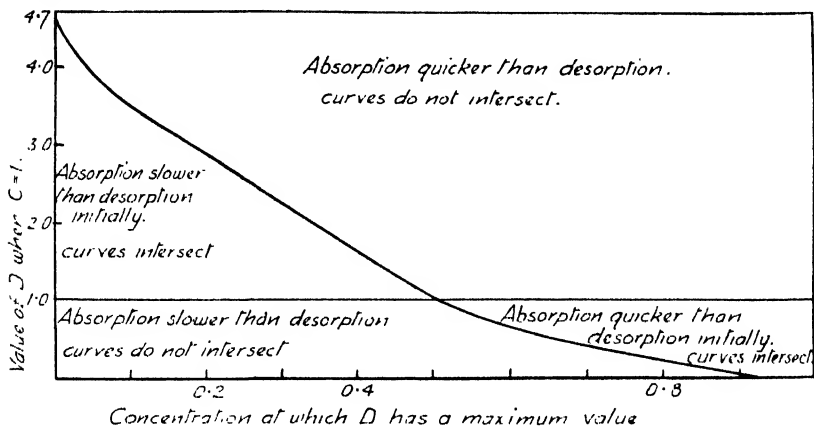


FIG. 7.

maximum is plotted as a function of the value of  $D$  at  $c = 1.0$ . The critical position is seen to move towards  $c = 0$  as the value of  $D$  at  $c = 1$  is increased.

The points at each end of the curve of Fig. 7 were arrived at by general reasoning and the intermediate points by calculation. Thus considering first the case where the value of  $D$  at  $c = 1$  is very close to 4.7, which is the value of the maximum  $D$  for this family of curves, it is clear that in general for a  $D$ - $c$  curve of this type the diffusion coefficient is effectively increasing over the whole range of concentration and absorption will be quicker than desorption throughout. This is true for all positions of the maximum except when the maximum is so near to  $c = 0$  that the diffusion coefficient is effectively constant over the whole range of concentration, in which case the absorption and desorption-time curves coincide and  $c = 0$  is therefore the limiting position of the maximum when  $D = 4.7$  at  $c = 1$ .

By an extension of this argument the critical position of the maximum can be determined when  $D = 0$  at  $c = 1$ . It was seen above that the absorption-time curve obtained when  $D$  is a certain function of  $c$  is the same as the desorption-time curve when  $D$  is the same function of  $(1 - c)$

and vice versa. It follows immediately that if, when  $D$  is a certain function of  $c$ , the initial rates of absorption and desorption are equal, they will also be equal when  $D$  is the same function of  $(1 - c)$ , i.e. if the critical position of the maximum value of  $D$  is  $c = c_m$  in the first case, it will be  $c = 1 - c_m$  in the second case. Now if  $D$  is a function of  $c$  such that  $D$  is very small when  $c = 1$ , the corresponding function of  $(1 - c)$  is such that the ratio of the maximum value of  $D$  to the value at  $(1 - c) = 0$ , is almost the same as the ratio of the value of  $D$  at  $(1 - c) = 1$  to the value at  $(1 - c) = 0$ . This relation approximates to the type just considered above and the critical position of the maximum value of  $D$  is at  $(1 - c) = 0$  and therefore at  $c = 1$  for the original  $D$ - $c$  curve.

For any  $D$ - $c$  curve of the general family under discussion the relative behaviour of the absorption and desorption-time curves can be deduced from Fig. 7 if the value of  $D$  at  $c = 1$  and the position of the maximum are known. Four regions are to be distinguished, in two of which the absorption and desorption-time curves intersect at some time satisfying  $t > 0$ , and in the other two they do not intersect when  $t > 0$ . When the value of  $D$  at  $c = 1$  is greater than 1.0, the initial rate of desorption is more rapid than that of absorption if the curves intersect, and vice versa when  $D < 1.0$  at  $c = 1$ .

The position of the critical maximum no doubt depends on the magnitude of the maximum value of  $D$ , and also for a given maximum value, it will depend to some extent on the detailed shape of the diffusion coefficient-concentration curve. An examination of these effects is clearly possible along the lines of the present paper. There is little indication, however, that the results obtained would be of sufficient interest to justify the considerable amount of labour involved in a general investigation of this kind, and so no attempt has yet been made to carry the work beyond the stage already described.

##### 5. A New Method of Measuring a Variable Diffusion Coefficient.—

When the diffusion coefficient is constant and equal to  $D_0$ , say, the absorption and desorption curves coincide and are given by the formal solution,

$$\frac{M_t}{M_\infty} = 1 - \sum_{n=0}^{\infty} \frac{8}{(2n+1)^2\pi^2} e^{-D_0\pi^2(n+\frac{1}{2})^2t/l^2}, \quad (39)$$

where  $M_t$  is the amount absorbed or desorbed as the case may be.

If an experimental absorption-time curve is obtained for a system in which the diffusion coefficient is constant, the value of this constant can be determined by comparing the experimental curve with the one calculated using (39). If the diffusion coefficient is not constant, however, this comparison yields some mean value  $\bar{D}$  of the coefficient. The particular mean measured depends on how the comparison is made. A simple comparison is to choose  $\bar{D}$  such that the calculated and experimental curves coincide at 50 % absorption, i.e.  $M_t/M_\infty = 0.5$ .

In order to discover the significance of  $\bar{D}$  measured in this way the calculated absorption curves for the variable diffusion coefficients discussed above have been compared with the formal solution for a constant diffusion coefficient and a value of  $\bar{D}$  obtained in each case. In Table VI the values of  $\bar{D}$  are compared with corresponding values of  $\int_{c=0}^{c=1} D dc$ , which are readily calculated in each case from the known relation between  $D$  and  $c$ . Here  $c = 1$  is the concentration of penetrant at the surface of the sheet in the reduced variables.

It is seen that when  $\bar{D}$  is measured from the absorption data alone it provides an approximation to

$$\int_0^1 D dc = (1/C_0) \int_0^{C_0} D dC$$

i.e. to the integrated mean of the diffusion coefficient between the extreme



## 650 EFFECT OF VARIABLE DIFFUSION COEFFICIENT

limits of concentration existing at the start of diffusion. The greatest error in this approximation for the diffusion coefficients examined in Table VI is about 23 %. When the desorption data alone are used to estimate  $\bar{D}$  the errors are slightly greater on the whole, the largest being about 26 %, the two errors being in opposite senses. By taking the mean of the values of  $\bar{D}$  estimated from absorption and desorption data separately these % errors are considerably reduced, the largest being about 3 %.

TABLE VI  
 $D = 1 + f(c)$

$f(c)$	$\int_0^1 D dc$	Absorption		Desorption		Mean of Adsorption and Desorption	
		$\bar{D}$	% Error *	$\bar{D}$	% Error *	$\bar{D}$	% Error *
10c . . . .	6.00	7.14	+19	4.44	-26	5.79	-3
7.5c . . . .	4.75	5.66	+19	3.64	-23	4.65	-2
4.8c . . . .	3.40	4.15	+22	2.58	-24	3.36	-1
2.5c . . . .	2.25	2.77	+23	1.66	-26	2.22	-1
4.8c <sup>3</sup> . . . .	2.20	2.55	+16	1.80	-18	2.17	-1
4.8c <sup>1/3</sup> . . . .	4.60	4.88	+6	4.20	-9	4.54	-1
100c <sup>2</sup> e <sup>-10c<sup>2</sup></sup> . . . .	2.38	1.98	-17	2.62	+10	2.31	-3
14.8c(1-c) . . . .	3.47	3.42	-1	3.42	-1	3.42	-1
4.06 erf (14.5c) - 2.5c . . . .	3.84	3.48	-9	4.08	+6	3.78	-2
4.62 erf (6.1c) - 3.1c . . . .	3.65	3.45	-5	3.74	+2	3.59	-2

The data of Table VI suggest a method of deriving the relationship between diffusion coefficient and concentration. Thus suppose absorption-time curves are measured for several values of surface concentration  $C_0$ . A value of  $\bar{D}$  can be obtained for each curve as above and hence, by assuming as a first approximation that

$$\bar{D} = \frac{1}{C_0} \int_0^{C_0} D dC, \quad . \quad . \quad . \quad (40)$$

a graph showing the integral as a function of  $C_0$  can be plotted. Differentiation of this curve yields a first approximation to the diffusion coefficient. If now absorption-time curves are calculated by the methods of this paper for several values of  $C_0$  and using the first approximation to the diffusion coefficient, the error involved in use of (40) can be estimated and a second approximation to the diffusion coefficient deduced. The process is repeated till two successive approximations agree to within the order of accuracy justified by the experimental data.

A practical example of the use of this method is described in ref. 6 and the process was found to converge satisfactorily after only three approximations.

*Courtaulds, Limited,  
Maidenhead, Berks.*

\* This is the difference between  $\bar{D}$  and  $\int_0^1 D dc$  expressed as a percentage of  $\int_0^1 D dc$ .

<sup>6</sup> Crank and Park, *Trans. Faraday Soc.*, 1949, **45**, 240.

# A NEW TECHNIQUE FOR THE DETERMINATION OF DYNAMIC SURFACE TENSIONS

BY A. M. POSNER AND A. E. ALEXANDER

*Received 9th February, 1949*

The technique for determining dynamic surface tensions described here utilizes the changes in surface potential to follow the adsorption of solute molecules upon a freshly formed surface. Three different types of apparatus are described, a simple trough suitable for systems in which adsorption equilibrium requires a time greater than a few minutes, a Perspex channel suitable for times between *ca.* 0.01 and 1 sec., and a jet suitable for times between *ca.* 0.001 and 0.01 sec. Most attention has been given to the last two methods for obvious reasons. The hydrodynamics of the jet and channel are outlined to show how the age of the surface can be calculated from various known parameters.

Methods for converting the measured surface potentials into surface tensions and surface concentrations, utilizing data from equilibrium static systems, are discussed. A number of typical results for aqueous solutions of *iso*amyl alcohol and *sec.*-octyl alcohol are presented graphically.

---

The kinetics of adsorption and desorption processes at interfaces are of interest in connection with the general problem of diffusion, and are particularly pertinent to any detailed analysis of the formation and decay of foams and emulsions. Since the amount of adsorption can usually be obtained from the lowering of the surface tension, the problem is thus none other than that of determining a dynamic surface tension.

Almost all the common methods for surface tension determination are of very limited value for dynamic studies, since the times necessary are much too long, many adsorptions being effectively complete in *ca.* 0.1 sec. or less. Two methods capable of extension to such short times are the oscillating jet, an old method recently developed by Addison,<sup>1, 2</sup> and the flowing sheet method of Bond.<sup>3, 4</sup> Both, however, suffer from certain inherent difficulties of a practical and theoretical nature.

The present method, which utilizes the changes in contact potential to determine the dynamic surface tension and hence the amount of adsorption, arises very directly from the study of insoluble monolayers. The contact potential of water, or of a dilute solution of acid, is first measured in some suitable apparatus (depending on the time-scale of the adsorption under study), followed by the solution of the capillary active substance. The difference in contact potentials gives the so-called "surface potential"  $\Delta V$ , from which the surface tension can be readily found after suitable static calibration measurements. So far the shortest time interval studied has been *ca.* 0.001 sec., but there seems no fundamental reason why smaller times could not be reached, if necessary.

## Experimental

Three different types of apparatus are described below, each suitable for a particular range of times.

<sup>1</sup> Addison, *J. Chem. Soc.*, 1943, 543 *et seq.*

<sup>2</sup> Addison, *Phil. Mag.*, 1945, (7) **36**, 73.

<sup>3</sup> Bond, *Proc. Physic. Soc.*, 1935, **47**, 549.

<sup>4</sup> Bond and Puls, *Phil. Mag.*, 1937, (7) **24**, 864.

(a) **Surface Trough Apparatus.**—If the time for half-adsorption is more than a minute or so, it is possible to use a simple adaptation of the ordinary surface trough, as shown diagrammatically in Fig. 1. The surface of the trough can be swept by means of waxed glass slides and after thorough cleaning in this way, the contact potential of the water or dilute acid ( $V_{aq.}$ ) is measured by means of the potentiometer, utilizing a valve or suitable high-resistance electrometer.

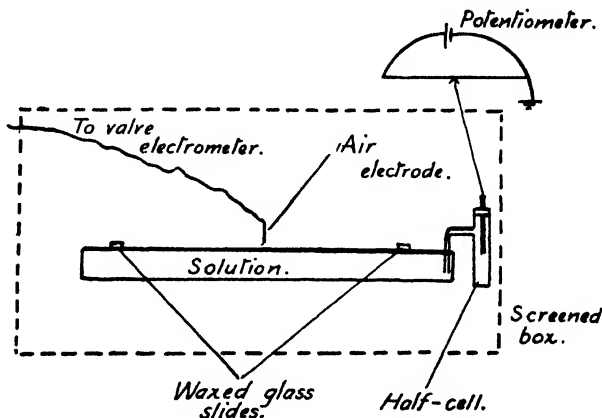


FIG. 1.—Trough apparatus for determining surface potentials for surface ages greater than *ca.* 1 min.

In the work described here a silver wire coated with silver chloride formed the half-cell and it was found preferable to use N/100 or N/1000 HCl rather than pure water. Having determined  $V_{aq.}$  the trough is emptied and refilled with the solution under test. Its surface is then cleaned as above, and its contact potential ( $V_{soln.}$ ) measured as a function of time. From the surface potential so found ( $\Delta V = V_{soln.} - V_{aq.}$ ), the dynamic surface tension follows at once after measuring  $\Delta V$  and  $\gamma$  for suitable systems at equilibrium. For relatively slow adsorptions it is possible to obtain both  $\Delta V$  and  $\gamma$  on the same system, measuring the latter by the ring method for example.<sup>5</sup>

(b) **"Channel" Apparatus.**—Fig. 2 shows the principle of the channel apparatus, as it may be termed, which enables the surface tension to be measured for times greater than *ca.* 0.01 sec. The apparatus, constructed entirely of Perspex, is tilted slightly so as to maintain a uniform depth over the

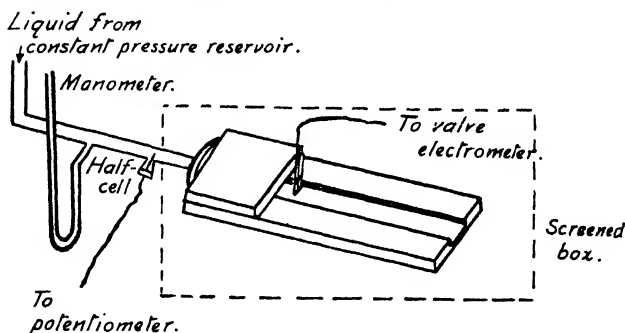


FIG. 2.—Channel apparatus for determining surface potentials for surface ages between 0.02–1.0 sec.

whole length of the channel. The half-cell, consisting of a chloridized silver wire as above, is inserted into a side-arm as shown in Fig. 2. By means of a constant pressure-head device, in conjunction with a manometer, constant rates of flow could be readily maintained. In general it was found more convenient to vary the velocity of the liquid (by varying the pressure head), rather than to move the air-electrode to various positions along the channel.

<sup>5</sup> Alexander, *Trans. Faraday Soc.*, 1941, 37, 15.

After the whole apparatus had been thoroughly cleaned, the dilute (N/100) HCl solution was run through and the contact potential measured over the possible range of flow rates. By means of a Y connection the capillary active solution (also containing N/100 HCl) was then substituted and the measurements repeated under otherwise identical conditions. Some typical curves obtained in this way are shown in Fig. 3. The average rate of flow was found

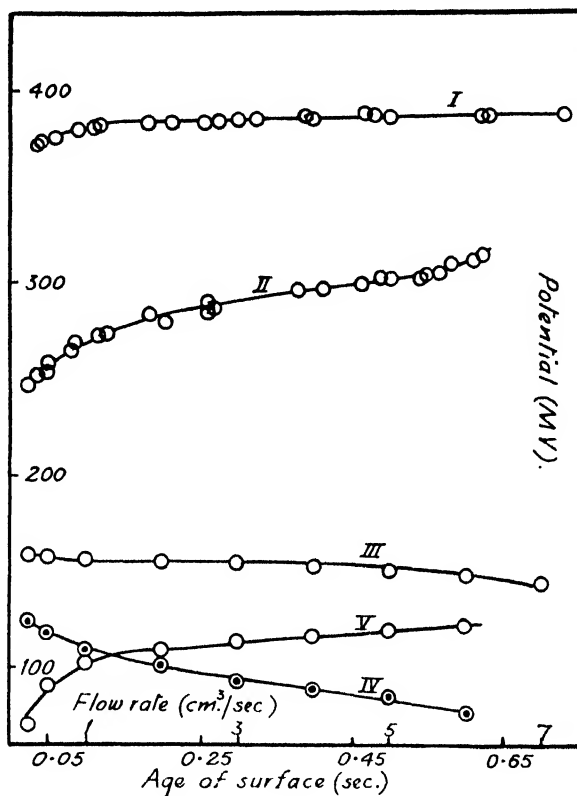


FIG. 3.—I. Contact potential of N/100 HCl plotted against flow rate.  
 II. Contact potential of 0.01 % *sec.*-octyl alcohol in N/100 HCl plotted against flow rate.  
 III. Surface potential of 0.01 % *sec.*-octyl alcohol in N/100 HCl plotted against flow rate.  
 IV. Surface potential of 0.02 % *sec.*-octyl alcohol in N/100 plotted against flow rate.  
 V. Surface potential of 0.01 % *sec.*-octyl alcohol in N/100 HCl plotted against surface age.

directly by timing the outflow into a graduated cylinder. Fresh solution was used for each experiment so as to reduce the risk of contamination, and at least four repeat runs were made with each system.

In order to find the true age of the surface it was necessary to examine in some detail the hydrodynamics of the flowing liquid in the channel. According to the usual treatment of Newtonian fluids (e.g. Prandtl and Tietjens,<sup>6</sup>) flow will be laminar provided the Reynolds number for the particular system does not exceed a certain critical value (*ca.* 1,000). The Reynolds number  $R$ , a dimensionless quantity, is defined as

$$R = \bar{u}r/\nu,$$

<sup>6</sup> Prandtl and Tietjens, *Applied Hydro- and Aero-Mechanics* (McGraw-Hill, 1934), p. 14.

where  $\bar{u}$  is the mean rate of flow (i.e. rate in  $\text{cm.}^3/\text{sec.} \div$  cross-sectional area of channel),  $\nu$  is the kinematic viscosity and  $r$  the hydraulic radius of the system. In the case of a channel the hydraulic radius is equal to  $2A/W$ , where  $A$  is the cross-sectional area of the channel and  $W$  the length of the wetted periphery. (It reduces to  $r$  when the channel becomes a circular tube.) The kinematic viscosity  $\nu = \eta/\rho$ , where  $\eta$  is the ordinary viscosity coefficient and  $\rho$  the density, and for the dilute aqueous systems considered here will not be sensibly different from the value for pure water.

For the Perspex channel used,  $r = 0.369/1.53 = 0.24$  cm., and in view of the volumes which would be required, flow rates greater than about  $7 \text{ cm.}^3/\text{sec.}$  are undesirable. The maximum average velocity will thus be *ca.*  $38 \text{ cm.}^3/\text{sec.}$ , and the maximum Reynolds number *ca.* 910, so that for rates below *ca.*  $7 \text{ cm.}^3/\text{sec.}$  flow will be laminar in this particular channel.

The simplest method of calculating the surface age at any point along the surface of the flowing liquid is to assume that the flow is uniform and that the velocities of the bulk liquid and surface are identical and equal to the average velocity as defined above. In this case at a distance  $x$  from the point of formation the surface age equals  $xA/V$ , where  $A$  = cross-sectional area of channel and  $V$  is the flow rate in  $\text{cm.}^3/\text{sec.}$  It will be shown below that these assumptions are reasonable and that the velocity of the surface at the point where the contact potential is measured (1 cm. along the open channel) is equal to the average velocity of the bulk liquid.

Consider first the effect of the two parallel walls and the orifice upon the velocity distribution at the surface. Before the entrance to the channel the velocity distribution will be parabolic, but then, owing to the change in cross-section and the sharp edges involved in the transition from the circular glass tube to the rectangular Perspex channel, this distribution will be destroyed. Under such conditions the velocity can be considered to be sensibly uniform, and hence equal to the mean velocity. As the liquid flows down the channel, flow will tend to assume a parabolic velocity distribution once again, and the distance  $x$  required for this transition is given approximately by the equation,

$$x/(rR) = 0.26$$

(Prandtl and Tietjens<sup>7</sup>). Thus if  $R = 1,000$  (the critical value),  $x = 63$  cm. For the results given here, measurements were made at  $x = 6$  cm. so that the velocity distribution will still be non-parabolic at this point, provided  $R < \text{ca. } 100$ . ( $x = 6$  cm. corresponds to a point 1 cm. along the open surface of the channel.) A Reynolds number of 100 corresponds to  $\bar{u} = 4 \text{ cm.}/\text{sec.}$ , i.e. a rate of flow of  $0.8 \text{ cm.}^3/\text{sec.}$  Hence for flow rates exceeding this value, corresponding to surface ages less than *ca.* 0.3 sec., the velocity of the surface can be taken as the mean velocity  $\bar{u}$ . (See also later.)

(c) **Jet Apparatus.**—For studying adsorption at much shorter times, down to *ca.* 0.001 sec., it was essential to reduce the volume flow of liquid, otherwise

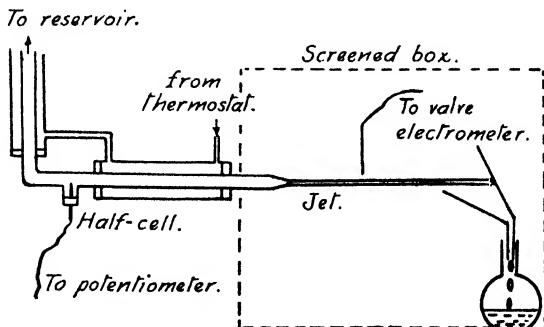


FIG. 4.—Jet apparatus for determining surface potentials for surface ages between 0.001 and 0.01 sec.

the requisite amounts would have become prohibitive. This was achieved in a very simple way, by means of a fine jet issuing from a circular orifice (Fig. 4). The half-cell was inserted as before, and in order to ensure good

<sup>7</sup> Prandtl and Tietjens, *Applied Hydro- and Aero-Mechanics* (McGraw-Hill, 1934), p. 25.

temperature control the supply tubes were thermostatted by a circulating water system. In this case it was found more convenient to keep the pressure head fixed and to move the air-electrode along the jet by means of a fine graduated movement. As before dilute HCl was first run through, followed by the solution under test. The average rate of flow was measured directly as with the channel apparatus. Some typical results are shown in Fig. 5.

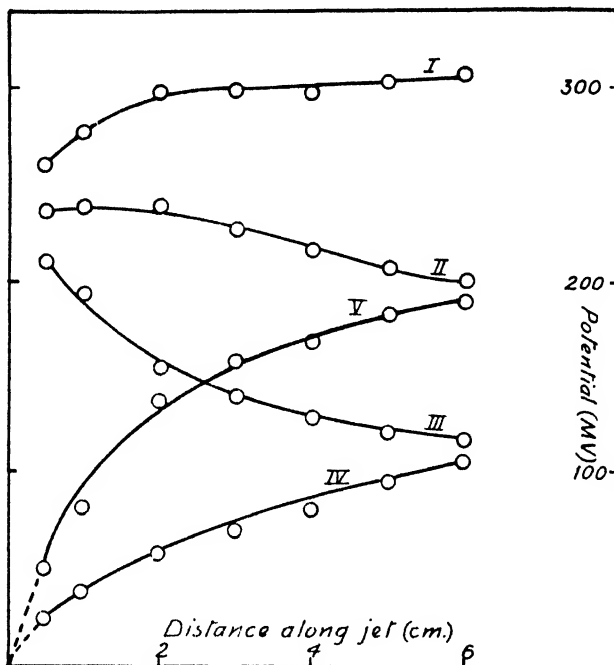


FIG. 5.—I. Contact potential of N/100 HCl plotted against distance from orifice of jet.

II. Contact potential of 0.01 % *sec.*-octyl alcohol in N/100 HCl plotted against distance from orifice.

III. Contact potential of 0.02 % *sec.*-octyl alcohol in N/100 HCl plotted against distance from orifice.

IV. Surface potential of 0.01 % *sec.*-octyl alcohol in N/100 HCl plotted against distance from orifice.

V. Surface potential of 0.02 % *sec.*-octyl alcohol in N/100 HCl plotted against distance from orifice.

The requisite diameter of the jet was calculated as follows (see Prandtl and Tietjens,<sup>6</sup>). As pointed out above, for laminar flow

$$R = 1,000 \div ur'\nu,$$

where  $u$  = rate of flow in cm./sec. and  $\nu = 0.01$  in c.g.s. units; also

$$u = V'/\pi r^2.$$

Therefore,

$$1,000 = V'/\pi r \times 0.01, \text{ i.e. } V = 10\pi r.$$

It was desired to have a surface age of 1/500 sec. at a distance of 1 cm. from the orifice.

$$\therefore 0.002 = \frac{\pi r^2}{V}, \quad \therefore 1,000 = \frac{r}{0.01 \times 0.002}, \quad \therefore r = 0.02 \text{ cm.}$$

$$\therefore V = 10\pi \times 0.02 = 0.63 \text{ cm.}^3/\text{sec.}$$

An approximate estimate of the head required to give this flow was obtained by putting

$$mgh = \frac{1}{2}mu^2,$$

where  $h$  = head of liquid, and  $u$  = rate of flow. For aqueous solutions this gave  $h \approx 130$  cm.

In calculating the surface potential it is necessary to take the difference between the contact potentials for the N/100 HCl solution and the solution under test at definite distances along the jet. Considerable discrepancy might thus arise if the diameter of the jet varied a great deal with the solution. Experiment shows, however, that such a discrepancy is small and often negligible, as shown for example by the results for N/100 HCl and 0.025 % cetyl trimethyl ammonium bromide at corresponding lengths given in Table I.

TABLE I

N/100 HCl	0.025 % Cetyl Trimethyl Ammonium Bromide in N/100 HCl
Equilibrium $\gamma$ = 72.8 dynes/cm. Flow Rate = 0.55 cm. <sup>3</sup> /sec.	Equilibrium $\gamma$ = 36 dynes/cm. Flow Rate = 0.548 cm. <sup>3</sup> /sec.

Distance from Orifice (cm.)	Diam. (mm.)	Diam. (mm.)
0.5	0.400	0.393
1	0.401	0.395
2	0.400	0.398
3	0.398	0.398
4	0.385	0.388
5	0.380	0.377
6	0.370	0.370

(The jet begins to break up soon after 6 cm.)

It is possible to allow for discrepancies in the rate and diameter of the two jets by plotting the contact potentials against time, calculated using the rate of flow and the mean diameter. A jet such as the one used here, moving with a high velocity, deviates only slightly from the horizontal, and any allowance to be made is very small.

As before the surface age was calculated from the average rate of flow, assuming the velocity to be uniform across the thickness of the jet. Such an assumption seems reasonable for the free jet since the air friction will be slight, but the presence of boundary layers in the glass tube might introduce some errors at points close to the orifice. If such effects are appreciable the calculation of surface ages would not be nearly so simple as the method given above. Since very little work of a practical or theoretical nature appears to have been done on these residual boundary layers, it was decided to try a few experiments to indicate their importance in the present work. The most obvious method was to vary the conditions widely and to see if the same potential-time curve was obtained.

The first test involved reducing the rate of flow of the liquid by altering the head. This would be expected to increase the thickness of the boundary layer, which should thus exist for a longer time on the surface of the free jet, so that if boundary effects are appreciable the surface potentials at corresponding times should be greater (due to a closer approach to adsorption equilibrium) than the previously found values. In another test the shape of the tip of the tube was varied. The glass one used previously was replaced by one of a very different shape, made out of Perspex, and cemented to a glass tube (see Fig. 6, inset). In this modification only the central core of liquid emerges and this should be relatively unaffected by the boundary layer in the wider tube. In addition, no appreciable layer should form during the passage of the liquid through the Perspex orifice, since this is only *ca.* 0.1 mm. thick.

Solutions of *sec.*-octyl alcohol were used in these experiments, and the results are shown graphically in Fig. 6. It can be seen that all variations tried gave essentially the same result, indicating that the effect of boundary layers is too small to invalidate seriously our present method of calculating surface

ages. A rather similar problem arises when considering the calculation of surface ages in the channel apparatus. Very little is known about boundary layers in such a system, but since the results obtained fit well with those from the jet, it seems likely that the errors are again negligible.

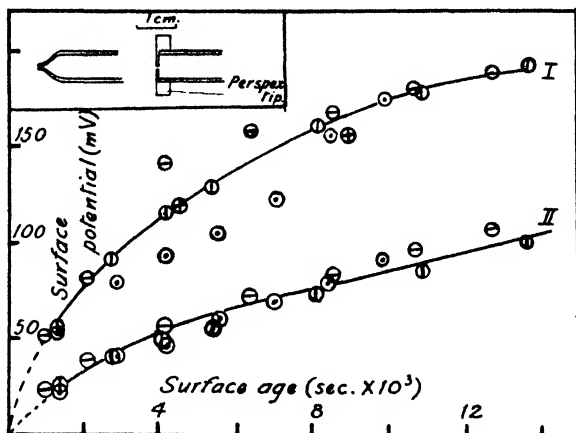


FIG. 6.—Effect of variation of flow-rate and tip upon the surface potential.

I. 0.02 % *sec.*-octyl alcohol solution.

II. 0.01 % *sec.*-octyl alcohol solution.

- Results using glass tip and full head (flow-rate 0.56 cm.<sup>3</sup>/sec.).
- ⊙ Results using glass tip and half head (flow-rate 0.40 cm.<sup>3</sup>/sec.).
- ⊕ Results using larger glass tip and full head (flow-rate 2.65 cm.<sup>3</sup>/sec.).
- ⊗ Results using Perspex tip and half head (flow-rate 0.44 cm.<sup>3</sup>/sec.).

*Inset.* Left—glass tip.

Right—Perspex tip.

## Results and Discussion

**Translation of Surface Potentials into Surface Tensions and Amounts of Adsorption.**—By means of the above apparatus it is possible to determine the surface potential  $\Delta V$  as a function of the age of the surface for any times greater than about 0.001 sec. Fig. 3 and 5 show a few typical results. The values of  $\Delta V$  have then to be translated into corresponding surface tensions and, what is of more importance, into amounts adsorbed.

The relationship between  $\Delta V$  and  $\gamma$  can be found very simply by measurements of both quantities upon solutions at equilibrium, using the large trough shown in Fig. 1. The ring method for surface tension, utilizing the simple technique developed in this laboratory,<sup>8</sup> has been found very suitable.

In the case of the channel apparatus a discrepancy was found between the equilibrium surface potential obtained by extrapolating the  $\Delta V$ -rate curve to zero rate and that determined experimentally on the large trough. This difference is ascribed to electrical effects from charges on the surrounding Perspex. The difficulty was overcome by determining the static surface potentials used in the  $\Delta V$ - $\gamma$  curve on the Perspex channel itself, when the agreement became reasonable, as shown by the following figures of Table II.

Such a discrepancy is small in the case of the jet, as can be seen by studying the adsorption of *isoamyl* alcohol which is complete before the jet breaks up (see Table III).

<sup>8</sup> Alexander, *Recent Advances in Surface Chemistry* (Bordeaux Conference, 1947) (in press).



When constructing the complete  $\Delta V$ -time curve, utilizing the results from both apparatus, the charge effects on the Perspex channel are allowed

TABLE II

Substance	Concentration (weight %)	$\Delta V$ (mV)		Value on Perspex Channel
		Found by Extrapolation	Value on Glass Trough	
<i>sec.</i> -Octyl alcohol	0.02	160	241	159
" "	0.01	131	205	127
<i>iso</i> Amyl alcohol	0.189	135	197	135
" "	0.05	50	65	50

for by displacing the relevant  $\Delta V$ 's by the difference between the static values from the Perspex channel and the glass trough. As Fig. 7 shows,

TABLE III.—ADSORPTION OF *iso*AMYL ALCOHOL

Conc. (g. mole/l.)	$\Delta V$ (mV)	
	Equilibrium from Jet	From Glass Trough
0.083	234	226
0.0184	162	170
0.0046	78	85
0.0023	50	37

a continuous curve is thus obtained. Typical  $\gamma$ -time curves determined from the static  $\Delta V$ - $\gamma$  calibration and the dynamic  $\Delta V$ -time curves are shown in Fig. 7. Table IV below compares the surface tension values

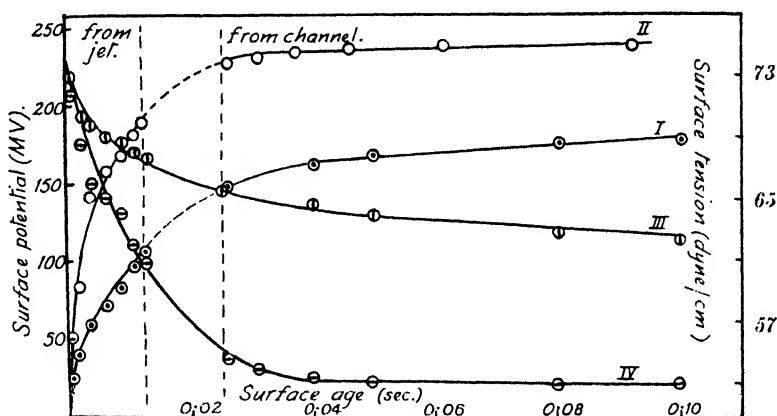


FIG. 7.—I. Surface potential for 0.01 % *sec.*-octyl alcohol plotted against surface age.

II. Surface potential for 0.02 % *sec.*-octyl alcohol plotted against surface age.

III. Surface tension for 0.01 % *sec.*-octyl alcohol plotted against surface age.

IV. Surface tension for 0.02 % *sec.*-octyl alcohol plotted against surface age.

so found with those found by Addison<sup>9, 10</sup> from the oscillating jet method. A considerable divergence between the two techniques is apparent from Table IV, and further work is necessary for its clarification, although we feel that the present method, with its freedom from the theoretical difficulties associated with the oscillatory jet technique, is more likely to give the correct results.

TABLE IV

0.162 % isoAmyl Alcohol			0.02 % sec.-Octyl Alcohol		
Time $\times 10^3$ (sec.)	Present Method ( $\gamma_t - \gamma_E$ )* dyne/cm.	Addison ( $\gamma_t - \gamma_E$ )† dyne/cm.	Time (sec.)	Present Method ( $\gamma_t - \gamma_E$ )‡ dyne/cm.	Addison ( $\gamma_t - \gamma_E$ )§ dyne/cm.
1	5.4	9.6	0.08	0.3	0.8
3	2.3	8.8	0.06	0.7	1.7
5	1.4	7.6	0.04	1.7	3.5
7	0.4	6.6	0.03	2.6	5.5

\*  $\gamma_E = 59.9$  dynes/cm.

†  $\gamma_E = 62.5$  dynes/cm. estimated from Addison.<sup>9</sup>

‡  $\gamma_E = 53.1$  dynes/cm.

§  $\gamma_E = 56.0$  dynes/cm<sup>10</sup>

For determining the amount of adsorption ( $n$  or  $\Gamma$ ) (where  $n$  is the number of molecules and  $\Gamma$  the number of g. moles/cm.<sup>2</sup> of surface), recourse must be had either to the Gibbs adsorption isotherm or to an assumed equation of state. The former, for the dilute systems considered here, can be written in the form,

$$\Gamma = -\frac{1}{RT} \times \frac{d\gamma}{d \ln cf}, \quad (1)$$

where  $c$  and  $f$  are respectively the concentration and activity coefficient of the solute.

With non-electrolytes such as alcohols the activity coefficient is approximately independent of concentration, so that eqn. (1) reduces to

$$\Gamma = -\frac{1}{RT} \times \frac{d\gamma}{d \ln c} = -\frac{1}{2.3RT} \times \frac{d\gamma}{d \log_{10} c} \quad (2)$$

From the  $\gamma - \log_{10} c$  curve the adsorption can thus be found in g. moles/cm.<sup>2</sup>. Assuming the adsorption to be confined to a layer uni-molecular in thickness, for which the evidence seems fairly conclusive,<sup>11</sup> the area per molecule can readily be found since

$$\Gamma NA = 1 \text{ and } n = 1/A,$$

where  $A$  is the area per molecule in cm.<sup>2</sup> and  $N$  is Avogadro's number.

With ionized solutes such as soaps and dyes the variation of activity coefficient with concentration is given approximately by the usual Debye-Hückel expression provided micelles are absent, but above the critical micellar concentration the deviations become too great for this to be of value. For colloidal electrolytes in the micellar range it therefore becomes necessary to obtain the adsorption from an assumed equation of state, as outlined below.

The study of adsorbed films of non-electrolytes such as alcohols has shown that over most concentration ranges the following equation of state is obeyed:

$$\Pi(A - A_0) = \pi kT \quad (3)$$

<sup>9</sup> Addison, *J. Chem. Soc.*, 1944, p. 252.

<sup>10</sup> *Idem, ibid.*, p. 277.

where the surface pressure  $\pi = \gamma_{\text{aq.}} - \gamma_{\text{soln.}}$ .  $A_0$  is the co-area and  $\kappa$  is a constant. In any given homologous series  $A_0$  is constant, whereas  $\kappa$  decreases with increasing chain-length. For any given compound  $\kappa$  can usually be estimated from the chain-length, and  $A_0$  from the study of insoluble monolayers of the higher homologues. With colloidal electrolytes (soaps and dyes) in the micellar range (i.e. at the higher surface pressures), it is sometimes preferable to use the following equation of state :

$$(\Pi - \Pi_0)(A - A_0) = \kappa kT \quad . \quad . \quad . \quad (4)$$

where  $\Pi_0$  is the (negative) spreading pressure of the hydrocarbon chains.  $\Pi_0$ ,  $A_0$  and  $\kappa$  can usually be estimated from the study of monolayers of related compounds (see for example Alexander<sup>11</sup>). From the equation of state, and assuming as before that the adsorbed film is unimolecular in thickness, the adsorption follows at once.

If the polar groups of the adsorbed molecules exert no mutual influence then  $\Delta V$  should be directly proportional to  $n$ , the molecular density in the surface. The study of insoluble monolayers shows that this is indeed often the case with unionized polar groups, the results frequently being expressed by the relation :

$$\Delta V = k'n, \text{ or } \Delta V = 4\pi n\mu, \quad . \quad . \quad . \quad (5)$$

where  $k'$  or  $\mu$  depends upon the nature of the polar group, and is approximately independent of  $n$ . Hence if the proportionality constant is known from insoluble monolayers of the higher homologues it is clear that adsorptions can be calculated directly from the surface potentials of the solutions.

Fig. 8 gives a plot of  $\Delta V - n$  in the case of *sec.*-octyl alcohol, the values

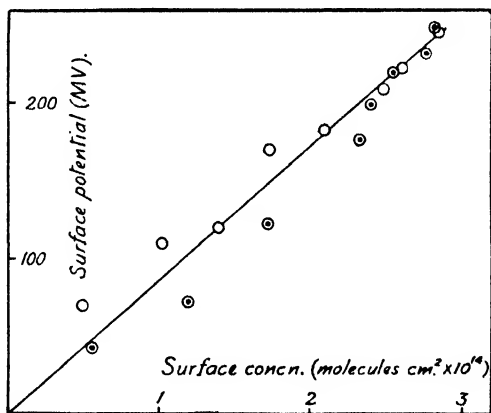


FIG. 8.—○ Surface concentration calculated from the Gibbs adsorption isotherm.

⊙ Surface concentration calculated from the equations of state.

of  $n$  being calculated from the Gibbs equation and from the equation of state

$$\Pi(A - 25) = 0.4 kT.$$

It will be seen that the  $\Delta V - n$  relationship is linear within the experimental error, the slope giving a value of 226 mD for  $\mu$ , which agrees very closely with the value of *ca.* 230 found from insoluble monolayers of the higher homologues, and from other soluble alcohols.<sup>12, 13</sup>

<sup>11</sup> Alexander, *Trans. Faraday Soc.*, 1942, **38**, 248.

<sup>12</sup> Adam, *The Physics and Chemistry of Surfaces* (Oxford Univ. Press, 1941, 3rd ed.), p. 136.

<sup>13</sup> Sawai, *Trans. Faraday Soc.*, 1935, **31**, 765.

The bearing of the results obtained by the above technique upon current theories of adsorption will be discussed in further publications. It may be pointed out, however, that in the case of the lower alcohols so far examined, the  $\log (\Delta V_E - \Delta V) - t$  curve is linear within the experimental error, as shown in Fig. 9 ( $\Delta V_E$  is the equilibrium surface potential,

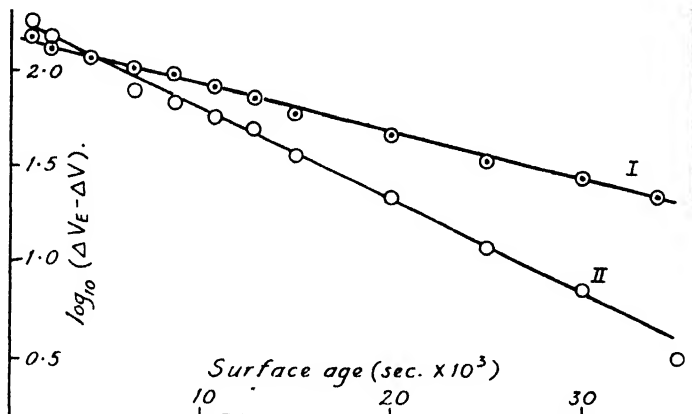


Fig. 9.— $\log_{10} (\Delta V_E - \Delta V)$  plotted against surface age.

I. 0.01 % *sec.*-octyl alcohol in N/100 HCl.

II. 0.02 % *sec.*-octyl alcohol in N/100 HCl.

i.e. when  $t = \infty$ ). Since  $\Delta V$  is directly proportional to  $n$  in these systems (Fig. 8), the kinetics of adsorption thus obey a first-order equation.

The authors would like to thank the Wm. S. Merrell Company, U.S.A., for a supply of pure cetyl trimethyl ammonium bromide, and Mr. A. M. Binnie for helpful discussions on boundary layers. One of us (A. M. P.) is indebted to the Brighton Education Committee for the award of a research scholarship during the tenure of which most of the present work was carried out, and to the D.S.I.R. for subsequent assistance.

*Department of Colloid Science,  
Cambridge.*

## THE HEAT OF FORMATION OF BORON TRIOXIDE

BY W. EGGERSGLUESS, A. G. MONROE AND W. G. PARKER

*Received 7th November, 1947; as revised 11th February, 1949*

The heat of formation of boron trioxide has been determined by a modified calorimetric method and found to be  $281.1 \pm 3.1$  kcal./mole. This result supports an early value of 279.9 kcal./mole calculated by Berthelot (1897) from experiments of Troost and Hautefeuille (1876) and disagrees with the more recent values of 349 kcal./mole and 335 kcal./mole published by Roth and Boerger (1937) and by Todd and Miller (1946) respectively. It is considered that a value of approx. 280 kcal./mole is correct and that the higher values cited can be attributed to the use in both instances of boron containing some combined hydrogen. Using the corrected value for the oxide the heat of formation of diborane ( $B_2H_6$ ) is calculated to be  $-26$  kcal./mole and not  $+44$  kcal./mole as stated by Roth. Diborane is therefore an endothermic substance.

The first thermochemical determinations of the heat of formation of  $B_2O_3$  were made by Troost and Hautefeuille,<sup>1</sup> who determined the heat of formation and of hydrolysis of boron trichloride in a mercury calorimeter. Their value of 312 kcal./mole was corrected by Berthelot<sup>2</sup> to 279.9 kcal./mole. This value of Berthelot was generally accepted for 40 years. In 1931 Pohland,<sup>3</sup> who determined the heat of formation of boron tribromide pointed out that Berthelot gave his corrected value only as "approximate" and that since this value was very uncertain, a new determination was desirable. In 1937 Roth and Boerger<sup>4</sup> made a new and more direct determination by burning boron and paraffin simultaneously in separate crucibles in oxygen in an isothermal bomb calorimeter. The heat of formation of  $B_2O_3$  was calculated on the weight of  $B_2O_3$  determined by analysis after combustion and found to be  $349 \pm 3$  kcal./mole. Recently, Todd and Miller<sup>5</sup> burned spectroscopically pure boron together with benzoic acid in oxygen in a Parr isothermal bomb calorimeter and obtained the value  $335.8 \pm 0.8$  kcal./mole at 25°C. Neither group of investigators could explain their large deviation from the old value, and there is therefore a choice of three values viz., 280, 349 and 335 kcal./mole. This is unsatisfactory and we have made a fresh determination and have considered the reasons for the deviations mentioned. This work suggests that the Berthelot figure may be nearer to the correct value than the others.

### Experimental

In all our experiments we used a 300 ml. Kroecker bomb and calibrated it with pure benzoic acid. The apparatus was kept in a room maintained at  $20^\circ C \pm 1^\circ C$  and temperature changes in the bomb calorimeter were observed with a Beckmann thermometer. The bomb was filled initially with oxygen at 400 lb./in.<sup>2</sup> (28.1 atm.) pressure and in our preliminary experiments we adopted the method of Roth and Boerger using medicinal paraffin oil in a separate crucible below the crucible containing the boron. It is perhaps necessary to explain that boron alone does not burn satisfactorily in oxygen owing to the formation of viscous  $B_2O_3$  in the initial stages which forms a protective layer round the remainder of the boron. If it is burned with a substance which is more readily combustible e.g. medicinal paraffin oil, the  $B_2O_3$  layer is less effective and the reaction is more complete. The heat of combustion of the additive must be known (from a separate determination) and it is essential to base the calculation for the heat of formation of  $B_2O_3$  on the weight of  $B_2O_3$  determined by analysis after combustion and not on the weight of boron put into the bomb. The  $B_2O_3$  formed was determined by titration with N/10 NaOH after addition of glycerol. The accuracy of this method was found to be 0.2-0.3 % in agreement with Roth. A correction for the formation of nitric acid was found to be unnecessary provided the bomb was carefully flushed with oxygen before filling to pressure.

We used the purest sample of boron available (Merck) which contained 93.8 % boron and 5.2 % boric acid. A spectroscopical examination showed that Si and Mg were the only significant impurities. Subsequent examination by X-ray powder crystallography showed that apart from the lines attributable to boric acid there were a few rather weak lines indicating the presence of some other crystalline constituent. These lines could not be identified with published data on either silicon or magnesium compounds or any likely impurity except crystalline boron. It is not possible to state definitely that the lines were due to crystalline boron, however, since truly reliable data are not available for the element. Removal of boric acid by leaching out with water was not attempted although subsequent tests showed that this could be done satisfactorily with cold water. Hot water extraction caused a slow and progressive oxidation of the boron. In this investigation the determination of boric acid was made under identical conditions in both the original sample of boron and in the products

<sup>1</sup> Troost and Hautefeuille, *Ann. Chim. Phys.*, 1876, **9**, (5), 70.

<sup>2</sup> Berthelot, *ibid.*, 1878, **15**, (5), 215, and *Thermochimie* (Paris, 1897), Vol. II, p. 122.

<sup>3</sup> Pohland, *Z. anorg. Chem.*, 1931, **201**, 282.

<sup>4</sup> Roth and Boerger, *Ber., B*, 1937, **70**, 48, 971.

<sup>5</sup> Todd and Miller, *J. Amer. Chem. Soc.*, 1946, **68**, 530.

of each combustion. Boric acid in the latter was that derived from the hydration of  $B_2O_3$  formed in combustion as well as that associated with the quantity of boron used.

In three preliminary experiments, which were made before we were aware of the recent determination of Todd and Miller, we obtained a mean value for the heat of formation of  $B_2O_3$  of  $284 \pm 6$  kcal./mole at constant volume or of approx.  $285 \pm 6$  kcal./mole at constant pressure. The error shown, viz.  $\pm 6$  kcal./mole, is the root mean square error calculated in the usual way.

The method has two disadvantages because (1) only a small part of the total heat evolved in the bomb is contributed by the boron viz. 8-10 % in our experiments, 15-19 % in those of Roth and Boerger and 11-14 % for Todd and Miller, and (2) the correction which must be made for the heat of hydration of  $B_2O_3$  is uncertain since  $B_2O_3$  only reacts slowly with water. Todd and Miller considered this to be the greatest error in their calculations. We sought to overcome these disadvantages by intimately mixing the boron with a readily combustible additive which did not contain hydrogen. Sulphur and red phosphorus which have acidic oxides were tried and in excess gave complete combustion with 100-200 mg. of boron. Boride formation probably occurs, however, since after the addition of water,  $H_2S$  or  $PH_3$  could be detected. Graphite did not burn completely and different samples of charcoal were found to contain large percentages of hydrogen even after strong drying. Lampblack after heating for half an hour at  $1000^\circ C$  contained only 0.80 % of hydrogen and it proved satisfactory in the bomb. A fresh series of experiments in which mixtures of boron and lampblack were burnt was undertaken. The quantities of lampblack used are given in Table I together with the heat of hydration which would be evolved if all water (from the hydrogen of the lampblack) is used for hydration according to the equation,

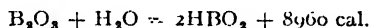
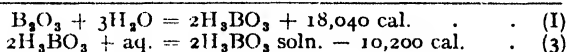
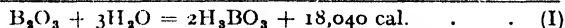
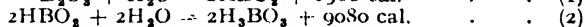
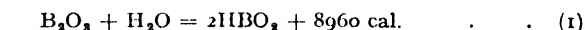


TABLE I

QUANTITIES OF LAMPBLACK USED AND POSSIBLE HEAT OF HYDRATION

Expt. No.	Lampblack (mg.)	Hydrogen (mg.)	Water Formed (millimole)	Heat of Hydration of $B_2O_3$ (cal.)
1	307.40	2.46	1.22	10.9
2	356.45	2.85	1.41	12.6
3	437.50	3.50	1.74	15.6
4	394.70	3.16	1.57	14.1
5	429.50	3.44	1.71	15.3
6	557.50	4.46	2.21	19.8
7	394.90	3.16	1.57	14.1

As the quantity of  $B_2O_3$  is much greater than that of  $H_2O$  we may assume that in our experiments only this step in the hydration of  $B_2O_3$  occurs and not steps (2) and (3) in the following :<sup>6</sup>



Reactions (1) to (3) are single steps whereas (I) is the summary reaction for total hydration and (II) for the total dissolution.

As stated above we have used the figure of 8960 cal. for 1 mole of water in our calculations (reaction (I) would only yield 6013 cal. for 1 mole of water).<sup>7</sup>

<sup>6</sup> Roth and Boerger, *loc. cit.*<sup>4</sup>

<sup>7</sup> Todd and Miller used a value of 10,800 cal./mole for assessing this correction. In their experiments reaction (I) can proceed quantitatively (they used boron mixed with benzoic acid) but only a relatively small amount of the boric acid can be dissolved as its solubility in water is small. We therefore think that in their work the value of the correction should approach 18,040 rather than 7,820 kcal./mole, and this would reduce their final value.

If all the water formed during combustion of the lampblack is used up in the hydration of  $B_2O_3$ , an appreciable quantity of heat is released as shown in the last column of Table I.

In Table II the initial quantities of boron are given and the quantities of  $B_2O_3$  determined after combustion. As the boron already contained a small amount of boric acid (1 g. contained 0.84 millimole) this was subtracted according to the quantity of boron used. No evidence was obtained of a sub-oxide being present in either the original sample of boron or in the products of combustion. Neither showed any reducing properties.

TABLE II

Expt. No.	Initial Wt. of Boron (g.)	Initial Quantity of Boron (millimole $B_2$ )	Total $B_2O_3$ by Analysis after Combustion (millimole)	$B_2O_3$ in Boron Initially (millimole)	$B_2O_3$ Formed in Combustion (millimole)	Boron Burnt (%)
1	212.00	9.80	6.209	0.089	6.120	62.5
2	123.10	5.69	3.673	0.052	3.621	63.6
3	124.45	5.75	3.312	0.052	3.260	56.7
4	238.50	11.02	6.210	0.100	6.110	55.5
5	274.95	12.70	6.970	0.115	6.855	54.0
6	247.75	11.45	6.602	0.104	6.498	56.8
7	120.00	5.54	2.818	0.050	2.768	50.0

The results of all our calorimetric determinations with boron and lampblack are given in Table III. The water equivalent of the calorimeter was  $3139 \pm 5$  cal. (error =  $\pm 0.16$  %) and the heat of combustion of the lampblack was  $7795 \pm 16$  cal./g. (error =  $\pm 0.21$  %).

TABLE III.—HEAT OF FORMATION OF  $B_2O_3$  AT CONSTANT VOLUME

Expt. No.	Total Heat Evolved (cal.)	Heat Contributed by the Boron		Heat Contributed by the Boron* (%)	Heat of Formation of $B_2O_3$ kcal./mole	
		No Hydration Assumed (cal.)	Assuming Hydration (cal.)		No Hydration Assumed	Assuming Hydration
1	4219.4	1775.2	1764.3	41.8	290.1	288.3
2	3860.0	1035.0	1022.4	26.5	285.8	282.4
3	4392.7	935.2	919.6	20.9	286.9	282.1
4	4889.3	1765.8	1751.7	35.8	289.0	286.7
5	5268.8	1873.8	1858.5	35.3	273.3	271.1
6	6171.7	1779.0	1759.2	28.5	273.8	270.7
7†	3974.2	850.2	836.1	21.0	307.2	302.1

\* With hydration; the figures without hydration would be higher.

† Boron treated with hydrogen.

The average of the first 6 experiments gives for the heat of formation of  $B_2O_3$  from amorphous boron at 20° C (28.1 atm.  $O_2$  pressure):

(a) Without correction for hydration,

const. volume :  $283.2 \pm 3.1$  kcal./mole,  
 const. pressure (calc.) :  $284.1 \pm 3.1$  kcal./mole,  
 (error =  $\pm 1.10$  %).

(b) After correcting for hydration—assuming all the water formed during combustion combines with the  $B_2O_3$ ,

const. volume :  $280.2 \pm 3.1$  kcal./mole,  
 const. pressure (calc.) :  $281.1 \pm 3.1$  kcal./mole,  
 (error =  $\pm 1.11$  %).

We consider that the true value lies between the values of (a) and (b) and approximates more closely to the value of  $281.1 \pm 3.1$  kcal./mole since in the conditions of the experiment the  $B_2O_3$  is uniformly deposited in a very fine state of division together with the moisture on the sides of the bomb. Conditions are favourable for rapid and complete combination of the two. We also assume, as do the other investigators, that the  $B_2O_3$  is formed as a glass and is not truly crystalline, and we have adopted in our calculation the appropriate value for the heat of solution.

A greater overall accuracy than  $\pm 3.1$  kcal. in these experiments was not possible on account of the limitations imposed by the type of calorimeter available and in reading a Beckmann thermometer ( $\pm 0.005^\circ C$ ). In comparison with previous investigations, however, this somewhat lower accuracy is partly compensated by the greater percentage of the total heat evolved which is contributed by the boron, viz. 20.9-41.8 % compared with 11.19 % in previous works.

### Discussion

Our value of 281.1 kcal./mole supports Berthelot's value of 279.9 kcal./mole and disagrees with the results of Roth and Boerger and of Todd and Miller. Agreement between the latter two groups of workers is poor, viz. 349 and 335 kcal./mole respectively, and we have examined their papers closely. Roth prepared his boron by hydrogen reduction of  $BCl_3$  on a glowing tungsten filament and Todd obtained boron by thermal decomposition of  $B_2H_6$ . No details are given in either case of the final treatment of the boron produced, except that Todd examined the product spectroscopically and found it to be pure. We suggest that neither of these methods produces pure boron but a mixture of boron and boron hydrides, the higher homologues of which are solids. The composition of the product would be indefinite, which may explain the discrepancy between the results of the two groups of workers. By analogy with carbon, contamination with hydrogen compounds is very probable, since amorphous carbon produced by the decomposition of hydrocarbons contains a relatively high proportion of hydrogen, and complete removal of this hydrogen is a difficult matter requiring a temperature of more than 2000 C. The best sample of amorphous carbon we could procure contained 0.8 % hydrogen: 1 % hydrogen in boron could produce an error of 8 kcal./mole in calculating the heat of formation of  $B_2O_3$ . Hydrides are not detected by spectroscopic examination and the emission spectra of the samples are therefore no guarantee that the boron is pure. In order to support this explanation of the high values of Roth and Todd, we heated some of the boron we used in a stream of hydrogen at 400° C for  $\frac{1}{2}$  hr. and then, without further treatment of this product made a calorimetric determination as before. We found that the value for the heat of formation of  $B_2O_3$  had substantially increased to 302.1 kcal./mole (see Table III, Expt. 7). This increase is much greater than the experimental error and is attributed to the presence of hydrogen in the boron. The purity of our own sample of boron (Merck) has already been discussed and the method of determination is described below. The presence of Si and Mg also makes the apparent value higher than the true value but the error is very much smaller than with hydrogen. Similarly, a small quantity of crystalline boron if present would have only a secondary effect on the result. In the boron used these impurities did not exceed 1 % so that the maximum error in experiments 1 to 6 is not greater than 1.4 kcal.

The method which we adopted of mixing the boron with amorphous carbon of very low hydrogen content has two advantages over previous methods, because (1) a greater proportion of boron is burnt and as much as 40 % of the heat evolved may be due to the boron, and (2) only a very small quantity of water is produced and the necessary correction for hydration of the  $B_2O_3$  is relatively small. Todd and Millers' method of mixing boron with benzoic acid has the advantage of eliminating one

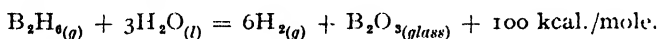


step in the procedure, namely, a separate determination of the calorific value of the additive, but it is subject to both the disadvantages already mentioned and also to possible intermediate compound formation. Roth and Boerger in experiments with boron mixed with vaseline noted the disagreeable smell of boron hydrides when the bomb was opened.

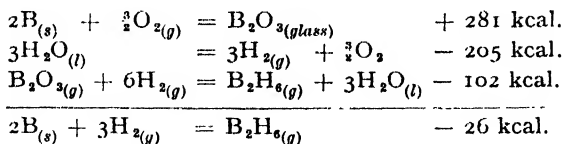
If we assume that in our experiments some of the carbon reacted with boron instead of burning to  $CO_2$ , we would have a large error in our calculation. For example, 10 % of the carbon forming boron carbide would give an apparent increase in the heat of formation of  $B_2O_3$  of approximately 40 kcal./mole. We have, however, several reasons to believe that the combination of carbon with boron does not occur in the conditions of our experiments :

- (1) In one experiment in which we analyzed the gaseous products we found practically all the carbon as  $CO_2$ , the quantity of CO was negligible ;
- (2) in our preliminary experiments in which we used the two crucible method and in which the formation of boron carbide seems to be impossible we found a similar low value ;
- (3) in three experiments not mentioned hitherto (two crucible method) with an impure boron which contained only 56 % of boron, we found for the heat of formation of  $B_2O_3$  the values 386, 394 and 395 kcal. calculated per mole  $B_2O_3$  formed. The principal impurities were found to be Al, Mg and Si, whose heats of combustion per g. are 7.05, 6.01 and 7.25 kcal. respectively. Assuming therefore that these impurities are burned in similar proportions to the boron and have an average heat of combustion of 6.5 kcal./g. we can make suitable corrections to the heat of formation of  $B_2O_3$  given above. The recalculated values then become 285, 295 and 295 kcal./mole respectively, which also favour the lower value.

As we consider that the high values of Roth and Todd are due to the contamination of the boron with hydrogen or boron hydrides, it was of interest to calculate the thermochemical data for these compounds. Roth and Boerger had found



With the value of 7820 cal. for the heat of total dissolution of  $B_2O_3$ , according to the above equation (II) we calculated the heat of reaction of diborane with water to be 102 kcal./mole. With this value and the value for  $B_2O_3$  established here we have



Diborane ( $B_2H_6$ ) is therefore shown to be an endothermic compound with - 26 kcal./mole and not an exothermic compound with a heat of formation of + 44 kcal./mole as stated by Roth and Boerger. This result is more compatible with the reactive nature of this compound (it is not very surprising that  $B_2H_6$  is an endothermic compound compared, for instance, with  $SbH_3$  which is also endothermic).

We have tried to explain the high value of Todd and of Roth as being due to contamination of the boron with hydrogen. Assuming that the bonds in the higher boron-hydrogen compounds are of the same strength as in diborane (which may not be true in all cases) we can calculate the approximate heat of combustion of such compounds if the hydrogen con-

tent is known. If  $x$  is the percentage of hydrogen we get for the heat of combustion of such compounds :

$$\frac{\text{Heat of combustion of mixture}}{\text{mole } B_2O_3} = \frac{x \frac{68.3 + 26/3}{2.016} + (100 - x) \frac{281}{21.64}}{(100 - x)} \\ = \frac{545x + 28,100}{(100 - x)}.$$

We have calculated from this equation the heats of combustion for several values of  $x$  and plotted the results in Fig. 1 (curve I). Assuming that

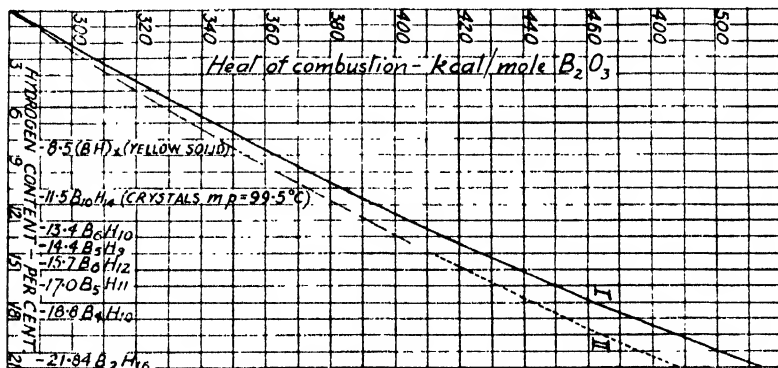


FIG. 1.—Heat of Combustion of Boron Hydrides.

higher hydrides may not be endothermic compounds we have calculated in a similar way, assuming the heat of formation to be zero, and obtained the expression  $\frac{453x + 28,100}{(100 - x)}$  for the heat of combustion of the mixture per mole  $B_2O_3$ . The results of this calculation are plotted in Fig. 1 (curve II, dotted line).

According to curve I therefore a hydrogen content of 1 % would give an increase of 8 kcal./mole for the heat of combustion of  $B_2O_3$ . In order to explain a value of 330 kcal./mole which we calculated from the experiments of Todd and Miller, a hydrogen content of 5.6 % would be necessary. This seems to be rather high but it is possible that the residual unburned "boron" (50-60 % in their experiments) was cracked and that this hydrogen was also burnt, so that a contamination of only 2.3 % hydrogen would explain their high value. This suggestion may also explain why the heat of formation of  $B_2O_3$  appears to increase with the amount of  $B_2O_3$  formed in the experiments of Roth and Boerger.

When we had completed this work we found a new publication of Roth<sup>8</sup> in which he has made a recalculation of his old value and that of Todd and Miller using better values for the heat of hydration of  $B_2O_3$ . He then obtained an average value of  $339.8 \pm 2.3$  kcal./mole. These considerations do not alter any of our conclusions. Some of his suggestions are already described in our work (e.g. the use of hydrogen-free substances, such as phosphorus or sulphur, for assisting the combustion of the boron). We cannot agree with his corrections for the heats of hydration and of solution (see our own discussion on this problem).

**Determination of the Purity of Boron.**—Winslow and Liebafsky<sup>9</sup> state that there is no accurate method for the determination of the boron

<sup>8</sup> Roth, *Z. Naturforsch.*, 1946, 1, 574.

<sup>9</sup> Winslow and Liebafsky, *J. Amer. Chem. Soc.*, 1942, 64, 2725.

content of commercial boron. They tried to determine the boron content after fusing with sodium peroxide or carbonate-nitrate mixtures or by chlorination and say that their results were not exact.

We have made a number of experiments in an attempt to oxidize boron by using oxides, peroxides, nitrates, nitrites, bromates, chlorates, perchlorates, and persulphates. We found PbO very convenient for the oxidation of small amounts of boron (approximately 20 to 50 mg.) in quartz test-tubes heated in a Bunsen flame. But in order to get a slow reaction the PbO must be fused and cooled before the boron is added. The reaction product was difficult to dissolve, however, and the quartz tube was corroded during fusion. Determination of the boric acid was also difficult in the presence of a large excess of lead salts. We therefore reverted to sodium peroxide and found that 20-30 mg. of boron mixed with approx. 500 mg. of sodium peroxide was completely oxidized after fusion for 10 min. The melt was white. After cooling the product was dissolved in water. Part of the solution was acidified, boiled to expel CO<sub>2</sub>, cooled and neutralized. The boric acid content of this was determined by titration with N/10 NaOH after addition of neutral glycerol solution.

This paper contains the opinions of the authors; the views expressed are not to be construed as official or reflecting those of the Ministry of Supply. Crown Copyright is reserved. It is published with the permission of the Controller of H.M. Stationery Office.

*Chemistry Department,  
Royal Aircraft Establishment,  
South Farnborough, Hants.*

## A STUDY OF THE FINE STRUCTURE OF CARBONACEOUS SOLIDS BY MEASUREMENTS OF TRUE AND APPARENT DENSITIES

### PART II.—CARBONIZED COALS

BY ROSALIND E. FRANKLIN

*Received 15th February, 1949*

Measurements of the true and apparent densities and adsorptive properties of coals carbonized at 600-1,650° C have been used to study the variation of the colloidal structure with the temperature of carbonization. It is shown that the true density increases with increasing carbonization temperature, reaching about 2.1 g./cm.<sup>3</sup> at 1,100-1,200° C.

The porosity of particles small enough to pass a 240 B.S. sieve is large (from 7 % to 23 %) and increases with increasing carbonization temperature in the range 600° to 1,000° C. The specific surface increases with increasing carbonization temperature between 600° and 800° C. The accessibility of the pores and inner surfaces to liquids and gases decreases with increasing carbonization temperature in the range 600° to 1,600° C and is governed by the width of fine constriction in the pore system rather than by the mean diameter of pores which are uniform along their length. As a result of this pore structure, the solids function as molecular sieves, the width of the constrictions in the pore system being of the same order as the diameters of the simple molecules used for the density

measurements (i.e. 2 to 6 Å). This molecular sieve structure must be of importance in determining both the chemical behaviour of the solid and the composition of the gas evolved during carbonization.

The industrial behaviour of coke prepared from any given coal is highly dependent on the maximum carbonization temperature. In particular, there is loss of reactivity when the temperature of carbonization rises above 650° C (the exact temperature varies from coal to coal), and the change is reflected in many of the physical and chemical properties of the material. For example, the adsorption of carbon dioxide, the reactivity to sulphuric acid, the dispersibility in sulphuric acid, the ignition temperature and the "combustibility" of a number of carbonized coals all decrease rapidly with increasing carbonization temperature above 700° C.<sup>1</sup> In an attempt to investigate the underlying structural changes, Cannon, Griffith and Hirst<sup>2</sup> made an extensive survey of the internal surface areas of carbonized coals, as measured by their heat of wetting in methanol. They found that there was apparently a marked loss of inner surface above 550°-650° C. This change in structure was further investigated by Maggs,<sup>3</sup> who studied the adsorption of methyl, ethyl and propyl alcohol vapours and showed that the apparent decrease in surface area resulted from a decrease in the accessibility of the inner surfaces. This is in accord with the earlier work of Macpherson, Slater and Sinnatt,<sup>4</sup> who found that the moisture content of laboratory-carbonized coals after exposure to the atmosphere for 48 hr. was greatest for samples carbonized at about 700° C and that the rate of adsorption and desorption of moisture decreased rapidly with further increase in carbonization temperature.

The measurements of the true and apparent densities of carbonized coals given in this paper make clearer the nature of the structural changes which occur between 600° and 1,000° C and which result in the changes in properties mentioned above. In particular, it will be shown that carbonized coals contain a large volume of very fine pores and a large internal surface area, even after heating to temperatures above 1,000° C. The porosity of the solid, due to these fine pores alone, increases with increasing carbonization temperature at least up to 1,000° C. The loss of reactivity and the apparent decrease in porosity and in internal surface area arise from the diminished accessibility of the pores.

The fine-structure porosity of a carbonized coal may be as high as 20 %. It must be emphasized, however, that it is in no way related to the bubble-structure developed by coking coals in what is called the "plastic" range. It is, in fact, much smaller in the products obtained from good coking coals than in those from anthracite and low-rank, weakly-caking coals which give no bubble-structure. Moreover, the greater part of the porosity is developed at temperatures above the plastic range, when the carbonized coal has already acquired a rigid structure and no further bubble-formation can occur.

A considerable number of measurements of the apparent densities of carbonized coals have been previously reported.<sup>5</sup> Although the influence of both carbonization temperature and method of density measurement was in no case systematically investigated, the results all appear to be

<sup>1</sup> South Metropolitan Gas Co., *The Solid Products of Carbonisation of Coal* (London, 1934).

<sup>2</sup> Cannon, Griffith and Hirst, *Proc. Conf. on Ultra-fine Structure of Coals and Cokes* (B.C.U.R.A., 1944), p. 131.

<sup>3</sup> Maggs, *ibid.*, p. 147.

<sup>4</sup> Macpherson, Slater and Sinnatt, *Fuel*, 1928, 7, 444.

<sup>5</sup> Rose, *Ind. Eng. Chem.*, 1922, 14, 1047; Drakeley and Wilkins, *J. Soc. Chem. Ind.*, 1931, 50, 331T; Hiles and Mott, *Fuel*, 1937, 16, 64; Smith and Howard, *Ind. Eng. Chem.*, 1942, 34, 43; Milner, Spivey and Coff, *J. Chem. Soc.*, 1943, 578.

consistent with those of the present work. This suggests that structural changes similar to those described below occur during the carbonization of all coals, and are not peculiar to the specimens studied here.

### Experimental

**Materials.**—CARBONIZED COALS. Samples were prepared from the following four coals.

- ANTHRACITE C: S. Wales anthracite, Group A1, 94.2 % carbon (dry, mineral-free).  
 COAL F: S. Wales coking coal, Meta-bituminous, 89.7 % carbon (dry, mineral-free).  
 COAL H: Yorkshire caking coal, Meta-lignitous, 83.5 % carbon (dry, mineral-free).  
 COAL K: Northumberland weakly caking coal, Meta-lignitous, 82.4 % (dry, mineral-free).

For carbonization at temperatures up to 1020° C samples ground to pass a 72 B.S. sieve were heated in nitrogen in Nichrome-wound furnaces at 5° C/min. and held for 2 hr. at the maximum temperature.

For carbonization at temperatures higher than 1020° C a molybdenum-wound tube furnace was used. The sample was first carbonized at 1000° C as above, and, if coherent, re-ground to pass a 72 B.S. sieve. It was then packed into a  $\frac{1}{4}$  in.-bore carbon tube through which nitrogen was passed. The molybdenum furnace was brought to the desired maximum temperature, and the tube containing the sample was then advanced through the furnace in steps so that each part of the sample remained for 2 hr. in the zone of maximum temperature. During the initial stages, and again at the completion of the process, the closed end of a carbon sighting-tube was situated in the zone of maximum temperature, and the temperature was measured with an optical pyrometer.

**Analyses.**—Proximate and ultimate analyses of the carbonized samples are given in Tables I to IV.

TABLE I.—ANALYSIS OF CARBONIZED COAL C

Carboniza- tion Temp., ° C	Proximate Analysis					Ultimate Analysis (Parr's basis)			
	Moisture	Volatile less Moisture	Fixed Carbon	Ash	Volatile Matter (dry, ash-free)	Carbon	Hydro- gen	Nitrogen	Oxygen + Errors
—	2.6	4.7	90.6	2.1	4.9	94.2	2.9	1.2	1.7
305	1.6	4.9	91.4	2.1	5.1	94.1	2.8	1.0	2.1
410	2.0	4.5	91.2	2.3	4.7	94.6	2.7	0.9	1.8
510	2.2	4.3	91.3	2.2	4.5	94.7	2.6	0.9	1.8
605	2.9	3.9	91.1	2.1	4.1	94.7	2.4	0.8	2.1
700	4.4	3.0	90.5	2.1	3.2	95.5	1.7	0.9	1.9
805	5.0	2.5	90.5	2.0	2.7	96.3	1.0	0.8	1.9
910	4.9	1.5	91.5	2.1	1.6	96.9	0.6	0.6	1.9
1,015	0.1	0.3	97.3	2.3	0.3	98.6	0.5	0.6	0.3

**Liquids.**—METHANOL, BENZENE, ACETONE, ETHER, CHLOROFORM, CARBON TETRACHLORIDE: Analar reagents were used.

*n*-HEXANE boiling at 67–69° was supplied by B.D.H.

CARBON DISULPHIDE was purified by treatment with potassium permanganate, mercury and mercuric sulphate according to the method of Hammick and Howard<sup>6</sup> and was subsequently dried and distilled.

**Gases.**—HYDROGEN was prepared by electrolysis of 10 % caustic potash solution saturated with baryta, and was purified by diffusion through a palladium tube.

OXYGEN, METHANE.—Cylinder gases were used without purification.

<sup>6</sup> Hammick and Howard, *J. Chem. Soc.*, 1932, 2915.

TABLE II.—ANALYSIS OF CARBONIZED COAL F

Carboniza- tion Temp., ° C	Proximate Analysis					Ultimate Analysis (Parr's basis)			
	Moisture	Volatile less Moisture	Fixed Carbon	Ash	Volatile Matter (dry, ash-free)	Carbon	Hydro- gen	Nitrogen	Oxygen + Errors
—	0.8	24.0	71.1	4.1	25.2	89.7	5.0	1.8	3.5
405	0.6	19.6	75.3	4.5	20.7	89.7	4.7	1.8	3.8
510	1.2	12.0	81.7	5.1	12.8	91.2	3.2	1.8	3.8
605	3.0	6.0	85.2	5.3	6.6	93.9	2.4	1.8	1.9
700	3.4	4.0	87.1	5.5	4.4	95.3	1.7	1.9	1.1
915	0.7	1.9	91.1	6.3	2.0	97.5	0.6	1.6	0.3

TABLE III.—ANALYSIS OF CARBONIZED COAL H

Carboniza- tion Temp., ° C	Proximate Analysis					Ultimate Analysis (Parr's basis)			
	Moisture	Volatile less Moisture	Fixed Carbon	Ash	Volatile Matter (dry, ash-free)	Carbon	Hydro- gen	Nitrogen	Oxygen + Errors
—	5.9	34.9	57.3	1.9	37.9	83.5	5.4	2.2	8.9
300	1.6	34.0	62.5	1.9	35.3	87.8	5.1	1.9	10.2
400	1.3	21.9	74.5	2.3	22.7	84.8	4.5	2.3	8.4
500	2.4	11.3	83.3	3.0	11.9	88.0	3.1	2.2	5.8
605	3.3	—	—	2.2	—	90.7	2.2	—	—
710	5.6	4.2	87.6	2.0	4.0	93.6	1.5	2.0	2.9
760	6.1	2.8	88.6	2.5	3.1	94.7	1.2	2.0	2.1
800	6.2	—	—	3.0	—	95.5	0.8	—	—
855	6.0	—	—	2.9	—	96.5	0.8	—	—
905	2.8	—	—	2.9	—	96.8	0.6	1.1	1.5
950	2.2	—	—	3.4	—	96.7	0.7	—	—
1,000	1.3	0.9	94.4	3.4	0.9	96.7	0.4	1.5	0.4

TABLE IV.—ANALYSIS OF CARBONIZED COAL K

Carboniza- tion Temp., ° C	Proximate Analysis					Ultimate Analysis (Parr's basis)			
	Moisture	Volatile less Moisture	Fixed Carbon	Ash	Volatile Matter (dry, ash-free)	Carbon	Hydro- gen	Nitrogen	Oxygen + Errors
—	10.5	33.8	54.7	1.0	38.2	82.4	5.1	1.9	10.6
300	2.0	33.5	63.4	1.1	34.6	82.2	5.1	2.0	10.7
400	2.2	24.9	72.0	0.9	26.0	83.2	4.5	2.2	10.1
495	1.9	13.7	83.0	1.4	14.2	88.4	3.3	2.3	6.0
550	3.6	8.9	86.0	1.5	9.4	90.7	2.9	2.4	4.0
620	2.6	7.2	88.3	1.9	7.5	92.1	2.5	2.3	3.1
680	—	—	—	1.9	—	92.1	2.2	—	—
720	5.4	5.6	87.3	1.7	6.0	95.3	1.6	2.0	1.1
820	6.2	4.1	88.0	1.7	4.5	97.1	0.7	1.5	0.7
915	6.7	2.1	89.0	2.2	2.3	97.5	0.4	1.8	0.3

**Measurement of Density.**—The apparatus and methods used for the measurements of densities in helium and in liquids have been described in a preceding paper.<sup>7</sup>

**Density "Drift."**—The "density drift," or increase of apparent density with time, was investigated by making measurements 2 hr. and 24 hr. after immersing the solid in the liquid. In helium, measurements were normally continued until no further drift occurred in 24 hr.; in a few cases the density drift in helium continued for many days and was not followed to completion.

**Correction for Mineral Matter.**—The density values recorded have in all cases been corrected for the mineral content of the samples by use of the correction formula of Wandless and Macrae.<sup>8</sup> Although the mineral content of carbonized coals is somewhat greater than that of raw coals, the uncertainty in the density correction is less since the composition of the mineral matter differs less from that of the ash whose density was determined. The correction did not exceed 3 % for any of the carbonized coals used.

## Results

**APPARENT DENSITIES OF COALS CARBONIZED AT TEMPERATURES UP TO 1650° C.**—Measurements of the densities of coals C, F, H and K carbonized at temperatures from 300-1650° C were made with helium, methanol, water and *n*-hexane. With coal H, carbon disulphide was also used and with coal K,

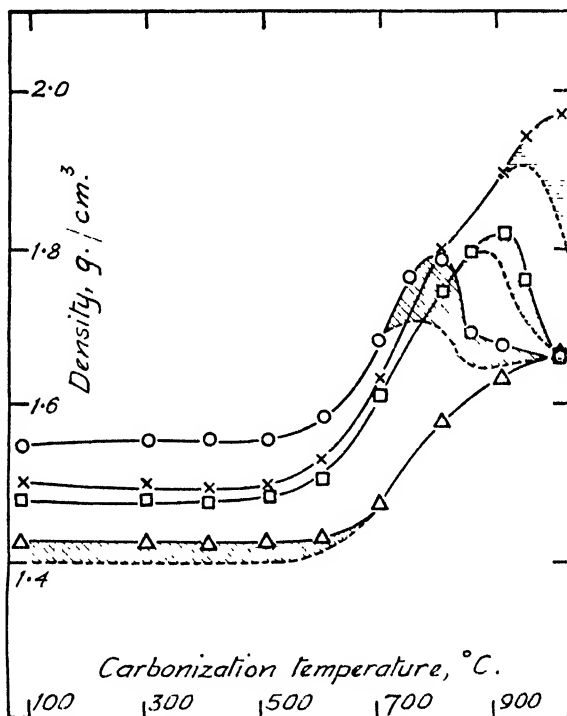


FIG. 1.—Anthracite C.

× Helium.      O Methanol.      □ Water.      Δ *n*-Hexane.

benzene. In Fig. 1 to 4, densities are plotted against carbonization temperature for temperatures up to 1020° C. The full-line curves in the Figures represent density values after 24 hr. immersion in the liquids and the final values obtained with helium, and the broken line curves represent apparent densities

<sup>7</sup> Franklin, *Trans Faraday Soc.*, 1949, **45**, 274.

<sup>8</sup> Wandless and Macrae, *Fuel*, 1934, **13**, 4.

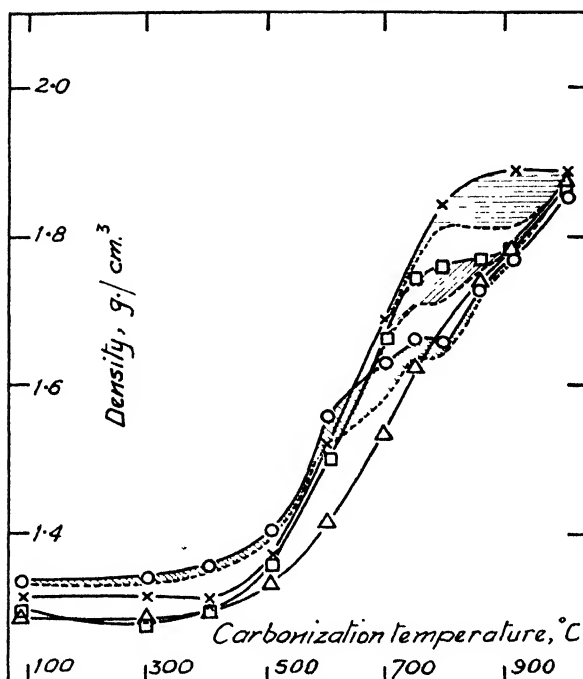


FIG. 2.—Coal F.

Helium.      ○ Methanol.      □ Water.      Δ n-Hexane.

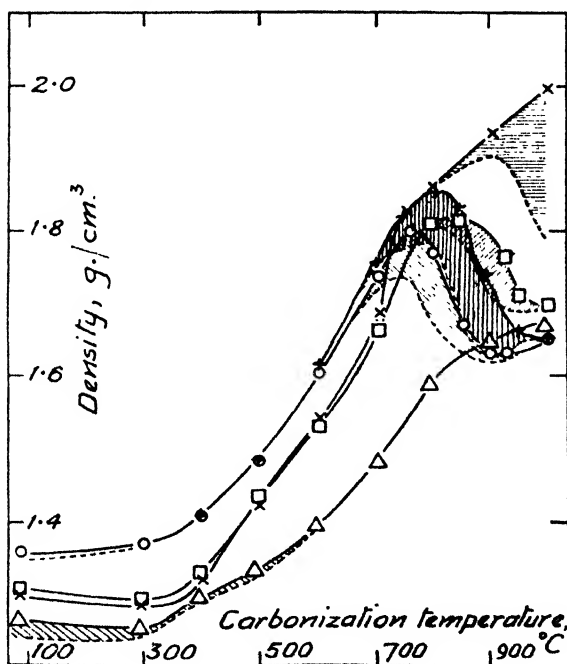


FIG. 3.—Coal H.

× Helium.      ○ Methanol.      □ Water.      Δ n-Hexane.      + Carbon disulphide.



after 2-hr. immersion in liquids and the first recorded values in helium. The height of the shaded areas is a measure of the density drifts. (The initial values recorded here and elsewhere for samples which show a large drift in helium refer to measurements made as quickly as possible after admitting the gas to the sample; they have only qualitative significance.\*)

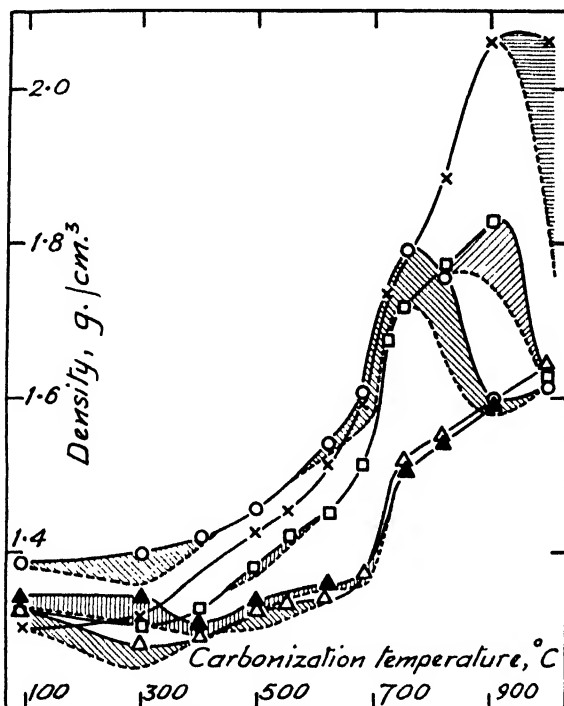


Fig. 4—Coal K

× Helium.    O Methanol.    □ Water    Δ *n*-Hexane.    ▲ Benzene.

**TEMPERATURES BELOW 500° C.**—Below 500° C the variation of apparent density with carbonization temperature is different for each of the four coals investigated. For the anthracite c there is no appreciable change. The apparent densities of coal F in water, of coal H in water, *n*-hexane and helium, and of coal K in water and in *n*-hexane are slightly *decreased* by heating to 300° C, and apparent densities in methanol in all cases increase continuously with increasing carbonization temperature.

**TEMPERATURE RANGE 500° C TO 600° C.**—Between 500° C and 600° C an increase in the apparent densities of the anthracite c sets in and the densities of the other coals all increase.

**TEMPERATURE RANGE 600° C TO 1020° C.**

(i) *Coals c, H and K.*—Fig. 1 to 4 show clearly that large and significant structural changes occur in all four coals between 600° C and 1000° C. The results for coals c, H and K may be summarized as follows.

*n*-Hexane gives a low density value which increases continuously with increasing carbonization temperature and shows no appreciable drift. The results obtained with benzene for coal K are similar. Helium gives a density which is from 7 % to 23 % in excess of the *n*-hexane value and which increases more rapidly with increasing carbonization temperature. When the temperature of treatment rises above about 900° C the density in helium begins to show some drift, and at 1000° C the drift is large and the initial density is only slightly in excess of the density in *n*-hexane.

\* In all cases sufficient time elapsed to ensure that thermal equilibrium between the sample and the thermostat was established before the helium was admitted.

The density in methanol exceeds that in helium for all carbonization temperatures up to 700° C. Between 600° C and 750° C a density drift in methanol begins to appear and increases with increasing carbonization temperature. At about 800° C the density in methanol (measured after 24-hr. immersion) passes through a maximum, and between 800° and 900° C it decreases sharply to a value approximately equal to the *n*-hexane value. At 1,000° C the densities in methanol and in *n*-hexane are equal and show no drift.

The variation of the apparent density in water is similar to that observed with methanol, except that the corresponding changes occur about 100° C higher. Up to 800° C the density in water shows no drift and is only slightly less than that in helium. Between 800° and 900° C a density drift develops, and the density after 24-hr. immersion is at a maximum at about 900° C. After carbonization at 1,000° C the densities of the coals c and k in water are equal to the low, *n*-hexane values and show no drift, while with coal h the density is only slightly higher than the *n*-hexane value and the drift is small.

Carbon disulphide gives apparent densities for the carbonized coal h which are identical with the methanol values for carbonization temperatures up to 600° C. Between 600° and 900° C the apparent densities in carbon disulphide are rather higher than in methanol, although a density drift is observed in approximately the same temperature range for the two liquids. After carbonization at 1,000° C the apparent density in carbon disulphide is equal to the low, *n*-hexane value and shows no drift.

(ii) *Coal F*.—The density changes which occur in the coal F in the temperature range 600–1,000° C are fundamentally similar to those described above for coals c, h, and k, but differ significantly in two respects.

Firstly, the density of this coal in *n*-hexane increases more rapidly with carbonization temperature, and the difference between the densities in helium and *n*-hexane for any one carbonization temperature is less; in methanol and water the maxima which appear in the curves for the other three coals are flattened into strong inflexions. Secondly, all the changes occur about 100° C lower for the coal F than for the coals c, h and k. The drift in density in methanol sets in below 600° C and at 800° C the density in methanol has fallen to the *n*-hexane value. At 900° C the density in water is equal to that in *n*-hexane. A density drift in helium begins below 800° C and at 1,000° C the density in helium too has fallen to the *n*-hexane level and shows no drift.

The results described above show clearly that after heating to 600° there is, in all four coals, a large pore volume which is accessible to helium but inaccessible

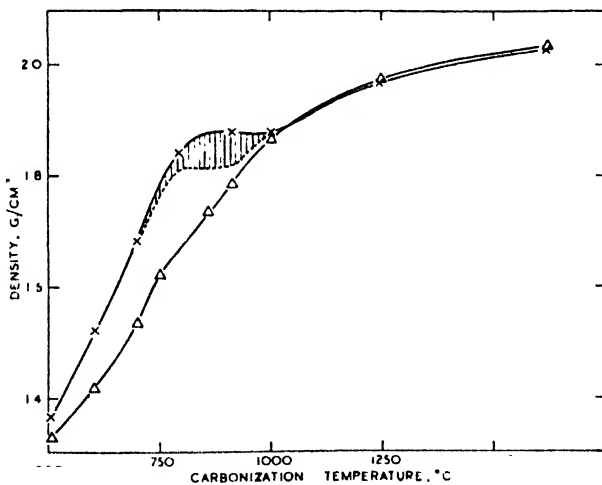


FIG. 5.—Coal F.

× Helium

Δ *n*-Hexane

to *n*-hexane. As the carbonization temperature is increased above 600° this pore volume is increased; at the same time, however, it becomes less accessible to fluids. Methanol, carbon disulphide and water are successively excluded, and, after carbonization at 1,000°, helium too is excluded from the pores of coal F and penetrates only slowly in the other coals.

The low values obtained with *n*-hexane for the coals carbonized above 600° are sharply defined and the apparent density in this liquid appears to represent a real characteristic of the solid material. There is no appreciable drift, and when apparent densities in water, methanol and carbon disulphide fall to the *n*-hexane level, these too show no drift. On the other hand, apparent densities intermediate between the *n*-hexane and helium values are associated with large drifts, showing that penetration of the pores by the liquids is slow and incomplete.

RANGE 1,000° C to 1,650° C.—The general pattern of the results outlined above is further clarified by measurements made on samples carbonized at temperatures above 1,000° C. Results for coals F and H are shown in Fig. 5 and 6. For each of the three coals c, F and H carbonized at 1,000°, the densities

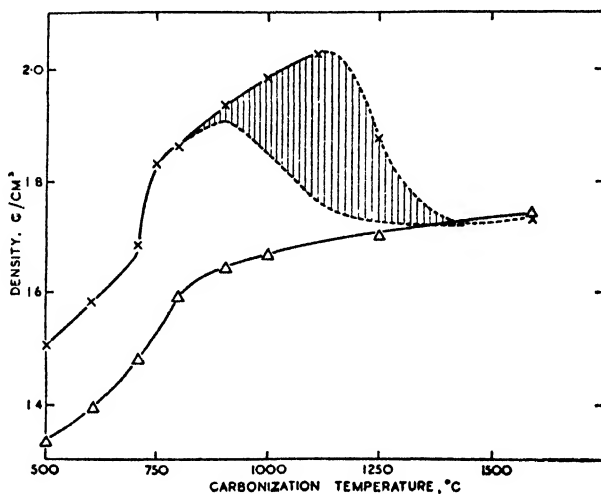


FIG. 6.—Coal H.

× Helium.

Δ *n*-Hexane.

given by methanol, water and *n*-hexane are equal and show no drift, and this is true also of higher carbonization temperatures. For the coal F, the density in helium, too, continues equal to the value obtained with the liquids. With increasing carbonization temperature from 1,000° C to 1,650° C the apparent density of the carbonized coal F in helium and in liquids increases from 1.87 g./cm.<sup>3</sup> to 2.04 g./cm.<sup>3</sup>.

The density of the carbonized coal H, measured in methanol, water or *n*-hexane, increases only slowly above 1,000°, reaching 1.75 g./cm.<sup>3</sup> at 1,600° C. The density in helium at first increases, and then decreases to the low value given by the liquids.\* The highest densities in helium are associated with large and prolonged drifts. The maximum value recorded was 2.03 g./cm.<sup>3</sup> for a carbonization temperature of 1,100–1,130° but since the drift was not followed to completion, this figure is lower than the true density of the sample; a higher value was obtained when the sample was more finely ground (see below).

**The Influence of Particle Size on Apparent Density.**—All the results described above were obtained with samples ground to pass a 72 B.S. sieve. Measurements were also made on samples of coal H carbonized at temperatures above 600° C and ground to pass a 240 B.S. sieve. The results are shown in Table V. The density in methanol of the sample carbonized at 805° C and the densities in helium of those carbonized at 1,100° and 1,250° C were considerably

\* The density in helium of the anthracite c carbonized at 1,450° C shows no drift and is equal to the *n*-hexane value (obtained by interpolation) for coal H carbonized at the same temperature. Since the apparent densities of the anthracite c and of the coal H carbonized between 700° and 1,000° C and measured in helium, water and *n*-hexane are almost identical (see Fig. 1 and 3), it is probable that the density of coal H in helium after carbonization at 1,450° C would be equal to the low *n*-hexane value and would have no drift. This result was taken into account in drawing the broken part of the helium curve in Fig. 6.

increased by reducing the particle size. On the other hand, the results obtained with *n*-hexane for samples carbonized above 800° C and with helium for those prepared below 1,000° C were not altered. Thus, where no density drift was observed the density was not increased by grinding to the lower size limit. The density drift in helium of the sample carbonized at 1,000° C was completed in considerably less than 24 hr., and in this case, too, the density measured after 24 hr. was independent of the particle size. For samples which showed large and prolonged density drifts, the apparent density after a given time was highly dependent on the particle size of the material.

TABLE V.—INFLUENCE OF PARTICLE SIZE ON APPARENT DENSITY OF CARBONIZED COAL H

Carbonization Temp., ° C	Size	Helium			Methanol			<i>n</i> -Hexane	
		Density after 24 hr., g./cm. <sup>3</sup>	Final Density, g./cm. <sup>3</sup>	Drift, %	Density after 24 hr., g./cm. <sup>3</sup>	Drift, % (2 hr. to 24 hr.)	Drift, % (2 hr. to 72 hr.)	Density after 24 hr., g./cm. <sup>3</sup>	Drift, % (2 hr. to 24 hr.)
600	72 B.S.	1.542	1.542	0.0	1.600	0.2	—	1.364	0.3
	240 B.S.	1.543	1.543	0.0	—	—	—	1.384	0.6
805	72 B.S.	1.848	1.848	0.0	1.761	7.9	10.4	1.558	0.0
	240 B.S.	1.861	1.861	0.0	1.816	7.4	9.0	1.558	0.1
1,000	72 B.S.	2.001	2.001	10.7	1.655	0.0	—	1.663	0.0
	240 B.S.	2.005	2.005	7.6	—	—	—	1.665	0.0
1,100-1,130	72 B.S.	1.982	2.029	13.4	—	—	—	—	—
	240 B.S.	2.028	2.087	15.8	—	—	—	—	—
1,245-1,250	72 B.S.	1.875	—	8.0 (to 24 hr.)	1.723	0.0	—	1.724	0.0
	240 B.S.	1.979	2.056	11.0	—	—	—	—	—

The maximum density value recorded was 2.09 g./cm.<sup>3</sup> for coal H carbonized at 1,100° C. The true density of the material exceeds this value, since a slight drift was still observable after 9 days.

**Influence of Molecular Size.**—The order in which *n*-hexane, methanol, water and helium are excluded from the pores as the carbonization temperature is raised is the same for each of the four widely different coals C, F, H and K. It is, in fact, the order of decreasing molecular size. Further measurements were made on the carbonized coal H with acetone, ether, chloroform and carbon tetrachloride; these, together with the results obtained with carbon disulphide for coal H and with benzene for coal K confirm that molecular size is the principal factor determining the power of organic liquids to penetrate into the pores of carbonized coals. The results obtained with 8 liquids and with helium for coal H carbonized at temperatures between 700° and 1,000° C are given in Table VI, together with the molecular volumes of the liquids at 25° C. The 4 liquids which have the largest molecular volumes give apparent densities approximately equal to the low, *n*-hexane values. No apparent densities appreciably lower than the *n*-hexane values have been observed.

**Adsorption of Gases on Carbonized Coal.**—The density of fine-structured carbonaceous solids cannot be measured in gases other than helium since all other gases are to some extent adsorbed at room temperature. However, since physical adsorption is a very rapid process, measurements of the apparent rate of adsorption may serve to study qualitatively the rate of penetration of gases into the fine pores in carbonized coals. With this object, the room-temperature adsorption of hydrogen, methane and oxygen on coal H carbonized at 600°, 800° and 1,000° C was briefly investigated. The apparatus and method were the same as those used for the measurements of densities with helium. The true volume of the sample was first determined with helium, which was then pumped off, and the measurements repeated with one of the other gases. The difference between the apparent volumes of the sample in this gas and in helium gave the volume of the gas adsorbed.

TABLE VI

Material \ Temp.		700° C	750° C	800° C	950° C	1,000° C	Molecular Volume of Liquid at 25° C, cm. <sup>3</sup>
Helium . .	Density, g./cm. <sup>3</sup>	1.64*	1.831	1.861	1.96*	1.998	—
	Drift, %	—	0.0	0.0	—	10.6	—
Water . .	Density after 24 hr., g./cm. <sup>3</sup>	1.62*	1.75*	1.808	1.710	1.695	18
	Drift, % (2 hr. to 24 hr.)	—	—	0.1	2.8	0.9	—
Methanol .	Density after 24 hr., g./cm. <sup>3</sup>	1.70*	1.80*	1.759	1.64*	1.600	41
	Drift, % (2 hr. to 24 hr.)	—	—	7.9	—	0.2	—
Carbon disulphide .	Density after 24 hr., g./cm. <sup>3</sup>	1.757	1.828	1.855	1.663	1.656	61
	Drift, % (2 hr. to 24 hr.)	0.7	4.3	4.2	1.4	0.0	—
Acetone . .	Density after 24 hr., g./cm. <sup>3</sup>	—	1.810	—	1.629	—	74
	Drift, % (2 hr. to 24 hr.)	—	1.0	—	0.1	—	—
Chloroform .	Density after 24 hr., g./cm. <sup>3</sup>	1.480	—	1.552	—	1.659	81
	Drift, % (2 hr. to 24 hr.)	0.0	—	0.0	—	0.0	—
Carbon tetrachloride .	Density after 24 hr., g./cm. <sup>3</sup>	—	—	1.560	—	1.660	99
	Drift, % (2 hr. to 24 hr.)	—	—	0.0	—	0.0	—
Ether . .	Density after 24 hr., g./cm. <sup>3</sup>	—	1.533	—	—	—	105
	Drift, % (2 hr. to 24 hr.)	—	0.3	—	—	—	—
<i>n</i> -Hexane .	Density after 24 hr., g./cm. <sup>3</sup>	1.47*	1.53*	1.550	1.65*	1.663	128
	Drift, % (2 hr. to 24 hr.)	—	—	0.2	—	0.0	—

\* Obtained by interpolation.

**HYDROGEN:** The quantities of hydrogen adsorbed on the three samples are shown graphically in Fig. 7. The heat of adsorption, calculated from measurements made at 15° and 25° C, was about 1,800 cal./g.-mol. Since the isotherms shown in Fig. 7 are approximately linear, and the heat of adsorption is the same for each sample, the slopes of the isotherms give a relative measure of the specific surfaces. Between 600° and 800° C the specific surface increases by about 40 %.

Adsorption equilibrium was established immediately (i.e. in less than  $\frac{1}{2}$  min. the time required for making the first measurement) on the samples carbonized at 600° and 800° C. On the 1,000° C sample, a rapid initial adsorption was followed by a large adsorption drift, and equilibrium was established within 24 hr. Between 800° and 1,000° there is a small decrease in specific surface, and the good agreement between the results obtained with the 72 mesh and the 240 mesh sample suggests that this decrease is real.

**METHANE:** The results obtained with methane are given in Table VII. The heat of adsorption on the sample carbonized at 610°, calculated from measurements made between 12° and 30°, was 5,800 cal./g.-mol.

Much larger quantities of methane were adsorbed than of hydrogen, but the process was considerably slower. With the sample carbonized at 610° C there was a large initial adsorption, 81 % of the total occurring in the first

2 min.; equilibrium was established within 5 hr. On the 810° C sample less than 1 % of the total adsorption occurred in the first 2 min., and 5 days were

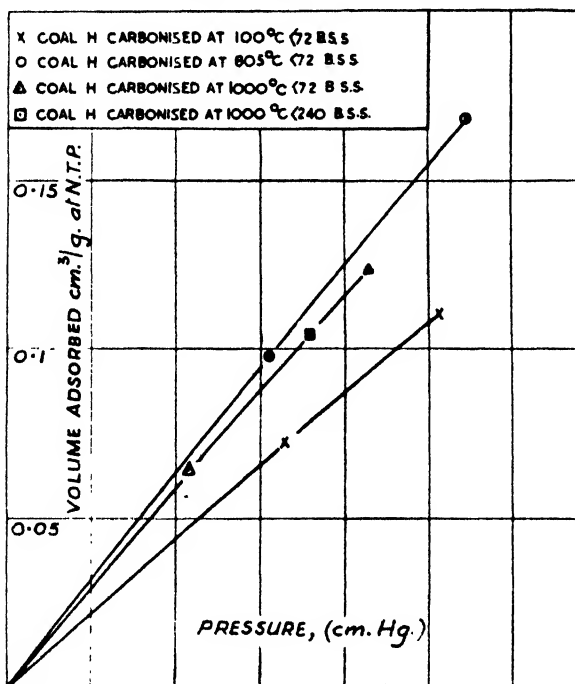


FIG. 7.

required for the establishment of equilibrium. Adsorption on the 1,010° C sample was very slow; a measurement made immediately after admitting the gas gave an apparent density little different from that in *n*-hexane.

TABLE VII.—ADSORPTION OF METHANE ON CARBONIZED COAL H

Carbonization Temperature, °C	Equilibrium Pressure, cm.	Volume Adsorbed cm. <sup>3</sup> /g. at N.T.P.
610	1.18	0.5
	6.86	2.33
810	2.76	0.39

**OXYGEN:** Oxygen was adsorbed in larger quantity than methane, and the adsorption proceeded, on the whole, more rapidly. For example, on the sample carbonized at 810° C, 55 % of the gas admitted was adsorbed in the first 2 min., as compared with 1 % for a similar quantity of methane. The rapid adsorption was, however, always followed by a long slow drift which is probably due, at least in part, to slow chemical adsorption. On the sample carbonized at 1,010° C the initial measurement with oxygen gave, as with methane, an apparent density approximately equal to the *n*-hexane value.

The above results show that the accessibility of the pores of the carbonized coal H to each of the four gases (helium, hydrogen, methane and oxygen) decreases with increasing carbonization temperature, and, as was found with

liquids, the larger the molecule of the gas, the lower the carbonization temperature for which it is first excluded from the pores. The results are summarized in Table VIII.

TABLE VIII

Gas	Molecular Diam.	Coal K Carbonized at		
		600° C	800° C	1,000° C
Helium	1.9	No drift, penetration complete	No drift, penetration complete	Large drift, penetration complete within 24 hr.
Hydrogen	2.4	No drift, penetration complete and adsorption rapid	No drift, penetration complete and adsorption rapid	Large drift, penetration and adsorption complete within 24 hr.
Oxygen	3.0	Large rapid adsorption followed by long slow drift. 82 % of total adsorption occurred in first 2 min.	As for 600° C but rather slower. 55 % of total adsorption occurred in first 2 min.	Penetration and adsorption very slow
Methane	4.0	Adsorption equilibrium established in 5 hr. 81 % of total adsorption occurred in first 2 min.	Adsorption equilibrium practically established in 5 days. 1 % of total adsorption occurred in first 2 min.	Penetration and adsorption very slow

It may be noted that the ease with which different fluids penetrate into the pores of carbonized coal increases with decreasing molecular size for both liquids and gases taken in a single series. Although strictly comparable values of the molecular diameters of all the fluids are not available, the general relationship is clear, and provides striking confirmation that the penetrating power does in fact depend primarily on molecular diameter and not on any other property of the liquids.

**Specific Surface.**—The specific surface of carbonized coals and its variation with the temperature of carbonization has been studied for a wide range of coals by Cannon, Griffith and Hirst,<sup>2</sup> who measured the heat of wetting of the materials in methanol. Further measurements on the carbonized coals C, F, H and K have been made by Griffith, and the results are shown in Fig. 8. The curves conform to the types previously described by Cannon, Griffith and Hirst, who have discussed their interpretation. In all cases the heat of wetting decreases with increasing carbonization temperature above 550–650° C. Maggs<sup>3</sup> has shown that this does not necessarily indicate a decrease in the true specific surface, since the accessibility of the pores also decreases—a result which is amply confirmed by the present work. Adsorption of hydrogen has shown that the increase in specific surface which occurs between 450° and 600° C and which is detected by methanol continues, also, at higher temperatures. The heat of wetting in methanol of coal H carbonized at 600° C is 12 cal./g.; on increasing the carbonization temperature to 800° C the heat of wetting is reduced to 2 cal./g. but adsorption of hydrogen is increased by about 40 %.

Cannon, Griffith and Hirst<sup>2</sup> have emphasized that the internal surface of coals is never entirely lost during carbonization and that coals which have large inner surfaces yield, in general, carbonized products with large inner surfaces. The present work provides further evidence that the fine-pore structure of a carbonized coal is directly related to that of the raw coal. Of the four coals investigated, coal K has the greatest porosity<sup>7</sup> and yields the most highly porous carbonized products. The raw coal F has a lower porosity and smaller specific surface than the coals C, H and K, and also a more highly constricted

pore system;<sup>7</sup> after carbonization, the fine-structure porosity, surface area and accessibility of the pores are all less than for the other coals carbonized at the same temperature.

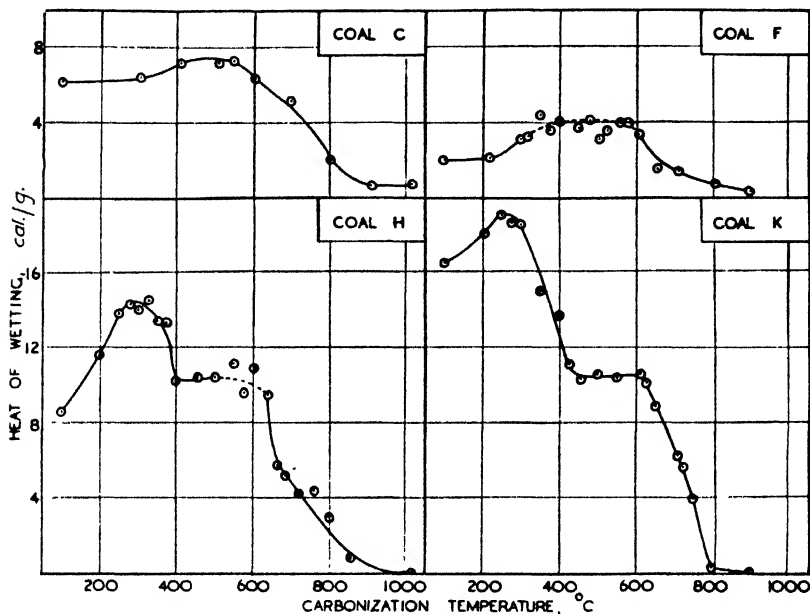


FIG. 8.

**Fine-Structure Porosity of Coals Carbonized above 600° C.**—It appears from the results described above that the low apparent density obtained for carbonized coals with *n*-hexane or with other liquids of large molecular size is substantially independent of the experimental conditions, and is a well-defined and significant property of the solids. There is considerable evidence that it is approximately equal to the lump density of the individual particles. Not only is it constant for a wide range of liquids, but it was also unchanged when samples of coal H pre-heated to 600° and 800° were exposed to dry air at room temperature for 1 hr. after evacuation and before admitting the liquid. The presence of air would obviously impede the diffusion of a liquid into fine pores, and the same treatment did, in fact, reduce considerably the apparent density of the same samples in methanol. Moreover, Maggs has measured the adsorption of *n*-hexane on coal K carbonized at 600°. The amount adsorbed at saturation pressure at 25° C corresponds approximately to that required to form a monolayer on the external surface of the powder.

Helium may be considered to measure the true density of carbonized coals when the carbonization temperature is not so high that the gas is excluded from the whole or a part of the pore space. This condition is fulfilled for coals C, H and K carbonized at temperatures up to 900° C and for coal F at temperatures up to 700° C. It follows that the fine-structure porosity of these materials is given by

$$P = (d_{\text{He}} - d_{\text{hex}})/d_{\text{He}},$$

where  $d_{\text{He}}$  and  $d_{\text{hex}}$  are the densities in helium and *n*-hexane respectively.

In Fig. 9,  $P$  is plotted against carbonization temperature. It is seen that throughout the range of carbonization temperature for which the true density is measurable (by helium) the fine-structure porosity increases with increasing temperature for all four coals.

Thus, the fine-structure porosity *increases* while the accessibility of the pores *decreases*. This leads to the conclusion that the accessibility of the pores is governed by the size and frequency of fine constrictions or "bottle-necks" in the pore system, and not by the mean diameter of pores which are uniform along their length. The alternative assumption of uniform pores would require that, with increasing temperature, the diameter of the pores steadily decreased



while their number increased rapidly, new pores formed at any one temperature being narrower than those formed at a lower temperature. In such a system, the increase in porosity would be accompanied by a still larger increase in specific surface. It has been shown, however, that between 800° and 1,000° C the specific surface *decreases* while the porosity increases.

The structural changes which accompany increasing carbonization temperature between 600° and 1,000° are associated with the loss of volatile decomposition products from a rigid solid. The existence of the decomposition products (mainly CO, CH<sub>4</sub> and H<sub>2</sub>) implies that there is a re-arrangement of surface atoms or small groups of atoms within the solid. This may be sufficient to account

for the creation of a more highly constricted pore system resulting from increased intermicellar contacts. A similar effect may perhaps account for the slight decrease in surface area between 800° and 1,000° by elimination of surface roughness. The increase in fine-structure porosity, on the other hand, shows that the rigidity of the structure is too great (or the carbonization temperature too low) to permit such large-scale re-arrangement as would be necessary to compensate for the loss of volatile matter and the increase in true density.

#### Molecular Sieve Properties of Carbonized Coals.

—The volume of fine pores in coals carbonized at 1,000° C or at higher temperatures may amount to more than 20 % of the volume of the solid. For carbonization temperatures between 600° and 1,000° C the solids behave as molecular sieves; in any given sample all molecules larger than a certain size are completely excluded from the pores. Carbonized coals may be compared in this respect with the zeolites studied by Barrer,<sup>9</sup> although their adsorption capacity is much less. The sieve "mesh" depends both

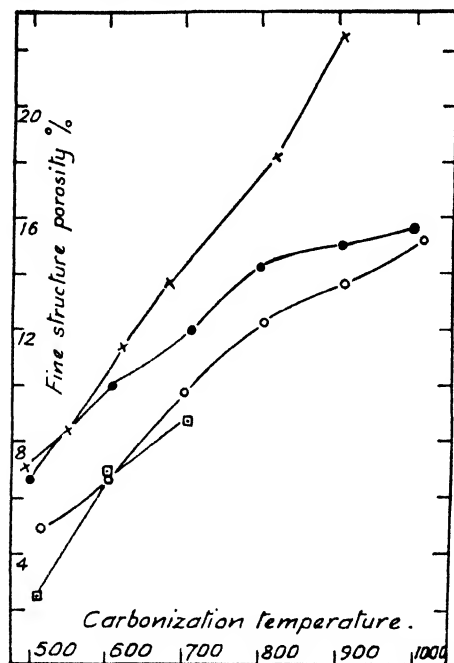


FIG. 9.

○ Coal c. □ Coal F. ● Coal H. × Coal K.

on the starting material and on the temperature of carbonization, and in the materials studied here it is never large enough to permit appreciable penetration of liquids with molecules as large as those of *n*-hexane and benzene.

The molecular sieve properties of carbonized coals must obviously be of considerable importance in determining the chemical behaviour of the materials, and probably also in determining the course of the later stages of the carbonization process. The principal volatile products of carbonization above 600° C are methane, hydrogen and carbon monoxide, and, above 700° C, hydrogen and methane, the proportion of hydrogen increasing with increasing temperature. It has been shown that methane penetrates the pore structure only slowly after carbonization at 600° C and still more slowly after carbonization at higher temperatures, whereas hydrogen penetrates freely after carbonization at 600° and 800° C. The very different rates of diffusion of the gaseous products may well have an important influence on the final composition of the gas evolved.

This work was carried out at the British Coal Utilization Research Association, and the author is grateful to Dr. D. H. Bangham for his interest and advice.

Laboratoire Central des Services Chimiques de l'Etat,  
12 quai Henri IV,  
Paris, IV,  
France.

<sup>9</sup> Barrer, *Diffusion in and through Solids* (C.U.P., 1941).

# THE BREAKDOWN AND REPAIR OF OXIDE FILMS ON IRON

By T. P. HOAR

*Received 18th February, 1949*

The mechanism of breakdown and repair of oxide films on metals is examined with special reference to the influence of the film-rupturing anions chloride and perchlorate, and the film-repairing anions carbonate, nitrite, and chromate, on the behaviour of iron. It is shown that film breakdown is often preceded by partial repair, and that it is caused by the action of the cell

O<sub>2</sub> on oxide-film surface | Electrolyte | Metal at base of film pores

producing precipitated hydroxide or oxide, but lowering the pH within the pore, so that partial repair caused by the precipitate occurs, followed by undermining and breakdown when the pore acidity has become sufficient to allow the corroding metal at the pore base to appear as a soluble product. Complete film repair occurs when precipitating anions such as OH<sup>-</sup>, CO<sub>3</sub><sup>-</sup>, NO<sub>2</sub><sup>-</sup> or CrO<sub>4</sub><sup>-</sup> are in sufficient supply within the pore and/or are replenished sufficiently well by transport from outside to produce complete pore plugging before the pore acidity becomes high enough to give breakdown.

It is suggested the "corrosive" anions are better characterized by their "film-rupturing" power, i.e. their ability to produce pore acidity, than by their "film-penetrating" power. Reasons are given for the belief that pores in oxide films that are potential points of incipient corrosion are easily and rapidly penetrated by all common anions. Cl<sup>-</sup> and ClO<sub>4</sub><sup>-</sup> are shown to have equal film-rupturing power in dilute solutions.

The nature and production of pores is discussed, and an analogy between the electrolytic properties of oxide-films and paint films is pointed out.

---

The resistance of metals to corrosive environments largely depends upon the protection afforded by superficial oxide films; the degree of protection is very variable for different metals and environments, a matter of obvious practical importance. Further, considerable theoretical interest attaches to the thermodynamics, kinetics and geometry of the reactions involved, and to the mechanism by which the films break down, remain stable, or build up, when metals bearing them are exposed to electrolytes. The detailed mechanism of film breakdown and repair is still not entirely clear, and the present investigation is an attempt to elucidate certain aspects of the matter that have not so far been fully explored.

**Previous Work.**—Of the factors leading to film breakdown or repair, the direct solubility or otherwise of the film substance in the corrosive environment is the most obvious and best understood. A film that is not directly soluble may, however, break down owing to the presence of places of weakness, such as cracks or pores extending through the film; if the corrosive material to which the metal is exposed can penetrate such pores and attack the metal at their base, the film may become undermined and flake off. In electrolytic environments, the nature of the anion is of crucial importance. If the anion forms easily soluble salts with the metal concerned, attack is likely, because the cell

O<sub>2</sub> on oxide-film | Electrolyte | Metal at base of film pore

comes into action, with cathodic reduction of  $O_2$  to  $OH^-$  on the film surface, anodic formation of the soluble metal salt within the pore, and subsequent undermining of the film by dissolution of metal. But if the anion forms *sparingly* soluble salts, no corrosion occurs, owing to the formation of the sparingly soluble anodic product within the pores of the film, which are thereby healed. This well-established rule, though of general applicability, is not entirely true in the simplest form just stated, and requires certain modifications. For instance, the influence of the pH of the electrolyte on the solubility of the product must be taken into account; it may be noted that it is the pH *within the pore* that is important, and that this is likely to become much lower than that of the bulk electrolyte, as explained below. Furthermore, application of the simple rule is not possible in cases of mixed electrolytes containing several anions, some forming easily soluble, others sparingly soluble, salts with the metal. Even a simple salt solution such as aqueous sodium chloride always contains hydroxyl ion, and this even when present in very small concentration at quite low pH values may precipitate metal hydroxides.<sup>1</sup>

Alkali-metal salts having anions that commonly form easily soluble salts with the heavy metals usually produce film breakdown and subsequent corrosion, but these salts show differences among themselves. Friend and Marshall<sup>2</sup> investigated the behaviour of iron in solutions of the "corrosive" sodium salts of  $Cl^-$ ,  $I^-$ ,  $Br^-$ ,  $NO_3^-$ ,  $SO_4^{2-}$ ,  $F^-$ , and  $CH_3CO_2^-$ , together with either sodium carbonate or borax as inhibitor. They found that the concentration of sodium carbonate required just to give inhibition of 0.05 or 0.01 N solutions of the "corrosive" salt diminished with the sequence of anions just listed; with borax as inhibitor, the sequence was  $Cl^-$ ,  $Br^-$ ,  $SO_4^{2-}$ ,  $I^-$ ,  $NO_3^-$ ,  $F^-$ ,  $CH_3CO_2^-$ . They pointed out that this sequence is approximately the same as the descending order of the strengths of the corresponding acids. Britton and Evans<sup>3</sup> measured the increase of current produced at aluminium and lead anodes in an "inhibiting" potassium chromate solution by the addition of standard amounts of "corrosive" salts, and thus estimated the "film-penetrating power" of the various anions to run in the descending order  $Cl^-$ ,  $Br^-$ ,  $I^-$ ,  $F^-$ ,  $SO_4^{2-}$ ,  $NO_3^-$ ,  $HPO_4^{2-}$  for aluminium, and  $NO_3^-$ ,  $Cl^-$ ,  $Br^-$ ,  $I^-$ ,  $HPO_4^{2-}$ ,  $SO_4^{2-}$  for lead. (The very low "penetrating power" of  $SO_4^{2-}$  at a lead anode was explained by reference to the sparing solubility of lead sulphate, which makes  $SO_4^{2-}$  actually "protective" towards lead.)

Brennert<sup>4</sup> found that the single electrode potential of tin corroding in salt solutions at first becomes more noble, and then falls, with onset of "black-spot" corrosion after the potential begins to fall. In a more detailed study,<sup>5</sup> I showed that this rise and fall—indicative of film repair followed by film breakdown—may be explained as follows. As soon as the metal is exposed to the electrolyte of approximately pH 7, the cell

$O_2$  on oxide-film surface | Electrolyte | Sn at base of film pores

comes into action, producing  $OH^-$  on the film surface and aquo-stannous and aquo-stannic ions within the pores. Owing to the exceptionally small solubility products of stannous and stannic hydroxides (or hydrous oxides),<sup>7</sup> the anolyte within the pores is at once supersaturated with respect to either or both of them at pH 7, so that precipitates tend to

<sup>1</sup> Britton, *Hydrogen Ions*, Vol. II (Chapman & Hall, 3rd ed., 1942), p. 35 *et seq.*, esp. p. 79; *Ann. Reports*, 1943, 40, 43.

<sup>2</sup> Friend and Marshall, *J. Chem. Soc.*, 1914, 105, 2776.

<sup>3</sup> Britton and Evans, *ibid.*, 1930, 1773.

<sup>4</sup> Brennert, *Tech. Pub. Int. Tin. Res. Council*, Series B, No. 2, 1935.

<sup>5</sup> Hoar, *Trans. Faraday Soc.*, 1937, 33, 1152.

<sup>6</sup> Bannister and Evans, *J. Chem. Soc.*, 1930, 1361.

<sup>7</sup> Latimer, *The Oxidation States of the Elements and their Potentials in Aqueous Solution* (Prentice-Hall, 1937).

form \* within the pores; this film repair explains the initial rise of the potential. The removal of  $\text{OH}^-$  from the anolyte † due to the formation of the hydroxide precipitate leads to a fall in pH, so that a moment is reached when the dissolving metal is no longer precipitated sufficiently to repair the pores further; on the contrary, metal dissolution to mainly *soluble* products undermines the film around the pores, film breakdown with fall of potential sets in, and corrosion considerably increases to form visible "black spots". This theory for tin is in harmony with the following additional experimental evidence.<sup>5</sup>

(i) The anions  $\text{Cl}^-$ ,  $\text{Br}^-$ ,  $\text{NO}_3^-$ ,  $\text{SO}_4^{2-}$ ,  $\text{ClO}_4^-$ , and  $\text{ClO}_3^-$ , all of which form "soluble" stannous salts provided that the pH is low enough, but giving precipitates of hydroxides and/or basic salts by hydrolysis above about pH 2, all behave in a qualitatively similar way in tin corrosion, producing the potential rise followed by the fall with onset of corrosion.

(ii) Increase of  $\text{Cl}^-$  concentration in the electrolyte leads to a more rapid rise of potential and attainment of the breakdown state—because (a) the lowered electrolytic resistance allows a larger current in the film-metal cell, with more rapid production of anodic products, and (b) the relatively greater  $\text{Cl}^-$  concentration in the electrolyte lessens the transport of cathodically produced  $\text{OH}^-$  into the pore, and of  $\text{H}^+$  out of it, so diminishing a factor favourable to repair.

The anions just listed as "corrosive" to tin all form strong acids. Clearly the anion of a *weak* acid, apart from other considerations, will not be favourable to film-breakdown because the now *buffered* anolyte will not attain the low pH necessary for the prevention of hydroxide precipitation. A probable reason for Friend and Marshall's ‡ finding, that anions of the stronger acids are the better corrosion promoters for iron, thus becomes apparent.

**Present Work.**—It is important to see how far the above theory can be extended to metals other than tin, and to inhibiting anions other than  $\text{OH}^-$ . In the present work, the attack of iron in chloride solutions containing also either carbonate, nitrite or chromate has been studied, and has been compared with that found in perchlorate solutions containing the same inhibiting anions. Perchlorate was chosen for this comparison because it is similar to chloride in all germane respects except two:

(i) The equivalent conductivities of sodium chloride and perchlorate in dilute solution are within 2 % of each other (0.01 M NaCl, 118.6 mhos/cm.; 0.01 M  $\text{NaClO}_4$ , 116.6, 25° C),<sup>§</sup> and thus the mobilities and diameters of the aquo-chloride and aquo-perchlorate ion are nearly identical (because of the much greater hydration of  $\text{Cl}^-$ ). However, in concentrated solution the conductivity of sodium perchlorate is appreciably less than that of sodium chloride (M NaCl, 74.19; M  $\text{NaClO}_4$ , 65.0, 18° C),<sup>§</sup> and hence the mobility of  $\text{ClO}_4^-$  is here less than that of  $\text{Cl}^-$ . This difference is important.

(ii) Both ions form very soluble ferrous and ferric salts.

(iii) Both ions are non-oxidizing to Fe and to  $\text{Fe}^{++}$  at ordinary dilutions and temperatures.

(iv) Both ions form strong acids.

(v)  $\text{Cl}^-$  is far more deformable than  $\text{ClO}_4^-$ , having a greater tendency to form covalent and adsorption complexes; this is the other important difference.

\* The formation of  $\text{Sn}(\text{OH})_2$  from (say)  $\text{Sn} \cdot 4\text{H}_3\text{O}^{++}$  may perhaps best be visualized, not as the replacement of the four water molecules round the cation by two hydroxyl ions, but rather as a loss of two water molecules and two protons—i.e. two  $\text{H}_3\text{O}^+$  ions—from the aquo-complex.

† Or production of  $\text{H}_2\text{O}^+$ , see preceding footnote.

‡ *Int. Crit. Tables*, Vol. V, pp. 233, 247.

### Experimental

The "iron" used was a cold-rolled mild steel strip (C 0.26, Si 0.21, S 0.031, P 0.038, Mn 0.36 %) of good surface, specially rolled for research purposes by The United Steel Companies Ltd., and kindly supplied by Dr. U. R. Evans from his stock; previous work<sup>9, 10</sup> has shown that iron and mild steel behave very similarly in nearly neutral salt solutions. It was abraded with Hubert IF emery paper, degreased with carbon tetrachloride, and stored over anhydrous calcium chloride for 24 hr. before use. The solutions were made from distilled water (condensed on Pyrex) and A.R. materials, stock sodium perchlorate of pH 7.0 being prepared from the acid and sodium hydroxide.

To economize material, the convenient "drop" technique was used. Solutions containing a wide range of concentrations of sodium chloride (or

perchlorate) and each of the three inhibitors were prepared in small quantities from freshly made stock solutions. 3 drops, each ca. 0.5 cm. in diameter, of each solution were placed on the experimental steel sheet (some 20 × 10 cm.), which was covered with a glass trough water-sealed with wet cotton-wool to a glass plate to prevent evaporation. After 24 hr., the onset or otherwise of corrosion was observed; reproducibility within the triplicate drops was remarkably good.

Some potential measurements were made with a modified drop technique, illustrated in Fig. 1. 12 small glass covers carrying corks and small tubes were set up on a prepared steel sheet, with chloridized silver wires dipping into each tube and attached through a twelve-way switch to a valve electrometer. Small amounts of various chloride-containing corrosive liquors were then run down the tubes, the drops formed on the steel sheet remaining in electrolytic

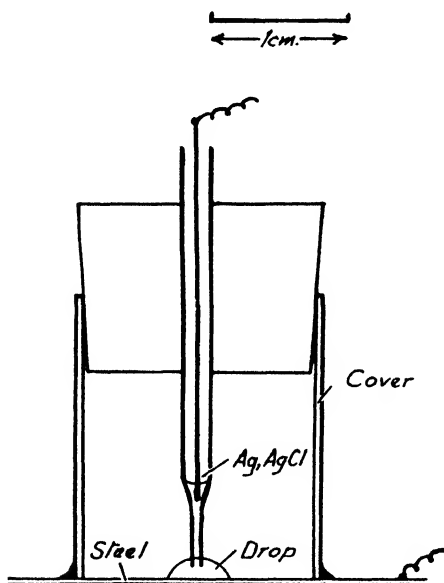


FIG. 1.—Measurement of corrosion potential in a drop.

connexion with the silver-silver-chloride electrodes by capillarity. The circuit to the electrometer being completed by a lead from the steel specimen, the potentials of each of the twelve drops could be measured from within a minute of application of electrolyte. In special experiments using one drop at a time and with two observers, readings could be taken within 5 sec. of the exposure of metal to electrolyte; it is hoped in future work to reduce this time to a small fraction of a second by the use of a recording oscillograph.

### Results

(a) **Occurrence of Corrosion.**—The onset or absence of corrosion after 24 hr. in the various chloride and perchlorate solutions is shown in Fig. 2 and 3 respectively. Near the border-line between corrosion and immunity pitting occurred, especially in the more concentrated carbonate- and chromate-inhibited solutions. The general similarity of the diagrams is evident; there are also some significant differences. The salient features are:

(i) The concentration of chloride or perchlorate necessary to give breakdown increases with inhibitor concentration; this is a confirmation of much previous work.

<sup>9</sup> Evans and Hoar, *Proc. Roy. Soc. A*, 1932, **137**, 343.

<sup>10</sup> Hoar and Evans, *J. Iron Steel Inst.*, 1932, **126**, 379.

(ii) At low chloride or perchlorate concentrations, the concentrations of chloride or perchlorate necessary to give breakdown in solutions containing a given amount of carbonate, nitrite or chromate are identical; at high concentrations, less chloride than perchlorate is necessary for breakdown.

(iii) Nitrite and chromate have approximately equal inhibiting power (at equal molarity), though nitrite is the better in concentrated solutions; carbonate is less effective, some 30 times the molar concentration of nitrite being required to give inhibition at any chloride or perchlorate concentration.

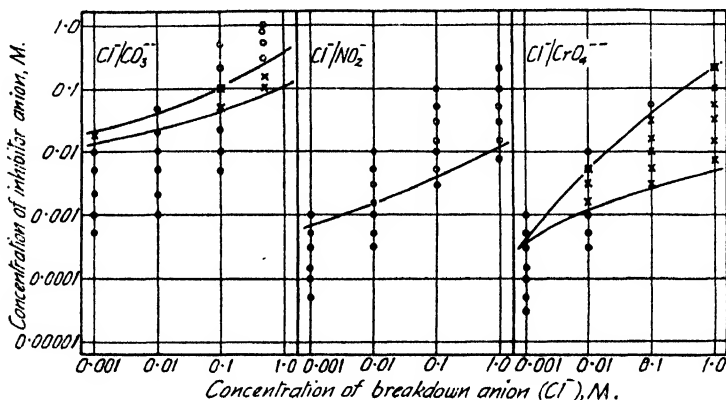


FIG. 2.—Incidence of corrosion in chloride solutions with inhibitors.  
○ No attack.    × Pitting.    ● General attack.

(iv) The conditions leading to pitting attack are much wider in chromate- and carbonate-containing solutions than in nitrite. This result is as yet unexplained; it should be mentioned that under other experimental conditions, quite a wide range of nitrite concentrations can give pitting.

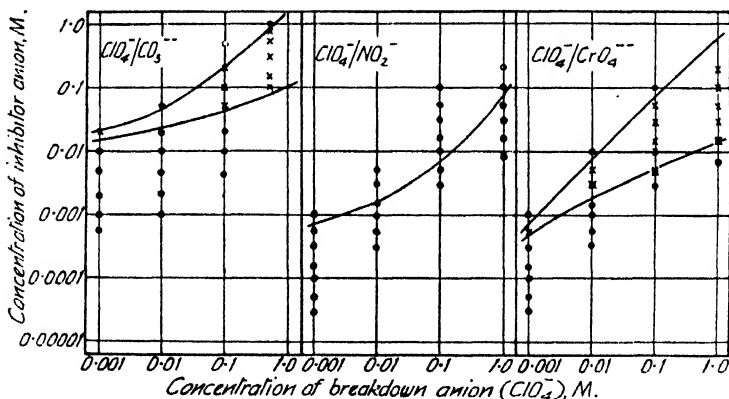


FIG. 3.—Incidence of corrosion in perchlorate solutions with inhibitors.  
○ No attack.    × Pitting.    ● General attack.

(b) **Potential-Time Curves.**—Fig. 4 shows typical potential\*-time curves obtained in nitrite-inhibited chloride solutions. They are similar to those previously found for tin in chloride and perchlorate solutions, except that the time-scales are much shorter and the initial potential rise less. Potential-time curves have also been given by Lochte and Paul<sup>11</sup> for a dead-mild steel

\* Potentials are given as mV on the normal hydrogen scale,  $E_H$  ("noble" potentials positive).

<sup>11</sup> Lochte and Paul, *Trans. Electrochem. Soc.*, 1933, 64, 23.

wire (C 0.11, P 0.06 %) totally immersed in stirred, aerated solutions of sodium chloride and hydroxide with various  $\text{Cl}^-/\text{OH}^-$  ratios; four of their curves, showing potential rise followed by fall, are replotted in Fig. 4, and the similarity they

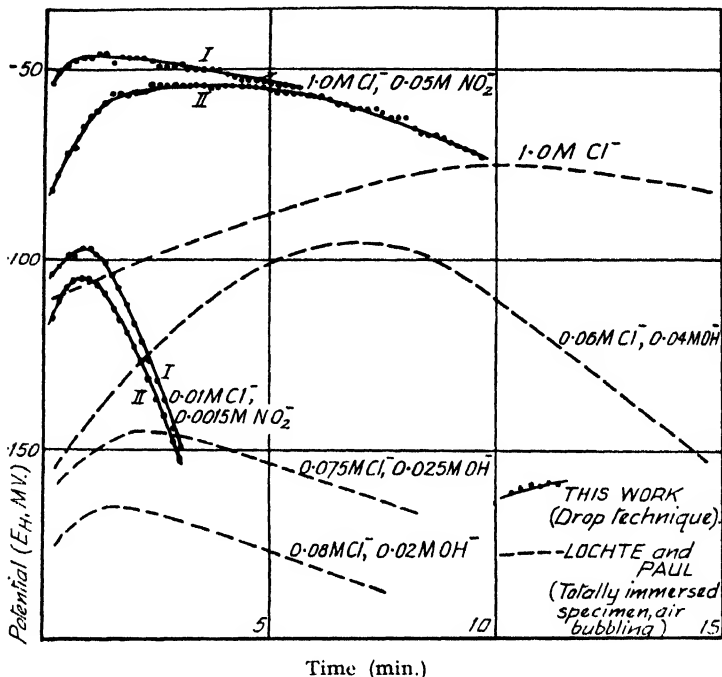


FIG. 4.—Potential-Time curves, steel (air-formed oxide-film) in solutions giving corrosion; film-repair followed by breakdown.

show to the present experimental curves, obtained by the "drop" technique with different steel and electrolytes, is noteworthy.

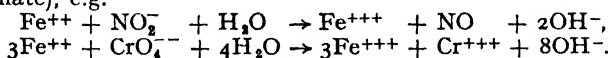
## Discussion

**Interpretation of Results.**—The results may be explained by an extension of the breakdown theory previously proposed for tin<sup>5</sup> and reviewed above.

We may picture the breakdown process, in solutions containing too large a  $\text{Cl}^-$  or  $\text{ClO}_4^-/\text{CO}_3^{2-}$ ,  $\text{NO}_2^-$ , or  $\text{CrO}_4^{2-}$  ratio to give immunity as follows:

1. Ferrous ions appear in the film pore by anodic dissolution.

1(a). Ferrous ions are oxidized to ferric by nitrite or chromate (not by carbonate), e.g.



2. Precipitation of basic ferrous carbonate, ferric hydroxide, or ( $\text{Fe}^{+++}$ ,  $\text{Cr}^{+++}$ ,  $\text{OH}^-$ ,  $\text{CrO}_4^{2-}$ )<sup>12</sup> occurs within the pore, tending to heal it and causing the corrosion potential of the metal to rise.

3. When the concentration of  $\text{CO}_3^{2-}$ ,  $\text{NO}_2^-$  or  $\text{CrO}_4^{2-}$  within the pore has been reduced by 1(a) and/or 2, and insufficiently replenished by transport from outside, ferrous hydroxide is precipitated and the pH falls.

<sup>12</sup> Hoar and Evans, *J. Chem. Soc.*, 1932, 2476.

4. When the pore pH has fallen to around 5,  $\text{Fe}^{++}$  is insufficiently precipitated<sup>1</sup> to give continued pore-healing, but on the contrary the continuing metal dissolution gives undermining and breakdown of the film near the pore, causing the corrosion potential to fall.

In solutions containing a high ratio of inhibiting to corrosive anions, the transport of inhibiting anions into the pore by electrolytic migration is evidently always sufficient to deal with all the  $\text{Fe}^{++}$  produced. In solutions containing a low ratio, the breakdown process can operate easily, since stage 4 above is reached quite quickly. For intermediate ratios, not quite high enough to give immunity, breakdown is slower; the onset of corrosion is in fact found to be delayed in such solutions, as compared with that in solutions with a low ratio of inhibiting to corrosive anions. The exhaustion of inhibiting anions envisaged in stage 3 must necessarily depend largely on the ratio of inhibiting to corrosive anion, since its replenishment by migration clearly depends on this ratio. Thus the fact that the concentration of chloride or perchlorate necessary to give breakdown increases with inhibitor concentration—result (i) of the previous section—is readily explained.

The rate of breakdown of the 24-hr. film formed in air at room temperature on abraded steel is much more rapid than that of the 100-hr. air-formed film on tin previously studied;<sup>5</sup> the potential maximum occurred at times varying from a few seconds to a few minutes. This is because the present films are much thinner and the pores shorter, and more especially because the pore anolyte need not become nearly so acid as in the case of tin, with its very sparingly soluble hydrous oxides.

We may now consider result (ii) of the previous section—the comparison of chloride and perchlorate as film-rupturing anions. At low concentrations the almost exact equivalence in their behaviour is evidently due to the near correspondence of their mobilities, sizes, solubilities of the ferric and ferrous salts, lack of oxidizing power, and proton affinities, referred to previously. At higher concentrations, the higher equivalent conductivity of a chloride solution as compared with a perchlorate will militate against replenishment of inhibiting anion by migration, so that a higher concentration of inhibiting anion will be necessary to prevent corrosion; furthermore, owing to the greater complex-forming tendency of chloride, this ion will produce at any given pH a higher ratio of soluble to insoluble iron compounds, since the formation of soluble ferric (and possibly ferrous) complexes will tend to prevent the precipitation of hydroxides and/or basic chromates. Thus the somewhat greater film-rupturing power of chloride ion as compared with perchlorate in the more concentrated solutions is well explained by the general theory.

The superior inhibiting power of nitrite and chromate ions as compared with carbonate (result (iii) above) is well known, and is almost certainly due to their oxidizing power for ferrous ion; the ferric compounds produced in the film pores have much smaller solubility products than the corresponding ferrous, and thus continue to give film repair at a much higher pore acidity.

Instead of the metal dissolution to soluble cations, followed by their precipitation, suggested as the initial processes within the film pore ((1) and (2) above), it is possible that a mechanism of direct anion reaction with metal to give a compact adherent film at the bottom of the pore occurs, somewhat as discussed by Evans and Hoar<sup>13</sup> in connection with magnesium corrosion, by Verwey<sup>14</sup> for the formation of oxide films on aluminium by anodic oxidation, by Pyke and Cohen<sup>15</sup> for nitrite inhibition of steel corrosion in natural waters, and by Mayne and Pryor<sup>16</sup> for the oxidation of a film-free steel surface by pure chromate solutions

<sup>13</sup> Evans and Hoar, *Trans. Faraday Soc.*, 1934, **30**, 424.

<sup>14</sup> Verwey, *Physica*, 1935, **2**, 1059.

<sup>15</sup> Pyke and Cohen, *Trans. Electrochem. Soc.*, 1948, **93**, 63.

<sup>16</sup> Mayne and Pryor, *J. Chem. Soc.* (in press).



with the production of a compact  $\gamma\text{-Fe}_2\text{O}_3$  film (shown by electron diffraction). Such a mechanism is attractive in that it does not need the postulate of an aqueous precipitation for the formation of insoluble compounds; the precipitation of hydrous ferric oxide from aqueous ferrous solution by nitrite is a rather slow reaction (though it may well be more rapid on an iron oxide surface such as the sides of a film-pore). The film-rupturing power of "corrosive" anions such as chloride and perchlorate in presence of (insufficient) inhibiting anion must be somewhat differently and less simply pictured if the latter acts by direct discharge; to account for it, it is necessary to postulate, instead of (3) and (4) above:

3(a). Production of pore acidity and the discharge of hydroxyl ion upon the compact film at the pore base, ferrous ions moving up from the metal through this film by lattice diffusion.

4(a). Dissolution of the film (now ferro-ferric) at the pore base when the pH in the pore has fallen sufficiently.

Present experimental evidence is scarcely sufficient to provide a decision between these alternative *kinetic* mechanisms of film repair followed by breakdown. On either view, however, the conception of repair or breakdown consequent on the relative transport of inhibiting or corrosive anions, and on the dependence of corrosion-product solubility upon the acidity within the pore, holds good; so does the explanation, on grounds of solubility, of the superior inhibiting powers of the oxidizing anions that produce ferric compounds. These essentially *thermodynamic* explanations based upon variations of solubility with pH (of which Pourbaix has given a generalized graphical treatment<sup>17</sup>) are a development of the arguments previously used in the case of tin.

Kabanov, Burstein and Frumkin,<sup>18</sup> studying the anodic behaviour of iron in alkaline chloride solutions, point out that hydroxyl ion passivates and chloride ion activates iron anodes. They explain this with reference to the film-forming power of hydroxyl ion and a "selective adsorption" of chloride ion that prevents film formation. It seems more precise to explain the influence of chloride in terms of the transport-solubility theory developed above, as already outlined in the discussion of Kabanov's paper.<sup>19</sup> It may be noted that Kabanov found an initial rise of anode potential followed by a fall, indicating film repair followed by film breakdown. Further, the quantity of electricity needed to reach the potential maximum of the anode was of the order of  $10^{-4}$  coulomb/cm.<sup>2</sup>, corresponding to a volume of ca.  $4 \times 10^{-8}$  cm.<sup>3</sup> of iron, or some  $10^{-9}$  cm.<sup>3</sup> of ferrous hydroxide; this is of the right order of magnitude to produce partial plugging of the pores of an oxide film, say, 100 Å thick, i.e. of volume  $10^{-8}$  cm.<sup>3</sup> per cm.<sup>2</sup> of surface.

**The Classification of "Corrosive" Anions.**—The term "film-rupturing power" has been used in this paper to describe the property of chloride, perchlorate and similar corrosive anions, rather than "film-penetrating power," in popular use following the work of Britton and Evans.<sup>3</sup> Emphasis is thus given to the view that the process associated with the onset of corrosion is the alteration of the film pores by partial plugging followed by undermining, the progress of this alteration being largely determined by the nature of the anion. The mere penetration of pores and cracks in oxide films on iron and mild steel by *any* anion, is, on this view, a relatively easy and rapid process because of the large width of the fissures compared with the diameters of the common anions, which may be assessed from the electrical mobilities as not widely different, perhaps owing to the higher degree of hydration of the halide as compared with other ions. It is not intended to imply that a real difference of

<sup>17</sup> Pourbaix, *Thermodynamique des Solutions Aqueuses Diluées* (Thesis, Delft, 1945; Béranger, Paris and Liège).

<sup>18</sup> Kabanov, Burstein and Frumkin, *Faraday Soc. Discussion*, 1947, 1, 259.

<sup>19</sup> Hoar, *ibid.*, 1947, 1, 299.

anion penetrating power *never* occurs—it may perhaps do so in the case of especially highly protective films such as those on aluminium anodes studied by Britton and Evans,<sup>8</sup> though it is at least possible that their measured increases in anodic current caused by chloride ion, etc., were really due to film breakdown by the mechanism discussed above; and we may note that Kabanov and his co-workers,<sup>17</sup> in the work discussed above, do not accept the film-penetrating power of chloride ion as sufficient explanation of its activating influence on iron anodes in alkaline solutions.

There are, in fact, other arguments that easy anion penetration is quite usual:

(i) In the great majority of cases of metals put into contact with electrolytes, movement of the measured potential from its initial value occurs quickly, sometimes to the extent of decivolts per second, even when no visible corrosion or film-growth occurs for minutes or hours afterwards. Thus the cell

O<sub>2</sub> on oxide-film surface | Electrolyte | Metal at base of film pores

is in action almost immediately the film surface is wetted; that is, the pores are rapidly penetrated by ions and solvent molecules alike.

(ii) If a pore is small enough to exert some kind of "sieving" effect on the common aqueous anions (diameters *ca.* 5-6 Å) it can at any instant contain only one anion and one outgoing metal cation sufficiently near one another to avoid the production of a charge-separation effect and a consequently very large polarization. Nor can there be more than a few solvent or solvating molecules nearby, and little or no space is provided for the electrolyte cation. Thus in pores of anion-sieve dimensions any partial penetration by an electrolyte must lead at once to high electrical polarization and complete mechanical plugging, so that such pores can play no part in the initiation of corrosion.

**What is a Pore?**—If we accept the view that pores effective in initiating corrosion are of such size as to be easily permeable by ions and solvent molecules, it is difficult to see how bare metal can exist at the base of such pores without being at once oxidized by atmospheric oxygen, on steel specimens exposed to air. When such specimens are immersed in electrolytes, however, local electrolytic action seems to begin immediately, as shown by the movement of the single potential, and the only possible electrolytic action seems to be that between film-covered metal and "bare" metal. Two possible explanations of this paradox can be offered.

(i) Contact with electrolyte tends to rupture the air-formed oxide film, e.g. by alteration of surface forces and hence mechanical stresses, leading to pores or fissures (*dissolution* of thin parts of film is ruled out on solubility-product as well as kinetic grounds).

(ii) The air-formed film is in a continual state of cracking and healing, due to its formation under mechanical stress, as argued by Evans;<sup>20</sup> thus, when the specimen is immersed in electrolyte, cracks—i.e. pores—appear constantly and provide bare metal from the first moments of immersion onwards.

Either initial process should produce a rapid *fall* of corrosion potential, even before the rise due to partial plugging already discussed. Such a fall is found in the case of tin,<sup>5</sup> but it has not yet been possible to observe it on mild steel covered with the 24-hr. oxide film formed in air at room temperatures, probably because with such a thin film it is exceedingly rapid. However, Fig. 5 shows duplicate potential-time curves obtained by the drop technique on a mild steel specimen carrying a fairly thick

<sup>20</sup> Evans, *Corrosion and Material Protection*, 1948, 5, No. 4, 15.

film (formed by heating in air at  $250^{\circ}\text{C}$  for 1 hr.) in which a preliminary fall of potential is found. These curves may be compared with the corresponding curves for the same electrolyte (0.01 M NaCl, 0.0015 M  $\text{NaNO}_3$ ) on specimens carrying the thin 24-hr. room-temperature film

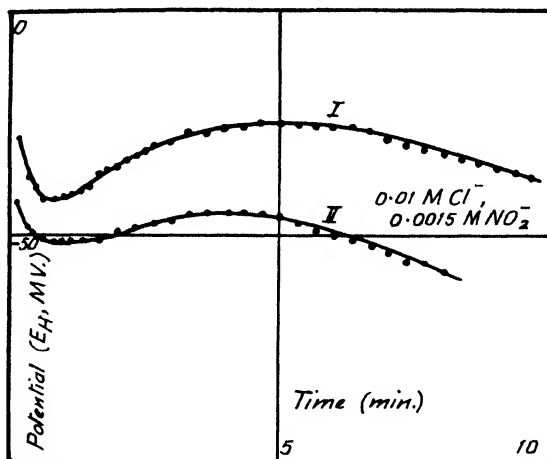


FIG. 5.—Potential-Time curves, steel (film formed 1 hr. at  $270^{\circ}\text{C}$ ) in solution giving corrosion; film penetration repair and breakdown.

(Fig. 4). It will be seen that the maximum due to partial pore-plugging occurs after *ca.* 1 min.—the general time-scale being increased for the thicker film, as would be expected.

**An Analogy between Paint Films and Oxide Films.**—Wormwell and Brasher,<sup>21</sup> following Blum and Haring<sup>22</sup> and Haring and Gibney,<sup>23</sup> have measured the change of potential of painted steel exposed to sea-water. They find that there is an initial fall, followed by a rise to a maximum in some 30 days, and then a final fall with onset of corrosion. This behaviour exactly parallels, on a much larger time-scale, that of the present specimens carrying an oxide film only, and a modified form of the present mechanism seems adequate to explain it. In the case of an organic paint film, the film surface cannot, of course, be a cathode; but it is likely that metal at the base of some of the pores in the paint film acts as cathode towards that at the base of other pores. Thus an electrolytic system very like that here postulated for oxide films is set up: the first potential fall is probably due to the breakdown of the oxide film at the bottom of the "anodic" paint pores, corresponding to the effect discussed above; the rise is due to the partial plugging of these pores, and the final fall to their complete breakdown. The time-scale is much longer than for the case of the oxide film because the paint film is much thicker, with much longer pores having high electrolytic resistance, as suggested by Mayne.<sup>24</sup>

The "cathodic" pores are presumably those that initially have oxide film at their base in relatively good repair; they will, of course, become alkaline and remain corrosion-free, though doubtless centres from which "alkaline peeling" of the paint begins.<sup>25</sup> It is noteworthy that alkaline

<sup>21</sup> Wormwell and Brasher, *Nature*, 1947, **159**, 678.

<sup>22</sup> Blum and Haring, *Trans. Electrochem. Soc.*, 1936, **69**, 169.

<sup>23</sup> Haring and Gibney, *ibid.*, 1939, **76**, 287.

<sup>24</sup> Mayne, *1st Int. Paint Conf.* (Paris, 1947), (in press).

<sup>25</sup> J. E. O. Mayne (private communication, Dec. 1947).

peeling is often relatively severe over the mill-scaled parts of partly de-scaled painted steel,<sup>26</sup> presumably because these become cathodic, as previously explained in general terms.<sup>27</sup>

My thanks are due to Mr. G. E. S. Eyles for careful assistance in the experimental work, and to Dr. U. R. Evans (in whose laboratories much of the work was carried out), Dr. J. N. Agar, Dr. J. E. O. Mayne, Mr. M. J. Pryor and Dr. M. Cohen for a number of stimulating discussions.

*Department of Metallurgy,  
University of Cambridge.*

<sup>26</sup> Footner, *J. Oil Col. Chem. Assoc.*, 1944, **27**, 32.

<sup>27</sup> Hoar, *ibid.*, 1944, **27**, 32.

---

## THE INFRA-RED SPECTRUM, AND THE ASSIGNMENT OF THE FUNDAMENTAL MODES OF VIBRATION OF THIOACETIC ACID

BY N. SHEPPARD

*Received 21st February, 1949*

The infra-red spectrum of thioacetic acid has been obtained and, with the help of the previously available Raman spectrum, has been used to obtain assignments for the fundamental modes of vibration of this molecule. A tentative frequency assignment has also been made for the closely related acetyl chloride molecule. The precise positions and intensities in the spectra of some of the fundamental modes of thioacetic acid have been used to draw conclusions about the polarity of the SH linkage, and the relative force constants of the methyl and C=O groups when compared with those in related molecules.

---

The infra-red spectrum of thioacetic acid has been obtained as part of a programme of work on the spectra of sulphur containing organic molecules. With the help of these data and the previously published Raman spectrum, it seemed worthwhile to attempt an assignment of the observed frequencies in terms of the normal modes of vibration of this molecule.

### Experimental

A pure sample of thioacetic acid, kindly supplied by the British Rubber Producers' Research Association, was evaporated into a previously evacuated gas cell with rocksalt windows. The infra-red spectrum was taken with a Hilger D209 double-beam spectrometer operating under standard conditions described previously.<sup>1</sup> Our observed infra-red spectrum is shown in Fig. 1. Fig. 2 shows a schematic representation of the Raman spectrum of this substance, and of the closely related acetyl chloride molecule, taken from the previous work of Kohlrausch and Pongratz.<sup>2</sup> The individual infra-red frequencies and intensities together with those found in the Raman spectrum of the liquid<sup>3</sup> are given in the first two columns of Table I.

**Assignment of the Spectrum.**—The maximum degree of symmetry that this molecule could possess would be a single plane of symmetry (symmetry group  $C_s$ ) and hence all the fundamental modes are allowed in both the infra-red and Raman spectra. There will be eighteen internal degrees of freedom

<sup>1</sup> Sheppard and Sutherland, *J. Chem. Soc.*, 1947, 1540.

<sup>2</sup> Kohlrausch and Pongratz, *Z. physik. Chem. B*, 1934, **27**, 176; *ibid.*, 1933, **22**, 373.

in all, sixteen of them corresponding to vibrational modes, and two of them to the restricted rotations of essentially the  $\text{CH}_3$  and  $\text{SH}$  groups about the neighbouring single linkages. The vibrational modes can be further subdivided into expected spectral regions according to well-established principles<sup>3</sup> as follows: 3500–1800  $\text{cm}^{-1}$  (four fundamentals; three  $\text{CH}$  stretching modes and one

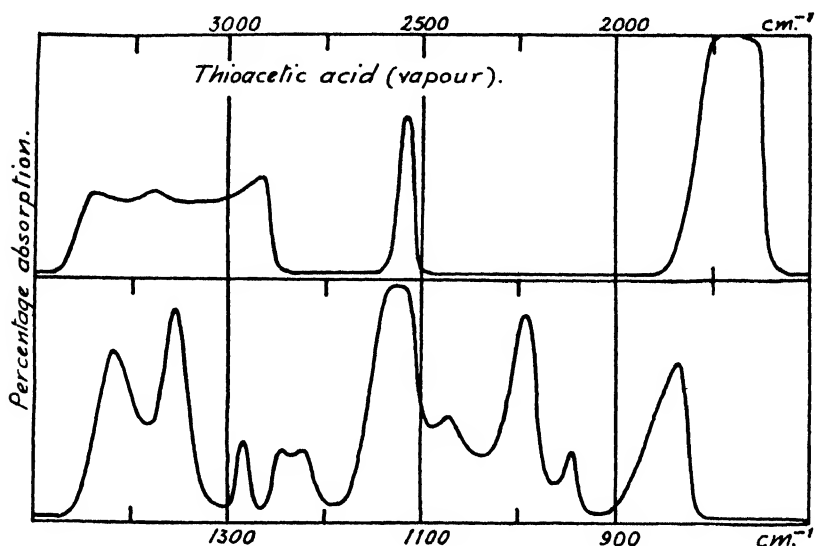


FIG. 1.—The infra-red spectrum of thioacetic acid vapour.

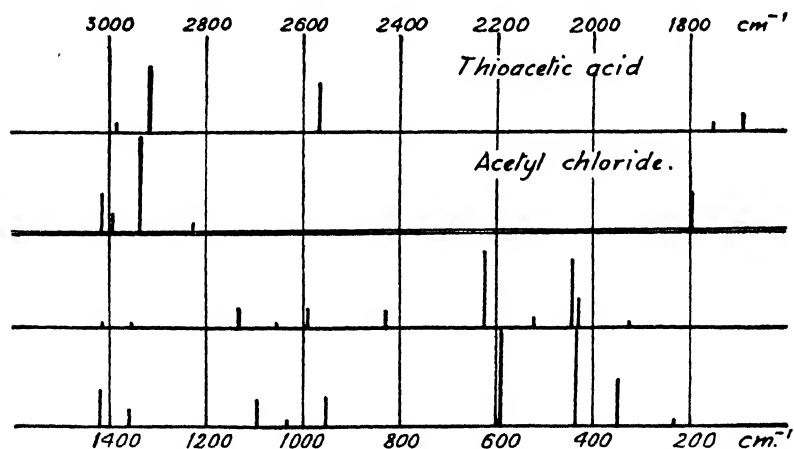


FIG. 2.—The Raman spectra of thioacetic acid and acetyl chloride (after Kohlrausch and Pongratz).<sup>2</sup>

$\text{SH}$  stretching mode), 1800–1600  $\text{cm}^{-1}$  (one fundamental; a  $\text{C}=\text{O}$  stretching mode), 1600–1300  $\text{cm}^{-1}$  (three fundamentals;  $\text{CH}_3$  deformation modes), 1300–550  $\text{cm}^{-1}$  (five fundamentals; one  $\text{C}-\text{C}$  stretching, one  $\text{C}-\text{S}$  stretching, two  $\text{CH}_3$  wagging, and one  $\text{SH}$  deformation mode) and <550  $\text{cm}^{-1}$  (two in-plane and one out-of-plane skeletal bending mode). With the help of these considerations and the strength and coincidences of the frequencies in absorption and

<sup>3</sup> Herzberg, *Infra-red and Raman Spectra of Polyatomic Molecules* (D. Van Nostrand Co., Inc., New York, 1945), p. 195, and discussions of individual molecules.

scattering (see Fig. 1 and 2, and Table I), the following frequencies have been chosen as being probably fundamentals: 2982 (2), 2920, 2568, 1696, 1415 (2), 1352, 1126, 1055, 993, 832, 626, 445, 432, 317  $\text{cm}^{-1}$ .

The prominent lines in the Raman spectrum at 2568 and 832  $\text{cm}^{-1}$ , which do not have counterparts in the very similar spectrum of acetyl chloride, are

TABLE I.—THE OBSERVED INFRA-RED AND RAMAN FREQUENCIES OF THIOACETIC ACID, AND THEIR ASSIGNMENT TO FUNDAMENTAL VIBRATIONS OF THE MOLECULE

Infra-red $\text{cm}^{-1}$	Raman <sup>a</sup> $\text{cm}^{-1}$	Assignment
3360 ( <i>m</i> )		$2 \times 1696$
3200 ( <i>m</i> )		(?)
	2982 (1)	$\text{CH}_3$ asymm. stretch (2)
2920 ( <i>m</i> )	2919 (7)	$\text{CH}_3$ symm. stretch
2550 ( <i>m</i> )	2568 (5)	SH stretch
	1756 (17)	$1126 + 626$ (?)
1696 ( <i>vs</i> )	1694 (2)	C=O stretch
1415 ( <i>m</i> )	1415 ( $\frac{1}{2}$ )	$\text{CH}_3$ asymm. deformation (2)
1352 ( <i>s</i> )		$\text{CH}_3$ symm. deformation
1287 ( <i>w</i> )		$828 + 445$
1227 ( <i>w</i> )		?
1126 ( <i>s</i> )	1130 (2)	$\text{CH}_3$ in-plane wag.
1071 ( <i>w</i> )		$626 + 445$
	1055 ( $\frac{1}{2}$ )	$\text{CH}_3$ out-of-plane wag.
993 ( <i>s</i> )	990 (2)	C—C stretch
947 ( <i>w</i> )		$626 + 317$
865 ( <i>w</i> )		$445 + 432$
838 ( <i>m</i> )	832 (2)	SH deformation
	626 (8)	C—S stretch
	522 (1)	$838 - 319$
Not investigated	445 (7)	Skeletal in-plane bend
	432 (3)	Skeletal in-plane bend
	317 ( $\frac{1}{2}$ )	Skeletal out-of-plane bend

(*vs*) very strong, (*s*) strong, (*m*) medium, (*w*) weak.

clearly the SH stretching and deformation modes respectively. Both of these frequencies agree well with values for such modes previously obtained in related molecules,<sup>4, 5, 6</sup> and have been previously assigned in this manner by Kohlrausch.<sup>7</sup> The assignment of the remainder of the fundamentals in the region 3000—1300  $\text{cm}^{-1}$  also follows previously well-established lines, while the 626  $\text{cm}^{-1}$  Raman line, and the frequencies below this value are clearly to be identified with the C—S stretching and skeletal bending vibrations respectively. The assignment of the remaining frequencies, viz. 1126, 1055, and 993  $\text{cm}^{-1}$ , will now be considered. These frequencies were chosen as fundamentals as they all occur in the Raman spectrum, and because an analogous trio of lines is also present in the corresponding acetyl chloride spectrum (Fig. 2). Two of them also have strong counterparts in the infra-red spectrum (see Table I). These frequencies have to be assigned to the in-plane and out-of-plane  $\text{CH}_3$  wagging modes, and the C—C stretching vibration. The correlation of the 1126  $\text{cm}^{-1}$  line with the in-plane  $\text{CH}_3$  wagging mode is in agreement with similar assignments in other molecules<sup>8, 9</sup> and with the fact that this is a completely symmetrical mode (assuming the molecule to have a plane of symmetry). For this reason it should be fairly strong in the Raman spectrum. It seems probable that the 993  $\text{cm}^{-1}$  line is also the C—C stretching mode on similar reasoning, and this is a likely value for such a mode. The 1055  $\text{cm}^{-1}$  line is therefore assigned to the out-of-plane wagging mode.

<sup>4</sup> Kohlrausch, *Ramanspektren* (Akademische Verlagsges., Becker and Erler, Leipzig, 1943), p. 211.

<sup>5</sup> Thompson and Skerrett, *Trans. Faraday Soc.*, 1940, **36**, 812.

<sup>6</sup> Sheppard, *J. Chem. Physics*, 1949, **17**, 79.

<sup>7</sup> Kohlrausch, *loc. cit.*, p. 248.

<sup>8</sup> Wu and Barker, *J. Chem. Physics*, 1941, **9**, 487.

<sup>9</sup> Szasz, Sheppard and Rank, *ibid.*, 1948, **16**, 704.

The results of the above assignments are summarized in the third column of Table I. There appear to be no features in the Raman spectra which can be attributed to the restricted rotation of the  $\text{CH}_3$  and  $\text{SH}$  groups, but such modes seem to be in general difficult to observe spectroscopically. Most of the remainder of the observed frequencies in the infra-red spectrum can all be explained reasonably as being summation or difference bands involving the already assigned fundamentals, as shown also in Table I. The infra-red frequencies at *ca.* 3200 and 1227  $\text{cm}^{-1}$  are exceptions to this. The fact that the 1227  $\text{cm}^{-1}$  band could not be satisfactorily explained in terms of the other fundamentals led to its reconsideration as fundamental. However, the only reasonable alternative seemed to be to substitute this for the weak 1055  $\text{cm}^{-1}$  Raman line already assigned to the out-of-plane  $\text{CH}_3$  wagging mode, and as 1227  $\text{cm}^{-1}$  appears to be an unusually high value for such a mode the possibility was rejected. It seems probable therefore that this infra-red absorption finds its explanation in terms of a combination frequency involving one of the non-assigned low lying torsional modes. There are several ternary combinations that can be assigned to the 3200  $\text{cm}^{-1}$  infra-red absorption, but as there is no satisfactory way of distinguishing between these, its assignment has been left open. Although some of the assigned combination levels do not agree too satisfactorily with the observed frequencies, the possible anharmonicities, and the fact that the Raman frequencies correspond to the liquid state, makes them appear reasonable.

It is clear from the general similarities of the Raman spectrum of thioacetic acid and acetyl chloride that the former predominantly exists in the form  $\text{CH}_3\text{CO} \cdot \text{SH}$ , and this has been assumed in the above discussion. However, it is perhaps possible that an equilibrium exists between this form and the isomeric  $\text{CH}_3\text{CS} \cdot \text{OH}$ , and that some of the weaker bands are due to the presence of a small percentage of the isomeric molecules. In particular, such a state of affairs would explain the difficulty in assigning the weak 1227  $\text{cm}^{-1}$  absorption in terms of fundamentals of the  $\text{CH}_3\text{CO} \cdot \text{SH}$  molecule, and furthermore one of the absorptions near 3300  $\text{cm}^{-1}$  could be caused by the presence of some OH linkages in such molecules. If this were the case the small proportion of  $\text{CH}_3\text{CS} \cdot \text{OH}$  molecules is presumably due to a higher energy content of these molecules, and the relative concentration of these should increase considerably with temperature. Such an effect would be observable as a temperature coefficient of some of the weak absorptions, relative to the stronger ones of the  $\text{CH}_3\text{CO} \cdot \text{SH}$  molecules.

### Discussion

Several of the assigned fundamentals differ notably in frequency from the constant values that such modes of vibration have in the spectra of hydrocarbons, and it seems worthwhile to consider these in turn. Thus the CH stretching modes of the  $\text{CH}_3$  group occur at 2982 and 2920  $\text{cm}^{-1}$  in contrast to their usual values of *ca.* 2960 and 2870  $\text{cm}^{-1}$  in saturated hydrocarbons.<sup>10</sup> As these modes are well known to interact to a negligible degree with the skeletal vibrations of a molecule (*i.e.* are independent of mass changes in the molecular skeleton) it seems that this must correspond to a rather higher value for the C—H stretching force constant than is applicable to purely hydrocarbon molecules.

Similarly the  $\text{CH}_3$  deformation modes occur at 1415 and 1352  $\text{cm}^{-1}$  in thioacetic acid as opposed to their usual values of *ca.* 1450 and *ca.* 1375  $\text{cm}^{-1}$  in hydrocarbon molecules. Although in this case the different masses of neighbouring skeletal atoms may play some part in this change in frequency, it seems probable also that the force constants controlling the angular deformation of the CH linkages are decreased in magnitude. Both the effects so far discussed are also apparent in the Raman spectrum of acetyl chloride, and it is probable that they are due to a change in the electronic structure of the CH linkages caused by the neighbouring C=O group. The observations on the  $\text{CH}_3$  deformation modes are also in line with a previous investigation in which CH deformation modes were found to decrease in frequency when an electronegative group was substituted nearby.<sup>11</sup> Kohlrausch<sup>12</sup> has previously made an extended

<sup>10</sup> Fox and Martin, *Proc. Roy. Soc. A*, 1940, **175**, 208.

<sup>11</sup> Sheppard and Sutherland, *ibid.* 1945, **196**, 195.

<sup>12</sup> Kohlrausch, *loc. cit.*, p. 250 *et. seq.*

study of the variation of the C=O stretching frequency with the nature of the substituent groups. However, it is interesting to note that this mode in the molecules acetyl chloride and thioacetic acid differs in frequency by  $100\text{ cm.}^{-1}$  ( $1798$  and  $1696\text{ cm.}^{-1}$ ). As in this case the structures of the two molecules are otherwise very closely related as shown by the similarity of their Raman spectra, a difference of this magnitude must arise from a change in the C=O stretching force constant. In this case the force constant has been notably increased by the substitution of the more electronegative chlorine atom for the SH group of thioacetic acid.

A further point of interest is the considerable strength in the infra-red of the  $2550\text{ cm.}^{-1}$  absorption caused by the SH stretching vibration. This fundamental is usually very weak in the infra-red (compare, for example, the relative strength of the SH and CH fundamentals in the ethyl mercaptan molecule,<sup>6</sup> which is of approximately equal size). The intensity of these SH bands in the infra-red will depend to a first approximation<sup>13</sup> on the square of  $\left(Q\frac{dM}{dr}\right)$ , where  $Q$  is the amplitude of

the SH stretching vibration,  $M$  is the dipole moment of the SH linkage, and  $r$  is the SH internuclear distance. It is very probable that for such a highly localized vibration,  $Q$  has approximately the same value in both thioacetic acid and ethyl mercaptan, and therefore that the value of  $dM/dr$  for the SH linkage in the latter molecule is abnormally high. As it seems more likely that a highly polar linkage (i.e. with a high value of  $M$ ) will have a greater  $dM/dr$  value than a relatively non-polar one (this is not necessarily true, as it depends on the precise shape of the  $M-r$  curve in question,<sup>13</sup> but the great strength in the infra-red of the stretching modes of many polar linkages such as O—H, N—H, C=O, etc., suggests that it is often the case) this observation may be an indication of a more polar SH linkage in proximity to the C=O group. In support of this contention is the fact that the SH deformation mode in this molecule (whose intensity depends directly on the dipole moment of the SH linkage) is much stronger in the infra-red than in the case of ethyl mercaptan.<sup>6</sup> On the other hand the polarity of the SH group is not sufficient to give rise to hydrogen bonding effects, as shown by the essentially normal position of the SH stretching frequency.<sup>4</sup>

**The Acetyl Chloride Spectrum.**—As a consequence of the assignment of the fundamentals of the thioacetic acid molecule and the similarity of the Raman spectra of these two molecules, it is possible to make a tentative assignment also for the fundamentals of acetyl chloride. This is given below, the frequencies in  $\text{cm.}^{-1}$  having been taken from the Raman spectrum of this substance obtained by Kohlrausch and Pongratz:<sup>2</sup>

$\text{CH}_3$  asymmetrical stretching,  $3016, 2991$ ;  $\text{CH}_3$  symmetrical stretching,  $2935$ ; C=O stretching,  $1798$ ;  $\text{CH}_3$  asymmetrical deformation,  $1418$  (2);  $\text{CH}_3$  symmetrical deformation,  $1358$ ;  $\text{CH}_3$  in-plane wagging,  $1096$ ;  $\text{CH}_3$  out-of-plane wagging,  $1038$ , C—C stretching,  $955$ ; C—Cl stretching,  $590$ ; skeletal in-plane bending,  $434, 348$ ; skeletal out-of-plane bending,  $236$ .

Although some of these frequencies might differ somewhat in the vapour phase, a more reliable assignment must await the investigation of the infra-red spectrum under these conditions.

The author is indebted to Dr. G. B. B. M. Sutherland for a valuable discussion. He would also like to thank the British Rubber Producers' Research Association for the sample of thioacetic acid, the Master and Fellows of St. Catharine's College, Cambridge, for a Senior Research Studentship held during the period of this work, and the Dunlop Rubber Co. Ltd., England, for financial assistance.

*Laboratory of Colloid Science,  
Free School Lane,  
Cambridge.*

<sup>13</sup> Herzberg, *loc. cit.*, pp. 240, 261.



# THE LATTICE SPACINGS OF SUBSTITUTIONAL SOLID SOLUTIONS

BY G. V. RAYNOR

*Received 10th December, 1948; as revised 17th March, 1949*

The lattice spacing relationships for substitutional solid solutions of various elements in copper, silver and gold have been analyzed in examination of the suggestion that the change in lattice spacing on alloy formation may be considered in terms of an atomic size factor and a valency factor operating together. If it is assumed that the contribution to the change of lattice spacing due to the difference between the valency of the solute and that of the solvent is the difference  $\Delta$  between the observed lattice spacing and that calculated from the atomic sizes of the components only, certain regularities are shown. Where the solute is in the same period as the solvent,  $\Delta \propto (V_{\text{solute}} - V_{\text{solvent}})(e - 1)$ , where  $V$  denotes valency and  $e$  the electron/atom ratio. Where the solute is in a period different from that of the solvent,

$$\Delta \propto (V_{\text{solute}} - V_{\text{solvent}} + C)(e - 1),$$

where  $C$  is a constant depending on the difference in the periods of the component metals. No such regularity appears to exist for solid solutions in magnesium and aluminium, but in general  $\Delta$  is positive where  $V_{\text{solute}} > V_{\text{solvent}}$ , and negative where  $V_{\text{solute}} < V_{\text{solvent}}$ . The results confirm the dual nature of lattice distortion effects in simple binary alloys.

---

**1. Introduction.**—The determination of the lattice spacings of alloys by precision X-ray techniques has led to the accumulation of many accurate data; it is clear that in general solid solution formation is accompanied by lattice spacing changes. The term "lattice distortion" is commonly used to denote the mean change of lattice spacing which occurs when a particular solid solution is formed. For cubic metals, such as copper, silver and gold, the lattice distortion takes the form of an average dilatation or contraction, owing to the presence of local centres of relatively intense dilatation or contraction. For non-cubic metals, relative changes in the dimensions of the unit cell may also occur.

It has been shown repeatedly that Vegard's law is of very limited validity, and that lattice distortion in substitutional solid solutions is intimately related to the solute valency, where this differs from that of the solvent. Information is particularly complete for the alloys of copper, silver and gold.<sup>1, 2</sup> Thus, according to Hume-Rothery, Lewin and Reynolds,<sup>1</sup> equal atomic percentages of cadmium, indium, tin and antimony expand the lattice of silver by amounts proportional to 2 : 3 : 4 : 6 respectively. In copper-rich alloys, equal atomic percentages of zinc, gallium and germanium expand the copper lattice by amounts proportional to 3 : 4 : 4.8. These relationships were confirmed by Owen and Roberts,<sup>3</sup> who reported that the factors for zinc, gallium, germanium and arsenic in copper were 3 : 4 : 5 : 7, and that the numerical relationships for both copper and silver alloys were valid at high temperatures.

<sup>1</sup> Hume-Rothery, Lewin and Reynolds, *Proc. Roy. Soc. A*, 1936, **157**, 167.

<sup>2</sup> Owen, *J. Inst. Metals*, 1947, **73**, 471.

<sup>3</sup> Owen and Roberts, *Phil. Mag.*, 1939 (vii), **27**, 294.

The atomic sizes of the solutes studied are all within the zone of favourable size-factors with respect to the appropriate solvents; since an increase in the valency of the solute leads to an increased lattice expansion at equal solute percentages, the distortion produced must depend markedly on the solute valency. The numerical relationships indicate that the effect of increasing valency is less marked in the copper series than in the silver series; increasing valency tends to expand the lattice, but this tendency appears to be opposed by some factor which is relatively more important in the copper series. It has been suggested<sup>1</sup> that this opposing factor is due to a contraction of the atom with increasing atomic number since the change in atomic number (A.N.) resulting from one step in the periodic table is relatively less for the elements following silver (A.N.=47) than for those following copper (A.N.=29).

It is now recognized, from the results of lattice spacing experiments and of correlations of solid-solubility relationships with lattice distortion,<sup>4</sup> that the general effect of the introduction of a solute atom on to the crystal lattice of the solvent is, broadly, composed of two main factors:

- (a) a valency factor, such that increasing valency of the solute produces an increased expansion of the lattice;
- (b) an atomic factor, which may produce either an expansion or a contraction of the lattice.

Thus, in a series of elements of regularly increasing valency, such as the series zinc, gallium, and germanium, the valency factor increases with increasing valency, but, owing to the general shrinkage of the electron shells with increasing atomic number, the atomic factor becomes smaller.<sup>5</sup> Although these two factors have been recognized, the nature of their interaction has not been established. It is the purpose of the present paper to point out that, if the atomic factor be identified with the expansion or contraction of the lattice produced by the size difference between the solute and solvent atoms, then the residual distortions, which may be ascribed to valency differences between the components, show interesting regularities.

**2. Lattice Spacing Effects in Alloys.**—A recent analysis of the lattice distortion produced by various solutes in aluminium<sup>6</sup> has emphasized the complexity of the problem, and has confirmed that, even where the two metals of a binary system have the same valency and crystal structure, Vegard's law is frequently invalid; the component atoms mutually influence each other. For alloys composed of metals of different valencies, additional effects, such as those involving Brillouin zone overlaps, may also be encountered, while the influences of the ionic radii and the volume per valency electron have also to be considered.

According to Vegard's law, the lattice spacing of a binary alloy may be expressed in such a way that the mean interatomic distance

$$d_m = nd_B + (1 - n)d_A,$$

where  $d_A$  and  $d_B$  are the inter atomic distances in the pure components, and  $n$  is the fraction of B atoms. Deviations from this relationship are often ascribed to differences between the A—B distances in the alloy and the mean of the A—A and B—B distances. Though this undoubtedly exists, as indicated by the changes in lattice spacing which occur when a disordered alloy becomes ordered, thereby changing the relative proportions of A—A, B—B, and A—B distances, this view is too simple. The solute valency, electrochemical differences and Brillouin zone characteristics all exert influences which might be important in a given case.

Certain alloys, however, in which such complicating factors are at a minimum, do show a relatively close approach to Vegard's law. Deviations from linearity are relatively small, and detailed analysis shows

<sup>4</sup> Hume-Rothery, *The Structure of Metals and Alloys* (Inst. Metals Monograph and Report Series, No. 1, 1944).

<sup>5</sup> Hume-Rothery, *Phil. Mag.*, 1936 (vii), 22, 1013.

<sup>6</sup> Axon and Hume-Rothery, *Proc. Roy. Soc. A*, 1948, 193, 1.

that the deviations which occur in systems where the solute and solvent valencies differ are very much bigger. In order to separate the valency factor in lattice distortion from the atomic factor, it would appear to be legitimate to assume that, to a first approximation, the expansion or contraction which would occur in the absence of any effect due to valency is given by an additive relationship between the interatomic distances in the component metals. Any residual distortion may then be attributed primarily to the valency factor. This procedure assumes that the atomic factor in lattice distortion is primarily an atomic size effect caused simply by the mixing together of differently sized atoms on a common lattice.

Assuming the relationship

$$d_m = nd_B + (1 - n)d_A,$$

the change in lattice spacing to be expected purely as a result of size effects may be calculated for any solute whose interatomic distance is known. For the purposes of this paper, the closest distance of approach in the crystal of the element is taken as a measure of the atomic diameter, irrespective of the co-ordination number of the particular crystal structure involved. The mean lattice spacing calculated in this manner for a particular composition differs from the observed value; the difference,

$$\Delta a = (a_{\text{observed}} - a_{\text{calculated}})$$

represents the contribution to the lattice spacing resulting mainly from valency effects, and may be referred to as the "valency contribution."  $\Delta a$  also includes the relatively small-scale effects which cause deviations from Vegard's law in the absence of valency differences, but for the dilute solutions to be considered, these may, to a first approximation, be neglected.

**3. Alloys of Copper, Silver and Gold with solutes of the Same Period as the Solvent.**—Accurate data exist for the lattice spacings of the solid solutions of zinc, gallium, germanium and arsenic in copper,<sup>1, 2, 3</sup>

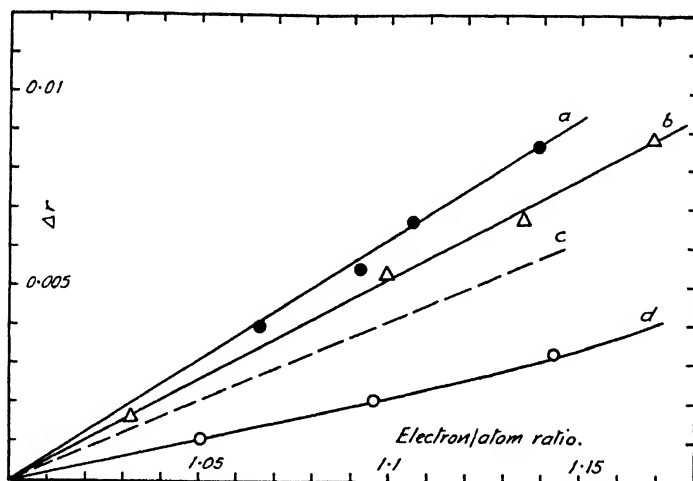


FIG. 1.—Curves of  $\Delta a$  against electron/atom ratio for zinc, germanium, arsenic (and gallium) in copper.

(a) CuGe.

(b) CuAs.

(c) (CuGa).

(d) CuZn.

and of cadmium, indium, tin, and antimony in silver.<sup>1, 3</sup> These alloys form a convenient series for the examination of the atomic and valency factors, since complicating effects are at a minimum. The solutes are all of relatively favourable size-factor with respect to the appropriate solvent, and electro-chemical differences are not important except for the

relatively electronegative elements arsenic and antimony. Except for these elements, the difference between the observed and calculated lattice spacings may be attributed to the effect of the solute valency.

Fig. 1 has been constructed from the data given by Hume-Rothery, Lewin and Reynolds,<sup>1</sup> and shows that, for zinc, germanium and arsenic in copper, the observed lattice spacing is greater than that calculated from atomic size differences only. In this figure, the difference has been expressed for convenience as

$$\Delta r = (r_{\text{observed}} - r_{\text{calculated}}),$$

where  $4/3 \pi r^3$  = the atomic volume, and  $\Delta r$  is plotted against the electron/atom ratio. The interatomic distances for zinc and germanium have been taken as 2.659 Å and 2.445 Å respectively; for gallium, the complex crystal structure involves interatomic distances of 2.437, 2.706, 2.736 and 2.795 Å, so that no reliable value for the appropriate interatomic distance is available. The curves of Fig. 1 are initially linear, and for low solute concentrations, the ratio of the slope of the copper-germanium curve to that of the copper-zinc curve is accurately 3/1 (see Table I). For a given solute, the valency contribution is proportional

TABLE I

System	Initial Slope of Curve of $\Delta r$ against $e \times 10^3$	$V_{\text{solute}} - V_{\text{solvent}}$
CuZn . . .	2.05	1
(CuGa) . . .	4.1	2)
CuGe . . .	6.15	3
AgCd . . .	2.3	1
(AgIn) . . .	4.54	2)
AgSn . . .	6.8	3
AgSb . . .	11.2	4
CuAs . . .	5.2	4
AuHg . . .	ca. 2.0	1
AuZn . . .	4.8	1
AuGa . . .	0.85 $\left. \begin{array}{l} > 2.05 \\ > 2.05 \end{array} \right\}$	2
AuGe . . .	8.9 $\left. \begin{array}{l} > 2.05 \\ > 2.05 \end{array} \right\}$	3
AuCd . . .	1.4	1
AuIn . . .	4.0 $\left. \begin{array}{l} > 2.6 \\ > 2.7 \end{array} \right\}$	2
AuSn . . .	6.7 $\left. \begin{array}{l} > 2.6 \\ > 2.7 \end{array} \right\}$	3
AgZn . . .	5.0 $\left. \begin{array}{l} > 1.6 \\ > 1.7 \end{array} \right\}$	1
AgGa . . .	6.6 $\left. \begin{array}{l} > 1.6 \\ > 1.7 \end{array} \right\}$	2
AgGe . . .	8.3 $\left. \begin{array}{l} > 1.6 \\ > 1.7 \end{array} \right\}$	3
AgAs . . .	6.6	4
CuCd . . .	2.1	1
CuIn . . .	23.5 $\left. \begin{array}{l} > 2.5 \\ > 2.5 \end{array} \right\}$	2
CuSn . . .	26 $\left. \begin{array}{l} > 2.5 \\ > 2.5 \end{array} \right\}$	3
AgHg . . .	ca. 2.8	1
CuSi . . .	4.7	3
AgMg . . .	-13.3	1

In this Table, the initial slope is expressed as  $\left( \frac{\Delta r}{e - 1} \right) \times 10^3$ .

to  $(e - 1)$ , where  $e$  is the electron/atom ratio, and at a given electron/atom ratio the valency contribution is proportional to  $(V_{\text{solute}} - V_{\text{solvent}})$ , where  $V$  denotes valency. The valency contribution thus depends on

the difference in the charges on the solvent and solute ions, and not merely on the increase in the energy of the conduction electrons caused by increasing their number; if the latter were true, the curves of  $\Delta r$  against electron/atom ratio for different solute valencies should coincide.

If these principles be accepted, the corresponding curve for gallium in copper should lie midway between those for the copper-zinc and copper-germanium systems, as shown by the broken line in Fig. 1. This allows a probable atomic diameter for gallium of 2.595 Å to be derived. This is closer to the mean distances of approach of atoms in the gallium structure (2.7 Å) than to the closest distance of approach, and confirms the suggestion made by Hume-Rothery, Reynolds and Raynor<sup>7</sup> that, for the study of alloy formation, the use of the closest distance of approach in this particular structure is unsound.

Similar curves of  $\Delta r$  against electron/atom ratio may be plotted for the alloys of cadmium, tin and antimony in silver;<sup>1</sup> the interatomic distances in the crystals of cadmium, tin and antimony have been taken

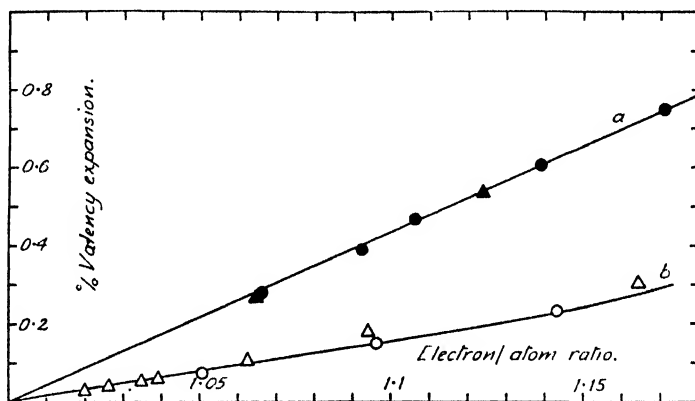


FIG. 2.—Curves of  $100 \Delta r/r$  against electron/atom ratio for copper and silver as solvents.

(a) CuGe (●) and AgSn (▲).

(b) CuZn (○) and AgCd (△).

as 2.9736, 2.797 (grey tin) and 2.898 Å respectively. No reliable estimate of the appropriate value to be used for indium is available, owing to incomplete ionization in the crystal of the element. The initial slopes of the curves obtained are summarized in Table I; although the absolute values are slightly different from those derived from Fig. 1, the ratio of the slopes for the silver-tin and silver-cadmium curves is again 3/1. As in the copper-gallium system, the slope of the silver-indium curve should lie midway between those for the silver-tin and silver-cadmium curves. The value of the atomic diameter of indium which would be consistent with such a slope is 2.926 Å, which is smaller than the closest distance of approach in the crystal, in agreement with the suggestion that indium metal is incompletely ionized. From a comparison of the interatomic distances in white tin (incompletely ionized) and grey tin (completely ionized) the atomic diameter for fully ionized indium would be expected to be about 0.3 Å less than that in the pure metal (3.24 Å). The newly derived value is in good agreement with this.

A comparison of the slopes of the curves of  $\Delta r$ , the valency contribution to the lattice expansion, against the electron/atom ratio for zinc and germanium in copper and for cadmium and tin in silver reveals a further important point with regard to the expansion of the copper and silver lattices produced by a given increase in the electron/atom ratio. Table I

<sup>7</sup> Hume-Rothery, Reynolds and Raynor, *J. Inst. Metals*, 1940, **66**, 191.

shows that the initial slopes are slightly larger for the silver alloys than for the copper alloys; the lattice spacing of silver, however, is slightly larger than that of copper. In Fig. 2, the percentage valency contributions, expressed as  $100\Delta r/r_{\text{solvent}}$ , have been plotted against the electron/atom ratio, and it is seen that, within the limits of experimental error, the points for zinc in copper and cadmium in silver lie on a single curve, while those for germanium in copper and tin in silver also fall on a single curve. For a given solute valency, a given increase in the electron/atom ratio produces the same percentage increase in the valency contribution to the lattice spacing for both copper and silver. Considering the valency contribution, therefore, the distortion effects produced, when allowance has been made for the atomic size factor, are the same for both solvents, and the puzzling differences noted by Hume-Rothery, Lewin and Reynolds, who considered the total distortion in the two series of alloys, disappear.

The regularities shown for the divalent and tetravalent solutes are lost for the electronegative solutes arsenic and antimony. The silver-antimony system gives a curve which has nearly five times the slope of the silver-cadmium curve (Table I). This is unexpected, since it is well known that the lattice spacings of alloys whose components differ markedly in electrochemical character are usually abnormally small. This factor probably accounts for the relatively small slope of the curve of  $\Delta r$  against electron/atom ratio for the copper-arsenic system, since arsenic is more electronegative than antimony, and copper is more electropositive than silver. It may be noted that the copper-arsenic system is not strictly comparable with the other systems studied, since the primary solid solution enters into equilibrium, not with an electron compound, but with an intermetallic compound  $\text{Cu}_3\text{As}$  of very limited homogeneity range. In this compound, it is possible that arsenic exhibits an electrovalency of 3.

For alloys of gold with elements of the same period, accurate data are available only for the gold-mercury system at  $18^\circ\text{C}$ . The interatomic distance in the mercury crystal at  $-46^\circ\text{C}$  is  $2.999\text{ \AA}$ ; this may be corrected to  $18^\circ\text{C}$  by the known thermal expansion coefficient to give an estimate of the change in lattice spacing to be expected purely as a result of size effects. The  $\Delta r$  values deduced are uncertain to the extent of the uncertainty in the temperature correction for the atomic diameter of mercury, but the curve of  $\Delta r$  against electron/atom ratio is close to those for zinc in copper and cadmium in silver (Table I).

**4. Alloys of Copper, Silver and Gold with Solutes of Different Periods from the Solvent.**—From data in the literature, curves of  $\Delta r$  against electron/atom ratio may be plotted for zinc, gallium, germanium, cadmium, indium and tin in gold, for zinc, gallium and germanium in silver, and for cadmium, indium and tin in copper. Data for certain other alloys are also available.

(a) **Gold with Zinc, Gallium and Germanium as Solutes.**—The lattice spacing data for these alloy systems<sup>a</sup> have been plotted in Fig. 3 as  $\Delta r$  against electron/atom ratio, the atomic diameter for gallium being taken as that derived from Fig. 1. The solubility of arsenic is too small for accurate comparison of lattice spacings with those of the other systems. The valency contribution produced by zinc in gold is much greater than that given by zinc in copper or cadmium in silver; the increase in slope, however, on passing from zinc to gallium is the same as that on passing from gallium to germanium (Table I). The valency contribution is again proportional to  $(e - 1)$  for a given solute, but, for different solutes at a given electron/atom ratio is proportional not to  $(V_{\text{solute}} - V_{\text{solvent}})$ , but to  $(V_{\text{solute}} - V_{\text{solvent}} + C)$ , where  $C$  is a constant depending on the differences in the electronic structures of the underlying ions of the solvent and solute metals.

<sup>a</sup> Owen and O'Donnell Roberts, *J. Inst. Metals*, 1945, **71**, 267.

(b) **Gold with Cadmium, Indium and Tin as Solutes.**—The slopes of the curves of  $\Delta r$  against the electron/atom ratio, constructed from the data of Owen and Roberts<sup>6</sup> for these alloys, are given in Table I. The solubility of antimony is too small for accurate comparison of lattice spacings. The interatomic distance used for indium is that derived by comparison with silver-cadmium and silver-tin alloys. The valency contribution in the case of cadmium is of the same order as that produced by zinc in copper and cadmium in silver. On passing from cadmium to indium, the increase in slope is the same as that obtained on passing from indium to tin. The same type of regularity is therefore observed as for zinc, gallium and germanium in gold.

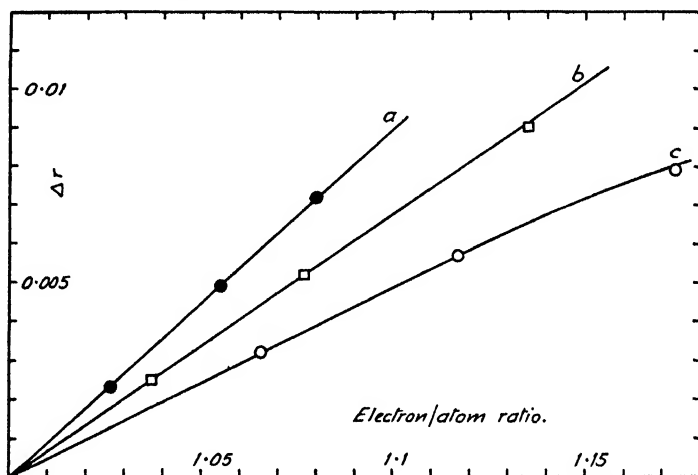


FIG. 3.—Curves of  $\Delta r$  against electron/atom ratio for zinc, gallium and germanium in gold.

(a) AuGe.

(b) AuGa.

(c) AuZn.

(c) **Silver with Zinc, Gallium, Germanium and Arsenic as Solutes.**—The lattice spacing data for these alloy systems are taken from the work of Owen and his collaborators,<sup>2</sup> and the curves of  $\Delta r$  against electron/atom ratio are similar to those shown in Fig. 3. The slopes for the various curves are given in Table I, which shows that the increase in slope on passing from zinc to gallium is the same as that on passing from gallium to germanium. The curve for the silver-arsenic alloys shows a considerably smaller valency contribution than would be expected for a pentavalent solute; it is almost superimposed on the curve for silver-gallium alloys.

(d) **Copper with Cadmium, Indium, Tin and Antimony as Solutes.**—According to Owen<sup>2</sup> the percentage increases in the lattice spacing of copper produced by 1 atomic % of cadmium, indium, tin and antimony are respectively 0.216, 0.259, 0.2805 and 0.3095. The lattice spacing-composition curves on which these values are based do not appear to have been published. From these values, however, calculation shows that the values of  $\Delta r$  at one atomic % of solute are, for cadmium, indium, and tin respectively, 0.007, 0.00157, and 0.0026. If, as in the other cases studied, the curve of  $\Delta r$  against electron/atom ratio is linear, then for a constant electron/atom ratio of 1.03 the corresponding  $\Delta r$  values are 0.0021, 0.00235 and 0.0026. The increase on passing from the divalent to the trivalent solute is again equal to that on passing from the trivalent to the tetravalent solute. As in the alloys previously considered, the valency contribution for antimony is anomalous, and somewhat lower than that produced by cadmium.

(e) **Other Solid Solutions in Copper and Silver.**—Data are available for the solid solutions of mercury,<sup>9</sup> magnesium<sup>10</sup> and aluminium<sup>11</sup> in silver, aluminium in gold,<sup>8</sup> and aluminium<sup>12</sup> and silicon<sup>13</sup> in copper. The alloys containing aluminium cannot, at present, be adequately discussed in terms of contributions due to atomic size and valency differences, owing to the uncertainty with regard to the appropriate atomic diameter for aluminium. The interatomic distance in the crystal of aluminium is abnormally large in comparison with the interatomic distances in the crystals of neighbouring elements in the periodic table, and, from systematic studies of alloy formation and lattice spacing effects, it has been suggested that the size of the aluminium atom in copper, silver and gold alloys is somewhat smaller than the interatomic distance in the crystal, and is of the order of 2.7 Å. The qualitative nature of this estimate, however, precludes quantitative analysis.

The atomic diameter of mercury may be assessed from the interatomic spacings at  $-46^{\circ}\text{C}$ , as described for the gold-mercury alloys, and the resulting curve for the silver-mercury system is closely similar to that for cadmium in silver (see Table I). The curve of  $\Delta r$  against electron/atom ratio for silicon in copper shows a positive slope (Table I), which is somewhat smaller than that of the copper-germanium curve. This may be accounted for by the fact that silicon is more electronegative than germanium, giving rise to a larger electrochemical factor. For the solid solution of magnesium in silver, however, there is a negative valency contribution. This is most probably due to the electropositive nature of magnesium; the resulting high electrochemical factor tends to contract the lattice spacings.

**5. Magnesium Alloys and Aluminium Alloys.**—For magnesium, the electronic state is more complex than for silver, copper or gold. The Brillouin zone for the magnesium structure, with two electrons per atom, is overlapped in the directions at right angles to the hexagonal axis.<sup>14</sup> According to Jones,<sup>15</sup> the effect of a small overlap across a face of the Brillouin zone is to tend to expand the structure in a direction at right-angles to the face concerned. Any increase in overlap, caused by the solution of elements of valency greater than 2, thus tends to expand the  $a$ -spacings of the crystal; this expansion will be superimposed on the lattice spacing changes caused by atomic size differences. Conversely, the solution of univalent elements should lead to a negative valency contribution.

When cadmium is dissolved in magnesium, there is no valency difference between solute and solvent, and the change in axial ratio is very small in dilute solution. This suggests that, in assessing the distortion due to atomic size differences only, it may be assumed that very little change in axial ratio will be caused purely as a result of these differences. The closest distance of approach in the magnesium structure is

$$d_{\text{Mg}} = (a^2/3 + c^2/4)^{1/2}.$$

In an alloy containing a proportion  $n$  of solute atoms, the closest distance of approach may, as previously, be expressed as

$$d_{\text{alloy}} = nd_{\text{solute}} + (1 - n)d_{\text{Mg}}.$$

and then, assuming a constant ratio of the  $c$ -axis to the  $a$ -axis, the  $a$

<sup>9</sup> Day and Mathewson, *Metals Tech.*, 1938, **51** (1); *Trans. Amer. Inst. Min. Met. Eng.*, 1938, **128**, 261.

<sup>10</sup> Andrews and Hume-Rothery, *J. Inst. Metals*, 1946, **69**, 485.

<sup>11</sup> Foote and Jette, *Trans. Amer. Inst. Min. Met. Eng.*, 1941, **143**, 151.

<sup>12</sup> Obinata and Wasserman, *Naturwiss.*, 1933, **21**, 382.

<sup>13</sup> Anderson, *Trans. Amer. Inst. Min. Met. Eng.*, 1940, **137**, 334.

<sup>14</sup> Raynor, *Proc. Roy. Soc. A*, 1940, **174**, 457.

<sup>15</sup> Jones, *ibid.*, 1934, **147**, 400.



spacing to be expected as a result of atomic size differences may be calculated from the relation

$$d_{\text{alloy}} = (a^2/3 + c^2/4)^{1/2}.$$

The valency contribution is then

$$\Delta a = (a_{\text{observed}} - a_{\text{calculated}}).$$

The data for indium, tin, gallium and silver<sup>14, 16</sup> are shown in Fig. 4; reliable estimates of the fully ionized atomic diameters for thallium and lead do not exist, so that curves for these solutes cannot be compared with those in Fig. 4. For comparison with the  $\Delta a$  values plotted,  $\Delta a$

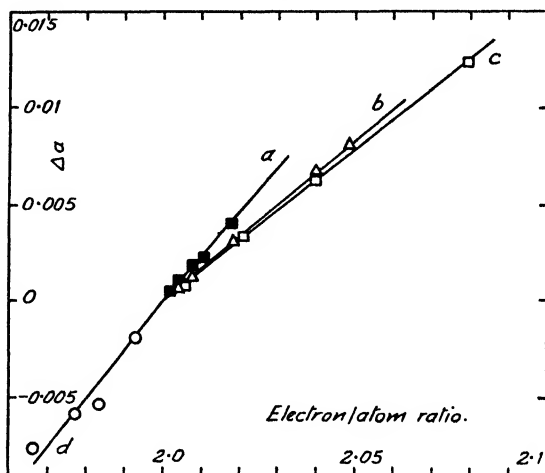


FIG. 4.—Curves of  $\Delta a$  against electron/atom ratio for gallium, tin, indium and silver in magnesium.

(a) MgGa.

(b) MgSn.

(c) MgIn.

(d) MgAg.

for the magnesium-cadmium system up to 10 atomic % cadmium does not exceed 0.0006 Å.

The curves for indium and tin do not differ greatly in slope, while that for gallium is relatively close but probably affected by the change in the period of the solute. In marked contrast, the curve for small amounts of silver in magnesium, where the electron/atom ratio is reduced, shows that the valency contribution is negative, and that the effect of reducing the electron/atom ratio is almost exactly the reverse of that of increasing the number of electrons per atom. For magnesium alloys, these curves suggest that the most important effect introduced by solutes of valency other than two is that due to alteration of the magnitude of the electronic overlap from the first Brillouin zone.

The electronic structure of aluminium is still more complex, and an analysis similar to that carried out for the copper, silver and gold alloys indicates that no well-defined regularities exist. The data of Axon and Hume-Rothery<sup>8</sup> show, however, that, where the solute is of higher valency than aluminium (i.e. silicon and germanium)  $\Delta a$  is positive, while solutes of lower valency, with the exception of zinc, give rise to a negative value of  $\Delta a$ , in agreement with the general principles discussed above.

**6. Summary and Discussion.**—The data presented above confirm that, for copper, silver and gold alloys, the change of lattice spacing on alloy formation may justifiably be considered in terms of an atomic size factor and a valency factor operating simultaneously. For all

<sup>16</sup> Raynor, *Proc. Roy. Soc. A*, 1942, **180**, 107.

systems studied, except silver-magnesium, the lattice spacing for a given composition is greater than that to be expected from a consideration of the atomic diameters of the components. The residual expansion,  $\Delta r$ , is intimately connected with the solute valency, except for the electro-negative elements of Group V of the periodic table. The relationships are most clearly shown for solutes of the same period as the solvent, but analogous relationships exist where the solvent and solute are not in the same period. This is summarized in Fig. 5, in which the slopes of the

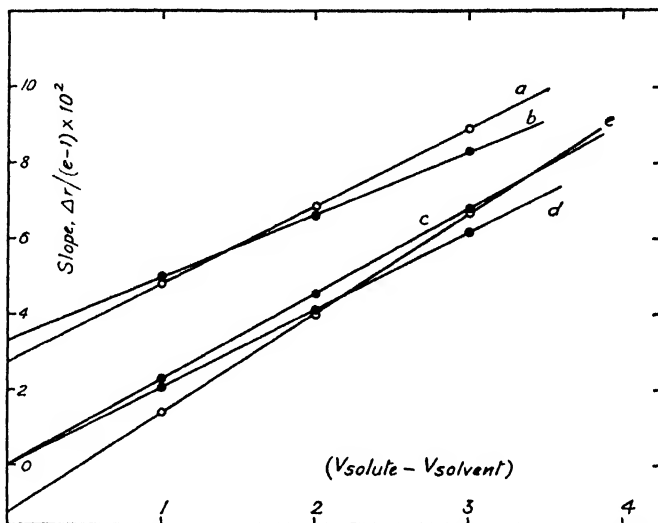


FIG. 5. —Slopes of the curves of  $\Delta r$  against electron/atom ratio, plotted against the valency difference between solute and solvent, for copper, silver and gold alloys.

- (a) Zinc, gallium and germanium in gold.
- (b) Zinc, gallium and germanium in silver.
- (c) Cadmium, indium and tin in silver.
- (d) Zinc, gallium and germanium in copper.
- (e) Cadmium, indium and tin in gold.

curves of  $\Delta r$  against electron/atom ratio are plotted against the difference in valency between the solute and solvent. Where the solute is in the same period as the solvent,

$$\Delta r/(e-1) \propto (V_{\text{solute}} - V_{\text{solvent}}),$$

but where the solute is in a period different from that of the solvent,

$$\Delta r/(e-1) \propto (V_{\text{solute}} - V_{\text{solvent}} + C),$$

where the constant  $C$  depends upon the difference in the periods of the component metals, and hence on the difference between the electronic structures of the respective ions. This indicates that the extra charge introduced by the solute atom is not the only factor involved in the valency contribution to the change in lattice spacing. It may particularly be noted that zinc in copper and cadmium in silver give rise to the same percentage valency contribution ( $100 \Delta r/r_{\text{solvent}}$ ) to the change in lattice spacing for a given increase in electron/atom ratio; the same behaviour is shown by germanium in copper and tin in silver.

The above relationship for alloys in which both solute and solvent belong to the same period implies that the valency contribution per unit increase in atomic composition  $\propto (V_{\text{solute}} - V_{\text{solvent}})^2$ , and thus takes the same form as the increase in electrical resistance brought about by 1 atomic % of a solute of the same period as the solvent.<sup>17</sup> The field

<sup>17</sup> Linde, *Ann. Physik.*, 1932, **15**, 219.

of the extra charge causes the electron scattering which gives rise to the increased resistance.

Regularity is lost for the electronegative solutes of Group V, which tend in general to give rise to a relative contraction of the lattice; similarly, where the solute is highly electropositive (e.g. silver-magnesium) the electrochemical effect leads to a tendency towards lattice contraction, which may overcompensate for the valency contribution to give a negative  $\Delta r$  value.

Little regularity is shown for the curves of valency contribution against electron/atom ratio for the magnesium and aluminium alloys which may be studied. It is, however, generally confirmed that positive values of the valency contribution are produced by solutes of valency greater than that of the solvent, while negative valency contributions are given by solutes of valency less than that of the solvent.

This research forms part of a general programme under the general supervision of Prof. D. Hanson, to whom the author's thanks are due for his interest and encouragement. The author must also express his gratitude to the Department of Scientific and Industrial Research, the Royal Society, the Chemical Society, and Imperial Chemical Industries Ltd., for financial contributions to the general programme.

*Department of Metallurgy,  
The University,  
Edgbaston,  
Birmingham, 15.*

---

## REVIEW OF BOOK

**Journal of the Electrodepositors' Technical Society, Vol. XXII, 1946-1947.** (The Society, at 27 Islington High Street, London, N.1.) Pp. 268. Price to non-members, 42s.

The new volume of this publication follows the same lines as its predecessors and a wide range of topics is presented. Of the papers devoted to specific depositions, nickel comes in for special attention, and the paper by G. E. Gardam on "Smoothing Action as a Mechanism in Bright Nickel Plating" is of particular interest. Four papers are devoted to the analysis of plating baths, and it is pleasing to note that two of these are concerned with the analysis of chromium plating baths by means of a photoelectric absorptiometer; it will be interesting to see to what extent these more rapid methods are adopted and whether their use results in a greater degree of control of the composition of plating baths.

Included amongst the more general papers are a review on the metallizing of glass and plastics and an article by A. W. Wallbank on "Electroplating Shop Costing" which represents the most comprehensive scheme yet devised and clearly merits thoughtful attention from industrial readers. A paper by N. A. Tope on "Factors Affecting the Distribution of Electrodeposits" once more focusses attention on current distribution, a problem encountered in all electrolytic work, but one that has largely been ignored or neglected by all except practical platers.

This volume marks the twenty-first anniversary of the Society, and the Society is to be congratulated on its coming-of-age and on the very important work that it has carried out over the last 21 years.

J. F. H.

# THE SLOW OXIDATION OF 2-METHYL PENTANE

BY C. F. CULLIS

*Received 24th September, 1948*

A study of the slow oxidation of 2-methyl pentane shows that, while the kinetics of the reaction are superficially similar to that involving normal paraffins, the yields of peroxides and aldehydes are lower, and that small quantities of ketones are also present. Ketones may arise from the breakdown of tertiary peroxides, which are probably formed in addition to primary and secondary compounds. In spite of the stability to oxidation of the ketones when formed, the yields obtained are low, which suggests that tertiary peroxide formation is relatively small. This indicates that attack at the CH group in this hydrocarbon is not important compared with attack at CH<sub>3</sub>.

In an earlier paper,<sup>1</sup> an account was given of the influence of structure on the ease of oxidation of some straight-chain and branched-chain paraffins. In addition, the kinetics of the oxidation of both *n*-hexane and *n*-pentane were examined in some detail and found to have certain well-defined characteristics. Mulcahy,<sup>2</sup> who studied the oxidation of *n*-butane, found that this compound behaved in a closely similar fashion.

It was thought desirable to examine in more detail the kinetics of the oxidation of a branched-chain paraffin to see whether any striking differences in behaviour were to be found. Attention has been directed not to constructing a full theory of hydrocarbon oxidation, but to providing the significant comparisons with the normal compounds previously studied; in particular, the question of ketone formation has been examined. Hitherto, comparatively few studies have been made of the slow oxidation of branched-chain paraffins. Pope, Dykstra and Edgar<sup>3</sup> compared the oxidation characteristics of five isomeric octanes with that of *n*-octane, and reached the conclusion that in general the behaviour of the straight-chain and branched-chain compounds is very similar. Beatty,<sup>4</sup> who studied the slow oxidation of 2:5-dimethyl hexane, detected acetone among the products, whereas ketones are not normally observed with straight-chain paraffins. Day and Pease,<sup>5</sup> who compared the rates of slow oxidation and the ignition temperatures of a number of hydrocarbons, noticed no fundamental difference in behaviour between the normal and *iso*-paraffins. As far as is known, however, no more detailed study of the kinetics of the oxidation of a branched-chain paraffin has yet been made, and in this paper some results are described relating to the slow oxidation of 2-methyl pentane.

## Experimental

The apparatus was of the same type as that used in the previous work,<sup>1</sup> the reaction being followed manometrically and by analysis for intermediate products. The formation not only of peroxides and aldehydes but also of methyl ketones was investigated. Messinger's iodoform method<sup>6</sup> was employed,

<sup>1</sup> Cullis and Hinshelwood, *Faraday Soc. Discussions*, 1947, **2**, 117.

<sup>2</sup> Mulcahy, *ibid.*, 128.

<sup>3</sup> Pope, Dykstra and Edgar, *J. Amer. Chem. Soc.*, 1929, **51**, 2203.

<sup>4</sup> Beatty, *Chem. Rev.*, 1937, **21**, 328.

<sup>5</sup> Day and Pease, *J. Amer. Chem. Soc.*, 1941, **63**, 912.

<sup>6</sup> Messinger, *Ber.*, 1888, **21**, 3366.

aldehydes being first removed by oxidation with silver oxide.<sup>7</sup> It was found in this work that formaldehyde, as well as higher aldehydes, was completely oxidized by the latter reagent, so that its presence does not affect the analysis.

**The Induction Period and the Maximum Oxidation Rate.**—The oxidation of 2-methyl pentane, like that of other hydrocarbons, is preceded by a somewhat variable induction period, after which the reaction accelerates rapidly to its maximum rate. In some cases, a small pressure decrease occurs before the normal pressure increase becomes apparent. In comparing the induction period and maximum oxidation rate with those of *n*-hexane under corresponding conditions (Table I), it is interesting to observe that the induction period varies more on passing from one hydrocarbon to the other than does the reaction rate.

TABLE I

Temperature, 202° C ; Hydrocarbon pressure, 50 mm. ; Oxygen pressure, 200 mm.

	2-Methyl Pentane	<i>n</i> -Hexane	Ratio
Induction period (min.)	23.0	5.0	4.6/1
Maximum rate (mm./min.)	0.455	1.25	1/2.8

The dependence of both these quantities on the initial reactant concentrations is given in Fig. 1 and 2. The reciprocal of the induction period is approximately proportional to oxygen and hydrocarbon pressure over the range

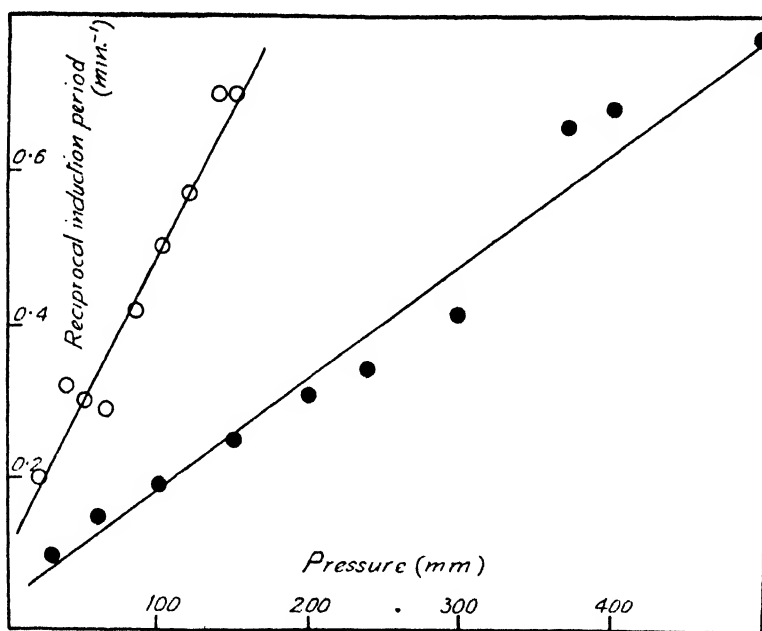


FIG. 1.—The variation of the induction period with the pressure of the reacting gases.

2-methyl pentane, 227° C.

Open circles : hydrocarbon pressure varied, oxygen pressure, 200 mm.

Full circles : oxygen pressure varied, hydrocarbon pressure, 50 mm.

of concentrations studied ; at lower pressures, this quantity must evidently decrease more rapidly, so that the induction period becomes infinite when the concentration of either reactant is reduced to zero. In contrast, the maximum reaction rate increases rather steeply with hydrocarbon concentration but is

<sup>7</sup> Hägglund, *Z. anal. Chem.*, 1914, 53, 433 ; Stepp and Fricke, *Z. Physiol. Chem.*, 1921, 116, 293.

much less dependent on oxygen concentration. These results are analogous to those found for *n*-hexane and *n*-pentane.

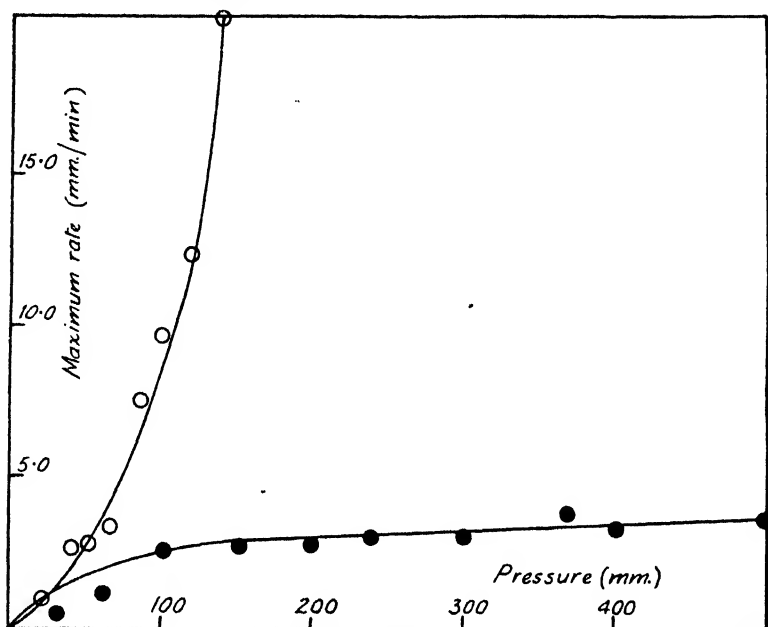


FIG. 2.—The variation of the maximum oxidation rate with the pressure of the reacting gases.

2-methyl pentane, 227° C.

(Open circles : hydrocarbon pressure varied, oxygen pressure, 200 mm.

Full circles : oxygen pressure varied, hydrocarbon pressure, 50 mm.

**Analytical Results.**—Analysis for peroxides and aldehydes showed that much smaller quantities of these substances are formed than in the oxidation of *n*-hexane. Since the amounts of both these intermediates present at any stage are approximately proportional to the rate of pressure increase, it is relevant to compare the relative quantities formed at a standard value of  $p_{\text{max.}} = 1.0$ . These are shown in Table II.

TABLE II

	2-Methyl Pentane	<i>n</i> Hexane
Peroxides (max.) . . .	0.55	2.88
Total aldehydes (max.) . .	1.28	5.55
Formaldehyde (max.) . . .	0.81	2.04

If pressure measurements constitute a reliable criterion of the progress of the reaction, it seems likely that with 2-methyl pentane other intermediates are being formed concurrently with those detected. Tests for methyl ketones showed that these substances are also present, their formation being very small initially but increasing fairly rapidly and reaching a limit when the reaction is complete. Table III shows the concentrations of the various intermediates present at different stages of the reaction. Since the quantities of these intermediate products are exceedingly small, the whole of each sample withdrawn was used for the analysis of one type of product only. Such samples were taken after definite pressure changes had occurred, rather than after fixed time intervals. This procedure was adopted so that the observed variability of the induction period had no influence.

TABLE III.—ANALYSIS OF PRODUCTS FROM OXIDATION OF 2-METHYL PENTANE  
AT 227° C

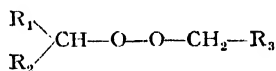
Hydrocarbon pressure, 50 mm.; oxygen pressure, 200 mm.

Pressure Change (mm.)	Peroxides	Formaldehyde	Aldehydes (Total)	Ketones
(All products are expressed in moles $\times 10^{-3}$ per initial mole $O_2$ )				
0.5	1.00	0.43	1.02	0.65
1.0	1.27	—	—	—
2.5	—	1.10	—	—
3.0	1.14	—	2.02	0.70
4.5	1.30	—	—	—
6.0	—	—	2.43	—
8.0	1.27	—	—	—
8.5	—	1.43	2.85	—
10.0	—	—	—	1.20
11.0	0.90	—	—	—
12.0	—	1.52	—	—
12.5	—	—	2.65	—
13.5	1.19	—	—	2.30
16.0	—	1.85	—	—
16.5	—	—	—	1.97
17.0	0.86	—	3.25	—
18.0	—	—	—	2.05
19.5	—	—	—	2.82
21.0	—	—	2.85	—
22.0	—	1.90	—	—
23.0	0.48	—	—	—
23.5	—	—	—	3.22
26.0	—	—	3.24	—
27.0	0.05	1.56	—	3.45
29.0 ( $\infty$ reading)	—	1.25	2.95	4.10

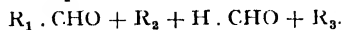
### Discussion

The general similarity of the kinetics of the oxidation of 2-methyl pentane suggests that the mechanism of the reaction is closely analogous to that occurring in the combustion of straight-chain paraffins, though some differences undoubtedly exist in the analytical results.

It was previously suggested<sup>1</sup> that an important step in hydrocarbon oxidation is the breakdown of intermediate peroxides, whose decomposition results in the production of aldehydes, e.g.



would give



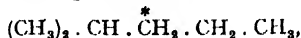
In the same way, ketones might be formed from tertiary peroxides; for there is considerable evidence that the breakdown of such compounds consists in the splitting of the O-O bond, followed by decomposition of the resulting radicals to give mainly ketones and saturated hydrocarbons.<sup>8</sup> Tertiary peroxides are, however, comparatively unreactive; thus, according to Milas and Surgenor,<sup>9</sup> di-*tert.*-butyl peroxide is unaffected even by concentrated hydriodic acid. The probable failure of such

<sup>8</sup> George and Walsh, *Trans. Faraday Soc.*, 1946, **42**, 94; Milas and Surgenor, *J. Amer. Chem. Soc.*, 1946, **68**, 205, 643, 1938; Raley, Rust and Vaughan, *ibid.*, 1948, **70**, 88.

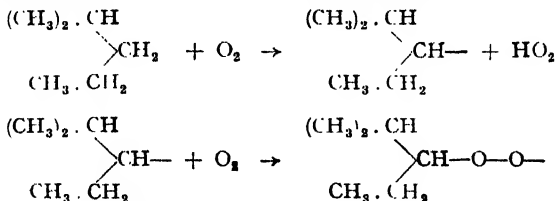
<sup>9</sup> Milas and Surgenor, *J. Amer. Chem. Soc.*, 1946, **68**, 205.

compounds to respond to the methods of analysis employed may partly account for the apparently low yield of peroxides.†

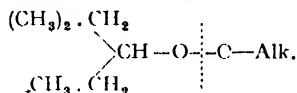
The formation of appreciable quantities of tertiary peroxides in the oxidation of 2-methyl pentane would be somewhat difficult to understand, for the most probable point of attack in the molecule,



is now thought to be that indicated by the asterisk.<sup>11</sup> The reaction with oxygen might therefore be initiated in the following way :

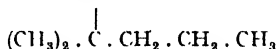


the latter radical resulting in the formation of a peroxide of the type,



On decomposing, the left-hand portion of the molecule would yield an aldehyde and a free radical but no ketone.

An essential feature of the reaction scheme previously proposed was the interaction of small alkyl radicals with fresh hydrocarbon molecules and the consequent regeneration of alkyl radicals of high carbon content. The work of Rice<sup>12</sup> has shown that in the reaction between hydrocarbons and alkyl radicals a tertiary carbon atom is the most likely point of attack, so that the radical produced would in this case probably be



and would ultimately form a peroxide containing a tertiary alkyl group. The formation of ketones would be only very small in the initial stages of the reaction, but would increase as the interaction of alkyl radicals with hydrocarbon molecules becomes appreciable.

Although comparison of the amounts of products formed shows that ketones are present in somewhat greater concentration than aldehydes at the end of the reaction, it must be remembered that ketones are relatively resistant to further attack by oxygen, whereas aldehydes are rapidly oxidized under the existing experimental conditions. The quantity of ketones finally present thus represents the total concentration produced during the entire course of the reaction, and amounts to only 3.3 % of the products formed ; the rate of ketone production, compared with that of aldehydes, is clearly small.

If ketones were produced in stoichiometrically considerable quantities, their formation might be an important factor contributing to a low apparent ease of combustion of branched paraffins, for effective oxidation might practically cease at this early stage. The absolute amounts present (corresponding to 2.5 mm. Hg in the reaction vessel when the rate is a

† The smaller amounts of aldehydes encountered would be expected to be accompanied by a lower yield of peroxides, for some of the peroxides present are undoubtedly aldehyde peroxides. In the oxidation of *n*-hexane, alkyl peroxides and aldehyde peroxides are present in approximately equal quantities.<sup>10</sup>

<sup>10</sup> Cullis (unpublished work).

<sup>11</sup> Cullis, Hinshelwood and Mulcahy, *Proc. Roy. Soc. A*, 1949, **196**, 160.

<sup>12</sup> Rice, *The Aliphatic Free Radicals* (Johns Hopkins, 1935).



maximum) are, however, so small that their formation is evidently unimportant in this respect. The low yields of ketones (and therefore probably of tertiary peroxides) suggest that attack at a  $\text{CH}_3$  group in 2-methyl pentane remains the general rule, but that for the reasons stated above attack may occasionally occur at CH.

The author would like to thank Prof. Sir Cyril Hinshelwood for much helpful discussion and advice, and Mr. F. J. Stubbs for considerable assistance with the analysis for ketones.

*Physical Chemistry Laboratory,  
South Parks Road,  
Oxford.*

## A PROPOSED SIMPLIFICATION IN THE PROCEDURE FOR COMPUTING ELECTRIC DIPOLE MOMENTS

BY E. A. GUGGENHEIM

*Received 8th November, 1948*

The usual procedure for computing the electric dipole moment of a polar solute in a non-polar solvent from Debye's formulae is unnecessarily complicated. A simpler method is described which incidentally eliminates the need of measuring densities accurately.

**1. Introduction.**—It is the object of this paper to show that the usual procedure for computing the electric dipole moment of a polar solute in a non-polar solvent from Debye's formulae is unnecessarily complicated. A simpler method is described which incidentally eliminates the need of measuring densities accurately.

**2. Notation.**—The following notation will be used :

- $d$  Density,
- $x$  Mole fraction of solute,
- $C$  Concentration of solute expressed as moles/volume,
- $\bar{V}$  Mean molar volume,
- $V_1$  Partial molar volume of solvent,
- $V_2$  Partial molar volume of solute.

The above quantities are identically related by

$$\bar{V} = (1 - x)V_1 + xV_2 = V_1 + x(V_2 - V_1), \quad (2.1)$$

$$C = x/\bar{V}. \quad (2.2)$$

Further,

- $\epsilon$  Dielectric constant of solution,
- $\epsilon_0$  Dielectric constant of pure solvent,
- $n$  Refractive index of solution,
- $n_0$  Refractive index of pure solvent,
- $\Delta \equiv (\epsilon - \epsilon_0) - (n^2 - n_0^2).$

Finally,

- $\gamma_e$  Electronic contribution to polarizability of solute molecule,
- $\gamma_a$  Atomic contribution to polarizability of solute molecule,
- $\mu$  Electric dipole moment of solute molecule,
- $k$  Boltzmann's constant,
- $N$  Avogadro's number.

**3. Debye's Formulae.**—We consider a solution of a polar solute 2 in a non-polar solvent 1 at a temperature  $T$ . Provided the solution is sufficiently dilute for mutual interaction between solute molecules to be negligible,  $V_1$  and  $V_2$  are constants. Debye<sup>1</sup> has shown that, subject to certain assumptions or approximations which we do not need to discuss here, the electric moment  $\mu$  of the solute molecule can then be derived from the pair of formulae,

$$\frac{\epsilon - 1}{\epsilon + 2} \bar{V} = \frac{\epsilon_0 - 1}{\epsilon_0 + 2} V_1(1 - x) + \frac{4\pi N}{3} \left( \gamma_s + \gamma_a + \frac{\mu^2}{3kT} \right) x, \quad (3.1)$$

$$\frac{n^2 - 1}{n^2 + 2} \bar{V} = \frac{n_0^2 - 1}{n_0^2 + 2} V_1(1 - x) + \frac{4\pi N}{3} \gamma_s x. \quad (3.2)$$

These formulae are the basis of the determination of  $\mu$  from measurements of  $\epsilon$  and  $n$ . Their derivation and foundation are admittedly open to criticism.<sup>2</sup> It is, however, the sole object of the present paper to consider the best way to use these formulae, not to criticize their derivation.

**4. Transformation of Formulae.**—There is no need to devote space to describing the usual well-known procedure for deriving a value of  $\mu$  from formulae (3.1) and (3.2). I shall rather straightway describe the alternative procedure which I recommend. I wish to emphasize here that this section contains nothing but elementary algebra. No new physical assumptions are made before § 7.

We begin by subtracting (3.2) from (3.1) obtaining

$$\left\{ \frac{\epsilon - 1}{\epsilon + 2} - \frac{n^2 - 1}{n^2 + 2} \right\} \bar{V} = \left\{ \frac{\epsilon_0 - 1}{\epsilon_0 + 2} - \frac{n_0^2 - 1}{n_0^2 + 2} \right\} V_1(1 - x) + \frac{4\pi N}{3} \left\{ \gamma_a + \frac{\mu^2}{3kT} \right\} x. \quad (4.1)$$

If there were no atomic contribution to the polarizability of either solvent or solute molecules, we should have  $\epsilon_0 = n_0^2$  and  $\gamma_a = 0$ , so that (4.1) would reduce to

$$\left\{ \frac{\epsilon - 1}{\epsilon + 2} - \frac{n^2 - 1}{n^2 + 2} \right\} \bar{V} = \frac{4\pi N}{3} \frac{\mu^2}{3kT} x, \quad (4.2)$$

or when we use (2.2)

$$\frac{\epsilon - 1}{\epsilon + 2} - \frac{n^2 - 1}{n^2 + 2} = \frac{4\pi N \mu^2}{9kT} C. \quad (4.3)$$

According to (4.3) if the experimental quantity

$$\frac{\epsilon - 1}{\epsilon + 2} - \frac{n^2 - 1}{n^2 + 2} \equiv \frac{3(\epsilon - n^2)}{(\epsilon + 2)(n^2 + 2)} \quad (4.4)$$

were plotted against  $C$  one should obtain a straight line through the origin having a slope equal to

$$\frac{4\pi N \mu^2}{9kT}. \quad (4.5)$$

Owing to the atomic polarizability of the solvent,  $\epsilon_0$  is not equal to  $n_0^2$  and so we have the more complicated relation (4.1) instead of (4.3). I shall now show that even when we take account of atomic polarizability, formula (4.1) can be transformed to a form almost as simple as (4.3).

I begin by defining for convenience a fictitious atomic polarizability  $\gamma'_a$  of the solute according to which the polarizabilities of solute and solvent would be in the ratio of their molar volumes. This definition of  $\gamma'_a$  can be expressed by the equation,

$$\frac{4\pi N}{3} \gamma'_a = \left\{ \frac{\epsilon_0 - 1}{\epsilon_0 + 2} - \frac{n_0^2 - 1}{n_0^2 + 2} \right\} \frac{V_2}{V_1}, \quad (4.6)$$

so that  $\gamma'_a$  is completely defined in terms of the experimental quantities  $\epsilon_0$ ,  $n_0$ ,  $V_1$ ,  $V_2$ .

<sup>1</sup> Debye, *Polar Molecules* (1929), § 11.

<sup>2</sup> See Onsager, *J. Amer. Chem. Soc.*, 1936, **58**, 1486.

When we substitute (4.6) into (4.1) using (2.1), we obtain

$$\left\{ \frac{\epsilon - 1}{\epsilon + 2} - \frac{n^2 - 1}{n^2 + 2} \right\} \bar{V} = \left\{ \frac{\epsilon_0 - 1}{\epsilon_0 + 2} - \frac{n_0^2 - 1}{n_0^2 + 2} \right\} \bar{V} + \frac{4\pi N}{3} \left\{ \gamma_a - \gamma'_a + \frac{\mu^2}{3kT} \right\} x. \quad (4.7)$$

Now, dividing (4.7) by  $\bar{V}$  and using (2.2) we obtain

$$\left\{ \frac{\epsilon - 1}{\epsilon + 2} - \frac{n^2 - 1}{n^2 + 2} \right\} = \left\{ \frac{\epsilon_0 - 1}{\epsilon_0 + 2} - \frac{n_0^2 - 1}{n_0^2 + 2} \right\} + \frac{4\pi N}{3} \left\{ \gamma_a - \gamma'_a + \frac{\mu^2}{3kT} \right\} C. \quad (4.8)$$

According to (4.8) if the experimental quantity

$$\frac{\epsilon - 1}{\epsilon + 2} - \frac{n^2 - 1}{n^2 + 2} \equiv \frac{3(\epsilon - n^2)}{(\epsilon + 2)(n^2 + 2)} \quad (4.9)$$

is plotted against  $C$  the curve has an initial height

$$\frac{3(\epsilon_0 - n_0^2)}{(\epsilon_0 + 2)(n_0^2 + 2)} \quad (4.10)$$

equal to  $4\pi N/3$  times the atomic contribution to the polarizability of the solvent molecule, and an initial slope

$$\frac{4\pi N}{3} \left\{ \gamma_a - \gamma'_a + \frac{\mu^2}{3kT} \right\}. \quad (4.11)$$

Incidentally this curve should be a straight line over the range of concentrations where the assumptions underlying Debye's formulae (3.1) and (3.2) are accurate.

**5. Further Simplification.**—We have seen that, when the experimental quantity (4.9) is plotted against  $C$ , the initial slope is (4.11). Since it is only this initial slope that is of interest, the procedure can be further simplified as follows.

If instead of (4.9), we plotted

$$\frac{3(\epsilon - n^2)}{(\epsilon_0 + 2)(n_0^2 + 2)} \quad (5.1)$$

against  $C$  we should, of course, obtain a different curve, but the initial height would be unchanged and the initial slope almost unaffected \* because  $\epsilon$  and  $n^2$  are at least roughly linear in  $C$  while  $\epsilon - n^2$  is roughly proportional to  $C$ .

We are thus led to the following strikingly simple procedure. We plot the experimental quantity  $\epsilon - n^2$  against  $C$  obtaining a curve having an initial height  $\epsilon_0 - n_0^2$  and an initial slope,

$$\frac{(\epsilon_0 + 2)(n_0^2 + 2)}{3} \frac{4\pi N}{3} \left\{ \gamma_a - \gamma'_a + \frac{\mu^2}{3kT} \right\}. \quad (5.2)$$

**6. Values of  $\epsilon_0$  and  $n_0^2$ .**—Whether we use the procedure just described or the usual procedure or any other procedure, the question

\* *Note added in Proof.*—As a result of comments made to me privately by Dr. J. W. Smith, to whom I am most grateful, I realize that this statement calls for amplification as follows. When we plot (5.1), instead of (4.9), against  $C$  the initial slope becomes

$$\frac{1}{(\epsilon_0 + 2)(n_0^2 + 2)} \left\{ \frac{\partial \epsilon}{\partial C} \left( 1 - \frac{\epsilon_0 - n_0^2}{\epsilon_0 + 2} \right) - \frac{\partial n^2}{\partial C} \left( 1 - \frac{\epsilon_0 - n_0^2}{n_0^2 + 2} \right) \right\}.$$

Thus the procedure described in the text implies neglecting the terms containing  $(\epsilon_0 - n_0^2)/(\epsilon_0 + 2)$  and  $(\epsilon_0 - n_0^2)/(n_0^2 + 2)$ . Of these the former is for polar solutes overwhelmingly more important than the latter. Typical values of the neglected factor are:

$$\text{Benzene :} \quad \frac{\epsilon_0 - n_0^2}{\epsilon_0 + 2} = \frac{2.2727 - 2.2580}{4.2727} = 0.0035.$$

$$\text{Carbon tetrachloride :} \quad \frac{\epsilon_0 - n_0^2}{\epsilon_0 + 2} = \frac{2.2277 - 2.1565}{4.2277} = 0.017$$

arises whether it is better to assign to  $\epsilon_0$  and  $n_0^2$  directly measured values or values obtained by smooth extrapolation of measured values of  $\epsilon$  and  $n^2$ .

This question can be controversial, but the following comments seem appropriate :—

(a) The wider the range of concentrations covered by the experimental data, the stronger the case for using extrapolated values of  $\epsilon_0$  and  $n_0^2$ . Conversely if the experimental data cover only a short range of concentrations, then the measured values of  $\epsilon_0$  and  $n_0^2$  are safer than extrapolated values.

(b) If the experimental data are good, the choice between the two alternatives will make little difference to the value obtained for  $\mu$ .

(c) This question is not directly related to our theme, namely, the comparison between the new procedure and the usual one for calculating  $\mu$ .

(d) In the numerical examples in § 8, I shall use the same values of  $\epsilon_0$  and  $n_0^2$  as were used by the experimenters in their calculations by the usual procedure. Any other choice would introduce a personal element which I prefer to avoid.

**7. Atomic Polarizability.**—In § 5 we saw that when  $\epsilon - n^2$  is plotted against  $C$  the initial slope is equal to the expression (5.2). We thus obtain an unambiguous value for

$$\gamma_a = \gamma'_a + \frac{\mu^2}{3kT} \quad (7.1)$$

without having made any physical assumptions or approximations beyond those inherent in Debye's formulae (3.1) and (3.2). It is to be recalled that  $\gamma'_a$  is also defined unambiguously in terms of experimental quantities. Hence  $\mu$  would be completely determined were it not for uncertainty of the value of  $\gamma_a$ .

We are thus left with the question what to do about  $\gamma_a$ . Before considering the best possible answer, I would point out that this question is equally present whether the usual method of calculating  $\mu$  is used or that recommended here. In fact every procedure contains an assumption either explicit or implicit concerning  $\gamma_a$ .

For non-polar substances by definition  $\mu$  is zero and so experiment determines  $\gamma_a$  and  $\gamma_e$ . It is found<sup>3</sup> that  $\gamma_a$  is nearly always less than one-tenth of  $\gamma_e$ , often about one-twentieth and sometimes less. For polar molecules quantitative information concerning  $\gamma_a$  is scanty, but there is no reason to suppose that it is greater in polar molecules than in similar non-polar ones. For polar solute molecules, at least those having  $\mu$  greater than one debye,  $\gamma_e$  is itself usually small compared with  $\mu^2/3kT$  and so *a fortiori*  $\gamma_a$  is likely to be small compared with  $\mu^2/3kT$ . Hence an accurate estimate of  $\gamma_a$  is not needed.

Under these circumstances the most sensible thing to do is to make the simplest assumption concerning  $\gamma_a$ , provided the assumption is reasonable and consistent with the scanty available experimental data. An assumption which will usually, if not always, fulfil these requirements is

$$\gamma_a = \gamma'_a \quad (7.2)$$

This assumption implies that in general  $\gamma_a$  is greater for big molecules than small ones; there is some experimental evidence<sup>3</sup> for this.

I accordingly recommend the use of (7.2) in the absence of better information concerning  $\gamma_a$ . But if anyone thinks he has a better estimate of  $\gamma_a$ , such as a specified fraction of  $\gamma_e$ , let him use this estimate in (7.1).

If we accept the approximation (7.2), then the procedure recommended reduces to the following: plot  $\epsilon - n^2$  against  $C$  and the initial slope is

$$\frac{(\epsilon_0 + 2)(n_0^2 + 2)}{3} \frac{3\pi N}{3} \frac{\mu^2}{3kT} \quad (7.3)$$

<sup>3</sup> See Sugden, *Trans. Faraday Soc.*, 1934, **30**, 739.

in which every quantity apart from  $\mu$  is known. Compared with this the usual method of calculation appears unnecessarily, nay ridiculously, complicated.

**8. Experimental Examples.**—There is necessarily some arbitrariness in the selection of experimental data by which to illustrate the recommended method of calculation. The choice is, however, considerably restricted by the fact that we require accurate values of  $\epsilon$  and  $n^2$  for each mixture.

Most experimenters do not publish values of  $n^2$ . Many do not even measure  $n^2$ , but assume that the mixing rule associated with the names Lorenz and Lorentz is valid over the whole range of compositions from pure solvent to pure solute. Experimenters seem to believe that this rule is supported by theory; theorists that it is supported by experiment. Neither belief has any secure foundation. Both theory and experiment indicate that the rule is but a rough approximation. It is certainly no more reliable than the rule of additivity for molar volumes, which, curiously enough, is usually not assumed. In short, for the procedure recommended we require accurate values of  $\epsilon$  and  $n^2$ , but, as we shall see, only rough values of the density.

TABLE I.—DICHLORONAPHTHALENES IN BENZENE AT 25° C

$10^3x$	$d$ g. cm. <sup>-3</sup>	$10^3C$ mole cm. <sup>-3</sup>	$\epsilon$	$n^2$	$\epsilon - n^2$	$\Delta$	$\Delta/10^3C$ cm. <sup>3</sup> mole <sup>-1</sup>
1 : 5-Dichloronaphthalene							
10.398	0.8815	0.1156	2.2809	2.2666	0.0143	-0.0004	—
9.691	0.8810	0.1079	2.2808	2.2659	0.0149	+0.0002	—
5.454	0.8777	0.0608	2.2766	2.2624	0.0142	-0.0005	—
0	—	—	2.2727	2.2580	0.0147	—	—
1 : 8-Dichloronaphthalene							
22.350	0.8912	0.2468	2.5337	2.2764	0.2573	0.2426	0.983
18.215	0.8879	0.2016	2.4803	2.2731	0.2132	0.1985	0.984
9.633	0.8812	0.1072	2.3870	2.2660	0.1210	0.1063	0.992
7.927	0.8798	0.0883	2.3682	2.2646	0.1036	0.0889	1.007
0	—	—	2.2727	2.2580	0.0147	—	0.99
2 : 7-Dichloronaphthalene							
12.554	0.8831	0.1394	2.3212	2.2671	0.0541	0.0394	0.283
11.712	0.8825	0.1301	2.3192	2.2666	0.0526	0.0379	0.291
8.653	0.8803	0.0963	2.3071	2.2645	0.0426	0.0279	0.290
5.546	0.8779	0.0619	2.2948	2.2619	0.0329	0.0182	0.294
0	—	—	2.2727	2.2580	0.0147	—	0.30
1 : 4-Dichloronaphthalene							
13.770	0.8841	0.1528	2.2879	2.2686	0.0193	0.0046	0.030
8.659	0.8802	0.0964	2.2823	2.2650	0.0173	0.0026	0.027
6.439	0.8785	0.0718	2.2797	2.2630	0.0167	0.0020	0.028
0	—	—	2.2727	2.2580	0.0147	—	0.029

Bearing these requirements in mind, I have selected for illustrative purposes the measurements made by Hampson and Weissberger<sup>4</sup> on the ten isomeric dichloronaphthalenes dissolved in benzene. For the sake of brevity details will be given for only four of these, selected as follows. The 1 : 5 isomer has zero electric moment, and is used rather to obtain evidence concerning the experimental accuracy. The 1 : 8 isomer has been chosen as having the greatest moment, and the 1 : 4

<sup>4</sup> Hampson and Weissberger, *J. Chem. Soc.*, 1936, 393, cf. Weissberger, Sängewald and Hampson, *Trans. Faraday Soc.*, 1934, 30, 891.

isomer the smallest non-zero moment. Finally the 2 : 7 isomer has been included as representative of a moment considerably smaller than the 1 : 8, but greater than the 1 : 4 isomer.

The data are collected in Table I. In order to use c.g.s. units throughout  $C$  is measured in mole  $\text{cm.}^{-3}$ , so that  $10^3 C$  is mole/l. The first and second columns give the published values of the mole fraction  $x$  and the density  $d$  respectively. These were used to calculate the volume concentrations  $C$  shown in the third column. The fourth and fifth columns give the published values of  $\epsilon$  and  $n^2$  respectively. The sixth and seventh columns contain values of  $\epsilon - n^2$  and of the quantity  $\Delta$  defined by

$$\Delta \equiv (\epsilon - n^2) - (\epsilon_0 - n_0^2). \quad (8.1)$$

As already mentioned I use the same values of  $\epsilon_0$  and  $n_0^2$  as the experimenters themselves. The sixth column gives values of  $\Delta/C$ .

The values of  $\Delta$  for the 1 : 5 isomer indicate that the experimental uncertainty is about  $\pm 0.0004$ . The fact that these values of  $\Delta$  are so near to zero is evidence that at least for this isomer  $\gamma_a - \gamma'_a$  is negligible. It therefore seems most reasonable to assume that  $\gamma_a - \gamma'_a$  is also negligible for the other isomers.

In order to eliminate personal judgment, the values of  $\Delta/C$  for  $C = 0$  were obtained for the 1 : 8 and 2 : 7 isomers by fitting a relation of the form,

$$\Delta = aC + bC^2, \quad (a, b \text{ const.}), \quad (8.2)$$

by least squares and taking  $a$  as the required limiting value of  $\Delta/C$ .

In the case of the 1 : 4 isomer owing to the smaller values of  $\Delta$  the relative experimental error is too great to warrant similar treatment. A relation of the simpler form,

$$\Delta = aC, \quad (a \text{ const.}) \quad (8.3)$$

was accordingly assumed and  $a$  was determined by least squares.

In view of the experimental uncertainty  $\pm 0.0004$  in  $\Delta$  revealed by the data on the 1 : 5 isomer, these extrapolations are as good as warranted by the experimental accuracy.

It is moreover clear that nothing is gained by having a higher accuracy in  $C$  than in  $\Delta$ . Consequently an accuracy of 0.1 % in  $x$  and in  $d$  is more than adequate in most cases. The customary measurements of  $d$  to ten times this accuracy become works of supererogation.

The extrapolated values of  $\Delta/C$  have been used to calculate the electric moments  $\mu$ . The computations are collected in Table II. The first

TABLE II.—DICHLORONAPHTHALENES IN BENZENE AT 25°C

ISOMER	1 : 8	2 : 7	1 : 4
$\frac{\Delta}{10^3 C} / \text{cm.}^3$	1.00	0.295	0.028
$\frac{\Delta}{C} \frac{3}{(\epsilon_0 + 2)(n_0^2 + 2)} / \text{cm.}^3$	1.03	49.5	4.8
${}_0P_2 / \text{cm.}^3$ , (H. and W.)	164.8	48.4	4.8
$\mu / \text{debye}$	2.82	1.56	0.48

line specifies the isomer and the second shows the values of  $\Delta/C$  extrapolated to  $C = 0$ . Multiplication by  $3/(\epsilon_0 + 2)(n_0^2 + 2)$  gives the quantity in the third line of the Table. This quantity is related to the electric moment  $\mu$  by

$$\left( \frac{\mu}{\text{debye}} \right)^2 = \frac{10^{38}}{N} \frac{9kT}{4\pi} \frac{3}{(\epsilon_0 + 2)(n_0^2 + 2)} \frac{\Delta}{C} \quad (8.4)$$

from which we see that it takes the place of the quantity usually denoted by  ${}_0P_2$ . The fourth line of the Table gives for comparison the values  ${}_0P_2$  published by Hampson and Weissberger.<sup>3</sup> We see that the calculations agree within the accuracy of extrapolation.

For the sake of completeness, values of  $\mu$  are given in the last line of the Table. If these differ slightly (less than 1 %) from the values computed by Hampson and Weissberger, this is partly due to uncertainty of extrapolation and partly to the use of more recent values of the universal constants  $N$  and  $k$ .

**9. Conclusion.**—The example of the preceding section shows that we can obtain the same answer by a considerably simpler calculation than the usual one. To guard against the possible objection that I have disregarded the computation of  $C$  from  $x$  and  $d$ , I would point out that this computation was necessitated entirely by the form in which the data were published. Whatever the method by which the mixtures are made up, it is no more trouble to compute  $C$  than to compute  $x$ . Since, moreover, in the recommended method  $C$  is required to an accuracy of at most 0.1 %, there is in fact further economy of effort.

*Chemistry Department,  
Reading University.*

## THE ANODIC OXIDATION OF PLATINUM

BY SIMON ALTMANN AND R. H. BUSCH

*Received 29th November, 1948*

Platinum electrodes were oxidized by means of an "undulant" current. It was found by chemical analysis that the product was practically pure  $\text{PtO}_2 \cdot n\text{H}_2\text{O}$ ; this was deposited in the anodic compartment (using 1 % sulphuric acid as electrolyte) at a rate of 0.025 g./hr. Details of optimum conditions are given.

A tentative theoretical explanation is offered which combines Ershler's theory of the passivity of platinum with the dispersion of the double layer capacity with A.C. frequency as found by Dolin and Ershler: A.C. diminishes the double layer capacity thereby increasing the potential drop to a value permitting the dissolution of the ion.

Early observations on the behaviour of platinum anodes during D.C. electrolysis are not conclusive.<sup>1</sup> Experiments by Marie<sup>2</sup> and Senter<sup>3</sup> indicated a gentle attack of the anode, and the production of a compound which the former assumed to be a peroxide. A detailed analysis of this product was not possible on account of the small quantity available. Massing and Laue<sup>4</sup> assumed it to be  $\text{PtO}_3$ . Alternating current electrolysis with platinum anodes has been studied by Drechsel,<sup>5</sup> Gerdes,<sup>6</sup> Brochet and Petit,<sup>7</sup> Ruer<sup>8</sup> and Marsh.<sup>9</sup>

<sup>1</sup> See Gmelins' *Handbuch der anorganischen Chemie*, 8th ed., 68C, p. 34 and 68B, p. 225.

<sup>2</sup> Marie, *Compt. rend.*, 1907, **145**, 117.

<sup>3</sup> Senter, *Trans. Faraday Soc.*, 1907, **2**, 142.

<sup>4</sup> Massing and Laue, *Z. physik. Chem. A*, 1937, **178**, 1.

<sup>5</sup> Drechsel, *J. prakt. Chem.*, 1879, **20**, 378; 1880, **22**, 476; 1884, **29**, 229.

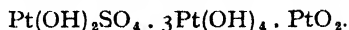
<sup>6</sup> Gerdes, *ibid.*, 1882, **26**, 257.

<sup>7</sup> Brochet and Petit, *Ann. Chim. Phys.*, 1904, (8), **3**, 433.

<sup>8</sup> Ruer, *Z. physik. Chem.*, 1903, **44**, 81.

<sup>9</sup> Marsh, *Proc. Roy. Soc. A*, 1920, **97**, 124. See also Marsh and Evans, *ibid.*, 1923, **102**, 328.

Margules<sup>10</sup> was the first to point out that platinum electrodes are dissolved under the influence of A.C. superposed on D.C. (undulant current). Ruer<sup>11</sup> studied the process in greater detail; by hydrolysis of the 66 % sulphuric acid solution which was used as electrolyte, he obtained a product the analysis of which suggested the formula



His interpretation of the process was discussed by Brochet and Petit.<sup>12</sup> Stuchlik<sup>13</sup> obtained crystals from the electrolytic solution (sulphuric acid,  $\rho = 1.84$ ), whose formula was  $\text{Pt}(\text{SO}_4)_2 \cdot \text{H}_2\text{O}$ , as found by chemical analysis. Ghosh,<sup>14</sup> Grube and Dulk,<sup>15</sup> Grube and Baumeister,<sup>16</sup> Malquori<sup>17</sup> and others, have made observations on similar processes.

Recently Briner and Yalda<sup>18</sup> observed, under conditions resembling closely those of Ruer, the formation of a brown layer on the electrode, and by chemical analysis found that it contained 4.1-4.2 % sulphur.

Some electrochemical theories, involving the oxidation of platinum electrodes, suggested other lines of investigation. Early studies were concerned with oxygen overpotential.<sup>19</sup> The phenomena which occur when an electrode is changed from a region of anodic potential to that of cathodic potential, were first examined by Bowden,<sup>20</sup> who assumed in explanation the formation of a film of  $\text{PtO}_2$  on the electrode. Butler *et al.*<sup>21</sup> concluded, using an analogous method, that it was a layer of oxygen adsorbed on the surface. On the other hand, Hickling<sup>22</sup> pointed out recently that  $\text{PtO}$  is formed during anodic polarization.

The results quoted above lead to the conclusion that the effect of undulant current on platinum anodes may offer a good means of obtaining more direct evidence concerning the oxidation of the electrode. It seemed necessary to arrive at a clear understanding of the following points: (i) the nature of the primary product formed by the attack of the electrode; (ii) the conditions under which that attack takes place; (iii) the possible theoretical interpretation of the process.

## Experimental

**Procedure.**—A circuit was used differing from the one described by Briner and Hoefler<sup>23</sup> in that the alternating current (from the town supply, 220 V, 50 c./sec.) was obtained from an auto-transformer, which made available a fairly wide range of intensities. In series with it was a lead accumulator, a regulating rheostat, an electrodynamic ammeter, a D.C. ammeter and the electrolytic cell. The total intensity  $i_t$  was read on the first ammeter and the D.C. intensity  $i_c$  obtained from the second. The electrolytic cell was similar to that of Briner and Yalda.<sup>18</sup> A porous vessel separated the anodic compartment.

Preliminary experiments were conducted under the optimum conditions quoted by Briner and Yalda, viz. total intensity 1.5 A, D.C. intensity 1 A, each electrode of 2 sq. cm. available surface, and an electrolyte of sulphuric acid 38 % by weight.

<sup>10</sup> Margules, *Wied. Ann.*, 1898, **65**, 629; 1898, **66**, 540.

<sup>11</sup> Ruer, *loc. cit.*, ref. 8. See also *Z. Elektrochem.*, 1903, **9**, 235; 1905, **11**, 10; 1905, **11**, 661.

<sup>12</sup> Brochet and Petit, *loc. cit.*, ref. 7. See *Z. Elektrochem.*, 1904, **10**, 909.

<sup>13</sup> Stuchlik, *Ber.*, 1904, **37**, 2913.

<sup>14</sup> Ghosh, *J. Amer. Chem. Soc.*, 1915, **37**, 733.

<sup>15</sup> Grube and Dulk, *Z. Elektrochem.*, 1918, **24**, 246.

<sup>16</sup> Grube and Baumeister, *ibid.*, 1924, **30**, 322.

<sup>17</sup> Malquori, *Atti della Reale Acc. Naz. Lincei*, 1924, **33**, 102.

<sup>18</sup> Briner and Yalda, *Helv. chim. Acta*, 1943, **26**, 1829.

<sup>19</sup> Gmelins, *loc. cit.*, ref. 1, 68B.

<sup>20</sup> Bowden, *Proc. Roy. Soc. A*, 1929, **125**, 446.

<sup>21</sup> Butler and Armstrong, *ibid.*, 1932, **137**, 604; Armstrong, Himsworth and Butler, *ibid.*, 1933, **143**, 89; Butler and Drever, *Trans. Faraday Soc.*, 1936, **32**, 427.

<sup>22</sup> Hickling, *ibid.*, 1945, **41**, 333.

<sup>23</sup> Briner and Hoefler, *Helv. chim. Acta*, 1943, **26**, 913.



The product obtained was very soluble in the anolyte, which property made its separation and filtration troublesome. A sintered-glass funnel to which the product adheres strongly was employed. 0.043 g. of the product was obtained in several experiments involving 24 hr. electrolysis. Several techniques tried were unsuccessful in improving the separation and filtration of the product. Later, the experimental conditions were modified by the use of 1 % sulphuric acid (by weight) as anolyte and in this circumstance: (i) the product is almost insoluble; \* (ii) the precipitate is coarse, easier to wash and filter, and does not adhere to the sintered glass. However, the yield was so poor that additional modifications were necessary before obtaining satisfactory results.

Optimum conditions (electrolysis No. 91) were found to be: anode 4 sq. cm. of available surface, d.c. intensity 1 A, total current intensity 2 A. The cell was submerged in an ice-water bath and the cathode had 2 sq. cm. of available surface. The last two factors were not critical. The yield was 0.025 g. of the product per hour of electrolysis (loss of weight of the anode, 0.017 g./hr.).

### Results

The product obtained from electrolysis with 38 % sulphuric acid as anolyte was investigated first. Its great solubility in water, implied by Briner and Yalda, was assigned to the high adsorption of sulphuric acid, thus making the wash liquors sufficiently acid to dissolve it. In fact, after several washings with cold water, dissolution is negligible. It was further washed with hot water until tests for the  $\text{SO}_4^-$  ion were negative. It was found by nephelometry that the sulphate concentration in the product was ca. 2 % (7 % S). The exceedingly high value of Briner and Yalda (4 %) was assigned to the inefficient washing with ethanol. The product was found to be amorphous by X-ray analysis.

TABLE I

Experimental Conditions				Results				Mean Values			Formula (Pt = 1)	
Anode Surface (sq. cm.)	D.C. Intensity (A)	Total Intensity (A)	Temperature (°C)	Pt %	O %	H <sub>2</sub> O %	Total	Pt %	O %	H <sub>2</sub> O %	O	H <sub>2</sub> O
4	2.6-	4.5	10-20°	76.3	12.4	11.3	100.0	76.7	12.4	11.4	1.98	1.62
	2.5			77.2	12.3	11.5	101.0					
4	2.5	4.5	60°	76.6	12.2	10.6	99.4	76.3	12.2	10.8	1.95	1.54
				76.0	12.2	11.1	99.3					
4	1	2	10-20°	75.8	12.5	11.0	99.3	75.8	12.5	11.0	2.01	1.57
1-4.6	0.5-	1.4	10-20°	76.8	12.5	10.5	99.8	76.4	12.5	10.6	1.99	1.51
	1.5			76.0	12.6	10.7	99.3					
4	2-	3.7	10-20°	76.5	12.1	11.1	99.7	76.2	12.2	11.4	1.96	1.62
	2.5			75.8	12.2	11.7	99.7					

Several samples of the product were separated during electrolysis using 1 % sulphuric acid as anolyte under different conditions of current density and temperature. They were washed until a negative  $\text{SO}_4^-$  reaction in the wash-liquors was obtained. The crude product from the electrolysis was almost pure: a sample (0.520 g.) which was washed with 6 l. water and dried, weighed 0.492 g. The samples were dried for 6 hr. at 120°, and analyzed for Pt, O and

\* This remarkable difference as compared with the product first quoted was due, once the analysis was known, to the 38 % sulphuric acid product being an hydrate  $\text{PtO}_2 \cdot n\text{H}_2\text{O}$  ( $n = 3 - 4$ ), soluble in dilute acid. Our product would be  $\text{PtO}_2 \cdot 2\text{H}_2\text{O}$ , which is only sparingly soluble. (See Gmelin, *loc. cit.*, 68, C 1, p. 50).

$\text{H}_2\text{O}$ . The method of analysis used was that of Wöhler<sup>24</sup> with slight modifications.<sup>25</sup> The oxide was decomposed by heat in a current of air-free carbon dioxide. The water evolved was absorbed by phosphorus pentoxide and the volume of oxygen measured in a nitrometer. The usual device of a combustion tube, boat and furnace was replaced by a glass bulb, in which the oxide was weighed and which could be heated first with a microburner and afterwards with a Bunsen burner. The analyses are given in Table I. The product showed no structure under X-ray examination.

Under our experimental conditions our results indicate that the product separating from the anode is  $\text{PtO}_2 \cdot n\text{H}_2\text{O}$ . Temperature and current density have no influence upon its composition. It seems, however, that further experimental work is required to establish the way in which platinum is initially attacked.

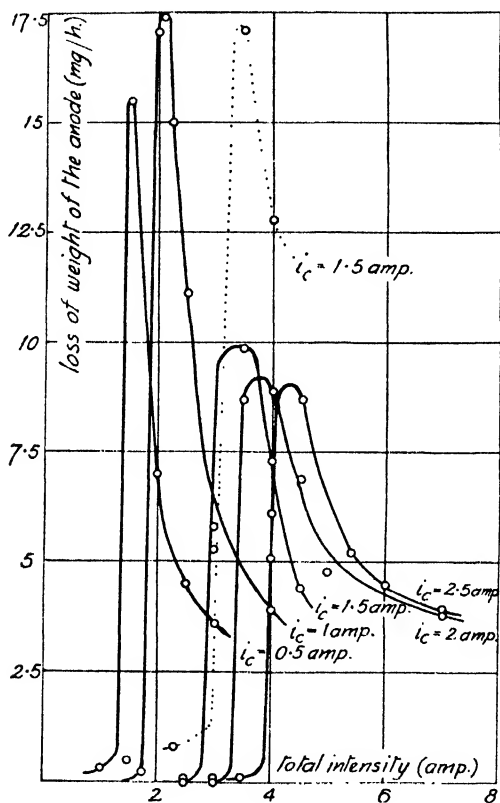


FIG. 1.

**Influence of the Experimental Conditions on the Yield.**—In studying the influence of D.C. and A.C. intensities with an anode of 4 sq. cm. of available surface, the curves of Fig. 1 were obtained, in which the loss of weight of the anode is plotted as a function of total intensity for several D.C. intensities. Their shape agrees with the results of Ruer.<sup>8</sup> Extrapolation of the ascending branches of the curves gives the threshold values of the total intensity  $i_t$  at which the electrode attack starts. Corresponding values of the root mean square intensity  $i_a$  were calculated from

$$i_a = (i_t^2 - i_c^2)^{1/2}$$

where  $i_c$  is the D.C. intensity. Threshold values of  $i_t$  and  $i_a$  were found to vary linearly with  $i_c$ . By the least squares method we obtained:

$$i_a = (0.6 + i_c) \pm 0.1 \text{ A.}$$

This is a more restrictive condition than that pointed out by Briner and Yalda.

<sup>24</sup> Wöhler, *Z. anorg. Chem.*, 1904, 40, 423.

<sup>25</sup> Raskovan and Pena, *Thesis* (Facultad de Ciencias Exactas, Físicas y Naturales, Buenos Aires, 1946). A. E. Cairo, personal communication.

The yield per sq. cm. of the anode depends on its surface. With the same current densities as quoted for electrolysis No. 91, the yields in g./hr. sq. cm., are 0.0009, 0.0043 and 0.0032 for anodes of 6, 4 and 1.88 sq. cm. of total surface respectively. The dotted curve of Fig. 1 corresponds to an anode of 6 sq. cm. ( $i_e = 1.5$  A).

With sulphuric acid 66 % in weight as anolyte, no layer was seen on the anode, and a loss of weight of 0.053 g./hr. was found, the other conditions being the same as for electrolysis No. 91. Varying the temperature from  $20 \pm 5^\circ$  to  $60 \pm 3^\circ$ , the yield decreased from  $8.7 \pm 0.3$  mg./hr. to  $6.4 \pm 0.1$  mg./hr. for an anode of 2 sq. cm. with  $i_e = 2.5$  A and  $i_a = 4.5$  A. It was found that the loss of weight per hour was, independent of the duration of the electrolysis from  $\frac{1}{2}$  to 6 hr.\*

### Discussion

The generally accepted interpretation of the process is that of Ruer :<sup>26</sup> i.e. D.C. causes the formation of a protective layer of an insoluble platinum oxide on the anode. The cathodic component of the A.C. reduces this to a soluble lower oxide.

This theory appears to be open to some criticism since (i) appreciable attack of the anode in conditions in which the product was sparingly soluble was observed and (ii) Ruer's first hypothesis involves a theory of platinum passivity not supported by the experimental facts recently obtained by Ershler.<sup>27</sup> The latter proposes a mechanism of the inhibitory action of oxygen on platinum dissolution in which he assumes that oxygen modifies the electrical field of the double layer and so increases the potential barrier that must be surmounted by the metal atoms that pass into solution. The expression given by Gurney<sup>28</sup> for the work of dissolution of a positive ion is

$$A = Y - W - neV$$

where  $A$  is the work of dissolution,  $Y$  is the work required to detach a positive core from the metal to a vacuum,  $W$  is the energy of hydration,  $V$  the potential of the double layer,  $e$  the charge of the electron and  $n$  the number of positive charges of the ion. The expression shows that diminution of the capacity of the double layer increases the work of dissolution of the metal.

Dolin and Ershler<sup>29</sup> found that the capacity of the platinum electrode diminishes rapidly with increasing A.C. frequency. With N sulphuric acid as electrolyte and 0.1 V polarizing potential, the capacity varied from ca. 1100 to ca. 700 F/sq. cm. as the frequency was increased from 10 to 50 c./sec.

The A.C. platinum depassivation described in this paper can be correlated with Ershler's results. The diminution of the double layer capacity would increase the potential drop in the double layer. Gurney's formula shows then that the work of dissolution of the ion diminishes.

This hypothesis requires that increasing A.C. frequency should increase the platinum dissolution, and in fact, Ruer<sup>30</sup> observed that by varying the speed of the rotary transformer from 2000 to 6000 rev./min. the quantity of platinum dissolved in  $\frac{1}{2}$  hr. varied from 0.0267 g. to 0.0394 g. This fact has not been explained till now. This tentative explanation requires, however, a more detailed elucidation.

*Facultad de Ciencias Exactas, Físicas y Naturales,  
Universidad de Buenos Aires,  
Buenos Aires,  
Argentina.*

\* As a control the cathode was weighed each time. In some cases a slight disintegration of the cathode was observed. After electrolysis the cathode was often covered with platinum black which could be rubbed off. Study of the loss of weight of the cathode showed that (i) it increases with increasing A.C. density and (ii) with constant A.C. density it decreases with increasing D.C. density.

<sup>26</sup> Ruer, ref. 11.

<sup>27</sup> Ershler, *Compt. rend. (Doklady)*, U.R.S.S., 1942, **37**, 226; 1942, **37**, 230; *Acta Physicochim.*, 1944, **19**, 139.

<sup>28</sup> Gurney, *Ions in Solution*, (Cambridge University Press, 1936), p. 83.

<sup>29</sup> Dolin and Ershler, *Acta Physicochim.*, 1940, **13**, 747. See also Rosenthal, Dolin and Ershler, *ibid.*, 1946, **21**, 213.

<sup>30</sup> Ruer, *loc. cit.*, ref. 8.

# THE KINETICS OF THE DEHYDROCHLORINATION OF SUBSTITUTED HYDROCARBONS

## PART IV. THE MECHANISM OF THE THERMAL DECOMPOSITION OF *tert*-BUTYL CHLORIDE

BY D. H. R. BARTON AND P. F. ONYON

Received 17th January, 1949

*tert*-Butyl chloride decomposes by a unimolecular mechanism over the temperature range 290–341° C to give stoichiometrically isobutene and hydrogen chloride. The pertinent first-order rate equation is

$$k = 10^{12.4 \pm 0.2} e^{-(41,400 \pm 600)/RT} \text{ sec.}^{-1}.$$

Reproducible results are only obtained when the reactor walls are coated with a carbonaceous film. With clean walled reactors a faster heterogeneous reaction supersedes the homogeneous decomposition. A general discussion distinguishes two homogeneous mechanisms for thermal dehydrochlorination and relates them to molecular structure.

In Parts II and III of this series<sup>1</sup> the mechanisms of thermal dehydrochlorination of ethyl chloride, 1:1-dichlorethane and 1:2-dichlorethane were established by kinetic measurements. In continuation of this work we have now studied the thermal decomposition of *tert*-butyl chloride. This reaction had already been examined from a similar point of view by Brearley, Kistiakowsky and Stauffer<sup>2</sup> who showed that it was homogeneous and exhibited first-order kinetics. Although it was concluded that the mechanism of the reaction was probably unimolecular, this was not in fact established, for no tests for a radical chain mechanism were applied.

The effect of quartz or glass in promoting the heterogeneous decomposition of organic compounds is well known. In many cases this heterogeneous reaction is replaced by a slower and homogeneous first-order process as the reactor walls become coated with a carbonaceous film.<sup>3</sup> We have noted similar effects with the chlorinated hydrocarbons so far employed in this series. Since it is usually only assumed, without proof, that the initial faster reactions are of a heterogeneous nature it seemed desirable to establish this point conclusively for one compound in our series. This we have now done for *tert*-butyl chloride.

### Experimental

**Materials.**—Technical, *tert*-butyl chloride was purified by the method used previously for other chlorinated hydrocarbons.<sup>1</sup> The following constants were recorded and are compared with the mean of the best literature values (in parentheses).

B.p. 50.6° C corr. (50.7° corr.); from: 51.0°;<sup>4</sup> 50.7°;<sup>5</sup> 50.7°;<sup>6</sup> 50.6°.<sup>7</sup>

<sup>1</sup> Barton and Howlett, *J. Chem. Soc.*, 1949, 155, 165.

<sup>2</sup> Brearley, Kistiakowsky and Stauffer, *J. Amer. Chem. Soc.*, 1936, **58**, 43.

<sup>3</sup> E.g. see Ramsperger and Leermakers, *ibid.*, 1931, **53**, 2067; Schultz and Kistiakowsky, *ibid.*, 1934, **56**, 395; Choppin, *et al.*, *ibid.*, 1939, **61**, 3176.

<sup>4</sup> Timmermans, *Bull. Soc. chim. Belg.*, 1921, **30**, 66.

<sup>5</sup> Norris and Rigby, *J. Amer. Chem. Soc.*, 1932, **54**, 2088.

<sup>6</sup> Timmermans, and Delcourt, *J. Chim. Phys.*, 1934, **31**, 85.

<sup>7</sup> Baker and Smyth, *J. Amer. Chem. Soc.*, 1939, **61**, 2798.

M.p. (sulphur dioxide vapour pressure thermometer),  $-27.85^{\circ}\text{C}$  ( $-26.4^{\circ}$ ); from:  $-28.5^{\circ}$ ; <sup>4</sup>  $-27.1^{\circ}$ ; <sup>8</sup>  $-25.4^{\circ}$ ; <sup>9</sup>  $-24.6^{\circ}$ .<sup>7</sup>  
 $d_{4}^{23^{\circ}}$  0.8375 (0.8401 interpolated); from  $d_{4}^{20^{\circ}}$  0.8457; <sup>10</sup>  $d_{4}^{25^{\circ}}$  0.8370; <sup>5</sup> 0.8347; <sup>11</sup> 0.8376.<sup>13</sup>  
 $n_{\text{D}}^{23^{\circ}}$  1.3835 (1.3837 interpolated); from:  $n_{\text{D}}^{25^{\circ}}$  1.3828; <sup>8</sup>  $n_{\text{D}}^{20^{\circ}}$  1.3839; <sup>13</sup> 1.3847; <sup>7</sup> 1.3853.<sup>14</sup>

**Apparatus.**—The apparatus and technique employed have already been described in detail by Barton and Howlett.<sup>1</sup> Modifications were not found necessary in the present work.

## Results

Brearley, Kistiakowsky and Stauffer<sup>2</sup> experienced difficulty in attaining reproducible results in their study of the *tert.*-butyl chloride decomposition and ascribed this to interference by a heterogeneous reaction at the reactor walls. We have confirmed this difficulty. Our initial experiments were carried out in a Pyrex glass reactor which had been coated by the thermal decomposition of 1:1:1:2-tetrachlorethane vapour, but which had subsequently been exposed to air at room temperature. In this reactor about 20 runs were required before reproducibility of results was attained. Accidental breakage of the spoon gauge and admission of air at the reaction temperature destroyed the effectiveness of the coating. Recoating of the walls was assisted by co-decomposition of *tert.*-butyl chloride with small quantities (*ca.* 10 %) of propylene, but even with this aid about 40 runs were required before the reproducibility of rate constants could be regained.

**Stoichiometry.**—That the reaction studied was the quantitative decomposition of *tert.*-butyl chloride to *isobutene* and hydrogen chloride was established in two ways. Firstly the final pressure in the reactor after many hours was close to twice the initial pressure (Table I). This also showed that the equilibrium

TABLE I

Temp. °K	Initial Pressure $p_0$ (mm.)	Time of Reaction (hr.)	Final Pressure $p_f$ (mm.)	$p_f/p_0$
577.5	105.7	13	212.5	2.01
586.8	120.2	14	243.7	2.03
585.7	167.5	22	330.0	1.97
587.4	119.3	13	237.6	1.99
587.6	97.4	15	199.1	2.04
604.5	127.3	17	257.7	2.02
598.2	133.0	18	261.0	1.96
596.1	114.4	17	228.1	1.99
598.0	122.6	17	244.9	2.00
597.0	96.6	16	191.0	1.99
597.2	92.1	60	176.7	1.92
579.6	116.5	17	235.2	2.02
571.8	105.6	15	216.1	2.05
563.7	116.4	15	230.0	1.98
561.4	108.3	16	216.3	2.00

in the *tert.*-butyl chloride-*isobutene*-HCl system was substantially 100 % on the side of the dissociation products over the temperature range employed. This can, indeed, be calculated from the equilibrium constants recorded by Kistiakowsky and Stauffer<sup>13</sup> for this system. Secondly, the amount of hydrogen chloride formed by the decomposition was given closely by the pressure increase.

<sup>8</sup> Timmermans, *Bull. Soc. chim. Belg.*, 1935, **44**, 17.

<sup>9</sup> Turkevich and Smyth, *J. Amer. Chem. Soc.*, 1940, **62**, 2468.

<sup>10</sup> Vogel, *J. Chem. Soc.*, 1943, 636.

<sup>11</sup> Quayle, Owen and Beavers, *J. Amer. Chem. Soc.*, 1939, **61**, 3107.

<sup>12</sup> Smyth and Dornie, *ibid.*, 1931, **53**, 545.

<sup>13</sup> Kistiakowsky and Stauffer, *ibid.*, 1937, **59**, 165.

<sup>14</sup> Mayo and Dolnick, *ibid.*, 1944, **66**, 985.

This is shown by the data illustrated in Fig. 1, where the line is drawn at the theoretical slope of  $45^\circ$ . Measurements of the pressure increase with time constitute, therefore, a satisfactory method of following the kinetics of the reaction.

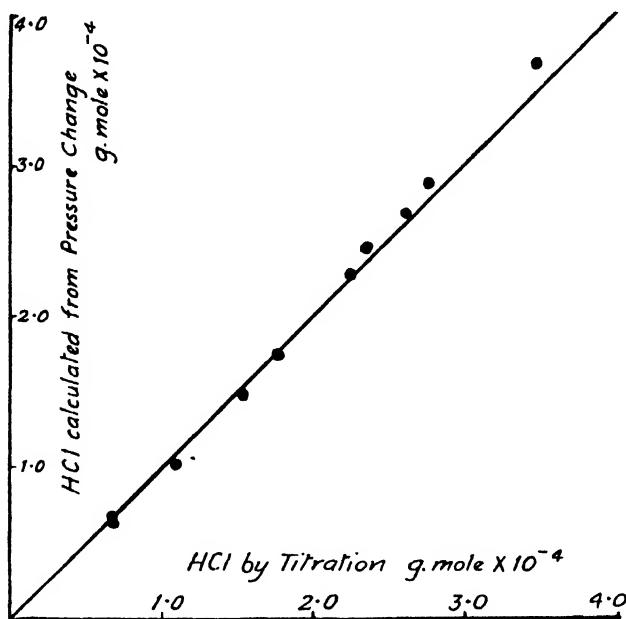


FIG. 1.

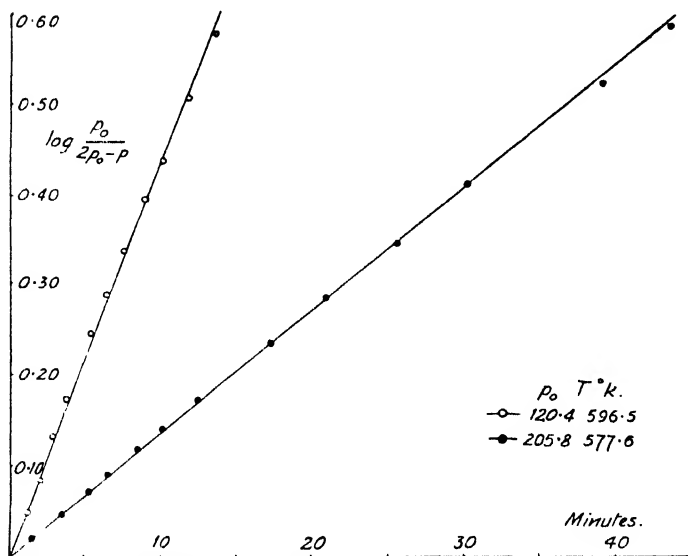


FIG. 2.

**Kinetics.**—In agreement with Brearley, Kistiakowsky and Stauffer,<sup>8</sup> the decomposition followed first-order kinetics. When reproducibility of results had been attained the reaction was first-order to at least 80% decomposition, as illustrated by the typical runs plotted in Fig. 2, but for runs before this the

## 728 DEHYDROCHLORINATION OF HYDROCARBONS

first-order rate tended to fall off at rather lower percentage decompositions. Even at the lowest temperatures studied there was no indication of any induction period, such as was found to be a characteristic feature of the 1:2-dichlorethane decomposition.

As with the chlorinated ethanes examined previously<sup>1</sup> the velocity constants of the *tert.*-butyl chloride decomposition showed no significant variation with initial pressure over the pressure range 40-240 mm. This is illustrated by the data in Table II, obtained at 614° K. The correlation coefficient<sup>16</sup>

$$\frac{\sum(x - \bar{x})(y - \bar{y})}{\sqrt{\sum(x - \bar{x})^2 \times \sum(y - \bar{y})^2}}$$

for the results in this Table was found to be -0.22. The probability of such a value being obtained by chance from 22 expt. is greater than 0.10 and it may, therefore, be concluded that there is no significant correlation.

TABLE II

$p_0$ (mm.)	$k \times 10^3$ (sec. -1)	$p_0$ (mm.)	$k \times 10^3$ (sec. -1)
50.2	4.72	123.7	4.70
52.9	4.24	126.7	4.95
60.6	5.01	130.8	4.85
70.9	4.75	135.7	4.65
82.2	4.61	143.8	4.47
96.5	4.78	143.9	4.54
100.9	4.30	149.1	4.68
103.0	4.70	154.9	4.46
104.4	4.56	178.1	4.62
112.9	4.40	194.1	4.46
119.5	4.67	202.7	4.39

For each set of runs over the temperature range 563-614 K the reproducibility of first-order rate constants was satisfactory. This is shown in the summarized data set out in Table III. At no temperature did the standard deviation of the mean exceed 1.6 % of the mean value.

TABLE III

Temp. (°K)	No. of Runs	Mean Velocity Constant (sec. -1)	% Standard Deviation of the Mean*
563.0	5	$0.22 \times 10^{-3}$	1.2
571.0	7	0.37	1.4
579.5	8	0.61	1.1
587.0	22	0.94	1.0
596.5	9	1.70	1.3
604.0	10	2.64	1.3
607.5	8	3.28	1.6
614.0	24	4.56	1.2

\* Given by  $100 \sqrt{\frac{\sum(x - \bar{x})^2}{n(n-1)}} / \bar{x}$  where the symbols have the obvious significance.

The logarithm of the mean rate constant plotted against the reciprocal of the absolute temperature gave a good straight line (Fig. 3). This line has been drawn by the least squares method giving the proper statistical weight to each point. The corresponding rate equation was found to be

$$k = 10^{12.4 \pm 0.2} e^{-(41,400 \pm 600)/RT} \text{ sec.}^{-1}.$$

The error limits in this equation were fixed as follows. It was assumed that all the error resided in the  $\log_{10} k$  values and none in the temperature measurements. The root mean square of the deviations of the logarithms of the mean

<sup>16</sup> See Fisher, *Statistical Methods for Research Workers* (Oliver and Boyd, 1934).

velocity constants from the least squares line (viz. 0.009) was then applied positively and negatively to the two ends of the least squares line at the extreme temperatures of the experimental range to give the error limits shown. Although this procedure may err in ascribing too high a degree of precision to our

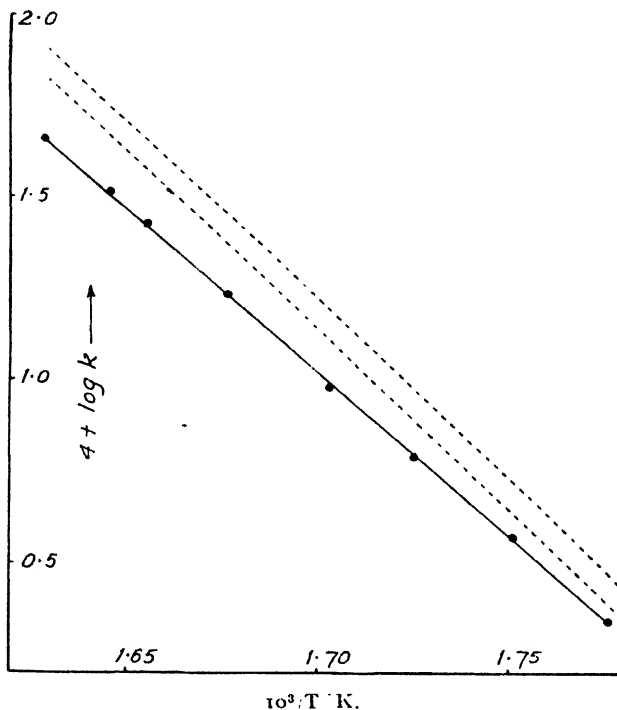


FIG. 3.

measurements, we intend to adopt it as a convenient method for comparing the agreement of our results from paper to paper and have, therefore, described it in detail on this occasion.

**Effect of Propylene.**—In previous parts of this series<sup>1</sup> and elsewhere<sup>18</sup> we have shown that propylene constitutes a powerful inhibitor for the decompositions of chlorinated hydrocarbons which proceed by a chain mechanism. The effect of adding propylene to decomposing *tert.*-butyl chloride was therefore studied. As with ethyl chloride and 1:1-dichlorethane, propylene had no influence on the rate of decomposition. This is illustrated in Fig. 4 where the *tert.*-butyl chloride initial pressures varied from 76 to 206 mm.

TABLE IV \*

Pressure of $Cl_2$ > 100 Initial Pressure of ( $C_2H_5$ ) <sub>2</sub> · CCl	Observed First Order Velocity Constant $k$ (sec. <sup>-1</sup> )	$k$ from Rate Equation (sec. <sup>-1</sup> )
0.82	$0.195 \times 10^{-3}$	} $0.205 \times 10^{-3}$
0.21	0.205	
8.0	Non-linear	
0.70	0.22	
1.66	0.23	

\* All experiments at 562.2° K.

**Effects of Chlorine and Oxygen.**—Small amounts of chlorine and oxygen are powerful inducing agents for the decomposition\* of 1:2-dichlorethane.<sup>21</sup> As the data summarized in Tables IV and V, which refer to chlorine and oxygen



respectively, show, these two elements have no significant effect on the course of the *tert.*-butyl chloride decomposition. For both addenda the kinetics were satisfactorily first order for less than 2 % additions.

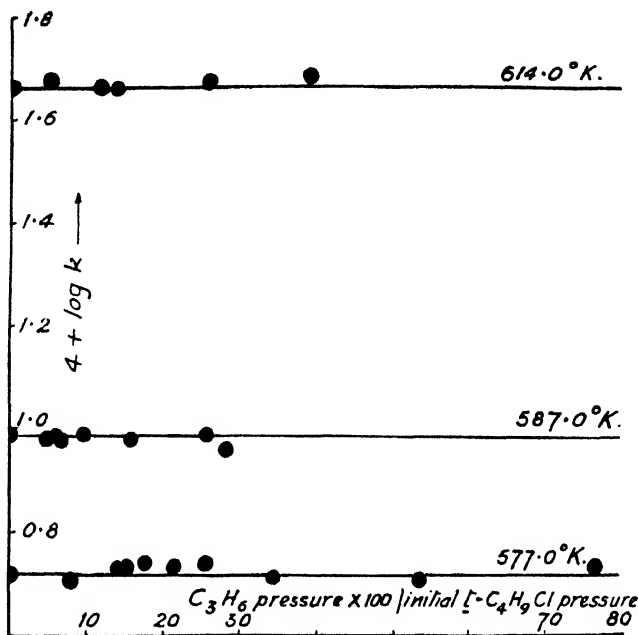


FIG. 4.

#### The Heterogeneous Decomposition of *tert.*-Butyl Chloride on Glass.—

Three series of experiments were carried out in the following reactors; series A, empty Pyrex glass reactor with a surface area to volume ratio of  $2.72 \text{ cm}^{-1}$ ; series B, Pyrex glass reactor packed with Pyrex tubing with a surface area to volume ratio of  $9.98 \text{ cm}^{-1}$ , and series C, Pyrex glass reactor packed with soft

TABLE V

Temp. °K	Pressure of $\text{O}_2 \times 100$ Initial Pressure of $(\text{CH}_3)_3\text{CCl}$	Observed First Order Velocity Constant $k$ ( $\text{sec}^{-1}$ )	$k$ from Rate Equation ( $\text{sec}^{-1}$ )
562.5	0.13	$0.20 \times 10^{-3}$	$0.21 \times 10^{-3}$
562.9	0.28	0.23	} 0.215
562.9	0.35	0.23	
563.1	1.15	0.225	} 0.22
563.1	1.91	0.225	

soda glass wool and having a very large surface area to volume ratio. The reactors were constructed from tubing that had been well washed with distilled water and before use each was evacuated at  $200^\circ$  under  $0.1 \text{ mm.}$  pressure for 16 hr.

The first runs in both series A and B showed zero-order kinetics. The runs immediately following proceeded at much faster rates but the apparent order of the reaction increased, in series B to predominantly first order, and in series A to an order varying between first and second. For comparison the results of series A, with the exception of the first zero-order run, have been expressed as first-order rate constants, calculated from the initial stages (first 25 %) of each experiment, where the deviation from first-order kinetics was not large.

The first eight runs all performed within the same day, for the two sets of experiments, are compared in Table VI. The series B in the packed reactor proceeded at 2-3 times the rate of the series A in the empty reactor. In both series the rate was considerably higher with the clean walled reactors than for the homogeneous reaction (calculated first-order velocity constant  $k = 1.44 \times 10^{-6} \text{ sec.}^{-1}$  at 496° K from the rate equation given above) in the coated reactor.

TABLE VI

Series A				Series B			
Temp. °K	Initial Pressure of (CH <sub>3</sub> ) <sub>2</sub> . CCl (mm.)	$t_{1/2}/t_{1/4}$	First-order Velocity Constant (sec. <sup>-1</sup> )	Temp. °K	Initial Pressure of (CH <sub>3</sub> ) <sub>2</sub> . CCl (mm.)	$t_{1/2}/t_{1/4}$	First-order Velocity Constant (sec. <sup>-1</sup> )
497.1	27.9	2.0	—	495.8	31.0	2.0	—
496.2	70.0	2.54	$0.88 \times 10^{-3}$	495.8	76.1	2.38	$2.77 \times 10^{-3}$
497.1	68.7	2.93	1.08	495.8	75.9	2.52	2.92
496.7	140.5	—	1.03	495.8	160.3	2.50	2.99
496.9	116.6	—	1.19	495.8	119.6	2.43	2.97
496.3	78.8	3.09	1.40	495.4	81.4	2.38	2.87
497.4	48.4	3.26	1.45	495.9	55.8	2.54	2.72
498.1	33.5	3.24	1.45	495.9	32.6	2.48	2.79

Whereas similar experiments with ethyl bromide showed<sup>16</sup> a rapid ageing of the glass surface this effect is very slow with chlorinated hydrocarbons as we have noted previously for 1:2-dichlorethane.<sup>1</sup> In series A the next 14 runs, made within 24 hr., although showing bad reproducibility from run to run, gave little indication of any overall downward trend in velocity constants.

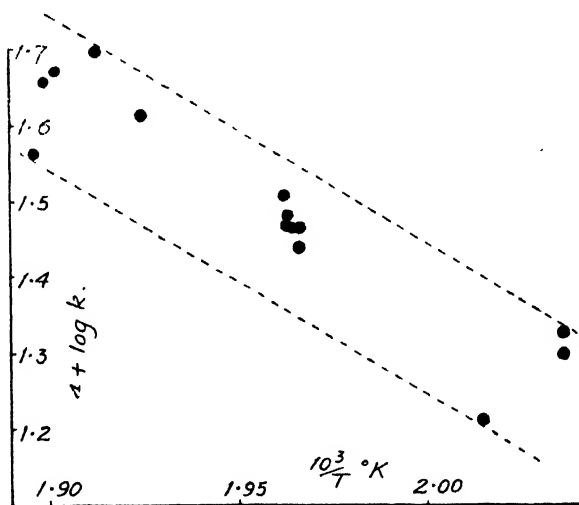


FIG. 5.

These results are summarized for various temperatures in Fig. 5, from which it may be deduced that the process studied had the low activation energy of roughly  $15,000 \pm 6,000$  cal.

Experiments to determine the effect of oxygen on the surface were made with the reactor used for series A. Immediately after the reaction products of a normal run had been pumped out of the reactor, a known pressure of oxygen

<sup>16</sup> Daniels and Veltman. *J. Chem. Physics*, 1939, 7, 756.

was admitted, allowed to remain in the reactor for 15 min., then pumped out and the test run started at once. The results, summarized in Table VII, show

TABLE VII

Pressure of Oxygen used for Pre-treatment (mm.) All experiments at 510° K	First Order Velocity Constant	
	Control Run (sec. <sup>-1</sup> )	Test Run (sec. <sup>-1</sup> )
8.0	$3.21 \times 10^{-3}$	$5.76 \times 10^{-3}$
5.9	2.94	6.08
0.6	3.60	4.71
0.7 (admitted with the <i>tert.</i> -butyl chloride)	3.31	3.35

that this pre-treatment with oxygen caused a marked increase in the velocity of heterogeneous decomposition. However, similar pressures of oxygen admitted with the *tert.*-butyl chloride at the beginning of a run did not increase the rate significantly (Table VII).

The initial runs at 490° K in series C were extremely fast, the *tert.*-butyl chloride decomposing as rapidly as it was admitted to the reactor. This was shown by allowing the pressure in the system to become steady (about 1 min.) condensing out the reaction products and titrating for hydrogen chloride. The pressure of the latter, calculated from the analysis, corresponded to half the final pressure in the system (Table VIII). Two runs were made at about 410° K, the lowest temperature attainable using mercury as thermostatic liquid. Even at this temperature the rate was so high that the initial pressure  $p_0$  had to be calculated from the time-pressure curve. This was done by adapting Guggenheim's method,<sup>17</sup> or in the following way. If  $p_0$  is the true initial pressure,  $p_1$  the first observed pressure at time  $t_0$ ,  $p_n$  the pressure at time  $t_{n-1}$  and  $\Delta t_{(n-1)} = t_{(n-1)} - t_0$ , then it is easily shown that, for a first-order reaction,

$$p_n \cdot e^{\Delta t_{(n-1)}} = e^{\Delta t_{(n-1)}} \cdot 2p_0 - (2p_0 - p_1)/e^k.$$

Thus by plotting  $p_n \cdot e^{\Delta t_{(n-1)}}$  against  $e^{\Delta t_{(n-1)}}$  the slope of the straight line gives  $2p_0$ . An average rate constant of  $11.7 \times 10^{-3}$  sec.<sup>-1</sup> was observed under these conditions.

TABLE VIII

Final Pressure $p_f$ (mm.)	$p_f/2$ (mm.)	HCl by Analysis (mm.)
132.6	66.3	69.5
215.2	107.6	104.0

## Discussion

The decomposition of *tert.*-butyl chloride corresponds by all experimental criteria with the similar reactions of ethyl chloride and of 1:1-dichlorethane.<sup>1</sup> Thus it is not inhibited by propylene, shows no induction period and from the experiments of Brearley, Kistiakowsky and Stauffer<sup>2</sup> is homogeneous. Furthermore its rate equation has a normal non-exponential term of  $10^{12.4}$  sec.<sup>-1</sup> and the reaction is not induced by chlorine or oxygen. By the arguments given previously<sup>1</sup> it must, therefore, be a unimolecular decomposition.

<sup>17</sup> Guggenheim, *Phil. Mag.*, 1926 [7], 2, 538.

Our rate equation for the reaction,

$$k = 10^{12.4 \pm 0.2} e^{-(41,400 \pm 600)/RT} \text{ sec.}^{-1}$$

is in fair agreement with that found previously,

$$k = 10^{13.9 \pm 0.7} e^{-(45,000 \pm 1,900)/RT} \text{ sec.}^{-1},$$

by Kistiakowsky.<sup>2, 13</sup> We consider that our result is the more reliable for the following reasons. Firstly, the error limits given by Kistiakowsky, indicated by the dotted lines in Fig. 3, are larger than those given here, though, of course, the method of calculation may be different. Secondly, Kistiakowsky's rate equation is based on 25 observations of which 15 were obtained over a 7° temperature range, whereas the results in this paper cover 93 observations spread over the whole temperature range studied.

We have shown above that the initial fast decomposition of *tert.*-butyl chloride in clean walled reactors is heterogeneous in origin and that the rates of reaction only approach complete reproducibility after many runs when the reactor walls have been uniformly coated. At the same temperatures as Kistiakowsky<sup>2, 13</sup> employed we have been able to obtain velocity constants identical with his, but on repeating the runs many times the constants have always fallen eventually to the values we give above.

#### General Mechanisms of Dehydrochlorination (with K. E. Howlett).

—We have now reached a stage in our investigations where it is convenient to summarize our views on the three general mechanisms of dehydrochlorination which we have established. The three mechanisms are (i) heterogeneous decomposition on glass surfaces as exemplified by our study on *tert.*-butyl chloride reported here and which is obviously of general application, (ii) homogeneous first-order unimolecular decomposition as exemplified by ethyl chloride,<sup>1</sup> 1:1-dichlorethane,<sup>1</sup> *tert.*-butyl chloride and isopropyl chloride<sup>18</sup> and (iii) homogeneous first-order decomposition by radical chains as exemplified by 1:2-dichlorethane<sup>1</sup> and 1:1:1:2- and 1:1:2:2-tetrachlorethanes.<sup>18</sup> It is now possible to predict which of the two homogeneous mechanisms (ii) and (iii) will be applicable to a particular chloro-compound from an inspection of its molecular structure. The correlation proceeds as detailed below.

A chloro-compound will decompose by a radical chain mechanism only so long as neither the compound itself nor the reaction products are inhibitors for the chains. In general the unimolecular mechanism will be of more universal application than the radical chain mechanism. The latter may be characterized by four steps comparable to those already shown to apply for the 1:2-dichlorethane decomposition.

(a) Initiating step or steps which are kinetically of the first-order and which lead to the production of chlorine atoms.

(b) First propagation step involving an attack of a chlorine atom on the substrate with abstraction of hydrogen and the formation of a "large" chlorine-containing radical.

(c) Decomposition of the "large" radical to give the olefine or chloro-olefine and a further chlorine atom which can participate again in step (b).

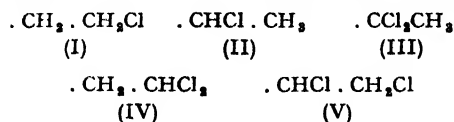
(d) Terminating step comprising the attack of a chlorine atom on the "large" radical to give non-radical products.

Steps (b) and (c) explain the stoichiometry of the reactions, step (d) the observed first-order kinetics. Inhibitors may suppress the reaction by interference in steps (b) and (c).

Now when ethyl chloride is attacked by chlorine atoms it affords not the 2-chlorethyl radical (I) but the 1-chlorethyl radical (II). This is

<sup>18</sup> To be published.

demonstrated by the formation of 1:1-dichlorethane by radical chlorination of ethyl chloride in the gas phase.<sup>19</sup> \* Similarly radical chlorination of 1:1-dichlorethane gives predominantly 1:1:1-trichlorethane as the trichloro-fraction.<sup>19</sup> This shows that the 1:1-dichlorethyl radical (III) must be formed as intermediate rather than the 2:2-dichlorethyl radical (IV). An analogous attack of chlorine atoms on 1:2-dichlorethane must, for structural reasons, furnish the 1:2-dichlorethyl radical (V).



Whereas the latter radical may furnish a chlorine atom and a stable olefine by fission of a single valency bond, radicals (II) and (III) can only give these reaction products provided the migration of a hydrogen atom accompanies the process. It is possible to understand, therefore, why ethyl chloride and 1:1-dichlorethane may act as inhibitors for their own radical chain decompositions. Similarly it is easily understood why the molecular structures of the two tetrachlorethanes permit them to decompose by the radical chain mechanism.

TABLE IX

Chloro compound	Predicted Homogeneous First-order Mechanism	
	Unimolecular	Radical Chain
Ethyl chloride . . .	× (already observed)	
1:1-Dichlorethane . . .	× (already observed)	
1:2-Dichlorethane . . .		× (already observed)
1:1:1-Trichlorethane . . .		×
1:1:2-Trichlorethane . . .		×
1:1:1:2-Tetrachlorethane . . .		× (already observed)
1:1:2:2-Tetrachlorethane . . .		× (already observed)
Pentachlorethane . . .		×
1-Chloropropane . . .	×	
2-Chloropropane . . .	× (already observed)	
1:2-Dichloropropane . . .	×	
1:2:3-Trichloropropane . . .		×
<i>n</i> -Butyl chloride . . .	×	
<i>tert.</i> -Butyl chloride . . .	× (already observed)	
2:2'-Dichlorethyl ether . . .		Possibly
β-Chloroethylbenzene . . .		Possibly
α-Chlorethylbenzene . . .	×	

*tert.*-Butyl chloride is an example of a molecule which should not, itself, be an inhibitor for the radical mechanism but its decomposition product, *isobutene*, should possess this power. *iso*Propyl chloride would be expected to exhibit both types of inhibition.

Table IX summarizes prediction and observation, so far as experiment has progressed in this field. We intend to examine the decomposition

\* It is an unexplained observation that attack by chlorine atoms on an alkyl chloride in solution<sup>20</sup> leads to substitution at a position remote from the chlorine atom originally present. In the gas phase exactly the opposite occurs.<sup>19</sup>

<sup>19</sup> Vaughan and Rust, *J. Org. Chem.*, 1940, 5, 449.

<sup>20</sup> Kharasch and Brown, *J. Amer. Chem. Soc.*, 1939, 61, 2142; compare Taft and Stratton, *Ind. Eng. Chem.*, 1948, 40, 1485.

characteristics of the various chloro compounds which we have not so far studied in order to test the validity of our suggestions.

It is attractive to speculate that only substances which can decompose by the radical chain mechanism can have their decomposition induced by oxygen or chlorine.<sup>21</sup> In the majority of the cases so far studied, such would appear to be the case.

We thank the Central Research Fund of London University for a grant in aid of this research. This work was carried out during the tenure of an I.C.I. Fellowship by one of us (D. H. R. B.). We also acknowledge a maintenance grant from the D.S.I.R. (P. F. O.).

*Chemistry Department,  
Imperial College,  
London, S.W.7.*

<sup>21</sup> Barton, *Nature*, 1946, **157**, 626; *J. Chem. Soc.*, 1949, 148.

---

## THE USE OF ACETALDEHYDE FOR THE DETECTION OF CHAIN REACTIONS

BY K. E. HOWLETT AND D. H. R. BARTON

*Received, 17th January, 1949*

Small amounts of acetaldehyde inhibit the decomposition of 1:2-dichloroethane but not that of ethyl chloride or of 1:1-dichloroethane. Hydrogen chloride induces the decomposition of acetaldehyde at 457° C. Relative to their own rates of decomposition ethyl chloride and 1:1-dichloroethane are ineffective as compared with 1:2-dichloroethane in catalyzing the decomposition of acetaldehyde at 457° C.

The mechanism of the thermal decomposition of acetaldehyde has been the subject of many investigations.<sup>1</sup> Although there have been conflicting views as to whether the reaction, in the absence of catalysts and inhibitors, is of the chain type or is molecular in character, it is generally agreed that the decomposition may be induced by the presence of substances which decompose to give free radicals.<sup>2</sup> The increase in rate of the acetaldehyde decomposition under these conditions can therefore be used as a test for free radicals. An example which is particularly relevant to this paper is the use of the method by Roof and Daniels<sup>3</sup> in their study of the pyrolysis of ethyl bromide.

Elsewhere<sup>4</sup> we have shown that while 1:2-dichloroethane undergoes thermal decomposition by a chain mechanism, the isomeric 1:1-compound, and also ethyl chloride, decompose by the unimolecular mechanism. It seemed worthwhile to us to apply the test of free radicals, provided by the acetaldehyde pyrolysis, to these three substances.

<sup>1</sup> Steacie, *Atomic and Free Radical Reactions* (A.C.S., Monograph, 1946).

<sup>2</sup> Sickman and Allen, *J. Amer. Chem. Soc.*, 1934, **56**, 1251; Allen and Sickman, *ibid.*, 1934, **56**, 2031; Fletcher, *ibid.*, 1936, **58**, 534; Fletcher and Rollefson, *ibid.*, 1936, **58**, 2129, 2135; Travers and Silcocks, *Nature*, 1937, **139**, 1018; Rice and Walters, *J. Amer. Chem. Soc.*, 1941, **63**, 1701; Wang and Winkler, *Can. J. Res. B*, 1943, **21**, 97.

<sup>3</sup> *J. Amer. Chem. Soc.*, 1940, **62**, 2912; 1944, **66**, 358.

<sup>4</sup> Barton, and Howlett, *J. Chem. Soc.*, 1949, 155, 165.

### Experimental

**Materials.**—Ethyl chloride and the 1:1- and 1:2-dichlorethanes were purified as described previously.<sup>4</sup> Acetaldehyde was prepared by depolymerization of paraldehyde and purified by distillation. It was stored over hydroquinone<sup>5</sup> before use. Otherwise no special precautions were taken to ensure its purity.

**Apparatus.**—Measurements were made in an all-glass apparatus of the type described previously.<sup>4</sup> Reaction rates were obtained from pressure measurements, the pressure increases being followed by the use of a spoon gauge. All measurements were made at 457° C. All experiments were carried out in reactors whose walls had been coated<sup>4</sup> with decomposition products from 1:2-dichlorethane.

### Results

In view of the uncertainty with regard to the order of the acetaldehyde decomposition all results have been expressed in terms of the initial rate of increase of pressure based on 100 mm. of acetaldehyde. Although acetaldehyde pressures remote from this figure were not used the results have been corrected, where indicated, to the 100 mm. basis by assuming the decomposition to be of the 3/2 order. In this procedure we follow the example of Morris.<sup>5</sup> Induction periods were not observed in any of the reactions where the acetaldehyde was in large excess.

**Decomposition of Acetaldehyde Alone.**—The mean initial rate of decomposition of 100 mm. of acetaldehyde was 0.65 mm. min.<sup>-1</sup> (Table I). Interpolation of the data of Morris<sup>5</sup> gives 0.62 mm. min.<sup>-1</sup> for untreated acetaldehyde and extrapolation 0.32 mm. min.<sup>-1</sup> for acetaldehyde treated with hydroquinone. The latter extrapolation is, however, not very reliable since it rests on data at only two temperatures giving the low activation energy of 43.5 kcal.

TABLE I

Initial Pressure of $\text{CH}_3 \cdot \text{CHO}$ ( $p_0(\text{CH}_3\text{CHO})$ ) (mm.)	Initial Rate Corr. to $p_0(\text{CH}_3\text{CHO}) = 100$ mm. (mm. min. <sup>-1</sup> )
103.5	0.68
123.5	0.58
101.0	0.67
107.0	0.68
92.0	0.61
100.0	0.65

**Decomposition of the Chlorinated Hydrocarbons in Presence of Small Amounts of Acetaldehyde.**—As shown previously<sup>4</sup> radical chain inhibitors, like propylene, have no effect on the rates of thermal decomposition of ethyl chloride and 1:1-dichlorethane. Similarly it has now been found that small amounts of acetaldehyde (Table II) do not inhibit the pyrolysis of these two

TABLE II

Chlorinated Hydrocarbons	Initial Pressures		First-order Vel. Constants $k$	
	Chlorinated Hydrocarbons (mm.)	$\text{CH}_3 \cdot \text{CHO}$ (mm.)	$k$ found (sec. <sup>-1</sup> )	$k$ from Rate eqn. <sup>4</sup> (sec. <sup>-1</sup> )
Ethyl chloride.	100	0	$24.7 \times 10^{-5}$	$26.3 \times 10^{-5}$
	100	8.0	25.0	—
1:1-Dichlorethane	100	5.5	220	186
1:2-Dichlorethane	100	0	57	56.2
	100	4.5	5.4	5.0

<sup>5</sup> Morris, *J. Amer. Chem. Soc.*, 1941, 63, 2535; 1944, 66, 584.

compounds. On the other hand a small amount of the aldehyde (Table II) strongly inhibits the decomposition of 1 : 2-dichlorethane and reduces the rate to the maximally inhibited value found previously<sup>4</sup> for propylene inhibition ( $k = 5.0 \times 10^{-8}$  sec.<sup>-1</sup>). In all cases when only small amounts of acetaldehyde were present the decompositions of the chlorinated hydrocarbons followed first-order kinetics, as found previously with propylene.<sup>4</sup> These experiments provide further confirmation for the difference in mechanism between the decompositions of 1 : 2-dichlorethane and ethyl chloride and 1 : 1-dichlorethane.

**Effects of Ethylene, Vinyl Chloride and Hydrogen Chloride on the Rate of Decomposition of Acetaldehyde.**—In agreement with Smith<sup>6</sup> small amounts of ethylene (Table III) had no effect on the rate of decomposition. The same

TABLE III

Addend	Initial Pressure of $\text{CH}_3\cdot\text{CHO}$ ( $p_0(\text{C}_2\text{H}_5\cdot\text{CHO})$ ) (mm.)	Initial Pressure of Addend (mm.)	Initial Rate Corr. to $p_0(\text{CH}_3\cdot\text{CHO}) = 100$ mm. (mm. min. <sup>-1</sup> )	Increase in Initial Rate per mm. of Addend (min. <sup>-1</sup> )
Ethylene	99.0	8.0	0.77	—
Vinyl chloride	100.0 98.5	9.5 9.5	0.63 0.68	
Hydrogen chloride	102.0 104.5 102.5 104.0	9.0 8.5 8.0 20.5	0.87 0.84 0.87 1.64	} mean 0.023  0.049
$\text{C}_2\text{H}_4 : \text{HCl}$	98.5	76.0 : 76.0	1.84	
$\text{C}_2\text{H}_3\text{Cl} : \text{HCl}$	105.5	41.0 : 41.0	2.95	0.016 0.056
Ethyl chloride	98.5 95.5 90.0 100.0 102.0 101.0 101.5 103.0 99.5 102.0	9.5 8.5 11.0 9.5 11.0* 10.5 9.5 9.5 5.0 21.0	0.75 0.85 0.60 0.71 0.70 0.70 0.70 0.71 0.62 0.62	mean 0.004
1 : 2-Dichlorethane	98.5 98.5 107.0 104.0	4.0 7.5 11.5 25.0	0.98 1.85 2.0 2.1	
1 : 1-Dichlorethane	95.0 100.5 87.5 97.5 101.5	9.0 12.0 9.0 7.5 18.0 †	1.80 2.5 1.46 1.30 2.2	mean 0.109

\* Acetaldehyde admitted 15 min. after the ethyl chloride.

† Acetaldehyde admitted 5 min. after the 1 : 1-dichlorethane.

applied to vinyl chloride. In contrast hydrogen chloride exerted a definite inducing action (Table III). Mixtures of ethylene and HCl and of vinyl chloride and HCl also caused induced decomposition.

**Effects of Ethyl Chloride and the 1 : 1- and 1 : 2- Dichlorethanes on the Rate of Decomposition of Acetaldehyde.**—The results are summarized in Table III. Ethyl chloride, which decomposes slowly at 457° C ( $k = 26.3 \times 10^{-8}$

<sup>6</sup> *Trans. Faraday Soc.*, 1939, **35**, 1328.



sec.<sup>-1</sup>), had no appreciable influence on the rate of decomposition. In contrast 1:2-dichlorethane, which decomposes more slowly ( $k = 5.0 \times 10^{-5}$  sec.<sup>-1</sup> for the maximally inhibited reaction), caused a marked catalysis of the decomposition. 1:1-Dichlorethane, which decomposes rapidly at 457° C ( $k = 186 \times 10^{-5}$  sec.<sup>-1</sup>) similarly caused a marked increase in the rate of decomposition. The figures in Table III for the latter compound have been corrected for the decomposition of the 1:1-dichlorethane itself but not for the inducing action of the hydrogen chloride formed in the reaction. The latter, though not negligible, is relatively small.

### Discussion

Besides compounds which decompose to give free radicals the acetaldehyde decomposition is also catalyzed by oxygen, iodine, bromine and similar substances which will react to give free radicals.<sup>1</sup> It is difficult, however, to explain the inducing action of hydrogen chloride, which has also been noted by Fromherz.<sup>7</sup>

The absence of any inducing effect by decomposing ethyl chloride is in agreement with the unimolecular mechanism already established for its decomposition. The relatively powerful effect of 1:2-dichlorethane in causing the decomposition is also in agreement with its established mechanism of decomposition. The inducing power of 1:1-dichlorethane, however, was not expected. It is important to realize that the use of the acetaldehyde decomposition is solely a method for detecting the presence of free radicals and does *not* prove to what extent a compound actually decomposes by a free-radical mechanism. The latter is only established by experiments with inhibitors and therefore the results recorded here do not necessarily constitute evidence against the mechanism we have already established for the decomposition of 1:1-dichlorethane.

Ethyl chloride and the two dichlorethanes decompose at different rates at 457° C. In order to take account of this difference it is best to compare their inducing action in terms of their own rates of decomposition.

TABLE IV

Chlorinated Hydrocarbon X	First Order Velocity Constant $k$ (sec. <sup>-1</sup> )	Increase ( $\Delta R$ ) in Initial Rate of $\text{CH}_3 \cdot \text{CHO}$ Decomp. per mm. of X	$\Delta R/k$
Ethyl chloride . . .	$26.3 \times 10^{-5}$	0.004	15
1:1-Dichlorethane . .	186	0.109	58
1:2-Dichlorethane . .	5.0	0.104	2100

This comparison is shown in Table IV. By this criterion 1:2-dichlorethane is far more effective than the two chlorinated hydrocarbons whose decompositions proceed by unimolecular mechanisms.

Imperial College,  
London, S.W.7.

<sup>7</sup> *Z. physik. Chem. B*, 1934, **25**, 301.

# THE NORMAL-STRESS COEFFICIENT IN SOLUTIONS OF MACRO-MOLECULES

By R. S. RIVLIN

Received 26th January, 1949

In a previous paper<sup>1</sup> it has been shown that if the stress components at a point of a fluid depend only on the state of flow in a small element about that point at the instant considered, then in general, two physical parameters are required to define completely the flow properties of the fluid. One of these is the viscosity and the other will be called the normal-stress coefficient. Each of these may or may not be dependent on the state of flow. In the present paper, a method similar to that adopted by Kramers<sup>2</sup> to calculate the intrinsic viscosity of a high-polymer solution has been employed to calculate its normal stress coefficient. It is shown that appreciable values of the normal-stress coefficient may be expected in concentrated solutions and that its non-vanishing results from the orientation of the molecules in the flowing solution.

**1. Introduction.**—In a previous paper<sup>1</sup> it has been shown that for an incompressible visco-elastic fluid, which is isotropic in its state of rest, the most general expressions that can be obtained for the stress components  $t_{xx}$ ,  $t_{yy}$ , . . .  $t_{zz}$ , in a rectangular Cartesian co-ordinate system ( $x$ ,  $y$ ,  $z$ ), in terms of the strain-velocity components  $a$ ,  $b$ , . . .  $\frac{1}{2}h$ , are

$$t_{xx} = 2\Theta a + 2\Psi A' + p, \text{ etc., and } t_{yz} = \Theta f + \Psi F', \text{ etc.,} \quad (1.1)$$

$$\text{where } a = \partial u / \partial x, \text{ etc. and } f = \partial v / \partial z + \partial w / \partial y, \text{ etc.} \quad (1.2)$$

( $u$ ,  $v$ ,  $w$ ) is the velocity of the element of the fluid at ( $x$ ,  $y$ ,  $z$ ).  $A'$ ,  $B'$ , . . .  $\frac{1}{2}H'$  are given by

$$A' = a^2 + \frac{1}{2}(g^2 + h^2), \text{ etc. and } F' = \frac{1}{2}gh + (b + c)f, \text{ etc.} \quad (1.3)$$

$p$  is a hydrostatic pressure.  $\Theta$  and  $\Psi$  are arbitrary functions of  $K_2$  and  $K_3$ , invariants of the strain-velocity, defined by

$$\begin{aligned} K_2 &= ab + bc + ca - \frac{1}{2}f^2 - \frac{1}{2}g^2 - \frac{1}{2}h^2 \\ K_3 &= abc + \frac{1}{2}fgh - \frac{1}{4}af^2 - \frac{1}{4}bg^2 - \frac{1}{4}ch^2. \end{aligned} \quad (1.4)$$

The equation (1.1) must also represent the stress-strain-velocity relations for a visco-elastic fluid in steady-state laminar flow. If  $\Psi = 0$  and  $\Theta$  is a constant, then (1.1) are the equations of classical hydrodynamics,  $\Theta$  being the viscosity of the fluid as normally defined.

In the present paper, it will be shown that a non-zero value of  $\Psi$ , which we shall call the *normal-stress coefficient* for reasons which will appear later, may obtain in solutions of macro-molecules or suspensions of rod-shaped particles. The method adopted is similar to that employed by Kramers<sup>2</sup> to calculate the intrinsic viscosity of a high-polymer solution.

It has been shown<sup>1</sup> that the non-vanishing of  $\Psi$  in the basic stress-strain-velocity relations (1.1) for the fluid would lead to its exhibiting a number of hydrodynamic effects which are not predicted by classical hydrodynamics. For example, if the fluid is contained between two coaxial cylinders which are rotated with respect to each other, at (say) a constant angular velocity, the fluid will rise up the inner cylinder.

<sup>1</sup> Rivlin, *Proc. Roy. Soc. A.*, 1948, **193**, 260.

<sup>2</sup> Kramers, *J. Chem. Physics*, 1946, **14**, 415.

Weissenberg<sup>3</sup> has recently drawn attention to the fact that a number of fluids exhibit such an effect.

**2. The Fundamental Formulae.**—Following Kramers,<sup>2</sup> we employ an idealized "pearl necklace" model for the high-polymer molecule. Each molecule is considered to consist of  $N$  equal massive points, each of mass  $M$ , connected by equal rigid links of length  $L$ , which are capable of some measure of rotation about the mass-points at their junctions. It is assumed that, in a solution of such molecules, the solvent exerts no force on the rigid links but that a force  $-\zeta \mathbf{v}$  is exerted on each mass-point, where  $\mathbf{v}$  is the vector velocity of the mass-point relative to the element of solvent in its immediate neighbourhood and  $\zeta$  is a constant depending on the nature of the high-polymer molecule and of the solvent.

We shall first consider the effect of a single dissolved high-polymer molecule per unit volume on the stress components which are associated with a specified steady irrotational state of flow in which the principal directions of flow are parallel to the rectangular Cartesian co-ordinate axes ( $x, y, z$ ), which will be taken as the axes of reference throughout this paper. The velocity components ( $u, v, w$ ) at any point ( $x, y, z$ ) may be written

$$u = \kappa_1 x, v = \kappa_2 y \text{ and } w = \kappa_3 z, \quad (2.1)$$

where, on account of the incompressibility of the fluid,

$$\kappa_1 + \kappa_2 + \kappa_3 = 0. \quad (2.2)$$

We shall assume that the flow configuration of the solvent is not altered by the introduction of the high-polymer molecule.

Let ( $x, y, z$ ) be the position of the centre of gravity of the macromolecule at time  $t$ . Let ( $x_i, y_i, z_i$ ) be the position at time  $t$  of the  $i$ th mass-point relative to the centre of gravity of the whole molecule. Then,

$$(x + x_i, y + y_i, z + z_i)$$

are the co-ordinates of the  $i$ th mass-point. Its velocity and acceleration are

$$(\dot{x} + \dot{x}_i, \dot{y} + \dot{y}_i, \dot{z} + \dot{z}_i) \text{ and } (\ddot{x} + \ddot{x}_i, \ddot{y} + \ddot{y}_i, \ddot{z} + \ddot{z}_i)$$

respectively. We have,

$$\sum_1^N x_i = \sum_1^N \dot{x}_i = \sum_1^N \ddot{x}_i = 0, \text{ etc.} \quad (2.3)$$

The viscous force exerted by the solvent on the  $i$ th mass-point is

$$[-\zeta(\dot{x} + \dot{x}_i - \kappa_1 x - \kappa_1 x_i), -\zeta(\dot{y} + \dot{y}_i - \kappa_2 y - \kappa_2 y_i), -\zeta(\dot{z} + \dot{z}_i - \kappa_3 z - \kappa_3 z_i)].$$

Let ( $X_i'', Y_i'', Z_i''$ ) be the resultant force exerted on the  $i$ th mass-point by the tensions in the links attached to it (i.e. the  $(i-1)$ th and  $i$ th links) and let ( $X_i', Y_i', Z_i'$ ) be a random force of such a nature that for a free particle equipartition would be maintained; i.e.  $X_i', Y_i'$  and  $Z_i'$  are independent of each other and of the positions of the mass-points and

$$\langle X_i' \rangle_{\Delta V} = \langle Y_i' \rangle_{\Delta V} = \langle Z_i' \rangle_{\Delta V} = 0.$$

Then, applying Newton's second law to the motion of the mass-point, we obtain the three equations

$$X_i'' = M(\ddot{x} + \ddot{x}_i) + \zeta(\dot{x} + \dot{x}_i - \kappa_1 x - \kappa_1 x_i) - X_i', \text{ etc.} \quad (2.4)$$

Now, if  $S_i (i = 1, \dots, (N-1))$  is the tension in the  $i$ th link and the direction-cosines of the  $i$ th link are ( $l_i, m_i, n_i$ ), we have

$$X_i'' = S_i l_i - S_{i-1} l_{i-1}, \text{ etc.}, \quad (2.5)$$

for each mass-point except the first and  $N$ th. For these,

$$X_1'' = S_1 l_1, \text{ etc. and } X_N'' = -S_{N-1} l_{N-1}, \text{ etc.} \quad (2.6)$$

<sup>3</sup> Weissenberg, *Nature*, 1947, **159**, 310.

From (2.5) and (2.6) we have

$$\sum_1^N X'_i = \sum_1^N Y'_i = \sum_1^N Z'_i = 0. \quad (2.7)$$

From (2.4) and (2.7) we obtain, bearing in mind the relations (2.3), the three equations

$$M\ddot{x} + \zeta\dot{x} - \zeta\kappa_1 x - X' = 0, \text{ etc.}, \quad (2.8)$$

where

$$X' = \frac{1}{N} \sum_1^N X'_i.$$

Equations (2.8) and (2.4) yield

$$X'_i = M\ddot{x}_i + \zeta\dot{x}_i - \zeta\kappa_1 x_i - X'_i + X', \text{ etc.} \quad (2.9)$$

The mean force which is exerted per unit area of a plane normal to the  $x$ -axis, on its negative side, by the high-polymer molecule, can be considered to consist of that due to the momentum transferred across the area by the high-polymer molecule, together with that due to the tensions in the links as they cross the area. We shall denote the former by  $(\delta_{xx}, \delta_{xy}, \delta_{xz})$  and the latter by  $(\delta'_{xx}, \delta'_{xy}, \delta'_{xz})$ .

Since the momentum of the  $i$ th mass-point is

$$[M(\dot{x} + \dot{x}_i), M(\dot{y} + \dot{y}_i), M(\dot{z} + \dot{z}_i)],$$

and when the velocity is

$$[(\dot{x} + \dot{x}_i), (\dot{y} + \dot{y}_i), (\dot{z} + \dot{z}_i)],$$

the number of times per second that it crosses the area considered is  $(\dot{x} + \dot{x}_i)$ , it can readily be seen that the mean rate of transfer of momentum across the area by the  $i$ th mass-point is

$$\langle M(\dot{x} + \dot{x}_i)^2 \rangle_{\Delta V}, \langle M(\dot{y} + \dot{y}_i)(\dot{x} + \dot{x}_i) \rangle_{\Delta V}, \langle M(\dot{z} + \dot{z}_i)(\dot{x} + \dot{x}_i) \rangle_{\Delta V} \quad (2.10)$$

where the average is taken over a sufficiently long interval of time. Summing these rates of transfer of momentum for all the  $N$  mass-points, we obtain

$$\delta_{xx} = \left\langle \sum_1^N M(\dot{x} + \dot{x}_i)^2 \right\rangle_{\Delta V}, \quad \delta_{xy} = \left\langle \sum_1^N M(\dot{x} + \dot{x}_i)(\dot{y} + \dot{y}_i) \right\rangle_{\Delta V}$$

$$\text{and} \quad \delta_{xz} = \left\langle \sum_1^N M(\dot{x} + \dot{x}_i)(\dot{z} + \dot{z}_i) \right\rangle_{\Delta V} \quad (2.11)$$

Employing the relations (2.3), equations (2.11) become

$$\delta_{xx} = \left\langle \sum_1^N M(\dot{x}^2 + \dot{x}_i^2) \right\rangle_{\Delta V}, \quad \delta_{xy} = \left\langle \sum_1^N M(\dot{x}\dot{y} + \dot{x}_i\dot{y}_i) \right\rangle_{\Delta V}$$

$$\text{and} \quad \delta_{xz} = \left\langle \sum_1^N M(\dot{x}\dot{z} + \dot{x}_i\dot{z}_i) \right\rangle_{\Delta V} \quad (2.12)$$

The force exerted by the  $i$ th link on the area considered is

$$(-S_l l_i, -S_m m_i, -S_n n_i),$$

when the link intersects the area. The probability for such an intersection to occur is  $Ll_i$ . Thus, the force exerted by the  $i$ th link on the area is

$$[-\langle LS_l l_i^2 \rangle_{\Delta V}, -\langle LS_m m_i l_i \rangle_{\Delta V}, -\langle LS_n n_i l_i \rangle_{\Delta V}].$$

Again the average must be taken over a sufficiently long time interval.

Summing the forces exerted by the  $(N - 1)$  links, we obtain

$$\delta'_{xx} = -L \sum_1^{N-1} \langle S_i l_i^2 \rangle_{\Delta V}, \quad \delta'_{xy} = -L \sum_1^{N-1} \langle S_i m_i l_i \rangle_{\Delta V},$$

$$\text{and} \quad \delta'_{xz} = -L \sum_1^{N-1} \langle S_i n_i l_i \rangle_{\Delta V}. \quad . \quad . \quad . \quad (2.13)$$

From (2.13), (2.5) and (2.6), we obtain

$$\delta'_{xx} = \sum_1^N \langle X_i' x_i \rangle_{\Delta V}, \quad \delta'_{xy} = \sum_1^N \langle Y_i' x_i \rangle_{\Delta V},$$

$$\text{and} \quad \delta'_{xz} = \sum_1^N \langle Z_i' x_i \rangle_{\Delta V}, \quad . \quad . \quad . \quad (2.14)$$

bearing in mind that  $x_{i+1} - x_i = Ll_i$ , etc. Denoting by  $t'_{xx}$ ,  $t'_{yy}$ , . . ., the parts of the stress components  $t_{xx}$ ,  $t_{yy}$ , . . ., which must be exerted as a result of the presence of the dissolved molecule, we have

$$t'_{xx} = -(\delta_{xx} + \delta'_{xx}), \text{ etc.},$$

$$\text{and} \quad t'_{yy} = -(\delta_{yy} + \delta'_{yy}), \text{ etc.} \quad . \quad . \quad . \quad (2.15)$$

From (2.15), (2.14) and (2.12) and further similar equations, we obtain

$$t'_{xx} = -\sum_1^N \langle M(\dot{x}^2 + \dot{x}_i^2) + X_i' x_i \rangle_{\Delta V}, \text{ etc.},$$

$$\text{and} \quad t'_{yy} = -\sum_1^N \langle M(\dot{y}^2 + \dot{y}_i^2) + Z_i' y_i \rangle_{\Delta V}, \text{ etc.} \quad . \quad (2.16)$$

Introducing the expressions (2.9) for  $X_i'$ ,  $Y_i'$  and  $Z_i'$  into (2.16), we obtain

$$t'_{xx} = -\sum_1^N \langle M\dot{x}^2 + M \frac{d}{dt}(x_i \dot{x}_i) + \frac{1}{2} \zeta \frac{d}{dt}(x_i^2) - \zeta \kappa_1 x_i^2 + (X' - X'_i) x_i \rangle_{\Delta V}, \text{ etc.},$$

and

$$t'_{yy} = -\sum_1^N \langle M\dot{y}^2 + M \frac{d}{dt}(y_i \dot{y}_i) + \zeta y_i(\dot{z}_i - \kappa_3 z_i) + (Z' - Z'_i) y_i \rangle_{\Delta V}, \text{ etc.} \quad (2.17)$$

$$\text{Now,} \quad \left\langle \frac{d}{dt}(x_i \dot{x}_i) \right\rangle_{\Delta V}, \quad \left\langle \frac{d}{dt}(x_i^2) \right\rangle_{\Delta V} \quad \text{and} \quad \langle (X' - X'_i) x_i \rangle_{\Delta V}$$

are all zero.

$$\text{Similarly,} \quad \left\langle \frac{d}{dt}(y_i \dot{y}_i) \right\rangle_{\Delta V} \quad \text{and} \quad \langle (Z' - Z'_i) y_i \rangle_{\Delta V}$$

are zero. Also

$$\langle y_i(z_i - \kappa_3 z_i) \rangle_{\Delta V} = \langle y_i \rangle_{\Delta V} \langle \dot{z}_i - \kappa_3 z_i \rangle_{\Delta V},$$

since the motion parallel to the  $z$ -axis is independent of the position of the centre of gravity parallel to the  $y$ -axis. The mean velocity of a particle at any point is equal to the velocity of the solvent at that point; i.e.

$$\langle \dot{z}_i - \kappa_3 z_i \rangle_{\Delta V} = 0.$$

Therefore,

$$\langle y_i(z_i - \kappa_3 z_i) \rangle_{\Delta V} = 0.$$

Employing these relations, (2.17) become

$$t'_{xx} = -NM\langle\dot{x}^2\rangle_{\Delta V} + \zeta\kappa_1 \sum_1^N \langle x_i^2 \rangle_{\Delta V}, \text{ etc.},$$

$$\text{and } t'_{yz} = -NM\langle\dot{y}\dot{z}\rangle_{\Delta V}, \text{ etc.} \quad (2.18)$$

Providing  $\zeta$  is sufficiently large, we can neglect the terms

$$-NM\langle\dot{x}^2\rangle_{\Delta V}, -NM\langle\dot{y}\dot{z}\rangle_{\Delta V}, \text{ etc.},$$

and we then obtain

$$t'_{xx} = \zeta\kappa_1 \sum_1^N \langle x_i^2 \rangle_{\Delta V}, \text{ etc.}, \text{ and } t'_{yz} = 0, \text{ etc.} \quad (2.19)$$

It should be noted that equations (2.9) can be re-written as

$$X'_i = M\ddot{x}_i + \zeta\dot{x}_i + \frac{\partial U}{\partial x_i} - X'_i + X', \text{ etc.}, \quad (2.20)$$

$$\text{where } U = -\sum_1^N \frac{1}{2} \zeta (\kappa_1 x_i^2 + \kappa_2 y_i^2 + \kappa_3 z_i^2). \quad (2.21)$$

Equations (2.20) describe the motion of a molecule relative to its centre of gravity, when situated in a force field given by (2.21).

**3. The Stress Components for a Flexible Chain—First-Order Approximation.**—( $x_i, y_i, z_i$ ) are given <sup>2</sup> by

$$x_i = \frac{L}{N} [l_1 + 2l_2 + \dots + (i-1)l_{i-1} - (N-i)l_i - \dots - l_{N-1}], \text{ etc} \quad (3.1)$$

Whence,

$$\sum_1^N x_i^2 = \frac{L^2}{N} \sum_1^{N-1} g_{ij} l_i l_j, \quad (3.2)$$

where

$$g_{ij} = \begin{cases} i(N-j) & \text{when } j > i \\ j(N-i) & \text{when } j \leq i \end{cases} \quad (3.3)$$

Now, the orientation of the  $i$ th link may be defined by two angles  $\theta_i$  and  $\phi_i$ .  $\theta_i$  is the inclination of the link to the  $x$ -axis and  $\phi_i$  is the inclination of its projection on the  $yz$ -plane to the  $y$ -axis. Then,

$$l_i = \cos \theta_i, m_i = \sin \theta_i \cos \phi_i \text{ and } n_i = \sin \theta_i \sin \phi_i \quad (3.4)$$

If the links are capable of perfectly free rotation about the mass-points at their junctions, then, when the fluid is at rest, the probability of the link having an orientation in the range  $(\theta_i, \theta_i + d\theta_i)$  and  $(\phi_i, \phi_i + d\phi_i)$  is given by

$$\frac{1}{4\pi} \sin \theta_i d\theta_i d\phi_i. \quad (3.5)$$

The probability of the  $(N-1)$  links having orientations in the ranges  $(\theta_i, \theta_i + d\theta_i)$  and  $(\phi_i, \phi_i + d\phi_i)$ , for  $i = 1, \dots, (N-1)$ , is

$$\prod_{i=1}^{N-1} \left\{ \frac{1}{4\pi} \sin \theta_i d\theta_i d\phi_i \right\} \quad (3.6)$$

If this is taken as the distribution of link orientations for the state of flow defined by (2.1), then

$$\begin{aligned} \sum_1^N \langle x_i^2 \rangle_{\Delta V} &= \frac{L^2}{N} \sum_1^{N-1} \langle g_{ij} l_i l_j \rangle_{\Delta V} \\ &= \frac{L^2}{N} \int_0^\pi \int_0^{2\pi} \sum_1^{N-1} (g_{ij} \cos \theta_i \cos \theta_j) \prod_1^{N-1} \left( \frac{1}{4\pi} \sin \theta_i \right) d\theta d\phi, \quad (3.7) \end{aligned}$$

where  $\int_0^\pi \dots d\theta = \int_0^\pi \dots \int_0^\pi \dots d\theta_1 d\theta_2 \dots d\theta_{N-1}$

and  $\int_0^{2\pi} \dots d\phi = \int_0^{2\pi} \dots \int_0^{2\pi} \dots d\phi_1 d\phi_2 \dots d\phi_{N-1}$  . (3.8)

Thus,

$$\begin{aligned} \sum_1^N \langle x_i^2 \rangle_{AV} = & \frac{L^2}{N} \sum_{i+j}^{N-1} \int_0^\pi \int_0^\pi \int_0^{2\pi} \int_0^{2\pi} \frac{1}{4} \left( \frac{1}{4\pi} \right)^2 g_{ij} \sin 2\theta_i \sin 2\theta_j d\theta_i d\theta_j d\phi_i d\phi_j \\ & + \frac{L^2}{N} \sum_1^{N-1} \int_0^\pi \int_0^{2\pi} \frac{1}{4\pi} g_{ii} \sin \theta_i \cos^2 \theta_i d\theta_i d\phi_i. \end{aligned} \quad (3.9)$$

The first of these integrals is zero. Thus,

$$\sum_1^N \langle x_i^2 \rangle_{AV} = \frac{L^2}{3N} \sum_1^{N-1} g_{ii} = \frac{1}{18} L^2 N^2, \text{ if } N \text{ is large.} \quad (3.10)$$

It can readily be seen, by symmetry, that

$$\sum_1^N \langle x_i^2 \rangle_{AV} = \sum_1^N \langle y_i^2 \rangle_{AV} = \sum_1^N \langle z_i^2 \rangle_{AV}. \quad (3.11)$$

Whence, substituting in (2.19), we have

$$t'_{xx} = \frac{1}{18} \zeta \kappa_1 L^2 N^2, \text{ etc.} \quad (3.12)$$

For the state of flow described by (2.1), equations (1.1) become, taking the hydrostatic pressure  $p = 0$ ,

$$t_{xx} = 2\theta\kappa_1 + 2\Psi\kappa_1^2, \text{ etc.} \quad (3.13)$$

Comparing (3.12) and (3.13), we see that with the assumptions made,

$$\theta = \frac{1}{36} \zeta L^2 N^2 \text{ and } \Psi = 0, \quad (3.14)$$

for the solution considered, in agreement with Kramers' calculation.

**4. The Stress Components for a Flexible Chain—Second-Order Approximation.**—We shall now reject the assumption that the uniform distribution of link orientations in space is not appreciably altered by the flow.

Suppose that  $(1 - p') \prod_{i=1}^{N-1} \left( \frac{1}{4\pi} \sin \theta_i d\theta_i d\phi_i \right)$

is the probability that the  $i$ th link lies in the orientation range

$(\theta_i, \phi_i)$  to  $(\theta_i + d\theta_i, \phi_i + d\phi_i)$  for  $i = 1, \dots, (N-1)$ .

$p'$  is a function of  $\kappa_1, \kappa_2$  and  $\kappa_3$ , the  $\theta$ 's and  $\phi$ 's, such that  $p' = 0$  when

$$\kappa_1 = \kappa_2 = \kappa_3 = 0.$$

Then,

$$t'_{xx} = \frac{1}{18} \zeta \kappa_1 L^2 N^2 - \frac{\zeta \kappa_1 L^2}{N} \int_0^\pi \int_0^{2\pi} \left( \sum_1^{N-1} g_{ii} l_i l_j \right) p' \prod_{i=1}^{N-1} \left( \frac{1}{4\pi} \sin \theta_i \right) d\theta d\phi, \quad (4.1)$$

where  $\int_0^\pi \dots d\theta$  and  $\int_0^{2\pi} \dots d\phi$  have the meanings defined by (3.8).

If, following Kramers,<sup>2</sup> we consider the effect of the flow of solvent on the dissolved molecule to be equivalent to a mechanical potential field  $U$  given by (2.21), we may write, from (2.21) and (3.2),

$$U = -\frac{1}{2} \frac{\zeta L^2}{N} \sum_1^{N-1} g_{ii} (\kappa_1 l_i l_j + \kappa_2 m_i m_j + \kappa_3 n_i n_j). \quad (4.2)$$

Then the Boltzmann formula gives

$$1 - p' = e^{-U/kT}, \quad (4.3)$$

where  $k$  and  $T$  are Boltzmann's constant and the absolute temperature respectively. If  $U \ll kT$ , (4.3) may be re-written

$$p' = U/kT. \quad (4.4)$$

Introducing this expression for  $p'$  into (4.1) and employing the expression (4.2) for  $U$ , we obtain

$$t'_{xx} = \frac{1}{18} \zeta L^2 N^2 \kappa_1 + \frac{1}{2} \frac{\zeta^2 L^4}{kTN^2} \kappa_1 (\kappa_1 I_1 + \kappa_2 I_2 + \kappa_3 I_3), \quad (4.5)$$

where

$$I_1 = \int_0^\pi \int_0^{2\pi} (\sum g_{ij} \cos \theta_i \cos \theta_j)^2 \prod_1^{N-1} \left( \frac{1}{4\pi} \sin \theta_i \right) d\theta d\phi,$$

$$I_2 = \int_0^\pi \int_0^{2\pi} (\sum g_{ij} \cos \theta_i \cos \theta_j) \prod_1^{N-1} \left( \frac{1}{4\pi} \sin \theta_i \right) (\sum g_{ij} \sin \theta_i \cos \phi_i \sin \theta_j \cos \phi_j) d\theta d\phi$$

and

$$I_3 = \int_0^\pi \int_0^{2\pi} (\sum g_{ij} \cos \theta_i \cos \theta_j) \prod_1^{N-1} \left( \frac{1}{4\pi} \sin \theta_i \right) (\sum g_{ij} \sin \theta_i \sin \phi_i \sin \theta_j \sin \phi_j) d\theta d\phi. \quad (4.6)$$

It can be shown, by carrying out the integrations indicated in (4.6) and summing the series so obtained, that, when  $N$  is large,

$$I_1 = \frac{1}{180} N^6 \text{ and } I_2 = I_3 = \frac{1}{324} N^6. \quad (4.7)$$

Introducing (4.7) into (4.5), and employing the relation (2.2), we find that

$$t'_{xx} = \frac{1}{18} \zeta L^2 N^2 \kappa_1 + \frac{1}{810} \frac{\zeta^2 L^4 N^4}{kT} \kappa_1^2. \quad (4.8)$$

$t'_{yy}$  and  $t'_{zz}$  are obtained from (4.8) by replacing  $\kappa_1$  by  $\kappa_2$  and  $\kappa_3$  respectively.

Comparing (4.8) with (3.13), we see that now

$$\Theta = \frac{1}{36} \zeta L^2 N^2 \text{ and } \Psi = \frac{1}{1620} \frac{\zeta^2 L^4 N^4}{kT}. \quad (4.9)$$

If there are  $\mathcal{N}$  high-polymer molecules per cm.<sup>3</sup> and we assume that the solution is sufficiently dilute for their interactions to be neglected we have

$$\Theta = \frac{1}{36} \zeta L^2 N^2 \mathcal{N} \text{ and } \Psi = \frac{1}{1620} \frac{\zeta^2 L^4 N^4 \mathcal{N}}{kT}. \quad (4.10)$$

From (4.10), we have

$$\Psi = \frac{4}{5} \frac{\Theta^2}{kT\mathcal{N}}. \quad (4.11)$$

**5. The Stress Components for a Straight Rigid Chain.**—In order to find qualitatively what effect the stiffness of the chain has on  $\Theta$  and  $\Psi$ , we can consider the extreme case in which each high-polymer molecule consists of  $N$  equal mass-points connected by rigid collinear links, which are weightless, offer no resistance to the motion of the solvent and are incapable of any rotation with respect to one another. The orientation of the chain may then be defined by two angles  $\theta$  and  $\phi$ . The direction-cosines ( $l, m, n$ ) of the molecule are then given by

$$l = \cos \theta, m = \sin \theta \cos \phi \text{ and } n = \sin \theta \sin \phi. \quad (5.1)$$

We now have

$$x_i = L[i - \frac{1}{2}(N+1)]l, \text{ etc.} \quad (5.2)$$



We obtain for the orientational potential energy of the molecule

$$U = -\frac{1}{2}\zeta L^2(\kappa_1 l^2 + \kappa_2 m^2 + \kappa_3 n^2) \sum_{i=1}^{N-1} [i - \frac{1}{2}(N+1)]^2, \text{ etc.} \quad (5.3)$$

Now, if  $N$  is large,

$$\sum_{i=1}^{N-1} [i - \frac{1}{2}(N+1)]^2 = \frac{1}{12}N^3. \quad (5.4)$$

Then,

$$U = -\frac{1}{24}\zeta L^2 N^3 (\kappa_1 l^2 + \kappa_2 m^2 + \kappa_3 n^2). \quad (5.5)$$

Also, from (2.19) and (5.2),

$$t'_n = \zeta \kappa_1 \sum_1^N \langle x_i^2 \rangle_{AV} = \zeta \kappa_1 L^2 \sum_{i=1}^{N-1} [i - \frac{1}{2}(N+1)]^2 \langle l^2 \rangle_{AV}. \quad (5.6)$$

Employing the relations (5.4) and (5.3) we obtain, in a manner similar to that of § 4,

$$t'_{zz} = \frac{1}{36}\zeta L^2 N^3 \kappa_1 + \frac{1}{2160} \frac{(\zeta L^2 N^3)^2}{kT} \kappa_1^2, \text{ etc.} \quad (5.7)$$

If now we have  $\mathcal{N}$  non-interacting high-polymer molecules per  $\text{cm}^3$ , then

$$t'_{zz} = \frac{1}{36}\zeta L^2 N^3 \mathcal{N} \kappa_1 + \frac{1}{2160} \frac{(\zeta L^2 N^3)^2 \mathcal{N}}{kT} \kappa_1^2, \text{ etc.} \quad (5.8)$$

Comparing equations (5.8) and (3.13), we see that

$$\Theta = \frac{1}{72}\zeta L^2 N^3 \mathcal{N} \text{ and } \Psi = \frac{1}{4320} \frac{(\zeta L^2 N^3)^2 \mathcal{N}}{kT}. \quad (5.9)$$

From (5.9), we have

$$\Psi = \frac{6}{5} \frac{\Theta^2}{kT\mathcal{N}}. \quad (5.10)$$

It is seen that although the assumption that the dissolved molecules are rigid increases considerably the values of  $\Theta$  and  $\Psi$ , yet the relation between  $\Theta$  and  $\Psi$  is not greatly altered.

**6. Relation to Kramers' Theory.**—The procedure followed has been basically the same as that adopted by Kramers. Unlike Kramers' procedure, however, the potential of the flow field has been introduced here only as a means of calculating the non-uniform distribution of chain orientations when the orientation of the molecules is appreciable. The contribution of dissolved high-polymer molecules to the viscosity, obtained in § 3, does not require the introduction of the notion of a flow field.

Instead of considering the general state of irrotational flow defined by (2.1), Kramers considers the special case when

$$u = \frac{1}{2}\kappa y, \quad v = \frac{1}{2}\kappa x \text{ and } w = 0, \quad (6.1)$$

in which the principal directions of flow are not parallel to the reference axes. For this case, he obtains (in our notation)

$$\Theta = -\frac{1}{2}\zeta \sum_{i=1}^{N-1} \langle (y + y_i)^2 \rangle_{AV} \quad (6.2)$$

and neglects  $y$ , the co-ordinate of the centre of gravity, apparently in a quite arbitrary manner.

**7. Discussion.**—In the theory which has been presented, the non-vanishing of  $\Psi$  arises essentially from the preferential orientation of the links along the stream-lines. Apart from the idealization of the molecules themselves, some assumptions have been made which are not strictly defensible.

It is assumed that the presence of a high-polymer molecule does not alter the flow configuration in its neighbourhood. It is, of course, extremely unlikely that this is so. However, it can readily be seen that the modification of the flow field will be such as to screen the central portions of the molecule from the full effect of the flow field, the effect of the flow in orienting the molecule being thereby somewhat reduced. Again, the replacement of the solvent-polymer interactions by a mechanical field of force in § 4 and § 5 is not strictly in accord with thermodynamic principles since the system considered is not one in thermodynamic equilibrium. It does, however, provide a method of estimating the degree of orientation of the links, which, if not correct in detail, should provide an order of magnitude for the effects considered.

In deriving equation (4.10) and (4.11), it is assumed that the solution is sufficiently dilute for interactions between the dissolved molecules to be negligible. This will be valid only at the lowest concentrations. For a 0.1 % solution of polystyrene in benzene and a state of flow defined by (6.1), we can calculate  $\nu_{xx} (= \frac{1}{2} \Psi \kappa^2)$ , taking the molecular weight of the polystyrene as  $10^5$ , and the contribution  $\Theta$  of the dissolved macromolecules to the viscosity of the solution as  $1.5 \times 10^{-3}$  poises, as

$$t_{xx} \approx \frac{1}{8} 10^{-8} \kappa^2 \text{ dynes/cm.}^2.$$

So, for such a solution,  $t_{xx}$  would be undetectably small, unless exceedingly high values of  $\kappa$  are employed.

As the concentration of the solution is increased, the interactions between molecules, either directly by entanglements, or through the disturbance of the flow field, can no longer be neglected. The effect of this is to produce (i) a non-linear dependence of the viscosity on concentration and (ii) dependence of the viscosity on the velocity gradient. We can conveniently consider these effects as arising in the following manner. Owing to the interactions of the molecules, they may be regarded as forming groups which act, for the purposes of our calculations, as single macro-molecules, in the sense that a force exerted on one molecule of the group will be transmitted to the others. For a given concentration of dissolved high-polymer, in g. cm.<sup>-3</sup>, the contribution to the viscosity will increase as the number of molecules in each group increases, as it depends linearly on the number of groups and more rapidly on the size of the group. The effective number of molecules in each group will, of course, depend on the velocity gradient, increasing as the velocity gradient decreases.

A rough estimate of the effective number of groups for a specified state of flow can be obtained by comparing the measured specific viscosity  $\eta'$  of the concentrated solution with the specific viscosity  $\eta''$  of a solution of equal concentration, in which the molecules do not interact.  $\eta''$  can be obtained from the measured intrinsic viscosity  $[\eta]$  for the solution. We have

$$\eta'' = [\eta]c, \quad . \quad . \quad . \quad . \quad . \quad . \quad (7.1)$$

where  $c$  is the concentration. Then, from (4.10), we have

$$\eta'' = \frac{1}{36} \zeta L^2 N^2 \mathcal{N} / \eta_0, \quad . \quad . \quad . \quad . \quad (7.2)$$

where  $\eta_0$  is the viscosity of the solvent.

Similarly, we have

$$\eta' = \frac{1}{36} \zeta L^2 N'^2 \mathcal{N}' / \eta_0. \quad (7.3)$$

where  $N'$  is the number of links in each effective flow group of molecules and  $\mathcal{N}'$  is the number of such groups.

Now,

$$N'\mathcal{N}' = N\mathcal{N} = \nu, \quad . \quad . \quad . \quad . \quad (7.4)$$

where  $\nu$  is the total number of links per cm.<sup>3</sup>.

From (7.2), (7.3) and (7.4), we obtain

$$\eta'/\eta'' = \mathcal{N}/\mathcal{N}'. \quad (7.5)$$

$\mathcal{N}$  can, of course, be obtained from the concentration and known molecular weight of the high-polymer.  $\Psi$  can then be calculated from the formula

$$\Psi = \frac{4}{5} \frac{\eta'^2}{kT\mathcal{N}'} \quad (7.6)$$

For a 25.7 % solution of polystyrene (of molecular weight 120,000) in xylene, Ferry<sup>4</sup> has found that the viscosity is 220 poises when the velocity gradient is 9 cm. sec.<sup>-1</sup>. The measurement was made with the fluid in a state of laminar flow. The intrinsic viscosity for such a solution would be about 2.5. Taking the viscosity of xylene as 0.006 poises, these figures give, from (7.5),

$$\mathcal{N}'/\mathcal{N} \approx 1.7 \times 10^{-3}. \quad (7.7)$$

Taking the value 120,000 for the molecular weight, we find that a 25.7 % solution contains approximately  $1.2 \times 10^{18}$  molecules per cm.<sup>3</sup>.

Thus,  $\mathcal{N}' \approx 2 \times 10^{15}$ .

Employing this, together with the measured viscosity (220 poises), in (7.6) and taking  $\kappa = 9$  sec.<sup>-1</sup>, we obtain for the state of flow considered

$$t_{xx} = t_{yy} = \frac{1}{2} \Psi \kappa^2 \approx 18 \text{ g./cm.}^2$$

and

$$t_{xy} = \eta' \kappa \approx 2.0 \text{ g./cm.}^2.$$

Thus, in this case, the calculated normal stress components are considerably greater than the tangential stress component. This contradicts the assumption made in the calculations that  $U \ll kT$ , but shows that normal stress components which are at any rate not greatly less than the tangential stress components should be obtainable in a concentrated high-polymer solution.

In the calculation, the effective flow group has been treated as though it consists of an unbranched chain of mass-points connected by rigid links. It might at first sight appear that it would be more realistic to treat it as a highly-branched molecule. The calculation for such a model would, however, be more complicated. The procedure that has been adopted assumes that for a particular velocity gradient the solution is equivalent from the point of view of its flow properties to one of equal concentration containing  $\mathcal{N}'$  non-interacting unbranched molecules.

It may be noticed, however, that the argument of § 2 is valid for the branched case and so, at any rate qualitatively, it is seen that orientation of the molecules as a result of the flow still results in non-zero values of  $\Psi$ , if we assume the flow groups to be branched.

Much of this work was carried out at the Mellon Institute of Industrial Research, Pittsburgh, Penn., while the author was on leave from the British Rubber Producers' Research Association and serving as a special consultant to the Institute's Multiple Fellowship on Synthetic Rubber sustained by the Office of the Rubber Reserve, Reconstruction Finance Corporation.

*Davy Faraday Laboratory,  
The Royal Institution,  
21 Albemarle Street,  
London W.1.*

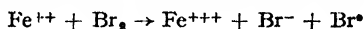
<sup>4</sup> Ferry, *J. Amer. Chem. Soc.*, 1942, 64, 1330.

# A STUDY OF THE CONVERSION OF MALEIC ACID TO FUMARIC ACID

BY D. H. DERBYSHIRE AND WILLIAM A. WATERS

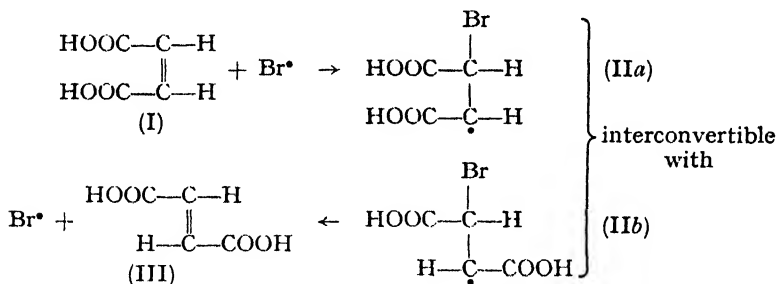
Received 14th February, 1949

It is shown that bromine atoms, generated in aqueous solution by the reaction



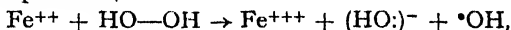
effect the conversion of maleic acid into fumaric acid by the simple mechanism of bromine addition followed by re-elimination subsequent to the occurrence of free rotation in the adduct.

The independent photochemical researches of Wachholtz and Eggert<sup>1</sup> and of Berthoud and his colleagues<sup>2, 3</sup> have shown that several geometrical isomerides, such as maleic and fumaric acids, can be interconverted by the action of free bromine atoms, which appear to act by adding on to the double bond of the less stable isomer (e.g. I) to give an organic radical (IIa or IIb) in which free rotation is possible, and then separating once more to give the more stable isomer (III):



The evidence for the existence of a transient organic radical (II) rests upon Berthoud's isolation of a dimeric product from  $\alpha$ -phenylcinnamitrile in a reaction of this type,<sup>4</sup> whilst that for the participation of bromine atoms in the change depends mainly upon a kinetic analysis of reaction velocities. Wachholtz,<sup>5</sup> however, showed that the reaction could also be effected in the dark by reducing free bromine, bromic acid, or hypobromous acid, with reagents such as ferrous sulphate, and pointed out that this evidence substantiated the view that uncharged bromine atoms were the true active catalysts. He did not, however, study the kinetics of the reaction in any detail.

In view of the close similarity between the reactions of ferrous salts with hydrogen peroxide,



and with molecular bromine (below) it appeared that the mechanism of

<sup>1</sup> Wachholtz and Eggert, *Z. physik. Chem.*, 1927, **125**, 1; *Z. Elektrochem.*, 1927, **33**, 542.

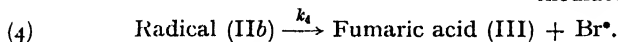
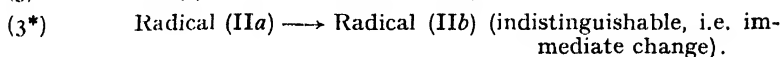
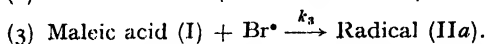
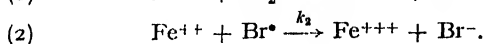
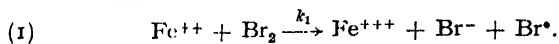
<sup>2</sup> *Z. physik. Chem.*, 1926, **120**, 174; *Helv. chim. Acta*, 1927, **10**, 289.

<sup>3</sup> *J. Chim. Phys.*, 1927, **24**, 213; 1930, **27**, 291.

<sup>4</sup> *Helv. chim. Acta*, 1930, **13**, 385.

<sup>5</sup> *Z. Elektrochem.*, 1927, **33**, 545.

this isomerization could be studied more clearly by examining the overall stoichiometry of the main chain reaction concerned by using the general technique of Merz and Waters.<sup>6</sup> The simplest reaction scheme can be written as follows :



Reactions (1) to (3) have already been well substantiated, but it has been uncertain hitherto as to whether reaction (4) occurs spontaneously, by solvent collision, or only upon a subsequent collision between a radical and a second maleic acid molecule. From eqn. (1)-(4), it follows that

$$[\text{Br}^\bullet] = k_1/k_2[\text{Br}_2],$$

$$[\text{Radical}] = k_3/k_4 \times [\text{Maleic acid}][\text{Br}_2],$$

and hence

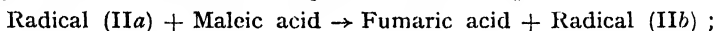
$$\frac{+d[\text{Fumaric acid}]/dt}{-d[\text{Fe}^{++}]/dt} = \frac{\frac{k_1 \times k_3}{k_2} [\text{Maleic acid}] \times [\text{Br}_2]}{2k_1 \times [\text{Fe}^{++}][\text{Br}_2]},$$

or

$$\frac{+d[\text{Fumaric acid}]}{-d[\text{Fe}^{++}]} = \frac{k_3}{2 \times k_2} \times \frac{[\text{Maleic acid}]}{[\text{Fe}^{++}]} \quad (A)$$

If, then, a dilute bromine solution is added, with stirring, to a prepared mixture of ferrous sulphate solution and maleic acid in such an amount that the changes in concentration  $\Delta[\text{Fe}^{++}]$  and  $\Delta[\text{Maleic acid}]$  are only a small fraction of the original concentrations,  $[\text{Fe}^{++}]$  and  $[\text{Maleic acid}]$ , then eqn. (A) should hold when the measurable quantities ( $-\Delta \text{Fe}^{++}$ ) and  $(+\Delta \text{Fumaric acid})$  are substituted for the differentials.

Fig. 1 shows that this is the case. The isomerization therefore does proceed according to eqn. (1) to (4) substantially, and requires neither the reduction of the radical (II) by another reagent (e.g.  $\text{Fe}^{++}$  ion) nor a halogen transfer between two organic molecules, e.g.



the second mechanism for instance would lead to a calculated consumption ratio ( $\Delta \text{Fumaric acid}/-\Delta \text{Fe}^{++}$ ) varying as  $[\text{Maleic acid}]^2$ .

The slope of the graph of Fig. 1 indicates that reaction (3) must be exceedingly fast, but no indication can be given of the rate of reaction (4). Reaction (3) presumably occurs easily with maleic acid because the energy of this  $p-p$  bond (ca. 62 kcal.) is less than the energy of formation of a C-Br bond (ca. 65 kcal.).<sup>7</sup> The occurrence of reaction (4) can only be facile if it is exothermic. Apparently it is the exact reverse of (3), but attention may be directed to the fact that the difference between the heats of combustion of maleic and fumaric acids (7 kcal.) is greater than the heat of reaction (3) as approximately computed above.

At high  $[\text{Maleic acid}]/[\text{Fe}^{++}]$  ratios, the final quantity of  $\text{Fe}^{+++}$  formed falls slightly below that equivalent to the bromine actually taken, presumably because a small amount of brominated acid (dibromosuccinic

<sup>6</sup> Merz and Waters, *Faraday Soc. Discussions*, 1947, **2**, 179; *J. Chem. Soc.* (in press).

<sup>7</sup> These approximations are the averages of recent bond-strength data, as collected by Steacie, *Atomic and Free Radical Reactions* (1946), pp. 72-85 compare Dewar, *The Electronic Theory of Organic Chemistry* (1949), p. 32.

acids or bromofumaric acid) is formed. This is so slight, however, that we have been unable to isolate the by-products or to decide exactly how they are formed. We satisfied ourselves, however, that in the dark, no significant *direct* addition of bromine to maleic acid occurs in the very short time which elapses in these isomerizations. In the presence of

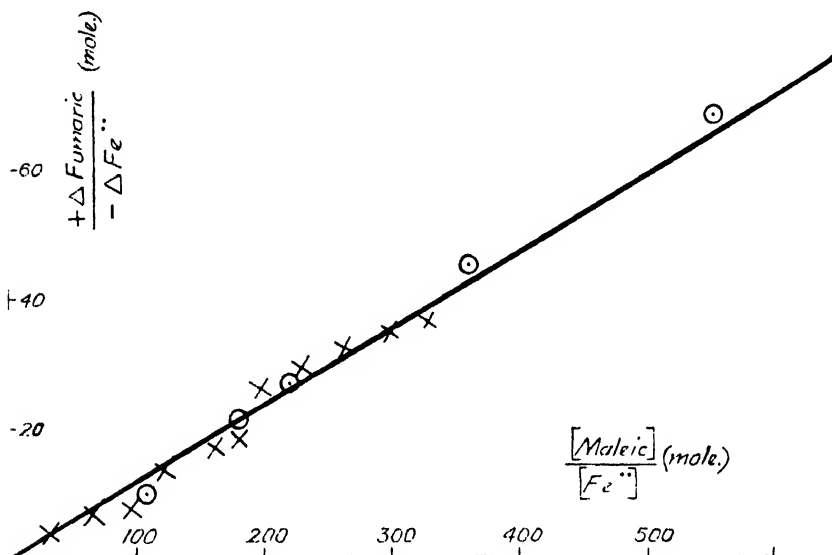


FIG. 1.

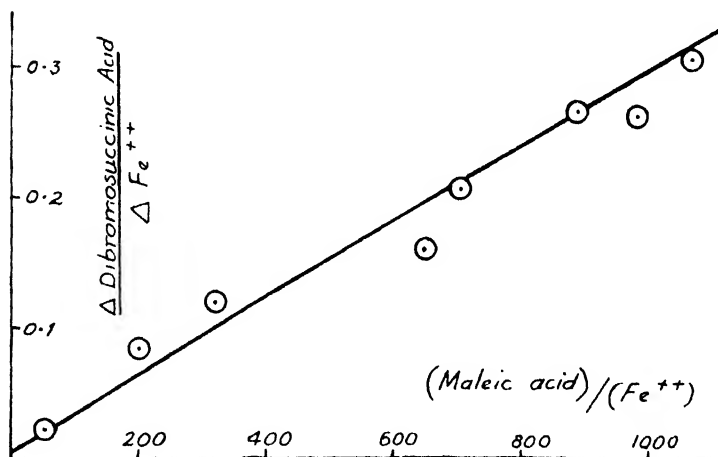


FIG. 2.

ferrous ions the isomerization is complete in a matter of seconds, whilst in its absence the decrease in the bromine concentration is measurable only after several minutes. This direct addition of bromine must therefore have an entirely different mechanism: it is not accompanied by any formation of fumaric acid.

## Experimental

All reactions were carried out at room temperature (*ca.* 19° C) in vessels surrounded by cardboard containers to exclude light. To secure a fairly constant pH, all solutions were prepared in 0.1 N H<sub>2</sub>SO<sub>4</sub>.

The ratio (+  $\Delta$  fumaric acid)/(-  $\Delta$  Fe<sup>++</sup>) was determined by taking prepared mixtures of maleic acid (1.5–3 M) and FeSO<sub>4</sub> (0.01–0.05 N) in 0.1 N H<sub>2</sub>SO<sub>4</sub> and adding to them dilute (*ca.* 0.03 N) aqueous bromine equivalent to no more than 40 % of the total Fe<sup>++</sup>, and often to much less. For instance, in two series of experiments (plotted separately as X and O in the Fig.) the mixtures were chosen as follows:

(a) 5.0 ml. of 0.04 N bromine were added to a series of mixtures each containing 5.0 ml. of 0.1 N FeSO<sub>4</sub> and from 5 to 50 ml. of 3 M maleic acid (i.e. the total volume of liquid varied); (b) 30.0 ml. of maleic acid were mixed with from 1 to 10 ml. of FeSO<sub>4</sub> solution, and the total volume was in each case made up to 40 ml. with 0.1 N H<sub>2</sub>SO<sub>4</sub> before adding bromine equivalent to 30 % of the Fe<sup>++</sup> present, and finally diluting to 50 ml.

Fumaric acid was determined by allowing the mixtures to stand overnight in the dark, when precipitation of this sparingly soluble reaction product reached completion. The deposits of fumaric acid were then separated on sintered-glass filters, washed with cold saturated fumaric acid in distilled water, and then dissolved in a known excess of standard baryta. The excess of alkali was then determined by titration with HCl using phenolphthalein as indicator. Data were finally corrected by taking into account the solubility of fumaric acid in cold 0.1 N mineral acid. This was found, by our measurements, to be 3.64 g./l., or 0.0314 M at 19° C, compared with a previously recorded solubility in pure water at this temperature of 0.0414 M.<sup>8</sup> The chemical identity and the purity of the precipitates were regularly checked. The linearity of the plot shows that the errors involved in this admittedly approximate method of estimating fumaric acid are only of second order.

(-  $\Delta$ Fe<sup>++</sup>) was throughout determined colorimetrically, as Fe<sup>+++</sup> produced, using the ferric thiocyanate colour, which was measured on a Hilger Spekker photo-electric absorptiometer.

We also evaluated the amounts of brominated acid produced during our reactions in terms of [Br<sub>2</sub>] (taken) - ( $\Delta$ [Fe<sup>++</sup>]) (found). This was always very small, and seemed to vary somewhat with the manner in which the bromine was added. Very approximately it rose as the ratio [Maleic acid]/[Fe<sup>++</sup>] was increased. The total amount of brominated acid was, however, only of the order of 10<sup>-4</sup> of the total acid taken, or of 10<sup>-2</sup> of the fumaric acid formed. This confirms our theoretical assumption—that chain-ending reactions other than (2) can be neglected in deriving the principal chain sequence from our analytical data. Clearly, too, the isolation of by-products in these small amounts is impracticable.

We thank the Royal Society for a grant for the purchase of the Spekker Absorptiometer. One of us (D. H. D.) thanks the Department of Scientific and Industrial Research for a maintenance grant.

*The Dyson Perrins Laboratory,  
Oxford.*

<sup>8</sup> Lange and Sink, *J. Amer. Chem. Soc.*, 1930, **52**, 2603.

## A NEW METHOD OF FORMING A LIQUID JUNCTION BETWEEN ELECTRODE VESSELS IN A THERMOSTAT

By G. S. SMITH

*Received 15th February, 1949*

A simple means of establishing and renewing a liquid junction between two electrode vessels, kept permanently in a thermostat, by means of operations wholly external to the thermostat, is described.

The apparatus \* to be described was designed to provide a simple means of establishing a liquid junction in a cylindrical tube between a calomel electrode and a polarographic half-cell, both of which were to remain permanently fixed in a thermostat, but the principle has obviously a wider application. Its special features are—(a) the calomel half-cell or other reference electrode and the liquid junction tube are completely immersed in the thermostat. (b) Taps for operating the flow of electrolyte etc., are completely outside the thermostat. (c) The liquid junction is easily formed and reproduced when necessary. (d) The electrode vessels and liquid junction tube can be kept permanently immersed in the thermostat. (e) The washing of connecting tubes, etc., can be carried out without any contact between the washing liquid, which could even be concentrated sulphuric acid if desired, and the liquid of the reference electrode.

### Experimental

The diagram of the apparatus in Fig. 1 shows the liquid junction tube in combination with a 3.5 N or saturated calomel electrode K. The tap funnel

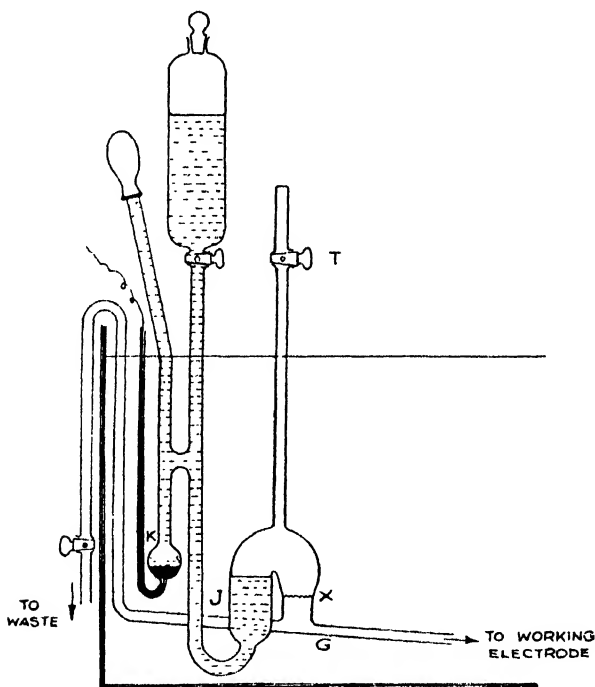


FIG. 1.

serves as a reservoir for the electrolyte. Its stem, which has a side-tube connected to a tube containing mercury overlaid with mercurous chloride-mercury mixture and potassium chloride solution, has its lower end bent upwards and joined to a wider tube J. The latter tube possesses a sharp downward bend and the end is connected at X by means of a fused joint, ground-glass joint or rubber tubing, to a short tube fused to the tube G which serves for connection to the working electrode and also to a siphon for carrying off waste liquid. The upper part of tube J carries a tube with a tap T. The tube containing the

\* The apparatus described forms part of the subject-matter of Provisional Patent Specification No. 14306/49, dated 27th May, 1949.



calomel half-cell K is closed with a rubber teat which is fitted after the tube has been nearly filled with the potassium chloride solution from the tap funnel. The potassium chloride solution is allowed to enter tube J until it overflows into the right side of J. The tap of the funnel is then closed and the teat momentarily squeezed to force a further quantity over, and to leave the surface of the liquid just below the bend in tube J as illustrated. The excess liquid is removed by slight suction when necessary at the waste end of tube G. With tap T closed and the waste tap open, tube G can be washed out with water or other suitable liquid from the working electrode side.

In forming the liquid junction the electrolyte from the working electrode vessel is allowed to flow along G, the waste tap is then closed and tap T is opened very carefully so that the electrolyte rises slowly past X and flows gently on top of the potassium chloride solution in J. Tap T is closed, and the apparatus is then ready for the taking of readings.

After use, gentle suction is applied at the waste tap, tap T is opened, and at the same time potassium chloride solution is allowed to flush out the junction liquid. Tap T is then closed, and the teat is pressed momentarily so as to leave the level in tube J as at the start of operations.

With the apparatus illustrated the liquid junction is formed in a relatively wide tube. A slight modification of J allows the junction to be formed in a narrow tube. For this purpose the upturned end of the delivery tube, in the form of a semi-capillary tube, is extended nearly to the position indicated by the liquid level in the diagram, and the left side of J is correspondingly shortened. The volume of the left side of J between the top of the narrow tube and the bend in the modified construction is arranged so that when the tap of the funnel is turned off after potassium chloride solution has been allowed to flow over into the right side of J, and a further amount of the solution has been forced over by pressure on the teat, the subsequent release of pressure leaves the surface of the solution somewhere within the semi-capillary tube. The potassium chloride solution ejected from J is, of course, allowed to flow to waste. To form the liquid junction the teat is pressed slightly to bring the potassium chloride solution just to the top of the narrow tube, the other electrolyte is allowed to flow gently into J by opening tap T as described above, and the pressure on the teat is then released so that the boundary of the two solutions is drawn into the narrow tube.

In electrochemical work it is sometimes convenient to be able to dip the end of a tube communicating with a calomel electrode into a solution in which another electrode is immersed. The electrode with the liquid junction vessel as described but terminating in an orifice at X may be used for this purpose. To form the liquid junction the apparatus is dipped into the solution, and tap T is opened so that the solution in the outside vessel flows into J. The junction is then formed in a cylindrical tube, i.e., in the left side of J, and not at the tip of a narrow tube as is usual with dipping electrodes. The necessary cylindrical symmetry of the junction is thus maintainable for a longer time.

The method is considered to be superior to others described: to that of Ingham and Morrison<sup>1</sup> in that it avoids the need for insertion and removal of a junction tube each time the apparatus is used; to that of Coates<sup>2</sup> in that an immersed tap is dispensed with, and to that of Smith and Speakman<sup>3</sup> in that the washing-out of the connecting tubes does not involve contact with the electrolyte of the reference electrode.

This paper is published by permission of the Ministry of Supply and the Controller of H.M. Stationery Office.

*Aeronautical Inspection Department,  
Test House,  
Harefield, Middlesex.*

<sup>1</sup> *J. Chem. Soc.*, 1933, 1200.

<sup>2</sup> *Trans. Faraday Soc.*, 1948, 44, 1031.

<sup>3</sup> *Ibid.*, 1945, 489.

# THE SOLUBILITY OF BENZYL PENICILLIN SALTS IN ACETONE

BY J. E. PAGE AND J. G. WALLER

*Received 2nd March, 1949*

An improved apparatus for solubility measurements is described. The solubilities of the ammonium, sodium, and potassium salts of benzylpenicillin in acetone containing 0.05 %, 1.0 % and 2.0 % of water have been measured over the temperature range  $-78^{\circ}$  to  $+40^{\circ}$  C. The solubilities showed unexpected increases at low temperatures.

In view of the claim<sup>1</sup> that acetone may be used for the crystallization of penicillin salts, we have measured over a wide temperature range the solubility in acetone of the purified ammonium, sodium, and potassium salts of benzylpenicillin (penicillin II or G).

In preliminary experiments,<sup>2</sup> saturated solutions were prepared by mixing acetone with excess sodium benzylpenicillin; they were then filtered through a sintered-glass plug, and the penicillin in the filtrate was assayed biologically. Unfortunately, it was difficult to control the solution temperature and there was evaporation of the acetone, making the filtrate usually cloudy or supersaturated. Better results were obtained by using a modification of Campbell's apparatus,<sup>3</sup> which enabled us to determine the solubility of benzylpenicillin salts in 5 ml. portions of acetone over the temperature range,  $-78^{\circ}$  to  $+40^{\circ}$  C.

## Experimental

Our solubility apparatus (Fig. 1) consisted of two test-tubes, A and B, that could be linked together through a ground-glass component C, through which passed two connecting tubes, D and E. Connecting tube E was constricted and packed with glass wool at the end opening into tube A. The end of connecting tube D reached to the middle of test-tube B and was drawn off to a capillary and bent round through  $180^{\circ}$  to prevent any liquid from splashing into it. A solution in test-tube B could be agitated by bubbling nitrogen through the side arm, F.

More than sufficient benzylpenicillin salt to produce saturation and about 5 ml. of acetone were placed in test-tube B, and nitrogen that had been saturated with acetone vapour at the temperature of the experiment was bubbled through the mixture. The ground-glass component C carrying tubes D and E was fitted to test-tube B, which was then placed inside a glass vessel containing either water or alcohol to preserve thermal contact, and mounted in a thermostat to keep it at the desired temperature. When temperature equilibrium had been reached (after 1-2 hr.), the solubility apparatus was removed from the thermostat, the nitrogen bubbling stopped and test-tube A fitted on to the ground-glass component, C. The apparatus was inverted and immediately returned to the thermostat. The solution filtered through the glass wool plug into test-tube A, the air being displaced out through connecting tube D. When filtration was complete, test-tube A was removed, tightly stoppered, and allowed to attain room temperature. A known volume of the supersaturated

<sup>1</sup> Clarke, Johnson and Robinson, *The Chemistry of Penicillin* (Princeton University Press, 1949), p. 85.

<sup>2</sup> *Ibid.*, p. 86.

<sup>3</sup> Campbell, *J. Chem. Soc.*, 1930, 179

or slightly cloudy solution was diluted to 20 ml. with a phosphate buffer solution of pH 7.0 (0.078 % of potassium dihydrogen phosphate and 0.10 % of dipotassium hydrogen phosphate) and assayed for penicillin by the cup plate method.<sup>4</sup> The accuracy of the replicate assays was probably better than 5 %.

For measurements at temperatures below 0° C, the apparatus was immersed in a partially frozen mixture of alcohol and water that had been cooled by the addition of solid carbon dioxide. The proportion of alcohol and water was adjusted so as to give the desired temperature. Special precautions were taken to prevent moisture entering the apparatus.

The acetone used was of A.R. quality and had been dried over and redistilled from anhydrous potassium carbonate. The moisture content of the acetone was determined by the Karl Fischer procedure.

The penicillin salts were supplied by Mr. W. K. Anslow of the Fermentation Division, Glaxo Laboratories Ltd.; the penicillin present was approximately 100 % benzylpenicillin.

## Results

Our data for the solubility of sodium, potassium and ammonium benzylpenicillin in acetone are set out in Tables I, II and III, respectively.

The solubility of the sodium salt in dry acetone is fairly constant between -20° and +25° C, but it increases with fall of temperature below -20° C. Acetone solutions containing 1.0 to 2.0 % of added water show a much greater increase in solubility with fall of temperature. By warming to 0° C acetone solutions saturated at -50° C, we obtained excellent crystals of sodium benzylpenicillin. The latter were isolated and on micro-analysis were found to consist of the anhydrous sodium salt (required: C, 53.9; H, 4.81; and N, 7.86; found: C, 52.8; H, 4.79; and N, 8.05 %). This unorthodox method of recrystallization may be of some general interest.

The solubility of potassium benzylpenicillin in anhydrous acetone and in acetone containing small amounts of water is fairly constant from +25° down to -40° C and then shows a small increase.

TABLE I.—SOLUBILITY OF SODIUM BENZYLPENICILLIN IN AQUEOUS ACETONE

Temperature in °C	Solubility in g. per 100 ml. of Acetone containing		
	<0.05 % Water	1.0 % Water	2.0 % Water
+40	0.008	0.038	0.10
+25	0.004	0.022	0.10
0	0.004	0.024	0.10
-20	0.006	0.040	1.2
-40	0.011	0.088	2.6
-78	0.015	0.23	1.6

The solubility of the ammonium salt in anhydrous acetone is, contrary to our observations on the sodium and potassium salts, reduced by the addition of small amounts of water, but, as for the other salts, is increased by lowering the temperature below -20° C.

Our observation that the ammonium salt is more soluble in anhydrous acetone than in acetone containing 1.0 % of water suggested that the addition of small amounts of water might precipitate ammonium benzylpenicillin from its solution in dry acetone. This was tried; the material that separated had

<sup>4</sup> Ref. 1, p. 1031.

the same melting point (140° C, with decomposition) as a specimen obtained by adding dry acetone to a saturated solution of the ammonium salt in acetone containing 10 % of water.

The phenomenon of increased solubility in acetone with fall in temperature

TABLE II.—SOLUBILITY OF POTASSIUM PENICILLIN

Temperature in °C	Solubility in g. per 100 ml. of Acetone containing		
	<0.5 % Water	1 % Water	2 % Water
+40	0.010	0.015	0.085
+25	0.004	0.020	0.090
0	0.004	0.020	0.085
-20	0.004	0.020	0.075
-40	0.004	0.015	0.070
-78	0.015	0.030	0.055

has been observed before with simple inorganic salts, but apparently has not been reported for organic salts. Thus Bell, Rowlands, Bamford, Thomas and Jones<sup>5</sup> found that the solubility of lithium chloride increased from 0.61 % at + 50° to 1.73 % at 0° C. On the other hand, the solubility of lithium bromide

TABLE III.—SOLUBILITY OF AMMONIUM PENICILLIN

Temperature in °C	Solubility in g. per 100 ml. of Acetone containing		
	<0.05 % Water	1 % Water	2 % Water
+40	1.8	0.50	0.90
+25	1.2	0.30	0.35
0	0.35	0.15	0.20
-20	0.27	0.080	0.15
-40	0.33	0.065	0.15
-78	0.45	0.15	0.25

fell from 0.40 % at 60° to 0.13 % at 10° C. The solubility of potassium iodide in acetone increases from 4.15 % at - 78.5° to 9.80 % at - 57.5° C and then decreases as the temperature is increased, being 1.33 % at 25° C and 0.84 % at 54.5° C.<sup>6</sup>

We wish to thank Mr. E. G. Cummins for technical assistance and Mr. G. L. F. Norris for the penicillin assays.

*Research Division,  
Glaxo Laboratories Ltd.,  
Greenford, Middx.*

<sup>5</sup> Bell, Rowlands, Bamford, Thomas and Jones, *J. Chem. Soc.*, 1930, 1927.

<sup>6</sup> Livingston and Halverson, *J. Physic. Chem.*, 1946, 50, 1.

# THE MEASUREMENT OF DIELECTRIC CONSTANTS OF LIQUIDS BY A FREQUENCY DEVIATION METHOD

BY W. L. G. GENT

*Received 10th March, 1949*

The measurement of dielectric constants of liquids by a frequency deviation method, which allows a continuous check on the standard capacity by calibration against a crystal oscillator, is described.

The determination of low dielectric constants ( $\sim 2$ ) of liquids and solutions by the heterodyne beat method usually involves <sup>1</sup> measurement of the capacity increment on filling a test cell in the grid circuit of a variable-frequency oscillator by the variation required on a parallel standard variable condenser to bring the oscillator back to its original frequency by reference to a crystal-controlled standard. The standard capacity requires fairly frequent re-calibration for measurements of high accuracy and to overcome this a method has been devised whereby a continuous check is obtained by calibration against a crystal oscillator, measurement of the frequency deviation on filling the test cell being made.

The block circuit (Fig. 1) shows the main layout. Power supplies are derived from a stabilized power pack <sup>2</sup> fed from a constant-voltage transformer and the filaments of the oscillators are run from accumulators.

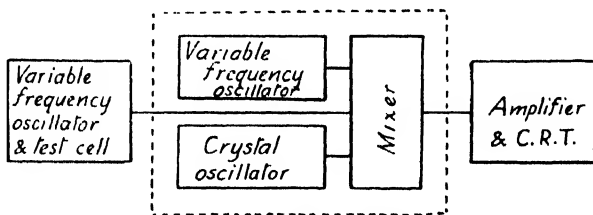


FIG. 1.—Block circuit.

By this means frequency drift due to changes in voltage and valve characteristics are reduced to relatively negligible proportions. The beat note is detected after amplification on a cathode-ray tube using the A.C. mains as 50 c./sec. time-base. Any convenient Lissajous figure may be used (e.g. the figure-of-eight at 100 c./sec. difference of the oscillators) or the zero-beat, since locking-in of the oscillators is very slight.

A transitron oscillator <sup>3</sup> is tuned (Fig. 2) by the test cell in parallel with a fixed capacity, the frequency being nominally 1 Mc./sec. Output is capacity coupled to a frequency meter (Bendix Radio BC-221-M). The tuning circuit of the variable-frequency oscillator of the meter is calibrated in the 1 Mc./sec. range at every 0.4 kc./sec. and the scale divided into 50,000 divisions. A change in the capacity of the calibrated condenser of the wave-meter is nullified by adjustment of a parallel

<sup>1</sup> Smyth, *Technique of Organic Chemistry*, Vol. II (1946), p. 989.

<sup>2</sup> *Amateur Radio Handbook*, 2nd ed. (1946), p. 157.

<sup>3</sup> Taylor, *Electronics*, 1946, 19, 142.

trimming capacitor each time the wave-meter is checked against the crystal oscillator. By this means the frequency of the transitron oscillator, and consequently the required change of capacity of the dielectric constant cell, can be measured unaffected by any change in circuit constants

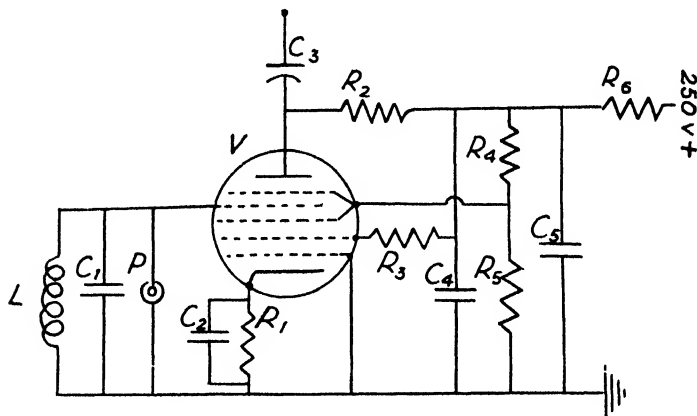


FIG. 2.—Transitron oscillator.

$C_1 = 80 \text{ pF}$	$R_1 = 450 \text{ ohms.}$	$R_6 = 25,000 \text{ ohms.}$
$C_2 = 0.01 \text{ } \mu\text{F}$	$R_2 = 50,000 \text{ ohms}$	$L = 290 \text{ } \mu\text{F}$
$C_3 = 0.15 \text{ pF}$	$R_3 = 50,000 \text{ ohms}$	$P = \text{coaxial plug}$
$C_4 = 0.002 \text{ } \mu\text{F}$	$R_4 = 15,000 \text{ ohms}$	$V = 6\text{ABG.}$
$C_5 = 8 \text{ } \mu\text{F}$	$R_5 = 7000 \text{ ohms}$	

other than that of the inductance of the transitron oscillator coil and the frequency of the quartz crystal. The crystal frequency was adjusted by reference to the transmission from station GMT.

Expressing the resonant frequency of the tuning circuit as

$$f = \frac{1}{2\pi} \left[ \frac{1}{L(\epsilon C_T + C_L)} - \frac{r^2}{4L^2} \right]^{\frac{1}{2}} \text{ c./sec.,}$$

where  $L$  = inductance in henries,  $\epsilon$  = dielectric constant of solution in test cell,  $C_t$  = air capacity of test cell in farads,  $C_0$  = parallel circuit capacity in farads, and  $r^2$  = resistance of inductance in ohms, it can be shown simply that

$$\frac{\epsilon_x - 1}{\epsilon_v - 1} = \frac{\frac{1}{f_x^2} - \frac{1}{f_0^2}}{\frac{1}{f_v^2} - \frac{1}{f_0^2}},$$

where  $f_0$  and  $f_0'$  are the frequencies of the circuit with empty test cell before filling with liquids of dielectric constant  $\epsilon_x$  and  $\epsilon_v$  respectively and with the actual circuit constants used. Test of the formula\* was made by substituting a variable condenser for the test cell and progressively adding capacity in steps by means of a small fixed capacitor (15 pF), measuring the frequency at each step. The relation between  $f^{-2}$  and  $n$ , the number of steps, was found to be linear to 1 part in 10,000, which for the scale-range used is one vernier division on the wave-meter. The capacity range in the tuning circuit of the transition oscillator over which the linearity holds is approximately 95-200 pF.

*Chemistry Department,  
Guy's Hospital Medical School,  
London Bridge, S.E.1.*

\* Measurements of the dipole moment of organo-platinum compounds will be reported elsewhere.

# REACTIONS BETWEEN FORMALDEHYDE AND NITROGEN DIOXIDE

## PART I.—THE KINETICS OF THE SLOW REACTION

BY F. H. POLLARD AND R. M. H. WYATT

*Received 17th March, 1949*

The non-explosive reaction between nitrogen dioxide and formaldehyde has been studied over a range of temperatures between 118° C and 184° C. It has been shown that up to 160° C the reaction is homogeneous and the rate proportional to  $P_{\text{HCHO}} \cdot P_{\text{NO}_2}$ . The value of  $k$  is given by

$$k = 10^{7.1} e^{-15,100/RT} \text{ l./mole sec.}$$

The products of the reaction are mainly NO, CO, CO<sub>2</sub> and H<sub>2</sub>O, with possibly some N<sub>2</sub> and N<sub>2</sub>O, but no hydrogen was observed among the gases. The ratio CO/CO<sub>2</sub> was practically constant throughout the course of the reaction. A possible mechanism is suggested to account for the experimental results, and attention is drawn to the low values of the  $B$  factor for other reactions involving NO<sub>2</sub>.

Above 160° C there appears to be some change in mechanism, for which  $k$  is estimated to be  $10^6 e^{-19,000/RT}$ , and at still higher temperatures the reaction becomes explosive.

In studies of gas-phase oxidative reactions, nitrogen dioxide, as the main oxidizing agent, has received very little attention, though of course it is well known that the addition of small quantities of nitrogen dioxide has a marked effect on the kinetics of the oxidation of hydrogen, carbon dioxide, etc., by oxygen. Only two reactions involving oxidation by nitrogen dioxide have been reported in any detail, namely the oxidation of carbon monoxide<sup>1</sup> and sulphur dioxide<sup>2</sup> respectively.

The oxidation of organic molecules by nitrogen dioxide is of particular interest in elucidating the mechanisms involved in the thermal decomposition of nitric esters. It has been suggested<sup>3, 4, 5, 6</sup> that the primary process in such decompositions is the breaking of the O—NO<sub>2</sub> bond. The remaining alkoxy fragments give rise to alcohols and aldehydes.<sup>7</sup> These alcohols and aldehydes react with the nitrogen dioxide formed in the primary process to give oxides of carbon, and lower oxides of nitrogen.

These papers deal with the slow and explosive oxidation of the simplest aldehyde, viz. formaldehyde by NO<sub>2</sub>.

## Experimental

**Materials.**—FORMALDEHYDE.—Monomeric formaldehyde was prepared by the method of Spence and Wild,<sup>8</sup> and stored at liquid air temperature.

NITROGEN DIOXIDE.—Liquid nitrogen tetroxide supplied by the I.C.I. Ltd. was sublimed *in vacuo*, and stored at — 80° C.

<sup>1</sup> Crist and Brown, *J. Chem. Physics*, 1941, **9**, 840.

<sup>2</sup> Illarionov, *J. Physic. Chem. Soc. Russ.*, 1940, **14**, 1428.

<sup>3</sup> Robertson, *J. Chem. Soc.*, 1909, 1241.

<sup>4</sup> Appin, Chariton and Todes, *Acta Physicochim.*, 1936, **5**, 655.

<sup>5</sup> Phillips, *Nature*, 1947, **160**, 753.

<sup>6</sup> Adams and Bawn (forthcoming publication).

<sup>7</sup> Steacie, *Atomic and Free Radical Reactions* (Reinhold, 1946), p. 141.

<sup>8</sup> Spence and Wild, *J. Chem. Soc.*, 1935, 338.

**Procedure.**—Since the reaction involved an increase in the number of molecules, a manometric method was used. The increase in pressure was observed at constant volume and temperature, using the apparatus as shown in Fig. 1.

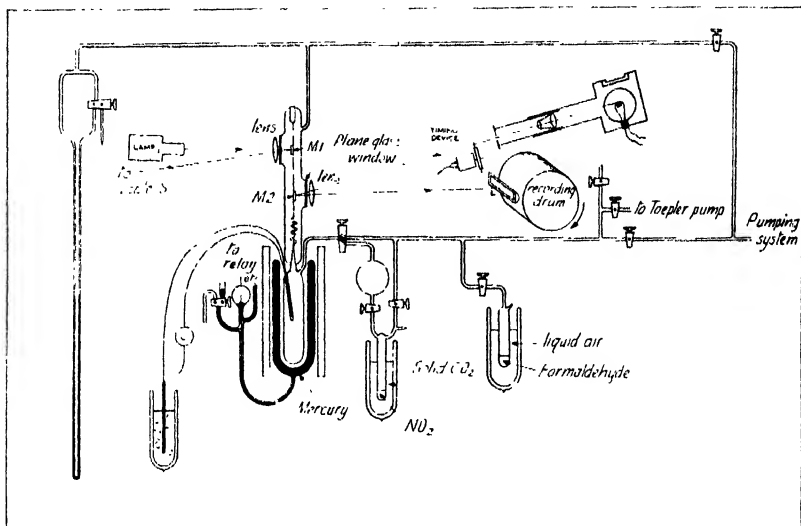


FIG. 1.

The reaction vessel was a double-walled one made of Hysil glass. Mercury was introduced into the space between the walls and this acted as a heating liquid and formed part of the thermostatic control. This vessel was placed in a wire-wound resistance furnace, and the temperature could be controlled to 0.2° or better during the course of an experiment, as indicated by the thermocouple in the centre of the reaction vessel.

Pressures were measured with a glass spiral gauge,<sup>9</sup> since nitrogen dioxide attacks mercury. This gauge was fitted with two mirrors,  $M_1$  and  $M_2$ : one mirror reflected on to an external scale for use when admitting gases and the other on to a revolving drum for photographically recording the increase of pressure during an experiment.

The procedure for an experiment was as follows. After thoroughly evacuating the whole system, a zero line was put on the recording paper. Air was admitted to the manometer side through a very fine jet until the required pressure was shown on the mercury manometer. The formaldehyde gas was admitted to the reaction vessel until the spiral returned to its zero position, as indicated by a light reflected on to the external scale S. This procedure was repeated with the  $\text{NO}_2$ , which was admitted as quickly as possible. A complete record of the pressure increase in the vessel was thus obtained, being time-marked every minute by a synchronous motor timing device. This timing was periodically checked with a stop-watch. Any correction for overshooting the admittance of nitrogen dioxide could be determined from the photographic trace.

The glass tubing leading from the reaction vessel to the tap T, and from there to the formaldehyde tube, was electrically heated above 100° C to prevent polymerization of the formaldehyde, and condensation of water produced in the reaction vessel. All taps which came into contact with nitrogen dioxide were greased with a special preparation of a mixture of polyisobutene and polythene in liquid paraffin, which was resistant to attack by this gas.

At the end of each reaction, or after any period of reaction, the hot gases were quickly admitted to a trap cooled in liquid air, when the non-permanent gases  $\text{CO}_2$ ,  $\text{H}_2\text{O}$ ,  $\text{CH}_3\text{O}$ ,  $\text{NO}_2$ , and some  $\text{NO}$  were condensed. The  $\text{CO}$  and the rest of the  $\text{NO}$  were pumped off with a Toepler pump and collected. The liquid air bath was replaced by an acetone-carbon dioxide bath, and the  $\text{CO}_2$  and the rest of the  $\text{NO}$  were pumped off and collected. In this way  $\text{H}_2\text{O}$  and unchanged

<sup>9</sup> Yorke, *J. Sci. Instr.*, 1945, **22**, 196 and 1948, **25**, 16.



CH<sub>2</sub>O and NO<sub>2</sub> were left behind in the traps, and no attempt was made to analyze this residue. The collected gases were analyzed for CO, CO<sub>2</sub> and NO; CO by oxidation to CO<sub>2</sub> by CuO at 500°, followed by absorption in KOH; CO<sub>2</sub> by absorption in KOH; and NO by chromous chloride solution. There was no convincing evidence of the presence of hydrogen.

### Results

Results obtained with different reaction vessels, and in vessels packed with small pieces of Hysil tubing, or coated with cryolite showed that the reaction was not dependent on the surface. No difference in the composition of the resultant gases was found in the packed or coated vessel. Additions of nitrogen, argon, and helium did not have any marked effects on the reaction rate.

TABLE I—I-CHO/2NO<sub>2</sub> MIXTURE.  
TEMP. 150° C

Rate in cm. Hg per min. Initially	$p_{\text{NO}_2} \cdot p_{\text{CH}_2\text{O}}$
0.25	14.9
0.41	20.9
0.63	30.0

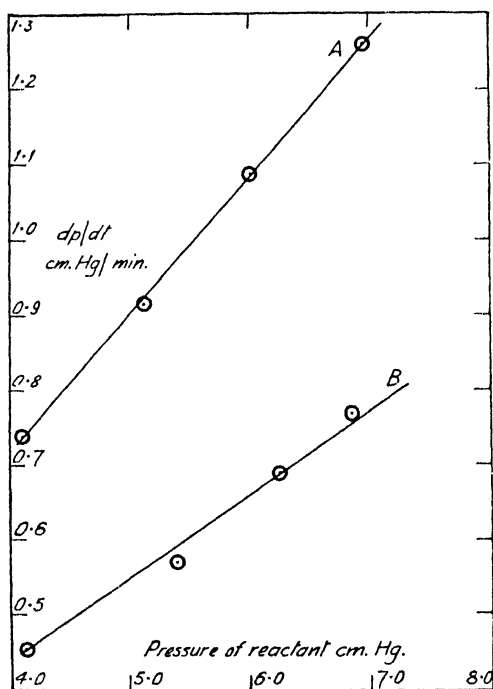


FIG. 2.

- A. Order with respect to nitrogen dioxide.  
B. Order with respect to formaldehyde.

Some experiments in vessels coated with potassium chloride did, however, show that the reaction rate was reduced to about one-third of that in the untreated vessel, but the gaseous products in general were the same.

**The Order of the Reaction.**—The course of the reaction at 150° C for a series of different initial pressures of a 1 CH<sub>2</sub>O/2NO<sub>2</sub> mixture showed that the total order of the reaction, as deduced from the influence of pressure on the

initial rate of reaction, is 2 (Table I). The effect of varying the initial concentration of one of the reactants while the other was in excess showed the rate to be proportional to the first power of the formaldehyde concentration and also to the first power of the nitrogen dioxide concentration (Fig. 2).

**Composition of the Gaseous Products.**—Analysis of the gases formed at different stages in a  $\text{CH}_3\text{O}/2\text{NO}_2$  mixture at  $154^\circ\text{C}$  showed that the ratio  $\frac{\text{CO}}{(\text{CO} + \text{CO}_2)}$  remained approximately constant throughout the course of the reaction. The average value of the ratio at this temperature was 0.60.

TABLE II

Time after start in min.	5	10	15	20	30	40	$\infty$
Ratio	0.58	0.61	0.59	0.62	0.60	0.61	0.59

It was also observed that the ratio  $\frac{\text{CO}}{(\text{CO} + \text{CO}_2)}$  had a slight tendency to increase as the temperature increased, from an average value of 0.58 at  $100^\circ\text{C}$  to 0.63 at  $220^\circ\text{C}$ . At the end of all experiments under different conditions of total pressure and temperature, the final gaseous products were analyzed, the average analysis being  $\text{NO}$ , 57.5 %;  $\text{CO}$ , 25.5 %;  $\text{CO}_2$ , 17.0 %. A check on the carbon balance at different temperatures showed that all the carbon in the initial formaldehyde was converted into carbon monoxide and carbon dioxide.

TABLE III

Temp. $^\circ\text{C}$	$p_{\text{CH}_2\text{O}}$ (cm. Hg)	$p_{\text{NO}_2}$	Total Volume in cm. <sup>3</sup> of Carbon Oxides	Calculated Volume in cm. <sup>3</sup> of Carbon Oxides
128	10.07	20.15	7.54	7.63
136	10.00	20.12	7.53	7.42
151	10.12	20.09	7.05	7.18
173	10.15	20.05	7.07	6.87

A similar check of the nitrogen balance indicated that most of the nitrogen dioxide formed nitric oxide, and there was always a small residue of unabsorbed permanent gas which was assumed to be nitrogen.

TABLE IV

Temp. $^\circ\text{C}$	$p_{\text{CH}_2\text{O}}$ (cm. Hg)	$p_{\text{NO}_2}$	Volume of $\text{NO}$ (cm. <sup>3</sup> )	Cal. Vol. of $\text{NO}$ (cm. <sup>3</sup> )
154	21.20	20.00	13.69	14.2
154	22.05	21.00	11.51	14.2

**Determination of the Velocity Constant and Activation Energy.**—The rates of reaction for the  $\text{CH}_3\text{O}/2\text{NO}_2$  mixture were studied over a range of temperatures from  $116$ – $184^\circ\text{C}$ . The increase of pressure was due to the formation of steam, since no volume change occurs when each molecule of formaldehyde is oxidized to oxides of carbon and each molecule of nitrogen dioxide is reduced to nitric oxide. The rate of pressure increase was therefore a measure of the rate of disappearance of  $\text{CH}_3\text{O}$ , and could be used as a measure of the reaction rate.

If  $\Delta P$  is the pressure increase after time  $t$ , for a reaction when the initial pressure of CH<sub>2</sub>O =  $P_c$  and the initial pressure of NO<sub>2</sub> =  $P_N$ , then the pressure of formaldehyde at time  $t$

$$= (P_c)_t = P_c - \Delta P.$$

The pressure of nitrogen dioxide at time  $t$

$$= P_N - (2 - \alpha)\Delta P,$$

where

$$\alpha = \frac{CO}{(CO + CO_2)}.$$

Values of the velocity constant  $k$  were thus determined by plotting  $dP/dt$  against the product  $(P_c)_t \cdot (P_N)_t$ , when straight lines were obtained. By the method of least squares, the following kinetic expression was obtained from Fig. 3:  $k = 10^{7.1} e^{-15,000/RT}$  l. mole<sup>-1</sup> sec.<sup>-1</sup>.

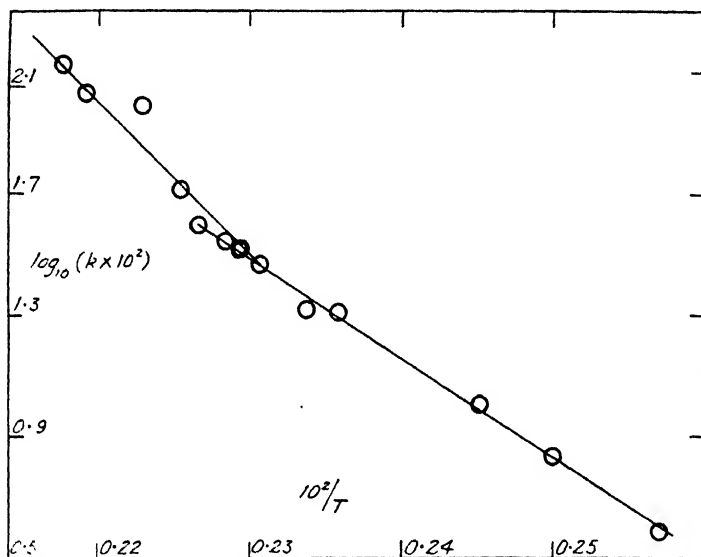
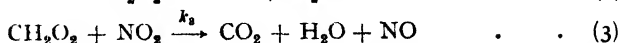
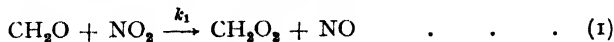


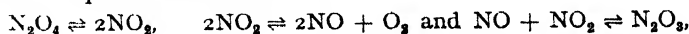
FIG. 3.—Influence of temperature on the speed of reaction.

### Discussion

Since this homogeneous reaction between nitrogen dioxide and formaldehyde is of first order with respect to each, the following mechanism was first proposed to account for the experimental results:



For the temperature range which is being considered, calculations from the known equilibrium constants for



showed that the gas present was essentially nitrogen dioxide.

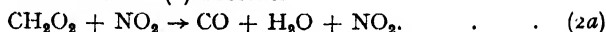
The intermediate, CH<sub>2</sub>O<sub>2</sub>, could be considered as either formic acid or a peroxide isomeric with formic acid. If it is the former, then one might have expected to find hydrogen in the products, especially as formic acid decomposes heterogeneously at 200° C in two ways, simultaneously yielding either carbon monoxide and water, or carbon dioxide and

hydrogen.<sup>10</sup> On the same grounds, an atom-radical mechanism like that proposed for the oxidation of formaldehyde with oxygen by Axford and Norrish<sup>11</sup> does not seem applicable at these temperatures, though of course this is not ruled out at higher temperatures. The slight decrease in rate using a potassium chloride surface might point to the intermediate having a peroxide nature, though this decrease could also be explained as due to the loss of nitrogen dioxide through the conversion of potassium chloride into potassium nitrate, a reaction which has recently been reported upon by Russian workers.<sup>12</sup>

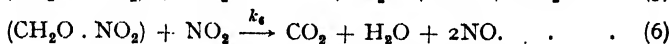
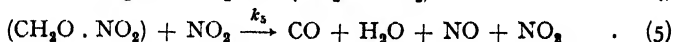
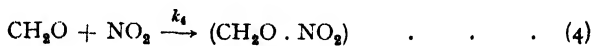
Since the ratio of  $\text{CO}/\text{CO}_2$  is almost constant throughout the course of the reaction, then reactions (2) and (3) proceed at a constant relative rate, and since the rate of the overall reaction has been shown to depend on the product of the concentration of  $\text{CH}_2\text{O}$  and  $\text{NO}_2$ , reaction (1) is the slow, rate-determining reaction, while reactions (2) and (3) are fast. If this is so, then

$$\frac{d(\text{CO})}{d(\text{CO}) + d(\text{CO}_2)} = \frac{k_2}{k_2 + k_3(\text{NO}_2)},$$

and since  $\text{CO}/(\text{CO} + \text{CO}_2) = 0.6$ , then  $k_2/k_3 = 3/2$ . Consequently the ratio would be expected to change as the reaction proceeded, or with different initial pressures of nitrogen dioxide. This was not so during the course of the reaction or with  $1\text{CH}_2\text{O}/1\text{NO}_2$  mixtures, when all the nitrogen dioxide is used up and some formaldehyde is left unoxidized. The reactions (2) and (3) do not satisfy the experimental results, unless one postulates that the breakdown of the intermediate is sensitized by nitrogen dioxide, when reaction (2) becomes



An alternative mechanism could involve the formation of a binary complex between formaldehyde and nitrogen dioxide, which can undergo sensitized decomposition by nitrogen dioxide, or oxidation by nitrogen dioxide, thus



There is some justification for (4) and (5) from unpublished work on the decomposition of ethyl nitrate.

Applying the stationary state principle to the intermediate complex:

$$k_4(\text{CH}_2\text{O})(\text{NO}_2) = (k_5 + k_6)(\text{CH}_2\text{O} \cdot \text{NO}_2)/(\text{NO}_2).$$

Since  $dp/dt = d(\text{H}_2\text{O})/dt = (k_5 + k_6)(\text{CH}_2\text{O} \cdot \text{NO}_2)/(\text{NO}_2),$

then  $dp/dt = k_4(\text{CH}_2\text{O})(\text{NO}_2),$

which agrees with the second-order relationships.

Also,

$$\begin{aligned} \frac{d(\text{CO})}{d(\text{CO}) + d(\text{CO}_2)} &= \frac{k_5(\text{CH}_2\text{O} \cdot \text{NO}_2)(\text{NO}_2)}{k_5(\text{CH}_2\text{O} \cdot \text{NO}_2)(\text{NO}_2) + k_6(\text{CH}_2\text{O} \cdot \text{NO}_2)(\text{NO}_2)} \\ &= \frac{k_5}{k_5 + k_6}, \end{aligned}$$

i.e. independent of nitrogen dioxide concentration, which would agree with our experimental results.

If, after a time  $t$ , a fraction  $\alpha$  of the formaldehyde is converted to carbon monoxide by reactions (4) and (5), then  $(1 - \alpha)$  will be converted into carbon dioxide by (4) and (6).  $(2 - \alpha)$  molecules of nitrogen dioxide

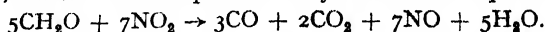
<sup>10</sup> Hinshelwood and Topley, *Proc. Roy. Soc. A*, 1922, **100**, 575.

<sup>11</sup> Oxford and Norrish, *ibid.*, 1948, **192**, 518.

<sup>12</sup> Epshtein, Chirkova and Papulova, *Khim. Prom.*, 1947, No. 4, 5.

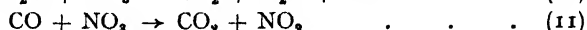
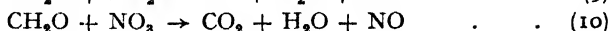
are needed, so that the pressure of unchanged formaldehyde at time  $t$  is  $P_0 - \Delta P$ , and the pressure of nitrogen dioxide is  $P_N - (2 - \alpha)\Delta P$ .

Since the value of  $\alpha$  is 0.60, then the stoichiometric mixture is 1CH<sub>2</sub>O/1.4NO<sub>2</sub>, that is, 42 % CH<sub>2</sub>O/58 % NO<sub>2</sub> (see typical gas analysis of products), which can be represented by the overall equation:



As has been mentioned before, the value of  $\alpha$  increases slightly with temperature. This presumably means that reaction (5) has a slightly higher activation energy than (6).

Many workers<sup>1, 13</sup> have attempted to explain the effect of nitrogen dioxide on the oxidation of hydrogen and carbon monoxide, by the use of the intermediate NO<sub>3</sub> in their suggested mechanisms. Consideration of such steps as



did not lead to relationships which could be explained by our present data.

The activation energy plot has a break at about 160° C. The value for the rate constant above this temperature, as far as the restricted data will allow, is given by

$$k = 10^9 e^{-19,000/RT}.$$

Above 180° C the slow reaction changes to an explosive oxidation characterized by fairly sharply defined limits of temperature and pressure, details of which are given in Part II.

Crist and co-workers<sup>1</sup> have found in their studies on the sensitization of carbon monoxide with nitrogen dioxide, that above a certain pressure of nitrogen dioxide (10 mm. Hg) the reaction becomes homogeneous. Over the temperature range of 225° C to 527° C the value of the kinetic expression for the reaction,  $\text{CO} + \text{NO}_2 \rightarrow \text{CO}_2 + \text{NO}$  is

$$k = 10^{8.68} e^{-27,800/RT} \text{ l. mole}^{-1} \text{ sec}^{-1}.$$

The decomposition of nitrogen dioxide<sup>14, 15</sup> is also homogeneous and follows a second-order law. The rate can be expressed by the equation,

$$k = 10^{8.9} e^{-25,000/RT} \text{ l. mole}^{-1} \text{ sec}^{-1}$$

over the temperature range 200-400° C.

The  $B$  factor for second-order reactions is usually  $10^{10}$ - $10^{12}$  when expressed in  $\text{l. mole}^{-1} \text{ sec}^{-1}$  units. Thus, all these reactions involving nitrogen dioxide have a rather low  $B$  factor.

A break in the activation energy plot has been observed by Illarionov<sup>4</sup> for the reaction between sulphur dioxide and nitrogen dioxide, at about 150° C, and the activation energy above 150° C is 24,500 cal. Below 150° C the activation energy is not given, but must be similar to our value of 15,000 cal. The temperature range 150-160° C coincides with that at which the decomposition of nitrogen dioxide into nitric oxide and oxygen is discernible but the rate is very slow.

For the photochemical oxidation of formaldehyde, Style and Sumners<sup>16</sup> found a change in mechanism and products for the reaction above 150° C, but there is no evidence for a change in products in the reaction we have studied. It is also interesting to note that Snowden and Style<sup>17</sup> found

<sup>13</sup> Lewis and von Elbe, *Combustion, Flames and Explosions of Gases* (Cambridge Univ. Press, 1938).

<sup>14</sup> Bodenstein and Ramstetter, *Z. physik. Chem.*, 1922, **100**, 106.

<sup>15</sup> Kassel, *Kinetics of Homogeneous Gas Reactions* (Reinhold, 1932), p. 156.

<sup>16</sup> Style and Sumners, *Trans. Faraday Soc.*, 1946, **42**, 388.

<sup>17</sup> Snowden and Style, *ibid.*, 1939, **35**, 426.

that vessels treated with concentrated nitric acid appeared to produce the least changeable surface in the oxidation of formaldehyde by oxygen.

Further work on the oxidation of organic molecules by nitrogen dioxide is being carried out in this laboratory, using a technique involving the simultaneous measurement of pressure increase and colorimetric estimation of nitrogen dioxide. Preliminary work with formaldehyde confirms the results reported in this paper.

*Dept. of Chemistry,  
University of Bristol.*

---

## REACTIONS BETWEEN FORMALDEHYDE AND NITROGEN DIOXIDE

### PART II. THE EXPLOSIVE REACTION

BY F. H. POLLARD AND P. WOODWARD

*Received 17th March, 1949*

In the region of  $180^{\circ}\text{C}$  the slow reaction between nitrogen dioxide and formaldehyde becomes explosive. Evidence is presented to show that this explosive reaction is thermal in character. Curves correlating the limiting explosion pressure with temperature are given, and analyses of the gaseous products show that the ratio of nitric oxide to nitrogen increases with increasing temperature, while the amount of carbon dioxide obtained remains approximately constant.

Nitrogen dioxide is one of the products formed in the thermal decomposition of nitric esters, and consequently the importance of its explosive reactions with other molecules also likely to be present in the decomposition, is self-evident. This paper describes the nature of the explosive oxidation of formaldehyde by nitrogen dioxide, and is complementary to the work of Pollard and Wyatt on the slow reaction between these two gases.

### Experimental

The gases were prepared and stored as described in Part I of this paper.<sup>1</sup> Reactions were carried out in a cylindrical reaction vessel, sealed at one end with an optically-plane glass face for purposes of observation. At the other end, a glass spiral pressure gauge was sealed, together with a single-way tap for admission of gases. The gauge was used as a null-point instrument, and in all experiments the formaldehyde was admitted *first*, owing to the difficulty of handling this material and of obtaining the large pressures which are necessary for rapid admission. A pre-determined quantity of nitrogen dioxide was then admitted as rapidly as possible and the result observed.

**The Critical Explosion Limit.**—With increasing temperature, the gaseous oxidation of formaldehyde by nitrogen dioxide increases in rate, and in the region of  $180^{\circ}\text{C}$  passes over into an explosive process characterized by sharply defined limits of temperature and pressure, below which no explosion occurs. The critical values depend upon the composition of the mixture. Considerable skill was necessary to admit the nitrogen dioxide, both quickly and accurately, using this technique, although the induction period before explosion is, of course, a maximum at the critical pressure. Consequently, if explosion occurred before all the nitrogen dioxide had been admitted, it was assumed that the pressure intended was almost certainly higher than the critical one. In all cases, the limit was obtained by finding the critical explosion pressure for a mixture of given composition at a fixed temperature; the limit was approached from both sides.

<sup>1</sup> Pollard and Wyatt. *Trans. Faraday Soc.* (preceding paper).

## Results

The critical pressures necessary for explosion to occur were first determined at several temperatures for a mixture of given composition. The points lie on a smooth curve. Similar series of points were then determined for other mixtures, and the curves in Fig. 1 are the graphical representation of results.

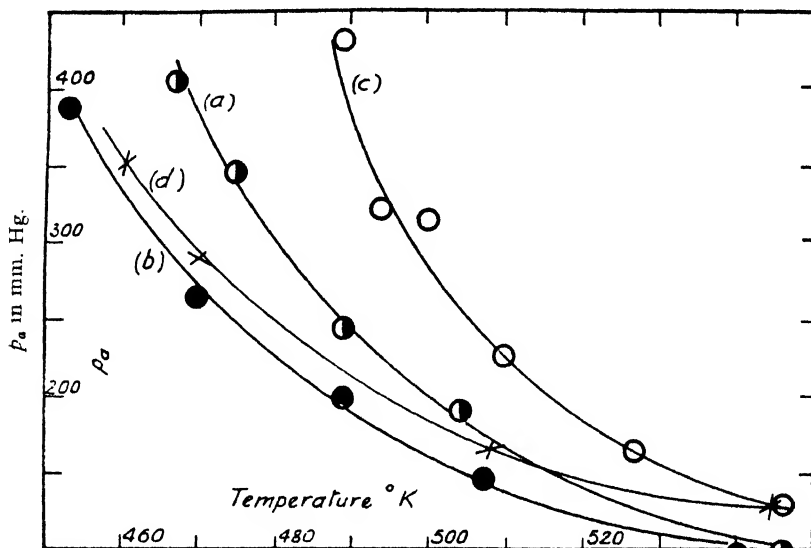


FIG. 1.—Explosion limits.

(a) 2NO<sub>2</sub>/1HCHO  
(c) 4NO<sub>2</sub>/1HCHO

(b) 1NO<sub>2</sub>/1HCHO  
(d) 1NO<sub>2</sub>/2HCHO.

To determine whether the explosion is the result of a thermal process or a branched-chain mechanism is by no means easy, since so many variables affect both in a similar way. The results so far obtained suggest, however, that a thermal process is more likely.

**Effect of Inert Gases.**—When the explosion limits are determined in presence of an inert gas, changes in the critical pressure are observed, as shown in Table I. Whereas helium has a very marked effect in raising the pressure

TABLE I.—EFFECT OF INERT GAS ADDITION

Temp. °C	Mixture HCHO/NO <sub>2</sub>	Pressure of Mixture (cm.)	Pressure of Inert Gas added (cm.)	Result	Explosion Limit in Absence of Inert Gas (cm.)
203	1/2	36.8	He 8.7	No flame	32.7
201	1/2	37.6	He 4.1	No flame	34.1
201	1/2	36.2	None	Flame	34.1
202	1/2	37.1	He 1.4	No flame	33.2
198	1/2	44.7	He 3.8	No flame	36.7
201	1/2	37.7	A 1.7	Flame	34.1
201	1/2	34.5	A 1.9	Flame	34.1
201	1/2	31.5	A 1.8	No flame	34.1
202	1/2	33.8	A 1.7	No flame	33.2

limit at any given temperature, argon, however, is by no means as effective. If the explosion is thermal, this is explained by the very high thermal conductivity of helium as compared with argon.

If the mechanism involved propagation by chains the reverse effect might be expected.

**Effect of the Nature of the Vessel Walls.**—Coatings of cryolite and of potassium chloride were put on the vessel walls and the experiments repeated. Practically no change in the explosion limits was observed, as the values given in Table II show. This again is evidence in favour of a thermal explosion.

TABLE II.—EFFECT OF VESSEL WALLS

Temp. °C	Mixture HCHO/NO <sub>2</sub>	Total Pressure (cm.)	Walls	Result	Explosion Limit in Glass Vessel (cm.)
201	1/2	35.9	KCl	No flame	34.1
201	1/2	38.7	KCl	Flame	
201	1/2	36.7	KCl	Flame	
201	1/2	36.0	KCl	No flame	
200	1/2	37.4	Cryolite	Flame	34.8
200	1/2	33.4	"	No flame	
200	1/2	36.3	"	Flame	
200	1/2	34.8	"	No flame	
200	1/2	35.4	"	Flame	
200	1/2	35.8	"	Flame	

**Gaseous Products of the Explosive Oxidation.**—Analyses were carried out after a few explosions, using 2NO<sub>2</sub>/1HCHO, according to the methods outlined in Part I of this paper. The gas obtained was analyzed for hydrogen, nitric oxide, carbon monoxide and carbon dioxide. The permanent-gas residue was assumed to be nitrogen.

In no case was any appreciable amount of hydrogen found, but the amounts of other gases showed a general trend—depending on the temperature—as Table III indicates.

TABLE III.—ANALYSIS OF GASEOUS PRODUCTS OF THE EXPLOSIVE OXIDATION

Temp. °C	Total Pressure (cm.)	% NO	% CO	% CO <sub>2</sub>	% N <sub>2</sub>
197	42.4	19.6	3.3	42.1	35.3
200	35.4	25.1	5.9	39.8	27.6
231	17.8	32.6	8.2	41.8	17.3
273	14.4	44.6	1.1	40.6	12.3

## Discussion

A thermal explosion occurs when the rate of transference of heat away from the reaction zone of a gas is insufficient to prevent the temperature of the gas rising, and thereby increasing the rate of reaction to an uncontrollable extent. Mathematical treatment of this process<sup>2</sup> leads to a relation of the type

$$\ln\left(\frac{p_a}{T_0}\right) = \frac{E}{2RT_0} + \text{const.},$$

where  $p_a$  is the critical pressure at temperature  $T_0$ . Unfortunately, the dependence of  $p_a$  on the absolute temperature according to the above law cannot be interpreted as an expression of the fact that the explosion has a purely thermal character, since the theory of branching chains leads to an equation of the same type.

<sup>2</sup> Semenov, *Z. physik.*, 1928, 48, 471.



Fig. 2 shows the result of plotting  $\log_{10} (p_a/T_0)$  as a function of  $1/T_0$  for the formaldehyde-nitrogen dioxide explosive oxidation. The points do not lie on a straight line even in the more accurately determined 1/1 mixtures. The curves are decidedly convex to the axis of  $1/T_0$ , although the departure from linearity is only slight in the 1/1 case. The curvature

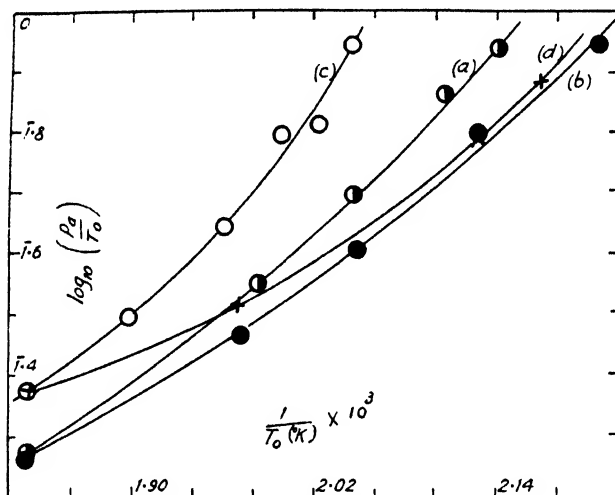


FIG. 2.—Plot of  $\log_{10} (p_a/T)$  against  $(1/T_0)$ .

cannot be explained as experimental error in this case, assuming the technique to be sound, although it is possible that slightly different curves would have been obtained by the use of a "premixing" method.

A similar curvature of the  $\log (p_a/T_0)$  against  $1/T_0$  curve was noticed by Appin, Chariton and Todes in their work on the thermal decomposition and explosion of methyl nitrate vapour.<sup>3</sup> In this paper the thermal nature of the explosion was established.

Acknowledgment is made to the Chief Scientist, Ministry of Supply, for permission to publish Parts I and II of this work.

Department of Chemistry,  
University of Bristol.

<sup>3</sup> Appin, Chariton and Todes, *Acta Physicochim.*, 1936, **5**, 655.

## THE EXTENT OF DISSOCIATION OF SALTS IN WATER

### PART XI. CALCIUM AND BARIUM THIOSULPHATES AND BARIUM BROMOACETATE

By C. W. DAVIES AND P. A. H. WYATT

Received 8th April, 1949

The dissociation constants in water of calcium and barium bromoacetates and thiosulphates are reported. From measurements at two temperatures values of  $\Delta H$  and  $\Delta S$  are derived for the electrolytic dissociation of barium thiosulphate.

The dissociation constants of these salts were required for the work reported in the following paper, and have been obtained by the solubility method described in earlier communications.<sup>1, 2</sup> Barium thiosulphate was studied at 25° and 35° C, the other salts at 25° only.

## Experimental

Barium iodate monohydrate crystals of suitable size for the solubility measurements were prepared by slow dropwise addition of solutions of A.R. BaCl<sub>2</sub> and KIO<sub>3</sub> to a large volume of water. Calcium iodate hexahydrate was prepared in a similar way. The Na<sub>2</sub>S<sub>2</sub>O<sub>3</sub> was an A.R. sample that had been recrystallized and dried over a saturated CaCl<sub>2</sub> solution. Sodium bromoacetate solutions were made up by neutralizing with standard NaOH solution a sample of the acid which had been redistilled at 15 mm. pressure and stored in the dark over conc. H<sub>2</sub>SO<sub>4</sub>.

The saturator was of the type used in previous work<sup>3</sup> and was immersed in a thermostat maintained at 25° ± 0.01°, or 35° ± 0.02°. Samples of saturated solution were withdrawn in warmed pipettes and analyzed volumetrically for iodate.

## Results

The experimental results are given, in millimoles per litre, in the first two columns of Tables I-IV; *s* is the solubility, *c* the concentration of added salt. Duplicate determinations of the calcium iodate solubilities agreed to within 0.1 %; with the less soluble barium salt the deviations were occasionally slightly larger. Solubilities in pure water were determined at intervals throughout the work, and are shown at the head of the Tables. That of calcium iodate is in complete agreement with previous work.<sup>3</sup> For barium iodate at 25° C the value  $8.12 \times 10^{-4}$  mole/l. was obtained; previous values in the literature are  $8.11$ <sup>4</sup> and  $8.177$ <sup>5</sup> × 10<sup>-4</sup>, and Macdougall and Davies<sup>1</sup> found  $8.10 \times 10^{-4}$  at 24.93° C.

It has been shown previously that saturated solutions of calcium and barium iodates contain small quantities of CaIO<sub>3</sub><sup>+</sup> and BaIO<sub>3</sub><sup>+</sup> respectively; and the dissociation constants of these intermediate ions have been determined from conductivity measurements.<sup>1, 2</sup> Further, it has been found<sup>6</sup> that if allowance is made for these, and in salt mixtures for any other association products, the solubilities of calcium and barium iodates are accurately expressed, up to an ionic strength of 0.1, by the equation:

$$\log [M''][\text{IO}_3] = \log S_0 - \log f_{\pm}^2 = \log S_0 + 3.0 \left\{ \frac{\sqrt{I}}{1 + \sqrt{I}} - 0.20I \right\}. \quad (1)$$

Here [M''] is the concentration in moles per litre of the calcium or barium ion, *S*<sub>0</sub> the solubility product and *I* the ionic strength. Our measurements in water give *S*<sub>0</sub> =  $7.119 \times 10^{-7}$  for calcium iodate, and *S*<sub>0</sub> =  $1.506 \times 10^{-9}$  for barium iodate at 25° C.

This equation is the basis of the calculations recorded in the later columns of the Tables. For instance, in sodium bromoacetate solutions saturated with barium iodate the possible products of ion-association are NaIO<sub>3</sub>, BaIO<sub>3</sub><sup>+</sup> and BaBrAc<sup>+</sup>; the further association of the intermediate ions will be negligible at the concentrations considered, and sodium bromoacetate, like the chloroacetate,<sup>7</sup> can be assumed to be completely dissociated. The dissociation constants of the two first-named are known from previous work,<sup>1, 8</sup>  $K_{\text{NaIO}_3} = 3.0$ ,  $K_{\text{BaIO}_3} = 0.08$ ,

<sup>1</sup> Macdougall and Davies, *J. Chem. Soc.*, 1935, 1416.

<sup>2</sup> Wise and Davies, *ibid.*, 1938, 273.

<sup>3</sup> Money and Davies, *ibid.*, 1934, 400.

<sup>4</sup> Keefer, Reiber and Bisson, *J. Amer. Chem. Soc.*, 1940, 62, 2951.

<sup>5</sup> Naidich and Ricci, *ibid.*, 1939, 61, 3268.

<sup>6</sup> Davies, *J. Chem. Soc.*, 1938, 2093.

<sup>7</sup> Saxton and Langer, *J. Amer. Chem. Soc.*, 1933, 55, 3638.

<sup>8</sup> Davies, *Trans. Faraday Soc.*, 1927, 23, 351.

and we therefore have three equations that must be simultaneously satisfied, eqn. (1) and the following :

$$\log [\text{Ba}^{++}][\text{IO}_3^-] = \log [\text{BaIO}_3^+] + \log 0.08 + 2 \left\{ \frac{\sqrt{I}}{1 + \sqrt{I}} - 0.20I \right\} \quad (2)$$

$$\log [\text{Na}^+][\text{IO}_3^-] = \log [\text{NaIO}_3] + \log 3.0 + \left\{ \frac{\sqrt{I}}{1 + \sqrt{I}} - 0.20I \right\} \quad (3)$$

Solving these three equations by successive approximations gives, by difference, the concentration of  $\text{BaBrAc}^+$ , and the dissociation constant of this intermediate ion is then obtained from an equation similar in form to eqn. (2). The dissociation constants calculated in this way are shown in the last columns of the Tables.

TABLE I.—SOLUBILITY OF BARIUM IODATE IN SODIUM BROMOACETATE SOLUTIONS AT 25° C

<i>c</i>	<i>s</i>	$[\text{NaIO}_3]$	$[\text{BaIO}_3^+]$	$[\text{BaBrAc}^+]$	<i>I</i>	$K_{\text{BaBrAc}^+}$
0	0.812	—	0.013	—	0.00241	—
10.00	0.920	0.005	0.013	0.010	0.01271	0.5 <sub>7</sub>
15.00	0.954	0.007	0.013	0.012	0.01781	0.6 <sub>9</sub>
20.00	0.986	0.010	0.013	0.021	0.02288	0.5 <sub>0</sub>
25.00	1.012	0.012	0.013	0.024	0.02795	0.5 <sub>4</sub>
Mean <i>K</i> :						0.5 <sub>7</sub>

To interpret the solubilities in sodium thiosulphate solutions the dissociation constant of the  $\text{NaS}_2\text{O}_3^-$  ion is required. This has not been determined, and we have assumed it to have the same value as the  $\text{NaSO}_4^-$  ion,<sup>9</sup> viz.  $K = 0.20$ .

TABLE II.—SOLUBILITY OF BARIUM IODATE IN SODIUM THIOSULPHATE SOLUTIONS AT 25° C

<i>c</i>	<i>s</i>	$[\text{NaIO}_3]$	$[\text{BaIO}_3^+]$	$[\text{NaS}_2\text{O}_3^-]$	$[\text{BaS}_2\text{O}_3]$	<i>I</i>	$K_{\text{BaS}_2\text{O}_3}$
5.025	1.022	0.005	0.012	0.138	0.217	0.01696	0.00609
8.030	1.097	0.008	0.012	0.317	0.288	0.02556	0.00605
10.050	1.137	0.011	0.012	0.479	0.321	0.03128	0.00615
15.080	1.223	0.016	0.011	0.933	0.398	0.04541	0.00606
20.090	1.295	0.022	0.011	1.503	0.463	0.05925	0.00590
Mean <i>K</i> :						0.0061	

This is supported by the roughly parallel conductivity curves of the two salts,<sup>10</sup> and we believe it to be sufficiently accurate for the purpose.

TABLE III.—SOLUBILITY OF CALCIUM IODATE IN SODIUM THIOSULPHATE SOLUTIONS AT 25° C

<i>c</i>	<i>s</i>	$[\text{NaIO}_3]$	$[\text{CaIO}_3^+]$	$[\text{NaS}_2\text{O}_3^-]$	$[\text{CaS}_2\text{O}_3]$	<i>I</i>	$K_{\text{CaS}_2\text{O}_3}$
0	7.840	—	0.482	—	—	0.0226	—
7.235	8.907	0.056	0.463	0.200	1.089	0.0427	0.00897
10.853	9.303	0.085	0.455	0.421	1.484	0.0527	0.00857
11.566	9.367	0.091	0.454	0.474	1.518	0.0548	0.00900
14.148	9.613	0.111	0.451	0.683	1.722	0.0620	0.00907
15.430	9.749	0.122	0.449	0.794	1.886	0.0654	0.00866
Mean <i>K</i> :						0.0089	

<sup>9</sup> Righellato and Davies, *ibid.*, 1930, 26, 592.

<sup>10</sup> *Int. Crit. Tables*, VI, 236, 247.

The results of the calculations at 35° are less reliable than those of the preceding Tables, as the necessary dissociation constants of  $\text{NaIO}_3$ ,  $\text{BaIO}_3^+$  and  $\text{NaS}_2\text{O}_3^-$  have not been determined. We have assumed them to be 10% lower than at 25°, an approximate rule that is in agreement with the data so far available for other salts.<sup>11</sup>

TABLE IV.—SOLUBILITY OF BARIUM IODATE IN SODIUM THIOSULPHATE SOLUTIONS AT 35° C

<i>c</i>	<i>s</i>	$[\text{NaIO}_3]$	$[\text{BaIO}_3^+]$	$[\text{NaS}_2\text{O}_3^-]$	$[\text{BaS}_2\text{O}_3]$	<i>I</i>	$K_{\text{BaS}_2\text{O}_3}$
0	1.049	—	0.023	—	—	0.00310	—
5.010	1.322	0.007	0.021	0.146	0.302	0.01745	0.0051
8.016	1.415	0.012	0.021	0.336	0.382	0.02603	0.0054
10.020	1.467	0.015	0.021	0.495	0.427	0.03171	0.0054
15.03	1.579	0.023	0.020	0.985	0.534	0.04569	0.0053
20.06	1.680	0.030	0.020	1.587	0.624	0.05948	0.0051
Mean <i>K</i> :							0.0053

### Discussion

The mean dissociation constants are collected in Table V, which also includes for comparison the dissociation constant of calcium bromoacetate.<sup>12</sup> As in previous work<sup>13</sup> the organic salt of barium is considerably stronger than that of calcium, whereas with the thiosulphates, like the nitrates and iodates, the order is reversed. The two determinations at 25° and 35° lead to the value  $\Delta H = -2600 \pm 400$  cal./g.-mole for the dissociation of barium thiosulphate, and combining this with  $\Delta G_{298.1} = -RT \ln K = 3020$  cal. gives  $\Delta S_{298.1} = -18.8$  cal./deg. for the dissociation.

TABLE V

Ion-Pair	Temp. °C	<i>K</i>	<i>a</i>
$\text{CaBrAc}^+ \quad . \quad . \quad .$	25	0.28	5.8
$\text{BaBrAc}^+ \quad . \quad . \quad .$	25	0.57	6.8
$\text{CaS}_2\text{O}_3 \quad . \quad . \quad .$	25	0.0089	6.4
$\text{BaS}_2\text{O}_3 \quad . \quad . \quad .$	25	0.0061	4.9 <sub>8</sub>
$\text{BaS}_2\text{O}_3 \quad . \quad . \quad .$	35	0.0053	4.8 <sub>0</sub>

The last column of the Table gives values in angstrom for the mean ionic diameters, derived from the *K*'s by Bjerrum's equation<sup>14</sup> for ion-pair formation. Individually they are of reasonable magnitude, but of course they reflect the reversal of order already noted. The two values for barium thiosulphate differ by more than the probable experimental error; in fact, the electrostatic treatment of ion-pair formation, using the normal value of the dielectric constant of water, predicts a  $\Delta H$  value less than one-half of that found experimentally and an entropy change much smaller than the figure quoted above.

Edward Davies Chemical Laboratories,  
Aberystwyth, Wales.

<sup>11</sup> Davies and James, *Proc. Roy. Soc. A*, 1948, **195**, 116; and unpublished results.

<sup>12</sup> Robertson (unpublished).

<sup>13</sup> Topp and Davies, *J. Chem. Soc.*, 1940, 87.

<sup>14</sup> Bjerrum, *Kgl. Danske Vid. Selsk. Math-fys. Medd.*, 1926, **7**, 9.

# IONIC REACTION RATES AND THE INCOMPLETE DISSOCIATION OF SALTS

## PART I. THE BROMOACETATE-THIOSULPHATE REACTION

BY P. A. H. WYATT AND C. W. DAVIES

*Received 8th April, 1949*

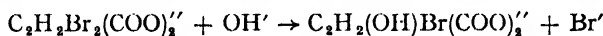
The kinetics of the reaction between barium bromoacetate and barium thiosulphate has been studied at 15° and 35° C, and the results have been combined with the published figures for the calcium and barium salts at 25° C. The results have been analyzed, using the dissociation data of the preceding paper, in terms of the three concurrent reactions:  $S_2O_3^{2-} + BrAc'$ ,  $BaS_2O_3 + BrAc'$ , and  $S_2O_3^{2-} + BaBrAc$ . The contribution of the third of these is insignificant, but the second gives concordant velocity constants and, in agreement with theory, shows a zero salt effect.  $BaS_2O_3$  and  $CaS_2O_3$  react at the same rate with the bromoacetate ion, the different catalytic efficiencies of the two metals being due to the different dissociation constants of the two salts. Both the velocity constant and the activation energy of the ion-pair-ion reaction fall between the values for the ion-ion reaction and the ion-molecule (ester) reaction.

The reaction between bromoacetates and thiosulphates has been extensively studied by LaMer, von Kiss and Vass and others.<sup>1-7</sup> It has proved to be uncomplicated and susceptible to accurate measurement in very dilute solutions, where the results are in excellent agreement with the Brönsted equation :

$$v = k[S_2O_3^{2-}][BrAc'] \frac{f_1 f_2}{f_3},$$

( $f_1$ ,  $f_2$ ,  $f_3$  being activity coefficients referring to 1-, 2- and 3-valent ions respectively). At higher concentrations, however, the reaction is influenced by the cation present, and, in particular, LaMer and Fessenden found that the presence of calcium, and still more barium, greatly enhanced the reaction rate.

Effects of this kind have been known for a long time. For instance Holmberg<sup>8</sup> in his studies of "cation catalysis" found that the reaction :



was greatly accelerated by bivalent cations, only in this case calcium has a much greater effect than barium.

Both LaMer and Kamner<sup>4</sup> and Scatchard<sup>9</sup> have discussed the anomalies in the bromoacetate-thiosulphate reaction in terms of the Bjerrum theory

<sup>1</sup> LaMer, *J. Amer. Chem. Soc.*, 1929, **51**, 3341, 3678.

<sup>2</sup> LaMer and Fessenden, *ibid.*, 1932, **54**, 2351.

<sup>3</sup> LaMer and Kamner, *ibid.*, 1931, **53**, 2832.

<sup>4</sup> LaMer and Kamner, *ibid.*, 1935, **57**, 2662.

<sup>5</sup> von Kiss and Vass, *Z. anorg. Chem.*, 1934, **217**, 305.

<sup>6</sup> Kappana, *J. Indian Chem. Soc.*, 1929, **6**, 45.

<sup>7</sup> Kappana and Patwardhan, *ibid.*, 1932, **9**, 379.

<sup>8</sup> Holmberg, *Z. physik. Chem.*, 1912, **79**, 147.

<sup>9</sup> Scatchard, *J. Chem. Physics*, 1939, **7**, 657.

of ion-pair formation,<sup>10</sup> but no attempt has been made to develop a quantitative treatment. To do so with profit clearly requires a knowledge from independent experiments of the extent of ion-association in the reaction mixtures, and our object in the present work was to use in this way the results of the general treatment of dissociation in salt solutions developed in the preceding and earlier papers. For the two reactions already quoted the most important effect of the presence of a bivalent cation will be its association with the bivalent anion, so that in the bromoacetate-thiosulphate reaction, for instance, an important contribution to the total velocity will be expected from the reaction between bromoacetate ions and the uncharged  $\text{MS}_2\text{O}_3$ . From electrostatic considerations this will be the faster process, thus explaining the catalytic effect of multi-valent cations. Moreover, barium thiosulphate is weaker than the calcium salt,<sup>11</sup> as required by LaMer's results, whereas for the succinates the opposite is true,<sup>12</sup> thus accounting for the reversal in the order of catalytic efficiency of the two cations in Holmberg's reaction.

In what follows we have attempted a detailed analysis of LaMer and Fessenden's results for the  $\text{BrAc-S}_2\text{O}_3$  reaction in the presence of calcium and barium at  $25^\circ\text{C}$ ; and we also report new kinetic measurements at  $15^\circ$  and  $35^\circ\text{C}$ , which enable us to extend the analysis to cover the effect of temperature on the barium-catalyzed reaction. We have taken into account all the association products that are present in significant amounts, and we have assumed that the separate reactions proceed independently by bimolecular mechanisms and contribute additively to the measured velocity. It is worth noting that these assumptions receive a searching test from the experimental data, for not only must the analysis lead to consistent values for the various  $k$ 's, but also these separate  $k$ 's—which refer to reactions of differing ionic type—must each show the characteristic salt effect required by the Brönsted equation.

## Experimental

**Materials.**—Bromoacetic acid was redistilled under 15 mm. pressure, and kept in the dark over strong sulphuric acid. Barium bromoacetate solutions were prepared from this by neutralizing weighed samples with a standard baryta solution, and making up with boiled-out distilled water. In this we followed the recommendations of earlier workers. We found, however, in parallel experiments that dilute solutions of bromoacetic acid are stable over many days, and barium salt solutions prepared by neutralizing these gave the same results as solutions prepared from the solid acid. The baryta was standardized with an HCl solution which had itself been standardized both with borax and with the thiosulphate used in the iodometric titrations. The barium thiosulphate, a B.D.H. reagent of formula  $\text{BaS}_2\text{O}_3 \cdot \text{H}_2\text{O}$ , was found to be 99.1 % pure in barium and thiosulphate, the remainder being ascribed to moisture; the concentrations of solutions were checked with 0.01 N iodine. 0.01 N solutions of  $\text{I}_2$  and  $\text{Na}_2\text{S}_2\text{O}_3$  were standardized daily against  $\text{KIO}_3$ .

**Method.**—In all experiments equimolar solutions of bromoacetate and thiosulphate were used. Suitable solutions were brought to thermal equilibrium in a thermostat at  $15^\circ$  or  $35^\circ \pm 0.02^\circ\text{C}$  before mixing, and aliquots were titrated at convenient intervals with iodine. As recommended by LaMer, the samples were run into an amount of iodine just insufficient to neutralize all the thiosulphate, and the remaining iodine added to the endpoint. For this final stage, 1 g. KI (iodate free) and 5 ml. of 1 % starch were added and the volume quickly made up to 200 ml.; under these standard conditions a consistent blank correction of 0.08 ml. of 0.01 N iodine was necessary.

The volumes of solutions were adjusted for temperature changes on the basis that the density differences were the same as that of water. In long experiments nitrogen was passed through the solutions after removal of samples.

<sup>10</sup> Bjerrum, *Kgl. Danske Vid. Selsk., Math-fys. Medd.*, 1926, 7, 9.

<sup>11</sup> Davies and Wyatt, *Trans. Faraday Soc.*, 1949 (preceding paper).

<sup>12</sup> Topp and Davies, *J. Chem. Soc.*, 1940, 84.

## Results

The course of a typical experiment is shown in Table I.

TABLE I

0.005 M  $\text{BaS}_2\text{O}_8$  + 0.0025 M  $\text{Ba}(\text{BrAc})_2$  at 35° C

$t$ (min.)	0	28.5	77.3	101.6	118.0	850.3	955.6	1148
$\text{I}_2$ titre (ml.)	27.55	23.02	17.18	15.45	14.27	3.59	3.25	2.80
$k$	—	(1.38)	1.56 <sub>1</sub>	1.54 <sub>2</sub>	1.57 <sub>7</sub>	1.57 <sub>0</sub>	1.56 <sub>8</sub>	1.54 <sub>6</sub>

The last row of figures gives :

$$\frac{I}{at} \left( \frac{x}{a-x} \right) = k \text{ (min.}^{-1} \text{ l. mol.}^{-1}\text{)}.$$

It illustrates an anomaly we have found throughout, especially at 35°: this is that measurements during the first 25 % conversion give abnormally low constants, even in the slowest runs. No mention of this is made in the literature, though LaMer and Kammer's constants<sup>4</sup> at 37.5° also appear to be based on measurements at conversions greater than 20 %.

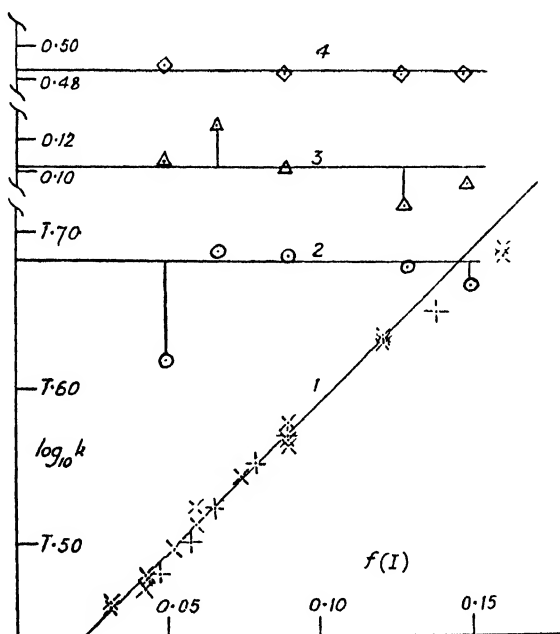


FIG. 1.— $\times$ , +. The ionic reaction; data of LaMer and Fessenden, and of von Kiss and Vass, respectively.

$\circ$ ,  $\Delta$ ,  $\diamond$ . The reaction  $(\text{BaS}_2\text{O}_8 + \text{BrAc}')$  at 15°, 25° and 35° C.

Complete results are given in the first two columns of Tables II and III; duplicate runs never differed from the mean value by more than 1 %.

TABLE II  
BARIUM SALTS AT 15° C

$M^*$	$k$	[BaS <sub>2</sub> O <sub>3</sub> ]	[BaBrAc·]	$I$	$f(I)$	$k_1 \cdot \frac{f_2 f_1}{f_3}$	$k'_2$	$k_2$
0.0005	0.142	0.0305	0.0004	0.002627	0.0482	0.1239	0.427	0.416
0.001	0.169	0.097	0.002	0.00511	0.0656	0.1337	0.505	0.489
0.002	0.199	0.289	0.005	0.00983	0.0883	0.1482	0.502	0.485
0.005	0.245	1.090	0.027	0.0231	0.1272	0.1774	0.489	0.477
0.0075	0.264	1.879	0.054	0.0336	0.1483	0.1955	0.477	0.465

\* [S<sub>2</sub>O<sub>3</sub>] total = [BrAc] total =  $M$ . Total Ba concn. = 1.5  $M$ .

TABLE III  
BARIUM SALTS AT 35° C

$M$	$k$	[BaS <sub>2</sub> O <sub>3</sub> ]	[BaBrAc·]	$I$	$f(I)$	$k_1 \cdot \frac{f_2 f_1}{f_3}$	$k'_2$	$k_2$
0.0005	0.917	0.0391	0.0006	0.00259	0.0479	0.731	3.14	3.08
0.001	1.03	0.123	0.002	0.00500	0.0650	0.793	(2.74)	(2.68)
0.002	1.27	0.357	0.007	0.00956	0.0871	0.877	3.11	3.05
0.005	1.57	1.298	0.034	0.0222	0.1256	1.045	3.10	3.04
0.0075	1.71	2.220	0.068	0.0323	0.1458	1.146	3.11	3.05

In addition, one experiment was carried out at 25° on a 0.005  $M$  mixture. The constant obtained, 0.625  $\pm$  0.002, was in satisfactory agreement with LaMer and Fessenden's value, 0.629. In Table IV our figures are combined with those

TABLE IV  
BARIUM SALTS AT 15°, 25° and 35° C

$M$	°C	Mean $k$	$\log k + 1$	$E$ (cal.)	$E$ (15-35) (cal.)
0.0005	15	0.142	0.152	16,930	16,450
	25	0.383	0.583	15,910	
	35	0.917	0.962		
0.001	15	0.169	0.228	16,770	(15,940)
	25	0.452	0.665	(15,030)	
	35	1.03	1.013		
0.002	15	0.199	0.299	16,460	16,350
	25	0.522	0.718	16,210	
	35	1.27	1.104		
0.005	15	0.245	0.389	16,100	16,390
	25	0.629	0.799	16,670	
	35	1.57	1.196		
0.0075	15	0.265	0.422	16,530	16,470
	25	0.696	0.843	16,380	
	35	1.71	1.233	*	



of LaMer and Fessenden at 25°, and in col. 5 activation energies for the two temperature intervals are calculated from the formula :

$$E = 2.303RT_m^2 \cdot \Delta \log_{10} k/\Delta T,$$

where  $T_m$  is the mean temperature. Our figure for the 0.001 M solution at 35° is clearly incompatible with the others. Neglecting this,  $E = 16,290 \pm 230$  cal. for the interval 25-30°, and  $16,560 \pm 230$  cal. for 15-25°. There is no significant variation of  $k$  with ionic strength for the concentrations studied, as is most clearly seen from the last column of the Table, which gives the activation energies calculated from our own measurements at 15° and 35° ( $E_{\text{mean}} = 16,415 \pm 45$  cal.).

**Calculations.**—The reaction in the presence of a bivalent cation may be analyzed into four parts involving the pairs of reactants ( $S_2O_8^{2-} + BrAc$ ), ( $MS_2O_3 + BrAc$ ), ( $S_2O_3^{2-} + MBrAc$ ) and ( $MS_2O_3 + MBrAc$ ). We assume that these four reactions proceed concurrently with the respective bimolecular constants  $k_1, k_2, k_3, k_4$ . It is shown later that the contribution of the ( $S_2O_3^{2-} + MBrAc$ ) reaction is only a minor one, and in view of this we can neglect the ( $MS_2O_3 + MBrAc$ ) reaction altogether; for the ratio  $[MS_2O_3]/[S_2O_3^{2-}]$  is always small, and also  $k_4$  may be expected to be less than  $k_3$  on account of the difference in the ionic type of these two reactions. If  $v$  is the experimentally observed rate of the reaction we can therefore write :

$$v = k_1[S_2O_8^{2-}][BrAc] \cdot \frac{f_2 f_1}{f_3} + k_2[MS_2O_3][BrAc] + k_3[S_2O_3^{2-}][MBrAc] \cdot \frac{f_2 f_1}{f_1} \quad (1)$$

By introducing the mass action constants :

$$\frac{[M''] [S_2O_3^{2-}]}{[MS_2O_3]} \cdot f_2^2 = K_1 \text{ and } \frac{[M''] [BrAc] f_2}{[MBrAc]} = K_2,$$

we can re-write the third term on the right-hand side of eqn. (1) and obtain :

$$v = k_1[S_2O_8^{2-}][BrAc] \cdot \frac{f_2 f_1}{f_3} + [MS_2O_3][BrAc] \left( k_2 + k_3 \cdot \frac{K_1}{K_2} \right) \quad (2)$$

It will be clear from eqn. (2) that  $k_2$  and  $k_3$  cannot be separately determined from our data; our primary object therefore will be to analyze the experimental rate into the two terms of eqn. (2), and this can be done by means of the dissociation constants reported in the preceding paper. In parenthesis, it may be noticed here that eqn. (2) cannot lead to a second-order overall reaction rate—such as is observed experimentally over the greater part of the course of the reaction—unless special conditions are fulfilled. These are that the dissociation constants of  $MS_2O_3$  and  $M(S_2O_3)Ac$  should be approximately the same, and similarly for  $MBrAc$  and  $MBr$ . If this is true, the values of  $[M'']$  and of the ionic strength will not vary during the course of a run,<sup>16</sup> and in the alternative form of eqn. (2),

$$v = [S_2O_8^{2-}][BrAc] \left\{ \frac{k_1 \cdot f_2 f_1}{f_3} + \frac{[M''] f_2^2}{K_1} \left( k_2 + k_3 \cdot \frac{K_1}{K_2} \right) \right\},$$

none of the terms within the braces will vary during the course of a run, and  $[S_2O_8^{2-}]$  and  $[BrAc]$  will remain constant fractions of the total concentration of the thiosulphate and bromoacetate radicals; the measured velocity will therefore obey a second-order equation in terms of total concentrations.

**The Reaction at 25° C.**—The velocity constant,  $k_1$ , for the reaction between the free ions is obtained from the available data for the sodium and potassium salts at high dilutions, where dissociation can be considered complete. LaMer and Fessenden pointed out that their sodium and potassium results were identical, and that when plotted against  $I^{\frac{1}{2}}$  they approached the theoretical limiting slope at high dilutions. In Curve 1 of the Figure the available  $\log_{10} k$  values are plotted against

$$f(I) = I^{\frac{1}{2}}/(1 + I^{\frac{1}{2}}) - 0.2I.$$

This gives a straighter line and enables more points to be taken into consideration. Curve 1 is drawn with the theoretical slope, 2.04, and leads to the value  $k_1 = 0.247$  (at zero ionic strength).

Considering now the reaction between the barium salts, the first two columns of Table V give LaMer and Fessenden's data. Col. 3 and 4 give the initial concentrations in millimoles per litre of the association products, obtained by successive approximations from the dissociation constants given in the preceding paper; the concentrations of the free ions can be found by difference. Col. 5 gives the ionic strength and Col. 6 gives values of  $f(I)$ . The contribution of the first term in eqn. (2), the rate of the reaction between the free ions, can now be calculated from the values of  $k_1 \cdot f_2 f_1 / f_3$ , read from Curve 1 and recorded in Col. 7; the contribution of the second term is next found by difference, and leads to the values of  $k'_2 = (k_2 + k_3 \cdot K_1/K_2)$  given in Col. 8.

As we have seen,  $k_2$  and  $k_3$  cannot be separated experimentally. But for the reaction ( $S_2O_8^{2-} + BrAc'$ )  $k_1$  is known to be 0.247 and an approximate value for the reaction ( $BaS_2O_8 + BrAc'$ ) is now known to be 1.2. For the reaction ( $S_2O_8^{2-} + BaBrAc'$ ) we can therefore infer on electrostatic grounds that the value of  $k_3$  will be very approximately 2.3. Taking the higher value and multiplying by  $K_1/K_2 = 0.011$  leads to the corrected values for the ( $BaS_2O_8 + BrAc'$ ) reaction given in the last column of the Table.

TABLE V  
BARIUM SALTS AT 25° C

M	$k_{obs.}$	[ $BaS_2O_8$ ]	[ $BaBrAc'$ ]	I	$f(I)$	$k_1 \frac{f_2 f_1}{f_3}$	$k'_2$	$k_2$
0.0005	0.383	0.0347	0.0005	0.00261	0.0481	0.312	1.32	1.28
0.001	0.452	0.110	0.002	0.00505	0.0653	0.337	1.38	1.35
0.002	0.522	0.323	0.006	0.009696	0.0877	0.373	1.30	1.27
0.005	0.629	1.192	0.030	0.02267	0.1264	0.447	1.23	1.20
0.0075	0.696	2.047	0.060	0.03294	0.1471	0.491	1.27	1.24

Exactly the same treatment has been applied to LaMer and Fessenden's data for the calcium salts, and the results are in Table VI.

TABLE VI  
CALCIUM SALTS AT 25° C

M	$k_{obs.}$	[ $CaS_2O_8$ ]	[ $CaBrAc'$ ]	I	$f(I)$	$k_1 \frac{f_2 f_1}{f_3}$	$k'_2$	$k_2$
0.0005	0.362	0.0248	0.0010	0.00265	0.0484	0.362	1.33	1.24
0.001	0.424	0.0797	0.0037	0.00517	0.0661	0.424	1.43	1.33
0.002	0.502	0.239	0.013	0.01002	0.0890	0.502	1.46	1.37
BrAc								
0.0033 $S_2O_8$	0.636	1.240	0.044	0.02660	0.1349	0.636	1.52	1.42
0.00667								

**The Reaction at 15° and 35° C.**—Our data for the barium salts at 15° and 35° have been treated in the same way, with the necessary adjustments in the values of the constants. Activation energies have been determined for the purely ionic reaction in dilute solutions,<sup>1-7</sup> and using the values

$$E(15-25^\circ) = 15,900 \text{ cal. and } E(25-35^\circ) = 15,700 \text{ cal.}$$

we obtain 0.0980 at 15° and 0.581 at 35° as the values of  $k_1$ . Dissociation constants were again taken from the preceding paper,  $K_{BaS_2O_8}$  at 15° being calculated by means of the  $\Delta H$  value there recorded. The total corrections for  $BaBrAc'$  are so small that the  $K$  value reported for 25° could be used at the other two temperatures without sensible error. The results of the calculations are in Tables II and III.

## Discussion

The quantitative interpretation of reaction rates in terms of incomplete dissociation clearly leads to reasonable results. The derived velocity constants at three temperatures for the reaction :



are plotted in Curves 2, 3 and 4 of the Figure, and in accordance with theory they are constant within experimental error and show a zero salt effect. So far as ionic atmosphere effects are concerned, therefore, the ion-pairs, as would be anticipated, behave like uncharged molecules. The  $k_2$  values derived for the calcium and barium salts are identical, within the error of the calculations, and so the difference in the catalytic efficiency of these two ions finds its explanation, as was suggested in the Introduction, in the different dissociation constants of the two thiosulphates and not in any marked difference in their reactivity.

The application of electrostatic theory to the thiosulphate reaction has been fully discussed by LaMer<sup>14</sup> and Moelwyn-Hughes.<sup>15</sup> If the electrical interaction energy (at infinite dilution) of two reacting ions is written  $z_A z_B e^2 / D r$ , where  $r$  is the critical separation of ionic centres for chemical change, then values of  $r$  can be derived from a consideration of the absolute reaction rate or from experimental study of changes in  $z$ ,  $D$  and  $T$ . In these ways  $r$  values have been derived which are plausible in themselves but vary by more than the experimental error according to the method of calculation or type of experimental result. The present work makes it possible to compare the constants for (a) the ionic reaction ( $\text{S}_2\text{O}_3^{2-} + \text{BrAc}'$ ), (b) the reaction between the thiosulphate ion and the methyl or ethyl ester of bromoacetic acid,<sup>3, 16</sup> and (c) the reaction between the bromoacetate ion and the calcium or barium thiosulphate ion-pairs. If the whole difference between (a) and (b) is attributed to the electrical interaction term a value  $r = 3.47 \text{ \AA}$  is derived.<sup>15</sup> Our value of  $\log k_2$  for the ion-pair-ion reaction falls approximately midway between the values for the ion-ion and the ion-molecule reactions. Qualitatively, this result seems a reasonable one; but it is clear that a quantitative interpretation would involve factors not considered in the simple electrostatic theory, and it is very doubtful if further discussion would be profitable until more independent evidence is available concerning the dimensions of the reactants and the values of  $D$  to be employed in calculations concerning their intimate interaction.

Our three values for the barium thiosulphate-bromoacetate reaction lead to the following values for the activation energy : 15-25°, 16,800 cal. ; 25-35°, 16,050 cal. ; mean, 16,400 cal. This value, again, falls between 15,800 cal., the mean energy of activation for the ionic reaction, and the value 17,400 cal. derived for the ion-molecule reaction from Slator's temperature coefficients.<sup>16</sup>

Edward Davies Chemical Laboratories,  
Aberystwyth, Wales.

<sup>14</sup> LaMer, *J. Franklin Inst.*, 1938, **225**, 709.

<sup>15</sup> Moelwyn-Hughes, *Kinetics of Reactions in Solution* (Clarendon Press, Oxford, 1947), 2nd ed., pp. 91-107.

<sup>16</sup> Slator, *J. Chem. Soc.*, 1905, **87**, 485.

# STRUCTURE AND STABILITY OF BURNER FLAMES

BY N. THOMAS

*Received 23rd March, 1948, as revised 25th April, 1949*

An attempt is made to develop a general theory of flame stability in stationary flames based on the assumption of steady-state heat balance. The heat balance equation for the flame is formulated, and approximate solutions obtained under certain specified conditions.

Certain experimental phenomena involving the stability limits of flames can be explained semi-quantitatively by this theory. It does not, however, take into account the chemical kinetics of the reactions, or aerodynamic effects which are of importance in dealing with high-velocity flames.

## 1. Introduction

The theories put forward in the past to explain the structure and stability of a stationary flame have been formulated mainly with specific reference to aerated flames of the Bunsen type and have been based on the idea that in a stable burner flame the flame velocity and gas feed velocity may be equated over the surface of the inner cone. This idea forms the basis of the work of Lewis and v. Elbe<sup>1</sup> on the physical structure of flames, and also that of Townend *et al.*<sup>2</sup>

In this paper only the physical aspects of combustion are dealt with, and no attempt has been made to deal with the chemical mechanism of the reactions occurring in flames. Aerodynamic factors are not treated in detail, and as these become extremely important in turbulent flames, their omission is an obvious limitation on the scope of the theory. The radiation equilibrium of the flame is also not considered, an assumption, which, while unjustified for flames containing large numbers of small radiating particles (e.g. poorly aerated benzene flames, aluminium flames), is true for ordinary gas flames which are not too poorly aerated.\*

The present theory starts from the assumption that a stationary flame is in a state of steady thermal equilibrium. In setting up the steady-state equations, a physical analogy, which may help in visualizing the process is introduced. The general equation is then modified for various special conditions, and approximate solutions are obtained. The theory is inapplicable to gas-rich flames for two reasons, the neglect of radiation equilibrium, mentioned above, and of the change of specific heat in combustion, which may be appreciable in such cases. Turbulent flames are not included in the scope of the theory.

It is considered that the thermal equilibrium theory is of more general application than the equilibrium treatment used by Lewis and v. Elbe. It was applied to the problem of propagation of flames in tubes by Holm<sup>4</sup> but this author did not attempt to generalize the treatment or to apply it to burner flames as such. Holm was, however, able to provide a satisfactory explanation of the fact that flame will not propagate in tubes

<sup>1</sup> Lewis and v. Elbe, *J. Chem. Physics*, 1943, **11**, 75; *Combustion, Flames and Explosions in Gases* (Cambridge, 1938).

<sup>2</sup> Garside, also Forsyth, Davies and Townend, *Inst. Gas Engr. Conm.* 244/102, 245/103 (published together).

<sup>3</sup> Fuidge, Dewhurst and Pleasance, *ibid.*, 266.

<sup>4</sup> Holm, *Phil. Mag.*, 1932 (7), **14**, 18.

\* Private communication from Dr. H. G. Wolfhard.

below a certain diameter (incidentally disproving the theory that this is due to heat loss through the tube surfaces), since the critical diameter was found to be independent of the thermal conductivity of the material of the tube. The general form of the theory is set out in the next section.

## 2. General Form of Theory

Symbols used are as follows :—

$H_c$  = Volume heat of combustion of gas mixture in flame,

$\lambda$  = Thermal conductivity of flame gases,

$dS$  = Unit surface area of flame,

$V$  = Volume of gas entering the flame,

$\frac{dV}{dt}$  = Flux of gas into the flame,

$\frac{\partial T}{\partial r}$  = Temperature gradient across external surface of flame,

$\frac{\partial T}{\partial x}$  = Temperature gradient across base of flame,

$\bar{c}_p$  = Mean sp. ht. of reaction products over range,

$\Delta T$  = Temperature difference between ignition temperature and temperature of inflowing gas,

$\bar{c}_p$  = Mean sp. ht. of gas mixture over range,

$\Delta T'$  = Difference between ignition and steady flame temperatures,

$H$  = Effective heat of combustion =  $[H_c - \bar{c}_p' \Delta T']$ .

Consider a flame and its surrounding envelope of burnt and partly burnt gases. We idealize the outer boundary in the model shown for, in practice, the cooling mechanism is not true conduction but some form of turbulent convection which, in a surrounding space large enough to act as a heat sink, quickly reduces the temperature of the outer cone gases to equilibrium.

On this assumption we see that the heat produced in the flame over a short period of time is removed (a) by conduction and convection across the outer cone boundary, (b) by the fresh gas mixture flowing in across the flame base and being raised to ignition temperature by the heat of the flame, (c) by the reaction products raised from ignition to flame temperature.

Thus, the heat of combustion equals the heat removed across the outer cone boundary + the heat used in raising fresh gas to the ignition temperature + the heat used in raising the reaction products from ignition to flame-temperature. Since the surroundings form a heat sink,  $H_c$  is taken as the heat of combustion at room temperature.

Then

$$H_c = \lambda \frac{\partial T}{\partial r} \oint dS + \bar{c}_p \Delta T \frac{dV}{dt} + \bar{c}_p' \Delta T'$$

over a short space of time, using volume variables for unit volume. In this case the concentration of reaction products and intermediates in the flame over the range  $\Delta T'$  is assumed independent of  $\frac{dV}{dt}$ . These

products are distributed throughout the flame system, not immediately dependent on increments to it. The heat balance of the flame might be regarded as being "perturbed" by the inflow of cold gas mixture.

If we transform to mass variables we get

$$m\bar{p}H_c = \text{conduction terms} + \bar{c}_{p,p} \Delta T \frac{dV}{dt} + m\bar{c}_{p,p}' \Delta T',$$

where  $m$  is the mass of combustible gas mixture present in the flame,

and  $\bar{\rho}$  the mean density. The term  $\rho H_c$  is, of course inverse of the mass heat of combustion  $H_c/\rho$  with respect to  $\rho$ . It will be seen in § 5 that this, rather than the volume heat of combustion, determines the stability of the flame to a large extent. Eliminating  $\bar{\rho}$  and  $m$  from the above equation we have

$$H_c = \text{conduction term} + \frac{\bar{c}_p}{m} \frac{dV}{dt} \Delta T + \bar{c}_p' \Delta T'.$$

We now define

$$H = (H_c - \bar{c}_p' \Delta T')$$

as our effective heat of combustion, which we use in the subsequent treatment and we have

$$H = \text{conduction terms} + \bar{c}_p \Delta T \frac{dV}{dt},$$

where  $m = 1$  or, more explicitly,

$$H = \lambda \frac{\partial T}{\partial r} \oint dS + \lambda A \frac{\partial T}{\partial x} + \bar{c}_p \Delta T \frac{dV}{dt}. \quad (1)$$

The conduction term is, rather arbitrarily, broken into two parts, one representing heat conduction across the outer flame surface, the other conduction across the flame base. This is convenient for a treatment of non-aerated flames. Equn. (1), though a simplification, seems adequate for our approximate treatment of flame stability.

We note that  $H$  is the sum of two terms, viz. (1) the heat derived from combustion of gas with primary air entrained in the gas stream, and (2) the heat derived from combustion of gas and air which have interdiffused, so we denote these by  $H_1$  and  $H_2$  respectively.  $H_2$  is dependent on the interdiffusion coefficient  $D$  of gas and air, and on the surface area of the flame;  $H_1$  is proportional to the percentage of air up to the stoichiometric limit. Below this we have

$$H = c_1 D \oint dS + c_2 \frac{dV}{dt}. \quad (2)$$

in which  $c_1, c_2$  are defined below. Combining (1) and (2) and neglecting the conduction term for the flame base, we have, on adding a term to allow for cooling due to air mixing across the flame surface, which we write  $K' \Delta T \oint dS$ ,

$$K' \Delta T \oint dS + \lambda \frac{\partial T}{\partial r} \oint dS + \bar{c}_p \Delta T \frac{dV}{dt} = c_1 D \oint dS + c_2 \frac{dV}{dt},$$

$$\begin{aligned} \text{or} \quad & \left( \oint dS \right) \left( \lambda \frac{\partial T}{\partial r} - c_1 D + K' \Delta T \right) = \frac{dV}{dt} (c_2 - \bar{c}_p \Delta T), \\ \therefore & \frac{\left( \oint dS \right)}{\frac{dV}{dt}} = \frac{[c_2 - \bar{c}_p \Delta T]}{\left[ \lambda \frac{\partial T}{\partial r} - c_1 D + K' \Delta T \right]}. \end{aligned}$$

Assuming  $\partial T / \partial r$  to be uniform over the whole surface (see ref. <sup>1</sup>), we may write

$$\frac{S}{U} = \frac{[c_2 - \bar{c}_p \Delta T]}{\left[ \lambda \frac{\partial T}{\partial r} - c_1 D + K' \Delta T \right]}. \quad (3)$$

Eqn. (3) bears some resemblance to Semenov's expression for the reaction rate in the theory of chain reactions. The rates become infinite when the denominator on the right-hand side becomes zero. From physical considerations we see that this condition will not arise in an

exposed flame, since the last term in the denominator, *allowing for cooling by air mixing across the surface, is dependent on  $D$ , and hence any increase in  $c_1 D$  is compensated by a corresponding increase in  $K'\Delta T$* . In closed vessels, however, the last term does not enter into the expression and if

$$c_1 D = \lambda \frac{\partial T}{\partial r}$$

then explosion will occur. This condition, of course, is realizable in practice.

One other point of some interest may be raised. We write the ratio

$$\frac{\text{Heat produced}}{\text{Heat lost}} \text{ as } \frac{H}{\left(K'\Delta T \frac{dV}{dt} + \lambda \frac{\partial T}{\partial r} \oint dS\right)}.$$

Now, writing the second term as constant and varying the remainder, we have

$$K' \cdot \frac{dM}{dt}$$

where  $M$  = mass and  $H$  heat produced in unit time.

This then becomes  $\left(\frac{\partial H}{\partial M}\right)$ , corresponding to the chemical potential  $\mu$  on a thermal theory; this term largely determines flame stability.

In the following sections the eqn. (1) is applied to account for various data on the stability of stationary flames. In § 5 an attempt is made to relate stability characteristics to other physical properties of the gases concerned; the earlier section dealt with simpler phenomena.

### 3. Application of the Theory to Various Cases

In this section the theory is further developed and applied to various cases of special interest.

(a) We shall first apply the theory to the case of flash-back in aerated burners. At certain gas-flow velocities and air/gas ratios, the flame propagates down the burner tube and the gas issuing from the injector nozzle ignites, giving a poorly aerated and noisy flame which is almost useless as a source of heat. Owing to its practical importance, thorough experimental investigations have been made into the nature of flash-back, particularly by Garside *et al.*,<sup>2</sup> and various devices have been suggested for its prevention, notably by Minchin.<sup>3</sup>

On the theory set forth by Lewis and v. Elbe,<sup>1</sup> flash-back is said to occur when the flame velocity at the inner cone surface exceeds the gas flow velocity, altering the pressure equilibrium set up at the flame front. From the thermal balance (eqn. (1)), we can set up a corresponding condition for flash-back. We write the equation for the steady state

$$H = \lambda \frac{\partial T}{\partial r} \oint dS + \lambda A \frac{\partial T}{\partial x} + K\Delta T \frac{dV}{dt},$$

where  $K = \bar{c}_p$  in the general equation.

Instead of Lewis and v. Elbe's condition, ours will be that flash-back occurs when  $H$  exceeds the right-hand side of the equation. The question of flash-back is, however, closely connected with the problem of the propagation of flame in tubes, which will now be considered in more detail.

(b) If we consider that a flame is propagated down a tube as a succession of Huyghens waves, we may develop and apply a simple model somewhat as follows. Assume that we have a sphere of combustible gas mixture, pushing a hemispherical flame front down the burner tube. As the flame front moves, it sweeps out a volume  $V$  in the tube against a pressure

<sup>3</sup> Minchin, *Gas J.*, 1939, **226**, 925.

difference  $dP$  per unit length. At the same time it is losing heat to the unignited gases in the tube at a rate given by  $\lambda A \frac{\partial T}{\partial r}$ , where  $A$  is the area of the flame front and  $\frac{\partial T}{\partial r}$  the thermal gradient set up. We then write the following heat balance equation,

$$H = \lambda A \frac{\partial T}{\partial r} + \int dP \cdot V \quad (1')$$

where  $H$  = heat generated in unit time by the burning gas. Eqn. (1') determines the condition for flame propagation.  $H$  is dependent on the volume of the sphere of burning gas, and on the air/gas ratio existing. Assuming the second of these factors to be constant,  $H$  can be written as

$$k \cdot \frac{4}{3} \pi r^3 = k_1 r^3.$$

Since  $A$ , the area of the hemispherical flame front is  $2\pi r^2$ , then

$$k_1 r^3 = k_2 r^2 \frac{\partial T}{\partial r} + V \int dP \quad (2')$$

The temperature gradient  $\frac{\partial T}{\partial r}$  is radial, and is evidently inversely proportional to  $r$ . So we have

$$k_1 r^3 = k_3 r + V \int dP \quad (3')$$

For flash-back, eqn. (3') becomes

$$k_1 r^3 > k_3 r + V \int dP.$$

The temperature gradient  $\frac{\partial T}{\partial r}$  may be determined from the "dead space" phenomenon observed in aerated burner flames. It was suggested by Smyth and Pickering,<sup>6</sup> that the space observed between a burner port and the flame base, the so-called "dead space," was a measure of the temperature gradient set up between the temperatures of the inflowing gas and the ignition temperature of the flame.

If the dead space distance =  $x$ , then the temperature gradient =  $\frac{\partial T}{\partial x}$  or  $k \cdot \frac{1}{x}$  putting  $T$  constant. In the case considered we have a radial temperature gradient, so if

$$\begin{aligned} \frac{\partial T}{\partial r} &= \frac{\partial T}{\partial x} \text{ then } \frac{\partial T}{\partial r} = k \cdot \frac{1}{x} \\ \therefore k_1 r^3 &= \frac{1}{x} \cdot k_2 r^2 + V \int dP \text{ from eqn. (2)} \quad (3a) \end{aligned}$$

If we neglect the pressure term, and assume flash-back is occurring,

$$k_1 r^3 > \frac{k_2 r^2}{x},$$

i.e. the probability of flash-back occurring is directly proportional to  $x$ .

Equating (3') and (3a) we have

$$\frac{k_2 r^2}{x} = k_3 r$$

at the critical condition for flash-back or

$$x = \frac{k_2}{k_3} \cdot r \quad (4)$$

If  $k_2$  and  $k_3$  are equal then  $x = r$  at the flash-back point.

<sup>6</sup> Smyth and Pickering, *J. Res. Nat. Bur. Stand.*, 1936, 17, 7.



We see from the above arguments that the probability of flash-back occurring decreases with the radius of the burner tube, hence with the diameter of the tube. Again neglecting the pressure term, we can write the flash-back condition as

$$k \cdot 2\pi r^2 < \frac{4}{3}\pi r^3 k'$$

and the ratio

$$\frac{\text{Heat lost}}{\text{Heat produced}} = k \cdot \frac{1}{r} \quad (5)$$

so that for small values of  $r$  the relative thermal loss will increase and hence flash-back will not occur below a certain value of  $r$ .

Flash-back in relation to the chemical composition of inflammable gas-mixtures will be considered in more detail later. The theory given for single tubes can be extended to groups of tubes in thermal contact with each other, such as are found in gauzes and in the "flame-proof" burner heads.

The probability of flash-back *not* occurring in a single tube can be seen from (5) to be inversely proportional to  $r$ , the radius of the tube, and we may write  $P = k \cdot \frac{1}{r}$ . In the case of groups of tubes we must make allowance for the mutual interaction effects, since each tube will receive a certain amount of heat from its neighbours. The form of the "interaction term" may be derived as follows.

Suppose we have a number of point sources of heat (Fig. 2) which are separated by a distance  $b$ . Now, if they are emitting heat uniformly

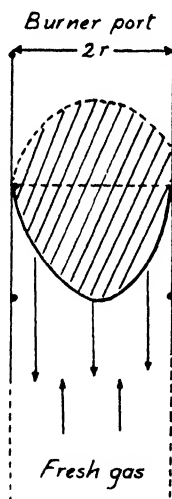


FIG. 1.

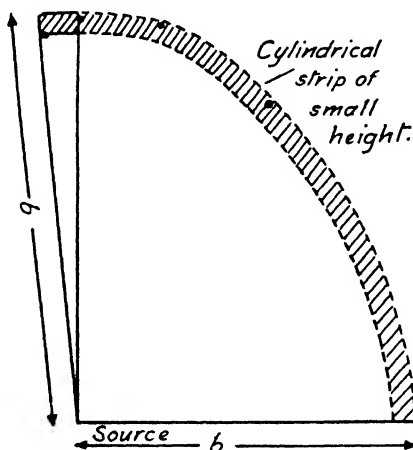


FIG. 2.

the heat traversing a small area  $dS$  of the receiving strip will be inversely proportional to the area of the strip, or

$$I = \frac{k}{\pi b^2} = k' \cdot \frac{1}{b^2}.$$

Now if the heat sources are considered as circles of radius  $r$ , then the radiative surface will be increased by a factor  $2\pi r$  (the circle perimeter): and hence we can write the heat flow at distance  $a$  as

$$k \cdot \frac{2\pi r}{\pi b^2} = k' \cdot \frac{2r}{b^2}.$$

This term represents the "interaction effect"; combining it with the expression for a single tube, we have

$$P = k \cdot \frac{1}{r} - k' \cdot \frac{2r}{b^2}.$$

(d) We now proceed to a further discussion of the stability limits of a flame. Writing the thermal balance equation in a shortened form

$$H = K \oint dS + K' \frac{dV}{dr},$$

(the heat loss through the base is included in the first term)—we note that when flash-back occurs, the value of  $H$  exceeds that of the right-hand side of the equation. However, it is possible for the condition of equality to be restored by an increase in  $\oint dS$  leading to a change in shape of the flame. No complete analysis of the nature of this change will be given; in practice, however, it is found that it takes the form of a tilting of the base of the inner cone down the burner tube and a distortion of the shape of the flame. If we assume this form of change, the problem can be treated quantitatively.

When tilt has occurred in a flame, we rewrite the thermal balance equation,

$$[H + \Delta H] = k \left[ \oint dS + \Delta \oint dS \right] = k' \frac{dV}{dt},$$

assuming that gas flow does not change during the tilting process, which, as the tilt only occupies a short space of time, seems a reasonable assumption, i.e.

$$\frac{\Delta H}{\Delta S} = K.$$

Now we determine  $\Delta S$ , the increase in area (see Fig. 3). If  $\Delta S$  is taken as proportional to the volume displaced in the burner tube by the tilting movement of the inner cone, i.e., the volume of the shaded half-cylinder in the figure, then

$$\Delta S = k' \frac{1}{2} \pi r^2 \times CB,$$

where  $CB = 2r \tan \theta$ , so  $\Delta S = \pi r^2 \tan \theta \times k'.$

We take  $\Delta H$  as proportional to the gas flow rate  $\frac{dV}{dt}$ , if the composition of the gas mixture is constant.

$$\therefore \frac{\Delta H}{\Delta S} = \frac{dV/dt}{\pi r^2 \tan \theta} = K.$$

When  $\theta$  is small,  $r \simeq \sigma$  so  $\Delta S = \pi r^2 \sin \theta$

or 
$$K = \frac{dV/dt}{\pi r^2 \sin \theta}.$$

(e) Finally we consider the relationship between flash-back and the composition of the air-gas mixture being used.

It should, of course, be noted that the term  $H$  in the fundamental equation is not only dependent on the total volume of burning mixture but on the air/gas ratio existing in that mixture. From physical considerations one would anticipate that  $H$  would reach a maximum as the

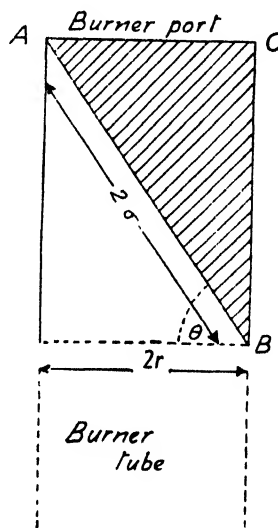


FIG. 3.

mixture approached stoichiometric proportions, and subsequently decline as the relative volume of air present exceeded that needed for complete combustion, if the total volume under consideration is stationary.

Let the stoichiometric air/gas ratio be  $\frac{1-x}{x}$ , where  $x$  is the gas percentage/100 at stoichiometric proportions:  $H$  is the heat of combustion of the mixture at this point. Suppose we have a mixture of ratio

$$\frac{1-(x-z)}{x-z},$$

then its heat of combustion is

$$H \cdot \frac{x-z}{x}.$$

Again, if we have an over-rich gas mixture of ratio  $\frac{1-x-z'}{x+z'}$  its heat of combustion will be  $H \cdot \frac{(1-x-z')}{(1-x)}$ . We see that  $H$  varies from  $\frac{x-z}{x}$  through unity to  $\frac{(1-x)-z'}{(1-x)}$ , where  $z, z'$  are arbitrary choices, i.e.,  $x$  varies linearly, while  $H$  has a maximum.

We saw previously that by eqn. (5), the ratio

$$\frac{\text{Heat loss}}{\text{Heat produced}} \propto \frac{1}{r}.$$

At the "limiting radius" for flash-back,  $r_c$ , we have,

$$\frac{\text{Heat loss}}{H} = \frac{k}{r_c} = 1,$$

$$\therefore H \propto \frac{1}{r_c}.$$

Now we had above a relation of type

$$y = \frac{x-z}{x}$$

between  $H$  and  $x$ . Inverting the right-hand side with respect to  $x$  this becomes

$$y = x^2 - zx,$$

which since  $H \propto \frac{1}{r_c}$  is the form of the relation between  $r_c$  and  $x$ . As  $H$  has a maximum at stoichiometric proportions, then  $r_c$  will have a minimum at this point. Thus we have a parabola with a minimum as the relation.

We now endeavour to determine the relation between  $H$  and the air/gas ratio, written as  $\frac{1-x}{x}$ ,  $x$  being the gas-fraction in the mixture and therefore  $< 1$ .

For values of  $x < 1$ ,  $\frac{1-x}{x}$  increases towards  $\infty$  with decreasing value of  $x$  it is a hyperbolic function of  $x$ .

Now we have a relation of the type  $H = \left(\frac{1}{x} + c\right)^2$  already, combining these we have

$$H = f\left(\frac{1}{x_1} + c\right)^2, \text{ where } x_1 = \frac{1-x}{x},$$

which is the general form. The curve is, of course, of the same type as the normal probability curve, in that it is exponential with a maximum at the stoichiometric air/gas ratio.

(f) The phenomenon of "blow-off", the disappearance of a burner flame when the gas feed velocity is raised above a certain value, is a well-known one and has been studied by Townend *et al.*<sup>2</sup> On the Lewis-v. Elbe theory of flame stability, blow-off occurs when the feed velocity over the surface of the inner cone exceeds the ignition velocity. As the present theory treats the thermal equilibrium of the flame, we set up a corresponding condition as follows.

When the blow-off occurs, the flame disappears and this fact in itself suggests that the heat produced in the flame is no longer sufficient to maintain equilibrium. At blow-off the fundamental equation may be written,

$$H < \lambda \frac{\partial T}{\partial r} \oint dS + \lambda A \frac{\partial T}{\partial x} + \bar{c}_p \Delta T \frac{dV}{dt},$$

the reverse of the condition for flash-back. When blow-off occurs, the volume of cold gas flowing into the flame in unit time is so great that the heat generated in unit time is insufficient to raise it to ignition temperature. Combustion actually ceases when this point is reached.

In the case where  $H$  is made up purely of heat derived from the combustion of gas with entrained air (the assumption tacitly made in the discussion on flash-back) we have already seen that  $x$  and  $H$  bear a relationship to each other of the form

$$\frac{1}{H} = K(x^2 + c).$$

Now in the equation of thermal equilibrium we may assume that at or near the blow-off point the  $\frac{dV}{dt}$  term on the right-hand side is large compared to the surface terms, so we have, approximately,

$$H < \bar{c}_p \Delta T \frac{dV}{dt}, \text{ while } \frac{1}{H} = k(x^2 + c),$$

so 
$$\frac{dV}{dt} = k(x^2 + c)$$

at equilibrium, since  $\frac{dV}{dt}$  increases with decreasing  $H$  around blow-off.

As with flash-back, we see from physical considerations that this parabola will have its maximum as  $x$  reaches the stoichiometric fraction for the mixture, since  $H$  will then reach a maximum for a given gas flow.

Where secondary air entrainment occurs, the equation assumes a different form. We must take into account the fact that, owing to inter-diffusion of gas and air, when the proportion of gas in the mixture exceeds the stoichiometric value all will be burnt. Assuming complete combustion we see that  $H$  is directly proportional to  $x$  (symbols as before), and since

$$H = K' \cdot \frac{dV}{dt} + \text{surface loss},$$

we can write

$$\frac{dV}{dt} = kx + c,$$

i.e. a linear relationship.

Now  $\frac{1-x}{x}$  is a hyperbolic function of  $x$  for values of  $x < 1$  and so, if as previously  $\frac{1-x}{x}$  is the air-gas ratio then we have

$$H = k \cdot f \left[ \frac{x}{(1-x)} + c \right],$$

which is similar to a logarithmic curve when  $x < 1$ .

#### 4. Non-aerated Flames

(a) The treatment of non-aerated flames given below is not complete for it deals only with the thermal aspects of such flames, and does not treat hydrodynamical problems.

The general equation may be applied in the form,

$$H = k \frac{dV}{dt} + \lambda \frac{\partial T}{\partial r} \oint dS,$$

where  $H$  is, as before, made up of two portions, one due to combustion with entrained air and the other to combustion of interdiffused gas and air. Rewriting the equation we have

$$c_1 \frac{dV}{dt} + c_2 \frac{\partial T}{\partial r} \int dS = k' \frac{dV}{dt} + \lambda \frac{\partial T}{\partial r} \int dS$$

or 
$$\frac{dV}{dt} (c_1 - k') = \int dS \times (\lambda - c_2) \frac{\partial T}{\partial r}.$$

Now, if we assume complete combustion, then the heat produced will be proportional to  $\frac{dV}{dt}$  as in the "blow-off" case previously treated, i.e. proportional to  $H\bar{\rho} \frac{dV}{dt}$  where  $\bar{\rho}$  is the mean gas density.

Then for equilibrium we have

$$H\bar{\rho} \frac{dV}{dt} = \lambda \oint dS + k \frac{dV}{dt},$$

to a first approximation. It is clear that the greater the value of  $H$ , the mass-heat of combustion of the gas, the less chance is there of the flame becoming unstable and blowing-off.

If  $\frac{dV}{dt} \propto P$ , the feed pressure, we have

$$P = k_1 \bar{\rho} H \frac{dV}{dt},$$

a linear relation if we neglect the surface loss term. The plot depends on the relation  $\oint \frac{dS}{dV/dt}$  which is dependent not only on  $P$  and  $\frac{1}{\bar{\rho}}$  but on other factors not so readily determined. Moreover, we have assumed combustion to be complete. This is not the case in non-aerated burners, except when they are burning hydrogen, which has a high diffusion coefficient and so mixes very thoroughly with air.

Whilst we shall not discuss hydrodynamical effects in detail in this section, we shall consider them in a qualitative way and also their influence upon the thermal balance equation.

(b) At certain definite feed pressures, a phenomenon occurs in non-aerated burners which is known as "lift". The burner flame rises a short distance from the port and remains suspended there. With some gases the lift point and blow-off coincide, or almost coincide, but this is not necessarily the case.

This phenomenon can only be understood from a consideration of the conditions of gas flow in non-aerated burners. The gas issues from the orifice in a narrow jet at high velocity and near the orifice it entrains air in appreciable quantity when the feed pressure, and hence the velocity of the emergent gas, is reasonably high. Thus, above a certain gas velocity enough air will be entrained to lower the temperature of the flame base below the ignition temperature of the mixture. Thus lift may be described as a "self-cooling" effect.

We may, in fact, state that the lift limit for any type of non-aerated flame is defined by the ratio  $\frac{\text{air entrained}}{\text{heat loss across burner base}}$  and there will be a linear relationship between the pressure at which lift occurs and this ratio.

The heat loss across the flame base has been defined as  $\lambda A \frac{\partial T}{\partial x}$ , where  $\lambda$  is the thermal conductivity of the gas,  $A$  the area of the flame base, and  $\frac{\partial T}{\partial x}$  the temperature gradient. The quantity of air entrained, relative to that of gas flowing from the orifice, is proportional to the area of the orifice for a given gas velocity. Hence for a given gas we can say, at the lift point,

$$\text{Area of orifice} = A \times (\text{air entrainment}).$$

On the other hand, since the gas velocity is dependent upon feed pressure, and since we assume that it is the drag of the moving gas which causes entrainment, we can write,

$$\text{Orifice area} = k'P,$$

i.e., a linear relation.

## 5. Further Development of Theory

The foregoing treatment of combustion, whilst giving a physical explanation of certain phenomena, did not correlate the behaviour of gases during combustion to their physical constants. An attempt to do this will now be made, in a form which may be applied to any one of the particular results covered in the preceding discussion.

The fundamental condition of equilibrium is

$$\text{Heat produced } (H) = \text{Surface loss } (\sigma) + k\Delta T \frac{dV}{dt},$$

$$\text{or} \quad \frac{H}{k\Delta T \frac{dV}{dt}} = \left[ \frac{\sigma}{k\Delta T \frac{dV}{dt}} \right] + 1.$$

Here  $H$  is the value  $(H_c - \bar{c}_p \Delta T)$  defined previously.

From this, the importance of the ratio  $\frac{H}{k\Delta T \frac{dV}{dt}}$  may be seen. If it

is small, then blow-off will readily occur. If it is large, there will be a tendency towards flash-back, unless  $\sigma$  also is large.

In the previous discussion we have determined  $H$  only in terms of the composition of the gas-mixture used but we now have to do this in terms of the physical constants of the gases. Also in our discussion we had not treated variations in  $\sigma$ , in dealing with combustion characteristics. In general we sought to determine the relationship between  $H$  and  $\frac{dV}{dt}$ . Accurate knowledge of this would enable us to predict the behaviour of any gas in a burner flame.

We note that in the thermal balance equation the relation between  $H$  and  $\frac{dV}{dt}$  is

$$\begin{aligned} H &= \sigma + k'\Delta T \frac{dV}{dt} \\ &= \sigma + k''\rho\Delta T \frac{dV}{dt}, \end{aligned}$$

where  $\rho$  = gas density.

We can take  $H$  as the volume heat of combustion of the gas in question,  $\rho$  its density, and  $\Delta T$  the ignition temperature of the inflammable mixture.

$$\therefore \frac{dV}{dt} = H \frac{k'}{\rho \Delta T} - \sigma$$

and we can substitute accordingly in the equations of the previous section.

It remains to determine the effect of the surface factor. Accurate determination of this by theoretical means is rather difficult. Now  $\sigma$  represents the heat given out by the flame, hence in a useful burner system  $\sigma$ , and therefore  $\frac{H}{\rho \Delta T}$ , must be as large as possible for the flame to be stable.

The surface area of the flame will be related to the feed pressure of the gas since an increase in this tends to enlarge the flame,  $\sigma$  will also depend on the thermal conductivity of the gas, the temperature and the interdiffusion coefficient of gas and air  $D$ . Thus

$$\sigma = f(\lambda, T, P, D).$$

It is clear that  $\sigma$  will be large for hydrogen, relatively small for ethylene, smaller still for the higher hydrocarbons. Methane will occupy an intermediate position. Introducing  $\sigma$  into our previous expressions we have

$$\bar{c}_p \bar{\rho} \Delta T \frac{dV}{dt} = (H - \sigma),$$

$$\text{or} \quad \frac{dV}{dt} = c(H - \sigma), \quad \text{if } c = \frac{1}{\bar{\rho} \Delta T \bar{c}_p},$$

$$\text{so} \quad \frac{dV}{dt} = \frac{1}{\bar{c}_p} \left\{ \frac{H}{\bar{\rho} \Delta T} - \frac{1}{\bar{\rho} \Delta T} f(\lambda, T, P, D) \right\}.$$

Thus the effective value of  $H$  will be reduced by a quantity which is a function of these fundamental characteristics, flame temperature, thermal conductivity, and diffusion coefficient.

This suggests that in flames with a large surface area, for instance, hydrogen flames, the blow-off will occur more readily, owing to the drop in  $H$ . For non-aerated flames it seems likely that the "surface factor" has little effect, since an expansion of the surface leads to more adequate mixing with air and hence to more complete combustion. In aerated flames, since  $H$  reaches a maximum relative to the input of mixture at stoichiometric proportions,  $\sigma$  will reach a minimum at this point, for a given gas.

Thus we have—

(a) For a non-aerated flame, neglecting surface factors :

$$\text{Stability} \propto \frac{H}{\bar{\rho} \Delta T} \quad . \quad . \quad . \quad . \quad (3e)$$

(b) For aerated burners, we adopt the expression from § 3(e) (symbols as previously), or

$$H = f\left(\frac{1}{\lambda_1^2} + c\right), \quad \text{where } \lambda_1 = \frac{1-x}{x},$$

for the flash-back condition ; and from § 3(f)

$$H = f\left(\frac{x}{1-x} + c\right)$$

for the blow-off of normal flames.

## 6. Experimental Evidence

The experimental evidence relating to the theory will now be dealt with. It falls under several heads, and will be considered in relation to the separate sections of the theory.

(a) **Flash-back.**—Garside <sup>3</sup> has carried out an investigation of flash-back in burner tubes of various diameters, and has plotted curves of gas composition against critical diameter for various gases. He obtains parabolic curves of the type indicated by the theory. Garside has also investigated the relation between "dead space". If the pressure term is neglected in the development in § 3(b), then we find the dead-space is equal to the critical radius of the tube. This was first assumed by Garside, but he subsequently suggested a linear relation.

Fuidge, Murch and Pleasance <sup>6</sup> have investigated the combustion characteristics of aerated burner flames using a method suggested by Smyth and Pickering. They plotted air/gas ratio against thermal throughput for various gases and types of burners. Curves obtained for the flash-back limits were of the general type,

$$y = S^2 x e - S^2$$

as indicated by the theoretical discussion in § 3(e).

Minchin <sup>5</sup> has discussed the so-called "flame-proof" burner heads consisting of gauzes placed over burner ports. He defines a "safety factor" for such burners, representing its susceptibility to flash-back, and obtains an empirical equation of the type,

$$S = \frac{1}{r} - \frac{2r}{b^2},$$

which is identical with the equation derived in § 3(f).

Tilted flames in aerated burners were investigated by v. Elbe and Mentser <sup>7</sup> who, as a result of their measurements, obtained an empirical equation which they express as

$$\frac{4V}{\pi r^3 \tan \theta} = \text{constant},$$

assuming  $\theta$  to be small. Here  $V$  is our  $\frac{dV}{dt}$ . This is the expression derived in § 3(d). The work of Garside <sup>3</sup> on critical diameters is an extension of earlier work by Holm, <sup>4</sup> who obtained a similar relationship.

Forsyth <sup>2</sup> plotted curves of gas flow against % gas in gas-air mixtures for various feed pressures. These curves increased roughly linearly to a maximum, then fell away in a similar way. At low pressures the curves are almost parabolic.

Writing the thermal balance equation,

$$\begin{aligned} H &= k\Delta T \frac{dV}{dt} + X \\ &= k'\rho\Delta T \frac{dV}{dt} + X, \end{aligned}$$

and knowing  $\frac{1}{H} = f(x + c)^2$  or  $\frac{1}{H} = kx^2 + c$ ,

where  $x$  is % gas in mixture, then we have, assuming  $x$  constant,

$$\frac{dV}{dt} = k''x^2 + c',$$

as in the treatment of § 3(f).

It will be noted that the constant  $k''$  includes  $\rho^2$  and as  $\rho \propto P$  we should expect the slope of the parabolas to vary with  $P^2$ , which is approximately true.

<sup>7</sup> v. Elbe and Mentser, *J. Chem. Phys.*, 1945, 13, 89.

<sup>6</sup> Fuidge, Murch and Pleasance, *Trans. Inst. Gas Engr.*, 1939-40, 283.



(b) **Blow-off.**—Garside <sup>2</sup> has made an experimental study of blow-off, plotting gas-flow velocity against mixture composition at the blow-off limit. The curves were obtained both for ordinary double-cone flames and the "separated cone" flames, in which only the double-cone flames gave straight lines. This is in accordance with the development of § 3(f). Fuidge *et al.*<sup>8</sup> have plotted curves of thermal throughput against air/gas ratio for various gases and obtain logarithmic curves as would be expected. The logarithmic character of these curves was not pointed out by Fuidge, but has been noted by American Gas Association workers.

(c) **Non-aerated Flames.**—The principal experimental work available on these is the paper of Fuidge, Dewhurst, and Pleasance <sup>3</sup> in which the orifice areas of non-aerated burners were plotted against corresponding thermal throughputs of the burner for the critical points, lift, blow-off, and roar. As the incidence of "roaring" seems to be a purely hydrodynamical phenomenon, it is not dealt with here. The reasons for the occurrence of "lift" and "blow-off" are treated qualitatively in § 4(a) and (b). A fuller treatment of these is given in a subsequent paper. However, the linear character of these curves is evident from the development in § 4(b). Also, the incidence of "lift" in non-aerated flames is given a physical explanation. Another experimental fact noted by Fuidge and his co-workers follows quite simply from the theory. They observed that when a non-aerated flame was burnt in strongly heated surroundings it was almost impossible to blow it off.

In the thermal balance equation, we may, in this special case, eliminate the heat loss term, since the surroundings are hot and

$$H = k\Delta T \frac{dV}{dt}.$$

But  $\Delta T$  will also be reduced by the heating of the surroundings, while  $H$  will be increased by radiation (in this case from hot firebricks surrounding the burner). Accordingly  $\frac{dV}{dt}$  will have to reach very large values to exceed  $H$ , which explains Fuidge's result.

## 7. Conclusion

The theory set out above is purely a thermal one, and is based on assumptions regarding heat transfer and *not* active centres as Lewis and v. Elbe have assumed in their work on flame propagation. This is a serious limitation as it is not possible to explain quantitatively the effects of various inerts on combustion characteristics of gases, notably flash-back, although it can readily be seen that the effect of such addition would be to reduce  $H$  by simple dilution of the inflammable mixture. Like most thermodynamical theories, the one given is of a general nature and does not deal with such questions as gas flow which becomes of importance in non-aerated burners.

I should like to thank Sir Alfred Egerton and Dr. J. H. Burgoyne for their help and encouragement, and particularly Dr. H. G. Wolfhard for reading the draft and for some helpful criticism.

*Department of Chemical Engineering and Applied Chemistry,  
Imperial College of Science and Technology,  
London, S.W.7.*

## REMARKS ON THE FORCE CONSTANTS IN TETRACHLORETHYLENE

BY JULES DUCHESNE

*Received, 15th May, 1949*

In a recent paper<sup>1</sup> Dr. Torkington has made an analysis of the vibrational potential function of tetrachlorethylene. He has reached the main conclusion that the C=C stretching force constant in this molecule takes a normal value if interaction forces between the C=C and C—Cl groups are used.

In this article the author refers to my paper<sup>2</sup> on this question and criticizes rightly the assignment proposed for the  $A_g$  frequencies of this molecule. However, this old assignment has been corrected later.<sup>3</sup> In these papers the potential function has been analyzed in detail. Among other results, there were found similar ones to those now given by Torkington, as far as the importance of the interaction forces and the normal value of the C=C bond force constant are concerned.

*University of Liège,  
Liège, Belgium.*

<sup>1</sup> *Trans. Faraday Soc.*, 1949, **45**, 445.

<sup>2</sup> *Nature*, 1938, **142**, 256.

<sup>3</sup> *Physica*, 1942, **9**, 249; *Mém. Soc. Roy. Sci. Liège*, 1943, **2**, 429; *V. Henri Mem. Vol.* (Desoer, Liège, 1947).

## REVIEWS OF BOOKS

**Compilation of Thermal Properties of Hydrogen in its Various Isotopic and Ortho-Para Modifications.** By HAROLD W. WOOLLEY, RUSSELL B. SCOTT and F. G. BRICKWEDDE. (Part of the Journal of Research of the National Bureau of Standards. Research Paper RP1932, vol. 41, 1948.) Pp. 97.

Some people would describe a diamond-studded watch as a necessity because they need to know the time; others would describe it as a luxury because a stainless steel watch would serve the same purpose; others might even claim that, as long as there is a clock within reach, a watch is redundant. This compilation calls to mind the diamond-studded watch.

In this report the available thermal data for  $H_2$ , HD and  $D_2$  in solid, liquid, and gaseous states have been brought together, including the distinctive properties of ortho and para forms of  $H_2$  and  $D_2$ . Some data not previously published have been added. The thermal data include thermodynamic functions for the ideal gas state, equilibrium constants, data of state, viscosity and thermal conductivity with dependence on the pressure, vapour pressure, solid-liquid equilibria, specific heats and latent heats. Values of state derivatives useful in thermodynamic calculations have been given for normal hydrogen, and the related differences

between thermodynamic functions for real and ideal gas states have been evaluated. A temperature-entropy diagram for normal  $H_2$  in the range of experimental data is also given. The compiled thermal properties of hydrogen are presented in 38 tables, 33 graphs and numerous equations. The sources of the data have been given in an extensive bibliography.

The reviewer for one is delighted to have all these useful data at hand in such a convenient form. He would, however, have known where and how to find most of it, admittedly in less convenient form, if he had needed it.

It is claimed that the computations of thermodynamic data are more accurate than previous ones, but, whereas the introduction states that the object of this report is utilitarian, this extra accuracy seems to the reviewer pure luxury. As a typical illustrative example, suppose one wanted to know at what temperature  $H_2$  at equilibrium contains equal parts of para and ortho forms. It would seem reasonable for a *practical* man to be satisfied if he knew the answer correct to the nearest degree. This would require the thermodynamic functions to be tabulated to the nearest  $0.1 \text{ cal. mole}^{-1} \text{ deg.}^{-1}$ . The computation of these functions is in fact reliably accurate to something approaching  $0.01 \text{ cal. mole}^{-1} \text{ deg.}^{-1}$ . In this report the functions are tabulated to  $0.001 \text{ cal. mole}^{-1} \text{ deg.}^{-1}$ .

In view of the acute shortage in this country of trained physical chemists, expert computers and skilled printers, not to mention paper, one cannot help gasping at the resources of the National Bureau of Standards.

The presentation of the data is excellent apart from one exception noticed by the reviewer. The text is far from clear as to what convention is used to fix the zero of entropy and it requires rather expert acquaintance with the subject to find out. In fact all molar entropies of  $H_2$  whether para, ortho or normal are relative to a value zero for *pure para*  $H_2$  at  $T = 0^\circ \text{ K}$ , while all molar entropies of  $D_2$  whether ortho, para or normal are relative to a value  $R \log_e 6$  for *pure ortho*  $D_2$  at  $T = 0^\circ \text{ K}$ . This convention is neither obvious nor even usual.

The reviewer regrets the effort wasted in converting joules, the now internationally recommended unit of energy, into calories. He regrets still more the effort that will be required to convert back to joules.

The reviewer is interested and rather pleased to note the tendency to use and tabulate  $-F/T$  rather than  $F$ . This function  $-F/T$  was first used by Massieu, who anticipated both Gibbs' and Helmholtz' use of  $F$ , and it was widely used by Planck.

E. A. G.

**Chemismus und Konstitution.** Vol. I. By BERND EISTERT. (Ferdinand Enke Verlag, Stuttgart.) Pp. ix + 387. Price DM. 41.50.

We learn from the author's preface that this book is effectively a new edition of his earlier monograph *Tautomerie und Mesomerie* but which, owing to the development of the subject during the intervening decade, has had to be considerably expanded. The outcome of this revision and enlargement is a work in two volumes of which the massive first one, published in November, 1948, with the Imprimatur of the U.S. Military Government, has reached us.

Volume I deals mainly with valency, molecular dimensions and physical properties of organic compounds, and ends with a short section on the reaction mechanisms (*Chemismus*) of addition, substitution and elimination reactions. The second volume will include tautomerism, molecular rearrangements and "mesomeric ions."

It appears to be the author's intention to give an up-to-date survey of the field of general and physical organic chemistry in order to enable his compatriot chemists and chemistry students to catch up again, in particular with the developments published during and since the war in inaccessible Western periodicals and books. Such an undertaking must have involved a patient study of the considerable output of scientific papers of that period, and author and publishers must be admired for their courage in producing a book which, in parts, aims at covering the literature up to the middle of 1948 and yet was published in November of the same year!

Under the circumstances it is not surprising that the review of British and American work between 1939 and 1947 lacks the clarity and balance of presentation which would, under more normal conditions, be demanded from a work on this scale. There are many places where the reader who is familiar with the subject under discussion will, for obvious and good reasons, disagree with the theory and sometimes even with the accuracy of the facts presented. As a teaching book it falls far short of the standard set by comparable English and American texts. However, even if it was not in the main meant for this purpose, the book does fulfil the useful function of what appears to be a fairly complete and up-to-date literature guide to German contributions in this field. It is therefore possible to extract from it with little trouble a list of references without having to go systematically through an accumulation of German periodicals, or having to wait for their ultimate publication in *British Abstracts*. For this reason—and it is a sufficient one—the reviewer is eagerly awaiting the appearance of the second volume.

V. G.

**The Theory of Solutions of High Polymers.** By A. R. MILLER.  
(Geoffrey Cumberlege at the Oxford University Press, 1948.) Pp. 118.  
Price 12s. 6d.

A precise expression for the number of arrangements of  $N_r$  molecules on the  $N$  sites of a lattice, in which each site has  $z$  neighbours and each molecule occupies  $r$  sites ( $rN_r < N$ ), is not known. An approximate expression for the case of a plane lattice and  $r = 2$  was given by Chang in 1939. In 1942 Dr. Miller extended Chang's result to three-dimensional lattices, for  $r = 2$  and  $r = 3$ , and proceeded to generalize the resulting formulae to find the corresponding approximate expression,  $g(N; N_r)$ , say, for any value of  $r$ , thereby opening an important chapter in the theory of polymer solutions. Each polymer molecule is taken to occupy  $r$  sites, where  $r$  is the number of monomer units in a polymer molecule (very large), the remaining sites being occupied by solvent molecules.

The present monograph recounts both the progress of this work and something of the history of other approximate treatments of the problem.

Miller's expression for  $g(N; N_r)$  was given a more satisfactory theoretical basis by Guggenheim. Knowing  $g(N; N_r)$ , and assuming that there is no effective energy of interaction between polymer and solvent systems, the thermodynamic properties of solutions of the rubber-benzene type can then be derived. The resulting expression for the free energy of mixing or, more precisely, the partial vapour pressure of the solvent, agrees surprisingly well with experimental measurements due to Gee and Treloar (rubber-benzene) and to Baughan (polystyrene in toluene and benzene).

It is, however, known that rubber-benzene solutions show a definite heat of mixing (though the experimental data are not particularly accurate). If entropies of dilution, calculated from experimental data, are compared with those predicted on the assumption of random mixing, i.e. on the basis of the expression derived for  $g(N; N_r)$ , the agreement between theory and experiment is much less satisfactory: and the situation is apparently only worsened when more proper theoretical account is taken, as in the work of Orr and Guggenheim (Bethe approximation, or method of quasi-chemical equilibrium), of the influence of interaction energies on the entropy of mixing. For this reason Orr suggested that the original formula for  $g(N; N_r)$  did not do adequate justice to the self-coiling, and self-obstruction, of individual polymer molecules which is of particular importance at low concentrations. Some rather beautiful work by Orr, in this connection, is mentioned, but not treated in detail, in Miller's book.

The story is an interesting one and a critical, coherent and up-to-date account was called for. Unfortunately the reviewer feels that this book, in its present form, barely fulfils these requirements. His judgement may be clouded by the rather large number of mistakes in formulae, including some quite serious ones, which have crept into the presentation (the more surprisingly since they are not to be found in the original papers by Miller, Guggenheim and others, to which references are given). But a monograph of this kind ought to be an authoritative introduction to the field for a new student, and such errors only confuse or mislead. There are, moreover, sections in which the statistical argument itself would seem at fault: notably § 3.21 where the situation appears to be saved by an error of sign in equation 3.62, and the detailed criticism of the work of Alfrey and Mark in § 2.6. Fortunately neither section is essential to the theme, but the reviewer feels they could have been omitted with profit. On the other hand the inclusion of a theoretical curve, on the basis of the work of Orr and Guggenheim, of the heat of dilution plotted against the volume fraction of polymer in a manner comparable with the experimental data exhibited in Fig. 9 would be valuable. It is also, at first sight, perplexing that Raoult's law should, without comment, be used in two quite different senses in Fig. 2 and Fig. 3, respectively.

It is only fair to add, however, that the reviewer is glad to have read the book, and hopes that others may derive an equal enjoyment from it.

G. S. R.

**The Electronic Theory of Organic Chemistry.** By M. J. S. DEWAR.  
(Geoffrey Cumberlege, Oxford University Press, 1949.) Pp. x + 324.  
Price 30s.

Dr. Dewar sets out "to give as complete an account as possible of organic chemistry in the light of modern quantum theory" using the molecular-orbital method of approach which he maintains (and many will probably disagree with him) "provides a picture of molecular structure closely akin to that of classical organic chemistry," in contrast to the resonance (valence-bond) method which is regarded as "most unsuitable" and involving "a new symbolism and a novel and uncongenial outlook." Many may find the consequent formulation of complex organic structures, in which the whole extent of the delocalization of electrons is denoted by dotted bond signs, not easy to interpret.

The author rejects Ingold's symbolism and convention that groups which, respectively, repel electrons (so *increasing* the electron density in the attached system) and attract electrons (giving a corresponding *decrease*) are regarded as exhibiting positive (+ *I*, + *T*) and negative (− *I*, − *T*) polar effects and reverts to Robinson's system in which these signs are reversed. Substituents are frequently referred to merely as

positive or negative so that, e.g. in the system  $-\overset{\curvearrowright}{\text{C}}=\text{C}\rightarrow\text{F}$ , the electro-negative element, fluorine, would be classified as a positive group with + *I*, − *E* effects. Reagents and reactions are classified as anionoid or cationoid. The usual symbolism  $S_1$  and  $S_2$  is retained for uni- and bi-molecular substitution but the terms − *S* and + *S* (for nucleophilic,  $S_N$ , and electrophilic,  $S_E$ ) are introduced without explanation (p. 69), whilst later (p. 118), in ester hydrolysis, the symbols −  $S_{CO_2}$ , −  $S_{CO_1}$ , −  $S_{R_2}$  appear for acyl- and alkyl-oxygen fission. There would seem to be little justification for such arbitrary changes from a symbolism which has become very widely adopted and understood, and they form one contributory cause to the creation of an impression that a rather ungenerous attitude to contributions by workers in other research schools pervades the book.

Dr. Dewar makes great use of his  $\pi$ -electron complex theory in formulating intermediates in reaction but many may feel that, though a fertile and suggestive hypothesis, it as yet lacks real experimental foundation. Thus cationoid (electrophilic) substitution of naphthalene and benzene is regarded (p. 176) as occurring through a  $\pi$ -complex but anionoid (nucleophilic) substitution "must . . . take place by a direct  $S_2$  replacement through a transition stage of the usual quinonoid type." There are good reasons for believing that the two types are similar and may best be consistently formulated as  $S_2$  replacements. Doubt may be cast on the validity of a number of statements in the book. Thus, for example, Hammick and Mason have already called attention (*Chem. and Ind.*, 1949, p. 193) to the misrepresentation of their views on the mechanism of the benzidine transformation (p. 236). The claim (p. 185) that Hammick *et al.* "have shown that picric acid forms complexes . . . with nitrobenzene and that the stability of the complexes is greater than that of benzene" has been denied by Dr. Hammick to Dr. Weiss (*ibid.* p. 226), who has also pointed out (*ibid.* p. 274) that the statement (p. 133), that

in the radical mechanism of the Cannizzaro reaction, "the chains must be long," is contrary to his published views. In the pinacol-pinacolone change groups are stated (p. 213) to migrate more readily, the more positive (i.e. electron-attracting) they are: actually the order seems to be that of electron-release.

Misprints, though not numerous, are often such as to add to the reader's difficulty in following the author's arguments.

These aspects (and other examples could be given) detract from a most stimulating and often original treatment of the mechanism of a whole range of heterolytic organic reactions on the basis of electronic theory (which is clearly explained in the earlier chapters), and a more brief, but adequate treatment of free-radical reactions in the concluding chapters. For the more advanced experienced worker, able to bring to the book a developed critical faculty, it is a valuable and stimulating work but, in the reviewer's opinion, it is less suited to the needs of students making a first approach to this treatment of organic chemistry.

Needless to say the production conforms to the high standards associated with the Oxford University Press.

J. W. B.

# CORRIGENDA

Page 687, Fig. 2. For  $\text{Cl}^-$  read  $\text{ClO}_4^-$  throughout.

" " " 3. For  $\text{ClO}_4^-$  read  $\text{Cl}^-$  throughout.

" 692, line 1. For  $250^\circ \text{C}$ . read  $270^\circ \text{C}$ .

" " " 6. For occurs after ca. 1 min. read occurs after ca. 5 min.

" 617. In Table 1, the column headings of the lower half.

For

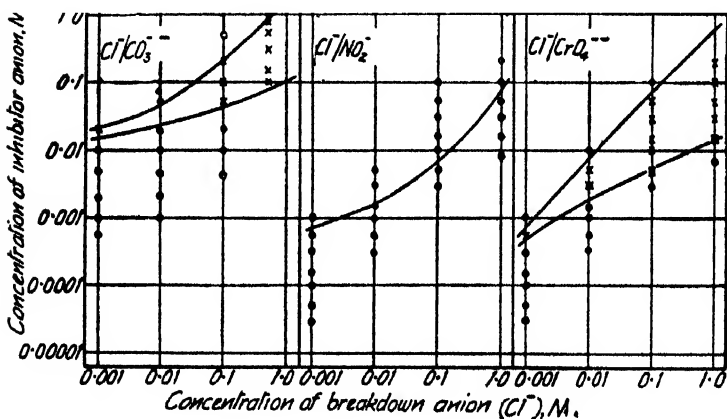
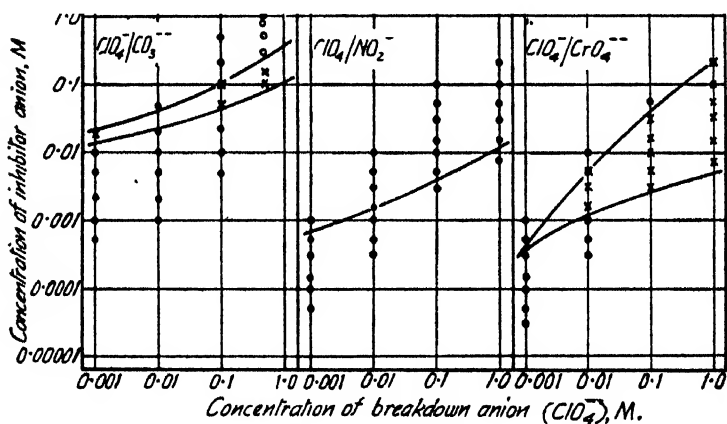
m	KAc	KIol	KCNS	$\text{KH}_2\text{PO}_4$	RbCl	RbBr	RI	$\text{RbNO}_3$	$\text{RbAc}$	CsOH	CsCl	CtBr
---	-----	------	------	--------------------------	------	------	----	-----------------	---------------	------	------	------

read

m	KAc	KIol	KCNS	$\text{KH}_2\text{PO}_4$	RbCl	RbBr	RbI	$\text{RbNO}_3$	$\text{PhAc}$	CsOH	CsCl	CsBr
---	-----	------	------	--------------------------	------	------	-----	-----------------	---------------	------	------	------

$270^\circ \text{C}$ .

ca. 5 min.







# SOME FUNDAMENTAL DEFINITIONS AND CONCEPTS IN DIFFUSION PROCESSES

BY G. S. HARTLEY AND J. CRANK

*Received 13th January, 1949*

The definition of a diffusion coefficient is examined critically, with particular reference to the necessity of defining clearly the section across which the rate of transfer of the diffusing substance is measured, and the units of concentration and space co-ordinate adopted. It is shown that, by suitable choice of these three factors, the one-dimensional diffusion behaviour of a two-component system can always be represented in terms of a single variable diffusion coefficient, even if the partial molal volumes of the two components vary with position.

The relations between the diffusion coefficients defined with respect to three different frames of reference of practical importance are established, and several standard methods of measuring diffusion coefficients are examined in order to see which coefficient is observed in each method. Some applications of the different frames of reference are discussed.

The physical nature of a pure diffusion process is discussed in terms of random molecular motions. It is suggested that, in a binary solution, the net rate of transfer of either component is the result of a transfer by pure diffusion coupled with a transfer of that component due to a mass-flow of the whole solution. The mass-flow is due to the fact that, in general, the intrinsic rates of pure diffusion of the two components will differ and hence there is a tendency to set up a hydrostatic pressure in the solution which is relieved by a mass-flow. Reference is made to an experimental demonstration of the mass-flow in a particular system, in which one component is a high polymer.

A tentative quantitative theory is proposed, incorporating the effect of mass-flow, and an expression for the mutual diffusion coefficient in a thermodynamically non-ideal binary solution is derived.

**1. Definition of a Diffusion Coefficient.**—Quantitative measurements of the rate at which a diffusion process occurs are usually expressed in terms of a diffusion coefficient. The present discussion is confined to diffusion in one dimension only, in which case the diffusion coefficient is defined as the rate of transfer of the diffusing substance across unit area of a section, divided by the space gradient of concentration of the substance at the section. Thus, if the rate of transfer is  $S$ ,  $C$  the concentration of diffusing substance and if  $x$  denotes the space co-ordinate, then

$$S = -D \frac{\partial C}{\partial x} \quad \dots \quad (1)$$

and (1) is a definition of the diffusion coefficient  $D$ . In order that this definition shall be unambiguous it is necessary to specify carefully the section used and the units in which  $S$ ,  $C$  and  $x$  are measured. Only the simplest system of practical importance is considered, which is a two-component system, since it is not possible to set up and observe a concentration gradient of a single substance in itself without introducing complicating features such as pressure gradients, etc. The diffusion of isotopes is best regarded as a special case of a two-component system.

**2. A Frame of Reference when the Total Volume of the System remains Constant.**—Consider the inter-diffusion of two liquids A and B in a closed vessel and assume that there is no overall change of volume

of the two liquids on mixing. Two diffusion coefficients  $D_A^v$ ,  $D_B^v$ , one for each liquid, may be defined by the relations

$$S_A = -D_A^v \frac{\partial C_A}{\partial x}, \quad . \quad . \quad . \quad . \quad (2)$$

$$S_B = -D_B^v \frac{\partial C_B}{\partial x}, \quad . \quad . \quad . \quad . \quad (3)$$

$C_A$  and  $C_B$  are the concentrations of A and B respectively, each expressed in the usual way in any convenient unit of amount (e.g. g. or, in the case of simple molecular substances, g. mole) per unit overall volume.  $S_A$  and  $S_B$  are the rates of transfer of A and B measured in the same units of amount per unit time, across a section which is defined by the condition that the total volume on either side of it remains constant as diffusion proceeds. In the particular case under consideration it is therefore fixed with respect to the containing vessel. The origin from which  $x$  is measured is such that the  $x$ -co-ordinate of the section is constant.  $x$  is measured in normal units of length, e.g. cm., and the same unit of length is used in measuring the volume which appears in the definition of concentration. If the unit of time adopted is the second it follows that the units of  $D_A^v$  and  $D_B^v$  are each  $\text{cm.}^2 \text{sec.}^{-1}$ . These somewhat obvious statements are made here in full because it will be seen later in § 4 below that other scales of length and alternative ways of measuring concentration are more suitable in some circumstances.

Let  $V_A$  and  $V_B$  denote the constant volumes of the unit amounts used in defining the concentrations of A and B. Thus if  $C_A$  is expressed in g. per unit volume,  $V_A$  is the volume of 1 g. of A. In dilute solutions, where the volume changes in the range of concentration concerned can be considered negligible,  $V_A$  and  $V_B$  will be the partial specific or molar volumes. That of the solute may be very different from the specific volume in the pure state. The volume transfer of A per unit time across unit area of the section defined is therefore

$$-D_A^v V_A \frac{\partial C_A}{\partial x},$$

and that of B is

$$-D_B^v V_B \frac{\partial C_B}{\partial x}.$$

By definition of the section as one across which there is no net transfer of volume we have immediately,

$$D_A^v V_A \frac{\partial C_A}{\partial x} + D_B^v V_B \frac{\partial C_B}{\partial x} = 0. \quad . \quad . \quad . \quad (4)$$

The volume of A per unit overall volume of solution is  $V_A C_A$  and of B is  $V_B C_B$ , so that, since only molecules of A and B are present, we have

$$V_A C_A + V_B C_B = 1, \quad . \quad . \quad . \quad . \quad (5)$$

which, following differentiation with respect to  $x$ , becomes

$$V_A \frac{\partial C_A}{\partial x} + V_B \frac{\partial C_B}{\partial x} = 0. \quad . \quad . \quad . \quad . \quad (6)$$

In order that (4) and (6) shall both be satisfied it follows that

$$D_A^v \equiv D_B^v, \quad . \quad . \quad . \quad . \quad (7)$$

or else that

$$V_A = 0, \text{ or } V_B = 0. \quad . \quad . \quad . \quad . \quad (8)$$

If  $V_A = 0$  and  $V_B \neq 0$ , it follows from (6) that

$$\frac{\partial C_B}{\partial x} = 0, \quad . \quad . \quad . \quad . \quad (9)$$

and further reference is made to this case in § 3(c) below. In either case the behaviour of a two-component system, satisfying the condition of zero volume change on mixing, may be described in terms of a single diffusion coefficient, which may vary with composition. It is convenient to refer to the single coefficient as the mutual diffusion coefficient, denoted henceforth by  $D^v$ . This coefficient is familiar in the interdiffusion of gases.<sup>1</sup> Its physical significance is discussed in § 6 below.

### 3. Some Standard Methods of Measuring Diffusion Coefficients.—

An examination of the standard methods of measuring diffusion coefficients reveals that for the most part they have been applied to systems in which the total volume remains constant, or can be assumed to do so with sufficiently good approximation, and that the diffusion coefficient measured is the coefficient  $D^v$  introduced above.

(a) GRAHAM'S SECOND METHOD.—The so-called second method of Graham<sup>2</sup> consists essentially in placing a solution of the diffusing substance, e.g. NaCl solution, beneath a long column of water and examining the concentrations of the diffusing substance in a number of different layers of the water column at subsequent times. This method has been elaborated by numerous workers and Stefan's tables<sup>3</sup> are commonly used to facilitate the calculation of a diffusion coefficient from the experimental data. Detailed reference to the various forms of apparatus based on this general method are to be found in a review article by Williams and Cady.<sup>4</sup> In all cases the origin from which the space co-ordinate is measured is the base of the containing vessel and so, provided there is no overall change of volume of the system, the diffusion coefficient  $D^v$  is measured.

(b) STEADY-STATE METHODS.—If a heavier-than-solvent solid is placed in the bottom of a vertical vessel and the whole vessel immersed in a larger one filled with solvent, diffusion occurs from the saturated solution at the base of the inner vessel to a concentration effectively zero at its open upper end. The dilute solution here "spills" over the rim and, if the outer vessel is large enough, the conditions in the inner vessel will remain effectively steady over a long period. This first, or "bath" method of Graham<sup>5</sup> has been elaborated by later workers and, by arrangement for upward as well as downward "spillage," an approximately steady-state diffusion layer can be maintained between any two concentrations (see e.g. Griffiths<sup>6</sup>). Clack<sup>7</sup>,<sup>8</sup> has described a formal correction for displacement of solvent to bring into line experiments where a solid is dissolving with those in which neither reservoir is saturated. The coefficient obtained by this correction is in effect our  $D_A^B$  (see below).

When the two solutions have only very small difference of density, a case of most practical interest in the study of dilute solutions, the method is very sensitive to disturbance by convection. This has largely been overcome in the porous disc method. Since this is normally applied to very dilute solutions, the ambiguities in definition due to volume change are small compared with purely experimental errors and the theoretical treatment as for constant volumes is adequate. The method was introduced by Northrop and Anson<sup>9</sup> and subsequently modified by McBain and Liu.<sup>10</sup> The diffusion cell consists essentially of a bell-shaped vessel, closed at the narrow top end by a stopcock and at the wide

<sup>1</sup> Jeans, *Kinetic Theory of Gases* (Cambridge, 1940).

<sup>2</sup> Graham, *Annalen*, 1862, **121**, 1.

<sup>3</sup> Stefan, *Akad. Wiss. Wien. Math. naturw., Klasse II*, 1899, **179**, 161.

<sup>4</sup> Williams and Cady, *Chem. Rev.*, 1934, **14**, 171.

<sup>5</sup> Graham, *Phil. Trans.*, 1850, **140**, 1.

<sup>6</sup> Griffiths, *Proc. Physic. Soc.*, 1915, **28**, 21.

<sup>7</sup> Clack, *ibid.*, 1916, **29**, 49.

<sup>8</sup> Clack, *ibid.*, 1921, **33**, 259.

<sup>9</sup> Northrop and Anson, *J. Gen. Physiol.*, 1929, **12**, 543.

<sup>10</sup> McBain and Liu, *J. Amer. Chem. Soc.*, 1931, **53**, 59.

bottom end by a sealed-in sintered-glass disc. The cell is filled with the solution, the diffusion rate of which is to be measured, and is immersed in the solvent. The function of the porous disc is to allow diffusion to proceed through it without interference from convection currents. The quantity observed is the rate of passage of solute through the disc in the steady state condition. The condition satisfied, because of the design of the apparatus, is that the volume of solution in the diffusion cell remains constant and therefore measurements of the rate of transfer relative to the disc are in effect relative to a section fixed so that the total volume on the cell side of it is constant during diffusion.

(c) OVERALL ABSORPTION BY A PLANE SHEET.—Suppose an infinite plane sheet of material B (in practice a sheet the area of whose plane surfaces is much greater than the area of its edge) is immersed in a bath of solution or in a vapour A. A comparatively simple observation to make is the rate of uptake of solution or vapour A by the sheet B. The simplest case is one in which the dimensions of the sheet do not change appreciably, i.e. the sheet does not swell, as A diffuses into it. This implies that  $V_A = 0$  in which case eqn. (8) and (9) hold. This state of affairs holds approximately for non-zero values of  $V_A$  if the concentration of A is very small. A method of dealing with the case where volume change is important is dealt with in § 4. In the former case the rate of diffusion of A is dependent on the coefficient  $D^v$  and is governed by the familiar equation of diffusion in one dimension,

$$\frac{\partial C_A}{\partial t} = \frac{\partial}{\partial x} \left( D^v \frac{\partial C_A}{\partial x} \right). \quad (10)$$

If  $D^v$  be assumed constant, (10) takes the simpler form

$$\frac{\partial C_A}{\partial t} = D^v \frac{\partial^2 C_A}{\partial x^2}. \quad (10a)$$

A convenient solution of this simpler equation for the boundary conditions

$$C_A = C_0 - \text{constant}, \quad x = \pm l, \quad t > 0, \quad (11)$$

and the initial condition

$$C_A = 0, \quad -l \leq x \leq l, \quad t = 0, \quad (12)$$

takes the form

$$\frac{M_t}{M_\infty} = 1 - \frac{8}{\pi^2} \sum_{m=0}^{\infty} \frac{1}{(2m+1)^2} \exp \{ -D^v(2m+1)^2 \pi^2 t / 4l^2 \}. \quad (13)$$

$M_t$  is the total amount of A absorbed by the sheet of thickness  $2l$  at time  $t$ , and  $M_\infty$  the equilibrium absorption attained theoretically after infinite time. By comparing the experimentally measured time at which  $M_t/M_\infty$  achieves a certain value, say 0.5, with the value of  $D^v t / 4l^2$  at which  $M_t/M_\infty$  calculated from (13) has the same value,  $D^v$  is readily determined if the thickness of the sheet is known. This method has been used to determine the rate of diffusion of direct dyes into cellulose sheet (Neale and Stringfellow<sup>11</sup>), and in studying the absorption of oxygen by muscle (Hill<sup>12</sup>).

(d) OPTICAL METHODS.—A number of optical methods have been devised for measuring the refractive index-distance relation or some more complicated relation, from which the diffusion coefficient can be calculated if the relation between concentration and refractive index is known. In some cases, following Wiener<sup>13</sup> and Thover<sup>14</sup> observations

<sup>11</sup> Neale and Stringfellow, *Trans. Faraday Soc.*, 1933, **29**, 1167.

<sup>12</sup> Hill, *Proc. Roy. Soc. B*, 1928, **104**, 39.

<sup>13</sup> Wiener, *Wied. Ann.*, 1893, **49**, 105.

<sup>14</sup> Thover, *Ann. Physik*, 1914, **2**, 369.

are made of the interference bands produced by light passing through different layers of the diffusion cell, or of the deviation of a narrow beam of light, while in others the blurring of an initially sharp boundary between two solutions in contact is observed (Svedberg<sup>15</sup>; Fürth<sup>16</sup>). A recent development in optical methods is reported by Coulson and others.<sup>17</sup> From the point of view of the present paper, however, the optical methods of measurement involve no new principle. In all cases the condition of zero volume change is considered to hold and measurements are made with reference to an initial boundary or fringe on both sides of which the volume remains constant, so that in these methods too,  $D^v$  is measured.

**4. Alternative Frames of Reference.** (a) GENERAL.—The definition of the volume-fixed section used in § 2 above is unambiguous only as long as the total volume of the diffusion system remains constant. If there is an overall change of volume of the two components on mixing, the side of the section on which the volume is to remain constant must be chosen arbitrarily, and the diffusion coefficient becomes equally arbitrary. In such a case some alternative frame of reference must be used in defining the section across which transfer of diffusing substance is to be measured. There are clearly several possible alternatives. Thus, for example, the total mass of the system will always be conserved even though volume is not, and a section can be defined consistently such that the mass of the system on either side of the section remains constant during diffusion.

Where a convention other than that of constant volume on either side is used in defining a section, the second-order differential equation describing diffusion may not take the standard form of eqn. (10). It is clearly convenient if it can be made to do so since the standard form has frequently been used as the starting point in calculations of diffusion behaviour. This can always be arranged by departing from the orthodox linear scale, e.g. cm., for measurement of the spacial co-ordinate so far denoted by  $x$ , and by measuring concentration in a certain way. Let some modified scale of length be denoted by  $\xi$ , and consider two sections, fixed on the same convention at  $\xi$ , and  $\xi + d\xi$ . The rate of entry of A into the volume enclosed between these sections is  $S_A$  and that of departure

$$\text{is} \quad S_A + \left( \frac{\partial S_A}{\partial \xi} \right) d\xi.$$

The rate of accumulation is therefore

$$- \left( \frac{\partial S_A}{\partial \xi} \right) d\xi,$$

and this is always true independently of how  $S_A$  and  $\xi$  are measured. It can only be equated to  $(\partial C_A / \partial t) d\xi$ , however, when  $C_A$  and  $\xi$  are measured in certain consistent units. Thus, if the sections are fixed with respect to total mass, then  $\xi$  must be measured so that equal increments of  $\xi$  always include equal increments of total mass, and  $C_A$  must be defined as the amount of A per unit total mass. Similarly, if the sections are fixed with respect to volume or mass of component B, equal increments of  $\xi$  must include equal increments of amount of B, and  $C_A$  must be expressed as the amount of A per unit amount of B. In general, for all values of  $\xi$  and  $t$ , the element of unit length in terms of  $\xi$ , and of unit cross-sectional area, is that which contains an amount of A equal to the unit used in defining the concentration  $C_A$ . When the quantities  $C_A$  and  $\xi$  satisfy this condition the usual relation

$$\frac{\partial C_A}{\partial t} d\xi = - \frac{\partial S_A}{\partial \xi} d\xi, \quad . \quad . \quad . \quad (14)$$

<sup>15</sup> Svedberg, *Colloid Chemistry* (Chemical Catalog. Co., New York, 1928), 2nd ed.

<sup>16</sup> Fürth *et al.*, *Kolloid-Z.*, 1927, **41**, 300.

<sup>17</sup> Coulson, *et al.*, *Proc. Roy. Soc. A*, 1948, **192**, 382.

follows at once and by substituting for  $S_A$  from the relation

$$S_A = -D \frac{\partial C_A}{\partial \xi}, \quad . \quad . \quad . \quad . \quad . \quad (15)$$

we derive the familiar form of the diffusion equation

$$\frac{\partial C_A}{\partial t} = \frac{\partial}{\partial \xi} \left( D \frac{\partial C_A}{\partial \xi} \right), \quad . \quad . \quad . \quad . \quad . \quad (16)$$

which reduces to the form (10a) when  $D$  is constant.

It is convenient that  $\xi$  should have the dimension of length and  $D$  the usual dimensions of (length)<sup>2</sup> (time)<sup>-1</sup>. This can be arranged without interfering with the generality or simplicity of eqn. (16), by multiplying the mass of component B (or the total mass of A and B together if this is the reference system being used) by an arbitrary constant specific volume. The volume represented by the product of a mass B, for example, and this arbitrary specific volume will be referred to for convenience as the basic volume of that mass of B.

The concentration of A was defined above as the amount of A per unit amount of B. We now re-define the concentration of A as the amount of A per unit basic volume of B, and unit  $\xi$  to contain unit basic volume of B per unit area. A convenient arbitrary specific volume is that of the pure component B, so that the basic volume of a certain mass of B is the volume that mass of B would occupy in the pure state.

The same arbitrary specific volume is used for concentrations expressed in the original definition per unit mass of A and B together, i.e. the basic volume of a mass of A and B together is obtained by multiplying the mass by the same arbitrary specific volume. This is true also for deriving the basic volume of A alone, so that the basic volume has a simple physical significance only in the case of the basic volume of B. Nevertheless the use of this particular basic volume has the convenience that all the concentrations measured in the different frames of reference tend to the same value in dilute solutions.

Concentration is, of course, frequently expressed in a number of different ways and so the symbol  $C_A$  is retained, but the appropriate index V, B or M as superscript is added, so that the concentration of A is written  $C_A^V$ ,  $C_A^B$  or  $C_A^M$  according as to whether the amount of A is contained in unit volume of solution, or in unit basic volume of B or in unit basic volume of total mass. According as to whether unit  $\xi$  contains, per unit area, unit basic volume of B or of A and B together the symbol  $\xi_B$  or  $\xi_M$  is used. The diffusion coefficients  $D_A^V$ ,  $D_A^B$ ,  $D_A^M$  also carry an index to indicate the frame of reference to which they refer. The arbitrary specific volume may be denoted by  $V_B^0$ , and then  $\xi_B$  and  $\xi_M$  are defined formally by the respective relations

$$d\xi_B = V_B^0 C_B^V dx, \quad . \quad . \quad . \quad . \quad . \quad (17)$$

$$d\xi_M = V_B^0 (C_A^V + C_B^V) dx. \quad . \quad . \quad . \quad . \quad (17a)$$

(b) SECTIONS FIXED WITH RESPECT TO TOTAL MASS AND MASS OF ONE COMPONENT.—It was found in § 2 that the behaviour of a two-component system satisfying the condition of zero volume change on mixing, can be represented in terms of a single diffusion coefficient  $D^V$ . A similar result follows readily for a system in which volume changes occur, provided the diffusion coefficients are defined with respect to a mass-fixed section. Thus the equation defining such a section is

$$D_A^M \frac{\partial C_A^M}{\partial \xi_M} + D_B^M \frac{\partial C_B^M}{\partial \xi_M} = 0, \quad . \quad . \quad . \quad . \quad (18)$$

and the definitions of  $C_A^M$  and  $C_B^M$  lead immediately to the equation

$$C_A^M + C_B^M = 1/V_B^0. \quad . \quad . \quad . \quad . \quad (19)$$

On differentiating (19) with respect to  $\xi_M$  and comparing with (18) we find

$$D_A^M \equiv D_B^M. \quad (20)$$

If a section fixed with respect to one component, say B, is used, then clearly  $D_B^B = 0$  and only the coefficient  $D_A^B$  is needed to describe the diffusion behaviour. Thus the statement that the diffusion behaviour of a two-component system can be described in terms of a single diffusion coefficient, is valid whether there is a change of volume of the whole system or not, provided the appropriate frame of reference is used in defining the diffusion coefficient. Frames of reference could be so chosen that the two coefficients are not identical and neither is zero, but they would be related through some function of the partial volumes and would not be independent measures of two separate diffusion processes. The possibility of measuring the diffusion of the two molecular species independently is discussed in § 7.

(c) RELATIONS BETWEEN THE DIFFUSION COEFFICIENTS:  $D_A^V, D_A^M, D_A^B$ .—The rate of transfer of A through a B-fixed section is greater than that through a total-mass-fixed section by an amount given by the concentration of A per unit mass of B multiplied by the flux of B across the mass-fixed section. Thus the flux of A across a B-fixed section in the direction of  $\xi$  increasing is

$$-D^M \frac{\partial C_A^M}{\partial \xi_M} + D^M \frac{C_A^M}{C_B^M} \frac{\partial C_B^M}{\partial \xi_M} = -\frac{D^M}{C_B^M V_B^0} \frac{\partial C_A^M}{\partial \xi_M}, \quad (21)$$

using (19).

But the rate of transfer across a B-fixed section is  $-D_A^B \partial C_A^B / \partial \xi_B$  so that we have

$$D_A^B = \frac{D^M}{V_B^0 C_B^M} \frac{\partial C_A^M}{\partial \xi_M} \frac{\partial \xi_B}{\partial C_A^B}. \quad (22)$$

From the definitions of  $C_A^M$  and  $C_A^B$  it is easy to show that

$$\frac{dC_A^M}{dC_A^B} = (V_B^0 C_B^M)^2. \quad (23)$$

Also since

$$d\xi_M = V_B^0 (C_A^V + C_B^V) dx, \quad d\xi_B = V_B^0 C_B^V dx, \quad (24)$$

we have

$$\frac{\partial \xi_B}{\partial \xi_M} = V_B^0 C_B^M, \quad (25)$$

so that finally, by substituting (25) and (23) in (22), we find,

$$D_A^B = D^M (V_B^0 C_B^M)^2. \quad (26)$$

since rearrangement of the partial derivatives in (22) is permissible. For a system in which there is zero volume change on mixing, so that  $V_A$  and  $V_B$  are constant, the relation between  $D_A^B$  and  $D^V$  can be similarly established. Thus the flux of A across a B-fixed section in the direction of  $\xi$  increasing is

$$-D^V \frac{\partial C_A^V}{\partial x} + D^V \frac{C_A^V}{C_B^V} \frac{\partial C_B^V}{\partial x} = -\frac{D^V}{V_B C_B^V} \frac{\partial C_A^V}{\partial x}, \quad (27)$$

using (5) and (6). But the rate of transfer of A across a B-fixed section is  $-D_A^B \partial C_A^B / \partial \xi_B$ , so that we have

$$D_A^B = \frac{D^V}{V_B C_B^V} \frac{\partial C_A^V}{\partial x} \frac{\partial \xi_B}{\partial C_A^B}. \quad (28)$$



From the definition of  $C_A^v$  and  $C_A^B$  it follows that

$$\frac{dC_A^v}{dC_A^B} = (V_B C_B^v)^{\frac{1}{2}}, \quad . \quad . \quad . \quad (29)$$

and from (24) we have immediately,

$$\frac{\partial \xi_B}{\partial x} = V_B C_B^v, \quad . \quad . \quad . \quad (30)$$

so that on substituting (29) and (30) in (28) we find

$$D_A^B = D^v (V_B C_B^v)^{\frac{1}{2}}. \quad . \quad . \quad . \quad (31)$$

Since (31) applies only when  $V_B$  is constant, and therefore when  $V_B = V_B^0$ , comparison of (31) and (26) shows that when there is no overall volume change accompanying diffusion

$$D^B = D^v (C_B^v / C_B^B)^{\frac{1}{2}} = D^v (\text{Basic total volume/true total volume})^{\frac{1}{2}}. \quad (32)$$

### 5. Applications of the New Scales of Length and Concentration.—

It is proposed to discuss briefly two examples which arise in practice where it is desirable to adopt one of the alternative frames of reference just discussed even though there is not necessarily a change of volume of the whole system.

(a) **STEADY-STATE DIFFUSION THROUGH A MEMBRANE.**—In order to study the rate of diffusion of a gas or a vapour A through a polymer B, a modified form of the porous disc method may be used, in which the disc is replaced by a membrane of the polymer and the steady rate of flow of A through it is observed. If the membrane swells as the steady state is established, and this is most likely to occur, then the thickness of the membrane in ordinary units of length, e.g. cm., will vary with time. In such a case the modified scale of length  $\xi_B$  may usefully be introduced since the thickness on this scale, being the basic volume of polymer per unit area of the membrane, remains constant and equal to its unswollen value. We are dealing here with transfer across a section fixed with respect to one component and the rate of transfer,  $S_A$ , of A through unit area of the membrane is given by

$$S_A = - D_A^B \frac{\partial C_A^B}{\partial \xi_B}. \quad . \quad . \quad . \quad (33)$$

Integrating (33) with respect to  $\xi_B$ , remembering that for steady state flow  $S_A$  is independent of  $\xi_B$ , we have

$$S_A = \frac{1}{a} \int_0^{C_0} D_A^B dC_A^B, \quad . \quad . \quad . \quad (34)$$

where  $a$  is the thickness of the unswollen membrane, and the concentrations of A at the two surfaces of the membrane are  $C_0$  and zero. By determining  $S_A$  experimentally for different values of  $C_0$  and differentiating the curve relating  $S_A$  to  $C_0$ , the diffusion coefficient  $D_A^B$  is obtained for various concentrations of A. This method has been applied by King<sup>18</sup> to the diffusion of water through a horn keratin membrane, though the swelling of the membrane and its effect on the diffusion coefficient measured was not discussed. If the swelling is in accordance with the condition of zero overall change of volume of the system, the coefficient  $D^v$  may be derived by use of eqn. (31).

(b) **ABSORPTION BY A SWELLING SHEET.**—The problem of the absorption of a vapour or liquid A by a sheet B has already been stated in § 3(c) for the case in which no swelling of the sheet occurs. Thus in the boundary condition (11) and the mathematical solution (13) the thickness  $2l$  of the sheet is assumed to remain constant. If swelling occurs, however, the condition (11) is to be applied on moving boundaries. Furthermore,

<sup>18</sup> King, *Trans. Faraday Soc.*, 1945, **41**, 479.

the motion of the boundaries is not known till the solution of the diffusion equation has been evaluated and this requires knowledge of the motion of the boundaries. The problem is therefore awkward and would, in this form, involve some method of successive approximations. When re-formulated in terms of the variable of length  $\xi_B$ , however, these difficulties are removed and the boundaries of the sheet correspond to constant values of  $\xi_B$ . The solution (13) then applies with  $2l$  denoting the unswollen thickness of the sheet and with  $D^v$  replaced by the coefficient  $D_A^B$  provided this is constant. In the likely event of  $D_A^B$  being dependent on the concentration of A, the comparison of experimental and calculated absorption-time curves suggested in § 3(c) yields some mean value of  $D_A^B$ . A method of deriving the concentration dependence of the diffusion coefficient from a number of mean values of this kind is described elsewhere (Crank and Park<sup>19</sup>).

(c) DIFFUSION OF ONE SUBSTANCE THROUGH A SECOND SUBSTANCE WHICH IS CONFINED BETWEEN MEMBRANES.—A case of considerable theoretical interest is the steady state of diffusion of one substance through another when the second substance is confined between membranes. Let the membranes be impermeable to B and let the concentrations of A in contact with the membrane be maintained by supply and removal of A through the membranes from and to reservoirs of vapour or of solution of A in B or other impermeant substance.

At the steady state, sections at fixed distances from the membranes are fixed with respect to amount of component B, and the rates of transfer of A across all such sections must be equal, so that

$$-D_A^B \frac{\partial C_A^B}{\partial \xi_B} = \text{const.} \quad (35)$$

We will assume that the partial volumes are constant. By substitution of (24), (29) and (31), (35) becomes

$$-\frac{D^v}{V_B C_B^v} \frac{\partial C_A^v}{\partial x} = \text{const.} \quad (36)$$

Substituting from (6) we have

$$-\frac{D^v}{V_A C_B^v} \frac{\partial C_B^v}{\partial x} = \text{const.} \quad (37)$$

If, instead, we maintain the steady state by substituting membranes permeable only to B and supplying and removing B in the reverse direction we find, by interchange of A and B in (36) and reversal of signs to allow for reversal of direction

$$\frac{D^v}{V_A C_A^v} \frac{\partial C_B^v}{\partial x} = \text{const.} \quad (38)$$

It is evident that eqn. (37) and (38) require different concentration-distance functions. The steady state is therefore different, even between the same concentration limits, according as to which component is constrained and which is free to diffuse.

This difference is particularly evident in dilute solutions. We shall assume here, in the interests of further simplicity, that  $D^v$  is constant. The concentration of A being very low,  $V_B C_B^v$  can be assumed to be unity. Eqn. (36) now becomes

$$D^v \frac{\partial C_A^v}{\partial x} = \text{constant rate of transfer of A.} \quad (36a)$$

This is valid for A diffusing and B restrained.

<sup>19</sup> Crank and Park, *Trans. Faraday Soc.*, 1949, **45**, 240.

Substituting from (6) we may modify (38) to

$$\frac{D^v}{V_B C_A^v} \frac{\partial C_A^v}{\partial x} = \frac{D^v}{V_B} \frac{\partial}{\partial x} (\log C_A^v) = \text{constant rate of transfer of B.} \quad (38a)$$

This is valid for A restrained and B diffusing between the same concentration limits.

It will be seen that, when the dilute component is diffusing, its concentration gradient, under these simple conditions, is linear. When the same limits are maintained by diffusing the "solvent" through membranes impermeable to the solute, the gradient of the logarithm of concentration of the latter is linear and hence the concentration itself varies exponentially with distance.

When the total fall of concentration  $\Delta C_A^v$  of the dilute constituent is small compared with its mean concentration, (36a) becomes

$$\text{rate of transfer of A} = \frac{D^v}{a} \Delta C_A^v. \quad (36b)$$

and (38a) becomes

$$\text{equivalent rate of transfer of B} = \frac{D^v}{a} \frac{\Delta C_A^v}{C_A^v V_B}. \quad (38b)$$

where  $a$  is the distance between the membranes. The rate of diffusion of water in such a system down a given small mean vapour pressure gradient is therefore expected not to be constant but to be inversely proportional to the mean concentration of the solute. It will further be proportional to the diffusion velocity of the solute given by (36b). Thus if water diffuses from 99.1 to 99.0 % relative humidity through a layer containing hydrogen chloride, it will do so about twice as rapidly as when the layer contains sodium chloride. If the diffusion occurs from 90.1 to 90.0 % relative humidity, each rate will fall to one-tenth of its former value.

These conclusions refer to the case where the membranes are separated by a fixed distance. If, as is more likely to be true in practice, the membranes confine a given amount of component A so that the volume between them will vary inversely as the mean concentration of A, the distance  $a$  in (38b) will be more nearly inversely proportional to  $C_A$  than constant. In this case the rate of transfer of B will be, to a first approximation, dependent on  $\Delta C_A$  only and not on the mean value of  $C_A$ . This result would be obtained directly of course from equations in § as in the treatment already given of the swelling membrane. Diffusion of solvent through a constant amount (per unit area) of solute is thus simpler than diffusion through a constant thickness. This conclusion is not at once obvious and may have some important applications in physiological processes.

A second conclusion of interest may be drawn if we consider what happens in such a steady state system, if the membranes are suddenly rendered completely impermeable. Sections fixed with respect to the membranes are now fixed with respect to volume of solution. The change of concentration with time will therefore from now on be governed by

$$\frac{\partial C_A^v}{\partial t} = \frac{\partial}{\partial x} \left( D^v \frac{\partial C_A^v}{\partial x} \right), \quad (39)$$

but, at the instant of change of membranes, eqn. (36) still holds if A has been the diffusing component, whence

$$\frac{\partial}{\partial x} \left( D^v \frac{\partial C^v}{\partial x} \right) = -\text{const.} \times V_B \frac{\partial C_B^v}{\partial x} = \text{const.} \times V_A \frac{\partial C_A^v}{\partial x}. \quad (40)$$

Combining (39) and (40) we obtain

$$\left(\frac{dx}{dt}\right)_c = -\text{const.} \times V_A \quad (41)$$

since 
$$\left(\frac{\partial C_A^v}{\partial t}\right)dt + \left(\frac{\partial C_A^v}{\partial x}\right)dx = dC_A^v = 0$$

for  $C_A^v$  constant. Now the constant in (35) and (41) is the rate of transfer of A at the steady state in standard units of amount. Multiplied by  $V_A$  it represents the volume rate of transfer of A, or, since we are always considering transfer across unit area, the linear apparent velocity with which A was passing through the system.

We thus find that, at the instant of cessation of flow through of A, the whole concentration-distance distribution commences to move backwards at the velocity with which substance A previously passed through the membrane. With increasing time, the distribution will, of course, flatten out from the low concentration upwards as the substance A diffusing down the gradient now accumulates.

It is evident, therefore, that in the steady state during the passage of substance A, there was superimposed on the statistical diffusion process a real flow of the whole system. The physical significance of compensating mass-flow is dealt with in § 6.

**6. Physical Picture of Pure Diffusion and Compensating Mass-flow.**—Probably a majority of students are first introduced to the subject of diffusion by way of the classical experiment in which a tall cylindrical vessel has the lower part filled with, say, iodine solution and a column of solvent is carefully placed on top so that no convection currents are set up. In this initial state there is a sharp, well-defined boundary separating the coloured solution from the pure solvent above it. On inspecting the system later it is found that the upper part has become coloured, the lower part being correspondingly less intensely coloured, and after sufficient time the whole solution appears uniformly coloured. It is therefore evident that a transfer of iodine molecules from the lower to the upper part of the vessel has occurred, this transfer taking place in the absence of convection currents. This is the process commonly referred to as diffusion, the iodine being said to have diffused into the solvent.

Now if it were possible to watch the individual molecules of iodine, and this can be done effectively by replacing them by particles small enough to share the molecular motions but just large enough to be visible under a microscope, it would be found that the motion of each molecule is a random one. In a dilute solution each molecule of iodine behaves independently of the others, which it seldom meets, and each is constantly undergoing collision with solvent molecules, as a result of which collisions it moves sometimes towards a region of higher, sometimes of lower, concentration, having no preferred direction of motion towards one or the other. The motion of a single molecule can be described in terms of the familiar "random walk" picture, and whilst it is possible to calculate the mean square distance travelled in a given interval of time it is not possible to say in what direction the molecule will move in that time. That is, if a molecule is observed at a given time the contours of equally probable displacements at successive times will be consecutive spheres with centre at the original position of the molecule, provided that the time between two successive observations is great compared with the time between two successive molecular collisions.

This picture of random molecular motions, in which no molecule has a preferred direction of motion, has to be reconciled with the fact that a transfer of iodine molecules from the region of higher to that of lower concentration is nevertheless observed. Consider any horizontal

section in the solution and two thin equal elements of volume one just below and one just above the section. Though it is not possible to say which way any particular molecule will move in a given interval of time, it can be said that on the average a definite fraction of the molecules in the lower element of volume will cross the section from below and the same fraction of molecules in the upper element will cross the section from above, in a given time. Thus, simply because there are more molecules in the lower element than in the upper one, there is a net transfer of molecules from the lower to the upper side of the section as a result of the random molecular motions.

Where the solution is thermodynamically non-ideal, the movement will not be entirely random, even apart from the effect of compensating mass flow referred to below. If the molecules, as is generally the case, find themselves in a less favourable molecular force environment in solution than in the pure state (or more concentrated solution), then, in a gradient of concentration, they will experience a real average force in the direction of higher concentration and therefore have a component of real velocity opposing the statistical flow.

Similarly, in the presence of a temperature gradient, a gradient of molecular force will arise which will not in general be the same for both components. This will give rise to a real velocity of the molecules which will cause a slight separation of the two components and a concentration gradient will be built up. This phenomenon, the Soret effect, is usually called "thermal diffusion". For the reasons discussed above, Toms and one of the present authors (G. S. H.<sup>20</sup>) have suggested that "thermal migration" would be a more correct name. In the corresponding phenomenon in gases the primary effect in the thermal separation is difference in mass of molecules and thermal diffusion may be a more correct term. There is no doubt, from the highly specific nature of the effect in liquids, that the force field effect predominates.

In the simplest case, where the molecules of A and B are identical in mass and size, the rates of transfer of the two components, due to random motion across a volume fixed section, may reasonably be expected to be equal and opposite. In general, however, differences of mass and size of A and B molecules result in the transfer of A by random motions being greater or less than that of B. Consequently a hydrostatic pressure tends to be built up in the region of the solution which contributes least to the volume rate of transfer. This pressure is relieved by a compensating mass-flow of A and B together, that is of the whole solution (Hartley<sup>21</sup>).

The overall rate of transfer, say of component A, across a volume-fixed section may thus be expressed as the combined effect of a mass-flow and a transfer due to pure diffusion, that is due to the random motions of non-uniformly distributed A molecules. Since the amount of A transferred by the mass-flow of the whole solution is proportional to the concentration of A, it follows that the diffusion coefficient  $D_A^v$  must necessarily be a function of the concentration of A, a result which was deduced above by a slightly different method.

Whilst the resolution of the overall transfer of matter into a mass-flow and a pure diffusion process, is mathematically simple, in the physical picture of such a combination it is not quite as easy to separate out diffusing molecules from those taking part in both processes simultaneously.

It is, however, possible to demonstrate the separate existence of pure diffusion and mass-flow in the case of gases, when diffusion occurs across a porous plate which offers considerable viscous resistance. In this case an increased pressure is found to arise in that part of the vessel occupied initially by the slower diffusing component. Similarly, in a

<sup>20</sup> Hartley and Toms, *Nature*, 1946, **158**, 451.

<sup>21</sup> Hartley, *Trans. Faraday Soc.*, 1946, **42B**, 6.

liquid system, the separation takes a tangible form if, between the two solutions, a membrane is inserted which is permeable to one component only. In this case diffusion occurs until a definite equilibrium pressure, familiar as the osmotic pressure, is built up and restrains further diffusion.

The interpretation for liquids and solids appears simpler if the current model of diffusion, in which it is assumed that a molecule spends most of its time oscillating within a cage or hole formed by the closely packed surrounding molecules is accepted. The molecule performing this oscillatory motion will occasionally acquire sufficient energy to break through the surrounding potential barrier and thus form a new constellation of neighbours. It is then said to undergo diffusion, and calculations of the energy required by a molecule before it can jump in this way show that, in a typical case, less than 1 % of the total number of molecules are undergoing a net displacement relative to the surrounding molecules at any time. Thus in this case it is permissible to think of the diffusing molecules, i.e. those undergoing jumps, as distinct from the surrounding oscillating molecules which take part in the mass flow, if any. The theoretical diffusion coefficient, calculated in terms of the frequency of the molecular jumps, thus gives the rate of diffusion relative to surrounding molecules, i.e. mass-flow is not included.

The distinction between jumping molecules and those which merely oscillate enables us to suggest a molecular mechanism for the compensating mass-flow. Molecules do not always jump into holes which are adequate to accommodate them. They may pass through a very unstable stage of high potential energy to a new position which, although it has lower energy than the barrier just passed, has higher energy than the space which has been vacated. As a result the new constellation of neighbours is pushed slightly further apart in order to reduce potential energy. This effect will be greater in general where it results from the molecules which are intrinsically capable of more rapid diffusion. The additive effect over a large number of such processes is the microscopic increase of hydrostatic pressure which is relieved by the mass-flow.

We have mentioned above that the microscopic picture of pure diffusion can be represented in terms of a series of contour shells about the initial position of any molecule, which represent equal probabilities of displacement after a finite time interval. In the general case, when mass-flow takes place concurrently with pure diffusion, these contours will assume an ellipsoidal form which can be resolved mathematically into the sum of a random displacement proportional to the square root of the time interval and a linear displacement proportional to the time interval.

**7. Intrinsic Diffusion Coefficients.**—From the point of view of interpreting diffusion coefficients in terms of molecular motions, the mutual diffusion coefficient,  $D^v$ , thus appears to be unnecessarily complicated by the presence of the mass-flow. It is desirable to define new diffusion coefficients,  $\mathcal{D}_A$  and  $\mathcal{D}_B$  in terms of the rate of transfer of A and B, respectively, across a section fixed so that no mass-flow occurs through it. Such a section may be in practice impossible to determine, except in special conditions mentioned below. It is fixed in a different way from any of the other sections previously dealt with, and it must follow the mass-flow although this flow is not normally directly observable. These new diffusion coefficients will be referred to as "intrinsic diffusion coefficients." When the partial volumes are constant they are related to the mutual diffusion coefficient in the following way.

On one side of a section fixed so that no mass-flow occurs through it, there is a rate of accumulation of total volume of solution, which may be denoted by  $\phi$ , where

$$\phi = V_A \mathcal{D}_A \frac{\partial C_A^v}{\partial x} + V_B \mathcal{D}_B \frac{\partial C_B^v}{\partial x}. \quad (42)$$

$\phi$ , as thus defined, is actually the rate of increase of volume on the side of smaller  $x$ , and this must be equal to the rate of transfer of total volume by mass-flow across a volume-fixed section. Such a mass-flow involves a rate of transfer of A of  $\phi C_A^v$ , so that, equating two expressions for the net rate of transfer of A across the volume-fixed section, we find

$$D^v \frac{\partial C_A^v}{\partial x} = \mathcal{D}_A \frac{\partial C_A^v}{\partial x} - \phi C_A^v. \quad (43)$$

On substituting for  $\phi$  from (42) and using (6) we have finally

$$D^v = V_A C_A^v (\mathcal{D}_B - \mathcal{D}_A) + \mathcal{D}_A. \quad (44)$$

If the molal volumes vary with composition, the coefficient  $D^v$  has no significance, but  $\mathcal{D}_A$ ,  $\mathcal{D}_B$  can still be defined in terms of the rates of transfer of A and B respectively across a section which moves so that there is no mass-flow of A and B together, through it. It is convenient in this case to relate the intrinsic diffusion coefficients to  $D_A^B$ . Since the net rate of transfer of B through a B-fixed section is, by definition, zero, it follows that the contributions to the transfer of B resulting from the overall mass-flow and from the true diffusion of B relative to the mass-flow, must be equal and opposite. The rate of transfer of B by true diffusion relative to the mass-flow is

$$\mathcal{D}_B \frac{\partial C_B^v}{\partial x}$$

in the direction of  $x$  increasing, and hence the volume transfer of the whole solution accompanying mass-flow with respect to the B-fixed section is given by

$$\left( \mathcal{D}_B \frac{\partial C_B^v / \partial x}{C_B^v} \right)$$

in the direction of  $x$  increasing.

This produces a rate of transfer of A through the B-fixed section of

$$\left( \frac{C_A^v}{C_B^v} \right) \mathcal{D}_B \frac{\partial C_B^v}{\partial x},$$

due to the mass-flow. This is to be combined with the rate of transfer of A relative to the mass-flow which is given by

$$- \mathcal{D}_A \frac{\partial C_A^v}{\partial x},$$

to give the net rate of transfer of A across a B-fixed section, which is simply

$$- \mathcal{D}_A^B \frac{\partial C_A^B}{\partial x_B}.$$

Thus we have the equation

$$- D_A^B \frac{\partial C_A^B}{\partial x_B} = - \mathcal{D}_A \frac{\partial C_A^v}{\partial x} + \frac{C_A^v}{C_B^v} \mathcal{D}_B \frac{\partial C_B^v}{\partial x}. \quad (45)$$

When the molal volumes are not constant, the relation

$$V_A C_A + V_B C_B = 1,$$

still holds, but the differentiated form (6) is to be replaced by

$$\left( V_A + C_A^v \frac{dV_A}{dC_A^v} \right) \frac{\partial C_A^v}{\partial x} + \left( V_B + C_B^v \frac{dV_B}{dC_B^v} \right) \frac{\partial C_B^v}{\partial x} = 0. \quad (46)$$

Since

$$\frac{dC_A^v}{dC_B^v} = V_B^0 V_B (C_B^v)^2,$$

it follows immediately from (30), (45) and (46) that

$$D_A^B = (V_B C_B^V)(V_B^0 C_B^V)^{-1} \left\{ \mathcal{D}_A + \mathcal{D}_B \frac{C_A V_A + C_A^V dV_A/dC_A^V}{C_B V_B + C_B^V dV_B/dC_B^V} \right\} \quad (47)$$

This reduces to (44) when  $V_A$  and  $V_B$  are constant.

It is not possible, therefore, to deduce the values of  $\mathcal{D}_A$  and  $\mathcal{D}_B$  separately, unless some other information is available or some approximation can be made. The frame of reference is not one which can normally be located experimentally. One of us (Hartley<sup>21</sup>) has introduced a technique which makes it possible to do so in certain special circumstances. We require reference points which move with the bulk of the solution as a whole and these can be provided by particles of inert solid, too large to diffuse, suspended in the solution, which must, however, be so viscous that the movement of the particles under gravity can be ignored. This is possible, in the case of a swelling polymer, over a considerable range of concentrations. The particles can be inserted into the original unswollen polymer in the form of a scale which can then be used as an experimental  $\xi$  scale for diffusion calculations. As it has been exploited so far, it is doubtful whether this method can be used in concentrations where the value of  $\mathcal{D}_B$  (referring to the polymer molecules) is distinguishable from zero. The method is capable of further refinement, however, and eventually it may be possible to use it for actual measurement of  $\mathcal{D}_B$ .

Where  $\mathcal{D}_B$  can be assumed zero, substitution in (44) gives

$$\mathcal{D}_A = \frac{D^V}{(1 - V_A C_A^V)} = \frac{D^V}{V_B C_B^V} \quad (48)$$

In this case, therefore, the intrinsic diffusion coefficient of A and its dependence on the concentration of A can be deduced from observations of  $D^V$ .

**8. A Tentative Quantitative Theory for all Concentrations of a Binary Solution.**—According to Nernst's method, the solute, in a concentration gradient, is considered to be driven down the gradient by a force determined by the gradient of osmotic pressure. The velocity of the solute molecules under the influence of this force is obtained by dividing by a resistance coefficient which, according to Einstein, can be taken to be that of a sphere of volume equal to the molecular volume. There is some disagreement about this derivation of the coefficient, e.g. it is considered that  $4\pi a$  gives a better fit for small molecules than the  $6\pi a$  of Stokes' law for macroscopic spheres of radius  $a$ . There is also good evidence that, for extremely unsymmetrical molecules, the estimate requires correction. These points, however, will not concern us here. We shall simply accept the resistance coefficient as  $\sigma\eta$ , where  $\sigma$  is a function of molecular size and shape without necessarily assuming it to be independent of the viscosity  $\eta$ . We might therefore replace  $\sigma\eta$  by a single symbol but we leave it as a product to indicate that, in simple solutions,  $\sigma$  is approximately independent of  $\eta$ .

The conception of an osmotic pressure gradient as a driving force is theoretically unsatisfactory for several reasons, not least of which is one noted above, that, in pure diffusion in a simple solution, no molecule has any finite average velocity in any preferred direction. The osmotic pressure method does, however, give the correct result and there follows below an equivalent treatment free from the theoretical objections.

Let the gradient of (low) concentration  $C_A$  of A be maintained in an equilibrium condition by the application of a force  $F_A$  per g. mole of A in the direction of increasing  $x$ . This is purely a hypothetical operation but can be realized in the case of large molecules much different in density from the solvent, by a centrifugal field. The condition for this thermodynamic equilibrium is, for an ideal dilute solution,

$$F_A = RT \frac{\partial \log C_A}{\partial x} \quad (49)$$





subject anew rather than to attempt to relate our conclusions to his equations.

According to the accepted definition of the activity coefficient  $f$ , the thermodynamic equilibrium equation (49) becomes, in its generalized form

$$F_A = RT \frac{\partial \log N_A f_A}{\partial x} \quad . \quad . \quad . \quad (54)$$

where  $N_A$  is the mol fraction of A.

Similarly

$$F_B = RT \frac{\partial \log N_B f_B}{\partial x} \quad . \quad . \quad . \quad (55)$$

We may note that the total force acting, at equilibrium, on a volume containing a total of 1 g. mole of A and B together, is

$$N_A F_A + N_B F_B = RT \left( \frac{d \log N_A f_A}{d \log N_A} \frac{\partial N_A}{\partial x} + \frac{d \log N_B f_B}{d \log N_B} \frac{\partial N_B}{\partial x} \right), \quad (56)$$

by (54) and (55).

Since the Duhem relationship gives

$$\frac{d \log N_A f_A}{d \log N_A} = \frac{d \log N_B f_B}{d \log N_B}, \quad . \quad . \quad . \quad (57)$$

and, since

$$N_A + N_B = 1$$

and therefore

$$\frac{\partial N_A}{\partial x} = - \frac{\partial N_B}{\partial x},$$

it follows from (56) that this total force is zero, as is of course necessitated by the condition of equilibrium. We have now to estimate the transfer rates of A and B produced by the forces  $F_A$  and  $F_B$  if acting in the absence of the balancing composition gradient.

The hydrodynamics of the movement of closely contiguous spheres is obviously a subject of great complexity. It is, however, unimportant, in the derivation of the condition of thermodynamic equilibrium between a concentration gradient and a maintaining force, whether this force operates uniformly over all the molecules or is unequally distributed between them, provided the distribution is entirely indiscriminate and changes with time. We shall therefore considerably simplify the hydrodynamic part of the calculation by considering the force,  $F_A$ , acting per g. mole of A, to operate at any one instant only on so small a fraction of the A molecules that the velocity of these molecules is uninfluenced by the numerous other A molecules in the vicinity.

Thus we replace the force  $F_A/N$  acting on every molecule (at a given value of  $x$ ) by a force  $kF_A/N$  acting on a small fraction,  $1/k$  only, of these molecules. These will have a velocity  $kv_A$  where

$$kv_A = \frac{kF_A}{N\sigma_A\eta}, \quad . \quad . \quad . \quad (58)$$

and the resulting rate of transfer of A is

$$\frac{1}{k} C_A \frac{kF_A}{N\sigma_A\eta} = \frac{C_A F_A}{N\sigma_A\eta} \text{ g. mole/sec.} \quad . \quad . \quad . \quad (59)$$

Since this is equal and opposite to the rate of transfer of A by diffusion, in absence of the force, relative to a section through which there is no mass-flow, we have on substituting for  $F_A$  from (54)

$$\mathcal{D}_A \frac{\partial C_A}{\partial x} = \frac{C_A RT}{N\sigma_A\eta} \frac{\partial \log N_A f_A}{\partial x}, \quad . \quad . \quad . \quad (60)$$

and hence,

$$\mathcal{D}_A = \frac{RT}{N\sigma_A\eta} \frac{d \log N_A f_A}{d \log C_A}. \quad . \quad . \quad . \quad (61)$$

By using the relations

$$C_A V_A + C_B V_B = 1, N_A + N_B = 1, N_A C_B = N_B C_A,$$

it can be shown that

$$\frac{d \log N_A}{d \log C_A} = \frac{N_A}{V_B C_A}, \quad (62)$$

so that (61) may be written

$$\mathcal{D}_A = \frac{RT}{N \sigma_A \eta} \frac{N_A}{V_B C_A} \frac{d \log N_A f_A}{d \log N_A}. \quad (63)$$

Similarly it can be shown that

$$\mathcal{D}_B = \frac{RT}{N \sigma_B \eta} \frac{N_B}{V_A C_B} \frac{d \log N_B f_B}{d \log N_B}. \quad (64)$$

On substituting from (63) and (64) in (44), recalling (57), we have finally

$$D^v = \frac{RT}{N} \frac{d \log N_A f_A}{d \log N_A} \left( \frac{N_B}{\sigma_A \eta} + \frac{N_A}{\sigma_B \eta} \right). \quad (65)$$

This is an expression for the mutual diffusion coefficient  $D^v$  in a binary solution, whose thermodynamic behaviour is non-ideal, when the effect of the overall mass-flow of the solution is included.

*Courtaulds Limited,  
Research Laboratory,  
Maidenhead.*

## HYDROGEN BONDING IN CERTAIN MONO-NITRONAPHTHYLAMINES

BY D. E. HATHWAY\* AND M. ST. C. FLETT

*Received 26th January, 1949*

Measurements have been made of the amino and nitro group frequencies of certain mono-nitronaphthylamines. It is concluded that whereas intramolecular hydrogen bonding occurs in the 1-nitro-2-amino and 2-nitro-1-amino-compounds, it is weak or absent in the 8-nitro-1-amino- and 3-nitro-2-amino-cases.

The ultra-violet spectra of thirteen of the fourteen possible mono-nitronaphthylamines have previously been reported<sup>1, 2</sup> and certain structural inferences drawn. It was thought that an examination of their infra-red spectra, particularly in those cases where the groups are adjacent and intramolecular hydrogen bonding is possible, might give further information. The detection of hydrogen bonding by observing changes in the frequencies and intensities of the bands associated with the groups involved is well known.<sup>3</sup> Accordingly, the two bands near 3500 cm.<sup>-1</sup> associated with NH<sub>2</sub> groups and the band near 1350 cm.<sup>-1</sup> associated with aromatic —NO<sub>2</sub> groups<sup>4</sup> have been examined. Dilute (0.1 %) solutions of the amines in carbon tetrachloride were used to eliminate the possibility of intermolecular interactions. The frequencies are listed in Table I.

\* Present address: Department of Organic Chemistry, The University, Liverpool.

<sup>1</sup> Hodgson and Hathway, *Trans. Faraday Soc.*, 1945, **41**, 115.

<sup>2</sup> *Ibid.*, 1947, **43**, 643.

<sup>3</sup> E.g. Pauling, *Nature of the Chemical Bond*, Ch. IX.

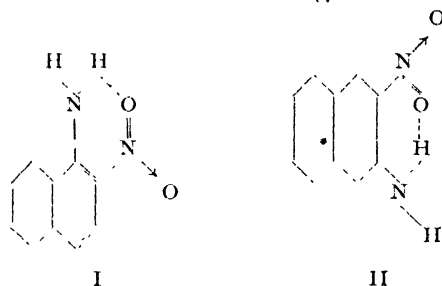
<sup>4</sup> Thompson, *J. Chem. Soc.*, 1948, p. 328.

It appears from these figures that intramolecular hydrogen bonding occurs to a marked extent in 2-nitro-1-naphthylamine, to a lesser extent in 1-nitro-2-naphthylamine, and is very weak or absent in 3-nitro-2- and 8-nitro-1-naphthylamines. Since the molecules are aromatic in nature, the substituents will (except probably in the 1:8 compound) be practically co-planar with the nucleus, and the explanation for bonding

TABLE I.—DATA FOR SUBSTITUTED NAPHTHALENES

Substituent (s)	N H Vibrations (cm. <sup>-1</sup> )	—NO <sub>2</sub> Vibrations (cm. <sup>-1</sup> )
1-Amino . . . .	3486, 3412	—
2-Amino . . . .	3490, 3410	—
1-Nitro . . . .	—	1341
2-Nitro . . . .	—	1347
2-Nitro-1-amino . . . .	3528, 3378	1350 (weak) 1300 (strong)
8-Nitro-1-amino . . . .	3485, 3410	1339
1-Nitro-2-amino . . . .	3513, 3398	1305, 1320
3-Nitro-2-amino . . . .	3497, 3413	1340
4-Nitro-2-amino . . . .	3498, 3515	1346 (strong) 1328 (weak)
5-Nitro-2-amino . . . .	3505, 3419	1340
7-Nitro-2-amino . . . .	3505, 3419	1345
8-Nitro-2-amino . . . .	3500, 3412	1335
3-Nitro-1-amino . . . .	3507, 3422	1345
5-Nitro-1-amino . . . .	3486, 3408	1343
6-Nitro-1-amino . . . .	3494, 3415	1343

in the C<sub>1</sub>C<sub>2</sub> substituted compounds and its absence from 3-nitro-2-naphthylamine may lie in the fact that the C<sub>1</sub>C<sub>2</sub> bond has the greater degree of double bond character.<sup>5, 6</sup> This is tantamount to saying that intramolecular hydrogen bonding is favoured by an increased degree of conjugation between the nucleus and chelate ring. If this conjugation were complete, the C<sub>1</sub>C<sub>2</sub> compound (I) would have a resonating system similar to that of phenanthrene (5 resonance forms) whereas the C<sub>2</sub>C<sub>3</sub> compound (II) would resemble anthracene (4 resonance forms):



A greater degree of stabilization would be expected in the former case.<sup>7</sup> The absence of bonding in the 1:8-derivative, where the groups are closer together than in the other cases, shows strikingly that conjugation between the nitro and amino group is necessary. The difference between the magnitude of the effect in 2-nitro-1-amino- and 1-nitro-2-amino-naphthalenes may be due in part to the different resonance forms thought to predominate in the two cases.<sup>1, 2</sup>

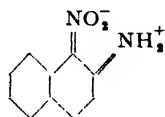
<sup>5</sup> Ref.<sup>3</sup>, Ch. IV.

<sup>6</sup> Baker, *et al.*, *J. Chem. Soc.*, 1934, 1684; 1935, 628; 1936, 274, 364.

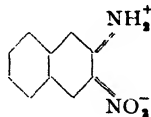
<sup>7</sup> Carter, *Trans. Faraday Soc.*, 1949, 45, 597.

It has been found<sup>8</sup> that 3-nitro-2-naphthylamine is a 10,000 times stronger base than the 2-nitro-1- and 1-nitro-2-naphthylamines. This may also result from the increased double bond character of the  $C_1C_2$  bond over the  $C_2C_3$  bond. The base form of 1-nitro-2-naphthylamine will, for example, be stabilized to a greater extent by resonance with form III, than 3-nitro-2-naphthylamine will be stabilized by resonance with IV. Such resonance stabilization of the ions is not of course possible.

Data on certain other mono-nitro-naphthylamines are also included.

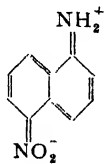


III

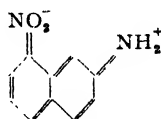


IV

The 4-nitro-1-amino- and 6-nitro-2-amino-compounds were insufficiently soluble for measurements to be made. It has been shown<sup>9</sup> that in substituted anilines, displacements of the  $NH_2$  frequencies provide some measure of the extent to which electrons are drawn from or donated to the amino group. Drifts in the  $NH_2$  frequencies of those nitro-naphthylamines where hydrogen bonding does not occur may have a similar significance. There is no evidence that this electron withdrawal is increased in such cases as 5-nitro-1-amino- and 8-nitro-2-amino- where resonance involving both groups is possible (V and VI):



V



VI

This suggests that such forms are not of outstanding importance.

Imperial Chemical Industries, Ltd.,  
Research Laboratories,  
Hexagon House,  
Blackley,  
Manchester, 9.

<sup>8</sup> Bryson, *Trans. Faraday Soc.*, 1949, **45**, 257.

<sup>9</sup> Flett, *ibid.*, 1948, **44**, 767.

## DIFFUSION AND SWELLING OF HIGH POLYMERS

### PART III.—ANISOTROPIC SWELLING IN ORIENTED POLYMER FILM

By G. S. HARTLEY

Received 11th February, 1949

The penetration of oriented cellulose acetate film in the plane of the film by various solvents and swellers has been examined qualitatively and roughly quantitatively. Penetration is much more rapid normal to the preferred direction of the macromolecular axes than parallel thereto, except in the case of certain "abnormal" solvents which are peculiar also in that they give rise to a sharply serrated front of attack in penetration of isotropic film.

The magnitude of the difference in penetration rates of normal substances is very great and it is doubtful whether there is any penetration at all parallel to the macromolecular axes in highly oriented film securely clamped against lateral expansion. With less oriented film and oblique penetration there is also a quantitative abnormality in that depth of penetration is initially more nearly proportional to time than to  $(\text{time})^{\frac{1}{2}}$ .

Whether this anisotropic penetration is due to anisotropy of the pure diffusion process itself or of the swelling that accompanies it cannot be decided by the present work but it is probable that both factors are operative.

In Part I<sup>1</sup> we noted that the penetration of a solvent or sweller into a polymer solid is characterized by a visible sharp front of advance. In Part II<sup>2</sup> Robinson gave some experimental examples of this phenomenon in dealing with the orientation produced by the swelling of cellulose acetate on penetration into it of a solvent or sweller. This orientation is due directly to the swelling, i.e. to the mass flow component of the mutual diffusion process, and commences at the inner boundary already sharply defined by refractive index discontinuity. In Part I the incorrect, or rather unnecessarily restricted, statement was made that the visible boundary indicated a rather abrupt change of refractive index and hence of concentration. Further work by Robinson<sup>3</sup> has now shown that the refractive index-distance curve is in some cases approximately linear with an abrupt termination to its slope, rather than abruptly sigmoid. The "step" which makes a boundary visible may therefore be in the refractive index itself or in its gradient. This does not affect the qualitative validity of the conclusion previously drawn that the diffusion coefficient must increase very rapidly with increasing concentration of solvent or sweller when this concentration is low.

The phenomenon of the sharp advancing front, although due to a complication in the diffusion process not present to so great an extent in solutions of simple liquids, offers also an experimental advantage. The progress of diffusive penetration can be measured very simply on the stage of a microscope by recording the variation with time of the distance between the advancing front and a convenient fixed point, or of the distance between two such fronts approaching one another from opposite sides of a specimen.

Although this paper is not primarily concerned with quantitative results but rather with an initial semi-quantitative survey of some peculiar features of diffusive penetration of polymer material, we must briefly discuss the significance of these measurements.

We will represent by  $x_n$  distance from some fixed point in the apparatus to a refractive index discontinuity and by  $x$  distance to a point at which the concentration of penetrating substance is  $C$  (measured on a volume scale). Denoting time by  $t$  and the diffusion coefficient by  $D$ , we find the time-distance-concentration behaviour governed by Fick's law,

$$\frac{\partial C}{\partial t} = \frac{\partial}{\partial x} \left( D \frac{\partial C}{\partial x} \right) \quad . \quad . \quad . \quad . \quad . \quad (1)$$

provided that there is no volume change on solution of the two components. This condition is only approximately valid for polymer-solvent systems but sufficiently so for the purposes of the present work, as is proved by measurements discussed below. Crank and the author have discussed elsewhere<sup>4</sup> a method of dealing with diffusion in a system where the overall volume is not constant, which enables an equation of the same form as (1) to be employed.

<sup>1</sup> Hartley, *Trans. Faraday Soc.*, 1946, **42B**, 6.

<sup>2</sup> *Ibid.*, p. 12.

<sup>3</sup> Not yet published.

<sup>4</sup> Crank and Hartley (in press).

Boltzmann<sup>5</sup> pointed out that eqn. (1) can be converted to express  $C$  as a function of  $D$  and a single combined parameter  $\alpha t$ , provided that  $D$  is a unique function of  $C$  and not independently influenced by  $t$  or  $dC/dx$ .

It follows from Boltzmann's theorem that, if  $\alpha$  is measured from the original line of separation of the two pure components, the value of  $\alpha$  for any one value of  $C$  is proportional to  $t$ , i.e.

$$\left(\frac{dx}{dt}\right)_c = f(D, C)t \quad . \quad . \quad . \quad (2)$$

Since the form of the  $C - \alpha$  curve is independent of  $t$ ,  $dC/dx$  and  $d^2C/dx^2$  will have maximum or minimum values at the same values of  $C$  for all values of  $t$ . Since refractive index can be expected to be approximately a linear function of  $C$  in the range of concentration of interest, regions of abrupt variation of refractive index, visible as boundaries under the microscope, will also correspond to constant values of  $C$ . Whence it is to be expected that

$$\frac{dx_n}{dt} = \text{const.} \quad . \quad . \quad . \quad (3)$$

The boundary defining the innermost limit of advance of the penetrating substance will correspond to some very low, but at present unknown, value of  $C$ .

It may here be mentioned that other "boundaries" may be visible by refractive index changes. In the case of non-solvent swellers, the outermost boundary is a perfectly sharp phase boundary. Even with solvents, a rather indefinite outer boundary can often be distinguished, due also, as was explained in Part I, to an enormous variation of diffusion coefficient with concentration. In some cases, a "middle" boundary is visible, which was not known when Part I was written. Between the inner and the middle boundaries the swollen polymer is always birefringent. The birefringence falls to zero when the swelling is sufficiently great, due to diffusional relaxation of the polymer molecules. Where a middle refractive index boundary occurs, the zone of birefringence terminates abruptly at this boundary.

In many simple cases of penetration into cellulose acetate sheet, it has been found that eqn. (3) is valid for the inner boundary and, where they are sufficiently sharp for measurement, for the other boundaries also. We can therefore conclude that the premises of the above brief discussion are valid and that, despite the very great and peculiar variation of  $D$  with  $C$ ,  $D$  is a single-valued function of  $C$  in any one system at any one temperature.

This is, however, only true for simple cases. Perhaps we should say that there are many cases in which it is true and these cases are the simplest from the diffusion point of view and may be regarded as representing normal behaviour. We shall here be concerned also with abnormal behaviour.

## Experimental

**Materials and Method of Observation.**— Commercial cellulose acetate film (Courtaulds Ltd.) was used in the greater part of this work but some observations were also made on a sample of commercial soluble Nylon film, polyvinyl alcohol film and films cast in the laboratory from polymethyl methacrylate.

The cellulose acetate had an acetyl content of approx. 2.3 groups per glucose residue and as supplied contained some 25 % by weight of phosphate and phthalate plasticizers. The plasticizers were removed prior to the penetration experiments by soaking the film in a methyl ethyl ketone-butyl acetate mixture (40/60 by volume) and then drying in an oven at 100° C to constant weight. There was some evidence that a small amount of butyl acetate was left in the film after this treatment. Later it was found that purer film could be obtained

<sup>5</sup> *Ann. Physik*, 1894, 53, 959.







PLATE 1

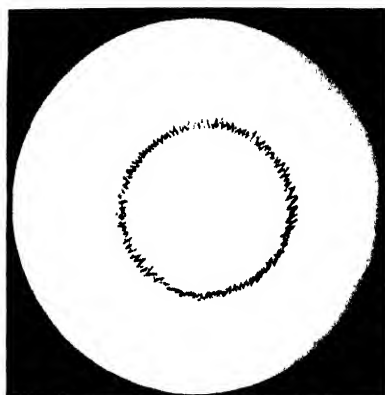


PLATE 2

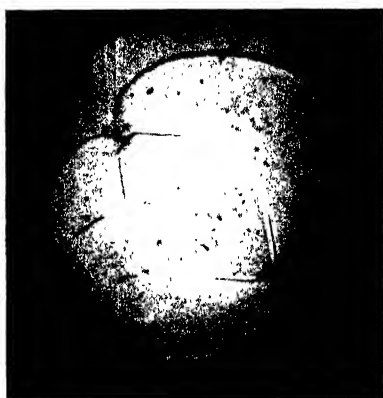


PLATE 3

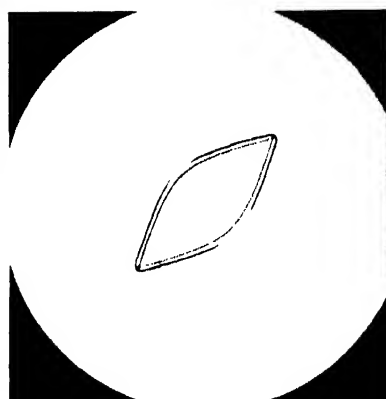


PLATE 4

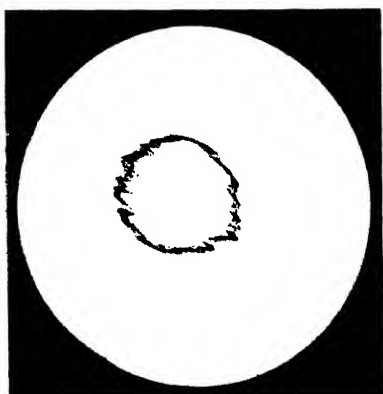


PLATE 5

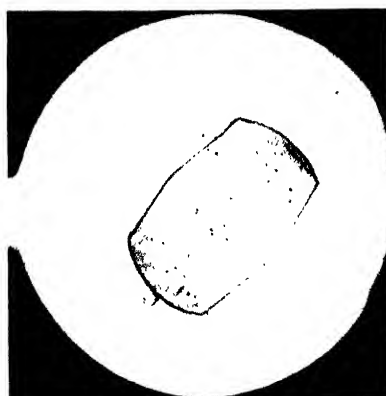


PLATE 6

$\text{CH}_2\text{Cl}_2$  Isotropic Polarized Light

[To face p. 823

by removing the plasticizer by soaking in methyl alcohol. One or two confirmatory experiments were done with this purer material.

As obtained in this way the film appears isotropic when viewed normally in polarized light but has an appreciable uniplanar orientation,<sup>6</sup> i.e. there is a tendency for the molecules to lie flat in the plane of the film. Measured by a method which will be described elsewhere, the difference in refractive index between light with electric vector in the plane of the film and light with the electric vector normal to the film was found to be 0.0012, as compared with a maximum attainable of 0.0035.

Observations were also made on film in which this uniplanar orientation had been substantially reduced by soaking the film in propyl acetate at 60° C for 30 min., which causes a significant decrease in area and increase in thickness. After drying, the difference of refractive index was found to have fallen 0.0004. This will be referred to as a fully isotropic film although it is evident that appreciable anisotropy was still present. The normal film will be referred to as uniplanar, although a more completely uniplanar film could in theory be obtained.

Much of the work refers to a film in which a measure of linear orientation had been produced by stretching to some 150 % of the original length when softened in the ketone ester mixture. The dried stretched film showed the second-order yellow colour between crossed polarizers at the average thickness of 0.23 mm. The corresponding difference of refractive index was found to be about 0.0038 as compared with a maximum attained in other experiments of 0.0070. Some observations were also made on the most highly stretched film but this is extremely difficult to handle owing to a very ready tendency to crack longitudinally. Some observations were also made on less stretched film.

The small specimens of film to be examined under a microscope were cut out as circles by a  $\frac{1}{4}$ -in. leather punch, or as small rectangular strips with a sharp knife, and clamped between glass plates by means of small brass screw clamps. The assembly was completely immersed in the solvent or swelling liquid in a small flat-bottomed glass trough. No disturbing effect of compression was noticed as long as an unattached core of hard material remained in the centre of the specimen. As soon as this disappeared, compression effects on the penetration became evident and these will be referred to later.

The glass trough was placed on the stage of a microscope and observations made with a low-power objective and an eyepiece fitted with a graduated scale. Magnification of 24 diameters was used. The boundaries were normally readily visible without special conditions of illumination. Where they were faint they could be brought out more sharply by inclining the mirror so that illumination was rather one-sided. The position of a boundary was not influenced by the conditions of illumination.

No control of temperature was attempted in these preliminary observations except that some, where mentioned, were made at elevated temperatures. All the film used was in equilibrium with ordinary atmospheric moisture and would therefore contain varying amounts of water, about 4 %. It has recently been found by Robinson<sup>8</sup> that the removal of this small amount of water has a profound effect on the rate of penetration.

## Results and Discussion

**An Irregular Advancing Front.**—A remarkable phenomenon noticed only in the later stages of this work will, for logical convenience, be mentioned first. In Plate 1 is shown a circular disc of isotropic film, partly penetrated by methylene chloride. This specimen was placed between parallel polaroids to make the inner boundary more distinct while leaving the outermost boundary of the swollen gel still visible. The orientation being radial a dark cross appears in the birefringent zone and it will be seen that this zone is limited outwardly by a rather indefinite middle boundary. All the boundaries are smooth concentric circles. They are much smoother than the original circumference of the circular punching.

In Plate 2 is shown the inner boundary only of a similar disc penetrated by pyridine. In this case neither outer nor middle boundaries are visible. The photograph is taken with unpolarized light. With polarization no significant difference would be revealed, the birefringent zone being very shallow or non-existent. The inner boundary is here no longer smooth but very sharply serrated. The serrations are fairly regular and bear no relation to roughness of

<sup>6</sup> See Sisson, article in *Chemistry of Cellulose* (Interscience Series on High Polymers, ed. Ott).

the original edge. If methylene chloride is replaced by pyridine after partial penetration of a disc by the former, serrations are developed after sufficient time in what was before a perfectly smooth inner boundary.

We consider the behaviour of methylene chloride as normal because it is evidently much more simple and is followed, with quantitative variations only, by many solvents and swellers. Moreover this behaviour is reproducible and little influenced by the conditions of clamping. The serrated front produced by pyridine is less exactly reproducible and more dependent on conditions of clamping.

Other solvents which give a similar picture to pyridine are dioxane and ethylene glycol diacetate. No non-solvent sweller was found which produced any serration of the inner boundary. The phenomenon is not apparently correlated with speed of penetration. Most of the normal penetrants advance more rapidly than the three abnormal ones investigated but some slower penetrants are also normal. Ethyl acetate (normal) is slower than pyridine and tetrachlorethane, *m*-cresol and cyclohexanone (all normal) are slower than any of the serrating penetrants. We have at present no explanation to offer of this very remarkable phenomenon but other observations noted below throw a little further light upon it.

**Anisotropic Normal Penetration.** (a)—THEORY.—It is to be expected, quite generally, that all vector properties of oriented material will show anisotropic behaviour. In diffusion, anisotropy may be anticipated from two closely related lines of argument.

There is a possibility of anisotropy of the pure diffusion process itself. An oriented film can be considered as an assembly of more or less parallel molecules each of which may be considered as a chain of rigid segments connected by links which have a limited flexibility by distortion of bond angles and rotation about single bonds. It is evident that oscillation of segments perpendicular to the chains will be of much greater amplitude than that parallel to the chains. Diffusion occurs by occasional exchange of places between molecules under the influence of thermal agitation. A small molecular substance penetrating a macromolecular matrix can be considered to diffuse by exchange of places between small molecules and segments of macromolecules. Pure diffusion will therefore be expected to occur more rapidly perpendicular to the macromolecular direction than parallel thereto. As the degree of swelling increases, the possibility of exchange in the parallel direction will become greater since more of the chains will assume a tortuous configuration.

We may also seek the explanation of anisotropy of diffusive penetration, as Mr. Crank has suggested to me, in anisotropy of the swelling associated with this penetration. Film, plasticized by swelling and then stretched exhibits pronounced toughening as stretching proceeds. Initially the stretching process is introducing a slight parallelism of previously crumpled and randomly distributed long molecules. As stretching progresses, increasing tension is required because there is decreasing possibility of extension by rotation of segments about connecting links, and stretching must occur mainly by sliding of aligned molecules one over another.

No measurements have been made of the anisotropy of plasticity of oriented film but it is evidently very great. It is much greater than is apparent in frequently noted<sup>7</sup> tensile strength measurements, because, in this case, an unoriented fibre is partly oriented before it is broken, and film stretched perpendicular to its orientation is partly re-oriented before breaking. The greater strength of well-oriented fibre or film is due to its orientation being effected under more favourable conditions than is the re-orientation when tensile strength is measured.

Since a mass flow (mechanical stretch) is an integral part of the process of diffusive penetration,<sup>1</sup> anisotropy of plasticity must be reflected in anisotropy of diffusive penetration. It is therefore to be expected that penetration will proceed much more easily perpendicular to the

<sup>7</sup> E.g. Mark, article in *Chemistry of Cellulose* (Interscience Series on High Polymers, ed. Ott), p. 1011.

molecular direction than parallel to it because the necessary swelling of the penetrated polymer can occur most easily in this direction.

Observations<sup>8</sup> on swollen oriented viscose sheet by a similar technique to that described have indicated that penetration of dyes from an external aqueous solution proceeded more rapidly parallel than perpendicular to the direction of stretch. More recently<sup>9</sup> it has been claimed that dyes penetrate oriented cellulose fibres more rapidly radially than longitudinally. It is to be expected that the behaviour of a highly crystalline polymer like cellulose will be more complicated than that of a non-crystalline one.

Measurement of the interdiffusion of similar, or preferably isotopic, small molecular substances, present in the same total concentration in an oriented non-crystalline polymer, will be necessary to establish definitely whether, and in which sense, anisotropy of pure diffusion occurs.

(b) OBSERVATION.—The phenomenon of anisotropic penetration can most readily be demonstrated by observations on circular discs cut from oriented film. The molecular direction in the disc can readily be found by observation between crossed polaroids in series with a piece of the original strip where the direction of the molecules is known.

Many such observations were made and it was quite generally found that penetration occurred more rapidly across than along the molecular direction. The magnitude of the effect was greater than expected. With all normal solvents and swellers penetration appeared to be exclusively lateral, the diameter parallel to the molecular direction being shortened only in the later stages of penetration by attack from the flanks. This is clearly shown in the penetration by methylene chloride (Plate 3) and in that by acetone (Plate 4), which was taken at a later stage. In the latter case, the lateral fronts have united to create (by a diffusion process!) sharp receding points. In the former case the irregular outline of the original cut edge is still just seen between the advancing lateral fronts, and the highly swollen isotropic gel is expanding over these unattacked edges.

It will be noticed in these photographs that the middle boundary is ill-defined with acetone and absent with methylene chloride in the region of most rapid penetration. As we proceed from the narrowing "equator" towards the unattacked "poles" this boundary becomes sharply defined. With isotropic film it is also clearly evident. The probable significance of this is mentioned below.

**Influence of Degree of Orientation.**—Reasonably good straight lines were obtained by plotting the half diameters of the unattacked residue of the disc at the "equator" against (time)<sup>1/2</sup>. Some rates of penetration obtained this way, expressed in mm. min.<sup>-1/2</sup> are given in Table I. Included are also some approximate figures for the penetration rate parallel to the molecular direction.

The presence of plasticizer increases the penetration rate if this can also be increased by further orientation. It was of interest to know whether also the small amount of residual butyl acetate might have a considerable effect. Accordingly, a specimen of film cast without plasticizer and stretched in methyl alcohol was dried to constant weight and then allowed to take up propyl acetate vapour. This was preferred to butyl acetate as being more mobile within the film. A comparison specimen was similarly treated but without stretching. Measurements were made of penetration by methylene chloride of small rectangular strips cut out at intervals while the propyl acetate was slowly drying out again. The results are given in Table II. Refractive index difference was 0.0042.

It thus appears that, without plasticizer, the penetration even of methylene chloride (the most rapid penetrant examined) is accelerated

<sup>8</sup> Boulton, Delph, Fothergill and Morton, *J. Text. Inst.*, 1933, **24**, 113.

<sup>9</sup> Frey-Wyssling, *J. Polymer Sci.*, 1947, **2**, 314.

by orientation of the film. The magnitude of the effect is worthy of comment. The ratio for lightly plasticized film (penetration normal to orientation) to unplasticized unstretched film is 24/1. Expressed in diffusion coefficient units this ratio would be squared, i.e. nearly 500/1.

TABLE I

Refractive Index Difference (Measure of Orientation)	CH <sub>2</sub> Cl <sub>2</sub> (20° C)		C <sub>4</sub> H <sub>8</sub> COCH <sub>3</sub> (30° C)	
	Normal	Parallel	Normal	Parallel
o (uniplanar, plasticized)	0.13		0.035	
o (uniplanar, deplasticized)	0.11		0.015	
0.0020	0.115	0.02	0.015	0.005
0.0032	0.12	0.00	—	—
0.0038	0.125	0.00	0.03	0.00
0.0045	0.125	—	0.075	—
0.0070	0.13	—	0.105	—

The results in the last row were obtained with the most highly oriented sheet obtained which was stretched in methyl alcohol vapour. They were obtained with a rectangular strip.

It will be seen that no great increase is obtained in the case of methylene chloride by stretching the film. The effect is mainly revealed in depressing the penetration rate parallel to the molecules. With methyl ethyl ketone on the other hand a high degree of orientation is necessary to get maximum penetration rate normal to the molecular direction.

TABLE II

Wt. % Propyl Acetate	Penetration Rate into	
	Stretched (Normal)	Unstretched
0	0.078	0.005
3	0.104	0.041
6	0.120	0.078
12	0.143	0.126

The result of attempts at more accurate measurements of the very much slower penetration parallel to the macromolecular direction will be dealt with in a later section.

**Anisotropic Penetration by Abnormal Solvents.**—In Plate 5, we have a picture of the advancing front when an abnormal solvent, dioxane, penetrates a circular disc of oriented film. The teeth are parallel to the molecular direction. The quantitative difference between the normal and parallel penetration rates is here largely reduced. Not the least remarkable result is that dioxane and pyridine, both of which penetrate film much more slowly from its faces (i.e. normal to the uniplanar orientation) than does methylene chloride, can penetrate oriented film parallel to the molecular direction much more rapidly.

The front which advances normal to the molecular direction reveals another abnormality when viewed between crossed polarizers. In all normal cases, the birefringence falls very sharply immediately behind the inner boundary. Where the unattacked film appears second-order yellow, the descending sequence of green, blue and red is telescoped into an effectively black line and only a white or pale yellow zone of reduced birefringence has appreciable width. With pyridine and dioxane

the whole zone of reduced birefringence is very shallow if the specimen is very firmly clamped, and, if it is not so firmly clamped, the zone is wider but the successive colour bands are then clearly spaced out and persist right round the specimen. If the specimen is rotated, light is extinguished over the whole field simultaneously. The orientation is thus not changed in direction by the swelling process as it is with normal solvents. Examined under greater magnification the explanation of both these abnormalities is at once seen to be that the early stages of swelling consist of a microscopic fragmentation. Small islands of slightly swollen material are being pushed outwards. This is evidently another manifestation of the serration phenomenon.

**Variation in the Zone of Reduced Birefringence.**—We may here interpolate some other observations on variations noticed in the zone of reduced birefringence. These refer to what we have called normal penetrating substances. Around the more or less elliptical residual core of the circular disc, this zone forms two crescent-shaped areas appearing only white or pale yellow (in the thickness usually examined, about 0.23 mm.). In their narrower parts they are abruptly bounded on the outside by the middle refractive index boundary. At their widest, corresponding to the most rapid penetration, the outer boundary is very diffuse and outside of it there is usually just detectable a small island of faint birefringence which examination with a Red I plate shows to be of opposite sign. Rotation of the specimen shows that the molecular direction in the narrow parts tends towards being parallel to the radius of the original specimen. This behaviour is entirely to be expected from the observations of Robinson <sup>3</sup> that orientation in the direction of diffusion is produced by the associated swelling process.

Where this swelling occurs perpendicular to the original molecular direction, the macromolecules will be separated out without rotation. Not until rotational diffusion has produced a more nearly random distribution can further swelling align the molecules in the new direction, but here the dilution and the high rate of relaxation restrict the associated birefringence to a very low value. Where swelling occurs obliquely to the original molecular direction, the molecules will be turned into the new direction without prior randomization. Why this should give rise to a sharp outer boundary of the birefringent zone will be made clear later.

The width of the zone of reduced birefringence in relation to the depth of penetration is very variable. The less the final equilibrium swelling, the broader the zone. A sufficiently poor sweller, e.g. methyl alcohol, shows no isotropic region. Where swelling is sufficient to permit relaxation of orientation and the development of an isotropic zone, we find that, in general, the more rapid the penetration, the broader the zone of reduced birefringence.

This is to be expected for the following reason. The rates of penetration, determined mainly by the diffusion conditions in the very dilute solution of penetrating substance in the polymer, are much more affected by the volume of the penetrating molecule than any ordinary diffusion coefficients in a liquid. This will be evident from a forthcoming paper by K. C. Smith. The penetration rates on our scale of measurement of acetone and cyclohexanone for example are in the ratio approximately 18/1 (diffusion coefficient ratio will be the square of this). The rates of relaxation of macromolecular orientation in the swollen state are more nearly dependent only on the viscosity. The diffusion coefficients are much less different in the high concentration of penetrating substance than in the near-solid polymer the variation of diffusion coefficient is therefore greater for slow penetration and the concentration gradient is thus steeper near the unchanged solid relative to that in the highly swollen region and the zone in which relaxation cannot occur much narrower.

Consistent with this explanation it was found that the zone of reduced birefringence was broadened by raising the temperature. The diffusion

in the near-solid polymer is accelerated relatively more than that in the highly swollen polymer.

A swollen oriented polymer can lose its orientation by two distinct mechanisms, (i) by rotational diffusion of the macromolecules, which can occur without change of shape, or (ii) by elastic recoil in which there is a contraction of the whole specimen in the direction of orientation and a corresponding expansion in the perpendicular direction. The latter process does not usually occur with cellulose acetate when clamped between glass plates as in our experiments. The crescents of reduced birefringence do not therefore contract along their length. Elastic behaviour of normally non-elastic polymers can usually be realized at higher temperatures. It was found that, with *m*-cresol penetrating a disc of oriented cellulose acetate at 100° C, the crescents had retreated from the slowly attacked tips of the unchanged core.

**Attempts to Measure the Rate of Penetration Parallel to the Molecules.**—This measurement is rendered difficult by the fact that the specimen, even if cut as a long strip with long faces perpendicular to the orientation, is consumed from the ends before appreciable advance has been observed from the sides. This difficulty was partly overcome by allowing the ends of the strip to project between the glass plates, subsequently cutting them off nearly flush with the plates and covering them over with fish glue which was allowed to dry before introduction into the swelling liquid. After some days, leakage of swollen filaments of cellulose acetate occurred through cracks in the protecting layer and attack of the whole strip from the ends then commenced.

Using a specimen not very highly oriented (refractive index difference = 0.0036), some measurements were made by this method in methylene chloride. The inner boundary appeared quite sharp between crossed polarizers where it was marked in this case by an *increase* of birefringence. A very sharp middle boundary was evident both by refractive index and by fall of birefringence to zero over a very short range.

Quite good straight lines were obtained for width against  $t$ , not  $t^{\frac{1}{2}}$ . The linear rate of advance was  $2.7 \times 10^{-4}$  mm./min. for the inner boundary, approximately zero for the outer boundary and  $1.0 \times 10^{-4}$  mm./min. outwards for the middle boundary. The temperature was 16° C and the corresponding rates for penetration perpendicular to orientation are 0.13 and 0.09 inwards and 0.19 mm./min. outwards. Thus in 10 min. the advance across the molecular direction would be 1400 times as far as along it: in 100 min., 140 times as far.

There is no doubt that, with more highly oriented film, the rates parallel to the molecules are much slower, but no consistent figures were obtained owing to the increase of the above-mentioned difficulties and the great sensitivity shown to the precision of clamping.

**The Mechanism of Anomalous Diffusion.**—This is the first case of which the writer is aware in which a departure from Fick's law in its most general form is found in a two-component system. Not only is  $D$  not constant but the failure of Boltzmann's equation makes it evident that  $D$  is no longer a single-valued function of  $C$ .  $D$  depends not only on  $C$  but also on the history of the particular diffusion process.

We have seen that the diffusion coefficient depends on molecular orientation and also that the swelling consequent on diffusive penetration modifies molecular orientation. Were there no relaxation of orientation by rotational diffusion of macromolecules at sufficiently high concentration of penetrating substance, then the orientation, for a given initial state of orientation and given degree of swelling in a given direction, would be fixed. The direction and extent of orientation would be uniquely determined by the initial state, the angle of penetration and the concentration of penetrating substance. All the factors controlling the diffusion coefficient would therefore be fixed for the particular system, at any one value of  $C$ , and  $D$  would therefore, for this system, be a unique

function of  $C$ . The basic condition for the Fick-Boltzmann law would therefore apply.

In general, however, the degree of orientation will be subject to decay by rotational diffusion of the macromolecules. Therefore in any element having concentration  $C$  at time  $t$  from the commencement of penetration, the degree of orientation will have fallen below that expected in the absence of rotational diffusion by an amount depending not only on  $C$  but on  $t$  also. The basic condition for validity of the Fick-Boltzmann law will now no longer obtain. The orientation will in general have a greater component in the direction of diffusion, at any one value of  $C$ , the earlier in the experiment this concentration is attained. Since this component has a retarding effect on diffusion, the rate of penetration will tend to be less rapid in the early stages of penetration than would be expected from observations at later stages. In the extreme limit, rotational diffusion may become the rate-determining process, and, being independent of  $dC/dx$ , this will tend to make  $dx/dt$  constant. Penetration distance may therefore be expected to commence proportionally to  $t$ , tending towards proportionality to  $t^{1/2}$  as penetration proceeds.

**Penetration Obliquely to the Molecular Direction.**—Several measurements were made on strips cut at various angles to the molecular direction. The results are somewhat confusing and more work would be necessary to clear up this subject.

At angular deviation from the normal (fastest direction) less than  $30^\circ$ , the behaviour is not distinguishable from normal penetration with methylene chloride, acetone or methyl alcohol. With methyl ethyl ketone, penetration appears to follow the Fick-Boltzmann law at  $30^\circ$ , but the rate on the  $t^{1/2}$  scale is about  $\frac{2}{3}$  of that at  $0^\circ$  (normal to molecules). This is the value which would be expected if the rate is a simple elliptical function of the angle  $\theta$  from the fastest direction, i.e.

$$\text{Rate} = (\text{fastest rate}) \cos^2 \theta + (\text{slowest rate}) \sin^2 \theta$$

and if the slowest rate is effectively zero.

At angles above  $45^\circ$ , penetration becomes different qualitatively in that the outer as well as inner boundary of the zone of modified birefringence becomes sharp. A rigidly clamped specimen then behaves as shown in Plate 3. The contraction of the unchanged central portion shows abnormal behaviour in that  $dx/dt$  increases for a short period before becoming constant at a value not much less than for normal penetration. The behaviour of the middle boundary is observed to be more markedly anomalous in the same sense. Anomalous expansion of the outermost boundary was not directly observed but extrapolation shows that a corresponding anomaly must exist. The behaviour of the other boundaries after the inner ones have met is due to the pressure of the clamping plates being applied to the swollen polymer after the hard core has disappeared. The isotropic gel is squeezed outwards and the swelling pressure of the anisotropic gel presumably reached, so that this can swell no further.

Rotation of the stage shows that the direction of orientation is changed in the middle zone, lying more nearly parallel to the direction of penetration and almost exactly parallel at its outer boundary. Since the effect of swinging the molecules into the direction of penetration will be to decrease the diffusion coefficient, we conclude that this effect must locally outweigh the opposed effect of dilution. The transient decrease of diffusion coefficient will cause a local increase of concentration gradient and it is this inflection in the concentration-distance curve which is visible as refractive index disturbance. This phenomenon of a middle refractive index line has been observed also in the penetration of unstretched uniplanar and isotropic film where it presumably has a similar explanation.



It is surprising, in view of the great difference in speed of attack parallel and perpendicular to the direction of orientation, that the rate of penetration does not fall off more rapidly with increasing deviation from the perpendicular direction. Except for the results with methyl ethyl ketone, one would be tempted to conclude that it is only the part of the diffusion process which deviates from the Fick-Boltzmann law which is anisotropic. Owing to its tendency to exaggerate itself by bringing molecules not at first parallel to the penetration direction into

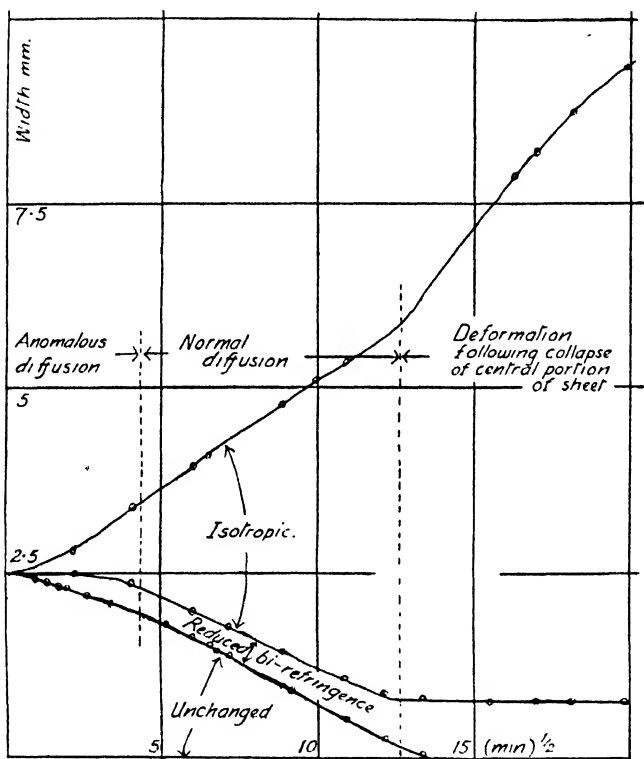


FIG. 1.—Cellulose acetate. Refractive index difference 0.0038 penetrated by methylene chloride at  $45^\circ$  to direction of orientation at  $19.5^\circ$  C.

this direction, the greatly retarded anomalous diffusion might become either dominant or negligible in effect. There is evidently a tendency towards this state of affairs, but it is not complete.

One might expect therefore that a simpler variation with direction of penetration would obtain, and non-Fickian diffusion disappear, if a very poor sweller were examined in which no diffusive relaxation of orientation occurred. No such relaxation can be observed with methyl alcohol. Although this substance penetrates very slowly parallel to the molecules, penetration at  $30^\circ$  to the normal is as fast as that in the normal direction itself. It is possible, however, that the very small molecules of this substance diffuse isotropically as soon as the macromolecular structure has been opened up by a relatively small concentration.

Another possible explanation of deviation from a simple elliptical velocity distribution is indicated by the remarkable behaviour of tetrachlorethane. In Plate 6 is shown the form of the unattacked core in an initially circular disc about half penetrated by tetrachlorethane. It will be seen that there are now obtuse angles where we should expect the

greatest rate of penetration. This must be due to the rate of penetration being *more* rapid in a direction making a small angle with the perpendicular to the orientation direction than in the perpendicular direction itself.

Tetrachlorethane is the only solvent studied in which these obtuse angles are unequivocally evident, but examination of Plate 4 (acetone) shows similar behaviour in less marked degree. Confirmation of the suggested explanation was found in the behaviour of a thin rectangular strip cut with its long side perpendicular to the molecular direction. Only the short fronts advanced. As is usual, the advance was at first more rapid near the corners, but, instead of remaining rounded, each front developed as two straight fronts at a small angle. At each end, one of these advanced more rapidly than the other, which was gradually eliminated. Thereafter, penetration proceeded by advance of a straight sloping front from either end. The asymmetry (but not the obliquity itself) was probably due to slight irregularity of the clamping pressure. In no other solvent was it possible to create the oblique advance by deliberate maladjustment of the clamping screws.

Reconsidering our proposed mechanism for anisotropy of pure diffusion, it is probable that, although exchange of position between macromolecular segments and small molecules will be at least probable in the direction of the macromolecular axis, it may not necessarily be true that exchange is most probable in the perpendicular direction. This may be modified by the geometrical disposition of the links whose rotation permits movement of the segments, and by the relative disposition of the segments of neighbouring chains.

**The Behaviour of Fully Isotropic Film.**—A few observations were made on film in which the uniplanar orientation had been reduced by treatment in hot propyl acetate. These indicated a much slower rate of penetration than in deplasticized uniplanar film.

Penetration normal to the surface of film suspended freely in solvent was also very much slower in the fully isotropic film. This is entirely consistent with the observations previously discussed, since in uniplanar film we have the molecules more or less perpendicular to the direction of penetration. That retardation also occurs in the plane of the film suggests that a different mechanism is also coming into play. It seems probable that freedom of movement of macromolecular segments will be reduced in all directions by the greater entanglement of chains in the fully isotropic state.

This property of isotropic film provides a simple demonstration of the importance of orientation effects in diffusion which makes it not surprising that the literature of permeability rates contains so many wide discrepancies. A specimen of commercial film is simultaneously made nearly isotropic and the plasticizer removed by soaking in propyl acetate at 60° for 30 min. It is soaked in cold methyl alcohol for 1 hr. to remove propyl acetate more quickly than by evaporation and dried in air for 1 hr. and in an oven at 100° C for 12 hr. It is then divided into strips and two of these are held in boiling methyl alcohol until soft. One is removed without stretching and dried as before. The other is quickly removed, stretched as far as possible immediately, and then dried.

The contrast between these specimens, identical in treatment except that one was stretched in the swollen state, is very marked. The stretched specimen is irretrievably softened and largely dissolved by immersion in acetone for less than 5 min. The unstretched specimen can be recovered almost intact after immersion for 1 hr. or more.

**The Generality of the Phenomena Discussed.**—So far in this series we have been concerned entirely with cellulose acetate. Some qualitative observations were made on some other transparent non-crystalline polymer films to confirm that the behaviour is by no means unique.

A specimen of unoriented polyvinyl alcohol film was examined with water as the penetrating substance. A sharp inner boundary was evident

with an anisotropic band outside it in which the orientation was radial. This had a rather indefinite outer boundary. A specimen of the film was then warmed and stretched. A disc cut out from this was found to be penetrated rapidly perpendicularly to the direction of stretch and hardly at all attacked parallel to this direction. The crescents of reduced double refraction were now sharply bounded on the outside towards the tips. The picture was very similar to the corresponding one for cellulose acetate and methylene chloride. A specimen of cresol-soluble Nylon film showed very similar behaviour in this solvent at 100° C.

A specimen of polymethyl methacrylate sheet, cast in the laboratory, could not be obtained in an optically anisotropic state by stretching. Correspondingly, no birefringence was induced by diffusive penetration. The inner boundary, both with benzene and acetone, was sharply defined but irregular in outline.

The author's best thanks are due to several colleagues with whom this work has been fruitfully discussed, in particular Mr. J. Crank, Dr. C. Robinson, Dr. G. S. Park and Mr. K. C. Smith, also Mr. J. W. G. McLaughlan for technical assistance and Mr. J. Goodwin for preparation of the photographs.

*Courtaulds Limited,  
Research Laboratories,  
Maidenhead.*

---

## MOLECULAR FORCE FIELDS

### PART X.—THE BENDING OF DOUBLE BONDS, WITH PARTICULAR REFERENCE TO ETHYLENE AND FORMALDEHYDE

BY J. W. LINNETT, D. F. HEATH AND P. J. WHEATLEY

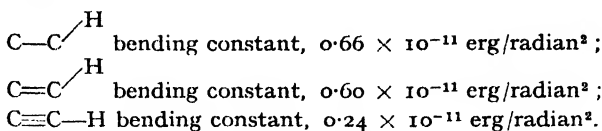
*Received 25th February, 1949*

We have applied the Orbital Valency Force Field (O.V.F.F.) to the formaldehyde and ethylene molecules, and their deuterium analogues, assuming that there is van der Waals' repulsion of the type  $V = a/R^{12}$  between the non-bonded hydrogen and oxygen and non-bonded hydrogen and carbon atoms respectively. Six constants are required for formaldehyde, and the vibration frequencies are predicted with an average error of 0.7 % if the HCH angle is taken as 120°. If the HCH angle is assumed to be less than 120° the accuracy is rather less. Ethylene requires nine constants, and the frequencies are predicted with an average error of 0.75 %. The most interesting feature of the results is that the O.V.F.F. used divided the bending of the double bond into two parts, one allowing for the bending of the  $\sigma$ -bond, and one for the bending of the  $\pi$ -bond. The constants associated with the bending of the  $\sigma$ -bond are positive, and, although the constant associated with the twisting of the  $\pi$ -bond in ethylene is positive, the other constants associated with different distortions of the  $\pi$ -bond are negative. From these results it is concluded that distortion of the  $\sigma$ -bond increases the potential energy of the molecules, that twisting of the  $\pi$ -bond increases the potential energy, but that, during other types of out-of-plane distortion, an increase in overlap of the  $\pi$  orbitals tends to lessen the increase of potential energy.

It has been pointed out previously that the bending constants of angles formed between a triple bond and a single bond are surprisingly small.<sup>1</sup>

<sup>1</sup> Linnett, *Quart. Rev.*, 1947, 1, 73.

The following Simple Valency Field Force (S.V.F.F.) bending constants illustrate this :



In this series the second constant is for in-plane distortion and during such bending the C=C  $\pi$ -bond, formed by the overlap of the two carbon  $2p\pi$  orbitals, is presumably unaffected to a major extent. In the bending of the C $\equiv$ C—H angle, however, at least one of the  $\pi$ -bonds is likely to be distorted to a major extent. This suggests that the explanation of the low bending constant for the C $\equiv$ C—H angle lies in the fact that bending occurs relatively easily when  $\pi$  orbitals are distorted.

There are two further points which tend to confirm the suggestion that when the  $\pi$  orbitals are distorted the bending constants are smaller. The first of these is that the smaller in-plane bending vibration frequency of formaldehyde (1280 cm.<sup>-1</sup>) is bigger than the out-of-plane bending vibration frequency (1167 cm.<sup>-1</sup>). Only in the out-of-plane vibration is there a major distortion of the  $\pi$ -orbitals. Similarly, in ethylene the two C=C—H in-plane bending vibration frequencies (1050 and 995 cm.<sup>-1</sup>) are bigger than the two C=C—H out-of-plane bending vibration frequencies (949 and 943 cm.<sup>-1</sup>). An examination of the treatment of Kilpatrick and Pitzer<sup>2</sup> shows that the in-plane constant is, as expected, greater than the out-of-plane constant.

The purpose of the present paper is to examine the application of the Orbital Valency Field Force (O.V.F.F.)<sup>3</sup> to formaldehyde and ethylene with the object of investigating in a little more detail the bending of bonds in which  $\pi$  orbitals are involved. We shall first consider the molecules H<sub>2</sub>CO and D<sub>2</sub>C(O) and then C<sub>2</sub>H<sub>4</sub> and C<sub>2</sub>D<sub>4</sub>.

**Formaldehyde.**—The application of the O.V.F.F. to H<sub>2</sub>CO and D<sub>2</sub>C(O) requires the consideration of four types of forces, if it is assumed that, to a first approximation, a distinction can still be drawn between  $\sigma$  and  $\pi$  molecular orbitals even when the molecule undergoes a small out-of-plane deformation: (a) bond stretching forces, (b)  $\sigma$ -bond bending forces, (c)  $\pi$ -bond bending forces, and (d) van der Waals' type forces between non-bonded atoms.

(a) We shall suppose that the variation of potential energy with bond length is given by

$$V_a = \frac{1}{2}k_1\Delta r_1^2 + B'\Delta r_1, \quad (1)$$

where  $\Delta r_1$  measures the change of the length of the bond from the equilibrium value. The second term in (1) arises because repulsion between the non-bonded atoms displaces the C—H bond length from its true equilibrium value. The first term in (1) is the usual valency force field term,  $k_1$  being the force constant of the bond.

(b) The treatment of  $\sigma$ -bond bending is the same as that described in Part III of this series. It is based on the assumption that directed bonds are formed by directed atomic orbitals, and that the potential energy is a minimum when the orbitals of the two atoms forming the bond overlap to the maximum possible extent. There are two O.V.F.F.  $\sigma$ -bond bending constants,  $k_H$  for the C—H bond, and  $k_\sigma$  for the  $\sigma$  member of the C=O bond. The variation of potential energy with bending is then given by

$$V_b = \frac{1}{2}k_H\Delta\beta^2 + \frac{1}{2}k_\sigma\Delta\theta^2 + B''\Delta\beta, \quad (2)$$

where  $\Delta\beta$  and  $\Delta\theta$  are the angles between the directions of maximum overlap in the equilibrium position and the corresponding directions in the distorted molecule.  $B''$  corresponds to  $B'$  in eqn. (1).

<sup>2</sup> Kilpatrick and Pitzer, *J. Res. Nat. Bur. Stand.*, 1947, **38**, 191.

<sup>3</sup> Heath and Linnett, *Trans. Faraday Soc.*, 1948, **44**, 873.

(c) The  $\pi$ -bond in formaldehyde is that formed by the "sideways" overlap of the carbon  $2p\pi$  orbital and the oxygen  $2p\pi$  orbital. It will be treated in a manner analogous to that used for the  $\sigma$ -bond. Suppose that, during a vibration, the carbon atom orbitals are directed to such a position that the carbon  $2p\pi$  orbital makes an angle  $\Delta\phi$  with a direction perpendicular to the line joining the carbon and oxygen atoms. Then the change of potential energy with distortion is given by

$$V_e = \frac{1}{2}k_\pi\Delta\phi^2 \quad (3)$$

The diagram in Fig. 1 which has been drawn to illustrate the similar case for ethylene may help the reader to appreciate this term. However, the case of formaldehyde is somewhat different from ethylene since, with formaldehyde, the oxygen  $2p\pi$  orbitals are free to orientate themselves so as to give the best possible overlap with the  $2p\pi$  orbitals of the carbon atom, whereas with ethylene there are the other two bonds to the hydrogen atoms to be considered.

(d) In previous papers we have shown that forces between non-bonded atoms in molecules such as  $\text{BF}_3$ ,  $\text{CCl}_4$  and  $\text{SF}_6$  must be taken into account when considering molecular distortions.<sup>4</sup> In formaldehyde one might expect that the crowding together of the non-bonded atoms would not be important since the hydrogen atom is so small. Linnett and Wheatley<sup>5</sup> have found it possible to treat  $\text{CH}_4$  assuming the  $\text{H}\cdots\text{H}$  repulsion to be negligible. Therefore in the present paper we have also assumed the  $\text{H}\cdots\text{H}$  repulsion to be negligible, although we would like to say that we feel that the assumption may perhaps be less justifiable than many people have assumed in the past. The case of the  $\text{H}\cdots\text{O}$  repulsion is different. Thompson and Linnett<sup>6</sup> have found that, to account for the vibration frequencies of formaldehyde using the S.V.F.F., it is necessary to include a cross-term between the  $\text{C}=\text{O}$  bond and the  $\text{HCO}$  angle, the sign of which indicates that the  $\text{HCO}$  angle tends to increase as the  $\text{C}=\text{O}$  bond length decreases. Such an effect would be expected if there were a considerable repulsion between the hydrogen and oxygen atoms. We have therefore included a term to take account of this repulsion. The change of potential energy due to repulsion, for each  $\text{H}\cdots\text{O}$  pair, is given by

$$V_4 = A \cdot \Delta R^2 + B \cdot \Delta R \quad (4)$$

as in Part IV.<sup>7</sup>  $\Delta R$  is the change in the  $\text{H}\cdots\text{O}$  distance from the value it has in the equilibrium configuration. For the same reasons as in Part IV we suppose that  $V = a/R^{12}$ , so that  $-B/R = 2A/13$ . Thus only one constant  $A$  is used to allow for the repulsion.

In the present treatment of formaldehyde we have assumed that there is no change in hybridization of the bond-forming orbitals of the carbon atom on distortion. It is assumed that the hybridization of the three  $sp^2\sigma$  orbitals remain constant and that the  $2p\pi$  orbital remains pure  $2p\pi$  throughout and always perpendicular to the plane of the three  $\sigma$  orbitals. This is possibly an undue simplification of the problem but, at present, there are insufficient data available to enable us to allow for changes in hybridization. We do not believe that the omission of the possibility of orbital-following by change of hybridization will obscure the main features of this problem.

There are six adjustable constants in our treatment :

- $k_1$ , the stretching force constant of the  $\text{C}-\text{H}$  bond,
- $k_2$ , the stretching force constant of the  $\text{C}=\text{O}$  bond,
- $A$ , allowing for  $\text{H}\cdots\text{O}$  repulsion,
- $k_H$ , the  $\text{C}-\text{H}$  bond O.V.F.F. bending constant,
- $k_\sigma$ , the  $\sigma$   $\text{C}=\text{O}$  bond O.V.F.F. bending constant,
- and  $k_\pi$ , the  $\pi$   $\text{C}=\text{O}$  bond O.V.F.F. bending constant.

<sup>4</sup> Heath and Linnett, *Trans. Faraday Soc.*, 1948, **44**, 561, 873.

<sup>5</sup> Linnett and Wheatley, *ibid.*, 1949, **45**, 39.

<sup>6</sup> Thompson and Linnett, *J. Chem. Soc.*, 1937, 1384.

<sup>7</sup> Heath and Linnett, *Trans. Faraday Soc.*, 1948, **44**, 878.

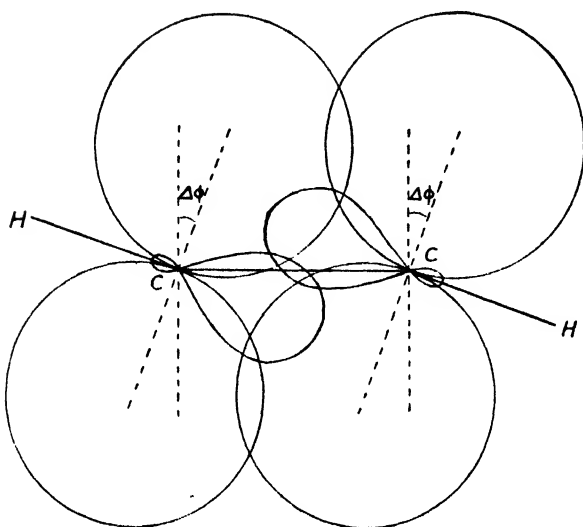


FIG. 1(a).

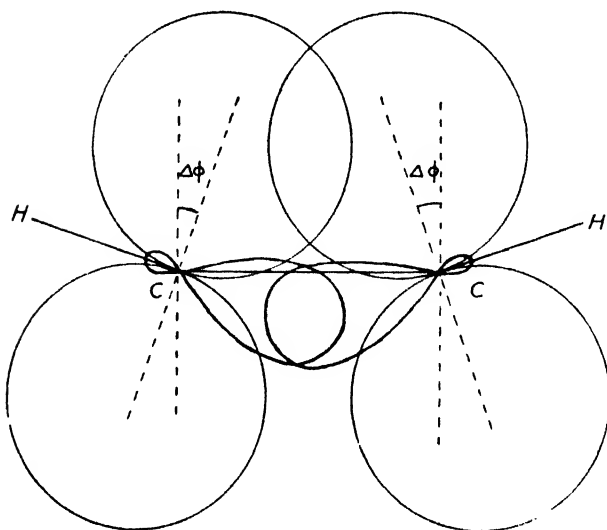


FIG. 1(b).

FIG. 1.—Two out-of-plane distortions of ethylene, showing the change in overlap in the  $\sigma$ - and  $\pi$ -bonds.

- (a) Symmetry class  $B_{2g}$ . The constants associated with this bending of the double bond are  $k_{\sigma}^b$  and  $k_{\pi}^b$ .
- (b) Symmetry class  $B_{1u}$ . The constants associated with this bending of the double bond are  $k_{\sigma}^u$  and  $k_{\pi}^u$ .

The first five constants appear in the expressions for the planar vibration frequencies, but  $k_\pi$  does not appear since the axis of the carbon  $2p\pi$  orbital must remain parallel to the axis of the oxygen  $2p\pi$  orbital and perpendicular to the line joining the carbon and oxygen atoms during all the planar vibrations. In the expression for the non-planar bending vibration frequency the last four constants appear. The algebraic expressions for the vibration frequencies in terms of the force constants, masses and geometric configuration of the molecule are given in Appendix I. In these expressions, the constant  $B$  (see formula (4)) is included though, in fact, we have always made  $-B/R$  equal to  $2/13$  of  $A$ . It will be noticed that the  $B'$  type constants for the C—H and C=O bonds (see formula (1)) do not appear in the formulae in the Appendix. They are absent because they are related to the constant  $B$ , and hence to  $A$ , by the requirement that, in the equilibrium configuration, the potential energy is a minimum. Or, alternatively, they disappear because the force of attraction between the bonded atoms must exactly balance the force of repulsion between the non-bonded atoms in the equilibrium configuration.

In making our calculations it is necessary to know the shape of the molecule. The two moments of inertia of  $\text{H}_2\text{CO}$ ,  $I_A = 21.65 \times 10^{-40}$  and  $I_B = 2.9768 \times 10^{-40}$  c.g.s. units,<sup>8</sup> are inadequate to enable an unequivocal calculation of the C—H and C=O bond lengths and of the HCH angle to be made. We have made our calculations, therefore, for three values of the latter :

- (A)  $\text{H}\hat{\text{C}}\text{H} = 120^\circ$ , giving  $r_{\text{CH}} = 1.0889$  and  $r_{\text{CO}} = 1.2162 \times 10^{-8}$  cm.,
- (B)  $\text{H}\hat{\text{C}}\text{H} = 115^\circ$ , giving  $r_{\text{CH}} = 1.1181$  and  $r_{\text{CO}} = 1.2027 \times 10^{-8}$  cm.,
- (C)  $\text{H}\hat{\text{C}}\text{H} = 110^\circ$ , giving  $r_{\text{CH}} = 1.1511$  and  $r_{\text{CO}} = 1.1874 \times 10^{-8}$  cm.

Molecular orbital theory might lead us to expect a value close to  $120^\circ$ , but this leads to a value of  $r_{\text{CH}}$  smaller than anticipated when it is considered that the C—H bond in  $\text{H}_2\text{CO}$  has an abnormally low force constant. If the HCH angle is less than  $120^\circ$ , the value deduced for  $r_{\text{CH}}$  is more reasonable. We believe, therefore, that the true shape must be within the range of shapes covered by (A), (B) and (C). For the atomic weights we used  $m_{\text{H}} = 1.00813$ ,  $m_{\text{D}} = 2.01473$ ,  $m_{\text{O}} = 12.00$  and  $m_{\text{C}} = 16.00$ . We took  $4\pi^2c^2/N$  to be  $5.890343 \times 10^{-2}$ . The frequencies used were taken from Herzberg.<sup>9</sup>

The results of our calculations are shown in Table I, where the calculated frequencies are compared with those observed. The values of the force constants used are also given in the Table. It will be seen that the force field reproduces the values of the observed frequencies well. The error increases somewhat on passing from  $\text{H}\hat{\text{C}}\text{H} = 120^\circ$  to smaller angles. For set (A) the twelve frequencies are calculated with an average error of 0.7 %. The maximum error is 2.9 % but that occurs for the planar antisymmetric bending vibration frequency of  $\text{D}_2\text{CO}$ , the exact value of which is uncertain. For all other vibrations the agreement is within 2 %. For  $\text{H}\hat{\text{C}}\text{H} = 115^\circ$  the average error has increased to 0.9 % and the maximum errors have also increased somewhat. For  $\text{H}\hat{\text{C}}\text{H} = 110^\circ$  the average error is 1.0 % and the maximum errors still greater.

The most interesting feature of the results is that  $k_\pi$  is negative ( $-0.88 \times 10^{-11}$  erg/radian<sup>2</sup>), indicating that there is an increase in the strength of the  $\pi$ -bond when it is distorted. We shall return to discuss this when we have considered ethylene.

**Ethylene.**—With the same assumptions as above the application of the O.V.F.F. to ethylene requires (a) two bond stretching constants, (b) one C—C  $\sigma$ -bond bending constant, and two C=C  $\sigma$ -bond bending

<sup>8</sup> Dieke and Kistiakowsky, *Physic. Rev.*, 1934, **45**, 4.

<sup>9</sup> Herzberg, *Infra-red and Raman Spectra of Polyatomic Molecules* (van Nostrand), p. 300.

TABLE I

	Obs. cm. <sup>-1</sup>	HCH = 120°		HCH = 115°		HCH = 110°	
		Calc. cm. <sup>-1</sup>	% Error	Calc. cm. <sup>-1</sup>	% Error	Calc. cm. <sup>-1</sup>	% Error
H <sub>2</sub> CO	2780	2822	+ 1.51	2835	+ 1.98	2843	+ 2.27
	1744	1748	+ 0.23	1748	+ 0.23	1754	+ 0.57
	1503	1512	+ 0.60	1513	+ 0.67	1514	+ 0.73
	2874	2882	+ 0.28	2882	+ 0.28	2876	+ 0.07
	1280	1280	—	1280	—	1280	—
	1167	1167	—	1167	—	1167	—
		Average	0.44		0.53		0.61
D <sub>2</sub> CO	2056	2062	+ 0.29	2078	+ 1.07	2093	+ 1.80
	1700	1699	- 0.06	1696	- 0.24	1696	- 0.24
	1106	1100	- 0.54	1100	- 0.54	1099	- 0.63
	2160	2127	- 1.51	2116	- 2.04	2113	- 2.18
	990	1019	+ 2.93	1030	+ 4.04	1034	+ 4.44
	938	932	- 0.65	938	—	944	+ 0.64
		Average	1.00		1.32		1.65

$k_1$	3.7135	3.7043	3.6799
$k_2$	10.9783	10.9585	11.0348
$k_H$	1.2190	1.3335	1.4540
$k_\sigma$	1.2644	1.3740	1.4751
$k_\pi$	-0.8793	-0.9038	-0.9104

Repulsion Constant  $A = 0.55 \times 10^5$  dyne/cm.

The units of the stretching constants ( $k_1$  and  $k_2$ ) are  $\times 10^5$  dynes/cm. and of the bending constants ( $k_H$ ,  $k_\sigma$  and  $k_\pi$ ) are  $\times 10^{-11}$  erg/radian<sup>2</sup>.

constants, (c) three C=C  $\pi$ -bond bending constants and (d) one constant, allowing for H...C repulsion (cf. formaldehyde). There are 22 observed frequencies of C<sub>2</sub>H<sub>4</sub> and C<sub>2</sub>D<sub>4</sub> to be accounted for by these nine constants. Fig. 1, which shows the distorted orbitals, illustrates why there are two C=C  $\sigma$ -bond bending constants. One applies to the bending vibrations which are symmetrical to the centre of symmetry when the two carbon  $2p\sigma$  orbitals rotate in the same sense (Fig. 1(a); vibration of symmetry  $B_{2g}$ ).<sup>14</sup> This constant will be designated  $k_\sigma$ . The other  $k_\sigma^u$  applies to the bending vibrations which are antisymmetrical to the centre of symmetry when the two carbon  $2p\sigma$  orbitals rotate in opposite senses (Fig. 1(b); vibration of symmetry  $B_{1u}$ ). Of the three C=C  $\pi$ -bond bending constants, one is involved in the twisting frequency  $k_\pi^t$  and has been



considered by Penney,<sup>10</sup> by Mulliken and Roothan<sup>11</sup> and by Parr and Crawford.<sup>12</sup> The other two C=C  $\pi$ -bond bending constants correspond to the two different C=C  $\sigma$ -bond bending constants ( $k_{\sigma}^u$  and  $k_{\sigma}^t$ ). The difference between them is similar to the difference between the two  $\sigma$ -bond constants and is illustrated in Fig. 1. The variation in potential energy is expressed in terms of the constants and distortions as for H<sub>2</sub>CO, and it is likewise assumed that there is no change of hybridization during

TABLE II

Symmetry Class	C <sub>2</sub> H <sub>4</sub>			C <sub>2</sub> D <sub>4</sub>		
	Obs. cm. <sup>-1</sup>	Calc. cm. <sup>-1</sup>	% Error	Obs. cm. <sup>-1</sup>	Calc. cm. <sup>-1</sup>	% Error
<i>A<sub>g</sub></i>	3019	3012	- 0.23	2251	2199	- 2.31
	1623	1604	- 1.17	1515	1514	- 0.07
	1342	1327	- 1.13	981	964	- 1.73
<i>A<sub>u</sub></i>	825	825	—	—	584	—
<i>B<sub>1g</sub></i>	3075	3113	+ 1.24	2304	2314	+ 0.43
	1050	1070	+ 1.90	883	871	- 1.36
<i>B<sub>1u</sub></i>	949	951	+ 0.21	720	719	- 0.14
<i>B<sub>2g</sub></i>	943	946	+ 0.32	780	778	- 0.26
<i>B<sub>2u</sub></i>	3106	3134	+ 0.90	2345	2333	- 0.51
	995	995	—	716-727	716	—
<i>B<sub>3u</sub></i>	2990	3039	+ 1.64	2200	2205	+ 0.23
	1445	1465	+ 1.38	1078	1080	+ 0.19
Average 0.84				Average 0.66		

Stretching Constants × 10 <sup>8</sup> dynes/cm.		Bending Constants × 10 <sup>-11</sup> ergs/radian <sup>2</sup>	
<i>k<sub>1</sub></i>	4.834	<i>k<sub>H</sub></i>	1.0891
		<i>k<sub>σ</sub><sup>g</sup></i>	0.6016
		<i>k<sub>σ</sub><sup>u</sup></i>	1.3571
		<i>k<sub>π</sub><sup>u</sup></i>	- 1.0355
		<i>k<sub>π</sub></i>	- 0.4188
<i>k<sub>2</sub></i>	7.16	<i>k<sub>π</sub><sup>t</sup></i>	1.2108

Repulsion Constant *A* = 0.275 × 10<sup>8</sup> dynes/cm.

the vibrations. The resulting algebraic expressions for the vibration frequencies in terms of the force constants, masses and shape of the molecule are given in Appendix II.

<sup>10</sup> Penney, *Proc. Roy. Soc. A*, 1934, 144, 166.

<sup>11</sup> Mulliken and Roothan, *Chem. Rev.*, 1947, 41, 219.

<sup>12</sup> Parr and Crawford, *J. Chem. Physics*, 1948, 16, 526.

In making the calculations the shape of the molecules have been taken to be

$$r_{CH} = 1.071 \text{ and } r_{CO} = 1.353 \times 10^{-8} \text{ cm., and } \hat{HCH} = 120^\circ.$$

Galloway and Barker<sup>13</sup> actually give  $\hat{HCH} = 119^\circ 55'$ , but the difference of this from  $120^\circ$  would not be significant in our calculations. The frequencies used were taken from Herzberg<sup>14</sup> and, while this may not be the finally accepted assignment, it seems to be the best available at the moment.

The results are shown in Table II where the calculated and observed frequencies are compared. It will be seen that the agreement is good, the average error being 0.75 %. For only one frequency is the error greater than 2 %.

The main results are :

- (1)  $k_\pi^u$  and  $k_\pi^g$  are both negative, like  $k_\pi$  for formaldehyde.  $k_\pi^u$  is about twice as big as  $k_\pi^g$ .
- (2)  $k_\pi^t$  has the value  $1.2108 \times 10^{-11}$  erg/radian<sup>2</sup>.
- (3)  $k_H$  for the bending of the C—H bond is  $1.0891 \times 10^{-11}$  erg/radian<sup>2</sup>, whereas  $k_H$  for the C—H bond in formaldehyde is bigger.
- (4)  $k_\sigma^u$  is about twice as big as  $k_\sigma^g$ .
- (5)  $A$  has the value  $0.275 \times 10^5$  dynes/cm., which is only half the value in formaldehyde.
- (6)  $k_1$  is  $4.834 \times 10^5$  dynes/cm. which is greater than  $k_1$  in formaldehyde.

## Discussion

The most interesting results of these calculations is that the O.V.F.F. leads to the conclusion that  $k_\pi$  of formaldehyde and  $k_\pi^u$  and  $k_\pi^g$  of ethylene are negative. The qualitative observations made in the introduction are reflected in this result. Let us consider  $k_\pi^u$  first (see Fig. 1(b)). We can see that, if this distortion were continued to the extent of rotating each  $2p\pi$  orbital through a right-angle, a C=C  $\sigma$ -bonding orbital would result. This C=C  $\sigma$ -bond would be stronger than the C=C  $\pi$ -bond. Hence we might expect that the change of overlap shown in Fig. 1(b) would lead to a decrease of energy and hence that  $k_\pi^u$  would be negative. This simple picture, therefore, gives a sign to  $k_\pi^u$  which is quite understandable. A similar argument cannot be used for  $k_\pi^g$ . Rotation of the  $2p\pi$  orbitals gives no change in overlap at first. It should not be concluded from this result that the sign of  $k_\pi^g$  is wrong, but rather that simple pictures do not necessarily give an accurate forecast of the precise electron distribution.<sup>15</sup> Preliminary wave-mechanical calculations have tended to confirm the conclusions reached here regarding the signs of both  $k_\pi^u$  and  $k_\pi^g$ . Furthermore it is important that the negative value of  $k_\pi$  for formaldehyde confirms the results obtained for ethylene, the value being of the same order as those of  $k_\pi^u$  and  $k_\pi^g$  in ethylene.

The value of  $1.21 \times 10^{-11}$  erg/radian<sup>2</sup> obtained here for  $k_\pi^t$  may be compared with the values obtained by Parr and Crawford<sup>13</sup> for this twisting constant. Their treatment assumes that, when the ethylene molecule twists, all the distortion occurs in the  $\pi$ -bond of the C=C bond, i.e. that  $k_H$  is infinite. We have presumed in this paper that the distortion is divided between a distortion of the C=C  $\pi$ -bond orbitals and a distortion of the four C—H bond orbitals. Since Parr and Crawford give only values of the frequency, we have deduced the values of  $k_\pi^t$  from their figures, from the formula in Appendix II, assuming that  $k_H$  is infinity. These values of  $k_\pi$  are given in Table III. Parr and Crawford state that  $Z$ , the screening constant, is probably slightly larger than 3.18.

<sup>13</sup> Galloway and Barker, *ibid.*, 1942, 10, 88.

<sup>14</sup> Ref. 9, p. 326; and footnote 173, on p. 327.

<sup>15</sup> cf. Walsh, *J. Chem. Soc.*, 1948, 404.

It will be seen that the function  $\psi_N$  (Heitler-London-Slater-Pauling (H.L.S.P.) function with added ionic terms) gives a value for  $k_\pi^i$  of about  $1 \times 10^{-11}$  erg/radian<sup>2</sup>.  $\psi_1$  (molecular-orbital function) gives about  $1\frac{1}{2} \times 10^{-11}$  and the simple H.L.S.P. treatment gives about  $\frac{1}{2} \times 10^{-11}$ . The agreement of the values obtained using  $\psi_N$  and  $\psi_1$  with our deduced value of  $k_\pi^i$  is very good indeed and much better than might have been expected. The value obtained using the H.L.S.P. approximation is rather smaller. However, the most important feature is that the order of magnitude of the observed constant is the same as that expected from wave-mechanical calculations.

TABLE III

	<i>Z</i>	$\nu$ cm. <sup>-1</sup>	$k_\pi \times 10^{-11}$ erg/radian <sup>2</sup>
$\psi_N$	2.35	1140	1.315
	3.18	995	1.002
	3.27	960	0.932
	3.91	715	0.517
$\psi_1$	2.35	1180	1.409
	3.18	1140	1.315
	3.27	1120	1.269
	3.91	1020	1.053
H.L.S.P.	1.96	738	0.551
	2.35	742	0.557
	2.74	698	0.493
	3.13	587	0.349
	3.91	374	0.142

Mulliken and Roothan <sup>11</sup> have made a semi-empirical wave-mechanical computation of the twisting frequency of ethylene. They have considered both the possibility that during twisting the distortion affects only the C=C  $\pi$ -bond and also the possibility that the C=C and C—H bond orbitals are simultaneously distorted. They considered various relative resistances to distortion of the C=C and C—H bonds. The values they obtain for the frequencies are in encouraging agreement with the observed value. It is of considerable interest that, if they allow no distortion of the C—H bonds (their case (a)), the value they obtain for the frequency is rather too high, indicating that it is correct to suppose, as we have done, that the distortion during twisting is divided between the C—H and C=C bond orbitals.

The third result is that the bending constant  $k_H$  for the C—H bond in ethylene is  $1.0891 \times 10^{-11}$  erg/radian<sup>2</sup>. This compares with 1.2 to  $1.45 \times 10^{-11}$  in formaldehyde. In formaldehyde the C—H bending constant is bigger. This may, in some way, be due to a drift of electrons towards the oxygen atom and away from the C—H links, although we might have expected this known drift to reduce the C—H bending constant. However, we are still rather ignorant regarding bending constants and perhaps our preconceived ideas are unreliable. Nevertheless, the main result is interesting: the C—H bending constant is of the same order of magnitude.

The fourth result is that  $k_\sigma^u = 1.357 \times 10^{-11}$  and  $k_\sigma^g = 0.602 \times 10^{-11}$  erg/radian<sup>2</sup>. These values are of the same order of magnitude as the bending constants of the C—H bond and therefore of reasonable size. However, we would certainly have expected that  $k_\sigma^g$  would have been greater than  $k_\sigma^u$  from Fig. 1 which indicates that the overlap decreases more during the distortion related to  $k_\sigma^g$  than during that related to  $k_\sigma^u$ . Four possible explanations of this apparent anomaly are that

- (i) the frequencies are wrongly assigned,
- (ii) in this case also, a simple picture is misleading,
- (iii) the simple O.V.F.F., used in this paper, is at fault,
- (iv) the assumption that no change in orbital hybridization occurs is incorrect.

We do not believe that the third possibility is very likely, nor have we any definite evidence that the frequencies are incorrectly assigned. The second explanation could readily be tested by a detailed wave-mechanical study. We have already commented on the fourth possibility.

The fifth result indicates that there is an appreciable repulsion between the non-bonded carbon and hydrogen atoms in ethylene, and between the oxygen and hydrogen atoms in formaldehyde. For ethylene  $\frac{1}{2} d^2V/dr^2 = 0.275 \times 10^5$  dynes/cm. and for formaldehyde  $0.55 \times 10^5$  dynes/cm. We would expect the repulsion to be bigger in formaldehyde than in ethylene for two reasons. In the first place the H...O distance is less than the H...C distance; and secondly, the drift of electrons to the oxygen atom means that this atom must have a larger electron cloud than if the atom carried a smaller negative charge. The charge on the carbon atom in ethylene must be small. Thus the two values of  $A$  are reasonable in relation to one another. As regards the absolute magnitude of  $A$  for ethylene, it is likely that it will be close to the geometric mean of the values of  $\frac{1}{2} d^2V/dr^2$  for He...He repulsion and Ne...Ne repulsion. We have calculated these repulsions from the figures of Buckingham<sup>16</sup> using only the  $a/R^{12}$  repulsion part since the attraction part is small at the distance with which we are concerned, 2.1 Å. At this distance, the geometric mean of the two values for  $\frac{1}{2} d^2V/dr^2$  for He...He and Ne...Ne repulsion is  $0.26 \times 10^5$  dynes/cm. We have made these calculations for ethylene because the linkages are only slightly polar in this molecule. We conclude finally therefore that the two values of  $A$  which it was found necessary to assume in these calculations are wholly reasonable in the light of other evidence regarding van der Waals' repulsion.

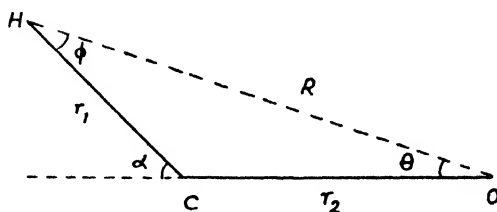
The sixth result shows that the stretching constant  $k_1$  of the C—H bond in formaldehyde is very much less than  $k_1$  in ethylene. The cause of this difference is probably the drift of electrons in formaldehyde towards the oxygen atom and away from the C—H bonds. It is surprising, however, that the smaller value of  $k_1$ , the stretching constant, occurs with the larger value of  $k_H$ , the bending constant. We would like to stress here that the stretching constants obtained when due allowance is made for repulsion between the non-bonded atoms by inclusion of the terms in  $\Delta R$  and  $\Delta R^2$ , as in this paper, cannot be compared with those obtained using potential energy functions which do not allow for such repulsion. We cannot compare the C—H stretching constants given here with many others that have been obtained using other force fields.

Lastly, the stretching constant  $k_2$  of the C=C bond in ethylene is 7.16 and that of the C=O bond in formaldehyde is  $11 \times 10^5$  dynes/cm. Both these are, as would be anticipated, bigger than the constants we have found for single bonds. They are smaller than values quoted elsewhere because the inclusion of necessary repulsion terms results in decreased bond force constants. Or, alternatively, the failure to include repulsion terms explicitly in the potential energy function results in the repulsion contributing to the bond force constants, thus making the deduced values of the bond constants too big. The way in which this happens may be seen by examining the formulae in Appendix I and II.

<sup>16</sup> Buckingham, *Proc. Roy. Soc. A*, 1938, **168**, 264.

## APPENDIX I

## Formaldehyde



## SYMMETRIC PLANAR

$$\begin{aligned} \lambda^2 - \lambda^2 \left\{ f_{11} \left[ \frac{1}{m_H} + \frac{2 \cos^2 \alpha}{m_C} \right] + f_{22} \left[ \frac{1}{m_O} + \frac{1}{m_O} \right] + f_{33} \left[ \frac{1}{m_H} + \frac{2 \sin^2 \alpha}{m_C} \right] \right. \\ \left. + f_{12} \left[ -\frac{4 \cos \alpha}{m_C} \right] + f_{13} \left[ \frac{4 \sin \alpha \cos \alpha}{m_C} \right] + f_{23} \left[ -\frac{4 \sin \alpha}{m_C} \right] \right\} \\ + \lambda \left\{ (f_{11} f_{22} - 2 f_{12}^2) \left[ \frac{1}{m_H m_C} + \frac{1}{m_H m_O} + \frac{2 \cos^2 \alpha}{m_C m_O} \right] + (f_{11} f_{33} - f_{13}^2) \left[ \frac{1}{m_H^2} + \frac{2}{m_H m_C} \right] \right. \\ \left. + (f_{22} f_{33} - 2 f_{23}^2) \left[ \frac{1}{m_H m_C} + \frac{1}{m_H m_O} + \frac{2 \sin^2 \alpha}{m_C m_O} \right] + f_{11} f_{23} - f_{12} f_{13} \left[ -\frac{4 \sin \alpha}{m_H m_C} \right] \right. \\ \left. + (f_{22} f_{13} - 2 f_{12} f_{23}) \left[ \frac{4 \sin \alpha \cos \alpha}{m_C m_C} \right] + (f_{33} f_{12} - f_{13} f_{23}) \left[ -\frac{4 \cos \alpha}{m_H m_C} \right] \right\} \\ - \left\{ (f_{11} f_{22} f_{33} - 2 f_{11} f_{23}^2 - f_{22} f_{13}^2 - 2 f_{33} f_{12}^2 \right. \\ \left. + 4 f_{12} f_{13} f_{23}) \left[ \frac{1}{m_H^2 m_C} + \frac{1}{m_H^2 m_O} + \frac{2}{m_H m_C m_O} \right] \right\} = 0, \end{aligned}$$

where

$$f_{11} = k_1 + 2A \cos^2 \phi + \frac{B}{R} \sin^2 \phi,$$

$$f_{22} = k_2 + 4A \cos^2 \theta + \frac{2B}{R} \sin^2 \theta,$$

$$f_{33} = \frac{k_H}{r_1^2} + 2A \sin^2 \phi - \frac{B}{R} \cdot \frac{r_2}{r_1} \cos \theta \cos \phi,$$

$$f_{12} = 2A \cos \theta \cos \phi - \frac{B}{R} \sin \theta \sin \phi,$$

$$f_{13} = 2A \sin \phi \cos \phi + \frac{B}{R} \cdot \frac{r_2}{r_1} \cos \theta \sin \phi,$$

$$f_{23} = 2A \cos \theta \sin \phi + \frac{B}{R} \sin \theta \cos \phi.$$

## ANTISYMMETRIC PLANAR

$$\begin{aligned} \lambda^2 - \lambda \left\{ f_{11} \left[ \frac{1}{m_H} + \frac{2 \sin^2 \alpha}{m_C} \right] + f_{22} \left[ \frac{1}{m_H} + \frac{2 \cos^2 \alpha}{m_O} \right] \right. \\ \left. + f_{22} \cdot \frac{r_1^2}{r_2^2} \left[ \frac{2}{m_C} + \frac{2}{m_O} \right] + f_{22} \frac{r_1}{r_2} \left[ \frac{4 \cos \alpha}{m_C} \right] \right. \\ \left. + f_{12} \left[ -\frac{4 \sin \alpha \cos \alpha}{m_C} - \frac{r_1}{r_2} \cdot \frac{4 \sin \alpha}{m_O} \right] \right\} \\ + \left\{ (f_{11} f_{22} - f_{12}^2) \left[ \left( \frac{1}{m_H^2} + \frac{2}{m_H m_C} \right) + \frac{r_1^2}{r_2^2} \left( \frac{2}{m_H m_C} + \frac{2}{m_H m_O} \right) + \frac{4 \sin^2 \alpha}{m_C m_O} \right] \right. \\ \left. + \frac{r_1}{r_2} \left( \frac{4 \cos \alpha}{m_H m_C} \right) \right\} = 0, \end{aligned}$$

where

$$f_{22} = \frac{k_H k_\sigma}{2k_H + k_\sigma} \cdot \frac{1}{r_1^2} - \frac{B}{R} \frac{r_2}{r_1} \cos \theta \cos \phi + 2A \sin^2 \phi.$$

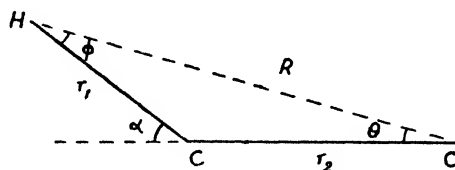
## NON-PLANAR

$$\lambda = \left[ \frac{k_H(k_\sigma + k_\pi)}{2k_H \cos^2 \alpha + k_\sigma + k_\pi r_1^2} - \frac{B}{R} \cdot \frac{r_2}{r_1 \cos \alpha} \right] \left\{ \left( \frac{1}{m_H} + \frac{2}{m_C} \right) + \cos^2 \alpha \cdot \frac{r_1^2}{r_2^2} \left[ \frac{2}{m_C} + \frac{2}{m_O} \right] + \cos \alpha \cdot \frac{r_1}{r_2} \left( \frac{4}{m_C} \right) \right\} = 0.$$

To obtain the secular equations for deuterioformaldehyde, replace  $m_H$  by  $m_D$ .

## APPENDIX II

## Ethylene

 $A_g$ 

$$\begin{aligned} \lambda^3 - \lambda^2 \left\{ f_{11} \left[ \frac{1}{m_H} + \frac{2 \cos^2 \alpha}{m_C} \right] + f_{22} \left[ \frac{2}{m_C} \right] + f_{33} \left[ \frac{2}{m_H} + \frac{2 \sin^2 \alpha}{m_C} \right] \right. \\ \left. + f_{12} \left[ -4 \frac{\cos \alpha}{m_C} \right] + f_{13} \left[ \frac{8 \sin \alpha \cos \alpha}{m_C} \right] + f_{23} \left[ -4 \frac{\sin \alpha}{m_C} \right] \right\} \\ + \lambda \left\{ (f_{11} f_{22} - f_{12}^2) \left[ -\frac{2}{m_H m_C} \right] + (f_{11} f_{33} - 4 f_{13}^2) \left[ \frac{1}{m_H^2} + \frac{2}{m_H m_C} \right] \right. \\ \left. + (f_{22} f_{33} - f_{23}^2) \left[ -\frac{2}{m_H m_C} \right] + (f_{11} f_{23} - 2 f_{12} f_{13}) \left[ -\frac{4 \sin \alpha}{m_H m_C} \right] \right. \\ \left. + (f_{33} f_{12} - 2 f_{13} f_{23}) \left[ -\frac{4 \cos \alpha}{m_H m_C} \right] \right\} \\ - \left\{ (f_{11} f_{22} f_{33} - f_{11} f_{23}^2 - 4 f_{22} f_{13}^2 - f_{33} f_{12}^2 + 4 f_{12} f_{13} f_{23}) \left[ \frac{2}{m_H^2 m_C} \right] \right\} = 0, \end{aligned}$$

where

$$\begin{aligned} f_{11} &= k_1 + \frac{B}{R} \sin^2 \phi + 2A \cos^2 \phi, \\ f_{22} &= k_2 - \frac{4B}{R} \sin^2 \theta + 8A \cos^2 \theta, \\ f_{33} &= \frac{k_H}{r_1^2} - \frac{B}{R} \cdot \frac{r_2}{r_1} \cos \theta \cos \phi + 2A \sin^2 \phi, \\ f_{12} &= -\frac{2B}{R} \sin \theta \sin \phi + 4A \cos \theta \cos \phi, \\ f_{13} &= \frac{B}{2R} \cdot \frac{r_2}{r_1} \sin \phi \cos \theta + A \sin \phi \cos \phi, \\ f_{23} &= \frac{2B}{R} \sin \theta \cos \phi + 4A \sin \phi \cos \theta. \end{aligned}$$

 $B_{3u}$ 

$$\begin{aligned} \lambda^2 - \lambda \left\{ f_{11} \left[ \frac{1}{m_H} + \frac{2 \cos^2 \alpha}{m_C} \right] + f_{33} \left[ \frac{1}{m_H} + \frac{2 \sin^2 \alpha}{m_C} \right] + f_{13} \left[ \frac{8 \sin \alpha \cos \alpha}{m} \right] \right\} \\ + \left\{ (f_{11} f_{33} - 4 f_{13}^2) \left[ \frac{1}{m_H^2} + \frac{2}{m_H m_C} \right] \right\} = 0. \end{aligned}$$

 $B_{2u}$ 

$$\begin{aligned} \lambda^2 - \lambda \left\{ f_{11} \left[ \frac{1}{m_H} + \frac{2 \sin^2 \alpha}{m_C} \right] + f_{33} \left[ \frac{1}{m_H} + \frac{2 \cos^2 \alpha}{m_C} \right] + f_{13} \left[ -\frac{8 \sin \alpha \cos \alpha}{m_C} \right] \right\} \\ + \left\{ (f_{11} f_{33} - 4 f_{13}^2) \left[ \frac{1}{m_H^2} + \frac{2}{m_H m_C} \right] \right\} = 0, \end{aligned}$$

where

$$f_{33} = \frac{1}{r_1^2} \cdot \frac{k_H k_\sigma^u}{2k_H + k_\sigma^u} - \frac{B}{R} \cdot \frac{r_2}{r_1} \cdot \cos \theta \cos \phi + 2A \sin^2 \phi.$$

$B_{1g}$ 

$$\lambda^2 - \lambda \left\{ f_{11} \left[ \frac{1}{m_H} + \frac{2 \sin^2 \alpha}{m_C} \right] + f_{33}^{11} \left[ \left( \frac{1}{m_H} + \frac{2 \cos^2 \alpha}{m_C} \right) + \frac{8}{m_C} \cdot \frac{r_1^2}{r_2^2} + \frac{8 \cos \alpha}{m_C} \cdot \frac{r_1}{r_2} \right] \right. \\ \left. + f_{13} \left[ \left( -\frac{8 \sin \alpha \cos \alpha}{m_C} \right) - \frac{16 \sin \alpha}{m_C} \cdot \frac{r_1}{r_2} \right] \right\} \\ + \left\{ (f_{11} f_{33}^{11} - 4 f_{13}^2) \left[ \left( \frac{1}{m_H} + \frac{2}{m_H m_C} \right) + \frac{8}{m_H m_C} \cdot \frac{r_1^2}{r_2^2} + \frac{8 \cos \alpha}{m_H m_C} \cdot \frac{r_1}{r_2} \right] \right\} = 0,$$

where

$$f_{33}^{11} = \frac{1}{r_1^2} \cdot \frac{k_H k_\pi^2}{2 k_H + k_\pi^2} - \frac{B}{R} \cdot \frac{r_2}{r_1} \cdot \cos \theta \cos \phi + 2 A \sin^2 \phi.$$

 $B_{1u}$ 

$$\lambda = \left[ \frac{k_H (k_\pi^u + k_\sigma^u)}{2 k_H \cos^2 \alpha + k_\pi^u + k_\sigma^u} \cdot \frac{1}{r_1^2} - \frac{B}{R} \cdot \frac{r_2}{r_1 \cos \alpha} \right] \left( \frac{1}{m_H} + \frac{2}{m_C} \right).$$

 $B_{2g}$ 

$$\lambda = \left[ \frac{k_H (k_\pi^g + k_\sigma^g)}{2 k_H \cos^2 \alpha + k_\pi^g + k_\sigma^g} \cdot \frac{1}{r_1^2} - \frac{B}{R} \cdot \frac{r_2}{r_1 \cos \alpha} \right] \left\{ \left( \frac{1}{m_H} + \frac{2}{m_C} \right) \right. \\ \left. + \frac{8 \cos \alpha}{m_C} \cdot \frac{r_1}{r_2} + \frac{8 \cos^2 \alpha}{m_C} \cdot \frac{r_1^2}{r_2^2} \right\}.$$

 $A_u$ 

$$\lambda = \left[ \frac{k_H k_\pi^t}{2 k_H \sin^2 \alpha + k_\pi^t} \cdot \frac{1}{r_1^2} \right] \left( \frac{1}{m_H} \right).$$

To obtain the secular equations for deuterioethylene, replace  $m_H$  by  $m_D$ .

**Conclusion.**—The present treatment of the vibrations of ethylene and formaldehyde has been made without introducing any cross-term constants which lack physical significance. All the terms introduced into the potential energy function can be related to particular distortions that occur when the molecule is vibrating and can be considered in terms of the theory of valency. Perhaps the most interesting result is that the force constant in the term measuring the effect of distorting the  $\pi$ -bond orbitals is negative. This means that when the C=C or C=O bonds are bent so as to distort the  $\pi$ -bond the increase in potential energy resulting from the distortion of the  $\sigma$ -bond is lessened by the decrease in potential energy resulting from the distortion of the  $\pi$ -bond.

We wish to thank Imperial Chemical Industries for providing us with a calculating machine. One of us (P. J. W.) would like to thank the Harmsworth Trust for a Senior Scholarship, and another (D. F. H.) the Department of Scientific and Industrial Research for a grant.

*Inorganic Chemistry Laboratory,  
Oxford.*

## MOLECULAR FORCE FIELDS

### PART IX.—A RELATION BETWEEN BOND INTERACTIONS DURING VIBRATIONS AND ON DISSOCIATION

By J. W. LINNETT AND M. F. HOARE

*Received 6th April, 1949*

The main object of this investigation is to relate the bond-bond cross-term constant  $k_{12}$  in a bonded system of atoms ABC to the change in the bond AB when the bond BC is broken. Theoretical considerations suggest that, if  $k_{12}$  is positive, the bond AB would become shorter and stronger when BC is broken; but if  $k_{12}$  is negative, AB would become longer and weaker. An examination of 10 symmetrical triatomic molecules ABA shows that this relation does exist.

There is a rough correlation between the change in length of the bond AB and the size of  $k_{12}$ . In all these cases, except possibly one ( $\text{SO}_2$ ) a positive cross-term is associated with the presence of electrons unlocalized over the region of the two bonds. This is also borne out by the study of another 12 molecules for which data are available. When only localized electrons are involved,  $k_{12}$  is always negative. The reason for this correlation is discussed.

The simplest potential energy (P.E.) functions, when applied to polyatomic molecules, do not make any allowance for the interaction between bonds. However, there is no doubt that such interactions do occur, i.e. when one bond in a molecule is distorted, the electronic structure of other bonds is affected and their properties changed. Allowance has usually been made for this by adding cross-terms to the P.E. function. That is, instead of writing the P.E. function as a sum of squared terms,

$$V = \frac{1}{2} \sum k_i \Delta r_i^2 + \text{an angular part,} \quad (1)$$

terms like  $k_{12} \Delta r_1 \Delta r_2$  are added and the function becomes

$$V = \frac{1}{2} \sum k_i \Delta r_i^2 + \frac{1}{2} \sum_{ij} k_{ij} \Delta r_i \Delta r_j + \text{an angular part.} \quad (2)$$

A number of suggestions have been made in attempts to clarify the situation with regard to these cross-terms.<sup>1</sup> The main purpose of this paper is to relate cross-terms to what happens when distortion is carried to the limit in the dissociation of the molecule. In the discussion we consider also the relation between the bond-bond cross-term and electronic structure.

Let us first consider how these cross-terms may be supposed to arise, by examining the P.E. function of a linear ABC molecule, limiting ourselves to the case when there are bond length distortions only.

The general P.E. function may be written

$$V = \frac{1}{2} k_1 (\Delta r_{AB})^2 + \frac{1}{2} k_2 (\Delta r_{BC})^2 + k_{12} \Delta r_{AB} \Delta r_{BC} \quad (3)$$

where

$$\Delta r_{AB} = r_{AB} - r_{AB}^e$$

$r_{AB}^e$  being the equilibrium length of the bond AB when  $\Delta r_{BC}$  is zero.

Now let us suppose that when the bond BC is distorted from  $r_{BC}^e$  to  $r_{BC}$ , there is an interaction effect between the electrons in the two bonds which results in the energy being a minimum when  $r_{AB} = r_{AB}^d$ ,  $r_{AB}^d$  being different from  $r_{AB}^e$ . If we then consider the distortions of AB occurring when BC is distorted to  $r_{BC}$ , we would write

$$V_{AB} = \frac{1}{2} k_1 (r_{AB} - r_{AB}^d)^2 \quad (4)$$

In this we suppose that the bond BC is held at  $r_{BC}$ , that  $V_{AB}$  is the potential energy in the bond AB only, and that  $k_1$  has not changed as a result of the distortion. We must likewise suppose that distortion of AB affects BC in the same way that distortion of BC affects AB. So we may write for the distorted molecule:

$$V = \frac{1}{2} k_1 (r_{AB} - r_{AB}^d)^2 + \frac{1}{2} k_2 (r_{BC} - r_{BC}^d)^2 \quad (5)$$

Now when

$$\Delta r_{BC} = 0, \quad r_{AB}^d = r_{AB}^e$$

and when

$$r_{BC} = \infty, \quad r_{AB}^d = r_{AB}^d$$

where  $r_{AB}^d$  is the length that the bond AB has in the diatomic molecule produced when the bond BC is broken. Similar conditions will apply for the effect of  $r_{AB}$  on  $r_{BC}^d$ .

It is reasonable to assume that  $r_{AB}^d$  changes smoothly and regularly from  $r_{AB}^e$  to  $r_{AB}^d$  as  $r_{BC}$  changes from  $r_{BC}^e$  to  $\infty$ . Let us suppose that the

<sup>1</sup> Coulson, Duschesne and Manneback, *Nature*, 1947, 160, 793.



change can be represented by the simplest form of relation, having the correct boundary conditions, namely :

$$\frac{r_{AB}^o - r_{AB}^e}{r_{AB}^d - r_{AB}^e} = \frac{r_{BC} - r_{BC}^e}{r_{BC}^e} = \frac{\Delta r_{BC}}{r_{BC}^e}, \quad (6)$$

or

$$r_{AB}^o = r_{AB}^e + \Delta r_{BC} \frac{r_{AB}^d - r_{AB}^e}{r_{BC}^e},$$

so that

$$(r_{AB} - r_{AB}^o) = \Delta r_{AB} - \Delta r_{BC} \frac{r_{AB}^d - r_{AB}^e}{r_{BC}^e} \quad (7)$$

But in molecular vibration problems we always consider vibrations to be of small amplitude and for these,  $r_{BC}$  is not appreciably different from  $r_{BC}^e$ . So (7) becomes

$$(r_{AB} - r_{AB}^o) = \Delta r_{AB} - \Delta r_{BC} \frac{r_{AB}^d - r_{AB}^e}{r_{BC}^e} \quad (8)$$

$$= \Delta r_{AB} - \Delta r_{BC} K_1,$$

where

$$K_1 = \frac{r_{AB}^d - r_{AB}^e}{r_{BC}^e} \quad (9)$$

Substituting this back into (4), and allowing for a similar effect of AB on BC, we have

$$V = \frac{1}{2} k_1 (\Delta r_{AB} - \Delta r_{BC} K_1)^2 + \frac{1}{2} k_2 (\Delta r_{BC} - \Delta r_{AB} K_2)^2, \\ = \frac{1}{2} (k_1 + k_2 K_1^2) (\Delta r_{AB})^2 + \frac{1}{2} (k_2 + k_1 K_2^2) (\Delta r_{BC})^2 - (k_1 K_1 + k_2 K_2) \Delta r_{AB} \Delta r_{BC} \quad (10)$$

But in most cases  $r_{AB}^d - r_{AB}^e$ , the difference between the equilibrium distances of AB in the diatomic molecule AB and in the triatomic molecule ABC is probably small compared with  $r_{BC}^e$ , so that  $K_1$  and similarly  $K_2$ , will be small. For this reason, terms involving  $K_1^2$  and  $K_2^2$  may be neglected to a first approximation, and (10) becomes

$$V = \frac{1}{2} k_1 \Delta r_{AB}^2 + \frac{1}{2} k_2 \Delta r_{BC}^2 - (k_1 K_1 + k_2 K_2) \Delta r_{AB} \Delta r_{BC} \quad (11)$$

or, for a symmetrical molecule ABA',

$$V = \frac{1}{2} k_1 (\Delta r_{AB}^2 + \Delta r_{A'B}^2) - 2k_1 K_1 \Delta r_{AB} \Delta r_{A'B} \quad (12)$$

Thus this picture would give  $k_{12}$  in eqn. (3) equal to  $-2k_1 K_1$ . Therefore, since  $k_1$  must be positive, the sign of  $k_{12}$  must have the opposite sign to that of  $K_1$ . From (9) we may say that when  $r_{AB}^d$  is greater than  $r_{AB}^e$  the cross-term constant will be negative; while when  $r_{AB}^d$  is greater than  $r_{AB}^e$  the cross-term constant will be positive.

That this is to be expected qualitatively, is easily demonstrated. When  $k_{12}$  is negative in the symmetrical molecule ABA' the P.E. increases less if  $\Delta r_{AB}$  and  $\Delta r_{A'B}$  are the same sign, (symmetric motion) than if  $\Delta r_{AB}$  and  $\Delta r_{A'B}$  are the opposite sign (anti-symmetric motion). This means that if the bond AB is stretched, the bond A'B may be expected to lengthen. If we extend this to the limit of breaking the bond AB completely, we may expect the A'B bond that is left to be longer than the AB of the triatomic molecule. This is the conclusion of the algebraic treatment. However, the latter has the advantage that it may help us not only to estimate the sign of the cross-term from a consideration of the diatomic and triatomic molecules, but also very roughly the magnitude.

In deducing the above formula, it was assumed that the  $k_1$  of AB did not change with the distortion of BC. This is adequate to the approximation required (second power terms only in  $\Delta r_{AB}$  and  $\Delta r_{BC}$ ). If the dependence of  $k_1$  on  $r_{BC} - r_{BC}^e$  were included, only third power terms would be introduced, and these contribute negligibly for small displacements.

So, in order to test the present idea we have to compare the change in bond length in passing from the diatomic to the triatomic molecule with the cross-term constant required in the triatomic molecule. Unfortunately the required bond lengths are not always known. In this event we may fall back on the Clark or Badger relationships.<sup>2</sup> The Clark relationship suggests that  $r_{AB}$  is inversely proportional to the sixth power of the force constant. As the bond energy changes regularly with the change in bond length and force constant, in certain cases it may be possible to compare change in bond energy with the cross-term constant.

Summarizing, we may say:

- (a) If  $r_{AB}^d > r_{AB}^e$  then  $k_{12}$  is expected to be negative.
- (b) If the force constant in the diatomic molecule is greater than the force constant in the triatomic molecule,  $k_{12}$  is expected to be positive.
- (c) If the bond energy in the diatomic molecule is greater than the bond energy in the triatomic molecule,  $k_{12}$  is expected to be positive.

## Results

The results for six linear symmetrical molecules are given in the first part of Table I, which lists the bond lengths, force constants, and bond energies of the triatomic and corresponding diatomic molecules. For such triatomic molecules, the bond force constant  $k_1$  and the cross-term constant  $k_{12}$  can both be determined from the frequencies of the two valency vibrations. The cross-term constants are listed in the last column.

The eighth column gives the difference between the bond lengths in the triatomic molecule and that in the diatomic molecule (see (a) above). This should be the same sign as  $k_{12}$ , and it will be seen that, in all cases where it is known, this is so. The corresponding force constant differences  $k(\text{di}) - k(\text{tri})$  and bond energy differences  $b(\text{di}) - b(\text{tri})$  (see (b) and (c) above), are shown in the ninth and tenth columns. These, likewise, should be the same sign as that of  $k_{12}$ . Again, in all cases it will be seen that the signs are the same.

The frequencies of five symmetrical non-linear triatomic molecules are also known with sufficient accuracy to enable force constant calculations to be made. Calculations for  $\text{H}_2\text{O}$  and  $\text{D}_2\text{O}$  were made by Heath and Linnett,<sup>3</sup> giving  $k_1$  and  $k_{12}$ . Those for  $\text{H}_2\text{S}$  and  $\text{H}_2\text{Se}$  have been made by Heath,<sup>4</sup> the bond-angle cross-term constant being arbitrarily put equal to zero. Similar calculations were made for  $\text{SO}_2$  and  $\text{NO}_2$ , the bond-angle cross-term constant again being put equal to zero, so that  $k_1$  and  $k_{12}$  were obtained. The values of  $k_{12}$  for these molecules are also given in the first part of Table I, and the bond length, force constant, and bond energy differences are given in columns 8, 9 and 10, as before. Again it will be seen that the signs of the figures in these three columns are the same as the sign of the corresponding  $k_{12}$  for all five molecules.

It must be realized that the results for the bent ABA molecules (except  $\text{H}_2\text{O}$ ) are less reliable than those for the linear ABA molecules, because we have had to fix an arbitrary value of  $\alpha$  for the bond-angle cross-term constant in order to solve the equations involved. However, it was found for  $\text{NO}_2$  that the sign of the bond-bond cross-term  $k_{12}$  was not altered by putting the bond-angle cross-term equal to  $+\frac{1}{2} \times 10^6$  or  $-\frac{1}{2} \times 10^6$  dyne/cm.

The results for some other linear molecules are given in the second part of Table I. With  $\text{N}_2\text{O}$  we can say that  $k_{12}$  is positive because any value less than 0.326 would give imaginary values for the main force constants. With the cyanogen halides we cannot fix the sign of the cross-term with certainty. The four valency vibrations of  $\text{HCN}$  and  $\text{DCN}$  lead to a negative value for  $k_{12}$ . In  $\text{C}_2\text{H}_2$  and  $\text{C}_2\text{D}_2$  the  $\text{C}\equiv\text{C}/\text{CH}$  and  $\text{C}\equiv\text{C}/\text{CD}$  cross-term constants were found to be negative. In  $\text{C}_2\text{N}_2$  a complete solution is possible and the  $\text{C}\equiv\text{N}/\text{C}-\text{C}$  cross-term is found to be positive. With  $\text{C}_3\text{O}_2$  also, both bond-bond cross-terms are positive. We have treated  $\text{HC}\equiv\text{C}-\text{C}\equiv\text{CH}$  by making the reasonable assumption that the  $\text{C}\equiv\text{C}/\text{CH}$  cross-term constant is the same as in acetylene. The four available frequencies then allow us to calculate the  $\text{C}\equiv\text{C}/\text{C}-\text{C}$  cross-term constant, which is found to be positive. Meister and Cleveland<sup>5</sup> have treated di-iodoacetylene and have calculated that the bond-bond cross-term is positive.

<sup>2</sup> Clark, *Phil. Mag.* 1934, 18, 459.

<sup>3</sup> Heath and Linnett, *Trans. Faraday Soc.*, 1948, 44, 556.

<sup>4</sup> Heath, *D.Phil. Thesis* (Oxford University 1948).

<sup>5</sup> Meister and Cleveland, *J. Chem. Physics*, 1940, 17, 212.

TABLE I.—SHOWING BOND LENGTHS IN Å, BOND ENERGIES IN KCAL./MOLE, FOR VARIOUS

† Molecule	$r_{AB}^e$	$r_{AB}^d$	$k_1$ Tri	‡ $k_1$ Di	$b$ Tri
CO <sub>2</sub> <sup>a</sup>	1.163 <sup>a</sup>	1.13 <sup>a</sup>	15.52	18.52	190.6 <sup>m</sup>
CS <sub>2</sub> <sup>a</sup>	1.55 <sup>f</sup>	1.53 <sup>g</sup>	7.53	8.32	138.3 <sup>m</sup>
N <sub>2</sub> <sup>-b</sup>	(1.15) <sup>f</sup>	1.09 <sup>g</sup>	13.46	22.40	—
HgCl <sub>2</sub> <sup>c</sup>	2.20 <sup>f</sup>	—	2.66	1.47	52.3 <sup>n</sup>
HgBr <sub>2</sub> <sup>c</sup>	2.40 <sup>f</sup>	—	2.37	1.14	43.9 <sup>n</sup>
HgI <sub>2</sub> <sup>c</sup>	2.55 <sup>f</sup>	—	1.81	0.69	34.5 <sup>n</sup>
SO <sub>2</sub> <sup>a</sup>	1.46 <sup>h</sup>	1.49 <sup>a</sup>	9.87	7.77	126.0 <sup>m</sup>
NO <sub>2</sub> <sup>a</sup>	1.21 <sup>h</sup>	1.15 <sup>a</sup>	10.80	15.50	110.0 <sup>m</sup>
H <sub>2</sub> O <sup>a</sup>	0.958 <sup>k</sup>	0.971 <sup>a</sup>	8.42 <sup>q</sup>	7.76	109.4 <sup>m</sup>
H <sub>2</sub> S <sup>a</sup>	1.35 <sup>k</sup>	1.334 <sup>a</sup>	4.03 <sup>q</sup>	—	86.5 <sup>m</sup>
H <sub>2</sub> Se <sup>a</sup>	1.6 <sup>p</sup>	—	3.15 <sup>q</sup>	—	—
N <sub>2</sub> O <sup>a</sup>	NN 1.12 <sup>f</sup> NO 1.19 <sup>f</sup>	1.09 <sup>g</sup> 1.14 <sup>f</sup>	14.68 < $k$ < 24.88 13.76 < $k$ < 23.32	22.40 15.50	*263.4 <sup>m</sup>
ClCN <sup>d</sup>	CCl 1.67 <sup>k</sup> CN 1.13 <sup>k</sup>	—	—	—	—
BrCN <sup>d</sup>	CBr 1.79 <sup>k</sup> CN 1.13 <sup>k</sup>	—	—	—	—
ICN <sup>d</sup>	—	—	—	—	—
HCN <sup>a</sup>	CH 1.06 <sup>k</sup> CN 1.15 <sup>k</sup>	—	5.51 18.74	4.09 14.74	—
C <sub>2</sub> H <sub>2</sub> <sup>a</sup>	CH 1.057 <sup>k</sup> CC 1.204 <sup>k</sup>	—	5.92 15.74	—	—
C <sub>2</sub> D <sub>2</sub> <sup>a</sup>	CD — CC —	—	5.99 15.85	—	—
C <sub>2</sub> N <sub>2</sub> <sup>a</sup>	CN 1.2 <sup>g</sup> CC 1.5 <sup>g</sup>	—	6.38 17.58	—	—
C <sub>2</sub> I <sub>2</sub> <sup>a</sup>	CI — CC —	—	3.26 <sup>e</sup> (15.80)	—	—
C <sub>3</sub> O <sub>2</sub> <sup>a</sup>	CO 1.20 <sup>k</sup> CC' 1.29 <sup>k</sup>	—	12.75 15.06	—	—
C <sub>4</sub> H <sub>2</sub> <sup>a</sup>	CH — CC' 1.19 <sup>k</sup> C'C' 1.36 <sup>k</sup>	—	5.58 18.02 3.15	—	—

<sup>a</sup> Herzberg, *Infra Red and Raman Spectra of Polyatomic Molecules* (Van Nostrand Co.).

<sup>b</sup> Sutherland and Penney, *Proc. Roy. Soc. A*, 1936, **156**, 678.

<sup>c</sup> Wehrli, *Helv. phys. Acta.*, 1938, **11**, 339.

<sup>d</sup> West and Farnsworth, *J. Chem. Physics*, 1933, **1**, 402.

<sup>e</sup> Meister and Cleveland, *J. Chem. Physics*, 1949, **17**, 212.

<sup>f</sup> Wells, *Structural Inorganic Chemistry* (O.U.P.).

<sup>g</sup> Spöner, *Molckulspektren*.

<sup>h</sup> Yost and Russell, *Systematic Inorganic Chemistry of the 5th and 6th Group Non-metallic elements* (O.U.P.).

<sup>k</sup> Wheland, *Theory of Resonance*.

BOND FORCE CONSTANTS AND BOND-BOND CROSS-TERMS IN DYNE/CM.  $\times 10^5$ , MOLECULES

$b_{Di}$	$r_{AB}^e - r_{AB}^d$	$k_1Di - k_1Tri$	$bDi - bTii$	$k_{12}$
256.1 <sup>m</sup>	+0.03	+3.00	+65.5	+1.63
166 <sup>m</sup>	+0.02	+0.79	+27.7	+0.623
225.1 <sup>m</sup>	(0.06)	+8.94	—	+1.568
24 <sup>n</sup>	—	-1.19	-28.3	-0.058
16.4 <sup>n</sup>	—	-1.23	-27.5	-0.0905
12.0 <sup>n</sup>	—	-1.11	-22.5	-0.0912
119.5 <sup>m</sup>	-0.03	-2.10	-6.5	-0.117
150 <sup>m</sup>	+0.06	+4.70	+40	+1.42
101 <sup>m</sup>	-0.013	-0.66	-8.4	-0.2008 <sup>q</sup>
<88 <sup>m</sup>	-0.016	—	—	-0.2188 <sup>q</sup>
—	—	—	—	-0.249 <sup>q</sup>
225.1 <sup>m</sup> 150 <sup>m</sup>	—	—	Positive	+0.326 $\leq k_{12} \leq$ +19.45
—	—	—	—	-3.39 $\leq k_{12} \leq$ +28.8
—	—	—	—	-4.29 $\leq k_{12} \leq$ +36.14
—	—	—	—	-4.45 $\leq k_{12} \leq$ +38.34
—	—	Negative	—	-0.72
—	—	—	—	-0.088
—	—	—	—	-0.067
—	—	—	—	+1.14
—	—	—	—	+0.85*
—	—	—	—	OC—CC + 1.257 CC—CC + 2.563
—	—	—	—	HC—CC (-0.088) CC—C'C' + 0.77

<sup>m</sup> Gaydon, *Dissociation Energies*.<sup>n</sup> Skinner, *Trans. Faraday Soc.*, 1940, **43**, 1.<sup>p</sup> Cameron, Sears and Nielsen, *J. Chem. Physics*, 1939, **7**, 994.<sup>q</sup> Heath, *D.Phil. Thesis* (Oxford University, 1948).† Figures in this column refer to the sources of the vibration frequencies used in the calculation of  $k_1$ .‡ Vibration frequencies for diatomic molecules were all taken from Herzberg, *Infra Red and Raman Spectra of Diatomic Molecules*. These were not corrected for anharmonicity.

\* Atomic Heat of Formation.

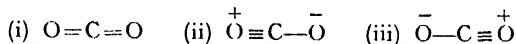
## Discussion

We propose first to consider the results for the ABA molecules since a more complete set of data is available for these than for the molecules in the second part of Table I.

The general conclusion is that with all of these symmetrical triatomic molecules, the sign of  $k_{12}$  is consistent with what happens when distortion is carried to the limit in the dissociation of the molecule. That is, when one bond in ABA is broken, the remaining bond is always a longer, weaker bond if  $k_{12}$  is positive (4 examples), but the remaining bond is always a shorter stronger bond if  $k_{12}$  is negative (6 examples). This is in agreement with the conclusions of our original discussion, which were summarized in (a), (b), and (c). These results therefore confirm the main thesis propounded at the beginning of the paper.

The case of  $\text{CO}_2$  requires further discussion. As Herzberg<sup>6</sup> and Gaydon<sup>7</sup> have pointed out, there are two possibilities for the dissociation of  $\text{CO}_2$ . Either it dissociates into CO in its ground state  $^1\Sigma$  and an oxygen atom in its excited state  $^1D$ , as suggested by Herzberg; or it dissociates into an oxygen atom in its ground state  $^3P$  and CO in an excited state  $^3\Pi$ , as suggested by Schmid.<sup>8</sup> The figures in Table I are those corresponding to the former possibility, for the figures for the diatomic molecule are those relating to carbon monoxide in its ground state. If the second possibility were the true one, as is advocated by Gaydon, the CO bond in  $\text{CO}_2$  would be stronger and shorter than the CO bond in the diatomic molecule left by the breaking of the other bond in the triatomic molecule, and  $k_{12}$  would be expected to be negative. The fact that  $k_{12}$  is undoubtedly positive in  $\text{CO}_2$ , together with the fact that in all other cases the sign of  $k_{12}$  is consistent with what occurs on dissociation, leads us to believe that, when one oxygen atom is removed from  $\text{CO}_2$  by an electronically adiabatic process, the CO molecule remaining is probably one having a smaller interatomic distance than the CO distance in  $\text{CO}_2$ . That is, we think that the present evidence supports the view that when  $\text{CO}_2$  in its ground state dissociates thermally, it produces a CO molecule in the ground state, and an oxygen atom in an excited singlet state.

Adel and Dennison<sup>9</sup> suggested that the positive sign of the cross-term in  $\text{CO}_2$  was due to repulsion between the oxygen atoms, but Thompson and Linnett<sup>10</sup> pointed out that resonance theory provided an explanation of the sign. That theory supposes that the electronic structure of  $\text{CO}_2$  can be represented as a combination of the three canonical structures:



This will lead us to expect a positive cross-term, for, if the left-hand CO bond is lengthened, the structure (iii) will be favoured relative to (ii) and the right-hand bond will tend to shorten. Moreover, if we now imagine this process to be continued further and further, we may suppose that (iii) eventually becomes of predominant importance. If this structure is then finally broken, the two electrons of the left-hand bond would have to pass as a pair into the carbon atom for the products to be electrically neutral, and all three lone pairs of the oxygen atom would be left intact. Though this resonance theory picture of the dissociation of  $\text{CO}_2$  may be over-simplified, it suggests that  $\text{CO}_2$  should dissociate into a normal CO molecule and an excited O atom.\* Before any definite conclusion

<sup>6</sup> Herzberg, *Chem. Rev.*, 1937, **20**, 145.

<sup>7</sup> Gaydon, *Spectroscopy and Combustion Theory* (1948), p. 188.

<sup>8</sup> Schmid and Gerö, *Z. physik. Chem. B*, 1937, **36**, 105.

<sup>9</sup> Adel and Dennison, *Physic. Rev.*, 1933, **44**, 99.

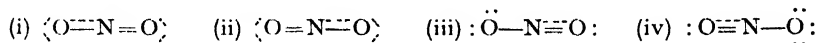
<sup>10</sup> Thompson and Linnett, *J. Chem. Soc.*, 1937, **2**, 1384.

\* In writing  $\text{X}-\text{Y}$ ,  $\text{X}=\text{Y}$  or  $\text{X}\equiv\text{Y}$  in these formulae we mean to signify only that there are two, four or six electrons in the bond and not that these are necessarily equally shared between the two atoms.

can be made, it is necessary that we should know with certainty the nature of the dissociation products of  $\text{CO}_2$ .

In the ion  $\text{N}_3^-$ , the cross-term is also positive as would be anticipated, because  $\text{N}_3^-$  is isoelectronic with  $\text{CO}_2$ . We would likewise expect  $\text{CS}_2$  to resemble  $\text{CO}_2$  and here also the cross-term is positive.

In  $\text{NO}_2$ ,  $k_{12}$  is positive. A similar resonance theory explanation can be given for this case also. The  $\text{NO}_2$  molecule may be supposed to be structurally a resonance combination of



If the left-hand bond is stretched, we may suppose that (i) increases in importance relative to (ii), and (iii) relative to (iv). As the stretching is continued, (iii) assumes the greatest importance and finally this splits into an oxygen atom and an NO molecule having the electronic structure  $\text{:N}\equiv\ddot{\text{O}}\text{:}$  which is that assigned to the ground state of NO by Pauling. This picture implies that the oxygen atom breaks away in the excited  $^1D$  state. However, it should be treated with the same reserve as the resonance picture of the dissociation of  $\text{CO}_2$ .

An alternative molecular-orbital way of describing the dissociation of these triatomic molecules with positive cross-terms may be expressed in the following manner. In all these molecules there are electrons which are non-localized. As one bond is lengthened, the P.E. of an electron in a space between the atoms forming this bond increases, and these un-localized electrons move out of the region of increasing P.E. towards the region of the other bond where the P.E. is not increasing. So that the electron cloud in that bond increases at the expense of the other. If this can be accommodated in a bonding orbital, and judging from the results this seems to be possible in all the cases considered here, the electron cloud will contribute further to the binding of that bond. Consequently the breaking of the one bond leaves the other stronger and shorter. This explanation is, of course, equivalent to that from the resonance theory.

The ABA molecules having a negative cross-term may be divided into three groups.  $\text{H}_2\text{O}$  and its analogues  $\text{H}_2\text{S}$  and  $\text{H}_2\text{Se}$ ,  $\text{HgCl}_2$  and its analogues  $\text{HgBr}_2$  and  $\text{HgI}_2$ , and  $\text{SO}_2$ .

We may note that the first six molecules are all supposed to possess localized binding electrons. In the dissociation of the water molecule into H and OH, for example, the situation is quite different from that obtaining when non-localized electrons are present in the molecule. When one H atom is broken off, the electron pair bond is split and one electron departs with the H atom and the other is left as a lone electron on the O atom. In  $\text{H}_2\text{O}$  there was a repulsion between the pair of electrons in one OH bond and the pair in the other. In the OH diatomic molecule left on dissociation, this repulsion is replaced by one between the lone electron on the O atom and the pair that remain in the OH bond that is left on dissociation. From the result that the OH bond is longer and weaker in the diatomic molecule than in  $\text{H}_2\text{O}$  (and that  $k_{12}$  is negative) it appears that the repulsion of the lone electron on the binding electrons of the OH bond in OH is greater than that of the shared pair in  $\text{H}_2\text{O}$ . An alternative way of expressing this is to say that the lone electron in OH has a larger screening effect than the shared pair in  $\text{H}_2\text{O}$ ; or that the effective electronegativity of the atom is greater in  $\text{H}_2\text{O}$  than in the OH radical. It is not unreasonable that this should be so because the orbital occupied by the lone electron on the O atom in OH will have its maximum value much nearer to the O atom than does the bonding orbital in  $\text{H}_2\text{O}$ , where the maximum is near the centre of the bond and well removed from the O atom.

This argument which has been applied here to  $\text{H}_2\text{O}$  is obviously a general one for molecules which contain only localized bonding electrons. So we would expect that the cross-term constant will always be negative when

non-localized bonding electrons are involved. This is a simple general rule which it is interesting to test. Of the ABA molecules,  $\text{H}_2\text{S}$  and  $\text{H}_2\text{Se}$  are like  $\text{H}_2\text{O}$  and have negative cross-terms as expected. The mercuric halides contain only localized bonding electrons and  $k_{12}$  is negative in agreement with the rule.\*  $\text{SO}_2$  seems to be anomalous, for it is supposed to contain non-localized electrons but the cross-term is negative. This will be considered in more detail later. So, of the eleven ABA molecules studied, ten obey the rule and one does not.

The molecules listed in the second part of Table I will now be considered. The structure of  $\text{N}_2\text{O}$  is always supposed to be a resonating combination of two basic canonical structures, i.e. it contains non-localized electrons. In agreement with the rule,  $k_{12}$  is positive. The three cyanogen halides contain non-localized bonding electrons and the cross-term would be expected to be positive. One cannot be certain of the sign of the cross-term, but Coulson, Duchesne and Manneback<sup>11</sup> have supposed it to be positive in  $\text{CNCl}$  in agreement with the above rule. In  $\text{C}_2\text{H}_2$ ,  $\text{C}_2\text{D}_2$  and  $\text{HCN}$ , the bonding electrons are localized and  $k_{12}$  is found to be negative as expected.  $\text{C}_2\text{N}_2$  is often represented as a resonance between three canonical structures, which implies the presence of non-localized bonding electrons. As would be expected from this,  $k_{12}$  is found to be positive. For  $\text{C}_3\text{O}_2$ , resonating canonical structures are also written, and the molecule is presumed to contain non-localized bonding electrons. Both the  $\text{CO/CC}$  and  $\text{CC/CC}$  cross-terms are found to be positive as would be expected from the rule. Non-localized bonding electrons assumed in the structure of  $\text{C}_2\text{I}_2$  are in agreement with the positive sign of the cross-term. Lastly, di-acetylene is isoelectronic with  $\text{C}_2\text{N}_2$ , and the central system of four carbon atoms is likely to resemble the atomic system of  $\text{NCCN}$ . So we may presume that as with  $\text{NCCN}$ , non-localized bonding electrons are present. This is confirmed by the positive value of the  $\text{CC/CC}$  cross-term constant.

Coulson and Longuet-Higgins<sup>12</sup> have made wave-mechanical calculations of cross-terms in hydrocarbons containing conjugated systems of single and double  $\text{C—C}$  bonds, and conclude that "the interactions between the unsaturated bonds arise primarily from the mobile electrons." It is noteworthy that in butadiene which is a system most like those we have studied, the cross-term constant is  $+2.1 \times 10^5$ . The considerations we have outlined above likewise suggest that this cross-term should be positive in sign.

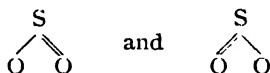
\* The great weakening of the  $\text{Hg-Hal}$  bond in the diatomic molecule compared with that in the triatomic, may require special treatment. When one halogen atom  $\text{X}$  is removed from  $\text{HgX}_2$ ,  $\text{HgX}$  is left in a doublet state. When the second halogen atom is removed from  $\text{HgX}$ , the  $\text{Hg}$  atom is left in a singlet state with no unpaired electrons. In  $\text{HgX}_2$  the mercury atom is usually regarded as being in the divalent state, i.e. the electronic structure is to be regarded as being constructed from a mercury atom with two unpaired electrons, in a pair of  $sp$  hybridized orbitals ( $6s6p$ ). So there is a transition of the state of the mercury atom from this to the singlet state ( $6s^2$ ) on passing from  $\text{HgX}_2$  through  $\text{HgX}$  to  $\text{Hg}$ . It is not unreasonable to suppose that the change in the state of the  $\text{Hg}$  atom occurs at the first stage rather than at the second. In that case  $\text{HgCl}$  would be regarded as a  $\text{Hg}$  atom with two  $6s$  electrons forming a single electron link with the chlorine atom. The alternative is to imagine  $\text{HgCl}$  to be constructed from  $\text{Hg}$  with two unpaired electrons in  $6s$  and  $6p$  orbits forming a pair bond with the unpaired electron of the chlorine atom. Either of the two alternative pictures is, of course, only an attempt to obtain an approximation to the true electronic structure of the molecule, but it may be that the formulation which involves a single electron bond provides a closer approximation to the true structure of  $\text{HgX}$ . It gives a clear explanation of the weakness of the  $\text{HgX}$  bond in the diatomic molecule.

<sup>11</sup> Coulson, Duchesne and Manneback, *Contribution a l'Etude de la structure Moleculaire* (Liège, 1948).

<sup>12</sup> Coulson and Longuet-Higgins, *Proc. Roy. Soc. A*, 1948, **193**, 456.

The general conclusion is therefore that of the 21 cross-terms, 20 obey the rule. The only one that fails is that in  $\text{SO}_2$ . The sign of  $k_{12}$  in  $\text{SO}_2$  is not certain, for with a value for the bond-angle cross-term slightly different from zero,  $k_{12}$  would be calculated to be positive. However, the comparison of the bond in  $\text{SO}_2$  and SO confirms the negative sign, so that it seems likely that  $k_{12}$  is really negative.

Pauling<sup>13</sup> has supposed  $\text{SO}_2$  to be a resonance hybrid of



This means that it contains non-localized electrons. We would therefore expect  $k_{12}$  to be positive instead of negative. When  $\text{SO}_2$  dissociates into SO and O, it is likely to produce both the atom and the molecule in their ground states rather than both in excited states. The ground states are  $\text{SO } ^3\Sigma$  and  $\text{O } ^3P$ . So we see that, in spite of the non-localized electrons,  $\text{SO}_2$  in some ways appears to behave in a similar manner to those molecules with localized electrons, where, on dissociation, a bonding pair is split, leaving one unpaired electron on the departing atom and one on the remaining molecule. In all cases of non-localized electrons so far considered, some non-localized pairs remain as pairs, and move as pairs into the bonds that remain after dissociation.

A possible alternative explanation may be that  $\text{SO}_2$  should be written as  $\text{O}=\text{S}=\text{O}$ , as suggested by Sutton,<sup>14</sup> in which the sulphur has an outer shell of 10 electrons—four localized shared pairs and one lone pair. This might be expected to dissociate so that two electron pairs become unpaired and SO and O are both produced in the triplet ground states.

Consequently we may say that, though  $\text{SO}_2$  may be an exception to the general rule, there do seem to be circumstances which provide some explanation of its abnormality—in particular, the probability of dissociation to an atom and a diatomic molecule, each containing unpaired electrons.

In the introduction it was suggested that the change of bond length on passing from ABA to AB, would enable us to calculate the value of the cross-term (see eqn. (3), (9) and (12)) which lead to

$$k_{12} = -2k_1 \cdot \frac{r_{AB}^e - r_{AB}^d}{r_{AB}^e} \quad (13)$$

This may be tested for  $\text{CO}_2$ ,  $\text{CS}_2$  and  $\text{H}_2\text{O}$ . For the other molecules the values of the constants are not sufficiently reliable or the appropriate bond lengths are not known. The figures used are those given in Table I. Results are given below.

	Calc. (dyne/cm.)	Obs. (dyne/cm.)
$\text{CO}_2$	$0.80 \times 10^5$	$1.33 \times 10^5$
$\text{CS}_2$	$0.19 \times 10^5$	$0.62 \times 10^5$
$\text{H}_2\text{O}$	$-0.23 \times 10^5$	$-0.20 \times 10^5$

Considering the nature of the calculation, the agreement between the calculated and observed values is surprisingly good. All the calculated values are of the right order of magnitude, and we may hope therefore that these may provide a means of estimating roughly the value of bond-bond cross-terms in molecules where it is not possible to calculate them.

<sup>13</sup> Pauling, *Nature of the Chemical Bond*, p. 247.

<sup>14</sup> Sutton, *Ann. Reports*, 1940, 37, 76.



In Fig. 1 we have plotted the value of  $(k_{12}/k_1)$  against  $(r_{AB}^e - r_{AB}^d)/r_{AB}^e$  for those ABA molecules for which figures are available. From eqn. (13) the points would be expected to lie on a straight line of slope 2, passing through the origin. It will be seen that they do in fact lie near a straight line, but the slope is 3. Therefore we may say that an empirical relationship,

$$k_{12} = 2\alpha k_1 \frac{r_{AB}^e - r_{AB}^d}{r_{AB}^e} \quad (14)$$

where

$$\alpha = 1.5,$$

would enable  $k_{12}$  to be calculated more accurately from the bond lengths than by (13).

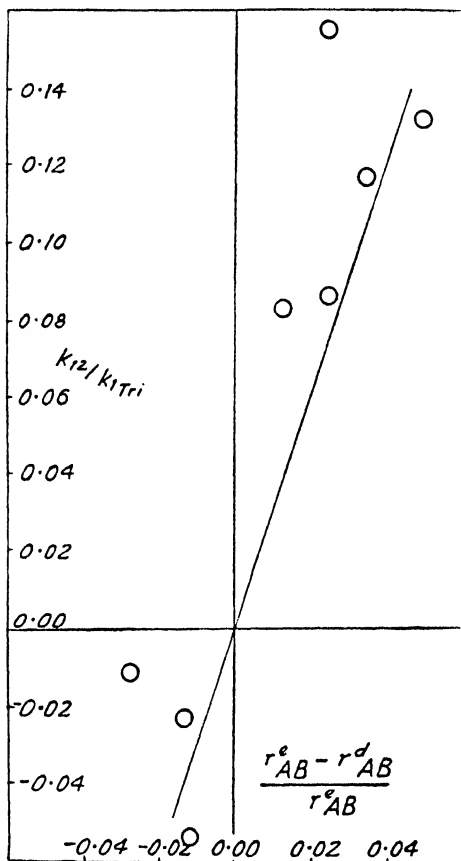


FIG. 1.—Graph showing values of  $(r_{AB}^e - r_{AB}^d)/r_{AB}^e$  plotted against  $k_{12}/k_1$  tri. (In drawing the line through the points, additional weight has been given to those of greater reliability.)

There is another interesting and surprising rule regarding  $k_{12}$ . This is, that the bond-bond cross-term constant  $k_{12}$  is always negative when the central atom has a higher atomic number than the mean of the atomic numbers of the outer atoms. Otherwise  $k_{12}$  is positive. This rule holds without exception for all the molecules studied. We believe that as more examples become available, this rule should be considered further to see whether it still continues to hold. It is very interesting that it should be obeyed by all the molecules studied in this paper, particularly as there is no obvious correlation between this and the rule relating the

sign of the cross-term to the presence or absence of non-localized bonding electrons.

In the above treatment we have ignored repulsion between non-bonded atoms which would obviously introduce cross-terms into the P.E. function. In the linear molecules we have considered, repulsion is not likely to be important because there is an atom in the line between the non-bonded atoms. In  $\text{H}_2\text{O}$ ,  $\text{H}_2\text{S}$  and  $\text{H}_2\text{Se}$ , repulsion between the hydrogen atoms is probably unimportant (cf. Heath and Linnett), but of course in other molecules such as  $\text{Cl}_2\text{O}$  or  $\text{F}_2\text{O}$ , repulsion would probably be important in contributing to the cross-terms. So in the present series of molecules we have restricted ourselves almost entirely to those in which only electronic interactions between bonds are important.

Our two general conclusions are, therefore :

(i) If, when one bond in a triatomic molecule is broken, the other is left weaker and longer,  $k_{12}$  is found to be negative ; on the other hand, if the bond left is stronger and shorter,  $k_{12}$  is found to be positive. This holds without exception, and there is a rough correlation between change in length of the bond, and the size of the cross-term.

(ii) If the two bonds involved in the cross-term contain only localized electrons, the cross-term is negative ; but if electrons are present which are unlocalized over the region of the two bonds, the cross-term constant is positive. This holds for all molecules studied except possibly for  $\text{SO}_2$ , i.e. certainly in 20 cases out of 21. With  $\text{SO}_2$  there seem to be additional factors to be taken into account. This has been discussed.

We wish to thank Imperial Chemical Industries and the Hope Department for making calculating machines available.

*Inorganic Chemistry Laboratory,  
Oxford.*

---

## THE CONDUCTIVITIES OF DILUTE AQUEOUS SOLUTIONS OF POTASSIUM FERROCYANIDE AND CALCIUM FERROCYANIDE

By J. C. JAMES

*Received 14th April, 1949*

The conductivities of dilute aqueous solutions of potassium ferrocyanide and calcium ferrocyanide have been measured at  $25^\circ\text{C}$ . The results indicate that considerable ion association occurs in potassium ferrocyanide solutions and a value for  $A_0$ , the conductivity at infinite dilution, has been derived from an extrapolation method based on this assumption. The behaviour of calcium ferrocyanide in dilute solution is that of a comparatively weak electrolyte, and the values  $K_1 = 3.7 \times 10^{-2}$ ,  $K_2 = 1.69 \times 10^{-4}$ , have been derived for the first and second dissociation constants.

The manner in which the conductivities very dilute solutions of multivalent electrolytes approach the limiting Onsager slope is of considerable theoretical interest, and accurate data for salts of this type provide a stringent test for the various methods which have been proposed for extrapolation to the equivalent conductivity at infinite dilution  $A_0$ . Also, Bjerrum's equation<sup>1</sup> predicts that extensive ion-pair formation

<sup>1</sup> Bjerrum, *Kgl. Danske Vid. Selsk.*, 1926, 7, No. 9.

should occur in such solutions and it is of interest to estimate the extent of such association.

Potassium ferrocyanide is one of the few 1-4 valency type electrolytes suitable for study, and accurate measurements on solutions of this salt have been made by Jones and Jelen.<sup>2</sup> No measurements were made at concentrations below 0.001 N, however, and in consequence a lengthy extrapolation to  $\Lambda_0$  was required. The results of this work were disappointing, as the authors could only conclude that the value of  $\Lambda_0$  was between 185 and 196. Swift<sup>3</sup> attempted to obtain a more precise  $\Lambda_0$  value from conductivity measurements on very dilute solutions, but the uncertainty due to experimental error was so considerable that no reliable extrapolation can be made from the results obtained.

Conductivity data for the 2-4 valency type salt, calcium ferrocyanide, have been reported by Shoch and Felsing<sup>4</sup> and calculations by Davies<sup>5</sup> based on these results indicate that dissociation is approximately 50 % complete at a concentration of 0.001 N. No measurements were made below this concentration, however, and an exact treatment of the dissociation equilibria was not possible.

In order to add to existing knowledge of such electrolytes, accurate conductivity measurements on very dilute solutions of potassium ferrocyanide and calcium ferrocyanide have therefore been made and are reported in this paper.

## Experimental

A.R. potassium ferrocyanide was recrystallized three times from conductivity water. Almost saturated solutions of the salt were prepared at 70-80° C, filtered, and allowed to crystallize; the crystals were dried to constant weight in a vacuum desiccator over the partially dehydrated salt. Conductivity measurements on the more concentrated solutions were in excellent agreement with the data of Jones and Jelen<sup>2</sup> and it was assumed therefore that the composition was accurately represented by the formula,  $K_4Fe(CN)_6 \cdot 3H_2O$ .

Kahlbaum calcium ferrocyanide was recrystallized three times from conductivity water, and dried to constant weight over the partially dehydrated salt. Some uncertainty has existed as to the exact degree of hydration; thus Roscoe and Schorlemmer,<sup>6</sup> and Colman<sup>7</sup> assign 11.5-12 molecules of  $H_2O$  to the salt, whereas Berkeley, Hartley and Burton<sup>8</sup> find 11. More recent work by Cumming,<sup>9</sup> and by Farrow,<sup>10</sup> indicates the formula  $Ca_2Fe(CN)_6 \cdot 11 H_2O$ , and the present work confirms this. (Found: Ca, 16.37 %,  $Fe(CN)_6$ , 43.22 %; calc. for  $Ca_2Fe(CN)_6 \cdot 11 H_2O$ ; Ca, 16.35 %,  $Fe(CN)_6$ , 43.14 %).

Conductivity measurements were made at 25° C, with the apparatus and technique described previously.<sup>11,12</sup> Measured conductivities were corrected for solvent conductivity, allowance being made in the correction for interionic attraction effects. Densities for the more concentrated potassium ferrocyanide solutions were taken from the data of Jones and Stauffer.<sup>13</sup>

Swift<sup>3</sup> has stated that with very dilute potassium ferrocyanide solutions "a continuous change in the resistance occurred during measurement, which was perhaps due to an unknown reaction of the material in the cell". In the present work, it was observed both with potassium and with calcium ferrocyanide solutions that a steady drift in the conductivity appeared to occur; gentle shaking of the cell caused the conductivity to rise and on standing a steady decrease again commenced. The conductivity as measured immediately after

<sup>2</sup> Jones and Jelen, *J. Amer. Chem. Soc.*, 1936, **58**, 2561.

<sup>3</sup> Swift, *ibid.*, 1938, **60**, 728.

<sup>4</sup> Shoch and Felsing, *ibid.*, 1916, **38**, 1926.

<sup>5</sup> Davies, *J. Chem. Soc.*, 1945, 460.

<sup>6</sup> Roscoe and Schorlemmer, *Treatise on Chemistry*, 1913, Vol. 2, p. 1256.

<sup>7</sup> Colman, *Analyst*, 1910, **25**, 299.

<sup>8</sup> Berkeley, Hartley and Burton, *Phil. Trans. A*, 1908, **209**, 177.

<sup>9</sup> Cumming, *J. Chem. Soc.*, 1924, 125.

<sup>10</sup> Farrow, *ibid.*, 1926, 50.

<sup>11</sup> Davies, *ibid.*, 1937, 432.

<sup>12</sup> Davies and James, *Proc. Roy. Soc. A*, 1948, **195**, 116.

<sup>13</sup> Jones and Stauffer, *J. Amer. Chem. Soc.*, 1936, **58**, 2558.

agitation of the cell remained almost constant for periods of up to 2 hr. and was taken as the true value. This behaviour is attributed to adsorption or decomposition of the electrolyte on the surface of the electrodes with a consequent decrease in conductivity in the immediate vicinity. On shaking, the solution concentration between the electrodes again becomes equal to the bulk concentration and the conductivity rises to the true value. This effect is only appreciable in very dilute solutions, becoming almost negligible for concentrations greater than 0.002 N. Similar drift effects have been observed with dilute potassium ferricyanide solutions by Hartley and Donaldson,<sup>14</sup> and with potassium iodate solutions by Monk,<sup>15</sup> and have been overcome in the same way.

### Discussion

**Potassium Ferrocyanide.**—Results are given in Table I and Fig. 1. Marked deviations from the limiting Onsager equation occur even in very dilute solution and it has been suggested by Davies<sup>16</sup> that these may be ascribed to the occurrence of first-stage association :

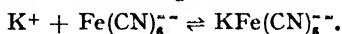


TABLE I

EQUIVALENT CONDUCTIVITIES OF POTASSIUM FERROCYANIDE SOLUTIONS AT 25° C

Run	$K_{\text{H}_2\text{O}} \times 10^6$ (ohm <sup>-1</sup> cm. <sup>-1</sup> )	$c \times 10^6$ (g. equiv./l.)	$\sqrt{c} \times 10^2$	$\Lambda$ (ohm <sup>-1</sup> cm. <sup>2</sup> g.-equiv. <sup>-1</sup> )
1	0.447	1.4210	1.192	179.78
		3.3624	1.834	175.76
		6.0115	2.452	171.80
		10.5480	3.248	166.70
2	0.339	0.8631	0.929	181.78
		2.0219	1.422	178.68
		3.9663	1.991	175.00
3	0.396	3.1981	1.788	176.11
		5.3843	2.320	172.63
4	0.447	3.0610	1.750	176.41
5	0.270	1.1335	1.065	180.71
		2.1798	1.476	178.17
		5.0385	2.245	173.14
6	0.275	1.9991	1.414	178.57
		4.1405	2.035	174.44
		5.7787	2.404	171.93
7	0.516	10.5950	3.255	166.68
8	0.277	0.9461	0.973	181.17
		1.6414	1.281	179.33
		3.5956	1.896	175.46
9	0.430	34.091	5.839	152.12
		48.227	6.944	146.88

The extrapolation method suggested by Onsager<sup>17</sup> has been shown<sup>18</sup> to be applicable only to very highly dissociated electrolytes ; with the present data, the plot of  $\Lambda + bc^{\frac{1}{2}}$  (where  $b$  is the limiting Onsager slope) against  $c$  shows considerable curvature, and cannot be satisfactorily extrapolated to zero concentration. To obtain an accurate  $\Lambda_0$  value, a method has therefore been used which takes into account the extensive association which occurs in potassium ferrocyanide solutions. If such

<sup>14</sup> Hartley and Donaldson, *Trans. Faraday Soc.*, 1937, **33**, 465.

<sup>15</sup> Monk, *J. Amer. Chem. Soc.*, 1948, **70**, 3281.

<sup>16</sup> Davies, *ibid.*, 1937, **59**, 1760.

<sup>17</sup> Onsager, *Physik Z.*, 1927, **28**, 277.

<sup>18</sup> Davies, *J. Chem. Soc.*, 1933, 645.

# 858 CONDUCTIVITIES OF FERROCYANIDE SOLUTIONS

association is governed by a mass-action equilibrium, then with the correct value for  $\Lambda_0$ , calculated dissociation constants will show no variation with concentration over the range studied and an accurate  $\Lambda_0$  value may

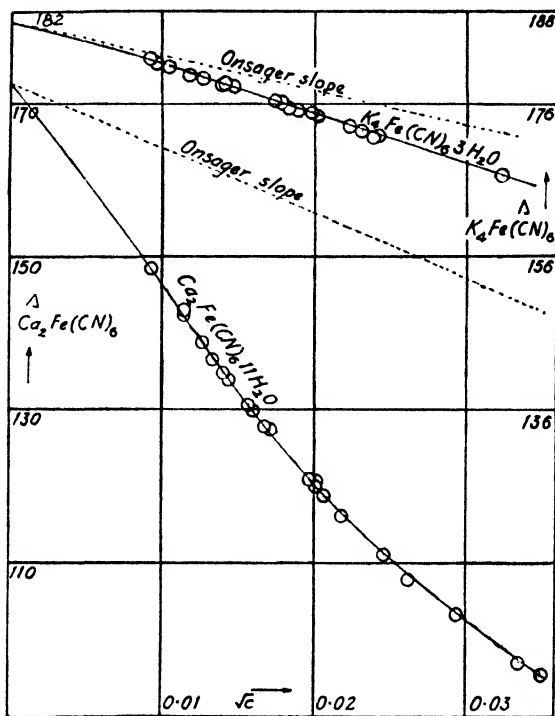


FIG. 1.—Conductivities of ferrocyanide solutions.

therefore be found by trial and error selection. Applying the treatment of Righellato and Davies,<sup>19</sup> if  $\alpha$  is the degree of dissociation of the intermediate ion  $\text{KFe}(\text{CN})_6^{--}$ , then the molar conductivity is given by

$$4\Lambda = 4\alpha \cdot \Lambda(\text{Fe}(\text{CN})_6^{--}) + 3(1-\alpha) \cdot \Lambda(\text{KFe}(\text{CN})_6^{--}) + (3+\alpha) \cdot \Lambda(\text{K}^+) \\ = 4\alpha[\Lambda(\text{K}^+) + \Lambda(\text{Fe}(\text{CN})_6^{--})] + 3(1-\alpha)[\Lambda(\text{K}^+) + \Lambda(\text{KFe}(\text{CN})_6^{--})],$$

where  $\Lambda(\text{Fe}(\text{CN})_6^{--})$ ,  $\Lambda(\text{KFe}(\text{CN})_6^{--})$ , and  $\Lambda(\text{K}^+)$  are the mobilities, at the concentration considered, of the three ions. The ionic strength of the solution is given by

$$I = 2m(3 + 2\alpha),$$

where  $m$  is the molar concentration; the mobility at infinite dilution of the intermediate ion  $\text{KFe}(\text{CN})_6^{--}$  has been assumed to be 80 by analogy with the mobilities for other trivalent ions. The mobility terms

$$[\Lambda(\text{K}^+) + \Lambda(\text{Fe}(\text{CN})_6^{--})] \text{ and } [\Lambda(\text{K}^+) + \Lambda(\text{KFe}(\text{CN})_6^{--})]$$

have been evaluated from the appropriate limiting Onsager equations and  $\alpha$  calculated by successive approximations. The dissociation constant is given by

$$\log K = \log \frac{\{\text{K}^+\} \{\text{Fe}(\text{CN})_6^{--}\}}{\{\text{KFe}(\text{CN})_6^{--}\}} = \log \frac{(3+\alpha)\alpha m}{(1-\alpha)} - 4.07I^{\frac{1}{2}}.$$

The value for  $\Lambda_0$  which is required to give consistent  $K$  values may be selected by a trial and error process to within 0.1 of a conductivity unit. As it is perhaps doubtful if the limiting equation can be applied, even at

<sup>19</sup> Righellato and Davies, *Trans. Faraday Soc.*, 1930, **26**, 592.

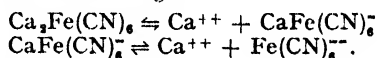
high dilutions to solutions containing a quadrivalent ion, Davies<sup>18</sup> has used an extended form of the Onsager equation to calculate the extent of association; values for  $\alpha$  have also been calculated from the present data in this way. The results obtained are summarized below.

Equation used	Intermediate ion mobility assumed $A_0 [\text{KFe(CN)}_6]^{4-}$	Mean $K \times 10^3$ (moles/l.)	$A_0$ (ohm <sup>-1</sup> cm. <sup>2</sup> g.-equiv. <sup>-1</sup> )
Limiting Onsager	80	6.8	186.45
Extended Onsager	80	5.7	186.50
Extended Onsager	100	4.3	186.50

It may be seen that the value obtained for  $A_0$  is dependent only slightly on the value assumed for the intermediate ion mobility and the form of the conductivity equation used in the evaluation of  $\alpha$ . The influence of these factors on the value obtained for  $K$  is, however, considerable, and it can only be concluded that the dissociation constant is of the order of 0.005, confirming the estimate made by Davies<sup>18</sup> from the three most dilute points of Jones and Jelen.<sup>2</sup>

Application of the extrapolation method suggested by Owen<sup>20</sup> gives the value  $A_0 = 186.7 \pm 0.05$ , in satisfactory agreement, and the mean value  $A_0 = 186.6$  has been adopted. It is of interest that the Owen method, which accounts for deviations from the limiting Onsager equation by the use of the theoretical extension due to Onsager and Fuoss,<sup>21</sup> should give a result in such good agreement with that obtained from a method which interprets the "conductivity deficiency" in terms of finite dissociation constants. Similar agreement has been observed with other multivalent electrolytes.<sup>12, 20</sup>

**Calcium Ferrocyanide.**—Results are given in Table II and Fig. 1. Large deviations from the limiting Onsager equation occur and unless the equation is quite inapplicable to this salt, it must be concluded that dissociation is far from complete even in dilute solutions. Calcium ferrocyanide will dissociate in two stages:



and

Approximate calculation indicates that even at a concentration of 0.0002 N, second-stage dissociation is only about 75 % complete. Such extensive association with an unsymmetrical valency type electrolyte would appear to render an accurate extrapolation to  $A_0$  impossible. The methods of Onsager<sup>17</sup> and of Owen<sup>20</sup> cannot be used satisfactorily, as plots of the extrapolation functions show marked curvature down to the lowest concentration studied, and the method of trial and error selection of a  $A_0$  value to satisfy the requirements of mass-action equilibrium for the ions present, can only give a very approximate estimate in this case, owing to the complex nature of the equilibria involved. An independent value  $A_0[\text{Ca}_2\text{Fe(CN)}_6] = 172.6$  has been obtained by combining the figure  $A_0[\text{K}_4\text{Fe(CN)}_6] = 186.6$  from the present work, with the values  $A_0[\text{K}^+] = 73.5$  and  $A_0[\text{Ca}^{++}] = 59.5$ , given by Shedlovsky and Brown.<sup>22</sup>

Taking  $\alpha$  to be the degree of first-stage dissociation, and  $\beta$  to be the degree of second-stage dissociation, then the concentrations in moles/l. are given by

$$[\text{Ca}_2\text{Fe(CN)}_6] = (1 - \alpha)m, [\text{CaFe(CN)}_6^-] = \alpha(1 - \beta)m, [\text{Fe(CN)}_6^{4-}] = \alpha\beta m,$$

$$\text{and } [\text{Ca}^{++}] = \alpha(1 + \beta)m,$$

where  $m$  is the molar concentration of the solution.

<sup>20</sup> Owen, *J. Amer. Chem. Soc.*, 1939, **61**, 1393.

<sup>21</sup> Onsager and Fuoss, *J. Physic. Chem.*, 1932, **36**, 2689.

<sup>22</sup> Shedlovsky and Brown, *J. Amer. Chem. Soc.*, 1934, **56**, 1066.

## 860 CONDUCTIVITIES OF FERROCYANIDE SOLUTIONS

TABLE II.—EQUIVALENT CONDUCTIVITIES OF CALCIUM FERROCYANIDE SOLUTIONS AT 25° C

Run	$K_{H_2O} \times 10^4$ (ohm <sup>-1</sup> cm. <sup>-1</sup> )	$c \times 10^4$ (g. equiv./l.)	$\sqrt{c} \times 10^2$	$\Lambda$ (ohm <sup>-1</sup> cm. <sup>2</sup> g.-equiv. <sup>-1</sup> )
1	0.717	1.2929 2.8187	1.137 1.679	142.10 127.85
2	0.564	2.0526 3.9854 6.8844 12.1670	1.433 1.996 2.624 3.488	133.84 119.92 107.76 95.21
3	0.337	2.4501 4.2776	1.567 2.068	130.66 118.59
4	0.451	4.7324 8.5889	2.175 2.931	116.02 102.90
5	0.635	2.8914 6.0254	1.700 2.455	126.90 110.90
6	0.586	1.9611 3.8370	1.400 1.959	134.65 120.86
7	0.593	1.5796 3.9019 11.3800	1.257 1.975 3.373	138.80 120.55 96.84
8	0.324	1.3065	1.143	142.33
9	0.346	1.7719 2.5065	1.331 1.583	136.43 129.83
10	0.400	0.8411	0.917	148.40

The molar conductivity is given by

$$4\Lambda = 4\alpha\beta \cdot \Lambda[\text{Fe}(\text{CN})_6^{4-}] + 2\alpha(1-\beta) \cdot \Lambda[\text{CaFe}(\text{CN})_6^{2-}] + 2\alpha(1+\beta) \cdot \Lambda(\text{Ca}^{++}) \\ = 4\alpha\beta[\Lambda \cdot [\text{Fe}(\text{CN})_6^{4-}] + \Lambda[\text{Ca}^{++}]] + 2\alpha(1-\beta)[\Lambda[\text{Ca}^{++}] + \Lambda[\text{CaFe}(\text{CN})_6^{2-}]] \quad (1)$$

and the dissociation constant for second-stage dissociation is given by

$$\log_{10} K_2 = \log_{10} \frac{\{\text{Ca}^{++}\}\{\text{Fe}(\text{CN})_6^{4-}\}}{\{\text{CaFe}(\text{CN})_6^{2-}\}} = \log_{10} \frac{(1+\beta)}{(1-\beta)} \alpha \beta m - 8.151t.$$

For dilute solutions,  $(1-\alpha)$  is small in comparison with  $(1+\beta)$  and values for  $K_2'$ , the apparent second-stage dissociation constant have been calculated assuming first-stage dissociation to be complete (i.e.  $\alpha=1$ ). The mobility at infinite dilution of the intermediate ion  $\text{CaFe}(\text{CN})_6^{2-}$  has been assumed to be 60, by analogy with the mobilities for other bivalent ions, and the mobility terms in eqn. (1) have been obtained from the appropriate limiting Onsager equations. The ionic strength of the solution is  $(4+8\beta)\alpha m$ ; values for  $\beta$  have been derived by a method of successive approximations. With decreasing concentration  $K_2'$  approaches  $K_2$ , and a short linear extrapolation of  $K_2'$  to zero concentration gives  $K_2 = 1.69 \times 10^{-4}$  moles/l.

For first-stage dissociation

$$\log_{10} K_1 = \log_{10} \frac{\{\text{Ca}^{++}\}\{\text{CaFe}(\text{CN})_6^{2-}\}}{\{\text{Ca}_2\text{Fe}(\text{CN})_6\}} \\ = \log_{10} \frac{\alpha^2(1+\beta)(1-\beta)m}{(1-\alpha)} - 4 \left[ \frac{\sqrt{I}}{1+\sqrt{I}} - 0.20I \right]$$

and using the value for  $K_2$  obtained above, calculation by a method of successive approximations gives  $K_1 = 3.7 \times 10^{-3} \pm 0.1 \times 10^{-3}$  moles/l. for the 5 most concentrated solutions studied. (The empirical extension of the Debye-Hückel limiting equation used in this treatment has been extensively tested for electrolytes of other valency types, and has been

shown to give good agreement with experimental data<sup>23</sup>). These values for  $K_1$  and  $K_2$  are necessarily rendered somewhat uncertain by the assumptions made as to the intermediate ion mobility, and the form of the conductivity equation, but their substantial correctness is indicated by an examination which has been made of solubility data for calcium iodate in calcium ferrocyanide solutions.<sup>6</sup>

In conclusion, the author wishes to thank Prof. C. W. Davies for his continued help and encouragement in this work.

*The University,  
Glasgow.*

*Battersea Polytechnic,  
London, S.W.11.*

<sup>23</sup> Davies, *J. Chem. Soc.*, 1938, 2093.

## THE EFFECT OF ADDITIVES ON ELECTRODE REACTIONS

### PART I. THE VARIATION OF HYDROGEN OVERVOLTAGE AT VARIOUS CATHODES ON THE ADDITION OF ETHYL ALCOHOL, ACÉTALDEHYDE, AND ACETIC ACID

BY ALLAN WETTERHOLM

*Received 29th January, 1948; as amended 3rd May, 1949*

The potential changes on the addition of some organic compounds at silver, copper, nickel, and platinum cathodes have been determined. The compounds were ethyl alcohol (irreducible), acetic acid (hardly reducible), and acetaldehyde (easily reducible) in an electrolyte of N sulphuric acid + 0.35 M sodium sulphate. The  $\eta$ -log c.d. curves were determined between  $2 \times 10^{-5}$  and  $2 \times 10^{-2}$  A/cm.<sup>2</sup>, with and without the addition of organic compound.

Potential changes on the addition of an organic compound were: (i) Sometimes an increase in overvoltage depending upon the added quantity of organic substance, as for Ag—C<sub>2</sub>H<sub>5</sub>OH, Ag—, Ni—, or Cu—CH<sub>3</sub>CHO, and Ag—, Ni—CH<sub>3</sub>COOH. The  $b$  value of the Tafel equation is changed little at low current densities by the presence of organic substance. (ii) Sometimes a depression of the original curve at low current densities with an increased gradient, e.g. Cu—, Pt—, or Ni—C<sub>2</sub>H<sub>5</sub>OH, Ni—CH<sub>3</sub>CHO, and Cu—CH<sub>3</sub>COOH. The cause of the complex nature of the overvoltage changes is discussed, and it is shown that a reduction potential cannot be interpreted without taking into the account both solvent and poison effects.

Many attempts have been made to use the potential of an organic electrolytic reduction as an indicator of the reducibility of the compound.<sup>1</sup> For irreversible processes the changes of potential caused by the addition of organic compounds are, however, more complicated than those associated with a simple depolarization because the organic compounds may affect the potential in other ways. A review of the literature shows that these additions may cause the hydrogen overvoltage to decrease or increase, or less frequently to remain the same.

**Decrease in Hydrogen Overvoltage.**—Haber and Russ<sup>2</sup> observed that the addition of nitrobenzene to alcoholic, alkaline solution caused a

<sup>1</sup> Russ, *Z. physik. Chem.*, 1903, 44, 641. Haber and Russ, *ibid.*, 1904, 47, 257. Hibbert and Read, *J. Amer. Chem. Soc.*, 1924, 46, 983. de Bottens, *Z. Elektrochem.*, 1902, 8, 305, 332. Tafel and Naumann, *Z. physik. Chem.*, 1905, 50, 713. Müller, *Chem. Rev.*, 1939, 24, 95.

<sup>2</sup> Haber and Russ, (ref.<sup>1</sup>).



depolarization at a working platinum cathode. The cathode potential could be expressed by the equation :

$$\eta = \eta_0 + x \frac{RT}{F} \ln \frac{I}{C_{R_0} \cdot k}$$

where  $R$ ,  $T$ , and  $F$  have their usual significance ;  $I$  is the current strength,  $C_{R_0}$  the concentration of the depolarizer,  $k$  a velocity constant, and  $x$  is attributed to a "reaction resistance." By analogy with the Tafel equation this may be written as

$$\eta = \alpha_1 + b_1 (\ln C_{R_0}),$$

from which the effect of the organic substance is easily seen. A lowered potential was found by Hibbert and Read<sup>3</sup> on adding aldehydes and ketones at a lead cathode, by Tafel and Naumann<sup>4</sup> with caffeine at a mercury cathode (less than 100 % yield), and by Leslie and Butler<sup>5</sup> with benzaldehyde at a mercury cathode. Herringshaw<sup>6</sup> investigated the reduction of maleic and crotonic acids and found a correlation between cathode potential drop and current yield. The work of Glasstone<sup>7</sup> indicated that the addition of methyl and ethyl alcohols (which are not reduced) lowered the hydrogen overvoltage at lead. Levina and Silberfarb,<sup>8</sup> and Novoselski<sup>9</sup> observed that the overvoltage at mercury cathodes was lower in pure non-aqueous solutions (methyl and ethyl alcohols and ether) than in pure non-aqueous solutions. In a comprehensive investigation of the overvoltages in solutions of HCl in various solvents including methyl and ethyl alcohols, ethylene glycol, formic and acetic acids, ether, dioxane, and in appropriate cases mixtures of these with water, Bockris<sup>10</sup> observed effects conforming to this group as well as to the two succeeding groups using lead, copper and nickel cathodes. The effect of very low concentrations ( $2 - 150 \times 10^{-6}$  mole/l.) of alkaloïds on the overvoltage is remarkable.<sup>11</sup> Although these substances lower the overvoltage at mercury and lead at low current densities, at high current densities they increase it, e.g. at mercury, tungsten, and platinum cathodes.

**Increase of Overvoltage.**—Evidence of a reducible substance increasing the potential is given by Tafel and Naumann,<sup>4</sup> who mention that succinimide increased the potential at lead and mercury cathodes. Leslie and Butler<sup>5</sup> observed a potential increase at a smooth platinum cathode on adding pyridine (at concentrations of M/10,000 to M/10 in  $\text{NH}_4\text{SO}_4$ , current densities  $10^{-3.5}$ – $10^{-2}$  A/sq. cm.) and the new  $\eta$ -log current density lines were parallel with the original ones.

The increase of polarization on adding an irreducible compound was first observed by Thiel and Breuning,<sup>12</sup> who measured the minimum overvoltage at platinum and tin cathodes and added small amounts of ether, amyl alcohol, heptyl alcohol, and butyric acid. Glasstone<sup>7</sup> found the addition of small quantities of isobutyl and isoamyl alcohols increased the potential, while larger amounts decreased it. Jofa *et al.*<sup>13</sup> investigated the mercury cathode and its behaviour on addition of surface-active cations and anions, the former increasing and the latter decreasing the overvoltage. Kolychev<sup>14</sup> reports a complex behaviour of isoamyl

<sup>3</sup> Hibbert and Read (ref. 1).

<sup>4</sup> Tafel and Naumann (ref. 1).

<sup>5</sup> Leslie and Butler, *Trans. Faraday Soc.*, 1936, **32**, 989.

<sup>6</sup> Herringshaw, *Thesis* (London, 1947).

<sup>7</sup> Glasstone, *Trans. Faraday Soc.*, 1925, **21**, 36.

<sup>8</sup> Levina and Silberfarb, *Acta physicochim.*, 1936, **4**, 275.

<sup>9</sup> Novoselski, *J. Physic. Chem. (Russ.)*, 1938, **11**, 369.

<sup>10</sup> Bockris, *Faraday Soc. Discussion*, 1947, **1**, 95.

<sup>11</sup> Bockris and Conway, *Nature*, 1947, **159**, 711.

<sup>12</sup> Thiel and Breuning, *Z. anorg. Chem.*, 1913, **83**, 329.

<sup>13</sup> Jofa, Kabanov, Kuchinsky and Chistiakov, *Acta physicochim.*, 1939,

**10**, 317.

<sup>14</sup> Kolychev, *Urhenye Zapiski Saratov Gosudarst Chernyshevskaya, Khim.*, 1940, **15**, 45.

alcohol at a mercury cathode, small concentrations giving an increase and larger concentrations a decrease. Small additions of tetrabutyl- or tetrapropyl-ammonium sulphate are effective, in raising the potential of a lead cathode.<sup>15</sup>

**No Change in Cathode Potential.**—According to Leslie and Butler,<sup>8</sup> the  $\eta$ -log current density curve for mercury is scarcely affected by the presence of pyriding (M/10), although this compound is readily reduced at a mercury cathode.<sup>16</sup> An irreducible substance not affecting the cathode potential is methyl alcohol at nickel.<sup>10</sup>

All the above-mentioned effects may occur simultaneously but there is as yet no method for their differentiation especially when reduction occurs.

The influence of high molecular weight substances on the hydrogen overvoltage has been known for a long time and utilized in practice, e.g. in the electrochemical deposition of metals. The increase of hydrogen overvoltage on addition of such substances has usually been ascribed to adsorption on the most active part of the electrode surface, which assumes a more uniform activity. For the influence of substances of high molecular weight, see ref. 17-22. Similar work to that discussed above for cathodic reactions has been carried out for anodic reactions by Bockris<sup>21</sup> and Hickling.<sup>22</sup>

In order to elucidate to some extent the mechanism involved in these apparently random effects, it seemed desirable to obtain results using relatively simple organic additives. Accordingly, in the series ethyl alcohol, acetic acid, acetaldehyde (in order of reducibility \*) were used with Cu, Ag, Ni, and Pt as cathodes. Furthermore, these organic compounds have the advantage of having similar values of surface energy (EtOH 22.3, CH<sub>3</sub>COOH 27.0, CH<sub>3</sub>CHO 21.2 dynes/cm.).

## Experimental

**APPARATUS.**—The measuring cell used was made up as a ring cell, according to a modified construction by Haber,<sup>23</sup> and was composed of glass rings pressed together (Fig. 1). The cell originally consisted of five rings comprising anode and cathode compartments, a middle ring continually washed with pure nitrogen during the measurements, and two rings for thermostating the system. The last two, however, proved superfluous since a room temperature of 20° C  $\pm$  2° C could be maintained. The surface area of the platinum sheet anode, the cathode, and the thick parchment paper diaphragms were 28 cm.<sup>2</sup>

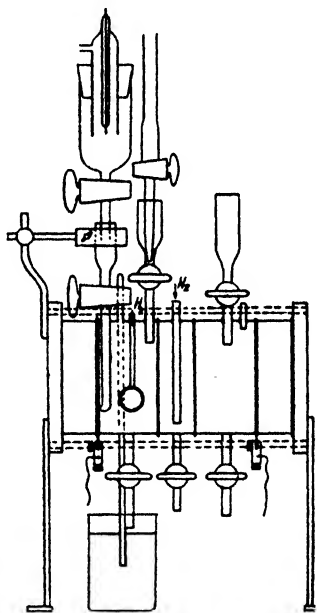


FIG. 1.—Diagram of apparatus.

The middle cell was necessary to prevent oxygen diffusion into the cathode compartment. The hydrogen was freed from

<sup>15</sup> Wanjukova and Kabanov, *J. Physic. Chem. (Russ.)*, 1940, **17**, 2620.

<sup>16</sup> Ahrens, *Z. Elektrochem.*, 1895, **2**, 577.

<sup>17</sup> Marie, *Compt. rend.*, 1908, **147**, 1400.

<sup>18</sup> Marie and Lejeune, *ibid.*, 1927, **179**, 679.

<sup>19</sup> Isgarischew and Berkmann, *Z. Elektrochem.*, 1922, **28**, 47.

<sup>20</sup> Newbery, *J. Chem. Soc.*, 1914, **105**, 2419.

<sup>21</sup> Bockris, *Faraday Soc. Discussion*, 1947, **1**, 229.

<sup>22</sup> Hickling, *ibid.*, 1947, **1**, 227.

\* Reduction experiments with M acetic acid in N H<sub>2</sub>SO<sub>4</sub> showed a reducibility of about 0.5 % at some cathode materials; c.d. 10<sup>-3</sup> to 5  $\times$  10<sup>-2</sup> A/cm.<sup>2</sup>

<sup>23</sup> Haber, *Z. physik. Chem.*, 1900, **32**, 193.

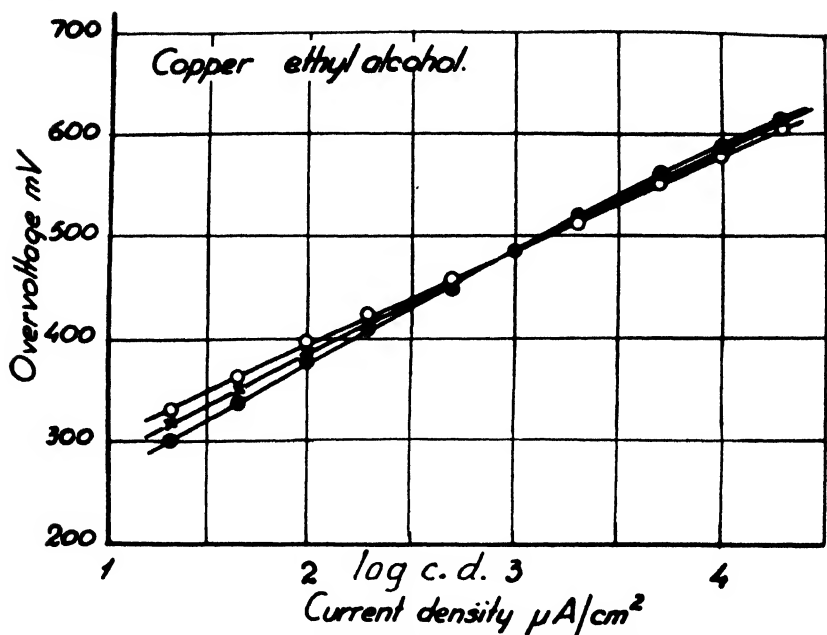


FIG. 2.—Overvoltage at a copper cathode with and without addition of ethyl alcohol.

○ Overvoltage without additive.  
 × " " with 1 mole/l. alcohol.  
 ● " " " 2 " " "

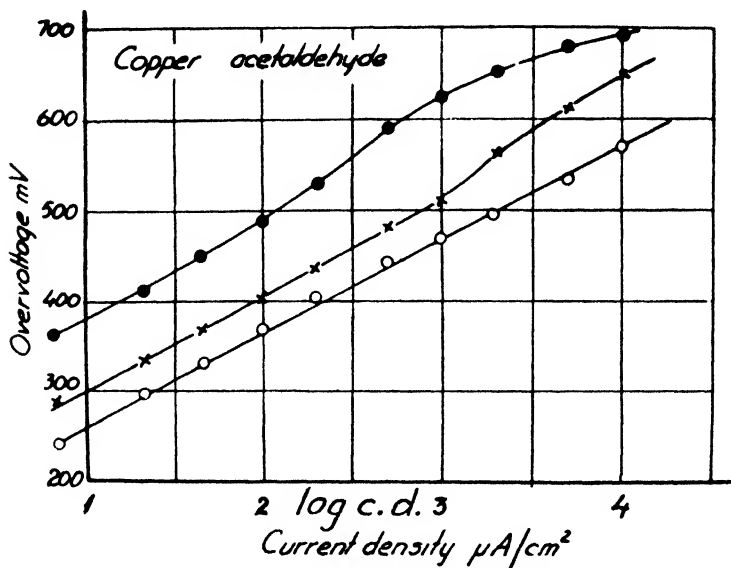


FIG. 3.—Overvoltage at a copper cathode with and without addition of acetaldehyde.

○ Overvoltage without additive.  
 × " " with 1 mole/l. acetaldehyde.  
 ● " " " 2 " " "

oxygen by passing it through a furnace at 600° C alternately packed with copper chips and 15 % platinized asbestos. The gas was then passed through a wash-bottle containing the same acid as the electrolyte and was conducted to the cell and the hydrogen electrode by all glass connections. The potential measurements made use of a valve bridge manufactured by the Cambridge Instrument Company, and the current was measured by a Hartmann and Braun precision milliammeter (accuracy  $\pm 1$  %). The measurements were made in the usual manner with the fine end of a glass tube, in electrolytic communication with the reference electrode, pressed against the surface of the cathode. As reference electrode a hydrogen electrode was employed in the same solution  $\text{N H}_2\text{SO}_4 + 0.35 \text{ M Na}_2\text{SO}_4$  (50 g./l.) \* as was used during the measurements.

**MATERIALS.**—The electrolyte was produced from A.R. sulphuric acid and NaOH and doubly-distilled water, prepared in an all-glass still. The ethyl alcohol used was 99.5 % alcohol. Commercial acetaldehyde is of varying purity due to polymerization on storage. Merck's P.A., Kahlbaum's and Eastman's C.P. acetaldehyde were therefore used, both being redistilled (over  $\text{CaCl}_2$ ) and analyzed after distillation.† In order to avoid polymers being carried over the distillation was carried out carefully since small amounts of polymers disturb the measurements. The receiver for the distillate was cooled in solid  $\text{CO}_2$  and the acetaldehyde, originally 70-90 %  $\text{CH}_3\text{CHO}$  was obtained 99.2-100 % pure. The distilled fractions were kept at  $-25^\circ \text{C}$  when formation of polymer is disclosed by crystallization. In the surface treatment the cathodes were moistened with distilled water and then ground with fine emery cloth. Each electrode was used only once or twice.

**Procedure.**—It is of primary importance for establishing the existence of a potential change to have an initial potential-c.d. curve ( $\eta$ -log c.d.) which is satisfactorily reproducible. It became evident that this condition was not easy to attain since the potential varied with the method of measurement (see below) and the time that the cathode had been charged or treated with hydrogen.

The methods of measurement which can be applied are :

(a) The potential, whether constant or not, is measured a fixed time after the adjustment of the current (see Knobel, Caplan and Eisemann,<sup>24</sup> who measured the potential 1 min. after the adjustment of the current. This method is rapid but not reliable).

(b) In principle the correct method of measurement would be to start from the zero current for every measuring point, then adjust it to the desired value, and await the constant potential. However, this introduces the risk of contaminating the solution by traces of the metal dissolved during the breaking of the current. This method of measurement was used by Masing and Laue,<sup>25</sup> by Hickling and Salt,<sup>26</sup> and by Bockris.<sup>27</sup>

(c) The cathode is prepolarized at a certain, usually low, current density, eventually the lowest current density used, for a relatively long time (up to 4 hr. or more). The values of potential at the higher current densities may then be measured rapidly (cp. Náray-Szabó<sup>28</sup> who used prepolarizing current  $5 \times 10^{-5} \text{ A/cm}^2$  for several hours and states that without this polarization no reproducible values could be obtained; see also Lukowzew, Lewina and Frumkin<sup>29</sup> and Legran and Lewina<sup>30</sup>).

In the present work method (c) was employed and found to give reproducible  $\eta$ -log c.d. plots. The object of this work was not so much to determine the overvoltage itself but the potential changes on the addition of organic compounds. Preliminary measurements showed that to obtain reproducible values the measurements must be done in the same manner and without delay between the separate runs. Consequently all measurements with one substance were carried out in one day.

\* The addition of  $\text{Na}_2\text{SO}_4$  was originally made in order to increase the conductivity of solutions of higher pH and was retained in the present studies. The presence of  $\text{Na}_2\text{SO}_4$  seemed to have no effect on the results in general.

† By Ripper's bisulphite method.

<sup>24</sup> Knobel, Caplan and Eisemann, *Trans. Amer. Electrochem. Soc.*, 1923, 43, 55.

<sup>25</sup> Masing and Laue, *Z. physik. Chem. A*, 1907, 178, 1.

<sup>26</sup> Hickling and Salt, *Trans. Faraday Soc.*, 1940, 36, 1226.

<sup>27</sup> Bockris, *ibid.*, 1947, 43, 417.

<sup>28</sup> v. Náray-Szabó, *Z. physik. Chem., A*, 1938, 181, 367.

<sup>29</sup> Lukowzew, Lewina and Frumkin, *Acta physicochim.*, 1939, 11, 21.

<sup>30</sup> Legran and Lewina, *ibid.*, 1940, 12, 243.

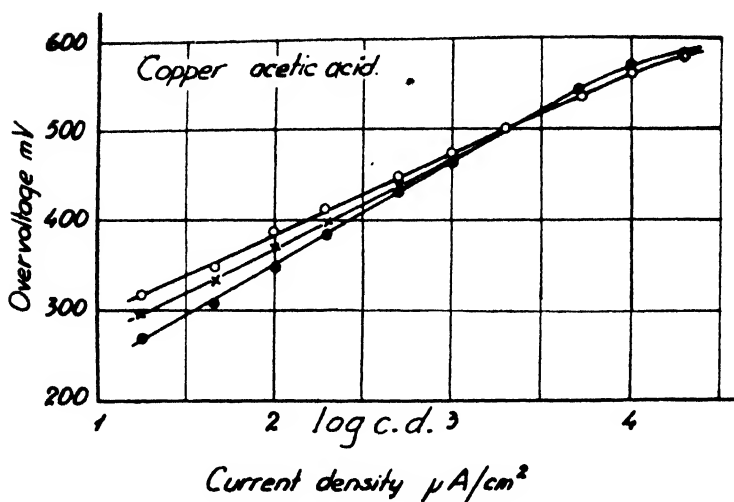


FIG. 4.—Overvoltage at a copper cathode with and without addition of acetic acid.

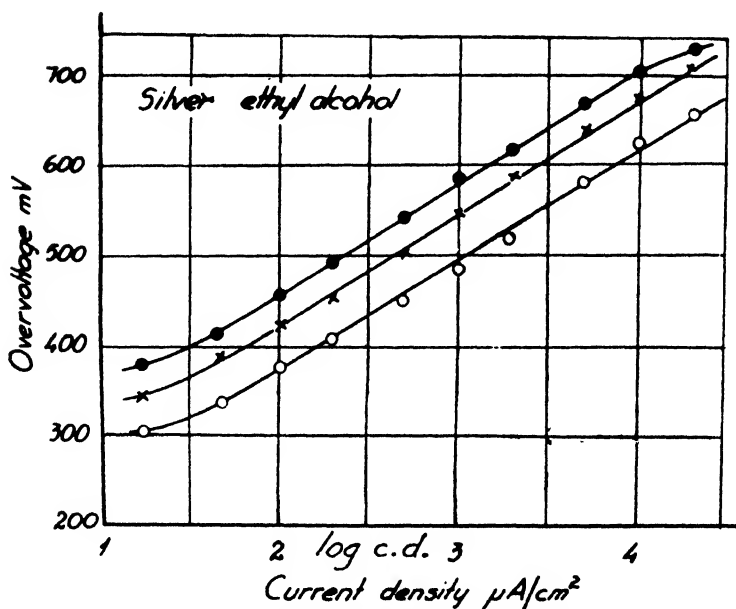


FIG. 5.—Overvoltage at a silver cathode with and without addition of ethyl alcohol.

The procedure used in the measurements was thus as follows. After previous hydrogen bubbling, prepolarization was commenced at  $2 \times 10^{-8}$  A/sq. cm. and continued until a steady potential value was attained, usually after 1-3 hr. Steady potentials at the higher current densities were then obtained within a few minutes after adjustment of current. This procedure was repeated until two series of measurements agreed within a few millivolts. The first addition of organic substance was then made (without switching off the current), prepolarization carried on to a stable potential value and the measurements repeated. Table I illustrates the procedure and the reproducibility obtained.

TABLE I.—OVERVOLTAGE AT A SILVER CATHODE WITH AND WITHOUT THE ADDITION OF ACETALDEHYDE (cp. FIG. 6)

Current density $i$ ( $\mu$ A/cm. <sup>2</sup> ). log $i$ . . .	21.1 1.33	42.3 1.66	100 2.00	200 2.30	500 2.70	1000 3.00	2000 3.30	5000 3.70	10000 4.00	20000 4.30
Overvoltage mV without additive										
Run No. 1 .	244	300	357	396	441	472	509	563	601	637
2 .	245	295	344	380	421	453	487	546	589	637
3 .	265	312	360	392	432	458	493	553	605	646
4 .	280	328	377	406	446	475	510	565	606	—
5 .	279	326	370	400	446	476	510	565	606	646
Overvoltage + 0.5 mole CH <sub>3</sub> CHO/l.										
1 .	333	380	420	449	492	526	567	617	657	689
2 .	333	377	415	445	491	528	577	655	692	716
Overvoltage + 1.0 mole CH <sub>3</sub> CHO/l.										
1 .	372	410	450	483	541	589	631	669	692	710
Overvoltage + 1.5 mole CH <sub>3</sub> CHO/l.										
1 .	410	444	480	520	587	632	666	693	711	726
After 10 hr. at 21.1 $\mu$ A/cm. <sup>2</sup>										
2 .	452	493	543	584	639	679	708	734	753	763
3 .	448	495	568	618	669	697	715	738	758	768
4 .	454	501	559	618	668	697	715	739	757	768
Overvoltage + 2.0 mole CH <sub>3</sub> CHO/l.										
1 .	503	557	614	646	676	694	705	725	734	742
2 .	508	560	616	653	680	700	714	735	746	755
Overvoltage + 3.0 mole CH <sub>3</sub> CHO/l.										
1 .	557	603	644	667	680	690	704	725	733	744
2 .	554	602	643	668	690	704	711	731	740	750

Adjustments to a lower current from a higher one always result initially in a far lower potential than was obtained in a previous run, but these lower potentials gradually increased to a steady value. It would be expected that adjustment of the current as above would lead to a higher potential; this is discussed later.

## Results

The results of the overpotential measurements with and without organic additions are presented diagrammatically.

As expected the overvoltage of platinum (cf. Masing and Laue <sup>25</sup>) reached its equilibrium value slowly especially at the lower current densities where several days may be required; consequently the lowest current density values were avoided. Table II shows the results on the addition of ethyl alcohol.

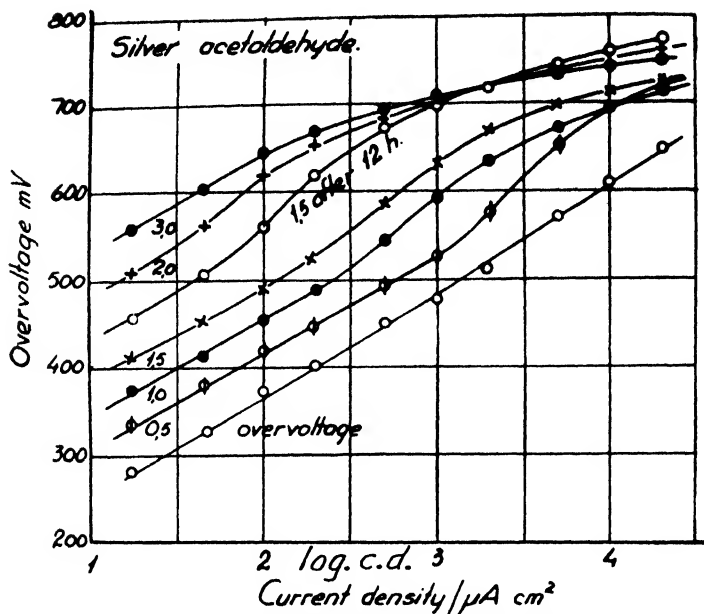


FIG. 6.—Overvoltage at a silver cathode with and without addition of acetaldehyde.

- Overvoltage without additive.  
 × " " with 1 mole/l. acetaldehyde.  
 ● " " " 2 " " "

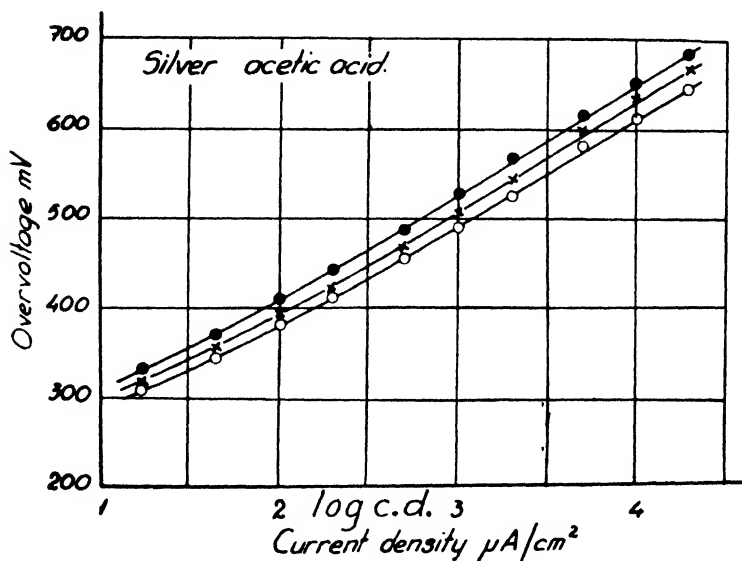


FIG. 7.—Overvoltage at a silver cathode with and without addition of acetic acid.

- Overvoltage without additive.  
 × " " with 1 mole/l. acetic acid.  
 ● " " " 2 " " "

TABLE II.—OVERVOLTAGE AT SMOOTH PLATINUM WITH AND WITHOUT THE ADDITION OF ETHYL ALCOHOL. Run No. 65

C.d. ( $\mu A/cm.^2$ ) log c.d.	Current Density							
	100 2'00	200 2'30	500 2'70	1000 3'00	2000 3'30	5000 3'70	10000 4'00	20000 4'30
Overvoltage mV *								
Run No. 2	407	484	508	525	545	591	641	696
3	410	445	474	498	525	595	654	714
4	421	470	502	531	566	618	674	711
1 mole $C_2H_5OH/l.^*$								
1	441	471	506	527	555	592	628	656
2	421	463	504	533	556	590	635	—

\* Prepolarized for 12 hr. at 100  $\mu A/cm.^2$ 

It is clear that the  $\eta$ -log. c.d. curve is approximately linear in the range  
 $2 \times 10^{-5} - 2 \times 10^{-2} A/cm.^2$

Generally, this agreement with a logarithmic course becomes more satisfactory with increasing number of runs and this is best illustrated in Fig. 11 which shows consecutive runs on platinum.

Calculation of the constants  $a$  and  $b$  (mean values) in Tafel's equation gives the following results :—

TABLE III(a).—VALUES OF CONSTANTS IN TAFEL'S EQUATION (DOUBLY-DISTILLED WATER USED)

Cathode Metal	No. of Expt.	$a$ (volt)	$b$ (volt)
Cu . . .	4	$0.75 \begin{smallmatrix} + 0.01 \\ - 0.01 \end{smallmatrix}$	$0.093 \begin{smallmatrix} + 0.011 \\ - 0.015 \end{smallmatrix}$
Ag . . .	3	$0.84 \begin{smallmatrix} + 0.00 \\ - 0.01 \end{smallmatrix}$	$0.119 \begin{smallmatrix} + 0.001 \\ - 0.002 \end{smallmatrix}$
Ni . . .	2	$0.78 \begin{smallmatrix} + 0.01 \\ - 0.02 \end{smallmatrix}$	0.118
Pt . . .	1	0.87	$0.112 - 0.15$

The influence of the very small amounts of impurities present in singly distilled water may clearly be seen by comparing Tables III(a) and III(b).

TABLE III(b)

Cathode Metal	No. of Expt.	$a$ (volt)	$b$ (volt)
Cu . . .	4	$0.75 \begin{smallmatrix} + 0.01 \\ - 0.00 \end{smallmatrix}$	$0.089 \begin{smallmatrix} + 0.008 \\ - 0.003 \end{smallmatrix}$
Ag . . .	2	$0.65 \begin{smallmatrix} + 0.01 \\ - 0.01 \end{smallmatrix}$	$0.108 \begin{smallmatrix} + 0.014 \\ - 0.014 \end{smallmatrix}$
Ni . . .	2	$0.57 \begin{smallmatrix} + 0.01 \\ - 0.01 \end{smallmatrix}$	$0.116 \begin{smallmatrix} + 0.001 \\ - 0.001 \end{smallmatrix}$



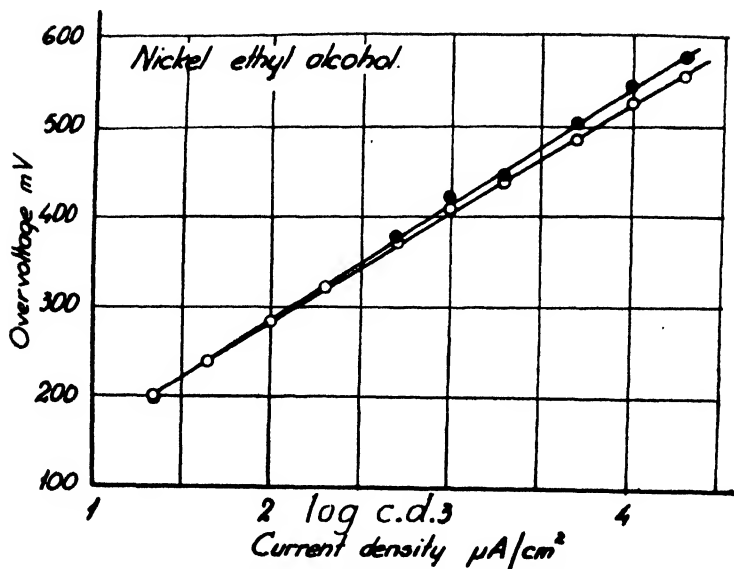


FIG. 8.—Overvoltage at a nickel cathode with and without addition of ethyl alcohol.

○ Overvoltage without additive.  
● " with 2 mole/l. alcohol.

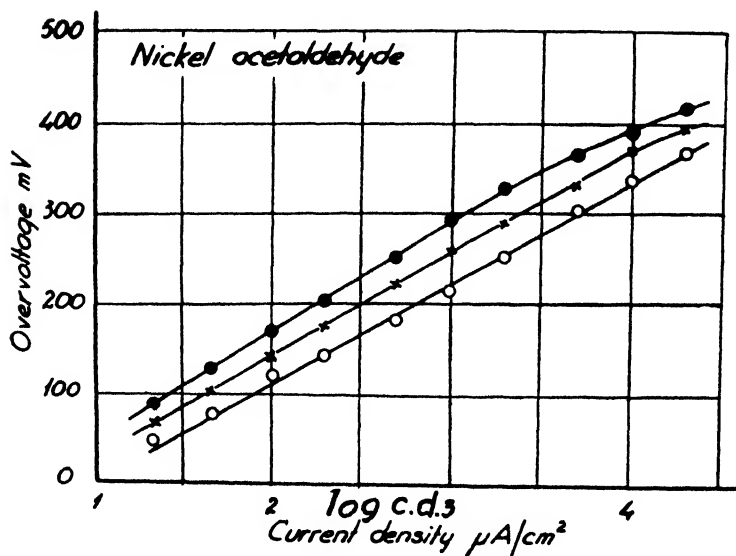


FIG. 9.—Overvoltage at a nickel cathode with and without addition of acetaldehyde.

○ Overvoltage without additive.  
× " with 1 mole/l. acetaldehyde.  
● " " 2 " "

Generally the  $a$  values are lower when using a less pure electrolyte. The values obtained are in agreement with Baars<sup>31</sup> who gives for copper  $a = 0.78$ ,  $b = 0.105$ , and for silver  $a = 0.95$ ,  $b = 0.120$ .

The effect of *addition* of an organic substance is sometimes to depress the original curve at lower current densities with an increased gradient of the Tafel line, and sometimes to increase the overvoltage at all current densities. A summary of the types of overvoltage change for different systems is given in the Table IV. (The word "turning" indicates an increased gradient was observed.)

TABLE IV

Cathode Metal	Behaviour on Organic Addition		
	Ethyl Alcohol	Acetaldehyde	Acetic Acid
Cu . . . .	Turning	Raising	Turning
Ag . . . .	Raising	Raising	Raising
Ni . . . .	Turning	Raising	Raising
Pt . . . .	Turning	—	—

The magnitudes of increase in overvoltage with addition of definite amounts of organic substances are given in Table V.

TABLE V.—INCREASE IN OVERVOLTAGE ON THE ADDITION OF EITHER  $C_2H_5OH$ ,  $CH_3CHO$ , OR  $CH_3COOH$ , AT  $10^{-3}$  A/CM.<sup>2</sup>

Cathode Metal-Organic Additive System	mV Increase on Addition of		Run No.
	1st (mole/l.)	2nd (mole/l.)	
Cu— $CH_3CHO$ . . .	39	83	33
	56	62	34
Ag— $C_2H_5OH$ . . .	29	28	40
	57	30	53
Ag— $CH_3CHO$ . . .	57	60	39
	80	70	70
Ag— $CH_3COOH$ . . .	18	18	62
Ni— $CH_3CHO$ . . .	15	17	57
Ni— $CH_3COOH$ . . .	30	30	46

Run 70 is interesting (Fig. 6). At the lower current densities the "additive" curves run parallel with the overvoltage curve but are displaced to more negative potentials. This is followed by a more rapid increase in potential, whilst at still higher current densities the curve rises less steeply. Further addition of acetaldehyde does not appear to effect any further increase of overvoltage above 730 to 740 mV.

## Discussion

The main effects of an organic compound on the cathode potential are :

- (i) A solvent effect on the overvoltage changing the overall velocity of hydrogen liberation reaction may decrease or increase the potential.
- (ii) An alternative hydrogen-consuming process at the cathode can only lower the potential (the reduction effect).
- (iii) An increase of the concentration of organic compound occurs at the metal-solution interface due to adsorption (the adsorption effect).

<sup>31</sup> Baars, *Sitz. ber. Ges. Naturwiss. Marburg*, 1928, **63**, 213.

No one hitherto has shown that the increase in potential is dependent on an adsorption process, although it is generally assumed to be so (cp. Leslie and Butler<sup>5</sup> and the so-called "poison effect" on overvoltage<sup>23</sup>).

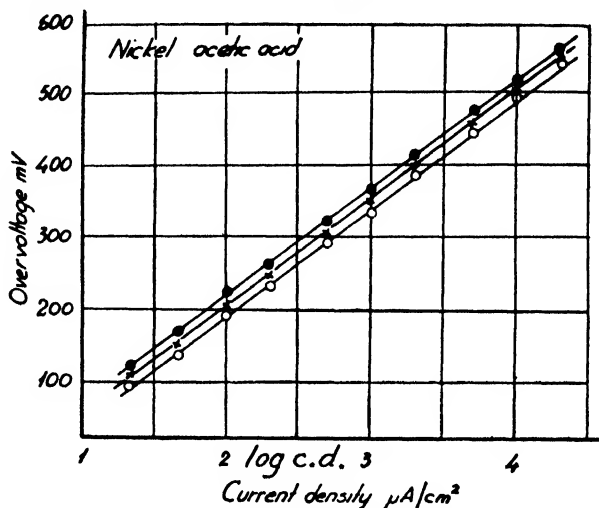


FIG. 10.—Overvoltage at a nickel cathode with and without addition of acetic acid.

- Overvoltage without additive  
 × " " with 1 mole/l. acetic acid.  
 ● " " " 2 " " "

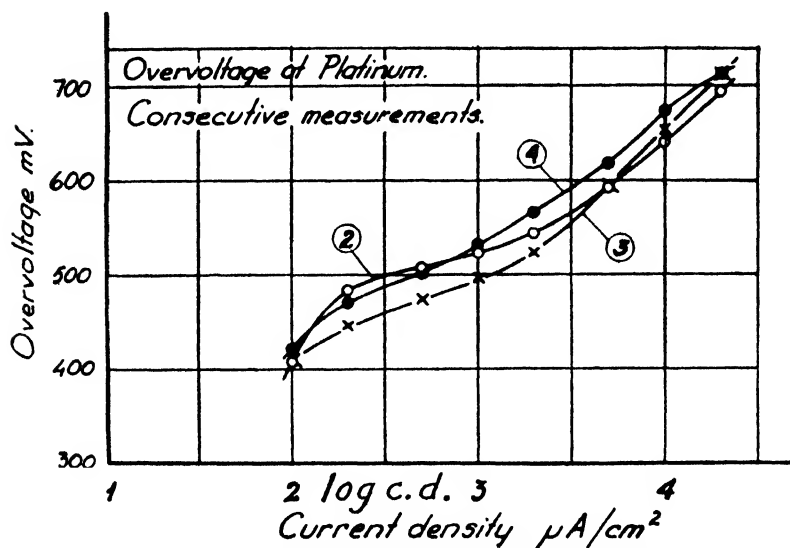


FIG. 11.—Attainment of a straight line at a platinum cathode without additives.

If, however, we try to use the depolarization effect of an organic substance to follow a reduction reaction or as an indicator of the reducibility of the compound then (i) and (iii) may be expected to influence the results. A reduction depolarization may thus be masked by other

<sup>23</sup> Bockris, *Chem. Rev.*, 1948, **43**, 526.

effects leading to higher or lower values than the real reduction depolarization. Sometimes an adsorption polarization conceals the depolarization completely, as with acetaldehyde. With irreducible substances the solvent and adsorption effects may give rise to the complicated course which the potential sometimes follows with increasing current density or concentration of organic compound. The existence of simultaneous effects, as considered above, may distort the potential relationships and render them difficult to interpret.

Although the number of systems, cathode metal-organic compound, studied is too low for general conclusions to be drawn it appears that the magnitude of the overvoltage increase bears some relation to the reducibility of the compound. Thus with acetaldehyde increases are found in 3 out of 3 metal cathodes, with acetic acid in 2 out of 3, and with ethyl alcohol in only 1 out of 3. These results are to be in accord with the prevailing view that the adsorption of the organic substance is mainly responsible for the observed increase in overvoltage.

The change of slope of the Tafel line which occurs in the presence of acetaldehyde may be ascribed to a depolarization reduction since the change of the slope occurs at approximately the same potential at all aldehyde concentrations. However, it must be noted that the current density at which the change occurs—which would therefore be identical with the limiting current of the depolarization process—decreases with increase in acetaldehyde concentration. Hence the explanation that the change of slope corresponds with the limiting current for the reduction process is inadequate.

As mentioned previously, on passing from a higher to a lower current density much lower  $\eta$ -values than expected from consideration of a preceding run are obtained, although the original values are gradually attained. An explanation of this behaviour may be found by applying Hickling and Salt's<sup>33</sup> theory of overvoltage. Masing and Laue<sup>25</sup> proved that the hydrogen content of platinum after charging depends on the previous cathode potential. At a higher potential we may thus expect a higher hydrogen content. This may hold for some other metals to a lesser degree. (A metal such as mercury which shows little or no variation of  $\eta$  with time would not be expected to contain hydrogen.) The amount of absorbed hydrogen in equilibrium with the cathode at high current densities is thus higher than that in equilibrium at low current densities. Because a new equilibrium with lower absorbed hydrogen is only slowly established, the probability of the combination of adsorbed hydrogen



is larger than that corresponding to equilibrium conditions for absorbed hydrogen. Gradually this excess of  $H_{ads.}$  over the equilibrium value disappears and the potential rises to its final value.

The author wishes to express his gratitude to Prof. G. Angel, Stockholm, for much good advice during the progress of this work, and to Dr. J. O'M. Bockris, Dr. J. F. Herringshaw, Dr. R. Parsons and Dr. B. Conway, and to Mr. E. C. Potter for valuable discussion during the preparation of the paper. He is also grateful to the Swedish State Council of Techn. Research for a grant.

*Royal Institute of Technology,  
Division of Applied Electrochemistry,  
Stockholm.*

<sup>33</sup> Hickling and Salt, *Trans. Faraday Soc.*, 1942, 38, 474.

# SOME APPLICATIONS OF INTENSITY MEASUREMENTS IN THE INFRA-RED

By R. E. RICHARDS AND W. R. BURTON

Received 19th May, 1949

Absolute extinction coefficients have been measured for the N—H absorption band near  $3400\text{ cm}^{-1}$ , and the C—O vibrations near  $1700\text{ cm}^{-1}$  in a number of compounds. The band areas were obtained by direct integration of an error function which was fitted to the absorption curves. By treating the N—H link as a harmonic oscillator with fixed charges on the nuclei, a value of 0.8D was obtained for the dipole moment of the N—H link. The extinction coefficient of the characteristic carbonyl band at  $1700\text{ cm}^{-1}$  is shown to be related to the polarity of the C—O link.

Previous applications of infra-red spectroscopy to the study of molecular structure have largely depended on the determination of the frequencies of the maxima of absorption bands;<sup>1</sup> this work is a preliminary investigation of the possibility of using absolute extinction coefficient determinations to study the molecular structure of polyatomic molecules. Relatively little work on these lines has been reported. Fox and Martin<sup>2, 3, 4</sup> have described the study of the hydrogen bond by measurement of the intensity of certain infra-red absorption bands of hydroxylic substances in solutions of different concentrations, and Bell, Thompson and Vago<sup>5</sup> have used the intensity of a C—H bending vibration of the aromatic ring to obtain a measure of the value and direction of the dipole moments in these compounds. Thorndike, Wells and Wilson<sup>6</sup> have made careful measurements of extinction coefficients in simple substances such as  $\text{N}_2\text{O}$  and  $\text{CO}_2$ .

The extinction coefficient of an absorption band in the infra-red can be shown to be a function of the change of dipole moment of the molecule during the vibration.<sup>7</sup> For a binuclear simple harmonic oscillator, it is easy to obtain an expression relating the area of an absorption band to the reduced mass of the link, and to the net charge  $e$  resident on each atom, this being assumed to remain constant during the vibration. This assumption is, of course, not valid for molecules, but if the dipole moment of the link is obtained in this way and compared with that obtained by other methods, it might be possible to discover how the charge distribution varies within the link during the vibration.

Now the area of an absorption band is given by<sup>7, 8</sup>

$$\int a_\nu d\nu = \frac{h\nu}{c_m} (B_{n \rightarrow m} \cdot N_n - B_{m \rightarrow n} \cdot N_m),$$

where  $a_\nu$  is the extinction coefficient at frequency  $\nu$  c./sec.,  $c_m$  is the velocity of light in the medium,  $N_n$  is the number of molecules per  $\text{cm}^3$  in the vibrational level  $n$ ,  $N_m$  is the number of molecules per  $\text{cm}^3$  in the level  $m$ , and  $B_{n \rightarrow m} = B_{m \rightarrow n}$  is the Einstein coefficient of absorption. At room

<sup>1</sup> E.g. Thompson, *J. Chem. Soc.*, 1944, 183; Barnes, Gore, Liddel and Williams, *Infra-red Spectroscopy*.

<sup>2</sup> Fox and Martin, *Proc. Roy. Soc. A*, 1937, **162**, 419.

<sup>3</sup> *Idem.*, *ibid.*, 1938, **167**, 257.

<sup>4</sup> *Idem.*, *Trans. Faraday Soc.*, 1940, **36**, 397.

<sup>5</sup> Bell, Thompson and Vago, *Proc. Roy. Soc. A*, 1948, **192**, 498.

<sup>6</sup> Thorndike, Wells and Wilson, *J. Chem. Physics*, 1946, **14**, 578; 1947, **15**, 157, 868.

<sup>7</sup> Pauling and Wilson, *Introduction to Quantum Mechanics*.

<sup>8</sup> Tolman, *Quantum Mechanics in Physics and Chemistry*.

temperatures,  $h\nu/kT$  is fairly large, so that  $N_n$  may be considered large compared with  $N_m$ , and we can write

$$\int a_\nu d\nu = \frac{h\nu N_n B_{n \rightarrow m}}{c_m}.$$

For a simple harmonic oscillator in a medium of dielectric constant  $\epsilon$ ,

$$B_{n \rightarrow n+1} = \frac{\pi e^2 (n+1)(\epsilon+2)^2}{3\mu h\nu \cdot 9\epsilon},$$

where  $\mu$  is the reduced mass of the link, and  $\nu$  is its vibration frequency. For this case, we have therefore,

$$\int a_\nu d\nu = \frac{N_n \pi e^2 (n+1)(\epsilon+2)^2}{3\mu c_m \cdot 9\epsilon}.$$

For the fundamental vibration frequency,  $n = 0$ .

It is well known<sup>9, 10</sup> that links between hydrogen and a heavy atom such as oxygen, nitrogen or carbon, behave to a considerable extent as independent oscillators, which are very little affected by variations of the masses of the groupings attached to the heavy atom. We have studied the extinction coefficient of the stretching vibration of the N—H link, and evaluated its dipole moment on the assumption that the charge distribution remains constant and that the link can be treated as a simple harmonic oscillator.

Another approach is to study the extinction coefficient of an absorption band known to be "characteristic" (ref. 9, p. 194) of a certain grouping in a related series of molecules, where the charge distribution within the group would be expected to vary along the series. We have chosen the carbonyl group for this investigation, and a correlation with current views on the structures of the compounds studied is obtainable.

## Experimental

All the measurements were carried out on a Hilger D209 double-beam spectrometer,<sup>11</sup> using a fluorite prism. The slit widths used were 0.14 mm. at 3250 cm.<sup>-1</sup>, and 0.50 mm. at 1700 cm.<sup>-1</sup>. The compounds studied were obtained commercially or prepared in this laboratory, and in all cases were purified by the appropriate methods. Two absorption cells were used; the one for use with the N—H compounds was made from a glass tube, 5.07 cm. long, with flanged ends to which rocksalt windows were sealed, and for the carbonyl compounds a rocksalt cell was used, of the usual kind provided with filling tubes which could be sealed off.<sup>12</sup> The thickness of the short cell was found to be about 0.03 mm., by measuring the absorption of a solution of azobenzene in benzene of known concentration and extinction coefficient, in light of wavelength 4360 Å. The concentrations used were within the ranges: (a) for the N—H compounds,  $1 - 10 \times 10^{-6}$  mole/cm.<sup>3</sup> in carbon tetrachloride, (b) for the C=O compounds  $1 - 20 \times 10^{-5}$  mole/cm.<sup>3</sup> in chloroform. The absorption cell was always replaced at a focus of the test beam of the spectrometer by means of positioning marks, and the reproducibility of this and of the instrument was checked by repeating each record at least twice. In order to obtain the position of the 0% absorption line, the record was repeated under exactly the same conditions using pure solvent in the absorption cell, and this record could then be super-imposed on that of the solution. For measurements near 1700 cm.<sup>-1</sup> chloroform was always used as a solvent, and near 3300 cm.<sup>-1</sup> carbon tetrachloride was the solvent.

Throughout the measurements the speed of the prism drive was maintained constant, so that a length of  $x$  cm. on the chart corresponded to a frequency

<sup>9</sup> Herzberg, *Infra-red and Raman Spectra*.

<sup>10</sup> Linnett, *Trans. Faraday Soc.*, 1945, **41**, 223.

<sup>11</sup> Thompson, Whiffen, Richards and Temple, *Report 17, Hydrocarbon Group, Inst. Petroleum*.

<sup>12</sup> Whiffen and Thompson, *J. Chem. Soc.*, 1945, 268.

## 876 INTENSITY MEASUREMENTS IN THE INFRA-RED

range of  $\pi c \bar{\nu}_k$  c./sec., where  $\bar{\nu}_k$  is the number of wave numbers corresponding to 1 cm. on the chart at the wavelength being studied. We have, therefore,

$$\frac{(\epsilon + 2)^2 N_n \pi e^2}{9\epsilon \cdot 3\mu c_m} = \int a_\nu \bar{\nu}_k c \cdot d\alpha.$$

For convenience in evaluating the results, we write

$$a_\nu = 1 - (\ln y)/d,$$

where  $y$  is the transmission at frequency  $\nu$ , and  $d$  cm. is the length of the absorbing path. Putting

$$K = \frac{-\log_{10} y}{C} = \frac{a_\nu d}{2.303 C},$$

where  $C$  is the concentration of the solution in mole/cm.<sup>3</sup>, we have

$$\int K d\alpha = \frac{(\epsilon + 2)^2 \cdot N \pi e^2 d}{9\epsilon \cdot 3\mu C c_m \bar{\nu}_k \cdot 2.303}$$

since  $N_n/C = N$ , the Avogadro number. The value of  $\int K d\alpha$  is therefore related to  $e^2$  for the simple case considered, the other quantities being known.

The value of this integral could be obtained by replottting the absorption band as a graph of  $K$  against  $\alpha$  for each solution, finding the areas by counting squares, and averaging the results. In order to reduce the labour involved in this method, we have fitted the absorption curve to an equation, from which the integral could then be obtained directly from the dimensions of the original record. The value of the integral  $\int K d\alpha$  is not altered by changing the position of the origin on the  $\alpha$  axis, so that we have taken the value of  $\alpha$  at the absorption maximum to be  $\alpha = 0$ . The majority of absorption bands studied were symmetrical about the peak, so  $K$  is an even function of  $\alpha$ , and may be written

$$K = f(\alpha^2).$$

The function

$$f(\alpha^2) = A/(1 + B\alpha^2)$$

was tried, but found to be unsatisfactory. Exponential functions have been found to be most suitable. The expression

$$f(\alpha^2) = Ae^{-B\alpha^2 - D\alpha^4}$$

was found to be no more satisfactory than the simple error function  $Ae^{-B\alpha^2}$ , which fitted every curve within the experimental error. Thus we may write

$$\int K d\alpha = \int_{-\infty}^{+\infty} Ae^{-B\alpha^2} d\alpha = A\sqrt{\pi/B}.$$

The constant  $A$  is identical with the value  $K_0$  of  $K$  at the peak, so that we have

$$\frac{\log_{10} K_0/K}{\alpha^2} = \frac{B}{2.303} = B',$$

so that the integral required is

$$K_0 \sqrt{\frac{\pi}{2.303 B'}}.$$

The value of  $B'$  can be found at any point on the curve. Its constancy along the curve is a measure of the closeness with which the error function represents the curve, and consequently is a good test of the accuracy of the area obtained, since a fractional variation  $g$  in the value of  $B'$  involves a variation of only  $\frac{1}{2}g$  in the value for the area obtained. It was usual to study about eight solutions, and values for the integral were obtained with a standard deviation of about 3%.

**The N—H Link.**—The values of  $\int K d\alpha$  for the N—H stretching vibration of three compounds, are given in Table I. Unfortunately it has not been possible to study a larger number of compounds of this type owing to limitations of solubility in carbon tetrachloride, which is the most convenient solvent for this region of the spectrum. The values of  $\int K d\alpha$  in Table I are comparable

to within 5 %, but may be subject to a greater absolute error. If the N—H link is treated as a binuclear harmonic oscillator as described above, we obtain the average values of the charges resident on each nucleus which are given in the last column of Table I. The dielectric constant is assumed to be that of carbon tetrachloride in all cases.

TABLE I.—N—H VALENCY VIBRATION NEAR 3400 CM.<sup>-1</sup>. SOLUTIONS IN CARBON TETRACHLORIDE

	$\bar{\nu}$ cm. <sup>-1</sup>	$K_0$	$\int K dx$	$\epsilon$ (electrons)
Methyl aniline	3430	95,000	305,000	0.16
Ethyl aniline	3430	89,000	300,000	0.16
Diphenylamine	3435	143,000	390,000	0.17 <sub>6</sub>

$K = \frac{-\log_{10} y}{x}$  where  $\nu$  = transmission  $C$  = concentration of solution in mole/cm.<sup>3</sup>.

$K_0$  = value of  $K$  at  $x = 0$ , i.e., at peak.  
 $x$  is measured in cm.

The larger value of  $\int K dx$  in diphenylamine shows that the change of moment of the N—H link in its stretching vibration is greater than with the other two compounds. For methyl and ethyl anilines, the moment of the N—H link is found to be about 0.8D, taking the N—H length as 1.01 Å.<sup>13</sup> From the dipole moment of ammonia (1.437D<sup>14</sup>), a value for the moment of the N—H link can be deduced by simple vector methods to be 1.28D. This is higher than the value obtained above for methyl and ethyl anilines, but it may be of interest to note that the electronegativity difference between hydrogen and nitrogen would suggest that the N—H bond has a moment of about 0.9D.<sup>15</sup> The neglect of anharmonicity of the N—H vibration in the above calculations cannot lead to very serious error, since its effect on the transition moment is small. This has been confirmed by second-order perturbation theory calculations for a diatomic molecule, using a potential function of the type :

$$V(x) = 2\pi^2\nu^2x^2 + ax^3 + bx^4.$$

Using plausible values<sup>16</sup> for the constants  $a$  and  $b$ , it is found that the transition moment differs only by about 3 % from that calculated on the basis of a harmonic oscillator. Rosenthal<sup>17</sup> has obtained a similar result using a Morse function. The low value of the moment of the N—H link found above is probably largely due to the fact that the fractional charges on the nitrogen and hydrogen atoms decrease as the link is stretched and increase as the link is compressed.

**The Carbonyl Link.**—The values of  $\int K dx$  for the C—O stretching vibration bands of a set of carbonyl compounds are given in Table II ; the estimated error is obtained from the closeness with which the absorption bands fit the error function used. The intensities show a steady variation from acetaldehyde to the amides, which have band areas nearly three times as great as the aldehydes.

Unfortunately, this link cannot be treated as an isolated harmonic oscillator in the same way as the N—H link, although there is evidence that this vibration is not greatly affected by the masses of the attached grouping.<sup>9, 18</sup> It is probable that this vibration is the one represented by  $\nu_1$  (Fig. 1<sup>19</sup>) except possibly in aldehydes, when the vibration might approach more closely to  $\nu_2$  (Fig. 1).

<sup>13</sup> Ref. <sup>9</sup>, p. 439.

<sup>14</sup> Van Itterbeek and De Clippeleier, *Physica*, 1946, **12**, 97.

<sup>15</sup> Malone, *J. Chem. Physics*, 1933, **1**, 197; Smyth, *J. Physic. Chem.*, 1937, **41**, 209; *J. Amer. Chem. Soc.*, 1938, **60**, 183.

<sup>16</sup> Linnett, *Trans. Faraday Soc.*, 1948, **44**, 556.

<sup>17</sup> Rosenthal, *Proc. Nat. Acad. Sci.*, 1935, **21**, 281.

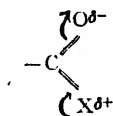
<sup>18</sup> Richards, Hartwell and Thompson, *J. Chem. Soc.*, 1948, 1436.

<sup>19</sup> Burkard, *Proc. Indian Acad. Sci.*, 1938, **8**, 365.



## 878 INTENSITY MEASUREMENTS IN THE INFRA-RED

It can be seen that for either mode, there would be expected a qualitative relationship between the charge separation in the molecule due to such mechanisms as



and the change of moment during the vibration, this being related to the band area. The results of Table II therefore suggest that the charge separation

TABLE II

Compound	$K_0$	$\int K dx$
Acetaldehyde . . . . .	2400	2200
Propionaldehyde . . . . .	1740	2200
Diethyl ketone . . . . .	1900	2150
Cyclohexanone . . . . .	2490	2900
Acetophenone . . . . .	2540	3000
Acetyl chloride . . . . .	2200	3300
Methyl propionate . . . . .	2620	3700
<i>n</i> -Amyl propionate . . . . .	2450	4050
Ethyl acetate . . . . .	2650	4200
Acetic acid . . . . .	3500	4400
Propionic acid . . . . .	3200	4400
Phenyl acetic acid . . . . .	3220	4500
Benzoic acid . . . . .	3930	5750
Acetanilide . . . . .	2220	4500
Methyl-aceto- <i>p</i> -toluidide . . . . .	4400	6300
Methyl-aceto- <i>o</i> -toluidide . . . . .	4320	6500
Diethyl formamide . . . . .	5315	7300

Estimated error = 10 %. For units see text.

due to electronic shifts of the kind suggested, increases along the series: aldehyde, ketone, acid-chloride, ester, acid, amide. This order fits well with that expected on other grounds,<sup>20</sup> although Walsh<sup>21</sup> suggests on the basis of ionization potential measurements that acetaldehyde possesses a more polar carbonyl group than acetyl chloride. This disagreement may arise from the uncertainty of the exact form of the vibrations of aldehydes being considered.

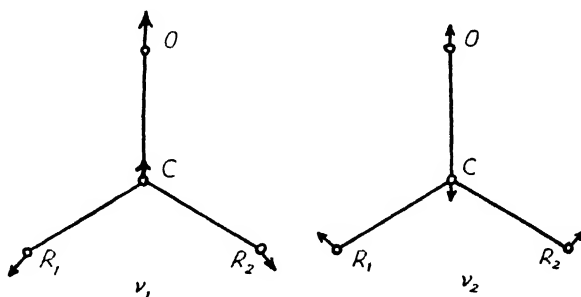


FIG. 1.

From the preliminary measurements on these two sets of molecules, it may be concluded that although the precise theoretical interpretation of the results is far from satisfactory, studies of this kind may well be of value when applied

<sup>20</sup> Walsh, *Trans. Faraday Soc.*, 1946, **42**, 56; *ibid.*, 1947, **43**, 158. Richards and Thompson, *ref.* <sup>18</sup>.

<sup>21</sup> Walsh, *Trans. Faraday Soc.*, 1946, **42**, 56.

in a semi-empirical way. For example, it may be possible to study variations in the properties of a grouping in a related set of molecules, or to estimate quantitatively the number of groupings of a particular kind in a molecule of unknown structure.

In conclusion we should like to express our<sup>\*</sup> appreciation to Dr. H. W. Thompson, F.R.S., for advice and the use of the spectroscopic equipment, and to Mr. T. L. Cottrell and Dr. D. H. Whiffen for helpful discussions.

*Physical Chemistry Laboratory,  
Oxford.*

---

## THE DETERMINATION OF THE SURFACE AREA OF A SOLID FROM AN ADSORPTION ISOTHERM

BY JAMES F. DUNCAN

*Received 22nd October, 1948; as revised 23rd May, 1949*

The Harkins method, and the Brunauer, Emmett and Teller method of estimating the surface area of a solid from the adsorption isotherm of a suitable gas are applied to isotherms of ethylene at liquid air temperature. It is shown that both methods lead to the same results for a given isotherm. The isotherm equation of Harkins, and the Brunauer, Emmett and Teller equation as modified by Anderson are reduced to the form  $p/p_0 = C(1 - V_m/(DV))$ ; it is shown that from the Anderson constant  $K$ , and assuming a given value for the area occupied by an adsorbed molecule, the Harkins constant  $k$  may be estimated approximately. A more accurate value of  $k$  is obtained from the plot of  $p/p_0$  against  $1/V$  for isotherms of nitrogen and ethylene. A quick method of determining the surface areas of large numbers of solids to about 20 % accuracy is suggested, based on the assumption of a value for the Anderson constant, and the linearity of the  $p/p_0 - 1/V$  plot over the range of  $p/p_0$  from 0.25 to 0.75.

The area of a porous solid is conveniently estimated from an adsorption isotherm of a suitable gas determined under conditions of physical adsorption. The work of Harkins<sup>1</sup> and also of Brunauer, Emmett and Teller<sup>2</sup> has provided alternative methods of estimating the surface area of a porous solid from a given isotherm, and the values obtained using the two different methods are in very good agreement.

The present paper gives some conclusions based on the determination of the surface areas of several different powders, estimated by measuring the adsorption of ethylene on the powder at liquid-air temperature. Both methods of calculating the surface area were used and in general good agreement was obtained. In the progress of this work, however, it was noticed that provided the constant  $c$  of the B.E.T. equation is large, the equations of state associated with the two methods could be reduced to identical form and another simpler method of calculation could be adopted. The number of samples of which it was necessary to determine the surface area was quite small, but if large numbers of surface area measurements are to be made a quick routine method could be developed which requires only one measurement of the quantity of gas adsorbed at an equilibrium pressure of about half the saturation vapour pressure.

<sup>1</sup> Harkins and Jura, *J. Amer. Chem. Soc.*, 1944, **66**, 1366.

<sup>2</sup> Brunauer, Emmett and Teller, *ibid.*, 1938, **60**, 309.

## Experimental

**Apparatus.**—The apparatus is shown in Fig. 1. The volume of ethylene adsorbed was measured at liquid-air temperatures; at this temperature the adsorption of ethylene is completely physical. The whole apparatus was pumped out with a mercury diffusion pump and the glass thoroughly flamed. Ethylene

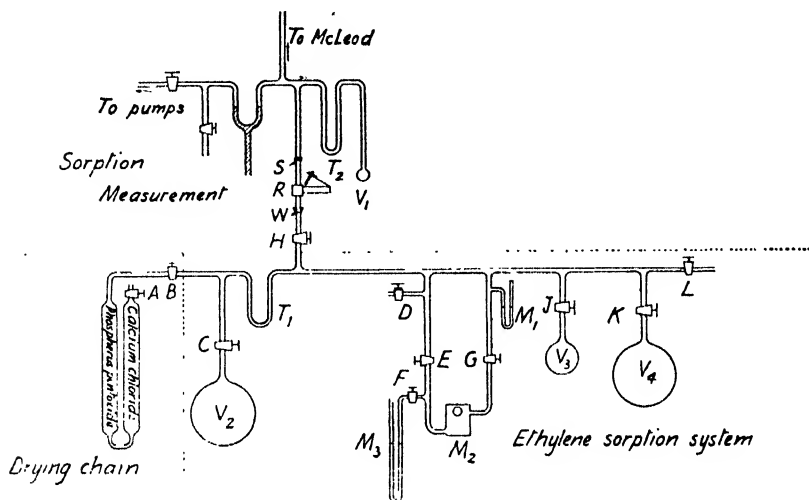


FIG. 1.—The sorption of ethylene at liquid air temperature.

A, B, C, D, E, F, G, H, J, K, L, Taps.  $M_1$ , Mercury manometer.  $M_2$ , Bellows manometer.  $M_3$ , Oil manometer. R, Fine control valve. S, Copper-glass seal.  $T_1$ ,  $T_2$ , Liquid air traps.  $V_1$ , Sorption vessel.  $V_2$ ,  $V_3$ ,  $V_4$ , Storage vessels (1½ l., 500 cm.<sup>3</sup> and 2 l. respectively). W, Black wax joint.

from a cylinder was introduced through a drying train until the pressure in the entire ethylene storage system (as measured in the mercury manometer  $M_1$ ) was about 10–15 cm. Hg. It was then frozen in the liquid-air trap  $T_1$  and any permanent gases were pumped away. The ethylene was successively evaporated and condensed in order to remove entrapped gases, which were pumped off. The drying train was then isolated and the trap immersed in a carbon dioxide-methanol mixture. The ethylene evaporated and filled the storage vessel; the flasks  $V_3$  and  $V_4$  were then isolated and the residue was pumped off after the trap  $T_1$  had been raised to room temperature. This procedure was repeated before each experiment.

The rate of entry of the ethylene into the adsorption vessel was controlled by a needle valve R, the needle of which was isolated from the atmosphere by means of a bellows.<sup>3</sup> A differential bellows manometer  $M_2$ , designed to measure pressures up to 15 mm. Hg with ½ % accuracy and previously calibrated against the oil manometer  $M_3$ , was used to measure the amount of ethylene let into the adsorption chamber. The gas in flask  $V_3$  or flask  $V_4$ , according to the adsorption expected, was allowed to fill both sides of the manometer and the entire volume from tap C to tap I and up to the needle valve (taps B, C, F, L and D and the needle valve being shut). Tap E was then closed and the pressure-drop occurring when gas was let into the adsorption chamber was determined.

The adsorption was measured on a McLeod gauge after about 2 hr. had been allowed for equilibrium to be established. Before the gas was admitted to the adsorption chamber the mercury cut-off was raised and liquid air was placed round trap  $T_2$  to prevent the back diffusion of mercury to the surface of the cooled powder.

**Errors Due to Thermal Transpiration.**—In measuring the adsorption of gases on solids many corrections must be made. For the measurement of sur-

<sup>3</sup> To be described in a forthcoming publication.

<sup>4</sup> Kuhn and East, *J. Sci. Instr.*, 1946, **33**, 185.

face areas most of these are small. The most serious error is that due to thermal transpiration. At very low pressures the relation between the pressures at the ends of a tube at temperatures  $T_1$  and  $T_2$  has been shown by Knudsen to be

$$p_1/p_2 = (T_1/T_2)^{1/2}.$$

This relation is true when  $2r/\lambda < 1$  (where  $r$  is the radius of the tube and  $\lambda$  is the mean free path of the gas). At higher pressures a dynamic equilibrium is set up due to the transfer of gas back along the centre of the tube. This state may also be treated theoretically for  $2r/\lambda > 10$ . At a pressure of  $10^{-3}$  mm. the mean free path is 32.4 mm. and at  $10^{-2}$  mm. it is 3.24 mm. Thus for the 8 mm. tubing used we are in the intermediate range between  $10^{-3}$  and  $10^{-2}$  mm. where the extent of the transpiration cannot easily be computed. In a theoretical treatment, Weber<sup>5</sup> has given a correction for this range for oxygen and hydrogen but not for ethylene. For 8 mm. tubing he predicts a difference of  $0.99 \times 10^{-3}$  mm. at an absolute pressure of  $10^{-2}$  mm. when one end is at room temperature and the other is immersed in liquid air; for 25 mm. tubing the correction is  $0.26 \times 10^{-3}$  mm. Thus, there should be a difference of observed pressure measured through 8 mm. tubing and through 25 mm. tubing. In actual fact, no difference was noticed for ethylene at  $10^{-2}$  mm. pressure, and not until pressures of less than  $3 \times 10^{-3}$  mm. was any difference greater than experimental error found. The effect of this error on surface area measurements is therefore small.

Errors such as the adsorption of ethylene on the cooled glass and on the metal parts of the apparatus were shown to be small from a "blank" experiment; thus, when 2 g. of powder was used the error was less than 1%. The same is true of the error due to the reduction in pressure of the gas on cooling the traps in liquid air. Applying the appropriate corrections the surface areas of the powders relative to each other (for the same method of calculation) should be obtained to  $\pm 5\%$ .

## Results

**Method of Calculation.**—The equation put forward by Brunauer, Emmett and Teller is

$$V \frac{p}{(p_0 - p)} = \frac{1}{V_m c} + \frac{c-1}{c} \cdot \frac{1}{V_m} \cdot \frac{p_0}{p}, \quad (1)$$

where  $V$  is the volume at N.T.P. adsorbed at a pressure  $p$ ,  $V_m$  is the volume at N.T.P. adsorbed when the entire surface is covered by a unimolecular layer,  $p_0$  is the saturation vapour pressure and

$$c = e^{(E_1 - E_L)/RT},$$

where  $E_1 - E_L$  is the difference in the heat of adsorption of the first layer and the latent heat of vaporization.

This equation was used as the basis of the calculation of the surface areas of the powders in the first instance, and the calculation was made by their method. The area occupied by one molecule of ethylene was taken as  $17.55 \text{ \AA}^2$ , as calculated by Wooten and Brown<sup>6</sup> from the density of solid ethylene. In the B.E.T. method of calculation it is necessary to know the adsorption of gas only over a range of  $0.1-0.3 p_0$  ( $28.8 \times 10^{-3}$  mm. for ethylene at liquid-air temperature), and this was the range used in the earlier experiments. In later experiments it was considered desirable to increase this range, however, in order to give more reliable data for Harkins method of calculation. Three only of the seven isotherms taken were over a range sufficiently large to enable them to be used in the calculations given later, although five could be used to give a Harkins plot over a reasonable range. The isotherm equation on which the Harkins method is based is

$$\log_{10} p/p_0 = X - Y/V^2, \quad (2)$$

where  $p$  is the equilibrium pressure when a volume  $V$  has been adsorbed and  $p_0$  is the saturation vapour pressure;  $X$  and  $Y$  are constants for a given gas and a given temperature. Harkins plotted  $\log p/p_0$  against  $1/V^2$  and determined  $X$  and  $Y$ , and showed that the surface area  $A$  of a powder is given by

$$A = kY^{1/2},$$

<sup>5</sup> Weber, *Leiden Comm.*, 1913, 137c, 32. Weber and Onnes, *ibid.*, 1915, 147b, 24.

<sup>6</sup> Wooten and Brown, *J. Amer. Chem. Soc.*, 1943, 65, 113.

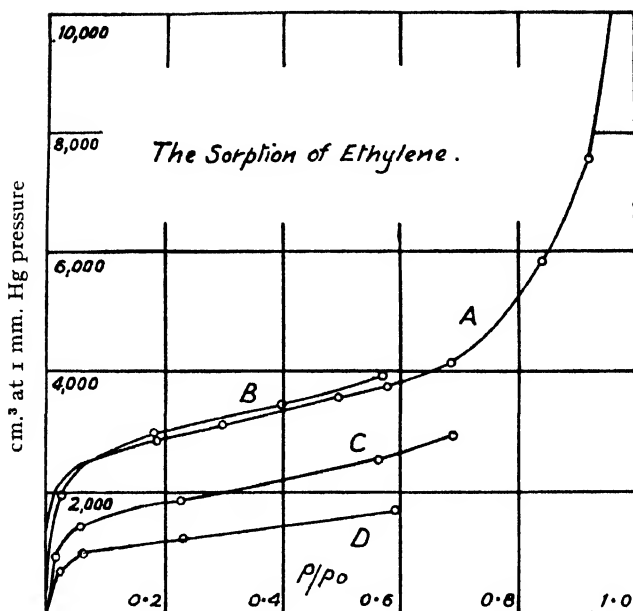


FIG. 2.

A, Adsorbent No. 2 degassed at 100° C. B, Adsorbent No. 2 degassed at 300° C.  
 C, Adsorbent No. 1 degassed at 100° C. D, Adsorbent No. 1 degassed at 300° C.

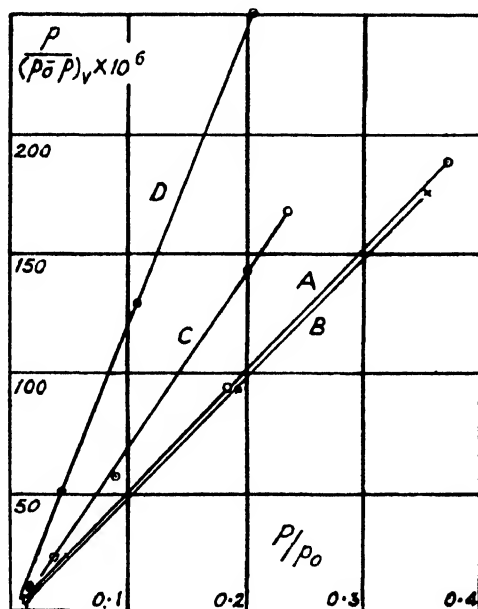


FIG. 3.—B.E.T. plot for isotherms of Fig. 2 (labelled correspondingly).

where  $k$  is a constant for a particular gas at a given temperature. Knowing an absolute value of one surface area, it was possible to calculate any other surface area relative to it. Harkins measured one absolute surface<sup>7</sup> using a crystalline solid which he covered with a film of water by putting it in contact with saturated water vapour. The surface of the water which is very nearly equal to that of the solid was then measured by dropping into liquid water and measuring the heat evolved when the liquid-vapour interface was destroyed.

Harkins then proceeded to calculate  $k$  at a given temperature for nitrogen, water, *n*-butane, and *n*-heptane, but not for ethylene. In the present discussion it was therefore necessary to assume that the B.E.T. method of calculation gave the correct surface area in one case, to obtain the value of  $k$  assuming this value, and to use it to calculate the surface areas in other cases by the Harkins method. The value of  $k$  used for ethylene at liquid-air temperature was 4.25 and was obtained for the set of results marked with an asterisk in Table I. The

TABLE I  
SURFACE AREA OF POWDERS CALCULATED FROM THE SAME ISOTHERMS  
IN DIFFERENT WAYS

ETHYLENE ISOTHERMS

Adsorbent	Harkins ( $k = 4.25$ ) (m. <sup>2</sup> )	B.E.T. (Cross-sectional Area of Molecule $= 17.55 \text{ \AA}^2$ ) (m. <sup>2</sup> )	$c$
Insoluble ionic crystallite No. 1 degassed at 100° C . . . . .	5.26	5.17	140
Insoluble ionic crystallite No. 1 degassed at 300° C . . . . .	3.16	3.08	180
Insoluble ionic crystallite No. 2 degassed at 100° C . . . . .	20.1 *	20.1 *	110
Insoluble ionic crystallite No. 2 degassed at 300° C . . . . .	20.1	20.5	110

remaining figures in the first column of Table I were calculated by the Harkins method, assuming this value of  $k$ . The actual isotherms upon which these results are based are shown in Fig. 2 and the B.E.T. and Harkins plots in Fig. 3 and 4 respectively.

Curve D

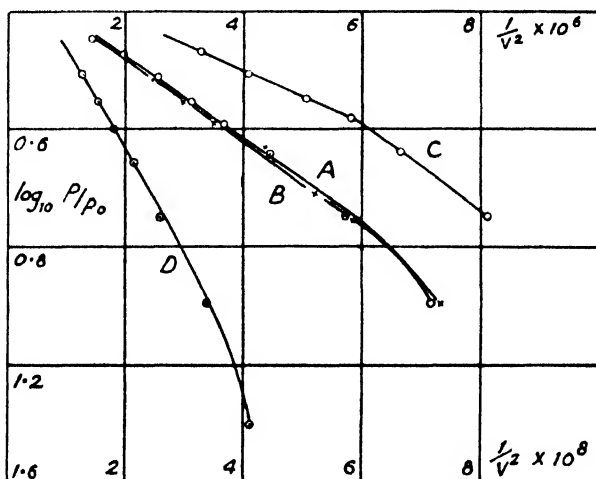


FIG. 4.—Harkins plot for isotherms of Fig. 2 (labelled correspondingly).

<sup>7</sup> Harkins, *J. Amer. Chem. Soc.*, 1944, **66**, 1362.

## Discussion

It may be noted that there is good agreement between the two methods of calculation using the isotherms of the liquid-air temperature adsorption of ethylene. It has been shown by Emmett<sup>8</sup> that an approximately straight-line Harkins plot is obtained only when the constant  $c$  of the B.E.T. theory is between 50 and 250. This is true in the present case as will be seen, and the above figures afford good confirmation of the conclusion of Harkins<sup>1</sup> that the two methods of calculation are in accord under conditions where only physical adsorption (van der Waals') is present. Since Emmett<sup>8</sup> showed that there are apparently some differences in the area occupied by adsorbed molecules for different values of  $c$ , the good agreement obtained is apparently fortuitous, and we might have had to assume a slightly different value from that given by Wooten and Brown for the area of an ethylene molecule to obtain agreement between the two methods.

**Comparison between the Two Methods of Calculation.**—In all the calculations which were performed to estimate the surface areas of powders by the B.E.T. method using ethylene adsorption isotherms, it was found that straight line plots were usually obtained over the range of  $p/p_0$  of 0.1 to 0.3. Above 0.3 and sometimes even below that value, the straight-line plot becomes curved.

In the B.E.T. treatment it is assumed that the heat of adsorption of the second to  $n$ th layers is the same as the heat of vaporization of the adsorbate. This is obviously untrue, since measured heats of adsorption are never independent of the quantity adsorbed. Nevertheless, it is a good approximation. But in making this assumption, Brunauer, Emmett and Teller attempt to describe the shape of the adsorption isotherm over the whole range of pressures up to  $p_0$ . From eqn. (1), it might be expected that straight-line plots would be obtained over the range  $p/p_0$  from 0.05 up to 1.0 (the former limit given by Brunauer since the heat of adsorption is rapidly altering during the first half layer). In general, this is far from true, and assuming the value of the surface area given by the linear portion, it seems that the B.E.T. equation is valid only over the range where the latter part of the first and the initial part of the second molecular layer is adsorbed; this is because of the approximate nature of the assumption of the equality of the heat of vaporization and the heat of adsorption of the second to  $n$ th layers. It has been shown by Anderson<sup>9</sup> that if  $\frac{p/p_0}{V(1 - Kp/p_0)}$  is plotted against  $p/p_0$ , where  $K$  has a

value of about 0.7 for nitrogen, a straight-line plot is obtained over the range of  $p/p_0$  from 0.05 to 0.7. He points out that this may be accounted for by assuming that the heat of adsorption of the second to higher layers is less than the heat of liquefaction by about 50 cal.

The findings of Anderson were in accordance with observations of the adsorption of ethylene, where it was found that the plot of  $p/(p_0 - Kp)V$  against  $p/p_0$  gave a good straight line for  $p/p_0$  values from 0.05 to 0.8 and  $K$  had a value of about 0.6. Three such plots are reproduced in Fig. 5.

When the Anderson modification is adopted, the equation can be used over the major part of the isotherm ( $0.05 < p/p_0 < 0.8$ ). The Harkins equation is also applicable for most of the same range (at least for  $0.3 < p/p_0 < 0.8$ , when  $c > 50$ ). Since both equations of state can be applied to the same results it is possible to reduce them to identical mathematical forms, and thus to obtain a relation between the constants of the two equations. Below are given mathematical treatments of the two equations showing that they can both be reduced to the form

$$\frac{p}{p_0} = C \left( 1 - \frac{V_m}{VD} \right) \quad . \quad . \quad . \quad (3)$$

<sup>8</sup> Emmett, *J. Amer. Chem. Soc.*, 1946, **68**, 1784. <sup>9</sup> Anderson, *ibid.*, 1946, **68**, 686.

where  $C$  and  $D$  are constant. There are no contradictory assumptions involved in the Harkins theory and the B.E.T. theory, which might vitiate such an attempt; one has a thermodynamic approach and the other is kinetically derived. There are, however, conditions introduced in the treatment given below which restrict the applicability of eqn. (3) to a range of  $p/p_0$  from about 0.25 to 0.75.

**Simplification of Harkins and B.E.T. Equations: Harkins Equation.**

Since  $A = kY^{\frac{1}{2}}$ ,

then 
$$V_m = \frac{FA}{k} = FY^{\frac{1}{2}},$$

where  $F$  is a constant, and if  $V_m$  is in  $\text{cm}^3$  N.T.P. per g. adsorbent,  $A$  in  $\text{m}^2/\text{g}.$  adsorbent,  $a$  is the area (in  $\text{\AA}^2$ ) of the surface of the adsorbent occupied by 1 molecule of the adsorbate in a completed monolayer, then

$$F = \frac{3.69k}{a},$$

the factor 3.69 being the conversion factor from  $\text{cm}^3$  gas at N.T.P. to  $\text{m}^2$  of surface.

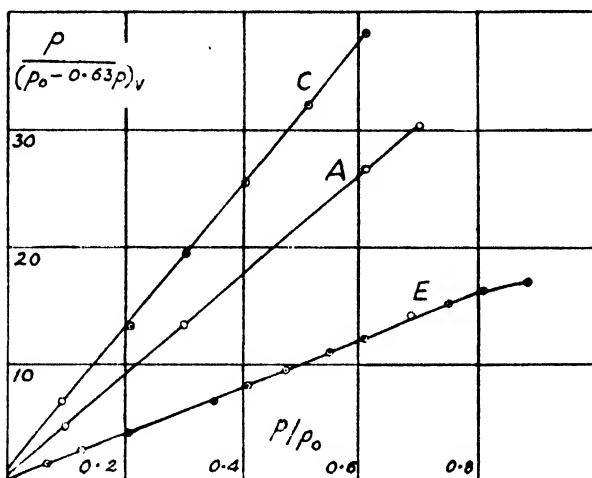


FIG. 5.—Anderson plot for ethylene.

A and C from corresponding isotherms of Fig. 2.

E from isotherm furnished by K. D. B. Johnson (see Table II).

Now since the Harkins plot is straight over the middle portion of the isotherm, putting

$$p/p_0 = \frac{1}{2}[1 + (p - \frac{1}{2}p_0)/\frac{1}{2}p_0] \quad (4)$$

and assuming that  $(p - \frac{1}{2}p_0)$  is small with respect to  $\frac{1}{2}p_0$ , then by eqn. (2),

$$\log_e p/p_0 = 2.303 \log_{10} p/p_0 = 2.303X - 2.303Y/V^2 \quad (5)$$

By (4), 
$$\log_e p/p_0 = \log_e \left\{ \frac{1}{2} \left[ 1 + (p - \frac{1}{2}p_0)/\frac{1}{2}p_0 \right] \right\},$$

$$= \log_e \frac{1}{2} + \log \{ 1 + (p - \frac{1}{2}p_0)/\frac{1}{2}p_0 \} \quad (6)$$

Therefore from (5) and (6) and expanding,

$$2.303X - 2.303Y/V^2 = -(\log_{10} 2) + (p - \frac{1}{2}p_0)/\frac{1}{2}p_0 \text{ approximately} \quad (7)$$

Since  $Y = V_m^2/F^2$ ,

substituting in (7) and transforming, we have

$$\begin{aligned} 2.303V_m^2/F^2V^2 &= 2.303(\log_{10} 2) + 2.303X - (p - \frac{1}{2}p_0)/\frac{1}{2}p_0 \\ &= 2.303 \left[ X + \log_{10} 2 \right] \left[ 1 - \frac{p - \frac{1}{2}p_0}{2.303 \cdot \frac{1}{2}p_0(X + \log_{10} 2)} \right] \quad (8) \end{aligned}$$



Since  $X$  is positive, the final term in the bracket is small; taking the square root of both sides and performing a binomial expansion,

$$V_m/FV = (X + \log_{10} 2)^{\frac{1}{2}} \left[ 1 - \frac{p - \frac{1}{2}p_0}{p_0} \cdot \frac{1}{2 \cdot 303 (X + \log_{10} 2)} \right] \text{ approx.} \quad (9)$$

This can be reduced to

$$p/p_0 = C[1 - V_m/VD] \quad (10)$$

where

$$C = 2 \cdot 303H + \frac{1}{2}, \quad (11)$$

$$D = (H + 0 \cdot 217)F/H^{\frac{1}{2}}, \quad (12)$$

and

$$H = X + \log_{10} 2. \quad (13)$$

This treatment is valid over the range where all but the first two terms of the logarithmic and binomial expansions may be neglected. When  $X$  has a value between 0.2 and 0.4 the error arising in the value of  $1/V$  is always less than 5 % over a range of  $p/p_0$  from 0.25 to 0.75. Over the greater part of this range the error is much smaller and can be regarded as negligible compared with experimental errors.

**The Equation of Brunauer, Emmett and Teller.**—The equation as modified by Anderson may be written as

$$\frac{1}{V(1/x - K)} = \frac{1}{cV_m} + \frac{c-1}{c} \cdot \frac{x}{V_m}$$

where  $K$  is the Anderson constant, and  $c$  is the Brunauer constant and

$$p/p_0 = x.$$

Where  $c$  is large,

$$\frac{V_x}{V_m} \left( \frac{1}{x} - K \right) = 1,$$

$$\text{or} \quad x = p/p_0 = \frac{1}{K} \left( 1 - \frac{V_m}{V_x} \right). \quad (14)$$

**Comparison of the Two Derivations.**—By comparing eqn. (10) and (14)  $D$  might be expected to have a value of unity. Further, the Anderson constant  $K$  is directly related to the Harkins constant  $X$  by the relation

$$1/K = 2 \cdot 303H + \frac{1}{2}, \quad (15)$$

where

$$H = X + 0 \cdot 3010.$$

Having determined  $X$  (or  $H$ ) and assuming that  $D$  is equal to unity, it is possible to estimate  $F = 3 \cdot 69k/a$  from eqn. (12). Thus, assuming for nitrogen that  $K = 0 \cdot 7$ , and that the area occupied by a nitrogen molecule at liquid-air temperature is  $16 \cdot 2 \text{ \AA}^2$  (as Brunauer, Emmett and Teller calculate) the value of  $X$  for nitrogen under these conditions is found to be 4.44. The value obtained by Harkins is 4.06. It will be seen later that the value of  $D$  is not exactly unity, as predicted above by the treatment of the B.E.T. equation. It is this which explains the above discrepancy.

Mathematical comparisons of the B.E.T. equation and the Harkins equation have been made by Emmett<sup>8</sup> and also by Livingston.<sup>10</sup> The former author was concerned with the value of the constant  $c$  of the B.E.T. equation and the alteration in the area occupied by the adsorbed molecule for different values of  $c$ . Livingston calculated values of the surface pressure from the B.E.T. adsorption equation and showed that over a wide range the calculated values were in approximate agreement with a two-dimensional equation of state; he has suggested that  $k$  is not in fact a true constant and has concluded that extremely accurate

<sup>10</sup> Livingston, *J. Chem. Physics*, 1947, **15**, 617.

experimental work would be required for an assessment of which equation is the more nearly correct.

The derivations of eqn. (10) and (14) are valid for the same range of  $c$  values as Livingston and Emmett showed to be applicable to the simultaneous validity of the Harkins and the B.E.T. equations. Eqn. (14) has been derived from the Anderson modified B.E.T. equation, the validity of which rests on firm experimental grounds, but which has received no theoretical justification as yet. Dole<sup>11</sup> derived an equation on a statistical model which is similar to the Anderson equation, by assuming the heat of vaporization of the second to the  $n$ th layers to be equal, but different from that of the heat of liquefaction.

It will be noticed that if the B.E.T. equation gives a reasonable value for  $V_m$ , eqn. (14) is valid over that range of pressure ( $0.3 < p/p_0 < 0.75$ ) where sufficient gas has been adsorbed to complete at least a monolayer. Brunauer, Emmett and Teller do not make any assumption as to whether a given layer has been completed before adsorption in a further layer is commenced, but if the heat of adsorption of the first layer is large compared with that in the second to  $n$ th layers (i.e.  $c$  is large), it would be reasonable to suppose that the greater part of the first layer is complete before any further layers begin to be formed. If one assumes that the second to  $n$ th layers are adsorbed on top of an initially completed first layer, then one may derive an equation describing the adsorption of gas after the completion of a monolayer.

Transforming eqn. (14),

$$\text{or} \quad \frac{V - V_m}{V_m} = \frac{Kx}{1 - Kx} \quad (16)$$

Now  $V - V_m$  is the amount of gas adsorbed after the completion of a monolayer, and may be set equal to  $V_x$ .

Hence 
$$V_x = \frac{V_m K x}{1 - K x} \quad . \quad . \quad . \quad . \quad (17)$$

Eqn. (17) has been derived by Dole (his eqn. (10)) on the assumption that the partition function in the liquid state is a certain fraction  $K$  of the pure liquid state partition function (for an infinite number of adsorption layers). Thus, to a first approximation at least, it appears that all layers except the first have the same partition function, which is different from that in the liquid state by an amount given by the Anderson constant  $K$ , equal to the ratio of the partition function in these layers and in the liquid state. This statement is true only when the heat of vaporization of the first layer is much larger than that of the remaining layers (i.e.  $c$  is large) but under such conditions adsorption seems to occur on top of an initially adsorbed first layer, which is only slightly affected by wide changes in pressure. This presumably accounts for the absence of  $c$  from eqn. (10), valid over a pressure range ( $0.3 < p/p_0 < 0.75$ ), where the initially adsorbed layer is substantially complete.

Eqn. (3) also predicts that the plot of  $p/p_0$  against  $1/l$  should give a straight line over the range of  $p/p_0$  where the derivation is valid. A series of such plots were therefore made using isotherms for which the value of the B.E.T. constant  $c$  was known to be large (cf. Fig. 6 and 7). From each plot

- (i) the value of  $V_0$  given by the reciprocal of the intercept on the  $I/V$  axis: and
- (ii) the constant  $D$  equal to  $V_m/V_0$  were evaluated.

<sup>11</sup> Dole, *J. Chem. Physics*, 1948, 16, 25.

For this it was necessary to use the best value of  $V_m$ . In most cases this was the value obtained using the simple B.E.T. eqn. (1). In order to increase the scope of the treatment, several isotherms of Harkins, and also of Brunauer, Emmett and Teller were included in these calculations. Since most of their papers do not give actual experimental results it was possible only to interpolate the data used from the graphs given. However, for the nitrogen isotherm on anatase it was possible to assume the value of  $V_m$  which was calculated by Harkins<sup>7</sup> using his absolute method of determining the surface from the heat of immersion in water of anatase. The value obtained by this independent method was in good agreement with the nitrogen isotherm measurement using the same powder. For the results marked† in Table II, the area of the solid calculated by Harkins did not agree very closely with the nitrogen isotherm value;

TABLE II  
RESULTS OF CALCULATIONS FROM THE PLOT  $p/p_0$  AGAINST  $1/V$

Adsorbate	Adsorbent	$V_m$ (B.E.T.) cm. <sup>3</sup> at 1 mm. Hg press.	Inter- cept $V_0$ cm. <sup>3</sup> at 1 mm. Hg press.	$D$	Inter- cept $C$	And- er- son Con- stant $K$	Harkins Con- stant $X$	$F$	Harkins Con- stant $A$
Ethylene at -195.8° C	Insoluble ionic crystallite No. 2 degassed at 100° C.	3800	3850	0.99	1.56	0.64	0.16	0.99	4.66
	Insoluble ionic crystallite No. 3 degassed at 300° C	3500	3782	0.96	1.54	0.65	0.15	0.96	4.75
	Insoluble ionic crystallite No. 1	912	956	0.98	1.57	0.64	0.16	0.98	4.65
	Insoluble ionic crystallite No. 4 §	5000	5260	0.98	1.72	0.58	0.23	0.96	4.60
				Average		0.63			4.65
Nitrogen at -195.8° C	Anatase <sup>6</sup>	(cm. <sup>3</sup> at N.T.P.) 3.23	(cm. <sup>3</sup> at N.T.P.) 3.54	0.91	1.49	0.60	0.43	0.92	4.03
	(Surface treated Anatase <sup>5</sup> )	(2.20)†	(2.75)	(0.80)	(1.56)	(0.58)	(0.46)	(0.80)	(3.50)
	Fe—Al <sub>2</sub> O <sub>3</sub> catalyst <sup>2</sup>	144.0	147.2	0.98	1.30	0.77	0.35	1.02	4.57
	Unpromoted Fe Catalyst No. 973-1 <sup>8</sup>	5.5*	6.68	0.83	1.48	0.67	0.41	0.85	3.75
	Unpromoted Fe Catalyst No. 973-11 <sup>8</sup>	14.5*	16.5	0.88	1.38	0.73	0.38	0.91	3.99
	Single-promoted Catalyst No. 954-1 <sup>8</sup>	12.8*	15.4	0.86	1.36	0.73	0.37	0.88	3.88
	Doubly-promoted Catalyst No. 931 <sup>8</sup>	46.4*	51.0	0.91	1.37	0.72	0.38	0.94	4.12
	Singly-promoted Catalyst No. 930 <sup>8</sup>	6.4*	7.70	0.83	1.50	0.67	0.43	0.85	3.75
		Average (excluding results in parenthesis)					0.70		4.01

this latter value was therefore used instead since Harkins himself considered the water isotherms to be less reliable in these cases. The value of  $V_m$  was calculated from the corresponding area of the solid using the value of 16.2 Å<sup>2</sup> for the area of a nitrogen molecule. The results for nitrogen which are marked with an asterisk are taken from Emmett and Brunauer.<sup>12</sup> The exact values of  $V_m$  for these isotherms are not given by the authors since at the date of publication they had not put forward their theory of multimolecular adsorption. In view of this the value given for the point  $B$  in the paper † in which the isotherms appeared was taken

† This is the point  $B$  as defined by Brunauer and Emmett.<sup>12</sup>

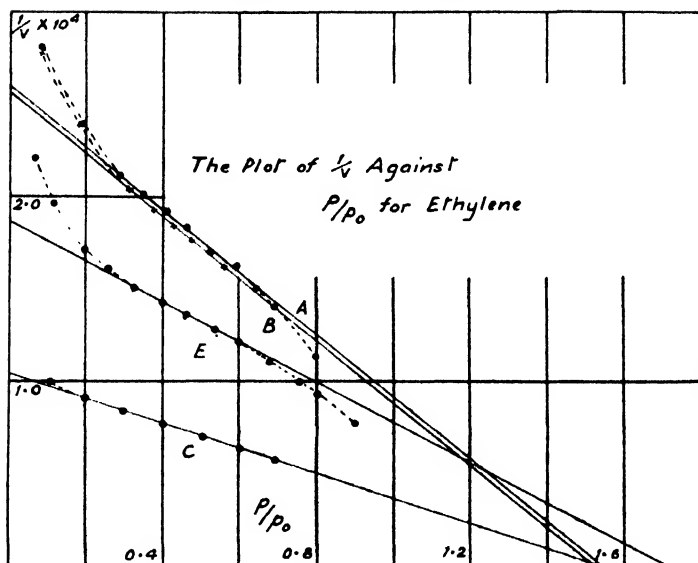


FIG. 6.

A, B and C from corresponding isotherms of Fig. 2.  
E from isotherm furnished by K. D. B. Johnson.

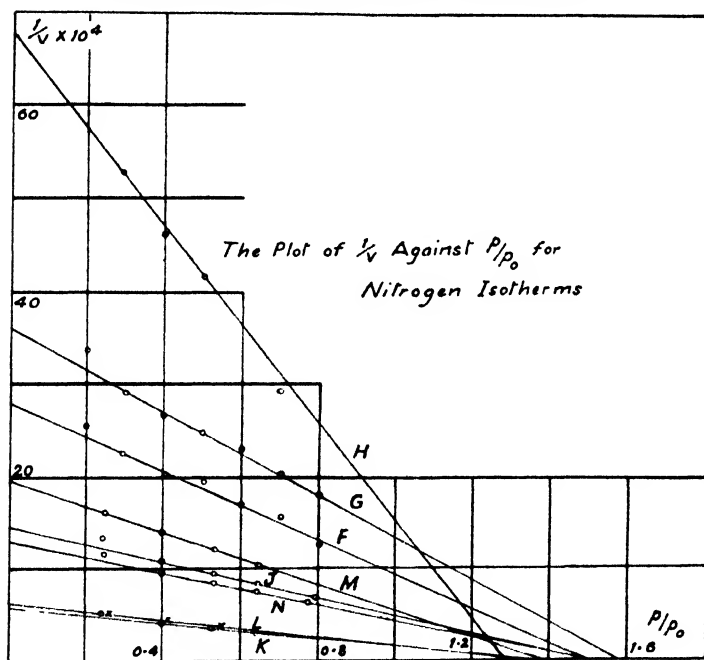


FIG. 7

F, Anatase (Harkins<sup>7</sup>). G, Surface treated anatase (Harkins<sup>7</sup>). H, Fe—Al<sub>2</sub>O<sub>3</sub> catalyst (B.E.T.<sup>12</sup>). J, Unpromoted Fe catalyst No. 973-I (B.E.T.<sup>12</sup>). K, Unpromoted Fe catalyst No. 973-II (B.E.T.<sup>12</sup>). L, Singly promoted Fe catalyst No. 954-I (B.E.T.<sup>12</sup>). M, Doubly promoted Fe catalyst No. 931-I (B.E.T.<sup>12</sup>). N, Singly promoted Fe catalyst No. 930 (B.E.T.<sup>12</sup>).

For the sake of simplicity only those points on the linear portion of the plots are included.

as the value of  $V_m$ . It has been shown by Brunauer, Emmett and Teller that this differs from the theoretical value of  $V_m$  by less than 10 %.

Having determined the constant  $D$  from this value of  $V_m$  we may use it as a criterion of the correspondence of the two equations. If  $D$  is unity, the Harkins and Anderson equations are in accord. Table II shows that whilst  $D$  is very close to unity it is significantly different from it.

The constant  $C$  of eqn. (3) is equal to the intercept on the  $p/p_0$  axis and its reciprocal is equal to the Anderson constant  $K$ . It will be seen that  $K$  has usually a value of about 0.7 but is significantly lower for ethylene than it is for nitrogen. *A priori* one would not expect the Anderson constant to be the same for all gases.

Eqn. (11) and (13) can now be employed to estimate the constant  $X$  of eqn. (2). This is usually positive and small.

From eqn. (12),  $F$  may be determined and the Harkins constant  $k$  obtained. It will be noticed that  $F$  has a value near unity also, though this is purely fortuitous; if  $F$  is assumed to be unity it is possible to determine  $k$  to about 20 % accuracy simply by assuming a corresponding value of  $a$ , the area occupied by the adsorbed molecule. Thus, if we assumed Emmett's value of 56.6 and 64 Å<sup>2</sup> for *n*-butane and *n*-heptane respectively, and take  $F$  as unity we obtain  $k$  as 15.3 and 17.4 respectively. The values given by Harkins are 13.6 and 16.9. This method gives only an approximate value. For ethylene and nitrogen at liquid-air temperature, the more exact calculation gives 4.65 and 4.01. The ethylene value is a little high by comparison with the value used in Table I.

Eqn. (3) above does not in itself provide any further information than could have been obtained using eqn. (1) and (2), except that it shows the relation between the constants which different authors have found it necessary to assume. It is, however, possible to utilize eqn. (3) as the basis of a simple method for determining surface areas. Assuming that the value of  $D$  is unity, eqn. (3) may be written

$$p/p_0 = C(1 - V_m/V)^* \quad (18)$$

Hence, if one plots  $p/p_0$  against  $1/V$ , the intercept on the  $1/V$  axis is equal to  $1/V_m$  from which the area of the solid may be determined. Further, it will be seen from Table II that for a given gas, Anderson's  $K$  is sensibly constant. If the value of this is known, then in Fig. 8 the intercept  $C$  is known and it is necessary to determine only one experimental point in order to extrapolate back to  $V_m$ ; for reliable results, the point  $P$  should be determined in the range of  $p/p_0$  between 0.3 and 0.7. In certain cases this might be a distinct advantage. For a gas whose saturation pressure at room temperature is of the order of an atmosphere (e.g. sulphur dioxide, or possible carbon tetrachloride, or water vapour at a higher temperature) about 5000 mm.<sup>3</sup> gas N.T.P. would be adsorbed ( $p/p_0$  about 0.2) by a solid of surface area about 20 m.<sup>2</sup>. In an apparatus of volume, say, 100 cm.<sup>3</sup> this would lead to a drop in pressure of about 4 cm. Hg, which could be measured with accuracy using a differential bellows manometer or possibly a differential oil manometer. Further, since it is not necessary to employ a high-vacuum technique, prolonged degassing of the adsorbent before the adsorbate is introduced into the adsorption chamber would be avoided.

Because (i)  $D$  is assumed to be unity, (ii) variations might occur in the value of the Anderson constant from adsorbent to adsorbent due to different heats of adsorption and (iii) errors will be introduced in the extrapolation, the method suggested is probably not accurate to nearer than 20 %. Corrections can be made for the above errors but for many purposes an accuracy of 20 % is quite near enough. In such cases, and

\* If the Anderson equation is assumed to be true, then eqn. (18) follows directly, without any assumption as to the value of  $D$ , other than that implicit in the Anderson equation.

especially when the surface areas of large numbers of samples must be estimated, this method would be valuable in view of the simpler experimental technique. The method should be applied with caution, as it is only applicable to the determination of areas of simpler or related adsorbents for which  $c$  is known to be large and  $k$  approximately constant.

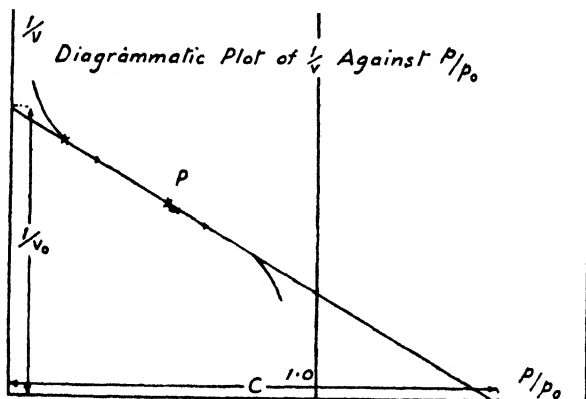


FIG. 8.

Finally, it will be noticed from Fig. 6 and 7 that a straight-line plot is obtained over the range  $p/p_0$  from about 0.3 to 0.7. This is as predicted from the treatment of the Harkins equation given above, although the derivation of eqn. (14) (from the B.E.T. theory) does not assume any upper limit. It is often stated that the Harkins method has the merit that it is unnecessary to assume any value for the area of the adsorbed molecule. It will be seen, however, that  $k$  is equal to  $Fa/3.69$ ; since  $F$  may be uniquely determined without any assumption as to the value of  $F$  or  $a$ , implicit in a given value for the Harkins constant is an assumption of the area occupied by a single molecule.

My thanks are due to Mr. D. L. Chapman, F.R.S., of Jesus College, Oxford for his helpfulness in discussion and to the Ministry of Supply for permission to publish this paper.

*Jesus College,  
Oxford.*

## REVIEWS OF BOOKS

**Advances in Electronics.** Vol. I. By I. L. MARTON (Academic Press Inc., N.Y., 1948). Pp. xi + 475. Price \$9.00.

Text-books in general serve two very useful purposes. They are an essential aid to the student who requires a complete account of the fundamentals of his subject. To the research worker they provide a convenient means of acquiring detailed information on subjects lying outside his own particular field of research but which he may decide have some important bearing on his own speciality.

In his own field the experienced research worker will be familiar with original papers in the various scientific periodicals; but the beginner in research wants an up-to-date review of the subject, much more complete than is found in the usual text-book. This publication aims at meeting this need in Electronics. It is proposed to publish further volumes annually. The editor claims that this series will enable the research worker to keep abreast of developments in the various branches of Electronics. It must, of course, be recognized that limitations of space will necessitate rather long intervals between reviews in any particular branch and it is only in a few selected topics each year that information can be really up-to-date. For this reason the present reviewer would prefer to consider these publications as an introduction to the literature rather than as a means of keeping abreast of developments in Electronics.

Vol. I is written by ten authors, each a recognized authority in his own particular subject. This procedure of joint publication has much to commend it; all too often text-books, while being excellent in some special branch of the subject, are very inadequate when, as often happens, a rather wide field is covered.

The first contribution is on "Oxide Coated Cathodes" by A. S. Eisenstein. This is an excellent 62-page report and deals with this subject very fully. The modern theories of the emission process are well covered and there is a comprehensive list of reference. "Secondary Electron Emission" is dealt with by K. G. McKay. In addition to secondary emission from metallic surfaces the important problem of emission from insulators is also fully discussed. "Television Pick-up Tubes" is the subject of a valuable contribution by A. Rose. This is one of the best sections in this volume and deals with the fundamentals of the subject in a very satisfactory manner. The questions of bandwidth, signal-to-noise ratio, and ideal performance are discussed.

"The Deflection of Beams of Charged Particles" by R. G. E. Hutter, "Modern Mass Spectroscopy" by M. G. Inghram and "Particle Accelerators" by M. S. Livingston are all three very excellent reports in rather specialized branches of Electronics and the justification for such a high degree of specialization undoubtedly lies in the fact that in each of these branches progress has been very rapid just recently. "Cosmic Radio Noise" by S. W. Herbstreit falls into the same category. This is a very interesting and clear account of a very new subject. The remaining sections are "Ionospheric Research" by A. G. McNish, "Propagation in the F.M. Broadcast Band" by K. A. Norton and "Electronic Aids to Navigation" by J. A. Pierce. In the limited space allocated to these three authors it would be impossible to give a complete account of the recent progress in such subjects. Better balance in this publication would have been achieved had more specialized topics been chosen and dealt with in greater detail.

J. S.

**Metal Rectifiers.** By H. K. HENISCH (Oxford, at the Clarendon Press, 1949). Pp. xi + 156. Price 15s.

There has long been a need for a readable account of the theory and practice of dry electrical rectifiers, and this book admirably fulfils this need. Until fairly recently the field was a difficult one to survey, since

there were many different types of metal rectifier, still more different ways of manufacturing them, and an embarrassing number of different theories to account for their behaviour. The field has now, however, been reduced to some sort of order, and the author is able to confine himself to the four types of rectifier at present commercially available—cuprous oxide, selenium, magnesium-cupric sulphide and germanium. Without going into great practical detail an account is given in fifty pages of their manufacture and operating characteristics, and this section of the book should be of the greatest use to engineers, physicists and even chemists who want to use metal rectifiers. In particular applications, it is of importance to know which type of rectifier is most likely to be suitable and also to know what is and what is not practically possible. The basic principles underlying practical application are simply and adequately stated, and will enable one to read manufacturers' literature with the required critical eye.

The remainder of the book is largely a survey of the surviving modern theories of contact rectification. A simplified treatment is used throughout, and the reader is referred to the original literature for more complete accounts. The similar theories of Mott and Schottky seem now to give an adequate explanation of all the rectifiers met with in practice, and the author gives perhaps too much space to describing other theories; although, as he rightly points out, under special conditions other theories such as Fairweather's may become applicable. This section of the book will be of great interest to scientists concerned in the manufacture or development of metal rectifiers. It is easily read since most of the more complicated mathematics and quantum mechanics are omitted.

The book finishes with a chapter on possible future developments in rectifiers, the author's faith in the possibilities of titanium dioxide being quite touching. A most valuable bibliography on semi-conductors and rectifiers containing over 500 references since 1925 is included, and experts in the field will find this bibliography alone well worth the price of the book.

J. T. K.

✓ **Surface Active Agents : Their Chemistry and Technology.** BY ANTHONY M. SCHWARTZ AND JAMES W. PERRY. (Interscience Publishers, New York and London.)

This book will be welcomed by the large number of scientists who use surface active agents in one way or another and the authors are to be congratulated on producing the first critical account of a subject whose literature consists mainly of patents. The make-up of the book is instructive; the chemistry of synthetic agents occupies 206 pages; the physical chemistry of surface active agents in theory and practice forms Part II of the book and receives 149 pages, while a further 120 of Part III lists rather superficially a very wide range of practical applications. These substances now form an important branch of applied preparative chemistry and the book should be as welcome to organic chemists as to physical.

The authors suggest that something akin to the *Colour Index* will be needed: the situation is similar in that these materials are sold under trade names, but this will not be enough: many agents are mixtures of



homologues and isomers and their surface activity is more important than their chemical make-up. Where is this information? The weakness is shown up in the second part of the book: the authors have traced their way through this complex and confused field with skill and judgment but the need for great increase of publication of reliable research is apparent. The chief difficulty is probably not desire for secrecy but the difficulty of interpreting or even of placing any value upon measurements made with anything but rigorously pure single compounds. These are very rare.

It is remarkable that references to B.I.O.S. and C.I.O.S. reports are not in evidence: because, I think, that German advances during the war, as in some other fields, consisted only of expansion of processes known and patented before the war. It is a pity that the authors have not given dates to their patent references. The book is to be commended highly but it leaves the reviewer with the depressing thought that it seems to be easier to produce 300 million pounds of synthetic agents of considerable complexity than it is to organize the comparatively small amount of fundamental research so obviously needed.

A. S. C. L.

**Introduction to Statistical Mechanics.** By G. S. RUSHBROOKE. (Oxford University Press, 1949.) Pp. 324. Price 21s.

Since Tolman wrote *Statistical Mechanics with Applications to Physics and Chemistry* in 1926 (just too soon to make use of the new quantum mechanics) no elementary book on statistical mechanics has been written in English by an expert in the subject. Tolman himself has written two *magna opera* on the subject, but he never again wrote an elementary book. The admirable exposition of the subject by Mayer and Mayer is considered by many teachers too advanced or too long for students of physical chemistry. Other attempts at elementary expositions have indeed been perpetrated by authors ready, indeed eager, to write on any and every subject, but the less said of these the better. Now at last we have an elementary book written by an expert. In this respect the book is unique and its publication is an important and welcome event.

The strategy of the exposition is summarized by the author on page 313: "Throughout the past chapters we have looked upon statistical mechanics as a bridge, or set of bridges, between mechanics and thermodynamics, and we have consciously built these bridges from both ends." This is the author's taste; it is not the reviewer's. The reviewer regards statistical mechanics as something he understands, or thinks he understands; but he regards thermodynamics as something which he can only understand through statistical mechanics. He accordingly has a strong preference for deriving thermodynamics from statistical mechanics, that is, for one-way traffic across the bridge or bridges. Holding this view, the reviewer finds it strange to have to wait until page 174 for a statistical derivation of the zeroth law of thermodynamics, namely, that two systems in mutual equilibrium have the same temperature.

The book is based on a course of lectures given by the author. In the reviewer's opinion there is far too much evidence of this on reading the book. For example, a digression on how to convert wave-numbers

to electron-volts is in order at any time during any lecture; in a textbook it should occur either in a preamble or in an appendix instead of in chapter 8. Again, there are far too many footnotes concerning points which have obviously been omitted from the text by accident, not design. The indication of some formulae by a dashed number out of the normal sequence is irritating.

On page 33 the contrast between Einstein's and Debye's curves is deceptive. These should be compared at values of the characteristic frequencies giving the best possible superposition instead of at equal values. It would then be seen that the discrepancy between the two curves is appreciable only at the lowest temperatures.

In reading the book hurriedly the only non-trivial misprints noticed were the following:—

- p. 173. The unnumbered formula between (15) and (16). A factor  $-T$  on the left or  $-T^{-1}$  on the right has been omitted.  
p. 260. Last line of footnote: (30) should be (20).

These are all small defects which can easily be removed in a later edition, for which the reviewer confidently predicts there will be a demand within a few years. He will certainly do his utmost to create this demand.

E. A. G.

**Colloid Science.** Vol. I and II. A. E. ALEXANDER and P. JOHNSON. (Geoffrey Cumberlege, Oxford, at the Clarendon Press, 1949.) Pp. xxii + 837. Price 6os.

There has long been a need for a broad, modern and authoritative treatment of the subject of colloid physics and chemistry from the fundamental rather than from the phenomenological viewpoint. Many physical chemists and biophysicists have also long cherished the hope that such a book would be written at Cambridge. The present two volumes, appropriately named after the Department of Colloid Science at Cambridge, will, therefore, be heartily welcomed—and justly praised. The book contains 28 chapters which fall into three parts—a historical and general survey, experimental methods and their theoretical basis, and the principal colloidal systems. It is a great pity, but clearly inevitable, that the length of the complete book has necessitated a high price of publication. There can be no doubt, however, that there is good value here, but because these two volumes are such valuable additions to the literature and will have such a large effect on the development of colloid science, it is tempting to suggest that the authors and publishers be induced to issue at some later date a shorter version at a more moderate price. This new volume would then be read with profit by many whose primary interests are not in the colloidal field.

Thus, much of the historical survey of Part I is adequately covered in other well-known texts, and much of the material in the chapter on the principal advances since 1910 is treated by the authors in greater detail in Parts II and III. Similarly, without withholding praise for the masterly condensation of the chapter on thermodynamic functions and recognizing their purpose in emphasizing the value and power of the thermodynamic approach to colloidal problems, it is felt that there are

quite a few books on thermodynamics which give a clearer and more useful presentation. An alternative suggestion is that Part II, which is regarded as the most valuable of the three parts, might be bound as a separate volume and that this and Part III be priced separately.

Part II has a chapter on osmotic pressure and membrane phenomena, two chapters on sedimentation equilibrium and sedimentation velocity, both of which deserve special praise; one on electrophoresis and allied phenomena wherein there is an excellent survey of the experimental techniques now available. There are also chapters on translational and rotational diffusion, viscosity, plastic flow and elasticity, and optical X-ray, electron diffraction and other methods; in each the reader will find well-written and clear accounts of the most important aspects. The section on the study of the interface is short, being only about 60 pages, and there has been a tendency to concentrate more on the broader and more elementary aspects with a consequent loss in the treatment of later developments.

Part III has chapters on sols, gels and pastes, foams, emulsions, colloidal electrolytes, clays and zeolites, proteins, polymers and membranes. Such a wide field must, of necessity, be treated in certain parts rather sketchily in so small a space as 300 pages, but the authors have selected the material with critical minds and mature judgment. Outlines of available techniques, the main trends of modern developments and selected bibliographies are given in each chapter. It would be difficult to select any one chapter for special mention, but few authors, it is suggested, could have used the 50 pages devoted to polymers, or the 20 and 30 pages to clays and zeolites and proteins to greater advantage.

However, the true value of this book is in the approach adopted by the authors—at last, here is a successful attempt to break away from those stereotyped, descriptive and often unco-ordinated treatments normally found in books on this subject.

The authors are to be congratulated on the achievement of writing the first book on *Colloid Science*.

# CORRIGENDA

P. 623, Table IV—

In column 3 the type has been displaced. The Table IV should read :

TABLE IV.—OSMOTIC AND ACTIVITY COEFFICIENTS OF SUCROSE AT 25° C

<i>m</i>	0.1	0.2	0.3	0.4	0.5	0.6	0.7	0.8	0.9	1.0	1.2	1.4
$\phi$	1.008	1.017	1.024	1.033	1.041	1.050	1.060	1.068	1.079	1.088	1.108	1.129
$\gamma$	1.017	1.034	1.051	1.068	1.085	1.105	1.125	1.144	1.165	1.188	1.233	1.283
<i>m</i>	1.6	1.8	2.0	2.5	3.0	3.5	4.0	4.5	5.0	5.5	6.0	
$\phi$	1.150	1.169	1.189	1.240	1.288	1.334	1.375	1.414	1.450	1.482	1.511	
$\gamma$	1.335	1.387	1.442	1.590	1.751	1.924	2.101	2.310	2.481	2.680	2.878	

P. 715—

In formula (4.6) the last factor  $V_1$  in the denominator should be omitted so that the formula reads :

$$\frac{4\pi N}{3} \gamma_a = \left\{ \frac{\epsilon_0 - 1}{\epsilon_0 + 2} - \frac{n_0^2 - 1}{n_0^2 + 2} \right\} V_2 \quad (4.6)$$

P. 724, line 31—

For capacity *read* potential drop.



# MOLECULAR FORCE FIELDS

## PART XI.—A WAVE-MECHANICAL TREATMENT OF THE CHANGE WITH DISTORTION OF THE INTERACTION ENERGY OF CARBON $2p\pi$ ORBITALS

Pauling  
change  
then the  
r to th  
ie same  
suggested  
n fre-  
ie fre-  
hange  
n, are

in

...ment of  
...toothan.<sup>2</sup> In the  
ilar calculations which consider

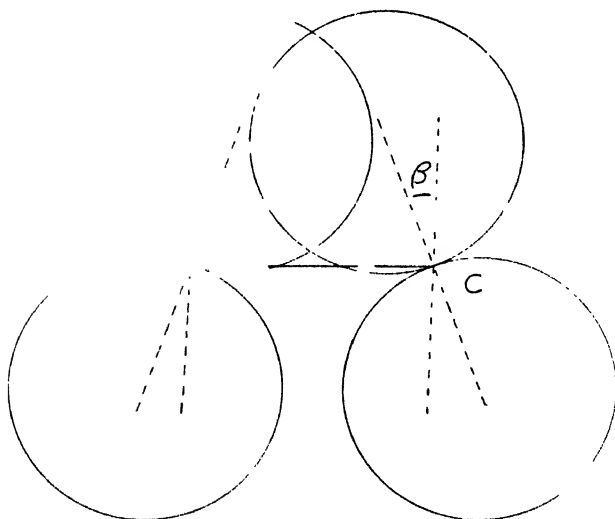


FIG. 1 (a).—Rotation of the carbon  $2p\pi$  orbitals in opposite senses ( $u$ -distortion).

<sup>1</sup> Parr and Crawford, *J. Chem. Physics*, 1948, 16, 526.

<sup>2</sup> Mulliken and Roothan, *Chem. Rev.*, 1947, 41, 219.

the change in interaction energy occurring when the two carbon  $2p\pi$  orbitals are rotated relative to one another about two parallel axes perpendicular to the  $C=C$  bond. In Fig. 1 (a) the rotation of the two carbon  $2p\pi$  orbitals are in opposite senses, while in Fig. 1 (b) they are in the same sense. Both cases will be examined.

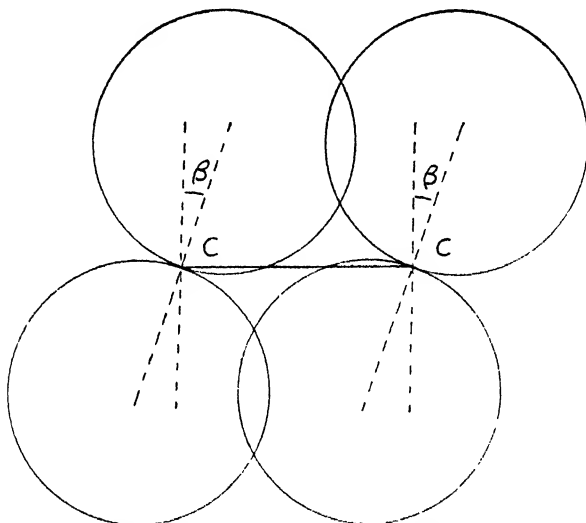


FIG. 1 (b).—Rotation of the carbon  $2p\pi$  orbitals in the same sense ( $g$ -distortion).

In the present calculations we have used the H.L.S.P. (Heitler-London-Slater-Pauling) approximation in writing down the wave function of the two electrons. Thus, if  $\psi(A1)$  is the atomic wave function of electron 1 of atom A and similarly for electron 2 and atom B, the wave function of the two electrons is

$$\Psi = \psi(A1)\psi(B2) + \psi(A2)\psi(B1). \quad (1)$$

The co-ordinate system that will be used is shown in Fig. 2. In the equilibrium position the  $\pi$ -bond is produced by the "sideways" overlap of the  $2p_z$  orbitals. We will represent the  $2p_z$  atomic orbital by  $\psi_z$ . Then for the undistorted position the wave function is

$$\Psi = \psi_z(A1)\psi_z(B2) + \psi_z(A2)\psi_z(B1). \quad (2)$$

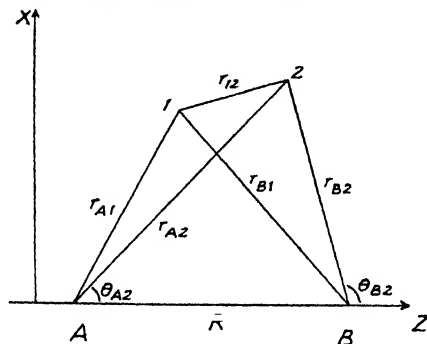


FIG. 2.—The co-ordinate system used.

Suppose the carbon  $2p$  atomic orbitals change their orientation in the manner shown in Fig. 1 (a) ( $u$ -distortion), and are rotated through an angle  $\beta$ , the rotation being in the opposite sense on the two atoms.

It is now convenient to represent the carbon  $2p$  atomic orbitals which make an angle  $\beta$  with the perpendicular to the line joining the two carbon atoms by the following :

$$\begin{aligned}\text{For atom A,} \quad \psi(A1) &= \psi_x(A1) \cos \beta + \psi_z(A1) \sin \beta, \\ \text{For atom B,} \quad \psi(B1) &= \psi_x(B1) \cos \beta - \psi_z(B1) \sin \beta.\end{aligned}\quad (3)$$

In using this representation the  $x$  and  $z$  axes are kept perpendicular to and along the line joining the two carbon atoms respectively. The wave function of the two electrons in the new electron pair bond is then

$$\begin{aligned}\Psi_u &= \{\psi_x(A1) \cos \beta + \psi_z(A1) \sin \beta\} \{\psi_x(B2) \cos \beta - \psi_z(B2) \sin \beta\} \\ &\quad + \{\psi_x(A2) \cos \beta + \psi_z(A2) \sin \beta\} \{\psi_x(B1) \cos \beta - \psi_z(B1) \sin \beta\}\end{aligned}\quad (4)$$

By a similar argument we may write for the wave function associated with the distortion shown in Fig. 1(b) ( $g$ -distortion) :

$$\begin{aligned}\Psi_g &= \{\psi_x(A1) \cos \beta + \psi_z(A1) \sin \beta\} \{\psi_x(B2) \cos \beta + \psi_z(B2) \sin \beta\} \\ &\quad + \{\psi_x(A2) \cos \beta + \psi_z(A2) \sin \beta\} \{\psi_x(B1) \cos \beta + \psi_z(B1) \sin \beta\}\end{aligned}\quad (5)$$

Returning to  $\Psi_u$ , the energy is now calculated by applying

$$\mathcal{H} \Psi_u = W \Psi_u \quad (6)$$

from which

$$W = \frac{\int \Psi_u \mathcal{H} \Psi_u dv_1 dv_2}{\int \Psi_u \Psi_u dv_1 dv_2} \quad (7)$$

In order to apply (7) we have to write down the Hamiltonian  $\mathcal{H}$ . We took this to be

$$\begin{aligned}\mathcal{H} &= \hbar^2/8\pi^2m\nabla_1^2 \Psi_u + \hbar^2/8\pi^2m\nabla_2^2 \Psi_u \\ &\quad + e^2(Z^2/R + 1/r_{12} - Z/r_{A1} - Z/r_{A2} - Z/r_{B1} - Z/r_{B2}).\end{aligned}$$

This makes the assumption that each carbon atom produces a field like that of a point charge  $+Ze$  when the electron which it contributes to the bond considered has been removed. This is obviously a drastic assumption, since in any given case the carbon atoms will be joined to other atoms. However, we are not interested in determining the absolute energy of the bond, but only in obtaining an idea of how its energy changes during the distortions that we are considering. Some assumption has to be introduced at this stage, since we are dealing with an electron pair that would be part of a polyatomic system, and this seems to be the most sensible in view of what is required. We are now in a position to solve the integrals in the numerator and denominator of (7). The details of this are given in the Appendix.

The energy for small distortions is finally obtained in the form

$$W_u = W_0 + k^u(\beta)^2 \quad (8)$$

for the distortion shown in Fig. 1(a), and similarly for  $W_g$  in terms of  $k^g$  when the change of orientation is that shown in Fig. 1(b). The results of our work are represented, therefore, by expressions for  $k^u$  and  $k^g$ , the force constants of the two distortions.

The values of  $k^u$  and  $k^g$  depend on  $R$ , the distance between the two atoms and  $Z$ , the effective charge on the two nuclei. We have made calculations for the same case as Parr and Crawford,<sup>1</sup> namely the C=C bond in the ethylene molecule. Three values of  $R$  have been used: 1.353 Å the value given by Gallaway and Barker;<sup>2</sup> 1.331 Å, suggested by Thompson;<sup>4</sup> and an intermediate value of 1.34 Å. The value that should be used for  $Z$  is less certain. Zener<sup>5</sup> suggested that a value of about 3.6 is appropriate for the ionized carbon atom, but in order to discover whether there was a considerable variation of the force constants

<sup>2</sup> Gallaway and Barker, *J. Chem. Physics*, 1942, **10**, 88.

<sup>4</sup> Thompson, *Trans. Faraday Soc.*, 1939, **35**, 697.

<sup>5</sup> Zener, *Physic. Rev.*, 1930, **36**, 51.



with  $Z$ , we have made calculations with  $Z$  varying from 2.74 to 3.97. The deduced values of  $k^u$ ,  $k^v$  and their ratio for the different values of  $R$  and  $Z$  are given in Table I. The most important feature of these results is that the wave-mechanical calculations indicate that both  $k^u$  and  $k^v$  are negative.

TABLE I

$\frac{R}{\text{\AA}}$	$\frac{ZR}{a_0}$	$Z$	$k^u$ $\times 10^{-11}$ erg/radian <sup>2</sup>	$k^v$ $\times 10^{-11}$ erg/radian <sup>2</sup>	$\frac{k^u}{k^v}$
1.331	7	2.78	-1.459	-0.767	1.90
	8	3.18	-1.746	-0.795	2.20
	9	3.58	-1.898	-0.866	2.19
	10	3.97	-1.945	-0.987	1.97
1.340	7	2.76	-1.431	-0.759	1.89
	8	3.16	-1.715	-0.786	2.18
	9	3.55	-1.866	-0.856	2.18
	10	3.95	-1.913	-0.975	1.97
1.353	7	2.74	-1.393	-0.747	1.86
	8	3.13	-1.671	-0.775	2.16
	9	3.52	-1.820	-0.841	2.16
	10	3.91	-1.875	-0.956	1.96

In a previous paper Linnett, Heath and Wheatley<sup>6</sup> made a study of the vibration frequencies of ethylene and deuterioethylene. They pointed out that it is easier to distort the molecules in an out-of-plane deformation than in a corresponding in-plane deformation, with the result that the potential energy increases more rapidly with in-plane distortion than with out-of-plane distortion. This implies that, in the out-of-plane deformation, there is some additional factor (or factors) tending to lower the potential energy as the molecules are bent. The present calculations show that the change in interaction energy of the two  $2p_x$  electrons of the carbon atoms is one of these factors, since this energy decreases as the relative orientation of the two  $2p_x$  orbitals are changed in the manners shown in Fig. 1(a) and 1(b). Although this result is of considerable interest, it should be stressed that the present calculations do not provide values of the force constants  $k_\pi^u$  and  $k_\pi^v$  used in the paper of Linnett, Heath and Wheatley,<sup>6</sup> since changes in other interactions would have to be considered.

### Appendix

In order to obtain an expression for the change of energy on distortion, it is first necessary to substitute values of  $\psi_x$  and  $\psi_z$  in formula (4) or (5). We have assumed that the carbon  $2p\pi$  orbitals are hydrogen-like in character and that their wave functions are given by

$$\psi_x = (Z^5/32\pi a_0^5)^{1/2} \exp(-\alpha r) \sin \theta \cos \phi,$$

$$\psi_z = (Z^5/32\pi a_0^5)^{1/2} \exp(-\alpha r) \cos \theta,$$

where

$$\alpha = Z/2a_0.$$

The resulting expression for  $\Psi_u$  or  $\Psi_v$  is then substituted, together with the Hamiltonian  $\mathcal{H}$ , in formula (7). Expansion of the resulting equations yields:

$$W_u = W_0 + [1 + I_{xx}^2 - 2I_{xx}(I_{zz} + I_{zz})\beta^2]^{-1} \{ [K_{xxxx} + L_{xxxx} - 2Z(G_{xx} + I_{xx}J_{xx})] \\ + \beta^2 \{ 2K_{zzxx} - 4K_{zzxx} - 2L_{zzxx} - 2L_{zzxx} + 2L_{zzxx} - 2K_{zzxx} - 2L_{zzxx} \\ - 2Z(G_{zz} - G_{zz} - 2I_{xx}J_{xx} - I_{zz}J_{xx} - I_{xx}J_{zz}) \} ]$$

$$W_v = W_0 + [1 + I_{xx}^2 + 2I_{xx}(I_{zz} - I_{zz})\beta^2]^{-1} \{ [K_{xxxx} + L_{xxxx} - 2Z(G_{xx} + I_{xx}J_{xx})] \\ + \beta^2 \{ 2K_{zzxx} + 4K_{zzxx} + 2L_{zzxx} + 2L_{zzxx} + 2L_{zzxx} - 2K_{zzxx} - 2L_{zzxx} \\ - 2Z(G_{zz} - G_{zz} - 2I_{xx}J_{xx} + I_{zz}J_{xx} + I_{xx}J_{zz}) \} ]$$

<sup>6</sup> Linnett, Heath and Wheatley, *Trans. Faraday Soc.*, 1949, **45**.

The symbols  $G$ ,  $I$ ,  $J$ ,  $K$  and  $L$  and their subscripts refer to the integrals listed below. When these integrals are evaluated and the figures substituted in the above expressions, the coefficient of  $\beta^2$  is  $k^u$  or  $k^v$ , the force constant (cf. eqn. (8)).

### Integrals

$$G_{zz} = \int \psi_z^2(A1)/r_{B1} dv_1$$

$$G_{xx} = \int \psi_x^2(A1)/r_{B1} dv_1$$

$$I_{zz} = \int \psi_z(A1)\psi_z(B1) dv_1$$

$$I_{xx} = \int \psi_x(A1)\psi_x(B1) dv_1$$

$$J_{zz} = \int \psi_z(A1)\psi_z(B1)/r_{A1} dv_1$$

$$J_{xx} = \int \psi_x(A1)\psi_x(B1)/r_{A1} dv_1$$

$$K_{zzzz} = \iint \psi_z^2(A1)\psi_z^2(B2)/r_{12} dv_1 dv_2$$

$$K_{zzxx} = K_{xxzz} = \iint \psi_z^2(A1)\psi_x^2(B2)/r_{12} dv_1 dv_2$$

$$K_{zzzz} = K_{zzzz} = \iint \psi_z(A1)\psi_x(A1)\psi_z(B2)\psi_x(B2)/r_{12} dv_1 dv_2$$

$$K_{xxxx} = \iint \psi_x^2(A1)\psi_x^2(B2)/r_{12} dv_1 dv_2$$

$$L_{zzzz} = \iint \psi_z(A1)\psi_z(B1)\psi_z(A2)\psi_z(B2)/r_{12} dv_1 dv_2$$

$$L_{zzxx} = L_{xxzz} = \iint \psi_z(A1)\psi_x(B1)\psi_z(A2)\psi_x(B2)/r_{12} dv_1 dv_2$$

$$L_{xxxx} = L_{xxxx} = \iint \psi_x(A1)\psi_x(B1)\psi_x(A2)\psi_x(B2)/r_{12} dv_1 dv_2$$

$$L_{zzzz} = L_{zzzz} = \iint \psi_z(A1)\psi_x(B1)\psi_x(A2)\psi_z(B2)/r_{12} dv_1 dv_2$$

Of these integrals  $G_{zz}$ ,  $I_{zz}$ ,  $J_{zz}$ ,  $K_{zzzz}$  and  $L_{zzzz}$  are to be found in a paper of Rosen.<sup>7</sup>  $G_{xx}$ ,  $I_{xx}$  and  $J_{xx}$  can readily be derived from a collection of integrals given by Coulson.<sup>8</sup> All the  $K$  integrals can be found in Bartlett's paper.<sup>9</sup> There are a number of inaccuracies in the latter paper, and the solutions had to be carefully checked before they were used. Approximate forms of the  $L$  integrals are also available in this paper of Bartlett,<sup>9</sup> but we preferred to obtain the full solutions by the standard method developed by Rosen,<sup>7</sup> rather than use these approximate values. The complete expressions for the  $L$  integrals are given below.

$$L_{zzzz} = 1/15120R \cdot (\alpha R)^{10} [147H(6, 6) - 315H(6, 4) + 252H(6, 2) - 63H(6, 0) + 225H(4, 4) - 675H(4, 2) + 180H(4, 0) + 837H(2, 2) - 459H(2, 0) + 63H(0, 0) - 294S(5, 6) + 315S(5, 4) - 252S(5, 2) + 63S(5, 0) + 217S(3, 6) - 240S(3, 4) + 213S(3, 2) - 54S(3, 0) - 189S(1, 6) + 225S(1, 4) - 243S(1, 2) + 63S(1, 0)].$$

$$L_{zzxx} = 1/30240R \cdot (\alpha R)^{10} [-147H(6, 6) + 420H(6, 4) - 126H(6, 2) - 75H(4, 4) - 360H(4, 2) + 90H(4, 0) + 297H(2, 2) - 108H(2, 0) + 9H(0, 0) + 294S(5, 6) - 322S(5, 4) + 70S(5, 2) - 420S(5, 4) + 10S(3, 4) + 80S(1, 4) + 126S(5, 2) - 402S(3, 2) - 186S(1, 2) - 162S(3, 0) + 36S(1, 0)].$$

$$L_{xxxx} = 1/30240R \cdot (\alpha R)^{10} [-147H(6, 6) + 420H(6, 4) - 126H(6, 2) - 525H(4, 4) + 720H(4, 2) - 90H(4, 0) - 351H(2, 2) + 108H(2, 0) - 9H(0, 0) + 294S(5, 6) - 322S(5, 4) + 70S(5, 2) - 420S(5, 4) + 910S(3, 4) - 280S(1, 4) + 126S(5, 2) - 678S(3, 2) + 246S(1, 2) + 90S(3, 0) - 36S(1, 0)].$$

$$L_{zzxx} = 1/60480R \cdot (\alpha R)^{10} [-294H(6, 6) + 735H(6, 4) - 378H(6, 2) + 63H(6, 0) - 225H(4, 4) - 585H(4, 2) + 180H(4, 0) + 864H(2, 2) - 405H(2, 0) + 45H(0, 0) + 588S(5, 6) - 539S(5, 4) + 217S(5, 2) - 735S(3, 4) - 735S(3, 4) + 625S(3, 4) - 240S(1, 4) + 378S(5, 2) - 297S(3, 2) - 3S(1, 2) - 63S(5, 0) + 51S(3, 0) + 18S(1, 0)].$$

$$L_{zzzz} = 1/120960R \cdot (\alpha R)^{10} [441H(6, 6) - 1470H(6, 4) + 630H(6, 2) - 42H(6, 0) + 1725H(4, 4) - 2250H(4, 2) + 270H(4, 0) + 945H(2, 2) - 270H(2, 0) + 21H(0, 0) - 882S(5, 6) + 1176S(5, 4) - 182S(5, 2) + 1470S(3, 4) - 2120S(3, 4) + 410S(1, 4) - 630S(5, 2) + 1032S(3, 2) - 258S(1, 2) + 42S(5, 0) - 88S(3, 0) + 30S(1, 0)].$$

<sup>7</sup> Rosen, *Physic. Rev.*, 1931, **38**, 2099.

<sup>8</sup> Coulson, *Proc. Camb. Phil. Soc.*, 1941, **38**, 210.

<sup>9</sup> Bartlett, *Physic. Rev.*, 1941, **37**, 507.

The  $H$  and  $S$  functions are simpler integrals defined by

$$H(m, n, \rho) = \int_1^\infty \lambda_1^m \exp(-\rho\lambda_1) Q_0(\lambda_1) d\lambda_1 \int_1^{\lambda_1} \lambda_2^n \exp(-\rho\lambda_2) d\lambda_2 \\ + \int_1^\infty \lambda_1^n \exp(-\rho\lambda_1) Q_0(\lambda_1) d\lambda_1 \int_1^{\lambda_1} \lambda_2^m \exp(-\rho\lambda_2) d\lambda_2,$$

$$S(m, n, \rho) = \int_1^\infty \lambda_1^m \exp(-\rho\lambda_1) d\lambda_1 \int_1^{\lambda_1} \lambda_2^n \exp(-\rho\lambda_2) d\lambda_2,$$

where  $\rho = \alpha R$ , and  $Q_0(\lambda)$  is the Legendre function of the second kind and is given by

$$Q_0(\lambda) = \frac{1}{2} \log_n (1 + \lambda)/(1 - \lambda).$$

We are indebted to Prof. J. O. Hirschfelder for providing us with a copy of Rosen's figures for the  $H$  and  $S$  integrals.

We have obtained numerical values for all the fifteen basic integrals with values of  $R$  equal to 1.331, 1.340 and 1.353 Å, and with values of  $ZR/a_0$  equal to 7, 8, 9 and 10. In Table II are listed the values of the integrals for  $R$  equal to 1.353 Å. It will be noticed that these values are, in some cases, slightly different from those given by Parr and Crawford<sup>10</sup> in a paper that was published after this present work was completed. The differences are due to the fact that there are no approximations involved in the solution of our integrals.

TABLE II

$ZR/a_0$	7	8	9	10
$G_{zz}$	0.84743	0.84230	0.83171	0.81986
$G_{xx}$	0.65179	0.67101	0.68481	0.69493
$I_{zz}$	-0.26486	-0.31869	-0.33258	-0.31893
$I_{xx}$	0.37017	0.28695	0.21857	0.16396
$J_{zz}$	-0.38244	-0.44221	-0.45954	-0.44405
$J_{xx}$	0.33524	0.27977	0.22630	0.17845
$K_{zzzz}$	0.76404	0.81057	0.83863	0.85184
$K_{zzxz}$	0.67881	0.70937	0.72931	0.74115
$K_{xxzz}$	-0.01604	-0.01718	-0.01650	-0.01438
$K_{zzzx}$	0.60180	0.62864	0.64865	0.66377
$L_{zzzz}$	0.19630	0.23194	0.23457	0.21043
$L_{zzxz}$	-0.09665	-0.08658	-0.07069	-0.05360
$L_{xxzz}$	0.05545	0.04401	0.03245	0.02249
$L_{zzzx}$	-0.11687	-0.11080	-0.09168	-0.06899
$L_{xxzx}$	0.11760	0.07817	0.04673	0.02866
$Z$	2.737	3.128	3.519	3.910

The  $I$  integrals are dimensionless. All the other integrals are expressed in Å<sup>-1</sup>.  $a_0$  was taken as 0.529 Å.

The  $K$  and  $L$  integrals were checked by obtaining numerical values with the same value of  $Z$  for decreasing values of  $R$ , when corresponding  $K$  and  $L$  integrals should tend to the same limiting value. As a final check, this limiting value was obtained for each pair of  $K$  and  $L$  integrals by taking  $R$  equal to zero, when the problem becomes a mononuclear one.

Since each pair of  $K$  and  $L$  integrals tended to the same limiting value, and since this limiting value was confirmed by independent means, we have every reason to believe that the values quoted for the  $K$  and  $L$  integrals are completely accurate.

We wish to thank Imperial Chemical Industries for providing us with a calculating machine, and one of us (P. J. W.) would like to thank the Harmsworth Trust for a Senior Scholarship.

*Inorganic Chemistry Laboratory,  
Oxford.*

<sup>10</sup> Parr and Crawford, *J. Chem. Physics*, 1948, **16**, 1049.

# THE KINETICS OF THE PHOTOCHEMICAL INTERACTION OF HYDROGEN WITH CHLORINE

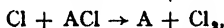
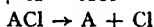
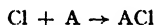
BY W. J. KRAMERS AND L. A. MOIGNARD

Received 28th January, 1949; as revised, 21st March, 1949

The rate of photochemical interaction between purified hydrogen and chlorine is proportional to the square root of the intensity of the light, in accordance with Nernst's prediction, providing the light intensity and also the chlorine pressure are not too low. The rate is independent of the chlorine pressure (hydrogen approximately 0.1 mm.) when it is greater than about 200 mm., providing the intensity is not too low and is rendered uniform throughout the actinometer by using light having a small extinction coefficient.

At low intensities and at chlorine pressures below about 200 mm., the rate of reaction becomes proportional to the intensity of the light and to the chlorine pressure. It is shown that this change is not caused by removal of the chain carriers at the walls of the reaction vessel under these conditions. It appears to be due to the presence in the chlorine of a certain kind of inhibitive impurity which is not completely destroyed by light and so not removed in the purification process to which the chlorine is submitted. The inhibitor is probably derived from impurities in the phosphoric acid used to lubricate the taps.

The Nernst hypothesis appears to be a special case of a more complete theory in which it is postulated that the chain carriers are removed by inhibitors which are not completely destroyed by light. The discussion is limited to the case where the removal is mainly of chlorine atoms and the following reactions are tentatively suggested:



where A is an inhibitor molecule. If  $\text{A} = \text{Cl}_2$  (so that the chlorine molecule is itself one kind of inhibitor) and  $\text{Cl}_2$  is very unstable the theory leads to the required kinetic expression in which  $\frac{d[\text{HCl}]}{dt} \propto I^{\frac{1}{2}}$  and independent of the chlorine pressure. If another inhibitor forming a relatively stable compound ACl is present in the chlorine in amounts unaffected by variations in the chlorine pressure, it can be shown that chain termination by this inhibitor becomes more significant relative to that by  $\text{Cl}_2$  as the chlorine pressure or light intensity is reduced and leads to the kinetic expression  $\frac{d[\text{HCl}]}{dt} \propto I/[\text{Cl}_2]$ .

Berthoud<sup>1</sup> in 1924 and later Chapman<sup>2</sup> pointed out that Nernst's<sup>3</sup> theory of the photochemical interaction of chlorine and hydrogen required that the rate of reaction should be proportional to the square root of the intensity of the light. This conclusion, however, was directly opposed to the experimental evidence at the time, since all reliable investigations<sup>4</sup> of the influence of the intensity of the light had shown that within the limits of experimental error a linear law held. The linear relationship appeared to be confirmed by certain subsequent re-investigations<sup>5</sup> and

<sup>1</sup> Berthoud, *Helv. chim. Acta*, 1924, **7**, 324.

<sup>2</sup> Chapman, *Trans. Faraday Soc.*, 1925, **21**, 547.

<sup>3</sup> Nernst, *Z. Elektrochem.*, 1916, **22**, 62; 1918, **24**, 335.

<sup>4</sup> E.g. (a) Draper, *Phil. Mag.*, 1843, **23**, 401. (b) Bunsen and Roscoe, *Phil. Trans.*, 1857, **147**, 355. (c) Chapman, *J. Chem. Soc.*, 1924, **125**, 1521.

<sup>5</sup> E.g. (a) Kornfeld and Müller, *Z. physik. Chem.*, 1925, **117**, 242. (b) Allmand and Beesley, *J. Chem. Soc.*, 1930, 2693.

the discrepancy was the major objection to the unqualified acceptance of the theory.

One possible cause of it was that, in spite of the care usually taken to purify the reactants, the gases had not been sufficiently freed from impurities to avoid nearly all the chains being terminated by collision of either hydrogen atoms, or chlorine atoms, or both, with inhibitor molecules. This explanation was suggested by Berthoud<sup>6</sup> who had previously<sup>7</sup> been the first to give a convincing experimental demonstration of the occurrence of photochemical reactions in which the rate of change is proportional to the square root of intensity of the illumination. It was later verified experimentally by Chapman and Gibbs<sup>8</sup> in 1931 after the discovery that a square-root relationship held in the otherwise closely analogous photo-reaction between bromine and hydrogen.<sup>9</sup> Previously it had been assumed by Bodenstein and Lütkemeyer,<sup>10</sup> but not shown experimentally, that this photochemical reaction obeyed the square-root relationship.

In investigating the dependence of the reaction velocity on the respective concentrations of the interacting gases it is necessary to eliminate two other possible sources of error. Firstly a relatively rapid removal of atoms by the walls of the container must be avoided and this was accomplished by employing an actinometer of at least 1 litre capacity. Secondly, light having a low coefficient of extinction has to be used, in order to ensure that there is no appreciable decrease of intensity of illumination of the contents of the actinometer remote from the points of entry of the rays as the concentration of the chlorine is increased. The correction for this effect by computation is not easy but the difficulty can be overcome by operating with light which has passed through a long column of chlorine at atmospheric pressure.

It was found at first by Evans<sup>11</sup> that when the purified chlorine and hydrogen mixture was illuminated in a large actinometer with light which had passed through the column of chlorine, the rate of combination was no longer proportional to the square root of the intensity of the light but directly proportional to it. The same behaviour, however, was observed with white light when its intensity was reduced to such an extent that the rate of combination had become as slow as that observed with the filtered light. By increasing the intensity of the filtered light sufficiently by the use of a more powerful source of light the square-root relation was again obeyed. It has since been found that if the chlorine pressure is sufficiently reduced the square-root intensity relation again degenerates to that of direct proportionality.

Accordingly, at low intensities of the light or at low concentrations of the chlorine the rate of photochemical change is given by  $kI\sqrt{[H_2][Cl_2]}$  and not by  $k'I/[H_2][Cl_2]$  in which expressions  $k$  and  $k'$  are constants. These changes in the relationship between the intensity of the light and the rate of chemical change can be attributed to the breaking of single chains either at the walls of the container or by molecules of a suitable inhibitor.

The first of these causes was unlikely because of the large actinometer in use and is shown not to be responsible since the sensitivity of a comparatively low pressure of chlorine was not substantially altered when it was mixed in the actinometer with carbon dioxide at a pressure several times greater than that of the chlorine. Moreover, the reaction rate remained directly proportional to the intensity of the light although with chlorine alone in the actinometer at the same total pressure and with

<sup>6</sup> Berthoud, *Helv. chim. Acta.*, 1924, 7, 324.

<sup>7</sup> Berthoud and Bellenot, *ibid.*, 307.

<sup>8</sup> Chapman and Gibbs, *Nature*, 1931, 127, 854.

<sup>9</sup> Briers and Chapman, *J. Chem. Soc.*, 1928, 1802.

<sup>10</sup> Bodenstein and Lütkemeyer, *Z. physik. Chem. A*, 1925, 114, 208.

<sup>11</sup> Evans, *Thesis* (Oxford, 1934).

light of similar intensity the reaction rate is proportional to a power of the intensity near to 0.6. The presence of an inhibitor also seemed unlikely since the samples of chlorine used attained the same maximum sensitivity after purification in various ways. These, however, always involved long exposure to the white light of a tungsten filament lamp as the final stage and it is shown that an inhibitor can form in the chlorine used by the action of light rich in ultraviolet rays. It is probable that although most inhibitors are destroyed by the treatment to which the gas is subjected, an inhibitor (or mixture of inhibitors) is at the same time formed and destroyed by the action of the white light until its concentration becomes constant after the attainment of equilibrium.

The investigation of the kinetics of the change has been conducted with mixtures of chlorine and hydrogen which, before exposure to light, contained chlorine at pressures varying from about an atmosphere to a few millimetres and hydrogen at a pressure of about 0.1 mm. The rate of photochemical change is then almost exactly proportional to the pressure of the hydrogen,<sup>14</sup> so that when the intensity of the light was high and the concentration of the chlorine was not too low the rate of interaction was given by the expression  $kI[H_2]/[Cl_2]$ . It has been found, when using filtered light, that the rate of interaction is independent of the pressure of the chlorine under these conditions; but when white light was used the rate of interaction rose rapidly as the pressure of the chlorine was reduced owing to the second source of error mentioned above.

### Experimental

**Apparatus.**—This is shown diagrammatically in Fig. 1. The reaction vessel P (and also Q) was a spherical quartz globe of about 1 litre capacity which terminated in a tubulure into which condensable gases could be liquefied. The

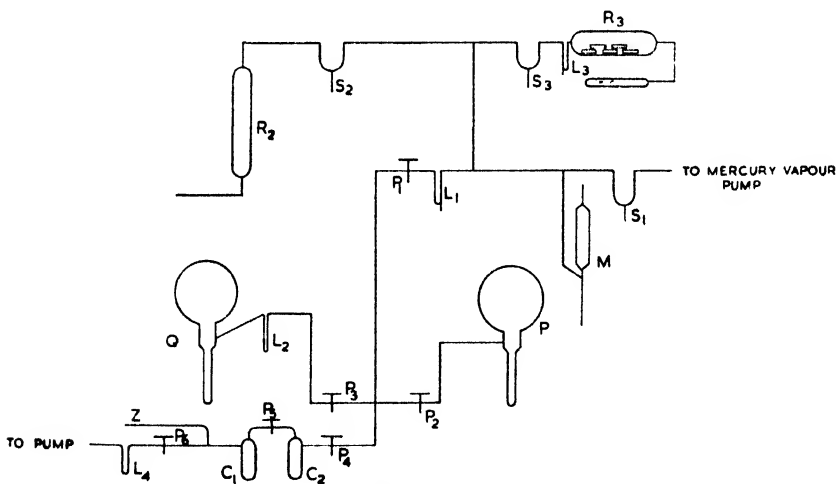


FIG. 1.—Diagram of Apparatus.

<sup>12</sup> E.g. Rollefson and Burton, *Photochemistry* (Prentice-Hall, 1939), p. 327.

<sup>13</sup> Cf. Allmand, Cunliffe and Maddison, *J. Chem. Soc.*, 1925, **127**, 822. Chapman, and Macmahon, *J. Chem. Soc.*, 1910, **97**, 845. Beaven, *Thesis* (Oxford, 1934).

<sup>14</sup> (a) Chapman and Macmahon, *J. Chem. Soc.*, 1910, **97**, 845. (b) Beaven, *Thesis* (Oxford, 1934).

<sup>15</sup> (a) Chapman and Underhill, *J. Chem. Soc.*, 1913, **103**, 496. (b) Chapman, *ibid.*, 1923, **123**, 3062. (c) Chapman and Watkins, *ibid.*, 1933, 743.

<sup>16</sup> (a) Chapman and Underhill, *loc. cit.* (b) Bodenstein and Dux, *Z. physik. Chem.*, 1913, **85**, 297. (c) Chapman, *loc. cit.* (d) Squire and Allmand, *J. Chem. Soc.*, 1936, 1869. (e) Potts and Rollefson, *J. Amer. Chem. Soc.*, 1935, **57**, 1027.

remainder of the apparatus was constructed of soft glass, P being connected by means of a graded seal.  $P_1$ ,  $P_2$ ,  $P_3$ ,  $P_4$ ,  $P_5$  and  $P_6$  were taps constructed and lubricated with phosphoric acid as described by Chapman and Moignard.<sup>17</sup>  $L_1$ ,  $L_2$ ,  $L_3$  and  $L_4$  were conventional liquid-air traps and  $S_1$ ,  $S_2$  and  $S_3$  mercury seals of the constant-level type. The reservoirs  $R_1$  and  $R_2$  each of about 500 ml. capacity were used to store hydrogen and oxygen respectively and the McLeod gauge M was calibrated to measure pressures up to about 5 mm. The seal  $S_1$  was always kept closed when the pumps were not in use; and the U-tube  $L_1$  was kept surrounded by liquid air whenever  $P_1$  was open. Before assemblage all parts were treated with hot chromic acid, washed and dried. Then, with the apparatus evacuated and P and Q outgassed at red heat, cleaning was completed by passage of silent electric discharges alternately in oxygen and hydrogen (using external aluminium electrodes) until the amount of condensable matter collecting in  $L_1$  after each discharge fell to a very low value. This procedure was repeated whenever air had been admitted to the apparatus.

**Materials.**—HYDROGEN was generated in a Kipp's apparatus from arsenic-free zinc and 5-10 %  $H_2SO_4$  and admitted slowly to  $R_2$  through a heated palladium diffusion tube. OXYGEN was prepared by cautiously heating dried recrystallized potassium permanganate. Freshly prepared gas was allowed to stand some time over potash sticks contained in  $R_3$ , and  $L_3$  was surrounded by liquid air for as long as conveniently possible before lowering  $S_3$  to admit any gas into A or B. CHLORINE was prepared by electrolysis of pure hydrogen chloride solution in "inhibitor-free" water,<sup>18</sup> and also by electrolysis of saturated aqueous cupric chloride which had previously been freed from inhibitive impurity by boiling under reflux with chlorine for 50 hr. in an all-glass apparatus. Iridium electrodes were used and the liberated chlorine was condensed as a liquid in  $C_1$ . When sufficient had collected the generator was sealed off at Z and permanent gas removed through  $P_6$ . A "middle" fraction, collected in  $C_2$  was then introduced at the desired pressure into P through  $P_4$  by surrounding  $C_2$  with a suitable refrigerant (see Table III). CARBON DIOXIDE was prepared by heating an intimate mixture of A.R. sodium carbonate and metaphosphoric acid in an evacuated tube connected at Z and the gas collected in  $C_1$ . After removing traces of permanent gas and collecting a "middle" fraction in  $C_2$ , a pressure of approx. 170 mm.  $CO_2$  was collected in Q by surrounding  $C_2$  with a mixture of solid and liquid toluene.

**Reaction Velocity Measurements.**—The chlorine together with any other condensable gases contained in it, such as HCl and  $CO_2$ , was condensed out in tubulure P with liquid air, 1 hr. being allowed for completion of the process. Meanwhile the leads were thoroughly evacuated.  $P_2$  was then opened and any trace of permanent gas pumped out. Sometimes P was now washed out with hydrogen but this step had little influence and was usually omitted. A pressure of hydrogen of about 0.1 mm. was introduced and measured accurately on the McLeod gauge after which  $P_2$  was shut and the chlorine evaporated ( $\frac{1}{2}$  hr.) with the laboratory in darkness. The gases were then exposed for a known time to one of the standard sources of illumination after which the condensable gases including any extra HCl formed photochemically were recondensed. From the change in hydrogen pressure measured after opening  $P_2$  the percentage of hydrogen S which has combined photochemically with the chlorine can be calculated. S is not a linear measure of the sensitivity for the rate at which hydrogen is consumed is known to be directly proportional to the pressure of the hydrogen under the experimental conditions,<sup>19</sup> i.e.  $-\frac{d[H_2]}{dt} = k[H_2]$  in

which  $k$  is a constant. The  $K$  values for the reaction rate recorded in this investigation are the values of  $k \times 10^3$  calculated from this expression,  $t$  being expressed in minutes and common logarithms used. The measurements of the reaction rate were made at the temperature of the laboratory which normally varied little from 18° C. Errors due to fluctuation in reaction temperature were minor since the temperature coefficient is small; <sup>19</sup> we have found it to be only 1.36 per 10° C. between 7° and 30° C for light of high intensity and 1.24 for light of very low intensity.

#### Sources of Illumination used for Measuring Reaction Velocity.—

The low intensity of light consisted of an aged 100-W lamp operated with galvanometer control at approx. 80 % of its rated voltage. It was placed (with the filament about 40 cm. from the centre of P) in a blackened container so that

<sup>17</sup> Chapman and Moignard, *J. Chem. Soc.*, 1939, 1936.

<sup>18</sup> Burgess and Chapman, *ibid.*, 1906, 89, 1399.

<sup>19</sup> Craggs and Allmand, *ibid.*, 1936, 241.

the light falling on the actinometer passed through a 7-cm. diam. hole covered with an opalescent white plate which transmitted only about  $1/10$ th of the total light. In some experiments in which light of very low intensity was used the 100-W lamp was replaced by a 10-W lamp. The light of high intensity was obtained by the use of a 500-W lamp, similarly arranged and controlled. In experiments requiring the use of a high intensity of light which is only weakly absorbed by the chlorine in the actinometer the opalescent plate was replaced by a filter consisting of a glass container 20 cm. long, of which a length of 8 cm. contained chlorine. Variation in intensity of illumination was achieved by placing a perforated metal screen behind the opalescent plate. This screen was calculated by Summers<sup>20</sup> and also shown directly by Dr. C. Hurst to reduce the light intensity 3.62-fold.

## Results

**The Preparation of Chlorine of Maximum Sensitivity.**—Chapman and Gibbs<sup>8</sup> boiled chlorine with inhibitor-free water in order to purify it. As this method has several disadvantages an exhaustive study has been made of other possible purification treatments, including (a) fractional distillation, (b) distillation through a low pressure of oxygen or hydrogen undergoing silent electric discharge, (c) heating with oxygen (by surrounding the tubulure P or Q with an electric furnace) and (d) prolonged illumination to strong light, e.g. 200-W tungsten lamps. The sequence of treatments has been varied and different specimens of chlorine have been used. From several hundred experiments<sup>21</sup> the following conclusions have been drawn.

(i) Chlorine immediately after preparation is always comparatively insensitive. Unless very great precautions are taken during the preparation to avoid contamination, the initial sensitivity may be several hundredfold less than the maximum obtainable.

(ii) On purification the sensitivity of the chlorine with light of the standard of low intensity rises to a maximum which is always the same ( $K \sim 20$ ). That is, the maximum sensitivity is independent of the initial sensitivity of the chlorine and of the method by which the specimen was prepared.

(iii) The most important stage in the purification of the chlorine is the exposure of the gas to strong illumination from tungsten filament lamps and, providing sufficient precautions are taken, the other treatments described were unnecessary.

(iv) It is difficult to avoid the introduction of inhibitive impurities into the chlorine during its transference from one part of the apparatus to another and consequently mere fractionation of the chlorine does not yield a specimen of maximum sensitivity.

The simplest method of obtaining chlorine of maximum sensitivity is to prepare the gas by electrolysis of a strong aqueous solution of cupric chloride (as described above) and then expose it to illumination from ordinary tungsten lamps. However, to purify chlorine in this manner it was necessary to boil the phosphoric acid solution used to prepare the lubricant for the taps for a prolonged period with chlorine. The initial sensitivity of the most carefully prepared chlorine has been as high as  $K = 13$  and rose to the maximum after exposure for about 150 hr. to two 200-W tungsten filament lamps (arranged on opposite sides of the actinometer and with the filaments of each about 23 cm. from its centre). After the addition of carbon dioxide to the chlorine, purification by prolonged illumination had to be repeated.

**The Influence of Variation in Intensity of Light on the Reaction Velocity of Chlorine of Maximum Sensitivity.**—Typical results are shown in Table I which gives values for  $K_1$ ,  $K_2$  and  $n$  in the expression  $K_1/K_2 = (I_1/I_2)^n$  at different intensities of white light and at different pressures of chlorine.

$K_1$  and  $K_2$  are respectively the reaction velocities at the intensities  $I_1$  and  $I_2$ , where  $I_2 = I_1/3.62$ .  $K_1'$  and  $K_2'$  and  $n'$  are the corresponding values with a fixed pressure of  $\text{CO}_2$  of approx. 170 mm. admixed with the chlorine. Table I shows:

(i) at constant chlorine pressure the value of  $n$  increases from about 0.5 to approximately unity as the intensity of the light is diminished. It is noteworthy that the same relationship has been observed in other photochemical

<sup>20</sup> Summers, *Thesis* (Oxford, 1932).

<sup>21</sup> Some of these experiments were performed by Plummer, *Thesis* (Oxford, 1935).



## 908 INTERACTION OF HYDROGEN WITH CHLORINE

reactions involving the halogens, e.g. the interaction of hydrogen and bromine.<sup>22</sup> Values for  $n$  less than 0.5 were not observed (cp. Squire and Allmand<sup>16d</sup>);

(ii) with light of high intensity the value of  $n$  increases from about 0.5 to approximately unity when the chlorine pressure is reduced from about 200 mm. to about 45 mm.;

(iii) with light of high intensity the value of  $n'$  is the same as that of  $n$  at the same pressure of chlorine, i.e. the addition of 170 mm. CO<sub>2</sub> to a low pressure of chlorine (45 mm.) at which  $n$  is approximately unity does not decrease the value of  $n$ .

TABLE I

Approx Chlorine Pressure mm.	Intensity of White Light	Reaction Rate			Corresponding Reaction Rate in Presence of 170 mm. CO <sub>2</sub>		
		$K_1$	$K_2$	$n$	$K_1'$	$K_2'$	$n'$
600	High *	598	201	0.52	—	—	—
600	High	324	153	0.58	286	133	0.585
260	High	364	172	0.58	—	—	—
170	High	363	159	0.64	—	—	—
45	High	181	51.7	0.98	95.3	25.7	1.016
600	Low	20.3	—	—	20.2	7.2	0.81
600	Very low	1.48	0.390	1.05	—	—	—

\* This light was from a line filament lamp as used in the experiments reported in Table II. In this experiment  $I_1/I_2 = 8$ .

The reduced chlorine pressures were achieved by the use of suitable refrigerants (see Table III) surrounding the tubulure of the actinometer. The actual pressures quoted are thus only approximate; especially so in the presence of carbon dioxide since this may have affected the partial pressure of the chlorine. In the experiment in which  $n$  was measured at approx. 45 mm. Cl<sub>2</sub> pressure the result was the same whether  $1\frac{1}{2}$  hr. or 7 hr. was allowed for equilibrium to be attained.

TABLE II

Experiment No.	Conditions	$K$	$n$	Mean Life (sec.)
351	Disc not rotated Light passed through open sector	619	0.52	0.26
352		577		
348	Disc rotated very rapidly $\frac{1}{8}$ sectors out	196		
349		206		
347	One rotation of disc in 8.5 sec. $\frac{1}{8}$ sectors out	156		
350		146		

Since  $n$  varies with the intensity of the light the value recorded is the mean for the two intensities employed. It can readily be shown, however, that for a 3.62-fold variation in intensity the difference in  $n$  at the two intensities is not appreciable except when  $n$  lies between 0.6 and 0.9. If  $n$  is the mean value and  $n_1$  and  $n_2$  the values at  $I_1$  and  $I_2$  respectively then when  $n = 0.82$ ,  $n_1$  can be calculated to be 0.76 and  $n_2 = 0.88$ .

The value of  $n$  nearest to 0.5 was obtained using light of high intensity from a 500-W line filament and was made in connection with a determination of the "mean duration" of a reaction chain (see Table II) by the rotating disc method as developed by Briers, Chapman and Waters.<sup>23</sup> The disc used measured 15 in.

<sup>22</sup> Boller, *Thesis* (Oxford, 1929).

<sup>23</sup> Briers, Chapman and Waters, *J. Chem. Soc.*, 1926, 562.

diam. and was divided equally into sectors by drawing sixteen equally spaced diameters and concentric circles, one  $10\frac{1}{2}$  in. and the other 13 in. from the centre.

**Formation of an Inhibitor in Purified Chlorine under the Influence of Light Rich in Ultraviolet Rays.**—This is shown in Fig. 2, in which curve A is for 600 mm. chlorine and curve B for a mixture of 600 mm. chlorine with approx. 170 mm. carbon dioxide. The mercury lamp was a 250-W Hanovia model of the high-pressure type with a quartz U-shaped arc tube placed normally at a distance of 18 cm. from the centre of the actinometer. New arc tubes were in

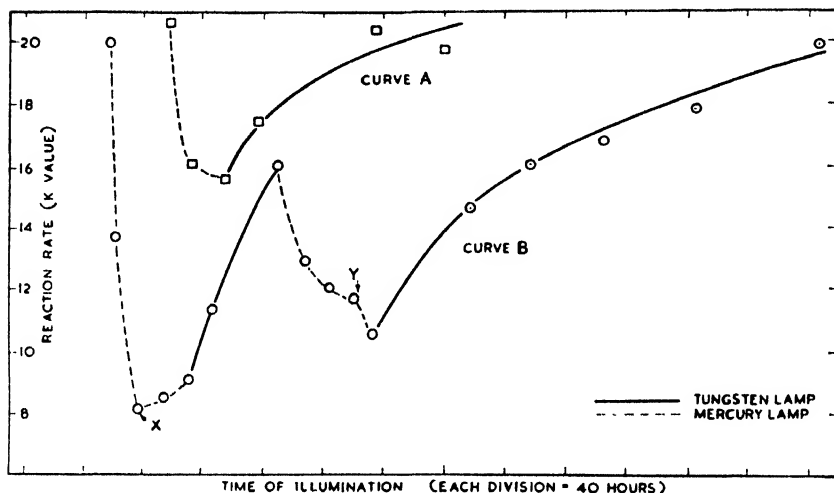


FIG. 2.—The formation of an inhibitor in purified chlorine under the influence of light rich in ultra-violet rays.

use at the commencement of each of the series of experiments comprising curves A and B. At X the distance of the mercury lamp from the actinometer was increased to 25 cm. and at Y decreased to 12 cm. The conclusions from the results contained in Fig. 2 and from other experiments are that :

- (i) on exposure to the rays from the mercury lamp the sensitivity of purified chlorine falls to a constant value ;
- (ii) on re-exposure to illumination from tungsten lamps the sensitivity rises again to the usual maximum value ;
- (iii) the influence of the mercury lamp apparently diminishes as the tube ages but the effect of the lamp appears to be intensified after addition of moisture to the chlorine in spite of the tendency of the lamp to age. Thus chlorine of maximum sensitivity containing 2 mm. water vapour (the latter prepared in the globe Q by heating hydrogen and oxygen) gave, on exposure for 12 hr., a 50 % greater fall in sensitivity than was previously obtained with the same lamp ;
- (iv) the addition of carbon dioxide has no influence on the general effect of the mercury lamp ;
- (v) the ultraviolet rays from the mercury lamp are responsible for the decrease in sensitivity since the effect is not observed if these are absorbed in a filter of sodium nitrite solution.

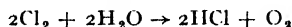
The constant maximum sensitivity obtained after exposure to tungsten illumination appears to be independent of the intensity of the light and is not significantly influenced by the addition of 1-2 mm. of either water or hydrogen chloride. Some evidence was, however, obtained of a reduction in sensitivity of about 10 % on illuminating (with tungsten lamps) the purified gas maintained at about 50° C by the passage of hot water over the actinometer. Other cases of photochemical equilibria dependent on the wavelength of the light used have been reported.<sup>12</sup>

**The Action of Heat on the Sensitivity of the Chlorine.**—The chlorine has been heated by surrounding the tubulure of the actinometer with an electric furnace maintained at a maximum temperature of about 800° C. Some oxygen was always formed by interaction with traces of moisture present in the chlorine and derived from the tap lubricant. Because of the solubility of oxygen in

## 910 INTERACTION OF HYDROGEN WITH CHLORINE

liquid chlorine, it was often desirable to evaporate and recondense the chlorine in order to reduce the concentration of oxygen to a low value before commencing a sensitivity determination although, of course, under the experimental conditions oxygen has no effect on the rate of reaction.<sup>15b</sup> Heatings varied in duration from a few hours to more than 50 hr. The hydrogen chloride simultaneously produced with the oxygen was removed from time to time by prolonged vacuum distillation between P and L<sub>1</sub>, these being maintained at the temperatures of liquid oxygen and liquid nitrogen respectively. Its removal had no effect on the reaction rate.

When purified chlorine is subjected to heat treatment in P the sensitivity falls from  $K \approx 20$  to a minimum value of  $K \approx 7$ . On further heating the sensitivity increases gradually, especially if the hydrogen chloride content is small. Removal of hydrogen chloride facilitates the reaction



on subsequent heating. After raising the sensitivity to  $K = 14.2$  by prolonged heat treatment it was found that after the addition of 1.7 mm. moisture the sensitivity was again reduced to  $K \approx 7$  after heating.

**The Influence of Variation in Chlorine Pressure on the Rate of Reaction.**

—This is shown in Fig. 3. The pressure of the purified chlorine was varied by surrounding the tubulure of the actinometer with pure liquids maintained at their melting point by the presence of crystals of solid. The liquids used and the corresponding approximate vapour pressures of chlorine at the melting

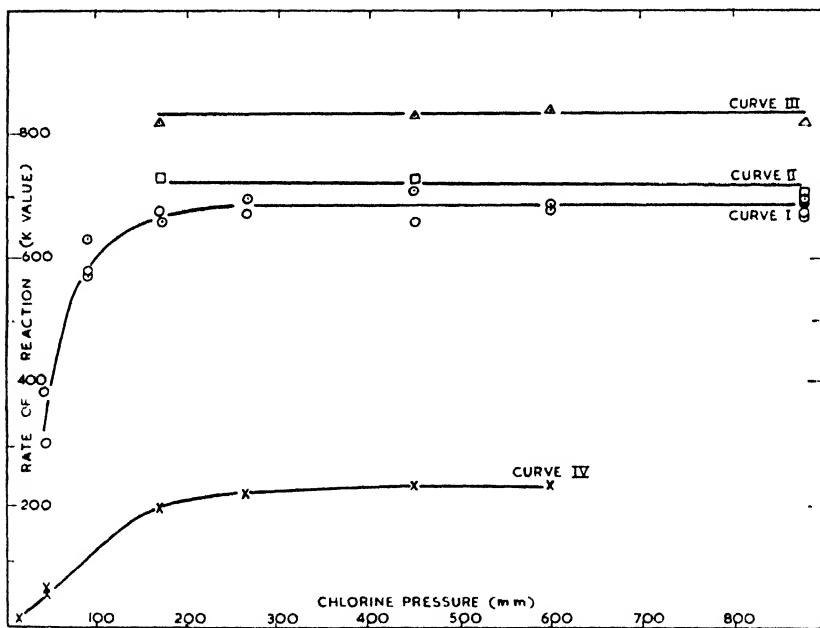


Fig. 3.—The influence of variation in chlorine pressure on the rate of reaction.

points were as shown in Table III. The specimen of chlorine with which curves I and II and III were obtained was estimated to have a total pressure of about 880 mm. from the volume of liquid condensed by benzyl chloride and the absence of any condensate when bromobenzene was used as refrigerant. In curve I the reaction rate was measured with a high intensity of filtered light, the pressure of chlorine in the 20 cm.-long filter being atmospheric.

Curves II and III differ from curve I in that the pressure of chlorine in the filter was reduced to 0.8 and 0.5 atm. respectively. Curve IV is for another sample of purified chlorine in which the light was passed not only through 20 cm. chlorine at atmospheric pressure but also through 3 cm. of an approx.  $\frac{1}{2}$  saturated solution of chlorine in carbon tetrachloride.

The results show that the use of light which is progressively more weakly absorbed in the actinometer does not alter the character of the curves and that :

(i) at pressures of chlorine in the actinometer greater than about 200 mm. the reaction rate is independent of the chlorine pressure ;

(ii) when the chlorine pressure is reduced below about 200 mm. so that  $n$  is then approx. unity (Table I), the rate of reaction becomes directly proportional to the pressure of the chlorine.

TABLE III

Refrigerant	Approximate Chlorine Pressure in mm.
Bromobenzene . . . . .	940
Benzyl chloride . . . . .	600
Monochlorobenzene . . . . .	450
Benzaldehyde . . . . .	260
Chloroform . . . . .	170
Acetic anhydride . . . . .	90
Ethyl acetate . . . . .	45

The fact that the absorption of light in the actinometer was adequately uniform throughout its length at each chlorine pressure has also been confirmed by calculations based on the extinction data for chlorine given by von Halban and Siedentop.<sup>24</sup> Furthermore, when *white*, and hence a relatively strongly absorbed, light was used for measuring the reaction velocity a totally different behaviour was observed, there being a pronounced maximum in the reaction velocity with reduction in chlorine pressure in this case, as shown in Table IV.

TABLE IV

Cl <sub>2</sub> Pressure (mm.)	Reaction Rate ( $K$ value) at Different Intensities of White Light				
	$I_1$	$I_2$	$I_3$	$I_4$	$I_5$
880	1330	—	—	—	—
600	—	240	109	324	153
450	1424	281	126	—	—
260	—	—	—	304	172
170	1680	—	—	303	159
45	—	—	—	181	51.7

$I_1, I_2$ , etc. indicate different intensities of white light varied either by variation in the distance of the lamp from the actinometer or by insertion of intensity reducing screen.

From  $\frac{1}{2}$  to  $1\frac{1}{2}$  hr. was always allowed for the equilibrium chlorine pressure to be set up in the actinometer and the results were not influenced by whether the equilibrium was approached from larger or smaller chlorine pressures. Reduction in chlorine pressure by repeated expansion of the contents of P into Q (the chlorine transferred to Q being removed to another part of the apparatus between expansions) also indicated that there was no marked variation in the reaction velocity until the chlorine pressure fell below about 220 mm.

**The Influence of Carbon Dioxide on the Rate of Reaction.**—Table I shows that whilst the addition of 170 mm. carbon dioxide appears to have little influence on  $K_1$  at low intensities, there is apparently some reduction in  $K_1$  at the high intensity of light. A preliminary attempt has been made to study the influence of carbon dioxide at high intensities of light in more detail by

<sup>24</sup> Von Halban and Siedentopf, *Z. physik. Chem.*, 1922, **103**, 71.

## 912 INTERACTION OF HYDROGEN WITH CHLORINE

investigating the influence of variation in chlorine pressure on the reaction rate in the presence of a fixed amount of carbon dioxide. Some of the results obtained are given in Table V.

TABLE V

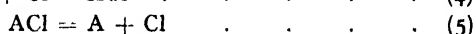
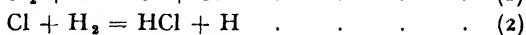
Experiment No.	Approx. Pressures in mm.		Reaction Rate K Value
	Chlorine	Carbon Dioxide	
303 } 366 } 304 }	600	170	{ 339 328 259
305 }	260	170	{ 255

These preliminary experiments, in which the reduced chlorine pressure was obtained by the use of a refrigerant, appear to confirm that carbon dioxide is an inhibitor of Class I. By the application of the theory given below for the case when the system contains two inhibitors of Class I ( $\text{Cl}_2$  and  $\text{CO}_2$ ) and an unknown inhibitor of Class II it can be deduced from these results (and with the aid of data given in Table I), that  $\text{CO}_2$  is apparently more effective as an inhibitor than  $\text{Cl}_2$ .

### Discussion

The results described above suggest that the simple Nernst mechanism of mutual chain carrier recombination is probably a special case of a more complete theory which appears to account satisfactorily for the experimental observations. It can readily be shown that in the Nernst theory it is a matter of indifference whether the removal of the chain carriers is accomplished in the presence of a hydrogen or chlorine molecule as third body or by the combination of chlorine atoms or hydrogen atoms with themselves or with one another. Further discussion of the hypotheses is limited to those cases in which the termination of the Nernst chains is accomplished solely by the removal of the chlorine atoms and any substance or substances which promote this recombination are not destroyed. In other words inhibitors such as nitrogen chloride<sup>18, 25</sup> which are destroyed by light in the presence of chlorine are assumed to be absent and the reaction vessel is assumed to be sufficiently large to minimize the influence of the walls.

Denoting the stable inhibitor by the symbol A, the series of chemical changes which take place in the presence of this inhibitor are assumed provisionally to be those indicated by the following equations :



from which, in the stationary state,

$$\frac{d[\text{HCl}]}{dt} = 2k_2[\text{Cl}][\text{H}_2] \quad . \quad . \quad . \quad . \quad (10)$$

The rate of formation of hydrogen chloride can therefore be found if  $[\text{Cl}]$  can be expressed as a function of  $[\text{Cl}_2]$  and of the atoms of A (combined and uncombined) present in the reacting mixture.

Letting  $[\alpha] = [A] + [ACl]$ ,  
then we can deduce that

$$k_1 I [Cl_2] = \frac{2k_4 k_6 [\alpha] [Cl]^2}{k_5 + (k_4 + k_6) [Cl]} \quad (11)$$

This equation leads to a simple expression for the rate of formation of hydrogen chloride (eqn. (10)) if  $k_5$  is either large or small in comparison with  $k_4 + k_6$ , i.e. according as the inhibitor forms a relatively unstable or stable compound ACl.

CASE I.— $k_5$  large in comparison with  $k_4 + k_6$  (i.e. ACl very unstable). In this case

$$[Cl] = \frac{k_1 k_5 I [Cl_2]}{2k_4 k_6 [\alpha]} \quad (12)$$

and an inhibitor of this class therefore leads to an expression,

$$\frac{d[HCl]}{dt} \propto I^{\frac{1}{2}}.$$

If we assume that  $Cl_2$  can take the place of A and that  $Cl_2$  is very unstable eqn. (12) becomes

$$[Cl] = \sqrt{\frac{k_1 k_5 I}{2k_4 k_6}} = \text{const.} \times I^{\frac{1}{2}}.$$

This expression is in agreement with the experimental observation that the rate of formation of hydrogen chloride is independent of the concentration of the chlorine molecules when it is proportional to the square root of the light intensity. It will be observed that this special case of  $k_5$  being large implies that the chlorine atoms are removed by reaction (6) closely following reaction (4). In the limit this is the Nernst mechanism modified to include a molecule A as third body viz. :



CASE II.— $k_5$  small in comparison with  $k_4 + k_6$  (i.e. ACl a stable compound). In this case the theory demands that the concentration of the chlorine atoms should be proportional to the intensity of the light and to the concentration of the chlorine molecules, and inversely proportional to  $[\alpha]$ . This conclusion can be verified by assuming that the chlorine atoms are removed in accordance with the reactions :



We can then deduce that

$$k_1 I [Cl_2] = \frac{2k_4 k_6 [\alpha] [Cl]^2}{(k_4 + k_6) [Cl]} \quad (13)$$

which is identical with eqn. (11) when  $k_5$  is zero.

For the photochemical reaction between hydrogen and chlorine no inhibitor of Class II has been discovered so far as we know, but the experimental evidence given above suggests that an inhibitor of this kind does exist. Moreover, for the reaction between bromine and hydrogen a compound is known which displays the required characteristics. Thus Boller<sup>22</sup> has discovered that nitric oxide is a powerful inhibitor of the photochemical reaction between bromine and hydrogen, that it is not removed by the action of light, and when present in small quantities causes the photochemical reaction of bromine and hydrogen to be directly proportional to the intensity of the light.

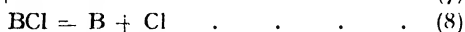
The inhibitor of Class II present in the chlorine appears to be derived from the tap lubricant. This was prepared from commercial glacial phosphoric acid which is a mixture of metaphosphoric acid and sodium metaphosphate. In the normal procedure the acid was dissolved in water

<sup>22</sup> Rollefson and Eyring, *J. Amer. Chem. Soc.*, 1932, **54**, 3876.

and evaporated until the boiling point of the solution was  $360^{\circ}\text{C}$ . At the temperature of the laboratory this lubricant is a soft glassy solid which adheres firmly to the ground surface of the bore of tap and effectively prevents any leakage. When the tap is warmed the lubricant becomes a very viscous liquid, and this permits it to be turned without appreciable displacement of the lubricant. The lubricant has the disadvantage that concentrating a solution of phosphoric acid until its boiling point is  $360^{\circ}\text{C}$ . does not remove the water to a sufficient degree to prevent its supporting a very slight pressure of water vapour. This condenses in the tubulure of the actinometer whenever the chlorine is condensed within it by the application of liquid air so that the contents of the actinometer are not completely dry after a series of measurements have been made. A method of overcoming this has since been discovered by Wynne.<sup>27</sup> He found that the commercial glacial phosphoric acid which is a solid even at  $100^{\circ}\text{C}$  contains as much as 10 % sodium salt but that if this proportion is reduced a satisfactory lubricant can be prepared. Pure metaphosphoric acid which has been fused in a gold dish at a high temperature so as to make it a powerful desiccating agent is too mobile at the temperature of the laboratory to be of use. But if the metaphosphoric acid is mixed with from 3 to 4 % of sodium metaphosphate before being fused in the gold dish it furnishes an excellent lubricant which is a glassy solid at the temperature of the laboratory and liquid of the right degree of viscosity at  $100^{\circ}\text{C}$ . It is also possible that an acid prepared from pure re-crystallized sodium phosphate might not contain other impurities which may be present in the commercial acid and may be the actual source of the inhibitor. Metaphosphoric acid can be prepared from a concentrated solution of sodium metaphosphate by adding concentrated hydrochloric acid when sodium chloride is precipitated out.

If the inhibitor is derived from the water present in the lubricant one possibility is that it is an oxide or oxyacid of chlorine formed photochemically.<sup>13, 14</sup> Evidence has been given that an inhibitor is formed under conditions when chlorine is *heated* with water vapour. Oxygen and hydrochloric acid are formed at the same time, but the inhibitor is not oxygen because this gas could be completely removed and also because at the low pressure of the hydrogen (0.1 mm.) used to test the sensitivity it would have had no effect on the rate of photochemical change even if its pressure had been equal to that of the hydrogen.<sup>15</sup>

The above theory can readily be extended to include the case when the system contains two stable inhibitors. Let the free inhibitors be designated by A and B. Then the reactions which terminate the chains are:



In the stationary state:

$$0 = k_1 I [\text{Cl}_2] - 2k_6 [\text{ACl}][\text{Cl}] - 2k_9 [\text{BCl}][\text{Cl}].$$

Putting  $[\alpha] = [\text{A}] + [\text{ACl}]$ , as before, and  $[\beta] = [\text{B}] + [\text{BCl}]$ , and eliminating A, ACl, B and BCl from the above equations we obtain eqn. (15) corresponding to eqn. (11).

$$k_1 I [\text{Cl}_2] = \frac{2k_4 k_6 [\alpha] [\text{Cl}]^2}{k_6 + (k_4 + k_6) [\text{Cl}]} + \frac{2k_7 k_9 [\beta] [\text{Cl}]^2}{k_9 + (k_7 + k_9) [\text{Cl}]} \quad . \quad . \quad (15)$$

<sup>27</sup> Wynne, *Thesis* (Oxford, 1942).

As before, this equation leads to a simple expression for  $\frac{d[\text{HCl}]}{dt}$  according to the class of the inhibitors A and B.

#### A AND B BOTH OF CLASS I.

In this case  $\text{ACl}$  and  $\text{BCl}$  are both very unstable so that  $k_8$  is large in comparison with  $k_4 + k_6$ , and  $k_8$  large in comparison with  $k_7 + k_9$ , whence eqn. (15) can be expressed as

$$[\text{Cl}] = \sqrt{\frac{\frac{1}{2}k_1k_5k_8I[\text{Cl}_2]}{k_4k_6k_8[\alpha] + k_7k_9k_8[\beta]}} \quad (16)$$

#### A = CLASS I, B = CLASS II.

In this case  $\text{ACl}$  is very unstable and  $k_8 \gg k_4 + k_6$ , whilst  $\text{BCl}$  is a stable compound and  $k_8 \ll k_7 + k_9$ . Hence eqn. (15) becomes

$$k_1 I[\text{Cl}_2] = \frac{2k_4k_6[\alpha][\text{Cl}]^2}{k_8} + \frac{2k_7k_9[\beta][\text{Cl}]}{k_7 + k_9} \quad (17)$$

When  $A = \text{Cl}_2$  this equation becomes

$$k_1 I[\text{Cl}_2] = \frac{2k_4k_6[\text{Cl}_2][\text{Cl}]^2}{k_8} + \frac{2k_7k_9[\beta][\text{Cl}]}{k_7 + k_9} \quad (17a)$$

This can be expressed in the form :

$$I[\text{Cl}_2] = K[\text{Cl}]^2[\text{Cl}_2] + K'[\beta][\text{Cl}] \quad (17b)$$

where  $K$  and  $K'$  are constants. The first term,  $K[\text{Cl}]^2[\text{Cl}_2]$  is assumed to be large in comparison with  $K'[\beta][\text{Cl}]$  providing the intensity of the light is high and the concentration of the chlorine not too low. Reduction in either of these quantities will increase the relative importance of the second term so that either at low light intensities or if the chlorine pressure is reduced sufficiently,  $[\text{Cl}]$  becomes proportional to  $I[\text{Cl}_2]$ , which is in accordance with the experimental observations.

Although it is practically certain that the presence of carbon dioxide has no appreciable effect on the rate of interaction of hydrogen and chlorine at low intensities of light, so that it cannot be an inhibitor of Class II, it appears nevertheless to be true, as described above, that carbon dioxide acts like  $\text{Cl}_2$  as an inhibitor of Class I. However, the experiments concerned were not performed under conditions specially devised for testing the question and too much reliance should not be placed on the conclusion drawn. In fact the work on this aspect of the reaction demands repetition under ideal conditions.

This investigation was carried out in the Sir Leoline Jenkins Laboratories, Jesus College, Oxford. We are very much indebted to Mr. D. L. Chapman, F.R.S., for his constant help and guidance both in the experimental work and in the preparation of this paper. Our thanks are also due to the Governing Body of the College for facilities and financial support and by one of us (L. A. M.) to the Governors of the Howard Leopold Davis Trust, for a Scholarship.

*Jesus College,  
Oxford.*



# THE KINETICS OF THE HYDROGEN EVOLUTION REACTION AT MERCURY CATHODES

## THE EFFECT OF TEMPERATURE, pH, AND PRESSURE ON HYDROGEN OVERPOTENTIAL IN AQUEOUS, MIXED AND METHANOLIC SOLUTIONS

By J. O'M. BOCKRIS AND ROGER PARSONS

Received 25th March, 1949

The constants of the Tafel equation ( $\eta = a - b \log i$ ) at 20° C for a mercury electrode in aqueous N/10 HCl solution are  $a = -1.395 \pm 0.002$ ,  $b = 0.113 \pm 0.001$ . These values correspond to overpotential values in the range actually measured agreeing to 20 mV with those considered by Frumkin<sup>45</sup> to be the most satisfactory obtained in the Karpov Institute. Both the parameter  $\alpha = 2.303 \frac{RT}{bF}$  and the heat of activation of the evolution reaction vary with temperature. The mean heat of activation in aqueous solution is  $21.1 \pm 0.3$  kcal./mole.

The overpotential at a given c.d. decreases continuously as the methanol content of the solvent increases. The heat of activation increases to  $23.6 \pm 0.5$  kcal./mole in 36 mole % methanol and then decreases to  $19.7 \pm 0.2$  kcal. in pure methanolic solutions. The pH effect on overpotential at a Hg cathode is more pronounced in methanolic than in aqueous solutions in that the region in which  $\partial\eta/\partial(\text{pH})$  is constant extends only up to 0.1 N solutions. The cathode potential of a working hydrogen electrode is independent of the partial pressure of hydrogen above the solution. The resolution of the anomaly of the pH effect at static and dropping electrodes shows that the effect is identical at both electrodes. A detailed account of the results cannot be given in terms of the theories of the kinetics of the hydrogen evolution reaction so far proposed. Qualitatively, however, the results support the view that the rate-determining step is the discharge of the solvated proton.

Some of the important factors governing the kinetics of a reaction are the temperature, pressure, concentration of reactant and the medium. Reliable studies of the hydrogen evolution reaction at mercury cathodes have been carried out under limited conditions in aqueous media<sup>1, 2, 3, 4</sup> only in respect of the third of these factors. More extensive information is needed before a quantitative theory of the kinetics of this electrode reaction can be attempted. In this paper the effect of the above factors is reported, special care having been taken to remove trace impurities which are known to vitiate results (cp. <sup>6</sup>).

Although the effect of pH on hydrogen overpotential in aqueous solution has been examined before,<sup>1, 2, 3, 6, 7, 8</sup> an anomaly exists between the value of  $\partial\eta/\partial(\text{pH})$  recorded at some mobile and static mercury surfaces.<sup>9</sup> This coefficient has been re-examined at the dropping mercury electrode.

<sup>1</sup> Levina and Sarinsky, *Acta Physicochim.*, 1937, **6**, 491.

<sup>2</sup> *Idem*, *ibid.*, 1937, **7**, 485.

<sup>3</sup> Jofa, *ibid.*, 1939, **10**, 903.

<sup>4</sup> Agar and Llopis, *Anal. fis. y quim.*, 1947, **43**, 1087.

<sup>5</sup> Azzam, Bockris, Conway, Rosenberg and Parsons (in course of publication).

<sup>6</sup> Herasymenko, *Rec. trav. chim.*, 1925, **44**, 499.

<sup>7</sup> Herasymenko and Slendyk, *Z. physik. Chem. A*, 1930, **149**, 123.

<sup>8</sup> Bowden, *Trans. Faraday Soc.*, 1928, **24**, 473.

<sup>9</sup> Gatty and Spooner, *The Electrode Potential Behaviour of Corroding Metals in Aqueous Solutions* (Oxford, 1938), Appendix III.

### Experimental

(a) **Static Mercury Electrode.**—The cell is illustrated in Fig. 1. The entire apparatus was cleaned with cleaning mixture followed by washing overnight with rapid-streaming water. The system was then rinsed several times with conductivity water. To reduce the amount of oxygen in the system to a minimum, it was evacuated three times, filling again each time with pure hydrogen. All joints and taps were sealed with conductivity water to eliminate grease from the system. Conductivity water was refluxed under reduced pressure of hydrogen for 2 hr. and distilled in a stream of hydrogen into the anode compartment (conductivity accepted:  $3.5 \times 10^{-7}$  mho cm.<sup>-2</sup>). Hydrogen chloride, prepared from KCl baked in a stream of H<sub>2</sub> at 550° was passed into the solvent after purification by passage through glass helices maintained at - 80° C. The solution concentration was determined conductimetrically.

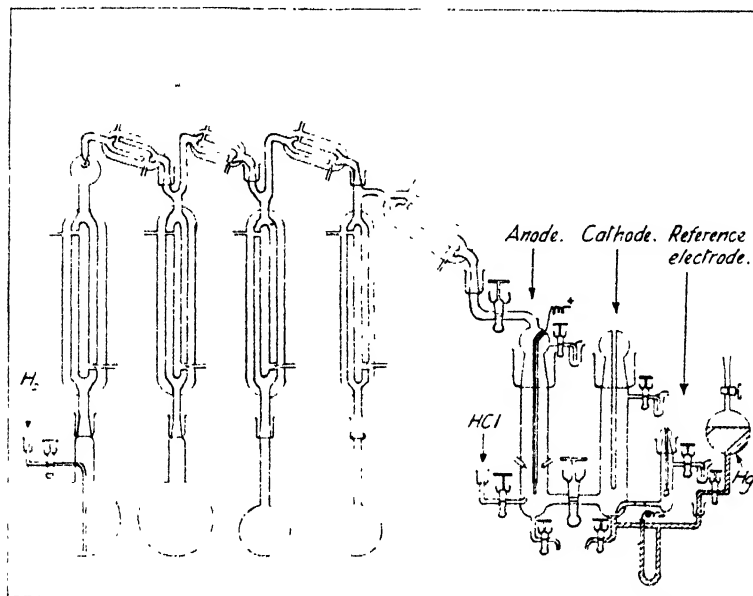


FIG. 1.—Methanol purification system and electrolytic cell.

For anhydrous solutions the apparatus was dried by rinsing with redistilled ethanol followed by sodium-dried ether. Joints and taps were sealed with purified methanol. 99.5 % acetone-free methanol was prepared from A.R. methanol by the method of Bates, Mullaly and Hartley<sup>10</sup> and was allowed to stand over *m*-phenylene diamine for a week,<sup>11</sup> after which it was introduced into the final purification system (Fig. 1). This consisted of a set of four distillation sections connected directly to the cell. Using this system the methanol could be distilled in a current of H<sub>2</sub> from the *m*-phenylene diamine onto magnesium methoxide<sup>12</sup> (prepared *in situ*) with which the methanol was refluxed for 30 min. The dry methanol was distilled first into the third flask and then redistilled twice in hydrogen, finally into the anode compartment. The first fraction was neglected and that accepted had a specific conductivity of  $1.4 \times 10^{-7}$  mho cm.<sup>-2</sup> (cp.<sup>13</sup>). This methanol gave a slight pink colour with Schiff's reagent after standing for  $\frac{1}{2}$  hr. in air, but appeared to give less than that prepared by other means.\*<sup>14, 15</sup>

<sup>10</sup> Bates, Mullaly and Hartley, *J. Chem. Soc.*, 1923, **123**, 401.

<sup>11</sup> Rowe and Phelps, *J. Amer. Chem. Soc.*, 1924, **46**, 2078.

<sup>12</sup> Lund and Bjerrum, *Ber.*, 1931, **64**, 210.

<sup>13</sup> Copley and Hartley, *J. Chem. Soc.*, 1930, 2488.

<sup>14</sup> Szilard, *Z. Elektrochem.*, 1906, **12**, 393.

<sup>15</sup> Pearce and Mortimer, *J. Amer. Chem. Soc.*, 1918, **40**, 509.

<sup>16</sup> Levina and Silberfarb, *Acta Physicochim.*, 1936, **4**, 275.

\* Levina and Silberfarb<sup>16</sup> do not appear to have obtained ethyl alcohol which gave no colour with Schiff's reagent.

For the mixed solvents the water-still and the methanol purification system were both attached directly to the anode compartment of the cell. In order to prepare solvent mixtures of known composition in hydrogen without contact with the outside atmosphere a small glass float was introduced into the anode compartment before the apparatus was set up. The floats were calibrated with known methanol-water mixtures. Approximately the correct quantity of methanol was distilled into the anode compartment, followed by water which was distilled in until the float became suspended in the liquid: mixtures so prepared were accurate to within about 1 %.

All solutions were finally purified by electrolysis for about 20 hr. at  $10^{-4}$  A/cm.<sup>2</sup> using a mercury cathode which was renewed every 4 hr. The measurements were carried out using a fresh cathode surface by varying the c.d. in steps, and observing the potential difference (p.d.) between the working electrode and a reversible hydrogen electrode in the same solution. Measurements were made at room temperature (18°-20° C) unless otherwise stated. A study of experimental technique in the measurement of overpotential will be published later.<sup>5</sup>

The partial pressure of hydrogen above the solution was varied by introducing purified nitrogen into the hydrogen stream (cp. for the reversible electrode<sup>17</sup>).

The relation between overpotential and c.d. was studied at constant temperature in the range 0-40° C by immersing the cell to above the level of the solution in a water-filled thermostat.\* The temperature inside the cell could be controlled within  $\pm 0.50^\circ$  C, in which range the variation of the overpotential is less than the normal error of measurement. The bath was cooled to the lower temperatures by the addition of solid CO<sub>2</sub> which was used because of the impurities present in commercial ice. The mercury cathode was renewed between each run at a given temperature.

**(b) The Dropping Mercury Electrode.**—The cell used was similar to that described by Bockris and Parsons<sup>18</sup> except for modifications to the cathode compartment (Fig. 2). A dropping electrode capillary *c*, internal diam. 0.000 cm., was inserted into the stopper and sealed by means of a mercury cup *j*. The auxiliary Pt electrode *a* and the cup for collecting Hg drops<sup>19</sup> *b* were fitted into the stopper by means of gas-tight sleeves. Mercury which fell to the bottom of the cell was kept at a negative potential (to prevent dissolution) by means of an auxiliary circuit to *e* and could be removed by means of a tap *f*. The effective height of the mercury column was varied by means of the reservoir CC (cp. 19) in order that the electrode mercury would not be contaminated by contact with rubber. The maximum area of the drops was estimated for each overpotential measurement by collecting a known number of drops in the cup *b*. These could then be drawn into *d*, washed, dried and weighed.

The aqueous solutions were prepared as described by Bockris and Parsons<sup>18</sup> but hydrogen was passed through them for 12 hr. before introduction to the cell. Methanol was first purified by the method of Bates, Mullaly and Hartley,<sup>10</sup> and then dried as described by Lund and Bjerrum.<sup>12</sup> After distilling from AgNO<sub>3</sub>,<sup>14</sup> the methanol was finally distilled into the solution preparation vessel in a stream of hydrogen. Hydrogen was then passed through the solution for 12 hr. and the HCl introduced immediately before the solution was forced into the cell. This method of preparing solutions was adopted since the measurements could not be extended far below  $10^{-4}$  A/cm.<sup>2</sup> because at this c.d. the charging current becomes comparable to the total current. The rigorous deoxygenation used for the work using static electrodes is therefore unnecessary here.

The cathode capillary was not filled with mercury when the solution was forced into the cell. The Pt electrode *a* was polarized cathodically at a c.d. of  $10^{-2}$  A/cm.<sup>2</sup> and the solution pre-electrolyzed for 12-16 hr. with hydrogen bubbling in all three compartments. The Pt electrode was then raised above the level of the solution (without opening the external circuit) and the cathode capillary filled with mercury.

The dropping mercury electrode was polarized using a circuit with a high series resistance to ensure a constant current. The mean potential difference

<sup>17</sup> Romann and Chang, *Bull. Soc. Chim.*, 1932, **51**, 932.

<sup>18</sup> Bockris and Parsons, *Trans. Faraday Soc.*, 1948, **44**, 860.

<sup>19</sup> Kolthoff and Lingane, *Polarography* (Interscience, New York, 1946).

\* Some trouble in the early stages of the work due to leakage currents through the bath was successfully overcome; the results presented here are in good agreement with those obtained later using an air thermostat.

between the dropping electrode and a reversible hydrogen electrode was measured using a Cambridge potentiometer.

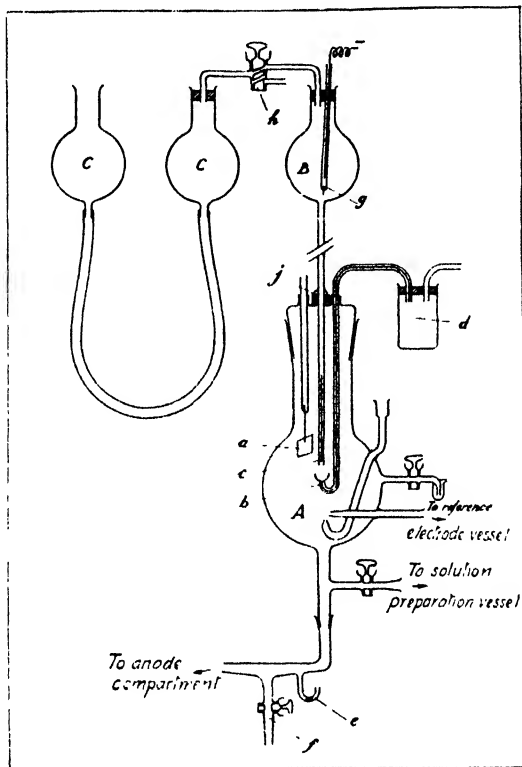


Fig. 2.—Cathode compartment showing dropping mercury electrode.

In order to allow free dropping, the cathode was about 1 cm. from the Luggin<sup>20</sup> capillary. Correction for the ohmic overpotential was made \* using the formula,

$$\eta_{r.d.} = \frac{2r_0 i}{\kappa d} (d - r_0), \quad (1)$$

where  $r_0$  is the radius of the drop,  $d$  is the distance between the drop and the Luggin capillary,  $i$  is the current density and  $\kappa$  the specific conductivity of the solution. This equation was derived by assuming that the current lines are radically symmetrical over half of the dropping electrode and may be neglected over the other half.†

## Results

### Stationary Cathode

**Effect of Solvent.**—Hydrogen overpotential at a stationary mercury cathode was measured in 0.1 N solutions of hydrogen chloride in methanol, water and a series of six methanol-water mixtures.

<sup>20</sup> Luggin, *Z. physik. Chem. A*, 1900, **32**, 208.

<sup>21</sup> Azzam, *Thesis* (London, 1949).

\* The value of the correction exceeded 0.1 V only for the 0.01 N methanolic solution at  $5 \times 10^{-3}$  A/cm.<sup>2</sup>.

† See the discussion of the correction of ohmic errors in overpotential measurements by Azzam.<sup>21</sup>

(a) THE EFFECT OF SOLVENT ON THE TAFEL LINE (Fig. 3).—It can be seen that the overpotential is decreased by the addition of the non-aqueous component. Also the slope  $b$  of the Tafel line decreases on addition of methanol.

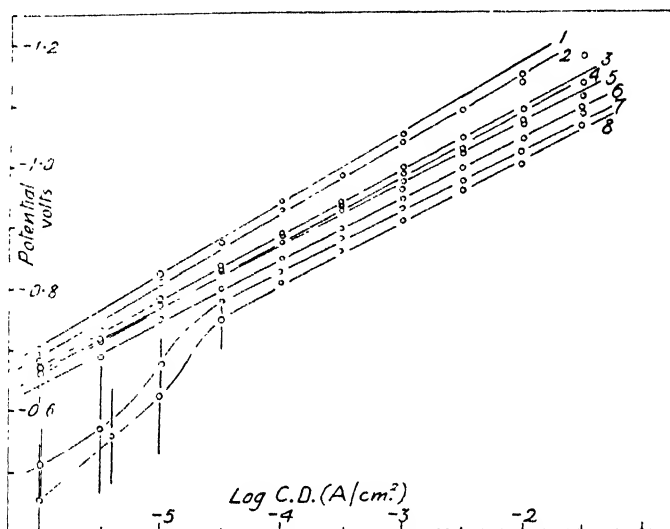


FIG. 3.—Hydrogen overpotential at a mercury cathode in 0.1N HCl solutions in methanol-water mixtures.\*

Solvent: 1. Pure  $\text{H}_2\text{O}$  4. 36 mole %  $\text{CH}_3\text{OH}$  7. 95 mole %  $\text{CH}_3\text{OH}$   
 2. 6 mole %  $\text{CH}_3\text{OH}$  5. 56 mole %  $\text{CH}_3\text{OH}$  8. Pure  $\text{CH}_3\text{OH}$   
 3. 20 mole %  $\text{CH}_3\text{OH}$  6. 84 mole %  $\text{CH}_3\text{OH}$

This is more clearly illustrated in Fig. 4, where  $\alpha$  ( $= 2.303 RT/bF$ ) is plotted against solvent composition. Here  $\alpha$  increases until the solvent contains about 30 mole % methanol but on further addition of methanol remains approximately constant.

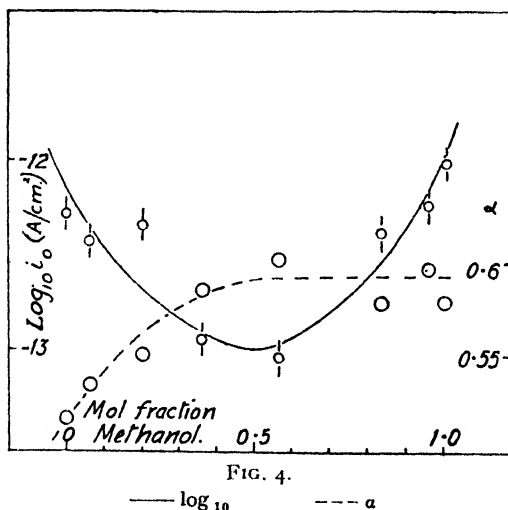


FIG. 4.

—  $\log_{10}$       ---  $\alpha$

\* In the graphical representation of all results the probable error

$$(\gamma = 0.675 \sqrt{28^2/n(n-1)})$$

of each is indicated by the length of the vertical bar of the cross corresponding to each experimental measurement.

The parameter  $i_0$  varies in an unexpected way with solvent composition (Fig. 4). The probable error of each value is indicated. Hence it can be seen that the minimum value of  $i_0$  at intermediate solvent composition is significantly different from the values in the pure solvents which differ only slightly. This indicates that the electrode process is more irreversible in the mixed solvent than in either of the pure solvents.

(b) THE EFFECT OF SOLVENT ON OVERPOTENTIAL AT CONSTANT C.D. (Fig. 5).—The values of overpotential at  $10^{-6}$ ,  $10^{-5}$ ,  $10^{-4}$ ,  $10^{-3}$  and  $10^{-2}$  A cm.<sup>-2</sup> are plotted against solvent composition in Fig. 5. Each line may be divided into three sections: a decrease of overpotential from 0 to 20 mole % methanol, a horizontal part from 20 to 70 or 80 mole %, and a further decrease to 100 mole %. At  $10^{-6}$  and  $10^{-5}$  A cm.<sup>-2</sup> this final decrease of overpotential is accentuated and corresponds to the deviations from the Tafel line found in 95 and 100 mole % methanol at low c.d. (see later).

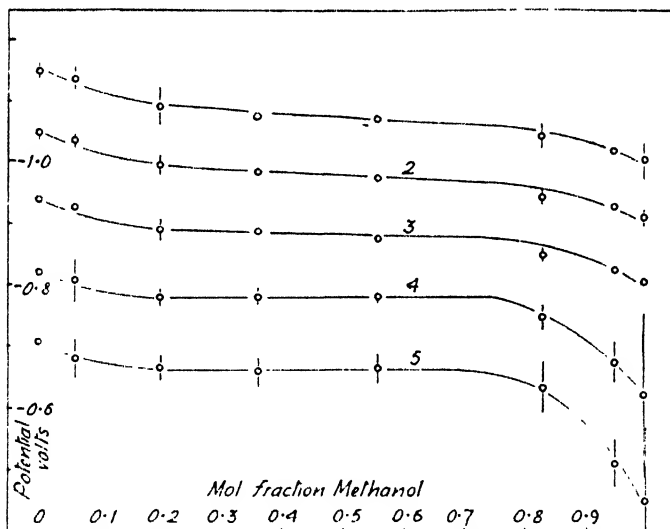


FIG. 5.—Overpotential at a mercury cathode in methanol-water mixtures.

Current and density:  $\left\{ \begin{array}{lll} (1) 10^{-2} \text{ A/cm.}^2 & (3) 10^{-4} \text{ A/cm.}^2 & (5) 10^{-6} \text{ A/cm.}^2 \\ (2) 10^{-3} \text{ A/cm.}^2 & (4) 10^{-5} \text{ A/cm.}^2 & \end{array} \right.$

(c) COMPARISON WITH PREVIOUS WORK.—No previous results for the overpotential at a mercury cathode in mixed solvents are available but results of a similar form for other high overpotential electrode materials were obtained in the high c.d. range by Bockris,<sup>23</sup> and Bockris and Ignatowicz.<sup>24</sup> The values of overpotential observed in pure aqueous solution are in good agreement with those obtained by other workers using suitable experimental conditions.<sup>1, 4</sup>

Results for the overpotential at a mercury cathode in pure methanolic solution were obtained by Novoselski.<sup>25</sup> Over the narrow range of c.d. covered by the Russian worker ( $2 \times 10^{-5}$  to  $3 \times 10^{-4}$  A cm.<sup>-2</sup>) the results are in good agreement ( $\pm 0.02$  V). The higher slope of the Tafel line (0.125) obtained by Novoselski may be ascribed to the inclusion of a small ohmic overpotential since this worker did not use a Luggin capillary.<sup>†</sup>

\* The overpotential—log c.d. line (Tafel line) may be represented by  $\eta = a - b \log i$ , or  $\eta = b(\log i_0 - \log i)$ , where  $\eta$  is the overpotential,  $i$  the current density, and  $a$ ,  $b$  and  $i_0$  are constants for the given line.  $i_0$  is thus the cathodic current which would flow at zero overpotential if the mechanism of the process remained unchanged.<sup>23</sup>

<sup>23</sup> Bockris, *Chem. Rev.*, 1948, **43**, 525.

<sup>24</sup> Bockris, *Faraday Soc. Discussions*, 1947, **1**, 95.

<sup>25</sup> Bockris and Ignatowicz, *Trans. Faraday Soc.*, 1948, **44**, 519.

<sup>†</sup> Novoselski, *J. Physic Chem. (U.S.S.R.)*, 1938, **11**, 369.

The potential gradient in 0.1 N HCl in methanol near a cathode surface at which the c.d. is  $3 \times 10^{-4}$  A cm.<sup>-2</sup> is of the order of 0.03 V cm.<sup>-1</sup>.

The results of Bowden and Grew<sup>26</sup> may be represented between  $10^{-6}$  and  $10^{-7}$  A cm.<sup>2</sup> by

$$\eta = -1.054 - 0.10 \log i$$

and between  $5 \times 10^{-7}$  and  $5 \times 10^{-8}$  A cm.<sup>2</sup> by

$$\eta = -1.45 - 0.14 \log i.$$

Neither of these results is in very good agreement with those of the present work. It must be noted, however, that Bowden and Grew, using the same apparatus, obtained results in aqueous solution corresponding to the equation

$$\eta = -1.46 - 0.14 \log i$$

which is in poor agreement with the corresponding result in the present work and also with other work carried out in pure solutions (Levina and Sarinsky,<sup>1</sup> Jofa, Kabanov, Chistyakov and Kuchinski,<sup>27</sup> Agar and Llopis<sup>4</sup>). The work of Bowden and Grew is also open to the criticism that in methanolic solutions an internal Pt anode was used at the higher c.d.'s with no provision for the prevention of diffusion of the anode products (particularly Pt which readily dissolves anodically in methanolic HCl) to the cathode surface.

(d) OVERPOTENTIAL IN METHANOL AT LOW C.D.'S.—The deviations from the linear  $\eta$ — $\log$  c.d. relation which were observed at c.d.'s between  $10^{-6}$  and  $10^{-8}$  A cm.<sup>2</sup> in the present work\* may be compared with the break in the Tafel line observed at c.d.'s between  $10^{-7}$  and  $10^{-8}$  A cm.<sup>2</sup> by Bowden and Grew. These authors suggest that this effect may be due to the participation of both the hydroxonium and the methoxonium ion in the proton discharge. Alternatively the effect might be due to the presence of aldehyde in the methanol which may cause depolarization under such conditions. However, neither of these explanations lead readily to the conclusion that the effect is approximately equally marked in 95 mole % and 100 mole % methanol but disappears altogether in 84 mole % methanol which is the experimental observation.

The results of the effect of  $H^+$  concentration in methanolic solution reported in this paper show that the dependence of overpotential on pH is more marked in methanolic solutions than in aqueous solutions. In aqueous solutions the dependence of overpotential on pH in concentrated solutions is ascribed by Jofa and Frumkin<sup>28</sup> to the presence of anions in the double layer. Following this assumption it would appear that the chloride ion has a greater surface activity in methanolic than in aqueous solution. The results of Jofa, Kabanov, Chistyakov and Kuchinski<sup>27</sup> in aqueous solutions containing the surface-active anions  $I^-$  and  $Br^-$  are strikingly similar to those obtained here in 95 and 100 mole % methanolic solutions. Hence it appears possible that the break in the Tafel line may be due to the slow adsorption of chloride ions (cf. Jofa *et al.*<sup>27</sup>).

Although no definite conclusion can be made as yet as to the cause of this effect it may be noted that pre-electrolysis appeared to have no significant effect on the overpotential results in this range. Consequently it appears more likely that the effect is an intrinsic property of the system rather than a result of the presence of impurities.

**Effect of Pressure.**—The experiments were carried out by discontinuing the bubbling in the reference electrode compartment. (A hydrogen electrode in a pure hydrogen-saturated solution will maintain the equilibrium potential for many hours.<sup>29</sup>) The hydrogen in the cathode compartment was then replaced by pure nitrogen. During 2 hr. of nitrogen bubbling no change (i.e. less than 2 mV) in the potential difference between the cathode and the reference electrode was observed. It thus appears that the potential of a working hydrogen electrode does not depend on the hydrogen pressure above the solution and hence the variation of the overpotential (i.e. the p.d. between a working electrode and a reversible electrode in the same solution and in the same atmosphere) is due entirely to the variation in the potential of the reversible hydrogen electrode.

Previous work on the effect of pressure on the overpotential at a mercury cathode has been confused. Bircher and Harkins<sup>30</sup> in 1923 using a mercurous

<sup>26</sup> Bowden and Grew, *Faraday Soc. Discussions*, 1947, **1**, 88.

<sup>27</sup> Jofa, Kabanov, Chistyakov and Kuchinski, *Acta Physicochim.*, 1939, **10**, 317.

<sup>28</sup> Jofa and Frumkin, *ibid.*, 1943, **18**, 183.

<sup>29</sup> Ellis, *J. Amer. Chem. Soc.*, 1916, **38**, 737.

<sup>30</sup> Bircher and Harkins, *ibid.*, 1923, **45**, 2810.

\* The results plotted are the mean values for runs in which the c.d. was increased and those in which it was decreased. A hysteresis was observed, the extent of which may be seen from the length of the vertical bars at each point.

sulphate reference electrode found that the p.d. between this electrode and the working electrode was independent of pressure; Harkins and Adams<sup>31</sup> in 1925, however, reporting earlier work of Harkins,<sup>32</sup> found that the potential between a mercury electrode evolving hydrogen and a reversible hydrogen electrode was independent of pressure. Thus the results are contradictory though obtained by the same worker. The present results show that the cathode potential of a mercury electrode evolving hydrogen is independent of the hydrogen pressure.

The result obtained enables a clear distinction to be made between theories of overpotential in which the free energy of activation of the deposition reaction is affected by a term proportional to the *overpotential* and those in which it is affected by a term proportional to the *cathode potential*.<sup>33</sup> In the former the overpotential is independent of hydrogen pressure while in the latter the cathode potential is independent of pressure. The present results are in agreement with the latter prediction. Theories of the former type, notably that of Eyring, Glasstone and Laidler,<sup>34</sup> must therefore be regarded as erroneous. The same conclusion must apply to the concept of the structure of the electrode double layer implied by these authors.<sup>34</sup> It has been shown that the theory of Eyring, Glasstone and Laidler is theoretically improbable<sup>35, 36</sup> but the above constitutes the first direct experimental proof of its invalidity.

**Effect of Temperature.**—The variation of overpotential with temperature at a stationary mercury electrode was investigated in 0.1 N HCl solutions in water, in a 50 % w/w methanol water mixture (35 mole % methanol) and in pure methanol.

(a) **THE EFFECT OF TEMPERATURE ON THE TAFEL LINE**—The values of the coefficients *a* and *b* in the Tafel equation are summarized in Table I. It

TABLE I

Mole fraction Methanol	Temp. °C	<i>a</i> Volt	$\pm \gamma$	<i>b</i> volt	$\pm \gamma$
0	0	— 1.455	0.0075	0.116	0.0025
	11	— 1.440	0.0035	0.117	0.0011
	20.5	— 1.395	0.0019	0.113	0.001
	30	— 1.376	0.0010	0.119	0.0030
	40	— 1.325	0.0081	0.114	0.0026
0.36	2.1	— 1.356	0.0021	0.105	0.0006
	13.0	— 1.313	0.0026	0.102	0.0005
	21.7	— 1.280	0.0040	0.100	0.0010
	31	— 1.242	0.0032	0.100	0.0009
	41	— 1.222	0.0024	0.101	0.0007
1.00	2.2	— 1.288	0.00124	0.108	0.0031
	12	— 1.241	0.00063	0.106	0.0014
	20.5	— 1.216	0.00084	0.104	0.0025
	30	— 1.201	0.00031	0.107	0.0008
	39.3	— 1.175	0.00019	0.106	0.0017

can be seen that the overpotential decreases by about 0.003 V per degree rise in temperature. This value of the temperature coefficient does not appear to vary with c.d. The mean value of the temperature coefficient in aqueous and 50 % w/w methanolic solution is

$$(\partial\eta/\partial T)_i = 0.0030 \pm 0.0001 \text{ V/}^\circ\text{C.},$$

while that in the pure methanolic solution is significantly different

$$(\partial\eta/\partial T)_i = 0.0025 \pm 0.0001 \text{ V/}^\circ\text{C.}$$

The observation of the constancy of the temperature coefficient with current density is supported by the fact that the coefficient *b* does not appear to vary with temperature. Fisher's *t*-test<sup>36</sup> was therefore applied to the experimental

<sup>31</sup> Harkins and Adams, *J. Physic. Chem.*, 1925, **29**, 215.

<sup>32</sup> Harkins, *Thesis* (Chicago, 1914).

<sup>33</sup> Eyring, Glasstone and Laidler, *J. Chem. Physics*, 1939, **7**, 1053.

<sup>34</sup> Kimball, Glasstone and Glassner, *ibid.*, 1941, **9**, 91.

<sup>35</sup> Frumkin, *Acta Physicochim.*, 1940, **12**, 481.

<sup>36</sup> Fisher, *Statistical Methods for Research Workers* (Oliver and Boyd, 1930).



results (cp.<sup>37</sup>). It was found that for all systems investigated the variation of  $\alpha$  ( $= \frac{2.3RT}{F}b$ ) with temperature is highly significant. The results were then analyzed statistically for the variation of  $\alpha$  with temperature. It was found that the temperature coefficient of  $\alpha$  in the systems investigated was not significantly different, the mean value being  $(2.34 \pm 0.19) \times 10^{-3}^\circ\text{C}^{-1}$ .

(b) THE HEAT OF ACTIVATION OF THE ELECTROLYTIC EVOLUTION OF HYDROGEN.—The heat of activation  $\Delta H^\ddagger$  at a given overpotential  $\eta$  is given by

$$\left(\frac{\partial \ln i}{\partial T}\right)_\eta = \frac{\Delta H^\ddagger}{RT^2} \quad . \quad . \quad . \quad (2)$$

$$\text{or} \quad \left(\frac{\partial \eta}{\partial T}\right)_i = \frac{\Delta H^\ddagger}{\alpha FT} \quad (\text{cf. Agar.})^{38} \quad . \quad . \quad . \quad (3)$$

Hence the heat of activation at the reversible potential is

$$\Delta H_0^\ddagger = \alpha F \left[ T \left( \frac{\partial \eta}{\partial T} \right)_i - \eta \right]^* \quad . \quad . \quad . \quad (4)$$

Since  $\alpha$  has been found to vary with temperature it would be expected from (4) that  $\Delta H_0^\ddagger$  would also vary with temperature. Also since  $(\partial \eta / \partial T)_i$  remains approximately constant with c.d. (which follows if  $\alpha$  is directly proportional to the absolute temperature) the quantity  $(T \partial \eta / \partial T)_i - \eta$  will vary with c.d. Hence a different value for  $\Delta H_0^\ddagger$  will be obtained for each temperature and c.d. The results are therefore presented as mean values for the region of the measurements. These values are shown in Table II together with their statistical "probable errors" which give a measure of the degree of variation of  $\Delta H_0^\ddagger$  in this region; they are, of course, considerably larger than the deviations resulting from experimental variations.

TABLE II

Solution	$\Delta H_0^\ddagger$ kcal. g. -ion <sup>-1</sup>
N/10 HCl — H <sub>2</sub> O . . .	21.1 $\pm$ 0.6
N/10 HCl 36 mole % MeOH . . .	23.2 $\pm$ 1.0
N/10 HCl — MeOH . . .	19.7 $\pm$ 0.4

(c) COMPARISON WITH OTHER WORKERS.—No measurements of the temperature coefficient of hydrogen overpotential have been previously reported for the systems investigated here. Bowden<sup>39</sup> found  $\alpha$  to be constant with temperature for a Hg cathode in N/5 aqueous H<sub>2</sub>SO<sub>4</sub>. His values of overpotential, however, differ considerably from those of the best modern work.

Jofa and Mikulin<sup>40</sup> found  $\alpha$  to be constant with temperature in N/4 aqueous H<sub>2</sub>SO<sub>4</sub> but Jofa and Stepanova<sup>41</sup> observed a decrease in  $\alpha$  with rise in temperature in aqueous N HCl. A more complex variation of  $\alpha$  was obtained in more concentrated HCl solutions. The difference in the effect of temperature on  $\alpha$  between results in H<sub>2</sub>SO<sub>4</sub> and in HCl solutions may arise from the comparatively greater difficulty in removing small quantities of impurities from H<sub>2</sub>SO<sub>4</sub>. An increase of  $\alpha$  with temperature has been reported by Roiter and Jampolskaya<sup>42</sup> for the electro-reduction of oxygen and by Stout<sup>37</sup> for the overpotential of azide deposition.

The few values of heat of activation recorded in the literature are all based on measurements of cathode potential with respect to a standard half-cell at

<sup>37</sup> Stout, *Trans. Faraday Soc.*, 1945, **41**, 75.

<sup>38</sup> Agar, *Faraday Soc. Discussions*, 1947, **1**, 81.

<sup>39</sup> Bowden, *Proc. Roy. Soc., A*, 1929, **126**, 107.

<sup>40</sup> Jofa and Mikulin, *J. Physic. Chem. (U.S.S.R.)*, 1944, **18**, 137.

<sup>41</sup> Jofa and Stepanova, *ibid.*, 1945, **19**, 125.

<sup>42</sup> Roiter and Jampolskaya, *Acta Physicochim.*, 1937, **7**, 247.

\* The symbol  $\Delta H_0^\ddagger$  refers to the standard heat of activation of the deposition reaction at the reversible potential derived from measurements using as a reference electrode a reversible hydrogen electrode at the same temperature as the working cathode. The symbol  $\Delta H_0^\ddagger$  is used when the reference electrode is a standard half-cell maintained at a constant temperature.

a constant temperature, i.e.  $\Delta H_0^{\ddagger}$ .<sup>38</sup> These values are thus connected to the true heat of activation by a term containing the temperature coefficient of the reversible hydrogen potential together with the thermojunction potential which is unknown. Jofa and Mikulin,<sup>40</sup> however, give values of  $(\partial\eta/\partial T)_t$  for a mercury cathode in aqueous  $N/4$   $H_2SO_4$ . With the aid of interpolated values of  $\eta$  from the graph given by these authors  $\Delta H_0^{\ddagger}$  has been found to be  $20.7$  kcal. g.-ion<sup>-1</sup> which is in good agreement with the value of  $21.1 \pm 0.3$  kcal. g.-ion<sup>-1</sup> found here for aqueous  $0.1$  N HCl.

## The Dropping Electrode

**The Effect of Hydrogen Ion Concentration in Aqueous and Methanolic Solution.**—(a) THE EFFECT OF pH ON THE TAFEL LINE.—Overpotential was measured at the dropping mercury electrode in solutions of  $0.01$ ,  $0.1$ ,  $1.0$  and  $5.0$  N HCl in pure water and pure methanol at c.d.'s from  $10^{-4}$  to  $10^{-1}$  A cm.<sup>-2</sup>.

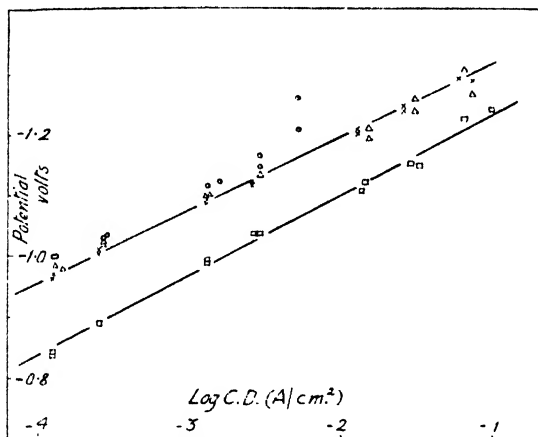


FIG. 6.—Overpotential at the dropping mercury cathode pH effect in aqueous solution.

□ 5 N HCl      × 1 N HCl      △ 0.1 N HCl      ○ 0.01 N HCl

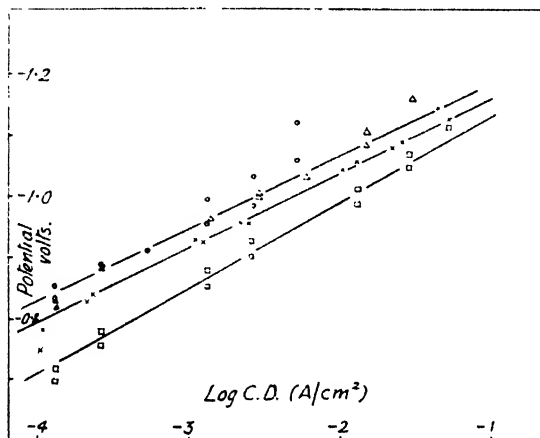


FIG. 7.—Overpotential at the dropping mercury cathode pH effect in methanolic solution.

□ 5 N HCl      × 1 N HCl      △ 0.1 N HCl      ○ 0.01 N HCl

The results are shown graphically in Fig. 6 and 7. It can be seen that change of  $H^+$  concentration in aqueous solution from  $0.01$  N to N does not affect the overpotential while further increase in concentration causes it to decrease.

In methanolic solution the overpotential remains constant only from 0.01 to 0.1 N and decreases as the HCl concentration increases from 0.1 N to 5.0 N. In spite of this apparently more marked pH effect in methanolic than in aqueous solution the change in overpotential between 1.0 and 5.0 N in the former is less than in the latter. This may be due to a trace of water in the 5 N solution produced by the esterification reaction which, though occurring very slowly in dilute solution,<sup>48</sup> will become appreciable in 5 N solution. Results at the stationary electrode reported above indicate that the presence of water would increase the overpotential thus causing the decrease in overpotential between 1 N and 5 N solutions to be less than would be expected.

(b) COMPARISON WITH PREVIOUS RESULTS.—The only previous investigation of the pH effect in pure acid solution at a dropping electrode is that of Herasymenko and Slendyk.<sup>7</sup> This work led to the anomaly referred to above. These authors found that the overpotential was independent of pH in concentrated solutions but in dilute solutions the overpotential increased with increase of pH, the change approaching  $RT/F$  volts per ten-fold dilution. This is in contradiction to the results obtained by Levina and Sarinsky<sup>1</sup> and by Jofa<sup>8</sup> using a static electrode, according to which the overpotential remains constant with pH in dilute solution and a variation with pH is first observed in solutions of acid concentrations greater than 1 N.

The results reported here are in good agreement with those obtained at a stationary electrode.<sup>1,8</sup> Hence it appears that there is no essential difference between the pH dependence of overpotential at dropping and stationary cathodes in pure solutions and that the anomaly must be due to earlier inadequacies in the measurement of overpotential at the dropping electrode. Such inadequacies might be of two types: firstly, and more likely, in the purification of the solution and secondly, in the measurement of overpotential (e.g. the method by which Herasymenko and Slendyk arrive at the  $\eta$ -log c.d. is not made clear). These authors do not mention the corrections necessary for the variation of the size of the drops with applied potential which are essential for the accurate measurement of a Tafel line under these conditions.

**A Comparison of the Dropping and Stationary Electrodes.**—Jofa, Kolychev and Shtifman<sup>44</sup> showed by considering the variation of current density at constant potential during growth of a drop that the Tafel line obtained and the dropping electrode should lie at  $\frac{2}{3} \frac{RT}{\alpha F}$  volt (or 34 mV, if  $\alpha = 0.5$ ) more

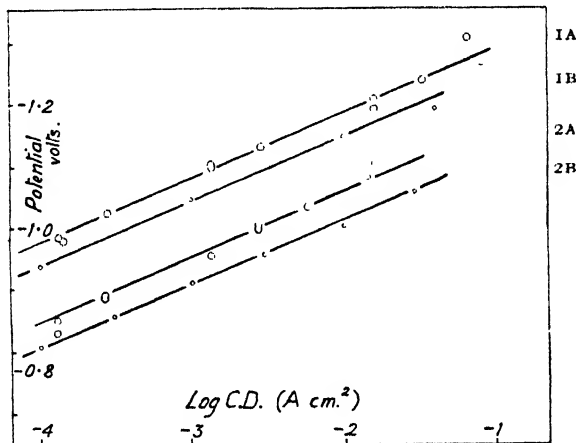


FIG. 8.—Potential at stationary and dropping mercury cathodes.

o Stationary Cathodes. O Dropping Cathodes.

1A, 1B 0.1N HCl in H<sub>2</sub>O

2A, 2B 0.1N HCl in CH<sub>3</sub>OH

negative than that obtained at a stationary electrode. The results shown in Fig. 8 support this, the difference found here being about 40 mV for both aqueous

<sup>48</sup> Woolcock and Hartley (unpublished work).

<sup>44</sup> Jofa, Kolychev and Shtifman, *Acta Physicochim.*, 1940, 12, 231; *idem.*, *J. Physic. Chem. (U.S.S.R.)*, 1940, 14, 58.

and methanolic solutions. It may also be noted that a similar difference is obtained between the results reported here for the dropping electrode in N and 5 N and those reported for the stationary electrode by Jofa and Stepanova.<sup>41</sup>

### Discussion

The agreement between the constants of the Tafel equation for mercury in aqueous acid solution reported here and those reported by Russian workers<sup>1, 4, 42</sup> appears to resolve the controversy concerning these values. The present values were obtained after many experiments concerned with the most satisfactory method of eliminating trace impurities from the solution, notably by pre-electrolysis. A detailed report of the investigations of the experimental conditions required for reliable overpotential determinations will be published later.<sup>5</sup>

A second important result of the present work is the observation of the variation of the term  $\alpha \left( = 2.303 \frac{RT}{bF} \right)$  with temperature. Many authors have tacitly assumed in their theoretical discussions of overpotential that  $\alpha$  would remain constant with temperature. The validity of the small experimental justification for this has been discussed above. Three types of theories have included rational interpretations of  $\alpha$ ; the (energy level) slow discharge<sup>43, 47</sup> theory, the slow prototropic transfer theory<sup>33</sup> and the catalytic theories.<sup>48</sup> Essentially two interpretations of  $\alpha$  are suggested: that it is the ratio of the slopes of the potential energy curves of the initial and final states of the system; that it is the exponential in a Freundlich type of isotherm. The solvation energy, the adsorption energy and the thickness of the electrode double layer are known to vary with temperature and since these factors determine the position and slope of the potential energy curves it would appear unlikely that these variations would cancel out in so far as they affect the relative slopes of the potential energy curves at their point of intersection. Since the exponential of the Freundlich isotherm also varies with temperature a variation of  $\alpha$  with temperature would be expected. Similarly  $\Delta H_0^\ddagger$  as defined in eqn. (4), would be expected to vary with temperature.

A theory of the effect of the solvent on hydrogen overpotential when this is due to a delay in the atom combination reaction has been developed by one of us.<sup>44</sup> This indicates that the overpotential at a given current density would be less in methanolic than in aqueous solution, in agreement with the experimental results reported. In mixed solvents containing primary alcohols and water, however (e.g. the methyl alcohol—water mixtures of the present experiments) the solvent layer theory indicates a rise in overpotential which disagrees with the experimental facts for mercury cathodes. This evidence therefore strongly supports the view that the hydrogen atom combination is a rapid stage in the evolution reaction (see also the evidence concerning the concentration of adsorbed hydrogen on mercury cathodes in acidic media<sup>39</sup>).

Some discussion of the effect of the medium upon the discharge stage of the evolution reaction has already<sup>18</sup> been given. According to a modification of the energy level type of slow discharge theory discussed the variation of the overpotential of a high overpotential metal with change of solvent is primarily due to the effect of the solvent on the adsorption energy of hydrogen at the reversible electrode. It has been shown that for metals such as Ni and Pt, the number of solvent molecules attached to the cathode should be similar when the solvent is either methanol or water. The area of cathode surface occupied will be somewhat larger

<sup>45</sup> Frumkin, *Acta Physicochim.*, 1943, **18**, 23.

<sup>46</sup> Horiuti and Polanyi, *ibid.*, 1935, **2**, 505.

<sup>47</sup> Butler, *Proc. Roy. Soc. A*, 1936, **157**, 423.

<sup>48</sup> Horiuti and Okamoto, *Sci. Pap. Inst. Phys. Chem. Res. Tokyo*, 1936, **29**, 223.

in methanolic than aqueous solutions because of the larger size of the methanol molecule. The adsorption energy of hydrogen will consequently be lowered and the reversible potential will be more negative in methanol than in aqueous solution. This conclusion is qualitatively supported by the fact that the reversible hydrogen electrode is more negative in methanolic than in aqueous solution by about 0.1 V if measured with respect to the electrocapillary maximum (which is an approximation to an electrode with zero electrode-solution p.d.).<sup>4b</sup>

The lowering of overpotential at a mercury electrode in methanolic solution can thus be qualitatively accounted for on the basis of this theory. A detailed discussion of the variation in mixed solvents and a quantitative interpretation of the solvent effect, however, do not appear to be possible at the present time.

Many thanks are due to Professor H. V. A. Briscoe for his interest in this work. One of us (R. P.) wishes to thank the Scholarship Committee of the University of London for a Postgraduate Studentship during the tenure of which this work was carried out. Thanks are also due to the administrators of the Dixon Fund of London University for a grant for apparatus used in the work.

*Department of Inorganic and Physical Chemistry,  
Imperial College of Science,  
London, S.W.7.*

## A NOTE ON INTERSTITIAL DIFFUSION

BY R. M. BARRER AND W. JOST

*Received 12th April, 1949*

In zeolitic diffusion described by the general diffusion equation

$$\frac{\partial c}{\partial t} = \frac{\partial}{\partial x} \left[ D' \frac{d \ln a}{d \ln c} \frac{\partial c}{\partial x} \right]$$

in which each unit diffusion process involves only a single jump from one sorption site to the next, it has been shown that the concentration dependance in the diffusion coefficient  $D'$  and the departure from ideality in the mixture expressed

by  $\frac{d \ln a}{d \ln c}$  exactly compensate, to give Fick's law  $\frac{\partial c}{\partial t} = D_0 \frac{\partial^2 c}{\partial x^2}$ .

However, existing data show that  $D' \frac{d \ln a}{d \ln c}$  decreases in some zeolites as the concentration increases at least for smaller values of concentration. This can be so if  $n$ -fold as well as single jumps occur in some unit diffusion processes. It is further shown, however, that in this event diffusion should begin according to the generalized diffusion equation and then tend to Fick's law as the interstitial concentration approaches saturation.

Barrer and co-workers<sup>1</sup> have observed certain features of diffusion in zeolites, for which they advanced an explanation. These characteristics are

(i) diffusion coefficients in zeolites decrease at least in some crystals as the interstitial concentration of sorbate increases;

(ii) the rate of sorption tends to become independent of the pressure of gaseous sorbate in contact with the crystals as this pressure rises.

<sup>1</sup> Barrer and Ibbitson, *Trans. Faraday Soc.*, 1944, **40**, 206. Barrer and Riley, *J. Chem. Soc.*, 1948, 133. Barrer, *Trans. Faraday Soc.*, 1941, **37**, 590.

An interpretation of the first characteristic was given as follows. The probability of migration of a sorbed particle is proportional to the probability of finding an unoccupied neighbouring sorption site, and this is equal to  $1 - \theta$ , if  $\theta$  is the fraction of available sites occupied by sorbed molecules.<sup>2</sup> Consequently, the diffusion coefficient decreases with increasing sorption ( $D = D_0(1 - \theta)$ ).

The second feature was explained in terms of the sorption isotherm. The intracrystalline sorption is governed by a Langmuir type of isotherm,<sup>3</sup>

$$p = k\theta/(1 - \theta), \quad (1)$$

as demonstrated experimentally. Therefore, for sufficiently high pressure the crystal will be almost saturated near its surface, and a further increase in pressure cannot increase the concentration near the surface, and consequently the rate of sorption becomes independent of pressure.

Interstitial mobility of a sorbate within a zeolite may also be modified if all sites are not of the same kind. There is then a tendency for sites of highest sorption potential to be occupied first, and for molecules sorbed at these sites to be held more firmly. However, this would operate in the opposite direction to the factor  $(1 - \theta)$  in the relation  $D = D_0(1 - \theta)$ , and so the explanation of decreasing mobility given in the first paragraph is no doubt essentially correct. Nevertheless, it is of interest to extend the theory to meet difficulties which emerge when a more detailed analysis is made.

Since the diffusion coefficient in the systems under consideration sometimes depends on concentration and since the solution near saturation is not ideal, we must use the diffusion equation in its most general forms, such as \*

$$\frac{\partial c}{\partial t} = \frac{\partial}{\partial x} \left( D' \frac{d \ln a}{d \ln c} \frac{\partial c}{\partial x} \right), \quad (2)$$

if we consider the one-dimensional problem. In (2),  $c$  is the concentration of the diffusing substance,  $a$  its activity,  $D'$  is a diffusion coefficient which still may depend on concentration, but does not contain factors due to non-ideality of the mixture under consideration. If (2) is applied to diffusion in the vicinity of the surface of the crystal, near saturation, it is seen that by a further increase in pressure the concentration and therefore  $\partial c / \partial x$  cannot be changed considerably in accordance with the above explanation of the experiments. But the activity  $a$  depends on pressure too, and may be increased considerably by an increase of pressure, without noticeable change in concentration. Therefore the term

\* Barrer, ref. 1.

<sup>2</sup> E.g. Barrer, *Ann. Reports*, 1914, 41, 31.

\* It is usual to write  $D = D' \frac{d \ln a}{d \ln c}$ , thus transforming eqn. (2) into eqn. (6).

Eqn. (2) may be derived as follows. The force acting on a single molecule and tending to cause diffusion is proportional to the gradient in chemical potential  $\partial \mu / \partial x$ . The force on all the molecules at a point where their concentration is  $c$  is proportional to  $c \frac{\partial \mu}{\partial x}$  and the flux through unit area at this point is then

$P = D^* c \cdot \frac{\partial \mu}{\partial x}$ , leading in the usual way to  $\frac{\partial c}{\partial t} = \frac{\partial}{\partial x} \left[ D^* c \cdot \frac{\partial \mu}{\partial x} \right]$ . However,  $\partial \mu = RT d \ln a$ , and so the diffusion equation becomes

$$\begin{aligned} \frac{\partial c}{\partial t} &= \frac{\partial}{\partial x} \left\{ D^* c \frac{RT}{a} \cdot \frac{\partial a}{\partial x} \right\} \\ &= \frac{\partial}{\partial x} \left\{ D^* \cdot RT \cdot \frac{d \ln a}{d \ln c} \cdot \frac{\partial c}{\partial x} \right\} \\ &= \frac{\partial}{\partial x} \left\{ D' \frac{d \ln a}{d \ln c} \cdot \frac{\partial c}{\partial x} \right\} \text{ where } D' = D^* \cdot RT. \end{aligned}$$

$d \ln a / d \ln c$  might partly upset the explanation given so far. It can be shown, however, that this is not the case. Putting

$$D' = D_0(1 - \theta), \quad (3)$$

$$\text{and} \quad a \propto p = k\theta/(1 - \theta) \quad (4)$$

(which involves only the assumption of sufficiently ideal behaviour of the gas phase) we obtain

$$\frac{d \ln a}{d \ln \theta} = \frac{d \ln a}{d \ln c} = \frac{1}{(1 - \theta)},$$

and so from (2)

$$\frac{\partial c}{\partial t} = D_0 \frac{\partial^2 c}{\partial x^2} \quad (5)$$

This means we are dealing with the interesting case where there are strong deviations from ideality of the mixture and from constancy of  $D'$ , but where the final result is identical with that obtained for ideal solution and constant diffusion coefficient  $D$ .

Now we have, however, a new difficulty with which the theory must be reconciled. The results mentioned in the beginning under (i) indicate that for concentrations sufficiently below saturation the equation which holds is

$$\frac{\partial c}{\partial t} = \frac{\partial}{\partial x} \left( D \frac{\partial c}{\partial x} \right) \quad (6)$$

with  $D$  decreasing for increasing  $c$ . This is in contradiction with eqn. (5). But it is possible to modify the underlying picture to give eqn. (6) as the limiting case for small concentrations, and eqn. (5) as the limiting case for concentrations near saturation. A particle, moving in the interstitial channels of a zeolite, may, if once activated, jump over several elementary distances of length  $d$ , before it is deactivated.\* As a first approximation a diffusion coefficient, involving  $n$ -fold jumps, is obtained:†

$$D_n \simeq (nd)^2 \cdot \nu \cdot (1 - \theta)^n \exp(-E_n/RT), \quad (7)$$

where  $\nu$  is of the order of magnitude of the oscillation frequency of a sorbed molecule,  $(1 - \theta)^n$  gives the probability of finding a vacant neighbouring site  $n$  times in succession, and the energy of activation  $E_n$  may or may not depend on  $n$ .† Therefore at the point where  $\theta$  is the fraction of occupied sites one has an effective diffusion coefficient  $D'$  given approximately by the relation:

$$D' \simeq \sum_{n=1}^{\infty} D_n \phi_n; \quad \sum_{n=0}^{\infty} \phi_n = 1, \quad (8)$$

where  $\phi_n$  is the fraction of occupied sites from which at any instant  $n$ -fold jumps occur.

Now, unless  $E_n$  is increasing strongly with increasing  $n$ , it is obvious on comparing the relative magnitudes of  $(nd)^2 \times (1 - \theta)^n$  and  $d^2(1 - \theta)$  that for small  $\theta$  values of  $D_n$  with  $n \geq 2$  may give a considerable contribution to  $D'$ , while for  $\theta$  close to 1 only the term with  $n = 1$  will be of importance. Thus (7) and (8) lead exactly to the limiting cases (5) and (6), as required.

The picture, outlined above for the case of zeolites, might be of value for other examples of interstitial diffusion such as that of hydrogen in transition metals.

Chemistry Department,  
Marischal College,  
Aberdeen.

Physikal.-Chem. Institut d.  
Universität, Marburg.

\* For a derivation of a similar equation for the case of a single jump see Barrer,<sup>1</sup>.

†  $d$  is the distance between adjacent sorption sites along the interstitial channel.

†  $E_n$  is constant for all values of  $n$  in a zeolite where all the sorption sites have the same sorption potential. In such a homogeneous zeolite  $E_n$  is then a measure of the energy needed to surmount the energy barrier between adjacent equilibrium sites.

# THE CHANGE OF ENTROPY, VOLUME AND BINDING STATE OF THE ELEMENTS ON MELTING

BY O. KUBASCHEWSKI

Received 4th May, 1949

It is known from crystallographical considerations that the stability of the lattices of the solid elements may be due to metallic, homopolar, or van der Waals' binding forces. The structure of the solid elements may be represented by the co-ordination numbers, which are a measure of the participation of the different bonds maintaining the lattice. One may classify elements into several groups: true metals, meta-metals, semi-metals, and non-metals. In the true metals, pure metallic bondings are responsible for the stability, in the meta-metals and semi-metals an increasing participation of homopolar bonding occurs. The physical properties of the elements, such as electrical conductivity and magnetic susceptibility, depend on the binding mechanism.

It is shown that the molar heat capacity at the melting point  $C_p$  divided by the absolute temperature of fusion  $T_m$  and the cubic coefficient of expansion at the melting point  $\alpha$  is also a measure of the bonding mechanism. The ratio  $C_p/(T_m\alpha)$  is nearly constant for the true metals and the meta-metals, but is much greater and varies within wide limits for the semi-metals, and is generally smaller for the non-metals.

It is concluded from the co-ordination numbers in the liquid state and the ratio  $C_p/(T_m\alpha)$  (liq.) that the semi-metals partially lose their homopolar bonds on melting. This is also evident from the change of entropy and of conductivity on melting. The ratio  $\Delta S_m/\Delta V_m$  is again constant for the true metals and the meta-metals, but is much greater or negative for the semi-metals and smaller for the non-metals. Combining this result with Clapeyron's equation a relation is found between the lowering of melting point by pressure and the atomic volume ( $\Delta V$ ):  $dp/dT \rightarrow (\Delta V)/\delta_m$ , holding true as far as it can be compared with experimental measurements.

---

The entropy of fusion is the quotient of the heat of fusion divided by the absolute melting temperature,  $L_m/T_m = \Delta S_m$ . Alternatively entropy is a measure of the state of order, and so the entropy of fusion represents the difference in the state of order of melt and crystal lattice. Using this conception it has been possible to estimate the degree of order of alloys from the measured entropies of fusion.<sup>1</sup> It was found that the difference between the measured entropy of fusion and that obtained by adding the entropies of fusion of the constituents represents a measure of the degree of order of the respective alloy at its melting point.

The entropies of evaporation of many compounds and elements are nearly constant (21.5 cal./deg.; Trouton-Pictet rule). Divergences are observed only with substances whose molecules associate in the gaseous state or which vaporize at very low temperatures.<sup>2</sup> In comparison the entropies of fusion even of the elements alone show a much greater variation, though a certain regularity is perceptible (Richards-Crompton rule). According to Tammann<sup>3</sup> the entropies of fusion of metals are scattered about the value of 2.2 cal./deg.

<sup>1</sup> Kubaschewski, *Z. Elektrochem.*, 1941, **47**, 475; *Z. physik. Chem.*, 1943, **192**, 292.

<sup>2</sup> Eucken, *Lehrbuch der chemischen Physik*, II (Leipzig, 1944), pp. 865-870, 891-894.

<sup>3</sup> Tammann, *Z. physik. Chem.*, 1913, **85**, 273.



This mean value is much lower than the entropy of evaporation. This is due to the greater similarity between the solid and liquid state compared with the change from liquid to gas. On the other hand the differences in structure between the various solid crystal lattices must have a relatively large percentage effect on the entropy of fusion.

Now the binding mechanism in any aggregate decides its state of order. In the elements we have to consider mainly the homopolar and the metallic bonds (compensation of electron spins or formation of the electron gas) and possibly the dispersion forces. There already exists considerable evidence of the binding mechanism of metals (see for instance the monographs by Pauling,<sup>4</sup> Dehlinger<sup>5</sup> and Hume-Rothery<sup>6</sup>). Thus the atoms of carbon, silicon and germanium are kept together by homopolar bonds, those of the alkaline earth metals by metallic bonds, and the condensed rare gases by dispersion binding. The considerations which led to this classification, based on the structure of the crystal lattice concerned, takes into account the number of neighbouring atoms of any atom in the lattice, i.e. the so-called co-ordination number.

Structures made up entirely by metallic bonding have high co-ordination numbers (up to 12); homopolar structures have lower numbers (e.g. C, Si, Ge: 4). Thus the co-ordination number should give some indication of the extent of homopolar binding in the crystal in question.

In melting a crystal a complete break-up of the lattice occurs, and changes in the bonding are expected. The co-ordination numbers of several liquid elements obtained by high-temperature X-ray methods are known. In Table I the co-ordination numbers (C. No.) in the solid and liquid state, the atomic distances (AD) between one atom and its nearest neighbour, the change in co-ordination number on melting ( $\Delta C. No. = C. No._{liq.} - C. No._{sol.}$ ) and the entropies of fusion are tabulated.

It is perhaps premature to discuss each anomaly in Table I, since owing to the difficulties of measurement some of the co-ordination numbers may be unreliable. Taken broadly, however, the table gives some significant indications.

Thus the high co-ordination numbers (12 and 8) in the solid state of the metals exhibiting metallic bonding do not change on melting, or decrease slightly:  $\Delta C. No. = 0$  to  $-1$ . This indicates a slight change in the binding state on melting. This is borne out by the retention of electrical conductivity on melting, with only a slight lowering.<sup>7</sup> The entropies of fusion are nearly constant at 1.7 cal./deg. for the alkali elements (C. No. = 8) or at 2.0 to 2.4 for the metals of C. No. 12. On the other hand, the (semi-)metals with low co-ordination, such as gallium, germanium and bismuth, which are bound largely by homopolar bonds, show an appreciable increase in co-ordination number on melting. The rigid homopolar bonds holding the atoms in the solid state are obviously replaced partly or totally by a metallic binding. This transition is further marked by the great increase in electrical conductivity on melting which is characteristic of this type of element.

We may try to make some predictions from Table I. Thus we may expect the co-ordination number of liquid Rb and Cs to be about 8. The co-ordination numbers of copper and silver should be nearly the same as that of gold (C. No. = 11). The entropies of fusion are easier to obtain than the "structures" of molten substances, and using these values it appears possible to estimate the co-ordination numbers of liquid elements by such comparisons as Table I, if the numbers for the solid state are known.

The co-ordination numbers and the interatomic distances govern the value of the atomic volume. This quantity includes not only the

<sup>4</sup> Pauling, *The Nature of the Chemical Bond* (London, 1945).

<sup>5</sup> Dehlinger, *Chemische Physik der Metalle und Legierungen*, Leipzig, 1939.

<sup>6</sup> Hume-Rothery, *Atomic Theory* (Institute of Metals, London, 1947).

<sup>7</sup> Grube and Dietrich, *Z. Elektrochem.*, 1938, **44**, 755.

volume occupied by the atoms themselves but also the interatomic space. The entropy of fusion can now be defined more exactly as a measure of the increase in disorder and of volume expansion. Eucken<sup>2</sup> discusses the correlation of these quantities starting from the melting theory of

TABLE I.—ENTROPY OF FUSION OF SOME ELEMENTS AND THEIR CO-ORDINATION NUMBERS IN THE SOLID AND LIQUID STATE

Element	Crystal Lattice		Molten State		Ref.	$\Delta C$ . No.	$\Delta S_m$ in Cal./deg.	Ref.
	C. No.	AD in Å	C. No.	AD in Å				
A	12	3.82	7	3.00	8	-5	—	—
			10	3.80	9	-2	3.35	10
Li	8	3.04	9.8	3.24	11	+1.8	1.53	12
Na	8	3.72	8	3.85	13	0	1.70	12
K	8	4.58	8	4.64	14	0	1.70	12
Rb	8	4.9	—	—	—	—	1.68	12
Cs	8	5.3	—	—	—	—	1.65	12
Mg	12	3.20	—	—	—	—	2.25	12
Cu	12	2.55	—	—	—	—	2.20	12
Ag	12	2.88	—	—	—	—	2.22	12
Au	12	2.88	11	2.86	15	-1	2.20	12
Zn	6+6	2.65; 2.94	11	2.94	11	-1	2.48	12
Cd	6+6	2.97; 3.30	8	3.06	11	-4	2.57	12
Hg	6+6	3.00; 3.47	—	—	—	—	2.37	12
Al	12	2.86	10.6	2.96	11	-1.4	2.70	12
Ga	1+6	2.43; 2.71 to 2.79	11	2.77	15	+4	4.42	12
In	4+8	3.24; 3.37	8+4	3.17; 3.88 3.30	15 11	0 (-4)	1.82	12
Tl	12	3.45	8+4	3.30; 4.22	15	0	1.79	12
Si	4	2.35	—	—	—	—	6.5	12
Ge	4	2.43	8	2.77	15	+4	6.0	12
Sn	4+2	3.02; 3.15; 3.76	10	3.20	15	0	3.35	12
	+4	3.76	—	—	—	—	—	—
Pb	12	3.49	8+4	3.40; 4.37	15	0	1.98	12
Sb	3+3	2.87; 3.80	—	—	—	—	5.25	12
Bi	3+3	3.09; 3.46	7.5	3.32	15	+1.5	4.78	12

Lennard-Jones and Devonshire.<sup>16</sup> It is argued that the interlattice energy, defined by Lennard-Jones and Devonshire, should be proportional to the volume increase on melting and also to the entropy of fusion and that therefore proportionality between these two quantities should exist. It can be shown that this proportionality, predicted by Eucken, is confirmed for any element whose solid lattice is held by the same bonding mechanism.

The entropies of fusion and volume changes on fusion critically selected from the literature or obtained from the author's measurements are

<sup>8</sup> Eisenstein and Gingrich, *Physic. Rev.*, 1940, **58**, 307.

<sup>9</sup> Miller and Lark-Horowitz, *Physic. Rev.*, 1940, **58**, 207.

<sup>10</sup> Landolt-Börnstein-Roth-Scheel, *Physikalisch-chemische Tabellen*, III, Suppl. Vol., 1936, pp. 2212, 2237, 2245, 2697, 2685.

<sup>11</sup> Gamertsfelder, *Physic. Rev.*, 1939, **55**, 1116; 1940, **57**, 1055; 1941, **59**, 926.

<sup>12</sup> Kubaschewski, *Z. Elektrochem.*, 1949, **53**; *Z. Metallkunde*, 1949, **40** (in press).

<sup>13</sup> Trimble and Gingrich, *Physic. Rev.*, 1938, **53**, 278.

<sup>14</sup> Thomas and Gingrich, *J. Chem. Physics*, 1938, **6**, 411.

<sup>15</sup> Hendus, *Z. Naturforsch.*, 1947, **2a**, 505.

<sup>16</sup> Lennard-Jones and Devonshire, *Proc. Roy. Soc. A*, 1938, **169**, 317; 1939, **170**, 464.

TABLE II.—CHANGE OF ENTROPY AND VOLUME ON MELTING OF THE ELEMENTS

Element	$\Delta S_m$ cal./deg.	Ref.	$\Delta V_m$	Ref.	$\delta_m$ cal./deg.
Li	1.53	12	0.0165	19, 20	(93)
Na	1.70	12	0.025	21, 22, 23,	68
K	1.70	12	0.0255	24, (20), (25)	67
Rb	1.68	12	0.025	22, 20, 25, 20, (23)	67
Cs	1.65	12	0.026	20, 25, 26	64
Cu	2.29	12	0.0415	20, 22, 27, 28	55
Ag	2.22	12	0.038 (0.05)	28, (20), (22)	58
Au	2.29	12	0.051	20, 22, 29	45
Mg	2.25	12	0.041	22, 30, 31, 32	55
Zn	2.48	12	0.042	33, 34, (23), (27)	(59)
Cd	2.57	12	0.047	22, (23), (24)	55
Hg	2.57	12	0.037	22, 24	64
Al	2.70	12	0.060	32, (28), (23), (35)	45
Ga	4.42	12	-0.032	10	-138
In	1.82	12	(0.027)	*	(67)
Tl	1.79	12	0.032	22, (23), (24)	56
Si	6.5	12	—	—	—
Ge	6.0	12	—	—	—
Sn	3.35	12	0.028	21, 22, 23, 24, 28, 33	120
Pb	1.98	12	0.035	22, 23, 24, 33	57
P	0.47	12	0.035	36	13
Sb	5.25	12	-0.0095	37	-560
Bi	4.78	12	-0.0335	21, 22, 23, 24, 28, 33	-134
S	0.82	12	(0.055)	21	(15)
Se	3.04	12	0.159/0.072	38	19/42
Te	5.80	12	—	—	—
Fe	2.01	12	0.007-0.044	39	?
Ni	2.45	12	—	—	—
Ar	3.35	10, 18	0.125	10, 17	27

\* Estimated from the change in the co-ordination number and interatomic distance on melting (see Table I).

<sup>17</sup> Bridgman, *Physic. Rev.*, 1934, **46**, 930.

<sup>18</sup> Landolt-Börnstein-Roth-Scheel, *Physikalisch-chemische Tabellen*, I, Suppl. Vol., 1927, p. 682.

<sup>19</sup> Kleiner and Thum, *Beibl. Ann. Physik.*, 1907, **31**, 539, 1042.

<sup>20</sup> Losana, *Gazz. Chim. Ital.*, 1938, **68**, 836; 1935, **65**, 851.

<sup>21</sup> Block, *Z. Physik. Chem.*, 1912, **78**, 385.

<sup>22</sup> Endo, *Sci. Rep. Tōhoku*, 1925, **13**, 193, 219; *Bull. Chem. Soc. Japan*, 1927, **2**, 134.

<sup>23</sup> Töpler, *Wied. Ann.*, 1894, **53**, 351, 376.

<sup>24</sup> Vicentini and Omodei, *Beibl. Ann. Physik.*, 1888, **12**, 176, 177; 1892, **16**, 67.

<sup>25</sup> Hackspill, *Compt. rend.*, 1911, **152**, 259.

<sup>26</sup> Eckardt and Graefe, *Z. anorg. Chem.*, 1900, **23**, 382; *Ann. Physik.*, 1900, **1**, 79.

<sup>27</sup> Pelzel and Schneider, *Z. Metallkunde*, 1943, **35**, 121.

<sup>28</sup> Sauerwald, *ibid.*, 1922, **14**, 145, 254, 329, 457.

<sup>29</sup> Krause and Sauerwald, *Z. anorg. Chem.*, 1929, **181**, 347.

<sup>30</sup> Edwards and Taylor, *Trans. Amer. Inst. Min. Met. Eng.*, 1923, **69**, 1074.

<sup>31</sup> Honda and Masumoto, *Sci. Rep. Tōhoku*, 1931, **20**, 346.

<sup>32</sup> Pelzel, *Z. Metallkunde*, 1940, **32**, 7.

<sup>33</sup> Goodrich, *Trans. Faraday Soc.*, 1929, **25**, 531.

<sup>34</sup> Pelzel and Sauerwald, *Z. Metallkunde*, 1941, **33**, 229.

<sup>35</sup> Edwards and Moormann, *Z. Metallkunde*, 1921, **13**, 384.

<sup>36</sup> Hoather, *Proc. Physic. Soc.*, 1930, **48**, 699.

<sup>37</sup> Matuyama, *Sci. Rep. Tōhoku*, 1928, **17**, 1; 1929, **18**, 733.

<sup>38</sup> Gmelin, *Handbuch der anorg. Chem.*, Syst. 10 (Se), 1942, pp. 179, 181.

<sup>39</sup> *Idem.*, *ibid.*, Vol. Eisen.

collected in Table II. The volume change on fusion is expressed by the quantity

$$\Delta V_m = \frac{AV_{liq.} - AV_{sol.}}{AV_{sol.}}, \quad (1)$$

where the atomic volume of the element in the solid state at the melting point is designated by  $AV_{sol.}$  and that of the liquid state by  $AV_{liq.}$  (also at the melting point).

It will be noted that the quotient of the entropy of fusion and the volume change on fusion

$$\delta_m = \Delta S_m / \Delta V_m \quad (2)$$

is nearly constant for a considerable number of metals (alkali and alkaline earth, Cu, Ag, Au, Mg, Zn, Cd, Hg, Al, In, Tl, Pb) and amounts to an average of 60 cal./deg., or, considering metals with C. No. 8 and 12 separately, 67 and 56 cal./deg. respectively. The deviations (particularly for Li, Au, and Al) can well be caused by inaccuracies in measurement, especially of the volume change at fusion.

The large divergences of the  $\Delta V_m$  values measured by various observers in particular cases indicate the difficulty of an exact determination of the change in volume. Differences of 25 % are not rare, and sometimes even this discrepancy is exceeded. The critical mean compensates these errors to some extent, but it is not always possible to estimate.

Extending the scope of the discussion, we show in Tables III and IV the specific heats per g.-atom at the melting point divided by the absolute temperature of fusion ( $C_p/T_m$ ) and the coefficient of cubic expansion  $\alpha$  for the solid and liquid states respectively. The expression,

$$C_p/(T_m\alpha) = \delta_{sol.} \text{ or } \delta_{liq.} \quad (3a, b)$$

which is obtained empirically, has the same dimension as  $\delta_m$ , namely cal./deg.

While the increase in entropy on melting is due to the increase in disorder *and* volume change, the quantities  $\delta_{sol.}$  and  $\delta_{liq.}$  represent only the increase in entropy due to expansion.<sup>2</sup> It is observed that nearly all the metals with a constant value for  $\delta_m$  have an almost constant value for  $\delta_{sol.}$  and  $\delta_{liq.}$  of 86 and 73 cal./deg. Other elements, such as silicon, germanium, bismuth, phosphorus, etc., show divergences well outside experimental error. Actually, all these are elements in which the bond is not purely metallic. The same elements also show deviations in the value of the quotient  $\delta_m$  given in Table II. In many examples the variations in volume  $\Delta V$  exhibit the well-known negative effect.

On summarizing the information in Tables II, III and IV the following qualitative picture of the nature of the bonds and bond structure of liquid and solid elements can be deduced.

In solid elements in which the lattice is preserved mainly by metallic bonding forces, a given increase in volume is always associated with a certain absorption of energy.\* A rise in temperature from 1 degree below the melting temperature results in an increase in the kinetic and the potential energy of the oscillating units of about  $3R$  per mole. The whole of the increase can be measured macroscopically as the atomic heat. On increasing the kinetic energy the amplitude of oscillation is increased and volume expansion results. If the bonding mechanism of the atoms is the same, entropy and volume increases are proportional to each other. On the other hand the coherence of atoms is much

\* The atomic heat has approximately the same value for all metals. The Dulong-Petit value amounts to about 7.25 cal./deg. at the melting point. This leads to a constant value for  $\alpha T_m$  of the elements with metallic bondings of approx. 0.078. This regularity is already known and is consistent with Grüneisen's rule whereby the total volume change of the normal metals amounts to 7 % between absolute zero and the melting point.

stronger with homopolar bonding. The same increase in entropy <sup>13</sup> is therefore accompanied by a smaller increase of the amplitude of oscillation and hence a smaller volume expansion; the quotient  $\delta_{\text{sol}}$  must therefore

TABLE III.—ATOMIC HEAT AND COEFFICIENT OF EXPANSION OF SOLID ELEMENTS AT THE MELTING TEMPERATURE

Element	$C_p/T_m$ cal./deg. $\times 10^3$	Ref.	$\alpha$ deg. $\times 10^3$	Ref.	$\delta_{\text{sol}}$ cal./deg.
Li	15.3	12	0.18	19, 42	85
Na	19.0	40	0.22	24, 42	86
K	20.8	40	0.25	24, 25, 42	83
Rb	23.0	40	0.27	25, 43	85
Cs	24.4	40	0.29	25	84
Cu	5.5	40	0.070	43, 44, 45, (46)	79
Ag	6.05	12	0.081	43, 47, (46)	75
Au	5.5	12	0.058	45, 48, (10)	95
Mg	8.2	12	0.110	10, 49, 50	75
Zn	10.2	40	0.113	47, 49, 51, 52	90
Cd	11.6	40	0.126	49	92
Hg	29.0	10	0.171	10	170
Al	8.4	12	0.099	35, 43, 45, 49, 50, 53, 63	85
Ga	21.1	41	0.054	10	384
In	15.4	40, 41	0.125	54, 55, 56	123
Tl	12.4	12	0.126	49	99
Si	3.9 (1000° C)	40	0.0096 (1000°)	49	(406)
Ge	4.6 (0-400° C)	40	0.023 (0-400°)	49	(200)
Sn	14.2	40	0.095	49	150
Pb	11.6	40	0.12	46, 49, (24)	97
P	17.9	12	0.375	24, 43	48
Sb	7.1 (0°-m.p.)	40	0.033 (0°-m.p.)	57	(215)
Bi	12.6 (20-270° C)	12	0.040 (20-270°)	10, 18, 24, 49	315
S	13.5	40	(0.30)	43	(38)
Se	12.8	40	0.18	38	71
Te	8.7 (0-100° C)	12	0.053 (50° C)	42, 54	(164)
Fe	5.8	12	?	—	—
Ni	4.6 (1000° C)	12	0.057 (1000°)	43, 45	82

be larger than with a metallic bond. According to Table III, this actually occurs. The lattice structures of metals such as silicon and germanium, which crystallize in the diamond structure are the result of spin compensation. The same applies, though to a lesser extent, to the distorted

<sup>40</sup> Kelley, *U.S. Bur. Mines Bull.*, No. 371, 1934.

<sup>41</sup> Roth, Mayer and Zeumer, *Z. anorg. Chem.*, 1933, **214**, 309; 1934, **216**, 303.

<sup>42</sup> Bridgman, *Proc. Amer. Acad. Sci.*, 1911, **47**, 348; 1925, **60**, 305; 1935, **70**, 71.

<sup>43</sup> Landolt-Börnstein-Roth-Scheel, *Physikalisch-chemische Tabellen*, 1923, pp. 1217, 1228.

<sup>44</sup> Haring and Davey, *Physic. Rev.*, 1935, **47**, 337.

<sup>45</sup> Nix and MacNair, *Physic. Rev.*, 1941, **60**, 597.

<sup>46</sup> Eucken and Dannöhl, *Z. Elektrochem.*, 1934, **40**, 814.

<sup>47</sup> Owen and Yates, *Phil. Mag.*, 1934, **17**, 113.

<sup>48</sup> Müller, *Physik. Z.*, 1916, **17**, 29.

<sup>49</sup> Landolt-Börnstein-Roth-Scheel, *Physikalisch-chemische Tabellen*, II, Suppl. Vol., 1931, pp. 1151, 1221, 1478.

<sup>50</sup> Bollenrath, *Z. Metallkunde*, 1934, **26**, 62.

<sup>51</sup> Bocharov and Sviderskaja, *A.C.S. Abstr.*, 1946, **40**, 2369.

<sup>52</sup> Sieglerschmidt, *Metallwirtsch.*, 1938, **17**, 155.

<sup>53</sup> Taylor, Willay, Smith and Edwards, *Metals Alloys*, 1938, **9**, 189.

<sup>54</sup> Fizeau, *Compt. rend.*, 1869, **68**, 1125.

<sup>55</sup> Frevel and Ott, *J. Amer. Chem. Soc.*, 1935, **57**, 228.

<sup>56</sup> Shinoda, *Mem. Sci. Kyoto Univ.*, 1933, **16**, 198.

<sup>57</sup> Hidnert, *Z. Metallkunde*, 1935, **27**, 286.

diamond structure of white tin. A homopolar bond participation most probably occurs also in the layer lattice structure of antimony and bismuth. The spiral chain of the atoms about the triangular axis in metallic selenium and tellurium is assumed to be of homopolar nature, whilst the cohesion of the chains to each other is attributed to the metallic bond.<sup>69</sup>

TABLE IV.—ATOMIC HEAT AND COEFFICIENT OF EXPANSION OF LIQUID ELEMENTS AT THE MELTING POINT

Element	$C_p/T_m$ cal./deg.-° × 10 <sup>3</sup>	Ref.	$\alpha$ deg.- <sup>1</sup> × 10 <sup>3</sup>	Ref.	$\delta_{liq.}$ cal./deg.
Li	15.4	12	—	—	—
Na	20.2	40	0.275	24, 25, 43, 59	73
K	22.8	40	0.29	24, 25, 43, 59	78
Rb	25.2	40	0.34	25	74
Cs	26.4	40	0.365	25, 26	73
Cu	5.7	10	0.095	60	60
Ag	6.7	40	0.105	28, 61	64
Au	5.2	40	0.060	29	(76)
Mg	8.8	12	0.125	32	70
Zn	11.1	58, 40, 12	0.154	34, 37, 62, 63	72
Cd	12.0	40, 58	0.165	24, 37, 61, 62, 64, (65)	73
Hg	28.3	10	0.182	24, 43, 66	155
Al	8.7	40	0.122	32, 35	71
Ga	22.5	10	0.126	36	179
In	16.4	10	—	—	—
Tl	11.7	10	0.150	24	78
Si	—	—	—	—	—
Ge	—	—	—	—	—
Sn	13.1	40	0.115	24, 37, 60, 62, (65)	114
Pb	12.5	40	0.13	24, 37, 62, 64, 65	96
P	19.2	12	0.53	24, 43, 67	36
Sb	7.9	40	0.10	28, 64	79
Bi	14.0	12	0.12	24	117
S	16.2	10	0.47	24, 43	35
Se	14.2	12	0.40	38	36
Te	12.4	12	—	—	—
Fe	5.2 ± 0.7	39	0.03-0.14	39	?
Ni	—	—	—	—	—
Ar	125.0	18	4.54	68	28

It is possible to take the argument a stage further and, using the  $\delta_{01}$  values, set up a qualitative table arranged according to the participation of a homopolar bond in the bond structure. According to such an arrangement gallium should be below silicon. This is an interesting result as crystallographic considerations alone have failed to establish the bonding mechanism of gallium with certainty.<sup>5</sup> Even indium in the solid state exhibits some degree of homopolarity.

<sup>58</sup> Braune, *Z. anorg. Chem.*, 1920, **111**, 124.

<sup>59</sup> Rinck, *Ann. Chim.*, 1932, **18**, 395.

<sup>60</sup> Widawski and Sauerwald, *Z. anorg. Chem.*, 1930, **192**, 145.

<sup>61</sup> Jouniaux, *Bull. Soc. Chim. France*, 1930, **47**, 524, 682; 1932, **51**, 677.

<sup>62</sup> Hogness, *J. Amer. Chem. Soc.*, 1921, **43**, 1621.

<sup>63</sup> Saeger and Ash, *Bur. Stand. J. Res.*, 1932, **8**, 37.

<sup>64</sup> Greenaway, *J. Inst. Metals*, 1947, **74**, 133.

<sup>65</sup> Arpi, *Z. Metallographie*, 1914, **5**, 142.

<sup>66</sup> Harlow, *Phil. Mag.*, 1929, **7**, 674.

<sup>67</sup> Dobinski, *Bull. intern. acad. polon., Cl. sci. math. nat.*, A, 1935, 253.

<sup>68</sup> Baly and Donnan, *J. Chem. Soc.*, 1902, **81**, 907.

<sup>69</sup> Halla, *Kristallchemie und Kristallphysik metallischer Werkstoffe* (Leipzig, 1939).

The exceptional behaviour of the elements possessing a homopolar bond is also shown in the  $\delta_m$  values. This indicates that the nature of the bond in the solid phase is at least partially changed on melting. It might therefore be expected that, for example, the spin compensation in liquid bismuth or antimony is less pronounced and that in its place more quasi-free electrons are produced: the bond after melting would therefore be more metallic than in the lattice. The  $\delta_m$  value for antimony is actually found to approach very closely that of liquid elements possessing a metallic bond. This is in agreement with the observation that the electrical conductivity of antimony and bismuth markedly increases during melting;<sup>7</sup> and is in contrast to the normal metals, which exhibit the reverse effect and that only to a lesser extent.\* Gallium, too, shows an increase in conductivity; its  $\delta_{liq.}$  value is therefore correspondingly lower than  $\delta_{sol.}$ . However, the homopolar forces appear to be still operative to some extent in liquid gallium. The same apparently applies to tin and probably to germanium and silicon.

The homopolar bond requires a low co-ordination (see Table I). The displacement of the homopolar bond by the metallic bond results in some instances in a closer packing and hence in a contraction of volume during fusion. The negative  $\Delta V$  values of antimony, bismuth, tellurium and gallium can be explained in this manner. Silicon and germanium probably also contract on melting.<sup>70</sup>

Other elements, such as phosphorus, selenium, sulphur or argon, have much lower  $\delta$  values than correspond to the average in Tables II, III and IV. The absorption of energy, associated with a certain change in volume, is therefore lower than that of an element in which a metallic bond is operative. This is especially easy to understand in the case of the rare gases, in which the weak van der Waals' forces maintain the lattice structure. The same is true for the other elements mentioned. In sulphur, for instance, the molecular unit is maintained during expansion and melting and the volume changes are due to the widening of the spaces between the molecules which are kept together by van der Waals' forces.

No complete explanation can as yet be given for the exceptional behaviour of mercury, which behaves as if possessing a metallic bond during fusion, except that the  $\delta_{sol.}$  and  $\delta_{liq.}$  values are twice as high as the average in Tables III and IV.

The results described above are supported by Klemm,<sup>70</sup> who has recently arrived at results similar to the above, from consideration of magnetic behaviour. He classifies elements on the basis of the co-ordination number, electrical conductivity, and the chemical character of the oxides and hydroxides, into the following groups: true metals, meta-metals, semi-metals and non-metals (see Table VI). In non-metals each of the valency electrons belong to one pair of atoms, and in meta-metals Klemm postulates a tendency towards such an attachment. The electrons, almost free in the true metals, are confined, as it were, to great "orbits" surrounding groups of atoms in the meta-metals. The attachment of electrons to single pairs of atoms is not complete in the semi-metals, since these elements have an appreciable electrical conductivity. The great orbits postulated should affect the magnetic behaviour of the elements concerned; thus, whereas the electrons of the electron cloud show a weak paramagnetism, independent of temperature, the bound electrons lead to diamagnetism, the magnitude of which is proportional to the size of the orbit. The anomalous diamagnetism due to "giant orbits" is pronounced in the Group V elements, antimony and bismuth.

\* The proportional change in the electrical conductivity value is not great if the volume change during melting is considered as well, i.e. if the conductivity is related to equal numbers of atoms and not to 1 cm.<sup>3</sup>.

<sup>70</sup> Klemm, paper read before the *Deutsche Chemische Gesellschaft* (Feb., 1944).

It is exhibited in the diamond structure, in gallium at low temperatures and possibly in grey tin. It is strongly marked in graphite and there are indications of it in thallium.

Finally, another conclusion arising from the relationships described, may be mentioned. For the true metals the ratio

$$\frac{\Delta S_m}{\Delta V_m} = \frac{L_m}{T_m} \frac{AV_{sol.}}{AV_{liq.} - AV_{sol.}} = \delta_m \quad (2)$$

is constant. Combining this equation with that of Clapeyron for the change of melting point with pressure

$$\frac{T_m (AV_{liq.} - AV_{sol.}) dp}{L_m} = dT \quad (4)$$

we obtain

$$AV_{sol.} dp = \delta_m dT \quad (5)$$

Using this equation the lowering of the melting point by pressure may be calculated in the range of lower pressures, using only the atomic volumes of the true metals at the melting point. Here is a pronounced analogy to the equation of ideal gases, except that the constants  $R$  and  $\delta$  have different values.

TABLE V.—COMPARISON OF THE CALCULATED AND MEASURED VALUES OF THE LOWERING OF MELTING POINT BY PRESSURE

Element	M.p. °C.	$AV_{sol.}$ cm. <sup>3</sup> /g.-atom	$\frac{dp}{dT}$ (measured) atm./deg.	$\frac{dp}{dT} - \frac{\delta_m}{AV}$ atm./deg.
Na	97.6	24.0	119.0	116.0
K	62.5	45.7	61.0	61.0
Rb	38.7	56.0	50.0	49.5
Cs	29.7	71.0	43.0	39.0
Cd	320.5	13.3	159.0	174.0
Hg	-38.8	14.1	185.0	164.0
Pb	327.2	18.7	124.0	124.0

Values of the inverse ratio of the melting point lowering,  $dp/dT$ , measured by Bridgman,<sup>71</sup> Tammann,<sup>72</sup> and Johnston and Adams<sup>73</sup> are collected in Table V. Lithium is not considered, since an incorrect value of its heat of fusion results from Bridgman's measurements,<sup>12</sup> nor are those metals possessing a partly homopolar bond. In the last column are the  $dp/dT$  values calculated from eqn. (5). The mean values in Table II,  $\delta_m = 67$  cal./deg. (C. No. 8),  $\delta_m = 56$  cal./deg. (C. No. 12) (or in other units,  $\delta_m = 2770, 2310$  cm.<sup>3</sup> atm./deg. respectively) are used for the calculation. The calculated and measured values agree fairly well.\* The error of measurement has, of course, to be considered in this comparison. For deriving the  $dp/dT$  (or rather  $\Delta p/\Delta T$ ) values, depressions of freezing point by pressure differences as high as 1000 kg./sq. cm. had to be used. Thus formula (5) is thus approximate and subject to this limitation.

<sup>71</sup> Bridgman, *Physic. Rev.*, 1926, **27**, 68.

<sup>72</sup> Tammann, *Z. anorg. Chem.*, 1904, **40**, 54.

<sup>73</sup> Johnston and Adams, *ibid.*, 1911, **72**, 11.

\* The values of the melting point lowering can, of course, be calculated by means of Clapeyron's equation if the volume change on melting is known. Eqn. (5) allows a calculation if the atomic volume of the solid at the melting point only is known.



TABLE VI.—CLASSIFICATION OF ELEMENTS. THEIR PHYSICAL CONSTANTS IN THE SOLID AND LIQUID STATE

Property	True Metals	Meta-metals	Semi-metals	Non-metals
C. No. (sol.)	12 or 8	6+6, 4+8	$\leq 6$	low
$\kappa$ (sol.)	$3 \times 10^4$ - $7 \times 10^5$	$10^4$ - $10^5$	$10^{-5}$ - $10^4$	$< 10^{-6}$
$\chi$ (sol.)	Para- to ferro-magnetic (weak diamagnetic)	Weak dia-magnetic	Weak to strong diamagnetic	Diamagnetic
$\delta$ (sol.)	85	90-120	150-400	$< 70$
$\kappa_{\text{liq.}} - \kappa_{\text{sol.}}$	Weakly negative		Positive	
$\delta_m$	65	65	Negative	$< 40$
C. No. (liq.)	8-11	8-11	7.5-11	Varying
$\delta$ (liq.)	75	75	80-180	$< 50$
Elements	Li, Na, K, Rb, Cs, Cu, Ag, Au, Mg, Ca, Al, Co, Ni, Ti, Pb	Zn, Cd, Hg, In	C, Si, Ge, Sn, Sb, Bi, Te, Ga, Se, P	P, S, Se, F, Cl, Br, I

A summary of the conclusions of this paper is presented in Table VI. The elements may be classified as true metals, meta-metals, semi-metals and non-metals. For each of these classes there is a characteristic range of values for some of their physical constants: electrical conductivity  $\kappa$ , magnetic susceptibility  $\chi$ , co-ordination number C. No., and the entropy/volume ratios  $\delta$ . Typical examples are given of each group.

It is intended that similar considerations should be applied to alloy phases and compounds.

The author is indebted to Mr. E. LI. Evans who kindly assisted him in writing the English script of this paper.

*National Physical Laboratory,  
Teddington,  
Middlesex.*

## THE MAGNITUDE OF THE PROBABILITY FACTORS IN RADICAL REACTIONS

BY M. G. EVANS AND M. SZWARC

*Received 6th May, 1949*

The experimental data relating to the rate constants and the temperature coefficients of various reactions involving radicals or atoms are collected. In the light of this compilation it is found that the probability factors of the reactions examined are "normal". The problem of the probability factors is treated theoretically. The reasons which led Steacie and his co-laborators to the assumption of abnormally low probability factors are analyzed.

The magnitude of the probability factors of some simple gas reactions involving radicals or atoms has recently been discussed by Steacie, Darwent and Trost.<sup>1</sup> These authors tentatively suggested \* that the probability factors of such reactions should generally be very low and in some cases they proposed values as low as  $10^{-5}$  or  $10^{-6}$ . The idea of low probability factors in such reactions has been further emphasized by Bamford and Dewar,<sup>2</sup> who made the statement: "It seems reasonable to infer that organic radical reactions with activation energies less than 20 kcal. *in general* have frequency factors of the order of  $10^7$  and not  $10^{12}$  as is commonly assumed. Steacie has tentatively suggested that this is also true in gas reactions."

We think, therefore, that this matter needs careful examination and the present communication reviews the experimental evidence relevant to this problem. The evidence is supplied by two kinds of reactions: metathesis, in which an atom or radical reacts with a molecule to form two particles, and association or recombination reaction involving atoms or radicals.

The most reliable information about the magnitude of the probability factors of such processes would be provided by investigations of simple systems in which the number of possible secondary reactions is reduced to a minimum and for which measurements of the temperature coefficient of the rate of reaction have led to a knowledge of the activation energy of the process in question. It should be noted that an evaluation of the probability factor  $P$  is obtained from the relationship

$$k = PZc - E/RT$$

and that owing to the uncertainty in the estimation of the collision diameter which is required for the calculation of the collision frequency the probability factor  $P$  is likely to be uncertain by a power of 10.†

Table I summarizes the experimental evidence on metathesis reactions of the type:



where  $X$  represents an atom. All the systems listed in this Table are very simple and the results seem to be unambiguous, demonstrating that the most probable value of  $P$  for such reactions is of the order of 0.1 to within a factor of 10.

The best argument in favour of "normal" probability factor for reactions between an atom and a molecule is provided by those reactions which take place at nearly every collision. Table Ia lists some of these

<sup>1</sup> Steacie, Darwent and Trost, *Faraday Soc. Discussions*, 1947, **2**, 80.

<sup>2</sup> Bamford and Dewar, *Nature*, 1949, **163**, 256.

\* In a private communication Dr. Steacie remarks "that the main object of the paper by Trost, Darwent and myself was to draw attention to the very serious discrepancies between existing experimental results for the reactions of hydrogen atoms and of methyl radicals with the paraffin hydrocarbons. It was shown that the assumption of low steric factors was a possible way of bringing the results into line. It is, of course, also possible that the experimental results are in error.

"We wished to emphasize the lack of knowledge of the steric factors, and the frequency with which experimental "activation energies" are merely the result of calculations which assume steric factors of unity. The widespread assumption that such factors are almost always unity appears to be a dangerous one. What is needed is much more detailed *experimental* information for a few important reactions. Until such information is available it seems impossible to obtain an adequate verification of theory. On our part we hope to be able to provide more accurate experimental information in the near future on the reactions of methyl radicals with the paraffins."

† The collision diameter is usually computed either from molecular dimensions furnished by electron diffraction or X-ray diffraction measurements, or from data based on physical properties of gases such as viscosity, which are interpreted by the kinetic theory of gases.

TABLE I

No.	Reaction	E kcal./mole	P	Reference
1	$H + p\text{-}H_2 \rightarrow o\text{-}H_2 + H$	5.5	0.07	a
2	$D + o\text{-}D_2 \rightarrow p\text{-}D_2 + D$	6.0	0.07	a
3	$H + D_2 \rightarrow HD + D$	6.5	0.07	a
4	$D + H_2 \rightarrow HD + H$	4.9	0.07	a
5	$D + NH_3 \rightarrow H + NH_2D$	10.7	0.3	b
6	$D + PH_3 \rightarrow H + PH_2D$	14.4	0.25	b
7	$Br + CH_4 \rightarrow CH_3 + HBr$	15.6	0.1-0.2	d
8	$H + N_2H_4 \rightarrow H_2 + N_2H_3$	7.2	0.01	c
9	$Br + H_2 \rightarrow HBr + H$	17.6	0.2	e
10	$H + Br_2 \rightarrow HBr + Br$	1.2	1	f, g
11	$H + HBr \rightarrow H_2 + Br$	1.2	0.1	f, g
12	$Cl + H_2 \rightarrow HCl + H$	6.7	0.1	h
13	$H + Cl_2 \rightarrow HCl + Cl$	2	1	i
14	$H + HCl \rightarrow H_2 + Cl$	4.5	0.1	i
15	$H + I_2 \rightarrow HI + I$	0	1	i
16	$CH_3Cl + Na \rightarrow CH_3 + NaCl$	7.5	~1	k
17	$C_6H_5Br + Na \rightarrow C_6H_5 + NaBr$	3.8	~1	l

a. Farkas and Farkas, *Proc. Roy. Soc. A*, 1935, **155**, 124.

b. Melville and Bolland, *ibid.*, 1937, **160**, 384.

c. Birse and Melville, *ibid.*, 1940, **175**, 164.

d. Kistiakowsky and van Artsdalen, *J. Chem. Physics*, 1942, **12**, 469.

e. Jost, *Z. physik. Chem. B*, 1929, **3**, 118.

f. Schumacher, *Chemische Gasreaktionen* (Steinkopff, 1938), p. 416.

g. Bodenstein and Lütkemeyer, *Z. physik. Chem.*, 1924, **114**, 208.

h. Rodebush and Klingelhoffer, *J. Amer. Chem. Soc.*, 1933, **55**, 141.

i. Schumacher, *Chemische Gasreaktionen* (Steinkopff, 1938), p. 352.

k. Hartel and Polanyi, *Z. physik. Chem. B*, 1930, **11**, 97.

l. Warhurst, *Trans. Faraday Soc.*, 1939, **35**, 674.

reactions, and it should be noted that this class includes atomic reactions with large and complicated organic molecules. Obviously the probability factor of all these reactions cannot be smaller than 0.1.

TABLE Ia

Reaction	Number of Efficient Collisions — Total Number of Collisions	Reference
$Na + Cl_2 \rightarrow NaCl + Cl$	1/1	a, b
$Na + Br_2 \rightarrow NaBr + Br$	1/1	a, b
$K + Cl_2 \rightarrow KCl + Cl$	1/1	a, b
$CH_3I + Na \rightarrow CH_3 + NaI$	1/1.5	c
$C_6H_5I + Na \rightarrow C_6H_5 + NaI$	1/2	d
$CCl_4 + Na \rightarrow CCl_3 + NaCl$	1/5	e
$C_2H_5I + Na \rightarrow C_2H_5 + NaI$	1/2.5	f
$C_6H_5 \cdot CH \cdot CH \cdot CH_2Br + Na$ $\rightarrow C_6H_5 \cdot CH = CH \cdot CH_2 + NaBr$	1/1	f
$CNCl + Na \rightarrow CN + NaCl$	1/4.7	f
$CNBr + Na \rightarrow CN + NaBr$	1/4.2	f

a. Polanyi, *Atomic reactions* (London, 1932).

b. Schumacher, *Chemische Gasreaktionen* (Steinkopff, 1938), p. 340.

c. Hartel and Polanyi, *Z. physik. Chem. B*, 1930, **11**, 97.

d. Fairbrother and Warhurst, *Trans. Faraday Soc.*, 1935, **31**, 987.

e. Haresnape, Stevens and Warhurst, *ibid.*, 1939, **36**, 405.

f. Evans and Walker, *ibid.*, 1944, **40**, 384.

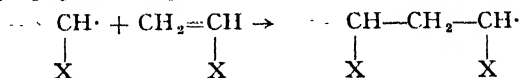
Direct experimental evidence for the bimolecular association reactions is scanty. We can, however, obtain indirect information from the relationship between the velocity constants and the equilibrium constants of reactions of the type,  $A + B \rightarrow AB$ , provided we possess a knowledge of the unimolecular velocity constant. The evidence which has accumulated in recent years from careful studies of unimolecular decomposition reactions of the type  $AB \rightarrow A + B$  has shown that in the majority of cases the frequency factor is  $10^{12}$  to  $10^{13}$  sec.<sup>-1</sup>. Using this value which we now consider to be securely established, we calculated the rate constants for the unimolecular dissociation of a number of diatomic molecules. It was then possible to compute the velocity constants of the "true" bimolecular associations from a knowledge of the appropriate equilibrium constants, and it should be noted that the latter reactions must be kinetically bimolecular under the conditions for which the dissociation processes are kinetically unimolecular. Inspection of Table II, which contains the results obtained in this way for a number of association reactions, reveals that the frequency factors for these bimolecular associations are between  $10^{11}$  and  $10^{13}$ . Hence the steric factor as defined above cannot be smaller than  $10^{-2}$ .

TABLE II

Calculation of  $P$  for reactions  $A + A \rightarrow A_2$ . It is assumed that the reaction proceeds under the conditions in which  $A_2$  decomposes *unimolecularly*;  $k_1$  being  $10^{13} \exp(-D/RT)$  sec.<sup>-1</sup>.  $D$  = dissociation energy of  $A_2$ .  $k_2 = K_{eq}/k_1$ . Calculated for  $T = 1000^\circ$  K.  $D$  and  $K_{eq}$  taken from spectroscopic data.

Reaction	$K_{eq}$ . (atm.)	$k_1$ (sec. <sup>-1</sup> )	$k_2$ (sec. <sup>-1</sup> cm. <sup>3</sup> mole <sup>-1</sup> )
H + H $\rightarrow$ H <sub>2</sub>	$6.4 \times 10^{-18}$	$5 \times 10^{-10}$	$6 \times 10^{12}$
D + D $\rightarrow$ D <sub>2</sub>	$9 \times 10^{-19}$	$2 \times 10^{-10}$	$15 \times 10^{12}$
O + O $\rightarrow$ O <sub>2</sub>	$3 \times 10^{-20}$	$2.5 \times 10^{-13}$	$0.6 \times 10^{12}$
Cl + Cl $\rightarrow$ Cl <sub>2</sub>	$2 \times 10^{-7}$	4	$2 \times 10^{12}$
Br + Br $\rightarrow$ Br <sub>2</sub>	$5 \times 10^{-6}$	$1.6 \times 10^3$	$24 \times 10^{12}$
I + I $\rightarrow$ I <sub>2</sub>	$2 \times 10^{-3}$	$2 \times 10^6$	$8 \times 10^{12}$

It has been found, however, that the association reactions between two big radicals correspond to a very small probability factor. For example, as direct measurements have been made on the rate of the unimolecular decomposition and equilibrium constant of hexaphenyl ethane,<sup>3</sup> one is able to calculate the rate of the bimolecular recombination of triphenyl methyl radicals at  $10^3$  sec.<sup>-1</sup> cm.<sup>3</sup> mole<sup>-1</sup>. This recombination process involves an activation energy of about 7 kcal./mole.<sup>4</sup> Hence the frequency factor for recombination of triphenyl methyl radicals appears to be of the order  $10^8$  only, thus indicating a low probability factor. Another example is furnished by Melville's study on the kinetics of the photo-initiated polymerization of vinyl acetate.<sup>5</sup> From this investigation a value of  $10^6$  sec.<sup>-1</sup> cm.<sup>3</sup> mole<sup>-1</sup> was obtained for the frequency factor of the propagation step,



**Theoretical Discussion.**—A clear understanding of the magnitude of the probability factors is possible in terms of the transition state method.<sup>6</sup>

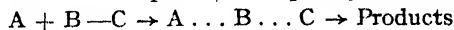
<sup>3</sup> Ziegler and Ewald, *Annalen*, 1929, **473**, 163. Ziegler *et al.*, *ibid.*, 1942, **551**, 161.

<sup>4</sup> Ziegler, *Trans. Faraday Soc.*, 1934, **30**, 10.

<sup>5</sup> Melville, *Nature*, 1945, **156**, 661.

<sup>6</sup> Glasstone, Laidler and Eyring, *The Theory of Rate Processes* (McGraw Hill, New York, 1941).

This method enables us to express the frequency factor for the reaction



Transition State  
Complex

as

$$PZ = \left\{ \frac{m_a + m_b + m_c}{m_a(m_b + m_c)} \right\}^{3/2} \cdot \frac{I_{abc}}{I_{bc}} \cdot \frac{h^2}{(2\pi)^{3/2} \cdot (kT)^{3/2}} \cdot \frac{\nu_{bc}}{\nu_\phi} \cdot \left( \frac{kT}{h\nu_\phi} \right)^2 \quad (1)$$

In this equation  $m_a$ ,  $m_b$  and  $m_c$  refer to the masses of the centres A, B, C respectively,  $I_{bc}$  and  $I_{abc}$  the moments of inertia of the molecule BC and the transition state complex ABC, and  $\nu_{bc}$ ,  $\nu_i$  and  $\nu_\phi$  to the frequencies of the normal modes of vibration of the molecule BC and the transition state complex. The frequency factor corresponding to collision between the centres A and BC is given by the kinetic theory as

$$Z = \left\{ \frac{m_a + m_b + m_c}{m_a(m_b + m_c)} \right\}^{3/2} \cdot I_{abc} \cdot \frac{8\pi^2 kT}{h^2} \cdot \frac{h^2}{(2\pi kT)^{3/2}} \cdot \frac{kT}{h} \quad (2)$$

From eqn. (1) and (2) we can express the probability factor  $P$  as

$$P = \frac{1}{I_{bc}} \cdot \frac{kT}{8\pi^2} \cdot \frac{\nu_{bc}}{\nu_i \cdot \nu_\phi^2} \quad (3)$$

Eqn. (3) shows that the factors influencing  $P$  are mainly the moment of inertia of the molecule BC and the bending frequency of the transition state complex. The larger the moment of inertia and the higher the bending frequency, the smaller will be the probability factor. These

TABLE III

$P$  calculated from eqn. (3).  
 $\nu_\phi$  assumed  $5 \times 10^{12} \text{ sec}^{-1}$ .

Reaction	$I_{bc} \times 10^{40}$	$P$
X + HCl	2.5	0.22
X + HBr	3.3	0.17
X + HI	4.3	0.13
X + CH <sub>3</sub> Cl	54	0.01
X + CH <sub>3</sub> Br	71	0.008
X + CH <sub>3</sub> I	87	0.006
X + C <sub>2</sub> H <sub>4</sub>	25	0.025
X + C <sub>2</sub> H <sub>6</sub>	53	0.01
X + iso-C <sub>4</sub> H <sub>8</sub>	75	0.008

conclusions are illustrated by Table III which gives the values of the probability factors calculated on the basis of (3) assuming  $\nu_{bc} = \nu_s$  and reasonable values for  $I_{bc}$  and  $\nu_\phi$ . Again we note that for relatively simple bimolecular association reactions involving atoms this theoretical treatment would lead to values of  $P$  ranging from  $10^{-1}$  to  $10^{-2}$ .

The much smaller probability factors which are characteristic of the bimolecular association reaction of large and complicated radicals are also understandable in terms of this treatment. In these cases three degrees of rotational freedom are lost in the formation of the transition

state. In terms of this loss of rotational freedom the low frequency factor for the dimerization of triphenyl methyl radicals, for the growth of a polymer chain, for chain transfer, and for chain termination have been described and understood.<sup>7</sup>

We would conclude from this discussion, therefore, that if one is measuring a true bimolecular reaction involving radicals no new features affect the frequency factor which cannot be understood in terms of the above discussion. It may be, however, that in association reactions involving atoms or small radicals the energy transfer from the newly-formed bond becomes the rate-determining step. Under such conditions the reverse decomposition reaction cannot be truly unimolecular and probably not kinetically of the first order. To such cases the above discussion cannot apply. All the reactions discussed by Steacie and his collaborators are metathesis reactions, and it is difficult to see how in such cases energy

<sup>7</sup> Baxendale and Evans, *Trans. Faraday Soc.*, 1947, **43**, 1.



is quite normal, being of the order  $10^{-3}$  which is to be expected on the basis of the considerations we have given above.

**Conclusion.**—From this discussion we would conclude that there is no experimental evidence of abnormally small probability factors for metathesis reactions involving atoms. We think also that on the basis of the theoretical treatment of bimolecular and unimolecular reactions there is no justification for assuming abnormally low probability factors for such reactions. Small probability factors will occur in reactions involving two complex radicals or molecules. This is not new, and has frequently been discussed in terms of the loss of rotational freedom of the reacting centres.

*Chemistry Dept.,  
University of Manchester.*

---

## ZERO-POINT ENERGIES IN THE DECOMPOSITION OF PARAFFIN MOLECULES

BY R. P. BELL

*Received 9th May, 1949*

Calculations have been made, using a simple model, to investigate the effect of changes in zero-point energy on the activation energy for the fission of a chain molecule. The results indicate a significant decrease of activation energy with increasing chain-length, but the effect is too small to account for the observed variations in the rate of pyrolysis of paraffin molecules. It is concluded that these variations must be mainly due to differences in the nature of the carbon-carbon links, though the zero-point energies may be important in determining the relatively small differences in the probabilities of fission at different points of the same molecule.

It is well established experimentally<sup>1</sup> that the rate of pyrolysis of the normal paraffins in the gas phase increases rapidly in the series ethane, propane, butane, and that in paraffins with more than three carbon atoms the probability of breaking the chain is different at different points. If the force constants and dissociation energies of all the carbon-carbon links are assumed to be the same, then a classical treatment on the basis of simple harmonic motion (neglecting the small difference in mass between  $\text{CH}_2$  and  $\text{CH}_3$ ) predicts that the probability of breaking a given link should be independent of the length of the chain, and the same for all the links in a molecule.<sup>2</sup> This is contrary to experiment, and probably shows that the carbon-carbon links differ from one another, perhaps on account of hyperconjugation.

It is, however, possible that a quantal rather than a classical treatment would modify the above theoretical conclusions, and it is the purpose of the present paper to investigate this point. The breaking of a bond involves high quantum numbers, and it is unlikely that a change from classical to quantum statistics would make any difference. On the other hand, the vibrational zero-point energies will contribute to the energy of the molecule in its ground state and may therefore affect the activation energies differently for different types of fission, even when the interatomic forces are identical in all the links. The observed activation energies for hydrocarbon pyrolysis are close to the accepted

<sup>1</sup> E.g. Partington, *Faraday Soc. Discussion*, 1947, 43B, 114.

<sup>2</sup> The most general proof of this has been given recently by Slater, *Proc. Roy. Soc. A*, 1948, 194, 112; *Proc. Leeds Phil. Soc.*, 1949, 5 (ii), 75.

value for the energy of a carbon-carbon link, and it will therefore be a good approximation to assume that the relevant bond is completely broken in the transition state. The formation of the transition state will therefore be accompanied by a loss of zero-point energy, which will serve to decrease the activation energy of the reaction.

The zero-point energies could, in principle, be calculated from the observed Raman and infra-red frequencies. However, the allocation of these frequencies is uncertain, even for propane, and I have therefore preferred to make a theoretical calculation on the basis of a simple model in order to estimate the magnitude of the effect. The model treated is a chain of equal masses with tetrahedral angles in its equilibrium position: this ignores the small mass difference between  $\text{CH}_3$  and  $\text{CH}_2$ , and enables the fragments to be treated in the same way as the paraffin molecules. It also ignores the C—H vibrations, which are assumed to be unaffected by the fission of the molecule. A simple valence-force field was used, with a stretching force constant derived from the stretching frequency of ethane ( $990\text{ cm}^{-1}$ ), and a bending force constant one-tenth of this.<sup>3</sup>

The conclusions arrived at would be essentially the same for any reasonable choice of force constants. Table I contains the calculated frequencies for ethane, propane and butane. Butane can assume a variable configuration in space, and the calculation has been made for the extreme *cis* and *trans* planar configurations.

TABLE I.—SKELETAL FREQUENCIES OF PARAFFIN MOLECULES

(*s* and *a* denote respectively symmetry and antisymmetry with respect to the plane or centre of symmetry)

Molecule	Frequencies ( $\text{cm}^{-1}$ )	$\sum h\nu$	
		joules/mole	cal./mole
Ethane . .	990	590	1408
Propane . .	1069 ( <i>a</i> ), 937 ( <i>s</i> ), 410 ( <i>s</i> )	1439	3436
<i>cis</i> -Butane . .	1109 ( <i>s</i> ), 1026 ( <i>a</i> ), 881 ( <i>s</i> ), 401 ( <i>a</i> ), 228 ( <i>s</i> )	2171	5184
<i>trans</i> -Butane . .	1084 ( <i>s</i> ), 990 ( <i>a</i> ), 907 ( <i>s</i> ), 393 ( <i>s</i> ), 314 ( <i>a</i> )	2199	5250

The loss of zero-point energy in the various fission reactions is thus as follows (taking the ethane value for  $\text{C}_2\text{H}_6$  and the propane value for  $\text{C}_3\text{H}_8$ ).

Reaction	Loss of Zero-point Energy	
	joules/mole	cal./mole
$\text{C}_2\text{H}_6 \rightarrow 2\text{CH}_3$ . . . . .	590	1410
$\text{C}_3\text{H}_8 \rightarrow \text{CH}_3 + \text{C}_2\text{H}_5$ . . . . .	840	2030
<i>cis</i> - $\text{C}_4\text{H}_{10} \rightarrow \text{CH}_3 + \text{C}_3\text{H}_7$ . . . . .	730	1750
<i>trans</i> - $\text{C}_4\text{H}_{10} \rightarrow \text{CH}_3 + \text{C}_3\text{H}_7$ . . . . .	760	1810
<i>cis</i> - $\text{C}_4\text{H}_{10} \rightarrow 2\text{C}_2\text{H}_5$ . . . . .	990	2370
<i>trans</i> - $\text{C}_4\text{H}_{10} \rightarrow 2\text{C}_2\text{H}_5$ . . . . .	1020	2430

There should thus be significant differences between the activation energies, and both propane and butane should pyrolyze faster than ethane. However, the differences are not nearly great enough to account for the

<sup>3</sup> Cf. Sutherland and Simpson, *J. Chem. Physics*, 1947, **15**, 153.



observed increase in rate, and doubtless the main effect is due to differences in the nature of the bonds. On the other hand, the zero-point energy would have to be taken into account in any quantitative treatment, and may be important in determining the relatively small differences in the probabilities of fission at different points of the same molecule.

My thanks are due to Professor Sir Cyril Hinshelwood for calling my attention to this problem and for valuable discussion.

*Physical Chemical Laboratory,  
Oxford.*

---

## THE THERMODYNAMICS OF THE IRON-NICKEL ALLOYS

BY O. KUBASCHEWSKI AND ORTRUD VON GOLDBECK

*Received 23rd May, 1949*

The partial and integral thermodynamic data of the formation of  $\gamma$  iron-nickel alloys have been derived from equilibrium measurements between  $H_2O$ ,  $H_2$  and alloys of various composition. The entropy of formation is almost ideal, and the heat of formation is slightly negative ( $\Delta H_{max} = -260$  cal./g.-atom). The corresponding data for the  $\alpha$  phase have been derived from published work on heat-content measurements. Thus the free energy curves for  $\alpha$  and  $\gamma$  iron-nickel alloys have been calculated and the accuracy estimated. From these curves the phase boundaries  $\alpha/\alpha + \gamma/\gamma$  have been derived. Comparison of the results with the most reliable data from the literature shows good agreement within the normal errors which generally occur in thermochemical experiments and calculations. The results are discussed from a general aspect.

The complete thermodynamic data of the iron-nickel system have not yet been worked out in spite of the great technical significance of both the binary and ternary alloys. It can, however, be expected from general considerations that the binary alloys behave almost ideally.<sup>1, 2</sup> The slow rate of attaining equilibrium in the  $\alpha$ - $\gamma$  region also suggests that the differences in free energy of the two phases are rather small. Further information on these questions has been obtained in this work by applying the results of equilibrium measurements and evaluating the data available from the literature. It is also shown that the  $\alpha$  and  $\gamma$  phase-boundaries can be determined from the data obtained.

### Experimental

The choice of a suitable method of investigation requires some consideration. In the first place, vapour-pressure measurements cannot be applied to iron-nickel alloys since both metals have extremely low vapour pressures at the temperatures under consideration. Moreover, electromotive force measurements may give rise to erroneous results due to the relatively large influence of the localized concentration cell effects when the difference between the standard potentials of the two metals is low.<sup>3</sup> A difference of 0.7 V should be taken as a minimum. Another method recently worked out by Grube and Flad<sup>4</sup> for the chromium-nickel system appeared to be suitable for investigating the iron-nickel system, although certain disadvantages affecting the accuracy of measurement must be taken into account.

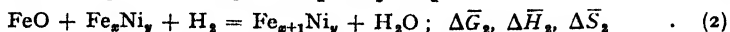
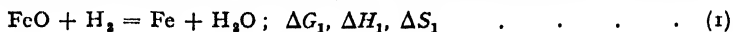
<sup>1</sup> Chipman in *Basic Open-Hearth Steel-Making* (New York, 1944), p. 480.

<sup>2</sup> Jones and Pumphrey, *J. Iron Steel Inst.*, 1949, **163**, 121.

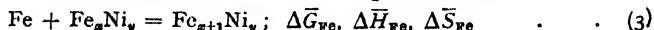
<sup>3</sup> See Weibke and Kubaschewski, *Thermochemie der Legierungen* (Berlin, 1943).

<sup>4</sup> Grube and Flad, *Z. Elektrochem.*, 1942, **48**, 377.

The principle of the method is as follows. The reaction between water vapours and pure iron and iron-nickel alloys of various composition is observed:\*



The difference between these two equations gives the solution of 1 g.-atom of iron in a (theoretically) unlimited amount of the respective alloy:



Consequently,

$$\Delta \bar{G}_{\text{Fe}} = \Delta \bar{G}_2 - \Delta G_1; \Delta \bar{H}_{\text{Fe}} = \Delta \bar{H}_2 - \Delta H_1; \Delta \bar{S}_{\text{Fe}} = \Delta \bar{S}_2 - \Delta S_1 \quad (4)$$

The amount of alloy is assumed to be so great that the compounds  $\text{Fe}_x\text{Ni}_y$  and  $\text{Fe}_{x+1}\text{Ni}_y$  are of equal composition. Thus the over-lined terms represent partial molar thermodynamic functions for the solution of iron in iron-nickel alloys. Since the  $\alpha$ - $\gamma$  field is in the iron-rich part of the diagram it would be more advantageous to determine the corresponding values for nickel; no method, however, of observing these directly is known. The differences  $\Delta \bar{G}_2 - \Delta G_1$ , etc., are so small in the  $\alpha$ - $\gamma$  region that any uncertainty becomes serious. The complete activity curve over the whole range of concentration was therefore determined and the integral values of free energy calculated.

A simple static method originally developed by St. Claire-Deville was selected in preference to the dynamic method adopted by Grube and Flad.<sup>4</sup> The main disadvantage of the static method, namely the effect of thermal diffusion, does not affect the results seriously when small differences are investigated, as will be seen later. The apparatus and procedure were similar to those used by Eastman and Evans<sup>5</sup> who measured the equilibria between iron and water vapour. A short description of the method is given here. A sketch of the apparatus is shown in Fig. 1.

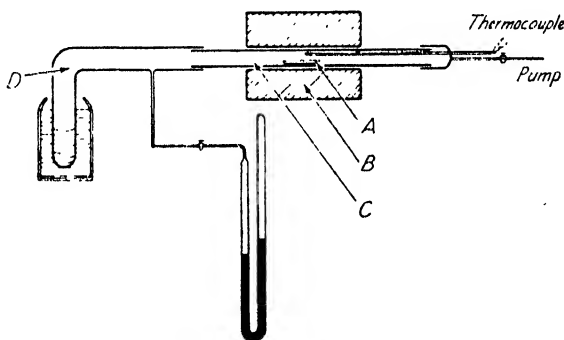


FIG. 1.

About 1 g. of millings of iron-nickel alloy contained in an alumina boat A is heated in an electric furnace B. The boat is placed in a silica tube C, connected to a closed bent Pyrex tube D, containing distilled water (kept at 0°C by a jacket of melting ice), and to a rotary vacuum pump. By this means a water vapour pressure of 4.56 mm. is maintained in the reaction tube after evacuation. The tube C is also connected to a mercury manometer with which the pressure due to the reaction could be measured with an accuracy of  $\pm 0.05$  mm. Hg. The temperature was measured to an accuracy of  $\pm 1^\circ$  by means of a Pt/Pt-Rh thermocouple, protected by an alumina tube. The couple was calibrated at the melting points of Zn, Ag and the eutectics of Ag—Cu, Al—Fe and Al—Cu.

The alloys were prepared from very pure metals. The analysis of those containing 1 to 34 % nickel are given in a previous publication.<sup>6</sup> Additional alloys, containing 50, 70 and 85 % nickel respectively were prepared and analyzed in the Metallurgy Division of the National Physical Laboratory. To avoid

\* Bars over the symbols denote partial molar thermodynamic functions.

<sup>4</sup> Eastman and Evans, *J. Amer. Chem. Soc.*, 1924, 46, 888.

<sup>6</sup> Bristow, *Iron Steel Inst., 2nd Report, Alloy Steel Res. Comm.*, No. 24 (1939).

spurious pressure readings due to water, etc., adsorbed on the walls of the tube, the latter was evacuated and heated several times above the reaction temperature between each measurement.

The course of an experiment was as follows. The alumina boat with the metal millings was placed in the silica tube. The tube was then sealed, evacuated, and the vapour pressure of the ice-cooled water read on the manometer. Small deviations from 4.56 mm. Hg were applied as a correction during the experiment. The tube was then heated and the equilibrium pressure noted at a series of temperatures.

The water vapour reacts with the iron of the alloy to form FeO until the hydrogen formed reaches its equilibrium value corresponding to a constant value of the ratio  $p_{H_2O}/p_{H_2}$  for any one alloy at a given temperature. The total pressure recorded by the manometer equals the sum  $p_{H_2O} + p_{H_2} = P$ . As the water vapour pressure is determined by the temperature of the water and is thus constant, the hydrogen pressure was obtained by subtracting 4.56 mm. Hg from the (corrected) total pressure, and the equilibrium constant was thus obtained by the relationship

$$K_p = \frac{p_{H_2O}}{p_{H_2}} = \frac{4.56}{P - 4.56} \quad (6)$$

The complete results of measurements taken in one experiment (with the alloy containing 8 % Ni) are given as an example in Table I. The  $H_2O$  pressures are of the order of several mm. Hg. The total pressure readings are probably accurate to  $\pm 0.1$  mm. Hg. This may cause a maximum error of  $\pm 0.005$  at  $\log K_p = -0.15$  or, in the extreme case, the error may be  $\pm 0.01$ . The average error, however, is about  $\pm 0.004$ . It is considered that this order of accuracy, although not high, should be sufficient in view of other sources of error.

TABLE I

$$p_B = 4.1 \text{ mm.}$$

At. %	Time	Temp. (°C)	Total P (mm.)	$p_{H_2}$	$p_{H_2O}$	$\log K_p$	$1/T \times 10^{-4}$
7.50	10.45	715	10.0	5.9	4.56	-0.112	10.11
	11.30	715	11.0	6.9	4.56	-0.180	10.11
	12.00	715	11.3	7.2 <sub>8</sub>	4.56	-0.197	10.11
	13.00	715	11.7	7.6	4.56	-0.221	10.11
	13.30	715	11.7	7.6	4.56	-0.221	10.11
	15.00	815	10.9	6.8	4.56	-0.173	9.23
	16.05	815	10.6	6.5	4.56	-0.153	9.23
	16.25	815	10.6	6.5	4.56	-0.153	9.23
	16.50	900	9.9	5.8	4.56	-0.104	8.52
	17.10	900	9.7	5.6	4.56	-0.089	8.52
	17.30	900	9.75	5.6 <sub>8</sub>	4.56	-0.096	8.52

The formation of nickel oxide in addition to iron oxide would, of course, affect the evaluation of the data on alloy formation. Since, however, the dissociation pressure of NiO is considerably higher than that of FeO, errors due to its formation should not occur up to relatively high concentrations of nickel. Moreover an electron diffraction study of oxide films formed on alloys of iron and nickel (some of them also containing chromium) up to 700° C at an oxygen pressure of 1 mm. Hg by Hickmann and Gulbranssen<sup>7</sup> shows that NiO never occurs in the oxide films, even with percentages as high as 50 % nickel (Hipernik) and 80 % nickel (Inconel, Nichrome). In the authors' experiments the equilibrium values measured were not reproducible with an alloy containing 85 % nickel, a difficulty which did not arise with any of the other alloys containing up to 70 %. It was therefore concluded that up to this percentage the oxidation is expressed completely by eqn. (2) and that no appreciable amount of NiO, which could affect the equilibrium values, is formed.

<sup>7</sup> Hickman and Gulbranssen, *J. Amer. Inst. Min. Met. Eng.*, Techn. Publ. No. 2069 (1946).

For evaluation, all the measurements corresponding to the reaction in eqn. (2) must be related to (i.e. subtracted from) the equilibrium on pure iron (eqn. (1)). The equilibrium corresponding to this reaction therefore needs detailed discussion. Measurements involving the system  $\text{Fe}_3\text{O}_4\text{—FeO—Fe—H}_2\text{O—H}_2$  (or  $\text{—CO}_2\text{—CO}$ ) are numerous. For example, work on these systems has been carried out by Darken and Gurry, Cirilli, Chipman and Marshall, Emmett and Shultz,<sup>8,9</sup> and Eastman and Evans.<sup>5</sup> The results vary within relatively wide limits due probably to the wide phase-fields of the oxides, to sensitivity of the equilibrium constants to small amounts of impurities in the iron used, and to the effect of thermal diffusion, mainly in static measurements. The results of the authors' measurements are close to those of Eastman and Evans; the slope in the  $\log K_p - 1/T$  curve is, however, somewhat different for the two allotropic forms of iron.

The final curve was drawn in the following way. At  $1200^\circ\text{K}$  ( $927^\circ\text{C}$ ) the values given by the observers mentioned<sup>5, 8, 9</sup> vary within the limits

$$\log \frac{p_{\text{H}_2\text{O}}}{p_{\text{H}_2}} = -0.035 \text{ to } 0.230.$$

In any binary system Raoult's law should apply to the solvent within a certain high concentration range which in a system such as iron-nickel should extend from 100 % at least down to 90 % iron ( $N_{\text{Fe}} = 0.9$  to  $1.0$ ). Applying Raoult's law to the results obtained with the alloys containing 4, 7, 8 and 10 % nickel an equilibrium value for pure iron (at  $1200^\circ\text{K}$ ) of  $\log K_p = -0.108$  is obtained.

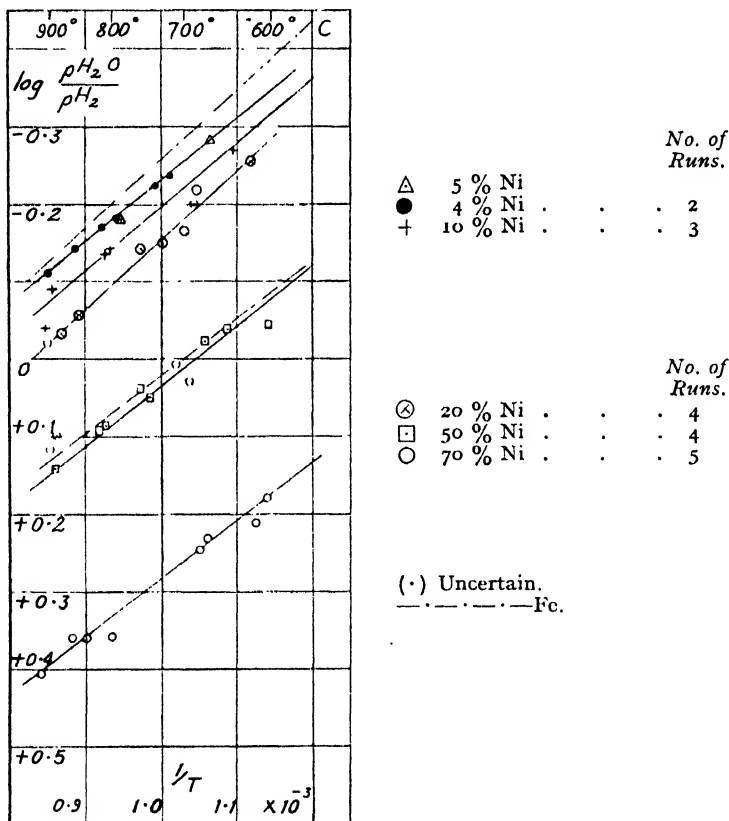


FIG. 2.

<sup>8</sup> All these results are collected and discussed in a recent publication by Richardson and Jeffes, *J. Iron Steel Inst.*, 1948, **160**, 261.

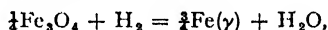
<sup>9</sup> See also *Landolt-Börnstein-Roth-Scheel*, including supplementary volumes.

This fixes one value. Although the absolute positions of the  $\log K_p - 1/T$  curves of the various observers show relatively large divergences the slopes are similar. The weighted mean of the slopes of all the curves given by Chipman and Marshall, Emmett and Shultz, Darken and Gurry, Cirilli,<sup>8</sup> Neumann and Göhler, Hofmann,<sup>9</sup> Eastman and Evans,<sup>8</sup> and the authors amounts to  $-845 \pm 25$  for the  $T^{-1}$  term in the  $\log K_p$  equation. This is consistent with the authors' measurements on the iron-nickel alloys at low nickel percentages. Thus the equilibrium constant  $p_{H_2O}/p_{H_2}$  in the reduction of solid FeO to  $\gamma$ -iron is represented by

$$\log K_p(\text{FeO/Fe}) = -845 \cdot T^{-1} + 0.596 \quad (6)$$

The following calculations with the iron-nickel oxidation equilibria are based upon this equation for pure iron. It must be emphasized, however, that eqn. (6) is a relationship obtained from and expressing the results of the present measurements. It does not necessarily represent the true equilibrium constant for reaction (1). For this a correction must be applied for the effect of thermal diffusion.

The free energy values for the reduction of  $\text{Fe}_3\text{O}_4$  to  $\gamma$ -iron at the temperatures under consideration, according to the equation,



are rather similar to those of reaction (1), the slope of the  $\Delta G-T$  curve, however, is steeper and cannot be accepted if the authors' values for low concentration of nickel are taken into consideration. Thus, the possibility of the formation of  $\text{Fe}_3\text{O}_4$  must be omitted from the thermodynamic calculation. The  $\text{O}_2$  pressure, i.e. the  $\text{H}_2\text{O}/\text{H}_2$  ratio, is determined by the FeO phase as long as some of it is present.

The curve thus obtained for pure iron (eqn. (1)) and the curves determined for iron-nickel alloys (eqn. (2)) are represented in Fig. 2 in the form of a  $\log \frac{p_{H_2O}}{p_{H_2}}$  against  $1/T$  diagram. For the sake of clarity, results from only half the number of concentrations investigated are plotted. The deviations are the same for the other concentrations, and increase with increasing nickel content.

The equilibrium constants proved to be more reproducible when a series of measurements was made at decreasing temperatures, i.e. at increasing oxidation; more weight was therefore given to these measurements. In a few cases the oxidation remained almost constant during the whole series without obvious reason; these results were rejected. The results on the 85 % nickel alloy could not be evaluated, as was mentioned above. The complete set of results is summarized in the form of the thermochemical data in Table II.

TABLE II

Concentration of Ni (Weight %)	$N_{\text{Fe}}$	Number of Runs	Activity $a_{\text{Fe}}$		Activity Coefficient $\gamma_{\text{Fe}}$		Entropy of Solution cal./deg.		Heat of Solution $\Delta \bar{H}_{\text{Fe}}$ (calc.)
			1000° K	1200° K	1000° K	1200° K	$\Delta \bar{S}_{\text{Fe}}$ (obs.)	$\Delta \bar{S}_{\text{Fe}}$ (ideal)	
0	1.0	—	1.0	1.0	1.0	1.0	0	0	0
3.98	0.962	2	0.959	0.981	0.996	1.020	(-0.16)	0.07	(-275)
5.12	0.951	1	0.959	—	1.007	—	—	0.10	—
7.00	0.932	1	—	(0.945)	—	(1.014)	—	—	—
7.85	0.925	1	0.918	0.924	0.992	0.999	0.11	0.16	-85
7.85	0.925	1	(0.824)	(0.814)	(0.891)	(0.880)	(0.52)	0.16	—
10.16	0.902	3	0.892	0.898	0.989	0.996	0.16	0.20	-85
15.40	0.852	3	0.799	0.806	0.938	0.947	0.34	0.32	-140
20.43	0.804	4	0.804	0.794	1.000	0.987	0.57	0.43	+140
33.94	0.672	3	0.650	0.650	0.976	0.967	0.85	0.79	0
50.05	0.500	4	0.520	0.536	1.040	1.072	1.00	1.38	-330
50.05	0.500	(3)	(0.535)	(0.562)	(1.070)	(1.124)	(0.76)	1.38	(-580)
70.08	0.310	4	0.292	0.304	0.942	0.981	2.07	2.32	-470
70.08	0.310	1	(0.250)	(0.261)	(0.813)	(0.842)	(2.12)	2.32	-520

### Discussion

**Evaluation.**—From the  $\log K_p - 1/T$  curves for pure iron  $(p_{\text{H}_2\text{O}}/p_{\text{H}_2})_1$  and those for the various alloys,  $(p_{\text{H}_2\text{O}}/p_{\text{H}_2})_2$ , the activities of iron ( $a_{\text{Fe}}$ ) in the alloys are first calculated at  $1000^\circ\text{C}$  and  $1200^\circ\text{K}$ , by means of the relationship

$$a_{\text{Fe}} = \frac{(p_{\text{H}_2\text{O}}/p_{\text{H}_2})_1}{(p_{\text{H}_2\text{O}}/p_{\text{H}_2})_2} \quad (7)$$

These values are given in Table II and plotted against the molar fraction ( $N_{\text{Fe}}$ ) in Fig. 3. It is seen that the activities  $a_{\text{Fe}}$  lie close to Raoult's line

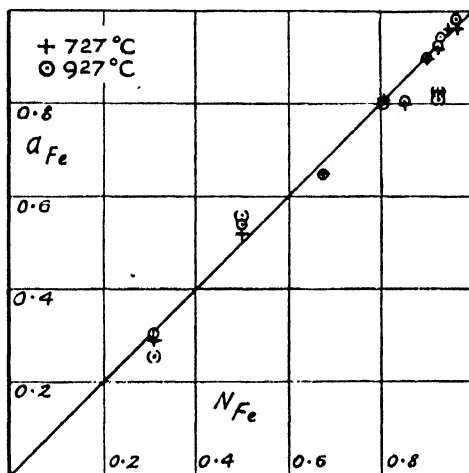


FIG. 3.

thus indicating almost ideal solution. Therefore the activity coefficients, calculated for  $1200^\circ\text{K}$  in Table II,

$$\gamma_{\text{Fe}} = a_{\text{Fe}}/N_{\text{Fe}} \quad (8)$$

are not far from unity.

Further calculations involve the partial molar entropy and heat of solution. The entropy of solution is obtained from

$$\Delta \bar{S}_{\text{Fe}} = -4.57 \left( T \frac{d \log a}{dT} + \log a \right) \quad (9)$$

and the heat of solution from

$$\Delta \bar{H}_{\text{Fe}} = -4.57 T^2 \frac{d \log a}{dT} \quad (10)$$

The values thus obtained from the straight lines in the  $\log K_p - 1/T$  diagrams are also tabulated in Table II.

In column 9 the entropies are calculated from the formula

$$\Delta \bar{S}_{\text{Fe}} = -4.57 \log N_{\text{Fe}} \quad (11)$$

which applies to, and is indeed characteristic of, regular and ideal solutions. It should be emphasized that the values obtained for the entropy changes in alloy formation more so than the other thermodynamical functions are very sensitive to the slightest inaccuracy in their determination and it may be concluded that within the limits of accuracy of the authors' measurements the entropies observed indicate a regular behaviour. The values appear to be a little lower at the high concentrations of nickel. A similar deviation has been observed in activity determinations on the

silver-gold system.<sup>11</sup> These activities could be obtained more accurately by electromotive force measurements. It was concluded, however, that measurements tend to give values somewhat too low and that the equation for ideal solutions (11) must be applied. It must, therefore, be assumed that the best representation of the entropies of solution in iron-nickel alloys is also that given by the ideal equation (11) and that the error thus involved can be only small.

The accuracy of the calculated heats of solution in column 10 (Table II) is probably no better than  $\pm 300$  cal. for the single value. Such an order of accuracy is normal for measurements of this kind, but since the values of  $\Delta\bar{H}$  are not far from zero, the percentage error is very great. A tendency to negative values of  $\Delta\bar{H}$  can, however, be observed in spite of the error involved. It would appear, therefore, to be more accurate to use the small negative values observed in calculating the results, instead of assuming a zero heat of formation, i.e. a completely ideal solution.

The possible error caused by the effect of thermal diffusion in the  $\text{H}_2\text{O}-\text{H}_2$  mixture can be deduced from experimental measurements. Emmett and Shultz<sup>10</sup> have determined the decomposition due to thermal diffusion at  $400^\circ$  to  $500^\circ\text{C}$  by a few measurements and have estimated further values for  $700^\circ$  to  $1000^\circ\text{C}$  from comparison of the results of various observers, obtained with either the static or the dynamic method. A far more extensive study of thermal diffusion in  $\text{H}_2\text{O}-\text{H}_2$  mixtures has been carried out by Shibata and Kitagawa.<sup>12</sup> These observers studied the temperature range  $400^\circ$  to  $1020^\circ\text{C}$  with various compositions of gas, making 150 single measurements. These results can be represented with good accuracy by the equation

$$\log \left( \frac{p_{\text{H}_2\text{O}}}{p_{\text{H}_2}} \right)_{T_2} = 1.035 \times \log \left( \frac{p_{\text{H}_2\text{O}}}{p_{\text{H}_2}} \right)_{T_1} - 0.21 \times 10^{-3} (T_2 - T_1),$$

where  $T_1$  is the temperature of the cold end ( $20^\circ$ – $25^\circ\text{C}$ ) and  $T_2$  that of the hot zone. Although the application of these values results in a considerable modification of the *absolute* equilibrium values, it affects the *differences* in the  $\text{H}_2\text{O}/\text{H}_2$  ratios very little. It will be found that the alterations required in the activities and consequently in the entropy and heat of reduction data remain well within the limits of accuracy stated in the present paper and that they do not affect the calculations and the statements that a slight negative heat of solution though not very accurate is still sufficiently pronounced to prefer it to the assumption of a zero heat of formation.

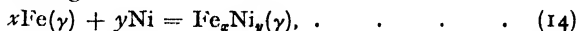
The partial molar values are therefore integrated to obtain the integral molar values of alloy formation<sup>13</sup> applying respectively

$$\Delta H_f = \int_0^{N_{\text{Fe}}} \Delta\bar{H}_{\text{Fe}} \cdot d\frac{N_{\text{Fe}}}{N_{\text{Ni}}}, \quad . \quad . \quad . \quad (12)$$

$$\text{and } \Delta S_f = \int_0^{N_{\text{Fe}}} \Delta\bar{S}_{\text{Fe}} \cdot d\frac{N_{\text{Fe}}}{N_{\text{Ni}}} = -4.57(N_{\text{Fe}} \log N_{\text{Fe}} + N_{\text{Ni}} \log N_{\text{Ni}}) \quad (13)$$

The curve for  $\Delta H_f$  calculated by means of eqn. (12) and mainly with the  $\Delta\bar{H}_{\text{Fe}}$  values at high concentrations (70, 50 and 34 % nickel) is given in Fig. 4. Its accuracy is estimated at about  $\pm 150$  cal.

The values of  $\Delta S_f$  can be obtained directly for any concentration by means of eqn. (13). These data refer to the formation of  $\gamma$  Fe—Ni alloys from  $\gamma$  Fe and Ni, according to



wherein  $x$  and  $y$  are equal to the molar fractions  $N_{\text{Fe}}$  and  $N_{\text{Ni}}$  respectively.

<sup>10</sup> Emmett and Shultz, *J. Amer. Chem. Soc.*, 1932, **54**, 3780.

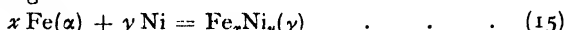
<sup>11</sup> Kubaschewski and Huchler, *Z. Elektrochem.*, 1948, **52**, 170.

<sup>12</sup> Shibata and Kitagawa, *J. Fac. Sci. Hok. Imp. Univ.* (II), 1938, **2**, 223.

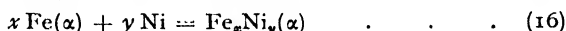
<sup>13</sup> See Weibke and Kubaschewski, *Thermochemie der Legierungen* (Berlin, 1943).

**Free Energies of the  $\alpha$  and  $\gamma$  Phases.**—The measurements and calculations above do not involve the  $\alpha$  iron-nickel phase. The curve of the 4 % nickel alloy in Fig. 2 extends into the  $\alpha$  field and should therefore show a break due to the free energy of  $\gamma$ — $\alpha$  transformation. This break, however, can only be slight since the differences in free energy between the  $\alpha$  and  $\gamma$  phases are very small (as is shown below). Moreover, the accuracy of measurement is not sufficient to determine the difference in the slope. In fact, it is considered that sufficient accuracy cannot be attained by any method involving equilibrium measurements, to justify this evaluation. The authors therefore used the following method to derive integral free energies of formation of the  $\alpha$  and  $\gamma$  phases.

The temperature range of main interest is that from room temperature to about 750° C, i.e. the range of existence of  $\alpha$  iron. The calculations therefore may be related to the formation of either  $\alpha$  or  $\gamma$  alloys from  $\alpha$  iron and nickel, according to



and



respectively, when  $x$  and  $y$  are again in the ratio of the atomic proportions of iron and nickel which are present in the alloys.

**$\gamma$  PHASE.**—The free energies of formation for eqn. (15) can be obtained from the results above, applying the Gibbs equation and considering the free energy of transformation of  $\gamma$  to  $\alpha$  iron. In the equation,

$$\Delta G_{15} = \Delta H_f - T\Delta S_f - \Delta G_{tr} \quad . \quad . \quad . \quad (17)$$

$\Delta H_f$  represents the heat of  $\gamma$  Fe—Ni formation from  $\gamma$  Fe (given in Fig. 4),

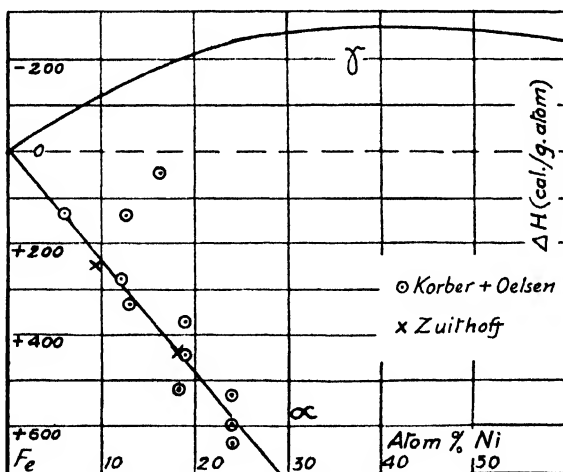


FIG. 4.

$\Delta S_f$ , the corresponding entropy of formation (given by eqn. (13), and  $\Delta G_{tr}$  is the free energy of the transformation:  $[\text{Fe}]_\gamma = [\text{Fe}]_\alpha$ . The latter value is obtained from the available data for the heat capacities of  $\alpha$  iron,  $\beta$  iron and  $\gamma$  iron<sup>8</sup> and the heats of transition  $\alpha$ — $\beta$  and  $\beta$ — $\gamma$ .<sup>9</sup> The most probable equation which is obtained from all measurements, but of which the evaluation cannot be discussed in detail here, is:

$$[\text{Fe}]_\gamma \rightarrow [\text{Fe}]_\alpha: \Delta G_{tr} = -460 + 8.19T \log T - 2.8 \times 10^{-3}T^2 - 21.40T \quad (18)$$

Since eqn. (17) will be applied to various temperatures the heat capacity terms of the iron nickel alloy formation

$$\int_0^T \Delta C_p \cdot dT \quad \text{and} \quad \int_0^T \frac{\Delta C_p}{T} \cdot dT$$



should be involved. The heat capacities of iron-nickel alloys can, however, be calculated almost additively from those of the constituent elements as was shown by Zuithoff<sup>14</sup> who determined these values at various compositions between 100° and 1400° C. From his measurements Zuithoff even calculated a  $C_p$  curve of "irreversible" iron, that is a curve excluding the deviations in  $C_p$  due to the two transformations. The possible deviations from additive  $C_p$  values cannot affect the following calculations appreciably and thus may be neglected. It was also found by Kawakami<sup>15</sup> that the heat contents of iron-nickel alloys at temperatures between 30° and 250° C, are independent of whether they were obtained on normalized samples or on those quenched from 1000° C. Although quenching need not necessarily completely retain the  $\gamma$  structure, some  $\gamma$  should remain, and no indication is found that the two states have a different heat capacity except between 15 and 25 % nickel. The deviations found in that range require a small correction in the following calculations which need not be explained in detail, and might even be neglected.

Eqn. (17) can therefore be applied to various temperatures without any further correction and the free energy of formation of  $\gamma$  iron-nickel (according to eqn. (15)) is obtained. The method of calculation may be shown by an example, say for 800° K (= 527° C) and 10 atomic % nickel.

$\Delta H_f$  is - 125 cal. (Fig. 4),  $\Delta S_f$  is calculated (eqn. (13)) to be 0.647, and consequently  $T\Delta S_f = + 518$  cal.  $\Delta G_{tr}$  for pure iron (eqn. (18)) is found to be - 350 cal./g. atom, so the corresponding  $\Delta G_{tr}$  for the mole fraction,  $x = N_{Fe} = 0.9$ , according to eqn. (15), is - 350  $\times$  0.9 = - 315; consequently (eqn. (17))

$$\Delta G_{15} = - 125 - 518 + 315 = - 328 \text{ (800° K, } N_{Fe} = 0.9).$$

The complete  $\Delta G_{15}$  curves of alloys of compositions up to 50 atomic % nickel are calculated in this manner and are plotted in Fig. 5-7 (designated  $\gamma$ ).

$\alpha$  PHASE.—As there are no equilibrium data for the  $\alpha$  phase of the iron-nickel system, the free energy of formation of this phase, according to eqn. (16), must be calculated from the heat and entropy of formation.

The heat of formation of  $\alpha$  iron-nickel alloys is not known to have been determined directly. Körber, Oelsen, and Lichtenberg<sup>16</sup> have, however, measured the change in heat contents of iron-nickel alloys of various compositions on heating from 20° C to 1000° and 1600° C. The difference between their values for 1000° C. and the values obtained additively from the heat contents of the pure metals in the same atomic proportion is equal to the differences in the heats of formation of the reactions in eqn. (14) and (16) (according to Hess's and Kirchhoff's laws).<sup>\*</sup> The numerical values of these differences may thus be deducted from the corresponding heats of formation of the  $\gamma$  iron-nickel alloys obtained in the present paper to give the heats of formation of the  $\alpha$  iron-nickel alloys. These are plotted as circles in Fig. 4. Although their values appear to be somewhat scattered, the work of Körber, Oelsen and Lichtenberg may be regarded as reliable. The results are given support by some values, plotted as crosses, derived from measurements by Zuithoff. In computing these, the present authors have chosen mean values for the range 25° to 1000° C, and have made allowance for Zuithoff's use of the heat contents of pure iron determined by Jaeger, Rosenbohm and Zuithoff<sup>17</sup> with the same apparatus.

<sup>14</sup> Zuithoff, *Rec. trav. chim.*, 1940, **59**, 131.

<sup>15</sup> Kawakami, *Sci. Rep. Tôhoku*, 1926, **27**, 614.

<sup>16</sup> Körber, Oelsen and Lichtenberg, *Mitt. K.W.I. Eisenforschung, Düsseldorf*, 1937, **19**, 131.

<sup>17</sup> Jaeger, Rosenbohm and Zuithoff, *Rec. trav. chim.*, 1938, **57**, 1313.

<sup>\*</sup> It may be noted that this is numerically equal to the corresponding difference in the values at 1600° C, which implies that the heat of formation of the liquid alloy from its components in the liquid state is the same as that of the solid alloy in the  $\gamma$  iron state.

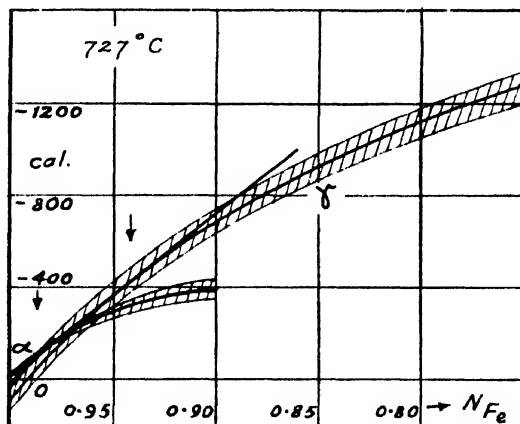


FIG. 5.

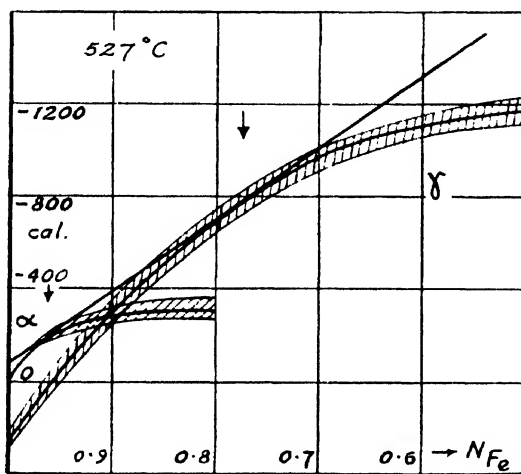


FIG. 6.

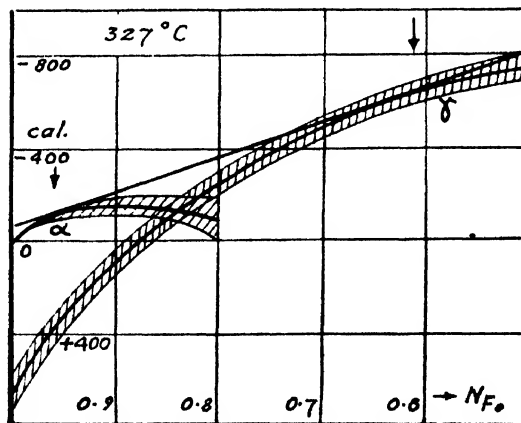


FIG. 7.

These two series of figures agree satisfactorily. The most serious objection which may arise is whether the  $\alpha$  iron-nickel alloys formed in the experiments were in a state of equilibrium, as the calorimetric method applied involves relatively rapid cooling from 1000° C to room temperature. An error may be expected due to this cause, but the curve of heat of formation of  $\alpha$  iron-nickel alloys up to 25 % nickel in Fig. 4 will be used for further calculation.

Finally, the entropy of formation of  $\alpha$  Fe—Ni must be derived. Since the entropy of formation of the  $\gamma$  phase approaches ideal behaviour and since the heat of formation of the  $\alpha$  phase is more positive than that of the  $\gamma$  phase, one may assume the validity of the ideal law also for the  $\alpha$  phase. It is a general experience that systems with small positive heats of formation conform with the relationships in eqn. (11) and (13).

It has been stated above that the heat capacities of the  $\alpha$  and  $\gamma$  phases of the iron-nickel alloys are equal (with a small exception at 20 % nickel) and that they are almost additive. The free energy of the  $\alpha$  phase is therefore obtained by the relationship :

$$\Delta G_{1\alpha} = \Delta H_{\alpha} - T\Delta S_{\alpha} \quad . \quad . \quad . \quad (19)$$

where the heat of formation  $\Delta H_{\alpha}$  is given by the lower curve in Fig. 4 and  $\Delta S_{\alpha}$  is calculated by eqn. (13).

For the atomic fraction  $N_{\text{Fe}} = 0.90$  and a temperature of 800° K,  $\Delta H_{\alpha}$  is + 238 cal., according to Fig. 4 and  $\Delta S_{\alpha}$  is calculated to be 0.647, consequently  $T\Delta S_{\alpha} = + 518$  cal. The free energy of formation results from (19) :

$$\Delta G_{1\alpha} = 238 - 518 = - 280 \quad (800^{\circ} \text{ K} ; N_{\text{Fe}} = 0.90).$$

The complete  $\Delta G_{1\alpha}$  curves up to 20 atomic % nickel are calculated in this manner for various temperatures and are also drawn in Fig. 5-7 (designated  $\alpha$ ).

The actual errors will not affect the final conclusions unless they are more than a few hundred calories. The significant error is that found in the *differences* of the free energy curves for the two phases. The accuracy of the differences in the two  $\Delta H$  curves (Fig. 4) is determined by the accuracy of the heat content measurements. Although these values were checked by two independent observers, the uncertainty of the nature of the product after rather rapid cooling must be considered and it may be assumed that this error is not less than 5 cal. per 1 atomic % nickel (e.g. 50 cal. at 10 atomic % nickel). The entropy of formation is calculated with the same formula for both  $\alpha$  and  $\gamma$  phases ; the difference in the  $T\Delta S$  term is therefore zero. This may introduce another, but smaller, error : about 0.002 cal. per 1 atomic % nickel may be assumed. The fact that the heat capacities are possibly not *quite* additive must also be taken into account :  $\pm 1$  cal. per 1 atomic % nickel is estimated. The free energy of transformation of  $\alpha$  to  $\gamma$  iron (eqn. (18)) introduces another source of error of which the accuracy is estimated and represented by 0.001 (1100 -  $T$ ) % Fe. From these figures the shaded areas in Fig. 5-7 are derived, which represent (as mentioned above) not the absolute but the relative average errors.

From the free energy curves in Fig. 5-7 the probable boundaries of the  $\alpha$ — $\gamma$  field can be determined. Since no concave break should occur in the free energy diagram of stable alloys, the tangent must be drawn to the two curves of  $\alpha$  and  $\gamma$ , thus defining the phase boundaries  $\alpha/\alpha + \gamma$  and  $\alpha + \gamma/\gamma$ . It is seen that the differences in free energy of the two phases are very small. This explains the very slow attainment of equilibrium at low temperatures as the "driving force" to attain it is rather small. The small differences between  $\Delta G_{1\alpha}$  and  $\Delta G_{1\gamma}$  cause also a relatively large error in the phase boundaries obtained from the tangential

<sup>18</sup> Kubaschewski and Schneider, *Z. Elektrochem.*, 1942, **48**, 671.

points. These boundaries are therefore shaded in Fig. 8 and are compared with the boundaries obtained by Owen and Sully.<sup>10</sup> The agreement is as good as can be expected, considering that the free energy curves are obtained quite independently of any measurement concerning directly the phase boundaries of the equilibrium diagram.

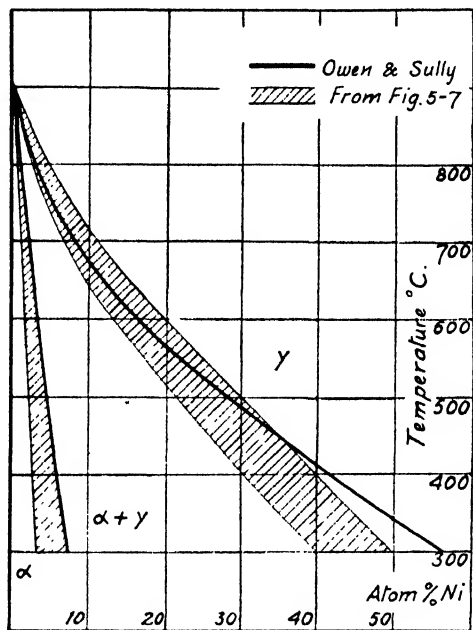


FIG. 8.—Iron-nickel equilibrium diagram.

**General Conclusions.**—The possibilities of the application of thermochemical measurements for the determination of phase boundaries of intermetallic systems is briefly discussed.

If vapour pressure or electromotive force measurements are applicable (i.e. if the components differ widely enough in their standard potentials, or if one component has a considerable vapour pressure at normal temperatures) relatively accurate results may be expected. The Grube-Flad method is generally less accurate. None of these methods can be used to establish the unstable branches of the free energy curves so in order to locate the points of contact of the tangential portions of the curves, the stable branches must be determined with extreme accuracy especially in systems of low affinity. The highest accuracy is required in thermochemical measurements for determining the phase boundaries in equilibrium diagrams. Generally, heat capacity measurements (including the heats of transition) must also be applied. Here again a difficulty arises for systems of low affinity: the usual "drop" method, which was applied by Körber, Oelsen and Zuithoff, does not necessarily lead to equilibrium as the samples are cooled relatively rapidly. True heat capacity measurements should be applied and the heats of transformation should be determined at the transformation temperature.

The conditions of measurements may vary from system to system; generally, however, it should be pointed out that the investigation is rather complicated and a general improvement in thermochemical methods is required. The accuracy of the numerical data obtained for alloy

<sup>10</sup> Owen and Sully, *Phil. Mag.*, 1939, **27**, 614.

formation by vapour pressure, electromotive force, and calorimetric measurements is frequently over-estimated, and the data obtained by such methods cannot be applied without supplementation with a considerable general knowledge of the thermodynamics of alloy formation.

The work described above has been carried out as a part of the research programme of the National Physical Laboratory, and this paper is published by permission of the Director of the Laboratory. The authors desire to acknowledge the suggestions made by Dr. N. P. Allen in initiating this investigation, and the assistance of Mr. C. A. Bristow, B.Sc., and Mr. A. J. Cook who prepared the iron-nickel alloys.

*National Physical Laboratory,  
Teddington,  
Middlesex.*

---

## SPATIAL INTERFERENCE IN POLYMERIZATION REACTIONS

BY G. M. BURNETT, L. VALENTINE AND H. W. MELVILLE

*Received 30th May, 1949*

In computing the value of velocity coefficients for radical-radical interactions it is usually assumed that the radicals are uniformly distributed throughout the reaction space. It is therefore important to devise a method which demonstrates whether or not radical production is localized. A simple means of settling the matter for any given reaction system, geometry and source of radiation, is described and the results obtained with a number of monomers discussed.

The rapid developments in recent years in determining the absolute values of the velocity coefficients of polymerization and oxidation reactions following the realization that the determination of the life-time of radicals in such systems was the clue to the solution of the problem, have raised many questions of technique. Whereas in previous studies of such mechanisms it has been sufficient to establish the general kinetic features, i.e. variation of rate with reactant concentrations, with temperature, etc., it is now essential to carry out the reactions under closely controlled conditions if the numerical values of the rate coefficients are to have any real value.

Some time ago<sup>1</sup> in the study of the photochemical vapour-phase polymerization of methyl acrylate, a method was described for estimating the size of the zone of reaction surrounding the zone of illumination of the system. This method was based on the principle of using a double source of illumination in which one beam of radiation could be moved relative to a second beam. In this way the zones of reactivity could be separated by any desired distance. In this particular reaction the rate of polymerization is proportional to the square root of incident intensity. When, therefore, the two zones of reactivity are brought into close proximity there is a diminution in the total rate of reaction due to the mutual interference between the radicals produced in the two zones of illumination. While this method can be used quantitatively to measure the average life-time of the radicals it also emphasizes the importance of the geometry of the system in photochemical reactions

<sup>1</sup> Jones and Melville, *Proc. Roy. Soc. A*, 1940, **175**, 392.

of this type. Thus, if for any reason, there is a localized concentration of radicals in part of a reaction system then the rate of disappearance of these radicals may become abnormally fast. This effect may become important in liquid-phase polymerizations where optical absorption coefficients may have high values. The result would be that the radicals are confined to a thin layer near the position at which the radiation enters the system. In computing the value of velocity coefficients for radical-radical interactions it is usually assumed that the radicals are in fact uniformly distributed throughout the reaction space.

In comparing the velocity coefficients for such processes from a variety of sources there are very considerable discrepancies. For example, in the vinyl acetate polymerization Bartlett claims, on the basis of entirely inadequate evidence, that the discrepancy between his and Melville and Burnett's<sup>3</sup> results is due to this factor and that in the latter's experiments this "skin" effect is present. There are, however, many other factors which can give rise to discrepancies and these need not be discussed in this paper. It is, however, important to devise a method which will demonstrate whether radical production is in fact localized. This trouble could, of course, be avoided by working with monochromatic radiation which is only weakly absorbed, but as usual in photochemical experiments it is essential to use polychromatic light sources to get measurable rates of reaction. The method described below provides a simple means of settling the matter for any given reaction system, geometry, and source of radiation. Two sources of light of similar intensity are placed at about equal distances on opposite sides of a reaction vessel. Three experiments are then carried out. First the rate of polymerization  $R_1$ , due to lamp No. 1 is measured, then that due to lamp No. 2,  $R_2$ , and finally the rate with both lamps together,  $R_3$ . If the zone of reaction is confined to a region at the entrance windows of the reaction cell then  $R_1 + R_2$  will be equal to  $R_3$ . On the other hand if reaction is spread uniformly throughout the vessel  $R_3 = (R_1^2 + R_2^2)^{1/2}$  by virtue of the fact that the rate of polymerization is proportional to the square-root of the incident intensity.

In the work described in this laboratory unit polymerizations are carried out in cylindrical vessels with an internal diameter not exceeding 1 cm. The following experiments, using a variety of systems, have been carried out using a 10 atm. type of capillary mercury arc, and are simply to illustrate the application of the method.

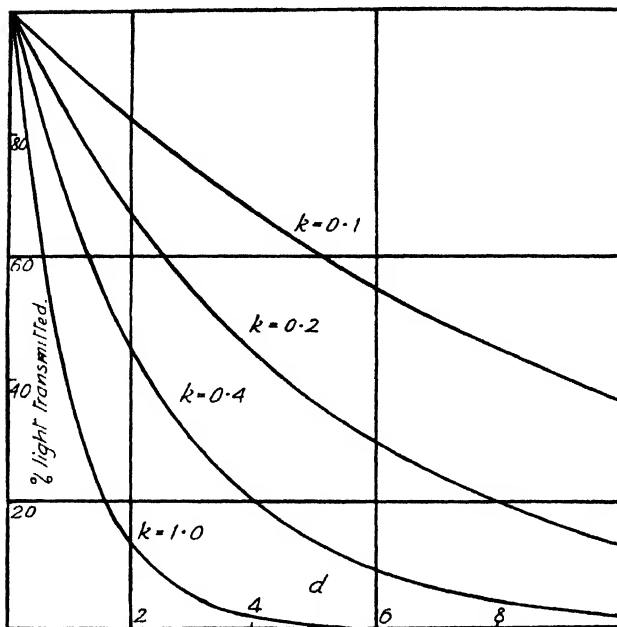
**Theory.**—The absorption of light by a liquid medium can be assumed to obey the law,

$$I = I_0 e^{-kx},$$

where  $I_0$  and  $I$  are the intensities of the incident and transmitted light,  $x$  the length of the light path and  $k$  an extinction coefficient, which is, in effect the product of the normal extinction coefficient and the concentration of the liquid under examination. Fig. 1 is drawn to show the absorption of light at values of vessel diameters and extinction coefficients commonly used. If a photo-reaction is carried out in a reaction vessel whose depth is  $d$  then the light absorbed in the vessel will be  $I_0(1 - e^{-kd})$ . If, therefore,  $k$  be large there is the possibility that the absorption of light will take place in a depth of liquid less than  $d$  so that non-uniform conditions would exist. Since it is of the utmost importance that such a situation should not arise in polymerization reactions, the "two-lamp test" has been devised. The theory is relatively simple. If two lamps are arranged so that the intensities of illumination  $I_0$  of opposite sides of a reaction vessel are equal then the total light intensity at a point in the vessel will be

$$I_t = I_0(e^{-kx} + e^{-k(d-x)}).$$

In a reaction in which the termination mechanism is by the interaction of two of the propagating chains, the concentration of active species is

FIG. 1.—Absorption of light according to  $I = I_0 e^{-kd}$ 

proportional to the square root of the light intensity so that for one lamp the concentration for the whole system will be

$$(P)_I = KI_0^{\frac{1}{2}} \int_0^d e^{-\frac{kx}{2}} dx, \quad . \quad . \quad . \quad (1)$$

where  $K$  is a proportionality constant. In the same way with two lamps the actual concentration will be given by

$$(P)_{II} = KI_0^{\frac{1}{2}} \int_0^d (e^{-kx} + e^{-k(d-x)})^{\frac{1}{2}} dx, \quad . \quad . \quad . \quad (2)$$

where  $d$  is the length of the light path. The evaluation of eqn. (2) was carried out by plotting the function and measuring the areas under the curves by means of a planimeter. A typical set of curves (for  $k = 1$ ) is shown in Fig. 2. It is evident, from kinetic analysis that the overall reaction rate is proportional to the concentration of the active centres so that experiments can readily be carried out by determining the rate of reaction with two separate lamps and with both together. Now it is obvious that if the light is completely absorbed (for practical purposes) within a very small distance the effect of two lamps will be to double the rate, or in general, to give a rate equal to the sum of the separate rates. On the other hand, if there is only extremely weak absorption of the light the rate with two lamps will be  $\sqrt{R_1^2 + R_2^2}$ , where  $R_1$  and  $R_2$  are the separate rates. It is of interest to find the amount of interference and relate this to the fraction of the reaction vessel which is effectively filled by the light. The fractional amount of interference,  $Z$ , has been shown to be <sup>1</sup>

$$Z = \frac{\frac{R_1 + R_2}{R_1 + R_2} - 1}{\frac{R_1 + R_2}{\sqrt{R_1^2 + R_2^2}} - 1}. \quad . \quad . \quad . \quad (3)$$

If the lamps give identical intensities at the opposite ends of the reaction vessel then eqn. (3) will reduce to

$$Z = \frac{2R_1 - R_{1+2}}{0.414 R_{1+2}} \quad (4)$$

Fig. 3 shows the relationship between  $Z$  and the light path  $d$  for various values of  $k$ . Theoretically, of course, there will be 100 % interference only when  $k$  is zero. Fig. 4 represents the correlation between the volume of the reaction system effectively occupied and the amount of interference. The former was assumed to be proportional to the area under

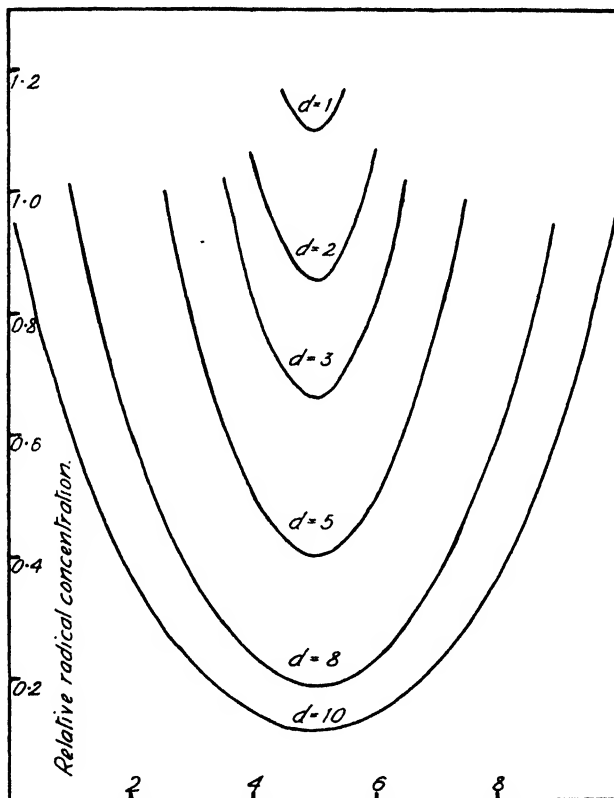


FIG. 2 —Radical distribution for two light sources for various path lengths ( $k = 1$ )

the requisite absorption curve shown in Fig. 1. From this relationship it is possible to find what proportion of the volume of the vessel is effectively occupied by the free radicals propagating the reaction. In this way correction for the fundamental constants can be readily effected.

In the foregoing, it has been assumed that (i) the distance of diffusion of the polymer chain is negligible and (ii) the convection currents which must be present due to the quite considerable heat of reaction will have a negligible transport effect so that the radicals will be confined to the volume occupied by the light. This is especially important in high absorption since it is possible that the reaction rate is very high in an exceptionally small volume.



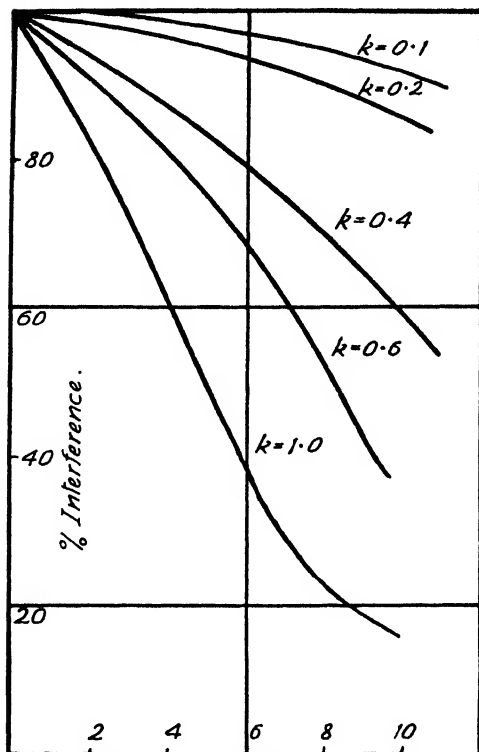


FIG. 3.—Relationship between % interference and the path length for various values of  $k$

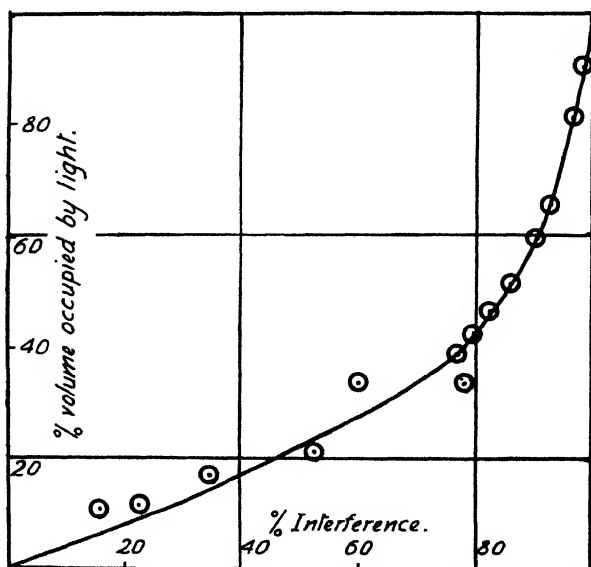


FIG. 4.—Relation between % interference and effective volume in which reaction occurs

## Results and Discussion

The experiments were carried out in silica reaction vessels having a diameter of about 1 cm. and fitted with a capillary of 3.5 mm. bore, the volume of monomer being 3.4 ml. The rate of reaction was measured dilatometrically using a cathetometer to follow the fall in the meniscus level. Two G.E.C. Osira 125-W lamps were used as sources of illumination and were arranged to give approximately equal rates of polymerization. Purified, outgassed monomer was distilled into the reaction vessels which were then sealed off under high vacuum. Results are shown in Table I.

TABLE I.—"SKIN EFFECT" FOR A NUMBER OF MONOMERS

Monomer	Rate for Lamp 1	Rate for Lamp 2	Rate for both Lamps	% Interference
Vinyl acetate (c) . . .	0.0458	0.0543	0.0848	44
Vinyl acetate (a) . . .	0.0218	0.0253	0.0392	52
Methyl methacrylate (c) .	0.0202	0.0214	0.0290	100
Methyl methacrylate (a) .	0.0168	0.0170	0.0233	100
Styrene (b) . . . . .	0.085	0.093	0.114	100
Vinylidene chloride (c) .	0.0178	0.0198	0.0282	80

(a) A filter of 2 cm. of 50 % acetic acid was used. Difficulty was experienced in the case of vinyl acetate due to the warming up of the filter, it being noted that the rate increased during this period. Using cold acid as in the original experiments<sup>3</sup> there is little doubt that the figure of 52 % could be raised.

(b) The polymerization was effected using benzoyl peroxide ( $5.8 \times 10^{-3}$  mole/l.) as photosensitiser. For these requirements the wavelength was in excess of 2900 Å.

It will be seen that in the case of methyl methacrylate the interference is complete and that the results for the rate coefficients<sup>4</sup> are therefore not complicated by localized absorption. Similarly, in this case, the methods used in this laboratory are such as to eliminate a factor of this kind. Even with vinylidene chloride using the whole spectrum of the mercury arc there is only a relatively small tendency for the system to exhibit localized absorption.

From the results of Table I the figures for the termination coefficient of vinyl acetate photo-polymerization need a little adjustment. If Bartlett and Swain's<sup>2</sup> suggestion is correct that their terminations are 1/40 of Burnett and Melville's<sup>3</sup> on account of localized absorption this would imply that 95 % of the radiation would be absorbed in a layer about 0.7 mm. thick so that there would be no detectable interference in the above experiments. Taking the value of 52 % interference from Table I, the percentage effective volume for reaction is 25 %. This corresponds to a factor of 4.0 and hence  $k_t = 4 \times 10^8$  which is still in excess of Bartlett and Swain's results by a factor of about 10.

In making these modifications to rate constants there is another factor which must be mentioned. In some reactions mono-radicals are involved, in others di-radicals. Kinetically the important matter is the interaction of a *radical end* with monomer or other molecules and with other radical ends. In the original vinyl acetate work the calculations were based on the rate of production of di-radicals. Adopting the above convention, therefore, the rate of initiation should be multiplied by a factor of 2.

<sup>2</sup> Swain and Bartlett, *J. Amer. Chem. Soc.*, 1946, **68**, 2381.

<sup>3</sup> Burnett and Melville, *Proc. Roy. Soc. A*, 1947, **189**, 456.

<sup>4</sup> Mackay and Melville, *Trans. Faraday Soc.*, 1949, **45**, 323.

The old and new methods of calculations are shown in Table II. The termination is also further corrected for localized photochemical action giving the final result shown in that Table.

TABLE II

Temp. 25° C

	$k_p$ mole/l.sec.	$k_t$ mole/l.sec.
Di-radical . . . . .	1100	$3 \cdot 10 \times 10^9$
Mono-radical . . . . .	780	$1 \cdot 55 \times 10^9$
Mono-radical corrected for localized absorption . . . . .	780	$3 \cdot 92 \times 10^8$

There is one other factor which will tend to counteract localized absorption effects and that is convection. Although the temperature rise owing to reaction is kept at a minimum the effect cannot wholly be avoided. Convection currents are thus set up. Further, since radical life-times may be as high as  $10^3$  sec. the polymer radical can be transported quite considerable distances during its period of growth. This will tend to even out radical concentration gradients. The calculation of this effect is very complicated but experimentally it could readily be estimated by introducing small opaque particles into the polymerizing system and observing their motion. This technique has already been successfully used in the much more difficult problem of delineating infrared spectra.<sup>5</sup>

We thank the Department of Scientific and Industrial Research for a Senior Award to G.M.B. and a maintenance allowance to L.V. The vinylidene chloride used during these experiments was kindly supplied by the Distillers Company Limited.

*Chemistry Department,  
University of Birmingham.*

<sup>5</sup> Sutherland and Lee, *Report Prog. Physics*, 1948, **2**, 144.

## MOLECULAR INTERACTION IN MIXTURES OF ESTERS

### PART I.—THE VOLUME CHANGES ON MIXING

BY P. MEARES

*Received 20th January, 1949; as revised, 13th June, 1949*

Three mechanisms are suggested as contributing to the volume changes on mixing. There is always a contribution due to the difference between the cohesive energy of the components in the separated and mixed states. A geometric effect occurs only when there is a large difference between the molecular sizes of the components. The magnitude of each of these contributions is estimated from data for related mixtures of esters. In a few cases a third contribution to the volume change is important; this arises from a large difference between the cohesive energy densities and compressibilities of the pure components.

In general, when two different liquids are allowed to mix at constant pressure there is a change in the total volume of the system. While the influence of this volume change on the thermodynamic properties of the system has been considered by Hildebrand<sup>1</sup> and a quantitative treatment has been given by Scatchard<sup>2</sup> little attention has been devoted to the underlying physical processes. X-ray investigations have established that most molecules in a liquid have a certain fixed number of neighbours situated at a well-defined average distance. The molecules of non-associated liquids at a temperature not too close to the freezing point may, to a first approximation, be regarded as occupying spherical volumes, since the absence of strong localized forces enables them to rotate freely in all directions. Molecules in the liquid state tend therefore to be hexagonally close-packed.

In a mixture, when the ratio of the molecular diameters of the two components is less than 1.25/1 the molecules can freely replace each other without seriously disrupting this arrangement. When the molecular diameter ratio is larger, there may be a geometrical rearrangement. If the molecules can be arranged so as to increase the number of nearest neighbour contacts between them or increase the area of molecular surface effective in each contact, then the volume will decrease. The volume of a pure liquid also depends upon the nature of the chemical groups determining the attractive forces between neighbouring molecules. Weakening the attractive forces without changing the shape and arrangement of the molecules would lead to an increase in their average separation, since equilibrium must be maintained between the attractive and repulsive forces.

When two liquids are mixed, changes may occur in both intermolecular forces and geometrical arrangement, hence both effects contribute to the volume change. If, as is frequently assumed, the interaction energy between a pair of unlike molecules is the geometric mean of the interaction between each molecule and another of its own kind, then the total energy of molecular interaction is not greater in the mixture than in the pure components and the liquids tend to expand on mixing. When there is a geometrical rearrangement this will usually act so as to bring the molecules into close contact over a larger area of their surfaces. Thus the two processes contributing to the change in volume will frequently act in opposition to each other.

It was the purpose of this investigation to determine the relative importance of these two effects. By using a homologous series of compounds it has been possible to vary gradually the intermolecular forces without greatly affecting the size and shape of the molecules. The liquids examined were all esters; these are normal liquids but have moderately polar groups contributing to the intermolecular forces.

## Experimental

The volume changes on mixing were obtained from the densities of the pure components and of the mixtures. A pycnometer of about 1 ml. capacity, calibrated at 20° C with freshly distilled water, was used. The components of the mixtures were buretted into small weighed bottles fitted with carefully ground stoppers. The bottles were reweighed after each addition and the densities of the pure components used to calculate the volume compositions of the mixtures. Buoyancy corrections were applied to all weighings; these were recorded to 0.0001 g. though the accuracy was considerably greater than this. The thermostat was set at 20° ± 0.05° C and maintained constant to ± 5 × 10<sup>-4</sup>° C. At 20° C the temperature coefficient of the densities of esters is about 0.001 g./ml. deg., hence the uncertainty in the mean thermostat temperature caused an uncertainty in the absolute values of the densities of 0.0001 g./ml.; they were repeatable to ± 0.0001 g./ml.

<sup>1</sup> Hildebrand, *Solubility* (Chemical Catalogue Co., New York, 1st Ed. 1924), Chap. VI, p. 63.

<sup>2</sup> Scatchard, *Trans. Faraday Soc.*, 1937, **33**, 160.

The esters were dried with anhydrous potassium carbonate and purified by fractional distillation; they were always freshly dried and redistilled before being used for density measurements. The ethyl acetate was Hopkin and Williams A.R. grade; the fraction used boiled at 77.1° C at 758 mm. 1:3-Butanediol diacetate (this will be abbreviated to BDA) was supplied by Canadian Resins and Chemicals Ltd. The purified product distilled between 92° and 94° C at 13 mm. (cp. Kulpinski and Nord<sup>3</sup>). The diethyl esters were pure materials and were treated as described above. The dibutyl esters and the dialkyl phthalates were specially prepared materials supplied by the Geigy Colour Co. Ltd. Their specimens of dimethylglycol and di- $\beta$ -chloroethyl phthalates were dried and distilled under reduced pressure.

## Results

The densities and molar volumes of the pure esters are presented in Table I.

TABLE I.—DENSITIES AND MOLAR VOLUMES OF ESTERS AT 20° C

Ester	Density (g./ml.)	Molar Volume (ml.)
Ethyl acetate . . . . .	0.9002	97.88
1:3-Butanediol diacetate . . . . .	1.0328	168.67
Diethyl oxalate . . . . .	1.0785	135.51
Diethyl malonate . . . . .	1.0544	151.92
Diethyl succinate . . . . .	1.0413	167.29
Diethyl adipate . . . . .	1.0128	190.70
Diethyl diethylmalonate . . . . .	0.9886	218.78
Diethyl sebacate . . . . .	0.9655	267.60
Dibutyl oxalate . . . . .	0.9884	204.63
Dibutyl malonate . . . . .	0.9827	220.10
Dibutyl succinate . . . . .	0.9770	235.73
Dibutyl adipate . . . . .	0.9620	268.58
Dibutyl sebacate . . . . .	0.9367	335.73
Dimethyl phthalate . . . . .	1.1908	163.08
Diethyl phthalate . . . . .	1.1183	198.74
Di- <i>n</i> -propyl phthalate . . . . .	1.0767	232.47
Di- <i>n</i> -butyl phthalate . . . . .	1.0465	265.99
Di-isobutyl phthalate . . . . .	1.0412	267.35
Di- <i>n</i> -amyl phthalate . . . . .	1.0243	299.14
Dimethylglycol phthalate . . . . .	1.1698	241.32
Di- $\beta$ -chloroethyl phthalate . . . . .	1.3268	219.44

Two series of mixtures have been investigated; in the first BDA was mixed with each of the esters of the dicarboxylic acids and in the second ethyl acetate was mixed with each of these esters. The mixture of BDA with ethyl acetate has also been examined. The fractional volume changes ( $\Delta V/V_0$ ) for mixtures containing equal volumes of the two components are presented in Table II; an expansion on mixing is designated positive. Six mixtures have been investigated over a range of concentrations; these data are shown graphically in Fig. 2.

## Discussion

It is generally recognized that the cohesive forces between molecules may be regarded as composed of three contributions. These are the London dispersion forces, the interaction of dipoles with dipoles and of dipoles with induced dipoles. In the absence of electrostatic long-range forces, such as exist between ions, the intermolecular energies in a liquid all diminish as  $r^{-6}$ , where  $r$  is the distance between the interacting centres,

<sup>3</sup> Kulpinski and Nord, *J. Org. Chem.*, 1943, 8, 256.

i.e. the separate atoms which form each molecule. Owing to the short-range character of the forces the potential energy of attraction between two neighbouring molecules is due almost entirely to the interaction of the one or two adjacent atoms at the molecular surfaces in contact. Thus, from the point of view of the intermolecular forces, the surface of a molecule is made up of different areas representing the various chemical groups in the molecule.

TABLE II.—FRACTIONAL VOLUME CHANGES ON MIXING EQUAL VOLUMES OF COMPONENTS AT 20° C

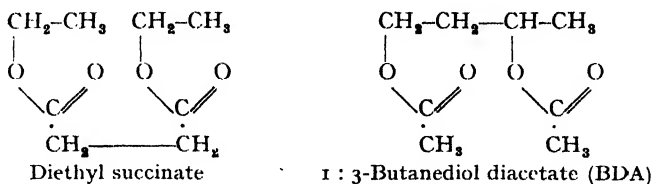
Ester	Mixed with Ethyl Acetate	Mixed with 1:3-Butanediol Diacetate	Difference (Geometrical Contribution)
1:3-Butanediol diacetate . . .	— 0.0025	—	— 0.0025
Diethyl oxalate . . .	— 0.0028	— 0.0005	— 0.0023
Diethyl malonate . . .	— 0.0020	0.0001	— 0.0019
Diethyl succinate . . .	0.0025	+ 0.0001	— 0.0026
Diethyl adipate . . .	— 0.0028	+ 0.0003	— 0.0031
Diethyl diethylmalonate . . .	— 0.0023	+ 0.0002	— 0.0025
Diethyl sebacate . . .	— 0.0018	+ 0.0011	— 0.0029
Dibutyl oxalate . . .	— 0.0020	+ 0.0001	— 0.0021
Dibutyl malonate . . .	— 0.0020	+ 0.0003	— 0.0023
Dibutyl succinate . . .	— 0.0020	+ 0.0006	— 0.0026
Dibutyl adipate . . .	— 0.0016	+ 0.0011	— 0.0027
Dibutyl sebacate . . .	— 0.0009	+ 0.0022	— 0.0031
Dimethyl phthalate . . .	— 0.0075	— 0.0012	— 0.0063
Diethyl phthalate . . .	— 0.0047	— 0.0001	— 0.0048
Di- <i>n</i> -propyl phthalate . . .	— 0.0038	— 0.0006	— 0.0044
Di- <i>n</i> -butyl phthalate . . .	— 0.0027	+ 0.0011	— 0.0038
Di- <i>isobutyl</i> phthalate . . .	— 0.0026	— 0.0009	— 0.0035
Di- <i>n</i> -amyl phthalate . . .	— 0.0018	+ 0.0012	— 0.0030
Dimethylglycol phthalate . . .	— 0.0074	— 0.0011	— 0.0063
Di- $\beta$ -chloroethyl phthalate . . .	— 0.0078	— 0.0014	— 0.0064

In esters there are two types of molecular surface, the non-polar hydrocarbon groups and the polar carboxyl residues,  $-\text{COO}-$ . Since a methylene group,  $-\text{CH}_2-$ , and an oxygen atom each have the same number of electrons in the outer shell, Slater and Kirkwood's <sup>4</sup> treatment shows that the dispersion forces are almost equal for any contact between two ester molecules. When two carboxyl residues approach close to one another there is an extra attractive force arising from the interaction between the dipoles in these two groups. The cohesion between a carboxyl residue and a methylene group will be slightly greater than the contribution of the dispersion forces alone owing to the small polarizability of the hydrocarbon group. Thus the molar cohesive energy of the members of a homologous series of esters changes gradually in ascending the series as the proportion of hydrocarbon groups to carboxyl residues varies.

When two esters have equal ratios of hydrocarbon to carboxyl residue, their intermolecular forces will be similar, and hence there will be no change in the forces on mixing. When the molecules of the esters are also similar in size and shape there should be no volume change on mixing; when there is a size difference the volume will change if a more compact arrangement of the molecules is possible in the mixture. These conclusions can be verified from the data in Table II. BDA and diethyl succinate are isomeric and differ only in the position of the bond between the

<sup>4</sup> Slater and Kirkwood, *Physic. Rev.*, 1931, **37**, 682.

symmetrical halves of the molecules ; their molecules may be regarded as two molecules of ethyl acetate joined by the eliminations of two hydrogen atoms :



No volume change would be expected on mixing these two liquids and this is confirmed by the result. Ethyl acetate has a hydrocarbon to carboxyl residue ratio equal to that of BDA and diethyl succinate but its molecules are about half as large as those of these diesters. On mixing ethyl acetate with either, there should be a volume change resulting from a geometrical rearrangement and a contraction of 0.0025 was observed in both these mixtures.

When a modification of the intermolecular forces and a geometrical rearrangement both contribute to the volume change it is desirable to be able to differentiate between these two effects. For liquids which mix without a molecular rearrangement Scatchard<sup>2</sup> has predicted an expansion quantitatively related to the energy of mixing. In Part II it is shown that, with one exception, this hypothesis is obeyed by the mixtures of BDA with the aliphatic diesters. Since the molar volumes of these diesters are not very different from that of BDA, no geometrical rearrangement is probable and it may be concluded that the volume change is determined only by the intermolecular forces. Since ethyl acetate and BDA have similar intermolecular force fields, when either is mixed with a diester the modification of these forces will be closely related. Thus the volume change in the mixture containing BDA, due only to this change in forces, also occurs in the mixture containing ethyl acetate, but in the latter case there is a further change due to a molecular rearrangement. Thus the difference between the volume change on mixing BDA with an aliphatic diester and that on mixing ethyl acetate with the same diester gives the contribution due to this geometrical effect.

The fractional volume change for mixtures containing equal volumes of the two components (Table II, columns 2 and 3) is a suitable quantity for comparison. The fourth column of Table II, which is the difference between the second and third columns, gives the volume change due to the molecular rearrangement on mixing the diesters with ethyl acetate. This quantity is fairly constant for the mixtures with the eleven aliphatic diesters and agrees with the value of the geometrical effect found for the mixture of ethyl acetate with BDA. The effect appears to increase slightly in ascending the homologous series which is to be expected since the extent of the molecular rearrangement will increase as the size disparity of the component molecules increases.

The theory of Scatchard predicts from the energies of mixing an expansion for these mixtures containing ethyl acetate, whereas in every case a contraction has been observed. This disagreement is explained by the fact that there is a geometrical contraction which, in every case, is larger than the expansion due to the change in the intermolecular forces. This latter effect increases as the series is ascended while the geometrical effect remains constant so that the magnitude of the resultant contraction decreases. The extent of the geometrical rearrangement must be small since the contraction is only 0.25 % ; it is due to local changes rather than a fundamental change in the system of packing of the molecules. Since the molecules are not perfect spheres there will be some gaps in the hexagonally close-packed arrangement not caused by thermal agitation. The ethyl acetate molecules, being smaller, are

able to fit on mixing into some of these holes in the liquid diesters, restoring the ordered arrangement in otherwise imperfectly ordered regions.

The contraction in the mixture of BDA with diethyl oxalate is caused by a strengthening of the intermolecular forces on mixing. There is a strong attractive force between the two electropositive carboxyl carbon atoms of the oxalate and the electronegative carbonyl oxygen atoms of the neighbouring ester molecules. This produces orientating forces which tend to pull the molecules closer together and so decrease the volume of the mixture. Since the difference between the volume changes on mixing diethyl oxalate with BDA and with ethyl acetate gives the expected value for the geometric contribution these orientating forces have the same effect in the latter mixture. Dibutyl oxalate does not behave similarly since the butyl groups are large enough to screen the carboxyl carbon atom of the residue to which they are not attached.

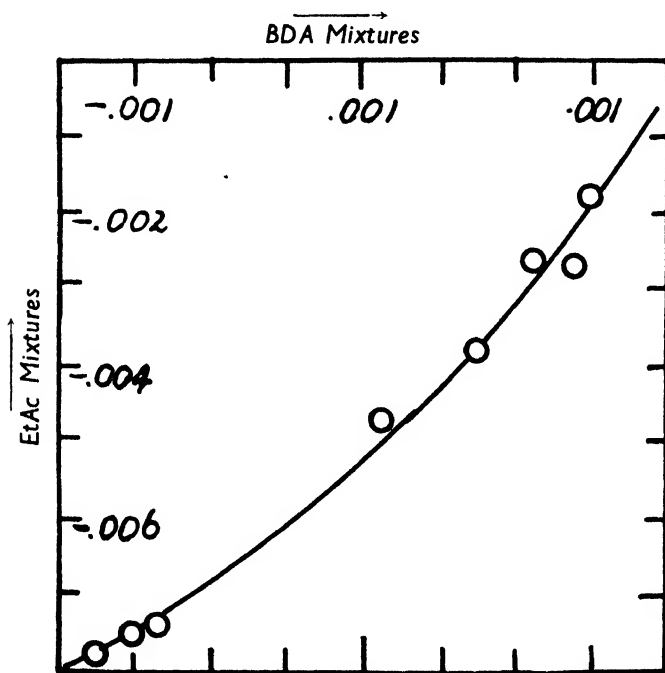


FIG. 1.—Volume changes on mixing the phthalates with ethyl acetate (EtAc) and with 1 : 3-butanediol diacetate (BDA).

Data for the volume changes in mixtures of ethyl acetate and BDA with the phthalates are also presented in Tables I and II. The molecules of BDA are comparable in size with those of the phthalates, and the ethyl acetate molecules are about half as large so the same considerations as with the aliphatic diesters should apply regarding a geometrical rearrangement on mixing. However, in three of the eight mixtures of BDA with phthalates there was a contraction; this is in disagreement with the theory of Scatchard. It is shown in Part II that the expansions in the mixtures from di-*n*-amyl to di-*n*-propyl phthalate bear the predicted relation to the energies of mixing, while the expansion with diethyl phthalate is much too small. The contractions with the dimethyl ester and with dimethylglycol phthalate are quite irregular and that with di- $\beta$ -chloroethyl phthalate is larger than expected from the small negative energy of mixing. Table II shows that there was a contraction for all mixtures of ethyl acetate with the phthalates. These volume changes



are parallel to those in the BDA series, a decreasing contraction being equivalent to an increasing expansion. The existence of a quantitative connection between the two sets of values is indicated by the smooth curve obtained by plotting the data for the ethyl acetate series against those for the BDA series (Fig. 1).

The difference between the volume changes for the two series of mixtures (Table II, column 4) is not constant. It decreases as the series of phthalates is ascended to a value not very different from that found with the aliphatic diesters. Since the fixation of the ester groups on the benzene ring will make the phthalate molecules cylindrical rather than spherical, the geometric contribution may be somewhat larger in these mixtures and the value of about  $-0.0037$  for the phthalates from di-*n*-propyl to di-*n*-amyl is therefore quite reasonable. The very large difference ( $-0.0063$ ) found for the mixtures containing dimethyl, dimethylglycol and di- $\beta$ -chlorethyl phthalates is not a simple geometrical effect. The cohesive energy densities or energies of evaporation per ml. at  $20^\circ\text{C}$  of the phthalates, given in Table III, have been obtained for four phthalates

TABLE III.—COHESIVE ENERGY DENSITIES (C.E.D.) OF THE PHTHALATES

Substance	C.E.D. (cal./ml.)
Dimethyl phthalate . . .	109.8
Diethyl phthalate . . .	98.6
Di- <i>n</i> -propyl phthalate . . .	93.3
Di- <i>n</i> -butyl phthalate . . .	90.6
Di- <i>n</i> -amyl phthalate . . .	85.0
Dimethylglycol phthalate . . .	107.7
Di- $\beta$ -chlorethyl phthalate . . .	116.2
1 : 3-Butanediol diacetate . . .	83.0

from the data of Small, Small and Cowley<sup>5</sup> and for the remainder from Hildebrand's rule with correction from the boiling point to  $20^\circ\text{C}$ . The difference between the cohesive energy densities (C.E.D.) of dimethyl, and diethyl phthalates is much larger than that between di-*n*-propyl, di-*n*-butyl and di-*n*-amyl phthalates. The molecular size and shape of dimethylglycol and di-*n*-butyl phthalates are very similar, but the substitution of  $-\text{O}-$  for  $-\text{CH}_2-$  increases the C.E.D. by 17 cal./ml. There is a similar increase when two hydrogen atoms in diethyl phthalate are replaced by chlorine atoms. The C.E.D. of BDA is included in Table III for comparison.

A mixture of components of widely different cohesive energies usually shows positive deviations from Raoult's law, the binding forces between unlike molecules being comparatively weak an expansion on mixing would be expected. However, substances of low cohesive energy have high compressibilities and vice-versa, thus the molecules of the liquid of low cohesive energy become compressed by the surrounding molecules of the other component. This explains the contraction in mixtures of BDA with dimethyl, dimethyl glycol and di- $\beta$ -chlorethyl phthalates and the very small expansion in the mixture with diethyl phthalate. Ethyl acetate molecules are smaller than BDA molecules and, although they have similar cohesive energies, ethyl acetate is more compressible. This accounts for the large difference between the volume changes in the two series of mixtures, the extra compression in the ethyl acetate mixture augmenting the geometrical effect. Contraction in mixtures of components having very different cohesive energies is a general phenomenon. For example, in mixtures of hydrocarbons with alcohols there is a contraction accompanied by an absorption of energy and positive deviations from Raoult's law.

<sup>5</sup> Small, Small and Cowley, *Trans. Faraday Soc.*, 1948, **44**, 810.

**The Concentration Dependence of the Volume Changes.**—Let the volume fraction in the mixture of the component of smaller molecules be  $v_1$  and of the other component  $v_2$ . For unit volume of mixture, the volume of holes initially in the component of larger molecules is proportional to  $v_2$ , and the probability of a hole being filled in the mixture is proportional to  $v_1$ . Hence the fractional volume change due to the geometrical effect  $\Delta V_g$  is given by

$$\Delta V_g = k_g v_1 v_2,$$

where  $k_g$  is a constant for the mixture.

The volume change due to the modification of the intermolecular forces on mixing  $\Delta V_f$  has been investigated by Scatchard<sup>2</sup> who found the expression :

$$\Delta V_f = k_f \kappa_0 v_1 v_2 ;$$

$k_f$  is a constant, and  $\kappa_0$ , the compressibility of the isolated components is given by

$$\kappa_0 = v_1 \kappa_1 + v_2 \kappa_2$$

where  $\kappa_1$  and  $\kappa_2$  are the compressibilities of the pure components.

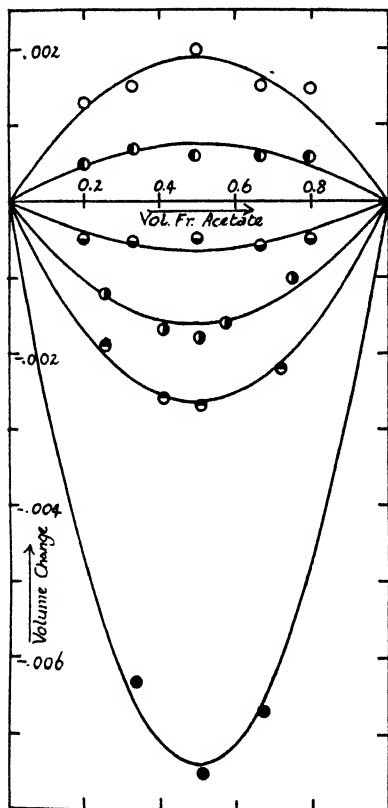


FIG. 2.—Concentration dependence of volume changes.

- Ethyl acetate and dimethyl phthalate.
- Ethyl acetate and di-*n*-butyl phthalate.
- Ethyl acetate and di-*n*-amyl phthalate.
- 1 : 3-Butanediol diacetate and diethyl oxalate.
- 1 : 3-Butanediol diacetate and di-*n*-propyl phthalate.
- 1 : 3-Butanediol diacetate and dibutyl sebacate.

When the C.E.D. of the two components differ markedly let component 1 have the lower C.E.D. The excess cohesive energy in the mixture over its value in pure component 1 is

$$v_2(L_2 - L_1),$$

where  $L_1$  and  $L_2$  are the C.E.D. of the pure components. This expression is not exact since it neglects the energy of mixing but the error is less

than 1 % in all these mixtures. Thus the compression of component 1 in the mixture is

$$\beta_1 v_1 (L_2 - L_1),$$

where  $\beta_1$  is the compressibility of a small cluster of molecules of component 1 (this will be smaller than the macroscopic compressibility  $\kappa_1$ ). An identical expression with the subscripts interchanged may be derived for the corresponding expansion of component 2. The difference between these two expressions is the volume change due to the compressibility and cohesive energy difference between the components and may be written as

$$\Delta V_e = k_e v_1 v_2, \\ k_e = (L_1 - L_2)(\beta_1 - \beta_2).$$

where

Thus two of the contributions to the volume change have the form  $kv_1 v_2$ , while the contribution due to the intermolecular forces is affected by the concentration dependence of  $\kappa_0$ . Since the compressibilities of organic liquids do not differ greatly, this dependence is only slight. The fractional volume changes for six mixtures plotted against the composition by volume appear in Fig. 2. The curves are all drawn to the form  $kv_1 v_2$  and coincide with the experimental points within the limits of error. The data are not sufficiently accurate to determine the precise form of the curves.

The author wishes to thank Prof. E. K. Rideal for many useful discussions and for his interest in this work which was carried out during the tenure of a D.S.I.R. Senior Award. The author is also grateful to the Managers of the Royal Institution for the facilities of the Davy-Faraday Research Laboratory.

*The Davy-Faraday Research Laboratory,  
The Royal Institution,  
London, W.1.*

## THE SECOND VIRIAL COEFFICIENTS OF POLAR GASES

By J. S. ROWLINSON

*Received 24th March, 1949; as revised 23rd June, 1949*

An expression is calculated for the second virial coefficient of a gas composed of spherical molecules whose intermolecular potential has a repulsive term proportional to  $r^{-12}$ , an attractive term proportional to  $r^{-6}$ , and which have point dipoles at their centres. The method is that used by Stockmayer. A Table is given for this function for suitable values of the temperature and the dipole moment. The calculated values fit the experimental results for nine polar gases. The dipole energies of interaction and equilibrium distances of separation are calculated. The results are compared with those derived previously by an alternative treatment, using the law of mass action. In both cases, molecules that can form hydrogen bonds differ significantly from other polar molecules.

**1. Introduction.**—The second virial coefficient of a polar gas can yield useful information about the forces acting between the molecules. Two methods, apparently very different, have been used to interpret such measurements. In this paper the method of Stockmayer is applied, with slight modification, to the observed values of the second virial coefficients for the nine polar gases for which reliable results are available, viz., water, ammonia, methyl alcohol, acetonitrile, acetaldehyde, acetone, methyl chloride, ethyl chloride, and chloroform. The results are com-

pared with the interpretation offered by Lambert, Roberts, Rowlinson, and Wilkinson<sup>1</sup> and by earlier authors.<sup>2, 3</sup>

The method of Stockmayer<sup>4</sup> is an exact treatment of the second virial coefficient of a gas composed of spherical molecules which attract according to the 6th power of their separation, repel according to the power  $s$ , and have, in addition, a point dipole at their centre. He used classical methods throughout but showed that quantum corrections were negligibly small. If this is a satisfactory model for the molecule in question, there is no doubt about the validity of his result. Stockmayer worked both with  $s$  infinite (hard-sphere model) and equal to 24. He fitted the experimental results for water and ammonia at relatively high temperatures to his expression for the virial coefficient. Hirschfelder, McClure and Weeks<sup>5</sup> repeated Stockmayer's calculations with the more usual value of  $s = 12$ , but also only for high temperatures. Before this treatment can be extended to the seven other gases considered here, Stockmayer's expression must first be evaluated for lower temperatures.  $s$  will be put equal to 12.

The second method of interpretation was originally applied by Alexander and Lambert to their results on acetaldehyde.<sup>3</sup> Here use is made of the experimental fact that the Berthelot equation appears to account for all the forces acting between molecules except the dipole-dipole forces. The difference between the observed virial coefficient and that calculated by the Berthelot equation is therefore ascribed to these forces, which are assumed to cause a small reversible dimerization which may be treated by the law of mass action. This treatment fails for acetone and methyl alcohol. A more detailed description has been given elsewhere,<sup>1</sup> and is further amplified below.

**2. Stockmayer's expression for the second virial coefficient.**—Stockmayer starts from the expression for the second virial coefficient given by statistical mechanics,

$$B = \frac{N}{4} \int_0^\infty \int_0^\pi \int_0^\pi \int_0^{2\pi} (1 - e^{-E/RT}) r^2 \cdot \sin \theta_1 \sin \theta_2 \cdot dr d\theta_1 d\theta_2 d\phi,$$

where  $E$  is the potential energy of two molecules (referred to  $E = 0$  at infinite separation). In general,  $E$  is a function of  $r$ , the distance of separation, of  $\theta_1$  and  $\theta_2$ , the angles made by the dipoles with the line joining their centres, and of  $\phi$ , the angle between the planes which pass through the line of centres and contain the two axes. For non-polar molecules it is usually assumed that  $E$  is so little dependent on orientation that an average value may be taken and the integration is performed for only one co-ordinate, the distance of separation. The triple integral over  $\theta_1$ ,  $\theta_2$  and  $\phi$  then becomes  $8\pi$ . This is not so for polar molecules, where  $E$  now depends so strongly on the mutual orientation that these co-ordinates must be considered separately. Following the method of Lennard-Jones, Stockmayer expands the integral as a series of  $F$ -functions, and gives an expression for  $B$  that reduces to the following when  $s = 12$ ,

$$B = \frac{2}{3} \pi N d^3 \cdot 2^{\frac{1}{2}} \theta^{-\frac{1}{2}} \left[ \Gamma\left(\frac{3}{2}\right) - \frac{1}{4} \sum_{n=1}^{\infty} \frac{2^n}{n!} \sum_{\kappa=0}^{n \leq n/2} \frac{\binom{n}{2\kappa} \Gamma\left(\frac{2n-2\kappa-1}{4}\right)}{2\kappa+1} \cdot \frac{G \cdot \Gamma(2\kappa)}{\theta^{(\eta+\kappa)/2}} \right], \quad (2.1)$$

where  $G = \sum_{m=0}^{\kappa} \frac{\binom{\kappa}{m} 3^m}{2m+1}$ , and  $\binom{\kappa}{m}$  etc. denote binomial coefficients.

<sup>1</sup> Lambert, Roberts, Rowlinson and Wilkinson, *Proc. Roy. Soc. A*, 1949, 196, 113. <sup>2</sup> Alexander and Lambert, *Trans. Faraday Soc.*, 1941, 37, 421.

<sup>3</sup> Schäfer and Foz Gazulla, *Z. physik. Chem. B*, 1942, 52, 299. Foz (Gazulla) and Vidal, *Anal. Fis. Quim.*, 1947, 43, 842.

<sup>4</sup> Stockmayer, *J. Chem. Physics*, 1941, 9, 398, 863.

<sup>5</sup> Hirschfelder, McClure and Weeks, *ibid.*, 1942, 10, 201.

$d$  is the collision diameter, defined as the distance of separation at which  $E$  would be zero in the absence of the dipole forces (cf. Fig. 1) ;

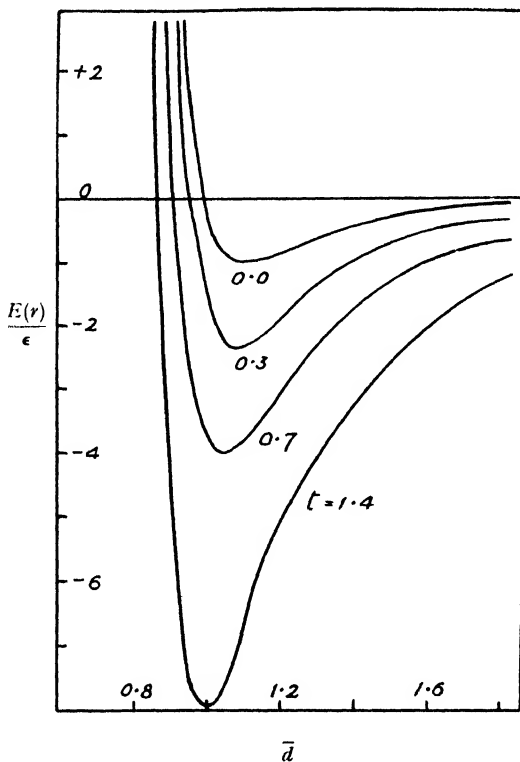


FIG. 1.—The energy of interaction of two molecules with the dipoles in the attractive end-on position, for different values of  $t$ , the reduced dipole energy as defined in eqn. (2.2). When  $t = 0$ , the minimum value of  $E(r)$  is  $-\epsilon$  and  $E(r) = 0$  when  $r$  (the distance of separation)  $= d$ .

$\theta$  is the “reduced temperature”, given by  $kT/\epsilon$ , where  $\epsilon$  would be the maximum energy of interaction in the absence of the dipole forces.

$t$  is a pure number which may be called the “reduced dipole energy”. It is defined by

$$t = 8^{-\frac{1}{2}} \cdot (\mu^2/\epsilon d^3), \quad (2.2)$$

where  $\mu$  is the dipole moment. It is a measure of the relative contribution to  $B$  of the dipole and non-polar forces, since it is the ratio of a dipole energy term ( $\mu^2/d^3$ ) to  $\epsilon$ . The factor  $8^{-\frac{1}{2}}$  is introduced solely for mathematical convenience.

Eqn. (2.1) may be written,

$$B = (2/3)\pi N d^3 \cdot F(\theta, t),$$

and before any use may be made of it,  $F(\theta, t)$  must be evaluated for all likely values of  $\theta$  and  $t$ . The only computation of this kind that exists, is that of Hirschfelder, McClure and Weeks,<sup>5</sup> which is confined to the range  $\theta > 1$ . The experimental results used in this paper require  $F(\theta, t)$  at much lower temperatures. Here, unfortunately, the series converge very slowly, but by taking 25 terms in the summation for  $n$ , it was possible to find  $F(\theta, t)$  for all reasonable values of  $t$  in the range  $0.3 < \theta \leq 2.0$ . The results are given in Table I, where the accuracy aimed at was 1 part in 1000. The figures for  $\theta > 1$  agree with the calculations of Hirschfelder, McClure and Weeks.

TABLE I.— $F(\theta, t)$ 

$\frac{t}{\theta}$	0.0	0.1	0.2	0.3	0.4	0.5	0.6	0.7	0.8	0.9	1.0	1.2	1.4
0.30	27.88	31.13	42.97	72.03									
0.35	18.75	20.35	25.88	38.07									
0.40	13.80	14.71	17.77	24.09	60.39								
0.45	10.75	11.34	13.24	16.98	35.92		58.75						
0.50	8.720	9.120	10.40	12.84	24.11		36.36	58.39					
0.55	7.275	7.564	8.479	10.18	17.53		24.92	37.28					
0.60	6.197	6.415	7.099	8.349	13.48		18.33	26.01					
0.70	4.710	4.840	5.267	6.018	8.897		11.39	15.05	58.76	59.74	41.80		
0.80	3.734	3.837	4.112	4.611	6.444		7.948	10.04	38.55	28.80	23.20	45.78	
0.90	3.047	3.114	3.319	3.675	4.943		5.946	7.293	20.50	17.15	14.93	26.30	50.27
1.00	2.538	2.589	2.744	3.010	3.940		4.657	5.595	12.98	11.50	10.54	17.18	29.77
1.20	1.836	1.868	1.965	2.131	2.695		3.115	3.647	6.820	5.154	6.204	9.201	14.11
1.40	1.376	1.398	1.465	1.578	1.958		2.235	2.580	4.316	3.519	4.147	5.839	8.380
1.60	1.052	1.068	1.117	1.200	1.474		1.671	1.913	2.207	2.559	2.978	4.009	5.616
1.80	0.8120	0.8245	0.8618	0.9250	1.133		1.280	1.461	1.677	1.934	2.236	3.002	4.047
2.00	0.6275	0.6374	0.6670	0.7167	0.8798		0.9951	1.135	1.302	1.498	1.726	2.296	3.052
$(v_0/d)^3$	1.414	1.352	1.300	1.257	1.220	1.187	1.158	1.132	1.109	1.087	1.068	1.033	1.002
$\Delta U/\epsilon$	0.000	0.409	0.837	1.279	1.736	2.207	2.690	3.184	3.689	4.204	4.730	5.807	6.920

**3. The Dipole Energy of Interaction.**—The two quantities which it will be most useful to calculate are the maximum value of the dipole energy of interaction and the equilibrium distance apart of the molecules. The attractive energy of two dipoles has its minimum value of  $-2\mu^2/r^3$  when the dipoles are in the end-on position. The total energy will then be given by

$$\frac{E(r)}{4\epsilon} = \left(\frac{d}{r}\right)^{12} - \left(\frac{d}{r}\right)^6 - i\sqrt{2} \cdot \left(\frac{d}{r}\right)^3. \quad (3.1)$$

Some of these curves are shown in Fig. 1. On putting  $\frac{dE(r)}{dr} = 0$ , a cubic equation in  $(d/r_0)^3$  is obtained, where  $r_0$  is the stationary value. This has only one real root if  $t > 2/\sqrt{27}$ , and it may be shown that it has only one real *positive* root if  $t < 2/\sqrt{27}$ . The real positive values of  $r_0$  are given by

$$\left(\frac{r_0}{d}\right)^3 = \frac{\sqrt{3}}{\sqrt{2}} \cdot \frac{\sec \phi}{\operatorname{sech} \phi}, \text{ where } \frac{\cos \phi}{\cosh 3\phi} = 2t/\sqrt{27}.$$

This equation was used to calculate the values of  $r_0$  in Table I. The maximum energy of interaction  $E_0$  is found by putting  $r = r_0$  in eqn. (3.1), which gives

$$E_0 = \frac{4}{3}\epsilon \cdot \frac{\cos \phi}{\cosh \phi} \left( \frac{\cos \phi}{\cosh \phi} + \frac{\cos 3\phi}{\cosh 3\phi} \right).$$

The *dipole* energy of interaction,  $\Delta U$ , given in Table I, is  $(E_0 - \epsilon)$ .

**4. Treatment of the Experimental Results.**—The three variable parameters in the expression for the virial coefficient are  $d$ ,  $\epsilon$  and  $t$ . The experimental facts that must be known to determine these are the absolute value of  $B$ , its variation with temperature, and the dipole moment. Two further tables were calculated from Table I (not reproduced). First, a table for  $H(\theta, t)$ , where  $H(\theta, t) \equiv (\theta/t) \cdot F(\theta, t)$ , and secondly a logarithmic difference table which gave the mean slope over each interval of

$$\log_{10} [-F(\theta, t)]/\log_{10} \theta.$$

From the definition of  $t$  (eqn. (2.2)), it follows that

$$\frac{B}{F(\theta, t)} = \frac{2}{3}\pi N d^3 = \frac{3231\mu^2\theta}{T \cdot t},$$

where  $B$  and  $Nd^3$  are measured in ml./mole,  $\mu$  in debye, and  $T$  in °K. Therefore,

$$\frac{BT}{3231\mu^2} = H(\theta, t).$$

The left-hand side of this equation contains only observable quantities and so can be evaluated from the experimental results. Values of  $H(\theta, t)$  compiled in this way were compared with the Table and a fit found for values of  $\theta$  and  $t$  so not only was  $H(\theta, t)$  correct, but also the slope of a plot of  $\log_{10} (-B)/\log_{10} T$  agreed with the value of

$$\log_{10} [-F(\theta, t)]/\log_{10} \theta.$$

In this way, the virial coefficients shown in Table II were calculated. The values chosen for the parameters, together with  $r_0$  and  $\Delta U$ , are shown in Table III. The experimental data for water and ammonia are taken from the equations of Keyes, quoted by Stockmayer.<sup>4</sup> The values for ammonia are confirmed by recent measurements in this laboratory by Mr. E. D. T. Strong. The results for methyl chloride are those quoted by Hirschfelder, McClure and Weeks.<sup>5</sup> Those for acetaldehyde are from the measurements of Alexander and Lambert,<sup>2</sup> and those for acetonitrile,

methyl alcohol, acetone, ethyl chloride and chloroform from the measurements of Lambert, Roberts, Rowlinson and Wilkinson.<sup>1</sup> The calculated values are very sensitive to the value used for the dipole moment. The figures used are shown in Table III.

TABLE II

(All values of  $B$  in ml./mole)

<i>Water</i>										
$T^{\circ}\text{C}$	.	40	70	100	150	200	300	400		
$-B$ (expt.)	.	976	638	450	284	197	112	72		
$-B$ (calc.)	.	980	635	460	290	202	115	74		
$-B$ (Berthelot)	.	421	348	292	223	175	114	77		
<i>Ammonia</i>										
$T^{\circ}\text{C}$	.	-30	0	30	60	100	150	200	250	
$-B$ (expt.)	.	560	367	261	197	143	103	77	59	
$-B$ (calc.)	.	560	370	265	195	145	105	78	60	
$-B$ (Berthelot)	.	327	255	203	165	127	94	71	54	
<i>Methyl Alcohol</i>										
$T^{\circ}\text{C}$	.	60	80	100	120					
$-B$ (expt.)	.	1220	1000	790	620					
$-B$ (calc.)	.	1270	980	760	590					
(The calc. value at 60° C depends on a small extrapolation.)										
<i>Acetonitrile</i>										
$T^{\circ}\text{C}$	.	50	70	90	110	130				
$-B$ (expt.)	.	4000	2840	2110	1690	1330				
$-B$ (calc.)	.	3760	2750	2160	1740	1410				
<i>Acetaldehyde</i>										
$T^{\circ}\text{C}$	.	15	20	25	30	35	40	70	100	165
$-B$ (expt.)	.	1460	1300	1230	1125	1050	960	770	540	320
$-B$ (calc.)	.	1410	1300	1210	1130	1050	980	730	530	320
<i>Acetone</i>										
$T^{\circ}\text{C}$	.	30	50	70	90	110	130			
$-B$ (expt.)	.	1800	1560	1280	1040	850	700			
$-B$ (calc.)	.	1900	1530	1230	1010	850	730			
<i>Methyl chloride</i>										
$T^{\circ}\text{C}$	.	-34	-23	-18	10	38	65	93	121	149
$-B$ (expt.)	.	764	668	637	500	401	320	265	214	184
$-B$ (calc.)	.	770	675	640	482	380	310	260	210	185
<i>Ethyl chloride</i>										
$T^{\circ}\text{C}$	.	50	70	90	110	130				
$-B$ (expt.)	.	580	510	450	390	350				
$-B$ (calc.)	.	560	500	450	410	370				
<i>Chloroform</i>										
$T^{\circ}\text{C}$	.	50	70	90	110					
$-B$ (expt.)	.	1000	840	730	630					
$-B$ (calc.)	.	1010	850	730	630					

For the nine compounds in Table II, the difference between the observed and calculated values of  $B$  in no case exceeds the experimental error. It is noticeable that the agreement is best for those substances where the data are most accurate and over the widest temperature range,



viz., water, ammonia, acetaldehyde and methyl chloride. The poorest agreement is found where the experimental results are least accurate, i.e. acetonitrile and methyl alcohol.

TABLE III

VALUES OF THE PARAMETERS USED TO CALCULATE  $B$  IN TABLE II

	$\mu$ debye	$t$	$\frac{1}{2}\pi N d^3$ ml./mole	$\epsilon$ cal./mole	$r_0$ Å	$\Delta U$ cal./mole
Chloroform .	1.05	0.1	33.45	2110	3.30	860
Ethyl chloride	2.02	0.2	199.7	640	5.41	530
Methyl chloride	1.89	0.6	50.73	750	3.60	2020
Acetone .	2.74	0.7	66.87	1030	3.91	3280
Methyl alcohol.	1.66	0.8	17.48	1200	2.49	4660
Ammonia .	1.47	1.0	22.12	630	2.66	2960
Water .	1.83	1.2	23.42	760	2.68	4440
Acetonitrile .	3.5	1.2	82.04	800	4.07	4640
Acetaldehyde .	2.7	1.4	62.75	530	3.68	3680

**5. Discussion.**—The constants of Table III give excellent agreement with the experimental results. Their significance will now be considered and they will be compared with the constants derived from the other interpretation that has been proposed for the same results.

The parameter  $t$ , the effective polarity of the molecule, is found to increase in a very reasonable manner from the halides to those molecules commonly regarded as highly polar. The values given for  $\epsilon$ , the non-polar energy of interaction, have little significance for two reasons. Firstly, they will include a term for the polarization of one molecule by the dipole of another (also proportional to  $r^{-6}$ ), which London estimates<sup>6</sup> to be about 20 % of  $\epsilon$  for water and 10 % for ammonia. Secondly, a much more serious source of error will be the fact that when  $t > 0.6$  the dipole energy is so large compared with  $\epsilon$  (Fig. 1) that any effect of the non-polar forces on the virial coefficient will be masked, and so  $\epsilon$  will be more subject to error.

The two quantities that have most significance are  $r_0$ , the equilibrium separation of the molecules, and  $\Delta U$ , the maximum value of the dipole-dipole energy of interaction. For non-polar molecules,  $r_0$  and  $d$  have a constant ratio and each is proportional to the actual physical space occupied by the molecule. This will not be so for polar molecules. When the interaction energy is due largely to the dipoles, then  $r_0$  will be determined not so much by the size of the molecules as by the equilibrium separation of the *dipoles*. If the model chosen were perfectly correct then this would make no difference, for the dipoles are supposed to be at the centre of the molecules. But if data for molecules whose dipoles are not symmetrically arranged (e.g. methyl alcohol), are fitted to  $F(\theta, t)$ , then the more correct interpretation of  $r_0$  is as the equilibrium separation of the dipoles. From this point of view, the results in Table III are particularly illuminating. Much of the lowest values of  $r_0$  are those for methyl alcohol (2.49 Å), ammonia (2.66 Å) and water (2.68 Å), which are the three molecules that would be expected to show hydrogen bonding. These are the distances between the centres of the dipoles and so are slightly less than the O—H . . . O and N—H . . . N distances found in the solid state. On this model the hydrogen bond would be interpreted as an interaction between two dipoles at unusually short distances, which are possible only when the electron density is a minimum near the hydrogen atom. The bonds in water and methyl alcohol have almost the same energy. Chloroform (3.30 Å) has the next largest value of  $r_0$ . Here

<sup>6</sup> London, *Trans. Faraday Soc.*, 1937, **33**, 8.

again the dipole will cause a fall of electron density around the hydrogen atom. The chance of forming hydrogen bonds will be much reduced as  $\Delta U$  is so small (860 cal./mole). Although methyl chloride is a smaller molecule, the value of  $r_0$  (3.60 Å) is larger than for chloroform, as would be expected, since the charge on any one hydrogen atom is now much reduced. The two molecules with carbonyl groups, acetaldehyde and acetone, show similar values for both  $r_0$  (3.68, 3.91 Å) and for  $\Delta U$  (3680, 3280 cal./mole). This would suggest that the association in both is of the same kind, and would not support the hydrogen-bonded ring structure that has been proposed for the former. Nevertheless, it is the increased positive charge and exposure of the hydrogen atom in an aldehyde group that causes  $r_0$  to be slightly lower for acetaldehyde. In acetonitrile it is the very large dipole moment, rather than close interaction, that leads to the large value of  $\Delta U$ .

#### 6. The dipole association treated by the law of mass action.—

The second virial coefficient is an equilibrium property of a gas. Properly interpreted, it will give information about the possible energies of interaction of two molecules and the chance of the molecules assuming the necessary configuration. No information is obtained about the length of time two molecules spend in association before they separate again,

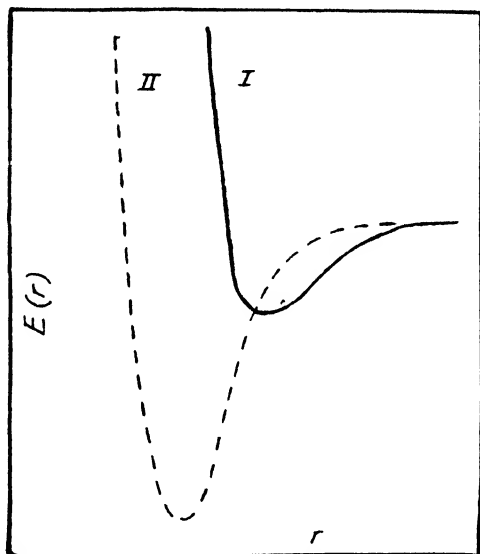


FIG. 2.

for that is a rate process, which cannot be investigated without going outside the equilibrium properties and measuring some dynamical property such as the thermal conductivity. It is true that the treatment of the dipole association by the law of mass action has been used in cases where it has been thought that dimers of long life have been formed (see especially Schäfer and Foz Gazulla<sup>3</sup>), but this is not a necessary restriction. In general, it is not correct to divide the second virial coefficient into two parts and say that each represents a different kind of interaction, but such a procedure is quite sound in certain circumstances. In the present case the restrictive condition is that the dipole forces are only effective in configurations for which the non-polar energy is negligible. This may easily arise with asymmetric molecules, as shown schematically in Fig. 2. Here the full line (I) represents the non-polar energy of interaction which gives rise to one part of the virial coefficient. However, when the dipoles are not at the centres of the molecules it is possible that,

for certain mutual orientations, they can approach much more closely, giving rise to the interaction curve shown by the dotted line (II). In this case it is allowable to represent the dipole interaction by an additional term in the virial coefficient. An equilibrium constant may be used for this term, when the energy factor will represent the depth of the trough and the entropy factor the restrictions imposed on the mutual orientations for the interaction to follow curve II rather than curve I.

The value of the virial coefficient given by the Berthelot equation is used to represent the non-polar forces. This is justified by the excellent agreement of the observed values with the Berthelot equation for non-polar molecules<sup>1</sup> and for water and ammonia at high temperatures (see Table II). For the other gases, measurements have not been taken to high enough temperatures to decide unambiguously whether the virial coefficient is approaching the Berthelot value, but the published diagrams<sup>1</sup> show that the behaviour of water and ammonia is probably typical. It is satisfactory to find that the values of the equilibrium constants given below would lead to only 7.8 % of dimerization for water and ammonia at the critical point, indicating that  $T_c$  and  $p_c$ , which are used to calculate  $B$  from Berthelot's equation, will not be greatly affected by the supposed dimerization.

In the treatment given in the first part of this paper, the important quantities were the maximum energy of interaction  $\Delta U$  and the equilibrium distance of separation  $r_0$ . If the law of mass action is used then the important quantities will be  $\Delta U$  and the standard entropy of association  $\Delta S^\circ$ . The equilibrium constant for the association is given by<sup>1</sup>

$$B(\text{expt.}) - B(\text{Berthelot}) = -RT/K_p.$$

As there are now only two adjustable parameters ( $\Delta U$  and  $\Delta S^\circ$ ) this equation does not always fit the experimental results as well as Stockmayer's expression. It will, however, give values of  $B$  that agree fairly closely with the observed values if  $K_p$  is given by:

Acetonitrile . . . . .	$\log_{10} K_p = 4.505 - 1147/T$
Methyl chloride . . . . .	$\log_{10} K_p = 4.533 - 555/T$
Acetaldehyde . . . . .	$\log_{10} K_p = 4.871 - 986/T$
Water . . . . .	$\log_{10} K_p = 5.650 - 1250/T$
Ammonia . . . . .	$\log_{10} K_p = 5.809 - 967/T$

( $K_p$  in atm.)

For chloroform and ethyl chloride ( $t = 0.1$  and  $0.2$ ), the difference between the observed and Berthelot values for  $B$  is negligible. An equation of this kind will not represent the results for acetone and methyl alcohol.<sup>1</sup> The values for acetonitrile and acetaldehyde are those given previously.<sup>1</sup> The Berthelot equations for the other three gases were calculated from the following values of the critical constants:

Methyl chloride . . . . .	$T_c = 143.1^\circ \text{C}$	$p_c = 65.9 \text{ atm.}$
Water . . . . .	$T_c = 374.2^\circ \text{C}$	$p_c = 218.5 \text{ atm.}$
Ammonia . . . . .	$T_c = 132.5^\circ \text{C}$	$p_c = 112.3 \text{ atm.}$

The energy of interaction at  $100^\circ \text{C}$  ( $\Delta U_{273}$ ) and the standard entropy of association ( $\Delta S^\circ$ ) have been calculated from  $K_p$ .

TABLE IV

	$\Delta U_{273}$	$U$ (§ 4)	$\Delta S^\circ$ (expt.)	$\Delta S^\circ$ (calc.)	Diff.
	cal./mole		cal./mole deg.		
Acetonitrile . . . . .	4500	4640	20.6	21.4	+ 0.8
Methyl chloride . . . . .	2390	2020	20.7	22.1	+ 1.4
Acetaldehyde . . . . .	3790	3680	22.3	21.9	- 0.4
Water . . . . .	4980	4440	25.8	22.2	- 3.6
Ammonia . . . . .	3680	2960	26.8	22.1	- 4.7

In the second column of Table IV are the values of  $\Delta U$  found above by Stockmayer's method. They are generally smaller than  $\Delta U_{\text{exp}}$ , though the difference is not large. The values found for the entropy of association (third column) are compared with those calculated from a very simple model (fourth column). If it is assumed that the dipole association will not affect the internal vibrations of each molecule, then the entropy of association will be the following product of partition functions,

$$\frac{{}_1f_T \cdot {}_1f_R \cdot 2}{{}_2f_T \cdot {}_2f_R \cdot {}_2f_V}$$

where the numerical subscripts denote monomer and dimer, and  $T$ ,  $R$  and  $V$  stand for the translational, rotational and vibrational partition functions. The symmetry of the dimer is 2. To proceed further it is necessary to make some drastic approximations. A comparison of the observed and calculated  $\Delta S^0$  will then show how sound these are. Firstly, it will be assumed that  ${}_2f_R$  for the rotation of the whole dimer about the axis of the "dipole bond" may be cancelled with one of the  ${}_1f_R$  of the numerator. Secondly, the dipole bond will be assumed to be completely stiff in compression or tension (one of the  ${}_2f_V = 1$ ), but so little resistant to deformation that the remaining five  ${}_2f_V$  may be cancelled with the five  ${}_1f_R$  of the numerator. These last assumptions will both be wrong, but the errors they introduce will be in the opposite directions. The product of partition functions is now reduced to that for the association of two atoms to form a rigid molecule, where  $\Delta S^0$  depends only on the masses and the internuclear distance. The calculated values of  $\Delta S^0$  were obtained in this way, by using the usual expression for the partition functions<sup>7</sup> and values of  $r_0$  from Table III for the distance of separation, and correcting for the difference between expressions at constant pressure and constant volume. It can be seen at once that the agreement between the observed and calculated values is surprisingly good, in view of the crudity of the partition functions. The differences that remain may throw some light on the structure of the dimers. For methyl chloride, the calculated  $\Delta S^0$  is too high. Probably the  ${}_2f_V$  for the stretching of the dipole bond is here very much greater than 1, as the bond is very weak (2400 cal./mole). The agreement is good for acetonitrile and acetaldehyde. Here there must be a satisfactory cancellation of errors in the assumptions made about the rigidity of the dipole bond. The calculated values for water and ammonia are too low, showing that, here again, there is a quantitative difference of behaviour between those molecules that can form hydrogen bonds and those that cannot. The difference here is an increased entropy of formation of the dimer, which implies a more rigid structure with less relative motion of the component molecules. It is satisfactory that the results for these gases should confirm the conclusions drawn from Trouton constants concerning entropies of association of polar molecules, where ability to form a hydrogen bond is a much more potent factor than mere polarity.<sup>8</sup>

**7. Conclusion.**—It has been shown that the two methods of interpreting the virial coefficient results are both useful in elucidating the nature of dipole forces. In particular, it is found that molecules where hydrogen bonding is possible (water, ammonia, and methyl alcohol) behave as other polar molecules but that their association is characterized

<sup>7</sup> Fowler and Guggenheim, *Statistical Thermodynamics* (C.U.P., 1939), pp. 165-7.

<sup>8</sup> Hildebrand, *Proc. Phys. Soc.*, 1944, **56**, 221.

by unusually short dipole-dipole distances and unusually large entropies of association. The hydrogen bond strengths found are:  $\text{O}-\text{H} \dots \text{O}$ , 4440 or 4980 cal./mole in water, and 4640 cal./mole in methyl alcohol;  $\text{N}-\text{H} \dots \text{N}$  2960 or 3680 cal./mole in ammonia.

I would like to thank Mr. J. D. Lambert, Mr. R. P. Bell and Prof. E. A. Guggenheim for most helpful discussions.

*Physical Chemistry Laboratory,  
Oxford.*

## REVIEWS OF BOOKS

**Niels Bjerrum, Selected Papers Edited on the Occasion of his 70th Birthday.** (Munksgaard, Copenhagen, 1949). Pp. 295. Kr. 18.

Niels Bjerrum was born on 11th March, 1879. His seventieth birthday has been celebrated by his colleagues in Copenhagen by the publication in English of this collected edition of some of his most important papers. This publication was made possible by generous support from various Danish scientific societies and industrial concerns, to whom physical chemists throughout the world will be grateful. The translations into English were done by members of the editorial committee, all Danes, and the result is remarkably good. There is a foreword by the chairman of the editorial committee, Niels Bohr.

Niels Bjerrum is recognized as one of the great masters of physical chemistry; in my opinion he is the greatest of his generation. Note that I am speaking of physical chemistry, not of any one or more particular specialized branches of the subject. Those of us who have had the privilege of working in Bjerrum's laboratory know, as some others less fortunate may not know, the exceptional width and depth of his grasp of physical chemistry. His original contributions extend from the colloid chemistry of soils and brewing to applications of quantum theory and statistical mechanics. But, the most amazing feature brought to light by this collection of papers is that this exceptional versatility had already been revealed before Bjerrum was thirty-five. Let me give a few examples.

In the period 1906-1908 Bjerrum was determining the structure of various chromium complexes, incidentally discovering how to make monochlorochromic dichloride, correcting a mistaken view of Werner on the structure of monochlorochromic sulphate and measuring hydrogen ion concentrations before the expression pH had yet been invented by Sørensen.

In 1909 at the London meeting of the International Union of Chemistry, Bjerrum produced experimental evidence, which now seems indisputable, that in dilute aqueous solution salts are completely dissociated into ions. It is well known how Debye in 1923 obtained satisfactory quantitative formulae for the effect of the interionic forces and so finally proved the non-existence of any "anomaly of strong electrolytes". The earlier history of this subject is much less well known and I take this opportunity to throw light on the matter by a few quotations, which I give in inverse chronological order.

Milner, *Phil. Mag.*, 1913, **25**, 743: ". . . can be completely accounted for by the effect of the interionic forces . . . on the assumption that the dissociation is complete."

Noyes and Falk, *J. Amer. Chem. Soc.*, 1912, **34**, 489: "There appears however, to be no chemical explanation which would account for both these anomalies; and it seems therefore probable that physical deviations must enter as a complicating factor."

G. N. Lewis, *Z. physik. Chem.*, 1910, **70**, 215, 218: "*If we had no other criterion\** for the degree of dissociation, these facts would undoubtedly lead us to regard salts, up to a concentration of normal or half normal as completely dissociated. . . . I believe that we shall make no great error in assuming that the degree of dissociation calculated from the conductivities is in most cases substantially correct."

Bjerrum, *Proc. 7th Inter. Cong. Pure Applied Chem.* (London, 1909), § x, p. 56: "We suppose that the strong electrolytes always are completely separated into ions, and this is the reason why they always have the same colour in all concentrations. . . . the decrease in molecular conductivity and in molecular depression of the freezing-point that accompanies the increase in concentration must be due to the action of the electric charges of the ions on each other."

So much for Bjerrum in 1909. In 1911 he published a joint paper with Perrin on measurements of Brownian movement connected with the determination of Avogadro's number. In the same year he was making the first application of quantum theory to the specific heat of gases and in 1912 was doing pioneer work on the quantal interpretation of infra-red spectra.

The period 1916-1920 was largely devoted to the application of thermodynamics to electrolyte solutions. In 1923 came the revolutionary, but convincing argument that the form of an amino-acid, such as glycine, having zero net charge is a zwitter-ion  $\text{NH}_2^+ \cdot \text{CH}_2 \cdot \text{CO}_2^-$ . This period also included theoretical work on the effect of electric charge on acid constants.

It would take too much space to refer in any detail to the more recent work. Suffice it to say that out of nearly a hundred published papers twenty seven are included in this collection. Although several important papers have been omitted, the choice is admirable as every paper included, without exception, makes interesting reading. Apart from several papers of fundamental importance and others of great historical importance, I would call attention to the especial usefulness of two papers for teaching purposes, namely a paper "On Acid and Basic Reaction" (1917), and another, "Acids, Salts and Bases" (1931). The former contains the most complete, accurate and clear treatment of acid-base titration with indicators.

No one worthy of the designation physical chemist can fail to find palatable food for thought somewhere in this excellently varied menu.

E. A. G.

\* The italics are mine. Confusion has been increased by a misquotation of this sentence in one of the best introductory textbooks on physical chemistry.

**Tables of Scattering Functions for Spherical Particles.** (National Bureau of Standards, Applied Mathematics Series, 4. Washington, D.C., 1948.) Price 45 cents.

The scattering of a plane wave by spherical particles is a phenomenon found in almost every branch of physics, chemistry and even biology. Here are some numerical Tables that will certainly prove useful to workers actually using observed scattering intensities to estimate the size of particles with which they are concerned.

These Tables are based on Mie's theory of the scattering of light by particles with a radius comparable in magnitude with the wavelength of light. They give the angular distribution of intensity and the total light scattered by a small, spherical particle—such as a fog droplet—in terms of size of particle and wavelength of the incident light. Thus the Tables permit both the concentration and diameter of spherical particles in suspension to be determined from measurements of the attenuation of an incident beam due to scattering, provided the particles are of uniform size.

The first of the four parts of the Tables gives the angular distribution of the intensities of the two incoherent, plane-polarized components scattered by a transparent particle illuminated with natural light. In Part II the total scattering coefficient is given for a transparent material of refractive index 1.5. In Part III the total scattering (and absorbing) coefficient, may be obtained for absorbing materials of extinction coefficient varying from 0 to 0.1, and of real refractive index varying from 1.44 to 1.55. In Part IV the Tables have been extended to certain values of complex arguments for a problem in the application of microwave radar in the wavelength region in the order of 10 cm. and shorter, where a dispersion by liquid water sets in, making the index of refraction complex and a function of wavelength.

These Tables are beautifully got up and all the figures are extremely clear. We have to thank the National Bureau of Standards for subsidizing publications like this so that the price is only a few shillings. Why can we not do things like this in Britain?

C. A. C.

**Klockmann's Lehrbuch der Mineralogie.** By P. RAMDOHR. 13th ed. (F. Enke Verlag, Stuttgart, 1948). Pp. xii + 674. Price 50 German marks.

This new edition of a well-known German textbook on mineralogy incorporates the substantial increase in exact knowledge won during the last two decades by the application of recent techniques, particularly X-ray diffraction and the study of polished ores by reflected polarized light. The author himself has made extensive studies of minerals by this last technique and no-one is more capable than he of proceeding beyond determinative mineralogy to the wider aspects of mineral chemistry, mineral paragenesis, geochemistry, and the evolution of rock types. The first part of the book on general mineralogy includes sections on the physical properties of minerals: crystal form, crystal structure and

mineral physics (including optical and other physical characters), a section on mineral chemistry and crystal chemistry (including lists of blowpipe and microchemical reactions), an account of mineral formation, mineral deposits and paragenesis with an alphabetical list of well-known mineral localities illustrating the more familiar types of mineral association and finally a brief section on the technical and ornamental uses of minerals. The second and larger part of the book gives a systematic and well-illustrated description of minerals classified as follows :

I. Elements ; II. Sulphides ; III. Halogen salts ; IV. Oxides and hydroxides (including quartz and its polymorphs) ; V. Oxygen salts with oxygen in three-fold co-ordination (nitrates, iodates, carbonates and borates) ; VI. Sulphates, chromates, molybdates and tungstates ; VII. Phosphates, arsenates and vanadates ; VIII. Silicates ; IX. Organic compounds.

The arrangement within each class follows closely on what is known so far of the crystal structure as well as the chemical nature of each species. Unnecessary mineral names and synonyms are listed together with those minerals whose classification still remains doubtful.

F. A. B.

**A Survey of General and Applied Rheology.** By G. W. SCOTT BLAIR.  
(Pitman, London, 1949.) Pp. xv + 314. Price 40s.

The new edition (1st edition, 1943 ; 2nd edition, 1949) enhanced by a comprehensive survey of recent advances by rheologists in different fields of science and of the results of war investigations released by the Services, will be of great value to those who wish to be informed on the latest ideas on the nature of viscosity, plastic flow, thixotropy, etc. The book is especially useful to industrial research workers who deal with plastic masses, doughs and pastes, bituminous or rubber mixes, adhesives, greases or thickened liquids and need information on the measurement or control of the rheological properties.

The book has been written from a new angle, and 20 pages are given to the evidence, of psycho-physics ; there is also a section on *gestalt* psychology and the non-Newtonian time-scale. The conclusions of the "analytical school" which notes deviations from the classical laws, as Trouton did in his study of the flow of pitch and of the "integrative school" which regards the properties of complex materials as intermediate between those of fluid and solid and is obliged to forego the advantage of dimensionally simple rheological properties, are presented succinctly together with the principles of rheological measurement from the time of Galileo (1638), Hooke (1676), and Newton (1687), when modern rheology began.

The author has included the modern concepts on the superfluidity of helium II, high elasticity, spinnbarkeit, stress hardening, etc., and direction is given where to find original papers ; also included are summaries of rheological papers on special subjects (20 pages) and a bibliography (30 pages). There are four important chapters (60 pages) in which are listed and described a wide range of industrial methods and



instruments used in practice for control of manufacture and in general research. Dr. Scott Blair distinguishes between empirical tests and fundamental measurements and wisely indicates that results from *ad hoc* instruments should be interpreted with considerable care.

There is an interesting chapter on orientation and surface phenomena dealing with mesomorphism, the smectic and nematic states, the sigma phenomenon and the rheological properties of thin films; this should be of help to the lubricant technologist and students of surface chemistry.

The book is an excellent guide when information is required on problems of anomalous flow behaviour not explicable by hydrodynamics or the classical laws.

E. W. J. M.

# STUDIES IN HYDROGEN OVERPOTENTIAL

## THE EFFECT OF CATALYTIC POISONS AT PLATINIZED PLATINUM AND NICKEL

BY J. O'M. BOCKRIS AND B. E. CONWAY

*Received 3rd May, 1949*

The effect of As (as  $\text{As}_2\text{O}_3$  in HCl) on H overpotential set up at platinized platinum electrodes has been examined. The effect of the presence in solution of traces of  $\text{As}_2\text{O}_3$ , CO,  $\text{CS}_2$ , KCN and  $\text{PtCl}_4$  on the rate of the hydrogen evolution reaction at a Ni cathode has been determined. Negative deviations from the Tafel equation at higher current densities were not observed in pure solutions but were produced by the presence of traces of poison ( $\text{As}_2\text{O}_3$ ).

At high (0.1 M) concentration of  $\text{As}_2\text{O}_3$  a limiting current occurs at about  $3 \times 10^{-3}$  A/cm.<sup>2</sup> in N aqueous HCl solution.

The variation of hydrogen overpotential with time at constant c.d. is negligible at platinized platinum and Ni electrodes in the absence of impurities but is considerable, erratic and of long duration in the presence of traces of impurities. This variation in impure solution can be considerably reduced by pre-electrolysis of the solutions used. Impurities at concentrations of the order of  $10^{-10}$  mole/l. affect the rate of the hydrogen evolution reaction on Ni cathodes at a given overpotential. The effect of these poisons is experimentally analogous in a number of respects to poison effects in heterogeneous catalysis.

Although the general direction of the effects of catalytic poisons on overpotential has been established <sup>1, 2, 3, 6, 7, 8</sup> little information concerning the dependence of the effect upon poison concentration is available and in particular no determination of the theoretically important critical low concentration limit for poisoning has been made. The latter determination is of importance in relating the overpotential behaviour of metals to their catalytic power for H atom recombination, or for adsorption of atomic hydrogen, and also in assessing the necessity for ultra-purification <sup>9-13</sup> of solutions.

In this paper, therefore, an investigation of the nature of the dependence of the poison effect upon poison concentration and the determination of the lower limiting concentration for the onset of poisoning of an electrode by a series of catalytic poisons is reported.

<sup>1</sup> Bockris, *Chem. Rev.*, 1948, **3**, 525.

<sup>2</sup> Bowden and Agar, *Ann. Reports*, 1938, 63.

<sup>3</sup> Volmer and Wick, *Z. physik. Chem. A*, 1935, **171**, 429.

<sup>4</sup> Aten and Zieren, *Rec. trav. chim.*, 1929, **48**, 984.

<sup>5</sup> Aten and Zieren, *ibid.*, 1930, **49**, 641.

<sup>6</sup> Raeder and Nilson, *Norges Tek. Hiskole, Anh. til. 25 Jub.* 1935, 263.

<sup>7</sup> Kobosew and Nekrassov, *Z. Elektrochem.*, 1930, **36**, 519.

<sup>8</sup> Hickling and Salt, *Trans. Faraday Soc.*, 1941, **37**, 333.

<sup>9</sup> Bockris and Conway (in press).

<sup>10</sup> Bockris, Azzam, Conway and Parsons (in course of publication).

<sup>11</sup> Lewis and Jackson, *Z. physik. Chem.*, 1906, **56**, 1207.

<sup>12</sup> Schroeder, *Ann. Physik*, 1909, **29**, 125.

<sup>13</sup> Jaffe, *Ann. Physik*, 1909, **28**, 326.

## Experimental

**POISONING OF PLATINIZED PLATINUM BY ARSENIC.**—For apparatus and experimental technique, see previously.<sup>14</sup> Platinized platinum test electrodes, 2 cm.<sup>2</sup> in area and reference electrodes were prepared by the method of Ellis.<sup>16</sup>

For the determination of hydrogen overpotential in the presence of arsenic oxide the electrolyte of N HCl was made by dissolving As<sub>2</sub>O<sub>3</sub> in N HCl prepared (cp. <sup>14</sup>) but before transference of the electrolyte to the cell was made. The electrolyte in the reference electrode vessel was aqueous N HCl. Diffusion of poison to this electrode was prevented by closing the tap of the electrode vessel.

Overpotential measurements were made by the direct method.

Potential measurements were accurate to  $\pm 2$  mV and polarizing current could be measured to within  $\pm 2$  %. The measurements of apparent electrode areas were accurate to  $\pm 5$  %.

**POISONING OF THE Ni ELECTRODE BY AS, CS<sub>2</sub>, CO, KCN AND ITS ACTIVATION BY Pt.**—The most satisfactory procedure for establishing the lower concentration limit for the onset of poisoning would involve establishing a constant overpotential or a constant trend of overpotential with time, and adding quantities of poison solution until this caused a significant change in the behaviour. Accordingly, the time variation of overpotential at nickel electrode at a fixed current density was investigated first in pure solutions. Since it was intended to study very low concentrations of additives it was necessary rigorously to purify all solutions by pre-electrolysis<sup>9, 10, 11</sup> and stringent deoxygenation of cells and solution.

The cell used was an all-glass three-compartment type (described elsewhere<sup>1</sup>) equipped with ground-glass water-sealed taps and joints.

Conductivity water was first heated to the boiling point in an all-glass apparatus passing through which was a rapid stream of hydrogen and refluxed in a slower stream of hydrogen for 5 hr. 50 ml. water were then withdrawn and rejected. Water of conductivity  $5.8 \times 10^{-7}$  mhos was then distilled into the anode compartment of the cell.

Hydrochloric acid gas (prepared from A.R. sulphuric acid and A.R. ammonium chloride) was passed through a trap to eliminate spray, a tube of calcium chloride and finally two glass spirals cooled to  $-80^\circ\text{C}$ . The gas mixed with hydrogen was then passed into the water in the anode compartment of the cell until electrolyte of required concentration (determined conductometrically by means of the two platinum points in the anode compartment of the cell) was obtained. This solution was then pre-electrolyzed.

Electrolytic hydrogen was led into the train via a special trap\* through Telcothene plastic tubing. The latter was used owing to possible contamination of hydrogen with sulphurous compounds from rubber. The gas was dried over silica gel and magnesium perchlorate, and passed through a tube of Hopcalite for removal of traces of CO by catalytic oxidation to CO<sub>2</sub> by the trace of O<sub>2</sub> present in the H<sub>2</sub>. The CO<sub>2</sub> formed was removed by passage through a tube of soda-lime and the H<sub>2</sub> was then passed through a furnace containing 5 % palladized asbestos maintained at  $450^\circ\text{C}$  to effect complete deoxygenation, and dried by passage through several liquid nitrogen traps containing alternately glass wool and charcoal.<sup>16</sup> The train was of Hysil glass to avoid contamination of hydrogen by arsenic compounds from Pyrex glass.

Nickel electrodes 0.4 cm.<sup>2</sup> in area (Hilger spectroscopically pure) were heat treated and annealed in hydrogen at  $600^\circ\text{C}$  and sealed into glass bulbs in an hydrogen atmosphere.<sup>17</sup> These electrodes were kept in the cell during pre-electrolysis until breakage<sup>16, 17</sup> of the bulb when the polarization was commenced.

**THE OVERPOTENTIAL-TIME BEHAVIOUR AT  $10^{-3}$  A/CM.<sup>2</sup> IN ULTRA-PURE 0.1 N HCl.**—In preliminary experiments the maximum pre-electrolysis at a Pt auxiliary cathode, consistent with a change of concentration of HCl not greater than 10 % was used, i.e. electrolysis at  $3 \times 10^{-3}$  A for 15 hr. The time variation of overpotential was no longer erratic (see Fig. 1 and 2) as in experiments with no, or less, pre-electrolysis, but still showed steady slow increase of overpotential during 6-10 hr., which behaviour was unsuitable for study of trace additions of poisons (see Fig. 1).

<sup>14</sup> Bockris, *Trans. Faraday Soc.*, 1947, **43**, 417.

<sup>15</sup> Ellis, *J. Amer. Chem. Soc.*, 1916, **38**, 737.

\* A mercury blow-off safety valve (see Conway, *Thesis* (London, 1949)).

<sup>16</sup> Bockris and Conway (in press).

<sup>17</sup> Bockris and Conway, *J. Sci. Instr.*, 1948.

Increase of the strength of the pre-electrolyzing current to  $4 \times 10^{-3}$  A for 15-17 hr. led to an important result. The protracted time variation was eliminated and a slow build-up, lasting  $\frac{1}{2}$ -2 hr. to a value constant (i.e. variation less than 20 mV) for more than 12 hr. was observed. An initial solution of 0.3 N in strength was used which during electrolysis became diluted to 0.1 N in 17 hr.

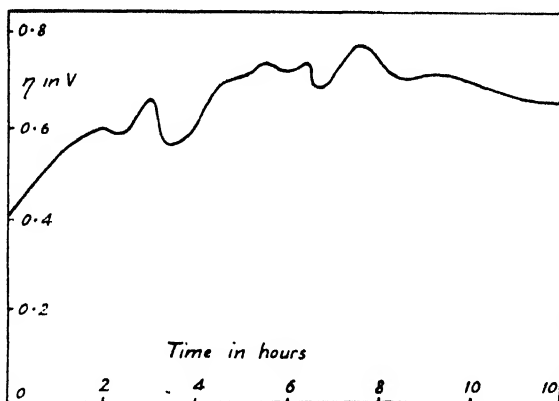


FIG. 1.—Typical time variation of  $\eta$  at Ni cathode in 0.1 N HCl at  $10^{-2}$  A/sq. cm. in simple cell with no pre-electrolysis.

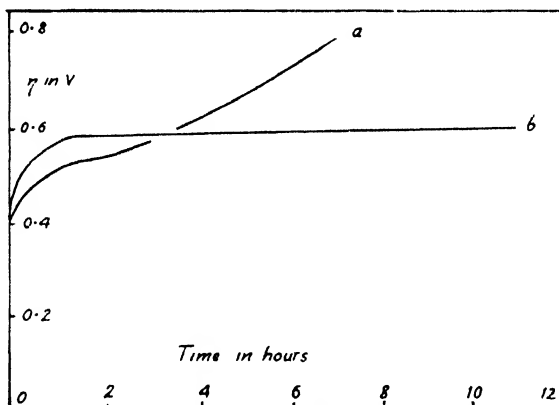


FIG. 2.—Time variation of  $\eta$  at Ni at  $10^{-2}$  A/sq. cm. in all-glass cell. Effect of pre-electrolysis:

- (a) At  $2 \times 10^{-3}$  A/sq. cm. for 12 hr.
- (b) At  $6 \times 10^{-3}$  A/sq. cm. for 15 hr.

.. 4

The constancy of overpotential with time (see Fig. 2) under these conditions was reproducible but the period of initial build-up varied from 30 to 120 min. and although the initial potential was reproducible the final constant overpotential was less reproducible. This accounts for the smaller reproducibility of overpotential values obtained by the slow or resting methods.<sup>10</sup>

Having thus obtained a constancy of overpotential with time at  $10^{-2}$  A/cm.<sup>2</sup>, poison concentrations of  $10^{-15}$ - $10^{-3}$  mole/l. were introduced successively into the solution. The poison solutions had been previously subjected to an analogous purification to that of the main electrolyte.

Before poison additions were made complete blank experiments on solutions containing no poison were carried out. No significant effects of the blank solutions were observed. In the poison experiments a blank of 50 drops (2 ml.)

of the pre-electrolyzed HCl solution, before poison had been added, was added to the catholyte to check in each experiment the initial purity of the basic solution.

The following poisons were used:  $\text{As}_2\text{O}_3$ ,  $\text{CS}_2$ , KCN, CO and also the activator (cf. <sup>18, 19</sup>)  $\text{H}_2\text{I}^+\text{tCl}_6$ .

### Results

**Poisoning of Pt by As.**—The  $\eta$ -log  $i$  relationship for the polarization of platinized platinum in N HCl in the presence of As concentrations zero, 0.0001, 0.0002, 0.001, 0.005, 0.02, 0.1 and 0.2 mole/l., are shown in Fig. 3. The curve

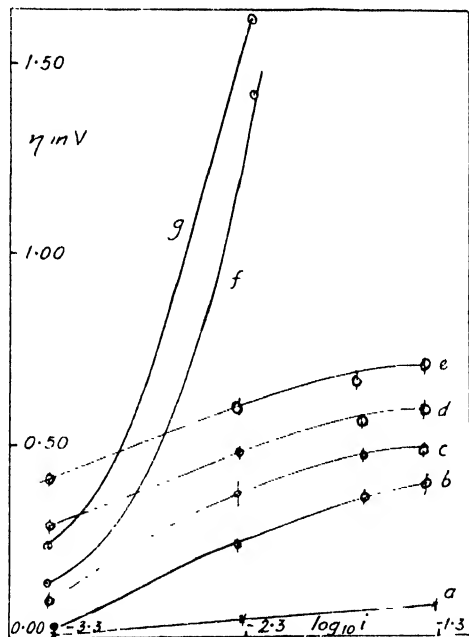


FIG. 3.— $\eta$ - $\log_{10} i$  curves for platinized platinum. Effect of poisoning by  $\text{As}_2\text{O}_3$  in N HCl. (a) Pure, (b) 0.0001 M, (c) 0.0002 M, (d) 0.0005 M, (e) 0.02 M, (f) 0.1 M, (g) 0.2 M.

for platinized platinum in pure solution is linear with a slope  $b$  of 0.03. In the solution with lowest arsenic concentration, a rise in the  $\eta$ -log  $i$  line occurs and the slope between  $10^{-2}$  and  $10^{-3}$  increases to  $b = 0.20$ . At high c.d.'s (c.d.  $\equiv$  current density) of  $10^{-2}$  to  $5 \times 10^{-2}$  A/cm.<sup>2</sup> the overpotential approaches a constant limiting value. At higher As concentrations 0.0002-0.005 M, a steady increase of overpotential at a given c.d. occurs and the initial slopes of the lines are slightly lower ( $b = 0.17$ ) than those in solutions with less poison.

In 0.1 M and 0.2 M solutions of  $\text{As}_2\text{O}_3$  the character of the  $\eta$ -log  $i$  relation is radically different. It shows large deviations from the Tafel equation towards more negative potentials whilst in As solutions an approach to a limiting current in the region  $i = 10^{-2}$  A/cm.<sup>2</sup> is observed. At low c.d. the overpotential in 0.1 and 0.2 M solutions is lower than that for corresponding c.d.'s in 0.001, 0.005 and 0.02 M As solution.

If the overpotential at a given c.d. is plotted against molar concentration of arsenic (Fig. 4) curves similar to adsorption isotherms are obtained. At concentrations of arsenic between 10 and  $50 \times 10^{-4}$  mole/l. the  $\eta$ -concentration graphs are linear with approximately the same slope for each c.d. The poison is seen to have relatively greater effects at high c.d.'s.

In Fig. 5 overpotential values at given c.d. are plotted as a function of  $\log_{10}[\text{As}]$ . In the concentration range  $10^{-4}$ - $10^{-2}$  mole/l. of As these plots are

<sup>18</sup> Herazymenko and Slendyk, *Z. physik. Chem.*, 1932, **162**, 223.

<sup>19</sup> Slendyk, *Coll. Czech. Chem. Comm.*, 1932, **4**, 335.

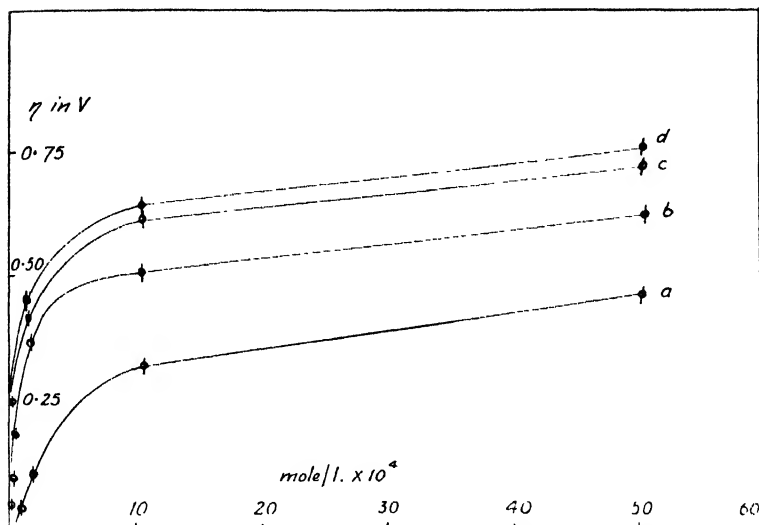


FIG. 4.— $\eta$  as a function of As conc. at constant current density.

- (a)  $5 \times 10^{-4}$  A/sq. cm. (b)  $5 \times 10^{-3}$  A/sq. cm.  
 (c)  $2.5 \times 10^{-2}$  A/sq. cm. (d)  $5 \times 10^{-2}$  A/sq. cm.

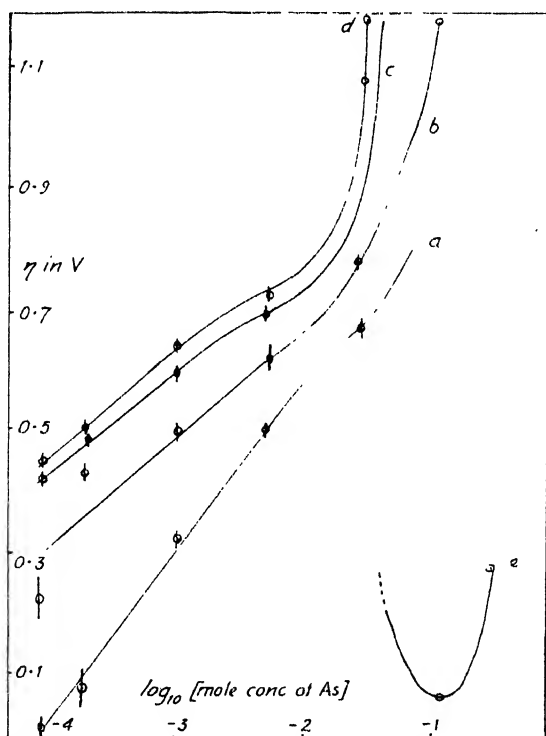


FIG. 5.— $\eta - \log$  (As conc.) curves for polarization at platinized platinum.

- (a)  $5 \times 10^{-4}$  A/sq. cm. (b)  $5 \times 10^{-3}$  A/sq. cm.  
 (c)  $2.5 \times 10^{-2}$  A/sq. cm. (d)  $5 \times 10^{-2}$  A/sq. cm.  
 (e) Depolarization by As  $\cdots$  at  $5 \times 10^{-4}$  A/sq. cm.

essentially linear but show a decrease in slope with increasing c.d. For concentrations greater than  $10^{-3}$  M the tendency for approach to a limiting current causes a marked rise in the  $\eta$ -log [As] lines in the c.d. range  $10^{-2}$ - $0.5 \times 10^{-1}$  A/cm.<sup>2</sup> At  $5 \times 10^{-3}$  A/cm.<sup>2</sup> in the strongest As solutions, anomalous low overpotential values occur which give rise to a maximum and minimum in the  $\eta$ -log [As] curve.

Since the  $\eta$ -log  $i$  behaviour was studied by the resting method, data were obtained on the build-up, decay and static potential of the electrodes. The

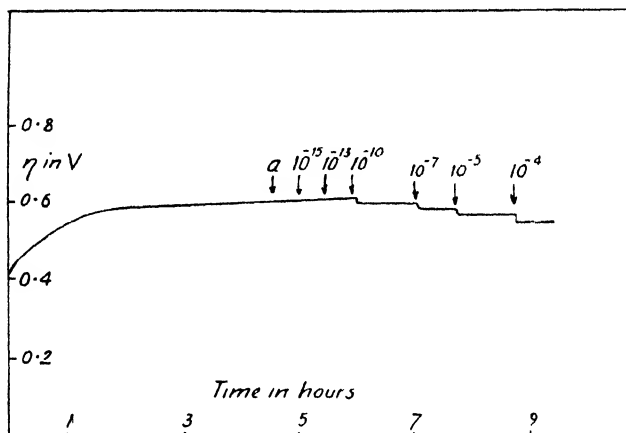


FIG. 6.—Poisoning of Ni by  $\text{As}_2\text{O}_3$  in 0.1 N aq. HCl at  $10^{-3}$  A/sq. cm. (a) 50 drops of 0.1 N HCl added as blank. Arrows show conc. of  $\text{As}_2\text{O}_3$  in mole/l.

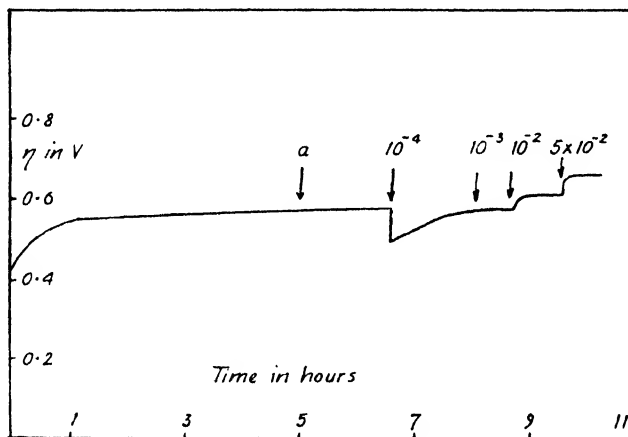


FIG. 7.—Poisoning of Ni by  $\text{As}_2\text{O}_3$  in 0.1 N HCl at  $10^{-3}$  A/sq. cm. for higher conc. of As. (a) 50 drops of 0.1 N HCl added as blank. Arrows show conc. of As in mole/l.

static potential of the platinized platinum electrode in poisoned solutions was positive to the normal hydrogen electrode, the positive potential being greater the stronger the poison solution (see Fig. 4 and 5).

In pure solutions the time variation of overpotential at a given c.d. was imperceptible after the first 1-2 sec. of polarization, but in poisoned solutions a long time variation was observed, constancy being attained in 1-2 hr. At  $10^{-3}$  A/cm.<sup>2</sup> the initial potentials observed were underpotentials which after some minutes became overpotentials.

The decay of overpotential in poisoned solutions was very rapid during the

first minute after terminating polarization; a potential of 0.03 to 0.1 V was reached. This then changed slowly to a constant, more positive value.

**Poisoning of Ni by As, CS<sub>2</sub>, CO, KCN: Effect of PtCl<sub>4</sub>.** OVERPOTENTIAL-TIME BEHAVIOUR AT A CONSTANT C.D. OF  $10^{-3}$  A/CM.<sup>2</sup>—Prior to addition of traces of poisons, two runs were conducted with *blank addition solutions* of

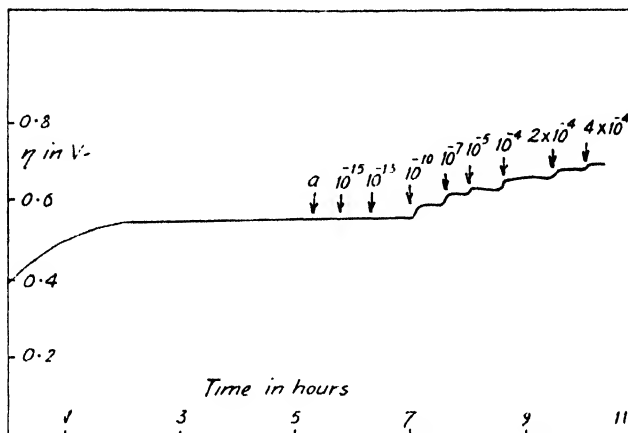


FIG. 8.—Onset of poisoning of Ni by CO at  $10^{-3}$  A/sq. cm. in 0.1 N HCl. (a) 50 drops of 0.1 N HCl added as blank. Arrows show conc. of CO in mole/l.

0.1 N HCl prepared in the same way as were the poison solutions. Additions of volumes of these solutions equal to the volumes used in poison additions had no effect.

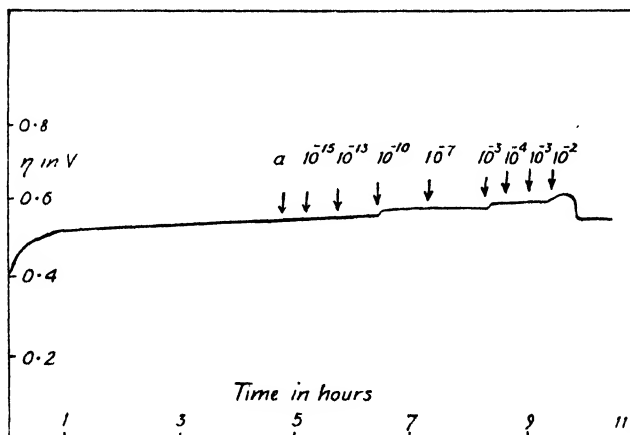


FIG. 9.—Poisoning of Ni by KCN in 0.1 N HCl at  $10^{-3}$  A/sq. cm. 50 drops of 0.1 N HCl added as blank. Arrows show conc. of KCN in mole/l.

The low concentration limit for onset of poisoning was studied by introducing  $10^{-15}$ – $9 \times 10^{-3}$  mole CS<sub>2</sub>,  $10^{-15}$ – $5 \times 10^{-3}$  As<sub>2</sub>O<sub>3</sub>,  $10^{-15}$ – $10^{-2}$  KCN,  $10^{-15}$ – $4 \times 10^{-4}$  CO and  $10^{-15}$ – $10^{-3}$  M H<sub>2</sub>PtCl<sub>6</sub>. Successive additions were made to give the concentrations indicated on the graphs (6–11), and after each addition time was allowed for constant overpotential to be attained before further addition was made.

For the five additives studied no effect was found at concentrations from  $10^{-15}$  to  $10^{-13}$  M. At  $10^{-10}$  M, however, an increase of 0.006 to 0.012 V was observed for the poisons CS<sub>2</sub>, KCN and CO; although a lowering of overpotential



of 0.006 V was observed for  $\text{As}_2\text{O}_3$  solutions at this concentration. The onset of activation by  $\text{H}_2\text{PtCl}_6$  was not apparent until a concentration of  $10^{-6}$  M had been reached; but at this concentration a marked lowering of overpotential towards that of a platinized platinum electrode at  $10^{-2}$  A/cm.<sup>2</sup> was observed.

Further additions of  $\text{CS}_2$  to give a  $10^{-7}$  M solution caused a further increase of overpotential. At  $10^{-5}$  M, however, a lowering of 0.05-0.06 V occurred whilst

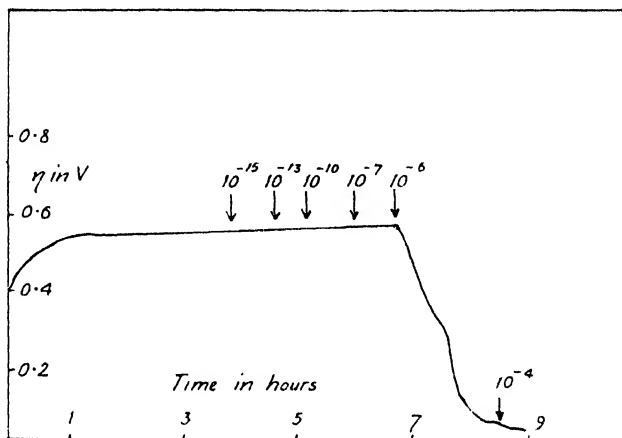


FIG. 10.—Activation of Ni by  $\text{PtCl}_4$  in 0.1 N HCl at  $10^{-2}$  A/sq. cm. Arrows show conc. of added Pt in mole/l.

at  $10^{-4}$  M a further lowering of 0.05-0.1 V was observed. An increase of concentration of  $\text{CS}_2$  to  $3 \times 10^{-3}$  and  $6 \times 10^{-3}$  M then made no significant difference. The adsorption of  $\text{CS}_2$  tending to saturation at high concentrations appears to be reversible since on vigorous bubbling in the cathode compartment

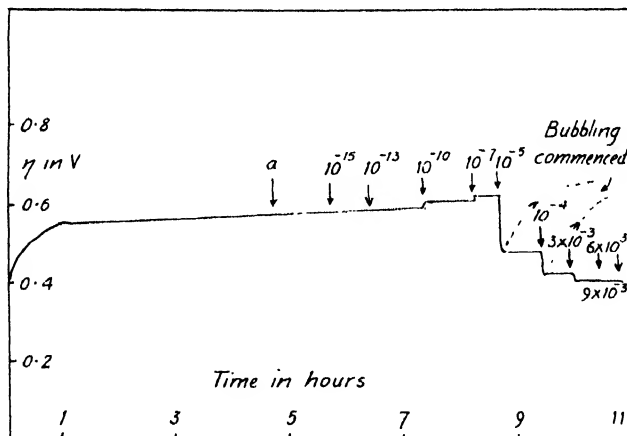


FIG. 11.—Poisoning of Ni by  $\text{CS}_2$  at  $10^{-2}$  A/sq. cm. in 0.1 N HCl. (a) 50 drops of 0.1 N HCl added as blank. Arrows show conc. of  $\text{CS}_2$  in mole/l.

(thus removing  $\text{CS}_2$  from the solution phase) the electrode again approached its initial constant overpotential.

The activation by As which began to be apparent at  $10^{-10}$  M, increased with concentration up to  $10^{-4}$  M solution. At this concentration addition of the appropriate volume of solution caused an activation of ca. 0.05 V which was, however, temporary. The activation at this concentration appeared to be overcome in 1.15 hr. and a further addition of As to give  $10^{-3}$  M solution

had neither an activating nor a poisoning effect.\* At greater concentrations of As ( $10^{-2}$  and  $5 \times 10^{-2}$  M) a marked poisoning corresponding to overpotential changes of 0.05-0.06 V was observed. The behaviour was reproducible to 1.5 cV.

Confirmation of this activating and poisoning effect by As is obtained from two independent sources. Thus, Polukarov *et al.*<sup>20</sup> found that As acts both as a corrosion inhibitor and activator at similar concentrations for which As acts as an overpotential poison or activator respectively. Similarly, Slygin and Ershler<sup>21</sup> found that low concentrations of As increase adsorption of atomic hydrogen at platinum whilst increased quantities of As diminish this.

Carbon monoxide appears to poison nickel throughout the range  $10^{-10}$ - $4 \times 10^{-6}$  M. At the highest concentration the increase of overpotential is approximately 0.07 V. No tendency for saturation adsorption was observed which by analogy with the effect of  $CS_2$ , may not occur until concentrations greater than  $10^{-2}$  M are attained. This concentration was not realized owing to the limited solubility of CO in aqueous HCl.

## Discussion

The poisoning of platinized platinum by fairly large concentrations of As (see Fig. 4) has been shown to be related to poison concentration in a manner characteristic of adsorption saturation with increasing poison concentration. Slygin and Ershler<sup>21</sup> showed that the strength of binding of adsorbed hydrogen is increased by the poison (contrast effect of KCN<sup>21</sup>) but the actual surface concentration is diminished. This implies that the activation energy for both the electrochemical and catalytic<sup>1</sup> desorption reactions would be increased, and since at these poison concentrations the surface activity of hydrogen is also diminished an increase in overpotential would be observed. According to Lukovsev<sup>22</sup> and Horiuti *et al.*<sup>24</sup> the factor  $\alpha$  for the recombination-controlled process for Ni is  $0 < \alpha < 2$ , where  $\alpha$  tends to 2 for very sparsely covered surfaces and is zero for a saturated surface. Since the second effect of the As poison is to diminish the concentration of adsorbed hydrogen<sup>21</sup> the factor  $\alpha$  would thus tend to diminish from 2 to a lower value as poisoning occurs (see Fig. 3).

Negative deviations from the Tafel equation (see Fig. 3) occur when quite small amounts of As are present in the solution, although the Tafel line is quite straight in their absence. This is important in connection with the work of Hickling and Salt<sup>8</sup> whose theory of hydrogen overpotential was supported largely by negative deviations from the Tafel equation at high c.d.'s. These deviations were considered by Frumkin to be due to errors arising from the use of a thyatron commutator for measuring overpotential by the indirect method. Bockris<sup>14, 25</sup> found, however, that results similar to those of Hickling and Salt could also be obtained by the direct method *so long as the solution was prepared in the same way as that of Hickling and Salt*. The results reported here imply that negative deviations from the Tafel equation at high c.d.'s are due to the presence of impurities in the solution.† Azzam and Bockris,<sup>21</sup> working in pre-electrolyzed solution, recently confirmed this by showing that the Tafel equation is valid up to more than 100 A/cm.<sup>2</sup> on several metals for which Hickling and Salt claimed negative deviations.

\* At platinized platinum investigations were not carried out for concentrations  $< 10^{-4}$  M in As so that for the electrode any possible dual activation and poisoning has not yet been established.

<sup>20</sup> Polukarov and Polukarova, *Uchenye. Zap. Molotov Gosudarst Univ.*, 1939, 3, 101.

<sup>21</sup> Slygin and Ershler, *Acta Physicochim.*, 1939, 11, 45.

<sup>22</sup> Knorr and Schwartz, *Z. physik. Chem. A*, 1936, 176, 161.

<sup>23</sup> Lukovsev, *J. Phys. Chem. Russ.*, 1947, 21, 589.

<sup>24</sup> Horiuti, Okamoto and Hirota, *Inst. Phys. Chem. Res. Tokyo*, 1936, 29, 223.

<sup>25</sup> Azzam and Bockris (in course of publication).

† In recent unpublished work Miss H. Rosenberg has shown that addition of traces of  $H_2S$  to the solution causes the negative deviations or "bend-over" effect.

The variation of overpotential with time is absent in purified solutions at platinized platinum electrodes but when As is present even in minute traces, variation with time is considerable. At platinum electrodes, therefore, much of the reported variation of overpotential with time is due to the use of inadequately purified solutions (see <sup>8, 10</sup>).

The limiting current in the region of  $5 \times 10^{-3}$  A/cm.<sup>2</sup> observed at platinized Pt electrodes in 0.1 M As<sub>2</sub>O<sub>3</sub> solutions may be true limiting current due to activation overpotential brought about by the poisoning or it may be due to an ohmic resistance error, caused by the covering of the electrode surface with a film of deposited As. The resistance of the adsorbed film would have to be of the order of  $10^4$  ohms/cm.<sup>2</sup> (which is unlikely) to account for the effect observed. Similar approaches to a limiting current observed at Fe electrodes in the presence of corrosion inhibitors have been shown by Bockris and Conway<sup>32</sup> not to be due to film-resistance error.

On Ni electrodes, the irregular time variation is also eliminated by pre-electrolysis<sup>9, 10, 33, 34, 35</sup> and hence (see also <sup>12, 13</sup>) it can be concluded that pre-electrolysis is usually a necessary technique in preparation of solutions sufficiently pure for the purposes of measurement of overpotential.

The effect of the small amounts of impurities is small but outside the experimental error. The limiting concentration corresponds to  $5 \times 10^{-12}$  mole of poison present in the cathode compartment.

If every atom of Ni ( $r = 1.25$  Å) adsorbed one molecule of poison on a 1 cm.<sup>2</sup> electrode we should have  $6.4 \times 10^{15}$  molecules/cm.<sup>2</sup>, i.e.  $1.1 \times 10^{-8}$  mole/cm.<sup>2</sup> attached to the electrode. It appears, therefore, that if all the available poison were attached to the electrode the latter would be approx. 0.1 % covered by poison (since the electrode area was ca. 0.5 cm.<sup>2</sup>). Since it is improbable that all the poison present in the solution becomes adsorbed, this figure represents an upper limit for the coverage by poison. The rate-determining process at Ni is therefore highly sensitive to surface contamination.

The above behaviour is similar that of specific poisoning in heterogeneous catalysis. Thus, (i) an amount only sufficient to cover about one Ni atom in 1000 is effective in poisoning (or activating). This behaviour is analogous to that observed by Benton and White<sup>28, 33</sup> who found that CO inhibits adsorption of H<sub>2</sub> on nickel in a way such that much less CO is required for the inhibition than corresponds to a monolayer coverage. Similarly Pease<sup>29</sup> has found that the activity of Cu as a dehydrogenation catalyst is markedly inhibited by a trace of mercury.

(ii) The effect of the various additives is specific in that some act as accelerators whilst others act as a poison, depending on their concentration. For some additives (e.g. As) there is at first an activating effect at very low concentrations and then a poisoning effect at higher concentrations.<sup>28, 30</sup> This behaviour resembles that in heterogeneous catalytic gas reactions in that in both systems the behaviour depends upon the effect of the poison on the free energy of adsorption which is a governing factor in the rates of reaction at gas-metal interfaces.\*

<sup>28</sup> Lukovsev, Levina and Frumkin, *Acta Physicochim.*, 1939, **11**, 21.

<sup>29</sup> Bockris and Watson (unpublished).

<sup>30</sup> Benton and White, *J. Physic. Chem.*, 1931, **35**, 1784.

<sup>31</sup> Pease, *J. Amer. Chem. Soc.*, 1923, **45**, 1196, 2235, 2297.

<sup>32</sup> Griffin, *ibid.*, 1927, **49**, 2136.

<sup>33</sup> Schwab, *Catalysis* (van Nostrand, 1937), p. 242.

<sup>34</sup> Bockris and Conway, *J. Physic. Chem.*, 1949, **53**, 527.

<sup>35</sup> Berkman, Morell and Egloff, *Catalysis* (Rheinhold, 1940), p. 389.

<sup>36</sup> Lewina and Sarinsky, *Acta Physicochim.*, 1937, **6**, 491, and **7**, 485.

<sup>37</sup> Lukovsev, Lewina and Frumkin, *Acta Physicochim.*, 1939, **11**, 21.

\* Thus the free energy of adsorption of the reacting materials appear to determine amongst other factors the activation energy and hence the rate of the heterogeneous reaction.<sup>31</sup>

Poisoning effects by As on Ni are anomalous in that the initial portions decrease the overpotential whilst larger concentrations cause an increase. In an examination of the charging curves on Pt in acid solutions and the effect of poisons on them, Slygin and Ershler<sup>21</sup> have observed a similar behaviour. At low concentrations an increase in the amount of adsorbed hydrogen occurred whilst at higher concentrations ( $1.5 \times 10^{-5}$  g. atom. As adsorbed on the electrode) the strength of binding of hydrogen was increased. The poisoning effect at Ni by As appears to be connected with similar facts. If the initial ( $10^{-10}$ - $10^{-6}$  mole/l. of As) quantities of As increase the concentration of H at the Ni surface, processes involving atomic adsorbed hydrogen as a reactant, i.e. the recombination or electrochemical desorption processes will be accelerated and a diminution of overpotential would be noticed as is observed at small As concentrations. If, on Ni as on Pt, larger quantities of poison increase the *strength* of binding of hydrogen then the *energy of activation* for the electrochemical or recombination processes will be increased and the overpotential will be raised as observed.

At the highest concentration of As, viz. 0.3 M, a diminution in overpotential at the lowest c.d. ( $0.5 \times 10^{-3}$  A./cm.<sup>2</sup>) compared with the corresponding overpotential value for 0.1 M As solution was observed.

For complete concentration polarization\* of the As<sup>+++</sup> the limiting current is  $i_d = 0.09$  A./cm.<sup>2</sup> for stirred solutions. This is a maximum value for the diffusion current since  $c_0$ , the concentration of As<sup>+++</sup> at the electrode surface, may not be zero; the comparative diminution in overpotential in 0.3 M As solution at low c.d. would appear, therefore, to be due to depolarization of the electrode by deposition of As<sup>+++</sup> ions.

Other work<sup>24, 25, 26</sup> indicates that the most probable mechanism for the hydrogen evolution process at a Ni cathode is the rapid discharge of a solvated proton followed by an alternative slow electrochemical or H atom catalytic recombination desorption process. The striking effect of traces of poisons and the similarity of this effect to that of poisons in heterogeneous catalysis provides cogent evidence in support of the effective presence of a *catalytic* rate-determining stage at the Ni electrode. It is not immediately obvious how such small traces of poison could affect the kinetics of the electrochemical desorption. It will be noticed, however, that the effect of traces of poisons though definite, is small. This probably indicates the presence of a dual catalytic and electrochemical desorption, only the first of which is affected by the trace poisons.

The hydrogen evolution reaction at a Ni cathode is comparatively insensitive to Pt (see Fig. 10). This depends simply on the deposition potential of Pt onto Ni which is not reached until the comparatively high concentration of  $10^{-6}$  mole/l. This is confirmed by the greater sensitivity to Pt of the H<sub>2</sub> evolution reaction at a Hg solution interface, at which the potential is more negative, so that Pt can deposit at lower concentrations.<sup>27</sup>

It is desired to thank Professor H. V. A. Briscoe for his interest in this work. The administrators of the Dixon Fund (London University) and the Grants Committee of the Chemical Society are also thanked for financial support.

*Department of Inorganic and Physical Chemistry,  
Imperial College of Science,  
London, S.W.7.*

\* I.e. for zero As<sup>+++</sup> concentration in the solution at the electrode surface.

# SOME APPLICATIONS OF THE VALENCE-BOND METHOD TO PROBLEMS OF MOLECULAR STRUCTURE

## PART III.—CALCULATIONS OF THE LENGTHS OF BONDS IN MOLECULES WHICH CONTAIN A POLYVALENT CENTRAL ATOM

BY JOHN SCANLAN AND ERNEST WARHURST

*Received 12th May, 1949*

The method described previously by one of us for the calculation of the lengths of covalent single bonds which possess partial ionic character has been extended to include the bonds in molecules of the type  $MX_n$ , for which the ionic state is degenerate. A bond length equation has been obtained from the first derivative of the secular equation. This bond length equation, applied to certain series of molecules which are considered to be free from complications arising from partial double-bond character, gives results which are in satisfactory agreement with experimental data. It has been shown that, as the number of M—X bonds increases in a series of molecules, the calculated M—X bond length decreases, in agreement with observation, but the ionic character per bond progressively *decreases*, corresponding to a decrease in bond dipole moment. Some aspects of this treatment of  $MX_n$  molecules have been applied to the polyhalides of certain elements of the second and higher rows of the Periodic Table. A qualitative explanation of the bond lengths in these molecules has been given which entails much smaller contributions from multiple-bonded structures than Pauling suggested originally. The interpretation removes certain difficulties with regard to the charge distribution in these molecules.

---

**Introduction.**—In Part I of this series of papers<sup>1</sup> one of us has discussed the available experimental data for the lengths of single bonds between atoms of different electronegativity in cases for which the partial double-bond character can be assumed to be negligible. On the basis of the valence-bond method which treats such covalent bonds with partial ionic character in terms of resonance between pure covalent\* and ionic structures (Pauling<sup>2</sup>) it was concluded that this type of resonance causes appreciable bond contractions, the magnitudes of which bear a very rough linear relationship to the ionic resonance energy of the bonds. From the first derivative of the secular equation with respect to inter-nuclear separation a bond length equation was derived which was shown to yield satisfactory results when applied to the hydrogen halides.

The present paper describes an extension of the theoretical method to include cases of resonance between pure covalent and ionic structures for molecules of the type  $MX_n$ , where M is a polyvalent central atom. In these cases the first excited ionic structures form an  $n$ -fold degenerate set. One feature of considerable interest is the behaviour of the M—X bond length along the series of systems  $MX$ ,  $MX_2$ , . . .  $MX_n$ , i.e. as the number of M—X bonds increases. There are two types of series available for the consideration of this effect. In the first instance the  $n$  valence

<sup>1</sup> Warhurst, *Trans. Faraday Soc.*, 1949, **45**, 461 and 476.

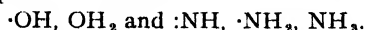
\* The terms "pure covalent structure" and "pure covalent bond" have been defined in Part I.

<sup>2</sup> Pauling, *The Nature of the Chemical Bond*, chap. II.

electrons of the atom M are all used in bond formation and the increase in the number of M—X bonds is achieved at the expense of another type of bond, which, to avoid further complexity in ionic structures, is assumed to possess negligible ionic character. The series  $\text{CH}_3\text{F}$ ,  $\text{CH}_2\text{F}_2$ ,  $\text{CHF}_3$ ,  $\text{CF}_4$  is an example of this kind. The second type of series consists of  $(n-1)$  radicals and one saturated molecule, the last member, e.g.



Examples of this type are the series



Although a number of qualitative conclusions arrived at in this paper apply to cases in which the M—X bonds possess partial double-bond character as well as to the cases in which the bonds possess partial ionic character, numerical calculations have been attempted only in the latter cases, since there appears to be no plausible method for estimating the energy of the  $\text{M}^- = \text{X}^+$  configuration.

The experimental data are not very extensive for the lengths of bonds in molecules and radicals for which resonance between pure covalent and ionic structures can be safely assumed to constitute the predominating effect. The above series for O—H and N—H bonds clearly fulfil this requirement and we also consider, for reasons which are presented in the discussion, that the above series for the C—F bond is a further example of this type.\* The series  $\cdot\text{O}-\text{CH}_3$ ,  $\text{CH}_3-\text{O}-\text{CH}_3$  is also considered to belong to this type; unfortunately, the C—O bond length is only known for the case of dimethyl ether. The bond lengths of the polyhalides of Si, Sn, P and other elements of the second and higher periods of the Periodic Table have not been dealt with quantitatively since the empty *d* orbitals of the central atom introduce the likelihood of partial double-bond character.

There are two common features displayed by the data for the series for the O—H, N—H and C—F bonds. Firstly, the mono-derivative possesses a bond length which shows a contraction relative to the appropriate covalent radius sum. Secondly, there is a distinct, but small, decrease in the M—X bond length as the number of such bonds increases. These effects are evident from Tables III and IV. The contraction exhibited by the mono-derivative can be quite easily accounted for on the basis of the work described in Part I.<sup>1</sup> The second feature is more difficult to understand. It might be argued that if, in accordance with the conclusions arrived at in Part I, the contraction of an M—X bond increases in magnitude with the ionic character of the bond, then the further contraction in bond length with increase in the number of bonds could be ascribed to an increase in the ionic character of *each* bond along the series. There are, however, a number of objections to this simple view.

In the first place, the electronic configuration  $\text{MX}^+$  is less stable than  $\text{M}^+ : \text{X}$ , so that along the series  $\text{MX} \rightarrow \text{MX}_n$ , an increase in ionic character *per bond*, would entail the curious consequence that the more the unfavourable net positive charge on the central atom the more easy it becomes to increase it still further. (For a similar argument, see Skinner and Sutton.<sup>2</sup>)

Secondly, difficulties can arise in discussing the ionic character of  $\text{MX}_n$  molecules in certain cases. It has become customary to refer to the percentage ionic character of a bond in a molecule. For a given bond this may be defined as  $100 \times$  the square of the coefficient of the wave function for the structure in which this bond assumes an ionic configuration; the wave function for the actual state of the molecule

\* The reasons for the omission of the similar series for C—Cl, C—Br and C—I bonds (for which bond length data are available) are dealt with in the discussion.

<sup>2</sup> Skinner and Sutton, *Trans. Faraday Soc.*, 1944, **40**, 164.

being presented by the usual type of linear combination. For the case of an  $n$ -valent atom M, in the mono-derivative MX, if the percentage ionic character were greater than  $100/n$ , then along the series  $MX \rightarrow MX_n$ , unless the percentage ionic character per bond decreased, the total percentage ionic character of the molecule  $MX_n$  would be greater than 100.

Finally, this view that the ionic character per bond increases with  $n$  would entail a parallel increase in the M—X bond moment. There are, of course, no data for the OH and NH series and, unfortunately, no measurements other than that for  $CH_3F$ , have been made on the C—F series. However, data for the C—Cl series exist and show a pronounced fall in moment from the mono- to the tri-halide.<sup>4</sup> Although there are difficulties in the description of the chloromethanes simply in terms of resonance between pure covalent and ionic structures, it is felt that this fall in dipole moment casts a certain amount of doubt on the view that the ionic character of the C—F bond increases from  $CH_3F$  to  $CF_4$ .

In the following treatment the above difficulties are overcome and it is shown that, on account of the degeneracy in the ionic state, as the number of M—X bonds increases a contraction in bond length and a decrease in the coefficients of the wave functions which represent the excited structures are quite compatible with each other.

**Development of the Equations.**—Consider the case of an  $MX_n$  molecule, for which the actual or ground state is described in terms of resonance between a pure covalent structure and an  $n$ -fold degenerate set of excited structures each of which corresponds to  $(n-1)$  pure covalent

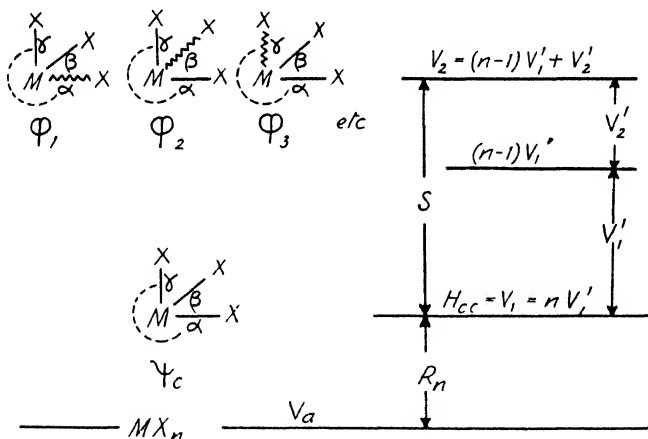


FIG. 1.—Energy zero  $M + nX$ .

M—X bonds and one "non-covalent" M—X bond. The general term "non-covalent" bond has been introduced because a number of the equations derived in this section are independent of the nature of this bond and, for example, apply equally well to the treatment of both partial ionic character and partial double-bond character. In the former instance

the non-covalent bond is  $\overset{+}{M}\overset{-}{X}$  and in the latter it is  $\overset{+}{M}=\overset{-}{X}$ . It is important to realize that the pure covalent structure and the  $n$  excited structures all correspond to a nuclear configuration in which all the M—X bond lengths are equal. Fig. 1 shows the structures diagrammatically. The non-covalent bonds are represented by wavy lines, the pure covalent bonds by straight lines. The  $n$  bonds originating from the central atom are distinguished by the notation  $\alpha, \beta, \gamma$  etc. The zero

<sup>4</sup> Maryott, Hobbs and Gross, *J. Amer. Chem. Soc.*, 1941, **63**, 659

to which all energies are referred corresponds to dissociation into  $M + nX$  neutral atoms.

The conventional approximation for  $(\psi_a)_n$ , the wave function for the actual state of the molecule is

$$(\psi_a)_n = a_n \psi_c + b_n (\phi_1 + \phi_2 + \dots \phi_n), \quad (1)$$

in which  $\psi_c$  is the wave function for the pure covalent structure,  $\phi_1 \dots \phi_n$  the wave functions for the excited structures and  $a_n$  and  $b_n$  the participation coefficients. The suffix  $n$ , throughout, indicates the number of  $M-X$  bonds, i.e. the degeneracy of the excited structures. The functions  $\phi_1 \dots \phi_n$  represent completely equivalent bond configurations and hence the same participation coefficient  $b_n$  has been used for each function in the linear combination. Assuming  $(\psi_a)_n$  is normalized and  $\psi_1, \phi_1 \dots \phi_n$  are normalized and mutually orthogonal,\* then

$$a_n^2 + nb_n^2 = 1. \quad (2)$$

On account of the equivalence of the  $\phi$ 's the secular equation can be expressed in a quadratic form. This is most conveniently dealt with by representing  $(\psi_a)_n$  as follows:

$$(\psi_a)_n = a_n \psi_c + \beta_n \psi_s. \quad (3)$$

The normalizing condition for  $(\psi_a)_n$  leads to the relationships:

$$a_n^2 + \beta_n^2 = 1, \quad (4)$$

hence

$$\beta_n = \sqrt{n} \cdot b_n, \quad (5)$$

and thus

$$\psi_s = \frac{1}{\sqrt{n}} \sum_i \phi_i. \quad (6)$$

The energy  $V_a$  for the actual state of the molecule is given by the lower root of the secular equation corresponding to the use of eqn. (3) as an approximation for  $(\psi_a)_n$ :

$$V_a = \frac{H_{cc}}{2} + \frac{H_{ss}}{2} - \left\{ \left( \frac{H_{ss} - H_{cc}}{2} \right)^2 + H_{cs}^2 \right\}^{\frac{1}{2}} \quad (7)$$

In this equation

$$H_{cc} = \int \bar{\psi}_c H \psi_c d\tau = V_1 = nV_1', \quad (8)$$

where  $V_1$  is the energy of the pure covalent structure, and  $V_1'$  is the energy of a pure covalent  $M-X$  bond,

$$H_{ss} = \int \bar{\psi}_s H \psi_s d\tau \text{ and } H_{cs} = \int \bar{\psi}_c H \psi_s d\tau.$$

Using eqn. (6) the last two integrals can be expanded as follows:

$$H_{ss} = \frac{1}{n} \int \left( \sum_i \bar{\phi}_i \right) H \left( \sum_i \phi_i \right) d\tau = \frac{1}{n} \left[ \sum_i h_{ii} + \sum_i \sum_j h_{ij} \right], \quad (9)$$

$$\text{and } H_{cs} = \frac{1}{\sqrt{n}} \int \bar{\psi}_c H \left( \sum_i \phi_i \right) d\tau = \frac{1}{\sqrt{n}} \sum_i h_{ci}, \quad (10)$$

\* It is realized that these functions are not necessarily orthogonal and that neglect of this may be a serious matter. However, it has been shown in Part I of this series, for the case of resonance between one covalent and one ionic structure, that the use of empirical resonance energies and energies of separation to evaluate parameters in the bond length equation, to some extent allows for the effect of non-orthogonality of the functions. In any case, if non-orthogonality integrals are included in the present problem the equations become unmanageable and we feel that it is worth while making the simplifying assumptions and seeing how the results of calculations agree with the experimental observations.



in which

$$h_{ii} = \int \bar{\phi}_i H \phi_i d\tau,$$

$$h_{ij} = \int \phi_i H \phi_j d\tau, \quad (i \neq j)$$

and

$$h_{ei} = \int \bar{\psi}_e H \phi_i d\tau.$$

There are  $n$  integrals of the type  $h_{ii}$ ,  $n(n-1)$  of the type  $h_{ij}$  and  $n$  of the type  $h_{ei}$ . Since the  $n$  excited structures are degenerate we have

$$h_{11} = h_{22} = \dots h_{nn} = V_2 = (n-1)V_1' + V_2', \quad (11)^*$$

where  $V_2$  is the common energy, possessed by all these structures, and  $V_2'$  is the energy of a non-covalent M—X bond referred to the zero corresponding to dissociation into the neutral particles  $MX_{n-1} + X$ , which clearly lies below the zero  $M + nX$  by an amount  $(n-1)V_1'$ , see Fig. 1. In the case of ionic structures  $V_2'$ , unlike  $V_a$ ,  $V_1$ ,  $V_1'$  and  $V_2$ , is usually positive.

The "cross" integrals  $h_{ij}$  are clearly all equal:

$$h_{12} = h_{13} = h_{23} \dots = Y. \quad (12)$$

Similarly, the "cross" integrals  $h_{ei}$  are all equal:

$$h_{e1} = h_{e2} = \dots = W. \quad (13)$$

Eqn. (9) and (10) thus simplify to

$$H_{..} = V_2 + (n-1)Y = (n-1)V_1' + V_2' + (n-1)Y, \quad (9a)$$

and

$$H_{ee} = \sqrt{n} \cdot W \quad (10a)$$

Substituting for  $H_{ee}$ ,  $H_{..}$  and  $H_{e.}$  in eqn. (7) gives †

$$V_a = \frac{V_1}{2} + \frac{V_2 + (n-1)Y}{2} - \left\{ \left( \frac{V_2 - V_1 + (n-1)Y}{2} \right)^2 + nW^2 \right\}^{\frac{1}{2}}. \quad (14)$$

Using the relationships,

$$R_n = V_1 - V_a = nV_1' - V_a \quad (15)$$

= resonance energy referred to the pure covalent state, and

$$S = V_2 - V_1 = V_2' - V_1' \quad (16)$$

= energy of separation, eqn. (14) assumes the form

$$R_n = -\frac{S + (n-1)Y}{2} + \left\{ \left( \frac{S + (n-1)Y}{2} \right)^2 + nW^2 \right\}^{\frac{1}{2}}. \quad (14a)$$

The expression for the participation coefficients can be shown to be

$$(1 - a_n^2) = \beta_n^2 = nb_n^2 = \frac{R_n}{2R_n + S + (n-1)Y} \quad (17)$$

\*Eqn. (8) and (11) take no explicit account of the interactions between non-bonded electrons. For the equations to hold approximately it must be assumed either that this factor is small compared with the interaction between bonded electrons or that it is roughly proportional to the number of bonds present. We think the assumption that this non-bonding interaction (though not entirely negligible) is considerably smaller than the bonding interaction and probably increases in a roughly proportional manner with the number of bonds present may not be far from the truth, and is worth introducing in order to avoid further complexity in the equations.

† It can easily be shown, generally, that the  $(n+1)$  solutions corresponding to the use of  $(n+1)$  functions  $\psi_e, \phi_1, \dots, \phi_n$ , with the equalities expressed in eqn. (11), (12) and (13), are the two solutions of eqn. (14) and the  $(n-1)$ -fold degenerate solution,  $V_a = V_2 - Y$ .

The behaviour of the right-hand side of (17) with changes in  $n$  is of some interest. As  $n$  increases  $R_n$  increases,  $S$  and  $Y$  (see below) remain constant. Thus, remembering that  $R_n$  and  $S$  are positive but  $Y$  is negative, it is clear that  $\beta_n^*$  increases as  $n$  increases. This increase in the coefficient of the combined excited state is to be expected since the energy of this state,  $H_{nn} (= V_2 + (n-1)Y)$ , decreases and hence  $H_{nn} - H_{oo}$ , the energy of separation, also decreases as  $n$  increases. Thus the total non-covalent character of the molecule, as given by  $\beta_n^*$ , increases. But,

$$\text{since} \quad \psi_n = \frac{1}{\sqrt{n}} \sum_i \phi_i,$$

the non-covalent character of *each bond* in the *combined excited state* falls proportionally to  $1/n$ , hence it can be seen that the non-covalent character per bond in the *actual state of the molecule*, i.e.  $b_n^*$ , may actually decrease as  $n$  increases. We shall see later that this, indeed, is the case for most molecules.

Eqn. (14a) and (17) will be used to discuss all the members of the series  $MX \rightarrow MX_n$ , hence it is necessary to examine the values of the parameters  $S$ ,  $W$  and  $Y$  in relation to  $n$ , the number of bonds present.\* It is clear from eqn. (16) that  $S = V_2' - V_1'$  is independent of  $n$ . For the discussion of the behaviour of  $W$  and  $Y$  with regard to changes in  $n$  it is of some assistance to examine more closely the nature of the wave functions which form the linear combination given in eqn. (1). The functions are all bond eigenfunctions and have important connections with each other in respect of their numerical values over the whole region of configuration space. The relationship between  $\psi_n$  and any one of the  $\phi$ 's, say  $\phi_1$ , is such that the two functions have identical values throughout all space *except for the region in and around one bond*, within which  $\psi_n$  and  $\phi_1$  have non-zero values which differ. This is the "bond region"  $\alpha$  in this instance. In other words, the two structures to which  $\psi_n$  and  $\phi_1$  refer, possess electron distributions which only differ in the bond region  $\alpha$  and have identical distributions throughout all the remaining regions of space. Similarly, any two of the  $\phi$  functions are related in such a way that the functions have identical values throughout the whole of configuration space *except for the region in and around two bonds*. These features are important in discussing the dependence of  $W$  and  $Y$  on  $n$  and their dependence on internuclear separation.

Each of the integrals  $h_{\alpha}$  (denoted, generally, by  $W$ ) is a "cross" integral involving  $\psi_n$  and one of the  $\phi$ 's. From the foregoing discussion, it is clear that the magnitude of such an integral is determined solely by the values of  $\psi_n$  and  $\phi_1$  in *one* "bond region" and hence is independent of

\* The discussion, in this section, of the integrals of the types  $W$  and  $Y$  and their dependence on the internuclear separation of a particular M-X bond may be clarified by the use of the following abbreviated notation. The notation is very similar to that used in the H.L.S.P. treatment of unsaturated hydrocarbons. Let  $x$  denote the wave function for *one* pure covalent bond and  $y$  that for *one* non-covalent bond. Then we may write

$$\begin{aligned}\psi_n &= (x_\alpha x_\beta x_\gamma \dots), \\ \phi_1 &= (y_\alpha x_\beta x_\gamma \dots), \\ \phi_2 &= (x_\alpha y_\beta x_\gamma \dots), \text{ etc.}\end{aligned}$$

$$\text{Then} \quad h_{\alpha 1} = \int \bar{\psi}_n H \phi_1 d\tau = \int (x_\alpha x_\beta x_\gamma \dots) H (y_\alpha x_\beta x_\gamma \dots) d\tau$$

may be abbreviated to  $h_{\alpha 1} = (xy)_\alpha$ .

$$\text{Similarly,} \quad h_{12} = \int \phi_1 H \phi_2 d\tau = \int (y_\alpha x_\beta x_\gamma \dots) H (x_\alpha y_\beta x_\gamma \dots) d\tau$$

may be abbreviated to  $h_{12} = (xy)_\alpha (xy)_\beta$ . This notation brings out the fact that  $h_{\alpha 1}$  integrals each depend on perturbations confined to one bond and  $h_{ij}$  integrals depend on perturbations confined to two bonds.

the number of other bonds present, which will, of necessity, be pure covalent bonds in both the structures to which  $\psi_e$  and  $\phi_i$  refer. This conclusion is, of course, only strictly valid for a series  $\text{MX} \rightarrow \text{MX}_n$  provided the bond angles and lengths remain constant. This is very nearly true in the cases of the series for which we shall present numerical calculations.\*

Similarly, the magnitude of the "cross" integrals of the type  $k_{ij}$  (denoted generally by  $Y$ ) is determined by the values of the functions  $\phi_i$  and  $\phi_j$  in *two* bond regions only; this, likewise, is clearly independent of the number of other bonds present provided the bond angles and lengths remain constant. It is concluded, therefore, that eqn. (14a) and (17) can be applied to all the members of a series  $\text{MX} \rightarrow \text{MX}_n$  with constant values for  $S$ ,  $W$  and  $Y$ . The appropriate value of  $W$  in terms of  $R_1$  and  $S$  is obtained from eqn. (14a) with  $n = 1$ , i.e.

$$W = -\{R_1(R_1 + S)\}^{\frac{1}{2}}. \quad (18)$$

Eqn. (1) to (18) are valid for all values of  $r$ . The bond length equations which are derived below apply, of course, specifically to  $r = r_a$ , the normal internuclear separation for the M—X bonds in the actual state of the molecule.

The derivation of a bond length equation necessitates differentiation of the secular equation. This has been carried out in the following way. Attention has been confined to one particular bond, the bond  $\alpha$ , and the secular equation has been differentiated with respect to  $r_\alpha$ . It is clear that eqn. (14) and (14a), which do not distinguish between the different  $h_{ii}$ ,  $h_{ij}$  and  $h_{ji}$  integrals cannot be used for this partial differentiation. For example, it is evident from the notation shown in Fig. 1 that

$$\frac{\partial}{\partial r_\alpha} \int \bar{\phi}_1 H \phi_1 d\tau + \frac{\partial}{\partial r_\alpha} \int \bar{\phi}_2 H \phi_2 d\tau,$$

since the first expression corresponds to the stretching of a non-covalent bond and the second to a pure covalent bond. Accordingly, the bond length equation has been derived by differentiation of eqn. (7) together with eqn. (8), (9) and (10).

In relation to the differentiation with respect to  $r_\alpha$  the integrals fall into a number of distinct classes.

CLASS (a).—The integrals which represent structures with the bond  $\alpha$  pure covalent. These comprise

$$H_{ee} \text{ and } h_{ii} (i \neq 1).$$

There are  $(n - 1)$  examples of the type  $h_{ii}$ . Assuming that the potential energy of the covalent bond  $\alpha$ , for relatively small displacements, is given by a parabolic expression, we have

$$\left(\frac{\partial H_{ee}}{\partial r_\alpha}\right)_{r_a} = \left(\frac{\partial h_{ii}}{\partial r_\alpha}\right)_{r_a} = \left(\frac{\partial V_1'}{\partial r_\alpha}\right)_{r_a} = k_1(r_a - r_1),$$

in which  $r_1$  is the normal internuclear separation of a pure covalent bond

and  $k_1 = \left(\frac{d^2 V_1'}{dr^2}\right)_{r_1}$  is its force constant.

CLASS (b).—The only member of this class is the integral  $h_{11}$ , which represents the energy of an excited structure with the bond  $\alpha$  non-covalent. Assuming a parabolic form for the potential energy of a "non-covalent" bond, we have

$$\left(\frac{\partial h_{11}}{\partial r_\alpha}\right)_{r_a} = \left(\frac{\partial V_2'}{\partial r_\alpha}\right)_{r_a} = k_2(r_a - r_2),$$

\* If this were not true then the calculations described in this paper should be considered as the first stage in a method of successive approximations.

in which  $r_1$  is the normal internuclear separation of a "non-covalent" bond and  $k_2 = \left( \frac{d^2 V_2}{dr^2} \right)_{r_1}$  is its force constant.

CLASS (c).—The "cross" integrals in which the two eigenfunctions concerned correspond to structures for which the bond  $\alpha$  is different in the two cases, i.e. covalent in one structure and non-covalent in the other. This class comprises of  $h_{c1}$  and  $2(n-1)$  examples of the type  $h_{1k}$  and  $h_{k1}$ , ( $k \neq 1$ ).

CLASS (d).—The "cross" integrals in which the two eigenfunctions concerned correspond to structures for which the bond  $\alpha$  is the same, i.e. pure covalent, in both cases. This class consists of  $(n-1)$  examples of the type  $h_{cp}$  ( $p \neq 1$ ) and  $(n-2)(n-1)$  of the type  $h_{lm}$  ( $l \neq 1, m \neq 1, l \neq m$ ).

Differentiation of eqn. (7) and introduction of the condition  $\left( \frac{\partial V_\alpha}{\partial r_\alpha} \right)_{r_\alpha} = 0$ , gives

$$0 = (1 - nb_n^2) \frac{\partial H_{cc}}{\partial r_\alpha} + nb_n^2 \frac{\partial H_{nn}}{\partial r_\alpha} - \frac{2nb_n^2 H_{cn}}{R_n} \cdot \frac{\partial H_{cn}}{\partial r_\alpha} \quad (19)$$

Substituting the derivatives of eqn. (8), (9) and (10) and classifying the integrals as described above this equation\* becomes

$$\begin{aligned} (r_\alpha - r_1) = -\Delta_n = & \frac{1}{\left( \frac{1 - b_n^2}{b_n^2} \right) \frac{k_1}{k_2} + 1} \left\{ (r_2 - r_1) \right. \\ & - \frac{1}{k_2} \left[ 2(n-1) \frac{\partial h_{1k}}{\partial r_\alpha} + (n-1)(n-2) \frac{\partial h_{1m}}{\partial r_\alpha} \right] \\ & \left. + \frac{2n}{k_2} \left( \frac{W}{R_n} \right) \left[ \frac{\partial h_{c1}}{\partial r_\alpha} + (n-1) \frac{\partial h_{cp}}{\partial r_\alpha} \right] \right\} \quad (20) \end{aligned}$$

This equation can be simplified in a number of aspects which are discussed below.

**The Integrals of Class (c),  $h_{c1}$  and  $h_{1k}$ .**—The magnitude of the integral  $h_{c1}$  is dependent on the values of the bond eigenfunctions  $\psi_c$  and  $\phi_1$  in the region of space in which these functions differ. In this instance the region is the bond  $\alpha$ . Accordingly, stretching this bond will alter the overlap of  $\psi_c$  and  $\phi_1$ , hence  $\left( \frac{\partial h_{c1}}{\partial r_\alpha} \right)_{r_\alpha} \neq 0$ . Similarly, the magnitude of the integrals  $h_{1k}$  is determined by the values of  $\phi_1$  and  $\phi_k$  in two bond regions, one of which, in each case, is the bond  $\alpha$ , hence  $\left( \frac{\partial h_{1k}}{\partial r_\alpha} \right)_{r_\alpha} \neq 0$ .

**The Integrals of Class (d),  $h_{cp}$  and  $h_{lm}$ .**—Although  $h_{cp} = h_{c1} = W$  and  $h_{lm} = h_{1k} = Y$ , the derivatives of class (d) integrals with respect to  $r_\alpha$  are clearly different from those of class (c). The magnitude of the "cross" integrals  $h_{cp}$  is determined by the values of  $\psi_c$  and  $\phi_p$  in the region of space in which these functions differ, i.e. in one bond region which, in none of these instances, is the bond  $\alpha$ . Accordingly, stretching the bond has no effect on the overlap of  $\psi_c$  and  $\phi_p$  in the region which is critical in the determining of the magnitude of  $h_{cp}$ . Hence it is concluded that

$$\left( \frac{\partial h_{cp}}{\partial r_\alpha} \right)_{r_\alpha} = 0. \text{ Similarly, the magnitude of the cross integrals } h_{lm} \text{ is}$$

\* This equation can also be obtained by performing a differentiation on eqn. (7) which corresponds to the simultaneous equal stretching of all the  $n$  bonds in the molecule (as in a symmetrical breathing frequency). The above classification of integrals and of their dependencies on internuclear separation are used.

determined by the values of the bond eigenfunctions  $\phi_l$  and  $\phi_m$  in two bond regions. Since for all examples of  $h_{lm}$  neither of the critical bond regions happens to be the bond  $\alpha$ , then it is concluded that  $\left(\frac{\partial h_{lm}}{\partial r_\alpha}\right)_{r_\alpha} = 0$ .\*

**The Resonance Energy,  $R_n$ .**—There is a good deal of evidence to show that, in cases of resonance between a pure covalent structure and an increasing number of *degenerate* ionic structures, the resonance energy is roughly proportional to the number of ionic structures, i.e.  $R_n \approx nR_1$ .

Such a condition for the series  $MX \rightarrow MX_n$  means that the average bond energy, or the bond energy term  $\frac{Q_a(MX_n)}{n}$  remains approximately constant, where  $Q_a(MX_n)$  is the heat of formation of  $MX_n$  from gaseous atoms. The evidence will be discussed in detail in a later section of this paper. In this section the condition  $R_n \approx nR_1$  will be used to simplify eqn. (17) and (20). Substitution of  $R_n = nR_1$  into eqn. (14a) for  $n = n$ , and comparison with the equation for  $n = 1$ , yields the following simple relationships between the integral  $Y$  and  $R_1$ :

$$Y = -R_1 = +S/2 - \{(S/2)^2 + W^2\}^{1/2}.$$

Substitution of  $R_n = nR_1$  and  $Y = -R_1$  into eqn. (17) gives

$$b_n^2 = \frac{R_1}{2R_1 + S + (n-1)R_1},$$

hence

$$b_n^2 = \frac{b_1^2}{1 + (n-1)b_1^2}. \quad (21)$$

From eqn. (21) it can now be seen that if  $R_n \approx nR_1$  the ionic character per bond decreases as  $n$  increases, whereas the total ionic character of the molecule, i.e.  $\beta_n^2$  increases, as mentioned previously.

It follows from (21) that

$$\left(\frac{1 - b_n^2}{b_n^2}\right) \frac{k_1}{k_2} + 1 = f(b_1) + (n-1) \frac{k_1}{k_2},$$

where

$$f(b_1) = \left(\frac{1 - b_1^2}{b_1^2}\right) \frac{k_1}{k_2} + 1$$

is independent of  $n$ . This result is a considerable simplification of the term outside the brackets in eqn. (20).

Substitution of the above simplifications into eqn. (20) gives the following expression:

$$(r_\alpha - r_1) = -\Delta_n = \frac{1}{f(b_1) + (n-1)k_1/k_2} \left\{ (r_2 - r_1) - \frac{2}{k_2} \left( \frac{R_1 + S}{R_1} \right)^{1/2} \frac{\partial h_{c1}}{\partial r_\alpha} - \frac{2(n-1)}{k_2} \cdot \frac{\partial h_{1k}}{\partial r_\alpha} \right\} \quad (22)$$

in which  $W$  has been eliminated by means of eqn. (18).

\* Using the abbreviated notation, these conclusions with regard to the dependence of the different types of cross integrals on the internuclear separation of a particular M—X bond may be summarized as follows: if  $\alpha$ ,  $m$  and  $n$  denote three particular bonds, then

$$\frac{\partial}{\partial r_\alpha}(h_{cm}) = \frac{\partial}{\partial r_\alpha}(xy)_m = 0,$$

unless  $\alpha \equiv m$ , i.e. unless  $\alpha$  is identical with  $m$ , and

$$\frac{\partial}{\partial r_\alpha}(h_{mn}) = \frac{\partial}{\partial r_\alpha}(xy)_m(xy)_n = 0,$$

unless  $\alpha \equiv m$  or  $\alpha \equiv n$ .

\* Butler and Polanyi, *Trans. Faraday Soc.*, 1943, **39**, 19.

In Part I of this series of papers it was shown that for the case of resonance between a pure covalent structure and one ionic structure, the expression

$$W_r = W_{r_i} \exp(-\gamma(r - r_i)) \quad (23)$$

was a satisfactory approximation for the dependence of the cross integral  $W$  on internuclear separation. Since  $h_{e1}$  is the same integral (when the excited structures are ionic), eqn. (23) will be used for the evaluation of

$\left(\frac{\partial h_{e1}}{\partial r_\alpha}\right)_{r_a}$ . The value of the positive constant  $\gamma$  will be discussed later.

Although the integrals  $h_{1k}$  are not equal to  $h_{e1}$  (since the former are determined by overlaps in two bond regions and the latter in only one bond region) it is clear that the derivatives of  $h_{1k}$  and  $h_{e1}$  with respect to  $r_\alpha$  will be closely related. This is determined by the fact that the dependencies in both cases arise from the alteration in overlap in one bond region, in which region both the bond eigenfunctions concerned differ. We have used two approximate formulations of this close connection.

$$\text{ASSUMPTION I.} \quad \frac{\partial h_{1k}}{\partial r_\alpha} = \frac{\partial h_{e1}}{\partial r_\alpha}.$$

This is independent of the nature of the non-covalent bond. If the excited structures are ionic, this may be formulated more specifically, using eqn. (18) and the derivative of eqn. (23) as follows:

$$\left(\frac{\partial h_{1k}}{\partial r_\alpha}\right)_{r_a} = \left(\frac{\partial h_{e1}}{\partial r_\alpha}\right)_{r_a} = -\gamma W = \gamma\{R_1(R_1 + S)\}^{\frac{1}{2}}.$$

ASSUMPTION II.—This slightly different approximation applies specifically to cases in which the excited states are ionic. It is assumed that the dependence of  $h_{1k}$  on  $r_\alpha$  has the same form as that for  $h_{e1}$ , i.e. is given by an equation of the type (23) with same value for the constant  $\gamma$ . Hence,

$$\left(\frac{\partial h_{1k}}{\partial r_\alpha}\right)_{r_a} = -\gamma Y = \gamma R_1.$$

These two assumptions, for the case of ionic excited structures, when incorporated into eqn. (22), yield the following bond length equations, respectively:

$$-\Delta_n = \frac{1}{f(b_1) + (n-1)k_1/k_2} \left\{ (r_2 - r_1) - \frac{2\gamma(R_1 + S)}{k_2} - \frac{2(n-1)\gamma\{R_1(R_1 + S)\}^{\frac{1}{2}}}{k_2} \right\}, \quad (24 \text{ I})$$

and

$$-\Delta_n = \frac{1}{f(b_1) + (n-1)k_1/k_2} \left\{ (r_2 - r_1) - \frac{2\gamma(nR_1 + S)}{k_2} \right\} \quad (24 \text{ II})$$

**Experimental Evidence for the Relationship  $R_n \approx nR_1$ .**—In this section the following terminology will be used. The dissociation energy of a bond A—B will be denoted by  $D(\text{A—B})$ , i.e. the difference between the energy of the molecule AB in its ground state and the sum of the energies of the radicals A and B in their respective ground states. The bond energy term  $^s$  of the bond A—B will be denoted by  $T(\text{A—B})$ . The energy of a pure covalent bond A—B in a pure covalent structure will be denoted by  $P(\text{A—B})$ . It is assumed that this latter quantity can be obtained approximately by application of Pauling's geometric mean rule. All the energy terms given in this section are in kcal. mole<sup>-1</sup>.

**C—F BONDS.**—Unfortunately, there are no data for the CH<sub>3</sub>F molecule from which either  $D(\text{C—F})$  or  $T(\text{C—F})$  can be estimated. The nearest approach to  $D(\text{C—F})$  for CH<sub>3</sub>F is the corresponding quantity

for the molecule  $\text{F}-\text{CH}_2 \cdot \text{CH}_2\text{OH}$ . Assuming that  $D(\text{C}-\text{H})$  for one hydrogen atom on the  $\beta$  carbon atom of  $\text{CH}_3 \cdot \text{CH}_2\text{OH}$  is the same as  $D(\text{C}-\text{H})$  for ethane (which will be very nearly true, since the resonance structures arising from the  $-\text{OH}$  group will contribute almost equally in the  $\text{CH}_3 \cdot \text{CH}_2\text{OH}$  molecule and the  $\cdot \text{CH}_2 \cdot \text{CH}_2\text{OH}$  radical) then  $D(\text{C}-\text{F})$  is given by

$$D(\text{C}-\text{F}) = Q_a(\text{FCH}_2 \cdot \text{CH}_2\text{OH}) - Q_a(\text{CH}_3 \cdot \text{CH}_2\text{OH}) + D(\text{C}-\text{H}),$$

in which  $Q_a$  denotes the heat of formation from gaseous atoms, data for which have been taken from the book of Rossini and Bichowsky.<sup>6</sup> The value of  $D(\text{C}-\text{H})$  has been taken from Baughan and Polanyi.<sup>7</sup> It is clear that  $D(\text{C}-\text{F})$  is independent of the value for the latent heat of sublimation of carbon. However,  $D(\text{C}-\text{F})$  does depend on the dissociation energy of fluorine. Rossini and Bichowsky<sup>6</sup> give  $D(\text{F}_2) = 63.5$ . Recent work<sup>8</sup> has led to a value in the neighbourhood of 33. Accordingly, two parallel sets of calculations concerning  $\text{C}-\text{F}$  bonds have been made; one, indicated throughout by (a) is based on  $D(\text{F}_2) = 63.5$ ; the other, indicated by (b), is based on  $D(\text{F}_2) = 33$ . The values obtained for  $D(\text{C}-\text{F})$  are 117.4(a) and 102.1(b). Application of the geometric mean rule, using for  $D(\text{C}-\text{C})$  the ethane value given by Baughan and Polanyi,<sup>7</sup> gives  $P(\text{C}-\text{F}) = 74.6(a)$  and 53.9(b). Hence

$$R_1 - D(\text{C}-\text{F}) - P(\text{C}-\text{F}) = 42.8(a) \text{ and } 48.2(b).$$

The data given by Rossini and Bichowsky,<sup>6</sup> lead to the following values for  $Q_a(\text{CF}_4)$ :  $(290 + L)(a)$  and  $(229 + L)(b)$ , in which  $L$  is the latent heat of sublimation of carbon. Hence  $T(\text{C}-\text{F})$ , in  $\text{CF}_4$ , which is equal to  $Q_a/4$ , is  $(72.5 + \frac{1}{4}L)(a)$  and  $(57.3 + \frac{1}{4}L)(b)$ . The correct value for  $L$  is still uncertain, but recent evidence<sup>9</sup> adds further support to a value of about 170. On this basis we obtain:  $T(\text{C}-\text{F})$ , in  $\text{CF}_4$ , is 115.0(a) and 99.8(b). Combining these with the values for  $P(\text{C}-\text{F})$  gives  $R_4/4 = 40.4(a)$  and 45.9(b). Thus  $R_4/4$  is very nearly equal to  $R_1$ .

It is, perhaps, more strictly correct to compare  $T(\text{C}-\text{F})$  in  $\text{FCH}_2 \cdot \text{CH}_2\text{OH}$  with the corresponding quantity in  $\text{CF}_4$ . This can be done by making use of Pauling's bond energy values<sup>10</sup> (which are really bond energy terms, see ref. <sup>5</sup>) for  $\text{C}-\text{H}$ ,  $\text{C}-\text{O}$ ,  $\text{C}-\text{C}$  and  $\text{O}-\text{H}$  bonds. This gives

$$T(\text{C}-\text{F}) \text{ in } \text{FCH}_2 \cdot \text{CH}_2\text{OH} = (76.1 + \frac{1}{4}L)(a) \text{ and } (60.8 + \frac{1}{4}L)(b).$$

Thus  $T(\text{C}-\text{F})$  for  $n = 1$  and  $n = 4$  are approximately equal. The same procedure applied to  $\text{F}_2\text{CH} \cdot \text{CH}_2\text{OH}$  gives

$$T(\text{C}-\text{F}) = (81.6 + \frac{1}{4}L)(a) \text{ and } (66.3 + \frac{1}{4}L)(b).$$

Considering the difficulties in the accurate measurement of the heats of formation of fluorine compounds, the above results are considered to be a satisfactory example of the condition,  $R_n \approx nR_1$ . Since the two alternative values obtained above for  $D(\text{C}-\text{F})$  are independent of  $L$ , they, and the corresponding values of  $R_1$ , have been used in the bond length calculations.

**O—H BONDS.**—A value for the energy of a pure covalent  $\text{O}-\text{O}$  single bond, i.e.  $P(\text{O}-\text{O})$ , is required in order to evaluate the resonance energies of the  $\cdot\text{OH}$  radical and  $\text{H}_2\text{O}$  molecule. This can be obtained in the following way:

$$Q_a(\text{H}_2\text{O}_2) = 2P(\text{O}-\text{H}) + P(\text{O}-\text{O}) + R(\text{H}_2\text{O}_2),$$

<sup>6</sup> Bichowsky and Rossini, *The Thermochemistry of the Chemical Substances* (New York, 1936).

<sup>7</sup> Baughan and Polanyi, *Nature*, 1940, **146**, 685.

<sup>8</sup> Schmitz and Schumaker, *Z. Naturforsch.*, 1947, **2a**, 359 and 362.

<sup>9</sup> Brewer, Gilles and Jenkins, *J. Chem. Physics*, 1946, **16**, 797.

<sup>10</sup> *Loc. cit.*,<sup>2</sup> p. 53.

in which  $R(\text{H}_2\text{O}_2)$  is the resonance energy of the  $\text{H}_2\text{O}_2$  molecule, i.e. the difference in energy between the actual state of the molecule and the pure covalent state. Similarly,

$$Q_a(\text{H}_2\text{O}) = 2P(\text{O—H}) + R(\text{H}_2\text{O}).$$

Eliminating  $P(\text{O—H})$  gives

$$P(\text{O—O}) = Q_a(\text{H}_2\text{O}_2) - Q_a(\text{H}_2\text{O}) - \{R(\text{H}_2\text{O}_2) - R(\text{H}_2\text{O})\}.$$

$R(\text{H}_2\text{O}_2)$  and  $R(\text{H}_2\text{O})$  will be very nearly equal. In both cases the first excited ionic structures form a doubly degenerate set, which will possess almost identical energies of separation with respect to the corresponding pure covalent states. Owing to the close similarity of the structures involved in the two cases, the cross integrals are probably nearly the same. Hence, it is considered that

$$P(\text{O—O}) \approx Q_a(\text{H}_2\text{O}_2) - Q_a(\text{H}_2\text{O})$$

is likely to prove a fairly good approximation. Evaluating the  $Q_a$ 's from the data given in Rossini and Bichowsky\* gives

$$P(\text{O—O}) \approx 34.9. \quad (11)$$

This happens to be identical with the value which Pauling<sup>11</sup> terms the O—O bond energy in hydrogen peroxide. It should be distinguished from the *dissociation energy* of the O—O bond in hydrogen peroxide as, for example, obtained by Skinner.<sup>12</sup> Using the above value for  $P(\text{O—O})$ , application of the geometric mean rule gives:

$$P(\text{O—H}) = 50.2,$$

hence

$$R_1 = D(\cdot\text{O—H})^{13} - P(\text{O—H}) = 40.8,$$

for the  $\cdot\text{OH}$  radical, and

$$R_2/2 = \frac{1}{2}Q_a(\text{H}_2\text{O}) - P(\text{O—H}) = 50.2$$

for the  $\text{H}_2\text{O}$  molecule. It is seen that the relationship  $R_n \approx nR_1$  does not hold quite so well as in the case of C—F bonds. This may be due to neglect of the second excited structure  $\text{HOH}^{++}$  and to a small degree of  $sp$  character in the O—H bonds, the contribution varying as the number of bonds is increased.

**N—H BONDS.**—Evaluations of resonance energies requires a knowledge of the energy of a pure covalent N—N single bond. An approximate value for this can be obtained by a method similar to that used to derive  $P(\text{O—O})$ :

$$Q_a(\text{N}_2\text{H}_4) = 4P(\text{N—H}) + P(\text{N—N}) + R(\text{N}_2\text{H}_4),$$

and

$$Q_a(\text{NH}_3) = 3P(\text{N—H}) + R(\text{NH}_3).$$

Elimination of  $P(\text{N—H})$  gives

$$P(\text{N—N}) = Q_a(\text{N}_2\text{H}_4) - \frac{4}{3}Q_a(\text{NH}_3) - [R(\text{N}_2\text{H}_4) - \frac{4}{3}R(\text{NH}_3)].$$

In  $\text{N}_2\text{H}_4$  and  $\text{NH}_3$  the energies of separation between the first excited ionic structures and the corresponding pure covalent structures will be approximately equal, as will the cross integrals. Since there is one extra ionic structure in the case of  $\text{N}_2\text{H}_4$ , then  $R(\text{N}_2\text{H}_4)$  will probably be somewhat greater than  $R(\text{NH}_3)$ . Hence it is concluded that

$$R(\text{N}_2\text{H}_4) \approx \frac{4}{3}R(\text{NH}_3)$$

may be a tolerably close approximation. Thus

$$P(\text{N—N}) \approx Q_a(\text{N}_2\text{H}_4) - \frac{4}{3}Q_a(\text{NH}_3).$$

<sup>11</sup> *Loc. cit.*,<sup>2</sup> p. 54.

<sup>12</sup> Skinner, *Trans. Faraday Soc.*, 1945, 41, 645.

<sup>13</sup> Gaydon, *Dissociation Energies and Spectra of Diatomic Molecules* (London, 1947).



Using the value of 225 for the dissociation energy of the nitrogen molecule,<sup>13</sup> together with data in Rossini and Bichowsky,<sup>6</sup> the  $Q_a$ 's can be evaluated. This gives

$$P(\text{N—N}) \approx 38.0.$$

Hence

$$P(\text{N—H}) = 62.8$$

and

$$R_3/3 = \frac{1}{3}Q_a(\text{NH}_3) - P(\text{N—H}) = 30.3.$$

A plot of  $D$  against  $r_a$  (or plots such as  $\log D$  against  $\log r_a$ , which reduce the curvature, somewhat for) the diatomic systems HF,  $\cdot\text{OH}$  and  $\cdot\text{CH}$  enables an approximate value for  $D(\text{N—H})$  in the  $\cdot\text{NH}$  radical to be interpolated. These methods give an average value of 87.3. (By a more elaborate treatment of the same series Glockler<sup>14</sup> has derived a value of 86.2.) This gives  $R_1 = 87.3 - P(\text{N—H}) = 24.5$ , which is approximately equal to  $R_3/3$ . The situation for the N—H bonds in the series  $\cdot\text{NH}$ ,  $\cdot\text{NH}_2$  and  $\text{NH}_3$  may be complicated, as with O—H bonds, by contributions from second excited ionic structures and by changes in the  $sp$  character of the bonds.

**The Resonance Energies of Carbonium Ions.**—The series of positive ions  $(\text{CH}_3\text{CH}_2)^+$ ,  $[(\text{CH}_3)_2\text{CH}]^+$  and  $[(\text{CH}_3)_3\text{C}]^+$  provides an example of resonance between a single pure covalent structure (with the positive charge located on the carbon atom) and an increasing number of members of a degenerate set of excited hyperconjugation structures all of which possess the same energy of separation relative to the pure

covalent structure. The excited structures are of the type  $\text{CH}_2=\overset{\text{H}}{\underset{|}{\text{C}}}$ .

Although these ions do not constitute examples of resonance between ionic and covalent structures, since the excited structures involve protons it is considered that the relationship between the resonance energy and the degeneracy of the excited state is of some relevance to the present problem. A. G. Evans<sup>15</sup> has drawn attention to the marked fall in ionization potential along the series of radicals, ethyl, isopropyl, *tert.*-butyl, and has pointed out that this entails a pronounced increase in the resonance energies of the corresponding positive ions. Approximate values for the resonance energy may be obtained from the following relationship:

$$R(\text{R}^+) = I(\text{CH}_3\cdot) + R(\text{R}\cdot) - I(\text{R}\cdot)$$

in which  $I(\text{CH}_3\cdot)$  and  $I(\text{R}\cdot)$  are the ionization potentials of the methyl and  $R$  (ethyl, isopropyl and *tert.*-butyl) radicals, respectively, and  $R(\text{R}^+)$  and  $R(\text{R}\cdot)$  are the resonance energies of the  $\text{R}^+$  ion and  $\text{R}\cdot$  radical, respectively. The values of  $R(\text{R}^+)$  and  $R(\text{R}^+)/n$ , in which  $n$  is the number of excited hyperconjugation structures, are given in Table I. It can be seen that  $R_n = nR_1$  holds approximately for these carbonium ions and,

TABLE I

Radical	$I(\text{R}\cdot)$ <sup>16</sup>	$R(\text{R}\cdot)$ <sup>16</sup>	$R(\text{R}^+)$	$R(\text{R}^+)/n$	$R(\text{R}\cdot)/n$
Methyl	232	0	0	—	—
Ethyl	200	7.2	39.2	13.1	2.4
<i>iso</i> Propyl	179	12.6	65.6	10.9	2.1
<i>tert.</i> -Butyl	165	16.7	83.7	9.3	1.9

<sup>14</sup> Glockler, *J. Chem. Physics*, 1948, **16**, 602.

<sup>15</sup> Evans, *Trans. Faraday Soc.*, 1946, **42**, 719.

<sup>16</sup> Baughan, Evans and Polanyi, *ibid.*, 1941, **37**, 377.

indeed, applies equally well to the corresponding series of neutral radicals,  $R^\cdot$ .

From the above examples it is evident that the relationship  $R_n = nR_1$  is a fairly good approximation, but does not hold rigorously. Indeed, it is not expected to do so and small changes in average bond energy along a series  $MX \rightarrow MX_n$  may prove of great importance in certain problems. However, such variations in the cases dealt with in this paper do not have any serious effect on the bond length calculations.

**Details of the Calculations.**—The method, by means of which eqn. (24I) and (24II) have been used to calculate bond lengths, is that which has been designated method I in Part I.<sup>1</sup> This method, which gives satisfactory results for the hydrogen halides, uses the approximations:

$$R_1 = V_{0. M} - D_0 = P(M-X) - D(M-X), \quad S = (V_2)_{r_1} - V_{0. M},$$

and  $k_1 = k_a$ , in which  $k_a$  is the restoring force constant of an  $M-X$  bond in the actual state of the molecule. It has been pointed out<sup>1</sup> that these approximations for  $R$  and  $S$  involve errors which are opposite in sign and about equal in magnitude to those introduced by assuming that the energy curves for the pure covalent and ionic bonds are parabolic over the relevant region of internuclear separation.

The values of  $R_1$  and  $R_n/n$  for the case of  $C-F$ ,  $O-H$  and  $N-H$  bonds have been discussed in the previous section. For  $C-O$  bonds the quantity  $R_2/2$  may be obtained from the following:

$$R_2 = \Sigma D(C-O) - 2P(C-O) = Q_a(CH_3OCH_3) - 2Q_a(CH_4) + 2D(C-H) - 2P(C-O),$$

in which  $\Sigma D(C-O)$  is the energy required to dissociate both  $C-O$  bonds in dimethyl ether, and  $D(C-H)$  is the dissociation energy of the first  $C-H$  bond in methane. For the latter quantity a value of 102 has been used, the average of three independent determinations.<sup>17</sup> The  $Q_a$  values have been evaluated from data given by Rossini and Bichowsky.<sup>6</sup> This value of  $R_2$  is clearly independent of the latent heat of sublimation of carbon.

The parameters  $k_2$  and  $V_2$  of the ionic structures have been obtained by means of the Born and Mayer equation.<sup>18</sup> The use of this equation in this type of calculation has been discussed fully in Part I.<sup>1</sup> The following values of ionization potentials and electron affinities have been employed:  $I_H = 312.2$ ,<sup>6</sup>  $I_{CH_3} = 232$ ,<sup>15</sup>  $E_F = 96^*$ ,  $E_{OH} = 45$ ,<sup>†</sup>  $E_{OCH_3} = 45$ <sup>†</sup> and  $E_{NH_3} = 35$ .<sup>‡</sup>

For the ionic configurations  $\overset{+}{O}H$  and  $NH\overset{+}{}$ , in which the positive ion is a proton, the constant  $\rho$  in the Born and Mayer equation has been given the value 0.400, as recommended in Part I<sup>1</sup> for this type of ion pair.

For the configurations  $\overset{+}{C}O$  and  $CF\overset{+}{}$ , in which the  $C$  ion possesses an inner shell, the constant has been given the value 0.333, i.e. very close to that derived by Born and Mayer from a study of the alkali metal halides. It must be emphasized that the calculated bond contractions, as in Part I,<sup>1</sup> are very insensitive to changes in this parameter  $\rho$ .

<sup>17</sup> Baughan and Polanyi<sup>7</sup>; Kistiakowski, van Artsdalen and Anderson, *J. Chem. Physics*, 1942, **10**, 305; Severson, *J. Chem. Physics*, 1942, **10**, 291.

<sup>18</sup> Born and Mayer, *Z. Physik*, 1932, **75**, 1.

\*  $E_F = 96$  corresponds to the value of 95.3 obtained by Mayer and Helmholz, *Z. Physik*, 1932, **75**, 19, increased slightly to give weight to the higher value of 98.5 obtained by Sherman, *Chem. Rev.*, 1932, **11**, 93.

† For the electron affinity of  $OH$  the value of 40<sup>16</sup> has been increased to 45 to give some weight to the much higher values derived by Goubeau (see ref. 16).  $E_{OCH_3}$  has been assumed to be the same as  $E_{OH}$ .

‡ A value of  $E_{NH_3} = 35$  has been assumed, merely on the grounds that the smaller electronegativity of nitrogen relative to oxygen will probably entail a lower electron affinity for  $NH_3$  than that for  $OH$ .

The values of  $r_2$ , the normal internuclear separation for an ionic bond, have been derived as follows. For the  $\overset{+}{\text{C}}\overset{-}{\text{F}}$  and  $\overset{+}{\text{C}}\overset{-}{\text{O}}$  configurations,  $r_2$  has been obtained from the sum of gaseous ionic radii. Baughan and Polanyi<sup>19</sup> have obtained a set of gaseous ionic radii for a number of halogen and alkali metal ions, by utilizing the observed internuclear separations in ion pairs to correct the crystal radii. We have extrapolated their method of correction to derive a gaseous ionic radius for  $\text{F}^-$ . The crystal radius of  $\text{F}^-$  is 1.36 Å;<sup>20</sup> the extrapolated value of the correction is 0.20 Å, giving a gaseous ionic radius of 1.16 Å. The crystal radius of  $\text{O}^-$  is 1.40 Å.<sup>20</sup> This is not widely different from the crystal radius of  $\text{F}^-$ , and on these grounds we have also applied the correction of 0.2 Å to the  $\text{O}^-$  crystal radius in order to arrive at an approximate value for the gaseous ionic radius of oxygen in the structure  $\overset{+}{\text{C}}\text{H}_3\overset{-}{\text{O}}-\overset{+}{\text{C}}\text{H}_3$ , i.e. a value of 1.20 Å has been used. The radius of  $\overset{+}{\text{C}}$  appropriate for this type of calculation has been taken as 0.56 Å, the value derived by Baughan and Polanyi.<sup>19</sup> For the structure  $\overset{+}{\text{H}}\overset{-}{\text{O}}-\text{H}$  we have decreased the above value for the gaseous ionic radius of oxygen in order to allow for the penetration of the proton into the electron density of the oxygen. The extent of this penetration is very uncertain.<sup>21</sup> It has been taken to be the same as that applied to the case of  $\text{HF}$  (Part I<sup>1</sup>), i.e. about 0.05 Å, giving  $r_2 = 1.15$  Å for the structure  $\overset{+}{\text{H}}\overset{-}{\text{O}}-\text{H}$ . An appropriate value of  $r_2$  for the configuration  $\overset{+}{\text{H}}\overset{-}{\text{N}}$  is even more difficult to assess. We have assumed a value of  $r_2 = 1.30$  Å based, merely, on the view that it seems plausible to take a value somewhat larger than the one used for the configuration  $\overset{+}{\text{H}}\overset{-}{\text{O}}$ . These estimates are admittedly open to great uncertainties, but it should be noted that the calculated bond contractions, like those presented in Part I,<sup>1</sup> are very insensitive to changes in this parameter. The values of  $k_s$  have been taken from the following sources:

C—F bonds, the value for  $\text{CH}_3\text{F}$  given by Herzberg,<sup>22</sup>

O—H bonds, calculated from the fundamental frequency of vibration in the OH radical,<sup>23</sup>

N—H bonds, the value given by Herzberg<sup>24</sup> for the :NH radical,

C—O bonds, the value calculated by Bonner<sup>25</sup> for  $\text{CH}_3-\text{O}-\text{CH}_3$ .

The value of  $r_1$ , the normal internuclear separations of pure covalent bonds, have been obtained from the sums of the appropriate covalent radii. These radii have been taken from the paper of Schomaker and Stevenson<sup>26</sup> except for hydrogen for which the value of 0.32 Å, suggested in Part I,<sup>1</sup> has been used.

The value of the constant  $\gamma$ , in eqn. (23), which governs the dependence of the cross integrals upon internuclear separation, requires some comment. For O—H and N—H bonds, the ionic structures, in so far as they involve protons, are very similar to those which arise in the hydrogen halides. Satisfactory calculated values of bond contractions were obtained by the use of the same value of  $\gamma$  for all four hydrogen halides. It seems a very

<sup>19</sup> Baughan and Polanyi, *Trans. Faraday Soc.*, 1941, **37**, 648.

<sup>20</sup> *Loc. cit.*,<sup>2</sup> p. 350.

<sup>21</sup> Warhurst, *Trans. Faraday Soc.*, 1944, **40**, 26.

<sup>22</sup> Herzberg, *Infrared and Raman Spectra of Polyatomic Molecules* (New York, 1945).

<sup>23</sup> *Molecular Spectra and Molecular Structure. I. Diatomic Molecules* (New York, 1939).

<sup>24</sup> Bonner, *J. Chem. Physics*, 1937, **5**, 293.

<sup>25</sup> Schomaker and Stevenson, *J. Amer. Chem. Soc.*, 1941, **63**, 37.

<sup>26</sup> *Loc. cit.*<sup>23</sup>

plausible step to extend the use of this value of  $\gamma$  ( $\approx 1.5$ ) to the case of O—H and N—H bonds. For C—F bonds the procedure, which follows strictly that used in Part I<sup>1</sup> for the evaluation of  $\gamma$  for the hydrogen halides, would be to plot  $\log W$  against  $r_1$  for the series  $\text{CH}_3\text{F}$ ,  $\text{CH}_3\text{Cl}$ ,  $\text{CH}_3\text{Br}$  and  $\text{CH}_3\text{I}$ . However, as will be illustrated briefly in the discussion, there are good reasons for considering that this method cannot be expected to give a satisfactory result in the case of this series. Failing this approach we have calculated the bond contractions for C—F bonds (and also for C—O bonds) using the simple assumption that the value of  $\gamma$  is the same as that which has been derived for the hydrogen halides in Part I, i.e.  $\gamma \approx 1.5$ .

### Discussion

**Bonds with Partial Ionic Character.**—The calculated and observed values of  $\Delta$ , the bond contraction, and the squares of the participation coefficients of the ionic structures are shown in Tables III and IV.

TABLE II

Bond	$R_n/n$	$R_1$	$S$	$r_1$	$r_2$	$k_a$	$k_b$
C—F	(a) { 40.4 (b) { 45.9	42.8 48.2	62.6 41.7	1.49 1.49	1.72 1.72	864 864	206 206
O—H	50.2	40.8	140	1.06	1.15	1125	191
O—C	48.7	—	98.2	1.51	1.76	661	200
N—H	30.3	24.5	170	1.06	1.30	874	189

In all the Tables  $r_a$ ,  $r_1$ ,  $r_2$  and  $\Delta$  are given in Å,  $R$  and  $S$  in kcal. mole<sup>-1</sup>,  $k_a$  and  $k_b$  in kcal. mole<sup>-1</sup> Å<sup>-2</sup>.

TABLE III

Molecule	$r_a$ (obs.)	$\Delta$ (obs.) ( $r_1 - r_a$ )	$\Delta$ (calc.)				$b_n^2$		$nb_n^2$	
			Assumption I		Assumption II		(a)	(b)	(a)	(b)
			(a)	(b)	(a)	(b)				
CH <sub>3</sub> F	$\left\{ \begin{array}{l} 1.39 \text{ (a)} \\ 1.384 \text{ (b)} \\ 1.38 \text{ (c)} \end{array} \right\}$	$\left\{ \begin{array}{l} 0.10 \\ 0.10_6 \\ 0.11 \end{array} \right\}$	0.11 <sub>5</sub>	0.12 <sub>3</sub>	0.11 <sub>5</sub>	0.12 <sub>3</sub>	0.288	0.349	0.288	0.349
CH <sub>2</sub> F <sub>2</sub>	$\left\{ \begin{array}{l} 1.32 \text{ (d)} \\ 1.36 \text{ (a)} \end{array} \right\}$	$\left\{ \begin{array}{l} 0.17 \\ 0.13 \end{array} \right\}$	0.14 <sub>6</sub>	0.15 <sub>7</sub>	0.13 <sub>0</sub>	0.13 <sub>7</sub>	0.224	0.259	0.448	0.518
CHF <sub>3</sub>	1.322 (b)	0.16 <sub>8</sub>	0.16 <sub>5</sub>	0.17 <sub>4</sub>	0.12 <sub>9</sub>	0.14 <sub>4</sub>	0.183	0.206	0.549	0.618
CF <sub>4</sub>	1.36 (a)	0.13	0.17 <sub>6</sub>	0.18 <sub>6</sub>	0.13 <sub>2</sub>	0.14 <sub>9</sub>	0.155	0.171	0.620	0.684

(a) Wheland, *The Theory of Resonance* (New York, 1944).

(b) Gordy, *Rev. Mod. Physics*, 1948, **20**, 712.

(c) Herzberg and Bernstein, *J. Chem. Physics*, 1948, **16**, 36.

(d) Stewart and Nielsen, *Physic. Rev.*, 1949, **75**, 640.

The values of the latter parameter  $b_n^2$  have been obtained from eqn. (21) and are thus based on the condition  $R_n \approx nR_1$ . It is seen that for all the series the first member exhibits a bond contraction and that, as the number of bonds increases, there is a further slight contraction in bond lengths. As pointed out in the introduction, these are the two main features shown by the experimental data. The agreement between the calculated and observed values of  $\Delta$  is very satisfactory in view of the complexity of the problem, with the exception of the series for N—H

TABLE IV

Molecule	$r_a$ (obs.)	$\Delta$ (obs.) ( $r_1-r_a$ )	$\Delta$ (calc.)				$b_n^2$
			Assumption I		Assumption II		
$\cdot\text{OH}$ $\text{OH}_2$	0.971 (a) 0.958 (b)	0.089 0.102	(0.10 <sub>1</sub> ) (0.12 <sub>2</sub> )	0.12 <sub>4</sub> 0.15 <sub>1</sub>	(0.10 <sub>1</sub> ) (0.10 <sub>3</sub> )	0.12 <sub>4</sub> 0.12 <sub>6</sub>	0.209 0.173
$\cdot\text{O}-\text{CH}_3$ $\text{CH}_3-\text{O}-\text{CH}_3$	— 1.42 (c)	— 0.09	— —	0.10 <sub>6</sub> 0.13 <sub>5</sub>	— —	0.10 <sub>6</sub> 0.11 <sub>0</sub>	0.185 0.156
$\cdot\text{NH}$ $\cdot\text{NH}_2$ $\text{NH}_3$	1.038 (a) — 1.010 (b)	0.022 — 0.05	(0.07 <sub>6</sub> ) (0.09 <sub>3</sub> ) (0.10 <sub>7</sub> )	0.09 <sub>3</sub> 0.11 <sub>5</sub> 0.13 <sub>2</sub>	(0.07 <sub>6</sub> ) (0.07 <sub>6</sub> ) (0.07 <sub>8</sub> )	0.09 <sub>3</sub> 0.09 <sub>4</sub> 0.09 <sub>5</sub>	0.132 0.116 0.104

(a) Herzberg.<sup>23</sup>(b) Herzberg.<sup>22</sup>(c) Wheland, *The Theory of Resonance* (New York, 1944).

The values of  $\Delta$  given in parenthesis for O—H and N—H bonds are those calculated on the basis of  $R = R_1$ .

bonds, for which the method considerably overestimates the contractions. This satisfactory agreement is considered to justify the assumptions and approximations which have been made in the treatment. It should be noted that the rough agreement between calculated and observed bond contractions for both the molecules discussed in this paper and those dealt with in Part I has been obtained using the *same approximation for the dependence of resonance or cross integrals on internuclear separation*. Eqn. (23) with the *same* value of  $\gamma$ , viz. 1.50, has been used throughout for this dependence of resonance integrals which arise in the perturbation of a pure covalent bond by an ionic component. It would thus appear that this approximation, although very rough, is of fairly wide applicability for this type of integral. The calculations also reveal another point which is very striking. In each series, as  $n$  increases,  $\Delta$  increases in magnitude slightly, but  $b_n^2$ , i.e. the ionic character per bond, *decreases*. Thus the treatment results in the interesting consequence that the further contraction in the C—F bond length from  $\text{CH}_3\text{F}$  to  $\text{CF}_4$  runs parallel to a decrease in the C—F bond moment. The latter, as mentioned earlier, has not been investigated experimentally but the effect certainly exists in the correspondening series  $\text{CH}_3\text{Cl} \rightarrow \text{CHCl}_3$ .<sup>4</sup> The quantity  $nb_n^2$  is a measure of the total positive charge on the central atom M. This, it can be seen from eqn. (21), increases with  $n$ , but the increase is less rapid than that corresponding to direct proportionality and it shows a saturation effect. We consider that this is the most plausible behaviour of the unstable charge distribution (see also ref. 3).

Eqn. (21) and (22) are quite general and do not depend on the type of excited structure, provided for each excited structure the excitation is confined to one bond only of the pure covalent structure. The only special condition attached to eqn. (21) is that the average M—X bond energy remains approximately constant along the series. It is clear from eqn. (21) that the decrease of  $b_n^2$  with increase in  $n$  is more marked the larger the value of  $b_1^2$ , that is, for example, the greater the ionic character or double-bond character in the bond of the first member of the series. This is illustrated for a number of values of  $b_1^2$  in Fig. 2. The broken curves labelled (a) and (b) are the actual values of  $b_n^2$  for the series  $\text{CH}_3\text{F} \rightarrow \text{CF}_4$ , based on the two alternative values for  $D(\text{F}_2)$ .

Eqn. (22) shows that the behaviour of the bond contractions along a series is the result of two opposing factors. As  $n$  increases,  $b_n^2$  decreases and this causes a decrease in the value of the multiplier outside the brackets

on the right-hand side of the equation. This factor acts in the direction of increasing the bond length along the series. The first two terms within the brackets,  $(r_2 - r_1)$ , and the term involving the derivative of the cross integrals  $W$  between the pure covalent structure and individual excited structures, are independent of  $n$ . Thus, if the effect of resonance integrals

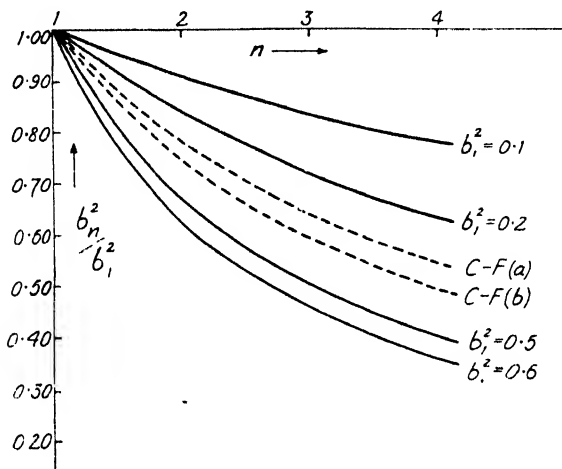


FIG. 2.

$Y$  between members of the set of excited structures is neglected, then the net result would be an *increase* in bond length as  $n$  increases. However, as  $n$  increases, it is clear that an increasing number of negative terms (derivatives of cross integrals ( $Y$ ) with respect to internuclear separation) make their appearance inside the brackets and this offsets the first factor. In the series treated in this paper the latter effect is always slightly larger in magnitude than the former. From the discussion, given in an earlier section, concerning the nature of the cross integrals and their derivatives it is clear that the *structural* relationships between the integrals  $W$  and  $Y$  and their derivatives  $\partial W/\partial r_\alpha$  and  $\partial Y/\partial r_\alpha$  are independent of the nature of the non-covalent bond which characterizes the excited structures. Hence it follows that the approximation

$$\left(\frac{\partial Y}{\partial r_\alpha}\right)_{r_a} \approx \left(\frac{\partial W}{\partial r_\alpha}\right)_{r_a}$$

should be applicable to cases involving any type of excited structure, for example, those which contain the configuration  $M = \overset{+}{X}$ . It therefore seems plausible to conclude that in the case of double-bonded excited structures also, as  $n$  increases, the effect of the increased number of negative terms within the brackets in the bond length equation will probably out-weigh the effect of the decrease in  $b_n^2$ , and thus result in a further contraction in the bond length.

**Bonds with Partial Double-Bond Character.**—The above considerations are of great use in removing a number of serious difficulties attached to the usual explanation of the contracted bonds in polyhalide molecules solely in terms of partial double-bond character.<sup>27</sup> For halides of the type  $M\overset{+}{X}_n$ , in which  $M$  is an element of the second or higher rows of the Periodic Table, there are two possible types of first excited structure.

These are, the ionic structures  $X_{n-1}\overset{+}{M}X$  and the double-bond structures

<sup>27</sup> *Loc. cit.*,<sup>2</sup> chap. VII.

$X_{n-1}M = \overset{+}{X}$ . In any individual case it is difficult to assess the relative importance of these two types of excited structure and detailed calculations of the kind described in this paper, are not possible in such a complicated case. However, an incorporation of certain aspects of this theoretical treatment in a more empirical approach leads to some consequences of interest. A few examples will suffice to illustrate this.

**Si—Cl BONDS.**—The observed Si—Cl bond lengths in the chlorosilanes are as follows:<sup>28</sup>  $\text{SiH}_3\text{Cl}$ ,  $2.06 \pm 0.05 \text{ \AA}$ ;  $\text{SiH}_2\text{Cl}_2$ ,  $2.02 \pm 0.03 \text{ \AA}$ ;  $\text{SiHCl}_3$ ,  $2.01 \pm 0.03 \text{ \AA}$ ; and  $\text{SiCl}_4$ ,  $2.00 \pm 0.02 \text{ \AA}$ . The sum of the covalent single bond radii of silicon and chlorine is  $2.16 \text{ \AA}$ . In discussing  $\text{SiCl}_4$ , Pauling uses a curve connecting bond length with partial double-bond character derived from his well-known curve for carbon-carbon bonds<sup>29</sup> and from this he concludes that the bond contraction in  $\text{SiCl}_4$  ( $0.16 \text{ \AA}$ ) corresponds to each Si—Cl bond possessing 50 % double-bond character.<sup>30</sup> In order to ensure the correct polarity of the bonds, i.e. silicon positive, it is assumed that the ionic structures, which involve

the configuration  $\overset{+}{\text{Si}} \overset{-}{\text{Cl}}$  make an *even greater* contribution to the actual state of the molecule. This does not seem to be a satisfactory description of the molecule. Since we have shown that, for this type of molecule,  $b_s^2$  and the bond contraction can change in opposite directions along a series, it is not permissible to use a bond-length — % double-bond curve in the case of a tetrahalide for the purpose of estimating the percentage double-bond character from the bond length; the mono-halide should be used.\* Further, since there is a considerable electronegativity difference between silicon and chlorine the bond contraction arising from resonance between pure covalent and ionic structures cannot be neglected.

A much more plausible description of this series of molecules, which accounts qualitatively for the bond contractions, can be made on the following lines. In Part I<sup>1</sup> it was shown that, for single covalent bonds, for which the predominant perturbing influence is partial ionic character, a very rough linear relationship holds between the bond contraction and the ionic resonance energy,  $R_{ic}$ . This can be used to estimate approximately the contraction in an Si—Cl bond which arises from the ionic character. The value of  $R_{ic}$ , based on the geometric mean rule, is  $36.2 \text{ kcal. mole}^{-1}$ . This gives  $\sim 0.10 \text{ \AA}$  for the "ionic contraction".

This figure is as large as the observed contraction in  $\text{SiH}_3\text{Cl}$ . It might be concluded, then, that the above series of Si—Cl bonds constitutes a case like the C—F series, i.e. one in which the predominating effect on the bond length is the ionic character. In this case there is no difficulty in accounting for the net polarity of the bonds, nor in accounting for the fact that the Si—Cl bond moment decreases along the series† since the percentage ionic character per bond will decrease from  $\text{SiH}_3\text{Cl}$  to  $\text{SiCl}_4$ .

<sup>28</sup> Brockway and Beach, *J. Amer. Chem. Soc.*, 1938, **60**, 1836; Brockway and Coop, *Trans. Faraday Soc.*, 1938, **34**, 1429.

<sup>29</sup> *Loc. cit.*,<sup>3</sup> p. 174.

<sup>30</sup> *Loc. cit.*,<sup>3</sup> p. 228 *et seq.*

\* Even in this case this procedure assumes that the formal charges across the double bond, i.e.  $M = \overset{+}{X}$ , have no effect on the bond length. If the effect

of these formal charges is similar to that which operates in the case of the  $\overset{+}{M}\overset{-}{X}$  configuration, then, in the bond length equation (for  $n = 1$ ), the importance of the negative term containing the derivative of the cross integral will be increased relative to that of the term  $r_2 - r_1$  (see Warhurst, *Trans. Faraday Soc.*, 1944, **40**, 26, also ref. 1). The result will be that, for a given bond contraction, the percentage double-bond character estimated from the above curve will be too large. This effect merely adds further weight to the conclusions reached in this section, namely, that Pauling's treatment of this type of molecule seriously overestimates the percentage double-bond character in attempting to account for the bond lengths.

† Brockway and Coop, *Trans. Faraday Soc.*, 1938, **34**, 1429.

However, it must be noted that the above linear relationship is only very approximate and, further, the experimental accuracy ( $\pm 0.05 \text{ \AA}$ ) of the determination of the Si—Cl bond length in  $\text{SiH}_3\text{Cl}$  is not very high. So that it is possible that a part of the observed contraction is due to double-bond character. It seems safe to conclude that certainly not more than one-half of the observed contraction in  $\text{SiH}_3\text{Cl}$  should be attributed to partial double-bond character. Taking this as an upper limit, the bond length—% double-bond curve gives 10 % double-bond character for a contraction of  $0.05 \text{ \AA}$ . Thus  $b_1^2 < 0.1$ . Substituting this in eqn. (21) gives  $b_1^2 < 0.077$ . The detailed calculations for a number of molecules presented in this paper have shown that, despite a decrease in ionic character per bond, as  $n$  increases the bond length decreases and we have also shown that this feature probably also applies to partial double-bond character. Thus the contracted bond length in  $\text{SiH}_3\text{Cl}$  and the further contraction along the series can be accounted for qualitatively on the basis of somewhat less than 8 % double-bond character per bond in the case of the tetrahalide. With such small contributions there is no difficulty in accounting for the net polarity of the bonds in terms of greater contributions from the ionic structures. The fall in bond moment along the series also can be accounted for satisfactorily. The decrease in partial double-bond character per bond, corresponding to a decrease in the polarity  $\overset{\leftarrow}{\text{M}}-\overset{+}{\text{X}}$ , along the series tends to cause an increase in net polarity  $\overset{+}{\text{M}}-\overset{\leftarrow}{\text{X}}$ . However, since the ionic character per bond is greater than the partial double-bond character for any member, its decrease with  $n$  will be faster (eqn. (21)), and thus the net polarity  $\overset{+}{\text{M}}-\overset{\leftarrow}{\text{X}}$  will decrease along the series.

**Si—F BONDS.**—The Si—F bond length in  $\text{SiF}_4$  is  $1.54 \pm 0.02 \text{ \AA}$ .<sup>21</sup> Using the revised value for the covalent radius of fluorine,<sup>22</sup> the sum of the covalent single bond radii is  $1.89 \text{ \AA}$  and that for the double-bond radii is  $1.69 \text{ \AA}$ . The observed distance is thus  $0.35 \text{ \AA}$  less than the pure single-bond length *and even less than the pure double-bond length*. There can be little doubt that a considerable part of this contraction arises from the large partial ionic character of the bonds. The ionic resonance energy,  $R_{\text{ion}}$ , for an Si—F bond is  $91 \text{ kcal. mole}^{-1}$ . Using the graph given in Part I, this value corresponds to an "ionic" contraction of  $\sim 0.26 \text{ \AA}$ . Thus, of the total contraction, only about  $0.09 \text{ \AA}$  arises from partial double-bond character. Referring this to a bond length—percentage double-bond curve, gives a figure for the double-bond character of 30 %. For reasons given above this figure is an over-estimate since the molecule is a tetrahalide and not a monohalide. Hence  $b_1^2 < 0.3$ . From eqn. (21) we obtain  $b_1^2 < 0.15$ . This result, that the bonds in  $\text{SiF}_4$  possess something less than 15 % partial double-bond character, goes a long way towards removing the difficulty of accounting for the net polarity of the Si—F bonds in terms of greater contributions from ionic structures.

Eqn. (21) and (22) could also provide a qualitative explanation of the results obtained by Skinner and Sutton<sup>2</sup> for the Sn—X bond lengths in the series of molecules  $(\text{CH}_3)_{4-n}\text{SnX}_n$ ,  $\text{X} = \text{Cl, Br, I}$  and  $n = 1, 2, 3, 4$ . It is clear that, by means of these equations, the progressive decrease in the Sn—X bond length, as  $n$  increases, can be understood without the necessity of assuming an increase in percentage double-bond character per bond and consequently an improbable behaviour of the charge on the Sn atom.<sup>3</sup>

The decrease in C—F bond length along the series  $\text{CH}_3\text{F} \rightarrow \text{CF}_4$  has been attributed by Brockway<sup>23</sup> to the participation of structures of the type  $\overset{+}{\text{F}}\text{C} = \overset{-}{\text{F}}$ . At the time this hypothesis was put forward, it was

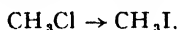
<sup>21</sup> *Loc. cit.*,<sup>2</sup> p. 233.

<sup>22</sup> *Loc. cit.*,<sup>2</sup> p. 235.



considered that the C—F bond length in  $\text{CH}_3\text{F}$  was identical with the covalent radius sum. However, the revised radius for fluorine together with recent electron diffraction and spectroscopic results for the bond length in  $\text{CH}_3\text{F}$  has shown that this bond exhibits a contraction (0.11 Å) which is much larger than the further contraction. This large contraction shown by  $\text{CH}_3\text{F}$  is quite inexplicable on Brockway's theory. Further, it does not seem inevitable that the above type of structure should produce a bond contraction, since one of the C—F bonds can only achieve double-bond character by reducing the binding force between the carbon atom and the second fluorine atom to very weak polarization forces. In view of these comments, together with the fact that the treatment described in this paper gives satisfactory results for the bond lengths of *all* the members of this series, we have concluded that, while such "no-bond" structures may have some significance in the general description of the molecules, they have a negligible effect on the bond lengths in the actual states of the molecules.

SOME GENERAL CONSIDERATIONS.—From Pauling's work<sup>2</sup> and the empirical data and calculations presented in this paper and Parts I and II, it appears that there are a number of properties that are characteristic of single bonds which possess partial ionic character. These properties are: (a) the bond possesses "extra ionic" resonance energy,<sup>2</sup> (b) the bond is shorter than the corresponding covalent radius sum, the contraction being roughly proportional to the ionic resonance energy,<sup>1</sup> (c) the bond possesses a dipole moment<sup>2</sup> and (d) the frequency of vibration, corresponding to stretching the bond, decreases when the molecule which contains the bond is liquefied or dissolved in a non-ionizing medium.<sup>1, 21</sup> The sensitivity of this latter change is greater the greater the ionic character. However, it should be realized that an examination of the relevant empirical data for  $\text{CH}_3\text{Cl}$ ,  $\text{CH}_3\text{Br}$ ,  $\text{CH}_3\text{I}$  indicates serious discrepancies with regard to the above generalizations particularly in the case of  $\text{CH}_3\text{I}$ . We are inclined to the view that the description of the carbon-halogen bonds in the methyl halides simply in terms of resonance between ionic and covalent structures is a satisfactory approximation only in the case of  $\text{CH}_3\text{F}$ , for which the partial ionic character is relatively large. With the remaining molecules some addition factor makes an increasingly important contribution along the series



These discrepancies constitute the main reasons why we have not considered it worth while to carry out bond length calculations for C—Cl, C—Br and C—I bond series. Nor have we thought it justifiable to use the series  $\text{CH}_3\text{F}$ ,  $\text{CH}_3\text{Cl}$ ,  $\text{CH}_3\text{Br}$  and  $\text{CH}_3\text{I}$  for an approximate evaluation of the constant  $\gamma$  in eqn. (23) by the method which was used in Part I for the hydrogen halides. There is also a further factor which will impair the value of bond length calculations for these series. It is clear from the force constant work of Badger<sup>22</sup> and Linnett<sup>24</sup> that, in the case of chloro-, bromo- and iodo-methanes which contain two or more halogen atoms, the repulsion forces between halogen atoms are probably by no means negligible.\* These forces will tend to lengthen the carbon halogen bond length relative to that in the methyl derivative (cf. ref. 34).

In spite of discrepancies in certain cases it seems justifiable to conclude that, on the whole, the concept of resonance between ionic and covalent structures can be applied with considerable success to a fairly wide field and can be very useful in establishing connections of considerable interest between otherwise unrelated phenomena.

<sup>22</sup> Badger, *J. Chem. Physics*, 1935, **3**, 710.

<sup>24</sup> Heath and Linnett, *Trans. Faraday Soc.*, 1948, **44**, 561 and 878.

\* This effect, of course, may operate, to a smaller extent, in the series  $\text{CH}_3\text{F}_2 \rightarrow \text{CF}_4$ .

In conclusion, we wish to express our thanks to Prof. M. G. Evans, F.R.S., for much helpful discussion and to the D.S.I.R. for a grant to one of us (J. S.).

*Chemistry Department,  
The University,  
Manchester.*

## ELECTRIC DIPOLE MOMENT STUDIES

### PART I.—AN ANALYSIS OF THE MOMENTS OF ETHYLENE OXIDE AND ITS HOMOLOGUES

By W. L. G. GENT

*Received 13th May, 1949*

The moments of ethylene oxides and its homologues have been calculated employing (i) the model of Frank (as used by Groves and Sugden) in two ways, viz. by treating the methylene group as a compound atom (Model I) or as a group (Model II), and (ii) that of Smallwood and Herzfeld in a modified form (Model III). It is concluded that the dipole moments of dimethyl ether, ethylene oxide and the homologues may be explained by assuming the bond moments of  $\mu(\overset{+}{\text{C}}-\overset{-}{\text{O}}) = 1.7\text{D}$  and  $\mu(\overset{+}{\text{C}}-\text{H}) = 0.4\text{D}$  and by modifying the vector sum of the bond moments by contributions from secondary moments caused by electrostatic induction in all of the atoms by the (C—O) group moments.

The magnitude and direction of the electric dipole moment of a molecule are expressions of the electric dissymmetry over the whole aggregate of atoms. Electric moment studies during the period 1923-1930 were dominated by the idea that the molecular dipole moment is no more than the vectorial sum of the independent moments of pairs of atoms. By 1929 sufficient experimental data had accumulated for it to become clear that simple vectorial addition of either group moments, as derived by Williams,<sup>1</sup> or of bond moments, as calculated by Eucken and Meyer,<sup>2</sup> were only of limited value for the prediction of molecular dipole moments. The critical survey of van Vleck<sup>3</sup> indicated the limits of validity of this treatment.

The causes of these defects are clearly interactions between different atoms or groups of atoms in the molecule. Where mesomeric and similar effects<sup>4</sup> are absent or of small magnitude the most obvious deviation from the simple vectorial addition will be caused by what may be described in terms of classical physics as electrostatic induction of secondary moments by the primary dipoles in a molecule.

Höjendahl<sup>5</sup> recognized the probably important effect of secondary moments induced by polar groups on the summation for the molecular moment and also that, as Thomson<sup>6</sup> had suggested, two polar groups close together would interact to cause distortion of valency angles. This being so it became apparent that the determination of the geometry of molecules by analysis of dipole moment data is unlikely to be a satisfactory procedure. As a consequence of this, electric moment studies

<sup>1</sup> *Physik. Z.*, 1929, **30**, 391.

<sup>2</sup> *Ibid.*, p. 397.

<sup>3</sup> *Theory of Electric and Magnetic Susceptibilities* (1932).

<sup>4</sup> See Gent, *Quart. Rev.*, 1948, **2**, 383.

<sup>5</sup> *Physik. Z.*, 1929, **30**, 390.

<sup>6</sup> *Phil. Mag.*, 1923, **46**, 513.

after 1930 have been largely concerned with estimation of inductive effects and of mesomerism in molecules whose geometry has been determined by one or the other of the more certain methods. The problem of geometrical distortion by interplay of polar groups has also disappeared except in certain special cases such as that of restricted rotation about a bond as in 1 : 2-dichloroethane.<sup>7</sup>

The earliest attempt to calculate the magnitude of induction effects was made by Smallwood and Herzfeld<sup>8</sup> in an analysis of the electric moments of the disubstituted benzenes. The basic assumption which these authors made is that the electrostatic laws describing the behaviour of bulk dielectrics can be applied to molecules. The moment induced in an atom or group is defined by  $\mu_i = \alpha E$  where  $\alpha$  is the polarizability of the group at a point where the field intensity is  $E$ . The field strength, at any point, generated by a primary dipole directed along one axis of a set of rectangular co-ordinates can be expressed in terms of its  $x$  and  $y$  components and the polar co-ordinates of the point. Combination of these two relationships leads to equations for the  $x$  and  $y$  components of the induced moment. It was found necessary, in order to give coherent results, to locate the primary dipoles at the points of contact of the atoms taken as spheres with normal covalent radii.

Using this model Smallwood and Herzfeld found that the difference between the calculated and observed values of the electric moments of many disubstituted benzenes could be reduced to the order of experimental errors. Smyth<sup>9</sup> applied the method to simple derivatives of methane with some success and later made more systematic application of these ideas to a variety of molecules, ultimately forming a table of bond moments<sup>10</sup> and interpreting it in terms of Pauling's electronegativity system.

On the same assumptions but using a different molecular model, Groves and Sugden<sup>11</sup> calculated group moments in aliphatic compounds with a view to estimating the magnitude of the mesomeric effect in benzene derivatives. These calculations depend on a theory put forward by Frank<sup>12</sup> and his solution of the practical problem of computation.

In considering the nature of solvent effects on the measurement of dipole moments in solution Frank suggested that the component atoms of molecules could be treated as spheres of solid dielectric material. Since the field strength at a point varies inversely as the cube of the distance from the dipole it is necessary to make allowance for this effect in calculating the moment induced in an atom since the field intensity will not be the same at all points within the sphere. Furthermore, if the molecule is treated as a solid dielectric there will be a reduction of field intensity at any point. Under the conditions imposed by such a model the induced moment in any element of an atom is a function of the polar co-ordinates  $r$ ,  $\theta$  of the element and its extension  $l$ , the primary moment being situated at the origin of the co-ordinate system and along one of the axes. Frank showed that the triple integral expressing the moment induced in a whole atom can be solved graphically.

In applying this treatment to the problem of intramolecular induction, Groves and Sugden overcame the two defects of the earlier method. Allowance is made for the field intensity variation over the volume of the atom and the reduction of field strength by dielectric behaviour of the molecule. In their calculations Groves and Sugden considered only one or two aliphatic molecules containing the same polar bond whose moment it was desired to estimate and it seemed desirable to test the method more fully.

<sup>7</sup> Smyth, Dornte and Wilson, *J. Amer. Chem. Soc.*, 1931, **53**, 4242.

<sup>8</sup> *Ibid.*, 1930, **52**, 1919.

<sup>9</sup> *Trans. Faraday Soc.*, 1934, **30**, 752.

<sup>10</sup> *J. Physic. Chem.*, 1937, **41**, 209; *J. Amer. Chem. Soc.*, 1938, **60**, 183.

<sup>11</sup> *J. Chem. Soc.*, 1937, 1992.

<sup>12</sup> *Proc. Roy. Soc. A*, 1935, **152**, 171.

Simple homologous series would provide the most suitable data for analysis, but the difficulties of treating the dynamic geometry of chain molecules of more than two carbon atoms in length suggested that cyclic compounds of which the geometry is either known or determinable are to be preferred. The moments of the cyclic ethers are recorded in the literature and have been used for an exploration of the possibilities of Frank's and other models. It was early appreciated that since for each molecule the observed moment would be expressed in terms of the primary moment between carbon and oxygen and the moment of the H—C linkage it might be possible to derive a magnitude and direction for the H—C bond.

**Description of the Models.**—Two types of model were used in calculating the induced component of the molecular moment :

- (i) that of Frank as used by Groves and Sugden, either treating the methylene group as a compound atom (Model I) or as a group (Model II) ;  
 (ii) that of Smallwood and Herzfeld in a modified form (Model III).

TABLE I.—ANALYSIS OF MOLECULAR MOMENTS

(Model I)

Substance	$\mu_D$	(i)	(ii)	(iii)	(iv)	(v)	(vi)
		$a$	$b$	$c$	$\mu(\text{CH}_2\text{-O})_D$	$\mu(\text{H-C})_D$	$\mu(\text{CH}_2\text{-O})_D$
Dimethyl ether . . . . .	1.28	1.134	-0.388	1.932			2.50
Ethylene oxide . . . . .	1.88	1.685	-0.808	—	(2.14)	(-0.16)	2.14
					2.47	(-0.02)	
Trimethylene oxide . . . . .	2.01	1.360	-0.410	1.152	1.56	(-0.28)	2.48
					3.17	-0.29	
Tetramethylene oxide . . . . .	1.71	1.134	-0.106	1.782		+0.06	2.18
						-0.87	
Average Value					2.40	-0.37	

TABLE II.—ANALYSIS OF MOLECULAR MOMENTS

(Model II)

Substance	(i)	(ii)	(iii)	(iv)	(v)	(vi)
	$a$	$b$	$c$	$\mu(\text{CH}_2\text{-O})_D$	$\mu(\text{H-C})_D$	$\mu(\text{CH}_2\text{-O})_D$
Dimethyl ether . . . . .	1.134	-0.154	1.932			2.20
Ethylene oxide . . . . .	1.685	-0.495	—	(1.58)	(-0.14)	1.58
				2.18	(+0.16)	
Trimethylene oxide . . . . .	1.360	-0.204	1.152	2.17	(-0.08)	2.15
				2.26	-0.44	
Tetramethylene oxide . . . . .	1.134	0.014	1.782		-0.44	2.20
					-0.49	
Average Value				2.20	-0.46	

TABLE III.—ANALYSIS OF MOLECULAR MOMENTS

(Model III)

Substance	(i)	(ii)	(iii)	(iv)	(v)	(vi)
	<i>a</i>	<i>b</i>	<i>c</i>	$\mu(\text{CH}_2\text{-O})$ D	$\mu(\text{H-C})$ D	$\mu(\text{CH}_2\text{-O})$ D
Dimethyl ether . . .	1.134	0.766	1.932			1.80
Ethylene oxide . . .	1.685	-0.654	—	(2.02)	(-0.58)	2.02
				1.69	(-0.78)	
Trimethylene oxide . .	1.360	0.084	1.152	2.06	(-0.46)	1.72
				1.59	-0.38	
Tetramethylene oxide .	1.134	0.220	1.782		-0.61	1.74
					-0.23)	
Average value				1.78	-0.41	

For Models I and II the equations connecting induced and inducing moments are

$$\left. \begin{aligned} \mu_{ix} &= \mu \cdot \alpha \cdot \frac{\epsilon + 2}{3\epsilon_0} \cdot \frac{\sum A_x}{\pi r^2 r_x} \\ \mu_{iy} &= \mu \cdot \alpha \cdot \frac{\epsilon + 2}{3\epsilon_0} \cdot \frac{\sum A_y}{\pi r^2 r_y} \end{aligned} \right\} \quad \text{. . . . . (I)}$$

The inducing moment  $\mu$  is considered to act along the  $x$ -axis of a system of rectangular co-ordinates,  $\mu_{ix}$  and  $\mu_{iy}$  are the  $x$  and  $y$  components of the induced moment,  $\alpha$  is the atom or group polarizability,  $\epsilon$  and  $\epsilon_0$  the atom or group and intra-molecular dielectric constants respectively and  $r$  is the covalent radius of the atom polarized.  $r_x$  and  $r_y$  are the co-ordinates of the centre of the atom or group and the quantities  $\sum A_x$  and  $\sum A_y$  are dependent on the equations:

$$\left. \begin{aligned} A_x &= \frac{a^3}{d^2} \cdot \sin \theta (3 \cos^2 \theta - 1) \\ A_y &= \frac{a^3}{d^2} \cdot 3 \cos^2 \theta \cdot \sin \theta \end{aligned} \right\} \quad \text{. . . . . (2)}$$

$d$  and  $\theta$  are the polar co-ordinates of a square element of side  $a$  in the cross-section of the polarized atom. The area between the axes of the co-ordinates is divided into such elements each of which has an  $A$  value. The calculations were made with square mosaics in which  $a = 0.5 \text{ \AA}$ .<sup>\*</sup> It was considered that the assumption by Groves and Sugden of spherically symmetrical polarizability for the methyl and methylene groups would cause a relatively large error and in Model II, therefore, the calculation was made for separate C and H inductions.

Calculations were made with Smallwood's model modified (Model III) as the assumption of uniform polarizability over a spherical atom in Models I and II seemed extreme in view of the fact that the polarizability of an atom depends almost entirely on the binding electrons. It is equally certain, of course, that the bonding pair is not concentrated at one point so that Model III is the opposite extreme to Models I and II.

<sup>\*</sup> A mosaic of  $A_x$  and  $A_y$  for  $0.25 \text{ \AA}$  squares was constructed and the induced moment computed for two of the molecules (dimethyl ether and ethylene oxide). Although a different value of the induced moment was obtained, the direction also differed and the net contribution to the molecular moment was not appreciably different to that computed from the  $0.5 \text{ \AA}$  mosaics.

In the same symbols as eqn. (1) the relations between induced and inducing moment is given by

$$\left. \begin{aligned} \mu_{ix} &= \frac{\mu \cdot \alpha \cdot (3 \cos^2 \theta - 1)}{\epsilon_0 r^3} \\ \mu_{iy} &= \frac{\mu \cdot \alpha \cdot 3 \cos \theta \sin \theta}{\epsilon_0 r^3} \end{aligned} \right\}, \quad (3)$$

where  $\alpha$  is now the bond polarizability, that is the sum of the parts derived from each atom. For the C—O bond it is assumed that the unbonded pairs of the oxygen atom are equally as polarizable as the bonding pairs so that

$$\alpha(\text{C—O}) = \frac{1}{2}\alpha(\text{C}) + \frac{1}{2}\alpha(\text{O}).$$

In a few cases, such as for the C—H bond, it may be possible to derive a true bond moment, but whenever one of the atoms possess unbonded electrons the moment is best termed a group moment. A similar designation is given to the moment of a chemical group such as  $\text{CH}_2\text{—O}$  and written  $\mu(\text{CH}_2\text{—O})$ .

In the first part of the present investigation it is this quantity which has been calculated rather than  $\mu(\text{C—O})$  to avoid the inclusion of induction terms from the hydrogen atoms attached to the carbon atom. At the short distances (less than 1 Å) the errors will be relatively much greater than for the induced moments in the rest of the atoms of the molecule. This moment,  $\mu(\text{CH}_2\text{—O})$ , has been directed along the axis of the C—O bond whereas, in fact, the resultant moment of the group is at an angle to this direction. In effect, the moment calculated is the component of the group moment parallel to the C—O bond, the normal component being neglected. This is made up of the normal components of the two H—C moments and of the induced moments in the hydrogen, both of which are expected to be small compared to  $\mu(\text{C—O})$  and directed oppositely. The error, therefore, would be of the same order as that caused by omission of secondary inductions and inductions by C—H moments.

**Data Pertaining to Geometry, Dipole Moment and Polarizability of the Molecules.**—Internuclear distances were derived from the normal covalent radii quoted by Pauling.<sup>13</sup> The oxygen valency angle was found to be  $111^\circ$  in dimethyl ether by Sutton and Brockway<sup>14</sup> and in tetramethylene oxide by Beach.<sup>15</sup> It has the calculated value of  $65.2^\circ$  in ethylene oxide according to Ackermann and Meyer.<sup>16</sup> The value of  $94.3^\circ$  was calculated for trimethylene oxide according to the method of least strain suggested by de Vries Robles.<sup>17</sup> Applied to a planar model of tetramethylene oxide this method gives  $111^\circ$  in agreement with the experimental value. Values of dipole moments have been taken from tables<sup>18</sup> and that of dimethyl ether from the publication of Groves and Sugden.<sup>19</sup>

The values for trimethylene and tetramethylene oxides are from solution measurements, but the error involved by not using vapour phase measurements is not great enough to be of importance.\* Polarizability values are derived from the collections in Landolt-Börnstein.

**Limitations of the Methods.**—Considerable approximations are made in the calculations, the chief of which are as follows:

- (i) The primary dipole is situated at the point of "contact" of

<sup>13</sup> *Nature of the Chemical Bond*, 2nd ed. (1941).

<sup>14</sup> *J. Amer. Chem. Soc.*, 1935, **57**, 473.

<sup>15</sup> *Ibid.*, 1936, **4**, 377.

<sup>16</sup> *Trans. Faraday Soc.*, 1934, **30**.

<sup>17</sup> *J. Chem. Physics*, 1940, **9**, 54.

<sup>18</sup> *Rec. trav. chim.*, 1939, **58**, 111.

<sup>19</sup> *J. Chem. Soc.*, 1937, 1779.

\* In general  $\mu_{\text{gas}}/\mu_{\text{sol.}} > 1$  for molecules in which the dipolar axis lies along the greatest length axis.† For trimethylene and tetramethylene oxides the length axes are about equal so that an error of  $> 10\%$  is not likely.

† Frank, *loc. cit.*

spherical atoms defined by normal covalent radii. The additivity of covalent radii implies that they represent the mean position of the bonding electron pair from the nucleus; the general contraction of these radii in a period of typical elements, e.g. Li to F, supports this. For a primary bond moment of 1 D this polar separation will be about 0.1 Å so that the electrical centre of the bond would be displaced about 0.05 Å towards the more electropositive atom. In the absence of any data as to the magnitude of primary bond moments and since the effect is so small the electrical centre of gravity is best sited as the position of the electron pair.

(ii) The electrostatic law pertaining to a point dipole is applicable. The configuration of a field generated by a point dipole is not likely to be very different from that caused by a dipole of length 0.1 Å (see above).

(iii) The field operates in an isotropic medium of dielectric constant equal to that of the material in bulk freed from extra-molecular components. The real meaning of this assumption is that allowance is made for the reaction field of the molecule as a whole other than the particular atom under consideration. Undoubtedly some diminution of the field takes place but the value of  $\epsilon$  ascribed to this is rather arbitrary.

(iv) An atom may be treated as a sphere of uniform polarizability. There are two implications, firstly that the electronic density has a spherically symmetrical distribution and, secondly, that such a sphere is defined by the covalent radius. For a classical model both assumptions are considered to be valid in the first instance.

(v) Induction due to induced moments and to C—H moments may be neglected. These effects will be dealt with in a later paper but are small enough to be neglected for the present considerations.

**Calculations.**—A summary of the calculations based on the three models is given in Tables I, II and III. The molecular moment may be expressed as the sum of three component vectors:

$$\mu = a\mu(\text{CH}_2\text{—O}) + b\mu(\text{CH}_2\text{—O}) + c\mu(\text{H—C})$$

in which  $a$  (column (ii)) depends on the direction of the primary moments,  $b$  (column (ii)) on the magnitude and direction of the total induced moment and  $c$  (column (iii)) on the direction of the H—C moments relative to the molecular moment axis. Since  $a$  and  $b$  can be summed the set of equations in three terms can be solved to yield values of  $\mu(\text{CH}_2\text{—O})$  (column (iv)) and  $\mu(\text{C—H})$  (column (v)). Relatively small errors in the coefficients cause appreciable alteration of the apparent group moments, so that the individual values were averaged and  $\mu(\text{C—H})$  substituted back to give estimates of  $\mu(\text{CH}_2\text{—O})$ . Figures in parenthesis refer to ethylene oxide and are not included in the averages for reasons considered in a later paragraph.

A few modifications of the methods were required for individual cases.

(a) Dimethyl Ether: In order that  $\mu(\text{CH}_2\text{—O})$  shall be equivalent to that derived from the moments of other molecules one of the hydrogen atoms of the methyl of the inducing group is considered to make a contribution to the induced moment. With tetrahedral disposition of the three hydrogen atoms the resultant vector acts in the direction of the C—O linkage and is equal in magnitude to  $\mu(\text{H—C})$ .

With Model II it was assumed that the methyl group freely rotates about the C—O axes, the hydrogen atoms describing thereby a ring. The moment induced in this was calculated, assuming that the polarizability of the three hydrogen atoms is contained in the ring-shaped atom, using a modified form of eqn. (1).

With Model III the locus of the three H—C bonds is defined by the circle of rotation of a carbon covalent radius set at the tetrahedral angle to the C—O bond. The induced moment due to these bonds is a fluctuating quantity and it is difficult to compute the mean value of the moment by an exact treatment. An approximation was made, therefore, by

considering the three bond points to be situated at the centre of the circle of rotation.

(b) Ethylene Oxide: With Models I and II the carbon atom is cut by the  $y$ -axis of the mosaic co-ordinates so that on rotation of the cross-section about the axis an apple-shaped volume is formed instead of the usual ring, the inner and outer parts of which generate moment components of opposite direction. A modified form of eqn. (1) was used to compute the net component.

**Complete Analysis.**—A complete analysis of the molecular moments of all the molecules is possible in terms of  $\mu(\text{C—O})$  and  $\mu(\text{H—C})$  but it was found that the coefficients of these quantities are so nearly identical that solution of the equations would be uncertain. For dimethyl ether and tetramethylene oxide, however, there seemed to be a reasonable difference and, accordingly, the equations have been constructed.

#### MODEL II

$$\begin{aligned} 1.28 &= 0.916 \mu(\text{C—O}) + 1.132 \mu(\text{H—C}) \\ 1.71 &= 1.094 \mu(\text{C—O}) + 1.041 \mu(\text{H—C}) \\ \mu(\text{C—O}) &= 2.13 \text{ D}; \mu(\text{H—C}) = -0.60 \text{ D.} \end{aligned}$$

#### MODEL III

$$\begin{aligned} 1.28 &= 1.236 \mu(\text{C—O}) + 1.132 \mu(\text{H—C}) \\ 1.71 &= 1.386 \mu(\text{C—O}) + 1.041 \mu(\text{H—C}) \\ \mu(\text{C—O}) &= 1.52 \text{ D}; \mu(\text{H—C}) = -0.37 \text{ D.} \end{aligned}$$

These values are in reasonable agreement with those calculated from  $\mu(\text{CH}_2\text{--O})$  (Tables II and III) by allowing for the  $\mu(\text{H—C})$  primary and induced components:

Model II,  $\mu(\text{C—O}) = 1.97 \text{ D}$ ; Model III,  $\mu(\text{C—O}) = 1.43 \text{ D}$

which suggests that neglect of the vertical component of  $\mu(\text{CH}_2\text{--O})$  is not important. Taking the mean of results from the application of the two methods

$$\mu(\text{C—O}) = 1.7 \text{ D}, \mu(\text{H—C}) = -0.4 \text{ D.}$$

**Ethylene Oxide.**—The anomalous values (Tables I-III) of  $\mu(\text{CH}_2\text{--O})$  derived from the dipole moment of ethylene oxide are in part due to the displacement of the hydrogen atoms, in the  $\text{CH}_2\text{--O}$  group, relative to the  $\text{C—O}$  bond. This will alter not only the induced moment but also the contribution of the  $(\text{H—C})$  moments as a result of distortion of  $\text{H—}\hat{\text{C}}\text{—H}$ . A rough calculation putting  $\text{H—}\hat{\text{C}}\text{—H} = 120^\circ$  and the plane of the hydrogen atoms defined by the bisector of  $\text{C—}\hat{\text{C}}\text{—O}$  gives:

$$\text{Model II, } \mu(\text{C—O}) = 1.80 \text{ D}$$

$$\text{Model III, } \mu(\text{C—O}) = 1.76 \text{ D.}$$

In both cases there is a convergence towards the values of  $\mu(\text{C—O})$  found in the unstrained molecules.

**Conclusions.**—It appears from the analysis that the dipole moments of dimethyl ether, ethylene oxide and the homologues may be accounted for by assuming bond moments  $\mu^+(\text{C—O}) = 1.7 \text{ D}$ ,  $\mu^+(\text{C—H}) = 0.4 \text{ D}$ , using a model of the molecules in which the vector sum of the bond moments is modified by contributions from secondary moments caused by electrostatic induction in all of the atoms by the  $(\text{C—O})$  group moments. It is clear that the validity of the procedures may be tested by the sign of the  $(\text{C—H})$  moment found, for a reverse polarity would allow of no concordance between the individual values of  $\mu(\text{C—O})$ .

The problem of the polarity of the  $\text{C—H}$  bond (and the magnitude of its moment) has been examined at length recently<sup>4</sup> and it appears to be almost certainly  $\overset{+}{\text{C}}\text{—}\overset{-}{\text{H}}$  in saturated aliphatic compounds. That the



magnitude of the moment is also close to measured values is additional evidence of the correctness of the results obtained. The C—F group moment has been computed by a similar method and the magnitudes in aliphatic compounds  $\mu(\text{C—F}) = 1.9 \text{ D}$  assigned. The value of  $1.7 \text{ D}$  for  $\mu(\text{C—O})$  is of the expected order relative to that of  $\mu(\text{C—F})$ .

A later paper will describe the application of these methods to the moments of some other simple molecules.

*Chemistry Department,  
Guy's Hospital Medical School,  
London Bridge, S.E.1.*

## THE DENSITY OF LIQUID ARSINE

BY A. L. G. REES AND K. STEWART

*Received 20th May, 1949*

The determination of the liquid density of carefully purified arsine over the temperature range  $-85^{\circ}$  to  $+48^{\circ} \text{C}$  is reported. The liquid density is found to be expressed by the equation:

$$\rho_t = 1.413 - 3.602 \times 10^{-3}t - 4.321 \times 10^{-6}t^2.$$

The published data on the density of liquid arsine comprise measurements at five temperatures between  $-112^{\circ} \text{C}$  and  $-60^{\circ} \text{C}$  by Johnson and Pechukas<sup>1</sup> and at seven temperatures between  $-60^{\circ} \text{C}$  and  $0^{\circ} \text{C}$  by Durrant, Pearson and Robinson.<sup>2</sup> The agreement between these two sets of data is not good and a complete redetermination of the density over a wider temperature range is desirable. Furthermore, Durrant, Pearson and Robinson made no allowance for the mass of arsine in the vapour phase in their pycnometers, with the result that their density values diverge progressively from the true values with increase in temperature. This statement is confirmed by the results of work recorded here. Considerable care has been taken in obtaining arsine of high purity and in handling the gas and liquid under high-vacuum conditions.

### Experimental

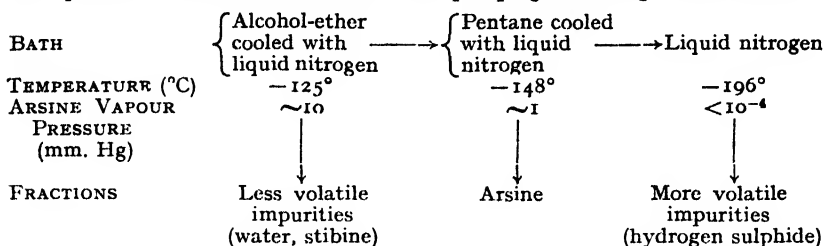
**Preparation and Purification of Arsine.**—The arsine used in this work was obtained by the reaction of 10 % hydrochloric acid on powdered zinc arsenide,  $\text{Zn}_3\text{As}_2$ . This method has been shown to be the most convenient in the laboratory; the yield is good ( $\sim 86\%$  theoretical) and the subsequent purification of the product relatively straightforward. The gas evolved contained 91–93 % arsine, the remainder being mainly hydrogen and water vapour, although small amounts of stibine and hydrogen sulphide are likely to be present.

Powdered zinc arsenide, prepared by direct combination of the elements in stoichiometric proportions in a Rose crucible of Battersea ware in a stream of hydrogen, was reacted with 10 % hydrochloric acid in a stream of hydrogen. The evolved gases were passed through lead acetate solution to remove sulphur compounds, through glacial phosphoric acid to remove water vapour and unprecipitated spray, and collected in two internally sealed traps, cooled to  $-180^{\circ} \text{C}$  in liquid air. Uncondensed hydrogen left the system through a concentrated sulphuric acid safety bubbler. After sweeping the system with hydrogen at the completion of the reaction, the system was pumped free of non-condensable gases and the condensables distilled *in vacuo* into a U-trap.

<sup>1</sup> *J. Amer. Chem. Soc.*, 1937, **59**, 2065.

<sup>2</sup> *J. Chem. Soc.*, 1934, 730.

This product was then fractionated with pumping according to the scheme :



Part of the arsine was lost in the tail and head fractions, which were rejected. The process may be repeated with the middle fraction, without the system being under continuous evacuation. The purity of the sample was checked by taking a series of vapour pressure measurements with head and tail fractions obtained from it by simple distillation. Two separate preparations of zinc arsenide were used in this work and both lots of purified arsenic gave identical vapour pressure-temperature data.

**The Density Determinations.**—Three pycnometers of the same design were used : each consisted of a thick-walled capillary of  $\sim 1$  mm. bore with a bulb of 1.2 cm.<sup>3</sup> capacity blown on one end. The wall thickness of the bulb was comparable with that of the capillary so that the glass would have sufficient strength to withstand 30-40 atm. pressure. A thick scratch toward the bottom of the capillary served as a reference mark. The whole pycnometer was annealed thoroughly and uniformly to relieve any strain in the glass. Each pycnometer was calibrated for volume up to the reference mark and for uniformity of bore over the whole range of the capillary using redistilled Merck's thiophen-free benzene over freshly-cut sodium. The density and coefficient of expansion were derived from published data<sup>3</sup> and the calibration performed with the benzene always within the temperature range of these data, so that extrapolation of the density-temperature relation was unnecessary.

Volume measurements were made with the pycnometer immersed in a large silvered Dewar vessel having an unsilvered vertical slot, through which the pycnometer could be observed by means of a cathetometer capable of measurement of differences in length of 0.001 cm. Between  $-90^\circ$  and  $-70^\circ$  the bath was of acetone cooled with liquid nitrogen ; between  $-70^\circ$  and  $+10^\circ$ , acetone cooled with solid carbon dioxide and between  $+10^\circ$  and  $+50^\circ$ , water. The bath was stirred mechanically. Temperatures were measured by (i) a carbon dioxide vapour-pressure thermometer in the range  $-90^\circ$  to  $-70^\circ$ , (ii) an ammonia vapour-pressure thermometer in the range  $-70^\circ$  to  $-20^\circ$  and (iii) standard mercury thermometers, graduated in  $0.1^\circ$ , in the range  $-20^\circ$  to  $+50^\circ$ .

Following calibration, the pycnometers were filled with the requisite amount of arsine by high-vacuum distillation, care being taken to exclude mercury vapour completely from the system. The pycnometers were sealed off under vacuum and the seals carefully annealed. Volume measurements were made over a range of temperature. The capillaries were then carefully marked with a glass knife near to the tips to facilitate opening of the tubes. The pycnometers were allowed to come to room temperature, when they were carefully weighed. The arsine was then frozen solid in liquid nitrogen and the tip of each capillary broken off sharply at the file mark. The arsine was allowed to evaporate, the tube evacuated, dried in an air oven and the two pieces of the pycnometer weighed. The weight of arsine was obtained by difference.

## Results

Three pycnometers, two from the same length of capillary, were calibrated as indicated previously. All capillaries proved to be uniform in bore to within 1 part in 2000, and the volume unit length therefore to 1 part in 1000, over the entire length. The relevant data for the pycnometers used are given for  $20^\circ\text{C}$ .

In calculating densities from the measured volume of liquid arsine, three corrections must be considered (i) the elastic deformation of the glass under vapour pressures of the order encountered in the temperature range, (ii) the

<sup>3</sup> *Landolt-Börnstein Tabellen* (Berlin, 1936).

## DENSITY OF LIQUID ARSINE

TABLE I

Pyknometer	Volume to Reference Line (cm. <sup>3</sup> )	Volume/unit length of capillary (cm. <sup>3</sup> /cm.)
1	1.2962	0.1940
2	0.8008	0.02848
3	1.9479	0.02848

TABLE II.—DENSITY OF LIQUID ARSINE

<i>t</i> (°C)	Pyknometer	$\rho_t$ (obs.)	$\rho_t$ (calc.)	Deviation
— 84.9	1	1.689	1.688	— 0.001
— 80.6	1	1.676	1.675	— 0.001
— 74.4	1	1.659	1.657	— 0.002
— 70.3	1	1.648	1.645	— 0.003
— 67.5	1	1.639	1.637	— 0.002
— 64.5	1	1.629	1.628	— 0.001
— 63.6	1	1.624	1.625	— 0.001
— 62.8	2	1.622	1.622	0
— 61.6	2	1.619	1.619	0
— 60.8	2	1.616	1.616	0
— 59.6	2	1.612	1.613	+ 0.001
— 58.3	2	1.609	1.609	0
— 57.3	2	1.605	1.605	0
— 55.5	2	1.601	1.600	— 0.001
— 54.7	2	1.596	1.597	+ 0.001
— 53.5	2	1.591	1.594	+ 0.003
— 50.7	1	1.585	1.585	0
— 50.6	2	1.583	1.584	+ 0.001
— 45.0	2	1.563	1.567	+ 0.004
— 39.1	2	1.545	1.547	+ 0.002
— 35.3	2	1.532	1.535	— 0.003
— 35.0	1	1.535	1.534	— 0.001
— 30.9	2	1.517	1.520	+ 0.003
— 24.8	2	1.498	1.500	+ 0.002
— 19.1	2	1.479	1.480	+ 0.001
— 14.1	2	1.460	1.463	+ 0.003
— 10.0	2	1.446	1.449	+ 0.003
— 4.1	2	1.427	1.428	+ 0.001
— 2.8	1	1.425	1.423	— 0.002
+ 0.6	2	1.411	1.411	0
+ 5.3	2	1.392	1.394	+ 0.002
+ 6.4	3	1.395	1.390	— 0.005
+ 7.3	2	1.385	1.387	+ 0.002
+ 10.0	3	1.381	1.377	— 0.004
+ 11.0	2	1.372	1.373	+ 0.001
+ 15.0	3	1.363	1.358	— 0.005
+ 19.8	3	1.344	1.340	— 0.004
+ 20.0	1	1.339	1.339	0
+ 21.5	3	1.337	1.334	— 0.003
+ 22.3	3	1.333	1.331	— 0.002
+ 23.4	3	1.330	1.327	— 0.003
+ 24.0	3	1.328	1.324	— 0.004
+ 25.0	3	1.324	1.320	— 0.004
+ 38.0	3	1.267	1.270	+ 0.003
+ 41.4	3	1.256	1.257	+ 0.001
+ 43.0	3	1.249	1.250	+ 0.001
+ 45.9	3	1.236	1.239	+ 0.003
+ 48.0	3	1.223	1.230	+ 0.007

change in volume of the pyknometers with temperature, (iii) the mass of arsine in the gaseous phase. Durrant, Pearson and Robinson<sup>3</sup> neglected any correction for change in volume under pressure, since, after subjection to the vapour pressures of the order of 10-20 atm., no change in volume of the pyknometer could be detected. However, one must consider the elastic deformation of the pyknometer, giving rise to a change in volume  $\Delta V = \frac{Vp}{k}$  cm.<sup>3</sup>, where

$k$  is the bulk modulus of elasticity of the glass,  $p$  the pressure difference in dyne cm.<sup>-2</sup> and  $V$  the original volume. For a pyknometer of 2 cm.<sup>3</sup> capacity, constructed of glass of bulk modulus  $5 \times 10^{11}$  dyne cm.<sup>-2</sup>, the change in volume  $\Delta V \sim 10^{-4}$  cm.<sup>3</sup> at the highest pressures encountered ( $\sim 26$  atm.) is negligible and no correction need be applied. On the other hand, the change in volume of the pyknometer due to thermal changes amounts to 0.005 cm.<sup>3</sup> for a 2 cm.<sup>3</sup> pyknometer at the lowest temperatures and corrections must be made throughout. The coefficient of cubical expansion<sup>4</sup> of the soft glass used was taken as  $2.55 \times 10^{-6}$ . Since the total mass of arsine in the pyknometer is not wholly in the liquid phase, a correction (negative) must be applied to the weight of arsine. This correction amounts to

$$\Delta m = \frac{vpM}{22414 T} \frac{273.2}{T}$$

where

$v$  is volume of vapour phase,

$p$  the vapour pressure of arsine in atmospheres,

$M$  the molecular weight of arsine,

and

$T$  the absolute temperature,

amounts to some 2 % of the total mass under some of the experimental conditions and cannot be neglected. Corrections were applied in the calculation of the densities.

The density was measured at 48 temperatures in the range; the results are tabulated in Table II and plotted in Fig. 1.

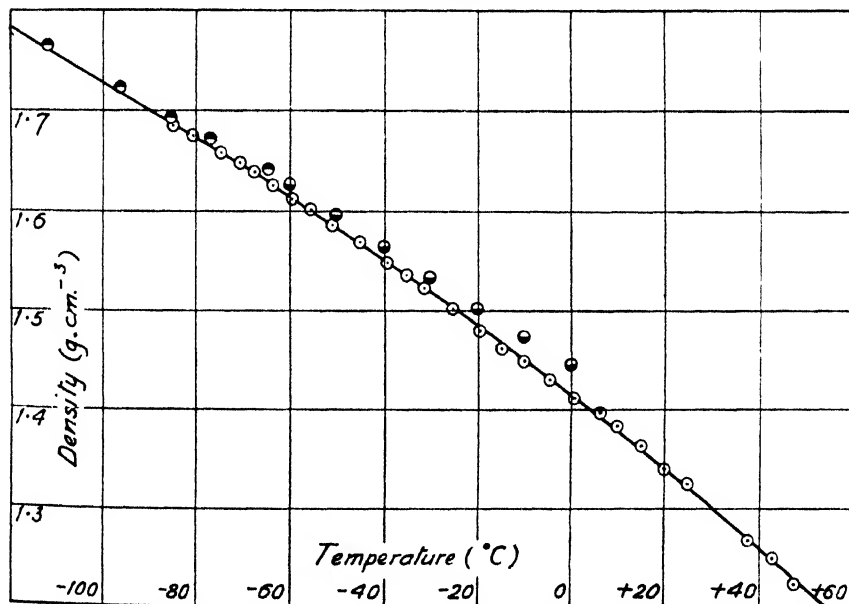


FIG. 1.—Density-temperature relation for liquid arsine. Experimental points : ● Johnson and Pechukas ; ◐ Durrant, Pearson, and Robinson ; ○ this work. Continuous curve calculated from least squares expression.

The empirical relationship—

$$\rho_t = 1.413 - 3.602 \times 10^{-3}t - 4.321 \times 10^{-6}t^2,$$

<sup>4</sup> Kaye and Laby, *Tables of Physical and Chemical Constants*, 9th ed. (1944).

obtained by applying the method of least squares to the experimental data, has been used to calculate the density at each temperature; these are tabulated in Table II and the continuous curve in Fig. 1 has been drawn from this relation. The standard error is

$$\sqrt{\frac{\sum d_i^2}{n}} = 0.0027.$$

Experimental points obtained by other observers shown in Fig. 1, diverge progressively from our data as the temperature increases, due evidently to the failure to correct for the mass of arsine in the vapour phase.

This work constituted part of a study of arsine carried out at the Imperial College of Science and Technology for the Ministry of Supply in 1940. Permission to publish, given by the Chief Scientist, Ministry of Supply, is acknowledged. The authors wish to thank Prof. H. V. A. Briscoe for his friendly advice.

*Council for Scientific and Industrial Research,*  
*Industrial Chemistry Division,*  
*Melbourne.*  
*Chemistry Faculty,*  
*Military College of Science,*  
*Shrivenham, Nr. Swindon,*  
*Wilts.*

## THE EFFECT OF AROMATIC COMPOUNDS ON THE VAPOUR-PHASE OXIDATION OF FUELS

### PART I.—THE EFFECT ON THE VAPOUR-PHASE OXIDATION OF ETHERS

By G. H. N. CHAMBERLAIN AND A. D. WALSH

*Received 20th May, 1949*

The effects of a wide range of aromatic additives on the vapour-phase slow oxidation of diisopropyl ether at 360°C are reported. It is found possible to correlate the efficacy of the inhibiting action with the electronic properties of the benzene ring in the inhibitor. Experiments are also reported on the effects of aromatic additives on the slow oxidation of diisopropyl ether in the cool flame temperature range and on the ignition of diethyl ether to both cool and hot flames. It appears that aromatic inhibitors react with radical chain carriers, the reaction not being limited to a single type of radical and being greatly facilitated by increasing spread of the electronic cloud of the ring.

A number of reactions in solution are known which involve aromatic compounds and where changes in rate can be correlated with electronic properties. This paper is thought to report the first case of such an effect in a gas-phase reaction.

In a series of papers <sup>1, 2, 3, 4</sup> an extensive investigation of the vapour-phase oxidation of ethers has been described, including the effect of a wide range of additives upon the oxidation in various pressure-temperature regions. Such a systematic study of the effect of additives has the

<sup>1</sup> Chamberlain and Walsh, *Colloque sur la cinétique et le mécanisme des réactions d'inflammation et de combustion en phase gazeuse* (Paris, April, 1948).

<sup>2</sup> Chamberlain and Walsh, *Third Symposium on Combustion and Flame and Explosion Phenomena* (Madison, U.S.A., Sept., 1948).

<sup>3</sup> Chamberlain and Walsh, *ibid.*

<sup>4</sup> Chamberlain and Walsh (in course of publication).

twofold advantage of shedding light on the reactions involved in ether oxidation and on the behaviour of the additives. The latter may be important for engine practice since impurities are often added to the fuel with the object of improving engine performance.

The first part of this paper reports experiments on the effect of aromatic compounds on the slow oxidation and ignition of ethers. The second part considers further the results obtained and applies them to explain the mode of action of aromatic anti-knocks in engines. Ethers were chosen as fuels partly because their vapour-phase oxidation can be studied (i) at such low pressures that the difficulty of introducing at room temperature an appreciable proportion of such involatile additives as aromatic compounds is reduced; and (ii) at such low temperatures that complications due to decomposition or oxidation of such additives as aromatic compounds are reduced.

### Experimental and Results

The apparatus and procedure were the same as previously described.<sup>2</sup>

**The Slow Oxidation of Diisopropyl Ether at 360° C.**—The main results relating to the combustion of diisopropyl ether-oxygen mixtures at 360° C have already been reported. At this temperature, the so-called "high" temperature mode of oxidation is dominant. The  $\Delta p$ -time curves show a slow rise to a maximum slope attained after an interval of several minutes and then a gradual falling-off of the rate of pressure rise. We shall here be concerned solely with the effect upon these curves of various aromatic compounds. The curves shown below were repeatedly checked for reproducibility.

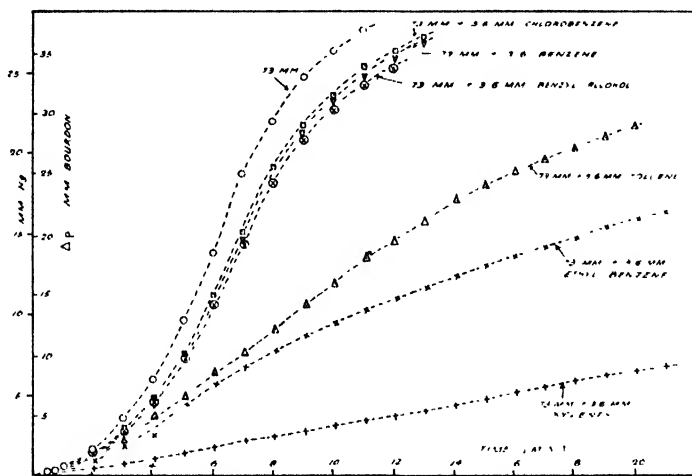


FIG. 1.—Slow oxidation of diisopropyl ether at 360° C. Effect of ca. 5 % additions of benzene, toluene, ethyl benzene, xylene, chlorobenzene and benzyl alcohol. 30 % ether-oxygen. Quartz vessel. 1.33 mm. Bourdon = 1 mm. Hg.

Fig. 1 shows the  $\Delta p$ -time curve for 73 mm. of a 30 % diisopropyl ether-oxygen mixture and the effect upon it of an addition of 3.6 mm. (i.e. ca. 5 %) benzene. Addition of 5 % of inert gas would have negligible effect (see<sup>2</sup>). The benzene has a small inhibiting action, the maximum rate of pressure rise being attained some 60 sec. later than without the additive and the maximum rate of pressure rise being reduced. Fig. 1 also shows the effect of chlorobenzene, benzyl alcohol, toluene, ethyl benzene and xylenes. The first two of these had effects practically indistinguishable from that of benzene. The addition of 5 % toluene instead of benzene produced a much larger inhibiting effect. With ethyl benzene the effect was somewhat greater still, the difference increasing with time. Addition of 5 % mixed xylenes caused a further big increase of inhibiting effect.

Variations in vapour pressure and large variations in magnitude of effect

made it impossible to compare satisfactorily the effect of all the aromatics at the same concentration. They were therefore all compared with benzene as standard. Fig. 2 shows the results obtained with certain additives in ca. 3 %

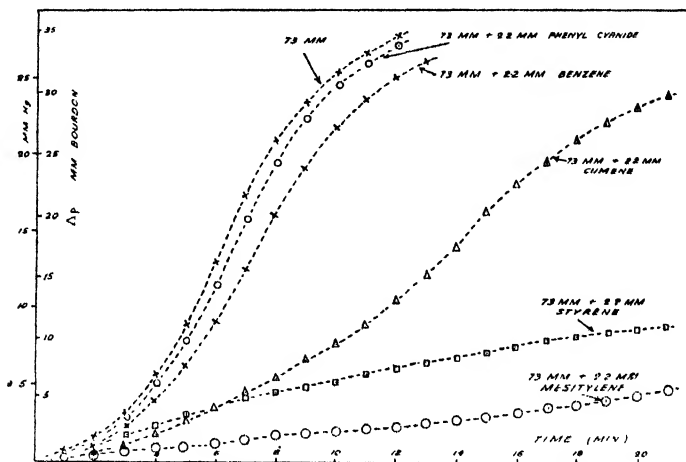


FIG. 2.—Slow oxidation of diisopropyl ether at 360° C. Effect of ca. 3 % additions of benzene, phenyl cyanide, cumene, mesitylene and styrene. 30 % ether-oxygen. Quartz vessel. 1.24 mm. Bourdon = 1 mm. Hg.

concentration. Phenyl cyanide has an even smaller inhibiting effect than the already small effect of benzene. Cumene has a much greater effect and mesitylene a much greater one still. Styrene also has a large effect, but since our specimen contained about 20 % ethyl benzene as impurity, Fig. 2 does not afford a quantitative comparison with the other substances shown. However, the effect of styrene was evidently comparable to that of mesitylene.

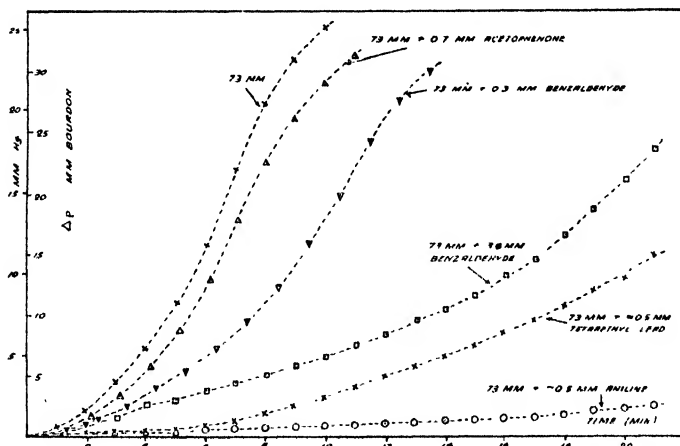


FIG. 3.—Slow oxidation of diisopropyl ether at 360° C. Effect of acetophenone, benzaldehyde, aniline and tetraethyl lead. 30 % ether-oxygen. Quartz vessel. 1.33 mm. Bourdon = 1 mm. Hg.

Fig. 3 shows the effect of acetophenone and aniline at concentrations close to 1 %. At this concentration the effect of benzene is very small and that of acetophenone is not much greater. The effect of aniline, however, is very great. In Fig. 3 there is included also a curve showing the effect of the addition of a small concentration of lead tetra-ethyl. Not much stress should be put upon the exact position of this curve relative to that of aniline, since absorption in

tap grease makes it difficult, particularly with lead tetraethyl, to be sure just how much additive has entered the reaction vessel. But Fig. 3 makes it probable that, under these conditions, at least, the effects of lead tetraethyl and aniline are much more comparable than they are as engine knock inhibitors: in an engine lead tetraethyl is enormously more effective than a similar concentration of aniline in raising the knock-limited compression ratio.<sup>5</sup>

Fig. 3 also shows the effect of benzaldehyde. To our surprise (see below) this was a much greater inhibitor than benzene. The result was confirmed with benzaldehyde that had been specially purified by the preparation and decomposition of its bisulphite compound. It was noticed that some condensation of the benzaldehyde occurred on the walls of the capacity vessel when the mixture was given its routine time of standing before admission to the reaction vessel so that it is possible that the actual amount of benzaldehyde entering the mixture was greater than the measured pressure indicated; but even so the large inhibiting effect appears to be a real one.

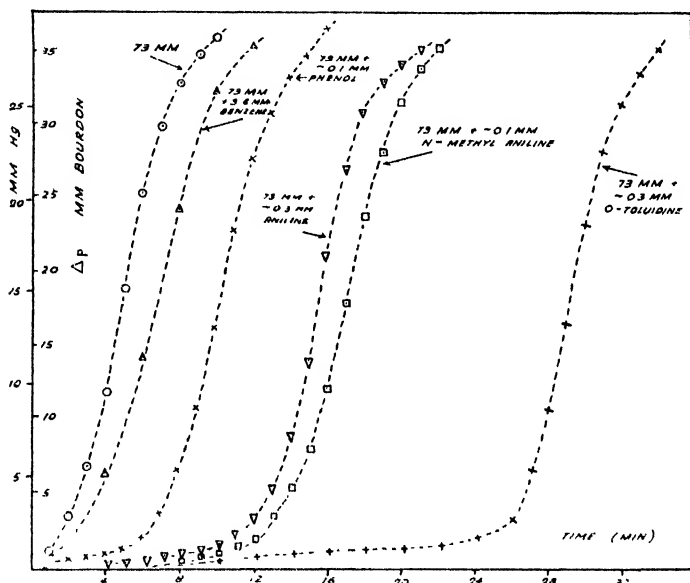


FIG. 4.—Slow oxidation of diisopropyl ether at 360°C. Effect of small quantities of phenol, aniline, *N*-methyl aniline and *o*-toluidine. 30 % ether-oxygen. Quartz vessel. 1.24 mm. Bourdon = 1 mm. Hg.

Fig. 4 shows the effect of aniline in a rather smaller concentration. It is clear that very little pressure rise occurs at all until, after about 12 min., the aniline appears to become exhausted. Similar results are shown in Fig. 4 for *N*-methyl aniline (which, compared with an equal concentration of aniline, is clearly much more effective) and *o*-toluidine which is also much more effective than aniline. *N*-dimethyl aniline was similarly shown to be more effective than aniline. The effect of addition of ca. 0.3 mm. *N*-dimethyl aniline was to give a curve almost identical with that for the addition of ca. 0.1 mm. *N*-methyl aniline. For purposes of comparison, Fig. 4 shows the effect of benzene in much larger concentration. The figure also shows the effect of phenol to be considerable, though much less than that of *N*-methyl aniline. In all these curves the order of efficacy is the same whether judged from the pressure rise before the steep portion of the curve occurs or from the time required to attain the steep portion. Just as for aniline, the steep portion of the curves for phenol, *N*-methyl aniline, *N*-dimethyl aniline, and *o*-toluidine all have slopes that are practically identical with that of the curve for no additive present. Evidently, after a time these very effective inhibitors become used up and then the  $\Delta p$ -time curve rises normally. Lead tetraethyl by contrast is not used up, the

<sup>5</sup> See Downs and Walsh (in course of publication).



inhibited curve never attaining the same rate as the uninhibited one. Presumably an induced oxidation of the aromatic substances occurs and this destroys their inhibiting effect.

Fig. 5 shows that pyridine is an inhibitor similar in efficacy to benzene and anisole somewhat more effective.

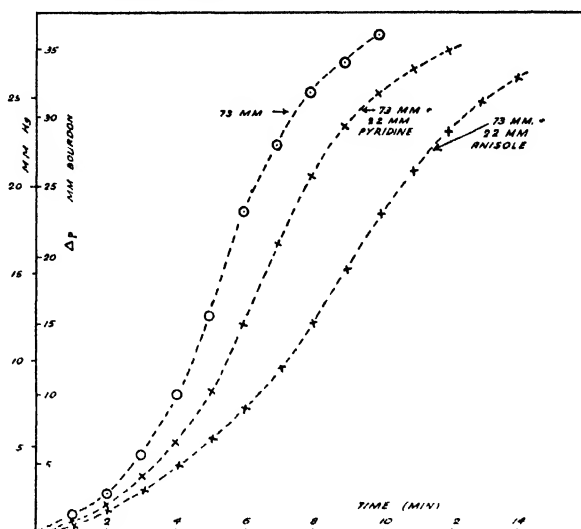


FIG. 5.—Slow oxidation of diisopropyl ether at 360°C. Effect of pyridine and anisole. 30 % ether-oxygen. Quartz vessel. 1.24 mm. Bourdon = 1 mm. Hg.

**The "Low" Temperature Slow Oxidation of Diisopropyl Ether.**—Fig. 6 shows the effect of xylene, in a concentration of *ca.* 3.5 %, on the slow oxidation

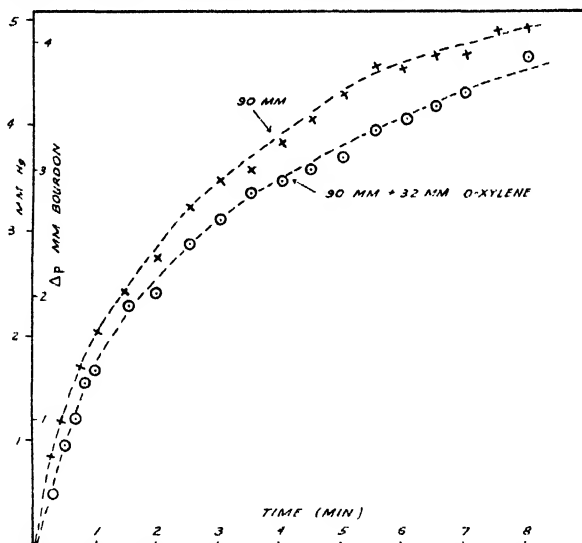


FIG. 6.—The effect of xylene on the slow oxidation of diisopropyl ether at 220°C. 30 % ether-oxygen. Quartz vessel. 0.832 mm. Bourdon = 1 mm. Hg.

of diisopropyl ether at 220°C. This temperature lies within the "low" temperature region of diisopropyl ether oxidation (see 2,3) where the slope

of the  $\Delta p$ -time curves reaches its maximum practically at once and then continuously falls off. Xylene produced a small inhibition. A curve plotted to show the effect of addition of *ca.* 0.2 % *N*-dimethyl aniline lay almost on top of the 3.5 % xylene curve, showing the much greater inhibition by *N*-dimethyl aniline. These results suggest that, in general, the order of efficacy of inhibition by aromatic compounds is the same in the "low" temperature zone as in the "high". Owing to the greater experimental difficulty of obtaining reliable "low" temperature curves and the smaller effect observed, these "low" temperature experiments were therefore not pursued and attention was concentrated on the determination of the order of inhibiting efficacy from the experiments at 360° C reported above.

It should be noted, however, that additions of benzaldehyde had virtually no effect at 220° C. Further, Fig. 7 shows the effect of *ca.* 0.4 % aniline on the slow oxidation of diisopropyl ether at 210° C. Instead of an inhibition,

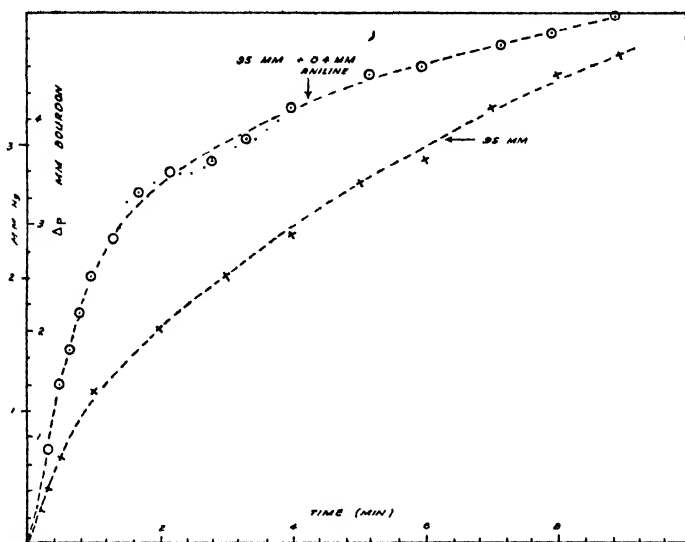


FIG. 7.—The effect of aniline on the slow oxidation of diisopropyl ether at 210° C. 30 % ether-oxygen. Quartz vessel. 1.24 mm. Bourdon = 1 mm. Hg.

an acceleration of the pressure rise took place, this acceleration being most marked in the early stages of the reaction and the two curves later approaching each other. At first sight this seems surprising, but a simple explanation is given below.

**Cool Flames of Diethyl Ether.**—Xylene was found to raise the minimum pressure required for the appearance of a cool flame in a 30 % diethyl ether-oxygen mixture at 200° C (Fig. 8) and to lengthen the time required for that cool flame to appear (Fig. 9). A fairly rapid increase of these inhibiting effects occurred with increasing xylene concentration, but the curves of Fig. 8 and 9 should probably be taken as qualitative only, since (i) rapid absorption in tap grease always occurred, and (ii) on account of the low vapour pressure of xylene, the "doser" technique (see \*) of introduction could not be employed, the additive having to be measured directly into the capacity vessel and an additional uncertainty in concentration thereby introduced.

Fig. 10 shows the effect of aniline on both the "flash" and "Bourdon" (for the explanation of these terms, see \*) cool flame limit curves of diethyl ether. At the lowest temperatures, the effect of the aniline is to push the "Bourdon" limit curve to higher pressures. At temperatures above the tip of the most prominent peninsula of the limit curve, a shift to slightly lower pressures takes place. Obviously this is connected with the accelerating effect of aniline noticed on the slow oxidation in this temperature region. It is clear from Fig. 10 that aniline is exerting two effects: (i) an inhibiting action, presumably by virtue of its aromatic character, and (ii) a promoting effect

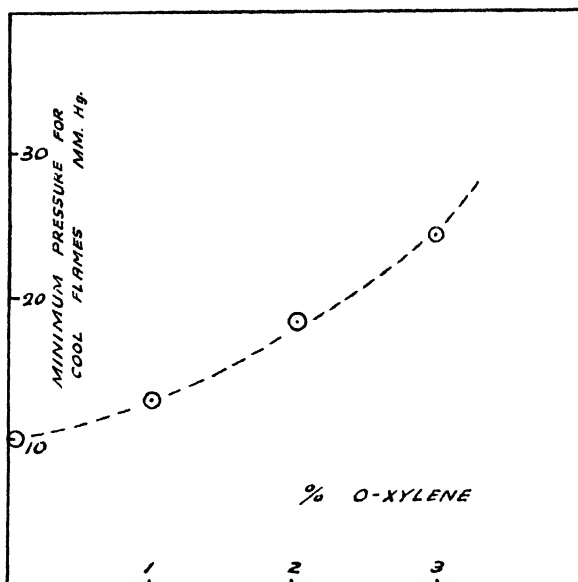


FIG. 8.—The effect of xylene on the minimum pressure required for a cool flame in a 30 % diethyl ether-oxygen mixture at 200° C. Quartz vessel.

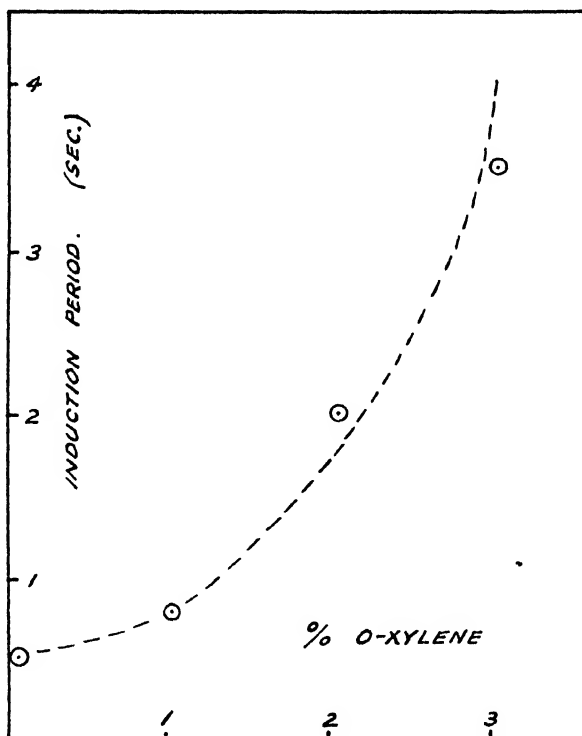


FIG. 9.—The effect of xylene on the induction period preceding a cool flame in a 30 % diethyl ether-oxygen mixture at 200° C. Quartz vessel.

which under certain circumstances can outweigh (i). The key to an understanding of (ii) was obtained when it was noticed that, during work with aniline, a greenish material appeared on the tubing leading from the reaction vessel. Tests showed that, on treatment with hydrochloric acid, this deposit yielded formaldehyde and aniline hydrochloride. Almost certainly the material was

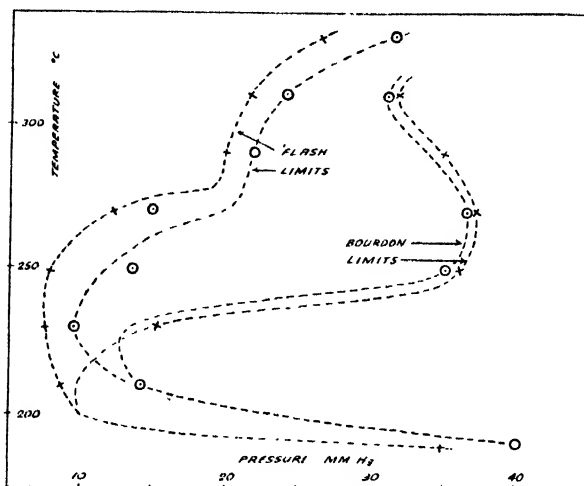


FIG. 10.—The effect of aniline on cool flames of diethyl ether. 30 % ether-oxygen. Quartz vessel. —x—x— undoped. —o—o— + ~ 0.4 mm. aniline.

a polymer of methylene aniline,  $\phi-N=CH_2$ , the reaction forming it occurring on the cold surfaces of the tubes leading to the reaction vessel. Aniline was therefore removing formaldehyde produced during these experiments. Since we have shown<sup>2,3</sup> (i) that formaldehyde inhibits "low" temperature slow oxidation of diisopropyl ether, (ii) that formaldehyde raises the pressure limits required for diethyl ether cool flames and (iii) that the production of formaldehyde in the flash accompanying admission of the ether-oxygen mixture to the reaction vessel at temperatures above that of the tip of the main cool flame limit peninsula must push the "Bourdon" cool flame limit curve to higher pressures than would otherwise be the case, it is clear that the anomalous promoting effect of aniline on "low temperature" oxidation is due to its removal of formaldehyde. In agreement with (iii), aniline raised the "flash" limit curve to higher pressures throughout its course: there was no formaldehyde to remove before the flash occurred. These experiments confirm the explanation given earlier<sup>3</sup> of the "flash" and "Bourdon" limit curves.

**Hot Flames of Diethyl Ether.**—Aniline raised slightly the minimum pressure required for a hot flame in a 30 % diethyl ether-oxygen mixture at both 200 and 400° C. (Table I). Xylene appeared ineffective. It should be

TABLE I

Additive	Aniline		o-Xylene	
	200	400	240	400
Temp. °C . . . . .	200	400	240	400
Limit in absence of additive mm. Hg	182.8	168.5	183.0	168.5
Limit in presence of additive mm. Hg	184.0	173.7	183.0	167.0
Additive concentration % . . .	0.3	0.3	1.0	1.0

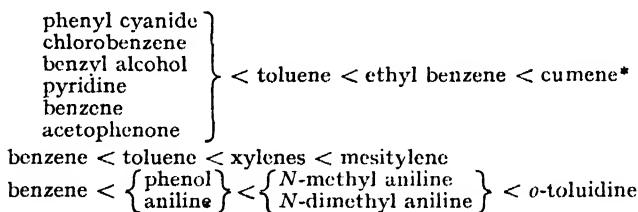
remembered, however, that with ignition requiring a total pressure approaching 200 mm. Hg, only very small percentages of aromatic additives could be introduced, owing to their low vapour pressures.

## Discussion

The experimental work reported above falls into two main divisions—first, a survey of the effect of one or two aromatic compounds on all the five broad regions into which vapour-phase oxidation can be divided<sup>\*</sup> and wherein we have previously established (for ethers) the main facts; and second, a survey of the effect of a wide range of aromatic compounds on one particular pressure-temperature region. For the first survey, xylene and aniline were chosen and the effect of each determined on the slow oxidation in the "high" temperature zone, on the ignition to hot flames in the "high" temperature zone, on the slow oxidation in the "low" temperature region, on the ignition to cool flames and on the ignition to hot flames in the "low" temperature zone. Systematic work of this sort is a powerful method of attacking the problem of how a given additive produces its effect. In this case, apart from the easily explained anomalous effect of aniline under certain conditions in the "low" temperature zone, the experiments suggest that aromatic compounds have an inhibiting effect in all the five main pressure-temperature regions. This result is to be contrasted with that obtained for formaldehyde<sup>2, 3</sup> where inhibition was found in the "low" temperature region but promotion in the "high"; and for lead oxide where in one of the five regions (namely, that of the cool flame limits) the additive had little effect. With aromatic compounds the inhibition does not appear to be specific to particular chain processes.

The value of the second survey is that it enables the order of efficacy of the aromatic substances among themselves to be determined. The fact that such a wide range of aromatic compounds is effective, makes it practically certain that they all exert their effect by virtue of the benzene ring they contain. Benzene itself is a weak inhibitor, a fact connected with the knowledge<sup>6</sup> that in the vapour-phase oxidation of benzene the reaction chains are broken in the gas phase—presumably in part by the unchanged benzene molecules.

Though it has not been possible to test all the additives at the same concentration, the order of efficacy appears to be :



This order suggests a correlation with the electronic properties of the benzene ring. It appears in general to be the order of the first ionization potentials expected for the  $\pi$  electrons of the benzene ring. Only a few of these (Table II) are definitely known, but most can be roughly predicted relative to benzene from general considerations of molecular structure. The two main causes lowering the ionization potential are charge transfer (as, e.g., in the alkyl benzenes) and conjugation effects (as, e.g., in styrene).<sup>7</sup>

The lower the expected first ionization potential, the greater the inhibiting effect. For alkyl benzenes, the order is that of electron release from the side chains to the benzene ring: the greater the negative charge

\* Fort and Hinshelwood, *Proc. Roy. Soc. A*, 1930, **129**, 294.

\* Based on the inhibition observed in the first 10 min., after which the cumene begins to be quickly used up.

<sup>7</sup> Price and Walsh, *Proc. Roy. Soc. A*, 1947, **191**, 22; Walsh, *ibid.*, 1947, **191**, 32.

on the benzene ring, the lower the  $\pi^{-1}$  ionization potential<sup>6</sup> and the greater the inhibiting effect. As H of benzene is exchanged for CH<sub>3</sub>, the methyl group releases electrons to the benzene ring and so toluene is a better

TABLE II

Substance	First $\pi^{-1}$ Ionization Potential <sup>7</sup> (V)
Pyridine .	~ 9.7
Benzene .	9.24
Toluene .	8.82
Ethyl benzene .	~ 8.75
Cumene .	~ 8.6
<i>o</i> -Xylene .	8.4

inhibitor than benzene, *o*-xylene better than toluene and mesitylene better than *o*-xylene. As CH<sub>3</sub> is exchanged for C<sub>2</sub>H<sub>5</sub>, a further electron transfer takes place and ethyl benzene is a better inhibitor than toluene. Similarly, cumene is a better inhibitor still.

There is a partial correlation with the direction of the dipole moment in the side chain. If this is directed so that its negative end lies towards the ring<sup>9</sup> (e.g. alkyl benzenes, phenol, aniline), there occurs an increased inhibiting effect relative to benzene. Side chains which *remove* electrons from the benzene ring cause the inhibiting effect to become less than that of benzene, or at least to remain very small. (Experimentally, it is difficult to be sure of the exact order among the molecules whose effects differ only slightly: the curve in the absence of additive is itself liable to small fluctuations in position and slope and we have already referred to the difficulty of absorption by tap grease. No stress can be put on small differences of effect.) Examples are phenyl cyanide, chlorobenzene, benzyl alcohol, acetophenone. A rule similar to that of Crum Brown for the orientating effect of substituents can be stated to cover many of the cases. In mono-substituted benzenes, those side chains that cause *o-p* orientation of a subsequent entering group have a greater inhibiting effect than benzene; those side chains that cause *m* substitution do not have a greater inhibiting effect than benzene itself. Chlorobenzene would, of course, be an exception to such a rule, just as it is a well known exception to the correlation of sign of dipole moment and orientating effect. It is interesting that the action of chlorobenzene correlates with its known dipole moment (which moment has its positive end on the benzene ring) and not with the properties of an hypothetical  $^+Cl = \text{benzene ring}^-$  molecule.

The results described suggest the following order of efficacy:

aniline < *N*-dimethyl aniline < *N*-methyl aniline.

It is noteworthy that this is also the order of the dipole moments measured in benzene solution, the values being: aniline 1.52 D at 20° C; *N*-dimethyl aniline 1.58 D at 25° C; *N*-methyl aniline 1.64 D at 25° C.

There is also a partial correlation between the order of the inhibiting effect and the order of the wavelength shifts in the absorption corresponding to the 2600 Å system of benzene. Table III lists values of  $\lambda_{\text{max}}$ , for some of the inhibitors tested. The position of the absorption maximum, however, depends not only upon the ground state but also upon the excited state; so that, while in general, shifts in  $\lambda_{\text{max}}$  reflect shifts in the  $\pi^{-1}$  ionization potential, there are exceptions. Ethyl benzene and cumene

<sup>6</sup> See Price, *Chem. Rev.*, 1947, 41, 257, for the first ionization potentials of the alkyl benzenes.

<sup>7</sup> See Sidgwick, *The Covalent Link in Chemistry* (Cornell, 1933).

are known examples; <sup>10</sup> chlorobenzene and phenyl cyanide may be others.

According to the correlation between inhibiting effect and ionization potential, benzaldehyde would be expected to have an effect less than"

TABLE III

Substance $\phi = C_6H_5$	In <i>n</i> -hexane Solution (Å)	In <i>n</i> -heptane Solution (Å)
Pyridine . . .	—	2510
$\phi$ -H . . .	2560	—
$\phi$ -Me . . .	2620	2620
<i>o</i> -Xylene . . .	—	2630
$\phi$ -Cl . . .	2650	—
$\phi$ -OH . . .	2750	—
$\phi$ -NH <sub>2</sub> . . .	2800	—
Styrene . . .	—	2820

that of benzene. The reason for its considerable effect at 360° C remains unexplained. Presumably it is due to some reaction involving the CHO group rather than the aromatic nucleus. It was thought possible that some reaction might take place between acetaldehyde and benzaldehyde. Acetaldehyde, a product of the reaction at 360° C, is known to have a strong promoting effect on the pressure rise, so that its removal would represent an inhibition of the oxidation. However, no reaction of benzaldehyde and acetaldehyde within 6 min. was observed on admitting mixtures of benzaldehyde and acetaldehyde to the reaction vessel at 360° C.

This correlation of inhibitor efficacy with the electronic properties of the benzene ring confirms the deduction that the aromatic compounds exert their effect by virtue of the benzene ring they contain. The variation of effect is due in the main \* to the indirect action of the side chains in enhancing or diminishing the fundamental property of the benzene ring.

A further fact to emerge from the work at 360° C is that the aromatic additives, while exerting their inhibiting effect, are subject to an induced oxidation. The latter presumably occurs by attack of radicals produced in the ether oxidation. It is probable that the inhibiting effect can be ascribed to the same reaction of radicals with the benzene ring. The fact that the inhibiting effect is found in all the five main pressure-temperature regions of oxidation suggests that the benzene ring can react with more than one type of radical. The facts that benzene <sup>12</sup> and *N*-methyl aniline <sup>5</sup> inhibit the oxidation of carbon disulphide, that benzene inhibits the hydrogen-oxygen reaction <sup>12</sup> and that benzene and toluene (toluene being more effective than benzene) inhibit the polymerization of isoprene, <sup>13</sup> further suggest that the benzene ring can react with a wide variety of free radicals.

If the inhibiting effect involves free radicals attacking the benzene ring, it is to be expected that the ease of their reaction with a benzene ring will be greater the greater the spread of the electronic cloud of the ring, i.e. the lower the first  $\pi^{-1}$  ionization potential. Since in the well-known kinetic theory expression

$$\text{rate} = pZe^{-E/RT}$$

<sup>10</sup> See Walsh, *Ann. Reports*, 1947, 44, 32.

\* There may, of course, be superimposed a *direct* effect of certain side chains. The aromatic amines may provide examples, since methyl amine has been reported <sup>11</sup> to inhibit cool flame propagation and aliphatic amines may have an engine anti-knock effect.

<sup>11</sup> Neiman, Rubina and Schnol, *J. Physic. Chem. Soc. Russ.*, 1948, 22, 641.

<sup>12</sup> Mardles, *Aer. Res. Comm. Rep.*, 1930, No. 1374.

<sup>13</sup> Bolland, *Proc. Roy. Soc. A*, 1941, 178, 24.

the frequency factor  $p$  is hardly likely to change greatly from one simple benzene derivative to another, changes in inhibiting efficiency might be expected to be due to changes in activation energy of the reaction between radical chain carriers and the benzene ring. A low activation energy for a reaction between a free radical and the benzene ring would be expected when, owing to the diffuse nature of the electronic cloud of the ring, that reaction takes place at a comparatively large distance from the nuclei of the ring: repulsion between the nuclei is then very much less.

The following paper provides a little further information on the nature of the reaction taking place during the inhibition.

The authors desire to thank the Shell Petroleum Company who made it possible for one of the authors (G. H. N. C.) to take part in this work at Cambridge and who defrayed the costs of the research.

*Laboratory of Physical Chemistry,  
Cambridge.*

## THE EFFECT OF AROMATIC COMPOUNDS ON THE VAPOUR-PHASE OXIDATION OF FUELS

### PART II.—THE ANTI-KNOCK EFFECT OF AROMATIC COMPOUNDS IN ENGINES

BY A. D. WALSH

*Received 20th May, 1949*

A survey is made of the anti-knock effect of aromatic compounds in internal combustion engines. This, combined with the results described in the preceding paper, enables conclusions to be drawn as to the mode of action of aromatic anti-knocks. There exists a correlation between the anti-knock effect of aromatic compounds and the influence of the side chains upon the electronic properties of the benzene rings. The anti-knock effect increases with decreasing binding of the ring electrons. The effect is exerted by the unchanged molecules and anomalies are explicable as due to pyrolysis or oxidation of the anti-knocks. A considerable mass of previously incoherent data can be reduced to comparative order using these ideas. The observed anti-knock effect of hexamethyl benzene suggests that the reaction between radical chain carriers and the benzene ring, which is responsible for inhibition by aromatic compounds, is best regarded as the temporary formation of a complex between the radical and the electronic cloud of the ring.

This paper is concerned with the effect of aromatic compounds on the behaviour of fuels in internal combustion engines, in particular on knock. Knock may be defined as an explosion of the fuel-air mixture in the last part of the cylinder charge to burn, and propagated with a speed comparable with that of a true detonation wave. Anti-knocks and pro-knocks are substances which respectively decrease and increase the tendency to the knock explosion. Increase of engine compression ratio usually increases the tendency to knock. Measurement of the compression ratio at which knock is just noticeable (the "highest useful compression ratio" or H.U.C.R.) in the presence and absence of an additive in the fuel permits comparison of the anti-knock effects of different additives.



The anti-knock effect of aromatics has been known since the pioneer work of Midgley and Boyd in the early nineteen twenties; but in spite of the great economic importance of aromatic compounds as additives and fuels in internal combustion engines, hitherto there has been no satisfactory theory of their action. There can be little doubt that the knock action of aromatic compounds is to be considered as a whole and that therefore the seat of the action is the benzene nucleus. Anilines and phenols exert their anti-knock effect essentially as benzene exerts its slight anti-knock effect: the side groups, in the main, merely increase or decrease the property of the benzene ring. Taken in conjunction with the preceding paper, it is the purpose of the following discussion to show that the anti-knock effect of benzene derivatives can be correlated with the electronic properties of the side chains, as long as allowance is made for the complicating effects of pyrolysis and oxidation of the compounds.

**Collection of Data.**—Callendar<sup>1</sup> measured the % change in highest useful compression ratio for a 5 % (liquid) volume addition of various additives to a fuel. It would be best to compare the action of additives at the same mole fraction concentration. However, since the simple benzene derivatives do not differ greatly in density and molecular weight, a 5 % volume addition can be taken roughly as a constant mole fraction. Boyd<sup>2</sup> studied the substituted anilines and measured the molecular effectiveness relative to aniline, based on concentrations up to 3 % by

TABLE I

Substance	% Increment in H.U.C.R. for 5 % Vol. Addition— Callendar	Relative Mole Effectiveness up to 3 % Vol. Addition—Boyd	Aniline Equiv./100— Spiers
Benzene . . . . .	1.0	0.685	0.10
Toluene . . . . .	2.0	0.112	0.15
Xylene (unspecified isomer) . . . . .	0.6	0.142	—
<i>o</i> - . . . . .	—	—	0.17
<i>m</i> - . . . . .	—	—	0.23
<i>p</i> - . . . . .	—	—	0.26
Ethyl benzene . . . . .	—	—	0.19
<i>n</i> -Propyl benzene . . . . .	—	—	0.24
<i>n</i> -Butyl benzene . . . . .	—	—	0.20
Mesitylene . . . . .	—	—	0.31
Phenol . . . . .	4.4	—	—
Cresol (unspecified isomer) . . . . .	5.8	—	—
Anisole . . . . .	1.1	—	—
Phenetole . . . . .	1.3	—	—
Benzyl alcohol . . . . .	0.4	—	—
Benzaldehyde . . . . .	0	—	—
Bromo benzene . . . . .	— 1.7	—	—
Aniline . . . . .	21.7	1.00	1.00
<i>N</i> -methyl aniline . . . . .	22.2	1.4	—
<i>N</i> -ethyl aniline . . . . .	10.4	1.02	—
<i>N-n</i> -propyl aniline . . . . .	—	0.75	—
<i>N-n</i> -butyl aniline . . . . .	—	0.52	—
<i>N-isoamyl</i> aniline . . . . .	—	0.25	—
<i>N</i> -dimethyl aniline . . . . .	—	0.21	—
Toluidine (unspecified isomer) av. of <i>o</i> -, <i>m</i> -, <i>p</i> - . . . . .	18.3	1.22	—
<i>m</i> -Xyldine . . . . .	22.3	1.4	—
Cumidine . . . . .	—	1.51	—
Pyridine . . . . .	1.2	—	—
Phenyl hydrazine . . . . .	— 5.9	—	—

<sup>1</sup> Callendar, *Aer. Res. Comm. Rep.*, 1925, No. 1018.<sup>2</sup> Boyd, *Ind. Eng. Chem.*, 1924, 16, 893.

volume of the fuel (kerosene). The handbook compiled by Spiers<sup>3</sup> lists the "aniline equivalents" of a number of aromatics, this quantity being defined as the reciprocal of the number of moles of substance required to give the same anti-knock effect as one mole of aniline, i.e. the greater the aniline equivalent, the better the anti-knock properties. The aniline equivalent of Spiers is approximately  $100 \times$  the relative mole effectiveness of Boyd. Table I summarizes the data given by Callendar, Boyd and Spiers.

**Discussion of Data.**—Some disagreement between the various sets of results is evident, but in view of the different factors of engine concentration, mixture strength, expression of results, etc., this is to be expected and is not serious.

Inspection of Table I makes it evident that, to a large extent, the order of the anti-knock effect of aromatic compounds is that of their inhibition of the slow oxidation of diisopropyl ether at  $360^\circ\text{C}$  recorded in the previous paper. Thus the list of Spiers shows the anti-knock effect to have the order :

benzene < toluene < ethyl benzene

and benzene < toluene < xylenes < mesitylene ;

while the lists of Callendar and Boyd show :

benzene < -phenol < aniline < *N*-methyl aniline  
benzyl alcohol < benzene

and pyridine slightly more effective than benzene.

Again there appears a correlation between inhibiting effect and electronic properties of the benzene ring. Exceptions are dealt with below. The less the binding of the  $\pi$  electrons of the benzene ring, the greater tends to be the anti-knock effect. In the alkyl benzenes transfer of negative charge from the side chains to the ring reduces the  $\pi$ - $\pi^*$  ionization potential and tends to increase the anti-knock action. In phenol the operation of the so-called mesomeric effect reduces the binding of the most weakly bound  $\pi$  electrons still further and phenol is a considerably more powerful anti-knock. Similarly, hydroquinone is expected to be, and is, capable of exerting an anti-knock action.<sup>4</sup> Addition of an alkyl group, as in the cresols, adds to the negative charge density in the benzene ring and improves the anti-knock effect. In aniline the expected large mesomeric effect correlates with the particularly large anti-knock effect. Addition of the charge transfer effect of alkyl groups is capable of enhancing further the anti-knock value. Thus the toluidines on Boyd's scale are better than aniline ; *N*-methyl aniline and *m*-xylydine are better still and cumidine best of all.

If the benzene ring bears a positive charge relative to benzene, then the aromatic is less effective as an anti-knock than benzene : that is, its effect is either practically zero or even pro-knock. This can be seen from the effects of benzyl alcohol, benzaldehyde and bromobenzene (Table I) ; and from the facts that, relative to benzene, fluorobenzene, chlorobenzene, phenyl cyanide, acetophenone, nitrobenzene and nitrosobenzene all have zero or slight pro-knock effects.<sup>5</sup> The action of benzaldehyde (confirmed by later work<sup>5</sup>) is especially noteworthy in view of the anomalous result obtained in the oxidation of diisopropyl ether at  $360^\circ\text{C}$ . With the exception of the halogen compounds, for the monosubstituted benzenes one can say (as for inhibition of the diisopropyl ether oxidation) that substances which are *o-p* directing are good anti-knocks ; while substances which are *m* directing are pro-knocks relative to benzene. Even pyridine, which is weakly *o-p* directing and (according to Callendar) a slightly

<sup>3</sup> Spiers, *Technical Data on Fuel*, British Nat. Comm. Wld. Power Conference (London, 1935).

<sup>4</sup> Mardles, *Aer. Res. Comm. Rep.*, 1930, No. 1374.

<sup>5</sup> Downs and Walsh (in course of publication).

better anti-knock than benzene, fits this rule. Alternatively, we may say that, without exception, simple side chains which activate the benzene ring (in the sense of facilitating nitration, etc.) are anti-knocks relative to benzene; while those that deactivate the ring are pro-knocks relative to benzene.

One proviso has to be made. To say that the anti-knock effect of aromatics is determined by the binding of the  $\pi$  electrons of the benzene ring implies that the effect is one of the unchanged molecules. This is quite plausible, since simple aromatics have in general considerable stability both to pyrolysis and to oxidation. Whereas aliphatic compounds that influence knock (alkyl nitrites and nitrates, peroxides, metallic alkyls, etc.) all decompose at temperatures under 250° C and therefore at an early stage in the compression stroke, the simple aromatic compounds do not decompose at atmospheric pressure until temperatures of about 500° C or more. Whereas it is *necessary* for such an anti-knock as lead tetraethyl to decompose and/or oxidize in order to exert its effect,<sup>6</sup> the simple aromatics exert their anti-knock effect as undecomposed molecules.\* If decomposition or oxidation *does* occur, then a reduced anti-knock or even a pro-knock effect will result, for side-chain fragments may be split off that have profound effects of their own on the knock reactions and the correlation with the properties of the undisturbed benzene ring can no longer hold.

Certain anomalies to the correlation between anti-knock effect and ring electronic properties can now readily be understood. The qualifying adjective "simple" applied to the aromatic compounds in the above statements on anti-knock effect is to be stressed. As the length or complexity of the side chains is increased, in general its tendency to split or to oxidize will increase. One *expects* deviations from the correlation of knock effect and ring properties as the side chain length is increased. This is exactly what is found. According to the list of Spiers, benzene, toluene, ethyl benzene, *n*-propyl benzene, form a regular series in their increasing anti-knock effect, but *n*-butyl benzene, instead of being as good as or a little better than *n*-propyl benzene, is a little inferior.† Similarly, in the lists of Boyd and Callendar, *N*-methyl aniline is better than aniline, but *N*-ethyl is worse than *N*-methyl and *N*-*n*-propyl, *N*-*n*-butyl, *N*-*iso*-amyl, *N*-dimethyl, progressively worse still. So, too, phenyl hydrazine, instead of being an anti-knock like aniline, is actually a pro-knock. If it were not for this disturbance with increasing side-chain size, the basic strengths of the anilines could have been taken as a reflection of the negative charge on the benzene ring (an equal positive charge being present on the nitrogen atom) and a graph plotted of anti-knock effect against base strength. Such a graph for aniline, the toluidines, *N*-methyl aniline and cumidine is indeed smooth.

One sees now the value of studying the inhibiting effect of aromatic compounds on such an oxidation reaction as that of diisopropyl ether at 360° C, for the ether oxidizes so readily that the temperature at which this comparative study can conveniently be carried out is much lower than the end gas temperatures reached in engines (perhaps 500-600° C at "top dead centre").

<sup>6</sup> See Chamberlain and Walsh (in course of publication).

\* In the case of aniline, Sokolik and Jantovsky <sup>7</sup> supposed the exact opposite of this, viz., that aniline exerts its anti-knock effect by virtue of the free radicals to which its decomposition gives rise.

<sup>7</sup> Sokolik and Jantovsky, *Acta Physicochim.*, 1944, 19, 329.

† Relative to *n*-butyl benzene, one would expect *tert*-butyl benzene to be a much better anti-knock fuel since (i) the *tert*-butyl group has a larger effect in reducing the  $\pi$ -<sup>-1</sup> ionization potential of the ring, (ii) containing only 1° CH bonds in the side chain, it will have a lower tendency to oxidize. This expectation is borne out <sup>8</sup> by the observed critical compression ratios.

<sup>8</sup> Boord, 9th Ann. Report, Amer. Petroleum Inst., 1948.

Consequently any anomalies to the correlation of inhibiting efficacy with electronic properties of the benzene ring should be less marked. This is just what is found and the fact can be used as further support for the present theories. Thus, by the simple correlation *N*-dimethyl aniline should be a better inhibitor than aniline. In fact, *N*-dimethyl aniline, according to Boyd, is a much less effective engine anti-knock than aniline; but as an inhibitor of diisopropyl ether slow oxidation at 360° C is considerably more effective than aniline.

Since anomalies to the correlation of electronic properties and anti-knock effect are attributed to thermal decomposition or oxidative destruction of the aromatic compounds, the corollary may be formulated that the action of an aromatic compound (especially those with the bigger or more numerous side chains) will be at its best under the coolest possible engine running conditions. This agrees with general experience of engine behaviour. It should be possible to correlate the different effectiveness of aromatic substances in different engines, or in different fuels, with the operating temperatures and speeds. Some of the minor discrepancies in Table I between the different columns are no doubt to be explained in this way.

**Further Work.**—The ideas of this paper were first evolved in the middle years of the war. In subsequent years, during and after the war, in collaboration with Messrs. Ricardo and the Shell Petroleum Company, a great deal of engine work has been carried out to test them. The results of this work will be published in detail elsewhere.<sup>5</sup> In general the data obtained confirm, or can be understood in terms of, the above ideas.

A result of especial importance, however, may be referred to here. This is that hexamethyl benzene has a considerable anti-knock effect. It shows the effect that would be expected in view of the simple correlation between anti-knock action and  $\pi^{-1}$  ionization potential. In the previous paper it was concluded that aromatic inhibitors react with radical chain carriers. There is no apparent anomaly in the effect of hexamethyl benzene, in spite of the absence of hydrogen atoms directly attached to the ring; this shows that reaction of free radicals with ring hydrogen atoms is not a necessary part of the anti-knock action. It seems best to conceive of the inhibiting action as the formation of a temporary complex between a radical chain carrier and the electronic cloud of the benzene ring. Such a complex may decompose again to the original aromatic molecule and radical chain carrier or break down to yield new products; \* but in either case, if it has an appreciable lifetime, its formation results in a reduction of concentration of radical chain carriers with a consequent inhibiting effect. The ease of formation of the complex will increase with increasing spread of the electronic cloud of the benzene ring (and so with decreasing strength of binding of the ring electrons) as explained in the previous paper. The correlation of anti-knock and electronic properties therefore appears a natural one.

The action of hexamethyl benzene, with its bulky methyl groups, also suggests that the free radicals reacting with the benzene ring approach from above or below the plane of the ring. It is probable that the inhibiting effect of an olefin on free radical reactions takes place in a very similar way to that of benzene: each molecule contains comparatively weakly bound  $\pi$  electrons. Now one can think of molecules such as ethylene oxide and cyclopropane as built from ethylene molecules and oxygen atoms or  $\text{CH}_2$  radicals respectively. According to this point of

\* It is known, for example, that in the inhibition by aromatic compounds of liquid-phase polymerizations, chain transfer may occur,<sup>6</sup> i.e. the aromatic molecule may terminate a chain (becoming itself incorporated in the polymer) with simultaneous initiation of a new chain centre. Similarly, the phenols yielded by the vapour-phase oxidation of benzene may be formed in part by hydroxyl radicals exchanging for hydrogen atoms of the benzene ring.

<sup>5</sup> See, e.g. Cuthbertson, Gee and Rideal, *Proc. Roy. Soc. A*, 1939, 179, 309.

view, which has many advantages,<sup>10</sup> the observed symmetry of these molecules forces one to conceive of their formation taking place by the approach of the oxygen atom or  $\text{CH}_3$  radical from a direction vertically above or below the centre of the nuclear plane of the ethylene molecule. It is therefore not surprising that when the benzene ring forms a complex with a free radical, the latter approaches from above or below the ring plane. Conversely, the deduction from the observed anti-knock effect of hexamethyl benzene could be used as evidence of the value of thinking of such a molecule as ethylene oxide as built from an oxygen atom and an ethylene molecule. The existence of the tendency for complexes to form between free radicals and the  $\pi$  electrons of olefinic or benzene ring groups must be of great importance for the oxidation of such fuels as benzene and ethylene. The oxidation chains of ethylene, like those of benzene, will be short.\* With both fuels, initiation of oxidation chains is likely to occur, at least in part, by the formation in the first place of a complex between the  $\pi$  electrons and the oxygen molecule (which has a diradical structure). It is not surprising that an important product of the vapour-phase oxidation of ethylene is ethylene oxide.<sup>11</sup>

**General Conclusions.**—The main conclusions are (i) that the anti-knock effect of aromatic compounds is an effect of undissociated molecules, (ii) that their anti-knock effect increases with decreasing strength of binding of the electrons in the benzene ring, (iii) that deviations from (ii) are due to decomposition or oxidative destruction under the conditions used and therefore the more likely to occur the higher the temperature.

These three conclusions provide a working knowledge of the anti-knock action of aromatic compounds. Broadly, it can be predicted whether a hitherto untried aromatic substance will be effective. In the first place one considers its likelihood of stability with temperature rise in an oxidizing atmosphere. No aromatic molecule with a very large side chain is likely to be effective because collisions will readily detach that side chain. Nor must the bonds attaching the side chain to the ring be weak. Given stability, the side chain, in order to confer the best anti-knock properties, must be such as to cause the greatest spread of the electronic cloud of the ring. If the aromatic additive is being used near the temperature limit of its thermal stability, then it will be more effective if the mixture strength, fuel, engine and general running conditions be such as to give the coolest possible operation. The primary factor determining response in paraffins is not so much the fuel as the operating temperature. Response in a naphthenic fuel may be less than in paraffins because of hotter running.

Benzene derivatives, if only they were more effective, would be in many ways the ideal anti-knock additives, since they burn away completely, leaving no deleterious deposits as do the metallic alkyls. It is unfortunate that the conclusions above do not leave much hope that any more effective aromatic compound remains to be discovered.

*The Chemistry Department,  
The University,  
Leeds.*

<sup>10</sup> Walsh, *Nature*, 1947, **159**, 165 and 712; 1947, **160**, 902; Linnett, *ibid.*, 1947, **160**, 162; Skinner, *ibid.*, 1947, **160**, 902; for some disadvantages of the viewpoint, see Robinson, *ibid.*, 1947, **159**, 400; 1947, **160**, 162.

<sup>11</sup> See Lewis and von Elbe, *Combustion, Flames and Explosions of Gases* (Cambridge, 1938).

\* Note added in proof. The oxidation chains of ethylene will not be so short as those of benzene because the  $\pi^{-1}$  ionization potential is considerably higher for ethylene (10.50 V) than for benzene (9.24 V). The propylene ionization potential is much lower (9.7 V) than that of ethylene and correspondingly there is evidence that vapour phase chain ending is more important in propylene oxidation.

# DETERMINATION OF THE VELOCITY COEFFICIENTS FOR POLYMERIZATION PROCESSES

## THE POLYMERIZATION OF BUTYL ACRYLATE

BY H. W. MELVILLE AND A. F. BICKEL

*Received 30th May, 1949*

The polymerization of liquid butyl acrylate has been investigated with a view to the determination of the rate coefficients for polymer growth and termination of growth. The reaction falls into the generally accepted type for radical polymerization. The rate of initiation of polymerization has been determined by the molecular weight method (in absence of transfer) and by the use of tetraphenyl hydrazine as an inhibitor. The results are in good agreement. The photo-reaction is accelerated and not retarded by the conventional inhibitors such as quinones and amino compounds. If  $k_p$  and  $k_t$  are the growth and termination coefficients then at 25°C,  $k_p = 13$  l. mole<sup>-1</sup> sec.<sup>-1</sup> and  $k_t = 1.8 \times 10^4$  l. mole<sup>-1</sup> sec.<sup>-1</sup>. The frequency factors are  $4.4 \times 10^4$  and  $1.8 \times 10^4$  respectively. The energy of activation for propagation is 2 kcal./mole and that for termination, zero.

This paper is one of a series dealing primarily with the determination of the absolute velocity coefficients in vinyl polymerizations. The mechanism of this kind of polymerization is now without doubt a free-radical process and the general kinetic features are sufficiently well established. The problem of measuring rates of initiation and life-times of radicals is still a matter for experimentation and there is much to be done in trying to measure such quantities as accurately as possible. The polymerization of butyl acrylate is the first of the acrylate series to be studied.

Apart altogether from the problem of developing the techniques for the determination of coefficients the values are important in the general study of radical-double interactions and of radical-radical interactions. The establishment of a quantitative chemistry of these processes is of interest both theoretically and practically. Since the principle, and to some extent the practice, of measuring coefficients is a subject of study it is of further importance to be able to tackle the problem of polymerization kinetics. Here all the individual coefficients need to be known for each monomer before any attempt is made to put copolymerization reactions on an absolute basis. Butyl acrylate copolymerizes easily with a large number of vinyl derivatives and hence the study of its polymerization opens up a considerable field in copolymerization kinetics.

### Experimental

Butyl acrylate containing 0.1 % inhibitor was obtained from The Resinous Products and Chemical Company (Philadelphia, Pa.). It was shaken several times with 10 % sodium hydroxide solution and with distilled water, dried over sodium sulphate and distilled *in vacuo* (b.p., 59.3°C, 24 mm.). Monomer received from Imperial Chemical Industries Ltd. was treated in the same way and gave the same experimental results.

Benzoyl peroxide which was used as a catalyst was purified by dissolving

in a small amount of chloroform and precipitating with an excess of methanol. It was kept in a vacuum desiccator over calcium chloride.

The inhibitors used were purified in the following manner. Benzoquinone was steam-distilled and sublimed. Hydroquinone was recrystallized from a mixture of benzene and ethanol. Phenyl  $\beta$ -naphthylamine and *o*- and *p*-phenylene diamine were sublimed *in vacuo*. Tetraphenyl hydrazine was recrystallized from acetone.

In order to avoid the presence of oxygen all polymerizations were carried out *in vacuo* and the monomer was carefully freed from air before use. The apparatus was evacuated by means of a mercury diffusion pump backed by a rotary oil pump. A reservoir of the monomer and reaction tubes made of Pyrex glass were attached to the main vacuum line by means of ground glass joints. Catalysts or inhibitors were introduced by pouring a known volume of a standard solution in a suitable solvent into the reaction tube and removing the solvent in the vacuum of a water pump. Butyl acrylate was distilled into the tubes under high vacuum and the tubes were sealed off. The rate of polymerization was followed dilatometrically.

The light source used for the photopolymerizations was a high-pressure mercury arc from which the outer glass envelope had been removed. It was fed by a constant voltage transformer. The beam was directed on the dilatometer placed in a copper thermostat fitted with silica windows. The distance between lamp and reaction tube was the same in all experiments.

When short periods of light and dark were required, intermittent illumination was obtained by the use of a disc, cut with sectors, which was rotated at a constant speed in the path of the light. For periods of the order of minutes a shield was used which was placed in position and removed manually.

## Results and Discussion

**The Polymerization of Butyl Acrylate by Benzoyl Peroxide.**—The overall rate of the reaction was determined by measuring the volume contraction. The density of the polymer being 1.0315 g. cm.<sup>3</sup> and that of the monomer 0.8934 at 25° and 0.8841 at 35°, the volume contraction for 100 % polymerization is 13.39 % at 25° and 14.29 % at 35°. Checks were made by weighing the quantity of polymer formed.

The thermal rate at 35° was found to be negligible compared with the catalyzed one. In general the overall rate of reaction proved to be linear with time up to about 8 % polymerization. Thereafter the rate increases owing to the "gel" effect. The rates of polymerization using peroxide

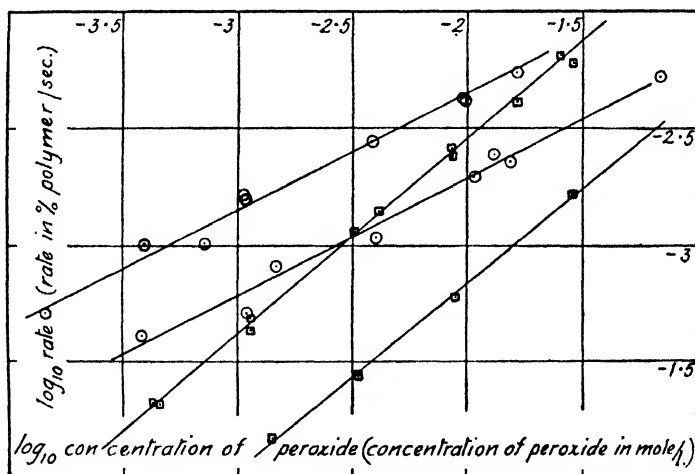


FIG. 1.—The polymerization of butyl acrylate by benzoyl peroxide, at 25° and 35° C; ○ pure butyl acrylate; □ butyl acrylate purified by distillation only.

concentrations from  $1.5 \times 10^{-4}$  to  $1.5 \times 10^{-2}$  mole/l. were determined at  $25^\circ$  and  $35^\circ$ . Fig. 1 represents the results, showing clearly that the rate of polymerization is strictly proportional to the square root of the concentration of peroxide, indicating that the termination reaction involves the mutual destruction of two of the growing polymer molecules.

Fig. 1 gives a value of 15.6 kcal. mole for the apparent energy of activation of the polymerization.

Butyl acrylate which had been distilled but not purified by shaking with a solution of sodium hydroxide, shows a different behaviour. In this case it was found that the relation between rate and peroxide concentration at  $25^\circ$  as well as at  $35^\circ$  may be represented by

$$R = k \cdot C_{\text{bpo}}^{0.82},$$

where  $R$  is the rate,  $k$  a proportionality constant and  $C_{\text{bpo}}$  the concentration of benzoyl peroxide. Fig. 1 shows these results. The formula holds accurately for peroxide concentrations varying from  $4 \times 10^{-4}$  to  $3 \times 10^{-2}$  mole/l. Obviously the inhibitor present in butyl acrylate cannot be completely removed by distillation only.

From the fact that the exponent in the above expression is 0.82 it must be presumed that termination of the chains occurs by the reaction of butyl acrylate radicals with the inhibitor in such a way that the resulting radical is so unreactive that it cannot take any further part in the polymerization reaction. It is worth noting that the exponent is apparently constant over quite a large range of peroxide concentration. It might have been expected that the exponent would have tended to decrease at the higher concentrations.

**The Molecular Weight of the Polymer.**—If mutual termination occurs the overall rate of polymerization is given by

$$-\frac{d(M)}{dt} = \frac{k_p}{k_t^{1/2}} \cdot I^{1/2}(M), \quad . \quad . \quad . \quad (1)$$

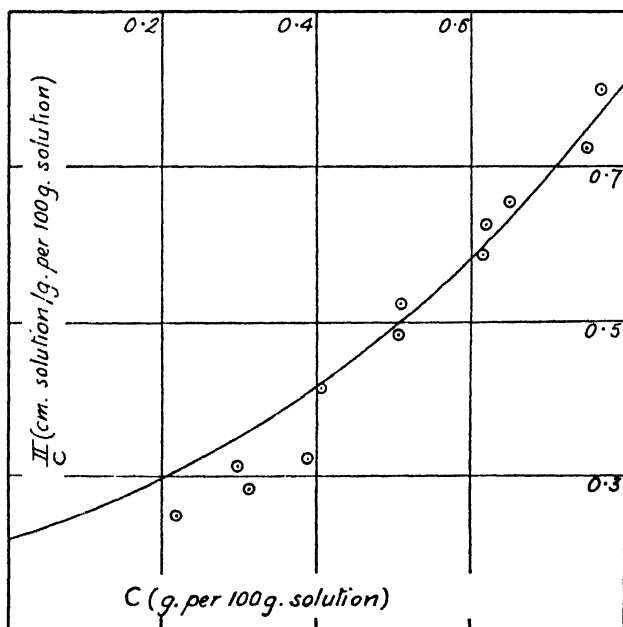


FIG. 2.—Osmometric determination of molecular weight ( $M = 1,120,000$ ;  $\overline{DP} = 8750$ ).



where  $(M)$  is the concentration of the monomer,  $I$  the rate of initiation and  $k_p$  and  $k_t$  the velocity coefficients for propagation and termination respectively. In order to be able to calculate the ratio  $k_p/k_t^{1/2}$  it is, therefore, necessary to know the rate of initiation of chains. It should be possible to obtain a value for this quantity by determining the molecular weight of the polymer. The dependence of the molecular weights on the concentration of peroxide will give an indication about the magnitude of transfer.

Osmometric measurements were carried out on five samples of polybutyl acrylate dissolved in benzene. The osmometer used was of the Fuoss and Mead type<sup>1</sup> employing bacterial cellulose<sup>2</sup> as a membrane. The experimental results for one sample are shown in Fig. 2.

The molecular weights proved to be extremely high and the results, therefore, are liable to have a larger error than usual, especially those of the samples prepared with small concentrations of benzoyl peroxide.

If chain transfer occurs the kinetic chain length  $\bar{v}_k$  is not the same as the average degree of polymerization  $\overline{DP}$ . These quantities are given by

$$\bar{v}_k = \frac{k_p(P)(M)}{k(P)^2}, \quad (2)$$

and

$$\overline{DP} = \frac{k_p(P)(M)}{k_t(P)^2 + k_f(P)(M)}, \quad (3)$$

where  $(P)$  is the concentration of the active polymer molecules and  $k_f$  the velocity coefficient for chain transfer. It follows that

$$\frac{I}{\overline{DP}} = \frac{I}{\bar{v}_k} + \frac{k_f}{k_p}. \quad (4)$$

The ratio  $k_f/k_p$  is the transfer constant. Using the value of  $(P)$  derived from the stationary state equation,

$$\frac{d(P)}{dt} = I - k_t(P)^2 = 0,$$

(3) may be written as

$$\frac{I}{\overline{DP}} = \frac{k_t^{1/2}}{k_p} \cdot \frac{I^{1/2}}{(M)} + \frac{k_f}{k_p}. \quad (5)$$

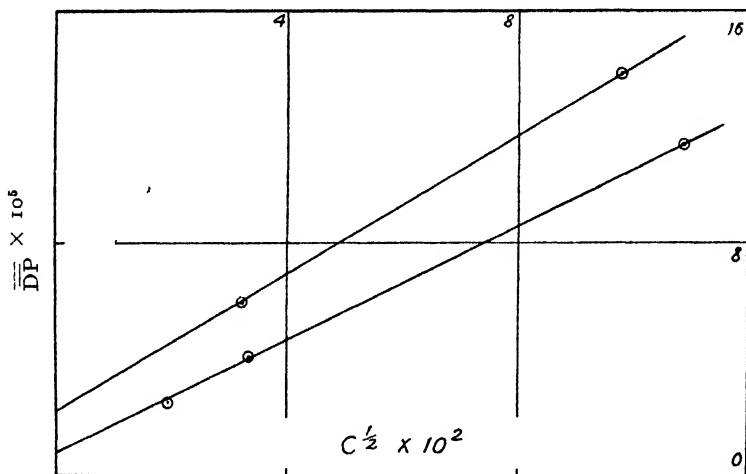


FIG. 3.—The transfer constant.

<sup>1</sup> Fuoss and Mead, *J. Physic. Chem.*, 1943, **47**, 59.

<sup>2</sup> Cruickshank, Masson, Melville and Menzies, *Nature*, 1946, **157**, 74.

The value of the transfer constant may therefore be obtained as the intercept on the  $1/\overline{DP}$ -axis in a plot of  $1/\overline{DP}$  against the square root of the concentration of peroxide (Fig. 3).

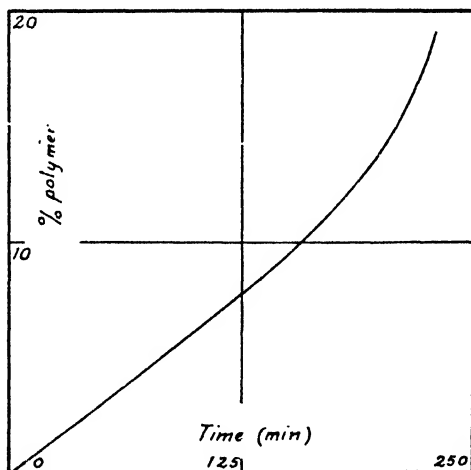
Due to the large errors in the molecular weights the values of the transfer constant are not very accurate. Their main importance is to show the small order of magnitude of transfer. Table I summarizes the results obtained from these experiments;  $v_k$  has been calculated using (4),  $I$  using  $-d(M)/dt = Iv_k$  and  $k_p/k_t^{\frac{1}{2}}$  by means of (1).

TABLE I

$C_{\text{ppo}}$ mole/l. $\times 10^4$	$T$ $^{\circ}\text{C}$	$\overline{DP}$	$v_k$	$k_f/k_p$ $\times 10^6$	$\frac{d(M)}{dt}$ mole/l. sec. $\times 10^4$	$I$ mole/l. sec. $\times 10^8$	$k_p/k_t^{\frac{1}{2}}$ mole $^{-\frac{1}{2}}$ l. $^{\frac{1}{2}}$ sec. $^{-\frac{1}{2}}$
119	25	8750	9400	0.75	1.47	1.56	0.17
11.0	—	24200	29600	—	0.441	0.149	0.16
3.85	—	39000	55000	—	0.261	0.048	0.17
96.2	35	7200	8550	2.2	3.06	3.57	0.23
10.7	—	16400	25600	—	1.015	0.396	0.23

The next stage is to obtain separate values for  $k_p$  and  $k_t$  and for this purpose it is necessary to study the photopolymerization with a view to determining the lifetime of the polymer radicals.

**The Photopolymerization of Butyl Acrylate.**—The rate of reaction proved to be linear with time up to about 10% polymerization and thereafter increased (Fig. 4). The average value at  $25^{\circ}\text{C}$  was found to be  $10.4 \times 10^{-4} \% \text{ sec.}^{-1}$  ( $0.72 \times 10^{-4}$  mole/l. sec.) and at  $35^{\circ}$ ,  $11.65 \times 10^{-4} \% \text{ sec.}^{-1}$  ( $0.805 \times 10^{-4}$  mole/l. sec.), giving an energy of activation of 2.1 kcal./mole.

FIG. 4.—The photopolymerization of butyl acrylate ( $25^{\circ}\text{C}$ ).

In order to verify whether mutual termination of the growing radicals is also operative in the photopolymerization, the intensity of the light was varied by means of a perforated screen whose transmission was 40.8%. The rates under the total illumination  $R$  and with the screen in position  $R_s$  were measured. From the experiments the average value of the intensity exponent  $n$  is 0.52 at  $25^{\circ}$  and 0.53 at  $35^{\circ}$ , thus proving that

the termination mechanism is the same as in the polymerization by peroxide (Table II).

TABLE II

$T$ ( $^{\circ}\text{C}$ )	$R_p/R$	$n$
25	0.65	0.48
—	0.61	0.55
—	0.63	0.52
35	0.62	0.53

**Action of Inhibitors on the Photopolymerization of Butyl Acrylate.**—Due to the very high molecular weights the rate of initiation of the polymerization by peroxide could not be obtained very accurately and, therefore, it was thought desirable to try to estimate the number of chains started by means of the action of an inhibitor. The reaction with several inhibitors was investigated and the results are shown in Fig. 5. It appears that benzoquinone causes no inhibition or

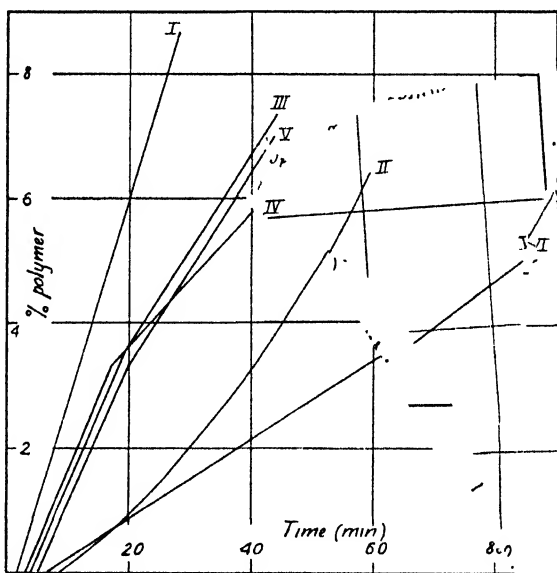


FIG. 5.—Action of inhibitors ( $25^{\circ}\text{C}$ ). I. Benzoquinone  $1.7 \times 10^{-3}$  mole/l. II. Hydroquinone  $1.7 \times 10^{-3}$  mole/l. III. Phenyl- $\beta$ -naphthylamine  $0.19 \times 10^{-3}$  mole/l. IV. *p*-Phenylene diamine  $0.41 \times 10^{-3}$  mole/l. V. *o*-Phenylene diamine  $0.44 \times 10^{-3}$  mole/l. VI. No inhibitor.

retardation but, on the contrary, a large acceleration of the polymerization; the rate is strictly linear up to 20 % polymerization. Hydroquinone shows no inhibition either, but a gradually increasing rate, again larger than that of the "uninhibited" reaction. Furthermore the action of phenyl  $\beta$ -naphthylamine, *p*- and *o*-phenylene diamine was investigated. All these compounds prove to be accelerators of the reaction. In some cases the intensity exponents were determined. The polymerizations with phenyl  $\beta$ -naphthylamine and *o*-phenylene diamine have a value of 0.5 and that with *p*-phenylene diamine a value of 1.0, showing that the termination reaction mechanism is not always the same. No explanation can, as yet, be offered for the above figures, except that all

these molecules would appear to act as photosensitizers and some of them as retarders at the same time. Since none of the usual types of inhibitors or retarders appear to function, the remaining type would be a free radical itself or a free-radical-producing substance. For this purpose tetraphenyl hydrazine appears to be more suitable.

In experiments with tetraphenyl hydrazine it appeared that this compound causes retardation of the polymerization. The results at

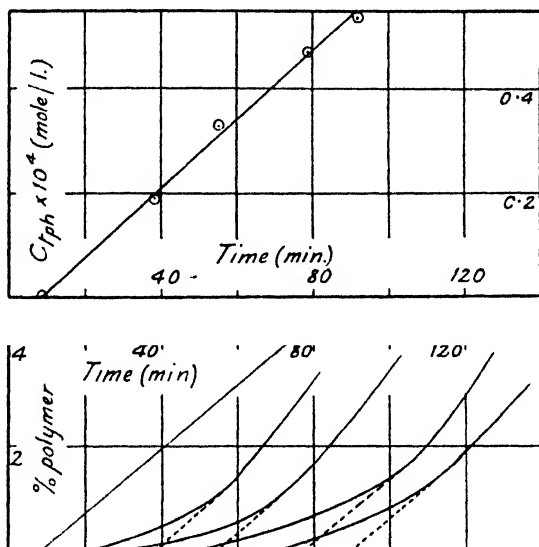


FIG. 6.—Inhibition by tetraphenyl hydrazine (*tph*) at 25°C.

25° are shown in Fig. 6; those at 35° are similar. The curves do not represent ideal inhibition as known from investigations by Foord<sup>3</sup> on styrene and by Burnett and Melville<sup>4</sup> on vinyl acetate. With butyl acrylate the polymerization starts after a period of complete inhibition and the rate increases gradually to a value larger than the rate of the uninhibited process. Moreover, this value is not always the same. In order to obtain comparable results, tangents parallel to the straight line representing the uninhibited rate were drawn to each rate curve, the intercepts on the time-axis being taken as the inhibition time. Of course, it is doubtful whether this arbitrary measure is justifiable.

In calculating the value of *I*, it has been assumed that the photo-reaction involves the growth of a polymer diradical and that the termination reaction occurs by the addition of a diphenyl nitrogen radical at each end of the diradical. The same result would have been obtained if it had been assumed that the butyl acrylate had, in fact, been split into two single radicals, each of which grows as a polymer radical this growth being stopped by interaction with a diphenyl nitrogen radical.

The fact that in the presence of an inhibitor the reaction does not suddenly proceed at full speed at the end of the induction period shows that, even with this very powerful inhibitor, the propagation reaction must compete very effectively, which fact points to a rather high value for *k<sub>p</sub>*.

The rates of initiation at  $1.11 \times 10^{-8}$  mole/l. sec. 25° and  $1.15 \times 10^{-8}$  mole/l. sec. at 35°. Hence the rate of initiation determined

<sup>3</sup> Foord, *J. Chem. Soc.*, 1940, 48.

<sup>4</sup> Burnett and Melville, *Proc. Roy. Soc. A*, 1947, 189, 456.

in this manner is temperature independent. Using the values of the overall rate already given, the ratio  $k_p/k_t^{1/2}$  has been calculated (Table III).

TABLE III

$T$ (°C)	$-\frac{d(M)}{dt}$ (mole/l. sec. $\times 10^8$ )	$I$ (mole/l. sec. $\times 10^8$ )	$k_p/k_t^{1/2}$ (mole $^{-1/2}$ l. $^{1/2}$ sec. $^{-1}$ )
25	0.72	1.13	0.097
35	0.805	1.13	0.110

Comparison of the values of  $k_p/k_t^{1/2}$  with those mentioned in Table I shows that they differ by a factor 2, while the temperature dependence is not the same in both cases. Considering the large possible error in the osmometric molecular weights and the uncertainties involved in the evaluation of the inhibition experiments the accordance of the figures is not worse than could be expected.

**The Lifetime of the Active Polymer.**—The lifetime of the growing radical was determined by measuring the rate of polymerization under steady and intermittent illumination. The theoretical treatment and the experimental technique of this method have already been described by Burnett and Melville.<sup>4</sup> These authors defined the lifetime  $\tau$  as

$$\frac{\text{number of polymer radicals per unit volume}}{\text{number of polymer radicals disappearing per unit volume and per unit time}} = \frac{(P)_0}{k_t(P)_s^{1/2}}$$

The steady state equation is

$$\frac{d(P)}{dt} = I - k_t(P)_s^{1/2} = 0,$$

which gives

$$\tau = I^{-1/2} k_t^{-1/2}.$$

They also derived a relation between the ratio  $(P)_0/(P)_s$  (where  $(P)_0$  is the average concentration of active particles over the light and dark periods) and  $m = t/\tau$  (where  $t$  is time of flash). The ratio  $(P)_0/(P)_s$  is obviously the same as the ratio of the rates under intermittent and steady illumination. Fig. 7 shows the values of  $(P)_0/(P)_s$  as a function of  $m$  for equal periods of light and darkness.

The experimental results for butyl acrylate are shown in Fig. 8. Change in temperature does not appreciably affect the position of the curve, in other words the lifetime and also the velocity coefficient for termination are temperature independent within the limits of experimental error. Using the values of  $m$  from the theoretical curve of Fig. 7, the lifetime  $\tau$  may be calculated. Applying this procedure, it is found that the lifetime decreases rapidly with decreasing relative rate; in other words, the experimental curves fall off much faster than would be expected theoretically. It is worth emphasizing that the limiting values of the ratio at extreme times of flash are in accord with the square-root intensity relation. To find the best value for the lifetime available under these circumstances  $\tau$  values taken from the upper, probably more reliable, part of the curves of Fig. 8, were used to draw the experimental curves in Fig. 7. Accordingly, a value of 70 sec. for  $\tau$  appears to be the best approximation. No explanation can, as yet, be offered for the discrepancies observed.

**The Velocity Coefficients for Propagation and Termination.**—By inhibition with tetraphenyl hydrazine the rate of initiation at 25° as well as at 35° was found to be  $1.13 \times 10^{-8}$  mole/l. sec. Hence

$$k_i = 1.8 \times 10^4 \text{ l. mole}^{-1} \text{ sec.}^{-1}$$

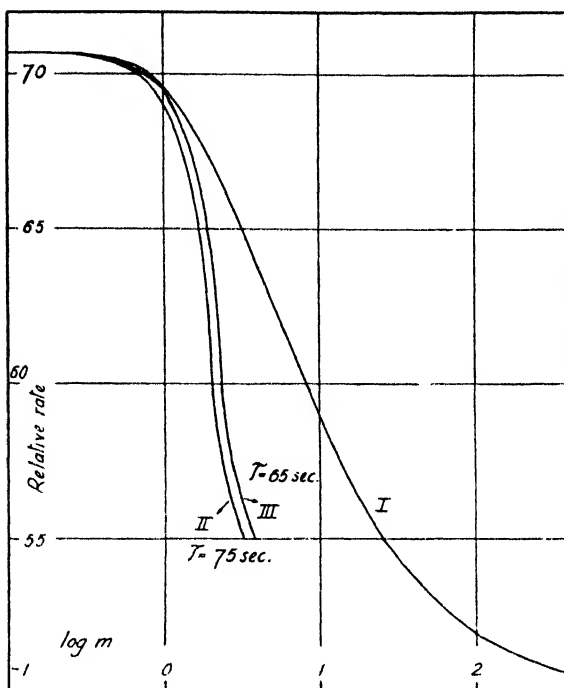


FIG. 7.—I. Theoretical curve; II and III. Experimental curves.

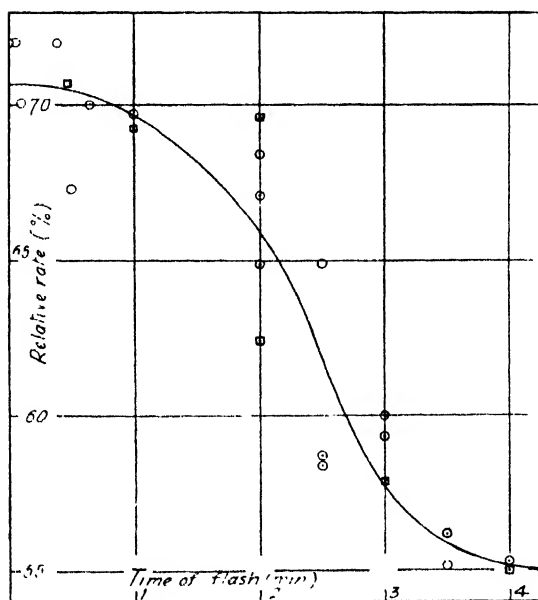


FIG. 8.—Rate of reaction as a function of duration of flash (○ 25°; □ 35°)

and with the respective values of  $k_p/k_t^{\frac{1}{2}}$

$$k_p = 13 \text{ l. mole}^{-1} \text{ sec.}^{-1} \text{ at } 25^\circ,$$

$$k_p = 14.5 \text{ l. mole}^{-1} \text{ sec.}^{-1} \text{ at } 35^\circ \text{ C.}$$

Since the temperature coefficient of  $k_t$  is directly calculable from the measurement of  $\tau$  at different temperatures there seems little doubt that  $k_t$  is not dependent on temperature. The values of  $k_p$  calculated above show a temperature dependence corresponding to an energy of activation of 2.1 kcal./mole, the rate of photo initiation being independent of temperature. Taking the maximum possible value of a bimolecular coefficient as  $10^{11} \text{ l. mole}^{-1} \text{ sec.}^{-1}$ , the steric factor therefore amounts to  $5 \times 10^{-9}$  for propagation and  $10^{-7}$  for termination ( $A_p = 4.4 \times 10^4$ ,  $A_t = 1.8 \times 10^6$ ).

In view of the difficulty of obtaining accurate absolute values of the rate of initiation by inhibition experiments the absolute values of  $k_p$  and  $k_t$  may be in error. It is therefore of interest to utilize the value of  $k_p/k_t^{\frac{1}{2}}$  from the peroxide experiments and, bearing in mind that the rate of initiation is obtained from molecular weight measurements, to calculate another set of values for  $k_p$ . These are

$$22.5 \text{ l. mole}^{-1} \text{ sec.}^{-1} \text{ at } 25^\circ,$$

$$31 \text{ l. mole}^{-1} \text{ sec.}^{-1} \text{ at } 35^\circ.$$

The energy of activation thus is 6.0 kcal./mole which is somewhat larger than that from the photo results. The reason is that it is more difficult to obtain an accurate value of the temperature coefficient of the propagation reaction when already the temperature coefficient of the initiation reaction is as high as 30 kcal. According to these calculations the steric factor comes out at  $5 \times 10^{-6}$  ( $A_p = 5.1 \times 10^5$ ).

One of the authors (A. F. B.) is indebted to the Management of the Koninklijke/Shell-Laboratorium, Amsterdam, for having been given the opportunity to carry out this investigation. The experimental work was carried out in the Chemistry Department of the University of Aberdeen.

*Chemistry Department,  
University of Birmingham.*

## THE REACTION KINETICS OF WOOL WITH CHLORINE SOLUTIONS

### PART I.—DIFFUSION ACROSS A LIQUID LAYER

BY P. ALEXANDER, D. GOUGH AND R. F. HUDSON

*Received 30th May, 1949*

It is shown that the rate-controlling step in the reaction of a solution with wool is either diffusion through a liquid film or diffusion in the fibre, the two processes being characterized by activation energies of 6 and 12 kcal./mole respectively. The conditions of film diffusion are determined and the effect of agitation and temperature on film thickness calculated and related with experiment. It is deduced that the temperature coefficient of the film diffusion-controlled reaction should be greater than that of diffusion of chlorine in water.

The process of reaction in a heterogeneous system involves the following steps, one of which may be rate determining :

- the transport of reactant to the surface,
- the sorption of reactant,
- diffusion of reactant through solid phase,
- reaction at specific sites,
- diffusion of products of reaction to the surface of the solid,
- the diffusion of reaction products away from the surface into the bulk of the solution.

For diffusion processes, rate of stirring of solution is all important and with low stirring rates the overall rate of reaction may be governed by (a) or (f). This point has recently been made by Boyd, Myers and Adamson<sup>1</sup> who studied the rate of diffusion of ions into a synthetic resin. They have shown that increase in concentration causes the rate-determining process to change from diffusion in solution to diffusion through the resin.

The classical approach of Noyes and Whitney,<sup>2</sup> Nernst<sup>3</sup> and Brunner<sup>4</sup> considered a stationary layer of solution close to the solid surface across which diffusion proceeds according to the law of Fick. Then the rate of transport  $P$  across unit area of the layer is given by

$$P = D\Delta c / \delta \quad . \quad . \quad . \quad . \quad . \quad . \quad (I)$$

where  $D$  is the diffusion coefficient, and  $\Delta c$  the change in concentration across the layer of width  $\delta$ . It is usual to assume that owing to rapid reaction at the surface the concentration of reactant near the surface is negligible compared with that of the bulk of the solution. This leads to the general relation

$$t = \frac{\delta V}{DA} \ln \frac{c}{c-x}, \quad (2)$$

where  $c$  is the initial concentration of the solution,  $c - x$  the concentration at time  $t$ , and  $V$  the volume of solution in contact with an area  $A$ .

From this equation,  $\delta$  is found to be of considerable magnitude whereas Fage<sup>6</sup> observed experimentally that the liquid close to the surface is in motion. The limitations and apparent invalidity of the simple theory led Eucken<sup>6</sup> to attempt to develop a strictly hydrodynamic theory. The treatment is very complex and formal solutions have been obtained in two simple systems only.<sup>7</sup> A more general, although semi-empirical treatment has been developed by Coburn *et al.*<sup>8</sup> and recently applied to rate processes at an electrode by Agar.<sup>9</sup> This treatment will be applied below to an investigation of the effect of temperature on the width of the diffusion layer which is of importance when the measured activation energy of the reaction of wool with chlorine at low stirring speeds is compared with the activation energy of diffusion in aqueous solution.

## Experimental

**Preparation of Reactants.**—Pure sodium hypochlorite solutions of known concentration and alkali content were prepared by passing chlorine into sodium hydroxide solution at 0° C following the procedure of Cuttania and Rannucci.<sup>10</sup> Knitted fabric of fine botany wool was used which had received no prior treatment other than mild scouring in soap and ammonia. Samples of this fabric

<sup>1</sup> Boyd, Myers and Adamson, *J. Amer. Chem. Soc.*, 1947, **69**, 2836.

<sup>a</sup> Noyes and Whitney, *Z. physik. Chem.*, 1897, **23**, 689.

<sup>3</sup> Nernst, *ibid.*, 1904, 47, 52.

<sup>4</sup> Brunner, *ibid.*, 1904, 47, 56.

<sup>5</sup> Fage, *Proc. Roy. Soc. A*, 1932, 135, 828.

<sup>6</sup> Eucken, *Z. Elektrochem.*, 1932, 38, 341.

<sup>7</sup> Levich, *Acta Physicochim.*, 1942, 17, 257; *ibid.*, 1944, 19, 117, 133; *Faraday Soc. Discussion*, 1947, 1, 37.

<sup>8</sup> Colburn, *Ind. Eng. Chem.*, 1930, **22**, 967; *Trans. Amer. Inst. Chem. Eng.*, 1933, **29**, 174; Chiltern and Coburn, *Ind. Eng. Chem.*, 1934, **26**, 1183.

<sup>9</sup> Agar, *Faraday Soc. Discussions*, 1947, 1, 26.

<sup>10</sup> Cattania and Rannucci, *Ann. Chim. Appl.*, 1915, 3, 161.



were extracted by refluxing with alcohol and ether in a Soxhlet apparatus for several hours. The degreased sample was then dried at  $102^{\circ}$ – $105^{\circ}$  C for one hour, cooled and weighed in a dry condition.

**Procedure.**—The reaction was performed in an air-tight flask into which were fitted a thermometer, automatic pipette and stirrer, Fig. 1. To prevent

obstruction of the stirrer by other apparatus, the three-necked litre flask A was constructed with a wide central neck 55 mm. diam. and 70 mm. long, and with two small necks on either side approximately 100 mm. diam.

The stirrer B was constructed of solid glass rod, the side of the square being 42 mm. and the length 70 mm. These dimensions were such that the stirrer frame could be drawn into the large neck of the flask out of contact with the liquid before a run was started. The stirrer was led into the flask through a mercury seal C and connected to an electric motor, the speed of which was varied by means of a rheostat and measured by a tachimeter.

Finally, the specially constructed automatic pipette E was inserted and samples of known volume of the reacting solution could be removed. The tube F was connected to a filter pump through a wash-bottle trap, with G open to the air. The procedure for taking a sample was first to connect the bulb of the pipette to the pump, and then the bulb to the tube leading into the reaction vessel by turning  $T_1$ . When the liquid in the pipette had risen almost to  $T_1$ ,  $T_2$  was closed,  $T_1$  opened to the air, and the liquid run out through exit tube H to an upper graduation. The calibrated volume was then collected in a small flask containing acidified potassium iodide solution and the residual liquid in the pipette run back into the reaction vessel.

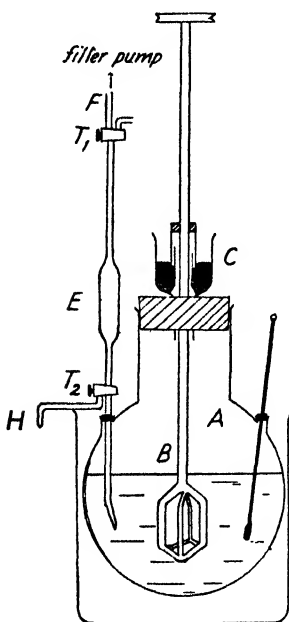


FIG. 1.—Apparatus for rate of reaction determinations.

tion mark, was to enable the residual liquid in H from a previous sample to be driven out before the following sample was taken.

In stating the concentrations of reactants in this heterogeneous system, three variables must be specified, viz. the quantity of chlorine in solution, the volume of solution, and weight of fibres immersed. In all the experimental work described below the weight of fibres in a volume of solution was kept at a fixed ratio of 1/150. Consequently, the amount of chlorine used may be referred either to the volume of solution, i.e. as molarity, or to the weight of fibres. In the results below this concentration is expressed as the % weight of chlorine per weight of fibres.

In a typical experiment a known weight of fabric (3.4 g.) was weighed, and from the dry weight the correct volume of reaction solution calculated to give the required ratio 1/150. The required volume of buffer solution was introduced into the flask and the calculated quantity of sodium hypochlorite solution added. The weighed piece of fabric was then fixed uniformly round the stirrer cage and immersed in buffer solution overnight at the reaction temperature. After the initial pH of the reaction mixture had been taken the stirrer and fabric were fitted into the flask so that the fabric remained out of contact with the solution. A zero time reading was taken by withdrawing an initial sample in the manner described above and titrating the liberated iodine with standard sodium thiosulphate solution. The stirrer motor was then started and reaction initiated by lowering the stirrer frame into the liquid. Samples were then withdrawn and the stirring rate noted periodically. After 10–15 samples had been collected, reaction was stopped by withdrawing the stirrer and the final pH taken. In no case did the pH vary by more than 0.1 pH unit.

The reactions were all performed at pH 2. As no satisfactory buffer applies to this low pH, it was found to be satisfactory to use the calculated quantity of sulphuric acid and adjust the pH by small additions of acid to give the required value.

## Results

Table I gives a brief summary of the measured rate of reaction with 0.01 M chlorine the results being given in half-life values as the kinetics are of the first order. In all these experiments at pH 2, a fibre/solution ratio of 1/150 (wt./vol.) was employed.

TABLE I

Stirring Rate rev./min.	$t_{\frac{1}{2}}$ min. at 25° C	$t_{\frac{1}{2}}$ min. at 0° C	$\frac{t_{\frac{1}{2}} 0^{\circ} \text{C}}{t_{\frac{1}{2}} 25^{\circ} \text{C}}$	E cal.
80	3.6	10.7	3.0	4150
90	[6.6]*	10.0	—	6370
110	3.0	7.8	2.6	6220
200	1.5	4.0	2.7	6460
300	1.1	2.9	2.6	6220
400	0.57	—	—	—

\* For 10° C.

To demonstrate that the method of stirring used was efficient, limited experiments were performed holding the wool on a stationary frame and agitating the solution with a 3-cm. paddle-type stirrer. The results given in Table II show that the former method is some 8-10 times as efficient as the latter process, judged on rate of reaction.

TABLE II  
0.01 M chlorine; 0° C

Stirring Rate rev./min.	$t_{\frac{1}{2}}$ min.
110	67.5
420	14.6
600	11.5

The effect of concentration of chlorine at 0° C is given in Table III. The half-life values recorded are the mean for two or three individual experiments.

The course of these reactions is represented graphically in Fig. 2, 3 and 4 as plots of  $\log_{10} \frac{c}{c-x}$  against  $t$ . It is seen that with low con-

centrations of chlorine at low and high stirring rates, these graphs are linear in agreement with eqn. (2). As the concentration is increased at low stirring rates deviations are noted suggesting an accumulation of chlorine at the surface. With increasing concentration at high stirring rates, however, the law is no longer

TABLE III

Stirring Rate rev./min.	$t_{\frac{1}{2}}$ Values for Concentrations *						
	25 %	15 %	10 %	5 %	3 %	1 %	$\frac{1}{2}$ %
100	—	—	8.9	—	5.3	—	5.0
600	3.2	2.5	2.7	1.64	1.6	1.7	1.5

\* Expressed as % wt. of chlorine per wt. of fabric.

obeyed (Fig. 3); this is discussed in Part II in terms of a change in mechanism. With 10 % chlorine on the weight of wool this change occurs at 300 rev./min. at 0° C and 500 rev./min. at 25° C and with lower chlorine concentrations at correspondingly higher stirring rates. At the higher temperatures (e.g. 25° C), there was an unavoidable loss of chlorine when the fabric was introduced into the flask, which explains the failure of the graphs shown in Fig. 4 to pass through the origin.

## Discussion

The observation that the rate of reaction is highly dependent on the rate of stirring (Fig. 6), together with the logarithmic form of the rate curve and the comparatively low activation energy of ca. 6 kcal./mole

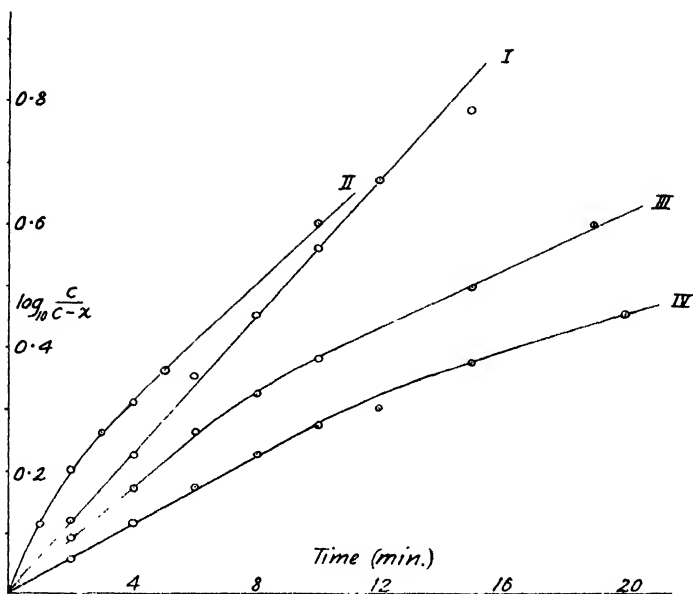


FIG. 2.—Graphs of  $\log_{10} \frac{c}{c-x}$  against  $t$  for low stirring rates at  $0^{\circ}\text{C}$ .  
 I. 3 % and 0.5 %  $\text{Cl}_2$  solutions at 100 rev./min. II. 10 %  $\text{Cl}_2$  at 300 rev./min.  
 III. 10 %  $\text{Cl}_2$  at 200 rev./min. IV. 10 %  $\text{Cl}_2$  at 115 rev./min.

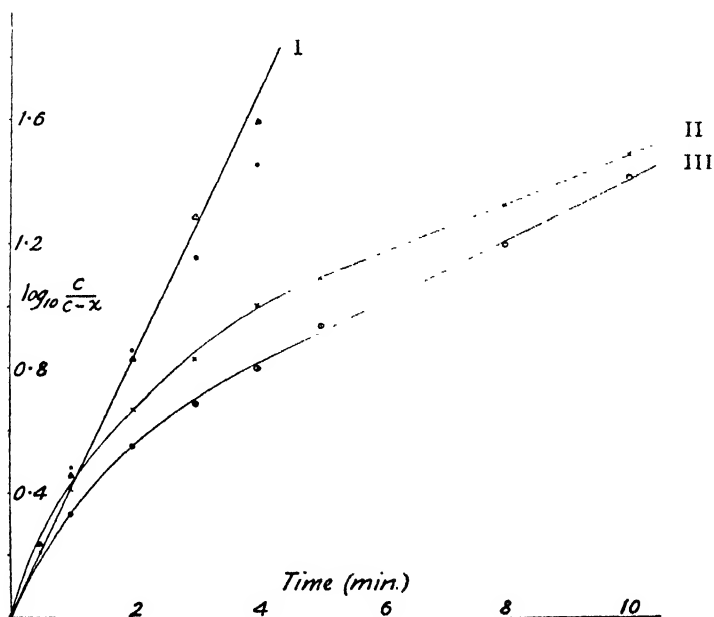


FIG. 3.—Graphs of  $\log_{10} \frac{c}{c-x}$  against  $t$  at 600 rev./min. at  $0^{\circ}\text{C}$ . I. 5 %  $\text{Cl}_2$   
 3 %, 1 % and  $\frac{1}{2}$  %  $\text{Cl}_2$ . II. 15 %  $\text{Cl}_2$ . III. 25 %  $\text{Cl}_2$ .

supports the conclusion that diffusion of chlorine through the liquid governs the rate of reaction. This mechanism is promoted by low stirring

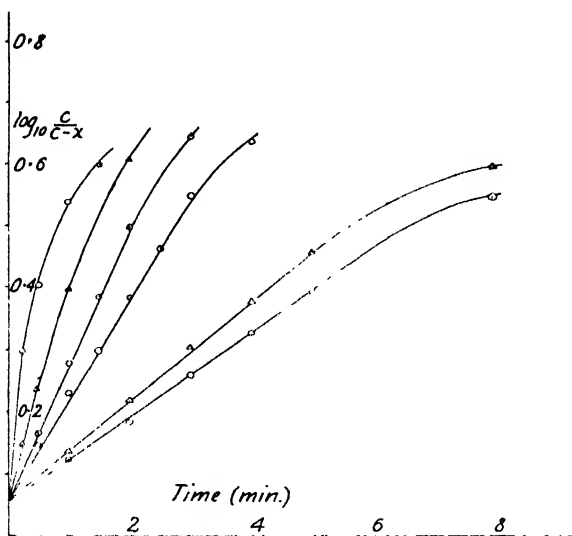


FIG. 4.—Graphs of  $\log_{10} \frac{c}{c-x}$  against  $t$  at  $25^\circ \text{C}$  with 10 %  $\text{Cl}_2$  at stirring rates of 80 to 600 rev./min.

rates, low concentrations and high temperatures, and changes to an alternative process characterized by an apparent activation energy of 12 kcal./mole on changes of these conditions (Fig. 5). In the latter

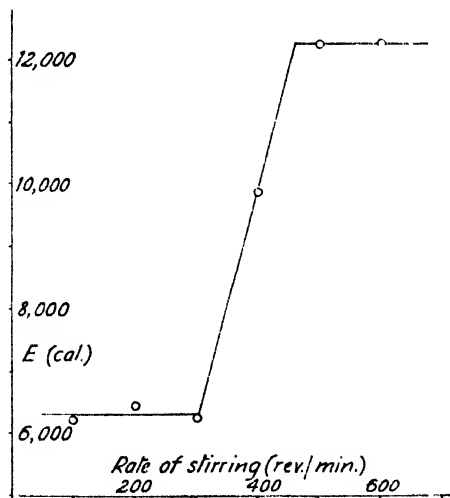


FIG. 5.—Apparent activation energy and stirring rate for 10 %  $\text{Cl}_2$ .

case the rate of reaction is independent of the rate of stirring and consequently must be due to a rate process within the fibre. This process is considered in Part II.

Values of  $\delta$  were calculated from the eqn. (2) using data for chlorine

solutions of concentration 10 %. An approximate value of  $D$  of  $0.5 \times 10^{-5}$  cm.<sup>2</sup>/sec. at 0° C, derived from the Stokes-Einstein equation and from a comparison of  $D$  for similar molecules, was assumed, and the surface area <sup>11</sup> of the fibres taken to be 3 to 10 cm.<sup>2</sup>/g. A linear relationship is found to exist between  $l$  and rate of stirring (Fig. 6). The values

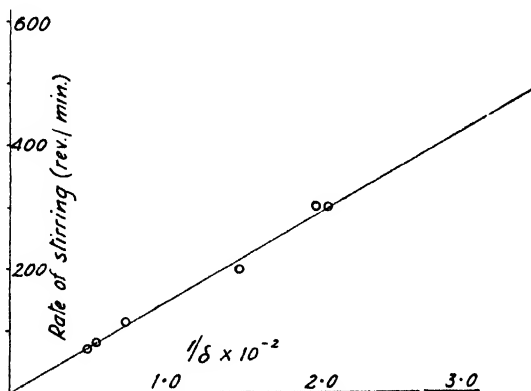


FIG. 6.—The effect of rate of stirring on the thickness of the diffusion layer, calculated from rate measurements.

of  $\delta$  compare favourably with other values calculated from rate measurements of physical,<sup>12</sup> chemical<sup>13</sup> and electrochemical processes.<sup>14</sup> It has been observed in many cases<sup>15</sup> that a general relationship between  $\delta$  and rate of stirring  $U$  of the following type holds,

$$\delta = \frac{\text{const.}}{U^a}, \quad (3)$$

where  $a$  varies from 0.5 to 1.0 depending on mode of stirring. In many studies of the rate of dissolution of crystals, Gutman *et al.*<sup>16</sup> has found that the rate is proportional to stirring rate (i.e.  $a = 1$ ). King and Bravermann<sup>17</sup> studying the rate of solution of zinc in acids found that  $a$  varies initially from 0.5 to 1.0, after which the rate of reaction increases in direct proportion to the rate of stirring.

**The Effect of Temperature.**—The calculated activation energy of the diffusion of chlorine across a liquid layer at the fibre surface is found to be approximately 6 kcal./mole as compared with values between 4.0 and 4.5 kcal./mole for the diffusion of solutes in water.<sup>18</sup> This difference indicates that the value of  $\delta$  decreases with increase in temperature, which effect is incorporated in the experimental activation energy. This

<sup>11</sup> Sullivan and Hertel, *Textile Res.*, 1940, 11, 30.

<sup>12</sup> (a) King *et al.*, *J. Amer. Chem. Soc.*, 1935, 57, 828; *ibid.*, 1937, 59, 1375; *Ind. Eng. Chem.*, 1937, 29, 75; (b) Gutman, *et al.*; see ref. 16; also ref. 15.

(c) Wilderman, *Phil. Mag.*, 1929, 18, 558.

<sup>13</sup> (a) Jablczyński, *Z. anorg. Chem.*, 1929, 180, 184; (b) King and Bravermann, *J. Amer. Chem. Soc.*, 1932, 54, 1744 (see also ref. 15).

<sup>14</sup> See review by Glasstone and Hickling, *Electrolytic Oxidation and Reduction* (Chapman and Hale, 1935), and ref. 4.

<sup>15</sup> Hixson and Crowell, *Ind. Eng. Chem.*, 1931, 23, 1160; Van Name, *Z. physik. Chem.*, 1910, 73, 97; Wilderman, *ibid.*, 1909, 66, 445; King and Schack, *J. Amer. Chem. Soc.*, 1935, 57, 1212.

<sup>16</sup> Gutman, *et al.*; *Rocz. Chem.*, 1928, 8, 445; 1932, 12, 9; Jablczyński, Gutman and Walczuk, *Z. anorg. Chem.*, 1931, 202, 403.

<sup>17</sup> King and Bravermann, *J. Amer. Chem. Soc.*, 1932, 54, 1744.

<sup>18</sup> Kincaid, Eyring and Stearn, *Chem. Rev.*, 1941, 28, 301; Kincaid and Eyring, *J. Chem. Physics*, 1939, 43, 37.

condition has so far not been examined, as it is usual practice to identify the activation energy of the heterogeneous process with that of liquid diffusion.

The width of a hypothetical diffusion layer  $\delta$  may be represented in terms of hydrodynamic properties as follows :<sup>9</sup>

$$\delta = \text{const.} \left( \frac{\eta}{U\rho} \right)^a \left( \frac{\rho D}{\eta} \right)^b \quad (4)$$

where  $\eta$  is the viscosity and  $\rho$  the density of the solution. The velocity of the heterogeneous process may be given in terms of a first-order constant  $k$  such that

$$k = D/\delta \quad (5)$$

so that

$$k = \text{const.} D \left( \frac{U\rho}{\eta} \right)^a \left( \frac{\eta}{\rho D} \right)^b \quad (6)$$

It has been seen (Fig. 6) that  $a \sim 1$  but there is little direct information on the value of  $b$ . Theoretical calculations of Levich<sup>7</sup> require a value of 0.3, although experimental values for several processes<sup>19</sup> have suggested values lying between 0.3 and 0.5. For the diffusion of a wide variety of solutes in water it is observed that the temperature coefficient for diffusion is almost equal to the energy of viscous flow. Thus, for the 0°-20° C range, the energy of activated diffusion of many solutes in water lies between 4 and 5 kcal./mole, the energy of viscous flow being 4.6 kcal./mole.

From eqn. (6) the velocity constants  $k_1$  and  $k_2$  at two temperatures are given by

$$\frac{k_1}{k_2} = \frac{D_1}{D_2} \frac{\rho_1}{\rho_2} \frac{\eta_2}{\eta_1} \left( \frac{\eta_1 \rho_2 D_2}{\eta_2 \rho_1 D_1} \right)^b \quad (7)$$

Neglecting the change in density of water and assuming that  $\eta_2/\eta_1 \sim D_1/D_2$ , values of the apparent activation energy are calculated for the extreme values for  $b$  of 0.3 and 0.5 (Table IV). Thus, values of the apparent activation energy somewhat greater than the activation energy for diffusion in solution are to be expected. The available experimental data reviewed in Table V support this deduction.

These results show that apparent activation energies of the order of 6000-7000 cal./mole can be interpreted

TABLE IV

$a$	$b$	$E$ (cal./mole.)
1.0	0.5	4500
1.0	0.3	6500

TABLE V

Diffusion Process	$E$ (cal./mole.)
Solution of benzoic acid . . . . .	5700 <sup>13</sup>
" " CuSO <sub>4</sub> . . . . .	6300 <sup>16</sup>
" " NiSO <sub>4</sub> . . . . .	7200 <sup>16</sup>
" " K <sub>2</sub> Cr <sub>2</sub> O <sub>7</sub> . . . . .	5180 <sup>16</sup>
" " picric acid . . . . .	7000 <sup>16</sup>
" " activated Al in HCl . . . . .	5800 <sup>13a</sup>
" " Cu in ammonia . . . . .	7000 <sup>13</sup>
" " Zn in HCl . . . . .	4500 <sup>17</sup>
Reaction of KMnO <sub>4</sub> with wool . . . . .	8000 <sup>20</sup>
Dyeing of wool in very dilute solutions . . . . .	6000 <sup>21</sup>

<sup>19</sup> Hixson and Baum, *Ind. Eng. Chem.*, 1941, **33**, 478; 1942, **34**, 120; King and Howard, *ibid.*, 1937, **29**, 75; McAdams, *Heat Transmission* (McGraw Hill, 1942).

<sup>20</sup> Alexander and Hudson, *J. Physic. Chem.*, 1949, **53**, 733.

<sup>21</sup> Alexander and Hudson (in press).

<sup>22</sup> Yamasaki, *Int. Cong. Pure Appl. Chem.*, 1909, **10**, 172.

on a diffusion basis only and that observed values of this order do not necessarily mean that the rate is controlled by a chemical process.

The relatively high value of the apparent activation energy of the reaction between wool and chlorine when controlled by liquid diffusion is thus in agreement with theoretical expectations and observed values in a variety of widely differing processes also controlled entirely by diffusion in solution.

The authors wish to thank Messrs. Wolsey Ltd. Leicester, for financial support which made this investigation possible and Prof. H. V. A. Briscoe for his help and interest.

*Dept. of Inorganic and Physical Chemistry,  
Imperial College of Science,  
London, S.W.7.*

---

## MOLECULAR INTERACTION IN MIXTURES OF ESTERS

### PART II.—THE HEAT AND ENERGY CHANGES ON MIXING

BY P. MEARES

*Received 20th January, 1949; as amended 13th June, 1949*

A calorimeter is described for the measurement of heats of mixing and data are presented for thirty-nine mixtures of esters. The cohesive energies, coefficients of thermal expansion and isothermal compressibility of the esters have been obtained and used to derive the energies of mixing at constant volume.

These energies are examined in terms of the regular solution theory and the assumption of random mixing is found to be a good approximation for most of the mixtures. Energies of mixing predicted by the theory from the cohesive energies do not agree with the experimental values. Some agreement is obtained using cohesive energies at the boiling point and this is discussed in terms of the theory of corresponding states. There is a close connection between the energy of mixing of an ester with ethyl acetate and of the same ester with 1:3-butanediol diacetate.

The theory of Scatchard relating the volume changes and energies of mixing is examined for mixtures conforming to the necessary assumptions and a close agreement found with the experimental results.

Solutions with a non-zero heat but an ideal entropy of mixing have been considered by Scatchard<sup>1</sup> and Hildebrand<sup>2</sup> by whom they have been named regular solutions. The heat of mixing is due to the interaction of the potential energy fields surrounding the different types of constituent molecules. The regular solution theory expresses the energy change on mixing in terms of the concentrations and physico-chemical properties of the constituents. With the assumption that, in a binary mixture, molecules of the first species can replace those of the second without changing the molecular arrangement an expression has been derived by a number of authors<sup>3, 4, 5</sup> for the molar energy of mixing,  $\Delta U_v$ ,

<sup>1</sup> Scatchard, *Chem. Rev.*, 1931, **8**, 321.

<sup>2</sup> Hildebrand, *Solubility of Non-electrolytes* (Reinhold, New York, 1936), 2nd ed., p. 65.

<sup>3</sup> Heitler, *Ann. Physik.*, 1926, **80** (4), 630.

<sup>4</sup> Hildebrand and Salstrom, *J. Amer. Chem. Soc.*, 1932, **54**, 4257.

<sup>5</sup> van Arkel, *Rec. trav. chim.*, 1936, **55**, 407.

equivalent to

$$\Delta U_0 = -x_1 x_2 (\Delta U_{1\text{vap.}} + \Delta U_{2\text{vap.}} - 2Ne_{12}). \quad (1)$$

$\Delta U_{1\text{vap.}}$  and  $\Delta U_{2\text{vap.}}$  are the molar energies of vaporization and  $x_1$  and  $x_2$  the mole fractions of the two components,  $N$  is the Avogadro number and  $e_{12}$  the potential energy of a molecule of one species completely surrounded by molecules of the other species. It is usual to set

$$Ne_{12} = (\Delta U_{1\text{vap.}} + \Delta U_{2\text{vap.}})^{\frac{1}{2}}$$

though this is only approximately true. Eqn. (1) then reduces to

$$\Delta U_0 = x_1 x_2 [(\Delta U_{1\text{vap.}})^{\frac{1}{2}} - (\Delta U_{2\text{vap.}})^{\frac{1}{2}}]^2. \quad (2)$$

The assumption of random mixing without change of arrangement can only be justified when the molecules of both species are alike in size and shape, when they differ in these respects Scatchard<sup>1</sup> and Hildebrand and Wood<sup>2</sup> have derived equivalent formulae for the energies of mixing:

$$\Delta U_0 = \frac{x_1 V_1^0 x_2 V_2^0}{x_1 V_1^0 + x_2 V_2^0} \left[ \left( \frac{\Delta U_{1\text{vap.}}}{V_1^0} \right)^{\frac{1}{2}} - \left( \frac{\Delta U_{2\text{vap.}}}{V_2^0} \right)^{\frac{1}{2}} \right]^2, \quad (3)$$

where  $V_1^0$  and  $V_2^0$  are the molar volumes of the pure components. Here the geometric-mean assumption for the interaction energies is introduced in a form involving  $(\Delta U_{\text{vap.}}/V_0)$ , the cohesive energy densities of the components.

It has been pointed out by Guggenheim<sup>7</sup> that it is unlikely that the conditions required for a regular solution can ever be realized in practice. Equations have been derived by a number of authors which take account of the non-randomness in the arrangement of the molecules due to a finite energy of mixing.<sup>7, 8, 9, 10</sup> The existence of this effect is generally accepted,<sup>2, 11, 12, 13</sup> but it is agreed<sup>10, 14, 15, 16</sup> that in many cases its extent is so small as to have little effect on the energy of mixing, except for a small range just above the critical solution temperature. Scatchard and Hamer<sup>11</sup> have found that the regular solution eqn. (3) is in some cases more satisfactory than the refined ones and the simple theory has been used successfully by Hildebrand and his co-workers to explain the behaviour of a large number of binary mixtures containing non-polar or slightly polar components.

The energy of mixing may be obtained from determinations of the heat of mixing at constant pressure together with data on the volume changes. Heat and energy of mixing data are presented in this paper for a number of related mixtures and the validity of eqn. (3) examined.

## Experimental

**The Calorimeter.**—The calorimeter, developed from one described by Ferry, Gee and Treloar,<sup>17</sup> is depicted in Fig. 1 which is drawn to scale. The liquids were mixed in the double bulb A. To minimize evaporation loss from the outer bulb a rubber ring B fitted tightly into a brass collar C, the hole in which

<sup>6</sup> Hildebrand and Wood, *J. Chem. Physics*, 1933, **1**, 817.

<sup>7</sup> Guggenheim, *Proc. Roy. Soc. A*, 1935, **148**, 304.

<sup>8</sup> Rushbrooke, *ibid.*, 1938, **166**, 290.

<sup>9</sup> Fowler and Guggenheim, *Statistical Thermodynamics* (Cambridge Univ. Press), p. 358.

<sup>10</sup> Kirkwood, *J. Chem. Physics*, 1939, **43**, 97.

<sup>11</sup> Scatchard and Hamer, *J. Amer. Chem. Soc.*, 1935, **57**, 1805.

<sup>12</sup> Scatchard, *Chem. Rev.*, 1949, **44**, 7.

<sup>13</sup> Hildebrand, *ibid.*, 1938, **44**, 37.

<sup>14</sup> *Op. cit.*, ref. 9, p. 356.

<sup>15</sup> Hildebrand, *Science*, 1939, **90**, 1.

<sup>16</sup> Hildebrand and Negishi, *J. Amer. Chem. Soc.*, 1937, **59**, 339.

<sup>17</sup> Ferry, Gee and Treloar, *Trans. Faraday Soc.*, 1945, **41**, 340.



just allowed free passage of the inner bulb tube; this was closed with a rubber cap D. The first liquid, introduced into the outer bulb from a burette with a

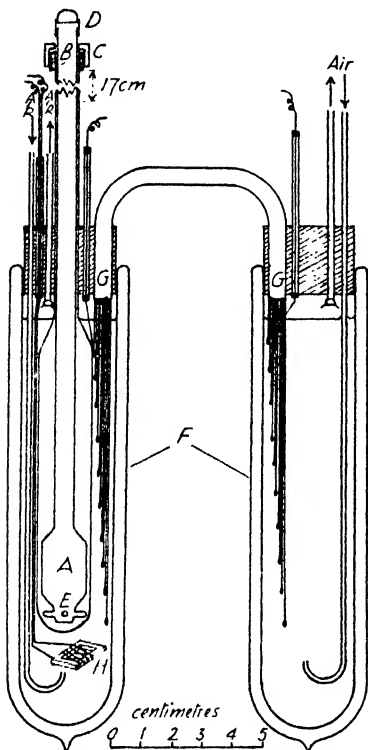


FIG. 1.—The calorimeter.

of 0.01 cal. required. The thermal capacity of the apparatus was about 80 cal./deg. so that 0.01 cal. corresponded to approximately  $5 \times 10^{-8}$  V. A null method of measurement was devised, a diagram of the circuit appears in Fig. 2. The commutator was arranged so that the P.D. across the 0.02 ohm resistance opposed the thermopile E.M.F., and the variable resistance adjusted until the galvanometer, a Kipp and Zonen Zernicke Zc, returned to its zero point. Then the ratio of the P.D. across the 1000 ohm resistance to the thermopile E.M.F. was 50,000/1. A heat of mixing of 1 cal. corresponded to a P.D. of 0.25 V, measured on a potentiometer, and the required accuracy of 2.5 mV was well within the limits of the potentiometer using a needle-type galvanometer.

**Method of Operation.**—The potentiometer reading was taken at the start of each experiment to ensure that the calorimeter had reached thermal equilibrium. After mixing the liquids, potentiometer readings were taken at intervals of 0.5 min. or 1 min. for 14 min. and a cooling curve constructed (Fig. 3). The heat change was always complete in 1-2 min. and the cooling curve of such small

long delivery tube which reached through the inner bulb, was separated by a pool of mercury from the second liquid which was in the inner bulb. Mixing was effected by raising the inner bulb and rotating it, the glass spikes E acting as stirrers.

This mixing bulb fitted centrally through a rubber bung into an unsilvered Dewar vessel F filled with water and stirred by a stream of air saturated with water vapour. The air exit tube was covered at the bottom by a glass disc to prevent water splashing out. The temperature changes were measured with a twenty junction thermopile G of 20 s.w.g. constantan and 34 s.w.g. copper. The constant temperature level was a second Dewar vessel, placed close to the first and stirred with the air stream. The thermojunctions were arranged alternately in the two Dewars so as to be distributed at 1 cm. intervals throughout their depths. The wires and junctions were insulated with cloth sleeving painted with a solution of polystyrene in benzene incorporating some plasticizer. This coating did not deteriorate during long immersion in water. The heat capacity of the calorimeter was determined by the introduction of measured amounts of electrical energy through the Nichrome coil H of resistance about 12.5 ohm. The calorimeter and air saturators were immersed, so that only the leads and the mixing bulb tubes projected, in a water thermostat at 20° C, kept constant to  $\pm 5 \times 10^{-4}$ ° C.

Heats of mixing from 0.1 cal. to 3.0 cal. were anticipated and an accuracy of

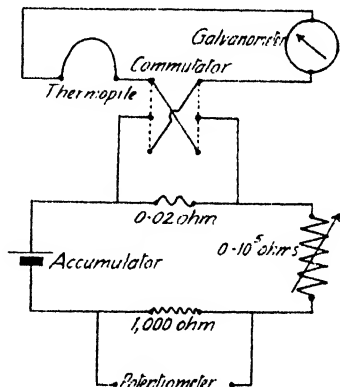


FIG. 2.—The thermopile circuit.

slope that extrapolation was simple. The cooling correction, applied assuming Newton's law, was never greater than 2 % of the total heat change. The thermal capacity was determined for each run using an amount of electrical energy

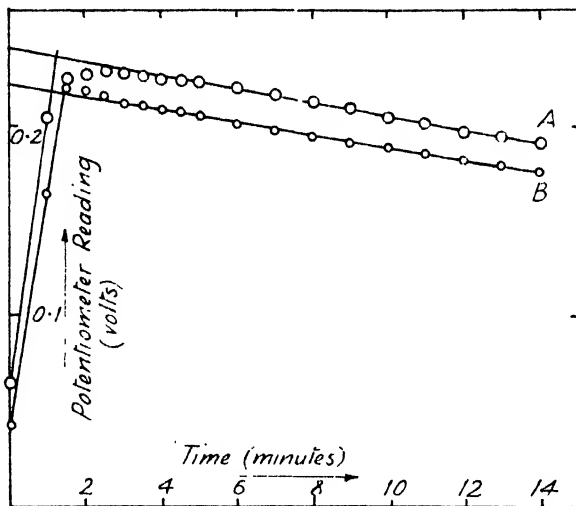


FIG. 3.—Typical cooling curves.

A—Mixing experiment.

B—Thermal capacity determination

approximately equal to the heat of mixing, and a cooling correction applied as before. The resistance of the heating coil was checked in a Wheatstone net circuit and the P.D. across the coil measured on the potentiometer during the time of operation of the heating current which was usually 1 min. A stirring correction for the mixing was obtained by stirring the already mixed liquids according to a standard technique. This was never greater than 0.02 cal. The apparatus was cleaned by sucking out the contents of the mixing bulb, flushing three times with acetone and drawing through a stream of dry air.

It was frequently required to determine the heat of mixing of equal volumes of components, A and B. Parallel runs were carried out except that in the first case A was in the outer bulb and in the second case B was in the outer bulb. The average of the results was taken as the true heat of mixing. When either or both of the components were fairly volatile errors arose and it was necessary to employ a method of differences. There was about 12 ml. of free air space in the outer bulb saturated with vapour in equilibrium with the liquid in that bulb. After mixing, evaporation of one component and condensation of the other occurred in order to maintain this equilibrium and the heat effects did not in general counter-balance. To overcome this, the heat of mixing of  $a$  ml. of A and  $b$  ml. of B was measured with  $(2 + a + b)$  ml. of mercury in the pool; then the heat of mixing of  $2a$  ml. of A and  $2b$  of B was measured with 2 ml. of mercury in the pool. The total volume of the contents,  $2(a + b + 1)$  ml., and hence the volume of free air space, was equal in both experiments and so was the composition of the mixture, thus the evaporation heat effects were also equal. The difference between the two results gives, therefore, the heat of mixing of  $a$  ml. of A with  $b$  ml. of B. Heat determinations were repeatable to  $\pm 0.02$  cal. or, for heats greater than 1 cal.,  $\pm 2$  %.

The materials were identical with those used in Part I.<sup>18</sup>

## Results

**Heats of Mixing.**—The same series of mixtures as in Part I was investigated. For mixtures containing ethyl acetate the difference method was employed. The heats of mixing per mole of mixture, for equal volumes of the two components, together with the molar volumes of the mixtures at 20° C, ( $x_1 V_1^\circ + x_2 V_2^\circ$ ),

<sup>18</sup> Meares, *Trans. Faraday Soc.*, 1949, **45**, 966.

are given in Tables I and II in which heat absorbed is recorded as positive. The same mixtures as in Part I were investigated over a range of concentrations and the data are presented in Fig. 4.

TABLE I.—HEATS AND ENERGIES OF MIXING AT 20° C FOR MIXTURES CONTAINING ETHYL ACETATE (1 cal. = 4.184 joules.)

Substance	Mole Fr. EtAc	Molar Vol. Mixture (ml.)	$\Delta H_p$ (cal./mole)	$\Delta U_v$ (cal./mole)
1 : 3-Butanediol diacetate . . .	0.633	123.9	-0.4	25.5
Diethyl oxalate . . .	0.581	113.7	-19.9	8.2
Diethyl malonate . . .	0.608	119.1	6.4	27.0
Diethyl succinate . . .	0.631	123.5	0.0	26.2
Diethyl adipate . . .	0.671	131.4	-5.5	25.1
Diethyl diethylmalonate . . .	0.691	135.3	6.2	30.6
Diethyl sebacate . . .	0.732	143.3	28.5	49.9
Dibutyl oxalate . . .	0.676	132.4	-7.9	13.4
Dibutyl malonate . . .	0.692	135.5	-5.0	16.9
Dibutyl succinate . . .	0.707	138.4	8.3	31.0
Dibutyl adipate . . .	0.733	143.5	31.6	50.3
Dibutyl sebacate . . .	0.774	151.6	75.5	86.8
Dimethyl phthalate . . .	0.625	122.3	-6.1	80.1
Diethyl phthalate . . .	0.670	131.2	5.9	61.3
Di- <i>n</i> -propyl phthalate . . .	0.704	137.7	20.4	65.9
Di- <i>n</i> -butyl phthalate . . .	0.731	143.1	32.9	66.6
Di- <i>isobutyl</i> phthalate . . .	0.732	143.3	17.1	48.4
Di- <i>n</i> -amyl phthalate . . .	0.753	147.6	62.0	84.7
Dimethylglycol phthalate . . .	0.711	139.6	45.9	141.3
Di- $\beta$ -chloroethyl phthalate . . .	0.692	135.4	-60.2	40.5

TABLE II.—HEATS AND ENERGIES OF MIXING AT 20° C FOR MIXTURES CONTAINING 1 : 3-BUTANEDIOL DIACETATE (BDA) (1 cal. = 4.184 joules.)

Substance	Mole Fr. BDA	Molar Vol. Mixture (ml.)	$\Delta H_p$ (cal./mole)	$\Delta U_v$ (cal./mole)
Diethyl oxalate . . .	0.446	150.3	-20.1	-12.6
Diethyl malonate . . .	0.474	159.9	9.4	11.1
Diethyl succinate . . .	0.498	168.0	6.7	5.0
Diethyl adipate . . .	0.542	182.9	22.5	18.4
Diethyl diethylmalonate . . .	0.565	190.5	65.3	62.2
Diethyl sebacate . . .	0.613	206.9	88.6	69.9
Dibutyl oxalate . . .	0.548	184.9	10.2	8.6
Dibutyl malonate . . .	0.566	191.0	32.7	27.8
Dibutyl succinate . . .	0.583	196.6	57.0	47.2
Dibutyl adipate . . .	0.614	207.2	85.2	66.8
Dibutyl sebacate . . .	0.666	224.5	170.9	135.6
Dimethyl phthalate . . .	0.492	165.8	15.4	34.3
Diethyl phthalate . . .	0.541	182.5	44.0	42.2
Di- <i>n</i> -propyl phthalate . . .	0.580	195.5	61.0	50.6
Di- <i>n</i> -butyl phthalate . . .	0.612	206.4	101.4	81.6
Di- <i>isobutyl</i> phthalate . . .	0.613	206.9	81.3	65.4
Di- <i>n</i> -amyl phthalate . . .	0.639	215.8	128.7	107.0
Dimethylglycol phthalate . . .	0.589	198.6	70.7	90.9
Di- $\beta$ -chloroethyl phthalate . . .	0.565	190.7	-47.3	-21.3

**Estimation of Cohesive Energies.**—In order to test eqn. (3) the cohesive energy densities of the esters at 20° C are required. The molar cohesive energy of the liquid is generally regarded as the energy  $\Delta U_{vap}$  required to vaporize one mole into the perfect gas state. If the vapour is treated as behaving

ideally this is related to the molar latent heat of vaporization,  $\Delta H_{\text{vap.}}$ , by

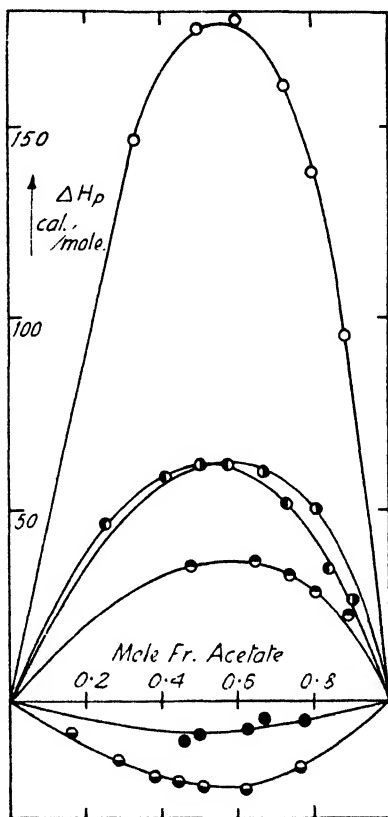
$$\Delta U_{\text{vap.}} = \Delta H_{\text{vap.}} - RT. \quad (4)$$

There are apparently no calorimetric data for the latent heats of diesters so alternative approaches must be adopted. The latent heats of some dialkyl

Fig. 4.—Concentration dependence of heat of mixing.

KEY TO FIG. 4, 5, 6 and 7

- Ethyl acetate and dimethyl phthalate.
- Ethyl acetate and di-*n*-butyl phthalate.
- Ethyl acetate and di-*n*-amyl phthalate.
- 1:3-Butanediol diacetate and diethyl oxalate.
- 1:3-Butanediol diacetate and di-*n*-propyl phthalate.
- 1:3-Butanediol diacetate and dibutyl sebacate.



phthalates have been obtained, for temperatures ranging from 40° C for dimethyl phthalate to 85° C for the di-*n*-amyl ester, from the vapour pressure data of Small, Small and Cowley,<sup>19</sup> using the Clausius-Clapeyron equation. Latent heats may be estimated using Hildebrand's extension of Trouton's rule.<sup>20</sup> This rule, the fundamental basis of which has been established by a number of theoretical studies, shows that the dependence of  $\Delta H_{\text{vap.}}$  upon  $t_b$ , the boiling point on the Centigrade scale, is almost linear over a wide range. The values of the latent heats refer to a temperature close to the boiling point. The latent heats of about thirty esters of monocarboxylic acids have been measured at their boiling points.<sup>21, 22</sup> The esters range from methyl formate (b.p. 32° C) to ethyl nonylate (b.p. 227° C), and the data are fitted within  $\pm 2\%$  by

$$\Delta H_{\text{vap.}} = 20.60t_b + 6,103, \quad (5)$$

$\Delta H_{\text{vap.}}$  is in cal./mole. In two-thirds of the cases the deviation from (5) is less than 1%. This equation has been used to calculate the latent heats of the diesters at their boiling points (Table III, col. 3).

<sup>19</sup> Small, Small and Cowley, *Trans. Faraday Soc.*, 1948, **44**, 810.

<sup>20</sup> Hildebrand, *J. Amer. Chem. Soc.*, 1915, **37**, 970; *ibid.*, 1918, **40**, 45; *op. cit.*, ref. 3, p. 102.

<sup>21</sup> Brown, *J. Chem. Soc.*, 1903, **83**, 987.

<sup>22</sup> Matthews, *J. Amer. Chem. Soc.*, 1926, **48**, 562.

The variation of the latent heat of evaporation with temperature is determined, very approximately, by

$$\Delta H_{\text{vap.}(t_1)} \simeq \Delta H_{\text{vap.}(t_b)} + \int_{t_1}^{t_b} \Delta C_p \cdot dT, \quad (6)$$

where

$$\Delta C_p = C_p(\text{liq.}) - C_p(\text{vap.}).$$

$C_p$  is a molar specific heat at constant pressure, and if  $\Delta C_p$  is treated as independent of temperature,  $t_1$  is 20° C and  $t_2$  is the boiling point,  $t_b$ , then (6) becomes

$$\Delta H_{\text{vap.}(20^\circ)} \simeq \Delta H_{\text{vap.}(t_b)} + \Delta C_p(t_b - 20). \quad (7)$$

Suitable specific heat data are almost entirely lacking, but  $\Delta C_p$  (cal./deg. g.) for certain diesters may be estimated from (7) by comparing the latent heats

TABLE III.—LATENT HEATS AND EVAPORATION ENERGIES OF ESTERS

Substance.	Boiling Pt. °C	$\Delta H_{\text{vap.}}$ (b.p.) (cal./mole)	$\Delta H_{\text{vap.}}$ (20° C) (cal./mole)	$\Delta U_{\text{vap.}}$ (b.p.) (cal./mole)	$\Delta U_{\text{vap.}}$ (20° C) (cal./mole)
Ethyl acetate . . . . .	77.1	7,711	8,522	7,015	7,940
1 : 3-Butandiol diacetate . . . . .	208.0	10,388	14,600	9,432	14,000
Diethyl oxalate . . . . .	186.1	9,937	13,100	9,025	12,500
Diethyl malonate . . . . .	198.9	10,200	13,900	9,262	13,300
Diethyl succinate . . . . .	216.5	10,563	15,000	9,590	14,400
Diethyl adipate . . . . .	241.0	11,068	16,900	10,047	16,300
Diethyl diethylmalonate . . . . .	226.0	10,759	16,500	9,767	15,900
Diethyl sebacate . . . . .	308.0	12,448	22,100	11,294	21,500
Dibutyl oxalate . . . . .	243.4	11,117	17,000	10,091	16,400
Dibutyl malonate . . . . .	251.5	11,284	17,800	10,242	17,200
Dibutyl succinate . . . . .	274.5	11,758	19,400	10,670	18,800
Dibutyl adipate . . . . .	305.0	12,386	21,900	11,238	21,300
Dibutyl sebacate . . . . .	344.0	13,189	26,400	11,063	25,800
Dimethyl phthalate . . . . .	282.0	11,912	18,500	10,809	17,900
Diethyl phthalate . . . . .	296.1	12,203	20,200	11,072	19,600
Di- <i>n</i> -propyl phthalate . . . . .	317.5	12,644	22,300	11,741	21,700
Di- <i>n</i> -butyl phthalate . . . . .	340.0	13,107	24,700	11,889	24,100
Di-isobutyl phthalate . . . . .	327.0	12,839	23,900	11,647	23,300
Di- <i>n</i> -amyl phthalate . . . . .	344.0	13,189	26,100	11,963	25,500
Dimethylglycol phthalate . . . . .	358.0	13,478	26,600	12,224	26,000
Di- $\beta$ -chlorethyl phthalate . . . . .	355.0	13,416	26,100	12,168	25,500

from the vapour pressure data<sup>19</sup> with those at the boiling points from Hildebrand's rule. An almost constant value  $\Delta C_p = 0.13$  cal./deg. g., obtained by this means, has been used to reduce all the values of  $\Delta H_{\text{vap.}}$  at the boiling points for the diesters to 20° C (Table III, col. 4). Taking the same value of  $\Delta C_p$  for all the diesters is a very crude approximation and the use of the rough eqn. (6) is therefore justified. It is clear that the values of  $\Delta H_{\text{vap.}}$  (20° C) are considerably less accurate than  $\Delta H_{\text{vap.}}$  (b.p.). For ethyl acetate  $\Delta H_{\text{vap.}}$  (20° C) has been obtained from the vapour pressure data in the International Critical Tables.

The energies of evaporation at the boiling points and at 20° C (Table III, col. 5 and 6) have been obtained from the heats of evaporation using eqn. (4).

**Determination of the Coefficients of Thermal Expansion and Isothermal Compressibility.**—In order to obtain the energies of mixing at constant volume from the heats of mixing at constant pressure the coefficients of thermal expansion ( $\alpha = 1/V(dV/dT)_p$ ) and isothermal compressibility ( $\kappa = -1/V(dV/dp)_T$ ) are necessary.

Using the technique of Part I, the densities of all the esters have been determined at 25° C. In conjunction with the densities at 20° C (Part I, Table I), these have been used to calculate the coefficients of thermal expansion. These are presented in Table V, col. 3.

There are few published values of the isothermal compressibilities of the

diesters, and the data of different observers frequently disagree. It can be shown thermodynamically that <sup>23</sup>

$$T\alpha/\kappa \simeq \Delta U_{\text{vap.}}/V^\circ. \quad (8)$$

The values of  $(\Delta U_{\text{vap.}}/V^\circ)$  at 20° C, obtained from the energies of vaporization in Table III and the molar volumes (Part I, Table I), are given in Table V, col. 2. The isothermal compressibility of ethyl acetate has been measured at 20° C by Tyrer <sup>24</sup> and for diethyl oxalate and malonate the compressibilities may be obtained from the data of Gay. <sup>25</sup> These compressibilities have been used to test eqn. (8); it is clear from Table IV that it is closely obeyed.

TABLE IV

Substance	$\alpha$	$\kappa$ (Mbarye) <sup>-1</sup>	$T\alpha/\kappa$ (cal./ml.)	$\Delta U_{\text{vap.}}/V^\circ$ (cal./ml.)
Ethyl acetate . . . . .	$1.32 \times 10^{-3}$	$113 \times 10^{-6}$	81.6	80.7
Diethyl oxalate . . . . .	0.99	75	92.4	92.2
Diethyl malonate . . . . .	0.95	75	88.6	87.5

The values of  $\kappa$  for the other diesters and for 1 : 3-butanediol diacetate have been obtained from eqn. (8) (Table V, col. 4).

TABLE V.—COHESIVE ENERGY DENSITIES, COEFFICIENTS OF THERMAL EXPANSION AND ISOTHERMAL COMPRESSIBILITY OF ESTERS AT 20° C

Substance	$\frac{\Delta U_{\text{vap.}}}{V^\circ}$ (cal./ml.)	$\alpha$	$\kappa$ (Mbarye) <sup>-1</sup>
Ethyl acetate . . . . .	80.7	$1.32 \times 10^{-3}$	$113 \times 10^{-6}$
1 : 3-Butanediol diacetate . . . . .	83.0	0.89	75
Diethyl oxalate . . . . .	92.2	0.99	75
Diethyl malonate . . . . .	87.5	0.95	75
Diethyl succinate . . . . .	86.1	1.02	83
Diethyl adipate . . . . .	81.6	0.91	78
Diethyl diethylmalonate . . . . .	72.7	0.91	88
Diethyl sebacate . . . . .	80.3	0.81	71
Dibutyl oxalate . . . . .	80.1	0.87	76
Dibutyl malonate . . . . .	78.1	0.88	79
Dibutyl succinate . . . . .	79.8	0.84	74
Dibutyl adipate . . . . .	79.3	0.81	72
Dibutyl sebacate . . . . .	76.8	0.81	74
Dimethyl phthalate . . . . .	109.8	0.76	49
Diethyl phthalate . . . . .	98.6	0.72	51
Di- <i>n</i> -propyl phthalate . . . . .	93.3	0.75	56
Di- <i>n</i> -butyl phthalate . . . . .	90.6	0.69	53
Di- <i>isobutyl</i> phthalate . . . . .	87.1	0.77	62
Di- <i>n</i> -amyl phthalate . . . . .	85.0	0.69	57
Dimethylglycol phthalate . . . . .	107.7	0.65	42
Di- $\beta$ -chloroethyl phthalate . . . . .	116.2	0.68	41

The adiabatic compressibilities of many liquids, including the diethyl esters of oxalic, malonic, succinic, adipic and phthalic acids, have been determined by a velocity of sound method. <sup>26</sup> The isothermal compressibilities obtained from these data are low compared with those from direct methods and have been disregarded.

<sup>23</sup> Glasstone, *Physical Chemistry* (Macmillan, 1946), 2nd ed., p. 479.

<sup>24</sup> Tyrer, *Z. physik. Chem.*, 1914, **87**, 182.

<sup>25</sup> Gay, *Ann. Chim. Phys.*, 1916, **6**, 127.

<sup>26</sup> Parthasarathy, *Proc. Indian Acad. Sci. A*, 1935, **2**, 497; *ibid.*, 1936, **3**, 285.

## Discussion

**The Reduction of Thermodynamic Quantities from Constant Pressure to Constant Volume.**—The relation, at constant temperature, between the energy change on mixing at constant volume,  $\Delta U_v$ , and the heat of mixing at constant pressure,  $\Delta H_p$ , derived by purely thermodynamic means,<sup>27</sup> is given, for small volume changes, by

$$\Delta H_p - \Delta U_v = \frac{\Delta VT\alpha_0}{\kappa_0} - \frac{1}{2V_0\kappa} \left[ 1 + \frac{d(\ln \kappa_0)}{dT} \right] \Delta V^2, \quad (9)$$

where  $\Delta V$  is the volume change on mixing at constant pressure, and  $V_0$  the volume of the separated components. If  $\alpha_1$  and  $\alpha_2$  are the coefficients of thermal expansion and  $\kappa_1$  and  $\kappa_2$  the coefficients of isothermal compressibility of the pure components, whose volume fractions in the mixture are  $v_1$  and  $v_2$ , then

$$\alpha_0 = v_1\alpha_1 + v_2\alpha_2, \quad \kappa_0 = v_1\kappa_1 + v_2\kappa_2.$$

For practical purposes the compressibility of the mixture,  $\kappa \simeq \kappa_0$ .

In the derivation of eqn. (3) the average co-ordination number of the molecules is assumed identical in the unmixed and in the mixed states. In a mixture in which there is a contraction due to a molecular rearrangement this average co-ordination number is slightly increased. In order to compare  $\Delta H_p$  for such a mixture with the theoretical value of  $\Delta U_v$  from eqn. (3) it is necessary to convert  $\Delta H_p$  not only to constant volume but to a state in which the number of nearest neighbour contacts between molecules is equal to the number of such contacts in the isolated components. The molecular rearrangement involves the filling of holes in the component of larger molecules by molecules of the other component and is akin to condensation. Thus the energy change due to this rearrangement is equal to the energy of condensation of a volume of mixture equal to the geometrical contraction. Using eqn. (3) for the energy of mixing, the condensation energy of 1 ml. of mixture,  $L_M$ , is given by

$$L_M = (v_1L_1^{\frac{1}{2}} + v_2L_2^{\frac{1}{2}})^2,$$

where  $L_1 = -(\Delta U_{1\text{vap.}}/V_1^0)$  etc. Since the energies of mixing are small, for all the mixtures considered in this investigation  $L_M$  differs from the cohesive energy of the isolated components,  $(v_1L_1 + v_2L_2)$ , by less than 1 % so that it is permissible to use this simpler expression as an approximation.

**Estimation of the Energies of Mixing at Constant Volume.**—The volume change in the mixtures containing 1:3-butanediol diacetate (abbreviated as BDA) is due only to the intermolecular forces<sup>18</sup> and eqn. (9) may be used to obtain  $\Delta U_v$ . For the mixtures containing ethyl acetate there is a geometrical contribution to the volume change. This must be corrected for as a condensation in order to obtain energies of mixing for comparison with eqn. (3). In fact, it is found that, for the series of mixtures examined here, the difference between this method and the use of eqn. (9) for the total volume change is always less than 2 % of the total correction. This error is negligible with that in determining  $\Delta V$ . The values of  $\Delta H_p$  have been corrected to  $\Delta U_v$  using the volume changes in Part I, Table I. The energies of mixing are included in the last columns of Tables I and II. The value of  $(d(\ln \kappa_0)/dT)$  obtained from the data of Tyrer for ethyl acetate and Gay for diethyl oxalate has been used for all the mixtures containing ethyl acetate. For the mixtures containing BDA  $(d(\ln \kappa)/dT)$  for pure diethyl oxalate has been used throughout.

The heats of mixing have been measured for six mixtures at various

<sup>27</sup> Scatchard, *Trans. Faraday Soc.*, 1937, **33**, 171.

concentrations; the corresponding volume change data have been discussed in Part I. These values of  $\Delta H_v$  and  $\Delta V$  have been plotted against mole fraction in Fig. 4 and 5 and from the curves the values at mole fraction intervals of 0.1 have been interpolated. Eqn. (9) has been used to obtain, from these, values of  $\Delta U_v$  at mole fraction intervals of 0.1, presented graphically in Fig. 6.

**The Regular Solution Approximation.**—The assumption of complete randomness of orientation and distribution of the molecules, which is fundamental to the regular solution theory, is identifiable with the concentration dependent terms on the right-hand side of eqn. (3).<sup>14</sup> The validity of this assumption can, therefore, be examined by comparing the concentration dependence of  $\Delta U_v$  from eqn. (3) with the experimental data. A test of this nature has been carried out by Ferry, Gee and Treloar<sup>17</sup> who found the form of eqn. (3) to be obeyed by a number of mixtures of non-polar components but departures were observed with polar substances.

In order to examine the data for the six ester mixtures it is convenient to transform eqn. (3) to

$$\frac{\Delta U_v(x_1 V_1^0 + x_2 V_2^0)}{x_2 V_1^0 V_2^0} = x_1 B_V, \quad (10)$$

where 
$$B_V = \left[ \left( \frac{\Delta U_{1vap.}}{V_1^0} \right)^{\frac{1}{2}} - \left( \frac{\Delta U_{2vap.}}{V_2^0} \right)^{\frac{1}{2}} \right]^2. \quad (11)$$

Since  $B_V$  is a constant for each mixture, the left-hand side of (10) plotted against  $x_1$  should give a straight line from the origin intersecting the ordinate  $x_1 - 1$  at  $B_V$ . In Fig. 7 energy of mixing data for these six mixtures are plotted against the mole fraction of acetate in this way. In every case a good linear relation is observed; five of these lines extrapolate to the origin, the exception being BDA with diethyl oxalate. In these five cases the assumption of random mixing of the molecules is justified over the whole concentration range. Since BDA with dibutyl sebacate and ethyl acetate with di-*n*-amyl phthalate are the mixtures with the largest energies of mixing, they are the mixtures in which departure from randomness is most probable. It may be concluded, therefore, that the regular solution approximation is justified for the other mixtures provided no special orientating influences are present.

The mixture of BDA with diethyl oxalate is exceptional in having a negative energy of mixing. This suggests that orientational forces play a part, and these must affect the randomness of the mixture. In this mixture there is a linear relation, as required by (10) for mole fractions of acetate greater than about 0.3. It appears that there is some molecular orientation in diethyl oxalate which has to be disrupted, involving an absorption of energy, and that this process of disorientation is complete when the mole fraction of BDA has reached 0.3, so that beyond this range the arrangement of the molecules in the mixture is effectively random, the energy of mixing being very small. Extrapolation of the linear part of the curve back to  $x_1 = 0$  gives, from the intercept on this ordinate, a

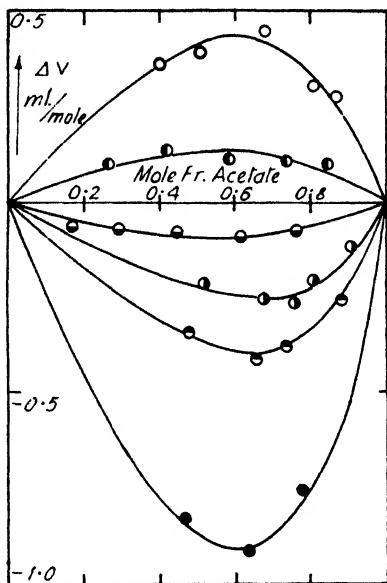
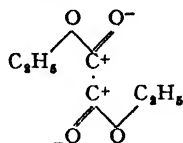


FIG. 5.—Concentration dependence of volume change on mixing



measure of the energy required for the complete disorientation of the pure diethyl oxalate. The reason for this orientation can be seen from the dipolar structure of diethyl oxalate :



The two electropositive carboxyl carbon atoms being directly attached to one another form a centre of electropositivity far more intense than

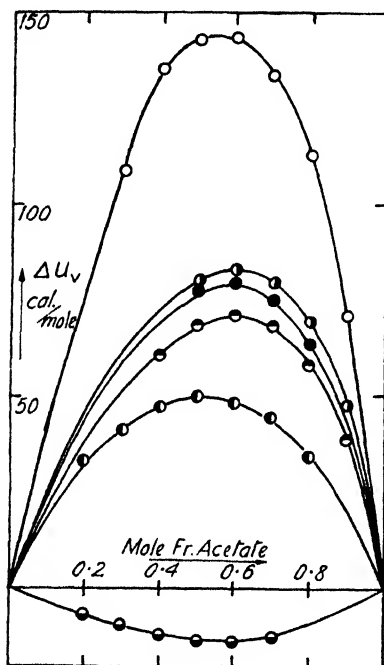


FIG. 6.—Concentration dependence of energy of mixing.

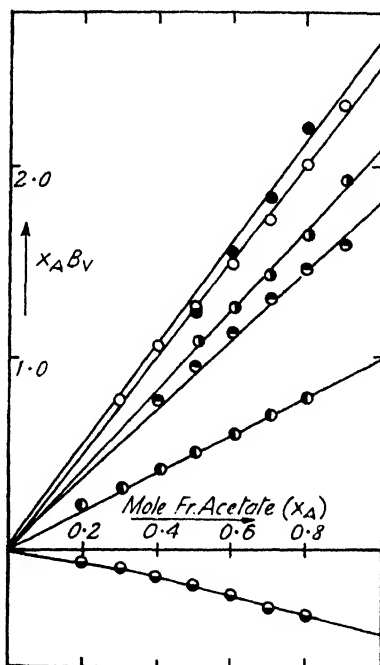


FIG. 7.—Test of the regular solution approximation.

in other esters where the carboxyl carbon atoms are attached to alkyl groups over which the positive charge is largely distributed by means of an inductive mechanism. This centre of electropositivity in an oxalate tends to become associated with the negative carbonyl carbon atoms of neighbouring ester groups, a tendency which is opposed by the thermal motions of the molecules.

**A Quantitative Test of the Regular Solution Equation.**—The value of  $B_v$  for each mixture may be obtained from the observed values of  $\Delta U_v$  using eqn. (10). It may also be obtained from the cohesive energy densities in Table V using eqn. (11). The values from the former method, designated " $B_v$  obs.," are compared in Table VI with those from the latter method, " $B_v$  calc. (20°)". It is clear that there is no systematic correspondence between the two sets of values.

The reliability of  $B_v$  obs. depends upon the accuracy of  $\Delta U_v$ , which is determined both by the accuracy of the  $\Delta H_v$  measurements and of the correction for the volume change on mixing. The uncertainty in  $\Delta H_v$

causes an uncertainty in  $B_V$  obs. of  $\pm 0.02$  or  $\pm 2\%$  for values greater than 1. The volume change correction is largely governed by the first term on the right-hand side of eqn. (9) since this is always much larger

TABLE VI.—QUANTITATIVE TEST OF THE REGULAR SOLUTION EQUATION

Substance	Mixed with Ethyl Acetate			Mixed with 1:3-Butanediol Diacetate		
	$B_V(20^\circ\text{C})$ calc.	$B_V$ obs.	$B_V$ (b.p.) calc.	$B_V(20^\circ\text{C})$ calc.	$B_V$ obs.	$B_V$ (b.p.) calc.
1:3-Butanediol diacetate	0.0	0.8	1.0	—	—	—
Diethyl oxalate . . .	0.4	0.3	0.1	0.2	-0.3	0.5
Diethyl malonate . . .	0.1	0.9	0.4	0.1	0.3	0.1
Diethyl succinate . . .	0.1	0.9	0.8	0.0	0.1	0.0
Diethyl adipate . . .	0.0	0.8	1.9	0.0	0.4	0.2
Diethyl diethylmalonate .	0.2	0.9	3.2	0.3	1.3	0.6
Diethyl sebacate . . .	0.0	1.4	3.9	0.0	1.4	1.0
Dibutyl oxalate . . .	0.0	0.4	2.1	0.0	0.2	0.2
Dibutyl malonate . . .	0.0	0.5	2.7	0.1	0.6	0.4
Dibutyl succinate . . .	0.0	0.9	3.0	0.0	1.0	0.6
Dibutyl adipate . . .	0.0	1.4	4.0	0.0	1.3	1.0
Dibutyl sebacate . . .	0.1	2.3	6.3	0.1	2.4	2.3
Dimethyl phthalate . . .	2.3	2.6	0.1	1.9	0.8	0.4
Diethyl phthalate . . .	0.9	1.9	1.0	0.7	0.9	0.0
Di- <i>n</i> -propyl phthalate . .	0.5	1.9	2.1	0.3	1.0	0.2
Di- <i>n</i> -butyl phthalate . .	0.3	1.9	3.2	0.2	1.6	0.6
Di- <i>isobutyl</i> phthalate . .	0.1	1.4	3.5	0.1	1.3	0.8
Di- <i>n</i> -amyl phthalate . .	0.1	2.3	4.6	0.0	2.0	1.4
Dimethylglycol phthalate	1.9	4.1	1.9	1.6	1.8	0.1
Di- $\beta$ -chlorethyl phthalate	3.2	1.2	1.0	2.8	-0.5	0.0

than the second term. Thus the experimental error in the volume change determinations creates, in  $B_V$  obs., an uncertainty of  $\pm 0.03$ . The largest source of error is in  $T\alpha_0/\kappa_0$ , which depends upon the estimated values of  $(\Delta U_{\text{vap.}}/V^\circ)$  for the pure components. These cannot be less reliable than  $\pm 10\%$  so that for each multiple of 0.0003 in the fractional volume change on mixing a further uncertainty of  $\pm 0.01$  is introduced into  $B_V$  obs. Hence for the series of mixtures containing BDA,  $B_V$  obs. is accurate to  $\pm 0.1$ , while for the ethyl acetate mixtures the reliability, on account of the larger volume changes, is nearer  $\pm 0.2$ . The effect of the uncertainty in  $(\Delta U_{\text{vap.}}/V^\circ)$  upon  $B_V$  calc. ( $20^\circ$ ) is more serious and difficult to estimate since the errors in the individual values of  $(\Delta U_{\text{vap.}}/V^\circ)$  are not entirely random and will tend to cancel when  $B_V$  is calculated. It seems clear that the differences between the values of  $(\Delta U_{\text{vap.}}/V^\circ)$ † for the individual esters are generally too small to account for the observed energies of mixing on the basis of eqn. (3).

It has been pointed out in a theoretical discussion<sup>28</sup> that when comparing the properties of liquids they should be in corresponding states, as defined by van der Waals. Since the critical pressures of most substances lie between 50 and 100 atm., the boiling point at atmospheric pressure is approximately a corresponding state. The fourth and seventh columns of Table VI, headed " $B_V$  calc. (b.p.)", have been calculated from the energies of evaporation at the boiling points and the molar volumes at  $20^\circ\text{C}$  (the number of molecules per ml. at the temperature of the mixture is required). For the BDA series of mixtures there is a fair agreement between  $B_V$  obs. and  $B_V$  calc. (b.p.). For the mixtures containing ethyl acetate the calculated values increase too rapidly with

<sup>28</sup> Pitzer, *J. Chem. Physics*, 1939, **7**, 583.

ascent of the homologous series.  $B_V$  calc. (b.p.) increases in each homologous series, in agreement with the experimental results, whereas the trend in  $B_V$  calc. (20°) is the reverse of this.

If the values of  $B_V$  obs. are compared for corresponding mixtures containing ethyl acetate and BDA a good agreement is observed throughout the whole range. This agreement was expected since ethyl acetate and BDA contain the same chemical groups in the same proportion and their molecules are therefore characterized by similar force fields. The problem of mixtures containing polar molecules should more properly be treated by an extension of the theory of independent surface action;<sup>29</sup> this will be the subject of a subsequent communication.

**The Relation between Internal Energy and Volume Changes.**—With the aid of certain assumptions Scatchard<sup>27</sup> has derived a relation between the change in internal energy and volume on mixing. Expressed in terms of the notation used here this is

$$\Delta V = \kappa_0 \Delta U_{\text{m}} \quad . \quad . \quad . \quad (12)$$

An important assumption is that the geometrical arrangement of the molecules is similar in the separated components and in the mixture. This assumption is approximately justified in the mixtures containing BDA, and eqn. (12) has been examined for these. The values of  $\Delta V$  in ml./mole calculated from (12) using  $\Delta U_{\text{m}}$  from Table II are compared in Table VII with the observed values of  $\Delta V$  (Part I, Table II). The

TABLE VII.—COMPARISON OF THEORETICAL AND OBSERVED VOLUME CHANGES FOR MIXTURES CONTAINING 1:3-BUTANEDIOL DIACETATE

Substance	$\kappa_0$ (Mbarye) <sup>1</sup>	$\Delta V$ Theor. ( $\frac{\text{ml.}}{\text{mole}}$ )	$\Delta V$ Obs. ( $\frac{\text{ml.}}{\text{mole}}$ )
Diethyl oxalate . . .	$75 \times 10^{-6}$	-0.04	-0.08
Diethyl malonate . . .	75	0.03	-0.02
Diethyl succinate . . .	79	0.02	0.02
Diethyl adipate . . .	77	0.06	0.05
Diethyl diethylmalonate	82	0.21	0.04
Diethyl sebacate . . .	73	0.21	0.23
Dibutyl oxalate . . .	76	0.03	0.02
Dibutyl malonate . . .	77	0.09	0.06
Dibutyl succinate . . .	75	0.15	0.12
Dibutyl adipate . . .	74	0.21	0.23
Dibutyl sebacate . . .	75	0.43	0.45
Dimethyl phthalate . . .	62	0.09	-0.20
Diethyl phthalate . . .	63	0.11	0.02
Di- <i>n</i> -propyl phthalate . . .	66	0.14	0.12
Di- <i>n</i> -butyl phthalate . . .	64	0.22	0.23
Di- <i>isobutyl</i> phthalate . . .	69	0.19	0.19
Di- <i>n</i> -amyl phthalate . . .	66	0.29	0.26
Dimethylglycol phthalate	59	0.22	-0.22
Di- $\beta$ -chlorethyl phthalate	58	-0.05	-0.27

accuracy of the observed values is about  $\pm 0.03$  ml./mole. The mixtures containing dimethyl, diethyl, dimethylglycol and di- $\beta$ -chlorethyl phthalates have been discussed in Part I, and the negative or low values of  $\Delta V$  explained in terms of the large cohesive energy density differences between these substances and BDA. There is a similar effect in the mixture of BDA with diethyl diethylmalonate; in this case BDA is the component of higher cohesive energy density. The standard deviation for the difference between the observed and theoretical values of  $\Delta V$  for the remaining

<sup>29</sup> Langmuir, *Colloid Symp. Monogr.*, 1925, 3, 48.

fourteen mixtures in Table VII is 0.0234. Applying the *t*-test for significance it is found that  $t = 1.22$ . With thirteen degrees of freedom, a value of *t* less than 1.77 ( $P = 10\%$ ) is definitely not statistically significant. The deviations for the five mixtures with large cohesive energy density differences are all highly significant. The assumption of mixing without change of arrangement is not justified for the mixtures containing ethyl acetate. For these mixtures  $\Delta V$  is negative and  $\Delta U_v$  positive so that eqn. (12) cannot apply.

From eqn. (10),

$$\Delta U_v = \frac{B_V x_1 V_1^0 x_2 V_2^0}{x_1 V_1^0 + x_2 V_2^0}$$

Thus with (12),

$$\Delta V = \frac{\kappa_0 B_V x_1 V_1^0 x_2 V_2^0}{x_1 V_1^0 + x_2 V_2^0} \quad (13)$$

When  $\kappa_0$  is almost independent of concentration, (13) becomes

$$\Delta V = \frac{k x_1 V_1^0 x_2 V_2^0}{x_1 V_1^0 + x_2 V_2^0} \quad (14)$$

where *k* is a constant, and this is the form of the concentration dependence of  $\Delta V$  found previously.<sup>18</sup> When this is not the case the departure of  $\Delta V$  from the form of (14) should be appreciable. In the mixtures of BDA with diethyl oxalate and dibutyl sebacate the variation of  $\kappa_0$  with concentration is negligible, but with di-*n*-propyl phthalate it is considerable. For this mixture, values of  $\Delta V$  calculated from eqn. (12) using  $\Delta U_v$  at mole fraction intervals of 0.1 (Fig. 6), are compared, in Table VIII,

TABLE VIII.—COMPARISON OF THEORETICAL AND OBSERVED VOLUME CHANGES FOR MIXTURES OF 1:3-BUTANEDIOL DIACETATE WITH DI-*n*-PROPYL PHTHALATE

Mole Fr. Acetate	$\kappa_0$ (Mbarre) <sup>-1</sup>	$\Delta V$ Theor. ( $\frac{\text{ml.}}{\text{mole}}$ )	$\Delta V$ Obs. ( $\frac{\text{ml.}}{\text{mole}}$ )
0.2	$59 \times 10^{-6}$	0.08	0.08
0.3	61	0.11	0.11
0.4	62	0.12	0.12
0.5	64	0.13	0.13
0.6	66	0.13	0.13
0.7	68	0.13	0.12
0.8	70	0.10	0.10

with the observed values from Fig. 5 at the same concentrations. The very good agreement is closer than could be obtained from an equation of the form of (14). Thus the theory of volume changes suggested by Scatchard is in good agreement with experiment for mixtures where the necessary assumptions are acceptable.

The author is grateful to the Managers of the Royal Institution for permission to use the Davy-Faraday Research Laboratory, where part of this work was carried out. He has pleasure in expressing his thanks to Prof. E. K. Rideal for advice and encouragement and also to Dr. R. F. Tuckett for many helpful suggestions when this investigation was begun in the Department of Colloid Science, Cambridge University.

*The Davy-Faraday Research Laboratory,  
The Royal Institution,  
London, W.1.*

## REVIEWS OF BOOKS

**Ion Exchange. Theory and Application.** Ed. F. C. NACHOD. (Academic Press Inc., New York, 1949.) Pp. xii + 411. Price \$8.50.

This is the first comprehensive monograph on ion exchange. It consists of 16 articles, dealing with diverse aspects of the subject, written by leading American specialists. The work as a whole admirably illustrates the editor's thesis that "ion exchange now takes its place among the more common unit processes such as distillation, adsorption and filtration".

The articles are largely in the nature of reviews of published work, and range from the almost purely mathematical treatment of "Kinetics of Fixed-Bed Ion Exchange" by H. C. Thomas to descriptions of plant construction in M. E. Gilwood's article on "Ion Exchange Equipment Design." The articles are not unnaturally tinged by the views of the individual authors and there is a good deal of overlap between them. Consequently the book lacks the unity of an authoritative textbook. The range of the articles is so wide, however, that no one person could have covered the subject adequately. In any case, few readers will wish to study more than a small selection of the aspects dealt with.

The physico-chemical theory of ion exchange is fully reviewed in articles by H. F. Walton and W. C. Bauman. Taken together, these give a correct picture of the present state of the subject—namely, a great deal of fragmentary, superficial information covers our fundamental ignorance. This is well illustrated, for example, by the variety of different semi-empirical approaches which have been used to treat cation-exchange equilibria. On the other hand, not a single equilibrium constant can be predicted from fundamental theory with any confidence. There is still much to be learned concerning the structure of exchangers, but the problem of calculating interionic energies in such systems presents more formidable difficulties and has not yet been touched.

Ion exchange is best known, of course, from its application to water treatment. This topic is thoroughly described in the book under review, but it is very significant that about two-thirds of the book is devoted to existing or potential applications to *other* fields of chemistry.

The following list of articles must suffice to give some idea of the wide range of applications which have already been found or suggested for ion exchange: separations of inorganic cations (J. Schubert); as a tool in analytical chemistry (W. Rieman III); metal concentration and recovery (S. Sussman and F. C. Nachod); catalytic applications (S. Sussman); biochemical and physiological studies (N. Applezweig); separation of amino acids (R. J. Block); sugar refining and by-product recovery (A. B. Mindler); recovery of alkaloids (N. Applezweig and F. C. Nachod); miscellaneous applications, classified under eleven heads (F. H. Lindsay and D. G. Braithwaite).

Every chemist, whatever his "brand", should dip into appropriate chapters of this book. The potentialities of ion exchange are not yet sufficiently appreciated in this country, and it is safe to predict that every reader will find something of real interest to his own line of work.

The defects of the book are few and minor. The statement on page 175 that "the affinity of a cation for the cation exchanger increases with increasing valence" is too sweeping and is now out of date; there is, in fact, a great overlap between ions of different valency groups. (Incidentally, a prompt revision of this book will be essential if it is to keep pace with the progress of research.) There are not many typographical errors, but there are *six* places where the reader may learn that Adams and Holmes (1935) were pioneers in introducing synthetic resin exchangers. British readers may flinch at the unconscious "salesmanship" for ion exchange which has crept into one or two sections, and the industrialist may doubt the economic soundness of some of the reported applications. Similarly, the research man may regard a half-page picture devoted to a "jackleg tank support" (p. 82) or the chart on page 276 as slightly ridiculous, and a numerical table of capacities of anion exchangers which are characterized only by letters A, B, C, etc. (p. 135) as worthless.

Such minor blemishes do not detract appreciably from the great usefulness of the work. The production is excellent, but since few individuals will be prepared to pay \$8.50 for the privilege of looking through the two or three chapters which concern them, this is clearly a book which should be added to every chemical departmental library at once.

J. A. K.

**Les Spectres Moléculaires.** (Le Centre National de la Recherche Scientifique, 13 Quai Anatole-France et 45 Rue d'Ulm, Paris, 1947.) Pp. 176. Price 150 fr. or 16s. (H. K. Lewis & Co. Ltd.)

This is a collection of papers presented at the International Conference on Molecular Spectra held in Paris in May, 1947. The papers have previously appeared in various 1948 numbers of *J. Physique* and *J. Chim. Phys.* but are collected for convenience in this publication. The conference was the first important international conference of molecular spectroscopists to be held in Europe since the war. It afforded the opportunity of reviewing progress and presenting work done in this field since 1940. Papers were given by many American and British as well as Continental scientists attending the meeting.

The articles are classified into seven groups as follows: (1) Papers dealing with electronic band spectra, (2) The Raman effect in crystals, (3) Techniques and applications of infra-red and Raman spectra, (4) Molecular spectra and molecular energies—dissociation and excitation energies, potential functions, force constants, etc., (5) Raman effect and molecular structure, (6) Hydrogen bonding and related questions, (7) Reports on molecular spectroscopic research in the French zones of Germany and Austria.

All the papers are by leading authorities and the volume shows how much important fundamental work it was possible to do under the difficult conditions of the war years and provides under one cover some record of that work. It is to be hoped that in view of the great scientific and industrial importance of spectroscopy that it may be possible to hold conferences of this nature more frequently in the future.

W. C. P.

**Advances in Catalysis and Related Subjects, Vol. I.** Edited by W. G. FRANKENBURG, V. I. KOMAREWSKY and E. K. RIDEAL. Editorial Board, P. H. EMMETT and H. S. TAYLOR. (Academic Press, Inc., New York, 1948.) Pp. xiii + 321. Price, \$7.80.

The editors of this series have, in Vol. I, begun to close the gap between the text-book presentation and the current themes of Catalysis. The book contains eight reviews by authors describing the state (in early 1948) of their especial topics. Among techniques, P. H. Emmett provides a critical account of specific area measurement by the now "standard" Brunauer-Emmett-Teller procedure and by other gas absorption methods. M. H. Jellinek and I. Fankuchen describe the application of X-ray diffraction to solid catalyst research with emphasis upon its use in particle size and phase analysis; lattices with extensive defects are easily recognized by this method but the important "micro"-defect demands a subtler tool.

Some catalysts of the petroleum and organic chemical industries are discussed by V. N. Ipatieff and L. Schmerling ("Alkylation of Iso-paraffins"), H. Pines ("Isomerization of Alkanes") and H. H. Storch ("The Fischer-Tropsch and Related Processes"). The first two items outline the experimental bases of established processes catalyzed by strong acids and metal halides; they illustrate the unity attainable through ionic mechanisms in suitable form. On the other hand the carbon monoxide-hydrogen reactions, although technically developed and chemically similar among themselves on Storch's showing, contain a more elusive motif.

R. H. Griffith, in an excellent statement of the geometric "factor" in catalysis, is unable to establish its uniqueness, either as cause or adjunct of activity in the complicated catalysts of industrial processes; the significance of the geometry as a factor cannot be doubted, but the contemporary tendency to imply that the part is the whole arises from the neglect of other correlations. The heterogeneity of the complex surface is well brought out by H. S. Taylor in some activated adsorption studies, which ought now to be compared with the work of Beeck, Ritchie and Wheeler (*J. Colloid Sci.*, 1948, **3**, 505). By way of contrast, in "The Catalytic Activation of Hydrogen", D. D. Eley is primarily concerned with simple, "clean", metal surfaces but includes more intricate (even biological) systems. The power of the methods used in research on the reactions of ortho- and para-hydrogen or the hydrogen isotopes, and the weight of the results, are conveyed largely through the geometric approach taken by the original workers; nevertheless the author is aware of the importance of the electron properties of the solid in catalytic activity.

Without exception, the articles are illuminating, easy to read and well supplied with illustrations and references; the book is pleasant in the hand and contains only a few minor misprints. The editors have certainly accomplished their purposes in Vol. I, and the proposed contents of Vol. II compel the liveliest interest.

D. A. D.

**Laboratory and Workshop Notes.** Ed. RUTH LANG (for Institute of Physics), (Arnold and Co., 1949). Pp. v + 272. Price 21s.

The Laboratory and Workshop Notes of the *J. Sci. Instr.* are well known and widely read. The majority of readers, however, do not possess the complete series of this Journal, but for the price of 21s. they may at least possess a selected list of these Notes over the past 25 years.

As the Editor emphasized, the book is not intended to cover a complete range of laboratory and workshop practice, but it is full of many simple, ingenious and elegant solutions of those practical problems which are constantly engaging the attention of experimentalists. To assist in guiding the reader there is a good index and the book is broadly classified into eight sections.

Each of the 181 Notes has the appropriate reference to the original article in the Journal. The royalties from the sales will be placed to the credit of the Institute's Benevolent Fund, and subject to favourable reception of this volume a further volume of these Notes is contemplated. The book can be heartily recommended to experimental physical chemists.

F. C. T.

**Techniques of Histo- and Cytochemistry.** BY DAVID GLICK. (London, Interscience Publishers, 1949.) Pp. 531. Price 48s.

This book marks a milestone in science, the virtual coalescing of physics and chemistry with cytology. As Dr. Glick remarks in his preface: "The day is past when our vision cannot penetrate beyond the architecture of the cell. The wealth of knowledge that has been, or can still be gleaned by purely descriptive microscopic anatomy is not to be minimized, but under the new illuminations we begin to discern the chemical patterns in the cellular architecture." On the one hand the cytologist has been provided with a wealth of new methods which give precise information about the composition and physical state of cell structures; on the other, the physicist and the chemist can come to grips with the actual participants of the extraordinary happenings in living cells. For the latter to continue to work on crude models of what might be considered to represent living matter is entirely unjustified. Their efforts might be better devoted to determining what are the actual components of living cells. Even then caution is necessary, for, as Prof. Bensley remarks in his foreword: "The belief that in the complex colloidal matrix of protoplasm reactions occur as they do in more simplified systems *in vitro* is responsible for many mistakes."

Dr. Glick's book is a most useful reference book for all who are working on the chemical or physical anatomy of cells. It is remarkably comprehensive. Besides the micro-chemical and enzymological tests suitable for histological use, it describes most of the newer physical methods, such as visible, u.-v. and X-ray absorption spectroscopy, radioautographs and electron micrographs. It is to be noted, however, that there is no reference to phase contrast microscopy. The Cartesian diver techniques on the micro-litre scale, developed by Linderstrøm-Lang in the Carlsberg laboratory are described at some length and the book closes with a short account of the methods which have been recently



developed by Claude, Dounce, Bensley and others, of separating the particulate constituents of cells by differential centrifuging.

As is now usually the case with U.S. publications, the price is too high, and is out of keeping with that of British books of similar size. It ought to be possible to sell a book of just over 500 pages for less than 48 shillings, notwithstanding the excellent production. The price in the United States is \$8 and it is not evident why it should be increased 20 % (at the current rate of exchange) in crossing the Atlantic. It appears to the writer that the present methods of exchange of scientific books across the Atlantic are disadvantageous to us both ways. We import complete books for sale here at an enhanced price, but our books are usually bought by the U.S. in sheet form at what can only be described as bargain prices—namely, at 30-40 % of the published price, whatever they are sold at there.

J. A. V. B.

**Theory of Dielectrics, Dielectric Constant, and Dielectric Loss.** By H. FRÖHLICH (Oxford, at the Clarendon Press, 1949). Pp. viii + 180. Price 18s.

Since Debye in 1928 and Van Vleck in 1932 produced their monographs on the molecular theory of dielectrics there have been important advances which have not been adequately surveyed in any book. Onsager's and Kirkwood's treatment, of internal fields and of molecular interactions, Kauzmann's application of Eyring's theory of rate processes, and other developments have caused big changes in the non-quantum part of the theoretical picture. The great accumulation of experimental material has brought to light some new phenomena for the theorists to treat. By undertaking the task of collation and systematization Prof. Fröhlich has put us in his debt, more especially because in doing it he has made valuable original contributions. His treatment of the subject is broad, yet thorough and critical. There is only one omission worth noting: the theory of inhomogeneous dielectrics is of some practical importance, and a section devoted to it would be welcome.

The author has written intentionally for applied scientists, a term which, in this context, includes chemists; so it is pertinent to consider how far he succeeds in the difficult task of making the subject intelligible to those who do but lisp the language of mathematical physics. For them the book is not easy reading. The mathematical manipulation is not very heavy, but the difficulty of grasping the concepts and of following the rather condensed physical arguments is considerable. The book is relatively brief; and the author has freely used the popular device of putting supposedly technical steps of the argument in appendices. The book would gain in clarity if, in the next edition, these latter (or some of them) were expanded and given as early chapters or brought into the main text. Nevertheless, it should be emphasized that, although it is hard going, this book holds the reader by its unmistakable quality.

The book is up to the usual high standard of the Clarendon Press. There are a few misprints but these are very minor.

L. E. S.

# DIFFUSION PHENOMENA IN GASES

## PART I.—THE THERMAL DIFFUSION OF OXYGEN— EXPERIMENTAL

BY E. WHALLEY, E. R. S. WINTER AND H. V. A. BRISCOE

*Received 1st April, 1949*

The thermal diffusion factor of oxygen gas has been determined at three temperatures. The construction and operation of a thermal diffusion column designed to enrich  $^{18}\text{O}$  in oxygen gas is described and the results detailed.

The theory of the thermal diffusion column, first used by Clusius and Dickel,<sup>1</sup> has been discussed in detail by Furry and Jones<sup>2</sup> who give references to all the important work on the subject up to 1946. The separation achieved depends upon the dimensions of the column, upon the physical properties of the gas used and its pressure, and upon the temperature difference in the column. The effect of the dimensions of the column has been studied principally by Clusius and Dickel and the results are in good accord with theory.<sup>2</sup> A few workers have studied the effect of certain of the other variables, the most satisfactory examinations being those of Nier and Bardeen<sup>3a, b</sup> of the separation of the carbon isotopes in methane, and Simon<sup>3c</sup> of the separation of the argon isotopes. This paper and Part II report a similar investigation of the separation of the oxygen isotopes. Three investigations upon the separation of the oxygen isotopes by gaseous thermal diffusion<sup>4</sup> have been reported but no attempt has been made to test the theory experimentally; it is of particular interest to do this since oxygen is one of the few light elements without a long-lived radioactive isotope suitable for tracer studies.

### **The Determination of the Thermal Diffusion Factor of Oxygen Gas.—**

In order to compare the operation of a thermal diffusion column with the theory of Jones and Furry, it is necessary to know the values and temperature variations of certain physical properties of the gas. In the case of oxygen sufficient information for our purpose is available for all these properties except that of thermal diffusion; we have therefore measured the thermal diffusion factor of oxygen at three temperatures and the results, which are presented below, will be discussed and used in Part II. The method used was that of Nier.<sup>5</sup>

If a temperature gradient is maintained in a gas of two components we have

$$D_{12} \text{ grad } c_2 = - \frac{D_T}{T} \cdot \text{grad } T, \quad . \quad . \quad . \quad (1)$$

where  $c_2$  is the concentration of one component ( $c_1 + c_2 = 1$ ),  $T$  is the temperature, and  $D_T$  is the coefficient of thermal diffusion, and  $D_{12}$  that

<sup>1</sup> Clusius and Dickel, *Naturwiss.*, 1938, **26**, 546; *Z. physik. Chem.*, 1938, **44**, 397.

<sup>2</sup> Jones and Furry, *Rev. Mod. Physics*, 1946, **18**, 153.

<sup>3</sup> (a) Nier, *Physic. Rev.*, 1940, **57**, 30. (b) Bardeen, *ibid.*, 1940, **57**, 35. (c) Simon, *ibid.*, 1946, **69**, 596.

<sup>4</sup> Wells, *ibid.*, 1941, **59**, 679. Clusius, Dickel and Becker, *Naturwiss.*, 1943, **31**, 210. Lauder, *Trans. Faraday Soc.*, 1947, **43**, 620.

<sup>5</sup> Nier, *Physic. Rev.*, 1939, **56**, 1009.

of ordinary diffusion in the gas mixture at the temperature  $T$ . We may also write

$$\frac{D_T}{D_{12}} = k_T = \alpha c_1 c_2, \quad (2)$$

where  $k_T$  is the thermal diffusion ratio and  $\alpha$  is the thermal diffusion factor. If the temperature gradient is maintained between two bulbs of equal volume at temperatures  $T_1$  and  $T_0$ , connected by a relatively narrow tube, then if  $c_2^1$  is the concentration of the second component, at equilibrium, in the bulb at temperature  $T_1$  we have

$$\alpha = \frac{c_2^1 - c_2}{c_1 c_2} \cdot \frac{\frac{T_0}{T_1} + 1}{\ln(T_1/T_0)} \quad (3)$$

where  $c_1$  and  $c_2$  are the initial concentrations. With isotopic mixtures the separation thus obtained will in general be very small after one operation: but if the two bulbs are isolated and that at  $T_0$  then evacuated, the gas from the other allowed to fill both bulbs, and the system again allowed to come to equilibrium the concentration difference  $c_2^1 - c_2$  will be doubled. In general we have instead of (3),

$$\alpha = \frac{(c_2^1)_n - c_2}{nc_1 c_2} \cdot \frac{\frac{T_0}{T_1} + 1}{\ln(T_1/T_0)} \quad (4)$$

where  $(c_2^1)_n$  is the concentration in the one bulb after  $n$  operations. This equation is only approximate as it neglects the volume of gas in the connecting tube and does not allow for the case when the volumes of the bulbs are not equal; a more general expression is, for the case that the lower (cold) bulb is evacuated each time,

$$\frac{(c_2^1)_n - c_2}{nc_1 c_2 \ln((T_1/T_0))} = \alpha \left[ \frac{V_1 T_1 + \frac{1}{2} V_c T_1 T_0 / \bar{T}}{V_1 T_1 + V_2 T_0 + V_c T_1 T_0 / \bar{T}} \right], \quad (5)$$

where  $V_1$ ,  $V_2$  are the volumes of the cold and hot bulbs respectively, and  $V_c$  is the volume of the connecting tube;  $\bar{T}$  is the mean temperature in the connecting tube, assuming a linear gradient. Eqn. (5) or its equivalent, depending on the method of operation used, i.e. which bulb was evacuated,\* has been employed in calculating the values for  $\alpha$  given below.

## Experimental

The procedure adopted was thus to set up the two-bulb apparatus with  $V_1 = 1085$  ml.,  $V_2 = 940$  ml., and  $V_c = 63.5$  ml. The vertical connecting tube was about 22 cm. long, including the tap, and about 2.0 cm. diam.; the tap was about 1.5 cm. bore. The upper bulb was surrounded by a furnace which was kept at  $T_1 \pm 5^\circ$  throughout each run, the furnace being specially made and carefully checked for uniform temperature distribution inside; the lower bulb was immersed in a well-lagged thermostat which was filled with water or solid  $\text{CO}_2$ , as required, and kept at  $T_0 \pm 3^\circ$ . The oxygen used was prepared by electrolysis from water containing about 1.3 %  $^{18}\text{O}$ ; it contained about 1 % of impurity, presumably nitrogen, giving mass 28 in the mass spectrometer. The apparatus was filled with the oxygen to a pressure of about 70 cm. Hg and a sample taken of the initial gas: with the bulbs at  $T_1$  and  $T_0$  the system was allowed to reach equilibrium allowing at least five times the relaxation time for the system as given by Jones and Furry.<sup>6</sup> The tap connecting the two bulbs was closed and the gas in the lower bulb transferred by means of a Töpler pump to a storage bulb; the gas in the upper bulb was allowed to expand and fill both bulbs by opening the connecting tap and the system allowed to reach equilibrium again. This procedure was repeated a number of times and the small quantity of gas finally remaining in one bulb was recovered for analysis.

\* See footnote to Table I.

<sup>6</sup> Jones and Furry, ref. 2, eqn. (38).

TABLE I

Run No.	Temp. °K	No. of Operations	Mass 32/Mass 34, Ratio		$\Delta c \times 10^4$	$\alpha \times 10^3$
			Initial	Final		
I *	195-373	6 {	38.25 $\pm$ 0.11 35.75 $\pm$ 0.08	39.00 $\pm$ 0.02 36.33 $\pm$ 0.05	4.7 4.2	9.9 $\pm$ 0.8
II *	195-373	6 {	37.79 $\pm$ 0.01 38.04 $\pm$ 0.04	38.58 $\pm$ 0.03 38.66 $\pm$ 0.02	5.1 4.2	
II †	195-373	6 {	36.82 $\pm$ 0.04	37.52 $\pm$ 0.06	4.9	
III †	295-528	6 {	37.50 $\pm$ 0.02 36.90 $\pm$ 0.03	38.61 $\pm$ 0.02 38.02 $\pm$ 0.02	7.4 7.5	12.8 $\pm$ 0.6
IV *	296-703	5 {	37.47 $\pm$ 0.03 37.92 $\pm$ 0.03	38.70 $\pm$ 0.03 39.19 $\pm$ 0.07	8.2 8.2	

\* Analyses by A.E.R.E. Mass Spectrometer Division.

† Analyses by us.

$\Delta c$  is the change in mass 34 concentration.

Runs I, II and IV were performed by evacuating the cold bulb each time and taking the final sample from the cold bulb at the end of the 6th operation (5th in the case of run IV); run III was similar but the final sample was taken from the hot bulb.

The results for three temperature ranges are given in detail in Table I. The analysis by mass spectrometer gives the ratio of mass 32 to mass 34 in the samples; these ratios are quoted as arithmetic means of about 20 determinations with the error as standard deviation. Certain of these analyses were performed by the Mass Spectrometer Division A.E.R.E., Harwell; this has been indicated. The remainder were analyzed in this Department. It is of interest to note that the two mass spectrometers give concordant results in run (2) where samples were analyzed both by us and by A.E.R.E.

**Analysis of Isotopic Mixtures.**—In order to carry through the work reported here, it was necessary to construct and use a mass spectrometer for the isotope abundance analyses: this has been done by one of us (E. R. S. W.). The instrument is a Nier-type 60° sector model, with a tube of resolving power 110 very similar to that described by Graham, Harkness and Thode,<sup>7</sup> and with electronic controlling and measuring circuits developed by these workers: the circuits have proved as good in performance as is claimed by Thode *et al.*, and to be quite free from trouble in operation. The machine has been briefly described elsewhere by one of us.<sup>8</sup> Fig. 1 shows a typical mass spectrum, for a sample containing 2.67 % <sup>18</sup>O.

**The Thermal Diffusion Column.**—At the commencement of this work no facilities were readily available for mass spectrometer analyses; for this reason, and also to save time, it was necessary to proceed with the design and construction of the column without waiting for accurate knowledge of the thermal diffusion constant for oxygen gas. The design of a suitable cylindrical thermal diffusion column for any given purpose has been discussed in great detail by Jones and Furry,<sup>9</sup> but this paper was not published when we were designing our column, and our dimensions had to be based upon their earlier calculations for a planar column. We were not interested in getting the best overall thermal efficiency, but merely wished to erect a column which would yield oxygen containing some 15 % <sup>18</sup>O, and also to study the performance of the column. In practice it has been found that our column will produce a maximum of 21.9 % <sup>18</sup>O, but the enrichment reached at a reasonable production rate is around 15 %. In making our preliminary calculations we deliberately underestimated  $\alpha$ , and allowed for possible asymmetries in construction (which would reduce the maximum separation attainable), by writing  $K_p = 0.5 K_d$  (cf. Part II). It was as well that we did so since it appears that our column does contain some serious defect of this type (cf. Part II).

<sup>7</sup> Graham, Harkness and Thode, *J. Sci. Instr.*, 1947, **24**, 119.

<sup>8</sup> Winter, *Analyst*, 1948 (in press).

The column is of the concentric tube type (Fig. 2), and consists of a copper tube,  $\frac{7}{8}$  in. int. diam.,  $\frac{1}{8}$  in. wall thickness, 34 ft. (1060 cm.) long, made by butting together two shorter lengths with an external sleeve, care being taken to keep the inside smooth and symmetrical at the junction. This tube is surrounded by a water jacket made similarly from two lengths of 2 in. int. diam. copper tubing of  $\frac{1}{8}$  in. wall thickness; flanges were brazed to the inner tube near the ends and the water jacket brazed to these as shown. Two side-tubes near the top of the inner tube allow for sampling or for the passage of gas across the top of the column. The heating element is a brass tube of  $\frac{7}{8}$  in. ext. diam. and of length (when cool) about 34 ft.; down the centre of this tube passes a wire of 19 gauge Nichrome, which is crimped and silver-soldered into a plug at the bottom of the brass tube; the heating current passing down the wire (contact with the brass tube being prevented by ceramic bead spacers covering the whole

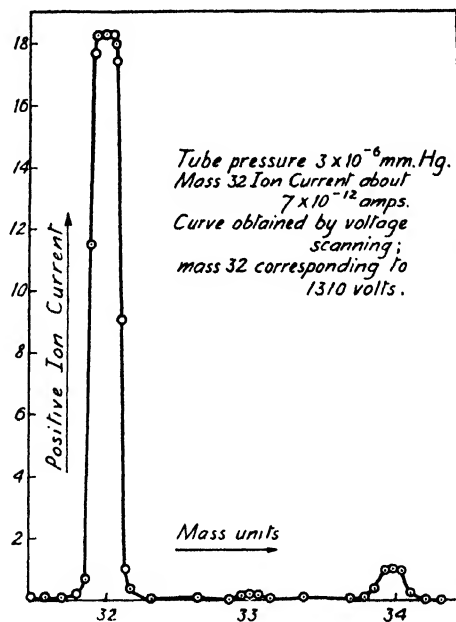


FIG. 1.

length) and to earth through the column. The differential expansion of the wire and tube on heating is taken up by an insulated metal spring attached to the Nichrome wire as it emerges from the top of the column. The brass tube is constructed from pieces about 10 ft. in length, turned on a lathe to give ends fitting one inside the other, and brazed together and filed to give a uniform ext. diam. of  $\frac{7}{8}$  in., this very inconvenient method of construction being necessary because of space restrictions at the bottom and top of the column, the first heating element having to be replaced after the column had been erected. Each joint was tested for vacuum tightness before making the next. The brass tube is kept central inside the copper tube by metal spacers, placed every 3 ft., which were accurately made so as to allow just sufficient play for ready extension of the brass when heated. Metal spacers are used because they can be machined more accurately than asbestos or ceramic spacers, which also were found unsuitable for prolonged use as they became brittle very quickly. The total heat transfer across all our spacers under the conditions of operation was calculated as about 30 W compared with a total consumption of some 2 kW; this calculation gives the maximum possible transfer assuming perfect metal-metal contact throughout, which certainly does not occur.

For convenience in dismantling, the ends of the gas space are closed by bolting together reeded brass flanges with washers of silicone rubber; this silicone rubber stands up well to the temperatures involved and we found it much superior

to lead or leather, lead being too hard and inelastic and leather deteriorating rapidly with the heat. At the top the flanges are brazed to the brass tube near its end, and to the end of the copper tube, which projects some 2 in. from the water jacket, so that the brass tube hangs from this flange. Similarly, at the bottom the copper tube projects from the water jacket and has a flange at the end, but here the other flange is attached to a short length of copper tubing leading to a copper-glass seal and so to the manometer, sampling tubes, vacuum pumps and oxygen preparation train. When cold, the end of the heater tube is just above the copper-glass seal and a metal pointer screwed into the plug

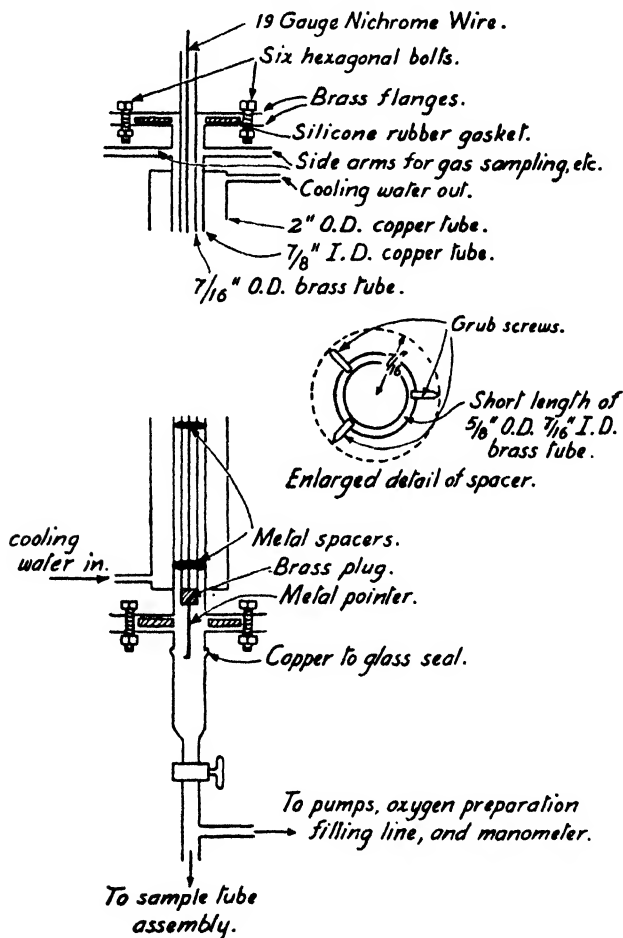


FIG. 2.

at the end gives an accurate indication of its expansion on heating, its movement being measured by means of a graduated glass scale fixed behind the glass tube; this expansion is used to calculate the temperature of the brass tube. The power consumption of the column is about 3 kW and is measured by a voltmeter and ammeter: the cooling water rises 5° C in temperature in passing up the column when it is operated with the brass tube at about 420° C.

The column was evacuated and made vacuum-tight: sample tubes were then attached top and bottom and the column outgassed by raising the temperature of the brass tube to 420° C and pumping with a two-stage mercury diffusion pump for 12 hr. Oxygen was prepared by heating A.R. potassium permanganate *in vacuo* and passing the gas through a drying train into the column. The column was filled with gas to the required pressure, with the

brass tube heated to  $417^{\circ}\text{C}$ , and samples taken from the top and bottom until equilibrium was reached. This procedure was repeated for a number of working pressures and the samples analyzed; the detailed results are given in Table II.

TABLE II

$p$ (atm.)	Time (hr.)	$^{18}\text{O}$ %		Separation Factor $q$
		Top	Bottom	
0.391	17.5	0.106	0.386	3.64
0.391	30.0	0.066	0.467	7.03
0.391	78.2	0.038	0.500	13.0
0.391	108.5	0.038	0.497	13.0
0.538	43.5	0.036	0.65	18.0
0.538	69.0	0.023	0.76	33.0
0.538	91.5	0.015	0.79	53.0
0.538	120.0	0.015	0.79	53.0
0.869	7.25	0.17	0.44	2.6
0.869	24.5	0.074	0.74	10.0
0.869	48.0	0.022	0.83	37.7
0.869	72.7	0.016	—	(~60.0)
0.869	120.0	0.014	0.84	60.0
1.41	12.5	0.084	0.43	5.12
1.41	24.0	0.05	0.49	9.9
1.41	96.5	0.05	0.52	10.4
1.41	120.0	0.05	0.52	10.4
0.255	120.0	0.096	0.340	3.54
1.18	120.0	0.02	0.71	35.5

Since normal oxygen was used in these studies the abundance of the  $^{18}\text{O}$  isotope was in many cases reduced to a rather low figure at the top of the column; for this reason, in spite of great care in the analyses, it is considered that in general the values quoted for the separation factor may have an error of  $\pm 5\%$ .

For producing a quantity of enriched oxygen, electrolytic oxygen from a cylinder was passed over heated palladized asbestos, through a drying train and across the top of the column by means of the two side-arms fixed in the  $\frac{1}{4}$  in. int. diam. copper tube; the rate of flow was regulated by a needle valve and flowmeter to twice the speed calculated to be necessary to maintain effectively the normal  $^{18}\text{O}$  concentration at the top of the column. A small reservoir and a few sampling tubes were attached to the bottom of the column. The optimum working pressure (see Part II) is calculated to be 55 cm., giving a maximum of some 21.9%  $^{18}\text{O}$ ; for convenience, up to the present, the column has been operated at atmospheric pressure, where the maximum possible concentration is about 10.4%  $^{18}\text{O}$ : a concentration of 8.7% has been obtained but the run was curtailed by a failure of the power supply.

We wish to express our gratitude to the Mechanical Engineering Department of this College for assistance in the construction of the thermal diffusion column, to Mr. R. L. Graham for advice upon the construction and operation of the mass spectrometer, and to Dr. E. R. Roberts of this Department and Mr. E. Vero and Dr. J. F. Martin of Messrs Genatosan Ltd. for the construction of various parts of the mass spectrometer. Also to the Mass Spectrometer Division, A.E.R.E. Harwell, for some of the analyses given in Table I, to the Department of Scientific and Industrial Research for a maintenance grant to one of us (E. W.) and to Imperial Chemical Industries Ltd., for financial assistance.

*Department of Inorganic and Physical Chemistry,  
Imperial College,  
S.W.7.*

# DIFFUSION PHENOMENA IN GASES

## PART II.—THE THERMAL DIFFUSION OF OXYGEN— THEORETICAL

BY E. WHALLEY (in part) AND E. R. S. WINTER

*Received 1st April, 1949*

Experimental values for the thermal diffusion factor of oxygen gas agree well with those calculated using the 13/7 intermolecular force model. The performance of the thermal diffusion column described in Part I is in reasonable agreement with theory. It is shown that the performance of Lauder's thermal diffusion column is not in agreement with theory and it is concluded that the probable reasons for this are the presence of turbulence in the gas flow, and the inadequacy of the molecular model used by Furry and Jones in deriving the general theory of the thermal diffusion column.

**The Thermal Diffusion Constant of Oxygen.**—It is well known that the thermal diffusion constant  $\alpha$  of a gas varies with temperature; in general  $\alpha$  has a low, or negative, value at temperatures close to the boiling point of the gas and becomes greater as the temperature is increased, approaching at high temperatures the value calculated using the theory of Chapman and Enskog in which the gas molecules are assumed to be perfectly elastic smooth spheres. The custom has arisen of comparing the experimental value of  $\alpha$  with that calculated for elastic spheres,  $\alpha_{es}$ , giving a ratio

$$R_T = \alpha_{obs.}/\alpha_{es} \quad . \quad . \quad . \quad (1)$$

$R_T$  therefore increases with temperature and approaches unity, the highest recorded values being about 0.8. Our results for oxygen follow the normal trend in this respect (Table I): the results are given in full in Part I.

TABLE I

$T_r$ , °K*	264	389	443
$\alpha_{obs.}$	$9.9 \times 10^{-3}$	$1.28 \times 10^{-2}$	$1.45 \times 10^{-2}$
$\alpha_{es}$	$2.7 \times 10^{-2}$	$2.7 \times 10^{-2}$	$2.7 \times 10^{-2}$
$R_T$ (obs.)	0.367	0.482	0.537
$\alpha_{13/7}$	$9.47 \times 10^{-3}$	$1.34 \times 10^{-2}$	$1.36 \times 10^{-2}$

\*  $T_r$  is given by  $T_r = \frac{T_1 T_2}{T_1 + T_2} \cdot \ln \left( \frac{T_2}{T_1} \right)$ , see ref.<sup>9</sup>

The introduction of  $R_T$  is useful in order to provide some basis for the comparison of experimental figures since theoretical calculations of  $\alpha$  are difficult using any molecular model which is at all realistic; calculations have been performed using the Sutherland model, the inverse-power model and its special case, the Maxwell model (here  $\alpha = 0$  at all temperatures) and the Lennard-Jones 9/5 force model; none of these models is successful in predicting the value and temperature variation of  $\alpha$ .<sup>1, 10</sup> It is known that the best procedure which could be made the basis of

<sup>1</sup> Jones and Furry, *Rev. Mod. Physics*, 1946, **18**, 153.



such computations (without discussing refinements such as an exponential repulsion which make the labour involved prohibitively great) is to use the Lennard-Jones 13/7 model, which gives the interaction energy of two molecules separated by a distance  $r$  (from centre to centre) as  $E(r)$ , where

$$-E(r) = E(o)\{2(r_0/r)^{12} - (r_0/r)^6\}. \quad (2)$$

In this equation,  $E(o)$  is the minimum value of  $E(r)$ , which occurs at separation  $r_0$ . This equation has been successfully used in a variety of calculations.<sup>2</sup>

The evaluation of the Enskog and Chapman collision integrals for molecules which obey the above law has recently been reported by Hirschfelder *et al.*,<sup>3</sup> so that it is possible to test this model. Using Hirschfelder's tables and the general equations of Chapman and Cowling,<sup>4</sup> a variety of experimental data upon thermal diffusion and diffusion in gases has been compared with theory by one of us and this will be dealt with in a later paper in this series. We quote here the results of the calculations for oxygen and compare them with the experimental figures, full details of which are given in Part I.

The agreement between the first and last lines is remarkably good—much better than has previously been obtained in such calculations using other models. We must, however, state that the results with other gases do not in general show such good concordance when a wider range of temperature is considered; even so the agreement is impressive. It is to be noted that the above results and calculations refer to the separation of the molecules of mass 34 ( $^{18}\text{O } ^{18}\text{O}$ ) from those of mass 32 ( $^{16}\text{O}_2$ ); under the conditions used changes in the concentration of the mass 33 species ( $^{17}\text{O } ^{18}\text{O}$ ) or in the mass 36 ( $^{18}\text{O}_2$ ) are not determinable with sufficient accuracy to merit consideration.

**The Performance of the Thermal Diffusion Column.\***—Theory predicts<sup>1</sup> that the equilibrium separation factors  $q_e$  obtained with a thermal diffusion column should vary with the operating pressure according to the expression:

$$\ln q_e = \frac{ap^{-\frac{1}{2}}}{1 + bp^{-\frac{1}{2}}}. \quad (3)$$

Our results (Table II, Part I) satisfy this relationship, as is seen by Fig. 1. By the method of least squares, the best straight line through the experimental points gives us

$$a/b = 18.3; \quad a = 5.0. \quad (4)$$

Similar agreement with theory has been reported by a number of workers.<sup>1</sup>

Since we have determined  $\alpha$  for the mean temperature at which the column was operated we may enquire more closely into the agreement of theory and experiment. Using the notation of Furry and Jones,<sup>1</sup> eqn. (3) becomes

$$\ln q_e = 2AL = \frac{HL}{K_e + K_s + K_p}, \quad (5)$$

where  $A$ ,  $H$ ,  $K_e$  and  $K_s$  are functions which have been given by Furry and Jones,<sup>1</sup> and  $K_p$  is a term introduced to allow for parasitic remixing effects due to asymmetries in the column geometry—in particular, to lack of perfect centring of the heated tube inside the gas space.  $K_p$ , of course, cannot be calculated. Using the equations of Jones and Furry, correcting

<sup>1</sup> See Fowler and Guggenheim, *Statistical Thermodynamics*, (C.U.P.), Ch. 7 and 8.

<sup>2</sup> Hirschfelder, Bird and Spotz, *J. Chem. Physics*, 1948, 16, 968.

<sup>4</sup> Chapman and Cowling, *The Mathematic Theory of Non-uniform Gases* (C.U.P., 1939).

\* With E. Whalley.

as indicated by them for the cylindricity of the column and employing our experimental value of  $\alpha$ , we calculate

$$\begin{aligned} H &= 2.86 \times 10^{-5} p^2 \text{ g. sec.}^{-1}, \\ K_e &= 2.44 \times 10^{-3} p^4 \text{ g. cm. sec.}^{-1}, \\ K_d &= 1.18 \times 10^{-3} \text{ g. cm. sec.}^{-1}, \end{aligned} \quad (6)$$

with  $p$  in atmospheres.

Eqn. (5) and (6) give us, neglecting  $K_d$ ,

$$\ln q_e = \frac{12.4 p^{-2}}{1 + 0.484 p^{-4}} \quad (7)$$

from which the calculated ratio  $a/b$  (eqn. (3) and (4)) is 25.6, in only moderate agreement with the observed value of 18.3. Better agreement than this has been obtained in the case of methane.<sup>5</sup> In assessing the significance of this discrepancy, it is necessary to bear in mind that the

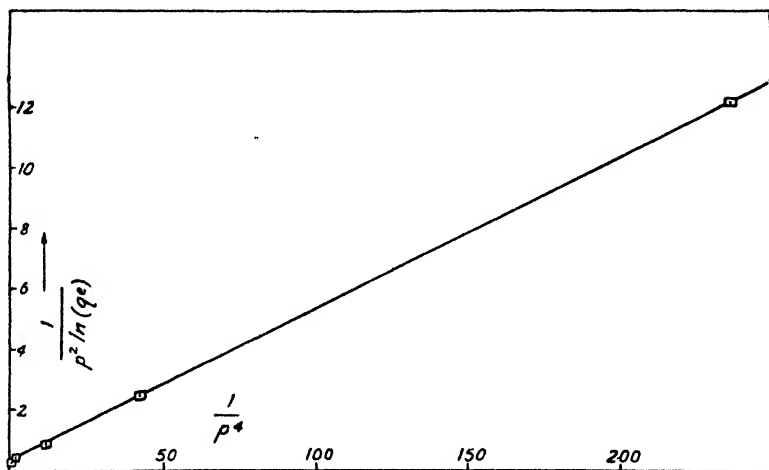


FIG. 1.

calculations of the functions  $H$ ,  $K_e$  and  $K_d$  by Furry and Jones are only for the cases that the viscosity, thermal conductivity, and self-diffusion coefficients of the gas have the temperature dependence of Maxwellian molecules, i.e.

$$\eta \propto T; \quad \lambda \propto T \text{ and } D_{11} \propto T^2 \quad (8)$$

and that  $\alpha$  is either independent of  $T$ , or varies directly as  $T$ . In arriving at eqn. (6) we used the results for  $\alpha$  proportional to  $T$ , which is clearly the best approximation of the two in our case, but since the relationships of eqn. (8) do not hold for oxygen, the values of eqn. (6) cannot be correct. The error involved is difficult to assess without carrying through some lengthy numerical integrations, and since in addition our value of  $\alpha$  is probably correct only to  $\pm 5\%$  it seems best, for further comparison, to arrange the experimental equation so that the discrepancies between the calculated and the observed coefficients of  $p^{-2}$  and  $p^{-4}$  are approximately equal. This yields

$$\ln q_e = \frac{10.8 p^{-2}}{2.09 + 0.057 p^{-4}} \quad (9)$$

from which it appears that in our column  $K_p = 1.09 K_e$ . This is a high value for  $K_p$ ; Nier<sup>5</sup> found a value of  $0.283 K_e$ <sup>1</sup> for his 20 ft. concentric

<sup>5</sup> Nier, *Physic. Rev.*, 1940, **57**, 30.

cylinder column using methane. This large value is probably reasonable in view of the sectional nature of the construction of our column and it is clearly desirable to work in shorter units—say 12 to 15 ft. in length—using only single lengths of tubing throughout.

By differentiating eqn. (9) with respect to pressure and equating the result to zero, we may derive the operating pressure for maximum separation  $P_{\text{opt.}}$ , and also this maximum separation  $(q_e)_{\text{max.}}$  by substituting  $P_{\text{opt.}}$  in eqn. (9):

$$P_{\text{opt.}} = 0.723 \text{ atm.}; (q_e)_{\text{max.}} = 140.$$

Thus at this working pressure the column will produce a maximum of 21.9 %  $^{18}\text{O}$  from normal oxygen, and operated at atmospheric pressure about 10.4 %  $^{18}\text{O}$ : in both cases the figures quoted are for no rate of production; if enriched material is continually removed from the heavy end the enrichment achieved will be less than the possible maximum.

**Rate of Approach to Equilibrium.\***—The approach to equilibrium for a column operating with both ends closed, i.e. with no reservoirs, is theoretically exponential and characterized by a relaxation time  $t_r$ ,<sup>1</sup>

$$t_r = \frac{2\mu}{AH \left(1 - \frac{\pi^2}{A^2 L^2}\right)}, \quad (10)$$

where  $\mu$  = the mass of gas in 1 cm. of the column,  $L$  is the length of the column in cm., and  $A$  and  $H$  have been defined above;  $t_r$  is the time required for the column to attain  $(1 - 1/e)$  of its equilibrium separation: eqn. (10) holds for  $AL < 2$ .

We have seen above that the calculated values of  $H$ ,  $K_e$  and  $K_d$  are not likely to be accurate; also the experimental equation (9) will only give us the ratio  $H/K_d$  and not the absolute value of either. The value for  $H$  obtained by substituting  $(K_d)_{\text{calc.}}$  into eqn (9) is  $2.01 \times 10^{-5} p^2$  g. sec.<sup>-1</sup>: since we have no means of deciding between this figure and that given in eqn. (6) it seems best in what follows to use the mean, i.e.  $H = 2.43 \times 10^{-5} p^2$  g. sec.<sup>-1</sup>, retaining of course, the experimental expression for  $A$ . The use of either of the other two values for  $H$  does not alter the general course of the discussion below.

TABLE II

$p$ (atm.)	$q_e$	$(1 - 1/e)q_e$	$t_r$ (hr.)	
			Expt.	Theor.
0.391	13	8.4	34	16.2
0.538	53	34	70	15.1
0.869	60	39	48	9.7
1.41	10.4	6.7	14.2	4.2

Examination of our results (Table II) shows that the rate of approach to equilibrium does not accord with theory, and a plot shows that it is in the initial stages that the separation is much slower than would be expected. The difference is partly due to the dead space at top and bottom of the column, amounting in all, including the sample tubes, to some 100 ml., most of which volume is at the bottom. The presence of this dead space means that much more heavy isotope than is considered in the theory of the column has to be transported to the bottom. Calculation of the error involved is difficult, but qualitatively it is evident that this volume will cause the relaxation (and effective equilibrium)

\* With E. Whalley.

time to be greater in practice than in theory. Our form of spacers will impose some restriction on the gas flow, and this also will increase the equilibrium time.

If the concentration of heavy isotope at the top of the column is kept at 0.2 % by continual replenishment, i.e. by circulating normal oxygen gas across the top, the rate of approach to equilibrium, with no reservoir at the bottom, is governed (when  $AL > 0.5$ ) by a relaxation time  $t_r$ ,

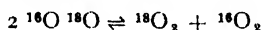
$$t_r = \frac{\mu L}{H} \left\{ \frac{\exp(2AL) - 1}{2AL} - 1 \right\}. \quad (11)$$

Thus, operated at 1 atm. the relaxation time would be 400 hr., and operated at the optimum pressure (0.723 atm.) it would be 1030 hr. Continuous runs of this duration have not up to the present been possible owing to interruptions of the power supply, but results so far obtained indicate that here also the rate of approach to equilibrium is somewhat slower than theory predicts.

#### Some Comments upon the Operation of Thermal Diffusion Columns.

—We wish now to comment upon a recent paper by Lauder<sup>6</sup> in which a study was made of the separation of the oxygen isotopes by thermal diffusion, and also upon some calculations by Davies<sup>7</sup> dealing with Lauder's experimental data.

The column used was of the hot-wire type in which the heated surface was a Nichrome wire at 1100° K; it is possible that at this temperature the catalytic exchange reaction



may become fast enough to effect appreciably the observed separation;<sup>8</sup> production of molecules of mass 36 in place of molecules of mass 34 would increase the  $^{18}\text{O}$  concentration at the bottom of the column above that calculated below.

Using again the equations and tabulations of Jones and Furry, with the gas constants evaluated at 293° K (since in this case the greater part of the gas will be at room temperature<sup>1</sup>) and employing our experimental value of  $\alpha$  (Table I) we obtain  $H = 2.07 p^2 \times 10^{-5}$  g. sec.<sup>-1</sup>;  $K_s = 8.59 \times 10^{-4}$  g. cm. sec.<sup>-1</sup>;  $K_e = 3.35 p^4 \times 10^{-3}$  g. cm. sec.<sup>-1</sup>;

$$\text{and} \quad \ln q_e = 2AL = \frac{2.47 p^{-2}}{1 + 0.257 p^{-4}}. \quad (12)$$

Eqn. (12) has been calculated for the separation of molecules of mass 34 from those of mass 32. This gives us a value of  $q_e = 4.37$  at 31.25 cm. pressure which is in very fair agreement with Lauder's figure of 5. This calculation has been performed by Davies, using an estimated value of  $\alpha$ , with results essentially the same as ours: Davies concluded that because of the agreement between theory and experiment at 31.25 cm. pressure the column used by Lauder was without parasitic currents. The argument upon which this conclusion is based is wrong and Davies has not considered properly the full consequences of eqn. (12). As already noted the calculations ignore the possibility of catalytic formation of  $^{18}\text{O}_2$  molecules: this reaction almost certainly occurs at the temperature of the wire in the presence of oxides,<sup>9</sup> as is stated by Lauder, and could, if efficient, have the effect of increasing  $H$  to about  $4.1 p^2 \times 10^{-5}$  g. sec.<sup>-1</sup>, i.e. twice that for molecules of mass 34. That  $H$  is in fact greater than  $2.07 p^2 \times 10^{-5}$  g. per sec. is evidenced by the mean daily transport rate

<sup>6</sup> Lauder, *Trans. Faraday Soc.*, 1947, **43**, 620.

<sup>7</sup> Davies, *ibid.*, 1949, **45**, 145.

<sup>8</sup> E. R. S. Winter, unpublished results on the interaction of  $^{18}\text{O } ^{16}\text{O}$  gas with various oxides; rapid exchange of oxygen occurs with many oxides at temperatures in the range 350–600° C.

of 0.56 ml. N.T.P. per day of pure  $^{18}\text{O}$  found by Lauder when running his four columns concurrently. Due to hold-up in the connecting tubing, slight inaccuracies in the matching of the columns, etc., this figure is probably considerably less than the practical maximum for any one column but the mean rate calculated from the theoretical values of  $H$  at the various pressures used by Lauder amounts to 0.48 ml. N.T.P. per day over the 24 weeks' operation; the observed transport rate should certainly be no more than this if molecules of mass 34 only are involved. A much more serious reason for rejecting Davies' arguments is that eqn. (12) predicts a maximum separation of 11.4 at a pressure of 54 cm.

(the optimum pressure is obtained by putting  $\frac{\partial \ln q_s}{\partial p} = 0$ , and the maximum separation by substituting this value of  $p$  in eqn. (12)). Examination of Lauder's results, and in particular his Fig. 2, shows that this is impossible: it follows that eqn. (12) does not describe the performance of the column in any important respect (except the general nature of the dependence of  $q_s$  upon pressure) and that the presence or otherwise of parasitic remixing currents in the apparatus is not determinable with the data given. It would be most surprising if no such effect were present.

Lauder's method of finding the optimum operating pressure is not good. He determined the separation at various pressures after 24 hr. operation and decided that the pressure which gave the highest separation in that time was the correct optimum pressure. Lauder states that this is liable to give a result which is slightly too high, but in fact the error may be considerable: the only safe way to find the optimum pressure is to do as we have done, and measure the *equilibrium* separation at a number of pressures and proceed as above. Lauder used a single column with a 10 l. reservoir of oxygen at the light end; the concentration of  $^{18}\text{O}$  in this reservoir did not change much after 3 days (to 0.18 %) so that the change in 24 hr. may be neglected to a first approximation; under these conditions we may regard the case as equivalent to operation with an infinite reservoir at one end. That being so, the separation is governed by a relaxation time given by eqn. (11) so long as  $2AL > 1.0$ : it is of interest to examine in detail what error may then be involved in using the separation after 24 hr.,  $q_{24}$ , to determine  $p_{\text{opt}}$ . Table III gives the results of calculations to this end, using for purposes of illustration eqn. (12).

TABLE III

$p$ (atm.)	$2AL$	$q_e$	$t_r$ (hr.)	$q_{24}$
0.25	0.72	2.07	16.5	1.55
0.368	1.22	3.38	22.6	2.20
0.411	1.47	4.32	26.7	2.55
0.447	1.66	5.29	31.1	2.80
0.553	2.15	8.63	40.5	3.88
0.632	2.37	10.7	43.8	4.60
0.711	2.43	11.4	40.6	5.13
0.790	2.39	10.9	35.1	5.34
0.868	2.25	9.56	28.4	5.35
0.947	2.09	8.05	22.0	5.31
1.00	1.96	7.13	18.7	5.06

It is seen that by considering only  $q_{24}$  the value of  $p_{\text{opt}}$  will be predicted as 0.868 atm. ( $q_s = 9.56$ ) compared with the true value of 0.711 atm. ( $q_s = 11.4$ ) so that a serious loss of efficiency would in this case be involved. The error involved in practice depends, of course, upon the values of the numerical factors in the practical equation which is the

analogue of the theoretical eqn. (12) and the error may well be increased by the presence of an appreciable dead volume at the heavy end.

Attempts have been made by calculations similar to these to find an expression for  $q_s$  of the form of eqn. (12) which fits Lauder's results for  $q_{s4}$ , but this is not possible even allowing for possible changes in  $H$  (i.e. replacing  $H$  by values up to  $2H$  as discussed above) and for the presence of a  $K_s$  term of any reasonable magnitude, without departing considerably from the calculated values of  $K_c$  and  $K_d$ . These two coefficients should not be greatly changed by the formation of a small concentration of  $^{18}\text{O}_2$  molecules near the hot wire.\* In all cases the plot of  $q_{s4}$  against pressure gives a much broader maximum than that obtained by Lauder: these discrepancies are curious and merit further consideration and investigation. It may be that because of the greater temperature difference in the hot wire column the deficiencies in the theory are magnified sufficiently to produce serious errors in the final expression: these deficiencies are likely to be chiefly due to the inadequate molecular force model used by Furry and Jones. Another likely source of trouble is turbulent gas flow in the column: turbulence should not occur until <sup>1</sup>

$$\frac{K_c}{K_d} > 25, \quad . \quad . \quad . \quad . \quad . \quad (13)$$

while from eqn. (12) we find that the calculated value of  $K_c/K_d$  is  $\approx 4$ , so that turbulence should be absent. However, Lauder reports that he used spacers in the form of crosses of mica cemented upon porcelain beads, and spaced every 3 in. along the wire. Whatever the design of these spacers (a drawing is not given) such a close array will certainly impose severe restrictions upon the gas flow and probably upset the normal working of the column. The chance of turbulence occurring will increase very rapidly with pressure and this may well be the cause of the rapid falling-off of the separation above 31.25 cm. Hg. An investigation of the performance of a similar column with reference to the design and number of spacers would be interesting.

\* Brown, *Physic. Rev.*, 1940, **58**, 661.

<sup>10</sup> Stier, *ibid.*, 1942, **62**, 548.

\* It may be noted however that Simon <sup>11</sup> found it necessary to introduce semi-empirical correction factors of considerable magnitude in order to obtain reasonable agreement with theory in the case of his hot-wire column used in separating argon isotopes. Such procedures cannot be attempted here owing to lack of experimental data.

<sup>11</sup> Simon, *ibid.*, 1946, **69**, 596.

*Department of Inorganic and Physical Chemistry,  
Imperial College,  
S.W.7.*

# KINETICS OF OPEN REACTION SYSTEMS

## CHAINS OF SIMPLE AUTOCATALYTIC REACTIONS

BY MARGARET J. MOORE

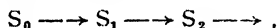
*Received 8th April, 1949*

An open reaction system is considered, which consists of a chain of successive autocatalytic reactions. The precursor to the chain is supposed to enter the system by a rapid first-order process, so as to remain almost constant, and all the reactants to leave by similar but much slower processes. It is found that if a non-zero steady state exists, the concentrations do not settle down to their steady-state values but instead oscillate about them, with a slight degree of damping depending on how far from constant is the concentration of precursor. If the reactants leave the system too rapidly for a completely non-zero steady state to exist, the later reactants may vanish, leaving a shorter chain with oscillating concentrations.

In the special case when there is no first-order removal of intermediate reactants, and the number of autocatalytic reactions is odd, conditions may be chosen so that alternate reactants (beginning with the second after the precursor) show damped oscillations with lengthening period about fixed values, while the other reactants vanish from the system.

In a previous report <sup>1</sup> a general discussion was given on the concentration changes occurring in open reaction systems, i.e. those systems in which there is continuous supply and removal of the reactants. It was shown that in an open system of first-order reactions, there is always an upper limit to the number of maxima and minima that can occur in the concentration of a given species as a function of time, that is, the possibility of true oscillation is ruled out. On the other hand, Lotka <sup>2</sup> has developed differential equations for a rather idealized system of two autocatalytic reactions, which give undamped oscillations in the concentrations of both autocatalysts. More recently, Frank-Kamenetzky <sup>3</sup> and Walsh <sup>4</sup> have used very similar equations in treating the mechanism of two-stage ignition, where something resembling undamped oscillation is seen in fact.

The system of Lotka is as follows :



- where
- (a) Concentration of  $S_0$  is constant.
  - (b) Reaction  $S_0 \longrightarrow S_1$  is catalyzed by  $S_1$ .
  - (c) Reaction  $S_1 \longrightarrow S_2$  is catalyzed by  $S_2$ .
  - (d) Reaction removing  $S_2$  from the system is first order.

Lotka showed that this system produced true oscillations in the concentrations of  $S_1$  and  $S_2$ , about a fixed centre and with a fixed period, the amplitude depending on the initial conditions. The oscillations are not harmonic, as both concentrations move further from the central position when above this value than when below it.

An attempt is made here to extend Lotka's case to a series of any number of autocatalytic reactions. Lotka's rather artificial condition

<sup>1</sup> Denbigh, Hicks (Moore), Page, *Trans. Faraday Soc.*, 1948, **44**, 479.

<sup>2</sup> Lotka, *J. Amer. Chem. Soc.*, 1920, **42**, 1595.

<sup>3</sup> Frank-Kamenetzky, *J. Physic. Chem. (U.S.S.R.)*, 1940, **14**, 1.

<sup>4</sup> Walsh, *Trans. Faraday Soc.*, 1947, **43**, 305.

—that the concentration of the precursor (called  $S_0$  by him) is constant —has been modified to the more natural condition that the precursor enters the system by a first-order transfer process, as for example by diffusion, and allowance is also made for the other reactants to be removed from the system—perhaps also by diffusion.

### Notation

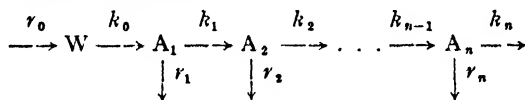
W, precursor,  
 $A_1, A_2 \dots A_n$ , autocatalysts,  
 $w, a_i$ , concentrations of W,  $A_i$ ,  
 $\bar{w}, \bar{a}_i$ , steady state (or central) values of  $w, a_i$ ,  
 $w_0, a_{0i}$ , initial values of  $w, a_i$ ,  
 $k_0$ , reaction constant of the autocatalytic reaction  $W \rightarrow A_1$ ,  
 $k_1$ , " " " " autocatalytic reaction  $A_j \rightarrow A_{j+1}$ ,  
 $k_n$ , " " " " first-order reaction  $A_n \rightarrow$ ,  
 $r_0, r_j$ , rate of exit of W,  $A_j$  per unit quantity in the system,  
 $r_0 w^0$ , rate of entry of W per unit volume of the system,

so that  $r_0(w^0 - w)$  is the net rate of entry of W per unit volume.

Here  $r, w^0$  are constants whose meaning depends on the method by which W enters and W,  $A_j$  leave the system. If it is by mass transfer, all the  $r$ 's are alike equal to the flow-rate divided by the volume of the system, while  $w^0$  is the concentration of W in the inflow. If it is by diffusion to and from an external solution,  $w^0$  is the concentration of W in the external solution, and the several  $r$ 's depend on the rate constants of diffusion of the various reactants as well as the area and nature of the walls of the vessel and the volume of the system. Alternatively, W may enter and leave the system by some other mechanism which gives a net rate of entry  $r_0(w^0 - w)$ , while  $A_j$  may be removed only by reaction to  $A_{j+1}$ , so that  $r_1 = r_2 = \dots = r_n = 0$ .

Throughout the paper,  $j$  represents any integer and  $2m$  any even integer between 1 and  $n$ .

### The System to be Considered



The differential equations defining the change of the various concentrations of the system with time are given below (D). In certain parts of the paper, two simplifying assumptions are made: firstly (Lotka's assumption) that the rate of entry of W is such that  $w$  remains constant; secondly, that the intermediate reactants are not removed from the system, i.e.  $r_1 = \dots = r_{n-1} = 0$ , in which case, for convenience, the removal rate of  $A_n$  is incorporated in its first-order reaction rate  $k_n$ , and  $r_n$  is also taken as zero.

$$\left. \begin{aligned} dw/dt &= r_0(w^0 - w) - k_0 w a_1, & (o) \\ da_1/dt &= k_0 w a_1 - k_1 a_1 a_2 - r_1 a_1, & (i) \\ da_2/dt &= k_1 a_1 a_2 - k_2 a_2 a_3 - r_2 a_2, & (ii) \\ &\vdots & \vdots \\ da_n/dt &= k_{n-1} a_{n-1} a_n - k_n a_n - r_n a_n & (n) \end{aligned} \right\} \quad \dots \quad (D)$$

### 1. Solution for a Modified System in which $w$ is Constant

For this system, (D, o) does not apply, but instead

$$\left. \begin{aligned} dw/dt &= 0 & (o) \\ \text{Let } K &\text{ be the fixed value of } k_0 w. \\ \text{Then (D, i) becomes} & & \\ da_1/dt &= K a_1 - k_1 a_1 a_2 - r_1 a_1, & (i) \\ \text{Eqn. (ii) to (n) of (D) are unchanged.} & & \end{aligned} \right\} \quad \dots \quad (M)$$

It is proposed first to decide under what conditions a set of values  $\bar{a}_1, \bar{a}_2$  etc. of the concentrations, each greater than zero, can be found



which will make the whole system invariant with time; such a set of values is termed a "non-zero steady state". The solution of (M) for these cases, when the concentrations are not initially at the steady-state values, will then be discussed; this gives the way in which the system ordinarily evolves with time. Finally, the cases where the concentrations can only remain stationary if some at least are zero, will be considered.

**A. Steady-State Values of the Concentrations.**—FOR  $n$  EVEN. The non-zero steady-state values are obtained by equating to zero in succession,

$$\frac{1}{a_1} \frac{da_1}{dt}, \frac{1}{a_2} \frac{da_2}{dt} \dots \frac{1}{a_{n-1}} \frac{da_{n-1}}{dt},$$

to give  $\bar{a}_2 = (K - r_1)/k_1$  and so on, up to

$$\bar{a}_n = \left\{ Kk_2k_4 \dots k_{n-2} - \sum_{m=1}^{\frac{1}{2}n} k_1k_3 \dots k_{2m-3}r_{2m-1}k_{2m} \dots k_{n-2} \right\} / k_1k_3 \dots k_{n-1}$$

and then equating to zero.

$$\frac{1}{a_n} \frac{da_n}{dt}, \frac{1}{a_{n-2}} \frac{da_{n-2}}{dt}, \dots \frac{1}{a_2} \frac{da_2}{dt}, \text{ to give}$$

$$\begin{aligned} \bar{a}_{n-1} &= (k_n + r_n)/k_{n-1}, \dots \bar{a}_1 \\ &= \left\{ k_2k_4 \dots k_n + \sum_{m=1}^{\frac{1}{2}n} k_2 \dots k_{2n-2}r_{2m}k_{2m+1} \dots k_{n-1} \right\} / k_1k_3 \dots k_{n-1}. \end{aligned}$$

The existence of a non-zero steady state evidently depends on the value given for  $\bar{a}_n$  above being positive, i.e.

$$Kk_2k_4 \dots k_{n-2} > \sum_{m=1}^{\frac{1}{2}n} k_1 \dots k_{2m-3}r_{2m-1}k_{2m} \dots k_{n-2}. \quad (1)$$

This condition implies in general that the rates of removal of the different reactants  $r$  shall be small compared with  $K$ .

FOR  $n$  ODD, the procedure is modified slightly.

Writing  $\frac{1}{a_j} \frac{da_j}{dt} = 0$  for even values of  $j$  gives

$$\left. \begin{aligned} k_1\bar{a}_1 &= k_2\bar{a}_3 + r_2, \\ k_3\bar{a}_3 &= k_4\bar{a}_5 + r_4, \\ &\vdots \\ k_{n-2}\bar{a}_{n-2} &= k_{n-1}\bar{a}_n + r_{n-1}. \end{aligned} \right\} \quad (2)$$

These are  $\frac{1}{2}(n-1)$  equations in  $\frac{1}{2}(n+1)$  unknowns, and are therefore indeterminate; but for a given value of  $a_1$ , all the other odd-numbered steady-state concentrations may be found, provided that

$$\bar{a}_1 > \sum_1^{\frac{1}{2}(n-1)} \frac{k_2k_4 \dots k_{2m-2}r_{2m}}{k_1k_3 \dots k_{2m-1}}.$$

If  $r_2 = r_4 = \dots = 0$ , the ratio of odd-numbered steady-state concentrations may be found from (2).

Writing  $\frac{1}{a_j} \frac{da_j}{dt} = 0$  for odd values of  $j$  gives

$$\left. \begin{aligned} K &= k_1\bar{a}_2 + r_1, \\ k_2\bar{a}_2 &= k_3\bar{a}_4 + r_3, \\ &\vdots \\ k_{n-1}\bar{a}_{n-1} &= k_n + r_n. \end{aligned} \right\} \quad (3)$$



Returning again to the original differential equations (M) these may be summed and integrated (see Appendix, § II) to give

$$\sum_1^n (a_i - a_{0,i}) = \sum_1^n \bar{a}_i \ln (a_i/a_{0,i}), \quad (6)$$

where, if  $n$  is odd, any set of values  $\bar{a}_1, \bar{a}_3, \dots, \bar{a}_n$  satisfying (2) may be used.

Also, for  $n$  odd, another summation and integration will give

$$\frac{1}{2} \sum_0^{n-1} \frac{k_1 k_3 \dots k_{2m-1}}{k_2 k_4 \dots k_{2m}} \ln (a_{2m+1}/a_{0,2m+1}) = 0. \quad (7)$$

The absolute values of  $\bar{a}_1, \bar{a}_3$  etc. for  $n$  odd may reasonably be taken now as those which satisfy (7) as well as (2).

Considering (6) it will be seen that, as  $a_{0,i}$  can have any value between 0 and saturation, the equation will only be satisfied by the steady-state concentrations for exceptional initial conditions. Thus the steady state cannot generally be attained.

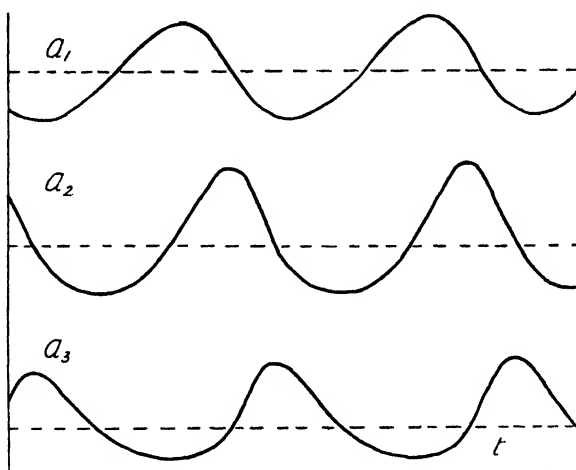


FIG. 1

If the  $a_i$ 's  $\rightarrow 0$ , the left-hand side of (6)  $\rightarrow$  a finite limit, the right-hand side  $\rightarrow -\infty$ ; and if the  $a_i$ 's  $\rightarrow \infty$  the left-hand side of (6) tends to an infinity of a higher order than the right-hand side. In either case, the left-hand side tends to a value infinitely greater than the right-hand side, so that no arrangement of  $a_i$ 's tending some to zero and some to infinity would satisfy (6).

Since the system cannot tend to its steady state or to zero or infinite concentration, there remains only the possibility of oscillation about the steady state. The approximate solution given above must therefore give a fair picture even for large values of  $\alpha_i$ , except that the components of the oscillation will not be simple harmonic but (as in the case of two equations described by Lotka<sup>2</sup>) will show greater movement from the steady state above than below.

Fig. 1 and 2 are differential analyser solutions of (M). Fig. 1 is the case  $n = 3$ ,  $Kk_3 - k_1k_3 = r_1k_2 + k_1r_3$  and shows oscillations having one component of the type described. Within the limits of accuracy of the machine these oscillations are periodic, i.e. there is no variation in shape from one wave to the next. Fig. 2 is the case,  $n = 4$  for  $r_1 = 0$ . What was expected in this case was oscillations having two components each

not quite harmonic, and the curiously irregular shape of the curves is in accordance with expectation.

**C. Cases where no Complete Non-Zero Steady State Exists.**—First consider the case where  $n$  is even and (1) does not obtain. Supposing, for the moment, that all the  $k$ 's are equal and so are all the  $r$ 's, (1) reduces to

$$K > \frac{1}{2}nr.$$

That is, the rate of formation of the first reactant is greater than the total rate of removal of half the reactants. If the  $k$ 's and  $r$ 's are not all alike, (1) still has a similar significance.

When (1) does not obtain, then the reactants are being removed too fast. As the only entry into the system is at the beginning of the chain ( $A_1$ ), one would expect the too great removal rates to affect the last reactants most, and these might well vanish from the system, beginning with the last and working forward, until stability is reached with a shorter chain for which (1) does obtain.

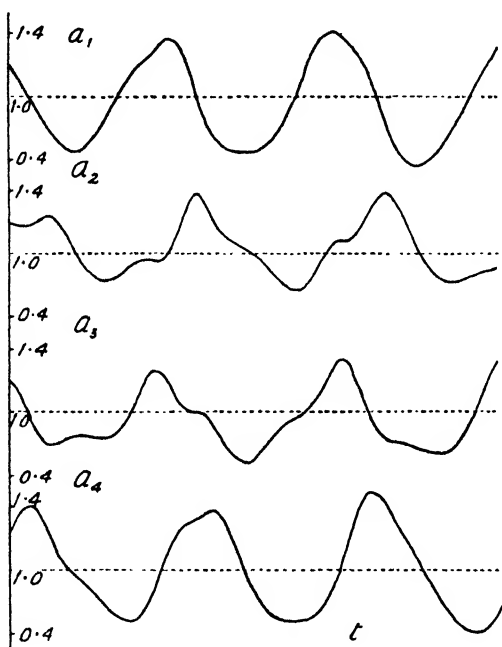


FIG. 2

Now consider the conditions mathematically. If (1) does not obtain, the odd-numbered reactants cannot be kept steady without making *either* some of the odd-numbered steady-state concentrations zero, *or* some of the even-numbered ones negative (which is, of course, impossible). It may be possible, however (see Appendix, § III), to choose positive values for some of the even-numbered steady-state concentrations—say  $\bar{a}_2, \bar{a}_4, \dots, \bar{a}_{2m}$ —although no such values can be found for the later ones. Then a corresponding set  $\bar{a}_1, \bar{a}_3, \dots, \bar{a}_{2m-1}$  can also be found, but  $\bar{a}_{2m+1} = \bar{a}_{2m+2} = \dots = \bar{a}_n = 0$ . The effect will be, as was suggested above, that the end of the chain will gradually disappear, while the beginning will oscillate in much the same way as would a chain of length  $2m$  instead of  $n$ . There will, however, be complications in the oscillations of the lower-numbered reactants while the others are disappearing. On further examination of condition (1) it is seen that there is one unexpected feature; only the odd-numbered  $r$ 's affect the situation. It may appear,

however, that if the even-numbered  $r$ 's are too great,  $\bar{a}_1$  as calculated in § A may turn out to be greater than the saturation value of  $a_1$ , which would equally well invalidate the steady state as found.

Now consider the case where  $n$  is odd and (4) does not obtain (which will generally be the case). (M, i, iii, v) etc. may be summed and integrated (see Appendix, § IIB) to give

$$\begin{aligned} & \sum (k_1 k_2 \dots k_{2m-1} k_{2m+2} \dots k_{n-1}) \ln (a_{2m+1}/a_{0, 2m+1}) \\ &= \left\{ K k_2 \dots k_{n-1} - k_1 k_2 \dots k_n \right. \\ & \quad \left. - \sum k_1 k_2 \dots k_{2m-1} k_{2m+2} \dots k_{n-1} r_{2m+1} \right\} t. \quad (8) \end{aligned}$$

If the right-hand side of (8) is negative, the general tendency is for odd-numbered  $a$ 's to decrease to zero, and if it is positive, the tendency is to increase, apparently to infinity, in fact to saturation. (If (4) obtains, the right-hand side of (8) is zero, so (8) reduces to (7).) Eqn. (8), however, gives no indication as to what happens to the even-numbered concentrations, or, indeed, as to what happens individually to the odd-numbered ones.

Further information may, however, be obtained when every  $r_j = 0$ . In this case, although there is no non-zero steady state, what might be termed a "half-steady state" exists, i.e. conditions may be chosen so that even-numbered concentrations only are steady. Writing  $\bar{a}_{2m}$  for these values and  $\bar{a}_{2m+1}$  for corresponding changing values of the odd-numbered concentrations, we obtain, since  $r_j = 0$

$$\bar{a}_{2m} (k_{2m-1} \bar{a}_{2m-1} - k_{2m} \bar{a}_{2m+1}) = 0$$

at all times.

$$\therefore k_{2m-1} \bar{a}_{2m-1} = k_{2m} \bar{a}_{2m+1}, \quad (9)$$

and

$$k_{2m-1} \frac{d}{dt} (\bar{a}_{2m-1}) = k_{2m} \frac{d}{dt} (\bar{a}_{2m+1}). \quad (10)$$

Dividing the left-hand side and the right-hand side of (10) by the left-hand side and the right-hand side of (9) we have

$$\frac{d}{dt} (\bar{a}_{2m-1}) / \bar{a}_{2m-1} = \frac{d}{dt} (\bar{a}_{2m+1}) / \bar{a}_{2m+1},$$

or

$$\left. \begin{aligned} K - k_1 \bar{a}_1 &= k_2 \bar{a}_2 - k_3 \bar{a}_3, \\ &= k_{2m} \bar{a}_{2m} - k_{2m+1} \bar{a}_{2m+1}, \\ &= k_{n-1} \bar{a}_{n-1} - k_n. \end{aligned} \right\} \quad (11)$$

The set (11) comprise  $\frac{1}{2}(n-1)$  equations in  $\frac{1}{2}(n-1)$  unknowns,  $\bar{a}_2, \bar{a}_4$ , etc., so that these may be determined.

Putting  $\epsilon$  for all the equal quantities of (11) we have, for odd-numbered concentrations,

$$\begin{aligned} \frac{d}{dt} (\bar{a}_{2m+1}) &= \epsilon \bar{a}_{2m+1}, \\ \therefore \bar{a}_{2m+1} &= \bar{a}_{0, 2m+1} e^{\epsilon t}. \quad (12) \end{aligned}$$

Thus, if the odd-numbered  $a$ 's are initially in the proportion given by (9), while  $a_{0, 2m} = \bar{a}_{2m}$  as defined by (11),  $a_{2m+1}$  will follow the path given by (12) and  $a_{2m}$  will remain steady.

When  $K k_2 \dots k_{n-1} < k_1 k_2 \dots k_n$  (i.e.  $=$  is replaced by  $<$  in (4)),  $\epsilon < 0$  so that (12) defines a negative exponential path decreasing to zero. When  $K k_2 \dots k_{n-1} > k_1 k_2 \dots k_n$ , on the other hand,  $\epsilon > 0$  and (12) defines an increasing exponential curve.

When the conditions (9) and (11) giving the half-steady state do not obtain initially, which is, of course, usually the case, the solution may

still be related to a corresponding half-steady state. The latter, however, is not completely defined by (9) and (11), as (9), like (2), are indeterminate, so that an additional condition in the  $\tilde{a}_{0, 2m+1}$  must be obtained.

Eqn. (8) now reduces to

$$\sum (k_1 k_2 \dots k_{2m-1} k_{2m+2} \dots k_{n-1}) \ln (a_{2m+1}/a_{0, 2m+1}) = (K k_2 \dots k_{n-1} - k_1 k_3 \dots k_n) t, \quad (13)$$

which must also be true if  $\tilde{a}_{2m+1}/\tilde{a}_{0, 2m+1}$  be substituted for  $a_{2m+1}/a_{0, 2m+1}$ , so that

$$\sum (k_1 \dots k_{2m-1} k_{2m+2} \dots k_{n-1}) \ln (a_{2m+1} \cdot \tilde{a}_{0, 2m+1}/a_{0, 2m+1} \cdot \tilde{a}_{2m+1}) = 0.$$

It seems reasonable, therefore, to complete the definition of the associated half-steady state by supposing

$$\sum (k_1 \dots k_{2m-1} k_{2m+2} \dots k_{n-1}) \ln (a_{2m+1}/\tilde{a}_{2m+1}) = \sum (k_1 \dots k_{2m+1} k_{2m+2} \dots k_{n-1}) \ln (\tilde{a}_{0, 2m+1}/a_{0, 2m+1}) = 0. \quad (14)$$

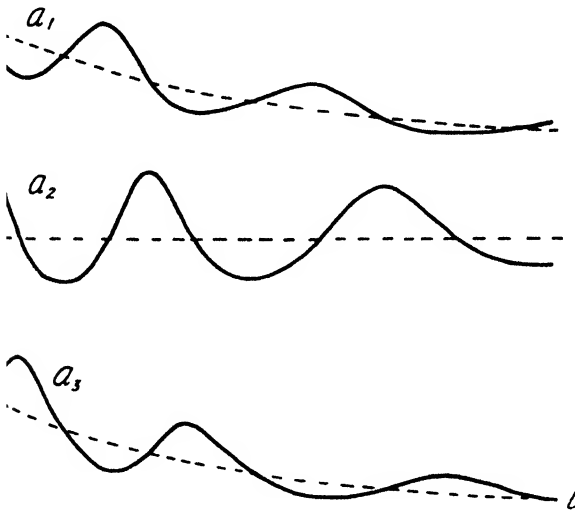


FIG. 3.

Considering (14), and also the question of continuity when (4) very nearly obtains, the most probable solution is that of oscillations about the  $\tilde{a}_{2m}$  and the  $\tilde{a}_{2m+1}$ . Since, when (4) obtains, the period is smaller the greater the absolute values of  $\tilde{a}_1$  etc., it seems reasonable to suppose that when (4) does not obtain the oscillations will not be periodic, but will speed up if  $\tilde{a}_{2m+1}$  increases, and slow down if  $\tilde{a}_{2m+1}$  decreases. Further consideration also suggests that the oscillations must be damped in the decreasing case, and that they will therefore expand in the increasing case.

Fig. 3 is a differential analyser solution for (M) with  $n = 3$ ,  $r_1 = 0$ ,  $Kk_2 = \frac{1}{2}k_1k_3$ . It shows the three concentrations oscillating with increasing "period" and decreasing amplitude,  $a_1$  and  $a_3$  each about a decreasing exponential curve, and  $a_2$  about a fixed value. The theoretical paths of  $\tilde{a}_1$  and  $\tilde{a}_3$  and the level  $\tilde{a}_2$  are put in as dotted lines for comparison.

Fig. 4 is the case in which

$$n = 3, r_2 = 1 \text{ and } (K - r_1)k_2 = \frac{1}{2}k_1(k_3 + r_3).$$

This shows no resemblance to the case considered above—instead, it appears that  $A_3$  rapidly vanishes from the system, which afterwards behaves as if  $n = 2$ . It seems probable that this is what happens for any odd number of equations if  $r_j \neq 0$  and the equality in (4) is replaced by a  $<$  sign.

**II. Solution of the Original Equations (D), by Comparing them with the Modified Equations (M). A. Non-Zero Steady States of (D).—**The steady states of (D) are the same as those of (M) with the following provisions:

FOR  $n$  EVEN.

$$\bar{w} = r_0 k_1 k_3 \dots k_{n-1} w^0 / \left\{ k_0 k_2 \dots k_n + \sum_{m=0}^{\frac{1}{2}n} k_0 k_2 \dots k_{2m-2} k_{2m+1} \dots k_{n-1} r_{2m} \right\}.$$

$K$  is replaced by  $k_0 \bar{w}$  in all the even-numbered concentrations. Replacing  $K$  by  $k_0 \bar{w}$  in  $a_n$  gives as the condition of existence for the steady state,

$$r_0 k_1 k_2 \dots k_{n-1} w^0 > \left\{ k_0 k_2 \dots k_n + \sum_{m=0}^{\frac{1}{2}n} k_0 k_2 \dots k_{2m-2} k_{2m+1} \dots k_{n-1} r_{2m} \right\} \\ \times \sum_{1}^{\frac{1}{2}n} k_1 k_3 \dots k_{2m-3} k_{2m} \dots k_{n-2} r_{2m-1}. \quad (I')$$

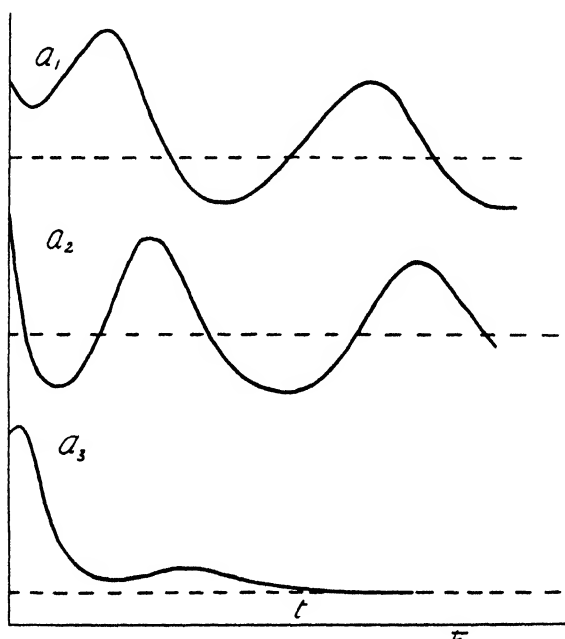


FIG. 4.

Roughly speaking, this requires that  $r_0$  should be very large compared with all the other  $r$ 's, and also  $w^0$  should be large.

FOR  $n$  ODD.

$$\bar{w} = \left\{ k_1 k_3 \dots k_n + \sum_{m=1}^{\frac{1}{2}(n+1)} k_1 k_3 \dots k_{2m-3} k_{2m} \dots k_{n-1} r_{2m-1} \right\} / k_0 k_1 \dots k_{n-1} \quad (15)$$

provided that this is  $< w^0$ .

Now  $K = k_0 \bar{w}$  so that

$$K k_2 \dots k_{n-1} = k_0 k_2 \dots k_{n-1} \bar{w} \\ = \left\{ k_1 k_3 \dots k_n + \sum_{1}^{\frac{1}{2}(n+1)} k_1 k_3 \dots k_{2m-3} k_{2m} \dots k_{n-1} r_{2m-1} \right\}$$

i.e. (4) always obtains provided that  $\bar{w}$  above exists.

$\bar{a}_1$  is no longer indeterminate, but is given by  $r_0(w^0 - \bar{w})/k_0\bar{w}$ .

$$\bar{a}_n = \left\{ k_1 k_2 \dots k_{n-2} r_0 w^0 - \bar{w} \sum_{m=0}^{\frac{1}{2}(n-1)} k_0 \dots k_{2m-2} k_{2m+1} \dots k_{n-2} r_{2m} \right\} / k_0 \bar{w}. \quad (16)$$

There are now two conditions for the existence of a non-zero steady state :

$$\begin{aligned} w^0 &> \bar{w}, \\ \bar{a}_n &> 0. \end{aligned}$$

The latter resembles the condition (1) for  $n$  even, and roughly speaking, implies that  $r_0$  is large and all other  $r$ 's are small.

If the value of  $\bar{w}$  given by (15) is greater than  $w^0$ ,  $w$  will not tend to this, but instead to  $w^0$ , or to some value less than  $w^0$ .  $K$  will then have to be taken  $< k_0 w^0$ , and condition (4) will have its equality replaced by a  $<$  sign. It is impossible to find a case of (D) corresponding to that of (M) where the equality in (4) is replaced by a  $>$  sign.

**B. Variation with Time of System (D).**—The basic assumption for taking (M) as an approximation to (D) is that the constants of (D, o)

$$dw/dt = r_0(w^0 - w) - k_0 w a_1$$

are such that  $w$  remains nearly steady while the other concentrations,  $a_i$ , vary much more. The condition for this is that  $r_0$  should be very large compared with  $k_0$ , so that a small change in  $w$  affects  $dw/dt$  more than a change of the same proportion in  $a_1$ . If this is so, after a short time, to allow  $w$  to approach its steady state value, the system represented by (D) should approximate very nearly to that represented by (M). The effect of having  $w$  not quite constant will probably be a slight damping of the oscillations.

**Conclusion.**—In a system such as is typified by (D), i.e. a chain of autocatalytic reactions, where the precursor is introduced by a first-order process and the other substances are removed by first-order processes, there will in general be almost undamped oscillations provided that

- the rate of entry of precursor is great enough ;
- the rate of removal of the other substances is small enough (see (1) for  $n$  even, (17), (16), (15) for  $n$  odd) ;
- in the case where there is an odd number of autocatalytic reactions, the quantity which has been termed the " external concentration " of precursor is greater than a fixed value, determined by the other constants of the system.

If condition (a) above does not obtain, it will probably only mean that there is a much higher degree of damping, although the effect may well be in extreme cases that there is no evidence of oscillation at all.

If condition (b) does not obtain, or, in general, if (c) does not for  $n$  odd, the later reactants of the series will vanish from the system, but it may be found that a smaller chain is left, with an even number of reactants  $a_j$ , for which condition (b) does apply.

If condition (c) only does not obtain for the case  $n$  odd, and  $r_j = 0$ , ( $1 < j < n$ ), the  $a_{2m}$  will oscillate about a fixed value and the  $a_{2m+1}$  about negative exponential curves, all the oscillations being damped, and of lengthening period.

## Appendix

I. The auxiliary equation for (5) is

$$\Delta(\lambda) \equiv \begin{vmatrix} \lambda & k_1 \bar{a}_1 & 0 & \dots & 0 & 0 \\ -k_1 \bar{a}_2 & \lambda & k_2 \bar{a}_2 & \dots & 0 & 0 \\ 0 & -k_2 \bar{a}_3 & \lambda & \dots & 0 & 0 \\ 0 & 0 & -k_3 \bar{a}_4 & \dots & 0 & 0 \\ \vdots & \vdots & \vdots & \ddots & \vdots & \vdots \\ 0 & 0 & 0 & \dots & \lambda & k_{n-1} \bar{a}_{n-1} \\ 0 & 0 & 0 & \dots & -k_{n-1} \bar{a}_n & \lambda \end{vmatrix} = 0. \quad (18)$$



When  $n$  is even,  $\Delta(\lambda)$  reduces to a polynomial of degree  $\frac{1}{2}n$  in  $\lambda^2$ , which has  $\frac{1}{2}n$  linear factors of the form  $(\lambda^2 + \text{a positive constant})$ . Thus (18) has  $n$  purely imaginary roots. If  $n$  is odd,  $\Delta(\lambda)$  has one factor  $\lambda$  and  $\frac{1}{2}(n-1)$  of the form  $(\lambda^2 + \text{a positive constant})$ , so that (18) has  $(n-1)$  imaginary and one zero root.

This means that the solution to (5) gives every  $a_j$  as the sum of  $\frac{1}{2}n$  or  $\frac{1}{2}(n-1)$  simple harmonic terms. For  $n$  odd there is also a constant term, but there seems no reason why this cannot be incorporated in  $\bar{a}_j$ .

II. (a) The equations of (M) are first summed as they stand, to give

$$\sum_1^n da_j/dt = Ka_1 - k_n a_n - \sum_1^n r_j a_j. \quad (19)$$

Each equation of (M) is now multiplied by  $\bar{a}_j/a_j$ , with the appropriate value for  $j$ , and the equations are summed, to give

$$\sum_1^n \frac{\bar{a}_j}{a_j} \times \frac{da_j}{dt} = \bar{a}_1(-r_1 K - k_1 \bar{a}_2) + \sum_2^{n-1} \bar{a}_j(k_{j-1} \bar{a}_{j-1} - k_j \bar{a}_{j+1} - r_j) + \bar{a}_n(k_{n-1} \bar{a}_{n-1} - k_n - r_n) \quad (20)$$

(If  $n$  is odd, any values of  $\bar{a}_1$ ,  $\bar{a}_2$ , etc., which satisfy (2) are taken.)

The steady-state values are now introduced into (19) in place of the variable concentrations, so that every  $da_j/dt = 0$ , giving

$$0 = K\bar{a}_1 - k_n \bar{a}_n - \sum r_j \bar{a}_j \quad (21)$$

(21) is now added to, and (20) subtracted from, (19) to give

$$\sum_1^n \frac{da_j}{dt} - \sum_1^n \frac{\bar{a}_j}{a_j} \frac{da_j}{dt} = a_1(K - r_1 - k_1 \bar{a}_2) + \sum_2^{n-1} a_j(k_{j-1} \bar{a}_{j-1} - k_j \bar{a}_{j+1} - r_j) + a_n(k_{n-1} \bar{a}_{n-1} - k_n - r_n) = 0 \quad (22)$$

Eqn. (22) may be integrated to give

$$\sum (a_j - a_{0,j}) - \sum \bar{a}_j \ln(a_j/a_{0,j}) = 0.$$

(b) When  $n$  is odd, the odd-numbered equations may also be summed in the following way to give an integrable result. The equation (M,  $2m+1$ ), for  $m=0, 1, \dots, \frac{1}{2}(n-1)$  is divided by  $a_{2m+1}$  and multiplied by

$$k_1 k_3 \dots k_{2m-1} k_{2m+2} k_{2m+3} \dots k_{n-1}.$$

The resulting equations are then added to give

$$\begin{aligned} \frac{1}{2}(n-1) \sum_0 \frac{1}{a_{2m+1}} \frac{da_{2m+1}}{dt} \cdot k_1 k_3 \dots k_{2m-1} k_{2m+2} \dots k_{n-1} \\ = K k_2 k_4 \dots k_{n-1} - k_1 k_3 \dots k_n \\ - \sum_0^{\frac{1}{2}(n-1)} r_{2m+1} k_1 k_3 \dots k_{2m-1} k_{2m+2} \dots k_{n-1} \quad (23) \end{aligned}$$

When (4) obtains, right-hand side of (23) is zero.

On integration, (23) gives, for (4) obtaining

$$\sum_0^{\frac{1}{2}(n-1)} (k_1 k_3 \dots k_{2m-1} k_{2m+2} \dots k_n) \ln(a_{2m+1}/a_{0,2m+1}) = 0$$

and for (4) not obtaining

$$\begin{aligned} \frac{1}{2}(n-1) \sum_0 (k_1 k_3 \dots k_{2m-1} k_{2m+2} \dots k_n) \ln(a_{2m+1}/a_{0,2m+1}) \\ = \left\{ K k_2 \dots k_{n-1} - k_1 k_3 \dots k_n - \sum_0^{\frac{1}{2}(n-1)} r_{2m+1} k_1 k_3 \dots k_{2m-1} k_{2m+2} \dots k_n \right\} t. \end{aligned}$$

### III. Incomplete Non-Zero Steady State.

The analytical values of the even-numbered non-zero steady-state concentrations are obtained in succession by the formulae,

$$\bar{a}_2 = (K - r_1)/k_1$$

$$\bar{a}_{2m} = (k_{2m-1}\bar{a}_{2m-2} - r_{2m-1})/k_{2m-1} \text{ for } 2 \leq m \leq \frac{1}{2}n. \quad (24)$$

so that if the value found for  $\bar{a}_{2m}$  is positive, so are  $\bar{a}_{2m-2}$  and all preceding values, while if  $\bar{a}_{2m+2}$  is zero or negative,  $\bar{a}_{2m+4}$  and all successive values are negative. Suppose that this is the case, assuming first that (24) gives  $\bar{a}_{2m+2}$  negative rather than zero; then non-zero steady-state values really exist up to  $\bar{a}_{2m}$ , and do not from  $\bar{a}_{2m+2}$  onward since a real concentration cannot be negative.

Now, from (M,  $2m+1$ ),  $a_{2m+1}$  will be stationary if

$$\bar{a}_{2m+1}(k_{2m}\bar{a}_{2m} - k_{2m+1}\bar{a}_{2m+2} - r_{2m+1}) = 0.$$

But no positive value of  $\bar{a}_{2m+2}$  will make the bracketed term zero, so that  $\bar{a}_{2m+1} = 0$ .

To make  $a_{2m+2}$  stationary,  $\bar{a}_{2m+2}(k_{2m+1}\bar{a}_{2m+1} - k_{2m+2}\bar{a}_{2m+3} - r_{2m+2}) = 0$ , so that  $\bar{a}_{2m+2} = 0$ .

Similarly, all subsequent steady-state values are zero.

Returning to equation (M,  $2m$ ), since  $\bar{a}_{2m+1} = 0$ ,  $a_{2m}$  is stationary for

$$\bar{a}_{2m}(k_{2m-1}\bar{a}_{2m-1} - r_{2m}) = 0,$$

and a non-zero value for  $\bar{a}_{2m-1}$  is given by

$$\bar{a}_{2m-1} = r_{2m}/k_{2m-1}.$$

The earlier odd-numbered steady-state values may be found as in § IA of the text.

Thus the chain of length  $n$  may be reduced to a shorter chain of length  $2m$  for which a steady state exists.

If (24) gives  $\bar{a}_{2m+2} = 0$ , instead of negative, it is possible that a non-zero steady state may be found for the chain of reactants up to and including  $a_{2m+1}$ , and if so, this chain will presumably survive after the later reactants have vanished. This case will, however, be rare.

*Imperial Chemical Industries Ltd.,  
Butterwick Research Laboratories,  
The Frythe,  
Welwyn.*

## THE REACTION KINETICS OF WOOL WITH CHLORINE SOLUTIONS

### PART II.—DIFFUSION WITHIN THE FIBRE

BY P. ALEXANDER, D. GOUGH AND R. F. HUDSON

*Received 30th May, 1949*

The conditions under which the reaction is controlled by diffusion within the fibre are determined. It is shown that the rate is almost proportional to initial concentration (i.e.  $t_{\frac{1}{2}}$  constant) and it is concluded that diffusion proceeds from a changing surface concentration. A kinetic expression for these conditions is derived and compared with the diffusion equation of Wilson. The mechanism of fibre diffusion is discussed and the high energy of activation step is considered to be hole formation in the fibre-water gel.

The limiting conditions under which the reaction of wool with chlorine solutions may be controlled by the rate of transport of solute in solution have been discussed fully in the previous paper. On changing experimental conditions such as rate of stirring or concentration, it is possible for the migration of reactant through the solid to become the rate-controlling factor and the experimental data recorded here are interpreted in this way.

The apparent energy of activation of the oxidation reaction when controlled by diffusion in solution (ca. 6000 cal./mole) is of the same order as the energy of activation of diffusion in aqueous solution (see Part I). The fibre-controlled process, however, is characterized by a much greater apparent activation energy (ca. 12,000 cal./mole) which thus provides an excellent criterion for differentiating between the two mechanisms. This value for the apparent activation energy has also been obtained for the oxidation of wool by potassium permanganate<sup>1</sup> where the observed rate is governed by the rate of diffusion through the fibre, although in this case the rate is modified by the deposit of manganese dioxide on the fibre.

We are considering in all cases complete reaction of the chlorine in solution so that the solution concentration decreases from the initial value almost to zero. It follows, therefore, that the surface concentration of chlorine, which governs the rate of diffusion into the fibre, continually decreases. This, of course, implies the assumption that chlorine distributes uniformly between liquid and solid phase according to the distribution law. Although solutions of the general Fick equation for diffusion into a solid from a constant surface concentration are well known,<sup>2</sup> treatment of the case of varying surface concentration has proved to be extremely complex. Recently a formal solution for a surface concentration varying linearly with solution concentration has been given by Wilson<sup>3</sup> assuming that a certain constant proportion of the solute within the solid phase is mobile and is responsible for diffusion, the remainder being deposited on absorption sites. For diffusion into a cylinder of infinite length compared with the radius, Wilson gives the following solution,

$$\frac{Q_t}{Q_\infty} = 1 - \sum_n \frac{4\alpha(1+\alpha)e^{-q_n^2\beta t}}{4+4\alpha+\alpha^2q_n^2},$$

where  $Q_t/Q_\infty$  is the fractional attainment of equilibrium,  $q_n$  represents the positive roots other than zero of the equation

$$\alpha q_n J_0(q_n) + 2J_1(q_n) = 0.$$

The constants  $\alpha$  and  $\beta$  are given by

$$\alpha = \frac{A}{a^2\pi(R+1)} \quad \text{and} \quad \beta = \frac{D}{(R+1)a^2}.$$

This applies only for a linear distribution between absorbed and mobile solute. For a general isotherm, e.g. of the Freundlich type, a numerical method<sup>4</sup> has to be employed, as in this case the diffusion equation cannot be solved formally.

Barrer<sup>5</sup> has considered the diffusion of gases into a sorbent in a constant volume sorption system in which the equilibrium distribution of sorbate between gas phase and sorbent follows Henry's law. Using the standard methods of solution as applied to heat conduction<sup>6</sup> he gives a complete solution<sup>7</sup> which leads to the following approximation,

$$\frac{Q_t}{Q_\infty} = \frac{6}{a} \cdot \frac{Q_0}{Q_0 - Q_\infty} \sqrt{\frac{Dt}{\pi}},$$

where  $Q_0$  is the quantity of gas present initially in the gas phase. This shows that a parabolic law may be followed under some circumstances even though the surface concentration is changing rapidly as in the reaction discussed in this paper.

<sup>1</sup> Alexander and Hudson, *J. Physic. Chem.*, 1949, **53**, 733.

<sup>2</sup> Barrer, *Diffusion in and through Solids* (Cambridge Univ. Press, 1941); Barrer, *Symposium on Fibrous Proteins* (Leeds, 1946).

<sup>3</sup> Wilson, *Phil. Mag.*, 1948, **39**, 48.

<sup>4</sup> Crank, *ibid.*, 1948, **39**, 140.

<sup>5</sup> Barrer, *Trans. Faraday Soc.*, 1949, **45**, 358.

<sup>6</sup> Carslaw and Jaeger, *Conduction of Heat* (O.U.P., 1947), p. 205.

<sup>7</sup> Paterson, *Proc. Physic. Soc.*, 1947, **59**, 50.

## Experimental

(1) RATE MEASUREMENTS have been described in detail in Part I. In addition to fabric, several samples of equivalent amounts of loose wool fibres were fitted to the frame stirrer and the rate of reaction determined as before. It was found to be difficult to obtain the same degrees of agitation owing to the large bulk of the fibres and the values can only be taken as indicative. The maximum rate of stirring which could be employed was 600-700 rev./min., as with greater speeds vortexing of the liquid led to unreliable results.

(2) RETAINED CHLORINE.—At the end of several experiments the quantity of chlorine in the fabric was determined by rinsing the sample in cold water for 5 min., i.e. until the washings gave no coloration with dilute potassium iodide solution. The fabric was then shaken with excess of standard ferrous ammonium sulphate solution which was titrated with standard potassium dichromate. From the results the percentage of strongly absorbed chlorine was calculated.

An alternative method leading to similar results was to immerse the wool after rinsing in an acidified solution of potassium iodide and titrate the liberated iodine immediately with thiosulphate. It was shown that the iodine liberated does not react with the wool in the short time required for the analysis.

(3) CYSTINE CONTENT OF TREATED WOOL.—Wool samples were reacted with varying quantities of chlorine in the same way as in the kinetic experiments. The samples were hydrolyzed and their cystine content determined colorimetrically.<sup>8</sup>

## Results

(1) RATE MEASUREMENTS.—Table I illustrates the fact that the rate of reaction of 10 % chlorine becomes independent of stirring at high stirring speeds. Rates are expressed in half-life values which may be used as a measure of fibre diffusion rate for reactions proceeding largely to exhaustion as will be shown in the discussion. Fig. 3 shows the rate of reaction in terms of  $t_{\frac{1}{2}}$  values with 10 % chlorine per weight of wool at different stirring speeds at 0° and 25°.

TABLE I

Stirring Rate rev./min.	$t_{\frac{1}{2}}$ min. 25°	$t_{\frac{1}{2}}$ min. 10°	$t_{\frac{1}{2}}$ min. 0°	$E_{0-25}$ cal./mole	$E_{0-10}$ cal./mole
300	—	—	2.9	—	—
400	0.57	—	2.6	9,900	—
500	0.4	—	2.7	12,400	—
600	0.4	1.0	2.6	12,200	14,100

TABLE II.—EXPERIMENTS WITH LOOSE FIBRES

Stirring Rate rev./min.	$t_{\frac{1}{2}}$ at 0° C
600	3.4
650	2.2
750	1.8

Loose fibres were used in the place of fabric to show that the rate of reaction remains the same for loosely and tightly packed fibres. Complete agreement is not to be expected as loose fibres are more difficult to agitate evenly than fabric.

The effect of changing concentration is shown graphically by the relation  $t_{\frac{1}{2}}$  against  $Q_0$  and  $t$  against  $\ln \left( \frac{c}{c-x} \right) - \frac{x}{c}$ , where  $c$  is the initial concentration in solution and  $c-x$  concentration at time  $t$ . These graphs are approximately

<sup>8</sup> Shinohara, *J. Biol. Chem.*, 1935, 109, 665.

linear, whereas for concentrations less than 10 % the rate of reaction is proportional to bath concentration (see Part I). It should be noted here that  $t_{\frac{1}{2}}$  is almost independent of initial concentration, although the rate appears to be controlled by diffusion within the fibre (i.e.  $t_{\frac{1}{2}} = 2.7, 2.5$ , and  $3.2$  for 10 %, 15 % and 25 % at 0° C).

(2) **RETAINED CHLORINE.**—The analyses of chlorine retained by the fibres at the end of the reaction for varying initial concentrations of chlorine are given in Tables III and IV.

TABLE III

Initial $\text{Cl}_2$ conc. %	Wt. of $\text{Cl}_2$ (g.) in Reaction soln.	Wt. of $\text{Cl}_2$ (g.) retained by Fibres	% $\text{Cl}_2$ (of total $\text{Cl}_2$ ) Retained
10	0.290	0.00415	1.4
7	0.194	0.00275	1.4
5	0.154	0.00195	1.3
3	0.096	0.00098	1.02
1	0.0359	0.00062	1.73

TABLE IV

Treatment of Chlorinated Fibres (10 %)	Wt. of $\text{Cl}_2$ applied (g.)	Wt. of Residual $\text{Cl}_2$ (g.)	% $\text{Cl}_2$ Retained
Dried at 80° C for 75 min. . . . .	0.301	0.000089	0.03
Distilled water at 20° C for 60 min. . . . .	0.299	0.00399	1.34
Jet of running water for 10 min. . . . .	0.285	0.00399	1.4
Distilled water at 50° C for 30 min. . . . .	0.270	0.00133	0.49

TABLE V

Initial $\text{Cl}_2$ conc. %	% Cystine Oxidized
3	13
5	22
10	43
15	57
25	75

These results show that the quantity of free chlorine remaining in the fibres is proportional to the quantity of chlorine reacted. This chlorine appears to be sorbed on the fibres, as immersion in distilled water for some time does not affect removal. Treatment with water at elevated temperatures or the action of heat alone destroys the oxidizing power. These observations suggest that the chlorine is present as an adsorbate rather than as an organic chloro compound.

(3) **CYSTINE CONTENT OF TREATED WOOL.**—The relation between the quantity of chlorine reacting and the amount of cystine removed is shown in Table V. The cystine oxidized in each case is expressed as a proportion of that of the original sample and not as a proportion of the cystine present in the reacted wool sample.

### Discussion

Two observations indicate that the rate process under observation is connected with the fibre and not the solution.

(i) With increasing stirring rate, rate of reaction increases rapidly and suddenly becomes constant above a critical value.

(ii) The measured activation energy simultaneously changes from 6000 to 12,000 cal./mole.

It has been shown<sup>9</sup> that the rate of reaction of chlorine with individual amino acids (except glycine) in solution is extremely rapid, so it is likely that migration of reactant to reaction sites is the slower process. In a similar system<sup>10</sup> it has been shown that the rate of exchange of ions on a synthetic resin is governed by diffusion of ions through the solid.

The linear relation between  $t^{\frac{1}{2}}$  and quantity diffused, which holds in the initial stages of the reaction (Fig. 2) is typical for diffusion into a semi-infinite solid from constant surface concentration. Owing to the change in concentration of the solution during reaction, it is improbable that in the course of the reaction the surface concentration remains constant. This is supported by the observed constancy in the half-life values with increasing concentration. Whereas for constant  $C_s$  from the general relation,<sup>10</sup> for reaction proceeding to completion,

$$Q_t = 2C_s A \sqrt{Dt/\pi},$$

i.e.

$$(x/c)Vc = 2C_s A \sqrt{Dt/\pi},$$

it is seen that  $t^{\frac{1}{2}} \propto c^2$ , where  $c$  is the initial bath concentration,  $c - x$  the concentration at time  $t$ , and  $V$  the volume of solution in contact with area  $A$  of fibres. This is in agreement with the conclusion of Barrer<sup>8</sup> discussed in the introduction, that linear  $t^{\frac{1}{2}} - Q_t$  plots do not necessarily require a constant surface concentration. In an analogous system Wagner and Hammen<sup>11</sup> have observed, in the oxidation of copper, that  $t^{\frac{1}{2}} - Q_t$  plots are linear, although the rate of reaction increases with pressure of oxygen, in contrast to the oxidation of zinc, the rate of which is independent of oxygen pressure.

**Derivation of a Semi-Empirical Relation.**—As the reaction results in removal of reactant a semi-empirical approach can be made, similar to that which has been adopted in the study of surface reactions of gases and solids, with the formation of a layer of product.<sup>12</sup> Thus, Wagner *et al.* have found in the oxidation of metals and for the reaction of silver with sulphur, the thickness of the layer of product increases proportionally to  $\sqrt{2At}$ . This can be derived theoretically by applying the simple law of Fick.<sup>13</sup>

Booth<sup>14</sup> has recently pointed out that this derivation is not strictly valid, although interpreting experimental results satisfactorily. The assumption of a linear diffusion gradient leads to the anomaly that

$$\partial^2 c / \partial x^2 = 0.$$

This can only hold for a stationary state, i.e. where the width of the diffusion layer does not vary with time. However, Booth obtained a rigorous solution and showed that the diffusion gradient is approximately linear if the diffusing concentration is small compared with the density of the product.

This condition is satisfied in the reaction under consideration as reaction is extensive, and although mathematically unsatisfactory, application of the pseudo-steady state concept gives results in agreement with experiment.

The rate of transport of reactant at any particular time across the layer of product of width  $d$  may be given by

$$\frac{d(xV)}{dt} = D_s A \frac{c_1 - c_2}{d},$$

<sup>9</sup> Alexander, Gough and Hudson (unpublished).

<sup>10</sup> Hill, *Proc. Roy. Soc. B*, 1929, **104**, 39.

<sup>11</sup> Wagner and Hammen, *Z. physik. Chem. B*, 1938, **40**, 197.

<sup>12</sup> Wagner, *ibid.*, 1933, **21**, 25.

<sup>13</sup> Mott and Gurney, *Electronic Processes in Ionic Crystals* (O.U.P., 1940), Ch. VIII.

<sup>14</sup> Booth, *Trans. Faraday Soc.*, 1948, **44**, 796.

where  $c_1$  and  $c_2$  are concentrations at the inner and outer boundaries,  $x$  the decrease in bath concentration in time  $t$ , and  $V$  the volume of solution. At any particular time,  $d$  is a function of the extent of reaction, i.e. the amount of product formed per given unit area. We may consider two extreme cases:

(a) Reaction is virtually complete within the product layer as in the case of metals forming oxides or sulphides. If  $C_f$  is the concentration

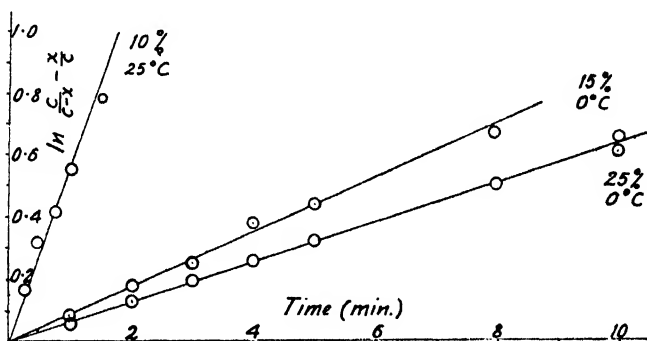


FIG. 1.—Graphs of  $\ln \frac{c}{c-x} - \frac{x}{c}$  against  $t$  for 10 %, 15 %, 25 %  $\text{Cl}_2$ .

of product formed, the distance penetrated is given by  $d = xV/AC_f$ ,

so that

$$\frac{d(xV)}{dt} = \frac{D_s A^2 (c-x) C_f}{xV},$$

i.e.

$$D_s \cdot C_f \left( \frac{A}{V} \right)^2 \cdot t = c \left( \ln \frac{c}{c-x} - \frac{x}{c} \right).$$

It is seen that in this case the half-life value is proportional to initial concentration of reactant in solution.

(b) It was seen from the results that the half-life values are almost independent of initial concentration. This may be interpreted in terms of incomplete reaction within the product layer. It is assumed that the layer  $d$  increases in proportion to the extent of the reaction, i.e.

$d = \frac{x}{c} d_0$ , where  $d_0$  represents the final penetration distance. Thus,

$$t = \frac{d_0 V}{D_s A} \left( \ln \frac{c}{c-x} - \frac{x}{c} \right)$$

and under such circumstances  $t_{\frac{1}{2}}$  becomes independent of initial concentration.

In both (a) and (b) a linear relationship holds between  $t$  and

$$\ln \frac{c}{c-x} - \frac{x}{c}.$$

Fig. 1 shows that such an expression applies to the experimental data. In addition, it is readily seen by expansion of the logarithmic term that if this relation holds, then the plot of  $t^{\frac{1}{2}}$  against  $Q_t$  must be linear for the initial stages of the reaction.

The concept of  $d_0$  implies that the diffusing species advances in the form of a well-defined front at which reaction occurs very rapidly. This has been demonstrated experimentally by Hermans<sup>16</sup> for the diffusion

<sup>16</sup> Hermans, *Contribution to the Physics of Cellulose Fibres* (Elsevier, 1946), p. 31.

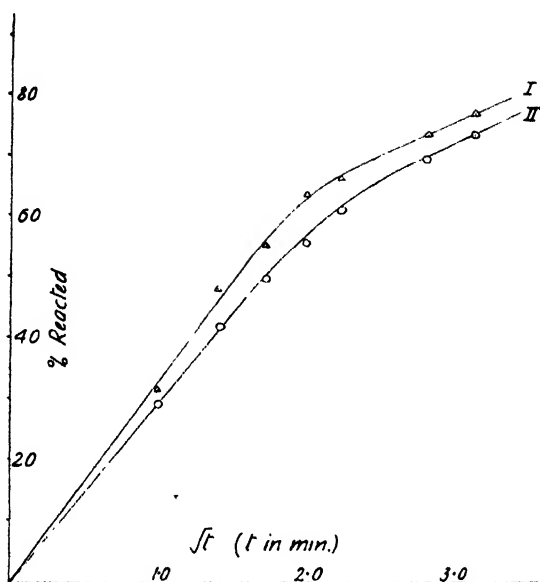


FIG. 2.—Graphs of  $t^{\frac{1}{2}}$  against % reacted for (I) 15 %, (II) 25 %  $\text{Cl}_2$  at  $0^\circ\text{C}$ .

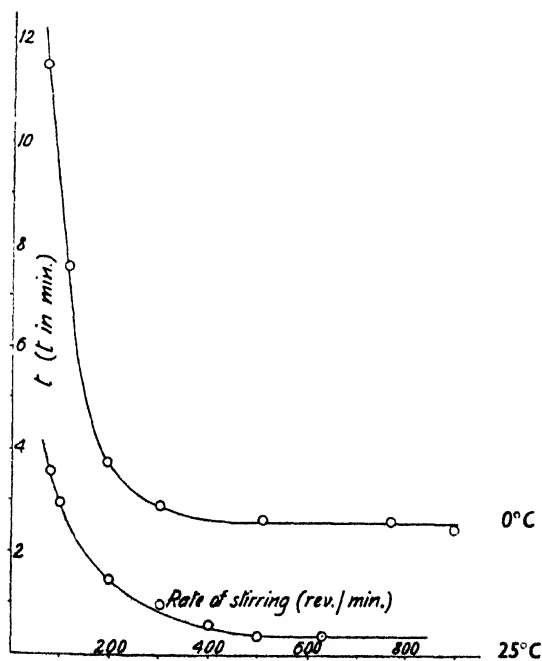


FIG. 3.—The effect of stirring on half-life values for 10 %  $\text{Cl}_2$  at  $0^\circ$  and  $25^\circ\text{C}$ .



of water into cellulose, and photomicrographs show clearly that in the case of dyeing of wool, cellulose and Nylon fibres diffusion proceeds in this way.<sup>16</sup> Some knowledge of the approximate value of  $d_0$  may be obtained in the present case from analyses of the treated fibres. The most reactive grouping, cystine, is rapidly attacked by chlorine,<sup>17</sup> the results of analyses with varying initial chlorine concentrations are given in Table V. The percentage cystine oxidized is proportional to the chlorine concentration until approximately 50 % has been removed (i.e. with 15 % chlorine solutions). Above this concentration the proportionality no longer exists, and the half-life value of the reaction increases. Thus, it would appear that  $d_0$  may be identified approximately with half the radius of the fibre. Assuming the radius of the fibre<sup>18</sup> to be  $10^{-3}$  cm. a value of the diffusion coefficient of  $10^{-7}$  cm.<sup>2</sup>/sec. at 0° C is obtained. This is of the same order as values of the diffusion coefficient of similar molecules through fibres, e.g.  $D$  for water at high regains approaches  $10^{-7}$  cm.<sup>2</sup>/sec. at room temperature.<sup>19</sup> Values of the order of  $10^{-6}$  cm.<sup>2</sup>/sec. were obtained by Boyd, Myers and Adamson for the exchange of small cations on a synthetic resin.<sup>20</sup>

Finally, this value may be compared with that obtained from the complete treatment of Wilson.<sup>3</sup> Difficulty is encountered in assigning a value to  $R$  which represents the ratio of concentration reacting to concentration diffusing. It has been seen from analysis of retained chlorine that approximately 1.0 to 1.5 %  $\text{Cl}_2$  remains unreacted at the end of the reaction, which leads to a value of approximately  $10^3$  for  $R$  (Table III). The constant  $\alpha$  (the actual value does not affect the form of the curve materially) thus approximates to unity as in this case  $\frac{A}{\pi a^2} = 150$ . The solution of Wilson's equation for  $\alpha = 1$  is given in Fig. 4. The dotted curve compares this solution with the semi-empirical relation

$$t \propto \left( \ln \frac{c}{c-x} - \frac{x}{c} \right),$$

from which it is seen that agreement is excellent. The calculated value of  $D_s = 0.3 \times 10^{-7}$  cm.<sup>2</sup>/sec. at 0° C agrees reasonably well with the value obtained from the semi-empirical treatment, when the difficulty of assigning correct values of  $R$  and  $d_0$  respectively in the two treatments is appreciated. The assumption in the semi-empirical treatment of an approximately linear diffusion gradient is supported by the calculated values of Crank<sup>21</sup> shown in Fig. 5 for the change in concentration with distance from the surface. It is seen that a linear diffusion gradient is a good approximation for 60 % of the reaction.

**The Effect of Temperature.**—The above discussion has been limited to the reaction at constant temperature. Owing to the high value of the apparent activation energy, 12,000 cal./mole, for fibre diffusion and the lower value, 6000 cal./mole for film diffusion, it follows that the mechanism governing the overall rate of reaction is highly dependent on temperature. Thus, if under a given set of conditions the mechanism is fibre-diffusion controlled, then increase in temperature favours the change-over to liquid-film diffusion. This is shown clearly by the graph of half-life values against stirring rate at 0° and 25° C (Fig. 3). Conversely, as soon as a build-up of concentration occurs at the surface the activation energy rises to 12,000 cal./mole, even though the rate is governed by

<sup>16</sup> Millson, Watkins and Royer, *Amer. Dyestuff Reprtr.*, 1947, **36**, 45; Morton, *Textil. Rundschau*, 1949, **4**, 39.

<sup>17</sup> Alexander, Hudson and Fox, *Biochem. J.* (in press).

<sup>18</sup> Sullivan and Hertel, *Textile Res.*, 1940, **11**, 30.

<sup>19</sup> King, *Trans. Faraday Soc.*, 1945, **41**, 326, 479.

<sup>20</sup> Boyd, Myers and Adamson, *J. Amer. Chem. Soc.*, 1947, **69**, 2836.

<sup>21</sup> Crank (private communication).

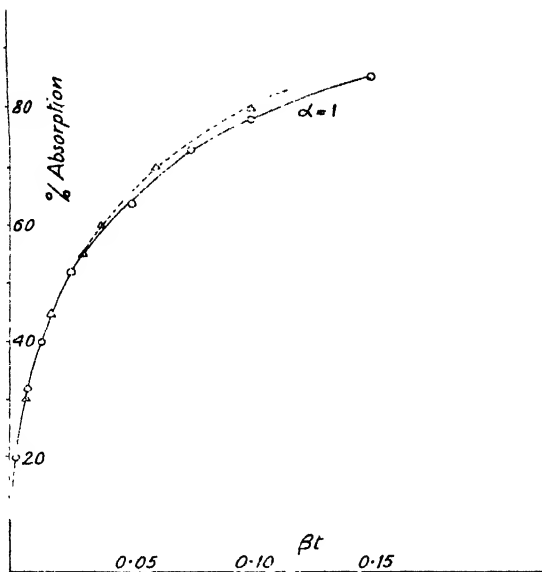


FIG. 4.—% Absorption-time graph calculated from the solution given by Wilson for  $\alpha = 1$ .

— Calculated from the equation of Wilson

$$\alpha = \frac{A}{\pi a^2} \frac{1}{R+1} = 1; \beta = \frac{D}{a^2(R+1)}.$$

- - - Calculated from the relation

$$t - \frac{d_0 V}{D.A} = \ln \left( \frac{c}{c-x} \right) - \frac{x}{c}$$

The graphs are fitted to 50 % reaction.

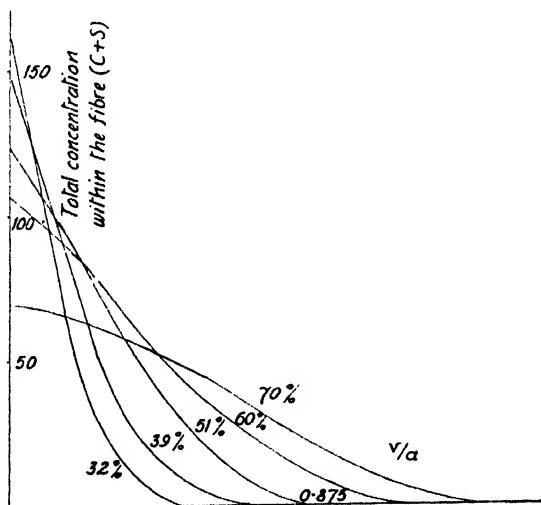


FIG. 5.—Diffusion gradients calculated by the method of Crank<sup>4</sup> for linear absorption with bath exhausting to 90 % for various degrees of exhaustion. Solution to fibre ratio (volumes), i.e.  $A/\pi a^2 = 25$ .

diffusion in both phases at the higher temperature. This accounts for the rapid change of temperature coefficient with changing conditions.

Before the significance of this activation energy can be examined the mode of diffusion in the solid must be considered. The reacting molecules may be rapidly absorbed on the solid surface and diffuse through a solid lattice of molecular chains to the reaction centres. This is unlikely as the fibres possess a high water content and are highly swollen, so that diffusion probably occurs through the aqueous phase within the fibre. To support this contention the diffusion of water and alcohols through keratin in the form of wool and horn may be quoted.<sup>19</sup> It is shown that the diffusion coefficient is highly dependent on moisture regain so that at low humidities  $D = 10^{-10}$  cm.<sup>2</sup>/sec., rising to ca.  $10^{-7}$  cm.<sup>2</sup>/sec. Thus, it seems highly probable that diffusion proceeds through an aqueous phase. It has been suggested<sup>22</sup> that the reactant diffuses through micropores of the fibre and is rapidly absorbed and subsequently reacts on the internal surface. This would imply a diffusion coefficient and activation energy of the same order as the corresponding quantities in aqueous solution. Alternatively, if adsorption were rate determining the activation energy would be a function of the heat of absorption. The remarkably constant values of  $E$  for widely varying diffusing species, given in Table VI tend to discount this theory.

TABLE VI

Diffusing Species	Diffusion Media	E. App. (cal./mole)
Anions: $\text{HSO}_3^-$ , $\text{Cl}^-$ , $\text{NO}_3^-$ . . .	Wool	10,500 <sup>23</sup>
$\text{SO}_4^{2-}$ , $\text{C}_6\text{H}_5\text{SO}_3^-$ . . .	"	11,500 <sup>23</sup>
$\text{KMnO}_4$ . . .	"	12,000 <sup>1</sup>
$\text{Cl}_2$ . . .	"	12,000
Dyes . . .	"	12,000-14,000 <sup>24</sup>
Water . . .	Cellulose	13,000 <sup>15</sup>
Dyes . . .	"	14,000 <sup>25</sup>

These  $E$  values vary slightly and increase with molecular size, thus indicating that diffusion alone through an isotropic medium governs the rate. The swollen fibre can thus be regarded as a uniform gel the component molecules undergoing restricted motion compared with molecules in aqueous solution. Neale<sup>26</sup> has advanced the possibility that this high activation energy indicates that desorption must precede diffusion, but considers it more likely to be merely the energy of hole formation opposing inter-molecular attraction forces which are greater than in a true solution. This mechanism is in agreement with the above activation energy values, the lower diffusion coefficient, and the greater entropy of activation of the fibre diffusion process calculated from  $D$ , and  $E$ <sup>23, 24</sup> compared with diffusion in aqueous solution.

The authors wish to thank Messrs. Wolsey Ltd., Leicester, for financial support which made this investigation possible and Prof. H. V. A. Briscoe for his help and interest.

Department of Inorganic and Physical Chemistry,  
Imperial College of Science,  
London, S.W.7.

<sup>22</sup> Morton, *Trans. Faraday Soc.*, 1935, **31**, 262; Neale, *ibid.*, 1935, **31**, 282; Valko, *ibid.*, 1935, **31**, 278. <sup>23</sup> Hudson and Schmeidler (unpublished).

<sup>24</sup> Alexander and Hudson (in press).

<sup>25</sup> Neale and Stringfellow, *Trans. Faraday Soc.*, 1933, **29**, 1167; Hanson, Neale and Stringfellow, *ibid.*, 1935, **31**, 1718.

<sup>26</sup> Neale, *Trans. Faraday Soc.*, 1948, **44**, 1027.

# DIFFUSION IN MEDIA WITH VARIABLE PROPERTIES

## PART II.—THE EFFECT OF A VARIABLE DIFFUSION COEFFICIENT ON THE CONCENTRATION-DISTANCE RELATIONSHIP IN THE NON-STEADY STATE

BY J. CRANK AND M. E. HENRY

*Received 17th June, 1949*

Concentration-distance curves are calculated for diffusion coefficients which depend on concentration in three different ways, and which may have a range of as much as 200-fold. The results are presented graphically in a form convenient for interpolation.

A method is suggested by which an approximate concentration-distance curve can be obtained, with relatively little labour, for any diffusion coefficient which depends on concentration, not necessarily in one of the ways for which the detailed results are presented.

The importance of the results in connection with a recently proposed method of measuring variable diffusion coefficients is discussed. Some insight into the nature of the sharp advancing boundary observed in many systems is provided, and the significance of the mean diffusion coefficient, deduced from the rate of advance of such a boundary, is considered.

---

**1. Introduction.**—In a recent paper Barrer<sup>1</sup> obtained formal solutions of the diffusion equation for conditions corresponding to steady-state diffusion through a membrane. The diffusion coefficient was considered to be variable and to be a function either of the concentration of the diffusing substance or of the space co-ordinate. A number of concentration-distance curves were shown for various types of variable diffusion coefficients. The shape and properties of the concentration-distance curves in the non-steady state are also of considerable interest. The task of calculating such curves, however, is a much more formidable one because of the lack of formal solutions of the diffusion equation in the non-steady state and the consequent necessity of employing graphical, numerical or mechanical methods of integration. In the present paper concentration-distance curves for the non-steady state are obtained by numerical methods for diffusion coefficients varying in different ways with the concentration of the diffusing substance. The results are restricted to one-dimensional diffusion into a medium which is essentially semi-infinite. These are effectively the conditions of diffusion into a plane sheet of finite thickness in the early stages of diffusion before the concentration has changed appreciably at the centre of the sheet. It has been seen<sup>2</sup> that, for diffusion coefficients which increase considerably with concentration increasing, the concentration-distance curve is of such a shape that the sheet is often behaving as a semi-infinite one when the overall absorption is over 50 % of the final equilibrium value. Thus the semi-infinite condition is an important one in practice.

The results are presented in such a way that concentration-distance curves can be obtained by interpolation for diffusion coefficient-concentration relationships which are of the same algebraic form as those for which

<sup>1</sup> Barrer, *Proc. Physic. Soc.*, 1946, **58**, 321.

<sup>2</sup> Crank and Park, *Trans. Faraday Soc.*, 1949, **45**, 240.

actual calculations have been performed but for which the numerical values of the parameters are different. A method is also suggested by which a reasonably good approximation to the concentration-distance curve can be obtained, with relatively little labour, for any diffusion coefficient which increases with concentration increasing. This method is not restricted to diffusion coefficients which behave in one of the ways for which detailed calculations have been performed.

Apart from the general interest in the form of the concentration-distance curves the results have an important bearing on the evaluation of variable diffusion coefficients by the new method described recently.<sup>3</sup>

The method is based on an approximate relation between  $\int Ddc$  and a mean diffusion coefficient which can be obtained readily from simple absorption measurements. Originally the method involved successive approximations to the integral by an iterative process necessitating somewhat laborious calculations. By using the results of the present paper much of the labour is avoided and the method becomes a much more amenable one.

A relatively simple observation to make in many systems is the rate of advance of a fixed concentration of diffusing substance and this affords a measure of the diffusion coefficient provided it is constant. When it is not constant the same observation yields some mean diffusion coefficient over the relevant range of concentration. The present results indicate, it is thought for the first time, the significance of the mean which is observed in this way.

## 2. The Equations and a Previous Method of Evaluating Solutions.

—Part I<sup>3</sup> of this series was concerned with the evaluation of numerical solutions of the diffusion equation for concentration-dependent diffusion coefficients having a range of approximately 5-fold in most cases. Recent measurements on the chloroform-polystyrene system<sup>2</sup> suggest that diffusion coefficients in polymer-liquid systems may vary much more violently than this. The diffusion coefficients dealt with in the present paper therefore have a range of as much as 200-fold.

The equations and boundary conditions for diffusion in one dimension in a semi-infinite medium at whose surface the concentration is constant were developed previously<sup>3</sup> and so they can be introduced here with a minimum of explanation. In the earlier paper it was seen that for these conditions the concentration becomes a function of a single variable only, and the diffusion equation reduces to an ordinary differential equation of the form

$$-2\eta \frac{dc}{d\eta} = \frac{d}{d\eta} \left( D \frac{dc}{d\eta} \right) \quad (2.1)$$

We are interested in solutions of (2.1) which satisfy the conditions

$$c = 1, \quad \eta = 0, \quad c \rightarrow 0, \quad \eta \rightarrow \infty. \quad (2.2)$$

Here  $c$  is the concentration of diffusing substance so expressed that the concentration is constant and equal to unity at the surface of the semi-infinite sheet,  $\eta = 0$ ; and  $\eta$  is defined by the relation

$$\eta = x/2(D_0 t)^{1/2}, \quad (2.3)$$

where  $x$  is the space co-ordinate measured from the surface of the sheet,  $t$  is the time, and  $D_0$  the value of the true diffusion coefficient when  $c = 0$ .  $D$  is a function of  $c$  and is the ratio of the true diffusion coefficient to  $D_0$  so that  $D$  is non-dimensional and  $D = 1$  when  $c = 0$ .

Solutions of (2.1) were obtained in Part I by an iterative evaluation of the expression

$$c = 1 - A \int_D^1 \exp \left\{ - \int_D^{\frac{1}{D}} d\eta \right\} d\eta, \quad (2.4)$$

<sup>3</sup> Crank and Henry, *Trans. Faraday Soc.*, 1949, **45**, 636.

where  $A$  is a constant determined by conditions (2.2). Values of  $c$  calculated from

$$c = 1 - \operatorname{erf} \eta, \quad (2.5)$$

were used as the first approximation in the iterative process. When the same procedure was tried for more widely varying types of  $D$ - $c$  relationships, the convergence of the iterative process was found to be prohibitively slow and it was clearly necessary either to find a new method of solution or to obtain a much better first approximation to the solution. The present results have been obtained by adopting the latter alternative.

**3. An Improved First Approximation to the Solution.**—Inspection of several  $c$ - $\eta$  curves obtained in the course of calculating the absorption-time curves of Part I, shows that the  $c$ - $\eta$  curves vary considerably with the  $D$ - $c$  relationship, even for moderately varying  $D$ . Thus it is not easy to obtain a good first approximation to the  $c$ - $\eta$  curve especially when  $D$  varies considerably with  $c$ .

In the steady-state flow through a membrane between two fixed concentrations of diffusing substance, the shape of the concentration-distance curve is very dependent on the  $D$ - $c$  relationship, but the product  $D(dc/dx)$  is constant at all points of the membrane. This suggests that, although we are here concerned with the non-steady state and hence  $D(\partial c/\partial x)_t$  cannot be strictly constant, nevertheless the results may assume a simpler form in terms of a variable which includes such a product. We define a new variable  $s$  by the relation

$$s = \left( \int_0^c D dc \right) / \left( \int_0^1 D dc \right), \quad (3.1)$$

so that

$$\frac{ds}{d\eta} = \frac{D}{D_1} \frac{dc}{d\eta}, \quad (3.2)$$

and

$$s = 1, \quad c = 1, \quad \eta = 0, \quad (3.3)$$

$$s \rightarrow 0, \quad c \rightarrow 0, \quad \eta \rightarrow \infty \quad (3.4)$$

where

$$D_1 = \int_0^1 D dc. \quad (3.5)$$

For certain types of  $D$ - $c$  relation it will be possible to evaluate  $s$  and  $D_1$  by formal integration, but otherwise the integrals of (3.1) can be evaluated numerically. The transformation (3.1) is essentially the one suggested by Eyres, Hartree and others<sup>4</sup> in a different context. When the  $s$ - $\eta$  curves are plotted for the  $D$ - $c$  relationships considered in Part I it is found that they all have the same general shape. They all approximate to straight lines over the range  $1 > s > 0.2$ , and furthermore the gradient of each straight line is approximately  $-2/\pi^{\frac{1}{2}} D_1^{\frac{1}{2}}$ . This is the gradient the  $s$ - $\eta$  curves would have at  $\eta = 0$ , if  $D$  were constant and equal to  $D_1$ , for then

$$s = 1 - \operatorname{erf}(\eta D_1^{\frac{1}{2}}), \quad (3.6)$$

and  $-2/\pi^{\frac{1}{2}} D_1^{\frac{1}{2}}$  is the first term in the expansion of the right-hand side of (3.6) for small  $\eta$ .<sup>5</sup> The  $s$ - $\eta$  curves calculated for the diffusion of chloroform into polystyrene, where  $D$  is an exponential function of  $c$  with a range of 200, show a similar behaviour.

These earlier results suggest the following method of obtaining a first approximation from which to start the iterative process. For  $s > 0.2$ ,  $s$  is assumed to be a linear function of  $\eta$ , the gradient of the line being  $-2/\pi^{\frac{1}{2}} D_1^{\frac{1}{2}}$ . Below  $s = 0.2$ ,  $s$  is tailed off to approach  $s = 0$  with zero gradient at a value of  $\eta$  slightly greater than that at which the straight

<sup>4</sup> Eyres, Hartree, Ingham, Jackson, Sarjant and Wagstaff, *Phil. Trans.*, 1946, **240**, 1.

<sup>5</sup> *Tables of Probability Functions* (Works Projects Administration, New York, 1941), Vol. I.

line intersects the  $\eta$ -axis. A rough guide to the value of  $\eta$  at which  $s$  should approach zero to within, say, 3 decimal places is afforded by use of the asymptotic expansion for the error function.<sup>5</sup> Since the linear dependence of  $s$  on  $D_1$  has been found to break down for  $s < 0.2$  it is reasonable to suppose that the asymptotic approach to zero depends mainly on a mean value of  $D$  taken over the range  $s < 0.2$ . On the basis of this supposition the value of  $\eta$  at which  $s$  takes a low value, say, 0.001, is given approximately by the first term in the expansion

$$s = \frac{2}{\pi^{\frac{1}{2}}} \frac{e^{-\eta^2}}{2\eta_1} \left\{ 1 - \frac{1}{2\eta_1^2} + \frac{1.3}{(2\eta_1^2)^2} - \dots \right\}, \quad (3.7)$$

where  $\eta_1 = \eta/D_1^{\frac{1}{2}}, \quad (3.8)$

and  $D_1^{\frac{1}{2}} = \int_{s=0}^{s=0.2} D dc. \quad (3.9)$

An indication of the self-consistency of the first approximation to the  $s$ - $\eta$  curve is provided by a comparison of two expressions for  $M_t$ , the total amount of diffusing substance which has crossed  $\eta = 0$  at time  $t$  per unit area. Thus

$$M_t = \int_0^\infty c dx = 2(D_0 t)^{\frac{1}{2}} \int c d\eta, \quad (3.10)$$

and also

$$\frac{dM_t}{dt} = - \left( DD_0 \frac{\partial c}{\partial x} \right)_{\eta=0} = - \frac{DD_1^{\frac{1}{2}}}{2t^{\frac{1}{2}}} \left( \frac{dc}{d\eta} \right)_{\eta=0} = - \frac{D_1 D_1^{\frac{1}{2}}}{2t^{\frac{1}{2}}} \left( \frac{ds}{d\eta} \right)_{\eta=0}, \quad (3.11)$$

so that on integrating

$$M_t = - D_1 (D_0 t)^{\frac{1}{2}} \left( \frac{ds}{d\eta} \right)_{\eta=0} \quad (3.12)$$

Thus, if the first approximation to the complete  $s$ - $\eta$  curve is consistent with the initial gradient we must have

$$2 \int_0^\infty c d\eta = - D_1 \left( \frac{ds}{d\eta} \right)_{\eta=0} \quad (3.13)$$

In terms of the variable  $s$ , (2.4) takes the slightly simpler form

$$s = 1 - A \int \exp \left\{ - \int \frac{2\eta}{D} d\eta \right\} d\eta. \quad (3.14)$$

The iterative treatment of (3.14), by which  $s$  is evaluated as a function of  $\eta$  when  $D$  is a known function of  $s$ , follows closely that of (2.4) with the slight modification due to the disappearance of the factor  $1/D$ . The first approximation to the  $s$ - $\eta$  relation, from which to start the iteration, is obtained in the manner described above instead of by using (2.5). For some  $D$ - $c$  relationships  $s$  is a slowly varying function of  $c$  for small  $c$  so that a small error in  $s$  corresponds to a much larger error in  $c$ . For this reason, when the values of  $s$  in two successive stages of the iteration agree reasonably well, it is desirable to convert the  $s$  values into  $c$  values and to finish the iterative process in terms of  $c$  using (2.4).

The final solution resulting from the iterative process usually approaches zero at a value of  $\eta$  less than that given by (3.7). If, however, at any stage of the iteration  $s$  or  $c$  becomes zero although  $ds/d\eta$  or  $dc/d\eta$  is not zero to the desired order of accuracy, it means that the solution has not been extended far enough in  $\eta$  and a new approximation should be made in which  $s$  or  $c$  tends to zero with zero gradient at a higher value of  $\eta$ . Sometimes (3.13) provides a useful check on the iterative solutions. Thus, if at any stage of the iteration (3.13) is not satisfied, convergence cannot be complete. This does not imply, of course, that a solution satisfying (3.13) is necessarily the correct one.

#### 4. Calculated Concentration-distance Curves.—Numerical solutions

of the diffusion eqn. (2.1) subject to conditions (2.2) have been obtained for the following  $D$ - $c$  relationships:

$$D = 1 + ac, \quad (4.1)$$

$$D = e^{bc}, \quad (4.2)$$

$$D = 1 + 50 \log(1 + kc), \quad (4.3)$$

In every case  $D = 1$  when  $c = 0$  and the value of  $D$  when  $c = 1$  is determined by choice of the parameters  $a$ ,  $b$  or  $k$ . With one exception the present calculations are restricted to a maximum range of about 200-fold in  $D$ . One solution has been evaluated for an exponentially varying  $D$  having a range of about 400-fold. The choice of the factor 50 in (4.3) is arbitrary and merely gives  $D$ - $c$  curves convenient for present purposes.

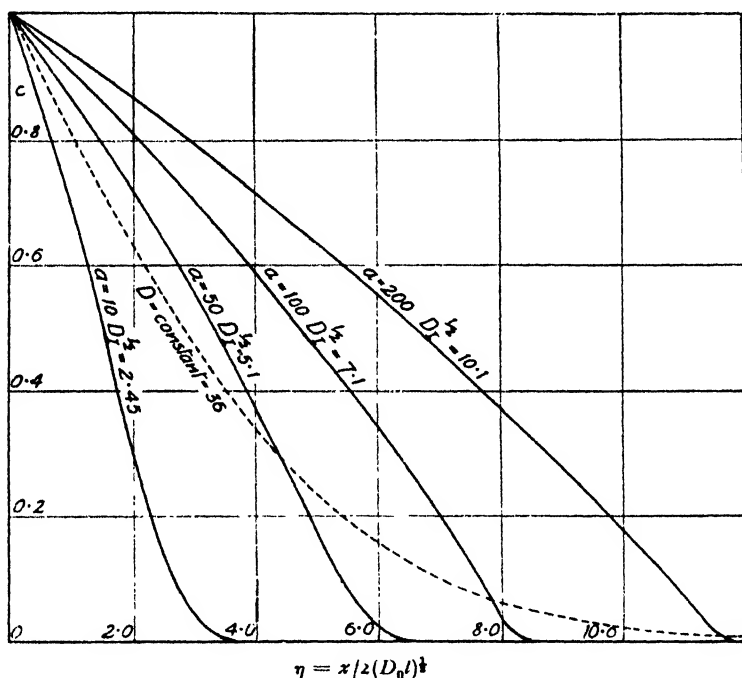


FIG. 1.—Concentration-distance curves for  $D = 1 + ac$ .

Fig. 1, 2 and 3 show concentration-distance curves for each type of diffusion coefficient represented by (4.1), (4.2) and (4.3). The curves are plotted as functions of  $\eta$  but since  $\eta = x/2(D_0 t)^{1/2}$  they are readily converted into concentration-distance curves at any time  $t$  by multiplying  $\eta$  by the appropriate factor  $(D_0 t)^{1/2}$ . The curves of Fig. 1, relating to  $D$  a linear function of  $c$ , are drawn for chosen values of  $a$ , namely  $a = 10, 50, 100, 200$ . The corresponding values of  $D_1^{1/2}$  are 2.45, 5.1, 7.1, 10.1, which are approximately equally spaced values. The curves of Fig. 2 and 3 are drawn for values of  $D_1^{1/2}$  which are exactly equally spaced, i.e.  $D_1^{1/2} = 3.0, 4.0, 5.0, 6.0$  in Fig. 3 and  $D_1^{1/2} = 3.0, 7.0, 10.0, 13.0$  in Fig. 4. The reason for this is clear from Fig. 4, 5 and 6. Here, for each type of  $D$ , the value of  $\eta$  at which  $c$  has a certain value, e.g.  $c = 0.1$ , is plotted as a function of  $D_1^{1/2}$ . In each figure, the graphs for each value of  $c$  are seen to be linear within the degree of accuracy of the present calculations and over the range of  $D_1^{1/2}$  considered. This means that, given



a  $D$ - $c$  relationship of any of the types (4.1), (4.2) or (4.3) and having a value of  $D_1$  intermediate between those for which detailed  $c$ - $\eta$  curves are shown, the  $c$ - $\eta$  curve can be obtained by linear interpolation in terms of  $D_1^{\frac{1}{2}}$  either on the data of one of the Fig. 1, 2 and 3, or of Fig. 4, 5 and 6.

One example of the way in which  $s$  varies with  $\eta$  is shown in Fig. 7 for each type of  $D$ - $c$  relation. These curves are of the simpler shape anticipated earlier in the paper. The degree of approximation provided by the straight lines of gradient  $-2/\pi^{\frac{1}{2}}D_1^{\frac{1}{2}}$  (shown in the figure as broken lines) for  $s > 0.2$  is also indicated. The value of  $\eta$  at which  $c = 0.001$  according to the asymptotic formula (3.7) using  $D_1$  given by (3.9), is indicated by a cross, showing that a useful estimate of the end point of the curve is provided by this means.

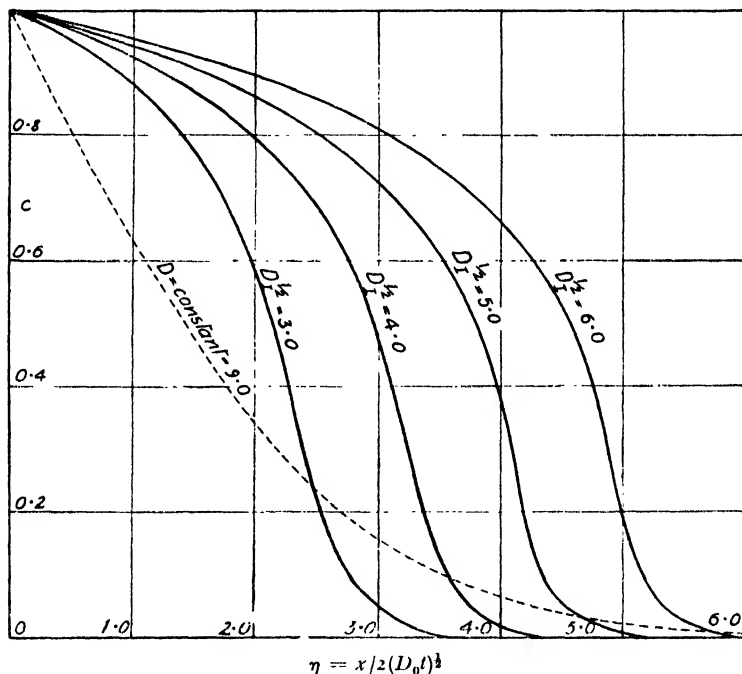


FIG. 2.—Concentration-distance curves for  $D = e^{bc}$ .

**5. (a) Shape of the Concentration-distance Curves.**—The shapes of the concentration-distance curves are characteristic of the diffusion coefficients to which they relate. They do not conform to quite such a simple classification as do the corresponding curves in the steady-state. Thus Barrer<sup>1</sup> is able to write, with regard to the results of his steady-state calculations, that whenever  $D$  increases as  $c$  increases, concentration-distance curves are convex away from the distance axis. Fig. 1 and 2 show that this general statement is also true over the greater part of the concentration range in the non-steady state when  $D$  increases with concentration either linearly or at a rate which steadily increases as  $c$  increases, e.g. an exponential rate of increase of  $D$  with  $c$ . When  $D$  increases with concentration at a steadily decreasing rate, however, the concentration-distance curve may become convex downwards as in Fig. 3.

In the region of low concentration there is an important difference in behaviour of the concentration-distance curves in the steady and non-steady states. This difference is a direct consequence of the difference in

boundary conditions. In the steady state the condition is that the concentration shall have some fixed value, possibly zero, at the emergent face of the membrane through which the diffusion is proceeding. When the diffusion occurs into a semi-infinite medium, however, the condition that the concentration shall approach zero at infinity means that the gradient of concentration tends to zero at the limit of penetration into the sheet. This produces a point of inflexion in any concentration-distance curve which is convex away from the distance axis at high concentrations, as in Fig. 1 and 2.

The shape of the curves at low concentrations is of some practical interest. It has been observed<sup>6</sup> that when, for example, an organic liquid is diffusing into a high polymer solid, a sharp advancing boundary is visible. The same phenomenon has been observed when water diffuses

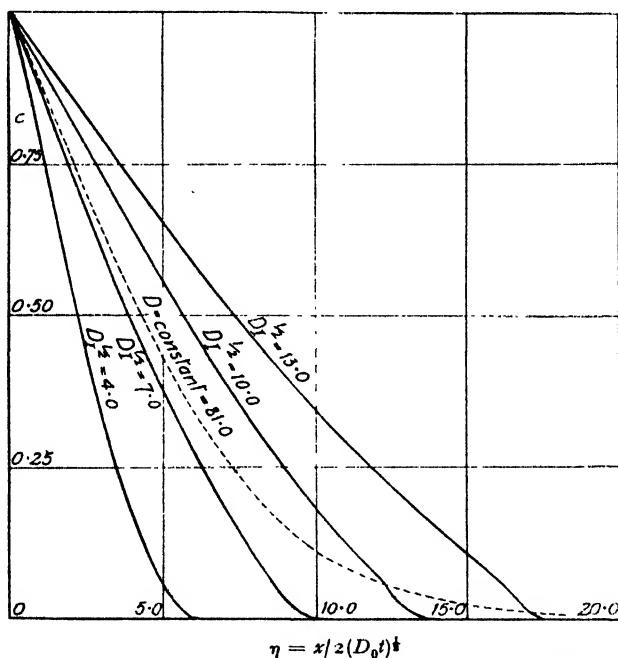


FIG. 3.—Concentration-distance curves for  $D = 1 + 50 \log(1 + kc)$ .

into dry cellulose.<sup>7</sup> In some systems, e.g. the diffusion of various substances into gels, a similar sharp boundary appears to be due to the fact that the diffusing particles react with the medium to form a precipitate and are thus withdrawn from the diffusion process.<sup>8</sup> This can hardly be the cause in the liquid-polymer systems, however. In this case Hartley<sup>6</sup> has associated the visible boundary with the presence of a high gradient of concentration, and hence of refractive index, caused by a considerable variation of diffusion coefficient in the neighbourhood of the boundary. The present results, however, offer no evidence of locally steep concentration gradients at low concentrations either for exponentially varying diffusion coefficients or for the other types, which vary more rapidly at low concentrations for the same overall range. There is, on the other hand, a marked tendency for the gradient of concentration to change

<sup>6</sup> Hartley, *Trans. Faraday Soc.*, 1946, **42B**, 6.

<sup>7</sup> Hermans and Vermaas, *J. Polymer Sci.*, 1946, **1**, 149.

<sup>8</sup> Hermans, *J. Colloid Sci.*, 1947, **2**, 387.

rapidly at low concentrations, i.e. the concentration distribution terminates more abruptly when  $D$  is an increasing function of  $c$  than when it is constant. This effect is least marked for an exponentially varying  $D$  but even there the rate of increase of gradient is much greater than for a constant  $D$  for which the rate of penetration is comparable, as shown by the broken line on Fig. 2. A complete explanation of the sharp advancing boundary involves a knowledge not only of the concentration-distance distribution but also of the refractive index concentration relation. It seems likely, however, that the boundary can be associated with an abrupt termination of the concentration distribution not necessarily accompanied by a locally steep concentration gradient.

(b) **Rate of Penetration of a Fixed Concentration.**—In any system in which the diffusion coefficient is constant its value can be determined by observing the rate of penetration of any known concentration. Thus for a constant coefficient  $D_0$  we have the relation

$$c = 1 - \operatorname{erf} \{x/2(D_0 t)^{\frac{1}{2}}\}, \quad . \quad . \quad . \quad (5.1)$$

from which  $x/(D_0 t)^{\frac{1}{2}}$  can be calculated for any known value of  $c$ . If

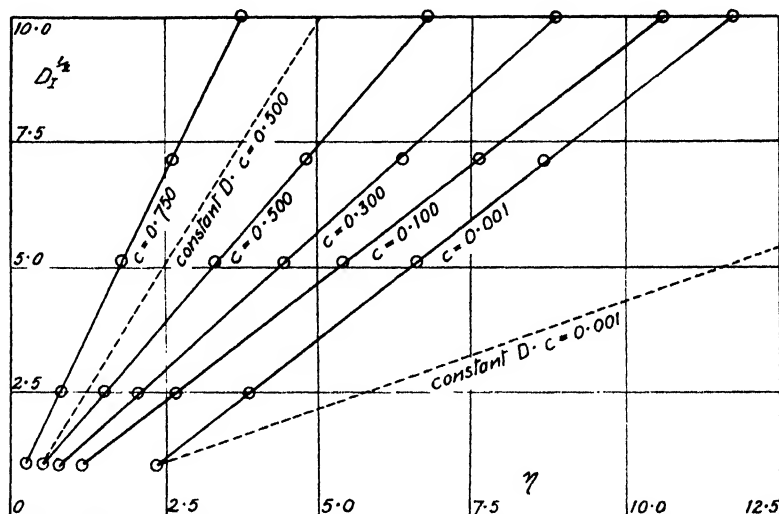


FIG. 4.—Constant concentration lines for  $D = 1 + ac$ .

now  $x/t^{\frac{1}{2}}$  is measured experimentally by observing the depth of penetration of the concentration concerned at successive times, the coefficient  $D_0$  is determined. Earlier in the paper  $D_0$  has been used to denote the value of the diffusion coefficient at zero concentration of diffusing substance. The rate of penetration of the same concentration for any other constant diffusion coefficient, say  $DD_0$ , is determined by the condition that  $x/2(DD_0 t)^{\frac{1}{2}}$  is constant and the plot of  $D^{\frac{1}{2}}$  against  $x/2(D_0 t)^{\frac{1}{2}}$  is a straight line. The gradient of the line depends on the particular concentration considered according to (5.1). Examples for  $c = 0.5$  and  $0.001$  are shown as broken lines in Fig. 4. They have a practical significance of some interest.

Thus if the rate of penetration of a fixed concentration, indicated perhaps by a sharp boundary, is observed in a system in which the diffusion coefficient is not constant but is concentration dependent, the value of the coefficient derived by use of (5.1) as above represents some mean value over the relevant concentration range. In the past it has not been possible to assess the significance of the mean observed in this way, but some useful conclusions can be drawn from Fig. 4. Thus, suppose a

concentration of 0.001 is observed to advance at a rate for which  $\pi/2(D_0 t)^{1/2} = 5.0$ . The mean value of  $D$ , on the assumption of no concentration dependence, would be read off the broken line for  $c = 0.001$  and would be  $(2.15)^2 = 4.62$ . If the diffusion coefficient actually varies linearly with concentration, however, the integrated mean over the whole concentration range, which has been denoted by  $D_1$ , is equal to

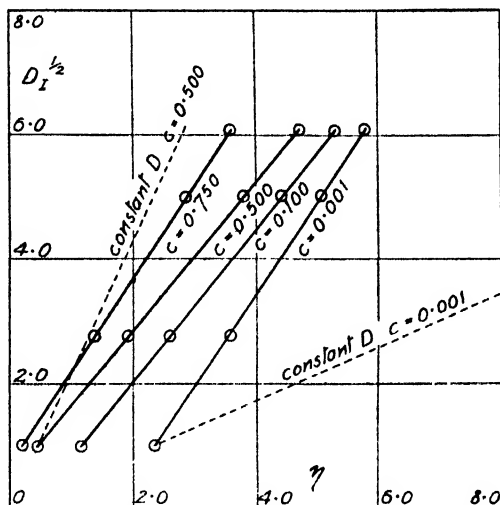


FIG. 5.—Constant concentration lines for  $D = e^{kc}$ .

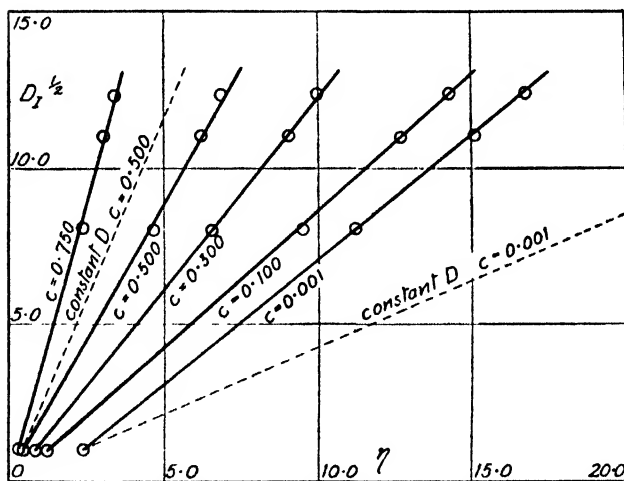


FIG. 6.—Constant concentration lines for  $D = 1 + 50 \log(1 + kc)$ .

$(3.55)^2 = 12.60$ , as indicated by the full line curve in Fig. 4 for  $c = 0.001$  and  $\pi/2(D_0 t)^{1/2} = 5.0$ . This value of  $D_1$  implies that  $D = 1 + 23.20c$  and hence the mean value of  $D$  deduced from the penetration observation is the integrated mean over the concentration range  $0 < c < 0.24$ . From Fig. 5 and 6 it is clear that the mean value of  $D$  measured by the rate of penetration of a low concentration,  $c = 0.001$ , is always weighted towards the low end of the concentration range. The discrepancy between the result of the penetration experiment for this concentration

and  $D_1$  is greater for an exponentially varying  $D$  than for either of the other types. The penetration experiment yields a coefficient closer to the value of the variable coefficient at  $c = 0.001$  than to  $D_1$ .

When the corresponding broken line is plotted for  $c = 0.5$  it is found to lie above the plot of  $D_1^\dagger$  against  $\eta$  for the same concentration. Thus a penetration experiment in which a concentration of 0.5 is observed yields a mean weighted towards the higher end of the concentration range. In general, the significance of the mean diffusion coefficient obtained by a penetration experiment depends very much on the concentration observed and on the way in which the diffusion coefficient varies with concentration. Clearly for each  $D$ - $c$  relation there is some concentration between 0.001 and 0.5 for which the penetration experiment yields  $D_1$  exactly. This concentration depends somewhat on the  $D$ - $c$  relation but the results suggest that if the rate of penetration of a concentration about 0.2 is observed the constant diffusion coefficient deduced will be a reasonable approximation to  $D_1$  for each of the above  $D$ - $c$  relations.

(c) **A Method of Measuring Variable Diffusion Coefficients.**—A new method of evaluating concentration-dependent diffusion coefficients was proposed in Part I and has since been applied successfully in practical cases.<sup>\*,\*</sup> The experimental technique involved is comparatively simple and consists in measuring the overall rates of absorption of penetrant by plane sheets of material suspended in penetrant vapour at different pressures. The mathematical analysis of the sorption-time curves, by which the diffusion coefficient is derived, consists in obtaining successive approximations to  $\int_0^{C_0} D dC$  for a number of values of the upper limit  $C_0$  which is the concentration at the surface of the sheet. Differentiation of the graph of the integral against  $C_0$  then yields  $D$  as a function of  $C$ . A mean diffusion coefficient  $\bar{D}$  is deduced from each sorption-time curve, the mean chosen being the constant diffusion coefficient for which the theoretical sorption-time curve reaches 50 % equilibrium sorption at the same time as the experimental curve. It is shown<sup>†</sup> that

$$\bar{D} = 0.04939 / (D_0 t / l^2)_{\frac{1}{2}} \quad . \quad . \quad . \quad . \quad (5.2)$$

where  $(t/l^2)_{\frac{1}{2}}$  denotes the value of  $t/l^2$  at which 50 % sorption is attained and  $l$  is the thickness of the sorbing sheet. As originally proposed the method was to obtain a first approximation to  $D$  by assuming that

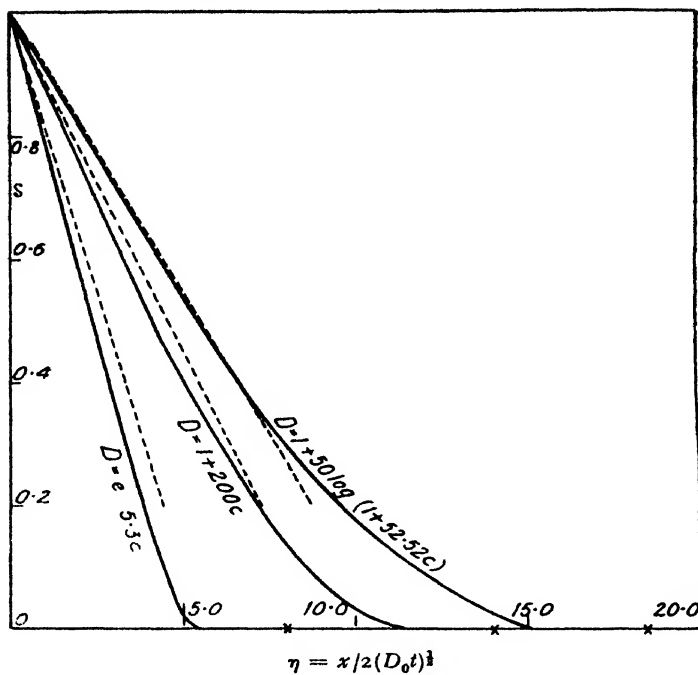
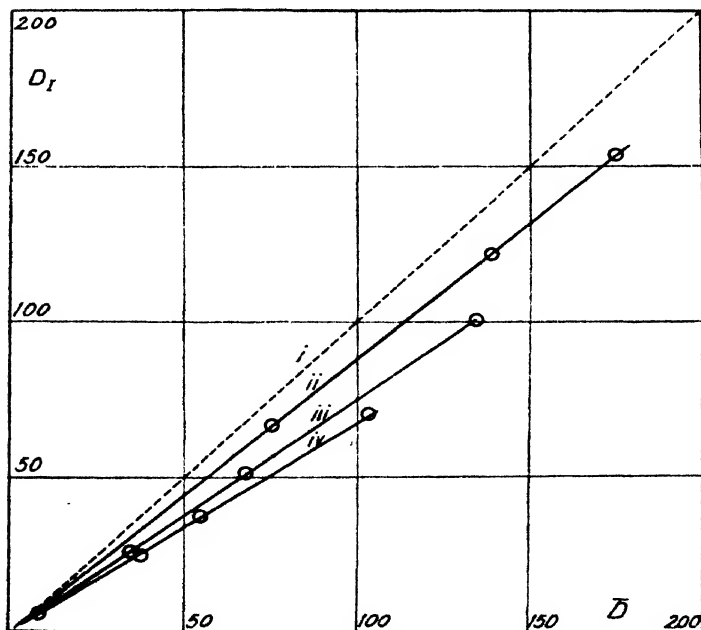
$$\bar{D} = (1/C_0) \int_0^{C_0} D dC \quad . \quad . \quad . \quad . \quad (5.3)$$

It was then necessary to carry out quite extensive calculations in order to obtain a better approximation to the integral, for the  $D$  just derived, than is afforded by (5.3). By using the data presented in Fig. 8 much of the calculation can be avoided. The three graphs show the relation

between  $\bar{D}$  and  $\frac{1}{C_0} \int_0^{C_0} D dC$ , which is  $D_1$  in the present nomenclature, for

the three types of  $D$  considered above. Thus suppose the first approximation to  $D$  obtained by using (5.3) is exponential in form, second approximations to  $D_1$  for the observed values of  $\bar{D}$  can be obtained from the appropriate curve of Fig. 8. The second approximation to the  $D$ - $c$  relation follows by differentiation but without extensive calculation. Unless particularly high accuracy is required a sufficiently good approximation to  $D_1$  can be obtained from Fig. 8 even if the  $D$ - $c$  relation is not exactly one of the 3 types considered above. Thus the difference in  $D_1$  between the exponential and linear types for a given  $\bar{D}$  is about 10 % of  $\bar{D}$  so that the error in interpolating for an intermediate type of  $D$  is probably less than 5 %.

\* Park, *Trans. Faraday Soc.* (in preparation).

FIG. 7.— $s - \eta$  relationships.FIG. 8.—Relation between  $D_I$  and  $\bar{D}$ .

- (i) Constant  $D$ .
- (ii)  $D = 1 + 50 \log(1 + kc)$ .
- (iii)  $D = 1 + ac$ .
- (iv)  $D = e^{bc}$ .

Along the broken line  $D_1 = \bar{D}$  in Fig. 8,  $D$  takes a succession of constant values. This line, therefore, appears to be the limiting position of the graphs of Fig. 8 since it corresponds to diffusion coefficients which increase instantaneously at  $c = 0$  to their final value and then remain constant over the whole of the concentration range. Thus the error involved in interpolating for any  $D$  which increases with  $c$  increasing at a steadily decreasing rate is also small.

(d) **A Simple Method of Calculating Approximate Concentration-Distance Curves**—Fig. 8 can also be used to obtain a good approximation to the concentration-distance curve for any  $D$  which increases with  $c$  increasing, by a refinement of the method described in § 3 for obtaining a first approximation in the iterative process. Thus for a finite sheet of thickness  $l$  we have

$$\frac{M_t}{M_\infty} = \frac{1}{l} \int_0^{l/2} c dx = 4 \left( \frac{D_0 t}{l^2} \right)^{\frac{1}{2}} \int_0^\infty c d\eta, \quad (5.4)$$

provided the sheet is still behaving as a semi-infinite one. Under such conditions, for a constant diffusion coefficient,  $\bar{D}D_0$ , there is the well-known solution<sup>10</sup>

$$\frac{M_t}{M_\infty} = \frac{4}{\pi^{\frac{1}{2}}} \left( \frac{\bar{D}D_0 t}{l^2} \right)^{\frac{1}{2}}, \quad (5.5)$$

and when

$$M_t/M_\infty = 1/2, \quad (5.6)$$

this becomes

$$\bar{D} = (\pi/64)/(D_0 t/l^2)^{\frac{1}{2}}, \quad (5.7)$$

which is numerically equivalent to (5.2). Combining (5.7) with (5.6) and (5.4) gives

$$\int_0^\infty c d\eta = (\bar{D}/\pi)^{\frac{1}{2}}. \quad (5.8)$$

Finally by substituting (5.8) in (3.13) we obtain

$$\left( \frac{ds}{d\eta} \right)_{\eta=0} = - \frac{2}{\pi^{\frac{1}{2}}} \frac{\bar{D}^{\frac{1}{2}}}{\bar{D}_1} \quad (5.9)$$

The approximation to the initial gradient used in § 3 was  $-2/\pi^{\frac{1}{2}}\bar{D}$  which follows from (5.9) on writing  $\bar{D} = D_1$ . Fig. 8, however, provides a better estimate of  $\bar{D}$  and hence of the initial gradient of the  $s$ - $\eta$  curve. Thus an approximate  $s$ - $\eta$  curve, and hence of course a  $c$ - $\eta$  curve, can be obtained by following the procedure described in § 3 but using (5.9) for the initial gradient instead of  $-2/\pi^{\frac{1}{2}}\bar{D}_1^{\frac{1}{2}}$ . The remainder of the  $s$ - $\eta$  curve should be drawn so that (3.13) is satisfied.

*Courtaulds, Limited,  
Research Laboratory,  
Maidenhead, Berks.*

<sup>10</sup> McKay, *Proc. Physic. Soc.*, 1930, **42**, 547.

# RELATIVE INTENSITIES IN THE RAMAN SPECTRA OF SOME GROUP IV TETRAHALIDES

BY L. A. WOODWARD AND D. A. LONG

Received 11th July, 1949

Considerations based on the Placzek theory show that, when the usual Wood's tube method of Raman excitation is used, the calculation of relative mean derived polarizabilities  $a$  from observed relative Raman intensities is only possible for specially selected molecules and vibrational modes. The Group IV tetrahalides and their symmetrical breathing modes satisfy the requisite conditions. Values of  $a$  for a number of these compounds are deduced from the corresponding Raman intensities, as determined relative to  $\text{CCl}_4$  by photographic photometry of the spectra of suitable binary mixtures. The results are quite at variance with the assumption, previously made by Hansen-Damaschun, that  $a$  is simply proportional to the degree of covalent character of the bond involved. The measured values for the typical and Group IVB tetrahalides  $\text{XY}_4$  conform approximately to the simple empirical rule that  $a$  is proportional to the product of (i) the sum of the atomic numbers of X and Y and (ii) the percentage covalency of the X—Y link as obtained by Pauling's relation from the electronegativities. The tetrachloride of titanium, the only Group IVA compound investigated, does not obey the rule.

According to the Placzek theory<sup>1</sup> an important quantity determining the intensity of a vibrational Raman line is the derived polarizability  $\alpha'$  which is defined as  $(\partial\alpha/\partial q)_0$ , where  $\alpha$  is the polarizability of the molecule,  $q$  is the normal co-ordinate of the vibration and the subscript denotes that the value is taken at the equilibrium configuration. The view has been expressed by Placzek<sup>2</sup> and others that when the chemical bonds affected by the vibration are of the covalent type, i.e. when the electrons involved are shared by the nuclei,  $\alpha'$  (and consequently the Raman intensity) will be greater than when the bonds are of the ionic type, i.e. when the electrons belong entirely to their respective nuclei. Placzek goes so far as to say<sup>3</sup> that in the ionic case the polarizability will be independent of internuclear distance, so that no Raman effect will appear. The latter conclusion cannot be strictly true, however: the polarizability of an assemblage of ions will not be merely the sum of the polarizabilities of the separate ions, since the magnitude of the dipole produced in any particular ion by an external field will be modified by the fields of the dipoles produced in the other ions. Since this mutual effect depends on the distances between the ions, the polarizability of the whole assemblage will not be strictly independent of these distances, i.e. the derived polarizability and hence the intensity of the vibrational Raman effect will not be expected completely to vanish.

The observations of Krishnamurti<sup>4</sup> have been taken as providing qualitative support for the general expectation that covalently linked molecules will give strong Raman spectra and ionically linked molecules weak or unobservable Raman spectra.

Apparently only one quantitative investigation has hitherto been undertaken, in which Hansen-Damaschun<sup>5</sup> measured the relative intensities of certain Raman lines of a number of compounds using the

<sup>1</sup> Placzek, *Handbuch d. Radiologie*, 1934, 6, (ii), 205.

<sup>2</sup> Placzek, *loc. cit.*<sup>1</sup>, p. 366.

<sup>3</sup> Placzek, *Leipziger Vorträge*, 1931, p. 92.

<sup>4</sup> Krishnamurti, *Indian J. Physics*, 1930, 5, 113.

<sup>5</sup> Hansen-Damaschun, *Z. physik. Chem. B*, 1933, 22, 97.



conventional Wood's tube arrangement\* and deduced therefrom the relative mean-value invariant  $a$  of  $\alpha'$  (see below). The relative degrees of covalent character of the bonds involved were then calculated on the assumption of simple proportionality to  $a$ .

This work of Hansen-Damaschun is open to several criticisms. In the first place the use of a Wood's tube, for which there is no well-defined relation between directions of illumination and observation, destroys the significance of measured relative intensities, except when the molecular species and vibrational modes to be compared are specially selected. Secondly, it follows from the Placzek theory that certain not inconsiderable factors, omitted by Hansen-Damaschun, should be taken into account in deducing the value of  $a$  from the observed intensity. Lastly, it appears desirable to investigate the validity of the assumption that  $a$  is a direct measure of degree of covalent character of chemical binding.

In the present paper the principles of the determination of relative  $a$  values from observed relative Raman intensities are examined on the basis of the Placzek theory; an account is then given of determinations on a number of Group IV tetrahalides; and finally the relation of  $a$  to bond character is discussed. The assumption of Hansen-Damaschun, that the degree of covalent character is simply proportional to  $a$ , is not borne out by the results; and an alternative approximate empirical regularity is put forward.

**Raman Effect Intensity and Derived Polarizability.**—In this section is given a brief derivation, based on the Placzek theory, of the relation to be used for the calculation of relative  $a$  values from experimentally determined relative intensities of vibrational Raman lines. Let the irradiation be with light of frequency  $\nu_0$ , assumed to lie sufficiently far from any absorption region of the substance under investigation. Consider a Raman line arising from a transition in the molecule (considered for the present as unable to rotate) from an initial state characterized by a set of vibrational quantum numbers  $n$  to a final state characterized by a set  $m$ . Let the frequency of this line be designated by  $\nu_0 - \nu_{nm}$ . The intensity  $I_{nm}$  of this line can then be written

$$I_{nm} = KM(\nu_0 - \nu_{nm})^4 [P]_{nm}^2 \quad (1)$$

in which  $K$  is a constant,  $M$  is the molar concentration of the scattering substance and the transition probability factor is given by

$$[P]_{nm} = \int \psi_n^* P \psi_m d\tau,$$

where  $P$  is the induced dipole moment vector,  $\psi_n$  and  $\psi_m$  are the time-independent portions of the vibrational wave functions for the initial and final states and the integral is to be extended over the whole of co-ordinate space.

In general the polarizability  $\alpha$  of the molecule is a (symmetrical) tensor of components

$$\begin{array}{ccc} \alpha_{xx} & \alpha_{xy} & \alpha_{xz} \\ \alpha_{yx} & \alpha_{yy} & \alpha_{yz} \\ \alpha_{zx} & \alpha_{zy} & \alpha_{yz} \end{array}$$

with  $\alpha_{xy} = \alpha_{yx}$  etc., the subscripts referring to a co-ordinate system fixed in the molecule and in space. Application of an electric field whose strength has the components  $E_x$ ,  $E_y$  and  $E_z$  will produce in the molecule a dipole moment whose  $x$  component  $P_x$  is given by

$$P_x = E_x \alpha_{xx} + E_y \alpha_{xy} + E_z \alpha_{xz}.$$

Analogous expressions may be written for  $P_y$  and  $P_z$ . In the case of

\* Wood, *Physic. Rev.*, 1930, **36**, 1421.

incident light exciting the Raman line involving the transition  $n \rightarrow m$  the corresponding expression for  $[P_{xx}]_{nm}$  is

$$[P_{xx}]_{nm} = E_x[\alpha_{xx}]_{nm} + E_y[\alpha_{xy}]_{nm} + E_z[\alpha_{xz}]_{nm}, \quad (2)$$

where  $E_x$ ,  $E_y$ , and  $E_z$  are now the amplitudes of the electric vector of the incident light and

$$[\alpha_{xx}]_{nm} = \int \psi_n^* \alpha_{xx} \psi_m d\tau, \text{ etc.}$$

In general each of the tensor components  $\alpha_{xx}$  etc. changes when the nuclei are displaced from their equilibrium positions and, following Placzek, we may write

$$\alpha_{xx} = (\alpha_{xx})_0 + \sum_i \left( \frac{\partial \alpha_{xx}}{\partial q_i} \right)_0 q_i + \dots$$

in which  $q_i$  is a normal co-ordinate of displacement and the zero subscripts refer to the equilibrium position. Neglecting higher powers of the small displacements  $q_i$ , we obtain

$$[\alpha_{xx}]_{nm} = (\alpha_{xx})_0 \int \psi_n^* \psi_m d\tau + \sum_i \left( \frac{\partial \alpha_{xx}}{\partial q_i} \right)_0 \int \psi_n^* q_i \psi_m d\tau. \quad (3)$$

in which  $\psi_n$  and  $\psi_m$  are functions of all the  $q_i$ . The first term on the right-hand side obviously vanishes because of the mutual orthogonality of  $\psi_n$  and  $\psi_m$ .

Let the initial and final states be characterized respectively by the sets of vibrational quantum numbers  $n_1, n_2, \dots, n_i, \dots$  and  $m_1, m_2, \dots, m_i, \dots$ . Then assuming the vibrations to be simple harmonic, we can write

$$\psi_n = \psi_{n_1}(q_1) \psi_{n_2}(q_2) \dots \psi_{n_i}(q_i) \dots,$$

and

$$\psi_m = \psi_{m_1}(q_1) \psi_{m_2}(q_2) \dots \psi_{m_i}(q_i) \dots$$

Inserting these values of  $\psi_n$  and  $\psi_m$  into the eqn. (3) and bearing in mind that all integrals of the type  $\int \psi_{n_j}(q_j) \psi_{m_j}(q_j) dq_j$  vanish unless  $n_j = m_j$ ,

and that all those of the type  $\int \psi_{n_i}(q_i) q_i \psi_{m_i}(q_i) dq_i$  vanish unless  $m_i = n_i \pm 1$ , it follows that  $[\alpha_{xx}]_{nm}$  vanishes unless for only one normal vibration the quantum number changes by unity, i.e. only fundamentals are allowed in the Raman effect.

Consider now the Stokes Raman line corresponding to the fundamental of the  $k$ th normal mode of vibration, i.e. to the transition for which  $n_k = m_k - 1$  and  $n = m$  for all other modes. We obtain in this case,

$$[\alpha_{xx}]_{n_k m_k} = \left( \frac{\partial \alpha_{xx}}{\partial q_k} \right)_0 \int \psi_{n_k}(q_k) q_k \psi_{m_k}(q_k) dq_k \quad (4)$$

Omitting the subscripts  $k$  for simplicity, writing  $\alpha'_{xx}$  for the component  $(\partial \alpha_{xx} / \partial q_k)_0$  of the derived tensor  $\alpha'$ , and inserting the known value of the integral,<sup>7</sup> eqn. (4) becomes

$$[\alpha_{xx}]_{nm} = \alpha'_{xx} \sqrt{\frac{(n+1)\hbar}{8\pi^2\mu\nu}},$$

where  $\mu$  and  $\nu$  are respectively the reduced mass and the fundamental frequency of the  $k$ th vibrational mode.

Using the above value of  $[\alpha_{xx}]_{nm}$  and the analogous values of the other components, eqn. (2) may be written

$$[P_{xx}]_{nm} = \sqrt{\frac{(n+1)\hbar}{8\pi^2\mu\nu}} \{ E_x \alpha'_{xx} + E_y \alpha'_{xy} + E_z \alpha'_{xz} \} \quad (5)$$

<sup>7</sup> See, e.g., Pauling and Wilson, *Introduction to Quantum Mechanics* (McGraw Hill Book Co., New York, 1935), p. 82.

Thus far we have considered the molecule as unable to rotate, the co-ordinate system  $x, y, z$  being fixed relative to the molecule (as well as in space). At ordinary temperatures, however, rotational states will be strongly excited. We therefore go over to a co-ordinate system  $X, Y, Z$  fixed in space. The appropriate value of the intensity of Raman scattering is then obtained by averaging over all orientations of the molecule. For this purpose it is convenient to introduce two quantities associated with the derived tensor  $\alpha'$ , viz. the mean value  $a$  and the anisotropy  $\gamma$ :

$$a = \frac{1}{3}(\alpha'_{xx} + \alpha'_{yy} + \alpha'_{zz})$$

$$\gamma^2 = \frac{1}{2} \left\{ \sum (\alpha'_{xx} - \alpha'_{yy})^2 + 6(\alpha'_{xy}^2 + \alpha'_{yz}^2 + \alpha'_{zx}^2) \right\}.$$

Both  $a$  and  $\gamma$  are invariants of the derived tensor, i.e. their values are independent of the orientation of the molecule relative to the co-ordinate system  $X, Y, Z$ . For the averaging of scattered intensity over all orientations of the molecule, we require the corresponding average values of the squares of the components of the derived tensor relative to the co-ordinate system fixed in space. These may be shown to be given by:

$$\overline{(\alpha'_{xx})^2} = \overline{(\alpha'_{yy})^2} = \overline{(\alpha'_{zz})^2} = \frac{1}{45}(45a^2 + 4\gamma^2), \quad . \quad . \quad (6)$$

$$\overline{(\alpha'_{xy})^2} = \overline{(\alpha'_{yz})^2} = \overline{(\alpha'_{zx})^2} = \frac{1}{15}\gamma^2 \quad . \quad . \quad . \quad (7)$$

Consider now irradiation along the positive  $Z$  axis by natural light. In this case we have  $E_x = E_y = E$  and  $E_z = 0$ . The intensity and state of polarization of the scattering depend on the average values of the squares of the components of  $[P]_{nm}$  which, by (5), (6) and (7) are

$$[P_x]_{nm}^2 = \frac{(n+1)\hbar}{8\pi^2\mu\nu} \left\{ E^2 \overline{(\alpha'_{xx})^2} + E^2 \overline{(\alpha'_{xy})^2} \right\} = \frac{(n+1)\hbar E^2}{8\pi^2\mu\nu} \frac{1}{45} (45a^2 + 7\gamma^2),$$

$$[P_y]_{nm}^2 = \frac{(n+1)\hbar}{8\pi^2\mu\nu} \left\{ E^2 \overline{(\alpha'_{yy})^2} + E^2 \overline{(\alpha'_{xy})^2} \right\} = \frac{(n+1)\hbar E^2}{8\pi^2\mu\nu} \frac{1}{45} (45a^2 + 7\gamma^2),$$

$$[P_z]_{nm}^2 = \frac{(n+1)\hbar}{8\pi^2\mu\nu} \left\{ E^2 \overline{(\alpha'_{zx})^2} + E^2 \overline{(\alpha'_{zy})^2} \right\} = \frac{(n+1)\hbar E^2}{8\pi^2\mu\nu} \frac{1}{15} \cdot 2\gamma^2.$$

Hence we may deduce at once an expression for the degree of depolarization  $\rho_n$  for scattering at right-angles to the direction of irradiation—a quantity to which reference will be made again below. Taking the direction of scattering as along the  $X$  axis, the effective components of  $[P]_{nm}$  are  $[P_z]_{nm}$  and  $[P_y]_{nm}$ . Hence  $\rho_n$ , defined as the ratio of the intensities of the corresponding polarized components of the scattered light, is given by

$$\rho_n = \frac{6\gamma^2}{45a^2 + 7\gamma^2}. \quad . \quad . \quad . \quad (8)$$

The irradiation being still with natural light and along the positive  $Z$  axis, consider the intensity of scattering in any selected direction making the angle  $\theta$  with the direction of irradiation. We resolve the components  $[P_x]_{nm}$ ,  $[P_y]_{nm}$ ,  $[P_z]_{nm}$  at right-angles to the direction of scattering and add the mean square contributions, thus obtaining the following effective value of  $[P]_{nm}^2$ :

$$\frac{(n+1)\hbar E^2}{8\pi^2\mu\nu} \frac{1}{45} \left\{ (45a^2 + 7\gamma^2)(1 + \cos^2 \theta) + 6\gamma^2 \sin^2 \theta \right\}. \quad . \quad (9)$$

At ordinary temperatures the majority of the scattering molecules will be in the lowest vibrational level ( $n = 0$ ), but some will be in higher vibrational levels for which the probability of the Raman transition, being proportional to  $n + 1$ , is greater. This must be taken into account in calculating the intensity of scattering. Let  $f_0, f_1, \dots, f_r, \dots$  be the fractions of the molecules with  $n = 0, 1, \dots, r, \dots$ . Then the

intensity will be proportional to the total number of molecules present (i.e. to the molar concentration  $M$ ) and also to  $\sum_r f_r(r+1)$ . Since

$$f_r = e^{-(r+\frac{1}{2})h\nu/kT} / \sum_r e^{-(r+\frac{1}{2})h\nu/kT}$$

it may easily be shown that

$$\sum_r f_r(r+1) = [1 - e^{-h\nu/kT}]^{-1} \quad (10)$$

From (1), (9) and (10) it follows that the intensity  $I_\theta$  of Raman scattering in the direction  $\theta$  will be

$$I_\theta = \frac{K'I_0 M(\nu_0 - \nu)^4}{\mu\nu(1 - e^{-h\nu/kT})} \left\{ (45a^2 + 7\gamma^2)(1 + \cos^2 \theta) + 6\gamma^2 \sin^2 \theta \right\}, \quad (11)$$

where  $I_0$  (proportional to  $E^2$ ) is the incident light intensity and  $K'$  is a universal constant.

When the convenient Wood's tube technique is used (as by Hansen-Damaschun and in the present work) there is no defined angle  $\theta$  between the directions of irradiation and scattering. If we consider only light which is "observed" by the spectrograph, then for each volume element of the scattering liquid there is a range of  $\theta$  values; and for each  $\theta$  there is a range of directions of irradiation, summation over which gives a certain effective intensity of irradiation. Summation over the volume of the Wood's tube will then give a certain effective intensity of irradiation  $(I_0)_\theta$  for each value of  $\theta$ . The observed intensity is obtained by integrating over the whole range of  $\theta$ .

For the determination of relative intensities the device adopted in the present work is to use a mixture containing the two substances to be compared in known molar ratio, so that in the integration  $(I_0)_\theta$  is identical for both. Using subscripts 1 and 2 to denote the two substances, the expression for the observed intensity ratio is then

$$\frac{I_2}{I_1} = \frac{M_2}{M_1} \left( \frac{\nu_0 - \nu_2}{\nu_0 - \nu_1} \right)^4 \frac{\mu_1 \nu_1}{\mu_2 \nu_2} \frac{1 - e^{-h\nu_1/kT}}{1 - e^{-h\nu_2/kT}} \frac{\int (I_0)_\theta ((45a_2^2 + 7\gamma_2^2)(1 + \cos^2 \theta) + 6\gamma_2^2 \sin^2 \theta) d\theta}{\int (I_0)_\theta ((45a_1^2 + 7\gamma_1^2)(1 + \cos^2 \theta) + 6\gamma_1^2 \sin^2 \theta) d\theta} \quad (12)$$

Since the dependence of  $(I_0)_\theta$  upon  $\theta$  is not known, the two integrals cannot be evaluated and the result can only have meaning provided that cancellation occurs. This will be so if  $\gamma_1^2/a_1^2 = \gamma_2^2/a_2^2$ . Reference to (8) shows that this is equivalent to the condition that  $(\rho_n)_1 = (\rho_n)_2$ .

An important special case in which this condition is fulfilled is when  $(\rho_n)_1 = 0 = (\rho_n)_2$ . This is in fact realized if, as in the present work, we select for investigation the symmetrical breathing mode of vibration of spherically symmetrical molecules such as the Group IV tetrahalides. In this case  $\gamma_1 = 0 = \gamma_2$  and the value of the observed intensity ratio (12) reduces to

$$\frac{I_2}{I_1} = \frac{M_2}{M_1} \left( \frac{\nu_0 - \nu_2}{\nu_0 - \nu_1} \right)^4 \frac{\mu_1 \nu_1}{\mu_2 \nu_2} \frac{1 - e^{-h\nu_1/kT}}{1 - e^{-h\nu_2/kT}} \left( \frac{a_2}{a_1} \right)^2 \quad (13)$$

This is the expression which is used below to calculate relative mean values  $a$  of derived polarizabilities from experimentally determined relative Raman intensities.

It may be noted that, with the above special choice of molecular and vibrational symmetry, the state of polarization is identical for both the lines under investigation, so that no "apparatus correction" is required on this account in the measurement of their relative intensities.

### Experimental

The spectrograph used was a Hilger constant-deviation glass instrument fitted with a special F/6 camera. The linear dispersion in the region of the Raman lines excited by Hg 4358 Å was approximately 63 Å/mm. Special care was taken, by the interposition of suitable screens, etc., to prevent light reflected inside the instrument from reaching the photographic plate.

The liquid mixture under investigation was contained in a glass Raman vessel of the Wood's tube type (capacity about 60 ml.) fitted with a glass jacket through which a suitable filter liquid could be passed continuously during an experiment, thus maintaining a constant temperature. The actual temperature ranged from 20 to 25° C in different experiments. The exciting light source was a straight Hanovia 250-W mercury arc run off the A.C. mains. Source and Raman tube were surrounded by an elliptical metal reflector, the whole assembly being mounted on adjustable legs to enable the Raman tube to be carefully aimed relative to the spectrograph collimator. The window of the tube was placed directly in front of the spectrograph slit, suitable stops being interposed to prevent primary light from entering the instrument. The exposure times for the Raman spectra were from 5 to 10 min. The plates chosen were Ilford Press Ortho (Series II). A glycine developer was used under standardized conditions.

By means of a tungsten band lamp, supplied from the A.C. mains by a suitable transformer, a set of continuous spectra were photographed on each plate to serve as calibration marks. An image of the central portion of the tungsten band was produced on the spectrograph slit by means of two lenses arranged so that the light between them was parallel. The standard intensity marks were obtained by interposing successively into the parallel beam, six wire gauze screens whose transmissions (ranging from 10 to 60 %) had been previously determined under analogous conditions by the National Physical Laboratory. Up to four Raman spectra were photographed on each plate, the time of exposure being the same as for the standard continuous spectra. Thus reciprocity failure of the plate was avoided.

It may be noted that, since an A.C. mercury arc was used, the exciting light and consequently the Raman scattering were pulsating at 100 c./sec.: for the band lamp, on the other hand, this pulsation was relatively small. Reference to the data of Webb,<sup>8</sup> however, shows that this cannot give rise to any appreciable "intermittency" error in the intensity measurements.

A Cambridge Instrument Company recording microphotometer was used to determine for each plate the characteristic curves at the wave-lengths  $\lambda_1$  and  $\lambda_2$  of the two Raman lines whose relative intensities were to be measured. The intensity scales of the two curves are not the same because of the wave-length dependence of the emission from the tungsten band lamp. In order to take this into account the optical temperature of the central portion of the band was determined (within  $\pm 5^\circ$  C) by means of an optical pyrometer of the disappearing-filament type using a selective filter ( $\lambda$  6600 Å). From this optical temperature the true temperature of the band was calculated from the Wien law, taking into account the transmission of the glass envelope of the lamp and the emissivity of tungsten at 6600 Å.<sup>9</sup> From the true temperature so obtained the ratio of the intensities of emission at  $\lambda_1$  and  $\lambda_2$  was computed from the Wien law, using the appropriate values of the emissivity of tungsten.<sup>9</sup> This ratio was duly taken into account in the relative intensity determinations.

It may be noted that, in the use of continua as standard marks for the measurement of the relative intensities of lines at different wave-lengths, correction should be made for the effect upon the densities of the former due to variation of the dispersion of the spectrograph with wave-length. However, in the present work the wave-length difference of the pairs of lines investigated was always so small that no appreciable correction was in fact necessary on this account.

The microphotometer traces of the Raman spectra excited by Hg 4358 Å showed that the lines to be measured were always superimposed upon a relatively weak continuous background. The peak intensity of each line was determined by subtracting the background intensity (as determined from the appropriate characteristic curve) from the similarly determined total intensity at the peak. Then by reversing the above procedure the ordinate of the photometer trace corresponding to half the line peak intensity above the background

<sup>8</sup> Webb, *J. Opt. Soc. Amer.*, 1933, **23**, 157 and 316.

<sup>9</sup> Forsythe and Adams, *ibid.*, 1945, **35**, 108.

was calculated, and the width of the line trace at this ordinate measured with a travelling microscope. The product of line peak intensity and half-intensity width was taken as a measure of line intensity.

The Raman lines chosen were those corresponding to the symmetrical breathing modes  $\nu_1$  of the tetrahalides. The intensities were all measured relative to carbon tetrachloride. The method adopted in all cases except that of germanium tetrachloride, to which special reference will be made below, was to prepare mixtures with carbon tetrachloride in known molar ratios, so that the Raman lines to be compared were excited under identical conditions.

A.R.  $\text{CCl}_4$  was fractionally distilled for use. The other compounds investigated were  $\text{SiCl}_4$ ,  $\text{GeCl}_4$ ,  $\text{SnCl}_4$ ,  $\text{CBr}_4$  and  $\text{TiCl}_4$ . All the liquids were fractionally distilled: the  $\text{CBr}_4$  was recrystallized from ethyl alcohol and sublimed *in vacuo* before use. Suitable precautions for the exclusion of moisture were taken in preparing the mixtures involving the tetrachlorides of Si, Ge, Sn and Ti. Preliminary tests were carried out to discover in each case the approximate molar ratio which would give densities of the two  $\nu_1$  lines on the photographic plate favourable for the photometric measurements. Then mixtures of suitable molar ratios were prepared by weighing. All the mixtures were quite clear and colourless. At least two different molar ratios were investigated for each compound (except  $\text{TiCl}_4$ ). In no case was there any significant difference between the measured values of  $(I_2/I_1)(M_1/M_2)$  at different molar ratios.

In the particular case of  $\text{GeCl}_4$  the  $\nu_2$  line coincides approximately with the  $\nu_1$  line of  $\text{CCl}_4$ , and so the desired relative intensity of the  $\nu_1$  line of  $\text{GeCl}_4$  could not be determined, as for the other compounds, by direct comparison. Its intensity relative to the corresponding line of  $\text{CBr}_4$  was therefore measured, the intensity of the  $\text{CBr}_4$  line relative to the  $\nu_1$  line of  $\text{CCl}_4$  being known from another determination. Preliminary tests indicated that the solubility of  $\text{CBr}_4$  in  $\text{GeCl}_4$  might not be sufficient to enable binary mixtures to be prepared with molar ratios that would give suitable line densities. Accordingly some  $\text{CCl}_4$  was mixed with the  $\text{GeCl}_4$  before the  $\text{CBr}_4$  was dissolved in it. In this way mixtures were prepared containing  $\text{GeCl}_4$  and  $\text{CBr}_4$  in suitable known molar ratios.

In order to absorb ultra-violet and so prevent possible slight fluorescence due to traces of impurity in the substances under investigation, an acidified ferric alum filter solution was passed continuously through the cooling jacket of the Raman tube during the exposures. In the experiments involving  $\text{CBr}_4$ , however, it was necessary to take special measures to prevent the liberation of free bromine by photochemical decomposition. The cooling and filter liquid here used was a solution of sodium nitrite (750 g./l.). Even with this filter a small amount of photochemical decomposition was inevitable. Preliminary tests were accordingly made with  $\text{CBr}_4$ — $\text{CCl}_4$  mixtures to which known small amounts of allyl alcohol had been added. These mixtures were irradiated under the same conditions as for the actual Raman exposures, and from the time required for the appearance of free bromine it was concluded that the percentage of  $\text{CBr}_4$  photochemically decomposed in the course of an actual experiment would be only a small fraction of 1 % and therefore quite negligible. For the Raman exposures from which the relative intensity determinations were made, two drops of allyl alcohol were added to each of the mixtures in order to remove the small amount of bromine formed.

The results obtained may be exemplified by giving the experimentally determined values of  $(I_2/I_1)(M_1/M_2)$  for the mixtures of  $\text{GeCl}_4$  (subscript 2) and  $\text{CBr}_4$  (subscript 1). Two different molar ratios were investigated. At the first ( $M_1/M_2 = 0.526$ ) the following 10 values were obtained from spectra upon 3 different plates: 0.772, 0.758, 0.815, 0.887, 0.894, 0.857, 0.843, 0.806, 0.890, 0.937. The mean of these is 0.846. The greatest individual deviation from the mean is about 11 % and the average absolute deviation is about 5½ %. At the other molar ratio ( $M_1/M_2 = 1.16$ ) the following 14 values were obtained from spectra upon 4 plates: 0.796, 0.948, 0.910, 0.951, 0.811, 0.796, 0.792, 0.799, 0.836, 0.880, 0.929, 0.793, 0.744, 0.774. The mean is here 0.840, the maximum individual deviation being 13 % and the average absolute deviation 7 %. There is satisfactory agreement between the two mean values at the two different molar ratios. The grand mean of all the determinations is 0.843. The limits of experimental error in this value are not easy to assess, but may perhaps not unreasonably be taken as  $\pm 5$  %.

For  $\text{CBr}_4$  (subscript 2) relative to  $\text{CCl}_4$  (subscript 1 here and subsequently) the mean value of  $(I_2/I_1)(M_1/M_2)$  from determinations at two molar ratios ( $M_1/M_2 = 5.42$  and 8.21) was 3.80. Combination of this result with that given

above for  $\text{GeCl}_4$  relative to  $\text{CBr}_4$  gives the value 3.20 for  $\text{GeCl}_4$  relative to the chosen standard  $\text{CCl}_4$ .

For  $\text{SiCl}_4$  relative to  $\text{CCl}_4$  the mean of determinations at two molar ratios ( $M_1/M_2 = 1.01$  and  $2.00$ ) was 1.04. For  $\text{SnCl}_4$  the mean of determinations at three molar ratios ( $M_1/M_2 = 3.04, 5.55$  and  $7.24$ ) was 4.76. Lastly, for  $\text{TiCl}_4$  the mean of determinations at  $M_1/M_2 = 5.84$  was 7.48. The  $\nu_1$  line of  $\text{CCl}_4$  taken as reference standard is well known to be a strong one; the corresponding line for  $\text{TiCl}_4$  is very strong indeed.

In connection with the probable accuracy of the above results it is to be borne in mind that we have taken the product of line peak intensity and half-intensity width as a measure of line intensity. This is admittedly an approximation. Ideally it would be preferable to take the integrated area on an energy-wave-length curve. In fact the photometer trace does not provide such a curve, on account mainly of the characteristics of the photographic plate. Nor is it feasible in practice to construct from the photometer trace an intensity-wave-length curve from which the desired area can be obtained with accuracy. The compromise adopted should, however, give reasonably good results in the comparison of the intensities of lines of similar profile, such as are here involved; but uncertainty is introduced when (as in general was the case) the lines are superimposed upon a continuous background which has a pronounced slope.

There is also a further circumstance that may detract to some extent from the quantitative significance of the measured intensity ratios. Only  $\nu_1$  lines were investigated for which, in the spectra of the mixtures, there was no fortuitous superposition of any other Raman line excited by  $\text{Hg } 4358 \text{ \AA}$ . As is well known, however, this strong exciting line is accompanied by a relatively feeble companion at  $4348 \text{ \AA}$  (and an even more feeble one at  $4340 \text{ \AA}$ ). The correspondingly weak Raman lines to which these must give rise are not ordinarily observed in photographic work; but with our mixtures they may in certain cases be fortuitously superimposed on one or other of the  $\nu_1$  lines excited by  $4358 \text{ \AA}$  and so have an effect on the measured intensity ratios. For instance, in a mixture of  $\text{SiCl}_4$  and  $\text{CCl}_4$  the  $\nu_1$  line of  $\text{SiCl}_4$  excited by  $4358 \text{ \AA}$  may have a certain contribution from the approximate coincidence of the relatively weak  $\nu_1$  line of  $\text{CCl}_4$  excited by  $4348 \text{ \AA}$ . This would cause the measured relative intensity for  $\text{SiCl}_4$  to be somewhat too high. Also in a mixture of  $\text{CBr}_4$  and  $\text{CCl}_4$  there is an approximate coincidence of the relatively weak  $\nu_1$  line of  $\text{CCl}_4$  excited by  $4348 \text{ \AA}$  with the  $\nu_1$  line of  $\text{CBr}_4$  excited by  $4358 \text{ \AA}$ , and so a similar effect on the measured relative intensity may be present. The magnitude of this effect will in all cases vary with the molar ratio of the substances in the mixture; and since no appreciable difference was found in the measured values for different molar ratios, it was concluded that the effect was small, and no correction for it was applied. In principle, of course, this effect could be avoided by determining the relative intensities from successive irradiations of the single substances, instead of by using binary mixtures. But it was felt that the results obtained by the former method would be less reliable owing to the impossibility of reproducing exactly the same conditions of irradiation for the two substances to be compared. This identity of irradiation, essential to the measurement, is of course realized perfectly by the procedure actually adopted.

Altogether it is clear from what has been said above that the experimental intensity ratios cannot be very precise. The rounded values, relative to  $\text{CCl}_4$  as unity, are:  $\text{SiCl}_4$ , 1.04;  $\text{GeCl}_4$ , 3.2;  $\text{SnCl}_4$ , 4.8;  $\text{TiCl}_4$ , 7.5;  $\text{CBr}_4$ , 3.8.

Only one comparison with a result of other workers is apparently possible. Welsh, Crawford and Scott<sup>10</sup> have recently given the value 5.0 for  $\text{SnCl}_4$  with the estimated error limits  $\pm 5\%$ . The agreement with our result is seen to be satisfactory. The same workers also give the value 14 for  $\text{SnBr}_4$ , a compound that we have not yet investigated.

Using eqn. (13) the relative mean values ( $a_2/a_1 = a$ ) of the derived polarizabilities may be calculated from the measured values of  $(I_2/I_1)(M_1/M_2)$  just given. For  $\text{SnBr}_4$  the temperature  $T$  was taken as  $25^\circ \text{C}$ . The  $a$  values so obtained are:  $\text{CCl}_4$ , 1.00 (standard);  $\text{SiCl}_4$ , 0.96;  $\text{GeCl}_4$ , 1.6;  $\text{SnCl}_4$ , 1.9;  $\text{TiCl}_4$ , 2.4;  $\text{CBr}_4$ , 2.0;  $\text{SnBr}_4$ , 3.3. It may be noted that, since the calculation involves taking the square root, the limits of percentage error of the  $a$  values are smaller than for the relative intensities.

<sup>10</sup> Welsh, Crawford and Scott, *J. Chem. Physics*, 1948, 16, 97.

### Discussion

Each of the values of  $a$  given above is the relative mean value of the derived polarizability of the molecule as a whole for the symmetrical breathing mode of nuclear displacement. If we regard the polarizability of each molecule as made up of four equal contributions from its four bonds, then it follows from the regular tetrahedral symmetry that the relative  $a$  values apply equally well to the individual bonds.

A glance at the  $a$  values shows that they are quite out of harmony with the assumption made by Hansen-Damaschun (see above) that  $a$  is directly proportional to the degree of covalent character of the bond. There is plenty of evidence that the degree of covalency of the bonds in  $\text{CCl}_4$  is greater than that of those in  $\text{SnCl}_4$ : yet the  $a$  value is much greater for the latter compound than for the former.

If we exclude the tetrachloride of titanium (which alone of the compounds investigated belongs to Group IVA and will be considered below) and confine ourselves to the tetrahalides of the typical Group IV elements carbon and silicon and of the Group IVB elements germanium and tin, it appears that the value of  $a$  for a compound  $\text{XY}_4$  depends mainly upon the position of X and Y in the periodic table. Thus with the single exception of  $\text{SiCl}_4$ , the value of  $a$  is always increased if either X or Y is replaced by an element of higher atomic number. In this connection it is interesting that also in the series  $\text{SF}_6$ ,  $\text{SeF}_6$ ,  $\text{TeF}_6$  it has been observed qualitatively<sup>11</sup> that the Raman effect intensity increases in the order given.

Nevertheless, it appears that the degree of covalent character of the bonding also plays a part. Thus for  $\text{SiCl}_4$  we may suppose that the increase of  $a$  to be expected from the replacement of carbon by silicon of larger atomic number is offset and, in fact, just outweighed by the decrease of  $a$  due to the smaller degree of covalent character of the Si—Cl bond. In order to deal with this sort of effect in a more quantitative manner, it is desirable to have some measure of degree of covalent character. Such a measure, at least approximate, has been suggested by Pauling.<sup>12</sup> From bond energy considerations he has ascribed to each element an electronegativity  $x$  and has proposed the empirical equation  $p = 100 e^{-\frac{1}{4}(x_X - x_Y)^2}$  for the percentage covalent character  $p$  of the bond X—Y. Using Pauling's electronegativity values, we hence calculate the following values of  $p$  for the bonds in the molecules under consideration:  $\text{CCl}_4$ , 94;  $\text{SiCl}_4$ , 70;  $\text{GeCl}_4$ , 65.5;  $\text{SnCl}_4$ , 65.5;  $\text{CBr}_4$ , 98;  $\text{SnBr}_4$ , 74. From the nature of their derivation these values will be expected to be only approximate and to refer to ordinary single bonds between the elements.

If the measured  $a$  values are plotted against these values of  $p$ , no sort of regularity is apparent: this is an expression of the invalidity of the Hansen-Damaschun assumption. In order to take account of the dependence of  $a$  upon the atomic numbers of the elements involved, the simplest course is to try putting  $a$  proportional to the sum of the atomic numbers  $Z_X$  and  $Z_Y$  for the compound  $\text{XY}_4$  and to ignore for the moment any influence of the percentage covalent character  $p$ . The constant of proportionality is of course fixed by making  $a$  equal to unity for  $\text{CCl}_4$ . The values of  $a$  for the other compounds calculated in this simple and obviously imperfect manner are plotted in Fig. 1 (points denoted by crosses) against the experimentally observed  $a$  values. The dotted line at  $45^\circ$  to the co-ordinate axes represents the locus of exact agreement between calculated and observed values. By contrast with a plot of observed  $a$  against  $p$ , a certain measure of regularity is apparent despite the neglect of any influence of bond character; thus indicating that the derived polarizability and hence the Raman intensity are to a large extent determined by atomic number.

<sup>11</sup> Yost, Steffens and Gross, *ibid.*, 1934, 2, 314.

<sup>12</sup> Pauling, *Nature of the Chemical Bond* (Cornell Univ. Press, 1940), p. 69.



An interesting result is obtained if, in order to take account in the simplest possible manner of the degree of covalent character of the bonds involved, we try putting  $a$  directly proportional, not only to  $Z_x + Z_y$ , but also to  $p$ . Again making  $a$  equal to unity for the reference compound  $\text{CCl}_4$ , the calculated values of  $a$  for the other compounds are as given in the following Table, in which for comparison the observed values are also included.

	$\text{CCl}_4$	$\text{SiCl}_4$	$\text{GeCl}_4$	$\text{SnCl}_4$	$\text{CBr}_4$	$\text{SnBr}_4$
$a_{\text{obs.}}$	1.00	0.96	1.6	1.9	2.0	3.3
$a_{\text{calc.}}$	(1.00)	1.0	1.5	2.0	1.9	2.9

The calculated values of  $a$  are plotted in the Fig. 1 (points in circles), the arrows indicating the effect of including the  $p$  factor. It is seen that the empirical relation

$$a = Cp(Z_x + Z_y) \quad (14)$$

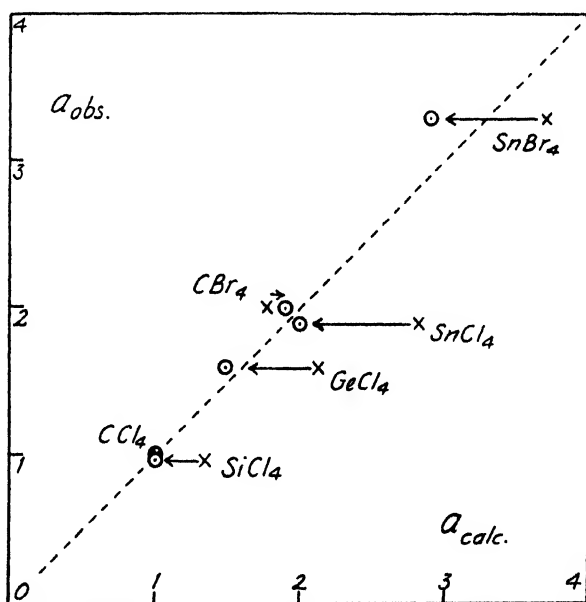


FIG. 1.

in which  $C$  is a constant, gives a remarkably good general account of the experimental observations. The rule is a very simple one and probably only approximate; but the number and accuracy of the data do not appear to justify elaborations. The agreement is least satisfactory for  $\text{SnBr}_4$ : the value of  $a_{\text{obs.}}$  for this compound was not determined in the present work, but is taken from Welsh, Crawford and Scott (see above).

The rule obviously cannot be extended to the limiting case of a hypothetical  $\text{XY}_4$  molecule with purely ionic bonds ( $p = 0$ ). For such a molecule the rule would give  $a = 0$  and zero Raman intensity, which is not in accordance with the conclusion reached in the opening paragraph of this paper.

The theoretical basis of our empirical rule remains obscure. The tendency of the derived polarizability to increase with increase of the

atomic number of the central atom X might be thought to be connected with back-co-ordination from the halogen atom and consequent partial double-bond character of the linkage. The shortening of the bond length in such compounds as  $\text{SiCl}_4$ , as compared with the sum of the single-bond atomic radii, is taken by Pauling<sup>13</sup> as evidence for this. But such back-co-ordination would not be expected with carbon as central atom in  $\text{CBr}_4$ , nor is there evidence of bond-shortening in this case. (For electron diffraction data on  $\text{CBr}_4$  vapour, see Wierl.<sup>14</sup>) Yet the replacement of Cl by Br in  $\text{CCl}_4$  produces a very marked increase in Raman intensity and derived polarizability.

Another conceivable explanation of the observed variation of the experimentally determined  $a$  values from molecule to molecule might be the inapplicability of the Placzek theory, upon which their derivation from the observed relative intensities is based. It is a condition for the validity of the theory that the frequency of the exciting radiation shall lie sufficiently far from any region of absorption of the substance concerned. It might therefore be thought that the increase of intensity in passing, say, from  $\text{CCl}_4$  to  $\text{CBr}_4$  or  $\text{SnCl}_4$  could be due to a shift in the ultra-violet absorption region towards the blue line of mercury which has been used for excitation in the present work. The existence of such a disturbing effect could be detected experimentally by determining the relative Raman intensities as excited by lines of other frequencies, or alternatively by investigating the relative intensities of the Stokes and anti-Stokes lines of the individual compounds excited by 4358 Å. As far as  $\text{CCl}_4$  is concerned the evidence<sup>15</sup> indicates that the Placzek theory is obeyed in the visible region. Published data for the other compounds are lacking, but preliminary measurements by the present authors<sup>16</sup> on the Stokes/anti-Stokes intensity ratios for the  $\nu_1$  lines of  $\text{CCl}_4$ ,  $\text{SiCl}_4$  and  $\text{SnCl}_4$  excited by 4358 Å indicate that the Placzek theory is obeyed for the last two compounds as well as for the first.

The case of  $\text{TiCl}_4$  has so far been excluded from the discussion. The experimental value for this compound,  $a_{\text{obs.}} = 2.4$ , shows no agreement with the value,  $a_{\text{calc.}} = 1.1$ , obtained from the empirical rule that has been seen to apply to the other compounds. This is probably due to the fact that in all the tetrahalides studied (with the exception of  $\text{TiCl}_4$ ) the central atoms belong to Group IVB and in their normal state have the arrangement  $s^2p^2$  of valency electrons; whereas Ti, the sole member of Group IVA that we have studied, has the arrangement  $d^2s^2$ . The type of hybridization for  $\text{TiCl}_4$  will therefore be expected to be different from the  $sp^3$  type common to all the other compounds, and this may well explain the failure of  $\text{TiCl}_4$  to conform to the rule which the others follow.

The authors wish to express their thanks to Mr. K. H. Jones and Mr. D. J. Perkins of Jesus College, Oxford, for their assistance in carrying out some of the intensity measurements, and to Messrs. Johnson and Matthey and Co. Ltd. for the supply of specially prepared samples of pure  $\text{TiCl}_4$  and  $\text{GeCl}_4$ . They are also very grateful to Prof. Pearse for permission to make use of the recording microphotometer at the Imperial College of Science and Technology, London.

*Inorganic Chemistry Laboratory,  
Oxford.*

<sup>13</sup> Pauling, *op. cit.*<sup>12</sup>, p. 229.

<sup>15</sup> See Placzek, *loc. cit.*<sup>1</sup> p. 369.

<sup>16</sup> Woodward and Long (unpublished work using a recording photoelectric Raman spectrometer).

<sup>14</sup> Wierl, *Ann. Physik*, 1931, 8, 521.

# PHASE RELATIONSHIPS IN POLYMER SOLUTIONS

BY H. TOMPA

Received 12th July, 1949

The existing statistical theories of polymer solutions are applied to the elucidation of the phase relationships of three component systems with at least one polymer component.

**1. Introduction.**—A great amount of experimental work has been published on the precipitation and fractionation of high polymeric substances but much less work has been done on the theoretical investigation of their phase relationships. Brønsted<sup>1</sup> has considered the solubility of polymers, but he only took energies of interaction into consideration, neglecting entropy effects, and Schulz<sup>2</sup> has discussed his experimental data on the same lines.

The phase relationships of any number of components can be deduced if an analytical expression for the free energy of mixing is available. Such expressions have been derived for solutions of high polymers by several authors, notably Flory,<sup>3</sup> Huggins<sup>4</sup> and Guggenheim<sup>5</sup>; they all use the methods of statistical mechanics and base the derivation on the lattice model of a liquid. The expressions derived by Guggenheim are the most comprehensive; it has been shown by Guggenheim<sup>5,6</sup> that his expressions reduce to those of Flory for the case of binary mixtures if the co-ordination number of the lattice is allowed to approach infinity, and also under certain less stringent conditions, while Huggins' formula is formally identical with Flory's, but the interaction constant (see eqn. (2) later) denotes different quantities in the two cases.

Flory<sup>7</sup> has made a study, based on his expression for the free energy of mixing, of the separation of a solution of high polymers into two phases; the method is only applicable if both phases are dilute solutions. Scott<sup>8</sup> has treated the system solvent + non-solvent + polymer with the assumption that a mixture of liquids can be considered as equivalent to a single liquid and has obtained valuable qualitative results. Gee<sup>9</sup> has considered several aspects of the phase relationships of polymers.

It is the purpose of this paper to derive the phase relationships of systems of three components, whose free energy of mixing is given by Flory's or Huggins' formulae; it is planned to extend the treatment to systems of four components later.

**2. Systems of Three Components: Analytical Treatment.**—Before considering in detail the compositions of co-existing phases, it is useful to consider under what conditions critical phenomena can appear. The general treatment of this problem is essentially due to Gibbs; we

<sup>1</sup> Brønsted, *C. R. Lab. Carlsberg, Ser. chim.*, 1938, **22**, 99.

<sup>2</sup> Schulz, *Z. physik. Chem. B*, 1940, **46**, 137.

<sup>3</sup> Flory, *J. Chem. Physics*, 1941, **9**, 660; 1942, **10**, 51.

<sup>4</sup> Huggins, *ibid.*, 1941, **9**, 440; *Ann N.Y. Acad. Sci.*, 1942, **43**, 1.

<sup>5</sup> Guggenheim, *Proc. Roy. Soc. A*, 1944, **183**, 203, 213.

<sup>6</sup> Guggenheim, *Trans. Faraday Soc.*, 1948, **44**, 1007.

<sup>7</sup> Flory, *J. Chem. Physics*, 1944, **12**, 425.

<sup>8</sup> Scott, *ibid.*, 1945, **13**, 178.

<sup>9</sup> Gee, *Trans. Faraday Soc.*, 1944, **40**, 468; *Quart. Rev.*, 1947, **1**, 265.

shall recapitulate the beautiful manner in which it has been applied by van der Waals<sup>10</sup> to divariant systems of two components. Shreinemakers<sup>11</sup> has extended the treatment to divariant systems of three components, i.e. systems at constant temperature and pressure.

We plot concentrations in the usual triangular diagram and construct the "free energy surface" by plotting free energy  $G$  at right-angles to it. If the free energy surface is concave throughout, a mixture of any composition forms a single, homogeneous phase. If, however, there are vertical cross-sections with points of inflection, separation into two phases will occur, and the compositions of the co-existing phases are given by the points of contact of a plane of double contact. These points (and their projections on the concentration diagram) are called nodes, the line joining them a tie line and their locus the binodial. The space between the free energy surface and the ruled surface which is the locus of the tie lines is called a plait and van der Waals and Kohnstamm develop their treatment from a consideration of the geometrical properties of plaits. Phases with representative points inside the binodial are not stable, but there is a metastable region consisting of the points at which the free energy surface is still concave. The inner boundary of this region is given by

$$(\partial^2 G / \partial n_1^2) \cdot (\partial^2 G / \partial n_2^2) - (\partial^2 G / \partial n_1 \partial n_2) = 0 \quad (1)$$

if we use the numbers of molecules of any two components as concentration variables. This is the equation of a curve called the spinodial. As  $\partial G / \partial n_i = \mu_i$ , the chemical potential of kind  $i$ , this curve is the locus of the points at which the curves  $\mu_i = \text{const.}$  have common tangents.

Plaits terminate if successive tie lines decrease in length until two corresponding nodes coincide; these points are the plait points or critical points. As the spinodial lies wholly within the binodial, it must touch the binodial at these points. Moreover, a detailed geometrical consideration shows that the curves  $\mu_i = \text{const.}$  touch the spinodial there and have contact of the second order with each other.

If we now change one of the parameters of the system, say the temperature, continuously, the positions of the binodial, the spinodial and the critical point (if any) also change continuously. It is shown in the theory of plaits that at a certain temperature a small new binodial may form around one of the points of the spinodial. At first the new binodial lies wholly within the old one, but on further changing the temperature, it can project through the old binodial. The general features are shown in Fig. 1; corresponding nodes are lettered with the same letter. It has been shown by van der Waals and Kohnstamm that the corresponding nodes of points at which binodial and spinodial intersect, are cusps. The new binodial contains two critical points (points of contact of binodial and spinodial), one of which, C, lies first in the metastable and later in the stable region, while the binodial near the other, B, is always in the unstable region. For this reason the point at which the new binodial starts to form and at which two critical points may be regarded to coincide, is called a heterogeneous double plait point (HDPP). The points of intersection of the binodials, D' and D'', are corresponding nodes, and are also nodes of D'''; we thus have here three co-existing phases and mixtures whose compositions lie within the triangle D'D''D''' split into three phases—D'D''D''' is a three-phase region and the compositions of the co-existing phases are given by D', D'' and D'''.

The further development of the small binodial can take several different forms; for solutions of polymers A and C ultimately interchange their roles, A and B then contract into a HDPP and vanish, leaving the system with one critical point at C. At a HDPP the curves  $\mu_i = \text{const.}$  not

<sup>10</sup> Van der Waals and Kohnstamm, *Lehrbuch der Thermo- und Kalorik* (Leipzig, 1927).

<sup>11</sup> Schreinemakers, Vol. 3 of Roozeboom, *Die Heterogenen Gleichgewichte* (Braunschweig, 1911/1913).

only touch the spinodal, but have second order contact with it, and have third order contact with each other. For proofs of these statements and further details the reader must consult van der Waals and Kohnstamm, especially the second volume.

**3. The System Solvent + Non-solvent + Polymer.**—The treatment in this paper will be based on the Flory-Huggins expression for the free energy of mixing; for a multicomponent system this is (cf. eqn. 11<sup>1</sup> and (15) of ref. 7)

$$\Delta G/kT = \sum_i n_i \ln y_i + \alpha y_i(1 - y_i) \sum_i r_i n_i. \quad (2)$$

Here  $n_i$  denotes the number of molecules of kind  $i$ ,  $y_i$  the site fraction, defined by

$$y_i = r_i n_i / \sum_i r_i n_i,$$

and  $r_i$  the number of sites occupied by a molecule of kind  $i$ ;  $\alpha$  is the familiar interaction constant. The assumption is implicit in eqn. (2)

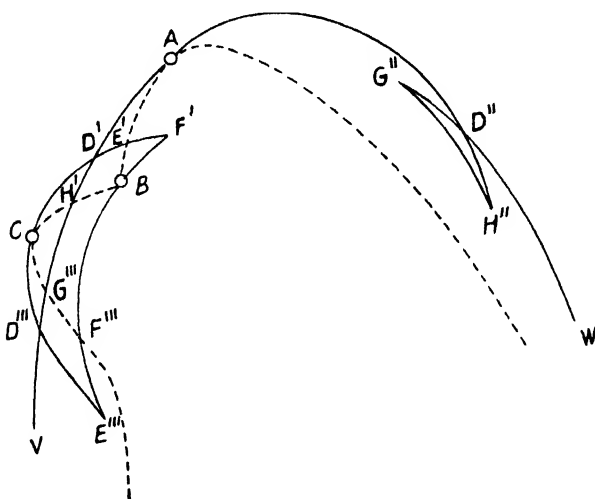


FIG. 1.—Ternary phase diagram with three critical points. VAH''G''W old binodal, E'''CF'BE''' new binodal, projecting through the old at D' and D''' --- spinodal, O critical points.

that the energies of interaction between molecules or segments of kind 1 and any other kind are equal, and that all other energies of interaction are zero. It can be shown that Guggenheim's expression for the free energy of mixing reduces to eqn. (2) for this case as well as for binary mixtures.

Consider a system of three components, a "non-solvent" (component 1,  $r_1 = 1$ ), a solvent (component 2,  $r_2 = 1$ ) and a polymer of definite chain length (component 3,  $r_3 = r$ ). Assume that there is no interaction between solvent and polymer,  $\alpha_{23} = 0$ , and that  $\alpha_{12} = \alpha_{13} = \alpha$ . Then the free energy of mixing is given by eqn. (2). Let the calculation be based on the free energy of mixing of "one mole of sites", so that  $\sum_i r_i n_i = 1$ , and denote this value of  $\Delta G/kT$  simply by  $G$ :

$$G = y_1 \ln y_1 + y_2 \ln y_2 + (1/r)y_3 \ln y_3 + \alpha y_1(1 - y_1). \quad (3)$$

We represent the composition of a system by taking  $y_1$ ,  $y_2$  and  $y_3$  as coordinates in a triangular diagram and use  $y_1$  and  $y_3$  as independent

variables. Then

$$(\partial G / \partial y_1)_{y_3} = \phi = \ln y_1 - \ln y_2 + \alpha(1 - 2y_1), \quad (4)$$

$$(\partial G / \partial y_3)_{y_1} = \psi = (1/r) \ln y_3 - \ln y_2 - (r - 1)/r,$$

and

$$\partial^2 G / \partial y_1^2 = 1/y_1 + 1/y_2 - 2\alpha, \quad (5)$$

$$\partial^2 G / \partial y_1 \partial y_3 = 1/y_2,$$

$$\partial^2 G / \partial^2 y_3 = 1/(ry_3) + 1/y_2.$$

The equation of the spinodal is

$$(\partial^2 G / \partial y_1^2) \cdot (\partial^2 G / \partial y_3^2) - (\partial^2 G / \partial y_1 \partial y_3)^2 = 0, \quad (6)$$

cf. eqn. (1), and reduces to

$$y_1 + (1 - 2\alpha y_1)[1 - y_1 + (r - 1)y_3] = 0. \quad (7)$$

By writing this in the form

$$(1 - 2\alpha y_1)[1 - 2\alpha(y_2 + ry_3)] = 1, \quad (8)$$

the spinodal is seen to be a hyperbola, whose asymptotes are

$$y_1 = 1/(2\alpha), \quad y_2 + ry_3 = 1/(2\alpha). \quad (9)$$

The spinodal is shown on the diagram for  $\alpha = 1.5$ ,  $r = 100$ , Fig. 4. At the critical point

$$(\partial y_1 / \partial y_3)_\phi = (\partial y_1 / \partial y_3)_{\psi}$$

(the suffix *sp* to mean along the spinodal); eliminating  $y_3$  from this equation and the equation of the spinodal gives

$$r(1 - 2\alpha y_1)^2(1 - 2\alpha y_1 + 2\alpha^2 y_1^2) - 4\alpha y_1^2(1 - \alpha y_1). \quad (10)$$

Eqn. (7) and (10) together determine the critical point; it is easily verified that the condition

$$(\partial^2 y_1 / \partial y_3^2)_\phi = (\partial^2 y_1 / \partial y_3^2)_\psi$$

is satisfied there.

For given  $r$ , the critical point for any  $\alpha$  can now be calculated. It is found that the lowest  $\alpha$  for which the critical point lies within the triangular diagram, and for which there is a two-phase region, is the value  $\alpha_c$ , given by eqn. (11) (cf. 5), at which components 1 and 3 mix critically, and which is for large  $r$  slightly larger than  $\frac{1}{2}$ :

$$\alpha_c = \frac{1}{2}(1 + r^{-\frac{1}{2}})^2. \quad (11)$$

For  $\alpha = 2$ , components 1 and 2 mix critically, and the two phase region cuts across the whole diagram. Now one of the roots of the quartic (10) is below  $1/(2\alpha)$  and the corresponding critical point lies outside the base triangle and has no physical meaning. For small  $r$ , and large  $r$  at  $\alpha$  well below two, eqn. (10) has one more real root, and there is therefore one critical point. For large  $r$  and  $\alpha = 2$  there are three critical points, corresponding to A, B and C in Fig. 1, so that for a certain  $\alpha$ , less than two, there must be a HDPP. This value of  $\alpha$  can be calculated from

$$(\partial^2 y_1 / \partial y_3^2)_\phi = (\partial^2 y_1 / \partial y_3^2)_{\psi},$$

or from

$$(\partial^2 y_1 / \partial y_3^2)_\phi = (\partial^2 y_1 / \partial y_3^2)_\psi,$$

by eliminating  $y_1$  and  $y_3$  from it with the help of eqn. (7) and (10). The resulting equation is

$$108(\alpha r)^3 - 4(99r + 43)(\alpha r)^2 - (4r^3 - 383r^2 - 298r - 91)(\alpha r) + 2(r - 2)^3(4r + 1) = 0, \quad (12)$$

and determines this  $\alpha$  as a function of  $r$ . For large  $r$  this equation has one negative (physically irrelevant) and two positive solutions, one just below two and one usually above two.

The picture we thus get for the position of the critical point and the binodal, for given not too small  $r$ , in systems with increasing  $\alpha$  is this:

at  $\alpha = \alpha_c$ , given by eqn. (11), the binodal consists of the critical point on the 1-3 side of the diagram. At larger  $\alpha$  the critical point is inside the triangle, and there is a finite two-phase region, Fig. 2a. When  $\alpha$  equals the smaller positive root of eqn. (12), a HDPP appears and at  $\alpha = 2$  the physically relevant part of the diagram is like Fig. 2b; there is a critical point at  $y_1 = y_2 = \frac{1}{2}$ ,  $y_3 = 0$ . It is to be noted that the binodal near this point and the three-phase region are extremely small. For  $\alpha > 2$  one of the critical points is outside the triangle, Fig. 2c, and when  $\alpha$  is greater than the larger root of eqn. (12) there is no critical point within the triangle, the remaining critical point having disappeared in another HDPP, Fig. 2d. For small values of  $r$ , eqn. (12) has no positive roots; the smallest  $r$  for which it has two (coincident) roots can be found by the usual methods of algebra. The resulting equation for  $r$  is of the

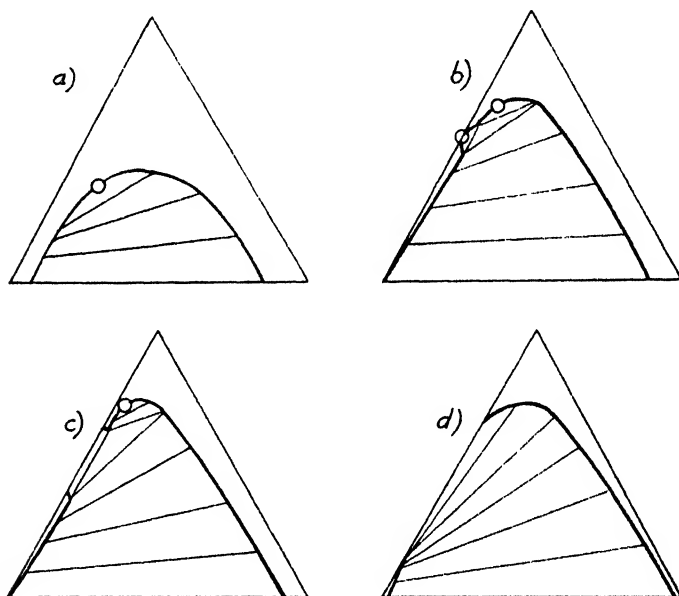


FIG. 2.—Ternary phase diagrams for increasing values of  $\alpha$ .  
— binodal. O critical points.

ninth degree, but has  $3r^2 - 47r + 1$  as a factor (see later), and this contains the only relevant root,  $r = 15.645$ ; the corresponding value of  $\alpha$  is 1.9838. A three-phase region appears only for  $r > 16$ , for smaller  $r$  diagrams of the type 2a go over continuously into type 2d without the appearance of a three-phase region. For  $r = 100$ , the HDPP are at  $\alpha = 1.9998$  and 2.8915.

The detailed shape of the binodal must be calculated from the conditions  $\mu_i' = \mu_i''$ . By differentiating  $\Delta G/kT$ , eqn. (2),

$$(r_1 = r_2 = 1, r_3 = r)$$

with respect to  $n_i$ , one gets

$$\begin{aligned} \mu_1/kT &= \ln y_1 + y_3(r-1)/r + \alpha(1-y_1)^2, \\ \mu_2/kT &= \ln y_2 + y_3(r-1)/r + \alpha y_1^2, \\ \mu_3/kT &= \ln y_3 - (1-y_3)(r-1) + r\alpha y_1^2, \end{aligned} \quad (13)$$

and by putting  $\mu_i' = \mu_i''$ , one obtains three equations in  $y_1'$ ,  $y_2'$ ,  $y_3''$  and  $y_3''$ . It has not been possible to find the equation of the binodal explicitly from this, and the following numerical method was used to obtain corresponding nodes: a suitable value of  $y_1''$  was chosen and a trial

value of  $y_1'$  assumed. From  $\mu_1' = \mu_1''$ ,  $y_3'' - y_3'$  was calculated :

$$y_3'' - y_3' = [r/(r-1)]\{[\ln y_1' + \alpha(1-y_1')^2] - [\ln y_1'' + \alpha(1-y_1'')^2]\} \quad (14a)$$

and  $y_3''/y_3'$  from  $\mu_3' - \mu_1'/r = \mu_1'' - \mu_3''/r$ ,

$$\ln (y_3''/y_3') = r[-\ln y_1' + 2\alpha y_1'] - [-\ln y_1'' + 2\alpha y_1''], \quad (14b)$$

and thus  $y_3''$  and  $y_3'$ . From  $\Sigma y_i' = 1$ ,  $y_1'$  was obtained and  $y_2''$  from

$$\mu_2' - \mu_3'/r = \mu_3'' - \mu_2''/r,$$

$$\ln (y_2''/y_2') = (1/r) \ln (y_3''/y_3'). \quad (14c)$$

$\Sigma y_i''$  should now be equal to one; if it was not, another value of  $y_1'$  was

tried, using the values of  $\Sigma y_i''$  as a guide to choose as near as possible the

correct value and the process repeated to obtain the  $y$ 's to the desired degree of accuracy. Some nodes for  $\alpha = 1, 1.5$  and  $2$  were thus calculated at  $r = 10, 100, 1000$  and are shown in Fig. 3, 4, 5, together with

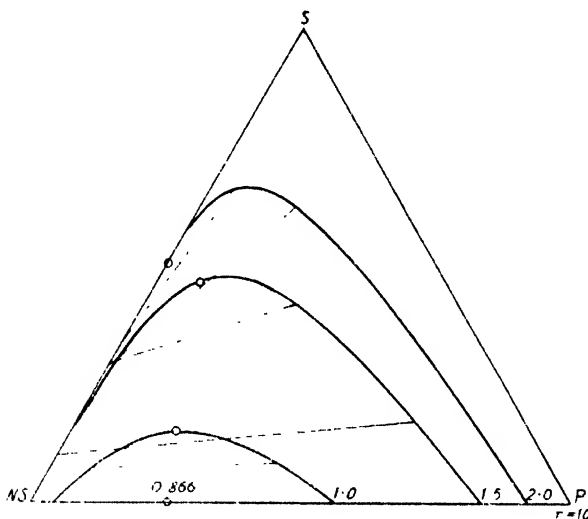


FIG. 3.—Phase diagrams solvent S + non-solvent NS + polymer P,  $r = 10$ , for values of  $\alpha$  indicated. O critical points.

their tie lines and the binodials which have been drawn to pass through them and the critical points, calculated from eqn. (7) and (10); tangents to the binodials at the critical points were calculated by differentiating eqn. (7). The points of intersection of the binodials with the 1-3 axis were obtained as the compositions of the coexisting phases in the binary system non-solvent + polymer; numerical evaluation was aided by the knowledge that in most cases one of the phases contains practically no polymer. For  $\alpha = 2$  and  $r \geq 16$  the exact position of the three-phase region can be found by drawing the binodial near  $y_1 = y_2 = \frac{1}{2}$  in detail and calculating the small binodial with the assumptions  $y_3' \ll 1$ ,  $y_3'' \ll 1$ . The points of intersection are two of the corners of the three-phase triangle and the corresponding node on the other side of the binodial is the third. The positions of these are marked on the binodials. For  $r = 100$ , two of the points are  $y_1 = 0.5 \pm 1.06 \times 10^{-6}$ ,  $y_2 = 1.5 \times 10^{-11}$ , and the third is  $y_1 = 0.2139$ ,  $y_2 = 0.1143$ .

The composition of the swollen polymer which precipitates from a given solution on adding non-solvent can be read off these diagrams, if sufficient tie lines are calculated; the general shape of the curves is as



expected, and is consistent with the experimental fact that except near the critical point, one of the phases contains practically no polymer. The curves also show how far, at least within the assumptions of the

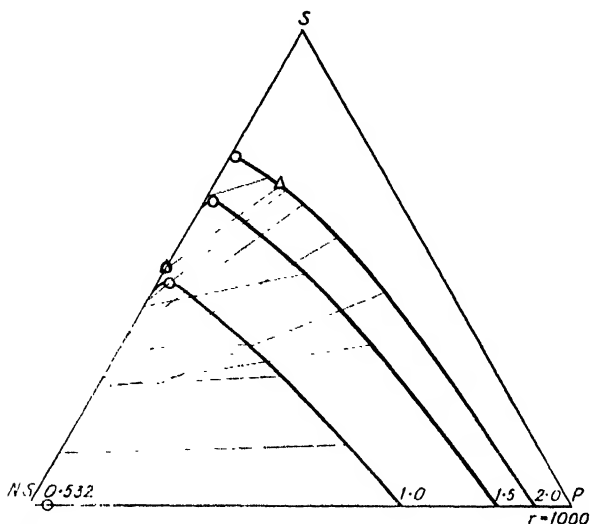


FIG. 4.—Phase diagrams solvent S + non-solvent NS + polymer P,  $r = 1000$ , for values of  $\alpha$  indicated. --- spinodal for  $\alpha = 1.5$ , O critical points,  $\Delta$  corners of three-phase triangle.

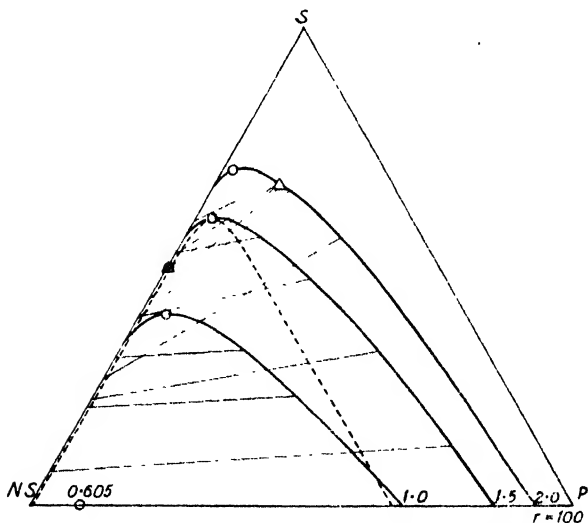


FIG. 5.—Phase diagrams solvent S + non-solvent NS + polymer P,  $r = 1000$ , for values of  $\alpha$  indicated. O critical points,  $\Delta$  corners of three-phase triangle.

model, one is justified in the usual assumption<sup>7, 8, 9</sup> that the ratio of solvent to non-solvent is the same in both phases.

**4. The System Solvent and Two Polymer Homologues.**—Another case which can be treated similarly is  $r_1 = 1$ ,  $r_2 = s$ ,  $r_3 = r$ ; if again  $\alpha_{12} = \alpha_{13} = \alpha$  and  $\alpha_{23} = 0$ , then this represents a solvent and two polymers

of a homologous series, the energy of interaction between solvent and a polymer segment being  $\alpha$ . The phase diagrams of this case are relevant to fractionation by preferential solution in a single solvent and are also interesting as being one of the four faces of the tetrahedron which must be used to represent the possible compositions of a four component system, consisting of non-solvent, solvent and two polymers.

The equation of the spinodal is

$$(1 - 2\alpha y_1)[1 - 2\alpha(sy_2 + ry_3)] = 1 \quad (15)$$

and represents again a hyperbola; the critical points are determined from the equation

$$rs(1 - y_1)(1 - 2\alpha y_1)^3 + (r + s)y_1(1 - 2\alpha y_1)^2 - y_1 = 0, \quad (16)$$

which is again of the fourth degree and has one irrelevant solution and one or three solutions within the triangle of reference.

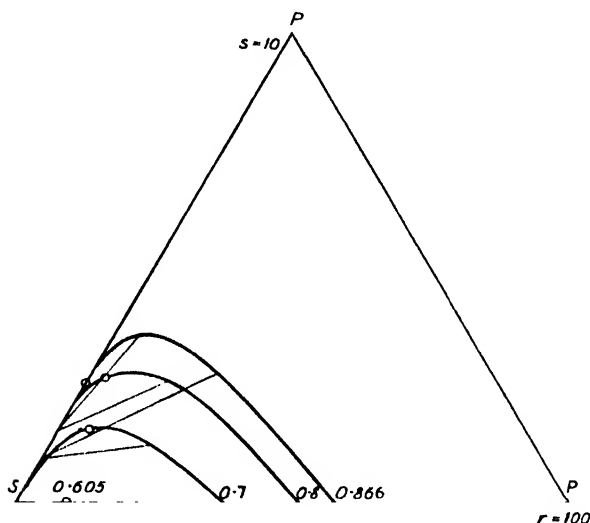


FIG. 6.—Phase diagrams solvent S and two polymer homologues P(s) and P(r),  $s = 10$  and  $r = 100$ , for values of  $\alpha$  indicated. O critical points.

The relation corresponding to eqn. (12) giving  $\alpha$  as a function of  $r$  and  $s$ , at which a HDPP appears, is involved algebraically, but it has been possible to find an equation giving critical values of  $r$  for the appearance of HDPP as a function of  $s$ ; these are the values at which two HDPP coincide.

The substitution  $v = 2\alpha y_1 - 1$ , transforms eqn. (16) into

$$rsv^4 - \lambda v^3 + (r + s)v^2 - v - 1 = 0, \quad (17)$$

where  $\lambda = (2\alpha - 1)rs - (r + s)$ . At a HDPP this equation has two coincident solutions, i.e. it has a root common with

$$4rsv^3 - 3\lambda v^2 + 2(r + s)v - 1 = 0. \quad (18)$$

The  $v$ -eliminant of these two equations is the relation referred to above giving  $\lambda$  (or  $\alpha$ ) as a function of  $r$  and  $s$ . At this value of  $\lambda$  the  $v$ -axis is a tangent to the curve obtained by plotting the left-hand side of eqn. (17) against  $v$ . The limits of  $r$  and  $s$ , at which the  $v$ -axis can be a horizontal tangent, are given by the case where there is a horizontal point of inflection on it, i.e. where

$$12rsv^2 - 6\lambda v + 2(r + s) = 0 \quad (19)$$

as well. We can now eliminate from eqn. (17), (18) and (19) first  $\lambda$  and then  $v$ , obtaining the required relation between  $r$  and  $s$ :

$$3(r^3 - 10rs + s^3)^2 + (r + s)(r^3 - 106rs + s^3) - 27rs = 0. \quad (20)$$

For  $s = 1$  this has  $(r - 2)^3$  as a factor, and dividing by it we get

$$3r^3 - 47r + 1 = 0, \quad (21)$$

the equation mentioned earlier. For large  $r$  and  $s$  the solutions are those of the first term, i.e.  $r/s = 9.90$  or  $0.101$ , so that there is no HDPP and no three-phase region unless  $r$  and  $s$  differ by a factor larger than ten.

Numerical calculation of the binodials was carried out on the same lines as for  $s = 1$  and curves are shown in Fig. 6 and 7. The highest values of  $\alpha$  used were those at which the system 1-2 shows critical mixing.

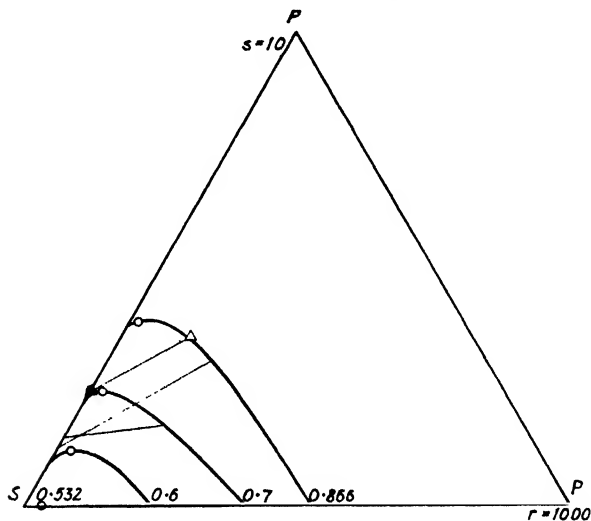


FIG. 7.—Phase diagrams solvent S and two polymer homologues P( $s$ ) and P( $r$ ),  $s = 10$  and  $r = 1000$ , for values of  $\alpha$  indicated. O critical points.

**5. The System Solvent + Polymer + Polymer.** An interesting application is to the case of a solvent and two polymers which do not belong to the same homologous series. It is to be expected that this will throw some light on Dobry's work<sup>18</sup> on the incompatibility of high polymers and on precipitating power as function of molecular size. In order to make our model applicable, we assume that there is no interaction between the solvent (component 2,  $r_2 = 1$ ) and one of the polymers (component 3,  $r_3 = r$ ) and that the interaction between a segment of the other polymer (component 1,  $r_1 = p$ ) and a solvent molecule is the same as that between segments of the two polymers. The free energy of mixing is again given by eqn. (2) and the complete phase relationship can be elucidated.

The spinodal is given by

$$(1 - 2\alpha py_1)[1 - 2\alpha(y_2 + ry_3)] = 1 \quad (22)$$

and is still a hyperbola, the critical point is determined from

$$r(1 - y_1)(1 - 2\alpha py_1)^2 + (r + 1)py_1(1 - 2\alpha py_1)^2 - p^2y_1 = 0. \quad (23)$$

It has not been thought worth while to investigate the conditions under which HDPP and three-phase regions appear, but binodials have been calculated for various cases as before and phase diagrams are shown in Fig. 8 and 9.

<sup>18</sup> Dobry and Boyer-Kawenoki, *J. Polymer Sci.*, 1947, **2**, 90. Dobry, *ibid.*, 1947, **2**, 623.

The low values of  $\alpha_c$ , corresponding to eqn. (11), at which 1 and 3 mix critically, is to be noted :

$$\alpha_c = \frac{1}{2}(p^{-1} + r^{-1})^{\frac{1}{2}}. \quad (24)$$

In fact  $\alpha_c$  is practically zero for large  $p$  and  $r$  and this is on the whole in agreement with Gee's remarks.<sup>8</sup> This means that polymers which have a positive energy of interaction do not mix at all ; and on adding solvent,

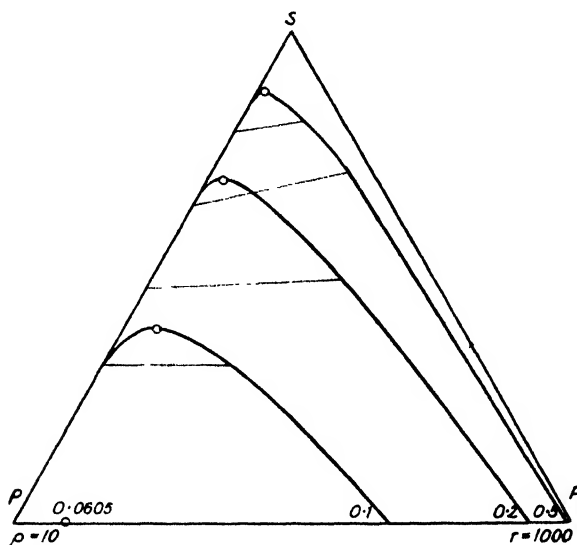


FIG. 8.—Phase diagrams solvent S + polymer P( $p$ ) + polymer P( $r$ ),  $p = 10$ ,  $r = 1000$ , for values of  $\alpha$  indicated. O critical points.

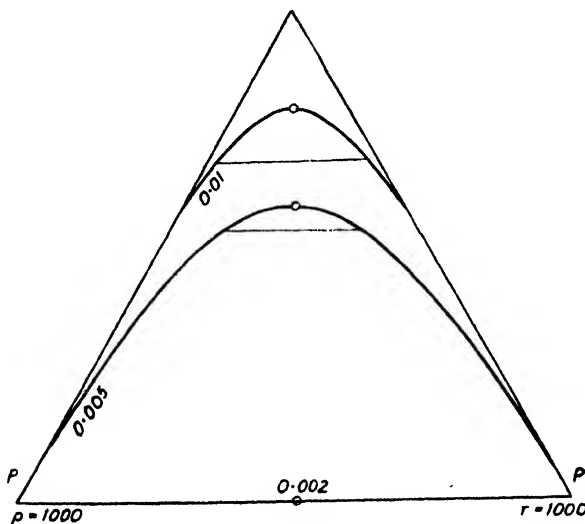


FIG. 9.—Phase diagrams solvent S + polymer P( $p$ ) + polymer P( $r$ ),  $p = 1000$ ,  $r = 1000$  for values of  $\alpha$  indicated. O critical points.

the two-phase region fills practically the whole of the diagram for values of  $\alpha$  which are still very small; this is in qualitative agreement with Dobry's experiments. Another noteworthy feature is the increase in the size of the two-phase region with increasing  $p$ , at constant  $r$  and  $\alpha$ ; e.g. in the case of the system 1-1-1000, there is no two-phase region below  $\alpha = 0.532$ , but in the case of 10-1-1000, the two-phase region already extends over most of the concentration diagram for  $\alpha = 0.5$ , again in agreement with Dobry's experiments.

The continuous change of the curves with increasing  $p$  (as also with increasing  $r$ , cf. Fig. 3, 4 and 5) is noteworthy. As the view is sometimes expressed that, especially in the realm of solubility and phase relationships, solutions of high polymers show "specific behaviour", the author thinks it worth while to point out that the behaviour of polymer solutions is a continuous function of  $r$  and there is nothing in any of the diagrams which could support the view that there is a discontinuity, even at  $r = \infty$ .

After the manuscript of this paper had been finished, two papers by Scott<sup>13</sup> were published which deal with the same problem. The general conclusions of Scott are the same as here presented. Briefly, the main difference between Scott's treatment and the one here given is that Scott starts from an expression for the free energy of mixing which is derived for a more general case; but just because of this he can carry the calculation further only for polymers of infinite chain length. By putting down an expression for the free energy for a more restricted case, as in this paper, the complete phase diagram for any value of  $r$  can be established, and has in fact been done for several cases. Naturally, there is a certain amount of incidental detail given in Scott's paper but not here, and vice versa.

The author is indebted to Mr. J. Crank and Miss M. E. Henry for some of the numerical calculations, and to Dr. C. H. Bamford and Dr. J. G. Oldroyd for many helpful discussions.

Courtaulds, Limited,  
Research Laboratory,  
Lower Cookham Road,  
Maidenhead, Berks.

<sup>13</sup> Scott, *J. Chem. Physics*, 1949, **17**, 268, 279.

## THE EFFECT OF PRESSURE ON THE BURNING VELOCITY OF ETHYLENE-AIR MIXTURES

BY P. J. WHEATLEY AND J. W. LINNETT

*Received 25th July, 1949*

Using the burner method we have found that, in ethylene-air flames, the burning velocity for a given mixture increases as the pressure is reduced below atmospheric. In the range from  $\frac{1}{2}$  to 1 atm. the burning velocity is inversely proportional to about the fourth root of the pressure. This is in agreement with the prediction of Tanford and Pease. The results do not agree with the predictions of Gaydon and Wolfhard, or with the behaviour suggested by the formula of Boys and Corner.

Recently several new theories of flame propagation have been proposed.<sup>1, 2, 3</sup> These theories are necessarily tentative, adopting different

<sup>1</sup> Tanford and Pease, *J. Chem. Physics*, 1947, **15**, 861. Tanford, *ibid.*, 1947, **15**, 433, 861.

<sup>2</sup> Gaydon and Wolfhard, *Proc. Roy. Soc. A*, 1949, **196**, 105.

<sup>3</sup> Boys and Corner, *ibid.*, 1949, **197**, 90.

approaches to the subject and neglecting certain effects. They all, however, predict the effect of pressure on burning velocities, but the predictions differ. It is therefore a matter of considerable theoretical, as well as practical, importance to discover the effect of pressure on the burning velocity of explosive gas mixtures. Several attempts have been made to do this<sup>4</sup> but the conclusions are conflicting. We have constructed an apparatus, similar to that described by Garside, Forsyth and Townend,<sup>5</sup> with which we have measured the burning velocities of ethylene-air mixtures at reduced pressures by the burner method.

### Experimental

The ethylene was prepared by dropping pure ethyl alcohol on to phosphoric acid at 200° C, the resulting vapours being passed through a furnace filled with pumice soaked in phosphoric acid at 220° C. The gases were dried by passing over pumice soaked in sulphuric acid, then through a calcium chloride tube and condensed in a liquid air trap. The ethylene was then slowly distilled into a second liquid air trap, leaving any ether behind. The ethylene could be boiled off from the second trap at any desired rate by means of a small heating coil. The air was taken from the compressed air supply without any preliminary treatment.

The gas flow and pressure were controlled by means of blow-offs and stabilizers, and their rates of flow measured on flowmeters, using glycol as the manometric fluid. The gases came together at a Y-piece and were led through safety- and reducing-valves to the burner tube. The water-jacketed burner tube of 0.988 cm. diam. was of sufficient length to ensure laminar flow. The top of the burner tube was surrounded by a large brass chimney in which the pressure could be controlled by means of an oil pump. The chimney had two plane glass windows on opposite sides at the level of the top of the burner tube, through which the flames could be photographed. Beneath and around the window frames was placed a heating coil to obviate fogging of the glass.

The flames were photographed by the shadow method described by Sherratt and Linnett,<sup>6</sup> and the burning velocity calculated from the dimensions of the flame as detailed in the same paper.

It was found impossible to eradicate a slight vertical flicker of the flame. It was concluded that the flicker was caused by aerodynamic effects within the chimney, since perfectly steady flames could be obtained without the pump or windows on. The flicker necessarily means that there is an alternate increase and decrease in the apparent burning velocity and hence a spread of points is to be expected. It was decided, therefore, to obtain as many readings at each pressure as practicable and to focus attention on the maximum of the burning velocity curve, since maximum burning velocity mixtures give minimum errors.

### Results

A smooth and consistent burning velocity curve has been obtained at atmospheric pressure without the pump operating or the windows in position. The maximum in this curve occurs at 7½ % ethylene. At lower pressures all the points were plotted and a smooth curve drawn through them assuming (a) that the position of the maximum is the same, and (b) that the general shape of the curve is the same as at atmospheric pressure. The results for three pressures are shown in Fig. 1. It will be seen that the assumptions are unlikely to introduce much error, provided the steep sides of the burning velocity curves are not considered. Values of the burning velocity were then read off for 7 %, 8 % and 9 % ethylene-air mixtures. These are given in Table II. The values at 17 cm. are in brackets since their degree of accuracy is considerably less than those at higher pressures. Furthermore, the values of the burning velocity quoted for 9 % mixtures are likely to be less accurate, since 9 %

<sup>4</sup> Wolfhard, *Z. tech. Phys.*, 1943, **24**, 206. Ubbelohde and Koelliker, *J. Gasbel.*, 1916, **59**, 49. Khitrin, *Tech. Phys. U.S.S.R.*, 1936, **3**, 926. Kolodtsev and Khitrin, *ibid.*, 1936, **3**, 1034. Ubbelohde and Andwandler, *J. Gasbel.*, 1917, **60**, 225. Stevens, *N.A.C.A. Reports*, 1931, **372**, Fiock and Roeder *ibid.*, **532**, 1935. Garside, Forsyth and Townend, *J. Inst. Fuel*, 1945, **18**, 175.

<sup>5</sup> Garside, Forsyth and Townend, *ibid.*, 1945, **18**, 175.

<sup>6</sup> Sherratt and Linnett, *Trans. Faraday Soc.*, 1948, **44**, 596.

mixtures lie on the beginning of the steep portion. We have reason to believe that the absolute values quoted may be a few per cent. too high throughout, but they should be proportional to the correct values.<sup>7</sup>

In order to apply any theory of flame propagation to these results, it is necessary to know the flame temperatures. These have been calculated for all mixtures at all pressures used and the results are given in Table II. The method used was that described by Lewis and von Elbe<sup>8</sup> and no account has been taken of the equilibrium

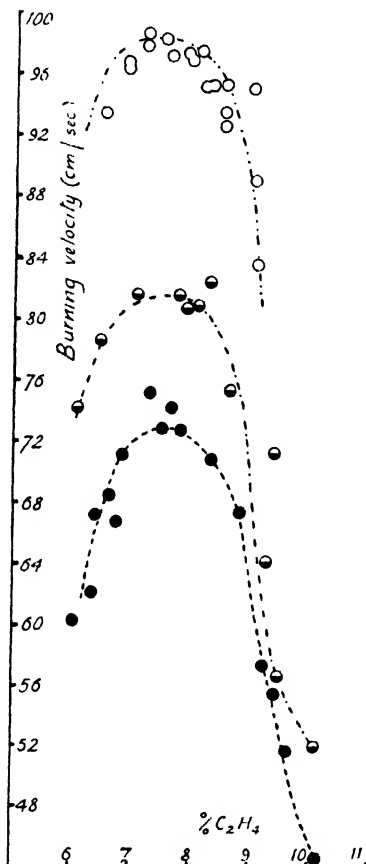


TABLE I

Pressure (cm. Hg)	7 %	8 %	9 %
77	71	71	59
70	72	72	61
64.5	70	72	65
56	76	77	66
49	81	81	67
37	89	91	81
27	97	98	87
(17)	(109)	(108)	(103)

Burning velocities in cm./sec. of 7 %, 8 % and 9 % ethylene-air mixtures.

FIG. 1.—A plot of the burning velocity, in cm./sec., of ethylene-air mixtures against the volume percentage of ethylene.

- (A) ● at 70 cm. Hg.  
 (B) ◐ at 49 cm. Hg.  
 (C) ○ at 27 cm. Hg.

The inclusion of this reaction would not lower the calculated flame temperatures by more than 10° C. In calculating these temperatures values were obtained for the concentrations of O, H and OH radicals. Only the figures for 7 %, 8 % and 9 % mixtures are given here (Tables III, IV and V).

### Discussion

We believe that the direct shadow or, better, the *Schlieren* method of photography is superior to direct photography for locating a flame front. In this we agree with van de Poll and Westerdijk.<sup>9</sup> Not only are the photographs more defined, and hence susceptible to more accurate measurement, but they, by virtue of a rapid change of refractive index,

<sup>7</sup> Subsequent work in this laboratory (to be published later).

<sup>8</sup> Lewis and von Elbe, *Phil. Mag.*, 1935, 20, 44.

<sup>9</sup> van de Poll and Westerdijk, *Z. Tech. Phys.*, 1941, 22, 29.

mark the onset of rapidly changing conditions. For the gases to be luminous, they must have passed through or be passing through the

TABLE II.—CALCULATED FLAME TEMPERATURES IN °K

Pressure (cm. Hg)	Pressure (atm.)	Volume percentage of ethylene						
		4 %	5 %	6 %	7 %	8 %	9 %	10 %
76.0	1.0000	1806.5	2106.0	2322.5	2417.0	2363.0	2256.0	2143.0
70.0	0.9211	1806.5	2105.0	2320.0	2413.0	2361.5	2255.0	2143.0
64.5	0.8487	1806.5	2104.0	2317.5	2410.0	2360.5	2254.0	2142.5
56.0	0.7368	1806.5	2103.0	2314.0	2405.0	2358.0	2252.5	2142.0
49.0	0.6447	1806.5	2102.0	2309.0	2398.0	2356.0	2250.5	2141.0
37.0	0.4868	1806.5	2100.5	2301.0	2388.0	2351.5	2248.0	2140.0
27.0	0.3553	1806.5	2096.5	2288.0	2376.0	2345.0	2245.0	2138.0
17.0	0.2237	1806.5	2091.0	2275.0	2356.0	2335.5	2240.0	2133.5

TABLE III.—CALCULATED RADICAL CONCENTRATIONS

Pressure (atm.)	7 % Mixture		
	$p_H \times 10^{-3}$	$p_{OH} \times 10^{-3}$	$p_O \times 10^{-4}$
1.0000	1.59	4.42	7.23
0.9211	1.52	4.08	7.25
0.8487	1.45	3.80	7.16
0.7368	1.31	3.41	6.44
0.6447	1.20	3.01	6.15
0.4868	1.01	2.40	5.17
0.3553	0.82	1.84	4.35
0.2237	0.61	1.29	2.74

TABLE IV.—CALCULATED RADICAL CONCENTRATIONS

Pressure (atm.)	8 % Mixture		
	$p_H \times 10^{-3}$	$p_{OH} \times 10^{-3}$	$p_O \times 10^{-4}$
1.0000	2.03	1.88	1.55
0.9211	1.93	1.78	1.52
0.8487	1.84	1.70	1.54
0.7368	1.71	1.56	1.53
0.6447	1.62	1.48	1.63
0.4868	1.39	1.25	1.53
0.3553	1.15	0.98	1.38
0.2237	0.85	0.72	1.13

reaction zone, and hence luminosity is not necessarily a satisfactory criterion of the flame front. Moreover, it has been observed that the visible cone lies well outside the shadow <sup>9</sup> or *Schlieren* cone,<sup>10</sup> and the distance between them increases as the pressure is lowered. It is this difference which probably accounts for the lack of agreement between our results and those of Garside, Forsyth and Townend <sup>8</sup> regarding the effect of pressure on the burning velocity (they use the term ignition velocity) of ethylene-air mixtures. For a 7½ % ethylene-air mixture they find that the burning velocity increases from about 53 to about 60 cm./sec. on lowering the pressure from 70 to 30 cm. Hg. For other mixtures in the 7 to 9 % range the increase in burning velocity found by them is smaller than this. So they do not find as big a change in

TABLE V.—CALCULATED RADICAL CONCENTRATIONS

Pressure (atm.)	9 % Mixture		
	$p_H \times 10^{-3}$	$p_{OH} \times 10^{-4}$	$p_O \times 10^{-3}$
1.0000	1.68	5.83	2.06
0.9211	1.60	5.54	1.96
0.8487	1.53	5.30	2.19
0.7768	1.41	4.94	2.29
0.6447	1.31	4.61	2.15
0.4868	1.14	4.00	2.13
0.3553	0.96	3.30	2.23
0.2237	0.74	2.54	1.87

<sup>10</sup> Klaukens and Wolfhard, *Proc. Roy. Soc. A.*, 1948, 193, 512.



burning velocity with pressure as we do. It is probable that Garside *et al.* obtain smaller values for the burning velocities than we do because the area of the visible cone is greater than the area of the shadow cone, since the former is outside the latter. Moreover the difference in the area of the two cones increases as the pressure is lowered because the distance between them increases. Consequently the differences between our results and theirs increases as the pressure is lowered and the increase in burning velocity found by their method will be expected to be less than that found by our method. As pointed out earlier, the shadow cone marks the zone where the conditions of the gas begin to change rapidly and this seems to be the most suitable zone to regard as the flame front. The zone where light is emitted is less suitable because it is in a region where the gases have reacted to a considerable extent and consequently in a region in which considerable expansion has already occurred. It is this expansion that causes the luminous cone to be larger in area than the shadow cone.

We will now consider our results in relation to the various predictions that have been made recently regarding the effect of pressure on burning velocity. Tanford and Pease<sup>1</sup> predict that the burning velocity will increase as the pressure falls, the burning velocity being inversely proportional to the fourth root of the pressure. Gaydon and Wolfhard<sup>2</sup> predict that the burning velocity will be virtually independent of the pressure if the chemical reaction is proportional to the total number of two-body collisions occurring per unit volume per second. Both the above theories are based on very simple radical diffusion pictures of flame propagation. They differ in the assumptions they make regarding the way in which the degree of dissociation in a flame varies with the pressure. Boys and Corner<sup>3</sup> predict that the burning velocity is proportional to  $P^{\frac{1}{2}(m-2)}$ , where  $P$  is the total pressure and  $m$  is the order of the reaction.\* Their theory is purely thermal. It predicts that the burning velocity is independent of pressure if  $m$  is 2. Only if  $m$  is less than 2 will the burning velocity increase as the pressure is lowered. The observations of Thompson and Hinshelwood,<sup>11</sup> and of Steacie and Plewes<sup>12</sup> showed that, around 450° C,  $m$  is about three. However, it may well be that this is not relevant to the present discussion because of the very different conditions existing in the flame. Nevertheless, it seems unlikely that  $m$  will be less than 2 as there are two reacting components; and this will be equally true if the reaction goes by a chain mechanism, since the order is usually high for chain reactions.<sup>13</sup> Therefore, the result that we obtain, that the burning velocity increases as the pressure is lowered, appears to be inconsistent with the formulae of Boys and Corner. In fact, the result agrees only with the prediction of Tanford and Pease. Moreover, the burning velocity does vary inversely as about the fourth root of the pressure as suggested by them. This is demonstrated in Fig. 2. It is important that the purely thermal theory of Boys and Corner, which does not contain the arbitrary features of the older thermal theories, suggests a behaviour which is different from what we find here. This definitely implies that a *purely* thermal theory is inadequate to account for the propagation of flame in these ethylene-air mixtures. It is

\* Boys and Corner state that "if the homogeneous reaction velocity varies as  $P^n$  the mass flame velocity will vary as  $P^{\frac{1}{2}(n+1)}$ ." In this paper they define reaction velocity in terms of fractional change so that the order, in the usual sense of the word, is  $(n + 1)$ . For this, commonly understood, order we have used the symbol  $m$ , so that  $n = m - 1$ . Since the mass flame velocity is proportional to the product of the burning velocity and the pressure, the burning velocity will be proportional to  $P^{\frac{1}{2}(m-1)}$ .

<sup>11</sup> Thompson and Hinshelwood, *ibid.*, 1929, 125, 277.

<sup>12</sup> Steacie and Plewes, *ibid.*, 1934, 146, 72.

<sup>13</sup> Hinshelwood, *Kinetics of Chemical Change in Gaseous Systems* (O.U.P., 1933), 272.

interesting in this connection that the burning velocity is linearly related to  $p_H/P$ , to  $p_O/P$ , and to  $p_{OH}/P$  for all three mixtures studied ( $p_H$ ,  $p_O$  and  $p_{OH}$  are the calculated equilibrium partial pressures of H, O and OH

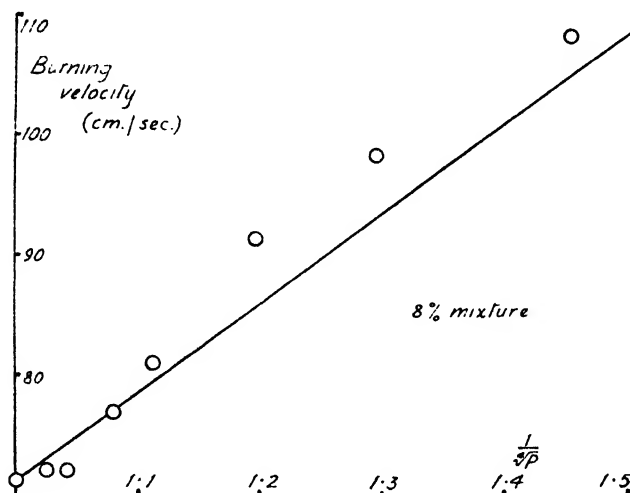


FIG. 2.—A plot of the burning velocity of an 8 % ethylene-air mixture against the reciprocal of the fourth root of the pressure. The line is drawn so as to pass through the origin, and thus show the direct proportionality between the two quantities.

at the flame temperatures, and  $P$  is the total pressure). Examples of these are shown in Fig. 3. Since the rates of diffusion are inversely

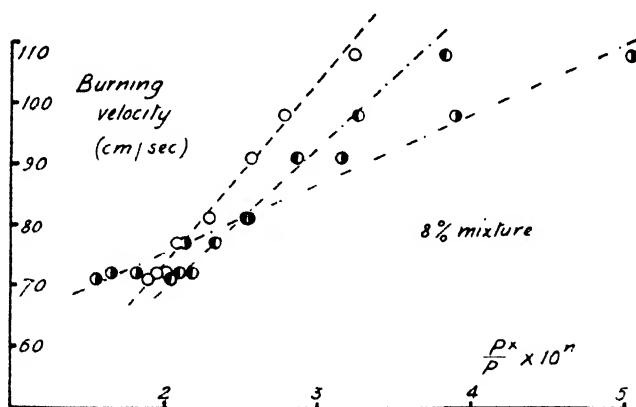


FIG. 3.—A plot of the burning velocity of an 8 % ethylene-air mixture against  $P_x/P \times 10^n$ .

- (A) ●  $P_H/P \times 10^{-3}$ ,  $n = 3$ .
- (B) ◐  $P_{OH}/P \times 10^{-3}$ ,  $n = 3$ .
- (C) ●  $P_O/P \times 10^{-4}$ ,  $n = 4$ .

proportional to the total pressure for a mixture of a given composition this result is very reasonable on a simple radical diffusion theory (cf. the calculations of Tanford and Pease for flames in  $\text{CO}-\text{O}_2-\text{N}_2$ ,  $\text{H}_2-\text{H}_2\text{O}$  mixtures). However, though we find that the burning velocity varies

with the pressure in the way predicted by Tanford and Pease, we are not of the opinion that a purely diffusion theory, like that of Tanford and Pease, can explain *all* the intricacies of flame propagation.

Some criticism has been levelled at the burner method as a means of measuring accurate burning velocities. Consequently, though there is no doubt that, with the burner tube and gas mixture used in the present investigation, the burning velocity increased as the pressure was lowered, we are now constructing an apparatus which should yield accurate values at all pressures and will not be subject to many of the criticisms of the burner method. We hope, therefore, to settle quite unambiguously how burning velocities depend on the pressure for a variety of mixtures.

*Inorganic Chemistry Laboratory,  
Oxford.*

## NOTE CONCERNING SOME RECENT STATEMENTS ON THE LATENT HEAT OF VAPORIZATION OF CARBON

BY L. H. LONG AND R. G. W. NORRISH

*Received 10th July, 1949*

The purpose of this note is to point out the misleading nature of some recently published statements relating to an earlier paper of ours on the thermochemistry of carbon.<sup>1</sup>

The statement of E. C. Baughan,<sup>2</sup> that according to Long and Norrish's view the *whole* of the  $^5S \rightarrow ^3P$  transition of carbon would appear in the process  $CH_3 \rightarrow CH_2 + H$  as energy of reorganization, is incorrect. In point of fact we clearly state<sup>3</sup> that we regard the energy as being divided into three parts, two of which are absorbed in the weakening of the two remaining C—H bonds. Nor is it true, as Baughan further states,<sup>2</sup> that the C—H bond strength in ethane is assumed to be *identical* with the dissociation energy into  $C_2H_5 + H$ . The bond energy was calculated from heats of combustion to be 1 kcal. less<sup>4</sup> than the C—H bond strength in methane, that is, 4 kcal. more than the experimental value for

$$D(C_2H_5-H) \text{ (99} \pm 2 \text{ kcal.)}$$

Likewise incorrect is the statement by H. A. Skinner<sup>5</sup> that the argument of Long and Norrish regarding the true value for the heat of sublimation of graphite is based on the "tacit assumption" that the C—H bond energies in  $CH_4$  and  $CH_3$  are of similar magnitude. We do not use any such assumed similarity of magnitude to calculate the heat of sublimation of carbon. Our arguments rest on an examination of all the diverse data available at the time of writing, and lead to a value of  $L_2$  ( $= L + X$  in Skinner's notation) with the limits 182 and 200 kcal.,<sup>6</sup> from which it may be calculated that the said bond energies do not differ by more than 2 kcal.

*Dept. of Physical Chemistry,  
Cambridge.*

<sup>1</sup> Long and Norrish, *Proc. Roy. Soc. A*, 1946, **187**, 337.

<sup>2</sup> Baughan, *Trans. Faraday Soc.*, 1948, **44**, 849.

<sup>3</sup> Long and Norrish, *op. cit.*, p. 341.

<sup>4</sup> *Ibid.*, p. 348 and Table III.

<sup>5</sup> Skinner, *Trans. Faraday Soc.*, 1949, **45**, 32.

<sup>6</sup> Long and Norrish, *op. cit.*, pp. 348 ff.

# THERMOCHEMISTRY OF METAL ALKYLs

## PART II.—THE BOND DISSOCIATION ENERGIES OF SOME Zn—C AND Cd—C BONDS, AND OF Et—I.

By A. S. CARSON, K. HARTLEY AND H. A. SKINNER

Received 15th July, 1949

Measurements of the heats of reaction of  $\text{CdEt}_2$ ,  $\text{ZnMe}_2$ , and  $\text{ZnEt}_2$  with dilute acid and water, and of  $\text{ZnEt}_2$  and  $\text{CdEt}_2$  with iodine, are reported, leading to the following values for the heats of formation  $Q_f$  of the liquids at room temperature:

$$\begin{aligned}Q_f(\text{CdEt}_2) &= -14.5 \text{ kcal. mole}^{-1} (\pm 0.5 \text{ kcal.}) \\Q_f(\text{ZnMe}_2) &= -6.3 \text{ kcal. mole}^{-1} (\pm 1 \text{ kcal.}) \\Q_f(\text{ZnEt}_2) &= -4.3 \text{ kcal. mole}^{-1} (\pm 1 \text{ kcal.}) \\Q_f(\text{EtI}) &= 9.1 \text{ kcal. mole}^{-1} (\pm 1 \text{ kcal.}).\end{aligned}$$

Assuming the values  $D(\text{CH}_3\text{—H}) = 102.0$  kcal., and  $D(\text{C}_2\text{H}_5\text{—H}) = 97.5$  kcal., these data lead to 52.8 kcal. for the dissociation energy of the C—I bond in EtI, and to 52.9 kcal., 81.9 kcal., and 68.7 kcal. respectively for the sum of the metal-carbon bond dissociation energies in  $\text{CdEt}_2$ ,  $\text{ZnMe}_2$  and  $\text{ZnEt}_2$ .

In a previous paper (Part I of this series), Carson, Hartley and Skinner<sup>1</sup> described an adiabatic calorimetric system in which they measured the heats of some reactions involving cadmium dimethyl. This paper reports some further thermochemical studies on the metal alkyls of Group II, using the same calorimeter and techniques as described earlier. The measurements here reported are of the heats of hydrolysis (at 20° C) of  $\text{CdEt}_2$ ,  $\text{ZnMe}_2$  and  $\text{ZnEt}_2$ , and of the heats of iodination of  $\text{CdEt}_2$  and  $\text{ZnEt}_2$ . These data provide values for the heats of formation (from elements in standard states, the  $Q_f$  values) of the metal alkyls and of EtI. Taken in conjunction with accepted values for the C—H bond dissociation energies in  $\text{CH}_4$  and  $\text{C}_2\text{H}_6$ , the  $Q_f$  values yield absolute values for the dissociation energies of the metal-alkyl bonds in the Zn and Cd alkyls, and for the C—I bond in EtI.

### Experimental

**Preparation of Compounds.**—(a)  $\text{CdEt}_2$ : prepared according to the method described by Krause,<sup>2</sup> by reacting anhydrous  $\text{CdI}_2$  with  $\text{EtMgI}$  in ethereal solution. The bulk of the ether was separated from the  $\text{CdEt}_2$ -ether mixture by distillation at normal pressure, and the residue removed by careful fractionation at reduced pressure using an efficient gauze-packed column. Final traces of ether were removed by repeated bulb-to-bulb distillations *in vacuo*. The pure product was collected and sealed in weighed glass phials and used almost immediately in experiment, as  $\text{CdEt}_2$  decomposes on standing and slowly deposits a blue-grey metallic precipitate.

(b)  $\text{ZnMe}_2$ : prepared in similar manner to that recommended by Renshaw and Greenlaw,<sup>3</sup> by long refluxing of a mixture of methyl iodide with excess Zn—Cu couple. The crude product was fractionally distilled in an efficiently packed column in an atmosphere of pure dry  $\text{N}_2$ , and finally *in vacuo* (b.p. 44° C, 760 mm.).

(c)  $\text{ZnEt}_2$ : prepared by Noller's method,<sup>4</sup> from Zn—Cu couple and a mixture of EtI and EtBr. It was purified by fractionation in an efficient column in an atmosphere of pure dry  $\text{N}_2$ , and finally by repeated bulb-to-bulb fractionation *in vacuo* (b.p. 117.7° C, 760 mm.).

<sup>1</sup> Carson, Hartley and Skinner, *Proc. Roy. Soc. A*, 1949, **195**, 500.

<sup>2</sup> Krause, *Ber.*, 1917, **50**, 1813.

<sup>3</sup> Renshaw and Greenlaw, *J. Amer. Chem. Soc.*, 1920, **42**, 1472.

<sup>4</sup> Noller, *Organic Syntheses*, vol. XII.

## Results and Discussion

**Heats of Hydrolysis, and of Reaction with Dilute Acid.**—(a)  $\text{CdEt}_2$ :

Unlike  $\text{CdMe}_2$ , which decomposes fairly rapidly when treated with water,  $\text{CdEt}_2$  is hydrolyzed only slowly at room temperature. The decomposition of  $\text{CdEt}_2$  by aqueous  $\text{N H}_2\text{SO}_4$ , however, proceeds rapidly to completion, giving  $\text{CdSO}_4$  (aq.) and ethane as the sole products. The heat of the reaction

$\text{CdEt}_2$  (liq.) +  $\text{H}_2\text{SO}_4$  (aq.)  $\rightarrow$   $\text{CdSO}_4$  (aq.) +  $2\text{C}_2\text{H}_6$  (gas) +  $Q_1$  kcal. (1) was measured in like manner as described previously for the corresponding reaction with  $\text{CdMe}_2$ . Analysis of the gaseous products showed ethane only: there was no detectable amount of  $\text{C}_2\text{H}_4$  or  $\text{H}_2$  in the gases collected.

The purity of the  $\text{CdEt}_2$  samples used (generally found to be from 99-100 % pure) was determined by measurement of the total volume of ethane produced in each experiment. To ensure a complete conversion of  $\text{CdEt}_2$  to  $\text{CdSO}_4$ , we have usually taken a twofold excess of  $\text{N H}_2\text{SO}_4$  in each experiment.

Results from 7 experiments are set out in Table I. The heat of reaction (i.e.  $Q_1$  of eqn. (1)) is related to the thermochemical heat of formation,  $Q_f$  ( $\text{CdEt}_2$  (liq.)) by the equation

$Q_1 = Q_f(\text{CdSO}_4, \text{aq.}) + 2Q_f(\text{C}_2\text{H}_6, \text{gas}) - Q_f(\text{H}_2\text{SO}_4, \text{aq.}) - Q_f(\text{CdEt}_2) + M$ , (2) where  $M$  is the heat of mixing of  $\text{CdSO}_4$  (aq.) with the excess  $\text{H}_2\text{SO}_4$ . The heat of mixing corrections are given in column 8 of Table I. As the reactions were carried out *in vacuo* in a sealed reaction vessel (see ref. 1 for further details), the observed heats of reaction give the  $-\Delta E$  (not  $-\Delta H$ ) of reaction: the  $-\Delta E$  values are transformed to  $-\Delta H$  values in column 7. Substituting the following published data for the various  $Q_f$  terms in eqn. (2),

$$Q_f(\text{CdSO}_4, 100 \text{ aq.})^5 = 232.41 \text{ kcal. mole}^{-1},$$

$$Q_f(\text{H}_2\text{SO}_4, 100 \text{ aq.})^5 = 211.59 \text{ " "}$$

$$Q_f(\text{C}_2\text{H}_6, \text{gas})^5 = 20.24 \text{ " "}$$

the equation becomes

$$Q_1 = -\Delta H = 61.30 - Q_f(\text{CdEt}_2, \text{liq.}) + M \text{ kcal.} \quad (3)$$

This latter equation was used to calculate the  $Q_f(\text{CdEt}_2, \text{liq.})$  given in column 9.

TABLE I.—HEAT OF REACTION OF  $\text{CdEt}_2$  WITH AQUEOUS  $\text{H}_2\text{SO}_4$

Expt.	Wt. $\text{CdEt}_2$ (g.)	Water equiv. (cal./°C)	$\Delta T^\circ \text{C.}$ (obs.)	Purity %	$-\Delta E$ (kcal.)	$-\Delta H$ (kcal.)	$M$ (kcal.)	$Q_f(\text{CdEt}_2, \text{liq.})$ (kcal. mole <sup>-1</sup> )
1	2.764	1270	0.967	99.6	76.0	74.8	-0.75	-14.25
2	2.810	1270	0.969	99.0	75.35	74.15	-0.75	-13.6
3	1.865	1272	0.660	99.9	76.85	75.65	-0.7	-15.0
4	2.740	1270	0.968	99.8	76.6	75.4	-0.75	-14.85
5	2.194	1270	0.773	99.8	76.4	75.2	-0.75	-14.65
6	3.086	1280	1.083	99.9	76.6	75.4	-0.80	-14.9
7	2.829	1275	0.985	99.8	75.8	74.6	-0.75	-14.05

Mean value of  $Q_f(\text{CdEt}_2, \text{liq.}) = -14.5 \text{ kcal. mole}^{-1}$ .

Maximum deviations from mean: 0.5 kcal., -0.9 kcal.

Standard error of mean  $\pm 0.18 \text{ kcal.}$

**(b)  $\text{ZnMe}_2$  and  $\text{ZnEt}_2$ :**

The decomposition of the Zn alkyls by water (or aqueous acids), takes place with extreme violence, so much so that the hydrolysis reaction,

$$\text{ZnR}_2 + 2\text{H}_2\text{O} \rightarrow \text{Zn(OH)}_2 + 2\text{RH},$$

<sup>5</sup> *Tables of Selected Values of Chemical Thermodynamic Constants* (Bureau of Standards, Washington, 1948).

may not completely express the mode of decomposition. Under the experimental conditions used in our reaction vessel—in which glass phials containing  $\frac{1}{2}$  g. or more of  $\text{ZnR}_2$  were quickly broken into a relatively large volume of water or dilute  $\text{H}_2\text{SO}_4$ —some small amount of thermal decomposition of the dialkyl would seem to accompany the main hydrolysis reaction. With  $\text{ZnEt}_2$ , for example, the gaseous products resulting from hydrolysis showed small amounts of  $\text{H}_2$  and  $\text{C}_2\text{H}_4$  admixed with  $\text{C}_2\text{H}_6$ . Furthermore, in the aqueous decomposition of  $\text{ZnEt}_2$ , the  $\text{Zn(OH)}_2$  precipitate was contaminated with numerous black specks, which we have not identified but presume to be specks of metallic Zn. A similar blackening of the  $\text{Zn(OH)}_2$  precipitate was observed in the aqueous decomposition of  $\text{ZnMe}_2$ .

The relative extent of the side-reaction (or side-reactions) was found to be much reduced by decreasing the amount of Zn alkyl introduced into the water at one time: e.g. much less  $\text{H}_2$  was produced by breaking two phials one after the other, each containing  $\frac{1}{2}$  g.  $\text{ZnEt}_2$ , than by breaking a single phial containing 1 g.  $\text{ZnEt}_2$ . It seems probable that the side-reactions are the net result of an initial thermal disruption,  $\text{ZnR}_2 \rightarrow \text{ZnR} + \text{R}$ , or of  $\text{ZnR}_2 \rightarrow \text{Zn} + \text{R} + \text{R}$ , caused by the intense *local* heating at the instant of breakage of the glass phials.

The aqueous hydrolyses (and the acid decompositions) are thus rather less satisfactory reactions for thermochemical study in the case of the Zn alkyls than in that of the Cd alkyls, where, if side reactions occur at all, they do so to a much smaller extent. To counter the violence of the reactions with the Zn alkyls, we have investigated the hydrolyses in *aqueous ether solutions*. Under these conditions, the hydrolyses proceed at a more leisurely pace, and the  $\text{Zn(OH)}_2$  precipitate produced is white and clean.

The result of 6 experiments on the aqueous ethereal hydrolysis of  $\text{ZnMe}_2$  are set out in Table II. Analyses of the  $\text{Zn(OH)}_2$  precipitates remaining in the reaction vessel after each experiment indicated that the  $\text{ZnMe}_2$  samples used were *ca.* 99 % pure: the volumes of  $\text{CH}_4$  produced indicated rather higher purity than this, and the results given in Table II are based upon an average purity figure of 99.5 %.

TABLE II.—HYDROLYSIS OF  $\text{ZnMe}_2$  IN AQUEOUS ETHERIAL SOLUTION

Expt.	Wt. $\text{ZnMe}_2$ (g.)	Water equiv. (cal./° C)	$\Delta T^\circ \text{C}$ (obs.)	$-\Delta E$ (kcal.)	$-\Delta H$ (kcal.)	$Q_f(\text{ZnMe}_2, \text{liq.})$ (kcal. mole <sup>-1</sup> )
1	1.509	1236	0.767	60.2	59.0	-6.4
2	1.370	1236	0.700	60.5	59.3	-6.7
3	1.4774	1232	0.763	61.0	59.8	-7.2
4	1.6703	1238	0.850	60.4	59.2	-6.6
5	1.265	1235	0.640	59.9	58.7	-6.1
6	1.406	1238	0.718	60.6	59.4	-6.8

Average purity of  $\text{ZnMe}_2$  samples: 95.5 %.

Mean value of  $-\Delta H = 59.2$  kcal.

Mean value of  $Q_f(\text{ZnMe}_2, \text{liq.}) = -6.6$  kcal. mole<sup>-1</sup>.

Maximum deviation from mean:  $\pm 0.6$  kcal.

Standard error of mean:  $\pm 0.14$  kcal.

The values of  $Q_f(\text{ZnMe}_2, \text{liq.})$  given in column 7 are calculated from the equation:

$$Q_f(\text{ZnMe}_2, \text{liq.}) = \Delta H + Q_f(\text{Zn(OH)}_2, \text{ppt.}) + 2Q_f(\text{CH}_4, \text{gas}) - 2Q_f(\text{H}_2\text{O}, \text{liq.}) \quad (4)$$

The values of the last two terms in eqn. (4) are well-established, viz.

$$Q_f(\text{CH}_4, \text{gas})^\circ = 17.89 \text{ kcal. mole}^{-1}.$$

$$Q_f(\text{H}_2\text{O}, \text{liq.})^\circ = 68.32 \text{ " "}$$

On the other hand, the term in  $Q_f(\text{Zn(OH)}_2)$  is less accurately known

From the work of Fricke and Meyring,<sup>6</sup> it seems that the heat of formation of precipitated  $\text{Zn}(\text{OH})_2$  is not a precise thermochemical constant, as it may vary with the mode of preparation and age of the sample. We have used the value for  $Q_f(\text{Zn}(\text{OH})_2, \text{ppt.})$  recommended by Rossini<sup>5</sup> (i.e. 153.5 kcal. mole<sup>-1</sup>) but it should be emphasized that there is some doubt attached to this figure, and the values derived for  $Q_f(\text{ZnMe}_2, \text{liq.})$  carry any error that may be present in  $Q_f(\text{Zn}(\text{OH})_2, \text{ppt.})$ . Substitution of the above  $Q_f$  values into eqn. (4) yields

$$Q_f(\text{ZnMe}_2, \text{liq.}) = \Delta H + 52.6 \text{ kcal.} \quad (5)$$

from which the  $Q_f$  values of column 7 are obtained.

Table III gives the results from 5 experiments on the hydrolysis of  $\text{ZnEt}_2$  in aqueous ether solution. The analytical tests showed the  $\text{ZnEt}_2$  samples to be of high purity, and the results given are based on an average purity of 99.9 %. The values of  $Q_f(\text{ZnEt}_2, \text{liq.})$  given in column 7 are derived from the equation :

$$Q_f(\text{ZnEt}_2, \text{liq.}) = \Delta H + 57.3 \text{ kcal.} \quad (6)$$

which is the equation corresponding to (5).

TABLE III.—HYDROLYSIS OF  $\text{ZnEt}_2$  IN AQUEOUS ETHER SOLUTION

Expt.	Wt. $\text{ZnEt}_2$ (g.)	Water equiv. (cal./° C)	$\Delta T^\circ \text{C}$ (obs.)	$-\Delta E$ (kcal.)	$-\Delta H$ (kcal.)	$Q_f(\text{ZnEt}_2, \text{liq.})$ (kcal. mole <sup>-1</sup> )
1	1.547	1237	0.645	63.7	62.5	- 5.2
2	1.417	1237	0.590	63.6	62.4	- 5.1
3	1.339	1237	0.561	64.0	62.8	- 5.5
4	1.4846	1240	0.618	63.7	62.5	- 5.2
5	2.259	1238	0.942	63.8	62.6	- 5.1

Average purity of  $\text{ZnEt}_2$  samples: 99.9 %.

Mean value of  $-\Delta H = 62.56 \text{ kcal. mole}^{-1}$ .

Mean value of  $Q_f(\text{ZnEt}_2, \text{liq.}) = -5.26 \text{ kcal. mole}^{-1}$ .

Maximum deviation from mean:  $\pm 0.25 \text{ kcal.}$

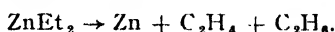
We have made several measurements of the heat of reaction of  $\text{ZnEt}_2$  with dilute (usually N)  $\text{H}_2\text{SO}_4$ . Most of our earlier observations proved of little thermochemical value, because of the appreciable side-reactions accompanying the main reaction (in some cases, the side-reactions amounted to as much as 5 % of the total). Later, it was found that the side-reactions are much reduced by using smaller quantities of  $\text{ZnEt}_2$  in each phial (ca.  $\frac{1}{2}$  to  $\frac{3}{4}$  g.). Some of the later results are collected together in Table IV.

As in the experiments with  $\text{CdEt}_2$ , an excess of  $\text{H}_2\text{SO}_4$  was employed in each run, necessitating corrections for the heat of mixing  $M$ , given in column 6 of Table IV. The values for  $Q_f(\text{ZnEt}_2, \text{liq.})$ , listed in column 8, are derived from the equation

$$Q_f(\text{ZnEt}_2, \text{liq.}) = \Delta H + 81.03 + M, \quad (7)$$

which is obtainable from an equation analogous to (2), on substituting the value  $Q_f(\text{ZnSO}_4, 100 \text{ H}_2\text{O}) = 252.14 \text{ kcal.}$  (see ref. 5).

Earlier results than those listed in Table IV gave smaller values for  $-\Delta H$ , corresponding to less negative values (by 1 or 2 kcal.) for  $Q_f(\text{ZnEt}_2)$ . One would expect the observed heats of reaction to be reduced by the occurrence of side-reactions such as



<sup>6</sup> Fricke and Meyring, *Z. anorg. Chem.*, 1937, **230**, 357.

Since, even in the later experiments listed in Table IV, side-reactions were not completely eliminated, the  $-\Delta H$  values represent *lower* limits, and the true  $Q_f(\text{ZnEt}_2)$  should be still more negative than those found in Table IV.

TABLE IV.—HEAT OF REACTION OF  $\text{ZnEt}_2$  WITH AQUEOUS  $\text{H}_2\text{SO}_4$ 

Expt.	Wt. $\text{ZnEt}_2$ (g.)	Water equiv. (cal./°C)	$\Delta T^\circ \text{C}$ (obs.)	$-\Delta E$ (kcal.)	$-\Delta H$ (kcal.)	$M$ (kcal.)	$Q_f$ ( $\text{ZnEt}_2$ , liq.) (kcal. mole <sup>-1</sup> )
1	1.3373	1277	0.718	84.6	83.4	-0.9	-3.3
2	1.4392	1277	0.772	84.6	83.4	-0.75	-3.1
3	1.5474	1277	0.839	85.5	84.3	-0.9	-4.2
4	1.4112	1277	0.764	85.35	84.15	-0.8	-3.9
5	1.3337	1270	0.710	83.5	82.3	-0.9	-2.2

\* Maximum deviations from mean :  $\pm 0.5$  kcal.

\* Mean value of  $Q_f(\text{ZnEt}_2, \text{liq.}) = -3.6$  kcal. mole<sup>-1</sup>.

\* From data of Expt. 1-4 only.

Some results on the heat of reaction of  $\text{ZnMe}_2$  with aqueous  $\text{H}_2\text{SO}_4$  are given in Table V. In these experiments we were not able to make reliable estimates of the extent of side-reactions, but we would presume they occurred to similar extent (i.e. 1-2 %) to those in the reactions with  $\text{ZnEt}_2$ , listed in Table IV. The  $Q_f(\text{ZnMe}_2, \text{liq.})$  values are calculated from

$$Q_f(\text{ZnMe}_2, \text{liq.}) = \Delta H + 76.3 + M, \quad (8)$$

which is the equation corresponding to (7)

As previously stated, the  $Q_f(\text{ZnR}_2)$  values derived from heats of acidification are probably too *large* (due to side-reactions). On the other hand, the heats of hydrolysis in ethereal solution give  $Q_f$  values which are probably too *small*. The reactions were carried out in a *sealed* reaction vessel, and corrections should be made to the observed  $-\Delta E$  to allow for spurious heat effects due to solution of a portion of the gaseous products in the solvent medium. In the acid reactions, the solution effects are quite small, and the heat corrections have been considered unimportant. But in the ether hydrolyses, both  $\text{CH}_4$  and  $\text{C}_2\text{H}_6$  (particularly the latter) dissolve to an appreciable extent in the ether solvent. We would expect the observed heats of reaction to be increased by solution of the gases, leading to *smaller* observed values for  $Q_f$  than the true values. The solution heat corrections would be expected to be larger in the experiments using  $\text{ZnEt}_2$ , than in those using  $\text{ZnMe}_2$ , but lack of solution heat data prevents an estimation of the magnitude of the corrections.

TABLE V.—HEAT OF REACTION OF  $\text{ZnMe}_2$  WITH AQUEOUS  $\text{H}_2\text{SO}_4$ 

Expt.	Wt. $\text{ZnMe}_2$ (g.)	Water equiv. (cal./°C)	$\Delta T^\circ \text{C}$ (obs.)	$-\Delta E$ (kcal.)	$-\Delta H$ (kcal.)	$M$ (kcal.)	$Q_f$ ( $\text{ZnMe}_2$ , liq.) (kcal. mole <sup>-1</sup> )
1	1.6108	1287	1.070	82.0	80.8	-0.8	-5.3
2	1.541	1287	1.025	82.1	80.0	-0.9	-5.5
3	1.463	1267	0.958	82.3	81.1	-0.9	-5.7

Average purity of  $\text{ZnMe}_2$  samples taken as 99.5 %.

Mean value of  $Q_f(\text{ZnMe}_2, \text{liq.}) = -5.5$  kcal. mole<sup>-1</sup>.

Average deviation from mean :  $\pm 0.2$  kcal.

A rough estimate of the amount by which the heats of acidification are too small (due to *ca.* 2 % side-reactions) suggests that *ca.* 1 kcal.



may be involved. Making due allowance for the various corrections, we propose

$$\begin{aligned} Q_f(\text{ZnMe}_2, \text{liq.}) &= -6.3 \pm 1 \text{ kcal. mole}^{-1}. \\ Q_f(\text{ZnEt}_2, \text{liq.}) &= -4.3 \pm 1 \text{ kcal. mole}^{-1}. \end{aligned}$$

as the best values given by our data. The limits of error ( $\pm 1$  kcal.) cover the range over which the *mean* values of  $Q_f(\text{ZnR}_2)$  lie, as determined by both sets of experiments.

These values agree very well with those recently reported by Long and Norrish<sup>7</sup> from measurements of the heats of combustion of zinc dimethyl and zinc diethyl ( $-6.5$  kcal. mole<sup>-1</sup> and  $-4.1$  kcal. mole<sup>-1</sup> respectively).

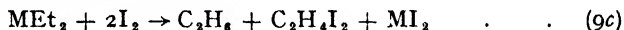
**Heats of Iodination of  $\text{ZnEt}_2$  and  $\text{CdEt}_2$ .**— $\text{ZnEt}_2$  reacts rapidly with a solution of excess  $\text{I}_2$  in benzene at room temperature.  $\text{CdEt}_2$  reacts similarly, but much less rapidly; in etherial  $\text{I}_2$  solution, however,  $\text{CdEt}_2$  reacts very quickly. The principal reaction between the di-alkyls and  $\text{I}_2$  is the formation of  $\text{EtI}$ :



Under the experimental conditions we have used, some small amounts of side-reaction accompanied the main reaction. The iodine balance indicated that the reaction,



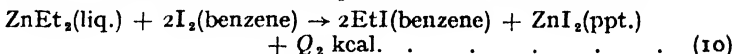
occurred to some extent, and the formation of small quantities (a few ml.) of  $\text{C}_2\text{H}_6$  suggests that the reaction



also contributed together with (9b).

In the absence of side-reactions the observed heat of iodination would correspond to the heat of reaction (9a), and enable a value for  $Q_f(\text{EtI})$  to be obtained directly. The occurrence of side-reactions requires that some correction be made to the observed heats of iodination, so that the true heat of (9a) can be assessed. Fortunately, the side-reactions (9b) and (9c) occur only to a small extent, and the corrections (which are difficult to assess exactly) are not large. Whilst the presence of these side-reactions prevents a highly accurate determination of the heat of reaction (9a) by this method, a value lying well within the limits  $\pm 2$  kcal. can be obtained.

(a) **HEAT OF IODINATION OF  $\text{ZnEt}_2$ .**—The heat of the reaction



is related to the heat of formation of  $\text{EtI}$  by the equation

$$\begin{aligned} 2Q_f(\text{EtI benzene}) &= Q_2 - Q_f(\text{ZnI}_2, \text{ppt.}) + Q_f(\text{ZnEt}_2, \text{liq.}) \\ &+ 2Q_f(\text{I}_2, \text{benzene}) \end{aligned} \quad (11)$$

Substituting the values:

$$\begin{aligned} Q_f(\text{ZnI}_2, \text{ppt.})^6 &= 49.98 \text{ kcal. mole}^{-1} \\ Q_f(\text{ZnEt}_2, \text{liq.}) &= -4.3 (\pm 1) \text{ kcal. mole}^{-1}. \\ Q_f(\text{I}_2, \text{benzene})^6 &= -4.3 \quad \text{,,} \quad \text{,,} \end{aligned}$$

in eqn. (11), one obtains

$$Q_f(\text{EtI benzene}) = Q_2/2 - 31.45 (\pm \frac{1}{2}) \text{ kcal.} \quad (12)$$

The experimental values of  $Q_2$ , obtained from 6 experiments, are listed in Table VI. In column 6 the estimated amounts of the side-reactions 9(b) and 9(c) are given to the nearest %. The corrections applied to  $-\Delta H_{\text{obs}}$  in order to arrive at  $Q_2$  are based on the correction figures:  $-0.12$  kcal. for each unit % of side-reaction 9(b), and  $-0.04$  kcal. for each unit % of side-reaction 9(c). Whilst both the estimates of the %

<sup>7</sup> Long and Norrish, *Phil. Trans. A*, 1949, **241**, 587.

<sup>6</sup> Hartley and Skinner (unpublished results).

TABLE VI.—HEAT OF IODINATION OF  $\text{ZnEt}_2$ 

Expt.	Wt. $\text{ZnEt}_2$ (g.)	Water equiv. (cal./°C)	$\Delta T^\circ \text{C}$ (obs.)	$-\Delta H_{\text{obs.}}$ (kcal.)	% side-reaction		$Q_3$ (kcal.)
					g (b)	g (c)	
1	1.311	1242	0.704	82.4	3	2	82.0
2	1.165	1242	0.622	81.9	3	2	81.5
3	1.292	1242	0.692	82.2	3	2	81.8
4	1.448	1242	0.764	81.2	2	1	80.9
5	1.562	1241	0.847	83.0	5	2	82.2
6	1.4690	1242	0.776	81.1	2	1	80.8

Mean value of  $Q_3 = 81.5 \text{ kcal. mole}^{-1}$ .

Maximum deviations from mean =  $\pm 0.7 \text{ kcal.}$

Standard error of mean =  $\pm 0.22 \text{ kcal.}$

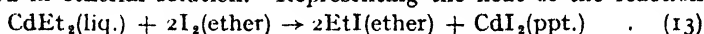
side-reaction, and the correction terms to be applied for each unit % of side reaction, are not very exact, the corrections are fortunately relatively small. In our view, the conclusion

$$Q_3 = 81.5 \pm 1.0 \text{ kcal.}$$

allows for the uncertainty in our observed heats of reaction due to the experimental and side-reaction errors. Substituting this value for  $Q_3$  into eqn. (12), we obtain

$$Q_f(\text{EtI, benzene}) = 9.3 \pm 1 \text{ kcal. mole}^{-1}$$

(b) HEAT OF IODINATION OF  $\text{CdEt}_2$ .—The reaction of  $\text{CdEt}_2$  with  $\text{I}_2$  was studied in ethereal solution. Representing the heat of the reaction



by  $Q_3 \text{ kcal.}$ , the equation

$$Q_f(\text{EtI, ether}) = Q_3/2 - 33.05 (\pm \frac{1}{2}) \text{ kcal.} \quad (14)$$

(corresponding to eqn. (12)) may be obtained assuming the following  $Q_f$  values:

$$Q_f(\text{CdI}_2, \text{ppt.})^6 = 48.0 \text{ kcal. mole}^{-1}$$

$$Q_f(\text{CdEt}_2, \text{liq.}) = -14.5 (\pm \frac{1}{2}) \text{ kcal. mole}^{-1}$$

$$Q_f(\text{I}_2, \text{ether})^6 = -1.8 \text{ kcal. mole}^{-1}.$$

Several experimental measurements of  $Q_3$  were made, from which a representative selection of 6 are given in Table VII. The final recommended value,

$$Q_3 = 84.4 \pm 1 \text{ kcal. mole}^{-1}$$

substituted into eqn. (14) gives

$$Q_f(\text{EtI, ether}) = 9.15 \pm 1 \text{ kcal. mole}^{-1}.$$

TABLE VII.—HEAT OF IODINATION OF  $\text{CdEt}_2$ 

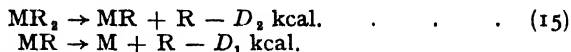
Expt.	Wt. $\text{CdEt}_2$ (g.)	Water equiv. (cal./°C)	$\Delta T^\circ$ (obs.)	$-\Delta H_{\text{obs.}}$ (kcal.)	% side-reaction		$Q_3$ (kcal.)
					g (b)	g (c)	
4	1.4606	1230	0.590	84.7	ca. 4	ca. 2	84.0
7	1.956	1239	0.800	86.3	ca. 5	ca. 2	85.5
9	2.251	1243	0.902	84.9	ca. 5	ca. 2	84.1
11	1.989	1240	0.809	85.9	ca. 5	ca. 2	85.1
12	1.982	1243	0.793	84.8	ca. 5	ca. 3	84.0
13	2.236	1243	0.891	84.4	ca. 5	ca. 2	83.6

Mean value of  $Q_3 = 84.4 \text{ kcal. mole}^{-1}$ .

Max. deviations from mean =  $+1.1, -0.8 \text{ kcal. mole}^{-1}$ .

Standard deviation from mean =  $\pm 0.28 \text{ kcal.}$

**Dissociation Energies of Zn—C and Cd—C Bonds**—Denoting the bond dissociation energies of the two M—R bonds in  $MR_2$  by  $D_1$  and  $D_2$ , viz.



the thermal relationship between  $D_1$ ,  $D_2$  and the heats of formation of  $MR_2$ , M and R is

$$(D_1 + D_2) = Q_f(MR_2) - Q_f(M) - 2Q_f(R). \quad (16)$$

All the terms in  $Q_f$  in eqn. (16) refer to *gaseous* states.

Values for  $Q_f(R)$  (where R = Me or Et) have been given elsewhere by Roberts and Skinner.<sup>9</sup> Values for  $Q_f(M)$  (M = Cd or Zn) follow from the heats of sublimation of the metals, given by Kelley.<sup>10</sup> The values of  $Q_f(MR_2, \text{gas})$  are obtainable from the  $Q_f(MR_2, \text{liq.})$  of this paper and published heats of vaporization of the di-alkyls. The relevant data are summarized in Table VIII.

TABLE VIII.—BOND DISSOCIATION ENERGIES IN Zn AND Cd ALKYLs

Molecule	$Q_f(MR_2, \text{liq.})$ (kcal.)	$Q_f(MR_2, \text{gas})$ (kcal.)	$Q_f(M)$ (kcal.)	$Q_f(R)$ (kcal.)	$(D_1 + D_2)$ (kcal.)	$\frac{1}{2}(D_1 + D_2)$ (kcal.)
CdMe <sub>2</sub>	-16.7 <sup>a</sup>	-25.2 <sup>b</sup>	-26.8 <sup>c</sup>	-32.1 <sup>d</sup>	65.8	32.9
CdEt <sub>2</sub>	-14.5 <sup>e</sup>	-24.5 <sup>f</sup>	-26.8 <sup>c</sup>	-25.3 <sup>d</sup>	52.9	26.5
ZnMe <sub>2</sub>	-6.3 <sup>g</sup>	-13.5 <sup>h</sup>	-31.2 <sup>c</sup>	-32.1 <sup>d</sup>	81.9	41.0
ZnEt <sub>2</sub>	-4.3 <sup>g</sup>	-13.1 <sup>h</sup>	-31.2 <sup>c</sup>	-25.3 <sup>d</sup>	68.7	34.4

a. Carson, Hartley and Skinner.<sup>1</sup> The value given here ( $Q_f, \text{liq.} = -16.7$ ) differs by -0.4 kcal. from that quoted in ref. 1. The reason for this change lies in the difference of -0.4 kcal. between the value of  $Q_f(\text{CdI}_2, \text{cryst.})$  used here (ref. 5) and that used in ref. 1.

b. Bamford, Levi and Newitt,<sup>11</sup>  $\lambda_{\text{vap.}}(\text{CdMe}_2) = 8.5$  kcal.

c. Kelley.<sup>10</sup>

d. Roberts and Skinner.<sup>9</sup>

e. This research.

f. We have estimated  $\lambda_{\text{vap.}}(\text{CdEt}_2) \sim 10.0$  kcal.

g. Bamford, Levi and Newitt,<sup>11</sup>  $\lambda_{\text{vap.}}(\text{ZnMe}_2) = 7.2$  kcal.

h. Hein and Schramm,<sup>12</sup>  $\lambda_{\text{vap.}}(\text{ZnEt}_2) = 8.8$  kcal.

The absolute values quoted for  $(D_1 + D_2)$  in Table VIII carry the experimental errors present in both  $Q_f(MR_2, \text{gas})$  and  $Q_f(R)$ . The former probably lie well within  $\pm 2$  kcal., and an error of similar magnitude may be present in the  $Q_f(R)$  values (which depend upon two assumed values, viz.  $D(\text{CH}_3-\text{H}) = 102.0$  kcal., and  $D(\text{C}_2\text{H}_5-\text{H}) = 97.5$  kcal.). The overall error in the *mean* bond dissociation energies (i.e. in  $\frac{1}{2}(D_1 + D_2)$ ) is thus of the order  $\pm 2$  kcal.

Elsewhere, one of us<sup>13</sup> has pointed out that there is no reason to expect  $D_1 = D_2 = \frac{1}{2}(D_1 + D_2)$ , and that, more probably,  $D_2 > D_1$  for the di-alkyls of Group 11B. None the less, the marked fall in the *mean* bond dissociation energies in  $MR_2$ , as we pass from R = Me to R = Et, almost certainly implies a fall at least as large in  $D_2$ . In this event, one would expect the  $\text{MEt}_2$  compounds to be thermally *less* stable than  $\text{MMe}_2$ , in so far as the initial step in thermal disruption is the split into R + MR. In the case of  $\text{CdEt}_2$ , relative to  $\text{CdMe}_2$ , the thermal instability is most marked, for whereas  $\text{CdMe}_2$  can be distilled without decomposition

<sup>9</sup> Roberts and Skinner, *Trans. Faraday Soc.*, 1949, **45**, 339.

<sup>10</sup> Kelley, *U.S. Bur. Mines Bull.*, 383, 1935.

<sup>11</sup> Bamford, Levi and Newitt, *J. Chem. Soc.*, 1946, 468.

<sup>12</sup> Hein and Schramm, *Z. physik. Chem. A*, 1930, **149**, 408.

<sup>13</sup> Skinner, *Trans. Faraday Soc.*, 1949, **45**, 20.

at atmospheric pressure,  $\text{CdEt}_2$  decomposes violently under similar treatment, and can only be distilled satisfactorily under low pressure (20 mm. or less).  $\text{ZnEt}_2$  on the other hand is thermally stable, relative to  $\text{CdEt}_2$ , presumably due to the greater strength (by *ca.* 7-8 kcal.) of  $\text{Zn}-\text{C}$  relative to  $\text{Cd}-\text{C}$  bonds. The conclusion that the bond dissociation energies are higher in  $\text{MMe}_2$  than in  $\text{MEt}_2$  is consistent with the observations of Bamford and Newitt<sup>14</sup> on the rates of oxidation of the alkyls; the methyl derivatives react with oxygen much more slowly than the higher ones.

**Dissociation-energy of C—I in  $\text{C}_2\text{H}_5\text{I}$ .**—Making due allowance for the heats of solution of liquid  $\text{EtI}$  in benzene and in ether, the results of a previous section give

$$(a) Q_f(\text{EtI, liq.}) = 9.4 \text{ kcal. mole}^{-1} \quad (\pm 1 \text{ kcal.})$$

$$(b) Q_f(\text{EtI, liq.}) = 9.15 \text{ kcal. mole}^{-1} \quad (\pm 1 \text{ kcal.})$$

in which (a) is derived from the heat of iodination of  $\text{ZnEt}_2$ , and (b) from the heat of iodination of  $\text{CdEt}_2$ . The results agree reasonably well with one another, considering the difficulties due to side-reactions, and the uncertainties in some of the assumed data e.g.  $Q_f(\text{Zn}(\text{OH})_2)$ . Of the two values quoted, (b) seems the more reliable.

Recently, Springall and White<sup>15</sup> have reported a new measurement of the heat of combustion of liquid  $\text{EtI}$  ( $350.5 \pm 0.5 \text{ kcal. mole}^{-1}$ ), corresponding to  $Q_f(\text{EtI, liq.}) = 8.4 \pm 0.5 \text{ kcal. mole}^{-1}$ . The agreement between the combustion heat value, and the values given here, lies within the estimated experimental errors of the two separate determinations.

The value  $Q_f(\text{EtI, liq.}) = 9.1 \pm 1 \text{ kcal. mole}^{-1}$  corresponds to  $Q_f(\text{EtI, gas}) = 2.0 \pm 1 \text{ kcal. mole}^{-1}$ , and (assuming  $D(\text{C}_2\text{H}_5-\text{H}) = 97.5 \text{ kcal.}$  for the  $\text{C}-\text{H}$  dissociation energy in ethane<sup>9</sup>) leads to

$$D(\text{C}_2\text{H}_5-\text{I}) = 52.8 \pm 1 \text{ kcal.}$$

for the dissociation energy of the  $\text{C}-\text{I}$  bond in ethyl iodide.

In Part I, the present authors gave 55.0 kcal. for the  $\text{C}-\text{I}$  dissociation energy in  $\text{CH}_3\text{I}$ . This value we would now amend slightly to 54.8 kcal., in view of our new measurement ( $-1.8 \text{ kcal. mole}^{-1}$ ) of the heat of solution of  $\text{I}_2$  in ether.<sup>8</sup> Accordingly, the comparable experiments on the heats of iodination of  $\text{CdMe}_2$  and  $\text{CdEt}_2$  lead to a difference of 2 kcal. between  $D(\text{CH}_3-\text{I})$  and  $D(\text{C}_2\text{H}_5-\text{I})$ , relative to an assumed difference of 4.5 kcal. between  $D(\text{CH}_3-\text{H})$  and  $D(\text{C}_2\text{H}_5-\text{H})$ . The difference agrees precisely with that given by Baughan and Polanyi in their table of  $\text{C}-\text{I}$  bond energies, as derived from the pyrolysis experiments on alkyl iodides by Butler and Polanyi.<sup>16</sup>

The authors wish to express thanks to Prof. M. Polanyi, F.R.S., for his interest and encouragement during the course of this research.

*Chemistry Department,  
University of Manchester.*

<sup>14</sup> Bamford and Newitt, *J. Chem. Soc.*, 1946, 688, 695.

<sup>15</sup> Springall and White, *Research*, 1949, **2**, 290.

<sup>16</sup> Butler and Polanyi, *Trans. Faraday Soc.*, 1943, **39**, 19.

## REVIEWS OF BOOKS

**The Adsorption of Gases on Solids.** By A. R. MILLER. (Brooke Crutchley, at the Cambridge University Press, 1949.) Pp. ix + 133. Price 12s. 6d.

The years which have elapsed since the publication in 1939 of *Some Problem in Adsorption* by J. K. Roberts have seen further applications of the methods of statistical mechanics to the treatment of the adsorption of gases on solids. There has, however, been no corresponding output of refined experimental material with which to test the statistically derived expressions although in some cases the models assumed and the approximations made are such as to render impossible comparison of theory with experiment. Recently the non-uniformity of the adsorbent surface has been stressed, so although a change in emphasis can be expected the present is an opportune time to review the statistical developments of the past decade.

According to the preface Dr. Miller's book is a "revision of Roberts's tract on adsorption". Some revisions are known to result in the production of a totally new work, but this volume is not such an instance for it contains unaltered, except for rearrangement, about two-thirds of the contents of the original tract. Furthermore, since it is a monograph and not a handbook it is restricted to certain selected references and consequently the title does not give an accurate indication of the contents of the book.

In order to accomplish the revision, judicious pruning has been exercised to make room for the new material and hence the text has only increased by ten pages. With the exception of the new title of Chapter 3, the chapter headings have been retained. The main additions are in those parts of the work concerned with the energetics of the adsorption process, Chapter 2, for example, containing a consideration of the statistics of a geometrically random distribution of pairs of occupied sites. Previous treatments of the effect of forces between adsorbed particles assumed a fixed interaction energy which is negligible for distances apart greater than some critical value. In Chapter 3, however, there is a discussion of the dependence of the heat of adsorption on coverage which takes cognizance not only of the potential energy of an adsorbed particle as this varies continuously and periodically with its position on the surface, but also of the variation with distance apart of the mutual potential energy of adsorbed particles. Experiment shows that the dipole moment of the adsorbate is not a constant but decreases with increasing coverage and the contents of Chapter 7 show how this can be taken into account.

The subject matter is well arranged and presented and the book itself excellently produced. The subject index is well done but there is no author index. This volume will be welcomed by all workers in the field and can be recommended as containing a trustworthy account of the application of statistical mechanics to some problems in adsorption.

V. A. C.

**Crystals and X-rays.** By KATHLEEN LONSDALE. (G. Bell & Sons Ltd., London, 1948.) Pp. viii + 199. Price 21s.

This book is about the study of the structures of crystals by X-ray diffraction methods; the generation and properties of X-rays are described only in so far as the information is necessary for the effective use of these rays in crystallographic investigations: the crystals are the objects of study, the X-rays are the tools used. The book is a highly condensed survey, in some 200 pages, of the methods and some of the outstanding results of such studies.

It is based on a course of public lectures given at University College, London, in 1946, and the style retains some of the characteristics of this origin; the informality and clarity of the author's lecture style make it eminently readable, and explanations are illustrated by many diagrams and photographs and enlivened by homely analogies and humorous asides. Let it not be supposed, however, that because the book is semi-popular in style it is superficial; on the contrary, its explanations refer, as far as possible in a book of this type, to fundamental concepts, and a surprisingly large amount of information on a very wide range of subjects is packed into its moderate compass. Indeed, the principal criticism which arose in the reviewer's mind when reading it is that in trying to cover such an immense range, the author may have gone too fast for some readers, or have condensed an argument by making a jump which her readers may not be able to emulate.

The first chapter—a historical introduction which includes a thrilling account of the discovery of X-ray diffraction in 1912 and the way in which the phenomena were elucidated by Laue and his school and the Braggs—is, to the reviewer, one of the best in the book. The familiar epic is told in such a way as to show how incorrect ideas were eliminated by successive experiments and by following up clues which turned up unexpectedly; it is a stimulating lesson to all research workers. After a chapter on the generation and properties of X-rays which contains much practical information, there follow two chapters which deal in a highly compressed manner with unit cells, symmetries and space groups, and their determination by X-ray methods helped out by the reciprocal lattice concept; the essential ideas are here, but taken at such a speed that beginners may not be able to make the grade; the reviewer felt rather breathless. The fifth chapter, on "Extra-structural studies", deals with imperfections and the thermal motions of atoms and molecules in crystals (another high spot, this) and the last draws attention to the many chemical contributions of X-ray analysis.

No serious errors have been noticed; but there are inevitably some places where one would like to question the author's point of view. The assertion (p. 85) that the reciprocal lattice and the atomic model are equally real (or equally unreal) is difficult to accept; we think, with good reason, that there are entities called atoms actually at the places where calculations or electron density maps say they are; a similar thing would never be said about the reciprocal lattice, which is frankly a piece of mental scaffolding, a convenient fiction. On the same page, the generalization about the reciprocal relation between crystal habit and unit cell shape seems to be pushed too far; it is misleading to connect the octahedral habit of many cubic crystals with the fact that "the

reciprocal of a cube is an octahedron", for an octahedral habit is shown by many crystals with face-centred lattices but not by those with other types of cubic lattice. A better approach to crystal habit (in so far as it is justifiable to treat it geometrically without reference to forces) is by way of Bravais' generalization and its extension by Donnay and Harker. High polymer properties (p. 185) are not very happily treated; the impression may be given that the difference between the properties of rubber and gutta-percha is more far-reaching than the facts warrant; this shows the danger of mentioning polymer properties without reference to temperature changes. A statement that long-chain polymers are tough and horn-like when crystalline but become flexible and elastic above their melting points (if the molecules are long enough) would have been more helpful; the contrast between gutta-percha and rubber at room temperature then falls into line as an example, because the melting point of the former is above and the latter below room temperature.

These, however, are minor matters. The book is a rapid panorama of method and achievement in X-ray analysis, it is eminently readable (as scientific text books should be: it is an artistic necessity that important and interesting material should be worthily presented), and it communicates to the reader some of the author's enthusiasm. If at times it seems to go too fast or to be over-compressed, that is only to say it ought to have been longer. It is very warmly recommended to the attention of all who are interested in the structures of crystalline substances.

C. W. B.

**Photoelectric Methods in Clinical Biochemistry.** By G. E. DELORY. (Hilger and Watts, Ltd.) Pp. x + 90. Price 15s.

In a foreword to this book Prof. E. J. King states that the aim is three-fold: to give in a simple fashion the theoretical background needed for the intelligent use of photoelectric colorimeters; to give descriptions and instructions for the use of the Hilger Spekker and Biochem. Absorptionimeters, and to give practical details for the colorimetric procedures most commonly undertaken in clinical biochemical laboratories.

The first of these aims is dealt with in chapters 1-3. A short account is given of Lambert's and Beer's laws, technical terms in common use, and multiple absorption. Instruments of the visual type, e.g. Duboscq and Pulfrich are only briefly mentioned since they are not photoelectric colorimeters. Photo-emissive cells are dismissed in one short paragraph which is not altogether correct. More space is given to a description of barrier-layer photo-cells since these are the type employed in the Hilger instruments. Other designs of colorimeters are not described but three references are given. Data are also given for Ilford and Chance Filters. Regarding the data given for Ilford Spectrum Filters the reviewer would point out that in addition to the transmission bands shown all No. 601, 602, 604 and 605 filters examined by him show a secondary light band in the red centred at *ca.* 680, 730, 719 and 719  $m\mu$  respectively and that this may produce a "stray light" effect under certain conditions.

Under the heading, "Optimum instrument readings", the author points out that accuracy is greatest at an optical density of 0.43 but no

serious loss of accuracy is involved between 0.2 and 0.8. He then suggests that these considerations are concerned with a degree of accuracy outside the limits set by other factors, such as the chemical procedure involved. This view appears to be reflected in the method given (p. 31) for the selection of test tubes for the Biochem. Absorptiometer which the reviewer would criticize strongly. The method given is that of selection of  $6 \times \frac{1}{8}$  in. thin-wall tubes by filling them with distilled water and selecting those which give 100 % transmission (zero reading on the logarithmic scale). This is only a test that the tube filled with water is not seriously distorting the optical system and the reviewer suggests that it would be much more profitable subsequently to use a coloured solution together with a suitable filter so that the density reading is of the order of 0.43. This would result in the selection of tubes of uniform internal diameter.

Chapters 4 and 5 deal with the construction of the Spekker and Biochem. Absorptiometers respectively and give full details for their operation. Chapter 6 gives methods in suitable form for use with these two instruments for the determination of 22 substances encountered in clinical biochemistry. References to the original papers are given. Of 4 checked at random, one to King *et al.* (1937) has the page given as 866 instead of 886. In most cases, as the author says, the methods have been adapted into a form suitable for these instruments.

Typical calibration curves are given for 12 substances, but the author points out that these only illustrate the relationship between instrument readings and concentration, and that the operator must prepare calibration curves for his own instrument. Much space is taken up by these curves which are of limited value. Moreover, in many cases the values quoted, e.g. Bilirubin in plasma (0.3-0.8 mg./100 ml. but up to 1.7 mg. occasionally) would give densities as shown on the calibration curve below 0.2; the instruments would not therefore be used within their optimal working range.

The collection of methods given in this book should be of value to workers in hospital laboratories who have available one of these absorptiometers. The price, however, seems very high for a book of this kind.

✓ **Molecules and Crystals in Inorganic Chemistry.** By A. E. VAN ARKEL (English trans. by J. C. SWALLOW). (Butterworths Scientific Publications, 1949.) Pp. ix + 234. Price 17s. 6d.

This is a translation of the third Dutch edition of *Moleculen en Kristallen* (now in preparation). It is concerned with the subject of the correlation of structure and properties of inorganic compounds. The treatment is based on the distinction between "the electrostatic and homopolar bonds"; this generalization has its dangers but the author emphasizes throughout the limitations and the approximate nature of his exposition. It is intended for first-year science and medical students, but the value of the present volume is somewhat marred by lack of care in presentation. If the translation is a faithful representation of the original text, it is regrettable that it should have been published without



some editorial attention. There seems little excuse in an elementary text-book for the presence of many statements which are either misleading or ambiguous. To quote two of these: (i) page 146—"In  $\text{CCl}_4$  the field of the positive ion attracts the electrons of the  $\text{Cl}^-$  ion inwards"; (ii) page 214—with reference to Fig. 43 (an adsorption isotherm showing the amount adsorbed as a monotonically increasing function of the concentration)—". . . as the surface of the adsorbent becomes covered with molecules the amount adsorbed will diminish". On page 38 there is a peculiar reaction:  $\text{I} + \theta = \text{I}'$ , with  $\theta$  undefined in the text. Lack of care is also evidenced by the units given in many of the tables. In columns 2 and 3 of Table III, "radius  $\times 10^4$ " is meaningless; the units are missing from Table IV. Heats of formation in Tables XVIII and XX are given rather unusually in kcal./equivalent (presumably g. equivalent is meant), whereas in Table XIX the heats of formation are given in kcal.—possibly this time per mole!

There is a good subject-index and some suggestions for further reading.

F. C. T.

**Tables of Electric Dipole Moments.** Compiled by L. G. WESSON. (The Technology Press, Massachusetts Institute of Technology, 1949.) Pp. 90. Price \$2.50.

The value of compilations of physico-chemical data need not be stressed; so we welcome briefly but very warmly these new tables of electric dipole moments, the first complete list to appear for nearly fifteen years.

The present tables list inorganic and metallo-organic compounds alphabetically, and organic compounds by empirical formula, the systematic name following. After this description, the solvent used (if any) is specified, the temperature, or temperature range, of observation is given, next the moment, and finally the reference. Observations by different authors are given separately; and errors are quoted when authors estimate them, which they do but rarely. The literature is surveyed up to August 1948. Values for over two thousand substances have been collected. A number of omissions and errors have come to light, but this is to be expected in so big and arduous an undertaking. The photo-offset process used for printing gives a clear and quite hand some page.

It is to be regretted that this publication has not been announced in this country through the usual trade channels and consequently is hardly known over here, for it is much too useful to be missed. The price quoted is that charged by the publishers who will supply direct. Even to us, in our present depreciated state, it is good value.

L. E. S.

**Preparations and Characteristics of Solid Luminescent Materials.** Ed.

by F. SEITZ AND G. FONDA. (John Wiley & Sons, Inc., New York, and Chapman & Hall, Ltd., London, 1948.) Pp. xvi + 459. Price 30s.

In a review of this book (*Trans. Faraday Soc.*, 1949, **45**, 302) it was noted that all contributors except one from England were Americans and it was remarked: "If the reason is that the English scientist can afford neither time nor money for such meetings, then some responsible organization should help to alleviate such hardship. If, however, the scientists in the States feel that English and Continental workers have little to contribute, then, as the Faraday Society attempts to do by its Discussions, we must make every effort to encourage our American friends to come to England, and hope that we may disillusion them."

Dr. Fonda now writes: "Let me assure you that we shared the reviewer's regret that Garlick was the only British scientist who was able to attend and that Holland was completely unrepresented. We had sent invitations to individual British and Dutch scientists and also a blanket invitation" (through the British Admiralty).

"The Atlantic Ocean offers no longer the physical barrier of years ago, but it still remains a financial hurdle. Those of you who can make the leap, however, may always feel assured of a warm and appreciative welcome from us. And on our side, we are exceedingly jealous of the occasional American who succeeds in getting to you."

F. C. T.

**The Theory of Atomic Collisions, 2nd Ed.** By N. F. MOTT and H. S. W.

MASSEY. (Geoffrey Cumberlege, Oxford University Press, 1949.) Pp. 388. Price 35s.

The second edition of Mott and Massey's well-known treatise will be welcomed by all scientists interested in atomic and nuclear collision problems. In the main the material of the first edition has been retained, with the changes and additions necessary to bring the material up to date. Most of the very few misprints in the first edition have also been removed.

Since 1933, when the book originally appeared, there have been so many developments in the field of nuclear physics that a great deal of new matter had necessarily to be added; the topics discussed include proton-proton and neutron-proton scattering, resonance processes in nuclear reactions, particularly those involving slow neutrons. A very useful account is given of several derivations of the dispersion formula originally due to Breit and Wigner. Nuclear fission is, of course, also dealt with; it is, however, a relief to find that fission receives its proper place in a scientific treatise of this kind, being relegated to a small section at the end of a long chapter.

It is hardly necessary to add that the new edition will become, as the first edition has been, the standard reference book on the theory of atomic and nuclear collisions.

M. B.

**Viscometry.** By A. C. MERRINGTON. (Edward Arnold & Co. London, 1949.) Pp. viii + 142. Price 16s.

This book is intended to provide a "concise yet up-to-date" account of viscometry for the practical research worker, and it accordingly deals more with experimental methods than with theoretical aspects. It certainly provides a very concise account of practical methods, although it cannot be said to be entirely up to date, due perhaps to the usual printing delays.

After a brief introduction there are separate chapters devoted to capillary viscometers, rotational and oscillational viscometers, the falling-sphere method, technical viscometers and miscellaneous methods. The viscosity of gases is dealt with in some ten pages, and the final two chapters consider methods for very viscous materials and application to rheology.

A number of tables are given as appendices; of these 1 and 2, dealing with the dimensions of capillary viscometers and conversion tables for technical viscometers, are particularly useful. Appendix 5 seems unnecessary, and in Appendix 4 the choice of  $10^{-5}$  poise as the unit has little to commend it.

Since intended for the practical worker a great deal more might well have been said concerning the limitations of the various methods described. For its size and content this book is too highly priced.

A. E. A.

**Monomers: Section I.** Edited by E. R. BLOUT, W. P. HOHENSTEIN and H. MARK. (Interscience Publishers, New York and London.) Pp. 312. Price 45s.

During the last few years intense interest has developed in a class of organic compounds—known as monomers—from which macromolecules can be synthesized. This book comprises a series of comprehensive articles dealing with individual monomers. The information given includes methods of laboratory and large-scale preparation, physical data, purification, analysis, handling and storing, methods of polymerization, and an enumeration of the most outstanding chemical properties of the monomer. Whilst most of this information is scattered throughout the literature, the present volume is valuable in that the material presented is carefully sifted and its reliability checked by authors with special interest in this field. This volume contains separate articles on acrylonitrile, butadiene, isobutylene, isoprene, methyl methacrylate, styrene, vinyl acetate and vinyl chloride. They are collected in a convenient binder. The editors are continuing the series and new articles can be easily added to the present binder. The information presented seems to be very complete and to contain unpublished measurements from the editors' and authors' own laboratories. Since many of these monomers, e.g. acrylonitrile, are of importance other than in the polymer field the book has increased value and can be recommended as an excellent work of reference.

C. E. H. B.

# Transactions of the Faraday Society.

## SUBJECT INDEX—VOLUME XLV, 1949.

	PAGE
<b>Absorption</b> and Desorption, The Effect of a Variable Diffusion Coefficient on the Rates of. J. Crank and M. E. Henry . . . . .	636
— Experiments, An Evaluation of the Diffusion Coefficient for Chloroform in Polystyrene from Simple. J. Crank and G. S. Park . . . . .	240
<b>Acetaldehyde</b> , and Acetic Acid. The Variation of Hydrogen Overvoltage at Various Cathodes on the Addition of Ethyl Alcohol. Allan Wetterholm . . . . .	861
— for Detection of Chain Reactions, The Use of. K. E. Howlett and D. H. R. Barton . . . . .	735
<b>Acetic Acid</b> , The Variation of Hydrogen Overvoltage at Various Cathodes on the Addition of Ethyl Alcohol, Acetaldehyde, and. Allan Wetterholm . . . . .	861
<b>Acetone</b> , The Solubility of Benzylpenicillin Salts in. J. E. Page and J. G. Waller . . . . .	755
<b>Acrylate</b> , The Polymerization of Butyl. Determination of the Velocity Coefficients. H. W. Melville and A. F. Bickel. . . . .	1049
<b>Activity</b> Coefficients of Electrolytes in Aqueous Solution at 25°, Tables of Osmotic and. R. A. Robinson and R. H. Stokes . . . . .	612
<b>Adsorption</b> Isotherm, The Determination of the Surface Area of a Solid from an. James F. Duncan . . . . .	879
— of Long Chain Polar Compounds from Solution on Metal Surfaces, The. E. B. Greenhill . . . . .	625
<b>Affinity</b> of Conjugated and Resonating Hydrocarbons, The Residual. William Moffitt . . . . .	373
<b>Alkanes</b> , Bond Refractions in the. Part II of The Polarizabilities of Bonds. B. C. Vickery and K. G. Denbigh . . . . .	61
<b>Alkyls</b> , Thermochemistry of Metal. Part II of The Bond Dissociation Energies of some Zn—C and Cd—C Bonds, and of Et—I. A. S. Carson, K. Hartley and H. A. Skinner . . . . .	1159
<b>Alloys</b> , On Phase-Change Processes in Iron-Silicon. K. M. Guggenheimer and H. Heitler . . . . .	137
— Some New Aspects of the Strength of. George-Maria Schwab . . . . .	385
— The Thermodynamics of the Iron-Nickel. O. Kubaschewski and Ortrud von Goldbeck . . . . .	948
<b>Ammonium</b> Compounds, Di magnetic Susceptibility of. M. E. Bedwell, J. F. Spencer and V. C. G. Trew . . . . .	217
<b>Anodic</b> Oxidation of Platinum, The. Simon Altmann and R. H. Busch . . . . .	720
<b>Arsine</b> , The Density of Liquid. A. L. G. Rees and K. Stewart . . . . .	1028
<b>Aryloxypropanes</b> , The Surface Tension of Aqueous Solutions of $\alpha$ : $\beta$ -Dihydroxy- $\gamma$ . A. C. R. Dean and W. Bradley . . . . .	250
<b>Autocatalytic</b> Reactions, Chains of Simple. Kinetics of Open Reaction Systems. Margaret J. Moore . . . . .	1098
<b>Bacteria</b> , with particular reference to Soaps, and Soap-Phenol Mixtures, The Action of Colloidal Electrolytes on. Anne Agar and A. E. Alexander. . . . .	528
<b>Barium</b> Bromo-acetate, Calcium and Barium Thiosulphates. Part XI of. The Extent of Dissociation of Salts in Water. C. W. Davies and P. A. H. Wyatt. . . . .	770
— Thiosulphates and Barium Bromo-acetate, Calcium and. Part XI of. The Extent of Dissociation of Salts in Water. C. W. Davies and P. A. H. Wyatt. . . . .	770
<b>Basic Strengths</b> of the Mononitronaphthylamines, The. Part I of The Effects of Substituents in the Naphthalene Ring. Alexander Bryson . . . . .	257
<b>Benzylpenicillin</b> Salts in Acetone, The Solubility of. J. E. Page and J. S. Waller . . . . .	755
<b>Bond</b> Dissociation Energies in Polyatomic Molecules of the Type MX <sub>n</sub> . H. A. Skinner . . . . .	20
— Dissociation Energies of Some Zn—C and Cd—C Bonds, and of Et—I, The. Part II of Thermochemistry of Metal Alkyls. A. S. Carson, K. Hartley and H. A. Skinner . . . . .	1159

	PAGE
<b>Bond-Forming Orbitals and the Effect on Molecular Vibrations, Distortions of.</b> Part VI of Molecular Force Fields. J. W. Linnett and P. J. Wheatley . . . . .	33
— Interactions during Vibrations and on Dissociation, A Relation between. Part IX of Molecular Force Fields. J. W. Linnett and M. F. Hoare . . . . .	844
— Lengths of the Hydrogen Halides, Calculations of the. Ernest Warhurst. . . . .	461
— Orders and Other Criteria of Double-Bond Character. V. Gold . . . . .	191
— Refractions in the Alkanes. Part II of The Polarizabilities of Bonds. B. C. Vickery and K. G. Denbigh . . . . .	61
— in Molecules which contain a Polyvalent Central Atom, Calculations of the Lengths of. John Scanlan and Ernest Warhurst . . . . .	1000
— which possess Partial Ionic Character, Calculations of the Effect of Solvation on the Force Constants of. Ernest Warhurst. . . . .	476
<b>Boron Trioxide, The Heat of Formation of.</b> W. Eggersgluess, A. G. Monroe and W. G. Parker . . . . .	661
<b>Bromoacetate-Thiosulphate Reaction, The.</b> Part I of Ionic Reaction Rates and the Incomplete Dissociation of Salts. P. A. H. Wyatt and C. W. Davies . . . . .	774
<b>Butyl Acrylate, The Polymerization of.</b> Determination of the Velocity Coefficients for Polymerization Processes. H. W. Melville and A. F. Bickel . . . . .	1049
<b>Calcium and Barium Thiosulphates and Barium Bromo-acetate.</b> Part XI of The Extent of Dissociation of Salts in Water. C. W. Davies and P. A. H. Wyatt . . . . .	770
— Ferrocyanide, The Conductivities of Dilute Aqueous Solutions of Potassium Ferrocyanide and. J. S. James . . . . .	855
<b>Calorimeter and a Comparison of some Thermodynamic Properties of Methyl Alcohol and Methyl Deuterioxide, A Semi-Micro Low-Temperature.</b> L. A. K. Staveley and A. K. Gupta . . . . .	50
<b>Capillary Networks of Molecular Dimensions, Transient Flow of Gases in Sorbents providing Uniform.</b> R. M. Barrer. . . . .	358
<b>Carbonaceous Solids by Measurements of True and Apparent Densities.</b> Part I. Rosalind E. Franklin . . . . .	274
— Solids by Measurements of True and Apparent Densities. Part II. Rosalind E. Franklin . . . . .	668
<b>Carbon Bonds, and Resonance Energies in Hydrocarbon Radicals, Dissociation Energies of.</b> J. S. Roberts and H. A. Skinner . . . . .	339
— Note concerning some recent statements on the Latent Heat of Vaporization of. L. H. Long and R. G. W. Norrish . . . . .	1158
— $2p\pi$ orbitals, A Wave-mechanical Treatment of the Change with Distortion of the Interaction Energy of. Part XI of Molecular Force Fields. P. J. Wheatley and J. W. Linnett . . . . .	897
<b>Catalytic Poisons at Platinized Platinum and Nickel, The Effect of.</b> Studies in Hydrogen Overpotential. J. O'M. Bockris and B. E. Conway. . . . .	989
<b>Chain Propagation in the Oxidation of Polyisoprenes.</b> The Mechanism of. J. L. Bolland and P. ten Have . . . . .	93
— Reactions, The Use of Acetaldehyde for Detection of. K. E. Howlett and D. H. R. Barton . . . . .	735
<b>Chlorine Solutions, The Reaction Kinetics of Wool with.</b> Part II: Diffusion within the Fibre. P. Alexander, D. Gough and R. F. Hudson . . . . .	1109
— The Kinetics of the Photochemical Interaction of Hydrogen with. W. J. Kramers and L. A. Moignard . . . . .	903
<b>Chloroform in Polystyrene from Simple Absorption Experiments, An Evaluation of the Diffusion Coefficient for.</b> J. Crank and G. S. Park . . . . .	240
<b>Coals, Carbonized.</b> Part II of A Study of the Fine Structure of Carbonaceous Solids by Measurements of True and Apparent Densities. Rosalind E. Franklin . . . . .	668
<b>Cohesion and the Structure of Liquids, The Energies of Vaporization, Viscosity and.</b> L. Grunberg and A. H. Nissan . . . . .	125
<b>Colloidal Electrolytes on Bacteria, with particular reference to Soaps and Soap-Phenol Mixtures, The Action of.</b> Anne Agar and A. E. Alexander . . . . .	528
<b>Complexes, The <math>[\text{Fe}(\text{OH})]^{2+}</math> and <math>[\text{Fe}(\text{O}_2\text{H})]^{2+}</math>.</b> M. G. Evans, Philip George and N. Uri . . . . .	230
<b>Conductivities of Dilute Aqueous Solutions of Potassium Ferrocyanide and Calcium Ferrocyanide.</b> J. C. James . . . . .	855
<b>Conjugated and Resonating Hydrocarbons, The Residual Affinity of.</b> William Moffitt . . . . .	373

	PAGE
<b>Continuous Reaction System, The Kinetics of the Transient State in a.</b>	
J. D. Johnson and L. J. Edwards . . . . .	286
<b>Cordite by Hot Gases, The Ignition of.</b> R. C. Brian and C. A. McDowell. .	212
<b>Cupric Ferrocyanide, Activation Energy of Diffusion and Membrane Potentials of Potassium Chloride through.</b> J. D. Tolliday, E. F. Woods and E. J. Hartung . . . . .	148
<b>Cyclo-Octatetraene, Electronic Structure and Dipole Moment of the Hypothetical Cross-Conjugated Isomer of.</b> G. Berthier and B. Pullman . . . . .	484
<b>Cyclopropane, etc. and Related Molecules, The Structures of Ethylene Oxide.</b> A. D. Walsh . . . . .	179
<b>Cyclotetramethylenetetranitramine, Cyclotrimethylenetetrinitramine and. Part II of The Thermal Decomposition of Explosives.</b> A. J. B. Robertson . . . . .	85
<b>Cyclotrimethylenetetrinitramine and Cyclotetramethylenetetranitramine. Part II of The Thermal Decomposition of Explosives.</b> A. J. B. Robertson . . . . .	85
<b>Decomposition of Ethyl Nitrate, The Homogeneous.</b> G. K. Adams and C. E. H. Bawn . . . . .	494
— of Explosives, The Thermal. Part II: Cyclotrimethylenetetrinitramine and Cyclotetramethylenetetranitramine. A. J. B. Robertson . . . . .	85
— of Paraffin Molecules, Zero-point Energies in the. R. P. Bell . . . . .	946
— of <i>tert.</i> -Butyl Chloride, The Mechanism of the Thermal. D. H. R. Barton and P. F. Onyon . . . . .	725
<b>Dehydrochlorination of Substituted Hydrocarbons, The Kinetics of the. Part IV: The Mechanism of the Thermal Decomposition of <i>tert.</i>-Butyl Chloride.</b> D. H. R. Barton and P. F. Onyon . . . . .	725
<b>Densities, A Study of the Fine Structure of Carbonaceous Solids by Measurements of True and Apparent. Part I.</b> Rosalind E. Franklin . . . . .	274
— Part II: Carbonized Coals. Rosalind E. Franklin . . . . .	668
— of Liquid Arsine, The. A. L. G. Rees and K. Stewart. . . . .	1028
<b>Desorption, The Effect of a Variable Diffusion Coefficient on the Rates of Absorption and.</b> J. Crank and M. E. Henry . . . . .	636
<b>Deuteromethanes, The Application of the Concept of Orbital-following to Methane and the. Part VII of Molecular Force Fields.</b> J. W. Linnett and P. J. Wheatley . . . . .	39
<b>Diamagnetic Susceptibility of Ammonium Compounds.</b> M. E. Bedwell, J. F. Spencer and V. C. G. Trew. . . . .	217
<b>Dielectric Constants of Liquids by a Frequency Deviation Method, The Measurement of.</b> W. L. G. Gent . . . . .	758
— Constant of Ionic Crystals, Polarizability and. B. Szigeti . . . . .	155
— Loss in Swollen Rubber. A. Schallamach and P. Thirion . . . . .	605
— Polarization Data to Infinite Dilution and Recalculation of the Apparent Molecular Polarization, A New Method for Extrapolating. J. W. Smith and D. Cleverdon . . . . .	109
<b>Diffusion across a Liquid Layer. Part I of The Reaction Kinetics of Wool with Chlorine Solutions.</b> P. Alexander, D. Gough and R. F. Hudson . . . . .	1058
— and Membrane Potentials of Potassium Chloride through Cupric Ferrocyanide, Activation Energy of. J. D. Tolliday, E. F. Woods and E. J. Hartung . . . . .	148
— and Swelling of High Polymers. Part III: Anisotropic Swelling in Oriented Polymer Film. G. S. Hartley . . . . .	820
— A Note on Interstitial. R. M. Barrer and W. Jost . . . . .	928
— in Media with Variable Properties. Part I: The Effect of a Variable Diffusion Coefficient on the Rates of Absorption and Desorption. J. Crank and M. E. Henry . . . . .	636
— in Media with Variable Properties. Part II: The Effect of a Variable Diffusion Coefficient on the Concentration-Distance Relationship in the Non-Steady State. J. Cranks and M. E. Henry . . . . .	1119
— Coefficient for Chloroform in Polystyrene from Simple Absorption Experiments, An Evaluation of the. J. Crank and G. S. Park. . . . .	240
— of Oxygen—Theoretical, The Thermal. Part II of Diffusion in Gases. E. Whalley (in part) and E. R. S. Winter . . . . .	1091
— Phenomena in Gases. Part I: The Thermal Diffusion of Oxygen—Experimental. E. Whalley, E. R. S. Winter and H. V. A. Briscoe . . . . .	1085
— Processes, Some Fundamental Definitions and Concepts in. G. S. Hartley and J. Crank . . . . .	801

- Diffusion**, The Separation of the Oxygen Isotopes by Thermal. R. H. Davies 145  
 — within the Fibre. Part II of The Reaction Kinetics of Wool with Chlorine Solutions. P. Alexander, D. Gough and R. F. Hudson 1109
- $\alpha$ : $\beta$ -Dihydroxy- $\gamma$ -Aryloxypropanes**, The Surface Tension of Aqueous Solutions of. A. C. R. Dean and W. Bradley 250
- Dimethyl Mercury**, Active Methyl Radicals in the Photolysis of. M. K. Phibbs and B. de B. Darwent 541
- Dipole Moment** of Nitrobenzene in Various Solvents. A new Method for Extrapolating Dielectric Polarization Data to Infinite Dilutions. J. W. Smith and D. Cleverdon 109  
 — of the Hypothetical Cross-Conjugated Isomer of Cyclo-Octatetraene, Electronic Structure and. G. Berthier and B. Pullman 484  
 — A Proposed Simplification in the Procedure for Computing Electric. E. A. Guggenheim 714  
 — Studies, Electric. Part I: An Analysis of the Moments of Ethylene Oxide and its Homologues. W. L. G. Gent 1021
- Dissociation**, A Relation between Bond Interactions during Vibrations and on Dissociation. Part IX of Molecular Force Fields. J. W. Linnett and M. F. Hoare 844  
 — Constant of Hydrogen Peroxide and the Electron Affinity of the HO<sub>2</sub> Radical, The. M. G. Evans and N. Uri 224  
 — Energies in Polyatomic Molecules of the Type MX<sub>n</sub>, Bond. H. A. Skinner 20  
 — Energies of Carbon Bonds, and Resonance Energies in Hydrocarbon Radicals. J. S. Roberts and H. A. Skinner 339  
 — Energies of Some Zn—C and Cd—C Bonds and of Et—I, The Bond. Part II of Thermochemistry of Metal Alkyls. A. S. Carson, K. Hartley and H. A. Skinner 1159  
 — of Salts in Water, The Extent of. Part XI: Calcium and Barium Thiosulphates and Barium Bromo-acetate. C. W. Davies and P. A. H. Wyatt 770  
 — of Salts, Ionic Reaction Rates and the Incomplete. Part I: The Bromoacetate-Thiosulphate Reaction. P. A. H. Wyatt and C. W. Davies 774
- Distillation** and its Experimental Verification, The Molecular Theory of. R. S. Bradley and A. D. Shellard 501
- Distortions** of Bond-Forming Orbitals and the Effect on Molecular Vibrations. Part VI of Molecular Force Fields. J. W. Linnett and P. J. Wheatley 33  
 — of the Interaction Energy of Carbon  $2p\pi$  Orbitals, A Wave-mechanical Treatment of the change with. Part XI of Molecular Force Fields. P. J. Wheatley and J. W. Linnett 897
- Dropping-Mercury Cathode**, The Reduction of Nitrocompounds. Part III: The Nitroresorcinols. J. Pearson 199
- Dynamic Surface Tensions**, A New Technique for the Determination of. A. M. Posner and A. E. Alexander 651
- Electro-chemistry** of Uranium, Some Observations on the. H. G. Heal 1
- Electrode Reactions**, The Effect of Additives on. Allan Wetterholm 861
- Electrolytes** in Aqueous Solution at 25°, Tables of Osmotic and Activity Coefficients of. R. A. Robinson and R. H. Stokes 612  
 — Thermal Diffusion Potentials in Non-Isothermal. H. J. V. Tyrrell and G. L. Hollis 411
- Electrometric Measurement** of the Free Energy of Formation of Naphthalene Picrate. R. P. Bell and J. A. Fendley 121
- Electron Affinity** of the HO<sub>2</sub> Radical, The Dissociation Constant of Hydrogen Peroxide and the. M. G. Evans and N. Uri 224
- Electronic Structure** and Dipole Moment of the Hypothetical Cross-Conjugated Isomer of Cyclo-Octatetraene. G. Berthier and B. Pullman 484  
 — of Thiophene and Related Molecules, The. H. C. Longuet-Higgins 173
- Elements** on Melting, The Change of Entropy, Volume and Binding State of the. O. Kubaschewski 931
- Energy** in the Decomposition of Paraffin Molecules, Zero-point. R. P. Bell 946  
 — of Some Zn—C and Cd—C Bonds, and of Et—I, The Bond Dissociation. Part II of Thermochemistry of Metal Alkyls. A. S. Carson, K. Hartley and H. A. Skinner 1159

	PAGE
<b>Energy</b> of Vaporization, Viscosity and Cohesion and the Structure of Liquids, The. L. Grunberg and A. H. Nissan . . . . .	125
— Changes on Mixing, The Heat and. Part II of Molecular Interaction in Mixtures of Esters. P. Meares . . . . .	1066
— of Diffusion and Membrane Potentials of Potassium Chloride through Cupric Ferrocyanide, Activation. J. D. Tolliday, E. F. Woods and E. J. Hartung . . . . .	148
— of Polycyclic Aromatic Hydrocarbons, An Empirical Equation for the Resonance. (The late) P. G. Carter . . . . .	597
<b>Entropy</b> , Volume and Binding State of the Elements on Melting, The Change of. O. Kubaschewski . . . . .	931
<b>Esters</b> , Molecular Interaction in Mixtures of. Part I: The Volume Changes Mixing. P. Meares . . . . .	966
— Molecular Interaction in Mixtures of. Part II: The Heat and Energy Changes on Mixing. P. Meares . . . . .	1066
<b>Ethers</b> , The Effect on the Vapour-Phase Oxidation of. Part I of the Effect of Aromatic Compounds on the Vapour-Phase Oxidation of Fuels. G. H. N. Chamberlain and A. D. Walsh . . . . .	1032
<b>Ethylene</b> and Formaldehyde, The Bending of Double Bonds, with Particular Reference to. Part X of Molecular Force Fields. J. W. Linnett, D. F. Heath and P. J. Wheatley . . . . .	832
— Air Mixtures, The Effect of Pressure on the Burning Velocity of. P. J. Wheatley and J. W. Linnett . . . . .	1152
— Oxide and its Homologues, An Analysis of the Moments of. Part III of Electric Dipole Moment Studies. W. L. G. Gent . . . . .	1021
— Oxide, Cyclopropane, etc., and Related Molecules, The Structures of. A. D. Walsh . . . . .	179
<b>Ethyl Alcohol</b> , Acetaldehyde, and Acetic Acid, The Variation of Hydrogen Over-voltage at Various Cathodes on the Addition of. Allan Wetterholm . . . . .	861
— Nitrate, The Homogeneous Decomposition of. G. K. Adams and C. E. H. Bawn . . . . .	494
<b>Explosive Reaction</b> between $\text{NO}_2$ and $\text{HCHO}$ , The. Part II of Reactions between Formaldehyde and Nitrogen Dioxide. F. H. Pollard and P. Woodward . . . . .	767
— The Thermal Decomposition of Cyclotrimethylenetrinitramine and Cyclotetramethylenetetranitramine. A. J. B. Robertson . . . . .	85
<b>Fatty Acid</b> Soaps and their Hydrolysis in Aqueous Solutions, The. Part I of Studies of Soap Solutions. G. Stainsby and A. E. Alexander . . . . .	897
<b>Ferrous</b> Ions and Hydrogen Peroxide in Aqueous Solution, The Heat of the Reaction between. M. G. Evans, J. H. Baxendale and N. Uri . . . . .	236
<b>Flames</b> , Structure and Stability of Burner. N. Thomas . . . . .	781
<b>Force Constant</b> of the $\text{C}=\text{C}$ Bond in that Molecule, The Vibrational Assignment for Tetrachloroethylene and the. P. Torkington . . . . .	445
— in Tetrachloroethylene. Jules Duchesne . . . . .	795
— of Bonds which possess Partial Ionic Character, Calculations of the Effect of Solvation on the. Ernest Warhurst . . . . .	476
<b>Force Fields, Molecular.</b> Part VI: Distortions of Bond-Forming Orbitals and the Effect on Molecular Vibrations. J. W. Linnett and P. J. Wheatley . . . . .	33
— Part VII: The Application of the Concept of Orbital-following to Methane and the Deuteromethanes. J. W. Linnett and P. J. Wheatley . . . . .	39
— Part VIII: The Vibration Frequencies of Some Octahedral $\text{XY}_6$ Molecules. D. F. Heath and J. W. Linnett . . . . .	264
— Part IX: A Relation between Bond Interactions during Vibrations and on Dissociation. J. W. Linnett and M. F. Hoare . . . . .	844
— Part X: The Bending of Double Bonds with Particular Reference to Ethylene and Formaldehyde. J. W. Linnett, D. F. Heath and P. J. Wheatley . . . . .	832
— Part XI: A Wave-mechanical Treatment of the Change with Distortion of the Interaction Energy of Carbon $2p\pi$ Orbitals. P. J. Wheatley and J. W. Linnett . . . . .	897
<b>Formaldehyde</b> and Nitrogen Dioxide, Reactions between. Part I: The Kinetics of the Slow Reaction. F. H. Pollard and R. M. H. Wyatt . . . . .	760
— and Nitrogen Dioxide, Reactions between. Part II: The Explosive Reaction between $\text{NO}_2$ and $\text{HCHO}$ . F. H. Pollard and P. Woodward . . . . .	767



	PAGE
<b>Formaldehyde</b> , The Bending of Double Bonds, with Particular Reference to Ethylene and. Part X of Molecular Force Fields. J. W. Linnett, D. F. Heath and P. J. Wheatley . . . . .	832
<b>Free Energy</b> of Formation of Naphthalene Picrate, Electrometric Measurement of the. R. P. Bell and J. A. Fendley . . . . .	121
<b>Frequency</b> Deviation Method, The Measurement of Dielectric Constants of Liquids by a. W. L. G. Gent . . . . .	758
<b>Friedel-Crafts Polymerizations</b> . Part I: The Effect of Solvent on the Polymerization of Olefines by Stannic Chloride. D. C. Pepper . . . . .	397
— Part II: The Kinetics of Polymerization of Styrene by Stannic Chloride. D. C. Pepper . . . . .	404
<b>Fuels</b> , The Effect of Aromatic Compounds on the Vapour-Phase Oxidation of. Part I. G. H. N. Chamberlain and A. D. Walsh . . . . .	1032
— The Effect of Aromatic Compounds on the Vapour-Phase Oxidation of. Part II. A. D. Walsh . . . . .	1043
<b>Fumaric Acid</b> , A Study of the Conversion of Maleic Acid to. D. H. Derbyshire and William A. Waters . . . . .	749
<b>Gases</b> , Diffusion Phenomena in. Part I: The Thermal Diffusion of Oxygen —Experimental. E. Whalley, E. R. S. Winter and H. V. A. Briscoe . . . . .	1085
— in Sorbents providing Uniform Capillary Networks of Molecular Dimensions, Transient Flow of. R. M. Barrer . . . . .	358
— The Second Virial Coefficients of Polar. J. S. Rowlinson . . . . .	974
<b>Halogens</b> in Aqueous Solution, Induced Reactions of. Part I: Reactions in the System Iodine-Thiosulphate-Nitrite. R. O. Griffith and R. Irving . . . . .	305
— in Aqueous Solution, Induced Reactions of the. Part II: Reactions in the Systems $I_2-S_2O_3^{2-}-N_2^-$ and $I_2-S_4O_6^{2-}-N_2^-$ . G. Dodd and R. O. Griffith . . . . .	546
— in Aqueous Solution, Induced Reactions of the. Part III: Reactions in the Systems $N_2^-Br_2$ , $N_2^-Br_2-S_2O_3^{2-}$ and $N_2^-Br_2-S_4O_6^{2-}$ . R. O. Griffith and R. Irving . . . . .	563
<b>Heat</b> of Formation of Boron Trioxide, The. W. Eggersgluess, A. G. Monroe and W. G. Parker . . . . .	661
— of the Reaction between Ferrous Ions and Hydrogen Peroxide in Aqueous Solution, The. M. G. Evans, J. H. Baxendale and N. Uri . . . . .	236
— of Vaporization of Carbon, Note concerning some statements in recent papers on the Latent. L. H. Long and R. G. W. Norrish . . . . .	1158
<b>High Polymers</b> , Diffusion and Swelling of. Part III: Anisotropic Swelling in Oriented Polymer Film. G. S. Hartley . . . . .	820
<b>Hydrocarbons</b> , An Empirical Equation for the Resonance Energy of Polycyclic Aromatic. (The late) P. G. Carter . . . . .	597
— A Theoretical Study of Some Non-benzenoid. Part I. R. D. Brown . . . . .	296
— Radicals, Dissociation Energies of Carbon Bonds, and Resonance Energies in. J. S. Roberts and H. A. Skinner . . . . .	339
— The Kinetics of the Dehydrochlorination of Substituted. Part IV: The Mechanism of the Thermal Decomposition of <i>tert.</i> -Butyl Chloride. D. H. R. Barton and P. F. Onyon . . . . .	725
— The Oxidation of: Observations on the High-Temperature Reaction. M. F. R. Mulcahy . . . . .	537
— The Oxidation of. Some Observations on the Induction Period. M. F. R. Mulcahy . . . . .	575
— The Residual Affinity of Conjugated and Resonating. William Moffitt . . . . .	373
<b>Hydrogen</b> Bonding in Certain Mononitronaphthylamines. D. E. Hathway and M. St. C. Flett . . . . .	818
— Evolution Reaction at Mercury Cathodes, The Kinetics of the. J. O'M. Bockris and Roger Parsons . . . . .	916
— Halides, Calculations of the Bond Lengths of the. Ernest Warhurst . . . . .	461
— Overpotential, Studies in. The Effect of Catalytic Poisons at Platinized Platinum and Nickel. J. O'M. Bockris and B. E. Conway . . . . .	989
— Overvoltage at Various Cathodes on the Addition of Ethyl Alcohol, Acetaldehyde, and Acetic Acid, The Variation of. Allan Wetterholm . . . . .	861
— with Chlorine, The Kinetics of the Photochemical Interaction of. W. J. Kramers and L. A. Moignard . . . . .	903
<b>Hydrogen Peroxide</b> and the Electron Affinity of the $HO_2$ Radical, The Dissociation of. M. G. Evans and N. Uri . . . . .	224

	PAGE
<b>Hydrogen Peroxide</b> in Aqueous Solution, The Heat of the Reaction between Ferrous Ions and. M. G. Evans, J. H. Baxendale and N. Uri . . . . .	236
— in Dilute Aqueous Solutions, The Termination Reaction in the Photolysis of. (The late) D. E. Lea . . . . .	81
<b>Hydrolysis</b> in Aqueous Solutions, The Fatty Acid Soaps and their. Part I of Studies of Soap Solutions. G. Stainsby and A. E. Alexander. . . . .	585
<b><math>\gamma</math>-Hydroxystearic Acid</b> in a Monolayer, The Lactonization of. J. T. Davies. . . . .	448
<b>Ignition</b> of Cordite by Hot Gases, The. R. C. Brian and C. A. McDowell. . . . .	212
<b>Induced Reactions</b> of Halogens in Aqueous Solution. Part I: Reactions in the System Iodine-Thiosulphate-Nitrite. R. O. Griffith and R. Irving . . . . .	305
— of the Halogens in Aqueous Solution. Part II: Reactions in the Systems $I_2-S_2O_8^{2-}-N_2$ and $I_2-S_4O_6^{2-}-N_2$ . G. Dodd and R. O. Griffith . . . . .	546
— of the Halogens in Aqueous Solution. Part III: Reactions in the Systems $N_2-Br_2$ , $N_2-Br_2-S_2O_8^{2-}$ and $N_2-N_3-Br_2-S_4O_6^{2-}$ . R. O. Griffith and R. Irving . . . . .	563
<b>Induction Period</b> , Some Observations on the. The Oxidation of Hydrocarbons. M. F. R. Mulcahy . . . . .	575
<b>Infra-Red</b> , Some Applications of Intensity Measurements in the. R. E. Richards and W. R. Burton . . . . .	874
— Spectrum, and the Assignment of the Fundamental Modes of Vibration of Thioacetic Acid, The. N. Sheppard . . . . .	693
<b>Intensity</b> in the Raman Spectra of Some Group IV Tetrahalides, Relative. L. A. Woodward and D. A. Long . . . . .	1131
— Measurements in the Infra-Red, Some Applications of. R. E. Richards and W. R. Burton . . . . .	874
<b>Interaction</b> Energy of Carbon $2p\pi$ Orbitals, A Wave-mechanical Treatment of the Change with Distortion of the. Part XI of Molecular Force Fields. P. J. Wheatley and J. W. Linnett . . . . .	897
— in Mixtures of Esters, Molecular. Part I: The Volume Changes on Mixing. P. Meares . . . . .	966
— in Mixtures of Esters, Molecular. Part II: The Heat and Energy Changes on Mixing. P. Meares . . . . .	1066
<b>Interference</b> in Polymerization Reactions, Spatial. G. M. Burnett, L. Valentine and H. W. Melville . . . . .	960
<b>Iodine</b> , The Polymerization of Vinyl Octyl Ether Catalyzed by. D. D. Eley and A. W. Richards . . . . .	425
— Thiosulphate-Nitrite, Reactions in the System. Part I of Induced Reactions of Halogens in Aqueous Solution. R. O. Griffith and R. Irving . . . . .	305
<b>Ionic Character</b> , Calculations of the Effect of Solvation on the Force Constants of Bonds which possess Partial. Ernest Warhurst . . . . .	476
— Crystals, Polarizability and Dielectric Constant. B. Szigeti . . . . .	155
— Polymerizations, The Kinetics of. Part I: The Polymerization of Vinyl Octyl Ether catalyzed by Iodine. D. D. Eley and A. W. Richards . . . . .	425
— Polymerizations, The Kinetics of. Part II: The Polymerization of Vinyl Octyl Ether Catalyzed by Stannic Chloride and Other Catalysts. D. D. Eley and A. W. Richards . . . . .	436
— Reaction Rates and the Incomplete Dissociation of Salts. Part I: The Bromoacetate-Thiosulphate Reaction. P. A. H. Wyatt and C. W. Davies . . . . .	774
<b>Ions</b> of Quinquevalent Uranium, Unstable. H. G. Heal and J. G. N. Thomas . . . . .	11
<b>Iron Complexes</b> : $(Fe(OH))^{2+}$ and $(Fe(O_2H))^{2+}$ , The. M. G. Evans, Philip George and N. Uri . . . . .	230
— Nickel Alloys, The Thermodynamics of the. O. Kubaschewski and Ortrud von Goldbeck . . . . .	948
— Silicon Alloys, On Phase-Change Processes in. K. M. Guggenheimer and H. Heitler . . . . .	137
— The Breakdown and Repair of Oxide Films on. T. P. Hoar . . . . .	683
<b>Isotopes</b> by Thermal Diffusion, The Separation of the Oxygen. R. H. Davies . . . . .	145
<b>Kinetics</b> of Ionic Polymerizations, The. Part I: The Polymerization of Vinyl Octyl Ether Catalyzed by Iodine. D. D. Eley and A. W. Richards . . . . .	425

	PAGE
<b>Kinetics</b> of Ionic Polymerizations, The. Part II: The Polymerization of Vinyl Octyl Ether Catalyzed by Stannic Chloride and Other Catalysts. D. D. Eley and A. W. Richards . . . . .	436
— of Open Reaction Systems. Chains of Simple Autocatalytic Reactions. Margaret J. Moore . . . . .	1098
— of Polymerization of Styrene by Stannic Chloride, The. D. C. Pepper . . . . .	404
— of Reactions between Ions and Polar Molecules, The Influence of the Solvent on the. E. A. Moelwyn-Hughes . . . . .	167
— of the Dehydrochlorination of Substituted Hydrocarbons, The. Part IV: The Mechanism of the Thermal Decomposition of <i>tert</i> -Butyl Chloride. D. H. R. Barton and P. F. Onyon . . . . .	725
— of the Hydrogen Evolution Reaction at Mercury Cathodes, The. J. O'M. Bockris and Roger Parsons . . . . .	916
— of the Photochemical Interaction of Hydrogen with Chlorine, The. W. J. Kramers and L. A. Moignard . . . . .	903
— of the Slow Reaction, The. Part I of Reactions between Formaldehyde and Nitrogen Dioxide. F. H. Pollard and R. M. H. Wyatt . . . . .	760
— of the Transient State in a Continuous Reaction System, The. J. D. Johnson and L. J. Edwards . . . . .	286
— of Wool with Chlorine Solutions, The Reaction. Part I: Diffusion Across a Liquid Layer. P. Alexander, D. Gough, and R. F. Hudson . . . . .	1058
— of Wool with Chlorine Solutions, The Reaction. Part II: Diffusion within the Fibre. P. Alexander, D. Gough and R. F. Hudson . . . . .	1109
— Studies in the Chemistry of Rubber and Related Materials. Part VII: The Mechanism of Chain Propagation in the Oxidation of Polyisoprenes. J. L. Bolland and P. ten Have . . . . .	93
<b>Lactonization</b> of $\gamma$ -Hydroxystearic Acid in a Monolayer, The. J. T. Davies . . . . .	448
<b>Lattice Spacings</b> of Substitutional Solid Solutions, The. G. V. Raynor . . . . .	698
<b>Liquid-Junction</b> between Electrode Vessels in a Thermostat, A New Method of Forming a. G. S. Smith . . . . .	752
<b>Liquids</b> , The Energies of Vaporization, Viscosity and Cohesion and the Structure of. L. Grunberg and A. H. Nissan . . . . .	125
<b>Lubrication</b> of Metal Surfaces by Mono- and Multi-molecular Layers, The. E. B. Greenhill . . . . .	631
<b>Mechanism</b> of Chain Propagation in the Oxidation of Polyisoprenes, The. J. L. Bolland and P. ten Have . . . . .	93
<b>Melting</b> , The Change of Entropy, Volume and Binding State of the Elements on. O. Kubaschewski . . . . .	931
<b>Membrane</b> Permeability, Studies in. Part V: Activation Energy of Diffusion and Membrane Potentials of Potassium Chloride through Cupric Ferrocyanide. J. D. Tolliday, E. F. Woods and E. J. Hartung . . . . .	148
<b>Mercury</b> Cathodes, The Kinetics of the Hydrogen Evolution Reaction at. J. O'M. Bockris and Roger Parsons . . . . .	916
— Cut-offs for the Controlled Introduction of Gas. J. C. P. Mignolet . . . . .	271
<b>Metal Alkyls</b> , Thermochemistry of. Part II: The Bond Dissociation Energies of Some Zn—C and Cd—C Bonds, and of Et—I. A. S. Carson, K. Hartley and H. A. Skinner . . . . .	1159
— Surfaces by Mono- and Multi-molecular Layers, The Lubrication of. E. B. Greenhill . . . . .	631
— Surfaces, The Adsorption of Long Chain Polar Compounds from Solution on. E. B. Greenhill . . . . .	625
<b>Methane</b> and the Deuteromethanes, The Application of the Concept of Orbital-following to. Part VII of Molecular Force Fields. J. W. Linnett and P. J. Wheatley . . . . .	39
<b>Methanolic</b> Solutions, The Effect of Temperature, pH, and Pressure on Pressure on Hydrogen Overpotential in Aqueous, Mixed and. The Kinetics of the Hydrogen Evolution Reaction at Mercury Cathodes. J. O'M. Bockris and L. A. Moignard . . . . .	916
<b>Methyl Alcohol</b> and Methyl Deuterioxide, A Semi-Micro Low-Temperature Calorimeter and a Comparison of some Thermodynamic Properties of. L. A. K. Staveley and A. K. Gupta . . . . .	50
— Deuterioxide. A Semi-Micro Low-temperature Calorimeter and a Comparison of some Thermodynamic properties of Methyl Alcohol and. L. A. K. Staveley and A. K. Gupta . . . . .	50

	PAGE
<b>Methyl Methacrylate</b> , Rate Coefficients in the Polymerization. Part I. M. H. Mackay and H. W. Melville . . . . .	323
2- ——— Pentane, The Slow Oxidation of. C. F. Cullis . . . . .	709
—— Radicals in the Photolysis of Dimethyl Mercury, Active. M. K. Phibbs and B. de B. Darwent . . . . .	541
<b>Molecular Distillation</b> and its Experimental Verification, The Theory of. R. S. Bradley and A. D. Shellard . . . . .	501
—— Structure, Some Applications of the Valence-Bond Method to Problems of. Part I. Ernest Warhurst . . . . .	461
—— Structure, Some Applications of the Valence-Bond Method to Problems of. Part II. Ernest Warhurst . . . . .	476
—— Structure, Some Applications of the Valence-Bond Method to Problems of. Part III. John Scanlan and Ernest Warhurst . . . . .	1000
<b>Monolayer</b> , The Lactonization of $\gamma$ -Hydroxystearic Acid in a. J. T. Davies. ——— and Multi-molecular Layers, The Lubrication of Metal Surfaces by. E. B. Greenhill . . . . .	448
<b>Mononitronaphthylamines</b> , Hydrogen Bonding in certain. D. E. Hathway and St. C. Flett . . . . .	631
—— The Basic Strengths of the. Alexander Bryson . . . . .	818
<b>Multi-molecular Layers</b> , The Lubrication of Metal Surfaces by Mono- and. E. B. Greenhill . . . . .	257
<b>Macro-molecules</b> , The Normal-Stress Coefficient in Solutions of. R. S. Rivlin . . . . .	631
<b>Maleic Acid</b> to Fumaric Acid, A Study of the Conversion of. D. H. Derbyshire and William A. Waters . . . . .	739
<b>Naphthalene Picrate</b> , Electrometric Measurement of the Free Energy of Formation of. R. P. Bell and J. A. Fendley . . . . .	749
—— Ring, The Effects of Substituents in the. Part I: The Basic Strengths of the Mononitronaphthylamines. Alexander Bryson . . . . .	121
<b>Nickel</b> , The Effect of Catalytic Poisons at Platinized Platinum and. Studies in Hydrogen Overpotential. J. O'M. Bockris and B. E. Conway . . . . .	257
<b>Nitrite</b> , Reactions in the System Iodine-Thiosulphate-. Part I of Induced Reactions of Halogens in Aqueous Solution. R. O. Griffith and R. Irving . . . . .	989
<b>Nitrobenzne</b> in Various Solvents. A New Method for Extrapolating Dielectric Polarization Data to Infinite Dilution. J. W. Smith and D. Cleverdon . . . . .	305
<b>Nitrobenzene</b> in Various Solvents. A New Method for Extrapolating Dielectric Polarization Data to Infinite Dilution. J. W. Smith and D. Cleverdon . . . . .	109
<b>Nitrocompounds</b> at the Dropping-Mercury Cathode, The Reduction of. Part III: The Nitroresorcinols. J. Pearson . . . . .	109
<b>Nitrogen Dioxide</b> , Reactions between Formaldehyde and. Part I: The Kinetics of the Slow Reaction. F. H. Pollard and R. M. H. Wyatt . . . . .	199
—— Reactions between Formaldehyde and. Part II: The Explosive Reaction. F. H. Pollard and P. Woodward . . . . .	760
<b>Nitroresorcinols</b> , The. Part III of The Reduciton of Nitrocompounds at the Dropping-Mercury Cathode. J. Pearson . . . . .	767
<b>Normal-Stress Coefficient</b> in Solutions of Macro-molecules, The. R. S. Rivlin . . . . .	199
<b>Octahedral <math>XY_6</math></b> , The Vibration Frequencies of Some. Part VIII of Molecular Force Fields. D. F. Heath and J. W. Linnett . . . . .	739
<b>Olefines</b> by Stannic Chloride, The Effect of Solvent on the Polymerization of. D. C. Pepper . . . . .	264
<b>Orbital-following</b> to Methane and the Deuteromethanes, The Application of the Concept of. Part VII of Molecular Force Fields. J. W. Linnett and P. J. Wheatley . . . . .	397
<b>Osmotic and Activity Coefficients</b> of Electrolytes in Aqueous Solution at 25°. Tables of. R. A. Robinson and R. H. Stokes . . . . .	39
<b>Overpotential</b> in Aqueous, Mixed and Methanolic Solutions, The Effect of Temperature, pH, and Pressure on Hydrogen. The Kinetics of the Hydrogen Evolution Reaction at Mercury Cathodes. J. O'M. Bockris and Roger Parsons . . . . .	612
—— Studies in Hydrogen. The Effect of Catalytic Poisons at Platinized Platinum and Nickel. J. O'M. Bockris and B. E. Conway . . . . .	916
—— at Various Cathodes on the Addition of Ethyl Alcohol, Acetaldehyde, and Acetic Acid, The Variation of Hydrogen. Allan Wetterholm . . . . .	989
	861

	PAGE
<b>Oxidation of Fuels, The Effect of Aromatic Compounds on the Vapour-Phase.</b>	
Part I: The Effect on the Vapour-Phase Oxidation of Ethers. G. H. N. Chamberlain and A. D. Walsh	1032
— of Fuels, The Effect of Aromatic Compounds on the Vapour-Phase. Part II: The Anti-Knock Effect of Aromatic Compounds in Engines. A. D. Walsh	1043
— of Hydrocarbons: Observations on the High-Temperature Reaction. M. F. R. Mulcahy	537
— of Hydrocarbons, The. Some Observations on the Induction Period. M. F. R. Mulcahy	575
— of 2-Methyl Pentane, The Slow. C. F. Cullis	709
— of Platinum, The Anodic. Simon Altmann and R. H. Busch	720
— of Polyisoprenes. The Mechanism of Chain Propagation in the. J. L. Bolland and P. ten Have	93
— Reduction Potentials of Quinones, A Theoretical Study of the. M. G. Evans, J. Gergely and J. de Heer	312
<b>Oxide Films on Iron, The Breakdown and Repair of.</b> T. P. Hoar	683
<b>Oxygen</b> —Experimental, The Thermal Diffusion of. Part I of Diffusion Phenomena in Gases. E. Whalley, E. R. S. Winter and H. V. A. Briscoe	1085
— Theoretical. The Thermal Diffusion of. Part II of Diffusion Phenomena in Gases. E. Whalley (in part) and E. R. S. Winter	1091
— Isotopes by Thermal Diffusion. The Separation of the. R. H. Davies	145
<b>Paraffins</b> , Statistical Thermodynamics of Mixtures of Normal. H. Tompa	101
— Zero-point Energies in the Decomposition of. R. P. Bell	946
<b>Pentane</b> , The Slow Oxidation of 2-Methyl. C. F. Cullis	709
<b>Permeability</b> , Studies in Membrane. Part V: Activation Energy of Dif- fusion and Membrane Potentials of Potassium Chloride through Cupric Ferrocyanide. J. D. Tolliday, E. F. Woods and E. J. Hartung	148
<b>Phase-Change</b> Processes in Iron-Silicon Alloys, On. K. M. Guggenheimer and H. Heitler	137
— Relationships in Polymer Solutions. H. Tompa	1142
<b>Phenol-Soap Mixtures</b> , The Action of Colloidal Electrolytes on Bacteria, with particular reference to Soaps and. Anne Agar and A. E. Alexander	528
<b>Photochemical</b> Interaction of Hydrogen with Chlorine, The Kinetics of the. W. J. Kramers and L. A. Moignard	903
<b>Photolysis</b> of Dimethyl Mercury, Active Methyl Radicals in the. M. K. Phibbs and B. de B. Darwent	541
— of Hydrogen Peroxide in Dilute Aqueous Solutions, The Termination Reaction in the. (The late) D. E. Lea	81
<b>Picrate</b> , Electrometric Measurement of the Free Energy of Formation of Naphthalene. R. P. Bell and J. A. Fendley	121
<b>Platinum</b> and Nickel, The Effect of Catalytic Poisons at Platinized. Studies in Hydrogen Overpotential. J. O'M. Bockris and B. E. Conway	989
— The Anodic Oxidation of. Simon Altmann and R. H. Busch	720
<b>Polarizability</b> and Dielectric Constant of Ionic Crystals. B. Szigeti	155
<b>Polarizabilities</b> of Bonds, The. Part II: Bond Refractions in the Alkanes. B. C. Vickery and K. G. Denbigh	61
<b>Polarization</b> Data to Infinite Dilution and Recalculation of the Apparent Molecular Polarization and Dipole Moment, A New Method for Extrapolating Dielectric. J. W. Smith and D. Cleverdon	109
<b>Polyatomic</b> Molecules of the Type $MX_n$ , Bond Dissociation Energies in. H. A. Skinner	20
<b>Polymerization</b> of Methyl Methacrylate, Rate Coefficients in the. Part I. M. H. Mackay and H. W. Melville	323
— of Olefines by Stannic Chloride, The Effect of Solvent on the. D. C. Pepper	397
— of Styrene by Stannic Chloride, The Kinetics of. D. C. Pepper	404
— of Vinyl Octyl Ether Catalyzed by Iodine. D. D. Eley and A. W. Richards	425
— Processes, Determination of the Velocity Coefficients for, The Polymer- ization of Butyl Acrylate. H. W. Melville and A. F. Bickel	1049
— Reactions, Spatial Interference in. G. M. Burnett, L. Valentine and H. W. Melville	960
<b>Polymer Solutions</b> , Phase Relationships in. H. Tompa	1142
<b>Polystyrene</b> from Simple Absorption Experiments, An Evaluation of the Diffusion Coefficient for Chloroform in. J. Crank and G. S. Park	240

	PAGE
<b>Polythene</b> , The Effect of Pressure on the Volume, Thermodynamic Properties and Crystallinity of. W. Parks and R. B. Richards . . . . .	203
<b>Polysoprenes</b> , The Mechanism of Chain Propagation in the Oxidation of. J. L. Bolland and P. ten Have . . . . .	93
<b>Potassium Chloride</b> through Cupric Ferrocyanide, Activation Energy of Diffusion and Membrane Potentials of. J. D. Tolliday, E. F. Woods and E. J. Hartung . . . . .	148
— Ferrocyanide and Calcium Ferrocyanide, The Conductivities of Dilute Aqueous Solutions of. J. C. James . . . . .	855
— Ions between Muscle and the Surrounding Medium, The Transfer of Sodium and. E. J. Harris and G. P. Burn . . . . .	508
<b>Potentials</b> in Non-Isothermal Electrolytic Systems, Thermal Diffusion. H. J. V. Tyrrell and G. L. Hollis . . . . .	411
— of Potassium Chloride through Cupric Ferrocyanide. Activation Energy of Diffusion and. J. D. Tolliday, E. F. Woods and E. J. Hartung. . . . .	148
— of Quinones, A Theoretical Study of the Oxidation-Reduction. M. G. Evans, J. Gergely and J. de Heer. . . . .	312
<b>Probability</b> Factors in Radical Reactions, The Magnitude of the. M. G. Evans and M. Szwarc . . . . .	940
<b>Proteins</b> of the Ground Nut ( <i>Arachis Hypogaea</i> ), The Ultra-Violet Absorption of the. A. C. R. Dean . . . . .	487
<b>Quinones</b> , A Theoretical Study of the Oxidation-Reduction Potentials of. M. G. Evans, J. Gergely and J. de Heer . . . . .	312
<b>Radical</b> Reactions, The Magnitude of the Probability Factors in. M. G. Evans and M. Szwarc . . . . .	940
— The Dissociation Constant of Hydrogen Peroxide and the Electron Affinity of the $\text{HO}_2$ . M. G. Evans and N. Uri . . . . .	224
<b>Raman Spectra</b> of Some Group IV Tetrahalides, Relative Intensities in the. L. A. Woodward and D. A. Long . . . . .	1131
<b>Rate</b> Coefficients in the Polymerization of Methyl Methacrylate. Part I. M. H. Mackay and H. W. Melville . . . . .	323
— Chains of Simple Autocatalytic Kinetics of Open Reaction Systems. Margaret J. Moore . . . . .	1098
— in the Photolysis of Hydrogen Peroxide in Dilute Aqueous Solutions, The Termination. (The late) D. E. Lea . . . . .	81
<b>Reduction</b> of Nitrocompounds at the Dropping-Mercury Cathode, The. Part III: The Nitroresorcinols. J. Pearson . . . . .	199
<b>Resonance Energies</b> in Hydrocarbon Radicals, Dissociation Energies of Carbon Bonds, and. J. S. Roberts and H. A. Skinner . . . . .	339
— of Polycyclic Aromatic Hydrocarbons, An Empirical Equation for the. (The late) P. G. Carter . . . . .	597
<b>Rubber</b> , Dielectric Loss in Swollen. A. Schallamach and P. Thirion . . . . .	605
<b>Semi-micro</b> Low-temperature Calorimeter and a Comparison of some Thermodynamic Properties of Methyl Alcohol and Methyl Deuterioxide, A. L. A. K. Staveley and A. K. Gupta . . . . .	50
<b>Soaps</b> , and Soap-Phenol Mixtures, The Action of Colloidal Electrolytes on Bacteria, with particular reference to. Anne Agar and A. E. Alexander . . . . .	528
— and their Hydrolysis in Aqueous Solutions, The Fatty Acid. G. Stainsby and A. E. Alexander . . . . .	585
— Solutions, Studies of. Part I: The Fatty Acid Soaps and their Hydrolysis in Aqueous Solutions. G. Stainsby and A. E. Alexander . . . . .	585
<b>Sodium</b> and Potassium Ions between Muscle and the Surrounding Medium, The Transfer of. E. J. Harris and G. P. Burn . . . . .	508
<b>Solid Solutions</b> , The Lattice Spacings of Substitutional. G. V. Raynor. . . . .	698
<b>Solubility</b> of Benzylpenicillin Salts in Acetone, The. J. E. Page and J. G. Waller . . . . .	755
<b>Solvation</b> on the Force Constants of Bonds which possess Partial Ionic Character, The Effect of. Ernest Warhurst . . . . .	476
<b>Sorbents</b> providing Uniform Capillary Networks of Molecular Dimensions, Transient Flow of Gases in. R. M. Barrer . . . . .	358
<b>Spectra</b> of Some Group IV Tetrahalides, Relative Intensities in the Raman. L. A. Woodward and D. A. Long . . . . .	1131
<b>Stannic Chloride</b> and Other Catalysts, The Polymerization of Vinyl Octyl Ether by. D. D. Eley and A. W. Richards . . . . .	436
— The Effect of Solvent on the Polymerization of Olefines by. D. C. Pepper . . . . .	397
— The Kinetics of Polymerizations of Styrene by. D. C. Pepper . . . . .	404

- Statistical Thermodynamics** of Mixtures of Normal Paraffins. H. Tompa. 101
- Strength** of Alloys, Some New Aspects of the. George-Maria Schwab. 385
- Structure** of Carbonaceous Solids by Measurements of True and Apparent Densities, A Study of the Fine. Rosalind E. Franklin. 274
- and Stability of Burner Flames. N. Thomas. 781
- of Liquids. The Energies of Vaporization, Viscosity and Cohesion and the. L. Grunberg and A. H. Nissan. 125
- of Thiophene and Related Molecules, The Electronic. H. C. Longuet-Higgins. 173
- Some Applications of the Valence-Bond Method to Problems of Molecular Structure. Part III. John Scanlan and Ernest Warhurst. 1000
- of Ethylene Oxide, Cyclopropane, etc., and Related Molecules, The. A. D. Walsh. 179
- Styrene** by Stannic Chloride, The Kinetics of Polymerization of. D. C. Pepper. 404
- Surface** Activity, The Effect of Additives known to Influence. Anne Agar and A. E. Alexander. 528
- Area of a Solid from an Adsorption Isotherm, The Determination of the. James F. Duncan. 879
- Tension of Aqueous Solutions of  $\alpha$ : $\beta$ -Dihydroxy- $\gamma$ -Aryloxypropanes, The. A. C. R. Dean and W. Bradley. 250
- Tensions, A New Technique for the Determination of Dynamic. A. M. Posner and A. E. Alexander. 651
- Susceptibility** of Ammonium Compounds, Diamagnetic. M. E. Bedwell, J. F. Spencer and V. C. G. Trew. 217
- Swelling** of High Polymers, Diffusion and. Part III: Anisotropic Swelling in Oriented Polymer Film. G. S. Hartley. 820
- tert.-Butyl Chloride**, The Mechanism of the Thermal Decomposition of. Part IV of The Kinetics of the Dehydrochlorination of Substituted Hydrocarbons. D. H. R. Barton and P. F. Onyon. 725
- Tetrachlorethylene**, The Force Constants in. Jules Duchesne. 795
- and the Force Constant of the C=C Bond in that Molecule, The Vibrational Assignment for. P. Torkington. 445
- Thermal** Decomposition of Explosives. Part II: Cyclotrimethylenetetranitramine and Cyclotetramethylenetetranitramine, The. A. J. B. Robertson. 85
- Decomposition of *tert.*-Butyl Chloride, The Mechanism of the. D. H. R. Barton and P. F. Onyon. 725
- Diffusion Potentials in Non-Isothermal Electrolytic Systems. H. J. V. Tyrrell and G. L. Hollis. 411
- Diffusion, The Separation of the Oxygen Isotopes by. R. H. Davies. 145
- Thermochemistry** of Metal Alkyls. Part II: The Bond Dissociation Energies of Some Zn—C and Cd—C Bonds, and of Et—I. A. S. Carson, K. Hartley and H. A. Skinner. 1591
- Thermodynamics**, Properties and Crystallinity of Polythene, The Effect of Pressure on the Volume. W. Parks and R. B. Richards. 203
- Properties of Methyl Alcohol and Methyl Deuterioxide, A Semi-Micro Low-Temperature Calorimeter and a Comparison of Some. L. A. K. Staveley and A. K. Gupta. 50
- of Mixtures of Normal Paraffins, Statistical. H. Tompa. 101
- of the Iron-nickel Alloys, The. O. Kubaschewski and Ortrud von Goldbeck. 948
- Thioacetic** Acid, The Infra-red Spectrum, and the Assignment of the Fundamental Modes of Vibration of. N. Sheppard. 693
- Thiophene** and Related Molecules, The Electronic Structure of. H. C. Longuet-Higgins. 173
- Thiosulphate-Nitrite**, Reactions in the System Iodine-. Part I of Induced Reactions of Halogens in Aqueous Solution. R. O. Griffith and R. Irving. 305
- Reaction, The Bromoacetate-. Part I of Ionic Reaction Rates and the Incomplete Dissociation of Salts. P. A. H. Wyatt and C. W. Davies. 774
- Transient** Flow of Gases in Sorbents providing Uniform Capillary Networks of Molecular Dimensions. R. M. Barrer. 358
- State in a Continuous Reaction, The Kinetics of the. J. D. Johnson and L. J. Edwards. 286
- Ultra-Violet** Absorption of the Protein of the Ground Nut (*Arachis Hypogaea*), The. A. C. R. Dean. 487

	PAGE
<b>Uranium</b> , Some Observations on the Electro-chemistry of. H. G. Heal . . .	1
— Unstable Ions of Quinquavalent. H. G. Heal and J. G. N. Thomas . . .	11
<b>Valence-Bond Method</b> to Problems of Molecular Structure, Some Applications of the. Part I: Calculations of the Bond Lengths of the Hydrogen Halides. Ernest Warhurst . . .	461
— to Problems of Molecular Structure, Some Applications of the. Part II. Ernest Warhurst . . .	476
— to Problems of Molecular Structure, Some Applications of the. Part III. John Scanlan and Ernest Warhurst . . .	1000
<b>Vaporization</b> , Viscosity and Cohesion and the Structure of Liquids, The Energies of. L. Grunberg and A. H. Nissan . . .	125
<b>Velocity</b> Coefficients for Polymerization Processes. The Polymerization of Butyl Acrylate. H. W. Melville and A. F. Bickel . . .	1049
— of Ethylene-Air Mixtures, The Effect of Pressure on the Burning. P. J. Wheatley and J. W. Linnett . . .	1152
<b>Vibration</b> Frequencies of Some Octahedral $XY_6$ Molecules, The. Part VIII of Molecular Force Fields. D. F. Heath and J. W. Linnett . . .	264
— Distortions of Bond-Forming Orbitals and the Effect on. Part VI of Molecular Force Fields. J. W. Linnett and P. J. Wheatley . . .	33
— of Tetrachloroethylene and the Force Constant of the $C\equiv C$ Bond in that Molecule, The. P. Torkington . . .	445
— of Thioacetic Acid, The Infra-red Spectrum, and the Assignment of the Fundamental Modes of. N. Sheppard . . .	693
<b>Vinyl Octyl Ether</b> Catalyzed by Iodine, The Polymerization of. D. D. Eley and A. W. Richards . . .	425
— Catalyzed by Stannic Chloride and Other Catalysts, The Polymerization of. D. D. Eley and A. W. Richards . . .	436
<b>Virial Coefficients</b> of Polar Gases, The Second. J. S. Rowlinson . . .	974
<b>Viscosity</b> and Cohesion and the Structure of Liquids, The Energies of Vaporization. L. Grunberg and A. H. Nissan . . .	125
<b>Volume</b> Changes on Mixing, The. Part I of Molecular Interaction in Mixtures of Esters. P. Meares . . .	966
<b>Wave-Mechanical</b> Treatment of the Change with Distortion of the Interaction Energy of Carbon $2p\pi$ Orbitals, A. Part XI of Molecular Force Fields. P. J. Wheatley and J. W. Linnett . . .	897
<b>Wool</b> with Chlorine Solutions, The Reaction Kinetics of. Part I: Diffusion across a Liquid Layer. P. Alexander, D. Gough and R. F. Hudson . . .	1058



# AUTHOR INDEX—VOLUME XLV, 1949

	PAGE
<b>Adams, G. K., and Bawn, C. E. H.</b> The homogeneous decomposition of ethyl nitrate	494
<b>Agar, A., and Alexander, A. E.</b> The action of colloidal electrolytes on bacteria with particular reference to soaps and soap-phenol mixtures. Part V: The effect of additives known to influence surface activity.	528
<b>Alexander, A. E.</b> See <i>Agar, A.</i> , and	
— See <i>Posner, A. M.</i> , and	
— See <i>Stainsby, G.</i> , and	
<b>Alexander, P., Gough, D., and Hudson, R. F.</b> The reaction kinetics of wool with chlorine solutions. Part I: Diffusion across a liquid layer	1058
— Part II: Diffusion within the fibre	1109
<b>Altmann, S., and Busch, R. H.</b> The anodic oxidation of platinum	720
<b>Barrer, R. M.</b> Transient flow of gases in sorbents providing uniform capillary networks of molecular dimensions	358
— and <b>Jost, W.</b> A note on interstitial diffusion	928
<b>Barton, D. H. R.</b> See <i>Howlett, K. E.</i> , and	
— and <b>Onyon, P. F.</b> The kinetics of the dehydrochlorination of substituted hydrocarbons. Part IV: The mechanism of the thermal decomposition of <i>tert</i> -butyl chloride	725
<b>Bawn, C. E. H.</b> See <i>Adams, G. K.</i> , and	
<b>Baxendale, J. H.</b> See <i>Evans, M. G.</i> , <i>Baxendale, J. H.</i> , and <i>Uri, N.</i>	
<b>Bedwell, M. E., Spencer, J. F., and Trew, V. C. G.</b> Diamagnetic susceptibility of ammonium compounds	217
<b>Bell, R. P.</b> Zero-point energies in the decomposition of paraffin molecules	946
— and <b>Fendley, J. A.</b> Electrometric measurements of the free energy of formation of naphthalene picrate	121
<b>Berthier, G., and Pullman, B.</b> Electronic structure and dipole moment of the hypothetical cross-conjugated isomer of cyclo-octatetruene	484
<b>Bickel, A. F.</b> See <i>Melville, H. W.</i> , and	
<b>Bockris, J. O'M., and Conway, B. E.</b> Studies in hydrogen overpotential. The effect of catalytic poisons at platinized platinum and nickel	989
— and <b>Parsons, R.</b> The kinetics of the hydrogen evolution reaction at mercury cathodes. The effect of temperature, pH and pressure on hydrogen overpotential in aqueous, mixed and methanolic solutions	916
<b>Bolland, J. L., and Have, P. ten.</b> Kinetic studies in the chemistry of rubber and related materials. Part VII: The mechanism of chain propagation in the oxidation of polyisoprenes	93
<b>Bradley, R. S., and Shellard, A. D.</b> The theory of molecular distillation and its experimental verification	501
<b>Bradley, W.</b> See <i>Dean, A. C. R.</i> , and	
<b>Brian, R. C., and McDowell, C. A.</b> The ignition of cordite by hot gases	212
<b>Briscoe, H. V. A.</b> See <i>Whalley, E.</i> , <i>Winter, E. R. S.</i> , and	
<b>Brown, R. D.</b> A theoretical study of some non-benzenoid hydrocarbons. Part I	296
<b>Bryson, A.</b> The effects of substituents in the naphthalene ring. Part I: The basic strengths of the mononitronaphthylamines	257
<b>Burn, G. P.</b> See <i>Harris, E. J.</i> , and	
<b>Burnett, G. M., Valentine, L., and Melville, H. W.</b> Spatial interference in polymerization reactions	960
<b>Burton, W. R.</b> See <i>Richards, R. E.</i> , and	
<b>Busch, R. H.</b> See <i>Altmann, S.</i> , and	
<b>Carson, A. S., Hartley, K., and Skinner, H. A.</b> Thermochemistry of metal alkyls. Part II: The bond dissociation energies of some Zn—C and Cd—C bonds, and of Et—I	1159
<b>Carter, P. G. (the late).</b> An empirical equation for the resonance energy of polycyclic aromatic hydrocarbons	597
<b>Chamberlain, G. H. N., and Walsh, A. D.</b> The effect of aromatic compounds on the vapour phase oxidation of fuels. Part I: The effect on the vapour phase oxidation of ethers	1032
<b>Cleverdon, D.</b> See <i>Smith, J. W.</i> , and	
<b>Conway, B. E.</b> See <i>Bockris, J. O'M.</i> , and	

	PAGE
<b>Crank, J.</b> See <i>Hartley, G. S.</i> , and	
— and <b>Henry, M. E.</b> Diffusion in media with variable properties. Part I: The effect of a variable diffusion coefficient on the rates of absorption and desorption . . . . .	636
— Part II: The effect of a variable diffusion coefficient on the concentration-distance relationship in the non-steady state . . . . .	1119
— and <b>Park, G. S.</b> An evaluation of the diffusion coefficient for chloroform in polystyrene from simple absorption experiments . . . . .	240
<b>Cullis, C. F.</b> The slow oxidation of 2-methyl pentane . . . . .	709
<b>Darwent, B. de B.</b> See <i>Phibbs, M. K.</i> , and	
<b>Davies, C. W.</b> See <i>Wyatt, P. A. H.</i> , and	
— and <b>Wyatt, P. A. H.</b> The extent of dissociation of salts in water. Part XI: Calcium and barium thiosulphates and barium bromoacetate . . . . .	770
<b>Davies, J. T.</b> The lactonization of $\gamma$ -hydroxystearic acid in a monolayer . . . . .	448
<b>Davies, R. H.</b> The separation of the oxygen isotopes by thermal diffusion . . . . .	145
<b>Dean, A. C. R.</b> The ultra-violet absorption of the proteins of the ground nut ( <i>arachis hypogaea</i> ) . . . . .	487
— and <b>Bradley, W.</b> The surface tension of aqueous solutions of $\alpha$ : $\beta$ -dihydroxy- $\gamma$ -aryloxypropanes . . . . .	250
<b>Denbigh, K. G.</b> See <i>Vickery, B. C.</i> , and	
<b>Derbyshire, D. H., and <b>Waters, W. A.</b> A study of the conversion of maleic acid to fumaric acid . . . . .</b>	749
<b>Dodd, G., and <b>Griffith, R. O.</b> Induced reactions of the halogens in aqueous solution. Part II: Reactions in the systems <math>I_2</math>—<math>S_2O_3^{2-}</math>—<math>N_3^-</math> and <math>I_2</math>—<math>S_4O_6^{2-}</math>—<math>N_3^-</math> . . . . .</b>	546
<b>Duchesne, Jules.</b> Remarks on the force constants in tetrachlorethylene . . . . .	795
<b>Duncan, J. F.</b> The determination of the surface area of a solid from an adsorption isotherm . . . . .	879
<b>Edwards, L. J.</b> See <i>Johnson, J. D.</i> , and	
<b>Eggersgluess, W., <b>Monroe, A. G., and <b>Parker, W. G.</b> The heat of formation of boron trioxide . . . . .</b></b>	661
<b>Eley, D. D., and <b>Richards, A. W.</b> The kinetics of ionic polymerizations. Part I: The polymerization of vinyl octyl ether catalyzed by iodine . . . . .</b>	425
— Part II: The polymerization of vinyl octyl ether catalyzed by stannic chloride and other catalysts . . . . .	436
<b>Evans, M. G., <b>Baxendale, J. H., and <b>Uri, N.</b> The heat of the reaction between ferrous ions and hydrogen peroxide in aqueous solution . . . . .</b></b>	236
— <b>George, P., and <b>Uri, N.</b> The <math>[Fe(OH)]^{+2}</math> and <math>[Fe(O_2H)]^{+2}</math> complexes . . . . .</b>	230
— <b>Gergely, J., and <b>de Heer, J.</b> A theoretical study of the oxidation-reduction potentials of quinones . . . . .</b>	312
— and <b>Szwarc, M.</b> The magnitude of the probability factors in radical reactions . . . . .	940
— and <b>Uri, N.</b> The dissociation constant of hydrogen peroxide and the electron affinity of the $HO_2$ radical . . . . .	224
<b>Fendley, J. A.</b> See <i>Bell, R. P.</i> , and	
<b>Flett, M. St. C.</b> See <i>Hathway, D. E.</i> , and	
<b>Franklin, R. E.</b> A study of the fine structure of carbonaceous solids by measurements of true and apparent densities. Part I: Coals. . . . .	274
— Part II: Carbonized coals . . . . .	668
<b>Gent, W. L. G.</b> The measurement of dielectric constants of liquids by a frequency deviation method . . . . .	758
— Electric dipole moment studies. Part I: An analysis of the moments of ethylene oxide and its homologues . . . . .	1021
<b>George, P.</b> See <i>Evans, M. G.</i> , <i>George, P.</i> , and <i>Uri, N.</i>	
<b>Gergely, J.</b> See <i>Evans, M. G.</i> , <i>Gergely, J.</i> , and <i>de Heer, J.</i>	
<b>Gold, V.</b> Bond orders and other criteria of double-bond character . . . . .	191
<b>Goldbeck, von O.</b> See <i>Kubaschewski, O.</i> , and	
<b>Gough, D.</b> See <i>Alexander, P.</i> , <i>Gough, D.</i> , and <i>Hudson, R. F.</i>	
<b>Greenhill, E. B.</b> The adsorption of long chain polar compounds from solution on metal surfaces . . . . .	625
— The lubrication of metal surfaces by mono- and multi-molecular layers . . . . .	631
<b>Griffith, R. O.</b> See <i>Dodd, G.</i> , and	
— and <b>Irving, R.</b> Induced reactions of halogens in aqueous solution. Part I: Reactions in the system iodine-thiosulphate-nitrite . . . . .	305

	PAGE
Griffith, R. O., and Irving, R. Part III: Reactions in the systems $N_3^-Br_3$ , $N_3^-Br_3-S_2O_8^{2-}$ and $N_3^-Br_3-S_4O_6^{2-}$ . . . . .	563
Grunberg, L., and Nissán, A. H. The energies of vaporization, viscosity and cohesion and the structure of liquids . . . . .	125
Guggenheim, E. A. A proposed simplification in the procedure for computing electric dipole moments . . . . .	714
Guggenheimer, K. M., and Heitler, H. On phase-change processes in iron-silicon alloys . . . . .	137
Gupta, A. K. See <i>Staveley, L. A. K.</i> , and	
Harris, E. J., and Burn, G. P. The transfer of sodium and potassium ions between muscle and the surrounding medium . . . . .	508
Hartley, G. S. Diffusion and swelling of high polymers. Part III: Anisotropic swelling in oriented polymer film . . . . .	820
— and Crank, J. Some fundamental definitions and concepts in diffusion processes . . . . .	801
Hartley, K. See <i>Carson, A. S.</i> , <i>Hartley, K.</i> , and <i>Skinner, H. A.</i>	
Hartung, E. J. See <i>Tolliday, J. D.</i> , <i>Woods, E. F.</i> , and	
Hathway, D. E., and M. St. C. Flett. Hydrogen bonding in certain mononitronaphthylamines . . . . .	818
Have, P. ten. See <i>Bolland, J. L.</i> , and	
Heal, H. G. Some observations on the electrochemistry of uranium . . . . .	1
— and Thomas, J. G. M. Unstable ions of quinquavalent uranium . . . . .	11
Heath, D. F. See <i>Linnett, J. W.</i> , <i>Heath, D. F.</i> , and <i>Wheatley, P. J.</i>	
— and Linnett, J. W. Molecular force fields. Part VIII: The vibration frequencies of some octahedral $XY_6$ molecules . . . . .	264
de Heer, J. See <i>Evans, M. G.</i> , <i>Gergely, J.</i> , and	
Heitler, H. See <i>Guggenheimer, K. M.</i> , and	
Henry, M. E. See <i>Crank, J.</i> , and	
Hoar, T. P. The breakdown and repair of oxide films on iron . . . . .	683
Hoare, M. F. See <i>Linnett, J. W.</i>	
Hollis, G. L. See <i>Tyrrell, H. J. Y.</i> , and	
Howlett, K. E., and Barton, D. H. R. The use of acetaldehyde for detection of chain reactions . . . . .	735
Hudson, R. F. See <i>Alexander, P.</i> , <i>Gough, D.</i> , and	
Irving, R. See <i>Griffith, R. O.</i> , and	
James, J. C. The conductivities of dilute aqueous solutions of potassium ferrocyanide and calcium ferrocyanide . . . . .	855
Johnson, J. D., and Edwards, L. J. The kinetics of the transient state in a continuous reaction system . . . . .	286
Jost, W. See <i>Barrer, R. M.</i> , and	
Kramers, W. J., and Moignard, L. A. The kinetics of the photo-chemical interaction of hydrogen with chlorine . . . . .	903
Kubaschewski, O. The change of entropy, volume and binding state of the elements on melting . . . . .	931
— and Goldbeck, von O. The thermodynamics of the iron-nickel alloys . . . . .	948
Lea, D. E. (the late). The termination reaction in the photolysis of hydrogen peroxide in dilute aqueous solutions . . . . .	81
Linnett, J. W. See <i>Heath, D. F.</i> , and	
— See <i>Wheatley, P. J.</i> , and	
— Heath, D. F., and Wheatley, P. J. Molecular force fields. Part X: The bending of double bonds, with particular reference to ethylene and formaldehyde . . . . .	832
— and Hoare, M. F. Part IX: A relation between bond interactions during vibrations and on dissociation . . . . .	844
— and Wheatley, P. J. Part VI: Distortions of bond-forming orbitals and the effect on molecular vibrations . . . . .	33
— Part VII: The application of the concept of orbital following to methane and the deuteromethanes . . . . .	39
Long, D. A. See <i>Woodward, L. A.</i> , and	
Long, L. H., and Norrish, R. G. W. Note concerning some recent statements on the latent heat of vaporization of carbon . . . . .	1158
Longuet-Higgins, H. C. The electronic structure of thiophene and related molecules . . . . .	173
Meares, P. Molecular interaction in mixtures of esters. Part I: The volume changes on mixing . . . . .	966
— Part II: The heat and energy changes on mixing . . . . .	1066

- Melville, H. W. See *Burnett, G. M., Valentine, L., and*  
 — See *Mackay, M. H., and*  
 — and *Bickel, A. F.* Determination of the velocity coefficients for polymerization processes. The polymerization of butyl acrylate . . . 1049
- Mignolet, J. C. P. Mercury cut-off designs for the controlled introduction of gas . . . 271
- Moelwyn-Hughes, E. A. The influence of the solvent on the kinetics of reactions between ions and polar molecules . . . 167
- Moffitt, W. E. The residual affinity of conjugated and resonating hydrocarbons . . . 373
- Moignard, L. A. See *Kramers, W. J., and*  
 Monroe, A. G. See *Eggersgluess, W., Monroe, A. G., and Parker, W. G.*
- Moore, Margaret, J. Kinetics of open reaction systems. Chains of simple autocatalytic reactions . . . 1098
- Mulcahy, M. F. R. The oxidation of hydrocarbons: Observations on the high temperature reaction . . . 537  
 — — — The oxidation of hydrocarbons: Some observations on the induction period . . . 575
- McDowell, C. A. See *Brian, R. C., and*  
 Mackay, M. H., and Melville, H. W. Rate coefficients in the polymerization of methyl methacrylate. Part I . . . 323
- Nissan, A. H. See *Grunberg, L.*  
 Norrish, R. G. W. See *Long, L. H., and*  
 Onyon, P. F. See *Barton, D. H. R., and*  
 Page, J. E., and Waller, J. G. The solubility of benzylpenicillin salts in acetone . . . 755
- Park, G. S. See *Crank, J., and*  
 Parker, W. G. See *Eggersgluess, W., Monroe, A. G., and*  
 Parks, W., and Richards, R. B. The effect of pressure on the volume, thermodynamic properties and crystallinity of polythene . . . 203
- Parsons, R. See *Bockris, J. O'M., and*  
 Pearson, J. The reduction of nitrocompounds at the dropping-mercury cathode. Part III: The nitroresorcinols . . . 199
- Pepper, D. C. Friedel-Crafts polymerizations. Part I: The effect of solvent on the polymerization of olefines by stannic chloride . . . 397  
 — — — Part II: The kinetics of polymerization of styrene by stannic chloride . . . 404
- Phibbs, M. K., and Darwent, B. de B. Active methyl radicals in the photolysis of dimethyl mercury . . . 541
- Pollard, F. H., and Wyatt, R. M. H. Reactions between formaldehyde and nitrogen dioxide. Part I: The kinetics of the slow reaction . . . 760  
 — and Woodward, P. Part II: The explosive reaction . . . 767
- Posner, A. M., and Alexander, A. E. A new technique for the determination of dynamic surface tensions . . . 651
- Pullman, B. See *Berthier, G., and*  
 Raynor, G. V. The lattice spacings of substitutional solid solutions . . . 698
- Rees, A. L. G., and Stewart, K. The density of liquid arsine . . . 1028
- Richards, A. W. See *Eley, D. D., and*  
 Richards, R. B. See *Parks, W., and*  
 Richards, R. E., and Burton, W. R. Some applications of intensity measurements in the infra-red . . . 874
- Rivlin, R. S. The normal-stress coefficient in solutions of macromolecules . . . 739
- Roberts, J. S., and Skinner, H. A. Dissociation energies of carbon bonds and the resonance energies in hydrocarbon radicals . . . 339
- Robertson, A. J. B. The thermal decomposition of explosives. Part II . . . 85
- Robinson, R. A., and Stokes, R. H. Tables of osmotic and activity coefficients of electrolytes in aqueous solution at 25° . . . 612
- Rowlinson, J. S. The second virial coefficients of polar gases . . . 974
- Scanlan, J., and Warhurst, E. Some applications of the valence-bond method to problems of molecular structure. Part III: Calculations of the lengths of bonds in molecules which contain a polyvalent central atom . . . 1000
- Schallamach, G., and Thirion, P. Dielectric loss in swollen rubber . . . 605
- Schwab, G. M. Some new aspects of the strength of alloys . . . 385
- Shellard, A. D. See *Bradley, R. S., and*  
 Sheppard, N. The infra-red spectrum, and the assignment of the fundamental modes of vibration of thioacetate acid . . . 693
- Skinner, H. A. Bond dissociation energies in polyatomic molecules of the type  $MX_n$  . . . 20

- Skinner**, See *Carson, A. S., Hartley, K., and*  
 — See *Roberts, J. S., and*  
**Smith, G. S.** A new method of forming a liquid junction between electrode vessels in a thermostat . . . . . 752  
**Smith, J. W., and Cleverdon, D.** A new method for extrapolating dielectric polarization data to infinite dilution and recalculation of the apparent molecular polarization and dipole moment of nitrobenzene in various solvents . . . . . 109  
**Spencer, J. F.** See *Bedwell, M. E., Spencer, J. F., and Trew, V. C. G.*  
**Stainsby, G., and Alexander, A. E.** Studies of soap solutions. Part I: The fatty acid soaps and their hydrolysis in aqueous solutions . . . . . 585  
**Staveley, L. A. K., and Gupta, A. K.** A semi-micro low-temperature calorimeter, and a comparison of some thermodynamic properties of methyl alcohol and methyl deuterioxide . . . . . 50  
**Stewart, K.** See *Rees, A. L. G., and*  
**Stokes, R. H.** See *Robinson, R. A., and*  
**Szigeti, B.** Polarizability and dielectric constant of ionic crystals . . . . . 155  
**Szwarc, M.** See *Evans, M. G., and*  
**Thirion, P.** See *Schallamach, G., and*  
**Thomas, J. G. M.** See *Heal, H. G., and*  
**Thomas, N.** Structure and stability of burner flames . . . . . 781  
**Tolliday, J. D., Woods, E. F., and Hartung, E. J.** Studies in membrane permeability. Part V: Activation energy of diffusion and membrane potentials of potassium chloride through cupric ferrocyanide . . . . . 148  
**Tompa, H.** Statistical thermodynamics of mixtures of normal paraffins . . . . . 101  
 — Phase relationships in polymer solutions . . . . . 1142  
**Torkington, P.** The vibrational assignment for tetrachlorethylene and some remarks on the force constant of the C=C bond in that molecule . . . . . 445  
**Trew, V. C. G.** See *Bedwell, M. E., Spencer, J. F., and*  
**Tyrell, H. J. V., and Hollis, G. L.** Thermal diffusion potentials in non-isothermal electrolytic systems . . . . . 411  
**Uri, N.** See *Evans, M. G., and*  
 — See *Evans, M. G., Baxendale, J. H., and Uri, N.*  
**Valentine, L.** See *Burnett, G. M., Valentine, L., and Melville, H. W.*  
**Vickery, B. C., and Denbigh, K. G.** The polarizabilities of bonds. Part II: Bond refractions in the alkanes . . . . . 61  
**Waller, J. G.** See *Page, J. E., and*  
**Walsh, A. D.** The structures of ethylene oxide, cyclopropane and related molecules . . . . . 179  
 — The effect of aromatic compounds on the vapour phase oxidation of fuels. Part II: The anti-knock effect of aromatic compounds in engines . . . . . 1043  
 — See *Chamberlain, G. H. N., and*  
**Warhurst, E.** Some applications of the valence-bond method to problems of molecular structure. Part I: Calculations of the bond lengths of the hydrogen halides . . . . . 461  
 — Part II: Calculations of the effect of solvation on the force constants of bonds which possess partial ionic character . . . . . 476  
**Warhurst, E.** See *Scanlan, J., and*  
**Waters, W. A.** See *Derbyshire, D. H., and*  
**Wetterholm, A.** The effect of additives on electrode reactions. Part I: The variation of hydrogen overvoltage at various cathodes on the addition of ethyl alcohol, acetaldehyde and acetic acid . . . . . 861  
**Whalley, E., and Winter, E. R. S.** Diffusion phenomena in gases. Part II: The thermal diffusion of oxygen—Theoretical . . . . . 1091  
 — **Winter, E. R. S., and Briscoe, H. V. A.** Part I: The thermal diffusion of oxygen—Experimental . . . . . 1085  
**Wheatley, P. J.** See *Linnett, J. W., and*  
 — See *Linnett, J. W., Heath, D. F., and*  
 — and *Linnett, J. W.* Molecular force fields. Part XI: A wave-mechanical treatment of the change with distortion of the interaction energy of carbon  $2p\pi$  orbitals . . . . . 897  
 — The effect of pressure on the burning velocity of ethylene-air mixtures . . . . . 1152  
**Winter, E. R. S.** See *Whalley, E., and*  
 — See *Whalley, E., Winter, E. R. S., and Briscoe, H. V. A.*  
**Woods, E. F.** See *Tolliday, J. D., Woods, E. F., and Hartung, E. J.* . . . . . 1131

- Woodward, L. A., and Long, D. A.** Relative intensities in the Raman spectra of some group IV tetrahalides . . . . . 1131
- Woodward, P.** See *Pollard, F. H.*, and
- Wyatt, P. A. H.** See *Davies, C. W.*, and
- and **Davies, C. W.** Ionic reaction rates and the incomplete dissociation of salts. Part I: The bromoacetate-thiosulphate reaction . . . 774
- Wyatt, R. M. H.** See *Pollard, F. H.*, and

## INDEX TO REVIEWS—VOLUME XLV, 1949

- Advances in catalysis and related subjects.** Vol. I. Edited by W. G. Frankenburg, V. I. Komarkewsky, and E. K. Rideal . . . . . 1082
- Alexander, A. E., and Johnson, P.** Colloid science, Vol. I and II . . . . . 895
- Arkel, A. E. van.** Molecules and crystals in inorganic chemistry . . . . . 1171
- Bawn, C. E. H.** The chemistry of high polymers . . . . . 214
- Bjerrum, Niels.** Selected papers . . . . . 984
- Blair, G. W. Scott.** A survey of general and applied rheology . . . . . 987
- Bolen, Marjorie, and Weil, B. H.** Literature search on dry cell technology . . 304
- Bouma, P. J.** Physical aspects of colour . . . . . 603
- Brickwedde, F. G.** See *Woolley, H. W.*, *Scott, R. B.*, and
- Catalytic, photochemical, electrolytic reactions.** Technique of organic chemistry. Vol. II. Edited by Arnold Weissberger . . . . . 423
- Chemical Society, The.** Annual reports on the progress of chemistry for 1947 . 214
- Delory, G. E.** Photoelectric methods in clinical biochemistry . . . . . 1170
- Dewar, M. J. S.** The electronic theory of organic chemistry . . . . . 799
- Eistert, B.** *Chemismus und Konstitution.* Vol. I . . . . . 796
- Flagg, John F.** Organic reagents used in gravimetric and volumetric analysis (Chemical analysis, Vol. 4) . . . . . 500
- Fonda, G.** See *Seitz, F.*, and
- Frankenburg, W. G.** See *Advances in catalysis and related subjects*
- Fröhlich, H.** Theory of dielectrics, dielectric constant and dielectric loss . . 1084
- Glick, David.** Techniques of histo- and cyto-chemistry . . . . . 1083
- Henisch, H. K.** Metal rectifiers . . . . . 892
- Honeyman, John.** An introduction to the chemistry of carbohydrates . . . 215
- Hume-Rothery, W.** Electrons, atoms, metals and alloys . . . . . 303, 604
- Johnson, P.** See *Alexander, A. E.*, and
- Journal of the Electrodepositors' Technical Society,** Vol. XXII, 1946-1947 . . . . . 708
- Komarkewsky, V. I.** See *Advances in catalysis and related subjects*
- Laboratory and workshop notes.** Edited by Ruth Lang . . . . . 1083
- Lang, Ruth.** See *Laboratory and workshop notes*
- Lonsdale, K.** Crystals and X-rays . . . . . 1169
- Marton, L.** Advances in electronics. Vol. I . . . . . 891
- Merrington, A. C.** Viscometry . . . . . 1174
- Miller, A. R.** The theory of solutions of high polymers . . . . . 797
- — — The adsorption of gases on solids . . . . . 1168
- Mitchell, A. D.** British chemical nomenclature . . . . . 301
- Monomers: Section I.** Edited by E. R. Blout, W. P. Hohenstein and H. Mark . . . . . 1174
- Mott N. F., and Massey, H. S. W.** Theory of Atomic Collisions, 2nd Edn. . . 1173
- Nachod, F. C.** Ion exchange. Theory and application . . . . . 1080
- Perry, James W.** See *Schwartz, A. M.*, and
- Philosophical Magazine, The.** Natural philosophy through the eighteenth century and allied topics . . . . . 122
- Preparations and Characteristics of Solid Luminescent Materials.** Edited by F. Seitz, and G. Fonda . . . . . 1173
- Ramdohr, P.** Klockmann's Lehrbuch der Mineralogie . . . . . 986
- Rushbrooke, G. S.** Introduction to statistical mechanics . . . . . 894
- Rideal, E. K.** See *Advances in catalysis and related subjects*
- Scott, R. B.** See *Woolley, H. W.*, *Scott, R. B.*, and *Brickwedde, F. G.*

	PAGE
<b>Schwartz, A. M., and Perry, J. W.</b> Surface active agents . . . . .	893
<b>Seitz, F., and Fonda, G.</b> Preparations and characteristics of solid luminescent materials . . . . .	302
<b>Spectres Moleculaires, Les</b> (Centre National de la Recherche Scientifique, Paris, 1947) . . . . .	1081
<b>Symposium on internal stresses in metals and alloys</b> (Institute of Metals, 1948) . . . . .	603
<b>Tables of electric dipole moments</b> . . . . .	1172
<b>Tables of scattering functions for spherical particles</b> . . . . .	986
<b>Textile Institute, The.</b> Handbook of textile technology, No. 3. The identification of textile materials . . . . .	124
<b>Tolansky, S.</b> Multiple-beam interferometry of surfaces and films . . . . .	215
<b>Weil, B. H.</b> See <i>Bolen, Marjorie</i> , and	
<b>Weissberger, Arnold.</b> See <i>Catalytic, photochemical, electrolytic reactions</i>	
<b>Woolley, H. W., Scott, R. B., and Brickwedde, F. G.</b> Compilation of thermal properties of hydrogen in its various isotopic and ortho-para modifications . . . . .	795
<b>Wyckoff, R. W. G.</b> Crystal structures (first section). . . . .	300
<b>Zener, C. M.</b> Elasticity and anelasticity of metals . . . . .	602

## MINUTES OF THE 43RD ANNUAL GENERAL MEETING

Held on Friday, 23rd September, 1949, at The University, Reading.

The President, Sir John Lennard-Jones, F.R.S., was in the Chair.

1. The Minutes of the 42nd Annual General Meeting were taken as read and were confirmed.
2. ANNUAL REPORT AND STATEMENT OF ACCOUNTS.

In presenting the Annual Report for the year 1948 (Session 1948-49), the President referred to the great increase in the volume of publications. This showed the increasing importance of the Society, but with the additional cost of printing it had had serious repercussions on the financial side. Members were now receiving the monthly issues of the *Transactions* and two Discussion numbers a year at a cost to the Society of approximately 50s., apart from administration expenses, although their subscription had been maintained at 40s. Council had therefore, after long consideration, very reluctantly been compelled to recommend an increase in the annual subscription as from January 1950.

**MEMBERSHIP.** Fortunately there had been a substantial increase in membership. At the end of 1948 the total membership was 1783, and one could confidently anticipate that the 2000 mark would be reached at the end of 1949. There had also been a gratifying increase in the number of Junior Members, and the Society might justifiably feel that it was taking a great part in bringing to the attention of young scientists recent advances in physical chemistry.

The Hon. Treasurer was then asked to present his accounts for 1948.

**FINANCE.** In proposing the adoption of the Accounts, Dr. Slade drew the attention of Members to the fact that during the war it had not been possible to print all the papers received, and money had been saved. At the beginning of 1948 about £4500 was available for the cost of printing the back lag of accumulated papers. During 1948 this sum, together with an additional £75, had been spent for this purpose. Expenditure had been particularly heavy because the 1948 Accounts included the cost of printing the Reports of two General Discussions which had been held in 1947.

He was glad that it had been possible to delay increasing the Society's subscriptions for so long, but it was now inevitable. Some help in meeting the increased costs of publication had been received from the Chemical Council's fund for scientific societies, and he hoped that more would be forthcoming.

The Annual Report and Statement of Accounts were then unanimously adopted.

3. ELECTION OF COUNCIL.

The Officers and Members of Council were elected to take office on the 1st of October as follows:—

### *President*

PROF. SIR JOHN LENNARD-JONES, K.B.E., D.Sc., F.R.S.

### *Vice-Presidents who have held the Office of President*

PROF. N. V. SIDGWICK, Sc.D., D.Sc., F.R.S.

PROF. M. W. TRAVERS, D.Sc., F.R.S.

PROF. E. K. RIDEAL, M.B.E., D.Sc., F.R.S.

PROF. W. E. GARNER, C.B.E., D.Sc., F.R.S.

PROF. A. J. ALLMAND, D.Sc., F.R.S.



## 1196 MINUTES OF THE ANNUAL GENERAL MEETING

### *Vice-Presidents*

PROF. C. E. H. BAWN, PH.D.	G. GEE, SC.D.
R. P. BELL, M.A., F.R.S.	PROF. SIR CYRIL HINSHELWOOD, SC.D., F.R.S.
PROF. H. J. EMELÉUS, D.Sc., F.R.S.	G. S. HARTLEY, D.Sc.
PROF. M. G. EVANS, D.Sc., F.R.S.	

### *Hon. Treasurer*

O. H. WANSBROUGH-JONES, O.B.E., M.A., PH.D.

### *Chairman of the Publications Committee*

PROF. E. A. GUGGENHEIM, M.A., SC.D., F.R.S.

### *Ordinary Members of Council*

F. P. BOWDEN, SC.D., D.Sc., F.R.S.	W. G. PENNEY, O.B.E., D.Sc., F.R.S.
PROF. C. A. COULSON, M.A., PH.D., D.Sc.	PROF. J. T. RANDALL, D.Sc., F.INST.P., F.R.S.
J. FERGUSON, PH.D.	J. H. SCHULMAN, O.B.E., SC.D.
SIR CHARLES GOODEVE, O.B.E., D.Sc., F.R.S.	R. E. SLADE, D.Sc.
R. LESSING, PH.D.	H. W. THOMPSON, M.A., D.PHIL., F.R.S.

It was requested that Members be specifically reminded each year at the appropriate time that nominations for Officers and Members of Council should be sent to the Secretary.

- The thanks of the Society were accorded with acclamation to the retiring Members of Council, to Dr. Slade for his services during the past ten years, including the difficult and anxious years of war, to the Members of the Publications and Finance Committees and to all those who had refereed papers during the year.
- The Society's Auditors, Messrs. Knox, Cropper & Co., were re-appointed.

This concluded the business of the meeting.

## MINUTES OF A SPECIAL GENERAL MEETING

Held at The University, Reading, on the 23rd September, 1949, at the conclusion of the Annual General Meeting.

The notice convening the meeting having been read by the President, it was resolved to make the following addenda to the Rules of the Society :

### *Honorary Life Membership*

- ADDENDUM 1. The Council shall have the power to elect to Honorary Life Membership any of its Members who have rendered outstanding services to the Society and to Physical Chemistry. Such Members shall enjoy all the privileges of Membership under Rule 6. The total number of Honorary Life Members shall not at any time exceed ten.
- ADDENDUM 2. Rules 15 and 16 of the Rules of the Faraday Society shall be amended so as to effect an increase by 50 % of the subscriptions mentioned in these two Rules.





**L.A.R.1. 75**

INDIAN AGRICULTURAL RESEARCH  
INSTITUTE LIBRARY, NEW DELHI.

[illegible]